Lipids (2011) 46:1
DOI 10.1007/s11745-010-3505-1

ANNOUNCEMENT

Springer in the International Year of Chemistry 2011

As a leading international publisher in Chemistry, Springer enthusiastically supports the goals of the International Year of Chemistry 2011. The objectives of the IYC include enhancing the public appreciation of chemistry in meeting world needs and also celebrating the achievements of chemistry and its contribution to the well-being of mankind. As a step towards these objectives, Springer constantly develops innovative ways to bring information about chemistry and related sciences to a wide audience, not only of specialists in a given area, but also to researchers and teachers in other areas, students and others. Increasingly online media play the key part in worldwide dissemination of Springer's publications. Springer's online Chemistry and Materials Science package provides 24/7 access to 200 peer-reviewed journals and over 2,000 eBooks, with some 200 new eBook titles added per year. Additionally, Springer offers publications in the area of chemical and molecular sciences that are included in Springer's other eBook collections in areas such as life sciences, medicine, environment and energy. Overall, Springer currently offers over 2,000 online journals and 40,000 ebooks.

Springer has a range of new products to support students and young scientists.

- A newly launched book series "Lecture Notes in Chemistry" will make information at the forefront of research accessible to advanced students.
- Springer Theses, publishes exceptional theses from leading research institutions around the world, providing an international forum for outstanding young scientists at the start of their careers.
- Students and staff of institutions in North America and several European countries, that have purchased one or more Springer eBook collections, are now offered the opportunity to order their personal printed copy of an eBook at a fixed price of 24.95 USD/EUR. These so-called MyCopy books are black-and-white, paperback, print-on-demand books, and can be ordered directly from SpringerLink.

Through its extensive range of journals, books, reference works and databases, Springer plays a leading part in the broad dissemination of information on chemistry and its applications in all areas of human activity.

Ken Derham
Editorial Director Springer Chemistry

Marion Hertel
Executive Editor Springer Chemistry

Lipids (2011) 46:3–23
DOI 10.1007/s11745-010-3496-y

REVIEW

Oxidative Stability of Marine Phospholipids in the Liposomal Form and Their Applications

F. S. Henna Lu · N. S. Nielsen · M. Timm-Heinrich · C. Jacobsen

Received: 31 March 2010 / Accepted: 26 October 2010 / Published online: 19 November 2010

Abstract Marine phospholipids (MPL) have attracted a great deal of attention recently as they are considered to have a better bioavailability, a better resistance towards oxidation and a higher content of eicosapentaenoic (EPA) and docosahexaenoic acids (DHA) than oily triglycerides (fish oil) from the same source. Due to their tight intermolecular packing conformation at the *sn*-2 position and their synergism with α-tocopherol present in MPL extracts, they can form stable liposomes which are attractive ingredients for food or feed applications. However, MPL are still susceptible to oxidation as they contain large amounts polyunsaturated fatty acids and application of MPL in food and aquaculture industries is therefore a great challenge for researchers. Hence, knowledge on the oxidative stability of MPL and the behavior of MPL in food and feed systems is an important issue. For this reason, this review was undertaken to provide the industry and academia with an overview of (1) the stability of MPL in different forms and their potential as liposomal material, and (2) the current applications and future prospects of MPL in both food and aquaculture industries with special emphasis on MPL in the liposomal form.

F. S. Henna Lu · N. S. Nielsen · C. Jacobsen (✉)
Division of Seafood Research, Lipids and Oxidation Group, National Food Institute, Technical University of Denmark, Søltofts Plads, Building 221, 2800 Kgs, Lyngby, Denmark
e-mail: cja@food.dtu.dk

F. S. Henna Lu
e-mail: fshl@food.dtu.dk

M. Timm-Heinrich
BASF A/S, Production unit Ballerup, Malmparken 5, 2750 Ballerup, Denmark

Keywords Marine phospholipids · Antioxidants · n-3 PUFA · Eicosapentaenoic acid · Docosahexaenoic acid · Oxidative stability · *sn*-2 Position · Liposome · Food industry · Aquaculture industry

Abbreviations

AA	Arachidonic acid
BHT	Butylated hydroxytoluene
CHO	Cholesterol
CL	Cardiolipin
DAG	Diacyglycerols
DHA	Docosahexaenoic acid
DP	Diacetyl phosphate
EE	Encapsulation efficiency
EFA	Essential fatty acid
EPA	Eicosapentaenoic acid
LA	Linoleic Acid
LPC	Lysophosphatidylcholine
LUV	Large unilamellar vesicles
MLV	Multilamellar vesicles
MPL	Marine phospholipids
n-3 PUFA	Omega-3 polyunsaturated fatty acid(s)
PA	Palmitic acid
PC	Phosphatidylcholine(s)
PE	Phosphatidylethanolamine
PG	Phosphatidylglycerol
PI	Phosphatidylinositol
PL	Phospholipid(s)
PS	Phosphatidylserine
SA	Stearylamine
SPM	Sphingomyelin
TAG	Triacyglycerols
TL	Total lipids
NL	Neutral lipids

Introduction

The present imbalance in the intake of n-3 and n-6 polyunsaturated fatty acids (PUFA) has a serious negative impact on health in the general population [1–3] and there is a strong desire to improve the situation by introducing new products on the market with a higher level of n-3 PUFA and a lower level of n-6 PUFA. Currently, the global food and dietary supplement market for n-3 fatty acids (EPA and DHA) is estimated to be 15,000–20,000 tons, derived from a total world production of fish oil of approximately 300,000 tons per year. Marine phospholipids (MPL) from, e.g., krill represents an alternative source of n-3 PUFA, but the market for MPL is still in its infancy even though an increasing activity in this field has been observed recently [4]. A number of companies are preparing market introduction of either natural MPL, derivatives of natural MPL, or synthetic MPL. The leading MPL product on the market at the moment is a krill extract with approximately 35% PL [5]. There are also MPL products that are made from fish processing by-products and salmon roe. It is expected that the MPL market will follow the general trends of n-3 fish oils. MPL are new on the market and their range of applications has yet to be determined. However, MPL are believed to have potential applications in human and animal nutrition, in pharmacology, and in drug delivery. The most well-documented applications of MPL are related to liposomes. Liposomes made from MPL have been developed as a test system for antioxidants and as model systems for oxidation of biological membranes [6–9].

Many studies have been performed on n-3 triacyglycerols (TAG) enriched functional foods [10] while limited studies have been carried out on MPL enriched functional foods either in their pure form or in liposomal form. Furthermore, the current applications of phospholipid liposomes are limited to lecithin from soy bean or phosphatidylcholine (PC) from egg yolk and no attempts to use MPL based liposomes for food purposes have been reported in the literature [11–13]. However, some studies [14–19] have investigated the use of MPL such as herring roe or krill PL for larvae feed in the aquaculture industry. The limited application of MPL and liposomes in both food and aquaculture industries can be attributed to several reasons (1) lack of knowledge especially related to the behavior of MPL in food and feed systems, (2) limitations in large scale production of liposomes without using organic solvents and (3) the requirement of expensive equipment for liposome production. Nevertheless, there is ongoing research in this area [20–28]. With the growing understanding of the following areas regarding (1) the physicochemical properties of MPL, (2) the oxidative stability of MPL or MPL based liposomes under gastrointestinal condition and (3) emerging technologies for liposome production without using organic solvents such as microfluidization and pro-liposomes method [29], it may soon become feasible to use MPL in both the food and aquaculture industries. This review gives an overview of our current knowledge on the above mentioned aspects.

Classification and Sources of MPL

PL can be divided into three classes: glycerophospholipids, ether glycerolipids and sphingophospholipids. Glycerophospholipids represent the most widespread phospholipid class and they differ in their polar head groups. For example, phosphatidylcholine (PC) has choline as a head group, while phosphatidylethanolamine (PE) has ethanolamine as a head group, etc. as shown in Fig. 1. In addition, PL from different sources also have different fatty acid profiles in the *sn*-1 and *sn*-2 positions (Fig. 2a). Thereby, the chain length and degree of unsaturation may vary from source to source. For example, PL originating from plants such as soy bean do not have fatty acid chain lengths longer than 18 carbon atoms and contain only one to three double

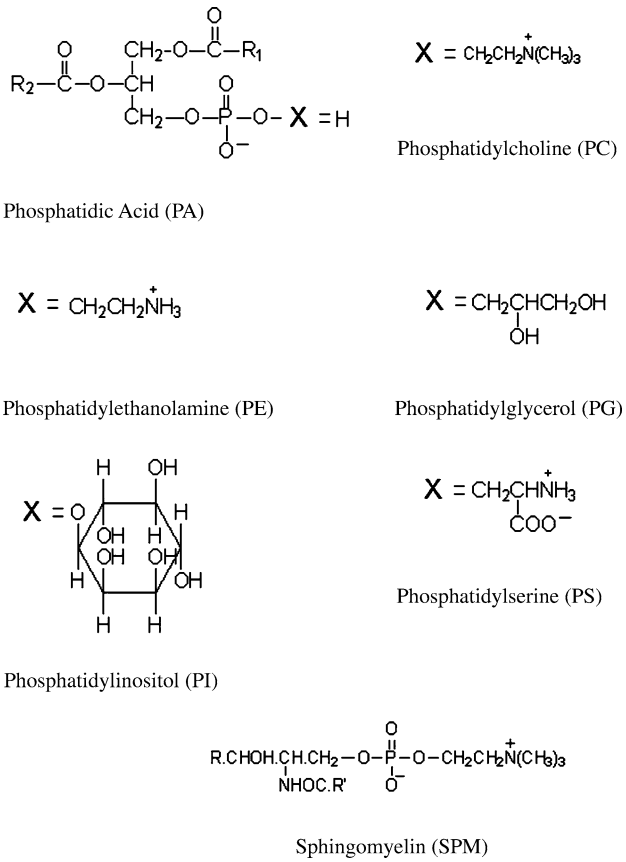

Fig. 1 Chemical structures of PL compounds with names and abbreviations

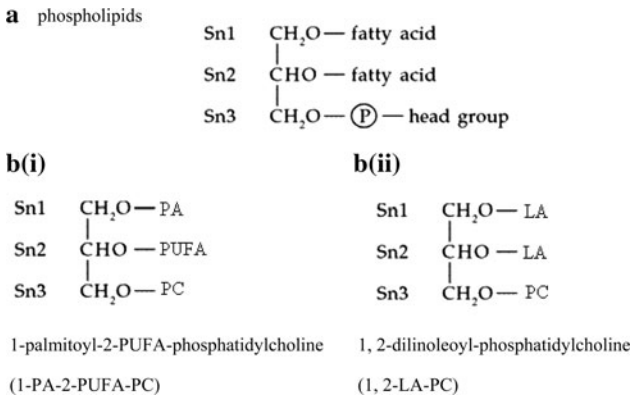

Fig. 2 **a** General structure of a phospholipid, **b** i) 1-palmitoyl-2-PUFA-phosphatidylcholine ii) 1,2-dilinoleoyl-phosphatidylcholine.

bonds, while PL originating from egg yolk or marine sources additionally have chain lengths of 20 and 22 carbon atoms with four to six double bonds e.g. as found in fatty acids of EPA and DHA. However, egg yolk only contains small amounts of EPA and DHA while marine sources are high in EPA and DHA. As far as marine sources are concerned, PL are found relatively abundant in roe, fish heads and offal such as viscera [30]. The most predominant PL in marine source such as salmon, tuna, rainbow trout and blue mackerel is phosphatidycholine (PC) as shown in Table 1. The second most abundant is phosphatidylethanolamine (PE). Phosphatidylinositol (PI), phosphatidylserine (PS), sphingomyelin (SPM) and lysophosphatidylcholine (LPC) are usually found in smaller amounts in marine sources, except for the relatively high level of sphingomyelin (SPM) found in tuna species [31–36]. Furthermore, krill such as *Euphausia superba* and *Euphausia pacifica* are other rich source of MPL [37, 38]. Almost half the lipid content of both types of krill is present in phospholipid form, mainly around 35% PC and 16% PE in *Euphausia superba* and 29% PC and 26% PE in *Euphausia pacifica*, respectively. Currently, Neptune Krill oil (a concentrate of MPL from *Euphausia superba*) is a leading commercial krill oil on the market.

Similar to the production of egg yolk PL, production of MPL in industry uses a combination of organic solvents such as hexane and acetone, isopropanol and ethanol for extraction of wet or dried biomass [36]. Non-polar solvents are used to extract TAG while polar solvents are used to extract PL. However, extraction of lipids using organic solvents may bring adverse health effects. Recently, a more promising method without using an organic solvent, supercritical fluid extraction (SFE) has been used for the extraction and fractionation of lipids [39–42]. The extraction can be carried out at low temperature by using CO_2. However, CO_2 can only extract neutral lipids from lipid mixtures, and a generally recognized as safe (GRAS) co-solvent such as ethanol must also be used to extract PL for the food industry. For instance, the addition of about 5–10% of ethanol to CO_2 is necessary to achieve the extraction of PL from egg yolk [42–44]. Additionally, krill oil has been extracted by a patented cold vacuum extraction process that can protect the biomass from exposure to heat, light or oxygen. Thereby, the oil is protected throughout the production process and the original nutrients of the krill are maintained intact.

Health Benefits of MPL

Many studies have shown that MPL are more efficient carriers of n-3 PUFA than TAG (normal fish oils) in terms of n-3 PUFA absorption in different tissues [45–47]. Thus, MPL not only contains more n-3 PUFA than TAG from the same source [31, 48, 49], but also provide better absorption in most tissues. This may be due to the amphiphilic properties of PL resulting in better water dispersability and

Table 1 Phospholipid composition (%) of marine sources

PL classes	Salmon head lipids	Rainbow trout fillet lipids	Bigeye muscle lipids	Bluefin muscle lipids	Bonito muscle lipids	Frigate muscle lipids	Skipjack muscle lipids	Yellowfin muscle lipids	Krill	Salmon roe
PC	54.7	53.6	42.1	42.2	53.9	47.4	51.5	37.9	87.5	86.0
PE	14.0	22.9	18.8	18.9	20.1	21.8	20.2	21.0	6.3	6.0
PI	2.5	8.3	5.8	6.7	2.3	10.9	4.9	8.5	0.5	2.0
PS	10.4	4.1	5.4	4.8	2.2	5.1	5.0	5.4	0.5	ND
SPM	8.3	4.9	3.3	5.6	7.6	3.0	0.5	4.0	1.3	2.0
LPC	1.4	ND	22.1	15.4	13.8	12.0	18.3	21.5	ND	2.0
Cardiolipin	ND	6.2	ND	ND	ND	ND	ND	ND	ND	ND
Other	ND	ND	4.4	6.6	Trace	1.7	1.5	2.8	3.9	1.0

Data compiled from references [5, 31–36]

PC phosphatidylcholine, *PE* phosphatidylethanolamine, *PI* phosphatidylinositol, *PS* phosphatidylserine, *SPM* sphingomyelin, *LPC* lysophosphatidylcholine, *ND* not determined

their greater reactivity towards phospholipases compared to the glycerolysis of triglycerides [49]. For this reason, supplementation of foods with n-3 PUFA rich PL has recently emerged as an interesting way of increasing the assimilation and thereby the health benefits of EPA and DHA. EPA and DHA have numerous well-documented health benefits, which have been reviewed extensively by Narayan et al. [50]. The more recent studies on these health benefits include a reduction of coronary heart diseases, inflammation, autoimmune diseases, hypertension, cancer, diabetes, susceptibility to mental illness and neurological diseases such as depression and Alzheimer's disease, as well as improved brain and eye functions in infants [51–59].

Apart from the benefits obtained from their favorable fatty acid composition, MPL may also provide health benefits due to their polar head groups [60, 61] or to a unique combination of the two in the same molecules. The latter explanation is supported by the following observations; the use of n-3 fatty acids (EPA and DHA) in PL form (either from marine or synthetic origin), instead of the triglyceride form, together with a vegetable oil containing n-6 fatty acids in a nutritive lipid emulsion, gave even lower blood triglyceride and cholesterol levels of patients as compared to the same amount of n-3 fatty acids given as fish oil [62]. The same observation was also obtained by Bunea et al. [63] who investigated the effect of krill oil (mainly present as PL) on hyperlipidemia. In addition, they reported that high doses of krill oil significantly reduced low-density lipoproteins (LDL) level and increased high-density lipoproteins (HDL). Their study concluded that krill oil was more effective at improving blood lipids and lipoproteins than fish oil. Apart from that, several studies have also shown that krill oil has many beneficial health effects such as it may has therapeutic value for metabolic syndrome, non-alcoholic fatty liver disease, attention deficit/hyperactivity deficit disorder (AD/HD), premenstrual syndrome (PMS) and it also showed anti-inflammatory effect [64–68]. Sampalis et al. [67] reported that phospholipid krill oil was more effective than triglyceride fish oil at improving both the physical and emotional symptoms of PMS while Deutsch [66] reported that the intake of krill oil at a daily dose of 300 mg can significantly inhibit inflammation and reduce arthritic symptoms within a short treatment period of 7 and 14 days. According to Maki et al. [64], 4 weeks of krill oil supplementation increased plasma EPA and DHA of overweight and obese men and women and was well tolerated without adverse effects on safety parameters. Besides that, Hayashi et al. [69] also showed that n-3 PUFA from salmon roe phosphatidylcholine may be beneficial in treatment of chronic liver diseases while Taylor et al. [70] showed that MPL is a promising new dietary approach to tumor-associated weight loss. Due to these numerous health benefits, there is an increasing desire to offer MPL containing n-3 PUFA to a wider market, e.g. for human foods and also to the general feed and aquaculture industry.

Introduction to Liposomes

Liposomes or lipid vesicles are aggregates formed from aqueous dispersions of amphiphylic molecules such as polar lipids that tend to produce bilayer structures [71]. They are useful microscopic carriers for nutrients and have a great potential for applications in both food and aquaculture industries. Besides that, liposomes have been recognized as a powerful tool in the treatment of diseases by the pharmaceutical industry. Their use as drug delivery vesicles and their medical applications such as in anticancer therapy, vaccination, gene therapy, and diagnostics have been reported in literature [72]. According to Watwe et al. [73], liposomes can be divided into three main classes: (a) multilamellar vesicles (MLV), contain more than a single bilayer membrane with a size range of 0.1–6.0 μm, (b) small unilamellar vesicles (SUV) and (c) large unilamellar vesicles (LUV) which both contain only a single bilayer membrane with sizes range of 0.02–0.05 μm and >0.06 μm, respectively. LUV are the most useful liposomes because they are more homogeneous than MLV and have higher encapsulation efficiency [74]. MPL or MPL based liposomes have obtained considerable attention and their oxidative stability has been studied extensively as shown in Table 2. Generally, MPL have been found to have a higher oxidative stability than TAG as will be discussed in the following.

Oxidative Stability of MPL

Mechanism of Oxidation for MPL

The PUFA chains in PL are the primary targets of oxidation. Similar to the oxidation of TAG, phospholipid oxidation may occur through radical and non-radical reactions involving enzymes such as lipoxygenase and myeloperoxidase or non-enzymatic systems such as ·OOH, ·OH, Fe^{2+}, Cu^{+} and radiation [75]. Due to the low dissociation energy of bisallylic carbon–hydrogen in double bonds of PUFA, a hydrogen atom can easily be removed. The first steps in the lipid peroxidation consist of hydrogen abstraction, rearrangement of double bonds and addition of triplet oxygen leading to highly reactive peroxyl radicals. These radicals can undergo a large variety of consecutive reactions including further reaction with other PL, fragmentation and generation of truncated PL and different

Table 2 Chemical and physical stability of MPL and MPL-based liposomes

Sources of phospholipids (PL)	Brief summary of findings	References
TL, NL and PL (from muscle of blue fish)	Antioxidant activity in salmon oil system supplemented with: 2.5% or 5% PL > 0.02% BHT 5% PL > 5% TL or 5% NL	King et al. [87]
Lipid fractions (from muscle, viscera and skin of sardine and mackerel fish)	Oxidative stability of lipid fractions: Muscle > viscera and skin Presence of higher PL (PE and PC) and α-Toc in muscle and synergistic effect of PE with α-Toc	Ohshima et al. [105]
Salmon roe PC, soybean PC	Oxidative stability of both PC in aqueous solution 1) Catalyzed by Fe^{2+}-ascorbic acid; salmon roe PC > soybean PC 2) Under influence of emulsifier: egg albumin > Tween 20 > deoxycholic acid sodium salt Reason: high stability of salmon roe PC is due to the conformation of PC molecule and the phase behavior of PC aggregation	Miyashita et al. [90]
Squid: muscle TL, viscera TL, eye TL; Tuna orbital TL, trout egg TL and bonito TAG	Oxidative stability of lipids fraction: Squid viscera TL or squid muscle TL > squid eye TL > trout egg TL > bonito TAG > tuna orbital TL Reason: higher stability is due to the presence of PL in squid tissue lipids and trout egg TL	Cho et al. [21]
DHA, PC, PE, TG	Oxidative stability of DHA in lipids: 1-DHA-2-palmitoyl-PE or 1-palmitoyl-2-DHA-PE or 1-DHA-2-palmitoyl-PC or 1-palmitoyl-2-DHA-PC > DHA + 1,2-palmitoyl-PC (1:1) > 1,2-diDHA-PC + 1,2-dipalmitoyl-PC (1: 1) or 1,2,3-triDHA-TAG DHA was most protected against oxidation when it was incorporated at one position of either PC or PE	Lyberg et al. [9]
Fish roes: salmon and herring, commercial fish oils: crude tuna oil and sardine oil	Oxidative stability of lipids Herring roe lipids > salmon roe lipids > commercial fish oils The higher oxidative stability is mainly due to the presence of PL in fish roe lipids and the synergistic effect of PL on the antioxidant activity of α-tocopherol	Moriya et al. [25]
Salmon roe PC, chicken egg PC and commercial soybean PC	Oxidative stability of PC in: a) Aqueous micelles: Salmon roe PC > chicken egg PC > soybean PC b) Liposomes: Chicken egg PC and salmon roe PC > soybean PC Reason: Higher stability is due to the presence of PUFAs in chicken egg PC and salmon roe PC which are esterified at the *sn*-2 position	Nara et al. [6]
Salmon roe PC, chicken egg PC and commercial soybean PC	Oxidative stability of liposomes containing DHA enriched TAG: Salmon roe PC > chicken egg PC and commercial soybean PC Addition of CHO; DP, SA, chicken egg albumin and Toc improved oxidative stability of salmon roe PC liposomes	Nara et al. [7]
68% PC, 23% PE, 2% PI, 2% PS and 1% SPM, 27% CHO and 4% TAG	Low pH led to an instantaneous vesicle aggregation of MPL-liposomes and shortened the release time of vitamin B1	Cansell et al. [20]
68% PC, 23% PE, 14% EPA, 31% DHA	MPL-liposomes exhibited relative high membrane physical and chemical stability in the gastric digestion condition indicating that MPL-liposomes could be used as oral administration vectors	Nacka et al. [28]
68% PC, 23% PE, 2% PI, 2% PS and 1% SPM	Acidification caused liposomes size and shape changes while maintaining the bilayer structure indicating that MPL-liposomes could be used as oral administration vectors	Nacka et al. [27]
68% PC, 23% PE, 14% EPA, 31% DHA	α-Toc uptake after oral delivery: MPL liposomes > sardine oil digestion Under gastrointestinal condition, α-Toc incorporation improved chemical stability of liposome suspension with best oxidative stability at (5 mol%)	Nacka et al. [26]

Table 2 continued

Sources of phospholipids (PL)	Brief summary of findings	References
Cod roe PL	Lipids oxidation is proportional to [Fe^{2+}] and [PL] but was dependent on pH with a maximum between pH 4 and 5 Addition of salt decreased the rate of lipid oxidation	Mozuraityte et al. [22]
Cod roe PL	Cations did not influence the rate of oxidation in ionic strength 0–0.14 M. Phosphate was more effective in reducing the oxidation rate than chloride. Salts and pH affected the zeta potential of the liposomes	Mozuraityte et al. [23]

TL total lipids, *NL* neutral lipids, *PL* phospholipids, *PC* phosphatidylcholine, *TAG* triacyglycerols, *PE* phosphatidylethanolamine, *CHO* cholesterol, *DP* diacetyl phosphate, *SA* stearylamine, *TOC* tocopherol

types of low molecular weight compounds such as aldehydes and ketones. However, enzymatic oxidation of PL can be eliminated in the MPL during their thermal production. Besides that, different PL oxidation products can be formed depending on the predominating oxidative process [76]. Oxidation products can be classified into three main categories such as: (1) long chain products that preserve the PL skeleton, and which may result from insertion of oxygen followed by rearrangement or cleavage of the PL hydroperoxides leading to epoxy, polyhydroxy, hydroxy, or keto derivatives of PL, (2) short-chain or truncated products, formed by cleavage of the unsaturated fatty acids. These products include ketones, aldehydes, unsaturated carboxylic acids, (keto)hydroxyl-aldehydes, (keto)hydroxyl-carboxylic acids, lyso-phospholipids and lyso-phospholipid halohydrins, and (3) adducts, formed by reaction between oxidation products and molecules containing nucleophilic groups, this include the products usually formed by cross-linking reactions between PL oxidation products with carbonyl groups and amino groups present in neighboring biomolecules such as peptides, proteins and phosphatidylethanolamine.

Dangers of Auto-Oxidation of MPL

Oxidation of MPL can not only deteriorate the quality of MPL enriched foods and affect the flavor, but also promote the development of neurodegenerative diseases. Many reported studies [75, 77–83] have shown that oxidized PL cause harmful effects to human health as they play physiopathological roles in developing diseases such as age-related and chronic diseases, acute lung injury, atherosclerosis, inflammation and decrease immune response. PL oxidation products such as hydroperoxyl, hydroxyl, aldehyde and epoxy groups that are potentially important in the progression of atherosclerosis and inflammation [80]. For instance, by activating the receptor for the platelet-activating factor (PAF), oxidized PL induce platelet aggregation [84–86]. Oxidized PL can also induce monocyte adhesion to endothelial cells, accumulate in atherosclerotic lesions, and play a role in inflammation and signaling inflammatory response. The dangers of the oxidized PL have been reviewed extensively and will not be further discussed in this review.

Antioxidant Effect of PL

King et al. [87] investigated the role of PL and the degree of fatty acid unsaturation on lipid oxidation in a salmon oil model system. Their findings showed that addition of a 2.5% (wt/wt) or a 5% (wt/wt) PL fraction extracted from bluefish to salmon oil increased its stability during heating at 55 and 180 °C as compared to the control salmon oil, or salmon oil to which 0.02% (wt/wt) of BHT or 5% (wt/wt) of other lipid fractions from bluefish such as total lipid or neutral lipid had been added. The PL fraction with 34% DHA was found to exhibit higher oxidative stability than other lipid fractions with 15% DHA. Subsequently, they investigated the antioxidant properties of individual PL in a salmon oil model system [88]. They found that nitrogen-containing PL such as PE, PC, LPC, and SPM were equally effective as antioxidants and they were more effective than PS, PG and PI. Their studies did not postulate any mechanism or reasons for the antioxidant properties of the different PL classes. In both studies by King and colleagues, the oxidative stability of the salmon oil model system was investigated through 2-thiobarbituric acids (TBARS) assay and the decreases in the ratio of DHA to PA (C22:6/C16:0). Boyd et al. [89] investigated the effect of 0.5% (by weight) PL toward lipid oxidation of 2.5 g salmon oil and menhaden oil model systems respectively, through the more sensitive headspace gas chromatographic analysis. Their study also showed that addition of PL significantly reduced the production of volatile compounds in both oil model systems.

Conformations of PUFA at the *sn*-2 Position of PL

Miyashita et al. [90] showed that salmon roe PC had a higher oxidative stability than soybean PC in an aqueous solution dispersed with chicken egg albumin although the degree of unsaturation in the salmon roe PC was higher

than in the soybean PC. They suggested that the high stability of salmon roe PC was mainly correlated with the conformation of the PC molecule and the phase behavior of PC aggregation. The main molecular species of soybean PC was 1,2-dilinoleoyl-phosphatidylcholine (1,2-diLA-PC), while for salmon roe PC it was 1-palmitoyl-2-PUFA-phosphatidylcholine (1-PA-2-PUFA-PC) as shown in Fig. 2b. Hence, the presence of this main molecular species in salmon roe PC (with most of the PUFA located at the *sn*-2 position of PC) may provide a more tightly packed molecular conformation as compared to the soybean PC and thereby increase resistance of PC towards oxidation. The findings of Miyashita et al. [90] corroborated the original work of Applegate and Glomset [91] who reported that DHA in the *sn*-2 position of diacylglycerol (DAG) containing a saturated acyl chain in the *sn*-1 position could form a tighter intermolecular packing conformation as will be further discussed below.

Conformations of DHA at the *sn*-2 Position in a DAG Model

Applegate and Glomset (1986) used a molecular modeling approach to search for conformations of DHA that might uniquely influence acyl chain packing in cell membranes. Their DHA conformations of lowest energy as shown in Fig. 3 were extended conformations in which six double bonds projected outward from the methylene axis (a) in two nearly perpendicular planes to form an extend angle-iron shaped structure or (b) at nearly 90° intervals to form a helical structure, respectively. Studies of packed arrays of these hexaenes with or without saturated hydrocarbons showed that tight packing arrangements were possible especially for angle iron-shaped molecules as a consequence of back-to-back, intermolecular contacts involving these chains. Applegate and Glomset [92, 93] further concluded that different unsaturated fatty acids at the *sn*-2 position of *sn*-1,2-diacylglycerols (DAG) may promote different packing and conformations. For instance, 1-stearoyl-2-DHA-DAG and 1-stearoyl-2-AA-DAG can assume a regular shape and tight packing while 1-stearoyl-2-oleoyl-DAG adopt a highly irregular shape and much looser packing. The simulations by Applegate and Glomset were done without reference to potential effects of polar headgroups, water of hydration and applied thermal energy. However, the molecular areas obtained for the model of DAG are in good agreement with that of the *sn*-2 polyunsaturated phosphoglycerides [94, 95]. This raises the possibility that corresponding natural phosphoglycerides may be able to pack closely together in monolayers and bilayers if their headgroups do not interfere. The findings of Applegate and Glomset were supported by Albrand et al. [96] who also agreed with the existence of the extended-helical conformations of DHA in PL. However, they also suggested several coiled conformations for DHA, tightly back-folded helical conformations with 1.2 and 1.5 spirals appearing to be the most stable as shown in Fig. 3.

More Recent Studies on the Conformation of PUFA at the *sn*-2 Position of PL

Nara et al. [6, 7] further compared the oxidative stability of PC from salmon roe, soybean and chicken egg in aqueous micelles and also in the form of liposomes with and without encapsulation of lipophilic substances. In aqueous

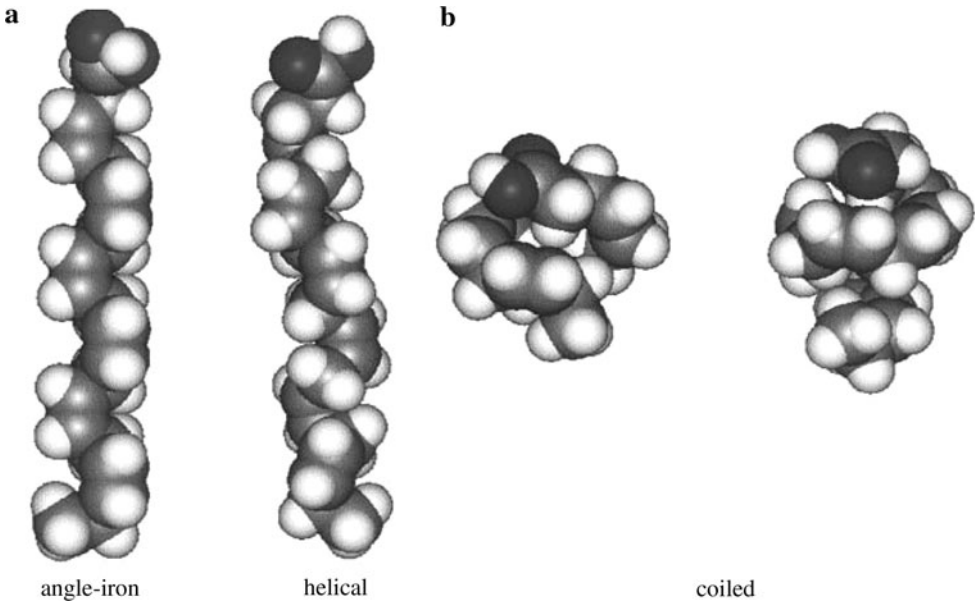

Fig. 3 Extended conformations of DHA in (**a**) angle-iron shaped and helical form, (**b**) coiled form

micelles, salmon roe PC was found to have the highest oxidative stability as evaluated by the highest content of un-oxidized PUFA, followed by chicken egg PC and soybean PC. Their findings are in agreement with the findings of Miyashita et al. [90]. No significant difference was found in oxidative stability between chicken egg PC and salmon roe PC when in the pure form of liposomes. However, for liposomes encapsulating with DHA enriched TAG resulted in the highest oxidative stability of both TAG and PC when salmon roe PC was used as the encapsulation material [7]. This unusual order of oxidative stability could be expected to be closely related to the conformation of PUFA at the *sn*-2 position in PC molecules as mentioned earlier [91]. Consequently, it is difficult for free radicals and oxygen to attack PUFA in bilayers of tighter conformation in salmon roe PC liposomes. Nara et al. [7] also suggested the possibility of using salmon egg PC as a liposomal material for the prevention of the oxidation of encapsulated fish oils.

Furthermore, Araseki et al. [8] also reported the characteristic oxidative stability of PC liposomes prepared from synthesized PC containing palmitic acid (PA), linoleic acid (LA), arachidonic acid (AA) and docosahexaenoic acid (DHA) in known positions. When the oxidative stability of 1-PA-2-LA-PC or 1-PA-2-AA-PC was compared with that of a 1:1 (mol ratio) mixture of 1,2-diPA-PC + 1,2-diLA-PC, or 1,2-diPA-PC + 1,2-diAA-PC respectively, the PC were more oxidatively stable than the latter corresponding PC mixtures in all oxidation systems despite the fact that the degree of unsaturation was the same in 1-PA-2-PUFA-PC and the corresponding mixture of PC. This was suggested to be due to the different conformation of PC bilayers which refer to the location of PUFA at the *sn*-2 position and the different rate of hydrogen abstraction by free radicals from intermolecular and intramolecular acyl groups. Their finding did not support a study by Lyberg et al. [9] who reported that the stability of DHA was improved independent of its position (*sn*-1 or *sn*-2) in PC or PE. Besides that, the more recent experiments and simulations [97–102] emphasized various degrees of flexibility of the DHA chain that gives looser packing of lipids bilayer. Their NMR analysis showed that the mobility of the hydrophobic part of the DHA molecule is higher than that of LA in liposome formation. These two competing views were portrayed in a review by Gawrish et al. [103]. However, according to Saiz and Klein [100], the flexibility of DHA chain conformation gives looser packing of the membrane at the lipid water interface and causes high water permeability. The presence of water molecules near DHA molecules lowers the density of the bisallylic hydrogen and inhibits the hydrogen abstraction from double bonds of PUFA during the propagation stage of autoxidation. As a conclusion, the higher water permeability of DHA and its specific conformation may be a reason for higher oxidative stability of DHA or other PUFA containing liposomes.

However, as compared to the study mentioned earlier by Miyashita et al. [90], contradictory results have also been reported by Monroig et al. [15, 16, 19] in their efforts to develop PUFA-rich liposomes for fish feed. They found that liposomes made from krill PL with 67% PC, 9% PE and a high content of PUFA showed lower oxidative stability as compared to liposomes made from soybean lecithin with 95% PC. The contradictory findings may be due to the different experimental conditions in the two studies, liposomes in model system versus liposomes in *Artemia* enrichment condition. In the model system, liposomes were formulated with pure PC containing fatty acid chains in known positions of the glycerol moiety and the oxidation was carried out in a very well-defined condition (temperature of 37 °C, in the dark and without agitation). On the contrary, the *Artemia* enrichment conditions were as follows: enrichment was carried out at 28 °C with strong aeration and 21 h of incubation.

Synergism Between PL and α-Tocopherol

Many studies have shown that the higher stability of PL may be due to the presence of antioxidants such as α-tocopherol in the PL mixture or synergistic effects of PL together with α-tocopherol [21, 25, 87, 88, 104–107]. The mechanism responsible for the synergy of tocopherols and PL is not very well understood. However, Hildebrand et al. [108] postulated that the mechanism involved in synergism of PE, PC and PI with tocopherol in the autoxidation of soybean oils were as follows: (1) amino groups of organic bases in PE and PC molecules and reducing sugar in the PI molecule facilitate hydrogen or electron donation to tocopherol and (2) these PL extend the antioxidant efficacy of tocopherol by delaying the irreversible oxidation of tocopherol to tocopherylquinone. Additionally, Saito et al. [106] reported that antioxidant activity of PL was found to be attributable not only to side chain amino groups such as choline and ethanolamine, but also to the hydroxyl group in the side chain.

Oshima et al. [105] studied the oxidative stability of sardine and mackerel lipids with respect to synergism between phospholipids and α-tocopherol. They investigated the oxidative stability of lipid fractions from different parts of sardine and mackerel; tissue from white and red muscles, viscera and skin of the fish. The oxidative stability was determined through the measured changes of the peroxide value (PV), fatty acid composition, α-tocopherol content and the oxygen uptake of lipids during an incubation period at 37 °C. Muscle lipids, which contain α-tocopherol and larger amounts of PL (PE and PC) than

other tissues, showed good oxidative stability despite their high content of PUFA. It was postulated that the synergistic effect of PE with α-tocopherol was the main reason for this phenomenon. Cho et al. [21] compared the oxidative stability of lipid fractions from marine organisms, squid muscle total lipids (TL), squid viscera TL, squid eye TL, tuna orbital TL, trout egg TL and bonito TAG. The fatty acid compositions, lipid classes, tocopherol contents and average number of bisallylic positions in each lipid fraction are shown in Table 3. Higher oxidative stabilities of three kinds of squid tissue TL and trout egg TL compared to those of bonito TAG and tuna orbital TL were observed as shown in Fig. 4. The authors suggested that the presence of PL in lipid fractions from squid tissue and trout egg was responsible for this increased oxidative stability. In addition, bonito TAG was found to be less susceptible to oxidation than tuna orbital TL and this could be due to the presence of a higher tocopherol content in bonito TAG.

Moriya et al. [25] compared the oxidative stability of fish roe lipids (salmon roe and herring roe) with that of lipids from commercial fish oils (crude tuna oil and crude sardine oil). As shown in Table 4, fish roe lipids contain higher levels of PL, EPA and DHA, and lower levels of tocopherol while lipids from commercial fish oils contain higher levels of TAG, tocopherol and lower EPA and DHA levels. Judging from these data, fish roe lipids were presumed to have lower oxidative stability. However, the opposite was observed as shown in Fig. 5 and it was proposed that the higher oxidative stability of fish roe lipids was mainly due to their high content of PL. It was also suggested that the synergistic effect of PL on the antioxidant activity of tocopherol was the main reason for this phenomenon. The higher oxidative stability of herring roe as compared to salmon roe was suggested to be due to synergism between PE and tocopherol. As shown in Table 4, the PE content in herring roe lipids was 6.6%, but there was no PE in salmon roe. Furthermore, herring roe also contained higher levels of PS and lysoPC than salmon roe and this may also have caused differences in their oxidative stability. The presence of antioxidants other than tocopherols in fish roe lipids such

Table 3 Composition of lipids from marine sources

Fatty acids (wt%)	Squid muscle TL	Squid viscera TL	Squid eye TL	Tuna orbital TL	Trout egg TL	Bonito TAG
14:0	2.1	4.4	0.9	2.9	3.6	3.3
16:0	32.7	15.9	23.2	17.0	10.7	16.3
18:0	4.4	2.9	5.6	3.0	3.0	4.1
18:1n-7	1.3	3.1	1.6	2.9	3.3	2.4
18:1n-9	1.3	8.7	0.2	23.8	15.8	13.8
20:1n-7	ND	2.8	ND	ND	1.7	ND
20:1n-9	2.5	4.2	3.4	1.8	1.8	0.9
18:2n-6	0.2	1.3	1.4	ND	1.1	3.6
18:3n-3	0.1	ND	0.2	ND	1.5	ND
20:3n-3	ND	ND	4.8	0.5	2.7	ND
20:4n-6	1.9	1.7	ND	2.0	0.7	ND
20:5n-3	10.6	12.3	15.1	4.8	18.4	0.6
22:6n-3	38.1	22.5	37.7	21.0	19.8	26.1
No. of bisallylic positions[a]	2.51	2.11	2.77	1.65	2.19	1.92
Lipid class (% of total lipids)						
Triacyglycerols	ND	95.5	ND	99.3	76.8	99.6
Free fatty acids	ND	ND	ND	0.4	ND	0.1
Glycolipids	ND	ND	6.8	ND	ND	ND
Sterols	23.7	0.7	28.3	ND	2.2	0.3
Phospholipids	75.6	3.8	66.4	0.2	23.1	ND
Tocopherol content (μg g^{-1} lipid)						
α-tocopherol	649.8	212.5	1198.8	541.3	215.5	253.4
β-tocopherol	ND	ND	ND	ND	ND	193.3
γ-tocopherol	ND	ND	ND	ND	ND	703.6
δ-tocopherol	ND	ND	9.2	ND	9.2	496.3
Total tocopherol	649.8	212.5	1208.0	541.3	215.5	1646.6

Data from reference [21]

ND not detected

[a] Per one fatty acid molecule

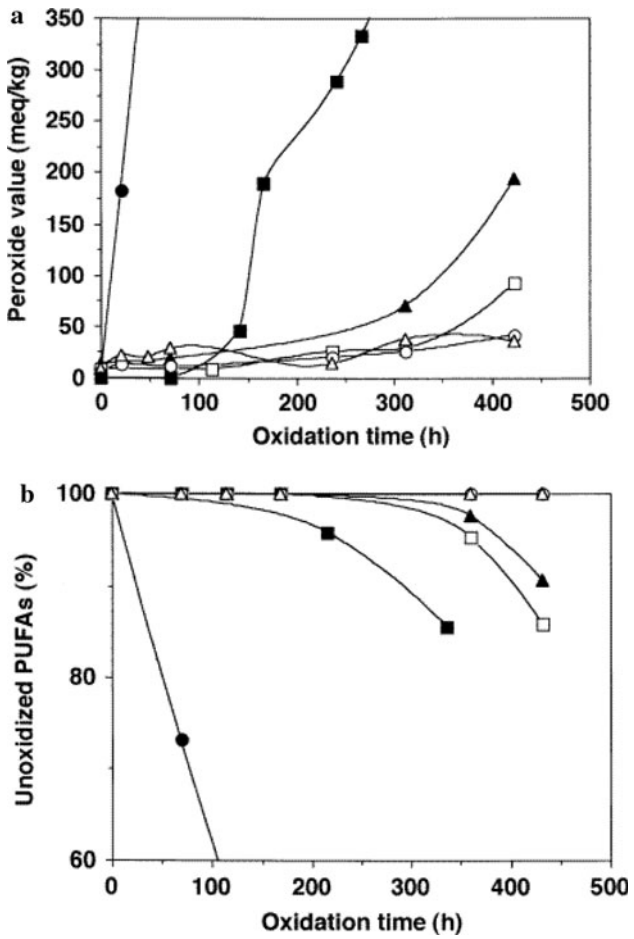

Fig. 4 **a** Changes in the peroxide value (PV) and **b** unoxidized PUFA in lipids from marine organisms during auto-oxidation at 37 °C. (*open triangle*) Squid viscera total lipids (TL); (*open circle*) squid muscle TL; (*open square*) squid eye TL; (*filled circle*) tuna orbital TL; (*filled triangle*) trout egg TL; (*filled square*) bonito oil. Reproduced from Cho et al. [18] with permission from John Wiley & Sons Ltd

as astaxanthin, coenzyme Q10 and lutein might contribute to this extraordinary stability as well.

Other studies [104, 107, 109] reported that the synergistic effect of PE with α-tocopherol was higher than that of PC. Bandarra et al. [104] investigated the antioxidant synergy of α-tocopherol (0.04%) with several PL fractions (0.5%) such as PE, PC and cardiolipin (CL) in a refined sardine oil model system. Their results showed that PC was the most effective individual antioxidant when it was compared to PE, CL and α-tocopherol while PE provided the highest synergistic effect with α-tocopherol. Higher synergism of PE as compared with that of PC could be due to the easier hydrogen transfer from the amino group of PE to tocopheroxyl radical and regeneration of tocopherol or the secondary antioxidant action of PE in reducing quinones formed during oxidation of tocopherols [109]. Since MPL may contribute to better oxidative stability than marine TAG, it can be expected that enrichment of foods or food emulsions with MPL could lead to n-3 PUFA enriched foods that have better oxidative stability than foods enriched with n-3 TAG.

Stability of MPL Based Liposomes Under Gastrointestinal Conditions

MPL based liposomes were designed with the purpose of increasing the PUFA bioavailability and also to protect entrapped compounds from digestive degradation. However, liposome characterization with respect to vesicle composition and membrane integrity under various gastrointestinal conditions are needed before considering liposomes as a useful oral dosage form. Many studies have shown that MPL liposomes could be used as an oral administration vector [6, 7, 20, 26–28]. This is because bilayer structures of MPL based liposomes were still maintained even under acid stress or gastrointestinal conditions despite of slight morphological modifications. Nacka et al. [28] investigated the in vitro behavior of MPL based liposomes under the influence of pH from 1.5–2.5 (stomach) to 7.4 (intestine) at physiological temperature (37 °C) in the presence of bile salts and phospholipase A_2 (Table 2). Their study showed that acidification induced instantaneous vesicle aggregation of MPL based-liposomes, which was partially reversed when the external medium was neutralized. Acidification also caused a complex morphological bilayer rearrangement and led to the formation of small aggregates. Nevertheless, Nacka et al. [27, 28] reported that the pH and temperature dependent structural rearrangement is mainly due to the osmotic shock and chemical lipid alterations such as oxidation and hydrolysis. Hydrolysis of the liposomes was amplified under the influence of an acid medium and high temperatures (Table 2).

Cansell et al. [20] investigated the physical stability of MPL-based liposomes containing vitamin B1 under acidic conditions simulating the stomach conditions. Encapsulation of vitamin B1 in the liposomes was carried out through passive encapsulation and active loading methods. They observed that vitamin B1 was totally released from liposomes after 24 h storage in a neutral medium and the time of release was shortened to 1 h in acidic condition (pH 1.5). According to their study, this liposome instability could result from the external medium osmolarity that forced water to flow out of the liposomes and simultaneously dragged vitamin B1 molecules through the bilayer. Furthermore, protons may also destabilize the lipid membrane by their interaction with PL via structural membrane rearrangement as previously mentioned. However, their study also proved that addition of xanthan gum improved the encapsulation efficiency and also the retention of vitamin B1 in liposomes regardless of the encapsulation

Table 4 Composition of marine lipids used for oxidation

Lipid class (% of total lipids)	Crude tuna oil	Crude sardine oil	Salmon roe	Herring roe
Triacyglycerols	99.6	99.8	71.8	9.3
Free fatty acids	0.1	0.2	ND	3.8
Phospholipids	ND	ND	23.1	73.6
Sterols + monoacylglycerols	0.3	ND	7.2	12.3
% of phospholipids				
PC	ND	ND	97.0	72.3
PE	ND	ND	ND	6.6
PS	ND	ND	2.6	8.7
LysoPC	ND	ND	ND	11.8
Fatty acid profiles				
14:0	3.3	4.1	3.6	2.1
16:0	16.3	8.0	10.7	25.8
18:0	4.1	1.4	3.0	2.2
18:1n-7	2.4	2.0	3.3	5.1
18:1n-9	13.8	10.9	15.8	13.2
20:4n-6	–	1.3	0.7	1.0
20:5n-3 (EPA)	0.6	21.8	18.4	14.4
22:6n-3 (DHA)	26.1	13.7	19.8	21.6
EPA + DHA	26.7	35.5	38.2	36.0
Tocopherol content (μg g^{-1} lipid)				
α-tocopherol	253.4	60.2	19.6	22.9
β-tocopherol	193.3	45.7	214.1	258.0
γ-tocopherol	703.6	376.7	11.6	7.7
δ-tocopherol	496.3	2670.9	11.3	11.5
Total tocopherol	1472.6	3153.5	256.6	300.1
Other antioxidants (μg g^{-1} lipid)				
Astaxanthin	ND	ND	156	ND
Coenzyme Q10	ND	ND	24	100
Lutein	ND	ND	ND	6.4

Data from reference [25]

ND not determined, *LysoPC* lysophosphatidylcholine, *PE* phosphatidylethanolamine, *PL* phospholipids, *PS* phosphatidylserine

method used. They suggested that this increase is due to the adsorption of hydrocolloid to the outer surface of the liposomes that not only trapped part of the external vitamin but also formed a strong xanthan gum coating around the liposome surface. They postulated that this coating resulted from strong lipid–hydrocolloid interactions occurring during the centrifugation steps of liposome preparation.

The Effect of Lamellarity, pH, Temperature, Ionic Strength, Presence of Pro-oxidants and Chelators on MPL-Based Liposomes' Stability

Chemical and physical stability of liposomes are closely related to the mechanical strength and lipid bilayer conformation. Strong and well-packed lipid bilayers or multilamellar layers can protect the entrapped substance, decrease the changes of size distribution, fusion or other changes in the mechanical properties of lipid bilayers. For this reason, factors such as lamellarity, pH, temperature, ionic strength, dissolved oxygen content within the formulation, the presence of antioxidants and chelators are believed to affect mechanical properties of lipid bilayers and thereby affect the physical and chemical stability of MPL-based liposomal products [22, 23].

Nacka et al. [27] showed that the sensitivity of MPL based liposomes towards harsh condition such as acidic condition depends on their size and lamellarity (Table 2). They found that filtered liposomes with higher lamellarity and a protective effect against aggregation showed a slower size rearrangement. This finding supported a study by Monroig et al. [19] who, in addition, reported that liposomes with multilamellar vesicles seem to be more suitable than liposomes with unilamellar vesicles in the encapsulation of free methionine. They found that methionine dissolved in the more internal intermembrane spaces of multilamellar liposomes would remain encapsulated, whereas methionine from the aqueous compartments located between the more outer membranes would leak out

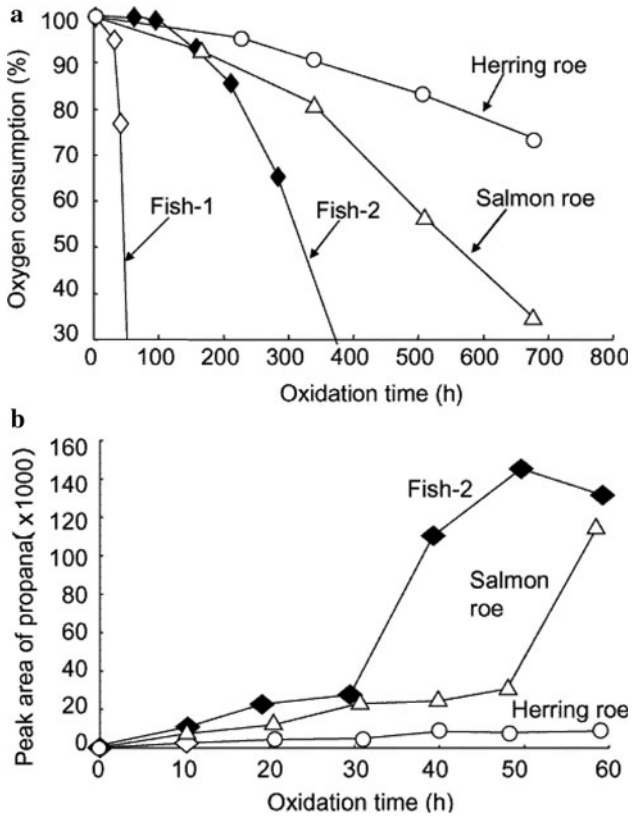

Fig. 5 **a** Oxygen consumption during the oxidation of fish lipids at 37 °C in the dark. (*open diamond*) fish-1; (*filled diamond*) fish-2; (*open triangle*) salmon roe lipids; (*open circle*) herring roe lipids. **b** Propanal formation during the oxidation of fish lipids at 37 °C in the dark. (*filled diamond*) fish-2; (*open triangle*) salmon roe lipids; (*open circle*) herring roe lipids. Reproduced from Moriya et al. [22] with permission from John Wiley & Sons Ltd.

into the external medium when the liposomes were subjected to harsh conditions. However, this result contradicts another study by this group [15] where unilamellar liposomes were found to be more stable than multilamellar liposomes. The apparent discrepancy in these two studies is probably due to different experimental conditions and materials used for the liposomes preparation.

Mozuraityte et al. [22] examined the lipid oxidation rate of liposomes made from cod PL under influence of factors such as the temperature, the amount of added Fe^{2+}, the lipid concentration, pH, the concentration of NaCl, and the dissolved oxygen. Their study showed that the rate of lipid oxidation was proportional to the iron and lipid concentrations. Furthermore, lipid oxidation was dependent on pH, with a maximum observed between pH 4 and 5. Addition of NaCl decreased the rate of lipid oxidation. However, contradictory results were reported in another study [110] which showed that addition of NaCl had no effect or even increased iron-catalyzed oxidation of a sodium dodecyl sulfate-stabilized salmon oil emulsion.

Mozuraityte et al. [23] examined the effect of zeta potential on the lipid oxidation rate of liposomes made from cod PL under the influence of pH and different cations such as Na^+, K^+, Ca^+, Mg^+ and anions such as $H_2PO_4^-$ and Cl^- (Table 2). Their data showed that cations did not influence the rate of oxidation in the tested range of the ionic strength from 0 to 0.14 M whereas the opposite was the case for anions. Both phosphate and chlorides have an additive antioxidative effect on the oxidation in liposomes. Phosphate was shown to be more effective in reducing the oxidation rate than chloride. The inhibition of Fe^{2+} induced oxidation of liposomes by phosphate might be due to the phosphate chelation of iron [111, 112]. Furthermore, they also concluded that addition of salts and changes in pH affected the zeta potential of the liposomes. However, absolute values of the zeta potential alone cannot be used to predict oxidation rates.

Improvement of MPL Based Liposomes' Oxidative Stability

Many studies have been conducted to improve the oxidative stability of liposomes. Most of the studies focus on the use of cholesterol in improving the oxidative stability of liposomes [12, 113–115]. For example, a study conducted by Nara et al. [7] showed that addition of cholesterol and ingredients such as diacetyl phosphate (DP) and stearylamine (SA) improved the oxidative stability of salmon roe PC liposomes. Furthermore, in the effort of developing liposomes as feed supplement in larva culture. Monroig et al. [15] also showed that addition of cholesterol to liposomes made from krill PL or 1,2-PA-PC or soy PC improved the oxidative stability of the liposomes. Cholesterol has a condensing effect on the PC bilayer arrangement over its phase transition temperature and thus improves the physical stabilization of PC liposomes [116]. Addition of cholesterol can increase the rigidity of 'fluid state' liposomal bilayers and the retention of entrapped hydrophilic substances [117]. It counteracts lipids phase transition and increases resistance to in vivo liposomes degradation [118–120]. An interaction mechanism between bilayer forming PL and cholesterol has been proposed. This is due to the formation of hydrogen bonds between the three hydroxyl group of cholesterol and fatty acyl esters of PL at both *sn*-1 and *sn*-2 positions [121, 122]. These physico-chemical effects of cholesterol on liposomes may contribute to the increased oxidative stability in liposomes with cholesterol.

α-Tocopherol is widely known for its antioxidative effect [123]. However addition of high concentrations of α-tocopherol may also cause prooxidative effects [124, 125]. The most effective concentration of α-tocopherol in the prevention of lipid oxidation in salmon roe PC liposome

suspensions was 0.25 μM in a study conducted by Nara et al. [7]. Nacka et al. [26] investigated the most efficient amount of α-tocopherol for liposomes incorporation under gastrointestinal-like conditions. Their findings showed that the best oxidative stability was obtained for liposomes that were prepared at a ratio of 5 mol% of α-tocopherol of the total marine lipids. This concentration of α-tocopherol produced liposomes with the lowest concentration of propanal as an oxidation product of n-3 PUFA and required the longest time of oxidation induction phase. They also found that incorporation of α-tocopherol induced liposome structural modifications, evidenced by turbidity and the production of lysophospholipids from PL chemical hydrolysis.

Nara et al. [6, 7] investigated the effect of addition of diacetyl phosphate (DP), stearylamine (SA) and chicken egg albumin, and soybean protein on improving the oxidative stability of MPL based-liposomes. DP and SA give a negative or positive charge to the liposomes respectively and thus protect the liposomes from aggregation. An improved oxidative stability of liposomes after addition of this ingredient was observed and suggested that it was due to the physical stabilization of the PC liposomes. Furthermore, added proteins such as chicken egg albumin and soybean protein improved the oxidative stability of liposomes by protecting the PC bilayer from the attack of free radicals. Proteins have the ability to absorb at PC–water interfaces and this adsorption of proteins would closely relate to its antioxidant activity [6]. However, albumin acted as a more effective inhibitor of the oxidation of PC containing DHA than PC containing LA [90].

Determination of Oxidation Products from MPL

As discussed above MPL has been found to exert antioxidative effects toward lipids oxidation. However, many of the lipid oxidation studies [6–8, 21, 90, 105] were performed using simple analyses such as TBARS, PV, determination of the un-oxidized lipids (PUFAs) content through gas chromatography, or determination of only one secondary volatile compound, propanal (as a marker of n-3 PUFA oxidation) by headspace GC–MS analysis [25], etc. In many of these oxidative stability studies, there is a lack of determination of the entire spectrum of volatile oxidation products or identification of specific oxidation products which are responsible for sensory off-flavors of the marine lipids. Furthermore, there are no studies providing the sensory data or statistical correlation between instrumental analysis and sensory data for oxidation of MPL. These data are particularly important in the studies of MPL for foods enrichment and additional studies in this area are clearly needed. Due to the low odor threshold, the presence of volatile secondary oxidation products, even at low concentrations, can significantly decrease the sensory quality of marine lipids or marine lipids containing foods.

In the recent years, the oxidation products of PL have attracted intensive research interest due to their biological functions in human pathophysiology. Similar to other lipids such as TAG, many methods can be used to study the oxidation of PUFA containing PL such as (1) measurement of lipid hydroperoxides through spectrophotometric determination of PV or conjugated dienes (CD). Lipid hydroperoxides may also be determined by sample derivatization followed by HPLC with chemiluminescence detection, (2) measurement of breakdown products of hydroperoxides, such as the aldehydes, malondialdehyde, etc. through anisidine value (AV), 2-thiobarbituric acid value (TBARS), etc., (3) measurement of secondary volatile compounds through more sensitive instrumental methods such as GC–MS, (4) measurement of long chain oxidation derivatives of PL through MS. Electrospray ionization (ESI) is gaining in popularity in this area nowadays for this purpose [76]. ESI is a soft ionization technique that does not cause fragmentation and allows detection of intact PL classes without sample derivatization. ESI can readily be coupled to reverse phase LC and allow the analysis of oxidized PL [126–129]. Interfacing reverse phase LC to ESI–MS has the advantage as oxidized PL elutes earlier than their native counterparts due to their higher hydrophilicity. Spickett et al. [127] used the positive ion ESI–MS for detection of hydroperoxide in PC vesicles after treatment with *tert*-butylhydroperoxide and Fe^{2+} while Yin et al. [129] used ultra performance liquid chromatography (UPLC) coupled with negative ion electrospray ion trap MS to identify the intact oxidation products of glycerophospholipids in vitro and in vivo such as hydroxyeicosatetraenoates (HETE) and isoprostanes (IsoP). Other soft ionization methods include matrix-assisted laser desorption ionization (MALDI) and tandem mass spectrometry (MS/MS). As a conclusion, the future direction for research and development could focus on the investigation of oxidative stability for MPL by using advanced MS analysis.

Potential of MPL as Liposomal Material

A variety of liposome preparation methods are available nowadays ranging from traditional methods using solvent extraction such as thin film hydration, detergent dialysis, reverse-phase evaporation, etc. to emerging technologies without using an organic solvent such as pro-liposome, supercritical fluid extraction, and microfluidization. Each method has its own advantages and drawbacks as reviewed by Taylor et al. [130]. Among these technologies, pro-liposome and microfluidization are recommended to produce liposomes for food applications. Pro-liposome is a

simple method for mass production of liposomes without using large amounts of energy, solvents and complex equipment. This method is based on the idea that addition of water to an appropriate mixture of ingredients leads to the spontaneous formation of liposomes [29]. On the other hand, microfluidization is a method using a microfluidizer (a high pressure homogenizer) that can rapidly produce large volumes of liposomes in a continuous and reproducible manner. The average size of the liposomes can be adjusted through this technology and the solutes to be encapsulated are not exposed to sonication, detergents or organic solvents. Furthermore, this technology enables the production of stable liposomes with high encapsulation efficiency [74]. Recently, Thompson et al. [131–133] used a microfluidization technique to produce liposomes from milk fat globule membrane PL in the food industry. Studies showed that liposomes prepared via microfluidization have high encapsulation efficiencies, smaller size, a narrower size distribution and a higher proportion of unilamellar vesicles as compared to methods such as thin film hydration. PL from soybean and egg yolk, either in purified form, crude form or hydrogenated form are widely used for liposome production in both the food and aquaculture industries. The use of MPL-based liposomes has gained attention recently in the aquaculture industry and there is much ongoing research in this area as shown in Table 5. Several studies have shown the use of MPL such as herring roe or krill PL for larvae feed in the aquaculture industry [14–19] but no attempts to use MPL based liposomes for food purposes have been reported in the literature so far.

One potential advantage of using MPL-based liposomes for food application is that they may provide better bioavailability of encapsulated nutrients [26, 134, 135] as compared to TAG. Nacka et al. [26] showed that MPL-based liposomes facilitated α-tocopherol uptake after oral delivery as compared to sardine oil digestion. Furthermore, Hossain et al. [136] also showed that MPL-based PC liposomes (squid PC and starfish PC) enhanced the permeability, transportation and uptake of PL in Caco-2-cells. It is also known that the fluidity of liposomes increases with increasing contents of highly unsaturated PUFA such as AA and DHA, showing the advantage of PC containing AA or DHA for use in drug or nutrient delivery systems [100, 101].

Application of PL Liposomes in the Food Industry

The uses of liposomes in the food industry can be summarized as follows (1) use of liposomes to encapsulate food ingredients in order to provide better protection or to hide the bitter taste of entrapped substances and (2) use of liposomes to control the delivery of functional components by delaying the release of the encapsulated materials. Liposomes have been used to entrap thermally sensitive compounds such as vitamins, enzymes, flavorings, PUFA from fish oils, antimicrobial peptides (lysozyme, nisin) and other nutrients [13, 137–144]. Hydrophilic substances can be entrapped in the internal water core of the liposomes while lipophilic compounds can be efficiently enclosed in the PL bilayer at the same time through a pro-liposomes approach [29]. For this reason, liposomes can be used for the formulation of functional foods or drinks such as energy drinks, sport drinks, fortified milk, etc. Arnaud et al. [145] reported that PC from egg or soybean has been used in development of liposome-based functional drinks. With the use of PC-based liposomes in food industry, consumers not only benefit from the health benefits of water soluble nutrients that are entrapped in the liposomes but also benefit from the nutritional benefits of PL in liposomes. In the production of cheese, PL liposomes may be used to delay the release of encapsulated proteinases [146, 147] or to protect encapsulated enzyme such as protease and lipases with the purpose of improving the texture and sensory properties of cheese [148–152]. Liposomes have also been used to encapsulate vitamin D with the purpose of increasing the vitamin D content of cheese [153].

Application of PL Liposomes in the Aquaculture Industry

Besides food incorporation, recent studies have also indicated that liposomes rich in n-3 PUFA can offer a range of benefits when used for fish larvae feed. Due to the high consumer demand and limited natural stocks of fish species such as salmon, trout and eel, much effort has recently been spent by researchers on developing cost effective aquaculture methods for farming such species. Generally, the main problems faced by aquaculture industry are low survival rate of the hatched fish larvae of the farmed species and the difficulty in supplying live prey organisms which provide nutritionally adequate feed for these larvae. Live prey such as Rotifers *Brachionus plicatilis* and *Artemia* nauplii provide adequate amounts of protein and energy. However, they do not provide lipid profiles that cover the requirements for EPA and DHA, which are essential for optimum survival, growth and development of larvae [154–157]. Thus, to provide prey organisms with such a composition of n-3 PUFA, it is necessary to cultivate these organisms in the presence of enrichment products with high EPA and DHA contents, preferably in an easily digestible, highly bio available form, such as MPL. During the enrichment process, enrichment products are passively filtered by *Artemia* nauplii and their digestive tract becomes loaded with these enrichment products. A wide

Table 5 Application of liposomes in the aquaculture industry

Sources of liposomes	Brief summary of findings			References
Purified PC, CHO, PG, menhaden oil	It is feasible to use liposomes for *Artemia* nauplii enrichment with PL and free amino acids such as glycine, liposomes were readily ingested and assimilated by *Artemia* nauplii as indicated by ^{14}C-glycine and ^{14}C-PC			Ozkizilcik and Chu [169]
1,2-PA-PC, egg PC, bovine brain PS	It is feasible to use liposomes in aquaculture as a delivery system through *Artemia* nauplii. PUFA rich liposomes were stable at least for 3 days at room temperature without agitation and freeze drying could stabilize liposomes for long term storage			Hontoria et al. [170]
PE, CHO, Toc	It is feasible to use liposomes as a delivery system of water soluble antibiotics, oxytetracycline for marine larvae			Touraki et al. [167]
1,2-PA-PC, herring roe PC, CHO	*Artemia* nauplii enrichment with MPL emulsion or MPL-liposomes significantly increased:			McEvoy et al. [165]
	DHA level (% of TL)	DHA:EPA ratio:	Polar lipids content:	
	PT (14%) > SS (6.3%) > L (2%)	PT (1.8) > SS (0.4) > L(0.3)	L (40.1 mg g^{-1}) > PT (32.4 mg g^{-1}) = SS (34.7 mg g^{-1})	
Egg yolk lecithin (60%PC), CHO	Consumption rate of liposomes in gilthead seabream (*Sparus aurata*) and white grouper (*Epinephelus aenaeus*) larvae:			Koven et al. [163]
	Liposomes containing CFE (238.5 ng liposome $larva^{-1}$ n^{-1}) > liposomes containing PHS (54.3 ng liposome $larva^{-1}$ n^{-1})			
	It is feasible to use liposomes as a nutrient supplement in first feeding marine fish larvae			
Crude egg yolk PC (>60%)	Content of methionine in *Artemia* nauplii after different enrichment methods:			Tonheim et al. [168]
Purified egg yolk PC (> 99%), CHO	Purified egg PC liposomes > crude egg PC liposomes > direct enrichment with free methinone > unenriched control			
1,2-PA-PC, Krill PL, soy PC, CHO	Oxidative stability of formulated liposomes:			Monroig et al. [15]
	(100%)Soy PC > (100%)Krill PL			
	(40%)1,2-PA-PC (40%)Krill PL(20%)CHO > (80%)Krill PL(20%)CHO			
	LUV > MLV			
	Addition of CHO improved oxidative stability			
Krill PL (mainly PC, PE)	EFA bioencapsulation depends on methods preparation and structure of vesicles:			Monroig et al. [18]
	LUV detergent > LUV extrusion > MLV extrusion			
Krill PL (mainly PC, PE)	Maximal bioencapsulation is achieved:			Monroig et al. [17]
	Nauplii densities: 300 nauplii ml^{-1}, number of doses of liposomes dispersion: single, product concentration: 0.5 g l^{-1}			
1,2-PA-PC, Krill PL, soy PC, CHO	Types of liposomes, membrane composition (w/w) and findings:			Monroig et al. [19]
	Encapsulation of vitamin A:		Encapsulation of vitamin A:	
	LUV: (98%)Krill PL(2%) vit. A		LUV: (98%)Krill PL(2%) vit. A	
	Increase of retinol content in *Artemia* nauplii		Increase of retinol content in *Artemia* nauplii	
	Encapsulation of methionine:			
	LUV: 80% soy PC20% CHO or 80% 1,2-PA-PC 20% CHO			
	MLV: 80% soy PC20%CHO			
	Efficiency of methionine delivery to *Artemia*: MLV > LUV			
1,2-PA-PC, Krill PL, soy PC, CHO	Oxidative stability of formulated liposomes:			Monroig et al. [16]
	(100%)Soy PC > (80%)1,2-PA-PC (20%)CHO > (80%)soy PC(20%)CHO > (100%)Krill PL (2%) vit A > (100%)Krill PL			
	No size changes of liposomes during the experimental period			

1,2-PA-PC, dipalmitoyl phosphatidylcholine; *PL*, phospholipids; *CHO*, cholesterol; *LUV*, large unilamellar vesicles; *MLV*, multilamellar vesicles; *EFA*, essential fatty acids; *PG*, phosphatidylglycerol; *SS*, Super Selco (Artemia Systems, INV E, Ghent) as control; *PT*, Tuna oil orbital oil emulsified with 12% herring roe polar lipids; *L*, liposomes with the composition, (40%)1,2-PA-PC (40%)PC(20%)CHO; *PS*, phosphatidylserine; *CFE*, cod fish extract; *PHS*, physiological saline; *Toc*, α-tocopherol

variety of enrichment products are available nowadays such as microalgae, microcapsules [158] and oil emulsion products [159].

PL especially MPL are considered to be a better way for providing EPA and DHA for larvae than TAG fish oil due to reasons such as: (1) marine fish larvae commonly ingest and assimilate better natural diets rich in PL than TAG [160–162]. The ratio of DHA:EPA in the PL naturally consumed by larvae is generally higher as compared to the corresponding ratio in TAG fish oil [156], (2) studies also showed that PL facilitate the absorption of lipids in the larvae gut [163] and thus promote growth and survival of larvae [164], and (3) PL have been shown to exert antioxidant properties against oxidation [87, 88].

Mcevoy et al. [14, 165] showed the advantage of using PC from soybean and marine fish eggs in enrichment of *Artemia* nauplii. They found that a mixture of DHA rich fish oil and PC (90:10) resulted in *Artemia* nauplii which were markedly enriched in DHA, and with minimal peroxidation in an aerated mixture during 18 h of enrichment. This is because the added PC functions as a natural emulsifying agent and a natural protectant against oxidation. They also showed that PC from marine egg sources was superior to soy PC in terms of n-3 PUFA content. This is presumably due to the presence of readily assimilable DHA and EPA in a ratio of 2:1 in marine roe lipids as compared to LA in soy PC. Their study corroborated the original work of Kanazawa et al. [166] using soy and bonito PC as feed supplements for larval sea bream and aye.

As mentioned earlier, there are several forms of enrichment products commercially available nowadays for live prey. However, as compared to an emulsion, liposomes provide more advantages. This is due to their ability to encapsulate lipids as well as water soluble components. For example, liposomes have been successfully used to encapsulate vitamin C [19] or water soluble antibiotics [167] in *Artemia* nauplii enrichment. In addition, liposomes can also be used to encapsulate hydrophobic components such as vitamin A [19] and free amino acids such as methionine [19, 168] or glycine [169]. Many studies have also shown that it is possible to encapsulate considerable amounts of n-3 PUFA into liposomes for *Artemia* enrichment [14, 15, 170].

Future Prospects and Conclusion

MPL may offer more advantages to consumer, food, and aquaculture industries as compared to fish oils. Particularly, the use of MPL-based liposomes is expected to provide benefits such as better oxidative stability, higher bioavailability and higher fluidity as compared to other PL-based liposomes. However, the use of MPL-based liposomes is just starting to be explored in both aquaculture and food industries and no current use of MPL-based liposomes for food applications has been reported. The next frontier in liposome application in the food industry will probably focus on the use of MPL for the development of n-3 PUFA enriched functional foods or the use of MPL-based liposomes as nutrient delivery system in foods and feed. Additionally, another area of study that needs further exploration is the use of liposomes for encapsulation of flavor, aroma and natural coloring compound in foods. However, due to the high content of n-3 PUFA in MPL, foods containing MPL are highly susceptible to lipid oxidation, which results in oxidative products that not only cause deterioration of food quality but also increase the risk of certain degenerative diseases as mentioned earlier. Therefore, it is expected that many more studies will be carried out in the future to explore the oxidative stability and sensory properties of MPL or MPL liposomes prior their potential uses in both food and aquaculture industries.

Acknowledgments The authors wish to acknowledge the financial support from the European Regional Development Fund, Væksforum Hovedstaden through Øresund Food's 'Healthy Growth' project and also Technical University of Denmark.

References

1. Okuyama H (2001) High n-6 to n-3 ratio of dietary fatty acids rather than serum cholesterol as a major risk factor for coronary heart disease. Eur J Lipid Sci Technol 103:418–422
2. Hibbeln JR, Nieminen LRG, Blasbalg TL, Riggs JA, Lands WEM (2006) Healthy intakes of n-3 and n-6 fatty acids: estimations considering worldwide diversity. Am J Clin Nutr 83:1483S–1493S
3. Simopoulos AP (2008) The importance of the omega-6/omega-3 fatty acid ratio in cardiovascular disease and other chronic diseases. Exp Biol Med 233:674–688
4. Løvaas E (2006) Marine phospholipids (MPL) resources, applications and markets. In: Luten JB, Jacobsen C, Bekaert K, Saebo A, Oehlenschlager J (eds) Seafood research from fish to dish, 1st ed. edn. Wageningen Academic Publishers, The Netherlands, pp 17–28
5. Neptune Technologies & Bioresources (2001) Natural phospholipids of marine origin containing flavonoids and polyunsaturated phospholipids and their uses [EP 1417211]
6. Nara E, Miyashita K, Ota T (1997) Oxidative stability of liposomes prepared from soybean PC, chicken egg PC, and salmon egg PC. Biosci Biotechnol Biochem 61:1736–1738
7. Nara E, Miyashita K, Ota T, Nadachi Y (1998) The oxidative stabilities of polyunsaturated fatty acids in salmon egg phosphatidylcholine liposomes. Fish Sci 64:282–286
8. Araseki M, Yamamoto K, Miyashita K (2002) Oxidative stability of polyunsaturated fatty acid in phosphatidylcholine liposomes. Biosci Biotechol Biochem 66:2573–2577
9. Lyberg AM, Fasoli E, Adlercreutz P (2005) Monitoring the oxidation of docosahexaenoic acid in lipids. Lipids 40:969–979
10. Jacobsen C (2008) Omega-3s in food emulsions: overview and case studies. Agro Food Ind Hi Tech 19:9–12

11. Rodriguez-Nogales JM, Perez-Mateos M, Busto MD (2004) Application of experimental design to the formulation of glucose oxidase encapsulation by liposomes. J Chem Technol Biotechnol 79:700–705
12. Xia SQ, Xu SY (2005) Ferrous sulfate liposomes: preparation, stability and application in fluid milk. Food Res Int 38:289–296
13. Taylor TM, Gaysinsky S, Davidson PM, Bruce BD, Weiss J (2007) Characterization of antimicrobial-bearing liposomes by zeta-potential, vesicle size, and encapsulation efficiency. Food Biophys 2:1–9
14. Mcevoy LA, Navarro JC, Hontoria F, Amat F, Sargent JR (1996) Two novel *Artemia* enrichment diets containing polar lipid. Aquaculture 144:339–352
15. Monroig O, Navarro JC, Amat I, Gonzalez P, Amat F, Hontoria F (2003) Enrichment of *Artemia* nauplii in PUFA, phospholipids, and water-soluble nutrients using liposomes. Aquacult Int 11:151–161
16. Monroig O, Navarro JC, Amat F, Gonzalez P, Hontoria F (2007) Oxidative stability and changes in the particle size of liposomes used in the *Artemia* enrichment. Aquaculture 266:200–210
17. Monroig O, Navarro JC, Amat F, Gonzalez P, Hontoria F (2006) Effects of nauplial density, product concentration and product dosage on the survival of the nauplii and EFA incorporation during *Artemia* enrichment with liposomes. Aquaculture 261:659–669
18. Monroig O, Navarro JC, Amat F, Gonzalez P, Bermejo A, Hontoria F (2006) Enrichment of *Artemia* nauplii in essential fatty acids with different types of liposomes and their use in the rearing of gilthead sea bream (*Sparus aurata*) larvae. Aquaculture 251:491–508
19. Monroig O, Navarro JC, Amat F, Hontoria F (2007) Enrichment of *Artemia* nauplii in vitamin A, vitamin C and methionine using liposomes. Aquaculture 269:504–513
20. Cansell M, Moussaoui N, Lefrancois C (2001) Stability of marine lipid based-liposomes under acid conditions. Influence of xanthan gum. J Liposome Res 11:229–242
21. Cho SY, Joo DS, Choi HG, Nara E, Miyashita K (2001) Oxidative stability of lipids from squid tissues. Fish Sci 67:738–743
22. Mozuraityte R, Rustad T, Storro I (2006) Pro-oxidant activity of Fe^{2+} in oxidation of cod phospholipids in liposomes. Eur J Lipid Sci Technol 108:218–226
23. Mozuraityte R, Rustad T, Storro I (2006) Oxidation of cod phospholipids in liposomes: effects of salts, pH and zeta potential. Eur J Lipid Sci Technol 108:944–950
24. Mozuraityte R, Rustad T, Storro I (2008) The role of iron in peroxidation of polyunsaturated fatty acids in liposomes. J Agric Food Chem 56:537–543
25. Moriya H, Kuniminato T, Hosokawa M, Fukunaga K, Nishiyama T, Miyashita K (2007) Oxidative stability of salmon and herring roe lipids and their dietary effect on plasma cholesterol levels of rats. Fish Sci 73:668–674
26. Nacka F, Cansell M, Meleard P, Combe N (2001) Incorporation of alpha-tocopherol in marine lipid-based liposomes: in vitro and in vivo studies. Lipids 36:1313–1320
27. Nacka F, Cansell M, Gouygou JP, Gerbeaud C, Meleard P, Entressangles B (2001) Physical and chemical stability of marine lipid-based liposomes under acid conditions. Colloids Surf B 20:257–266
28. Nacka F, Cansell M, Entressangles B (2001) In vitro behavior of marine lipid-based liposomes, influence of pH, temperature, bile salts, and phospholipase A(2). Lipids 36:35–42
29. Arnaud JP (1995) Liposomes in the agro food-industry. Agro Food Ind Hi Tech 6:30–36
30. Falch E, Rustad T, Jonsdottir R, Shaw NB, Dumay J, Berge JP, Arason S, Kerry JP, Sandbakk M, Aursand M (2006) Geographical and seasonal differences in lipid composition and relative weight of by-products from gadiform species. J Food Compost Anal 19:727–736
31. Gbogouri GA, Linder M, Fanni J, Parmentier M (2006) Analysis of lipids extracted from salmon (*Salmo salar*) heads by commercial proteolytic enzymes. Eur J Lipid Sci Technol 108:766–775
32. Striby L, Lafont R, Goutx M (1999) Improvement in the Iatroscan thin-layer chromatographic-flame ionisation detection analysis of marine lipids. Separation and quantitation of monoacylglycerols and diacylglycerols in standards and natural samples. J Chromatogr A 849:371–380
33. Medina I, Aubourg SP, Martin RP (1995) Composition of phospholipids of white muscle of 6 tuna species. Lipids 30:1127–1135
34. Body DR, Vlieg P (1989) Distribution of the lipid classes and eicosapentaenoic (20-5) and docosahexaenoic (22-6) acids in different sites in blue mackerel (*Scomber australasicus*) fillets. J Food Sci 54:569–572
35. Hazel JR (1985) Determination of the phospholipid-composition of trout gill by Iatroscan TLC/FID—effect of thermal-acclimation. Lipids 20:516–520
36. Schneider M (2008) Major sources, composition and processing. In: Gunstone FD (ed) Phospholipid technoloy and applications. The Oily Press, Bridgewater, pp 21–40
37. Saito H, Kotani Y, Keriko JM, Xue CH, Taki K, Ishihara K, Ueda T, Miyata S (2002) High levels of n-3 polyunsaturated fatty acids in *Euphausia pacifica* and its role as a source of docosahexaenoic and icosapentaenoic acids for higher trophic levels. Mar Chem 78:9–28
38. Le Grandois J, Marchioni E, Zhao MJ, Giuffrida F, Ennahar S, Bindler F (2009) Investigation of natural phosphatidylcholine sources: separation and identification by liquid chromatography-electrospray ionization-tandem mass spectrometry (LC–ESI-MS2) of molecular species. J Agric Food Chem 57:6014–6020
39. Boselli E, Caboni MF (2000) Supercritical carbon dioxide extraction of phospholipids from dried egg yolk without organic modifier. J Supercrit Fluids 19:45–50
40. Kang KY, Ahn DH, Jung SM, Kim DH, Chun BS (2005) Separation of protein and fatty acids from tuna viscera using supercritical carbon dioxide. Biotechnol Bioprocess Eng 10:315–321
41. Letisse M, Rozieres M, Hiol A, Sergent M, Comeau L (2006) Enrichment of EPA and DHA from sardine by supercritical fluid extraction without organic modifier—I. Optimization of extraction conditions. J Supercrit Fluids 38:27–36
42. Aro H, Jarvenpaa E, Konko K, Sihvonen M, Hietaniemi V, Huopalahti R (2009) Isolation and purification of egg yolk phospholipids using liquid extraction and pilot-scale supercritical fluid techniques. Eur J Lipid Sci Technol 228:857–863
43. Froning GW, Wehling RL, Cuppett SL, Pierce MM, Niemann L, Siekman DK (1990) Extraction of cholesterol and other lipids from dried egg-yolk using supercritical carbon dioxide. J Food Sci 55:95–98
44. Rossi M, Spedicato E, Shiraldi A (1990) Improvement of supercritical carbon dioxide extraction of egg lipids by means of ethanolic entrainer. Ital J Food Sci 2:249–256
45. Lemaitre-Delaunay D, Pachiaudi C, Laville M, Pousin J, Armstrong M, Lagarde M (1999) Blood compartmental metabolism of docosahexaenoic acid (DHA) in humans after ingestion of a single dose of [C^{-13}]DHA in phosphatidylcholine. J Lipid Res 40:1867–1874
46. Amate L, Gil A, Ramirez M (2001) Feeding infant piglets formula with long-chain polyunsaturated fatty acids as triacylglycerols or phospholipids influences the distribution of these fatty acids in plasma lipoprotein fractions. J Nutr 131:1250–1255

47. Wijendran V, Huang MC, Diau GY, Boehm G, Nathanielsz PW, Brenna JT (2002) Efficacy of dietary arachidonic acid provided as triglyceride or phospholipid as substrates for brain arachidonic acid accretion in baboon neonates. Pediatr Res 51:265–272
48. Peng JL, Larondelle Y, Pham D, Ackman RG, Rollin X (2003) Polyunsaturated fatty acid profiles of whole body phospholipids and triacylglycerols in anadromous and landlocked Atlantic salmon (*Salmo salar* L.) fry. Comp Biochem Phys B 134:335–348
49. Phares Pharmaceutical Research N.V. (2004) Marine Lipid Compositions [WO/2004/047554]
50. Narayan B, Miyashita K, Hosakawa M (2006) Physiological effects of eicosapentaenoic acid (EPA) and docosahexaenoic acid (DHA)—a review. Food Rev Int 22:291–307
51. Leaf A (2008) Historical overview of n-3 fatty acids and coronary heart disease. Am J Clin Nutr 87:1978S–1980S
52. Virtanen JK, Mozaffarian D, Chiuve SE, Rimm EB (2008) Fish consumption and risk of major chronic disease in men. Am J Clin Nutr 88:1618–1625
53. Calon F, Cicchetti F (2009) Omega-3 fatty acid in Parkinson disease. Agro Food Ind Hi Tech 20:7–9
54. Fotuhi M, Mohassel P, Yaffe K (2009) Fish consumption, long-chain omega-3 fatty acids and risk of cognitive decline or Alzheimer disease: a complex association. Nat Clin Pract Neurol 5:140–152
55. Ramakrishnan U, Imhoff-Kunsch B, DiGirolamo AM (2009) Role of docosahexaenoic acid in maternal and child mental health. Am J Clin Nutr 89:958S–962S
56. Boudrault C, Bazinet RP, Ma DWL (2009) Experimental models and mechanisms underlying the protective effects of n-3 polyunsaturated fatty acids in Alzheimer's disease. J Nutr Biochem 20:1–10
57. Tinoco SMB, Sichieri R, Setta CL, Moura AS, Do Carmo MGT (2009) n-3 polyunsaturated fatty acids in milk is associate to weight gain and growth in premature infants. Lipids Health Dis 8:23
58. Adkins Y, Kelley DS (2010) Mechanisms underlying the cardioprotective effects of omega-3 polyunsaturated fatty acids. J Nutr Biochem 21:781–792
59. Lopez-Huertas E (2010) Health effects of oleic acid and long chain omega-3 fatty acids (EPA and DHA) enriched milks. A review of intervention studies. Pharmacol Res 61:200–207
60. Wilson TA, Meservey CM, Nicolosi RJ (1998) Soy lecithin reduces plasma lipoprotein cholesterol and early atherogenesis in hypercholesterolemic monkeys and hamsters: beyond linoleate. Atherosclerosis 140:147–153
61. Zeisel SH (1992) Choline—an important nutrient in brain-development, liver-function and carcinogenesis. J Am Coll Nutr 11:473–481
62. Pharmacia AB (1995) Phospholipids containing omega-3 fatty acids [US Patent 5434183]
63. Bunea R, El Farrah K, Deutsch L (2004) Evaluation of the effects of Neptune krill oil on the clinical course of hyperlipidemia. Altern Med Rev 9:420–428
64. Maki KC, Reeves MS, Farmer M, Griinari M, Berge K, Vik H, Hubacher R, Rains TM (2009) Krill oil supplementation increases plasma concentrations of eicosapentaenoic and docosahexaenoic acids in overweight and obese men and women. Nutr Res 29:609–615
65. Tandy S, Chung RWS, Wat E, Kamili A, Berge K, Griinari M, Cohn JS (2009) Dietary krill oil supplementation reduces hepatic steatosis, glycemia, and hypercholesterolemia in high-fat-fed mice. J Agric Food Chem 57:9339–9345
66. Deutsch L (2007) Evaluation of the effect of Neptune krill oil on chronic inflammation and arthritic symptoms. J Am Coll Nutr 26:39–48
67. Sampalis F, Bunea R, Pelland MF, Kowalski O, Duguet N, Dupuis S (2003) Evaluation of the effects of Neptune krill oil on the management of premenstrual syndrome and dysmenorrhea. Altern Med Rev 8:171–179
68. Ierna M, Kerr A, Scales H, Berge K, Griinari M (2010) Supplementation of diet with krill oil protects against experimental rheumatoid arthritis. BMC Musculoskelet Disorders 11:136
69. Hayashi H, Tanaka Y, Hibino H, Umeda Y, Kawamitsu H, Fujimoto H, Amakawa T (1999) Beneficial effect of salmon roe phosphatidylcholine in chronic liver disease. Curr Med Res Opin 15:177–184
70. Taylor LA, Pletschen L, Arends J, Unger C, Massing U (2010) Marine phospholipids—a promising new dietary approach to tumor-associated weight loss. Support Care Cancer 18:159–170
71. Lasch J, Weissing V, Brandi M (2003) Preparation of liposomes. In: Torchilin VP, Weissing V (eds) Liposomes: a practical approach, 2nd edn. Oxford University Press, New York, pp 3–30
72. Lasic DD (1998) Novel applications of liposomes. Trends Biotechnol 16:307–321
73. Watwe RM, Bellare JR (1995) Manufacture of liposomes—a review. Curr Sci 68:715–724
74. Kim HY, Baiau IC (1991) Novel liposome microencapsulation techniques for food applications. Trends Food Sci Tech 2:55–61
75. Fruhwirth GO, Loidl A, Hermetter A (2007) Oxidized phospholipids: from molecular properties to disease. BBA Mol Basis Dis 1772:718–736
76. Domingues MRM, Reis A, Domingues P (2008) Mass spectrometry analysis of oxidized phospholipids. Chem Phys Lipids 156:1–12
77. Subbanagounder G, Deng YJ, Borromeo C, Dooley AN, Beliner JA, Salomon RG (2002) Hydroxy alkenal phospholipids regulate inflammatory functions of endothelial cells. Vascul Pharmacol 38:201–209
78. Leitinger N (2003) Oxidized phospholipids as modulators of inflammation in atherosclerosis. Curr Opin Lipidol 14:421–430
79. Leitinger N (2005) Oxidized phospholipids as triggers of inflammation in atherosclerosis. Mol Nutr Food Res 49:1063–1071
80. Spickett CM, Dever G (2005) Studies of phospholipid oxidation by electrospray mass spectrometry: from analysis in cells to biological effects. Biofactors 24:17–31
81. Spiteller G (2006) Peroxyl radicals: inductors of neurodegenerative and other inflammatory diseases. Their origin and how they transform cholesterol, phospholipids, plasmalogens, polyunsaturated fatty acids, sugars, and proteins into deleterious products. Free Radic Bio Med 41:362–387
82. Bochkov VN (2007) Inflammatory profile of oxidized phospholipids. Thromb Haemost 97:348–354
83. Imal Y, Kuba K, Neely GG, Yaghubian-Malhami R, Perkmann T, van Loo G, Ermolaeva M, Veldhuizen R, Leung YHC, Wang H, Liu H, Sun Y, Pasparakis M, Kopf M, Mech C, Bavari S, Peiris JS, Slutsky AS, Akira S, Hultqvist M, Holmdahl R, Nicholls J, Jiang C, Binder CJ, Penninger JM (2008) Identification of oxidative stress and toll-like receptor 4 signaling as a key pathway of acute lung injury. Cell 133:235–249
84. Subbanagounder G, Leitinger N, Shih PT, Faull KF, Berliner JA (1999) Evidence that phospholipid oxidation products and/or platelet-activating factor play an important role in early atherogenesis—in vitro and in vivo inhibition by WEB 2086. Circ Res 85:311–318
85. Androulakis N, Durand H, Ninio E, Tsoukatos DC (2005) Molecular and mechanistic characterization of platelet-activating factor-like bioactivity produced upon LDL oxidation. J Lipid Res 46:1923–1932
86. Gopfert MS, Siedler F, Siess W, Sellmayer A (2005) Structural identification of oxidized acyl-phosphatidylcholines that induce platelet activation. J Vasc Res 42:120–132

87. King MF, Boyd LC, Sheldon BW (1992) Effects of phospholipids on lipid oxidation of a salmon oil model system. J Am Oil Chem Soc 69:237–242
88. King MF, Boyd LC, Sheldon BW (1992) Antioxidant properties of individual phospholipids in a salmon oil model system. J Am Oil Chem Soc 69:545–551
89. Boyd LC, Nwosu VC, Young CL, MacMillian L (1998) Monitoring lipid oxidation and antioxidant effects of phospholipids by headspace gas chromatographic analyses of rancimat trapped volatiles. J Food Lipids 5:269–282
90. Miyashita K, Nara E, Ota T (1994) Comparative-study on the oxidative stability of phosphatidylcholines from salmon egg and soybean in an aqueous-solution. Biosci Biotechnol Biochem 58:1772–1775
91. Applegate KR, Glomset JA (1986) Computer-based modeling of the conformation and packing properties of docosahexaenoic acid. J Lipid Res 27:658–680
92. Applegate KR, Glomset JA (1991) Effect of acyl chain unsaturation on the conformation of model diacylglycerols—a computer modeling study. J Lipid Res 32:1635–1644
93. Applegate KR, Glomset JA (1991) Effect of acyl chain unsaturation on the packing of model diacylglycerols in simulated monolayers. J Lipid Res 32:1645–1655
94. Feng SS, Brockman HL, Macdonald RC (1994) On osmotic-type equations of state for liquid-expanded monolayers of lipids at the air–water-interface. Langmuir 10:3188–3194
95. Brockman HL, Applegate KR, Momsen MM, King WC, Glomset JA (2003) Packing and electrostatic behavior of *sn*-2-docosahexaenoyl and -arachidonoyl phosphoglycerides. Biophys J 85:2384–2396
96. Albrand M, Pageaux JF, Lagarde M, Dolmazon R (1994) Conformational-analysis of isolated docosahexaenoic acid (22/6 N-3) and its 14-(S) and 11-(S) hydroxy derivatives by force-field calculations. Chem Phys Lipids 72:7–17
97. Koenig BW, Strey HH, Gawrisch K (1997) Membrane lateral compressibility determined by NMR and X-ray diffraction: effect of acyl chain polyunsaturation. Biophys J 73:1954–1966
98. Eldho NV, Feller SE, Tristram-Nagle S, Polozov IV, Gawrisch K (2003) Polyunsaturated docosahexaenoic vs docosapentaenoic acid—differences in lipid matrix properties from the loss of one double bond. J Am Chem Soc 125:6409–6421
99. Feller SE, Gawrisch K, MacKerell AD (2002) Polyunsaturated fatty acids in lipid bilayers: intrinsic and environmental contributions to their unique physical properties. J Am Chem Soc 124:318–326
100. Saiz L, Klein ML (2001) Structural properties of a highly polyunsaturated lipid bilayer from molecular dynamics simulations. Biophys J 81:204–216
101. Huber T, Rajamoorthi K, Kurze VF, Beyer K, Brown MF (2002) Structure of docosahexaenoic acid-containing phospholipid bilayers as studied by H-2 NMR and molecular dynamics simulations. J Am Chem Soc 124:298–309
102. Everts S, Davis JH (2000) H^{-1} and C^{-13} NMR of multilamellar dispersions of polyunsaturated (22:6) phospholipids. Biophys J 79:885–897
103. Gawrisch K, Eldho NV, Holte LL (2003) The structure of DHA in phospholipid membranes. Lipids 38:445–452
104. Bandarra NM, Campos RM, Batista I, Nunes ML, Empis JM (1999) Antioxidant synergy of alpha-tocopherol and phospholipids. J Am Oil Chem Soc 76:905–913
105. Ohshima T, Fujita Y, Koizumi C (1993) Oxidative stability of sardine and mackerel lipids with reference to synergism between phospholipids and alpha-tocopherol. J Am Oil Chem Soc 70:269–276
106. Saito H, Ishihara K (1997) Antioxidant activity and active sites of phospholipids as antioxidants. J Am Oil Chem Soc 74:1531–1536
107. Kashima M, Cha GS, Isoda Y, Hirano J, Miyazawa T (1991) The antioxidant effects of phospholipids on perilla oil. J Am Oil Chem Soc 68:119–122
108. Hildebrand DH, Terao J, Kito M (1984) Phospholipids plus tocopherols increase soybean oil stability. J Am Oil Chem Soc 61:552–555
109. Weng XC, Gordon MH (1993) Antioxidant synergy between phosphatidyl ethanolamine and alpha-tocopherylquinone. Food Chem 48:165–168
110. Mei LY, Decker EA, McClements DJ (1998) Evidence of iron association with emulsion droplets and its impact on lipid oxidation. J Agric Food Chem 46:5072–5077
111. Kuzuya M, Yamada K, Hayashi T, Funaki C, Naito M, Asai K, Kuzuya F (1991) Oxidation of low-density-lipoprotein by copper and iron in phosphate buffer. Biochim Biophys Acta 1084:198–201
112. Djuric Z, Potter DW, Taffe BG, Strasburg GM (2001) Comparison of iron-catalyzed DNA and lipid oxidation. J Biochem Mol Toxicol 15:114–119
113. Were LM, Bruce BD, Davidson PM, Weiss J (2003) Size, stability, and entrapment efficiency of phospholipid nanocapsules containing polypeptide antimicrobials. J Agric Food Chem 51:8073–8079
114. Laridi R, Kheadr EE, Benech RO, Vuillemard JC, Lacroix C, Fliss I (2003) Liposome encapsulated nisin Z: optimization, stability and release during milk fermentation. Int Dairy J 13:325–336
115. Sulkowski WW, Pentak D, Nowak K, Sulkowska A (2005) The influence of temperature, cholesterol content and pH on liposome stability. J Mol Struct 744:737–747
116. Finean JB (1990) Interaction between cholesterol and phospholipid in hydrated bilayers. Chem Phys Lipids 54:147–156
117. Fiorentini D, Landi L, Barzanti V, Cabrini L (1989) Buffers can modulate the effect of sonication on egg lecithin liposomes. Free Radic Res Commun 6:243–250
118. Kirby C, Clarke J, Gregoriadis G (1980) Effect of the cholesterol content of small unilamellar liposomes on their stability in vivo and in vitro. Biochem J 186:591–598
119. Senior J, Gregoriadis G (1982) Stability of small unilamellar liposomes in serum and clearance from the circulation—the effect of the phospholipid and cholesterol components. Life Sci 30:2123–2136
120. Papahadj D, Jacobson K, Nir S, Isac T (1973) Phase-transitions in phospholipid vesicles—fluorescence polarization and permeability measurements concerning effect of temperature and cholesterol. Biochim Biophys Acta 311:330–348
121. Brockerh H (1974) Model of interaction of polar lipids, cholesterol, and proteins in biological-membranes. Lipids 9:645–650
122. Huang CH (1977) Structural model for cholesterol–phosphatidylcholine complexes in bilayer membranes. Lipids 12:348–356
123. Frankel EN (1993) In search of better methods to evaluate natural antioxidants and oxidative stability in food lipids. Trends Food Sci Tech 4:220–225
124. Cillard J, Cillard P, Cormier M, Girre L (1980) Alpha-tocopherol prooxidant effect in aqueous-media—increased autoxidation rate of linoleic-acid. J Am Oil Chem Soc 57:252–255
125. Bazin BC, Cillard J, Koskas JP, Cillard P (1984) Arachidonic acid autooxidation in an aqueous media effect of α-tocopherol, cystein and nucleic acids. J Am Oil Chem Soc 61:1212–1215
126. MacMillan DK, Murphy RC (1995) Analysis of lipid hydroperoxides and long-chain conjugated keto acids by negative ion

electrospray mass spectrometry. J Am Soc Mass Spectrom 6:1190–1201
127. Spickett CM, Pitt AR, Brown AJ (1998) Direct observation of lipid hydroperoxides in phospholipid vesicles by electrospray mass spectrometry. Free Radical Biol Med 25:613–620
128. Spickett CM, Rennie N, Winter H, Zambonin L, Landi L, Jerlich A, Schaur RJ, Pitt AR (2001) Detection of phospholipid oxidation in oxidatively stressed cells by reversed-phase HPLC coupled with positive-ionization electroscopy MS. Biochem J 355:449–457
129. Yin HY, Cox BE, Liu W, Porter NA, Morrow JD, Milne GL (2009) Identification of intact oxidation products of glycerophospholipids in vitro and in vivo using negative ion electrospray ion trap mass spectrometry. J Mass Spectrom 44:672–680
130. Taylor TM, Davidson PM, Bruce BD, Weiss J (2005) Liposomal nanocapsules in food science and agriculture. Crit Rev Food Sci 45:587–605
131. Thompson AK, Hindmarsh JP, Haisman D, Rades T, Singh H (2006) Comparison of the structure and properties of liposomes prepared from milk fat globule membrane and soy phospholipids. J Agric Food Chem 54:3704–3711
132. Thompson AK, Haisman D, Singh H (2006) Physical stability of liposomes prepared from milk fat globule membrane and soya phospholipids. J Agric Food Chem 54:6390–6397
133. Thompson AK, Mozafari MR, Singh H (2007) The properties of liposomes produced from milk fat globule membrane material using different techniques. Lait 87:349–360
134. Cansell M, Nacka F, Combe N (2003) Marine lipid-based liposomes increase in vivo FA bioavailability. Lipids 38:551–559
135. Cansell M, Moussaoui N, Petit AP, Denizot A, Combe N (2006) Feeding rats with liposomes or fish oil differently affects their lipid metabolism. Eur J Lipid Sci Technol 108:459–467
136. Hossain Z, Kurihara H, Hosokawa M, Takahashi K (2006) Docosahexaenoic acid and eicosapentaenoic acid-enriched phosphatidylcholine liposomes enhance the permeability, transportation and uptake of phospholipids in Caco-2 cells. Mol Cell Biochem 285:155–163
137. Kirby CJ, Whittle CJ, Rigby N, Coxon DT, Law BA (1991) Stabilization of ascorbic-acid by microencapsulation in liposomes. Int J Food Sci Tech 26:437–449
138. Chang HM, Lee YC, Chen CC, Tu YY (2002) Microencapsulation protects immunoglobulin in yolk (IgY) specific against *Helicobacter pylori* urease. J Food Sci 67:15–20
139. Rao DR, Chawan CB, Veeramachaneni R (1995) Liposomal encapsulation of beta-galactosidase—comparison of 2 methods of encapsulation and in vitro lactose digestibility. J Food Biochem 18:239–251
140. Hsieh YF, Chen TL, Wang YT, Chang JH, Chang HM (2002) Properties of liposomes prepared with various lipids. J Food Sci 67:2808–2813
141. Lee SC, Yuk HG, Lee DH, Lee KE, Hwang YI, Ludescher RD (2002) Stabilization of retinol through incorporation into liposomes. J Biochem Mol Biol 35:358–363
142. Lee SK, Han JH, Decker EA (2002) Antioxidant activity of phosvitin in phosphatidylcholine liposomes and meat model systems. J Food Sci 67:37–41
143. Lee SC, Lee KE, Kim JJ, Lim SH (2005) The effect of cholesterol in the liposome bilayer on the stabilization of incorporated retinol. J Liposome Res 15:157–166
144. Thapon JL, Brule G (1986) Effects of pH and ionic-strength on lysozyme-caseins affinity. Lait 66:19–30
145. Arnaud JP (1998) Liposome-based functional drinks. Agro Food Ind Hi Tech 9:37–40
146. Alkhalaf W, Piard JC, Elsoda M, Gripon JC, Desmazeaud M, Vassal L (1988) Liposomes as proteinase carriers for the accelerated ripening of Saint-Paulin type cheese. J Food Sci 53:1674–1679
147. Kirby CJ, Brooker BE, Law BA (1987) Accelerated ripening of cheese using liposome-encapsulated enzyme. Int J Food Sci Tech 22:355–375
148. Picon A, Gaya P, Medina M, Nunez M (1994) The effect of liposome encapsulation of chymosin derived by fermentation on Manchego cheese ripening. J Dairy Sci 77:16–23
149. Picon A, Gaya P, Medina M, Nunez M (1997) Proteinases encapsulated in stimulated release liposomes for cheese ripening. Biotechnol Lett 19:345–348
150. Benech RO, Kheadr EE, Laridi R, Lacroix C, Fliss I (2002) Inhibition of *Listeria innocua* in Cheddar cheese by addition of nisin Z in liposomes or by in situ production in mixed culture. Appl Environ Microbiol 68:3683–3690
151. Kheadr EE, Vuillemard JC, El Deeb SA (2000) Accelerated Cheddar cheese ripening with encapsulated proteinases. Int J Food Sci Tech 35:483–495
152. Matsuzaki M, Mccafferty F, Karel M (1989) The effect of cholesterol content of phospholipid-vesicles on the encapsulation and acid resistance of beta-galactosidase from *Escherichia coli*. Int J Food Sci Technol 24:451–460
153. Banville C, Vuillemard JC, Lacroix C (2000) Comparison of different methods for fortifying Cheddar cheese with vitamin D. Int Dairy J 10:375–382
154. Navarro JC, Bell MV, Amat F, Sargent JR (1992) The fatty-acid composition of phospholipids from brine shrimp, *Artemia* sp., eyes. Comp Biochem Physiol B 103:89–91
155. Bell MV, Batty RS, Dick JR, Fretwell K, Navarro JC, Sargent JR (1995) Dietary deficiency of docosahexaenoic acid impairs vision at low-light intensities in Juvenile herring (*Clupea harengus* L.). Lipids 30:443–449
156. Sargent JR, Mcevoy LA, Bell JG (1997) Requirements, presentation and sources of polyunsaturated fatty acids in marine fish larval feeds. Aquaculture 155:117–127
157. Navarro JC, Amat F, Sargent JR (1992) Lipid-composition of cysts of the brine shrimp *Artemia* sp. from Spanish populations. J Exp Mar Biol Ecol 155:123–131
158. Southgate PC, Lou DC (1995) Improving the eta-3 Hufa composition of *Artemia* using microcapsules containing marine oils. Aquaculture 134:91–99
159. Narciso L, Pousao-Ferreira P, Passos A, Luis O (1999) HUFA content and DHA/EPA improvements of *Artemia* sp. with commercial oils during different enrichment periods. Aquac Res 30:21–24
160. Salhi M, Hernandez-Cruz CM, Bessonart M, Izquierdo MS, Fernandez-Palacios H (1999) Effect of different dietary polar lipid levels and different n-3 HUFA content in polar lipids on gut and liver histological structure of gilthead seabream (*Sparus aurata*) larvae. Aquaculture 179:253–263
161. Izquierdo MS, Tandler A, Salhi M, Kolkovski S (2001) Influence of dietary polar lipids' quantity and quality on ingestion and assimilation of labelled fatty acids by larval gilthead seabream. Aquacult Nutr 7:153–160
162. Cahu CL, Infante JLZ, Barbosa V (2003) Effect of dietary phospholipid level and phospholipid: neutral lipid value on the development of sea bass (*Dicentrarchus labrax*) larvae fed a compound diet. Br J Nutr 90:21–28
163. Koven W, Barr Y, Hadas E, Ben-Atia I, Chen Y, Weiss R, Tandler A (1999) The potential of liposomes as a nutrient supplement in first-feeding marine fish larvae. Aquacult Nutr 5:251–256
164. Kanazawa A, Teshima SI, Sakamoto M (1985) Effects of dietary lipids, fatty-acids, and phospholipids on growth and survival of prawn (*Penaeus japonicus*) larvae. Aquaculture 50:39–49

165. Mcevoy LA, Navarro JC, Amat F, Sargent JR (1997) Application of soya phosphatidylcholine in tuna orbital oil enrichment emulsions for *Artemia*. Aquacult Int 5:517–526
166. Kanazawa A, Teshima S, Sakamoto M (1985) Effects of dietary bonito-egg phospholipids and some phospholipids on growth and survival of the larval ayu, *Plecoglossus altivelis*. Z Angew Ichthyol 4:156–170
167. Touraki M, Rigas P, Kastritsis C (1995) Liposome mediated delivery of water soluble antibiotics to the larvae of aquatic animals. Aquaculture 136:1–10
168. Tonheim SK, Koven W, Ronnestad I (2000) Enrichment of *Artemia* with free methionine. Aquaculture 190:223–235
169. Ozkizilcik S, Chu FLE (1994) Uptake and metabolism of liposomes by *Artemia* nauplii. Aquaculture 128:131–141
170. Hontoria F, Crowe JH, Crowe LM, Amat F (1994) Potential use of liposomes in larviculture as a delivery system through *Artemia* nauplii. Aquaculture 127:255–264

Lipids (2011) 46:25–36
DOI 10.1007/s11745-010-3472-6

ORIGINAL ARTICLE

Elucidation of Phosphatidylcholine Composition in Krill Oil Extracted from *Euphausia superba*

Bjørn Winther · Nils Hoem · Kjetil Berge · Léon Reubsaet

Received: 9 June 2010 / Accepted: 30 August 2010 / Published online: 17 September 2010

Abstract High performance liquid chromatography-electrospray tandem mass spectrometry was used to elucidate the phospholipids in krill oil extracted from *Euphausia superba*, an emerging source for human nutritional supplements. The study was carried out in order to map the species of the choline-containing phospholipid classes: phosphatidylcholine and lyso-phosphatidylcholine. In addition, the prevalent phosphatidylcholine class was quantified and the results compared with prior analysis. The qualification was performed with separation on a reverse phase chromatography column, while the quantification was obtained with class separation on a normal phase chromatography column. An Orbitrap system was used for the detection, and pulsed-Q dissociation fragmentation was utilized for the identification of the species. An asymmetrical exclusion list was applied for detection of phospholipid species of lower concentration, significantly improving the number of species observed. A total of 69 choline-containing phospholipids were detected, whereof 60 phosphatidylcholine substances, among others seven with probable omega-3 fatty acids in both *sn*-1 and *sn*-2. The phosphatidylcholine concentration was estimated to be 34 ± 5 g/100 g oil ($n = 5$). These results confirm the complexity of the phospholipid composition of krill oil, and the presence of long chained, heavily unsaturated fatty acids.

B. Winther · L. Reubsaet (✉)
Department of Pharmaceutical Chemistry,
School of Pharmacy, University of Oslo, Oslo, Norway
e-mail: j.l.reubsaet@farmasi.uio.no

N. Hoem · K. Berge
Aker BioMarine ASA, Fjordalléen 16, Vika,
P.O. Box 1423, 0115 Oslo, Norway

Keywords Fish oil · Krill oil · Mass spectrometry · Omega-3 · Phosphatidylcholine · Phospholipid

Abbreviations

EPA	Eicosapentaenoic acid
DHA	Docosahexaenoic acid
lyso-PtdCho	Lyso-phosphatidylcholine
NPLC	Normal phase liquid chromatography
PtdCho	Phosphatidylcholine
PtdEtn	Phosphatidylethanolamine
PtdIns	Phosphatidylinositol
PtdSer	Phosphatidylserine
PL	Phospholipid
RPLC	Reverse phase liquid chromatography

Introduction

Krill oil has emerged as an important source of omega-3 fatty acids for human consumption during the last decade, and the amount sold on the world market is rapidly increasing. In contrast to traditional omega-3 supplements on today's market, which are based on omega-3 fatty acids bound to triglycerides (such as cod liver oil and fish oil) or bound as ethyl esters (Omacor/Lovaza), krill oil contains a high proportion of omega-3 fatty acids bound to phospholipids.

Krill oil has been investigated in several preclinical and clinical studies [1–4], and there is growing evidence that the molecular form of the omega-3 fatty acids (i.e. triglycerides, ethyl-esters, phospholipids) might be of importance for their biological effect as well as distribution of the omega-3 fatty acids in the body. In one animal study,

it was demonstrated that when krill oil and fish oil were administrated to Zucker rats with an equimolar dose eicosapentaenoic acid (EPA) + docosahexaenoic acid (DHA), krill oil had stronger and in some instances different effects than fish oil on specific parameters related to the metabolic syndrome [1]. The lipid level in both heart and liver was significantly lower in rats treated with krill oil, when compared to rats fed the fish oil diet. The authors suggest that this difference may be linked to differences in the incorporation of omega-3 fatty acids into membranes, and consequently a reduction of inflammatory molecules and endocannabinoids, which might be relevant for the differences observed between fish oil and krill oil. Further, in the same study, it was demonstrated that the level of DHA in the brain increased significantly after krill oil administration, but not after fish oil administration, when compared to control animals [2]. Thus, omega-3 fatty acids linked to phospholipids may be differently distributed in the body compared to omega-3 fatty acids in other molecular forms. Moreover, in a clinical safety study, the presence of EPA and DHA in the blood plasma was determined after daily administration of 2 g krill oil or 2 g menhaden oil for 4 weeks [3]. The authors concluded that EPA and DHA from krill oil are absorbed at least as well as that from menhaden oil.

The aim of the current study was to characterize the phospholipids in krill oil in more detail to evaluate the composition of the fatty acids present in the phospholipids. The composition was determined using LC/ESI–MS(/MS), a technique which has lately played an important role in characterization of the lipidome in tissues and organisms [5]. An inherent limitation in the use of ESI for the ionization of long chained fatty acids has been described by Koivusalo et al. [6]. The study showed that the instrument response is affected by the acyl chain length. This is a consideration which is important particularly in the quantification of the lipids.

The elucidation of the phospholipid species is often performed either by doing a precursor ion scan or a neutral loss scan with triple quadrupole instrumentation [7–9], or with MS^n fragmentation with systems based on ion traps [10–13]. Normal phase liquid chromatography (NPLC) and reverse phase liquid chromatography (RPLC) are both frequently used for the separation of the components [10, 14–17]. Of these two separation techniques, RPLC has been shown to be more suitable for species separation and characterization [8].

Different ionization and fragmentation techniques can be used for the evaluation of phospholipids. Ionization of the phospholipids may be performed in negative- and positive-ionization mode. In general, fragmentation of phospholipids in the positive mode provides information about the phospholipid head group, while fragmentation in the negative mode is the source of structural information. For phospholipids containing choline-headgroups, the choline-specific fragment *m/z* 184 has been used in precursor ion scanning operating in the positive ionization mode for class determination [7, 18]. Also in the negative mode, class-specific fragments may be used in the characterization. All phospholipid classes, except those containing choline, yield molecular ions $[M-H]^-$ when a formate-based mobile phase is used. On the other hand, the choline-containing classes form stable adducts with formic acid in the mobile phase, yielding $[M + FA-H]^-$ ions ($m/z = M + 45$) [19, 20]. With fragmentation, this adduct dissociates with the loss of ($HCOO + CH_3$) into the fragment ion $[M-CH_3]^-$. This is in particularly useful in methods utilizing RPLC for separation. Although the chromatographic class information is lost in such setups, the class-specific fragments may be used in the characterization of the species [11].

Two ion activation techniques may be used for MS analysis utilizing ion traps: collision-induced dissociation (CID) and pulsed-Q dissociation (PQD) techniques. While CID has a low mass cut off below 28% of the *m/z* for the precursor ion, the novel PQD technique eliminates the potential loss of low mass fragments [21, 22]. This difference could be crucial in the fragmentation of larger molecules into low mass, specific fragments, as shown with detection of iTRAQ fragments with a linear ion trap [23].

The fatty acid composition of phosphatidylcholine (PtdCho) from krill oil has previously been investigated by Le Grandois et al. [24]. This study was performed with a method based on the ESI operated in the positive mode with triple quadrupole detection of lithium adduct ions, and showed the presence of a higher number of PtdCho species with long chained unsaturated fatty acids, than seen in egg yolk, ox liver and soy.

We believe the current study verifies previously presented findings and offer new insights into the composition of krill oil. In addition; it shows the advantage of performing an additional fragmentation using an exclusion list in the identification of low prevalent species.

Experimental Procedures

Chemicals

Phospholipid standards of lyso-phosphatidylcholine (lyso-PtdCho), PtdCho, phosphatidylethanolamine (PtdEtn), phosphatidylinositol (PtdIns) and phosphatidylserine (PtdSer) were purchased from Sigma-Aldrich (St. Louis, MO, USA). Lyso-PtdCho, PtdCho and PtdEtn were lyophilized powders obtained from egg yolk, whereas the PtdIns source was *glycine max* and the PtdSer source was

bovine brain. EPAX 6000 TG® fish oil was donated by EPAX (Ålesund, Norway), and Superba™ krill oil was obtained from Aker BioMarine (Oslo, Norway). All other chemicals were of MS grade.

Instrumentation

The chromatography was carried out on a Dionex system consisting of an Ultimate 3000 pump, an Ultimate 3000 RS autosampler, and an Ultimate 3000 flow manager. Detection was obtained using a linear ion trap LTQ XL coupled to an Orbitrap Discovery, LC-operation, data acquisition and processing were carried out using Chromelion SDK 6.80 SP2 Build 2327 and Xcalibur version 2.0.7 coupled with DCMS^{Link} 2.5 (all Instrument-Teknikk AS, Østerås, Norway).

Mass Spectrometry

The LTQ Orbitrap system was operated with a spray voltage of 5.00 kV, nitrogen as the sheath gas with flow rate set to 30 arbitrary units, and helium as the collision gas. The quantification of the PtdCho class was performed with a scan from $m/z = 400$ to $m/z = 1{,}000$ operated in negative ionization mode. MS^n experiments for identification of the choline-containing phospholipids were performed using data dependent PQD for the first fragmentation step. The molecular ion selected for each fragmentation in this step, was the most intense ion detected by the Orbitrap analyzer with target mass resolution of 30,000 and a scan window from $m/z = 400$ to $m/z = 1{,}000$. The normalized collision energy was 200 and the isolation width 2.00 Da. Subsequently, the most intense fragment ion detected was further fragmented using CID, with the normalized collision energy at 35 and an isolation width of 2.00 Da (MS^3). The LTQ was utilized for the detection of the fragments and the m/z range was relative to the m/z of the molecular ion. An alternative method was used in order to be able to observe species that were not selected for fragmentation in this way. The overall setup of this method was as described above, with the distinction of adding an asymmetric exclusion list. The exclusion list was generated with the purpose of the LTQ to ignore already identified substances. The list was based on the m/z of the molecular ions, with an exclusion window from this mass-to-charge ratio, up to $m/z + 1$. The width of the exclusion window was selected in order to diminish the detection of isotopes of the molecular ions.

Chromatographic Conditions RPLC

Chromatographic separation was performed on a ZORBAX Eclipse Plus C18 column with particle diameter of 5 μm and the column dimensions were 150 × 2.1 mm i.d.

The mobile phase A consisted of 90 parts 1% TEA and 0.2% formic acid in water, and 10 parts mobile phase B (*v*/*v*). Mobile phase B consisted of 1% TEA and 0.2% formic acid in 60 parts methanol and 40 parts acetonitrile (*v*/*v*).

A linear gradient was used for the separation. The system was first kept isocratic at 65% mobile phase B for 5 min after injection of sample. The gradient was then run from 65 to 100% mobile phase B in 5 min and was kept isocratic at 100% mobile phase B for 20 min, before it was returned to the initial condition in 0.1 min. The column was regenerated with 65% mobile phase B for 16 min. The mobile phase flow was set to 0.2 mL/min and the injection volume was 20 μL throughout the study.

Chromatographic Conditions NPLC

NPLC was performed on a HiCHROM LiChrospher 100 DIOL column with a particle diameter of 5 μm and column dimensions of 250 × 2 mm i.d. Mobile phase C was 100% chloroform, and the mobile phase D consisted of 0.05% TEA, 0.05% ammonia and 0.1% formic acid in methanol (*v*/*v*). For the class separation of the phospholipids, a linear gradient was used. The gradient was run from 5 to 27.5% mobile phase D in 15 min, followed by a rise to 80% in 2 min to flush the column. This concentration was kept isocratic for 4 min, before it was returned to the initial condition in 2 min. The column was regenerated with 5% mobile phase D for 12 min. The mobile phase flow was set to 0.3 mL/min, and the injection volume was 20 μL throughout the study.

Sample Preparation

Samples of krill oil and stock solutions of standards were prepared by dissolving the lipids in a mixture of chloroform and methanol at a ratio of 2:1. These solutions were stored at −32°C and excessive heating cycles were avoided. Samples were prepared by further dilution with solvents compatible with the mobile phases used. For NPLC, this was achieved with chloroform:MeOH 95:5, while it was attained by dilution in mobile phase A for RPLC.

Calibration Curve

For the quantification, a calibration curve was established with samples of PL free fish oil (EPAX®) spiked with a PtdCho standard purified from egg yolk to concentrations of 100 μg/mL. The spiking of PL free fish oil was performed in order to produce comparable matrixes in the standards and the krill oil samples. Stock solutions were made by dissolving PtdCho standard, PL free fish oil and krill oil separately in mixtures of chloroform:MeOH 2:1. The concentration of krill oil and PtdCho standard was

1 mg/mL and for PL free fish oil 10 mg/mL for these solutions. Respectively, 100 μL of PtdCho standards and of krill oil was added to 900 μL of the PL free fish oil, producing samples with concentrations of 100 μg/mL. For the calibration curve, the PtdCho standard samples were consecutively diluted to the desired concentrations of 10.0, 5.00, 2.50, 1.00, 0.50, 0.25, and 0.10 μg/mL ($n = 5$) with a mixture of chloroform:MeOH 95:5. The krill oil samples were diluted in the same way to a concentration of 1.00 μg/mL in order to measure the PtdCho content within the linear area of response of the calibration curve.

Results

Selection of MS-Mode for PtdCho-Classification

Initial experiments with standards of PtdEtn, PtdIns, PtdSer, PtdCho and lyso-PtdCho, were performed in both positive- and negative- ion mode using the LTQ Orbitrap as a detector. Separation of these substances on a NPLC column yielded class-specific baseline separation (data not shown). The results of these tests indicated a minor difference in the signal intensities obtained between the two settings, with a slightly higher response in negative mode.

Identification of Choline-Containing Phospholipids in Krill Oil

Since krill oil, as established in Fig. 1, is predominantly composed of choline-containing phospholipids, the emphasis of the work was focused on the elucidation of the species in the PtdCho and lyso-PtdCho classes. In NPLC, class separation of the phospholipids is achieved. A clear tendency of the elution order from the column was seen from high *m/z* to lower *m/z*. PtdCho class species eluted from 6.5 to 8 min, and the elution of the lyso-PtdCho class occurred between 10.5 and 12 min. Some species separation

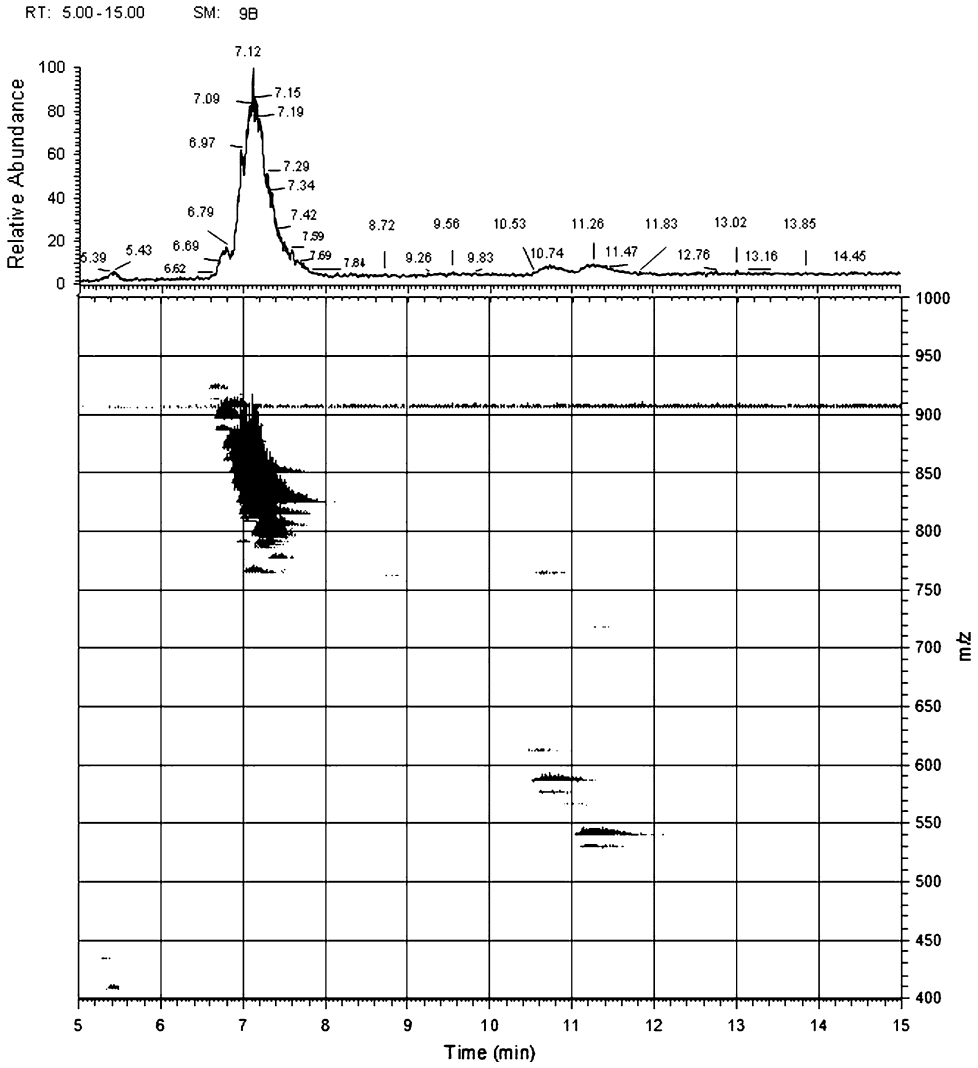

Fig. 1 Base peak chromatogram and three dimensional (*3D*) map of phospholipid class separation of krill oil, performed with a linear gradient NPLC/ESI–MS on a HiCHROM LiChrospher 100 DIOL column (250 × 2 mm i.d., 5 μm). MS was operated in the negative ionization mode and set to scan *m/z* 400–1,000. Only the relevant part of the chromatogram is shown (5–15 min). For the major part of the species, the map show adduct ions in the form of $[M + FA–H]^-$

was seen within the PtdCho class, however, this was not adequate for identification of the diverse species within the classes.

As the identification of the components is performed with data dependent fragmentation, chromatographic separations of the substances are critical for detection of the less prominent species. Hence, the separation for characterization of the species was performed utilizing a RPLC C18 column as described under "Experimental Procedures". This improved the chromatographic performance for species separation compared to NPLC (Fig. 2). As lyso-PtdCho only carry one fatty acyl group, these components elute earlier in the chromatogram than the PtdCho species. Lyso-PtdCho dominate the region between 12.0 min and 14.5 min in the chromatogram, while the heavier PtdCho components dominate the chromatogram after 14.5 min.

The identification of the species was performed utilizing a MS^3 data dependent fragmentation method, with an initial PQD fragmentation resulting in the loss of methyl formate, followed by a CID fragmentation. Analysis of the fragmentation spectra obtained typically revealed the identity of the substances without ambiguity. However, co-elution of isobaric compounds could potentially complicate the interpretation of the spectra. This challenge is minimized by applying a set of criteria for reliable identification. The following criteria were applied for reliable interpretation of a choline-containing phospholipid: based on the mass-to-charge ratio of the molecular ion, it is likely to be a choline-containing phospholipid (i.e. *m*/*z* being an even number). Following the first CID with PQD, a daughter ion should be produced by the loss of ($HCOO + CH_3$) as 60 Da. Further fragmentation with CID of the resulting product should produce specific fragments revealing the nature of the fatty acyl groups in both the *sn*-1 and the *sn*-2 position, either by the occurrence of the fragment for the fatty acyl group itself, or by the presence of the corresponding fragments of the lyso-compound. The sum of the fatty acyl groups elucidated in this matter should yield a mass matching the initial molecular mass. This is illustrated in Fig. 3, showing the elucidated fragment identity for the fragmentation of the 20:5–22:6 diacyl PtdCho.

The spectra were generally dominated by fatty acyl fragments from both the *sn*-1 and the *sn*-2 positions in addition to their corresponding fragments of the lyso-compound, ensuring identification of the species. The lyso-PtdChoand PtdCho substances identified by applying this method are presented in Tables 1 and 2. The relative intensity of the molecular ions is also presented.

As described earlier, the use of signal intensities in MS, for concentration comparison of the different substances, is only semi-quantitative. However, it provides a valuable indication of the composition of the PtdCho and lyso-PtdChoclasses. Chromatograms and fragmentation patterns are presented in Figs. 4 and 5 for the 10 foremost substances characterized from the PtdCho class.

As data dependent fragmentation methods are, by nature, biased in the selection of the most prevalent substances, the experiments where repeated with the use of an asymmetric exclusion list added to the MS-method. The exclusion list was based on the data sets obtained with the initial settings (i.e. Tables 1, 2). This method allowed the detection and identification of the additional substances presented in Table 3.

Quantification of PtdCho-Class in Krill Oil

Krill oil predominantly contains phospholipids from the PtdCho class (Fig. 1). It was therefore attempted to quantify the absolute concentration of this class by use of class separation with NPLC. Quantification of the PtdCho class was performed with a method developed "in-house" with a LTQ Orbitrap mass spectrometer for the detection.

In the construction of the calibration curve, PtdCho concentrations above 1.00 μg/mL resulted in a relative decrease in the MS signal response, yielding a quadratic polynomial curve ($y = ax^2 + bx + c$) where $a = -9{,}766$, $b = 330{,}360$ and $c = 4763.8$ with $r^2 = 0.9995$. From 0.10 μg/mL to 1.00 μg/mL, the calibration curve showed a high degree of linearity ($r^2 = 0.9995$) with a linear regression curve ($y = bx + c$) where $b = 368{,}737$ and $c = -16{,}547$.

The latter area was chosen for quantification purpose. From this, the PtdCho content of the undiluted krill oil was determined to be 34 ± 5% (*w*/*w*) ($n = 5$). Comparisons of the mass spectrum of the sample with the spectrum of the PtdCho standard indicated a difference in PtdCho class composition (Fig. 6). From the results, the average acyl chain lengths appear to be higher in krill oil than in egg yolk. This has also previously been shown by others [24]. As mentioned above, instrument response is affected by the acyl chain length of the PtdCho. These differences in chain lengths could therefore influence the quantification of the PtdCho class as discussed later. The quantitative results were compared with an earlier analysis of the krill oil, performed by the accredited analytical company Nofima (Bergen, Norway). They reported the PtdCho concentration in the krill oil sample to be 35 g/100 g oil.

Discussion

The fact that fatty acyl chain lengths of the PtdCho species are relatively long, affects both the choice of fragmentation technique and the effect of standards used for quantification purposes. Due to the low mass cut-off limit at 28% of the molecular ion mass with CID fragmentation in ion

traps, fragmentation utilizing PQD in the positive ionization mode was chosen as the first fragmentation step. In addition, utilizing PQD in the first fragmentation step of a MS^3 method, operating with negative mode ionization, also yields class elucidation of phospholipids with choline head groups. This is achieved by the detection of the $[M-CH_3]^-$ fragment formed after ($HCOO + CH_3$) loss from formate-molecular ion adducts. Consequently, performing a mode shift from the positive to the negative ionization mode is not necessary for the overall identification of lyso-PtdCho and PtdCho class phospholipids. PQD with a normalized collision energy at 200 produced the $[M-CH_3]^-$ fragments, without extensive fragmentation to secondary fragment ions. Higher collision energies produced secondary fragments that could be used as a source of structural information; however, this was better achieved with CID as a second fragmentation step. The CID was operated with a normalized collision energy of 35, for further fragmentation of the $[M-CH_3]^-$ ion. This value was not optimized for the individual species, and additional structural information could potentially have been achieved by specie specific optimization of this setting.

With the described method for separation and fragmentation of the phospholipids, typical fragmentation patterns were obtained, as shown in Fig. 3. The spectra were dominated by fatty acyl fragment ions originating

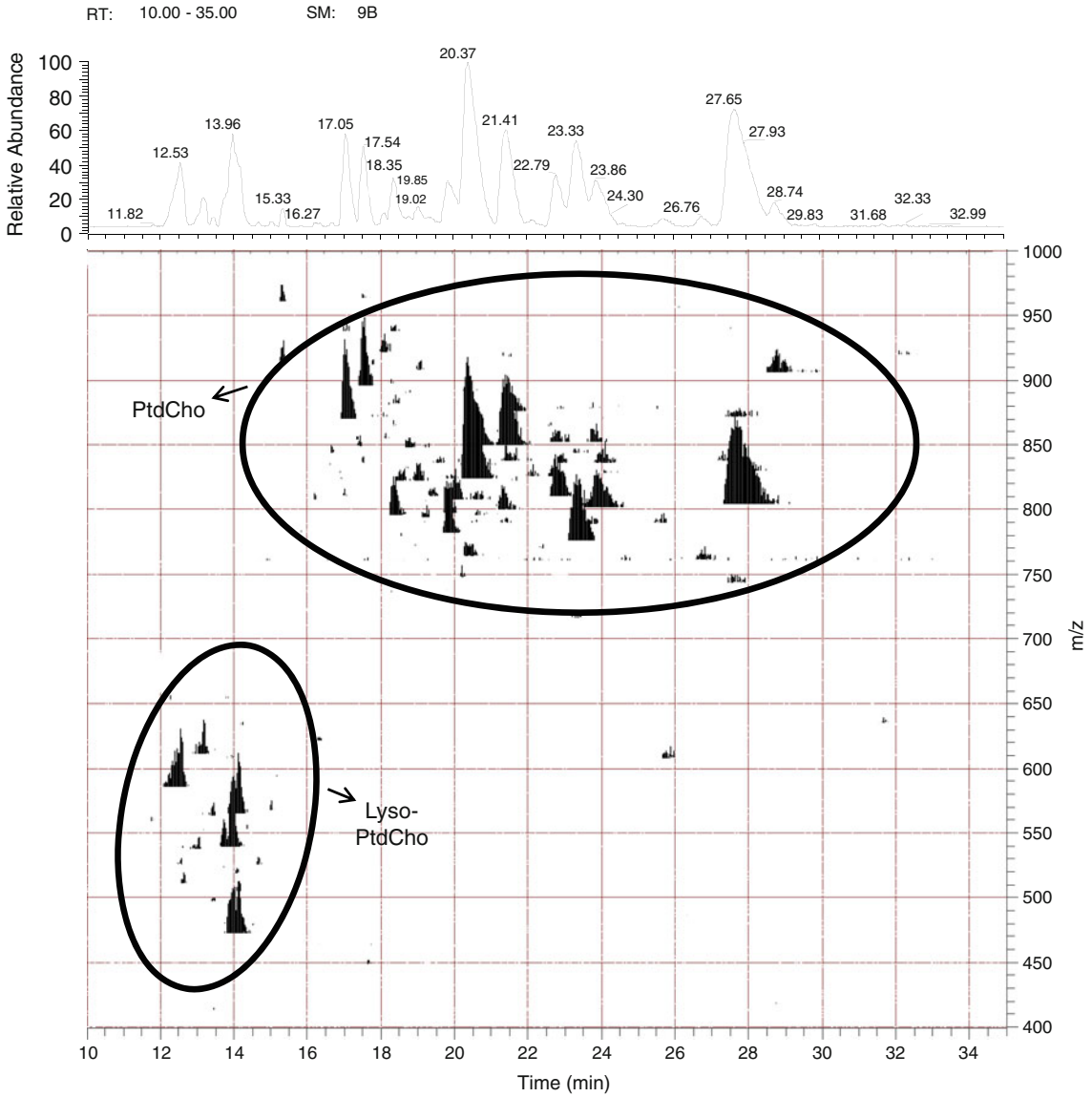

Fig. 2 Base peak chromatogram and three dimensional (*3D*) map of phospholipid specie separation of krill oil, performed with RPLC/ESI–MS on a ZORBAX Eclipse Plus C18 column (150 × 2.1 mm i.d., 5 μm). MS was run in negative the ionization mode and set to scan from *m*/*z* 400 to *m*/*z* 1,000. Only the most relevant part of the chromatogram is shown (10–35 min). Adduct ions in the form of $[M + FA–H]^-$ is seen throughout the map

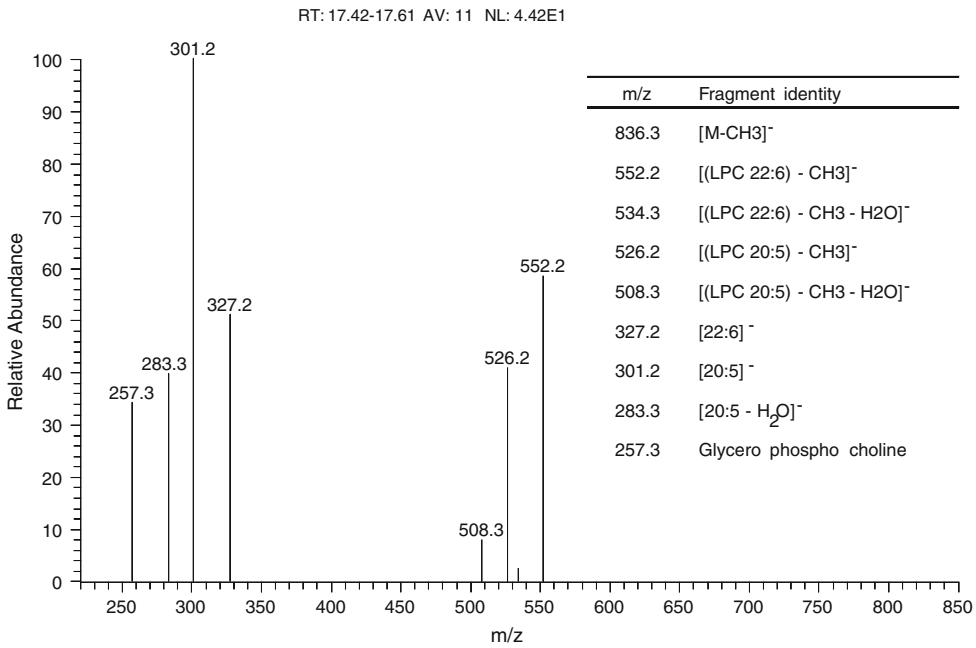

Fig. 3 MS^3 product ion spectrum of 22:6–20:5 diacyl PtdCho obtained in negative ionization mode. The molecular ion of *m/z* 896.6 was selected for PQD fragmentation; this yielded a fragment ion of *m/z* 836.3 which was further fragmented with CID resulting in the presented spectrum. Fragment identity is explained in the table on the *right hand side*, indicating the high level of certainty in the characterization

Table 1 Identified lyso-phospholipid species with choline head group in krill oil

Class	Mass	*m/z*[a]	Molecular specie	Relative intensity
Lyso-PtdCho	493.4	538.4	16:1	6.01
Lyso-PtdCho	495.4	540.4	16:0	32.42
Lyso-PtdCho	509.4	554.4	17:0	4.06
Lyso-PtdCho	521.4	566.4	18:1	23.21
Lyso-PtdCho	541.4	586.4	20:5	31.31
Lyso-PtdCho	563.4	608.6	21:1	16.70
Lyso-PtdCho	567.4	612.4	22:6	12.19

Data were obtained with RPLC/ESI–MS^3 operated in negative ionization mode and with data dependent fragmentation without exclusion list

[a] *m/z* for $[M + FA–H]^-$ adduct

from both *sn*-1 and *sn*-2, except in the fragmentation of alkyl–acyl species, where only a single fatty acyl fragment ion was observed. In addition, the corresponding fragment ions of the lyso-PtdCho compound were prevalent, confirming the characterization of the species. The fragments associated with the lyso-PtdCho compounds were either in the form of $[\text{lyso-PtdCho–CH}_3]^-$ or $[\text{lyso-PtdCho–CH}_3\text{–H}_2\text{O}]^-$. Furthermore, fragments specific for phospholipids carrying a choline head group were often registered. These dissociation products were *m/z* 257, *m/z* 242 and *m/z* 223, representing [Glycero phospho choline]$^-$, $[\text{Glycero phospho choline–CH}_3]^-$ and $[\text{Glycero phospho choline–CH}_3\text{–H}_2\text{O}]^-$, respectively. The identification of the phospholipid class was made based on the loss of 60 Da in the PQD fragmentation step. However, fragments specific for phospholipids carrying a choline head group affirms this interpretation. In spectra obtained from the dissociation of species carrying a 20:5 fatty acyl group, an ambiguous $[20:5–H2O]^-$ fragment ion with *m/z* 283 can often be detected. This ion can potentially be misinterpreted as the fatty acyl fragment $[18:0]^-$, but meeting the criteria for reliable identification will rule out this erroneous conclusion.

In some incidences, a molecular ion could be explained by either being a diacyl-, or an alkyl–acyl-compound. In these cases, the possible identification of alkyl–acyl PtdCho species was based on the presence of a relatively high MS-signal for a single fatty acyl fragment ion and the corresponding lyso-PtdCho compound. In addition, there should be a total absence of signals (i. e. both fatty acyl-, and lyso-PtdCho-ions) potentially explained by fragmentation of an ester bond in the opposite *sn*-position. An example of this is *m/z* 764.6 (spectrum shown in Fig. 5f) which could originate from both O16:0–20:5 alkyl–acyl PtdCho and 15:0–20:5 diacyl PtdCho. The presence *m/z* 466 $[\text{(lyso-PtdCho O16:0/15:0)–CH}_3]^-$, 448 $[\text{(lyso-PtdCho O16:0–15:0)–CH}_3\text{–H}_2\text{O}]^-$ and 301 $[20:5]^-$ indicate a fatty acyl group of 20:5, while there is no fragment indicating a fatty acyl group of 15:0 in the opposite *sn*-position. This is therefore assumed to be a PtdCho-specie with an alkyl-acyl composition of O16:0–20:5. Altogether, seven different potential alkyl-acyl PtdCho species were characterized. For all these species, the fatty alkyl chains were either hexadecanoic or octadecanoic, and either saturated or with a single double bond.

No further attempt was made to clarify the stereospecificity of the species. It is important to keep in mind that

Table 2 Identified phospholipid species with choline head group in krill oil

Class	Mass	m/z[a]	Molecular specie	Relative intensity
PtdCho	703.6	748.6	14:0–16:1	5.33
PtdCho	717.7	762.7	15:0–16:1	0.90
PtdCho	717.7	762.7	13:0–18:1	21.08
PtdCho	731.6	776.6	14:0–18:1	13.75
PtdCho	731.6	776.6	16:0–16:1	27.48
PtdCho	737.6	782.6	13:0–20:5	17.38
PtdCho	745.6	790.6	15:0–18:1	6.71
PtdCho	745.6	790.6	16:0–17:1	6.80
PtdCho	749.6	794.6	14:1–20:5	6.94
PtdCho	751.6	796.6	14:0–20:5	17.62
PtdCho	753.6	798.6	14:0–20:4	0.26
PtdCho	753.6	798.6	16:0–18:4	14.88
PtdCho	755.6	800.6	16:0–18:3	13.30
PtdCho	757.6	802.7	16:1–18:1	1.41
PtdCho	757.6	802.7	16:0–18:2	32.42
PtdCho	759.7	804.7	16:1–18:0	0.10
PtdCho	759.7	804.7	16:0–18:1	100.00
PtdCho	761.7	806.7	16:0–18:0	15.83
PtdCho	763.6	808.6	13:0–22:6	0.30
PtdCho	763.6	808.6	O16:1–20:5	20.17
PtdCho	765.6	810.7	O16:0–20:5	28.24
PtdCho	777.6	822.6	18:3–18:3	<0.01
PtdCho	777.6	822.6	12:4–24:2	0.03
PtdCho	777.6	822.6	18:1–18:5	0.07
PtdCho	777.6	822.6	16:1–20:5	4.85
PtdCho	777.6	822.6	14:0–22:6	12.25
PtdCho	779.6	824.6	18:1–18:4	0.10
PtdCho	779.6	824.6	16:0–20:5	96.57
PtdCho	781.6	826.6	16:0–20:4	24.23
PtdCho	783.7	828.7	18:1–18:2	7.69
PtdCho	785.6	830.7	18:1–18:1	14.69
PtdCho	789.6	834.7	O16:1–22:6	3.50
PtdCho	789.6	834.7	17:2–20:5	3.85
PtdCho	791.7	836.7	17:1–20:5	15.64
PtdCho	791.7	836.7	O16:0–22:6	22.97
PtdCho	793.6	838.6	O18:0–20:5	15.01
PtdCho	799.6	844.6	18:4–20:5	8.17
PtdCho	803.6	848.7	18:2–20:5	9.28
PtdCho	805.6	850.6	18:1–20:5	3.51
PtdCho	805.6	850.6	16:0–22:6	76.34
PtdCho	807.6	852.6	18:0–20:5	23.92
PtdCho	825.6	870.6	18:4–22:6	0.15
PtdCho	825.6	870.6	20:5–20:5	30.31
PtdCho	827.6	872.6	20:4–20:5	16.18
PtdCho	831.7	876.7	18:1–22:6	17.10
PtdCho	833.7	878.7	20:1–22:6	<0.01
PtdCho	851.6	896.6	20:5–22:6	24.80
PtdCho	861.7	906.7	20:5–22:1	20.80
PtdCho	867.6	912.7	20:5–23:5	<0.01
PtdCho	875.7	920.7	20:5–23:1	5.75
PtdCho	877.6	922.6	22:6–22:6	7.49

Data were obtained with RPLC/ESI-MS^3 operated in negative ionization mode and with data dependent fragmentation without exclusion list

[a] m/z for $[M + FA–H]^-$ adduct

stereoisomers would be difficult to separate and specifically identify. Therefore, the relative intensity values presented in Table 2 will in many cases be the sum of the signal intensities of the two stereoisomers. The ratio between the stereoisomers will vary among the different species. However, an interesting observation was that several of the *n*-3 acylated species appear to carry the *n*-3 fatty acyl group in the *sn*-1 position, based on the fragment ratios in the fragmentation spectra (e.g. 22:6–18:1 diacyl PtdCho).

In total, 58 species were characterized without the use of the exclusion list, whereof seven were from the lyso-PtdCho class and 51 from the PtdCho class. An additional 11 species were detected by applying the asymmetric exclusion list. Of these latter, two were identified as lyso-PtdCho and nine as PtdCho compounds, yielding an overall total of nine lyso-PtdCho class species and 60 PtdCho class species elucidated. Seven species yielded signals for highly probable fatty acyl *n*-3 groups in both the *sn*-1 and *sn*-2 positions (i.e. the diacyl PtdCho species 18:4–20:5, 18:4–22:6, 20:5–20:5, 20:5–22:6, 20:5–23:5, 22:6–22:6 and 20:5–22:5). Those species and the detection of more exotic species such as 22:6–23:5 and 20:5–26:4 diacyl PtdCho, show the complexity of krill oil.

Prior to analysis of the krill oil, the total fatty acid composition, wherein information on the concentration of individual fatty acids and their *n*-3 content was obtained and provided by Nofima, with the method AOCS Ce 1b-89 (data not shown). The sum of polyunsaturated (*n*-3) fatty acids was reported to be 18.5 g/100 g oil. The assumed homologous distribution of the fatty acid composition between triacylglycerols, free fatty acids, and the lyso-PtdCho- and PtdCho-classes, combined with the described relative intensities of the known species (Tables 1, 2), makes it possible to estimate the prevalence of *n*-3 fatty acids in one or both *sn* positions of the PtdCho species. For the PtdCho class, approximately 58% of the components contained a single *n*-3 fatty acid, and 10% held an *n*-3 fatty acid in both *sn*-1 and *sn*-2 positions. Of the species in the lyso-PtdCho class, approximately 35% contained an *n*-3

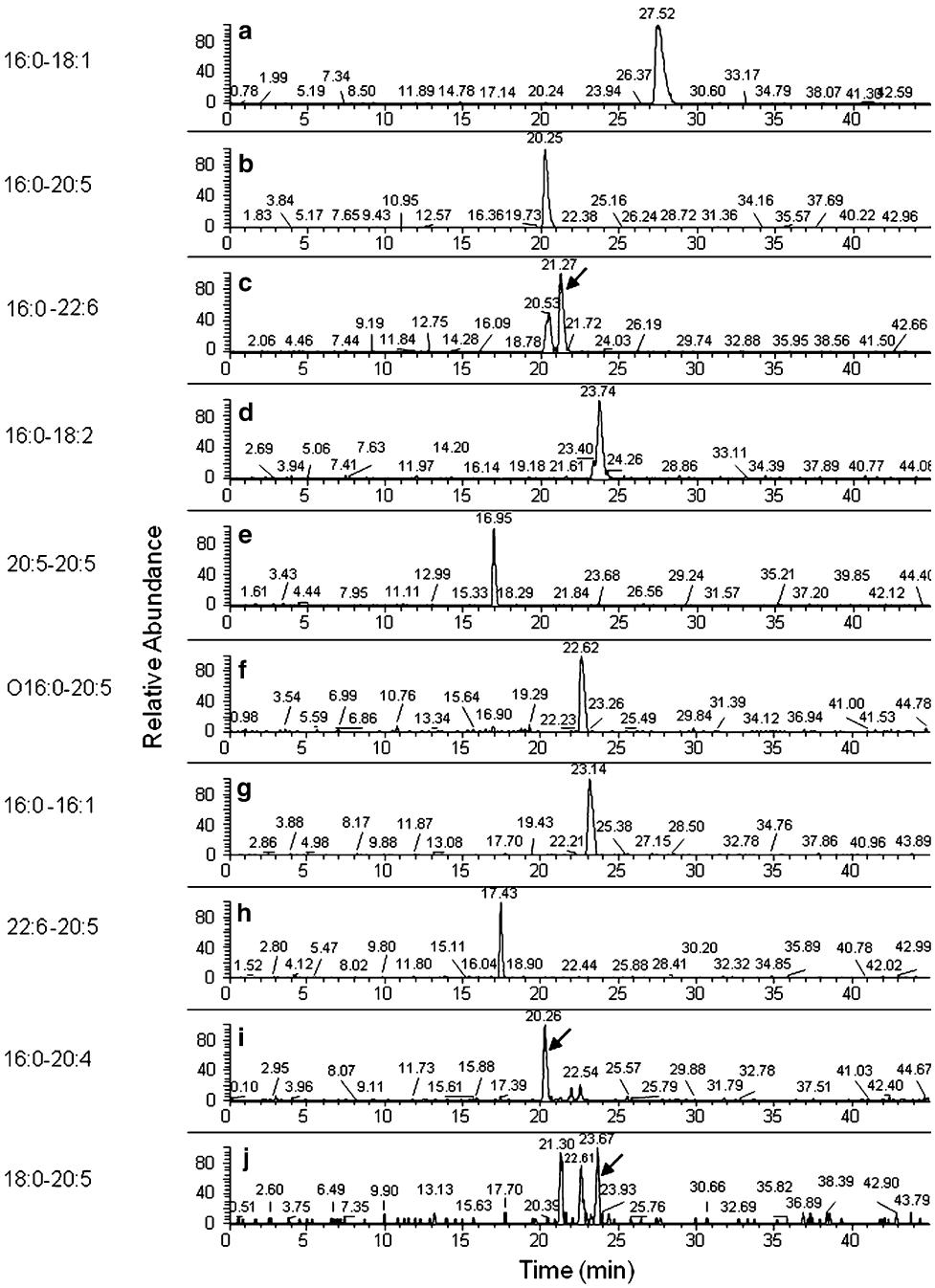

Fig. 4 Reconstructed ion chromatograms obtained for the 10 species with the highest relative intensities in falling order from **a** to **j**. The following *m*/*z* values for the adducts $[M + FA–H]^-$ were used for the reconstruction: **a** 804.6 **b** 824.6 **c** 850.6 **d** 802.6 **e** 870.6 **f** 810.6 **g** 776.6 **h** 896.6 **i** 826.6 **j** 852.6

fatty acid. The phospholipid composition might potentially give better insight into the mechanism and distribution of krill oil in the body.

In the analysis performed by Nofima, the PtdCho concentration of the same krill oil as was used in the current study was reported to be 35 g/100 g oil (Nofima internal method N A88, based on [25, 26]). With the method developed for this work, the PtdCho concentration was estimated to be 34 ± 5 g/100 g oil. This shows that, in spite of the difference between the methods, the correlation of the values obtained with the two methods is relatively high. Dissimilarity between the standards used for calibration and the actual composition of the phospholipid classes in the sample could influence the quantification. In this work, we utilized a PtdCho standard originating from egg yolk. The difference in the PtdCho profile between this standard and the krill oil (Fig. 6) could potentially result in an underestimation of the PtdCho content of the sample. This is a result of krill oil containing long chained fatty acids in the phospholipid components, which are less prone

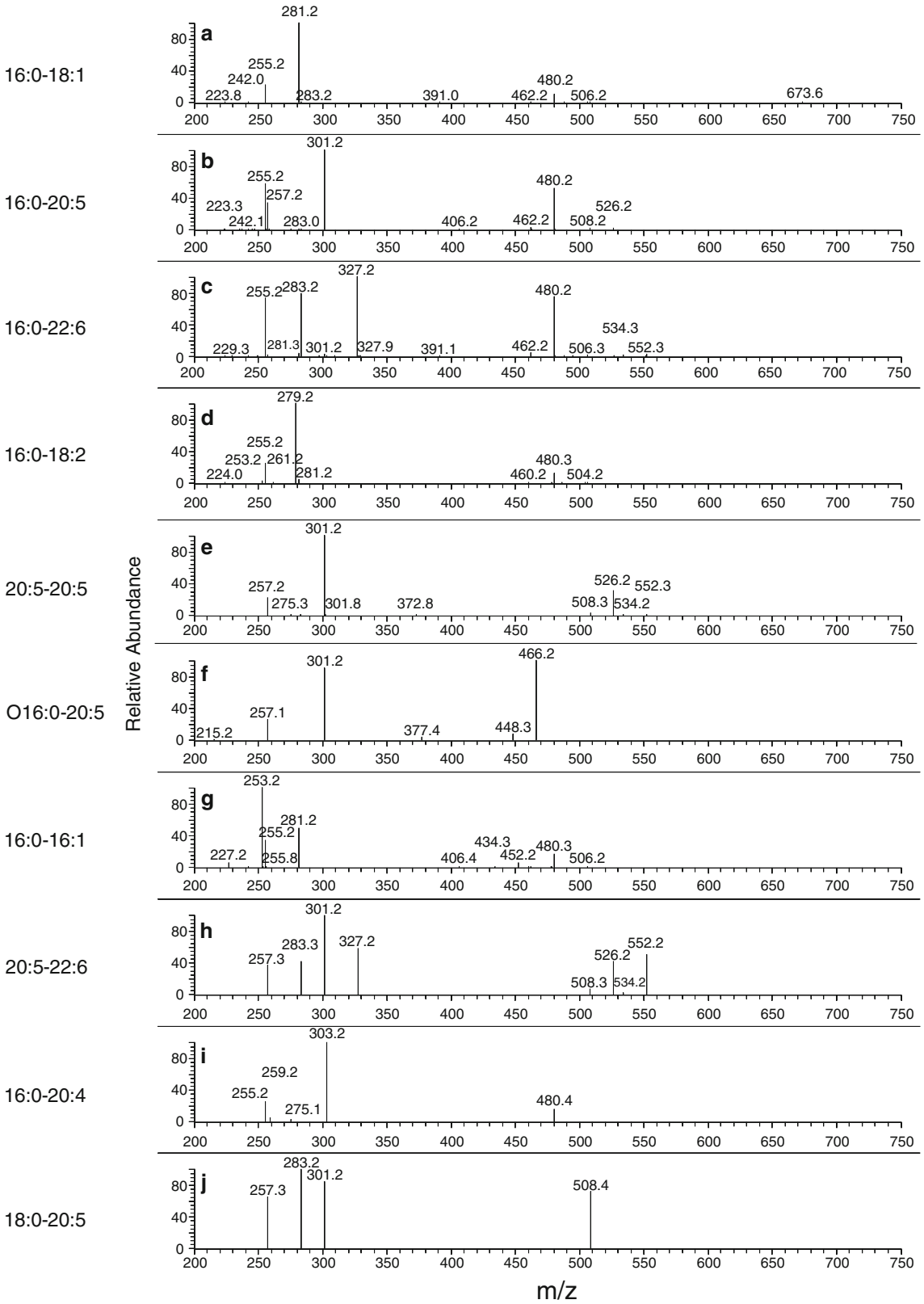

Fig. 5 MS^3 product ion spectrum for the 10 species with the highest relative intensities, obtained using RPLC for separation with data dependant fragmentation. Fig. 5 **a**–**j** corresponds to Fig. 4 **a**–**j**, respectively

Table 3 Identified lyso-phospholipid and phospholipid species with choline head group in krill oil

Class	Mass	m/z[a]	Molecular specie
Lyso-PtdCho	549.4	594.4	20:1
Lyso-PtdCho	569.4	614.4	22:5
PtdCho	771.3	816.3	O18:1–18:1
PtdCho	795.6	840.6	16:0–21:4
PtdCho	819.7	864.7	O18:0–22:6
PtdCho	829.5	874.5	18:2–22:6
PtdCho	845.6	890.6	20:5–21:2
PtdCho	853.2	898.2	22:6–23:5
PtdCho	853.2	898.2	20:5–22:5
PtdCho	893.6	938.6	20:4–22:6
PtdCho	911.6	956.6	20:5–26:4

Data were obtained with RPLC/ESI-MS^3 operated in negative ionization mode and with data dependent fragmentation with asymmetric exclusion list. Relative intensities for the two different methods cannot be compared

[a] m/z for $[M + FA–H]^-$ adduct

to ionization with ESI as described earlier. Hence, the use of a PtdCho standard originating from krill oil would have been preferred. However, this type of standard was not commercially available when the study was performed.

Krill oil has been analyzed by a novel method and numerous molecular species were found that were previously not known to be present in krill oil. To our knowledge, there has previously only been one report showing the fatty acid composition in PtdCho from krill oil [24] The method used in that study was comparable to the platform used in the current study, however, their detection was based on the formation of lithium adducts, detected with a triple quadrupole. The krill oil used in that study was delivered by Nestec SA (Lausanne, Switzerland), and the composition of the two krill oils might therefore not be directly comparable in respect to composition. However, in both studies the following three PtdCho species were among the five most prevalent: (16:0–20:5) (16:0–22:6), and (16:0–18:1). On the other hand, they detected high levels of other PtdCho species that are low or absent in our study, such as: (18:1–20:5) and (18:0–18:2). Le Grandois et al. detected neither fatty acids longer than 22 carbons nor ether-linked fatty acids. Moreover, in our study, a higher number of PtdCho species was detected. Whether these differences are due to a different composition of the two krill oils, or the methodology is not known, but might indicate that the detection method used in the current study is more sensitive.

The method used for quantification purposes in this study was optimized for specific quantification of the PtdCho class, and quantification of other PL classes was not attempted. However, it would be of great interests and an aid in the field of lipidomics, to develop standardized and validated LC–MS methods that meet the need for quantification of all phospholipid classes in complex matrixes like krill oil. One of the potential challenges in the development of such strategies would be the choice of suitable standards for the calibration curves.

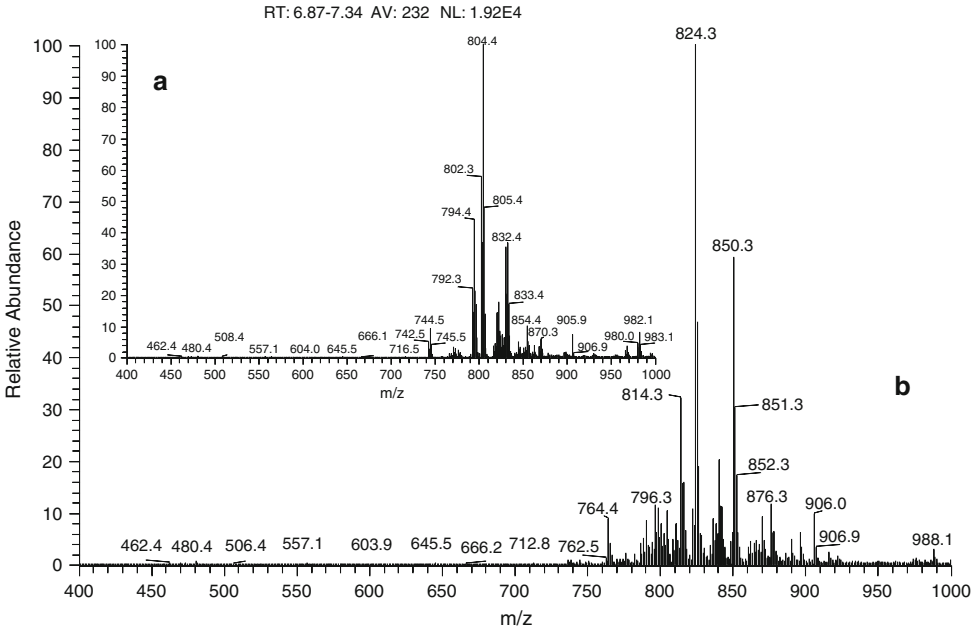

Fig. 6 **a** Mass spectrum of PtdCho class standard used as calibrant for quantification. **b** Mass spectrum of the krill PtdCho class. Both spectra were obtained with NPLC/ESI–MS operated with negative mode ionization, and show $[M + FA–H]^-$ adduct ions. The *mass spectra* indicate a higher occurrence of long chained fatty acyl groups in PtdCho species originating from krill than in the PtdCho standard from egg yolk

Acknowledgments The authors would like to thank Dr. Inge Bruheim and Dr. Åsmund Larsen for their helpful input and valuable discussions during the method development. This work was partially funded by Aker BioMarine ASA.

References

1. Batetta B, Griinari M, Carta G, Murru E, Ligresti A, Cordeddu L, Giordano E, Sanna F, Bisogno T, Uda S, Collu M, Bruheim I, Di Marzo V, Banni S (2009) Endocannabinoids may mediate the ability of (n-3) fatty acids to reduce ectopic fat and inflammatory mediators in obese Zucker rats. J Nutr 139:1495–1501
2. Di Marzo V, Griinari M, Carta G, Murru E, Ligresti A, Cordeddu L, Giordano E, Bisogno T, Collu M, Batetta B, Sanna F, Uda S, Berge K, Banni S (2010) Dietary krill oil increases docosahexaenoic acid and reduces 2-arachidonoylglycerol but not *N*-acylethanolamine levels in the brain of obese Zucker rats. Int Dairy J 20:231–235
3. Maki KC, Reeves MS, Farmer M, Griinari M, Berge K, Vik H, Hubacher R, Rains TM (2009) Krill oil supplementation increases plasma concentrations of eicosapentaenoic and docosahexaenoic acids in overweight and obese men and women. Nutr Res 29:609–615
4. Tandy S, Chung RWS, Wat E, Kamili A, Berge K, Griinari M, Cohn JS (2009) Dietary krill oil supplementation reduces hepatic steatosis, glycemia and hypercholesterolemia in high-fat fed mice. J Agric Food Chem 57:9339–9345
5. Han X, Gross RW (2005) Shotgun lipidomics: electrospray ionization mass spectrometric analysis and quantitation of cellular lipidomes directly from crude extracts of biological samples. Mass Spectrom Rev 24:367–412
6. Koivusalo M, Haimi P, Heikinheimo L, Kostiainen R, Somerharju P (2001) Quantitative determination of phospholipid compositions by ESI-MS: effects of acyl chain length, unsaturation, and lipid concentration on instrument response. J Lipid Res 42:663–672
7. Bruegger B, Erben G, Sandhoff FT, Wieland WD, Lehmann WD (1997) Quantitative analysis of biological membrane lipids at the low picomole level by nano-electrospray ionization tandem mass spectrometry. Proc Natl Acad Sci USA 94:2339–2344
8. Houjou T, Yamatani K, Imagawa M, Shimizu T, Taguchi R (2005) A shotgun tandem mass spectrometric analysis of phospholipids with normal-phase and/or reverse-phase liquid chromatography/electrospray ionization mass spectrometry. Rapid Commun Mass Spectrom 19:654–666
9. Lehmann WD, Koester M, Erben G, Keppler D (1997) Characterization and quantification of rat bile phosphatidylcholine by electrospray-tandem mass spectrometry. Anal Biochem 246:102–110
10. Beermann C, Mobius M, Winterling N, Schmitt JJ, Boehm G (2005) *sn*-Position determination of phospholipid-linked fatty acids derived from erythrocytes by liquid chromatography electrospray ionization ion-trap mass spectrometry. Lipids 40:211–218
11. Houjou T, Yamatani K, Nakanishi H, Imagawa M, Shimizu T, Taguchi R (2004) Rapid and selective identification of molecular species in phosphatidylcholine and sphingomyelin by conditional neutral loss scanning and MS3. Rapid Commun Mass Spectrom 18:3123–3130
12. Larsen A, Uran S, Jacobsen PB, Skotland T (2001) Collision-induced dissociation of glycero phospholipids using electrospray ion-trap mass spectrometry. Rapid Commun Mass Spectrom 15:2393–2398
13. Schwudke D, Hannich JT, Surendranath V, Grimard V, Moehring T, Burton L, Kurzchalia T, Shevchenko A (2007) Top-down lipidomic screens by multivariate analysis of high-resolution survey mass spectra. Anal Chem 79:4083–4093
14. Hvattum E, Hagelin G, Larsen A (1998) Study of mechanisms involved in the collision-induced dissociation of carboxylate anions from glycerophospholipids using negative ion electrospray tandem quadrupole mass spectrometry. Rapid Commun Mass Spectrom 12:1405–1409
15. Karlsson AA, Michelsen P, Larsen A, Odham G (1996) Normal-phase liquid-chromatography class separation and species determination of phospholipids utilizing electrospray-mass spectrometry tandem-mass spectrometry. Rapid Commun Mass Spectrom 10:775–780
16. Larsen A, Mokastet E, Lundanes E, Hvattum E (2002) Separation and identification of phosphatidylserine molecular species using reversed-phase high-performance liquid chromatography with evaporative light scattering and mass spectrometric detection. J Chromatogr B Analyt Technol Biomed Life Sci 774:115–120
17. Uran S, Larsen A, Jacobsen PB, Skotland T (2001) Analysis of phospholipid species in human blood using normal-phase liquid chromatography coupled with electrospray ionization ion-trap tandem mass spectrometry. J Chromatogr B Biomed Sci Appl 758:265–275
18. Ekroos K, Chernushevich IV, Simons K, Shevchenko A (2002) Quantitative profiling of phospholipids by multiple precursor ion scanning on a hybrid quadrupole time-of-flight mass spectrometer. Anal Chem 74:941–949
19. Harrison KA, Murphy RC (1995) Negative electrospray ionization of glycerophosphocholine lipids: formation of [M-15] ions occurs via collisional decomposition of adduct ions. J Mass Spectrom 30:1772–1773
20. Khaselev N, Murphy RC (2000) Structural characterization of oxidized phospholipid products derived from arachidonate-containing plasmenyl glycerophosphocholine. J Lipid Res 41: 564–572
21. Schwartz JC, Syka JP, Quarmby ST (2005) Improving the fundamentals of Msn on 2D ion traps: new ion activation and isolation techniques. In: 53rd ASMS Conference on Mass Spectrometry, San Antonio, Texas
22. Tyurin VA, Tyurina YY, Feng W, Mnuskin A, Jiang J, Tang M, Zhang X, Zhao Q, Kochanek PM, Clark RS, Bayir H, Kagan VE (2008) Mass-spectrometric characterization of phospholipids and their primary peroxidation products in rat cortical neurons during staurosporine-induced apoptosis. J Neurochem 107:1614–1633
23. Griffin TJ, Xie H, Bandhakavi S, Popko J, Mohan A, Carlis JV, Higgins L (2007) iTRAQ reagent-based quantitative proteomic analysis on a linear ion trap mass spectrometer. J Proteome Res 6:4200–4209
24. Le Grandois J, Marchioni E, Zhao M, Giuffrida F, Ennahar S, Bindler F (2009) Investigation of natural phosphatidylcholine sources: separation and identification by liquid chromatography-electrospray ionization-tandem mass spectrometry (LC–ESI–MS2) of molecular species. J Agric Food Chem 57:6014–6020
25. Homan R, Anderson MK (1998) Rapid separation and quantitation of combined neutral and polar lipid classes by high-performance liquid chromatography and evaporative light-scattering mass detection. J Chromatogr B Biomed Sci Appl 708:21–26
26. Moreau RA (2006) The analysis of lipids via HPLC with a charged aerosol detector. Lipids 41:727–734

Lipids (2011) 46:37–46
DOI 10.1007/s11745-010-3490-4

ORIGINAL ARTICLE

Metabolic Effects of Krill Oil are Essentially Similar to Those of Fish Oil but at Lower Dose of EPA and DHA, in Healthy Volunteers

Stine M. Ulven · Bente Kirkhus · Amandine Lamglait · Samar Basu · Elisabeth Elind · Trond Haider · Kjetil Berge · Hogne Vik · Jan I. Pedersen

Received: 7 July 2010 / Accepted: 9 October 2010 / Published online: 2 November 2010

Abstract The purpose of the present study is to investigate the effects of krill oil and fish oil on serum lipids and markers of oxidative stress and inflammation and to evaluate if different molecular forms, triacylglycerol and phospholipids, of omega-3 polyunsaturated fatty acids (PUFAs) influence the plasma level of EPA and DHA differently. One hundred thirteen subjects with normal or slightly elevated total blood cholesterol and/or triglyceride levels were randomized into three groups and given either six capsules of krill oil ($N = 36$; 3.0 g/day, EPA + DHA = 543 mg) or three capsules of fish oil ($N = 40$; 1.8 g/day, EPA + DHA = 864 mg) daily for 7 weeks. A third group did not receive any supplementation and served as controls ($N = 37$). A significant increase in plasma EPA, DHA, and DPA was observed in the subjects supplemented with n-3 PUFAs as compared with the controls, but there were no significant differences in the changes in any of the n-3 PUFAs between the fish oil and the krill oil groups. No statistically significant differences in changes in any of the serum lipids or the markers of oxidative stress and inflammation between the study groups were observed. Krill oil and fish oil thus represent comparable dietary sources of n-3 PUFAs, even if the EPA + DHA dose in the krill oil was 62.8% of that in the fish oil.

Keywords Plasma lipoproteins · Plasma lipids · Dietary fat · Nutrition, n-3 fatty acids · Lipid absorption · Phospholipids

Abbreviations

EPA	Eicosapentaenoic acid
DHA	Docosahexaenoic acid
FA	Fatty acid
PL	Phospholipids
PUFA	Polyunsaturated fatty acid
TG	Triglycerides

Introduction

An association between consumption of fish and seafood and beneficial effects on a variety of health outcomes has been reported in epidemiologic studies and clinical trials [1–5]. These effects are mainly attributed to the omega-3

Electronic supplementary material The online version of this article (doi:10.1007/s11745-010-3490-4) contains supplementary material, which is available to authorized users.

S. M. Ulven (✉) · E. Elind
Faculty of Health, Nutrition, and Management,
Akershus University College, 2001 Lillestrøm, Norway
e-mail: stinemarie.ulven@hiak.no

B. Kirkhus
Nofima Mat, Ås, Norway

A. Lamglait
Mills DA, Oslo, Norway

S. Basu
Department of Public Health and Caring Sciences,
Uppsala University, Uppsala, Sweden

T. Haider
Link Medical Research AS, Oslo, Norway

K. Berge · H. Vik
Aker BioMarine ASA, Oslo, Norway

J. I. Pedersen
Department of Nutrition, Institute of Basic Medical Sciences,
University of Oslo, Oslo, Norway

long-chain polyunsaturated fatty acids (n-3 PUFAs) abundant in fish and seafood, and in particular to eicosapentaenoic acid (EPA) and docosahexaenoic acid (DHA). The effects of marine n-3 PUFAs on various risk factors of cardiovascular disease (CVD) are in particular well documented. In large systematic reviews of the available literature, consistent reductions in triglyceride (TG) levels following consumption of n-3 PUFAs have been demonstrated as well as increases in levels of high-density lipoprotein (HDL) cholesterol [6, 7]. The net beneficial effects of these changes have been disputed, although several large intervention studies indicate that n-3 PUFAs reduce mortality in patients with high risk of developing coronary heart disease (CHD) [8]. Moreover, guidelines published by the American Heart Association for reducing CVD risk recommend fish consumption and fish oil supplementation based on the acknowledgement that EPA and DHA may decrease the risk of CHD, decrease sudden deaths, decrease arrhythmias, and slightly lower blood pressure [9].

Reports on health benefits have led to increased demand for products containing marine n-3 PUFAs. Since fish is a restricted resource, there is growing interest in exploiting alternative sources of marine n-3 PUFAs. Antarctic krill (*Euphausia superba*) is a rich source of n-3 PUFAs. Krill is by far the most dominant member of the Antarctic zooplankton community in terms of biomass, which is estimated to be between 125 and 750 million metric tons (according to the Food and Agriculture Organization of the United Nations; http://www.fao.org/fishery/species/3393/en), and thus attractive for commercial harvest. The DHA content of krill oil is similar to that of oily fish, but the EPA content is higher [10]. The overall fatty acid composition resembles that of fish. In fish, the fatty acids are mainly stored as TG, whereas in krill 30–65% of the fatty acids are incorporated into phospholipids (PL) [10]. Whether being esterified in TG or in PL impacts on the absorption efficiency of FAs into the blood and on effects on serum lipid levels are issues for discussion. In a study by Maki et al. [11] comparing the absorption efficacy of n-3 PUFAs from different sources it was shown that EPA and DHA from krill oil were absorbed at least as efficiently as EPA and DHA from menhaden oil (TG) [11], and studies in newborn infants have indicated that fatty acids in dietary PL may be better absorbed than those from TG [12–14]. Studies addressing the compartmental metabolism of dietary DHA have indicated that the metabolic fate of DHA differs substantially when ingested as TG compared with phosphatidylcholine, in terms of both bioavailability of DHA in plasma and accumulation in target tissues [15]. Only a limited number of studies addressing health outcomes following ingestion of krill oil as compared with fish oil are currently available, but some of these have shown promising effects of krill oil on serum lipids and on markers of inflammation and oxidative stress (reviewed in [10]).

The aim of this study is to investigate the plasma levels of EPA and DHA, and the effects on serum lipids and on some biomarkers of inflammation, oxidative stress, and hemostasis, after krill oil and fish oil administration in healthy subjects after a 7-week intervention period. Safety was evaluated based on assessment of hematology and biochemistry parameters, and registration of adverse events.

Experimental Procedures

Study Subjects

The 129 subjects included in the study were healthy volunteers of both genders with normal or slightly elevated total blood cholesterol (<7.5 mmol/L) and normal or slightly elevated blood triglyceride level (<4.0 mmol/L). Subjects with body mass index (BMI) >30 kg/m^2, hyperlipidemia, hypertension, coronary, peripheral or cerebral vascular disease were excluded from participating in the study. No concomitant medication intended to influence serum lipid level was permitted. All study subjects were informed verbally and in writing, and all subjects signed an informed consent form before entering the study. The study was approved by the Regional Ethics Committee.

Study Design

The study was an open single-center, randomized, parallel group designed study. Screening of subjects ($N = 149$) was performed at the first visit to include subjects that satisfied the eligibility criteria ($N = 129$). These were randomized into three study groups. Seven participants were lost before the baseline visit. The remaining 122 participants were given either 3 g krill oil daily ($N = 41$), 1.8 g fish oil daily ($N = 40$) or no supplementation ($N = 41$) for a period of 7 weeks. A total of 115 participants finished the study. The disposition of the subjects is illustrated in Fig. 1. None of the subjects regularly ate fatty fish more than once a week prior to inclusion or during the 7-week intervention period. None were using cod liver oil or other marine n-3 supplements during the study or at least 2 months prior to inclusion. All the participants were instructed by a nutritionist to keep their regular food habits during the study.

Study Products

The krill oil capsules contained processed krill oil extracted from Antarctic krill (*Euphausia superba*). The product was

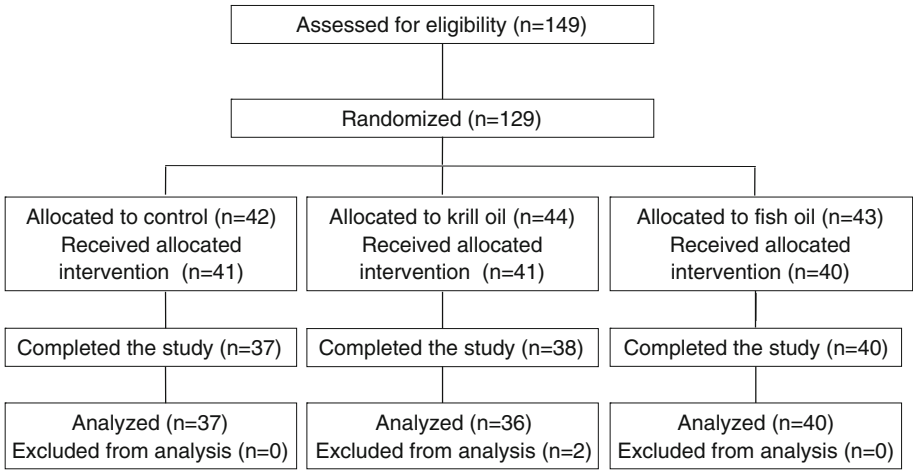

Fig. 1 Disposition of subjects

manufactured by Aker BioMarine ASA. Each capsule contained 500 mg oil that provided 90.5 mg EPA and DHA, and a total of 103.5 mg n-3 PUFAs. The capsules were made of gelatin softened with glycerol. The daily study dosage was six capsules (each of 500 mg oil). The comparator omega-3 fish oil product was manufactured by Peter Möller AS, Oslo, Norway. The daily study dosage was three capsules each containing 600 mg fish oil that provided 288 mg EPA and DHA, and a total of 330 mg n-3 PUFAs. The capsules were made of gelatin softened with glycerol. The fatty acid profile of the study products is presented in Table 1. The daily dose of EPA, DHA, and total n-3 PUFAs in the krill oil and fish oil groups is presented in Table 2. The daily EPA + DHA dose in the krill oil group was 62.8% of the dosage given in the fish oil group. DL-α-tocopheryl acetate (vitamin E), retinyl palmitate (vitamin A), and cholecalciferol (vitamin D) were added to the product.

Table 1 Relative content of fatty acids in the study products

Fatty acid	Fish oil (area %)	Krill oil (area %)
14:0	3.2	7.4
16:0	7.8	21.8
18:0	2.6	1.3
20:0	0.6	<0.1
22:0	0.4	0.2
16:1n-7	3.9	5.4
18:1n-9, -7, -5	6.1	18.3
20:1n-9, -7	2.0	1.2
22:1n-11, -9, -7	2.5	0.8
24:1n-9	<0.2	0.2
16:2n-4	0.7	0.5
18:2n-6	0.8	1.8
18:3n-6	<0.2	0.2
20:2n-6	0.3	<0.1
20:3n-6	0.2	<0.1
20:4n-6	1.5	0.5
22:4n-6	0.5	<0.1
18:3n-3	0.5	1.0
18:4n-3	1.9	1.6
20:3n-3	<0.2	<0.1
20:4n-3	<0.2	0.7
20:5n-3	27.0	19.0
21:5n-3	1.5	0.5
22:5n-3	4.8	0.5
22:6n-3	24.0	10.9
Other FA	7.2	6.4
Saturated FA	16.0	30.7
Monounsaturated FA	18.0	25.9
n-3	59.0	34.1
n-6	2.9	2.5

Clinical Assessment

Demographic characteristics (gender, age, height, and weight), concomitant medication, and medical history were recorded at the screening visit. In addition, all subjects went through a physical examination to confirm satisfaction of the eligibility criteria.

Changes in concomitant medication from screening, smoking and alcohol habits, and clinical symptoms before intake of the study products were also registered.

Serum Lipids and Blood Safety Parameters

Blood from venipuncture was collected after an overnight fast (≥12 h) at baseline and at final visit. The subjects were instructed to refrain from alcohol consumption and from vigorous physical activity the day before the blood sampling. Serum was obtained from silica gel tubes (BD Vacutainer), kept at room temperature for at least 30 min until centrifugation at 1,300 × *g* for 12 min at room temperature. Serum analysis of total, low-density lipoprotein

Table 2 n-3 fatty acid contents of the study products

Study product	Daily study dose	Daily dose EPA	Daily dose DHA	Daily dose EPA + DHA	Daily dose n-3 PUFAs
Fish oil	3 capsules (1.8 g oil)	450 mg	414 mg	864 mg	990 mg
Krill oil	6 capsules (3.0 g oil)	348 mg	195 mg	543 mg	621 mg

(LDL), and HDL-cholesterol, TG, apolipoprotein A1, and apolipoprotein B was performed at the routine laboratory at Department of Medical Biochemistry at the National Hospital, Norway using standard methods. Blood samples for analysis of hematology and serum biochemistry parameters including hemoglobin, leukocytes, erythrocytes, thrombocytes, hematocrit, glucose, calcium, sodium, potassium, urea, creatinine, alkaline phosphatase, alanine aminotransferase, bilirubin, albumin, and total protein were collected and analyzed at the routine laboratory at Department of Medical Biochemistry at the National Hospital, Norway using standard methods.

Plasma Fatty Acid Composition

Plasma was obtained from ethylenediamine tetraacetic acid (EDTA) tubes (BD Vacutainer) kept on ice immediately and within 12 min centrifuged at 1,300 × *g* for 10 min at 10°C. Plasma samples were kept frozen at −80°C until analysis. Plasma fatty acid composition was analyzed by Jurilab Ltd., Finland using a slight modification of the method of Nyyssonen et al. [16]. Plasma (250 μL), fatty acids, and 25 μL internal standard (eicosane 1 mg/mL in isopropanol) were extracted with 6 mL methanol–chloroform (1:2), and 1.5 mL water was added. The two phases were separated by centrifugation, and the upper phase was discarded. To the chloroform phase, 1 mL methanol–water (1:1) was added, and this extraction was repeated twice. The chloroform phase was evaporated under nitrogen. For methylation, the remainder was treated with 1.5 mL sulfuric acid–methanol (1:50) at 85°C for 2 h. The mixture was diluted with 1.5 mL water and extracted with light petroleum ether. The fatty acids from the ether phase were determined using a gas chromatograph (Agilent Technologies 6890)/mass spectrometer (Agilent Technologies 5973) with electron impact ionization and a HP-5ms capillary column (Hewlett Packard). For retention time and quantitative standardization, fatty acids purchased from Nu-Chek-Prep (Elysian, MN, USA) were used. All work was carried out under a certified ISO 9001/2000 quality system.

Plasma α-Tocopherol

Human plasma (100 μL) was diluted with 300 μL 2-propanol containing the internal standard tocol and butylated hydroxytoluene (BHT) as an antioxidant. After thorough mixing (15 min) and centrifugation (10 min, 4,000 × *g* at 10°C), an aliquot of 1 μL was injected from the supernatant into the high-performance liquid chromatography (HPLC) system. HPLC was performed with a HP 1100 liquid chromatograph (Agilent Technologies, Palo Alta, CA, USA) with a HP 1100 fluorescence detector (emission 295 nm, excitation 330 nm). Tocopherol isomers were separated on a 2.1 × 250 mm reversed-phase column. The column temperature was 40°C. A two-point calibration curve was made from analysis of a 3% albumin solution enriched with known concentration of tocopherols. Recovery is >95%, the method is linear from 1 to 200 μM at least, and the limit of detection is 0.01 μM. Relative standard deviation (RSD) is 2.8% (17.0 μM) and 4.6% (25.1 μM).

Urinary F2 Isoprostanes

Fasting urine samples were analyzed for 8-iso-prostaglandin $F_{2\alpha}$ (8-iso-$PGF_{2\alpha}$) by a highly specific and validated radioimmunoassay as described by Basu [17]. Urinary levels of 8-iso-$PGF_{2\alpha}$ were adjusted by dividing the 8-iso-$PGF_{2\alpha}$ concentration by that of creatinine.

Markers of Inflammation and Hemostasis

Plasma interleukin-6 (IL-6), tumour necrosis factor-alpha (TNFα), monocyte chemotactic protein-1 (MCP-1), thromboxane B_2 (TxB_2), interferon-gamma (INFγ), soluble E-selectin and P-selectin, soluble intracellular adhesion molecule-1 (ICAM-1), and vascular cell adhesion molecule-1 (VCAM-1) were determined by Fluorokine® MAP kits (R&D Systems, Inc., Minneapolis, MN, USA). Plasma leukotriene B_4 (LTB_4) and thromboxane B_2 (TxB_2) were assessed as described by Elvevoll et al. [18]. High-sensitivity C-reactive protein (hsCRP) evaluation was performed at the routine laboratory at Department of Medical Biochemistry at the National Hospital, Norway using standard method.

Statistics

All continuous variables were summarized by product group and visit number and described using standard statistical measures, i.e., number of observations, mean,

standard deviation (SD), median, minimum, and maximum. Absolute and percentage change from baseline to the week-7 visit are presented as summary statistics. All categorical (discrete, including ordinal) variables are presented in contingency tables showing counts and percentages for each treatment group at all time points. Continuously distributed efficacy laboratory parameters (lipids, EPA, DHA, and docosapentaenoic acid (DPA)) were analyzed by analysis of covariance (ANCOVA) using the following model: change in parameter value = baseline value + treatment + gender + age + error.

Change from baseline to week 7 was used as a dependent variable in the model. A linear model using SAS GLM with gender as fixed effect, subject as random effect, and baseline value and age as covariates was applied. A reduced ANCOVA model with baseline value and treatment was used for the secondary efficacy parameters. Significant treatment effects were analyzed by pairwise tests. Changes from baseline to end of intervention were tested by paired *t*-test.

Results

Subject Characteristics at Baseline

Figure 1 shows the disposition of all subjects. One hundred fifteen of 129 randomized subjects completed the study. Withdrawal rates were similar in all three groups (three withdrawals in the fish oil group, six withdrawals in the krill oil group, and five withdrawals in the control group). Three subjects discontinued the study due to clinical symptoms (all in the krill group), three subjects violated the exclusion criteria (two in the fish oil group and one in the krill oil group), and one subject in each group was lost to follow-up. Two subjects in the control group were withdrawn due to concomitant treatments, and three subjects withdrew their consent (one subject in the krill oil group and two subjects in the control group). Clinical symptoms included symptoms of common cold or gastrointestinal symptoms. During database clean-up, it was detected that two subjects (in the krill oil group) had been allowed to enter the study although they violated the entry criteria. They where therefore excluded from the per protocol subjects. The statistical analyses of efficacy were performed on the data collected from 113 per protocol subjects (Fig. 1).

The study groups were comparable in terms of weight, height, BMI, gender, and age at baseline (Table 3). Vital signs including systolic and diastolic blood pressure and heart rate were within normal ranges. More females than males were included in all study groups.

Table 3 Demographic information and body measurements

Parameter, mean (SD)	Study groups		
	Fish oil ($N = 43$)	Krill oil ($N = 44$)	Control ($N = 42$)
Age (years)	38.7 (11.1)	40.3 (14.8)	40.5 (12.1)
Height (cm)	171.2 (7.8)	171.3 (8.6)	172.2 (9.4)
Weight (kg)	71.7 (12.0)	69.8 (13.7)	71.7 (12.0)
BMI (kg/m^2)	24.4 (3.0)	23.6 (3.3)	23.9 (3.0)
Gender			
Female (*n*)	34 (79.1%)	31 (70.5%)	28 (66.7%)
Male (*n*)	9 (20.9%)	13 (29.5%)	14 (33.3%)

Fatty Acid Composition in Plasma

Plasma levels of EPA, DHA, and DPA increased significantly from baseline to the end of the intervention phase in the groups receiving fish oil and krill oil, but not in the control group. The changes in EPA, DHA, and DPA differed significantly between the subjects supplemented with n-3 PUFAs and the subjects in the control group, but there was no significant difference in the change in any of the n-3 PUFAs between the fish oil and the krill oil groups (Table 4).

There were significant within-group changes in individual FAs from start to end of intervention, but no clear trends in changes in the plasma FA composition were apparent in any of the study groups (Table 4).

The level of arachidonic acid (C20:4n-6) increased from baseline in the krill group, whereas a decrease was observed in the fish oil group. The changes in arachidonic acid between the fish oil and the krill oil groups, and the control group differed significantly ($p = 0.001$). Pairwise comparisons showed that the mean increase in arachidonic acid in the krill oil group was significantly different from the mean decreases in the fish oil and control groups, but there was no significant difference between the mean changes in arachidonic acid level between the fish oil and control groups.

Serum Lipids

Small changes in the levels of HDL-cholesterol, LDL-cholesterol, and TG were observed in all study groups from start to end of the intervention phase, but only the within-group increase in LDL-cholesterol seen in the fish oil group ($p = 0.039$) was statistically significant. The tests comparing the differences between the study groups gave no statistically significant results (Table 5). The HDL-cholesterol/TG ratio and the change from start to end of the intervention were calculated for all study groups. No significant changes in the HDL-cholesterol/TG ratio from start to end of the interventions were detected in the fish oil or

Table 4 Fatty acid composition in plasma

Parameter (μmol/L)	Treatment	*N*	Baseline	End of study	Change	*p*-Value[a] for change	*p*-Value[b] between groups
C14:0 myristic acid	Fish oil	40	67.4 ± 57.07	69.4 ± 62.32	2.0 ± 44.05	0.77	
	Krill oil	36	55.5 ± 32.43	57.8 ± 26.15	2.3 ± 30.93	0.65	0.71
	Control	37	60.5 ± 29.25	58.1 ± 38.01	−2.4 ± 35.46	0.69	
C15:0 pentadecanoic acid	Fish oil	40	18.2 ± 14.42	16.2 ± 8.22	−2.1 ± 12.01	0.28	
	Krill oil	36	14.7 ± 5.03	15.5 ± 3.69	0.8 ± 4.44	0.30	0.27
	Control	37	15.0 ± 5.02	15.0 ± 5.26	0.1 ± 4.32	0.94	
C16:0 palmitic acid	Fish oil	40	1,661.0 ± 496.5	1,522. ± 339.3	−139.0 ± 409.5	0.038	
	Krill oil	36	1,548.9 ± 477.9	1,547. ± 260.0	−2.3 ± 414.9	0.97	0.35
	Control	37	1,652.7 ± 374.2	1,578. ± 315.6	−74.6 ± 327.7	0.17	
C16:1n-7 palmitoleic acid	Fish oil	40	67.7 ± 35.41	63.0 ± 33.54	−4.7 ± 27.91	0.29	
	Krill oil	36	66.1 ± 49.18	61.8 ± 26.56	−4.4 ± 35.91	0.47	0.62
	Control	37	68.7 ± 32.98	63.9 ± 35.07	−4.8 ± 28.62	0.31	
C17:0 margaric acid	Fish oil	40	24.2 ± 8.38	23.9 ± 8.44	−0.3 ± 6.09	0.76	
	Krill oil	36	22.6 ± 5.85	24.0 ± 5.84	1.4 ± 5.49	0.14	0.089
	Control	37	23.3 ± 5.46	21.7 ± 5.84	−1.6 ± 4.85	0.048	
C18:0 stearic acid	Fish oil	40	580.6 ± 136.6	578.5 ± 130.2	−2.2 ± 133.2	0.92	
	Krill oil	36	548.5 ± 116.7	568.9 ± 112.6	20.4 ± 91.7	0.19	0.17
	Control	37	594.8 ± 103.5	562.4 ± 147.2	−32.4 ± 125.4	0.12	
C18:1n-9 oleic acid	Fish oil	40	558.9 ± 166.1	516.2 ± 146.8	−42.7 ± 154.0	0.087	
	Krill oil	36	532.8 ± 198.5	521.8 ± 109.1	−11.0 ± 191.0	0.73	0.71
	Control	37	570.2 ± 146.8	547.2 ± 156.1	−23.0 ± 151.9	0.36	
C18:2n-6 linoleic acid	Fish oil	40	829.3 ± 349.8	779.8 ± 254.5	−49.6 ± 251.3	0.22	
	Krill oil	36	742.0 ± 214.0	744.2 ± 187.9	2.2 ± 215.8	0.95	0.44
	Control	37	812.0 ± 219.6	735.7 ± 212.4	−76.3 ± 167.5	0.0088	
C18:3n-3 alpha-linoleic acid	Fish oil	40	61.7 ± 17.89	61.9 ± 20.22	0.2 ± 20.95	0.95	
	Krill oil	36	67.3 ± 25.24	68.4 ± 21.88	1.1 ± 20.08	0.73	0.15
	Control	37	68.3 ± 20.40	62.8 ± 22.07	−5.5 ± 19.55	0.094	
C20:3n-3 eicosatrienoic acid	Fish oil	40	39.6 ± 18.08	33.5 ± 17.97	−6.0 ± 10.00	0.0005	
	Krill oil	36	39.3 ± 19.20	34.9 ± 13.20	−4.4 ± 13.23	0.054	0.22
	Control	37	39.8 ± 18.24	37.7 ± 18.28	−2.1 ± 8.65	0.16	
C20:4n-6 arachidonic acid	Fish oil	40	192.6 ± 50.0	178.5 ± 45.3	−14.1 ± 29.6	0.0046	
	Krill oil	36	180.1 ± 52.4	192.1 ± 40.2	12.0 ± 32.8	0.035	0.0010
	Control	37	189.8 ± 44.2	182.8 ± 38.0	−7.0 ± 32.3	0.20	
C22:0 behenic acid	Fish oil	40	21.5 ± 6.05	21.8 ± 6.36	0.4 ± 3.30	0.49	
	Krill oil	36	20.2 ± 5.29	22.0 ± 6.25	1.9 ± 3.51	0.003	0.040
	Control	37	18.9 ± 6.02	18.3 ± 4.83	−0.6 ± 4.07	0.36	
C24:0 lignoceric acid	Fish oil	40	10.0 ± 4.07	10.3 ± 4.19	0.3 ± 1.71	0.22	
	Krill oil	36	9.7 ± 2.86	10.4 ± 3.15	0.7 ± 2.04	0.040	0.26
	Control	37	8.9 ± 3.37	8.5 ± 3.05	−0.4 ± 2.57	0.40	
C24:1n-9 neuronic acid	Fish oil	40	18.2 ± 6.88	18.9 ± 6.15	0.6 ± 3.75	0.29	
	Krill oil	36	16.7 ± 5.99	17.3 ± 5.87	0.6 ± 5.00	0.48	0.17
	Control	37	15.7 ± 5.39	16.7 ± 5.70	1.0 ± 5.67	0.30	
C20:5n-3 EPA	Fish oil	40	31.2 ± 23.11	76.3 ± 36.02	45.2 ± 29.65	<0.0001	
	Krill oil	36	30.4 ± 21.57	74.9 ± 38.66	44.5 ± 35.21	<0.0001	<0.0001
	Control	37	43.9 ± 40.74	37.2 ± 28.64	−6.6 ± 28.58	0.17	

Table 4 continued

Parameter (μmol/L)	Treatment	*N*	Baseline	End of study	Change	*p*-Value[a] for change	*p*-Value[b] between groups
C22:6n-3 DHA	Fish oil	40	47.0 ± 22.08	70.4 ± 25.70	23.4 ± 16.55	<0.0001	
	Krill oil	36	44.8 ± 21.36	64.2 ± 26.15	19.4 ± 23.75	<0.0001	<0.0001
	Control	37	57.4 ± 30.94	51.3 ± 23.70	−6.1 ± 21.25	0.088	
C22:5n-3 DPA	Fish oil	40	8.8 ± 3.98	12.7 ± 5.06	3.9 ± 3.24	<0.0001	
	Krill oil	36	8.2 ± 3.33	11.9 ± 3.56	3.6 ± 3.68	<0.0001	<0.0001
	Control	37	9.6 ± 5.09	8.6 ± 3.84	−1.0 ± 3.56	0.090	
Total fatty acids	Fish oil	40	4,250.7 ± 1,148.1	4,064.6 ± 890.8	−186.0 ± 921.8	0.21	
	Krill oil	36	3,958.1 ± 983.7	4,045.5 ± 662.5	87.4 ± 810.7	0.52	0.15
	Control	37	4,261.3 ± 804.2	4,016.8 ± 774.4	−244.5 ± 685.5	0.037	

[a] Test of within-group changes

[b] Test comparing change from start to end of intervention between the fish oil, krill oil, and control groups

control groups. In the krill oil group, however, there was a significant increase in the HDL-cholesterol/TG ratio. The test for differences between the study groups gave no significant results (Table 5).

Although the interventions did not significantly change TG levels a reduction was seen in those subjects in the krill oil group having the highest baseline values (Fig. 2).

The changes in levels of Apo B-100 from baseline to end of study were minor in all study groups. Moreover, the test for differences between the study groups in changes in Apo A1 was not significant. However, the within-group changes of Apo A1 levels from start to end of the interventions were statistically significant in the krill oil group.

Table 5 Serum lipids and lipoproteins

Parameter	Treatment	*N*	Baseline	End of study	Change	*p*-Value[a] for change	*p*-Value[b] between groups
HDL-cholesterol (mmol/L)	Fish oil	40	1.56 ± 0.384	1.61 ± 0.396	0.05 ± 0.157	0.063	
	Krill oil	36	1.50 ± 0.368	1.63 ± 0.517	0.13 ± 0.404	0.061	0.50
	Control	37	1.59 ± 0.354	1.63 ± 0.395	0.04 ± 0.228	0.29	
LDL-cholesterol (mmol/L)	Fish oil	40	2.96 ± 0.747	3.09 ± 0.827	0.13 ± 0.377	0.039	
	Krill oil	36	3.07 ± 0.724	3.16 ± 0.796	0.09 ± 0.390	0.18	0.45
	Control	37	2.98 ± 0.824	3.03 ± 0.802	0.05 ± 0.361	0.44	
Triglycerides (mmol/L)	Fish oil	40	0.95 ± 0.541	0.94 ± 0.542	−0.01 ± 0.462	0.84	
	Krill oil	36	1.10 ± 0.638	1.01 ± 0.649	−0.09 ± 0.417	0.21	0.65
	Control	37	0.92 ± 0.414	0.93 ± 0.523	0.02 ± 0.429	0.82	
HDL/triglycerides (%)	Fish oil	40	225.8 ± 151.08	216.8 ± 119.33	109.5 ± 44.62	0.19	
	Krill oil	36	196.9 ± 134.24	228.3 ± 146.62	129.2 ± 68.99	0.016	0.41
	Control	37	217.7 ± 138.65	234.4 ± 148.20	113.0 ± 49.28	0.12	
Total-cholesterol (mmol/L)	Fish oil	40	4.93 ± 0.778	5.13 ± 0.809	0.20 ± 0.424	0.0049	
	Krill oil	36	4.99 ± 0.815	5.20 ± 0.917	0.21 ± 0.496	0.014	0.78
	Control	37	4.95 ± 0.925	5.07 ± 0.861	0.12 ± 0.524	0.18	
Apo A1 (mmol/L)	Fish oil	40	1.64 ± 0.269	1.68 ± 0.250	0.04 ± 0.130	0.058	
	Krill oil	36	1.64 ± 0.241	1.73 ± 0.376	0.09 ± 0.267	0.047	0.70
	Control	37	1.68 ± 0.272	1.75 ± 0.272	0.07 ± 0.173	0.023	
Apo B-100 (mmol/L)	Fish oil	40	0.81 ± 0.184	0.80 ± 0.199	−0.01 ± 0.100	0.64	
	Krill oil	36	0.83 ± 0.208	0.81 ± 0.226	−0.02 ± 0.126	0.35	0.80
	Control	37	0.79 ± 0.197	0.78 ± 0.198	−0.01 ± 0.098	0.41	

[a] Test of within-group changes

[b] Test comparing change from start to end of intervention between the fish oil, krill oil, and control groups

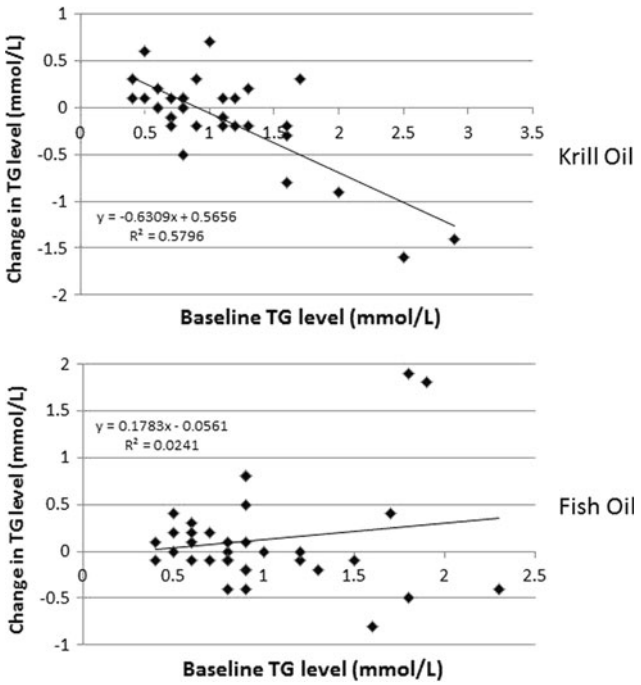

Fig. 2 Correlation between baseline TG levels and change in TG levels after 7 weeks of intervention with krill oil or fish oil

Oxidative Stress, Markers of Inflammation, and Hemostasis

α-Tocopherol is considered an antioxidant, and an increase in PUFAs may lead to increased oxidative stress. Although α-tocopherol was added to both supplements, no significant change in levels of α-tocopherol was detected (Supplementary Table). A tendency towards a reduced level of α-tocopherol was observed in all study groups. F2-isoprostanes, formed from free-radical-induced peroxidation of membrane-bound arachidonic acid, are considered a reliable biomarker of oxidative stress. However no differences were observed in urine F2-isoprostane, suggesting that there was not an increase in oxidative stress. No significant changes were observed in levels of hsCRP, markers of inflammation or hemostasis (Supplementary Table).

Discussion

The primary finding of the present study was that plasma concentrations of EPA, DPA, and DHA increased significantly in both the krill oil and fish oil groups compared with the control group following daily supplementation for 7 weeks. There was no statistically significant difference between these two groups in the levels of the increases in EPA and DHA. Since the subjects in the krill oil group received 62.8% of the total amount of n-3 PUFAs received by the subjects in the fish oil group, these findings indicate that the bioavailability of n-3 PUFAs from krill oil (mainly PL) is as, or possibly more, efficient as n-3 PUFA from fish oil (TG). This supports the results of a previous study with krill oil and menhaden oil in humans [11]. In the study performed by Maki et al., plasma EPA increased 90% and DHA increased 51% from baseline levels. In the current study EPA increased 146% and DHA increased 43% from baseline levels. The small discrepancy between these two studies might be related to different levels of EPA and DHA in the oils used, different treatment time (7 versus 4 weeks), and different dose used (3 g oil versus 2 g). It has been hypothesized that PL improve the bioavailability of lipids, which may facilitate absorption of EPA and DHA from marine PL compared with TG, but the extent to which this contributes to the efficient absorption observed in the krill oil group is unknown.

AHA dietary guidelines for long-chain n-3 PUFAs and fish for primary prevention of coronary diseases are two servings of fatty fish per week [9]. This recommendation will provide the order of 250–500 mg EPA + DHA per day [19]. In the present study we have shown that daily intake of 3 g krill oil containing 543 mg EPA + DHA increases the plasma level of EPA and DHA to the same extent as intake of fish oil containing 864 mg EPA + DHA. A food-based approach for achieving adequate intake of n-3 PUFAs is recommended [20]. However, for some individuals nutritional supplements may be needed, such as those who do not like fish or for other reasons choose not to include fish in their diet. This study demonstrates that supplementation with krill oil will be a good source of EPA and DHA in their daily diet.

Serum TG and HDL-cholesterol have been observed to be inversely related [21]. Although the metabolic relation that exists between HDL-cholesterol and TG is not fully understood, the ratio between TG and HDL-cholesterol has been shown to be a powerful risk predictor for CHD [22, 23]. In the present study, no statistically significant differences in HDL-cholesterol, TG or HDL-cholesterol/TG ratio were observed between the study groups. However, the change in the HDL-cholesterol/TG ratio in the krill oil group was statistically significant (Table 5). This observation supports the impression of a more pronounced effect of krill oil supplementation on HDL-cholesterol and TG compared with other n-3 PUFA supplements. However, to verify these effects of krill oil, they should be studied in a population with elevated blood TG levels and lowered HDL-cholesterol, i.e., in a population with markers of metabolic syndrome. The increase in HDL-cholesterol was slightly higher in the krill oil group than in the fish oil group (8.7% versus 3.2%), although not significantly so ($p = 0.061$). Compared with fish oil, krill oil contains a high amount of astaxanthin, which has been indicated to

increase HDL-cholesterol as well as decrease TG in humans [24]. Moreover, intake of PL may increase HDL-cholesterol [25]. The small increase in LDL-cholesterol, but no effect on HDL-cholesterol, in the fish oil group is in accordance with previous findings [7].

The analysis of the changes in the plasma fatty acid composition following 7 weeks of intervention with n-3 PUFAs showed that the levels of arachidonic acid and behenic acid significantly increased from baseline in the krill oil group as compared with the fish oil and control groups. Moreover, arachidonic acid was significantly decreased in the fish oil group. Intake of n-3 PUFAs from fish oil can be incorporated in cell PL in a time- and dose-dependent manner at the expense of arachidonic acid [26]. The explanation and importance of this finding are not clear. However, one possible explanation might be that arachidonic acid is mobilized from the cell membranes to the blood by EPA and DHA linked to the PL in the krill oil. However, the changes in plasma arachidonic acid were small compared with the changes in EPA and DHA, and there was no significant difference in the increase in EPA/arachidonic acid ratio between the two intervention groups.

The CRP level did not change during the study in any of the study groups, and no significant changes were observed in the other markers of inflammation and hemostasis (data not shown). This is in accordance with others who have examined the effect of fish oil among apparently healthy individuals [27–31]. Moreover, no statistically significant differences were found in α-tocopherol levels and F2-isoprostanes in urine, suggesting that no oxidative stress occurred.

The safety analysis revealed no clear patterns in the changes in any of the hematological or serum biochemical variables, vital signs or weight that might indicate a relation with administration of any of the studied products. Clinical symptoms registered during the study included mainly symptoms of common cold or gastrointestinal symptoms. However, one subject in the fish oil group experienced moderate bruises, and one subject in the krill oil group withdrew from the study because of an outbreak of rash that was possibly related to intake of the study products. Safety laboratory parameters and other safety observations such as occurrence of adverse events indicate that krill oil is well tolerated. There were no apparent differences in the rate of adverse events or blood safety parameters between the krill oil, fish oil or control groups.

In conclusion, the present study shows that n-3 PUFAs from krill oil in the form of PL are readily and effectively absorbed after ingestion and subsequently distributed in the blood. The krill oil supplement is safe and well tolerated. Krill oil thus represents a valuable source of n-3 PUFAs.

Acknowledgments The authors would like to thank the volunteers who participated in this study. This work was partially funded by Aker BioMarine ASA.

References

1. Burr ML, Fehily AM, Gilbert JF, Rogers S, Holliday RM, Sweetnam PM, Elwood PC, Deadman NM (1989) Effects of changes in fat, fish, and fibre intakes on death and myocardial reinfarction: diet and reinfarction trial (DART). Lancet 2:757–761
2. He K, Rimm EB, Merchant A, Rosner BA, Stampfer MJ, Willett WC, Ascherio A (2002) Fish consumption and risk of stroke in men. JAMA 288:3130–3136
3. He K, Song Y, Daviglus ML, Liu K, Van Horn L, Dyer AR, Greenland P (2004) Accumulated evidence on fish consumption and coronary heart disease mortality: a meta-analysis of cohort studies. Circulation 109:2705–2711
4. Kris-Etherton PM, Harris WS, Appel LJ (2002) Fish consumption, fish oil, omega-3 fatty acids, and cardiovascular disease. Circulation 106:2747–2757
5. Marckmann P, Gronbaek M (1999) Fish consumption and coronary heart disease mortality. A systematic review of prospective cohort studies. Eur J Clin Nutr 53:585–590
6. Balk EM, Lichtenstein AH, Chung M, Kupelnick B, Chew P, Lau J (2006) Effects of omega-3 fatty acids on serum markers of cardiovascular disease risk: a systematic review. Atherosclerosis 189:19–30
7. Harris WS (1997) n-3 fatty acids and serum lipoproteins: human studies. Am J Clin Nutr 65:1645S–1654S
8. GISSI-Prevenzione-Investigators (1999) Dietary supplementation with n-3 polyunsaturated fatty acids and vitamin E after myocardial infarction: results of the GISSI-Prevenzione trial Gruppo Italiano per lo Studio della Sopravvivenza nell'Infarto miocardico. Lancet 354:447–455
9. Lichtenstein AH, Appel LJ, Brands M, Carnethon M, Daniels S, Franch HA, Franklin B, Kris-Etherton P, Harris WS, Howard B, Karanja N, Lefevre M, Rudel L, Sacks F, Van Horn L, Winston M, Wylie-Rosett J (2006) Diet and lifestyle recommendations revision 2006: a scientific statement from the American Heart Association Nutrition Committee. Circulation 114:82–96
10. Tou JC, Jaczynski J, Chen YC (2007) Krill for human consumption: nutritional value and potential health benefits. Nutr Rev 65:63–77
11. Maki KC, Reeves MS, Farmer M, Griinari M, Berge K, Vik H, Hubacher R, Rains TM (2009) Krill oil supplementation increases plasma concentrations of eicosapentaenoic and docosahexaenoic acids in overweight and obese men and women. Nutr Res 29:609–615
12. Carnielli VP, Verlato G, Pederzini F, Luijendijk I, Boerlage A, Pedrotti D, Sauer PJ (1998) Intestinal absorption of long-chain polyunsaturated fatty acids in preterm infants fed breast milk or formula. Am J Clin Nutr 67:97–103
13. Morgan C, Davies L, Corcoran F, Stammers J, Colley J, Spencer SA, Hull D (1998) Fatty acid balance studies in term infants fed formula milk containing long-chain polyunsaturated fatty acids. Acta Paediatr 87:136–142
14. Ramirez M, Amate L, Gil A (2001) Absorption and distribution of dietary fatty acids from different sources. Early Hum Dev 65 Suppl:S95–S101

15. Lemaitre-Delaunay D, Pachiaudi C, Laville M, Pousin J, Armstrong M, Lagarde M (1999) Blood compartmental metabolism of docosahexaenoic acid (DHA) in humans after ingestion of a single dose of [(13)C]DHA in phosphatidylcholine. J Lipid Res 40:1867–1874
16. Nyyssonen K, Kaikkonen J, Salonen JT (1996) Characterization and determinants of an electronegatively charged low-density lipoprotein in human plasma. Scand J Clin Lab Invest 56:681–689
17. Basu S (1998) Radioimmunoassay of 15-keto-13, 14-dihydro-prostaglandin F2alpha: an index for inflammation via cyclooxygenase catalysed lipid peroxidation. Prostaglandins Leukot Essent Fatty Acids 58:347–352
18. Elvevoll EO, Barstad H, Breimo ES, Brox J, Eilertsen KE, Lund T, Olsen JO, Osterud B (2006) Enhanced incorporation of n-3 fatty acids from fish compared with fish oils. Lipids 41:1109–1114
19. Mozaffarian D, Rimm EB (2006) Fish intake, contaminants, and human health: evaluating the risks and the benefits. JAMA 296:1885–1899
20. Kris-Etherton PM, Innis S, Ammerican Dietetic Association, Dietitians of Canada (2007) Position of the American Dietetic Association and Dietitians of Canada: dietary fatty acids. J Am Diet Assoc 107:1599–1611
21. Thelle DS, Shaper AG, Whitehead TP, Bullock DG, Ashby D, Patel I (1983) Blood lipids in middle-aged British men. Br Heart J 49:205–213
22. da Luz PL, Favarato D, Faria-Neto JR Jr, Lemos P, Chagas AC (2008) High ratio of triglycerides to HDL-cholesterol predicts extensive coronary disease. Clinics (Sao Paulo) 63:427–432
23. Bittner V, Johnson BD, Zineh I, Rogers WJ, Vido D, Marroquin OC, Bairey-Merz CN, Sopko G (2009) The triglyceride/high-density lipoprotein cholesterol ratio predicts all-cause mortality in women with suspected myocardial ischemia: a report from the Women's Ischemia Syndrome Evaluation (WISE). Am Heart J 157:548–555
24. Yoshida H, Yanai H, Ito K, Tomono Y, Koikeda T, Tsukahara H, Tada N (2010) Administration of natural astaxanthin increases serum HDL-cholesterol and adiponectin in subjects with mild hyperlipidemia. Atherosclerosis 209:520–523
25. O'Brien BC, Andrews VG (1993) Influence of dietary egg and soybean phospholipids and triacylglycerols on human serum lipoproteins. Lipids 28:7–12
26. Gibney MJ, Hunter B (1993) The effects of short- and long-term supplementation with fish oil on the incorporation of n-3 polyunsaturated fatty acids into cells of the immune system in healthy volunteers. Eur J Clin Nutr 47:255–259
27. Geelen A, Brouwer IA, Schouten EG, Kluft C, Katan MB, Zock PL (2004) Intake of n-3 fatty acids from fish does not lower serum concentrations of C-reactive protein in healthy subjects. Eur J Clin Nutr 58:1440–1442
28. Vega-Lopez S, Kaul N, Devaraj S, Cai RY, German B, Jialal I (2004) Supplementation with omega3 polyunsaturated fatty acids and all-rac alpha-tocopherol alone and in combination failed to exert an anti-inflammatory effect in human volunteers. Metabolism 53:236–240
29. Madsen T, Christensen JH, Blom M, Schmidt EB (2003) The effect of dietary n-3 fatty acids on serum concentrations of C-reactive protein: a dose-response study. Br J Nutr 89:517–522
30. Yusof HM, Miles EA, Calder P (2008) Influence of very long-chain n-3 fatty acids on plasma markers of inflammation in middle-aged men. Prostaglandins Leukot Essent Fatty Acids 78:219–228
31. Fujioka S, Hamazaki K, Itomura M, Huan M, Nishizawa H, Sawazaki S, Kitajima I, Hamazaki T (2006) The effects of eicosapentaenoic acid-fortified food on inflammatory markers in healthy subjects—a randomized, placebo-controlled, double-blind study. J Nutr Sci Vitaminol (Tokyo) 52:261–265

Lipids (2011) 46:47–57
DOI 10.1007/s11745-010-3491-3

ORIGINAL ARTICLE

A High Omega-3 Fatty Acid Diet has Different Effects on Early and Late Stage Myeloid Progenitors

Melinda E. Varney · James T. Buchanan · Yulia Dementieva · W. Elaine Hardman · Vincent E. Sollars

Received: 24 May 2010 / Accepted: 18 October 2010 / Published online: 31 October 2010

Abstract The effects of the polyunsaturated omega-3 (n-3) and omega-6 (n-6) fatty acids (FA) on hematopoiesis are complex in that both FA forms are processed into leukotrienes, eicosanoids, and prostaglandins, which can have independent effects. These FA have antagonistic effects in that n-6 FA prostaglandins tend to be pro-proliferative and pro-inflammatory, while the effects of n-3 FA prostaglandins are the opposite. We have previously shown that diets high in n-3 FA reduce the size of the middle to later stage myeloid progenitor compartment in FVB X sv129 F_1hybrid mice. To assay the effects of high n-3 FA diets on earlier stages of myelopoiesis, we fed C57BL/6J mice diets high in n-3 FA or levels of n-3/n-6 FA similar to western diets and assayed the effects on myelopoiesis with flow cytometry and colony forming cell assays. Results indicate an expansion of the common myeloid progenitor cell compartment in high n-3 FA diets, which does not persist into later stages where the number of progenitor cells is actually lower in high n-3 FA fed animals. Investigations in vitro with the hematopoietic stem cell line EML-clone 1 indicate that cells cultured with eicosapentaenoic acid (n-3 FA) or arachidonic acid (n-6 FA) have no differences in cell viability but that arachidonic acid more rapidly produces progenitors with low levels of the macrophage developmental marker, F4/80.

M. E. Varney · J. T. Buchanan · W. Elaine Hardman · V. E. Sollars (✉)
Department of Biochemistry and Microbiology, Marshall University School of Medicine, One John Marshall Drive, Huntington, WV 25755, USA
e-mail: sollars@marshall.edu

Y. Dementieva
Department of Mathematics, Emmanuel College, 400 The Fenway, Boston, MA 02115, USA

Keywords Omega fatty acids · EPA · DHA · Immunology · Stem cells · Progenitor cells · Bone marrow · Nutrition

Abbreviations

n-3	Omega-3
n-6	Omega-6
ARA	Arachidonic acid
ALA	α Linolenic acid
AIN-76A diet	American institute of nutrition 76A diet
APC	Allophycocyanin
ATRA	all-*trans* Retinoic acid
BHK	Baby hamster kidney
CFC	Colony forming cell(s)
CFU-GM	Colony forming unit granulocyte–macrophage
CFU-M	Colony forming unit macrophage
CMP	Common myeloid progenitor(s)
COX	Cyclooxygenase
DHAn-3	Docosahexaenoic acid
DPA	Docosapentaenoic acid
EDTA	Ethylenediaminetetraacetic acid
EML	Erythroid myeloid lymphoid
EPA	Eicosapentaenoic acid
FA	Fatty acid(s)
$F_CR\gamma$	Fragment crystallizable receptor γ
FSC	Forward scatter
GMP	Granulocyte–macrophage progenitor(s)
HSC	Hematopoietic stem cell(s)
IL-3	Interleukin-3
IL-7Rα	Interleukin-7 receptor α
LNA	Linoleic acid
MEP	Megakaryocyte–erythrocyte progenitor
PE	Phycoerythrin

PBS	Phosphate-buffered saline
SCF	Stem cell factor
SSC	Side scatter

Introduction

The examination of omega-3 (n-3) and omega-6 (n-6) fatty acids (FA) effects on hematopoiesis is important to patient care. The inhibitory effect of n-3 FA on inflammation has led to the use of fish oils that are high in these FA in the management of several inflammatory and autoimmune diseases [1]. n-3 FA affect hematopoietic differentiation by influencing myeloid progenitor cells [2]. n-3 FA are known to affect immune system function by reducing several aspects of neutrophil, monocyte, and lymphocyte function [1]. Suppression of n-6 derived eicosanoids has been proposed as a strategy for chemoprevention and as an adjunct for treatment of cancer [3–6].

n-3 and n-6 FA are incorporated into cell membranes either directly or after elongation and then desaturation by Δ6 and Δ5 desaturases. Dietary linoleic acid (LNA, 18 carbons, n-6 FA) is generally considered to be the major source of tissue arachidonic acid (ARA, 20 carbons, n-6 FA) although meat fat can be a direct source of ARA [7]. n-3 FA have greater affinity for the Δ5 and Δ6 desaturases than n-6 FA. Consequently, increasing dietary intake of n-3 FA reduces the desaturation of LNA and reduces the production of ARA [8]. All three major n-3 FA—α linolenic acid (ALA, 18:3, n-3)—eicosapentaenoic acid (EPA, 20:5, n-3), and docosahexaenoic acid (DHA, 22:6, n-3), directly inhibit the production of ARA from LNA [8].

Both ARA and EPA can be cleaved from the cell membrane phospholipids stores by phospholipase A_2 and acted on by cyclooxygenases (either the constitutive COX1 or the inducible COX2) to produce prostaglandin precursors which are isomerized by prostaglandin synthases to produce prostaglandins. COX activity on ARA forms the two-series prostaglandins that tend to be pro-proliferative and pro-inflammatory in most tissues [9]. Micromolar concentrations of prostaglandin E2 increase human myeloid progenitor cell proliferation [2]. However, COX activity on EPA forms the three-series prostaglandins that tend to have anti-proliferative and anti-inflammatory properties [9]. In addition to prostaglandins, leukotrienes and eicosanoids are formed from FA through activity of various lipoxygenases. These have been shown to have varying and sometimes controversial effects on either hematopoietic stem cell or myeloid progenitor cell differentiation [2, 10]. A model system approach is needed to effectively dissect the net effect of dietary fatty acids on hematopoiesis in vivo.

In this study, we examined the effects of n-3 and n-6 fatty acids in vivo in the mouse, with an analysis at the level of stem and progenitor subtypes. Our results indicate that, compared to diets rich in n-6 FA, diets rich in n-3 FA induce lower levels of later stage myeloid progenitor cells in mice, but that there is a higher frequency of the earliest stage myeloid progenitor cells in these mice. Our in vitro results indicate that aspects of the in vivo effects of n-3 and n-6 FA can be modeled using the EML cell culture system to ascertain the mechanisms involved.

Materials and Methods

Animals

Mice were housed in the AAALAC accredited animal facilities of the Marshall Universitiy School of Medicine. All animal use and care was approved by the Marshall University Institutional Animal and Use Committee. The mice were housed 3–4 in a cage and individually numbered for identification. Mice were fed either a fish oil diet ($n = 8$) or a corn oil diet ($n = 8$) from 6 weeks of age until 20 weeks of age (100 days on diet).

Diet

The base diet was an AIN-76A diet modified by substitution of 5% sucrose for 5% more oils to contain a total of 10% w/w oil (Tables 1, 2). The fish oil diet contained 3.65% n-3 FA and 1.3% n-6 FA. The corn oil diet contained 0.1% n-3 FA and 6.1% n-6 FA. Diets were prepared in the Marshall University School of Medicine animal diet prep room. Diet composition is shown in Table 1 and was formulated to be isocaloric, isonutrient, and relevant to human consumption. The AIN-76A diet is adequate for the nutritional support of the mice [11]. The dry ingredients of the diet were obtained in bulk from MP Biomedicals (Solon, OH, USA), sugar, corn, and canola oil were purchased locally (100% canola oil, 100% corn oil, no additives or preservatives). The n-3 supplement (OmegaRx Liquid) was purchased from Zone Labs, Danvers, MA. Batches of diet were prepared as needed, about every 2 weeks. The diet mixture was pressed into trays. Food (25–30 g) was stored in sealed containers at −20 °C to prevent oxidation of the fat and bacterial growth in the food. Mice had free access to food and water and were fed fresh food 5 days per week. Food removed from cages was discarded.

Table 1 Modified AIN-76A diet composition

Ingredient	Diet composition	
	wt%	Amount/100 g
Casein (protein)	20	20
Sucrose	45	45
Corn starch (carbs)	15	15
Alphacel (fiber)	5	5
Choline bitartrate	0.2	0.2
DL-Methionine	0.3	0.3
Mineral mix	3.5	3.5
Vitamin mix	1.0	1
Fat	10	10
Total	100	100
Total fat		10
Total protein		20
Total carbohydrate		60

The base diet is an AIN-76A diet modified by substitution of 5% sucrose for 5% more oils to contain a total of 10% w/w oil. The mouse food recipe contains 10% fat in each diet supplied through these oils

Colony Forming Cell (CFC) Assays

CFC assays were performed upon bone marrow isolated from the mice as previously discussed [12, 13]. Briefly, bone marrow was harvested by flushing from the femurs with Iscove's modified Dulbecco's medium and cells were counted and seeded in 4-well plates at a density determined empirically by a pilot study conducted with a broad and consistent range of seeding densities. After linear response of colony production to seeding density was insured by the pilot study, seeding densities were chosen to produce 10–30 colonies for each well (4-well plates). Bone marrow was cultured in 1% semi-solid Methocult M3434 (StemCell Technologies), supplemented with 0.4% autochthonous sera. Cells were incubated for 6–7 days to allow colony formation. Colonies with a minimum cell number of 20 were scored as positive using an inverted microscope at 40× magnification. Colonies were counted based on morphological features that are associated with each progenitor type.

Cell Cycle Analysis

EML cells were seeded at 2×10^5 cells/mL and treated with vehicle, 60 μM ARA (Sigma–Aldrich, cat # A3555), and 60 μM EPA (Sigma–Aldrich, cat # E2011). Cell counts were taken at 24 and 48 h. After 48 h, cells were collected, centrifuged (500*g*) and washed once with PBS. The cells were then resuspended in PBS (without Ca^{2+} or Mg^{2+}) and incubated with 70% EtOH for >2 h, at which time they were again centrifuged (500*g*) and washed once with PBS. The cells were then resuspended in PBS (without Ca^{2+} or Mg^{2+}) containing 50 μg/mL of propidium iodide and 250 μg/mL of RNase A (both purchased from Sigma, St. Louis, MO, USA) and incubated at 37 °C for 30 min. Cells were then analyzed for fluorescence by flow cytometry on a BD FACSAria.

Flow Cytometry

The preparation of bone marrow for flow cytometry was performed as previously described [12]. EML cells were prepared by washing twice with FACS buffer (PBS supplemented with 0.5% bovine serum albumin and 2 mM EDTA) and collecting by centrifugation. Thereafter, samples of both type were incubated with 2% autochthonous sera obtained from cardiac puncture just before marrow harvest to prevent nonspecific binding by blocking the Fc receptors for half an hour at 4 °C. The cells were washed again and labeled with antibodies for 30 min on ice. The following antibodies were used in the bone marrow studies with Streptavidin-Pacific Blue to detect biotinylated antibodies: PE-Cy7 conjugated Sca-1 (clone D7, eBiosciences #25-5981-81), APC-eFluor 750 conjugated CD117 (clone 2B8, eBiosciences #47-1171-80), biotinylated lineage panel (BD Biosciences #559971), biotinylated IL-7Rα (clone B12-1, BD Biosciences #555288), APC conjugated $F_CR\gamma$ (clone 93, eBiosciences #17-0161-81), and PE

Table 2 Compositions of dietary fats (approximate %)

	Saturated FA	Linoleic acid (omega 6)	Total omega 3	Monounsaturated FA
Corn oil[a]	13	61	1	26
Canola oil[a]	6	20	10	62
n-3 supp[b]	9	6	63	21

The corn oil diet is the low n-3:n-6 FA diet containing 10% w/w corn oil as the source of all fat. The fish oil diet is our high n-3:n-6 FA diet containing 5% w/w canola oil and 5% w/w n-3 FA supplement. The corn oil diet contains 0.1% n-3 FA and 6.1% n-6 FA, which is a relative ratio of n-6 to n-3 of 61:1. The fish oil diet contains 3.65% n-3 FA and 1.3% n-6 FA, which is a relative ratio of 1:2.8

[a] From: http:\\www.canola-council.org/pubs/physprop.html

[b] From: manufacturer's certified analyses

conjugated CD34 (clone RAM34, BD Biosciences 551387). The following antibodies were used in labeling the EML-clone1 cells in labeling pairs with Streptavidin-APC (BD Biosciences #554067) to detect biotinylated antibodies: biotinylated Ly6G/C (clone RB6-8CS, BD Biosciences #553125) + PE conjugated CD117 (clone 2B8, BD Biosciences #553355), biotinylated CD11b (clone M1/70, BD Biosciences #553309) + PE conjugated Sca-1 (clone D7, BD Biosciences #553108), and biotinylated CD45 (clone RA3-6B2, BD Biosciences #553086) + PE conjugated F4/80 (clone BM8, Caltag #MF48004). Data acquisition was performed using BD FACS Aria I sorter and data analysis/compensation was performed using FlowJo v. 7.6 software (Treestar, Ashland, OR, USA) with super-enhanced *D*max subtraction analysis for determination of differences in histograms.

In Vitro Culture and Differentiation

EML C1 cells were the kind gift of Dr. Schickwann Tsai and were maintained in Iscove's modified Dulbecco medium (IMDM,) supplemented with 20% horse serum (American Type culture collection, ATCC, Manassas, VA, USA) and 10% BHK/MKL-conditioned medium [14]. For differentiation studies, EML cells were induced to differentiate into myeloid cells with 10 μM all-*trans* retinoic acid (ATRA; sigma, St. Louis, MO, USA), 10% BHK conditioned medium (source of stem cell factor) and 15% WEHI conditioned medium (source of interleukin-3a) for 3 days. EML-clone1 cells were seeded at 2×10^5 cells/mL and cultured for 24 h in 60 μM FA (same formulations as stated previously) in standard growth medium (20% horse serum, 70% Dulbecco's modified eagle medium, and 10% BHK conditioned medium). After 24 h cells were placed in differentiation medium with 60 μM FA at 2.0×10^5 cells/mL. Cell counts were performed using trypan blue at 24, 48, 72, and 96 h. After 96 h cells were processed for flow cytometry analysis.

FA Metabolism Studies

Cells were seeded at 2×10^5 cells/mL and treated with vehicle or 60 μM FA (same formulations as stated previously). Cell counts were performed at 24, 48, 72, and 96 h using trypan blue. At each time point, half the total volume of the culture was taken as a sample and replaced with untreated growth media. Each sample was centrifuged (500*g*), the supernatant removed and the pellet store at −20 °C until analyzed by gas chromatography.

At the time of gas chromatography, cells were homogenized in 0.1% butylated hydroxytoluene in 70% methanol/distilled water to prevent FA oxidation. Lipids were extracted with chloroform/methanol and methylated. Methylated lipids were separated and identified using gas chromatography as previously published [15]. FA methyl ester standards (Nu-Chek-Prep, Elysian, MN, USA) were used for peak identification. The FA methyl esters were reported as the percent of the total methylated FA (area under the curve).

Statistical Analysis

Statistical analyses were run using SAS software release 9.2 (SAS Institute Inc. Cary, NC, USA). Student's *t* tests were used to detect differences between the experimental groups (corn versus fish diet) of colony forming cells ($n = 8$ for each group) and between the experimental groups (corn vs. fish diet) in flow cytometry assays ($n = 8$ for each group). To determine statistical significance in gas chromatography experiments and differentiation studies the levels of fatty acids of a particular type were analyzed using either one-way analysis of variance (ANOVA) or by one-way Kruskal–Wallis analysis of variance on ranks. Dunnett multiple comparison tests were used for testing if any treatments are significantly different from a single control for all main effects means in the MEANS statement.

Results

Fish Oil Diets Induce Changes in the Frequency of Various Myeloid Progenitor Cell Types in the Bone Marrow

In our previous investigations of the effect of fish oil diets on murine hematopoiesis, we found a down-regulation in the frequency of myeloid progenitor cells in bone marrow in mice fed fish oil diets compared to those on corn oil diets [16]. Other investigators have reported that bone marrow of rodents readily changes composition based upon dietary FA sources [17]. However, our investigations using colony forming cell assays limited our ability to assay the frequency of more immature cell types, such as the common myeloid progenitor (CMP) and hematopoietic stem cell (HSC). In order to assay the effects of high n-3 FA diets on these cell types, we verified that the effects seen in hybrid F_1 animals were also seen in C57BL/6 mice where flow cytometry markers for examining these rare cell types have been verified [18]. In the experiments presented here, mice were fed diets rich in n-3 FA (fish oil diet) or rich in n-6 FA (corn oil diet) from 6 weeks of age until 20 weeks of age (Tables 1, 2, 100 days on diet). Bone marrow was then harvested and analyzed by colony forming cell assay and flow cytometry. There was no difference in density of cells in the bone marrow (Fig. 1a). Our results (Fig. 1b)

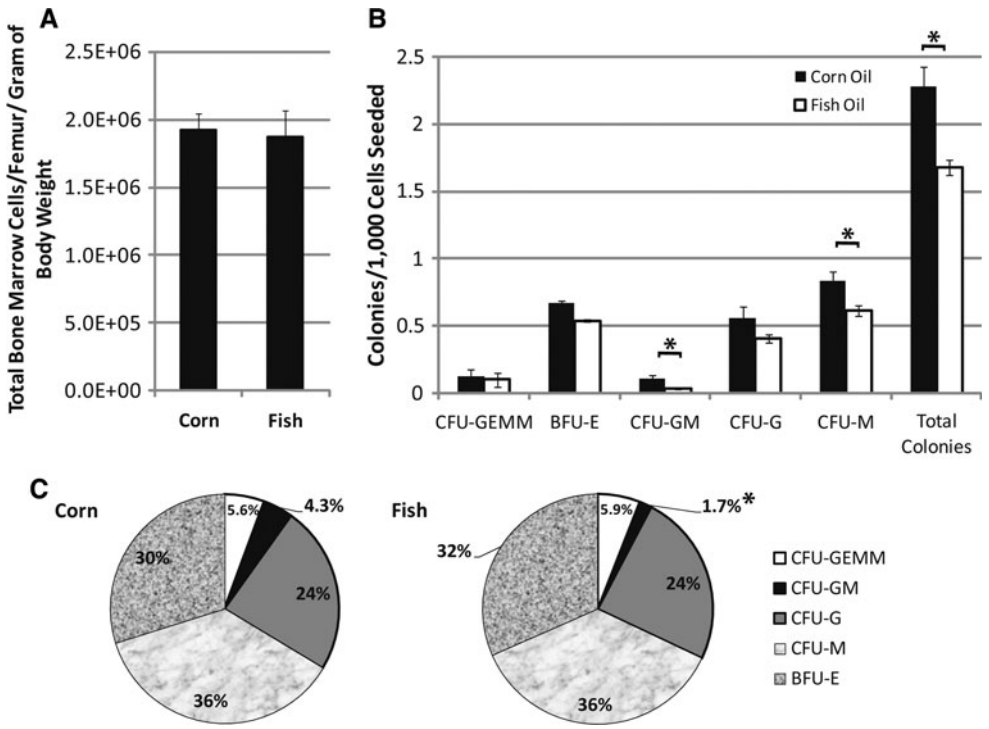

Fig. 1 Reduction in middle to latter stage myeloid progenitor cell types by high n-3 diet. Mice were fed either corn oil or fish oil diets for *x* days followed by harvesting of bone marrow from femurs. The number of cells harvested from the mice on the different diets were similar (**a**). Colony forming cell assays were performed to enumerate the frequency of middle to latter stage progenitor types. The frequency of each progenitor cell type (**b**) and the relative distribution of progenitor types (**c**) in the total progenitors assayed are shown. Significant differences as measured by Student's *t* tests ($p < 0.05$) are indicated by *asterisk*. *Error bars* represent SEM ($n = 8$). SEMs in **c** for the corn oil diet data are BFU-E, 2.4%, CFU-GEMM, 0.8%, CFU-GM, 1.1%, CFU-G, 2.7%, CFU-M, 1.8% and for the fish oil diet are BFU-E, 2.4%, CFU-GEMM, 0.6%, CFU-GM, 0.5%, CFU-G, 2.1%, CFU-M, 2.1%. *CFU* colony forming unit, *BFU* blast forming unit, *GEMM* granulocyte erythrocyte monocyte macrophage, *E* erythrocyte, *GM* granulocyte monocyte, *G* granulocyte, and *M* macrophage

indicated an overall lower frequency of mid to late stage progenitors when mice were fed n-3 FA rich diets compared to those that were fed diets rich in n-6 FA rich diets. There was a significantly lower (26%, $p < 0.01$) overall myeloid progenitor cell frequency, with significant reductions ($p < 0.05$) in colony forming unit granulocyte–macrophage (CFU-GM) and colony forming unit macrophage (CFU-M).

When we examined the relative contributions of each progenitor cell type to the overall myeloid progenitor cell pool in the bone marrow (Fig. 1c), we found that there is a significant reduction in CFU-GM proportion in mice on the fish oil diet ($p < 0.05$). The comparison of proportions of subtypes of myeloid progenitors is different than what we observed in FVB X sv129 F_1 hybrid mice [16], where we observed an overall shift to more later stage progenitor types [16]. Thus, though there was a reduction in myeloid progenitor cell frequencies in the marrow and a twofold reduction in proportion of CFU-GM, there was little shift in proportions of the other progenitor subtypes. This may be due to particular characteristics of the C57BL/6 inbred strain that are not seen in F_1 hybrid animals, due to the lessening of homozygous recessive mutations in hybrid animals. We have shown that mice vary significantly in myeloid progenitor cell frequencies in a previous publication [12]. These data indicate that C57BL/6 mice responded to high n-3 FA diets with a reduction in overall myeloid progenitors cell frequencies, and significantly altering the proportions of the CFU-GM present.

The Frequency of the Common Myeloid Progenitor Fraction is Increased in Mice Fed Fish Oil Diets

In order to assay the frequencies of earlier stage stem and progenitors cells in mice fed corn and fish oil diets, flow cytometry studies were conducted using established gating parameters for the assay of HSC, CMP, granulocyte–macrophage progenitors (GMP), and megakaryocyte–erythrocyte progenitors (HSC) in C57BL/6 mice[18] (Fig. 2a). Bone marrow was first gated by excluding high and low forward scatter cells along with those labeled positively for one of the differentiation antigens in the lineage panel or IL-7Rα, which marks lymphoid cells. These FSC^{mid}IL-7R$\alpha^{-}Lin^{-}$ were further separated into stem (FSC^{mid}IL-7R$\alpha^{-}Lin^{-}$Sca-1^{+}c-Kit^{+}) and progenitor (FSC^{mid}IL-7R$\alpha^{-}Lin^{-}$Sca-1^{-}c-Kit^{+}) cell fractions by

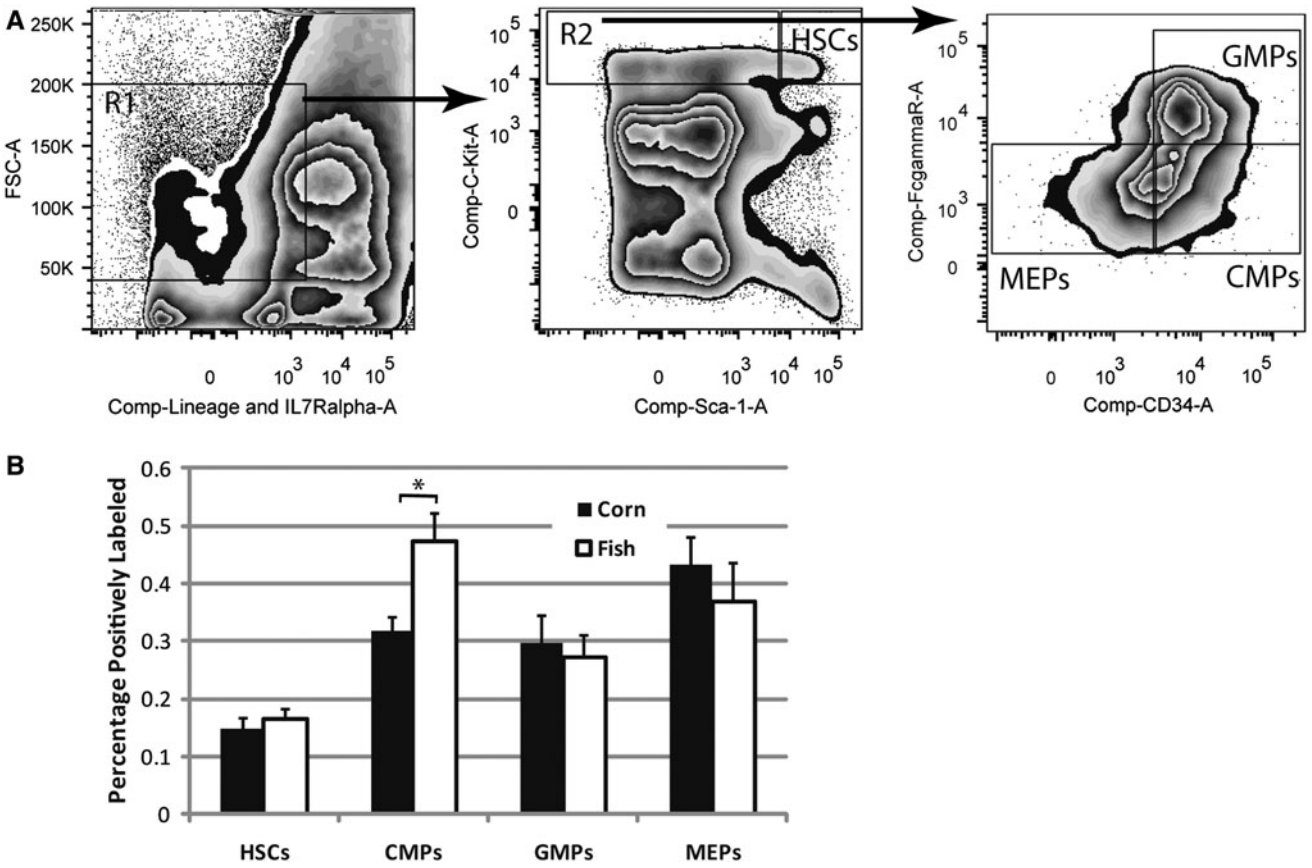

Fig. 2 Increase in early myeloid progenitors by high n-3 diets. Mice were fed either corn oil or fish oil diets for *x* days followed by harvesting of bone marrow from femurs. Bone marrow was analyzed by flow cytometry first by FSC X lineage panel + IL7Rα, then by C-kit and Sca-1 expression, followed by FcγR X CD34 expression to differentiate between various stem or progenitor cell types (**a**). The percentage of the total marrow cells labeling positive for each fraction are shown (**b**). Significant differences as measured by Student's *t* tests ($p < 0.05$) are indicated by *asterisk*. *Error bars* represent SEM ($n = 8$). *HSC* hematopoietic stem cells, *CMP* common myeloid progenitors, *GMP* granulocyte macrophage progenitors, and *HSC* megakaryocyte erythrocyte progenitors

expression of c-Kit and Sca-1 as shown. The progenitor pool was also separated based upon the expression of CD34 and FcγR to delineate CMP ($FSC^{mid}IL\text{-}7R\alpha^{-}Lin^{-}Sca\text{-}1^{+}$ $c\text{-}Kit^{+}Fc\gamma R^{lo}CD34^{+}$), GMP ($FSC^{mid}IL\text{-}7R\alpha^{-}Lin^{-}Sca\text{-}1^{+}$ $c\text{-}Kit^{+}Fc\gamma R^{hi}CD34^{+}$), and HSC ($FSC^{mid}IL\text{-}7R\alpha^{-}Lin^{-}$ $Sca\text{-}1^{+}c\text{-}Kit^{+}Fc\gamma R^{lo}CD34^{-}$). These data show a 50% increase ($p = 0.01$) in the frequency of the CMP fraction in mice fed fish oil diets (Fig. 2b). There were no significant differences in frequency of HSC, GMP, or MEP fractions indicated in these studies. These data suggest that the frequency of the CMP has been increased by administration of a diet containing high levels of n-3 FA.

FA Applied to EML Cell Culture Medium are Incorporated and Processed

In order to study the observed effects of n-3 versus n-6 FA on early myeloid progenitor cells in more detail, we examined the effects of the polyunsaturated fatty acids EPA and ARA on EML cells in culture. We chose to compare these two FA because EPA (20:5, n-3) is the fatty acid most molecularly similar to ARA (20 carbons, n-6 FA) available. DHAn-3 (22:6, n-3) has two more carbons in the chain. The EML cell line is a stem cell factor dependent multipotent cell line with erythroid (E), myeloid (M), and lymphoid (L) potential. It was established from DBA/2 mouse bone marrow infected with a retroviral vector (LRARα403SN) harboring a dominant negative retinoic acid receptor [14]. It is a suspension cell line consisting of mostly blast like cells with 20–30% hand mirror shaped cells. EML cells serve as an excellent model to study hematopoietic differentiation. It can be induced to differentiate towards granulocyte/monocyte progenitors by high concentration of all-*trans* retinoic acid (ATRA) in the presence of interleukin-3 (IL-3).

To verify the incorporation and processing by EML cells of FA placed in the culture medium, we spiked the culture medium with 60 μM ARA (Fig. 3a) or 60 μM EPA (Fig. 3b) and analyzed the levels of various FA present in the cells over the course of 4 days. Cells were analyzed

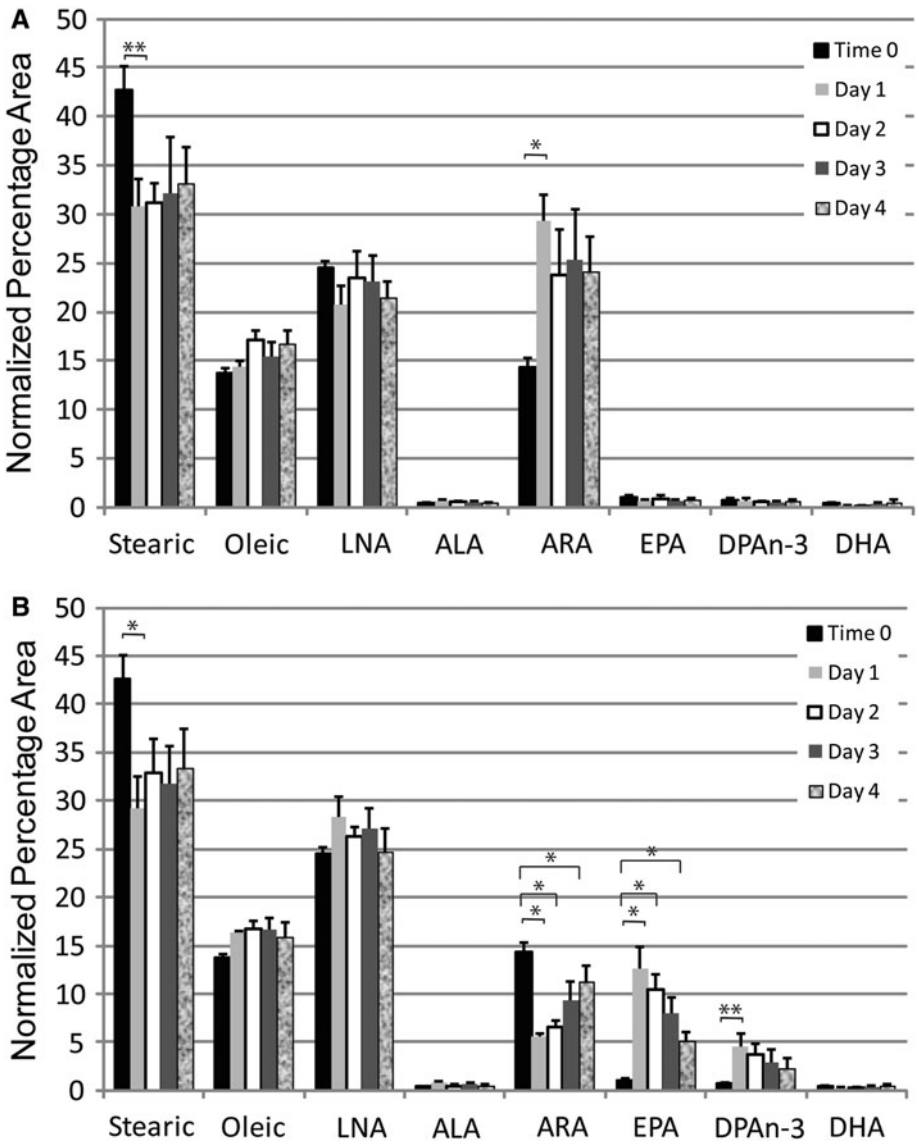

Fig. 3 EML cells take up and metabolize FA. EML cells were placed in growth medium containing 60 μM arachidonic (**a**) or eicosapentaenoic (**b**) acid. The uptake and processing of these FA was assayed over the course of 4 days. Samples were taken just before addition of the FA ($t = 0$), 24, 48, 72, and 96 h for analysis by gas chromatography. The gas chromatography data for each FA is shown above for the five data points in temporal order. Data displayed are the results of three independent experiments with the mean and SEM displayed. *LNA* linoleic acid, *ALA* alpha-linolenic acid, *ARA* arachidonic acid, *EPA* eicosapentaenoic acid, *DPA* docosapentaenoic acid, and *DHAn-3* docosahexaenoic acid. * indicate statistically significant ($p < 0.05$) differences based on one-way ANOVA test or Kruskal–Wallis test with Dunnett multiple comparisons adjustment. ** indicate statistically significant ($p < 0.05$) differences based on Student's *t* test or Mann–Whitney rank sum test without multiple comparison adjustment

with gas chromatography daily to determine the uptake and processing of FA. The major FA in untreated EML cell membranes are steric acid, oleic acid, LNA, and ARA (time 0). There are only faint traces of n-3 FA such as ALA, EPA, docosapentaenoic acid (DPA), and DHA in EML cell membranes under normal culturing conditions (time 0). In both cultures, the percentage of the major constituent of cell membranes (steric acid) is reduced as this is replaced by either ARA or EPA (Fig. 3a, b, 24 h). Thus, FA supplied in culture medium were being incorporated into cellular membranes and this occurs within 24 h. Supplementation of ARA in the medium caused an increase in the already substantial levels of ARA in cellular membranes (Fig. 3a). There was a significant ($p < 0.05$) two-fold increase in ARA at 24 h that drops to a 66% increase at 48 h and was maintained for the remainder of the 4 days. The addition of EPA to the culture medium caused a significant ($p < 0.001$) increase in the n-3 FA EPA and elevated levels (p value significant before correction for multiple comparisons) of the EPA elongation metabolite DPA, with a corresponding significant ($p < 0.001$) decrease in ARA by 24 h (Fig. 3b). Interestingly, there was no increase in DHA, which is the Δ4 desaturase metabolite of DPA, indicating EML cells do not have this enzymatic activity. Thus, addition of FA to the cell medium resulted in incorporation of these FA into cellular membranes and processing of these FA by 24 h.

Incubation of EML Cells with FA has Effects on Immunophenotype and Cell Viability

To determine if the effects of n-3 versus n-6 FA seen in our in vivo experiment are due to viability/proliferation differences induced by the FA, we analyzed the effect of n-3

and n-6 FA on EML cells in culture (Fig. 4a) for 2 days, since we have shown the greatest levels of incorporation of fatty acids supplied through the culture medium occur at 24 h according to the gas chromatography. EML cells in their native state are a model for hematopoietic stem cells. We found that cultures treated with 60 μM ARA had significantly reduced ($p < 0.05$) cell counts after 1 day compared to the vehicle control. EPA treated cultures had slightly lower cell counts at day one, but the difference was not statistically significant. Neither of the treated cultures had statistically significant differences from the control at day 2, indicating that the effects of treatment with ARA were transitory. These results are consistent with the in vivo results, where we saw no difference in the stem cell compartment of fish oil (high n-3) versus corn oil (high n-6) fed mice.

To observe cell autonomous effects of n-3 versus n-6 FA on cell viability and proliferation during the GMP myeloid progenitor cell differentiation stage we primed EML cells for 24 h with 60 μM EPA or ARA, then induced differentiation into macrophage/granulocytic lineages with ATRA, stem cell factor (SCF), and IL-3. After 72 h in the differentiation medium, cell counts were performed on these EML cell cultures. Viability/proliferation was measured by trypan blue exclusion (Fig. 4b). The viability of the cell cultures was very similar with the various treatments at each stage with a fairly consistent viability as the cultures differentiated (measured by non-stained cells/total cells, data not presented). All cultures were proliferating robustly with a doubling time starting at 18 h and shortening as differentiation proceeded (data not presented). The major finding of this study was a significant reduction ($p < 0.05$) in cell counts in the EPA treatment group at days 2 (11% reduction) and 3 (21% reduction) with a suggestive reduction at day 1 (Fig. 4b). There was no reduction in viability of the cultures at these time points, suggesting the difference was due to cell proliferation. These results are consistent with our in vivo results that show a higher frequency of middle-later stage myeloid progenitors with high n-6 diets.

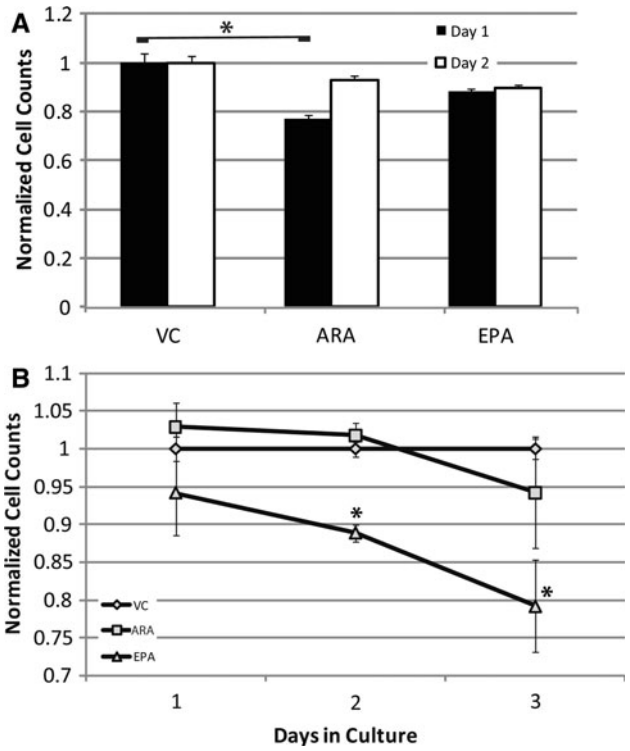

Fig. 4 In vitro culture of EML cells shows a slight increased viability in n-3 versus n-6 augmented cultures. EML cells in standard culture were augmented with either vehicle control, arachidonic acid (n-6), or eicosapentaenoic acid (n-3) for 48 h with cell counts performed at 24 and 48 h to determine viability (**a**). EML cells were cultured in either vehicle control, arachidonic acid (n-6), or eicosapentaenoic acid (n-3) for 24 h then induced to differentiate for another 72 h down myeloid lineages (**b**). Data displayed are the results of two (**a**) or three (**b**) independent experiments with the mean and SEM displayed of culture counts normalized to the vehicle control. * indicate statistically significant ($p < 0.05$) difference based on one-way ANOVA test with Dunnett multiple comparisons adjustment

Fig. 5 No significant differences in myeloid progenitor cell maturation rate between n-3 and n-6 FA. EML cells were cultured in either vehicle control, arachidonic acid (n-6), or eicosapentaenoic acid (n-3) for 24 h then induced to differentiate for another 72 h down myeloid lineages. Flow cytometry was performed analyzing the larger FSC population of non-apoptotic cells (**a**). The percentage of cells displaying various markers of differentiation are shown for each culture type (**b**). Representative histograms are displayed for the isotype control (*black*, *narrow line*), vehicle control (*dotted line*), EPA treated cultures (*gray line*), and ARA treated cultures (*black*, *thick line*) (**c**). Both fatty acid treated culture display a shift over to low level expression (a small increase in fluorescence) of the antigen, but the ARA treated cultures show a greater shift (more cells present in the higher fluorescence channels). Data represents the results from five independent experiments with the mean and SEM displayed. * indicates statistically significant ($p < 0.05$) difference based on one-way Kruskal–Wallis analysis of variance on ranks followed by Dunnett test. ** indicates statistically significant ($p < 0.05$) difference based on Student's *t* test without multiple comparison adjustment

To observe cell autonomous effects of n-3 versus n-6 FA on myeloid progenitor cell differentiation we primed EML cells for 24 h with 60 μM EPA or ARA, then induced differentiation into macrophage/granulocytic lineages with ATRA, stem cell factor (SCF), and IL-3. After 72 h in the differentiation medium, EML cells were immunophenotyped for the early markers Sca-1 and CD117, as well as the differentiation markers Ly6G, CD11b, CD45, and F4/80 (Fig. 5b). There were no significant decreases in Sca-1 levels (the first sign of differentiation in this model) with treatment, though the decrease with ARA treatment is suggestive (*p* value significant before correction for multiple comparisons, but not after the appropriate Dunnett multiple comparison correction) when comparing treatments to vehicle control. There was significant ($p < 0.05$)

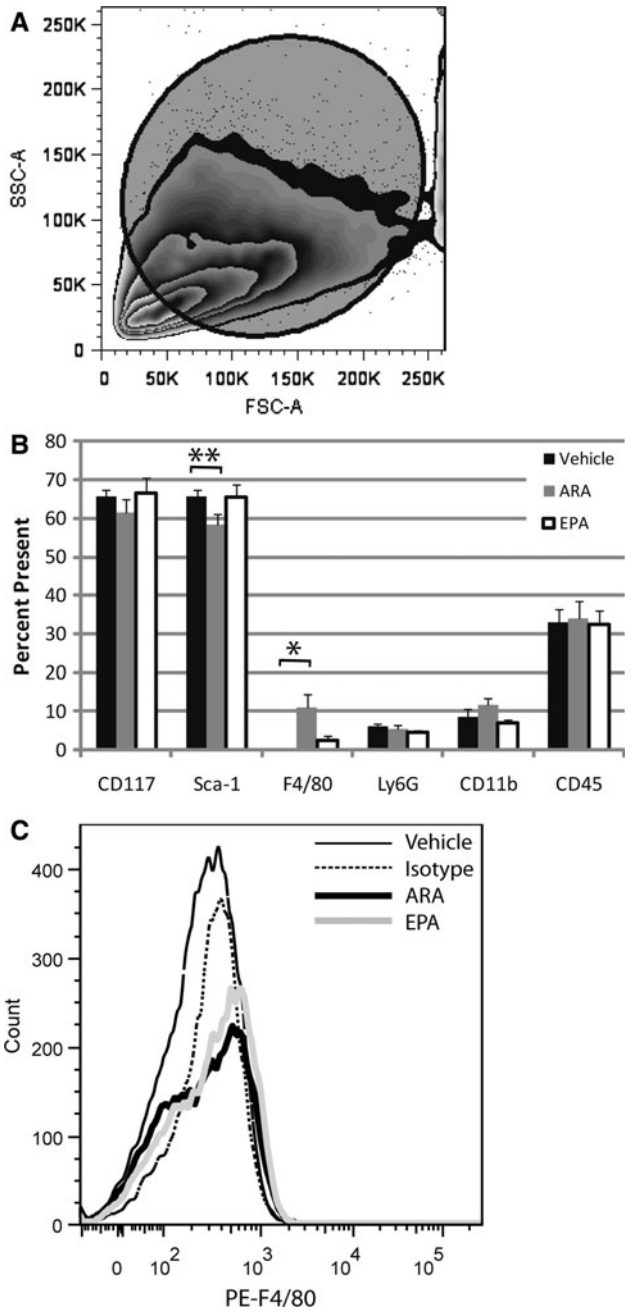

difference in the percentage of cells labeling with the F4/80 antigen in the ARA treatment group compared to the vehicle control. The sizeable increase in F4/80 positive cells coupled with the suggestive decrease for the Sca-1 antigen in the treatments with ARA compared to vehicle (Fig. 5b) indicates the production of a granulocyte/macrophage progenitor population with ARA treatment. These two results are consistent in that there is a lower frequency of the marker for stem cells and an increase in frequency of the differentiation marker F4/80. This result is also consistent with the in vivo data that found an increase in production of granulocyte and macrophage progenitor subtypes at later stages. The expression of F4/80 appears to be at a low abundance on a per cell basis in both ARA and EPA treated samples, but much more prevalent in ARA treated samples (Fig. 5c). Thus, our model suggests that the differences seen in the CMP compartment seen in our in vivo experiment are not due to changes in rate of differentiation in the bone marrow and that n-6 FA supplementation produces a shift to macrophage/granulocytic lineages as seen in vivo.

Discussion

Our primary objective in this study was to determine if the reduction of later myeloid progenitor subtypes by diets high in n-3 FA seen previously [12] was the continuation of differences induced at earlier stages of myeloid progenitor development. The data from these experiments indicate that this is not the case. The effect of lowering the frequency of myeloid progenitors of the later stages in mice fed n-3 FA rich diet was recapitulated in the present study, but we did not see a lowering of the stem/early progenitor cell fractions in the bone marrow. Conversely, we observed an increase in the common myeloid progenitor cell fraction with flow cytometry. Thus, the effects of n-3 FA on stem/progenitor cell biology in bone marrow are not a simple lowering of the overall frequency of these cell types. Determination of the exact mechanism of n-3 FA effects will entail studies at multiple levels of maturation in bone marrow. Possible mechanisms include effects through metabolites such as leukotrienes, resolvins, incorporation into cell signaling molecules such as hedgehog, or production of prostaglandins. Our data suggest that these mechanisms are eventually triggering a slowed differentiation between the early and middle myeloid progenitor phases resulting in an increase in early progenitors and a decrease in later stage progenitors in high n-3 diets. Understanding the mechanisms involved will enable targeted therapies to hematopoietic disorders involving problematic differentiation.

Our in vivo studies indicate that diets rich in n-3 FA when compared to n-6 FA have an effect of increasing the frequency of CMP, but no effect on HSC (Fig. 2). The changes seen in early stem/progenitor cell biology are then reversed, in that diets rich in n-6 FA produce more later stage progenitor cells of the granulocyte and macrophage lineage (Fig. 1). The results of our stem cell culture model found no lasting effects on stem cell viability or proliferation when cultured in n-3 versus n-6 fatty acids (Fig. 4a), similar to that seen in vivo. It is interesting that we did not see an increase in HSC with the corn oil diet containing high n-6 FA levels considering the recent results indicating one of the products of n-6 FA, prostaglandin E_2, can

increase HSC production in vivo [19–22]. This may be due to the complex metabolism of FA and use of them in biomolecules or the genetics of the C57BL/6 model. We found a low level expression of F4/80 antigen upon treatment with ARA treatment, characteristic of macrophage progenitor development [23–26], consistent with these progenitors being greater in vivo in corn oil fed mice compared to fish oil fed mice (Fig. 1). No other significant changes were seen in differentiation state upon treatment with ARA or EPA in comparison to vehicle controls. We observed a lower proliferation rate during differentiation of EML cells while cultured in EPA compared to vehicle controls that was not seen with ARA treatment. This is consistent with an overall lowering of middle-later stage myeloid progenitor cell numbers in mice fed fish oil diets relative to corn oil diets (Fig. 1). An important consideration in extrapolating these in vitro experiments to our in vivo results is that the EML cell model only takes into account cell autonomous factors. The stem cell niche is an important part of stem cell biology and this is not recapitulated in this model.

These data indicate that the effect of n-3 FA in the diet of mice on reducing later stage myeloid progenitors is not a simple reduction of HSC in the bone marrow relative to n-6 FA fed mice. n-3 FA appear to have a diverse effect depending upon the stage of progenitor cell development. Understanding the mechanisms involved will allow a more targeted approach to using n-3 FA clinically in differentiation therapies. We are currently investigating whether the use of n-3 fatty acids as a mechanism of induced differentiation is applicable to reduction of the progression of chronic myelogenous leukemia (CML) to the lethal blast crisis phase in a murine model as well as clinical trials with B-cell malignancies ([27] and unpublished results).

Acknowledgments This work was supported by NIH grants 1R03 CA129790 to VES, 1R01 CA114018 to WEH, COBRE (5P20RR020180) to Richard M. Niles, and the WV-INBRE Program (5P20RR016477) to Gary O. Rankin, as well as with support from the NASA WV Space Grant Consortium issued by NASA Goddard Space Flight Center, Grant Number NNG05GF80H. We would like to acknowledge John Wilkinson IV for assistance in discussion of results.

References

1. Kelley DS (2001) Modulation of human immune and inflammatory responses by dietary fatty acids. Nutrition 17(7–8):669–673
2. Dupuis F et al (1997) Effects of lipidic mediators on the growth of human myeloid and erythroid marrow progenitors. J Lipid Mediat Cell Signal 16(3):117–125
3. Germain E et al (1999) Dietary n-3 polyunsaturated fatty acids and oxidants increase rat mammary tumor sensitivity to epirubicin without change in cardiac toxicity. Lipids 34 Suppl: p S203
4. Hardman WE et al (1997) Effects of iron supplementation and ET-18-OCH3 on MDA-MB 231 breast carcinomas in nude mice consuming a fish oil diet. Br J Cancer 76(3):347–354
5. Karmali RA (1996) Historical perspective and potential use of n-3 fatty acids in therapy of cancer cachexia. Nutrition 12(1 Suppl):S2–S4
6. Oberley LW, Spitz DR (1984) Assay of superoxide dismutase activity in tumor tissue. Methods Enzymol 105:457–464
7. Li D et al (1998) Contribution of meat fat to dietary arachidonic acid. Lipids 33(4):437–440
8. Hagve TA, Christophersen BO (1984) Effect of dietary fats on arachidonic acid and eicosapentaenoic acid biosynthesis and conversion to C22 fatty acids in isolated rat liver cells. Biochim Biophys Acta 796(2):205–217
9. Rose DP, Connolly JM (1999) Omega-3 fatty acids as cancer chemopreventive agents. Pharmacol Ther 83(3):217–244
10. Rizzo MT (2002) The role of arachidonic acid in normal and malignant hematopoiesis. Prostaglandins Leukot Essent Fat Acids 66(1):57–69
11. Report of the American Institute of Nutrition ad hoc committee on standards for nutritional studies (1977) J Nutr 107(7): p 1340–1348
12. Sollars VE et al (2006) Analysis of expansion of myeloid progenitors in mice to identify leukemic susceptibility genes. Mamm Genome 17(8):808–821
13. Miller CL and Lai B (2005) Human and mouse hematopoietic colony-forming cell assays, in basic cell culture protocols In: Helgason CD & Miller (Eds) Humana Press Inc. Totowa, NJ, p 71–90
14. Tsai S et al (1994) Lymphohematopoietic progenitors immortalized by a retroviral vector harboring a dominant-negative retinoic acid receptor can recapitulate lymphoid, myeloid, and erythroid development. Genes Dev 8(23):2831–2841
15. Hardman WE, Ion G (2008) Suppression of implanted MDA-MB 231 human breast cancer growth in nude mice by dietary walnut. Nutr Cancer 60(5):666–674
16. Varney ME, Hardman WE, Sollars VE (2009) Omega 3 fatty acids reduce myeloid progenitor cell frequency in the bone marrow of mice and promote progenitor cell differentiation. Lipids Health Dis 8:9
17. Atkinson TG, Barker HJ, Meckling-Gill KA (1997) Incorporation of long-chain n-3 fatty acids in tissues and enhanced bone marrow cellularity with docosahexaenoic acid feeding in post-weanling Fischer 344 rats. Lipids 32(3):293–302
18. Akashi K et al (2000) A clonogenic common myeloid progenitor that gives rise to all myeloid lineages. Nature 404(6774):193–197
19. Frisch BJ et al (2009) In vivo prostaglandin E2 treatment alters the bone marrow microenvironment and preferentially expands short-term hematopoietic stem cells. Blood 114(19):4054–4063
20. Hoggatt J et al (2009) Prostaglandin E2 enhances hematopoietic stem cell homing, survival, and proliferation. Blood 113(22): 5444–5455
21. Goessling W et al (2009) Genetic interaction of PGE2 and Wnt signaling regulates developmental specification of stem cells and regeneration. Cell 136(6):1136–1147
22. Lord AM, North TE, Zon LI (2007) Prostaglandin E2: making more of your marrow. Cell Cycle 6(24):3054–3057
23. Gordon S et al (1986) Localization and function of tissue macrophages. Ciba Found Symp 118:54–67
24. McKnight AJ et al (1996) Molecular cloning of F4/80, a murine macrophage-restricted cell surface glycoprotein with homology to the G-protein-linked transmembrane 7 hormone receptor family. J Biol Chem 271(1):486–489
25. Torroella-Kouri M et al (2009) Identification of a subpopulation of macrophages in mammary tumor-bearing mice that are neither

M1 nor M2 and are less differentiated. Cancer Res 69(11): 4800–4809
26. Zhou Z et al (2010) Development and function of myeloid-derived suppressor cells generated from mouse embryonic and hematopoietic stem cells. Stem Cells 28(3):620–632
27. Witte TR et al (2010) RBC and WBC fatty acid composition following consumption of an omega 3 supplement: lessons for future clinical trials. Lipids Health Dis 9:31

Lipids (2011) 46:59–67
DOI 10.1007/s11745-010-3499-8

ORIGINAL ARTICLE

Omega-3 Index Correlates with Healthier Food Consumption in Adolescents and with Reduced Cardiovascular Disease Risk Factors in Adolescent Boys

Therese A. O'Sullivan · Gina L. Ambrosini · Trevor A. Mori · Lawrie J. Beilin · Wendy H. Oddy

Received: 22 July 2010 / Accepted: 21 October 2010 / Published online: 20 November 2010

Abstract The Omega-3 Index, a measure of long-chain omega-3 fats in red blood cell membranes, predicts heart disease mortality in adults, but its association with cardiovascular risk factors in younger populations is unknown. We determined the Omega-3 Index in adolescents participating in the Western Australian Pregnancy (Raine) Cohort, assessed associations with diet, lifestyle and socioeconomic factors, and investigated independent associations with cardiovascular and metabolic risk factors. Red blood cell fatty acid analysis was determined for 1,301 adolescents aged 13–15 years. Risk factors examined were blood pressure, fasting blood insulin and glucose concentrations, and fasting blood lipids including ratios. The mean Omega-3 Index was $4.90 \pm 1.04\%$ (range 1.41–8.42%). When compared with categories identified in adults, 15.6% of adolescents were in the high risk category (Index $< 4\%$). Age ($P < 0.01$), maternal education ($P < 0.01$) and BMI ($P = 0.05$) were positively associated with the Omega-3 Index. The Index was positively associated with dietary intakes of eicosapentaenoic and docosahexaenoic acid ($P < 0.01$), protein ($P < 0.01$), omega-3 fats ($P < 0.04$), and food groups of fish and wholegrains (both $P < 0.01$), and negatively associated with intakes of soft drinks and crisps (both $P < 0.01$). In boys, the Omega-3 Index was independently associated with total ($\beta = 0.06$, $P = 0.01$) and HDL-cholesterol ($\beta = 0.03$, $P = 0.01$), and diastolic blood pressure ($\beta = -0.68$, $P = 0.04$). The predictability of the Index for the risk of cardiovascular disease later in life warrants further investigation in the adolescent population.

Keywords Omega-3 Index · Adolescent · Cardiovascular disease · Cholesterol · Blood pressure · Diet · Raine Study

Abbreviations

EPA	Eicosapentaenoic acid
DHA	Docosahexaenoic acid
RBC	Red blood cell
HDL	High density lipoprotein
LDL	Low density lipoprotein

Introduction

The Omega-3 Index has been suggested as a physiologically relevant, modifiable, and independent risk factor for cardiovascular disease [1]. The Index is equal to the content of long-chain omega-3 fatty acids—eicosapentaenoic acid (EPA, 20:5n-3) and docosahexaenoic acid (DHA, 22:6n-3)—in red blood cell (RBC) membranes, as a percentage of the total fatty acids. The omega-3 fatty acid content of RBC membranes reflects the fatty acid content of cardiac membranes [2]. Dietary intake of fats is thought to modify the Index [3], and supplementation with long-chain omega-3

T. A. O'Sullivan (✉) · G. L. Ambrosini · W. H. Oddy
Telethon Institute for Child Health Research,
Centre for Child Health Research,
University of Western Australia, West Perth, Australia
e-mail: tosullivan@ichr.uwa.edu.au

G. L. Ambrosini
Elsie Widdowson Laboratory, Medical Research Council
Human Nutrition Research, Cambridge, UK

T. A. Mori · L. J. Beilin
Royal Perth Hospital Unit, School of Medicine
and Pharmacology, University of Western Australia,
Perth, Australia

fatty acids has been shown to increase the Omega-3 Index in a randomised trial [4]. Other factors such as age and smoking habits may also affect the Index [3].

Long-chain omega-3 fatty acids in RBC membranes exert beneficial metabolic effects, in part, by altering membrane characteristics and the activity of membrane-bound proteins [5]. They reduce the risk of cardiovascular disease through their strong anti-inflammatory effects, their capacity to reduce platelet adhesiveness, and by benefitting blood pressure and vascular reactivity, cardiac function, lipid metabolism, platelet and leukocyte function, cytokine production and oxidative stress [6–9]. Harris and von Schacky have shown, through analyses of epidemiological and randomised controlled trials, that an Omega-3 Index of <4% is associated with a high risk, 4–8% an intermediate risk and >8% a low risk of coronary heart disease mortality in adults [5].

Existing literature on investigations of the Omega-3 Index is predominantly focussed on adults [10–12]. To our knowledge, there have been no reports describing associations between the Omega-3 Index and cardiovascular and metabolic risk, dietary, lifestyle and socioeconomic factors in an adolescent population. To assess its potential value as an early predictor of adult cardiovascular and metabolic disease, we have investigated cross-sectional associations between cardiometabolic risk factors and the Omega-3 Index in a large population-based adolescent cohort in Western Australia.

Materials and Methods

Subjects

As a longitudinal observational study, the Raine Study recruited 2,900 pregnant women from May 1989 to November 1991 through the public antenatal clinic at the King Edward Memorial Hospital and private clinics in Perth, Western Australia. Further details on the Raine Study have been previously published [13]. Of the initial cohort of 2,868 live births, assessments occurred at birth and at ages one, two, three, five, eight, ten and 14 years. This study utilises data collected at the 14-year follow-up when assessments of RBC fatty acids and dietary intake were conducted. The ethics committees of King Edward Memorial Hospital and Princess Margaret Hospital approved the protocol for all aspects of the study. Each adolescent, as well as their parent or guardian, provided written consent for participation in the study.

Red Blood Cell Analysis

Fatty acids of interest for this study were EPA and DHA. RBC fatty acid analysis was performed as previously described [14]. Briefly, chloroform:methanol (2:1) was used to extract total lipids and fatty acid methyl esters were prepared by treatment of extracts with 4% H_2SO_4 in methanol at 90 °C for 20 min. Samples were analysed by gas chromatography using an Agilent 7890A gas chromatograph. The column was a BPX70 (25 m × 0.32 mm, 0.25 μm film thickness) (SGE, Ringwood, Victoria, Australia) with programmed temperatures of 150–210 °C at 4 °C/min. N_2 was used as the carrier gas at a split ratio of 30:1. Peaks were identified by comparison with a known standard mixture. Reproducibility for duplicate analysis was ~10–20%. Coefficients of variation were 2% for DHA and 4% for EPA. The fatty acids were expressed as a percentage of the total fatty acids measured (C_{14}–C_{22}).

Assessment of Cardiovascular Factors

Blood pressure readings were taken using a Dinamap ProCare 100 automatic oscillometric blood pressure recorder (GE Healthcare Technologies, Rydalmere, Australia) while subjects were seated after a 5-min rest. Over a 10-min period, six blood pressure measurements were taken. The first was disregarded and blood pressure was calculated as the mean of the next five measurements. Trained phlebotomists visited the adolescents at their homes and obtained fasting blood samples prior to breakfast. The biochemistry assays for the study were conducted by PathWest Laboratories at Royal Perth Hospital. Serum triglycerides were measured using the Cobas MIRA analyser (Roche Diagnostics, Basel, Switzerland). Glucose was measured using an automated Technicon Axon Analyzer (Bayer Diagnostics, Sydney, Australia) and insulin was measured on an Immunlite 2000 Insulin Analyzer (Siemens Medical Solutions Diagnostic, LA, USA). Insulin resistance was determined using the homeostasis model assessment of insulin resistance (HOMA-IR), calculated as fasting plasma insulin (mU/L) × plasma glucose (mmol/L)/22.5 [15]. High density lipoprotein (HDL) cholesterol was determined on a heparin–manganese supernatant [16]. Cholesterol ratios were calculated for total/HDL, low density lipoprotein (LDL)/HDL and triglycerides/HDL [17, 18].

Dietary Intake

Dietary intake at this follow-up was assessed from three-day food records in household measures, as previously reported [19]. In brief, subjects were provided with a record booklet with instructions and a set of metric measuring cups and spoons. Food records were individually checked by a dietitian as they were returned in order to clarify any ambiguous or potential omissions [20]. The Australian Food and Nutrient database through the

FoodWorks dietary analysis program (Professional Version 5, 2007, Xyris Software, Brisbane) was used to analyse the food record data. Individual nutrients as well as overall diet was considered from the food diaries, with dietary patterns used to investigate overall diet. Using exploratory factor analysis, two major dietary patterns were identified: a 'healthy' pattern high in fresh fruit, vegetables, whole grains and grilled or canned fish, and a 'western' pattern high in takeaway foods, confectionery, soft drinks, crisps and fried potato [21]. Each adolescent received a *z*-score for both western and healthy dietary patterns. A positive score indicated a greater intake of foods representative of that pattern. To assess differences in the Omega-3 Index due to early infant feeding, information on breastfeeding cessation was obtained from the year 1, 2 and 3 Raine follow-up questionnaires. At the time of these follow-ups it was not mandatory for infant formulas to be enriched with long-chain omega-3 fatty acids in Australia.

Additional Factors

Anthropometry and Puberty

Adolescents were dressed in running shorts and singlet tops for anthropometric measurements. Height was measured to the nearest 0.1 cm with a Holtain Stadiometer, and body weight was measured to the nearest 100 g using a Wedderburn Digital Chair Scale. The body mass index (BMI) was calculated as weight in kilograms divided by height in meters squared. The Tanner stages of pubic hair development [22, 23] was used to assess puberty; adolescents selected their corresponding developmental stage in a questionnaire completed privately. Adolescents were asked to choose from a set of standard drawings depicting the different Tanner stages from two (sparse) to five (adult) (stage one was omitted as this corresponds to pre-pubescent age younger than 10 years).

Sociodemographic and Family Characteristics

Family income, mother's age at conception and mother's education level were obtained by parent report. Maternal education was assessed by the highest school year completed. Current family income, defined as the annual income for the household before tax at the time of the follow-up, was determined as ($AUD): <$35,000 pa, $35,000–70,000 pa, or >$70,000 pa. Family history of cardiovascular disease was assessed as either yes or no, depending on whether a biological parent or sibling of the adolescent had been medically diagnosed with diabetes mellitus, hypertension, hypercholesterolemia, or other cardiac condition.

Fitness

The Physical Working Capacity 170 (PWC 170) test was applied to estimate aerobic fitness [24]. PWC170 was measured using a bicycle ergometer to determine the power output (watts) required at a heart rate of 170 beats per minute. This measure of fitness is highly correlated with self-reported physical activity level in the Raine cohort at the 14-year follow-up [25].

Statistical Analysis

Independent *t* tests or cross-tabs analysis were used to compare characteristics of Raine Study adolescents between Omega-3 Index risk categories, with low and intermediate categories combined due to the small number of subjects in the low category. Mann–Whitney tests were used to assess significance of dietary intakes of omega-3, the omega-6 to 3 ratio and EPA + DHA due to the skewed distribution of these variables. Associations between continuous variables and the Omega-3 Index were described with Pearson's or Spearman's correlations. Linear regression was used to examine associations between Omega-3 Index as a continuous independent variable and cardiovascular risk factors as dependent variables. General Linear Modelling was used to analyse associations with Omega-3 Index categories and cardiovascular risk factors. Log values were used for HOMA, triglycerides, and insulin due to their skewed distribution. To evaluate the relationship between the Omega-3 Index and cardiometabolic risk factors, parsimonious models were created which adjusted for age, sex, BMI, maternal education, total energy intake and family history of cardiovascular disease or diabetes, based on the relationship of the variables with the risk factors and the Omega-3 Index. Other variables considered for the model included puberty, aerobic fitness, physical activity, family income, single parent family, maternal age, but were excluded due to strong correlation between covariates or lack of association with risk factors and the Index. Subjects who were on cardiac or diabetes related medications ($n = 4$) or diagnosed with diabetes ($n = 9$) were excluded from analysis investigating cardiometabolic disease risk factors. The Statistical Package for Social Sciences for Windows, Rel.15.0.0. 2006 (Chicago: SPSS Inc) was used for analyses; statistical significance was set at $P \leq 0.05$.

Results

From the initial Raine Study cohort of 2,868 live births, 1,861 subjects completed at least one aspect of the 14-year

follow-up (mean age 14.0 ± 0.2 years, range 13.0–15.0 years), with the remainder lost to follow-up, withdrawn or temporarily deferred from the study ($n = 975$), or deceased ($n = 32$). RBC fatty acids were determined for 1,301 subjects. The mean ± SD Omega-3 Index was 4.90 ± 1.04% (range 1.41–8.42%). Relative to the published Omega-3 Index risk categories [5], 15.6% of adolescents were in the high risk category (<4%), 84.0% were in the intermediate risk category (4–8%) and 0.4% were in the low risk category (>8%). Omega-3 Index values in the population were normally distributed, while dietary intake of EPA and DHA was not (Fig. 1). Characteristics of this sample across high and low/intermediate Omega-3 Index risk categories are shown in Table 1.

When associations with subject characteristics were examined with the Omega-3 Index as a continuous variable, age at assessment ($r = 0.12$, $P < 0.01$) and maternal education ($r = 0.09$, $P < 0.01$) showed significant correlations with the Index. BMI showed borderline significance ($r = 0.05$, $P = 0.05$). The Omega-3 Index as a continuous variable showed significant positive associations with healthy eating pattern scores ($r = 0.14$, $P < 0.01$), energy adjusted dietary intakes of EPA + DHA ($r = 0.22$, $P < 0.01$), protein ($r = 0.12$, $P < 0.01$) and total omega-3 fats ($r = 0.08$, $P = 0.04$), and a significant negative association with western eating pattern scores ($r = -0.13$, $P < 0.01$) (data not shown). The significant association with EPA + DHA was also observed in comparison of Omega-3 Index risk categories ($P < 0.01$), along with a positive association with glycemic index ($P = 0.02$) (Table 1).

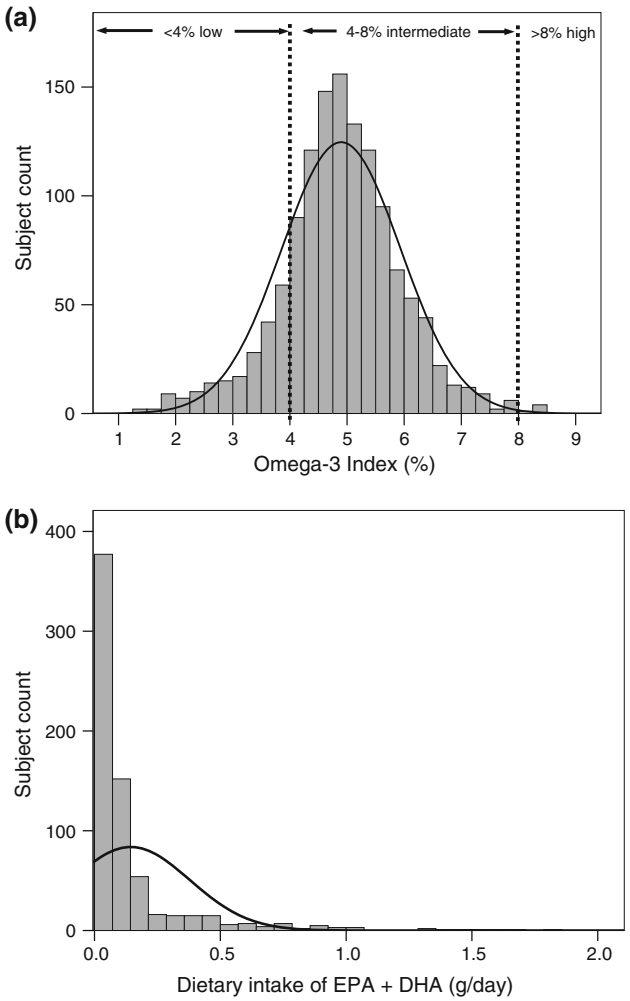

Fig. 1 **a** Histogram of Omega-3 Index in Raine Study adolescents ($n = 1{,}301$), showing Omega-3 Index risk categories (5), and **b** subjects who also reported dietary intake of EPA plus DHA from completed and followed-up 3-day food records ($n = 689$)

Several food group intakes were correlated with the Omega-3 Index (Fig. 2). Fish and seafood ($r = 0.18$, $P < 0.01$), wholegrain foods such as multigrain bread, brown rice and pasta ($r = 0.11$, $P < 0.01$) and vegetables ($r = 0.10$, $P < 0.01$) showed the strongest positive associations with the Omega-3 Index. Intakes of soft drinks ($r = -0.11$, $P < 0.01$) and crisps ($r = -0.10$, $P < 0.01$) were negatively correlated with the Omega-3 Index.

After adjustment for potential confounding factors in a linear regression model, the Omega-3 Index was positively associated with total cholesterol ($\beta = 0.064$, $P = 0.01$) and HDL-cholesterol ($\beta = 0.029$, $P = 0.01$) in boys and girls (Table 2). There were no significant associations with other cardiovascular or metabolic risk factors. When analysed according to gender, significant associations were observed with boys for total cholesterol ($\beta = 0.074$, $P = 0.03$), HDL-cholesterol ($\beta = 0.036$, $P = 0.01$) and diastolic blood pressure ($\beta = -0.684$, $P = 0.04$); insulin ($\beta = -0.019$, $P = 0.05$) and HOMA-IR ($\beta = -0.019$, $P = 0.07$) showed borderline significance. No significant associations were observed with girls. Associations with risk factors were also examined according to Omega-3 Index risk categories [5]. General linear modelling suggested boys and girls in the low/intermediate risk category were more likely to have lower HDL-cholesterol levels, with borderline significance ($\beta = -0.057$, $P = 0.07$); no other risk factors were significant when boys and girls were analysed together or separately (data not shown).

Discussion

Due to variation in the methods used for red blood cell analysis in different laboratories, direct comparison of results is not possible. However, we found that the mean Omega-3 Index in the Raine Study adolescents (4.9 ± 1.0%) was consistent with the value of 4.7 ± 0.4% previously reported in a smaller control sample of healthy Australian children and adolescents aged 9–18 years [26]. Our value is also similar in value to that reported in US

Table 1 Characteristics and energy adjusted dietary intakes of Raine Study adolescents in high risk ($n = 203$) compared with low/medium risk ($n = 1{,}098$) Omega-3 Index risk categories [5]

Characteristic	Omega-3 Index Category		P*
	High risk (<4%)	Low/intermediate risk (≥4%)	
Age at assessment (years)	13.94 ± 0.02	14.02 ± 0.01	<0.001
Body mass index (kg/m^2)	21.07 ± 0.30	21.40 ± 0.12	0.284
Puberty[a] (Tanner score range 2–5)	3.94 ± 0.07	3.91 ± 0.03	0.692
Aerobic fitness[b] (W)	114.4 ± 2.16	111.5 ± 0.92	0.212
Maternal age at birth (years)	29.09 ± 0.42	28.97 ± 0.17	0.796
Maternal education (school year completed, grades 7–12)	10.84 ± 0.08	11.00 ± 0.03	0.046
Male gender[c]	117 (57.6)[f]	563 (51.3)[f]	0.096
Single parent family[c]	40 (20.6)[f]	229 (21.4)[f]	0.797
Positive family history of diabetes or cardiovascular disease[c]	26 (13.4)[f]	206 (19.3)[f]	0.052
Annual family income ($AUD)[d]			
<$35,000	41 (21.4)[f]	266 (25.3)[f]	
$35,000–$70,000	70 (36.5)[f]	378 (35.9)[f]	0.235
>$70,000	81 (42.2)[f]	408 (38.8)[f]	
Dietary factors			
Energy (MJ/day)	9.76 ± 0.27	9.42 ± 0.10	0.199
Healthy diet pattern score[e]	−0.10 ± 0.08	0.00 ± 0.03	0.203
Western diet pattern score[e]	0.15 ± 0.07	−0.02 ± 0.03	0.051
Total fat (g)	80.76 ± 1.41	81.60 ± 0.51	0.538
Polyunsaturated fat (g)	10.18 ± 0.32	10.62 ± 0.13	0.199
Total omega-3 (g)	1.18 ± 0.06	1.23 ± 0.02	0.128◇
Total omega-6 (g)	7.87 ± 0.28	8.19 ± 0.12	0.290
Omega-6 to omega-3 ratio	7.42 ± 0.30	7.37 ± 0.14	0.495◇
EPA and DHA (g)	0.109 ± 0.02	0.154 ± 0.01	0.003◇
Monounsaturated fat (g)	27.16 ± 0.57	26.91 ± 0.21	0.663
Saturated fat (g)	34.17 ± 0.80	34.62 ± 0.29	0.565
Protein (g)	87.09 ± 1.49	89.09 ± 0.66	0.247
Carbohydrate (g)	286.8 ± 3.2	282.0 ± 1.3	0.175
Glycemic index (%)	59.13 ± 0.39	58.15 ± 0.16	0.023
Glycemic load	154.9 ± 2.3	151.2 ± 1.0	0.161
Age breastfeeding stopped (months)	7.6 ± 0.5	8.3 ± 0.2	0.215◇

Values are means ± SE

EPA eicosapentaenoic acid, *DHA* docosahexaenoic acid

* Independent t test for equality of means or Chi squared test for equality of proportions

◇ P value from Mann–Whitney test

[a] Puberty assessed using Tanner score for pubic hair development

[b] Aerobic fitness assessed using Physical Working Capacity 170

[c] Pearson's Chi square

[d] Linear-by-linear Association

[e] Each participant received a z-score for both Healthy and Western dietary patterns. A positive score indicates a greater intake of foods representative of that pattern

[f] Values are n (%)

adults (4.9 ± 2.1% [27] and 3.5 ± 1.2% [28]), but lower than that in young overweight and obese adults from Iceland, Spain and Ireland (7.0 ± 1.9% [29] and Korean preschool chidren (9.1 ± 0.8%) [30]. Although results are not directly comparable, dietary variations between cultures, particularly in regards to fish intake, may contribute to the variation in the Omega-3 Index observed in different populations.

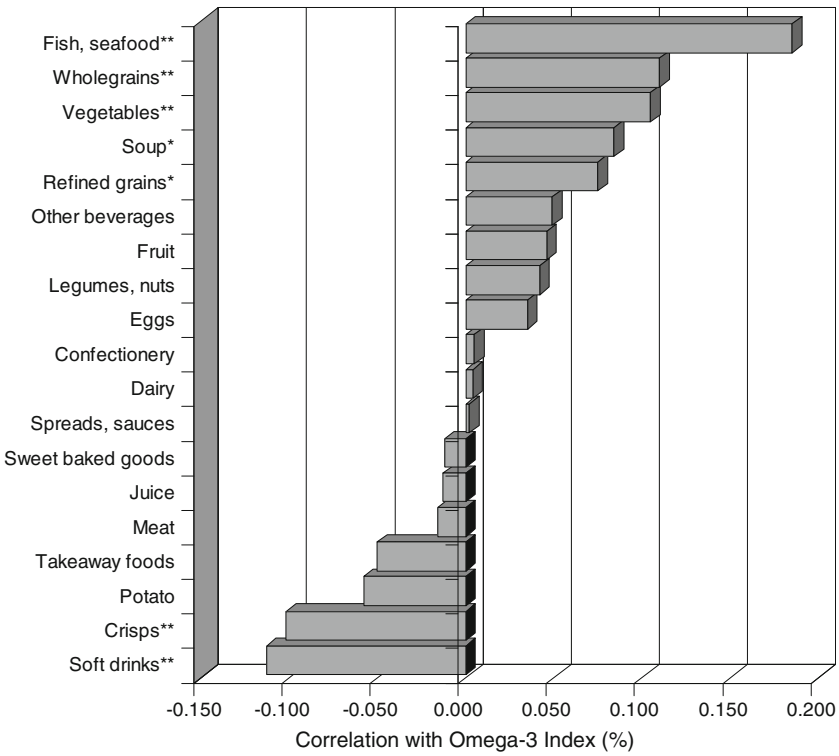

Fig. 2 Bivariate correlations between food group intakes (g/day) and the Omega-3 Index in Raine Study adolescents. $^{**}P < 0.01$, $^{*}P < 0.05$. *Wholegrains* includes wholegrain crackers and bread, oats, wholegrain breakfast cereal, brown rice and pasta. *Refined grains* includes white bread, crackers, rice and pasta, savory crackers. *Confectionery* includes ice and chocolate confection. *Takeaway foods* includes hamburgers, pizzas, fried chicken, savory pastries. *Sweet baked goods* includes cakes, biscuits, sweet pastries. *Crisps* includes popcorn, corn chips, extruded cheese snacks

Table 2 Linear regression analysis results for the Omega-3 Index as the independent variable with cardiovascular factors as the dependent variables, in Raine Study adolescents

	Girls and boys ($n = 1{,}288$)			Girls only ($n = 613$)			Boys only ($n = 675$)		
	Unstandardised β coefficient	Standardised β coefficient	P	Unstandardised β coefficient	Standardised β coefficient	P	Unstandardised β coefficient	Standardised β coefficient	P
Systolic BP (mm/Hg)	−0.464	−0.047	0.17	0.000	0.000	1.00	−0.821	−0.086	0.07
Diastolic BP (mm/Hg)	−0.331	−0.050	0.18	0.073	0.011	0.85	−0.684	−0.107	0.04
Glucose (mmol/L)	−0.010	0.014	0.44	−0.018	−0.050	0.38	−0.005	−0.015	0.77
Insulin (mmol/L)	−0.011	−0.055	0.10	−0.003	−0.016	0.75	−0.019	−0.086	0.05
HOMA	−0.012	−0.055	0.10	−0.005	−0.025	0.63	−0.019	−0.082	0.07
Total cholesterol (mmol/L)	0.064	0.093	0.01	0.031	0.042	0.46	0.074	0.115	0.03
HDL-cholesterol (mmol/L)	0.029	0.093	0.01	0.016	0.051	0.35	0.036	0.125	0.01
LDL-cholesterol (mmol/L)	0.041	0.067	0.08	0.038	0.058	0.30	0.036	0.061	0.24
Triglycerides (mmol/L)	−0.006	−0.037	0.32	−0.009	−0.056	0.31	−0.006	−0.033	0.52
Total/HDL-cholesterol	−0.003	−0.004	0.92	0.003	0.004	0.94	−0.017	−0.022	0.66
LDL/HDL-cholesterol	0.004	0.006	0.86	0.023	0.035	0.51	−0.015	−0.024	0.64
Triglycerides/HDL-cholesterol	−0.005	−0.036	0.33	−0.007	−0.053	0.33	−0.005	−0.035	0.50

Models adjusted for age, sex (where applicable), BMI, maternal education, daily energy intake, and family history of cardiovascular disease or diabetes

Dietary fish intake was the strongest food group predictor of the Omega-3 Index in the Raine adolescents ($P < 0.01$), and has previously been shown to be a determinant of the Index in older US adults [3]. Fish is a good source of dietary EPA and DHA, and this finding is consistent with trials showing increased dietary EPA and DHA leads to higher concentrations of RBC omega-3 fatty acids [4, 31]. Further, our results showed daily intake of EPA + DHA positively correlated with the Omega-3 Index ($P < 0.01$). Fish is also a good source of protein, along with legumes, nuts and eggs which may have contributed to the positive association observed with protein and Omega-3 Index. The wholegrain food group showed the next strongest positive association with the Omega-3

Index ($P < 0.01$). Wholegrains contain omega-3 fats in the form of alpha-linolenic acid (18:3n-3) in the bran outer layer of the grain. Interestingly, refined grain products that are missing the bran layer were also observed to have a significant positive association with the Omega-3 Index ($P < 0.05$). This may be partially due to the consumption of DHA enriched white bread observed in the Raine Study cohort at this follow up [19]. However, given the additional positive associations with vegetables and fruit, it is more likely that these associations with the Omega-3 Index are related to an overall 'healthy' pattern of eating. Similarly, a high intake of soft drinks and crisps, along with a high dietary glycemic index, may reflect a less 'healthy' eating pattern. This is reflected in the associations observed with the dietary pattern scores identified in this cohort: the Index showed a positive association with the healthy pattern score and a negative association with the western pattern score. Food groups loading on the healthy pattern included fresh fruit, vegetables, wholegrains and grilled or canned fish, while the 'western' pattern score represented a higher intake of takeaway foods, crisps and soft drinks [21]. Although soft drinks do not contain fat, their consumption has been shown to result in a rapid increase in glucose and insulin concentrations in adolescents [32], and the fructose component of sucrose in soft drinks may lead to enhanced fatty acid synthesis, contributing to higher circulating triglycerides [33]. Higher GI diets, as observed in subjects in the high risk Omega-3 Index category, may also contribute to higher plasma triglycerides [34]. Together, these dietary factors may play a role in alteration of the fatty acid content of RBC membranes.

Results of our study also extend the findings of previous research in adults [3, 31] by confirming that higher dietary intake of EPA and DHA through consumption of fish is associated with a higher Omega-3 Index in adolescents. However, the difference in distributions of dietary EPA and DHA compared to Omega-3 Index values (as shown in Fig. 1) highlight the contribution that non-dietary factors may also make in determination of the Omega-3 Index.

The Omega-3 Index has been proposed to predict coronary heart disease mortality in adults [5]. Our data show it is also associated with total and HDL-cholesterol concentrations and diastolic blood pressure in boys in our adolescent cohort. The positive relationship between increasing Omega-3 Index and higher HDL-cholesterol supports Australia's National Heart Foundation's position statement that marine omega-3 PUFA supplementation increases HDL-cholesterol levels [35]. This result is also consistent with previous research in adult populations [36]. In contrast, the Omega-3 Index was not significantly associated with HDL-cholesterol or other cardiovascular risk factors in a study of overweight and obese European adults [29], although borderline significance was observed with lower LDL. The findings, however, may have been influenced by weight status, as our results suggest that the BMI is positively associated with the Omega-3 Index ($P = 0.05$). Consistent with previous research showing a positive association between age and the Index [3], the adults in the European study had a noticeably higher Omega-3 Index than we observed in our adolescent population ($7.0 \pm 1.9\%$ vs. $4.9 \pm 1.0\%$), which may have affected associations with disease risk. Although high total cholesterol is commonly considered a risk factor for cardiovascular disease, high HDL-cholesterol is beneficial [37], and the two measures are related as HDL-cholesterol contributes to total cholesterol. Ratios may therefore be considered more useful as indicators of cardiovascular disease risk [17], however we found no significant associations between the Index and ratios of total/HDL-cholesterol, LDL/HDL-cholesterol or triglycerides/HDL-cholesterol.

The significant negative association observed with diastolic blood pressure in boys in our cohort supports a role for omega-3 fatty acids in optimisation of blood pressure. Omega-3 fatty acids have been shown to have a variety of actions that can lead to improved vasodilation and arterial compliance, including increased membrane fluidity, suppression of vasoconstrictors, and changes in mobilisation of intracellular calcium [9, 38, 39].

In our adolescent cohort, we observed a gender difference in the relationship between Omega-3 Index and risk factors for cardiovascular and metabolic disease. Analysis with boys showed significant or borderline associations with measures of cholesterol, blood pressure, and insulin resistance, whereas no significant associations were observed for measures in the girls analysis. Boys were more likely to be in the high risk category of Omega-3 Index (<4%) compared to the low risk (≥4%, $P = 0.10$), and similar gender differences have previously been identified in the long-chain omega-3 fatty acid composition of RBC membranes in rats, with a link between ovarian hormones and DHA composition proposed [40]. Sex hormones may play a role in modification of the omega-3 content of tissues, possibly by altering expression of enzymes in the liver [41], while also contributing to gender specific pathophysiological differences in cardiovascular and metabolic disease [42].

To our knowledge, this is the first study to evaluate the Omega-3 Index with cardiovascular and metabolic risk factors in a large cohort of adolescents. Interpretation of our study results is limited by the cross-sectional study design, however an important strength of our study is that it represents a large, population based cohort and has data on a wide range of cardiometabolic, socioeconomic and dietary variables. Our results demonstrate a significant and independent association between the Omega-3 Index and

total and HDL-cholesterol, as well as blood pressure, in Australian adolescent boys. Although the Omega-3 Index did not demonstrate a statistically significant association with the cholesterol ratios, it is considered to be a risk factor in its own right and has not been shown to mediate through effects on traditional risk factors. Therefore the Index may still be useful in the prediction of cardiovascular disease later in life, and our results support further long term investigation of this concept.

Acknowledgments We would like to express our gratitude to all the Raine Study participants and their families, and the Raine Study Team for cohort co-ordination and data collection. We thank Royal Perth Hospital laboratories for conducting biochemistry assays and Mr. Peter Jacoby for statistical assistance. We acknowledge the NH&MRC for their long term contribution to funding the study over the last 20 years, and the University of Western Australia (UWA), Raine Medical Research Foundation, UWA Faculty of Medicine, Dentistry and Health Sciences, The Telethon Institute for Child Health Research and the Women and Infants Research Foundation for providing funding for Core Management of the Raine Study. We also acknowledge support from the Telstra Research Foundation, the Western Australian Health Promotion Foundation, the Australian Rotary Health Research Fund and the National Heart Foundation of Australia and Beyond Blue. Biological specimens were funded by NH&MRC (Beilin et al., ID 403981) and RBC fatty acid analysis was funded from the NH&MRC Program Grant (Stanley et al., ID 003209).

Conflict of interest The authors have no conflict of interests to disclose.

References

1. Harris WS, von Schacky C (2004) The Omega-3 Index: a new risk factor for death from coronary heart disease? Prev Med 39:212–220
2. Harris WS, Sands SA, Windsor SL, Ali HA, Stevens TL, Magalski A, Porter CB, Borkon AM (2004) Omega-3 fatty acids in cardiac biopsies from heart transplantation patients: correlation with erythrocytes and response to supplementation. Circulation 110:1645–1649
3. Block RC, Harris WS, Pottala JV (2008) Determinants of blood cell omega-3 fatty acid content. Open Biomark J 1:1–6
4. Geppert J, Kraft V, Demmelmair H, Koletzko B (2005) Docosahexaenoic acid supplementation in vegetarians effectively increases Omega-3 Index: a randomized trial. Lipids 40:807–814
5. Harris WS (2008) The omega-3 index as a risk factor for coronary heart disease. Am J Clin Nutr 87:1997–2002
6. Mori TA, Watts GF, Burke V, Hilme E, Puddey IB, Beilin LJ (2000) Differential effects of eicosapentaenoic acid and docosahexaenoic acid on vascular reactivity of the forearm microcirculation in hyperlipidemic, overweight men. Circulation 102:1264–1269
7. Simopoulos AP (2008) The importance of the omega-6/omega-3 fatty acid ratio in cardiovascular disease and other chronic diseases. Exp Biol Med 233:674–688
8. Dyerberg J, Bang HO, Stoffersen E, Moncada S, Vane JR (1978) Eicosapentaenoic acid and prevention of thrombosis and atherosclerosis? Lancet 2:117–119
9. Mori TA, Beilin LJ (2001) Long-chain omega 3 fatty acids, blood lipids and cardiovascular risk reduction. Curr Opin Lipidol 12:11–17
10. Yongsoon P, Seonhye P, Hyeongjoong Y, Hyun Young K, Seok-Jae K, Juhan K, Hongyup A (2009) Low level of n-3 polyunsaturated fatty acids in erythrocytes is a risk factor for both acute ischemic and hemorrhagic stroke in Koreans. Nutr Res 29:825–830
11. Friedman AN, Saha C, Watkins BA (2008) Feasibility study of erythrocyte long-chain omega-3 polyunsaturated fatty acid content and mortality risk in hemodialysis patients. J Ren Nutr 18:509–512
12. Cohen BE, Garg SK, Ali S, Harris WS, Whooley MA (2008) Red blood cell docosahexaenoic acid and eicosapentaenoic acid concentrations are positively associated with socioeconomic status in patients with established coronary artery disease: data from the Heart and Soul Study. J Nutr 138:1135–1140
13. Newnham JP, Evans SF, Michael CA, Stanley FJ, Landau LI (1993) Effects of frequent ultrasound during pregnancy: a randomised controlled trial. Lancet 342:887–891
14. Mori T, Burke V, Puddey I, Watts G, O′Neal D, Best J, Beilin L (2000) Purified eicosapentaenoic acid and docosahexaenoic acid have differential effects on serum lipids and lipoproteins, LDL—particle size, glucose and insulin, in mildly hyperlipidaemic men. Am J Clin Nutr 71:1085–1094
15. Matthews D, Hosker J, Rudenski A, Naylor B, Treacher D, Turner RC (1985) Homeostasis model assessment: insulin resistance and beta cell function from fasting plasma glucose and insulin concentrations in man. Diabetologia 28:412–419
16. Warnick GR, Albers JJ (1978) A comprehensive evaluation of the heparin–manganese precipitation procedure for estimating high density lipoprotein cholesterol. J Lipid Res 19:65–76
17. Takahashi O, Glasziou PP, Perera R, Shimbo T, Suwa J, Hiramatsu S, Fukui T (2010) Lipid re-screening: what is the best measure and interval? Heart 96:448–452
18. da Luz PL, Favarato D, Faria-Neto JR Jr, Lemos P, Chagas ACP (2008) High ratio of triglycerides to HDL-cholesterol predicts extensive coronary disease. Clinics 63:427–432
19. O'Sullivan TA, Ambrosini GL, Beilin LJ, Mori TA, Oddy WH (2010) Dietary intake and food sources of fatty acids in Australian adolescents. Nutrition (in press) [Epub ahead of print]. doi: 10.1016/j.nut.2009.1011.1019
20. Di Candilo KG, Oddy WH, Miller M, Sloan N, Kendall GE, de Klerk NH (2007) Follow-up phone-calls increase nutrient intake estimated by three-day food diaries in 13 year old participants of the Raine study. Nutr Diet 64:165–171
21. Ambrosini G, O'Sullivan T, de Klerk N, Beilin LJ, Oddy WH (2010) Relative validity of adolescent dietary patterns: a comparison of a FFQ and 3 d food record. Brit J Nutr (in press)
22. Tanner J (1962) Growth at adolescence: with a general consideration of the effects of hereditary and environmental factors upon growth and maturation from birth to maturity. Blackwell, Oxford
23. Duke PM, Litt IF, Gross RT (1980) Adolescents' self-assessment of sexual maturation. Pediatrics 66:918–920
24. Rowland T, Rambusch J, Staab J, Unnithan V, Siconolfi S (1993) Accuracy of physical working capacity (PWC170) in estimating aerobic fitness in children. J Sports Med Phys Fitness 33:184–188
25. Hands B, Larkin D, Parker H, Straker L, Perry M (2009) The relationship among physical activity, motor competence and health-related fitness in 14-year-old adolescents. Scand J Med Sci Sports 19:655–663
26. Clayton E, Hanstock T, Hirneth S, Kable C, Garg M, Hazell P (2008) Long-chain omega-3 polyunsaturated fatty acids in the blood of children and adolescents with juvenile bipolar disorder. Lipids 43:1031–1038

27. Sands SA, Reid KJ, Windsor SL, Harris WS (2005) The impact of age, body mass index, and fish intake on the EPA and DHA content of human erythrocytes. Lipids 40:343–347
28. Friedman AN, Moe SM, Perkins SM, Li Y, Watkins BA (2006) Fish consumption and omega-3 fatty acid status and determinants in long-term hemodialysis. Am J Kidney Dis 47:1064–1071
29. Ramel A, Pumberger C, Martinéz JA, Kiely M, Bandarra NM, Thorsdottir I (2009) Cardiovascular risk factors in young, overweight, and obese European adults and associations with physical activity and omega-3 index. Nutr Res 29:305–312
30. Hwang I, Cha A, Lee H, Yoon H, Cho B, Lee S, Park Y (2007) N-3 polyunsaturated fatty acids and atopy in Korean preschoolers. Lipids 42:345–349
31. De Groote G, De Laporte A, Dhondt G, Christophe A (2008) Improvement in the plasma omega-3 index by the use of a fish oil-enriched spread. Ann Nutr Metab 53:23–28
32. Janssens JP, Shapira N, Debeuf P, Michiels L, Putman R, Bruckers L, Renard D, Molenberghs G (1999) Effects of soft drink and table beer consumption on insulin response in normal teenagers and carbohydrate drink in youngsters. Eur J Cancer Prev 8:289–296
33. Assy N, Nasser G, Kamayse I, Nseir W, Beniashvili Z, Djibre A, Grosovski M (2008) Soft drink consumption linked with fatty liver in the absence of traditional risk factors. Can J Gastroenterol 22:811–816
34. Liu S, Manson JE, Stampfer MJ, Holmes MD, Hu F, Hankinson S, Willett WC (2001) Dietary glycemic load assessed by food-frequency questionnaire in relation to plasma high-density-lipoprotein cholesterol and fasting plasma triacylglycerols in postmenopausal women. Am J Clin Nutr 73:560–566
35. National Heart Foundation (2008) Position statement: fish, fish oils, n-3 polyunsaturated fatty acids and cardiovascular health
36. Block RC, Harris WS, Reid KJ, Sands SA, Spertus JA (2008) EPA and DHA in blood cell membranes from acute coronary syndrome patients and controls. Atherosclerosis 197:821–828
37. Cooney MT, Dudina A, De Bacquer D, Wilhelmsen L, Sans S, Menotti A, De Backer G, Jousilahti P, Keil U, Thomsen T, Whincup P, Graham IM (2009) HDL cholesterol protects against cardiovascular disease in both genders, at all ages and at all levels of risk. Atherosclerosis 206:611–616
38. Abeywardena MY, Head RJ (2001) Longchain n-3 polyunsaturated fatty acids and blood vessel function. Cardiovasc Res 52:361–371
39. Cicero AFG, Ertek S, Borghi C (2009) Omega-3 polyunsaturated fatty acids: their potential role in blood pressure prevention and management. Curr Vasc Pharmacol 7:330–337
40. McNamara RK, Able J, Jandacek R, Rider T, Tso P (2009) Gender differences in rat erythrocyte and brain docosahexaenoic acid composition: role of ovarian hormones and dietary omega-3 fatty acid composition. Psychoneuroendocrinology 34:532–539
41. Childs CE, Romeu-Nadal M, Burdge GC, Calder PC (2008) Gender differences in the n-3 fatty acid content of tissues. Proc Nutr Soc 67:19–27
42. Regitz-Zagrosek V, Lehmkuhl E, Weickert M (2006) Gender differences in the metabolic syndrome and their role for cardiovascular disease. Clin Res Cardiol 95:136–147

Lipids (2011) 46:69–79
DOI 10.1007/s11745-010-3485-1

ORIGINAL ARTICLE

Biosynthesis of 14,15-Hepoxilins in Human L1236 Hodgkin Lymphoma Cells and Eosinophils

Åsa Brunnström · Mats Hamberg · William J. Griffiths · Bengt Mannervik · Hans-Erik Claesson

Received: 12 February 2010 / Accepted: 28 September 2010 / Published online: 29 October 2010

Abstract Hepoxilins are epoxy alcohols synthesized through the 12-lipoxygenase (12-LO) pathway in animal cells. The epidermis is the principal source of hepoxilins in humans. Here we report on the formation of novel hepoxilin regioisomers formed by the 15-LO pathway in human cells. The Hodgkin lymphoma cell line L1236 possesses high 15-lipoxygenase-1 (15-LO-1) activity and incubation of L1236 cells with arachidonic acid led to the formation of 11(*S*)-hydroxy-14(*S*),15(*S*)-epoxy 5(*Z*),8(*Z*),12(*E*) eicosatrienoic acid (14,15-HxA_3 11(*S*)) and 13(*R*)-hydroxy-14(*S*),15(*S*)-epoxy 5(*Z*),8(*Z*),11(*Z*) eicosatrienoic acid (14,15-HxB_3 13(*R*)). In addition, two hitherto unidentified products were detected and these products were collected and analyzed by positive ion electrospray tandem mass spectrometry. These metabolites were identified as 11(*S*),15(*S*)-dihydroxy-14(*R*)-glutathionyl-5(*Z*),8(*Z*),12(*E*)-eicosatrienoic acid (14,15-HxA_3-C) and 11(*S*),15(*S*)-dihydroxy-14(*R*)-cysteinyl-glycyl-5(*Z*),8(*Z*),12(*E*)-eicosatrienoic acid (14,15-HxA_3-D). Incubation of L1236 cells with synthetic 14,15-HxA_3 11(*S*) also led to the formation of 14,15-HxA_3-C and 14,15-HxA_3-D. Several soluble glutathione transferases, in particular GST M1-1 and GST P1-1, were found to catalyze the conversion of 14,15-HxA_3 to 14,15-HxA_3-C. L1236 cells produced approximately twice as much eoxins as cysteinyl-containing hepoxilins upon stimulation with arachidonic acid. Human eosinophils, nasal polyps and dendritic cells selectively formed 14,15-HxA_3 11(*S*) and 14,15-HxB_3 13(*R*) stereoisomers, but not cysteinyl-containing hepoxilins, after stimulation with arachidonic acid. Furthermore, purified recombinant 15-LO-1 alone catalyzed the conversion of arachidonic acid to 14,15-HxA_3 11(*S*) and 14,15-HxB_3 13(*R*), showing that human 15-LO-1 possesses intrinsic 14,15-hepoxilin synthase activity.

Keywords Arachidonic acid · L1236 · Hodgkin Reed-Sternberg cells · 15-Lipoxygenase · Glutathione conjugate · Glutathione transferase

Electronic supplementary material The online version of this article (doi:10.1007/s11745-010-3485-1) contains supplementary material, which is available to authorized users.

Å. Brunnström · H.-E. Claesson (✉)
Department of Medicine, Karolinska Institutet and Karolinska University Hospital Solna, 171 76 Stockholm, Sweden
e-mail: hans-erik.claesson@ki.se

M. Hamberg
Department of Medical Biochemistry and Biophysics, Karolinska Institutet, 171 77 Stockholm, Sweden

W. J. Griffiths
Institute of Mass Spectrometry, School of Medicine, Swansea University, Singleton Park, Swansea SA2 8PP, UK

B. Mannervik
Department of Biochemistry and Organic Chemistry, Uppsala University, Biomedical Center, 75123 Uppsala, Sweden

B. Mannervik
Department of Neurochemistry, Stockholms University, 106 91 Stockholm, Sweden

Å. Brunnström · H.-E. Claesson
Orexo AB, Box 303, 75105 Uppsala, Sweden

Abbreviations

EX	Eoxin
GST	Glutathione transferase
HPETE	Hydroperoxyeicosatetraenoic acid
HPLC	High performance liquid chromatography
Hx	Hepoxilin
LC–MS	Liquid chromatography–mass spectrometry
LO	Lipoxygenase

Introduction

Hepoxilins (Hx) are a family of hydroxy epoxides which are formed by rearrangement of 12(*S*)-HPETE [1]. Murine 12/15-lipoxygenase (LO) (earlier called leukocyte-type 12-LO), the ortholog to human 15-LO-1, can catalyze the metabolism of arachidonic acid via 12(*S*)-HPETE to 8(*R*/*S*)-hydroxy-11(*S*),12(*S*)-epoxy-5(*Z*),9(*E*),14(*Z*)-eicosatrienoic acid and 10(*R*/*S*)-hydroxy-11(*R*),12(*R*)-epoxy-5(*Z*),8(*Z*),14(*Z*)-eicosatrienoic acid, termed HxA_3 and HxB_3, respectively [2, 3]. Hydrolysis of these metabolites leads to the formation of trihydroxy-8,11,12-eicosatrienoic acid (trioxilin A_3, $TrxA_3$) and trihydroxy-10,11,12-eicosatrienoic acid ($TrxB_3$), respectively [4]. HxA_3 can also be converted into a glutathione conjugate, named HxA_3-C [5]. The enzyme γ-glutamyl transpeptidase catalyzes the conversion of HxA_3-C into HxA_3-D [6]. In contrast to murine 12/15-LO, human platelets which exhibit high 12(*S*)-LO activity can not convert arachidonic acid to HxA_3, probably due to low peroxide tonus in the cell [7]. However, 12(*R*)-LO and epidermal lipoxygenase-3 (eLOX3) are expressed in human skin and these enzymes are involved in the formation of the stereospecific HxA_3 8(*R*) in human epidermis [8–10].

The hepoxilins exert a variety of biological actions in different type of cells, likely mediated via changes in intercellular concentrations of calcium and potassium and alterations in the secondary messenger systems [2]. Several lines of evidence indicate that hepoxilins might play a role in the water-impermeable barrier of the outer epidermis [1, 11]. Genetic studies of inherited ichthyosis have demonstrated that mutations of 12(*R*)-LO and/or eLOX3 is connected to autosomal recessive congenital ichthyosis in man [12, 13]. Animal studies have also shown that 12(*R*)-LO deficiency leads to an ichthyosis form phenotype [14]. The formation of 12(*R*)-HETE and hepoxilins is increased in affected psoriatic skin [9, 15]. HxA_3 and HxB_3 have been reported to stimulate insulin secretion from rat langerhans islets [16] and calcium release [2]. HXA_3 has also been found to cause vascular contraction [17] and increased vascular permeability in rat [18]. In human neutrophils, the biological actions of HxA_3 are indicated to be receptor mediated [19], and this metabolite has been found to stimulate human neutrophils to migrate across intestinal epithelia [20]. HxA_3-C has been reported to induce vascular contraction in guinea pig isolated trachea [21] and increase vascular permeability in rat skin [18].

Human 15-lipoxygenase type 1 (15-LO-1) is mainly expressed in human airway epithelial cells, macrophages, reticulocytes, eosinophils and mast cells [22–26]. The amount and activity of 15-LO-1 is increased in the bronchial tissue of patients with asthma or chronic bronchitis compared to healthy subjects [26–29]. Eoxins (EX, also called 14,15-leukotrienes) are recently identified endogenous metabolites of arachidonic acid, formed through the 15-LO-1 pathway in human eosinophils, mast cells and nasal polyps [30]. 15-LO-1 catalyzes the conversion of arachidonic acid to EXA_4 which can be further metabolized to EXC_4, after conjugation with glutathione. EXC_4 and its metabolites EXD_4 and EXE_4 induce increased permeability of vascular endothelial cell monolayer in vitro, indicating that eoxins are pro-inflammatory mediators [31]. The Hodgkin cell line Ll236 possesses high 15-LO-1 activity and we have recently reported that these cells have a high capacity to produce EXC_4, EXD_4 and EXE_4 [31].

14,15-Hepoxilins of both A and B type are formed from arachidonic acid via the 15-lipoxygenase pathway in garlic root [32]. Human airway epithelial cells have been found to produce 14,15-HxB_3 [33]. Since most studies, however, have been focused on the formation of hepoxilins catalyzed by the animal enzyme 12/15-LO which possesses mainly 12-lipoxygenase activity, we thought it was of interest to reinvestigate which type of hepoxilins could be produced by human cells which express the ortholog 15-LO-1. In contrast to the animal 12/15-LO, the human enzyme possesses mainly 15-lipoxygenase activity. For that purpose, we used L1236 cells as a model system since this cell line possesses high 15-LO-1 activity [31]. Furthermore, we also investigated whether the corresponding metabolites were formed in human eosinophils, nasal polyps and dendritic cells.

Experimental Procedure

Materials

The [1-^{14}C] arachidonic acid (56.0 mCi/mmol) was obtained from Amersham Biosciences (Uppsala, Sweden) and unlabeled arachidonic acid was from Nu-Chek prep (Elysian, USA). Synthetic 14(*S*),15(*S*)-epoxy-5(*Z*),8(*Z*),10(*Z*),12(*E*)-eicosatetraenoic acid (EXA_4), 14(*R*)-glutathionyl-15(*S*)-hydroxy-5(*Z*),8(*Z*),10(*Z*),12(*E*)-eicosatetraenoic acid (EXC_4) and 14(*R*)-cysteinyl-glycyl-15(*S*)-hydroxy-5(*Z*),8(*Z*),10(*Z*),12(*E*)-eicosatetraenoic acid (EXD_4) were purchased from BIOMOL (Plymouth Meeting, USA). [1-^{14}C] 15(*S*)-hydroperoxy-5(*Z*),8(*Z*),11(*Z*),13(*E*)-eicosatetraenoic (15(*S*)-HPETE), 11(*S*)/(*R*)-hydroxy-14(*S*),15(*S*)-epoxy-5(*Z*),8(*Z*),12(*E*)-eicosatrienoic acid (14,15-HxA_3), 11(*S*),15(*S*)-hydroxy-14(*R*)-glutathionyl-5(*Z*),8(*Z*),12(*E*) eicosatrienoic acid (14,15-HxA_3-C), 13(*S*)/(*R*)-hydroxy-14(*S*),15(*S*)-epoxy-5(*Z*),8(*Z*),11(*Z*)-eicosatrienoic acid (14,15-HxB_3) was synthesized as described in the Supplement. 11(*S*)-hydroxy-14(*R*)-cys-gly-15(*S*)-hydroxy-5(*Z*),8(*Z*),12(*E*) eicosatrienoic acid (14,15-HxA_3-D) was made in house from 14,15-HxA3-C with γ-glutamyl transpeptidase (Sigma, Sweden). All solvents used were of HPLC grade.

Cell Experiment

The Hodgkin cell line L1236 (50–60 × 10^6 cells/sample) was suspended in PBS and pre-warmed for 2 min at 37 °C prior to addition of arachidonic acid (final concentration 30 μM) and labelled arachidonic acid (final concentration 9 μM). Incubation was stopped after 2 and 10 min, respectively, with the addition of one volume of cold methanol. L1236 cells were incubated, under similar experimental conditions, with EXA_4, 14,15-HxA_3 and 14,15-HxB_3, respectively. EXA_4 (37 μM) and 14,15-HxA_3 (42 μM) and 14,15-HxB_3 (48 μM) were incubated for 5, 10 and 10 min, respectively. Sonicated L1236 cells were incubated with [1-^{14}C]-15-HPETE (20 μM, 5 min). The sonicated cell suspensions were supplemented with glutathione (final concentration of 5 mM) and a protease inhibitor (Complete mini, Roche Diagnostics GmbH, Germany). Dendritic cells, eosinophils and nasal polyps (chopped up) were isolated as described [30, 34] and these cells/tissues were incubated in the same manner as described for the L1236 cells, with the addition of indomethacin (1 μM) to inhibit cyclooxygenase activity. This study was approved by the local ethic committee of the Karolinska University Hospital.

Enzyme Incubations

Human GST M1-1, M2-2, M3-3, M4-4, M5-5, P1-1(Ile105), P1-1(val105), T1-1, A1-1, A2-2, A3-3 and A4-4 are soluble recombinant glutathione transferases prepared by heterologous expression as previously described [35]. Two allelic forms of GST P1-1 were used [36]. Expression constructs (Bac-to-Bac Baculovirus expression system, Gibco/Life Technologies) for LTC_4 synthase was a kind gift from Dr. Jakobsson (Karolinska Biomic Center, Karolinska University Hospital and Karolinska Institutet, Sweden). The LTC_4 synthase membrane fraction was isolated as described [37]. Enzymatic conjugation of glutathione with 14,15-HxA_3 was studied as follows. Glutathione transferases (4 μg) in PBS (50 μL) were pre-warmed for 2 min at 37 °C followed by addition of 14,15-HxA_3 (228 μM) and glutathione (5 mM final concentration). Subsequently, the cells were incubated for 10 min and the incubation was terminated by addition of one volume acetonitrile/methanol/acetic acid (50:50:1, by vol).

Similar experimental conditions were used when recombinant 15-LO-1 (5 μg) was incubated with arachidonic acid (30 μM) and [1-^{14}C]-arachidonic acid (9 μM) combined. The incubation was stopped after 15 min by addition of one volume cold methanol.

HPLC-Analysis with UV and Radioactivity Detection

Cells and cell debris were removed by centrifugation (1,400×g, 6 min). The supernatant was diluted with water and then transferred to a washed and equilibrated extraction cartridge, Oasis HLB 1 cc 10 mg (Waters, Sweden). The extracted metabolites were washed with water and eluted with 200 μL methanol. Reverse-phase HPLC was performed on a Waters Alliance 2690 with a Nova Pak C18 column (2.1 × 150 mm, Waters AB, Sweden). The initial mobile phase was 100% A (0.01% acetic acid adjusted to pH 5.6 with ammonia) at a flow rate at 0.4 mL/min A linear gradient was started after 5 min, reaching 36% B (60:40 acetonitrile/methanol, by vol) at 20 min The mobile phase was isocratic at A/B (64:36, by vol) for 100 min. Column effluent was monitored using diode array detection (PDA 996, Waters AB, Sweden) and radioactivity monitoring (β-RAM, INUS-systems, USA). UV spectra were acquired between 200 and 340 nm. The eluting metabolites were collected with a fraction collector (FC II, Waters AB, Sweden) and further analyzed by mass spectrometry. The collected fractions were dried under N_2 and subsequently dissolved in methanol/water (1:1, by vol).

Nanospray Mass Spectrometry Analysis

Mass spectrometry was performed on a Quattro Ultima triple quadrupole mass spectrometer (Micromass, Manchester, UK) operating in positive ion mode for glutathione-containing metabolites and in negative ion mode for the other hepoxilins with a capillary voltage at 2.2 and 1.8 kV, respectively. MS/MS spectra were obtained using collision energy of 20 eV using argon as the collision gas.

Synthesis of Reference Substances

Four epoxy alcohols were prepared from 15(*S*)-hydroperoxy-5(*Z*),8(*Z*),11(*Z*),13(*E*)-eicosatetraenoic acid (15(*S*)-HPETE) by slight modification of a method previously described for synthesis of *erythro* and *threo* epoxy alcohols having trans epoxide stereochemistry [38], i.e. methyl 14(*S*),15(*S*)-epoxy-13(*S*)-hydroxy-5(*Z*),8(*Z*),11(*Z*)-eicosatrienoate and methyl 14(*S*),15(*S*)-epoxy-13(*R*)-hydroxy-5(*Z*),8(*Z*),11(*Z*)-eicosatrienoate. In addition to these major compounds, smaller quantities of the corresponding allylic epoxy alcohols, methyl 14(*S*),15(*S*)-epoxy-11(*S*)-hydroxy-5(*Z*),8(*Z*),12(*E*)-eicosatrienoate and methyl 14(*S*),15(*S*)-epoxy-11(*R*)-hydroxy-5(*Z*),8(*Z*),12(*E*)-eicosatrienoate, were also obtained. All four methyl esters were saponificated with lithium hydroxide to form the carboxylic acid. Glutathione conjugates, 11(*S*),15(*S*)-dihydroxy-14(*R*)-glutathionyl-5(*Z*),8(*Z*),12(*E*)-eicosatrienoic acid and 11(*R*),15(*S*)-dihydroxy-14(*R*)-glutathionyl-5(*Z*),8(*Z*),12(*E*)-eicosatrienoic acid, were prepared by reacting glutathione thiolate with 14(*S*),15(*S*)-epoxy-11(*S*)-hydroxy-5(*Z*),8(*Z*),12(*E*)-eicosatrienoic acid and 14(*S*),15(*S*)-epoxy-11(*R*)-hydroxy-5(*Z*),8(*Z*),12(*E*)-eicosatrienoic acid, respectively. For further information see supplementary information.

Quantification of 14,15-HxA_3-C and EXC_4 by LC–MS/MS

Quantification was performed on a Surveyor MS pump coupled to a TSQ Quantum Ultra triple quadrupole mass spectrometer (Thermo Scientific, Sweden). Reverse phase LC was performed using a Zorbax Eclipse Plus 3.5 μM C18 column 2.1 × 50 mm (ChromTech, Sweden) with the flow rate constantly held at 400 μL/min. Mobile phase A consisted of 2% acetonitrile in water and 0.1% acetic acid, and mobile phase B consisted of 80% acetonitrile in water and 0.1% acetic acid. Isocratic elution at 90% A for 1.5 min was followed by a 6.5 min linear gradient reaching 100% of B. The system was washed at 100% B for 4 min and subsequently equilibrated at 90% A for 4 min. The mass spectrometer was operated using an electrospray atmospheric pressure ionization source in positive mode. The spray voltage was set to 4,500 V, capillary temperature was 375 °C and sheath and auxiliary gas were optimal at 40 and 5, respectively (arbitrary units). Skimmer offset was at 10 V and tube lens 121 V. To quantify formed 14,15-HxA_3-C and EXC_4 multiple reaction monitoring, MRM, was utilized. The transitions utilized were 644.3 *m/z* to 526.0 and 479.2 *m/z* and 626.2 *m/z* to 301.0 and 205.0 *m/z* at collision energies between of 17 and 22 eV.

Standard calibration curve at ten levels was prepared in PBS (1 mL) and in the following interval; 2.5–1,000 nM for 14,15-HxA_3-C and 1–800 nM for EXC_4. Warfarin (Sigma, Sweden) was used as internal standard at 16 nM and one qualitative control in triplicate of 14,15-HxA_3-C and EXC_4 at 50 and 40 nM, respectively. The standard samples were extracted with the same solid phase method as the L1236 cell incubation samples. The following transitions was used for warfarin detection: 309.0 *m/z* to 251.2 and 163.1 *m/z* at a collision energy of 19 and 17 eV, respectively. One standard series was analyzed in the beginning and one at the end of the analysis list.

Results

Metabolism of Arachidonic Acid in L1236 Cells

The Hodgkin cell line L1236 has been found to produce eoxins and a series of 8,15-DiHETE metabolites after incubation with arachidonic acid [31]. In this study we detected other major unidentified metabolites in the radioactivity chromatogram after incubation of L1236 cells with ^{14}C-arachidonic acid (Fig. 1). These compounds were called metabolites I and II. Metabolites I and II did not have a UV-absorbance maximum above 200 nm, hence they did not contain any conjugated double bonds. Therefore, there were no corresponding metabolites detected in the UV chromatogram at 280 nm (Fig. 1). Maximal

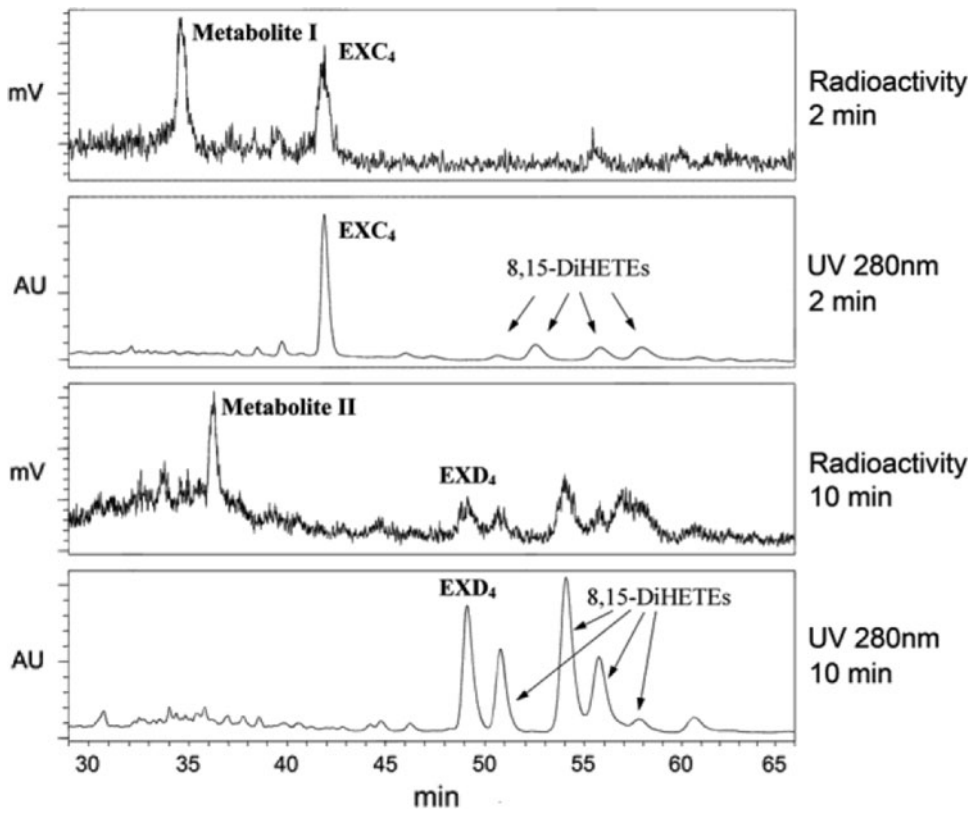

Fig. 1 L1236 cells incubated with arachidonic acid. Radioactivity and UV (280 nm) chromatograms of the products formed by L1236 after incubation with ^{14}C-labelled arachidonic acid (40 μM) for 2 and 10 min, respectively. The retention times of metabolites I and II, EXC_4, EXD_4 and 8, 15-DiHETEs are all indicated in the chromatograms. Metabolite I and EXC_4 dominated after 2 min of incubation and metabolite II and EXD_4 after 10 min. EXC_4 and EXD_4 were visible in the both UV and radioactivity chromatogram. Metabolites I and II were not detectable in the UV chromatogram at 280 nm

amounts of metabolites I and II were detected after 2 and 10 min of incubation, respectively. A similar time-course was observed for the formation of EXC_4 and EXD_4.

Incubation of L1236 cells with either arachidonic acid or 15(*S*)-HPETE, but not with EXA_4, led to the formation of metabolites I and II (data not shown). This indicates that the metabolites I and II are formed through the 15-LO-1 pathway but that these metabolites are not eoxins. Analyzing the two metabolites by mass spectrometry revealed that both metabolites I and II had a molecular weight of plus 18 (equivalent to H_2O) in comparison to EXC_4 and EXD_4, respectively. Together, these results suggest that the metabolites contain an additional hydroxyl group, in comparison to the eoxins, and contain three non-conjugated double bonds. Positive ion MS/MS spectrum of metabolite I showed a fragment ion with *m*/*z* 308 (Fig. 2), this may arise by cleavage of the carbon–sulfur bond with the charge retention on the peptide part as described for LTC_4 [39]. Analysis of the MS/MS spectra of metabolite II and EXD_4 demonstrated that both metabolites contain a fragment ion at *m*/*z* 179 (Fig. 3), representing the cysteinyl-glycine complex. These fragment ions make it clear that the material in metabolite I contains a conjugated glutathione metabolite and that the material in metabolite I is converted to metabolite II by the removal of glutamate, analogous to the conversion of EXC_4 to EXD_4. Since most fragments present in the MS/MS spectra for metabolite I and II are derived from the peptide and few from the lipid-containing part (as for EXC_4 and EXD_4 fragmentation), the position of the extra hydroxyl group in comparison to eoxins was not obvious.

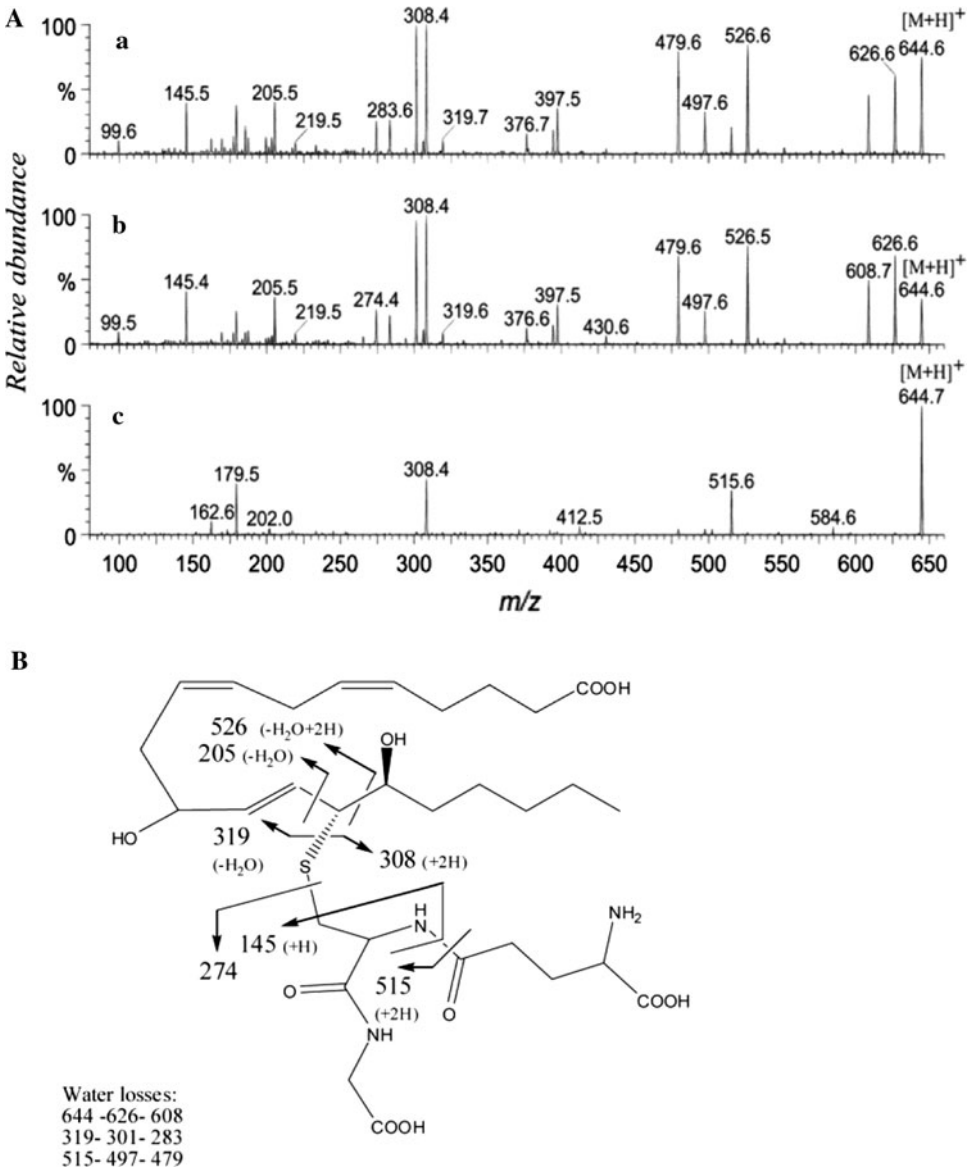

Fig. 2 **a** MS/MS spectra of metabolite I. Positive ion MS/MS spectra of $[M + H]^+$ at 644 *m*/*z* was recorded on a triple quadrupole mass spectrometer. MS/MS of (*A*) metabolite I formed by the L1236 cells compared to (*B*) synthetic 14,15-HxA_3-C and (*C*) synthetic 14,15-HxB_3-C. MS/MS spectra of 14,15-HxA_3-C and metabolite I were identical and show characteristic water losses. **b** Structure of the14,15-HxA_3-C with possible fragment ions present in the positive ion MS/MS spectrum indicated

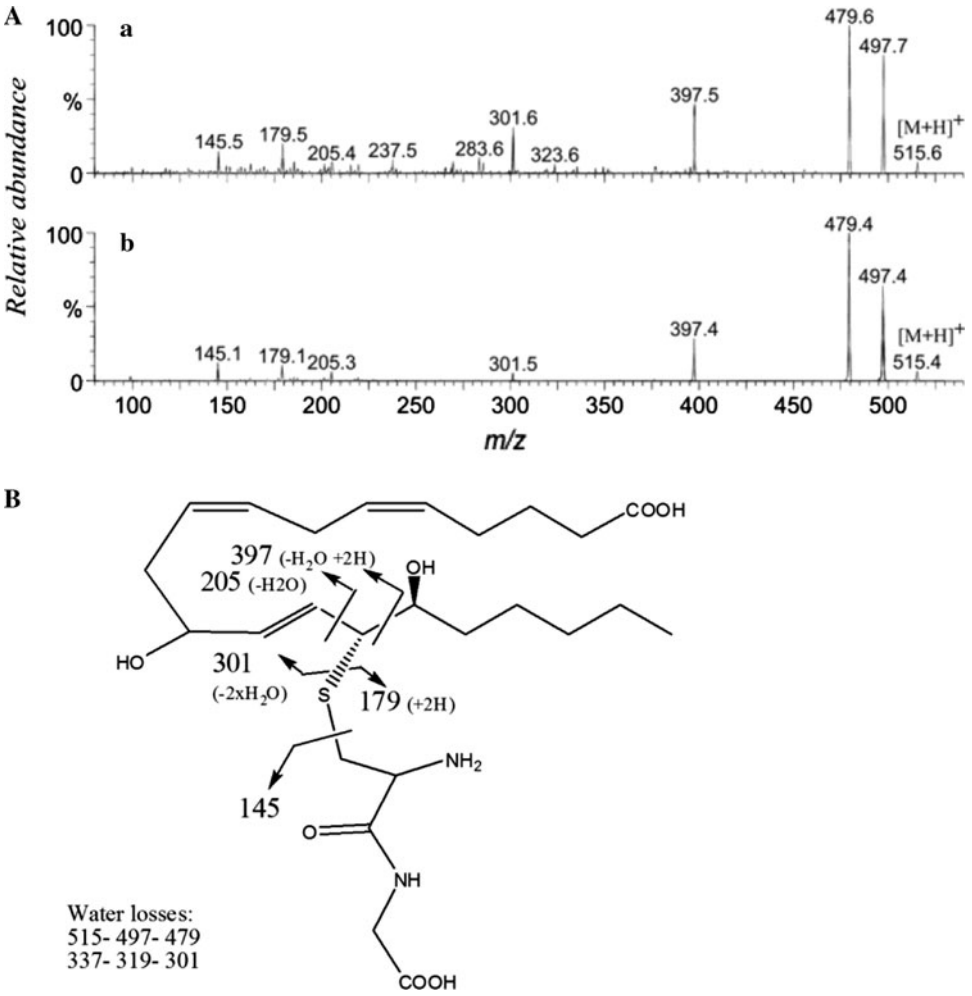

Fig. 3 **a** MS/MS spectra of metabolite II. Positive ion MS/MS spectra of $[M + H]^+$ at 515 *m/z* were recorded on a triple quadrupole mass spectrometer. MS/MS spectrum of (*A*) metabolite II formed by L1236 cells compared to (*B*) synthetic 14,15-HxA_3-D. **b** Structure of 14,15-HxA_3-D with possible fragment ions present in the positive ion MS/MS spectrum indicated

Chemical Structure of Metabolite I

13(*R*/*S*)-Hydroxy-14,15-epoxyeicosatrienoic acid also known as 14,15-Hepoxilin B_3 (14,15-HxB_3) is a previously characterized metabolite produced through the 15-LO-1 pathway in human airway epithelial cells [33]. A candidate structure for metabolite I was therefore 14,15-HxB_3 conjugated with a glutathione (14,15-HxB_3-C). Synthetic 14,15-HxB_3 with the hydroxyl group at position 13 in either *S* or *R* configuration was prepared. These compounds were incubated with L1236 cells leading to formation of 14,15-HxB_3-C. This metabolite, with the hydroxyl group in the 13(*R*) configuration, co-eluted with metabolite I but the MS/MS spectrum was not identical to the spectrum of metabolite I. Many fragments present in the MS/MS spectrum for metabolite I were not present in the 14,15-HxB_3-C spectrum such as losses of water from the protonated molecule (Fig. 2), showing that metabolite I was not identical to 14,15-HxB_3-C.

11(*R*/*S*)-Hydroxy-14,15-epoxyeicosatrienoic acid also known as 14,15-Hepoxilin A_3 (14,15-HxA_3) is also formed through the 15-LO-1 pathway, produced in garlic root [32]. 14,15-HxA_3 is more unstable than 14,15-HxB_3, and therefore more difficult to isolate since it is sensitive to acid and is easily degraded non-enzymatically to trihydroxy acids. Both enantiomers of 14,15-HxA_3 were synthesized containing the hydroxyl group at carbon 11 in either *S* or *R* configuration. These were then incubated with L1236. 14,15-HxA_3 with the hydroxyl group at position 11 in *S* configuration and a conjugated glutathione, 14,15-HxA_3-C 11(*S*), co-eluted and exhibited an essentially identical spectrum as metabolite I (Fig. 2). In contrast, 14,15-HxA_3-C with the hydroxyl group at position 11 in R configuration eluted faster than metabolite I. The structure of 14,15-HxA_3-C explains the facile losses of water evident in the MS/MS spectrum since removal of water produces a favourable conjugated double bond structure of a triene or a tetraene (Fig. 2).

14,15-HxA_3 is a *trans* epoxide in *S* configuration and the glutathione is probably conjugated in *R* orientation forming 11(*S*),15(*S*)-hydroxy-14(*R*)-glutathione-5(*Z*),8(*Z*),12(*E*) eicosatrienoic acid (14,15-HxA_3-C 11(*S*)) (**1**). This synthetic product co-eluted and had the same MS/MS spectrum as metabolite I produced endogenously in the cell line. In

comparison, the synthetic 11(*R*),15(*S*)-dihydroxy-14(*R*)-glutathionyl-5(*Z*),8(*Z*),12(*E*) eicosatrienoic acid (14,15-HxA_3-C 11(*R*)) did not co-elute with metabolite I. Incubation of 14,15-HxA_3 11(*S*) with purified enzyme GSTM1-1, a soluble glutathione transferase expressed in the L1236 cells (Feltenmark et al., to be published), also resulted in a identical MS/MS spectrum as for metabolite I.

Chemical Structure of Metabolite II

Metabolite II appeared to be formed by removal of glutamate from metabolite I. Therefore the identity of metabolite II was probably 11(*S*),15(*S*)-dihydroxy-14(*R*)-cysteinyl-glycine-5(*Z*),8(*Z*),12(*E*) eicosatrienoic acid (14,15-HxA_3-D) (**2**). The product formed after incubation of synthetic 14,15-HxA_3-C 11(*S*) with L1236 cells or γ-glutamyl transpeptidase had the same retention time on HPLC and similar MS/MS spectra as metabolite II (Fig. 3), demonstrating that the structure of the material in metabolite II was 14,15-HxA_3-D 11(*S*).

Comparison of the Amounts of 14,15-HxA_3-C and EXC_4 Formed by L1236 Cells

The amount 14,15-HxA_3-C and EXC_4 formed in arachidonic acid (40 μM) incubations with different L1236 cell densities (1, 5, 10, 20 and 50 million cells/mL) was quantified by LC–MS/MS. The amounts of 14,15-HxA_3-C and EXC_4 produced per million cell were similar at different cell densities but with a tendency to decreased ratio EXC_4 versus 14,15-HxA_3-C by increased cell density (Fig. 4). The L1236 cells produced 15.4 ± 8.5 pmol 14,15-HxA_3-C/million cell and 30.2 ± 8.2 pmol EXC_4/million cell ($n = 4$) at a cell density of 10 million cells/mL.

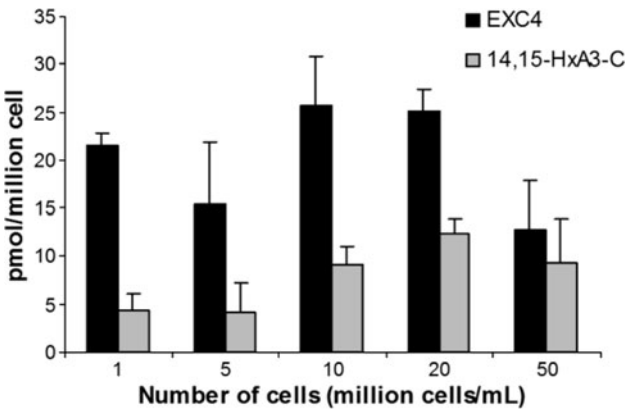

Fig. 4 Comparison of 14,15-HxA_3-C and EXC_4 formed from arachidonic acid by the L1236 cells. L1236 cells were incubated with arachidonic acid (40 μM) for 2 min at 37 °C at different cell densities i.e. 1, 5, 10, 20 and 50 million cells/mL. Quantification was performed by LC–MS/MS multiple reaction monitoring on a triple quadrupole mass spectrometer (TSQ Quantum). Each value represents the mean ± SD of three independent experiments

Soluble GSTs Catalyze the Conversion of 14,15-HxA_3 to 14,15-HxA_3-C

Subcellular fractionation of L1236 cells demonstrated that the 100,000 g supernatant but not the 100,000 g pellet converted 14,15-HxA_3 and EXA_4 to 14,15-HxA_3-C and EXC_4, respectively (data not shown). We therefore investigated the capacity of different soluble glutathione transferases to catalyze the conversion of 14,15-HxA_3 to 14,15-HxA_3-C. Earlier studies performed in our laboratory have shown that L1236 cells express high levels of GSTM1-1 (Feltenmark et al., to be published). Recombinant GST M1-1b, M2-2, M3-3, M4-4, M5-5, P1-1(Ile), P1-1(val), T1-1, A1-1, A2-2, A3-3 or A4-4 and LTC_4 synthase was solved in PBS followed by addition of 14,15-HxA_3 (228 μM) and glutathione (final concentration of 5 mM) followed by incubation for 15 min. GST M1-1 (520 pmol/μg), P1-1(Ile) (350 pmol/μg), M2-2 (250 pmol/μg) and P1-1(val) (230 pmol/μg) had the highest capacity to conjugate glutathione to 14,15-HxA_3 11(*S*). In comparison, LTC_4 synthase was less efficient than GST M1-1 to convert 14, 15-HxA_3 to 14,15-HxA_3-C (Fig. 5).

14,15-Hepoxilin Formation in Eosinophils, Nasal Polyps and Dendritic Cells

Besides the glutathione conjugated 14,15-hepoxilins, the L1236 cells also stereoselectively produced 14,15-HxA_3 11(*S*) and 14,15-HxB_3 13(*R*) upon challenge with arachidonic acid (Fig. 6b–c). These metabolites were identified by

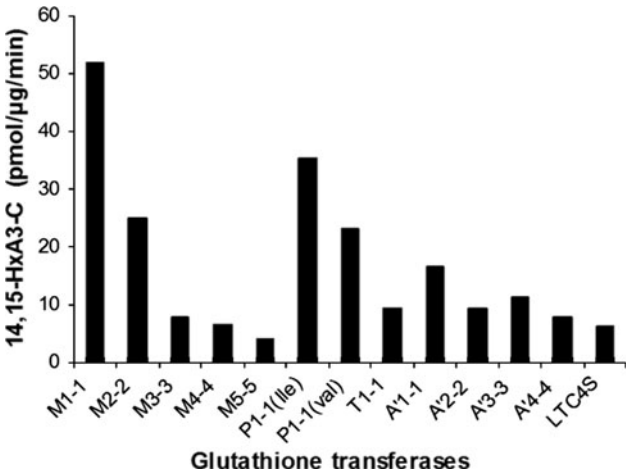

Fig. 5 Metabolism of 14,15-HxA_3 to 14,15-HxA_3-C by various glutathione transferases (GSTs). 14,15-HxA_3 11(*S*) (228 μM) was incubated with 12 different soluble glutathione transferases (4 μg), GST M1-1, M2-2, M3-3, M4-4, M5-5, P1-1(Ile), P1-1(val), T1-1, A1-1, A2-2, A3-3 and A4-4 and LTC_4 synthase for 10 min at 37 °C. The 14,15-HxA_3-C product was quantified by reverse phase HPLC coupled with UV detection (210 nm). Each value represents the mean of two independent experiments

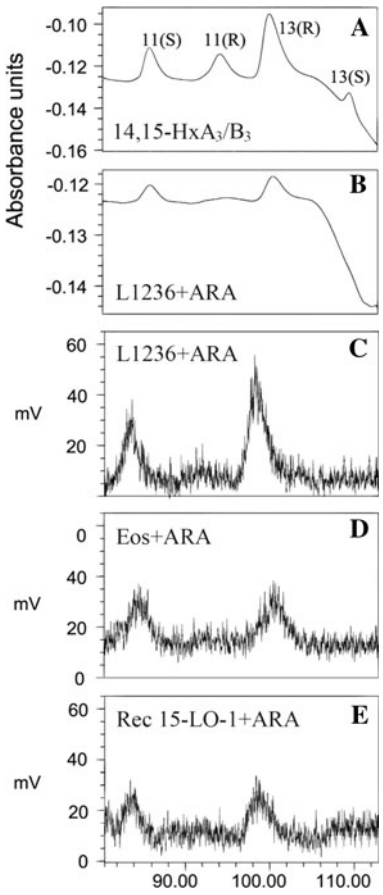

Fig. 6 Formation of isomers of 14,15-HxA_3 and 14,15-HxB_3. Standard 14,15-Hx isomers were separated as shown in the UV (210 nm) chromatogram (**a**). UV (210 nm) and radioactivity chromatograms of the L1236 cell line incubated with arachidonic acid are displayed in panels **b** and **c**, respectively. The cells produced exclusively 11(*S*)-hydroxy-14(*S*),15(*S*)-epoxy-5,8,12 (*Z*,*Z*,*E*)-eicosatrienoic acid (14,15-HxA_3 11(*S*)) and 13(*R*)-hydroxy-14(*S*),15(*S*)-epoxy-eicosatrienoic acid (14,15-HxB_3 13(*R*)). The same isomers were selectively formed in eosinophils and by recombinant 15-LO-1, and corresponding radioactivity chromatograms are shown in panel **d** and **e**

MS/MS spectra (data not shown) and retention times on column were compared with synthetic standards. In order to elucidate if other human cells or tissues, which express 15-LO-1, could produce 14,15-hepoxilins, eosinophils, dendritic cells and nasal polyps were incubated with [1-^{14}C] arachidonic acid, with or without glutathione, and analyzed using a radioactivity detector. The major formed hepoxilins in these cells/tissues were 14,15-HxA_3 11(*S*) and 14,15-HxB_3 13(*R*), however no glutathione-conjugated 14,15-hepoxilins were detected. Fig. 6d shows the formation of these metabolites in eosinophils. Similar results were obtained with dendritic cells and nasal polyps (data not shown). Incubation of recombinant 15-LO-1 with arachidonic acid also led to formation of 14,15-HxA_3 11(*S*) and 14,15-HxB_3 13(*R*) (Fig. 6e), demonstrating that human 15-LO-1 has an intrinsic hepoxilin A_3 and B_3 synthase activity. The hepoxilins represent 5–10% of the total peak area in the radio chromatograms.

Discussion

We had previously shown that the Hodgkin cell line L1236 exhibits high expression of 15-LO-1 and can convert arachidonic acid to eoxins [31]. In this study we have identified two other hitherto unknown cysteinyl-containing arachidonic acid metabolites formed through the 15-LO-1 pathway in L1236 cells. Based on MS/MS spectra of endogenous formed metabolites and corresponding synthetic compound, the unknown metabolites were identified as 11(*S*),15(*S*)-dihydroxy-14(*R*)-glutathionyl-5(*Z*),8(*Z*),12(*E*) eicosatrienoic acid (14,15-HxA_3-C) (**1**) and 11(*S*),15(*S*)-dihydroxy-14(*R*)-cys-gly-5(*Z*),8(*Z*),12(*E*) eicosatrienoic acid (14,15-HxA_3-D) (**2**) (Figs. 2, 3).

The 14,15-hepoxilins are described as hydroperoxide isomerase products [40] or as non-enzymatic degradation products of 15(*S*)-hydroperoxy-eicosatrienoic acid (15-HPETE) [41]. In rabbit aorta, a CYP2J2 is suggested to function as a 15-HPETE isomerase forming the 14,15-HxA_3 [42], and in the garlic root a hydroperoxide isomerase is described [32]. The origin of the 14,15-hepoxilins are enzymatic since formation of 14,15-HxA_3 and 14,15-HxB_3 is stereospecific. 14,15-HxA_3 11(*S*) and 14,15-HxB_3 13(*R*) were the major isomers formed in L1236 cells and also in eosinophils, dendritic cells and in nasal polyps (Fig. 6). This is consistent with the results from human epithelial cells where the 14,15-HxB_3 with the hydroxyl group in *R* configuration is the most prominent isomer [33]. These stereospecific products were formed when arachidonic acid was incubated with recombinant 15-LO-1, demonstrating that 15-LO-1 alone can catalyze the formation of the 14,15-hepoxilins. Thus, human 15-LO-1 possesses an intrinsic 14,15-hepoxilin activity without the presence of an isomerase. It had been demonstrated earlier that purified lipoxygenase from rabbit reticulocytes can convert arachidonic acid into 15-HPETE and 14,15-HxB_3 [43]. The 12-LO Fe^{3+} is described to catalyze the formation of the arachidonic acid peroxide radical which rearranges to give HxB_3 [10]. The biosynthesis of 14,15-hepoxilins was proposed to occur by a free radical mechanism. The 15-HPETE hydroperoxide forms an oxygen radical by homolytic cleavage catalyzed by the 15-LO-1 Fe^{2+}. Spontaneous cyclization forms an epoxyallylic radical having electron density principally at carbons 11 and 13. Oxygen rebound at these carbons results in the formation of 14,15-HxA_3 and 14,15-HxB_3, respectively. Although human epidermis appears to be the principal source of 12-lipoxygenate derived hepoxilins, there is evidence that human intestinal epithelial cell lines can also produce

HxA_3 [20, 44]. The enzyme which catalyzes the formation of this metabolite in these cells is not clear. However, it is possible that human 15-LO-1 also can, to a limited extent, catalyze the formation of hepoxilins, although human 15-LO-1 possesses a relatively low 12-lipoxygenase activity (ratio 15-HETE vs. 12-HETE 9:1 after incubation with arachidonic acid).

In summary, 14,15-HxA_3 and 14,15-HxB_3 were stereospecifically formed with the 11 or 13 hydroxyl group in *S* and *R* configuration, respectively, in human cells such as L1236, eosinophils, nasal polyps and dendritic cells. These metabolites were formed promptly upon stimulation with arachidonic acid. This fatty acid is mainly esterified in membranes in non-activated cells but during inflammatory processes, the level of free arachidonic acid can markedly increase. The metabolite 14,15-HxA_3 has not previously been described to be formed by human cells. The 14,15-HxA_3-C and the 14,15-HxA_3-D were novel identified metabolites of arachidonic acid produced by L1236 cells (Fig. 7). It is noteworthy that LTC_4 as well as EXC_4 in eosinophils are formed by membrane-bound LTC_4 synthase [30] but the synthesis of 14,15-HxA_3-C in L1236 cells is apparently catalyzed primarily by the soluble GST M1-1. This GST is abundant in this cell type, but in other cells GST P1-1 may be more important. GST M1-1 is polymorphic with a frequent null allele [45] and it is obvious that the relative contributions of the different GSTs expressed in a given cell will determined the amounts present. For clarification of the enzymology of 14,15-HxA_3-C formation in different tissues, it will be necessary to quantify the expression of soluble GSTs as well as the membrane-bound LTC_4 synthase in future studies.

The biological effects of the hepoxilins, formed by animal cells and in human epidermis, are still unclear although it has been reported to causes a rise in cytosolic calcium in human neutrophils [32], migration of neutrophils across intestinal epithelial [20], and relaxation of precontracted rabbit aorta [40]. HxA_3-C has been reported to induce vascular contraction of guinea pig isolated trachea

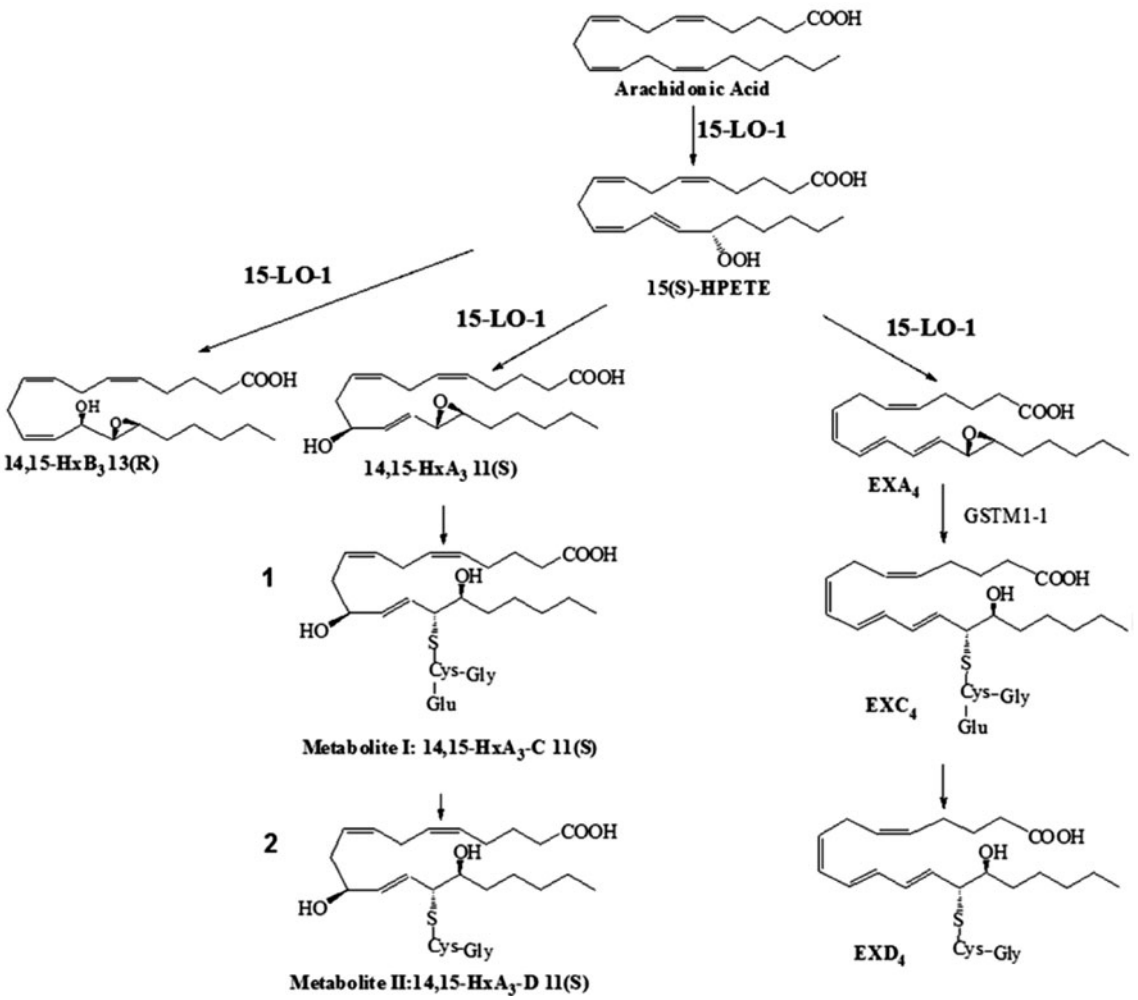

Fig. 7 Overview of the biosynthesis of 14,15-hepoxilins and eoxins in the Hodgkin lymphoma cell line L1236

and increase vascular permeability in rat skin [18, 21]. Therefore it will be of great interests to investigate the biological effects of these newly identified cysteinyl-containing 14,15-hepoxilins produced by human cells.

Acknowledgments This work was supported by grants from the Karolinska Institutet, the Swedish Research Council, the Swedish Cancer Society, Orexo AB, and European Commission Sixth Framework Programme Grant LSHM-CT-2004-005033.

References

1. Pace-Asciak CR (2009) The hepoxilins and some analogues: a review of their biology. Br J Pharmacol 158:972–981
2. Pace-Asciak CR (1994) Hepoxilins: a review on their cellular actions. Biochim Biophys Acta 1215:1–8
3. Nigam S, Shankaranarayanan P, Ciccoli R, Ishdorj G, Schwarz K, Petrucev B, Kuhn H, Haeggstrom JZ (2004) The rat leukocyte-type 12-lipoxygenase exhibits an intrinsic hepoxilin A3 synthase activity. J Biol Chem 279:29023–29030
4. Pace-Asciak CR, Granstrom E, Samuelsson B (1983) Arachidonic acid epoxides. Isolation and structure of two hydroxy epoxide intermediates in the formation of 8, 11, 12- and 10, 11, 12-trihydroxyeicosatrienoic acids. J Biol Chem 258:6835–6840
5. Pace-Asciak CR, Laneuville O, Chang M, Reddy CC, Su WG, Corey EJ (1989) New products in the hepoxilin pathway: isolation of 11-glutathionyl hepoxilin A3 through reaction of hepoxilin A3 with glutathione S-transferase. Biochem Biophys Res Commun 163:1230–1234
6. Laneuville O, Corey EJ, Couture R, Pace-Asciak CR (1991) Hepoxilin A3 (HxA3) is formed by the rat aorta and is metabolized into HxA3-C, a glutathione conjugate. Biochim Biophys Acta 1084:60–68
7. Sutherland M, Shankaranarayanan P, Schewe T, Nigam S (2001) Evidence for the presence of phospholipid hydroperoxide glutathione peroxidase in human platelets: implications for its involvement in the regulatory network of the 12-lipoxygenase pathway of arachidonic acid metabolism. Biochem J 353:91–100
8. Brash AR, Yu Z, Boeglin WE, Schneider C (2007) The hepoxilin connection in the epidermis. FEBS J 274:3494–3502 (Epub 2007 Jul 3492)
9. Anton R, Puig L, Esgleyes T, de Moragas JM, Vila L (1998) Occurrence of hepoxilins and trioxilins in psoriatic lesions. J Invest Dermatol 110:303–310
10. Anton R, Vila L (2000) Stereoselective biosynthesis of hepoxilin B-3 in human epidermis. J Invest Dermatol 114:554–559
11. Nigam S, Zafiriou MP, Deva R, Ciccoli R, Roux-Van der Merwe R (2007) Structure, biochemistry and biology of hepoxilins: an update. FEBS J 274:3503–3512
12. Eckl KM, Krieg P, Kuster W, Traupe H, Andre F, Wittstruck N, Furstenberger G, Hennies HC (2005) Mutation spectrum and functional analysis of epidermis-type lipoxygenases in patients with autosomal recessive congenital ichthyosis. Hum Mutat 26:351–361
13. Yu Z, Schneider C, Boeglin WE, Brash AR (2005) Mutations associated with a congenital form of ichthyosis (NCIE) inactivate the epidermal lipoxygenases 12R-LOX and eLOX3. Biochim Biophys Acta 1686:238–247
14. de Juanes S, Epp N, Latzko S, Neumann M, Furstenberger G, Hausser I, Stark HJ, Krieg P (2009) Development of an ichthyosiform phenotype in Alox12b-deficient mouse skin transplants. J Invest Dermatol 129:1429–1436. Epub 2009 Jan 1421
15. Hammarstrom S, Hamberg M, Samuelsson B, Duell EA, Stawiski M, Voorhees JJ (1975) Increased concentrations of nonesterified arachidonic acid, 12L-hydroxy-5, 8, 10, 14-eicosatetraenoic acid, prostaglandin E2, and prostaglandin F2alpha in epidermis of psoriasis. Proc Natl Acad Sci USA 72:5130–5134
16. Pace-Asciak CR, Martin JM, Corey EJ (1986) Hepoxilins, potential endogenous mediators of insulin release. Prog Lipid Res 25:625–628
17. Laneuville O, Couture R, Pace-Asciak CR (1992) Hepoxilins sensitize blood vessels to noradrenaline–stereospecificity of action. Br J Pharmacol 105:297–304
18. Laneuville O, Corey EJ, Couture R, Pace-Asciak CR (1991) Hepoxilin A3 increases vascular permeability in the rat skin. Eicosanoids 4:95–97
19. Sutherland M, Schewe T, Nigam S (2000) Biological actions of the free acid of hepoxilin A3 on human neutrophils. Biochem Pharmacol 59:435–440
20. Mrsny RJ, Gewirtz AT, Siccardi D, Savidge T, Hurley BP, Madara JL, McCormick BA (2004) Identification of hepoxilin A3 in inflammatory events: a required role in neutrophil migration across intestinal epithelia. Proc Natl Acad Sci USA 101:7421–7426
21. Laneuville O, Couture R, Pace-Asciak CR (1992) Neurokinin A-induced contraction of guinea-pig isolated trachea: potentiation by hepoxilins. Br J Pharmacol 107:808–812
22. Nadel JA, Conrad DJ, Ueki IF, Schuster A, Sigal E (1991) Immunocytochemical localization of arachidonate 15-lipoxygenase in erythrocytes, leukocytes, and airway cells. J Clin Invest 87:1139–1145
23. Gulliksson M, Brunnstrom A, Johannesson M, Backman L, Nilsson G, Harvima I, Dahlen B, Kumlin M, Claesson HE (2007) Expression of 15-lipoxygenase type-1 in human mast cells. Biochim Biophys Acta 1771:1156–1165. Epub 2007 Jun 1123
24. Hunter JA, Finkbeiner WE, Nadel JA, Goetzl EJ, Holtzman MJ (1985) Predominant generation of 15-lipoxygenase metabolites of arachidonic acid by epithelial cells from human trachea. Proc Natl Acad Sci USA 82:4633–4637
25. Turk J, Maas RL, Brash AR, Roberts LJ II, Oates JA (1982) Arachidonic acid 15-lipoxygenase products from human eosinophils. J Biolog Chem 257:7068–7076
26. Claesson HE (2009) On the biosynthesis and biological role of eoxins and 15-lipoxygenase-1 in airway inflammation and Hodgkin lymphoma. Prostaglandins Other Lipid Mediat 89:120–125
27. Chu HW, Balzar S, Westcott JY, Trudeau JB, Sun Y, Conrad DJ, Wenzel SE (2002) Expression and activation of 15-lipoxygenase pathway in severe asthma: relationship to eosinophilic phenotype and collagen deposition. Clin Exp Allergy 32:1558–1565
28. Bradding P, Redington AE, Djukanovic R, Conrad DJ, Holgate ST (1995) 15-Lipoxygenase immunoreactivity in normal and in asthmatic airways. Am J Respir Crit Care Med 151:1201–1204
29. Shannon VR, Chanez P, Bousquet J, Holtzman MJ (1993) Histochemical evidence for induction of arachidonate 15-lipoxygenase in airway disease. Am Rev Respir Dis 147:1024–1028
30. Feltenmark S, Gautam N, Brunnstrom A, Griffiths W, Backman L, Edenius C, Lindbom L, Bjorkholm M, Claesson HE (2008) Eoxins are proinflammatory arachidonic acid metabolites produced via the 15-lipoxygenase-1 pathway in human eosinophils and mast cells. Proc Natl Acad Sci USA 105:680–685
31. Claesson HE, Griffiths WJ, Brunnstrom A, Schain F, Andersson E, Feltenmark S, Johnson HA, Porwit A, Sjoberg J, Bjorkholm M (2008) Hodgkin Reed-Sternberg cells express 15-lipoxygenase-1 and are putative producers of eoxins in vivo: novel insight into the inflammatory features of classical Hodgkin lymphoma. FEBS J 275:4222–4234
32. Reynaud D, Ali M, Demin P, Pace-Asciak CR (1999) Formation of 14,15-hepoxilins of the A(3) and B(3) series through a

15-lipoxygenase and hydroperoxide isomerase present in garlic roots. J Biol Chem 274:28213–28218
33. Holtzman MJ, Hansbrough RJ, Rosen GD, Turk J (1988) Uptake, release and novel species-dependent oxygenation of arachidonic acid in human and animal airway epithelial cells. Biochim Biophys Acta 963:401–413
34. Andersson E, Schain F, Svedling M, Claesson HE, Forsell PK (2006) Interaction of human 15-lipoxygenase-1 with phosphatidylinositol bisphosphates results in increased enzyme activity. Biochim Biophys Acta 1761:1498–1505
35. Eklund BI, Moberg M, Bergquist J, Mannervik B (2006) Divergent activities of human glutathione transferases in the bioactivation of azathioprine. Mol Pharmacol 70:747–754
36. Johansson AS, Stenberg G, Widersten M, Mannervik B (1998) Structure-activity relationships and thermal stability of human glutathione transferase P1–1 governed by the H-site residue 105. J Mol Biol 278:687–698
37. Jakobsson PJ, Mancini JA, Ford-Hutchinson AW (1996) Identification and characterization of a novel human microsomal glutathione S-transferase with leukotriene C4 synthase activity and significant sequence identity to 5-lipoxygenase-activating protein and leukotriene C4 synthase. J Biol Chem 271:22203–22210
38. Corey EJ, Su W-G, Mehrotra MM (1984) A efficient and simple method for the conversion of 15-HPETE to 14, 15-EPETE (lipotriene A) and 5-HPETE to leukotriene A as the methyl esters. Tet Lett 25:5123–5126
39. Hevko JM, Murphy RC (2001) Electrospray ionization and tandem mass spectrometry of cysteinyl eicosanoids: leukotriene C4 and FOG7. J Am Soc Mass Spectrom 12:763–771
40. Pfister SL, Spitzbarth N, Nithipatikom K, Edgemond WS, Falck JR, Campbell WB (1998) Identification of the 11,14,15- and 11,12,15-trihydroxyeicosatrienoic acids as endothelium-derived relaxing factors of rabbit aorta. J Biol Chem 273:30879–30887
41. Narumiya S, Salmon JA, Cottee FH, Weatherley BC, Flower RJ (1981) Arachidonic acid 15-lipoxygenase from rabbit peritoneal polymorphonuclear leukocytes. Partial purification and properties. J Biol Chem 256:9583–9592
42. Pfister SL, Spitzbarth N, Zeldin DC, Lafite P, Mansuy D, Campbell WB (2003) Rabbit aorta converts 15-HPETE to trihydroxyeicosatrienoic acids: potential role of cytochrome P450. Arch Biochem Biophys 420:142–152
43. Bryant RW, Schewe T, Rapoport SM, Bailey JM (1985) Leukotriene formation by a purified reticulocyte lipoxygenase enzyme. J Biol Chem 260:3548–3555
44. Canny GO, McCormick BA (2008) Bacteria in the intestine, helpful residents or enemies from within? Infect Immun 76:3360–3373
45. Warholm M, Guthenberg C, Mannervik B (1983) Molecular and catalytic properties of glutathione transferase mu from human liver: an enzyme efficiently conjugating epoxides. Biochemistry 22:3610–3617

Lipids (2011) 46:81–85
DOI 10.1007/s11745-010-3489-x

COMMUNICATION

Two New Eicosanoids with a Unique Isovalerianic Acid Ester Moiety from the South China Sea Gorgonian *Dichotella gemmacea*

Chang-Yun Wang · Jie Zhao · Hai-Yan Liu · Chang-Lun Shao · Qing-Ai Liu · Yang Liu · Yu-Cheng Gu

Received: 12 April 2010 / Accepted: 11 October 2010 / Published online: 16 November 2010

Abstract Two new eicosanoids with a unique isovalerianic acid ester group at C-12, named dichotellates A (**1**) and B (**2**), were isolated from the gorgonian *Dichotella gemmacea* collected from the South China Sea using bioassay-guided fractionation. Their structures were established on the basis of extensive spectroscopic analysis including one-dimensional (1D) and two-dimensional (2D) NMR as well as high-resolution ESI-MS experiments. These two compounds were evaluated for their lethal activity toward brine shrimp *Artemia salina* and both showed weak activity.

Keywords Gorgonian · *Dichotella gemmacea* · Eicosanoid · Dichotellate A · Dichotellate B

Abbreviations

COSY	Correlation spectroscopy
DEPT	Distortionless enhancement by polarization transfer
ESI	Electrospray ionization
HMBC	Heteronuclear multiple bond correlation
HMQC	Heteronuclear multiple quantum correlation
IR	Infrared
MS	Mass spectrometry
NMR	Nuclear magnetic resonance

C.-Y. Wang (✉) · J. Zhao · H.-Y. Liu · C.-L. Shao · Q.-A. Liu · Y. Liu
Key Laboratory of Marine Drugs, The Ministry of Education of China, School of Medicine and Pharmacy, Ocean University of China, Qingdao 266003, People's Republic of China
e-mail: changyun@ouc.edu.cn

Y.-C. Gu
Syngenta, Jealott's Hill International Research Centre, Bracknell, Berkshire RG42 6EY, UK

Introduction

Polyunsaturated fatty acids (PUFA) have played important roles in the pharmaceutical and biochemical fields because of their biological properties including antimalarial activity, mycobactericidal activity, and antifungal activity [1–3]. They also have significant functions in animal systems as intermediate products, such as eicosanoids derived from C20 PUFA that regulate cell differentiation, immune responses, and homeostasis [4].

Coral is a notable source of eicosanoids, for example, cyclopropyl eicosanoids from the gorgonian *Plexaura homomalla*, (8*R*)-8-hydroperoxyeicosatetraenoic acid and 11(*R*)-hydroxy-eicosatetraenoic acid from *Plexaura homomalla* and *Plexaurella dichotoma*, respectively [5–7]. In the course of our program to search for bioactive metabolites from marine invertebrates, the petroleum ether extract of the gorgonian *Dichotella gemmacea* collected from the South China Sea showed lethal activity toward brine shrimp *Artemia salina*. Bioassay-guided fractionation of the active extract led to the isolation of two new eicosanoids, dichotellates A and B (**1**, **2**) (Scheme 1), containing a unique isovalerianic acid ester group at C-12. Herein, we report the isolation and structure elucidation of the two metabolites and their lethal activity toward the brine shrimp *A. salina*.

Materials and Methods

General Experimental Procedures

Optical rotations were measured with a Horiba SEAP-300 spectropolarimeter. IR (KBr) spectra were obtained on a Nicolet Nexus 470 infrared spectrophotometer. ^{1}H, ^{13}C, and 2D NMR spectra were recorded on a JEOL JNM-ECP

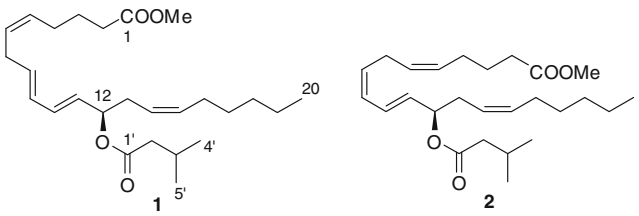

Scheme 1 Chemical structures of **1** and **2**

600-MHz NMR spectrometer with tetramethylsilane (TMS) as internal standard. MS spectral data were obtained on a Micromass Q-TOF spectrometer for ESI-MS. High-performance liquid chromatography (HPLC) separation was performed using a Waters 1525 preparative HPLC system coupled with a Waters 2996 photodiode array detector. A Kromasil C18 preparative HPLC column (250 × 10 mm, 5 μm) was used. Silica gel (200–300 mesh) for column chromatography and GF_{254} for TLC were made by the Qingdao Marine Chemical Factory, Qingdao, China.

Animal Material

The gorgonian *D. gemmacea* was collected at a coral reef in the South China Sea, Sanya, Hainan Province, China, in April 2006 and identified by Prof. Ren-Lin Zou, South China Sea Institute of Oceanology, Chinese Academy of Sciences, China. A voucher specimen was deposited in the Key Laboratory of Marine Drugs, Ministry of Education, School of Medicine and Pharmacy, Ocean University of China, Qingdao, China, with access code HN-SYM-20060032.

Extraction and Isolation

The fresh material (2.8 kg wet weight) was extracted with 95% EtOH three times (3 × 5 L) at room temperature, and the solution was evaporated to dryness under vacuum. The residue was suspended in H_2O (500 mL) and partitioned with petroleum ether (1,000 mL) three times. The petroleum ether extract (14.0 g) was subjected to silica gel column chromatography (CC), using petroleum ether/acetone (from 100:0 to 0:100) as eluent. The fractions were further subjected to Sephadex LH-20 CC and eluted with petroleum ether/$CHCl_3$/MeOH (2:1:1) and purified by semipreparative HPLC using MeOH/H_2O (90:10) as mobile phase to obtain compounds **1** (3.0 mg) and **2** (4.6 mg).

Dichotellate A (**1**)

Colorless oil, $[\alpha]_D^{25}$ −0.21° (*c* 0.5, $CHCl_3$). IR (KBr) ν_{max} 2,956, 2,927, 2,856, 1,736, 1,458, 1,370, 1,292, 1,242, 1,188, 1,096 cm^{-1}; NMR spectral data see Table 1; ESI-MS (+) *m/z*: 441 $[M + Na]^+$; High-resolution ESI-MS *m/z*: 441.2972 ($C_{26}H_{42}O_4Na$, calcd. 441.2981).

Dichotellate B (**2**)

Colorless oil, $[\alpha]_D^{25}$ −0.35° (*c* 0.5, $CHCl_3$). NMR spectral data see Table 1; ESI-MS (+) *m/z*: 441 $[M + Na]^+$; High-resolution ESI-MS *m/z*: 441.2983 ($C_{26}H_{42}O_4Na$, calcd. 441.2981).

Bioassays

The brine shrimp lethality assay was performed on *A. salina* according to the published protocols [8, 9].

The isolated compounds were screened for cytotoxic activity against KB and KBv200 cell lines using the method of microculture tetrazolium (MTT) [10].

Results and Discussion

The gorgonian *D. gemmacea*, collected from a coral reef of Sanya, Hainan Province, China, in April 2006, was extracted with 95% EtOH three times, and the extract was suspended in H_2O and partitioned with petroleum ether. The petroleum ether was subjected to silica gel column chromatography followed by separation on Sephadex LH-20. Further purification by semipreparative HPLC of fractions from petroleum ether extract yielded two new metabolites (**1**, **2**).

Compound **1**, isolated as a colorless oil, $[\alpha]_D^{25}$ −0.21° (*c* 0.5, $CHCl_3$), gave an $[M + Na]^+$ ion peak at *m/z* 441.2972 (calcd. 441.2981) by HR-ESI-MS, which indicated that the compound has molecular formula $C_{26}H_{42}O_4$ with 6° of unsaturation. The IR spectrum of **1** showed strong carbonyl group absorption at 1,736 cm^{-1}. In its ^1H NMR spectrum, eight olefinic proton signals were found at δ_H 6.23 (1H, dd, $J = 15.0$, 10.3 Hz), 6.02 (1H, dd, $J = 15.0$, 10.6 Hz), 5.70 (1H, m), 5.51 (1H, dd, $J = 15.4$, 7.4 Hz), 5.44 (2H, m), and 5.35 (2H, m), while three methyl groups signals were observed at δ_H 0.94 (6H, d, $J = 6.6$ Hz) and 0.88 (3H, t, $J = 7.0$ Hz) and one methoxyl group signal at δ_H 3.67 (3H, s). The ^{13}C NMR spectrum of **1** revealed 26 carbon signals. Furthermore, DEPT spectrum confirmed that this compound has 3 methyls, 1 methoxyl, 10 methylenes, 10 methines, and 2 quaternary carbon atoms. The six elements of unsaturation of **1** were accounted for eight olefinic carbon signals and two carbonyl groups (δ_C 174.0 and 172.4). A ^1H NMR spin system from H-2 to H-20 was completely revealed by analysis of its ^1H–^1H COSY spectrum (Table 1; Fig. 1). A sharp triplet at δ_H 2.31 with $J = 7.4$ Hz was caused by the C-2 methylene protons as in other oxylipins [11]. The above data implied that compound **1** is a long-chain unsaturated

Table 1 NMR spectroscopic data of dichotellate A (**1**) and dichotellate B (**2**)

Position	**1**				**2**	
	δ_C	δ_H (J in Hz)	^{1}H-^{1}H COSY	HMBC	δ_C	δ_H (J in Hz)
1	174.0 C	–	–	–	174.0 C	–
2	33.4 CH_2	2.31 t (7.4)	H_2-3	C-1, C-3	33.4 CH_2	2.31 t (7.3)
3	24.7 CH_2	1.69 m	H_2-2, H_2-4	C-1, C-2, C-4, C-5	24.7 CH_2	1.69 m
4	26.7 CH_2	2.08 m	H_2-3, H-5	C-2, C-3, C-5	26.7 CH_2	2.05 m
5	131.4 CH	5.44 m	H_2-4, H-6	–	131.7 CH	5.46 m
6	126.3 CH	5.35 m	H-5, H_2-7	–	126.9 CH	5.32 m
7	30.4 CH_2	2.82 t (7.0)	H-6, H-8	C-5, C-6, C-8	26.1 CH_2	2.92 t (7.0)
8	134.3 CH	5.70 m	H_2-7, H-9	C-10	131.5 CH	5.42 m
9	129.3 CH	6.02 dd (15.0, 10.3)	H-8, H-10	C-10	127.5 CH	5.95 t (11.0)
10	132.9 CH	6.23 dd (15.4, 10.3)	H-9, H-11	–	127.6 CH	6.54 dd (15.1, 11.0)
11	128.7 CH	5.51 dd (15.4, 7.4)	H-10, H-12	C-9, C-12	130.9 CH	5.61 dd (15.4, 7.3)
12	73.7 CH	5.29 q (7.0)	H-11, H_2-13	C-10	73.6 CH	5.35 m
13	32.5 CH_2	2.32 m, 2.41 m	H-12, H-14	C-12, C-14, C-15	32.6 CH_2	2.36 m, 2.43 m
14	125.0 CH	5.35 m	H_2-13, H-15	–	124.9 CH	5.37 m
15	131.4 CH	5.44 m	H-14, H_2-16	–	131.0 CH	5.46 m
16	27.1 CH_2	2.02 m	H-15, H_2-17	C-14, C-15, C-17	27.2 CH_2	2.02 m
17	29.3 CH_2	1.35 m	H_2-16, H_2-18	–	29.3 CH_2	1.36 m
18	31.5 CH_2	1.28 m	H_2-17	C-20	31.5 CH_2	1.30 m
19	22.6 CH_2	1.30 m	H_3-20	C-18	22.6 CH_2	1.27 m
20	14.1 CH_3	0.88 t (7.0)	H2-19	C-18, C-19	14.1 CH_3	0.89 t (7.0)
1′	172.4 C	–	–	–	172.6 C	–
2′	43.7 CH_2	2.17 m	H-3′	C-1′, C-3′, C-4′, C-5′	43.7 CH_2	2.18 m
3′	25.7 CH	2.08 m	H_2-2′, H_3-4′/5′	–	25.8 CH	2.08 m
4′/5′	22.4 CH_3	0.94 d (6.6)	H-3′	C-2′, C-3′	22.4 CH_3	0.95 d (6.6)
OMe	51.5 CH_2	3.76 s	–	C-1	51.5 CH_3	3.67 s

Spectra recorded in $CDCl_3$, ^{1}H NMR (600 MHz); ^{13}C NMR (150 MHz)

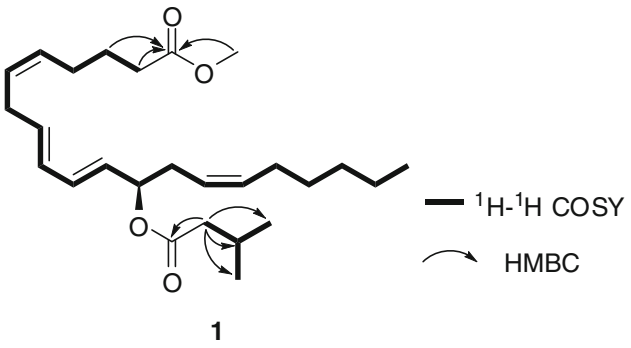

Fig. 1 ^{1}H–^{1}H COSY and selected HMBC correlations for **1**

eicosanoic acid derivative. From the HMQC spectrum data, all proton signals were assigned to their directly attached carbons, and the full assignments of chemical shift data of C-2 to C-20 were further confirmed by HMBC spectra (Table 1; Fig. 1). Since the HMBC correlation between the methoxyl group at δ_H 3.67 and C-1 at δ_C 174.0 was detected, compound **1** was presented as an methyl ester. The correlations of H-23/H-24/H-25, H-26 in the ^{1}H–^{1}H COSY spectrum together with the HMBC correlations from H-23 to C-22, C-24, C-25/C-26 and from H-25/H-26 to C-23, C-24 suggested that an isovalerate unit was located at C-12, an oxygenated carbon with chemical shift value at δ_C 73.7. The *trans–trans* relationships of H-8 and H-9, H-10 and H-11 were assigned by the coupling constants ($J_{8,9}$ = 15.0 Hz and $J_{10,11}$ = 15.4 Hz) while the *cis*-geometries of the other two double bonds were determined by the diallylic and allylic carbons, observed at δ_C 30.4 (C-7) and 27.1 (C-16), respectively [12, 13]. Based on the optical rotation of compound **1** together with those in the literatures for enantiomerically pure 12-HETE, its absolute configuration at C-12 was tentatively determined as *R* [14–16]. On the basis of these results, the full structure of **1** was elucidated as (5*Z*,8*E*,10*E*,12*R*,14*Z*)-methyl 12-(3-methyl-1-oxobutoxy)-5,8,10,14-eicosatetraenoate and named as dichotellate A.

Compound **2** was obtained as a colorless oil, $[\alpha]_D^{25}$ – 0.35° (*c* 0.5, $CHCl_3$) with a pseudomolecular ion peak

Scheme 2 Possible formation of **1** and **2** from arachidonic acid

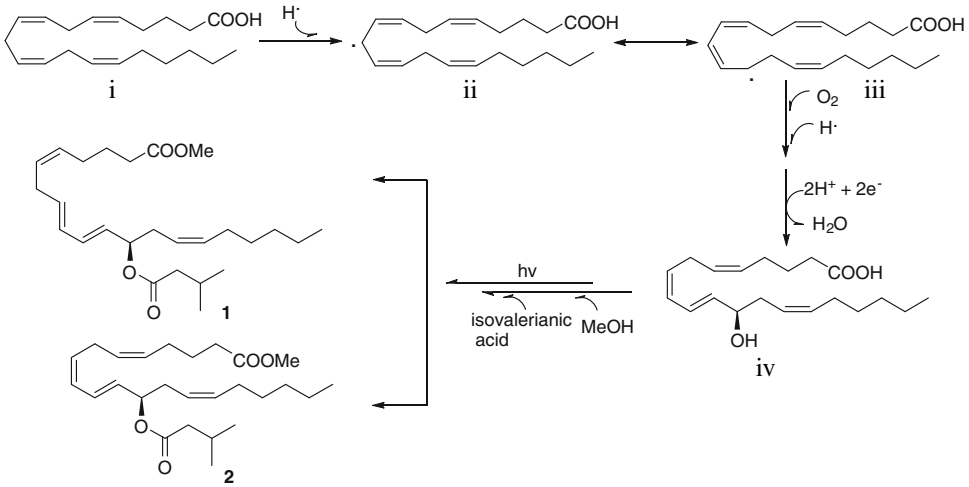

presented as an $[M + Na]^+$ ion at *m/z* 441 in ESI-MS. Its HR-ESI-MS ($[M + Na]^+$ *m/z* 441.2983, calcd. 441.2981) implied **2** has molecular formula $C_{26}H_{42}O_4$, which is the same as compound **1**. Possessing similar ^{1}H NMR data and patterns as for compound **1**, compound **2** has the same carbon skeleton as **1** (Table 1). The ^{13}C NMR and DEPT spectra revealed **2** has 26 carbon signals attributing to 3 methyls, 1 methoxyl, 10 methylenes, 10 methines, and 2 quaternary carbon atoms. The chemical shift value of C-7 at δ 26.1 and the H-8 and H-9 coupling constant of $J_{8,9} = 11.0$ Hz indicated that the configuration of C-8 and C-9 was at *cis* position to each other [13]. The carbons and protons were assigned unambiguously by analyzing its 2D NMR spectral data. The absolute configuration at C-12 in **2** was also tentatively determined as *R* [14–16]. Hence, the structure of compound **2** was established as (5*Z*,8*Z*,10*E*,12*R*,14*Z*)-methyl 12-(3-methyl-1-oxobutoxy)-5,8,10,14-eicosatetraenoate and named as dichotellate B.

A unique isovalerianic acid ester group at C-12 is the main characteristic of the two eicosanoids (**1** and **2**) isolated from gorgonian *D. gemmacea*. To the best of our knowledge, they are the first examples from nature of eicosanoids esterified by isovalerianic acid.

Taking into account the structures of compounds **1** and **2**, they may be derived from arachidonic acid, and a possible process for compounds **1** and **2** is proposed in Scheme 2 based on the literature [17–19]. The precursor arachidonic acid (**i**) was firstly abstracted at 10-*pro*-(*R*) hydrogen atom and converted into two resonance forms (**ii** and **iii**) with the radical at either C-10 or C-12. The resonance form **iii** was then oxidized at C-12, followed by peroxidase reduction, resulting in the corresponding hydroxyeicosatetraenoic acid (intermediate **iv**). After esterification and *cis–trans* isomerization, the intermediate **iv** was finally transformed into **1** and **2**.

Compounds **1** and **2** were evaluated for their lethal activity toward brine shrimp *A. salina*. At concentration of 50 μg/ml, compounds **1** and **2** showed weak lethality to the brine shrimp *A. salina* with lethal rates of 19% and 33%, respectively. These two compounds were also tested for cytotoxicity against KB and KBv200 tumor cell lines and shown to be inactive ($IC_{50} > 50$ μg/ml).

Two uncommon eicosanoid metabolites with a unique isovalerianic acid ester group at C-12 have been isolated and identified from gorgonian *D. gemmacea*. Their possible biosynthetic pathway was also proposed. The chemical investigation of *D. gemmacea* may be used as foundation for further studies on eicosanoid metabolites in gorgonian.

Acknowledgments This work was financially supported by the National Natural Science Foundation of China (Nos. 40976077; 30901879; 40776073), the Research Fund for Doctoral Program of Higher Education, Ministry of Education of China (No. 20090132110002), and the Basic Research Program of Science and Technology, Ministry of Science and Technology of China (No. 2007FY210500). We wish to thank Prof. R.-L. Zou. for identification of the coral material.

References

1. Krugliak M, Deharo E, Shalmiev G, Sauvain M, Moretti C, Ginsburg H (1995) Antimalarial effects of C18 fatty acids on *Plasmodium falciparum* in culture and on *Plasmodium vinckei petteri* and *Plasmodium yoelii nigeriensis* in vivo. Exp Parasitol 81:97–105
2. Carballeira NM, Cruz H, Kwong CD, Wan B, Franzblau S (2004) 2-Methoxylated fatty acids in marine sponges: defense mechanism against mycobacteria. Lipids 39:675–680
3. Carballeira NM, Sanabria D, Cruz C, Parang K, Wan B, Franzblau S (2006) 2, 6-hexadecadiynoic acid and 2, 6-nonadecadiynoic acid: novel synthesized acetylenic fatty acids as potent antifungal agents. Lipids 41:507–511
4. Kousaka K, Ogi N, Akazawa Y, Fujieda M, Yamamoto Y, Takada Y, Kimura J (2003) Novel oxylipin metabolites from the brown alga *Eisenia bicyclis*. J Nat Prod 66:1318–1323
5. Gerwick WH (1993) Carbocyclic oxylipins of marine origin. Chem Rev 93:1807–1823
6. Brash AR (1989) Formation of an allene oxide from (8*R*)-8-hydroperoxyeicosatetraenoic acid in the coral *Plexaura homomalla*. J Am Chem Soc 111:1891–1892

7. Di MV, Ventriglia M, Mollo E, Mosca M, Cimino G (1996) Occurrence and biosynthesis of 11(*R*)-hydroxy-eicosatetraenoic acid (11-*R*-HETE) in the Caribbean soft coral *Plexaurella dichotoma*. Experientia 52:834–838
8. Solis PN, Wright CW, Anderson MM, Gupta MP, Phillipson JD (1993) A microwell cytotoxicity assay using *Artemia salina* (brine shrimp). Planta Med 59:250–252
9. Meyer BN, Ferrigni NR, Putnam JE, Jacobson LB, Nicols DE, Mclaughlin JL (1982) Brine shrimp: a convenient bioassay for active plant constituents. Planta Med 45:31–34
10. Grever MR, Schepartz SA, Chabner BA (1992) The National Cancer Institute: cancer drug discovery and development program. Semin Oncol 19(6):622–638
11. Bernart MB, Gerwick WH (1994) Eicosanoids from the tropical red alga *Murrayella periclados*. Phytochemistry 36:1233–1240
12. Rossi R, Carpita A, Quirici MG, Veracini CA (1982) Insect pheromone components. Use of ^{13}C NMR spectroscopy for assigning the configuration of C=C double bonds of monoenoic or dienoic pheromone components and for quantitative determination of *Z*/*E* mixtures. Tetrahedron 38:639–644
13. Doi Y, Ishibashi M, Kobayashi J (1994) Isolation and structure of shimofuridins B–G from the okinawan marine tunicate *Aplidium multiplicatum*. Tetrahedron 50:8651–8656
14. Corey EJ, Niwa H, Knolle J (1978) Total synthesis of (S)-12-hydroxy-5,8,14-cis-10-trans-eicosatetraenoic acid (Samuelsson's HETE). J Am Chem Soc 100:1942–1943
15. Just G, Wang ZY (1985) A simple synthesis of methyl 11(*S*)- and 12(*S*)-HETE. Tetrahedron Lett 26:2993–2996
16. Rodríguez A, Nomen M, Spur BW, Godfroid JJ, Lee TH (2001) Total synthesis of 12(R)-HETE, 12(S)-HETE, 2H2-12(R)-HETE and LTB4 from racemic glycidol via hydrolytic kinetic resolution. Tetrahedron 57:25–37
17. Nugteren DH, Beerthuis RK, van Dorp DA (1966) The enzymatic conversion of all-cis 8,11,14-eicosatrienoic acid into prostaglandin El. Recl Trav Chim Pays Bas 85:405–418
18. Hamberg M, Samuelsson B (1967) Oxygenation of unsaturated fatty acids by the vesicular gland of sheep. J Biol Chem 242:5344–5354
19. Rouzer CA, Marnett LJ (2003) Mechanism of free radical oxygenation of polyunsaturated fatty acids by cyclooxygenases. Chem Rev 103:2239–2304

Lipids (2011) 46:87–93
DOI 10.1007/s11745-010-3500-6

ORIGINAL ARTICLE

Modeling the Primary Oxidation in Commercial Fish Oil Preparations

Jenna C. Sullivan · Suzanne M. Budge · Marc St-Onge

Received: 5 July 2010 / Accepted: 4 November 2010 / Published online: 23 November 2010

Abstract The quality of commercial fish oil products can be difficult to maintain because of the rapid lipid oxidation attributable to the high number of polyunsaturated fatty acids (PUFA), specifically eicosapentaenoic acid (EPA) and docosahexaenoic acid (DHA). While it is known that oxidation in fish oil is generally the result of a direct interaction with oxygen and fatty acid radicals, there are very few studies that investigate the oxidation kinetics of fish oil supplements. This study uses hydroperoxides, a primary oxidation product, to model the oxidation kinetics of two commercially available fish oil supplements with different EPA and DHA contents. Pseudo first order kinetics were assumed, and rate constants were determined for temperatures between 4 and 60 °C. This data was fit to the Arrhenius model, and activation energies (E_a) were determined for each sample. Both E_a agreed with values found in the literature, with the lower PUFA sample having a lower E_a. The oil with a lower PUFA content fit the first-order kinetics model at temperatures ≥20 °C and ≤40 °C, while the higher PUFA oil demonstrated first-order kinetics at temperatures ≥4 °C and ≤40 °C. When the temperature was raised to 60 °C, the model no longer applied. This indicates that accelerated testing of fish oil should be conducted at temperatures ≤40 °C.

Keywords Lipid chemistry · General area, lipid hydroperoxides · Oxidized lipids, fish oil · Specific lipids

J. C. Sullivan (✉) · S. M. Budge
Department of Process Engineering and Applied Science, Dalhousie University, Halifax, NS B3J 2X4, Canada
e-mail: jcsulliv@dal.ca

M. St-Onge
Ascenta Health Ltd., 4-15 Garland Avenue, Dartmouth, NS B3B 0A6, Canada

Introduction

Fish oil dietary supplements have been gaining popularity in recent years due to the health benefits provided by the polyunsaturated fatty acids (PUFA) they contain. The primary PUFA in fish oil are eicosapentaenoic acid (EPA) and docosahexaenoic acid (DHA). These fatty acids (FA) have been shown to be important factors in cardiovascular health as well as brain and eye development in babies [1–6] while deficiencies in PUFA have been associated with a number of negative health conditions including dermal conditions, attention deficit disorder and clinical depression [4]. Because most people do not consume the recommended 2–3 servings of fatty fish per week as recommended by the World Health Organization [7], fish oil supplements have become a popular alternative. Unfortunately, due to their large number of double bonds, PUFA in fish oil are subject to rapid oxidation which produces fishy off-flavors and can make supplements unpalatable.

The type of oxidation most commonly seen in commercial fish oil products is a result of direct interactions between fatty acid radicals and molecular oxygen. This process is initiated by reaction of singlet oxygen with lipids [8] to generate free radicals that in turn, initiate chain reactions of oxidation. Oxidation of PUFA leads to the formation of the primary oxidation products, lipid hydroperoxides, which then break down into secondary oxidation products including aldehydes, ketones, acids, and alcohols. Hydroperoxides are stable at room temperature, but readily decompose at elevated temperatures or in the presence of transition metals [9]. The rate of formation and degradation of hydroperoxides increases with increasing temperature [10]. Hydroperoxides are an important measure of oil quality as they are an indicator of the future levels of secondary oxidation products that negatively impact sensory

parameters. There are a variety of other factors, including fatty acid composition, lipid class composition, concentrations, and type of oxygen present, antioxidants and light, that can influence oxidation, and make accurate comparisons between oxidation studies difficult [9].

Tests of oxidative stability are commonly used to evaluate the shelf life of fish oils, but in order to complete testing in a reasonable amount of time, elevated temperature is frequently used to accelerate oxidation. The goal of this accelerated testing is to obtain results that can then be used to predict the shelf life of fish oil products that are stored under normal conditions [11]. For this to be possible, the kinetics of the oxidation reaction must be determined. Theoretically, oxidation rates can be monitored by following the degradation of specific FA. Though this has been attempted in fish oils [12], these oils have a complex FA profile and application of these techniques may not give an accurate representation of oxidation that is occurring in the oil as a whole. At normal oil storage temperatures the change in fatty acid profile happens very gradually and fatty acid analysis may not be sensitive enough to detect the minute changes in fatty acid concentration, making this method impractical to use for monitoring oxidation of fish oils. Rather than monitoring fatty acid composition of fish oils, other studies use oxygen concentrations to assess oxidation [e.g. 13, 14], a technique that may be more accurate for fish oil oxidation though it does not directly take into account the formation of oxidation products that could impart negative flavors into the oil. No studies could be found that attempt to decipher the kinetics of fish oil oxidation using a common oxidation indicator. The present study uses peroxide values (PV) to assess oxidation because these compounds are formed directly from lipids and therefore, the amount of hydroperoxides present can be directly related to the amount of oxidized lipid present at early stages of oxidation.

This study evaluates the stability of two commercially available liquid fish oil supplements for oxidative stability by monitoring hydroperoxide formation at a number of different temperatures, ranging from 4 °C to 60 °C to determine if oxidation of fish oil follows the Arrhenius model. This information is important to fish oil manufacturers as it will enable the application of accelerated stability data to real-time conditions, thereby reducing the time required to perform stability studies from years to weeks.

Experimental Procedures

Materials

Two different types of commercially available liquid fish oil supplements were obtained from a retail outlet. The first was NutraSea, a typical "18:12" fish oil, containing approximately 18% EPA and 12% DHA as proportions of total FA. The second was NutraSea HP, a fish oil "concentrate" containing approximately 30% EPA and 10% DHA. Both products were produced by Ascenta Health and contained winterized fish oil (97.86%), natural flavor (2%), alpha tocopherol (0.04%) and green tea catechins (0.1%). Amber bottles (200 ml) and lids were supplied by Ascenta Health. These products were marketed as fish oils and contained triacylglycerols (TAG) as the primary lipid at 70–75%. Monoacylglycerides (MAG) and diacylglycerides (DAG) were also preset at 20–25% and <5%, respectively.

Potassium iodide, 1% starch indicator, sodium chloride, butyl hydroxytoluene, boron trichloride-methanol, anhydrous sodium sulfate, Optima acetic acid and Optima isooctane were obtained from Fisher Scientific (Ottawa, ON). Optima chloroform was obtained from VWR (Mississauga, ON). An Isotemp 100 Series Model 126G oven (Fisher Scientific) was used to incubate samples. Methyl tricosenoate, methyl eicosapentaenoate, and methyl docosahexaenoate were obtained from Nu-Chek Prep (Elysian, MN).

Methods

Fatty Acid Analysis

Both fish oils were analyzed for EPA and DHA via GC-FID. Triacylglycerols were converted to methyl esters (ME) following the modified Global Organization for EPA and DHA Voluntary Monograph for Omega-3 [15], using methyl tricosenoate as an internal standard, as well as external standards for EPA and DHA. ME were separated using a column coated with (50% cyanopropyl)-methylpolysiloxane (30 m × 0.25 mm × 0.25 μm film thickness) and helium was used as the carrier gas at a flow rate of 1.0 ml/min. The oven temperature was initially held for 2 min at 153 °C then increased at 2.3 °C/min to 205 °C and held for 8.3 min. The total run time was approximately 32 min. The FID was maintained at 270 °C, and the injector (split mode 1:100, 4 mm liner) at 250 °C.

Stability Studies

Both oils were incubated in the dark at 4, 20, 40, and 60 °C. The 18:12 oil was also incubated at 30 °C. Three bottles were used for each incubation temperature. Bottles were capped but not purged with nitrogen after the initial opening. PV were measured in triplicate, with each bottle sampled at each time point, following AOCS Official Method Cd 8-53 [16]. Samples stored at 4 °C were initially tested weekly, but then were tested monthly after 3 months of testing. Samples stored at 20 °C were tested weekly, while samples stored at 30 and 40 °C were tested every 3 days. Samples stored at 60 °C were analyzed daily. Different

sampling periods were necessary to capture the variation in PV with changing oxidation rates. After removing an aliquot for sampling, each bottle was recapped and returned to the test temperature. Testing was stopped when an average peroxide value of 5 mequiv/kg was reached, as this is the maximum accepted value for fish oil as recommended by the Global Organization for EPA and DHA [15].

Determination of Rate Constants and Shelf Life Prediction

Kinetic analysis of data was carried out using methods adapted from Labuza [17], Labuza and Bergquist [18], Spears et al. [19] and Tan et al. [20]. Pseudo-first order conditions were assumed with the oil substrate in excess so that

$$-\mathrm{d}[\mathrm{O}_2] = \mathrm{d}[C]/\mathrm{dt} = kC \quad (1)$$

where C is the concentration of oxidation products, in this case the PV, and k is the rate constant. Integration leads to the classic relationship in first order kinetics:

$$\ln C = \ln C_\mathrm{o} + kt \quad (2)$$

where C_o is the initial concentration of oxidation products (PV at initial times) and t is time in days. Plots of ln PV versus time were linear with slopes of k for most trials. Rate constants derived from linear plots were then fit to an Arrhenius model:

$$\ln k = \ln A - E_\mathrm{a}/RT \quad (3)$$

where A is the prefactor, R is the universal gas constant, T is the absolute temperature and E_a is the activation energy in J/mol.

Because the ultimate goal of this study was to investigate the validity of shelf life prediction by extrapolating rate constants from high temperature to low temperature studies, we therefore examined the exponential relationship between the time require to reach the upper limit of acceptability (t_rej) and temperature, according to

$$t_\mathrm{rej} = ae^{T} \quad (4)$$

where a is a constant and t_rej is the time required to reach PV = 5 mequiv/kg, as the upper limit of acceptability for fish oil oxidation. Integration of this relationship gives

$$\ln t_\mathrm{rej} = a + \ln T \quad (5)$$

suggesting that a plot of ln t_rej versus T should be linear.

Results and Discussion

Fatty Acid Analysis

The amounts of EPA and DHA present in both the 18:12 and concentrate oils (Table 1) differed, as expected from their label claims. The 18:12 oil had a label specification of 269 mg/g while the concentrate specified 430 mg/g. Upon testing, both samples exceeded label claims for EPA and DHA with values of 286 and 499 mg/g, respectively. We therefore considered these oils to have significantly different PUFA contents. Complying with label claims was also important to establish that these oils were typical of commercial products currently available; the purpose of this study was to monitor oxidation in commercial products with added antioxidants and flavors that contained FA at expected levels.

Table 1 EPA and DHA content (mean ± SD) of 18:12 oil and concentrate oil compared to the label claim

	18:12	Concentrate
Omega-3 claim (mg/g)*	269	430
Actual EPA content (mg/g)	151 ± 0.97	349 ± 1.23
Actual DHA content (mg/g)	135 ± 1.23	150 ± 0.42
Total EPA + DHA content (mg/g)	286 ± 1.56	499 ± 1.30

* Manufacturer guarantees only the total sum of EPA+DHA, not the individual fatty acid content

Stability Studies

In the experimental design, pseudo-first order kinetics was assumed. For the initial setup, each bottle contained approximately 180 ml of fish oil with approximately 20 ml of headspace. This corresponds to approximately 0.6 mol of FA and 2×10^{-4} mol of O_2, with FA present in excess of 3,500 times the amount of O_2. This ensures that O_2 is limiting, a necessary criteria of pseudo-first order reactions. Even in the samples that had the longest testing period (22 time points, with 5 ml of oil being used at each point), this situation was maintained with 70 m of oil, and 130 ml of air. This is equivalent to 0.23 mol of FA and 1.3×10^{-3} mol of O_2, ensuring that FA were still present in excess of 176 times the amount of O_2. Resulting plots of PV versus time were therefore expected to increase exponentially over time (Fig. 1a, b) with linear fits for the corresponding regressions of ln PV versus time (Table 2). It should be noted that kinetics are typically modeled by monitoring the breakdown of reactants, while this study monitors the formation of oxidation products. Oxidation products have been used by a number of research groups including Labuza and Bergquist [18], Mancebo Campos et al. [21], and Gomez-Alonso et al. [22] to successfully model oxidation kinetics.

Despite ensuring that pseudo-first order conditions were met, the reaction was obviously not first order for several of the sample-temperature combinations. For example, at 4 °C the 18:12 oil showed a clear lag in the onset of oxidation (Fig. 1a) that did not fit the expected model. In fact,

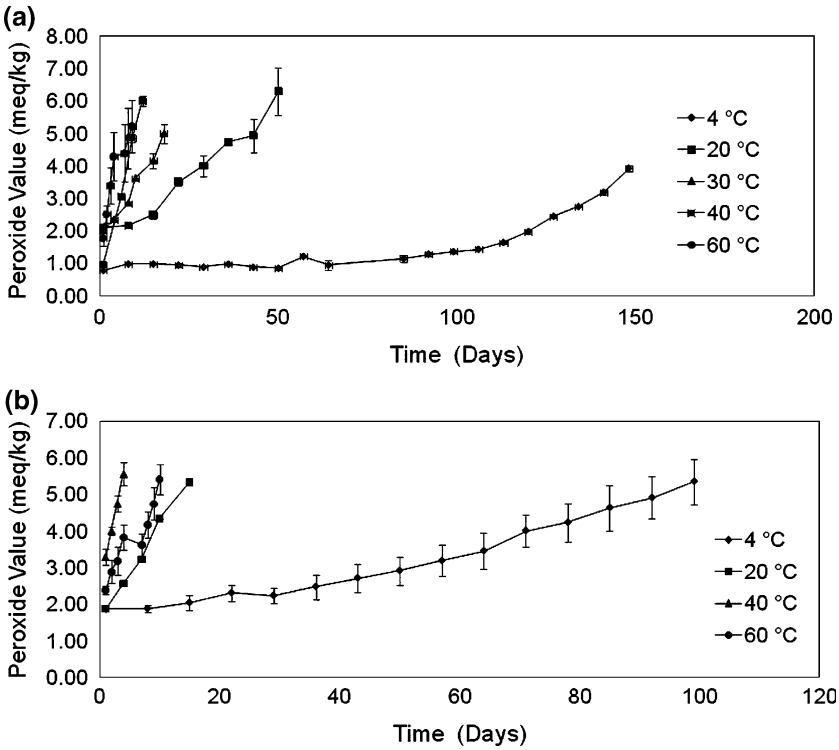

Fig. 1 Change in hydroperoxide value (mean ± SD, $n = 3$) at different temperatures over time. **a** 18:12 oil and **b** fish oil concentrate

Table 2 Testing temperatures, rate constants and coefficient of determinations for 18:12 oil and concentrate oil

Temperature (K)	18:12 oil		Concentrate oil	
	Rate constant (k days^{-1})	SD	Rate constant (k days^{-1})	SD
277	0.009	0.00	0.011	0.09
293	0.023	0.11	0.075	0.00
303	0.053	0.06	N/A	N/A
313	0.170	0.03	0.174	0.04
333	0.111	0.08	0.073	0.10
R^{2a}	0.822	–	0.524	–
R^{2b}	0.981	–	0.938	–

[a] Includes 60 °C data

[b] Excludes 4 and 60 °C data (18:12) or 60 °C data (concentrate)

modeling with zero and second order kinetics did not show any improvement at that temperature. Interestingly, the concentrate oil did follow a first order model quite well at 4 °C (Fig. 1b; Table 2), likely because of the absence of a prolonged lag phase. Both oils also deviated from the expected first-order model at 60 °C. This was less surprising as it is well accepted that the mechanisms for a complex chain reaction such as lipid oxidation may vary with increasing temperature [11]. For the purpose of this study, it was assumed that peroxide derivatives of fatty acids do not degrade; however, a large variety of secondary oxidation products are formed from these compounds as oxidation progresses. It may be that the increase in temperature increased the rate of both peroxide formation and breakdown; thus, the low rate constant derived at 60 °C for both oils suggests that peroxides are decomposing faster than they are being formed [9, 11]. Additionally, at elevated temperatures, lipid oxidation is more dependent on the concentration of oxygen. At high temperatures, the solubility of oxygen decreases, and becomes a limiting factor in lipid oxidation reactions as oxygen is rapidly consumed [11].

First-order kinetics were expected because of the experimental design, but all data was also evaluated for fit to a zero- and second-order model (Table 3). For a zero-order model, regression of PV versus time is linear, while for second-order models, one expects plots of 1/PV versus time to be linear. Coefficients of determination were simply used to assess fit (Table 3). In most cases it is quite obvious that a first-order model is as good as or better than other models (e.g., 18:12 oil at 20 and 30 °C). In other cases it is less obvious. For example, at both 40 and 60 °C for the 18:12 oil, a zero-order model has a slightly better fit to the data, while at 4 °C, the second order model has the best fit for the same oil. This is likely related to the high content of rapidly oxidizing PUFA that are present in fish oil.

Table 3 Coefficients of determination for 18:12 and concentrate fish oils when zero, first and second-order models were considered

Temperature (°C)	# of points	Zero-order	First-order	Second-order
18:12 Oil		r^2		
277	20	0.6993	0.8142	0.8648
293	8	0.9596	0.9429	0.9703
303	6	0.9752	0.9801	0.9572
313	4	0.9941	0.9539	0.8546
333	7	0.8777	0.8027	0.7052
Concentrate Oil		r^2		
277	15	0.9561	0.9876	0.9863
293	5	0.9429	0.9706	0.9105
313	4	0.9993	0.9969	0.9817
333	8	0.8812	0.8866	0.8603

All trials were stopped when the upper level for acceptability for fish oil, PV = 5 mequiv/kg, so that the duration of the experiment grew shorter as temperature increased. With daily sampling, this meant that fewer data points were acquired as temperature increased, making it difficult to fully capture the change in oil quality with time. The situation reached an extreme at 40 °C with both oils only requiring 4 days to exceed the upper limit of acceptability. Had sampling continued beyond this time point, the change in slope that is expected with first-order kinetics may have been captured. As plotted here, it is likely that only a small linear portion of a larger curve is being shown. Because we were only trying to model kinetics until the quality limit was reached and first-order kinetics fit well for 20 and 30 °C, it seemed appropriate to continue to model with first-order kinetics at the other temperatures. In addition, we were very reluctant to fit the data to a zero-order model in any situation. Zero-order kinetics dictates that reaction rate is independent of substrate concentration. Though both oils contain the same amount of fatty acid structures, the concentrate sample contained more PUFA, or substrate, that could be oxidized. Rates were obviously higher in the concentrate oil (Fig. 2; Table 2) so zero-order kinetics were ruled out immediately as an increase in PUFA increased the rate of peroxide formation. Finally, a first-order model was expected because others have found that oils containing antioxidants follow such models [17]. All this evidence pointed to the use of a first-order model when any ambiguity in model fit was encountered.

Arrhenius Behavior and Shelf Life Prediction

Rate constants for both oils were lower at 60 than at 40 °C; this result, combined with their poor fit to the first-order model, led to their exclusion from the Arrhenius plot. Similarly, because of the obvious lag time for onset of

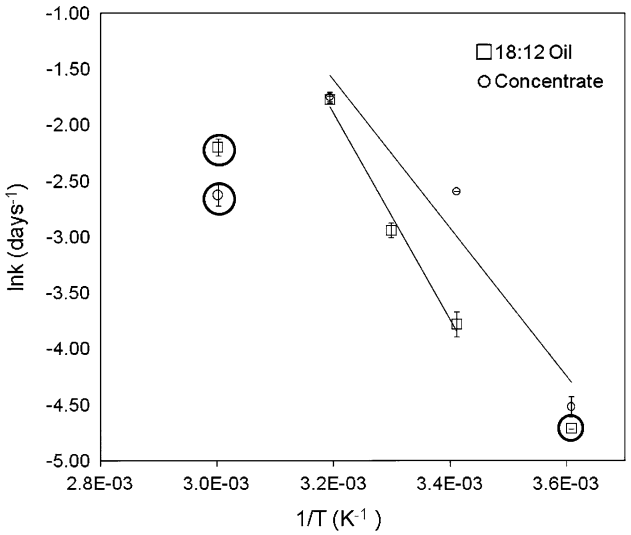

Fig. 2 Arrhenius plots for 18:12 oil (R^2 0.9871) and concentrate oil (R^2 0.9384). *Circled points* are not included in regression. Data are means ± SD

oxidation of 18:12 oil at 4 °C, the data collected at this temperature was also omitted from the plot for 18:12 oil, leaving only 3 data points for each oil. Despite the low sample numbers, we still see a good fit for both oils, with differing slopes. From the slopes, E_a of oxidation for the 18:12 and concentrate oils were calculated as 76 and 55 kJ/mol, respectively. The lower E_a for the concentrate oil was expected because less energy should be required to initiate oxidation due to the higher PUFA content. If the 4 °C data point is included in the 18:12 analysis (data not shown), the slopes are virtually identical, giving a very similar and highly unlikely E_a. This further points to the appropriateness of omitting the 4 °C data point in the 18:12 set. The E_a determined here are similar to those reported by Labuza [23] for lipid oxidation by free radical mechanisms (63–105 kJ\mol). With pure triglycerides (TAG), consisting of esterified DHA, Yoshii et al. [14] found similar E_a ranging from 77 to 97 kJ/mol, depending on the level of antioxidant added, and clearly showed that E_a increases with increased concentration of rosemary extract. With added antioxidants, both the fish oils examined here and those containing high levels of PUFA studied by Yoshii et al. [14], had E_a more similar to the stable vegetable oil from canola [24], pointing to the clear advantage of employing antioxidants to prevent oxidation.

The objective of this study was to determine the real time shelf life of these products by extrapolating from accelerated data. Data from experiments above 40 °C were therefore omitted from the shelf life plots (Fig. 3). This also agrees well with the recommendation by Frankel [11] that the temperature used for accelerated fish oil stability studies should not exceed 40 °C. This has obvious implications for fish oil stability studies that involve the use of

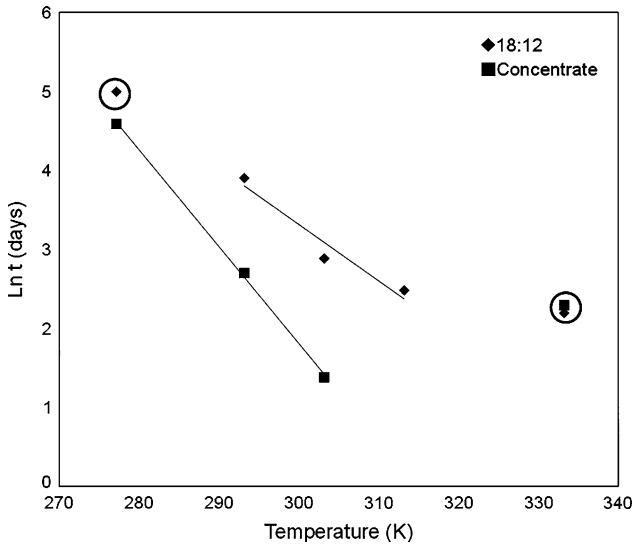

Fig. 3 Shelf life plots for 18:12 and concentrate fish oils. *Circled points* are not included in regression

oxygen absorption methods at elevated temperatures such as such as the Rancimat and Oxidative Stability Index (OSI) [25–27]. It is clear from the present study that PV of oils stored under Rancimat or OSI conditions will not be related to the PV of the same oils stored at temperatures <60 °C. Knowing that, the data for 4 °C in the 18:12 oil did not follow first order kinetics also led to its omission from the shelf life plot. Without that data, it is of course not possible to predict shelf life at temperatures <20 °C and >4 °C by interpolation. However, if the 4 °C data was included, the slope of the line would only change subtly so that the shelf life would be predicted at 143 days rather than the measured 148 days. This represents an error <4% and when considering data between 4 and 20 °C, the impact would be proportionally and absolutely less. Thus, one may cautiously extrapolate beyond the linear portion of the curve for 18:12 oil, knowing that the predicted shelf life would be under-estimated by no more than 4%. It is important to note that these equations only hold true for these specific products. Oils that have different fatty acid or lipid class profiles or use different antioxidants will likely have different rates of oxidation.

This study was designed to mimic the oxidation that might take place after a consumer has purchased a bottle of fish oil and has begun consuming it. The shelf lives measured here for storage at 4 °C for both oils (148 and 99 days for 18:12 and concentrate, respectively) agrees well with typical manufacturers' recommendations of 90 days in refrigeration. An obvious contrast is with freshly bottled fish oils, purged with inert gas, usually nitrogen. Exclusion of air in such products promotes much longer-term oxidative stability and we would not expect the kinetics of oxidation to be similar to those reported here. Studies to monitor such products would be logistically difficult to organize simply because sealed containers of oil could only be sampled once; after opening, the sample would be in contact with air and, even if again purged with nitrogen, rates of oxidation would be expected to vary. Thus, a very large amount of individually bottled oil would be required.

The lack of kinetic data between 4 and 20 °C is the largest flaw in this study. Had we included at least one data point in this range, we would have been much better able to characterize both the Arrhenius behavior and shelf life prediction. This is critical because it would have set a lower limit on temperatures to which we could interpolate without introducing a known minimum error. It would also have been useful to examine other measures of oxidation. Frankel [28] used volatile oxidation products to examine the kinetics of fish oil oxidation. Anisidine values are also recommended in the GOED Voluntary Monograph [15] as a quality measure of fish oil. These tests could allow us to investigate the relationship between primary and secondary oxidation and could help to determine if hydroperoxides are in fact breaking down at 60 °C. A substantial increase in either anisidines or volatile oxidation products would support our hypothesis of peroxide breakdown. Additionally, monitoring secondary oxidation would allow for the creation of shelf life plots that could potentially correlate with sensory characteristics of the oils and give a better indication of how consumers will perceive the oils. However, both parameters are difficult to accurately measure in commercial oils that have added flavors. Our experience has shown that flavor compounds co-elute with oxidation products in gas chromatographic analysis of volatiles, especially when headspace analysis techniques are utilized. While selective ion monitoring could potentially be used to monitor oxidation in co-eluting peaks, these techniques are beyond the scope of this paper. Flavor compounds also interfere with the *p*-anisidine test, causing drastic overestimation of the measure, sometimes outside the range of measurement. Thus, monitoring change in secondary kinetics with *p*-anisidine test would only be feasible in unflavored oils, which would not necessarily be relevant for shelf life studies of commercial dietary supplement.

Fish oil is a popular dietary supplement taken by many people for its health benefits. Because of the high PUFA content, the oil oxidizes rapidly. At temperatures ≥20 °C and ≤40 °C, 18:12 fish oil appears to follow first-order kinetics. Fish oil concentrate demonstrates first-order kinetics at temperatures ≥4 °C and ≤40 °C. At 60 °C both oils oxidized more rapidly, likely because of hydroperoxides breaking down faster than they could form. This confirms that accelerated stability studies using fish oil should be conducted at temperatures no higher than 40 °C. Accelerated temperature data can then be used to predict

shelf-life at lower temperatures; however, extrapolation of data should be done with caution as the rate of reaction may not hold true at low temperatures. This was the case for 18:12 oil as clearly demonstrated in this study.

References

1. Simopoulos AP (1991) Omega-3 fatty acids in health and disease and in growth and development. Am J Clin Nutr 54:438–463
2. Hu FB, Bronner F, Willet WC, Stampfer MJ, Rexrode KM, Albert CM, Hunter D, Manson JE (2002) Fish and omega-3 intake and risk of coronary heart disease in women. JAMA 287:1815–1821
3. Kris-Etherton PM, Harris WS, Appel LJ (2002) Fish consumption, fish oil, omega-3 fatty acid, and cardiovascular disease. Circulation 106:2747–2757
4. Lands WE (2005) Fish, Omega-3 and Human Health, 2nd edn, AOCS Press, Champaign
5. Leaf A (2006) Prevention of sudden cardiac death by n-3 polyunsaturated fatty acids. Fundam Clin Pharmacol 20:525–538
6. Innis SM (2008) Dietary omega-3 fatty acids and the developing brain. Brain Res 1237:35–43
7. World Health Organization (accessed Sept. 2008) Avoiding heart attacks and strokes
8. Min DB, Boff JM (2002) Chemistry and reaction of singlet oxygen in food. Comp Rev Food Sci F 1:58–71
9. Choe E, Min DB (2006) Mechanisms and factors for edible oil oxidation. Comp Rev Food Sci F 5:169–186
10. Shahidi F, Spurvey SA (1996) Oxidative stability of fresh and heat-processed dark and light muscles of mackerel (*Scomber scombrus*). J Food Lipids 3:13–25
11. Frankel EN (2005) Lipid oxidation, 2edn. The Oily Press Bridgewater, England
12. Bórquez R, Koller WD, Wolf W, Spieß W (1997) A rapid method to determine the oxidation kinetics of n-3 fatty acid in fish oil. Lebensm-Wiss Technol 30:502–507
13. Cho SY, Miyashita K, Miyazawa T, Fujimoto K, Kaneda T (1987) Autoxidation of ethyl eicosapentaenoate and docosahexaenoate. JAOCS 64:876–879
14. Yoshii H, Furuta T, Siga H, Moriyama S, Baba T, Maruyama K, Misawa Y, Hata N, Linko P (2002) Autoxidation kinetic analysis of docosahexanoic acid ethyl ester and docosahexanoic triglyceride with oxygen sensor. Biosci Biotechnol Biochem 66: 749–753
15. Global Organization for EPA and DHA (Accessed May 2008) Voluntary monograph for omega-3. http://www.goedomega3.com/
16. Official Methods and Recommended Practices of the American Oil Chemists' Society (1997) 4th edn., Firestone D (ed), Method Cd 8-53, American Oil Chemists' Society, Champaign
17. Labuza TP (1971) Kinetics of lipid oxidation in food. Crit Rev Food Technol 2:355–405
18. Labuza TP, Bergquist S (1983) Kinetics of oxidation of potato chips under constant temperature and Sine wave temperature conditions. J Food Sci 48:712–715
19. Spears RA, Tung MA, Jackman RL (1987) Prediction of colour deterioration in strawberry juice. Can I Food Sc Tech J 20:15–18
20. Tan CP, Che Man YB, Selamat J, Jusoff MSA (2001) Application of Arrhenius kinetics to evaluate oxidative stability in vegetable oils by isothermal differential scanning calorimetry. JAOCS 78:1133–1138
21. Mancebo-Campos V, Fragapane G, Desamparados Salvador M (2008) Kinetic study for the development of an accelerated oxidative stability test to estimate virgin olive oil potential shelf life. Eur J Lipid Sci 110:969–976
22. Gómez-Alonso S, Mancebo-Campos V, Descamparados Salvador M, Fregapane G (2004) Oxidation kinetics in olive oil triacylglycerols under accelerated shelf-life testing (25–75 °C). Eur J Lipid Sci 106:369–375
23. Labuza TP (1984) Application of chemical kinetics to deterioration of foods. J Chem Ed 61:348–358
24. Orlien V, Risbo J, Rantanen H, Skibsted LH (2006) Temperature-dependence of rate of oxidation of rapeseed oil encapsulated in a glassy food matrix. Food Chem 94:37–46
25. Méndez E, Sanhueza J, Speisky H, Valenzuela A (1996) Validation of the Rancimat test for the assessment of relative stability of fish oils. JAOCS 73:1033–1037
26. Luther M, Parry J, Moore J, Meng J, Zhang Y, Cheng Z, Yu L (2007) Inhibitory effect of Chardonnay and black raspberry on lipid oxidation in fish oil and their radical scavenging and antimicrobial properties. Food Chem 104:1065–1073
27. Yu L, Haley S, Perret J, Harris M (2002) Antioxidant properties of hard winter wheat extracts. Food Chem 4:457–461
28. Frankel EN (1993) Formation of headspace volatiles by thermal decomposition of oxidized fish oils vs. oxidized vegetable oils. JAOCS 70:767–772

Lipids (2011) 46:95–103
DOI 10.1007/s11745-010-3494-0

METHODS

Rapid Quantitative Analysis of Lipids Using a Colorimetric Method in a Microplate Format

Yu-Shen Cheng · Yi Zheng · Jean S. VanderGheynst

Received: 11 August 2010 / Accepted: 15 October 2010 / Published online: 11 November 2010

Abstract A colorimetric sulfo-phospho-vanillin (SPV) method was developed for high throughput analysis of total lipids. The developed method uses a reaction mixture that is maintained in a 96-well microplate throughout the entire assay. The new assay provides the following advantages over other methods of lipid measurement: (1) background absorbance can be easily corrected for each well, (2) there is less risk of handling and transferring sulfuric acid contained in reaction mixtures, (3) color develops more consistently providing more accurate measurement of absorbance, and (4) the assay can be used for quantitative measurement of lipids extracted from a wide variety of sources. Unlike other spectrophotometric approaches that use fluorescent dyes, the optimal spectra and reaction conditions for the developed assay do not vary with the sample source. The developed method was used to measure lipids in extracts from four strains of microalgae. No significant difference was found in lipid determination when lipid content was measured using the new method and compared to results obtained using a macro-gravimetric method.

Keywords Sulfo-phospho-vanillin · Microalgae · Macro-gravimetric

Abbreviations

SPV	Sulfo-phospho-vanillin
ATCC	American type culture collection
UTEX	The culture collection of algae
ANCOVA	Analysis of covariance
HSD	Honestly significant differences
vvm	Volume per volume per minute

Y.-S. Cheng · Y. Zheng · J. S. VanderGheynst (✉)
Department of Biological and Agricultural Engineering, University of California, One Shields Avenue, Davis, CA 95616, USA
e-mail: jsvander@ucdavis.edu

Introduction

Lipids are an important group of compounds that provide several biological functions such as energy storage, cell membrane structure and signaling [1, 2]. For this reason, lipid analyses are performed routinely in many different research areas. For example, the screening of oleaginous organisms has extensive application in both research and industry settings for identifying and producing food supplements and renewal biofuels [3–5]. In addition, in aquaculture processes analysis of lipid content in animals and microorganisms assists with monitoring the health conditions of the culture and developing growth strategies [6, 7]. Several methods have been developed to quantify total lipids. The most common approach is a macro-gravimetric method in which lipids are extracted from a sample, the extraction solvent is evaporated and the retained material is measured as the lipid content [8, 9]. This traditional gravimetrical method requires a relatively large quantity of sample and is time-consuming and labor-intensive when analysis of many samples is needed. Spectrofluorometric analysis of lipid, which uses the fluorescent dye Nile red, was originally developed by Greenspan et al. [10] and has also been modified for quantification of total lipids [11–14]. While this approach is high-throughput, environmental factors and other components in the cell cytoplasm, such as proteins and pigments, interfere with the assay and the fluorescence intensity varies between samples [14–16]. For

this reason accurate quantification of lipids using this approach requires that the optimal spectra and reaction conditions be determined for each type of sample prior to fluorescent measurements [13, 17].

The colorimetric sulfo-phospho-vanillin (SPV) method developed by Chabrol et al. [15, 18] is an attractive alternative for lipid measurement because of its fast response and relative ease in sample handling. The SPV method has been modified for diverse applications such as the determination of total lipids in serum, food and ecological samples [16, 19–23]. A micro scale modification of the SPV assay was developed by Van Handel [24] for determination of total lipids in a single mosquito, and assessed by several investigators as a more time and labor efficient approach compared to gravimetric methods [25–27]. In Inouye's report [25], 0.25 ml sample, 0.1 ml sulfuric acid and 2.4 ml vanillin reagent (1.2 mg vanillin per ml 68% phosphoric acid) were required for the micro-colorimetric assay. Similarly, in a report published by Lu et al. [27] 0.1 ml sample, 2.5 ml sulfuric acid and 5 ml vanillin reagent were needed to conduct the SPV assay on a micro scale. Both methods were completed in 13 × 100 mm culture tubes. Transfer of reactants to proper containers was required for absorbance measurement. Since color develops continuously, careful sample handing and control of color development are critical using this micro-scale approach.

The present work reports on an adaptation of the SPV method for completion of lipid quantification in a 96-well microplate for higher throughput and reduced costs. The adapted method involves an assay in which the reagent mixture is confined to one microplate for the entire assay. This enables faster measurement of multiple samples with easy background correction and more consistent monitoring of color development. As an example, total lipids in extracts from microalgae, which contain a dark green background, was successfully measured using this assay approach with corn oil as a standard.

Materials and Methods

Materials

Concentrated sulfuric acid, *o*-phosphoric acid (85%), chloroform and methanol, all ACS grade, were purchased from Thermo Fisher Scientific Inc (Waltham, MA, USA). Vanillin (≥98%) was purchased from Sigma-Aldrich (St. Louis, MO, USA). Commercial corn oil, canola oil, flax oil, sunflower oil and cod liver oil were obtained from local markets. A cholesterol standard for clinical work was purchased from MP biomedicals (Solon, OH, USA). Flat bottom, polystyrene 96-well microplates (Costar 3370) were obtained from Corning Incorporated (Corning, NY, USA).

Preliminary Assessment of General Assay Conditions

A preliminary microplate test was performed to determine the initial assay conditions. The general assay steps followed are presented in Fig. 1. The volume of reagents per well in the preliminary study included 100 µl of concentrated sulfuric acid and 100 µl vanillin–phosphoric acid reagent. Three concentrations of vanillin were examined (1, 0.5, and 0.1 mg vanillin per ml 68% phosphoric acid) to determine the suitable concentration for assay in a microplate format. Standard samples were prepared by mixing corn oil in solvent (chloroform:methanol = 1:1) at 15 mg/ml. Standards were added into each well of the microplate by varying the volume (0.5–30 µl) and then 100 µl concentrated sulfuric acid was added after the solvent was evaporated at 90 °C for about 10 min. The microplate was then incubated on a dry heating bath (Isotemp 125D, Thermo Fisher Scientific Inc.) at 90 °C for 10 min and cooled to room temperature on ice water (~2 min). A microplate reader (Model VMax, Molecular Device, Sunnyvale, CA, USA) with compatible software, Softmax v 2.43, was used to measure background absorbance. Then, 100 µl vanillin–phosphoric acid reagent was added for

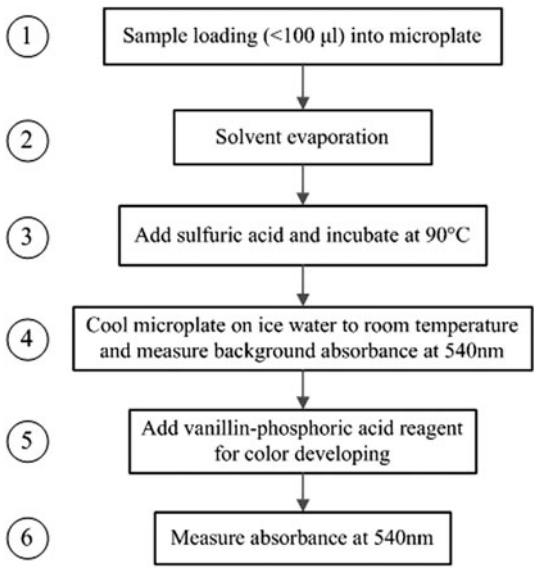

Fig. 1 General analysis procedures of SPV method in a microplate. Volumes of sulfuric acid and incubation times in *step 3*, and vanillin–phosphoric acid reagent levels and color development time in *step 5* were varied to determine the ideal assay conditions for high throughput microplate analysis of lipid

color development. Absorbance at 540 nm was measured after 5 min of color development.

Examination of Solvent Ratios for Sample Preparation

Solvent mixtures including four different ratios of chloroform and methanol (chloroform only, chloroform:methanol = 2:1, 1:1 and 1:2) were tested to determine the effect of sample preparation on the assay. Samples containing corn oil in solvent mixtures (15 mg corn oil per ml solvent) were pipetted into the microplate wells by varying the volume from 1 to 15 μl. The solvent was evaporated at 90 °C (~10 min), and then 100 μl concentrated sulfuric acid was added. The microplate was then incubated on a dry heating bath at 90 °C for 20 min. Absorbance at 540 nm was measured as background after the microplate was cooled to room temperature on ice water. Then, 100 μl vanillin–phosphoric acid reagent (0.5 mg vanillin per ml 68% phosphoric acid) was added for color development. Absorbance at 540 nm was measured after 5 min of development.

Examination of Vanillin and Phosphoric Acid Concentrations

After the sample preparation method was determined, concentrations of vanillin and phosphoric acid were investigated to determine their influence on the assay and if lower concentrations could be used in a high-throughput format. All assays used 100 μl vanillin–phosphoric acid reagent for color development. Four vanillin concentrations in 68% phosphoric acid were first tested at 0.5, 0.375, 0.25 and 0.125 mg/ml. After an ideal concentration of vanillin (0.25 mg/ml) was determined, four different concentrations of phosphoric acid (17, 34, 51 and 68%) were tested. To examine the possibility of further reducing vanillin in the assay, the vanillin concentration was optimized after the suitable concentration of phosphoric acid had been determined.

Volume of Vanillin Phosphoric Acid Reagent and Concentrated Sulfuric Acid

In an attempt to reduce water use and final volume, different volumes of vanillin phosphoric acid reagent were tested. Four volumes of vanillin phosphoric acid reagent (20, 25, 50, 100 μl) containing an equivalent amount of vanillin were first investigated to determine whether the volume of the reagent could be reduced by increasing the vanillin concentration. After the vanillin concentration in the phosphoric acid reagent and volume of vanillin phosphoric reagent in the assay were determined, the effect of concentrated sulfuric acid volume (100, 150 and 200 μl) on digestion was tested.

Examination of Reaction Time and Stability of Absorbance Linearity

To investigate the effect of reaction time on the assay, standard samples (10 mg corn oil per ml solvent) were loaded at varying volumes (12, 8, 4, 1 μl) in the assay with 100 μl concentrated sulfuric acid. The reaction time was varied from 10 to 60 min by carefully transferring samples from the original microplate to a new one at 10 min intervals. The new microplate was maintained on ice water until all the samples were transferred. After all samples had been cooled and background absorbance had been measured, 50 μl of vanillin–phosphoric acid reagent (0.2 mg vanillin per ml 17% phosphoric acid) was added to each well. To test the stability of absorbance linearity, absorbance measurements made at 540 nm were recorded from 5 min to 3.5 h after vanillin–phosphoric acid reagent addition.

Relative Absorbance and Linearity of Different Lipid Samples

To survey the applicability of the assay, six different lipid samples, including corn oil, canola oil, flax oil, sunflower oil, cod liver oil and cholesterol, were tested in the range 5–150 μg by varying loading volume of standard solutions (10 mg lipid per ml solvent). After the solvent was evaporated, 100 μl concentrated sulfuric acid was added to each well and then the microplate was incubated at 90 °C for 20 min. 50 μl of vanillin–phosphoric acid reagent (0.2 mg vanillin per ml 17% phosphoric acid) was added to each well for color development. Absorbance at 540 nm was measured after 10 min of development.

Applicability of the Assay for Measuring Lipid Extracted from Microalgae

Four different strains of microalgae, *Chlorella vulgaris* UTEX 259, *Chlorella sorokiniana* UTEX 2805, *Chlorella minutissima* UTEX 2341 and *Chlorella* sp. NC64A were obtained from The Culture Collection of Algae (UTEX) and American Type Culture Collection (ATCC). *Chlorella* UTEX 259 and UTEX 2805 were cultured in inorganic N8 medium, and *Chlorella* UTEX 2341 and NC64A were cultured in N8Y medium prepared by adding 0.1% yeast extract in N8 medium. All strains were cultured at 25 °C with either ambient air supply at 1 vvm or 2% CO_2 at 0.5 vvm in 1-l glass bottles and irradiated with fluorescent light at ~2,000 Lux on a 16:8 h light/dark cycle. Cultures were harvested in the late log phase of growth, centrifuged

at 2,000*g* and the retained pellet was lyophilized. The lipid extraction and purification methods were according to Folch [9] with slight modifications. Samples of purified lipid extracts were mixed with twice the volume of methanol for the colorimetric assay in a microplate, and the results were compared with the total lipid measured using the macro-gravimetric method [25].

Data Analysis

Linearity was determined by plotting absorbance versus lipid amount in the assay and examining the R^2 value upon linear regression of the data. Analysis of covariance (ANCOVA) and Tukey's HSD test were used to assess differences in the mean slope obtained upon linear regression of absorbance versus lipid amount. A paired *t* test and a graphical statistic paired test based on Bland's method [28] were performed to evaluate the agreement between the developed method and the macro-gravimetric method when lipid samples from microalgae were analyzed. Paired *t* tests, ANCOVA and Tukey's HSD tests were performed using JMP IN v.8.0 (SAS Institute Inc. Cary, NC, USA).

Results and Discussion

Preliminary Test of Assay Conditions

A preliminary microplate test was performed to determine a suitable range of vanillin in the assay. All tested concentrations (1, 0.5, and 0.1 mg vanillin per ml 68% phosphoric acid) gave good linearity of absorbance ($R^2 > 0.95$) at 540 nm in the range of 15–120 μg lipid (Data not shown). Vanillin concentration at 0.5 mg/ml gave a sufficient and relatively linear result, and therefore was selected as the starting point for optimization. Although the preliminary test showed very good linearity, there were some samples with noticeable film development and corrosion in the bottom of the wells of the microplate that might interfere with the reaction between lipid and sulfuric acid and affect color development. Therefore, different solvent ratios were also included in the development of the method.

Development of Reaction Conditions

Sample Preparation in Different Solvent Combinations

Only the samples prepared in a chloroform:methanol ratio of 2:1 had clear reactions and differences in color development (Fig. 2). In some of the tests using chloroform:methanol ratios of 2:1 and 1:1, corrosion and film development occurred in the bottom of wells. The corrosion might indicate intolerance of polystyrene to these solvent combinations, although the solvent was completely evaporated in a very short time (<10 min). The test of lipid measurement using chloroform only did not show any corrosion, however, a very thick and sticky layer formed when sulfuric acid was added, and color development was less than tests of lipid in other solvent combinations (Fig. 2). This phenomenon was also observed when the assay was performed in polypropylene microtubes, which suggests that the lipid layer might form because of overdrying when the solvent is evaporated rather than solvent intolerance of the assay container. Although the thick and sticky lipid layer could be dissolved after intensive mixing, this would not be suitable for an assay in a microplate where intensive mixing may be difficult to perform.

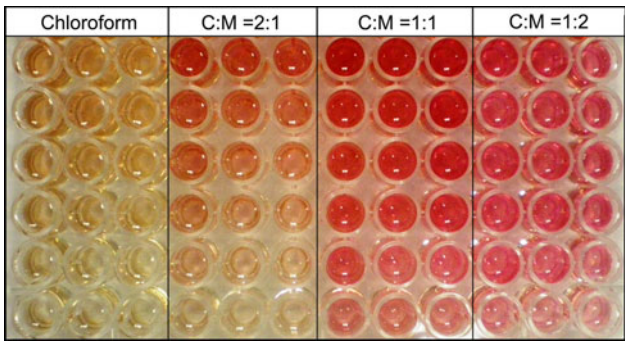

Fig. 2 Influence of solvent combinations on reaction and color development. *C* chloroform, *M* methanol. Samples (corn oil in solvent, 15 mg/ml) were added from 1 to 15 μl and incubated with 100 μl concentrated H_2SO_4 at 90 °C for 20 min. 100 μl vanillin–phosphoric acid reagent (0.5 mg vanillin per ml 68% phosphoric acid) was added for color development. Absorbance measurements were made after 5 min of color development. Sample loading volumes from top to bottom are 15, 12, 9, 6, 3, and 1 μl)

Concentration of Vanillin and Phosphoric Acid

Four different vanillin concentrations were tested based on the results from the preliminary test described earlier. When concentrated sulfuric acid addition was fixed at 100 μl, all concentrations of vanillin in 68% phosphoric acid tested in this study gave an even linearity of absorbance at 540 nm in the range 7.5–120 μg lipid (Fig. 3). In order to balance the conservation of vanillin use and sufficiency of absorbance, 0.25 mg/ml vanillin in 68% phosphoric acid was selected for the following optimization of phosphoric acid concentration. The purpose of testing different phosphoric acid concentrations was to investigate the possibility of using a lower amount of phosphoric acid while retaining linearity and sufficient absorbance. According to a previous report [18], when phosphoric acid concentration was varied between 17.6 and 70.4%, the

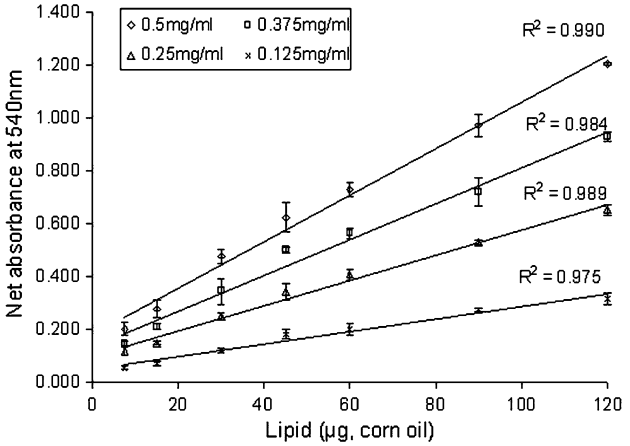

Fig. 3 Influence of vanillin concentration in vanillin–phosphoric acid reagent on color development. The vanillin–phosphoric acid reagent was prepared with 68% phosphoric acid. Samples were incubated with 100 µl concentrated H_2SO_4 at 90 °C for 20 min. 100 µl vanillin–phosphoric acid reagent was added for color development. Absorbance measurements were made after 5 min of color development. *Data points* and *error bars* represent the mean and standard deviation of three replicate samples

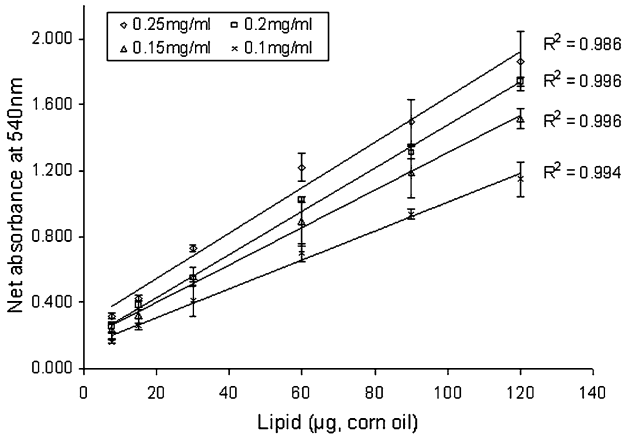

Fig. 5 Optimization of vanillin concentration in vanillin–phosphoric acid reagent for color development. The vanillin–phosphoric acid reagent was prepared with 17% phosphoric acid. Samples were incubated with 100 µl concentrated H_2SO_4 at 90 °C for 20 min. 100 µl vanillin–phosphoric acid reagent was added for color development. Absorbance measurements were made after 5 min of color development. *Data points* and *error bars* represent the mean and standard deviation of three replicate samples

higher concentration provided a greater and more stable color response. Thus, four different concentrations in this range were selected for testing. Figure 4 shows that lower phosphoric acid concentration gave a higher absorbance. This is in contrast to previous reports. The result suggests that the water content in the reagent might play a role in promoting the color response and an increase in the stability. Based on this result, the concentration of vanillin was further optimized. Figure 5 shows that the reduced vanillin concentration in 17% phosphoric acid provided equivalent absorbance linearity at 540 nm. Thus, vanillin concentration at 0.1 mg/ml was selected for the next study.

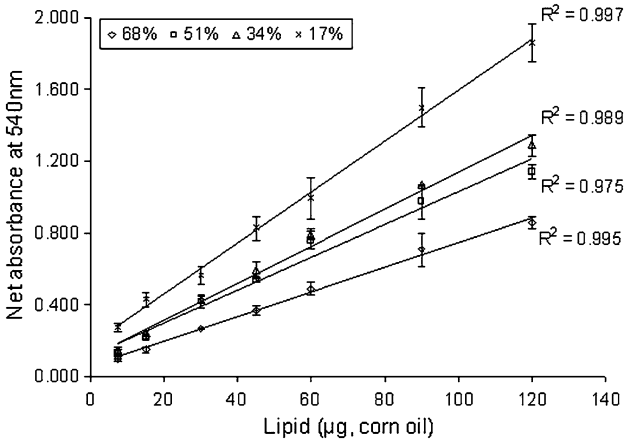

Fig. 4 Influence of phosphoric acid concentration in vanillin–phosphoric acid reagent on color development. The vanillin concentration was fixed at 0.25 mg/ml. Samples were incubated with 100 µl concentrated H_2SO_4 at 90 °C for 20 min. 100 µl vanillin–phosphoric acid reagent was added for color development. Absorbance measurements were made after 5 min of color development. *Data points* and *error bars* represent the mean and standard deviation of three replicate samples

Volumes of Vanillin–Phosphoric Acid Reagent and Concentrated Sulfuric Acid

In an attempt to reduce water use associated with the vanillin reagent, four volumes containing an equivalent amount of vanillin in 17% phosphoric acid were examined. Volumes of 100 µl (0.1 mg/ml) and 50 µl (0.2 mg/ml) provided fairly even linearity of absorbance compared to 20 µl (0.4 mg/ml) and 25 µl (0.5 mg/ml) (Fig. 6).

The volume of concentrated sulfuric acid might affect the reaction quality. In one report, the results were more consistent when the volume of concentrated sulfuric acid was more than 100 µl [25]. Therefore, sulfuric acid volumes of 100, 150 and 200 µl were examined to determine the effect of sulfuric acid loading volume on the color response and stability. Figure 7 shows that higher sulfuric acid volume did not result in better linearity and color development. The results suggest that a moderate ratio between water and sulfuric acid is important for color development.

Reaction Time and Stability of Absorbance Linearity

In the published format of the micro-scale assay, samples were incubated with concentrated sulfuric acid at 100 °C for 10 min. Previous reports also indicated that the heating temperature will affect the color response [19]. Because of

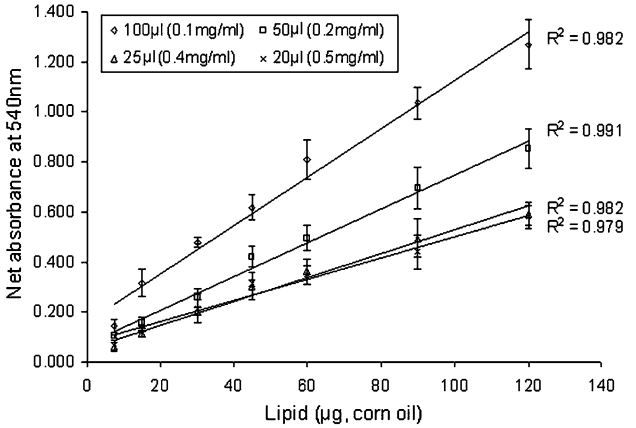

Fig. 6 Influence of the volume of vanillin–phosphoric acid reagent for color development. Vanillin–phosphoric acid reagents were prepared in 17% phosphoric acid. Samples were incubated with 100 μl concentrated H_2SO_4 at 90 °C for 20 min. Vanillin–phosphoric acid reagent was added for color development. Absorbance measurements were made after 5 min of color development. *Data points* and *error bars* represent the mean and standard deviation of three replicate samples

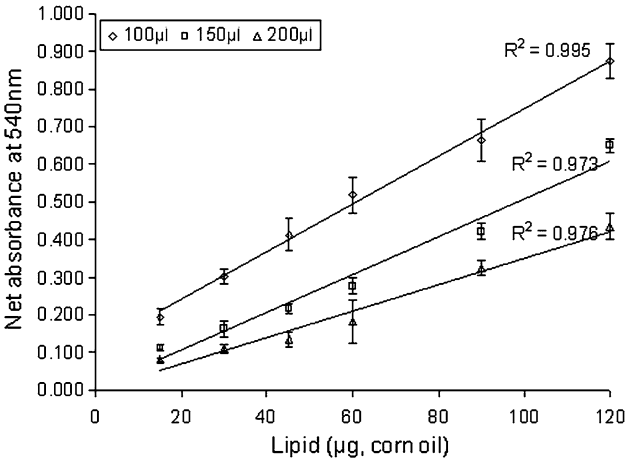

Fig. 7 Influence of volume of concentrated sulfuric acid for color development. Samples were incubated at 90 °C for 20 min. 50 μl Vanillin–phosphoric acid reagent (0.2 mg vanillin per ml 17% phosphoric acid) was added for color development. Absorbance measurements were made after 5 min of color development. *Data points* and *error bars* represent the mean and standard deviation of four replicate samples

the temperature limitation of polystyrene, the reaction temperature was set at 90 °C and longer incubation times were used to compensate for the temperature difference. Figure 8a shows that at a reaction time of 20 min, the absorbance increased with color development time. Linearity in absorbance was stable for 3.5 h and the results from different reaction times showed a similar pattern. While longer reaction times produced higher background absorbance (Data not shown), the total absorbance was only slightly increased (Fig. 8b). Since color develops

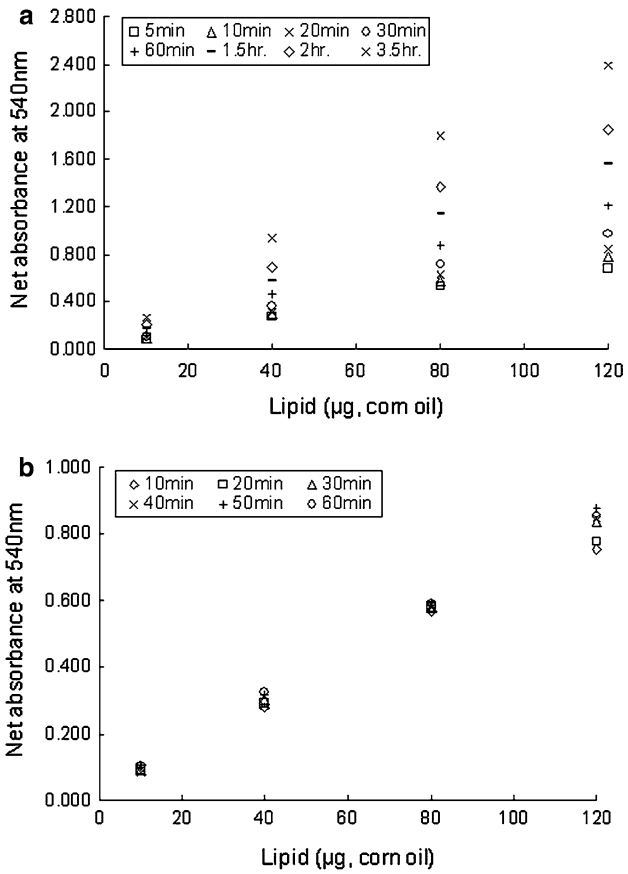

Fig. 8 Test of reaction time and stability for color development. **a** 20 min reaction time with color development from 5 min to 3.5 h, **b** 10–60 min reaction time with 10 min color development. 50 μl vanillin–phosphoric acid reagent (0.2 mg vanillin per ml 17% phosphoric acid) was added for color development. *Data points* represent the mean of three replicate samples

continuously, laborious transfer of the reaction mixture for absorbance readings causes considerable error when large numbers of samples need to be measured. In the developed assay, because the samples and standards are on the same sample plate and read at the same time, the timing error is minimized.

Relative Absorbance and Linearity of Pure Lipid Samples

Previous reports indicated that selecting an appropriate standard was important for assessing lipid content in different types of samples [18, 19, 29]. Thus, different types of oil and cholesterol were tested using the new assay format (Fig. 9). The slope of the standard curve was significantly affected by lipid type ($p < 0001$). Standard slopes for cod liver oil and cholesterol were significantly lower than slopes for plant oils (Table 1). There were no significant differences in slopes among the plant oils, except flax oil which was different from all other oils

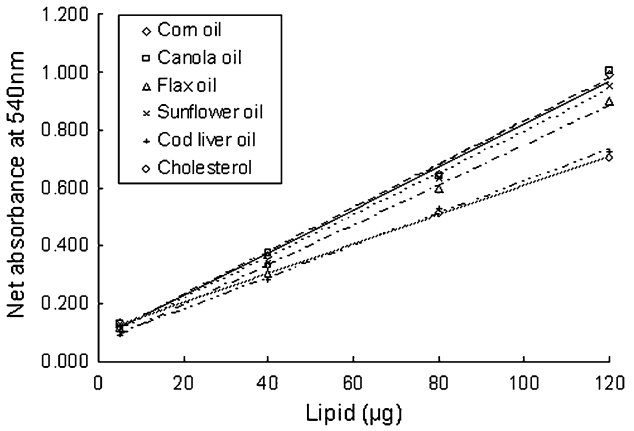

Fig. 9 Absorbance linearity of different lipid types. Samples were incubated with 100 µl concentrated H_2SO_4 at 90 °C for 20 min. 50 µl vanillin–phosphoric acid reagent (0.2 mg vanillin per ml 17% phosphoric acid) was added for color development. Absorbance measurements were made after 10 min of color development. Data points represent the mean of three replicate samples

Table 1 Mean slopes from standard curves measured using developed method

Lipid type	Mean slope (Au/µg)*
Canola oil	0.00755 A
Corn oil	0.00746 A
Sunflower oil	0.00721 AB
Flax oil	0.00685 B
Cholesterol	0.00502 C
Cod liver oil	0.00554 C

* Means followed by the same letter within columns are not significantly different according to Tukey's HSD means comparison test ($n = 3$), $p < 0.05$

except sunflower oil. Cod liver oil and cholesterol were also statistically equivalent (Table 1). Like other methods, standard selection should be based on the source of the sample (i.e., plant or animal) for the microplate method.

Final Microplate Procedure

The final procedure involves the addition of <100 µl of samples and standards that contain 5–120 µg lipids directly into the bottom of microplate wells. After the solvent is evaporated at 90 °C, 100 µl of concentrated sulfuric acid is added to each well. Then, the microplate is incubated at 90 °C for 20 min. Background absorbance at 540 nm is measured when the microplate is cooled to room temperature on ice water (~2 min). 50 µl of vanillin–phosphoric acid reagent (0.2 mg vanillin per ml 17% phosphoric acid) is added to each well for color development for 10 min, and then absorbance is measured at 540 nm. Since the heating and cooling steps will affect the absorbance, evenly heating and cooling the reaction mixtures are critical for having good absorbance linearity. Thus, performing the incubation in a microplate dry heating module or on a water bath with careful handling is recommended.

Applicability of the Assay for Measuring Solvent Extracted Lipid from Microalgae

Since the SPV method has been reported to have a variable response to varying sources of lipids [30], lipids extracted from four different strains of green microalgae were analyzed using the macro-gravimetric method and compared to the new microplate assay. Corn oil was used as the standard for the colorimetric method because microalgal lipids usually have a higher unsaturated ratio and are relatively close in composition to vegetable oil [16, 31–34]. The determined total lipids were converted to lipid percentage of dry algal biomass. Figure 10a shows the correlation of lipid percentage between the microplate format of the SPV method and the macro-gravimetric

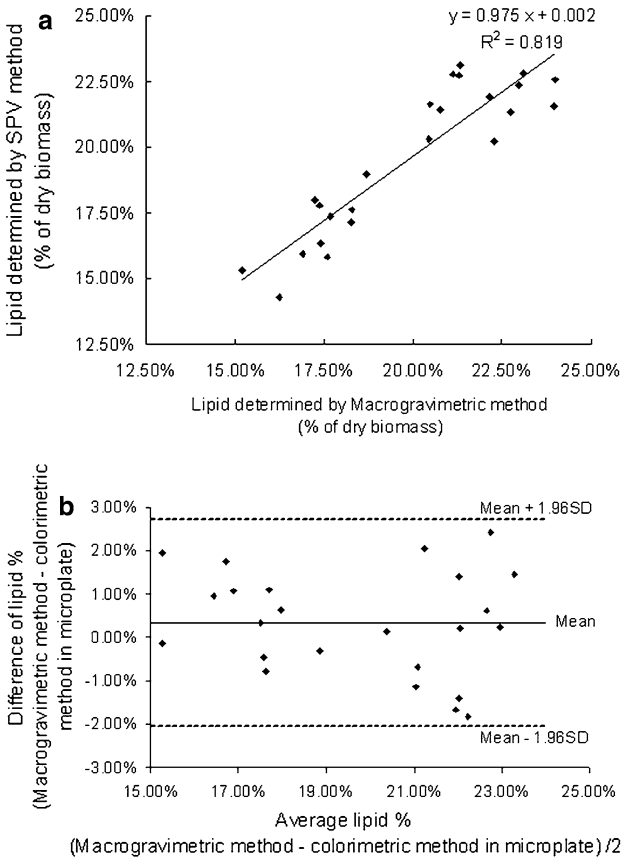

Fig. 10 **a** The correlation between lipid percentage of algae determined using the microplate colorimetric method and macro-gravimetric method. **b** Difference against average of macro-gravimetric and microplate format colorimetric measurement of lipid percentage with 95% limits of agreement (*dashed lines*)

method; there is a strong correlation between the macro-gravimetric method and the microplate format SPV method ($R^2 = 0.819$, $F = 99.72$, $p < 0.0001$). Figure 10b shows that the mean difference and standard deviation are 0.33 and 1.21% (test pairs = 24), respectively, and all differences fall between the 95% limits of agreement. Moreover, the matched paired t test is 1.35 ($p = 0.19$, two tails), which provides evidence that there is no significant difference between the microplate format of the SPV method and the macro-gravimetric method. This result is consistent with an earlier report [29] and suggests that the new SPV method in a microplate format can be applied for the quantification of total lipids from different types of microalgae samples with proper standard selection.

Conclusion

Total lipid quantification is frequently performed in many research areas with different types of samples. The present work reports on a modified colorimetric method for quantitative analysis of total lipid using a high-throughput microplate format. The presented method uses extracted and purified lipid samples. The extraction step minimizes interferences associated with other components in the sample and allows different samples from a variety of research areas to be analyzed using the same conditions. This approach could be very useful when screening the lipid content in different cell cultures and plants. With the development of high-throughput cell disruption technologies such as 96-well plate bead beaters and microwave extraction [35], lipid extraction from large numbers of samples could be done in minutes.

The new assay method possesses many advantages: (1) it requires a small amount sample and the sample volume can be adjusted to fit in the standard range, (2) it requires less time (<1 h) and less labor when a large number of samples is analyzed, and (3) the color development is more consistent with modifications of reagent concentrations. Moreover, the reagents are confined in the microplate through the entire assay procedure, which enables fast and accurate reading of multiple samples. In the final procedure, it is recommended that the volume of the sample should be less than 100 µl in order to ensure a complete reaction with the sulfuric acid. In addition, uniform heating and cooling are important for consistency in the reaction. The method was validated against the macro-gravimetric method. When corn oil was used as a standard, statistically equivalent results were achieved when both methods were used to measure total lipids in four different strains of *Chlorella*.

Acknowledgments Support for this research was provided by Chevron Technology Ventures and the University of California Energy Institute. The authors wish to thank Orn-u-ma Tanadul for assistance with preparation of algae and assays.

References

1. Wang X (2004) Lipid signaling. Curr Opin Plant Biol 7(3): 329–336
2. Wymann MP, Schneiter R (2008) Lipid signalling in disease. Nat Rev Mol Cell Biol 9(2):162–176
3. Colin R, Zvi C (2008) Microbial and algal oils: do they have a future for biodiesel or as commodity oils? Lipid Technol 20(7):155–160
4. Papanikolaou S, Komaitis M, Aggelis G (2004) Single cell oil (SCO) production by *Mortierella isabellina* grown on high-sugar content media. Bioresour Technol 95(3):287–291
5. Ratledge C (2002) Regulation of lipid accumulation in oleaginous micro-organisms. Biochem Soc Trans 30(Pt 6):1047–1050
6. Post JR, Parkinson EA (2001) Energy allocation strategy in young fish: allometry and survival. Ecology 82(4):1040–1051
7. Rinchard J, Czesny S, Dabrowski K (2007) Influence of lipid class and fatty acid deficiency on survival, growth, and fatty acid composition in rainbow trout juveniles. Aquaculture 264(1–4): 363–371
8. Bligh EG, Dyer WJ (1959) A rapid method of total lipid extraction and purification. Can J Biochem Physiol 37(8):911–917
9. Folch J, Lees M, Sloane-Stanley GH (1957) A simple method for the isolation and purification of total lipids from animal tissues. J Biol Chem 226(1):497–509
10. Greenspan P, Mayer E, Fowler S (1985) Nile red: a selective fluorescent stain for intracellular lipid droplets. J Cell Biol 100(3):965–973
11. Chen W, Zhang C, Song L, Sommerfeld M, Hu Q (2009) A high throughput Nile red method for quantitative measurement of neutral lipids in microalgae. J Microbiol Methods 77(1):41–47
12. Fowler S, Greenspan P (1985) Application of Nile red, a fluorescent hydrophobic probe, for the detection of neutral lipid deposits in tissue sections: comparison with oil red O. J Histochem Cytochem 33(8):833–836
13. Huang G-H, Chen G, Chen F (2009) Rapid screening method for lipid production in alga based on Nile red fluorescence. Biomass Bioenergy 33(10):1386–1392
14. Kimura K, Yamaoka M, Kamisaka Y (2004) Rapid estimation of lipids in oleaginous fungi and yeasts using Nile red fluorescence. J Microbiol Methods 56(3):331–338
15. Chabrol E, Charonnet R (1937) Une novelle reaction pour l'etude des lipides. Presse Med 45:1713
16. Desvilettes CH, Bourdier G, Amblard CH, Barth B (1997) Use of fatty acids for the assessment of zooplankton grazing on bacteria, protozoans and microalgae. Freshw Biol 38(3):629–637
17. Greenspan P, Fowler S (1985) Spectrofluorometric studies of the lipid probe, Nile red. J Lipid Res 26(7):781–789
18. Johnson KR, Ellis G, Toothill C (1977) The sulfophosphovanillin reaction for serum lipids: a reappraisal. Clin Chem 23(9): 1669–1678
19. Knight JA, Anderson S, Rawle JM (1972) Chemical basis of the sulfo-phospho-vanillin reaction for estimating total serum lipids. Clin Chem 18(3):199–202
20. Nakamatsu Y, Tanaka T (2004) Food resource use of hyperparasitoid *Trichomalopsis apanteloctena* (Hymenoptera: Pteromalidae), an idiobiotic ectoparasitoid. Ann Entomol Soc Am 97(5): 994–999

21. Visavadiya NP, Narasimhacharya AVRL (2007) Asparagus root regulates cholesterol metabolism and improves antioxidant status in hypercholesteremic rats. eCAM:nem091
22. Turlo J, Gutkowska B, Herold F (2010) Effect of selenium enrichment on antioxidant activities and chemical composition of *Lentinula edodes* (Berk.) Pegl. mycelial extracts. Food Chem Toxicol 48(4):1085–1091
23. Haskins SD, Kelly DG, Weir RD (2010) Novel pressurized solvent extraction vessels for the analysis of polychlorinated biphenyl congeners in avian whole blood. Anal Chim Acta (in press, corrected proof)
24. Van Handel E (1985) Rapid determination of total lipids in mosquitoes. J Am Mosq Control Assoc 1(3):302–304
25. Inouye LS, Lotufo GR (2006) Comparison of macro-gravimetric and micro-colorimetric lipid determination methods. Talanta 70(3):584–587
26. Landrum PF, Gedeon ML, Burton GA, Greenberg MS, Rowland CD (2002) Biological responses of *Lumbriculus variegatus* exposed to fluoranthene-spiked sediment. Arch Environ Contam Toxicol 42(3):292–302
27. Lu Y, Ludsin SA, Fanslow DL, Pothoven SA (2008) Comparison of three microquantity techniques for measuring total lipids in fish. Can J Fish Aquat Sci 65(10):2233–2241
28. Martin Bland J, Altman DG (1986) Statistical methods for assessing agreement between two methods of clinical measurement. Lancet 327(8476):307–310
29. Ahlgren G, Merino L (1991) Lipid analysis of freshwater microalgae: a method study. Archiv für Hydrobiologie 121(3): 295–306
30. Barnes H, Blackstock J (1973) Estimation of lipids in marine animals and tissues: detailed investigation of the sulphophosphovanilun method for 'total' lipids. J Exp Mar Biol Ecol 12(1):103–118
31. Isik O, Sarihan E, Kusvuran E, Gul O, Erbatur O (1999) Comparison of the fatty acid composition of the freshwater fish larvae *Tilapia zillii*, the rotifer *Brachionus calyciflorus*, and the microalgae *Scenedesmus abundans*, *Monoraphidium minitum* and *Chlorella vulgaris* in the algae-rotifer-fish larvae food chains. Aquaculture 174(3–4):299–311
32. Khasanova VM, Gusakova SD, Taubaev TT (1978) Composition of the neutral lipids of *Chlorella vulgaris*. Chem Nat Comp 14(1):37–40
33. Tsuzuki M, Ohnuma E, Sato N, Takaku T, Kawaguchi A (1990) Effects of CO_2 concentration during growth on fatty acid composition in microalgae. Plant Physiol 93(3):851–856
34. Hill AM, Feinberg DA (1984) Fuel from microalgae lipid products. p Medium, ED, Size, pp 17–30
35. Lee J-Y, Yoo C, Jun S-Y, Ahn C-Y, Oh H-M (2010) Comparison of several methods for effective lipid extraction from microalgae. Bioresour Technol 101(Suppl 1):S75–S77

Lipids (2011) 46:105–119
DOI 10.1007/s11745-010-3501-5

REVIEW

The Health Promoting Properties of the Conjugated Isomers of α-Linolenic Acid

Alan A. Hennessy · R. Paul Ross · Rosaleen Devery · Catherine Stanton

Received: 3 September 2010 / Accepted: 3 November 2010 / Published online: 15 December 2010

Abstract The bioactive properties of the conjugated linoleic acid (CLA) isomers have long been recognised and are the subject of a number of excellent reviews. However, despite this prominence the CLA isomers are not the only group of naturally occurring dietary conjugated fatty acids which have shown potent bioactivity. In a large number of in vitro and in vivo studies, conjugated α-linolenic acid (CLNA) isomers have displayed potent anti-inflammatory, immunomodulatory, anti-obese and anti-carcinogenic activity, along with the ability to improve biomarkers of cardio-vascular health. CLNA isomers are naturally present in high concentrations in a large variety of seed oils but can also be produced in vitro by strains of lactobacilli and bifidobactena through the activity of the enzyme linoleic acid isomerase on α-linolenic acid. In this review, we will address the possible therapeutic roles that CLNA may play in a number of conditions afflicting Western society and the mechanisms through which this activity is mediated.

Keywords CLA · Catalpic · Eleostearic · Calendic · Punicic · Cancer · Obesity · Atherosclerosis · Inflammation

A. A. Hennessy · R. P. Ross · C. Stanton (✉)
TEAGASC, Moorepark Food Research Centre,
Fermoy, Co. Cork, Ireland
e-mail: catherine.stanton@teagasc.ie

R. Devery
National Institute for Cellular Biotechnology,
Dublin City University, Dublin, Ireland

A. A. Hennessy · R. P. Ross · C. Stanton
Alimentary Pharmabiotic Centre, Cork, Ireland

Abbreviations

CLNA	Conjugated α-linolenic acid
CLA	Conjugated linoleic acid
COX-2	Cyclooxygenase-2
HDL	High density lipoprotein
IFN-γ	Interferon-γ
Ig	Immunoglobulin
LDL	Low density lipoprotein
LETO	Long–Evans Tokusima Otsuka
NF-kB	Nuclear factor kappa B
OLETF	Otsuka Long Evans Tokushima Fatty
PPAR	Peroxisome proliferator-activated receptor
SREBP	Sterol regulatory element binding protein(s)
TAG	Triacylglycerol
TNF-α	Tumor necrosis factor α
VLDL	Very low density lipoprotein

Introduction

Numerous investigations have attributed bio-functional properties to a range of conjugated fatty acids of which the conjugated linoleic acid (CLA) isomers are best characterized [1–3]. The health promoting attributes of the CLA isomers have been reported in detail, however, there are currently few reviews which address the other major group of naturally occurring conjugated fatty acids, the conjugated α-linolenic acid (CLNA) isomers. CLNA isomers combine the conjugated double bond system of CLA with the octadecatrienoic fatty acid (C18:3) structure of α-linolenic acid, conferring these fatty acids with a high bioactive potential. Structurally, CLNA isomers are positional and geometric isomers of α-linolenic acid, and similar to

CLA isomers, are characterized by having one or more double bonds in the *cis* (*c*) or *trans* (*t*) conformation, which are separated by simple carbon–carbon linkage as opposed to being separated by a methylene group (Fig. 1).

In nature, CLNA isomers are readily found in abundance in pomegranate seed (*c*9,*t*11,*c*13 CLNA), tung seed (*c*9,*t*11,*t*13 CLNA), bitter gourd seed (*c*9,*t*11,*t*13 CLNA), snake gourd seed (*c*9,*t*11,*t*13 CLNA), parwal seed (*c*9,*t*11,*t*13 CLNA), catalpa seed (*t*9,*t*11,*c*13 CLNA), and pot marigold seed (*t*8,*t*10,*c*12 CLNA) (Table 1). The presence of these conjugated fatty acids in seed oils is primarily as a result of the action of divergent forms of the enzyme, fatty acid conjugase on linoleic or α-linolenic acids [4, 5] (Fig. 2). Additionally, the *c*9,*t*11,*c*15 CLNA and *t*9,*t*11,*c*15 CLNA isomers may be produced through the isomerisation of α-linolenic acid by intestinal and ruminal bacteria via the action of the enzyme linoleic acid isomerase [6–8].

Research has shown that conjugated fatty acids are associated with potent anti-carcinogenic, anti-inflammatory and anti-atherosclerotic properties both in vitro and in vivo, and how their efficacy against a particular condition may vary substantially between the individual isomers [1–3, 9]. Thus, the conjugation process can result in the production of a range of fatty acids with diverse biogenic profiles [1–3, 9]. The mechanisms behind the health promoting properties of conjugated fatty acids range from their ability to modulate the expression of genes associated with disease pathogenesis, to their ability to compete with pro-inflammatory ω-6 fatty acids such as linoleic and arachidonic acids for incorporation into the cell membrane. In addition, there is evidence to suggest that CLNA isomers may undergo elongation and desaturation reactions similar to α-linolenic acid [10, 11]. This process results in the production of conjugated derivatives of EPA and DHA, which may also possess potent biogenic properties [9, 12]. Indeed, synthetically produced conjugated EPA isomers have displayed potent anti-carcinogenic and anti-adipogenic properties [9, 13–15], while conjugated DHA isomers have shown potent anti-carcinogenic properties [16].

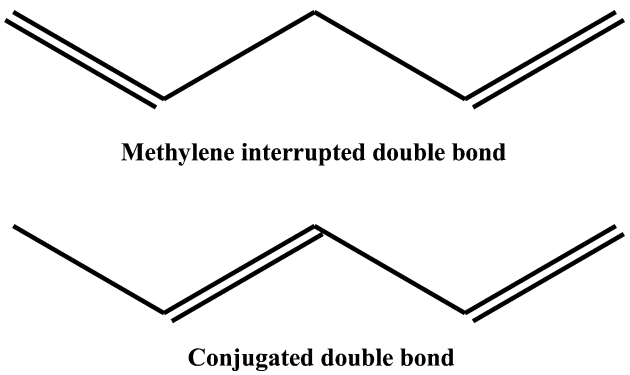

Fig. 1 Structure of conjugated double bonds

The Role of CLNA in Inflammatory Response and Immune Function

Structurally, CLNA isomers have much in common with the ω-3 fatty acid, α-linolenic acid, and the group of fatty acids known as the CLA isomers (*c*9,*t*11 and *t*10,*c*12 CLA isomers). In a number of studies, α-linolenic acid and the CLA isomers have been directly associated with anti-inflammatory and immune enhancing properties [17–19]. Investigations into the mechanisms through which these activities are mediated have highlighted the importance of (a) the down-regulation of eicosanoid production (prostaglandins and leukotrienes) [20, 21]; (b) increased peroxisome proliferator-activated receptor (PPAR) mediated anti-inflammatory response [22]; (c) suppression of inflammatory response through the regulation of the cell transcription factor Nuclear factor kappa B (NF-kB) [23, 24]; and (d) the reduced expression of pro-inflammatory proteins such as Tumor necrosis factor α (TNF-α), interleukin-6, and interleukin-1 beta, [22, 25, 26]. Additionally, both α-linolenic acid and the CLA isomers have been associated with improving the immune response in both animals and humans. In this regard, CLA isomers have been associated with reducing mitogen-induced T lymphocyte activation in humans [27] and improving immunoglobulin (Ig) profiles in both humans and animals [28, 29]. Similarly, α-linolenic acid has also been associated with improving immune response, reducing the proliferation of peripheral blood mononuclear cells without impacting on the concentration of helper and suppressor cells or T and B lymphocytes [30, 31].

The extent and range of the anti-inflammatory and immune enhancing activities shown by α-linolenic acid and the CLA isomers have prompted investigations into what impact, if any, CLNA isomers have on inflammation and immune response (Table 2). It was found that pomegranate seed oil (83% *c*9,*t*11,*c*13 CLNA) enhanced the function of B-cells, which play a prominent role in the humoral immune response [32]. In the study, increased production of IgG and IgM, two key immunoglobulins involved in the antigenic response and produced by B-cells was observed. During investigations into the affect of feeding a range of vegetables to mice on interferon-γ (IFN-γ) and interleukin-4, Ike et al. (2005) discovered the ability of bitter gourd to induce IFN-γ production in mice treated with heat inactivated *Propionibacterium acnes* [33]. IFN-γ is directly associated with Th1 T-helper cells, which play a crucial role in the cellular immune response, maximizing the killing efficacy of the macrophages and the proliferation of

Table 1 The principal conjugated α-linolenic acid isomers (CLNA) and their sources

	Source	Conc. (%)	Comments	Reference
CLNA isomer				
*c*9,*t*11,*c*13	Pomegranate seed	83		[142]
	Milk fat	≤0.03	Canadian milk fat	[7]
	Rapeseed oil	2.50	GMO rapeseed	[60]
*c*9,*t*11,*t*13	Tung seed	67.7		[142]
	Bitter gourd seed	56.2		[142]
	Snake gourd seed	30–50		[143]
	Parwal seed	30–50		[143]
	Sugihiratake mushroom	N.S.	Edible Japanese mushroom	[141]
*t*9,*t*11,*c*13	Catalpa seed	42.3		[142]
*t*9,*t*11,*t*13	Chemosynthesised	>97	Larodan Fine Chemicals, Sweden	[133]
*t*8,*t*10,*c*12	Pot marigold seed	62.2		[142]
*t*8,*t*10,*t*12	Pot marigold seed	4.7		[144]
*c*9,*t*11,*c*15	*Lactobacillus plantarum* AKU 1009a	67	At an α-linolenic acid conc. of 63 mg/ml	[145]
*c*9,*t*11,*c*15	Intestinal bifidobacteria	75	At an α-linolenic acid conc. of 0.24 mg/ml	[8]
*c*9,*t*11,*c*15	Milk fat	≤0.03	Canadian milk fat	[7]
*t*9,*t*11,*c*15	*Lactobacillus plantarum* AKU 1009a	33	At an α-linolenic acid conc. of 63 mg/ml	[145]

N.S. Not stated

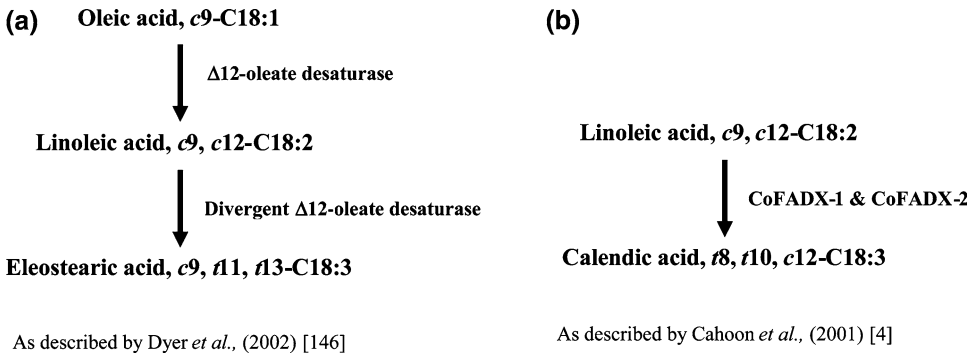

Fig. 2 Biosynthesis of conjugated fatty acids by **a** *Calendula officinalis* and **b** *Aleurites fordii* Hemsl (Tung tree)

cytotoxic CD8+ T cells [33]. Further investigations into the activity of bitter gourd demonstrated that while the pulp yielded the highest increases in IFN-γ, the peel and seed (sources of the *c*9,*t*11,*t*13 CLNA isomer) also resulted in increased IFN-γ production. Given these observations, more detailed investigations into the effect of the CLNA isomers on inflammation and immune response merit further study, particularly in light of the activity displayed by α-linolenic acid and the CLA isomers.

The Role of CLNA in Obesity

As one of the major health concerns facing the Western World, obesity and strategies to combat the condition have received substantial attention. In a number of studies, both α-linolenic acid and in particular the *t*10,*c*12 CLA isomer have proven themselves to be effective anti-adipogenic agents [3, 34–36]. The anti-adipogenic activity of α-linolenic acid has been attributed to factors such as (a) the high proportion of the fatty acid which undergoes β-oxidation [37–39], (b) the less efficient storage of α-linolenic acid in adipose tissue [40, 41], (c) the higher mobilization of stored α-linolenic acid from adipose tissue relative to linoleic acid [42] and d) the ability of α-linolenic acid to regulate genes associated with fatty acid metabolism [43–48]. Similarly, the anti-adipogenic activity of CLA has been attributed to (a) increased cellular β-oxidation [34], (b) the ability of the fatty acid to modulate the production of enzymes involved in fatty acid metabolism (particularly lipoprotein lipase and carnitine palmitoyltransferase) [49, 50], and (c) reduced proliferation and differentiation of preadipocytes [51, 52]. Interestingly, despite the strong evidence of the anti-adipogenic activity of the *t*10,*c*12 CLA isomer, the *c*9,*t*11 isomer has been significantly less effective in mediating anti-adipogenic activity [53–56].

Table 2 Assessing the effect of the conjugated isomers of α-linolenic acid (CLNA) on immune function and growth

Model	Isomer (purity)	Dose and duration	Function	Potential mechanism of action	References
Immune function					
Male 4 week old C57BL/6 N mice	Pomegranate seed oil (*c*9,*t*11,*c*13 CLNA) (83.1%)	0.12–1.2% wt diet, N.S.	↑ production of IgG and IgM	Potential ↑ B-cell function	[32]
Female ddY mice (intraperitoneal injection)	Bitter gourd seed (*c*9,*t*11,*t*13 CLNA) (N.D.)	0.5 ml of a 2.6×10^{-6} mg/ml stock, 7 days	↑ production of interferon-gamma	Potentially through increased production of Th1 T-helper cells	[33]
Growth promotion					
OLETF obese rats	Pomegranate seed oil (*c*9,*t*11,*c*13 CLNA)	1.0% wt diet, 2 weeks	May promote growth	↑ food effiency	[59]

N.D. Not determined, *N.S.* Not stated

The promise shown by α-linolenic acid and CLA isomers in the control of obesity has prompted investigations into the effect of the various CLNA isomers on the condition [1, 3, 57] (Table 3). Koba et al. (2002) found that the dietary intake of CLNA, prepared from α-linolenic acid via alkaline isomerisation, by Sprague–Dawley rats resulted in reductions in perirenal and epididymal adipose tissue and increased mitochondrial and peroxisomal *β*-oxidation [58]. Dietary pomegranate seed oil, rich in the *c*9,*t*11,*c*13 CLNA isomer has also been shown to reduce omental white adipose tissue weights in lean Long–Evans Tokusima Otsuka (LETO) rats but not abdominal white adipose tissue weights in obese, hyperlipidemic Otsuka Long Evans Tokushima Fatty (OLETF) rats [59]. Studies into the mechanisms behind the anti-adipogenic activity of the *c*9,*t*11,*c*13 CLNA isomer, using genetically modified rapeseed (2.5% of total fat was *c*9,*t*11,*c*13 CLNA) and ICR CD-1 mice, highlighted that dietary exposure to the isomer reduced leptin production and increased carnitine palmitoyl-transferase activity relative to the non-genetically modified control [60]. There is also evidence that the *t*8,*t*10,*c*12 CLNA isomer may decrease the body fat content of male mice [61]. Indeed, mice fed the isomer had a significantly lower percentage body fat than animals on the control diet. However, when the effects achieved with the *t*8,*t*10,*c*12 CLNA isomer were compared to those achieved with the *t*10,*c*12 CLA isomer, the reductions in body fat observed with the *t*10,*c*12 CLA isomer were found to be significantly greater.

There is some evidence to suggest that the anti-adipogenic activity of CLNA may stem not only from its ability to affect proteins such as leptin but also based on its ability to activate the nuclear receptor proteins, PPARs, and in particular PPARα. PPARα plays a key role in the activation of enzymes involved in lipid catabolism, and both the *c*9,*t*11,*t*13 CLNA isomer and *t*9,*t*11,*c*13 CLNA isomer have been directly associated with its activation [62]. Moreover, these CLNA isomers have been shown to increase the activity of acetyl-CoA carboxylase, a key enzyme involved in the peroxisomal *β*-oxidation of lipids under the control of PPARα.

The Role of CLNA in Cardio-Vascular Health

The dietary intake of α-linolenic acid, the non-conjugated parent form of the CLNA isomers has been associated with improving platelet function, cardiac arrhythmia, and atherosclerosis, all of which lend themselves to improved cardiovascular health [37, 38, 63–65]. Indeed, claims for this health promoting activity have been supported by a number of epidemiological studies, dietary trials and meta-analyses [37, 38, 66, 67]. These activities have been

Table 3 Assessing the effect of the conjugated isomers of α-linolenic acid (CLNA) on obesity

Model	Isomer (purity)	Dose and duration	Function	Potential mechanism of action	References
Obesity and diabetes					
Male Sprague–Dawley rats	Conjugated C18:3 (49.1%)	1.0% wt diet, 4 weeks	↓ perirenal and epididymal adipose tissue weight	↑ mitrocondrial and peroxisomal β-oxidation, ↑ carnitine palmitoyl-transferase activity, ↓ leptin conc.	[58]
Male OLETF obese rats	Pomegranate seed oil (*c*9,*t*11,*c*13 CLNA) (N.D.)	1.0% wt diet, 2 weeks	↓ omental white adipose tissue weight (27%), ←on abdominal white adipose tissue	↓ conc of MUFA in plasma, ↓ activity of SCD	[59]
Male ICR CD-1 mice	GM rapeseed oil (*c*9,*t*11,*c*13 CLNA) (2.5%)	0.25% wt diet, 4 weeks	↓ perirenal and epididymal adipose tissue weight, lower hepatic triglyceride conc	↑ carnitine palmitoyl-transferase activity, ↓ serum leptin concentration	[60]
Male and female ICR CD-1 mice	Calendic acid oil (*t*8,*t*10,*c*12 CLNA) (11.9%)	1.0% wt diet, 6 weeks	↓ percentage body fat	N.D.	[61]
H4IIEC3 murine hepatoma	Bitter gourd seed oil extract (*c*9,*t*11,*t*13 CLNA) (>50.2%)	180 μM, 72 h	Activated PPARα, ↑ acetyl-CoA oxidase	N.D.	[94]

N.D. Not determined

attributed to the impact of the fatty acid on eicosanoid production, sodium ion channels and low density lipoprotein (LDL) receptor activity [68–76]. Despite this evidence, further dietary trials and meta-analyses have drawn into question the claims of improved cardiovascular health while others have questioned the design of a number of the existing epidemiological studies [77–81]. In a number of in vitro and in vivo studies, the CLA isomers have displayed anti-atherosclerotic activity, though a consensus on the significance of this activity in humans is yet to be reached [82–85]. The existing evidence would suggest that any anti-atherosclerotic activity is mediated through effects on the expression of genes such as the LDL receptor gene and on acyl-coenzyme A:Cholesterol acyltransferase [86–88] and/or by their impact on the production of pro-inflammatory eicosanoids [21, 89, 90].

Like α-linolenic acid and the CLA isomers, the CLNA isomers have shown properties associated with improved cardiovascular health and in particular anti-hypercholesterolemic activity. In one such study, the *c*9,*t*11,*t*13 CLNA isomer was associated with significantly lowering total and non-high density lipoprotein (HDL) cholesterol in diabetic rats [91]. This activity may be mediated through the impact of the CLNA isomers on the secretion of apo-lipoprotein B100 and on PPARα (Table 4). Apo-lipoprotein B100 is an essential component of both very low density lipoprotein (VLDL) and LDL cholesterol types, which are associated with increased risk of coronary artery disease. Human hepatoma cells treated with the *c*9,*t*11,*c*13 CLNA isomer have been shown to produce less apo-lipoprotein B100 than cells treated with an equivalent concentration of α-linolenic acid [92]. Perhaps more significant is the increased activation of PPARα by CLNA given its role in lipid uptake and metabolism [93, 94]. Indeed, activators of PPARα such as fibrates have been directly associated with lowering serum cholesterol levels [95]. However, other studies such as that of Dhar et al. (1999) [96] have found no differences in plasma total, HDL, and non-HDL cholesterol when rats were fed *c*9,*t*11,*t*13 CLNA, relative to animals on the control diet. These results may suggest that the positive impact of CLNA on plasma cholesterol is limited to diabetic subjects.

Lipoprotein oxidation in vivo has been increasingly associated with the development and progression of atherosclerosis [97]. A number of natural compounds such as garlic oil, fenugreek, ferulic acid and CLA have been shown to possess antioxidant properties which may combat the oxidation of these lipoproteins. These observations have prompted investigations into the potential of CLNA to reduce lipoprotein oxidation during in vitro and in vivo studies (Table 4). In one such study, male albino rats fed a diet containing 0.5% by weight *c*9,*t*11,*t*13 CLNA were found to be significantly less susceptible to lipoprotein

Table 4 Assessing the effect of the conjugated isomers of α-linolenic acid (CLNA) on cardio-vascular disease

Model	Isomer (purity)	Dose and duration	Function	Potential mechanism of action	References
Cardio-vascular disease					
Male albino rats with alloxan induced diabetes	Bitter gourd seed oil (*c*9,*t*11,*t*13 CLNA) (55.7%)	0.5% wt diet, 6 weeks	↓ plasma total and non-HDL cholesterol, ↓ LDL and erythrocyte lipid peroxidation	Free radical scavenging	[91]
Male 4 week old C57BL/6 N mice	Pomegranate seed oil (*c*9,*t*11,*c*13 CLNA) (83.1%)	0.12–1.2% wt diet, N.S.	↑ plasma total cholesterol, significantly ↑ plasma TAG	N.D.	[32]
HepG2 human hepatoma	Bitter gourd seed oil (*c*9,*t*11,*t*13 CLNA)	100 μM/ml, 6–24 h	↓ apolipoprotein B100 secretion, ↓ TAG synthesis	Potentially reduces VLDL production	[92]
Male albino rats with alloxan induced diabetes	Bitter gourd seed oil (*c*9,*t*11,*t*13 CLNA) (51.1%)	0.5–10% wt diet, 4 weeks	↓ lipoprotein peroxidation, ↓ erythrocyte lipid peroxidation	Free radical scavenging	[96]
Diabetic and non diabetic human blood samples	Bitter gourd seed oil (*c*9,*t*11,*t*13 CLNA) (57.7%)	0.05–0.1% wt diet, N.S.	↓ plasma lipid peroxidation, lipoprotein peroxidation and erythrocyte membrane lipid peroxidation in both	Free radical scavenging	[98]
F344 rats with azoxymethane induced colonic aberrant crypt foci	Catalpa seed oil (*t*9,*t*11,*c*13 CLNA)	1.0% wt diet, 4 weeks	↓ serum triglyceride conc	N.D.	[138]

N.D. Not determined, *N.S.* Not stated

peroxidation and peroxidation of erythrocyte membrane lipids [96]. In rats with alloxan-induced diabetes mellitus, the *c*9,*t*11,*t*13 CLNA isomer also proved effective in reducing the oxidation of LDL cholesterol and of erythrocyte membrane lipids [91]. The antioxidant effect of *c*9,*t*11,*t*13 CLNA in relation to plasma lipoprotein is not exclusive to murine models. In a recent study, the in vitro antioxidant activity of the isomer in the blood of diabetic and non-diabetic humans was assessed [98]. The results showed that *c*9,*t*11,*t*13 CLNA significantly reduced plasma lipid peroxidation, lipoprotein peroxidation and erythrocyte membrane lipid peroxidation in both diabetic and non-diabetic blood samples.

The Role of CLNA in Cancer

α-Linolenic acid displays potent inhibitory effects on various cancer cell lines, such as colon cancer cells [99, 100], mammary cancer cells [101–104], melanoma cells [105] and hepatoma cells [106]. While reductions in the expression or cellular concentrations of cyclooxygenase-2 (COX-2) and prostaglandin synthesis were reported as contributing factors in the anti-carcinogenic activity of α-linolenic acid against most tumor types, other various tissue specific mechanisms were also identified [100, 103, 106, 107]. Reductions in the incidence of colon cancer in mice as a result of dietary inclusion of α-linolenic acid have been inversely associated with the concentration of *β*-catenin and protein kinase C-ζ [100]. Redistribution of *β*-catenin to its more 'normal' location in the membrane impairs activation of the nuclear Tcf/Lef transcription factor targeting proliferative genes. The anti-carcinogenic activity of α-linolenic acid against mammary cancer has been associated with reductions in expression of the oncogenes fatty acid synthase and human epidermal growth factor receptor 2 [108, 109] and also with the down-regulation of insulin-like growth factor 1 [102, 110, 111]. Vecchini et al. (2004) [106] associated the apoptotic activity of α-linolenic acid against hepatoma cells with reductions in the expression of sterol regulatory element binding proteins (SREBP), nuclear transcription factors which regulate lipid metabolism and lipogenic enzymes including fatty acid synthase. Interestingly, although the evidence pertaining to the anti-proliferative activity of α-linolenic acid is strong, a number of studies and meta-analysis have highlighted the potential increased risk of prostate cancer associated with increased α-linolenic acid intake [67, 112–114]. However, a large number of studies have found no significant relationship between dietary, blood and adipose tissue concentrations of α-linolenic acid and prostate cancer [115–118].

The CLA isomers have also been strongly linked with anti-carcinogenic properties against a range of tumors including those of the mammary gland, colon, skin and liver [1, 3, 119]. Much work has been conducted with regard to elucidating the mechanisms behind this anti-carcinogenic activity. The results have identified CLA isomers as effective modulators of (a) the expression of pro and anti-apoptotic oncogenes such as bcl-2, bax, bak, bad, p53, and p21, (b) eicosanoid synthesis (via their impact on COX-2 and cell membrane composition), and (c) the activity of cell transcription factors such as NF-kB and PPAR [1, 3, 119]. Additionally, conjugated fatty acids such as the CLA isomers, when incorporated into the membranes of cancer cells, can undergo lipid peroxidation leading to cellular apoptosis as a result of the increased oxidative stress [120, 121].

In light of the potent activity which both α-linolenic acid and the CLA isomers have displayed against a range of cancer types, much research has been directed towards identifying the effect that the various CLNA isomers have on cancer, both in vitro and in vivo. These investigations indicate that the various CLNA isomers differ substantially in their anti-carcinogenic properties and in the mechanisms through which this anti-carcinogenic activity is mediated (Table 5).

Pomegranate seed oil, rich in *c*9,*t*11,*c*13 CLNA, has been associated with inhibiting the incidence and multiplicity of chemically induced colonic aberrant crypt foci in male F344 rats via increased concentrations of the *c*9,*t*11 CLA isomer and expression of PPARγ in the colonic mucosa [122]. Pomegranate seed oil has also been associated with reducing the proliferation and invasion of the MCF-7 mammary cancer cell line and increasing apoptosis of the MDA-MB-435 mammary cancer cell line [123]. This anti-carcinogenic activity was potentially mediated through the anti-angiogenic properties of pomegranate seed oil and its ability to inhibit prostaglandin synthesis [124, 125]. Hora et al. (2003) [126] suggested that pomegranate seed oil could be a safe and effective chemopreventive agent against skin cancer. During their investigations, the oil was found to significantly reduce the incidence and multiplicity of chemically induced skin cancer, potentially through reduced ornithine decarboxylase activity.

Interestingly, pomegranate oil has also been associated with suppressing the proliferation and invasion of human prostate cancer despite the association of α-linolenic acid with the condition [67, 127] (Table 5). In one such study, dietary pomegranate seed oil rich in *c*9,*t*11,*c*13-CLNA was found to possess anti-proliferative activity against a range of prostate cancers in vivo, while in another, *c*9,*t*11,*c*13-CLNA was found to significantly reduce the invasiveness of the PC-3 prostate cancer cell line [128, 129].

One of the first investigations into the anti-carcinogenic activity of CLNA found that tung seed oil (67.7% *c*9,*t*11,*t*13 CLNA) was cytotoxic to a range of cancer cell lines at concentrations greater than 25 μM [130] (Table 5). Since that time, a range of further investigations have demonstrated that oils rich in *c*9,*t*11,*t*13 CLNA have anti-proliferative and apoptosis inducing activity against a range of cancers and in particular those of the colon [131–134]. A number of mechanisms have been suggested for this activity including the increased expression of PPARγ and the cell cycle arrest genes GADD45 and p53, along with decreased expression of the apoptosis suppressor Bcl-2 [131–133, 135]. In addition, increased lipid peroxidation within cancer cells, as a result of the uptake of *c*9,*t*11,*t*13 CLNA, has been proposed as contributing to the anti-carcinogenic effect of the isomer [134, 136]. A number of studies have compared the anti-carcinogenic properties of the *c*9,*t*11,*t*13 CLNA isomer or oils rich in the *c*9,*t*11,*t*13 CLNA isomer with that of CLA or certain anti-cancer drugs. When *c*9,*t*11,*t*13 CLNA was compared with both the *c*9,*t*11 and *t*10,*c*12 CLA isomers, the CLNA isomer was found to have stronger anti-carcinogenic activity against the DLD-1 colon cancer cell line than the CLA isomers [134]. Similarly, the *c*9,*t*11,*t*13 CLNA isomer was found to have a higher anti-carcinogenic activity than the PPARγ ligand, troglitazone [131, 132]. However, not all studies have observed the anti-carcinogenic properties of the *c*9,*t*11,*t*13 CLNA isomer. Kitamura et al. (2006) [137] assessed the impact of the isomer on chemically induced mammary and colon carcinogenesis in female Sprague–Dawley rats. The results indicated that treatment with the isomer resulted in only slight reductions in the incidence, multiplicity and volume of tumors.

The *t*9,*t*11,*c*13 CLNA isomer, the predominant conjugated fatty acid found in catalpa seed oil, has also been shown to possess anti-carcinogenic properties (Table 5). One of the first studies to highlight this anti-carcinogenic activity reported the cytotoxicity of the *t*9,*t*11,*c*13 CLNA isomer on transformed mouse fibroblast cell lines and on the human monocytic leukemia cell line U-937 [136]. Further investigations by the same group into this anti-carcinogenic activity showed the *t*9,*t*11,*c*13 CLNA isomer reduced the incidence of chemically induced colonic aberrant crypt foci in rats, increasing apoptosis and reducing proliferation of cancer cells [138]. These studies have inferred the role of increased lipid peroxidation and reduced expression of the enzyme COX-2 as mechanisms for this anti-carcinogenic activity. Interestingly, dietary supplementation of rats with catalpa seed oil (*t*9,*t*11,*c*13 CLNA rich) resulted in increased concentrations of *t*9,*t*11 CLA isomer in the colonic mucosa and liver. The *t*9,*t*11 isomer has previously been shown to decrease expression of Bcl-2, the anti-apoptotic oncogene, and may play a role

Table 5 Assessing the effect of the conjugated isomers of α-linolenic acid (CLNA) on cancer

Model	Isomer (purity)	Dose and duration	Function	Potential mechanism of action	References
Cancer					
(1) Transformed SV-T2 mouse fibroblast cells. (2) U-937 human monocytic leukemia	*c*9,*t*11,*c*13 CLNA (99%)	(1) ≥10 μM, (2) ≥5 μM, 24 h	Cytotoxic	↑ lipid peroxidation, supported by the ↓ in cytoxicity on addition of BHT and high susceptibility of the oil to lipid peroxidation	[136]
F344 rats with azoxymethane induced colonic aberrant crypt foci	Pomegranate seed oil (*c*9,*t*11,*c*13 CLNA) (>70%)	0.01–1.00% wt diet, 32 weeks	↓ incidence (38–56%) and multiplicity (0.50 ± 0.73 to 0.88 ± 0.96) of azoxymethane induced colonic aberrant crypt foci (control diet: 81% and 1.88 ± 1.54, respectively)	↑ *c*9,*t*11 CLA conc and PPARγ expression in the non-lesional colonic mucosa	[122]
(1) MCF-7 breast cancer. (2) MDA-MB-435 breast cancer	Pomegranate seed oil (*c*9,*t*11,*c*13 CLNA) (N.D.)	(1a) 100 μg/ml, (1b) 10 μg/ml. (2) 50 μg/ml supercritical fluid pomegranate seed oil	(1a) 90% ↓ in proliferation, (1b) 75%↓ in invasiveness. (2) Induced 54% apoptosis	N.D.	[123]
(1) MCF-7 breast cancer, (2) MCF-10A immortalised breast epithelial cells, (3) MDA-MB-231 breast cancer	Pomegranate seed oil (*c*9,*t*11,*c*13 CLNA) (N.D.)	(1) >100 μg/ml, (2) ≥10 μg/ml, (3) ≥10 μg/ml supercritical fluid pomegranate seed oil, 24 h	↓ angiogenesis	(1 and 2) Downregulation of the angiogenic promoter "vascular endothelial growth factor". (3) Upregulation of the angiogenic suppressors "migration inhibitory factor"	[124]
(1) Transformed SV-T2 mouse fibroblast cells. (2) U-937 human monocytic leukemia	*c*9,*t*11,*c*13 CLNA (99%)	(1) ≥10 μM, (2) ≥5 μM, 24 h	Cytotoxic	↑ lipid peroxidation, supported by the ↓ in cytoxicity on addition of BHT and high susceptibility of the oil to lipid peroxidation	[136]
F344 rats with azoxymethane induced colonic aberrant crypt foci	Pomegranate seed oil (*c*9,*t*11,*c*13 CLNA) (>70%)	0.01–1.00% wt diet, 32 weeks	↓ incidence (38–56%) and multiplicity (0.50 ± 0.73 to 0.88 ± 0.96) of azoxymethane induced colonic aberrant crypt foci (control diet: 81% and 1.88 ± 1.54, respectively)	↑ *c*9,*t*11 CLA conc and PPARγ expression in the non-lesional colonic mucosa	[122]
(1) MCF-7 breast cancer. (2) MDA-MB-435 breast cancer	Pomegranate seed oil (*c*9,*t*11,*c*13 CLNA) (N.D.)	(1a) 100 μg/ml, (1b) 10 μg/ml. (2) 50 μg/ml supercritical fluid pomegranate seed oil	(1a) 90% ↓ in proliferation, (1b) 75%↓ in invasiveness. (2) Induced 54% apoptosis	N.D.	[123]
(1) MCF-7 breast cancer, (2) MCF-10A immortalised breast epithelial cells, (3) MDA-MB-231 breast cancer	Pomegranate seed oil (*c*9,*t*11,*c*13 CLNA) (N.D.)	(1) >100 μg/ml, (2) ≥10 μg/ml, (3) ≥10 μg/ml supercritical fluid pomegranate seed oil, 24 h	↓ angiogenesis	(1 and 2) Downregulation of the angiogenic promoter "vascular endothelial growth factor". (3) Upregulation of the angiogenic suppressors "migration inhibitory factor"	[124]
(1) Transformed SV-T2 mouse fibroblast cells. (2) U-937 human monocytic leukemia	*c*9,*t*11,*c*13 CLNA (99%)	(1) ≥10 μM, (2) ≥5 μM, 24 h	Cytotoxic	↑ lipid peroxidation, supported by the ↓ in cytoxicity on addition of BHT and high susceptibility of the oil to lipid peroxidation	[136]

Table 5 continued

Model	Isomer (purity)	Dose and duration	Function	Potential mechanism of action	References
F344 rats with azoxymethane induced colonic aberrant crypt foci	Pomegranate seed oil (*c*9,*t*11,*c*13 CLNA) (>70%)	0.01–1.00% wt diet, 32 weeks	↓ incidence (38–56%) and multiplicity (0.50 ± 0.73 to 0.88 ± 0.96) of azoxymethane induced colonic aberrant crypt foci (control diet: 81% and 1.88 ± 1.54, respectively)	↑ *c*9,*t*11 CLA conc and PPARγ expression in the non-lesional colonic mucosa	[122]
(1) MCF-7 breast cancer. (2) MDA-MB-435 breast cancer	Pomegranate seed oil (*c*9,*t*11,*c*13 CLNA) (N.D.)	(1a) 100 μg/ml, (1b) 10 μg/ml. (2) 50 μg/ml supercritical fluid pomegranate seed oil	(1a) 90% ↓ in proliferation, (1b) 75%↓ in invasiveness. (2) Induced 54% apoptosis	N.D.	[123]
(1) MCF-7 breast cancer, (2) MCF-10A immortalised breast epithelial cells, (3) MDA-MB-231 breast cancer	Pomegranate seed oil (*c*9,*t*11,*c*13 CLNA) (N.D.)	(1) >100 μg/ml, (2) ≥10 μg/ml, (3) ≥10 μg/ml supercritical fluid pomegranate seed oil, 24 h	↓ angiogenesis	(3 and 2) Downregulation of the angiogenic promoter "vascular endothelial growth factor". (3) Upregulation of the angiogenic suppressors "migration inhibitory factor"	[124]
(1) Transformed SV-T2 mouse fibroblast cells. (2) U-937 human monocytic leukemia	*c*9,*t*11,*c*13 CLNA (99%)	(1) ≥10 μM, (2) ≥5 μM, 24 h	Cytotoxic	↑ lipid peroxidation, supported by the ↓ in cytoxicity on addition of BHT and high susceptibility of the oil to lipid peroxidation	[136]
F344 rats with azoxymethane induced colonic aberrant crypt foci	Pomegranate seed oil (*c*9,*t*11,*c*13 CLNA) (>70%)	0.01–1.00% wt diet, 32 weeks	↓ incidence (38–56%) and multiplicity (0.50 ± 0.73 to 0.88 ± 0.96) of azoxymethane induced colonic aberrant crypt foci (control diet: 81% and 1.88 ± 1.54, respectively)	↑ *c*9,*t*11 CLA conc and PPARγ expression in the non-lesional colonic mucosa	[122]
(1) MCF-7 breast cancer. (2) MDA-MB-435 breast cancer	Pomegranate seed oil (*c*9,*t*11,*c*13 CLNA) (N.D.)	(1a) 100 μg/ml, (1b) 10 μg/ml. (2) 50 μg/ml supercritical fluid pomegranate seed oil	(1a) 90% ↓ in proliferation, (1b) 75%↓ in invasiveness. (2) Induced 54% apoptosis	N.D.	[123]
(1) MCF-7 breast cancer, (2) MCF-10A immortalised breast epithelial cells, (3) MDA-MB-231 breast cancer	Pomegranate seed oil (*c*9,*t*11,*c*13 CLNA) (N.D.)	(1) >100 μg/ml, (2) ≥10 μg/ml, (3) ≥10 μg/ml supercritical fluid pomegranate seed oil, 24 h	↓ angiogenesis	(4 and 2) Downregulation of the angiogenic promoter "vascular endothelial growth factor". (3) Upregulation of the angiogenic suppressors "migration inhibitory factor"	[124]

N.D. Not determined

in the apoptotic effect found with catalpa seed oil [120]. Yasui et al. (2006b) [133] compared the anti-proliferative and pro-apoptotic properties of the *t*9,*t*11,*t*13 CLNA isomer with that of the *c*9,*t*11,*c*13 CLNA isomer using the Caco-2 colon cancer cell line. Comparatively, the *t*9,*t*11,*t*13 CLNA isomer was significantly more cytotoxic to the Caco-2 colon cancer cell line than the *c*9,*t*11,*c*13 CLNA isomer. In this study, it was found that exposure of the Caco-2 cells to the *t*9,*t*11,*t*13 CLNA isomer stimulated cellular apoptosis via increases in cellular DNA fragmentation, increased expression of the pro-apoptotic oncogene bax, and decreased expression of Bcl-2. Increased lipid peroxidation was also shown to play a role in this anti-carcinogenic activity. However, the observation that the *t*9,*t*11,*t*13 CLNA isomer remained active even in the presence of elevated concentrations of the anti-oxidant α-tocopherol is suggestive that cancer cell apoptosis triggered by increased cellular lipid peroxidation is not at least the predominant mechanism behind the anti-carcinogenic activity of the *t*9,*t*11,*t*13 CLNA isomers.

The *t*8,*t*10,*c*12 and *t*8,*t*10,*t*12 CLNA isomers derived from pot marigold have also been shown to possess some anti-carcinogenic properties (Table 5). The *t*8,*t*10,*c*12 CLNA isomer has displayed apoptotic activity against a range of cancers including the human monocytic leukaemia cell line U-937 and the Caco-2 colon cancer cell line [133, 136]. Investigations into the oxidative stability of the fatty acid and the impact of the antioxidants BHT and α-tocopherol led the authors to conclude that the anti-carcinogenic activity of the isomer was related to lipid peroxidation (Table 5). The anti-carcinogenic activity of the *t*8,*t*10,*t*12 CLNA isomer has also been investigated using the Caco-2 cell line [133]. In this study,*t*8,*t*10,*t*12 CLNA exhibited substantial cytotoxicity to the Caco-2 cell line and caused a substantial increase in the level of DNA fragmentation. However, the mechanism behind this anti-carcinogenic activity remained unclear and could only partially be attributed to increased cellular lipid peroxidation, as the *t*8,*t*10,*t*12 CLNA isomer remained active even in the presence of α-tocopherol.

Comparatively, the anti-carcinogenic activity of the CLNA isomers varies substantially. When the cytotoxicity of the *c*9,*t*11,*c*13, the *c*9,*t*11,*t*13, and the *t*9,*t*11,*c*13 CLNA isomers were compared to that of the *t*8,*t*10,*c*12 CLNA isomer using the U-937 monocytic leukemia cell line and the SV-T2 transformed mouse fibroblast cell line, the 9, 11, 13-CLNA isomers displayed much greater activity [136]. Yasui et al. (2006b) assessed the impact that the trans content of CLNA had on its apoptotic activity using the Caco-2 cancer cell line. The results showed that all trans CLNA isomers (*t*9,*t*11,*t*13 and *t*8,*t*10,*t*12) were more inhibitory to Caco-2 growth than their partial trans counterparts (*t*9,*t*11,*c*13 and *t*8,*t*10,*c*12). When compared to the CLA isomers (*c*9,*t*11 and/or *t*10,*c*12 CLA), tung and bitter gourd seed oils (rich in the *c*9,*t*11,*t*13 CLNA isomer) and pomegranate seed oil (rich in the *c*9,*t*11,*c*13 CLNA isomer) displayed higher anti-carcinogenic activities against colon cancers than the CLA isomers [122, 131, 134]. These investigations highlight the impact of bond position, bond number and bond conformation on the properties of these conjugated fatty acids.

CLNA Metabolism in Vivo

Investigations into the metabolism of CLNA have suggested that mammals rapidly convert 9,11,13-CLNA isomers to 9,11-CLA via a Δ^{13}-saturation reaction catalyzed by a NADPH dependent enzyme [122, 135, 138–140]. Hence, it may be CLA rather than CLNA which exerts its bioactivity in vivo. Interestingly, when rats were supplied with equivalent concentrations of CLA or CLNA, it was CLNA which caused the highest increase in CLA concentrations in both the non-lesional mucosa and liver, potentially explaining the higher anti-carcinogenic activity seen with CLNA. Despite this evidence, not all studies have witnessed the high conversion of CLNA to CLA in vivo. Plourde et al. (2006) [11] found that when Wistar rats were fed a mixture of CLNA isomers (i.e. *c*9,*t*11,*c*15 and *c*9,*t*13,*c*15 isomers), CLNA could be detected in the liver, blood plasma and adipose tissue, while the *c*9,*t*11 CLA isomer could not. This might suggest that n-5 CLNA isomers such as the 9,11,13-CLNA typically found in plants and seed oils, and n-3 CLNA isomers such as 9,11,15-CLNA produced by bacteria may have very different metabolic fates and hence, their activity on disease and health may differ substantially.

Conclusions

The ability to produce conjugated fatty acids is shared by certain plants and microbes, which though different in their chemical structure, often share common bioactivity. This is also true of the various conjugated isomers of CLNA which have been shown to display potent inflammatory and immune modulating properties, reduce the risk of obesity, improve cardiovascular health, and mediate strong anti-carcinogenic activity during in vitro studies and in animal models. These diseases represent some of the greatest mortality risks to humans in the Western world and have been inextricably linked with diet. Thus far, the information pertaining to the mechanisms through which the CLNA isomers impart their bioactivity show strong parallels to that of the CLA isomers. Indeed, in this regard both the CLNA isomers and the CLA isomers have been

shown to impart activity both at an endoplasmic (eicosanoid synthesis) and nuclear levels.

Although there is a plethora of evidence from in vitro studies and animal models to support the bioactive properties of CLNA, there are very limited data from human studies involving these isomers. Consequently, it is difficult to clearly establish the role of biologically active CLNA isomers in improving human health. Moreover, as certain CLA isomers have previously been associated with adverse activities in humans, a better understanding of the impact of CLNA isomers in the human diet is of paramount importance before any recommendations regarding their dietary intake can be made. In conclusion, better controlled human studies are required before CLNA or CLNA enriched foods can be recommended to humans with any degree of certainty that improved health and well-being can be achieved without any negative effects [128, 141–146].

Acknowledgments The financial assistance of the Alimentary Pharmabiotic Centre (APC) is gratefully acknowledged. A. A. Hennessy is in receipt of a Teagasc Walsh Fellowship. This research was also funded by EU project QLK1-2001-02362.

References

1. Wahle KW, Heys SD, Rotondo D (2004) Conjugated linoleic acids: are they beneficial or detrimental to health? Prog Lipid Res 43(6):553–587
2. Igarashi M, Miyazawa T (2005) Preparation and fractionation of conjugated trienes from alpha-linolenic acid and their growth-inhibitory effects on human tumor cells and fibroblasts. Lipids 40(1):109–113
3. Bhattacharya A, Banu J, Rahman M, Causey J, Fernandes G (2006) Biological effects of conjugated linoleic acids in health and disease. J Nutr Biochem 17(12):789–810
4. Cahoon EB, Ripp KG, Hall SE, Kinney AJ (2001) Formation of conjugated delta8, delta10-double bonds by delta12-oleic-acid desaturase-related enzymes: biosynthetic origin of calendic acid. J Biol Chem 276(4):2637–2643
5. Cahoon EB, Dietrich CR, Meyer K, Damude HG, Dyer JM, Kinney AJ (2006) Conjugated fatty acids accumulate to high levels in phospholipids of metabolically engineered soybean and *Arabidopsis* seeds. Phytochemistry 67(12):1166–1176
6. Ogawa J, Kishino S, Ando A, Sugimoto S, Mihara K, Shimizu S (2005) Production of conjugated fatty acids by lactic acid bacteria. J Biosci Bioeng 100(4):355–364
7. Destaillats F, Trottier JP, Galvez JM, Angers P (2005) Analysis of alpha-linolenic acid biohydrogenation intermediates in milk fat with emphasis on conjugated linolenic acids. J Dairy Sci 88(9):3231–3239
8. Coakley M, Banni S, Johnson MC, Mills S, Devery R, Fitzgerald G, Ross RP, Stanton C (2009) Inhibitory effect of conjugated α-linolenic acid (CALA) from bifidobacteria of intestinal origin on SW480 cancer cells. Lipids 44(3):249–256
9. Tsuzuki T, Kambe T, Shibata A, Kawakami Y, Nakagawa K, Miyazawa T (2007) Conjugated EPA activates mutant p53 via lipid peroxidation and induces p53-dependent apoptosis in DLD-1 colorectal adenocarcinoma human cells. Biochim Biophys Acta 1771(1):20–30
10. Destaillats F, Berdeaux O, Sebedio JL, Juaneda P, Gregoire S, Chardigny JM, Bretillon L, Angers P (2005) Metabolites of conjugated isomers of alpha-linolenic acid (CLnA) in the rat. J Agric Food Chem 53(5):1422–1427
11. Plourde M, Sergiel JP, Chardigny JM, Gregoire S, Angers P, Sebedio JL (2006) Absorption and metabolism of conjugated alpha-linolenic acid given as free fatty acids or triacylglycerols in rats. Nutr Metab (Lond) 3:8
12. Tsujita-Kyutoku M, Yuri T, Danbara N, Senzaki H, Kiyozuka Y, Uehara N, Takada H, Hada T, Miyazawa T, Ogawa Y, Tsubura A (2004) Conjugated docosahexaenoic acid suppresses KPL-1 human breast cancer cell growth in vitro and in vivo: potential mechanisms of action. Breast Cancer Res 6(4):R291–R299
13. Igarashi M, Miyazawa T (2000) Do conjugated eicosapentaenoic acid and conjugated docosahexaenoic acid induce apoptosis via lipid peroxidation in cultured human tumor cells? Biochem Biophys Res Commun 270(2):649–656
14. Tsuzuki T, Igarashi M, Miyazawa T (2004) Conjugated eicosapentaenoic acid (EPA) inhibits transplanted tumor growth via membrane lipid peroxidation in nude mice. J Nutr 134(5): 1162–1166
15. Yonezawa Y, Hada T, Uryu K, Tsuzuki T, Eitsuka T, Miyazawa T, Murakami-Nakai C, Yoshida H, Mizushina Y (2005) Inhibitory effect of conjugated eicosapentaenoic acid on mammalian DNA polymerase and topoisomerase activities and human cancer cell proliferation. Biochem Pharmacol 70(3):453–460
16. Danbara N, Yuri T, Tsujita-Kyutoku M, Sato M, Senzaki H, Takada H, Hada T, Miyazawa T, Okazaki K, Tsubura A (2004) Conjugated docosahexaenoic acid is a potent inducer of cell cycle arrest and apoptosis and inhibits growth of colo 201 human colon cancer cells. Nutr Cancer 50(1):71–79
17. Reynolds CM, Roche HM (2010) Conjugated linoleic acid and inflammatory cell signalling. Prostaglandins Leukot Essent Fatty Acids 82(4–6):199–204
18. Zhao G, Etherton TD, Martin KR, Gillies PJ, West SG, Kris-Etherton PM (2007) Dietary alpha-linolenic acid inhibits proinflammatory cytokine production by peripheral blood mononuclear cells in hypercholesterolemic subjects. Am J Clin Nutr 85(2):385–391
19. Ambrose DJ, Kastelic JP, Corbett R, Pitney PA, Petit HV, Small JA, Zalkovic P (2006) Lower pregnancy losses in lactating dairy cows fed a diet enriched in alpha-linolenic acid. J Dairy Sci 89(8):3066–3074
20. Chang HH, Chen CS, Lin JY (2008) Dietary perilla oil inhibits proinflammatory cytokine production in the bronchoalveolar lavage fluid of ovalbumin-challenged mice. Lipids 43(6):499–506
21. Belury MA (2002) Dietary conjugated linoleic acid in health: physiological effects and mechanisms of action. Annu Rev Nutr 22:505–531
22. Yang S, Zhu H, Li Y, Lin H, Gabrielson K, Trush MA, Diehl AM (2000) Mitochondrial adaptations to obesity-related oxidant stress. Arch Biochem Biophys 378(2):259–268
23. Ren J, Chung SH (2007) Anti-inflammatory effect of alpha-linolenic acid and its mode of action through the inhibition of nitric oxide production and inducible nitric oxide synthase gene expression via NF-kappaB and mitogen-activated protein kinase pathways. J Agric Food Chem 55(13):5073–5080
24. Cheng WL, Lii CK, Chen HW, Lin TH, Liu KL (2004) Contribution of conjugated linoleic acid to the suppression of inflammatory responses through the regulation of the NF-kappaB pathway. J Agric Food Chem 52(1):71–78
25. Jiang C, Ting AT, Seed B (1998) PPAR-gamma agonists inhibit production of monocyte inflammatory cytokines. Nature 391(6662):82–86
26. Nelson TL, Hickey MS (2004) Acute changes in dietary omega-3 fatty acid intake lowers soluble interleukin-6 receptor in

healthy adult normal weight and overweight males. Cytokine 26(5):195–201
27. Tricon S, Burdge GC, Kew S, Banerjee T, Russell JJ, Grimble RF, Williams CM, Calder PC, Yaqoob P (2004) Effects of cis-9, trans-11 and trans-10, cis-12 conjugated linoleic acid on immune cell function in healthy humans. Am J Clin Nutr 80(6):1626–1633
28. O'Shea M, Bassaganya-Riera J, Mohede IC (2004) Immunomodulatory properties of conjugated linoleic acid. Am J Clin Nutr 79(6 Suppl):1199S–1206S
29. Turpeinen AM, Ylonen N, von Willebrand E, Basu S, Aro A (2008) Immunological and metabolic effects of *cis*-9,*trans*-11-conjugated linoleic acid in subjects with birch pollen allergy. Br J Nutr 100(1):112–119
30. Bjerve KS, Fischer S, Wammer F, Egeland T (1989) Alpha-linolenic acid and long-chain omega-3 fatty acid supplementation in three patients with omega-3 fatty acid deficiency: effect on lymphocyte function, plasma and red cell lipids, and prostanoid formation. Am J Clin Nutr 49(2):290–300
31. Kelley DS, Branch LB, Love JE, Taylor PC, Rivera YM, Iacono JM (1991) Dietary alpha-linolenic acid and immunocompetence in humans. Am J Clin Nutr 53(1):40–46
32. Yamasaki M, Kitagawa T, Koyanagi N, Chujo H, Maeda H, Kohno-Murase J, Imamura J, Tachibana H, Yamada K (2006) Dietary effect of pomegranate seed oil on immune function and lipid metabolism in mice. Nutrition 22(1):54–59
33. Ike K, Uchida Y, Nakamura T, Imai S (2005) Induction of interferon-gamma (IFN-gamma) and T helper 1 (Th1) immune response by bitter gourd extract. J Vet Med Sci 67(5):521–524
34. Keim NL (2003) Conjugated Linoleic Acid and Body Composition. In: Sebedio JL, Christie WW, Adlof R (eds) Advances in conjugated linoleic acid research. AOCS Press, Champaign
35. Javadi M, Everts H, Hovenier R, Kocsis S, Lankhorst AE, Lemmens AG, Schonewille JT, Terpstra AH, Beynen AC (2004) The effect of six different C18 fatty acids on body fat and energy metabolism in mice. Br J Nutr 92(3):391–399
36. Ikemoto S, Takahashi M, Tsunoda N, Maruyama K, Itakura H, Ezaki O (1996) High-fat diet-induced hyperglycemia and obesity in mice: differential effects of dietary oils. Metabolism 45(12):1539–1546
37. Li D, Bode O, Drummond H, Sinclair AJ (2003) Omega-3 (n-3) fatty acids. In: Gunstone FD (ed) Lipids for functional foods and nutraceuticals. The Oily Press, Bridgewater, pp 225–262
38. Sinclair AJ, Attar-Bashi NM, Li D (2002) What is the role of alpha-linolenic acid for mammals? Lipids 37(12):1113–1123
39. Cunnane SC, Anderson MJ (1997) The majority of dietary linoleate in growing rats is beta-oxidized or stored in visceral fat. J Nutr 127(1):146–152
40. Lin DS, Connor WE, Spenler CW (1993) Are dietary saturated, monounsaturated, and polyunsaturated fatty acids deposited to the same extent in adipose tissue of rabbits? Am J Clin Nutr 58(2):174–179
41. Yeom K-H, van Trierum G, Hovenier R, Schellingerhout AB, Lee KW, Beynen AC (2002) Fatty acid composition of adipose tissue in goat kids fed milk replacers with different contents of alpha-linolenic and linoleic acid. Small Rumin Res 43:15–22
42. Raclot T, Langin D, Lafontan M, Groscolas R (1997) Selective release of human adipocyte fatty acids according to molecular structure. Biochem J 324(Pt 3):911–915
43. Iritani N, Komiya M, Fukuda H, Sugimoto T (1998) Lipogenic enzyme gene expression is quickly suppressed in rats by a small amount of exogenous polyunsaturated fatty acids. J Nutr 128(6):967–972
44. Kim HK, Choi S, Choi H (2004) Suppression of hepatic fatty acid synthase by feeding alpha-linolenic acid rich perilla oil lowers plasma triacylglycerol level in rats. J Nutr Biochem 15(8):485–492
45. Kim HK, Choi H (2005) Stimulation of acyl-CoA oxidase by alpha-linolenic acid-rich perilla oil lowers plasma triacylglycerol level in rats. Life Sci 77(12):1293–1306
46. Takahashi Y, Ide T (2000) Dietary n-3 fatty acids affect mRNA level of brown adipose tissue uncoupling protein 1, and white adipose tissue leptin and glucose transporter 4 in the rat. Br J Nutr 84(2):175–184
47. Ide T, Kobayashi H, Ashakumary L, Rouyer IA, Takahashi Y, Aoyama T, Hashimoto T, Mizugaki M (2000) Comparative effects of perilla and fish oils on the activity and gene expression of fatty acid oxidation enzymes in rat liver. Biochim Biophys Acta 1485(1):23–35
48. Ikeda I, Cha JY, Yanagita T, Nakatani N, Oogami K, Imaizumi K, Yazawa K (1998) Effects of dietary alpha-linolenic, eicosapentaenoic and docosahexaenoic acids on hepatic lipogenesis and beta-oxidation in rats. Biosci Biotechnol Biochem 62(4):675–680
49. Park Y, Albright KJ, Liu W, Storkson JM, Cook ME, Pariza MW (1997) Effect of conjugated linoleic acid on body composition in mice. Lipids 32(8):853–858
50. Park Y, Albright KJ, Storkson JM, Liu W, Cook ME, Pariza MW (1999) Changes in body composition in mice during feeding and withdrawal of conjugated linoleic acid. Lipids 34(3):243–248
51. Satory DL, Smith SB (1999) Conjugated linoleic acid inhibits proliferation but stimulates lipid filling of murine 3T3–L1 preadipocytes. J Nutr 129(1):92–97
52. Brodie AE, Manning VA, Ferguson KR, Jewell DE, Hu CY (1999) Conjugated linoleic acid inhibits differentiation of pre- and post- confluent 3T3–L1 preadipocytes but inhibits cell proliferation only in preconfluent cells. J Nutr 129(3):602–606
53. Declercq V, Zahradka P, Taylor CG (2010) Dietary *t*10,*c*12-CLA but not *c*9,*t*11 CLA reduces adipocyte size in the absence of changes in the adipose renin-angiotensin system in fa/fa Zucker rats. Lipids 45(11):1025–1033
54. Henriksen EJ, Teachey MK, Taylor ZC, Jacob S, Ptock A, Kramer K, Hasselwander O (2003) Isomer-specific actions of conjugated linoleic acid on muscle glucose transport in the obese Zucker rat. Am J Physiol Endocrinol Metab 285(1):E98–E105
55. Kelley DS, Erickson KL (2003) Modulation of body composition and immune cell functions by conjugated linoleic acid in humans and animal models: benefits versus risks. Lipids 38(4):377–386
56. House RL, Cassady JP, Eisen EJ, Eling TE, Collins JB, Grissom SF, Odle J (2005) Functional genomic characterization of delipidation elicited by *trans*-10,*cis*-12-conjugated linoleic acid (t10c12-CLA) in a polygenic obese line of mice. Physiol Genomics 21(3):351–361
57. Navarro V, Fernandez-Quintela A, Churruca I, Portillo MP (2006) The body fat-lowering effect of conjugated linoleic acid: a comparison between animal and human studies. J Physiol Biochem 62(2):137–147
58. Koba K, Akahoshi A, Yamasaki M, Tanaka K, Yamada K, Iwata T, Kamegai T, Tsutsumi K, Sugano M (2002) Dietary conjugated linolenic acid in relation to CLA differently modifies body fat mass and serum and liver lipid levels in rats. Lipids 37(4):343–350
59. Arao K, Wang YM, Inoue N, Hirata J, Cha JY, Nagao K, Yanagita T (2004) Dietary effect of pomegranate seed oil rich in 9*cis*, 11*trans*, 13*cis* conjugated linolenic acid on lipid metabolism in obese, hyperlipidemic OLETF rats. Lipids Health Dis 3:24

60. Koba K, Imamura J, Akashoshi A, Kohno-Murase J, Nishizono S, Iwabuchi M, Tanaka K, Sugano M (2007) Genetically modified rapeseed oil containing cis-9, trans-11, cis-13-octadecatrienoic acid affects body fat mass and lipid metabolism in mice. J Agric Food Chem 55(9):3741–3748
61. Chardigny JM, Hasselwander O, Genty M, Kraemer K, Ptock A, Sebedio JL (2003) Effect of conjugated FA on feed intake, body composition, and liver FA in mice. Lipids 38(9):895–902
62. Hontecillas R, Diguardo M, Duran E, Orpi M, Bassaganya-Riera J (2008) Catalpic acid decreases abdominal fat deposition, improves glucose homeostasis and upregulates PPAR alpha expression in adipose tissue. Clin Nutr 27(5):764–772
63. Mozaffarian D (2005) Does alpha-linolenic acid intake reduce the risk of coronary heart disease? A review of the evidence. Altern Ther Health Med 11(3):24–30; quiz 31, 79
64. Djousse L, Arnett DK, Carr JJ, Eckfeldt JH, Hopkins PN, Province MA, Ellison RC (2005) Dietary linolenic acid is inversely associated with calcified atherosclerotic plaque in the coronary arteries: the National Heart, Lung, and Blood Institute Family Heart Study. Circulation 111(22):2921–2926
65. Djousse L, Pankow JS, Eckfeldt JH, Folsom AR, Hopkins PN, Province MA, Hong Y, Ellison RC (2001) Relation between dietary linolenic acid and coronary artery disease in the National Heart, Lung, and Blood Institute Family Heart Study. Am J Clin Nutr 74(5):612–619
66. de Lorgeril M, Salen P (2004) Alpha-linolenic acid and coronary heart disease. Nutr Metab Cardiovasc Dis 14(3):162–169
67. Brouwer IA, Katan MB, Zock PL (2004) Dietary alpha-linolenic acid is associated with reduced risk of fatal coronary heart disease, but increased prostate cancer risk: a meta-analysis. J Nutr 134(4):919–922
68. Ander BP, Hurtado C, Raposo CS, Maddaford TG, Deniset JF, Hryshko LV, Pierce GN, Lukas A (2007) Differential sensitivities of the NCX1.1 and NCX1.3 isoforms of the Na+ –Ca2+ exchanger to alpha-linolenic acid. Cardiovasc Res 73(2): 395–403
69. Rupp H, Turcani M, Ohkubo T, Maisch B, Brilla CG (1996) Dietary linolenic acid-mediated increase in vascular prostacyclin formation. Mol Cell Biochem 162(1):59–64
70. Ferretti A, Flanagan VP (1996) Antithromboxane activity of dietary alpha-linolenic acid: a pilot study. Prostaglandins Leukot Essent Fatty Acids 54(6):451–455
71. Bierenbaum ML, Reichstein R, Watkins TR (1993) Reducing atherogenic risk in hyperlipemic humans with flax seed supplementation: a preliminary report. J Am Coll Nutr 12(5): 501–504
72. Mandasescu S, Mocanu V, Dascalita AM, Haliga R, Nestian I, Stitt PA, Luca V (2005) Flaxseed supplementation in hyperlipidemic patients. Rev Med Chir Soc Med Nat Iasi 109(3):502–506
73. Cintra DE, Costa AV, Peluzio Mdo C, Matta SL, Silva MT, Costa NM (2006) Lipid profile of rats fed high-fat diets based on flaxseed, peanut, trout, or chicken skin. Nutrition 22(2):197–205
74. Dupasquier CM, Dibrov E, Kneesh AL, Cheung PK, Lee KG, Alexander HK, Yeganeh BK, Moghadasian MH, Pierce GN (2007) Dietary flaxseed inhibits atherosclerosis in the LDL receptor-deficient mouse in part through antiproliferative and anti-inflammatory actions. Am J Physiol Heart Circ Physiol 293(4):H2394–H2402
75. London B, Albert C, Anderson ME, Giles WR, Van Wagoner DR, Balk E, Billman GE, Chung M, Lands W, Leaf A, McAnulty J, Martens JR, Costello RB, Lathrop DA (2007) Omega-3 fatty acids and cardiac arrhythmias: prior studies and recommendations for future research: a report from the National Heart, Lung, and Blood Institute and Office of dietary supplements omega-3 fatty acids and their role in cardiac arrhythmogenesis workshop. Circulation 116(10):e320–e335
76. Munoz S, Merlos M, Zambon D, Rodriguez C, Sabate J, Ros E, Laguna JC (2001) Walnut-enriched diet increases the association of LDL from hypercholesterolemic men with human HepG2 cells. J Lipid Res 42(12):2069–2076
77. Oomen CM, Ocke MC, Feskens EJ, Kok FJ, Kromhout D (2001) Alpha-linolenic acid intake is not beneficially associated with 10-y risk of coronary artery disease incidence: the Zutphen Elderly Study. Am J Clin Nutr 74(4):457–463
78. Wendland E, Farmer A, Glasziou P, Neil A (2006) Effect of alpha linolenic acid on cardiovascular risk markers: a systematic review. Heart 92(2):166–169
79. Wang C, Harris WS, Chung M, Lichtenstein AH, Balk EM, Kupelnick B, Jordan HS, Lau J (2006) n-3 Fatty acids from fish or fish-oil supplements, but not alpha-linolenic acid, benefit cardiovascular disease outcomes in primary- and secondary-prevention studies: a systematic review. Am J Clin Nutr 84(1):5–17
80. Albert CM, Oh K, Whang W, Manson JE, Chae CU, Stampfer MJ, Willett WC, Hu FB (2005) Dietary alpha-linolenic acid intake and risk of sudden cardiac death and coronary heart disease. Circulation 112(21):3232–3238
81. Harris WS (2005) Alpha-linolenic acid: a gift from the land? Circulation 111(22):2872–2874
82. Mitchell PL, McLeod RS (2008) Conjugated linoleic acid and atherosclerosis: studies in animal models. Biochem Cell Biol 86(4):293–301
83. Eder K, Ringseis R (2010) Metabolism and actions of conjugated linoleic acids on atherosclerosis-related events in vascular endothelial cells and smooth muscle cells. Mol Nutr Food Res 54(1):17–36
84. Cooper MH, Miller JR, Mitchell PL, Currie DL, McLeod RS (2008) Conjugated linoleic acid isomers have no effect on atherosclerosis and adverse effects on lipoprotein and liver lipid metabolism in apoE-/- mice fed a high-cholesterol diet. Atherosclerosis 200(2):294–302
85. McLeod RS, LeBlanc AM, Langille MA, Mitchell PL, Currie DL (2004) Conjugated linoleic acids, atherosclerosis, and hepatic very-low-density lipoprotein metabolism. Am J Clin Nutr 79(6 Suppl):1169S–1174S
86. Ringseis R, Konig B, Leuner B, Schubert S, Nass N, Stangl G, Eder K (2006) LDL receptor gene transcription is selectively induced by t10c12-CLA but not by c9t11-CLA in the human hepatoma cell line HepG2. Biochim Biophys Acta 1761(10):1235–1243
87. Yu-Poth S, Yin D, Zhao G, Kris-Etherton PM, Etherton TD (2004) Conjugated linoleic acid upregulates LDL receptor gene expression in HepG2 cells. J Nutr 134(1):68–71
88. Lam CK, Chen J, Cao Y, Yang L, Wong YM, Yeung SY, Yao X, Huang Y, Chen ZY (2008) Conjugated and non-conjugated octadecaenoic acids affect differently intestinal acyl coenzyme A: cholesterol acyltransferase activity. Atherosclerosis 198(1):85–93
89. Bassaganya-Riera J, Hontecillas R, Beitz DC (2002) Colonic anti-inflammatory mechanisms of conjugated linoleic acid. Clin Nutr 21(6):451–459
90. Nakamura YK, Flintoff-Dye N, Omaye ST (2008) Conjugated linoleic acid modulation of risk factors associated with atherosclerosis. Nutr Metab (Lond) 5:22
91. Dhar P, Bhattacharyya D, Bhattacharyya DK, Ghosh S (2006) Dietary comparison of conjugated linolenic acid (9 *cis*, 11 *trans*, 13 *trans*) and alpha-tocopherol effects on blood lipids and lipid peroxidation in alloxan-induced diabetes mellitus in rats. Lipids 41(1):49–54

92. Arao K, Yotsumoto H, Han SY, Nagao K, Yanagita T (2004) The 9cis, 11trans, 13cis isomer of conjugated linolenic acid reduces apolipoprotein B100 secretion and triacylglycerol synthesis in HepG2 cells. Biosci Biotechnol Biochem 68(12):2643–2645
93. Berger J, Moller DE (2002) The mechanisms of action of PPARs. Annu Rev Med 53:409–435
94. Chuang CY, Hsu C, Chao CY, Wein YS, Kuo YH, Huang CJ (2006) Fractionation and identification of 9*c*, 11*t*, 13*t*-conjugated linolenic acid as an activator of PPARalpha in bitter gourd (*Momordica charantia* L.). J Biomed Sci 13(6):763–772
95. Stahlberg D, Reihner E, Rudling M, Berglund L, Einarsson K, Angelin B (1995) Influence of bezafibrate on hepatic cholesterol metabolism in gallstone patients: reduced activity of cholesterol 7 alpha-hydroxylase. Hepatology 21(4):1025–1030
96. Dhar P, Ghosh S, Bhattacharyya DK (1999) Dietary effects of conjugated octadecatrienoic fatty acid (9 *cis*, 11 *trans*, 13 *trans*) levels on blood lipids and nonenzymatic in vitro lipid peroxidation in rats. Lipids 34(2):109–114
97. Esterbauer H, Gebicki J, Puhl H, Jurgens G (1992) The role of lipid peroxidation and antioxidants in oxidative modification of LDL. Free Radic Biol Med 13(4):341–390
98. Dhar P, Chattopadhyay K, Bhattacharyya D, Roychoudhury A, Biswas A, Ghosh S (2007) Antioxidative effect of conjugated linolenic acid in diabetic and non-diabetic blood: an in vitro study. J Oleo Sci 56(1):19–24
99. Dwivedi C, Natarajan K, Matthees DP (2005) Chemopreventive effects of dietary flaxseed oil on colon tumor development. Nutr Cancer 51(1):52–58
100. Oikarinen SI, Pajari AM, Salminen I, Heinonen SM, Adlercreutz H, Mutanen M (2005) Effects of a flaxseed mixture and plant oils rich in alpha-linolenic acid on the adenoma formation in multiple intestinal neoplasia (Min) mice. Br J Nutr 94(4):510–518
101. Numata M (1995) Antitumor effects of alpha-linolenic acid on the human tumor transplanted in nude mice and on the metastasis of Vx-7 tumor in rabbit. Hokkaido Igaku Zasshi 70(1):183–193
102. Chen J, Stavro PM, Thompson LU (2002) Dietary flaxseed inhibits human breast cancer growth and metastasis and downregulates expression of insulin-like growth factor and epidermal growth factor receptor. Nutr Cancer 43(2):187–192
103. Fritsche KL, Johnston PV (1990) Effect of dietary alpha-linolenic acid on growth, metastasis, fatty acid profile and prostaglandin production of two murine mammary adenocarcinomas. J Nutr 120(12):1601–1609
104. Hardman WE (2007) Dietary canola oil suppressed growth of implanted MDA-MB 231 human breast tumors in nude mice. Nutr Cancer 57(2):177–183
105. Yan L, Yee JA, Li D, McGuire MH, Thompson LU (1998) Dietary flaxseed supplementation and experimental metastasis of melanoma cells in mice. Cancer Lett 124(2):181–186
106. Vecchini A, Ceccarelli V, Susta F, Caligiana P, Orvietani P, Binaglia L, Nocentini G, Riccardi C, Calviello G, Palozza P, Maggiano N (2004) and P. Di Nardo, Dietary alpha-linolenic acid reduces COX-2 expression and induces apoptosis of hepatoma cells. J Lipid Res 45(2):308–316
107. Horia E, Watkins BA (2005) Comparison of stearidonic acid and alpha-linolenic acid on PGE2 production and COX-2 protein levels in MDA-MB-231 breast cancer cell cultures. J Nutr Biochem 16(3):184–192
108. Menendez JA, Vazquez-Martin A, Ropero S, Colomer R, Lupu R (2006) HER2 (erbB-2)-targeted effects of the omega-3 polyunsaturated fatty acid, alpha-linolenic acid (ALA; 18:3n–3), in breast cancer cells: the "fat features" of the "Mediterranean diet" as an "anti-HER2 cocktail". Clin Transl Oncol 8(11):812–820
109. Menendez JA, Ropero S, Mehmi I, Atlas E, Colomer R, Lupu R (2004) Overexpression and hyperactivity of breast cancer-associated fatty acid synthase (oncogenic antigen-519) is insensitive to normal arachidonic fatty acid-induced suppression in lipogenic tissues but it is selectively inhibited by tumoricidal alpha-linolenic and gamma-linolenic fatty acids: a novel mechanism by which dietary fat can alter mammary tumorigenesis. Int J Oncol 24(6):1369–1383
110. Chen J, Power KA, Mann J, Cheng A, Thompson LU (2007) Flaxseed alone or in combination with tamoxifen inhibits MCF-7 breast tumor growth in ovariectomized athymic mice with high circulating levels of estrogen. Exp Biol Med (Maywood) 232(8):1071–1080
111. Chen J, Power KA, Mann J, Cheng A, Thompson LU (2007) Dietary flaxseed interaction with tamoxifen induced tumor regression in athymic mice with MCF-7 xenografts by down-regulating the expression of estrogen related gene products and signal transduction pathways. Nutr Cancer 58(2):162–170
112. Gann PH, Hennekens CH, Sacks FM, Grodstein F, Giovannucci EL, Stampfer MJ (1994) Prospective study of plasma fatty acids and risk of prostate cancer. J Natl Cancer Inst 86(4):281–286
113. Ramon JM, Bou R, Romea S, Alkiza ME, Jacas M, Ribes J, Oromi J (2000) Dietary fat intake and prostate cancer risk: a case-control study in Spain. Cancer Causes Control 11(8):679–685
114. De Stefani E, Deneo-Pellegrini H, Boffetta P, Ronco A, Mendilaharsu M (2000) Alpha-linolenic acid and risk of prostate cancer: a case-control study in Uruguay. Cancer Epidemiol Biomarkers Prev 9(3):335–338
115. Mannisto S, Pietinen P, Virtanen MJ, Salminen I, Albanes D, Giovannucci E, Virtamo J (2003) Fatty acids and risk of prostate cancer in a nested case-control study in male smokers. Cancer Epidemiol Biomarkers Prev 12(12):1422–1428
116. Simon JA, Tanzman JS, Sabate J (2007) Lack of effect of walnuts on serum levels of prostate specific antigen: a brief report. J Am Coll Nutr 26(4):317–320
117. Freeman VL, Meydani M, Yong S, Pyle J, Flanigan RC, Waters WB, Wojcik EM (2000) Prostatic levels of fatty acids and the histopathology of localized prostate cancer. J Urol 164(6): 2168–2172
118. Meyer F, Bairati I, Fradet Y, Moore L (1997) Dietary energy and nutrients in relation to preclinical prostate cancer. Nutr Cancer 29(2):120–126
119. Banni S, Heys SD, Wahle KW (2003) Conjugated linoleic acid as anticancer nutrients: studies in vivo and cellular mechanisms, In: SebedioJL, Christie WW, Adlof R (eds). Advances in Conjugated Linoleic Acid Research, AOCS Press, Champaign, pp 267–282
120. Beppu F, Hosokawa M, Tanaka L, Kohno H, Tanaka T, Miyashita K (2006) Potent inhibitory effect of *trans* 9,*trans* 11 isomer of conjugated linoleic acid on the growth of human colon cancer cells. J Nutr Biochem 17(12):830–836
121. Devery R, Miller A, Stanton C (2001) Conjugated linoleic acid and oxidative behaviour in cancer cells. Biochem Soc Trans 29(Pt 2):341–344
122. Kohno H, Suzuki R, Yasui Y, Hosokawa M, Miyashita K, Tanaka T (2004) Pomegranate seed oil rich in conjugated linolenic acid suppresses chemically induced colon carcinogenesis in rats. Cancer Sci 95(6):481–486
123. Kim ND, Mehta R, Yu W, Neeman I, Livney T, Amichay A, Poirier D, Nicholls P, Kirby A, Jiang W, Mansel R, Ramachandran C, Rabi T, Kaplan B, Lansky E (2002) Chemopreventive and adjuvant therapeutic potential of pomegranate (*Punica granatum*) for human breast cancer. Breast Cancer Res Treat 71(3):203–217
124. Toi M, Bando H, Ramachandran C, Melnick SJ, Imai A, Fife RS, Carr RE, Oikawa T, Lansky EP (2003) Preliminary studies

on the anti-angiogenic potential of pomegranate fractions in vitro and in vivo. Angiogenesis 6(2):121–128
125. Nugteren DH, Christ-Hazelhof E (1987) Naturally occurring conjugated octadecatrienoic acids are strong inhibitors of prostaglandin biosynthesis. Prostaglandins 33(3):403–417
126. Hora JJ, Maydew ER, Lansky EP, Dwivedi C (2003) Chemopreventive effects of pomegranate seed oil on skin tumor development in CD1 mice. J Med Food 6(3):157–161
127. Brouwer IA (2008) Omega-3 PUFA: good or bad for prostate cancer? Prostaglandins Leukot Essent Fatty Acids 79(3–5): 97–99
128. Albrecht M, Jiang W, Kumi-Diaka J, Lansky EP, Gommersall LM, Patel A, Mansel RE, Neeman I, Geldof AA, Campbell MJ (2004) Pomegranate extracts potently suppress proliferation, xenograft growth, and invasion of human prostate cancer cells. J Med Food 7(3):274–283
129. Lansky EP, Harrison G, Froom P, Jiang WG (2005) Pomegranate (*Punica granatum*) pure chemicals show possible synergistic inhibition of human PC-3 prostate cancer cell invasion across Matrigel. Invest New Drugs 23(2):121–122
130. Igarashi M, Miyazawa T (2000) Newly recognized cytotoxic effect of conjugated trienoic fatty acids on cultured human tumor cells. Cancer Lett 148(2):173–179
131. Yasui Y, Hosokawa M, Sahara T, Suzuki R, Ohgiya S, Kohno H, Tanaka T, Miyashita K (2005) Bitter gourd seed fatty acid rich in 9c, 11t, 13t-conjugated linolenic acid induces apoptosis and up-regulates the GADD45, p53 and PPARgamma in human colon cancer Caco-2 cells. Prostaglandins Leukot Essent Fatty Acids 73(2):113–119
132. Yasui Y, Hosokawa M, Kohno H, Tanaka T, Miyashita K (2006) Troglitazone and 9cis, 11trans, 13trans-conjugated linolenic acid: comparison of their antiproliferative and apoptosis-inducing effects on different colon cancer cell lines. Chemotherapy 52(5):220–225
133. Yasui Y, Hosokawa M, Kohno H, Tanaka T, Miyashita K (2006) Growth inhibition and apoptosis induction by all-*trans*-conjugated linolenic acids on human colon cancer cells. Anticancer Res 26(3A):1855–1860.
134. Tsuzuki T, Tokuyama Y, Igarashi M, Miyazawa T (2004) Tumor growth suppression by alpha-eleostearic acid, a linolenic acid isomer with a conjugated triene system, via lipid peroxidation. Carcinogenesis 25:1417–1425
135. Kohno H, Yasui Y, Suzuki R, Hosokawa M, Miyashita K, Tanaka T (2004) Dietary seed oil rich in conjugated linolenic acid from bitter melon inhibits azoxymethane-induced rat colon carcinogenesis through elevation of colonic PPARgamma expression and alteration of lipid composition. Int J Cancer 110(6):896–901
136. Suzuki R, Noguchi R, Ota T, Abe M, Miyashita K, Kawada T (2001) Cytotoxic effect of conjugated trienoic fatty acids on mouse tumor and human monocytic leukemia cells. Lipids 36(5):477–482
137. Kitamura Y, Yamagishi M, Okazaki K, Umemura T, Imazawa T, Nishikawa A, Matsumoto W, Hirose M (2006) Lack of chemopreventive effects of alpha-eleostearic acid on 7, 12-dimethylbenz[a]anthracene (DMBA) and 1, 2-dimethylhydrazine (DMH)-induced mammary and colon carcinogenesis in female Sprague-Dawley rats. Food Chem Toxicol 44(2): 271–277
138. Suzuki R, Yasui Y, Kohno H, Miyamoto S, Hosokawa M, Miyashita K, Tanaka T (2006) Catalpa seed oil rich in 9t, 11t, 13c-conjugated linolenic acid suppresses the development of colonic aberrant crypt foci induced by azoxymethane in rats. Oncol Rep 16(5):989–996
139. Tsuzuki T, Tokuyama Y, Igarashi M, Nakagawa K, Ohsaki Y, Komai M, Miyazawa T (2004) Alpha-eleostearic acid (9Z11E13E–18:3) is quickly converted to conjugated linoleic acid (9Z11E–18:2) in rats. J Nutr 134(10):2634–2639
140. Tsuzuki T, Igarashi M, Komai M, Miyazawa T (2003) The metabolic conversion of 9,11,13-eleostearic acid (18:3) to 9,11-conjugated linoleic acid (18:2) in the rat. J Nutr Sci Vitaminol (Tokyo) 2003(3):195–200
141. Amakura Y, Kondo K, Akiyama H, Ito H, Hatano T, Yoshida T, Maitani T (2006) Characteristic long-chain fatty acid of *Pleurocybella porrigens*. Shokuhin Eiseigaku Zasshi 47(4):178–181
142. Takagi T, Itabashi Y (1981) Occurrence of mixtures of geometrical isomers of conjugated octadecatrienoic acids in some seed oils: Analysis by open-tubular gas liquid chromatography and high performance liquid chromatography. Lipids 16(7): 546–551
143. Dhar P, Bhattacharyya DK (1998) Nutritional characteristics of oil containing conjugated octadecatrienoic fatty acid. Ann Nutr Metab 42(5):290–296
144. Nagao K, Yanagita T (2005) Conjugated fatty acids in food and their health benefits. J Biosci Bioeng 100(2):152–157
145. Kishino S, Ogawa J, Ando A, Shimizu S (2003) Conjugated alpha-linolenic acid production from alpha-linolenic acid by *Lactobacillus plantarum* AKU 1009a. Eur J Lipid Sci 105(10): 572–577
146. Dyer JM, Chapital DC, Kuan JC, Mullen RT, Turner C, McKeon TA, Pepperman AB (2002) Molecular analysis of a bifunctional fatty acid conjugase/desaturase from tung. Implications for the evolution of plant fatty acid diversity. Plant Physiol 130(4):2027–2038

Lipids (2011) 46:121–130
DOI 10.1007/s11745-010-3486-0

ORIGINAL ARTICLE

Lipid Classes and Fatty Acid Patterns are Altered in the Brain of γ-Synuclein Null Mutant Mice

Irina Guschina · Steve Millership · Valerie O'Donnell · Natalia Ninkina · John Harwood · Vladimir Buchman

Received: 7 May 2010 / Accepted: 2 October 2010 / Published online: 21 October 2010

Abstract The well-documented link between α-synuclein and the pathology of common human neurodegenerative diseases has increased attention to the synuclein protein family. The involvement of α-synuclein in lipid metabolism in both normal and diseased nervous system has been shown by many research groups. However, the possible involvement of γ-synuclein, a closely-related member of the synuclein family, in these processes has hardly been addressed. In this study, the effect of γ-synuclein deficiency on the lipid composition and fatty acid patterns of individual lipids from two brain regions has been studied using a mouse model. The level of phosphatidylserine (PtdSer) was increased in the midbrain whereas no changes in the relative proportions of membrane polar lipids were observed in the cortex of γ-synuclein-deficient compared to wild-type (WT) mice. In addition, higher levels of docosahexaenoic acid were found in PtdSer and phosphatidylethanolamine (PtdEtn) from the cerebral cortex of γ-synuclein null mutant mice. These findings show that γ-synuclein deficiency leads to alterations in the lipid profile in brain tissues and suggest that this protein, like α-synuclein, might affect neuronal function via modulation of lipid metabolism.

Keywords Lipid composition · Synuclein · Midbrain · Cortex · Phosphatidylserine · Docosahexaenoic acid · γ-Synuclein null mutant mice

Abbreviations

ARA	Arachidonic acid
AD	Alzheimer's disease
alphaKO	α-Synuclein null mutant
Ptd_2Gro	Cardiolipin (diphosphatidylglycerol)
CNS	Central nervous system
DHA	Docosahexaenoic acid
DLB	Dementia with Lewy bodies
DMA	Dimethylacetal
ESI–MS-MS	Electrospray ionisation tandem mass spectrometry
FAME	Fatty acid methyl ester(s)
gammaKO	γ-Synuclein null mutant
LIT	Linear ion trap
LnA	α-Linolenic acid
PD	Parkinson's disease
PtdCho	Phosphatidylcholine
PtdEtn	Phosphatidylethanolamine
PtdGro	Phosphatidylglycerol
PtdIns	Phosphatidylinositol
PNS	Peripheral nervous system
PtdSer	Phosphatidylserine
PUFA	Polyunsaturated fatty acid(s)
CerPCho	Sphingomyelin
TAG	Triacylglycerol(s)
WT	Wild-type

I. Guschina (✉) · S. Millership · N. Ninkina · J. Harwood · V. Buchman
School of Biosciences, Cardiff University, Museum Avenue, Cardiff CF10 3AX, UK
e-mail: GuschinaIA@cf.ac.uk

V. O'Donnell
School of Medicine, Cardiff University, Cardiff CF14 4XN, UK

Introduction

The synuclein family comprises three small, closely-related, natively unfolded proteins, α-, β- and γ-synuclein, that are expressed predominantly in neural tissues. Alpha- and β-synucleins are abundant in the neurons of the central

nervous system (CNS) and concentrated within presynaptic terminals where they are loosely associated with synaptic vesicles. γ-Synuclein is mainly cytosolic and expressed in the neurons of the peripheral nervous system (PNS) and certain populations of CNS neurons. γ-Synuclein is also expressed in some malignant tumours and may be involved in tumorigenesis and metastasis [1].

Aggregated and fibrillated forms of α-synuclein are major components of Lewy bodies, histological hallmarks of hereditary and idiopathic forms of Parkinson's disease (PD). Moreover, several mutations in SNCA, a gene encoding α-synuclein, are associated with early onset autosomal dominant PD [2–7] and polymorphisms of this gene are risk factors for PD and other diseases associated with α-synuclein aggregation [8–12]. The accumulation of aggregation intermediates, i.e. partially or fully soluble oligomeric forms of α-synuclein, is believed to be the principle pathogenic event responsible for neuronal dysfunction [13–16] and interactions with lipids play an important role in oligomerisation of α-synuclein [17–19]. Interestingly, β- and γ-synucleins may act to suppress α-synuclein aggregation and toxicity [20].

In immortalised cell lines and primary neuronal cultures, both WT and PD mutant α-synuclein could be found associated with the phospholipid surface layer of lipid droplets [21] and are enriched in lipid rafts [22]. In the rafts, α-synuclein was associated with specific PtdSer species containing polyunsaturated fatty acids (PUFA) [23] or with gangliosides [24, 25]. Moreover, polyunsaturated fatty acyl groups were shown to promote multimerisation of α-, β-, and γ-synucleins [26] and lipid-associated oligomers of α-synuclein have been detected in the brain of patients with α-synucleinopathies [27, 28]. It has been suggested that α-synuclein—PUFA interactions can reciprocally regulate neuronal PUFA levels and the oligomerisation stage of α-synuclein in normal and disease nervous system [27, 28].

The importance of PUFA in brain structure and functions is well established [29]. These fatty acids, especially arachidonic acid (C20:4n-6, ARA) and docosahexaenoic acid (C22:6n-3, DHA), are enriched in certain brain phospholipids, for example, in PtdIns and PtdEtn, respectively [30]. In animal models, an inadequate supply of n-3 fatty acids during prenatal and early postnatal development decreases DHA levels in the brain. As a result, adult animals develop learning and memory deficits, which can be improved by dietary supplementation of DHA or other n-3 PUFA, e.g. α-linolenic acid (C18:3n-3, LnA) [31–33]. In humans, mental development may be improved by dietary DHA supplementation during infancy [34]. Conversely, low levels of DHA in human brains are associated with the risk of developing neurological diseases such as generalised peroxisomal disorders [35] and Alzheimer's disease (AD) [36, 37]. In contrast, elevated levels of DHA, docosatetraenoic acid and linoleic acid have been shown in those brain areas of PD patients that contain α-synuclein inclusions [28].

Although the precise mechanism of DHA-enriched phospholipid action on cognitive function is still poorly understood, possible effects on the blood–brain barrier, membrane fluidity, activity of certain enzymes, neural signalling, ionic channels, and control of nerve growth factor have all been suggested [38]. Recently, a neuroprotective action of the n-3 PUFA, DHA and LnA, in PD has been also demonstrated using rat and mice models of this disease [39, 40]. Interestingly, expression of genes encoding α-synuclein and γ-synuclein increased in brains of rats fed high n-3 PUFA diets [38]. In turn, an important role of α-synuclein in brain lipid metabolism as well as for fatty acid uptake and metabolism has been documented [41–43].

In contrast to the well-studied role of α-synuclein in lipid metabolism in the normal and diseased nervous systems, very little is known about the involvement of γ-synuclein in these processes. Nevertheless, some recent studies demonstrated that γ-synuclein is directly involved in lipid metabolism in mature adipocytes ([44, 45] and our unpublished observations). Therefore it was logical to investigate a possible link between γ-synuclein and lipids in the nervous system.

Here we analysed lipid composition and fatty acid patterns of individual lipids from brain regions of γ-synuclein null mutant (gammaKO) mice. We found that the level of PtdSer is increased in the midbrain whereas no changes in the relative proportions of membrane lipid classes were observed in the cerebral cortex of these animals. In addition, higher percentages of DHA were found in both PtdSer and PtdEtn from the cerebral cortex of gammaKO mice. These data suggest a role for γ-synuclein in lipid metabolism in the nervous system and are discussed in relation to what is known about alterations of lipid metabolism in α-synuclein-deficient animals.

Experimental Procedures

Materials

FA standards were obtained from Nu-Chek-Pre. Inc. (Elysian, MN) and silica gel G plates were from Merck KGaA (Darmstadt, Germany). Lipid standards were from Sigma (Poole, UK). Other reagents were of the best available grades and were from Fisher Scientific (Loughborough, UK).

Experimental Animals

All animal work was carried in accordance with the United Kingdom Animals (Scientific Procedures) Act (1986). Production of γ-synuclein null mutant mice on a pure (C57Bl6J, Charles River) genetic background and the method of animal genotyping by PCR have been described previously [46, 47]. For this study, male γ-synuclein null mutant mice and their WT littermates were kept in individual cages from the age of 9 weeks with access to water and food ad libitum. Animals were fed special diet DOI 58Y2 with 10% energy from fats (LabDiets). No significant differences in animal weight and food uptake were observed between groups of mutant and WT animals throughout the experimental period. In order to evaluate the effect of γ-synuclein deficiency on the lipid composition in the fully-developed nervous system, tissues of young but fully mature (21 week-old) adult mice were analysed.

Lipid Analysis

At the age of 21 weeks animals were fasted for 4 h before killing by lethal injection of phenobarbital. Lipids were extracted immediately from dissected brain regions by a modified Folch method [48]. In this procedure [originally developed for mitochondrial lipids such as cardiolipin (Ptd_2Gro)] efficient extraction even of highly polar compounds is ensured.

Polar lipids were separated by two-dimensional TLC on 10 × 10 cm 1.2% boric acid-impregnated silica gel G plates using chloroform: methanol: ammonium hydroxide (65:25:4; v/v/v) in the first dimension and then *n*-butanol: acetic acid: water (90:20: 20; v/v/v) in the second. Plates were sprayed with 0.05% (wt/vol) 8-anilino-4-naphthosulphonic acid in methanol and viewed under UV light to reveal lipids. Preliminary identification was made by reference to authentic standards and confirmed using specific colour reagents [49]. Additionally, the structural identification of lipids was confirmed by mass spectrometry (see next paragraph for details). Non-polar lipids were separated using 1-dimensional TLC on 10 × 10 cm silica gel G plates with double development using toluene: hexane: formic acid (140:60:1, v/v/v) for the entire plate followed by hexane: diethyl ether: formic acid (60:40:1, v/v/v) to half height. Individual lipids were scraped from the TLC plates and their fatty acid compositions and contents were determined by gas chromatography using an internal standard of pentadecanoate (for details, see "Fatty Acid Analysis" section below) [49].

Mass spectrometry was performed on an Applied Biosystems 4000 Q-Trap. Lipid extracts were diluted in methanol and introduced at 10 μl/min into the electrospray source operating in the negative ion mode. All scans were obtained using an ionspray voltage of −4,500 V and a declustering potential of −140 V. Q1 scans were performed scanning a mass range of 600–1,000 amu over 4 s, with 10 scans acquired and averaged. MS/MS scans using the ion trap mode of the Q-Trap were run at a scan rate of 1,000 amu/s with collision energies of −50 and −60 V, and a linear ion trap (LIT) fill time of 150 ms with Q0 trapping enabled. Again 10 scans were acquired and averaged and the data analysed using the software Analyst 1.4.1.

Fatty Acid Analysis

Fatty acid methyl esters (FAME) were prepared by transmethylation with 2.5% H_2SO_4 in dry methanol/toluene (2:1, by vol.). FAME were separated using a Clarus 500 gas chromatograph (Perkin-Elmer, Norwalk, Connecticut) fitted with a 30 m × 0.25 mm i.d. capillary column (Elite 225, Perkin Elmer). The oven temperature was programmed: 170 °C for 3 min, heated to 220 °C at 4 °C/min, held at 220 °C for 15 min. FAME were identified routinely by comparing retention times with fatty acid standards (Nu-Chek Prep. Inc., Elysian, USA) but confirmation of the structure of the major fatty acids had also been made by MS. Quantification was made with an internal standard of pentadecanoate.

Statistics

Statistical significance between groups was assessed by Student's *t* test.

Results

Fatty Acid Composition of Diet

The fatty acid composition of the diet used is presented in Table 1. It contained oleic acid as a major compound (35% of total diet FA) followed by linoleic (25%), palmitic (20%) and stearic (13%) acids. The relative amount of α-linolenic (an essential n-3 fatty acid) was low and did not exceed 2.5% of total FA. Thus, the ratio of n-6/n-3 fatty acids was high giving a value of 13 whereas a balanced human diet is believed to range from 1:1 to 1:4 [50]. Lipids accounted for 10% of total energy in this diet.

Fatty Acid Composition of Plasma

Fatty acid composition of plasma from WT and γ-synuclein null mutant mice (gammaKO) is present in Table 1. Palmitic, stearic, oleic, linoleic and arachidonic acids were the

Table 1 Fatty acid composition (% total acids) of the diet and the plasma from wild-type (WT) and γ-synuclein null mutant (gammaKO) mice

Fatty acid	Diet	Plasma	
		WT	gammaKO
C14:0	0.5 ± 0.1	tr.	tr.
C16:0	20.3 ± 2.6	17.8 ± 4.7	19.8 ± 2.6
C16:1 (n-7)	1.0 ± 0.2	2.0 ± 0.7	3.1 ± 0.8
C18:0	12.6 ± 2.1	13.0 ± 2.2	13.0 ± 4.8
C18:1 (n-9)	35.0 ± 1.3	16.0 ± 1.9	20.5 ± 2.8*
C18:1 (n-7)	2.0 ± 0.1	2.2 ± 0.2	3.0 ± 0.8
C18:2 (n-6)	24.9 ± 6.0	17.3 ± 1.8	15.1 ± 1.8
C18:3 (n-3)	2.2 ± 0.6	0.5 ± 0.2	0.5 ± 0.3
C20:1 (n-9)	0.6 ± 0.2	tr.	tr.
C20:3 (n-6)	n.d.	1.6 ± 0.8	2.0 ± 0.7
C20:4 (n-6)	n.d.	20.3 ± 4.5	15.9 ± 4.4
C22:6 (n-3)	n.d.	7.3 ± 2.4	5.2 ± 1.9

Data as means ± SD ($n = 3$ for diet and $n = 5$ for plasma)

Fatty acids are indicated with the number before colon showing the number of carbon atoms, the figure afterwards denoting the number of double bonds. The position of the first double bond is shown in brackets. Only the major fatty acids (≥0.5%) are listed

n.d. none detected; *tr* trace <0.5%

The asterisk (*) indicates a significant effect of γ-synuclein deficiency when compared with WT ($p < 0.05$)

major fatty acids in plasma together with a moderate amount of DHA in both, WT and gammaKO mice. The relative amount of oleic acid was increased significantly in the plasma of gammaKO mice compared to WT (Table 1).

Cortex and Midbrain Fatty Acid Composition of the Total Polar Lipids in WT and γ-Synuclein Null Mutant Mice

Table 2 shows the FA profile of the total polar lipid fractions from cortex or midbrain in WT and gammaKO mice. Palmitic and stearic acids were dominant FA in cortex followed by DHA, oleic acid and ARA. In midbrain, stearic and oleic acids were the major compounds followed by palmitic, DHA and ARA. The percentages of palmitic, arachidonic and DHA in total polar lipids were significantly higher in the cortex region compared to midbrain in both WT and gammaKO mice, whereas proportions of oleic and nervonic (C24:1) acids were higher in this lipid fraction from midbrain. There were no statistically significant differences in the relative proportions of fatty acids from the total polar lipid fraction between WT and gammaKO mice in either brain region.

Table 2 Fatty acid composition (% of total fatty acids) of the total polar lipid fraction from cortex or midbrain of wild-type (WT) and γ-synuclein null mutant (gammaKO) mice

FA	CORTEX		MIDBRAIN	
	WT	gammaKO	WT	gammaKO
C16:0	22.2 ± 0.5	22.6 ± 0.8	16.8 ± 0.2#	17.5 ± 0.8
C16:1 (n-7)	1.3 ± 0.2	1.4 ± 0.2	0.1 ± 0.0#	0.2 ± 0.0
C18:0	22.6 ± 0.4	22.8 ± 0.4	21.8 ± 2.3	21.6 ± 2.4
C18:1 (n-9)	15.9 ± 0.2	15.6 ± 0.3	21.7 ± 0.6#	21.1 ± 1.1
C18:1 (n-7)	3.8 ± 0.4	4.0 ± 0.3	4.7 ± 1.3	5.0 ± 0.5
C18:2 (n-6)	0.9 ± 0.1	0.8 ± 0.1	2.8 ± 0.9#	2.8 ± 0.8
C18:3 (n-3)	10.4 ± 0.5	10.5 ± 0.3	7.7 ± 0.9#	7.4 ± 1.2
C20:3 (n-6)	2.4 ± 0.1	2.4 ± 0.1	3.0 ± 0.9	3.7 ± 2.0
C20:4 (n-6)	16.5 ± 2.0	16.0 ± 0.6	12.1 ± 1.7#	11.5 ± 1.0
C22:6 (n-3)	0.8 ± 0.2	0.8 ± 0.2	2.5 ± 0.6#	2.6 ± 0.6

Data as means ± SD ($n = 6$–8)

See legend to Table 1 for other details

The hash (#) indicates significant differences between midbrain and cortex in WT animals ($p < 0.05$)

Polar Lipid Composition of Cortex and Midbrain Regions from WT and gammaKO Mice

The relative proportions of different polar lipids in the two brain regions are shown in Fig. 1. Three phospholipids, namely phosphatidylcholine (PtdCho), ethanolamine phospholipids and PtdSer, were the major polar lipids in both brain regions (accounting for about 70–80% of the total polar lipids). Phosphatidylinositol (PtdIns), sphingomyelin (CerPCho), Ptd_2Gro as well as sulfatide and cerebroside were present in smaller proportions and were each less than 5% of the total polar lipids. Sulfatides and cerebrosides were identified by electrospray ionisation tandem mass spectrometry (ESI–MS-MS) [51, 52]. The relative amounts of polar lipids did not vary much between midbrain and cortex samples from WT animals, although the levels of sulfatides and PtdCho were higher and lower, respectively, in the midbrain region (Fig. 1). In this brain region, γ-synuclein deficiency resulted in a statistically significant (∼40%) increase in the relative proportion of PtdSer compared to WT animals, whereas the proportions of other lipids were not altered significantly (Fig. 1). No differences in the polar lipid composition were found in the cortex of WT compared to gammaKO mice (Fig. 1). Also, no differences in the concentrations of total polar lipids and triacylglycerols (TAG) were observed for these brain regions as a result of γ-synuclein deficiency (data not shown).

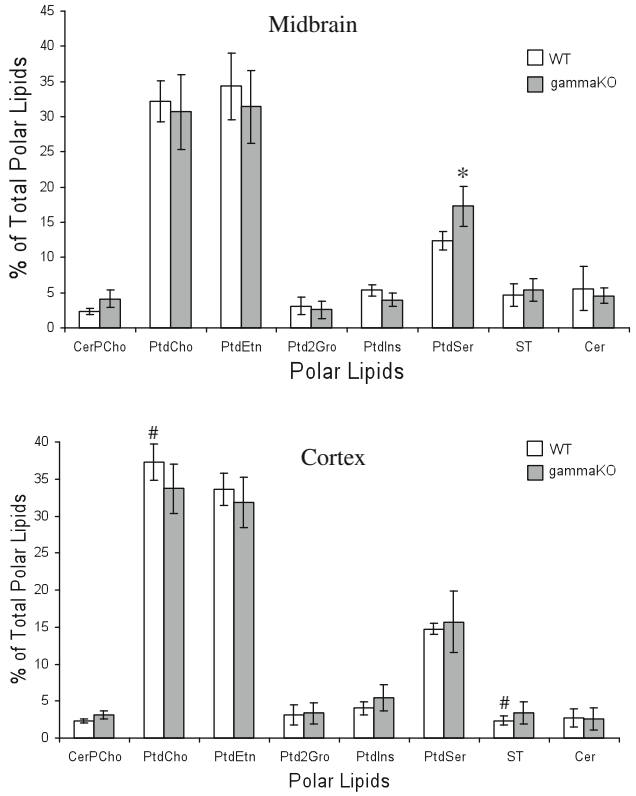

Fig. 1 Midbrain and cortex polar lipid composition (% of total polar lipids) from wild-type (WT) and γ-synuclein null mutant (gammaKO) mice. Values represent mean ± SD, $n = 5$. The *asterisk* (*) indicates a significant effect of γ-synuclein deficiency when compared with WT, and the *hash* (#) indicates significant differences between midbrain (*top panel*) and cortex (*bottom panel*) in WT animals ($p < 0.05$ for both). *CerPCho* sphingomyelin, *PtdCho* phosphatidylcholine, *PtdEtn* phosphatidylethanolamine, *Ptd$_2$Gro* cardiolipin, *PtdIns* phosphatidylinositol, *PtdSer* phosphatidylserine, *ST* sulfatide, *Cer* cerebroside

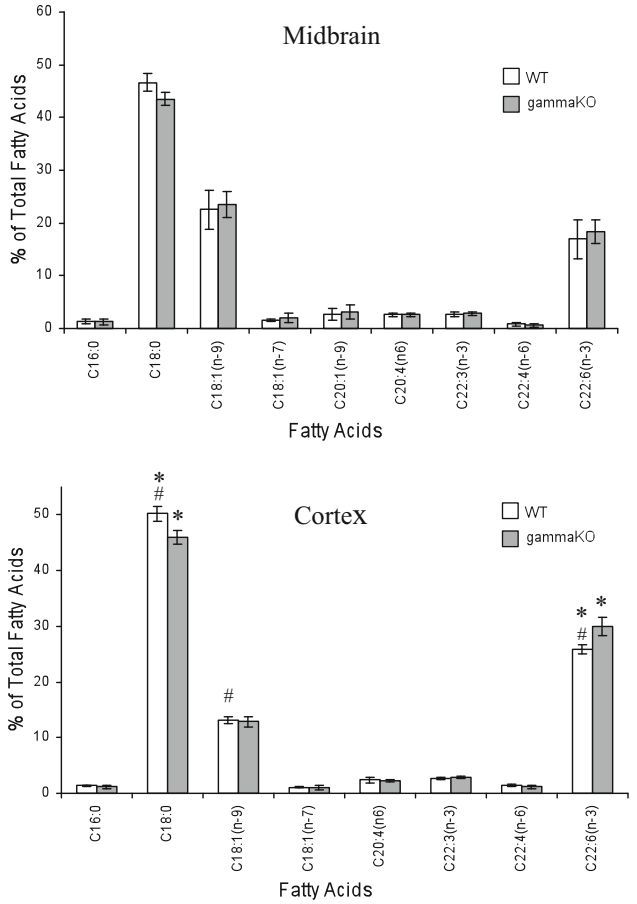

Fig. 2 Fatty acid composition of phosphatidylserine from midbrain or cortex in wild-type (WT) and γ-synuclein null mutant (gammaKO) mice. Values represent mean ± SD, $n = 5$. The *asterisk* (*) indicates a significant effect of γ-synuclein deficiency when compared with WT, and the *hash* (#) indicates significant differences between midbrain (*top panel*) and cortex (*bottom panel*) in WT animals ($p < 0.05$ for both). See legend to Table 1 for identification of fatty acids

Effect of γ-Synuclein Deficiency on the Fatty Acid Composition of Individual Polar Lipid Classes in Cortex and Midbrain

Figures 2, 3 and Table 3 show data on the fatty acid composition for the major polar lipids in cortex and midbrain from WT and gammaKO mice. These data show a fatty acid distribution typical of that for murine brain tissues.

PtdCho in both cortex and midbrain is characterised by a domination of palmitate (about 48 and 40% in cortex and midbrain, respectively), stearate (14 and 16%) and oleate (21 and 24%) with much lower levels of the two major brain long-chain polyunsaturated fatty acids, ARA and DHA (Table 3). In the cortex, the relative concentrations of ARA and DHA in PtdCho were about 6 and 3%, respectively. In the midbrain, about 4% of each of ARA and DHA was found in PtdCho. The levels of all above mentioned fatty acids were significantly different between the two brain regions. In contrast, there were no significant differences in these parameters between WT and gammaKO mice.

PtdIns is enriched with two fatty acids, stearic (around 44% in both cortex and midbrain) and ARA (37 and 34% in cortex and midbrain, respectively). DHA is a minor component in PtdIns and its relative concentration was about 2% in cortex and 4% in midbrain, these being significantly different. γ-Synuclein deficiency resulted in an increased level of ARA in PtdIns in cortex but did not affect the fatty acid profiles of this lipid in midbrain (Table 3).

Oleic and ARA were the major acids found in brain Ptd$_2$Gro. In this lipid, another C18:1 isomer, *cis*-vaccenic acid, was also present in appreciable amounts especially in the midbrain (around 11 vs. 7% in cortex). The relative concentration of ARA was higher in Ptd$_2$Gro from the cortex than in Ptd$_2$Gro from the midbrain (18 and 13%,

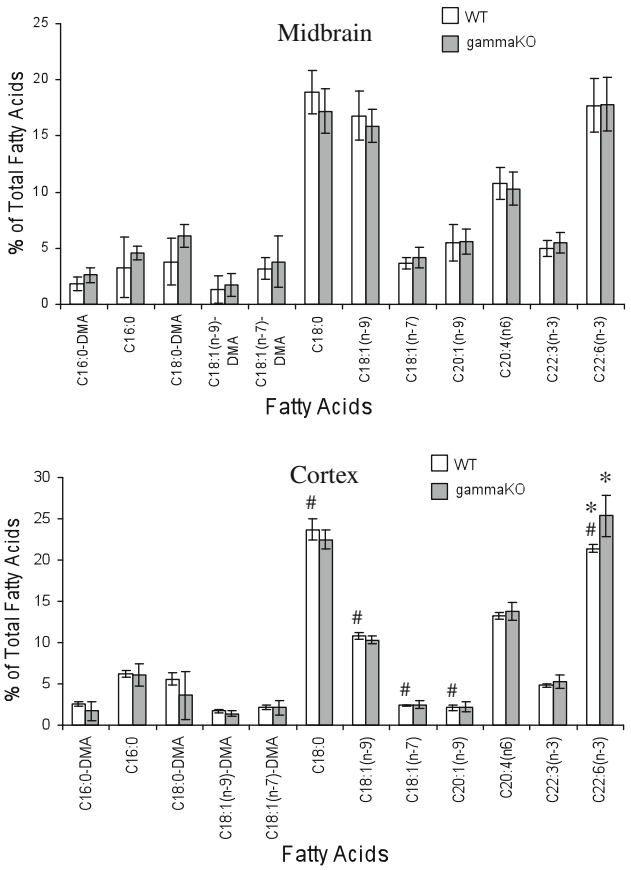

Fig. 3 Fatty acid and dimethylacetal composition of ethanolamine phospholipids from midbrain or cortex in wild-type (WT) and γ-synuclein null mutant (gammaKO) mice. Values represent mean ± SD, $n = 5$. The *asterisk* (*) indicates a significant effect of γ-synuclein deficiency when compared with WT, and the *hash* (#) indicates significant differences between midbrain (*top panel*) and cortex (*bottom panel*) in WT animals ($p < 0.05$ for both)

respectively). In comparison to other polar lipids isolated from the brain, Ptd_2Gro contains higher levels of C16 and C18 monoenic acids, namely C16:1n-7 (up to 5%), C18:1n-9 (up to 38%) and C18:1n-7 (up to 15%). The proportion of the latter was significantly higher in the midbrain than in cortex at the expense of arachidonic acid (Table 3). No statistically significant changes were found when comparing Ptd_2Gro fatty acid profiles in the cortex between WT and gammaKO animals, whereas in midbrain the proportion of C18:1n-7 was increased in gammaKO mice compared to WT (Table 3).

CerPCho from both cortex and midbrain contains stearic acid as its main fatty acid (up to 81% of total FAs in cortex, and up to 65% of that in midbrain). The presence of two very long chain acids, lignoceric (C24:0) and nervonic (C24:1n-6), is also characteristic for this lipid. Their levels were higher in midbrain than cortex. CerPCho fatty acids were unchanged as a response to γ-synuclein deficiency in

Table 3 Fatty acid composition (% of total fatty acids) in individual polar lipid classes from cortex or midbrain of wild-type (WT) and γ-synuclein null mutant (gammaKO) mice

FA	CORTEX		MIDBRAIN	
	WT	gammaKO	WT	gammaKO
Phosphatidylcholine				
C16:0	48.0 ± 2.7	45.2 ± 1.9	39.2 ± 3.5#	39.2 ± 2.6
C16:1 (n-7)	0.7 ± 0.1	0.8 ± 0.3	0.7 ± 0.2	0.9 ± 0.2
C18:0	3.7 ± 0.7	13.0 ± 0.7	16.5 ± 1.2#	15.1 ± 1.6
C18:1 (n-9)	20.6 ± 0.8	20.9 ± 1.1	24.1 ± 1.6#	23.9 ± 1.1
C18:1 (n-7)	5.1 ± 2.0	6.8 ± 0.9	7.2 ± 0.6	8.1 ± 1.6
C20:1 (n-9)	0.7 ± 0.1	0.7 ± 0.1	1.7 ± 0.5#	1.6 ± 0.3
C20:4 (n-6)	5.7 ± 0.6	6.4 ± 0.5	3.9 ± 0.7#	4.1 ± 0.6
C22:6 (n-3)	3.2 ± 0.5	3.8 ± 0.4	3.7 ± 0.6	4.3 ± 0.6
Phosphatidylinositol				
C16:0	8.2 ± 1.8	6.7 ± 1.9	7.3 ± 1.8	9.4 ± 2.1
C18:0	44.1 ± 3.2	40.7 ± 1.1	44.9 ± 3.2	40.7 ± 2.1
C18:1 (n-9)	5.1 ± 0.8	5.1 ± 0.6	5.5 ± 0.5	8.4 ± 2.4*
C18:1 (n-7)	2.2 ± 0.2	2.5 ± 0.4	2.5 ± 0.4	3.4 ± 0.7
C20:4 (n-6)	36.8 ± 3.5	41.8 ± 2.4*	33.5 ± 3.6	32.4 ± 1.1
C22:6 (n-3)	2.0 ± 0.8	2.2 ± 0.5	4.6 ± 1.7#	4.2 ± 1.3
Cardiolipin				
C16:0	6.7 ± 2.2	6.1 ± 2.2	7.8 ± 1.3	8.5 ± 1.9
C16:1 (n-7)	5.3 ± 1.1	5.1 ± 1.1	4.1 ± 2.6	4.8 ± 1.6
C18:0	8.1 ± 3.4	8.2 ± 3.5	10.6 ± 3.3	6.8 ± 2.9
C18:1 (n-9)	38.1 ± 2.2	36.4 ± 2.2	36.8 ± 2.3	33.9 ± 3.2
C18:1 (n-7)	6.9 ± 0.7	5.8 ± 0.9	10.5 ± 2.3#	15.4 ± 3.0*
C18:2 (n-6)	5.7 ± 2.1	4.8 ± 0.4	3.9 ± 0.6	4.2 ± 0.5
C20:3 (n-6)	1.9 ± 0.2	2.3 ± 0.4	1.7 ± 0.2	1.8 ± 0.2
C20:4 (n-6)	17.7 ± 2.3	19.4 ± 2.1	13.1 ± 2.2#	13.4 ± 0.8
C22:6 (n-3)	9.4 ± 2.3	11.5 ± 3.3	10.4 ± 2.9	10.7 ± 1.4
Sphingomyelin				
C16:0	4.8 ± 2.1	5.2 ± 2.0	5.2 ± 2.3	6.9 ± 4.0
C16:1 (n-7)	0.8 ± 0.2	0.7 ± 0.4	1.2 ± 0.6	1.6 ± 0.6
C18:0	80.6 ± 3.4	77.8 ± 1.7	65.0 ± 8.4#	55.1 ± 5.8*
C18:1 (n-9)	0.5 ± 0.2	1.2 ± 0.5	0.7 ± 0.3	1.7 ± 0.8
C20:0	2.3 ± 0.3	2.3 ± 0.3	2.8 ± 0.4	2.4 ± 0.2
C22:0	2.7 ± 0.5	2.4 ± 0.5	5.0 ± 2.1	4.6 ± 1.6
C24:0	2.1 ± 0.4	1.7 ± 0.4	4.5 ± 2.5	3.9 ± 1.0
C24:1 (n-6)	4.1 ± 2.1	7.3 ± 1.9	11.1 ± 5.7	19.9 ± 9.3
Sulfatide				
C16:0	6.9 ± 3.1	8.6 ± 1.8	7.9 ± 2.4	8.4 ± 2.4
C16:1 (n-7)	1.7 ± 0.2	1.8 ± 0.5	1.7 ± 1.0	1.6 ± 0.9
C18:0	20.7 ± 2.9	23.6 ± 2.4	19.0 ± 2.8	16.5 ± 3.5
C18:1 (n-9)	11.5 ± 1.7	13.2 ± 3.6	13.3 ± 1.4	14.1 ± 2.8
C18:1 (n-7)	1.4 ± 0.4	1.7 ± 0.4	2.2 ± 0.7	1.5 ± 0.9
C20:0	1.6 ± 0.2	1.5 ± 0.3	1.5 ± 0.4	1.3 ± 0.2
C20:1 (n-9)	1.6 ± 0.5	1.5 ± 0.7	2.2 ± 0.7	1.9 ± 0.6
C20:4 (n-6)	2.1 ± 1.1	2.3 ± 1.3	2.0 ± 0.5	2.2 ± 0.6
C22:0	6.6 ± 1.1	5.8 ± 0.8	6.0 ± 0.8	5.4 ± 0.8

Table 3 continued

FA	CORTEX		MIDBRAIN	
	WT	gammaKO	WT	gammaKO
C24:0	14.4 ± 2.0	11.5 ± 2.1*	12.9 ± 2.6	11.7 ± 1.2
C24:1 (n-6)	28.8 ± 4.9	27.7 ± 4.3	29.2 ± 3.7	34.5 ± 5.2
Cerebroside				
C16:0	3.1 ± 0.7	5.3 ± 2.7	3.7 ± 1.3	5.0 ± 2.5
C16:1 (n-7)	1.7 ± 0.2	1.7 ± 0.8	1.4 ± 0.7	0.8 ± 0.1
C18:0	11.4 ± 4.2	13.2 ± 4.4	12.1 ± 2.9	9.1 ± 3.0
C18:1 (n-9)	2.8 ± 1.1	4.6 ± 2.8	4.0 ± 0.7	7.0 ± 3.1
C18:1 (n-7)	0.4 ± 0.1	0.4 ± 0.2	0.8 ± 0.5	1.2 ± 0.5
C20:0	2.5 ± 0.1	2.0 ± 0.4	1.8 ± 0.5	1.6 ± 0.7
C20:1 (n-9)	0.4 ± 0.2	0.6 ± 0.3	0.8 ± 0.3	1.4 ± 0.5
C20:4 (n-6)	1.5 ± 0.9	2.3 ± 1.0	1.7 ± 1.0	2.2 ± 0.4
C22:0	12.0 ± 1.6	9.1 ± 1.7	10.2 ± 1.6	7.5 ± 0.8*
C22:1	1.9 ± 0.8	2.5 ± 0.2	2.0 ± 0.2	2.3 ± 0.3
C24:0	22.8 ± 4.0	15.7 ± 3.7*	21.4 ± 4.3	15.2 ± 2.8
C24:1 (n-6)	39.6 ± 6.5	42.4 ± 5.5	40.2 ± 6.3	46.9 ± 4.7

Data as means ± SD ($n = 6$–7)

See legend to Table 1 for other details

The asterisk (*) indicates a significant effect of γ-synuclein deficiency when compared with WT ($p < 0.05$). The hash (#) indicates significant differences between midbrain and cortex in WT animals ($p < 0.05$)

the cortex whereas in the midbrain decreased percentages of C18:0 was found.

Fatty acids from both sulfatides and cerebrosides did not show any differences between cortex and midbrain. γ-Synuclein deficiency resulted in a decreased proportion of lignoceric acid in sulfatides and cerebrosides in the cortex (Table 3). In midbrain region, a reduced relative proportion of behenic acid (C22:0) was found in cerebrosides in gammaKO mice (Table 3).

The fatty acid composition of PtdSer and PtdEtn which, in brain tissues, represent two lipid classes significantly enriched with the n-3 PUFA, DHA, are shown in Figs. 2 and 3, respectively. For PtdSer, the levels of both C18:0 and DHA were higher in cortex compared to midbrain while oleate was reduced (Fig. 2). Moreover, the level of DHA in PtdSer was significantly increased in the cortex of gammaKO mice compared to WT animals (30.0 and 25.8% of total FA, respectively) with a concomitant decrease in the proportion of stearate (C18:0) (Fig. 2). PtdEtn contained both ARA and DHA as major fatty acids and, similar to PtdSer, the proportion of DHA was enhanced significantly in cortex tissue (25.4%) in gammaKO mice as compared to control (21.4%). The proportions of ARA were unaffected by γ-synuclein deficiency in PtdEtn from both cortex and midbrain tissues (Fig. 3). In addition to fatty acids from the diacyl form of PtdEtn, we also analysed the profile of dimethylacetal (DMA) derivatives that represent aliphatic chains from ether derivatives (mainly plasmalogens) of PtdEtn (Fig. 3). Four DMA were identified with a domination of C18:0-DMA, but no significant changes in the relative proportion of these compounds in cortex and midbrain were found between WT and gammaKO mice.

In addition to the polar lipid classes described above, a C2-ceramide, *N*-acetylsphingosine, was present in lipid extracts from both cortex and midbrain in small but significant amounts [53]. The structure of this ceramide was elucidated by using ESI–MS (data not shown).

Discussion

The importance of lipids in neural tissue physiology and cell signalling has been demonstrated by the association of lipid imbalances and/or deregulated lipid metabolism with the development of various CNS disorders, including Alzheimer's disease, Parkinson's disease, Niemann–Pick disease, multiple sclerosis, Huntington's disease, amyotrophic lateral sclerosis, schizophrenia, bipolar disorders and epilepsy [54]. Recently, relationships between glucosylsphingosine accumulation due to mutations in the glucocerebrosidase gene (*GBA*) and Parkinsonism as well as dementia with Lewy bodies, have been reported [55, 56]. Because alterations in brain lipid biochemistry have been previously linked to the α-synuclein deficiency [41, 57] and since γ-synuclein and α-synuclein are closely-related proteins, whose functions are potentially redundant [47, 58, 59], it was clearly important to evaluate if γ-synuclein might also be involved in brain lipid homeostasis. In our study we examined the lipid composition of two brain regions, the midbrain that exhibits relatively high level of γ-synuclein expression, and the cerebral cortex, where expression level of this protein is substantially lower [46, 60].

No effect of γ-synuclein deficiency on the total polar lipid content and TAG accumulation in the cerebral cortex and midbrain was revealed in our work (data not shown). This contrasts to studies with α-synuclein deficient mice where an increase in TAG content of the whole brain has been demonstrated [41].

The mitochondria-specific phospholipid, Ptd_2Gro, which was found in both regions studied (4% of the total polar lipids), was not affected by γ-synuclein deficiency (Fig. 1). The fatty acid profile of Ptd_2Gro was also almost the same (Table 3). This was different from α-synuclein deficient mice that had a reduced total brain Ptd_2Gro content with a strongly altered acyl chain composition, a mitochondrial lipid abnormality possibly associated with electron transport chain impairment in the brain of PD patients [42].

Therefore, it is unlikely that the γ-synuclein deficiency affects mitochondrial function in the nervous system.

Similar to α-synuclein deficiency [41], γ-synuclein deficiency did not change the level of ethanolamine phospholipids (Fig. 1). The plasmenyl species of PtdEtn are important phospholipid components of most electroactive cellular membranes, such as cardiac sarcolemma and neuronal cell membranes. Between one-half and two-thirds of the ethanolamine phospholipids in the whole brain are in plasmalogen form, and 11–12% of myelin phospholipids are plasmalogens [61]. A deficiency of ethanolamine plasmalogens has been shown to be associated with aging and some degenerative diseases, especially those associated with peroxisomal disorders [62–64]. The absence of ethanolamine plasmalogen alterations is consistent with only mild alterations in normal neural function in both α-synuclein and γ-synuclein deficient mice. However, further comparative studies of aging mice would be important, due to various effects of aging on their nervous systems [65].

Among polar lipids, only the relative proportion of PtdSer changed in gammaKO in comparison to WT mice (Fig. 1). This change was evident only in the midbrain region where expression of γ-synuclein is much higher than in the cerebral cortex [46]. Although this increase was relatively minor in the whole midbrain tissue, the changes in PtdSer content may be much more pronounced in specific neuronal populations since γ-synuclein has been shown to be expressed only in a subset of midbrain neurons [46]. Previously, increases in PtdSer have been noted in plasma membrane phospholipids from affected regions of AD brains [63] where they may induce formation of amyloid fibers [66]. It is also of note, that PtdSer has roles in apoptosis, in the regulation of many enzymes and in control of the channel function of the acetylcholine receptor [62, 67, 68]. Thus, alteration in PtdSer may have implications for neuronal cell functions. However, the changes observed were not sufficient for triggering pathological alterations in the nervous system of γ-synuclein deficient mice [46, 47, 59].

Three lipid classes in brain contain high levels of PUFA. Whereas PtdSer and PtdEtn are enriched in DHA, PtdIns contains substantial amounts of ARA. When comparing midbrain and cortex regions, the latter was enriched in ARA but depleted in DHA (Table 2). These differences may be partly explained by higher content of PtdCho (Fig. 1), which possesses elevated levels of ARA, in the cerebral cortex (Table 3). Interestingly, statistically significant changes were found in the relative amount of PtdSer in the midbrain region of γ-synuclein null mutant mice (Fig. 1) and in the DHA content of both PtdSer (Fig. 2) and ethanolamine phospholipids (Fig. 3) in the cerebral cortex. Because only a limited number of cortical neurons normally express γ-synuclein, changes of DHA levels in these cells might be much more profound than those revealed by analysis of total cortex phospholipids. It is noteworthy that although α-synuclein null mutant mice had slightly decreased levels of DHA in the whole brain PtdEtn and PtdSer, an increased uptake of this fatty acid into brain phospholipids has also been reported [69]. It is well known that DHA is essential to perinatal neurological development during which it increases in the CNS. The high demand for DHA in the brain is maintained either by dietary supply or by biosynthesis from α-linolenate within the liver [33]. Since no very long-chain PUFA were present in the diet, and no changes in the liver (data not shown) or plasma PUFA profiles (Table 1) were found, we suggest that the differences in DHA levels are most likely related to possible effects of γ-synuclein deficiency on DHA metabolism in the developing brain. Alternatively, complete absence of γ-synuclein might trigger systemic changes, including alterations in adipose and other tissues normally expressing this protein, that activate compensatory mechanisms during brain development.

There is a growing body of evidence about the importance of PUFA in brain function where its deficiency is associated with cognitive decline during aging and with neurodegenerative diseases [70]. The beneficial neurophysiological role of DHA most probably relates to metabolites such as eicosanoids and other autacoids which are important as modulators of membrane microdomain composition, receptor signalling and gene expression [71]. Recent studies demonstrated a role for neuroprotectin D1 (NPD1) in the homeostatic regulation of brain cell survival and repair involving neurotrophic, anti-apoptotic and anti-inflammatory signalling in AD [70]. Unfortunately, there is no information about the possible involvement of such DHA metabolites in PD. But the gammaKO mutants, which exhibit higher levels of DHA accumulation in certain brain regions, may be a useful model for future research in this area.

Acknowledgments This work was supported by the Wellcome Trust Programme Grant to VLB. We are also grateful for equipment funding provided by the Wellcome Trust (VO'D, JLH).

References

1. Lavedan C (2008) The synuclein family. Genome Res 8:871–880
2. Polymeropoulos MH, Lavedan C, Leroy E, Ide SE, Dehejia A, Dutra A, Pike B, Root H, Rubenstein J, Boyer R, Stenroos ES,

Chandrasekharappa S, Athanassiadou A, Papapetropoulos T, Johnson WG, Lazzarini AM, Duvoisin RC, Di Iorio G, Golbe LI, Nussbaum RL (1997) Mutation in the alpha-synuclein gene identified in families with Parkinson's disease. Science 276:2045–2047
3. Kruger R, Kuhn W, Muller T, Woitalla D, Graeber M, Kosel S, Przuntek H, Epplen JT, Schols L, Riess O (1998) Ala30Pro mutation in the gene encoding alpha-synuclein in Parkinson's disease. Nat Genet 18:106–108
4. Singleton AB et al (2003) alpha-Synuclein locus triplication causes Parkinson's disease. Science 302:841
5. Chartier-Harlin MC, Kachergus J, Roumier C, Mouroux V, Douay X, Lincoln S, Levecque C, Larvor L, Andrieux J, Hulihan M, Waucquier N, Defebvre L, Amouyel P, Farrer M, Destee A (2004) Alpha-synuclein locus duplication as a cause of familial Parkinson's disease. Lancet 364:1167–1169
6. Ibanez P, Bonnet AM, Debarges B, Lohmann E, Tison F, Pollak P, Agid Y, Durr A, Brice A (2004) Causal relation between alpha-synuclein gene duplication and familial Parkinson's disease. Lancet 364:1169–1171
7. Zarranz JJ, Alegre J, Gomez-Esteban JC, Lezcano E, Ros R, Ampuero I, Vidal L, Hoenicka J, Rodriguez O, Atares B, Llorens V, Gomez Tortosa E, del Ser T, Munoz DG, de Yebenes JG (2004) The new mutation, E46K, of alpha-synuclein causes Parkinson and Lewy body dementia. Ann Neurol 55:164–173
8. Kay DM, Factor SA, Samii A, Higgins DS, Griffith A, Roberts JW, Leis BC, Nutt JG, Montimurro JS, Keefe RG, Atkins AJ, Yearout D, Zabetian CP, Payami H (2008) Genetic association between alpha-synuclein and idiopathic Parkinson's disease. Am J Med Genet B Neuropsychiatr Genet 147B:1222–1230
9. Mizuta I, Tsunoda T, Satake W, Nakabayashi Y, Watanabe M, Takeda A, Hasegawa K, Nakashima K, Yamamoto M, Hattori N, Murata M, Toda T (2008) Calbindin 1, fibroblast growth factor 20, and alpha-synuclein in sporadic Parkinson's disease. Hum Genet 124:89–94
10. Pankratz N, Wilk JB, Latourelle JC, DeStefano AL, Halter C, Pugh EW, Doheny KF, Gusella JF, Nichols WC, Foroud T, Myers RH (2009) Genomewide association study for susceptibility genes contributing to familial Parkinson disease. Hum Genet 124:593–605
11. Scholz SW et al (2009) SNCA variants are associated with increased risk for multiple system atrophy. Ann Neurol 65:610–614
12. Sutherland GT, Halliday GM, Silburn PA, Mastaglia FL, Rowe DB, Boyle RS, O'Sullivan JD, Ly T, Wilton SD, Mellick GD (2009) Do polymorphisms in the familial Parkinsonism genes contribute to risk for sporadic Parkinson's disease? Mov Disord 24:833–838
13. Caughey B, Lansbury PT (2003) Protofibrils, pores, fibrils, and neurodegeneration: separating the responsible protein aggregates from the innocent bystanders. Annu Rev Neurosci 26:267–298
14. Dev KK, Hofele K, Barbieri S, Buchman VL, van der Putten H (2003) Part II: alpha-synuclein and its molecular pathophysiological role in neurodegenerative disease. Neuropharmacology 45:14–44
15. Fink AL (2006) The aggregation and fibrillation of alpha-synuclein. Acc Chem Res 39:628–634
16. Uversky VN (2007) Neuropathology, biochemistry, and biophysics of alpha-synuclein aggregation. J Neurochem 103:17–37
17. Jo E, McLaurin J, Yip CM, St George-Hyslop P, Fraser PE (2000) α-Synuclein membrane interactions and lipid specificity. J Biol Chem 275:34328–34334
18. Davidson WS, Jonas A, Poon AW, Conway KA, Browne G (1998) Stabilization of α-synuclein secondary structure upon binding to synthetic membranes. J Biol Chem 273:9443–9449
19. Ramakrishnan M, Jensen PH, Marsh D (2003) α-Synuclein associated with phosphatidylglycerol probed by lipid spin labels. Biochemistry 42:12919–12926
20. Uversky VN, Li J, Souillac P, Millett IS, Doniach S, Jakes R, Goedert M, Fink AL (2002) Biophysical properties of the synucleins and their propensities to fibrillate. J Biol Chem 277: 11970–11978
21. Cole NB, Murphy DD, Grider T, Rueter S, Brasaemle D, Nussbaum RL (2002) Lipid droplet binding and oligomerization properties of the Parkinson's disease protein α-synuclein. J Biol Chem 277:6344–6352
22. Fortin DL, Troyer MD, Nakamura K, Kubo S-I, Anthony MD, Edwards RH (2004) Lipid rafts mediate the synaptic localization of α-synuclein. J Neurosci 28:6715–6723
23. Kubo S, Nemani VM, Chalkley RJ, Anthony MD, Hattori N, Mizuno Y, Edwards RH, Fortin DL (2005) A combinatorial code for the interaction of α-synuclein with membranes. J Biol Chem 280:31664–31672
24. Martinez Z, Zhu M, Han S, Fink AL (2007) GM1 specifically interacts with α-synuclein and inhibits fibrillation. Biochem 46:1868–1877
25. Pasquale ED, Fantini J, Chahinian H, Maresca M, Taïeb N, Yahi N (2010) Altered ion channel formation by the Parkinson's-disease-linked E46K mutant of α-synuclein is correlated by GM3 but not GM1 gangliosides. J Mol Biol 397:202–218
26. Perrin RJ, Woods WS, Clayton DF, George JM (2001) Exposure to long chain polyunsaturated fatty acids triggers rapid multimerization of synucleins. J Biol Chem 276:41958–41962
27. Sharon R, Bar-Joseph I, Frosch MP, Walsh DM, Hamilton JA, Selkoe DJ (2003) The formation of highly soluble oligomers of α-synuclein is regulated by fatty acids and enhanced in Parkinson's disease. Neuron 37:583–595
28. Sharon R, Bar-Joseph I, Mirick GE, Serhan CN, Selkoe DJ (2003) Altered fatty acid composition of dopaminergic neurons expressing α-synuclein and human brains with α-synucleinopathies. J Biol Chem 278:49874–49881
29. Valentine RC, Valentine DL (2004) Omega-3 fatty acids in cellular membranes: a unified concept. Prog Lipid Res 43:383–402
30. Maldjian A, Cristofori C, Noble RC, Speake BK (1996) The fatty acid composition of brain phospholipids from chicken and duck embryos. Comp Biochem Physiol B Biochem Mol Biol 115: 153–158
31. Salem N Jr, Moriguchi T, Greiner RS, McBride K, Ahmad A, Catalan JN, Slotnick B (2001) Alterations in brain function after loss of docosahexaenoate due to dietary restriction of n-3 fatty acids. J Mol Neurosci 16:299–308
32. Bourre JM, Francois M, Youyou A, Dumont O, Piciotti M, Pascal G, Durand G (1989) The effects of dietary alpha-linolenic acid on the composition of nerve membranes, enzymatic activity, amplitude of electrophysiological parameters, resistance to poisons and performance of learning tasks in rats. J Nutr 119:1880–1892
33. Barceló-Coblijn G, Murphy EJ (2009) Alpha-linolenic acid and its conversion to longer chain n-3 fatty acids: benefits for human health and a role in maintaining tissue n-3 fatty acid levels. Prog Lipid Res 48:355–374
34. Willatts P, Forsyth JS, Di Midugno MK, Varma S, Colvin M (1998) Effect of long-chain polyunsaturated fatty acids in infant formula on problem solving at 10 months of age. Lancet 352:688–691
35. Martinez M (1990) Severe deficiency of docosahexaenoic acid in peroxisomal disorders: a defect of delta 4 desaturation? Neurology 40:1292–1298
36. Soderberg M, Edlund C, Kristensson K, Dallner G (1991) Fatty acid composition of brain phospholipids in aging and Alzheimer's disease. Lipids 26:421–425
37. Hooijmans CR, Kiliaan AJ (2008) Fatty acids, lipid metabolism and Alzheimer pathology. Eur J Pharm 585:176–196

38. Kitajka K, Puskas LG, Zvara A, Hackler L, Barcelo-Coblijn G, Yeo YK (2002) The role of n-3 polyunsaturated fatty acids in brain: modulation of rat brain gene expression by dietary fatty acids. PNAS 99:2619–2624
39. Cansev M, Ulus IH, Wang L, Maher TJ, Wurtman RJ (2008) Restorative effects of uridine plus docosahexaenoic acid in a rat model of Parkinson's disease. Neurosci Res 62:206–209
40. Bousquet M, Saint-Pierre M, Julien C, Salem C Jr, Gicchetti F, Calon F (2008) Beneficial effects of dietary omega-3 polyunsaturated fatty acid on toxin-induced neuronal degeneration in an animal model of Parkinson's disease. FASEB J 22:1213–1225
41. Barceló-Coblijn G, Golovko MY, Weinhofer I, Berger J, Murphy EJ (2007) Brain neutral lipid mass is increased in α-synuclein gene-ablated mice. J Neurochem 101:132–141
42. Ellis CE, Murphy EJ, Mitchell DC, Golovko MY, Scaglia FS, Barceló-Coblijn G, Nussbaum RL (2005) Mitochondrial lipid abnormality and electron transport chain impairment in mice lacking α-synuclein. Mol Cell Biol 25:10190–10201
43. Golovko MY, Rosenberger TA, Faergeman NJ, Feddersen S, Cole NB, Pribill I, Berger J, Nussbaum RL, Murphy EJ (2006) Acyl-CoA synthetase activity links wild-type wild type but not mutant alpha-synuclein to brain arachidonate metabolism. Biochem 45:6956–6966
44. Oort PJ, Knotts TA, Grino M, Naour N, Bastard J-P, Clément K, Ninkina N, Buchman VL, Permana P, Luo X, Pan G, Dunn TN, Adams SH (2008) γ-Synuclein is an adipocyte-neuron gene coordinately-expressed with leptin and increased in human obesity. J Nutr 135:841–848
45. Frandsen PM, Madsen LB, Bendixen C, Larsen K (2009) Porcine gamma-synuclein: molecular cloning, expression analysis, chromosomal localization and functional expression. Mol Biol Res 36:971–976
46. Ninkina N, Papachroni K, Robertson DC, Schmidt O, Delaney L, O'Neill F, Court F, Rosenthal A, Fleetwood-Walker SM, Davies AM, Buchman VL (2003) Neurons expressing the highest levels of γ-synuclein are unaffected by targeted inactivation of the gene. Mol Cell Biol 23:8233–8245
47. Robertson DC, Schmidt O, Ninkina N, Jones PA, Sharkey J, Buchman VL (2004) Developmental loss and resistance to MPTP toxicity of dopaminergic neurons in substantia nigra pars compacta of γ-synuclein, α-synuclein and double α/γ-synuclein null mutant mice. J Neurochem 89:1126–1136
48. Garbus J, De Luca HF, Loomans ME, Strong FM (1963) The rapid incorporation of phosphate in mitochondrial lipids. J Biol Chem 238:59–63
49. Kates M (1986) Techniques of lipidology: isolation, analysis and identification of lipids, 2nd edn. Elsevier, Amsterdam
50. Simopoulos AP, Leaf A, Salem N Jr (2000) Workshop statement on the essentiality of and recommended dietary intakes for omega-6 and omega-3 fatty acids. Prostag Leukotr Ess Fatty Acids 63:119–121
51. Hsu F-F, Bohrer A, Turk J (1998) Electrospray ionization mass spectrometric analysis of sulfatide. Determination of fragmentation patterns and characterization of molecular species expressed in brain and in pancreatic islets. Biochim Biophys Acta 1392:202–216
52. Han X, Cheng H (2005) Characterization and direct quantitation of cerebroside molecular species from lipid extracts by shotgun lipidomics. J Lipid Res 46:163–175
53. Van Overloop H, Denizot Y, Baes M, Van Veldhoven PP (2007) On the presence of C_2-ceramide in mammalian tissues: possible relationship to etherphospholipids and phosphorylation by ceramide kinase. Biol Chem 388:315–3244
54. Adibhatla RM, Hatcher JF (2007) Role of lipids in brain injury and diseases. Future Lipidol 2:403–422
55. Aharon-Peretz J, Rosenbaum H, Gershoni-Baruch R (2004) Mutation in the glucocerebrosidase gene and Parkinson's disease in Ashkenazi Jews. N Engl J Med 351:1972–1977
56. Clark LN, Kartsaklis LA, Gilbert RW, Dorado B, Ross BM, Kisselev S, Verbitsky M, Mejia-Santana H, Cote LJ, Andrews H, Vonsattel J-P, Fahn S, Mayeux R, Honig LS, Marder K (2009) Association of glucocerebrosidase mutations with dementia with Lewy bodies. Arch Neurol 66:578–583
57. Rappley I, Myers DS, Milne SB, Ivanova PT, LaVoie MJ, Brown HA, Selkoe DJ (2009) Lipidomic profiling in mouse brain reveals differences between ages and genders, with smaller changes associated with α-synuclein genotype. J Neurochem 111:15–25
58. Chandra S, Fornai F, Kwon HB, Yazdani U, Atasoy D, Liu X, Hammer RE, Battaglia G, German DC, Castillo PE, Sudhof TC (2004) Double-knockout mice for alpha- and beta-synucleins: effect on synaptic functions. Proc Natl Acad Sci USA 101:14966–14971
59. Senior SL, Ninkina N, Deacon R, Bannerman D, Buchman VL, Cragg SJ, Wade-Martins R (2008) Increased striatal dopamine release and hyperdopaminergic-like behaviour in mice lacking both alpha-synuclein and gamma-synuclein. Eur J Neurosci 27:947–957
60. Abeliovich A, Schmitz Y, Farinas I, Choi-Lundberg D, Ho WH, Castillo PE, Shinsky N, Verdugo JM, Armanini M, Ryan A et al (2000) Mice lacking alpha-synuclein display functional deficits in the nigrostriatal dopamine system. Neuron 25:239–252
61. Nagan N, Zoeller RA (2001) Plasmalogens: biosynthesis and functions. Prog Lipid Res 40:199–229
62. Farooqui AA, Horrocks LA, Farooqui T (2000) Glycerophospholipids in brain: their metabolism, incorporation into membranes, functions, and involvement in neurological disorders. Chem Phys Lipids 106:1–29
63. Farooqui AA, Rapoport SI, Horrocks LA (1997) Membrane phospholipid alterations in Alzheimer's disease: deficiency of ethanolamine plasmalogens. Neurochem Res 22:523–527
64. Dragonas C, Bertsch T, Sieber CC, Brosche T (2009) Plasmalogens as a marker of elevated systematic oxidative stress in Parkinson's disease. Clin Chem Lab Med 47:894–897
65. Al-Wandi A, Ninkina N, Millership S, Williamson SJ, Jones PA, Buchman VL (2010) Absence of alpha-synuclein affects dopamine metabolism and synaptic markers in the striatum of aging mice. Neurobiol Aging 31:796–804
66. Zhao H, Tuominen EKJ, Kinnunen PKJ (2004) Formation of amyloid fibers triggered by phosphatidylserine-containing membranes. Biochem 43:10302–10307
67. Mozzi R, Buratta S, Goracci G (2003) Metabolism and functions of phosphatidylserine in mammalian brain. Neurochem Res 28:195–214
68. Sunshine C, McNamee MG (1992) Lipid modulation of nicotinic acetylcholine receptor function: the role of neutral and negatively charged lipids. Biochim Biophys Acta 1108:240–246
69. Golovko MY, Rosenberger TA, Feddersen S, Faergeman NJ, Murphy EJ (2007) Alpha-synuclein gene ablation increases docosahexaenoic acid incorporation and turnover in brain phospholipids. J Neurochem 101:201–211
70. Lukiw WJ, Bazan NG (2008) Docosahexaenoic acid and the aging brain. J Nutr 138:2510–2514
71. Kim H-Y (2007) Novel metabolism of docosahexaenoic acid in neural cells. J Biol Chem 282:18661–18665

Lipids (2011) 46:131–142
DOI 10.1007/s11745-010-3502-4

ORIGINAL ARTICLE

COX-2 Inhibition and Inhibition of Cytosolic Phospholipase A2 Increase CD36 Expression and Foam Cell Formation in THP-1 Cells

Kamran Anwar · Iryna Voloshyna · Michael J. Littlefield · Steven E. Carsons · Peter A. Wirkowski · Nadia L. Jaber · Andrew Sohn · Sajan Eapen · Allison B. Reiss

Received: 2 August 2010 / Accepted: 4 November 2010 / Published online: 22 December 2010

Abstract Cardiovascular safety of cyclooxygenase (COX)-2-selective inhibitors and nonselective nonsteroidal anti-inflammatory drugs (NSAIDs) is of worldwide concern. COX-2 inhibitors and NSAIDs act by inhibiting arachidonic acid metabolism to prostaglandins. They confer a cardiovascular hazard manifested as an elevated risk of myocardial infarction. Mechanisms underlying these cardiovascular effects are uncertain. Here we determine whether interference with cytosolic phospholipase A2 (cPLA-2) or COX-2 through pharmacologic blockade or silencing RNA impacts expression of scavenger receptor CD36 and scavenger receptor A, both involved in cholesterol uptake in monocytes and macrophages. THP-1 human monocytes and human peripheral blood mononuclear cells were exposed to celecoxib, a COX-2 selective inhibitor currently in clinical use, and to arachidonyl trifluoromethyl ketone (AACOCF3), an arachidonic acid analog that selectively inhibits cPLA-2. Celecoxib and AACOCF3 each upregulated expression of CD36, but not scavenger receptor A, as determined by quantitative PCR and immunoblotting. Silencing of cPLA-2 or COX-2 had comparable effects to pharmacologic treatments. Oil red O staining revealed a profound increase in foam cell transformation of THP-1 macrophages exposed to either celecoxib or AACOCF3 (both 25 μM), supporting a role for the COX pathway in maintaining macrophage cholesterol homeostasis. Demonstration of disrupted cholesterol balance by AACOCF3 and celecoxib provides further evidence of the possible mechanism by which COX inhibition may promote lipid overload leading to atheromatous lesion formation and increased cardiovascular events.

Keywords Cyclooxygenase · Atherosclerosis · Gene transcription · Cholesterol · Arachidonic acid

Abbreviations

AACOCF3	Arachidonyl trifluoromethyl ketone
COX	Cyclooxygenase
cPLA-2	Cytosolic phospholipase A2
FCS	Fetal calf serum
GAPDH	Glyceraldehyde-3-phosphate dehydrogenase
IFN	Interferon
HRP	Horseradish peroxidase
LDL	Low density lipoprotein
NSAIDs	Nonsteroidal anti-inflammatory drugs
PBMC	Peripheral blood mononuclear cells
PMA	Phorbol 12-myristate 13-acetate
RCT	Reverse cholesterol transport
ScR-A	Scavenger receptor A
TGF	Transforming growth factor

Introduction

Atherosclerosis is a leading cause of death and impairment in developed countries and is the underlying cause of myocardial infarction, stroke, and peripheral artery disease

Electronic supplementary material The online version of this article (doi:10.1007/s11745-010-3502-4) contains supplementary material, which is available to authorized users.

K. Anwar · I. Voloshyna · M. J. Littlefield · S. E. Carsons · P. A. Wirkowski · N. L. Jaber · A. Sohn · S. Eapen · A. B. Reiss (✉)
Department of Medicine, Winthrop-University Hospital, 222 Station Plaza North, Suite 502, Mineola, NY 11501, USA
e-mail: AReiss@winthrop.org

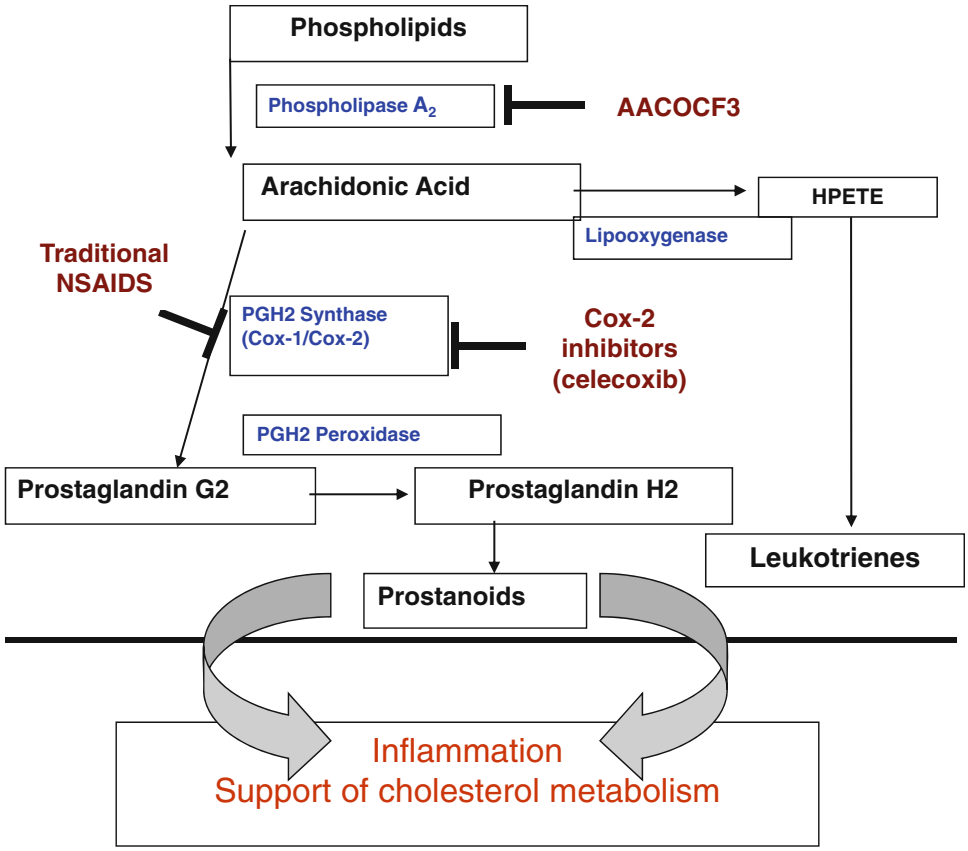

Fig. 1 Molecular pathway for formation of eicosanoids and prostanoids and where different drugs have their effects. cPLA-2 catalyzes the release of arachidonic acid from cell membrane phospholipids. Specific blockade of cPLA-2 with AACOCF3 abrogates eicosanoid synthesis through the arachidonic acid pathway. COX converts arachidonic acid to endoperoxide-containing intermediates to produce prostanoids–prostaglandins and thromboxanes. NSAIDs and COX-2 specific inhibitors reduce formation of these prostanoids, bioactive lipid mediators that support normal cholesterol flux

[1, 2]. It is characterized by accumulation of cholesterol and its esters in the vessel wall, either within macrophage foam cells or as extracellular lipids, including free cholesterol crystals. Unlike the classical low density lipoprotein (LDL) receptor, which is downregulated by increasing cellular cholesterol levels, the ability of scavenger receptors on the macrophage surface to take up modified LDL is not inhibited by increasing cellular cholesterol [3]. Substantial quantities of modified forms of LDL may be internalized by macrophages via scavenger receptors whose expression is not controlled by cholesterol loading, leading to foam cell formation [4, 5]. Lipid-laden foam cells are found within the sub-endothelial space of the arteries in fatty streak lesions, which are the first recognizable atherosclerotic lesions, as well as in more-advanced unstable atherosclerotic plaques.

It is now well-established that endocytic uptake of atherogenic lipoproteins by macrophages or macrophage-derived cells is mainly mediated by scavenger receptors, including scavenger receptor A (ScR-A) and CD36 [6]. The CD36 scavenger receptor is specific for nitrated LDL and oxidized LDL, the most atherogenic forms of modified LDL.

Inhibition of cyclooxygenase (COX) by either non-steroidal anti-inflammatory drugs (NSAIDs), which inhibit both COX-1 and COX-2 isoforms, or by COX-2 specific inhibitors (coxibs) provides analgesia and anti-inflammatory efficacy [7]. Coxibs and NSAIDs have been associated with increased frequency of cardiovascular toxicity and an elevated risk of acute myocardial infarction [8, 9]. The COX-2 inhibitors rofecoxib and valdecoxib have been withdrawn from the market, and two other coxibs failed to receive approval due to cardiovascular concerns [10–12].

The mechanisms underlying cardiovascular effects of coxibs are uncertain [13]. Our laboratory has previously demonstrated that both the NSAID indomethacin and the COX-2-selective inhibitor NS398 suppress expression of cholesterol 27-hydroxylase and ABCA1, proteins involved in reverse cholesterol transport (RCT) from the periphery to the liver for metabolism [14, 15]. This observation led us to propose that interference with normal cholesterol outflow from macrophages accelerates atheroma development, contributing to the cardiovascular consequences of coxib administration and that these effects may be reversible. In the present study, we extend our examination to determine whether interference with the COX/arachidonic acid pathway impacts expression of scavenger receptor genes involved in cholesterol uptake in human monocytes/macrophages. Our study used the COX-2 specific inhibitor celecoxib as well as arachidonyl trifluoromethyl ketone (AACOCF3), a cell-permeable trifluoromethyl ketone analog of arachidonic acid that selectively inhibits cytosolic phospholipase A2 (cPLA-2) (Fig. 1).

The effect of COX-2 and cPLA-2 inhibition on CD36 is measured against known effects of specific cytokines. In a follow-up to our previous reports that the pro-atherogenic cytokine interferon (IFN)-γ suppresses RCT proteins and increases foam cell formation in THP-1 human macrophages [16–18], we compare the impact of IFN-γ to COX/arachidonic acid pathway inhibition on the expression of CD36 and ScR-A1. Since the cytokine TGF-β may be involved in cardiovascular pathophysiology and has been reported to downregulate expression of scavenger receptors ScR-A and CD36, in human macrophages [19, 20], TGF-β was used as a known control in these studies.

Experimental Procedures

Cell Culture

THP-1 monocytes (American Type Culture Collection, Manassas, VA) were cultured in RPMI 1640 supplemented with 10% fetal calf serum (FCS), 2 mM L-glutamine and 50 μg per ml of penicillin–streptomycin at 37 °C in a 5% CO_2 atmosphere to a density of 10^6 cells per ml. Cell culture media and supplementary reagents were obtained from Invitrogen (Grand Island, NY). Differentiation of the monocytic THP-1 cells into adherent macrophages was stimulated by 48 h of exposure to 100 nM phorbol 12-myristate 13-acetate (PMA), obtained from Sigma–Aldrich (St. Louis, MO). When differentiated phenotype was achieved, the PMA-containing medium was removed, and replaced with complete RPMI 1640, supplemented with 10% FCS. The macrophages were cultured for another 24 h before treatment. THP-1 in both monocyte and macrophage states were subjected to the experimental conditions described below.

Human peripheral blood mononuclear cells (PBMC) were isolated from fresh blood obtained from healthy donors. The investigation conforms with the principles outlined in the Declaration of Helsinki. Approval for use of human blood was granted by the Winthrop University Hospital Institutional Review Board. Blood was collected in EDTA treated tubes, adjusted to a density of 1.120 g/ml with the addition of OptiPrep Density Gradient Media (Sigma–Aldrich, St. Louis, MO), according to the manufacturer's instructions. The blood was then overlaid with a 1.074 g/ml density solution composed of complete RPMI 1640 containing 10% FCS and OptiPrep Gradient Media. A layer of complete RPMI containing 10% FCS was then overlaid on top to prevent monocytes from sticking to the plastic tube. The blood was centrifuged at 750*g* for 30 min at 4 °C, then the monocyte interphase was collected from between the 1.074 g/ml and RPMI layers. The collected cells were diluted with two volumes of complete RPMI and harvested by centrifugation. The pellet was resuspended in complete RPMI. The monocytes were then counted with a hemocytometer and plated at a density of 2×10^6 cells/well in 6-well plates. Cells were maintained in complete RPMI 1640, supplemented with 10% FCS and were subjected to the experimental conditions described below.

Experimental Conditions

THP-1 monocytes, THP-1 macrophages and PBMC were incubated in six-well plates at 37 °C in a 5% CO_2 atmosphere for 18 and 24 h in RPMI media under the following six conditions: (1) no additions (untreated control); (2) DMSO vehicle (solvent control); (3) IFN-γ (500 U/ml); (4) celecoxib (25 μM); (5) AACOCF3 (25 μM); (6) transforming growth factor (TGF)-β (120 pg/ml).

AACOCF3 was purchased from Sigma–Aldrich (St. Louis, MO). Recombinant human IFN-γ and TGF-β were purchased from R&D Systems, Inc. (Minneapolis, MN). Celecoxib was obtained from Pfizer (New York, NY). AACOCF3 and celecoxib were dissolved in DMSO (Sigma, Indianapolis, IN) to form 100X stock solutions [21, 22].

Immediately after the incubation period, the cells were collected and centrifuged at 1,500 rpm at room temperature, media was aspirated, and cell protein and RNA were isolated.

Transfection of Small Interfering (si) RNA

Transfection of THP-1 monocytes was carried out when they achieved 70% confluence, approximately 24 h after seeding. Transfection was performed in serum-free medium using siRNA transfection reagent (Santa Cruz, CA, sc-29528). Cells were transfected for 6 h with 100 nM of human COX-2 and cPLA-2 small interfering RNA (siRNA) (Santa Cruz, CA, sc-29528 and sc-29280), or irrelevant non-targeting control siRNA-A (Santa Cruz, CA, sc-37007) according to the manufacturer's protocol. Cells were then further incubated for 24–72 h under standard growth conditions. At 24–72 h post-transfection, depletion of COX-2 was confirmed and expression of CD36 and ScR-A1 were analyzed by quantitative real-time (QRT)-PCR and immunoblotting.

RNA Isolation and cDNA Preparation

Total RNA was isolated using 1 ml per 10^6 cells of Trizol reagent (Invitrogen, Grand Island, NY). The quantity of total RNA from each condition was measured by absorption at 260 and 280 nm wavelengths by ultraviolet spectrophotometry (Hitachi U2010).

All reverse transcription reactions were carried out in an Eppendorf Mastercycler®-personal PCR thermocycler (Eppendorf, Hamburg, Germany). All reagents for reverse transcription and PCR were purchased from Applied Biosystems (Chicago, IL). For each reverse transcription reaction, 1 μg of total RNA was reverse transcribed using 50 units of Murine Leukemia Virus (MuLV) reverse transcriptase in the presence of 20 units of RNase inhibitor in a final volume of 20 μl. The reaction mixture contained 5 mM $MgCl_2$, 0.4 mM of each dNTP, 2.5 μM oligo dT primers and random hexamers. The reaction mixtures were incubated at 42 °C for 90 min. This was followed by heating at 95 °C for 5 min and cooling to 4 °C for 5 minutes. Final cDNA was diluted 10 times for the following QRT-PCR reaction.

Analysis of CD36 and ScR-A1 Message by QRT-PCR

QRT-PCR analysis was performed using the FastStart SYBR Green Reagents Kit according to the manufacturers' instructions on the Roche Light Cycler 480 (Roche Applied Science, Indianapolis, IN). 8 μl of cDNA were amplified using CD36 (forward primer 5′-GAGAACTGTTATGG GGCTAT-3′, reverse primer 5′-TTCAACTGGAGAG-G CAAAGG-3′) [23, 24] and ScR-A1 (forward primer 5′-CT CGTGTTTGCAGTTCTCA-3′; reverse primer 5′-CCATG TTGCTCATGTGTTCC-3′) [25] specific primers. Primers used in amplification reactions were generated by Sigma-Genosys (The Woodlands, TX).

Each reaction was done in triplicate. The amounts of PCR products were estimated using software provided by the manufacturer (Roche Applied Science). To correct for differences in cDNA load among samples, the target PCRs were normalized to a reference PCR involving the endogenous housekeeping gene glyceraldehyde-3-phosphate dehydrogenase (GAPDH). Specific primers were used for GAPDH amplification: forward primer 5′-ACCATCATC CCTGCCTCTAC-3′, reverse primer 5′-CCTGTTGCTGT AGCCAAAT-3′.

Non-template controls were included for each primer pair to check for significant levels of any contaminants. A melting-curve analysis was performed to assess the specificity of the amplified PCR products.

Protein Isolation and Western Blot

Cellular extracts were prepared for Western immunoblotting using radioimmunoprecipitation assay (RIPA) lysis buffer (98% PBS, 1% Igepal, 0.5% sodium deoxycholate, 0.1% SDS), supplemented with 10 μl per ml of protease inhibitor cocktail (Sigma–Aldrich). Protein content was measured in triplicate using the BCA Protein Assay Kit by absorption at 562 nm (Pierce Biotechnology Inc., Rockford, IL).

Protein samples (10 μg/lane) were boiled for 5 min, and fractionated on 8% SDS-PAGE, and transferred onto a nitrocellulose membrane (Bio-Rad, Hercules, CA). The membrane was stained with Ponceau red (Sigma–Aldrich) to verify uniformity of protein loading in each lane.

The membrane was blocked for 1 h at room temperature in blocking solution [3% nonfat dry milk (Bio-Rad) in 1X Tris-buffered saline/1% Tween 20 (TTBS)] and then immersed in a 1:500 dilution of primary antibody overnight at 4 °C. The following day, the membrane was washed and then incubated in a 1:5,000 dilution of ECL horseradish peroxidase (HRP)-linked species-specific whole antibody in blocking solution.

The immunoreactive proteins were detected using Pierce ECL Western Blot substrate system, and film development in SRX-101A (Konica Minolta Holdings, Inc., Tokyo, Japan). Stripping and reprobing of the membranes were performed according to the manufacturer's protocol (ECL kit instructions, Thermoscientific, Rockford, IL).

Mouse anti-human CD36 IgM primary antibody (sc-7309) and goat anti-mouse HRP conjugated IgM secondary antibody (sc-2064) were obtained from Santa Cruz Biotechnology (Santa Cruz, CA).

Goat anti-human macrophage ScR-A1 IgG polyclonal antibody (P21757) was purchased from Millipore (Billerica, MA). Donkey anti-goat IgG-HRP conjugated secondary antibody (sc-2020) was obtained from Santa Cruz Biotechnology (Santa Cruz, CA).

As a loading control, on the same transferred membrane, β-actin was detected using mouse anti-β-actin (diluted in 1:1,000) (Abcam, Cambridge, UK). IgG-HRP conjugated antibody was used as a secondary antibody (GE Healthcare Biosciences, Piscataway, NJ).

Band intensities for Western blot protein samples were quantified using Kodak Digital Science 1D, version 2.0.3, after imaging with Kodak Digital Science Electrophoresis Documentation and Analysis System 120.

Foam Cell Formation

THP-1 cells (10^6 cells per ml) were transferred into 8-well glass-chamber slides, then treated with PMA (100 nM, 48 h, 37 °C) to stimulate differentiation into macrophages. Cells were cholesterol-loaded with 50 μg/ml acetylated LDL or 50 μg/ml oxidized LDL (Inracel, Frederick, MD), then further incubated in RPMI 1640 for 48 h under the following five conditions: (1) untreated control, (2) IFN-γ (500 U/ml); (3) celecoxib (25 μM); (4) AACOCF3 (25 μM); (5) TGF-β (120 pg/ml). Following incubation, media was aspirated, slides were washed with PBS and fixed in 4% paraformaldehyde in water for 10 min. Cells were then washed in distilled water and stained with 0.2%

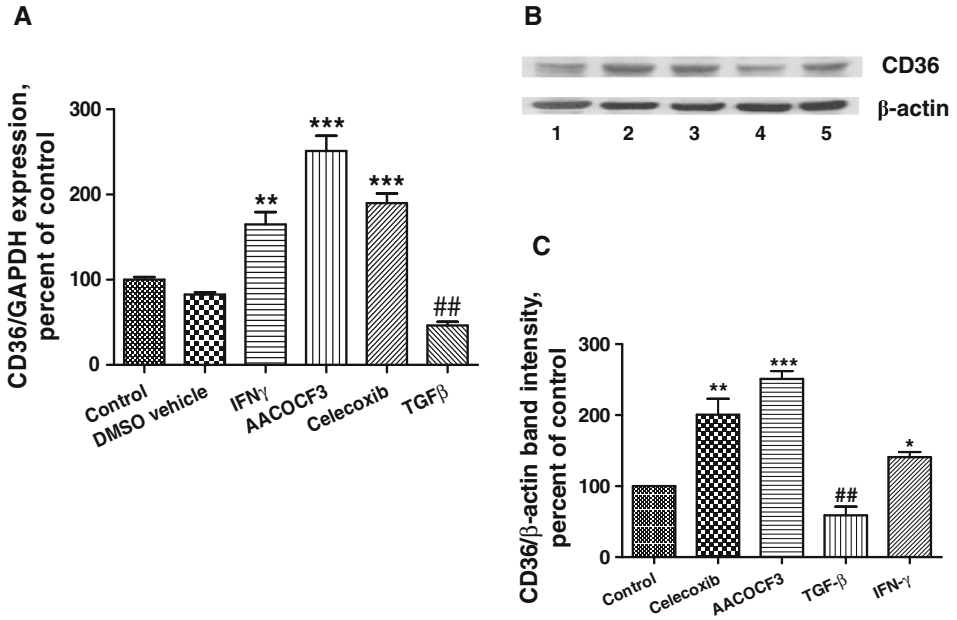

Fig. 2 Effect of COX-2 inhibition by celecoxib and cPLA-2 inhibition by AACOCF3 on CD36 expression in THP-1 macrophages. **a**. Relative CD36 mRNA abundance increases upon exposure to celecoxib or AACOCF3. THP-1 macrophages were incubated for 18 h under the following six conditions: (1) media alone, (2) vehicle (DMSO), (3) IFN-γ (500 U/ml), (4) AACOCF3 (25 μM), (5) celecoxib (25 μM), (6) TGF-β (120 pmol/ml). Total RNA was isolated from cells exposed to each condition. RNA was reverse transcribed and CD36 message was analyzed by QRT-PCR. Gene expression levels were graphed as relative mRNA expression. The expression of CD36 was normalized to that of GAPDH. The data represent the mean and SEM of five independent experiments ($n = 5$). $^{**}P < 0.01$ versus controls, $^{***}P < 0.001$ versus controls, $^{\#\#}P < 0.01$ versus IFN-γ, celecoxib, AACOCF3. **b** Western blot analysis using CD36-specific antibody. Total protein extracts were analyzed by Western blot for CD36 protein expression. THP-1 macrophages were incubated for 24 h under the following five conditions: (1) media alone, (2) celecoxib (25 μM), (3) AACOCF3 (25 μM), (4) TGF-β [120 pmol/ml], (5) IFN-γ (500 U/ml). β-Actin was detected on the same membrane as a loading control. **c** Graphic representation of immunoblot results for CD36 protein expression with normalization to β-actin. Conditions are the same as in part B. The data represent the mean and SEM of three independent experiments ($n = 3$). $^{*}P < 0.05$ versus control, $^{**}P < 0.01$ versus control, $^{***}P < 0.001$ versus control, $^{\#\#}P < 0.01$ versus IFN-γ, celecoxib, AACOCF3

Oil Red O (Sigma) for 30 min. After the PBS wash, cell nuclei were stained with hematoxylin (Sigma) for 5 min. After a final wash with PBS, coverslips were mounted on slides using Permount solution (Sigma).

Foam cells, recognized as macrophages stained with Oil Red O, were visualized via light microscopy (Axiovert 25; Carl Zeiss, Gottingen, Germany) with 40× magnification and photographed using a DC 290 Zoom digital camera (Eastman Kodak, Rochester, NY). Number of foam cells formed in each condition was calculated in triplicate manually and presented as a percentage of the total cells.

Data Analysis

Statistical analysis was performed using Graphpad Prism, version 5.01 (GraphPad Software, San Diego, CA). All data were analyzed by one-way analysis of variance, and pairwise multiple comparisons were made between control and treatment conditions using Bonferroni correction. P values less than 0.05 were considered significant.

Results

Celecoxib and AACOCF3 Exposure Increase CD36, But Not ScR-A1 Expression in THP-1 Macrophages and Monocytes

Celecoxib significantly increased CD36 message in THP-1 macrophages. In these mRNA and protein studies, we compared treated THP-1 macrophages to untreated control cells with mRNA and protein expression for untreated control set at 100%. Celecoxib (25 μM) raised CD36 mRNA to 186.77 ± 25.43% of control ($P < 0.001$, $n = 5$). Solvent control reduced CD36 message slightly to 87.64 ± 4.6% (Fig. 2a). AACOCF3 treatment had an effect comparable to celecoxib on CD36 expression in THP-1 macrophages. 25 μM AACOCF3 at 18 h of incubation markedly stimulated expression of CD36 (251.03 ± 39.99%, $P < 0.001$, $n = 5$) (Fig. 2a).

The concentration of celecoxib used was in the range of prior in vitro cell culture studies [26, 27]. Significant upregulation of CD36 message in THP-1 macrophages was

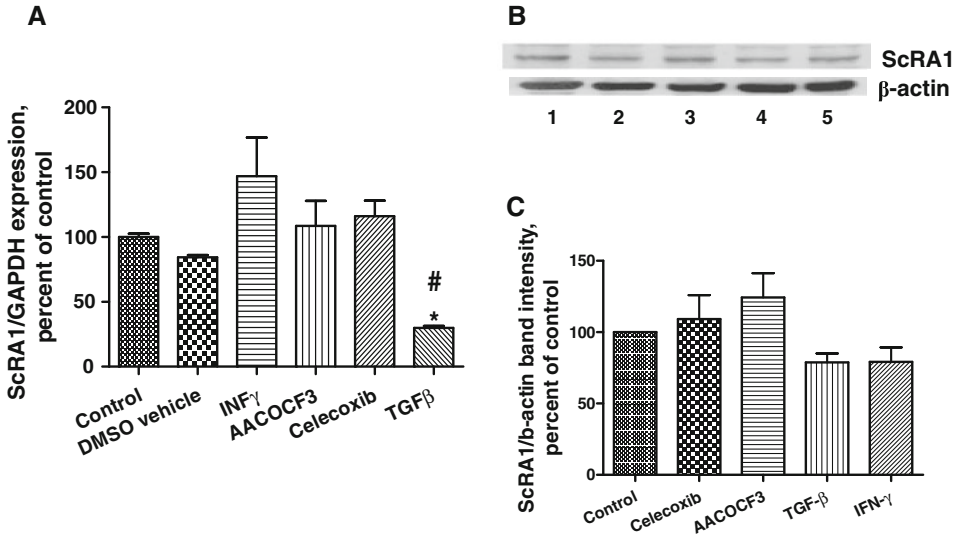

Fig. 3 Effect of COX-2 inhibition by celecoxib and cPLA-2 inhibition by AACOCF3 on ScR-A1 expression in THP-1 macrophages. **a** Relative ScR-A1 mRNA abundance is not significantly altered upon exposure to celecoxib or AACOCF3. THP-1 macrophages were incubated for 18 h under the following six conditions: (1) media alone, (2) vehicle (DMSO), (3) IFN-γ (500 U/ml), (4) AACOCF3 (25 μM), (5) celecoxib (25 μM), (6) TGF-β (120 pmol/ml). Total RNA was isolated from cells exposed to each condition. RNA was reverse transcribed and ScR-A1 message was analyzed by QRT-PCR. Gene expression levels were graphed as relative mRNA expression. The expressions of ScR-A1 was normalized to that of GAPDH. The data represent the mean and SEM of five independent experiments ($n = 5$), $^{*}P < 0.05$ versus control, $^{\#}P < 0.05$ versus IFN-γ, celecoxib, AACOCF3. **b** Western blot analysis using ScR-A1-specific antibody. Total protein extracts were analyzed by Western blot for ScR-A1 protein expression. THP-1 macrophages were incubated for 24 h under the following five conditions: (1) media alone, (2) celecoxib (25 μM), (3) AACOCF3 (25 μM), (4) TGF-β (120 pmol/ml), (5) IFN-γ (500 U/ml]. β-actin was detected on the same membrane as a loading control. **c** Graphic representation of immunoblot results for ScR-A1 protein expression with normalization to β-actin. Conditions are the same as in part B. The data represent the mean and SEM of three independent experiments ($n = 3$), NS

detected at celecoxib concentrations as low as 10 μM, simultaneously with abrogation of COX-2 expression (supplementary data Figure 1, not shown). Incubation of THP-1 macrophages with celecoxib at concentrations exceeding 25 μM had a toxic effect on the cells.

Protein expression, as determined by Western blot, confirmed the same pattern of alterations in CD36 expression after celecoxib and AACOCF3 treatment. Thus, celecoxib increased protein expression of CD36 by 100.7 ± 12.9% and AACOCF3 by 151.1 ± 11.9% versus expression in untreated THP-1 macrophages, as normalized to β-actin expression ($P < 0.01$ and $P < 0.001$, $n = 3$, respectively) (Fig. 2b, c).

Consistent with the previously shown pro-atherogenic properties of IFN-γ [17, 18, 28], incubation of THP-1 macrophages with IFN-γ for 18 h resulted in upregulation of CD36 expression to 164.9 ± 32.1% ($P < 0.01$, $n = 5$) for the message and to 140.9 ± 12.6% ($P < 0.05$, $n = 3$) for the protein (Fig. 2).

In contrast to the documented changes in CD36 expression in THP-1 macrophages after celecoxib and AACOCF3 treatment, ScR-A1 expression was not significantly affected by these compounds. Only incubation of THP-1 macrophages with TGF-β, our known control, for 48 h had a significant impact on the ScR-A1 message. We observed a decrease in ScR-A1 expression to 29.93 ± 3.38% of untreated THP-1 macrophages and 91.1 ± 0.29% of DMSO vehicle ($P < 0.05$, $n = 5$) (Fig. 3a). Nevertheless, none of the treatments significantly changed the protein expression of ScR-A1 (Fig. 3b, c).

Equivalent results were obtained in THP-1 monocytes under the conditions described above (supplemental data Figure 2, not shown).

Celecoxib and AACOCF3 Treatment Increases CD36, but Not ScR-A1 in PBMC

Exposure to either celecoxib or AACOCF3 caused a significant increase in CD36 message in human PBMC (Fig. 4a). In these mRNA studies, we compared treated PBMC to untreated control PBMC with mRNA for untreated control set at 100%. Incubation with celecoxib (18 h, 25 μM) resulted in upregulation of the CD36 message to 206.550 ± 32.3% versus untreated PBMC ($P < 0.01$, $n = 3$). AACOCF3 (18 h, 25 μM) stimulated expression of CD36 to 214.83 ± 36.2% ($P < 0.01$, $n = 3$).

Incubation of PBMC with IFN-γ for 18 h upregulated CD36 mRNA expression to 176.90 ± 17.6% ($P < 0.05$, $n = 5$) (Fig. 4a).

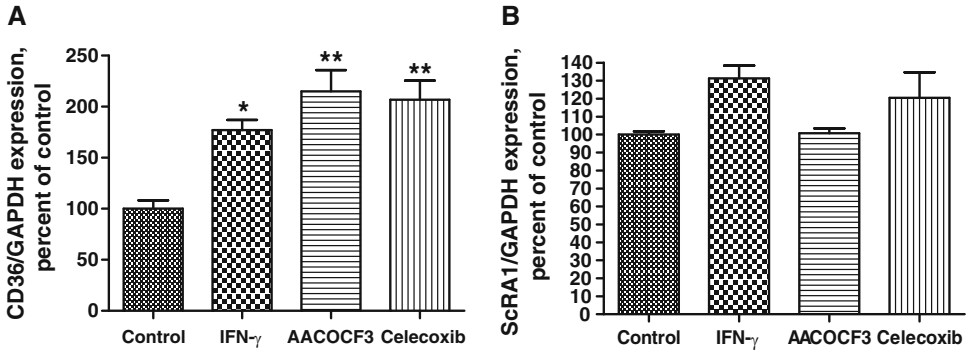

Fig. 4 Effect of COX-2 inhibition by celecoxib and cPLA-2 inhibition by AACOCF3 on CD36 and ScR-A1 mRNA expression in human PBMC. Monocytes from human peripheral blood were incubated for 18 h under the following four conditions: (1) media alone, (2) IFN-γ (500 U/ml), (3) AACOCF3 (25 μM), (4) celecoxib (25 μM). Following incubation, total RNA was isolated from cells exposed to each condition. RNA was reverse transcribed, CD36 and ScR-A1 messages were analyzed by QRT-PCR. The expressions of target genes were normalized to that of GAPDH. **a** CD36 gene expression graphed as relative mRNA expression and compared with results obtained from untreated PBMC. The data represent the mean and SEM of three independent experiments ($n = 3$), $^{*}P < 0.05$ versus PBMC control cells in media alone, $^{**}P < 0.01$ versus control cells. **b** ScR-A1 gene expression graphed as relative mRNA expression and compared with results obtained from untreated PBMC. The data represent the mean and SEM of three independent experiments ($n = 3$), NS

As in the THP-1 monocyte/macrophage system, incubation of PBMC with either celecoxib or AACOCF3 had no significant effect on the expression of ScR-A1 (Fig. 4b).

COX-2 or cPLA-2 Silencing in THP-1 Monocytes Upregulates CD36

Treatment of THP-1 monocytes with 100 nM of COX-2 and cPLA-2 siRNAs (48 h) downregulated the expression of COX-2 mRNA to 45.6 ± 3.48% and 48.97 ± 5.31% respectively, compared to control siRNA transfected cells ($P < 0.01$ and 0.01, $n = 3$ for each, respectively,) (data not shown). Both silencing of COX-2 and silencing of cPLA-2 resulted in upregulation of CD36 message to 156.7 ± 13.68% and 169.5 ± 15.77% respectively, versus mock transfected cells ($P < 0.01$ and 0.01, $n = 3$ for each, respectively) (Fig. 5a).

Incubation of THP-1 cells with COX-2 siRNA and cPLA-2 siRNA for 56 h resulted in significant stimulation of CD36 protein expression (Fig. 5b, c). Thus, transfection with COX-2 siRNA resulted in enhancement of CD36 expression to 139.2 ± 10.68% of mock-transfected control ($P < 0.01$, $n = 3$), which is comparable to the effect of celecoxib treatment on THP-1 monocytes for 24 h (150.1 ± 12.56%, $P < 0.01$, $n = 3$). cPLA-2 siRNA-mediated pathway inhibition and AACOCF3 treatment for 24 h resulted in 197.3 ± 34.67% and 192.7 ± 24.77% upregulation of CD36 protein expression, respectively ($P < 0.001$ and 0.001, $n = 3$ for each). Again, the pharmacologic blockade achieved enhancement of CD36 almost equivalent to the effect observed with silencing of the same target.

Celecoxib and AACOCF3 Augment Foam Cell Transformation in Lipid-laden THP-1 Macrophages

Acetylated LDL-treated THP-1 macrophages showed a significant increase in foam cell transformation in the presence of either celecoxib or AACOCF3 (Figs. 6, 7). Incubation of lipid-laden THP-1 macrophages with celecoxib resulted in 49.7 ± 5.773% of macrophages becoming foam cells vs. 25.57 ± 7.37% foam cells formed in untreated THP-1 macrophages, ($P < 0.01$, $n = 4$) (Fig. 7a). AACOCF3 treatment similarly promoted foam cell transformation in 59.11 ± 3.83% versus 25.57 ± 7.37% of cells in untreated THP-1 macrophages, ($P < 0.001$, $n = 4$) (Fig. 7). Comparable results were observed when THP-1 macrophages were pre-incubated with oxidized LDL (supplementary data Figure 3, not shown).

As additional evidence for the pro-atherogenic nature of IFN-γ, consistent with our previous reports [16, 17], we observed a significant elevation of foam cells to 50.37 ± 3.83% in IFN-γ treated THP-1 macrophages versus 25.57 ± 7.37% of foam cells formed in untreated THP-1 macrophages ($P < 0.01$, $n = 4$) (Figs. 6, 7).

Exposure of lipid-laden macrophages to TGF-β did not significantly alter the percentage of foam cells (Fig. 7).

Discussion

We report here that CD36 expression in human monocytes increases with inhibition of the arachidonic acid/COX pathway and specifically by celecoxib. To our knowledge,

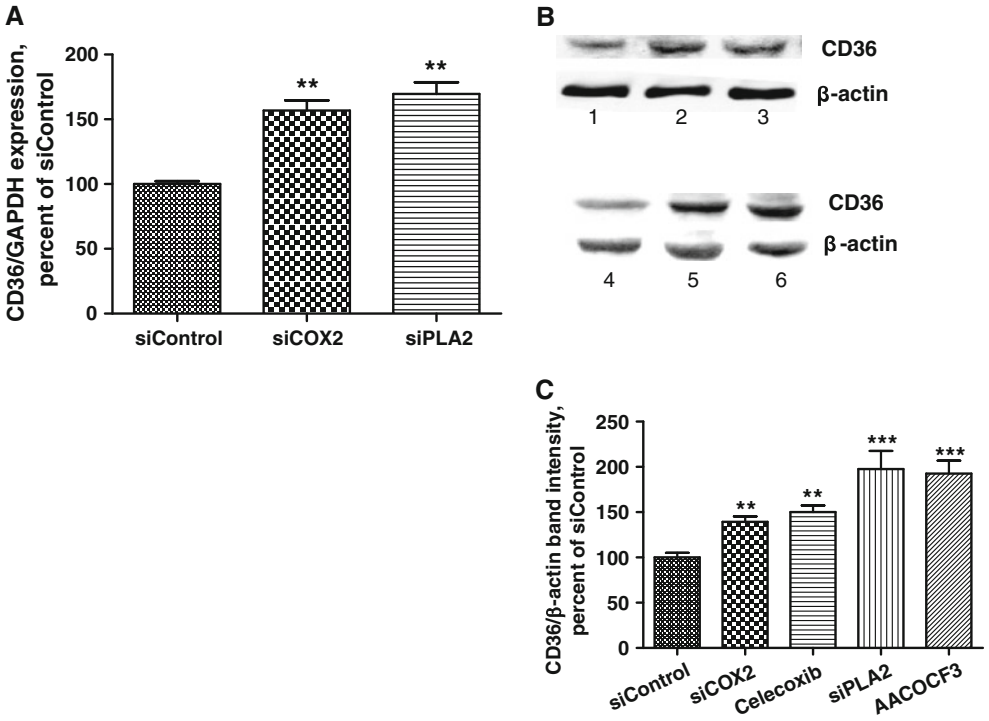

Fig. 5 Effect of COX-2 knockdown by COX-2 and PLA-2 siRNA on CD36 expression in THP-1 monocytes. **a** Relative CD36 mRNA abundance increases upon exposure to siCOX-2 and siPLA-2. THP-1 monocytes were transfected with 100 nM of: (1) siControl, (2) siCOX-2, (3) siPLA-2 and cultured for 48 h. Total RNA was isolated from cells exposed to each condition. RNA was reverse transcribed and CD36 message was analyzed by QRT-PCR. Gene expression levels were graphed as relative mRNA expression. The expression of CD36 was normalized to that of GAPDH. The data represent the mean and SEM of three independent experiments ($n = 3$). $^{**}P < 0.01$ versus siControl transfected cells. **b** Western blot analysis using human CD36-specific antibody. THP-1 monocytes were incubated for 56 h post-transfection of siControl, siCOX-2, siPLA-2 and for 24 h in the presence of celecoxib and AACOCF3. Total protein extracts were analyzed by Western blot for CD36 protein expression: (1) siControl, (2) siCOX-2, (3) celecoxib (25 μM), (4) siControl, (5) siPLA-2, (6) AACOCF3 (25 μM). β-actin was detected on the same membrane as a loading control. **c** Graphic representation of immunoblot results for CD36 protein expression with normalization to β-actin. Conditions are the same as in part B. The data represent the mean and SEM of three independent experiments ($n = 3$). $^{**}P < 0.01$ versus siControl, $^{***}P < 0.001$ versus siControl

this is the first demonstration that CD36 is regulated by a COX-2 inhibitor currently in use in humans. CD36 is a transmembrane, highly N-linked glycosylated glycoprotein expressed on the cell surface of monocytes/macrophages where it is the major receptor responsible for high-affinity recognition of oxidized LDL by macrophages and where it is thought to play important functions in inflammation and vascular biology [29, 30]. CD36 is responsible for over 50% of total modified LDL uptake into human monocyte-derived macrophages [31, 32]. In transgenic mice, knocking out CD36 on the pro-atherogenic apoE-null background reduces atherosclerosis [33]. These double-null mice show a 70–80% reduction in aortic lesion size when compared to apoE null mice. Further, macrophages from CD36-deficient mice exhibit a reduced uptake of modified LDL and are resistant to foam cell formation [33, 34]. Peripheral monocyte-derived macrophages from humans with genetic deficiency of CD36 have reduced uptake and degradation of oxidized LDL. Cholesteryl ester mass accumulation following exposure to oxidized LDL was reduced by approximately 40% in the macrophages from CD36-deficient subjects as compared to cells from normal controls [31]. Anti-CD36 monoclonal antibody reduced by 50% the specific binding of oxidized LDL to human peripheral blood monocyte-derived macrophages [35]. Upregulation of CD36 may contribute to the pathological process of atherosclerosis by promoting macrophage lipid overload and also by fostering cytoskeletal rearrangements that enhance cell spreading and inhibit emigration from lesions [31, 36]. It is likely that the observed phenotype of COX2/cPLA-2 inhibition is the result of multiple lipid regulation pathways gone awry. We previously reported on the suppression of lipid efflux by COX-2 inhibition [14]. Now, additionally, we report CD36 upregulation with COX2/cPLA-2 inhibition. This upregulation has the potential to further exacerbate the cellular lipid load.

Demonstration of disrupted cholesterol homeostasis by AACOCF3 and celecoxib provides further evidence of the possible mechanism through which COX inhibition by traditional NSAIDs or COX-2 specific inhibitors may cause

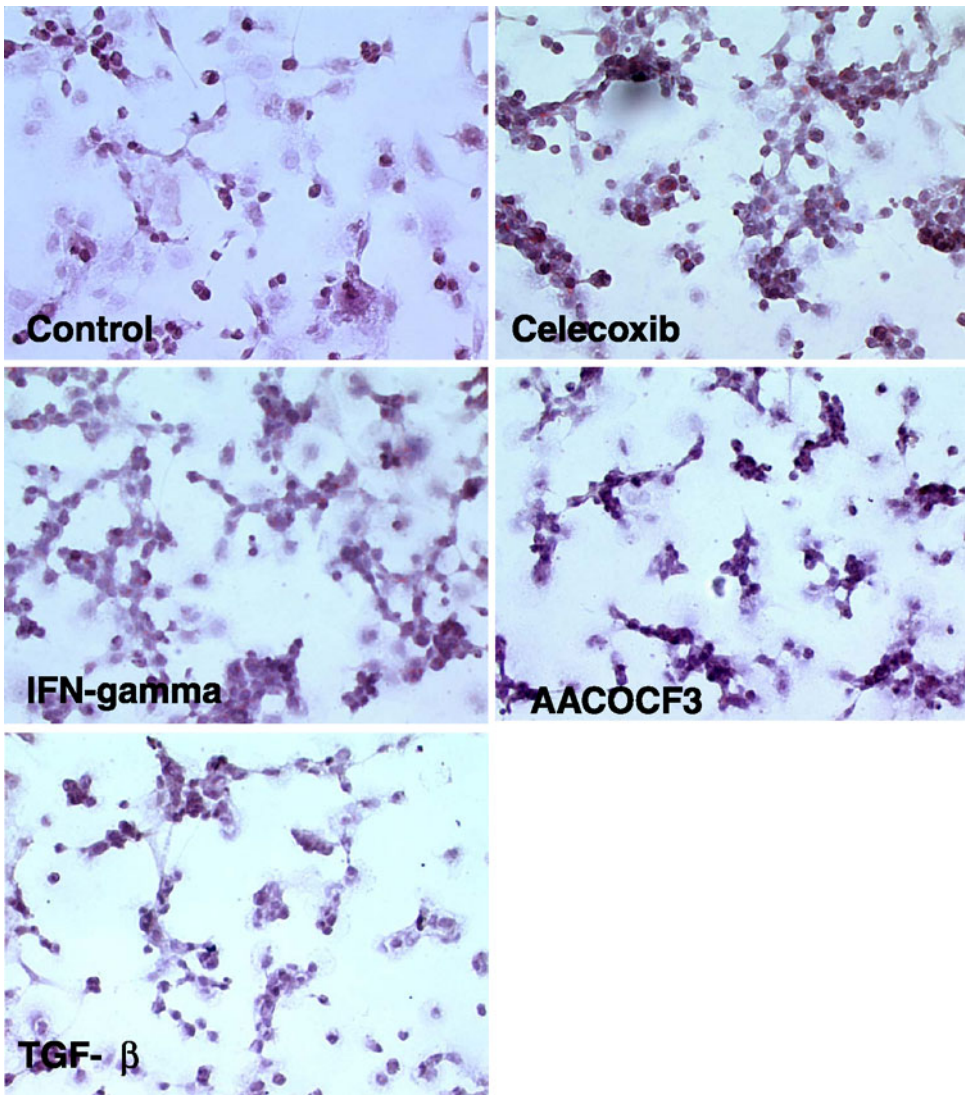

Fig. 6 Foam cell formation in THP-1 macrophages under cholesterol loading conditions is augmented by celecoxib or AACOCF3. THP-1 differentiated macrophages were treated with acetylated LDL (50 μg/ml, 48 h). Cells were then exposed for 48 h to the following five conditions: (1) untreated control, (2) IFN-γ (500 U/ml); (3) celecoxib (25 μM); (4) AACOCF3 (25 μM); (5) TGF-β (120 pg/ml). Representative light photomicrograph at magnification ×40 of Oil red O staining to detect foam cells

early atheromatous lesions leading to increased cardiovascular events.

The contribution of the leukotriene pathway, generated from arachidonic acid and not blocked by COX-2 inhibitors, must be considered. Although the role of leukotrienes in atherosclerosis is not clearly defined, they play a key role in aneurysm formation in mice [37, 38]. It has been shown that enzymes responsible for the biosynthesis of leukotrienes are highly expressed in human atherosclerotic lesions. There is also evidence that the 5-lipoxygenase and leukotriene A4 hydrolase expression, and hence, leukotriene production, are higher in patients with vulnerable atherosclerotic plaques as opposed to patients with stable lesions [39, 40]. Furthermore, it has been reported that all human cell types involved in atherosclerosis have leukotriene B4 receptors. Future studies involving specific blockade of the leukotriene pathway will illuminate its importance in macrophage lipid homeostasis.

One noted consequence of COX-2 inhibition that has been implicated in cardiovascular toxicity is disruption of the balance of thromboxane/prostaglandin I2 [41]. Namely, COX-2 inhibition suppresses prostaglandin I2 and prolonged suppression of prostaglandin I2 leads to deletion of its specific Gs-coupled I prostanoid receptor. A balance between thromboxane and prostaglandin I2 modulates vascular wall-platelet interactions. Thromboxane amplifies the aggregatory responses of platelets to all known agonists, whereas prostaglandin I2 impedes aggregation. Additionally, prostaglandin I2 has been shown to afford protection against oxidant injuries. Prostaglandin I2 appears to contribute to atheroprotection.

The relationship between COX and CD36 has been explored previously. In 2003, Sennlaub and colleagues [42]

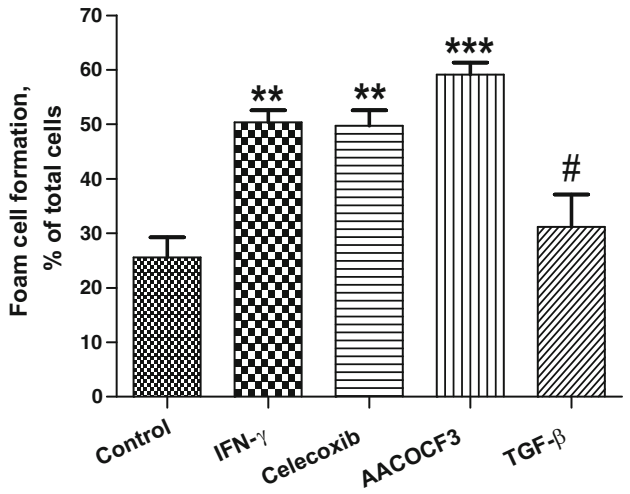

Fig. 7 Effect of celecoxib and AACOCF3 on foam cell transformation in THP-1 macrophages under cholesterol loading conditions. THP-1 macrophages were treated with acetylated LDL (50 μg/ml, 48 h). Cells were then exposed for 48 h to the following five conditions: (1) untreated control; (2) IFN-γ (500 U/ml); (3) celecoxib (25 μM); (4) AACOCF3 (25 μM); (5) TGF-β (120 pg/ml). Cells were stained with Oil red O to detect foam cells. Graphic representation of percentage foam cells shows a significant increase in foam cell transformation with celecoxib, AACOCF3 or IFN-γ ($n = 4$). $^{**}P < 0.01$ versus control cells, $^{***}P < 0.001$ versus control cells, $^{\#}P < 0.05$ versus celecoxib, AACOCF3

reported CD36 upregulation by the COX-2 inhibitor etodolac in a rat model of ischemic proliferative retinopathy. Our present results are consistent with the study by Viñals et al. [43] demonstrating that aspirin produces an increase of CD36 expression in THP-1 macrophages, possibly by decreasing production of PGE2 and the study by Chuang et al. [44] showing that CD36 levels are reduced in peritoneal macrophages derived from endometriosis patients, possibly due to excess prostaglandin E2. In the Chuang study, COX-1 or COX-2 inhibition increased CD36 message in cultured murine peritoneal macrophages.

In what may be a protective homeostatic mechanism, Bujold et al. [45] found that in cultured murine peritoneal macrophages activation of CD36 increases the expression of COX-2 through the activation of the extracellular signal-regulated kinase 1/2 pathway. Enhanced COX-2 expression then promotes cholesterol efflux, possibly by increasing intracellular levels of the PPARγ activator 15-deoxy-Δ12, 14-prostaglandin J2. PPARγ activation transcriptionally upregulates genes involved in cholesterol efflux including liver X receptors, ATP binding cassette transporters and cholesterol 27-hydroxylase [46].

The mechanisms of CD36 upregulation by COX inhibition are unknown. Further studies are needed to define the pathways involved and to determine which specific prostaglandin(s) are responsible for keeping CD36 levels in check.

Strategies to prevent atherosclerosis aimed at blocking upregulation of CD36 activity in patients taking NSAIDs or coxibs long-term may provide a novel therapeutic approach to improving the safety profile of these drugs. Further studies are needed to define the pathways involved and to determine whether CD36 expression may have prognostic value in evaluating cardiovascular toxicity of specific drugs in individuals. CD36 may be a feasible and attractive target for pharmacologic intervention [47, 48].

Acknowledgments This work was supported by an Innovative Research Grant from the Arthritis Foundation and by a Winthrop University Hospital Pilot and Feasibility Grant.

Conflict of interest None declared.

References

1. Lloyd-Jones D, Adams RJ, Brown TM, Carnethon M, Dai S, De Simone G et al (2009) Heart disease and stroke statistics—2009 update: a report from the American Heart Association Statistics Committee and Stroke Statistics Subcommittee. Circulation 119: 480–486
2. Yusuf S, Reddy S, Ounpuu S, Anand S (2001) Global burden of cardiovascular diseases part I: general considerations, the epidemiologic transition, risk factors, and impact of urbanization. Circulation 104:2746–2753
3. Goldstein JL, Brown MS (2009) The LDL receptor. Arterioscler Thromb Vasc Biol 29:431–438
4. Silverstein RL (2009) Inflammation, atherosclerosis, and arterial thrombosis: role of the scavenger receptor CD36. Cleve Clin J Med 76(Suppl 2):S27–S30
5. Platt N, Gordon S (2001) Is the class A macrophage scavenger receptor (SR-A) multifunctional?—The mouse's tale. J Clin Invest 108:649–654
6. Kunjathoor VV, Febbraio M, Podrez EA, Moore KJ, Andersson L, Koehn S, Rhee JS, Silverstein R, Hoff HF, Freeman MW (2002) Scavenger receptors class A-I/II and CD36 are the principal receptors responsible for the uptake of modified low density lipoprotein leading to lipid loading in macrophages. J Biol Chem 277:49982–49988
7. Bunimov N, Laneuville O (2008) Cyclooxygenase inhibitors: instrumental drugs to understand cardiovascular homeostasis and arterial thrombosis. Cardiovasc Hematol Disord Drug Targets 8:268–277
8. Bombardier C, Laine L, Reicin A, Shapiro D, Burgos-Vargas R, Davis B, Day R, Ferraz MB, Hawkey CJ, Hochberg MC, Kvien TK, Schnitzer TJ (2000) Comparison of upper gastrointestinal toxicity of rofecoxib and naproxen in patients with rheumatoid arthritis. VIGOR Study Group N Engl J Med 343:1520–1528
9. Vardeny O, Solomon SD (2008) Cyclooxygenase-2 inhibitors, nonsteroidal anti-inflammatory drugs, and cardiovascular risk. Cardiol Clin 26:589–601
10. Wong D, Wang M, Cheng Y, FitzGerald GA (2005) Cardiovascular hazard and non-steroidal anti-inflammatory drugs. Curr Opin Pharmacol 5:204–210
11. Farkouh ME, Kirshner H, Harrington RA, Ruland S, Verheugt FW, Schnitzer TJ et al (2004) Comparison of lumiracoxib with naproxen and ibuprofen in the Therapeutic Arthritis Research and

Gastrointestinal Event Trial (TARGET), cardiovascular outcomes: randomized controlled trial. Lancet 364:675–684
12. Ott E, Nussmeier NA, Duke PC, Feneck RO, Alston RP, Snabes MC, Hubbard RC, Hsu PH, Saidman LJ, Mangano DT (2003) Efficacy and safety of the cyclooxygenase-2 inhibitors parecoxib and valdecoxib in patients undergoing coronary artery bypass surgery. J Thorac Cardiovasc Surg 125:1481–1492
13. Dajani EZ, Islam K (2008) Cardiovascular and gastrointestinal toxicity of selective cyclo-oxygenase-2 inhibitors in man. J Physiol Pharmacol 59(Suppl 2):117–133
14. Chan ES, Zhang H, Fernandez P, Edelman SD, Pillinger MH, Ragolia L, Palaia T, Carsons S, Reiss AB (2007) Effect of COX inhibition on cholesterol efflux proteins and atheromatous foam cell transformation in THP-1 human macrophages: a possible mechanism for increased cardiovascular risk. Arthritis Res Ther 9:R4
15. Reiss AB, Anwar F, Chan ES, Anwar K (2009) Disruption of cholesterol efflux by coxib medications and inflammatory processes: link to increased cardiovascular risk. J Investig Med 57:695–702
16. Reiss AB, Rahman MM, Chan ES, Montesinos MC, Awadallah NW, Cronstein BN (2004) Adenosine A2A receptor occupancy stimulates expression of proteins involved in reverse cholesterol transport and inhibits foam cell formation in macrophages. J Leukoc Biol 76:727–734
17. Reiss AB, Patel CA, Rahman MM, Chan ES, Hasneen K, Montesinos MC, Trachman JD, Cronstein BN (2004) Interferon-gamma impedes reverse cholesterol transport and promotes foam cell transformation in THP-1 human monocytes/macrophages. Med Sci Monit 10(11):BR420–BR425
18. Reiss AB, Awadallah N, Malhotra S, Montesinos MC, Chan ESL, Javitt NB, Cronstein BN (2001) Immune complexes and interferon-γ decrease cholesterol 27-hydroxylase in human arterial endothelium and macrophages. J Lipid Res 42:1913–1922
19. Grainger DJ (2004) Transforming growth factor-β and atherosclerosis: so far, so good for the protective cytokine hypothesis. Arterioscler Thromb Vasc Biol 24:399–404
20. Draude G, Lorenz RL (2000) TGF-beta1 downregulates CD36 and scavenger receptor A but upregulates LOX-1 in human macrophages. Am J Physiol Heart Circ Physiol 278:H1042–H1048
21. Basu GD, Pathangey LB, Tinder TL, Gendler SJ, Mukherjee P (2005) Mechanisms underlying the growth inhibitory effects of the cyclo-oxygenase-2 inhibitor celecoxib in human breast cancer cells. Breast Cancer Res 7(4):R422–R435
22. Lee EJ, Kim SH, Kwark YE, Kim J (2006) Heterogeneous nuclear ribonuclear protein C is increased in the celecoxib-induced growth inhibition of human oral squamous cell carcinoma. Exp Mol Med 38(3):203–209
23. Pietsch A, Erl W, Lorenz RL (1996) Lovastatin reduces expression of the combined adhesion and scavenger receptor CD36 in human monocytic cells. Biochem Pharmacol 52:433–439
24. Han S, Sidell N (2002) Peroxisome-proliferator-activated-receptor gamma (PPARgamma) independent induction of CD36 in THP-1 monocytes by retinoic acid. Immunology 106:53–59
25. Takeda N, Manabe I, Shindo T, Iwata H, Iimuro S, Kagechika H (2006) Synthetic retinoid Am80 reduces scavenger receptor expression and atherosclerosis in mice by inhibiting IL-6. Arterioscler Thromb Vasc Biol 26:1177–1183
26. Davies NM, McLachlan AJ, Day RO, Williams KM (2000) Clinical pharmacokinetics and pharmacodynamics of celecoxib: a selective cyclo-oxygenase-2 inhibitor. Clin Pharmacokinet 38:225–242
27. Elrod HA, Yue P, Khuri FR, Sun SY (2009) Celecoxib antagonizes perifosine's anticancer activity involving a cyclooxygenase-2-dependent mechanism. Mol Cancer Ther 8:2575–2585
28. Whitman SC, Ravisankar P, Elam H, Daugherty A (2000) Exogenous interferon-gamma enhances atherosclerosis in apolipoprotein E−/− mice. Am J Pathol 157:1819–1824
29. Podrez EA, Febbraio M, Sheibani N, Schmitt D, Silverstein RL, Hajjar DP, Cohen PA, Frazier WA, Hoff HF, Hazen SL (2000) Macrophage scavenger receptor CD36 is the major receptor for LDL modified by monocyte-generated reactive nitrogen species. J Clin Invest 105:1095–1108
30. Silverstein RL, Febbraio M (2000) CD36 and atherosclerosis. Curr Opin Lipidol 11:483–491
31. Nozaki S, Kashiwagi H, Yamashita S, Nakagawa T, Kostner B, Tomiyama Y, Nakata A, Ishigami M, Miyagawa J, Kameda-Takemura K (1995) Reduced uptake of oxidized low density lipoprotein in monocyte-derived macrophages from CD36-deficient subjects. J Clin Invest 96:1859–1865
32. Sugano R, Yamamura T, Harada-Shiba M, Miyake Y, Yamamoto A (2001) Uptake of oxidized low-density lipoprotein in a THP-1 cell line lacking scavenger receptor A. Atherosclerosis 158: 351–357
33. Febbraio M, Podrez EA, Smith JD, Hajjar DP, Hazen SL, Hoff HF, Sharma K, Silverstein RL (2000) Targeted disruption of the class B scavenger receptor CD36 protects against atherosclerotic lesion development in mice. J Clin Invest 105:1049–1056
34. Kuchibhotla S, Vanegas D, Kennedy DJ, Guy E, Nimako G, Morton RE, Febbraio M (2008) Absence of CD36 protects against atherosclerosis in ApoE knock-out mice with no additional protection provided by absence of scavenger receptor A I/II. Cardiovasc Res 78:185–196
35. Nicholson AC, Frieda S, Pearce A, Silverstein RL (1995) Oxidized LDL binds to CD36 on human monocyte-derived macrophages and transfected cell lines. Evidence implicating the lipid moiety of the lipoprotein as the binding site. Arterioscler Thromb Vasc Biol 15:269–275
36. Park YM, Febbraio M, Silverstein RL (2009) CD36 modulates migration of mouse and human macrophages in response to oxidized LDL and may contribute to macrophage trapping in the arterial intima. J Clin Invest 119:136–145
37. Cao RY, St Amand T, Gräbner R, Habenicht AJ, Funk CD (2009) Genetic and pharmacological inhibition of the 5-lipoxygenase/leukotriene pathway in atherosclerotic lesion development in ApoE deficient mice. Atherosclerosis 203:395–400
38. Funk CD, Cao RY, Zhao L, Habenicht AJ (2006) Is there a role for the macrophage 5-lipoxygenase pathway in aortic aneurysm development in apolipoprotein E-deficient mice? Ann NY Acad Sci 1085:151–160
39. Riccioni G, Back M, Capra V (2010) Leukotrienes and atherosclerosis. Curr Drug Targets 11:882–887
40. Qiu H, Gabrielsen A, Agardh HE, Wan M, Wetterholm A, Wong CH et al (2006) Expression of 5-lipoxygenase and leukotriene A4 hydrolase in human atherosclerotic lesions correlates with symptoms of plaque instability. Proc Natl Acad Sci USA A103:8161–8166
41. Graff J, Skarke C, Klinkhardt U, Watzer B, Harder S, Seyberth H et al (2007) Effects of selective COX-2 inhibition on prostanoids and platelet physiology in young healthy volunteers. J Thromb Haemost 5:2376–2385
42. Sennlaub F, Valamanesh F, Vazquez-Tello A, El-Asrar AM, Checchin D, Brault S, Gobeil F, Beauchamp MH, Mwaikambo B, Courtois Y, Geboes K, Varma DR, Lachapelle P, Ong H, Behar-Cohen F, Chemtob S (2003) Cyclooxygenase-2 in human, experimental ischemic proliferative retinopathy. Circulation 108:198–204
43. Viñals M, Bermúdez I, Llaverias G, Alegret M, Sanchez RM, Vázquez-Carrera M, Laguna JC (2005) Aspirin increases CD36, SR-BI, and ABCA1 expression in human THP-1 macrophages. Cardiovasc Res 66:141–149

44. Chuang PC, Lin YJ, Wu MH, Wing LY, Shoji Y, Tsai SJ (2010) Inhibition of CD36-dependent phagocytosis by prostaglandin E2 contributes to the development of endometriosis. Am J Pathol 176:850–860
45. Bujold K, Rhainds D, Jossart C, Febbraio M, Marleau S, Ong H (2009) CD36-mediated cholesterol efflux is associated with PPARγ activation via a MAPK-dependent COX-2 pathway in macrophages. Cardiovasc Res 83:457–464
46. Reiss AB, Vagell ME (2006) PPARgamma activity in the vessel wall: anti-atherogenic properties. Curr Med Chem 13:3227–3238
47. Greaves DR, Gordon S (2009) The macrophage scavenger receptor at 30 years of age: current knowledge and future challenges. J Lipid Res 50:S282–S286
48. Reiss AB, Wan DW, Anwar K, Merrill JT, Wirkowski PA, Shah N, Cronstein BN, Chan ES, Carsons SE (2009) Enhanced CD36 scavenger receptor expression in THP-1 human monocytes in the presence of lupus plasma: linking autoimmunity and atherosclerosis. Exp Biol Med 234:354–360

Lipids (2011) 46:143–149
DOI 10.1007/s11745-010-3514-0

ORIGINAL ARTICLE

Short Term Dietary Fish Oil Supplementation Improves Motor Deficiencies Related to Reserpine-Induced Parkinsonism in Rats

Raquel Cristine Silva Barcelos · Dalila Moter Benvegnú · Nardeli Boufleur · Camila Pase · Angélica Martelli Teixeira · Patrícia Reckziegel · Tatiana Emanuelli · João Batista T. da Rocha · Marilise Escobar Bürger

Received: 14 May 2010 / Accepted: 1 December 2010 / Published online: 16 December 2010

Abstract Fish oil (FO) supplementation could cause an increase in the concentration of plasmatic free fatty acids and, consequently, could compete with pro-inflammatory arachidonic acid (ARA) derived from brain biomembranes metabolism in the cerebrospinal fluid. Essential fatty acids (EFA) (n-3) have been reported by their antioxidant and neuroprotective properties, and therefore the influence of the FO supplementation on the reserpine-induced motor disorders was studied. Wistar rats were orally treated with FO solution for 5 days, and co-treated with reserpine (*R*; 1 mg/kg/mL) or its vehicle for 3 days (every other day). Reserpine-induced orofacial dyskinesia and catalepsy ($P < 0.05$) were prevented by FO ($P < 0.05$). Biochemical evaluations showed that reserpine treatment increased the lipid peroxidation in the cortex and striatum ($P < 0.05$), while the FO supplementation prevented this oxidative effect in both brain regions ($P < 0.05$). Our results showed the protective role of FO in the brain lipid membranes, reinforcing the beneficial effect of n-3 fatty acids in the prevention of degenerative and motor disorders.

Keywords Fish oil · n-3 Essential fatty acids · Reserpine · Motor disorders · Lipid peroxidation

Abbreviations

ALA	α-Linolenic acid
ARA	Arachidonic acid
DA	Dopamine
DHA	Docosahexaenoic acid
DPA	Docosapentaenoic acid
EFA	Essential fatty acid(s)
EPA	Eicosapentaenoic acid
FO	Fish oil
FT	Facial twitching
LNA	Linoleic acid
MAO	Monoamine oxidase
NF-κB	Nuclear factor kappa-light-chain-enhancer of activated B cells
PUFA	Polyunsaturated fatty acids
SO	Soybean oil
TBARS	Thiobarbituric acid reactive substances
VCM	Vacuous chewing movements
VMAT	Vesicular monoamine transporter

Introduction

Families of n-3 and n-6 fatty acids are important constituents of neuron cell membranes and are considered essential fatty acids (EFA) because mammals are incapable of synthesizing fatty acids with a double bond past the Δ-9

N. Boufleur · C. Pase
Departamento de Fisiologia e Farmacologia, Universidade Federal de Santa Maria (UFSM), Santa Maria, RS, Brazil

R. C. S. Barcelos · D. M. Benvegnú · A. M. Teixeira · P. Reckziegel · T. Emanuelli · M. E. Bürger (✉)
Programa de Pós-Graduação em Farmacologia, Centro de Ciências da Saúde, Universidade Federal de Santa Maria (UFSM), Santa Maria, RS 97105-900, Brazil
e-mail: mariliseeb@yahoo.com.br

T. Emanuelli · J. B. T. da Rocha · M. E. Bürger
Programa de Pós-Graduação em Bioquímica Toxicológica, UFSM, Santa Maria, RS, Brazil

T. Emanuelli
Programa de Pós Graduação em Ciência e Tecnologia dos Alimentos, Centro de ciências Rurais, UFSM, Santa Maria, Brazil

position [1–3]. These EFA include α-linolenic acid (ALA, 18:3) and its metabolites docosahexaenoic acid (DHA, 22:6n-3) and eicosapentaenoic acid (EPA, 20:5n-3), which are members of the n-3 series, as well linoleic acid (LNA 18:2n-6) and its metabolite arachidonic acid (ARA; 20:4n-6), which are members of the n-6 series. While the n-3 polyunsaturated fatty acids (n-3 PUFA) are abundant in fish oil (FO) (EPA and DHA) and in smaller amounts in vegetable oils (ALA), the n-6 fatty acids are abundantly obtained from most types of vegetable oils including soybean oil. The intake of these EFA in the diet can affect the brain physiological functions [4]. An unbalanced diet in EFA may change cell permeability, synaptic membrane fluidity [5], density of receptors and function of ion channels. Furthermore, the activity of neurotransmitters is particularly modified [6], especially the dopamine (DA) system [7, 8]. In this sense, experimental studies correlated behavioral abnormalities with diets unbalanced in PUFA [9], while human studies showed a relation between abnormal levels of PUFA in the plasma and/or erythrocytes of subjects suffering from diseases of the central nervous system, such as motor disorders [10], confirming the influence of the diet in the function of neuronal membranes and their functions [11]. Furthermore, a connection between the EPA levels in liquor and Parkinson's disease was recently observed, suggesting the involvement of this fatty acids in neurodegenerative motor processes [12].

Reserpine is a catecholamine depletor that exerts a blockade on the vesicular monoamine transporter (VMAT) for neuronal transmission or storage, promoting dopamine-autoxidation and oxidative catabolism by monoamine oxidase (MAO) [13], which has been closely related to the oxidative stress process [14, 15]. Due to these effects, reserpine has been experimentally used to study movement disorders [16–22] as well as to evaluate new therapeutic approaches [23]. Of particular importance, basal ganglia are brain areas rich in monoamines and consequently more vulnerable to oxidative damage [24], which is frequently related to the development of movement diseases such as Huntington, Parkinson and tardive dyskinesia [25–27]. In this sense, the brain is more susceptible to OS when compared to other systems [28] due to its high level of membrane lipids and autoxidizable neurotransmitters. The neuronal phospholipid membrane is formed by PUFA which are more prone to lipid peroxidation by reactive oxygen species than other lipids such as cholesterol and saturated fatty acids [29]. On the other hand, the enzyme action on n-3 EFA generates less inflammatory docosanoids and eicosanoids than that originated from n-6 ARA [30]. Thus, the n-3 fatty acid supplementation becomes especially important because the majority of the diets contain abundance of n-6 and scarcity of n-3 fatty acids. Considering that n-3 has showed protective action on the neuronal lipid membranes, here we propose to study the effects of FO on reserpine-induced oxidative stress in an animal model. Behavioral and biochemical evaluations were performed to quantify the development of movement disorders and oxidative damage in brain tissues involved in motor control.

Methods

Twenty-eight male Wistar rats weighing 270–320 g (about 3 months of age) were kept in Plexiglas cages with free access to food and water in a room with controlled temperature (22–23°C) and in a 12 h-light/dark cycle with lights on at 7:00 a.m. The animals were maintained and used in accordance with the guidelines of the Committee on Care and Use of Experimental Animal Resources, School of Veterinary Medicine and Animal Science of the University of São Paulo, Brazil, which are in accordance with the National Institute of Health Guide for the Care and Use of Laboratory Animals (NIH Publications No 80-23) revised in 1996.

In order to assess the influence of n-3 fatty acids on the reserpine-induced movement disorders, FO was used as source of n-3 EFA, and SO, which contains high levels of n-6 fatty acids, was used as control. FO capsules (Softcaps®, Cotia (SP), Brazil) contained 1 g of oil/capsule rich in n-3 PUFA (35%), which are formed of EPA (20%; 20:5n-3), DHA (6%; 22:6n-3), ALA (0.4%; 18:3n-3) and DPA n-3 (1.2%; 22:5n-3), besides a low content of n-6 PUFA (1.7%) and undetectable levels of *trans* fatty acids. The SO had a high content of ω-6 PUFAs (about 50%), a low content of n-3 PUFA, and a very low content of *trans* fatty acids. Both FO and SO were evaluated by capillary gas chromatography (in the Núcleo Integrado de Desenvolvimento em Análises Laboratoriais-NIDAL-UFSM). Thus, FO and SO were incorporated daily in tap water through a 1% polysorbate 80 (Tween 80®) and offered to the rats in place of drinking water in dark bottles, avoiding contact with the light. Considering the daily intake of each rat (average 40 mL/rat/day), the n-3 fatty acids daily dose was estimated at 14 mg/rat/day for FO-treated rats. This dosage is equivalent to the daily recommendations for human consumption (between 3 and 4 g/adult/day) of n-3 fatty acids.

Reserpine (methyl reserpate 3,4,5-trimethoxybenzoic acid ester-Sigma Chemical) was dissolved in glacial acetic acid and then diluted to a final concentration of 0.5% acetic acid with distilled water. The vehicle consisted of a 0.5% acetic acid solution.

Wistar rats were divided into two groups of 14 animals each and treated with FO or SO solution for 5 days. In the 6th day the groups were re-divided and treated with

reserpine solution (1 mg/kg/mL; sc) (R and FO + R groups) or vehicle (C and FO groups) for 3 days (every other day). During this time the rats were maintained with FO solution or SO solution. One day (24 h) after the last injection of R or V, the rats were placed individually in cages (20 × 20 × 19 cm) containing a mirror under the floor and another one behind the back wall of the cage to allow behavioral quantification when the animal was facing away from the observer. To quantify the occurrence of orofacial dyskinesia, which is characterized by involuntary movements of the orofacial region, observers blinded to the drug treatment recorded the vacuous chewing movement frequency (VCM) and facial twitching time (FT) for three sets of 6 min with intervals of 5 min (a total of 18 min). In a preliminary study (using 5 control and 10 rats treated with reserpine) of interrater reliability, we found that the use of this method of observation for the parameters evaluated usually resulted in >93 agreement between the three different observers. The calculated value was significant for $P < 0.05$.

Immediately after the orofacial dyskinesia observation, rats treated with reserpine (R and FO R) were individually placed on the inclined wire grid (25 × 30 cm, inclined 45° relative to the bench top) for quantification of catalepsy time. This behavioral parameter is characterized by positional passivity, which is observed through failure to correct an uncomfortable imposed posture. Each rat was placed with its forepaws near the edge of the grid and the amount of time spent in this atypical position was recorded for three times, with an interval of 5 min between them. At the end of the three replications, the mean time spent by the rat without moving was calculated for each test. One day (24 h) after the behavioral observations the rats were anesthetized with thiopental (50 mg/kg of body weight, i.p.) and euthanized by exsanguination (blood was collected by cardiac puncture). After removal, the brains were put on ice and cut coronally at the caudal border of the olfactory tubercle. Lipid peroxidation was determined through the pink chromogen produced by the reaction of thiobarbituric acid (TBA) with aldehydes, measured spectrophotometrically at 535 nm, in accordance with Ohkawa et al. [31]. The cortex and striatum were homogenized in Tris/acetic acid buffer (pH 7.4) and centrifuged at 1,310×g for 10 min. The supernatants (10% w/v) were boiled (100 °C) in trichloroacetic acid (TCA-10%) and thiobarbituric acid (TBA-0.67%) for 60 min, cooled and centrifuged. The absorbance of the supernatant was read at 535 nm.

Data were analyzed by one or two-way ANOVA followed by Duncan's multiple range test when appropriate. Pearson's correlation coefficient was calculated between the orofacial dyskinesia parameters (VCM frequency and TF duration) and lipid peroxidation (TBARS levels). Data were analyzed using Statistica 11.0 and expressed as means + SEM. P-values lower than 0.05 were considered statistically significant.

Results

Rats' body weight gain and food/suspension intake were not different among the treatments, and no mortality occurred during the study (data not shown).

The effects of reserpine treatment on orofacial movements are shown in Table 1. Two-way ANOVA revealed a significant main effect of reserpine [$F(1,24) = 74.25$; $P < 0.001$], FO [$F(1,24) = 7.36$; $P < 0.05$], and a significant reserpine × FO interaction [$F(1,24) = 6.42$; $P < 0.05$] for VCM frequency. For duration of FT, two-way ANOVA revealed a significant main effect of reserpine and a significant reserpine × FO interaction [$F(1,24) = 36.62$; $P < 0.001$ and 8.38; $P < 0.05$, respectively].

Univariate ANOVA followed by Duncan's test showed that reserpine treatment (1 mg/kg) caused evident signs of orofacial dyskinesia, which were observed by an increase in the VCM frequency and FT duration (Table 1). The co-administration of FO solution (FO + R group) caused a reduction of 36% and 52% of these behavioral parameters, respectively. In fact, rats treated with FO showed similar VCM and FT as compared to the control group.

One-way ANOVA showed that reserpine treatment (1 mg/kg) caused catalepsy in rats and co-treatment with FO reduced about 21% of this immobility time (Table 1). In this behavioral evaluation, rats not treated with reserpine (C and FO groups) showed no catalepsy and therefore were not included in the "Results" and "Discussion" section.

Two-way ANOVA of cortical TBARS levels revealed a significant effect of reserpine [$F(1,24) = 10.50$; $P < 0.001$] and FO [$F(1,24) = 22.27$; $P < 0.001$], as well

Table 1 Effects of fish oil oral treatment on behavioral parameters (vacuous chewing movements, facial twitching and catalepsy time) of rats treated with reserpine solution (1 mg/kg, sc, every other day, for 3 days)

Groups	VCM (frequency)	FT (seconds)	Catalepsy (seconds)
C	26.7 ± 4.9	0.42 ± 0.4	–
FO	25.3 ± 7.6	1.50 ± 0.9	–
R	116.4 ± 10.8$^{**,\#\#}$	9.82 ± 1.4$^{**,\#\#}$	49.9 ± 2.3
FO + R	74.2 ± 8.6$^{**,\#\#,+}$	4.74 ± 1.1$^{*,\#,+}$	39.3 ± 4.0$^{\#}$

Values are means ± SEM ($n = 7$)

VCM vacuous chewing movements; *FT* facial twitching; *C* control, *FO* fish oil and *R* reserpine

$^{*}P < 0.05$, $^{**}P < 0.001$, differences from control group (C); $^{\#}P < 0.05$, $^{\#\#}P < 0.001$, differences from fish oil (FO) and $^{+}P < 0.05$, differences from reserpine group (R)

as a significant reserpine × FO interaction [$F(1,24) = 12.15$; $P < 0.05$]. Two-way ANOVA of striatal TBARS levels revealed a significant main effect of FO [$F(1,24) = 31.21$; $P < 0.001$] and a reserpine × FO interaction tendency ($P = 0.059$). Duncan's multiple range test showed that reserpine treatment (1 mg/kg) caused an increase in the cortical and striatal TBARS levels (Fig. 1a, b). The co-treatment with FO caused a reduction of 61% and 53% of this lipid peroxidation measure in both brain regions, respectively. Interestingly, statistical analyses revealed a significant positive correlation between VCM frequency ($r = 0.47$, $P < 0.0.05$, Fig. 2a) and FT duration ($r = 0.45$, $P < 0.05$, Fig. 2b) with striatal lipid peroxidation, confirming that motor disturbances and oxidative stress may result from the pro-inflammatory and oxidative cascade induced by reserpine.

Discussion

Our results demonstrate that FO rich in n-3 fatty acids reduced the reserpine-induced parkinsonism symptoms, observed through orofacial dyskinesia parameters, catalepsy time and lipid peroxidation. Sarsilmaz et al. [1] hypothesized that n-3 EFA could affect the oxidant/antioxidant status of the brain by stabilizing the neuronal membranes, acting as an antiapoptotic agent in brain neurons [32] with neuroprotective functions [33, 34]. In fact, n-3 fatty acids have a potential to reduce damages in the neuronal membranes, whose dysfunction may affect the dopaminergic and serotonergic neurotransmission [35]. In dopaminergic structures such as striatum, DA itself may be one of the key contributors to oxidative stress, mainly because it generates dopamine-quinones and hydrogen peroxide by autoxidation and MAO metabolism. In this sense, reserpine is known to exert a monoamine-depleting action by blocking the ATP-dependent uptake mechanism of the storage organelles, resulting in the accelerated presynaptic turnover of the cytoplasmic DA. This mechanism of reserpine was studied by Sussman et al. [36], who showed that reserpine administration causes a decrease in striatal DA levels and an increase in the metabolites of DA ratios (DOPAC/DA and HVA/DA) in rats. The reserpine-induced movement disorders have been suggested as a putative animal model of tardive dyskinesia and parkinsonism [14, 37] which has been used by different research groups [17–19, 38].

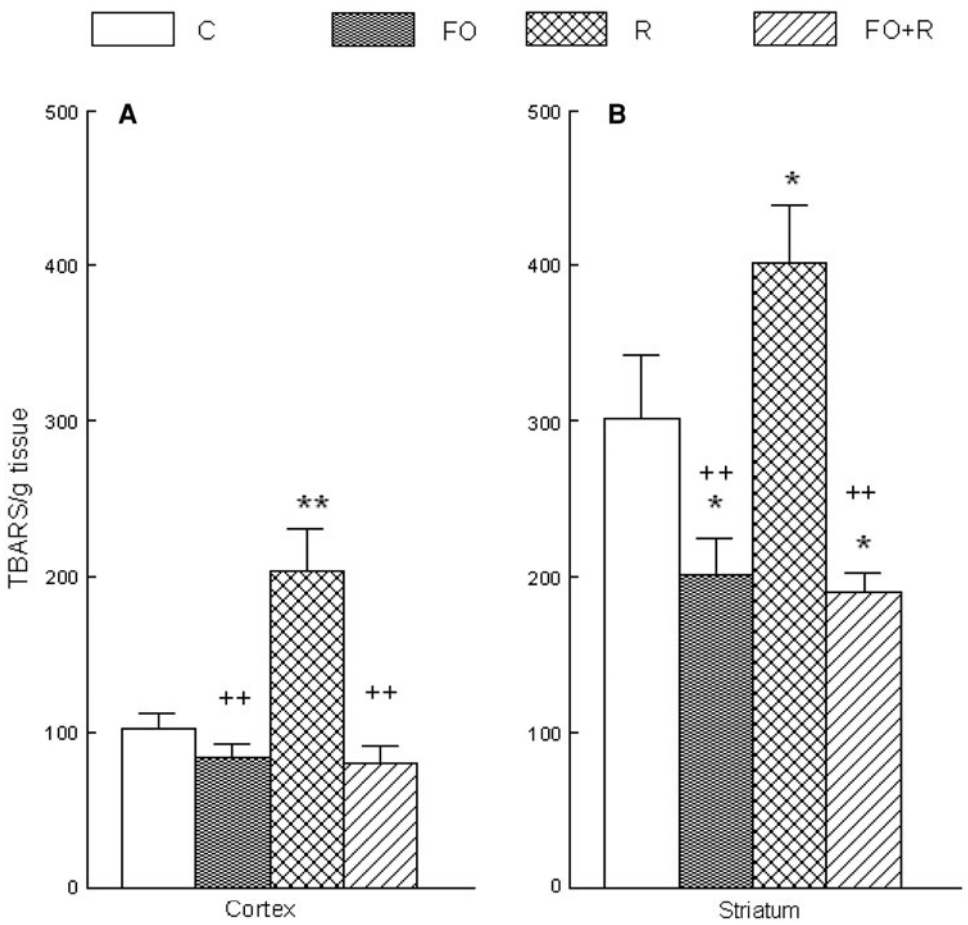

Fig. 1 Effects of fish oil oral treatment on TBARS levels in the cortex (**a**) and striatum (**b**) of rats treated with reserpine (1 mg/kg, sc, every other day, for 3 days). Abbreviations: control (*C*); fish oil (*FO*); reserpine (*R*). Data are reported as means + SEM. $^{*}P < 0.05$, $^{**}P < 0.001$, difference from C group; $^{++}P < 0.001$, difference from *R* group

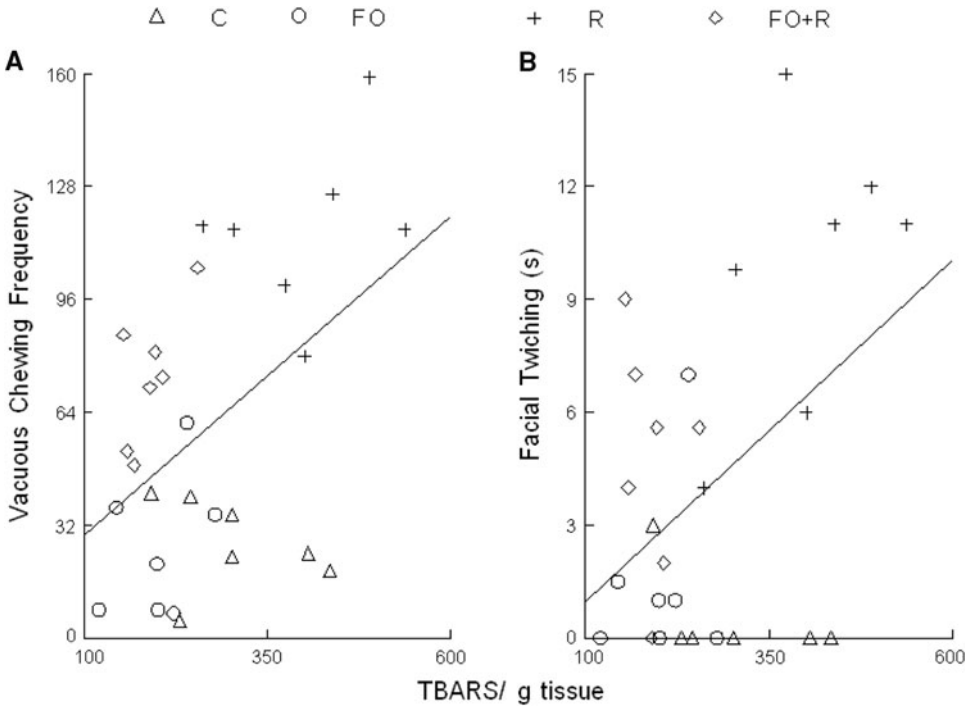

Fig. 2 Linear regression analysis between vacuous chewing frequency, facial twitching and striatal lipid peroxidation induced by reserpine treatment (1.0 mg/kg, sc, every other day, for 3 days) following 5 days of oral treatment with fish oil (ad libitum). Abbreviations: control (*C*); fish oil (*FO*); reserpine (*R*). Linear regression was evidenced by Pearson's coefficient ($r = 0.47$ and 0.45, respectively, $P < 0.05$)

In addition, it has also been used as an animal model of brain oxidative stress [13, 15, 23]. Apart from the names, these animal models are not contradictory, mainly because parkinsonism and tardive dyskinesia are closely related to oxidative stress and neurotoxicity [19, 39]. Recently, we showed a negative relationship between the glutamate transporter and the manifestation of orofacial dyskinesia in rats exposed to reserpine or haloperidol [19], strengthening the relation between oxidative stress, excitotoxicity and movement disorders.

Some studies have shown that deficiencies of n-3 PUFA may decrease the vesicular monoamine transporter (VMAT-2) [40] as well as alter DA vesicle density in frontal cortex [41] and mesolimbic pathway [42] but not in striatum [43, 44]. Unlike these results, our study was not conducted with a lack but with a supplementation of n-3 fatty acids, which showed a beneficial effect on reserpine-induced behavioral and biochemical parameters. Since reserpine acts on the VMAT-2 [13], we can assume that n-3 PUFA supplementation does not prevent its monoamine depleting effects, but attenuates the oxidative cascade resulting from monoamine metabolism. Our findings suggest that n-3 EFA plays a role as an neuroprotective agent. N-3 fatty acids supplementation allows its higher bioavailability for enzymatic activities (cyclooxygenase and lipoxygenase), which degrade the ARA (n-6 EFA) displaced from neuronal phospholipid membranes. So, both n-3 (from supplementation or diet) and n-6 EFA (from membrane phospholipids) compete for the common cyclooxygenase and lipoxygenase enzymes, but ARA produces more potent inflammatory and pro-aggregatory eicosanoids [45], which are also related to the generation of free radicals and development of oxidative damage, while the neuroprotectins derived from these n-3 EFA retard neuroinflammation, oxidative stress and apoptotic cell death in brain tissue [46]. Up to now, different hypotheses have been raised to explain the influence of n-3 EFA on inflammatory and oxidative processes: DHA (and, to a lesser degree, EPA) reduces chronic inflammation by attenuating nuclear factor kappa-light-chain-enhancer of activated B cells (NF-$_\kappa$B), in turn modulating the expression of pro-inflammatory cytokines. These fatty acids may decrease the phosphorylation of specific interleukins (I$_\kappa$B) modulating the availability of NF-$_\kappa$B. Importantly, this process can modulate the expression of the pro-inflammatory genes for COX-2 beyond other molecules of adhesion and signalizing [47]. These genes control the availability of lipid mediators such as prostaglandins, leukotrienes and thromboxanes, which modulate the intensity and duration of immune responses, which are also involved in neuroinflammatory processes. Of particular importance, DHA and its derivatives are themselves intimately involved in cell signaling processes [48]. Although EPA has been explored as a therapeutic agent to treat neurological diseases in recent years [49, 50], its uptake and incorporation in the brain is not clear. A recent study showed a low concentration of EPA in brain phospholipids after intracerebroventricular infusion of ^{14}C-EPA in rats, suggesting a fast β-oxidation (14% per day) of this fatty acid [51]. In this sense, FO, which contains DHA and other EFA, has

shown beneficial effects. A recent study on Parkinson's disease showed that short-term administration of DHA reduced the extent of levodopa-induced dyskinesia by about 40% in a non-human primate model of parkinsonism [52]. On the other hand, animal models showed the involvement of prostaglandins derived from ARA in orofacial dyskinesia [53] and cataleptic behavior [54] development. In addition, we recently showed the beneficial effect of FO on orofacial dyskinesia and oxidative stress induced by typical neuroleptics [55], confirming the protective role of n-3 fatty acids on brain phospholipid membranes [56].

Concerning the length of FO supplementation, different studies have shown the therapeutic properties of n-3 fatty acids after short-term treatment (5–14 days) [10, 32, 57]. Besides these experimental designs, a human study performed during antidepressant treatment showed the beneficial effects of 3 week FO supplementation [58]. In this sense, it is important to emphasize that, as the temporal relationship between humans and animals is very different, a relatively longer time of treatment is needed for animals as compared to humans. In fact, we believe that the demonstration of n-3 fatty acids incorporation in neuronal membranes may be conclusive, but the mechanisms by which the brain uptakes PUFA are not agreed upon. Several models regarding the uptake of PUFA by the brain have been proposed: via receptor mediated transporter (esterified PUFA in the form of a lipoprotein) or via passive diffusion (unesterified PUFA), whose rates of incorporation in brain membrane phospholipids vary with experimental conditions [59, 60]. In short, although brief treatment with n-3 fatty acids is not supposed to change significantly the composition of brain membranes (although this possibility cannot be ruled out), it could cause an increase in the concentration of plasmatic free fatty acids and, consequently, in the cerebrospinal fluid, that could compete with pro-inflammatory ARA derived from brain bio-membranes metabolism.

In conclusion, here we have shown that n-3 fatty acids may protect brain motor structures against reserpine-induced oxidative damage, and its supplementation or inclusion in the diet may prevent the development of motor disorders related to oxidative damages.

Conflict of interest The authors report no conflicts of interest.

References

1. Sarsilmaz M, Songur A, Ozyurt H, Kus I, Ozen OA, Ozyurt B, Sogut S, Akyol O (2003) Potential role of dietary ω-3 essential fatty acids on some oxidant/antioxidant parameters in rats' corpus striatum. Prostaglandins Leukot Essent Fatty Acids 69:253–259
2. Songur A, Sarsilmaz M, Sogut S, Ozyurt B, Ozyurt H, Zararsiz I, Turkoglu AO (2004) Hypothalamic superoxide dismutase, xanthine oxidase, nitric oxide, and malondialdehyde in rats fed with ω-3 fatty acids. Prog Neuropsychopharmacol Biol Psychiatry 28:693–698
3. Zararsiz I, Kus I, Akpolat N, Songur A, Ogeturk M, Sarsilmaz M (2006) Protective effects of omega-3 essential fatty acids against formaldehyde-induced neuronal damage in prefrontal cortex of rats. Cell Biochem Funct 24:237–244
4. Haag M (2003) Essential fatty acids and the brain. Can J Psychiatr 48:195–203
5. Jump DB (2002) Dietary polyunsaturated fatty acids and regulation of gene transcription. Curr Opin Lipidol 13:155–164
6. Yehuda S, Rabinovitz S, Mostofski DI (2005) Essential fatty acids and stress. In: Yehuda S, Mostofsky DI (eds) Nutrition, stress and medical disorders. Humana Press, Totowa, pp 99–100
7. Chalon S, Delion-Vancassel S, Belzung C, Guilloteau D, Lequisquet AM, Besnard JC, Durand G (1998) Dietary fish oil induces affects in monoaminergic neurotransmission and behavior in rats. J Nutr 128:2512–2519
8. Wainwright PE (2002) Dietary essential fatty acids and brain function: a development perspective on mechanisms. Proc Nutr Soc 61:61–69
9. Wainwright PE, Xing HC, Mutsaers L, McCutcheon D, Kyle D (1997) Arachidonic acid offsets the effects on mouse brain and behavior of a diet with a low (n-6)/(n-3) ratio and very high levels of docosahexaenoic acid. J Nutr 127:184–193
10. Éthier I, Kagechika H, Shudo K, Rouillard C, Lévesque D (2004) Docosahexaenoic Acid Reduces Haloperidol-Induced Dyskinesias in Mice: Involvement of *Nur77* and Retinoid Receptors. Biol Psychiatry 56:522–526
11. Yehuda S (1989) Behavioral effects of dietary fats. In: Chandra RK (ed) Health effects of fish and fish oils. ARTS St John's, Canada, pp 327–335
12. Lee PH, Lee G, Paik MJ (2008) Polyunsaturated fatty acids levels in the cerebrospinal fluid of patients with Parkinson's disease and multiple system atrophy. Mov Disord 23:309–310
13. Fuentes P, Paris I, Nassif M, Caviedes P, Segura-Aguilar J (2007) Inhibition of VMAT-2 and DT-diaphorase induce cell death in a substantia nigra-derived cell Line - an experimental cell model for dopamine toxicity studies. Chem Res Toxicol 20:776–783
14. Bilska A, Dubiel M, Sokolowska-Jez'ewicz M, Lorenc-Koci E, Wlodek L (2007) Alpha-lipoic acid differently affects the reserpine-induced oxidative stress in the striatum and prefrontal cortex of rat brain. Neuroscience 146:1758–1771
15. Teixeira AM, Reckziegel P, Müller L, Pereira RP, Roos DH, Rocha JBT, Bürger ME (2009) Intense exercise potentiates oxidative stress in striatum of reserpine-treated animals. Pharmacol Biochem Behav 92:231–235
16. Hallet PJ, Brotchie JM (2007) Striatal delta opioid receptor binding in experimental models of Parkinson's disease and dyskinesia. Mov Disord 22:28–40
17. Abilio VC, Silva RH, Carvalho RC, Grassl C, Calzavara MB, Registro S, D′Almeida V, Ribeiro R de R, Frussa-Filho R (2004) Important role of striatal catalase in aging- and reserpine-induced oral dyskinesia. Neuropharmacology 47:263–272
18. Bürger ME, Alves A, Callegari L, Athaide FR, Nogueira CCW, Zeni G, Rocha JBT (2003) Ebselen attenuates reserpine-induced orofacial dyskinesia and oxidative stress in rat striatum. Progr Neuropharmacol Biol Psychiatry 27:135–140
19. Bürger ME, Fachinetto R, Alves A, Callegari L, Rocha JBT (2005) Acute reserpine and subchronic haloperidol treatments change synaptosomal brain glutamate uptake and elicit orofacial dyskinesia in rats. Brain Res 1031:202–210
20. Naidu PS, Singh A, Kulkarni SK (2004) Reversal of reserpine-induced orofacial dyskinesia and cognitive dysfunction by quercetin. Pharmacology 70:59–67
21. Hughes NR, McKnight AT, Woodruff GN, Hill MP, Crossman AR, Brotchie JM (1998) *Kappa*-opioid receptor agonists increase

locomotor activity in the monoamine-depleted rat model of parkinsonism. Mov Disord 13:228–233
22. Hubbard A, Trugman JM (1993) Reversal of reserpine-induced catalepsy by selective D1 and D2 dopamine agonists. Mov Disord 8:473–478
23. Teixeira AM, Trevizol F, Colpo G, Garcia SC, Charo M, Pereira RP, Fachinetto R, JBT Rocha, Bürger ME (2008) Influence of chronic exercise on reserpine-induced oxidative stress in rats: Behavioral and antioxidant evaluations. Pharmacol Biochem Behav 88:465–472
24. Lohr JB, Kuczenski R, Niculescu AB (2003) Oxidative mechanisms and tardive dyskinesia. CNS Drugs 17:47–62
25. Lohr JB, Kuczenski R, Bracha HS (1990) Increased indices of free radical activity in the cerebrospinal fluid of patients with tardive dyskinesia. Biol Psychiatry 28:535–539
26. Andreassen OA, Jorgensen HA (2000) Neurotoxicity associated with neuroleptic-induced oral dyskinesias in rats. Implications for tardive dyskinesia? Prog Neurobiol 61:525–541
27. Gilgun-Sherki Y, Melamed E, Offen D (2001) Oxidative stress induced-neurodegenerative diseases: the need for antioxidants that penetrate the blood barrier. Neuropharmacology 40:959–975
28. Halliwel B, Gutteridge JMC (1999) Free radicals in biology and medicine. Oxford University Press, Oxford
29. Evans DR, Parikh VV, Khan MM, Coussons C, Buckley PF, Mahadik SP (2003) Red blood cell membrane essential fatty acid metabolism in early psychotic patients following antipsychotic drug treatment. Prostaglandins Leukot Essent Fatty Acids 69:393–399
30. Bazan N (2009) Cellular and molecular events mediated by docosahexaenoic acid-derived neuroprotectin D1 signaling in photoreceptor cell survival and brain protection. Prostaglandins Leukot Essent Fatty Acids 81:205–211
31. Ohkawa H, Ohishi N, Yagi K (1979) Assay for lipid peroxides in animal tissues by thiobarbituric acid reaction. Anal Biochem 95:351–358
32. Ozyurt B, Sarsilmaz M, Akpolat N, Ozyurt H, Akyol O, Herken H, Kus I (2007) The protective effects of omega-3 fatty acids against MK-801-induced neurotoxicity in prefrontal cortex of rat. Neurochem Int 50:196–202
33. Bazan NG (2006) The onset of brain injury and neurodegeneration triggers the synthesis of docosanoid neuroprotective signaling. Cell Mol Neurobiol 26:899–911
34. Bazan NG (2007) Omega-3 fatty acids, pro-inflammatory signaling and neuroprotection. Clin Nutr Metab Care 10:136–141
35. Fenton WS, Hibbeln J, Knable M (2000) Essential fatty acids, lipid membrane abnormalities, and the diagnosis and treatment of schizophrenia. Biol Psychiatry 47:8–21
36. Sussman AN, Tran-Nguyen LTL, Neisewander JL (1997) Acute reserpine administration elicits long-term spontaneous oral dyskinesia. Eur J Pharmacol 337:157–160
37. Neiswander JL, Castañeda E, Davis DA (1994) Dose-dependent differences in the development of reserpine-induced oral-dyskinesia in rats: support for a model of tardive dyskinesia. Psychopharmacology 116:79–84
38. Raghavendra V, Naidu PS, Kulkarni SK (2001) Reversal of reserpine-induced vacuous chewing movements in rats by melatonin: involvement of peripheral benzodiazepine receptors. Brain Res 904:149–152
39. Colpo G, Trevisol F, Teixeira AM, Fachinetto R, Pereira RP, Athayde ML, Rocha JBT, Bürger ME (2007) *Ilex paraguariensis* has antioxidant and attenuates haloperidol-induced orofacial dyskinesia and memory dysfunction in rats. Neurotox Res 12:1–10
40. Zimmer L, Durand G, Guilloteau D, Chalon S (1999) n-3 polyunsaturated fatty acid deficiency and dopamine metabolism in the rat frontal cortex. Lipids 34:S251
41. Zimmer L, Delpal S, Guilloteau D, Aïoun J, Durand G, Chalon S (2000) Chronic n-3 polyunsaturated fatty acid deficiency alters dopamine vesicle density in the rat frontal cortex. Neurosci Lett 284:25–28
42. Zimmer L, Vancassel S, Cantagrel S, Breton P, Delamanche S, Guiloteau D, Durand G, Chalon S (2002) The dopamine mesocorticolimbic pathway is affected by deficiency in n-3 polyunsaturated fatty acids. Am J Clin Nutr 75:662–667
43. Delion S, Chalon S, Herault J, Guilloteau D, Besnard JC, Durand G (1994) Chronic dietary alpha-linolenic acid deficiency alters dopaminergic and serotoninergic neurotransmission in rats. J Nutr 124:2466–2476
44. Delion S, Chalon S, Guilloteau D, Besnard JC, Durand G (1996) Alpha-linolenic acid dietary deficiency alters age-related changes of dopaminergic and serotoninergic transmission in the rat frontal cortex. J Neurochem 66:1582–1591
45. Calder PC (2001) Omega 3 polyunsaturated fatty acids, inflammation and immunity. World Rev Nutr Diet 88:109–116
46. Farooqui AA, Horrocks LA (2006) Phospholipase A2-generated lipid mediators in the brain: the good, the bad and the ugly. Neuroscientist 12:245–260
47. De Caterina R, Massaro M (2005) Omega-3 fatty acids and the regulation of expression of endothelial pro-atherogenic and pro-inflammatory genes. J Membr Biol 206:103–116
48. Farooqui AA, Horrocks LA, Farooqui T (2000) Glycerophospholipids in brain: their metabolism, incorporation into membranes and involvement in neurological disorders. Chem Phys Lipids 106:1–29
49. Burgess JR, Stevens L, Zhang W, Peck L (2000) Long-chain polyunsaturated fatty acids in children with attention-deficit hyperactivity disorder. Am J Clin Nutr 71:327S–330S
50. Sorgi PJ, Hallowell EM, Hutchins HL, Sears B (2007) Effects of an open-label pilot study with high-dose EPA/DHA concentrates on plasma phospholipids and behavior in children with attention deficit hyperactivity disorder. Nutr J 6:16
51. Chen CT, Liu Z, Bazinet RP (in press) Rapid de-esterification and loss of eicosapentaenoic acid from rat brain phospholipids: an intracerebroventricular study. J Neurochem. doi:10.1111/j.1471-4159.2010.07116.x
52. Samadi P, Gregoire C, Rouillard C, Bedard PJ, Di Paolo T, Levesque D (2006) Docosahexaenoic acid reduces levodopa-induced dyskinesias in 1-methyl-4-phenyl-1, 2, 3, 6-tetrahydropyridine monkeys. Ann Neurol 59:282–288
53. Naidu P, Kulkarni SK (2001) Possible involvement of prostaglandins in haloperidol-induced orofacial dyskinesia in rats. Eur J Pharmacol 430:295–298
54. Ono N, Abiru T, Sugiyama K, Kamiya H (1992) Influence of cyclooxygenase inhibitors on the cataleptic behaviour induced by haloperidol in mice. Prostaglandins Leukot Essent Fatty Acids 46:59–63
55. Barcelos RCS, Benvegnú DM, Boufleur N, Reckziegel P, Müller LG, Pase CS, Bürger ME (2010) Effects of n-3 essential fatty acids (n-3 EFA) on motor disorders and memory dysfunction typical neuroleptic-induced: behavioral and biochemical parameter. Neurotox Res 17:228–237
56. Mills SC, Windsor AC, Knight SC (2005) The potential interactions between polyunsaturated fatty and colonic inflammatory processes. Clin Exp Immunol 142:216–228
57. Wu A, Ying Z, Gomez-Pinilha F (2004) Dietary omega-3 fatty acids normalize BDNF levels, reduce oxidative damage, and counteract learning disability after traumatic brain injury in rats. J Neurotrauma 21:1457–1467
58. Nemets B, Stahl Z, Belmaker RH (2002) Addition of omega-3 fatty acid to maintenance medication treatment for recurrent unipolar depressive disorder. Am J Psychiatry 159(3):477–479
59. Robinson PJ, Noronha J, DeGeorge JJ, Freed LM, Nariai T, Rapoport SI (1992) A quantitative method for measuring regional in vivo fatty-acid incorporation into and turnover within brain phospholipids: review and critical analysis. Brain Res 17:187–214
60. DeMar JC Jr, Ma K, Bell JM, Rapoport SI (2004) Half-lives of docosahexahenoic acid in rat brain phospholipids are prolonged by 15 weeks of nutritional deprivation of n-3 polyunsaturated fatty acids. J Neurochem 91:1125–1137

Lipids (2011) 46:151–161
DOI 10.1007/s11745-010-3511-3

ORIGINAL ARTICLE

Low Levels of the Omega-3 Index are Associated with Sudden Cardiac Arrest and Remain Stable in Survivors in the Subacute Phase

Hildegunn Aarsetoey · Reidun Aarsetoey · Thomas Lindner · Harry Staines · William S. Harris · Dennis W. T. Nilsen

Received: 6 April 2010 / Accepted: 20 November 2010 / Published online: 14 January 2011

Abstract In previous studies, low blood levels of n-3 fatty acids (FA) have been associated with increased risk of cardiac death, and the omega-3 index (red blood cell (RBC) eicosapentaenoic acid (EPA) and docosahexaenoic acid (DHA) expressed as weight percentage of total FA) has recently been proposed as a new risk factor for death from coronary artery disease, especially following sudden cardiac arrest (SCA). As blood samples often haven been harvested after the event, the aim of our study was to evaluate the stability of RBC fatty acids following SCA. The total FA profile, including the omega-3 index, was measured three times during the first 48 h in 25 survivors of out-of-hospital cardiac arrest (OHCA), in 15 patients with a myocardial infarction (MI) without SCA and in 5 healthy subjects. We could not demonstrate significant changes in the FA measurements in any of the groups, this also applied to the omega-6/omega-3 ratio and the arachidonic acid (AA)/EPA ratio. Furthermore, we compared the omega-3 index in 14 OHCA-patients suffering their first MI with that of 185 first-time MI-patients without SCA; mean values being 4.59% and 6.48%, respectively ($p = 0.002$). In a multivariate logistic regression analysis, a 1% increase of the omega-3 index was associated with a 58% (95% CI: 0.25–0.76%) reduction in risk of ventricular fibrillation (VF). In conclusion, the omega-3 index remained stable after an event of SCA and predicted the risk of VF.

Keywords n-3 fatty acids · Eicosapentaenoic acid · Docosahexaenoic acid · Red blood cell membranes · The omega-3 index · Fatty acid stability · Sudden cardiac arrest · Ventricular fibrillation · Myocardial infarction

H. Aarsetoey (✉) · R. Aarsetoey
Department of Medicine, Stavanger University Hospital, PB 8100, 4068 Stavanger, Norway
e-mail: aahi@sus.no

D. W. T. Nilsen
Division of Cardiology, Stavanger University Hospital, Stavanger, Norway

H. Aarsetoey · D. W. T. Nilsen
Institute of Medicine, University of Bergen, Bergen, Norway

T. Lindner
Department of Anaesthesia and Intensive Care Medicine, Stavanger University Hospital, Stavanger, Norway

H. Staines
Sigma Statistical Services, Balmullo, Scotland, UK

W. S. Harris
Sanford Research/USD and Sanford School of Medicine, University of South Dakota, Sioux Falls, USA

Abbreviations

AA	Arachidonic acid
ACS	Acute coronary syndrome
AMI	Acute myocardial infarction
CAD	Coronary artery disease
DHA	Docosahexaenoic acid
ECG	Electrocardiography
EF	Ejection fraction
EPA	Eicosapentaenoic acid
FA	Fatty acid(s)
hsCRP	High-sensitivity C-reactive protein
ICD	Implantable cardioverter defibrillator
MI	Myocardial infarction
NSTEMI	Non-ST-elevation myocardial infarction
OHCA	Out-of-hospital cardiac arrest
PCI	Percutaneous coronary intervention
RBC	Red blood cell(s)
ROSC	Return of spontaneous circulation

SCA	Sudden cardiac arrest
SCD	Sudden cardiac death
STEMI	ST-elevation myocardial infarction
TnT	Troponin-T
VF	Ventricular fibrillation
VT	Ventricular tachycardia

Introduction

The first clinical evidence of a possible protective effect of n-3 fatty acids (FA) against sudden cardiac death (SCD) came from the publication of the GISSI-Prevenzione trial in 1999 [1]. In this study, supplementation with 1 g/day of n-3 FA following a myocardial infarction (MI) resulted in a 45% reduction of sudden deaths during 3.5 years of follow-up. This finding has been supported by the demonstration of low levels of blood n-3 FA in patients suffering SCD [2, 3] or a fatal cardiac event [4]. In addition, our research group has recently presented evidence for an increased risk of ventricular fibrillation (VF) during the acute ischemic phase of an MI in patients with low levels of cellular n-3 FA [5]. In our study, as well as in a previous investigation [3], blood samples were harvested after the episode of sudden cardiac arrest (SCA). To obtain a reliable result with this method, we have to assume that the blood composition of FA remains stable following the event, or else we need to correct for changes induced by the event itself in selected case–controls.

Previous studies have demonstrated significant changes in FA composition of serum [6] and plasma lipids [7] in the early stage of an MI. Recently, the red blood cell (RBC) FA composition has been found to reflect the cardiac omega-3 content [8, 9]. Even though stable in rats for 24 h after the induction of an MI [7], the only evaluation of post-MI RBC FA in humans demonstrated a statistically significant change in the investigated FA during a 7 day period [10]. As most episodes of cardiac arrest appear during the early course of an MI, these findings are of interest when assessing the FA profile of SCD/SCA-patients.

In patients with SCA, the event itself, as well as the resuscitation, might potentially affect the measurements. Stress-induced or injected adrenalin can activate phospholipases, releasing FA from cell membrane phospholipids leading to falsely low post-resuscitation measurements. The only evaluation of this question has so far been performed in animal studies, in which no significant effect of adrenalin on the FA composition in RBC [3] or serum lipids [11] has been observed. FA stability after an episode of cardiac arrest has previously not been reported in humans, and this was the primary aim of our study.

Based on the proposed post-MI changes in FA, we wanted to compare the time-related profile of RBC FA in SCA-patients with that of MI-patients without a cardiac arrest. We also wanted to evaluate whether the level of RBC eicosapentaenoic acid (EPA) + docosahexaenoic acid (DHA) (the omega-3 index) might be related to VF, as previously demonstrated in another group of SCA patients [5].

Materials and Methods

Study Subjects and Design

This study was performed at Stavanger University Hospital, Stavanger, Norway. The inclusion criteria were; age >18 years and out-of-hospital cardiac arrest (OHCA) of assumed cardiac origin. Patients with permanent return of spontaneous circulation (ROSC) had 6 mL of EDTA-blood drawn on hospital admission. Further blood sampling was repeated after 8–12 h and after 24–48 h. At this point, most patients were on a respirator at the intensive care unit, and blood samples were collected from an already established arterial crane. For the few patients who woke up immediately after resuscitation, blood sampling was performed as part of the hospital's routine. Echocardiography was performed shortly after admission for the evaluation of the ejection fraction (EF). Survivors gave written informed consent before discharge. If the patient stayed unconscious until death, the family was asked for consent on the patient's behalf.

From February 2007 until June 2009, blood samples for evaluation of RBC FA were collected from 25 patients with documented VF. Patients were divided into three groups based on the mechanism of their ventricular arrhythmia; (1) SCA without a present MI, (2) SCA with a first-time MI and (3) SCA with recurrent MI. The presence or absence of an MI was determined from the release pattern of troponin-T (TnT), using ST-segment analysis of the electrocardiogram (ECG) for the definition of ST-elevation MI (STEMI) or non-ST-elevation MI (NSTEMI). For one case, there were only two in-hospital samples available, and this patient was only included in the analysis of risk.

For the evaluation of MI related FA changes, 15 subjects with an acute MI (AMI) without SCA were recruited. In this group, MI was defined by a maximal TnT >0.03 μg/L and a typical release pattern. EDTA-blood from most of these patients was collected as part of the hospital's routine at admission or at coronary angiography and during the subsequent 48 h, employing the same time points as described for the SCA-patients. After collection of blood and baseline characteristics, the identity of these patients was destroyed and all samples treated anonymously. The

selection of the MI-patients was not sufficiently random for them to serve as controls for the assessment of risk.

To rule out a biological variation of the FA profile, we also analyzed a subsequent set of three blood samples in 5 healthy subjects, 3 men and 2 women, with an age of 34–72 years. The first and last (after 24 h) blood samples were drawn after an overnight fast, the second sample was in the fed state 8–12 h after the first one.

For risk evaluation, we compared the admission omega-3 index in the SCA-patients with first-time MI with our previous control-population of 185 first-time MI patients from the Risk factors in Acute Coronary Syndrome (RACS, ClinicalTrials.gov identifier: NCT00521976) study [5]). In that study, patients with chest pain or otherwise suspected acute coronary syndrome (ACS) were included at the same hospital from November 2002 until September 2003. Blood samples for the analysis of the omega-3 index were harvested immediately after admission, without subsequent sampling during hospitalization. Controls were selected based on the absence of VF or sustained ventricular tachycardia (VT) for at least 30 days of follow-up.

The present study was approved by the Regional Board of Research Ethics and the Norwegian Health Authorities and conducted in accordance with the Helsinki Declaration of 1975, as revised in 1983.

Laboratory Methods

Storage of blood samples prior to preparation was allowed for 24 h at room-temperature and 48 h in a refrigerator. RBC for analysis of FA were prepared from EDTA-blood after centrifugation at 2,500*g* for 10 min in room temperature. Plasma was extracted and the buffy coat discarded, after which sedimented RBC were washed twice with phosphate buffered saline (PBS), followed each time by centrifugation at 2,500*g* for 3 min. All samples were stored at –70 °C until extraction of FA could be performed. At this temperature, the composition of RBC FA has been demonstrated to remain stable for at least 4 years [12].

For the FA analysis a 50-μL sample of thawed packed RBC was placed on a filter paper disc (Whatman grade 1, 3.0 cm diameter) that had been pre-treated with butylated hydroxytoluene (50 mg/L) according to Marangoni et al. [13]. Dried blood spots were shipped to the US and the FA composition analyzed in the laboratory of W. S. Harris by flame ionization gas chromatography (GC9A, Shimadazu Corporation, Columbia, MD, USA), as previously described [5]. FA in dried RBC-samples remain stable during storage and shipment in cooled conditions for at least 1 week, as previously described [14]. We have also shown that dried RBC-samples can be stored at −70 °C for 1.5 years with no reduction in the omega-3 index ($n = 22$) (unpublished data). The coefficient of variation (CV) for the omega-3 index was 6%. Laboratory personnel performing the analyses were blinded with respect to clinical events.

Statistical Analyses

Characteristics of cases and controls are given as means ± standard deviations (SD) for normally distributed variables and as medians with interquartile range (25th–75th percentile) when the assumption of normality was violated. Differences between groups at baseline were tested by the Mann–Whitney *U* Test and the Kruskal–Wallis Test for non-normally distributed variables with the independent samples *t* test and the one-way between group analysis of variance (ANOVA) as the parametric alternative. Categorical variables were evaluated using the Chi-square test, or in the case of few expected observations, the *p* value was derived from Fisher's exact probability test. The sample sizes of the subgroups of SCA-patients were, however, too small to test for differences in inter-group frequencies.

For the evaluation of FA stability following an event of SCA and/or AMI we used one-way repeated measures ANOVA to compare the omega-3 index and individual FA at admission, after 8–12 h and after 24–48 h in the four different groups of patients; (1) SCA without an AMI ($n = 6$), (2) SCA with an AMI (both first and recurrent) ($n = 18$), (3) AMI without SCA ($n = 15$) and (4) healthy subjects ($n = 5$). The analysis was performed for each group with time as the only within-subject factor at three levels. The Mauchly's test of sphericity was used to check that the correlations and variances of the observations remained constant at all time points. The within-subject CV was calculated from the mean and SD of the three subsequent omega-3 index measurements, according to the method described by Harris and Thomas [15].

To evaluate the association between the omega-3 index and risk of VF we performed logistic regression analyses adjusting for age and sex. In addition, high-sensitivity C-reactive protein (hsCRP), EF and previous angina pectoris were included as potential confounders in a backward elimination procedure, and stayed in the final model if they were significant in the first step. Based on the existing knowledge of STEMI and anterior location as potential risk factors for VF during the course of an AMI [16, 17], we performed separate analyses for STEMI-patients only and for patients with anterior location of their infarction. We chose not to include maximal TnT as a measure of infarct size due to the possibility of this parameter being differentially affected by the mechanical manipulation of the heart, by coronary hypoperfusion during resuscitation [18, 19] as well as by later percutaneous coronary intervention (PCI) therapy [20]. The Odds Ratio (OR) for VF is

presented with 95% confidence interval (CI). The statistical analyses were performed with the statistical package SPSS version 17.0, with p values derived from the logistic regressions using the Wald chi-square test. All tests were 2-sided with a significance level of 5%.

Results

Characteristics of SCA-Patients

Out of the 25 patients admitted after an event of OHCA, 19 experienced their VF during the initial course of an AMI. The remaining 6 patients had no evidence of a present MI and their arrhythmia was classified as primary VF with the need for an implantable cardioverter defibrillator (ICD) prior to discharge. Patient characteristics for the different SCA-groups are given in Table 1.

Fourteen out of the 19 AMI-patients, 12 men and 2 women, experienced their first MI. These patients were relatively young (median age 52.5 years, range 41–78 years) and had a predominance of STEMI located to the anterior wall of the heart and mainly one-vessel disease evaluated by coronary angiography (Table 1). Retrospectively, 3 patients had evidence of pre-infarction angina, but none of them had received any treatment for this condition.

Characteristics of Control Subjects

The characteristics of the 185 control subjects (134 men and 51 women) are presented in Table 2. As compared to the group of SCA-patients with first-time MI they were significantly older, had a higher frequency of NSTEMI at admission, and at baseline hsCRP was significantly higher and s-glucose significantly lower. For the remaining baseline characteristics, including infarct location, previous history, presence of risk factors, use of medication, EF and degree of coronary artery disease (CAD), there were no statistically significant differences among the two groups.

Serial Measurements of Individual FA and the Omega-3 Index

A plot of the means of the omega-3 index with 95% CI in SCA patients with and without an AMI, in AMI-patients without SCA and in healthy subjects is presented in Fig. 1. Among patients with SCA, mean time from event to first sample was 1.3 ± 0.6 h. The time from admission until first, second and third sample was 0.5 ± 0.4, 11.1 ± 2.3 and 39.3 ± 6.0 h, respectively. After removing from the analysis one patient with chest pain for at least 74 h before the occurrence of cardiac arrest, patients with SCA during the course of their AMI had a mean duration of symptoms of 3.3 ± 5.7 h (range 0.6–21.0 h) at the time of the first sample. For AMI-patients without SCA, time from symptom onset until first sample was 3.4 ± 2.5 h (range 0.8–9.7 h) and from admission to subsequent sampling 0.3 ± 0.4, 10.2 ± 3.1 and 35.6 ± 6.8 h, respectively. Healthy subjects had samples taken at time 0, after 8.1 ± 0.1 and 23.4 ± 0.4 h. The repeated measures ANOVA (sphericity assumed) showed no statistically significant time-dependent effect on the omega-3 index in any of the groups. The within-subject CV differed from 16.7% in SCA-patients with an AMI to 10.4% in SCA-patients with no AMI. The corresponding values for AMI-patients without SCA and for healthy subjects were 11.7 and 12.9%, respectively.

Similar comparisons were performed for the individual FA. As shown in Table 3 the FA profile remained stable irrespective of sampling time in each subject group. Accordingly, the ratio between the omega-6 and omega-3 FA was also found to be stable, including the arachidonic acid (AA) to EPA ratio.

Omega-3 Index and Risk of VF

The mean omega-3 index among SCA-patients with first-time AMI was 4.59% as compared to 6.48% in controls. In the main logistic regression analysis age, sex, hsCRP and EF were included as covariates, 12 cases and 177 controls were enrolled based on available measurements. The omega-3 index turned out to be a highly significant predictor of VF during the course of a first-time AMI with an OR of 0.42 (95% CI; 0.24–0.75, $p = 0.003$). Of the other covariates included in the analysis, only EF (OR 0.94, 95% CI: 0.89–0.99) and hsCRP (OR 0.61, 95% CI: 0.39–0.95) contributed to the risk of VF.

When restricting the analysis to patients admitted with STEMI and to those with anterior location of their infarction, the omega-3 index still remained an independent predictor of VF with an OR of 0.53 (95% CI: 0.29–0.96), $p = 0.037$, in STEMI-patients ($n = 91$) and 0.50 (95% CI: 0.27–0.93), $p = 0.028$, among those with anterior infarctions ($n = 92$) (Fig. 2).

Discussion

We have demonstrated that the RBC FA, including the omega-3 index, remained stable after SCA and during the post-MI period. In healthy subjects, we have also ruled out any significant biological variability, largely confirming previous observations on reproducibility over time [15].

There has been diverging results in previous studies regarding the effect of an AMI on FA composition of phospholipids [6, 7, 10]. Our findings are consistent with

Table 1 Characteristics of patients suffering SCA

	First myocardial infarction ($n = 14$)	Recurrent myocardial infarction ($n = 5$)	Primary arrhythmia ($n = 6$)	p value
Men	12 (86%)	5 (100%)	5 (83%)	nd
Women	2 (14%)	0	1 (17%)	
Age (median, years)	52.5 (46.8–59.5)	68.0 (58.0–77.5)	73.5 (62.5–81.5)	0.006
BMI (mean ± SD, kg/m^2)	26.6 ± 3.9[b]	26.4 ± 3.3[c]	26.9 ± 4.3	0.017
Symptoms prior to SCA				
Chest pain	10 (71%)	3 (60%)	0	nd
Dyspnea	0	0	1 (17%)	
Asymptomatic	0	2 (40%)	4 (67%)	
Unknown	4 (29%)	0	1 (17%)	
ECG findings				
STEMI	11 (79%)	3 (60%)	0	nd
NSTEMI	3 (21%)	2 (40%)	0	
Infarct location				
Anterior wall	10 (71%)	3 (60%)	0	nd
Inferior wall	3 (21%)	1 (20%)	0	
Lateral wall	1 (7%)	1 (20%)	0	
TnT max (median, μg/L)	4.55 (1.21–6.99)	4.53 (2.61–11.99)	0.16 (0.04–0.74)	0.005
Ejection fraction (median, %)	58 (36–60)[d]	35 (30–50)	40 (20–43)[e]	ns
Coronary angiography				
Normal	0	0	2 (33%)	nd
1-vessel disease	9 (64%)	1 (20%)	1 (17%)	
2-vessel disease	3 (21%)	2 (40%)	0	
3-vessel disease	2 (14%)	2 (40%)	3 (50%)	
Coronary intervention				
LAD	9 (64%)	3 (60%)	1 (17%)	nd
RCA	2 (14%)	1 (20%)	1 (17%)	
CX	3 (21%)	1 (20%)	0	
Hypothermic treatment	10 (71%)	4 (80%)	5 (83%)	nd
Implantation of ICD	0	0	6 (100%)	nd
Death prior to discharge	2 (14%)	2 (40%)	0	nd
Previous history				
Angina pectoris	3 (21%)	0	1 (17%)	nd
Myocardial infarction	0	5 (100%)	5 (83%)	
Heart failure	0	1 (20%)	5 (83%)[a]	
Previous CABG	0	1 (20%)	2 (33%)	
Previous PTCA	0	3 (60%)	2 (33%)	
Hypertension	4 (29%)	2 (40%)	4 (67%)	
Aortic stenosis	0	0	0	
Mitral insufficiency	0	2 (40%)	4 (67%)	
Diabetes mellitus	0	0	0	
Hypercholesterolemia	10 (71%)	3 (60%)	2 (33%)	
Current smoking	4 (29%)	1 (20%)	1 (17%)	
Ex-smoker	6 (50%)[d]	3 (75%)[c]	4 (67%)	
Family history	7 (70%)[f]	2 (50%)[c]	4 (67%)	
Medication prior to admission				
Beta-blocker	1 (7%)	1 (25%)[c]	3 (50%)	nd
Ca-blocker	1 (7%)	1 (25%)[c]	2 (33%)	
ACE/AT II-inhibitor	1 (7%)	2 (50%)[c]	6 (100%)	

Table 1 continued

	First myocardial infarction ($n = 14$)	Recurrent myocardial infarction ($n = 5$)	Primary arrhythmia ($n = 6$)	p value
Diuretics	1 (7%)	0[c]	6 (100%)	
ASA	1 (7%)	4 (100%)[c]	0	
Warfarin	0	0[c]	6 (100%)	
Statin	2 (14%)	3 (75%)[c]	6 (100%)	
Antiarrhythmics	0	0[c]	0	
Baseline blood samples (median)				
Hemoglobin (g/L)	14.7 (13.5–15.8)	14.0 (13.0–17.0)	13.3 (11.1 15.1)	ns
Sodium (mmol/L)	140 (136–142)	143 (142–144)	138 (136–144)	0.045
Calcium (mmol/L)	4.0 (3.9–4.6)	4.0 (3.8–4.6)	3.5 (3.1–4.6)	ns
Creatinine (μmol/L)	92 (80–115)	110 (89–118)	107 (81–154)	ns
Total-cholesterol (mmol/L)	6.4 (4.8–6.9)	3.8 (3.6–4.1)	3.7 (2.9–5.1)	0.014
HDL-cholesterol (mmol/L)	1.4 (1.0–1.7)	1.3 (0.9–1.8)	1.4 (0.7–1.8)	ns
Triglyceride (mmol/L)	2.2 (1.0–3.2)[g]	1.5 (0.6–1.7)[h]	1.1 (1.0–1.4)[h]	ns
Glucose (mmol/L)	15.1 (8.7–22.5)[b]	12.0 (9.4 -18.9)	13.8 (8.1 14.9)[e]	ns
hsCRP (mg/L)	1.7 (1.1–3.1)	1.8 (1.1–2.9)	3.2 (2.3–28.3)	ns
Number of fish meals				
<1 × per month	1 (11%)[b]	0	0	nd
2–3 × per month	4 (44%)[b]	2 (100%)[i]	3 (50%)	
1 × per week	2 (22%)[b]	0	1 (17%)	
2–3 × per week	1 (11%)[b]	0	2 (33%)	
>3 × per week	1 (11%)[b]	0	0	
Omega-3 supplementation				
Cod-liver oil	0[b]	0[h]	2 (33%)	nd
Fish-oil capsules	1 (11%)[b]	1 (33%)[h]	1 (17%)	
Omega-3 index at admission (mean ± SD, %)	4.59 ± 1.58	5.26 ± 1.59	7.15 ± 1.77	0.014

Categorical data are given as n (%). Median values of continuous data given with 25th and 75th percentiles in parentheses (interquartile range)

Nd no data, p values not available, too small groups to test for differences for categorical variables. *ns* not significant

ACE angiotensin converting enzyme, *ASA* acetylsalicylic acid, *AT II* angiotensin II receptor, *BMI* body mass index, *CABG* coronary artery bypass grafting, *HDL* high density lipoprotein, *hsCRP* high-sensitivity C-reactive protein, *ICD* implantable cardioverter defibrillator, *LAD* left anterior descending artery, *RCA* right coronary artery, *CX* circumflex, *NSTEMI* non-ST-elevation myocardial, *PTCA* percutaneous transluminal coronary angioplasty, *SCA* sudden cardiac arrest, *SD* standard deviation, *STEMI* ST-elevation myocardial infarction, *TnT* troponin-T

[a] For one of the patients the diagnosis of dilated cardiomyopathy was first established after admission and this information is therefore not included in the baseline characteristics; [b] $n = 9$; [c] $n = 4$; [d] $n = 12$; [e] $n = 5$; [f] $n = 10$; [g] $n = 13$; [h] $n = 3$; [i] $n = 2$

results from an experimental study in rats by Shearer et al. [7]. Kark et al. [10] sampled 20 MI-patients up to 7 days after the event. Decreasing values of EPA were evident after 42 h, whereas DHA started to increase 7 h after admission. In that study there were no statistical analyses for composite indexes, but we would expect that increasing values of DHA (the major contributor to the sum of EPA + DHA) would reflect an increasing omega-3 index after the initial 7 h of admission, a finding not confirmed in our study. The observed decrease in EPA after 42 h could, however, have been missed by our investigation, as our mean time to last sample was 35.6 h following admission. The time between onset of symptoms and first blood sample was similar in the two studies. In contrast to the study of Kark et al., our STEMI patients were treated invasively, but there is no indication that this difference in the treatment strategy may influence the FA composition in phospholipids.

Unique to our study is a separate evaluation of the effect of SCA on FA composition in humans. The so-far existing research has been performed on primates [3] and rats [11]. In the study by Siscovick et al. [3] RBC membrane levels of EPA + DHA (corresponding to our omega-3 index) were altered only slightly (0.33%) from the pre-mortem to the post-mortem state, suggesting a non-significant effect on these FA by the cardiac arrest itself. Jurand et al. [11] injected rats with noradrenaline, but could not demonstrate any variation in serum FA. Our study confirms the findings

Table 2 Characteristics of cases and controls

	Case-patients ($n = 14$)	Control patients ($n = 185$)	p value
Men	12 (86%)	134 (72%)	ns
Women	2 (14%)	51 (28%)	
Age (median, years)	52.5 (46.8–59.5)	64 (53.5–73.0)	0.003
BMI (mean ± SD, kg/m^2)	26.6 ± 3.9[a]	25.9 ± 4.5	ns
ECG findings at admission			
STEMI	11 (79%)	85 (46%)[b]	0.026
NSTEMI	3 (21%)	98 (54%)[b]	
Infarct location			
Anterior wall	10 (71%)	85 (45%)	ns
Inferior wall	3 (21%)	64 (35%)	
Lateral wall	1 (7%)	0	
Unidentifiable	0	36 (20%)	
Ejection fraction (median, %)	58 (36–60)[c]	55 (50–60)[d]	ns
Coronary angiography			
1-vessel disease	9 (64%)	55 (39%)[e]	ns
2-vessel disease	3 (21%)	39 (28%)[e]	
3-vessel disease	2 (14%)	47 (33%)[e]	
Death prior to discharge	2 (14%)	1 (0.5%)	0.013
Previous history			
Angina pectoris	3 (21%)	56 (30%)	ns
Heart failure	0	12 (7%)	ns
Previous CABG	0	6 (3%)	ns
Previous PTCA	0	8 (4%)	ns
Hypertension	4 (29%)	61 (33%)	ns
Diabetes mellitus	0	21 (11%)	ns
Hypercholesterolemia	10 (71%)	92 (50%)	ns
Current smoking	4 (29%)	84 (45%)	ns
Ex-smoker	6 (50%)[c]	55 (40%)[f]	ns
Family history	7 (70%)[g]	121 (69%)[h]	ns
Medication prior to admission			
Beta-blocker	1 (7%)	31 (17%)	ns
Ca-blocker	1 (7%)	22 (12%)[i]	ns
ACE/AT II-inhibitor	1 (7%)	32 (17%)	ns
Diuretics	1 (7%)	17 (9%)	ns
ASA	1 (7%)	32 (17%)	ns
Warfarin	0	8 (4%)	ns
Statin	2 (14%)	36 (20%)	ns
Baseline blood samples (median)			
Hemoglobin (g/dL)	14.7 (13.5–15.8)	14.1 (13.1–15.0)	ns
Creatinine (μmol/L)	92 (80–115)	89 (75–98)	ns
Total-cholesterol (mmol/L)	6.4 (4.8–6.9)	5.6 (5.0–6.2)	ns
HDL-cholesterol (mmol/L)	1.4 (1.0–1.7)	1.2 (1.0–1.5)	ns
Triglycerides (mmol/L)	2.2 (1.0–3.2)[j]	1.4 (1.0–2.0)	ns
Glucose (mmol/L)	15.1 (8.7–22.5)[a]	6.5 (5.6–8.6)[b]	<0.001
hsCRP (mg/L)	1.7 (1.1–3.1)	4.4 (2.0–13.5)[b]	0.002
Omega-3 index (mean ± SD, %)	4.59 ± 1.58	6.48 ± 2.20	0.002

Categorical data given as n (%). Median values of continuous data given with 25th and 75th percentiles in parentheses (interquartile range)

ACE angiotensin converting enzyme, *ASA* acetylsalicylic acid, *AT II* angiotensin II receptor, *BMI* body mass index, *CABG* coronary artery bypass grafting, *HDL* high density lipoprotein, *hsCRP* high-sensitivity C-reactive protein, *NSTEMI* non-ST-elevation myocardial, *PTCA* percutaneous transluminal coronary angioplasty, *SD* standard deviation, *STEMI* ST-elevation myocardial infarction

[a] $n = 9$; [b] $n = 183$; [c] $n = 12$; [d] $n = 178$; [e] $n = 141$; [f] $n = 139$; [g] $n = 10$; [h] $n = 175$; [i] $n = 184$; [j] $n = 13$

in these animal studies, and is strengthened by similar results obtained in SCA-patients both with and without an AMI. Although the latter group only consisted of 6 patients, these subjects represent a population in which we could evaluate the effect of the cardiac arrest itself without any interference from an AMI. Also, there was no evidence

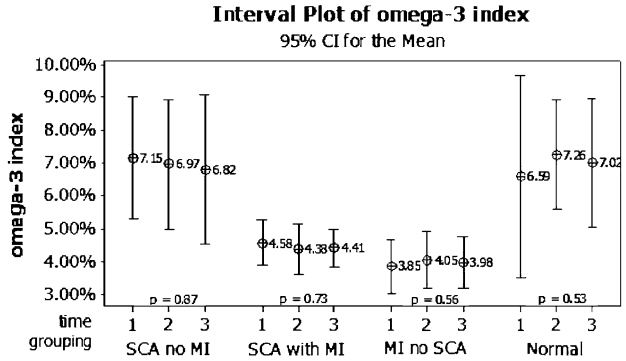

Fig. 1 Mean of the omega-3 index with 95% confidence interval (CI) at admission (time 1), after 8–12 h (time 2) and 24–48 h (time 3). Values given for sudden cardiac arrest (SCA) patients with and without an acute myocardial infarction (MI), MI-patients without SCA and healthy subjects (normal). *p* values for variance of the omega-3 index in each group derived from the ANOVA analysis with time as the only within-subject factor at three levels

of a decreased omega-3 index at admission in patients given adrenaline prior to hospitalization (5.60%, $n = 14$) as compared to those not receiving this medication (5.01%, $n = 11$).

Our findings suggest that any sample obtained within the first 48 h after an event of cardiac arrest, is representative of the total FA status, including the omega-3 index and AA/EPA ratio, of the individual prior to the event. Proof of that assumption would, however, require a measurement just prior to the event, but that would hardly be achievable in a clinical setting. The other option would be blood samples obtained in advance in large prospective cohort studies, but in those settings dietary changes may have taken place between the time of sampling and the event. As a second-best choice, our study was designed to harvest the first sample as close to the event as possible, based on the assumption that it may take some time for the cellular changes to appear. The first sample taken at admission was harvested at a mean time of only 1.3 h after the SCA event. Furthermore, the mean time from symptom onset was 3.3 h in AMI-patients with SCA as compared to 3.4 h in AMI-patients without a cardiac arrest. A possible effect of the cardiac arrest on the FA profile, has been one of the main objections to case–control studies demonstrating an increased risk of SCD/SCA with low levels of n-3 FA [3, 5]. However, these objections are not supported by our present results.

We had previously demonstrated that a 1% increase of the omega-3 index reflects a 48% reduction in risk of VF during the ischemic phase of an AMI [5]. In the present case–control study we have recruited a similar group of SCA-patients with first-time MI, with the use of the same control subjects in both study settings. As in our previous investigation, we found a large difference in the omega-3 index values between cases and controls at admission. Furthermore, the logistic regression analysis confirms an inverse relation between the omega-3 index and risk of VF; a 1% increase in this index reflecting a 58% reduced risk of VF (95% CI: 25–76%). Even though EF and hsCRP contributed to the risk of VF, the omega-3 index was the strongest predictor. The omega-3 index also remained an independent predictor of risk, but was slightly attenuated, in the subgroup analyses of STEMI-patients and anterior infarctions. Contrary to other investigations, both of our studies have documented ventricular fibrillation at the time of resuscitation, supporting the proposed antiarrhythmic mechanism of n-3 FA [21–23], especially in ischemia-induced VF. Theoretically, the antiarrhythmic mechanism of n-3 FA is based on an increase of the arrhythmic threshold in the ischemic zone of the myocardium, due to an indirect effect of the FA on sodium and calcium ion-channels in the myocardial membrane [22, 24].

The group of SCA patients without the presence of an AMI is highly different from the first-time MI population. Their high omega-3 index of 7.15% does not contradict the above finding, as their VF is mainly considered to be a result of myocardial scarring and heart failure. For arrhythmias generated by such mechanisms, n-3 FA might not be protective, as suggested by the discrepant results of n-3 FA in ICD-patients [25, 26]. Also, chronically ill patients may have changed their lifestyle according to an assumed protection by n-3 FA, ingesting an increased amount of fish and omega-3 supplements.

Limitations

Our evaluation of a time-dependent change in the FA profile following an event of SCA and/or AMI is limited by the relative low number of patients in each category, reducing our power to confidently exclude a small change. Statistically, power calculations are difficult to perform with repeated sampling, but the use of serial samples without any detectable change in healthy individuals and in different patient groups strengthen our conclusion. As our patient populations had highly different omega-3 index values, the present study furthermore supports the stability of this analysis in patients with both high and low n-3 FA levels.

The main objection to the present case-control study might be the different time-periods for inclusion of cases and controls. Whereas controls were participants in the RACS-study [5], sampled between November 2002 and September 2003, our new cases had their blood samples taken between February 2007 and June 2009. Both studies were, however, performed at Stavanger University Hospital, the only hospital available for the CAD and SCA

Table 3 Fatty acid profiles from red blood cells

Patient group	At admission	8–12 h	24–48 h	*p*
SCA without MI ($n = 6$)				
Myristic acid (C14:0)	3.56 (2.12–5.01)	5.00 (2.21–7.80)	5.29 (3.39–7.20)	0.276
Palmitic acid (C16:0)	23.10 (21.55–24.66)	22.59 (20.48–24.69)	22.98 (21.44–24.52)	0.843
Stearic acid (C18:0)	21.01 (18.36–23.66)	20.14 (17.42–22.87)	20.43 (18.43–22.44)	0.660
Oleic acid (C18:1n-9)	15.68 (13.93–17.43)	15.69 (14.40–16.98)	15.11 (14.08–16.14)	0.544
Linoleic acid (C18:2n-6)	8.32 (6.34–10.31)	8.19 (6.38–9.99)	8.04 (6.44–9.63)	0.427
α-Linolenic acid (C18:3n-3)	0.10 (0.03–0.17)	0.08 (0.04–0.12)	0.08 (0.03–0.12)	0.560
AA (C20:4n-6)	12.03 (9.96–14.11)	12.07 (9.72–14.43)	12.14 (10.16–14.12)	0.980
EPA (C20:5n-3)	1.42 (0.78–2.07)	1.36 (0.64–2.08)	1.24 (0.47–2.01)	0.429
DPA (C22:5n-3)	2.35 (1.83–2.86)	2.34 (1.80–2.88)	2.26 (1.92–2.60)	0.876
DHA (C22:6n-3)	5.73 (4.41–7.05)	5.61 (4.25–6.97)	5.58 (3.93–7.23)	0.949
Total n-3 FA	7.15 (5.30–9.01)	6.97 (4.98–8.96)	6.82 (4.54–9.09)	0.866
n-6 FA/n-3 FA	2.62 (1.93–3.31)	2.68 (1.99–3.37)	2.82 (1.98–3.66)	0.669
SCA with MI ($n = 18$)				
Myristic acid (C14:0)	4.27 (3.21–5.32)	4.90 (3.88–5.92)	4.98 (3.27–6.70)	0.569
Palmitic acid (C16:0)	24.28 (22.95–25.60)	24.44 (23.09–25.78)	25.01 (24.07–25.94)	0.356
Stearic acid (C18:0)	20.47 (19.32–21.61)	20.71 (19.79–21.64)	20.93 (20.05–21.82)	0.552
Oleic acid (C18:1n-9)	15.34 (14.43–16.25)	15.27 (14.59–15.96)	15.22 (14.38–16.06)	0.933
Linoleic acid (C18:2n-6)	9.55 (9.02–10.09)	9.37 (8.81–9.92)	9.27 (8.61–9.93)	0.144
α-Linolenic acid (C18:3n-3)	0.10 (0.08–0.12)	0.10 (0.07–0.13)	0.09 (0.06–0.11)	0.470
AA (C20:4n-6)	11.12 (9.87–12.37)	10.56 (9.49–11.63)	10.24 (9.49–10.99)	0.101
EPA (C20:5n-3)	0.79 (0.60–0.97)	0.70 (0.47–0.92)	0.74 (0.54–0.95)	0.283
DPA (C22:5n-3)	1.91 (1.67–2.15)	1.87 (1.61–2.12)	1.76 (1.51–2.01)	0.218
DHA (C22:6n-3)	3.91 (3.34–4.48)	3.80 (3.19–4.42)	3.68 (3.21–4.15)	0.591
Total n-3 FA	4.70 (4.03–5.37)	4.50 (3.72–5.28)	4.43 (3.82–5.03)	0.576
n-6 FA/n-3 FA	3.95 (3.48–4.42)	4.00 (3.45-4.56)	4.04 (3.46–4.62)	0.891
MI without SCA ($n = 15$)				
Myristic acid (C14:0)	5.91 (4.59–7.23)	6.33 (4.92–7.74)	7.13 (5.61–8.66)	0.380
Palmitic acid (C16:0)	25.79 (24.90–26.67)	25.40 (24.59–26.22)	24.99 (24.23–25.75)	0.135
Stearic acid (C18:0)	21.79 (21.03–22.54)	21.42 (20.76–22.09)	21.18 (20.41–21.95)	0.214
Oleic acid (C18:1n-9)	14.82 (14.11–15.54)	14.61 (13.98–15.23)	14.43 (13.81–15.06)	0.499
Linoleic acid (C18:2n-6)	9.22 (8.32–10.11)	9.20 (8.32–10.08)	8.82 (8.00–9.64)	0.053
α-Linolenic acid (C18:3n-3)	0.12 (0.09–0.15)	0.15 (0.10–0.20)	0.16 (0.10–0.23)	0.335
AA (C20:4n-6)	8.23 (7.40–9.06)	8.46 (7.65–9.27)	8.52 (7.54–9.49)	0.616
EPA (C20:5n-3)	0.68 (0.44–0.92)	0.69 (0.43–0.95)	0.63 (0.43–0.84)	0.361
DPA (C22:5n-3)	1.65 (1.47–1.84)	1.66 (1.51–1.80)	1.69 (1.57–1.82)	0.804
DHA (C22:6n-3)	3.18 (2.55–3.80)	3.36 (2.69–4.03)	3.34 (2.71–3.98)	0.421
Total n-3 FA	3.85 (3.03–4.67)	4.05 (3.18–4.92)	3.98 (3.18–4.77)	0.562
n-6 FA/n-3 FA	4.09 (3.35–4.83)	4.03 (3.21–4.85)	3.88 (3.21–4.56)	0.239
Healthy subjects ($n = 5$)				
Myristic acid (C14:0)	7.00 (2.87–11.13)	5.18 (1.64–8.71)	4.45 (2.88–6.02)	0.207
Palmitic acid (C16:0)	23.90 (21.87–25.93)	23.47 (22.48–24.46)	23.73 (22.25–25.20)	0.904
Stearic acid (C18:0)	21.09 (18.69–23.49)	20.88 (20.03–21.72)	21.06 (20.06–22.06)	0.956
Oleic acid (C18:1n-9)	13.86 (12.63–15.08)	15.34 (13.08–15.59)	14.70 (13.72–15.69)	0.232
Linoleic acid (C18:2n-6)	9.74 (8.58–10.91)	10.27 (8.74–11.81)	10.14 (9.08–11.21)	0.312
α-Linolenic acid (C18:3n-3)	0.17 (0.01–0.33)	0.12 (0.08–0.15)	0.13 (0.09–0.17)	0.613
AA (C20:4n-6)	9.04 (7.23–10.85)	9.99 (8.12–11.86)	9.98 (7.85–12.11)	0.409
EPA (C20:5n-3)	1.53 (0.53–2.53)	1.73 (0.87–2.59)	1.69 (0.79–2.59)	0.393

Table 3 continued

Patient group	At admission	8–12 h	24–48 h	*p*
DPA (C22:5n-3)	2.26 (1.55–2.97)	2.53 (2.20–2.85)	2.48 (1.94–3.03)	0.340
DHA (C22:6n-3)	5.06 (2.85–7.27)	5.53 (4.47–6.59)	5.33 (4.14–6.51)	0.599
Total n-3 FA	6.59 (3.50–9.69)	7.26 (5.56–8.96)	7.02 (5.06–8.97)	0.532
n-6 FA/n-3 FA	2.67 (1.24–4.10)	2.40 (1.61–3.19)	2.47 (1.74–3.20)	0.505

Means of red blood cell membrane fatty acids (FA) (given as percent of total FA) with 95% confidence interval (CI) at admission, after 8–12 h and 24–48 h. Values given for sudden cardiac arrest (SCA) patients with and without an acute myocardial infarction (MI), MI-patients without SCA and healthy subjects. *p* values for variance of the FA in each group derived from the ANOVA analysis with time as the only within-subject factor at three levels

AA arachidonic acid, *EPA* eicosapentaenoic acid, *DPA* docosapentaenoic acid, *DHA* docosahexaenoic acid

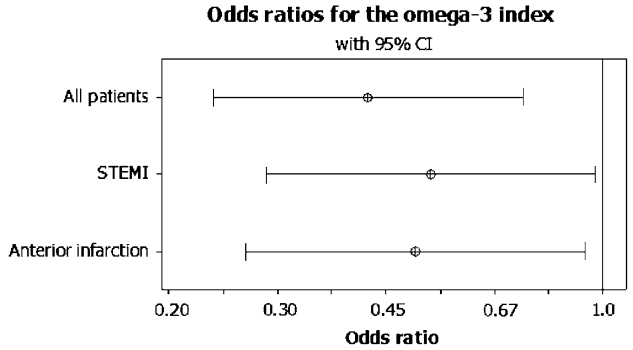

Fig. 2 Result of the multivariate logistic regression analysis in the total population (all patients) and in the subgroups of ST-elevation myocardial infarctions (STEMI) and anterior infarct location adjusting for age, sex, high sensitivity C-reactive protein and ejection fraction. Odds ratios (ORs) given with 95% confidence interval (CI)

populations in this region of Norway. The source-population should therefore be similar for both studies and there is no reason to believe that their way of living, including diet, would have changed significantly during a 5 year period. The results of our study are, however, only valid for the range of omega-3 index values included in the analyses.

Furthermore, we do not know for certain whether the omega-3 index in admitted SCA-patients differ from those of OHCA-patients where ROSC was not obtained. Also, the urgent situation during resuscitation and admission sometimes resulted in missing samples for admitted SCA-patients.

Conclusion

Our study supports an association between low levels of n-3 FA and the risk of VF during the ischemic phase of an AMI in hospitalized patients. The results are strengthened by our demonstration of the stability of RBC FA within the first 48 h after an episode of SCA or AMI, suggesting that the validity of risk assessment is maintained within this time frame.

Acknowledgments Study grants from the Regional Health Authorities in Western Norway, The Research Foundation at Stavanger University Hospital and The Laerdal Foundation for Acute Medicine are gratefully acknowledged. The FA analyses were performed by William S. Harris who is a consultant to companies with interests in omega-3 FA, including GlaxoSmithKline, Reliant Pharmaceuticals and the Monsanto Company. No pharmaceutical company supported this study financially. There are otherwise no financial or other relationships associated with the manuscript that might lead to a conflict of interest.

References

1. Investigators GISSI-Prevenzione (1999) Dietary supplementation with n-3 polyunsaturated fatty acids and vitamin E after myocardial infarction: results of the GISSI-Prevenzione trial. Lancet 354:447–455
2. Albert CM, Campos H, Stampfer MJ, Ridker PM, Manson JE, Willett WC et al (2002) Blood levels of long-chain n-3 fatty acids and the risk of sudden death. N Engl J Med 346:1113–1118
3. Siscovick DS, Raghunathan TE, King I, Weinmann S, Wicklund KG, Albright J et al (1995) Dietary intake and cell membrane levels of long-chain n-3 polyunsaturated fatty acids and the risk of primary cardiac arrest. JAMA 274:1363–1367
4. Lemaitre RN, King IB, Mozaffarian D, Kuller LH, Tracy RP, Siscovick DS (2003) n-3 Polyunsaturated fatty acids, fatal ischemic heart disease, and nonfatal myocardial infarction in older adults: the Cardiovascular Health Study. Am J Clin Nutr 77:319–325
5. Aarsetøy H, Pönitz V, Nilsen OB, Grundt H, Harris WS, Nilsen DWT (2008) Low levels of cellular omega-3 increase the risk of ventricular fibrillation during the acute ischaemic phase of a myocardial infarction. Resuscitation 78:258–264
6. Kirkeby K (1972) Disturbances in serum lipids and in their fatty acid composition following acute myocardial infarction. Acta med scand 192:523–528
7. Shearer GC, Chen J, Chen Y, Harris WS (2009) Myocardial infarction does not affect fatty acid profiles in rats. Prostaglandins Leukot Essent Fatty Acids 81:411–416
8. Harris WS, Sands SA, Windsor SL, Ali HA, Stevens TL, Magalski A et al (2004) Omega-3 fatty acids in cardiac biopsies

from heart transplantation patients correlation with erythrocytes and response to supplementation. Circulation 110:1645–1649
9. Owen AJ, Peter-Przyborowska BA, Hoy AJ, McLennan PL (2004) Dietary fish-oil dose and time-response effects on cardiac phospholipid fatty acid composition. Lipids 39:955–961
10. Kark JD, Manor O, Goldman S, Berry EM (1995) Stability of red blood cell membrane fatty acid composition after acute myocardial infarction. J Clin Epidemiol 48:889–895
11. Jurand J, Oliver M (1970) Effects of acute myocardial infarction and of noradrenaline infusion on fatty acid composition of serum lipids. Atherosclerosis 11:157–170
12. Hodson L, Skeaff CM, Wallace AJ, Arribas GL (2002) Stability of plasma and erythrocyte fatty acid composition during cold storage. Clin Chem Acta 321:63–67
13. Marangoni F, Colombo C, Galli C (2004) A method for the direct evaluation of the fatty acid status in a drop of blood from a fingertip in humans: applicability to nutritional and epidemiological studies. Anal Biochem 326:267–272
14. Aarsetoey H, Pönitz V, Grundt H, Staines H, Harris WS, Nilsen DWT (2009) (N-3) fatty acid content of red blood cells does not predict risk of future cardiovascular events following an acute coronary syndrome. J Nutr 139:507–513
15. Harris WS, Thomas RM (2010) Biological variability of blood omega-3 biomarkers. Clin Biochem 43:338–340
16. Gheeraert PJ, De Buyzere ML, Taeymans YM (2006) Risk factors for primary ventricular fibrillation during acute myocardial infarction: a systematic review and meta-analysis. Eur Heart J 27:2499–2510
17. Gheeraert PJ, Henriques JPS, De Buyzere ML (2000) Out-of-hospital ventricular fibrillation in patients with acute myocardial infarction coronary angiographic determinants. Am Coll Cardiol 35:144–150
18. Grubb NR, Fox KAA, Cawood CP (1996) Resuscitation from out-of-hospital cardiac arrest: implication for cardiac enzyme estimation. Resuscitation 33:35–41
19. Müller M, Hirschl MM, Herkner H (1996) Creatine kinase-MB fraction and cardiac troponin-T to diagnose acute myocardial infarction after cardiopulmonary resuscitation. J Am Coll Cardiol 28:1220–1225
20. Morrow DA, Cannon CP, Jesse RL, Newby K, Ravkilde J, Storrow AB et al (2007) National academy of clinical biochemistry laboratory medicine practice guidelines: clinical characteristics and utilization of biochemical markers in acute coronary syndromes. Clin Chem 53:552–574
21. Matthan NR, Jordan H, Chung M, Lichtenstein AH, Lathrop DA, Lau J (2005) A systematic review and meta-analysis of the impact of omega-3 fatty acids on selected arrhythmia outcomes in animal models. Metabolism 54:1557–1565
22. Leaf A, Xiao YF, Kang JX, Billman GE (2003) Prevention of sudden cardiac death by n-3 polyunsaturated fatty acids. Pharmacol Ther 98:355–377
23. Reiffel JA, McDonald A (2006) Antiarrhythmic effects of omega-3 fatty acids. Am J Cardiol 98(Suppl.):50i–60i
24. Xiao YF, Ke Q, Chen Y, Morgan JP, Leaf A (2004) Inhibitory effect of n-3 fish oil fatty acids on cardiac $Na^{+}/Ca2^{+}$ exchange currents in HEK293t cells. Biochem Biophys Res Commun 321:116–123
25. Brouwer IA, Raitt MH, Dullemeijer C, Kraemer DF, Zock PL, Morris C et al (2009) Effect of fish oil on ventricular tachyarrhythmia in three studies in patients with implantable cardioverter defibrillators. Eur Heart J 30:820–826
26. Metcalf RG, Sanders P, James MJ, Cleland LG, Young GD (2008) Effect of dietary n-3 polyunsaturated fatty acids on the inducibility of ventricular tachycardia in patients with ischemic cardiomyopathy. Am J Cardiol 101:758–761

Lipids (2011) 46:163–170
DOI 10.1007/s11745-010-3503-3

ORIGINAL ARTICLE

Increasing DHA and EPA Concentrations Prolong Action Potential Durations and Reduce Transient Outward Potassium Currents in Rat Ventricular Myocytes

Hong-Xia Li · Ru-Xing Wang · Xiao-Rong Li · Tao Guo · Ying Wu · Su-Xia Guo · Li-Ping Sun · Zhen-Yu Yang · Xiang-Jun Yang · Wen-Ping Jiang

Received: 13 March 2010 / Accepted: 12 November 2010 / Published online: 8 December 2010

Abstract The goal of this study was to determine the mechanisms of n-3 polyunsaturated fatty acids (n-3 PUFA) on anti-arrhythmias and prevention of sudden death. The calcium-tolerant Sprague–Dawley rat ventricular myocytes were isolated by enzyme digestion. Effects of docosahexaenoic acid (DHA) and eicosapentaenoic acid (EPA) on action potentials and transient outward potassium currents (I_{to}) of epicardial ventricular myocytes were investigated using whole-cell patch clamp techniques. Action potential durations (APDs) and I_{to} were observed in different concentrations of DHA and EPA. APD_{25}, APD_{50}, and APD_{90} with 0.1 μmol/L DHA and EPA were prolonged less than 15% and 10%. However, APDs were prolonged in concentration-dependent manners when DHA and EPA were more than 1 μmol/L. APD_{25}, APD_{50}, and APD_{90} were 7.7 ± 2.0, 21.2 ± 3.5, and 100.1 ± 9.8 ms respectively with 10 μmol/L DHA, and 7.2 ± 2.5, 12.8 ± 4.2, and 70.5 ± 10.7 ms respectively with 10 μmol/L EPA. I_{to} currents were gradually reduced with the increased concentrations of DHA and EPA from 1 to 100 μmol/L, and their half-inhibited concentrations were 2.3 ± 0.2 and 3.8 ± 0.6 μmol/L. The results showed APDs were prolonged and I_{to} current densities were gradually reduced with the increased concentrations of DHA and EPA. The anti-arrhythmia mechanisms of n-3 PUFA are complex, however, the effects of n-3 PUFA on action potentials and I_{to} may be one of the important mechanisms.

Keywords n-3 Polyunsaturated fatty acid · Docosahexaenoic acid · Eicosapentaenoic acid · Action potential · Action potential duration · Transient outward potassium current

Abbreviations

PUFA	Polyunsaturated fatty acids
DHA	Docosahexaenoic acid
EPA	Eicosapentaenoic acid
I_{to}	Transient outward potassium currents
APDs	Action potential durations
APD_{25}	Action potential duration of 25% repolarization
APD_{50}	Action potential duration of 50% repolarization
APD_{90}	Action potential duration of 90% repolarization
HP	Holding potential
V_{max}	Maximal velocity of action potential depolarization
APA	Action potential amplitude
OS	Overshoot

Introduction

Fatty acids, especially polyunsaturated fatty acids (PUFA), play an important role in cardiac activities. For example,

H.-X. Li · X.-J. Yang · W.-P. Jiang
Department of Cardiology, First Affiliated Hospital of Soochow University, Suzhou 215006, China

R.-X. Wang (✉) · X.-R. Li · Y. Wu · S.-X. Guo · L.-P. Sun · Z.-Y. Yang
Department of Cardiology, Affiliated Hospital of Nanjing Medical University in Wuxi and People's Hospital of Wuxi City, Wuxi 214023, China
e-mail: ruxingw@yahoo.com.cn

T. Guo
Department of Cardiology, First Affiliated Hospital of Kunming Medical College, Kunming 650032, China

PUFA are essential fuels for mechanical, electrical, and synthetic activities of the heart; and the dietary PUFA are very beneficial to heart functions [1, 2]. Recently, the beneficial effects of PUFA, particularly the n-3 series, have been reported for cardiovascular diseases [3–6]. n-3 PUFA have been shown to reduce cardiovascular mortality, in part, due to their anti-arrhythmic mechanisms that are not fully understood up till now [7, 8].

n-3 PUFA mainly include docosahexaenoic acid (DHA) and eicosapentaenoic acid (EPA). The vital importance of the n-3 PUFA, so called because of the location of the first double bond (at carbon no.3, from the methyl end of the carbon chain), is becoming widely recognized in human physiology. Many studies suggest that n-3 PUFA have beneficial effects on human health. Recently, more attentions have been paid to their beneficial effects on cardiovascular diseases, especially in their anti-arrhythmias and prevention of sudden cardiac death [9–13]. Although the underlying mechanisms of which are still not completely known, the effects of n-3 PUFA on action potentials and ionic channels might contribute to this phenomenon [14].

The typical action potentials consist of 5 phases or stages, i.e., 0, 1, 2, 3, and 4. The transient outward potassium current (I_{to}) is a major repolarizing ionic current of action potentials in ventricular myocytes of many mammals. Because of its immediate activation by depolarization and its transient nature, I_{to} plays an important role in the early repolarization of action potentials. It influences the height of the plateau potential and the action potential durations (APDs), especially in the early phase. Accordingly, its inhibition leads to a significant prolongation of APDs. It has been reported that APDs magnitude depends on the origin of the myocytes and is regulated by a number of physiological and pathophysiological signals [15, 16].

To investigate the underlying mechanisms of n-3 PUFA in anti-arrhythmias and prevention of sudden cardiac death, the magnitude of I_{to} and APDs were studied in rat ventricular myocytes of endocardial, mid-myocardial and epicardial origin using whole-cell patch clamp recordings. The aim of this study was to test the hypothesis that a differential distribution of I_{to} is the most important cause of different action potential waveforms in endocardial, mid-myocardial and epicardial myocytes, and the effects of n-3 PUFA on action potentials and I_{to} may be one of the important mechanisms of anti-arrhythmias. Since I_{to} may not be uniformly expressed in the ventricle [17], we have only investigated the epicardial cardiomyocytes in order to avoid experiment errors. These results may provide some experimental evidences for rational applications of n-3 PUFA to prevent and treat arrhythmias in clinical practice.

Experimental Procedures

Major Experimental Instruments

The instruments used were: MultiClamp 700B patch clamp amplifier (Axon Instruments, USA), D/A and A/D converter (DigiData 1322, Axon Instruments, USA), Pclamp 9.0 pulse software (Axon Instruments, USA), MP-285 motorized micromanipulator (Sutter Instruments, USA), IX71 inverted microscope (Olympus, Japan), SA-OLY/2 and DH-35 culture dish heater (Warner Instruments, USA), P-97 micropipette puller (Sutter Instruments, USA).

Reagents, Solutions and Drugs

The reagents, solutions and drugs used were: DHA (Sigma, USA), molecular weight 328.5, and EPA (Sigma, USA), molecular weight 302.45; 100 mmol/L stock solutions were prepared respectively by being dissolved in absolute ethanol and protected from light in a refrigerator at −20 °C. The experimental concentrations of DHA and EPA were obtained by dilution of stock solutions before each experiment. For the recording of action potentials, the internal solution (in mmol/L) contained KCl 120, $CaCl_2$ 1, $MgCl_2$ 5, Na_2ATP 5, EGTA 11, HEPES 10, glucose 11, pH 7.3 adjusted with KOH. The external solution was Tyrode's solution [18]. For the recording of I_{to}, the external solution (in mmol/L) contained NaCl 140, KCl 4, $CaCl_2$ 1.5, $MgCl_2$ 1, $CdCl_2$ 0.5, HEPES 5, glucose 10, pH 7.4 adjusted with NaOH. The internal solution (in mmol/L) contained KCl 140,$MgCl_2$ 1,K_2ATP 5, EGTA 5, HEPES 10, pH 7.4 adjusted with KOH. KB solution (in mmol/L) contained L-glutamic acid 50, KCl 40, KH_2PO_4 20, Taurine 20, $MgCl_2$ 3, KOH 70, EGTA 0.5, HEPES 10, glucose 10, pH 7.4 adjusted with KOH.

Cell Isolation

The investigation was approved by our institute ethics committee and conformed to the Guide for the Care and Use of Laboratory Animals published by the US National Institutes of Health (NIH publication No. 85-23, revised 1996). Healthy Sprague–Dawley rats of both sexes, aged 8–12 weeks and weighing approximately 200 g, were provided by the Experimental Animal Center of Soochow University (Suzhou, China). Animals were anesthetized with pentobarbital sodium intraperitoneally (i.p.), Hearts were removed and retrograde perfusion through the aorta was performed as described previously [19]. After retrograde perfusion, epicardial, mid-myocardial, and endocardial ventricular myocardium were obtained respectively by cutting with eye scissors and plyers. Isolated cells were kept at room temperature in KB solution and used within 6 h; only relaxed, striated, and rod-shaped cells were used.

Recordings of Action Potentials and I_{to} with and Without DHA and EPA

Currents in whole-cell voltage clamp configuration were recorded following the method of Hamill et al. [20]. Cardiomyocytes were transferred to a 1-ml chamber (DH-35 culture dish heater, Warner Instruments, USA) with external solution on the stage of an inverted microscope. The chamber was continuously perfused at a rate of 1–2 ml/min with external solution. Electrodes were prepared from borosilicate glass (Clark Instruments, UK) using a P-97 micropipette puller with resistances typically between 2 and 4 MΩ when filled with internal solution. Whole-cell voltage-clamp experiments were performed with a MultiClamp 700B amplifier. Whole-cell capacitance and series resistance were compensated by 60–80%. Experiments were performed at 36–37 °C. Voltage clamp pulses were generated via an IBM-compatible computer connected to Digidata 1322. Data acquisition and analyses were performed using pCLAMP software. To obtain action potentials, a 5-ms depolarizing pulse with 900pA, 1 Hz in current-clamp configuration was applied. DHA and EPA at 0.01, 0.1 , 1, 10, and 100 μmol/L were perfused for 10 min respectively to observe the effects on APDs. To obtain I_{to}, 600-ms depolarizing pulses in the range −40 mV to +70 mV were applied to the ventricular myocytes every 5 s in +10 mV increments from −40 mV holding potential (HP). Recordings of action potentials and I_{to} were performed in the physiological temperature range (36–37 °C). DHA and EPA at various concentrations were applied to investigate the effects on I_{to}.

Statistical Analysis

Continuous variables were expressed as means ± standard error ($\bar{x}$ ± SE). SPSS11.5 SPSS Inc, Chicago, IL, USA) was used for statistical analysis. Comparisons among groups were performed by repeated measurement analysis of variance (ANOVA) and least-significant difference contrast. Control and drug data for individual groups were compared by a Paired t test. $P \leq 0.05$ was considered significant. OriginPro 7.5 software (OriginLab, USA) was utilized to calculate the half-inhibited concentration (IC_{50}).

Results

Characteristics of Action Potentials and I_{to} of Rat Ventricular Myocytes

Action potentials of epicardial, mid-myocardial and endocardial ventricular myocytes were recorded respectively with action potential stimulus protocol. The action potential configurations were different in epicardial, mid-myocardial and endocardial ventricular myocytes (Fig. 1). APD_{25}, APD_{50}, and APD_{90} were gradually prolonged from epicardial to endocardial ventricular myocytes. APD_{25}, APD_{50}, and APD_{90} were 3.6 ± 1.2, 10.3 ± 2.1, and 46.3 ± 4.8 ms in epicardial ventricular myocytes ($n = 50$); 6.4 ± 1.8, 14.7 ± 2.4, and 69.4 ± 8.3 ms in mid-myocardial ventricular myocytes ($n = 58$) and 13.8 ± 2.1, 45.3 ± 10.2, and 152.1 ± 33.4 ms respectively in epicardial ventricular myocytes ($n = 62$). There were statistical significance of APDs' variations in cardiomyocytes of different layers ($P < 0.05$); however, there were no remarkable changes in the maximal velocity of action potential depolarization (V_{max}), amplitude (APA), and overshoot (OS) in epicardial, mid-myocardial and endocardial ventricular myocytes. V_{max} were 228.3 ± 14.5 V/s ($n = 71$), 10.3 ± 2.1 V/s ($n = 63$), and 46.3 ± 4.8 V/s ($n = 70$) in epicardial, mid-myocardial and endocardial ventricular myocytes ($P > 0.05$). APA were 110.7 ± 10.1 mV ($n = 71$),

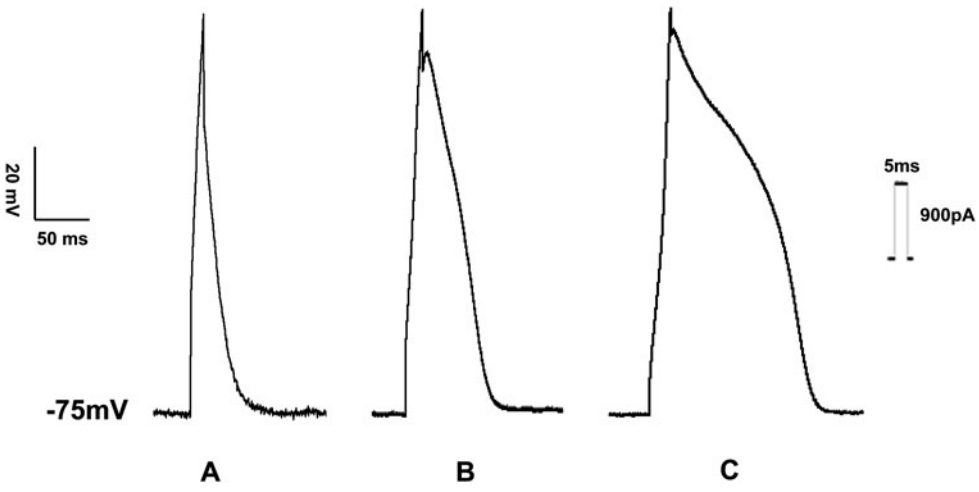

Fig. 1 Action potential configurations of rat ventricular myocytes. *A*, *B* and *C* were action potentials in epicardial, mid-myocardial and endocardial ventricular myocytes, respectively. Action potential durations were gradually increased from epicardial ventricular myocytes to endocardial ventricular myocytes

111.9 ± 9.3 mV ($n = 63$), and 109.8 ± 8.9 mV ($n = 70$) in epicardial, mid-myocardial and endocardial ventricular myocytes ($P > 0.05$). OS were 31.5 ± 5.4 mV/s ($n = 71$), 32.4 ± 6.3 mV ($n = 63$), and 30.8 ± 4.8 mV ($n = 70$) in epicardial, mid-myocardial and endocardial ventricular myocytes ($P > 0.05$). I_{to} current tracings at various test potentials were elicited by 600 ms depolarization in the range of −40 mV to +70 mV pulses applied to the ventricular myocytes every 5 s in +10 mV increments from −40 mV HP. The current densities of epicardial, mid-myocardial and endocardial ventricular myocytes at +70 mV were 59.5 ± 16.0 , 29.2 ± 5.5, and 12.3 ± 3.6 pA/pF, respectively.

The current–voltage curves of I_{to} were plotted with current densities at each test potential. The threshold potential of I_{to} channel opening was −30.3 ± 2.8 mV, i.e., I_{to} channel began to activate at more than −30 mV. I_{to} currents were gradually enhanced with the increase of test potentials. The activation of I_{to} channel was very rapid, and only needed about 10 ms, nonetheless, its inactivation was relatively slow. The time constants of epicardial, mid-myocardial, and endocardial ventricular myocytes were almost the same at each test potential. They were 31.8 ± 1.7, 32.9 ± 2.4, and 33.2 ± 2.9 ms, respectively, at +70 mV test potential ($P > 0.05$).

Effects of DHA and EPA on Action Potentials

DHA and EPA at 0.01, 0.1, 1, 10, and 100 μmol/L were applied to epicardial ventricular myocytes, respectively. The results showed that: ① APDs were gradually prolonged with the increase of DHA and EPA concentrations, whereas APD changes were not significant at low concentrations of DHA and EPA (<1 μmol/L). The prolongation of APD_{25}, APD_{50}, and APD_{90} was less than 15% compared with the control (0 min) when 0.1 μmol/L DHA was applied, and less than 10% with 0.1 μmol/L EPA application (Fig. 2). ② APDs were prolonged in concentration-dependent manners when DHA and EPA were more than 1 μmol/L. APD_{25}, APD_{50}, and APD_{90} were 7.7 ± 2.0, 21.2 ± 3.5, and 100.1 ± 9.8 ms respectively after 10 μmol/L DHA was used for 5 min (Fig. 3C), and 7.2 ± 2.5, 12.8 ± 4.2, and 70.5 ± 10.7 ms respectively with 10 μmol/L EPA application for 5 min (Fig. 3C1). APD_{25}, APD_{50}, and APD_{90} were 15.2 ± 4.0, 45.7 ± 6.8, and 215.6 ± 15.7 ms respectively when 100 μmol/L DHA was utilized for 5 min (Fig. 3D), and 13.1 ± 5.4, 48.2 ± 9.1, and 132.3 ± 21.2 ms respectively with 100 μmol/L EPA for 5 min (Fig. 3D1), which were significantly prolonged compared with those without addition of DHA and EPA ($P < 0.05$).

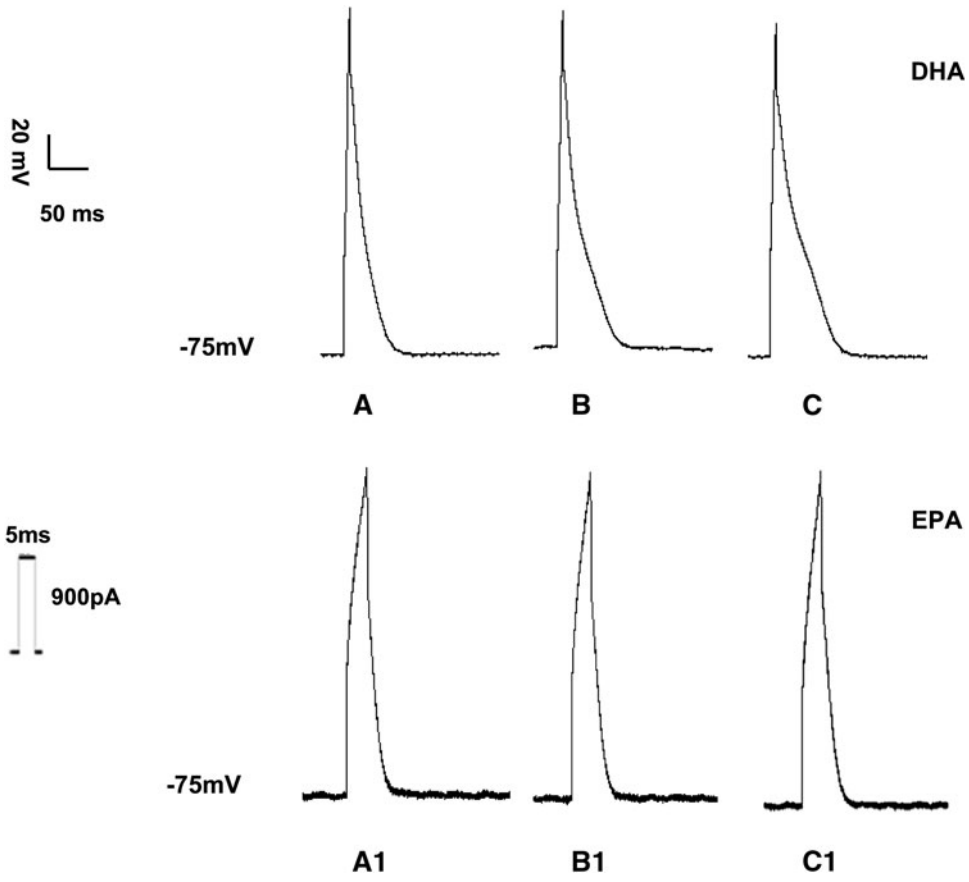

Fig. 2 Action potential changes of rat ventricular myocytes at 0.1 μmol/L DHA and EPA. *A*, *B*, and *C* were configurations of action potential when 0.1 μmol/L DHA was applied at 0, 1, and 5 min, respectively. The action potential duration was increased; however, compared with the control (0 min), the prolongation of action potential duration was less than 15%. *A1*, *B1*, and *C1* were configurations of action potential when 0.1 μmol/L EPA was applied at 0, 1, and 5 min, respectively. The action potential duration was increased; however, compared with the control (0 min), the prolongation of action potential duration was less than 10%

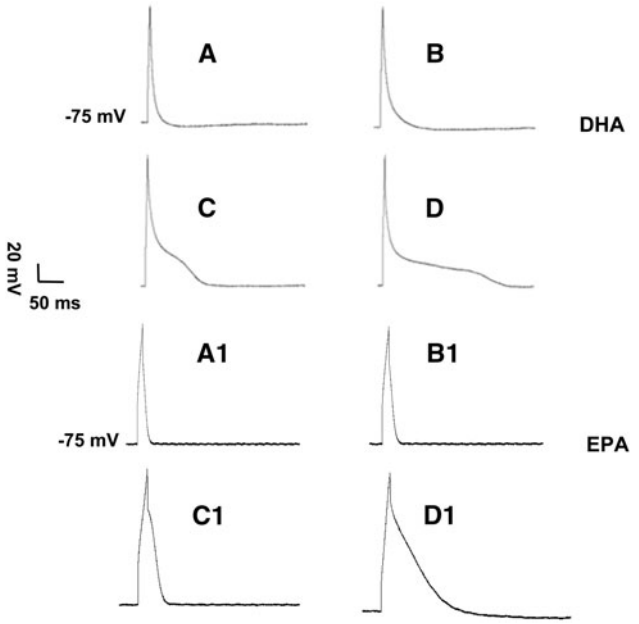

Fig. 3 Action potential changes of rat ventricular myocytes at different concentrations of DHA and EPA. *A*, *B*, and *C* were the applications of 10 μmol/L DHA at 0, 1, and 5 min. *D* was DHA at concentration of 100 μmol/L for 5 min. Action potential durations were significantly prolonged in concentration-dependent manners when DHA concentrations were more than 10 μmol/L. *A1*, *B1*, and *C1* were the applications of 10 μmol/L EPA at 0, 1, and 5 min. *D* was EPA at concentration of 100 μmol/L for 5 min. Action potential durations were significantly prolonged in a concentration-dependent manner when EPA concentrations were more than 10 μmol/L

Effects of DHA and EPA on I_{to}

DHA and EPA at 0.01, 0.1, 1, 10, and 100 μmol/L were applied, respectively. I_{to} currents were blocked by DHA and EPA in concentration-dependent manners. Current densities were gradually decreased with the increases of DHA and EPA concentrations. The I_{to} current densities at +70 mV in different concentrations of DHA and EPA were illustrated in Table 1. The representative current tracings blocked by DHA and EPA at 100 μmol/L were shown in Fig. 4. IC_{50} of DHA and EPA on I_{to} were fitted with Hill function and calculated by OriginPro 7.5 software, which were 2.3 ± 0.2 and 3.8 ± 0.6 μmol/L (Fig. 5).

Discussion

The typical action potentials consist of 5 phases or stages, i.e., 0, 1, 2, 3, and 4. The present study has showed that there are no typical action potential configurations of rat ventricular myocytes. APDs are the shortest in epicardial ventricular myocytes, and repolarization rapidly appears after depolarization, demonstrating no platform phase [21]. The phenomenon of "spike and dome" [22] sometimes can

Table 1 I_{to} current density changes in different concentrations of DHA and EPA

Concentrations (μmol/L)	I_{to} current densities (pA/pF)	
	DHA	EPA
0	59.5 ± 16.0	59.5 ± 16.0
0.01	58.4 ± 15.2	59.1 ± 14.3
0.1	57.1 ± 14.1	59.0 ± 13.2
1	49.3 ± 10.2	52.3 ± 10.5
10	35.4 ± 8.0	40.0 ± 9.2
100	30.1 ± 7.2	32.7 ± 8.1

be seen, however, this phenomenon does not appear in endocardial ventricular myocytes. Action potential repolarization in endocardial ventricular myocytes is slow, showing a relative standard action potential profile. The action potential configurations of mid-myocardial ventricular myocytes are between epicardial and endocardial ventricular myocytes [23, 24], but action potential repolarization is still rapid, and has the tendency of the platform phase, compared with the epicardial ventricular myocytes. The reasons why these alterations appear are that there are regional differences of I_{to} in epicardial, mid-myocardial and endocardial ventricular myocytes. The I_{to} channels are the most abundant in rat epicardial ventricular myocytes and then by turns in mid-myocardial and endocardial ventricular myocytes. The I_{to} current densities in epicardial, mid-myocardial and endocardial ventricular myocytes were different in this study, which further illustrates that I_{to} channels of rat ventricular myocytes have regional differences. I_{to} channels in epicardial myocytes are extremely abundant, and therefore, I_{to} currents are the largest, which makes action potential repolarization rapid, calcium inflow time and APDs short. In contrast, I_{to} channels in endocardial myocytes are few or absent, and therefore, APDs prolong. V_{max}, APA, and OS are formed mainly by 0 phase depolarization. Because regional differences of I_{to} channels do not affect depolarization of ventricular myocytes, and thus, there are no significant differences of V_{max}, APA, and OS in epicardial, mid-myocardial and endocardial myocytes [25].

The Ca^{2+}-insensitive but 4-aminopyridine-sensitive I_{to} currents play a major role in modulating cardiac electrical activity [26]. It underlies phase 1 repolarization, and thus, by setting the voltage of the early plateau phase, it influences activation and inactivation of other plateau currents that affect repolarization. It has also been reported in several studies that I_{to} channels are potentially important targets for both neuromodulatory control [27] and antiarrhythmic drug actions [28]. This current has been suggested to contribute significantly to the regional electrophysiological heterogeneity within the ventricular wall,

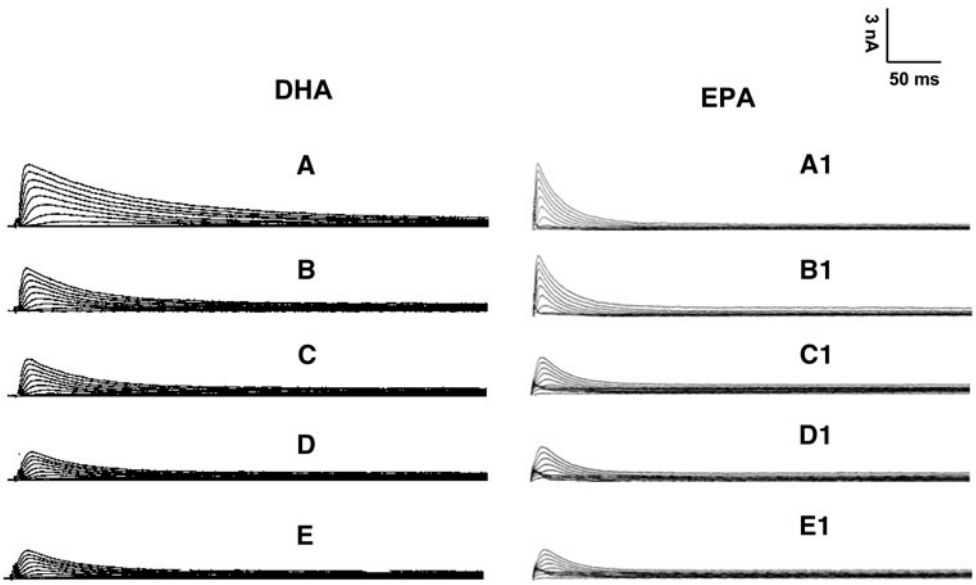

Fig. 4 Alterations of transient outward potassium currents after DHA and EPA at 100 μmol/L were applied. *A*, *B*, *C*, *D*, and *E* were representative transient outward potassium current tracings with DHA at 0, 1, 5, 10, and 15 min, respectively. Transient outward potassium currents were remarkably blocked by DHA. *A1*, *B1*, *C1*, *D1*, and *E1* were representative transient outward potassium current tracings with EPA at 0, 1, 5, 10, and 15 min, respectively. Transient outward potassium currents were significantly blocked by EPA

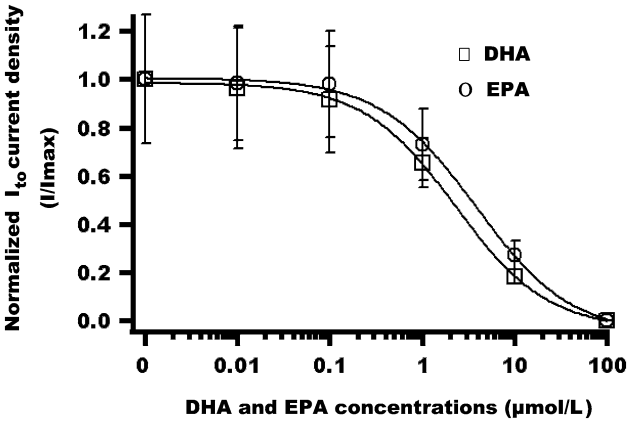

Fig. 5 Half-inhibited concentrations of DHA and EPA on transient outward potassium currents of rat ventricular myocytes. Half-inhibited concentrations of DHA and EPA on transient outward potassium currents were fitted with Hill function, which were 2.3 ± 0.2 and 3.8 ± 0.6 μmol/L

a fact considered to be responsible for T-wave polarity. The heterogeneous distribution of I_{to} thus appears to be essential in causing the transmural electrical gradients necessary for proper repolarization of cardiac action potentials. It is expected that changes in I_{to} distribution and availability can be expressed in the ECG by typical J-wave and T-wave alterations and may lead to cardiac arrhythmias during evolving heart diseases.

The present study results have shown that there are regional differences of action potentials and I_{to} amplitude and configuration of rat epicardial, mid-myocardial and endocardial myocytes. Regional differences of action potentials and I_{to} should be considered when rats are chosen as the experimental animal. We should try to obtain same regional ventricular myocytes to avoid experiment errors when we perform cellular electrophysiological studies. Consequently, in this study, we only chose epicardial myocytes to investigate the effects of DHA and EPA on action potentials and I_{to}.

There have been many reports about the electrophysiological effects of n-3 PUFA on potassium channels of cardiomyocytes and vascular smooth muscle cells in recent years [29–33]. Interestingly, it seems that n-3 PUFA inhibit or block potassium channels of cardiomyocytes [29–31], whereas they activate potassium channels of vascular smooth muscle cells [32, 33]. So far, n-3 PUFA protect against arrhythmia and sudden cardiac death using largely unknown mechanisms [34–36]. In order to investigate the mechanisms of n-3 PUFA on anti-arrhythmias and prevention of sudden death, we performed this experiment to study the effects of DHA and EPA on the action potential and I_{to} of rat ventricular myocytes. The reasons that we chose the rat as the experimental animal are not only because the rats have many advantages, e.g. cheap, strong vitality, and easily bred, but also because there are many similar electrophysiological characteristics between rat and human cardiomyocytes [17, 37].

After DHA and EPA at various concentrations were applied, APDs were gradually prolonged and I_{to} current densities were decreased by degrees with the increased concentrations of DHA and EPA. DHA and EPA could inhibit I_{to} currents, prolong APDs, and extend effective refractory period of cardiomyocytes [38]. The effects of DHA and EPA on action potentials and I_{to} may be one of their anti-arrhythmia mechanisms.

Figure 4 clearly showed that DHA and EPA could inhibit I_{to} currents. However, from the morphologic changes of action potentials in Fig. 3, we found that the morphologic changes of action potentials mainly appeared in phase 2 and phase 3 with the increased concentrations of

DHA and EPA. In contrast, there were no significant changes in phase 1 of action potential formed mainly by I_{to} current efflux. This means DHA and EPA may have effects on other ion currents in addition to the I_{to} current.

The present study has some limitations, e.g., we only investigated the effects of DHA and EPA on action potentials and I_{to} of rat ventricular myocytes. The effects of DHA and EPA on other ion currents such as I_{Na}, $I_{Ca\text{-}L}$, I_K, and I_{K1} still need to be studied further. Only if we explore the anti-arrhythmia mechanisms of n-3 PUFA completely, can we apply them correctly in clinical practice to prevent and treat cardiovascular diseases [39–43].

In summary, the present findings obtained by the patch-clamp technique have clearly shown that APDs are prolonged, and I_{to} current densities are gradually reduced with the increased concentrations of DHA and EPA. DHA and EPA have the similar effects on action potentials and I_{to} of ventricular myocytes. The effects of n-3 PUFA on action potentials and I_{to} may be one of the important mechanisms of anti-arrhythmias.

Acknowledgments This work was supported, in part, by a grant (CS20010015) from the Wuxi Science and Technology Bureau of Jiangsu Province, China; and by the Specialized Research Fund for the '135' Project (RC2007001) from Jiangsu Province of China. The authors thank Miss Lian-hua Han for her assistance in the preparation of this paper.

References

1. Lavie CJ, Milani RV, Mehra MR, Ventura HO (2009) Omega-3 polyunsaturated fatty acids and cardiovascular diseases. J Amer Coll Cardiol 54:585–594
2. Crumb JR, Munfakh N, Heck HA, Harrison LH (1999) Fatty acid block of the transient outward current in adult human atrium. J Pharmacol Exp Ther 289:386–391
3. Wilhelm M, Tobias R, Asskali F, Kraehner R, Kuly S, Klinghammer L, Boehles H, Daniel WG (2008) Red blood cell omega-3 fatty acids and the risk of ventricular arrhythmias in patients with heart failure. Amer Heart J 155:971–977
4. Arshad A, Mandava A, Kamath G, Musat D (2008) Sudden cardiac death and the role of medical therapy. Prog Cardiovasc Dis 50:420–438
5. Anand RG, Alkadri M, Lavie CJ, Milani RV (2008) The role of fish oil in arrhythmia prevention. J Cardiopulm Rehabil Prev 28:92–98
6. Metcalf RG, Sanders P, James MJ, Cleland LG, Young GD (2008) Effect of dietary n-3 polyunsaturated fatty acids on the inducibility of ventricular tachycardia in patients with ischemic cardiomyopathy. Amer J Cardiol 101:758–761
7. Von Schacky C (2008) Omega-3 fatty acids: antiarrhythmic, proarrhythmic or both? Curr Opin Clin Nutr Metab Care 11:94–99
8. He K (2009) Fish, long-chain omega-3 polyunsaturated fatty acids and prevention of cardiovascular disease—eat fish or take fish oil supplement? Prog Cardiovasc Dis 52:95–114
9. Smith CE, Freeman LM, Rush JE, Cunningham SM, Biourge V (2007) Omega-3 fatty acids in Boxer dogs with arrhythmogenic right ventricular cardiomyopathy. J Vet Intern Med 21:265–273
10. Leaf A (2007) Omega-3 fatty acids and prevention of arrhythmias. Curr Opin Lipidol 18:31–34
11. Leaf A (2006) Prevention of sudden cardiac death by n-3 polyunsaturated fatty acids. Fundam Clin Pharmacol 20:525–538
12. Von Schacky C, Harris WS (2007) Cardiovascular benefits of omega-3 fatty acids. Cardiovasc Res 73:310–315
13. Kottke TE, Wu La, Brekke LN, Brekke MJ, White RD (2006) Preventing sudden death with n-3 (omega-3) fatty acids and defibrillators. Amer J Prev Med 31:316–323
14. Bogdanov KY, Spurgeon HA, Vinogradova TM, Lakatta EG (1998) Modulation of the transient outward current in adult rat ventricular myocytes by polyunsaturated fatty acids. Amer J Physiol 274:H571–H579
15. Yang X, Salas PJ, Pham TV, Wasserlauf BJ, Smets MJ, Myerburg RJ, Gelband H, Hoffman BF, Bassett AL (2002) Cytoskeletal actin microfilaments and the transient outward potassium current in hypertrophied rat ventriculocytes. J Physiol 541:411–421
16. Volk T, Nguyen TH, Schultz JH, Ehmke H (1999) Relationship between transient outward K^+ current and Ca^{2+} influx in rat cardiac myocytes of endo- and epicardial origin. J Physiol 519:841–850
17. Bryant SM, Shipsey SJ, Hart G (1999) Normal regional distribution of membrane current density in rat left ventricle is altered in catecholamine-induced hypertrophy. Cardiovasc Res 42:391–401
18. Yazawa K, Kaibara M, Ohara M, Kameyama M (1990) An improved method for isolating cardiac myocytes useful for patch-clamp studies. Jap J Physiol 40:157–163
19. Tytgat J (1994) How to isolate cardiac myocytes. Cardiovasc Res 28:280–283
20. Hamill OP, Marty A, Nether E, Sakmann B, Sigworth FJ (1981) Improved patch-clamp techniques for high-resolution current recording from cells and cell-free membrane patches. Pflugers Arch 391:85–100
21. Shigematsu S, Kiyosue T, Sato T, Arita M (1997) Rate-dependent prolongation of action potential duration in isolated rat ventricular myocytes. Basic Res Cardiol 92:123–128
22. Hulme JT, Orchard CH (2000) Effect of acidosis on transient outward potassium current in isolated rat ventricular myocytes. Amer J Physiol Heart Circ Physiol 278:50–59
23. Stilli D, Berni R, Bocchi L, Zaniboni M, Cacciani F, Sgoifo A, Musso E (2004) Vulnerability to ventricular arrhythmias and heterogeneity of action potential duration in normal rats. Exp Physiol 89:387–396
24. Fauconnier J, Bedut S, Le Guennec JY, Babuty D, Richard S (2003) Ca^{2+} current-mediated regulation of action potential by pacing rate in rat ventricular myocytes. Cardiovasc Res 57:670–680
25. Orta-Salazar G, Bouchard RA, Morales-Salgado F, Salinas-Stefanon EM (2002) Inhibition of cardiac Na^+ current by primaquine. Br J Pharmacol 135:751–763
26. Antzelevitch C, Sicouri S, Litovsky SH, Lukas A, Krishnan SC, Di Diego JM, Gintant GA, Liu DW (1991) Heterogeneity within the ventricular wall: electrophysiology and pharmacology of epicardial, endocardial, and M cells. Circ Res 69:1427–1449
27. Fedida D, Braun AP, Giles WR (1993) α1-Adrenoceptors in myocardium: functional aspects and transmembrane signaling mechanisms. Physiol Rev 73:469–487
28. Duan D, Fermini B, Nattel S (1993) Potassium channel blocking properties of propafenone in rabbit atrial myocytes. J Pharmacol Exp Ther 264:1113–1123
29. Li GR, Sun HY, Zhang XH, Cheng LC, Chiu SW, Tse HF, Lau CP (2009) Omega-3 polyunsaturated fatty acids inhibit transient outward and ultra-rapid delayed rectifier K^+ currents and Na^+ current in human atrial myocytes. Cardiovasc Res 81:286–293

30. Guizy M, Arias C, David M, González T, Valenzuela C (2005) {Omega}-3 and {omega}-6 polyunsaturated fatty acids block HERG channels. Amer J Physiol Cell Physiol 289:C1251–C1260
31. Lai LH, Wang RX, Jiang WP, Yang XJ, Song JP, Li XR, Tao G (2009) Effects of docosahexaenoic acid on large-conductance Ca^{2+}-activated K^+ channels and voltage-dependent K^+ channels in rat coronary artery smooth muscle cells. Acta Pharmacol Sin 30:314–320
32. Wu KT, Huang CT, Wei J, Tsait LM, Hsu CH, Chen YC, Yangs JM, Lin CI (2007) Vasodilator action of docosahexaenoic acid (DHA) in human coronary arteries in vitro. Chin J Physiol 50:164–170
33. Xiao YF, Ke Q, Wang SY, Yang Y, Chen Y, Wang GK, Morgan JP, Cox B, Leaf A (2004) Electrophysiologic properties of lidocaine, cocaine, and n-3 fatty-acids block of cardiac Na+ channels. Eur J Pharmacol 485:31–41
34. Arnold C, Konkel A, Fischer R, Schunck WH (2010) Cytochrome P450-dependent metabolism of omega-6 and omega-3 long-chain polyunsaturated fatty acids. Pharmacol Rep 62:536–547
35. Pottala JV, Garg S, Cohen BE, Whooley MA, Harris WS (2010) Blood eicosapentaenoic and docosahexaenoic acids predict all-cause mortality in patients with stable coronary heart disease: the Heart and Soul study. Circ Cardiovasc Qual Outcomes 3:406–412
36. Galli C, Risé P (2009) Fish consumption, omega 3 fatty acids and cardiovascular disease. The science and the clinical trials. Nutr Health 20:11–20
37. He JY, Kargacin ME, Kargacin GJ, Ward CA (2003) Tamoxifen inhibits Na^+ and K^+ currents in rat ventricular myocytes. Amer J Physiol Heart Circ Physiol 285:661–668
38. Adamantidis MM (1995) Mechanisms of action of class III antiarrhythmia agents. Arch Des Maladies du Coeur et des Vaisseaux 88:33–40
39. Xiao YF, Sigg DC, Ujhelyi MR, Wilhelm JJ, Richardson ES, Iaizzo PA (2008) Pericardial delivery of omega-3 fatty acid: a novel approach to reducing myocardial infarct sizes and arrhythmias. Amer J Physiol Heart Circ Physiol 294:H1144–H1152
40. Den Ruijter HM, Berecki G, Verkerk AO, Bakker D, Baartscheer A, Schumacher CA, Belterman CN, de Jonge N, Fiolet JW, Brouwer IA, Coronel R (2008) Acute administration of fish oil inhibits triggered activity in isolated myocytes from rabbits and patients with heart failure. Circulation 117:536–544
41. Reiner E, Tedeschi-Reiner E, Stajminger G (2007) The role of omega-3 fatty acids from fish in prevention of cardiovascular diseases. Lijec Vjesn 129:350–355
42. Jacobson TA (2007) Beyond lipids: the role of omega-3 fatty acids from fish oil in the prevention of coronary heart disease. Curr Atheroscler Rep 9:145–153
43. Farzaneh-Far R, Lin J, Epel ES, Harris WS, Blackburn EH, Whooley MA (2010) Association of marine omega-3 fatty acid levels with telomeric aging in patients with coronary heart disease. JAMA 303:250–257

Lipids (2011) 46:171–178
DOI 10.1007/s11745-010-3519-8

ORIGINAL ARTICLE

Maternal Intake of Fish Oil but not of Linseed Oil Reduces the Antibody Response in Neonatal Mice

Lotte Lauritzen · T. M. R. Kjær · T. Porsgaard · M. B. Fruekilde · H. Mu · H. Frøkiær

Received: 25 May 2010 / Accepted: 15 December 2010 / Published online: 9 January 2011

Abstract Dietary levels of n-3 PUFA are believed to influence the immune system. The importance of the source of n-3 PUFA is debated. This study addressed how the content and source of n-3 PUFA in the maternal diet influenced tissue FA composition and the immune response to ovalbumin (OVA) in mice pups. From the day of conception and throughout lactation, dams were fed diets containing 4% fat from linseed oil (LSO), fish oil (FO) or a n-3 PUFA-deficient diet (DEF). Pups were injected with OVA within 24 h of birth and sacrificed at weaning (day 21). Overall, the content of n-3 PUFA in milk, liver and spleen reflected the source and only minor differences were observed in brain phospholipid 22:6n-3. The source had only limited influence on the n-3 PUFA accretion in peripheral tissue, with most pronounced differences in the spleen. The marine PUFA-group had reduced levels of total OVA-specific antibodies and OVA-IgG1 titers in the pup blood, while the response in the LSO-group did not differ from that in the DEF-group. There were no statistical differences in the cytokine responses to OVA-stimulated splenocytes, but the decrease in IgG1 was paralleled by an increase in IFNγ-production and a decrease in IL-6-production. Our results indicate that maternal intake of FO, but not of LSO, changes the offspring's antigen-specific response and potentially increases Th1-polarization.

Keywords n-3 long-chain polyunsaturated fatty acid · Tissue fatty acid incorporation · Immune maturation · Sensitization · Diet · Programming

Abbreviations

DEF	The n-3 PUFA-deficient group
20:5n-3	Eicosapentaenoic acid (individual fatty acids are named by number of carbon atoms: number of double bonds followed by the position of the last double bond)
FO	The fish oil group
Ig	Immunoglobulin
IL	Interleukin
IFNγ	Interferon-γ
LCPUFA	Long-chain PUFA
LSO	The linseed oil-group
OVA	Ovalbumin
PC	Phosphatidylcholine
PE	Phosphatidylethanolamine
TAG	Triacylglycerol
Th	T-helper lymphocytes
TNFα	Tumor necrosis factor-α

Introduction

An adequate supply of essential fatty acids during pregnancy and lactation is crucial for optimal fetal and

L. Lauritzen (✉)
Department of Human Nutrition, Faculty of Life Sciences, University of Copenhagen, Rolighedsvej 30, 1958 Frederiksberg C, Denmark
e-mail: ll@life.ku.dk

T. M. R. Kjær · T. Porsgaard · M. B. Fruekilde
Department of Systems Biology, Technical University of Denmark, Lyngby, Denmark

H. Mu
Department of Pharmaceutics and Analytical Chemistry, Faculty of Pharmaceutical Sciences, University of Copenhagen, Copenhagen, Denmark

H. Frøkiær
Department of Basic Sciences and Environment, Faculty of Life Sciences, University of Copenhagen, Frederiksberg, Denmark

postnatal development. It is well known that n-3 PUFA are required for growth and development of the central nervous system of the fetus and infant [1]. Long-chain n-3 PUFA (n-3 LCPUFA) have in studies with adults been shown to be immunosuppressive and to exert beneficial effects in a variety of inflammatory disorders [2]. Dietary n-3 LCPUFA have, in both human and animal experiments, been shown to affect a wide range of immune functions, including lymphocyte proliferation, cytokine production, NK-cell activity, adhesion molecules expression, and antigen presentation in adults [3]. However, the effect of maternal n-3 PUFA intake on immune function in the offspring is less well characterized and only few experimental studies have addressed this topic [4].

The immune system of the newborn has not fully matured and is believed to be more sensitive to environmental conditions, including diet. Such conditions have been hypothesized to influence the polarization of T-helper lymphocytes (Th1/Th2) of the immune system and accordingly the risk of allergy development [5]. The processes of importance for shaping the immune system take place already in utero and in the early postnatal period, and the immune system is therefore particularly susceptible to changes in diet and external stimuli to the fetus/newborn [6]. To this end, human studies with fish oil-supplementation of pregnant women have been shown to affect immune function in the neonate [7, 8]. We have previously shown that fish oil-supplementation during lactation resulted in a higher predisposition of the blood from the children to produce Interferon-γ (IFNγ) upon polyclonal stimulation [9, 10], indicating a higher intake of n-3 LCPUFA is associated with faster immune maturation and Th1-polarization. An association between a high maternal n-3 PUFA intake and a decreased risk of infant allergy is supported by recent randomized trials [11, 12]. In mice, maternal fish oil has been shown to lead to lower levels of prostaglandin E_2 in pups' lung and increased survival to infection compared to offspring of dams on a corn oil diet [13] and in another study manipulation of the ratio of n-6 to n-3 PUFA in the maternal diet showed better induction of oral tolerance in neonatal mice with a high relative intake of n-3 PUFA [14].

Even though mammals can convert α-linolenic acid (18:3n-3) to eicosapentaenoic acid (20:5n-3) and docosahexaenoic acid (22:6n-3), it is controversial whether a dietary intake of 18:3n-3 is as efficient as fish oil as a means to affect disease risk. Fish oil [11–13] as well as α-linolenic acid [14] have been used in the various human and animal studies, but since different doses and experimental designs have been used, the effect of the two sources is difficult to compare. In the present study, we hypothesized that maternal n-3 PUFA intake from fish oil0or plant oil during gestation and lactation affects the Th1/Th2-polarization early in life and that this is reflected in the antibody and cytokine production against food allergens encountered postnatally. We fed groups of female mice fish oil or linseed oil from mating until weaning of their offspring, and tested the antibody response to ovalbumin (OVA) injected in the offspring on day 1.

Experimental Procedure

Animals

The experiment was approved by the Danish Committee for Animal Experiments. BalbC mice from Taconic M&B (Ll. Skensved, Denmark) 8–10 weeks of age were housed in plastic cages in a temperature (21 °C) and humidity (50%) controlled environment on a 12 h/12 h light/dark cycle with a standard nonpurified diet (Altromin No. 1324, Chr. Petersen A/S, Ringsted, Denmark) and water freely available. They were acclimatized to the housing conditions for 7 days before conception. The mice were then allocated to individual cages and randomized to the three dietary treatments from the time of mating and throughout the pregnancy and lactation periods. In this feeding experiment, 3 dams on fish oil diet (FO) gave birth to 17 pups, 4 dams on n-3 PUFA-deficient diet (DEF) to 13 pups, and 2 dams on a linseed oil based diet (LSO) to 11 pups. An additional feeding experiment was performed with the same diets, since the first experiment resulted in fewer pregnancies than expected. This resulted in birth of further 12 pups in the FO groups, 11 in the DEF-group, and 10 in the LSO-group, from 2 dams in each of the groups. No differences were found in milk gland TAG fatty acid composition from the two feeding periods, so the results from the two experiments were pooled.

Diets

The overall composition of the three dietary groups was as follows: 56 g/100 g corn starch (Bestfoods Nordic A/S, Skovlunde, Denmark); 20 g/100 g casein (Miprodan milk-proteins, Arla Foods amba, Viby, Denmark), 10 g/100 g sucrose (Danisco Sugar, Copenhagen, Denmark), 5 g/100 g salt mixture (including trace elements), 4 g/100 g fat, 4 g/100 g cellulose powder (MN 100, Machery-Nagel GmbH & Co, Düren, Germany), 0.5 g/100 g vitamin mixture, and 0.5 g/100 g choline chloride (Merck, Darmstadt, Germany). The vitamin and salt mixtures were composed as described by Aaes-Jørgensen and Hølmer [15].

One group was given a DEF, in which fat was supplied as a 78:10-mix of coconut fat (Aarhus United A/S) and safflower oil (Urtekram A/S, Mariager, Denmark). The

other four groups were given n-3 PUFA sufficient diets with equal amounts of n-3 PUFA, but in the form of α-linoleic acid (18:3n-3) from linseed oil (Unikem, Copenhagen, Denmark) mixed with safflower oil, olive oil (FDB, Albertslund, Denmark), and coconut fat (43:13:25:19) (LSO) or n-3 LCPUFA from fish oil (Aarhus United A/S, Aarhus, Denmark) mixed with safflower oil (79:21) (FO). All diets had an equal content of n-6 PUFA (Table 1). All diets were supplied ad libitum. The diets were powdered, stored at –20 °C and provided fresh every day.

Immunization and Organ Collection

All neonatal mice were immunized both intraperitoneally and subcutaneously with 20 μL 10 mg/mL OVA within the first 24 h of life. 3 weeks after birth, blood from the offspring was drawn from retro-orbital venous plexus using calibrated 25 μL heparinized micropipettes. Blood was immediately diluted in 375 μL PBS and stored at −20 °C until antibody determination.

Dams and pups were weighed weekly and when pups were 3 weeks of age, all mice were anesthetized with 0.06 mL/10 g body weight of a mixture composed of Hypnorm (Janssen Pharmaceutica, Beerse, Belgium): Dormicum (Hoffmann-La Roche AG, Basel, Switzerland):sterile water (1:1:2), thereafter death was assured by cervical dislocation. Spleens were removed, and leucocytes were immediately after isolation and used for determination of the fatty acid composition and for OVA-specific cell proliferation and cytokine production. Brains, eyes, and livers were also removed from pups and milk glands from the dams and all organs were immediately frozen in liquid nitrogen. The organs were stored at −80 °C until analysis.

Table 1 Fatty acid composition of diets

	n-3 PUFA-deficient (DEF)	Linseed oil (LSO)	Fish oil (FO)
SFA	71.4	26.6	23.1
MUFA	10.0	30.5	34.3
n-6 PUFA	18.5	18.1	19.3
18:2n-6	18.5	18.1	18.9
20:4n-6	0.0	0.0	0.4
n-3 PUFA	0.1	24.6	23.2
18:3n-3	0.1	24.6	2.4
20:5n-3	0.0	0.0	6.1
22:6n-3	0.0	0.0	9.9
n-6/n-3 PUFA	185	0.7	0.8

Data are given as g/100 g

Analysis of Diets and Tissue Lipids

Lipid from diets and tissues were extracted with chloroform and methanol according to Folch et al. [16]. Fatty acid composition of the dietary fat and the structure of the TAG, represented by the fatty acid composition in *sn*-2 MAG, were measured as described previously [17]. TAG from milk glands were isolated by TLC with heptane–isopropanol–acetic acid (95:5:1, v/v/v) and methylated with a modified BF_3 procedure [18], as were the lipid extracts from the pup livers. Phospholipid classes in pup brain, eyes and spleen (from brain: phosphatidylcholine (PC), phosphatidylethanolamine (PE) and phosphatidylserine and PC and PE from eyes and spleen) were separated by TLC with chloroform–methanol–hexane–acetic acid–boric acid (40:20:30:10:1.8, v/v/v/v/w), visualized with 2,7-dichlorofluorescein (0.2% in ethanol), scraped off and methylated with BF_3 [19]. The resulting fatty acid methyl esters were analyzed by GLC in a Hewlett–Packard 5890 chromatograph equipped with a split/splitless injector, SP2380 capillary column (60 m, ID. 0.25 mm; Supelco Inc., Bellefonte, PA), flame-ionization detection and helium as carrier gas. The GLC conditions were as follows: injector temperature 270 °C, flame-ionization detector 270 °C, helium carrier gas at 1.2 mL/min, injector split ratio 1:11, initial oven temperature 70 °C, which was held for 5 min and the increased by 15 °C/min until 160 °C, 1.5 °C/min until 200 °C that was then maintained for 15 min followed by a finally temperature rise to 225 °C maintained for 10 min. The initial oven temperature for the fatty acid determinations in milk gland TAG was 50 °C. Peak areas were calculated using a Hewlett–Packard integrator and the fatty acids were identified by comparing the retention time with standards of known fatty acid composition (Nu-Chek-Prep, Elysian, MN).

Spleen Cell Preparation and Ex-Vivo-Stimulated Cytokine Production

Single-cell suspensions were prepared from spleens pooled from 2 to 3 offspring within a litter in DMEM (Gibco, Life Technologies, Scotland). Red blood cells were lyzed with ammonium chloride buffer (0.83% NH_4Cl). For the measurement of cytokine production, cells were washed and resuspended in X-VIVO 10 (serum free medium, Bio Whitaker, USA) at a final concentration of 2×10^6 cells/ mL and were cultured with 550 μL/well in flat-bottom 48-well tissue culture plates (Nunc, Denmark). Cells were stimulated with 0.5 mg OVA/well (0.9 mg/mL) or with medium in triplicates, and supernatants were collected after 72 h of culture. Supernatants were stored at −80 °C until determination of IFNγ, tumor necrosis factor-α (TNFα), interleukin (IL)-6, IL-10, IL-5 and IL-12 by commercial ELISA

kits from R&D systems Europe (Abingdon, UK) according to manufactures instructions (Duosets DY 485, DY 410, DY 406, DY 417, DY 405, DY 419). Cytokine concentrations were quantified relative to standard curves representing a range of dilutions of recombinant cytokine using 4-parameter curve fit analysis (Kineticalc software, version KC4 Rev 29, Biotek instruments). Limits of detection for these assays were 31 pg/mL (IFNγ), 16 pg/mL (TNFα), 16 pg/mL (IL-6), 31 pg/mL (IL-10), 16 pg/mL (IL-5) and 31 pg/mL (IL-12).

Determination of OVA-Specific Antibodies in Pups' Plasma

Presence of total immunoglobulins (Ig) and IgG_1 plasma antibodies specific for OVA was tested by ELISA. In brief, micro-titer plates (Nunc, Denmark) were coated with OVA overnight at 4 °C and plasma and controls were serially diluted in the washed plates. Bound OVA-specific Ig was detected with peroxidase-conjugated rabbit anti-mouse Ig (DAKO, Denmark). OVA-specific IgG_1 and IgG_{2a} were detected with rabbit anti-mouse IgG_1 and IgG_{2a} antibodies (Zymed, CA, USA) followed by peroxidase-conjugated swine anti-rabbit Ig (DAKO, Denmark). Hydrogen peroxide and tetramethylbenzidine (TMB, Merck, Germany) were used as substrates and the reaction was stopped after 10 min by the addition of phosphorous acid (2 M). Plates were measured spectrophotometrically at 450 nm using 690 nm as reference on an ELISA-reader (Bio-kinetics reader, EL 340, Biotek instruments). Controls, monoclonal antibodies against OVA (of IgG_1 and IgG_{2a} isotypes) and a pool of plasma from OVA-immunized animals were included on each plate. The antibody titers were expressed as $\log_2$ titers and defined as the interpolated dilution (4-parameter analysis, Kineticalc software, KC4 Rev 29, Biotek instruments) of a blood sample leading to an absorbance on 0.2 above background.

Statistics

Results were expressed as means ± standard errors (SEM). Differences in fatty acid compositions between groups were tested by one-way ANOVA (GraphPad PRISM version 3.02, GraphPad software, San Diego, CA). Tukey's Multiple Comparison post hoc test was used to determine the exact nature of the differences. The level of statistical significance was $P < 0.05$.

Results

Dams weighed 23 ± 0.5 g (mean ± SEM) at the beginning and 30 ± 0.6 g at the end of the 7 weeks study. During the course of the study all mice gained more weight due to pregnancy, which they lost again at delivery. The pups increased their weight by a factor 1.8–3.4 from birth until sacrifice at 3 weeks of age. The increase in weight was dependent on the number of pups in the litter, but there was no significant difference in pup litter size (3–7 pups/group in FO-group, 2–6 in DEF-groups, and 3–8 in the LSO-group) and weight between the dietary groups (results not shown).

The n-3 PUFA content in the milk gland TAG reflected the fatty acid composition of the maternal diets (Table 2). Milk gland TAG from both of the n-3 PUFA sufficient groups, LSO and FO, had a significantly higher content of n-3 PUFA relative to the DEF-group. In the LSO-group this was due to an increase in the content of 18:3n-3 and 20:5n-3, whereas also 22:6n-3 was increased in the FO-group. It is noteworthy that although approximately 25% of dietary fatty acids in the LSO-diet were 18:3n-3, only 2% of the milk gland TAG fatty acid was 18:3n-3. The n-6 PUFA-content of the milk glands was not affected by an increased intake of n-3 PUFA, whereas that of MUFA was decreased in the FO-group compared to that in the DEF-group. The composition of PUFA in the pup liver lipid in turn reflects that in the milk gland TAG (Table 3). Pups from both the FO- and the LSO-group had pronouncedly increased liver levels of n-3 PUFA, increased levels of PUFA as such, and lower levels of n-6 PUFA. These changes were more pronounced in the FO-group, but the two groups responded similar with respect to changes in

Table 2 Fatty acid composition of milk gland triacylglycerol in the dietary groups

	n-3 PUFA-deficient (DEF)	Linseed oil (LSO)	Fish oil (FO)
n	8	4	7
12:0	10.5 ± 0.6	8.7 ± 1.4	8.1 ± 1.2
14:0	13.4 ± 0.6	13.1 ± 2.1	13.3 ± 1.4
16:0	29.1 ± 0.5	28.3 ± 1.5	27.7 ± 0.7
18:1n-9	16.8 ± 0.7^{a,b}	19.3 ± 2.6^{a}	13.6 ± 0.8^{b}
18:1n-7	6.4 ± 0.4^{a}	4.5 ± 0.8^{b}	3.6 ± 0.2^{b}
n-6 PUFA	9.0 ± 0.7	7.1 ± 0.7	8.1 ± 0.7
18:2n-6	8.2 ± 0.7	6.5 ± 0.6	7.5 ± 0.7
n-3 PUFA	0.1 ± 0.0^{a}	4.7 ± 0.2^{b}	5.7 ± 0.5^{b}
18:3n-3	0.0 ± 0.0^{a}	3.2 ± 0.1^{c}	2.2 ± 0.2^{b}
20:5n-3	0.0 ± 0.0^{a}	0.3 ± 0.0^{b}	0.4 ± 0.1^{b}
22:6n-3	0.0 ± 0.0^{a}	0.3 ± 0.1^{a}	2.0 ± 0.2^{b}
n-6/n-3 PUFA	94.0 ± 9.5^{a}	1.5 ± 0.1^{b}	1.4 ± 0.0^{b}

Data are given as means ± SEM in g/100 g and the table shows single SFA and MUFA, which constitute >5%; and the main PUFA

Statistical analysis by ANOVA and post hoc group comparisons, if the overall $P < 0.05$: Groups with different superscripts differ significantly ($P < 0.01$)

Table 3 Fatty acid composition of liver lipids in the pups in the dietary groups

	n-3 PUFA-deficient (DEF)	Linseed oil (LSO)	Fish oil (FO)
n	13	8	16
Total PUFA	35.4 ± 0.8^{a}	42.5 ± 1.0^{b}	46.7 ± 0.7^{c}
n-6 PUFA	33.5 ± 0.7^{a}	21.4 ± 0.3^{b}	18.4 ± 0.2^{c}
20:4n-6	10.5 ± 0.6^{a}	6.7 ± 0.2^{b}	4.5 ± 0.2^{c}
22:4n-6	1.5 ± 0.1^{a}	0.0 ± 0.0^{b}	0.2 ± 0.0^{b}
22:5n-6	4.6 ± 0.2^{a}	0.0 ± 0.0^{b}	0.0 ± 0.0^{b}
n-3 PUFA	1.8 ± 0.1^{a}	21.2 ± 0.7^{b}	28.3 ± 0.6^{c}
18:3n-3	0.0 ± 0.0^{a}	2.9 ± 0.1^{c}	0.5 ± 0.0^{b}
20:5n-3	0.0 ± 0.0^{a}	1.9 ± 0.1^{b}	2.2 ± 0.1^{b}
22:5n-3	0.0 ± 0.0^{a}	2.9 ± 0.1^{b}	2.9 ± 0.1^{b}
22:6n-3	1.8 ± 0.1^{a}	12.4 ± 0.6^{b}	22.2 ± 0.5^{c}
n-6/n-3	19.2 ± 1.0^{a}	1.0 ± 0.0^{b}	0.7 ± 0.0^{b}

Data are given as means ± SEM g/100 g

Statistical analysis by ANOVA and post hoc group comparisons, if overall $P < 0.05$: values in a row with different superscripts differ significantly ($P < 0.0001$)

the overall n-6 to n-3 PUFA-ratio, the content of 20:5n-3 and 22:5n-3, and the observed deceases in the content of the n-3 PUFA-deficiency markers, 22:4n-6 and 22:5n-6.

The phospholipid PUFA-composition of pup tissues was also affected by the n-3 PUFA-content of the maternal diet. All types of n-3 LCPUFA were increased in both PC and PE in both brain and spleen, whereas the n-6 PUFA-content of the tissue phospholipids decreased. The n-6 PUFA-decrease was most pronounced for 22:5n-6, which is the dominant of the two n-3 PUFA-deficiency markers and which decreased to the same extent in the LSO- and FO-group (Table 4). The dietary n-3 PUFA-induced decrease in the tissue phospholipid n-6 PUFA-content was generally larger in the spleen than in the brain. The phospholipid PUFA-incorporation of the LSO- and FO-group only differed significantly in the PE-pool of the tissues, whereas the two groups were very comparable with respect to the composition in PC in brain but exhibited a minor difference in total n-3 PUFA in spleen PC (Table 4). Brain phosphatidylserine PUFA-incorporation was changed in the same way as that of PC and PE, with only minor differences between the LSO- and FO-group (data not shown). Furthermore, the observed diet-induced changes in eye PC and PE PUFA-composition were as those in the brain, except that no differences were found in the PUFA-composition of the LSO- and FO-group (data not shown).

OVA-immunization gave rise to a significant increase in the plasma concentration of OVA-specific antibodies and of OVA-IgG1, which in non-immunized mice of the same age was 6.0 ± 0.07 and 5.5 ± 0.06, respectively. The observed OVA-antibody titers reflect a Th2-polarization of the response, since the IgG1 titers corresponded to the titer measured for all antibody classes. It was not possible to obtain IgG2a titers (representing aTh1-polarization) that were significantly above the background (data not shown), possibly due to the much lower level of antibodies involved in this type of responses. The OVA-Ig titers were significantly reduced in FO group as compared to the DEF-group, whereas the LSO-group did not differ from the DEF-group ($P < 0.01$, Fig. 1). The results for OVA-IgG1 were similar to those of IgG (data not shown).

The cytokines produced in spleen cells from the same mice upon stimulation with OVA did not reveal any significant differences between the different groups (Table 5). The responses were for most of the analysed cytokines only slightly over the detection levels and rather variable and it was thus not possible to show any statistically significant differences between the groups. The high variation within groups may be ascribed to the fact that a proportion of cell cultures within each group did not result in cytokine productions above the background (for IFN-γ, 50, 60 and 40% were detectable in the FO, LSO and DEF-group, respectively). However, a trend towards an increasing IFNγ- and TNFα-production and a decreasing production of IL-6 with increasing incorporation of n-3 LCPUFA in spleen cells was observed. The production of IL-12 and IL-5 could not be detected in any of the groups. There were no significant differences in the spleen cell proliferation or in CD69-expression on the cultured spleen cells from the pups in the dietary groups (data not shown).

Discussion

The present study showed a reduction in total OVA-specific antibodies and in the IgG1 titers in the blood in the neonatal mice from dams in the fish oil-fed group. As we were not able to measure OVA-specific IgG_{2a} antibodies in the plasma, we cannot establish whether this reduction is caused by a general reduction in the ability to respond to an antigen or an increased Th1-polarization. However, although our results were not significant, the decrease in the Th2-facilitated IgG1-response was paralleled by an increase in IFNγ-production and a decrease in the production of IL-6 in OVA-stimulated spleen cells ex vivo, indicating an increase in Th1-cells in the spleen in FO-group compared to control. The response in the LSO-group did not differ from that in the DEF-group. This is supported by the study of Rayon et al. [13], who showed that maternal intake of menhaden oil resulted in a higher survival in rat pups towards group B *Streptococcal* infection. This was correlated with a lower PGE_2 production in the lungs as compared to the corn oil-fed group, indicative of conditions favoring a Th1- over Th2-polarization [20]. Korotkova

Table 4 Polyunsaturated fatty acid composition in PE and PC from pup spleen and brain in the dietary groups

	n-3 PUFA-deficient (DEF)		Linseed oil (LSO)		Fish oil (FO)	
	PE	PC	PE	PC	PE	PC
Brain						
n	13		8		16	
n-6 PUFA	34.0 ± 0.7[a]	8.3 ± 0.3[a]	19.5 ± 0.4[b]	6.1 ± 0.2[b]	16.1 ± 0.2[c]	5.8 ± 0.1[b]
20:4n-6	15.2 ± 0.3[a]	5.3 ± 0.1[a]	12.8 ± 0.2[b]	4.3 ± 0.2[b]	10.8 ± 0.2[c]	4.0 ± 0.1[b]
22:4n-6	6.7 ± 0.1[a]	0.5 ± 0.0[a]	4.3 ± 0.1[b]	0.3 ± 0.0[b]	2.9 ± 0.0[c]	0.2 ± 0.0[b]
22:5n-6	10.5 ± 0.4[a]	1.5 ± 0.1[a]	0.3 ± 0.0[b]	0.0 ± 0.0[b]	0.3 ± 0.0[b]	0.0 ± 0.0[b]
n-3 PUFA	14.8 ± 0.3[a]	1.7 ± 0.1[a]	26.8 ± 0.3[b]	3.0 ± 0.2[b]	31.1 ± 0.4[c]	3.7 ± 0.2[b]
20:5n-3	0.0 ± 0.0[a]	0.0 ± 0.0[a]	0.2 ± 0.0[b]	0.0 ± 0.0[a]	0.3 ± 0.0[c]	0.1 ± 0.0[b]
22:5n-3	0.1 ± 0.0[a]	0.1 ± 0.0	1.2 ± 0.0[b]	0.1 ± 0.0	1.1 ± 0.0[b]	0.1 ± 0.0
22:6n-3	14.6 ± 0.3[a]	1.6 ± 0.1[a]	25.5 ± 0.3[b]	2.9 ± 0.2[b]	29.7 ± 0.4[c]	3.5 ± 0.2[b]
n-6/n-3	2.3 ± 0.1[a]	4.9 ± 0.2[a]	0.7 ± 0.0[b]	2.0 ± 0.1[b]	0.5 ± 0.0[c]	1.6 ± 0.1[b]
Spleen						
n	6		5		7	
n-6 PUFA	53.4 ± 1.0[a]	25.8 ± 1.0[a]	19.4 ± 1.5[b]	14.3 ± 1.6[b]	17.2 ± 0.6[b]	15.6 ± 0.8[b]
20:4n-6	31.9 ± 0.5[a]	16.5 ± 0.8[a]	13.7 ± 1.4[b]	6.3 ± 0.7[b]	11.9 ± 0.4[b]	5.9 ± 0.3[b]
22:4n-6	10.1 ± 0.6[a]	2.0 ± 0.1[a]	1.3 ± 0.2[b]	0.4 ± 0.003[b]	0.8 ± 0.003[b]	0.3 ± 0.001[b]
22:5n-6	8.4 ± 0.3[a]	1.4 ± 0.0[a]	0.2 ± 0.0[b]	0.3 ± 0.1[b]	0.3 ± 0.0[b]	0.1 ± 0.0[b]
n-3 PUFA	3.9 ± 0.2[a]	0.8 ± 0.004[a]	24.7 ± 2.1[b]	7.6 ± 0.5[b]	36.2 ± 1.4[c]	10.9 ± 0.6[c]
20:5n-3	0.1 ± 0.04[a]	0.02 ± 0.001[a]	5.1 ± 0.2[b]	2.5 ± 0.1[b]	5.7 ± 0.3[c]	3.3 ± 0.2[c]
22:5n-3	0.7 ± 0.05[a]	0.2 ± 0.003[a]	10.1 ± 1.0[b]	2.7 ± 0.2[b]	8.0 ± 0.3[b]	2.6 ± 0.1[b]
22:6n-3	3.0 ± 0.2[a]	0.6 ± 0.003[a]	9.3 ± 1.0[b]	1.8 ± 0.2[b]	22.5 ± 0.8[c]	4.9 ± 0.3[c]

Data are given as means ± SEM in g/100 g

Statistical analysis by ANOVA and post hoc group comparisons, if the overall $P < 0.05$: groups with different superscripts in equivalent columns and rows differ significantly ($P < 0.05$)

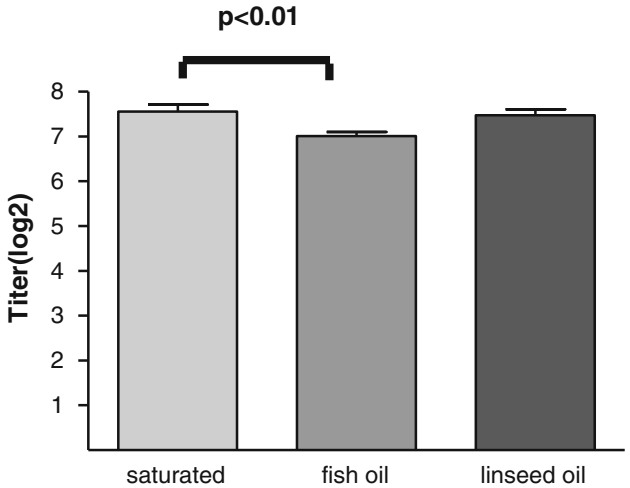

Fig. 1 Levels of OVA-specific antibodies in plasma of 3 weeks old mouse pups of mothers fed either fish oil (*white bars*, $n = 29$), linseed oil (*gray bars*, $n = 21$) or the n-3 PUFA-deficient diet (*black bars*, $n = 24$) during gestation and lactation. Results are shown as titer values (means ± SEM). Mice were immunized within 24 h after birth with OVA solubilized in PBS

Table 5 OVA-specific cytokine production in spleen cell cultures from pups in the different diet groups

	n-3 PUFA-deficient (DEF)	Linseed oil (LSO)	Fish oil (FO)
n	5	5	8
IFNγ (pg/mL)	100 ± 54	149 ± 79	175 ± 67
TNFα (pg/mL)	77 ± 8	80 ± 7	125 ± 17
IL-6 (pg/mL)	1,369 ± 456	1,136 ± 143	766 ± 106
IL-10 (pg/mL)	602 ± 130	688 ± 98	553 ± 67
IL-5 (pg/mL)	151 ± 87	153 ± 84	159 ± 44

Data are given as means ± SEM in *n* pools of spleen cells each obtained from 2 to 3 pups from 4 (DEF), 2 (LSO), and 3 (FO) dams, respectively. Statistical analysis by ANOVA showed no significant differences between the groups

et al. [14] have shown that a high maternal n-3 PUFA intake affected the induction of tolerance against orally administered OVA in neonatal rats, thus also supporting a critical need for n-3 PUFA in the perinatal period. Although the results of these two studies are not

comparable, they both point toward a role of n-3 PUFA in directing the immature immune system towards responses which are considered to be beneficial. Furthermore, our results also support our earlier findings in humans, where intake of fish oil in infancy or milk from fish oil-supplemented mother were associated with an increase in IFNγ-production in ex vivo stimulated blood cells also indicative of a Th1-polarization [9, 10]. As regards the effect of fish oil on allergy development in infancy, some studies suggest a protective role of n-3 LCPUFA [21, 22]. Whether a higher ex vivo IFNγ and a reduction in antigen-specific IgG1 antibodies directly can be compared to human studies on infant allergy is, however, purely speculative.

Not surprisingly we found that the milk gland TAG fatty acid composition was reflecting that of the diet, the PUFA-composition in the pup liver lipid in turn reflected that of the milk and that the tissue phospholipid PUFA-composition reflected that in the liver. Furthermore, the present study showed that the source of dietary n-3 PUFA, plant oil 18:3n-3 or marine n-3 LCPUFA, had only limited influence on the accretion of n-3 LCPUFA in the peripheral tissue, but with more pronounced differences in spleen than in brain. Intake of both fish oil and linseed oil gave rise to an increased incorporation of 22:6n-3 compared to that in the DEF-group, but the 22:6n-3 incorporation was more specific in the FO-group as intake of linseed oil also gave rise to pronounced increases in both 20:5n-3 and 22:5n-3. The accumulation of these intermediate n-3 LCPUFA is in agreement with many previous results and a key issue in the debate on whether intake of 18:3n-3 is an optimal way to fulfill requirements [23]. The difference in brain phospholipid 22-6n-3 content was however only minor, where as that in spleens was more pronounced. Brain phospholipid has been shown to saturate with 22:6n-3 at lower levels of intake than other tissues [24, 25]. The present study did not examine the dose response relationship but only compared the two sources of n-3 PUFA at levels well over levels of deficiency (2.5E% from n-3 PUFA) with that from a DEF (0.01E%, 2E% from n-6 PUFA). The level of 18:3n-3 and 22:5n-3 has been shown to increase in the brains of suckling rat pups when the mothers were fed diets with high compared to low levels of 18:3n-3 [26, 27]. A previous four-generation study in rats that compared incorporation of n-3 PUFA from marine oils with that from plant oils at an overall fat intake of 20 g/100 g (39 E% from fat, hereof around ¼ from n-3 PUFA) also found better n-3 LCPUFA-incorporation in brain PE and PS [28]. One of the strengths of this study is that we used intake levels that are similar to that in ordinary mouse chow (11E% from fat). We were unfortunately not able to get milk samples from the mice and used the fatty acid composition of mammary gland TAG as a proxy to the milk fatty acid composition. Several studies have determined the fatty acid composition of mouse milk after oxytocin injection and milking [25, 29, 30]. Although different dietary regimes were used in these studies the overall reported fatty acid composition of mice milk, including the relative content of the MCFA that are characteristic for milk, was comparable to the milk gland TAG composition in the present study. Most of the milk lipids are TAG, but there is however some phospholipid in milk and we expect these to be enriched in LCPUFA. It is therefore, possible that our results may be an exact estimate of the differences in milk-LCPUFA between the FO- and LSO-group. The levels of 22:6n-3 that we found in the milk glands of these mice and the range that we induce by the dietary changes are comparable to the variation in human milk. The average 22:6n-3 content in human milk in populations with a low fish intake such as the Australian or American is typically around 0.1–0.2% of the fatty acids [1] and has in some Chinese milk been found to be as high as 3.6% [31].

This study showed that maternal fish oil intake was associated with a decrease in plasma concentrations of OVA-induced IgG1in the pups and tended to show a Th1-polarization also in the ex vivo cytokine response to OVA in spleen cells, whereas no immuno-modulating effects were observed after intake of 18:3n-3 from linseed oil. Both types of n-3 PUFA were associated with an increase in milk and tissue n-3 LCPUFA-incorporation, although a slightly lower incorporation of 22:6n-3 was seen after 18:3n-3. Early growth is associated with a high n-3 LCPUFA accretion in the central nervous system and therefore a high requirement of n-3 PUFA. Other tissues may therefore be more susceptible to differences in the n-3 LCPUFA intake during the perinatal period than there are later in life. Since early processes play an important role in the long-term shaping of the immune system, the immune system may be especially vulnerable towards suboptimal intakes during the perinatal period. The acute and potential programming effects of an increased intake of n-3 LCPUFA early in life is not well characterized and this study indicate a need for more thorough investigation especially with respect to their potential effects on the immunological development.

Acknowledgments We acknowledge the late CE Høy, who was involved in the funding and planning of this study. We greatly appreciate the technical help of Karen Jensen, Lillian Vile, Charlotte Vajhøj, and Anni Mehlsen. The study was supported by The Danish Research and Development Program for Food and Technology (FELFO) and Center for Advanced Food Studies (LMC). None of the authors have any conflict of interest to disclose in connection with the submitted material.

References

1. Lauritzen L, Hansen HS, Jørgensen MH, Michaelsen KF (2001) The essentiality of long-chain n-3 fatty acids in relation to

development and function of the brain and retina. Prog Lipid Res 40:1–94
2. Calder PC (2010) The 2008 ESPEN Sir David Cuthbertson lecture: fatty acids and inflammation–from the membrane to the nucleus and from the laboratory bench to the clinic. Clin Nutr 29:5–12
3. Calder PC, Yaqoob P, Thies F, Wallace FA, Miles EA (2001) Fatty acids and lymphocyte functions. Br J Nutr 87(Suppl 1):S31–S48
4. Kremmyda LS, Vlachava M, Noakes PS, Diaper ND, Miles EA, Calder PC (2009) Atopy risk in infants and children in relation to early exposure to fish, oily fish, or long-chain omega-3 fatty acids: a systematic review. Clin Rev Allergy Immunol. doi: 10.1007/s12016-009-8186-2
5. Hanson LA, Korotkova M, Haversen L et al (2002) Breast-feeding, a complex support system for the offspring. Pediatrics Int 44:347–352
6. Garn H, Renz H (2007) Epidemiological and immunological evidence for the hygiene hypothesis. Immunobiol 212:441–452
7. Dunstan JA, Mori TA, Barden A et al (2003) Maternal fish oil supplementation in pregnancy reduces interleukin-13 levels in cord blood of infants at high risk of atopy. Clin Exp Allergy 33:442–448
8. Dunstan JA, Mori TA, Barden A et al (2003) Fish oil supplementation in pregnancy modifies neonatal allergen-specific immune responses and clinical outcomes in infants at high risk of atopy: a randomized, controlled trial. J Allergy Clin Immunol 112:1178–1184
9. Lauritzen L, Kjær TMR, Fruekilde MB, Michaelsen KF, Frøkiær H (2005) Fish oil supplementation of lactating mothers affects cytokine production in 2½-year-old children. Lipids 40:669–676
10. Damsgaard CT, Lauritzen L, Kjær TMR et al (2007) Fish oil supplementation modulates immune function in healthy infants. J Nutr 137:1031–1036
11. Furuhjelm C, Warstedt K, Larsson J et al (2009) Fish oil supplementation in pregnancy and lactation may decrease the risk of infant allergy. Acta Paediatr 98:1461–1467
12. Mihrshahi S, Peat JK, Webb K, Oddy W, Marks GB, Mellis CM (2004) Effect of omega-3 fatty acid concentrations in plasma on symptoms of asthma at 18 months of age. Pediatr Allergy Immunol 15:517–522
13. Rayon JI, Carver JD, Wyble LE et al. (1997) The fatty acid composition of maternal diet affects lung prostaglandin E2 levels and survival from group B streptococcal sepsis in neonatal rat pups. J Nutr 127:1989–1992
14. Korotkova M, Telemo E, Yamashiro Y, Hanson LA, Strandvik B (2004) The ratio of n-6 to n-3 fatty acids in maternal diet influences the induction of neonatal immunological tolerance to ovalbumin. Clin Exp Immunol 137:237–244
15. Aaes-Jørgensen E, Hølmer G (1969) Essential fatty acid-deficient rats. I. growth and testes development. Lipids 4:501–506
16. Folch J, Lees M, Sloane Stanley GH (1957) A simple method for the isolation and purification of total lipids from animal tissues. J Biol Chem 226:497–509
17. Porsgaard T, Høy CE (2000) Lymphatic transport in rats of several dietary fats differing in fatty acid profile and triacylglycerol structure. J Nutr 130:1619–1624
18. Porsgaard T, Xu XB, Gottsche J, Mu HL (2005) Differences in the intramolecular structure of structured oils do not affect pancreatic lipase activity in vitro or the absorption by rats of (n-3) fatty acids. J Nutr 135:1705–1711
19. Morrison WR, Smith LM (1964) Preparation of fatty acid methyl esters+dimethylacetals from lipids with boron fluoride-methanol. J Lipid Res 5:600–608
20. van der Pouw Krann TCTM, Boeije LCM, Smeenk RJT, Wijdenes J, Aarden LA (1995) Prostaglandin-E2 is a potent inhibitor of human interleukin 12 production. J Exp Med 181:775–779
21. Lowe AJ, Thien FCK, Stoney RM et al (2008) Associations between fatty acids in colostrum and breast milk and risk of allergic disease. Clin Exp Allergy 38:1745–1751
22. Giwercman C, Halkjær LB, Jensen SM, Bønnelykke K, Lauritzen L, Bisgaard H (2010) Increased risk of eczema but reduced risk of early wheezy disorder from exclusive breast-feeding in high-risk infants. J Allergy Clin Immunol 125:866–871
23. Gerster H (1998) Can adults adequately convert alpha-linolenic acid (18:3n-3) to eicosapentaenoic acid (20:5n-3) and docosahexaenoic acid (22:6n-3)? Int J Vitam Nutr Res 68:159–173
24. Ward GR, Huang YS, Bobik E et al (1998) Long-chain polyunsaturated fatty acid levels in formulae influence deposition of docosahexaenoic acid and arachidonic acid in brain and red blood cells of artificially reared neonatal rats. J Nutr 128:2473–2487
25. Wainwright PE, Huang YS, Bulmanfleming B et al (1992) The effects of dietary n-3/n-6 ratio on brain-development in the mouse–a dose-response study with long-chain n-3 fatty-acids. Lipids 27:98–103
26. Bowen RAR, Clandinin MT (2005) Maternal dietary 22:6n-3 is more effective than 18:3n-3 in increasing the 22:6n-3 content in phospholipids of glial cells from neonatal rat brain. Br J Nutr 93:601–611
27. Bowen RAR, Clandinin MT (2000) High dietary 18:3n–3 increases the 18:3n–3 but not the 22:6n–3 content in the whole body, brain, skin, epididymal fat pads, and muscles of suckling rat pups. Lipids 35:389–394
28. Jensen MM, Skarsfeldt T, Høy CE (1996) Correlation between level of (n-3) polyunsaturated fatty acids in brain phospholipids and learning ability in rats. A multiple generation study. Biochim Biophys Acta 1300(3):203–209
29. Silverman J, Stone DW, Powers JD (1992) The lipid-composition of milk from mice fed high or low fat diets. Lab Animals 26:127–131
30. Singh K, Hartley DG, McFadden TB, Mackenzie DDS (2004) Dietary fat regulates mammary stearoyl CoA desaturase expression and activity in lactating mice. J Dairy Res 71:1–6
31. Xiang M, Lei S, Li T, Zetterstrom R (1999) Composition of long-chain polyunsaturated fatty acids in human milk and growth of young infants in rural areas of northern China. Acta Pediatr 88:126–131

Lipids (2011) 46:179–187
DOI 10.1007/s11745-010-3512-2

ORIGINAL ARTICLE

Arachidonic Acid Induces Production of 17,20β-Dihydroxy-4-pregnen-3-one (DHP) via a Putative PGE2 Receptor in Fish Follicles from the Eurasian Perch

E. Henrotte · S. Milla · S. N. M. Mandiki · P. Kestemont

Received: 16 August 2010 / Accepted: 19 November 2010 / Published online: 24 December 2010

Abstract The effects of docosahexaenoic, eicosaenoic and arachidonic acids (DHA, EPA and ARA, respectively) on sex-steroid and prostaglandin (PG) production were investigated in Eurasian perch (*Perca fluviatilis*) follicles using an in- vitro incubation technique. Only ARA was able to induce the production of 17,20β-dihydroxy-4-pregnen-3-one (DHP), the hormone produced by vitellogenic follicles undergoing final meiotic maturation, as well as the production of PGE2 and PGF2α by the follicles. This work also investigated, using a preliminary pharmacological approach, the presence of a functional PGE2-like receptor in fish follicles. Exogenous PGE2 and butaprost (specific agonist of the EP2 receptor) stimulated DHP production. A second experiment assayed the cyclic adenosine monophosphate (cAMP) production by the follicles after 24 h of incubation with the agonist and antagonist of the EP2 receptor. As observed in mammals, we concluded that the cAMP produced in response to PGE2 was probably mediated by an intracellular mechanism via a PGE2-like receptor. This is the first pharmacological indication of this type of receptors in fish follicles. This study also indicates that ARA, and its derivatives, PGE2 and PGF2α, may act on final follicle maturation in Eurasian perch.

Keywords Eurasian perch · Follicle · 17,20β-Dihydroxy-4-pregnen-3-one · Prostaglandin receptor · Arachidonic acid

E. Henrotte · S. Milla · S. N. M. Mandiki · P. Kestemont (✉)
University of Namur, Unit of Research in Organismal Biology, 61 rue de Bruxelles, 5000 Namur, Belgium
e-mail: patrick.kestemont@fundp.ac.be

Abbreviations

ARA	Arachidonic acid
cAMP	Cyclic adenosine monophosphate
DHA	Docosahexaenoic acid
DHP	17,20β-Dihydroxy-4-pregnen-3-one
ELISA	Enzyme-linked immunosorbent assay
EPA	Eicosapentaenoic acid
FELASA	Federation of Laboratory Animal Science Associations
GVBD	Germinal vesicle break down
hCG	Human chorionic gonadotropin
MR	Mineralocorticoid receptor
PG	Prostaglandin
PUFA	Polyunsaturated fatty acid(s)
RIA	Radio-immuno assay

Introduction

Currently, difficulties in the supply of high quality eggs and fry are amongst the main constraints in the development of new species in aquaculture [1]. In an effort to improve egg quality and larval survival, attention should be given to establish the best dietary levels of docosahexaenoic acid (DHA), eicosapentaenoic acid (EPA) and arachidonic acid (ARA) for breeders [2]. DHA is particularly important during fish early ontogeny for normal development of neural and visual functions. Henrotte et al. [3] have shown that a high dietary EPA/ARA ratio could induce lower reproductive performances, especially regarding the larval survival and resistance to an osmotic stress in Eurasian perch, *Perca fluviatilis*. ARA is the chief precursor of the eicosanoids, including two-series prostaglandins (PGs).

However, EPA competitively interferes with eicosanoid production from ARA catalyzed by cyclooxygenase and lipoxygenase. In fish as in mammals, eicosanoid production is thus influenced by the cellular ratio of EPA/ARA [4].

Although several studies describe the action of ARA and its derivatives, on follicle ovulation and/or steroidogenesis in vitro in teleosts [5–10], nothing is known about the effects of those molecules on final follicle maturation and ovulation in the Eurasian perch, one of the most promising species for diversification in European inland aquaculture [11]. ARA alone stimulated sex-steroid production via its conversion into PGE2 and by increasing cAMP production in ovary and testis of goldfish *Carassius auratus* [7, 10], while EPA and DHA inhibited gonadotropin-stimulated testosterone production in goldfish and rainbow trout, *Oncorhynchus mykiss* [7]. In the European sea bass, *Dicentrarchus labrax,* ARA induced maturation in a dose- and time-dependent manner, while EPA and DHA were ineffective [9].

In mammals, pharmacological approaches have been used to demonstrate the existence of a variety of prostanoid receptors, which comprise five major subtypes: DP, FP, IP, TP and EP receptors named in accordance with their selectivity for the prostanoids PGD2, PGF2α, PGI2, TXA2 and PGE2, respectively. The actions of PGE2 are mediated by EP receptors comprising four subtypes: EP1, EP2, EP3 and EP4 [12]. Only few studies focused on those receptors in fish. Busby et al. [13] first demonstrated, by a pharmacological approach, the existence of the EP2 receptor in the liver of rockfish, *Sebastes caurinus*, involved in the regulation of glucose metabolism. PGE2, via EP1 and EP2, also interact with the NaCl transport across the opercular epithelium of killifish, *Fundulus heteroclitus* [14]. But there is no information yet on the presence of EP2 or FP receptors in ovarian follicles of fish linked to reproductive processes. In mammals, the effects associated with EP2 and EP4 receptors are considered relaxant and are believed to be associated with a stimulation of adenylate cyclase and an increase in the levels of intracellular cAMP [15, 16]. The role of cAMP in the stimulation of steroid hormone biosynthesis is well-recognized [17] and eicosanoid signal transduction pathways are highly conserved across vertebrate species [18]. Hizaki et al. [19] showed that ovulation was impaired and fertilization dramatically reduced in EP2-deficient mice, leading to the hypothesis that the reproductive failure during early pregnancy in COX-2 deficient mice was due to lack of PGE2 ligands available to bind to the EP2-receptor. Moreover, Narumiya and Fitzgerald [20] concluded thanks to knockout studies in mice that EP2, but not EP1, EP3 or EP4 was associated with reproductive failures. Given the reproductive stimulatory effects of PGs in fish and of PGs/EPs in mammals, one can suppose that such receptor exist in the gonad of fish and exert some positive actions in the final stages of oogenesis including sex-steroid synthesis in relation to cAMP production.

Our objective was to study the impact of polyunsaturated fatty acids (PUFA), and the derivatives of ARA, on sex-steroid and PG production by the Eurasian perch follicle, during the final stages of oogenesis, in order to understand their role on the follicle physiology. The second objective was to evaluate the presence of PGE2-like receptors in this fish species thanks to a pharmacological approach (use of the mammalian EP2 agonist butaprost and EP2 antagonist AH6809). This work was the first to investigate the presence of a PGE2-like receptor in fish ovary linked to the reproductive processes.

Materials and Methods

Research involving animal experimentation were conformed to the principles for the use and care of laboratory animals, in agreement with the Belgian and European regulations on animal welfare (FELASA).

Chemicals

All chemicals and fatty acids were purchased from Sigma–Aldrich (Belgium). Cortland medium was first selected to observe follicle maturational processes in response to a stimulation with hCG 100 UI mL^{-1}. Successful gonadotropin responsiveness of cultured follicles was observed by adapting the media composition, pH and duration of incubation (data not shown). Cortland medium chosen for follicle incubation consisted of the following (g/L): 7.25 NaCl, 0.38 KCl, 0.23 $CaCl_2$ $2H_2O$, 1.00 $NaHCO_3$, 0.41 NaH_2PO_4 H_2O, 0.23 $MgCl_2$ $6H_2O$, 0.23 $MgSO_4$ $7H_2O$, 5.20 Hepes, 1.00 BSA, 0.03 Penicillin and 0.05 Streptomycin, at pH 7.4. ARA, EPA, DHA, butaprost, AH6809 and PGE2 were first dissolved in ethanol and subsequently diluted with Cortland medium to the desired concentration. The final concentrations of ethanol in follicle incubation did not exceed 0.1%. Control incubations contained 0.1% ethanol.

Effect of PUFA and Derivatives on DHP and PG Production during the Final Follicle Maturation

Fish

Three sexually mature Eurasian perch fed with live food were collected in early March 2007 from a cage placed in a culture pond at the University of Namur (Belgium), maintained under natural conditions of temperature and photoperiod. Perch were killed by decapitation on the day

of sampling, and the ovaries were removed and dissected in Cortland medium adjusted to pH 7.4 at 15 °C.

Ovarian Follicle Incubations

The ovaries were dissected into small pieces containing 10–15 prematurational follicles attached to the surrounding extrafollicular tissue. Prematurational stage was defined as post-vitellogenic follicle, with no signs of yolk clarification or lipid droplet coalescence. Eight ovarian pieces per females were placed in triplicates in a 6-well plastic dish (Cellstar, Greiner Bio-One, Belgium) with 3 mL of Cortland medium per well. Follicles were allowed to stabilize at 15 °C for 30 min prior to treatment. All plates were then incubated at 15 °C under intermittent agitation for 48 h. Every 12 h, all from a group of 10–15 follicles of each replicate were treated with an follicle-clearing solution of ethanol:formalin:acetic acid (6:3:1) and examined immediately using an optical microscope to determine the survival of the follicles. A follicle was considered alive when the ooplasm was clear, tainted in light pink and in the center of the follicle, while dead cells were characterized by a grey color, with the outline of the ooplasm being heterogeneous. Survival was 96% after 48 h of follicle incubation, whatever the tested treatment. The media were replaced every 12 h with new experimental media and were placed in test tubes to be stored at −20 °C for a subsequent radioimmunoassay (RIA). Media tested were: ARA, EPA and DHA (100 μM); PGE2 (1, 100 and 1,000 ng mL^{-1}); butaprost (0.1, 1 and 10 μM) for hormone assays.

Hormone Assays

Sex-steroid hormone in culture media was assayed using RIA according to Fostier and Jalabert [21], following two extractions with cyclohexane/ethyl acetate (v/v). Goetz et al. [22] reported that yellow perch (*Perca flavescens*) follicles show first signs of ovulation predictably by approximate 34 h. We decided therefore to assay RIAs in the media after 36 h of incubation. Only 17,20β-dihydroxy-4-pregnen-3-one (DHP) was assayed, due to its important roles in final follicle maturation. The DHP antiserum and tracer were provided by Dr A. Fostier (INRA, Rennes, France). The intra-assay coefficients of variation was 9.60% ($n = 15$ replicates) and the detection limit was at 4–5 pg mL^{-1}.

Follicles were incubated with ARA, EPA or DHA 100 μM in order to assay PGs in the culture media after 36 h. PGE2 and PGF2α from the culture media were first purified on specific minicolumns (RPN 1903, Amersham, Biosciences) following the procedure of the manufacturer. RIA kits for PGE2 and PGF2α were purchased from Izotop (RK-25 M and RK-15 M, Hungary), the intra-assay coefficients of variation were 4.58 and 9.30% for PGE2 and PGF2α, respectively ($n = 15$).

Preliminary Pharmacological Study on the PGE2-Like Receptor

The study of PGE2-receptor was initiated in 2009 and completed in 2010.

Fish

Three sexually mature Eurasian perch were caught from a pond located in the north of France in early March 2009 and in total 12 females from the river Meuse in 2010. Perch were killed by decapitation few days before expected ovulation, and the ovaries were removed and dissected in Cortland medium adjusted to pH 7.4 at 15 °C.

Ovarian Follicle Incubations

Dissection and incubation conditions were performed as described in point 2. In a first set of experiments conducted in 2009, the media tested were: PGE2 (1,100 and 1,000 ng mL^{-1}); EP2 agonist, butaprost (0.1, 1 and 10 μM); EP2 antagonist, AH6809 (0.01, 1 and 10 μM) and the combination of AH6809 (0.01, 1 and 10 μM) with butaprost (1 μM). The incubation duration was 24 h in this set of experiments and the antagonist AH6809 was added 30 min prior to the addition of the agonist butaprost.

In a second set of experiments conducted in 2010, the treatments tested were: (1) PGE2 (1,000 ng mL^{-1}) in combination with AH6809 (1 μM). The antagonist AH6809 was added 30 min or 12 h prior to the addition of the agonist PGE2; (2) only butaprost (1 μM) testing three incubation periods (30 min, 3, 24 h) and the combination of AH6809 (1 μM) with butaprost (1 μM) when the antagonist AH6809 was added 30 min, 3 or 18 h prior to the addition of the agonist butaprost. The final concentrations of ethanol in follicle incubation did not exceed 0.1%.

cAMP Assay

After the incubation, the culture media were frozen to −80 °C and were diluted to 1:20 in 0.1 M HCl the day of the assay. cAMP concentration was quantified in the culture media by ELISA using a cAMP kit (Biovision, Gentaur, Belgium) according to the manufacturer's protocol. This method included an acetylation step which makes the cAMP assay much more sensitive and avoid the interferences of many components in unpurified samples.

Statistical Analysis

From three to eight females were used in these experiments. Measures in the follicle incubations were realized in triplicates for each females. The data were compared between treatments and over the time of incubation by analysis of variance (one-way ANOVA) followed by a Sheffé's test. A Hartley's test was used for homogeneity verification, and parameters that did not fulfill the assumptions of ANOVA were log-transformed before calculations by statistical software (STATISTICA 5.5). The effects of treatments on cAMP production were sometimes tested by a Wilcoxon non-parametric test because the assumption of normality and/of homogeneity of variance were not always obtained despite adequate transformations. Differences were considered significant at $P < 0.05$. Results are given as means ± standard error.

Results

Physiological Effects of PUFA

Ovarian fragments from sexually mature Eurasian perch were incubated with 100 µM ARA, EPA or DHA. ARA was the only FA able to stimulate DHP synthesis (Fig. 1), with DHP levels up to 25-fold higher to values found for DHA and EPA incubations ($P < 0.05$). As observed with DHP, PGE2 and PGF2α production were significantly higher than in controls only with incubation with ARA ($P < 0.05$) (Fig. 2).

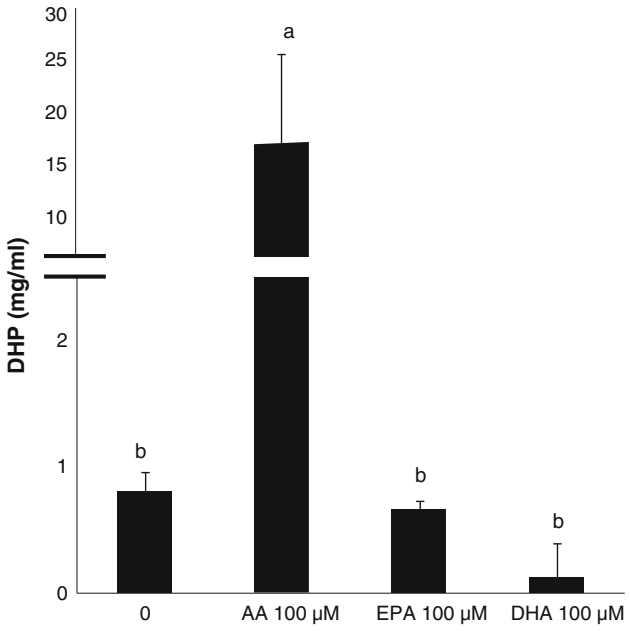

Fig. 1 17,20β-Dihydroxy-4-pregnen-3-one (DHP) levels in the media culture after 36 h of follicle incubation with arachidonic acid (AA), eicosaenoic acid (EPA) and docosahexaenoic acid (DHA) (100 µM). Values are means + SEM ($n = 3$). Significant differences ($P < 0.05$) are indicated with *different letters*

Physiological Effects of Prostaglandin

Follicles were incubated with different doses of PGE2 (1,100 and 1,000 ng mL^{-1}) during 36 h. PGE2 at a concentration of 1,000 ng mL^{-1} provided results comparable to ARA 100 µM in terms of DHP synthesis ($P > 0.05$) (Fig. 3). Nevertheless, due to a high variability, no significant differences were observed in terms of DHP production between the control and the different PGE2 concentrations.

Preliminary Results on the PGE2-Like Receptor

Firstly, one specific EP2 agonist was tested: butaprost (tested at 0.1, 1 and 10 µM). The results showed that DHP

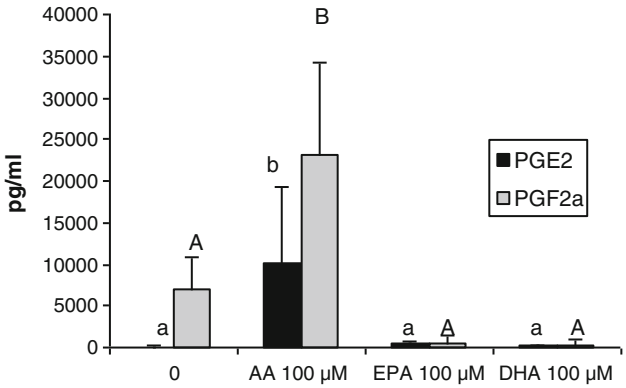

Fig. 2 Effects of arachidonic acid (AA), eicosaenoic acid (EPA) and docosahexaenoic acid (DHA) (100 µM) on the synthesis of PGE2 and PGF2α after 36 h of incubation. Values are means + SEM ($n = 3$). Significant differences ($P < 0.05$) are indicated with *different letters*. *Small letters* concerned PGE2, *capital letters* concerned PGF2α

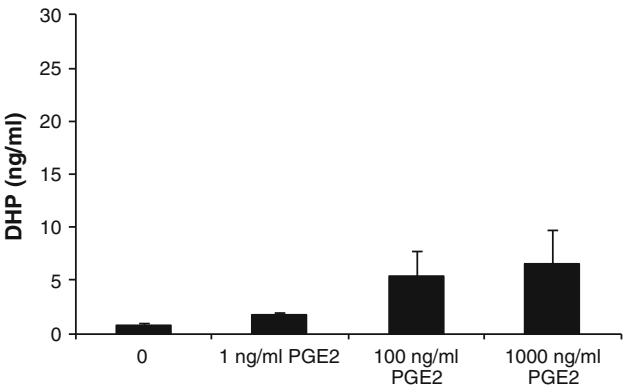

Fig. 3 17,20β-Dihydroxy-4-pregnen-3-one (DHP) levels in the media culture after 36 h of follicle incubation with PGE2 (1,100 and 1,000 ng mL^{-1}). Values are means + SEM ($n = 3$)

synthesis (Fig. 4) was significantly induced by 10 μM butaprost. Thereafter, cAMP production was measured in the media after incubation with PGE2, butaprost and AH6809. Increasing PGE2 or butaprost concentrations in the media increased the cAMP level in a dose-dependent way ($P < 0.05$) (Figs. 5 and 6). Unexpectedly, AH6809 enhanced cAMP production when added alone in the culture media (Fig. 6). But it significantly reduced the cAMP production when added together with butaprost (1 μM), after 30 min of incubation, whatever the antagonist concentration in the first set of experiment, and after 18 h of incubation in the second one (Fig. 8) ($P < 0.05$). During this latter, AH6809 decreased the cAMP production observed with an incubation of follicles with PGE2 1,000 ng mL^{-1}, when it was added 12 h before PGE2 ($P < 0.05$) (Fig. 7). The agonist effect of butaprost was verified by incubating the follicles with this molecule during 30 min, 3 or 24 h (Fig. 8), and the cAMP production was equally stimulated whatever the duration of the incubation period ($P < 0.05$).

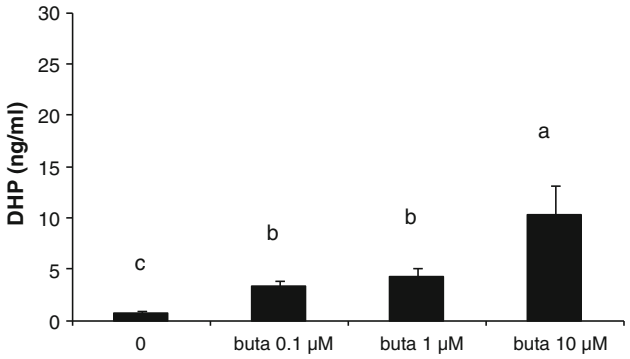

Fig. 4 17,20β-Dihydroxy-4-pregnen-3-one (DHP) levels in the media culture after 36 h of follicle incubation with butaprost (buta) at different concentrations. Values are means + SEM ($n = 3$). Significant differences ($P < 0.05$) are indicated with *different letters*

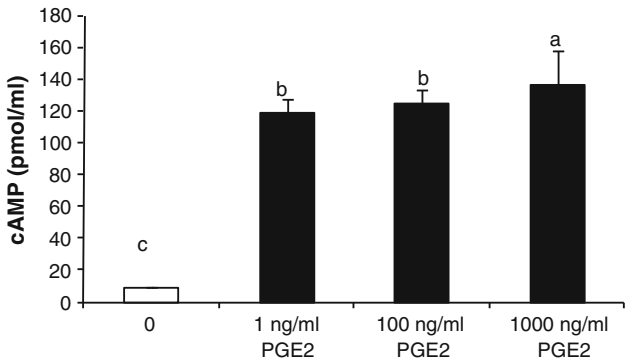

Fig. 5 cAMP levels in the media culture after 24 h of follicle incubation with PGE2 (1,100 and 1,000 ng mL^{-1}). Values are means + SEM ($n = 3$). Significant differences ($P < 0.05$) are indicated with *different letters*

Discussion

Follicle development in fish is divided into the phases of follicle growth and maturation. Vitellogenesis plays an important role in follicle growth and is estradiol-dependent, while the process of follicle maturation is characterized by the initiation of meiosis, migration, and breakdown of the germinal vesicle (GVBD), coalescence of lipid droplets and yolk globules in the cytoplasm, a rapid size increase of the follicle caused by hydration which is accompanied by an overall increase in follicle translucency [1]. In Eurasian perch, DHP seems to be the main steroid involved in the control of this final follicle maturation [23, 24]. Among the tested fatty acids tested in the present study, only ARA seemed to be able to participate in DHP production in vitro in Eurasian perch. Our results are consistent with previous studies on ARA and its metabolites, PGE2 and PGF2α, concerning their effects on steroidogenesis in goldfish [7, 8], European sea bass [9], and Atlantic croaker, *Micropogonias undulates* [6]. Studies on in vitro effects of EPA and DHA on follicle maturation and steroidogenesis are scarce. In the present study, both EPA and DHA were unable to induce the synthesis of DHP by the follicle, indicating that EPA and DHA were probably less active than ARA in participating to the triggering of final follicle maturation in perch. In agreement with this hypothesis, an in vitro study showed that EPA and DHA were ineffective to induce final follicle maturation at all doses tested in a marine teleost, the European sea bass [9]. Moreover, these FAs inhibited gonadotropin-stimulated testosterone production in the goldfish [7]. Thus, EPA and DHA does not appear to be strong regulators of fish follicle maturation and their respective roles in oogenesis are still confused. As EPA and DHA mainly constitute the PUFA composition in Eurasian perch eggs [25], they control the fluidity of membranes and consequently enzymatic activities, linkage between molecules and receptors, cellular interactions and nutrients transports [26]. In consequence, EPA and DHA could play a more energetic and structural role than ARA in fish membranes. Further studies are needed in order to understand the role of those two PUFA in the physiological process of oogenesis in teleosts. In vivo studies consisting in giving different dietary DHA/EPA/ARA ratios to perch breeders showed that fertilization and hatching rates were not influenced by the diets, but larval resistance to an osmotic stress was clearly lower for diets with a high EPA/ARA ratio [3] than in those with low dietary EPA/ARA ratio. High levels of EPA seem to have less impact on follicle maturation in Eurasian perch, but may interfere rather on larval survival.

ARA was the only FA able to stimulate PGE2 and PGF2α production by the follicles via the cyclooxygenase, as already demonstrated in vitro in goldfish by Mercure and

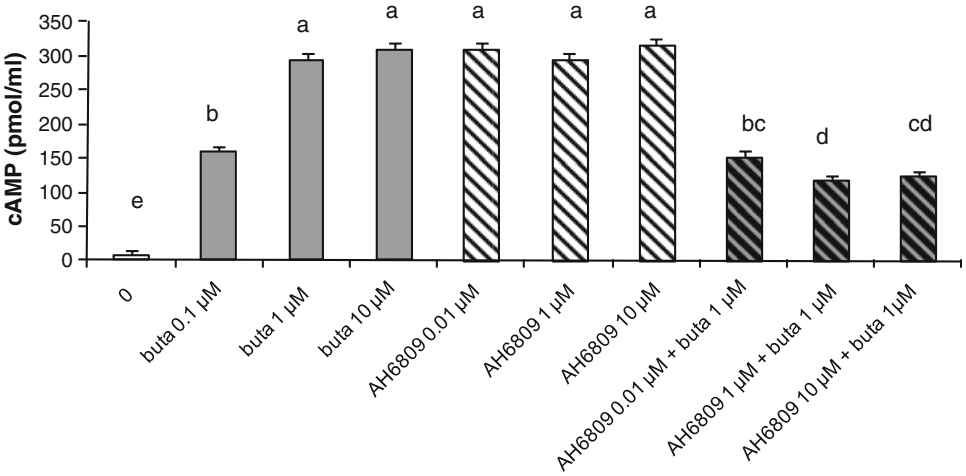

Fig. 6 cAMP levels in the media culture after 24 h of follicle incubation with the agonist of the EP2 receptor, butaprost (buta), with the antagonist of the EP2 receptor, AH6809 (AH), or with agonist and antagonist, at different concentrations. In the case of incubation with both agonist and antagonist, AH6809 was added 30 min before butaprost. Values are means + SEM ($n = 3$). Significant differences ($P < 0.05$) are indicated with *different letters*

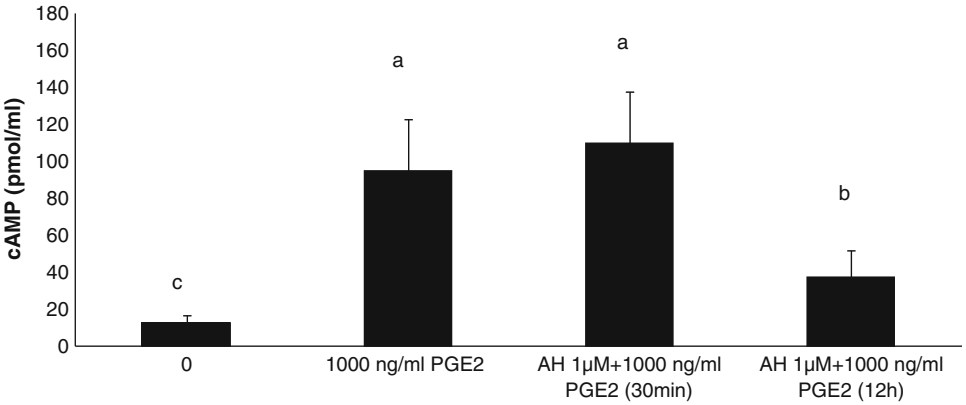

Fig. 7 cAMP levels in the media culture after 24 h of follicle incubation with PGE2 (1,000 ng mL^{-1}) with or without AH6809 (AH, the antagonist). In this case, AH6809 was added 30 min or 12 h before PGE2. Values are means + SEM ($n = 8$). Significant differences ($P < 0.05$) are indicated with *different letters*

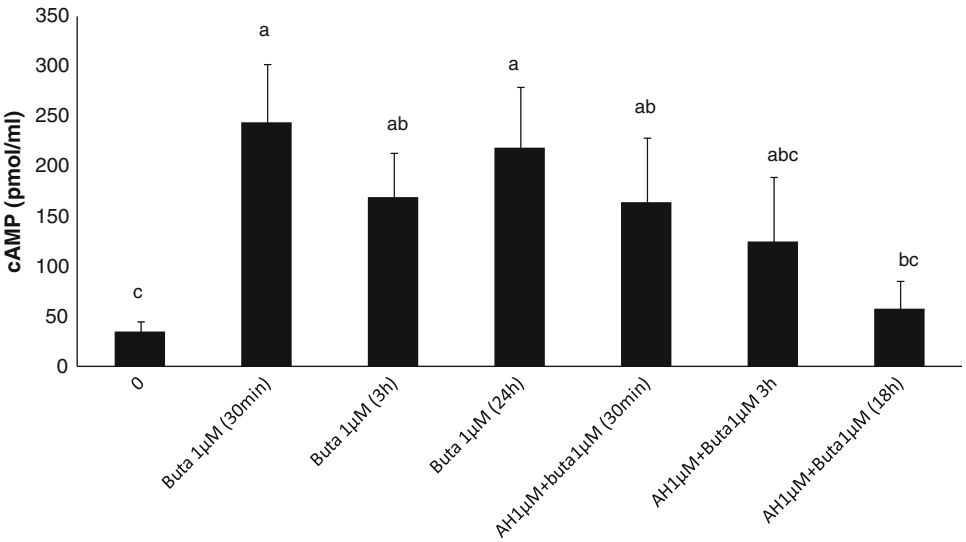

Fig. 8 cAMP levels in the media culture of follicle incubation with an agonist of the EP2 receptor, butaprost (buta, 1 µM) with or without AH6809 (AH, the antagonist). Follicles were incubated with butaprost alone during 30 min, 3 or 24 h. In the case of incubation with butaprost and AH6809, total incubation time was 24 h, and AH6809 was added 30 min, 3 or 18 h before butaprost. Values are means + SEM ($n = 4$). Significant differences ($P < 0.05$) are indicated with *different letters*

Van Der Kraak [8]. This was not surprising since ARA is the chief precursor of PGs from the two-series, not EPA and DHA. In agreement with this, in the present study, it appeared that ARA, but neither EPA and nor DHA, could enhance the follicle final maturation and ovulation, directly or indirectly (via PGE2), by stimulating the synthesis of DHP. PGE2 may also induce DHP production since PGE2 at a concentration of 1,000 ng mL^{-1} provided results comparable to ARA 100 µM. Studies using goldfish testicular tissue treated with PGs of the E-series indicated that they were the most potent stimulators of steroid production when compared to other cyclooxygenase-derived eicosanoids

[10], while lipooxygenase products of ARA metabolism had no effect on this production.

In mammals, ARA may be liberated from phospholipids by a Ca^{++}-dependent process involving phospholipase A2. PGE2 is a major metabolite of ARA synthesized by the cyclooxygenase pathway and regulates uterine functions such as contraction and relaxation of the uterine smooth muscles and the induction of labor [15, 27]. These actions of PGE2 are exerted through its binding to specific receptors on cellular membranes [28]. For example, the EP2 receptor plays critical roles in these processes, especially in ovulation and fertilization, in mice [29, 30]. The effects associated with EP2 and EP4 receptors are believed to be associated with a stimulation of adenylate cyclase and an increase in the levels of intracellular cAMP [31, 32]. In goldfish, ARA and PGE2 stimulated testosterone production in ovarian follicles by increasing cAMP production [7, 10]. From this, we can hypothesize that such type of receptors may exist in fish. Busby et al. (2002) [13] first demonstrated, by a pharmacological approach, the existence of the EP2 receptor in the liver of rockfish, *Sebastes caurinus*, involved in the regulation of glucose metabolism, but there is no information yet on the presence of EP2 receptor in ovarian follicles of fish linked to reproductive processes. In the present study, PGE2 and butaprost, the specific agonist of EP2 receptor in mammals, stimulated DHP synthesis in follicles. Moreover, PGE2 and butaprost both enhanced cAMP production. This is a first indication of PGE2-like receptors involvement in this process. The agonist effect of butaprost on cAMP induction was counteracted in presence of AH6809 when added after 30 min or 18 h of incubation. By contrast, our findings with this antagonist alone are unexpected because AH6809 appeared to be full agonist of the PGE2-like receptor in the absence of butaprost. The reason for this is unclear because AH6809 has been proven to be a specific antagonist of EP2 receptor in ovary of mammals [33, 34]. The agonist comportment of a molecule in fish which is normally considered in mammals as a specific antagonist is not new. For example, Sturm et al. (2005) [35] tested in rainbow trout the specific antagonist of mineralocorticoid receptor (MR), spironolactone, and observed that when the antagonist was tested alone, the transcription activity of MR was enhanced, and the transcription decreased if the antagonist was tested together with the agonist of the receptor (aldosterone). In the present study, as butaprost and PGE2 are less able to further induce cAMP rise in presence of AH6809, we also deduce that the regulation of cAMP by PGE2 implies, at least in part, the PGE2-like receptor transduction pathway in follicles, as observed in mammals. To support this conclusion, both cAMP and DHP production could be stimulated in a concentration-dependent manner by the EP2-selective agonist butaprost, as observed by Harris et al. [36], at least for the cAMP production, in human granulosa-lutein cells. All together, our data thus indicate the presence of PGE2-like receptors (probably including EP2 receptors) in perch ovary. It is the first pharmacological approach of this type of receptor in fish follicles, and further investigations are needed to confirm its existence, for example by using labeled antibodies or by studying the expression of those receptors by PCR analysis. Nevertheless, the failure of the EP2 antagonist AH6809 to completely abolish the cAMP response to butaprost indicates that this agonist may be acting through other receptor subtypes in fish follicles. EP4 is another receptor that could also be implied in those mechanisms, since this receptor is coupled to adenylate cyclase and generate cAMP that activates the protein kinase A signaling pathway [32]. In chicken, EP2 and EP4 were shown to be potently activated by PGE2 in vitro [37]. Otherwise, we can speculate that the level of butaprost used in the present work was in excess and mobilized a part of the available PGE2-like receptors, despite the fact that the antagonist was added more than 30 min before the agonist in the culture media. In mammals, it has been shown also that the affinity of AH6809 for the EP2 receptor was lower than affinity of butaprost [34]. This could explain why there was a remainder of cAMP in the medium when butaprost and AH6809 were added simultaneously. In that way, we observed that the duration of antagonist exposure influences the antagonist effect of AH6809. By contrast, the duration of agonist exposure does not seem to modify the stimulation of cAMP production by butaprost. In rockfish hepatocytes, cAMP production reached a maximum 2 min after PGE2 incubation and then remained high and steady during the 15 first minutes [13]. We can thus suspect significant changes in cAMP production within the first 30 min of agonist exposure of incubation, including a sudden and linear elevation in the first minutes. Finally, follicle incubations with butaprost together with the antagonist, AH6809, were done once in 2009, and another test with time points was done in 2010. Both experiments showed that AH6809 partly counteracted the stimulation of cAMP by PGE2 or butaprost. But the incubation time needed with the antagonist alone before the addition of butaprost, in order to observe such effect, differed in both experiments (30 min in 2009 vs. 18 h in 2010). The fact that the experimental conditions were not exactly the same (meteorology, fish origin,…) certainly explains this difference. The set of time points used in the present study, in order to evaluate the impact of our treatment on the cAMP production, allowed us to study these effects in a short time (30 min) or in a longer time.

In conclusion, the results of the present study confirm that PUFA act on the physiology of the follicle. Especially, ARA, via its conversion to PGE2 and PGF2α, may have a stimulating role in the final follicle maturation, by

enhancing the production of DHP. Moreover, this study allowed the observation of the stimulating and inhibiting effect of the EP2 receptor agonist and antagonist on DHP and cAMP production processes, which indicates the putative presence of PGE2-like receptor in the follicle membrane of Eurasian perch, as observed in mammals. This interaction has to be further studied in the future, and it remains to be determined whether fish follicles have different functional PGE2 receptor subtypes.

Acknowledgments Emilie Henrotte is grant holder of the "Fonds pour la Formation à la Recherche dans l'Industrie et dans l'Agriculture" (FRIA). Thanks are due to Jonathan Poncin, for his valuable help during data collection. The authors would like to express their gratitude to Dr Alexis Fostier for his comments on a first version of the manuscript.

References

1. Bromage NR, Roberts RJ (1995) Broodstock management and egg and larval quality. Blackwell, Oxford, p 424
2. Bell JG, Farndale BM, Ruce MP, Navas JM, Carillo M (1997) Effects of broodstock dietary lipid on fatty acid compositions of eggs from sea bass (*Dicentrarchus labrax*). Aquaculture 149: 107–119
3. Henrotte E, Mandiki SNM, Agbohessi TP, Vandecan M, Mélard C, Kestemont P (2010) Egg and larval quality and egg fatty acid composition of Eurasian perch breeders (*Perca fluviatilis*) fed different dietary DHA/EPA/ARA ratios. Aquacult Res. doi: 10.1111/j.1365-2109.2009.02455.x
4. Sargent J, Henderson RJ, Tocher DR (2002) The lipids. In: Halver JE, Hardy RW (eds) Fish nutrition. Academic Press, Seatle, pp 153–218
5. Goetz FW, Theofan G (1979) In vitro stimulation of germinal vesicle breakdown and ovulation of yellow perch (*Perca flavescens*) oocytes. Effects of 17α-hydroxy-20β-dihydroprogesterone and prostaglandins. Gen Comp Endocrinol 569:273–285
6. Patino R, yoshizaki G, Bolamba D, Thomas P (2003) Role of arachidonic acid and protein kinase C during maturation-inducing hormone-dependent meiotic resumption and ovulation in ovarian follicles of Atlantic Croaker. Biol Reprod 68:516–523
7. Mercure F, Van Der Kraak GJ (1995) Inhibition of gonadotropin-stimulated ovarian steroid production by polyunsaturated fatty acids in teleost fish. Lipids 30:547–554
8. Mercure F, Van Der aak G (1996) Mechanisms of action of free arachidonic acid on ovarian steroid production in the goldfish. Gen Comp Endocrinol 102:130–140
9. Sorbera LA, Asturiano JF, Carrillo M, Zanuy S (2001) Effects of polyunsaturated fatty acids and prostaglandins on oocyte maturation in a marine teleost, the European sea bass (*Dicentrarchus labrax*). Biol Reprod 64:382–389
10. Wade MG, Van Der Kraak GJ (1993) Arachidonic acid and prostaglandin E2 stimulate testosterone production by goldfish testis in vitro. Gen Comp Endocrinol 90:109–118
11. Kestemont P, Mélard C (2000) Aquaculture. In: Craig JF (ed) Percid fishes: systematics, ecology and exploitation. Blackwell, Dunscore, pp 191–224
12. Coleman RA, Smith WL, Narumiya S (1994) International Union of Pharmacology classification of prostanoid receptors: properties, distribution, and structure of the receptors and their subtypes. Pharmacol Rev 46:205–229
13. Busby ER, Cooper GA, Mommsen TP (2002) Novel role for prostaglandin E2 in fish hepatocytes: regulation of glucose metabolism. J Endocrinol 174:137–146
14. Evans DH, Rose RE, Roeser JM, Stidham JD (2004) NaCl transport across the opercular epithelium of *Fundulus heteroclitus* is inhibited by an endothelin to NO, superoxide, and prostanoid signaling axis. Am J Physiol Regul Integr Comp Physiol 286: 560–568
15. Dong YL, Yallampalli C (2000) Pregnancy of exogenous steroid treatments modulate the expression of relaxant EP2 and contractile FP receptors in the rat uterus. Biol Reprod 62:533–539
16. Wathes DC, Abayasekara DRE, Aitken RJ (2007) Polyunsaturated fatty acids in male and female reproduction. Biol Reprod 77:190–201
17. Leung PCK, Wang J (1989) Minireview: the role of inositol lipid metabolism in the ovary. Biol Reprod 40:703–708
18. Lord AM, North TE, Zon LI (2007) Prostaglandin E2 regulates vertebrate haematopoietic stem cells homeostasis. Cell Cycle 6:3054–3057
19. Hizaki H, Segi E, Sugimoto Y, Hirose M, Saji T, Ushikubi F, Matsuoka T, Noda Y, Tanaka T, Yoshido N, Narumiya S, Ishikawa A (1999) Abortive expansion of the cumulus and impaired fertility in mice lacking the prostaglandin receptor subtype EP (2). Proc Natl Acad Sci USA 96:10501–10506
20. Narumiya S, Fitzgerald GA (2001) Genetic and pharmacological analysis of prostanoid receptor function. J Clin Invest 108:25–30
21. Fostier A, Jalabert B (1986) Steroidogenesis in rainbow trout (*Salmo gairdneri*) at various preovulatory stages: changes in plasma hormone levels and in vivo and in vitro response of the ovary to salmon gonadotropin. Fish Physiol Biochem 2:87–89
22. Goetz FW, Duman P, Berndtson AK, Janowsky EG (1989) The role of prostaglandins in the control of ovulation in yellow perch (*Perca flavescens*). Fish Physiol Biochem 7:163–168
23. Nagahama Y (1987) 17α,20β-dihydroxy-4-pregnen-3-one: a teleost maturation-inducing hormone. Dev Growth Differ 29:1–12
24. Migaud H, Mandiki R, Gardeur J-N, Fostier A, Kestemont P, Fontaine P (2003) Synthesis of sex steroids in final oocyte maturation and induced ovulation in female Eurasian perch, *Perca fluviatilis*. Aquat Living Resour 16:380–388
25. Henrotte E, Lynne Overton J, Kestemont P (2008) Effects of dietary n-3 and n-6 fatty acids levels on egg and larval quality of Eurasian perch. Cybium 32:271–272
26. Breton J-C (1988) Triglycérides d'acides gras à chaîne moyenne. In: Douste-Blazy L, Mendy F (eds) Biologie des lipides chez l'homme, de la physiologie à la pathologie. Editions médicales internationales, Paris, pp 5–16
27. MacKenzie IZ, Castle BM, Mountford L, Ferguson L, Brennecke S, Embrey MP (1987) Prostaglandin release from preparations used vaginally for the induction of labor. Prostaglandins 34: 939–946
28. Adelantado JM, Lopez Bernal A, Turnbull AC (1998) Topographical distribution of prostaglandin E receptors in human myometrium. Br J Obstet Gynecol 95:348–353
29. Kennedy CRJ, Zhang Y, Brandon S, Guan Y, Coffee K, Funk CD, Magnuson MA, Oates JA, Breyer MD, Breyer RM (1999) Salt-sensitive hypertension and reduced fertility in mice lacking the prostaglandin EP2 receptor. Nat Med 5:217–220
30. Segi E, Sugimoto Y, Tsuji M, Tsunekawa H, Tamba S, Tsuboi K, Tanaka S, Ichikawa A (2003) Expression of messenger RNA for prostaglandin E receptor subtypes EP4/EP2 and cyclooxygenase isozymes in mouse preovulatory follicles and oviducts during superovulation. Biol Reprod 68:804–811
31. Negishi M, Sugimoto Y, Ichikawa A (1995) Molecular mechanisms of diverse actions of prostanoid receptors. Biochim Biophys Acta 1259:109–120

32. Arosh JA, Parent J, Chapdeleine P, Sirois J, Fortier MA (2002) Expression of cyclooxygenases 1 and 2 and prostaglandin E synthase in bovine endometrial tissue during the estrous cycle. Biol Reprod 67:161–169
33. Senior J, Sangha R, Baxter GS, Marshall K, Clayton JK (1992) In vitro characterization of prostanoid FP-, DP-, IP- and TP- receptors in the non-pregnant human myometrium. Br J Pharmacol 107:215–221
34. Tsuboi K, Sugimoto Y, Ichikawa A (2002) Prostanoid receptor subtypes. Prostag other Lipid Mediat 68–69:535–556
35. Sturm A, Bury N, Dengreville L, Fagart J, Flouriot G, Rafestin-Oblin ME, Prunet P (2005) 11-deoxycorticosterone is a potent agonist of the rainbow trout (*Oncorhynchus mykiss*) mineralocorticoid receptor. Endocrinology 146:47–55
36. Harris TE, Squires PE, Michael AE, Bernal AL, Abayasekara DR (2001) Human granulosa-lutein cells express functional EP1 and EP2 prostaglandin receptors. Biochem Biophys Res Commun 285:1089–1094

Lipids (2011) 46:189–199
DOI 10.1007/s11745-010-3521-1

ORIGINAL ARTICLE

Insulin Stimulates Lipogenesis and Attenuates Beta-Oxidation in White Adipose Tissue of Fed Rainbow Trout

S. Polakof · F. Médale · L. Larroquet · C. Vachot · G. Corraze · S. Panserat

Received: 23 September 2010 / Accepted: 20 December 2010 / Published online: 15 January 2011

Abstract As lipid deposition tissue in fish, the white adipose tissue (WAT) has important functions related to reproduction and the challenges of long-term fasting. In the study reported here, we infused fish fed a high-carbohydrate diet with two doses of insulin for 5 days in order to explore the effects of this hormone on lipogenesis and beta-oxidation-related enzymes. We demonstrated the presence of some of the main lipogenic enzymes at molecular, protein and activity levels (ATP-citrate lyase and fatty acid synthase). However, while ATP-citrate lyase was unexpectedly down-regulated, fatty acid synthase was up-regulated (at protein and activity levels) in an insulin dose-dependent manner. The main enzymes acting as NADPH donors for lipogenesis were also characterized at biochemical and molecular levels, although there was no evidence of their regulation by insulin. On the other hand, lipid oxidation potential was found in this tissue through the measurement of gene expression of enzymes involved in β-oxidation, highlighting two carnitine palmitoyltransferase isoforms, both down-regulated by insulin infusion. We found that insulin acts as an important regulator of trout WAT lipid metabolism, inducing the final stage of lipogenesis at molecular, protein and enzyme activity levels and suppressing β-oxidation at least at a molecular level. These results suggest that WAT in fish may have a role that is important not only as a lipid deposition tissue but also as a lipogenic organ (with possible involvement in glucose homeostasis) that could also be able to utilize the lipids stored as a local energy source.

Keywords Insulin · Fish · Dietary carbohydrates · White adipose tissue · Lipogenesis · Lipid oxidation

Abbreviations

6PGDH	6-Phosphogluconate dehydrogenase
ACLY	ATP citrate lyase
CPT	Carnitine palmitoyltransferase
EF1α	Elongation factor 1 alpha
FFA	Free fatty acids
G6PDH	Glucose 6-phosphate dehydrogenase
HOAD	3-Hydroxyacyl-CoA dehydrogenase
HSL	Hormone-sensitive lipase
ICDH	Isocitrate dehydrogenase
LPL	Lipoprotein lipase
ME	Malic enzyme
NAPDH	Nicotine adenine dinucleotide phosphate, reduced
TAG	Triacylglycerols
TNF	Tumor necrosis factor-alpha
WAT	White adipose tissue

Introduction

White adipose tissue (WAT) has a role in energy storage and as insulation from environmental temperature and trauma, storing lipids in the form of triacylglycerols (TAG)

S. Polakof (✉) · F. Médale · L. Larroquet · C. Vachot · G. Corraze · S. Panserat
INRA, UMR1067 Nutrition Aquaculture et Génomique, Pôle d'hydrobiologie, CD918, 64310 Saint-Pée-sur-Nivelle, France
e-mail: spolakof@st-pee.inra.fr

S. Polakof
Laboratorio de Fisioloxía Animal, Departamento de Bioloxía Funcional e Ciencias da Saúde, Facultade de Bioloxía, Universidade de Vigo, 36310 Vigo, Spain

and in mobilizing them via breakdown into free fatty acids (FFA) and glycerol [1]. In mammals, several studies have been able to document the presence of lipogenic enzymes and the conversion of glucose into fat in insulin-stimulated adipocytes [2], although very little is known about WAT lipid oxidation capacities [3]. FFA originating from dietary intake or de novo synthesis are stored as TAG. With its storage capacity and its ability to hydrolyze TAG, WAT provides a FFA buffering system for other organs [4].

WAT is one of the most important lipid stores in several teleosts, although the liver and muscle also constitute lipid storage organs in some species [5]. In salmonids, WAT is distributed primarily in the abdominal cavity, in association with the mesenteric and pyloric caeca [6]. In fish, as in mammals, the development of WAT and accumulation of lipids is a continuous process that depends on nutritional [7, 8] and reproductive status [9]. The WAT provides capital for fish reproduction [10] as well as for the challenges of long-term fasting [7].

As the enzymatic machinery responsible for lipid mobilization and deposition in fish, WAT is similar to that found in mammals [6], and both lipoprotein lipase (LPL) [11, 12] and hormone-sensitive lipase (HSL) [13, 14] have been characterized. However, other aspects of lipid metabolism such as the lipogenic and lipid oxidation potential have not been fully explored in fish WAT. Early studies have shown the presence of lipogenic enzyme activities in visceral fat in the eel [15], channel catfish [16] and coho salmon [17]. More recent studies have also investigated the presence of NADPH-donor enzymes involved in lipogenesis in gilthead seabream [18]. However, on the basis of findings in the rainbow trout, in which the liver accounts for more TAG synthesis than the adipose tissue [19], and the lower levels of lipogenic enzyme activity in WAT present in coho salmon [17], Henderson and Sargent [20] proposed a minor role for WAT in the whole fish lipogenic potential. The lipid oxidation capacities of fish WAT are poorly understood, although β-oxidation was recently reported to be regulated by different fatty acids in vivo [21] and in vitro [22] in Atlantic salmon. Functional data are scarce, and only gene expression of carnitine palmitoyltransferase (CPT) has been described in the WAT of rainbow trout [23] and salmon [24], while no expression was found in gilthead seabream [25]. Other enzymes involved in lipid oxidation are also expressed in salmon WAT, including acyl-CoA oxidase and acyl-CoA dehydrogenase, although they are not regulated by the nature of the oil present in the feed [24].

Lipid metabolism in fish WAT is regulated by several endocrine factors, such as insulin, GH and somatolactin, [26], glucagon [27] and norepinephrine [28], and also by other factors such as TNF-α [13, 29]. Clearly, most of the studies on endocrine control of lipid metabolism in fish WAT have been focused on the insulin action [12, 27, 30, 31]. Unfortunately, all these studies were carried out in order to understand the regulation of key enzymes involved in lipid storage and mobilization such as LPL and HSL (see above), and no information about hormone control of lipogenesis or lipid oxidation is available for fish WAT. On the other hand, insulin action on other tissues such as the liver and white skeletal muscle has been widely studied, with the predominant lipogenic and anti-lipolytic action of this hormone [30, 32]. We recently reported similar results at the molecular level in fasted rainbow trout infused with bovine insulin for 4 days [33], although details regarding the WAT were not available in that study. Insulin receptors have also been studied in rainbow trout WAT, showing the first evidence of insulin regulation of lipid metabolism in this tissue [34].

In order to characterize the lipogenic potential and its regulation by insulin in fish WAT, rainbow trout were infused with two different doses of bovine insulin for 5 days. We assessed two of the main enzymes involved in lipogenesis at enzymatic, protein and molecular levels (ACLY (ATP citrate lyase) and FAS (fatty acid synthase)) as well as the main enzymes acting as NADPH donors, including 6PGDH (6-phosphogluconate dehydrogenase), G6PDH (glucose 6-phosphate dehydrogenase), ICDH (isocitrate dehydrogenase) and ME (malic enzyme). RNA levels of two enzymes involved in lipid oxidation were also assessed, including HOAD (hydroxyacyl-CoA dehydrogenase) and CPT-1 isoforms. WAT insulin sensitivity was studied on the basis of the phosphorylation status of Akt, and fish were fed a high carbohydrate diet in order to counteract the insulin-induced hypoglycemia caused by the pump infusion [35] and to induce lipogenesis, as in other fish tissues [16, 36–38].

Materials and Methods

Fish

Rainbow trout (*Oncorhynchus mykiss* Walbaum) were obtained from the INRA experimental fish farm facilities of Donzacq (Landes, France). Fish were maintained in tanks with well-aerated water at 17 °C and a controlled photoperiod (LD12:12), and fed a standard trout commercial diet during the acclimatization period (T-3P classic, Trouw, France). Fish weight was 200 ± 10 g. The experiments were conducted in accordance with the Guidelines of the National Legislation on Animal Care of the French Ministry of Research (Decret N° 2001-464, May 29, 2001) and were approved by the Ethics Committee of INRA (according to INRA 2002-36, April 14, 2002).

Experimental Protocols

For sustained hormone infusions, fish were food-deprived for 48 h and then implanted with 1003D Alzet® mini-osmotic pumps (Alza, USA) containing either saline (control, $n = 6$) or bovine insulin solution at two different concentrations ($n = 6$) ($\sim$27 units/mg; Sigma Chemical Co.). Fish were first anesthetized and weighed, and pumps were then inserted into the peritoneal cavity through a 1.0-cm incision made in the ventral midline at ca. 2.0 cm rostral of the pelvic fins. The incision was closed with one stitch and an antibiotic gel was applied topically to the incision area. Pumps were implanted in the morning and fish were allowed to recover. The next morning (24 h later), fish were fed a diet containing a high-level of carbohydrate (30% dextrin, 57% fish meal and 10% fish oil) for 5 days and sampled 6 h after their last meal. Pump flow rate was established at 0.39 µl h^{-1}, which at 17 °C should provide sustained release of 0.35 (Ins1x) or 0.7 (Ins2x) IU kg^{-1} day^{-1} insulin for 11 days. The doses chosen were based on previous studies carried out in fasted rainbow trout [35, 39].

Tissue and Blood Sampling

Trout were sacrificed by a sharp blow on the head. Blood was removed from the caudal vessels and centrifuged (3,000*g*, 5 min); the plasma recovered was immediately frozen and kept at −20 °C pending analyses. Gut content of each fish was systematically checked to confirm that the fish sampled had in fact consumed the diet. The perivisceral WAT was collected and frozen in liquid nitrogen and kept at −80 °C pending analyses.

Molecular and Biochemical Analyses

Plasma glucose (Biomérieux, France), triglycerides (Biomérieux, France) and FFA (Wako Chemicals GmbH, Germany) levels were determined using commercial kits adapted to a microplate format. Bovine insulin levels were measured using a bovine-specific commercial ELISA kit (Mercodia, Sweden) as in [35].

Tissue mRNA levels of proteins involved in lipid metabolism were determined by real-time quantitative RT-PCR (q-PCR) [33]. The transcripts assessed FAS, G6PDH, ACLY, HOAD, CPTIA, CPTIB, CPTIC, CPTID, ME, 6PGDH and ICDH. Primers (Table 1) were designed to overlap an intron where possible (Primer3 software) using known sequences found in trout nucleotide databases (Genbank and INRA-Sigenae) as previously described [33]. Quantification of the target gene transcript level was performed using *ef1α* gene expression as reference [40], which was found to be stable in this study. Quantification of the target gene transcript in relation to the *ef1α* reference gene transcript was performed following the Pfaffl method [40].

Protein extraction (20 µg) and Western blotting were undertaken using anti-phospho-Akt Ser^{473} (Cell Signaling Technology), anti-FAS (Santa Cruz Biotechnology), anti-β-tubulin (Cell Signaling Technology) and anti-ACLY (Cell Signaling Technology) against human proteins.

Tissue used to assess enzyme activities was homogenized with 10 vol of ice-cold buffer consisting of 20 mmol l^{-1} Tris

Table 1 Sequences of the primer pairs used for real-time quantitative PCR determination of the transcript levels of several rainbow trout genes involved in lipid metabolism

Gene	5′–3′ forward primer	5′–3′ reverse primer	Annealing temperature (°C)
ACLY	CTGAAGCCCAGACAAGGAAG	CAGATTGGAGGCCAAGATGT	60
FAS	GAGACCTAGTGGAGGCTGTC	TCTTGTTGATGGTGAGCTGT	59
G6PDH	CTCATGGTCCTCAGGTTTG	AGAGAGCATCTGGAGCAAGT	59
6PGDH	ATGCCAGGGGGACACAAAGA	CAAAAGCCTGTGCCATCACG	60
ICDH	GACAGCACCAACAGGGCAA	AAGCCAGCCTCGATGGTCTC	59
ME	TACGTGCGGTGTGTGTGACG	GTGCCCACATCCAGCATGAC	60
CPT1A	TCGATTTTCAAGGGTCTTCG	CACAACGATCAGCAAACTGG	55
CPT1B	CCCTAAGCAAAAAGGGTCTTCA	CATGATGTCACTCCCGACAG	55
CPT1C	CGCTTCAAGAATGGGGTGAT	CAACCACCTGCTGTTTCTCA	59
CPT1D	CCGTTCCTAACAGAGGTGCT	ACACTCCGTAGCCATCGTCT	59
HOAD	GGACAAAGTGGCACCAGCAC	GGGACGGGGTTGAAGAAGTG	59
EF1α	TCCTCTTGGTCGTTTCGCTG	ACCCGAGGGACATCCTGTG	59

ACLY ATP citrate lyase, *FAS* fatty acid synthase, *G6PDH* glucose 6-phosphate dehydrogenase, *6PGDH* 6-phosphogluconate dehydrogenase, *ICDH* isocitrate dehydrogenase, *ME* malic enzyme, *CPT* carnitine palmitoyltransferase, *HOAD* 3-hydroxyacyl-CoA dehydrogenase, *EF1-α* elongation factor-alpha

(pH 7.4), 250 mM sucrose, 2 mmol l^{-1} EDTA, 10 mmol l^{-1} β-mercaptoethanol, 100 mM NaF and 0.5 mM EDTA. The homogenate was centrifuged for 20 min at 17,000*g* and the supernatant was used immediately for enzyme assays at 37 °C in pre-established conditions. HOAD was assessed as in [41], while G6PDH (final substrate concentration 0.5 mM glucose-6-phosphate) and FAS (final substrate concentration 50 μM malonyl-CoA) were assessed following the method described by Figueiredo-Silva et al. [42] adapted to trout tissues. ME, ICDH and 6PGDH were assessed as in [43], adapting the conditions to the WAT. ACLY activity was determined as in [44]. Levels of enzyme activity are expressed in terms of mg protein. Protein concentration was determined using a Bradford protein assay kit (Bio-Rad, Germany) with BSA as standard.

Statistical Analysis

The results are expressed as means ± SEM ($n = 6$). Data were analyzed by one-way ANOVA. When necessary, data were log-transformed to fulfill the conditions of the analysis of variance. Post-hoc comparisons were made using a Student–Newman–Keuls test, and differences were considered statistically significant at $P < 0.05$.

Results

Plasma triglyceride levels (Fig. 1a) were unaffected by the insulin infusion. In contrast, FFA levels in plasma (Fig. 1b) were reduced after the insulin infusion regardless of the dose. Bovine insulin levels were constant in all trout with insulin pumps, averaging 3.11 ± 0.34 and 6.36 ± 0.65 ng ml^{-1} for 1x and 2x, respectively. Plasma glucose levels were lower than in the controls in the Ins1x group (7.67 ± 0.42 mM), while glycemia was similar in the Ins2x group (9.02 ± 0.44 mM) to the saline-infused group (9.08 ± 0.42 mM).

The phosphorylation status of Akt (at Ser^{473}) is shown in Fig. 2. A twofold increase in phosphorylation of the kinase was observed when fish were infused with the higher insulin dose when compared with the saline-treated fish.

ACLY and FAS enzyme activity and protein and mRNA transcript levels are shown in Fig. 3. ACLY in particular was affected by insulin at the protein level, with lower levels in fish infused with either insulin dose than in the control group. In contrast, mRNA levels were only reduced with the Ins1x dose, while activity was down-regulated by the higher insulin dose. The main differences were found at the protein level, since insulin was able to reduce ACLY levels by more than 50%. In this study FAS was positively affected by insulin infusion at activity, protein and gene expression levels. The effect on activity was dose dependent, while

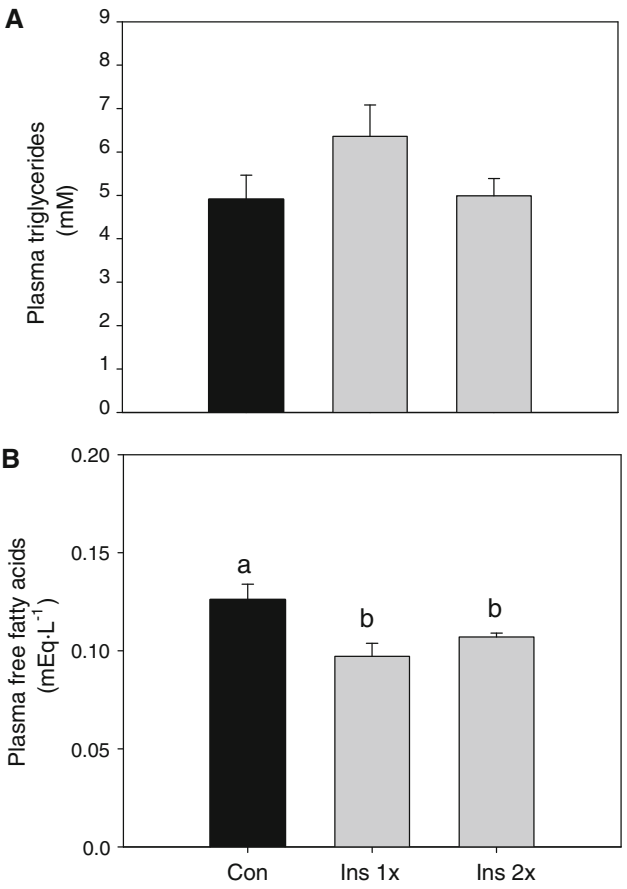

Fig. 1 Plasma triglyceride (**a**) and free fatty acid (**b**) levels in rainbow trout fed a carbohydrate-enriched diet and sacrificed 6 h after the last meal. Fish were implanted with pumps containing saline (control) or two insulin doses: Ins1x (0.35 IU kg^{-1} day^{-1}) and Ins2x (0.7 IU kg^{-1} day^{-1}) and then fed for 5 days. Results are expressed as means ± SEM ($n = 6$) and were analyzed by one-way ANOVA followed by Student–Newman–Keuls multiple comparison test. *Different letters* indicate significant differences among groups ($P < 0.05$)

mRNA levels were less affected. Protein FAS levels were increased up to fourfold when insulin was infused (regardless of the dose infused). On the other hand, WAT FAS activity (0.32–0.97 mU mg^{-1} protein = 4–11 mU g^{-1} tissue) was higher than in other studies involving fish liver [38, 41], although lower than in liver samples from the present study, ranging from 0.25 to 1 mU mg^{-1} protein = 29–86 mU g^{-1} tissue.

Changes in enzyme activity and mRNA levels of proteins acting as NADPH donors are shown in Fig. 4. The four enzymes studied were affected by insulin in different ways: no changes in 6PGDH or ICDH were found at either biochemical or molecular levels. G6PDH mRNA levels were reduced only with the Ins1x dose, with no impact on activity, which remained unchanged by the treatments. Finally, ME mRNA levels increased 2-fold when the Ins2x dose was infused in comparison with the control group.

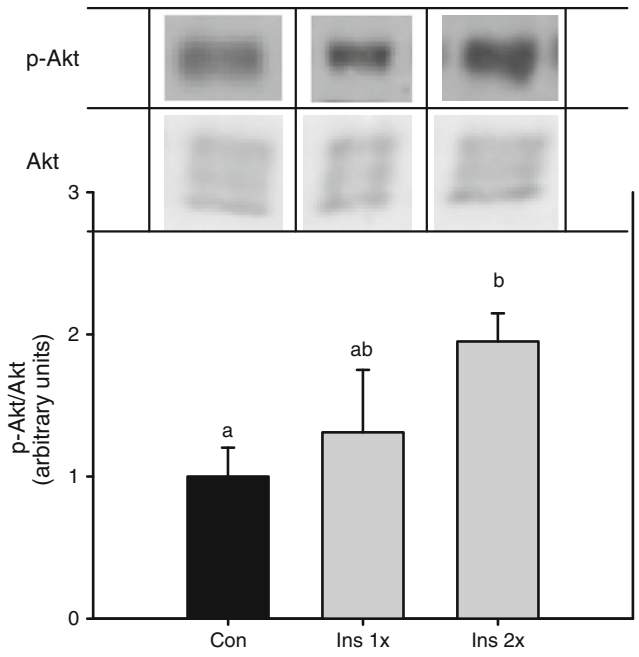

Fig. 2 Effects of insulin infusion (5 days) on WAT Akt phosphorylation status (Western blot analysis) in trout fed a high carbohydrate diet. Gels were loaded with 20 μg total protein per lane. Protein and phosphorylation levels were normalized to total tissue Akt levels and are indicated as fold-change compared with the saline-treated group. Results are expressed as means ± SEM ($n = 6$) and were analyzed by one-way ANOVA followed by Student–Newman–Keuls comparison test. *Different letters* indicate significant differences among groups ($P < 0.05$)

These changes were not followed by enzyme activity, that showed higher levels than the control group only when fish were infused with the Ins1x dose.

mRNA levels of the main enzymes involved in β-oxidation are presented in Fig. 5. No changes were observed in mRNA levels of HOAD. However, the different isoforms of CPT were regulated by insulin. No significant expression was found for CPT1A or CPT1B (data not shown). In contrast, the mRNA levels for CPT1C and D were affected by the treatment, an effect that was particularly clear in the latter isoform, responding to both insulin doses, while in the former reduced mRNA levels were found only with the Ins1x dose.

Discussion

The effects of insulin on fish WAT lipid metabolism are little known and, although the storage of TAG has been demonstrated, the lipogenic role of this tissue has been traditionally considered as minor compared with that of the liver [30]. In the present study we confirmed the presence of the main enzymes responsible for de novo lipid synthesis at a biochemical level in fish, and demonstrated important findings at both protein and molecular levels. We also present original findings showing the molecular expression of key enzymes involved in the β-oxidation of lipids in the WAT.

Insulin Effects on Plasma Parameters and Sensitivity of White Adipose Tissue

The main and well known effect of insulin in fish lipid metabolism is to decrease FFA levels in plasma (reviewed by [32]). The reduced levels of plasma FFA in our study confirm this insulin action as well as the physiological effects of insulin dose as applied in this experiment. Further confirmation of insulin action can be demonstrated by plasma glycemia and the phosphorylation status of a key protein in the insulin signalling pathway, such as Akt. In our study, Akt phosphorylation in the WAT was increased with the higher insulin dose, providing supporting evidence of insulin sensitivity of this tissue in the trout, as previously demonstrated by other authors [34, 45]. Bouraoui et al. (2010) [45] demonstrated the involvement of insulin in the development of adipocytes and also in glucose metabolism. The fact that Akt phosphorylation status can be significantly affected by insulin in vivo, as in the present study, confirms that insulin can activate its own signalling pathway in this tissue, suggesting an important role in WAT metabolism. It was recently demonstrated in rat adipocytes that Akt activity is required for the effects of insulin on lipid metabolism [46]. In this model, Akt was essential in the antilipolytic action of insulin and, when inhibited, the lipogenic role of insulin was counteracted. We can therefore hypothesize that the insulin-induced Akt phosphorylation in this fish model could be related to both increased lipogenic and decreased lipid oxidation potential in the WAT of rainbow trout, as discussed below.

Lipogenesis in White Adipose Tissue

Carbohydrates consumed in excess of energy requirements and of hepatic glycogen storage capacity must be converted into lipids for subsequent storage. De novo lipogenesis is the metabolic pathway that synthesizes fatty acids from excess carbohydrates to be incorporated into TAG for energy storage. In mammals the WAT is the main lipid-storing tissue [47], while in fish the liver has been traditionally considered as the main tissue responsible for lipogenesis [17, 20]. Due to this minor role in lipogenesis, this pathway has been little studied in fish WAT and therefore very little information is available in the literature.

Enzymes central to the process of lipogenesis are those that catalyze fatty acid biosynthesis, i.e. ACC, FAS and ACLY, which is involved in the transfer of acetyl-coenzyme A (acetyl-CoA) from the mitochondrion to the cytosol,

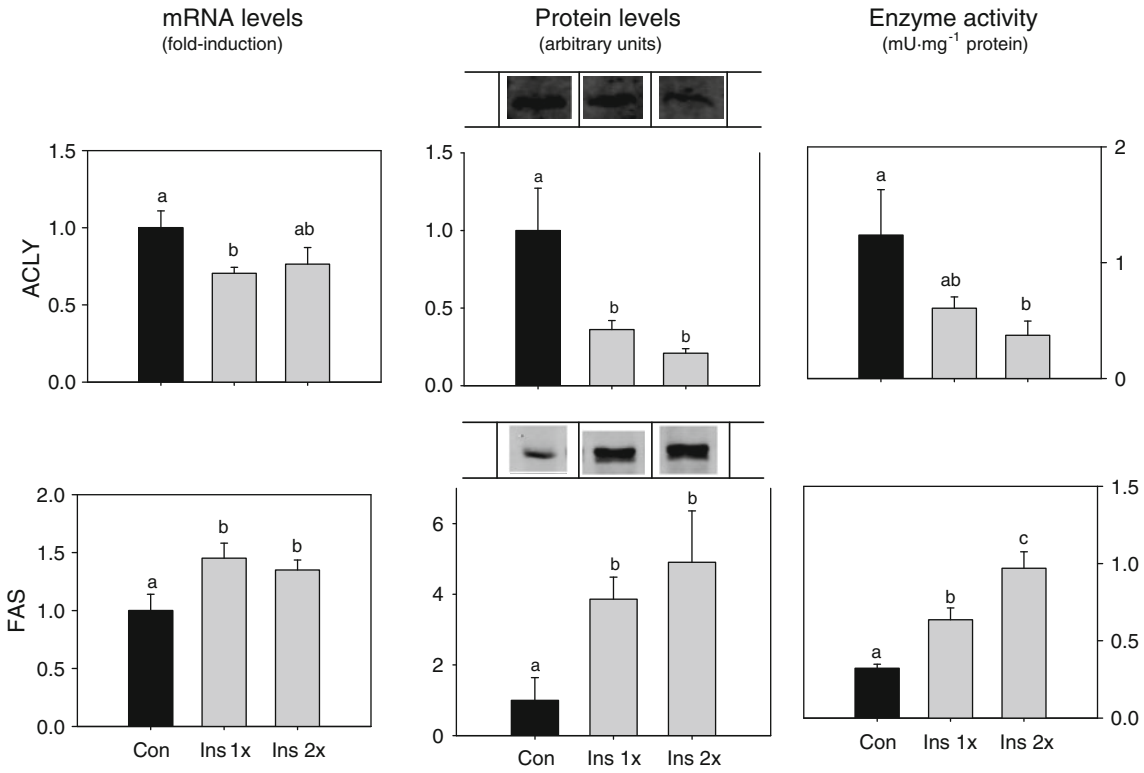

Fig. 3 Effects of insulin infusion (5 days) on ATP-citrate lyase (ACLY) and fatty acid synthase (FAS) mRNA levels, protein levels and levels of enzyme activity in WAT of trout fed a high-carbohydrate diet. mRNA levels were estimated using real-time RT-PCR. Expression levels were normalized to elongation factor 1α (EF1α)-expressed transcripts which did not change under the experimental conditions and are presented as fold-change against the saline solution-treated group set at 1. Enzyme activity units (mIU) are defined as nmol of substrate converted to product, per min, at 37 °C, were expressed/mg protein. Protein (20 μg per lane) and phosphorylation levels were normalized to tissue β-tubulin levels and are indicated as fold-change compared with the saline-treated group. Results are presented as means ± SEM ($n = 6$) and were analyzed by one-way ANOVA followed by Student–Newman–Keuls comparison test. *Different letters* indicate significant differences among groups ($P < 0.05$). More details in Fig. 1

where fatty acid synthesis occurs [48]. ACLY has only been described previously in coho salmon WAT, although its activity was unaffected by different diets [17]. In the present study ACLY was inhibited by insulin, especially at the protein level. This is the first time that this enzyme has been fully characterized in fish WAT. Insulin regulation of ACLY in mammals is not fully understood, and although this hormone is able to stimulate lipogenesis in rat adipocytes, ACLY activity and mRNA levels are often unaffected [49, 50]. Although intriguing, our results are not surprising in view of the fact that in other lipogenic tissue in the trout (the liver) ACLY is not regulated at the molecular level by either nutritional status [51] or insulin [33]. In fact, the inhibition of ACLY by insulin in the trout shows that this step of lipogenesis in fish WAT is regulated in a different way from that described in mammals. In mammals ACLY is phosphorylated by Akt into serine 455, abolishing the homotropic allosteric regulation by citrate and enhancing the catalytic activity of the enzyme [52]. This differential level of regulation compared to the mammalian model is further supported by the increased Akt phosphorylation with the higher insulin dose in the present study. We also analyzed FAS mRNA, protein and activity levels. Although FAS has been widely studied in the fish liver, information regarding the WAT is scarce [16, 17]. In the study presented here we showed similar levels of activity to those previously reported in salmon WAT [17] and higher levels than those reported in the trout liver, the traditional lipogenic organ in fish [38, 41]. Moreover, in accordance with the findings reported in mammals [47], FAS mRNA levels and protein and activity levels were stimulated by insulin, in line with the increased Akt phosphorylation status, which in mammals is considered to be essential to the insulin-stimulated lipogenesis in adipocytes [46]. This is the first time that insulin-induced lipogenic potential has been described in fish WAT, in agreement with the stimulating effects of dietary carbohydrates shown in catfish [16].

This study demonstrated that some of the main lipogenic enzymes are significantly expressed at both mRNA and protein levels in WAT and that the levels of activity are consistent with a biologically significant lipogenic pathway. Insulin-stimulated FAS regulation thus seems to be as

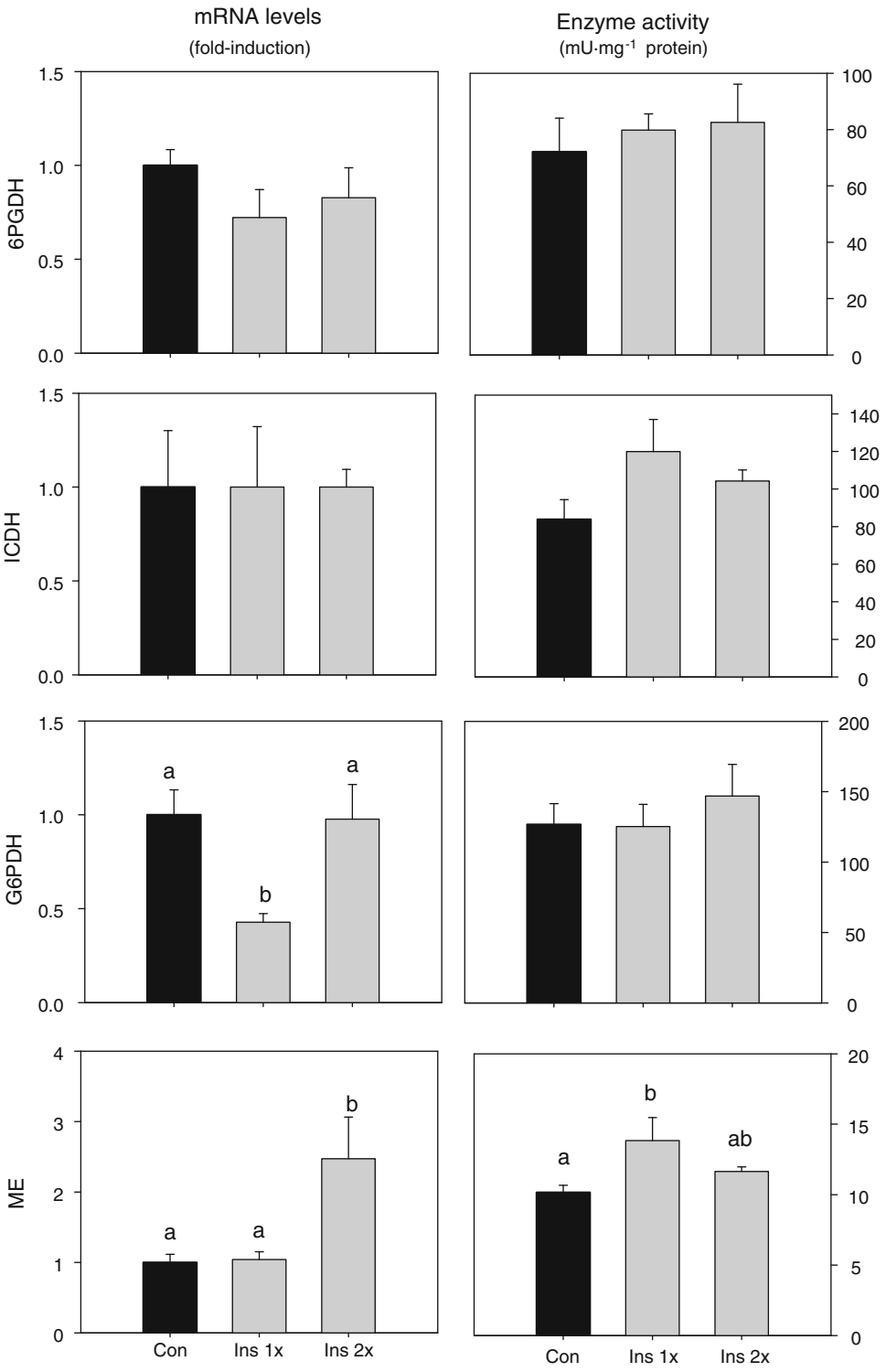

Fig. 4 Effects of insulin infusion (5 days) on glucose 6-phosphate dehydrogenase (G6PDH), 6-phosphogluconate dehydrogenase (6PGDH), isocitrate dehydrogenase (ICDH) and malic enzyme (ME) mRNA and levels of enzyme activity in WAT of trout fed a high-carbohydrate diet. mRNA levels were estimated using real-time RT-PCR. Expression levels were normalized to elongation factor 1α (EF1α)-expressed transcripts which did not change under the experimental conditions and are presented as fold-changes against the saline solution-treated group set at 1. Enzyme activity units (mIU) are defined as nmol of substrate converted to product, per min, at 37 °C, were expressed/mg protein. Results are presented as means ± SEM ($n = 6$) and were analyzed by one-way ANOVA followed by Student–Newman–Keuls comparison test. *Different letters* indicate significant differences among groups ($P < 0.05$). More details in Fig. 1

expected, in view of the anabolic action of insulin in fish [30] and the insulin-induced lipogenesis in hyperinsulinemic rats [53, 54]. However, the global inhibition of ACLY by insulin is surprising although consistent, since it was found at all the levels studied. More studies are needed to clarify whether this pathway is fully functional in fish WAT. On the other hand, the fact that lipogenesis can be up-regulated in trout WAT when fish are fed an excess of dietary carbohydrates also suggests a possible role in glucose metabolism and homeostasis. Lipogenesis in the liver in rainbow trout also fed with carbohydrates [38] was shown to be induced by the anti-diabetic drug metformin,

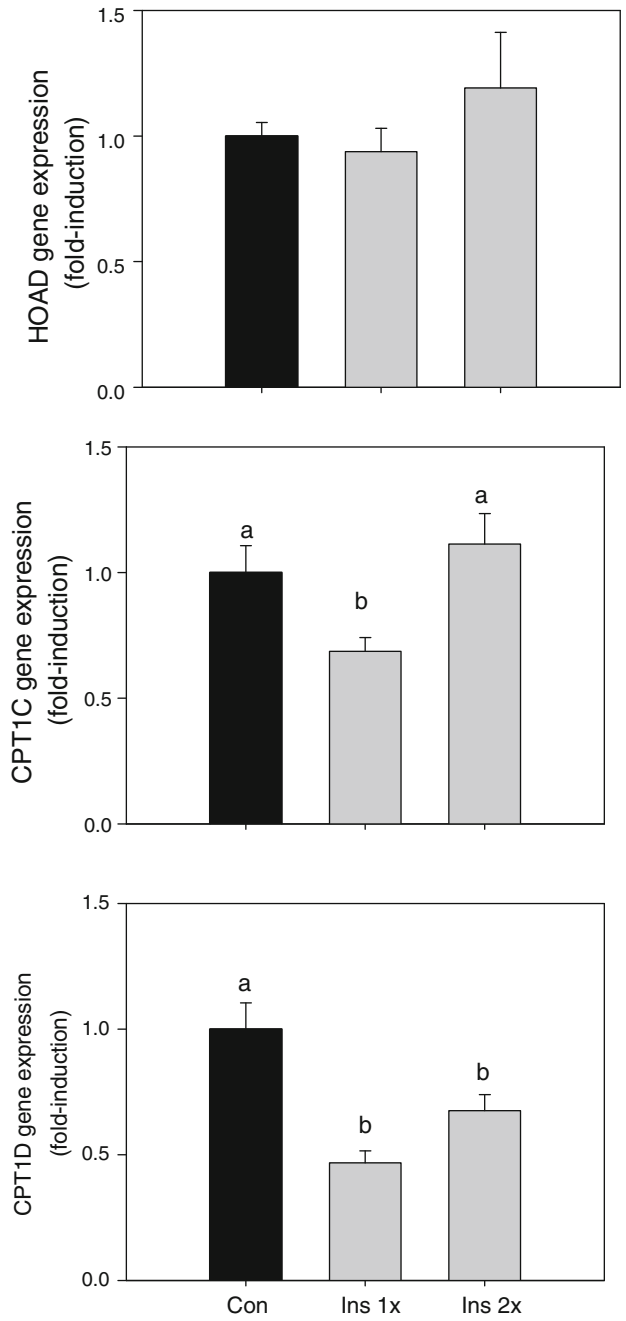

Fig. 5 Effects of insulin infusion (5 days) on 3-hydroxyacyl-CoA dehydrogenase (HOAD),carnitine palmitoyltransferase 1B (CPT1B), CPT1C and CPT1D and mRNA levels in WAT of trout fed a high-carbohydrate diet. mRNA levels were estimated using real-time RT-PCR. mRNA levels were normalized to elongation factor 1α (EF1α)-expressed transcripts which did not change under the experimental conditions and are presented as fold-changes against the saline solution-treated group set at 1. Results are presented as means ± SEM ($n = 6$) and were analyzed by one-way ANOVA followed by Student–Newman–Keuls comparison test. *Different letters* indicate significant differences among groups ($P < 0.05$). More details in Fig. 1

improving the glycemic profile and glucose homeostasis. The induction of WAT lipogenesis by the lower insulin dose in the present study may also be involved in the hypoglycemic effect of this hormone, thus improving control of glycemia in this "glucose intolerant" species [55].

NADPH Donors in White Adipose Tissue are Poorly Regulated by Insulin

The de novo synthesis of lipids in the cytoplasm of vertebrate tissues requires a carbon source (acetyl CoA), reducing equivalents (NADPH) produced by one or more of four cytoplasmic dehydrogenases (G6PDH, 6PGDH, ME and ICDH). We present here for the first time in fish the molecular and biochemical regulation by insulin of the four enzymes in the trout WAT. When compared with other fish species the reducing power generated in trout WAT (5.3 nmol NADPH min^{-1} g^{-1} = 347 nmol NADPH min^{-1} mg $protein^{-1}$) lipogenesis is variable and related to the species and the assay temperature. Trout WAT generates up to 4.5-fold more NADPH than the eel (assessed at 20 °C) [15] and catfish (assessed at 25 °C) [16] visceral adipose tissue. When compared with the salmon (assessed at 18 °C) [17], the difference is tenfold higher. Taking into account the assay temperatures and species-dependence of the findings described above, we can suggest that the WAT in trout has a similar lipogenic potential to other fish species such as the catfish and eel, but higher than that of other salmonids. Overall, it seems that the generation of reduction potential for lipogenesis in trout WAT is high enough to sustain lipogenic activity, although its potential is lower than in the liver. In view of the relative contributions of the different enzymes assessed as NAPDH donors, it should be noted that the ME activity was about 9.5-fold lower than that of the others, and thus its relative contribution to the total NADPH is probably low, as in the liver. These results are similar to those described in the fish species cited above, in which ME also presents low levels of activity. The activity levels of other enzymes involved in the generation of NADPH are relatively high, similar to levels found in the liver [41] and about tenfold higher than in other species studied [15–17]. However, despite this high potential NADPH production capacity, only minor changes in ME were found in trout WAT. The fact that the enzymes exhibiting higher levels of activity were unaffected by insulin suggests that the NADPH production pathway does not constitute the limiting step for lipogenesis in trout WAT.

Beta Oxidation Pathway in White Adipose Tissue: Regulation by Insulin

In this study, we examined two key enzymes involved in regulating FFA oxidation in trout WAT and the effects of insulin infusion at the molecular level. CPT-I is considered to be a key regulatory enzyme in FFA oxidation. It

catalyzes the formation of long-chain acyl-carnitine, the transportable form of activated FFAs, thus committing FFAs to oxidation in the mitochondria [56]. In fish, FFA oxidation takes place mainly in the liver and cardiac and skeletal muscle, where CPT-I is present [23, 25] and regulated by insulin [33]. However, information about CPT-I in fish WAT is limited: CPT-I gene expression has been described in the rainbow trout [23, 57], although no transcripts were found in seabream [25]. As far as we are aware, this is the first study in which WAT CPT-I regulation is explored in fish, especially in relation to insulin. Very interestingly, we found that the two major CPT-I isoforms expressed in the liver and muscle of rainbow trout (CPT-IA and CPT-IB) [33] were not significantly expressed in the WAT. Moreover, the main isoforms found in this tissue were CPT-IC (brain type) and D (larval type) (personal observations). The expression patterns of trout CPT-I compared to those of mammals, where the CPT-I-M (the muscle type) is the predominant isoform in the adipose tissue [58], were especially interesting. Overall, we found that the two isoforms expressed in the WAT were down-regulated by the insulin infusion, although no relationship with insulin dose was found. This finding agrees with the global anabolic role (anti-lipolytic effects) of insulin in fish [27, 59] and the down-regulation of CPT-IA and CPT-IB transcripts in muscle of fasted trout infused with insulin [33]. This is in accordance with the findings reported in rat adipocytes, in which the presence of insulin in the medium down-regulates CPT-I mRNA levels [3]. However, the relative contributions of the isoform transcripts studied to the total pool of CPT-I activity in WAT remain unidentified and further studies must therefore be conducted to clarify the regulation of this enzyme in fish WAT. Finally, we present here the presence of transcripts for the HOAD enzyme involved in the β-oxidation of lipids. Lipid oxidation in the WAT has been little explored in fish to date [21, 22] and, although the expression of HOAD does not seem to be regulated by insulin, its presence suggests the utilization of this substrate as a local energy source.

Conclusions and Perspective

Although the role of the WAT in fish as a lipid deposition organ is well recognized [6], both the lipogenic capacity and lipid energy metabolism have been traditionally considered to be of minor importance, and its biological significance and regulation have remained undemonstrated [20]. We present here original findings regarding lipid metabolism in the WAT of rainbow trout fed a high carbohydrate diet and infused with insulin that emphasize the functions of this tissue, mainly as energy storage for long-term periods of fasting [7] and for reproduction purposes [10]. In these conditions, we found the presence of some of the main enzymes required for lipogenesis at molecular, protein and activity levels, such as ACLY and FAS. The up-regulation of FAS activity by insulin in a dose-dependent manner reinforces the lipogenic role of WAT in the trout. We may thus hypothesize that this increased lipogenic potential can help trout to control glycemia when fed high-carbohydrate diets, as this pathway has been shown to be involved in control of glucose homeostasis in this species [38, 39]. Moreover, the presence of the major NADPH donors for lipogenesis with relatively high rates of activity (equivalent to those found in the liver in this species) supports this lipogenic role of WAT. However, the lack of response to insulin infusion suggests that NADPH production is not a lipogenesis limiting step in this tissue. On the other hand, lipid oxidation potential was found through the mRNA levels of enzymes involved in β-oxidation, such as HOAD, the brain isoform of CPT-IC, and an exclusive isoform of this tissue, CPT-ID. Although no levels of activity were assessed for these enzymes, a novel oxidation potential can be suggested in the WAT of rainbow trout, probably for local use. We found that insulin acts as an important regulator of trout WAT lipid metabolism as a whole, as recently proposed by Bouraoui et al. (2010) [45], inducing the final stage of lipogenesis and suppressing β-oxidation at a molecular level. Although preliminary, these results suggest that the WAT in fish may have an important role not only as lipid deposition tissue, but also as a lipogenic organ, that could also be able to utilize lipids stored as a local energy source.

Acknowledgments This study was supported by research grants from the Agence Nationale de la Recherche (ANR-08-JCJC-0025-01) and INRA PHASE Department. SP was recipient of a postdoctoral fellowship from the Xunta de Galicia (Program Ángeles Alvariño). We thank the technical stuff (Y. Hontang, F. Sandres, and F. Terrier) of the INRA experimental fish farm of Donzacq for supplying the experimental animals.

References

1. Bezaire V, Langin D (2009) Regulation of adipose tissue lipolysis revisited. Proc Nutr Soc 68:350–360
2. Minehira K, Bettschart V, Vidal H, Vega N, Di Vetta V, Rey V, Schneiter P, Tappy L (2003) Effect of carbohydrate overfeeding on whole body and adipose tissue metabolism in humans. Obes Res 11:1096–1103
3. Zang Y, Wang T, Xie W, Wang-Fischer YL, Getty L, Han J, Corkey BE, Guo W (2005) Regulation of acetyl CoA carboxylase and carnitine palmitoyl transferase-1 in rat adipocytes. Obes Res 13:1530–1539
4. Frayn KN (2002) Adipose tissue as a buffer for daily lipid flux. Diabetologia 45:1201–1210
5. Sheridan MA (1988) Lipid dynamics in fish: aspects of absorption, transportation, deposition and mobilization. Comp Biochem Physiol B Biochem Mol Biol 90:679–690
6. Sheridan MA, Harmon JS (1994) Adipose tissue. In: Hochachka PW, Mommsen TP (eds) Biochemistry and molecular biology of fishes, vol 3. Elsevier, Amsterdam, pp 305–311

7. Navarro I, Gutiérrez J (1995) Fasting and starvation. In: Hochachka PW, Mommsen TP (eds) Metabolic biochemistry, vol 4. Elsevier, Amsterdam, pp 394–434
8. Company R, Calduch-Giner JA, Kaushik S, Pérez-Sánchez J (1999) Growth performance and adiposity in gilthead sea bream (*Sparus aurata*): risks and benefits of high energy diets. Aquaculture 171:279–292
9. Sheridan MA (1989) Alterations in lipid metabolism accompanying smoltification and seawater adaptation of salmonid fish. Aquaculture 82:191–203
10. Tocher DR (2003) Metabolism and functions of lipids and fatty acids in teleost fish. Rev Fish Sci 11:107–184
11. Albalat A, Sánchez-Gurmaches J, Gutiérrez J, Navarro I (2006) Regulation of lipoprotein lipase activity in rainbow trout (*Oncorhynchus mykiss*) tissues. Gen Comp Endocrinol 146:226–235
12. Albalat A, Saera-Vila A, Capilla E, Gutiérrez J, Pérez-Sánchez J, Navarro I (2007) Insulin regulation of lipoprotein lipase (LPL) activity and expression in gilthead sea bream (*Sparus aurata*). Comp Biochem Physiol B Biochem Mol Biol 148:151–159
13. Cruz-Garcia L, Saera-Vila A, Navarro I, Calduch-Giner J, Perez-Sanchez J (2009) Targets for TNFalpha-induced lipolysis in gilthead sea bream (*Sparus aurata* L.) adipocytes isolated from lean and fat juvenile fish. J Exp Biol 212:2254–2260
14. Harmon JS, Rieniets LM, Sheridan MA (1993) Glucagon and insulin regulate lipolysis in trout liver by altering phosphorylation of triacylglycerol lipase. Am J Physiol Regul Integr Comp Physiol 265:R255–R260
15. Aster PL, Moon TW (1981) Influence of fasting and diet on lipogenic enzymes in the American eel, *Anguilla rostrata* LeSueur. J Nutr 111:346–354
16. Likimani TA, Wilson RP (1982) Effects of diet on lipogenic enzyme activities in channel catfish hepatic and adipose tissue. J Nutr 112:112–117
17. Lin H, Romsos DR, Tack PI, Leveille GA (1977) Influence of dietary lipid on lipogenic enzyme activities in coho salmon, *Oncorhynchus kisutch* (Walbaum). J Nutr 107:846–854
18. Bouraoui L, Sánchez-Gurmaches J, Cruz-Garcia L, Gutiérrez J, Benedito-Palos L, Pérez-Sánchez J, Navarro I (2010) Effect of dietary fish meal and fish oil replacement on lipogenic and lipoprotein lipase activities and plasma insulin in gilthead sea bream (*Sparus aurata*) Aquacult Nut 17:54–63. doi: 10.1111/j.1365-2095.2009.00706.x
19. Henderson RJ, Sargent JR (1981) Lipid biosynthesis in rainbow trout, *Salmo gairdneri*, fed diets of differing lipid content. Comp Biochem Physiol C Comp Pharmacol 69:31–37
20. Henderson RJ, JR Sargent (1985) Fatty acid metabolism in fish. In: Cowey CB, Mackie AM, Bell JG (eds) Nutrition and feeding in fish. Academic Press, New York, pp 349–364
21. Todorcevic M, Kjaer MA, Djakovic N, Vegusdal A, Torstensen BE, Ruyter B (2009) N-3 HUFAs affect fat deposition, susceptibility to oxidative stress, and apoptosis in Atlantic salmon visceral adipose tissue. Comp Biochem Physiol B Biochem Mol Biol 152:135–143
22. Todorcevic M, Vegusdal A, Gjoen T, Sundvold H, Torstensen BE, Kjaer MA, Ruyter B (2008) Changes in fatty acids metabolism during differentiation of Atlantic salmon preadipocytes; effects of n-3 and n-9 fatty acids. Biochim Biophys Acta 1781:326–335
23. Gutieres S, Damon M, Panserat S, Kaushik S, Medale F (2003) Cloning and tissue distribution of a carnitine palmitoyltransferase I gene in rainbow trout (*Oncorhynchus mykiss*). Comp Biochem Physiol B Biochem Mol Biol 135:139–151
24. Torstensen B, Nanton D, Olsvik P, Sundvold H, Stubhaug I (2009) Gene expression of fatty acid-binding proteins, fatty acid transport proteins (cd36 and FATP) and β-oxidation-related genes in Atlantic salmon (*Salmo salar* L.) fed fish oil or vegetable oil. Aquac Nutr 15:440–451
25. Boukouvala E, Leaver MJ, Favre-Krey L, Theodoridou M, Krey G (2010) Molecular characterization of a gilthead sea bream (*Sparus aurata*) muscle tissue cDNA for carnitine palmitoyltransferase 1B (CPT1B). Comp Biochem Physiol B Biochem Mol Biol 157:189–197
26. Mingarro M, Vega-Rubín de Celis S, Astola A, Pendon C, Valdivia MM, Pérez-Sánchez J (2002) Endocrine mediators of seasonal growth in gilthead sea bream (*Sparus aurata*): the growth hormone and somatolactin paradigm. Gen Comp Endocrinol 128:102–111
27. Harmon JS, Sheridan MA (1992) Effects of nutritional state, insulin, and glucagon on lipid mobilization in rainbow trout, *Oncorhynchus mykiss*. Gen Comp Endocrinol 87:214–221
28. Vianen GJ, Obels PP, van den Thillart GE, Zaagsma J (2002) Beta-adrenoceptors mediate inhibition of lipolysis in adipocytes of tilapia (*Oreochromis mossambicus*). Am J Physiol Endocrinol Metab 282:E318–E325
29. Albalat A, Liarte C, MacKenzie S, Tort L, Planas JV, Navarro I (2005) Control of adipose tissue lipid metabolism by tumor necrosis factor-α in rainbow trout (*Oncorhynchus mykiss*). J Endocrinol 184:527–534
30. Navarro I, Capilla E, Castillo A, Albalat A, Díaz M, Gallardo M A, Blasco J, Planas JV, Gutiérrez J (2006) Insulin metabolic effects in fish tissues. In: Reinecke M, Zaccone G, Kapoor BG (eds) Fish endocrinology Science Publishers Inc., Enfield, pp 15–48
31. Albalat A, Gutiérrez J, Navarro I (2005) Regulation of lipolysis in isolated adipocytes of rainbow trout (*Oncorhynchus mykiss*): the role of insulin and glucagon. Comp Biochem Physiol B Biochem Mol Biol 142:347–354
32. Mommsen TP, Plisetskaya EM (1991) Insulin in fishes and agnathans: history, structure, and metabolic regulation. Rev Aquat Sci 4:225–259
33. Polakof S, Medale F, Skiba-Cassy S, Corraze G, Panserat S (2010) Molecular regulation of lipid metabolism in liver and muscle of rainbow trout subjected to acute and chronic insulin treatments. Domest Anim Endocrinol 39:26–33
34. Planas JV, Méndez E, Banos N, Capilla E, Navarro I, Gutiérrez J (2000) Insulin and IGF-I receptors in trout adipose tissue are physiologically regulated by circulating hormone levels. J Exp Biol 203:1153–1159
35. Polakof S, Skiba-Cassy S, Choubert G, Panserat S (2010) Insulin-induced hypoglycaemia is co-ordinately regulated by liver and muscle during acute and chronic insulin stimulation in rainbow trout (*Oncorhynchus mykiss*). J Exp Biol 213:1443–1452
36. Dias J, Álvarez MJ, Díez A, Arzel J, Corraze G, Bautista JM, Kaushik S (1998) Regulation of hepatic lipogenesis by dietary protein/energy in juvenile European seabass (*Dicentrarchus labrax*). Aquaculture 161:169–186
37. Lin H, Romsos DR, Tack PI, Leveille GA (1977) Effects of fasting and feeding various diets on hepatic lipogenic enzyme activities in coho salmon (*Oncorhynchus kisutch* (Walbaum)). J Nutr 107:1477–1483
38. Panserat S, Skiba-Cassy S, Seiliez I, Lansard M, Plagnes-Juan E, Vachot C, Aguirre P, Larroquet L, Chavergnac G, Médale F, Corraze G, Kaushik S, Moon TW (2009) Metformin improves postprandial glucose homeostasis in rainbow trout fed dietary carbohydrates: a link with the induction of hepatic lipogenic capacities? Am J Physiol Regul Integr Comp Physiol 293:707–715
39. Polakof S, Skiba-Cassy S, Panserat S (2009) Glucose homeostasis is impaired by a paradoxical interaction between metformin and insulin in carnivorous rainbow trout. Am J Physiol Regul Integr Comp Physiol 297:1769–1776

40. Pfaffl MW (2001) A new mathematical model for relative quantification in real-time RT-PCR. Nucleic Acids Res 29:e45
41. Kolditz C, Borthaire M, Richard N, Corraze G, Panserat S, Vachot C, Lefevre F, Medale F (2008) Liver and muscle metabolic changes induced by dietary energy content and genetic selection in rainbow trout (*Oncorhynchus mykiss*). Am J Physiol Regul Integr Comp Physiol 294:R1154–R1164
42. Figueiredo-Silva AC, Corraze G, Borges P, Valente LMP (2010) Dietary protein/lipid level and protein source effects on growth, tissue composition and lipid metabolism of blackspot seabream (*Pagellus bogaraveo*). Aquac Nutr 16:173–187
43. Mommsen TP, Osachoff HL, Elliott ME (2003) Metabolic zonation in teleost gastrointestinal tract effects of fasting and cortisol in tilapia. J Comp Physiol B Biochem Syst Environ Physiol 173:409–418
44. Álvarez MJ, Díez A, López-Bote C, Gallego M, Bautista JM (2000) Short-term modulation of lipogenesis by macronutrients in rainbow trout (*Oncorhynchus mykiss*) hepatocytes. Br J Nutr 84:619–628
45. Bouraoui L, Capilla E, Gutierrez J, Navarro I (2010) Insulin and insulin-like growth factor I signaling pathways in rainbow trout (*Oncorhynchus mykiss*) during adipogenesis and their implication in glucose uptake. Am J Physiol Regul Integr Comp Physiol 299:33–41
46. Berggreen C, Gormand A, Omar B, Degerman E, Goransson O (2009) Protein kinase B activity is required for the effects of insulin on lipid metabolism in adipocytes. Am J Physiol Endocrinol Metab 296:E635–E646
47. Strable MS, Ntambi JM (2010) Genetic control of de novo lipogenesis: role in diet-induced obesity. Crit Rev Biochem Mol Biol 45:199–214
48. Towle HC, Kaytor EN, Shih HM (1997) Regulation of the expression of lipogenic enzyme genes by carbohydrate. Annu Rev Nutr 17:405–433
49. Saggerson ED, McAllister TW, Baht HS (1988) Lipogenesis in rat brown adipocytes effects of insulin and noradrenaline, contributions from glucose and lactate as precursors and comparisons with white adipocytes. Biochem J 251:701–709
50. Fukuda H, Iritani N (1999) Regulation of ATP citrate-lyase gene expression in hepatocytes and adipocytes in normal and genetically obese rats. J Biochem 126:437–444
51. Skiba-Cassy S, Lansard M, Panserat S, Medale F (2009) Rainbow trout genetically selected for greater muscle fat content display increased activation of liver TOR signaling and lipogenic gene expression. Am J Physiol Regul Integr Comp Physiol 297: 1421–1429
52. Potapova IA, El-Maghrabi MR, Doronin SV, Benjamin WB (2000) Phosphorylation of recombinant human ATP:citrate lyase by cAMP-dependent protein kinase abolishes homotropic allosteric regulation of the enzyme by citrate and increases the enzyme activity. Allosteric activation of ATP: citrate lyase by phosphorylated sugars. Biochemistry 39:1169–1179
53. Cusin I, Terrettaz J, Rohner-Jeanrenaud F, Jeanrenaud B (1990) Metabolic consequences of hyperinsulinaemia imposed on normal rats on glucose handling by white adipose tissue, muscles and liver. J.Biochem 267:99–103
54. Larue-Achagiotis C, Goubern M, Laury MC (1988) Concomitant food intake and adipose tissue responses under chronic insulin infusion in rats. Physiol Behav 44:95–100
55. Moon TW (2001) Glucose intolerance in teleost fish: fact or fiction? Comp Biochem Physiol B Biochem Mol Biol 129: 243–249
56. Louet JF, Le May C, Pegorier JP, Decaux JF, Girard J (2001) Regulation of liver carnitine palmitoyltransferase I gene expression by hormones and fatty acids. Biochem Soc Trans 29:310–316
57. Morash AJ, Bureau DP, McClelland GB (2009) Effects of dietary fatty acid composition on the regulation of carnitine palmitoyltransferase (CPT) I in rainbow trout (*Oncorhynchus mykiss*). Comp Biochem Physiol B Biochem Mol Biol 152:85–93
58. Esser V, Brown NF, Cowan AT, Foster DW, McGarry JD (1996) Expression of a cDNA isolated from rat brown adipose tissue and heart identifies the product as the muscle isoform of carnitine palmitoyltransferase I (M-CPT I): M-CPT I is the predominant CPT I isoform expressed in both white (epididymal) and brown adipocytes. J Biol Chem 271:6972–6977
59. Plisetskaya EM, Sheridan MA, Mommsen TP (1989) Metabolic changes in Coho and Chinook salmon resulting from acute insufficiency in pancreatic hormones. J Exp Zool 249:158–164

Lipids (2011) 46:201–206
DOI 10.1007/s11745-010-3510-4

COMMUNICATION

Stereochemistry of Hydrogen Removal During Oxygenation of Linoleic Acid by Singlet Oxygen and Synthesis of 11(*S*)-Deuterium-Labeled Linoleic Acid

Mats Hamberg

Received: 23 August 2010 / Accepted: 23 November 2010 / Published online: 16 December 2010

Abstract Exposure of unsaturated fatty acids to singlet oxygen results in the formation of hydroperoxides. In this process, each double bond in the acyl chain produces two regioisomeric hydroperoxides having an (*E*)-configured double bond. Although such compounds are racemic, the hydrogen removal associated with the oxygenation may, a priori, take place antarafacially, suprafacially or stereorandomly. The present study describes the preparation of [11(*S*)-^{2}H]linoleic acid by two independent methods and the use of this stereospecifically labeled fatty acid to reveal the hidden stereospecificity in singlet oxygenations of polyunsaturated fatty acids. It was found that linoleic acid 9(*R*)- and 13(*S*)-hydroperoxides formed from [11(*S*)-^{2}H] linoleic acid both retained the deuterium label whereas the 9(*S*)- and 13(*R*)-hydroperoxides were essentially devoid of deuterium. It is concluded that polyunsaturated fatty acid hydroperoxides produced in the presence of singlet oxygen in e.g., plant leaves are formed by a reaction involving addition of oxygen and removal of hydrogen taking place with suprafacial stereochemistry. This result confirms and extends previous mechanistic studies of singlet oxygen-dependent oxygenations.

Keywords Singlet oxygen · Oxygenation · Hydroperoxide · Linoleic acid · Oxylipins

Abbreviations

GC–MS	Gas–liquid chromatography–mass spectrometry
CP-HPLC	Chiral phase high performance chromatography
RP-HPLC	Reversed-phase high performance chromatography
SP-HPLC	Straight-phase high performance chromatography
Me_3Si	Trimethylsilyl
HPODE	Hydroperoxyoctadecadienoic acid
HODE	Hydroxyoctadecadienoic acid

M. Hamberg (✉)
Division of Physiological Chemistry II, Department of Medical Biochemistry and Biophysics, Karolinska Institutet, Stockholm, Sweden
e-mail: Mats.Hamberg@ki.se

Introduction

Lipoxygenases are non-heme dioxygenases which catalyze the incorporation of molecular oxygen at a 1(*Z*),4(*Z*)-pentadienyl moiety of polyunsaturated fatty acids forming optically active hydroperoxy fatty acids having a pair of (*E*),(*Z*)-configured conjugated double bonds [1–3]. The same type of fatty acid hydroperoxides is formed by autoxidation of polyunsaturated fatty acids by ground state (radical) dioxygen ($^{3}O_2$). In this case oxygenation takes place without control of regiochemistry and the hydroperoxides are racemic. A third possibility of generating hydroperoxides from unsaturated fatty acids is to expose them to singlet oxygen ($^{1}O_2$). This unstable, non-radical form of dioxygen can be generated from ground state oxygen by light irradiation in the presence of a photosensitizer. $^{1}O_2$ is also produced in certain oxygen-evolving reactions such as the oxidation of hydrogen peroxide by hypochlorite and during the thermal decomposition of phosphite ozonides and other oxygenated compounds (see Ref. [4] and references cited therein). In the process, each double bond in the acyl chain will produce two regioisomeric, racemic hydroperoxides.

Mechanistically, the vast majority of lipoxygenase-catalyzed oxygenations proceed with antarafacial stereochemistry, i.e. the initial hydrogen removal and the subsequent attack by $^3O_2$ take place from opposite sides of the plane of the 1,4-pentadiene moiety [2]. Autoxidation, on the other hand, is a stereorandom process where the carbon-centered radical formed following hydrogen removal can be attacked from both sides with equal probability [5]. Mechanistic studies of $^1O_2$ oxygenations of simple model alkenes have indicated a suprafacial process [6, 7], however, it was of interest to extend such studies to a biologically relevant substrate. The present report is concerned with singlet oxygenation of a polyunsaturated fatty acid having the characteristic methylene group-interrupted (*Z*),(*Z*)-diene partial structure. [11(*S*)-^{2}H]Linoleic acid prepared by two different methods was used for this purpose, and the regio- and stereoisomeric hydroperoxides formed during its exposure to $^1O_2$ were analyzed for isotope content using GC–MS.

Experimental Procedures

[11(*R*,*S*)-^{2}H]Linoleic Acid

The deuterated linoleic acid was synthesized by acetylene coupling followed by partial hydrogenation of the resulting deuterated octadecadiynoic acid. Briefly, 2-octynal (2.5 g; Sigma-Aldrich, Stockholm, Sweden) was reduced to [1-^{2}H]2-octyn-1-ol using sodium borodeuteride in methanol. The bromide (2.73 g) prepared by refluxing with PBr_3 was coupled to methyl 9-decynoate in the presence of CuI and Cs_2CO_3 [8]. Following purification on a silica gel column, 90% pure methyl [11(*R*,*S*)-^{2}H]9,12-octadecadiynoate (4.4 g; yield from 2-octynal, 75%) was obtained. An aliquot was subjected to partial hydrogenation using P-2 nickel as the catalyst [9]. The resulting deuterated methyl linoleate was purified by RP-HPLC, saponified, and further purified by a second RP-HPLC run to provide >99% pure [11(*R*,*S*)-^{2}H]linoleic acid.

[11(*S*)-^{2}H]Linoleic acid (**5**): Method A

It is well known from previous studies that soybean lipoxygenase-1 stereospecifically abstracts the *pro-S* hydrogen from the ω8 bisallylic methylene group of linoleic acid and other polyunsaturated fatty acids [10], and that substitution of this hydrogen for deuterium is accompanied by a large kinetic isotope effect (k_H/k_D about 40, see [11]). Thus, if [11(*R*,*S*)-^{2}H]linoleic acid is incubated with soybean lipoxygenase, the 11(*R*)-^{2}H-labeled enantiomer will be rapidly consumed whereas the 11(*S*)-^{2}H-labeled acid will largely remain not converted. Method A was based on these facts and involved stirring at 0 °C under oxygen atmosphere of [11(*R*,*S*)-^{2}H]linoleic acid (192 mg) in 300 mL of 0.1 M sodium borate buffer pH 10.4 with soybean lipoxygenase-1 (Sigma-Aldrich type IV, 60 μL (250,000 units) [unit definition: as defined by the manufacturer, 1 U will cause an increase in A_{234} of 0.001/min at pH 9.0 at 25 °C when linoleic acid is the substrate in 3.0 mL volume (1 cm light path)]. After 19 min, additional enzyme was added [20 μL (83,000 U)]. The reaction was followed spectrophotometrically by recording the absorbance at 234 nm and interrupted after 32 min (53% conversion according to UV spectrometry). From the mixture, [11(*S*)-^{2}H]linoleic acid was obtained in >99% pure form following preparative RP-HPLC. The isotope composition was 98.1% deuterated and 1.9% undeuterated molecules. In agreement with the labeling, re-incubation of an aliquot of the [11(*S*)-^{2}H]linoleic acid with soybean lipoxygenase-1 resulted in a very slow conversion and the formation of 13(*S*)-HPODE which was essentially devoid of deuterium.

The above method for enzymatic resolution of [11(*R*,*S*)-^{2}H]linoleic acid has been used in a previous study [11].

[11(*S*)-^{2}H]Linoleic acid (**5**): Method B

In Method B, a series of stereospecific transformations were used to convert the readily obtainable epoxy alcohol methyl 11(*S*),12(*S*)-epoxy-13(*S*)-hydroxy-9(*Z*)-octadecenoate (**1**) into the desired labeled linoleate (Scheme 1). Thus, **1** (250 mg [12]) in diethyl ether (10 mL) was stirred with lithium aluminium deuteride (155 mg, Sigma-Aldrich) at 23 °C for 5 h affording triol **2** as a white solid [214 mg (92%)]; mass spectrum (Me_3Si derivative) showing *m*/*z* 429 (2%; M^+–Me_3SiOH), 346 (26; M^+–Me_3SiO^+=CH–C_5H_{11}), 275 (100; Me_3SiO^+=CH–CH($OSiMe_3$)–C_5H_{11}), and 173 (Me_3SiO^+=CH–C_5H_{11}). Monoacetylation of **2** using acetyl chloride and 2,4,6-trimethylpyridine [13] afforded diol acetate **3** in quantitative yield; mass spectrum (Me_3Si derivative) showing *m*/*z* 474 (1%; M^+–CH_3), 316 (55; M^+–Me_3SiO^+=CH–C_5H_{11}), 275 (92; Me_3SiO^+=CH–CH($OSiMe_3$)–C_5H_{11}), and 173 (100; Me_3SiO^+=CH–C_5H_{11}). The *erythro*-12,13-diol function of **3** was deoxygenated via the cyclic thionocarbonate using previously described methodology [14]. Following saponification and purification on a silica gel column [1,1,11(*S*)-$^2H_3$]9(*Z*),12(*Z*)-octadecadienol **4** was obtained as a colorless oil [65 mg (32% from epoxy alcohol **1**)]; mass spectrum showing *m*/*z* 269 (7%; M^+), 251 (1; M^+–H_2O), 96 (59), 82 (87), and 68 (100). Oxidation using pyridinium dichromate (273 mg) in dimethylformamide (2.5 mL) containing water (26 mg) and butylated hydroxytoluene antioxidant (2 mg) at 40 °C for 15 h afforded the title compound **5** [23 mg (11% from **1**)]. The

pure compound was obtained following silica gel column chromatography and RP-HPLC. The mass spectrum (methyl ester) showed *m/z* 281 (20%; M^+), 250 (11; M^+–OCH_3), 96 (63), 82 (88), and 68 (100) and an isotopic composition of 2.0% unlabeled and 98.0% monodeuterated molecules. The purity of the sample was in excess of 99% as judged by GLC analysis (Fig. 1). Importantly, this analysis was carried out with the 9(*E*),12(*Z*)- and 9(*Z*),12(*E*)-octadecadienoate isomers as standards and proved that the two double bonds of **5** were both "*Z*".

High-Performance Liquid Chromatography (HPLC)

Purification of **5** and its methyl ester was performed by reversed-phase (RP) HPLC using a column of Nucleosil C_{18} 100-7 (250 × 10 mm; Macherey–Nagel, Düren, Germany) and solvent systems of acetonitrile–water (85:15, by vol) (**5** methyl ester) or acetonitrile–water–acetic acid (75:25:0.005, by vol) (**5**) at a flow rate of 4 mL/min. Regioisomeric hydroxyoctadecadienoic acids were separated by straight-phase (SP) HPLC using a column of Nucleosil 50-7 (250 × 10 mm, Macherey–Nagel, Düren,

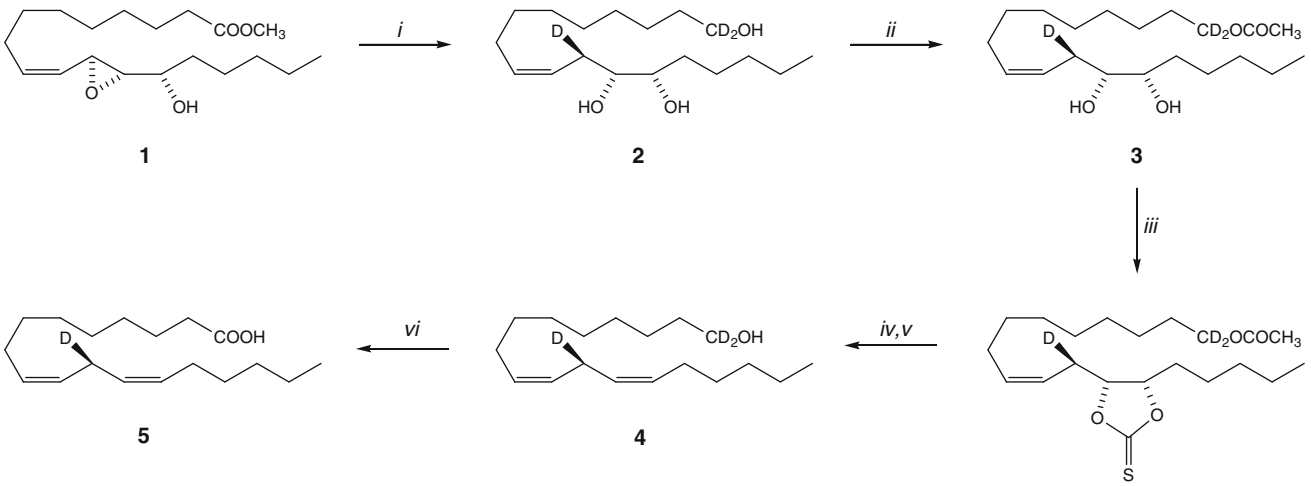

Scheme 1 Synthesis of [11(*S*)-^{2}H]linoleic acid **5** from epoxy alcohol **1**. (*i*) $LiALD_4$, diethyl ether; (*ii*) CH_3COCl, 2,4,6-trimethylpyridine; (*iii*) thiophosgene, 4-dimethylaminopyridine; (*iv*) 1,3-dimethyl-2-phenyl-1,3,2-diazaphospholidine; (*v*) NaOH, aq. ethanol; (*vi*) pyridinium dichromate, dimethylformamide, water

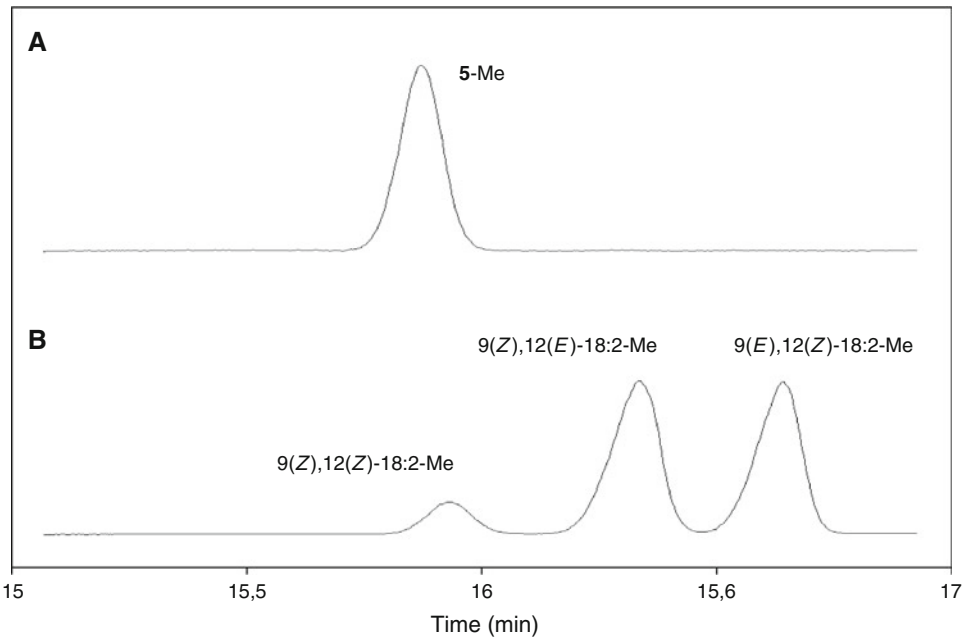

Fig. 1 GLC analysis of the methyl ester of **5** (**a**). The methyl esters of 9(*Z*),12(*Z*)-, 9(*Z*),12(*E*)- and 9(*E*),12(*Z*)-octadecadienoates were used as references (**b**). A methyl silicone capillary column (25 m, 0.33 μm film thickness) was used with helium as the carrier gas. Column temperature, 180 °C

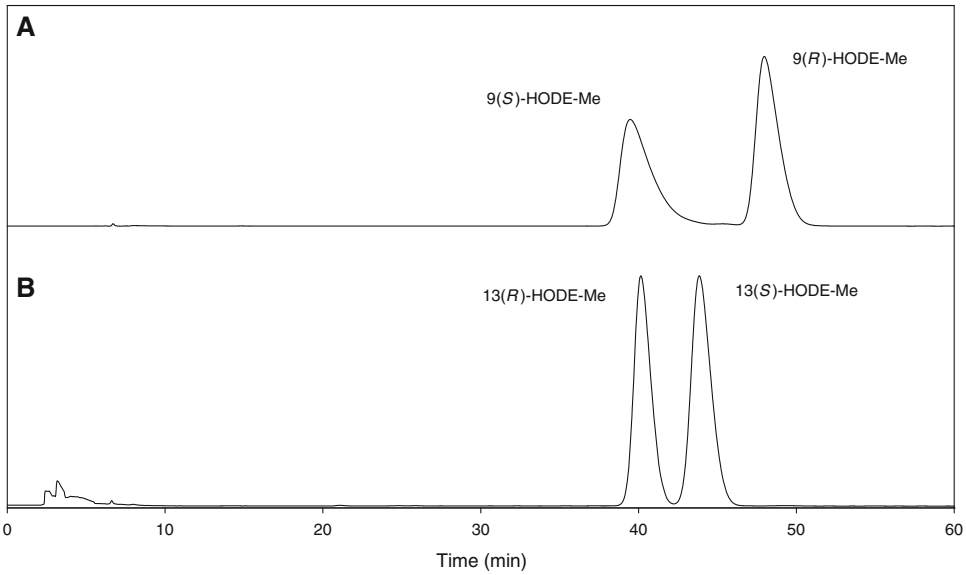

Fig. 2 Separation by CP-HPLC of the methyl esters of 9-HODE (**a**) and 13-HODE (**b**) obtained by singlet oxygenation of **5**. A Chiralcel OB-H column (250 × 4.6 mm) eluted with 2-propanol/hexane (1.5:98.5, v/v) at 0.5 mL/min was used. Detection by UV (234 nm)

Germany) and a solvent system of 2-propanol-hexane-acetic acid (2:98:0.01, by vol) at a flow rate of 4 mL/min. The column effluent was passed through serially connected detectors for measurement of UV absorbance (210 or 234 nm) and refractive index. Methodology for separation of enantiomers of the methyl esters of 9- and 13-HODE by chiral phase (CP) HPLC has been described in detail [15, 16].

Oxygenation Procedure and Isolation of Products

[11(*S*)-^{2}H]Linoleic acid (4.7 mg) was dissolved in methanol (6 mL) containing methylene blue (3 mg). The solution was stirred at 5–8 °C under continuous bubbling of O_2 and irradiated by a 250 W halogen lamp giving a light intensity of approximately 30,000 lx. After 100 min, the solution was cooled on ice and treated with $NaBH_4$ (15 mg). Water was added, and the material extracted with diethyl ether was subjected to SP-HPLC (refractive index detection). Four peaks were observed due to 13-HODE (29%; 42.7 mL effluent), 12-HODE (21%; 51.3 mL), 10-HODE (21%; 57.0 mL), and 9-HODE (29%; 73.1 mL). The 9- and 13-hydroxyoctadecadienoates were methyl-esterified and individually resolved into enantiomers using CP-HPLC (Fig. 2). Derivatization of the methyl esters into Me_3Si derivatives [16] was performed prior to analysis by GC–MS.

GC–MS

A Hewlett–Packard model 5970B mass selective detector connected to a Hewlett–Packard model 5890 gas chromatograph was used. For determination of the isotope content of methyl ester–Me_3Si derivatives, the instrument was operated in the selected ion monitoring mode using the following ions: *m/z* 382.3/383.3 (M^+), 311.2/312.2 (Me_3SiO^+=CH–CH=CH–CH=CH–$(CH_2)_7$–$COOCH_3$), and 225.1/226.1 (Me_3SiO^+=CH–CH=CH-CH=CH–$(CH_2)_4$–CH_3).

Results and Discussion

Shown in Table 1 are results of GC–MS analyses of 9- and 13-hydroxyoctadecadienoates isolated following exposure of [11(*S*)-^{2}H]linoleic acid to singlet oxygen. It is clear that most of the deuterium label was retained in the 9(*R*)-and 13(*S*)-hydroxy derivatives, and that the 9(*S*)- and 13(*R*)-hydroxy compounds had lost most of the label. Thus, the first-mentioned pair was formed by stereospecific elimination of the 11(*R*)-hydrogen, whereas the 11(*S*)-deuterium was lost in the formation of the latter pair. This means that the stereochemical relationship between oxygen addition and hydrogen abstraction is suprafacial in the formation of all four stereoisomers, a finding which confirms and extends previous studies carried out using simple synthetic

Table 1 Deuterium-content of 9- and 13-hydroxyoctadecadienoates formed by $^1O_2$ oxygenation of [11(*S*)-^{2}H]linoleic acid (**5**)

Hydroxyoctadecadienoate[a]	Monodeuterated molecules (%)	
	Exp 1[b]	Exp 2[c]
9(*R*)-HODE	97.1	96.9
9(*S*)-HODE	3.5	2.3
13(*R*)-HODE	3.4	2.5
13(*S*)-HODE	97.2	97.1

[a] The deuterium label was fully retained in the 10- and 12-hydroxyoctadecadienoates

[b] **5** prepared from [11(*R,S*)-^{2}H]linoleic acid was used

[c] **5** prepared from epoxy alcohol **1** was used

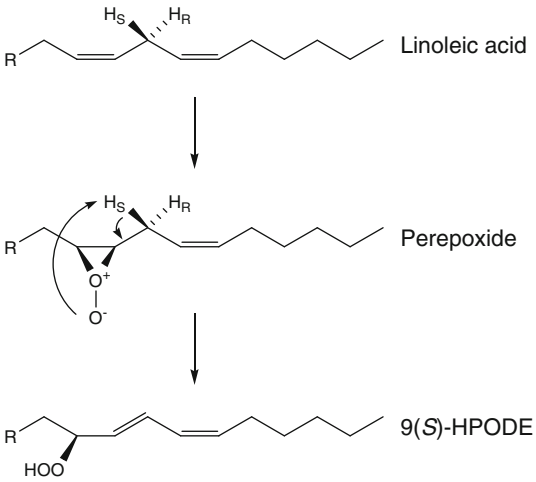

Scheme 2 Possible mechanism in the formation of 9(*S*)-HPODE from linoleic acid in the presence of singlet oxygen

alkenes [6, 7]. Although the detailed mechanism of singlet oxygenation is still being discussed [17–19], it appears that the most plausible one consists of initial addition of $^1O_2$ to the C=C bond to form a doubly charged perepoxide, in which the geometrical configuration of the two carbon atoms is retained (e.g., a (*Z*) double bond gives rise to a *cis*-configured epoxide group) [7]. As illustrated for the linoleic acid → 9(*S*)-HPODE conversion (Scheme 2), suprafacial abstraction of a proton from the allylic methylene by the negatively charged perepoxide oxygen, opening of the epoxide ring and creation of an (*E*)-configured double bond completes formation of the hydroperoxide.

Fatty acid peroxidation in biological systems can take place by lipoxygenase-catalyzed oxygenation, autoxidation, or oxygenation by singlet oxygen, and such oxygenations frequently take place in parallel. This has been best studied in plant leaves, which possess lipoxygenase activity, can initiate $^3O_2$-dependent autoxidation, and produce $^1O_2$ during photosynthesis [20, 21]. Whereas the first- and second-mentioned oxygenations take place antarafacially and stereorandomly, respectively, the present report shows that oxygenation of polyunsaturated fatty acids by singlet oxygen proceeds suprafacially. The distribution of regio- and stereoisomeric hydroperoxides formed by the three oxygenation pathways differ, and determination of specific hydroxide isomers by GC–MS or HPLC has been used to assess the relative importance of the different modes of fatty acid peroxidation in leaves [20]. Conceivably, a further aid in such studies could be provided by isotope analysis of the various hydroxide isomers if a stereospecifically deuterated fatty acid precursor is included as a probe.

Finally, singlet oxygenation has been reported to be accompanied by a weak intramolecular deuterium isotope effect (k_H/k_D 1.4 or less) [7]. An isotope effect would lead to a preponderance of the 10- and 12-hydroxyoctadecadienoates at the expense of the 9- and 13-hydroxy isomers, however, this was not observed using SP-HPLC (refractive index-based detection) or during analysis of the reaction product by GC–MS. Also, as seen in Fig. 2, the ratio of the enantiomers of 9- and 13-hydroxyoctadecadienoates observed on CP-HPLC was close to 1.

Acknowledgments The expert technical assistance by Mrs. G. Hamberg is gratefully acknowledged. This work was supported by a grant from the Swedish Research Council (project 2009-5078) and by Lipidox Co., Stockholm, Sweden.

References

1. Andreou A, Feussner I (2009) Lipoxygenases: structure and reaction mechanism. Phytochemistry 70:1504–1510
2. Schneider C, Pratt DA, Porter NA, Brash AR (2007) Control of oxygenation in lipoxygenase and cyclooxygenase catalysis. Chem Biol 14:473–488
3. Liavonchanka A, Feussner I (2006) Lipoxygenases: occurrence, functions and catalysis. J Plant Physiol 163:348–357
4. Richard JA (2009) Singlet oxygen. Synlett 7:1187–1188
5. Brash AR, Porter AT, Maas RL (1985) Investigation of the selectivity of hydrogen abstraction in the nonenzymatic formation of hydroxyeicosatetraenoic acids and leukotrienes by autoxidation. J Biol Chem 260:4210–4216
6. Alberti MN, Vassilikogiannakis G, Orfanopoulos M (2008) Stereochemistry of the singlet oxygenation of simple alkenes: a stereospecific transformation. Org Lett 10:3997–4000
7. Alberti MN, Orfanopoulos M (2010) Recent mechanistic insights in the singlet oxygen ene reaction. Synlett 7:999–1026
8. Caruso T, Spinella A (2003) Cs_2CO_3 Promoted coupling reactions for the preparation of skipped diynes. Tetrahedron 59:7787–7790
9. Brown CA, Ahuija VK (1973) Catalytic hydrogenation VI. The reaction of sodium borohydride with nickel salts in ethanol solution. P-2 nickel, a highly convenient, new, selective hydrogenation catalyst with great sensitivity to substrate structure. J Org Chem 38:2226–2230
10. Hamberg M, Samuelsson B (1967) On the specificity of the oxygenation of unsaturated fatty acids catalyzed by soybean lipoxidase. J Biol Chem 242:5329–5335
11. Rickert KW, Klinman JP (1999) Nature of hydrogen transfer in soybean lipoxygenase-1: separation of primary and secondary isotope effects. Biochemistry 38:12218–12228
12. Hamberg M (1987) Vanadium-catalyzed transformations of 13(*S*)-hydroperoxy-9(*Z*), 11(*E*)-octadecadienoic acid: structural studies on epoxy alcohols and trihydroxy acids. Chem Phys Lipids 43:55–67
13. Ishihara K, Kurihara H, Yamamoto H (1993) An extremely simple, convenient, and selective method for acetylating primary alcohols in the presence of secondary alcohols. J Org Chem 58:3791–3793
14. Corey EJ, Hopkins PB (1982) A mild procedure for the conversion of 1,2-diols to olefins. Tetrahedron Lett 23:1979–1982
15. Hamberg M (1998) Stereochemistry of oxygenation of linoleic acid catalyzed by prostaglandin-endoperoxide H synthase-2. Arch Biochem Biophys 349:376–380
16. Bannenberg G, Martínez M, Hamberg M, Castresana C (2009) Diversity of the enzymatic activity in the lipoxygenase gene family of *Arabidopsis thaliana*. Lipids 44:85–95

17. Alberti MN, Orfanopoulos M (2008) The cyclopropyl group as a hypersensitive probe in the singlet oxygen ene reaction mechanism. Org Lett 10:2465–2468
18. Leach AG, Houk KN, Foote CS (2008) Theoretical prediction of a perepoxide intermediate for the reaction of singlet oxygen with *trans*-cyclooctene contrasts with the two-step no-intermediate ene reaction for acyclic alkenes. J Org Chem 73:8511–8519
19. Sheppard AN, Acevedo O (2009) Multidimensional exploration of valley-ridge inflection points of potential-energy surfaces. J Am Chem Soc 131:2530–2540
20. Przybyla D, Göbel C, Imboden A, Hamberg M, Feussner I, Apel K (2008) Enzymatic, but not non-enzymatic, $^1O_2$-mediated peroxidation of polyunsaturated fatty acids forms part of the EXECUTER1-dependent stress response program in the *flu* mutant of *Arabidopsis thaliana*. Plant J 54:236–248
21. Vellosillo T, Vicente J, Kulasekaran S, Hamberg M, Castresana C (2010) Emerging complexity in reactive oxygen species production and signaling during the response of plants to pathogens. Plant Physiol 154:444–448

Lipids (2011) 46:207
DOI 10.1007/s11745-011-3529-1

EDITORIAL

Are You a Good Citizen of Science?

Eric J. Murphy

In the past I have pondered this important, but perhaps a bit nebulous question: Am I a good citizen of science? So I ask you: Are you a good citizen of science? This is an intriguing and interesting question on which we should all reflect and one that I would hope receives a resounding, "you bet I am!", from everyone. (For those unfamiliar with the movie Fargo, in the upper Midwestern part of the United States that would be a "you betcha!") But are you and I really good science citizens? What exactly does a good citizen of science do, or, on the contrary, not do?

Science citizenship can take on many different forms, from citing papers from a competing scientist to agreeing to review yet another paper on top of the many other commitments one has on hand; from mentoring young colleagues, to offering a colleague a helping hand, to sharing reagents with a no-strings-attached policy, and working to enhance one's own field by doing the drudgery of society work. In the end, good science citizenship is offering our precious time in a selfless manner to help others in our respective fields. Yet, are we good citizens?

This brings me to one of the fundamental cornerstones of science, peer-review. I wish I had a quarter, whether it be in Euros, US, or Canadian currency, every time someone uttered: "I have a grant due in 2 months, so I cannot review that manuscript." Or "I have a meeting in 2 weeks; sorry I just cannot review that manuscript." Amazingly, many individuals who are too busy and too overcommitted to review a manuscript, have no problem burdening the peer-review system with their own manuscripts. They have no problem if their equally busy peers who have meetings to attend, grants to write, and a family with which they might want to see, take time to review a manuscript of theirs. Yet, isn't this a profession in which being overcommitted, understaffed, and underfunded is the norm? So why do many of our colleagues think they should forgo participating in the peer-review process, yet subject others to reviewing their own manuscripts? Perhaps it is selfishness or just plain old-fashioned greed for more time devoted to their own pursuits? Regardless, this is a growing problem not just at *Lipids*, but at many other journals, and something with which editorial board members have repeatedly dealt and uttered complaints about dealing with so many reluctant reviewers.

So, to each reader I offer a suggestion to actively participate in the peer-review process. My "Golden Rule" for peer review is quite simple: Review at least four times the number of manuscripts that you submit in a year. When you are truly pressed for time, discuss with a young colleague, a student or a post-doctoral fellow in your lab the possibility of taking on a peer-review assignment. I have found that many early career scientists—including graduate students—make the best reviewers. Taking this approach will actually expand the vista of your citizenship as you help mentor a young scientist in the peer-review process. This helps educate them on the process as well as providing real experiential learning on how to write (or not to write) a manuscript.

So are you a good science citizen? I hope you are and if not, perhaps you'll see the value of being a good citizen and you'll start down the path of recovery so that you, too, can again feel that exhilaration of being a science citizen in good standing.

E. J. Murphy (✉)
Department of Pharmacology, Physiology, and Therapeutics, University of North Dakota, Grand Forks, ND, USA
e-mail: eric.murphy@med.und.edu

Lipids (2011) 46:209–228
DOI 10.1007/s11745-010-3524-y

REVIEW

Dietary Monounsaturated Fatty Acids Are Protective Against Metabolic Syndrome and Cardiovascular Disease Risk Factors

Leah G. Gillingham · Sydney Harris-Janz · Peter J. H. Jones

Received: 5 November 2010 / Accepted: 21 December 2010 / Published online: 10 February 2011

Abstract Over 50 years of research has sought to define the role dietary fat plays in cardiovascular disease (CVD) risk. Although optimal dietary fat quantity has been keenly pursued over past decades, attention has recently centered on the value of dietary fat quality. The purpose of the present review is to provide a critical assessment of the current body of evidence surrounding efficacy of dietary monounsaturated fatty acids (MUFA) for reduction of traditional risk factors defining metabolic syndrome (MetS) and CVD. Due to existing and emerging research on health attributes of MUFA rich diets, and to the low prevalence of chronic disease in populations consuming MUFA rich Mediterranean diets, national dietary guidelines are increasingly recommending dietary MUFA, primarily at the expense of saturated fatty acids (SFA). Consumption of dietary MUFA promotes healthy blood lipid profiles, mediates blood pressure, improves insulin sensitivity and regulates glucose levels. Moreover, provocative newer data suggest a role for preferential oxidation and metabolism of dietary MUFA, influencing body composition and ameliorating the risk of obesity. Mounting epidemiological and human clinical trial data continue to demonstrate the cardioprotective activity of the MUFA content of dietary fat. As the debate on the optimal fatty acid composition of the diet continues, the benefit of increasing MUFA intakes, particularly as a substitute for dietary SFA, deserves considerable attention.

L. G. Gillingham · S. Harris-Janz · P. J. H. Jones (✉)
Department of Human Nutritional Sciences,
Richardson Centre for Functional Foods and Nutraceuticals,
University of Manitoba, 196 Innovation Drive,
Winnipeg, MB R3T 2N2, Canada
e-mail: peter_jones@umanitoba.ca

Keywords Monounsaturated fatty acids · Metabolic Syndrome · Cardiovascular disease · Fatty acids · Lipids · Nutrition

Abbreviations

ALA	Alpha-linolenic acid
BMI	Body mass index
CHD	Coronary heart disease
CHO	Carbohydrate
CVD	Cardiovascular disease
DM	Diabetes mellitus
HDL-C	High-density lipoprotein cholesterol
LF	Lower fat
LNA	Linoleic acid
LDL-C	Low-density lipoprotein cholesterol
MetS	Metabolic syndrome
MF	Moderate fat
MUFA	Monounsaturated fatty acids
OLA	Oleic acid
PUFA	Polyunsaturated fatty acids
SFA	Saturated fatty acids
STA	Stearic acid
TAG	Triglyceride
TC	Total cholesterol
TFA	Trans fatty acids

Introduction

Considerable scientific interest has focused on the impact of dietary fat in the development of metabolic disorders, leading to cardiovascular disease (CVD) [1, 2]. The complications associated with metabolic syndrome (MetS) are the primary foundation of CVD morbidity and

mortality. Dyslipidemia, hypertension, hyperglycemia, insulin resistance and obesity, namely abdominal obesity, are critical factors contributing to MetS. As MetS is a combination of modifiable risk factors, dietary intervention is targeted in primary prevention and secondary treatment therapies. Cumulative scientific evidence suggests that dietary monounsaturated fatty acids (MUFA) effect reductions in key risk factors for MetS [3–5]. Dietary MUFA promote a healthy blood lipid profile, mediate blood pressure, and favorably modulate insulin sensitivity and glycemic control. Conversely, the detrimental effects of diets rich in saturated fatty acids (SFA) have been widely recognized [6, 7]. Thus, national dietary guidelines with a primary focus on cardiovascular health have emphasized the need to reduce consumption of SFA as compared to a decrease in total dietary fat. With emerging research on the health attributes of MUFA rich diets, and the low prevalence of chronic disease in populations consuming MUFA rich Mediterranean diets [8], recommendations have been made to replace SFA intakes with unsaturated fats [9]. However, questions still remain as to the optimal dietary replacement for SFA, comparing MUFA intakes to those of polyunsaturated fatty acids (PUFA) and carbohydrates (CHO). Despite PUFA numerous cardiovascular benefits, intakes have been limited to $\leq$10% of energy due to potential adverse effects, including reduction of high-density lipoprotein cholesterol (HDL-C) levels and increased susceptibility of low-density lipoprotein (LDL) to oxidation [4, 10]. Furthermore, the replacement of dietary SFA with CHO may result in challenges in glucose metabolism and insulin resistance, as well as blood triglyceride (TAG) and HDL-C levels [11, 12]. Thus, potential health attributes of increasing MUFA intakes, particularly at the expense of dietary SFA, deserve careful attention. In light of the recent attention challenging the cardioprotective benefits of MUFA [13, 14], professional organizations continue to recommend dietary MUFA for the prevention of CVD [15, 16]. The purpose of the present review, therefore, is to critically assess the current evidence from human clinical trials surrounding the efficacy of dietary MUFA in the reduction of risk factors for MetS, ultimately targeting a reduction in CVD.

Metabolic Syndrome; Definition and Prevalence

The rising prevalence of chronic disease is related to unhealthy lifestyle choices, including atherogenic diets and lack of physical activity. Metabolic syndrome is defined by a collection of metabolic disorders occurring in an individual and associates with an increased risk of developing type 2 diabetes mellitus (DM-II) and CVD [17–19]. The primary clinical endpoint of MetS is CVD morbidity and mortality. Since the term was first classified by Reaven [20], the definition has evolved to include specific diagnostic criteria by several professional organizations. Recently, the National Cholesterol Education Program's Adult Treatment Panel III (NCEP ATP III) defines MetS as an individual possessing any three or more of the following five risk factors; elevated TAG [$\geq$150 mg/dL (1.7 mmol/L)], reduced HDL-C [<40 mg/dL (1.03 mmol/L) in men or <50 mg/dL (1.29 mmol/L) in women], elevated fasting glucose [$\geq$100 mg/dL (5.6 mmol/L)], hypertension ($\geq$130/85 mmHg or drug treatment), or obesity [waist circumference $\geq$102 cm (40 in) in men or $\geq$88 cm (35 in) in women] [20], with ethnicity specific values for waist circumference outlined by the International Diabetes Federation [21]. Furthermore, emerging risk factors for MetS include a proinflammatory and prothrombotic state [20]. Initially it was hypothesized that insulin resistance was the main risk factor for MetS [22], however, recent definitions propose abdominal obesity to be the predominate risk factor underlying MetS [20, 21, 23, 24]. The prevalence of MetS ranges worldwide [25], impacted by cultural differences associated with population dietary and lifestyle patterns. For example, the prevalence of MetS in the United States (34.5%) is approximately threefold that of Mediterranean countries [25–27]; predominated by the epidemic growth of obesity in the United States [28]. Currently, approximately 66% of the United States population are classified as overweight (BMI > 25 kg/m^2) and 33% obese (BMI > 30 kg/m^2) [29]. The components of the Mediterranean diet are fundamental to the lower prevalence of MetS [30]. Although the Mediterranean diet is complex in nature, rich in fruits, vegetables, and whole-grains, the MUFA content of Mediterranean diets accounts for 16–29% of energy [4], with olive oil providing 15–30% of energy [8]. Therefore, incorporating MUFA into Western dietary patterns, particularly at the expense of SFA, may target a reduction in risk for MetS and CVD.

Monounsaturated Fat; Structure and Sources

Monounsaturated fatty acids are classified as fatty acid chains containing one double bond. Monounsaturated fatty acids possess higher melting points than PUFA, which contain two or more double bonds. Both MUFA and PUFA are liquid at room temperature, whereas MUFA exist as semi-solids or solids when refrigerated. Conversely, SFA contain no double bonds and are solid at room temperature. Structurally, the common MUFA, palmitoleic acid (16:1n-7) and oleic acid (OLA; 18:1n-9), are both *cis* isomers of MUFA. The major dietary *trans* isomer of MUFA is elaidic

acid (*trans*18:1n-9). Oleic acid is the predominate MUFA in the diet, representing ~92% of *cis*MUFA [4]. Table 1 outlines the fatty acid content of food rich in MUFA. Of the MUFA rich dietary oils, the most commonly consumed are olive and canola oil. Furthermore, over the last decade an increase has occurred in commercial production of high OLA modified dietary oils with increased stability for the use in food processing, as a replacement to dietary oils rich in SFA and *trans* fatty acids (TFA) [31].

Current and Recommended Intakes of Dietary Fatty Acids

The total fat intake from Western diets is similar to that of the Mediterranean diet (Table 2), however, the type of dietary fat, specifically MUFA, differs vastly. In the United States, MUFA intakes are 13–14% of energy, SFA intakes are in excess at 11–12% of energy, and PUFA intakes are ≤7% of energy, of which 85–89% of PUFA intakes are

Table 1 Fatty acid composition of oils, nuts, seeds and fruit high in monounsaturated fat

	Calories (kcal)	Total fat (g)	SFA (g)	MUFA (g)	PUFA (g)	n-6 PUFA (g)	n-3 PUFA (g)
Vegetable oil							
Almond oil	884	100	8.2	69.9	17.4	17.4	0.0
Apricot oil	884	100	6.3	60.0	29.3	29.3	0.0
Avocado oil	884	100	11.6	70.6	13.5	12.5	1.0
Canola oil	884	100	7.4	63.3	28.1	19.0	9.1
Hazelnut oil	884	100	7.4	78.0	10.2	10.1	0.0
Olive oil	884	100	13.8	73.0	10.5	9.8	0.7
High-oleic canola oil	884	100	6.5	72.0	17.1	14.5	2.6
High-oleic safflower oil	884	100	6.2	74.6	14.4	14.4	0.0
High-oleic sunflower oil	884	100	9.7	83.6	3.8	3.6	0.2
Mid-oleic sunflower oil	884	100	9.0	57.3	29.0	29.0	0.0
Nuts and seeds[a]							
Almonds	597	52.8	4.0	33.7	12.6	12.6	0.0
Cashews	574	46.4	9.2	27.3	7.8	7.7	0.2
Hazelnuts	646	62.4	4.5	46.6	8.4	8.4	0.1
Macadamia nuts	718	76.1	11.9	59.3	1.5	1.3	0.2
Mixed nuts	594	51.5	6.9	31.4	10.8	10.5	0.2
Peanuts	585	49.7	6.9	24.6	15.7	15.7	0.0
Peanut butter (smooth)	588	50.4	10.3	23.7	13.9	13.8	0.1
Pistachios	571	46.0	5.6	24.2	13.9	13.6	0.3
Pecans	710	74.3	6.3	44.0	20.6	19.6	1.0
Sesame seeds	565	48.0	6.7	18.1	21.0	20.7	0.4
Tahini (sesame butter)	595	53.8	7.5	20.3	23.6	23.1	0.4
Walnuts (black)	618	59.0	3.4	15.0	35.1	33.1	2.0
Walnuts (English)	654	65.2	6.1	8.9	47.2	38.1	9.1
Fruit							
Avocado, raw	160	14.7	2.1	9.8	1.8	1.7	0.1
Olives, ripe	481	10.7	1.4	7.9	0.9	0.8	0.1
Selected animal products							
Ground beef, regular 100 g	259	16.3	5.7	7.5	0.6	0.5	0.1
Chicken breast, boneless skinless 100 g	690	3.57	1.0	1.2	0.8	0.7	0.1
Egg, large whole 50 g	324	5.3	1.6	2.0	0.7	0.6	0.1
Fried bacon, 3 slices	529	9.6	3.2	4.3	1.1	1.0	0.1

Source: USDA National Nutrient Database for Standard Reference. United States Department of Agriculture Website (http://www.nal.usda.gov/fnic/foodcomp/search/) Accessed 18 August 2009

MUFA monounsaturated fatty acids, *PUFA* polyunsaturated fatty acids, *SFA* saturated fatty acids

[a] All nuts and seeds are dry roasted, without salted added

Table 2 Current nutrient intakes in the Mediterranean and United States as compared to the recommended intakes outlined by health professional organizations

	Current Intakes			Recommended intakes					
	Mediterranean (%)[a]	United States (%)[a,b]	United States (g)[c]	Dietary guidelines (%)[a]	ADA and DC (%)[a]	NCEP ATP III (%)[a]	USDA's MyPyramid (g)[c]	NHLBI's dash eating plan (g)[c]	Harvard health eating pyramid (g)[c]
Total fat	33–40	33	83–87	20–35	20–35	25–35	64.8	41.1	69.0
SFA	<8	11–12	28–30	<10	<10	<7	17.3	10.0	12.8
MUFA	16–29	13–14	32–33	–	≤25	≤20	23.5	15.0	24.8
PUFA	<7	<7	17–18	–	≤10	≤10	19.6	12.6	25.7

ADA American Dietetic Association, *DASH* Dietary Approaches to Stop Hypertension, *DC* Dietitians of Canada, *MUFA* monounsaturated fatty acid, *NCEP ATPIII* National Cholesterol Education Program Adult Treatment Panel III, *NHLBI* National Heart, Lung, and Blood Institutes, *PUFA* polyunsaturated fatty acids, *SFA* saturated fatty acids, *USDA* United States Department of Agriculture

– Not specified, however supports recommendations by other expert organizations

[a] Percent of daily energy

[b] Means of United States male and females (ages 20–59) from the NHANES, 1999–2000

[c] Based on a ~2,000 kcal/day

omega-6 PUFA, principally linoleic acid (LNA) [4, 32, 33]. Conversely, the majority of total fat intake (33–40% of energy) in the Mediterranean diet is represented by MUFA, ranging from 16 to 29% of energy, with olive oil as the principal fat [4, 34, 35]. The high MUFA intake of the Mediterranean diet is at the expense of SFA, with intakes of SFA <8% of energy. Thus, an inverse relationship between the Mediterranean diet and coronary heart disease (CHD) risk has been substantiated in both epidemiological studies and randomized clinical trails [1].

Cardiovascular disease, the clinical outcome of MetS, remains the leading cause of mortality in the Western population [29] and therefore, several professional health organizations have outlined target fatty acid intakes to reduce MetS, DM and CVD risk (Table 2) [9, 36–41]. Recently, the recommendations focus on dietary fat quality versus fat quantity with less emphasis on high CHO diets. The American Diabetes Association (ADA) have modified their previous dietary recommendations for individuals with diabetes, which consisted of high CHO intakes and restricted total fat to ≤30% of energy, with SFA, MUFA, and PUFA at ≤10% of energy [42]. The ADA currently recommends that 60–70% of total calories in diets of those affected with DM-I and -II should be obtained from MUFA and CHO, emphasizing individualization of macronutrients by healthcare professionals [43, 44]. Moreover, the most recent position statement on dietary fatty acids from the ADA and Dietitians of Canada allows for total fat between 20 and 35% of energy, enhancing MUFA intakes up to 25% of energy [36]. The upper limit of total fat at 35% of energy is to minimize intakes of SFA, as well as an upper limit of PUFA intake at 10% of energy due to inconclusive scientific evidence supporting higher intakes of LNA for individuals with DM. Furthermore, the NCEP ATP III, endorsed by the American Heart Association (AHA), has recommended dietary guidelines for primary and secondary prevention of CHD with emphasis on monitoring total dietary fat and targeting a reduction in SFA. Similar to the ADA, earlier recommendations by the AHA, NCEP Step I and II diets, limited total fat intake to ≤30% and MUFA intake to ≤15% of energy [45]. However, in 2001 the NCEP released revisions to the ATP III guidelines [9] increasing total fat to 25–35% of energy, allowing a specific increase in MUFA intakes of up to 20% of energy, with a recommendation for replacing CHO with unsaturated fats for individuals with DM or MetS. Of interest, the current NCEP ATP III recommendations mirror the dietary fat profile of the Mediterranean diet (Table 2) [4, 34, 35]. Recently, the Joint FAO/WHO Expert Consultation on Fats and Fatty Acids in Human Nutrition recommended that MUFA intakes be 15–20% of energy, according to total fat intakes [46]. Unlike other fatty acids with a recommended limit, MUFA intakes should be determined by calculating the difference, i.e. MUFA (% energy) = Total Fat (% of energy) − SFA (% of energy) − PUFA (% of energy) − TFA (% of energy). Thus, MUFA intakes will range with respect to the total fat and fatty acid composition of the diet.

As mentioned, olive oil is the predominate fat in the Mediterranean diet, and although olive oil use is not as common in Western diets, MUFA rich canola oil use in the United States has increased 5.5-fold from 1985 to 1994 [32]. Canola oil, originally naturally bred from rapeseed oil and low in erucic acid, has grown to become the third largest consumed vegetable oil in the world and, next to soybean oil, canola oil is the second most consumed

vegetable oil in the United States. Canola oil can be regarded as one of the most healthy consumed vegetable oils with an attractive fatty acid profile distinctively low in SFA, and rich in MUFA and n-3 PUFA α-linolenic acid (ALA) (Table 1). Consequently, in 2006 the United States Food and Drug Administration (FDA) authorized a qualified health claim stating that canola oil (~19 g daily) may reduce the risk of CHD due its unsaturated fat content, recommending direct caloric replacement of dietary SFA with canola oil [47]. A recent dietary modeling study revealed that replacing common dietary fats in the United States with canola oil and canola-based spreads would increase the percentage of Americans complying with current dietary intake recommendations for fatty acids, namely SFA, MUFA, and ALA, but not for LNA [48]. More specifically, a 50% substitution of fats with canola oil would decrease SFA intakes by 4.7%, whereas a 100% substitution would decrease SFA and LNA intakes by 9.4 and 44.9%, respectively, while increasing MUFA and ALA intakes by 27.6 and 73.0%, respectively. Based on the emphasis of increasing the intakes of MUFA in the diet, particularly at the expense of SFA, it is timely and appropriate to explore the efficacy of MUFA rich diets in the prevention of MetS and CVD.

Monounsaturated Fat and Blood Lipids

Numerous randomized controlled trials have investigated the impact of dietary intervention on changes in circulating lipids [49–52]. The NCEP ATP III guidelines have outlined risk factors that increase CHD risk over a 10 year period. Traditionally, elevated LDL-C [>100 mg/dL (2.6 mmol/L)] remains the strongest primary factor in predicting CHD and therefore is a primary target of therapy [53]. However, as circulating TAG and HDL-C concentrations are critical risk factors in MetS, the TC:HDL-C ratio has been considered a more valuable marker in determining CHD risk [52]. Although the hypolipidemic effect of reducing dietary SFA is well-known and remains the primary target of dietary intervention [7], the debate as to whether MUFA, PUFA or CHO should replace SFA in the diet continues.

Effects of Monounsaturated Fat Compared with Saturated Fat

Evidence from randomized controlled trials has substantiated the deleterious effects of dietary SFA on circulating lipids and lipoproteins [49–51]. When MUFA isocalorically replace SFA in the diet there are improvements in the TC:HDL-C ratio, namely associated with a decrease in serum LDL-C levels and preservation of HDL-C levels. Recently, attention has focused on the lipidemic effects of individual SFA, as stearic acid (STA, 18:0) is considered to have neutral or hypolipidemic effects on circulating lipids compared with other SFA, namely lauric (12:0), myristic (14:0) and palmitic (16:0) acids [52, 54]. Although only a few studies have directly compared OLA to STA intakes, Hunter et al. [54] collectively showed that when OLA replaced STA, LDL-C levels decreased by 5–13% in 3 of 8 studies, however, had no effect in 5 other studies. HDL-C levels increased in one study between 5 and 7%, with no effect in 7 of 8 studies. Triglycerides decreased 20–37% in 2 studies; with no effect in 6 other studies. Finally, an estimated directional decrease in TC:HDL-C ratio was observed in 6 of the 8 studies when OLA replaced STA. Overall compared to OLA, STA tended to increase LDL-C and TAG levels, lower HDL-C levels, and resulted in an increase in the TC:HDL-C ratio. Thus, novel modified dietary oils with a high OLA content have been developed by agricultural and food industries to replace partially hydrogenated oils rich in TFA and SFA for use in food preparation, including frying, baking, and blending with other fats [31]. However, as there are specific food applications that require a solid fat (i.e. shortenings and baked goods), a high STA fat may provide an alternative to fat-containing TFA [54].

Dietary Monounsaturated Fat Versus Carbohydrate for Replacement of Saturated Fat

The effects on CHD risk with substitution of SFA by other macronutrients continue to be a primary focus of public health agendas [14, 52, 55]. Diets rich in CHO, PUFA and MUFA have been compared to those rich in SFA in assessing the ability of each dietary strategy to favorably alter plasma lipids. In studies conducted with healthy subjects comparing high MUFA diets to high CHO diets, those on high MUFA diets showed significant reductions in TAG levels [56–58]. Likewise, overweight and obese subjects [59], those with DM-II [5, 60, 61], and MetS [62] also benefitted from the substitution of MUFA rich diets, as compared to CHO rich diets, in improving plasma TAG levels. One of the main cardioprotective activities of high MUFA diets is the ability of MUFA to either preserve or increase HDL-C levels when compared to CHO rich diets which mostly produce decreases in HDL-C levels [5, 56, 60, 62, 63]. As compared to high CHO diets, high MUFA diets more favorably affect the TC:HDL-C ratio, emphasized by a reduction in LDL-C and TAG levels, while increasing HDL-C levels [52]. Recently, Cao et al. [64] conducted a meta-analysis of 30 controlled-feeding studies in subjects with and without diabetes, comparing moderate fat (MF) (30.2–50% of energy; mean MUFA intake 23.6%

of energy) versus lower fat (higher CHO) diets (LF) (18.3–30.2% of energy; mean MUFA intake 11.4% of energy). In all subjects, reductions in LDL-C levels were similar between the MF and LF diets. However, the MF diet increased HDL-C levels (2.28 mg/dL; 95% CI 1.66–2.90 mg/dL) and decreased TAG levels (−9.36 mg/dL; 95% CI −12.16 to −6.08 mg/dL) versus the LF diet. Moreover, in subjects with diabetes, a further decrease in TAG levels (−24.79 mg/dL) was observed after the MF diet, as well as a decrease in the TC: HDL-C ratio (−0.62) and non-HDL-C (−5.39%) versus the LF diet. The authors concluded that MF diets reduced predicted CHD risk by 6.37% in men and 9.34% in women, including subjects with diabetes, compared with the LF diet. Therefore, MUFA versus CHO replacement for SFA may be more beneficial for individuals predisposed to MetS or with DM-II [5, 53].

Dietary Monounsaturated Fat Versus Polyunsaturated Fat for Replacement of Saturated Fat

Comparison studies and reviews have also examined the action of PUFA rich versus MUFA rich diets on plasma lipid modulation [4, 52, 65–67]. Evidence supports the notion that MUFA rich diets have slightly less or comparable TC and LDL-C lowering effects to those of PUFA rich diets. Whereas n-3 PUFA rich diets may additionally reduce serum TAG [68], MUFA rich diets have more favorable effects on HDL-C concentrations. The ability to effectively target an increase in plasma HDL-C is critical in patients with MetS, DM-II and the prevention of CVD [69, 70]. When PUFA and MUFA rich diets were compared for replacement of dietary SFA in healthy adult subjects, those consuming MUFA rich diets demonstrated a preservation of HDL-C levels to a greater extent with only a 4% decrease in HDL-C levels compared to those consuming PUFA rich diets, which decreased HDL-C levels by 14% [71]. Thus, due to the preservation of HDL-C with MUFA versus PUFA rich diets, effects on the TC:HDL-C ratio where comparable when either MUFA or PUFA replaced dietary SFA [52, 71].

Dietary Monounsaturated Fat and Blood Pressure

Evidence from human clinical studies have shown that dietary MUFA either have neutral or hypotensive effects when compared to diets rich in CHO, n-6 or n-3 PUFA, notably reporting consistent reductions in blood pressure when MUFA are compared to SFA rich diets (Table 3). A study comparing hypertensive subjects consuming MUFA and PUFA rich diets revealed that virgin olive oil high in OLA resulted in significant decreases in total blood pressure [72]. The hypotensive effect of MUFA also alleviated the need of anti-hypertensive drug therapy by 48%, whereas all subjects on a PUFA rich diet required further drug therapy. In contrast, a study conducted by Mutanen et al. [73] failed to observe hypotensive effects of either MUFA or PUFA rich diets in normotensive subjects. Among the studies comparing MUFA and PUFA rich diets, hypotensive benefits of MUFA rich diets are observed in individuals predisposed to MetS in 2 clinical trials, whereas 4 of 5 clinical trials observed no difference between MUFA and PUFA diets in healthy individuals (Table 3).

The effects of MUFA versus CHO rich diets on blood pressure were compared in a meta-analysis by Shah et al. [74]. Of the 10 intervention trials assessed, MUFA rich diets were associated with a slight reduction in blood pressure, specifically systolic blood pressure, compared to the CHO rich diets. Similarly, in this review, 3 of 6 clinical trials observed hypotensive benefits with MUFA rich diets compared to CHO rich diets in individuals predisposed to MetS (Table 3). Muzio et al. [75] compared consumption of high MUFA diets to high CHO diets in 100 obese subjects with MetS over 5 months. At study cessation, while both groups showed significant reductions in all components of MetS, only the diet high in MUFA produced a significantly lower systolic blood pressure, as well as lowered heart rate. In the large randomized, crossover Omni Heart Trial, 164 subjects with prehypertension or stage-1 hypertension consumed diets varying in dietary fats for 6 weeks to determine their subsequent risk of hypertension [76]. Compared to a high CHO diet, consumption of high protein and MUFA diets produced significant reductions in systolic blood pressure and additional benefits in TAG and HDL-C levels.

Considering prospective cohort studies, the SUN (Seguimiento Universidad de Navarra) study of nearly seven thousand subjects reported that high intake of olive oil for an average of 28.5 months was associated with a decrease in the incidence of hypertension in men, but not women [77]. Similarly, in the Greek EPIC (European Prospective Investigation into Cancer and Nutrition) study, olive oil consumption was a primary dietary factor in the Mediterranean diet preventing hypertension [78]. More specifically, a reduction in both systolic and diastolic blood pressure was noted with olive oil consumption, even after controlling for vegetable intake. Alongside, there was an inverse relationship between blood MUFA:SFA ratio and arterial blood pressure. Indeed, olive oil in Mediterranean diets has potent hypotensive effects [79]. However, the OLA content of olive oil, independent of its other components, has been shown to be directly associated with a reduction in blood pressure [80]. As such, strong support can be obtained from clinical trials of the blood pressure

Table 3 Human clinical trials investigating the effects of monounsaturated fat and hypertension

Reference	Subject characteristics	Study design/ duration	Diets	Outcome
Individuals predisposed to metabolic syndrome				
Gulseth et al. [125]	MetS subjects ($n = 486$)	Randomized, parallel 12 weeks	MUFA 39% fat; 10% SFA, 19% MUFA, 7% PUFA SFA 40% fat; 18% SFA, 13% MUFA, 6% PUFA H-CHO 30% fat; 9% SFA, 12% MUFA, 6% PUFA H-CHO + n-3 PUFA 29% fat; 9% SFA, 11% MUFA, 6% PUFA, 1.6 g/d EPA + DHA	No difference in systolic BP or diastolic BP between diets ↓ Pulse pressure with MUFA vs. SFA in men
Brehm et al. [94]	Overweight or obese with DM-II subjects ($n = 124$)	Randomized, parallel 12 months	MUFA 38% fat; 14% MUFA H-CHO 28% fat; 8% MUFA	No difference in diastolic BP between diets
Muzio et al. [75]	Hypercholesterolemic obese subjects with MetS ($n = 100$)	Randomized 5 months	H-CHO 22% fat; 5% SFA, 14% MUFA, 3% PUFA MUFA 33% fat; 9% SFA, 21% MUFA, 4% PUFA	↓ Systolic BP and HR with MUFA vs. H-CHO
Appel et al. [76]	Pre-HT or HT (stage 1) subjects ($n = 164$)	Randomized, crossover 6 weeks	H-CHO 27% fat; 6% SFA, 13% MUFA, 8% PUFA Protein 27% fat; 6% SFA, 13% MUFA, 8% PUFA MUFA 37% fat; 6% SFA, 21% MUFA, 10% PUFA	↓ Systolic and diastolic BP with MUFA and protein vs. CHO in all subjects
Shah et al. [126]	DM-II subjects ($n = 41$)	Randomized, crossover 6 weeks, then 14 weeks	H-CHO 30% fat; 10% SFA, 10% MUFA, 10% PUFA MUFA 45% fat; 10% SFA, 25% MUFA, 10% PUFA	No difference in BP between diets at 6 weeks ↑ Diastolic BP and heart rate at 14 weeks with H-CHO vs MUFA
Piers et al. [106]	Overweight or obese men ($n = 8$)	Randomized, crossover 4 weeks	SFA 40% fat; 24% SFA, 13% MUFA, 3% PUFA MUFA 40% fat; 11% SFA, 22% MUFA, 7% PUFA	↓ Mean arterial pressure and diastolic BP with MUFA vs. SFA
Ferrara et al. [72]	HT subjects ($n = 23$)	Randomized, crossover 6 months	MUFA 27% fat; 6% SFA, 17% MUFA, 4% PUFA PUFA 27% fat; 6% SFA, 11% MUFA, 11% PUFA	↓ Systolic and diastolic BP with MUFA vs. PUFA ↓ HT drug treatment with MUFA but not PUFA

Table 3 continued

Reference	Subject characteristics	Study design/ duration	Diets	Outcome
Thomsen et al. [127]	DM-II subjects ($n = 16$)	Randomized, crossover 3 weeks	MUFA 49% fat; 10% SFA, 30% MUFA, 7% PUFA PUFA 49% fat; 9% SFA, 10% MUFA, 27% PUFA	↓ Arterial BP with MUFA vs. PUFA
Walker et al. [128]	DM-II subjects ($n = 24$)	Randomized, crossover 12 weeks	H-CHO 23% fat; 9% SFA, 10% MUFA, 4% PUFA MUFA 36% fat; 11% SFA, 20% MUFA, 5% PUFA	No differences in BP between diets
Healthy individuals				
Rasmussen et al. [129]	Healthy subjects ($n = 162$)	Randomized, parallel 3 months	SFA 37% fat; 17% SFA, 14% MUFA, 6% PUFA MUFA 37% fat; 8% SFA, 23% MUFA, 6% PUFA Further randomization with n-3 PUFA (fish oil): 3.6 g/d	↓ Systolic and diastolic BP with MUFA from baseline ↔ BP with SFA from baseline ↓ Diastolic BP with MUFA vs. SFA ↔ BP with addition of fish oil supplementation
Aro et al. [130]	Healthy subjects ($n = 87$)	Randomized, parallel 8 weeks	Control 20% fat; 8% SFA, 8% MUFA, 3% PUFA MUFA 26% fat; 7% SFA, 14% MUFA, 3% PUFA PUFA 26% fat; 8% SFA, 8% MUFA, 8% PUFA	No differences in BP between diets
Lahoz et al. [131]	Healthy subjects ($n = 42$)	4 Consecutive diet phases 5 weeks	SFA 35% fat; 17% SFA, 14% MUFA, 4% PUFA MUFA 35% fat; 9% SFA, 21% MUFA, 4% PUFA n-6 PUFA 35% fat; 10% SFA, 12% MUFA, 13% PUFA n-3 PUFA 35% fat; 9%SFA, 12% MUFA, 13% PUFA (1.6% n-3 PUFA)	↓ Systolic BP with MUFA vs. SFA and n-6 PUFA

Table 3 continued

Reference	Subject characteristics	Study design/ duration	Diets	Outcome
Uusitupa et al. [132]	Healthy subjects ($n = 159$)	Randomized, parallel 6 months	SFA 35% fat; 14:19:4 SFA:MUFA:PUFA AHA diet 32% fat; 10:8:8 SFA:MUFA:PUFA MUFA 34% fat; 11:11:5 SFA:MUFA:PUFA Low-fat 30% fat; 12:8:3 SFA:MUFA:PUFA	↓ Systolic BP with AHA only ↑ BP with SFA in men only
Mutanen et al. [73]	Healthy subjects ($n = 59$)	Randomized, crossover 3.5 weeks	MUFA 38% fat; 13% PUFA PUFA 38% fat; 16% MUFA	No differences in BP between diets
Mensink et al. [133]	Healthy subjects ($n = 58$)	Randomized, parallel 5 weeks	MUFA 36% fat; 13% SFA, 15% MUFA, 8% PUFA PUFA 36% fat; 13% SFA, 11% MUFA, 13% PUFA	No differences in BP between diets
Mensink et al. [134]	Healthy subjects ($n = 47$)	Randomized, parallel 5 weeks	H-CHO 22% fat; 7% SFA, 9% MUFA, 5% PUFA MUFA 41% fat; 10% SFA, 24% MUFA, 5% PUFA	No differences in BP between diets

Direction of effect on biomarkers of hypertension (↑ increased; ↓ decreased; ↔ no effect)

AHA American Heart Association, *BP* blood pressure, *CHO* carbohydrate, *DM-II* Diabetes Mellitus-II, *H-CHO* high-carbohydrate, *HT* hypertensive, *HR* heart rate, *MetS* metabolic syndrome, *MUFA* monounsaturated fatty acids, *PUFA* polyunsaturated fatty acids, *SFA* saturated fatty acids, *vs* versus

lowering effects of MUFA rich diets in both normotensive and hypertensive individuals.

Monounsaturated Fats, Insulin Resistance and Diabetes Mellitus-II

With the rising prevalence of DM worldwide [81], MUFA have gained attention for their ability to regulate glycemic response and improve insulin sensitivity. Similar to the detrimental effects on circulating lipids, SFA have been shown to impair glycemic control and insulin sensitivity [12], specifically in skeletal muscle cells [82]. Therefore, clinical trials replacing dietary SFA with MUFA have noted improvements in insulin sensitivity and glycemic response in individuals predisposed to insulin resistance [83–86], as well as healthy people [87–91] (Table 4). The KANWU (Kuopio, Aarhus, Naples, Wollongong and Uppsala) Study of 162 healthy subjects reported a reduction in insulin sensitivity following consumption of a SFA rich diet for 3 months, and that replacement of SFA with a MUFA rich diet improved insulin sensitivity [89]. More specifically, when total daily fat intake was <37% of energy, an 8.8% increase in insulin sensitivity was observed with the MUFA rich diet, whereas the SFA rich diet decreased insulin sensitivity by 12.5%. However, these effects were not observed when total daily fat intakes exceeded 37% of energy. In the development of DM-II, pancreatic β-cells that secrete insulin to counteract postprandial rises in blood glucose become overwhelmed and as a result, fail to effectively provide the necessary insulin to regulate glucose levels [92]. Recently, MUFA was shown to have a direct action on β-cell function and lower

Table 4 Human clinical trials investigating the effects of monounsaturated fat on glucose and insulin responses

Reference	Subject characteristics	Study design/ duration	Diets	Outcome
Individuals predisposed to metabolic syndrome				
Brehm et al. [94]	Obese and overweight subjects with DM-II ($n = 124$)	Randomized 1 year	H-CHO 28% fat; 7–9% MUFA MUFA 38% fat; 14–15% MUFA	No differences in glucose and insulin sensitivity between groups
Due et al. [83]	Nondiabetic obese subjects ($n = 46$)	Randomized, parallel 6 months	SFA 32% fat; 15% SFA, 10% MUFA, 4% PUFA MUFA 39% fat; 7% SFA, 20% MUFA, 8% PUFA Low-fat 23% fat; 8% SFA, 8% MUFA, 5% PUFA	↓ Fasting glucose, insulin, and insulin resistance score with MUFA vs. other diets ↓ HOMA-IR with MUFA vs. other diets
Paniagua et al. [84]	Obese DM-II subjects ($n = 11$)	Randomized, crossover 28 days	SFA 38% fat; 23% SFA, 9% MUFA, 6% PUFA MUFA 38% fat; 9% SFA, 23% MUFA, 6% PUFA H-CHO 20% fat; 6% SFA, 8% MUFA, 6% PUFA	↓ Fasting glucose with MUFA and H-CHO vs. SFA ↑ Insulin sensitivity (↓ HOMA-IR) with MUFA vs. other diets ↑ Postprandial GLP-1 with MUFA vs. H-CHO
Shah et al. [85]	DM-II subjects ($n = 11$)	Randomized, crossover 15 days	SFA 50% fat; 26% SFA, 20% MUFA, 5% PUFA MUFA 50% fat; 7% SFA, 39% MUFA, 5% PUFA n-6 PUFA 50% fat; 4% SFA, 8% MUFA, 39% PUFA n-3 PUFA 50% fat; 9% SFA, 15% MUFA, 44% PUFA	↓ Postprandial insulin response with MUFA and n-3 PUFA vs. SFA and n-6 PUFA ↔ Postprandial glucose response between diets
Vega-Lopez et al. [135]	Hyperlipidemic subjects ($n = 15$)	Randomized, crossover 5 weeks	TFA 30% fat; 9% SFA, 10% MUFA, 8% PUFA, 4% TFA SFA 30% fat; 15% SFA, 11%MUFA, 4% PUFA MUFA 32% fat; 6% SFA, 15% MUFA, 9% PUFA PUFA 28% fat; 7% SFA, 8% MUFA, 12% PUFA	No difference in fasting insulin, fasting glucose, or HOMA between diets

Table 4 continued

Reference	Subject characteristics	Study design/ duration	Diets	Outcome
Gerhard et al. [136]	DM-II subjects ($n = 11$)	Randomized, crossover 6 weeks	Low-fat 20% fat; 4% SFA, 8% MUFA, 6% PUFA MUFA 40% fat; 6% SFA, 25% MUFA, 6% PUFA	No difference in fasting glucose, glycemic control or insulin sensitivity between diets
Thomsen et al. [137]	Overweight subjects with DM-II ($n = 12$)	Randomized, crossover $\geq$1 week	SFA MUFA	↔ Glucose or insulin responses between diets ↑ GLP-1 responses with MUFA vs. SFA
Lovejoy et al. [138]	Healthy, normal and overweight subjects ($n = 25$)	Randomized, crossover 4 weeks	SFA 28% fat; 9% SFA MUFA 28% fat; 9% MUFA TFA 28% fat; 9% TFA	↔ Insulin sensitivity between diets ↓ Insulin sensitivity with SFA vs. MUFA for overweight subjects
Lauszus et al. [139]	Pregnant women with gestational DM-II ($n = 27$)	Randomized From 33rd gestational week for 5 weeks	H-CHO 30% fat; 13% SFA, 11% MUFA, 6% PUFA MUFA 37% fat; 10% SFA, 22% MUFA, 5% PUFA	No difference in fasting insulin and glucose, insulin sensitivity between diets
Rodriguez-Villar et al. [140]	DM-II subjects ($n = 12$)	Randomized, crossover 12 weeks	CHO 29% fat; 6% SFA, 12% MUFA, 5% PUFA MUFA 40% fat; 8% MUFA, 25% MUFA, 5% PUFA	No differences in fasting or postprandial glucose and insulin between diets
Luscombe et al. [141]	DM-II subjects ($n = 21$)	Randomized, crossover 4 weeks	CHO (high GI diet) 21% fat; 8% SFA, 7% MUFA, 4% PUFA CHO (low GI diet) 23% fat; 8% SFA, 7% MUFA, 4% PUFA MUFA (high GI diet) 35% fat; 8% SFA, 18% MUFA, 7% PUFA	No difference in fasting insulin and glucose between diets
Christiansen et al. [86]	DM-II and obese subjects ($n = 16$)	Randomized, crossover 6 weeks	SFA 30% fat; 20% SFA, 5% MUFA, 5% PUFA MUFA 30% fat; 5% SFA, 20% MUFA, 5% PUFA TFA 30% fat; 5% SFA, 20% TFA, 5% PUFA	↔ Glycemic control or postprandial glycemic response between diets ↓ Postprandial insulinemia with MUFA vs. SFA and TFA

Table 4 continued

Reference	Subject characteristics	Study design/ duration	Diets	Outcome
Sarkkinen et al. [142]	IGM subjects ($n = 22$)	Randomized 8 weeks	SFA 37% fat; 18%SFA, 11% MUFA, 5% PUFA MUFA 40% fat; 11% SFA, 19% MUFA, 8% PUFA PUFA 34% fat; 11% SFA, 10% MUFA, 10% PUFA	↓ Fasting glucose with MUFA vs. SFA ↔ Fasting glucose with PUFA vs. SFA ↑ Glucose effectiveness with MUFA vs. PUFA
Parillo et al. [143]	DM-II subjects ($n = 10$)	Randomized 15 days	H-CHO 20% fat MUFA 40% fat	↓ Fasting glucose and insulin with MUFA vs. H-CHO
Bonanome et al. [144]	DM-II subjects ($n = 19$)	Consecutive diets 2 months	H-CHO 25% fat; 10% SFA, 10% MUFA, 5% PUFA MUFA 40% fat; 10% SFA, 25% MUFA, 5% PUFA	↔ Fasting glucose or insulin response between diets
Garg et al. [60]	DM-II subjects ($n = 10$)	Randomized 28 days	H-CHO 25% fat MUFA 50% fat; 33% MUFA	↓ Plasma glucose and insulin requirements with MUFA vs. H-CHO
Healthy individuals				
Lopez et al. [87]	Healthy men ($n = 14$)	Randomized, crossover Single meal 8 h	NCEP Step-I diet 29% fat Butter diet 38% fat; 0.48 MUFA:SFA High-palmitic sunflower oil diet 38% fat; 2.42 MUFA:SFA Refined olive oil diet 38% fat; 5.43 MUFA:SFA Vegetables/fish oil diet 38% fat; 7.08 MUFA:SFA	↑ Postprandial β-cell function and insulin sensitivity with an increase in the MUFA to SFA ratio of dietary fats
Perez-Jimenez et al. [88]	Healthy subjects ($n = 59$)	Randomized, crossover 28 days	SFA 20% SFA, 12% MUFA, 6% PUFA H-CHO 28% fat; 10% SFA, 12% MUFA, 6% PUFA MUFA 38% fat; 10% SFA, 22% MUFA, 6% PUFA	↑ Fasting insulin and mean glucose for the SFA vs. MUFA and H-CHO Improvement in insulin sensitivity with MUFA and H-CHO vs. SFA

Table 4 continued

Reference	Subject characteristics	Study design/ duration	Diets	Outcome
Vessby et al. [89]	Healthy subjects ($n = 162$)	Randomized 3 months	SFA 37% fat; 18% SFA, 13% MUFA, 5% PUFA MUFA 37% fat; 10% SFA, 21% MUFA, 5% PUFA	↓ Insulin sensitivity with SFA vs. MUFA ↔ Insulin secretion between diets
Salas et al. [90]	Healthy men ($n = 41$)	Consecutive diets 4 weeks	SFA 38% fat; 20% SFA MUFA 38% fat; 22% MUFA NCEP Step-I 47% CHO, 28% fat	↑ Insulin on SFA diet ↓ Fasting glucose and insulin with MUFA vs. NCEP Step-I diet
Thomsen et al. [95]	Healthy subjects ($n = 16$)	Randomized, crossover 4 weeks	H-CHO 28% fat; 9% SFA, 8% MUFA, 7% PUFA MUFA 42% fat; 9% SFA, 24% MUFA, 6% PUFA	↔ Insulin sensitivity between diets ↔ Fasting blood glucose between diets
Thomsen et al. [145]	Healthy subjects ($n = 10$)	Randomized Single meal 8 h	CHO SFA MUFA	↔ Postprandial glucose or insulin response between diets ↑ GLP-1 and GIP responses with MUFA vs. SFA
Louheranta et al. [146]	Healthy women ($n = 15$)	Randomized, crossover 4 weeks	SFA 39%fat; 19% SFA, 12% MUFA, 6% PUFA MUFA 41% fat; 13% SFA, 19% MUFA, 6% PUFA	↔ Glucose or insulin responses between diets ↔ Insulin sensitivity between diets
Joannic et al. [147]	Healthy men ($n = 8$)	Randomized, crossover Single meal 3 h	MUFA 47% fat; 4.3 MUFA:PUFA PUFA 47% fat; 0.4 MUFA:PUFA	↓ Postprandial glucose and insulin responses with PUFA vs. MUFA
Uusitupa et al. [91]	Healthy subjects ($n = 10$)	Randomized, crossover 3 weeks	SFA 39% fat; 20% SFA, 12% MUFA, 4% PUFA MUFA 40% fat; 9% SFA, 19% MUFA, 10% PUFA	↓ Glucose AUC with MUFA vs. SFA ↑ Glucose disappearance rate with MUFA vs. SFA

Direction of effect on biomarkers of glucose and insulin responses (↑ increased; ↓ decreased; ↔ no effect)

AUC area under curve, *CHO* carbohydrate, *DM-II* diabetes mellitus-II, *GI* glycemic index, *GIP* gastric inhibitory polypeptide, *GLP-1* glucagon-like peptide-1, *H-CHO* high-carbohydrate, *HOMA-IR* homeostasis model assessment of insulin resistance, *IGM* irregular glucose metabolism, *MUFA* monounsaturated fatty acid, *NCEP* National Cholesterol Education Program, *PUFA* polyunsaturated fatty acids, *SFA* saturated fatty acids, *TFA* trans fatty acids, *vs* versus

insulin resistance in a study of 14 healthy men using a randomized, crossover design [87]. Data revealed that MUFA improved insulin sensitivity and β-cell function when compared with SFA. With the incremental substitution of MUFA for SFA, direct linear decreases in insulin resistance were observed.

As a replacement for dietary SFA, high MUFA diets have been compared to high CHO diets for preventing insulin resistance and DM-II risk [3, 5]. An earlier meta-analysis of 10 randomized controlled trials by Garg [5], assessing the effects of high MUFA diets in patients with either DM-I or DM-II, reported improvements in glycemic control, as well as lipoprotein profiles, as compared to high CHO diets. Ros [3] reviewed the evidence on dietary MUFA and metabolic control in DM-II following the comprehensive meta-analysis by Garg [5] and observed similar beneficial metabolic effects of MUFA rich diets. Following these analyses, Paniagua et al. [84, 93] demonstrated that compared to SFA or CHO rich diets, insulin resistant subjects consuming a MUFA rich diet exhibited improvements in insulin sensitivity, as well as other hormonal and metabolic parameters. Similarly, when compared to high CHO and high SFA diets, diets high in MUFA have been shown to significantly decrease fasting glucose by 3% and insulin by 9.4%, and improve insulin sensitivity by 12.1% [83]. In contrast, clinical trials with healthy subjects have observed no difference between MUFA and CHO rich diets in markers of glucose–insulin homeostasis [88, 94, 95]. However, due to other metabolic abnormalities associated with high CHO diets, such as the deleterious effects on plasma TAG and HDL-C levels [11] high MUFA diets may be more beneficial for ameliorating the risk of DM-II. Taken together, evidence from prospective cohort studies have reported that dietary MUFA are not associated with increased risk of DM-II in men [96] or women [97] after adjustment for other dietary fats, age and BMI.

Monounsaturated Fat in Weight Maintenance and Obesity

There is a perception that fat, rich in calories as compared to CHO or protein, is associated with body weight gain leading to obesity [98]. However, a strong argument also exists that dietary fat is not the primary cause of the high prevalence of obesity [99, 100]. Moreover, fat quality may have a stronger correlation to weight gain than fat quantity [101]. Considering fat quality and specific effects of dietary fatty acids for risk of obesity, evidence from prospective cohort studies have reported that MUFA intake is not associated with increases in waist circumference or body weight gain [101, 102]. In the Health Professionals Study of 16,587 men over a 9 year period, replacement of 2% energy of PUFA or CHO with MUFA was not associated with any change in waist circumference, whereas replacement with TFA or SFA led to an increase [102]. Similarly, in the Nurses' Health Study, consumption of MUFA, as well as PUFA, was not associated with an increase in body weight, while TFA and SFA positively correlated with weight gain after 8 years [101]. Large prospective cohort studies in the Mediterranean region have revealed that high intakes of olive oil [103] or nuts [104], both rich sources of MUFA, or adherence to a Mediterranean diet [105] were not associated with an increase in weight or risk of obesity over the longer term [103, 104].

With respect to human clinical trials, Paniagua et al. [93] have demonstrated that compared to CHO rich diets, insulin resistant subjects consuming a MUFA rich diet showed significantly increased fat oxidation rates and decreased abdomen-to-leg adipose ratios, thus preventing central body fat distribution [93]. This finding has important implications for those at risk for MetS since the increase in central adiposity was associated with a reduction in adiponectin expression and insulin sensitivity following the CHO rich diet as compared to the MUFA rich diet. An inverse relationship has been shown between circulating adiponectin levels and body fat percentage as well as central body fat accumulation, specifically visceral adiposity. Similarly, Piers et al. [106] substituted a SFA rich diet with MUFA for 4 weeks in eight overweight and obese men using a randomized crossover design to determine the effects on body weight and composition. Assessment of body composition by dual energy X-ray absorptiometry (DEXA) revealed a significant decrease in body mass (-2.1 ± 0.4 kg; $p = 0.0015$) and fat mass (-2.6 ± 0.6 kg; $p = 0.0034$) following the MUFA compared to the SFA rich diet, albeit no differences in total energy or fat intake were noted between diets. Furthermore, the changes in body mass and fat mass were accompanied with a decrease in waist-to-hip ratio after the MUFA rich versus the SFA rich diets. The favorable modifications in body composition and amelioration of weight gain after consumption of MUFA compared to SFA have also been observed in healthy subjects [107].

Of interest and as extensively reviewed by Bergouignan et al. [82], MUFA is the primary fat composing adipose tissue, however, there appears to be no direct relation between MUFA intake and MUFA levels in adipose. Rather SFA intake seems to be more closely associated with endogenous MUFA levels [108, 109]. Bergouignan et al. [82] hypothesized that in vivo desaturation of SFA may be related to an increase in MUFA versus SFA in adipose tissue. Furthermore, OLA preferentially accumulates in subcutaneous fat versus visceral fat, whereas the reverse exists with palmitate [110, 111]. Thus, since a direct correlation exists between visceral fat and risk factors for metabolic syndrome [112], OLA concentrating in subcutaneous fat versus visceral fat may be less atherogenic. Moreover, dietary MUFA may be preferentially oxidized as compared to other dietary fatty acids, as the degree of fatty acid chain length and unsaturation may

contribute to the partitioning of dietary fat to energy expenditure versus energy storage [107, 113–116]. Furthermore, the metabolism of dietary fat stimulates behavioral changes in food intake preference [117]. Indeed, evidence suggests that different dietary fats may elicit varying effects on satiety and total energy intake [118]. Taken together, dietary MUFA consumption is associated with maintenance of body weight and favorable shifts in reducing central body fat adiposity, potentially ameliorating obesity risk.

Monounsaturated Fats and Cardiovascular Risk; Epidemiological Evidence

As effects on risk markers may not directly translate into effects on clinical outcomes of disease, it is thus critical to assess effects of dietary MUFA on the primary clinical endpoint of MetS, that is CVD morbidity and mortality. Randomized controlled trials are considered the gold standard for evaluating the causal relationship between dietary intervention and chronic disease endpoints in humans; however, to date no randomized controlled trials have investigated dietary MUFA on CVD morbidity and/or mortality as the clinical endpoint [1]. Consequently, Rudel et al. [119] have challenged the cardioprotective effects of MUFA, observing equal coronary artery atherosclerotic effects between dietary MUFA and SFA in nonhuman primates. However, it is acknowledged that results from experimental animal models may not always extrapolate to humans. Considering the substantial evidence presently reviewed supporting the beneficial effects of dietary MUFA on risk factors for MetS and CVD, additional evidence is needed to uncover the discrepancy between human epidemiological evidence and experimental animal models. The following literature discusses the evidence from ecological and prospective cohort studies on effects of MUFA and CVD risk.

Ecological Studies

In a landmark epidemiological trial of 11,579 men aged 40–59 in the Seven Countries study, Keys et al. [8] presented important data revealing that areas consuming a Mediterranean diet rich in OLA from olive oil, even though higher in total fat (33–40% of energy), exhibited lower incidence of CHD mortality. Indeed, in this 15 year follow-up trial, data continued to emphasize the strong inverse relationship between dietary MUFA, as well as the ratio of dietary MUFA to SFA, and incidence of CHD mortality. Conversely, Hegsted and Ausman [120] reported a positive correlation between dietary MUFA and CHD mortality in men aged 35–74 from 18 countries. It is important, however, to note the authors emphasized a rather high correlation between MUFA and SFA intakes and stated that SFA as a confounding variable compromised conclusions linking dietary MUFA with increase risk of CHD.

Prospective Cohort Studies

Large prospective cohort studies are considered to be the strongest source of evidence of the observational studies. Recently, a systematic review of 507 prospective cohort studies confirmed the relationship between a Mediterranean diet and decreased risk of CHD (RR = 0.66; 95% CI 0.57–0.75), evidence that was further confirmed as effective through pooled analysis of 94 randomized control trials [1]. Of interest, analysis of the prospective cohort studies revealed strong evidence of an inverse relationship between dietary MUFA and CHD risk (RR = 0.81; 95% CI 0.68–0.93). Conversely, Mente et al. also identified that consumption of foods high in TFA and glycemic load were attributed to increased CHD risk (RR = 1.32; 95% CI 1.16–1.48; and RR = 1.33; 95% CI 1.13–1.52, respectively). In a 14 year follow-up of 80,082 women in the Nurses' Health Study, a 5% increase in energy intake from MUFA was associated with a relative risk of CHD of 0.81 (95% CI 0.65–1.00) [121]. Furthermore, it was estimated that a 5 or 2% energy replacement of SFA or TFA with MUFA decreased risk of CHD by approximately 30 and 50%, respectively, whereas a 5% energy replacement of MUFA with CHO increased risk of CHD by approximately 25%. Results of the Finnish ATBC (Alpha-Tocopherol, Beta-Carotene) Cancer Prevention Study revealed that after adjustment for vitamin E, C, and β-carotene intakes, an inverse association existed between MUFA intakes and CHD mortality (RR between the extreme quintiles = 0.73; 95% CI 0.56–0.95) [122]. Conversely, a pooled analysis of 11 American and European cohort studies conducted by Jakobsen et al. [14] failed to identify a causal link between MUFA intake and decreased CHD risk. These authors reported that a 5% energy substitution of MUFA for SFA resulted in a hazard ratio of 1.19 (95% CI 1.00–1.42) for CHD events and 1.01 (95% CI 0.73–1.41) for CHD deaths. The authors, however, discussed that the association of MUFA intakes with CHD risk may be confounded by incomplete adjustments for TFA intakes, as MUFA intakes in Westernized diets are primarily from meat, dairy and hydrogenated oils [123]. Moreover, data from the Nurses' Health Study reported a strong correlation between MUFA intakes and SFA ($r = 0.81$) and TFA ($r = 0.55$) [121]. Taken together, observational evidence supports dietary MUFA for

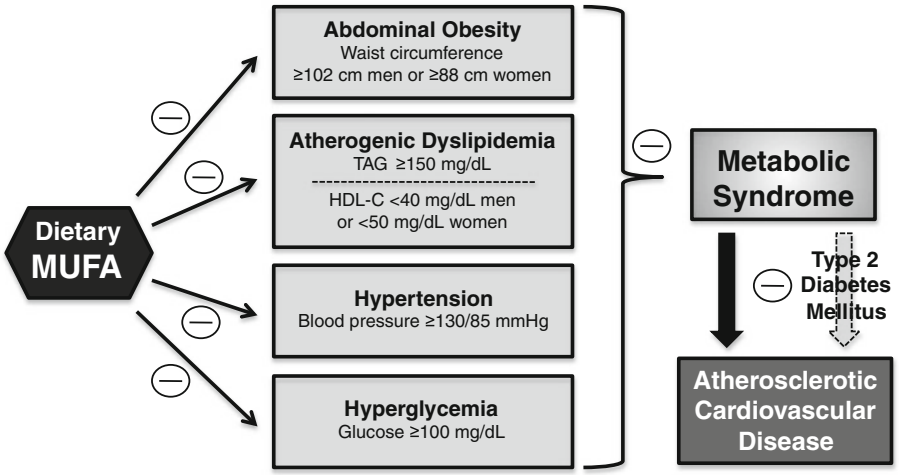

Fig. 1 Dietary monounsaturated fats for the prevention of metabolic syndrome and atherosclerotic cardiovascular disease risk

reduction of CVD risk, however, results from large randomized controlled trials are crucial to substantiate the cardioprotective effects of dietary MUFA.

Conclusion

As dietary intervention remains the primary strategy for the prevention of CVD risk, professional organizations continue to ascertain the optimal fatty acid profile for population intake recommendations. This critical assessment of randomized controlled trials demonstrates that dietary MUFA prevent or ameliorate MetS and CVD risk by favorably modulating blood lipids, blood pressure and insulin sensitivity. Moreover, MUFA preferential oxidation and metabolism influence body composition and potentially ameliorate the risk of obesity (Fig. 1). Considering dietary replacement of SFA, as compared to CHO, MUFA are effective at preserving HDL-C levels, lowering TAG levels, and improving insulin sensitivity; benefits which are especially important in individuals with MetS and DM. As compared to PUFA, MUFA have slightly less or comparable plasma LDL-C and TC lowering effects, however, ameliorate reductions in HDL-C levels, and potentially provide hypotensive effects. The majority of epidemiological data favor the cardioprotective activity of dietary MUFA. More specifically, strong evidence from prospective cohort studies suggests that dietary MUFA are associated with a 20% reduced risk in CHD events [1]. It has also been well established that the intake of a Mediterranean diet rich in MUFA contributes to reducing CHD in both healthy adults and those with established chronic disease.

In North America, where consumption of SFA and TFA are in excess, a dietary movement is occurring to reduce the content of these deleterious fats from commercial production of foods. With the escalating use of MUFA rich canola oil, replacing common dietary fats with canola oil and canola-based spreads would increase the percentage of North Americans complying with current dietary intake recommendations for fatty acids [48]. Consumer awareness of the health implication of dietary fats is increasing [124] and there is a demand for modified dietary oils with a high OLA content for the use in cooking and food preparation in replace of partially hydrogenated oils rich in TFA and SFA [31]. Novel dietary oils rich in OLA with enhanced oxidative stability, such as high-oleic canola oil, provide an attractive healthful alternative to increase dietary MUFA and reduce SFA in commercial food use. With epidemiological and human clinical research substantiating the cardioprotective value of dietary MUFA, increasing population consumption of MUFA, specifically as a substitute for SFA, will embark beneficial implication for MetS, CVD and overall health.

Conflict of interest The authors have no conflict of interest to declare.

References

1. Mente A et al (2009) A systematic review of the evidence supporting a causal link between dietary factors and coronary heart disease. Arch Intern Med 169(7):659–669
2. Salas-Salvado J et al (2008) Effect of a Mediterranean diet supplemented with nuts on metabolic syndrome status: one-year results of the PREDIMED randomized trial. Arch Intern Med 168(22):2449–2458
3. Ros E (2003) Dietary *cis*-monounsaturated fatty acids and metabolic control in type 2 diabetes. Am J Clin Nutr 78(3 Suppl):617S–625S
4. Kris-Etherton PM (1999) AHA Science Advisory. Monounsaturated fatty acids and risk of cardiovascular disease. American Heart Association. Nutrition Committee. Circulation 100(11): 1253–1258
5. Garg A (1998) High-monounsaturated-fat diets for patients with diabetes mellitus: a meta-analysis. Am J Clin Nutr 67(3):577S–582S

6. Krauss RM et al (2000) AHA Dietary Guidelines: revision 2000: a statement for healthcare professionals from the Nutrition Committee of the American Heart Association. Stroke 31(11): 2751–2766
7. American Heart Association Nutrition Committee et al (2006) Diet and lifestyle recommendations revision 2006: a scientific statement from the American Heart Association Nutrition Committee. Circulation 114(1):82–96
8. Keys A et al (1986) The diet and 15-year death rate in the seven countries study. Am J Epidemiol 124(6):903–915
9. Expert Panel on Detection, Evaluation, and Treatment of High Blood Cholesterol in Adults (2001) Executive Summary of The Third Report of The National Cholesterol Education Program (NCEP) Expert Panel on Detection, Evaluation, And Treatment of High Blood Cholesterol In Adults (Adult Treatment Panel III). JAMA 285(19):2486–2497
10. Moreno JJ, Mitjavila MT (2003) The degree of unsaturation of dietary fatty acids and the development of atherosclerosis (review). J Nutr Biochem 14(4):182–195
11. Reaven GM (2000) Diet and Syndrome X. Curr Atheroscler Rep 2(6):503–507
12. Vessby B (2000) Dietary fat and insulin action in humans. Br J Nutr 83(Suppl 1):S91–S96
13. Warensjo E et al (2008) Markers of dietary fat quality and fatty acid desaturation as predictors of total and cardiovascular mortality: a population-based prospective study. Am J Clin Nutr 88(1):203–209
14. Jakobsen MU et al (2009) Major types of dietary fat and risk of coronary heart disease: a pooled analysis of 11 cohort studies. Am J Clin Nutr 89(5):1425–1432
15. WRITING GROUP MEMBERS et al (2010) Heart disease and stroke statistics—2010 update: a report from the American Heart Association. Circulation 121(7):e46–e215
16. United States Department of Agriculture (2010) Dietary guidelines for Americans. http://www.cnpp.usda.gov/dietaryguidelines.htm. Accessed Dec 2010
17. Grundy SM et al (2004) Definition of metabolic syndrome: Report of the National Heart, Lung, and Blood Institute/American Heart Association conference on scientific issues related to definition. Circulation 109(3):433–438
18. Isomaa B et al (2001) Cardiovascular morbidity and mortality associated with the metabolic syndrome. Diabetes Care 24(4):683–689
19. Lakka HM et al (2002) The metabolic syndrome and total and cardiovascular disease mortality in middle-aged men. JAMA 288(21):2709–2716
20. Grundy SM et al (2005) Diagnosis and management of the metabolic syndrome: an American Heart Association/National Heart, Lung, and Blood Institute Scientific Statement. Circulation 112(17):2735–2752
21. International Diabetes Federation (2010) IDF worldwide definition of the metabolic syndrome. http://www.idf.org/idf-worldwide-definition-metabolic-syndrome. Accessed Dec 2010
22. Reaven GM (1988) Banting lecture 1988. Role of insulin resistance in human disease. Diabetes 37(12):1595–1607
23. Carr DB et al (2004) Intra-abdominal fat is a major determinant of the National Cholesterol Education Program Adult Treatment Panel III criteria for the metabolic syndrome. Diabetes 53(8): 2087–2094
24. Tong J et al (2007) Intra-abdominal fat accumulation predicts the development of the metabolic syndrome in non-diabetic Japanese-Americans. Diabetologia 50(6):1156–1160
25. Potenza MV, Mechanick JI (2009) The metabolic syndrome: definition, global impact, and pathophysiology. Nutr Clin Pract 24(5):560–577
26. Ford ES (2005) Prevalence of the metabolic syndrome defined by the International Diabetes Federation among adults in the US. Diabetes Care 28(11):2745–2749
27. Cameron AJ, Shaw JE, Zimmet PZ (2004) The metabolic syndrome: prevalence in worldwide populations. Endocrinol Metab Clin North Am 33(2):351–375
28. Grundy SM (2004) Obesity, metabolic syndrome, and cardiovascular disease. J Clin Endocrinol Metab 89(6):2595–2600
29. American Heart Association (2009) Heart disease and stroke statistics—2009 update. American Heart Association, Dallas
30. Babio N, Bullo M, Salas-Salvado J (2009) Mediterranean diet and metabolic syndrome: the evidence. Public Health Nutr 12(9):1607–1617
31. Tarrago-Trani MT et al (2006) New and existing oils and fats used in products with reduced *trans*-fatty acid content. J Am Diet Assoc 106(6):867–880
32. Kris-Etherton PM et al (2000) Polyunsaturated fatty acids in the food chain in the United States. Am J Clin Nutr 71(1):179S–188S
33. Briefel RR, Johnson CL (2004) Secular trends in dietary intake in the United States. Annu Rev Nutr 24:401–431
34. Willett WC et al (1995) Mediterranean diet pyramid: a cultural model for healthy eating. Am J Clin Nutr 61(6):1402S–1406S
35. Perez-Jimenez F, Lopez-Miranda J, Mata P (2002) Protective effect of dietary monounsaturated fat on arteriosclerosis: beyond cholesterol. Atherosclerosis 163(2):385–398
36. Kris-Etherton PM et al (2007) Position of the American Dietetic Association and Dietitians of Canada: dietary fatty acids. J Am Diet Assoc 107(9):1599–1611
37. National Heart, Lung and Blood Institute (2010) DASH eating plan. NHLBI Information for Patients & the Public. http://www.nhlbi.nih.gov/health/public/heart/hbp/dash/new_dash.pdf. Accessed Oct 2010
38. US Department of Agriculture (2010) MyPyramid. http://www.mypyramid.gov/. Accessed Oct 2010
39. US Department of Health and Human Services (2010) Dietary Guidelines for Americans 2005. http://www.health.gov/dietaryguidelines/dga2005/document/default.htm. Accessed Oct 2010
40. Willett WC (ed) (2005) Eat, drink, and be healthy: The Harvard Medical School guide to healthy eating. Simon and Schuster, New York
41. Reedy J, Krebs-Smith SM (2008) A comparison of food-based recommendations and nutrient values of three food guides: USDA's MyPyramid, NHLBI's dietary approaches to stop hypertension eating plan, and Harvard's healthy eating pyramid. J Am Diet Assoc 108(3):522–528
42. American Diabetes Association (1987) Nutritional recommendations and principles for individuals with diabetes mellitus: 1986. Diabetes Care 10(1):126–132
43. Franz MJ et al (2002) Evidence-based nutrition principles and recommendations for the treatment and prevention of diabetes and related complications. Diabetes Care 25(1):148–198
44. Expert Committee on the Diagnosis and Classification of Diabetes Mellitus (2003) Report of the expert committee on the diagnosis and classification of diabetes mellitus. Diabetes Care 26(Suppl 1):S5–S20
45. Krauss RM et al (1996) Dietary guidelines for healthy American adults. A statement for health professionals from the Nutrition Committee, American Heart Association. Circulation 94(7):1795–1800
46. The Joint FAO/WHO Expert Consultation on Fats and Fatty Acids in Human Nutrition November 10–14, 2008, Geneva, Switzerland (2010) Interim summary of conclusions and dietary recommendations on total fat & fatty acids. http://www.fao.org/ag/agn/nutrition/docs/Fats%20and%20Fatty%20Acids%20Summaryfin.pdf. Accessed Dec 2010

47. FDA U.S. Food and Drug Administration (2009) Qualified health claims: letter of enforcement discretion: unsaturated fatty acids from canola oil and reduced risk of coronary heart disease (Docket No. 2006Q-0091). http://www.fda.gov/Food/LabelingNutrition/LabelClaims/QualifiedHealthClaims/ucm072958.htm. Accessed Aug 2009
48. Johnson GH, Keast DR, Kris-Etherton PM (2007) Dietary modeling shows that the substitution of canola oil for fats commonly used in the United States would increase compliance with dietary recommendations for fatty acids. J Am Diet Assoc 107(10):1726–1734
49. Mensink RP, Katan MB (1992) Effect of dietary fatty acids on serum lipids and lipoproteins. A meta-analysis of 27 trials. Arterioscler Thromb 12(8):911–919
50. Hegsted DM et al (1993) Dietary fat and serum lipids: an evaluation of the experimental data. Am J Clin Nutr 57(6):875–883
51. Clarke R et al (1997) Dietary lipids and blood cholesterol: quantitative meta-analysis of metabolic ward studies. BMJ 314(7074):112–117
52. Mensink RP et al (2003) Effects of dietary fatty acids and carbohydrates on the ratio of serum total to HDL cholesterol and on serum lipids and apolipoproteins: a meta-analysis of 60 controlled trials. Am J Clin Nutr 77(5):1146–1155
53. National Cholesterol Education Program (NCEP) Expert Panel on Detection, Evaluation, and Treatment of High Blood Cholesterol in Adults (Adult Treatment Panel III) (2002) Third Report of the National Cholesterol Education Program (NCEP) Expert Panel on Detection, Evaluation, and Treatment of High Blood Cholesterol in Adults (Adult Treatment Panel III) final report. Circulation 106(25):3143–3421
54. Hunter JE, Zhang J, Kris-Etherton PM (2010) Cardiovascular disease risk of dietary stearic acid compared with *trans*, other saturated, and unsaturated fatty acids: a systematic review. Am J Clin Nutr 91(1):46–63
55. Mozaffarian D, Clarke R (2009) Quantitative effects on cardiovascular risk factors and coronary heart disease risk of replacing partially hydrogenated vegetable oils with other fats and oils. Eur J Clin Nutr 63(Suppl 2):S22–S33
56. Mensink RP, Katan MB (1987) Effect of monounsaturated fatty acids versus complex carbohydrates on high-density lipoproteins in healthy men and women. Lancet 1(8525):122–125
57. Archer WR et al (2003) High carbohydrate and high monounsaturated fatty acid diets similarly affect LDL electrophoretic characteristics in men who are losing weight. J Nutr 133(10):3124–3129
58. Kris-Etherton PM et al (1999) High-monounsaturated fatty acid diets lower both plasma cholesterol and triacylglycerol concentrations. Am J Clin Nutr 70(6):1009–1015
59. Colette C et al (2003) Exchanging carbohydrates for monounsaturated fats in energy-restricted diets: effects on metabolic profile and other cardiovascular risk factors. Int J Obes Relat Metab Disord 27(6):648–656
60. Garg A et al (1988) Comparison of a high-carbohydrate diet with a high-monounsaturated-fat diet in patients with non-insulin-dependent diabetes mellitus. N Engl J Med 319(13):829–834
61. Rodriguez-Villar C et al (2004) Comparison of a high-carbohydrate and a high-monounsaturated fat, olive oil-rich diet on the susceptibility of LDL to oxidative modification in subjects with Type 2 diabetes mellitus. Diabet Med 21(2):142–149
62. Berglund L et al (2007) Comparison of monounsaturated fat with carbohydrates as a replacement for saturated fat in subjects with a high metabolic risk profile: studies in the fasting and postprandial states. Am J Clin Nutr 86(6):1611–1620
63. Ashton EL, Best JD, Ball MJ (2001) Effects of monounsaturated enriched sunflower oil on CHD risk factors including LDL size and copper-induced LDL oxidation. J Am Coll Nutr 20(4):320–326
64. Cao Y et al (2009) Effects of moderate (MF) versus lower fat (LF) diets on lipids and lipoproteins: a meta-analysis of clinical trials in subjects with and without diabetes. J Clin Lipidol 3(1):19–32
65. Lada AT, Rudel LL (2003) Dietary monounsaturated versus polyunsaturated fatty acids: which is really better for protection from coronary heart disease? Curr Opin Lipidol 14(1):41–46
66. Gardner CD, Kraemer HC (1995) Monounsaturated versus polyunsaturated dietary fat and serum lipids. A meta-analysis. Arterioscler Thromb Vasc Biol 15(11):1917–1927
67. Grundy SM (1997) What is the desirable ratio of saturated, polyunsaturated, and monounsaturated fatty acids in the diet? Am J Clin Nutr 66(4):988S–990S
68. Harris WS (1997) N-3 fatty acids and serum lipoproteins: human studies. Am J Clin Nutr 65(5):1645S–1654S
69. Franceschini G (2001) Epidemiologic evidence for high-density lipoprotein cholesterol as a risk factor for coronary artery disease. Am J Cardiol 88(12A):9N–13N
70. Hausenloy DJ, Yellon DM (2008) Targeting residual cardiovascular risk: raising high-density lipoprotein cholesterol levels. Heart 94(6):706–714
71. Hodson L, Skeaff CM, Chisholm WA (2001) The effect of replacing dietary saturated fat with polyunsaturated or monounsaturated fat on plasma lipids in free-living young adults. Eur J Clin Nutr 55(10):908–915
72. Ferrara LA et al (2000) Olive oil and reduced need for antihypertensive medications. Arch Intern Med 160(6):837–842
73. Mutanen M et al (1992) Lack of effect on blood pressure by polyunsaturated and monounsaturated fat diets. Eur J Clin Nutr 46(1):1–6
74. Shah M, Adams-Huet B, Garg A (2007) Effect of high-carbohydrate or high-*cis*-monounsaturated fat diets on blood pressure: a meta-analysis of intervention trials. Am J Clin Nutr 85(5):1251–1256
75. Muzio F et al (2007) Effects of moderate variations in the macronutrient content of the diet on cardiovascular disease risk factors in obese patients with the metabolic syndrome. Am J Clin Nutr 86(4):946–951
76. Appel LJ et al (2005) Effects of protein, monounsaturated fat, and carbohydrate intake on blood pressure and serum lipids: results of the OmniHeart randomized trial. JAMA 294(19):2455–2464
77. Alonso A, Martinez-Gonzalez MA (2004) Olive oil consumption and reduced incidence of hypertension: the SUN study. Lipids 39(12):1233–1238
78. Psaltopoulou T et al (2004) Olive oil, the Mediterranean diet, and arterial blood pressure: the Greek European Prospective Investigation into Cancer and Nutrition (EPIC) study. Am J Clin Nutr 80(4):1012–1018
79. Lopez-Miranda J et al (2008) Olive oil and health: summary of the II international conference on olive oil and health consensus report, Jaen and Cordoba (Spain) 2008. Nutr Metab Cardiovasc Dis 20(4):284–294
80. Teres S et al (2008) Oleic acid content is responsible for the reduction in blood pressure induced by olive oil. Proc Natl Acad Sci USA 105(37):13811–13816
81. Wild S et al (2004) Global prevalence of diabetes: estimates for the year 2000 and projections for 2030. Diabetes Care 27(5):1047–1053
82. Bergouignan A et al (2009) Metabolic fate of saturated and monounsaturated dietary fats: the Mediterranean diet revisited

from epidemiological evidence to cellular mechanisms. Prog Lipid Res 48(3–4):128–147
83. Due A et al (2008) Comparison of the effects on insulin resistance and glucose tolerance of 6-mo high-monounsaturated-fat, low-fat, and control diets. Am J Clin Nutr 87(4):855–862
84. Paniagua JA et al (2007) A MUFA-rich diet improves postprandial glucose, lipid and GLP-1 responses in insulin-resistant subjects. J Am Coll Nutr 26(5):434–444
85. Shah M et al (2007) Lipid, glycemic, and insulin responses to meals rich in saturated, cis-monounsaturated, and polyunsaturated (n-3 and n-6) fatty acids in subjects with type 2 diabetes. Diabetes Care 30(12):2993–2998
86. Christiansen E et al (1997) Intake of a diet high in trans monounsaturated fatty acids or saturated fatty acids. Effects on postprandial insulinemia and glycemia in obese patients with NIDDM. Diabetes Care 20(5):881–887
87. Lopez S et al (2008) Distinctive postprandial modulation of beta cell function and insulin sensitivity by dietary fats: monounsaturated compared with saturated fatty acids. Am J Clin Nutr 88(3):638–644
88. Perez-Jimenez F et al (2001) A Mediterranean and a high-carbohydrate diet improve glucose metabolism in healthy young persons. Diabetologia 44(11):2038–2043
89. Vessby B et al (2001) Substituting dietary saturated for monounsaturated fat impairs insulin sensitivity in healthy men and women: The KANWU Study. Diabetologia 44(3):312–319
90. Salas J et al (1999) The diet rich in monounsaturated fat modifies in a beneficial way carbohydrate metabolism and arterial pressure. Med Clin (Barc) 113(20):765–769
91. Uusitupa M et al (1994) Effects of two high-fat diets with different fatty acid compositions on glucose and lipid metabolism in healthy young women. Am J Clin Nutr 59(6):1310–1316
92. Tierney AC, Roche HM (2007) The potential role of olive oil-derived MUFA in insulin sensitivity. Mol Nutr Food Res 51(10):1235–1248
93. Paniagua JA et al (2007) Monounsaturated fat-rich diet prevents central body fat distribution and decreases postprandial adiponectin expression induced by a carbohydrate-rich diet in insulin-resistant subjects. Diabetes Care 30(7):1717–1723
94. Brehm BJ et al (2009) One-year comparison of a high-monounsaturated fat diet with a high-carbohydrate diet in type 2 diabetes. Diabetes Care 32(2):215–220
95. Thomsen C et al (1999) Comparison of the effects of a monounsaturated fat diet and a high carbohydrate diet on cardiovascular risk factors in first degree relatives to type-2 diabetic subjects. Eur J Clin Nutr 53(10):818–823
96. van Dam RM et al (2002) Dietary fat and meat intake in relation to risk of type 2 diabetes in men. Diabetes Care 25(3):417–424
97. Salmeron J et al (2001) Dietary fat intake and risk of type 2 diabetes in women. Am J Clin Nutr 73(6):1019–1026
98. Bray GA, Popkin BM (1998) Dietary fat intake does affect obesity. Am J Clin Nutr 68(6):1157–1173
99. Willett WC (1998) Dietary fat and obesity: an unconvincing relation. Am J Clin Nutr 68(6):1149–1150
100. Willett WC, Leibel RL (2002) Dietary fat is not a major determinant of body fat. Am J Med 113(Suppl 9B):47S–59S
101. Field AE et al (2007) Dietary fat and weight gain among women in the Nurses' Health Study. Obesity (Silver Spring) 15(4):967–976
102. Koh-Banerjee P et al (2003) Prospective study of the association of changes in dietary intake, physical activity, alcohol consumption, and smoking with 9-y gain in waist circumference among 16,587 US men. Am J Clin Nutr 78(4):719–727
103. Bes-Rastrollo M et al (2006) Olive oil consumption and weight change: the SUN prospective cohort study. Lipids 41(3):249–256
104. Bes-Rastrollo M et al (2007) Nut consumption and weight gain in a Mediterranean cohort: The SUN study. Obesity (Silver Spring) 15(1):107–116
105. Mendez MA et al (2006) Adherence to a Mediterranean diet is associated with reduced 3-year incidence of obesity. J Nutr 136(11):2934–2938
106. Piers LS et al (2003) Substitution of saturated with monounsaturated fat in a 4-week diet affects body weight and composition of overweight and obese men. Br J Nutr 90(3):717–727
107. Kien CL, Bunn JY, Ugrasbul F (2005) Increasing dietary palmitic acid decreases fat oxidation and daily energy expenditure. Am J Clin Nutr 82(2):320–326
108. Garland M et al (1998) The relation between dietary intake and adipose tissue composition of selected fatty acids in US women. Am J Clin Nutr 67(1):25–30
109. Baylin A et al (2002) Adipose tissue biomarkers of fatty acid intake. Am J Clin Nutr 76(4):750–757
110. Garaulet M et al (2001) Site-specific differences in the fatty acid composition of abdominal adipose tissue in an obese population from a Mediterranean area: relation with dietary fatty acids, plasma lipid profile, serum insulin, and central obesity. Am J Clin Nutr 74(5):585–591
111. Sabin MA et al (2007) Depot-specific effects of fatty acids on lipid accumulation in children's adipocytes. Biochem Biophys Res Commun 361(2):356–361
112. Wajchenberg BL (2000) Subcutaneous and visceral adipose tissue: their relation to the metabolic syndrome. Endocr Rev 21(6):697–738
113. McCloy U et al (2004) A comparison of the metabolism of eighteen-carbon 13C-unsaturated fatty acids in healthy women. J Lipid Res 45(3):474–485
114. DeLany JP et al (2000) Differential oxidation of individual dietary fatty acids in humans. Am J Clin Nutr 72(4):905–911
115. Jones PJ, Jew S, AbuMweis S (2008) The effect of dietary oleic, linoleic, and linolenic acids on fat oxidation and energy expenditure in healthy men. Metabolism 57(9):1198–1203
116. Casas-Agustench P et al (2009) Acute effects of three high-fat meals with different fat saturations on energy expenditure, substrate oxidation and satiety. Clin Nutr 28(1):39–45
117. Friedman MI (1998) Fuel partitioning and food intake. Am J Clin Nutr 67(3):513S–518S
118. Lawton CL et al (2000) The degree of saturation of fatty acids influences post-ingestive satiety. Br J Nutr 83(5):473–482
119. Rudel LL, Parks JS, Sawyer JK (1995) Compared with dietary monounsaturated and saturated fat, polyunsaturated fat protects African green monkeys from coronary artery atherosclerosis. Arterioscler Thromb Vasc Biol 15(12):2101–2110
120. Hegsted DM, Ausman LM (1988) Diet, alcohol and coronary heart disease in men. J Nutr 118(10):1184–1189
121. Hu FB et al (1997) Dietary fat intake and the risk of coronary heart disease in women. N Engl J Med 337(21):1491–1499
122. Pietinen P et al (1997) Intake of fatty acids and risk of coronary heart disease in a cohort of Finnish men. The Alpha-Tocopherol, Beta-Carotene Cancer Prevention Study. Am J Epidemiol 145(10):876–887
123. Katan MB (2009) Omega-6 polyunsaturated fatty acids and coronary heart disease. Am J Clin Nutr 89(5):1283–1284
124. Eckel RH et al (2009) Americans' awareness, knowledge, and behaviors regarding fats: 2006–2007. J Am Diet Assoc 109(2):288–296
125. Gulseth HL et al (2010) Dietary fat modifications and blood pressure in subjects with the metabolic syndrome in the LIPGENE dietary intervention study. Br J Nutr: 1–4
126. Shah M et al (2005) Effect of a high-carbohydrate versus a high-*cis*-monounsaturated fat diet on blood pressure in patients with type 2 diabetes. Diabetes Care 28(11):2607–2612

127. Thomsen C et al (1995) Comparison of the effects on the diurnal blood pressure, glucose, and lipid levels of a diet rich in monounsaturated fatty acids with a diet rich in polyunsaturated fatty acids in type 2 diabetic subjects. Diabet Med 12(7): 600–606
128. Walker KZ et al (1995) Dietary composition, body weight, and NIDDM. Comparison of high-fiber, high-carbohydrate, and modified-fat diets. Diabetes Care 18(3):401–403
129. Rasmussen BM et al (2006) Effects of dietary saturated, monounsaturated, and n-3 fatty acids on blood pressure in healthy subjects. Am J Clin Nutr 83(2):221–226
130. Aro A et al (1998) Lack of effect on blood pressure by low fat diets with different fatty acid compositions. J Hum Hypertens 12(6):383–389
131. Lahoz C et al (1997) Effects of dietary fat saturation on eicosanoid production, platelet aggregation and blood pressure. Eur J Clin Invest 27(9):780–787
132. Uusitupa MI et al (1994) Long-term effects of four fat-modified diets on blood pressure. J Hum Hypertens 8(3):209–218
133. Mensink RP, Stolwijk AM, Katan MB (1990) Effect of a monounsaturated diet vs. a polyunsaturated fatty acid-enriched diet on blood pressure in normotensive women and men. Eur J Clin Invest 20(4):463–469
134. Mensink RP, Janssen MC, Katan MB (1988) Effect on blood pressure of two diets differing in total fat but not in saturated and polyunsaturated fatty acids in healthy volunteers. Am J Clin Nutr 47(6):976–980
135. Vega-Lopez S et al (2006) Palm and partially hydrogenated soybean oils adversely alter lipoprotein profiles compared with soybean and canola oils in moderately hyperlipidemic subjects. Am J Clin Nutr 84(1):54–62
136. Gerhard GT et al (2004) Effects of a low-fat diet compared with those of a high-monounsaturated fat diet on body weight, plasma lipids and lipoproteins, and glycemic control in type 2 diabetes. Am J Clin Nutr 80(3):668–673
137. Thomsen C et al (2003) Differential effects of saturated and monounsaturated fats on postprandial lipemia and glucagon-like peptide 1 responses in patients with type 2 diabetes. Am J Clin Nutr 77(3):605–611
138. Lovejoy JC et al (2002) Effects of diets enriched in saturated (palmitic), monounsaturated (oleic), or *trans* (elaidic) fatty acids on insulin sensitivity and substrate oxidation in healthy adults. Diabetes Care 25(8):1283–1288
139. Lauszus FF et al (2001) Effect of a high monounsaturated fatty acid diet on blood pressure and glucose metabolism in women with gestational diabetes mellitus. Eur J Clin Nutr 55(6):436–443
140. Rodriguez-Villar C et al (2000) High-monounsaturated fat, olive oil-rich diet has effects similar to a high-carbohydrate diet on fasting and postprandial state and metabolic profiles of patients with type 2 diabetes. Metabolism 49(12):1511–1517
141. Luscombe ND, Noakes M, Clifton PM (1999) Diets high and low in glycemic index versus high monounsaturated fat diets: effects on glucose and lipid metabolism in NIDDM. Eur J Clin Nutr 53(6):473–478
142. Sarkkinen E et al (1996) The effects of monounsaturated-fat enriched diet and polyunsaturated-fat enriched diet on lipid and glucose metabolism in subjects with impaired glucose tolerance. Eur J Clin Nutr 50(9):592–598
143. Parillo M et al (1992) A high-monounsaturated-fat/low-carbohydrate diet improves peripheral insulin sensitivity in non-insulin-dependent diabetic patients. Metabolism 41(12):1373–1378
144. Bonanome A et al (1991) Carbohydrate and lipid metabolism in patients with non-insulin-dependent diabetes mellitus: effects of a low-fat, high-carbohydrate diet vs. a diet high in monounsaturated fatty acids. Am J Clin Nutr 54(3):586–590
145. Thomsen C et al (1999) Differential effects of saturated and monounsaturated fatty acids on postprandial lipemia and incretin responses in healthy subjects. Am J Clin Nutr 69(6): 1135–1143
146. Louheranta AM et al (1998) A high-stearic acid diet does not impair glucose tolerance and insulin sensitivity in healthy women. Metabolism 47(5):529–534
147. Joannic JL et al (1997) How the degree of unsaturation of dietary fatty acids influences the glucose and insulin responses to different carbohydrates in mixed meals. Am J Clin Nutr 65(5):1427–1433

Lipids (2011) 46:229–238
DOI 10.1007/s11745-010-3515-z

ORIGINAL ARTICLE

Aerobic Training in Rats Increases Skeletal Muscle Sphingomyelinase and Serine Palmitoyltransferase Activity, While Decreasing Ceramidase Activity

Agnieszka Błachnio-Zabielska · Piotr Zabielski · Marcin Baranowski · Jan Gorski

Received: 11 September 2010 / Accepted: 1 December 2010 / Published online: 22 December 2010

Abstract Sphingolipids are important components of cell membranes that may also serve as cell signaling molecules; ceramide plays a central role in sphingolipid metabolism. The aim of this study was to examine the effect of 5 weeks of aerobic training on key enzymes and intermediates of ceramide metabolism in skeletal muscles. The experiments were carried out on rats divided into two groups: (1) sedentary and (2) trained for 5 weeks (on a treadmill). The activity of serine palmitoyltransferase (SPT), neutral and acid sphingomyelinase (nSMase and aSMase), neutral and alkaline ceramidases (nCDase and alCDase) and the content of sphingolipids was determined in three types of skeletal muscle. We also measured the fasting plasma insulin and glucose concentration for calculating HOMA-IR (homeostasis model assessment) for estimating insulin resistance. We found that the activities of aSMase and SPT increase in muscle in the trained group. These changes were followed by elevation in the content of sphinganine. The activities of both isoforms of ceramidase were reduced in muscle in the trained group. Although the activities of SPT and SMases increased and the activity of CDases decreased, the ceramide content did not change in any of the studied muscle. Although ceramide level did not change, we noticed increased insulin sensitivity in trained animals. It is concluded that training affects the activity of key enzymes of ceramide metabolism but also activates other metabolic pathways which affect ceramide metabolism in skeletal muscles.

A. Błachnio-Zabielska (✉) · P. Zabielski · M. Baranowski · J. Gorski
Department of Physiology, Medical University of Białystok, Mickiewicza 2C, 15-222 Białystok, Poland
e-mail: blacha@umwb.edu.pl

Keywords Serine palmitoyltransferase · Sphingomyelinase · Ceramidase · Sphingolipid intermediates · Skeletal muscle · Training

Abbreviations

Cer	Ceramide
dhCer	Dihydroceramide
Sph	Sphingosine
SPA	Sphinganine
S1P	Sphingosine-1-phosphate
SPA1P	Sphinganine-1-phosphate
SPT	Serine palmitoyltransferase
nCDase	Neutral ceramidase
alCDase	Alkaline ceramidase
nSMase	Neutral sphingomyelinase
aSMase	Acidic sphingomyelinase

Introduction

Sphingolipids are an important lipid class that is present in all higher organisms. Ceramide (Cer) is the key compound on the crossroads of sphingolipid metabolism. Ceramide mediates a number of biological processes, including apoptosis, proliferation, differentiation, growth arrest, inflammation and heat stress response [1–4]. The variety of cellular effects of ceramide can be attributed to its ability to alter the activity of kinases, phosphatases and transcription factors [5–7]. Other sphingolipid intermediates, such as sphingosine (Sph), sphingosine-1-phosphate (S1P), ceramide-1-phosphate are also important second messengers [8–12]. The cellular content of ceramide is determined by a balance between the rate of its formation and degradation.

There are two major types of ceramides production. One of them is hydrolysis of sphingomyelin and the other one is de novo biosynthesis. Sphingomyelin is located in the plasma membrane, in lysosomes, and in endosomes. Its hydrolysis is catalyzed by the neutral and acid sphingomyelinase (n- and aSMase). De novo synthesis is initiated by condensation of serine with palmitoyl-CoA to generate 3-ketosphinganine [13]. This, the rate-limiting step in de novo sphingolipid biosynthesis is catalyzed by the enzyme serine-palmitoyltransferase (SPT). 3-Ketosphingosine is rapidly reduced to sphinganine (SPA) by the action of the enzyme 3-ketosphinganine reductase. Next, SPA is acylated to form dihydroceramide by the action of dihydroceramide synthase. The last step of ceramide synthesis is conversion of dihydroceramide to ceramide by insertion of a 4,5-*trans*-double bond into dihydroceramide. This reaction is catalyzed by the enzyme dihydroceramide desaturase [13]. Ceramide is hydrolyzed by the enzyme ceramidase (CDase) to yield a free fatty acid and sphingosine. There are three isoforms of ceramidase: acid (aCDase), neutral (nCDase) and alkaline (alCDase). By the use of enzymatic assay and Northern blot analysis almost no activity or mRNA of aCDase was found in skeletal muscle [14].

Ceramide has been shown to be present in skeletal muscle [15–17]. Its content in the muscles depends on the muscle type. The higher content of ceramide was observed in muscle composed mostly of oxidative fibers than in muscle composed mostly of glycolytic fibers [16]. Skeletal muscles are responsible for 70–80% of whole body insulin-stimulated glucose uptake [18, 19]. Recent evidence suggests that the accumulation of intramuscular lipids is involved in the induction of insulin-resistance [20, 21]. One candidate for this action is ceramide [17]. The intracellular level of ceramide is increased in the muscles of obese, insulin-resistant Zucker rats [22] and obese insulin-resistant humans [17]. Adams et al. reported that ceramide content increased nearly twofold in skeletal muscles of obese humans. It is also well known that trained subjects are more insulin sensitive than sedentary subjects [23, 24].

A previous study showed that endurance training decreases the total content of sphingomyelin and ceramides, increases the content of sphinganine, does not affect the sphingosine content, and increases nSMase activity [25]. Moreover, sphingolipid content and the activity of enzymes of ceramide metabolism both depend on the duration of exercise and muscle type [26]. In the mentioned study, the ceramide level decreased after 30 min of running but increased after exhaustive exercise [26]. Data obtained from human skeletal muscle showed that training did not change either ceramide content or nSMase activity [27]. There was no data on the effect of training on the activity of SPT, acid sphingomyelinase and ceramidases in rat skeletal muscles. Therefore the aim of the present study was to examine the effect of training on the activity of key enzymes of ceramide metabolism and selected sphingolipid intermediates in skeletal muscle.

Materials and Methods

Animals and Study Design

The investigation was approved by the Ethical Committee for Animal Experiments at the Medical University of Bialystok. The experiments were carried out on male Wistar rats (200–250 g) fed ad libitum on commercial food pellets for rodents. Animals were housed in standard conditions (21 ± 2 °C, 12 h light/12 h dark cycle) with free access to tap water and food pellets. The animals were randomly divided into two groups ($N = 8$ in each group): (1) sedentary (control) (2) trained for 5 weeks on an electrically driven treadmill according to the following protocol [28]: 1st week 1 h daily at a speed of 960 m/h. The same running time was applied during successive weeks but the running speed was increased as follows: 2nd week 1,200 m/h, 3rd week 1,440 m/h, 4th–6th week 1,680 m/h. This type of training was previously found to affect ceramide metabolism in both cardiac and skeletal muscle of the rat [25, 29]. Twenty four hours after the last exercise bout in the training program, the rats were anaesthetized along with the controls with pentobarbital sodium administered intraperitoneally at a dose of 80 mg/kg. The soleus and the red and white sections of the gastrocnemius were excised, cleaned of any visible adipose tissue, nerves, and fascias and frozen in liquid nitrogen. These muscles are composed predominantly of slow-twitch oxidative, fast-twitch oxidative-glycolytic, and fast-twitch glycolytic fibers, respectively [30, 31]. We used a homeostasis model assessment for calculating insulin resistance (HOMA-IR) in both groups.

The Content of Sphingosine, Sphinganine and Sphingosine-1-phosphate

The content of Sph, SPA and S1P was measured using the method previously described by Min et al. [32]. Internal standards (C17-sphingosine and C17-S1P, Avanti Polar Lipids) were added to the samples before homogenization and ultrasonication. The dried lipid residues were redissolved in ethanol and sphingoid bases were converted to their *o*-phthalaldehyde derivatives and analyzed on an HPLC system (ProStar, Varian Inc.) equipped with a fluorescence detector and C18 reversed-phase column (Varian Inc. OmniSpher 5, 4.6 × 150 mm). The isocratic eluent composition of acetonitrile (Merck): water (9:1 v/v) and a flow rate of 1 ml/min were used. The column temperature

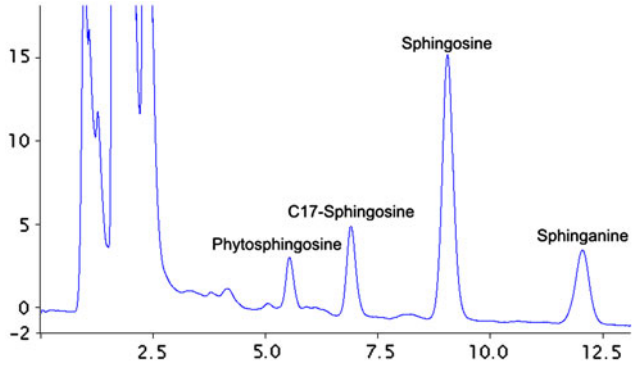

Fig. 1 HPLC chromatography separation of sphingolipids

was maintained at 33 °C. Figure 1 presents a chromatogram showing the separation of sphingolipids. Figure 2 shows the standard curve of SPA, Cer, Sph and S1P.

The Content of Ceramide and Dihydroceramide

A small volume of the chloroform phase containing lipids extracted as described above was transferred to a fresh tube containing 31 pmol of C17-sphingosine as an internal standard. The samples were evaporated under a nitrogen stream, redissolved in 1 M KOH in 90% methanol and heated at 90 °C for 60 min to convert ceramide into sphingosine. This digestion procedure does not convert complex sphingolipids, such as sphingomyelin, galactosylceramide or glucosylceramide, into free sphingoid bases [33]. Samples were then partitioned by the addition of chloroform and water. The upper phase was discarded and the lower phase was evaporated under nitrogen. The content of free sphingosine liberated from ceramide was then analyzed by means of HPLC as described above. The calibration curves were prepared using *N*-palmitoylsphingosine and *N*-palmitoylsphinganine (Avanti Polar Lipids, Alabaster, AL, USA) as standards. The chloroform extract used for the analysis of Cer and dhCer levels also contains small amounts of free sphingoid bases. Therefore, the content of ceramide and dihydroceramide was corrected for the level of free sphingosine and sphinganine, respectively, as determined in the same sample.

The Activity of Sphingomyelinases

The activity of n- and aSMase was determined according to Liu and Hannun [34]. The activity of both sphingomyelinases was measured with the use of radiolabeled substrate [*N*-methyl-^{14}C]-sphingomyelin (Perkin-Elmer Life Sciences). The product of reaction—^{14}C-choline phosphate—was extracted with $CHCl_3$:methanol (2:1, v/v), transferred to scintillation vials and counted using a Packard TRI-CARB 1900 TR scintillation counter.

The Activity of Ceramidases

The activity of alCDase and nCDase was measured by the method of Nikolova-Karakashian and Merrill [35]. The activity of the enzymes was determined with the use of radiolabeled [*N*-palmitoyl-1-^{14}C]-sphingosine (Moravek Biochemicals) as a substrate. Unreacted ceramide and liberated ^{14}C-palmitate were separated with basic Dole solution (isopropanol:heptane:1 N NaOH, 40:10:1, v/v/v). Radioactivity of the ^{14}C-palmitate was measured by scintillation counting.

The Activity of Serine Palmitoyltransferase

The activity of SPT was examined as described by Merrill [36] with the use of a radiolabeled substrate, [^{3}H]-L-serine (Moravek Biochemicals). Briefly, rat skeletal muscle microsomal fraction was obtained by ultracentrifugation at 150,000*g* for 40 min. Microsomes were incubated for 10 min at 37 °C in the reaction buffer (100 mM HEPES (pH 8.3), 5 mM DTT (dithiothreitol), 2.5 mM EDTA (pH 7.0), 50 μM pyridoxal phosphate, 200 μM palmitoyl-CoA and 2 mM L-serine, 44,000 dpm/nmol). The labeled lipid product 3-ketosphinganine was extracted with $CHCl_3$:methanol (1:2, v/v) and the radioactivity was measured by scintillation counting.

Plasma Insulin and Glucose Concentration

The plasma insulin concentration was determined using an ELISA kit (Mercodia Insulin ELISA kit). The plasma glucose concentration was measured using the Glucose Ox Liquid Kit (Pointe Scientific).

Plasma Free Fatty Acids (FFA) Concentration

The FFA concentration was determined using the Wako NEFA C kit (Wako Chemicals).

Statistical Analysis

All data are presented as means ± SD. Data were analyzed by one-way analysis of variance (ANOVA), followed by the Newman–Keuls post hoc test. p values <0.05 were taken to indicate statistical significance.

Results

Plasma FFA, Glucose and Insulin Concentration and HOMA-IR

The cellular ceramide level depends on the availability of plasma FFA. Circulating FFA must be converted to their

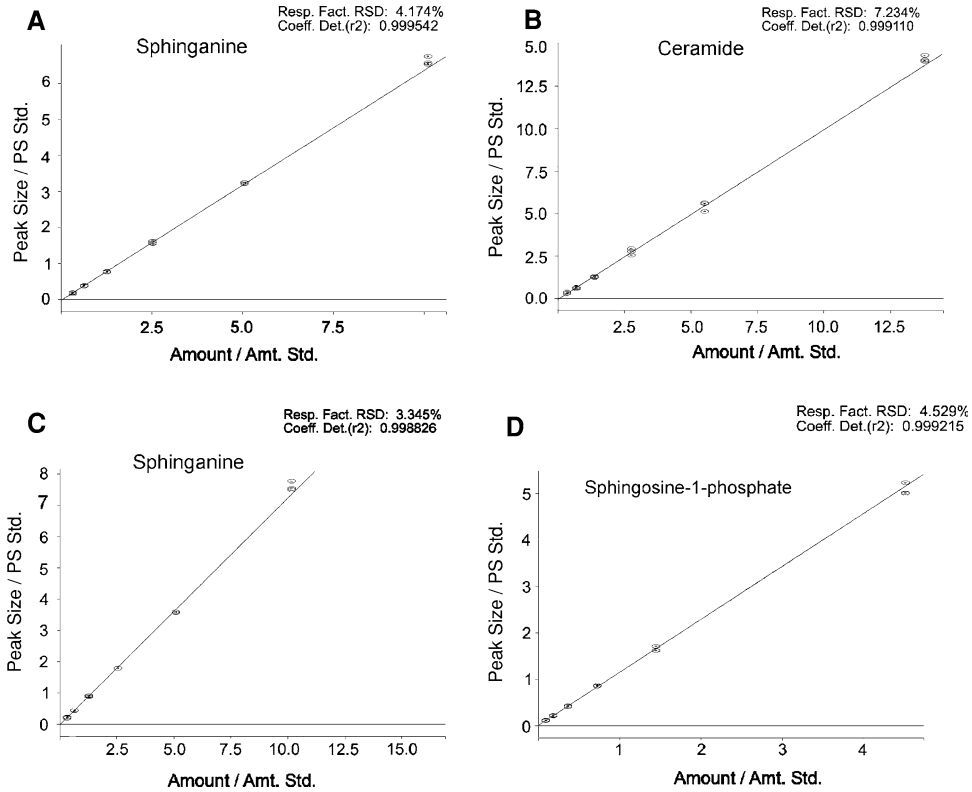

Fig. 2 Standard curve of sphinganine (**a**), ceramides (**b**), sphingosine (**c**), sphingosine-1-phosphate (**d**)

active form—fatty acyl coenzyme A—after entering the cell in order to participate in further metabolic processes. Acyl-CoA is used as a substrate in the de novo sphingolipids biosynthesis. In our study the plasma FFA concentration decreased from 260 ± 17 nmol × ml^{-1} (control group) to 111.06 nmol × ml^{-1} ($p < 0.01$) (training group) (Table 1). To estimate the insulin sensitivity we measured fasting plasma insulin and glucose concentration for HOMA-IR calculation. The equation for calculating HOMA-IR was as follows: HOMA-IR = (fasting plasma glucose × fasting plasma insulin)/2,430, where fasting plasma glucose was in mg/dl and fasting plasma insulin in μU/ml [37]. Both plasma glucose and insulin concentration were significantly lower in the trained group compared to the sedentary group (Table 1). We found that HOMA-IR values were lower in the trained group ($HOMA\text{-}IR_{trained}$ = 0.54) than in the sedentary group ($HOMA\text{-}IR_{sedentary}$ = 1.13) which means that exercised animals were more insulin sensitive than sedentary rats.

Table 1 Effect of training on plasma free fatty acid, glucose and insulin concentration

	Control	Training
Plasma FFA concentration (nmol × ml^{-1})	260 ± 17	111.06 ± 15[b]
Plasma glucose concentration (mg/dl)	140.76 ± 16.6	90.18 ± 11.8[a]
Plasma insulin concentration (μU/ml)	19.6 ± 2.4	14.6 ± 2.1[a]
HOMA-IR	1.13 ± 0.10	0.54 ± 0.04[b]

Values are means ± SD ($n = 8$ in each group). The rats were either sedentary (control) or trained on the electrically driven treadmill as described in the methods

HOMA-IR = [fasting glucose (mg/dl) × fasting insulin (μU/ml)]/2,430

FFA free fatty acids

[a] $p < 0.01$, [b] $p < 0.001$ versus the control group

The Content of Skeletal Muscle Sphingolipids (Table 2)

Sphingolipids, especially ceramides, are very active biologically and mediate a number of biological processes. It seems that ceramides play an important role in the induction of different diseases states such as insulin resistance [38, 39]. Data from our previous study showed that ceramide metabolism changes with the duration of single-bout exercise [26]. In the present study we wanted to examine how training affects sphingolipids content and enzymes activities implicated in ceramide metabolism in skeletal muscle. Therefore we measured the content of the following sphingolipids: sphingosine, sphingosine-1-phosphate, sphinganine, sphinganine-1-phosphate (SPA1P), ceramides and dihydroceramide (dhCer). The content of Sph (Fig. 3a) and S1P (Fig. 3b) did not change in any

Table 2 Effect of training on the content of sphingolipids in rat skeletal muscle

	Sphingosine		Sphinganine		S1P		Ceramide		SPA1P		dhCer	
	Control	Training	Control	Training	Control	Training	Control	Training	Control	Training	Control	Training
Soleus	1.00 ± 0.17	1.17 ± 0.21	0.39 ± 0.06	0.59 ± 0.11[a]	0.22 ± 0.04	0.27 ± 0.04	24.57 ± 3.53	28.70 ± 3.59	0.224 ± 0.07	0.202 ± 0.05	0.836 ± 0.19	0.891 ± 0.15
RG	1.00 ± 0.24	1.20 ± 0.26	0.38 ± 0.08	0.54 ± 0.09[a]	0.25 ± 0.06	0.28 ± 0.03	24.57 ± 3.63	24.60 ± 3.13	0.167 ± 0.06	0.269 ± 0.06[a]	0.990 ± 0.28	1.003 ± 0.24
WG	0.51 ± 0.08	0.59 ± 0.06	0.21 ± 0.02	0.27 ± 0.05	0.09 ± 0.01	0.11 ± 0.04	22.05 ± 3.97	23.32 ± 3.40	0.093 ± 0.04	0.337 ± 0.04[b]	1.059 ± 0.33	0.956 ± 0.26

Values are means ± SD ($n = 8$ in each group). The rats were either sedentary (control) or trained on the electrically driven treadmill as described in the methods

RG red section of the gastrocnemius, *WG* white section of the gastrocnemius, *S1P* sphingosine-1-phosphate, *SPA1P* sphinganine-1-phosphate, *dhCer* dihydroceramide

[a] $p < 0.01$, [b] $p < 0.001$ versus the control group

studied muscle after endurance training. SPA level increased by 52% ($p < 0.01$) and 41% ($p < 0.01$) in the soleus and red section of the gastrocnemius, respectively, compared to the control group. There was no difference in the SPA content in the white section of the gastrocnemius between trained and sedentary groups (Fig. 3c). The content of sphinganine-1-phosphate increased in both sections of the gastrocnemius in trained animals. In the red section of the gastrocnemius the SPA1P level was 50% ($p < 0.01$) higher than in the same muscle in the control group. In the white section of the gastrocnemius the SPA1P level was almost four times higher ($p < 0.001$) then in the same muscle from the sedentary group (Fig. 3d). The content of ceramide and dhCer did not change in any studied muscle from the trained group (Fig. 3e, f).

The Enzymes of Ceramide Metabolism (Table 3)

The activities of the key enzymes implicated in ceramides metabolism: SPT, nSMase, aSMase (enzymes responsible for ceramides generation) and nCDase and alCDase (enzymes responsible for ceramides degradation) were measured. There are limited data about the activity of the above-mentioned enzymes in skeletal muscle. The only available data on the activity of all the enzymes in muscle refer to the enzymes' activity at rest, after a single-bout of exercise [26], from diabetic and healthy animals with increased plasma FFA concentration [40] and from animals fed high fat diets [41]. In the present study the activity of SPT increased in each studied muscle in the trained group. The enzyme activity was almost two times ($p < 0.001$), three times ($p < 0.001$) and almost four times ($p < 0.001$) higher in the soleus, red, and white section of the gastrocnemius, respectively, compared to the control group (Fig. 4a).

In the soleus, there was no difference in nSMase activity between the control and trained groups. In the red and white sections of the gastrocnemius, the activity of nSMase increased by 30% ($p < 0.01$) and by 41% ($p < 0.001$), respectively, compared to the control group (Fig. 4b).

The activity of the aSMase increased in each studied muscle in the trained group. The enzyme activity was 1.5 ($p < 0.001$), 2.5 ($p < 0.001$) and 2.3 times ($p < 0.001$) higher in the soleus, red and white sections of the gastrocnemius respectively, compared to the control group (Fig. 4c).

The activity of nCDase decreased by 19% ($p < 0.05$) and by 30% ($p < 0.05$) in the soleus and white section of the gastrocnemius respectively, compared to the control group. The enzyme activity did not change in red section of the gastrocnemius (Fig. 5a).

The activity of alkaline ceramidase (alCDase) decreased by 21% ($p < 0.05$), 24% ($p < 0.05$) and 34% ($p < 0.01$) in

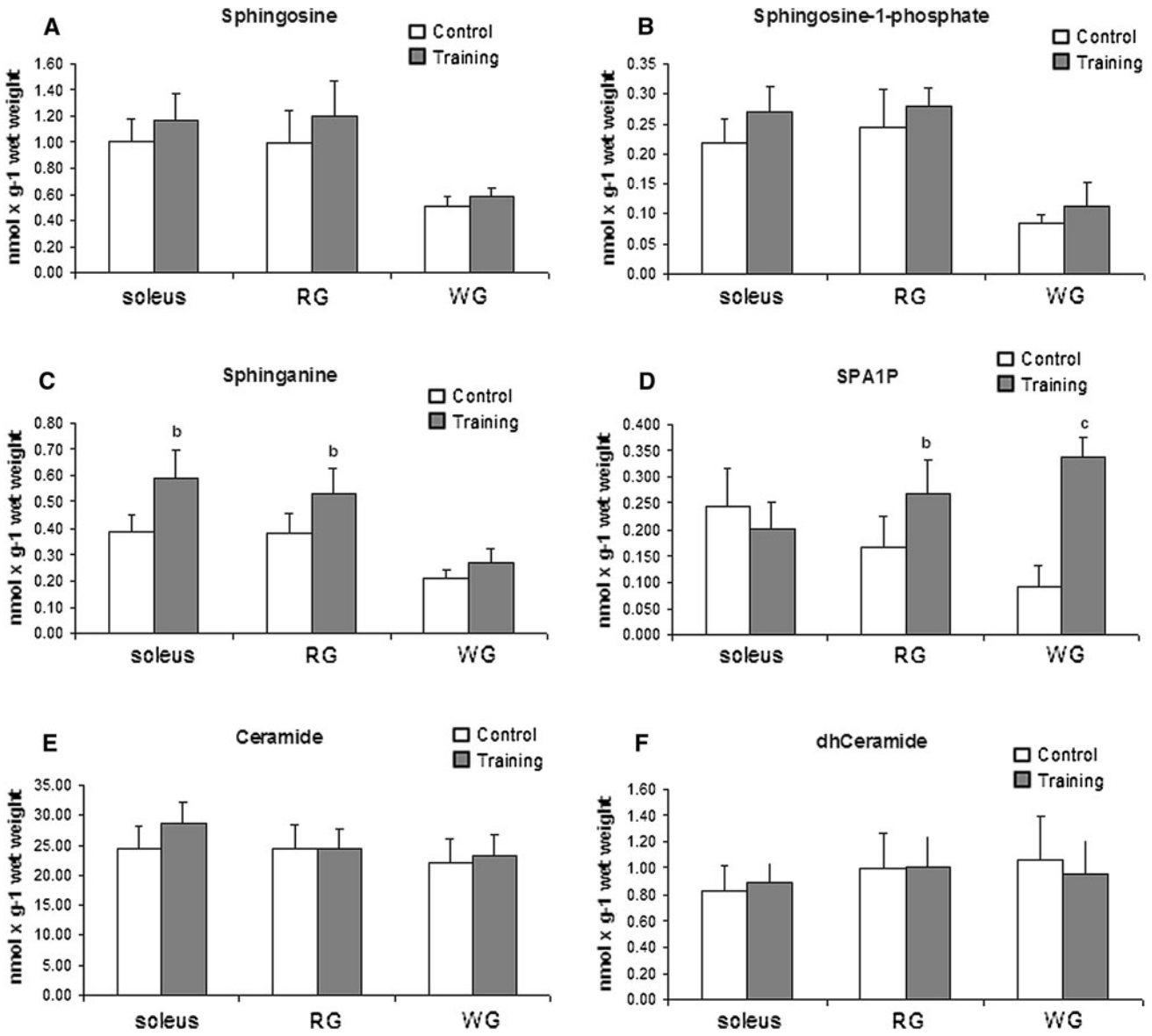

Fig. 3 Effect of training on the content of sphingosine (**a**), sphingosine-1-phosphate (**b**), sphinganine (**c**), sphinganine-1-phosphate (**d**), ceramide (**e**) and dihydroceramide (**f**) in three types of rat skeletal muscles. Values are means ± SD ($n = 8$ in each group). The rats were either sedentary (control) or trained on an electrically driven treadmill as described in the methods. $^{b}p < 0.01$, $^{c}p < 0.001$ versus the control group. RG, *red section* of the gastrocnemius; WG, *white section* of the gastrocnemius

the soleus, red and white sections of the gastrocnemius respectively, compared to the control group (Fig. 5b).

Discussion

Endurance training induces several changes in lipid metabolism in skeletal muscles. The major change is an increased capacity of the muscles to utilize free fatty acids as a source of energy. Certain changes in phospholipid content and composition and the content of triacylglycerols have been also described [42, 43]. Recent research has provided information on the role of sphingolipids in induction of insulin resistance. Therefore, knowledge of how the ceramide metabolism can be changed seems to be very important for the invention of new treatments to prevent ceramide accumulation. Ceramide metabolism is changed in muscle in rats fed a high fat diet [41], diabetic and healthy animals with increased plasma FFA concentration [40], and also after a single-bout of exercise [26]. There are very few data in the literature concerning the effect of training on the activity of the key enzymes of ceramide metabolism in skeletal muscle. Our results suggest that the regulation of ceramide metabolism depends on

Table 3 Effect of training on the activity of enzymes implicated in sphingolipids metabolism in rat skeletal muscle

	SPT		nSMase		aSMase		nCDase		alCDase	
	Control	Training	Control	Training	Control	Training	Control	Training	Control	Training
Soleus	9.79 ± 0.92	18.81 ± 2.29[c]	13.54 ± 1.35	12.71 ± 2.41	23.37 ± 3.13	35.12 ± 6.71[c]	1.19 ± 0.11	0.97 ± 0.14[a]	1.48 ± 0.22	1.16 ± 0.14[a]
Gastrocnemius	11.10 ± 1.40	36.51 ± 5.63[c]	16.54 ± 1.17	21.57 ± 3.73[b]	20.80 ± 3.75	52.47 ± 8.19[c]	1.17 ± 0.19	1.11 ± 0.14	1.53 ± 0.22	1.16 ± 0.20[a]
White section of the Gastrocnemius	10.73 ± 1.28	42.42 ± 5.98[c]	11.63 ± 1.23	16.38 ± 3.06[c]	9.13 ± 0.61	20.81 ± 3.90[c]	1.66 ± 0.19	1.15 ± 0.19[a]	1.90 ± 0.18	1.26 ± 0.15[b]

Values are means ± SD ($n = 8$ in each group). The rats were either sedentary (control) or trained on the electrically driven treadmill as described in the methods

[a] $p < 0.05$, [b] $p < 0.01$, [c] $p < 0.001$ versus the control group

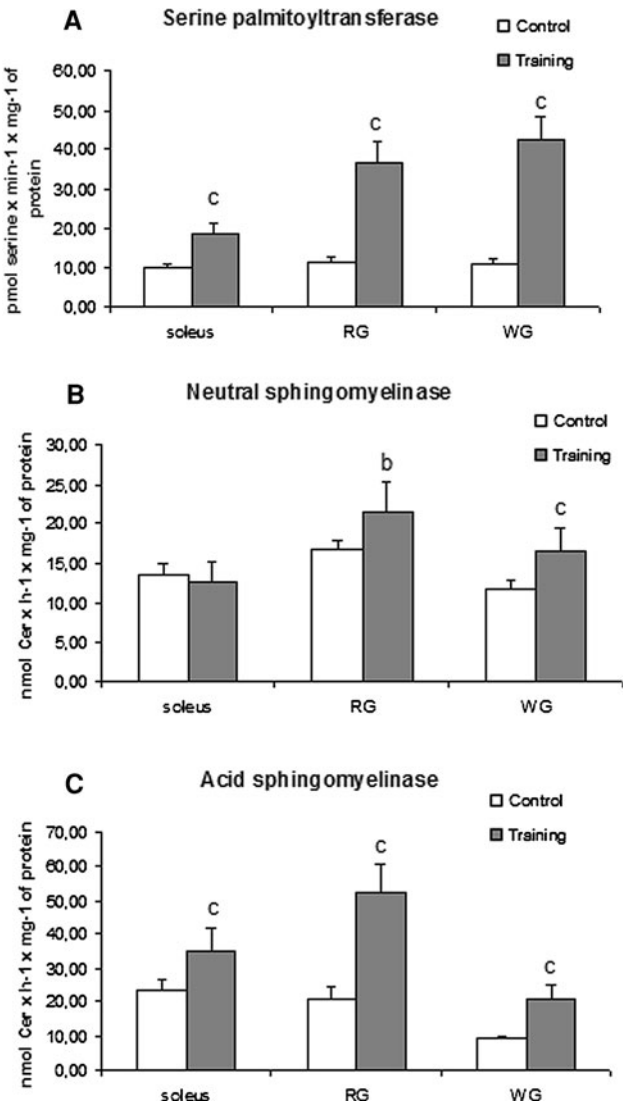

Fig. 4 Effect of training on the activity of **a** serine palmitoyltransferase, **b** neutral sphingomyelinase, **c** acid sphingomyelinase in three types of rat skeletal muscles. Values are means ± SD ($n = 8$ in each group). The rats were either sedentary (control) or trained on an electrically driven treadmill as described in the methods. [b] $p < 0.01$, [c] $p < 0.001$ versus the control group. RG, *red section* of the gastrocnemius; WG, *white section* of the gastrocnemius

the type of exercise. We found that the short-time exercise caused a reduction in ceramide content but exhaustive exercise led to an elevated ceramide content in muscle [26]. Data from the current study show that training affects the ceramide metabolism in a different way to single-bout exercise. The ceramide level does not change in the trained group although the activities of the key enzymes of ceramide metabolism changed. The data regarding the content of ceramide are in agreement with the results reported previously, where 8 week training did not affect the ceramide content in rat gastrocnemius muscle [44]. In human skeletal muscle, training did not change the total ceramide

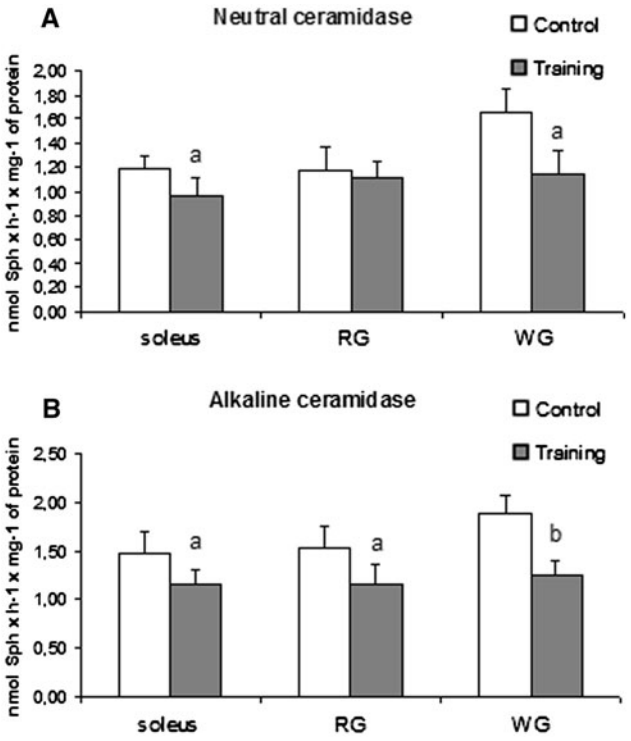

Fig. 5 Effect of training on the activity of neutral (**a**) and alkaline (**b**) ceramidase in rat skeletal muscle. Values are means ± SD ($n = 8$ in each group). The rats were either sedentary (control) or trained on the electrically driven treadmill as described in the methods. $^{a}p < 0.05$, $^{b}p < 0.01$, $^{c}p < 0.001$ versus the control group. RG, *red section* of the gastrocnemius; WG, *white section* of the gastrocnemius

content [27]. However, there are also conflicting data on the ceramide content in trained muscle. Experiments performed on obese subjects showed that endurance training reduces ceramide content and improves glucose tolerance [45, 46]. It must be mentioned that in these cases, obese people were examined and the ceramide metabolism in obesity can be different than in lean subjects. However, in the literature, there are also data showing that ceramide content decreases in muscle from trained rats [25]. The possible explanation of this discrepancy could be different analytical techniques used for measurement of the ceramide level in these two studies. In the mentioned work, ceramide content was measured by means of gas–liquid chromatography (GLC) after transmethylation of the ceramide fatty acids. Ceramide was purified by means of thin layer chromatography (TLC). The total content of different ceramides was measured including species containing: sphingosine, sphinganine, phytosphingosine, and homologs as a sphingoid base.

In our work, we have demonstrated that ceramide generation increased (increased activity of SPT, nSMase and aSMase) and decreased ceramides degradation (decreased activity of both CDases isoforms). Because of increased activity of enzymes responsible for ceramide production and decreased activity of enzymes responsible for ceramides degradation, we would expect to have an elevated ceramide content in the muscle, but we did not notice any changes in the ceramides level. We also did not observed any changes in muscle dihydroceramide content between trained and sedentary groups. This suggests that in the trained muscle other enzymes responsible for ceramides degradation/conversion are activated. We suspect that ceramide kinase, sphingomyelin synthase or glucosylceramide synthase are activated. Contribution of these pathways to regulation of ceramide content has not been recognized, so far.

Presently, we reported increased activity of SPT (enzyme catalyzing the reaction of condensation of serine and palmitoyl-CoA) and elevated content of sphinganine (main intermediate in sphingolipids de novo biosynthesis) in trained muscle. The elevation in the activity of SPT and the SPA content during exercise strongly indicates that physical exercise augments de novo sphingolipids synthesis in the muscles. The accumulation of SPA in the skeletal muscles of trained rats was observed also in the former study [25]. In our work we have observed an increased content of sphinganine-1-phosphate. It seems that sphinganine is directed to SPA1P instead of dhCer in the de novo synthesis pathway. Unfortunately, we have been unable to compare results from SPT activity and SPA1P content with any others because there is no information about SPT activity and SPA1P content in trained muscle.

Moreover, we also noticed increased activity of both isoforms of sphingomyelinases. We assume that increased nSMase activity is the effect of an increased content of TNF-α. During exercise TNF-α concentration increases and this agent is well known as an SMase activator [47]. Increased activity of nSMase was also previously observed in trained rat muscles [25]. In the literature there are also conflicting results related to nSMase activity. Data from trained muscle in human subjects showed that training does not affect nSMase activity [27].

Besides increased activities of enzymes responsible for ceramide production (SPT, n- and aSMase), we have simultaneously observed decreased activity of both isoforms of CDases. We cannot compare this result with any others studies because this is the only study when the enzymes activities were measured in trained muscles. In our work we did not observe any changes in Sph content and this result is in line with the results obtained previously [25].

It is well known that accumulation of ceramides, diacylglycerols and LCACoA in skeletal muscle is responsible for induction of insulin resistance. In our work, although ceramide content did not change in trained muscle, increased insulin sensitivity was observed—HOMA-IR

values were significantly lower in trained animals compared to sedentary rats (Table 1).

In summary, ceramide content does not change in the trained group although the animals were more insulin sensitive, Moreover, the activity of enzymes responsible for ceramide production (SPT, nSMase, aSMase) increased and the activity of enzymes responsible for ceramide degradation (nCDase, alCDase) decreased. These results suggest that in trained muscle other metabolic pathways are activated and have an effect on the ceramide content.

Acknowledgments This work was supported by the Ministry of Scientific Research and Information Technology, Grant: 2P05A 011 28 and Medical University of Bialystok, grant 3-18578, 3-18631 and 3-18610.

Conflict of interest There is no conflict of interest for this study.

References

1. Ohanian J, Ohanian V (2001) Sphingolipids in mammalian cell signalling. Cell Mol Life Sci 58:2053–2068
2. Kolesnick R, Fuks Z (2003) Radiation and ceramide-induced apoptosis. Oncogene 22:5897–5906
3. Oh HL, Seok JY, Kwon CH, Kang SK, Kim YK (2006) Role of MAPK in ceramide-induced cell death in primary cultured astrocytes from mouse embryonic brain. Neurotoxicology 27:31–38
4. MacRae VE, Burdon T, Ahmed SF, Farquharson C (2006) Ceramide inhibition of chondrocyte proliferation and bone growth is IGF-I independent. J Endocrinol 191:369–377
5. Verheij M, Bose R, Lin XH, Yao B, Jarvis WD, Grant S, Birrer MJ, Szabo E, Zon LI, Kyriakis JM, Haimovitz-Friedman A, Fuks Z, Kolesnick RN (1996) Requirement for ceramide-initiated SAPK/JNK signalling in stress-induced apoptosis. Nature 380:75–79
6. Wang YM, Seibenhener ML, Vandenplas ML, Wooten MW (1999) Atypical PKC zeta is activated by ceramide, resulting in coactivation of NF-kappaB/JNK kinase and cell survival. J Neurosci Res 55:293–302
7. Schubert KM, Scheid MP, Duronio V (2000) Ceramide inhibits protein kinase B/Akt by promoting dephosphorylation of serine 473. J Biol Chem 275:13330–13335
8. Spiegel S, Olivera A, Zhang H, Thompson EW, Su Y, Berger A (1994) Sphingosine-1-phosphate, a novel second messenger involved in cell growth regulation and signal transduction, affects growth and invasiveness of human breast cancer cells. Breast Cancer Res Treat 31:337–348
9. Pyne S, Pyne NJ (2000) Sphingosine 1-phosphate signalling in mammalian cells. Biochem J 349:385–402
10. Liang H, Yao N, Song JT, Luo S, Lu H, Greenberg JT (2003) Ceramides modulate programmed cell death in plants. Genes Dev 17:2636–2641
11. Pettus BJ, Bielawska A, Subramanian P, Wijesinghe DS, Maceyka M, Leslie CC, Evans JH, Freiberg J, Roddy P, Hannun YA, Chalfant CE (2004) Ceramide 1-phosphate is a direct activator of cytosolic phospholipase A2. J Biol Chem 279:11320–11326
12. Phillips DC, Martin S, Doyle BT, Houghton JA (2007) Sphingosine-induced apoptosis in rhabdomyosarcoma cell lines is dependent on pre-mitochondrial Bax activation and post-mitochondrial caspases. Cancer Res 67:756–764
13. Merrill AH Jr (2002) De novo sphingolipid biosynthesis: a necessary, but dangerous, pathway. J Biol Chem 277:25843–25846
14. Li CM, Hong SB, Kopal G, He X, Linke T, Hou WS, Koch J, Gatt S, Sandhoff K, Schuchman EH (1998) Cloning and characterization of the full-length cDNA and genomic sequences encoding murine acid ceramidase. Genomics 50:267–274
15. Turinsky J, Bayly BP, O'Sullivan DM (1990) 1, 2-Diacylglycerol and ceramide levels in rat skeletal muscle and liver in vivo. Studies with insulin, exercise, muscle denervation, and vasopressin. J Biol Chem 265:7933–7938
16. Dobrzyn A, Gorski J (2002) Ceramides and sphingomyelins in skeletal muscles of the rat: content and composition. Effect of prolonged exercise. Am J Physiol Endocrinol Metab 282:E277–E285
17. Adams JM 2nd, Pratipanawatr T, Berria R, Wang E, DeFronzo RA, Sullards MC, Mandarino LJ (2004) Ceramide content is increased in skeletal muscle from obese insulin-resistant humans. Diabetes 53:25–31
18. Kruszynska YT, Olefsky JM (1996) Cellular and molecular mechanisms of non-insulin dependent diabetes mellitus. J Investig Med 44:413–428
19. DeFronzo RA, Ferrannini E, Sato Y, Felig P, Wahren J (1981) Synergistic interaction between exercise and insulin on peripheral glucose uptake. J Clin Invest 68:1468–1474
20. Krssak M, Falk Petersen K, Dresner A, DiPietro L, Vogel SM, Rothman DL, Roden M, Shulman GI (1999) Intramyocellular lipid concentrations are correlated with insulin sensitivity in humans: a 1H NMR spectroscopy study. Diabetologia 42:113–116
21. Phillips DI, Caddy S, Ilic V, Fielding BA, Frayn KN, Borthwick AC, Taylor R (1996) Intramuscular triglyceride and muscle insulin sensitivity: evidence for a relationship in nondiabetic subjects. Metabolism 45:947–950
22. Turinsky J, O'Sullivan DM, Bayly BP (1990) 1,2-Diacylglycerol and ceramide levels in insulin-resistant tissues of the rat in vivo. J Biol Chem 265:16880–16885
23. Stallknecht B, Larsen JJ, Mikines KJ, Simonsen L, Bulow J, Galbo H (2000) Effect of training on insulin sensitivity of glucose uptake and lipolysis in human adipose tissue. Am J Physiol Endocrinol Metab 279:E376–E385
24. Teran-Garcia M, Rankinen T, Koza RA, Rao DC, Bouchard C (2005) Endurance training-induced changes in insulin sensitivity and gene expression. Am J Physiol Endocrinol Metab 288:E1168–E1178
25. Dobrzyn A, Zendzian-Piotrowska M, Gorski J (2004) Effect of endurance training on the sphingomyelin-signalling pathway activity in the skeletal muscles of the rat. J Physiol Pharmacol 55:305–313
26. Blachnio-Zabielska A, Baranowski M, Zabielski P, Gorski J (2008) Effect of exercise duration on the key pathways of ceramide metabolism in rat skeletal muscles. J Cell Biochem 105:776–784
27. Helge JW, Dobrzyn A, Saltin B, Gorski J (2004) Exercise and training effects on ceramide metabolism in human skeletal muscle. Exp Physiol 89:119–127
28. Langfort J, Czarnowski D, Pilis W, Wojcik B, Gorski J (1996) Effect of various types of exercise training on 5′-nucleotidase and adenosine deaminase activities in rat heart: influence of a single bout of endurance exercise. Biochem Mol Med 59:28–32

29. Dobrzyn A, Knapp M, Gorski J (2004) Effect of acute exercise and training on metabolism of ceramide in the heart muscle of the rat. Acta Physiol Scand 181:313–319
30. Sullivan TE, Armstrong RB (1978) Rat locomotory muscle fiber activity during trotting and galloping. J Appl Physiol 44:358–363
31. Dyck DJ, Peters SJ, Glatz J, Gorski J, Keizer H, Kiens B, Liu S, Richter EA, Spriet LL, van der Vusse GJ, Bonen A (1997) Functional differences in lipid metabolism in resting skeletal muscle of various fiber types. Am J Physiol 272:E340–E351
32. Min JK, Yoo HS, Lee EY, Lee WJ, Lee YM (2002) Simultaneous quantitative analysis of sphingoid base 1-phosphates in biological samples by *o*-phthalaldehyde precolumn derivatization after dephosphorylation with alkaline phosphatase. Anal Biochem 303:167–175
33. Bose R, Chen P, Loconti A, Grullich C, Abrams JM, Kolesnick RN (1998) Ceramide generation by the reaper protein is not blocked by the caspase inhibitor, p35. J Biol Chem 273:28852–28859
34. Liu B, Hannun YA (2000) Sphingomyelinase assay using radiolabeled substrate. Methods Enzymol 311:164–167
35. Nikolova-Karakashian M, Merrill AH Jr (2000) Ceramidases. Methods Enzymol 311:194–201
36. Merrill AH Jr (1983) Characterization of serine palmitoyltransferase activity in Chinese hamster ovary cells. Biochim Biophys Acta 754:284–291
37. Cacho J, Sevillano J, de Castro J, Herrera E, Ramos MP (2008) Validation of simple indexes to assess insulin sensitivity during pregnancy in Wistar and Sprague-Dawley rats. Am J Physiol Endocrinol Metab 295:E1269–E1276
38. Pickersgill L, Litherland GJ, Greenberg AS, Walker M, Yeaman SJ (2007) Key role for ceramides in mediating insulin resistance in human muscle cells. J Biol Chem 282:12583–12589
39. Teruel T, Hernandez R, Lorenzo M (2001) Ceramide mediates insulin resistance by tumor necrosis factor-alpha in brown adipocytes by maintaining Akt in an inactive dephosphorylated state. Diabetes 50:2563–2571
40. Blachnio-Zabielska A, Zabielski P, Baranowski M, Gorski J (2010) Effects of streptozotocin-induced diabetes and elevation of plasma FFA on ceramide metabolism in rat skeletal muscle. Horm Metab Res 42:1–7
41. Blachnio-Zabielska A, Baranowski M, Zabielski P, Gorski J (2010) Effect of high fat diet enriched with unsaturated and diet rich in saturated fatty acids on sphingolipid metabolism in rat skeletal muscle. J Cell Physiol 225:786–791
42. Gorski J (1992) Muscle triglyceride metabolism during exercise. Can J Physiol Pharmacol 70:123–131
43. Gorski J, Zendzian-Piotrowska M, de Jong YF, Niklinska W, Glatz JF (1999) Effect of endurance training on the phospholipid content of skeletal muscles in the rat. Eur J Appl Physiol Occup Physiol 79:421–425
44. Tsalouhidou S, Petridou A, Mougios V (2009) Effect of chronic exercise on DNA fragmentation and on lipid profiles in rat skeletal muscle. Exp Physiol 94:362–370
45. Bruce CR, Thrush AB, Mertz VA, Bezaire V, Chabowski A, Heigenhauser GJ, Dyck DJ (2006) Endurance training in obese humans improves glucose tolerance and mitochondrial fatty acid oxidation and alters muscle lipid content. Am J Physiol Endocrinol Metab 291:E99–E107
46. Dube JJ, Amati F, Stefanovic-Racic M, Toledo FG, Sauers SE, Goodpaster BH (2008) Exercise-induced alterations in intramyocellular lipids and insulin resistance: the athlete's paradox revisited. Am J Physiol Endocrinol Metab 294:E882–E888
47. Mathias S, Pena LA, Kolesnick RN (1998) Signal transduction of stress via ceramide. Biochem J 335(Pt 3):465–480

Lipids (2011) 46:239–247
DOI 10.1007/s11745-010-3477-1

ORIGINAL ARTICLE

Dietary Inclusion of Tea Catechins Changes Fatty Acid Composition of Muscle in Goats

C. Y. Tan · R. Z. Zhong · Z. L. Tan · X. F. Han · S. X. Tang · W. J. Xiao · Z. H. Sun · M. Wang

Received: 28 January 2010 / Accepted: 14 September 2010 / Published online: 13 October 2010

Abstract This study was conducted to examine dietary tea catechins (TC) supplementation on the fatty acid composition of muscle and ruminal bacteria in goats fed a maize stover-based diet. Forty goats, 8 months old (16.2 ± 1.2 kg), were randomly divided into four equal groups (10 animals in each group) and assigned to four experiment diets with TC supplementation at four levels (0, 2,000, 3,000 and 4,000 mg TC/kg feed, namely TC0, TC2000, TC3000 and TC4000, respectively). After a 60-day feeding period, all the goats were slaughtered and sampled. The results showed that dietary TC inclusion increased the average daily gain (ADG), protein content in the *semimembranosus* muscle and dry matter in the *longissimus dorsi* muscle (LD). Dietary TC supplementation increased the ratio of n-6 to n-3 fatty acid, the ratio of polyunsaturated fatty acids to saturated fatty acids was higher in TC3000 and TC4000 than in TC0 and TC2000 for LD. The current results implied that dietary inclusion of a suitable TC dose could improve the growth performance and increase the proportions of unsaturated fatty acids in muscle, and the biohydrogenation of ruminal microorganisms might change the profiles of fatty acids in the muscle of growing goats.

Keywords Goats · Tea catechins · Fatty acids · Biohydrogenation

Abbreviations

ADF	Acid detergent fiber
CLA	Conjugated linoleic acid
CP	Crude protein
DM	Dry matter
GM	Gluteus medius muscle
IMF	Intramuscular fat
LD	*Longissimus dorsi* muscle
MUFA	Monounsaturated fatty acid(s)
ME	Metabolizable energy
NDF	Neutral detergent fiber
OM	Organic matter
PUFA	Polyunsaturated fatty acid(s)
SFA	Saturated fatty acid(s)
SM	*Semimembranosus* muscle
TC	Tea catechins
UFA	Unsaturated fatty acid(s)

C. Y. Tan · R. Z. Zhong · Z. L. Tan (✉) · X. F. Han · S. X. Tang · Z. H. Sun · M. Wang
Key Laboratory of Agro-ecological Processes in Subtropical Region, Institute of Subtropical Agriculture, The Chinese Academy of Sciences, Changsha 410125, Hunan, People's Republic of China
e-mail: zltan@isa.ac.cn

C. Y. Tan · R. Z. Zhong · Z. H. Sun
Graduate University of the Chinese Academy of Sciences, Beijing 100039, People's Republic of China

W. J. Xiao
Hunan Agricultural University, Changsha 410128, Hunan, People's Republic of China

Introduction

Ruminants have a relatively high ratio of saturated to unsaturated fat acids in their body lipids. A low intake of saturated fat and an increased polyunsaturated to saturated fatty acid ratio (PUFA:SFA) in the diets are associated with a low risk of human coronary heart disease [1]. However, the level of PUFA consumed by the general population is

currently considered to be inadequate [2]. Hence, many animal scientists have been focusing on how to produce PUFA fortified animal products (meat, eggs and milk) for human beings.

In the past decades, the interest has been focused on the effects of antioxidants on nutrient digestibility, microbial nitrogen synthesis, and fatty acid profiles of meat in ruminants [3]. Dietary supplementation of antioxidants could improve total carbohydrate, neutral and acid detergent fiber (ADF and NDF) digestibility, and the amount of digested feed nitrogen converted to microbial nitrogen in dairy cows [4]. Furthermore, antioxidant supplementation could result in ruminal microbial metabolic changes, which were beneficial to cellulolytic activity [4] and growth of rumen microbes [5]. Researchers have demonstrated that dietary antioxidants might increase the PUFA content of meat in ruminants. Vázquez-Añón et al. [4] suggested that inclusion of dietary antioxidants could protect fatty acids from further peroxidation with a reduction in the toxic effect of unsaturated fatty acids on rumen microbes. Meanwhile, antioxidants might act as electron donors to provide the electrons for the reduction of some UFA, and be metabolized to these donors by microorganisms in the rumen [6].

Tea catechins (TC), a predominant group of polyphenols in green tea leaves (*Camellia sinensis* L.), comprise mainly four compounds namely (−)-epicatechin (EC), (−)-epicatechin gallate (ECG), (−)-epigallocatechin (EGC), and (−)-epigallocatechin gallate (EGCG) [7]. The TC have many biological functions, especially the anti-oxidative function. Its anti-oxidative properties as the dietary supplement have already been studied in dairy [5], chicken [8] and pig [9] using in vivo or vitro experiments. However, few trials have been conducted to study the effect of dietary TC supplementation on enhancing PUFA content of goat meat in a practical feeding system. The objective of this study was to investigate the effect of dietary TC supplementation on fatty acids profiles of ruminal bacteria and relevant tissues in goat kids.

Materials and Methods

The experiment was conducted according to the animal care and the use guidelines of the Animal Care Committee, Institute of Subtropical Agriculture, The Chinese Academy of Sciences, Changsha, China.

Reagent and Materials

All commercial kits used were obtained from Jiancheng Biology Co., Nanjing, China. All other general laboratory chemicals used for analysis were "AnalaR" grade. Tea catechins (TC) (purity of 80.86%) were extracted from green tea leaves (*Camellia sinensis* L.) by using high pressure liquid chromatography (HPLC) (Model Waters600, Waters Corp., Milford, USA) analysis according to the procedure reported previously [10] at Hunan Agriculture University, Changsha, Hunan, China. The TC were mainly composed of, by weight, caffeine (CAF) (0.75%), (+)-catechin and (−)-catechin (DL-C) (1.61%), EC (5.77%), EGC (0.47%), ECG (13.03%), (−)-gallocatechin gallate (GCG) (1.56%), and EGCG (57.67%).

Animal Management and Diet Preparation

Forty castrated Liuyang black male goats (a local breed) with an average age of 8 months ± 10 days, an average initial body weight of 16.2 ± 1.2 kg and the same genetic background were randomly divided into four equal groups (10 animals in each group) and assigned to four experiment diets for 60 days of the feeding trial, respectively. The control group (TC0) was fed the basal diet without TC supplementation. The other three groups were fed the basal diet with dietary TC supplementation at the levels of 2,000 (TC2000), 3,000 (TC3000) and 4,000 (TC4000) mg TC kg^{-1} feed (on DM basis). The ingredients and chemical composition of the basal diet, formulated according to NRC (1981) [11], are given in Table 1. Before the commencement of the trial, each group was allowed a 2-week adaptation period to the diets, respectively, and the average voluntary feed intake was measured. During the formal feeding period, each kid was fed twice daily (08:00 and

Table 1 The ingredients and chemical composition of the basal diet

Ingredient (% of DM)		Chemical composition	
Maize stover	45	DM (%)	89.8
Ground corn	25	OM (% of DM)	92.7
Soybean meal	15	ME (Mcal/kg DM)[b]	2.75
Wheat bran	11.2	CP (% of DM)	12.3
Urea	0.2	NDF (% of DM)	36.7
Calcium carbonate	0.9	ADF (% of DM)	24.2
Calcium bicarbonate	0.6	Calcium (% of DM)	0.92
Sodium chloride	0.6	Total phosphorus (% of DM)	0.74
Minerals and vitamins salt[a]	1.5		

DM dry matter, *OM* organic matter, *ME* metabolizable energy, *CP* crude protein, *NDF* neutral detergent fiber, *ADF* acid detergent fiber

[a] Contained per kg: 227 g $MgSO_4 \cdot H_2O$, 12.5 g $FeSO_4 \cdot 7H_2O$, 2.8 g $CuSO_4 \cdot 5H_2O$, 12.2 g $MnSO_4 \cdot H_2O$, 13.4 g $ZnSO_4 \cdot H_2O$, 20 mg Na_2SeO_3, 50 mg KI, 35 mg $CoCl_2 \cdot 6H_2O$, 90,000 IU vitamin A, 17,000 IU vitamin D, and 17,500 IU vitamin E.

[b] Metabolic energy (ME) was calculated according to NRC (1981) [11]

20:00 hour) with the amount of 578 g DM diets (determined by the average voluntary feed intake) and recorded the orts daily. Each goat was assigned to a single finishing barn as an experiment unit with an average room temperature of 24 ±1 °C with free access to fresh water. After 60 days of the feeding period, all goats were humanely slaughtered and samples were collected.

Slaughtering Procedure and Samples Preparation

After 60 days of feeding period, all kids were weighed (average weight was 17.5 ± 1.4 kg) and slaughtered under the commercial procedures, which was maintained according to the animal ethic committee of the Institute of Subtropical Agriculture. After slaughter, the goat carcasses were hung to remove the skin, head (at the occipito-atlantal joint), fore feet (at the carpal-metacarpal joint), hind feet (at the tarsal-metatarsal joint), gastrointestinal tract and visceral organs such as lung, liver, heart and kidney. About 1,000 g rumen fluid contents (mixed well) were collected from the rumen of the freshly slaughtered goat. Then, carcasses were cooled at 4 °C for 1 h in total darkness, and the left half-carcass was used for meat quality measurement. Muscles were separated from the carcass, and all external fat and connective tissue were removed within 24 h postmortem. About 200 g of left LD (from the 6th to 10th rib), 200 g gluteus medius muscle (GM) and 200 g *semimembranosus* muscle (SM) were sampled, respectively. Then, 100 g LD, GM and SM were, respectively, freeze-dried for analysis of intramuscular fat (IMF), crude protein (CP), ash and DM, and 50 g LD was taken and cut into slices and stored at −20 °C for determination of the fatty acid composition.

Analytical Procedure

At the beginning and end of the feeding trial, the weight of the goats was measured, which was used to measure the average daily gain of goats. The DM, CP, IMF and ash contents of LD, GM and SM were determined according to the method of the Association of Official Analytical Chemists [12]. Samples of LD were analyzed for fatty acid composition according to the following procedure. Tissue samples were homogenized and lipids were extracted from LD with chloroform/methanol (2:1). About 2 g of a muscle sample was combined with 10 ml of extraction solution (chloroform/methanol, 2:1, by vol) and 3 ml distilled water, and then extracted for 2 h at room temperature. After vacuum filtration, residues were rinsed with 10 ml of chloroform and then again filtered. The filtered solution was centrifuged at 5,000 rpm for 10 min. The upper layer (methanol and water layer) was removed and the bottom layer was sucked into the test tubes. These tubes were placed in a water bath at 37 °C for evaporating the chloroform using dry nitrogen. Then the extracts were stored at −40 °C until required for analysis. After extraction of the fat, fatty acid methyl esters were prepared for gas chromatography analysis. Briefly, 2 mg of extracted lipids were placed in a glass vial, and then 1.5 ml hexane, 100 µl methyl acetate and 100 µl sodium methoxide were added to the vial and thoroughly mixed. The mixture was kept for 20 min at 20 °C, and then 10 min at −20 °C in a refrigerator. Afterward, the vial was taken out of the refrigerator, and 60 µl of oxalic acid was added quickly. After centrifuging at 5,000 rpm for 10 min and discarding the deposit, the supernatant solution was dried over Na_2SO_4 and stored for future injection.

According to Kramer et al. [13], gas chromatography analyses of methyl esters were performed with the Agilent Technologies 6890N gas chromatograph (Agilent Technologies Inc., Palo Alto, CA, USA), fitted with a flame ionization detector. Separation was carried out on a CP-Sil88 fused silica open tubular capillary column (100 m × 0.25 nm) (Chrompack, Bridgewater, NJ, USA). The oven temperature started at 45 °C for 4 min, it was raised 13 °C/min to 175 °C; held for 27 min at 175 °C; increased 4 °C/min to 215 °C and held for 35 min at 215 °C. Injector and detector temperatures were 250 °C. The carrier gas was hydrogen at a flow rate of 30 ml/min. Identification of fatty acid methyl esters was accomplished by comparing their retention time with a GC reference standard (GLC 463, Nu-Chek Prer Inc, Elysian, MN).

Four specific isomers of conjugated linoleic acid (CLA) (18:2c9,t11, 18:2t10,c12, 18:2c9,c11 and 18:2t9,t11; Matreya LLC, USA) were used for CLA identification according to the procedure described by Destaillats and Angers [14]. Fatty acid methyl esters were quantified by determining areas under the identified peaks. Results were expressed as a proportion of each fatty acid methyl ester in relation to the total methyl esters detected.

The fatty acid composition of the ruminal solid-associated bacteria was measured according to the following procedure modified by Bas et al. [15]. 200 ml ruminal samples collected from each goat were pooled the rest of the group immediately and squeezed using four layers of cheesecloth. The liquid phase was centrifuged at 800×*g* for 15 min at 4 °C. The precipitate was added to the particles retained on the cheesecloth, then particles were blended (200 g of particles plus 200 ml of 0.9% cold NaCl) in a blender for 1 min, squeezed through four layers of cheesecloth, and then washed with 200 ml of 0.9% cold NaCl and squeezed again. The filtrates were centrifuged at 27,000×*g* for 30 min at 4 °C to obtain a pellet that contained solid-associated bacteria. Bacterial isolates were freeze-dried and ground using a mortar and pestle for later analysis of the fatty acid composition of the ruminal bacteria.

Table 2 Effect of dietary TC supplementation on chemical composition (fresh basis) of *longissimus dorsi* (LD), gluteus medius (GM) and *semimembranosus* (SM)

Item	Treatment				SEM	TC effect ($P \leq$)		
	TC0	TC2000	TC3000	TC4000		Linear	Quadratic	Cubic
Moisture (%)								
LD	76.6[a]	72.9[c]	74.8[b]	75.6[b]	0.33	**	***	***
SM	76.2	76.1	76.3	75.8	0.40	ns	ns	ns
GM	76.2	75.2	76.4	75.4	0.36	ns	ns	ns
IMF (g/kg)								
LD	23.0	32.8	25.5	28.2	0.32	ns	ns	ns
SM	22.9[a]	22.4[a]	17.4[b]	21.7[a]	0.11	ns	ns	**
GM	25.4	31.4	28.5	22.7	0.26	ns	ns	ns
Ash (%)								
LD	1.54[a]	1.31[b]	1.11[b]	1.15[b]	0.063	***	**	ns
SM	1.36[ab]	1.57[a]	1.44[a]	1.12[b]	0.093	ns	**	ns
GM	1.21	1.23	1.07	1.02	0.073	ns	ns	ns
CP (%)								
LD	18.5	21.2	19.7	19.2	0.08	ns	ns	ns
SM	18.6[b]	19.0[a]	19.0[a]	19.3[a]	0.11	*	ns	ns
GM	18.8	19.3	18.2	19.3	0.15	ns	ns	ns

Mean values with different superscripts in the same row differ significantly ($P < 0.05$)

SEM standard error of means, *TC0* No TC, *TC2000* 2,000 mg TC/kg feed, *TC3000* 3,000 mg TC/kg feed, *TC4000* 4,000 mg TC/kg feed, *IMF* intramuscular fat, *CP* crude protein, *ns* not significant

* $P < 0.05$, ** $P < 0.01$, *** $P < 0.001$

Statistical Analysis

All data were subjected to analysis of variance (ANOVA) using the generalized linear model procedure of SAS (2002). The main effect tested was the TC supplementation level for all variables. The following statistical model was used for data analysis:

$$Y_{ij} = \mu + T_i + e_{ij}$$

where Y_{ij} is dependent variables, μ is the overall mean, T_i is the effect of treatment ($i = 1, 2, 3, 4$), and e_{ij} is the random residual error. Where the effects of treatment were significant, differences among means were tested with Duncan's multiple range tests. Statistical significance was declared at $P \leq 0.05$.

Results

Chemical Composition of Fresh Meat

Effects of TC supplementation on chemical composition (fresh basis) of muscle are listed in Table 2. The TC supplementation decreased (linear, $P < 0.01$; quadratic and cubic, $P < 0.001$) moisture content of LD, and TC2000 treatment was found to have the highest DM content among all the groups. Dietary TC inclusion had a cubic effect ($P < 0.05$) on IMF content of SM, the least value occurred at TC3000 treatment. The ash content of LD in TC groups decreased significantly ($P < 0.05$) compared to control group, TC inclusion had a quadratic effect ($P < 0.01$) on ash content of SM. The CP content of SM linearly increased ($P < 0.05$) in response to TC supplementation, and control group had the lowest value. On the other hand, the average daily gains of TC0, TC2000, TC3000 and TC4000 groups were observed for 14.2, 17.2, 28.4 and 27.5 g/day, respectively. The results showed that TC supplementation had a linear and a cubic increase effect ($P < 0.001$) on the ADG of goats. All TC supplementation groups had a higher ADG than the control group ($P < 0.05$), and TC3000 and TC4000 had higher values than the TC2000 treatment.

Fatty Acid Composition of the *Longissimus Dorsi* Muscle

Effect of TC supplementation on the fatty acid composition of LD is presented in Table 3. For SFA, TC supplementation had no significant effect on the fatty acid proportions of 10:0, 12:0, 14:0, 16:0, 17:0, and 18:0, but the proportion of 15:0 decreased linearly ($P < 0.001$) with increasing TC supplementation levels; TC3000 and TC4000 had lower

Table 3 Effect of dietary TC supplementation on fatty acid composition of fresh *longissimus dorsi* (LD) (% total fatty acids)

Item	Treatment				SEM	TC effect ($P \leq$)		
	TC0	TC2000	TC3000	TC4000		Linear	Quadratic	Cubic
10:0	0.18	0.14	0.14	0.17	0.017	ns	ns	ns
12:0	0.11	0.08	0.13	0.10	0.014	ns	ns	ns
14:0	2.13	2.14	2.00	1.85	0.304	ns	ns	ns
15:0	0.62^{a}	0.56^{a}	0.39^{b}	0.29^{b}	0.038	***	ns	ns
16:0	26.8	27.2	26.0	26.0	0.54	ns	ns	ns
17:0	1.63	1.54	1.29	1.10	0.204	ns	ns	ns
18:0	17.9	15.4	15.6	15.9	1.37	ns	ns	ns
14:1	0.10	0.08	0.08	0.07	0.018	ns	ns	ns
16:1	2.54	2.56	2.54	2.29	0.305	ns	ns	ns
9t18:1	0.68	0.62	0.65	0.65	0.049	ns	ns	ns
11t18:1	0.72	0.49	0.77	0.68	0.142	ns	ns	ns
9c18:1	40.1^{b}	43.9^{a}	42.9^{a}	43.6^{a}	0.59	***	*	ns
11c18:1	0.07^{b}	0.04^{b}	0.29^{a}	0.04^{b}	0.076	*	**	***
12c18:1	1.56	1.53	1.54	1.58	0.113	ns	ns	ns
11c20:1	0.41^{a}	0.21^{b}	0.40^{a}	0.37^{ab}	0.054	ns	ns	*
9c12c18:2n-6	1.80^{ab}	1.15^{b}	2.36^{a}	2.18^{ab}	0.343	ns	ns	ns
9t12t18:2n-6	0.09^{c}	0.44^{a}	0.12^{b}	0.10^{c}	0.006	***	***	***
α-18:3n-3	0.17^{bc}	0.10^{c}	0.28^{a}	0.25^{ab}	0.034	*	ns	**
20:3n-6	0.07	0.06	0.08	0.06	0.018	ns	ns	ns
20:4n-6	1.23^{ab}	0.87^{b}	1.59^{ab}	1.92^{a}	0.269	ns	***	***
20:5n-3	0.30	0.30	0.27	0.28	0.054	ns	ns	ns
22:4n-6	0.03	0.13	0.07	0.06	0.011	ns	ns	ns
22:5n-3	0.24	0.18	0.28	0.19	0.040	ns	ns	ns
22:6n-3	0.06	0.04	0.03	0.04	0.012	ns	ns	ns
9c11tCLA	0.15^{a}	0.07^{b}	0.10^{ab}	0.08^{b}	0.020	*	ns	ns
11c13tCLA	0.10	0.07	0.07	0.08	0.014	ns	ns	ns
10t12cCLA	0.10^{a}	0.05^{b}	0.05^{b}	0.07^{ab}	0.012	*	*	ns
8c10c/11c13cCLA	0.04	0.05	0.03	0.02	0.007	ns	ns	ns
SFA	49.4^{a}	47.2^{ab}	45.5^{b}	45.4^{b}	0.87	**	ns	ns
MUFA	46.2^{b}	49.5^{a}	49.2^{a}	49.3^{a}	0.67	**	ns	ns
PUFA	4.39^{b}	3.50^{c}	5.30^{a}	5.33^{a}	0.293	**	*	**
Total CLA	0.38^{a}	0.24^{b}	0.25^{b}	0.25^{b}	0.061	***	*	ns
Total n-6	1.42^{b}	1.50^{b}	1.85^{ab}	2.14^{a}	0.148	**	ns	ns
Total n-3	0.78^{a}	0.62^{b}	0.84^{a}	0.76^{a}	0.032	ns	*	***
n-6/n-3	1.77^{b}	2.40^{a}	2.23^{ab}	2.81^{a}	0.192	**	ns	ns
PUFA/SFA	0.10^{b}	0.07^{c}	0.12^{a}	0.12^{a}	0.007	**	**	**
Total fatty acids g/kg	20.2	23.7	24.9	26.2	5.11	ns	ns	ns

Mean values with different superscripts in the same row differ significantly ($P < 0.05$)

SEM standard error of means, *TC0* No TC, *TC2000* 2,000 mg TC/kg feed, *TC3000* 3,000 mg TC/kg feed, *TC4000* 4,000 mg TC/kg feed, *t* trans, *c* cis, *CLA* conjugated linoleic acid, *SFA* saturated fatty acid, *MUFA* monounsaturated fatty acid, *PUFA* polyunsaturated fatty acid, *ns* not significant

* $P < 0.05$, ** $P < 0.01$, *** $P < 0.001$

proportions of SFA when compared to the control group. For MUFA, there was no significant effect on the fatty acid proportions of 14:1, 16:1, 9t18:1, 11t18:1 and 12c18:1 with TC supplementation; but TC3000 had higher proportion of 11c18:1, TC2000 had a lower proportion of 11c20:1, and all TC treatments had higher proportions of 9c18:1 and MUFA. For PUFA, TC supplementation had no significant effect on fatty acid proportions of 9c12c18:2, 20:3, 20:5,

22:4, 22:5 and 22:6; when compared to the control group, TC2000 had lower 20:4 and total n-3, TC3000 had higher proportion of α-18:3n-3, TC4000 had higher proportion of total n-6, TC2000 and TC3000 had higher proportions of 9t12t18:2, TC3000 and TC4000 had higher proportions of PUFA. For CLA, TC inclusion had no significant effect on fatty acid proportions of 11c13tCLA and 8c10c/11c13cCLA, whilst total CLA proportion decreased linearly ($P < 0.001$); TC2000 and TC3000 had lower proportions of 10t12cCLA when compared to the control group. In general, dietary TC supplementation increased (linear, $P < 0.001$) the ratio of n-6 to n-3 fatty acid in LD, the ratio of PUFA to SFA was higher ($P < 0.05$) in TC3000 and TC4000 than in TC0 and TC2000.

Fatty Acid Composition of Rumen Bacteria

Effect of TC supplementation on fatty acid composition of rumen bacteria attached to the solid particles is given in Table 4. For SFA, TC supplementation had no significant effects on the proportions of 14:0, 15:0, 16:0, 17:0 and SFA, but TC2000 had a higher ($P < 0.05$) proportion of 18:0, TC2000 and TC4000 had higher ($P < 0.05$) proportion of 20:0, and TC3000 and TC4000 had higher ($P < 0.05$) proportion of 12:0. For MUFA, there were no significant effects on fatty acid proportions of 16:1, 9t18:1, 9c18:1, 11c18:1, 12c18:1, 11c20:1 and MUFA among all experimental groups, but the proportion of 11t18:1 increased quadratically ($P < 0.05$) with increasing dietary TC levels. For PUFA, TC supplementation had no significant effects on fatty acid proportions of 20:3, 20:5, 22:4, and the ratio of n-6 to n-3; when compared to the control group, TC2000 had a higher proportion of 22:6, TC3000 had a lower proportion of 22:5, TC4000 had a higher proportion of total n-3, TC2000 and TC3000 had lower ($P < 0.05$) proportions of 9c12c18:2, TC2000 and TC4000 had higher ($P < 0.05$) proportions of 20:4, TC3000 and TC4000 had higher ($P < 0.05$) proportions of PUFA, n-6 and a higher ratio of PUFA to SFA. There were quadratic effects ($P < 0.05$) on the proportion of α-18:3n-3 with the greatest value being for TC2000 and TC4000. For CLA, TC inclusion had no significant effects on fatty acid proportions of 9c11tCLA and 8c10c/11c13cCLA; when compared to the control group, TC3000 had a higher proportion of 11c13tCLA, TC4000 had higher proportions of 10t12cCLA and total CLA.

Discussion

The ADG is the most important index which reflects the growth performance of animals. In this study, we found that the high TC dosage in the diets could improve the growth rate of growing goats. The reason for the increasing ADG may be attributed to TC supplementation, as a growth promoter, presumably acting on the intestinal and ruminal microorganism leading to higher nutrient digestion [5]. Tea polyphenols, especially the catechins, are effective antimicrobial and antioxidant agents [16]. Therefore, dietary TC inclusion could enhance the animal growth performance through regulating the physiological function of rumen microorganisms.

Consumers have given more attention to meat quality during recent years because of the high incidence of disease related to diet, especially related to fatty acid composition of meat. Our results demonstrated that TC supplementation could increase the CP content in SM. This might be supported by the previous results of Kondo et al. [17], in which dietary inclusion of green tea waste containing the rich antioxidant increased N retention in goats. Although it has been generally accepted that a higher IMF level is positively related to the sensory experience associated with meat [18], TC supplementation did not affect the IMF deposition in LD and GM in this study. The current results indicated that dietary antioxidant was not a main factor in regulating IMF content of muscle. It has been proven that TC has an antimicrobial property, which make it a potential alternative to antibiotics to manipulate microbial activity in the rumen [19]. Many plants can produce secondary metabolites which might have antimicrobial properties, e.g., tannin and saponin. These secondary metabolites have been shown to modulate the rumen fermentation to improve nutrient utilization [20]. Hence, it might be the potential explanation for the improvement of N retention when TC was added in the diets of ruminants. As for the increase of CP in SM but not in LD or GM, it might need further studies in the future.

Banskalieva et al. [21] reviewed similar results to this study concerning the main SFA, MUFA and PUFA of meat. Our results indicated that suitable dosages of dietary TC inclusion could increase the proportions of MUFA and PUFA in LD. These results were supported by the findings of Dal Bosco et al. [22], who reported that dietary antioxidant could increase PUFA and decrease SFA in rabbit meat. Sant'Ana et al. [23] also reported that addition of antioxidants in vivo could improve the composition of PUFA in fish fillets. According to our previous findings [24], TC addition in the diets was effective in inhibiting peroxidation in goat. If free radicals exceed the capacity of the cellular intrinsic free radical scavenging systems, they will become cytotoxic to cells by attacking fatty acids, and the reactions caused by exceeding radicals lead to lipid peroxidation of membranes. As an antioxidant, TC could protect the peroxidation of oxidative-labile MUFA and PUFA rather than that of more stable SFA. These results were consistent with the findings of Herlie et al. [25] in

Table 4 Effect of dietary TC supplementation on fatty acid composition of ruminal bacteria (% total fatty acid)

Item	Treatment				SEM	TC effect ($P \leq$)		
	TC0	TC2000	TC3000	TC4000		Linear	Quadratic	Cubic
10:0	0.32^{ab}	0.54^{a}	0.14^{b}	0.26^{ab}	0.098	ns	ns	**
12:0	2.33^{c}	2.08^{c}	4.20^{a}	3.16^{b}	0.099	***	ns	***
14:0	10.75	8.61	9.54	11.81	1.297	ns	ns	ns
15:0	7.09	5.10	6.34	6.45	0.490	ns	ns	ns
16:0	42.5	43.2	43.2	40.7	1.74	ns	ns	ns
17:0	1.31	1.12	1.33	1.33	0.105	ns	ns	ns
18:0	9.76^{b}	11.64^{a}	9.83^{b}	9.05^{b}	0.556	ns	**	ns
20:0	0.35^{b}	0.85^{a}	0.31^{b}	0.80^{a}	0.138	ns	ns	**
16:1	5.63	4.38	4.77	5.93	0.573	ns	ns	ns
9t18:1	0.52	0.42	0.50	0.55	0.083	ns	ns	ns
11t18:1	3.39^{ab}	5.61^{a}	2.90^{ab}	1.99^{b}	0.958	ns	*	ns
9c18:1	8.48	9.44	7.94	7.69	0.474	ns	ns	ns
11c18:1	0.46	0.44	0.35	0.61	0.095	ns	ns	ns
12c18:1	1.73	1.50	1.39	1.58	0.330	ns	ns	ns
11c20:1	0.47	0.20	0.21	0.34	0.098	ns	ns	ns
9c12c18:2n-6	0.31^{a}	0.19^{b}	0.18^{b}	0.25^{ab}	0.038	ns	*	ns
9t12t18:2n-6	2.92^{b}	2.96^{b}	5.17^{a}	4.86^{a}	0.534	**	ns	ns
α-18:3n-3	0.85^{ab}	0.57^{b}	0.68^{b}	1.25^{a}	0.144	ns	**	ns
20:3n-6	0.13	0.18	0.10	0.19	0.022	ns	ns	ns
20:4n-6	0.03^{c}	0.10^{b}	0.07^{bc}	0.16^{a}	0.020	***	ns	*
20:5n-3	0.07	0.03	0.06	0.15	0.028	ns	ns	ns
22:4n-6	0.09	0.09	0.12	0.15	0.028	ns	ns	ns
22:5n-3	0.13^{a}	0.12^{ab}	0.06^{b}	0.08^{ab}	0.021	*	ns	ns
22:6n-3	0.05^{b}	0.12^{a}	0.07^{b}	0.03^{b}	0.016	ns	**	ns
9c11tCLA	0.18	0.19	0.20	0.25	0.042	ns	ns	ns
11c13tCLA	0.04^{b}	0.04^{b}	0.09^{a}	ND	0.008	ns	***	***
10t12cCLA	0.10^{b}	0.22^{b}	0.22^{b}	0.39^{a}	0.053	***	ns	ns
8c10c/11c13cCLA	0.01	0.02	0.02	0.02	0.006	ns	ns	ns
SFA	74.4	73.2	74.9	73.5	1.83	ns	ns	ns
MUFA	22.0	20.7	18.1	18.7	1.57	ns	ns	ns
PUFA	4.91^{b}	4.83^{b}	7.04^{a}	7.80^{a}	0.545	***	ns	ns
Total CLA	0.33^{b}	0.47^{ab}	0.52^{ab}	0.67^{a}	0.077	**	ns	ns
Total n-6	3.17^{b}	3.33^{b}	5.47^{a}	5.38^{a}	0.546	**	ns	ns
Total n-3	1.10^{b}	0.85^{b}	0.87^{b}	1.51^{a}	0.167	ns	**	ns
n-6/n-3	3.60	3.96	6.57	3.79	0.912	ns	ns	ns
PUFA:SFA	0.07^{b}	0.07^{b}	0.09^{a}	0.10^{a}	0.005	***	*	ns

Mean values with different superscripts in the same row differ significantly ($P < 0.05$)

SEM standard error of means, *ND* not detected, *TC0* No TC, *TC2000* 2,000 mg TC/kg feed, *TC3000* 3,000 mg TC/kg feed, *TC4000* 4,000 mg TC/kg feed, *t* trans, *c* cis, *CLA* conjugated linoleic acid, *SFA* saturated fatty acid, *MUFA* monounsaturated fatty acid, *PUFA* polyunsaturated fatty acid, *ns* not significant

* $P < 0.05$, ** $P < 0.01$, *** $P < 0.001$

cultured cardiomyocytes. Alternatively, the extensive biohydrogenation of ingested PUFA by rumen microorganisms might lead to the low PUFA:SFA ratio in ruminant meat [26]. Chikunya et al. [6] reported that dietary antioxidant could protect the UFA in milk from biohydrogenation in the rumen, and they concluded that antioxidants might act as electron donors to provide the electrons for the reduction of some UFA and be metabolized to these donors by microorganisms in the rumen. Vasta et al. [27] also reported that the addition of

antioxidant could reduce the biohydrogenation through inhibiting the activity of rumen microorganisms. Therefore, we suggested that the possible mechanism should be that dietary TC inclusion exerts its function in the protection of polyunsaturated acids in feed and tissues. With high TC supplementation, the proportion of PUFA n-6 increased and the proportion of PUFA n-3 was not affected. A similar result was reported by Donaldson [28].

There was no more information about the effect of dietary TC inclusion on fatty acid composition of ruminal microorganism. Our results showed that suitable doses of TC supplements could increase the composition of PUFA, PUFAn-6, PUFAn-3 and CLA. The main fatty acid 18:1 as MUFA, 18:2 of rumen bacteria was close to the previous findings reported by Williams and Dinusson in bovine ruminal bacteria [29], but our results showed higher 16:0 and lower 18:0 proportions than those Williams and Dinusson reported. The higher 16:0 and lower 18:0 proportions might be a result of the different sources of rumen microorganisms which might be derived from different breeds of animals, and different feeding regimes, because the fatty acid composition is remarkably different for different sources of ruminal microorganisms and is significantly affected by feeding type [15].

Furthermore, numerous studies showed that different nutritional conditions can change lipid fatty acid composition of muscle, such as PUFA and total n-6 [30]. The profiles of fatty acids of digesta arriving at the proximal duodenum were different from those of the diets ingested in ruminants. The composition of fatty acids in muscle might partially be co-determined by the biohydrogenation and de novo synthesis by microorganisms in the rumen. The synchronous increase of UFA in muscle fat and ruminal bacteria, and the decrease of SFA in muscle with dietary TC inclusion in this study, probably implied that rumen microorganism could contribute a substantial part to the UFA of muscle.

Conclusion

In summary, dietary TC supplementation could improve the growth performance, and increase the proportions of MUFA and PUFA, and the ratio of PUFA to SFA in muscle, and increase the proportion of PUFA and the ratio of PUFA to SFA of ruminal bacteria in growing goats. As an antioxidant, dietary inclusion of the suitable TC dose (3,000 mg/kg) could change the fatty acid profile of goat meat through enhancing the contents of unsaturated fatty acids.

Acknowledgments The authors would like to express their sincere gratitude and appreciation to the Ministry of Science and Technology of China (2006BAD04A15; 2008BADA7B04) for providing the financial support.

References

1. Hu FB, Stampfer MJ, Manson JE, Ascherio A, Colditz GA, Speizer FE, Hennekens CH, Willett WC (1999) Dietary saturated fats and their food sources in relation to the risk of coronary heart disease in women. Am J Clin Nutr 70:1001–1008
2. Mantzioris E, Cleland LG, Gibson RA, Neumann MA, Demasi M, James MJ (2000) Biochemical effects of a diet containing foods enriched with n-3 fatty acids. Am J Clin Nutr 72:42–48
3. Salvatori G, Pantaleo L, Di Cesare C, Maiorano G, Filetti F, Oriani G (2004) Fatty acid composition and cholesterol content of muscles as related to genotype and vitamin E treatment in crossbred lambs. Meat Sci 67:45–55
4. Vázquez-Añón M, Jenkins T (2007) Effects of feeding oxidized fat with or without dietary antioxidants on nutrient digestibility, microbial nitrogen, and fatty acid metabolism. J Dairy Sci 90:4361–4367
5. Hino T, Andoh N, Ohgi H (1993) Effects of beta-carotene and alpha-tocopherol on rumen bacteria in the utilization of long-chain fatty acids and cellulose. J Dairy Sci 76:600–605
6. Chikunya S, Demirel G, Enser M, Wood JD, Wilkinson RG, Sinclair LA (2004) Biohydrogenation of dietary n-3 PUFA and stability of ingested vitamin E in the rumen, and their effects on microbial activity in sheep. Br J Nutr 91:539–550
7. Graham HN (1992) Green tea composition, consumption, and polyphenol chemistry. Prev Med 21:334–350
8. Tang SZ, Ou SY, Huang XS, Li W, Kerry JP, Buckley DJ (2006) Effects of added tea catechins on colour stability and lipid oxidation in minced beef patties held under aerobic and modified atmospheric packaging conditions. J Food Eng 77:248–253
9. Mason LM, Hogan SA, Sulliivan KO, Lawlor PG, Kerry JP (2005) Effects of restricted feeding and antioxidant supplementation on pig performance and quality characteristics of *longissimus dorsi* muscle from Landrace and Duroc pigs. Meat Sci 70:307–317
10. Nonaka G, Kawakami O, Nishioka I (1983) Tannins and related compounds. XV. A new class of dimeric flanan-3-ol gallates, theasineneins A and B, and proanthocyanidin gallates from green tea leaf. Chem Pharm Bull 31:3906–3910
11. RC N (1981) Nutrient requirements of goats: angora, dairy and meat goats in temperate and tropical countries. National Academy Press, Washington DC
12. AOAC 1996 Official methods of analysis. Washington DC, USA
13. Kramer JK, Hernandez M, Cruz-Hernandez C, Kraft J, Dugan ME (2008) Combining results of two GC separations partly achieves determination of all *cis* and *trans* 16:1, 18:1, 18:2 and 18:3 except CLA isomers of milk fat as demonstrated using Ag-ion SPE fractionation. Lipids 43:259–273
14. Destaillats F, Angers P (2003) Directed sequential synthesis of conjugated linoleic acid isomers from △7,9 to △12,14. Eur J Lipid Sci Technol 105:3–8
15. Bas P, Archimède H, Rouzeau A, Sauvant D (2003) Fatty acid composition of mixed-Rumen bacteria: effect of concentration and type of forage. J Dairy Sci 86:2940–2948
16. Almajano MP, Carbó R, Jiménez JAL, Gordon MH (2008) Antioxidant and antimicrobial activities of tea infusions. Food Chem 108:55–63
17. Kondo M, Kita K, Yokota HO (2004) Feeding value to goats of whole-crop oat ensiled with green tea waste. Anim Feed Sci Technol 113:71–81
18. van Laack RL, Stevens SG, Stalder KJ (2001) The influence of ultimate pH and intramuscular fat content on pork tenderness and tenderization. J Anim Sci 79:392–397
19. Benchaar C, Calsamiglia S, Chaves AV, Fraser GR, Colombatto D, McAllister TA, Beauchemin KA (2008) A review of plant-

derived essential oils in ruminant nutrition and production. Anim Feed Sci Technol 145:209–228
20. Hristov AN, McAllister TA, Van Herk FH, Cheng KJ, Newbold CJ, Cheeke PR (1999) Effect of *Yucca schidigera* on ruminal fermentation and nutrient digestion in heifers. J Anim Sci 77:2554–2563
21. Banskalieva V, Sahlu T, Goetsch AL (2000) Fatty acid composition of goat muscles and fat depots: a review. Small Rumin Res 37:255–268
22. Dal Bosco A, Castellini C, Bianchi L, Mugnai C (2004) Effect of dietary [alpha]-linolenic acid and vitamin E on the fatty acid composition, storage stability and sensory traits of rabbit meat. Meat Sci 66:407–413
23. Sant'Ana LS, Mancini-Filho J (2000) Influence of the addition of antioxidants in vivo on the fatty acid composition of fish fillets. Food Chem 68:175–178
24. Zhong RZ, Tan CY, Han XF, Tang SX, Tan ZL, Zeng B (2009) Effect of dietary tea catechins supplementation in goats on the quality of meat kept under refrigeration. Small Rumin Res 87:122–125
25. Hrelia S, Bordoni A, Angeloni C, Leoncini E, Toschi TG, Lercker G, Biagi PL (2002) Green tea extracts can counteract the modification of fatty acid composition induced by doxorubicin in cultured cardiomyocytes. Prostaglandins, Leukot Essent Fatty Acids 66:519–524
26. Jenkins TC (1993) Lipid metabolism in the rumen. J Dairy Sci 76:3851–3863
27. Vasta V, Makkar HP, Mele M, Priolo A (2009) Ruminal biohydrogenation as affected by tannins in vitro. Br J Nutr 102:82–92
28. Donaldson WE (1993) Effects of dietary lead, fish oil, and ethoxyquin on hepatic fatty-acid composition in chicks. Biol Trace Elem Res 36:319–326
29. Williams PP, Dinusson WE (1973) Amino acid and fatty acid composition of bovine ruminal bacteria and protozoa. J Anim Sci 36:151–155
30. Mandell IB, Buchanan-Smith JG, Campbell CP (1998) Effects of forage vs grain feeding on carcass characteristics, fatty acid composition, and beef quality in limousin-cross steers when time on feed is controlled. J Anim Sci 76:2619–2630

Lipids (2011) 46:249–261
DOI 10.1007/s11745-010-3482-4

ORIGINAL ARTICLE

N-Acylated Bacteriohopanehexol-Mannosamides from the Thermophilic Bacterium *Alicyclobacillus acidoterrestris*

Tomáš Řezanka · Lucie Siristova · Karel Melzoch · Karel Sigler

Received: 20 July 2010 / Accepted: 23 September 2010 / Published online: 21 October 2010

Abstract Identification of molecular species of various *N*-acylated bacteriohopanehexol-mannosamides from the thermophilic bacterium *Alicyclobacillus acidoterrestris* by semipreparative HPLC and by RP-HPLC with ESI is described. We used triple-quadrupole type mass spectrometer, ^{1}H and ^{13}C NMR for analyzing this complex lipid. CD spectra of two compounds (model compound—7-deoxy-D-*glycero*-D-*allo*-heptitol obtained by stereospecific synthesis, and an isolated derivative of hopane) were also measured and the absolute configuration of both compounds was determined. On the basis of all the above methods, we identified the full structure of a new class of bacteriohopanes, represented by various *N*-acylated bacteriohopanehexol-mannosamides.

Keywords *Alicyclobacillus acidoterrestris* · Negative RP-HPLC–ESI–MS/MS · Circular dichroism · *N*-Acylated bacteriohopanehexol-mannosamides · ω-Cyclohexyl fatty acids

Abbreviations

BH	Bacteriohopane
BHpolyols	Bacteriohopanepolyols
CD	Circular dichroism
CID	Collision-induced dissociation
COSY	Correlation spectroscopy
DMAP	Dimethylaminopyridine
FAME	Fatty acid methyl ester(s)
GC–MS	Gas chromatography–mass spectrometry
HMBC	Heteronuclear multiple bond coherence
HMQC	Heteronuclear multiple quantum coherence
HR-FAB-MS	High resolution fast atom bombardment mass spectrometry
LC–MS	Liquid chromatography–mass spectrometry
LC–MS/ESI SIM	Selected ion monitoring
NOE	Nuclear Overhauser effect
ROESY	Rotating-frame Overhauser effect spectroscopy
RP-HPLC/MS-ESI	Reversed phase liquid chromatography–electrospray ionization mass spectrometry
RP-HPLC–ESI–MS/MS	Reversed phase liquid chromatography–electrospray ionization tandem mass spectrometry
SPE	Solid phase extraction
TFFH	Fluoro-*N,N,N′,N′*-tetramethylformamidinium hexafluorophosphate
TLC	Thin layer chromatography
VVM	Air volume per volume of culture medium per minute

T. Řezanka (✉) · K. Sigler
Institute of Microbiology, Academy of Sciences of the Czech Republic, Vídeňská 1083, 142 20 Prague, Czech Republic
e-mail: rezanka@biomed.cas.cz

L. Siristova · K. Melzoch
Department of Fermentation Chemistry and Bioengineering, Institute of Chemical Technology Prague, Technická 5, 166 28 Prague, Czech Republic

Introduction

Bacteriohopanepolyols (BHpolyols) are pentacyclic triterpenoids, which are present as membrane constituents in

many bacteria [1]. They perform a regulating and rigidifying function in membranes analogous to that of some sterols in eukaryotes [2–4]. BHpolyol side chains form many structures, which differ in terms of the number, position and nature of the functional groups [2, 5]. The side chain is responsible for the charge and the function of the molecule [6].

The most commonly occurring BHpolyols in bacteria contain four functional groups in the side chain, typically three hydroxyl groups at 32*R*, 33*R*, 34*S* [7, 8] with the C-35 position occupied by either another OH or an amino group [2].

In numerous strains belonging to various taxonomic groups (e.g. purple nonsulfur bacteria, methylotrophs, or cyanobacteria) the bacteriohopane (BH) derivatives are not present as free polyols but are linked to various polar moieties like glucosamine or *N*-acylglucosamine, anhydrogalacturonopyranosides, α-amino acids such as tryptophan and ornithine, adenosine, cyclitol ethers or other polar entities the structures of which are still unidentified [2, 9]. BHpolyols have been found in many other structural variations including double bonds in the ring system or substitution by methyl groups in ring A. Furthermore, BHpolyols with five and six functional groups in the side chain, i.e. BHpolyols with additional one or two OH group(s) at C-30 and/or C-31 position(s) were identified [10–14, 40]. These structures are restricted to a limited number of organisms or occur in an explicit group of organisms and can serve as specific bacterial marker information [2, 5].

To date there have been only a few hexafunctionalized side chain structures reported from nature. The basic structure has five hydroxyl groups and NH_2 functionality at C-35, and has only been observed in Type I methanotrophic bacteria [14, 15]. Further, BHhexol cyclitol ether was identified in sediments of two lakes from Antarctica [16], soils from Northern England [17], and BHhexol in sediments from the popular Loch Ness (UK) [2].

This report is part of our investigation of thermophilic bacteria, mainly of the genus *Alicyclobacillus*. We extended our analysis from glycophospholipids [18], unusual acylphosphatidylglycerols [19], and *O*-acyl glycosylated cardiolipins [20] to hopanoids. The structure of *N*-acylated BHhexol-mannosamides was confirmed not only by ESI–MS, but, after isolation, also by measurement of ^{1}H-, ^{13}C-NMR, and CD spectra, including synthesis of a model compound.

Experimental

Instrumentation

The liquid chromatograph was the semipreparative Gradient LC System G-1 (Shimadzu, Kyoto, Japan) with two LC-6A pumps (0.5 ml/min), an SCL-6A system controller, an SPD ultraviolet detector an SIL-1A sample injector and a C-R3A data processor, with a preparative normal phase HPLC column Supelcosil LC-Si HPLC column 5 µm particle size, length × I.D. 25 cm × 21.2 mm with mobile phase containing hexane–isopropanol-0.05% triethylamine in water (99.5:0:0.5, v/v/v) to hexane–isopropanol-0.05% triethylamine in water (20:78:2 v/v/v) for 40 min, a flow rate of 9.9 ml/min, and monitored by a variable wavelength detector at 210 nm (HP 1040M Diode Array Detector).

The HPLC equipment consisted of a 1090 Win system, PV5 ternary pump and automatic injector (HP 1090 series, Hewlett Packard, USA) and two Ascentis® Express HILIC HPLC column 2.7 µm particle size, L × I.D. 15 cm × 2.1 mm (Supelco, Prague) in series were used. This setup provided us with a high-efficiency column—approximately 30,000 plates/30 cm. LC was performed at a flow rate of 300 µl/min with a linear gradient from the mobile phase containing methanol/acetonitrile/aqueous 1 mM ammonium acetate (60:20:20, v/v/v) to methanol/acetonitrile/aqueous 1 mM ammonium acetate (20:60:20, v/v/v) for 40 min. The whole HPLC flow (0.37 ml/min) was introduced into the ESI source without any splitting.

The detector was an Applied Biosystems Sciex API 4000 mass spectrometer (Applied Biosystems Sciex, Ontario, Canada) using electrospray mass spectra. The ionization mode was negative, the nebulizing gas (N_2) pressure was 345 kPa and the drying gas (N_2) flow and temperature were 9 l/min and 300 °C, respectively. The electrospray needle was at ground potential, whereas the capillary tension was held at 4,000 V. The cone voltage was kept at 250 V. The mass resolution was 0.1 Da and the peak width was set to 6 s. For an analysis, total ion currents (full scan) were acquired from 200 to 1,600 Da.

CID ions mass spectra were acquired by colliding the Q1 selected precursor ions with Ar gas at a collision target gas and applying collision energy of 50 eV in Q2. Scanning range of Q3 was *m/z* 200–1,600 with a step size of *m/z* 0.3 and a dwell time of 1 ms. A peak threshold of 0.3% intensity was applied to the mass spectra. The instrument was interfaced to a computer running Applied Biosystems Analyst version 1.4.1 software.

Gas chromatography–mass spectrometry of FAME was done on a GC–MS system consisting of Varian 450-GC, Varian 240-MS ion trap detector with electron impact ionization, and CombiPal autosampler (CTC, USA). The sample was injected onto a 25 m × 0.25 mm × 0.1 µm Ultra-1 capillary column (Supelco, Czech Republic) under a temperature program: 5 min at 50 °C, increasing at 10 °C/min to 320 °C and 15 min at 320 °C. Helium was the carrier gas at a flow of 0.52 ml/min. All spectra were scanned within the range *m/z* 50–600. The spectra was identified manually, se also Siristova et al. [18].

The oven temperature for identification of the acetylated alcohols BH (degradation products) was programmed from 50 to 275 °C at 10 °C/min and further at 5 °C/min to 350 °C and further with 8 min isothermal elution. The others conditions of GC–MS apparatus were identical.

Saccharides were separated on a single HILIC HPLC column (see above) by isocratic elution with acetonitrile and 0.1% acetic acid in water at a ratio of 40:60. They were identified by comparing their retention times with those of commercially obtained standards (galactosamine, glucosamine and mannosamine) and single ion monitoring at m/z 180 ($[M + H]^+$).

NMR spectra were recorded on a Bruker AMX 500 spectrometer (Bruker Analytik, Karlsruhe, Germany) at 500.1 MHz (^1H) and 125.7 MHz (^{13}C). Optical rotations were measured with a Perkin-Elmer 243 B polarimeter. The circular dichroism measurement was carried out under dry N_2 on a Jasco-500A spectropolarimeter at 24 °C. HR-FAB-MS (positive ion mode) were obtained with a PEG-400 matrix using a VG 7070E-HF spectrometer. All compounds were purchased from Sigma–Aldrich (Prague, Czech Republic).

Cultivation, Isolation and Identification

Alicyclobacillus acidoterrestris CCM 4660 (Czech Collection of Microorganisms, Brno, Czech Republic) was cultivated in an alicyclobacillus medium containing (g/l): yeast extract 6.0, glucose 5.0, $CaCl_2 \cdot 2H_2O$ 0.25, $MgSO_4 \cdot 7H_2O$ 0.5, $(NH_4)_2SO_4$ 0.2, KH_2PO_4 3.0 and 1 ml/l of trace element solution ($ZnSO_4 \cdot 7H_2O$ 0.1 g/l, $MnCl_2 \cdot 4H_2O$ 0.03 g/l, H_3BO_3 0.3 g/l, $CuCl_2 \cdot 6H_2O$ 0.2 g/l, $CaCl_2 \cdot 2H_2O$ 0.01 g/l, $NiCl_2 \cdot 6H_2O$ 0.02 g/l, $Na_2MoO_4 \cdot 2H_2O$ 0.03 g/l), pH was adjusted to 4. A volume of 600 ml of inoculum was prepared in 500-ml round-bottom flasks on a temperature controlled shaker at 45 °C and 200 rpm. The biomass was cultivated in a 5-l mechanically stirred fermentor with the aim of obtaining inoculum for a 50-l fermentor. Inoculum was cultivated for 12 h under aerobic conditions with aeration rate 0.8 VVM. The stirrer frequency was 300–400 rpm and the cultivation temperature was 45 °C.

The strain main cultivation was carried out in a 50-l mechanically stirred fermentor for 15 h, under aerobic conditions with an aeration rate of 1 VVM. The stirrer frequency was 350–400 rpm and the cultivation temperature was 45 °C. Cells were harvested in the log phase when the optical density of the culture was maximal. The dry biomass was 1.49 g/l media.

The extraction procedure was based on the method of Bligh and Dyer [21]. The alcohol-water mixture was cooled and one part chloroform was added and the lipids were extracted for 30 min. Insoluble material was sedimented by centrifugation and the supernatant was separated into two phases. The aqueous phase was aspirated off and the chloroform phase was washed three times with two parts 1 M KCl each. The resulting chloroform phase was evaporated to dryness under reduced pressure.

First, total lipid extracts were applied to Sep-Pak Cartridge Vac 35 cc (Waters; with 10 g of aminopropyl-silica-based polar bonded phase), and from the cartridge were subsequently eluted chloroform–methanol mixture (98:2) [22] for removing of non-polar lipids, and polar lipids, but not phospholipids were further eluted by an acetone. The eluate was reduced in volume and subjected to normal phase HPLC.

The aliquot of total BHs (5 mg) was stirred for l h at room temperature with periodic acid (H_5IO_6; 3 mg) in tetrahydrofuran/water (3 ml; 8:1 v/v). The vicinal diols were oxidized to yield aldehyde products. After addition of water (10 ml) the mixture was extracted with petroleum ether (3 × 5 ml). The combined extracts were evaporated and further stirred for l h at room temperature with sodium borohydride ($NaBH_4$; 1 mg) in ethanol (3 ml) to produce alcohols. The excess of $NaBH_4$ was destroyed by water and the mixture was extracted with petroleum ether (3 × 5 ml). The extracts were evaporated and acetylated, see below.

The total extract was acetylated overnight at room temperature with acetic anhydride/pyridine (30 ml; 1:1 v/v). The peracetylated BHs were evaporated and further analyzed.

The fraction of *N*-acylated BHhexol-glycoside after semipreparative HPLC was treated for 16 h at 100 °C with a 10% solution of dry HCl in CH_3OH. The reaction mixture was taken to dryness, suspended in water, the pH was regulated by 5% NaOH to 9, BHhexol was extracted by diethyl ether, the water mixture was acidified by 5% HCl to pH 4, free fatty acids were extracted by $CHCl_3$ and water phase was after lyophilization was silylated, see above. The fatty acid methyl esters were prepared by reaction of the free fatty acids with methanol, see Rezanka et al. [23].

Preparation of 7-Deoxyheptitol

D-*glycero*-D-*allo*-Heptose (**8a**) and D-*glycero*-D-*altro*-heptose (**8b**) were prepared from KCN and D-allose (**6**) according to procedures described previously [24, 25]. Briefly, the pH of an aqueous solution (15 ml) of potassium cyanide (269 mg, 4.14 mmol) was lowered to 7.2 by dropwise addition of aqueous acetic acid (3 M) with rapid stirring at room temperature. An aqueous solution (10 ml) of D-allose **6** (248 mg, 1.38 mmol) was slowly added, with addition of acetic acid (3 M) or sodium hydroxide (1 M) as appropriate to maintain a pH of 7.2–7.5 during addition of D-allose and subsequent reaction, which was allowed to proceed for 1.5 h. The reaction mixture was analyzed by TLC (cellulose sheets, 90:10 acetone–water) to reveal a

complete conversion of D-allose (**6**) (R_f 0.67) into the aldonitriles (**7a** and **7b**) (R_f 0.8–0.9). The pH of the aldonitrile solution was lowered to 4.7 by dropwise addition of acetic acid (3 M) and the solution was stored at 4 °C for ca. 1 h. Further, the pH of the solution was again lowered to 4.2 by dropwise addition of acetic acid (3 M). Following addition of prereduced 5% palladium on barium sulfate (86 mg = 4.3 mg, 0.04 mmol Pd), the flask was evacuated three times and flushed with hydrogen. Vigorous stirring under an atmosphere of hydrogen was then allowed to proceed at room temperature for ca. 15 h. The reaction mixture was analyzed by TLC (90:10 acetone–water) to reveal a complete reduction of the aldonitriles (**7a** and **7b**) (R_f 0.8–0.9) into the imines (R_f 0.4–0.6). The catalyst was removed over Celite and the pH of the resultant filtrate was lowered from pH 4.4 to ca. pH 3.0 by repeated batch-wise treatment with Dowex® 50WX2 hydrogen form 200–400 mesh (4 × 4 g). The final filtrate was analyzed by TLC (95:5 acetone–water) and no imine was detected. The water was removed by lyophilization to leave the epimeric mixture of **8a** and **8b** as a pale yellow oil; the yield of epimeric sugars was 243 mg (84%) and they were separated by semi-preparative TLC.

Aldrich Analtech TLC Uniplates™ with spherical particles (size 50 μm) of α-cellulose matrix, size 20 cm × 20 cm, layer thickness 250 μm, fluorescent indicator were used. The mobile phase was acetone–water (95:5, v/v), D-glucose being used as standard. Identification under UV light gave the following R_f values for the compounds: D-*glycero*-D-*allo*-heptose (**8a**) (0.35), D-glucose (0.51) and D-*glycero*-D-*altro*-heptose (**8b**) (0.63). The yield of D-*glycero*-D-*allo*-heptose (**8a**) was 106 mg, with $[\alpha]_D^{23}$ +12.8 (1 day, c = 0.15), lit. data: $[\alpha]_D^{21}$ +14.1 [26], $[a]_D$ +10.7 (24 h) (c 1.6, H_2O) [27], $[a]_D$ +7.2 (3 min) → +12.7 (24 h) (c 4.6, H_2O) [28]; ^{13}C NMR (125 MHz, D_2O) δ major: 93.8 (C-1), 73.8, 72.1, 71.3, 71.2, 67.7, 61.8; minor: 92.7 (C-1), 72.0, 71.7, 67.6, 67.1, 66.9, 62.1 [27, 28]; ^{13}C NMR δ 94.4, 72.9, 72.0, 71.9, 74.6, 68.5, 62.6 (the values for C-1 → C-7 of β-pyranose), the values for C-1 were 93.4 (α-pyranose), 94.4 (β-pyranose), 96.8 (α-furanose), and 101.4 (β-furanose) [29]. Our data measured for mixture of four forms at C-1 were 93.2 (α-pyranose), 94.5 (β-pyranose), 97.0 (α-furanose), and 101.5 (β-furanose) and the following values are for the major form: ^{13}C NMR (125 MHz, D_2O) δ 94.5 (C-1), 73.3 (C-2), 72.5 (C-3), 71.6 (C-4), 73.8 (C-5), 68.4 (C-6), and 62.2 (C-7); HR-FAB-MS (m/z): 211.0823 $[M + H]^+$, calc. for $[C_7H_{14}O_7 + H]^+$ 211.0818.

D-*glycero*-D-*allo*-Heptose diethyl thioacetal = (2*S*,3*R*,4*S*,5*S*)-7,7-bis(ethylthio)heptane-1,2,3,4,5,6-hexaol. A mixture of D-*glycero*-D-*allo*-heptose (**8a**) (105 mg) and concentrated HCl (5 ml) was shaken for about 10 min to dissolve most of the sugar and then, as the solution began to assume a reddish color, 5 ml of ethylthiol was added and shaking was continued for 2.5 h. The product was allowed to stand overnight in the refrigerator. About 5 ml of cold water was added, the dithioacetal filtered, and washed with cold ethanol. The yield, after one recrystallization from ethanol, was 100 mg (63.3%). Very surprisingly, this compound (**9**) has not yet been described. $[a]_D$ +10.7 (c 0.16, MeOH); ^{1}H-NMR (500 MHz, CD_3OD) δ 4.92 (1H, *d*, J = 1.6, H-7), 4.93 (1H, *dd*, J = 1.6, 5.5, H-6), 5.06 (1H, t, J = 5.5, H-5), 5.19 (1H, t, J = 5.5, H-4), 4.71 (1H, t, J = 5.5, H-3), 4.65 (1H, *ddd*, J = 5.5, 3.2, 8.2, H-2), 4.52 (1H, *dd*, H = 11.0, 3.2, H-1a), 4.42 (1H, *dd*, J = 11.0, 8.2, H-1b), 2.89 (2H, m, $SC\underline{H}_2$), 2.89 (2H, m, $SC\underline{H}_2$), 1.22 (6H, m, $CH_2C\underline{H}_3$); ^{13}C NMR (125 MHz, CD_3OD) 56.1 (C-7), 74.2 (C-6), 73.3 (C-5), 71.2 (C-4), 74.6 (C-3), 72.8 (C-2), 64.4 (C-1), 64.8 ($S\underline{C}H_2$), 15.0 ($CH_2\underline{C}H_3$); HR-FAB-MS (m/z): 317.1099 $[M + H]^+$, calc. for $[C_{11}H_{24}O_6S_2 + H]^+$ 317.1092.

7-Deoxy-D-*glycero*-D-*allo*-Heptitol, i.e. (2*R*,3*R*,4*S*,5*S*,6*S*)-heptane-1,2,3,4,5,6-hexaol (**10**). Reductive desulfurization of similar dithioacetals has already been described [30]. To a solution of the derivative **9** (95 mg, 0.30 mmol) in dioxane (5 ml) was added Raney Ni (300 mg). The suspension was heated at 80 °C for 1 h with stirring to give the derivative **9**. Crystallization from absolute ethanol yielded 43.5 mg (74%) of the desired desoxyheptitol as clusters of needles, with an m.p. at 124–125 °C and $[\alpha]_D$ +1.7 (c 0.16, MeOH); ^{1}H-NMR (500 MHz, CD_3OD) δ 3.65 (1 H, *dd*, J = 10.1, 11.5, 1a-H) and 3.84 (1 H, *dd*, J = 3.4, 11.5, 1b-H), 3.77 (1 H, *ddd*, J = 2.2, 3.4, 10.1, 2-H), 3.70 (1 H, *dd*, J = 3.9, 2.2, 3-H), 3.92 (1H, *dd*, J = 3.9, 3.4, 4-H), 3.62 (1 H, *dd*, J = 3.4, 5.2, 5-H), 3.94 (1 H, *dq*, J = 5.2, 6.5, 6-H), 1.21 (3 H, *d*, J = 6.5, 7-H); ^{13}C NMR (125 MHz, CD_3OD) 19.1 (C-7), 70.4 (C-6), 73.2 (C-5), 71.7 (C-4), 74.2 (C-3), 72.7 (C-2), 64.1 (C-1); HR-FAB-MS (m/z): 197.1025 $[M + H]^+$, calc. for $[C_7H_{16}O_6 + H]^+$ 197.1025. Again, though it is hard to believe, this compound has not yet been described.

General Procedure for Bichromophoric Derivatization

Anthroylation

To an ice cooled suspension of the 9-anthracenecarboxylic acid (0.1 mmol, 22.2 mg) and fluoro-*N,N,N′,N′*-tetramethylformamidinium hexafluorophosphate (TFFH, 0.1 mmol, 26.4 mg) in a minimum of CH_2Cl_2 (ca. 5 ml) was added Et_3N (0.5 mmol, 50.5 mg, 70 μl) resulting in a clear solution with some heat evolution. After stirring for 30 min at 20 °C the alcohol (**10**) (0.1 mmol, 19.6 mg) and a catalytic amount of DMAP (0.01 mmol, 1.22 mg) were added and the reaction mixture was stirred at 20 °C overnight. Water (5 ml) was added and the mixture extracted with CH_2Cl_2 (3 × 3 ml). The combined organic extracts were dried ($MgSO_4$),

filtered and concentrated in vacuo. The resulting crude residue was purified by SPE with silica gel (MeOH/CH_2Cl_2, 1:9) to yield the desired ester (**11**) [yield 33.6 mg (84%)]. HR-FAB-MS (*m/z*): 401.1606 $[M + H]^+$, calc. for $[C_{22}H_{24}O_7 + H]^+$ 401.1600. The eluate was concentrated, the mixture was separated by normal phase HPLC (Supelcosil™ LC-Si HPLC Column 5 µm particle size, L × I.D. 25 cm × 10 mm, EtOAc-hexane, 3:7; 2 ml/min; 311 nm UV detection), and used for the next step, cinnamoylation.

The preparation of the anthroyl derivative of BHhexol (**13**) was performed similarly as with (**11**). From the 9-anthracenecarboxylic acid (1 µmol, 222 µg), TFFH (1 µmol, 264 µg) in CH_2Cl_2 (200 µl), Et_3N (5 µmol, 505 µg, 0.7 µl) and the alcohol (**3**) (1 µmol, 578 µg) with catalytic amount of DMAP (1 µmol, 122 µg) compound **13** was obtained after purification by SPE with silica gel (MeOH-CH_2Cl_2, 2:98) in a yield of 610 µg (78%). HR-FAB-MS (*m/z*): 783.5199 $[M + H]^+$, calc. for $[C_{50}H_{70}O_7 + H]^+$ 783.5204.

Cinnamoylation

To an ice cooled suspension of the p-methoxycinnamic acid (712 mg, 4 mmol) and fluoro-*N,N,N′,N′*-tetramethylformamidinium hexafluorophosphate (TFFH, 5 mmol, 1.32 g) in a CH_2Cl_2 (35 ml) was added Et_3N (25 mmol, 2.52 g, 3.48 ml) resulting in a clear solution with some heat evolution. After stirring for 30 min at 20 °C the anthroyl derivative (**11**) (30 mg, 75 µmol) and a catalytic amount of DMAP (0.1 mmol, 12.2 mg) were added and the reaction mixture was stirred at 20 °C overnight. H_2O (10 ml) was added and the mixture extracted with CH_2Cl_2 (3 × 5 ml). The combined organic extracts were dried ($MgSO_4$), filtered and concentrated in vacuo. The resulting crude residue was purified by SPE with silica gel (MeOH/CH_2Cl_2, 1:9) to yield (66.6 mg, i.e. 74%) the desired ester (**12**). HR-FAB-MS (*m/z*): 1,201.4221 $[M + H]^+$, calc. for $[C_{72}H_{64}O_{17} + H]^+$ 1,201.4226.

The preparation of cinnamoyl derivative of BHhexol (**14**) was performed similarly as with the derivative (**12**). From the p-methoxycinnamic acid (712 µg, 4 µmol), TFFH (5 µmol, 1.32 mg) in CH_2Cl_2 (0.1 ml), Et_3N (25 µmol, 2.52 mg, 3.5 µl) and the alcohol (**13**) (0.77 µmol, 603 µg) with catalytic amount of DMAP (0.1 µmol, 12 µg), 915 µg (75%) of compound (**14**) was obtained after purification by SPE with silica gel (MeOH-CH_2Cl_2, 2:98). HR-FAB-MS (*m/z*): 1,583.7816 $[M + H]^+$, calc. for $[C_{100}H_{110}O_{17} + H]^+$ 1,583.7820.

Results

A. acidoterrestris was cultivated in a 50-l fermentor as described previously [20]. The total lipids were obtained by Bligh-Dyer extraction [21] of lyophilized cells and a part of the total lipids was cleaved by H_5IO_6 followed by $NaBH_4$ reduction. This releases mainly a mixture of alcohols arising from the BHpolyol derivatives, identical in GC retention times and mass spectra with the previously described alcohols which were used for the identification of BHpolyols from sediments [31]. Three alcohols were identified by GC–MS, i.e. bishomohopanol representing BHtetrols, homohopanol belonging to BHpentols, and the BHhexol hopanol. The detection of hopanol suggests the presence of a hopanoid with a hexafunctionalized side-chain in the total lipid extract.

Further, part of the total lipids was fractionated by means of cartridges with aminopropyl silica-based polar bonded phase, which were rinsed in a chloroform–methanol mixture (98:2) [22] for removing non-polar lipids. Polar lipids, but not phospholipids, were further eluted by acetone. Polar non-phospholipids (25% of total lipids, i.e. 385 mg) were further separated by normal phase HPLC, as described by Moreau et al. [22]. Briefly, non-phospholipids were subjected to semi-preparative normal phase HPLC with a linear gradient in for 40 min and with detection at 210 nm, as described by Fox et al. [1]. Table 1 gives the data obtained after normal phase semipreparative HPLC. The relative amounts of the C32, C31 and C30 alcohols, i.e. the relative contributions of tetra-, penta-, and hexafunctionalized side-chains were in a 2:1:1 ratio, which is in agreement with data from Table 1. This table also summarizes appropriate classes of hopanoids, i.e. tetrols, pentols, and hexols, whereas minority derivatives of BHs (up to 2% of total lipids) were omitted.

Table 2 gives the data obtained after RP-HPLC from the fraction of per-acetylated *N*-acylated BHhexol-glycosides,

Table 1 BH derivatives from *A. acidoterrestris* after normal phase semipreparative HPLC

Compound	%[a]
N-acyls glucosamine BHtetrol	29.3
N-acyls-mannosamine-BHpentol	5.9
N-acyls-mannosamine-BHhexol	11.2
BHtetrol	12.5
BHpentol	8.6
BHhexol	6.7
BHtetrol-glucosamine	4.5
BHpentol-mannosamine	9.4
BHhexol-mannosamine	9.8
BHtetrol-ether	2.1
∑ tetrols	48.4
∑ pentols	23.9
∑ hexols	27.7

[a] Minority derivatives of BHs (up to 2% of total lipids) were omitted

Table 2 Per-acetylated *N*-acylated BHhexol-glycosides separated by RP-HPLC and FAs content by GC–MS

Compound	%[a]	%[b,c]
N-C15-mannosamine-BHhexol	2.7	2.94
N-C17-mannosamine-BHhexol	30.8	31.13
N-C19-mannosamine-BHhexol	54.7	54.41
N-C21-mannosamine-BHhexol	5.8	6.11
N-C23-mannosamine-BHhexol	3.2	2.98
N-C25-mannosamine-BHhexol	1.7	1.52
N-C27-mannosamine-BHhexol	0.9	0.76
N-C29-mannosamine-BHhexol	0.2	0.15

[a] Determined by ESI

[b] Minority fatty acids up to 0.1% of total fatty acids were omitted

[c] Determined by GC–MS

which had the broadest interval of molecular weights. A total of 8 peaks were separated by LC–MS/ESI on narrow-bore columns connected in series. The chromatogram is given in Fig. 1.

Diagnostic fragment ions for hexafunctionalized bacteriohopane structures include the ion at *m/z* 771 resulting from the loss of the terminal group at C35 (either OH or any other moiety linked to C35 via oxygen [32]) and *m/z* 711, 651, 591, 531 and 471 from sequential loss of the remaining 5 acetylated OH groups from C30 to C34. The ESI/MS spectrum (Fig. 2) of a proposed acetylated *N*-acyls glycoside of BHhexol (**2**, $n = 3$) includes all these diagnostic ions as well as a further series *m/z* 579, 519, 459, 399, 339 and 279 from neutral loss of the A and B rings (i.e. loss of 192 Da) after a loss of one to six of the acetylated hydroxyls [32]. The composite hexafunctionalized structure **2** is proposed on the basis of observation of the diagnostic ions *m/z* 771 (etc.) and ions at *m/z* 554 (etc.), indicating the mass of the terminal group, and by comparison with spectra reported for the penta- and hexafunctionalized cyclitol ethers, see also Table 3.

The structure of pentacyclic nucleus including the side chain was essentially determined by ^{1}H-NMR spectroscopy using COSY, ROESY, HMQC, and HMBC experiments. The ^{1}H-NMR spectrum (data see Table 4) of acetylated hopanoids (**2**) showed signals in the methyl region typical of bacteriohopane derivatives. Both signals, including the ^{13}C NMR, are in agreement with previously published papers [7, 14, 33].

The ROESY spectrum displayed a number of correlation peaks between methyl groups and ring protons in the 1,3 diaxial relationship. Thus, 24-Me, H-6ax, 25-Me, 26-Me, and 13-H were shown to be all located on the upper face of

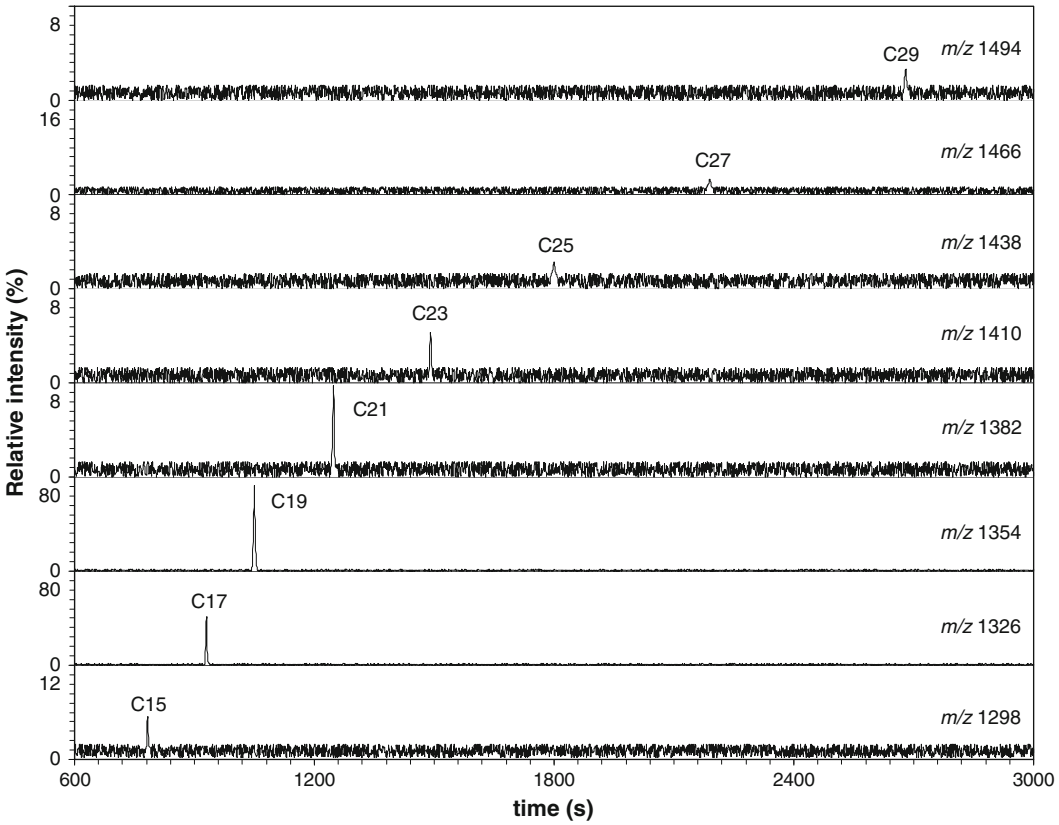

Fig. 1 LC–MS/ESI SIM chromatograms of *N*-acylated BHhexol glycosides from total lipids of *A. acidoterrestris* after normal phase HPLC; fraction of *N*-acyls-mannosamine-BHhexol is shown. The SIM traces depict $[M + H]^{+}$ masses, see *m/z* values

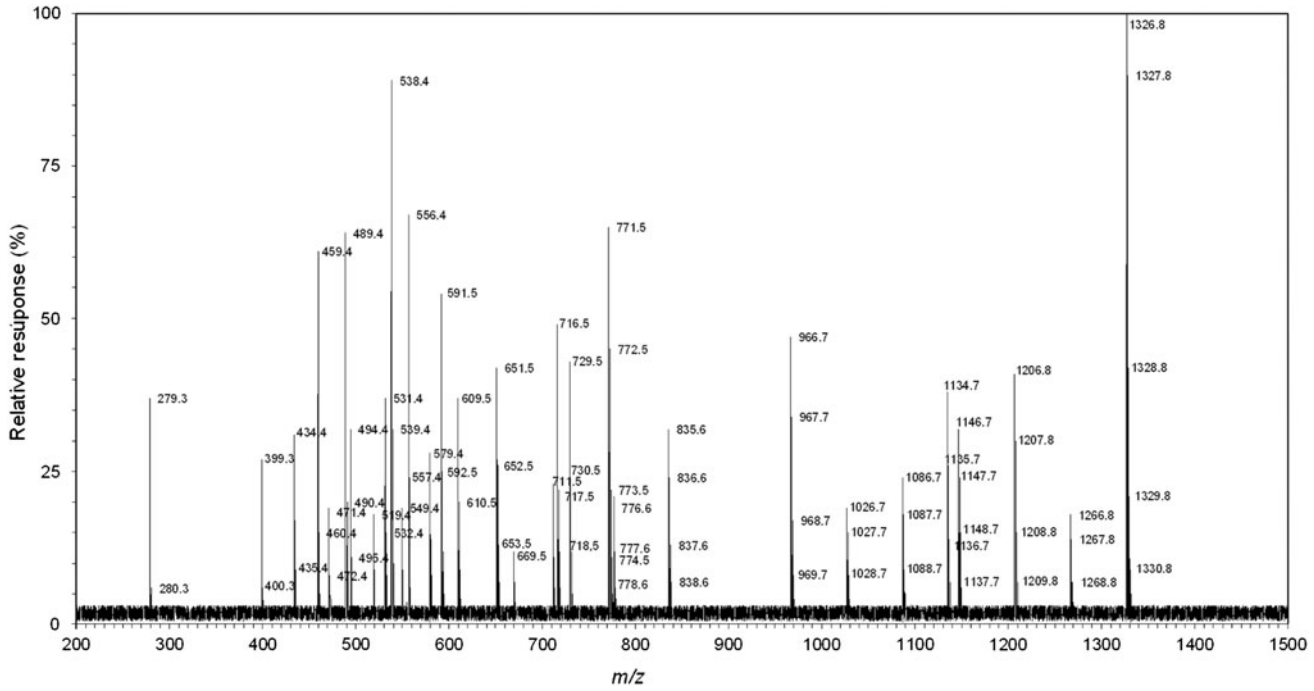

Fig. 2 The tandem quadrupole ESI product-ion spectrum of the $[M + H]^+$ ion of *N*-C17-mannosamine-BHhexol at *m/z* 1,326

the molecule, whereas 27-Me, 28-Me, H-5ax, and H-9ax were all on its lower face. Also the four-bond couplings (W coupling) of an angular methyl group with a ring proton in the COSY were observed. These couplings are only possible when the dihedral angle between the methyl group and the ring proton is near 180° and these couplings confirmed a trans connection of all the rings, hence the stereochemistry of compound **2** was the same as in previously isolated bacteriohopanoids. This was confirmed by HMBC correlations between Me groups and carbons of the ring system. Thanks to this fact the ^{13}C-resonance (see δ_C values in Table 5) of the five cycle moiety could be determined [7, 14, 33].

The ^{1}H-NMR spectrum of the octaacetate of compound (**2**) shows that the signals of the protons at C30 to C34 are nearly identical to those of the corresponding protons of the synthetic tetraacetate glycoside [33] and/or isolated pentaacetate of aminoBHtetrol [14] and are easily identifiable. Decoupling experiments performed on the C34 proton permitted an assignment of the signals of the two C35 protons which are nearly equivalent and appear as two doublets at 3.68 and 3.98 ppm. The fact that the signals of the C35 protons as well as the signal of the C35 carbon atom were shifted in comparison to the signals of the corresponding atoms of acetylated BHpolyol [9] indicated that a sugar moiety was located on the oxygen atom at C35. From the ^{1}H-NMR spectrum eight acetoxy groups are present: five at C30 to C34 and three on the residue linked at C35. Decoupling experiments initiated on the exchangeable NH proton of the acylamide group as well as dimensional proton/proton correlation allowed the whole pattern of the substituent to be established as compatible with the structure of an acylated sugar.

The large vicinal coupling constants, $^3J_{3',4'} = 9.5$ Hz and $^3J_{4',5'} = 9.5$ Hz, and the NOE between H-3′ and H-5′ indicated that H-3′, H-4′ and H-5′ protons were located at an axial position. The observation of NOE between H-4′ and 2′-NH proton suggested that 2′-NH was oriented in an axial position. These data indicate that the monosaccharide is a mannosamine in pyranose form; α configuration was determined by a large coupling constant, $^1J_{C\text{-}1',H\text{-}1'} = 166.1$ Hz [34] and small $^3J_{H\text{-}1'\text{-}H\text{-}2'} = 1.8$ Hz [35]. This implies also that the linkage between the BHhexol and the mannosamine moiety is an *O*-glycosidic bond.

HMBC analysis indicated that 2-NH′ of the mannosamine was esterified by a fatty acyl group by the correlation peak between H-2′ (δ 4.63) and C-1′′ (δ 172.8) of the fatty group and that 3-OH′, 4-OH′, and 6-OH′ of the mannosamine moiety were esterified by acetates by the correlation peaks between H-3′ (δ 5.38), H-4′ (δ 5.06), and H-6′ (δ 4.30, 4.14) and the other three carbonyl carbons (δ 170.7, 170.6, 170.2). The key HMBC are showed in Fig. 3.

The components of *N*-acylated BHhexol-mannosamide were also analyzed after hydrolysis (Fig. 4). The hydrolyzate contained BHhexol as the aglycone moiety and mannosamine was the only sugar which was detected by GC–MS in this fraction. Mannosamine had $[\alpha]_D^{25}$-4.1, compared to the literature data, $[\alpha]_D^{25}$ -4.2 for D-mannosamine

Table 3 The main molecular species of *N*-acylated BHhexol glycoside (**2**) from *A. acidoterrestris*

Ions	*m/z*	Abundance
M + H	1,326.8	100
M + H-AcOH	1,266.8	18
M + H-2AcOH	1,206.8	41
M + H-3AcOH	1,146.7	32
M + H-192	1,134.7	38
M + H-4AcOH	1,086.7	24
M + H-5AcOH	1,026.7	19
M + H-6AcOH	966.7	47
M + H-4AcOH-Acyl	836.6	32
M + H-5AcOH-Acyl	776.6	21
M + H-SC	771.5	65
M + H-SC-42	729.9	43
M + H-6AcOH-Acyl	716.5	49
M + H-SC-AcOH	711.5	23
M + H-SC-AcOH-42	669.5	12
M + H-SC-2AcOH	651.5	42
M + H-SC-2AcOH-42	609.5	37
M + H-SC-3AcOH	591.5	54
M + H-SC-192	579.4	28
SC + 18	556.4	67
SC	538.4	89
M + H-SC-3AcOH-42	549.4	19
M + H-SC-4AcOH	531.4	37
M + H-SC-AcOH-192	519.4	18
SC-AcOH	494.4	32
M + H-SC-4AcOH-42	489.4	64
M + H-SC-5AcOH	471.4	19
M + H-SC-2AcOH-192	459.4	61
SC-2AcOH	434.4	31
M + H-SC-3AcOH-192	399.3	27
SC-3AcOH	374.3	42
M + H-SC-4AcOH-192	339.3	27
M + H-SC-5AcOH-192	279.3	37

(2-amino-2-deoxy-D-mannopyranose) [36]. The mixture of homologous ω-cyclohexyl fatty acids, isolated from the hydrolyzate, was also determined by GC–MS. The fatty acid composition obtained by GC–MS was nearly identical with the results obtained from ESI analysis (see Table 2).

Bisseret and Rohmer [37], who synthesized the eight possible diastereomers of BHtetrols, established the absolute stereochemistry of the side chain on the basis of their ^{1}H-NMR spectra. Since the 32 diastereomers for BHhexols have not yet been synthesized, we had to use the CD exciton chirality method [38] that has been applied to sugar polyols [39] and/or different acyclic polyols such as BHpolyols [40] with up to five contiguous OH groups, or aminoBHpentols [41, 42]. These CD studies clearly showed that with flexible

Table 4 ^{1}H NMR of compound **2** (500 MHz, $CDCl_3$)

No.	^{1}H
22	2.23 (1H, *m*)
23	0.80 (3H, *s*)
24	0.83 (3H, *s*)
25	0.84 (3H, *s*)
26	0.94 (3H, *s*)
27	0.96 (3H, *s*)
28	0.69 (3H, *s*)
29	0.92 (3H, *d*, $J_{22,29} = 6.5$)
30	5.24 (1H, *dd*, $J_{22,30} = 2.1$; $J_{30,31} = 9.0$)
31	5.23 (1H, *dd*, $J_{30,31} = 9.0$; $J_{31,32} = 3.5$)
32	5.26 (1H, *dd*, $J_{31,32} = 3.5$; $J_{32,33} = 6.5$)
33	5.33 (1H, *dd*, $J_{32,33} = 6.5$; $J_{33,34} = 4.2$)
34	5.10 (1H, *ddd*, $J_{33,34} = 4.2$; $J_{34,35a} = 7.2$; $J_{34,35b} = 3.8$)
35a	3.68 (1H, *dd*, $J_{34,35a} = 7.2$; $J_{35a,35b} = 11.0$)
35b	3.98 (1H, *dd*, $J_{34,35b} = 3.8$; $J_{35a,35b} = 11.0$)
1′	4.78 (1H, *d*, $J_{1',2'} = 1.8$)
2′	4.63 (1H, *ddd*, $J_{1',2'} = 1.8$; $J_{2'3'} = 4.8$; $J_{2'NH} = 9.0$)
3′	5.38 (1H, *dd*, $J_{2',3'} = 4.8$; $J_{3'4'} = 9.5$)
4′	5.06 (1H, *t*, $J_{3'4'=4',5'} = 9.5$)
5′	3.96 (1H, *ddd*, $J_{4'5'} = 9.5$; $J_{5'6a'} = 4.5$; $J_{5'6b'} = 2.5$)
6a′	4.14 (1H, *dd*, $J_{5'6a'} = 4.5$; $J_{6a'6b'} = 12.5$)
6b′	4.30 (1H, *dd*, $J_{5'6a'} = 2.5$; $J_{6a'6b'} = 12.5$)
NH	6.45 (1H, *d*, $J_{2'NH} = 9.0$)
2‴	2.14 (2H, *t*, $J = 7.5$)
3‴	1.66 (2H, *m*)
4‴-ω8	1.23–1.45 (14H, *m*)
ω7	1.14 (2H, *m*)
Cyclohexyl's CH	1.36 (1H, *m*)
Cyclohexyl's CH_2	1.08–1.68 (*m*)
CH_3CO	2.018 (3H, *s*)
CH_3CO	2.023 (3H, *s*)
CH_3CO	2.029 (3H, *s*)
CH_3CO	2.036 (3H, *s*)
CH_3CO	2.036 (3H, *s*)
CH_3CO	2.049 (3H, *s*)
CH_3CO	2.054 (3H, *s*)
CH_3CO	2.054 (3H, *s*)

compounds it is preferable to explore the exciton coupling between two different chromophores such as anthroyl and cinnamoyl.

Based on the similarity of CD spectra of our compound (BHhexol, **14**) and the previously published aminoBHpentol derivative [41], we concluded that our compound is also a homolog of *allo* configuration. To verify this hypothesis, we consequently prepared from a commercially

Table 5 ^{13}C NMR of compound **2** (125 MHz, $CDCl_3$)

No.	^{13}C	No.	^{13}C
1	40.4t	33	71.6d
2	18.7t	34	71.0d
3	42.2t	35	64.5d
4	33.3s	1′	100.3d
5	56.2d	2′	55.4d
6	18.7t	3′	69.3d
7	33.2t	4′	71.4d
8	41.5s	5′	68.5d
9	50.5d	6′	62.1t
10	37.5s	1″	172.8s
11	20.8t	2″	34.1t
12	24.0t	3″	24.8t
13	49.3d	4″-ω8	27.4–30.0t
14	41.8s	ω7	38.5t
15	33.7t	Cyclohexyl's CH	29.1d
16	22.6t	Cyclohexyl's CH_2	26.6–34.6t
17	54.2d	C=O	172.8s
18	44.5s	C=O	170.7s
19	41.6t	C=O	170.6s
20	27.9t	C=O	170.5s
21	42.9d	C=O	170.2s
22	38.1d	C=O	169.7s
23	21.5q	C=O	169.5s
24	33.3q	C=O	169.4s
25	15.8q	$\underline{C}H_3CO$	21.1q
26	16.4q	$\underline{C}H_3CO$	21.1q
27	16.5q	$\underline{C}H_3CO$	20.9q
28	15.9q	$\underline{C}H_3CO$	20.8q
29	16.4q	$\underline{C}H_3CO$	20.7q
30	69.8d	$\underline{C}H_3CO$	20.6q
31	70.3d	$\underline{C}H_3CO$	20.5q
32	71.0d	$\underline{C}H_3CO$	20.4q

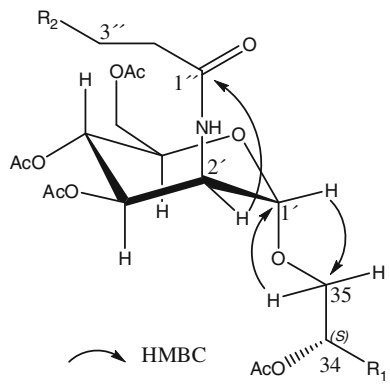

Fig. 3 Partial structure of a new compound (**2**). Only important HMBC correlations are shown

available saccharide D-allose (**6**) appropriate 7-deoxy-D-*glycero*-D-*allo*-heptitol (**10**) via the D-*glycero*-D-*allo*-heptose (**8a**) according to Fig. 5. This helped us remove the obstacle mentioned by Zhou et al. [41], viz. that configurational determination of aminoBHpentol is not straightforward due to the lack of reference hexols.

The original version of the Kiliani-Fischer synthesis was modified according to several authors [24, 25]. Instead of conversion of the cyanohydrin (aldonitrile) to a lactone, the cyanohydrin is reduced with hydrogen (palladium on barium sulfate) in water to an imine that quickly hydrolyzes at pH 4.2 to an aldehyde; thus the final sugars are produced in just two steps rather than three and, moreover, the final sugars are separated instead of the lactones. We used semipreparative TLC on cellulose plates and employed a previously described solvent system (acetone–water 95:5, v/v) with D-glucose as standard. The compound with an R_f lower than glucose was D-*glycero*-D-*allo*-heptose (**8a**) while that with an R_f higher than glucose was D-*glycero*-D-*altro*-heptose (**8b**), see also paper [25]. The measurement of ^{13}C-NMR spectra of (**8a**) showed that, in keeping with literature data [27], this compound is present as a mixture of four forms, i.e. α and β pyranoses and α and β furanoses in a ratio of 15:75:5:5. Experimental part gives only the values for the most copious form, i.e. β-pyranose.

Heptose (**8a**) was converted first to the diethyl thioacetal (**9**), and then, by reductive desulfurization with Raney nickel, to 7-deoxy-D-*glycero*-D-*allo*-heptitol (**10**). This desoxyheptitol was esterified by selective anthroylation of primary hydroxyl by anthracene-9-carboxylic acid to (2*R*, 3*R*, 4*S*, 5*S*, 6*S*)-2,3,4,5,6-pentahydroxyheptyl anthracene-9-carboxylate (**11**). To make sure that we had indeed the appropriate and pure epimer (viz. the separation of heptoses by TLC after reduction) we used a separation of this compound by means of normal phase HPLC, see also Wiesler and Nakanishi [43]. They reported that mixtures of saccharides (after cyanohydrin synthesis) could be directly subjected to anthroylation, after which separation of the fluorescent monoesters was greatly simplified. The secondary hydroxyls of anthroyl derivative (**11**) were per-p-methoxycinnamoylated to an appropriate "bichromophoric" derivative (**12**) and CD spectrum of this compound was measured, see Fig. 6. The curve for L-*allo* (**12**) is plotted as a mirror image of the D-series, see also Zhou et al. [39].

On the basis of all above mentioned spectra (including CD spectrum of synthetic compound **12**), we confirmed that the configuration of the side chain is 30*R*, 31*R*, 32*R*, 33*S*, 34*S* (D-*glycero*-D-*allo*) and the components of this fraction are *N*-acylated-mannosamine-BHhexols which contain—α-D-2-amino-2-deoxymannopyranose esterified by ω-cyclohexyl fatty acids from C-15 to C-29. The correct name of the glycoside with C-17 fatty acids is 11-cyclohexyl-*N*-((2*S*,3*S*,4*R*,5*S*,6*R*)-2-((2*S*,3*S*,4*R*,5*R*,6*R*,7*S*)-7-((3*S*,3a*S*,5a*R*,

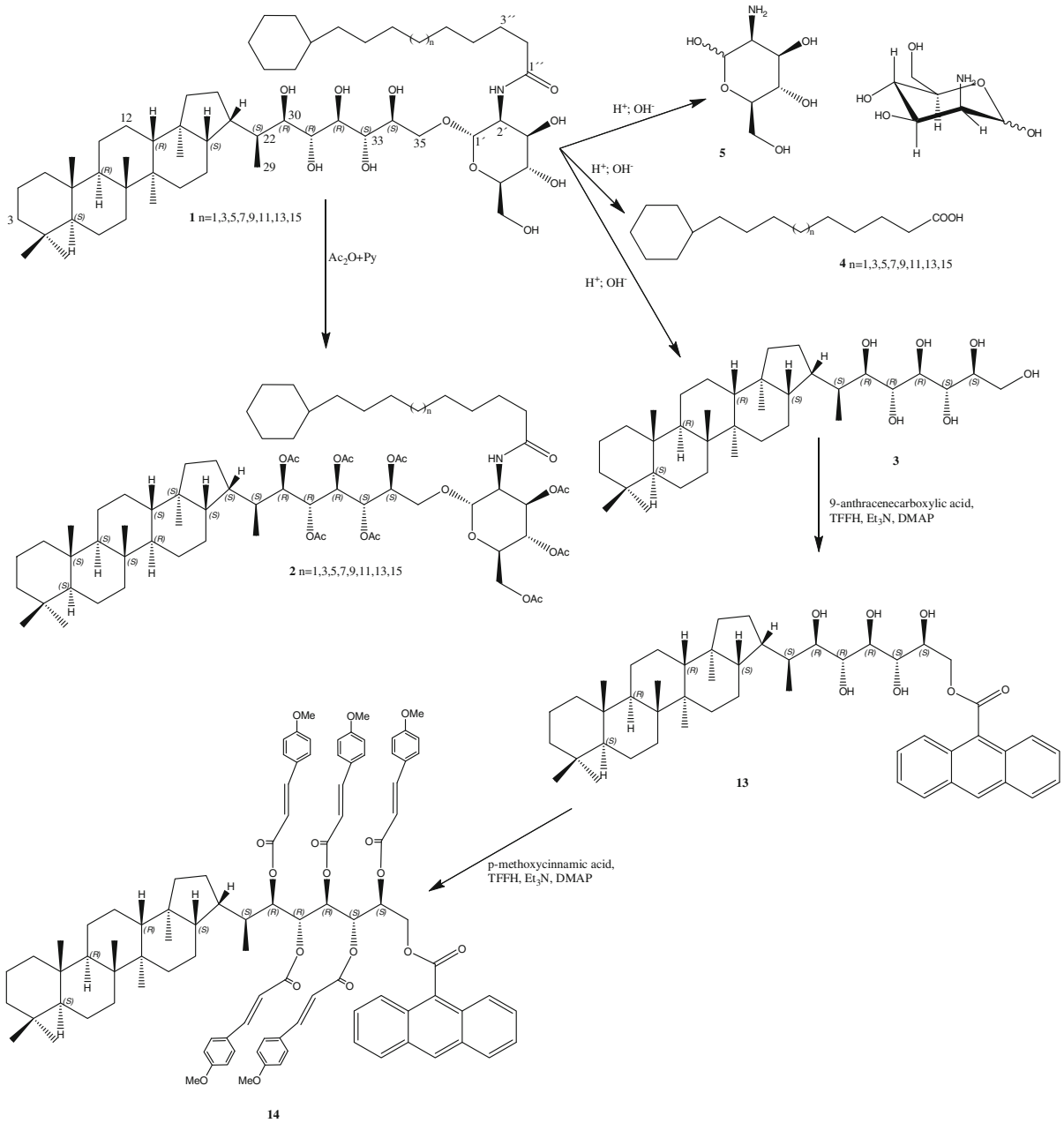

Fig. 4 Structure of **1** and synthesis of appropriate derivatives

5b*R*,7a*S*,11a*S*,11b*R*,13a*R*,13b*S*)-5a,5b,8,8,11a,13b-hexamethylicosahydro-1*H*-cyclopenta[a]chrysen-3-yl)-2,3,4,5,6-pentahydroxyoctyloxy)-4,5-dihydroxy-6-(hydroxymethyl) tetrahydro-2*H*-pyran-3-yl)undecanamide (**1**).

Discussion

To the best of our knowledge, this is the first report of BHhexol from a specific bacterium. Bacteriohopanoids having hexol in the side chain, including their composite derivatives, have so far been identified only in sediments but their configuration has been unknown [2, 16, 17]. Based on the comparison with the synthesized model compound (**12**), we determined its absolute configuration by using CD. Still, the identification of a novel hopanoid from *A. acidoterrestris* is not too surprising since only several tens of bacterial and cyanobacterial genera have been tested for the presence of hopanoids [16]. Although the biological significance of our compound is not yet clear; it is probable that in *A. acidoterrestris* the long chain ω-cyclohexyl FAs, which are bound by an amidic bond to

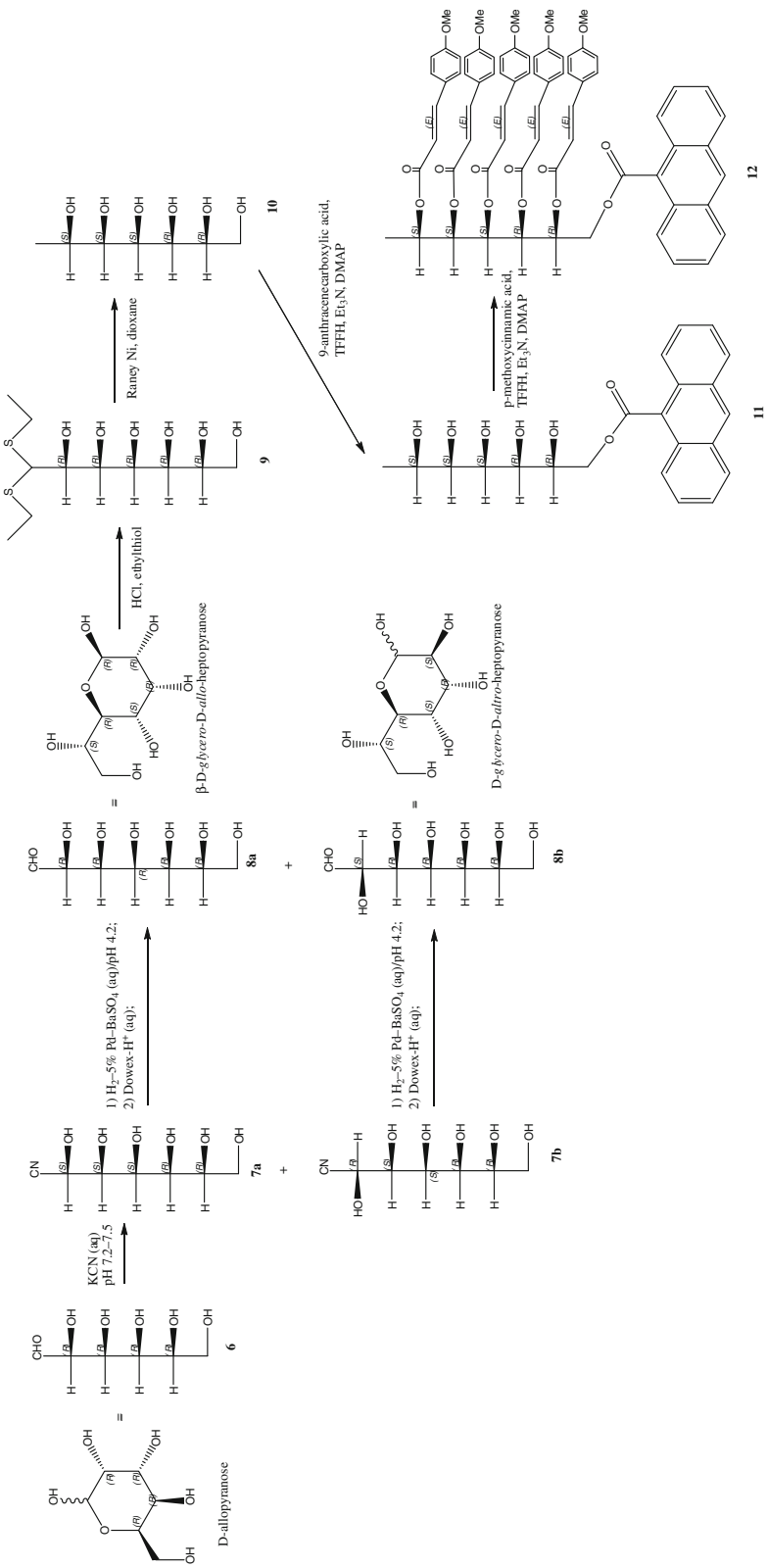

Fig. 5 Enantioselective synthesis of 7-deoxy-D-*glycero*-D-*allo*-heptitol (**10**) and its derivatives used for CD

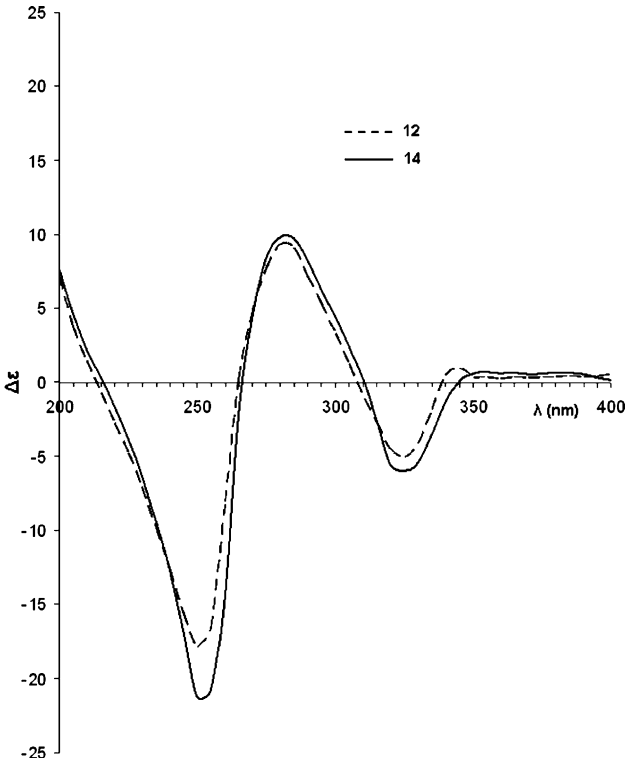

Fig. 6 CD spectra of compounds **12** (synthesized standard) and **14** (BHhexol)

the amino group in position 2 of the appropriate monosaccharide, play an important role in the thermophilicity of this bacterium.

Different monosaccharide derivatives have been found to be bound glycosidically to the primary C35 hydroxyl: Simonin et al. [44] described galacturonic and altruronic acids while all other studies describe 2-amino-2-deoxyglucose and one study reports on 6-amino-6-deoxyglucose [44]. We assume that the change in the configuration of the amino group on C2 (mannose is a 2-epimer of glucose), i.e. axial to equatorial, alters the planarity of the whole molecule.

The last result of our study is the heretofore undescribed large variability of chain lengths. Only ω-cyclohexyl FA with 17 and 19 carbon atoms have so far been described [18]. Solely in *N*-acyl glycoside of BHtetrol did Talbot et al. [5] succeeded in identifying by ESI also other homologues, one shorter (C15) and one longer (C21). We have extended the range of homologues by other longer-chain members—odd-numbered C23 to C29.

In conclusion we can state that, by using modern analytical methods, we succeeded in identifying one of the possible sources of BHhexol in sediments, i.e. *A. acidoterrestris*, and determined the absolute configuration of the side chain of BHhexol by CD and by its comparison with the synthetic model compound 7-deoxy-D-*glycero*-D-*allo*-heptitol, i.e. (2*R*,3*R*,4*S*,5*S*,6*S*)-heptane-1,2,3,4,5,6-hexaol (**10**), which has not yet been described.

Acknowledgments The research was supported by projects of the *Ministry of Education, Youth and Sports of the Czech Republic* (no. 1M06011; GACR P503/10/P182), and by *Institutional Research Concepts* AV 0Z 502 0910 and MSM6046137305.

References

1. Fox PA, Carter J, Farrimond P (1998) Analysis of bacteriohopanepolyols in sediment and bacterial extracts by high performance liquid chromatography/atmospheric pressure chemical ionization mass spectrometry. Rapid Commun Mass Spectrom 12:609–612
2. Talbot HM, Farrimond P (2007) Bacterial populations recorded in diverse sedimentary biohopanoid distributions. Org Geochem 38:1212–1225
3. Ourisson G, Rohmer M (1992) Hopanoids. 2. Biohopanoids: a novel class of bacterial lipids. Acc Chem Res 25:403–408
4. Kannenberg EL, Poralla K (1999) Hopanoid biosynthesis and function in bacteria. Naturwissenschaften 86:168–176
5. Talbot HM, Rohmer M, Farrimond P (2007) Rapid structural elucidation of composite bacterial hopanoids by atmospheric pressure chemical ionisation liquid chromatography/ion trap mass spectrometry. Rapid Commun Mass Spectrom 21:880–892
6. Stroeve P, Pettit CD, Vasquez V, Kim I, Berry AM (1998) Surface active behavior of hopanoid lipids: bacteriohopanetetrol and phenylacetate monoester bacteriohopanetetrol. Langmuir 14:4261–4265
7. Shatz M, Yosief T, Kashman Y (2000) Bacteriohopanehexol, a new triterpene from the marine sponge *Petrosia* species. J Nat Prod 63:1554–1556
8. Rohmer M (1993) The biosynthesis of triterpenoids of the hopane series in the eubacteria: a mine of new enzyme reactions. Pure Appl Chem 65:1293–1298
9. Costantino V, Fattorusso E, Imperatore C, Mangoni A (2000) The first 12-methylhopanoid: 12-methylbacteriohopanetetrol from the marine sponge *Plakortis simplex*. Tetrahedron 56:3781–3784
10. Pan W, Zhang Y, Liang G, Rohmer M, Sinay P, Vincent SP (2007) Diastereoselective synthesis of aminobacteriohopanetetrol, a biomarker for methanotrophic bacteria: confirmation of the absolute configuration. Chem Biodivers 4:2182–2189
11. Simonin P, Jurgens UJ, Rohmer M (1992) 35-*O*-β-6-amino-6-deoxyglucopyranosyl bacteriohopanetetrol, a novel triterpenoid of the hopane series from the cyanobacterium *Synechocystis* SP PCC-6714. Tetrahedron Lett 33:3629–3632
12. Herrmann D, Bisseret P, Connan J, Rohmer M (1996) A non-extractable triterpenoid of the hopane series in *Acetobacter xylinum*. FEMS Microbiol Lett 135:323–326
13. Joyeux C, Fouchard S, Llopiz P, Neunlist S (2004) Influence of the temperature and the growth phase on the hopanoids and fatty acids content of Frateuria aurantia (DSMZ 6220). FEMS Microbiol Ecol 47:371–379
14. Neunlist S, Rohmer M (1985) Novel hopanoids from the methylotrophic bacteria *Methylococcus capsulatus* and *Methylomonas methanica*. (22S)-35-aminobacteriophane-30, 31, 32, 33, 34-pentol and (22S)-35-amino-3β-methylbacteriophane-30, 31, 32, 33, 34-pentol. Biochem J 231:635–639
15. Cvejic JH, Bodrossy L, Kovacs KL, Rohmer M (2000) Bacterial triterpenoids of the hopane series from the methanotrophic bacteria *Methylocaldum* spp.: phylogenetic implications and first evidence for an unsaturated aminobacteriohopanepolyol. FEMS Microbiol Lett 182:361–365
16. Talbot HM, Summons RE, Jahnke LL, Cockell CS, Rohmer M, Farrimond P (2008) Cyanobacterial bacteriohopanepolyol signatures from cultures and natural environmental settings. Org Geochem 39:232–263

17. Cooke MP, Talbot HM, Farrimond P (2008) Bacterial populations recorded in bacteriohopanepolyol distributions in soils from Northern England. Org Geochem 39:1347–1358
18. Siristova L, Melzoch K, Rezanka T (2009) Fatty acids, unusual glycophospholipids and DNA analyses of thermophilic bacteria isolated from hot springs. Extremophiles 13:101–109
19. Rezanka T, Siristova L, Melzoch K, Sigler K (2009) Identification of (*S*)-11-cycloheptyl-4-methylundecanoic acid in acylphosphatidylglycerol from *Alicyclobacillus acidoterrestris*. Chem Phys Lipids 158:104–113
20. Rezanka T, Siristova L, Melzoch K, Sigler K (2009) Direct ESI–MS analysis of *O*-acyl glycosylated cardiolipins from the thermophilic bacterium *Alicyclobacillus acidoterrestris*. Chem Phys Lipids 161:115–121
21. Bligh EG, Dyer WJ (1959) A rapid method of total lipid extraction and purification. Can J Biochem Physiol 37:911–917
22. Moreau RA, Powell MJ, Osman SF, Whitaker BD, Fett WF, Roth L, O'Brien DJ (1995) Analysis of intact hopanoids and other lipids from the bacterium *Zymomonas mobilis* by high-performance liquid chromatography. Anal Biochem 224:293–301
23. Rezanka T (1990) Identification of very long polyenoic acids as picolinyl esters by Ag ion-exchange high-performance liquid chromatography, reversed-phase high-performance liquid chromatography. J Chromatogr 513:344–348
24. Patching SG, Middleton DA, Henderson PJF, Herbert RB (2003) The economical synthesis of [2′-13C, 1,3–15N2]uridine; preliminary conformational studies by solid state NMR. Org Biomol Chem 1:2057–2062
25. Snyder JR, Johnston ER, Serianni AS (1989) D-talose anomerization: NMR methods to evaluate the reaction kinetics. J Amer Chem Soc 111:2681–2687
26. Dmitriev BA, Chernyak AYa, Chizhov OS, Kochetkov NK (1972) Monosaccharides—communication 26. β-methyl-D-*allo*-heptopyranoside-4-ulose and syntheses based on it. Russ Chem B 21:2230–2235
27. Kim M, Grzeszczyk B, Zamojski A (2000) Homologation of protected hexoses with Grignard C1 reagents. Tetrahedron 56:9319–9337
28. Pratt JW, Richtmyer NK (1955) D-*glycero*-D-*allo*-Heptose, L-*allo*-Heptulose, D-*talo*-Heptulose and related substances derived from the addition of cyanide to D-allose. J Amer Chem Soc 77:6326–6328
29. Angyal SJ, Tran TQ (1983) Equilibria between pyranoses and furanoses. 5. The composition in solution and the C-13 NMR-spectra of the heptoses and the heptuloses. Aust J Chem 36:937–946
30. Fukase H, Horii S (1992) Synthesis of a branched-chain inosose derivative, a versatile synthon of *N*-substituted valiolamine derivatives from D-glucose. J Org Chem 57:3642–3650
31. Bravo J-M, Perzl M, Hartner T, Kannenberg EL, Rohmer M (2001) Novel methylated triterpenoids of the gammacerane series from the nitrogen-fixing bacterium *Bradyrhizobium japonicum* USDA 110. Eur J Biochem 268:1323–1331
32. Talbot HM, Squier AH, Keely BJ, Farrimond P (2003) Atmospheric pressure chemical ionisation reversed-phase liquid chromatography/ion trap mass spectrometry of intact bacteriohopanepolyols. Rapid Commun Mass Spectrom 17:728–737
33. Pan W, Zhang Y, Liang G, Vincent SP, Sinay P (2005) Concise syntheses of bacteriohopanetetrol and its glucosamine derivative. Chem Commun 27:3445–3447
34. Kasai R, Okihara M, Asakawa J, Mizutani K, Tanaka O (1979) Carbon-13 NMR study of α- and β-anomeric pairs of D-mannopyranosides and L-rhamnopyranosides. Tetrahedron 35:1427–1432
35. Lin C-H, Sugai T, Halcomb RL, Ichikawa Y, Wong C-H (1992) Unusual stereoselectivity in sialic acid aldolase-catalyzed aldol condensations: synthesis of both enantiomers of high-carbon monosaccharides. J Amer Chem Soc 114:10138–10145
36. Kaji E, Lichtenthaler FW, Nishino T, Yamane A, Zen S (1988) Practical syntheses of immunologically relevant β-glycosides of 2-acetamido-2-deoxy-D-mannopyranose. Methyl *N*-acetyl-β-D-mannosaminide, *N*-acetyl-β-D-mannosaminyl-(1 → 6)-D-galactose, and methyl *N*-acetyl-β-D-mannosaminyl-(1 → 4)-α-D-glucopyranoside. Bull Chem Soc Jpn 61:1291–1297
37. Bisseret P, Rohmer M (1989) Bacterial sterol surrogates. Determination of the absolute configuration of bacteriohopanetetrol side chain by hemisynthesis of its diastereoisomers. J Org Chem 54:2958–2964
38. Berova N, Nakanishi K, Woody RW (2000) Circular dichroism: principles and applications, 2nd edn. Wiley Blackwell, New York
39. Zhou P, Berova N, Wiesler WT, Nakanishi K (1993) Assignment of relative and absolute configuration of acyclic polyols and aminopolyols by circular dichroism-trends follow Fischer's sugar family tree. Tetrahedron 49:9343–9352
40. Zhao N, Berova N, Nakanishi K, Rohmer M, Mougenot P, Jurgens UJ (1996) Structures of two bacteriohopanoids with acyclic pentol side-chains from the cyanobacterium *Nostoc* PCC 6720. Tetrahedron 52:2777–2788
41. Zhou P, Berova N, Nakanishi K, Knani M, Rohmer M (1991) Microscale CD method for determining absolute configurations of acyclic amino tetrols and amino pentols. Structures of aminobacteriohopanepolyols from the methylotrophic bacterium *Methylococcus luteus*. J Amer Chem Soc 113:4040–4041
42. Zhou P, Berova N, Nakanishi K, Rohmer M (1991) Assignment of absolute stereochemistry of aminopolyols by the bichromophoric exciton chirality method. J Chem Soc Chem Commun, pp 256–258
43. Wiesler WT, Nakanishi K (1989) A simple spectroscopic method for assigning relative and absolute configuration in acyclic 1, 2, 3-triols. J Amer Chem Soc 111:3446–3447
44. Simonin P, Jurgens UJ, Rohmer M (1996) Bacterial triterpenoids of the hopane series from the prochlorophyte *Prochlorothrix hollandica* and their intracellular localization. Eur J Biochem 241:865–871

Lipids (2011) 46:263–270
DOI 10.1007/s11745-010-3497-x

ORIGINAL ARTICLE

The Absolute Configurations of Hydroxy Fatty Acids from the Royal Jelly of Honeybees (*Apis mellifera*)

Tetsuya Kodai · Takafumi Nakatani · Naoki Noda

Received: 20 June 2010 / Accepted: 22 October 2010 / Published online: 17 November 2010

Abstract 9-Hydroxy-2*E*-decenoic acid (9-HDA) is a precursor of the queen-produced substance, 9-oxo-2*E*-decenoic acid (9-ODA), which has various important functions and roles for caste maintenance in honeybee colonies (*Apis mellifera*). 9-HDA in royal jelly is considered to be a metabolite of 9-ODA produced by worker bees, and it is fed back to the queen who then transforms it into 9-ODA. Recently we found that 9-HDA is present in royal jelly as a mixture of optical isomers (*R*:*S*, 2:1). The finding leads us to suspect that chiral fatty acids in royal jelly are precursors of semiochemicals. Rather than looking for semiochemicals in the mandibular glands of the queen bee, this study involves the search for precursors of pheromones from large quantities of royal jelly. Seven chiral hydroxy fatty acids, 9,10-dihydroxy-2*E*-decenoic, 4,10-dihydroxy-2*E*-decenoic, 4,9-dihydroxy-2*E*-decenoic, 3-hydroxydecanoic, 3,9-dihydroxydecanoic, 3,11-dihydroxydodecanoic, and 3,10-dihydroxydecanoic acids were isolated. The absolute configurations of these acids were determined using the modified Mosher's method, and it was revealed that, similar to 9-HDA, five acids are present in royal jelly as mixtures of optical isomers.

Keywords Absolute configuration · *Apis mellifera* · Honeybees · Hydroxy fatty acid · Modified Mosher's method · Royal jelly

Abbreviations

COSY Two-dimensional ^{1}H-^{1}H shift correlation
HMBC Two-dimensional heteronuclear multiple-bond connectivity
MTPA 2-Methoxy-2-(trifluoromethyl)phenylacetic acid
TMS Tetramethylsilane

T. Kodai · T. Nakatani · N. Noda (✉)
Faculty of Pharmaceutical Sciences, Setsunan University, 45-1, Nagaotoge-cho, Hirakata, Osaka 573-0101, Japan
e-mail: noda@pharm.setsunan.ac.jp

Introduction

The so-called "queen substance," 9-oxo-2-decenoic acid (9-ODA), was isolated from the honeybee queen mandibular glands by Butler et al. [1]. This compound is a well-known semiochemical which has various important functions, such as queen recognition and inhibition of ovary development in worker bees for caste maintenance in honeybee colonies [2].

In 1965, Johnston and co-workers reported that 9-ODA was rapidly metabolized to 9-hydroxy-2*E*-decenoic (9-HDA) or 9-hydroxydecanoic acids [3]. They further postulated a "pheromone cycle," in which worker bees would receive 9-ODA from the queen and convert it into 9-HDA. The metabolite would then be transported to the worker mandibular glands where it would be passed back to the queen through royal jelly. The queen would then convert it back into the active oxo-form, 9-ODA. In fact, significant amounts of 9-HDA have been found in royal jelly, but 9-ODA has not yet been detected. Furthermore, our previous study revealed that 9-HDA is present as a mixture of optical isomers (*R*:*S*, 2:1) in royal jelly [4]. This interesting finding is important with regard to searching for precursors of unknown semiochemicals in royal jelly.

The present study was undertaken to examine the constituents of royal jelly in the hope of discovering precursors of unknown queen substances. We conducted a more

detailed survey of the components, particularly the fatty acid fraction, and isolated seven chiral fatty acids in the pure state. The absolute configurations of the chiral acids were determined using the modified Mosher's method [5–7]. Similar to 9-HDA found in royal jelly, five acids are present as mixtures of optical isomers.

Experimental Procedure

Materials

Lyophilized royal jelly powder was supplied by Yamada Apiculture Center Inc. (Okayama, Japan). A voucher specimen was deposited in the Faculty of Pharmaceutical Sciences, Setsunan University.

Instrumentation

Optical rotations were measured at 25 °C with a JASCO DIP-140 polarimeter (JASCO, Tokyo, Japan). ^{1}H- and ^{13}C-NMR spectra were recorded on JEOL JMN GX400 or ECA 600SN spectrometers (JEOL, Tokyo, Japan), using tetramethylsilane (TMS) as an internal reference. All samples were measured at a probe temperature of 35 °C. The two-dimensional heteronuclear multiple bond connectivity (HMBC) spectrum was recorded at 600 MHz with 64 scans ($^{2,3}J_{CH} = 8$ Hz). Fast atom bombardment mass spectrometry (FAB-MS) including high-resolution mass was recorded on a JEOL JMS-700T spectrometer (JEOL). (Accelerating voltage, 5 kV; matrix, glycerin or triethanolamine; collision gas, He). Column chromatography was carried out on Diaion HP-20 (Mitsubishi Chemical Co., Tokyo, Japan), Sephadex LH-20 (Amersham Pharmacia Biotech AB, Uppsala, Sweden), silica gel (Kiesergel 60, Merck), and Cosmosil 75C_{18}-OPN (Nacalai Tesque, Inc., Tokyo, Japan). Preparative HPLC was conducted over Mightysil RP-18 GP (5 μm, 4.6 × 250 mm, Kanto Chemical Co. Inc. Tokyo, Japan) and Inertsil ODS-3 (4 μm, 4.6 × 100 mm, GL Sciences Inc., Tokyo, Japan) columns with a JASCO 980-PU (JASCO, Tokyo, Japan). The elution profile was monitored by a refractive index detector, RI504R (GL Sciences Inc., Tokyo, Japan).

Isolation of Compounds, 1–7

Lyophilized royal jelly powder (1 kg) was percolated with chloroform to remove a major component, 10-hydroxy-2*E*-decenoic acid. The residue was extracted with chloroform/acetone (1:1, vol/vol), and the solvent was removed in vacuo to give an extract (36.1 g). This was chromatographed on silica gel and eluted successively with chloroform/methanol/water (7:2:0.2 → 7:3:0.5 → 6:4:1 by vol) to give four fractions, fr. 1 (30.0 g), fr. 2 (1.8 g), fr. 3 (0.9 g), and fr. 4 (0.5 g). Fr. 2 was chromatographed on Sephadex LH-20 (methanol) and Cosmosil 75C_{18}-OPN (methanol/water, 1:1 vol/vol → methanol) columns to give three fractions, fr. 5 (115 mg), fr. 6 (314 mg), and fr. 7 (340 mg). Fr. 5 was subjected to preparative HPLC on a reversed-phase column (Inertsil ODS-3) using acetonitrile/water/trifluoroacetic acid, 30:70:0.25 by vol to give compound **1** (7.6 mg). Fr. 3 was chromatographed on Sephadex LH-20 (methanol) and Cosmosil 75C_{18}-OPN (methanol/water, 3:7 → 1:1 by vol → methanol) columns to give four fractions, fr. 8–11. Fr. 8 (31.2 mg) was subjected to preparative HPLC on a reversed-phase column (Mightysil RP-18 GP) using a mobile phase (methanol/water/trifluoroacetic acid, 25:75:0.5 by vol) to give compounds **2** (11.7 mg) and **3** (1.3 mg). Fr. 9 (499 mg) was separated by an Inertsil ODS-3 column using a mobile phase (methanol/water/trifluoroacetic acid, 25:75:0.5 by vol) to give compounds **5** (5.4 mg) and **7** (118 mg). Fr. 10 was subjected to HPLC on an Inertsil ODS-3 column using a solvent (methanol/water/trifluoroacetic acid, 37:63:0.5 by vol) to give compounds **4** (3.4 mg) and **6** (4.2 mg). Compound **7** was identified as 3*R*,10-dihydroxydecanoic acid by comparison of the NMR and FABMS spectroscopic data with those of an authentic sample [4].

1: High resolution negative ion FABMS *m/z*: 201.1120 $[M-H]^-$ (calcd. for $C_{10}H_{17}O_4$: 201.1127). $[\alpha]_D$ −5.5° at 0.8 g/100 mL in methanol. **2**: High resolution negative ion FABMS *m/z*: 201.1118 $[M-H]^-$ (calcd. for $C_{10}H_{17}O_4$: 201.1127). **3**: High resolution negative ion FABMS *m/z*: 201.1117 $[M-H]^-$ (calcd. for $C_{10}H_{17}O_4$: 201.1127). $[\alpha]_D$ −3.1° at 0.2 g/100 mL in methanol. **4**: High resolution negative ion FABMS *m/z*: 187.1339 $[M-H]^-$ (calcd. for $C_{10}H_{19}O_3$: 187.1334). $[\alpha]_D$ +1.1° at 0.3 g/100 mL in methanol. **5**: High resolution negative ion FABMS *m/z*: 203.1291 $[M-H]^-$ (calcd. for $C_{10}H_{19}O_4$: 203.1283). $[\alpha]_D$ +3.3° at 0.5 g/100 mL in methanol. **6**: High resolution negative ion FABMS *m/z*: 231.1588 $[M-H]^-$ (calcd. for $C_{12}H_{23}O_4$: 231.1596). $[\alpha]_D$ +3.4° at 0.4 g/100 mL in methanol. ^{1}H- and ^{13}C-NMR spectroscopic data of **1**–**6** are shown in Tables 1 and 2.

Preparation of 2-Methoxy-2-(trifluoromethyl)phenylacetyl (MTPA) Ester Derivatives

Compounds **1** through **6** (*ca.* 1 mg) were each treated with diazomethane in diethyl ether. (−)- and (+)-MTPA Chlorides (Tokyo Kasei Kogyo Co. Ltd., 20 mg each) were separately added to a solution of the above product in carbon tetrachloride (0.3 mL) and pyridine (1.0 mL), and the mixture was stirred at room temperature for 12 h. After removal of the solvent under a nitrogen stream, the reaction

Table 1 ^{1}H-NMR chemical shifts of **1–6** (CD_3OD)

	1	2	3	4	5	6
H-2	5.80 (1H, d, 15.6)	5.97 (1H, d, 15.6)	5.97 (1H, d, 15.6)	2.36 (1H, dd, 8.0, 15.2)	2.39 (1H, dd, 8.4, 15.0)	2.36 (1H, dd, 8.0, 15.6)
				2.44 (1H, dd, 4.8, 15.2)	2.48 (1H, dd, 4.8, 15.0)	2.44 (1H, dd, 4.8, 15.6)
H-3	6.89 (1H, dt, 15.6, 6.8)	6.92 (1H, dd, 4.8, 15.6)	6.89 (1H, dd, 4.8, 15.6)	3.97 (1H, m)	3.97 (1H, m)	3.97 (1H, m)
H-4	2.21 (2H, dt, 6.8, 6.8)	4.22 (1H, m)	4.22 (1H, m)			
H-9	3.57 (1H, m)		3.72 (1H, m)		3.71 (1H, m)	
H-10	3.41 (1H, dd, 6.8, 11.2)	3.54 (2H, t, 6.6)	1.14 (3H, d, 6.6)	0.90 (3H, t, 6.8)	1.14 (3H, d, 6.6)	
	3.47 (1H, dd, 4.4, 11.2)					
H-11	–	–	–	–	–	3.70 (1H, m)
H-12	–	–	–	–	–	1.14 (3H, d, 6.4)

δ in ppm from TMS. Splitting patterns and coupling constants (J) in Hz are given in *parentheses*

Table 2 ^{13}C-NMR chemical shifts of **1–3** and **5–6** (CD_3OD)

	1	2	3	5	6
C-1	171.4	170.0	170.6	174.1	173.8
C-2	123.7	120.9	121.7	43.3	43.3
C-3	149.5	152.9	152.2	69.4	69.3
C-4	33.0	71.6	71.6		
C-9	73.1		68.6	68.6	
C-10	67.3	63.0	23.5	23.5	
C-11	–	–	–	–	68.5
C-12	–	–	–	–	23.5

δ in ppm from TMS

mixture was subjected to silica gel column chromatography (chloroform) to give a MTPA derivative.

Bis[(−)-MTPA] Ester of Methyl Ester of **1** (**1a**) ^{1}H-NMR ($CDCl_3$, 600 MHz) δ: 1.18–1.17 (8H, m, $CH_2 \times 4$), 2.12 (0.5H, dt, $J = 7.2$, 7.2 Hz, H_2-4 of *S*-form), 2.16 (1.5H, dt, $J = 7.2$, 7.2 Hz, H_2-4 of *R*-form), 3.42 (2.25H, m, OCH_3 of *R*-form), 3.44 (2.25H, m, OCH_3 of *R*-form), 3.48 (0.75H, m, OCH_3 of *S*-form), 3.49 (0.75H, m, OCH_3 of *S*-form), 3.73 (3H, s, CO_2CH_3), 4.27 (0.75H, dd, $J = 4.8$, 12.0 Hz, Ha-10 of *R*-form), 4.30 (0.25H, dd, $J = 6.0$, 12.0 Hz, Ha-10 of *S*-form), 4.54 (0.75H, dd, $J = 3.0$, 12.0 Hz, Hb-10 of *R*-form), 4.62 (0.25H, dd, $J = 3.0$, 12.0 Hz, Hb-10 of *S*-form), 5.28–5.32 (1H, m, H-9), 5.79 (0.25H, d, $J = 15.6$ Hz, H-2 of *S*-form), 5.80 (0.75H, d, $J = 15.6$ Hz, H-2 of *R*-form), 6.92 (0.25H, dt, $J = 15.6$, 7.2 Hz, H-3 of *S*-form), 6.93 (0.75H, dt, $J = 15.6$, 7.2 Hz, H-3 of *R*-form), 7.33–7.40 (6H, m, H-ph), 7.43–7.50 (4H, m, H-ph).

Bis[(−)-MTPA] Ester of Methyl Ester of **2** (**2a**) ^{1}H-NMR ($CDCl_3$, 400 MHz) δ: 1.22–1.72 (10H, m, $CH_2 \times 5$), 3.53–3.55 (6H, m, $OCH_3 \times 2$), 3.74 (1.5H, s, CO_2CH_3 of *R*-form), 3.76 (1.5H, s, CO_2CH_3 of *S*-form), 4.24–4.34 (2H, m, H_2-10), 5.57–5.60 (1H, m, H-4), 5.86 (0.5H, d, $J = 15.6$ Hz, H-2 of *R*-form), 5.98 (0.5H, d, $J = 15.6$ Hz, H-2 of *S*-form), 6.78 (0.5H, dd, $J = 6.0$, 15.6 Hz, H-3 of *R*-form), 6.84 (0.5H, dd, $J = 6.0$, 15.6 Hz, H-3 of *S*-form), 7.38–7.42 (6H, m, H-ph), 7.49–7.52 (4H, m, H-ph).

Bis[(−)-MTPA] Ester of Methyl Ester of **3** (**3a**) ^{1}H-NMR ($CDCl_3$, 400 MHz) δ: 0.86-1.61 (11H, m, H_3-10 and $CH_2 \times 4$), 3.52–3.57 (6H, m, $OCH_3 \times 2$), 3.74–3.76 (3H, m, CO_2CH_3), 5.04–5.13 (1H, m, H-9), 5.51–5.60 (1H, m, H-4), 5.85 (0.29H, d, $J = 15.6$ Hz, H-2 of 4*R*9*R*-form), 5.86 (0.21H, d, $J = 15.6$ Hz, H-2 of 4*R*9*S*-form), 5.96 (0.37H, d, $J = 15.6$ Hz, H-2 of 4*S*9*R*-form), 5.98 (0.13H, d, $J = 15.6$ Hz, H-2 of 4*S*9*S*-form), 6.76 (0.29H, dd, $J = 5.6$, 15.6 Hz, H-3 of 4*R*9*R*-form), 6.78 (0.21H, dd, $J = 5.6$, 15.6 Hz, H-3 of 4*R*9*S*-form), 6.81 (0.37H, dd, $J = 5.6$,

15.6 Hz, H-3 of 4*S*9*R*-form), 6.83 (0.13H, dd, $J = 5.6$, 15.6 Hz, H-3 of 4*S*9*S*-form), 7.39–7.43 (6H, m, H-ph), 7.50–7.53 (4H, m, H-ph).

(−)-MTPA Ester of Methyl Ester of **4** (**4a**) ^{1}H-NMR ($CDCl_3$, 400 MHz) δ: 0.88 (3H, t, $J = 7.2$ Hz, H_3-10), 1.18–1.58 (12H, m, $CH_2 \times 6$), 2.58 (1H, dd, $J = 4.8$, 16.0 Hz, Ha-2), 2.65 (1H, dd, $J = 8.0$, 16.0 Hz, Hb-2), 3.56 (3H, m, OCH_3), 3.59 (3H, s, CO_2CH_3), 5.48 (1H, m, H-3), 7.37–7.43 (3H, m, H-ph), 7.52–7.54 (2H, m, H-ph).

(+)-MTPA Ester of Methyl Ester of **4** (**4b**) ^{1}H-NMR ($CDCl_3$, 400 MHz) δ: 0.87 (3H, t, $J = 7.2$ Hz, H_3-10), 1.20–1.67 (12H, m, $CH_2 \times 6$), 2.61 (1H, dd, $J = 4.8$, 16.0 Hz, Ha-2), 2.70 (1H, dd, $J = 8.0$, 16.0 Hz, Hb-2), 3.55 (3H, m, OCH_3), 3.66 (3H, s, CO_2CH_3), 5.48 (1H, m, H-3), 7.37–7.41 (3H, m, H-ph), 7.52–7.54 (2H, m, H-ph).

Bis[(−)-MTPA] Ester of Methyl Ester of **5** (**5a**) ^{1}H-NMR ($CDCl_3$, 600 MHz) δ: 1.25 (2H, d, $J = 6.6$ Hz, H_3-10 of 3*R*9*S*-form), 1.33 (1H, d, $J = 6.6$ Hz, H_3-10 of 3*R*9*R*-form), 1.31–1.66 (10H, m, $CH_2 \times 5$), 2.55 (0.33H, dd, $J = 4.8$, 16.2 Hz, Ha-2 of 3*R*9*R*-form), 2.56 (0.67H, dd, $J = 4.8$, 16.2 Hz, Ha-2 of 3*R*9*S*-form), 2.63 (0.33H, dd, $J = 7.8$, 16.2 Hz, Hb-2 of 3*R*9*R*-form), 2.64 (0.67H, dd, $J = 7.8$, 16.2 Hz, Hb-2 of 3*R*9*S*-form), 3.51–3.56 (6H, m, $OCH_3 \times 2$), 3.59 (3H, m, CO_2CH_3), 5.10–5.14 (1H, m, H-9), 5.43–5.48 (1H, m, H-3), 7.37–7.42 (6H, m, H-ph), 7.50–7.53 (4H, m, H-ph).

Bis[(+)-MTPA] Ester of Methyl Ester of **5** (**5b**) ^{1}H-NMR ($CDCl_3$, 600 MHz) δ: 1.24 (1H, d, $J = 6.6$ Hz, H_3-10 of 3*R*9*R*-form), 1.32 (2H, d, $J = 6.6$ Hz, H_3-10 of 3*R*9*S*-form), 1.11–1.65 (10H, m, $CH_2 \times 5$), 2.58 (0.67H, dd, $J = 4.8$, 16.2 Hz, Ha-2 of 3*R*9*S*-form), 2.59 (0.33H, dd, $J = 4.8$, 16.2 Hz, Ha-2 of 3*R*9*R*-form), 2.68 (0.67H, dd, $J = 7.8$, 16.2 Hz, Hb-2 of 3*R*9*S*-form), 2.69 (0.33H, dd, $J = 7.8$, 16.2 Hz, Hb-2 of 3*R*9*R*-form), 3.53–3.56 (6H, m, $OCH_3 \times 2$), 3.66 (3H, m, CO_2CH_3), 5.08–5.13 (1H, m, H-9), 5.42–5.48 (1H, m, H-3), 7.36–7.40 (6H, m, H-ph), 7.51–7.54 (4H, m, H-ph).

Bis[(−)-MTPA] Ester of Methyl Ester of **6** (**6a**) ^{1}H-NMR ($CDCl_3$, 600 MHz) δ: 1.18–1.68 (14H, m, $CH_2 \times 7$), 1.25 (2.25H, d, $J = 6.0$ Hz, H_3-12 of 3*R*11*S*-form), 1.33 (0.75H, d, $J = 6.0$ Hz, H_3-12 of 3*R*11*R*-form), 2.57 (1H, dd, $J = 4.8$, 15.6 Hz, Ha-2), 2.64 (1H, dd, $J = 7.8$, 15.6 Hz, Hb-2), 3.52 (3H, m, OCH_3), 3.54 (3H, m, OCH_3), 3.59 (3H, s, CO_2CH_3), 5.11–5.16 (1H, m, H-11), 5.45–5.49 (1H, m, H-3), 7.38–7.41 (6H, m, H-ph), 7.52–7.53 (4H, m, H-ph).

Bis[(+)-MTPA] Ester of Methyl Ester of **6** (**6b**) ^{1}H-NMR ($CDCl_3$, 600 MHz) δ_H: 1.38–1.65 (14H, m, $CH_2 \times 7$), 1.25 (0.75H, d, $J = 6.0$ Hz, H_3-12 of 3*R*,11*R*-form), 1.33 (2.25H, d, $J = 6.0$ Hz, H_3-12 of 3*R*11*S*-form), 2.61 (1H, dd, $J = 4.8$, 15.6 Hz, Ha-2), 2.70 (1H, dd, $J = 8.4$, 15.6 Hz, Hb-2), 3.54 (3H, m, OCH_3), 3.57 (3H, m, OCH_3), 3.66 (3H, s, CO_2CH_3), 5.11–5.17 (1H, m, H-11), 5.44–5.49 (1H, m, H-3), 7.38–7.40 (6H, m, H-ph), 7.53–7.54 (4H, m, H-ph).

The ratio of *R* to *S* was determined by the intensity of the signals arising from both enantiomers.

Results

The total lipid fraction obtained from lyophilized royal jelly powder (1 kg) was separated repeatedly by silica gel column chromatography with various solvents to give the crude fatty acid fraction. This fraction was further separated with HPLC, and seven compounds **1**–**7** were isolated in pure form (see "Experimental Procedure").

The molecular formula of **1**, $C_{10}H_{18}O_4$, was established using high resolution FAB-MS. The ^{1}H-NMR spectrum of **1** showed *trans* olefinic (δ_H 5.80 and 6.89), oxymethine (δ_H 3.57), and allylic (δ_H 2.21) groups together with non-equivalent methylene signals. The ^{13}C-NMR spectrum showed one oxy methine (δ_C 73.1) and one oxy methylene (δ_C 67.3) units together with carboxyl (δ_C 171.4) and olefinic (δ_C 123.7 and 149.5) carbons. The COSY and HMBC spectra showed significant correlation peaks between H_2-10/H-9, H-2/C-1, and H-3/C-1, respectively. These findings revealed that **1** was 9,10-dihydroxy-2*E*-decenoic acid. The absolute configuration of C-9 was determined using the modified Mosher's method.[1]

Methylation of **1** with diazomethane, followed by treatment with (−)-MTPA chloride gave the (−)-MTPA ester (**1a**). The ^{1}H-NMR spectrum of **1a** showed two sets of signals in a ratio of *ca* 3:1 due to optical isomers. The $\Delta\delta$ values [δ (−)-MTPA ester – δ (+)-MTPA ester] of the major characteristic H-2 and H-3 protons were +0.011 and +0.013 ppm, respectively, whereas those of Ha-10 and Hb-10 were −0.025 and −0.076 ppm, respectively, indicating the 9*R* configuration. Hence, **1** was revealed to be a mixture of 9*R*,10- and 9*S*,10-dihydroxy-2*E*-decenoic acids in a ratio of *ca* 3:1 (Fig. 1).

The high resolution FAB-MS of **2** showed an $[M-H]^-$ ion peak at *m*/*z* 201.1118, consistent with the same molecular formula, $C_{10}H_{18}O_4$, as that of **1**, and indicating that **2** is an isomer of **1**. The ^{1}H-NMR spectrum of **2** showed similar *trans* olefinic (δ_H 5.97 and 6.92) signals due to protons H-2 and H-3, and equivalent H_2-10 (δ_H

[1] To establish whether the modified Mosher's method is applicable to compounds possessing a 1,2-diol, we firstly examined this method using 3-(octadecyloxy)-1,2*S*-propanediol. The $\Delta\delta$ values of the corresponding (−)- and (+)-MTPA esters were consistent with those predicted for *S* configuration.

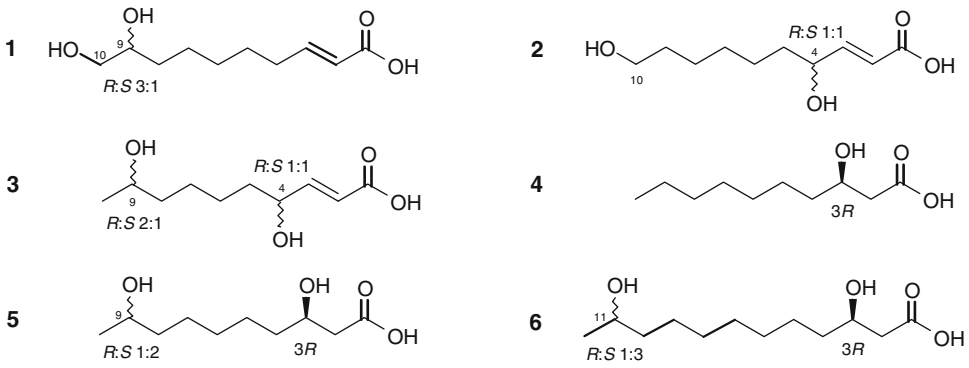

Fig. 1 Structures of chiral fatty acids **1–6**

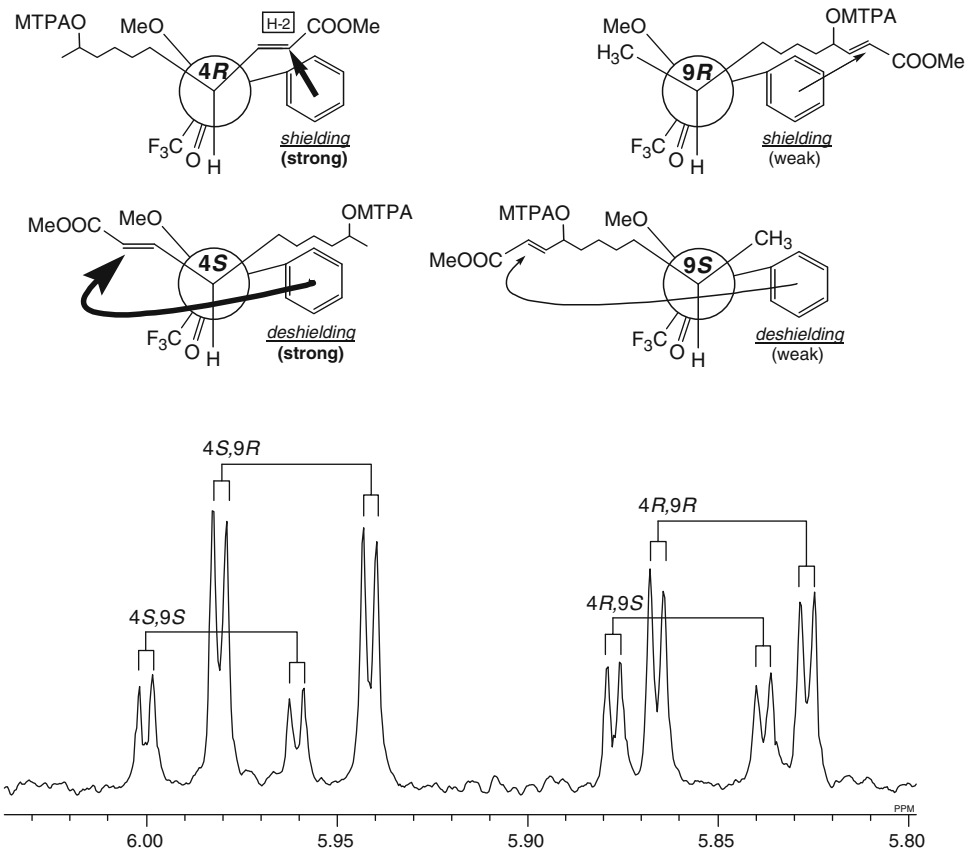

Fig. 2 ^{1}H-NMR spectrum of H-2 of **3a** and anisotropic effects of two MTPA groups

3.54) signals together with an oxy methine (δ_H 4.22) group coupled with H-3. These findings revealed that **2** was a positional isomer of **1**; that is, **2** differed in the position of the secondary hydroxyl group placed at C-4 instead of C-9 as in **1**, and hence the structure was determined to be 4, 10-dihydroxy-2*E*-decenoic acid. Methylation of **2** with diazomethane followed by esterification with (−)-MTPA chloride gave the (−)-MTPA ester (**2a**). The ^{1}H-NMR spectrum of **2a** showed, similar to that of **1a**, two sets of signals assignable to optical isomers, but, in a ratio of ca. 1:1. From these findings, it was determined that **2** was a mixture of 4*R*,10- and 4*S*,10-dihydroxy-2*E*-decenoic acids, in a ratio of ca. 1:1 (Fig. 1).

Compound **3** ($C_{10}H_{18}O_4$) was found, using two dimensional ^{1}H-NMR (COSY and HMBC) spectroscopic analyses, to be another isomer, 4,9-dihydroxy-2*E*-decenoic acid. The ^{1}H-NMR spectrum of (−)-MTPA ester (**3a**) showed, in contrast to those of **1a** and **2a**, four sets each of signals due to protons H-2 and H-3, indicating that **3a** is a mixture of four isomers (4*R*9*S*, 4*S*9*R*, 4*R*9*R*, and 4*S*9*S*). As can be seen in Fig. 2, the olefinic signal for proton (H-2) of the 4*R*9*R* isomer should appear at the highest field because of the anisotropic effect of the two phenyl groups of the MTPA esters (strong shielding by the near 4*R*-MTPA+ weak shielding by the far 9*R*-MTPA). The signal observed at the second highest field could be assigned as proton H-2

Fig. 3 ^{1}H-NMR spectrum of **5a**

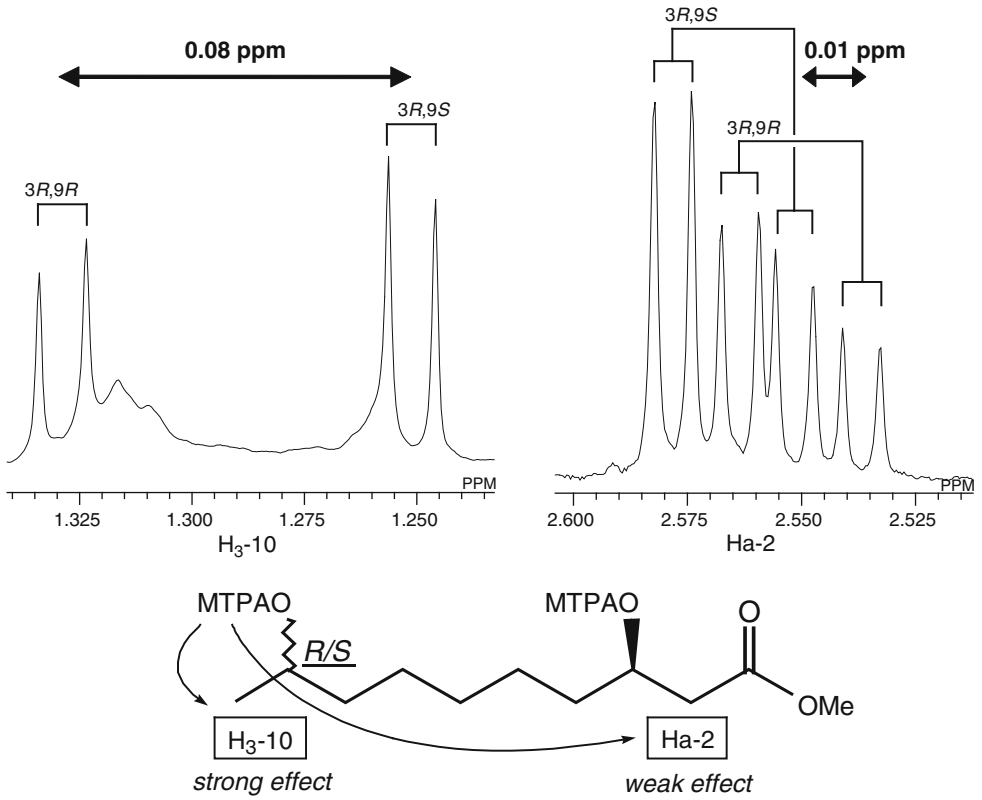

of the 4*R*9*S* isomer (strong shielding by the near 4*R*-MTPA + weak deshielding by the far 9*S*-MTPA). Again, employing the modified Mosher's method as described above, olefinic signals due to the four isomers were successively discriminated, and thus **3** was revealed to be a mixture of 4*S*9*R*-, 4*R*9*R*-, 4*R*9*S*-, and 4*S*9*S*-dihydroxy-2*E*-decenoic acids, in a ratio of ca. 9:7:5:3. On comparison with those of **2a**, the $\Delta\delta$ values for protons H-2 and H-3 were consistent with the assignment of configurations (Fig. 4).

Analysis of the NMR and FAB-MS spectra of **4** ($C_{10}H_{20}O_3$) revealed the structure to be 3-hydroxydecanoic acid. The ^{1}H-NMR spectrum of (−)-MTPA ester (**4a**) showed, unlike those of **1a**–**3a**, signals due to one optical isomer. We then prepared the (+)-MTPA ester (**4b**). The $\Delta\delta$ value for protons H_2-2 showed that the configuration at C-3 was *R* (Fig. 4).

The ^{1}H-NMR spectrum of **5** ($C_{10}H_{20}O_4$) showed two oxy methine signals (δ 3.71 and 3.97), and similar to that of **4**, no signals due to olefinic protons. One oxy methine was coupled with the terminal methyl, H_3-10, and the other was coupled with the nonequivalent protons, H_2-2. From this information, it was clear that the two hydroxyl groups were located at the C-3 and C-9 positions, and hence the structure of **5** was defined as 3,9-dihydroxydecanoic acid. To clarify the absolute configuration, **5** was converted into the (−)-MTPA derivative (**5a**). The ^{1}H-NMR spectrum of **5a**, in contrast to that of **3a**, showed two signals for protons H_2-2, and accordingly **5** was regarded as being a mixture of enantio- and/or diastereoisomers. We then prepared the (+)-MTPA ester (**5b**). If compound **5** was a mixture of enantiomers [(3*R*9*R* and 3*S*9*S*) or (3*R*9*S* and 3*S*9*R*)], the chemical shifts of all signals arising from the (+)- and (−)-MTPA esters would reverse each other, and similar to those of **2a**, the $\Delta\delta$ values would have the opposite sign (Fig. 4). However, the signals in the spectra of **5a** and **5b** gave different chemical shifts. Based on these findings, compound **5** was revealed to be a mixture of diastereomers. The anisotropic effect of the phenyl group of the MTPA ester decreases with increasing numbers of methylene groups between it and the chiral center. In the ^{1}H-NMR spectrum of **5a**, the difference in the chemical shifts for the Ha-2 group (0.01 ppm) was less than that for the H_3-10 group (0.08 ppm) (Fig. 3). Therefore it was determined that the C-9 position has two (*R* and *S*) configurations, while the C-3 carbon has only one. Since the $\Delta\delta$ values for the H_2-2 protons in both the (+)- and (−)-MTPA esters showed the same minus sign, the configuration of the C-3 position could be assigned as *R*. On the basis of the results obtained above, compound **5** was found to be a mixture of 3*R*9*R*- and 3*R*9*S*-dihydroxydecanoic acids, in a ratio of ca. 1:2.

The ^{1}H-NMR spectrum of **6** was quite similar to that of **5**, including signals due to two methines and one terminal methyl group. Its negative ion FAB-MS showed

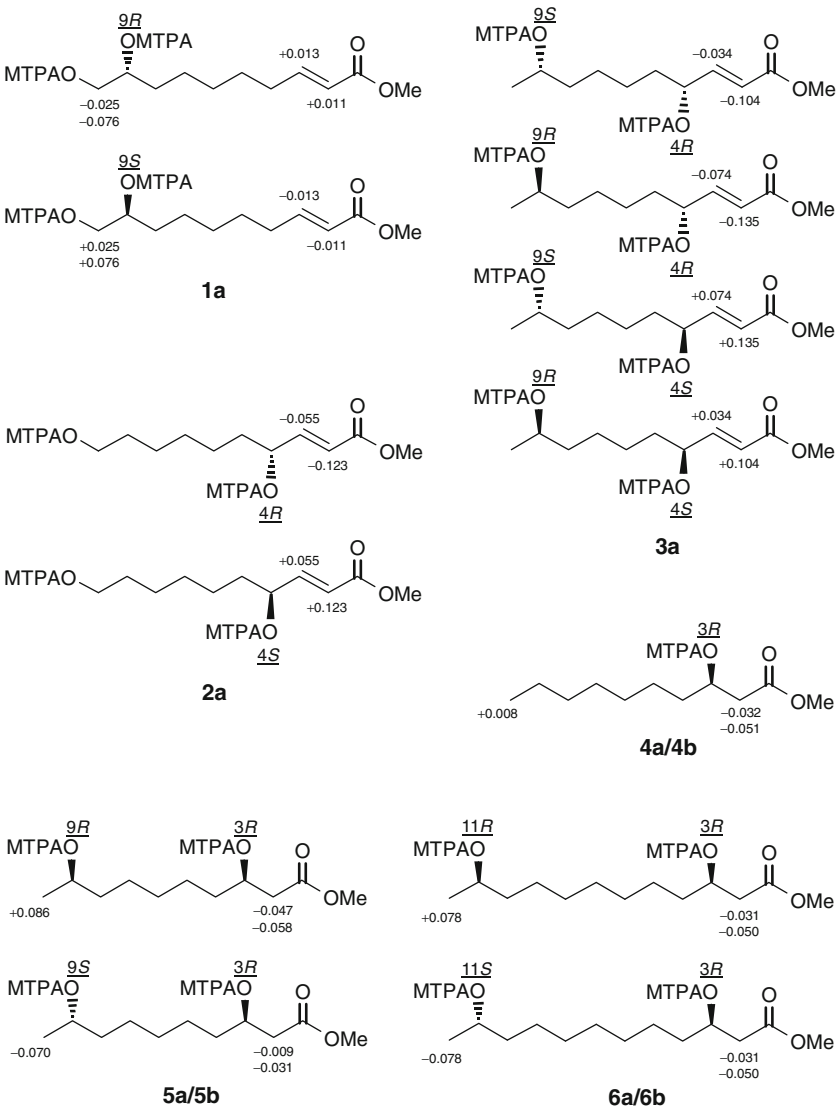

Fig. 4 $\Delta\delta$ values of ^{1}H-NMR chemical shift difference (ppm) for MTPA esters

an $[M-H]^-$ ion peak at *m/z* 231, which was 28 mass units more than that of **5**, while in the ^{13}C-NMR spectrum, two additional methylene signals were observed. From these findings, **6** was revealed to be 3,11-dihydroxydodecanoic acid. The absolute configurations of the two secondary hydroxy groups were determined in the same manner as described for **5**. With the $\Delta\delta$ values and signs of the diagnostic signals, similar to those of **5**, the C-3 position was determined to be the *R* configuration, while the C-11 carbon was found to have both forms (Fig. 4). Accordingly, **6** was identified as a mixture of the isomers, 3*R*11*R* and 3*R*11*S* in a ratio of 1:3.

Discussion

Seven hydroxy fatty acids were isolated in the pure state from the royal jelly of honeybees (*Apis mellifera*). Compounds **1**–**3** and **5** are the first hydroxy fatty acids isolated from royal jelly, although **5** has already been detected in human urine by Tserng et al. [8]. Compound **6**, was recently isolated from royal jelly, by Melliou and co-workers [9], however, the absolute configuration remains unclear. Similar to 9-HDA in royal jelly, the chiral acids obtained in this study are revealed to be mixtures of enantio- or diastereo-isomers (Fig. 4).

It should be noted that the absolute configurations of the secondary hydroxy groups located at C-3 of the chiral acids are all the *R* form, while those at positions C-4, C-9, and C-11 have both forms.

A recent study of the genome sequencing of the honeybee, *A. mellifera*, demonstrated that the species has more odorant receptors than other insects, such as *Drosophila melanogaster*, *Anopheles gambiae*, and *Bombyx mori*, indicating that the honeybee lifestyle involves enhanced pheromone communication [10].

Considering the above information together with the relationship between 9-ODA and 9-HDA, it is believed that the chiral acids isolated in the present study are precursors of unknown semiochemicals, and that their corresponding oxo-forms may play physiologically important functions and roles in the hierarchy of honeybee colonies. We are now synthesizing these oxo-derivatives in order to examine the biological activities of these compounds.

Acknowledgments The authors wish to thank Dr. K. Hashimoto, Institute for Bee Products & Health Science, for supplying the royal jelly. This study was supported in part by a Grant-in-Aid for Scientific Research from the Ministry of Education, Culture, Sports, Science and Technology of Japan.

References

1. Butler CG, Callow RK, Johnston NC (1962) The isolation and synthesis of queen substance, 9-oxodec-*trans*-2-enoic acid, a honeybee pheromone. Proc R Soc Lond B Biol Sci 155:417–432
2. Butler CG (1954) The method and importance of the recognition by a colony of honeybees (*A, mellifera*) of the presence of its queen. Trans R Ent Soc Lond 105:11–29
3. Johnston NC, Law JH, Weaver N (1965) Metabolism of 9-ketodec-2-enoic acid by worker honeybees (*Apis mellifera* L.). Biochemistry 4:1615–1621
4. Noda N, Umebayashi K, Nakatani K, Miyahara K, Ishiyama K (2005) Isolation and characterization of some hydroxy fatty and phosphoric acid esters of 10-hydroxy-2-decenoic acid from the royal jelly of honeybees (*Apis mellifera*). Lipids 40:833–838
5. Kusumi T, Ooi T, Ohkubo Y, Yabuuchi T (2006) The modified Mosher's method and sulfoximine method. Bull Chem Soc Jpn 79:965–980
6. Ohtani I, Kusumi T, Kashman Y, Kakisawa H (1991) High-field FT NMR application of Mosher's method. The absolute configurations of marine terpenoids. J Am Chem Soc 113:4092–4096
7. Ono M, Yamada F, Noda N, Kawasaki T, Miyahara K (1993) Determination by Mosher's method of the absolute configuration of mono- and dihydroxyfatty acids originated from resin glycosides. Chem Pharm Bull 41:1023–1026
8. Tserng K-Y, Jin S-J (1991) Metabolic origin of urinary 3-hydroxydicarboxylic acids. Biochemistry 30:2508–2514
9. Melliou E, Chinou I (2005) Chemistry and bioactivity of royal jelly from Greece. J Agric Food Chem 53:8987–8992
10. The honeybee genome sequencing Consortium (2006) Insights into social insects from the genome of the honeybee *Apis mellifera*. Nature 443:931–949

Lipids (2011) 46:271–276
DOI 10.1007/s11745-010-3506-0

ORIGINAL ARTICLE

A New Mechanism for Photo- and Radiation-Induced Decomposition of Sphingolipids

Alexandra G. Lisovskaya · Oleg I. Shadyro · Irina P. Edimecheva

Received: 2 October 2010 / Accepted: 10 November 2010 / Published online: 8 December 2010

Abstract Data have been obtained showing regularities in product formation following radiolysis of serinol, lysosphingomyelin and photolysis of *N*-(2-hydroxypropyl)hexanamide, sphingomyelin, which point to the possibility of photo- and radiation-induced destruction of the named substrates via a C–C bond rupture. The key stage of this process is the formation and decomposition of N-centered radicals generated from the starting compounds.

Keywords Lipid chemistry · General area · Free radicals · Oxidized lipids · Sphingomyelin · Specific lipids

Abbreviations

CerPCho	Sphingomyelin
D_2O	Deuterium oxide
GC–MS	Gas chromatography–mass spectrometry
HPHA	*N*-(2-Hydroxypropyl)hexanamide
HPLC	High performance liquid chromatography
LC	Liquid chromatography
SPPtdCho	D-*erythro*-sphingosine phosphocholine (lysosphingomyelin)
UV	Ultraviolet

A. G. Lisovskaya (✉) · O. I. Shadyro · I. P. Edimecheva
Department of Chemistry, Belarusian State University, Minsk, Belarus
e-mail: alexandra-lis@rambler.ru

O. I. Shadyro
e-mail: shadyro@open.by

Introduction

Lipids are known to undergo various free-radical transformations on irradiation. Of these processes, the most extensively studied one is lipid peroxidation [1]. In cases of hydroxyl-containing lipids, such as cardiolipin and phosphatidylinositol, the radiation may induce free-radical fragmentation, in which the key stage is the decomposition of α-hydroxyl-containing carbon-centered radicals formed from the starting molecules [2, 3]. Unlike glycerophospholipids, the radiation-induced transformations of sphingolipids have been studied to a much less extent, and only sporadic publications on this issue can be found in the literature. At the same time, sphingolipids, the structural components of which are sphingosine bases, represent one of the most diversified kinds of lipids, as regards chemical structure and functional activity. They are indispensable components of cell membranes and therefore play an important role in biosystem functioning. In plasmatic membranes of mammals, the major part of sphingolipids is localized, together with cholesterol, in definite areas of biomolecules, usually named "lipid rafts" [4]. The "lipid rafts" containing high concentrations of sphingomyelin (CerPCho) are believed to have the potential to accumulate significant amounts of CerPCho, which leads to the formation of high local concentrations of ceramide, an important participant in apoptosis processes [5]. Lysosphingolipids, such as lysosphingomyelin (SPPtdCho) and sphingosine-1-phosphate, are regarded as a new class of signaling molecules. They are formed during physiological and pathological processes and are responsible for activating various signaling cascades [6].

The aforesaid may serve as a serious motivation for studying photo- and radiation-induced transformations of sphingolipids.

Materials and Methods

Materials

In the present study, composition of the product mixtures formed on radiolysis of 2-aminoglycerol (serinol) or SPPtdCho was examined, as well as that of photolysis products of *N*-(2-hydroxypropyl)hexanamide (HPHA) and CerPCho. Structures of the compounds under study are shown in Fig. 1.

CerPCho from *Sigma* and serinol from *Aldrich* were used in the study. SPPtdCho was prepared by deacylation of CerPCho [7]. Synthesis of HPHA was performed according to a procedure based on acylation of amino alcohol with complex capric/*n*-butylcarbonic acid anhydride in a solvent system containing tetrahydrofuran and acetonitrile (1:2), with the addition of 15 μL of triethylamine per 10 mL of the mixture [8]. Structures of the synthesized compounds were confirmed by ^{1}H- and ^{13}C-NMR spectroscopy.

Preparation of Liposomes from Lipids

Multilayer liposomes were prepared by dispersing thin lipid films in phosphate buffer [9]. To do this, the solvent was removed on a rotor evaporator from solutions of the respective lipids in chloroform, and the film samples obtained were kept under a vacuum for at least 1 h to complete the process of solvent removal. To the lipid film thus obtained, a definite amount of phosphate buffer was added ($c = 0.05$ mol/L; pH 7.4), pre-deaerated by bubbling argon (99.9%) for 45 min. The mixture was shaken for 15 min on a Vortex mixer at 50 °C. The obtained multilayer liposomes were sonicated for 3 min at 24 kHz (50% vibration amplitude, cycling mode 0.3) on an ultrasound unit UP 200H. Lipid concentration in the liposomes was 2×10^{-2} mol/L.

Preparation of Solutions of the Compounds Under Study

Freshly twice-distilled water was used for preparation of 0.1 M aqueous solutions of serinol and HPHA. The necessary pH values of serinol solutions were achieved by adjusting with perchloric acid or sodium hydroxide. Oxygen was removed from the solutions obtained by bubbling argon through them for 45 min.

Irradiation of Samples

The prepared samples were irradiated on a γ-unit equipped with ^{60}Co source; the dose rate was 0.45 ± 0.1 Gy/s. The absorbed dose range for serinol solutions and SPPtdCho liposomes was 0.54–2.70 kGy.

CerPCho dispersions and HPHA solutions were irradiated with a continuous spectrum of a high pressure mercury arc lamp (DRT-100). The sample distance from the source was 20 cm. The dose rate in the wavelength range

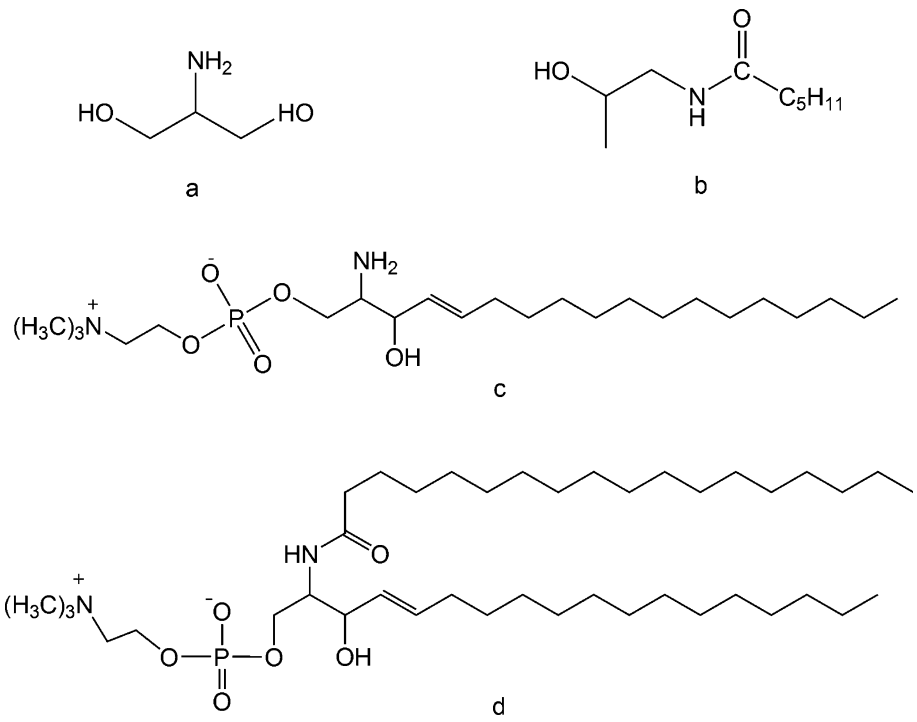

Fig. 1 Structures of the compounds studied, **a** serinol; **b** *N*-(2-hydroxypropyl) hexanamide (HPHA); **c** lysosphingomyelin (SPPtdCho); **d** sphingomyelin (CerPCho)

230–320 nm was 6.8×10^{15} photons s^{-1} mL^{-1}. The irradiation period for HPHA was varied from 10 to 100 min, and that for CerPCho liposomes was 15–160 min.

LC Analysis of Ammonia in Serinol Solutions

The ammonia content of serinol solutions was determined by means of the liquid chromatography technique as described in [10] using sodium citrate buffer pH 10.1 as eluent.

HPLC Analysis of Carbonyl-Containing Products

Analysis of carbonyl-containing products (formaldehyde, acetaldehyde, glycolic aldehyde, β-hydroxypropionic aldehyde, hydroxyacetone) formed on radiolysis or photolysis of the substrates being studied was carried out, after derivatization of the named compounds with 2,4-dinitrophenylhydrazine, by means of the high performance liquid chromatography technique using a Shimadzu LC-10AD_{VP} instrument equipped with a UV detector. The chromatographic conditions were as follows: NUCLEOSIL 120-5 C_{18} column (length 250 mm, ID 4 mm); eluent: methanol/water (60:40); eluent flow rate: 0.6 mL/min; temperature: 37 °C; detection wavelength 360 nm; injection volume: 4 μL.

GC–MS Analysis of Radiolysis Products Formed from Lipid Liposomes

2-Hexadecenal, stearamide and hydrocarbon contents of irradiated lipid liposomes were determined using the chromatography-mass spectrometry technique on a Shimadzu GCMS-QP2010 instrument (electron impact at 70 eV; ion source temperature 250 °C). The products were separated on an Equity™-5 capillary column (30 m, 0.25 mm ID, 025 μm thickness of the liquid phase layer). The GC oven temperature was increased from 60 to 280 °C at a rate of 5 °C/min. The samples were extracted from the liposomes with methanol.

Radiation-chemical yields of formation for the respective products were calculated from the data on radiolysis product accumulation as function of the dose absorbed. The figures given the tables are average values from at least three measurements. Within the absorbed dose range used, concentrations of radiolysis products increased linearly with the irradiation dose.

Results

The parent compound for sphingolipids is sphingosine, which contains a 2-aminoglycerol moiety in its structure (Fig. 1a). For this reason, we investigated the composition and determined yields of the products formed on radiolysis of deaerated 0.1 M serinol solutions in water and deuterium oxide (D_2O) as function of the solution pH (Table 1). The data obtained show that the main radiolysis products of serinol are ammonia and various carbonyl-containing substances, which are formed on deamination and C–C destruction of the starting compound. The yields of these products are significantly affected by pH of the starting solutions, as well as by replacement of H_2O by D_2O.

Radiolysis of aqueous SPPtdCho dispersions (Fig. 1c) results in formation of compounds with lower molecular mass than that of the starting substrate. Using the GC–MS method, we have detected 2-hexadecenal among radiolysis products formed in 0.02 M aqueous SPPtdCho dispersions. Figure 2 shows the mass spectrum of a product present in the reaction mixture obtained after radiolysis of SPPtdCho. The spectrum is consistent with the structure of 2-hexadecenal, an unsaturated C_{16} aldehyde [11].

Accumulation of 2-hexadecenal proceeds proportionally to the dose absorbed (Fig. 3). This fact indicates that the named compound is a primary product of SPPtdCho radiolysis.

Table 1 Radiation-chemical yields (G, molecule/100 eV) of product formation on radiolysis of deaerated 0.1 M serinol solutions in water and D_2O as function of pH

Products	G, molecule/100 eV	
	pH 7.0	pH 11.0
NH_3	2.94 ± 0.05	3.03 ± 0.12
$HOCH_2CH_2CHO$	(0.82 ± 0.06)/(1.54 ± 0.04)	(0.54 ± 0.04)/(0.24 ± 0.05)
$HOCH_2C(O)CH_3$	(0.03 ± 0.01)/–	(0.23 ± 0.01)/(0.01 ± 0.01)
CH_2O	(0.20 ± 0.03)/(0.05 ± 0.03)	(0.40 ± 0.06)/(0.14 ± 0.04)[a]
CH_3CHO	(0.04 ± 0.01)/(0.02 ± 0.01)	(0.29 ± 0.05)/(0.05 ± 0.02)
$HOCH_2CHO$	(0.05 ± 0.04)/(0.01 ± 0.02)	(0.36 ± 0.03)/(0.03 ± 0.01)

[a] The formaldehyde yield value given in the Table at pH 11.0 may be lower than the actual one since formaldehyde at alkaline pH values can undergo condensation reactions

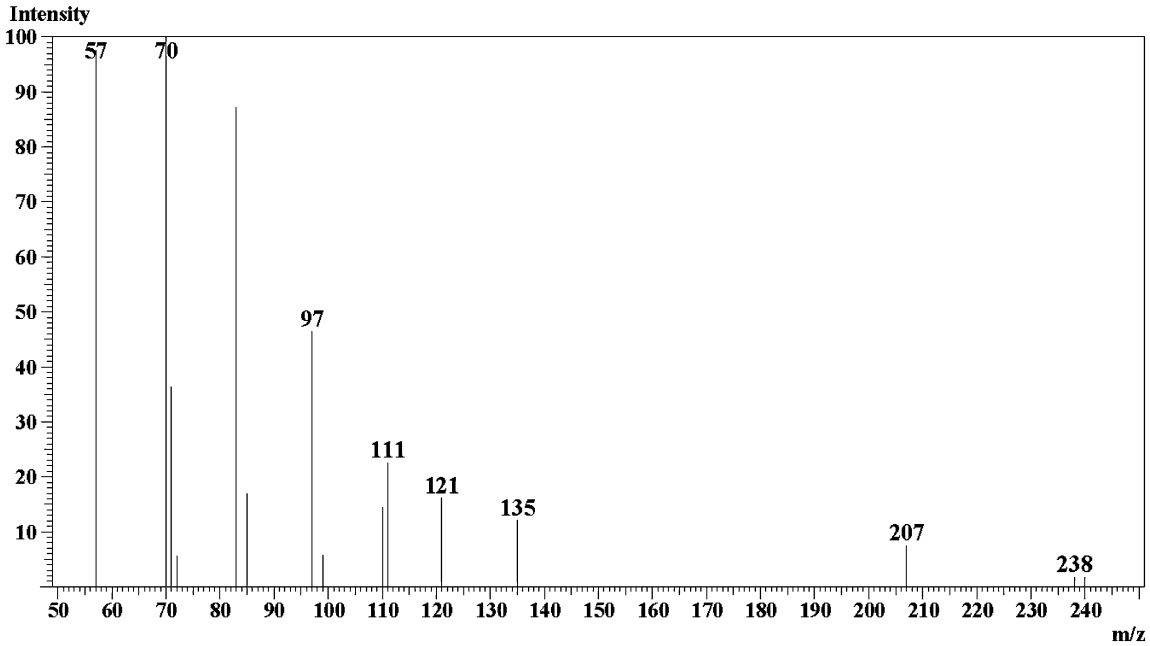

Fig. 2 Mass spectrum of 2-hexadecenal present in irradiated SPPtdCho dispersions

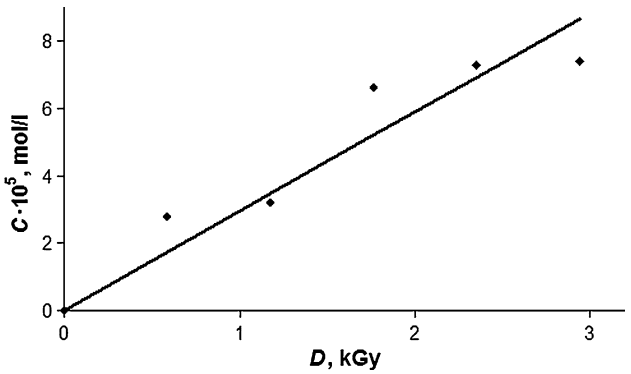

Fig. 3 Accumulation of 2-hexadecenal on irradiation of aqueous SPPtdCho dispersions ($c = 0.02$ mol/L, pH 7.4) as function of dose absorbed

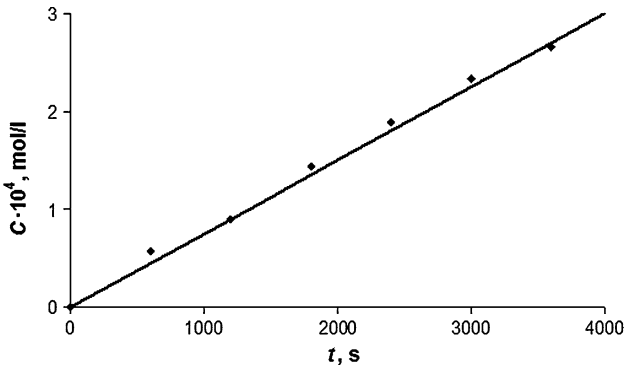

Fig. 4 Accumulation of acetaldehyde in UV-irradiated 0.1 M HPHA solutions as function of irradiation time

The radiation-chemical yield of 2-hexadecenal calculated from the data shown in Fig. 3 for 0.02 M aqueous SPPtdCho dispersions amounted to 0.22 ± 0.04 molecule/100 eV.

Furthermore, photolysis of 0.1 M HPHA solutions and 0.02 M CerPCho dispersions were performed in this study. Thereafter, composition of the product mixtures was examined and quantum yields determined for the respective photolysis products.

On photolysis of deaerated aqueous 0.1 M HPHA solutions, we have detected pentane and acetaldehyde. Accumulation of the latter occurred in direct proportion to UV irradiation time (Fig. 4).

Photolysis of deaerated aqueous 0.02 M CerPCho dispersions results in formation of the corresponding hydrocarbons and 2-hexadecenal.

Quantum yields of the photolysis products obtained after UV-irradiation of HPHA and CerPCho are presented in Table 2.

Along with the CerPCho destruction products formed via C–C bond cleavage, we have also detected stearamide, a deamidation product of the starting substance (Table 2).

Discussion

A characteristic feature of the chemistry of free radicals generated from bi- and polyfunctional organic compounds

Table 2 Quantum yields of formation (Φ, molecule/photon) of photolysis products for the compounds under study

Starting substances	Photolysis products	Φ, molecule/photon
Deaerated aqueous 0.1 M HPHA solution	Acetaldehyde	1.5×10^{-3}
	Pentane	3.2×10^{-4}
Deaerated aqueous 0.02 M CerPCho dispersions	2-Hexadecenal	3.5×10^{-4}
	Stearamide	5.3×10^{-5}
	Hydrocarbons	4.4×10^{-5}

is their tendency towards decomposition via the stage involving formation of carbon-centered radicals according to the following scheme [12]:

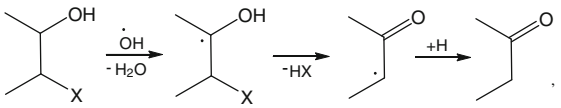

X= OH, NH_2, OR, OCOR (1)

Realization of reaction (1) on the radiolysis of serinol results in the formation of ammonia and 3-hydroxypropionic aldehyde. Based on the yields obtained for ammonia, one can conclude that the radiation-induced deamination is the prevailing process in the case of serinol. Radiation-induced deamination of serinol is accompanied by the formation of hydroxyacetone and 3-hydroxypropanal. This fact suggests the possibility of ammonia elimination by two pathways, and the pH of the starting solution appears to have a deciding influence on the probability of their realization.

At the same time, the probability of product formation via rupture of C–C bonds in serinol molecules appears to be quite high, especially in alkaline media.

It has been shown while studying radiolysis of amino alcohols and diamines [12] that the radiation-induced destruction of amino-containing bifunctional compounds proceeds according to a mechanism shown below:

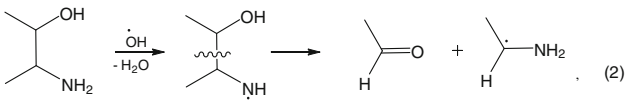

(2)

The probability of reaction (2) being realized should increase in alkaline media, where the amino group is deprotonated, making the abstraction of a hydrogen atom from it by the electrophilic ·OH radical easier. Indeed, the yields of serinol breakdown products such as formaldehyde, acetaldehyde and glycolic aldehyde increase significantly when changing to alkaline solutions. The probability of forming nitrogen-centered radicals should decrease if the radiolysis is performed in D_2O, because the amino group will be deuterated in this case, and abstraction of deuterium requires more energy.

The facts established in this study allow the following schemes to be proposed for the product formation resulting from the destruction occurring on radiolysis of serinol:

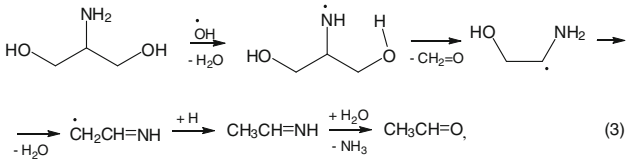

(3)

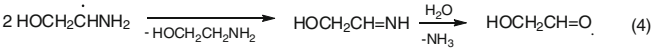

(4)

The attack of the ·OH radical formed on radiolysis of water on the amino group of SPPtdCho should also induce destruction of the latter involving cleavage of the C–C bond:

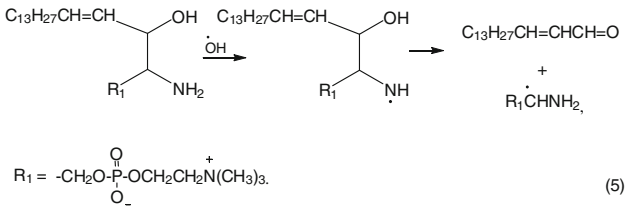

(5)

Identification of 2-hexadecenal among the products formed on the radiolysis of SPPtdCho may serve as a confirmation for the process of radiation-induced C–C destruction being realized with the starting substance.

Unlike substances belonging to the amino alcohol class, their amide analogues absorb UV radiation. This leads to their destruction according to the Norrish type I scheme, which, in the case of HPHA, can be represented in the following way:

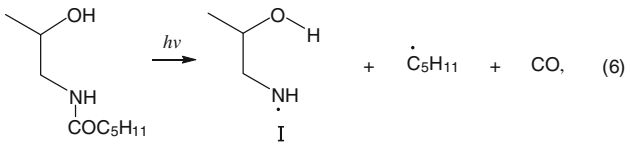

(6)

Realization of photochemical reaction (6) should lead to the generation of aminyl radicals (I), and hence to the appearance of products resulting from their subsequent destruction via C–C bond rupture.

Indeed (see Table 2), among the photolysis products of HPHA, we have identified pentane, evidencing realization of the Norrish destruction (6), as well as acetaldehyde. Formation of the latter is possible due to C–C destruction of the species I:

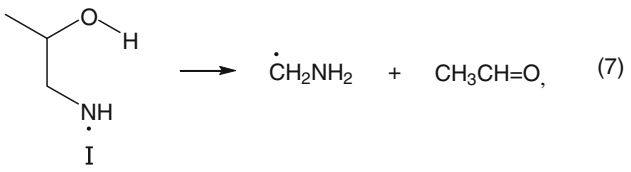

The established fact of photo-decomposition of CerP-Cho, due to the biological importance of this substance, is of particular interest. After photon absorption, CerPCho will undergo the Norrish type I decomposition:

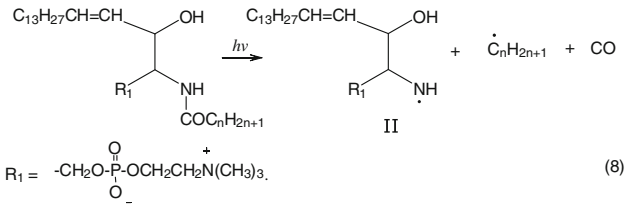

Subsequently, the nitrogen-centered radicals II should decompose to form 2-hexadecenal:

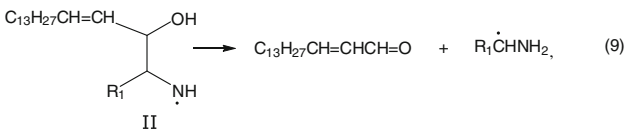

The alkyl radicals formed according to reaction (8) are capable of abstracting an H atom from the starting molecule and initiating the deamidation process, as described in [13].

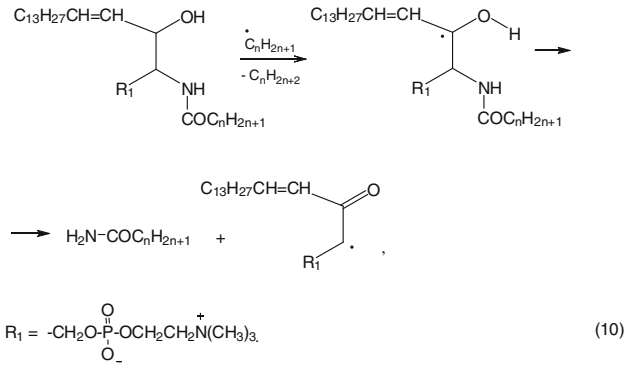

Analysis of the reaction mixture obtained after photo-induced destruction of CerPCho (see Table 2) revealed the presence of 2-hexadecenal, stearamide and hydrocarbons, which may serve as confirmation for the reactions (8–10) taking place.

Thus, the data presented in this paper point to the realization of γ- and UV-induced fragmentation of sphingolipids involving C–C bond cleavage, which has not been described previously.

References

1. Halliwell B, Gutteridge JMC (2007) Free radicals in biology and medicine, 4th edn. Clarendon Press, Oxford
2. Shadyro OI, Yurkova IL, Kisel MA, Brede O, Arnhold J (2004) Radiation-induced fragmentation of cardiolipin in a model membrane. Int J Radiat Biol 80:239–245
3. Shadyro OI, Yurkova IL, Kisel MA, Brede O, Arnhold J (2004) Radiation-induced free-radical transformations of phospholipids: MALDI-TOF MS study. Chem Phys Lipids 132:235–246
4. Won J, Singh I (2006) Sphingolipid signaling and redox regulation. Free Radical Biol Med 40:1875–1888
5. Cremesti AE, Goni FM, Kolesnick R (2002) Role of sphingomyelinase and ceramide in modulating rafts: do biophysical properties determine biologic outcome? FEBS Lett 531:47–53
6. Alewijnse AE, Michel MC (2006) Sphingosine-1-phosphate and sphingosylphosphorylcholine: two of a kind? Br J Pharmacol 147:347–348
7. Bittman R, Verbicky C (2000) Methanolysis of sphingomyelin: toward an epimerization-free methodology for the preparation of D-*erythro*-sphingosylphospocholine. J Lipid Res 41:2089–2093
8. Bezuglov VV, Gretskaia NM, Blazhenova AV, Adrianova EL, Akimov AV, MIu Bobrov, Nazimov IV, Kisel MI, Sharko OL, Novikov AV, Krasnov NV, Shevchenko VP, V'iunova TV, Miasoedova NF (2006) Arachidonoyl amino acids and arachidonoyl peptides: synthesis and properties. Bioorg Khim 32(3):258–267
9. Bangham AD, Standish MM, Watkins JC (1965) Diffusion of univalent ions across the lamellae of swollen phospholipids. J Mol Biol 13:238–252
10. Shadyro OI, Sosnovskaya AA, Vrublevskaya O (2003) C–N bond cleavage reactions on radiolysis of amino containing organic compounds and their derivatives in aqueous solutions. Int J Rad Biol 79:269–279
11. Brahmbhatt VV, Hsu F-F, Kao JL-F, Frank EC, Ford DA (2007) Novel carbonyl and nitrile products from reactive chlorinating species attack of lysosphingolipid. Chem Phys Lipids 145:72–84
12. Petryaev EP, Shadyro OI (1986) Radiation chemistry of bifunctional organic compounds. Universitetskoye Publ., Minsk (in Russian)
13. Akhrem AA, Edimecheva IP, Zaitsev AA, Kisel MA, Timoschuk MA, Shadyro OI (1991) Elimination of acylamides in radiation-induced free radical fragmentation of sphingomyelin. Dokl Acad Nauk SSSR 316:919–921 (in Russian)

Lipids (2011) 46:277–285
DOI 10.1007/s11745-010-3520-2

ORIGINAL ARTICLE

In Vitro Intestinal Bioaccessibility of Alkylglycerols Versus Triacylglycerols as Vehicles of Butyric Acid

Diana Martín · María I. Morán-Valero · Francisco J. Señoráns · Guillermo Reglero · Carlos F. Torres

Received: 30 August 2010 / Accepted: 17 December 2010 / Published online: 12 January 2011

Abstract Butyric acid has been the subject of much attention last years due to its bioactivity. However, the potential advantages of butyrate are limited by the problem to reach enough plasma concentrations; therefore, pro-drugs have been proposed as an alternative to natural butyrate. A comparative study on in vitro intestinal digestion of 2,3-dibutyroil-1-*O*-octadecyl glycerol (D-SCAKG) and tributyrin (TB), as potential pro-drugs of butyric acid, was performed. Aliquots were taken at different times of digestion for studying the extent and rate of hydrolysis of both substrates. The micellar phase (MP) and oily phase (OP) formed in the digestion media were separated and their composition in lipid products was analyzed. Initially, it was confirmed that the in vitro model reproduced physiological results by testing against olive oil as a standard lipid. The progress of in vitro intestinal digestion of D-SCAKG was slower than that of TB. TB hydrolyzed completely to butyric acid, whereas D-SCAKG mainly yielded 2-butyroil-1-*O*-octadecyl glycerol (M-SCAKG), followed by butyric acid and 1-*O*-octadecyl glycerol (AKG). The MP from both substrates mainly consisted of butyric acid. Minor levels of M-SCAKG and AKG were also found in the MP after hydrolysis of D-SCAKG, the M-SCAKG being mainly distributed in the OP. Therefore, D-SCAKG produced a stable form of esterified butyric acid as M-SCAKG after in vitro intestinal digestion, unlike TB. Additionally, such a product would integrate both bioactive compounds, butyric acid and alkylglycerol, within the same molecule. Free butyric acid and AKG would be also released, which are lipid products of interest as well.

Keywords Alkylglycerols · Butyric acid · Lipid digestion · Micellar phase · Structured lipids · Pro-drugs

Abbreviations

AKG	1-*O*-octadecyl glycerol
DAG	Diacylglycerol
DB	Dibutyrin
D-SCAKG	2,3-dibutyroil-1-*O*-octadecyl glycerol
MAG	Monoacylglycerol
MB	Monobutyrin
MP	Micellar phase
M-SCAKG	2-Butyroil-1-*O*-octadecyl glycerol
OP	Oily phase
TAG	Triacylglycerol
TB	Tributyrin

D. Martín · M. I. Morán-Valero · G. Reglero · C. F. Torres (✉)
Departamento de Producción y Caracterización de Nuevos Alimentos, Instituto de Investigación en Ciencias de la Alimentación (CIAL), Campus de la Universidad Autónoma de Madrid (CSIC–UAM), 28049 Cantoblanco, Madrid, Spain
e-mail: carlos.torres@uam.es

D. Martín · M. I. Morán-Valero · F. J. Señoráns · G. Reglero · C. F. Torres
Facultad de Ciencias, Sección Departamental de Ciencias de la Alimentación, Universidad Autónoma de Madrid, 28049 Cantoblanco, Madrid, Spain

Introduction

Butyric acid has been the subject of much attention over the last years due to its bioactivity. Besides having physiological role as the main metabolic fuel for colonocytes and control of colonic inflammation, butyrate seems to interfere with the pathogenesis of diverse cancers, such as colorectal cancer, hepatocarcinoma, leukemia, breast and

prostate cancer, by inhibiting cell proliferation or inducing apoptosis [1–5]. However, the potential application of butyrate as antitumor agent is limited by the problem to reach enough plasma concentrations required to exert its antiproliferative/differentiating actions. Moreover, it is rapidly metabolized, showing a short half-life [3, 6]. Therefore, there is a current interest on overcoming these drawbacks in order to allow its application as therapeutic agent. Pro-drugs, such tributyrin (TB), have been proposed as alternative of natural butyrate [3, 7].

Recently, structured triradylglycerols as potential vehicles of butyric acid in the form of alkylglycerols (2,3-dibutyroil-1-*O*-octadecyl glycerol; D-SCAKG) have been synthesized by Torres et al. [8] (Fig. 1). Besides butyrate, the own alkylglycerol backbone is of current interest by itself. Alkylglycerols, alkylglycerophospholipids and their derivatives, namely ether lipids, are membrane components and cellular signaling molecules. They have been related to antitumor, antineoplastic and cellular differentiation properties and increased immune responses. Furthermore, alkylacetylglycerols are precursors of the platelet-activating factor, which is biologically active phospholipid with diversity effects on cells and tissues [9–12]. Therefore, additionally to TB, the structured lipid in the form of D-SCAKG might have the double advantage of alkylglycerols as potential lipid vehicle of butyrate and the bioactivity of each individual compound, alkylglycerol and butyrate, within the same molecule.

One of the problems that arise is to elucidate which of these two lipids, alkylglycerols or triacylglycerols, would be more effectively transported and chemically stable in the plasma, diffuse through biological membranes, or show more effective intracellular metabolism and, specially, would be more bioaccessible during gastrointestinal digestion, as the first step before any other physiological action beyond colon or intestinal tissues.

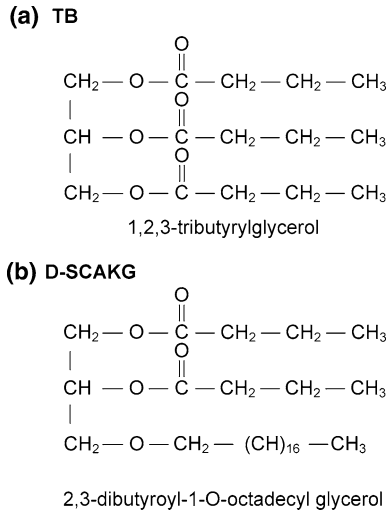

Fig. 1 Triradylglycerols sterified with butyric acid

In vitro intestinal models of lipid digestion are an interesting approach for obtaining preliminary and valuable information concerning digestion of lipid species. A huge diversity of in vitro intestinal models of lipid digestion can be found in the scientific literature trying to simulate pseudo-physiological conditions [13, 14]. However, the fact is that the composition of the reaction media used to be diverse concerning most variables, such as the ratio enzyme/substrate, bile salts/lecithin, the volume or time of reaction, the pH, or the composition and ionic strength of the used buffer. Since there is no standardized method, we considered that the selection of the model that closely simulate in vivo conditions was especially essential when performing in vitro lipid digestion of novel or unknown lipids, in order to accurately understand obtained results and to avoid misinterpretations due to the own used methodology.

The study of intestinal lipid digestion under in vitro conditions is frequently completed by the subsequent study of the different phases of the digestive media containing the released lipid products. During intestinal digestion of dietary fat, the intraluminal content has been shown to be structured as an oily phase (OP) dispersed in a micellar bile salt solution (MP) [15]. The OP mainly contains undigested triacylglycerols (TAG) and released diacylglycerols (DAG), whereas the MP contains bile salt and the poorly soluble end products of enzymatic hydrolysis, namely monoacylglycerols (MAG) and fatty acids, structured as mixed micelles, micelles, vesicles or emulsion droplets [13, 16]. Absorption of lipid products takes place supported by this MP, which enhances the transport of lipid products to enterocytes throughout the unstirred water layer close to the microvillus membrane, where they are absorbed [17]. The analysis of lipid products of these phases contributes to the study of bioaccessibility. The term bioaccessibility defined according to Fernandez-Garcia et al. [18], as the fraction of a compound that is released from its matrix in the gastrointestinal tract and thus becomes available for intestinal absorption. The intraluminal behavior of short-chain TAG during intestinal digestion is rather different. Thus, short-chain fatty acids released by pancreatic enzymes do not need to be included in the micellar structures, but they are easily solubilized in the aqueous media and the unstirred water layer close to enterocytes for absorption [17, 19]. On the other hand, to the best of our knowledge, previous information concerning the distribution of alkylglycerides, both free and esterified, within the intraluminal phases during intestinal digestion has not been previously reported. In fact, the general information on the process of intestinal absorption of alkylglycerides is scarce. Nevertheless, evidence that 1-*O*-alkyl-*sn*-glycerols derived

from dietary ether glycerolipids are completely absorbed by intestine without cleavage of the ether bond exists [20]. After reaching the targets, alkylglycerols were directly utilized to synthesize membrane alkylglycerolipids and plasmalogens, according to the normal metabolism described for this kind of lipids [20]. However, the exact mechanism of absorption is unknown.

The aim of the present research was to perform a comparative study about the intestinal digestion of TB and D-SCAKG under in vitro conditions, in order to show differences in the rate and extent of reaction, generation of lipid products and their potential bioaccessibility. Firstly, the in vitro intestinal digestion model was tested against a standard lipid, in order to be certain that the model reflected physiological intestinal lipid digestion and to reject that any artifact or the own conditions of the digestion method would not interfere with the results obtained for TB and D-SCAKG hydrolysis.

Materials and Methods

Reagents and Materials

The D-SCAKG was synthesized according to a methodology previously described by our group [8], TB (Ref. T8626) was purchased from Sigma-Aldrich Chemie GmbH (Steinheim, Germany) and olive oil as the standard lipid was from Inmaculada Murga Arenas (Toledo, Spain). Trizma (Ref. T1503), maleic acid (Ref. M0375), pancreatin (Ref. P1750), bile salts (Ref. B8756) and phosphatidyl choline from egg yolk (Ref. 61771) were purchased from Sigma-Aldrich Chemie GmbH (Steinheim, Germany). Hydrochloric acid, sodium sulfate anhydrous, sodium chloride (Ref. 141659.1211), calcium chloride (Ref. 141221.1211) were from Panreac (Barcelona, Spain). *n*-Dodecane for synthesis was purchased from Merck (Darmstadt, Germany). All solvents used were of HPLC grade from Lab-Scan (Dublin, Ireland).

In Vitro Lipid Digestion

The in vitro lipid digestion model was based on Martin et al. [21]. Since this model was rather preliminary and basic, some improvements were performed in the present study, in order to reach closer physiological results by using the closest physiological conditions. Such modifications included the increase in the ratio enzyme/substrate, bile salts and phospholipids concentrations, the preemulsion of the substrate and the preparation of fresh pancreatic extract [13]. On the other hand, in our former method [21] and in many in vitro models of lipid digestion [13], the pH of the process used to be maintained to that physiological by continuous addition of NaOH to the reaction media. Since we detected non-physiological acyl migration of 2-MAG to 1-MAG in the presence of NaOH (36.7 and 80.0% of total MAG as 2-MAG in presence and absence of NaOH, respectively), the use of alkali was avoided and the ionic strength of the pH 7.5 buffer was increased instead. Under this condition, a physiological ratio 2-MAG to 1-MAG was kept and the pH of the media varied from 7.2 to 6.5, which was within the optimum and physiological range of pancreatic lipase activity [15, 22].

The final conditions of the amended in vitro digestion model will be described briefly. Sample (1 g) was mixed with 0.5 g of bile salts, 0.2 g of lecithin, 5 mM $CaCl_2$, 150 mM NaCl and 54 mL of Trizma-maleate buffer (0.1 M for olive oil and 1 M for TB and D-SCAKG) pH 7.5. The mixture was homogenized (Ultra-Turrax IKA T18) for 20 min at 7,000 rpm. The homogenized mixture was placed in a thermostatically controlled vessel (37°C) under continuous stirring by magnetic stir bar at 1,000 rpm. Simulation of intestinal digestion was started by addition of fresh pancreatin extract (1 g of pancreatin in 6 mL of Trizma-maleate buffer pH 7.5 stirred for 10 min and centrifuged at 1,600×*g* for 15 min). In order to study the evolution of lipid products throughout the hydrolytic process, aliquots (450 mg) were taken at 0, 2, 4, 10, 20, 30 and 60 min of reaction. In vitro digestion of each sample was performed in triplicate.

Separation of Phases After In Vitro Lipid Digestion

The digestion medium was submitted to centrifugation at 4,000 rpm, for 40 min, at 20°C (5810R Eppendorf Iberica, Madrid, Spain) according to Soler-Rivas et al. [23]. After centrifugation, an upper OP, a lower aqueous phase (MP) and a minor precipitated pellet were obtained. Aliquots (450 mg from the aqueous phase or 50 mg from the oily phase) were taken for studying their composition on lipid products.

Lipid Extraction

The total lipids from samples were extracted by 1,450 μL of hexane/methyl-*tert*-butyl ether (50:50, by vol) in polypropylene tubes of 2,000 μL. Furthermore, this medium was acidified by hydrochloric acid (150 mM) in order to stop the enzymatic reaction and to enhance the recovery of butyric acid in the case of TB and D-SCAKG digestions [24]. *n*-Dodecane (10 mg) was added as internal standard for analysis of TB and D-SCAKG lipid products. The mixture was vortexed for 1 min and centrifuged for 10 min at 15,000 rpm. Organic phase containing separated lipids was collected and anhydrous sodium sulfate was added before further analysis. A second lipid extraction

was performed on the remaining aqueous phase in the polypropylene tube in the case of olive oil.

Analysis of Lipid Products

Hydrolysis products of olive oil were determined by high-performance liquid chromatography (HPLC) according to Torres et al. [25] on a Kromasil silica 60 column (250 mm × 4.6 mm, Analisis Vinicos, Tomelloso, Spain) coupled to a CTO 10A VP 2 oven, a LC-10AD VP pump, a gradient module FCV-10AL VP, a DGU-14A degasser, and an evaporative light scattering detector (ELSD-LT) from Shimadzu (IZASA, Spain). The column temperature was maintained at 35°C. 20 µL of the diluted samples (4 mg/mL) were injected. Quantification was based on calibration curves performed with appropriate standards (Sigma-Aldrich Chemie GmbH, Steinheim, Germany).

Hydrolysis products of TB and D-SCAKG were determined according to Torres et al. [26] by gas chromatography (GC) (Hewlett-Packard 5890 series II) with on-column injection using a 7 m 5% phenyl methyl silicone capillary column (Quadrex Corporation, New Haven, CT, USA), 0.25 µm i.d. A deactivated column of 12 cm 530 µm i.d. was used as pre-column. Injector and detector temperature was 43 and 360°C, respectively. The temperature program was as follows: starting at 40°C and then heating to 250°C at 42°C min^{-1} with 10 min hold, followed by heating from 250 to 325°C at 7.5°C min^{-1} with 30 min hold. Helium was used as the carrier gas at a pressure of 5.2 psi. The peaks were computed using GC chemstation software (Agilent Technologies, Santa Clara, CA, USA) and quantified according to the internal standard.

Results

In Vitro Intestinal Digestion of the Standard Lipid

Previous to in vitro digestion of D-SCAKG and TB, we first tested the intestinal digestion model on a standard lipid, in order to be certain that the in vitro model reflected more physiological intestinal lipid digestion, and to reject that any artifact or the own conditions of the digestion method would not interfere with the results obtained for TB and D-SCAKG hydrolysis. Olive oil was chosen as the standard lipid because it is a well-known, simple, natural and abundant oil. As reference of physiological levels of lipid products after in vivo intestinal digestion, we considered the outstanding results reported by Hofmann and Borgstrom [15] in one of the first relevant and complete studies performed on the lipid composition of the intraluminal phase during fat digestion in man.

A huge diversity of in vitro intestinal models of lipid digestion can be found in the scientific literature trying to simulate pseudo-physiological conditions, the complexity of the composition of the media being diverse [13, 14]. In a first attempt, the in vitro lipid digestion of the standard lipid was performed under an in vitro model previously reported by ourselves on fish oils [21]. Since such a model was rather preliminary and basic, some improvements were performed in the present study, in order to reach closer physiological results by using the closest physiological conditions. Such modifications, and the final conditions of the amended in vitro digestion model, were those described in "Material and Methods". The yield in lipid products of the adapted method closely reflected those physiological previously found in the intraluminal phase in man during fat digestion [15] (Fig. 2a, c), so this model was used for simulating lipid digestion of D-SCAKG and TB under pseudo-physiological conditions.

In Vitro Intestinal Digestion of D-SCAKG and TB

The course of in vitro intestinal digestion of D-SCAKG and TB is shown in Fig. 3a, b, respectively. The progress of the in vitro intestinal digestion of the standard lipid has

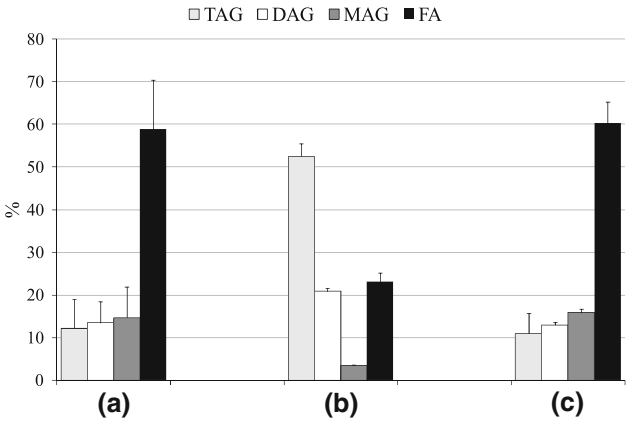

Fig. 2 Lipid products of **a** the in vivo intraluminal phase in man during fat digestion (adapted from Hofmann and Borgstrom [15]) (Mean of lipid products of samples taken from intraluminal content of five men during fat digestion at different collection interval and intestinal site.), **b** the in vitro intestinal digestion of olive oil following the method of Martin et al. [21] without modifications[2] (Mixture of 1 g of sample, 54 mL of 50 mM Trizma-maleate pH 7.5, 5 mM $CaCl_2$, 150 mM NaCl. Addition of fresh pancreatin solution (20 mg in 6 mL of Trizma-maleate buffer, 50 mg lecithin, 250 mg bile salts, stirred for 10 min). Continuous stirring at 37°C and continuous addition of NaOH 1 M to maintain pH at 7.5.) and **c** the in vitro intestinal digestion of olive oil after modification of the method of Martin et al. [21] (Homogenization of 1 g of sample, 54 mL of 100 mM Trizma-maleate pH 7.5, 5 mM $CaCl_2$, 150 mM NaCl, 200 mg lecithin, 500 mg bile salts. Addition of fresh pancreatin solution (1,000 mg in 6 mL of Trizma-maleate buffer, stirred for 10 min and centrifuged at 1,600×g 15 min). Continuous stirring at 37°C)

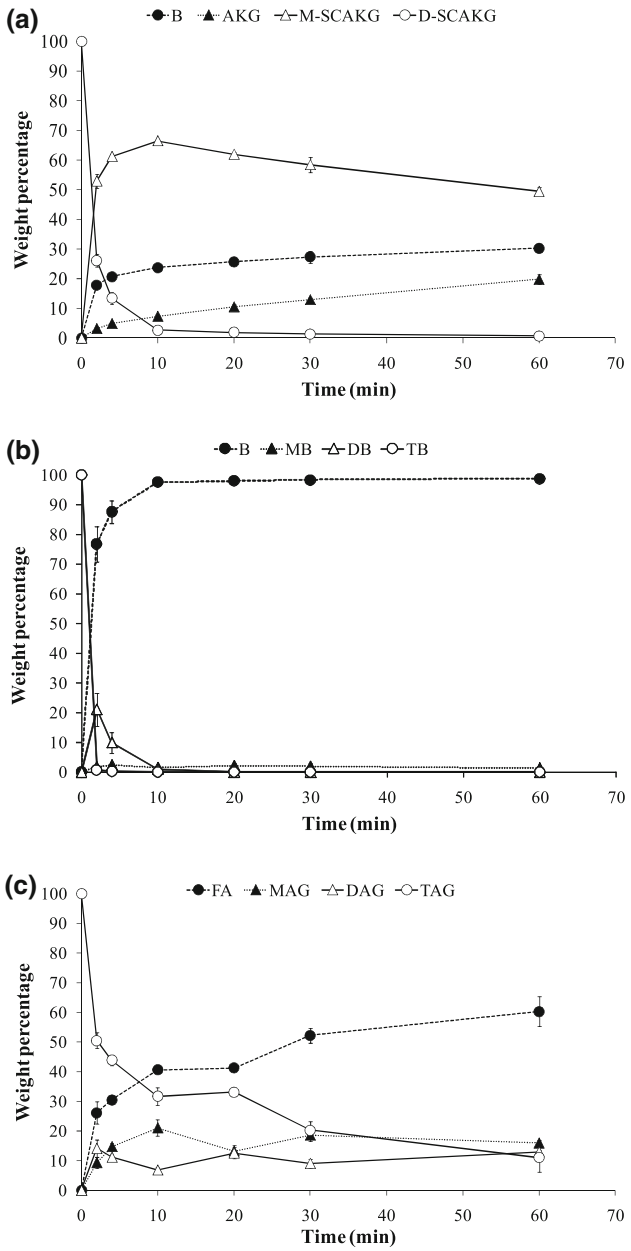

Fig. 3 Evolution of lipid products throughout in vitro intestinal digestion of **a** D-SCAKG, **b** TB and **c** olive oil. *D-SCAKG* 2,3-dibutyroil-1-*O*-octadecyl glycerol; *TB* tributyrin

been also included (Fig. 3c). Pancreatic enzymes effectively recognized the substrate D-SCAKG, but led to diverse differences on the course of hydrolysis respect to TB. The progress of in vitro intestinal digestion of D-SCAKG was slower than that of TB. An almost total hydrolysis of TB was detected just at 2 min of reaction (99.4%), whereas the extent of D-SCAKG hydrolysis was 73.9% at the same moment. After 20 min of in vitro intestinal digestion, the complete hydrolysis of TB and its derived glyceride products, namely dibutyrin (DB) and monobutyrin (MB), was reached, yielding butyric acid as the only final lipid product. In the case of alkylglycerols, the complete hydrolysis of D-SCAKG was also observed, but only after longer times of in vitro digestion (60 min), and yielding 2-butyroil-1-*O*-octadecyl glycerol (M-SCAKG) as the main lipid product, followed by butyric acid and 1-*O*-octadecylglycerol (AKG). Therefore, compared to MB, the released M-SCAKG was quite stable throughout the course of in vitro intestinal digestion, although a low, but progressive decrease after 10 min of reaction was observed. An additional in vitro digestion was performed for D-SCAKG beyond 60 min. After 240 min of in vitro digestion, the level of M-SCAKG was still 39.2%.

Lipid Composition of the Separated Phases After In Vitro Intestinal Digestion of D-SCAKG and TB

The lipid composition of the separated MP and OP after in vitro digestion of the standard lipid is shown in (Fig. 4a). Approximately, 94 and 6% of total lipids distributed in the MP and OP, respectively. The results obtained were in agreement with the lipid composition of the intraluminal phases during in vivo fat digestion in man [15].

The lipid composition of the separated MP and OP after in vitro digestion of D-SCAKG and TB is shown in Fig. 4b and c, respectively. Approximately, 40% of the total lipid products distributed in the MP in the case of the hydrolysis of D-SCAKG. Such MP mainly consisted of butyric acid and minor proportions of M-SCAKG and AKG. The remaining 60% of total lipid products from hydrolyzed D-SACKG distributed in the OP, the M-SCAKG being its major component. Concerning AKG, this lipid product seemed to be distributed in both MP and OP. Similar to D-SCAKG, the total butyric acid from hydrolyzed TB was found in the MP (Fig. 4c). Due to the complete hydrolysis of glycerides species from TB, there was no separation of OP [14].

Discussion

The course of in vitro intestinal digestion of TB observed in the present assay was in agreement with the classic described process of gastrointestinal digestion of short-chain TAG. These kinds of lipids are rapidly and completely hydrolyzed to fatty acids and glycerol by digestive enzymes, such as the *sn*-1,3 specific gastric lipase and pancreatic lipase, whereas long-chain TAG are mainly hydrolyzed by the *sn*-1,3 specific pancreatic lipase to yield 1,2-DAG, which is later on hydrolyzed to fatty acid and 2-MAG [27, 28]. Taking into account the specificity of digestive enzymes to *sn*-1,3 locations, the complete hydrolysis of short-chain TAG has been explained in most

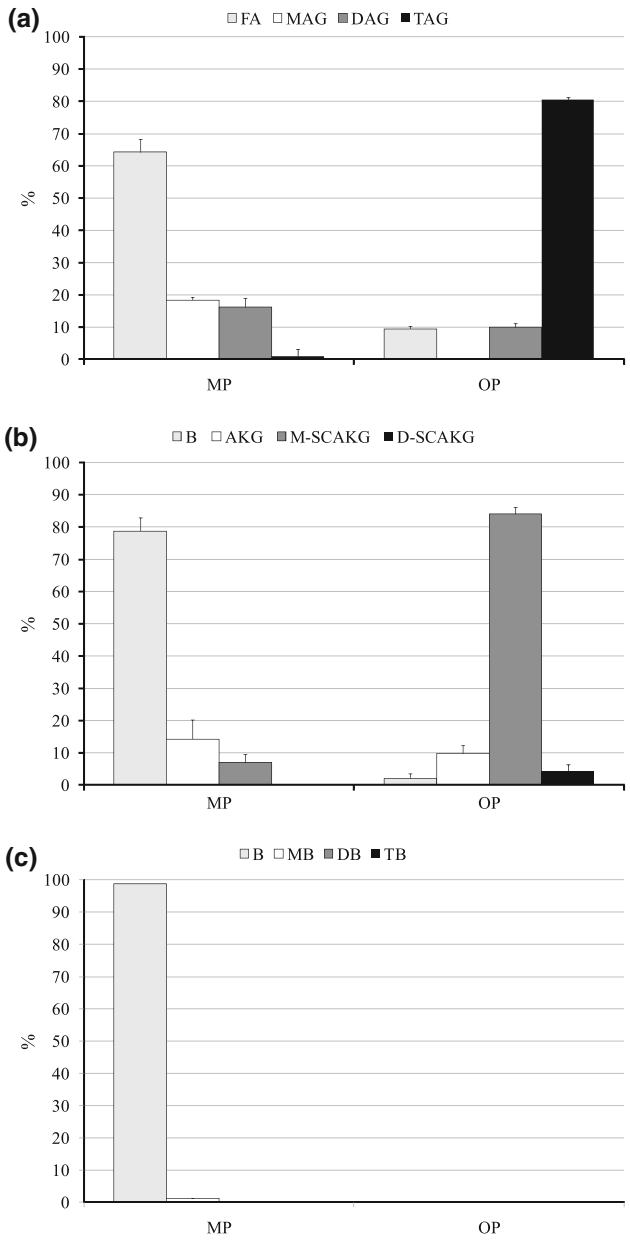

Fig. 4 Lipid composition of the MP and OP after in vitro intestinal digestion of **a** olive oil, **b** D-SCAKG and **c** TB. *D-SCAKG* 2,3-dibutyroil-1-*O*-octadecyl glycerol); *TB* tributyrin

studies by acyl migration phenomena. Thus, the formed 1,2-DAG or 2-MAG rapidly isomerizes to outer positions to give 1,3-DAG or 1-MAG, where the 1,3 specific pancreatic lipase acts, yielding fatty acids and glycerol [29].

Despite the gastric phase of lipid digestion was not being included in the in vitro model, it should be pointed out that the action of gastric lipase, previous to the hydrolysis by pancreatic lipase, might contribute to the overall hydrolysis of short-chain lipids, both TB and D-SCAKG. This is because gastric lipase shows a higher activity on short-chain lipids compared to longer fatty acids [27–29]. Further studies with a more complex in vitro model including simulation of the gastric phase of lipid digestion would contribute to the knowledge of the digestion of these molecules.

In the case of M-SCAKG, the progressive decrease observed after 10 min of in vitro intestinal digestion (Fig. 3a) might suggest that acyl migration of esterified butyric acid from the *sn*-2 to the *sn*-3 location could also take place, but after longer times and at slower rate than MB. Furthermore, the disappearance of M-SCAKG did not begin until the hydrolysis of D-SCAKG was almost complete, whereas the disappearance of MB was simultaneous to the hydrolysis of TB (Fig. 3b). This different course of hydrolysis/acyl migration between M-SCAKG and MB during in vitro intestinal digestion might be due to the own structure of the alkylglycerol backbone, in which the *sn*-1 location is not available due to the etherified octadecyl alcohol, and the *sn*-3 outer position of the M-SCAKG being the only chance of acylmigration for internal butyric acid. The proposed mechanism of acylmigration for explaining the hydrolysis of D-SCAKG is illustrated in Fig. 5, compared to the normal hydrolysis process of TB. Other reasons related to the own etherified alkyl chain, the hydrophobicity of the whole molecule or the steric structure, might influence the interaction of the enzyme with alkylglycerols and explain the different course of reaction respect to TB [30, 31].

Previous information concerning catalyzed-hydrolysis of alkylglycerols by pancreatic lipase is scarce. A lower rate of hydrolysis for long-chain PUFA diesterified alkylglycerols compared to the analogous TAG by pancreatic lipase was reported by Endo et al. [31], in agreement with the results obtained. Similarly, a resistance to pancreatic lipase of diacyl glyceryl ethers isolated form the muscle of the fish *Stromateus stellatus* was found by Sato et al. [32]. On the other hand, the lipase-catalyzed ethanolysis of the same substrates of the present study was previously performed by Vazquez et al. [33]. Despite this, such a trial was carried out in a simple non-aqueous media, unlike the aqueous and more complex media of the present study, these authors reported differences in the course of reactions of D-SCAKG and TB similar to those observed in the present study. Thus, the rate of lipase-catalyzed ethanolysis of D-SCAKG by lipase B from *Candida antarctica* was lower than that of TB, the ethanolysis of TB was more complete, the M-SCAKG was the major product from D-SCAKG and the level of this lipid product kept almost constant during the course of reaction.

Regardless of the specific mechanism of in vitro intestinal digestion of D-SCAKG, the observed differences in the present study between TB and D-SCAKG, in the course of hydrolysis and levels of lipid products, showed interesting implications. One of the problems of the application of butyrate as an antitumor agent is due to the limitation of

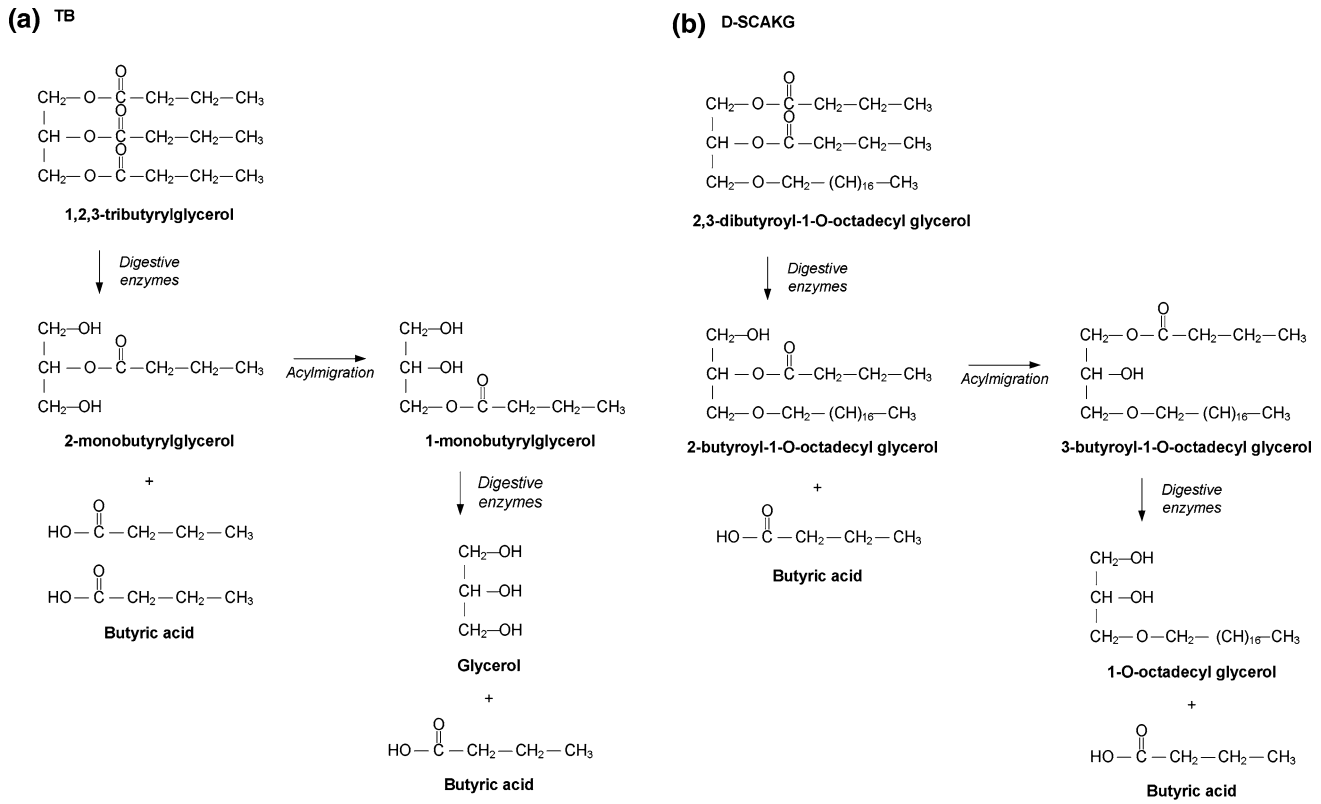

Fig. 5 Hydrolysis and released lipid products of triradylglycerols of butyric acid by digestive enzymes (proposed mechanism in the case of D-SCAKG). *TB* tributyrin; *D-SCAKG* 2,3-dibutyroil-1-*O*-octadecyl glycerol

reaching the enough plasma concentrations required to exert its antiproliferative/differentiating actions [3, 6]. This is because the normal metabolism of short-chain fatty acids inside enterocytes after absorption is the local use as a fuel for the enterocytes or their transport to the liver by the portal bloodstream, whereas only trace amounts enter the general blood circulation and they are rapidly oxidized in peripheral tissues where they arrive there [28, 34]. Diverse studies have successfully evidenced higher levels of butyrate in peripheral tissues after administration in the form of TB [35, 36], but the problem of the extremely short half-life of butyrate in plasma remained [28]. Efficient prodrugs of butyrate should have a sufficiently stable bond between the carrier and the drug molecule to increase its in vivo half-life [1]. The experimental D-SCAKG assayed in the present study showed such behavior during in vitro lipase-catalyzed hydrolysis, since most butyric acid remained esterified in the *sn*-2 location throughout digestion as M-SCAKG, unlike the analogous MB.

On the other hand, alkylglycerols are of interest by themselves due to their own functional properties [9–11]. Therefore, in addition to TB, the structured lipid in the form of D-SCAKG would have the double advantage of alkylglycerols as a potential lipid vehicle for butyrate and the bioactivity of each individual compound, alkylglycerol and butyrate, within the same molecule. Furthermore, the released AKG after in vitro intestinal digestion of D-SCAKG would be another option to take advantage of the bioactivity of alkylglycerols, this product being minor at initial times of digestion (3.2% at 2 min) but progressively increasing up to 19.8% at 60 min or 33.0% at 240 min of enzyme-catalyzed intestinal digestion.

Therefore, the present study showed that, after in vitro intestinal digestion of D-SCAKG, diverse potential bioactive products might be obtained, namely butyric acid, esterified butyric acid, mono-esterified alkylglycerol and non-esterified alkylglycerol, the proportion of each product being different at short-term or long-term times of digestion. Despite the interest in these molecules beyond the intestinal tract, it should be pointed out that, some of these breakdown metabolites might be of interest within the intestinal tract. Most of them might contribute to the intraluminal level of butyrate, with the importance of its implication as one of the main metabolic fuels for colonocytes, and interfere with the control of colonic inflammation or the pathogenesis of colorectal cancer [27, 28]. On the other hand, esterified butyrate with AKG, or the simultaneous presence of both lipid products as individual metabolites, might be evaluated on the bioactivity of these molecules within the intestinal tract.

Concerning the distribution of lipids products in the different phases of the digestion medium, the findings of the present study showed that the major hydrolysis product, namely M-SCAKG, was mainly distributed in the OP (Fig. 4b). This result might be partially explained by the poor solubility of this molecule in the micellar structures, related to the etherified octadecyl alcohol of the alkylglycerol moiety. It has been found that long-chain saturated fatty acids, either free or esterified, are poorly absorbed, because these fatty acids and their MAG are poorly solubilized in mixed micelles, and show a strong tendency to form insoluble calcium soaps at the alkaline pH of intestine [17, 37, 38]. Nevertheless, it has been shown that the absorption of insolubilized lipids might be increased when fed together with unsaturated fatty acids. This is because the inclusion in MP seems to be enhanced when micelles are expanded by the incorporation of MAG and fatty acids of unsaturated nature [13, 38]. This premise might be also considered for alkylglycerols. Thus, it could be hypothesized that the co-administration of D-SCAKG and unsaturated fats might enhance the incorporation of released M-SCAKG into micelles. In fact, this might be the likely situation in a real meal in which fats of diverse nature and saturation degree use to be ingested together. To the best of our knowledge, information concerning the distribution of alkylglycerides, both free and esterified, within the intraluminal phases during intestinal digestion has not been previously reported. In fact, the general information of the process of intestinal absorption of alkylglycerides is scarce. Nevertheless, there is evidence that 1-*O*-alkyl-*sn*-glycerols derived from dietary ether glycerolipids are completely absorbed by the intestine [20]. However, the exact mechanism of absorption is unknown. As example of effective absorption of alkylglycerols in rodents and human, Das et al. [20] showed that alkylglycerols liberated from dietary ether lipids in the lumen are readily absorbed without cleavage of the ether bond, transported to the liver and other organs, where they were directly utilized to synthesize membrane alkylglycerolipids and plasmalogens.

Concerning AKG, this lipid product seemed to be distributed in both MP and OP, regardless of the presence of octadecyl alcohol (Fig. 4b). The lack of esterified butyric acid might lead to a higher polarity of this molecule with respect to M-SCAKG, in which both esterified butyric acid and etherified octadecyl alcohol might contribute to the lower polarity of the whole molecule.

In conclusion, the present study showed that the structured lipid 2,3-dibutyroil-1-*O*-octadecyl glycerol might be proposed as a potential vehicle of butyrate, since it produced a stable esterified form of butyric acid as 2-butyroil-1-*O*-octadecyl glycerol after simulation of intestinal lipid digestion. In contrast, the analogous TB, was completely hydrolyzed to butyric acid. Furthermore, structured alkylglycerols would have additional properties, since they might integrate two bioactive compounds, alkylglycerol and butyrate, within the same molecule. Their own alkylglycerol backbone would be a third bioactive lipid product released after hydrolysis catalyzed by pancreatic enzymes.

Further in vivo studies concerning the potential of structured alkylglycerol as a pro-drug of butyrate are worthwhile, in order to elucidate whether these compounds, especially 2-butyroil-1-*O*-octadecyl glycerol, would be effectively absorbed, reach the plasma at high enough bioactive concentrations, would show an adequate half-life or if interactions on bioactivity between alkylglycerol and butyric acid exist. Specially, the bioaccessibility of lipid products containing the alkylglycerol moiety should be studied in depth, since the present research showed a limitation of their inclusion within the bioaccessible micellar structures. Whether this finding was a result of the sole presence of alkylglycerol in the digestion medium, and if the co-administration with fat of a different saturation degree would improve the bioaccessibility of lipid products, needs to be examined.

Acknowledgments The work was supported by the Ministerio de Ciencia e Innovacion, Spain (AGL2006-02031/ALI and AGL2008-05655) and the Community of Madrid, Spain (ALIBIRD-CM S-2009/AGR-1469). Diana Martin thanks the Ministerio de Ciencia e Innovacion and Fondo Social Europeo for funding her postdoctoral "Juan de la Cierva" contract.

References

1. Coradini D, Pellizzaro C, Miglierini G, Daidone M (1999) Hyaluronic acid as drug delivery for sodium butyrate: improvement of the anti-proliferative activity on a breast-cancer cell line. Int J Cancer 81:411–416
2. Avivi-Green C, Polak-Charcon S, Madar Z, Schwartz B (2000) Apoptosis cascade proteins are regulated in vivo by high intracolonic butyrate concentration: correlation with colon cancer inhibition. Oncol Res 12:83–95
3. Kuroiwa-Trzmielina J, de Conti A, Scolastici C, Pereira D (2009) Chemoprevention of rat hepatocarcinogenesis with histone deacetylase inhibitors: efficacy of tributyrin, a butyric acid prodrug. Int J Cancer 124:2520–2527
4. Kuefer R, Hofer M, Altug V, Zorn C (2004) Sodium butyrate and tributyrin induce in vivo growth inhibition and apoptosis in human prostate cancer. Br J Cancer 90:535–541
5. Ooi CC, Good NM, Williams DB, Lewanowitsch T, Cosgrove LJ, Lockett TJ, Head RJ (2010) Efficacy of butyrate analogues in HT-29 cancer cells. Clin Exper Pharm Physiol 37:482–489
6. Li Y, Le Maux S, Xiao H, McClements D (2009) Emulsion-based delivery systems for tributyrin, a potential colon cancer preventive agent. J Agric Food Chem 57:9243–9249
7. Clarke JM, Bird AR, Topping D, Young GP, Cobiac L (2006) Effect of resistant starch, butyrylated starch and tributyrin on colon cancer in rats. J Gastr Hepatol 21:A270–A270
8. Torres C, Vazquez L, Señorans F, Reglero G (2009) Enzymatic synthesis of short-chain diacylated alkylglycerols: a kinetic study. Process Biochem 44:1025–1031

9. Pedrono F, Saiag B, Moulinoux JP, Legrand AB (2007) 1-*O*-alkylglycerols reduce the stimulating effects of bFGF on endothelial cell proliferation in vitro. Cancer Lett 251:317–322
10. McIntyre T, Snyder F, Marathe G (2008) Ether-linked lipids and their bioactive species. In: Vance D, Vance J (eds) Biochemistry of lipids, lipoproteins and membranes. Elsevier, Oxford
11. Farooqui A, Farooqui T, Horrocks L (2008) Metabolism and function of bioactive ether lipids in the brain, Springer
12. Bams-Mengerink AM, Brites P, Vyth A, Duran M, Wanders RJA, Heymans HSA, Poll-The BT (2008) Butyl alcohol as a therapeutic option in rhizomelic chondrodysplasia punctata. J Inherited Met Dis 31:68-68
13. Porter C, Charman W (2001) In vitro assessment of oral lipid based formulations. Adv Drug Deliv Rev 50:s127–s147
14. Dahan A, Hoffman A (2008) Rationalizing the selection of oral lipid based drug delivery systems by an in vitro dynamic lipolysis model for improved oral bioavailability of poorly water soluble drugs. J Contr Release 129:1–10
15. Hofmann A, Borgstrom B (1964) The intraluminal phase of fat digestion in man: the lipid content of the micellar and oil phases of intestinal content obtained during fat digestion and absorption. J Clin Inv 43:247–257
16. Fatouros D, Bergenstahl B, Mullertz A (2007) Morphological observations on a lipid-based drug delivery system during in vitro digestion. Eur J Pharm Sci 31:85–94
17. Ramirez M, Amate L, Gil A (2001) Absorption and distribution of dietary fatty acids from different sources. Early Hum Develop 65:s95–s101
18. Fernandez-Garcia E, Carvajal-Lerida I, Perez-Galvez A (2009) In vitro bioaccessibility assessment as a prediction tool of nutritional efficiency. Nutr Res 29:751–760
19. Christensen M, Hoy C, Becker C, Redgrave T (1995) Intestinal absorption and lymphatic transport of eicosapentaenoic (EPA), docosahexaenoic (DHA) and decanoic acid: dependence on intramolecular triacylglycerol structure. Am J Clin Nutr 61:56–61
20. Das A, Holmes R, Wilson G, Hajra A (1992) Dietary ether lipid incorporation into tissue plasmalogens of humans and rodents. Lipids 27:401–405
21. Martin D, Nieto-Fuentes JA, Señorans FJ, Reglero G, Soler-Rivas C (2010) In vitro digestion of fish oils and ω3-concentrates as triacylglycerols and ethyl esters. Eur J Lipid Sci Technol 112:1315–1322
22. Zangenberg N, Mullertz A, Kristensen H, Hovgaard L (2001) A dynamic in vitro lipolysis model I controlling the rate of lipolysis by continuos addition of calcium. Eur J Pharm Sci 14:115–122
23. Soler-Rivas C, Marin F, Santoyo S, Garcia-Risco M, Señorans F, Reglero G (2010) Testing and enhancing the in vitro bioaccessibility and bioavailability of *Rosmarinus officinalis* extracts with a high level of antioxidant abietanes. J Agric Food Chem 58:1144–1152
24. Sek L, Porter C, Charman W (2001) Characterisation and quantification of medium chain and long chain triglycerides and their in vitro digestion products, by HPTLC coupled with in situ densitometric analysis. J Pharm Biomed Anal 25:651–661
25. Torres C, Vazquez L, Señorans F, Reglero G (2005) Study of the analysis of alkoxyglycerols and other non-polar lipids by liquid chromatography coupled with evaporative light scattering detector. J Chromatogr A 1078:28–34
26. Torres C, Tenllado D, Señorans F, Reglero G (2009) A versatile GC method for the analysis of alkylglycerols and other neutral lipid classes. Chromatographia 69:729–734
27. Takeuchi H, Sekine S, Kojima K, Aoyama T (2008) The application of medium-chain fatty acids: edible oil with a suppressing effect on body fat accumulation. Asia Pac J Clin Nutr 17:320–323
28. Wachtershauser A, Stein J (2000) Rationale for the luminal provision of butyrate in intestinal diseases. Eur J Nutr 39:164–171
29. Howard J, Jackson M, Smyth D (1970) Intracellular hydrolysis of short chain glycerides by rat small intestine in vitro and transfer of glycerol. J Physiol 208:461–471
30. Tsuzuki W, Ue A, Nagao A, Akasaka K (2002) Fluorometric analysis of lipase hydrolysis of intermediate- and long-chain glycerides. Analyst 127:127
31. Endo Y, Chiba T, Fujimoto K (1996) Oxidative and hydrolytic stability of synthetic diacyl glyceryl ether. Biosci Biotechnol Biochem 60:216–219
32. Sato T, Seo H, Endo Y, Fujimoto K (2002) Diacyl glyceryl ether as the major muscle lipid in *Stromateus stellatus* and its hydrolyzability by lipase and oral acute toxicity on mice. Nippon Suisan Gakkaishi 68:569–575
33. Vazquez L, Fernandez O, Blanco R, Señorans F, Reglero G, Torres C (2010) A kinetic study of the lipase-catalyzed ethanolysis of two short-chain triradylglycerols: alkylglycerols vs. triacylglycerols. J Mol Catal B Enzym 64:101–106
34. Mu H, Hoy C (2004) The digestion of dietary triacylglycerols. Prog Lipid Res 43:105–133
35. Conley B, Egorin M, Tait N, Rosen M, Sausville E, Dover G (1998) Phase I study of the orally administered butyrate prodrug, tributyrin, in patients with solid tumors. Clin Cancer Res 4:629–634
36. Newmark H, Lupton J, Young C (1994) Butyrate as a differentiating agent pharmacokinetics, analogues and current status. Cancer Lett 78:1–5
37. Renner R, Hill F (1961) Factors affecting the absorbability of saturated fatty acids in the chick. J Nutr 74:254–258
38. Dawson A (1971) The absorption of fat. J Clin Path 24:77–84

Lipids (2011) 46:287–295
DOI 10.1007/s11745-010-3495-z

ORIGINAL ARTICLE

Selectively Hydrogenated Soybean Oil Exerts Strong Anti-Prostate Cancer Activities

Mun Yhung Jung · Nak Jin Choi · Chan Ho Oh · Hyun Kyung Shin · Suk Hoo Yoon

Received: 2 May 2010 / Accepted: 19 October 2010 / Published online: 13 November 2010

Abstract Prostate cancer is the second leading cause of male deaths due to cancer in the United States. Hydrogenated vegetable oils have been suspected of inducing adverse health effects, including atherosclerosis and cancer. Here we report that a selectively hydrogenated soybean oil (SHSO) containing a high quantity of conjugated linoleic acids showed remarkably strong anticarcinogenic activity against prostate cancer in the rat model (Copenhagen rats with MAT-LyLu syngeneic rat prostate cancer cells) study in vivo and human prostate carcinoma cell lines studies in vitro, as compared with native soybean oil. A 5% dietary supplementation with SHSO inhibited the growth of prostate cancer by 80% in vivo. The TUNEL method and immunohistochemical staining assays of bax, bcl-2, and survivin clearly showed that SHSO induced prostate cancer cell apoptosis in the tested rats. DNA fragmentation analysis in vitro further confirmed the apoptotic activity of SHSO on the MAT-LyLu prostate cancer cells. The SHSO also showed strong cytotoxicity on human prostate cancer cells (DU145 and PC3). This represents the first report demonstrating the significant anticancer activities of hydrogenated vegetable oils at low levels of dietary supplementation.

M. Y. Jung · C. H. Oh
College of Food Science, Woosuk University, Samyre-Eup, Jeollabuk-Do, Republic of Korea

N. J. Choi · H. K. Shin
Division of Life Science and Silver Biotechnology, Hallym University, Chuncheon, Kangwon-Do, Republic of Korea

S. H. Yoon (✉)
Division of Innovative Technology Research, Korea Food Research Institute, Seongnam-Si, Kyunggi-Do, Republic of Korea
e-mail: shyoon@kfri.re.kr

Keywords Hydrogenated soybean oil · Anticancer activity · Prostate cancer · Apoptosis · Conjugated linoleic acids

Abbreviations

CLA	Conjugated linoleic acids
SHSO	Selectively hydrogenated soybean oil
FAME	Fatty acid methyl esters
TUNEL	Terminal deoxynucleotidyl transferase dUTP nick end labeling
MTT assay	Method of transcriptional and translational assay

Introduction

Prostate cancer is the second leading cause of male deaths due to cancer in the United States. Each year roughly 230,000 men are diagnosed with prostate cancer in the United States, with more than 30,000 deaths occurring [1]. Various environmental factors appear to influence the development and progression of prostate cancer. It has been generally accepted that the dietary amount of fat is the strongest environmental factor.

Hydrogenated vegetable oils are widely consumed worldwide in foods such as salad and cooking oils, margarines, shortenings and confectionery fats. The health effects of hydrogenated vegetable oils have been studied extensively [2, 3], with the previous studies showing their adverse effects on health such as hypercholesterolemia, atherogenesis and coronary heart disease. The hydrogenated vegetable oils have been also suspected to be related with cancer development [4–6]. Their reputations

for negative effects on health are mainly attributable to their high contents of *trans*-fatty acids and saturated fatty acids. The fatty acid composition of hydrogenated vegetable oils can be manipulated by controlling the hydrogenation conditions. We originally reported that an exceptionally high level of conjugated linoleic acids (CLA), which are beneficial functional compounds, can be formed during commercially selective hydrogenation of soybean oil, and that the quantity of CLA (98–230 mg/g oil) in the selectively hydrogenated soybean oil (SHSO) was the highest ever reported in foods [7–9]. CLA have been recognized for their ability to inhibit carcinogenesis in multiple systems at several levels, including initiation [10–13], promotion [14, 15], and progression [16] and metastasis [17, 18]. Other physiological benefits of CLA include a reduction in the severity of atherosclerosis [19, 20], improvement in glucose tolerance [21, 22], and reduction in body fat [22–26]. The major dietary source of CLA was ruminant animal meats and dairy product, which contain small quantities of CLA (4–7 mg/g oil) [9, 27]. Thus, normal food lipids containing CLA have not been used in tumorigenesis studies because their low concentration of CLA have prevented them from being added directly to experimental diets. The CLA used in the previous researches were obtained by the alkali-induced isomerization of linoleic acid. This isomerization induces almost exclusively two isomers (*cis*-9 *trans*-11- and *trans*-10 *cis*-12-) along with small portions of other minor isomers [28]. Most studies have focused on the functionalities of these two isomers. The composition of CLA isomers in SHSO differs greatly from that produced by alkali isomerization. Twenty-one different CLA isomers in a triacylglycerol form were found in SHSO, as determined by a combination of silver ion-impregnated HPLC and a GC-ion impacted mass spectrometry of DMOX derivatives of the CLA isomers [9, 31]. The individual CLA isomers reportedly have different activity on their biological functionalities [22, 24, 25, 29, 30]. Currently, the activities of most of the CLA isomers present in SHSO are not clearly defined. Moreover, although it has been reported that SHSO contains a high level of CLA, its anticancer activities has not been studied previously.

The objective of this research was to find out whether SHSO containing a large quantity of CLA exerts anticancer effects against prostate cancer in an animal model in vivo and in human prostate carcinoma cell lines in vitro, as compared with native soybean oil, which is the most consumed vegetable oil worldwide. The apoptotic activities of SHSO were also studied by TUNEL analysis, immunohistochemical analysis of bax, blc-2, and survivin, and DNA fragmentation analysis.

Materials and Methods

Materials

Six-week-old Copenhagen rats (body weight about 200 g) were obtained from Harlan Sprague–Dawley (Indianapolis, IN). A rat prostate cancer cell line of MAT-LyLu was purchased from the European Collection of Cell Cultures (ECACC). Human prostate carcinoma cell lines of PC-3 and DU145 were purchased from the Korean Cell Line Bank (Seoul, Korea). The antibodies of anti-bax and anti-blc-2 antibodies were obtained from Santa Cruz Biotechnology (Santa Cruz, CA), and anti-survivin antibodies were purchased from Alpha Diagnostic International Inc. (San Antonio, TX). Soybean oil was obtained from a local edible oil refinery (Heinz Korea, Incheon, Korea).

SHSO with High CLA

Hydrogenation was performed in a 1-L capacity hydrogenator equipped with temperature, pressure and stirring-rate controller to obtain the SHSO with a large quantity of CLA [8, 9]. Six hundred and fifty gram of soybean oil was hydrogenated for 40 min with a commercially available selective Ni catalyst (0.5%, nickel, based on the oil mass) under the condition of a reactor temperature of 230 °C, a hydrogen pressure of 0.5 kg/cm^2, and a 300-rpm stirring rate.

Fatty Acid Methyl Esterification

The fatty acids in the triacyl moiety of the SHSO were methylesterified with a 1.0 mL of 0.25 N sodium methoxide in methanol at 55 °C for 30 min [9]. The fatty acid methyl esters (FAME) were extracted from the reacted samples with 2,2,4-trimethyl pentane.

Gas Chromatography

For the separation and quantification of individual fatty acids and CLA, 2–6 μL FAME sample was injected into a gas chromatograph equipped with a flame ionization detector [9]. The column used was a highly polar fused silica capillary column (cyanopropyl siloxane phase, SP2380 100 m × 0.25 mm, 0.25 μm thickness, Supelco Inc., Bellefonte, PA). A 100:1 split injection was used for sample injection. Helium was used as carrier gas with a head pressure of 300 kPa. Temperature of the injector and detector were 230 and 250 °C, respectively. The initial oven temperature was 170 °C, which was held for 1 min and then increased at 0.8 °C/min to 200 °C.

Silver Ion-Impregnated High Performance Liquid Chromatography

Silver ion-high performance liquid chromatographic analysis of CLA was carried out with an HPLC (Shimazu, Tokyo, Japan) equipped with a 20 μL injection loop (Waters) and UV detector operated at 233 mm. Three analytical silver-impregnated columns (ChromSpher 5 Lipid, 250 mm × 4.6 mm i.d., 5 μm, Chrompak, Bridgewater, NJ) were used in series [9, 31, 32]. The mobile phase was 0.1% acetonitrile in hexane, operated isocratically at a flow rate of 1.0 mL/min.

In Vivo Anticancer Activity

The effects of the SHSO on prostate cancer growth were studied using the well-known model of male Copenhagen rats with syngeneic rat prostate cancer cells (MAT-LyLu). All animal experiments were carried out in Hallym University (Chuncheon-Si, Gangwon-Do, Korea) after the approval of Institutional Animal Care and Use Committee (IACUC) of Hallym University (IUCUC Approval Number, Hallym-1-60, 28 October, 2008). The 6-week-old rats were fed ad libitum with AIN-76A diet and water for 1 week before the experiments. The experiments were done in wire-bottomed cages in a temperature- (20–25 °C) and humidity-(60–70%) controlled room with a 12:12-h light:dark cycle. The 7-weeks-old rats were divided into four groups ($n = 10$ per group) by a randomized complete block design, and were fed isocaloric AIN-76A diets for 3 weeks with the following fat composition: 5% soybean oil (0% SHSO diet group), 1.5% SHSO + 3.5% soybean oil (1.5% SHSO diet group), 3% SHSO + 2% soybean oil (3% SHSO diet group) and 5% SHSO (5% SHSO diet group). On day 8 of the feeding program, 2×10^5 MAT-LyLu prostate cancer cells were injected subcutaneously into the right flank on each animal. After being fed the experimental diets for an additional 2 weeks, the rats were killed by cervical dislocation under general anesthesia with diethyl ether in the presence of a veterinarian. Tumors were excised and weighed, and tissue specimens from tumors were fixed in 10% buffered formalin and embedded in paraffin.

Immunohistochemistry for bcl-2, bax and Survivin Protein Expressions

The expression of bcl-2, bax, and survivin protein expressions were evaluated using an immunohistochemical staining assay. Paraffin-embedded thin sections (4 μm thickness) were mounted on slides, deparaffinized, rehydrated and washed with TBS-T. The intrinsic peroxidase activity was inhibited by 0.3% H_2O_2 for 20 min, and nonspecific binding was blocked with normal goat serum (1:5, DAKO kit, Dako co. Ltd, Kyoto, Japan) for 1 h. Primary antibodies were diluted 1:50 and incubated with the sections overnight at 4 °C. The primary antibodies used were anti-bax, anti-bcl-2, and anti-survivin. A secondary antibody, biotinylated link antibody (Dako Co. Ltd, Kyoto, Japan), was incubated with the sections for 20 min, and the sections were treated with streptavidin peroxidase for 15 min, and then stained with DAB. The sections were counterstained with Meyer's hematoxylin, and then washed with distilled water.

TUNEL Method

TUNEL staining was done with an in-situ apoptosis kit (Takara Shuzo Co., Kyoto, Japan), according to the manufacturer's instruction. The apoptosis index was determining by counting the percentage of TUNEL-positive cells in the total cell counts.

In Vitro Cell Proliferation

SHSO was dissolved in ethanol, and the solution was added into the DME media. Cancer cell lines were cultured for 48 h at 37 °C in CO_2 incubator. The proliferations of the cells were assayed by MTT [33] and trypan blue dye exclusion methods [34]. Apoptosis of cell line was determined by DNA fragmentation.

Statistical Analysis

Duncan's multiple range tests and paired *t* test were used to assess the statistical significance between the treated groups, using the SAS System [35].

Results

CLA Composition in SHSO

Native soybean oil did not contained detectable amounts of CLA. The manufactured SHSO contained CLA at 210.6 mg/g oil in its triacylglycerol moiety as measured by gas chromatography, which is about 40 times higher than the contents in dairy products and ruminant meats [8, 27]. Native soybean oil contained 11.33% palmitic acid, 4.29% stearic acid, 22.19% oleic acid, 1.33% *cis*-C18:1, 52.99% linoleic acid, 0% CLA, 0.63% unconjugated $C_{18:2}$, 6.17% linolenic acid, 0.37% arachidonic acid, and 0.70% behenic acid. The fatty acid composition of the SHSO was 11.53% palmitic acid, 6.18% stearic acid, 20.28% oleic acid, 5.56% *trans* $C_{18:1}$, 2.39% *cis* $C_{18:1}$, 20.70% linoleic acid, 22.97% CLA, 7.48% unconjugated $C_{18:2}$, 1.07% linolenic acid, 0.65% linolenic acid isomers, 0.42% arachidic acid, and 0.77%

behenic acid, as determined by gas chromatography. The individual isomers were identified by silver-ion impregnated HPLC and confirmed by ion-impacted mass spectroscopy of their DMOX derivatives (Table 1). The relative composition of individual CLA isomers in SHSO was as follow: 13t,15t (2.65%), 12t,14t (3.36%), 11t,13t (6.40%), 10t,12t (11.83%), 9t,11t (12.09%), 8t,10t (6.39%), 7t,9t (2.75%), 12t,14c (1.54%), 12c,14t (1.11%), 11t,13c (1.97%), 11c,13t (4.23%), 10t,12c; 10c,12t (14.33%), 9c,11t; 9t,11c (17.58%), 8t,10c; 9c,10t (4.91%), 7t,9c; 7c,9t (0.93%), 11c,13c (1.31%), 10c,12c (2.73%), 9c,11c (2.77%), and 8c,10c (1.10%).

In Vivo Inhibition of Prostate Cancer Growth

Figure 1a shows that the dietary SHSO supplements greatly inhibited the prostate cancer growth in vivo. The quantitative effects of dietary SHSO supplements on the growth of prostate cancer in the rats are shown in Fig. 1b. The SHSO supplements inhibited the prostate cancer growth in a dose-dependent manner: the tumor weights in the groups supplemented with the 0, 1.5, 3, and 5% SHSO were 8.07 ± 0.99, 7.91 ± 2.53, 5.05 ± 1.64, and 1.60 ± 0.29 g, respectively. No overt toxic symptoms were observed in these groups during the experiments. The effects of dietary SHSO on growth performance of rats inoculated with Mat-LyLu cancer cells are given in Table 2. The food intake of rats in the 0, 1.5, 3 and 5% SHSO dietary groups during the feeding experiment were

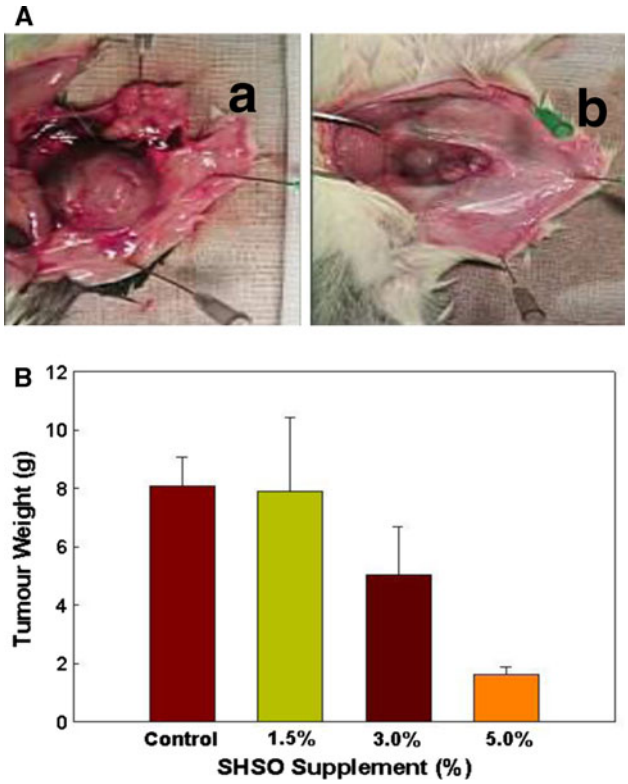

Fig. 1 Anticarcinogenic activity of selectively hydrogenated soybean oil (SHSO) in vivo rat model study. **a** Prostate cancer growth in rats treated with control diet (*a*) and 5% dietary SHSO (*b*), **b** Mean prostate tumor weight in rats treated with control diet, 1.5, 3, and 5% SHSO

Table 1 CLA composition in SHSO as determined by silver-ion impregnated HPLC

CLA isomers	Proportion (%)
13t,15t	2.65
12t,14t	3.36
11t,13t	6.40
10t,12t	11.83
9t,11t	12.09
8t,10t	6.39
7t,9t	2.75
12t,14c	1.54
12c,14t	1.11
11t,13c	1.97
11c,13t	4.23
10t,12c; 10c,12t	14.33
9c,11t; 9t,11c	17.58
8c,10t; 8t,10c	4.91
7c,9t; 7t,9c	0.93
11c,13c	1.31
10c,12c	2.73
9c,11c	2.77
8c,10c	1.10

17.43 ± 0.07, 16.66 ± 0.55, 16.79 ± 0.54, and 17.36 ± 0.54 g, respectively. The mean body weight gains in the 0, 1.5, 3, and 5% SHSO groups were 25.86 ± 1.64, 19.37 ± 3.16, 21.49 ± 2.29, and 16.85 ± 1.38 g, respectively.

Immunohistochemistry

To assess the modulation of the expression of proapoptotic and antiapoptotic proteins by SHSO, we performed immunohistochemical staining assays with tumor tissues obtained from control and SHSO treated groups (Fig. 2 and Table 3). Figure 2 shows the pictures of immunohistochemical staining for bax, blc-2 and survivin proteins with samples from control (a) and 5% SHSO groups (b). The SHSO treated groups showed greatly higher expression of bax (proapoptotic protein) than control. The increased amount of the SHSO treatment, the higher the expressions of bax were observed (Table 3). SHSO treated groups showed greatly lower expressions of bcl-2 and survivin (antiapoptotic protein) (Fig. 2). The down regulation activities of SHSO on the expressions of bcl-2 and survivin were dose-dependent (Table 3).

Table 2 Effects of SHSO on growth performance of rats inoculated with Mat-LyLu cancer cells

	Treatments			
	Control	1.5% SHSO	3% SHSO	5% SHSO
Initial body weight (g)	209.74 ± 4.49	207.66 ± 4.77	207.54 ± 3.09	207.66 ± 3.86
Final body weight (g)	235.60 ± 5.97	227.03 ± 3.07	229.03 ± 4.78	222.51 ± 4.59
Group intake (g)	58.09 ± 5.19	57.42 ± 1.59	61.55 ± 5.69	63.65 ± 1.15
Individual intake (g)	17.43 ± 0.07^{a}	15.66 ± 0.55^{b}	16.79 ± 0.54^{ab}	17.36 ± 0.54^{a}
Body gain (g)	25.86 ± 1.64^{a}	19.37 ± 3.16^{ab}	21.49 ± 2.29^{ab}	16.86 ± 1.38^{b}

Values are means ± SD

Values with different superscripts within a row are significantly different from each other at $p < 0.05$ by Duncan's multiple range ANOVA test

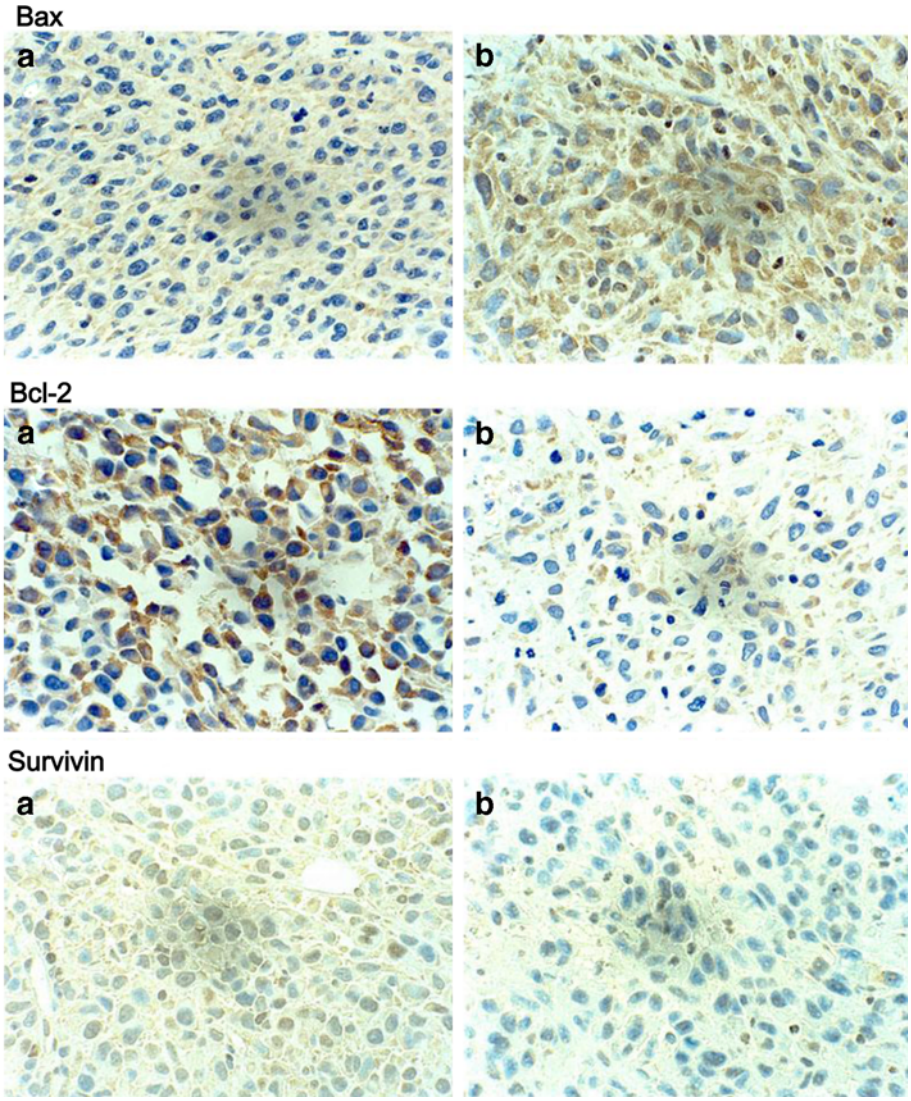

Fig. 2 Immunohistochemical staining of bax, bcl-2, and surviving obtained from tissues in prostate cancer from Copenhagen rats treated with different level of SHSO administrations: **a** tissues from control group, **b** tissues from 5% SHSO group

TUNEL Assay

Figure 3 shows the in situ TUNEL staining of tumor tissues obtained from the 0, 1, 3 and 5% SHSO groups. The results clearly show that the amount of apoptosis induced increased with SHSO, which is consistent with the result from the immunohistochemical staining assay. The apoptotic index was calculated by counting the percentage of apoptotic cell in total cell counts (Table 4). The apoptosis indexes of the 0% SHSO (control), 1.5% SHSO, 3.0%

Table 3 Intensity of immunohistochemical staining of Bax, Bcl-2, and Survivin (staining intensity)

Treatments	*n*	Bax	Bcl-2	Survivin
Control	5	−	+++	+++
1.5% SHSO	5	+	++	++
3.0% SHSO	5	++	+	+
5.0% SHSO	5	+++	−	−

− Not or rare expression, + Low expression, ++ Middle expression, +++ high expression

Table 4 Apoptotic index obtained from TUNEL assay from prostate cancer in rats

Diets	Number of samples	Apoptotic index[a,b] Mean ± SD (%)
Control diet	5	2.60 ± 1.19[a]
SHSO 1.5% diet	5	5.09 ± 0.39[b]
SHSO 3% diet	4	10.00 ± 0.90[c]
SHSO 5% diet	5	14.54 ± 1.16[d]

[a] Apoptotic index : (number of TUNEL-positive cell/number of total cell) × 100

[b] Values of different subscripts are significantly different at $p < 0.0001$ by Duncan's multiple range test

SHSO, and 5.0 SHSO groups were 2.60 ± 0.19, 5.09 ± 0.39, 10.0 ± 0.9 and 14.54 ± 1.16%, respectively. The results suggested that the in vivo anticancer activity of SHSO in the Copenhagen rat model with transgenic prostate cancer cell could be explained, at least in part, by the induction of apoptosis of the MAT-LyLu.

In Vitro Assays for Antiproliferation and Apoptosis in the MAT-LyLu Prostate Cancer Cell Line

To confirm the apoptotic activity of SHSO, we studied its antiproliferation and DNA fragmentation analysis of SHSO on the prostate cancer cell line. We incubated the prostate cancer cells (Mat-LyLu) with 300 μg/mL (equivalent to CLA TG 82 μM) of SHSO for 48 h to check the cytotoxicity of SHSO in vitro. The SHSO showed significant in vitro cytotoxicity at this concentration. The inhibitions of the MAT-LyLu cell proliferation by SHSO as measured by MTT and trypan blue assays were 11.3 ± 2.8 and 14.2 ± 1.1%, respectively. However, native soybean did not show any significant in vitro cytotoxicity on MAT-LyLu, showing 4.2 ± 3.1 and 2.9 ± 4.8% inhibitions at 300 μg/mL as measured by MTT and trypan blue assays, respectively. No cytotoxicity of the SHSO on normal, non-cancer cell line (3T3, fibroblasts) was observed at the tested concentration (300 μg/mL) (data not shown). Instead, SHSO slightly promoted the normal human cell (3T3) proliferation. The effect of CLA on DNA fragmentation in MAT-LyLu cells are shown in Fig 4. The results show that SHSO induced the apoptosis of the prostate cancer cell line at the levels of 200 and 300 μg/mL (equivalent to CLA TG 55 and 82 μM, respectively), as shown in Fig 4. However, native soybean oil at 300 μg/mL (equivalent to CLA TG 0 μM) did

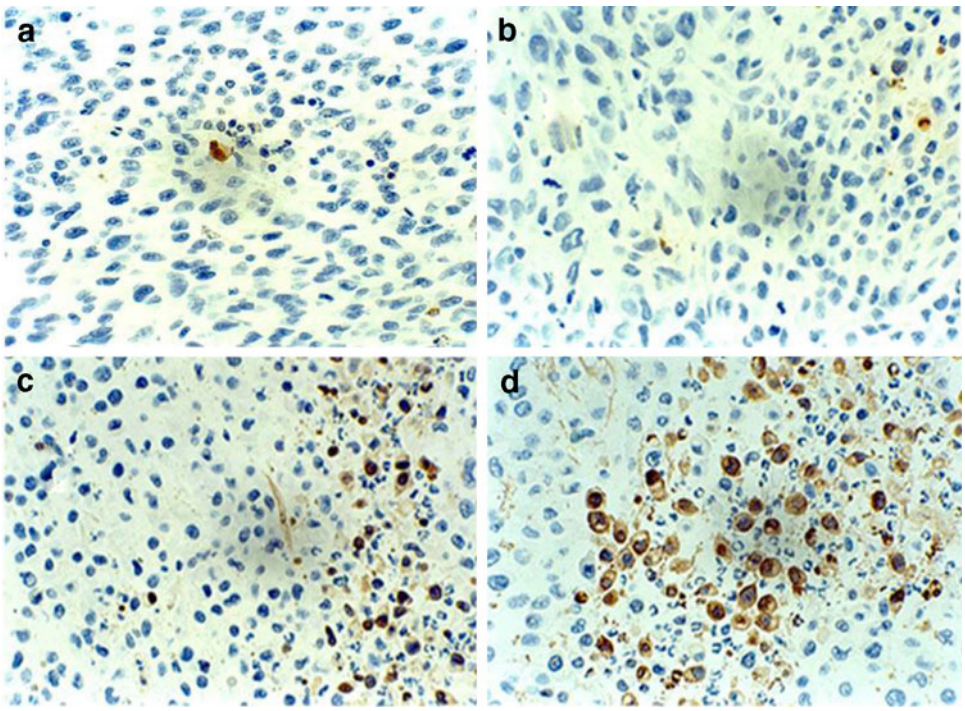

Fig. 3 Effects of different levels of SHSO-supplemented diet on apoptosis as measured by TUNEL assay: **a** control diet, **b** 1.0% SHSO diet, **c** 3% SHSO diet, **d** 5% SHSO diet

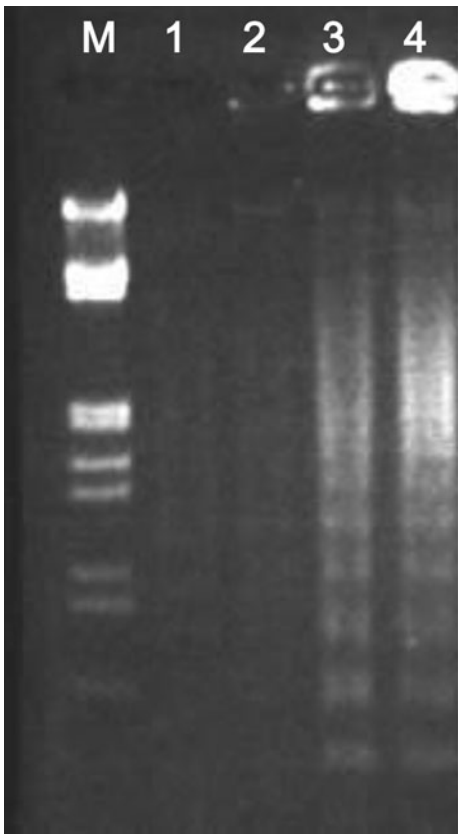

Fig. 4 Agarose gel electrophoresis of DNA extracted from MAT-LyLu cells exposed to SHSO (100–300 μg/mL) for 48 h was treated with cultured MAT-LyLu cell. DNA was electrophoresed in a 1.2% agarose gel stained with ethidium bromide and photographed by UV illumination. *Lane 1*: SHSO 0 μg/mL, *Lane 2*: CLA 100 μg/mL, *Lane 3*: CLA 200 μg/mL, *Lane 4*: CLA 300 μg/mL

not show DNA fragmentation, indicating no apoptotic activity (data not shown).

In Vitro Assays for Antiproliferation on Human Prostate Cancer Cell Lines

The effects of SHSO on the proliferation of human prostate cancer cell lines (DU145 and PC-3) were also studied to check the cytotoxic activity of SHSO on these human cancer cell lines. SHSO at 300 μg/mL (equivalent to CLA TG 82 μM) significantly reduced the proliferation of both DU145 and PC-3 cell lines in vitro: by 33.3 ± 1.7 and 43.3 ± 2.7%, respectively, as measured by MTT assay. In contrast, native soybean oil at of 300 μg/mL (equivalent to CLA TG 0 μM) inhibited the proliferation of DU145 and PC-3 by only 13.7 ± 5.0 and 18.8 ± 5.4, respectively, as measured by MTT assay. The cytotoxicity of SHSO on the DU145 and PC-3 cell lines was further confirmed by the trypan blue dye exclusion method, which showed that 300 μg/mL (equivalent to CLA-TG 82 μM) SHSO inhibited the proliferation of DU145 and PC-3 by 22.3 ± 2.7 and 27.4 ± 2.4%, respectively.

Discussion

Our study shows that SHSO exerted markedly strong anticancer effects on the prostate cancer in vivo, as compared with native soybean oil. Dietary supplementation with 5% SHSO induced an 80% inhibition of prostate tumor weight in rats. The individual food intakes of rats in 3 and 5% SHSO groups were not significantly different from those in control during the feeding experiment (Table 2). This result clearly showed that the anticarcinogenic activity of (SHSO) was not due to the changes in caloric intake. The mean body weight gains in the 3 and 5% SHSO groups were significantly lower than that in control group (0% SHSO), and this was mainly attributable to the differences in their tumor weights; there was no significant difference in body weight gains after correcting for the tumor weight. Note that the mean tumor weights of control, 3% SHSO, and 5% SHSO groups were 8.07 ± 0.99, 5.05 ± 1.64 and 1.60 ± 0.29 g, respectively (Fig. 1b). SHSO dietary supplementation up-regulated the expression of bax, and down-regulated the expressions of bcl-2 and survivin in a dose-dependent manner. The results obtained from the TUNEL assay were consistent with the immunohistochemical staining of bax, bcl-2, and survivin, indicating the positive in vivo apoptotic effects exerted by SHSO against Mat-LyLu prostate cancer cells.

SHSO also showed antiproliferation activity against the growth of MAT-LyLu and human prostate carcinoma cell lines (DU145 and PC-3) in vitro. The in vitro DNA fragmentation data further confirmed that SHSO possessed apoptotic activity on Mat LyLu. It is interesting that the antiproliferation activities of SHSO on human prostate carcinoma cell lines (DU145 and PC-3) were much higher than that on MAT-LyLu at the same concentration. This result suggests that SHSO might be also effective in reducing the risk of prostate cancer in human. SHSO showed cell-specific cytotoxicity, in that it did not inhibit the growth of the normal 3T3 cell lines (human fibroblasts), indicating that the SHSO was not cytotoxicity to a normal cell line.

This is the first report demonstrating significant anticancer and apoptotic properties of a hydrogenated vegetable oil on prostate cancer rat model in vivo and human cell line studies in vitro. Our in vitro result obtained from cell line proliferation studies showed that native soybean oil did not exert any significant antiproliferation activities on Mat-LyLu, and much lower effects on DU145 and PC-3 cells than SHSO. From these results, it is reasonable to postulate that the active components of SHSO are the CLA formed

during hydrogenation. The SHSO contained 22.97% CLA in their triacylglycerol structures, and so the 5% SHSO diet was equivalent to approximately 1.0% CLA supplementation. CLA are geometric and positional isomers of octadecadienoic acid that are known to be present in trace amounts in ruminant meats and dairy products. These fatty acids have been shown to be effective in inhibiting carcinogenesis in multiple systems and at several levels, including initiation, promotion, progression, and metastasis [10–18, 27, 29]. CLA supplementation as a fatty acid form at 1% level reportedly exerted anticancer effects independently from the level and types of other fat treated [15]. It also has been reported that 1% CLA sodium salt (mixture of c9,t11- and t10,c12) significantly reduced the growth of prostate tumors in SCID mice [17]. It has been reported that 100 mM CLA increased the level of mRNA for glutathione peroxidase and reduced the diacylglycerol contents in human prostate cancer cells (PC3) [35]. Ochoa et al. [36] reported that CLA mixture (c9 t11:t10 c12) was able to decrease PC-3 proliferation at 100 and 150 μM (19.9% of control and 59.3% of control, respectively). Masso-Welch et al. [37] reported that *cis*-9, *trans*-11 and *trans*-10, *cis*-12 CLA isomers were effective in inhibiting angiogenesis in a dose-dependent manner. Even though the CLA have been reported to have various anticancer activities with a single or a mixture of its isomers as a fatty acid form (obtained from alkali isomerization from linoleic acid), the anticancer activities of hydrogenated vegetable oils with a high quantity of CLA have not been previously reported. The CLA in SHSO used in this study were present as an esterified form in a triacylglycerol structure, not as a fatty acid. Furthermore, the SHSO was obtained by the hydrogenation of soybean oil, which is a classical food process that has been used for over a century for the production of margarine, shortening, and confectionery fats. The isomeric distribution of CLA in the SHSO used in our study was greatly different from those CLA isomers studied previously. The CLA produced by alkali isomerization from linoleic acid contains mainly two isomers of *cis*-9, *trans*-11 and *trans*-10, *cis*-12 isomers (more than 85%) along with minor proportion of other isomers [28]. But the SHSO contained various types of isomers with a wide distribution, as indicated in Table 2. It has been reported that the bioactivities of the CLA isomers were different with different isomers. The bioactivities of only few isomers (including c9,t11- and t10,c12- isomers) have been well elucidated. We previously identified 21 CLA isomers in SHSO [31], but the bioactivities of most of the CLA isomers present in SHSO have not been studied. The relative distributions of *trans/trans, cis/trans* or *trans/cis*, and *cis/cis* isomers in SHSO were 45.5, 46.6, and 7.9%, respectively (Table 2). The high proportion of *trans/trans* isomers in the CLA products in the present study is in contrast to trace of *trans/trans* isomers in CLA produced by alkali isomerization. The high distribution of *trans/trans* isomers in SHSO might play an important role in its anti-prostate cancer activity. Park et al. [30] compared the cytotoxic effects of four CLA isomer (10t,12c-, 9c,11t-, 10t-,12t- and 9t,11t-) on the gastric cancer cell line (NCI-N87). The authors reported that 9t,11t and 10t,12t- isomers (*trans/trans* isomers) showed stronger cytotoxic activity on the NCI-N87 cancer cell line proliferation than 10t, 12c- and 9c,11t-CLAs (*cis/trans* isomers). Hydrogenated vegetable oils have earned reputations for negative effects on human health mainly due to their high contents of *trans* fatty acids and saturated fatty acids. The increased concern about the effects of *trans* fatty acids on health led to regulations requiring the nutrition facts panel on all food labels to indicate the *trans* fat content by 1 January, 2006. It is interesting to note that CLA are a type of *trans* fatty acids, in a chemical view point. We previously demonstrated that the fatty acid composition of hydrogenated vegetable oils could be manipulated by controlling the reaction conditions such as temperature, catalyst type and amount, hydrogen pressure, and agitation rate [8, 9]. The present study showed a clear evidence that hydrogenated vegetable oils with high conjugated linoleic acids, which were obtained by carefully controlled hydrogenation condition, have great potential as a prototype functional food ingredient for the chemoprevention of prostate cancer. Previously, we reported that SHSO with CLA also showed body fat reducing activity (deleted—and antiatherosclerotic) properties in rats [38]. Prostate cancer is the second leading cause of male death due to cancer in the United States. Given that hydrogenated vegetable oils have been extensively consumed for about a century, this novel approach may be particularly appealing to those people who are unwilling to change their eating habits (in terms of fat consumption), but still desire alternative food choices for cancer prevention.

References

1. American Cancer Society (2005) Cancer facts and figures. Atlanta, GA
2. Judd JT, Clevidence BA, Muesing RA, Wettes J, Sunkin ME, Podczasy JJ (1994) Dietary *trans*-fatty acids: effects of plasma lipids and lipoproteins of healthy men and women. Am J Clin Nutr 59:861–868
3. Oomen CM, Ocke MC, Feskens EJM, Erp-Baart MJV, Kok FJ, Kromhout D (2001) Association between *trans*-fatty acid intake and 10-year risk of coronary heart disease in the Zutphen Elderly Study: a prospective population-based study. Lancet 357: 746–751
4. Enig MG, Munn RJ, Keeney M (1978) Dietary fat and cancer trends—a critique. Fed Proc 37:2215–2220

5. Hogan ML, Shamsuddin AM (1984) Large intestinal carcinogenesis. I. Promotional effects of dietary fatty acid isomers in the rat model. J Natl Cancer Inst 73:1293–1296
6. Awad AB (1981) *Trans*-fatty acids in tumor development and the host survival. J Natl Cancer Inst 67:189–192
7. Jung MY, Ha YL (1999) Conjugated linoleic acid isomers in partially hydrogenated soybean oil obtained during non-selective and selective hydrogenation processes. J Agric Food Chem 47: 704–708
8. Jung MO, Yoon SH, Jung MY (2001) Effects of temperature and agitation rate on the formation of conjugated linoleic acids in soybean oil during hydrogenation process. J Agric Food Chem 49:3010–3016
9. Jung MO, Ju JW, Choi DS, Yoon SH, Jung MY (2002) CLA formation in oils during hydrogenation process as affected by catalyst types, catalyst contents, hydrogen pressure, and oil species. J Am Oil Chem Soc 79:501–510
10. Ip C, Chin SF, Scimeca JA, Pariza MW (1991) Mammary cancer prevention by conjugated dienoic derivative of linoleic acid. Cancer Res 51:6124–6188
11. Ha YL, Grimm NK, Pariza MW (1987) Anticarcinogens from the fried ground beef: heat-altered derivatives of linoleic acid. Carcinogenesis 8:1881–1887
12. Ha YL, Storkson J, Pariza MW (1990) Inhibition of benzo(a)-pyrene-induced mouse forestomach neoplasia by conjugated dienoic derivatives of linoleic acid. Cancer Res 50:1097–1101
13. Liew C, Schut HAJ, Chin SF, Pariza MW, Dashwood RH (1995) Protection of conjugated linoleic acid against 2-amino-3-methylimidazo[4,5-f]quinoline-induced colon carcinogenesis in the F344 rat: a study of inhibitory mechanisms. Carcinogenesis 16:3037–3043
14. Belury MA, Nickel KP, Bird CE, Wu Y (1996) Dietary conjugated linoleic acid modulation of phorbol ester skin tumor promotion. Nutr Cancer 26:149–157
15. Ip C, Briggs SP, Haegele AD, Tompson HJ, Storkson J, Seimeca JA (1996) The efficacy of conjugated linoleic acid in mammary cancer prevention is independent of the level or type of fat in the diet. Carcinogenesis 17:1045–1050
16. Ip C, Jiang C, Thompson HJ, Scimeca JA (1997) Retention of conjugated linoleic acid in the mammary gland is associated with tumor inhibition during the post-initiation phase of carcinogenesis. Carcinogenesis 18:755–759
17. Cesano A, Visonneau S, Esimeca JA, Kritchevsky D, Santoli D (1998) Opposite effects of linoleic acid and conjugated linoleic acid on human prostate cancer in SCID mice. Anticancer Res 18:1429–1434
18. Hubbard NE, Lim D, Summers I, Erickson KI (2000) Reduction of murine mammary tumor metastasis by conjugated linoleic acid. Cancer Lett 150:93–100
19. Lee KN, Kritchevsky D, Pariza MW (1994) Conjugated linoleic acid and atherosclerosis in rabbits. Atherosclerosis 108:19–25
20. Nicolosi RJ, Rogers EJ, Kritchevsky D, Scimeca JA, Huth PJ (1997) Dietary conjugated linoleic acid reduced plasma lipoproteins and early aortic atherosclerosis in hypercholesterolemic hamsters. Artery 22:266–277
21. Houseknecht KL, Vanden Heuvel JP, Moya-Camarena SY, Portocarrero CP, Peck LW, Nickel KP, Belury MA (1998) Dietary conjugated linoleic acid normalizes impaired glucose tolerance in the Zucker diabetic fatty fa/fa rat. Biochem Biophys Res Commun 244:678–682
22. Ryder JW, Portocarrero CP, Song XM, Cui L, Yu M, Combatsiaris T, Galuska D, Bauman DE, Barbano DM, Charron MJ, Zierath JR, Houseknecht KL (2001) Isomer-specific antidiabetic properties of conjugated linoleic acid: improved glucose tolerance, skeletal muscle insulin action, and UCP-2 gene expression. Diabetes 50:1149–1157
23. Riserus U, Berglund L, Vessby B (2001) Conjugated linoleic acid (CLA) reduced abdominal adipose tissue in obese middle-aged men with signs of metabolic syndrome: a randomized controlled trial. Int J Obes 25:1129–1135
24. Belury MA, Mahon A, Banni S (2003) The conjugated linoleic acid (CLA) isomer, t10c12-CLA, is inversely associated with changes in body weight and serum leptin in subjects with type 2 diabetes mellitus. J Nutr 133:257S–260S
25. Evans ME, Brown JM, McIntosh MK (2002) Isomer-specific effects of conjugated linoleic acid (CLA) on adiposity and lipid metabolism. J Nutr Biochem 13:508–516
26. Terpstra AHM (2004) Effect of conjugated linoleic acid on body composition and plasma lipids in humans: an overview of the literature. Am J Clin Nutr 79:352–361
27. Chin SF, Liu W, Storkson JM, Ha YL, Pariza MW (1992) Dietary sources of conjugated dienoic isomers of linoleic acid, a newly recognized class of anticarcinogens. J Food Comp Anal 5:185–197
28. Yurawecz MP, Hood JK, Mossoba MM, Roach JAG, Ku Y (1995) Furan fatty acids determined as oxidation products of conjugated octadecadienoic acid. Lipids 30:595–598
29. Ip C, Dong Y, Ip MM, Banni S, Carta G, Angioni E, Murru E, Spada S, Melis MP, Saebo A (2002) Conjugated linoleic acid isomers and mammary cancer prevention. Nutr Cancer 43:52–58
30. Park SJ, Park CW, Kim SJ, Kim YR, Kim YS, Ha YL (2003) Divergent cytotoxic effects of conjugated linoleic acid isomers on NCI-N87 cells, Chapter 10. In: Food factors in health promotion and disease prevention. Oxford University Press, pp 111–118
31. Jung MY, Jung MO (2002) Identification of conjugated linoleic acid isomers in hydrogenated soybean oil by silver ion impregnated HPLC and GC-ion impacted mass spectrometry of their 4,4-dimethyloxazoline derivatives. J Agric Food Chem 50:6188–6193
32. Sehat N, Rickert R, Mossoba MM, Kramer JKG, Yurawecz MP, Roach JAG, Adlof RO, Morehouse KM, Fritsche J, Eulitz KD, Steinhart H, Ku Y (1999) Improved separation of conjugated fatty acid methyl esters by silver ion-high performance liquid chromatography. Lipids 34:407–413
33. Mosmann T (1983) Rapid colorimetric assay for cellular growth and survival: application to proliferation and cytotoxicity assays. J Immunol Methods 65:55–63
34. Kaltenbach JP, Kaltenbach MH, Lyons WB (1958) Nigrosin as a dye for differentiating live and dead ascites cells. Exp Cell Res 15:112–117
35. Farquharson A, Wu H-C, Grant I, Graf B, Choung J-J, Eremin O, Heys S, Wahle K (1999) Possible mechanisms for the putative antiatherogenic and antitumorigenic effects of conjugated polyenoic acids. Lipids 34:S343
36. Ochoa JJ, Farquharson JF, Grant I, Moffat LE, Heys SD, Wahle KWJ (2004) Conjugated linoleic acids (CLAs) decrease prostate cancer cell proliferation: different molecular mechanism for *cis*-9, *trans*-11 and *trans*-10, *cis*-12 isomers. Carcinogenesis 25: 1185–1191
37. Masso-Welch PA, Zangani D, Ip C, Vaughan MM, Shoemaker S, Ramirez RA, Ip MM (2002) Inhibition of angiogenesis by the cancer chemopreventive agent conjugated linoleic acid. Cancer Res 62:4383–4389
38. Choi NJ, Kown D, Yoon SH, Jung MY, Shin HK (2004) Selectively hydrogenated soybean oil with conjugated linoleic acid modifies body fat composition and plasma lipid in rats. J Nutr Biochem 15:411–417

Lipids (2011) 46:297–306
DOI 10.1007/s11745-011-3531-7

METHODS

Improved Methods for the Fatty Acid Analysis of Blood Lipid Classes

Ken'ichi Ichihara · Kumiko Yoneda · Ayuko Takahashi · Noriko Hoshino · Motoyoshi Matsuda

Received: 6 October 2010 / Accepted: 14 January 2011 / Published online: 7 February 2011

Abstract Two improved methods have been developed for preparation of fatty acid methyl esters (FAME) from major *O*-ester lipid classes in blood, i.e., cholesterol ester, triacylglycerol, and glycerophospholipids. The methods involve simple operations, and use neither harmful solvents such as chloroform or benzene nor highly reactive volatile reagents such as acetyl chloride. The FAME synthesis reaction proceeds under mild temperature conditions. The methods include (1) extraction of lipids from 0.2 ml of blood with 0.2 ml of *tert*-butyl methyl ether and 0.1 ml of methanol, (2) separation of the total lipids into lipid classes using a solid-phase extraction column or thin-layer chromatography, and (3) methanolysis of each lipid class at room temperature or at 45 °C. In all the operations, solvent concentration is performed only once prior to gas–liquid chromatography (GC). No noticeable differences in composition determined by GC have been found between FAME prepared by the present methods and those prepared by a conventional method involving lipid extraction with chloroform/methanol. The mild reaction and simplified procedures of the present methods enabled safe and reproducible analysis of the fatty acid compositions of the major ester-lipid classes in blood.

Keywords Fatty acid composition · Fatty acid methyl ester · Methanolysis · Cholesterol ester · Plasma · Phospholipid · Triacylglycerol · Blood lipids

K. Ichihara (✉) · K. Yoneda · A. Takahashi · N. Hoshino · M. Matsuda
Department of Biomolecular Chemistry, Graduate School of Life and Environmental Sciences, Kyoto Prefectural University, Shimogamo, Kyoto 606-8522, Japan
e-mail: ichihara@kpu.ac.jp

Abbreviations

tert-BME	*tert*-Butyl methyl ether
CE	Cholesterol ester(s)
FAME	Fatty acid methyl ester(s)
FFA	Free fatty acid(s)
GC	Gas–liquid chromatography
GPL	Glycerophospholipids
GroPCho	Glycerophosphocholine
GroPEtn	Glycerophosphoethanolamine
PtdCho	Phosphatidylcholine
PtdEtn	Phosphatidylethanolamine
SPE	Solid phase extraction
TAG	Triacylglycerol(s)
TLC	Thin-layer chromatography

Introduction

The major ester-lipid classes in blood are cholesterol esters (CE), triacylglycerols (TAG), and glycerophospholipids (GPL). The fatty acid compositions of these lipid classes are among the indicators related to human health and nutritional status, and they have been used in many clinical and epidemiological studies [1–6]. While convenient methods have been presented for preparation of fatty acid methyl esters (FAME) from blood total lipids [7–10], the preparation of FAME from individual lipid classes in blood is both labor-intensive and time-consuming. The first step in conventional preparation of FAME from lipid classes is extraction of total lipids from blood with chloroform–methanol, phase separation, and concentration of the chloroform solution. However, the trihalomethane solvent is toxic for humans and its carcinogenicity is a considerable

health risk for researchers in laboratories [11]. Chloroform may also contaminate the environment. It has been noted that labile lipid species can be chemically modified with the phosgene formed by decomposition of chloroform [12]. Chloroform has another disadvantage in phase separation, in that it forms a lower layer because of its high density (1.48 g/cm^3). When the lower solvent layer is collected with a pipette, it can be contaminated with solid impurities floating in the interface between the upper and lower layers [13]. Therefore, chloroform should be replaced with a less harmful, non-chlorinated, low-density solvent. The second step is isolation of individual lipid classes by silica gel thin-layer chromatography (TLC) or column chromatography. The procedure of this step varies between groups, and there is still no unified protocol for isolation. The third step is formation of FAME from the isolated individual lipid classes by methanolysis or by saponification followed by methylation. Although FAME have been mostly synthesized at temperatures higher than 70 °C, the operation of methanolysis under lower, mild temperatures must be adopted for safety of researchers and to allow simplification of the apparatus used. BF_3 and 3-(trifluoromethyl) phenyltrimethylammonium hydroxide are often used as catalysts for methanolysis of isolated lipid classes [14, 15], but fluorine compounds are restricted for the global environment by local drainage laws. Environmentally friendly alternatives to fluorine compounds should be used as catalysts. HCl is a widely used acid catalyst, and anhydrous HCl/methanol can be prepared from acetyl chloride and methanol [16]. However, the volatile acid halide is an extreme irritant to the eyes, and care must also be taken to prevent violent reaction with methanol. From a safety standpoint, it is desirable to avoid use of this reagent. Benzene, which has been used in the preparation and extraction of FAME [7, 17], may cause leukemia, and it should therefore be replaced by an alternative solvent. Purification of the synthesized FAME is necessary to remove impurities for capillary gas–liquid chromatography (GC) at the last step of preparation, but the procedure is variable and is not standardized. During these operations, concentration of solvents is often repeated, but the number of concentration steps must be minimized for simplification.

We attempted to develop and establish simplified procedures for routine fatty acid analysis of blood CE, TAG, and GPL, and also to minimize possible hazards during chemical manipulation in laboratories and to reduce environmental burden of waste products. Here, we propose two methods and the corresponding protocols for preparation of FAME derived from the blood lipid classes. The first includes a procedure using a solid-phase extraction (SPE) column for separation of blood lipids into lipid classes and is suitable for simultaneous treatment of many samples or robotic systems, and the other includes a TLC procedure, which has been used most frequently to date.

Materials and Methods

Reagents

Cholesteryl oleate and dierucoyl glycerophosphocholine (GroPCho) were purchased from Avanti Polar Lipids (Alabaster, AL, USA). Cholesteryl erucate, trierucoyl glycerol, and the FAME standard mixture for GC were purchased from Nu-Chek-Prep (Elysian, MN, USA). Trioleoyl glycerol was obtained from Sigma-Aldrich (St. Louis, MO, USA). Dioleoyl glycerophosphoethanolamine (GroPEtn) was from Wako Pure Chemical Industries (Osaka, Japan). Dioleoyl GroPCho was synthesized from GroPCho and oleic acid [18]. Acetone, chloroform, hexane, and methanol were purchased from Wako Pure Chemical Industries or Nacalai Tesque (Kyoto, Japan) as glass-distilled solvents for analysis of residual pesticides and herbicides. Metal Na, KOH, 50% BF_3 in methanol, *tert*-butyl methyl ether (*tert*-BME), methyl acetate, and heparin sodium salt were of reagent grade. Methanolic CH_3ONa solutions of 1.2 M and 2.0 M were prepared by diluting 25% (w/w; 4.37 M) methanolic CH_3ONa, which was purchased from Sigma-Aldrich, with methanol or prepared by dissolving metal Na in methanol. A reagent for methylation of FFA, 0.8 M HCl in 95% methanol, was prepared by diluting conc. HCl (12 M) 15-fold with methanol. TLC plates of silica gel (0.25 mm thick, No. 105715) and SPE columns packed with 200 mg of silica gel (LiChrolut, No. 102021) were products of Merck (Darmstadt, Germany). The SPE columns were previously washed with 10 ml of hexane and 6 ml of acetone to remove plasticizers and impurities, and then dried in vacuo (1.3 kPa) for 16 h. Microcentrifuge tubes (1.5 ml; Greiner Bio-One, Kremsmünster, Austria) made of homopolymer polypropylene and translucent were soaked in hexane overnight to remove plasticizers. Transparent tubes made of the copolymer polypropylene contained more plasticizers and were not used for lipid extraction. Most solvent systems for lipid extraction and TLC contained 0.001% 2,6-di-*tert*-butyl-*p*-cresol as an antioxidant. Small volumes ($\leq$1 ml) of organic solvents were measured with positive displacement pipettes (Microman M-100 and M-250; Gilson, Middleton, WI, USA). M-1000 was also used for solvents other than chloroform.

TLC and GC

Reaction products of methanolysis were analyzed by silica gel TLC. Developed lipids on TLC plates were visualized

by spraying with 50% (w/w) sulfuric acid and then heating at 137 °C. Phospholipids were also detected with the Dittmer and Lester reagent [19]. For preparation of FAME from lipid classes, methanolic 0.001% primulin was sprayed on plates and lipids were detected under ultraviolet light at 365 nm. FAME prepared were analyzed with a Shimadzu 2014 gas chromatograph equipped with flame ionization detectors and columns of DB-23 (0.25 mm × 30 m) and SUPELCOWAX 10 (0.53 mm × 30 m) at an isothermal column temperature of 200 °C or 215 °C in N_2 gas.

Conventional Method for Preparation of FAME from Blood Lipid Classes

Lipids were extracted from 0.2 ml of blood plasma containing heparin with 4 ml of chloroform/methanol (2:1, v/v) by the Folch method [20]. Total lipids thus obtained were developed on silica gel plates (5 cm in width × 10 cm in height) to 2 cm from the origin with acetone and then redeveloped with hexane/*tert*-BME (90:10, v/v) to 8 cm from the origin. Lipids were detected with primulin, and those located at the origin of the plate were regarded as GPL. Silica gel bands corresponding to lipid classes were scraped off and suspended in 2 ml of methanol/toluene (4:1, v/v). After addition of acetyl chloride (0.2 ml), the mixture was heated at 100 °C for 1 h in a screw-capped glass test tube [7]. FAME formed were extracted with hexane.

Method I (SPE Column Method)

Extraction of Lipids and SPE Column Fractionation (*Fig. 1a*)

Total lipids were extracted from 0.2 ml of whole blood in small glass test tubes or in 1.5-ml polypropylene microcentrifuge tubes by vortexing for 1 min with 0.2 ml of *tert*-BME and 0.1 ml of methanol. The tubes were centrifuged for 1 min and 0.1 ml of the upper ether layer formed was slowly applied at the center of the upper-frit surface of a dry SPE column packed with 200 mg of silica gel. The upper frit put on the silica gel matrix was washed with 0.02 ml of hexane. The silica gel charged with blood total lipids as a *tert*-BME solution containing methanol and water was allowed to stand for 5 min and dried for 1 h or overnight in vacuo (1.3 kPa). CE was eluted with 3.4 ml of 1% (v/v) methyl acetate in hexane, and the volume of eluate was 3.0 ml. TAG was then eluted with 3 ml of 2.5% (v/v) methyl acetate in hexane. After the column was washed with 3 ml of acetone to remove cholesterol and pigments, GPL were eluted with 4 ml of methanol.

(a) Extraction of blood total lipids and isolation of lipid classes by an SPE column

Blood 0.2 ml
- ← 0.2 ml of *tert*-BME and 0.1 ml of methanol
- vortexed for 1 min
- centrifuged for 1 min

tert-BME layer (0.1 ml from 0.14 ml in total)
- applied to a silica gel SPE column

Silica gel SPE column
- washed with 0.02 ml of hexane
- allowed to stand for 5 min
- dried in vacuo for 1 h or overnight
- eluted with 3.4 ml of 1% methyl acetate in hexane (CE)
- eluted with 3 ml of 2.5% methyl acetate in hexane (TAG)
- washed with 3 ml of acetone
- eluted with 4 ml of methanol (GPL)

CE, TAG, and GPL fractions

(b) Preparation of FAME from lipid classes

CE fraction (3 ml of 1% methyl acetate/hexane)
- ← 1.5 ml of acetone and 0.6 ml of 2 M CH_3ONa
- vortexed and allowed to stand for 30 min at room temperature
- ← 0.1 ml of acetic acid and 3 ml of water

Hexane layer
- washed twice with 3 ml each of water
- applied to an SPE column
- eluted with 3 ml of 1% methyl acetate/hexane

Eluate (FAME from CE)
- concentrated

GC

TAG fraction (3 ml of 2.5% methyl acetate/hexane)
- ← 0.1 ml of acetone and 0.1 ml of 2 M CH_3ONa
- vortexed for 30 s at room temperature
- ← 0.02 ml of acetic acid and 3 ml of water

Hexane layer
- washed twice with 3 ml each of water
- applied to an SPE column
- eluted with 3 ml of 1% methyl acetate/hexane

Eluate (FAME from TAG)
- concentrated

GC

GPL fraction (4 ml of methanol)
- ← 0.6 ml of 2 M CH_3ONa
- vortexed and allowed to stand for 7 min at room temperature
- ← 0.1 ml of acetic acid, 3 ml of hexane, and 3 ml of water

Hexane layer
- washed with 3 ml of water
- applied to an SPE column
- eluted with 3 ml of 1% methyl acetate/hexane

Eluate (FAME from GPL)
- concentrated

GC

Fig. 1 Flow chart for Method I

Preparation of FAME from Lipid Classes in Eluates (*Fig. 1b*)

The CE solution (3 ml) was mixed with 1.5 ml of acetone and 0.6 ml of 2 M CH_3ONa, the final concentration of which was 0.24 M. The mixed solution, which formed a single phase, was allowed to stand for 30 min at room temperature. Methanolysis was stopped with 0.1 ml of acetic acid, and then 3 ml of water was added to the solution. After mixing, the hexane layer formed was washed twice with 3 ml of water each time and applied to a silica gel SPE column conditioned with 2 ml of hexane for removal of the byproduct cholesterol and small amounts of FFA. The flow-through fraction was discarded, and FAME were then eluted with 3 ml of 1% methyl acetate in hexane. Cholesterol and FFA were retained in the column. The FAME solution was concentrated in vacuo for GC analysis.

To the TAG solution (3 ml) were added 0.1 ml of acetone and 0.1 ml of 2 M CH_3ONa, and the mixed solution of two separate phases was vortexed for 30 s at room temperature. The reaction was terminated by addition of 0.02 ml of acetic acid, and the solution was mixed with 3 ml of water. The hexane layer was washed twice with water and FAME were purified by the same procedures as described above.

The methanolic GPL solution (4 ml) was mixed with 0.6 ml of 2 M CH_3ONa. Methanolysis was completed within 7 min at room temperature. After addition of 0.1 ml of acetic acid and 3 ml of water to the reaction mixture, FAME were extracted with 3 ml of hexane. The separated hexane layer was washed with 3 ml of water and FAME were purified with a silica gel column to remove non-acylated compounds similar to GPL in polarity as described above.

Method II (TLC Method)

Extraction of Lipids and Fractionation by TLC (*Fig. 2a*)

An area (4 cm in width × 1 cm in height) of a 5 × 10 cm silica gel TLC plate was spotted with 0.1 ml of a *tert*-BME solution of total lipids extracted from 0.2 ml of whole blood by the same procedures as described for lipid extraction in Method I. The plate was dried in vacuo (1.3 kPa) for 15 min, developed with acetone to 3 cm from the bottom of the plate, dried in vacuo for 5 min, and redeveloped with hexane/*tert*-BME (90:10, v/v) to 9 cm from the bottom. Bands of CE and TAG were located by spraying with primulin solution followed by visualizing under an ultraviolet lamp at 365 nm, while GPL remained at the spotted area. Each silica gel band was scraped off and placed in a glass test tube (16.5 mm × 125 mm) for TAG and GPL or in a screw-capped glass test tube (16.5 mm × 105 mm) for CE.

Preparation of FAME from Lipid Classes on Silica Gel (*Fig. 2b*)

CE on silica gel was vortexed with 0.5 ml of toluene/acetone (1:1, v/v) and 1 ml of 1.2 M CH_3ONa for 10 s, and methanolysis was carried out at 45 °C for 30 min. To the reaction mixture was added 3 ml of 0.8 M HCl in 95% methanol, and the test tube was incubated at 45 °C for 20 min for methylation of FFA byproducts. Two phases were formed by the addition of 1 ml of hexane and 2 ml of water to the acidic solution, and the hexane layer was washed with 2 ml of water. The hexane solution thus obtained was applied to a silica gel SPE column. The adsorbed FAME were eluted with 3 ml of 1% methyl acetate in hexane, and the eluate was concentrated for GC analysis.

TAG on silica gel and GPL on silica gel were vortexed with 0.5 ml of toluene/acetone (1:1, v/v) and 1 ml of 1.2 M CH_3ONa for 30 s, and then the mixture was allowed to stand for 1 min at room temperature. Methanolysis was terminated by addition of 0.1 ml of acetic acid. Then, 1 ml of hexane and 2 ml of water were added to the solution for extraction of FAME. The hexane layer was washed with 2 ml of water, and FAME were purified by the same procedure as described for methanolysis of CE.

Assessment of Lipid Extraction with *tert*-BME/Methanol

Whole blood (0.2 ml) was vortexed with 0.2 ml of *tert*-BME and 0.1 ml of methanol, and the mixture was centrifuged. The upper *tert*-BME layer was removed, and the surface of the lower layer was gently washed with 0.1 ml of *tert*-BME. These *tert*-BME solutions were combined. Lipids that were not extracted with *tert*-BME and remained in the lower water/methanol layer were extracted twice with 0.2 ml and with 0.1 ml of chloroform. For comparison, blood (0.2 ml) was diluted with 0.3 ml of 0.5 M KH_2PO_4 and lipids were extracted with 1.5 ml of chloroform and 0.5 ml of methanol by vortexing for 2 min [21]. The chloroform layer was removed, and the surface of the water/methanol layer was gently washed with 1 ml of chloroform. The two chloroform solutions were combined. Lipids in the water/methanol layer were re-extracted twice with 1 ml and with 0.5 ml of chloroform. Extracted lipids were analyzed by TLC. The plate was first developed in chloroform/methanol/water/acetic acid (65:35:4:1, v/v/v/v) to 3 cm from the origin, dried in vacuo, and then redeveloped in hexane/*tert*-BME/acetic acid (85:15:0.5, v/v/v) to 8 cm from the origin.

(a) Extraction of blood total lipids and isolation of lipid classes by TLC

Blood 0.2 ml
- ← 0.2 ml of *tert*-BME and 0.1 ml of methanol
- vortexed for 1 min
- centrifuged for 1 min

tert-BME layer (0.10 ml from 0.14 ml in total)
- applied to a silica gel TLC plate

Lipids on the silica gel plate
- dried in vacuo for 15 min
- developed with acetone to 3 cm from the bottom
- dried in vacuo for 5 min
- developed with hexane/*tert*-BME (9:1, v/v)
- sprayed with 0.001% primulin/methanol
- located under UV light at 365 nm
- scraped off a test tube

CE, TAG, and GPL adsorbed on silica gel

(b) Preparation of FAME from lipid classes

CE on silica gel
- ← 0.5 ml of toluene/acetone (1:1, v/v)
- ← 1 ml of 1.2 M CH_3ONa
- vortexed and then incubated for 30 min at 45°C
- ← 3 ml of 0.8 M HCl/95% methanol
- incubated for 20 min at 45°C
- ← 1 ml of hexane and 2 ml of water
- vortexed and centrifuged

Hexane layer
- washed with 2 ml of water
- applied to a silica gel SPE column

FAME in the silica gel column
- eluted with 3 ml of 1% methyl acetate/hexane

Eluate (FAME from CE)
- concentrated

GC

TAG or **GPL** on silica gel
- ← 0.5 ml of toluene/acetone (1:1, v/v)
- ← 1 ml of 1.2 M CH_3ONa
- vortexed for 30 s
- allowed to stand for 1 min at room temperature
- ← 0.1 ml of acetic acid, 1 ml of hexane, and 2 ml of water
- vortexed and centrifuged

Hexane layer
- washed with 2 ml of water
- applied to a silica gel SPE column

FAME in the silica gel column
- eluted with 3 ml of 1% methyl acetate/hexane

Eluate (FAME from TAG or GPL)
- concentrated

GC

Fig. 2 Flow chart for Method II

Acid-Catalyzed Methanolysis

Although this study focused on the fatty acid analysis of ester lipids, FAME from both *O*-acyl and *N*-acyl lipids were also prepared (Fig. 3). An 8% (w/v) solution of HCl in methanol/water (85:15, v/v) was prepared by diluting 10 ml of conc. HCl with 42.8 ml of methanol [10]. Blood total lipids were extracted with *tert*-BME/methanol and lipid classes were isolated by TLC. Toluene (0.2 ml), methanol (1.5 ml), and the 8% HCl solution (0.3 ml) were added sequentially to each lipid class/silica gel. The final concentration of HCl was 1.2% (w/v), and the solution contained 2.2% (w/v) water derived from conc. HCl. Methanolysis was carried out at 100 °C for 1 h. The reaction mixture was neutralized with 2 ml of 0.5 M $NaHCO_3$, and products were extracted with chloroform for TLC. When FAME were analyzed by GC, they were extracted with hexane without neutralization.

Results and Discussion

Extraction of Total Lipids and Yields of FAME

tert-BME is immiscible with water and its density is lower than water. It has moderate polarity and moderate volatility with boiling point of 55 °C. Its toxicity is lower than chloroform. It is not prone to peroxide formation. It is commercially available as a reagent of high purity in reasonable prices. Thus, *tert*-BME was selected as an alternative solvent to chloroform for lipid extraction. The compositions of blood total lipids extracted by two

Preparation of FAME from lipid classes

CE, TAG, or GPL on silica gel
- ← 0.2 ml of toluene, 1.5 ml of methanol, and 0.3 ml of 8% HCl/85% methanol
- heated at 100°C for 1 h
- ← 1 ml of hexane and 2 ml of water
- vortexed and centrifuged

Hexane layer
- washed with 2 ml of water
- applied to a silica gel SPE column

FAME in the silica gel column
- eluted with 3 ml of 1% methyl acetate/hexane

Eluate (FAME)
- concentrated

GC

Fig. 3 Flow chart for an alternative TLC method utilizing acid-catalyzed methanolysis. See Fig. 2a for extraction of total lipids and isolation of lipid classes

different solvent systems, the present *tert*-BME/methanol system and a modified Folch method that uses chloroform/methanol, were compared by TLC, but no differences in lipid composition were found (Fig. 4). The lower water/methanol phase formed on extraction with *tert*-BME was extracted with chloroform to confirm lipid classes remaining in the lower phase that should be discarded. Small amounts of lipids were distributed to the lower layer, but the lipid compositions of the two layers were very similar to each other on the TLC plate. Matyash et al. [13] also reported that *tert*-BME gave good recoveries for extraction of major lipid classes and was comparable to chloroform used in the Folch method [20] or the Bligh and Dyer method [22].

Extraction efficiencies were compared between the above two solvent systems based on data from an experiment performed in triplicate. An internal standard, methyl erucate, in *tert*-BME or in chloroform was added to blood at the time of lipid extraction. FAME were prepared from the total lipids by HCl-catalyzed methanolysis at 45 °C [10] and analyzed by GC. There was no significant difference in total yield of FAME between *tert*-BME/methanol extraction and chloroform/methanol extraction, and the fatty acid compositions of these FAME preparations were very similar to each other. These findings indicated that *tert*-BME/methanol compares favorably with chloroform/methanol for extraction of blood total lipids as reported previously in lipidomics research [13].

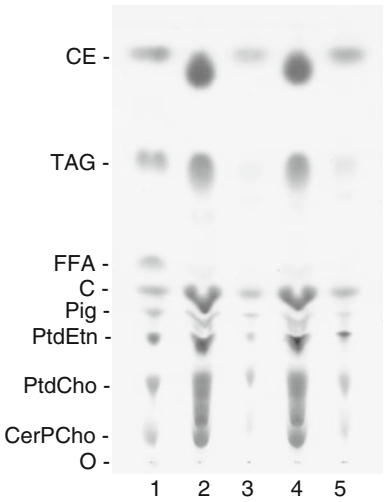

Fig. 4 Lipid extraction from blood with *tert*-BME/methanol and with chloroform/methanol. The TLC plate was first developed in chloroform/methanol/water/acetic acid (65:35:4:1, v/v/v/v) to 3 cm from the origin, dried in vacuo, and then redeveloped in hexane/*tert*-BME/acetic acid (85:15:0.5, v/v/v). *Lane 1* authentic lipids, *lane 2* lipids extracted with *tert*-BME, *lane 3* lipids in the water/methanol layer of *tert*-BME extraction, *lane 4* lipids extracted with chloroform, *lane 5* lipids in the water/methanol layer of chloroform extraction. *C* cholesterol, *Pig* pigments, *CerPCho* sphingomyelin, *O* origin

Methanolysis of Lipid Classes Separated by Silica Gel SPE Columns (Method I)

In the 1980s, SPE columns were used for separation between non-polar lipids and phospholipids [23]. Figure 5a shows that CE, TAG, and GPL could be fractionated from total lipids by SPE columns. Methanolysis was carried out at room temperature without concentration of the lipid solutions, and FAME derived from each lipid class were purified to a single spot on TLC (Fig. 5b).

Methanolysis of TAG proceeds in a solvent mixture of hexane and methanol containing a base catalyst, and it requires vortexing for 2 min at room temperature in the absence of acetone [24]. Addition of acetone to a mixture of the TAG eluate and CH_3ONa/methanol stimulated the reaction, and TAG was converted into FAME within 30 s by vortexing at room temperature (Fig. 5b, lanes 5, 6). Hexane and methanol are immiscible, while methanolysis occurs in the lower methanol phase in which a base catalyst, e.g., CH_3ONa or KOH, is dissolved. As TAG, which is a non-polar lipid, is soluble in hexane but slightly soluble in methanol, it is distributed unevenly to the hexane phase when dissolved in a mixed solvent of hexane and methanol. The concentration of TAG in the methanol phase is low, and hence methanolysis proceeds slowly. When a small volume of acetone is added to a mixture of hexane and methanol, acetone is miscible with methanol and the two polar solvents form a lower phase. As acetone is a good solvent for TAG, the concentration of TAG increases in the lower phase where methoxide ions are present and methanolysis occurs. FAME formed are more hydrophobic than TAG and are transferred immediately to the upper hexane phase. FAME are, therefore, not hydrolyzed by alkali dissolved in the methanol/acetone phase. This is probably why methanolysis of TAG is stimulated with acetone.

CE is more hydrophobic and less soluble in methanol than TAG, and methanolysis of CE does not proceed under the conditions for TAG [25, 26]. Various solvents have been used to increase the solubility of CE in methanol to enhance its reactivity. For example, good yields of FAME are obtained in 1 h at 37 °C or at room temperature by reaction in diethyl ether/methyl acetate/methanol containing 1 M CH_3ONa (50:1:1, v/v/v) or in methyl propionate/methanol containing 0.84 M NaOH (2:3, v/v), respectively [25, 26]. A mixture of CE eluate (3 ml of 1% methyl acetate in hexane), 1.5 ml of acetone, and 0.6 ml of 2 M CH_3ONa/methanol formed a single homogenous phase of the solvents, and methanolysis was completed in 30 min at room temperature (Fig. 5b, lane 2). This improved reactivity of CE was also due to its high solubility in the solution containing acetone.

To a methanol eluate (4 ml) of GPL was added 0.6 ml of 2 M CH_3ONa/methanol to form a 0.26 M CH_3ONa

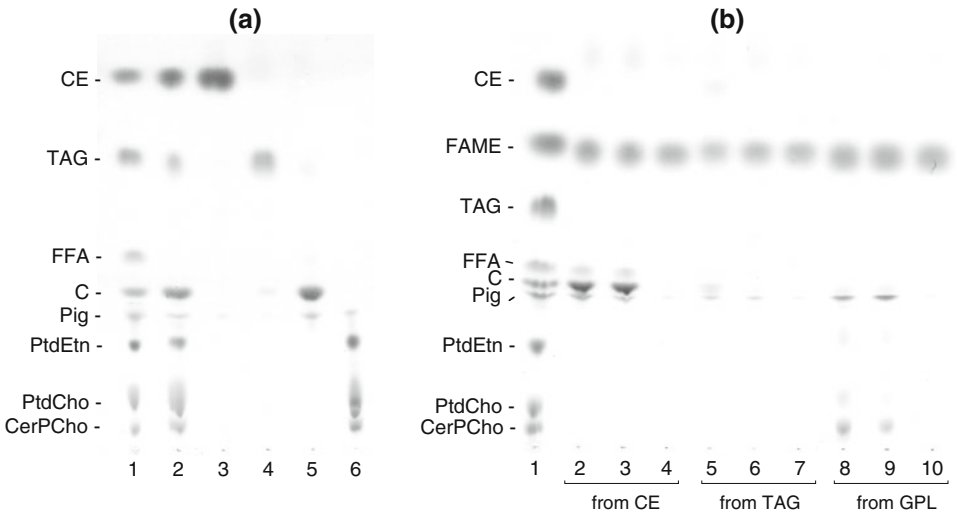

Fig. 5 **a** Isolation of CE, TAG, and GPL by a silica gel SPE column. Total lipids were extracted from whole blood with *tert*-BME/methanol (*lane 2*) and separated into three lipid classes, CE (*lane 3*), TAG (*lane 4*), and GPL (*lane 6*) by an SPE column. *Lane 5* is the acetone eluate that contains cholesterol and pigments. Reference lipids were developed in lane 1. **b** Preparation of FAME from lipid classes. Reaction products of the isolated lipid classes by methanolysis were extracted with chloroform (*lanes 2, 5, 8*) or with hexane (*lanes 3, 6, 9*). The hexane extracts were purified by SPE columns (*lanes 4, 7, 10*). Lane 1 is a mixture of authentic lipids. The conditions of TLC were the same as those in Fig. 4

solution, which was allowed to stand for 7 min at room temperature. As GPL are polar lipids and sufficiently soluble in methanol, the reaction proceeded rapidly in methanol (Fig. 5b, lane 8). The reaction time of 7 min at room temperature was sufficient for transesterification of GPL bearing *O*-ester linkages. The pale spot detected near the position corresponding to PtdEtn after methanolysis was not a phospholipid, and another pale spot found near the position of PtdCho was lysoplasmalogen. Sphingomyelin, which has no ester-linked acyl residue, remained unchanged as expected. The fatty acid composition of sphingomyelin is considerably different from those of glycerophospholipids, and it must be determined using acid-catalyzed methanolysis after isolation.

Acetone is known to reacts with aminophospholipids to form Schiff's bases under mild conditions [27, 28], but the influences of acetone complexes on the preparation of phospholipids and analysis of fatty acid composition were not considered in the present study.

Methanolysis of Lipid Classes Separated by Silica Gel TLC (Method II)

CE, TAG, and GPL were isolated by silica gel TLC from *tert*-BME extracts (Fig. 6). Methanolysis in the presence of silica gel has some disadvantages compared to the reaction in the absence of silica gel, especially for CE; i.e., the reaction proceeds slowly and FFA are produced. However, these disadvantages could be alleviated by optimizing reaction conditions. A reaction medium consisting of 0.25 ml of toluene, 0.25 ml of acetone, and 1 ml of methanolic 1.2 M CH_3ONa forms a single organic phase, in which the concentration of CH_3ONa is 0.8 M. This solvent system containing the base catalyst was able to dissolve all three lipid classes and was used for methanolysis.

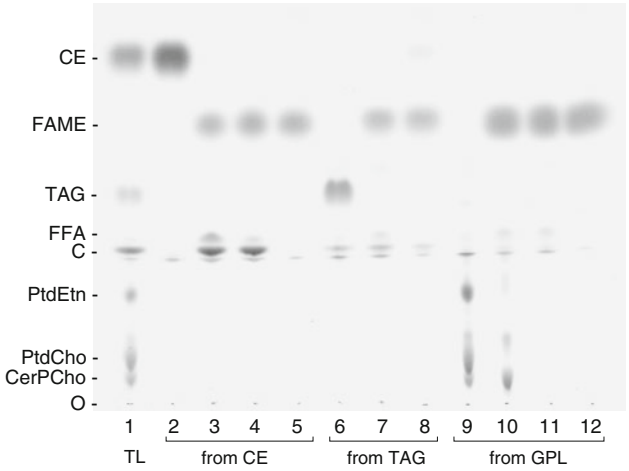

Fig. 6 Preparation of FAME from lipid classes isolated by TLC. *Lane 1* total lipids extracted with *tert*-BME/methanol, *lane 2* CE isolated by TLC, *lane 3* methanolysis products of CE/silica gel, *lane 4* products from CE on silica gel by methanolysis followed by methylation (methanolysis/methylation), *lane 5* FAME purified from methanolysis/methylation products corresponding to lane 4, *lane 6* TAG isolated by TLC, *lane 7* methanolysis products of TAG/silica gel, *lane 8* FAME purified from methanolysis products corresponding to lane 7, *lane 9* GPL isolated by TLC, *lane 10* chloroform extract of methanolysis products from GPL/silica gel, *lane 11* hexane extract of methanolysis products from GPL/silica gel, *lane 12* FAME purified from the hexane extract corresponding to lane 11. The conditions of TLC were the same as those in Fig. 4. *TL* total lipids

Table 1 Blood fatty acid compositions (%) determined by different methods

Lipid class	Fatty acid	Method I	Method II	Conventional method
CE	14:0	1.1 ± 0.2	0.9 ± 0.0	0.8 ± 0.0
	16:0	12.4 ± 0.1[a]	13.8 ± 0.4	13.7 ± 0.0[a]
	16:1	2.8 ± 0.1	2.5 ± 0.1	2.8 ± 0.0
	18:0	1.4 ± 0.1	1.0 ± 0.1	1.0 ± 0.0
	18:1	20.1 ± 0.1	19.9 ± 0.1	20.4 ± 0.0
	18:2	45.6 ± 0.1	45.6 ± 0.3	45.7 ± 0.1
	18:3 n-3	0.8 ± 0.0	0.8 ± 0.0	0.7 ± 0.0
	20:3 n-6	0.3 ± 0.0	0.4 ± 0.1	0.3 ± 0.0
	20:4 n-6	5.2 ± 0.1	5.2 ± 0.1	5.0 ± 0.0
	20:5 n-3	8.3 ± 0.1	7.9 ± 0.1	7.7 ± 0.0
	22:6 n-3	2.1 ± 0.1	2.0 ± 0.0	1.9 ± 0.0
TAG	14:0	3.0 ± 0.3	2.5 ± 0.1	3.3 ± 0.2
	16:0	25.7 ± 0.2	26.5 ± 0.2	27.2 ± 0.1
	16:1	3.9 ± 0.1	4.1 ± 0.0	4.2 ± 0.1
	18:0	6.6 ± 0.1[a,b]	5.8 ± 0.0[a]	5.7 ± 0.0[b]
	18:1	36.2 ± 0.1	35.5 ± 0.1	35.3 ± 0.1
	18:2	12.2 ± 0.1	12.6 ± 0.0[a]	12.1 ± 0.0[a]
	18:3 n-3	1.1 ± 0.1	1.3 ± 0.0[a]	1.0 ± 0.0[a]
	20:1	2.0 ± 0.1	1.6 ± 0.0	1.5 ± 0.0
	20:4 n-6	1.2 ± 0.0	1.3 ± 0.1	1.2 ± 0.0
	20:5 n-3	2.3 ± 0.0	2.5 ± 0.0	2.5 ± 0.0
	22:5 n-3	1.4 ± 0.0	1.3 ± 0.0	1.2 ± 0.0
	22:6 n-3	4.6 ± 0.1	5.0 ± 0.1	4.7 ± 0.0
GPL	14:0	0.3 ± 0.0	0.3 ± 0.0	0.3 ± 0.0
	16:0	24.6 ± 0.2	24.8 ± 0.3	24.1 ± 0.2
	16:1	0.4 ± 0.0	0.3 ± 0.0	0.5 ± 0.0
	18:0	15.8 ± 0.1	15.6 ± 0.2	16.4 ± 0.2
	18:1	14.2 ± 0.1	14.2 ± 0.1	14.2 ± 0.0
	18:2	13.0 ± 0.0[a]	12.9 ± 0.1[b]	11.6 ± 0.0[a,b]
	20:1	0.4 ± 0.0[a]	0.3 ± 0.0[b]	0.7 ± 0.0[a,b]
	20:3 n-6	1.1 ± 0.0	1.1 ± 0.0	1.1 ± 0.0
	20:4 n-6	9.0 ± 0.0[a]	9.0 ± 0.1[b]	10.0 ± 0.0[a,b]
	20:5 n-3	6.6 ± 0.0	6.6 ± 0.0	6.5 ± 0.1
	22:4 n-6	0.6 ± 0.0[a]	0.6 ± 0.0	0.8 ± 0.0[a]
	22:5 n-3	2.4 ± 0.0[a]	2.5 ± 0.0	2.8 ± 0.0[a]
	22:6 n-3	11.8 ± 0.1	11.7 ± 0.1	11.3 ± 0.1

Each value is the average obtained from three FAME preparations. Values that share common superscript letters in each row are significantly different at $P < 0.01$. Minor components and C_{24} acids are omitted

In the absence of silica gel, TAG can be readily derivatized to FAME in two solvent phases composed of hexane and methanol [24]. Acetone in the methanol phase enhances the reaction rate, as described for methanolysis of TAG isolated by SPE columns. Silica gel interfered with the reaction, and under the conditions used for the two-phase solvent system, conversion of TAG to FAME resulted in low yields. However, methanolysis of TAG was completed in 90 s at room temperature with trace amounts of FFA byproducts, when silica gel that adsorbed TAG was treated with the homogeneous solution of 0.8 M CH_3ONa in toluene/acetone/methanol (Fig. 6, lanes 6–8).

CE on silica gel was also incubated with CH_3ONa solution (Fig. 6, lanes 2–5). CE disappeared within 30 min at 45 °C or 45 min at 37 °C, but considerable amounts of FFA were produced, as reported previously [25]. The compositions of the FFA were not different from those of FAME formed by methanolysis. FFA in the reaction mixture were scavenged by adding 3 ml of 0.8 M HCl in 95% methanol. Most of the FFA were methylated at 45 °C for

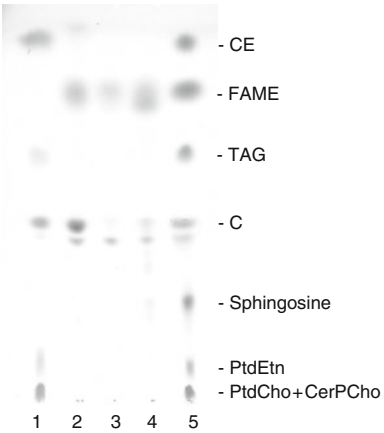

Fig. 7 Methanolysis of blood lipid classes with 1.2% HCl/methanol/toluene in the presence of silica gel. See "Materials and Methods" for details on preparation of FAME. The TLC plate was developed to 3.5 cm from the origin in chloroform/methanol/15 M NH_3 (80:20:1, v/v/v), and then redeveloped in hexane/*tert*-BME (90:10, v/v). *Lane 1* blood total lipids; *lanes 2–4* products of CE, TAG, and phospholipids, respectively; *lane 5* authentic lipids

20 min. Remaining FFA and cholesterol derived from CE were removed by SPE columns prior to GC.

FAME were formed from GPL within 90 s at room temperature by the same procedures as described for TAG, but they were contaminated with sphingomyelin, lysoplasmalogen, pigments, and other impurities (Fig. 6, lanes 9–12). Sphingomyelin and lysoplasmalogen in the reaction mixture showed little extraction by hexane. Pigments and other impurities were derived from the original GPL preparation and were removed by SPE columns.

Purification of FAME by Silica gel SPE Columns

Methanolysis of CE inevitably produces free cholesterol as a byproduct. As methanolysis of acyl lipids is accompanied by a side reaction, saponification or hydrolysis, in the presence of water, small amounts of FFA are formed during the reaction. FAME products obtained under the present conditions of methanolysis were contaminated by cholesterol, FFA, and other impurities, such as pigments. These impurities were removed by SPE columns (Figs. 5, 6). Purification of FAME is thus recommended, but FAME products can be injected immediately into GC columns without purification to speed up analysis as adopted in most methods reported previously [1–3, 7]. Reactions of blood lipids in HCl/methanol at high temperatures are accompanied by the formation of two major artifacts derived from CE and cholesterol [29, 30], i.e., 3,5-cholestadiene and cholesteryl methyl ether, the latter of which cannot be removed by silica columns. Base-catalyzed methanolysis used in the present method does not generate these artifacts.

Fatty Acid Compositions of Lipid Classes and Yields of FAME

The three major *O*-acyl lipids of blood, CE, TAG, and GPL, were isolated by silica gel SPE columns or TLC, and converted into FAME. The fatty acid compositions of these lipid classes were determined by GC and they were compared with each other and with those obtained by a conventional method (Table 1). There were no remarkable differences in fatty acid composition among these methods, although some small but significant differences were found. To assess the validity of the present methods, the yields of FAME were compared between the present methods and a conventional method including Folch extraction followed by isolation of lipid classes by TLC. Total lipids were extracted with the *tert*-BME or chloroform solvents containing three internal standards, i.e., cholesteryl erucate, glyceryl trierucate, and dierucoyl GroPCho. In GC analysis of the FAME thus prepared, similar yields were obtained for the two present methods and the conventional method (data not shown). These findings support the validity and reliability of the present methods. Although fatty acid analysis of lipid classes in whole blood was reported here, plasma and serum can also be analyzed.

Some fatty acid species are acid- and heat-labile. For example, conjugated linoleic acids that occur predominantly in dairy products and show physiological activities are associated human plasma lipids in small quantities [31]. As these acids are unstable under acidic conditions, Methods I and II, which include base-catalyzed methanolysis under mild temperature conditions, will be useful for determination of these acid-labile fatty acid species in plasma lipid classes.

When the combined fatty acid compositions of both *O*-acyl and *N*-acyl phospholipids including sphingomyelin are required, acid-catalyzed methanolysis must be used. Even in this case, a combination of lipid extraction from blood with *tert*-BME/methanol and methanolysis at 100 °C with 1.2% HCl/methanol prepared from aqueous conc. HCl and methanol [10] is recommended for safety and convenience (Fig. 3). Figure 7 shows methanolysis products obtained by this combination. A pale spot found near the solvent front in lane 2 is probably 3,5-cholestadiene, a decomposition product of cholesterol.

In conclusion, the present protocols for preparation of FAME from lipid classes of blood do not include chloroform in the lipid extraction and TLC steps. The reactions of all three lipid classes, CE, TAG, and GPL, proceed at room temperature or at 45 °C. Method I in which lipid classes isolated by SPE columns may be more readily automated than Method II in which silica gel bands corresponding to individual lipid classes on TLC plates must be manually

scraped off. TLC, on the other hand, has been commonly used for separation of blood total lipids into lipid classes. In each method, the protocols proposed are thus safer for researchers and have less impact on the environment than those adopted previously. Moreover, the reaction conditions are mild for lipids. In the future, it may be worthwhile to further develop these methods to simpler and time-saving direction.

Acknowledgments We thank Dr. Kouhei Yamamoto (Osaka Prefecture University) for his advice on GC analysis of blood fatty acids. This work was partially supported by the Kansai Bureau of Economy, Trade and Industry/Ministry of Economy, Trade and Industry Japan, the Kyoto Municipal Industrial Research Institute, and the Advanced Scientific Technology and Management Research Institute of Kyoto.

References

1. Lands WEM, Libelt B, Morris A, Kramer NC, Prewitt TE, Bowen P, Schmeisser D, Davidson MH, Burns JH (1992) Maintenance of lower proportions of (n-6) eicosanoid precursors in phospholipids of human plasma in response to added dietary (n-3) fatty acids. Biochim Biophys Acta 1180:147–162
2. Ma J, Folsom AR, Shahar E, Eckfeldt JH (1995) Plasma fatty acid composition as an indicator of habitual dietary fat intake in middle-aged adults. Am J Clin Nutr 62:564–571
3. Baylin A, Kim MK, Donovan-Palmer A, Siles X, Dougherty L, Tocco P, Campos H (2005) Fasting whole blood as a biomarker of essential fatty acid intake in epidemiologic studies: comparison with adipose tissue and plasma. Am J Epidemiol 162:373–381
4. Hodson L, Skeaff CM, Fielding BA (2008) Fatty acid composition of adipose tissue and blood in humans and its use as a biomarker of dietary intake. Prog Lipid Res 47:348–380
5. Steffen LM, Vessby B, Jacobs DR Jr, Steinberger J, Moran A, Hong C-P, Sinaiko AR (2008) Serum phospholipid and cholesteryl ester fatty acid and estimated desaturase activities are related to overweight and cardiovascular risk factors in adolescents. Int J Obes 32:1297–1304
6. Saadatian-Elahi M, Slimani N, Chajes V, Jenab M, Goudable J, Biessy C, Ferrari P, Byrnes G, Autier P, Peeters PHM, Ocke M, Bueno de Mesquita B, Johansson I, Hallmans G, Manjer J, Wirfält E, Gonzalez CA, Navarro C, Martinez C, Amiano P, Suarez LR, Ardanaz E, Tjønneland A, Halkjaer J, Overvad K, Jakobsen MU, Berrino F, Pala V, Palli D, Tumino R, Vineis P, de Magistris MS, Spencer EA, Crowe FL, Bingham S, Khaw K-T, Linseisen J, Rohrmann S, Boeing H, Noethlings U, Olsen KS, Skeie G, Lund E, Trichopoulou A, Oustoglou E, Clavel-Chapelon F, Riboli E (2010) Plasma phospholipid fatty acid profiles and their association with food intakes: results from a cross-sectional study within the European prospective investigation into cancer and nutrition. Am J Clin Nutr 89:331–346
7. Lepage G, Roy CC (1986) Direct transesterification of all classes of lipids in a one-step reaction. J Lipid Res 27:114–120
8. Ichihara K, Waku K, Yamaguchi C, Saito K, Shibahara A, Miyatani S, Yamamoto K (2002) A convenient method for determination of the $C_{20–22}$ PUFA composition of glycerolipids in blood and breast milk. Lipids 37:523–526
9. Bailey-Hall E, Nelson EB, Ryan AS (2008) Validation of a rapid measurement of blood PUFA levels in humans. Lipids 43:181–186
10. Ichihara K, Fukubayashi Y (2010) Preparation of fatty acid methyl esters for gas–liquid chromatography. J Lipid Res 51:635–640
11. Nagano K, Kano H, Arito H, Yamamoto S, Matsushima T (2006) Enhancement of renal carcinogenicity by combined inhalation and oral exposures to chloroform in male rats. J Toxicol Environ Health A 69:1827–1842
12. Schmid P, Hunter E, Calvert J (1973) Extraction and purification of lipids: III. Serious limitations of chloroform and chloroform–methanol in lipid investigations. Physiol Chem Phys 5:151–155
13. Matyash V, Liebisch G, Kurzchalia TV, Shevchenko A, Schwudke D (2008) Lipid extraction by methyl-*tert*-butyl ether for high-throughput lipidomics. J Lipid Res 49:1137–1146
14. Ackman RG (1998) Remarks on official methods employing boron trifluoride in the preparation of methyl esters of the fatty acids of fish oils. J Am Oil Chem Soc 75:541–545
15. McCreary DK, Kossa WC, Ramachandran S, Kurtz RR (1978) A novel and rapid method for the preparation of methyl esters for gas chromatography: application to the determination of the fatty acids of edible fats and oils. J Chromatogr Sci 16:329–331
16. Christie WW (2003) Lipid analysis, 3rd edn. The Oily Press, UK
17. De Vriese SR, Christophe AB, Maes M (2003) Fatty acid composition of phospholipids and cholesteryl esters in maternal serum in the early puerperium. Prostaglandins Leukot Essent Fatty Acids 68:331–335
18. Ichihara K, Iwasaki H, Ueda K, Takizawa R, Naito H, Tomosugi M (2005) Synthesis of phosphatidylcholine: an improved method without using the cadmium chloride complex of *sn*-glycero-3-phosphocholine. Chem Phys Lipids 137:94–99
19. Dittmer JC, Lester RL (1964) A simple, specific spray for the detection of phospholipids on thin-layer chromatograms. J Lipid Res 5:126–127
20. Folch J, Lees M, Sloane Stanley GH (1957) A simple method for the isolation and purification of total lipides from animal tissues. J Biol Chem 226:497–509
21. Cyberlipid Center (accessed October 2010) Techniques of analysis/extraction, handling of extracts/general methodology. http://www.cyberlipid.org
22. Bligh EG, Dyer WJ (1959) A rapid method of total lipid extraction and purification. Can J Biochem Physiol 37:911–917
23. Bitman J, Wood DL, Hamosh M, Hamosh P, Mehta NR (1983) Comparison of the lipid composition of breast milk from mothers of term and preterm infants. Am J Clin Nutr 38:300–312
24. Ichihara K, Shibahara A, Yamamoto K, Nakayama T (1996) An improved method for rapid analysis of the fatty acids of glycerolipids. Lipids 31:535–539; 31:889 (Erratum)
25. Christie WW (1982) A simple procedure for rapid transmethylation of glycerolipids and cholesteryl esters. J Lipid Res 23:1072–1075
26. Ichihara K, Yamaguchi C, Nishijima H, Saito K (2003) Preparation of fatty acid methyl esters from sterol esters. J Am Oil Chem Soc 80:833–834
27. Ando N, Ando S, Yamakawa T (1971) The structure and formation mechanism of *N*-acetone derivatives of phosphatidyl ethanolamine. J Biochem 70:341–348
28. Kuksis A, Ravandi A, Schneider M (2005) Covalent binding of acetone to aminophospholipids in vitro and in vivo. Ann NY Acad Sci 1043:417–439
29. Shapiro IL, Kritchevsky D (1965) Degradation of cholesterol during transesterification of cholesterol stearate. J Chromatogr 18:599–601
30. Kramer JKG, Hulan HW (1976) Artifacts produced during acid-catalyzed methanolysis of sterol esters. J Lipid Res 17:674–676
31. Shahin AM, McGuire MK, McGuire MA, Ritzenthaler KL, Shultz TD (2003) Determination of *c*9,*t*11-CLA in major human plasma lipid classes using a combination of methylation methodologies. Lipids 38:793–800

Lipids (2011) 46:307–309
DOI 10.1007/s11745-011-3543-3

EDITORIAL

Citations: The Rules They Didn't Teach You

Eric J. Murphy

Citations, so many citations, so what is right and what is wrong? As an editor-in-chief, as a reviewer, and as an author of my own journal articles I have personally dealt with this question on multiple levels. At times, the emergence of PubMed has resulted in a citation explosion and a resulting quagmire as many authors are just not selective about referencing papers and tend to be a bit over zealous in citing more and more papers many of which are not on the topic. In such cases, I often question whether these authors have read anything more than just the titles of these papers that they cite left and right to support their own work. Last August, Dr. William J. Pearce authored an intriguing opinion piece in *The Scientist* entitled "Citations: Too Many, or Not Enough" (*The Scientist* 24(8):29). In this piece he waxed somewhat nostalgic regarding the use of *Index Medicus,* bringing back fond memories of how we found citations in the "old days". Of course, of late, I have been referred to as a dinosaur. Although I am not "Singin' the Dinosaur Blues" (a reference to a Steven Fromholz song sung by Jerry Jeff Walker), I do think it is indeed an important point to understand what are the best practices for citing the literature. Dr. Pearce also brought forth additional points about the current use of citations in the literature such as the number of citations in a manuscript, the quality of citations used, the appropriateness of these citations, and the use of reviews as a substitute for the primary literature. These are all extremely important issues that are a concern for many in the field and are addressed herein.

E. J. Murphy (✉)
Department of Pharmacology, Physiology, and Therapeutics, University of North Dakota, Grand Forks, ND 58202-9037, USA
e-mail: eric.murphy@med.und.edu

How do you find a citation? How do you know if a citation is appropriate? Prior to the invention of PubMed and Google as a means to search the scientific literature and back when people recognized such names as *Index Medicus* or *Current Contents*, we would start with several papers on the topic of interest. After thoroughly reading and understanding the content of these papers, the references would lead us to the next round of papers from the literature that were deemed to be pertinent. Scampering off to the library and pulling these 20–30 new papers to read we determined if these papers could be used as citations in the burgeoning manuscript that we were composing. Someone skilled in the art of citation seeking would then have another round of papers to pull as these 20–30 papers would lead to new potentially citable papers in the literature.

There are several important themes in this process that may be absent today. First, papers were read completely because that was the only way to really determine if there were important references contained in the paper being read that could be potentially useful. Second, there was a need to really understand and comprehend what was being discussed in the paper being read to make an informed decision whether it was indeed worth citing in your manuscript. Hence, decisions were made based upon a lot of time devoted to reading and understanding the literature. What concerns me is the emerging practice of authors having not really read the papers that they cite, but an even greater concern is whether authors have read anything more than the title of a paper that they are citing. Hence, these authors have not really made any decision on citing a particular paper based upon a true comprehension of that paper, but rather are citing that paper based upon a rather superficial understanding of it based solely upon the title or abstract.

In this type of authors' defense, it is a really quick process to get the citation. But should it be? In the past, finding citations took time, but it also meant reading papers and being more judicious in selecting papers on the topic to cite, reducing the superfluous citations that are common today. As a graduate student coming of age at that time, the citations of another laboratory's work in the literature or the repeated reference to a particular paper would bolster my confidence that this paper was truly worth reading and that it might serve as a solid citation in my own manuscript. This confidence was a key point in teaching yourself to place a value on the quality of the work presented in potential citations and to pick only those that met an ever evolving selectivity.

Does this mean that Google and PubMed should not be used to find citations? Absolutely not as these are modern and useful tools for searching through the ever growing literature. However, there is something to be said about having to go the library to see the newest copy of *Lipids*, *Biochemistry*, *Journal of Neurochemistry*, or *Journal of Lipid Research* to see what the newest papers are in each issue. This used to be accomplished by a weekly trip to the library to actually look at something called a printed copy of these journals. Hence, there was an effort to actually look at the literature, not merely use a computer search to find a particular topic. In the past, this was how we often found important papers that otherwise might have been overlooked. Today of course we have the table of contents for our favorite journals sent to us by e-mail, which enables us to look through the various papers published in an issue and select ones to print off or to save as a PDF to our computer. The question then is whether or not these printed or saved papers are ever really read and fully digested by the reader.

This brings me to the ever increasing citation of reviews as if they were primary literature. In the past, reviews were written by absolute leaders in the field who where imparting to the readers years of knowledge in the field and putting the current status of the field into perspective. Hence, there was a sense of validation to the papers that were cited in the review as you knew that the author was indeed one of the world's leading experts on that topic. Is that still the case today? Over the past few years, I often find reviews written by people who I don't recognize as a leader in the field and may not recognize them at all. This causes a major credibility gap, but more importantly, it suggests that less well-known individuals recognize that reviews, good or bad, will get cited by individuals who are unwilling to bother with reading the primary literature.

Let me give you a personal example as I am currently composing a review on fatty acid binding proteins (FABP) in the brain. I have used PubMed to look for potential missing key papers, which was more or less not overly productive. However, reading the literature, which when combined with the PubMed search, led to about 35 novel papers. After reading these papers, I generated another list of about 15 or more papers to acquire and then read prior to initiating writing of that review. While I know this literature quite well, I was amazed by the number of papers I didn't have in my collection and these papers I came to via reading the literature and looking for unique citations in these papers that would be useful and pertinent to the review. However, this is a bit of a tangent, nonetheless an important one about composing a review, yet it includes the ideas of reading the papers being cited as well as using someone else's citations to find previously unknown literature to you on the topic of interest. This newly acquired literature was located despite doing a thorough PubMed search, which of course depended upon me picking the correct key words as well as the authors picking the correct key words. While I figure that the authors might have chosen correctly, my confidence in myself on this point is less than overwhelming.

However, does a review on, let's say FABP in the brain, suffice for a reference for the role of FABP3 in brain fatty acid uptake? No. A review might be useful to cite as a global vision on the role of FABP in brain function, yet the actual paper(s) in which the observation regarding fatty acid uptake was illuminated should be cited. This is where I find many authors repeatedly making this mistake, assuming that citing a review is sufficient, but it is absolutely not sufficient nor is such a citation correct.

Why is this so critical? Well for two overlapping reasons. First, it fails to give credit to the individuals who make a particular discovery and report this in the literature. The author of the review may not have made that observation, so why give them credit? So many times I see a repeated citation of a review by multiple authors over several years, yet when looking at the actual review I find it has little to do with what it is credited to report. Hence, it is especially important not to start an inappropriate base for others to continue to make an incorrect citation, but not giving credit where credit is due does exactly that. Second, citing a review does not permit an individual to grow the number of references to their work nor to the journal in which it was originally printed. This can impact many aspects of career development such as promotion and salary, but for a journal it impacts how well a journal is perceived by the greater science community. Thus, in the end, I guess the "Golden Rule" again comes into play, cite others' work properly as you hope others will cite your work properly.

Yet amazingly, editors love to publish reviews because this type of publication is often highly cited and that will drive up a journal's impact factor. Whether such a citation

is right or wrong is based upon the willingness of the individuals doing the citing actually to read the review and the primary literature cited therein. Well-written reviews offer an incredible resource to a novice in the field giving a historical background and a current perspective by a leader in the field. Well-written reviews offer readers an up-to-date literature review and a great starting-off point to begin collecting the most pertinent literature that they can begin to read. Undoubtedly, this will give them an additional insight into particular discoveries as well as offer a new source for potential pertinent references not contained in the review. Hence, reviews are crucial for every field in science, but the use of reviews as the key citation for this or that discovery is not proper as such citations should go back to the original literature.

While Dr. Pearce highlighted the increase in the number of citations per paper using the *American Journal of Physiology* as an example, he noted that the average number of citations per paper grew from 29 in 1989 to 37 in 1999 and then to 42 in 2009 [1], I really don't see much of a problem with this trend. As the literature expands, it is my expectation that authors will need to cite more and more papers from the literature to be complete. Adding an additional 13 papers cited on average over a 20 year period is not overwhelming nor is the growth of 5 papers over the last 10 years. I would rather see an author include 10–15 additional references in a manuscript that are all deemed important rather than pick and choose which work is cited or even worse use one or two reviews to fill this void. So, in the end I think it is important to cite papers that bring into perspective for the reader the important background required to introduce the topic properly, the methods used in the study, and the required citations to have a proper discussion of how the author's work fits into the field. This of course includes citations that both support the author's conclusions as well as those that might dispute the author's conclusions.

This editorial condenses down to my rather simple rules for citations. These rules may not be all-comprehensive, but I have done the best I can to be inclusive. Here they are:

1. Read and comprehend all of the literature that you are citing in your manuscript
2. Cite the primary literature and the actual papers to which a particular discovery is attributed; if multiple citations need to be made, do so
3. Cite the literature that agrees as well as that which disagrees with your point-of-view; be fair to multiple points-of-view
4. Be as inclusive as possible, but know where to draw the line, citing the most pertinent literature and the original papers
5. Use reviews judiciously in your manuscript and use them properly
6. Do NOT cite reviews in lieu of citing the original literature
7. Remember that PubMed goes back to 1966, but many worthwhile discoveries were made prior to that time and it is important to be historically accurate in your citations
8. When citing your own work, do so to support your point-of-view or to put the current work into the proper context for the reader. Do not attempt to grow your own citation base solely on the dreaded "self-citation"

Following these simple rules will certainly help limit the use of improper, superfluous citations because you have actually read the literature. An additional advantage is that by reading the literature, you will be able to find those elusive, yet important papers on your topic of interest. This adds importance and perhaps makes an Introduction and Discussion much more relevant and inclusive. By avoiding merely citing your own work and including work of others as well as those papers with a different point-of-view, you are in the end being a good citizen of science and working to recognize the contribution of your colleagues in the field. In the end, following these simple rules avoids many of the issues brought forth in this editorial and in the article by Dr. Pearce. So if you have been a citation abuser, try this 8-step program.

Reference

1. Pearce WJ (2010) Citations: too many, or not enough. Scientist 24(8):29

Lipids (2011) 46:311–321
DOI 10.1007/s11745-011-3540-6

ORIGINAL ARTICLE

Activation of AMP-kinase by Policosanol Requires Peroxisomal Metabolism

Subhashis Banerjee · Sarbani Ghoshal · Todd D. Porter

Received: 10 December 2010 / Accepted: 3 February 2011 / Published online: 27 February 2011

Abstract Policosanol, a well-defined mixture of very long chain primary alcohols that is available as a nutraceutical product, has been reported to lower blood cholesterol levels. The present studies demonstrate that policosanol promotes the phosphorylation of AMP-kinase and HMG-CoA reductase in hepatoma cells and in mouse liver after intragastric administration, providing a possible means by which policosanol might lower blood cholesterol levels. Treatment of hepatoma cells with policosanol produced a 2.5-fold or greater increase in the phosphorylation of AMP-kinase and HMG-CoA reductase, and increased the phosphorylation of Ca^{++}/calmodulin-dependent kinase kinase (CaMKK), an upstream AMP-kinase kinase. Intragastric administration of policosanol to mice similarly increased the phosphorylation of hepatic HMG-CoA reductase and AMP-kinase by greater than 2-fold. siRNA-mediated suppression of fatty aldehyde dehydrogenase, fatty acyl-CoA synthetase 4, and acyl-CoA acetyltransferase expression in hepatoma cells prevented the phosphorylation of AMP-kinase and HMG-CoA reductase by policosanol, indicating that metabolism of these very long chain alcohols to activated fatty acids is necessary for the suppression of cholesterol synthesis, presumably by increasing cellular AMP levels. Subsequent peroxisomal β-oxidation probably augments this effect.

S. Banerjee · T. D. Porter
Graduate Center for Toxicology, University of Kentucky, Lexington, KY 40536-0305, USA

S. Ghoshal · T. D. Porter (✉)
Department of Pharmaceutical Sciences, College of Pharmacy, University of Kentucky, Lexington, KY 40536-0596, USA
e-mail: tporter@email.uky.edu

Keywords Policosanol · AMP-kinase · Peroxisomes · HMG-CoA reductase · Hepatoma cells · Ca^{++}/calmodulin-dependent kinase kinase

Abbreviation
CaMKK Calcium-calmodulin-dependent kinase kinase

Introduction

Policosanol is a well-defined mixture of very long-chain alcohols (C26-C32) derived most commonly from the wax of processed sugar cane [1]. A number of early clinical studies indicated that policosanol at 5–20 mg/day could lower blood cholesterol levels [2–4], although several more recent, larger studies have been unable to replicate this benefit, even with doses up to 80 mg/day [5–7]. Our previous studies [8] showed that policosanol decreases cholesterol synthesis in rat hepatoma cells by up to 30% at concentrations relevant to clinical dosing regimens, providing a possible mechanism to lower blood cholesterol. This inhibition is mediated at or above HMG-CoA reductase, the regulatory step in cholesterol synthesis, but policosanol does not directly inhibit this enzyme nor does it decrease enzyme levels as measured by immunoquantitation [8]. Similar results were obtained with fibroblasts in vitro [9, 10], and two studies with whole animals similarly showed that policosanol treatment decreases hepatic cholesterol synthesis [11, 12]. However, two studies with hamsters were unable to demonstrate an effect of policosanol on cholesterol synthesis in vivo [13, 14].

Policosanol treatment of hepatoma cells increases the phosphorylation of AMP-kinase at Thr172 [8, 15], a

modification known to activate this kinase, providing a possible mechanism by which policosanol might down-regulate HMG-CoA reductase activity and decrease cholesterol synthesis without directly inhibiting the enzyme or reducing its expression: AMP-kinase is the principal regulatory kinase for HMG-CoA reductase, catalyzing the phosphorylation of HMG-CoA reductase at Ser872 [16]. This phosphorylation decreases HMG-CoA reductase activity by 70–80% [17] and is thought to provide a rapid means to modulate cholesterol synthesis in response to cellular ATP levels and other stimuli. The present studies were undertaken to test this hypothesis that policosanol treatment promotes the phosphorylation of HMG-CoA reductase and to identify the mechanism by which policosanol activates AMP-kinase.

Materials and Methods

Chemicals

Lesstanol Brand Natural Policosanol OCTA-60 was kindly provided by Garuda International, Inc. (Lemon Cove, CA). Alcohol content, determined by gas chromatography/flame ionization detection (average of two independent determinations), yielded 66% octacosanol (C28), 17% triacontanol (C30), 6% hexacosanol (C26), 5% dotriacontanol (C32), 2% tetracosanol (C24), and 1% tetratriacontanol (C34). Tricosanol (C23) and heptacosanol (C27) each constituted less than 1% of the mixture, and eicosanol (C20), docosanol (C22), and nonacosanol (C29) constituted less than 0.1%; total alcohol content was 98%. Dulbecco's modified Eagle's medium (DMEM), penicillin-streptomycin-glutamine (PSG), fetal bovine serum (FBS), and trypsin were purchased from Invitrogen (Carlsbad, CA). Acadesine (AICAR), 1,1-dimethylbiguanide hydrochloride (metformin), ionomycin, sodium acetate, and protease inhibitor cocktail were obtained from Sigma (St. Louis, MO). HALT phosphatase inhibitor and the BCA protein assay kit were purchased from Roche Diagnostics (Indianapolis, IN) and Pierce/Thermo Scientific (Rockford, IL) respectively. McA-RH7777 rat hepatoma cells were obtained from American Type Culture Collection (Manassas, VA) and used between passages 12 and 22.

Cell Culture and Preparation of Lysates

McA-RH7777 rat hepatoma cells were cultured in DMEM supplemented with 10% FBS and 1× PSG in six-well plates at 37 °C under a humidified atmosphere of 5% CO_2. After 48 h the medium was replaced with fresh medium with the addition of policosanol (10–25 μg/ml in 50% ethanol) and incubation was continued for 3 h. Control cells received an equal volume of 50% ethanol, which did not exceed 1% final concentration in the medium. Cells were washed once with phosphate-buffered saline (pH 7.4), scraped from the plates, pelleted by low-speed centrifugation, and lysed by two cycles of freeze-thawing (dry ice/ethanol and 37 °C water bath) in 0.25 M Tris–HCl buffer (pH 7.5) containing protease and phosphatase inhibitors at 2× standard concentration. The lysates were cleared by centrifugation (18,300×*g*, 10 min, at 4 °C) and the supernatant was stored in aliquots at −80 °C.

Animal Treatments

Experiments involving the use of animals were performed following protocols approved by the Institutional Animal Care and Use Committee of the University of Kentucky and were in accordance with all policies for the use and care of laboratory research animals as stipulated by the NIH. Seven-to-eight week-old female C57BL/6 J mice (∼15–17 g) were purchased from Jackson laboratories (Bar Harbor, ME) and maintained in a temperature-, humidity-, and light-controlled facility with free access to water and food for one week prior to experimentation. After an overnight fast, mice in groups of 5 were gavaged with 150 μl of policosanol in 50% ethanol in doses of 25, 50 or 100 mg/kg body weight. Control animals received an equal volume of 50% ethanol only. Access to food was restored, and at 0, 3, 6, 12, and 18 or 24 h the mice were euthanized by CO_2 asphyxiation and the liver and intestine were removed and portions promptly frozen in liquid nitrogen and stored at −80 °C until use.

Preparation of Tissue Homogenates

Hepatic and intestinal homogenates were prepared as follows: Approximately 25 mg of tissue was transferred into 4 volumes of ice-cold RIPA homogenization buffer (50 mM Tris–HCl, pH 7.4, 150 mM NaCl, 1 mM PMSF, 1 mM EDTA, 5 μg/ml aprotinin, 5 μg/ml leupeptin, 1% Triton X-100, 1% sodium deoxycholate, and 0.1% SDS) and homogenized using a Potter-Elvehjem homogenizer. The samples were then subjected to two cycles of freeze–thawing (dry ice/ethanol and 37 °C water bath) and then cleared by centrifugation (18,300×*g*, 10 min, 4 °C). The supernatant was stored in aliquots at −80 °C. Protein concentration was determined by BCA assay.

Gel Electrophoresis and Immunoblotting

Thirty micrograms of protein from cell lysate or tissue homogenate was fractionated by SDS-polyacrylamide gel electrophoresis on 8% gels and electroblotted to nitrocellulose (Bio-Rad, Hercules, CA). The membrane was

blocked with 0.05% Tween-20 and 5% defatted milk for 1 h at room temperature and then incubated in this same buffer with rabbit antibody to total AMP-kinase (anti-AMPK α-pan, 1:2000; Upstate/Millipore, Billerica, MA) or to phosphorylated AMP-kinase (anti-phospho-AMPKα, 1:500; Upstate/Millipore) overnight at 4 °C with gentle shaking. The immunoblot was developed with a secondary antibody conjugated to horseradish peroxidase for 1 h at room temperature and the chemiluminescent image (Supersignal West Pico Chemiluminescent Substrate, Pierce/Thermo Scientific) captured by autoradiography on a Kodak Image Station or on film and analyzed for mean intensity above background. Band intensity on film was measured with Image J software on the scanned image with background subtraction. The same procedure was followed for detecting total HMG-CoA reductase (anti-HMG-CoA reductase, 1:1000, Millipore) and phosphorylated HMG-CoA reductase (anti-phospho-HMG-CoA reductase, 1:500; Millipore).

Immunoprecipitation

To determine the level of phosphorylation of the kinases LKB1 and calcium-calmodulin-dependent kinase kinase (CaMKK), cell lysates or tissue homogenates were incubated for 1 h at 4 °C with 20 μl of mouse monoclonal antibody to phosphoserine/phosphothreonine/phosphotyrosine (Abcam, Cambridge, MA). Antibody conjugates were precipitated with 35 μl of protein A or G Plus-Agarose (Calbiochem/EMD Chemicals, Gibbstown, NJ) for 1 h at 4 °C as follows: After centrifugation at 12,000×*g* for 20 s at 4 °C, the immunoprecipitated phosphoproteins were released from the agarose beads by heating at 95 °C for 4 min in 25 μl of 2× gel loading buffer [0.5 M Tris–HCl, pH 6.8, 4.4% SDS, 20% (v/v) glycerol, 2% (v/v) 2-mercaptoethanol, and bromophenol blue in deionized water]. After removal of beads by centrifugation at 12,000×*g* for 20 s at 4 °C, the phosphoproteins were fractionated by SDS-gel electrophoresis and electroblotted to nitrocellulose as described above. Phosphorylated protein content was detected and quantified with an antibody to LKB1 (anti-LKB1, 1:1000; Sigma Chemical) or CaMKK (anti-CaMKK, 1:1000; BD Transduction, San Jose, CA) followed by a secondary antibody conjugated with horseradish peroxidase as described above.

siRNA Plasmid Transfection and RT-PCR Analysis of Expression

Plasmids for the expression of siRNA (SureSilencing™ shRNA, SABiosciences, Frederick, MD) to fatty aldehyde dehydrogenase 3A2 (ALDH3A2), peroxisomal acyl-CoA synthetase long-chain family member 4 (ACSL4), and peroxisomal acetyl-CoA acyltransferase 1 (β-ketothiolase, ACAA1) were prepared by standard techniques from *Escherichia coli* DH5α and used to transfect hepatoma cells plated in 6-well plates at a density of 8×10^4 cells per cm^2 as follows: On the day following plating, plasmid DNA was mixed with Fugene 6 transfection reagent (Roche Diagnostics) according to the manufacturer's instructions at a ratio of 1 μg DNA:5 μl reagent and complexes were allowed to form for a minimum of 30 min at room temperature. The cell culture medium then was replaced with antibiotic-free medium containing 10% FBS and the transfection mixture was added drop-wise to the cells with gentle swirling. Four plasmids with unique siRNA sequences were provided for each gene; all four were tested for efficacy by RT-PCR as described below (data not shown), and the plasmid providing the greatest suppression of mRNA expression for each gene was selected for use (Table 1). A plasmid containing a scrambled siRNA sequence served as the negative control.

Total RNA was isolated from cells with the use of TRIzol reagent (Invitrogen) at 2, 4, 6, 8, and 10 days post-transfection and the concentration of RNA was determined spectrophotometrically with the use of a Nanodrop instrument (Thermo Scientific). First strand cDNA synthesis was performed using 200 units of Superscript II Reverse Transcriptase (Invitrogen) with 200 ng of random primers, 1 μl RNaseOUT (Invitrogen), 5 μg of total RNA, 2 μl of 0.1 M DTT, and 1 μl of dNTP mix (200 μM each nucleotide) in a total volume of 12 μl in diethylpyrocarbonate-treated water.

Table 1 siRNA plasmid sequences and PCR primers

Gene	GeneID	siRNA sequence	PCR primers
ALDH3A2	65183	TCACTGATGTTGACCCTAACT	Fw: 5′-GCGAGAGAAGGACATCTTGG-3′
ALDH3A2	65183	GGGAGAGAGTGTTAACAAACT	Rv: 5′-TCGTCCATCATGGTAAGCAG-3′
ACSL4	113976	GAAGGTGGTTATACAGTTCAT	Fw: 5′-CACCATTGCCATTTTCTGTG-3′
			Rv: 5′-ATAATGCCGCCTTCAGTTTG-3′
ACAA1	24157	ATCTCTGTGGGTAACGTACTT	Fw: 5′-GGTCCAAGGCTGAAGAACTG-3′
			Rw: 5′-CAGTAGAGGGCCTGACTTGC-3′
Scrambled control		GGAATCTCATTCGATGCATAC	

The reaction was incubated at 25 °C for 10 min, followed by 50 min at 42 °C and then inactivated by incubation at 70 °C for 15 min. Synthesized single-stranded cDNA was quantified by Nanodrop measurement. Gene-specific primers for real-time polymerase chain reaction (PCR) were designed using Primer 3 software (http://frodo.wi.mit.edu/primer3/) and are shown in Table 1. Each 20-µl PCR reaction mixture contained 0.1 µg of single-stranded cDNA or template, 0.5 µl of gene-specific primers (10 µM each), 3 µl of dNTP mix (200 µM each nucleotide) and 1× SYBR Green PCR buffer (Applied Biosystems, Carlsbad, CA). Cycling conditions were: 2 min at 50 °C to activate, initial denaturation for 10 min at 95 °C, followed by 50 cycles of denaturation for 15 s at 95 °C and 1 min of annealing/extension at 55 °C. In order to detect nonspecific amplification, dissociation curves were established for each PCR product. The detection and quantitation of nucleic acid levels was done by using the comparative delta-delta ct method [18].

Statistical Analysis

Image intensity values for each blot were normalized, setting the control (untreated) value at 100 after background subtraction. Results are presented as the mean and standard deviation with significance determined by one-way analysis of variance (ANOVA) with either Dunnett's or Tukey's post-hoc test, setting $p < 0.05$, using Prism (GraphPad Software, La Jolla, CA).

Results

Previous results from our laboratory demonstrated that policosanol activates AMP-kinase in hepatoma cells [8]. To confirm and extend those findings, we carried out dose-response and time-course experiments. Policosanol increased AMP-kinase phosphorylation in hepatoma cells by more than 2.5-fold after a 3-h treatment (Fig. 1a), with maximal stimulation occurring between 15–25 µg/ml. These increases were comparable to those seen with AICAR and metformin, both of which are known to promote phosphorylation of AMP-kinase and served as positive controls. No change in the level of total AMP-kinase protein levels were observed over the 3-hr period of the experiment. As shown in Fig. 1b, policosanol treatment rapidly activated AMP-kinase, with an increase in phosphorylation evident at 30 min; phosphorylation peaked at 1.5 h and stayed elevated through 3 h.

The activation of AMP-kinase by policosanol was concomitant with the phosphorylation of HMG-CoA reductase in hepatoma cells, as shown in Fig. 2. HMG-CoA reductase phosphorylation was increased in a dose-dependent manner with 10–25 µg/ml of policosanol. Treatment of

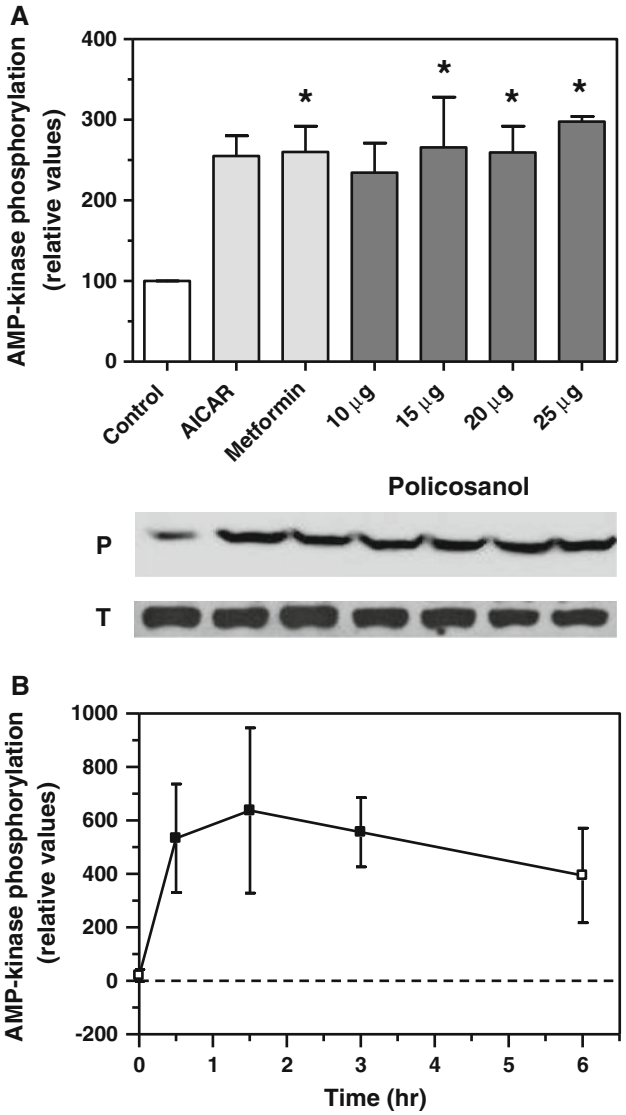

Fig. 1 Policosanol activates AMP-kinase in vitro. **a** Phosphorylated AMP-kinase in hepatoma cells was measured by immunoquantitation with an antibody specific for the phosphorylated protein after a 3-h treatment with 10–25 µg/ml of policosanol. The AMP-kinase activators AICAR and metformin (1 mM each) served as positive controls. Values represent the mean and standard deviation of three experiments; *asterisks* indicate values statistically different from control (ANOVA with Dunnett's post-hoc test, $p < 0.05$). Representative immunoblots of phosphorylated (P) and total (T) AMP-kinase are shown below the graph. **b** AMP-kinase phosphorylation in hepatoma cells at various times after treatment with 15 µg/ml of policosanol. Values represent the mean and standard deviation of three experiments; *closed symbols* are statistically different from the zero-time value

cells with AICAR or metformin yielded a similar increase in phosphorylated HMG-CoA reductase. Total HMG-CoA reductase protein levels did not change over the course of this experiment.

To extend these studies to whole animals in vivo, the phosphorylation of AMP-kinase and HMG-CoA reductase

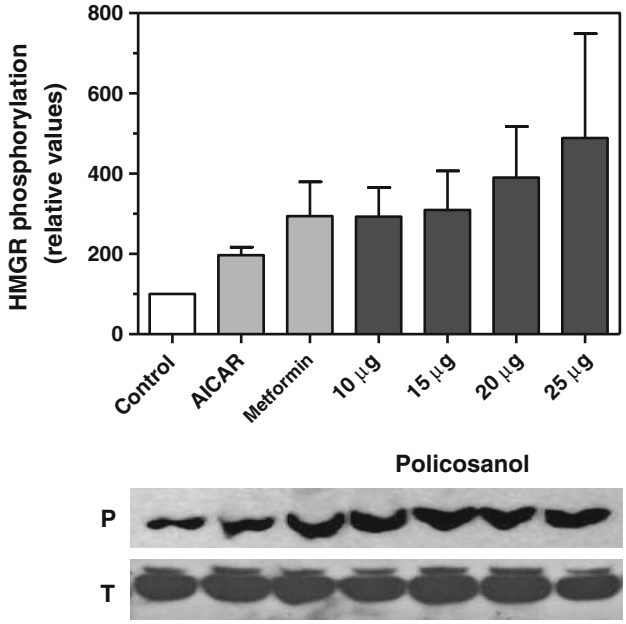

Fig. 2 Policosanol inactivates HMG-CoA reductase in vitro. Phosphorylated HMG-CoA reductase in hepatoma cells was measured by immunoquantitation with an antibody specific for the phosphorylated protein after a 3-h treatment with 10–25 μg/ml of policosanol. AICAR and metformin (1 mM each) served as positive controls. Values represent the mean and standard deviation of three experiments. Representative immunoblots of phosphorylated (P) and total (T) HMG-CoA reductase are shown below the graph

was assessed in the livers of mice gavaged with a single dose of policosanol at 10, 25, 50, and 100 mg/kg. As shown in Fig. 3, policosanol increased the phosphorylation of AMP-kinase and HMG-CoA reductase at 25 and 50 mg/kg by 2 to 4-fold as early as 3 h after dosing. No increase in phosphorylation was seen at lower (10 mg/kg) or higher doses (100 mg/kg), and no change in the total AMP-kinase or HMG-CoA reductase was observed at each of time points and the dosing regimens tested (data not shown). Policosanol had no effect on AMP-kinase in the duodenum of mice gavaged with 25 or 50 mg/kg (data not shown), suggesting that intestinal cholesterol synthesis, which can account for up to 25% of circulating cholesterol, is resistant to suppression by these fatty alcohols.

As AMP-kinase is itself activated by upstream kinases, we wanted to determine if policosanol acted on these upstream kinases. The principal AMP-kinase kinase is LKB1, but AMP-kinase can also be activated by CaMKKβ [19]. As both kinases are activated by phosphorylation, we monitored their phosphorylation in hepatoma cells and in mouse liver by immunoblotting after policosanol treatment. LKB1 phosphorylation was increased about 3-fold in hepatoma cells by policosanol (Fig. 4), slightly less than that seen with metformin, a known activator of LKB1, although neither increase was statistically significant. LKB1 phosphorylation was not increased in mouse liver after gavage with policosanol. CaMKK phosphorylation was increased in hepatoma cells about 2.5-fold by policosanol, and to a slightly greater extent than that seen with ionomycin, an activator of CaMKK; both increases were statistically significant. CaMKK phosphorylation also was increased up to 4-fold in mouse liver at 6 h post-dosing, and remained elevated up to 18 h, although these increases did not reach statistical significance. These results support the activation of AMP-kinase by policosanol both in cell culture and in vivo, and suggest that CaMKK contributes to this activation.

Long-chain fatty alcohols are substrates for the 'fatty alcohol cycle' which converts these alcohols to their corresponding fatty acids [20]. To determine if metabolism of policosanol by this pathway was necessary for the activation of AMP-kinase, we used siRNA to suppress the expression the second enzyme in this pathway, fatty aldehyde dehydrogenase 3A2, in hepatoma cells. As shown in Fig. 5, the siRNA plasmid suppressed ALDH3A2 mRNA expression nearly completely at 4 and 6 days post-transfection. The corresponding ability of policosanol to promote AMP-kinase phosphorylation at 4, 6, and 8 days post-transfection was reduced by greater than 50% in these cells, and phosphorylation of HMG-CoA reductase was nearly extinguished. These results reveal that the very long chain alcohols that make up policosanol must be converted to fatty acids in order to activate AMP-kinase.

To determine if peroxisomal metabolism of policosanol was also required for activation of AMP-kinase, we used siRNA to suppress the expression of peroxisomal acyl-CoA synthetase long-chain family member 4 (ACSL4) and peroxisomal acetyl-CoA acyltransferase 1 (β-ketothiolase, ACAA1) in hepatoma cells; these enzymes catalyze the activation of long-chain fatty acids and the last step in peroxisomal β-oxidation, respectively. As shown in Fig. 6, mRNA levels for both enzymes were suppressed by greater than 80% on days 4 and 6 post-transfection, similar to that seen with ALDH3A2. The ability of policosanol to stimulate the phosphorylation of AMP-kinase and HMG-CoA reductase was fully prevented in cells transfected with either siRNA plasmid. The ability of metformin to activate AMP-kinase and promote HMG-CoA reductase phosphorylation was not affected by these siRNAs, demonstrating that the AMP-kinase pathway itself was not impaired by the suppression of peroxisomal fatty acid catabolism.

As the principal metabolite of fatty acid β-oxidation is acetyl-CoA, we determined if addition of acetate to cells would similarly increase the phosphorylation of AMP-kinase. As shown in Fig. 7a, addition of sodium acetate (0.12 mM) increased AMP-kinase phosphorylation by 2–3-fold, similar to that seen with AICAR, metformin, and policosanol. To determine if acetate activated AMP-kinase

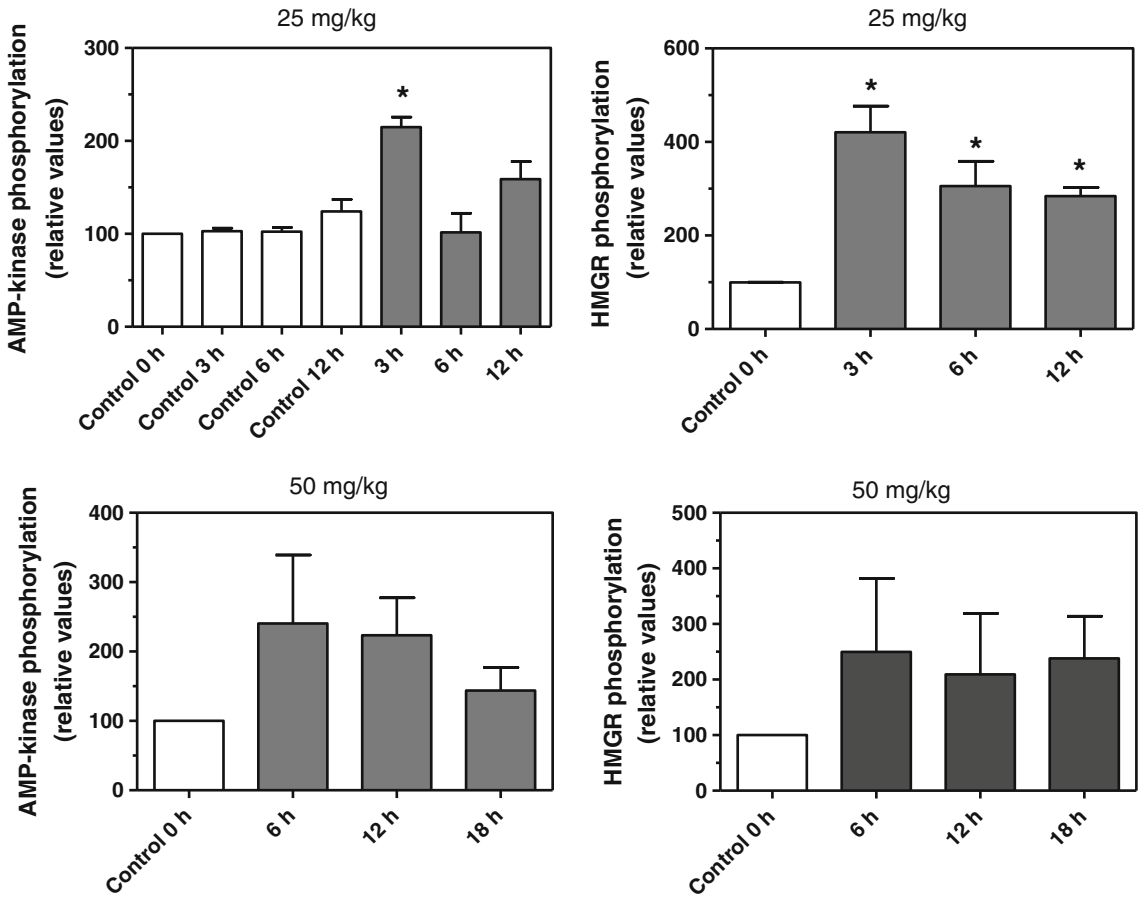

Fig. 3 Policosanol increases the phosphorylation of AMP-kinase and HMG-CoA reductase (HMGR) in vivo. Mice were gavaged with policosanol (25 or 50 mg/kg) and phosphorylated AMP-kinase and HMG-CoA reductase were measured in liver homogenates by immunoquantitation. Values represent the mean and standard deviation of 2–3 experiments; values that are statistically different from untreated controls are indicated with *asterisks*. Statistical significance was determined by ANOVA with Dunnett's post-hoc test, $p < 0.05$

by the same pathway as policosanol, the effect of acetate treatment on CaMKK phosphorylation and LKB1 phosphorylation was measured. As seen with policosanol, acetate increased CaMKK phosphorylation by nearly 3-fold (Fig. 7b), but did not increase LKB1 phosphorylation (Fig. 7c).

Discussion

The present studies reveal that the activation of AMP-kinase by policosanol is dependent upon the oxidation and peroxisomal metabolism of these very long-chain alcohols. It was anticipated that these alcohols would be metabolized by this route [21, 22]; moreover, the ability of long chain fatty acids to activate AMP-kinase is well established [23]. These findings thus provide a biochemical mechanism to explain the observed ability of policosanol to decrease cholesterol synthesis, through the activation of AMP-kinase and subsequent inactivation of HMG-CoA reductase [8, 15]. It is worth noting that D-003, a mixture of very long chain fatty acids also derived from sugarcane wax, has similarly been shown to decrease cholesterol synthesis in cultured fibroblasts [24]. These results do not exclude the possibility that policosanol acts through other HMG-CoA reductase kinases as well, such as a protein kinase C or a calmodulin-dependent protein kinase, as both have been shown to be capable of phosphorylating HMG-CoA reductase in vitro [25].

Metformin, a widely used drug in Type II diabetes, is a potent activator of AMP-kinase [26] and is well known to modestly lower blood lipid levels in patients. The present results are consistent with the possibility that policosanol could act via this same mechanism to lower blood cholesterol levels. However, although we show here that policosanol is able to increase the phosphorylation of HMG-CoA reductase in mouse liver after intragastric administration, the ability of therapeutically recommended doses of policosanol to decrease blood cholesterol levels by this pathway remains in doubt. The doses used in our study, ranging from

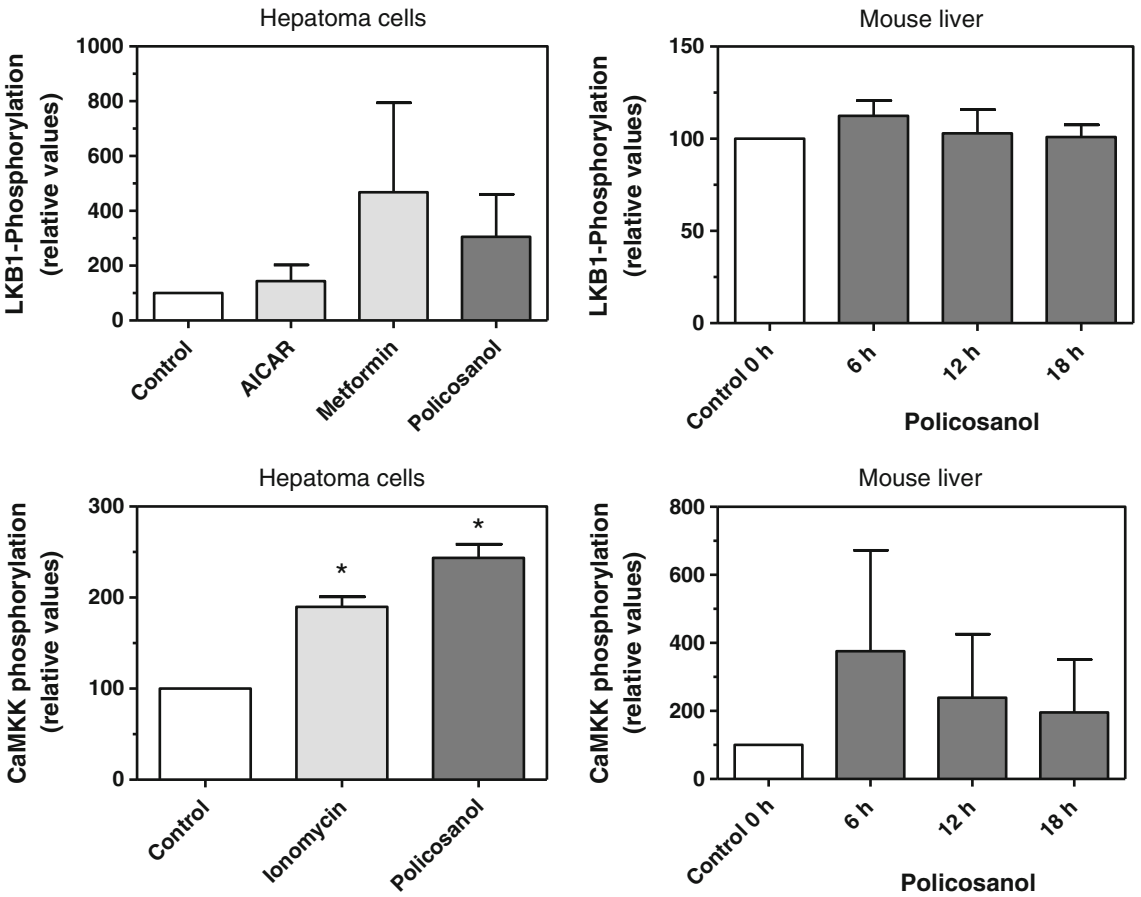

Fig. 4 Policosanol activates CaMKK and LKB1. Phosphorylated LKB1 and CaMKK were immunoprecipitated from hepatoma cell lysates or mouse liver homogenates with an antibody to phosphoserine/phosphothreonine/phosphotyrosine and then quantified by immunoblotting with an antibody to LKB1 or CaMKK. Metformin (1 mM) served as a positive control and AICAR (1 mM) as a negative control for the LKB1 assays; ionomycin (1 μg/ml) was a positive control for the CaMKK assay. Hepatoma cells were incubated with 15 μg/ml of policosanol for 3 h; mice were gavaged with 50 mg/kg body weight of policosanol and the livers removed at 6, 12, and 18 h post-dosing. Values represent the mean and standard deviation of 2–3 experiments; values that are statistically different from controls are indicated with *asterisks*. Statistical significance was determined by ANOVA with Dunnett's post-hoc test, $p < 0.05$

10 to 100 mg/kg by body weight, are considerably higher than those used in clinical studies, where the typical dose is between 5 to 80 mg per day. Assuming that the typical patient weighs 70 kg, a minimal 10 mg/kg dose would require a 35-fold higher dose than that typically used (up to 1 g/d), and this calculation does not consider differences in intestinal absorption between mice and men. Nonetheless, long-chain alcohols are a common constituent of human diets [27], and no significant adverse effects have been noted for policosanol in animal or clinical studies.

CaMKK is thought to be a principal AMP-kinase kinase in brain, but is considered to be an alternative to LKB1 in the liver [28]. In our studies policosanol produced a statistically significant increase in CaMKK phosphorylation in hepatoma cells, suggesting that activation of this upstream kinase by policosanol contributes to the phosphorylation of AMP-kinase. CaMKK phosphorylation was also increased 4-fold in mouse liver after gavage, although this increase was not statistically significant. CaMKK also appeared to be activated by addition of acetate to hepatoma cells, which would bypass the requirement for peroxisomal metabolism; either acetate per se, or its activation to acetyl-CoA or subsequent metabolism would appear to be sufficient to activate this kinase. Notably, Za'tara et al. [23] have shown that non-metabolizable analogs of long-chain fatty acids are also able to activate AMP-kinase, but that this requires activation with coenzyme A. The CoA synthetases that activate these fatty acids to acyl-CoAs generate AMP; AMP is an allosteric regulator of AMP-kinase that facilitates its phosphorylation by LKB1, but not, interestingly, by CaMKK [19, 28]. Thus, β-oxidation of very long chain fatty acids may not be required if they are present in sufficient abundance to generate elevated levels of AMP by activation with coenzyme A.

Our studies with siRNA-mediated suppression of fatty alcohol cycle (ALDH3A2) and peroxisomal enzymes

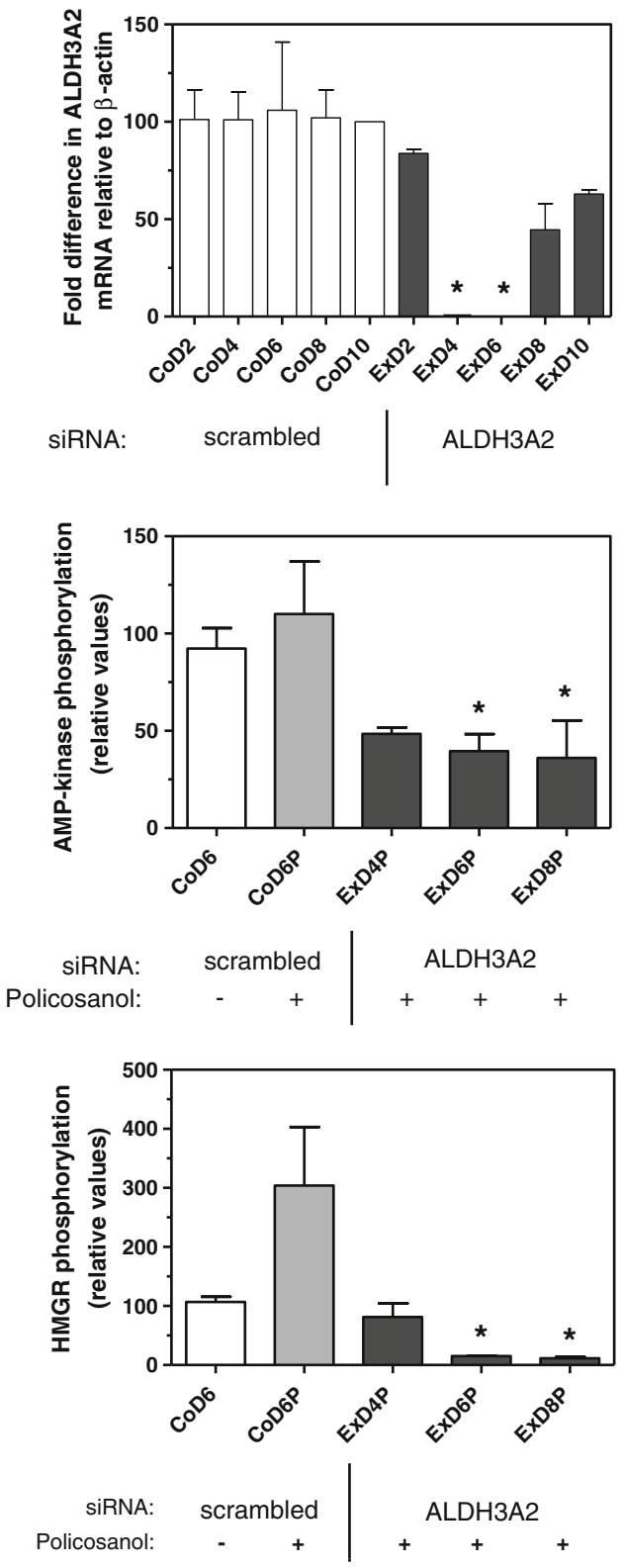

Fig. 5 siRNA-mediated suppression of fatty aldehyde dehydrogenase 3A2 (ALDH3A2) prevents the increase in phosphorylation of AMP-kinase and HMG-CoA reductase by policosanol. ALDH3A2 mRNA was quantified by RT-PCR with the primers listed in Table 1; control cells contained a plasmid with a scrambled siRNA sequence. Phosphorylated AMP-kinase and HMG-CoA reductase were measured by immunoquantitation. Cells were incubated with 15 μg/ml of policosanol for 3 h as indicated. Values represent the mean and standard deviation of 2–3 experiments; values that are statistically different from the corresponding day control (mRNA levels) or the policosanol-treated control are indicated with *asterisks*, as determined by one-way ANOVA with Tukey's post-hoc test, $p < 0.05$. *Co* control cells, *Ex* cells transfected with ALDH3A2 siRNA plasmid; 'D' indicates day post-transfection; 'P' indicates policosanol treatment

(ACSL4, ACAA1) demonstrate that peroxisomal metabolism of policosanol is necessary for the activation of AMP-kinase in hepatoma cells. This requirement for β-oxidation, as shown with ACAA1 suppression, suggests that repeated chain-shortening with subsequent activation by ketothiolase is necessary to generate sufficient AMP to increase AMP-kinase phosphorylation. However, the suppression of peroxisomal β-oxidation not only blocked the effect of policosanol, but also reduced the phosphorylation of AMP-kinase and HMG-CoA reductase below the level seen in non-suppressed (control) cells. This suggests that peroxisomal metabolism contributes to the basal level of AMP-kinase activation under normal physiological conditions. It is thus formally possible that the activation of policosanol-derived fatty acids to acyl-CoAs is sufficient to increase AMP-kinase phosphorylation and activity, without further metabolism by β-oxidation, as found by Za'tara et al. [23]. Nonetheless, under normal circumstances the subsequent peroxisomal metabolism of these activated very long chain fatty acids would greatly increase the generation of AMP and amplify this signaling pathway.

This peroxisomal pathway for the activation of AMP-kinase by policosanol in hepatoma cells can be extrapolated to the liver in an intact animal. However, the observation made here and earlier [29] that acetate, the product of β-oxidation, leads to the activation of AMP-kinase, raises the possibility that policosanol does not need to be absorbed intact to activate hepatic AMP-kinase. Although there is good evidence that the very long-chain alcohols of policosanol are absorbed into the systemic circulation, the fractional absorption is very low [22, 30, 31]. It can be considered that a significant portion of these alcohols may be metabolized in the colon by gut bacteria to generate chain-shortened metabolites, including acetate, propionate, and butyrate, which are readily absorbed and transported to the liver [reviewed in 32]. Moreover, a number of studies have reported that propionate produced in the gut can decrease hepatic cholesterol synthesis [32]. These chain-shortened metabolites would bypass peroxisomal metabolism and serve as direct substrates for cytosolic acyl-CoA synthases, thereby generating AMP; the ability of intraperitoneal administration of acetate to increase AMP levels in hepatocytes and in the liver [33, 34] supports this hypothesis. It was also reported that

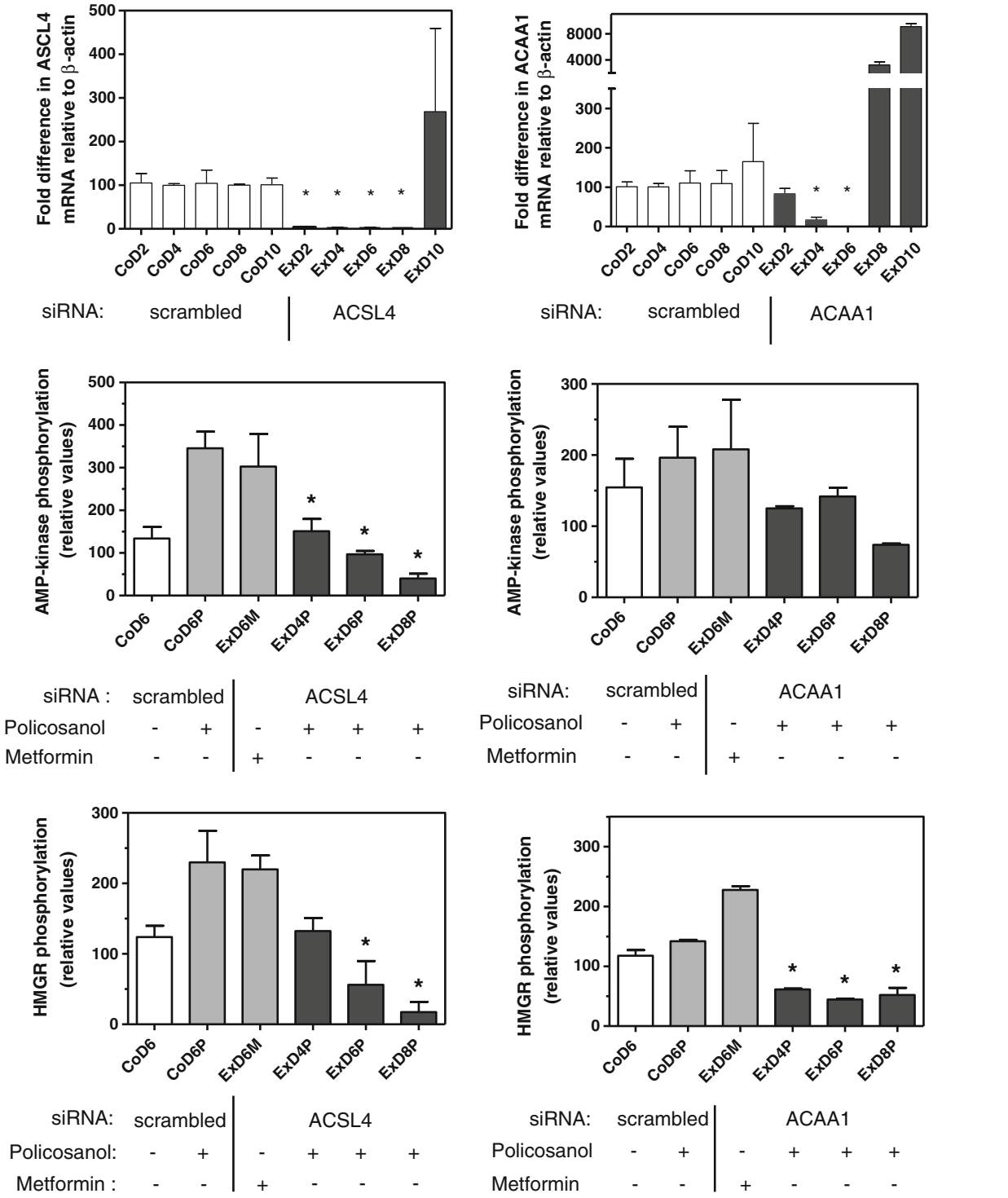

Fig. 6 siRNA-mediated suppression of peroxisomal fatty acyl-CoA synthetase 4 (ACSL4) or acetyl-CoA acyltransferase 1 (ACAA1) prevents the increase in phosphorylation of AMP-kinase and HMG-CoA reductase by policosanol. ACSL4 and ACAA1 mRNA was quantified by RT-PCR with the primers listed in Table 1; control cells contained a plasmid with a scrambled siRNA sequence. Phosphorylated AMP-kinase and HMG-CoA reductase were measured by immunoquantitation. Cells were incubated with 15 μg/ml of policosanol or 1 mM metformin for 3 h as indicated. Values represent the mean and standard deviation of 2 experiments; values that are statistically different from the policosanol-treated control are indicated with *asterisks*, as determined by one-way ANOVA with Tukey's post-hoc test, $p < 0.05$. *Co* control cells; *Ex* cells transfected with ACSL4 or ACAA1 siRNA plasmid; 'D' indicates day post-transfection; 'M' indicates metformin treatment; 'P' indicates policosanol treatment

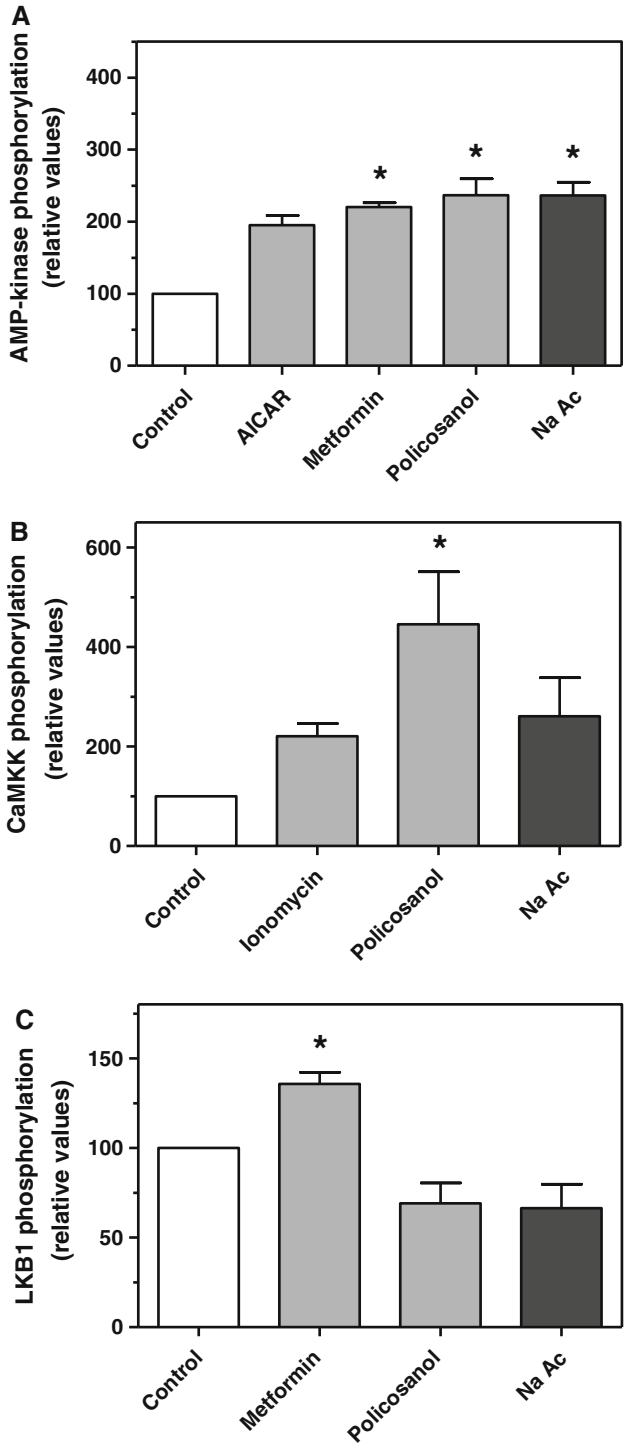

Fig. 7 Treatment of hepatoma cells with sodium acetate promotes the phosphorylation of AMP-kinase through CaMKK. Phosphorylated AMP-kinase (**a**), CaMKK (**b**), and LKB1 (**c**) were measured by immunoquantitation in hepatoma cells three hours after treatment with sodium acetate (0.12 mM), AICAR (1 mM), metformin (1 mM), policosanol (15 μg/ml) or ionomycin (1 μg/ml). Values represent the mean and standard deviation of 2–3 experiments; values that are statistically different from the control are indicated with *asterisks*, as determined by one-way ANOVA with Dunnett's post-hoc test, $p < 0.05$

acetate treatment of hepatocytes decreased SREBP-1 mRNA levels [29], which could lead to decreased expression of HMG-CoA reductase. Taken together, these observations suggest that there are multiple pathways by which policosanol might generate elevated hepatic acyl-CoA and AMP levels to activate AMP-kinase and suppress cholesterol synthesis.

Acknowledgments We thank Dr. Geza Bruckner for helpful insight and advice, and numerous anonymous reviewers for their comments and suggestions. This work was supported by the National Institutes of Health National Center for Complementary and Alternative Medicine [Grant AT003488].

References

1. Marinangeli CP, Jones PJ, Kassis AN, Eskin MN (2010) Policosanols as nutraceuticals: fact or fiction. Crit Rev Food Sci Nutr 50:259–267
2. Torres O, Agramonte AJ, Illnait J, Mas Ferreiro R, Fernandez L, Fernandez JC (1995) Treatment of hypercholesterolemia in NIDDM with policosanol. Diabetes Care 18:393–397
3. Arruzazabala ML, Molina V, Mas R, Fernandez L, Carbajal D, Valdes S, Castano G (2002) Antiplatelet effects of policosanol (20 and 40 mg/day) in healthy volunteers and dyslipidaemic patients. Clin Exp Pharmacol Physiol 29:891–897
4. Castano G, Mas R, Fernandez L, Illnait J, Gamez R, Alvarez E (2001) Effects of policosanol 20 versus 40 mg/day in the treatment of patients with type II hypercholesterolemia: a 6-month double-blind study. Int J Clin Pharmacol Res 21:43–57
5. Cubeddu LX, Cubeddu RJ, Heimowitz T, Restrepo B, Lamas GA, Weinberg GB (2006) Comparative lipid-lowering effects of policosanol and atorvastatin: a randomized, parallel, double-blind, placebo-controlled trial. Am Heart J 152:982 e981–e985
6. Berthold HK, Unverdorben S, Degenhardt R, Bulitta M, Gouni-Berthold I (2006) Effect of policosanol on lipid levels among patients with hypercholesterolemia or combined hyperlipidemia: a randomized controlled trial. Jama 295:2262–2269
7. Francini-Pesenti F, Beltramolli D, Dall'acqua S, Brocadello F (2008) Effect of sugar cane policosanol on lipid profile in primary hypercholesterolemia. Phytother Res 22:318–322
8. Singh DK, Li L, Porter TD (2006) Policosanol inhibits cholesterol synthesis in hepatoma cells by activation of AMP-kinase. J Pharmacol Exp Ther 318:1020–1026
9. Menendez R, Amor AM, Rodeiro I, Gonzalez RM, Gonzalez PC, Alfonso JL, Mas R (2001) Policosanol modulates HMG-CoA reductase activity in cultured fibroblasts. Arch Med Res 32:8–12
10. Menendez R, Fernandez SI, Del Rio A, Gonzalez RM, Fraga V, Amor AM, Mas RM (1994) Policosanol inhibits cholesterol biosynthesis and enhances low density lipoprotein processing in cultured human fibroblasts. Biol Res 27:199–203
11. Menendez R, Amor AM, Gonzalez RM, Fraga V, Mas R (1996) Effect of policosanol on the hepatic cholesterol biosynthesis of mormocholesterolemic rats. Biol Res 29:253–257
12. Menendez R, Arruzazabala L, Mas R, Del Rio A, Amor AM, Gonzalez RM, Carbajal D, Fraga V, Molina V, Illnait J (1997) Cholesterol-lowering effect of policosanol on rabbits with hypercholesterolaemia induced by a wheat starch-casein diet. Br J Nutr 77:923–932
13. Wang Y, Ebine N, Jia X, Jones PJ, Fairow C, Jaeger R (2005) Very long chain fatty acids (policosanols) and phytosterols affect

plasma lipid levels and cholesterol biosynthesis in hamsters. Metabolism 54:508–514
14. Wang YW, Jones PJ, Pischel I, Fairow C (2003) Effects of policosanols and phytosterols on lipid levels and cholesterol biosynthesis in hamsters. Lipids 38:165–170
15. Oliaro-Bosso S, Calcio Gaudino E, Mantegna S, Giraudo E, Meda C, Viola F, Cravotto G (2009) Regulation of HMGCoA reductase activity by policosanol and octacosadienol, a new synthetic analogue of octacosanol. Lipids 44:907–916
16. Clarke PR, Hardie DG (1990) Regulation of HMG-CoA reductase: identification of the site phosphorylated by the AMP-activated protein kinase in vitro and in intact rat liver. Embo J 9:2439–2446
17. Beg ZH, Stonik JA, Brewer HB Jr (1978) 3-Hydroxy-3-methylglutaryl coenzyme A reductase: regulation of enzymatic activity by phosphorylation and dephosphorylation. Proc Natl Acad Sci USA 75:3678–3682
18. Livak KJ, Schmittgen TD (2001) Analysis of relative gene expression data using real-time quantitative PCR and the 2(-Delta Delta C(T)) Method. Methods 25:402–408
19. Carling D, Sanders MJ, Woods A (2008) The regulation of AMP-activated protein kinase by upstream kinases. Int J Obes (Lond) 32(Suppl 4):S55–S59
20. Rizzo WB, Craft DA, Dammann AL, Phillips MW (1987) Fatty alcohol metabolism in cultured human fibroblasts. Evidence for a fatty alcohol cycle. J Biol Chem 262:17412–17419
21. Kabir Y, Kimura S (1993) Biodistribution and metabolism of orally administered octacosanol in rats. Ann Nutr Metab 37:33–38
22. Menendez R, Marrero D, Mas R, Fernandez I, Gonzalez L, Gonzalez RM (2005) In vitro and in vivo study of octacosanol metabolism. Arch Med Res 36:113–119
23. Za'tara G, Bar-Tana J, Kalderon B, Suter M, Morad E, Samovski D, Neumann D, Hertz R (2008) AMPK activation by long chain fatty acyl analogs. Biochem Pharmacol 76:1263–1275
24. Menendez R, Mas R, Amor AM, Rodeiros I, Gonzalez RM, Alfonso JL (2001) Inhibition of cholesterol biosynthesis in cultured fibroblasts by D003, a mixture of very long chain saturated fatty acids. Pharmacol Res 44:299–304
25. Beg ZH, Stonik JA, Brewer HB Jr (1987) Modulation of the enzymic activity of 3-hydroxy-3-methylglutaryl coenzyme A reductase by multiple kinase systems involving reversible phosphorylation: a review. Metabolism 36:900–917
26. Shaw RJ, Lamia KA, Vasquez D, Koo SH, Bardeesy N, Depinho RA, Montminy M, Cantley LC (2005) The kinase LKB1 mediates glucose homeostasis in liver and therapeutic effects of metformin. Science 310:1642–1646
27. Hargrove JL, Greenspan P, Hartle DK (2004) Nutritional significance and metabolism of very long chain fatty alcohols and acids from dietary waxes. Exp Biol Med (Maywood) 229:215–226
28. Hawley SA, Pan DA, Mustard KJ, Ross L, Bain J, Edelman AM, Frenguelli BG, Hardie DG (2005) Calmodulin-dependent protein kinase kinase-beta is an alternative upstream kinase for AMP-activated protein kinase. Cell Metab 2:9–19
29. Sakakibara S, Yamauchi T, Oshima Y, Tsukamoto Y, Kadowaki T (2006) Acetic acid activates hepatic AMPK and reduces hyperglycemia in diabetic KK-A(y) mice. Biochem Biophys Res Commun 344:597–604
30. Haim D, Berrios M, Valenzuela A, Videla LA (2009) Trace quantification of 1-octacosanol and 1-triacontanol and their main metabolites in plasma by liquid-liquid extraction coupled with gas chromatography-mass spectrometry. J Chromatogr B Analyt Technol Biomed Life Sci 877:4154–4158
31. Keller S, Gimmler F, Jahreis G (2008) Octacosanol administration to humans decreases neutral sterol and bile acid concentration in feces. Lipids 43:109–115
32. Wong JM, de Souza R, Kendall CW, Emam A, Jenkins DJ (2006) Colonic health: fermentation and short chain fatty acids. J Clin Gastroenterol 40:235–243
33. Kawaguchi T, Osatomi K, Yamashita H, Kabashima T, Uyeda K (2002) Mechanism for fatty acid "sparing" effect on glucose-induced transcription: regulation of carbohydrate-responsive element-binding protein by AMP-activated protein kinase. J Biol Chem 277:3829–3835
34. Zydowo MM, Smolenski RT, Swierczynski J (1993) Acetate-induced changes of adenine nucleotide levels in rat liver. Metabolism 42:644–648

Lipids (2011) 46:323–332
DOI 10.1007/s11745-010-3498-9

ORIGINAL ARTICLE

Presence of Apolipoprotein C-III Attenuates Apolipoprotein E-Mediated Cellular Uptake of Cholesterol-Containing Lipid Particles by HepG2 Cells

Shin-ya Morita · Atsushi Sakurai · Minoru Nakano · Shuji Kitagawa · Tetsurou Handa

Received: 15 September 2010 / Accepted: 26 October 2010 / Published online: 16 November 2010

Abstract Apolipoprotein C-III (apoC-III) decreases the apolipoprotein E (apoE)-mediated uptake of lipoprotein remnants by the liver, and a high plasma concentration of apoC-III in VLDL is associated with hypertriglyceridemia and the risk of coronary heart disease. In this study, we prepared lipid emulsions containing triolein, phosphatidylcholine and cholesterol as model particles of lipoproteins, and examined the roles of apoC-III in apoE-mediated uptake of emulsions by HepG2 cells. Cholesterol in emulsion particles enhanced the apoE-mediated uptake via heparan sulfate proteoglycan and LDL receptor-related protein pathways. The amount of apoE bound to emulsion particles was increased by the presence of cholesterol at the particle surface, whereas cholesterol had no effect on the binding amount of apoC-III. Surface cholesterol alleviated the inhibitory effect of apoC-III on apoE incorporation into the emulsion surface. However, ApoC-III almost completely inhibited the apoE-mediated uptake of cholesterol-containing emulsions despite sufficient binding of apoE to emulsions. These findings suggest that apoC-III attenuates the binding of apoE to the lipoprotein surface and apoE-mediated cellular uptake of lipoprotein remnants. Furthermore, cholesterol may affect these functions of apoC-III and apoE involved in the clearance of lipoprotein remnants.

Keywords Apolipoprotein C-III · Apolipoprotein E · Cholesterol · Lipid emulsions

Abbreviations

apoC-III	Apolipoprotein C-III
apoE	Apolipoprotein E
HSPG	Heparan sulfate proteoglycan
LRP	LDL receptor-related protein
PL	Phospholipid
PMC oleate	Pyrenemethyl 3β-(*cis*-9-octadecenoyloxy)-22,23-bisnor-5-cholenate
PtdCho	Phosphatidylcholine
TAG	Triacylglycerol

Introduction

Apolipoprotein C-III (apoC-III) in VLDL and LDL is an independent risk factor for coronary heart disease [1–3]. A high concentration of apoC-III-containing VLDL is associated with the delayed catabolism of triacylglycerol (TAG) in VLDL and hypertriglyceridemia [4, 5]. ApoC-III enhances the conversion from light LDL to dense LDL [6, 7]. ApoC-III deficiency (by ~50% of normal levels) confers a favorable lipid profile and reduced subclinical coronary artery atherosclerosis [8]. Recently, it has been reported that polymorphisms in the apoC-III gene promoter are associated with plasma apoC-III concentration, plasma TAG concentration, lipoprotein profile, cardiovascular health, nonalcoholic fatty liver disease, insulin sensitivity, and longevity [9, 10].

S. Morita (✉) · S. Kitagawa
Kobe Pharmaceutical University, Higashinada-ku, Kobe 658-8558, Japan
e-mail: smorita@kobepharma-u.ac.jp

A. Sakurai · M. Nakano · T. Handa
Graduate School of Pharmaceutical Sciences, Kyoto University, Sakyo-ku, Kyoto 606-8501, Japan

Present Address:
T. Handa
Faculty of Pharmaceutical Sciences, Suzuka University of Medical Science, 3500-3 Minami-Tamagaki-cho, Suzuka, Mie 513-8670, Japan

Apolipoprotein E (apoE), a 299-amino acid plasma apolipoprotein, is a ligand for the LDL receptor, LDL receptor-related protein (LRP) and the VLDL receptor, and binds to cell surface heparan sulfate proteoglycans (HSPG) [11]. The liver produces the vast majority of plasma apoE, and apoE promotes the internalization of TAG-rich lipoprotein remnants by hepatocytes. ApoE knockout mice have high levels of plasma cholesterol, which is a result of the impaired clearance of lipoprotein remnants, and readily develop atherosclerosis [12, 13].

ApoC-III is a 79-amino acid glycoprotein synthesized mainly in the liver and to a minor extent in the intestine as a component of chylomicrons, VLDL, LDL and HDL [11]. In normotriglyceridemic subjects, apoC-III is associated primarily with HDL, whereas there is redistribution of apoC-III to chylomicrons and VLDL in the postprandial state and hypertriglyceridemia [14, 15]. Human apoC-III transgenic mice exhibit markedly elevated levels of chylomicron and VLDL TAG [16]. In addition, a synergistic interaction between the human apoC-III transgene and LDL receptor defects produces large quantities of VLDL and LDL and enhances the development of atherosclerotic lesions in mice [17]. ApoC-III is known to be a potential inhibitor of lipoprotein lipase activity [18]. ApoC-III also inhibits the apoE-mediated hepatic uptake of TAG-rich lipoproteins through LDL receptor and LRP [19, 20], but the mechanism of this inhibition has not been characterized in detail.

Emulsion particles are used as protein-free models for plasma lipoproteins. Our previous studies demonstrated that apoC-III reduced the apoE-mediated uptake of emulsion particles by HepG2 cells [21]. We also showed that free cholesterol in the emulsion surface enhanced the apoE-mediated uptake by J774 macrophages by increasing the amount of apoE bound to emulsion particles [22]. In this study, to elucidate the influence of apoC-III on apoE-mediated uptake of lipoprotein remnants, we investigated the uptake of lipid emulsions by HepG2, human hepatoma, cells and the binding of apoE and apoC-III to the emulsion surface.

Materials and Methods

Materials

Egg yolk phosphatidylcholine (PtdCho) was generously provided by Asahi Kasei (Tokyo, Japan). Triolein, cholesterol, heparinase I, and BSA were purchased from Sigma-Aldrich (St. Louis, MO, USA). 1-Pyrenemethyl 3β-(*cis*-9-octadecenoyloxy)-22,23-bisnor-5-cholenate (PMC oleate) was obtained from Molecular Probes (Eugene, OR, USA). Bovine lactoferrin was purchased from Wako Pure Chemicals (Osaka, Japan). All other chemicals used were of the highest reagent grade.

Preparation of Emulsions

The lipid emulsions were prepared by the method described previously using a high-pressure emulsifier (Nanomizer System YSNM-2000AR; Yoshida Kikai, Nagoya, Japan) [23]. Briefly, mixtures of triolein, PtdCho and free cholesterol were suspended in 10 mM Tris–HCl buffer (pH 7.4), containing 150 mM NaCl, 1 mM EDTA, and successively emulsified under 100 MPa of pressure at 40–60 °C. Depending on the purpose of the experiment, PMC oleate, which has been used as a tracer of lipoprotein endocytosis and as a general nonexchangeable membrane marker [24, 25], was added to the lipid mixtures at a ratio of 1 mol% of triolein. After the removal of contaminating vesicles by ultracentrifugation (55,000*g*, 60 min), homogeneous emulsion particles were obtained. The mean particle diameter of each emulsions was about 120 nm determined from dynamic light scattering measurements using a Photal LPA-3000/3100 (Otsuka Electronics, Hirakata, Japan) equipped with a He–Ne laser at a wavelength of 632.8 nm. The concentrations of triolein, PtdCho and cholesterol were determined using enzymatic assay kits purchased from Wako. As a result, we confirmed that the composition of PtdCho and cholesterol in the isolated emulsions was the same as that in the starting lipid mixtures, and the isolated emulsions contained the expected amount of cholesterol (molar ratio of PtdCho/cholesterol = 3/2). The molar ratios of core triolein to surface PtdCho for isolated triolein-PtdCho and triolein-PtdCho/cholesterol (3/2) emulsions were 4.76 $\pm$ 0.29 and 4.99 $\pm$ 0.12, respectively.

ApoE and ApoC-III

Recombinant human apoE (isoform E3) was provided by PeproTech (London, UK). Recombinant apoE was previously shown to have similar physical and biological properties to native human plasma apoE [26]. Purified apoC-III from human plasma was purchased from Chemicon (Temecula, CA, USA). To minimize self-association, apoE and apoC-III were added to 6 M guanidine hydrochloride solution and dialyzed extensively against Tris–HCl buffer.

Cell Cultures

HepG2 cells were grown in a humidified incubator (5% CO_2) at 37 °C in DMEM supplemented with 10% heat-inactivated FBS, L-glutamine, penicillin, and streptomycin. The FBS was replaced with 1% BSA 15 min before each experiment. Experiments were carried out in DMEM containing 1% BSA.

Cell Uptake Assays

The lipid emulsions were preincubated with apoE and apoC-III at 37 °C for 30 min, allowing sufficient time for equilibrium binding [27]. Treatment with heparinase was performed by preincubating the cells at 37 °C for 45 min in the presence of 10 units/ml heparinase. HepG2 cells were incubated with PMC oleate-labeled emulsions (250 μM triolein) containing apolipoproteins at 37 °C for 2 h. After incubation, the cells were chilled on ice and washed twice with ice-cold Hepes buffer containing 0.2% BSA and then washed twice with ice-cold Hepes buffer alone. Cells were then dissolved in 0.2% Triton X-100. To evaluate the particle uptake, the fluorescence intensity of PMC oleate (excitation 342 nm, emission 377 nm) was measured with a Hitachi F-4500 spectrofluorometer, and the concentration of cellular protein was measured by the method of Lowry. By this method, uptake means binding and internalization by the cells.

Apolipoprotein Binding Assay

Lipid emulsions (250 μM triolein) were incubated with apoE and apoC-III at 37 °C for 30 min, which allowed sufficient time for equilibrium binding [27]. The mixtures were subjected to ultracentrifugation (55,000*g*, 60 min) to separate both emulsions and lipid-bound apolipoproteins from free apolipoproteins. The concentration of triolein in the top fraction was measured using an enzymatic assay kit. This apolipoprotein–emulsion complex was diluted to 2.5 mM triolein in 1% Triton X-100 and treated with sample buffer. Apolipoproteins were separated by 10–20% SDS PAGE. Following silver staining, the amounts of apoE and apoC-III were quantified by densitometric scanning calibrated with standard solution of each apolipoprotein. The binding of apolipoproteins had no effect on the size of emulsion particles [28].

Statistical Analysis

The statistical significance of differences between mean values was analyzed using the non-paired *t* test. Differences were considered significant at $P < 0.05$. Unless indicated otherwise, results are given as means ± SE ($n = 3$).

Results

ApoE-Mediated Uptake of Lipid Emulsions by HepG2 Cells

To investigate the role of cholesterol in the apoE-mediated uptake of emulsion particles by HepG2 cells, we prepared two types of emulsions: triolein-PtdCho and triolein-PtdCho/cholesterol (molar ratio of PtdCho/cholesterol = 3/2). Triolein-PtdCho/cholesterol emulsions were used as models for lipoprotein remnants. As shown in Fig. 1, apoE enhanced the uptake of both emulsions by HepG2 cells in a dose-dependent manner. There was no significant difference between triolein-PtdCho and triolein-PtdCho/cholesterol emulsion uptake in the absence of apoE. The uptake of triolein-PtdCho/cholesterol emulsions was 2.7-fold higher than that of triolein-PtdCho emulsions in the presence of 4 μg/ml apoE, indicating that the apoE-mediated uptake was markedly enhanced by the presence of cholesterol at the emulsion surface.

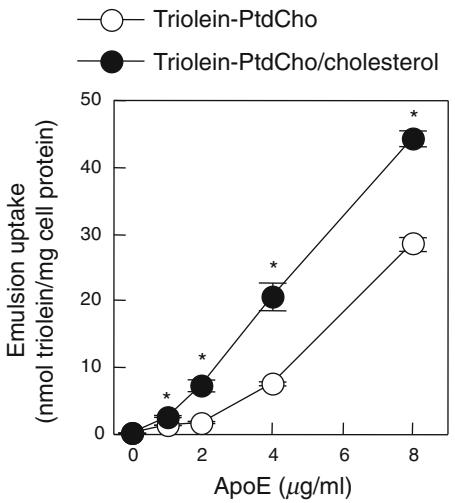

Fig. 1 ApoE-mediated uptake of emulsion particles by HepG2 cells. HepG2 cells were incubated for 2 h at 37 °C with triolein-PtdCho (*open circles*) or triolein-PtdCho/cholesterol (3/2) (*closed circles*) emulsions (250 μM triolein) in the presence of the indicated amounts of apoE. Values represent the means ± SE of three measurements. *$P < 0.05$, significantly different from triolein-PtdCho emulsions

To examine if known lipoprotein receptors on HepG2 cells are involved in the emulsion uptake, we conducted experiments using inhibitors of lipoprotein receptors. HSPG and LRP play important roles in apoE-enriched remnant uptake, and HSPG participate in the uptake, either associating with LRP or acting alone as a receptor [29]. Heparinase released the sulfated glycosaminoglycan side chains from HSPG [30]. In this study, heparinase treatment significantly inhibited both triolein-PtdCho and triolein-PtdCho/cholesterol emulsion uptake by HepG2 cells in the presence of 8 μg/ml apoE (Fig. 2). Lactoferrin interacts with HSPG and LRP, and inhibits the uptake of lipoprotein remnants by preventing their binding to HSPG and subsequent transfer to LRP [31]. In the presence of 8 μg/ml apoE, lactoferrin (5 mg/ml) also markedly prevented the uptake of triolein-PtdCho and triolein-PtdCho/cholesterol emulsions by HepG2 cells (Fig. 2). Thus, HSPG and LRP were mainly involved in the apoE-mediated uptake of triolein-PtdCho and triolein-PtdCho/cholesterol emulsions by HepG2 cells.

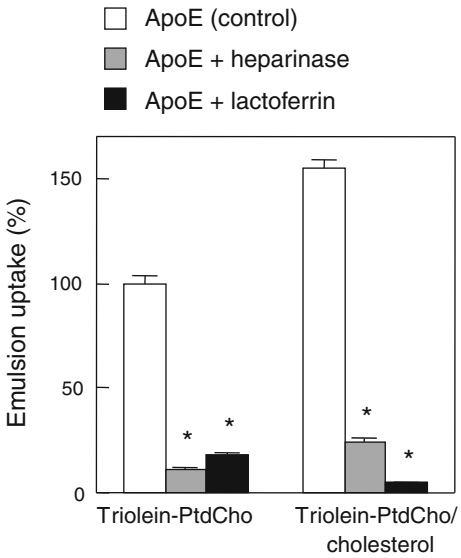

Fig. 2 Effects of heparinase and lactoferrin on apoE-mediated uptake of emulsion particles by HepG2 cells. Treatment with heparinase was performed by preincubating the cells at 37 °C for 45 min in the presence of 10 units/ml heparinase (*gray bars*). HepG2 cells were incubated for 2 h at 37 °C with triolein-PtdCho or triolein-PtdCho/cholesterol (3/2) emulsions (250 μM triolein) with 8 μg/ml apoE in the absence (control; *white bars*) or presence of 5 mg/ml lactoferrin (*black bars*). Results are expressed as the percentage of triolein-PtdCho emulsion uptake measured in the presence of 8 μg/ml apoE. Each *bar* represents the mean ± SE of three measurements. $^*P < 0.05$, significantly different from the control

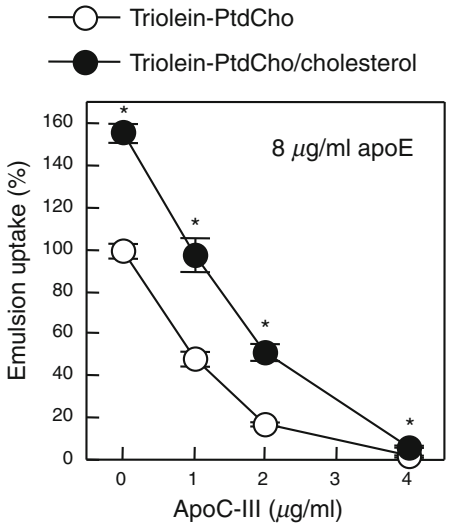

Fig. 3 Effects of apoC-III on apoE-mediated uptake of emulsion particles by HepG2 cells. HepG2 cells were incubated for 2 h at 37 °C with triolein-PtdCho (*open circles*) or triolein-PtdCho/cholesterol (3/2) (*closed circles*) emulsions (250 μM triolein) in the presence of 8 μg/ml apoE and the indicated amounts of apoC-III. Results are expressed as the percentage of triolein-PtdCho emulsion uptake measured in the presence of 8 μg/ml apoE without apoC-III. Values represent the means ± SE of three measurements. $^*P < 0.05$, significantly different from triolein-PtdCho emulsions

Effects of ApoC-III on ApoE-Mediated Uptake by HepG2 Cells

We assessed the uptake of triolein-PtdCho and triolein-PtdCho/cholesterol emulsions by HepG2 cells in the presence of apoE and apoC-III. Figure 3 shows that the apoE-mediated uptake of both emulsions decreased with the apoC-III concentration. The uptake of triolein-PtdCho/cholesterol emulsions was higher than that of triolein-PtdCho emulsions in the presence of both apoE and apoC-III. At a higher concentration (4 μg/ml) of apoC-III, the cellular uptake of triolein-PtdCho and triolein-PtdCho/cholesterol emulsions was very low (97.5 ± 0.1 and 95.8 ± 0.2% inhibition, respectively), indicating apoC-III almost completely abolished the stimulatory effect of apoE on the emulsion uptake. Possible mechanisms of the inhibition of apoE-mediated uptake by apoC-III are: (1) apoC-III displaces apoE from emulsion surfaces; (2) apoC-III directly interacts with apoE bound to emulsion particles.

Binding of ApoE and ApoC-III to Emulsion Particles

To examine the effects of surface cholesterol on the binding of apoE and apoC-III to the emulsion particles, we compared the amount of apoE or apoC-III bound to triolein-PtdCho and triolein-PtdCho/cholesterol emulsions. In accord with our previous report [22], the incorporation of cholesterol into the emulsion surface caused a significant increase in the binding amount of apoE (Fig. 4a). However, the amounts of apoC-III bound to triolein-PtdCho and triolein-PtdCho/cholesterol emulsions were nearly the same (Fig. 4b). These results indicated that the presence of cholesterol at the emulsion surface enhanced the binding of apoE. In contrast, the binding amount of apoC-III was not affected by surface cholesterol.

We next explored the competitive binding of apoE and apoC-III to emulsion particles. As shown in Fig. 5a, apoC-III reduced the binding of apoE to triolein-PtdCho and triolein-PtdCho/cholesterol emulsions. In the presence of 2 μg/ml apoC-III, the binding of apoE to triolein-PtdCho/cholesterol emulsions was significantly larger than that to triolein-PtdCho emulsions, whereas the binding amount of apoC-III was similar between triolein-PtdCho and triolein-PtdCho/cholesterol emulsions (Fig. 5b). At 4 μg/ml apoC-III, the apoC-III binding to triolein-PtdCho/cholesterol emulsions was slightly higher than triolein-PtdCho emulsions. Figure 5c shows that the binding amount of apoE was found to correlate inversely with the binding amount of apoC-III to triolein-PtdCho and triolein-PtdCho/cholesterol emulsions ($r = -0.980$ and $r = -0.988$, respectively). The slope of the plot for triolein-PtdCho emulsions (−3.45 ± 0.50) was lower than that for triolein-PtdCho/cholesterol emulsions (−2.00 ± 0.23), indicating that apoC-III inhibited the apoE binding to

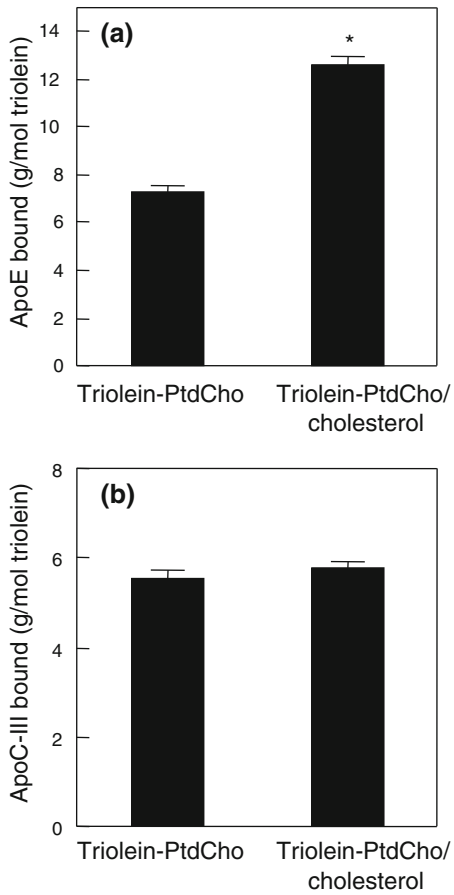

Fig. 4 Effects of cholesterol on the binding of apoE **a** and apoC-III **b** to emulsion particles. Triolein-PtdCho and triolein-PtdCho/cholesterol (3/2) emulsions (250 μM triolein) were incubated with 4 μg/ml apoE or 2 μg/ml apoC-III for 30 min at 37 °C. Each *bar* represents the mean ± SE of three measurements. $^*P < 0.05$, significantly different from triolein-PtdCho emulsions

triolein-PtdCho emulsions more effectively than that to triolein-PtdCho/cholesterol emulsions. ApoC-III decreased the total binding of apoE and apoC-III to triolein-PtdCho emulsions compared to the binding of apoE alone (Fig. 5d). The total binding amount of apoE and apoC-III to triolein-PtdCho/cholesterol emulsions was larger than that to triolein-PtdCho emulsions. The total binding of apoE and apoC-III to triolein-PtdCho/cholesterol emulsions was not significantly different from that of apoE alone (Fig. 5d), because the loss of apoE bound to triolein-PtdCho/cholesterol emulsions by apoC-III was largely offset by the amount of apoC-III bound to triolein-PtdCho/cholesterol emulsions (Fig. 5a, b).

Relationship between Cellular Uptake and Binding of ApoE and ApoC-III

To determine if the binding of apoE or apoC-III is responsible for the emulsion uptake, we studied the relationship between the emulsion uptake by HepG2 cells and the binding amounts of apoE and apoC-III. The apoE and apoC-III concentrations in the incubation media used in apolipoprotein binding assays and cell uptake assays are summarized in Table 1. As shown in Fig. 6a, excluding the case of triolein-PtdCho/cholesterol emulsions in the presence of both apoE and apoC-III (closed circle, closed inverted triangle and closed square), the emulsion uptake was positively correlated with the amount of apoE bound to emulsions ($r = 0.996$). Compared with triolein-PtdCho/cholesterol emulsions in the presence of 4 μg/ml apoE (emulsion uptake, 72.7 ± 7.0%; apoE bound, 12.6 ± 0.4 g/mol triolein; closed triangle), the uptake of triolein-PtdCho/cholesterol emulsions in the presence of 8 μg/ml apoE and 4 μg/ml apoC-III (closed square) was markedly lower (6.5 ± 0.3%) despite the fact that similar amount of apoE bound to the emulsions (12.2 ± 2.0 g/mol triolein). As depicted in Fig. 6b, at 8 μg/ml apoE, there were inverse correlations between the emulsion uptake and the binding of apoC-III ($r = -0.997$ for triolein-PtdCho and $r = -0.987$ for triolein-PtdCho/cholesterol emulsions). Thus, apoC-III bound to emulsion particles may prevent the apoE-mediated uptake.

Discussion

The concentrations of apoE and apoC-III in human plasma are 50–80 and 80–120 μg/ml, respectively [9, 10, 32, 33]. Homozygosity of the A-641C allele in the apoC-III gene promoter is associated with significantly lower serum levels of apoC-III [9], whereas the variant alleles in the apoC-III gene promoter (C-482T and T-455C) cause a 30% increase in the fasting plasma apoC-III concentration compared with the WT homozygotes [10]. The normal plasma TAG concentration is <1.5 mg/ml (<1.69 mM) in the fasting state. In the present study, the concentrations of apoE (0–8 μg/ml), apoC-III (0–4 μg/ml) and triolein (250 μM) in the media were not physiological but optimal conditions to investigate the functions of apoE and apoC-III [21–23].

In this study, we used the lipid emulsions as protein-free lipoprotein models. However, the emulsions may not necessarily represent the nature of TAG-rich lipoproteins owing to the lack of other apolipoproteins, notably apolipoprotein B. Apolipoprotein B plays a crucial role in the maintenance of the lipoprotein structure, the cellular uptake of lipoproteins through the LDL receptor, and the development of atherosclerosis [34, 35]. At present, apolipoprotein B cannot be properly reconstituted on emulsion particles. However, the lipid emulsions are useful to elucidate the roles of exchangeable apolipoproteins in lipoprotein metabolism because they enable easy control of the lipid and protein constituents and the size of the particles.

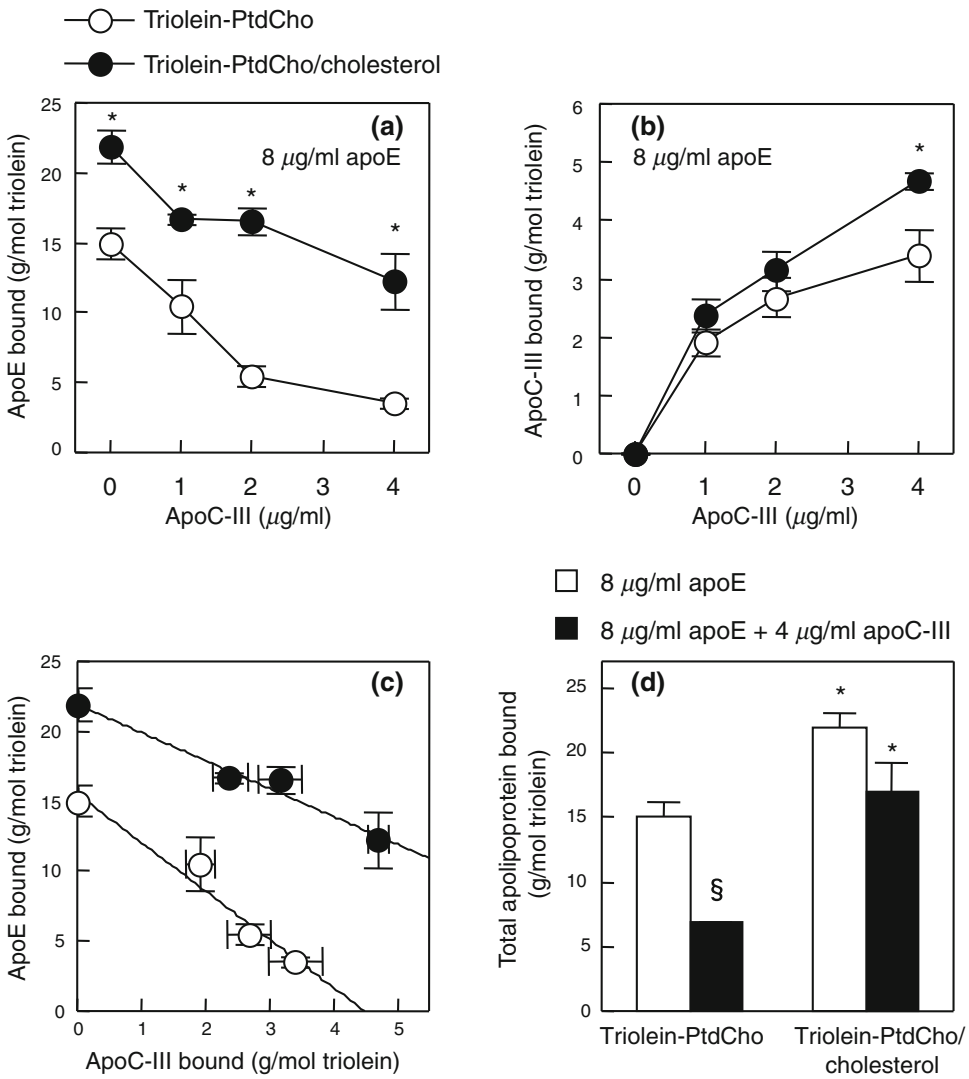

Fig. 5 Competitive binding of apoE and apoC-III to emulsion particles. Triolein-PtdCho and triolein-PtdCho/cholesterol (3/2) emulsions (250 μM triolein) were incubated with 8 μg/ml apoE and the indicated amounts of apoC-III for 30 min at 37 °C. **a** The amounts of apoE bound to triolein-PtdCho (*open circles*) and triolein-PtdCho/cholesterol (3/2) (*closed circles*) emulsions in the presence of apoC-III. **b** The amounts of apoC-III bound to triolein-PtdCho (*open circles*) and triolein-PtdCho/cholesterol (3/2) (*closed circles*) emulsions in the presence of apoE. **c** Plot of the binding of apoE versus the binding of apoC-III to triolein-PtdCho (*open circles*) and triolein-PtdCho/cholesterol (3/2) (*closed circles*) emulsions. Regression line between apoE bound and apoC-III bound to triolein-PtdCho ($r = -0.980$) or triolein-PtdCho/cholesterol (3/2) emulsions ($r = -0.988$). **c** Total binding of apolipoproteins to emulsion particles in the presence of 8 μg/ml apoE alone (*open bars*) or 8 μg/ml apoE and 4 μg/ml apoC-III (*filled bars*). Values represent the means ± SE of three measurements. The absence of an *error bar* signifies an SE value smaller than the graphic symbol. $^{*}P < 0.05$, significantly different from triolein-PtdCho emulsions. $^{\S}P < 0.05$, significantly different from 8 μg/ml apoE alone

It has been suggested that apoC-III is made of two helical domains. The N-terminal domain of apoC-III is important in the modulation of lipoprotein lipase activity, and the binding of apoC-III to surface phospholipid is mediated by the C-terminal helix [33, 36]. Gangabadage et al. [37] have reported the three-dimensional NMR structure of apoC-III in complex with SDS micelles, in which 6–10-residue amphipathic helices wrap around the micelle surface, three positively charged residues line the polar faces of helices 1 and 2, and an array of negatively charged residues lines the polar faces of helices 4 and 5 and the adjacent flexible loop.

It has been demonstrated that apoE contains two independently folded domains, the 22-kDa N-terminal domain and 10-kDa C-terminal domain [11]. The C-terminal domain has a high affinity for lipid and is responsible for lipoprotein binding and preference [38, 39]. The N-terminal domain exists in the lipid-free state as a four-helix bundle and contains the LDL receptor-binding region [40]. The cluster of arginine and lysine residues located

Table 1 ApoE and apoC-III concentrations in incubation media used in apolipoprotein binding assays and cell uptake assays

The molecular masses of apoE and apoC-III are 34.0 and 8.8 kDa, respectively

ApoE (μg/ml)	ApoC-III (μg/ml)	ApoC-III/apoE molar ratio	Symbols in Fig. 6	
			Triolein-PtdCho	Triolein-PtdCho/cholesterol
4	0	0	Open triangle	Closed triangle
8	0	0	Open diamond	Closed diamond
8	1	0.483	Open circle	Closed circle
8	2	0.966	Open inverted triangle	Closed inverted triangle
8	4	1.93	Open square	Closed square

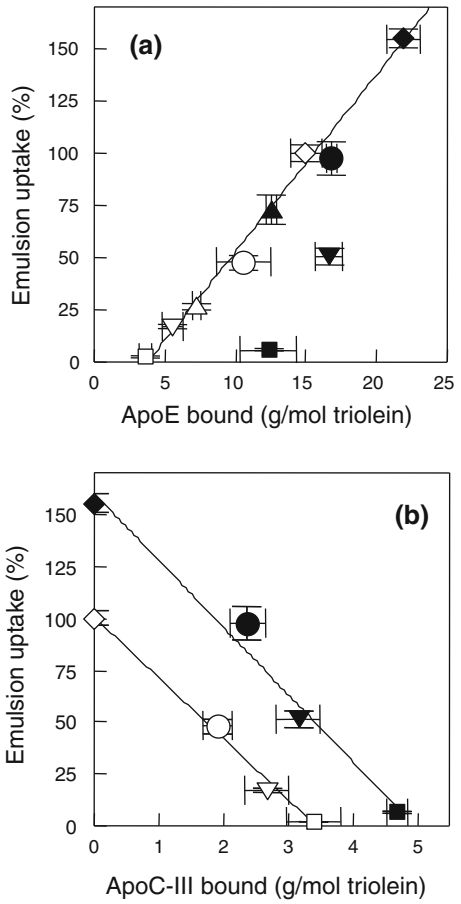

Fig. 6 Relationship between emulsion uptake by HepG2 cells and apoE binding or apoC-III binding. HepG2 cells were incubated for 2 h at 37 °C with triolein-PtdCho (*open symbols*) or triolein-PtdCho/cholesterol (3/2) (*closed symbols*) emulsions (250 μM triolein) in the presence of apoE and apoC-III. The concentrations of apoE and apoC-III in the incubation medium of each symbol are indicated in Table 1. **a** Regression line between cellular uptake and apoE binding to emulsions ($r = 0.996$) excluding triolein-PtdCho/cholesterol (3/2) emulsions with 8 μg/ml apoE and various amounts of apoC-III (*closed circle*, *closed inverted triangle*, and *closed square*). **b** Regression line between cellular uptake and apoC-III binding to triolein-PtdCho ($r = -0.997$) or triolein-PtdCho/cholesterol (3/2) emulsions ($r = -0.987$)

between residues 136–158 represents the binding site for LDL receptor. The segment comprising the receptor-binding portion of apoE (residues 130–149) interacts with ligand-binding clusters of LRP [41, 42]. Both domains of apoE contain heparin-binding sites, but the N-terminal site plays a dominant role in the binding to heparin [43]. The cluster of positively charged amino acids between residues 136–150 is also involved in the heparin interaction. The four-helix bundle in the N-terminal domain undergoes a conformational opening upon lipid binding, leading to the receptor-active conformation of apoE [11, 44]. In this conformation, the positive electrostatic potential in the receptor-binding region of apoE is enhanced [45, 46]. The leucine zipper motif confers stability to the helix bundle conformation of the N-terminal domain, which serves to maintain apoE in a receptor-inactive state [47].

The lipoprotein surface is mainly formed by phospholipids (PL) and cholesterol together with apolipoproteins. The amount of cholesterol in lipoproteins regulates their metabolism. The cholesterol/PL ratios in VLDL and LDL are 0.78 and 0.73, respectively [48]. When chylomicrons are converted to chylomicron remnants by the action of lipoprotein lipase, there is an increase in the relative content of cholesterol in the remnants [49]. The cholesterol/PL ratio of the remnant fraction of human serum in the postprandial state is close to 1 [50]. In the present study, triolein-PtdCho/cholesterol (3/2) emulsions can be applied as a model for TAG-rich lipoprotein remnants [22]. Emulsions rich in cholesterol were metabolized like chylomicron remnants [51]. Cholesterol can distribute between the surface and core phases in lipid emulsions and lipoproteins. From the surface-core phase equilibrium, over 80% of cholesterol is accommodated in the surface phase in TAG-PtdCho emulsions [52]. Cholesterol induces a motional restriction of PtdCho and a rigidification of the TAG-PtdCho emulsion surface with increasing content [52]. Cholesterol is associated with surface PL but located deep in the inner hydrocarbon region [52]. Our previous report showed that cholesterol enrichment on the emulsion surface led to PtdCho head group separation and hydration, and markedly increased the apoE binding maximum without changing the binding affinity [22]. There was a correlation between the degree of PL head group separation and the apoE binding maximum. It was also demonstrated that the acyl chain packing was not a determining factor in apoE binding, suggesting that apoE binds to emulsion particles through

insertion between the PL head groups but not deep penetration into the hydrocarbon interior [22]. In this study, cholesterol in the emulsion surface increased the amount of apoE bound to the particles, but had no effect on the binding amount of apoC-III (Fig. 4), suggesting that the binding of apoC-III is insensitive to the degree of PtdCho head group separation at the emulsion surface. Our current data also demonstrated that cholesterol reversed the inhibitory effect of apoC-III on apoE incorporation into the emulsion surface, and increased the total binding of apoE and apoC-III (Fig. 4). We consider that cholesterol at the emulsion surface increases the number of the apoE binding sites rather than the apoC-III binding sites.

Our results show that in the presence of apoE and apoC-III, the uptake of cholesterol-containing emulsions by HepG2 cells was higher compared with that of cholesterol-free emulsions (Fig. 3), consistent with the facilitated uptake of cholesterol-containing emulsions by the liver [53]. Increased levels of apoC-III on the lipoprotein particles would displace apoE, which would result in decreased remnant clearance [54]. It has been proposed that apoCs induce conformational alteration of the N-terminal domain of apoE and modulate the receptor binding properties [55]. ApoC-III completely abolishes the apolipoprotein B-mediated binding of lipoproteins to LDL receptor, suggesting that this inhibitory action of apoC-III on lipoprotein binding is due to a masking of the receptor domain of apolipoprotein B by apoC-III [56]. In the present study, we showed that despite sufficient amount of apoE bound to cholesterol-containing emulsions, apoC-III almost abolished the cellular uptake of the emulsions via HSPG and LRP pathways (Fig. 6a). It is possible that at the cholesterol-containing particle surface, apoC-III leads to the receptor-inactive conformation of the apoE-N-terminal domain or masks the cluster of positively charged amino acids of apoE involved in the binding to LRP and HSPG, in addition to the attenuation of apoE binding to the particle surface.

ApoC-III delays the metabolism of TAG-rich lipo proteins by inhibiting lipoprotein lipase activity and apoE-dependent hepatic uptake, which has been suggested to increase the probability of cholesterol deposition of lipoprotein particles in the vessel wall [3, 4]. ApoC-III may inhibit apoE incorporation into the lipoprotein surface and apoE-mediated cellular uptake of lipoprotein particles through HSPG and LRP pathways. In addition, cholesterol at the surface of lipoprotein remnants would modulate these atherogenic functions of apoC-III.

Acknowledgments This work was supported in part by Grants-in-Aid for Scientific Research and Young Scientists from the Japanese Ministry of Education, Culture, Sports, Science, and Technology (17390011 and 22790053), by the Program for the Promotion of Fundamental Studies in Health Science (04-8) of the National Institute of Biomedical Innovation (NIBIO), and a grant from Research Fellowships of the Japan Society for the Promotion of Science for Young Scientists.

References

1. Luc G, Fievet C, Arveiler D, Evans AE, Bard JM, Cambien F, Fruchart JC, Ducimetiere P (1996) Apolipoproteins C-III and E in apoB- and non-apoB-containing lipoproteins in two populations at contrasting risk for myocardial infarction: the ECTIM study. Etude Cas Temoins sur 'Infarctus du Myocarde. J Lipid Res 37:508–517
2. Sacks FM, Alaupovic P, Moye LA, Cole TG, Sussex B, Stampfer MJ, Pfeffer MA, Braunwald E (2000) VLDL, apolipoproteins B, CIII, and E, and risk of recurrent coronary events in the cholesterol and recurrent events (CARE) trial. Circulation 102:1886–1892
3. Lee SJ, Campos H, Moye LA, Sacks FM (2003) LDL containing apolipoprotein CIII is an independent risk factor for coronary events in diabetic patients. Arterioscler Thromb Vasc Biol 23:853–858
4. Lee SJ, Moye LA, Campos H, Williams GH, Sacks FM (2003) Hypertriglyceridemia but not diabetes status is associated with VLDL containing apolipoprotein CIII in patients with coronary heart disease. Atherosclerosis 167:293–302
5. Chan DC, Watts GF, Nguyen MN, Barrett PH (2006) Apolipoproteins C-III and A-V as predictors of very-low-density lipoprotein triglyceride and apolipoprotein B-100 kinetics. Arterioscler Thromb Vasc Biol 26:590–596
6. Mendivil CO, Zheng C, Furtado J, Lel J, Sacks FM (2010) Metabolism of very-low-density lipoprotein and low-density lipoprotein containing apolipoprotein C-III and not other small apolipoproteins. Arterioscler Thromb Vasc Biol 30:239–245
7. Zheng C, Khoo C, Furtado J, Sacks FM (2010) Apolipoprotein C-III and the metabolic basis for hypertriglyceridemia and the dense low-density lipoprotein phenotype. Circulation 121:1722–1734
8. Pollin TI, Damcott CM, Shen H, Ott SH, Shelton J, Horenstein RB, Post W, McLenithan JC, Bielak LF, Peyser PA, Mitchell BD, Miller M, O'Connell JR, Shuldiner AR (2008) A null mutation in human APOC3 confers a favorable plasma lipid profile and apparent cardioprotection. Science 322:1702–1705
9. Atzmon G, Rincon M, Schechter CB, Shuldiner AR, Lipton RB, Bergman A, Barzilai N (2006) Lipoprotein genotype and conserved pathway for exceptional longevity in humans. PLoS Biol 4:e113
10. Petersen KF, Dufour S, Hariri A, Nelson-Williams C, Foo JN, Zhang XM, Dziura J, Lifton RP, Shulman GI (2010) Apolipoprotein C3 gene variants in nonalcoholic fatty liver disease. N Engl J Med 362:1082–1089
11. Saito H, Lund-Katz S, Phillips MC (2004) Contributions of domain structure and lipid interaction to the functionality of exchangeable human apolipoproteins. Prog Lipid Res 43:350–380
12. Zhang SH, Reddick RL, Piedrahita JA, Maeda N (1992) Spontaneous hypercholesterolemia and arterial lesions in mice lacking apolipoprotein E. Science 258:468–471
13. Plump AS, Smith JD, Hayek T, Aalto-Setala K, Walsh A, Verstuyft JG, Rubin EM, Breslow JL (1992) Severe hypercholesterolemia and atherosclerosis in apolipoprotein E-deficient mice created by homologous recombination in ES cells. Cell 71:343–353
14. Batal R, Tremblay M, Barrett PH, Jacques H, Fredenrich A, Mamer O, Davignon J, Cohn JS (2000) Plasma kinetics of apoC-III and apoE in normolipidemic and hypertriglyceridemic subjects. J Lipid Res 41:706–718
15. Krauss RM (1998) Atherogenicity of triglyceride-rich lipoproteins. Am J Cardiol 81:13B–17B

16. de Silva HV, Lauer SJ, Wang J, Simonet WS, Weisgraber KH, Mahley RW, Taylor JM (1994) Overexpression of human apolipoprotein C-III in transgenic mice results in an accumulation of apolipoprotein B48 remnants that is corrected by excess apolipoprotein E. J Biol Chem 269:2324–2335
17. Masucci-Magoulas L, Goldberg IJ, Bisgaier CL, Serajuddin H, Francone OL, Breslow JL, Tall AR (1997) A mouse model with features of familial combined hyperlipidemia. Science 275:391–394
18. van Dijk KW, Rensen PC, Voshol PJ, Havekes LM (2004) The role and mode of action of apolipoproteins CIII and AV: synergistic actors in triglyceride metabolism? Curr Opin Lipidol 15:239–246
19. Kowal RC, Herz J, Weisgraber KH, Mahley RW, Brown MS, Goldstein JL (1990) Opposing effects of apolipoproteins E and C on lipoprotein binding to low density lipoprotein receptor-related protein. J Biol Chem 265:10771–10779
20. Sehayek E, Eisenberg S (1991) Mechanisms of inhibition by apolipoprotein C of apolipoprotein E-dependent cellular metabolism of human triglyceride-rich lipoproteins through the low density lipoprotein receptor pathway. J Biol Chem 266:18259–18267
21. Morita SY, Okuhira K, Tsuchimoto N, Vertut-Doi A, Saito H, Nakano M, Handa T (2003) Effects of sphingomyelin on apolipoprotein E- and lipoprotein lipase-mediated cell uptake of lipid particles. Biochim Biophys Acta 1631:169–176
22. Sakurai A, Morita SY, Wakita K, Deharu Y, Nakano M, Handa T (2005) Effects of cholesterol in chylomicron remnant models of lipid emulsions on apoE-mediated uptake and cytotoxicity of macrophages. J Lipid Res 46:2214–2220
23. Morita SY, Kawabe M, Sakurai A, Okuhira K, Vertut-Doi A, Nakano M, Handa T (2004) Ceramide in lipid particles enhances heparan sulfate proteoglycan and low density lipoprotein receptor-related protein-mediated uptake by macrophages. J Biol Chem 279:24355–24361
24. Heuser JE, Anderson RG (1989) Hypertonic media inhibit receptor-mediated endocytosis by blocking clathrin-coated pit formation. J Cell Biol 108:389–400
25. Denicola A, Batthyany C, Lissi E, Freeman BA, Rubbo H, Radi R (2002) Diffusion of nitric oxide into low density lipoprotein. J Biol Chem 277:932–936
26. Vogel T, Weisgraber KH, Zeevi MI, Ben-Artzi H, Levanon AZ, Rall SC Jr, Innerarity TL, Hui DY, Taylor JM, Kanner D, Yavin Z, Amit B, Aviv H, Gorecki M, Mahley RW (1985) Human apolipoprotein E expression in *Escherichia coli*: structural and functional identity of the bacterially produced protein with plasma apolipoprotein E. Proc Natl Acad Sci USA 82:8696–8700
27. Tajima S, Yokoyama S, Yamamoto A (1983) Effect of lipid particle size on association of apolipoproteins with lipid. J Biol Chem 258:10073–10082
28. Morita SY, Nakano M, Sakurai A, Deharu Y, Vertut-Doi A, Handa T (2005) Formation of ceramide-enriched domains in lipid particles enhances the binding of apolipoprotein E. FEBS Lett 579:1759–1764
29. Mahley RW, Ji ZS (1999) Remnant lipoprotein metabolism: key pathways involving cell-surface heparan sulfate proteoglycans and apolipoprotein E. J Lipid Res 40:1–16
30. Ji ZS, Sanan DA, Mahley RW (1995) Intravenous heparinase inhibits remnant lipoprotein clearance from the plasma and uptake by the liver: in vivo role of heparan sulfate proteoglycans. J Lipid Res 36:583–592
31. Ji ZS, Mahley RW (1994) Lactoferrin binding to heparan sulfate proteoglycans and the LDL receptor-related protein. Further evidence supporting the importance of direct binding of remnant lipoproteins to HSPG. Arterioscler Thromb 14:2025–2031
32. Curtiss LK, Boisvert WA (2000) Apolipoprotein E and atherosclerosis. Curr Opin Lipidol 11:243–251
33. Jong MC, Hofker MH, Havekes LM (1999) Role of ApoCs in lipoprotein metabolism: functional differences between ApoC1, ApoC2, and ApoC3. Arterioscler Thromb Vasc Biol 19: 472–484
34. Morita SY, Kawabe M, Nakano M, Handa T (2003) Pluronic L81 affects the lipid particle sizes and apolipoprotein B conformation. Chem Phys Lipids 126:39–48
35. Morita SY, Deharu Y, Takata E, Nakano M, Handa T (2008) Cytotoxicity of lipid-free apolipoprotein B. Biochim Biophys Acta 1778:2594–2603
36. Liu H, Talmud PJ, Lins L, Brasseur R, Olivecrona G, Peelman F, Vandekerckhove J, Rosseneu M, Labeur C (2000) Characterization of recombinant wild type and site-directed mutations of apolipoprotein C-III: lipid binding, displacement of ApoE, and inhibition of lipoprotein lipase. Biochemistry 39:9201–9212
37. Gangabadage CS, Zdunek J, Tessari M, Nilsson S, Olivecrona G, Wijmenga SS (2008) Structure and dynamics of human apolipoprotein CIII. J Biol Chem 283:17416–17427
38. Westerlund JA, Weisgraber KH (1993) Discrete carboxyl-terminal segments of apolipoprotein E mediate lipoprotein association and protein oligomerization. J Biol Chem 268:15745–15750
39. Sakamoto T, Tanaka M, Vedhachalam C, Nickel M, Nguyen D, Dhanasekaran P, Phillips MC, Lund-Katz S, Saito H (2008) Contributions of the carboxyl-terminal helical segment to the self-association and lipoprotein preferences of human apolipoprotein E3 and E4 isoforms. Biochemistry 47:2968–2977
40. Wilson C, Wardell MR, Weisgraber KH, Mahley RW, Agard DA (1991) Three-dimensional structure of the LDL receptor-binding domain of human apolipoprotein E. Science 252:1817–1822
41. Croy JE, Brandon T, Komives EA (2004) Two apolipoprotein E mimetic peptides, ApoE(130–149) and ApoE(141–155)2, bind to LRP1. Biochemistry 43:7328–7335
42. Guttman M, Prieto JH, Handel TM, Domaille PJ, Komives EA (2010) Structure of the minimal interface between ApoE and LRP. J Mol Biol 398:306–319
43. Saito H, Dhanasekaran P, Nguyen D, Baldwin F, Weisgraber KH, Wehrli S, Phillips MC, Lund-Katz S (2003) Characterization of the heparin binding sites in human apolipoprotein E. J Biol Chem 278:14782–14787
44. Sivashanmugam A, Wang J (2009) A unified scheme for initiation and conformational adaptation of human apolipoprotein E N-terminal domain upon lipoprotein binding and for receptor binding activity. J Biol Chem 284:14657–14666
45. Lund-Katz S, Zaiou M, Wehrli S, Dhanasekaran P, Baldwin F, Weisgraber KH, Phillips MC (2000) Effects of lipid interaction on the lysine microenvironments in apolipoprotein E. J Biol Chem 275:34459–34464
46. Lund-Katz S, Wehrli S, Zaiou M, Newhouse Y, Weisgraber KH, Phillips MC (2001) Effects of polymorphism on the microenvironment of the LDL receptor-binding region of human apoE. J Lipid Res 42:894–901
47. Yamamoto T, Ryan RO (2006) Role of leucine zipper motif in apoE3 N-terminal domain lipid binding activity. Biochim Biophys Acta 1761:1100–1106
48. Ben-Yashar V, Barenholz Y (1991) Characterization of the core and surface of human plasma lipoproteins. A study based on the use of five fluorophores. Chem Phys Lipids 60:1–14
49. Redgrave TG, Small DM (1979) Quantitation of the transfer of surface phospholipid of chylomicrons to the high density lipoprotein fraction during the catabolism of chylomicrons in the rat. J Clin Invest 64:162–171
50. Windler EE, Preyer S, Greten H (1986) Influence of lysophosphatidylcholine on the C-apolipoprotein content of rat and human triglyceride-rich lipoproteins during triglyceride hydrolysis. J Clin Invest 78:658–665

51. Maranhao RC, Tercyak AM, Redgrave TG (1986) Effects of cholesterol content on the metabolism of protein-free emulsion models of lipoproteins. Biochim Biophys Acta 875:247–255
52. Saito H, Minamida T, Arimoto I, Handa T, Miyajima K (1996) Physical states of surface and core lipids in lipid emulsions and apolipoprotein binding to the emulsion surface. J Biol Chem 271:15515–15520
53. Redgrave TG, Vassiliou GG, Callow MJ (1987) Cholesterol is necessary for triacylglycerol-phospholipid emulsions to mimic the metabolism of lipoproteins. Biochim Biophys Acta 921:154–157
54. Aalto-Setala K, Fisher EA, Chen X, Chajek-Shaul T, Hayek T, Zechner R, Walsh A, Ramakrishnan R, Ginsberg HN, Breslow JL (1992) Mechanism of hypertriglyceridemia in human apolipoprotein (apo) CIII transgenic mice. Diminished very low density lipoprotein fractional catabolic rate associated with increased apo CIII and reduced apo E on the particles. J Clin Invest 90:1889–1900
55. Narayanaswami V, Ryan RO (2000) Molecular basis of exchangeable apolipoprotein function. Biochim Biophys Acta 1483:15–36
56. Clavey V, Lestavel-Delattre S, Copin C, Bard JM, Fruchart JC (1995) Modulation of lipoprotein B binding to the LDL receptor by exogenous lipids and apolipoproteins CI, CII, CIII, and E. Arterioscler Thromb Vasc Biol 15:963–971

Lipids (2011) 46:333–340
DOI 10.1007/s11745-010-3517-x

ORIGINAL ARTICLE

Simvastatin Therapy Reduces Prooxidant-Antioxidant Balance: Results of a Placebo-Controlled Cross-Over Trial

Seyyed M. R. Parizadeh · Mahmoud R. Azarpazhooh · Mohsen Moohebati · Mohsen Nematy · Majid Ghayour-Mobarhan · Shima Tavallaie · Amir A. Rahsepar · Maral Amini · Amirhossein Sahebkar · Maryam Mohammadi · Gordon A. A. Ferns

Received: 16 March 2010 / Accepted: 10 December 2010 / Published online: 5 January 2011

Abstract Oxidative stress is thought to play an important role in atherogenesis. The statin group of cholesterol-lowering drugs have been shown to reduce cardiovascular events and possess antioxidant properties. We aimed to assess the effects of simvastatin on a novel measure of prooxidant–antioxidant balance (PAB) in dyslipidemic patients. The PAB assay can measure the prooxidant burden and the antioxidant capacity simultaneously in one assay, thereby giving a redox index. We treated 102 dyslipidemic individuals with simvastatin, or a placebo in a double-blind, cross-over, placebo-controlled trial. PAB values were measured before and after each treatment period. Seventy-seven subjects completed the study. We found that statin therapy was associated with a significant reduction in PAB values ($P < 0.001$). This effect appeared to be independent of the cholesterol-lowering effects of statins. We conclude that serum PAB values are decreased by simvastatin therapy. Regarding previous reports on the elevation of PAB in conditions associated with oxidative stress, the PAB assay, along with other markers of oxidative stress, may be applied to estimate the extent of oxidative stress in patients, assessment of the antioxidative efficacy of medication such as statins and perhaps also for the identification of those individuals who need antioxidant therapy.

Keywords Simvastatin · Prooxidant–antioxidant balance (PAB) · Dyslipidemia

Abbreviations

BMI	Body mass index
CVD	Cardiovascular disease
eNOS	Endothelial nitric oxide synthase
FBS	Fasting blood sugar
HDL-C	High-density lipoprotein cholesterol
HMG-CoA	3-Hydroxy-3-methylglutaryl-coenzyme A
LDL-C	Low density lipoprotein cholesterol
NADPH	Nicotinamide adenine dinucleotide phosphate

S. M. R. Parizadeh
Department of Biochemistry and Nutrition, Faculty of Medicine, Mashhad University of Medical Sciences, Mashhad, Iran

S. M. R. Parizadeh
Biochemistry and Nutrition Research Center, Avicenna (Bu-Ali) Research Institute, Mashhad University of Medical Sciences, Mashhad, Iran

M. Moohebati · M. Nematy · M. Ghayour-Mobarhan · S. Tavallaie · A. A. Rahsepar · A. Sahebkar · M. Mohammadi
Cardiovascular Research Center, Avicenna (Bu-Ali) Research Institute, Mashhad University of Medical Sciences, Mashhad, Iran

M. R. Azarpazhooh · A. A. Rahsepar
Department of Neurology, Faculty of Medicine, Mashhad University of Medical Sciences, Mashhad, Iran

M. Moohebati
Department of Cardiology, Faculty of Medicine, Mashhad University of Medical Sciences, Mashhad, Iran

M. Nematy · M. Ghayour-Mobarhan (✉)
Department of Nutrition, Faculty of Medicine, Mashhad University of Medical Sciences, Mashhad, Iran
e-mail: ghayourm@mums.ac.ir

M. Amini
Young Researchers Club, Mashhad Islamic Azad University, Mashhad, Iran

G. A. A. Ferns
Institute for Science and Technology in Medicine, University of Keele, Guy Hilton Research Centre, Thornburrow Drive, Stoke on Trent, Staffordshire ST4 7QB, UK

NF-κB	Nuclear factor kappa-light-chain-enhancer of activated B cells
NO	Nitric oxide
ox-LDL	Oxidized low density lipoprotein cholesterol
PAB	Prooxidant–antioxidant balance
ROS	Reactive oxygen species
SAS	Statistical analysis software
SD	Standard deviation
TC	Total cholesterol
TG	Triglycerides
TMB	3,3′,5,5′-Tetramethylbenzidine

Introduction

Oxidative stress is an imbalance between the production of pro-oxidants and antioxidant defenses in favor of pro-oxidants. Oxidative stress is usually related to the increased formation of reactive oxygen species (ROS), and is thought to play an important role in the pathogenesis of cardiovascular disease (CVD) and its complications. Recently oxidative stress [1] and inflammation [2] have been proposed to be significant risk factors for CVD, and the lipid oxidation hypothesis provides one mechanism by which oxidative stress may be implicated [3].

It is also suggested that oxidative stress may be a strong and independent prognostic predictor of cardiovascular events [4].

Low density lipoprotein cholesterol (LDL-C) has been associated with several pro-atherothrombotic processes through the development of endothelial dysfunction, inflammation and foam cell formation [5]. Indeed, individuals with relatively normal LDL levels but high exposure to oxidative stress such as those with hypertension [6], are at increased risk of developing CVD via the formation of pro-inflammatory and pro-atherogenic molecules associated with the formation of oxidized-LDL (ox-LDL). Ox-LDL has been shown to accumulate in the arterial wall and this is associated with the development of endothelial dysfunction [7, 8]. Thus, reduction in plasma levels of LDL and ox-LDL may represent a useful approach for preventing from atherosclerotic diseases.

Statins are a group of lipid-lowering agents which block the rate limiting step in cholesterol biosynthesis, the conversion of 3-hydroxy-3-methylglutaryl-coenzyme A (HMG-CoA) to mevalonic acid. The LDL-cholesterol lowering property of statins is associated with a reduction of cardiovascular endpoints including definite coronary events (specified as nonfatal myocardial infarction or death from coronary heart disease), definite nonfatal myocardial infarctions; death from definite plus suspected coronary heart disease and death from all cardiovascular causes [9]. However, it has been argued that the benefits obtained with statin therapy in patients with a wide range of cholesterol levels may be due to their "pleiotropic" non-cholesterol-lowering effects. These pleiotropic effects of statins include: improving endothelial function, decreasing oxidative stress (by lowering ROS production and increasing the resistance of LDL-C to oxidation), inhibiting platelet adhesion, reducing inflammation, and enhancing the stability of atherosclerotic plaques [10].

Until now, many methods have been developed that can separately determine the total pro-oxidant and antioxidant capacities and are therefore hard, time consuming, expensive, and imprecise. We have recently used a simple, rapid and inexpensive method [11] to measure the PAB directly, by using 3,3′,5,5′-tetramethylbenzidine (TMB) and two different kinds of reaction, an enzymatic reaction where the chromogen TMB is oxidized to a colored cation by peroxides, and a chemical reaction in which the colored TMB cation is reduced to a colorless compound by antioxidants. A redox index is thereby derived from these two reactions. The assay has been calibrated against the most significant known oxidants and antioxidants and its response has been found to be a linear decrease against antioxidants and a linear increase against oxidants. The method was also, validated in depth by other known oxidative stress markers [11]. In this study, we aimed to evaluate the effect of simvastatin on PAB values by a modified PAB assay [12] in a randomized, double blind, cross-over trial in dyslipidemic patients.

Methods

Subjects

One hundred and two men and women, aged 20–88 who were not originally taking lipid-lowering agents were recruited from the lipid clinics at the Qaem hospital, Mashhad, Iran. In addition to a history of not taking statins, other inclusion criteria were any of the following conditions (based on the NCEP-ATP III guidelines [13]): (1) patients with <2 risk factors (except diabetes mellitus) for coronary heart disease (CHD) and 160 mg/dL < LDL-C < 190 mg/dL, or (2) patients with ≥2 risk factors (except diabetes mellitus) for coronary heart disease (CHD) and 130 mg/dL < LDL-C < 160 mg/dL. Cardiovascular risk factors were defined as age >65 years, hypertension (defined as taking any anti-hypertensive medication; or systolic blood pressure ≥140 mmHg or diastolic blood pressure ≥90 mmHg), diabetes mellitus (defined as fasting blood sugar (FBS) ≥ 126 mg/dL), positive family history of CVD, smoking, male sex and obesity [defined as body mass index (BMI) ≥ 30 kg/m^2].

The exclusion criteria were; malignancy or history of malignancy, infections, connective tissue disorders or treatment with immunomodulatory drugs (e.g. corticosteroids), liver or renal disease, leukocytosis (white blood cell count >10,000 10^9/L), thrombocytosis (platelet count >450,000 10^9/L) and anemia (hematocrit <40%). Each subject gave informed written consent to participate in the study, which had previously been approved by the Mashhad University of Medical Science Ethics Committee. In addition, subjects were advised to continue their normal medication schedule.

Study Design

This study was designed as a randomized, double blind, cross-over trial in which each patient received simvastatin or a placebo and then crossed over to the alternate regimen. Each treatment period was 30 days and there was a 2-week washout interval in between the regimens. The dose of simvastatin and all other medication remained unchanged during the experimental period, and the patients were advised not to change their lifestyle during the study. At the first visit, patients were randomized for one of two treatment regimens, 51 patients were provided with simvastatin 40 mg/day for 30 days and other 51 patients received a placebo (simply prepared by filling empty capsules—which were matched for size and color with simvastatin capsules—with starch instead of simvastatin) for 30 days. After another 2-week wash-out period, patients crossed over to the other form of treatment.

Anthropometric Measurements

Anthropometric parameters including weight, height, and BMI were measured. Weight was measured with the subjects dressed in light clothing after an overnight fasting using a standard scale. BMI was calculated as weight (kg) divided by height squared (m^2).

Blood Sampling

Blood samples were collected four times for each subject (before and after starting each period). Blood samples for laboratory assays were obtained on the day of sampling after 12 h of fasting. Following venipuncture, blood samples were collected in Vacutainer® tubes and centrifuged at 10,000*g* for 15 min at 4 °C. After separation, aliquots of serum were frozen at −80 °C until analysis.

Routine Biochemical Analysis

A full fasted lipid profile comprising total cholesterol, triglycerides, high-density lipoprotein cholesterol (HDL-C) and LDL-C was determined for each subject. Serum lipid and FBS concentrations were measured enzymatically with the use of commercial kits.

Chemicals

TMB powder (3,3′,5,5′-tetramethylbenzidine, Fluka), peroxidase enzyme (Applichem: 230 U/mg, A3791,0005, Darmstadt, Germany), chloramine T trihydrate (Applichem: A4331, Darmstadt, Germany), hydrogen peroxide (30%) (Merck). These chemicals and all the other reagents used were reagent grade and were prepared in double distilled water.

Prooxidant–Antioxidant Balance (PAB) Assay

A modified PAB assay was applied based on a previously described method [11, 12]. The standard solutions were prepared by mixing varying proportions (0–100%) of 250 μM hydrogen peroxide with 3 mM uric acid (in 10 mM NaOH). TMB powder (60 mg) was dissolved in 10 mL DMSO. For preparation of the TMB cation, 400 μL of the TMB/DMSO solution was added to 20 mL of acetate buffer (0.05 M buffer, pH 4.5), and then 70 μL of fresh chloramine T (100 mM) solution was added to this 20 mL. The solution was mixed well and incubated for 2 h at room temperature in a dark place. Then 25 U of peroxidase enzyme solution was added to 20 mL of TMB cation solution, dispensed in 1 mL and stored at −20 °C. In order to prepare the TMB solution 200 μL of TMB/DMSO was added to 10 mL of acetate buffer (0.05 M buffer, pH 5.8) and the working solution was prepared by mixing 1 mL TMB cation with 10 mL of TMB solution. This working solution was incubated for 2 min at room temperature in a dark place and used immediately. Ten microliters of each sample, standard or blank (distilled water) were mixed with 200 μL of working solution in each well of a 96-well plate, which was then incubated in a dark place at 37 °C for 12 min. At the end of the incubation time, 100 μL of 2 N HCl was added to each well, and the optical density (OD) was measured in an ELISA reader at 450 nm with a reference wavelength of 620 or 570 nm. A standard curve was provided from the values relative to the standard samples. The values of the PAB are expressed in arbitrary units, this is the percentage of hydrogen peroxide in the standard solution. The values of the unknown samples were then calculated based on the values obtained from the above standard curve.

Statistical Analysis

Values were expressed as means ± SD or, in the case of non-normally distributed data, as median and inter-quartile

range. The comparison between pre and post treatments was done using the paired t test or the Wilcoxon signed rank test. Data obtained from independent variables analyzed using Student's t test (for those with normal distribution) or Mann–Whitney U test (for those without normal distribution). Categorical data were compared using χ^2 test. Correlations between changes in serum PAB and LDL-C levels were assessed using the Pearson correlation coefficient. Mixed model analysis of variance for 2×2 cross-over studies were fitted when assumption for normality were met. All analysis were performed with the Statistical Analysis Software (SAS version 8). A two-sided P value of <0.05 was considered statistically significant.

Results

From 102 subjects who entered our study, 25 (24.5%) did not complete the study, leading to a final sample size of 77 (78.18%). The reasons for drop-outs were non-compliance with the study protocol ($n = 21$), drug intolerance ($n = 2$) and moving to anothercity ($n = 2$) (Fig. 1). To rule out the possibility of a carryover effect from one treatment period to the other treatment period, we compared baseline values before the first treatment period to those before the second treatment period. No significant difference was found in the analysis ($P > 0.05$). The mean age and BMI of subjects were 46.61 ± 13.95 and 29.94 ± 6.08, respectively, with 72.1% being female. The prevalence of smoking, diabetes mellitus and hypertension were 7.0, 14.0 and 9.3%, respectively.

Effect of Administration of Simvastatin Versus Placebo on Weight, BMI and FBS

FBS was not significantly affected by simvastatin nor by the placebo ($P > 0.05$). However, mean baseline values for BMI and weight were significantly different between the first and second periods of treatment ($P = 0.019$ and $P = 0.003$, respectively) (Table 1).

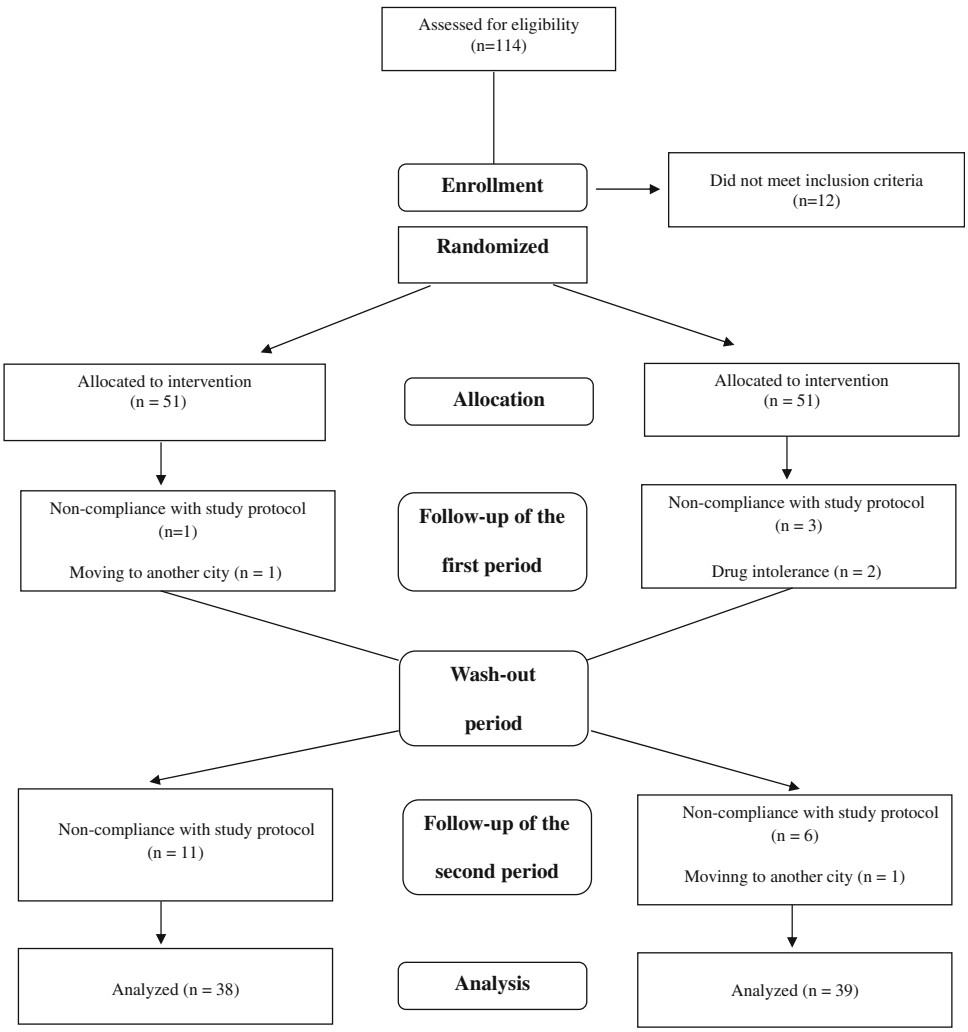

Fig. 1 Flow chart of the trial

Table 1 Effect of simvastatin and placebo therapy in two groups of subjects

	Study groups	First Pre treatment	Period Post treatment	Second Pre treatment	Period Post treatment	Period effect[a]	Treatment effect (S vs. P)
FBS (mg/dl)	Statin–placebo	86.46 ± 19.52	85.58 ± 17.12	81.28 ± 15.83	81.09 ± 13.65	($P > 0.05$)	($P > 0.05$)
	Placebo–statin	104.36 ± 47.61	101.71 ± 45.86	103.5 ± 45.55	99.10 ± 33.28		
Weight (kg)	Statin–placebo	71.59 ± 22.02	72.42 ± 19.24	73.80 ± 18.60	75.27 ± 18.55	($P = 0.003$)	($P > 0.05$)
	Placebo–statin	78.04 ± 16.63	77.17 ± 16.30	76.99 ± 15.50	76.71 ± 16.41		
BMI (kg/m^2)	Statin–placebo	28.83 ± 6.18	28.30 ± 6.19	28.95 ± 5.90	29.09 ± 5.91	($P = 0.019$)	($P > 0.05$)
	Placebo–statin	31.12 ± 6.41	30.83 ± 6.36	30.33 ± 7.41	31.25 ± 6.04		
TC (mg/dl)	Statin–placebo	203.02 ± 36.11	152.48 ± 41.60	181.69 ± 30.65	182.38 ± 37.64	($P > 0.05$)	($P < 0.001$)
	Placebo–statin	193.32 ± 39.65	191.06 ± 38.04	194.85 ± 37.75	160.37 ± 60.81		
LDL-C (mg/dl)	Statin–placebo	131.44 ± 28.46	87.35 ± 35.01	119.75 ± 26.44	121.09 ± 23.86	($P > 0.05$)	($P < 0.001$)
	Placebo–statin	118.38 ± 30.48	115.22 ± 35.03	121.75 ± 28.25	92.50 ± 46.48		
HDL-C (mg/dl)	Statin–placebo	44.08 ± 10.80	43.31 ± 12.19	40.36 ± 13.34	41.79 ± 14.97	($P > 0.05$)	($P > 0.05$)
	Placebo–statin	42.40 ± 11.92	42.64 ± 13.32	44.55 ± 12.42	45.96 ± 14.58		
TG (mg/dl)	Statin–placebo	137.23 ± 65.07	118.87 ± 57.20	128.11 ± 58.17	126.54 ± 59.14	($P > 0.05$)	($P < 0.001$)
	Placebo–statin	156.00 ± 84.11	151.35 ± 76.98	156.65 ± 93.07	132.37 ± 93.13		

Values are expressed as means ± SD for normally distributed data and median and interquartile range. Statin-placebo group took statin at first, while placebo-statin group received statin following placebo

BMI body mass index, *FBS* fasting blood sugar, *TC* total cholesterol, *HDL* high-density lipoprotein, *LDL* low-density lipoprotein, *TG* triglycerides, *PAB* prooxidant–antioxidant balance

[a] Defined as comparison of mean values between the first and second periods

Effect of Administration of Simvastatin Versus Placebo on Lipid Parameters

As expected, total cholesterol, LDL-C and triglycerides were reduced significantly after 4-weeks of treatment with simvastatin ($P < 0.001$). However, HDL-C did not change significantly with either treatment ($P > 0.05$) (Table 1).

Effect of Administration of Simvastatin Versus Placebo on PAB Values

Treatment with simvastatin 40 mg/day for 4 weeks caused a statistically significant reduction in the mean PAB values ($P < 0.001$) (Fig. 2).

Correlation Between Changes in PAB Values with Changes in LDL-C Levels

Statistical analysis showed that there was no significant correlation between changes in PAB values and serum LDL-C levels in any of the periods, neither in the placebo-statin nor in the statin-placebo group ($P > 0.05$, Table 2). The only exception was a significant correlation between PAB changes and serum total cholesterol changes in the placebo-statin group ($P < 0.05$, Table 2).

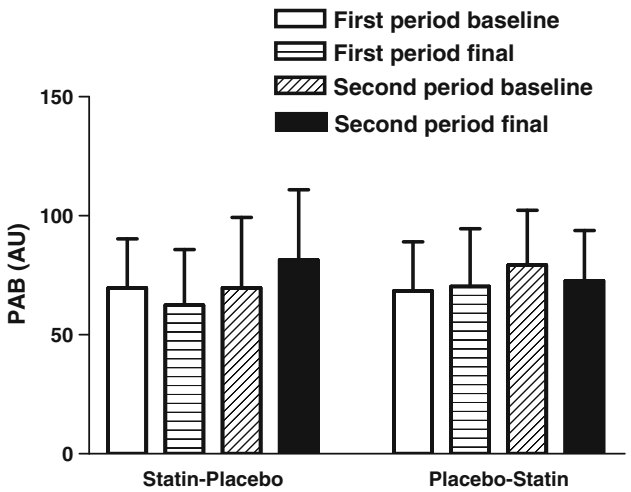

Fig. 2 Effect of simvastatin versus placebo on serum PAB values. Period effect: $P > 0.05$; treatment effect: $P < 0.001$

Discussion

In the present study we found that simvastatin therapy for 4 weeks caused a statistically significant reduction in mean PAB values, showing that statin therapy may be associated with a reduction in levels of oxidative stress. Our finding confirms the results of other studies evaluating the effect of statins on plasma measures of oxidation status. Fluvastatin therapy was found to reduce superoxide radical generation

Table 2 Correlations between changes in serum PAB and LDL-C levels

	LDL-C		Total cholesterol	
	r	*p*	*r*	*p*
Placebo–statin				
First period	0.197	>0.05	0.335	<0.05
Second period	0.005	>0.05	−0.016	>0.05
Statin–placebo				
First period	0.050	>0.05	0.031	>0.05
Second period	−0.356	>0.05	−0.360	>0.05

Correlations were assessed using the Pearson correlation coefficient

PAB prooxidant–antioxidant balance

and the susceptibility of LDL to oxidation in cholesterol-fed rabbits [14]. Moreover, simvastatin was reported to lower superoxide generation in human macrophages [15]. Furthermore, oxidative stress of different patients has been shown to decrease after treatment with atorvastatin, simvastatin, pravastatin, fluvastatin, and lovastatin [16–18]. In addition, treatment with these statins was followed by a prolonged lag time of LDL oxidation [19–21]. Statin therapy also causes a significant reduction in plasma levels of ox-LDL [17] and it has also been reported that in hypercholesterolemia or mixed type hyperlipidemia, atorvastatin can increase total plasma antioxidant status, leading to a lower LDL oxidation capacity [19].

There appear to be several mechanisms whereby statins may reduce oxidative stress. Apart from their hypocholesterolemic effects and the subsequent reduction of oxidation substrate, statins are known to exert radical scavenging activity and decrease the generation and release of ROS through different mechanism such as inhibition of Rac1GTPase and NADPH-oxidase [22].

Nicotinamide adenine dinucleotide phosphate (NADPH) oxidases are as one of the important sources of superoxide in human coronary artery, and their activities have been reported to be increased in patients with CVD [23]. Statins have been reported to reduce NADPH dependant superoxide formation by monocyte-derived cell lines in culture [24]. Atorvastatin has been reported to inhibit angiotensin II-induced superoxide formation by NADPH oxidase in rats in vivo [25]. Statin therapy has been also suggested to inhibit ox-LDL induced NADPH oxidase expression and superoxide anion formation [26]. The anti-inflammatory properties of statins make them able to inhibit macrophage growth and foam cell formation stimulated with ox-LDL [27], leading to a reduction in influx of inflammatory cells, which consecutively results in a decreased release of ROS and the LDL oxidation.

Statins may also act as an antioxidant via different mechanisms, for instance, there are some reports, though not consistent, indicating that statins are able to increase the activity and/or expression of antioxidant enzymes such as catalase, paraoxonase and glutathione peroxidase, while decreasing those of NADPH oxidase [28–31]. It is also reported that statins can increase the release of NO [32], and also several statins have the ability to increase eNOS expression in the blood vessels of treated animals [33], resulting in the restoration of endothelial function. Moreover, atorvastatin has been reported to increase paraoxonase activity and decrease the enhanced cellular uptake of ox-LDL of monocytes differentiating into macrophages [34]. Finally some statin metabolites are considered to possess antioxidant properties and prevent lipid peroxidation [35] (Fig. 3).

In our study, we did not find a significant correlation between changes in PAB values with changes in serum levels of LDL-C, implying that antioxidant activity of statins may be at least partly due to other pleiotropic properties rather than just lipid-lowering effects of these drugs. It is suggested that the underlying cholesterol independent effects relates to the inhibition of isoprenoid intermediates of the cholesterol synthesis pathway [36].

The aforementioned studies together with the findings of the present study support the notion that oxidative stress could be used as a significant risk predictor in the atherosclerotic process. Statins have pleiotropic properties as endothelial protective, anti-inflammatory, and antioxidative agents, and suggest that other markers such as

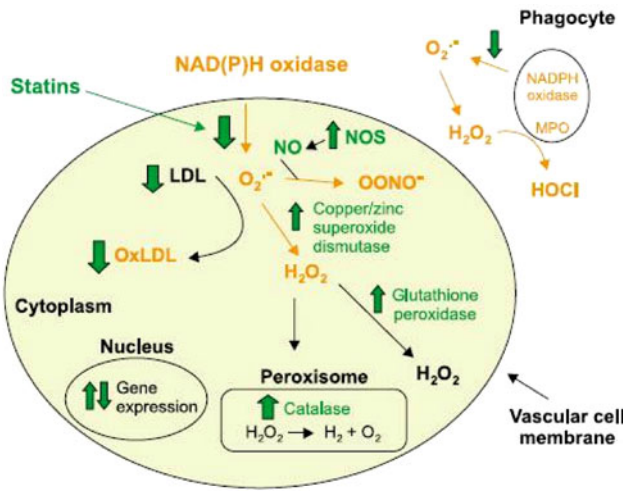

Fig. 3 Some antioxidant mechanisms of statins. Statins inhibit the assembly of NAD(P)H oxidase in both vascular cells and phagocytes, thus preventing the formation of superoxide ($O_2^{\cdot-}$). *Bi-directional arrows* associated with gene expression indicate upregulation of expression of antioxidant enzymes (eNOS and catalase) and down-regulation of oxidants (NAD[P]H components and cyclooxygenase-2). Permission from Drugs of Today [41] [Drugs of Today 2004;40(12):975–989. Copyright © 2004 Prous Science, S.A. All rights reserved.]

C-reactive protein, oxidative biomarkers and isoprenoid intermediates might be used in conjunction with serum cholesterol levels to assess the therapeutic benefits of statin therapy better.

In previous studies using the PAB assay, it was reported to be elevated in a number of conditions associated with oxidative stress including diabetes mellitus [11], coronary artery disease [12], acute coronary syndrome [37], exfoliative glaucoma [38], and stroke [39]. PAB values have been also reported to decrease following antioxidant vitamins (E and C) [11] and selenium consumption [40]. The PAB assay may be useful as a CVD risk predictor [12, 37] and could help to identify patients with higher oxidative stress in order to introduce interventions for the prevention of vascular disease earlier. In the present study, we showed that this assay may serve as a useful method to assess the effect of statin therapy in CVD, indicating that the PAB assay, along with other known markers of oxidative stress, may be used to estimate the extent of oxidative stress in high-risk groups, identify subjects who need antioxidant therapy, and evaluate the antioxidative efficacy of different supplements and medications. Finally, further clinical research is required based on a larger healthy population, as well as on various physiological and pathological states associated with oxidative stress, and by multiple laboratories in order to substantiate the potency of the assay to become a clinical laboratory test.

Study Limitations

The present study had several limitations. First, 25 subjects did not complete the study due to non-compliance with the study protocol or drug intolerance. Second, simvastatin was administered at a dose of 40 mg/day for a limited period (30 days), and longer term studies are necessary to show that this effect is sustained. Finally, using several doses of statins could have been useful to determine whether the observed effects of simvastatin are dose-dependent and whether higher doses exert more dramatic effects.

Acknowledgments We are particularly grateful to the patients and their family members who volunteered to participate in this study. This work was financially supported by the Iran National Science Foundation and Mashhad University of Medical Science (MUMS), Mashhad, Iran.

References

1. Cai H, Harrison DG (2000) Endothelial dysfunction in cardiovascular diseases: the role of oxidant stress. Circ Res 87:840–844
2. Osterud B, Bjorklid E (2003) Role of monocytes in atherogenesis. Physiol Rev 83:1069–1112
3. Singh U, Jialal I (2006) Oxidative stress and atherosclerosis. Pathophysiology 13:129–142
4. Walter MF, Jacob RF, Jeffers B, Ghadanfar MM, Preston GM, Buch J et al (2004) Serum levels of thiobarbituric acid reactive substances predict cardiovascular events in patients with stable coronary artery disease: a longitudinal analysis of the PREVENT study. J Am Coll Cardiol 44:1996–2002
5. Rosenson RS, Tangney CC (1998) Antiatherothrombotic properties of statins: implications for cardiovascular event reduction. JAMA 279:1643–1650
6. Giugliano D, Ceriello A, Paolisso G (1995) Diabetes mellitus, hypertension, and cardiovascular disease: which role for oxidative stress? Metabolism 44:363–368
7. Yla-Herttuala S, Palinski W, Rosenfeld ME, Parthasarathy S, Carew TE, Butler S et al (1989) Evidence for the presence of oxidatively modified low density lipoprotein in atherosclerotic lesions of rabbit and man. J Clin Invest 84:1086–1095
8. Thorne SA, Abbot SE, Winyard PG, Blake DR, Mills PG (1996) Extent of oxidative modification of low density lipoprotein determines the degree of cytotoxicity to human coronary artery cells. Heart 75:11–16
9. Shepherd J, Cobbe SM, Ford I, Isles CG, Lorimer AR, MacFarlane PW et al (1995) Prevention of coronary heart disease with pravastatin in men with hypercholesterolemia. West of Scotland Coronary Prevention Study Group. N Engl J Med 333:1301–1307
10. Ray KK, Cannon CP (2005) The potential relevance of the multiple lipid-independent (pleiotropic) effects of statins in the management of acute coronary syndromes. J Am Coll Cardiol 46:1425–1433
11. Alamdari DH, Paletas K, Pegiou T, Sarigianni M, Befani C, Koliakos G (2007) A novel assay for the evaluation of the prooxidant-antioxidant balance, before and after antioxidant vitamin administration in type II diabetes patients. Clin Biochem 40:248–254
12. Alamdari DH, Ghayour-Mobarhan M, Tavallaie S, Parizadeh MR, Moohebati M, Ghafoori F et al (2008) Prooxidant–antioxidant balance as a new risk factor in patients with angiographically defined coronary artery disease. Clin Biochem 41:375–380
13. Third Report of the National Cholesterol Education Program (NCEP) (2002) Expert Panel on detection, evaluation, and treatment of high blood cholesterol in adults (Adult treatment panel III). Final report. Circulation 106:3143
14. Rikitake Y, Kawashima S, Takeshita S, Yamashita T, Azumi H, Yasuhara M et al (2001) Anti-oxidative properties of fluvastatin, an HMG-CoA reductase inhibitor, contribute to prevention of atherosclerosis in cholesterol-fed rabbits. Atherosclerosis 154:87–96
15. Giroux LM, Davignon J, Naruszewicz M (1993) Simvastatin inhibits the oxidation of low-density lipoproteins by activated human monocyte-derived macrophages. Biochim Biophys Acta 1165:335–338
16. van den Akker JM, Bredie SJ, Diepenveen SH, van Tits LJ, Stalenhoef AF, van LR (2003) Atorvastatin and simvastatin in patients on hemodialysis: effects on lipoproteins, C-reactive protein and in vivo oxidized LDL. J Nephrol 16:238–244
17. Inami S, Okamatsu K, Takano M, Takagi G, Sakai S, Sano J et al (2004) Effects of statins on circulating oxidized low-density lipoprotein in patients with hypercholesterolemia. Jpn Heart J 45:969–975
18. Aviram M, Dankner G, Cogan U, Hochgraf E, Brook JG (1992) Lovastatin inhibits low-density lipoprotein oxidation and alters its fluidity and uptake by macrophages: in vitro and in vivo studies. Metabolism 41:229–235
19. Orem C, Orem A, Calapoglu M, Baykan M, Uydu HA, Erdol C (2002) Plasma fibronectin level and its relationships with lipids, lipoproteins and C-reactive protein in patients with dyslipidaemia during lipid-lowering therapy. Acta Cardiol 57:421–425
20. Sobal G, Sinzinger H (2005) Effect of simvastatin on the oxidation of native and modified lipoproteins. Biochem Pharmacol 70:1185–1191

21. Portal VL, Moriguchi EH, Vieira JL, Schio S, Mastalir ET, Buffe F et al (2003) Comparison of the effect of two HMG CoA reductase inhibitors on LDL susceptibility to oxidation. Arq Bras Cardiol 80:156–161
22. Stancu C, Sima A (2001) Statins: mechanism of action and effects. J Cell Mol Med 5:378–387
23. Guzik TJ, Mussa S, Gastaldi D, Sadowski J, Ratnatunga C, Pillai R et al (2002) Mechanisms of increased vascular superoxide production in human diabetes mellitus: role of NAD(P)H oxidase and endothelial nitric oxide synthase. Circulation 105:1656–1662
24. Delbosc S, Morena M, Djouad F, Ledoucen C, Descomps B, Cristol JP (2002) Statins, 3-hydroxy-3-methylglutaryl coenzyme A reductase inhibitors, are able to reduce superoxide anion production by NADPH oxidase in THP-1-derived monocytes. J Cardiovasc Pharmacol 40:611–617
25. Wassmann S, Laufs U, Baumer AT, Muller K, Ahlbory K, Linz W et al (2001) HMG-CoA reductase inhibitors improve endothelial dysfunction in normocholesterolemic hypertension via reduced production of reactive oxygen species. Hypertension 37:1450–1457
26. Rueckschloss U, Galle J, Holtz J, Zerkowski HR, Morawietz H (2001) Induction of NAD(P)H oxidase by oxidized low-density lipoprotein in human endothelial cells: antioxidative potential of hydroxymethylglutaryl coenzyme A reductase inhibitor therapy. Circulation 104:1767–1772
27. Sakai M, Kobori S, Matsumura T, Biwa T, Sato Y, Takemura T et al (1997) HMG-CoA reductase inhibitors suppress macrophage growth induced by oxidized low density lipoprotein. Atherosclerosis 133:51–59
28. Wassmann S, Laufs U, Müller K, Konkol C, Ahlbory K, Bäumer AT et al (2002) Cellular antioxidant effects of atorvastatin in vitro and in vivo. Arterioscler Thromb Vasc Biol 22:300–305
29. Luo JD, Zhang WW, Zhang GP, Zhong BH, Ou HJ (2002) Effects of simvastatin on activities of endogenous antioxidant enzymes and angiotensin-converting enzyme in rat myocardium with pressure-overload cardiac hypertrophy. Acta Pharmacol Sin 23:124–128
30. Deakin S, Leviev I, Guernier S, James RW (2003) Simvastatin modulates expression of the PON1 gene and increases serum paraoxonase: a role for sterol regulatory element-binding protein-2. Arterioscler Thromb Vasc Biol 23:2083–2089
31. Li J, Sun YM, Wang LF, Li ZQ, Pan W, Cao HY (2010) Comparison of effects of simvastatin versus atorvastatin on oxidative stress in patients with coronary heart disease. Clin Cardiol 33:222–227
32. Kaesemeyer WH, Caldwell RB, Huang J, Caldwell RW (1999) Pravastatin sodium activates endothelial nitric oxide synthase independent of its cholesterol-lowering actions. J Am Coll Cardiol 33:234–241
33. Laufs U, Gertz K, Dirnagl U, Bohm M, Nickenig G, Endres M (2002) Rosuvastatin, a new HMG-CoA reductase inhibitor, upregulates endothelial nitric oxide synthase and protects from ischemic stroke in mice. Brain Res 942:23–30
34. Fuhrman B, Koren L, Volkova N, Keidar S, Hayek T, Aviram M (2002) Atorvastatin therapy in hypercholesterolemic patients suppresses cellular uptake of oxidized-LDL by differentiating monocytes. Atherosclerosis 164:179–185
35. Adam O, Laufs U (2008) Antioxidative effects of statins. Arch Toxicol 82:885–892
36. Liao JK, Laufs U (2005) Pleiotropic effects of statins. Annu Rev Pharmacol Toxicol 45:89–118
37. Ghayour-Mobarhan M, Alamdari D, Moohebati M, Sahebkar A, Nematy M, Safarian M et al (2009) Determination of pro-oxidant-antioxidant balance after acute coronary syndrome using a rapid assay: a pilot study. Angiology 60:657–662
38. Koliakos GG, Befani CD, Mikropoulos D, Ziakas NG, Konstas AG (2008) Prooxidant-antioxidant balance, peroxide and catalase activity in the aqueous humour and serum of patients with exfoliation syndrome or exfoliative glaucoma. Graefes Arch Clin Exp Ophthalmol 246:1477–1483
39. Parizadeh SMR, Azarpazhooh MR, Mobarra N, Nemati M, Alamdari DH, Tavallaie S et al (2011) Prooxidant-antioxidant balance in stroke patients and 6-month prognosis. Clin Lab (Accepted)
40. Tara F, Rayman MP, Boskabadi H, Ghayour-Mobarhan M, Sahebkar A, Alamdari DH et al (2010) Prooxidant-antioxidant balance in pregnancy: a randomized double-blind placebo-controlled trial of selenium supplementation. J Perinat Med (Epub ahead of print). doi:10.1515/JPM.2010.068
41. Stoll LL, McCormick ML, Denning GM, Weintraub NL (2004) Antioxidant effects of statins. Drugs Today 40:975–989

Lipids (2011) 46:341–348
DOI 10.1007/s11745-011-3539-z

ORIGINAL ARTICLE

Ezetimibe Treatment Lowers Indicators of Oxidative Stress in Hypercholesterolemic Subjects with High Oxidative Stress

Michael S. Kostapanos · Athanasia T. Spyrou · Constantinos C. Tellis · Irene F. Gazi · Alexandros D. Tselepis · Moses Elisaf · Evangelos N. Liberopoulos

Received: 31 October 2010 / Accepted: 4 February 2011 / Published online: 26 February 2011

Abstract Ezetimibe effectively reduces low-density lipoprotein cholesterol (LDL-C). In this study, we tested the hypothesis that ezetimibe monotherapy may also decrease markers of oxidative stress in subjects with hypercholesterolemia. Subjects with hypercholesterolemia and no evidence of cardiovascular disease were randomly allocated to open-label ezetimibe monotherapy 10 mg/day (EZT group) or therapeutic lifestyle changes (TLC group). At baseline and 12 weeks post-treatment serum lipoprotein and apolipoprotein levels as well as oxidative stress parameters, including oxidized LDL (ox-LDL), 8-isoprostanes (8-epi-PGF2a) and reactive oxygen metabolites (d-ROMs) levels, were blindly determined. A total of 60 patients were included; 30 in each group. Despite a significant decrease in ox-LDL levels (by 20.8%, $p < 0.001$ vs. baseline; $p < 0.001$ vs. TLC group) in the EZT group no change in the ratio ox-LDL to LDL-C was noticed following ezetimibe treatment. No significant change in 8-epiPGF2a and d-ROMs levels was observed in the EZT group. Of note, a significant decrease in 8-epiPGF2a and d-ROMs levels (by 20.4% and 18.2%, respectively, $p < 0.01$ vs. baseline for both), was noted among patients in the EZT group who exhibited 'high oxidative stress' at baseline. No change in any of oxidative stress parameters was noted in the TLC group. Ezetimibe may decrease markers of oxidative stress in hypercholesterolemic subjects. This benefit may be more profound among patients who exhibit 'high oxidative stress' at baseline.

Keywords Ezetimibe · Oxidative stress · Oxidized LDL · 8-Isoprostanes · Reactive oxygen metabolites · Pleiotropic actions · Hypercholesterolemia

Abbreviations

ANCOVA	Analysis of covariance
Apo	Apolipoprotein
d-ROMs	Reactive oxygen metabolites
EZT	Ezetimibe
HDL-C	High-density lipoprotein cholesterol
HOMA	Homeostasis model assessment
LDL-C	Low-density lipoprotein cholesterol
NCEP	National Cholesterol Education Program
Ox-LDL	Oxidized low-density lipoprotein
RISCC	Ratio of ingested saturated fat and cholesterol to calories
TC	Total cholesterol
TAG	Triacylglycerol
TLC	Therapeutic lifestyle changes
8-epiPGF2a	8-Isoprostane

Introduction

Lowering levels of low-density lipoprotein cholesterol (LDL-C) plays an important role in cardiovascular disease prevention and comprises the main target of hypolipidemic therapy [1]. Statins are considered the most effective drugs in terms of improving serum lipid profile [2]. Treatment with statins has been associated with improved outcomes

M. S. Kostapanos · A. T. Spyrou · I. F. Gazi · M. Elisaf (✉) · E. N. Liberopoulos
Department of Internal Medicine, Medical School, University of Ioannina, 451 10 Ioannina, Greece
e-mail: egepi@cc.uoi.gr

C. C. Tellis · A. D. Tselepis
Laboratory of Biochemistry, Department of Chemistry, University of Ioannina, 451 10 Ioannina, Greece

either in the primary or the secondary prevention of cardiovascular disease [3]. This benefit has been attributed not only to the lipid-lowering potency, but also to various pleiotropic anti-atherosclerotic properties of these drugs (namely anti-inflammatory, anti-oxidative and anti-thrombotic) [4].

Ezetimibe potently inhibits the intestinal absorption of cholesterol from dietary and biliary sources by blocking the Niemann–Pick C1-like 1 protein for cholesterol transport [5]. Clinical studies showed that ezetimibe either as monotherapy or in combination with statins decreases LDL-C levels and beneficially modifies serum lipid profile [6, 7]. However, there is a lack of convincing evidence that ezetimibe may prevent cardiovascular disease [8–11]. It also remains questionable whether ezetimibe shares some of the pleiotropic properties of statins [12].

Oxidative stress, mostly by giving rise to endothelial dysfunction and pro-inflammatory processes, plays a major role in atherogenesis [13]. Several biomarkers, including oxidized LDL (ox-LDL), 8-isoprostane (8-epiPGF2a) and reactive oxygen metabolites (d-ROMs), are useful for the assessment of oxidative stress in clinical practice [14]. Hyperlipidemia and increased oxidative stress often coexist and their combined unfavorable effects may result in increased atherogenicity [13].

To date, limited data suggest that ezetimibe may reduce various markers of oxidative stress [15–17]. As with other possible pleiotropic actions, it remains unclear whether these effects are associated with the LDL-C lowering capacity of this drug. In the present study, we sought to investigate the effects of ezetimibe monotherapy on serum markers of oxidative stress in subjects with primary hypercholesterolemia.

Materials and Methods

Study Population

Subjects with mild-to-moderate hypercholesterolemia consecutively attending the Outpatient Lipid Clinic of the University Hospital of Ioannina, Ioannina, Greece, were included in the present study. Exclusion criteria consisted of: (1) age <18 years, (2) coronary heart disease (unstable angina, acute myocardial infarction, coronary artery bypass graft, or percutaneous transluminal coronary angioplasty within the last 3 months), (3) type 2 diabetes [fasting blood glucose >126 mg/dL (6.93 mmol/L)], (4) renal function impairment as defined by serum creatinine levels higher than 1.8 mg/dL (158.4 μmol/L) and/or total protein urinary (UTpr) excretion >150 mg/24 h, (5) liver disease (as defined by alanine and/or aspartate aminotransferase levels >3 times the upper limit of normal in more than two consecutive measurements), (6) raised thyroid-stimulating hormone (TSH) levels (>5 IU/mL), (7) childbearing potential for women, (8) psychiatric disease with defects in judgement, (9) known allergic reaction to ezetimibe, (10) heavy alcohol consumption (>3 drinks per day) or (11) lipid-lowering therapy (including statins, fibric acid derivatives, nicotinic acid, cholestyramine, or ω-3 fatty acids) or other treatment that could possibly affect lipid metabolism, renal or hepatic function, as well as parameters examined in this study.

After a 6 week dietary lead-in, eligible patients were randomly allocated to receive either open-label ezetimibe 10 mg/day (EZT group) or continue therapeutic lifestyle changes (TLC group). Compliance with study medication was assessed at week 12 with questionnaires and pill count; patients were considered compliant if they took 80–100% of the prescribed number of tablets. All patients gave written informed consent and the study protocol was approved by the Institutional Ethics Committee.

In order to validate the measurements of oxidative stress markers and distinguish patients with 'high oxidative stress' at baseline, we evaluated a 'control group' of 30 subjects who were selected among volunteers attending a Primary Care Family Screening Program. The same exclusion criteria were applied to the control group.

Clinical Evaluation

At baseline as well as 12 weeks post-treatment body weight and height measurements were performed in every individual to calculate body mass index [BMI = body weight (in kilograms)/height (in m^2)]. Waist circumference and blood pressure measurements were also obtained. A food record rating score was calculated from 3-day diaries kept by participants to assess compliance to dietary intervention throughout the study. The mean total daily intake of energy, carbohydrates, protein, fat, saturated fat, and cholesterol was calculated from these diaries by a modified Nutritionist V diet analysis (First Databank, San Bruno, CA, USA), which was amended to include traditional Greek recipes. From these data, the dietary RISCC (ratio of ingested saturated fat and cholesterol to calories) rating was determined [18]. The RISCC rating condenses the saturated fat, cholesterol, and energy intakes into one value, which summarizes the serum lipoprotein-raising potential of a diet [18]. For example, the RISCC rating of a typical diet (fat intake of 35–40% of total energy) is between 24 and 28. All participants were instructed to keep a dietary pattern similar to that of the NCEP (National Cholesterol Education Program) Step I diet, which is characterized by a reduced fat intake scoring from 13 to 18[19]. Stability in RISCC ratings over time provides evidence for stability of background dietary patterns.

Laboratory Investigations

Blood samples were obtained at baseline and after 12 weeks following a 12-h overnight fast to determine serum lipid and non-lipid metabolic parameters as well as oxidative stress markers. All samples were blindly assessed with regard to treatment allocation.

Non-Lipid Metabolic Parameters

Serum glucose, insulin, creatinine, creatine kinase, aminotransferases, and thyroid function tests were performed shortly after blood sampling by use of conventional methods. The Homeostasis Model Assessment (HOMA) a marker of insulin resistance (IR) [$HOMA_{IR}$ = insulin (μU/mL) × glucose (mg/dL)/405] was also assessed.

Lipid Determinations

Measurements of serum lipids [total cholesterol (TC), triacylglycerols (TAG) and high-density lipoprotein cholesterol (HDL-C)] were performed shortly after blood sampling. The concentrations of TC and TAG were determined enzymatically on the Olympus AU 600 clinical chemistry analyzer (Olympus Diagnostica, Hamburg, Germany). HDL-C was determined by a direct assay (Olympus Diagnostica, Hamburg, Germany). LDL-C was calculated using the Friedewald formula.

For the determination of apolipoprotein (apo) variables, samples were frozen and stored at −80 °C, and all samples were analyzed in the same run at the end of the study. ApoA1, apoB, apoE and Lp(a) were measured with a Behring Nephelometer BN100, and reagents (antibodies and calibrators) from Dade Behring Holding GmbH (Liederbach, Germany). The apoA1 and apoB assays were calibrated according to the International Federation of Clinical Chemistry (IFCC) standards.

Oxidative Stress Markers

To assess oxidative stress, serum levels of 8-epiPGF2a, ox-LDL and d-ROMs were measured. Serum levels of 8-epiPGF2a were determined by means of a competitive ELISA using a commercially available kit (Cayman Chemicals, Ann Arbor, MI, USA), as previously described [20]. This method has a specificity of 100% for 8-epiPGF2a, while having minimal cross-reactivity with other compounds, mostly 8-isoPGF3α. Concentrations of ox-LDL were assayed with the noncompetitive immunoassay (Mercodia AB, Uppsala, Sweden), which uses an antibody (4E6) that was obtained after immunization of mice with copper-oxidized LDL [21, 22]. As a measure of the equilibrium between free radical production and antioxidant defense, serum levels of d-ROMs were determined using a commercial kit (d-ROMs test Diacron International, Grosseto, Italy) on a Free Radical Analytical System (FRAS 4, Diacron, Grosseto, Italy) [23–25]. The reactive oxygen metabolites, primarily hydroperoxides are able to generate alkoxyl and peroxyl radicals in the presence of iron released from plasma proteins by an acidic buffer in accordance to the Fenton's reaction. Such radicals are, in turn, able to oxidize an alkyl-substituted aromatic amine (*N*,*N*-diethyl-*para*-phenylendiamine) to the corresponding radical cation, which can be quantified spectrophotometrically at 505 nm. The concentration of d-ROMs is positively directly correlated with color intensity and is expressed as Carratelli Units (1 CARR $U = 0.08$ mg hydrogen peroxide/dL). In normal subjects carr U values range from 250 to 300 [23, 24].

Statistical Analysis

It was estimated that a sample size of 54 would give a 95% power to detect a 15% difference in the reduction of 8-epiPGF2a between the 2 groups at an alpha of 0.05. We included 60 patients allowing for a drop-out rate of ∼10%.

Preliminary analysis was performed to ensure no violation of the assumptions of linearity and normality. The Shapiro–Wilk test was used to evaluate whether each parameter followed a Gaussian distribution. Values are expressed as mean ± standard deviation (SD) and median (range) for normally and non-normally distributed variables, respectively. In-group comparisons of continuous variable values prior to and post-treatment were performed by a paired two-tailed Student's test for parametric variables and Wilcoxon's ranks test for non-parametric distributed ones.

Relationships between variables were assessed by the Pearson's and Spearman correlations coefficients for parametric and non-parametric variables, respectively. Analysis of covariance (ANCOVA), adjusted for baseline values, was used for comparisons between treatment groups. Logarithmic transformations were performed for non-parametric variables. All comparisons were also held into subgroups of hypercholesterolemic patients either exhibiting 'high oxidative stress' or 'normal oxidative status' at baseline. In hypercholesterolemic patients, 'high oxidative stress' was defined as levels of 8-epiPGF2a equal or greater than the mean value of 8-epiPGF2a plus a standard deviation in controls.

Differences were considered significant at a value of $p < 0.05$. All analyses were carried out with SPSS 16.0 (SPSS Inc, Chicago, IL, USA).

Results

Demographics

A total of 60 subjects were enrolled, 30 in the EZT group and 30 in the TLC group. The demographic, clinical and laboratory characteristics of the study population are shown in Table 1. No differences between the EZT and TLC group were recorded with regard to baseline clinical and laboratory parameters.

Safety and Compliance

All patients completed the study protocol without any withdrawals. Small elevations of aminotransferase activities (<3 times the upper limit of normal) were observed in two patients in the EZT group and of creatine kinase (<5 times the upper limit of normal) in one patient in the same group. Enzyme activities returned to normal with continuing treatment in all cases. Mean compliance was above 90% during the study period.

Clinical Evaluation

No alterations in clinical parameters, including BMI, waist circumference and blood pressure were noted in either group. Likewise, RISCC scores remained unchanged at the end of the follow-up in both treatment arms (data not shown).

Changes in Lipids and Apolipoproteins (Table 1)

TC and LDL-C levels were reduced by 13.2 and 18.1%, respectively, following ezetimibe treatment ($p < 0.001$ vs. baseline and $p < 0.001$ vs. TLC group for both comparisons) (Table 1). No significant change with regard to HDL-C and TAG levels was observed in the EZT group. A decrease in non-HDL-C levels by 14.5% was recorded ($p < 0.001$ vs. baseline and $p < 0.05$ vs. TLC group) in the EZT group (Table 1). None of these variables was significantly altered from baseline in the TLC group. Ezetimibe induced significant reductions in apoB and apoE levels by 16.5% ($p < 0.001$ vs. baseline and $p < 0.01$ vs. TLC

Table 1 Baseline demographic, clinical and laboratory parameters of the study population as well as changes in these parameters at the end of the 12-week follow-up

Variable	Ezetimibe group ($N = 30$)			TLC group ($N = 30$)			Controls ($N = 30$)
	Baseline	Week 12	Change %	Baseline	Week 12	Change %	Baseline
Age (Years)	59 ± 9	–		56 ± 10	–		53 ± 10
Gender, male (%)	13 (43)	–		14 (47)	–		15 (50)
Current smokers (%)	8 (27)	8 (27)	0.0	9 (30)	9 (30)	0.0	9 (30)
TC (mg/dL)	258 ± 56	224 ± 49	−13.2***,‡	247 ± 38	238 ± 22	−4.1	202 ± 32
TAG (mg/dL)	144 (50–373)	139 (48–284)	−4.1	137 (74–281)	131 (58–301)	−3.9	80 (45–169)
HDL-C (mg/dL)	60 ± 14	58 ± 13	−3.3	59 ± 14	59 ± 10	−0.4	51 ± 9
LDL-C (mg/dL)	169 ± 43	138 ± 36	−18.1***,‡	163 ± 32	158 ± 27	−3.1	136 ± 26
Non-HDL-C (mg/dL)	197 ± 46	169 ± 40	−14.5***,†	191 ± 51	187 ± 38	−2.3	147 ± 31
ApoA1 (mg/dL)	167 ± 23	157 ± 18	−6.1	162 ± 19	158 ± 24	−2.1	152 ± 22
ApoB (mg/dL)	125 ± 37	105 ± 41	−16.5***,†	120 ± 28	114 ± 32	−5.5	89 ± 17
ApoE (mg/L)	46 (24–138)	38 (21–115)	−15.4*,†	51 (20–112)	43 (32–100)	−7.2	24 (10–52)
Ox-LDL (U/L)	108 ± 25¶	86 ± 25	−20.8***,‡	103 ± 32¶	96 ± 27	−5.7	42 ± 15
8-epiPGF2a (pg/mL)	71 (30–273)¶	61 (43–195)	−15.2	74 (23–302)¶	70 (34–159)	−4.2	45 ± 19
d-ROMs (carr U)	380 ± 98¶	343 ± 45	−10.0	375 ± 85¶	358 ± 99	−4.4	281 ± 29

To convert values for TC, LDL-C, non HDL-C and HDL-C levels to mmol/L, multiply by 0.02586; to convert TG levels to mmol/L multiply by 0.01129

TLC therapeutic lifestyle changes, *TC* total cholesterol, *TAG* triacylglycerols, *HDL-C* high-density lipoprotein cholesterol, *LDL-C* low-density lipoprotein cholesterol, *apo* apolipoprotein, *ox-LDL* oxidized low-density lipoprotein, *8-epiPGF2a* 8-isoprostane, *d-ROMs* reactive oxygen metabolites

* $p < 0.05$ versus baseline, ** $p < 0.01$ versus baseline, *** $p < 0.001$ versus baseline

† $p < 0.05$ for the comparison with the TLC group, ‡ $p < 0.001$ for the comparison with the TLC group

¶ $p < 0.01$ for the comparison with the control group

group) and 15.4% ($p < 0.001$ vs. baseline and $p < 0.01$ vs. TLC group), respectively, while apoA1 concentration remained unchanged (Table 1). No change in apolipoprotein levels was noted in the TLC group.

Evaluation of Baseline Oxidative Stress in Hyperlipidemic Patients and Controls

Hyperlipidemic patients exhibited higher levels of ox-LDL, 8-epiPGF2a and d-ROMs as compared with controls ($p < 0.01$ for all comparisons) (Table 1). 'High oxidative stress' as assessed by increased baseline 8-epiPGF2a levels (i.e., ≥64 pg/mL) was noted in 17/30 patients of the EZT group and 18/30 patients of the TLC group (57 vs. 60%, respectively, p = NS for the comparison between groups).

Changes in Oxidative Stress Markers

A significant reduction of ox-LDL levels by 20.8% was observed following ezetimibe treatment ($p < 0.001$ vs. baseline and $p < 0.001$ vs. TLC group) (Table 1). However, ezetimibe treatment, by producing comparable decreasing effects on ox-LDL and LDL-C levels, did not affect the ratio of ox-LDL to LDL-C (from 0.64 ± 0.23 to 0.62 ± 0.21, p = NS). No significant alterations in 8-epiPGF2a and d-ROMs levels were noted in the EZT group after 12 weeks of treatment (Table 1). No change was observed in the TLC group in any of the above measured oxidative stress markers.

Correlations of Oxidative Stress Markers

Baseline ox-LDL levels were correlated with baseline TC ($r = 0.72$, $p < 0.001$), non-HDL-C ($r = 0.74$, $p < 0.001$), LDL-C ($r = 0.65$, $p < 0.001$) and apoB ($r = 0.77$, $p < 0.001$) levels. The post-treatment decrease in ox-LDL levels observed in the EZT group was positively correlated with age ($r = 0.50$, $p < 0.05$), baseline levels of ox-LDL ($r = 0.41$, $p < 0.05$) as well as with the decreases in TC ($r = 0.48$, $p < 0.05$) and LDL-C levels ($r = 0.57$, $p < 0.01$). Baseline levels of 8-epiPGF2a were significantly correlated with baseline TC levels ($r = 0.41$, $p < 0.05$). Only baseline 8-epiPGF2a levels ($r = 0.52$, $p < 0.05$) were correlated with the reduction in 8-epiPGF2a concentration following ezetimibe treatment, which was independent of any post-treatment changes in lipid and apolipoprotein levels. Baseline d-ROMs concentration was correlated with baseline TAG ($r = 0.43$, $p < 0.05$), non-HDL-C ($r = 0.43$, $p < 0.05$) and Lp(a) ($r = 0.60$, $p < 0.01$) levels. The decrease in d-ROMs levels in the EZT group was positively correlated with age ($r = 0.498$, $p < 0.05$) and inversely with baseline TC levels ($r = -0.57$, $p < 0.01$).

Differential Changes of Oxidative Stress Parameters in Ezetimibe-Treated Patients Exhibiting 'High' or 'Normal' Oxidative Stress at Baseline (Table 2)

Both groups exhibited similar serum lipid profile at baseline. No differential effect of ezetimibe on serum lipid and apolipoprotein levels was observed between groups. In patients who exhibited 'high oxidative stress' at baseline ($n = 17$) ezetimibe treatment significantly reduced ox-LDL levels by 19.1% ($p < 0.01$ vs. baseline), whereas the ratio of ox-LDL to LDL-C did not change (from 0.64 ± 0.31 at baseline to 0.63 ± 0.29 post-treatment, p = NS). In the same subgroup of patients ezetimibe was associated with a significant decrease in the levels of 8-epiPGF2a and d-ROMs by 20.4 and 18.2% ($p < 0.01$ vs. baseline for all comparisons), respectively. Spearman's correlations coefficients revealed that the post-treatment decreases in 8-epiPGF2a and d-ROMs levels in the 'high oxidative stress' patients was independent of any change in lipid and apolipoprotein levels. The decrease in d-ROMs levels was significantly associated only with baseline d-ROMs concentration ($r = 0.68$, $p < 0.05$).

In the subgroup of patients with 'normal oxidative stress' at baseline ($n = 13$) ezetimibe treatment was associated with a significant decrease of ox-LDL levels by 18.9% ($p < 0.01$ vs. baseline). This decrease was not significantly different from that observed in patients with 'high oxidative stress'. Contrarily to the patients with 'high oxidative stress', no post-treatment changes in 8-epiPGF2a and d-ROMs levels were observed among hyperlipidemic patients with 'normal oxidative stress' at baseline ($p < 0.05$ for the comparison between groups). Also, TLC resulted in no significant changes in any of the examined oxidative stress markers in patients with either 'normal' ($n = 12$) or 'high' ($n = 18$) oxidative stress at baseline.

Discussion

The present study provides evidence that a 12-week ezetimibe treatment may reduce oxidative stress markers in subjects with primary hypercholesterolemia. This benefit is reflected by a decrease in the levels of 8-epiPGF2a and d-ROMs, which was observed among patients with 'high oxidative stress'. Decreases in ox-LDL levels following ezetimibe treatment were closely related with the degree of LDL-C lowering. Therefore, the levels of ox-LDL to LDL-C ratio did not change. No differential effect of ezetimibe on ox-LDL was detected in patients with either 'high' or 'normal' oxidative stress at baseline.

Ezetimibe is a potent inhibitor of cholesterol intestinal absorption and effectively decreases LDL-C levels. However, it remains uncertain whether this drug may affect

Table 2 Differential changes of laboratory parameters in ezetimibe-treated patients with 'high' or 'normal' oxidative stress at baseline

Variable	High oxidative stress ($n = 17$)			Normal oxidative stress ($n = 13$)		
	Baseline	Week 12	Change %	Baseline	Week 12	Change %
Age (Years)	60 ± 9	–	–	59 ± 9	–	–
Gender, male (%)	7 (41)	–	–	6 (46)	–	–
Current smokers (%)	5 (29)	5 (29)	–	3 (23)	3 (23)	–
TC (mg/dL)	259 ± 27	222 ± 35	–12.9*	245 ± 35	204 ± 36	−14.2*
TAG (mg/dL)	164 (119–212)	146 (129–284)	–5.7	126 (50–373)	122 (48–224)	−3.0
HDL-C (mg/dL)	61 ± 11	60 ± 13	–2.4	59 ± 12	57 ± 14	−3.4
LDL-C (mg/dL)	172 ± 33	140 ± 25	–17.2**	161 ± 27	128 ± 31	−20.5**
Non-HDL-C (mg/dL)	198 ± 50	169 ± 41	–14.9**	189 ± 53	163 ± 45	−14.1**
ApoA1 (mg/dL)	172 ± 45	162 ± 41	–5.8	170 ± 49	160 ± 52	−6.2
ApoB (mg/dL)	130 ± 32	109 ± 27	–15.5**	128 ± 27	108 ± 19	−15.2**
ApoE (mg/L)	43 (24–138)	38 (21–129)	–15.1*	47 (24–135)	37 (30–135)	−19.4*
Ox-LDL (U/L)	110 ± 37	88 ± 27	–19.1**	103 ± 25	84 ± 22	−18.9**
8-epiPGF2a (pg/mL)	102 (69–273)	83 (43–288)	–20.4**,†	50 (30–58)	56 (48–93)	+5.1
d-ROMs (carr U)	391 ± 86	318 ± 97	–18.2**,†	374 ± 77	352 ± 56	−5.9

To convert values for TC, LDL-C, non HDL-C and HDL-C levels to mmol/L, multiply by 0.02586; to convert TG levels to mmol/L multiply by 0.01129

TC total cholesterol, *TAG* triacylglycerols, *HDL-C* high-density lipoprotein cholesterol, *LDL-C* low-density lipoprotein cholesterol, *apo* apolipoprotein, *ox-LDL* oxidized low-density lipoprotein, *8-epiPGF2a* 8-isoprostane, *d-ROMs* reactive oxygen metabolites

* $p < 0.05$ versus baseline, ** $p < 0.01$ versus baseline

† $p < 0.05$ for the comparison between groups

atherosclerosis progression or improve clinical outcomes [8–11]. Given the potency of ezetimibe to effectively reduce LDL-C levels, the possible pleiotropic antiatherosclerotic actions of ezetimibe have been posed under question [12]. Several studies have come with contradictory results with regard to the effect of ezetimibe on inflammatory markers and endothelial function indices [12, 26, 27]. The anti-oxidative potential of this drug is also under consideration. In this study, we tested the hypothesis that ezetimibe treatment may decrease markers of oxidative stress in subjects with primary hypercholesterolemia. Markers used for the evaluation of oxidative stress were ox-LDL, 8-epiPGF2a and d-ROMs.

Ox-LDL, the product of oxidative modification of LDL, when impedes into the arterial wall induce endothelial dysfunction and gives rise to a cascade of inflammatory and proliferative processes leading to atherosclerotic plaque formation [14, 28]. High levels of ox-LDL have been recognized as an independent risk predictor for cardiovascular disease [29]. Ezetimibe treatment significantly decreased ox-LDL levels in our study (by 20.8%, $p < 0.001$) an observation that accords with recently published results showing that ezetimibe treatment reduced ox-LDL levels in 30 hyperlipidemic patients after a 3-month period [30]. Our results further showed that there is a significant positive correlation of post-treatment change in ox-LDL levels with the corresponding changes in LDL-C. Consequently, the ratio of ox-LDL to LDL-C remained unchanged, implying that the ezetimibe-induced decrease in ox-LDL levels may be primarily attributed to its effect on LDL-C levels.

8-epiPGF2a result from free-radical attack of cell membrane phospholipids or circulating LDLs. 8-epiPGF2a levels comprise a marker of lipid peroxidation and have been recognized as one of the most valid markers of in vivo oxidative stress. Increased levels of 8-epiPGF2a have been associated with increased risk for cardiovascular disease [31]. In our study a significant decrease of 8-epiPGF2a levels was observed in patients with 'high oxidative stress' (by 20.4%, $p < 0.01$ vs. baseline). This effect of ezetimibe was independent of the degree of LDL-C lowering. Our findings are consistent with a decrease in 8-epiPGF2a levels associated with a 3-month ezetimibe treatment in 30 hyperlipidemic patients in the previously mentioned study [30].

The d-ROMs test is a novel available test for the determination of organic peroxides [31]. High concentrations of lipid peroxides may produce an imbalance between nitric oxide and reactive oxygen species in vascular endothelium. This process results in endothelial dysfunction which comprises a critical step in the atherosclerotic process [32]. In the present study, ezetimibe induced a small (by 10%) but not significant decrease in d-ROMs levels. Of note, this decrease was significant in patients

with 'high oxidative stress' at baseline (by 18.2%, $p < 0.01$ vs. baseline). This effect was independent of any post-treatment change in lipid parameters. The ezetimibe-related reduction of d-ROMs in our study is comparable to that induced by a 22-week ezetimibe treatment (by 11%) in 14 high-risk patients with hypercholesterolemia who were on stable treatment with statins [16].

Study Limitations and Strengths

Limitations of the current study include the open-label design, the absence of a 'true' placebo group and the relatively short duration. Also, it should be acknowledged that it is very difficult to correctly quantify lipid peroxides and is impossible to quantify reactive oxygen species in vivo, due to their reactivity. We determined ox-LDL, dROMs and 8-epiPGF2a levels which are only markers of oxidative stress. In addition, 8-epiPGF2a levels would depend on the amount of arachidonic acid in the diet. To this regard, the determination of arachidonic acid would be useful and the concentration of 8-epiPGF2a should have been expressed per equivalent of plasma 20:4.

On the other hand, we assessed oxidative stress by the determination of various parameters, we included a TLC group and we blindly assessed endpoints.

Conclusion

In patients with primary hypercholesterolemia ezetimibe may reduce markers of oxidative stress, including ox-LDL, 8-epiPGF2a and d-ROMs levels, especially in those who exhibit 'high oxidative stress' at baseline. This action of ezetimibe, especially the decrease in ox-LDL levels, could be at least partially mediated through its lipid-lowering potency. However, the possibility that ezetimibe may decrease 8-epiPGF2a and d-ROMs levels independently of its lipid-lowering capacity cannot be excluded. Further studies are needed to explore the underlying mechanisms for the anti-oxidative actions of ezetimibe.

Conflict of interest This study was conducted independently; no company or institution supported it financially.

References

1. Third Report of the National Cholesterol Education Program (NCEP) expert panel on detection, evaluation, and treatment of high blood cholesterol in adults (Adult Treatment Panel III) final report (2002) Circulation 106:3143–3421
2. Ong HT (2005) The statin studies: from targeting hypercholesterolaemia to targeting the high-risk patient. QJM 98:599–614
3. Baigent C, Keech A, Kearney PM, Blackwell L, Buck G, Pollicino C, Kirby A, Sourjina T, Peto R, Collins R, Simes R (2005) Efficacy and safety of cholesterol-lowering treatment: prospective meta-analysis of data from 90,056 participants in 14 randomised trials of statins. Lancet 366:1267–1278
4. Kostapanos MS, Milionis HJ, Elisaf MS (2008) An overview of the extra-lipid effects of rosuvastatin. J Cardiovasc Pharmacol Ther 13:157–174
5. Garcia-Calvo M, Lisnock J, Bull HG, Hawes BE, Burnett DA, Braun MP, Crona JH, Davis HR Jr, Dean DC, Detmers PA, Graziano MP, Hughes M, Macintyre DE, Ogawa A, O'Neill KA, Iyer SP, Shevell DE, Smith MM, Tang YS, Makarewicz AM, Ujjainwalla F, Altmann SW, Chapman KT, Thornberry NA (2005) The target of ezetimibe is Niemann–Pick c1-like 1 (npc1l1). Proc Natl Acad Sci USA 102:8132–8137
6. Mikhailidis DP, Wierzbicki AS, Daskalopoulou SS, Al-Saady N, Griffiths H, Hamilton G, Monkman D, Patel V, Pittard J, Schachter M (2005) The use of ezetimibe in achieving low density lipoprotein lowering goals in clinical practice: position statement of a United Kingdom consensus panel. Curr Med Res Opin 21:959–969
7. Stein EA, Ballantyne CM, Windler E, Sirnes PA, Sussekov A, Yigit Z, Seper C, Gimpelewicz CR (2008) Efficacy and tolerability of fluvastatin XL 80 mg alone, ezetimibe alone, and the combination of fluvastatin XL 80 mg with ezetimibe in patients with a history of muscle-related side effects with other statins. Am J Cardiol 101:490–496
8. Kastelein JJ, Akdim F, Stroes ES, Zwinderman AH, Bots ML, Stalenhoef AF, Visseren FL, Sijbrands EJ, Trip MD, Stein EA, Gaudet D, Duivenvoorden R, Veltri EP, Marais AD, de Groot E (2008) Simvastatin with or without ezetimibe in familial hypercholesterolemia. N Engl J Med 358:1431–1443
9. Fleg JL, Mete M, Howard BV, Umans JG, Roman MJ, Ratner RE, Silverman A, Galloway JM, Henderson JA, Weir MR, Wilson C, Stylianou M, Howard WJ (2008) Effect of statins alone versus statins plus ezetimibe on carotid atherosclerosis in type 2 diabetes: the SANDS (stop atherosclerosis in native diabetics study) trial. J Am Coll Cardiol 52:2198–2205
10. Villines TC, Stanek EJ, Devine PJ, Turco M, Miller M, Weissman NJ, Griffen L, Taylor AJ (2010) The ARBITER 6-HALTS trial (arterial biology for the investigation of the treatment effects of reducing cholesterol 6-HDL and LDL treatment strategies in atherosclerosis): final results and the impact of medication adherence, dose, and treatment duration. J Am Coll Cardiol 55:2721–2726
11. Rossebo AB, Pedersen TR, Boman K, Brudi P, Chambers JB, Egstrup K, Gerdts E, Gohlke-Barwolf C, Holme I, Kesaniemi YA, Malbecq W, Nienaber CA, Ray S, Skjaerpe T, Wachtell K, Willenheimer R (2008) Intensive lipid lowering with simvastatin and ezetimibe in aortic stenosis. N Engl J Med 359:1343–1356
12. Kalogirou M, Tsimihodimos V, Elisaf M (2010) Pleiotropic effects of ezetimibe: do they really exist? Eur J Pharmacol 633:62–70
13. Madamanchi NR, Vendrov A, Runge MS (2005) Oxidative stress and vascular disease. Arterioscler Thromb Vasc Biol 25:29–38
14. Ridker PM, Brown NJ, Vaughan DE, Harrison DG, Mehta JL (2004) Established and emerging plasma biomarkers in the prediction of first atherothrombotic events. Circulation 109:IV6–IV19
15. Staprans I, Pan XM, Rapp JH, Moser AH, Feingold KR (2006) Ezetimibe inhibits the incorporation of dietary oxidized cholesterol into lipoproteins. J Lipid Res 47:2575–2580
16. Yamaoka-Tojo M, Tojo T, Kosugi R, Hatakeyama Y, Yoshida Y, Machida Y, Aoyama N, Masuda T, Izumi T (2009) Effects of ezetimibe add-on therapy for high-risk patients with dyslipidemia. Lipids Health Dis 8:41
17. Hussein O, Minasian L, Itzkovich Y, Shestatski K, Solomon L, Zidan J (2008) Ezetimibe's effect on platelet aggregation and

LDL tendency to peroxidation in hypercholesterolaemia as monotherapy or in addition to simvastatin. Br J Clin Pharmacol 65:637–645
18. Harris WS, Held SJ, Dujovne CA (1995) Comparison of two scoring systems used to monitor diets in outpatient clinical trials. J Cardiovasc Risk 2:359–365
19. Grundy SM, Cleeman JI, Merz CN, Brewer HB Jr, Clark LT, Hunninghake DB, Pasternak RC, Smith SC Jr, Stone NJ (2004) Implications of recent clinical trials for the National Cholesterol Education Program Adult Treatment Panel III guidelines. Circulation 110:227–239
20. Spirou A, Rizos E, Liberopoulos EN, Kolaitis N, Achimastos A, Tselepis AD, Elisaf M (2006) Effect of barnidipine on blood pressure and serum metabolic parameters in patients with essential hypertension: a pilot study. J Cardiovasc Pharmacol Ther 11:256–261
21. Holvoet P, Donck J, Landeloos M, Brouwers E, Luijtens K, Arnout J, Lesaffre E, Vanrenterghem Y, Collen D (1996) Correlation between oxidized low density lipoproteins and von Willebrand factor in chronic renal failure. Thromb Haemost 76:663–669
22. Tsouli SG, Kiortsis DN, Lourida ES, Xydis V, Tsironis LD, Argyropoulou MI, Elisaf M, Tselepis AD (2006) Autoantibody titers against oxLDL are correlated with Achilles tendon thickness in patients with familial hypercholesterolemia. J Lipid Res 47:2208–2214
23. Cornelli U, Terranova R, Luca S, Cornelli M, Alberti A (2001) Bioavailability and antioxidant activity of some food supplements in men and women using the d-ROMs test as a marker of oxidative stress. J Nutr 131:3208–3211
24. Kaneko K, Taniguchi N, Tanabe Y, Nakano T, Hasui M, Nozu K (2009) Oxidative imbalance in idiopathic renal hypouricemia. Pediatr Nephrol 24:869–871
25. Vassalle C (2008) An easy and reliable automated method to estimate oxidative stress in the clinical setting. Methods Mol Biol 477:31–39
26. Saougos VG, Tambaki AP, Kalogirou M, Kostapanos M, Gazi IF, Wolfert RL, Elisaf M, Tselepis AD (2007) Differential effect of hypolipidemic drugs on lipoprotein-associated phospholipase A2. Arterioscler Thromb Vasc Biol 27:2236–2243
27. Nakou ES, Filippatos TD, Georgoula M, Kiortsis DN, Tselepis AD, Mikhailidis DP, Elisaf MS (2008) The effect of orlistat and ezetimibe, alone or in combination, on serum LDL and small dense LDL cholesterol levels in overweight and obese patients with hypercholesterolaemia. Curr Med Res Opin 24:1919–1929
28. Hulthe J, Fagerberg B (2002) Circulating oxidized LDL is associated with subclinical atherosclerosis development and inflammatory cytokines (AIR study). Arterioscler Thromb Vasc Biol 22:1162–1167
29. Holvoet P, Mertens A, Verhamme P, Bogaerts K, Beyens G, Verhaeghe R, Collen D, Muls E, Van de Werf F (2001) Circulating oxidized LDL is a useful marker for identifying patients with coronary artery disease. Arterioscler Thromb Vasc Biol 21:844–848
30. Turfaner N, Uzun H, Balci H, Ercan MA, Karter YH, Caner M, Sipahioglu F, Genc H (2010) Ezetimibe therapy and its influence on oxidative stress and fibrinolytic activity. South Med J 103:428–433
31. Vassalle C, Petrozzi L, Botto N, Andreassi MG, Zucchelli GC (2004) Oxidative stress and its association with coronary artery disease and different atherogenic risk factors. J Intern Med 256:308–315
32. Bertuglia S, Giusti A (2005) Role of nitric oxide in capillary perfusion and oxygen delivery regulation during systemic hypoxia. Am J Physiol Heart Circ Physiol 288:H525–H531

Lipids (2011) 46:349–356
DOI 10.1007/s11745-010-3513-1

ORIGINAL ARTICLE

Serum Lipoprotein(a) Levels are Greater in Female than Male Patients with Type-2 Diabetes

Manouchehr Nakhjavani · Afsaneh Morteza · Alireza Esteghamati · Omid Khalilzadeh · Ali Zandieh · Reza Safari

Received: 9 August 2010 / Accepted: 24 November 2010 / Published online: 14 December 2010

Abstract Women with diabetes are faced with a higher risk of dyslipidemia and cardiovascular disorders than men with diabetes. We aimed to study the role of gender and menopausal status in serum Lp(a) levels in patients with type 2 diabetes. We quantified serum Lp(a) levels in a group of 477 patients with type 2 diabetes (men, premenopausal and postmenopausal women with diabetes), as well as in 105 controls. We stratified the patients into two groups of low Lp(a) levels (Lp(a) <35 mg/dl) and elevated Lp(a) levels (Lp(a) >35 mg/dl). Patients with diabetes had higher serum Lp(a) levels than the controls. Serum Lp(a) levels was significantly higher in women with diabetes than men with diabetes. Lp(a) levels did not differ between male and females in the control group. Premenopausal and postmenopausal women with diabetes did not differ significantly in serum Lp(a) levels. The odds ratio of having a serum Lp(a) level higher than 35 was 5.85 in premenopausal women with diabetes, 5.08 in postmenopausal women with diabetes, 2.41 in men with diabetes and 1.9 in the women in the control group compared to the men in the control group, after adjustment for age and BMI. This observational study clearly indicated that serum Lp(a) levels were significantly higher in women and men with diabetes. The increase in women was independent of menopause. The level of serum Lp(a) had no correlation with lipid parameters in men or women.

Keywords Lipoprotein(a) · Type 2 diabetes · Dyslipidemia · Women · Menopause

M. Nakhjavani (✉) · A. Morteza · A. Esteghamati · O. Khalilzadeh · A. Zandieh · R. Safari
Endocrinology and Metabolism Research Center (EMRC), Vali-Asr Hospital, Tehran University of Medical Sciences, P.O. Box: 13145-784, Tehran, Iran
e-mail: nakhjavanim@tums.ac.ir

A. Morteza
e-mail: aafsaneh03@gmail.com

A. Esteghamati
e-mail: esteghamati@tums.ac.ir

O. Khalilzadeh
e-mail: khalilzadeh@razi.tums.ac.ir

A. Zandieh
e-mail: ali_zandieh3@yahoo.com

R. Safari
e-mail: s_reza406@yahoo.com

Abbreviation

Apo (B)	Apoprotein B-100
BMI	Body mass index
HDL-C	High density lipoprotein cholesterol
LDL-C	Low density lipoprotein cholesterol
Lp(a)	Lipoprotein(a)
TG	Triglyceride
VLDL	Very low density lipoprotein cholesterol

Introduction

While cardiovascular disease mortality is currently decreasing in the general population [1], mortality in women with diabetes is increasing [2]. Both metabolic syndrome and diabetes pose a significant increase in the risk of mortality in postmenopausal women [3]. However, the traditional risk factors for coronary heart disease like, hypertension, elevated serum cholesterol, smoking habit and diabetes dyslipidemia [4], do not explain the excessive prevalence of coronary heart disease among women with diabetes [5–7].

Lipoprotein a [Lp(a)] is a modified form of low density lipoprotein in which apoprotein B-100 [apo (B)] is linked to a unique glycoprotein, named apoprotein (a) [8]. It is mainly determined genetically, depending on apoprotein (a) genotype [9, 10]. The direct association between serum Lp(a) levels and the risk of cardiovascular disorders is well established [11, 12]. Elevated levels of serum Lp(a) is also associated with an increased risk of coronary heart disease in patients with diabetes [13, 14]. It is also a predictor of non-proliferative retinopathy in these patients [15–19]. Lp(a) is present in the arterial wall at sites of atherosclerosis in humans and results in both atherogenesis and thrombosis (3). Elevated levels of Lp(a) are associated with aortic dissection [20], occlusion of large cerebrovascular arteries [21] and silent cerebrovascular infarction in hemodialysis patients [22].

To date, we are unaware of any study demonstrating the impact of diabetes and menopausal status on serum Lp(a) levels. This is debatable due to the wide variability of serum Lp(a) levels in the general population, its highly skewed distribution and the role of gender particularly on its association with diabetes [23–26]. In this observational study, we aimed to evaluate serum Lp(a) levels, in males, premenopausal and postmenopausal females with diabetes.

Method

We performed a cross-sectional analysis of the serum samples of 477 patients with type 2 diabetes who were consecutively selected from the diabetes clinic of Vali-Asr hospital affiliated with Tehran University of Medical Science plus 105 controls. Controls were healthy volunteers from the patients' concomitants or hospital staff. Healthy controls were selected from those without any known disease including type 2 diabetes, hyperlipidemia, ischemic heart disease, and malignancy. The patients were divided into 3 groups of 115 women in premenopausal state, 144 women in postmenopausal state and 218 men. Diabetes was diagnosed according to the criteria of the American Diabetes Association [27]. Exclusion criteria were pregnancy, acute or chronic renal failure, glomerulonephritis, congestive heart failure, thyroid disorders, acute infections, stroke, diabetic ketoacidosis, non-ketonic hyperosmolar diabetes and hospital admission in recent months. The age of menopause and the time of elapse after menopause were recorded in the questionnaire. None of the studied participants had overt diabetes complications; none of the studied patients had a history of ischemic heart disease. The frequency of insulin therapy was similar between men and women with type 2 diabetes (15–20%). Based on our clinical experience, we rarely have diabetic patients on either oral contraceptive agents or hormone replacement therapy. Therefore, we think this will not influence on our results. The groups were also matched according to statin therapy. Nearly 40–60% of the patients were on statin therapy. Furthermore, our clinical experiences indicate that niacin treatment may reduce Lp(a) levels at a very high doses. None of the participants in our study were using niacin at high doses.

Demographic and anthropometric data including age, sex, duration of diabetes, height, weight in light clothing and blood pressure in the sitting position were recorded. Blood pressure was remeasured twice after an average of 5 min. The body mass index (BMI; kg/m^2) was calculated according to the Quetelet formula. All participants gave written informed consent before participation. The research was carried out according to the principles of the Declaration of Helsinki; the local ethics review committee of Tehran University of Medical Science approved the study protocol.

Blood Samples

Blood samples were collected after 12 h of fasting and, serum creatinine, fasting blood sugar (FBS), total cholesterol, triglycerides (TG), high density lipoprotein cholesterol (HDL-C), low density lipoprotein cholesterol (LDL-C) and HbA1C were measured. Glucose measurements [intra-assay coefficient of variants (CV) 2.1%, inter-assay CV 2.6%] were carried out using the glucose oxidase method. Cholesterol, HDL-C, LDL-C and TG were determined using direct enzymatic methods (Parsazmun, Karaj, Iran). HbA1C was estimated by high-pressure liquid chromatography (HPLC) Method. Apo (B) and Lp(a) were measured by multiple standard non-linear immunoturbidimetry with a Cobas-Mira device. All the kits used were supplied by Parsazmun Co., Karaj, Iran.

Statistical Analysis

The statistical package SPSS 16 for Windows (Chicago, IL, USA), was used for analysis. The Kolmogorov–Smirnov test was employed to test the normality of the variables in each group. Variables distributed normally are presented as means ± standard deviation of mean (SD). Variables with skewed distribution are presented as the median [interquintile range]. For comparison of serum Lp(a) level, lipid profile and other variables between patients with type 2 diabetes and controls and also between men and women within in each group, Mann–Whitney *U* test (for variables deviated from normal distribution), and student *t* tests (for normally distributed variables), were employed. Partial correlation coefficients were calculated to demonstrate the

association of serum Lp(a) and apo (B) level with other studied variables, after adjustment for age and BMI. Plasma Lp(a) levels vary over 100 fold in the population, ranging from <0.1 mg/dl to >100 mg/dl [21]. Threshold levels of serum Lp(a) for the development of atherosclerosis varies from 20 to 45 mg/dl [21]. To provide a measure of association of high Lp(a) levels and cardiovascular risk factors the patients were stratified into two groups of low Lp(a) levels (<35 mg/dl) and elevated Lp(a) levels (>35 mg/dl). Logistic regression analysis was employed to predict the odds of a patient having a serum Lp(a) level higher than 35 mg/dl in each group, after adjustment for age and BMI. General linear models were employed to study serum Lp(a) levels in premenopausal and postmenopausal state when controlling for age, duration of diabetes and BMI. Significance was set at $p < 0.05$.

Results

Demographic data of participants are shown in Table 1. The mean of age, BMI, total cholesterol, LDL-C and diastolic blood pressure was similar for patients and controls. Patients with diabetes had significantly higher serum Lp(a), apo (B), TG and HDL-C levels than the controls (Table 1). Men and women in the control group were similar in all studied variables except that the women had a higher HDL-C level. There was a significant difference between men and women with diabetes in BMI, lipid profile and diastolic blood pressure. Women with diabetes had higher serum Lp(a) levels than men with diabetes (Table 1). The distribution of serum Lp(a) levels in controls, men with diabetes, premenopausal and postmenopausal women with diabetes are illustrated in Fig. 1.

Postmenopausal women had significantly higher levels of apo (B), LDL-C, total cholesterol, and systolic blood pressure than premenopausal women, however, they did not differ significantly in serum Lp(a), FBS, TG, HDL-C, diastolic blood pressure and HbA1C levels (Table 2). Serum Lp(a) levels did not differ significantly between premenopausal and postmenopausal women with diabetes, even after adjusting for age, duration of diabetes and BMI. There were no difference sin serum Lp(a) levels before ($n = 29$) and after ($n = 36$) menopause in controls.

Partial correlation analysis demonstrated that serum Lp(a) levels had a significant correlation with FBS in men and women of control group, when controlling for age and BMI (Table 3). It did not have any significant correlation with the lipid profile, HbA1c, systolic and diastolic blood pressure in the studied groups.

The Lp(a) level was more than 35 (mg/dl) in 31% of women in the control group, 21% of men in the control

Table 1 Characteristics of the participants

	Control ($n = 105$)		Diabetes ($n = 477$)		P value
	Men ($n = 40$)	Women ($n = 65$)	Men ($n = 218$)	Women ($n = 259$)	
Age (years)	52.8 ± 7.6	53.3 ± 7.8	56.5 ± 11.6	53.7 ± 10.19	NS
Body mass index (kg/m^2)	26.8 [25.6–28.3]	27.8 [26.4–29.1]	25.8 [24.3–26.1]	28.1 [27.3–29.5]*	NS
Duration of diabetes (years)	–	–	9.77 ± 7.1	8.1 ± 7.1	–
Lp(a) (mg/dl)	16.5 [17.0–29.34]	18 [24–42]	25.50 [31.3–51.1]	42 [46.3–58.6]**	<0.001
Apo (B) (mg/dl)	97.3 ± 23.3	97.2 ± 30.2	100.86 ± 26.58	117.8 ± 30.2**	<0.001
Cholesterol (mg/dl)	202.6 ± 31.7	201.95 ± 40.3	192.03 ± 5.215	233 ± 63.9**	NS
Triglyceride (mg/dl)	161 [149.2–196.1]	132 [129–193]	157.5 [159.7–194.1]	191 [211–251]**	<0.001
HDL-C (mg/dl)	37.3 ± 13.97	46.3 ± 14.9*	40.6 ± 14.05	47.2 ± 15.4**	<0.001
LDL-C (mg/dl)	130.9 ± 29.6	127.8 ± 35.3	117.13 ± 4.085	141 ± 48.8**	NS
HbA1c (%)	–	–	9.1 [8.6–9.9]	9.4 [9.0–9.8]	<0.001
FBS (mg/dl)	92.0 [87.7–95.6]	91.6 [89.0–95.3]	195 [187.5–215.6]	192 [190.7–213.2]	<0.001
Creatinine (mg/dl)	0.90 ± 0.15	0.94 ± 0.21	0.98 ± 0.09	0.91 ± 0.14	<0.001
Systolic blood pressure (mmHg)	120 [117–127.6]	130 [121.5–131.8]	129.0 [125.6–131.9]	130 [129.8–135.8]	<0.001
Diastolic blood pressure (mmHg)	80.0 [78.4–84.3]	80.0 [73.3–82.4]	80.3 [75.2–79.4]	80.0 [79.1–82.9]*	NS

Variables distributed normally are expressed as means ± SD, otherwise median [interquartile range]. Normally distributed variables were compared using the t test and variables deviating from the normal distribution were compared using the Mann–Whitney U test for comparison of men and women

P values were calculated for comparison of patients with type 2 diabetes and controls

NS not significant

* $P < 0.05$, ** $P < 0.01$, when comparing women with men in diabetes and control groups

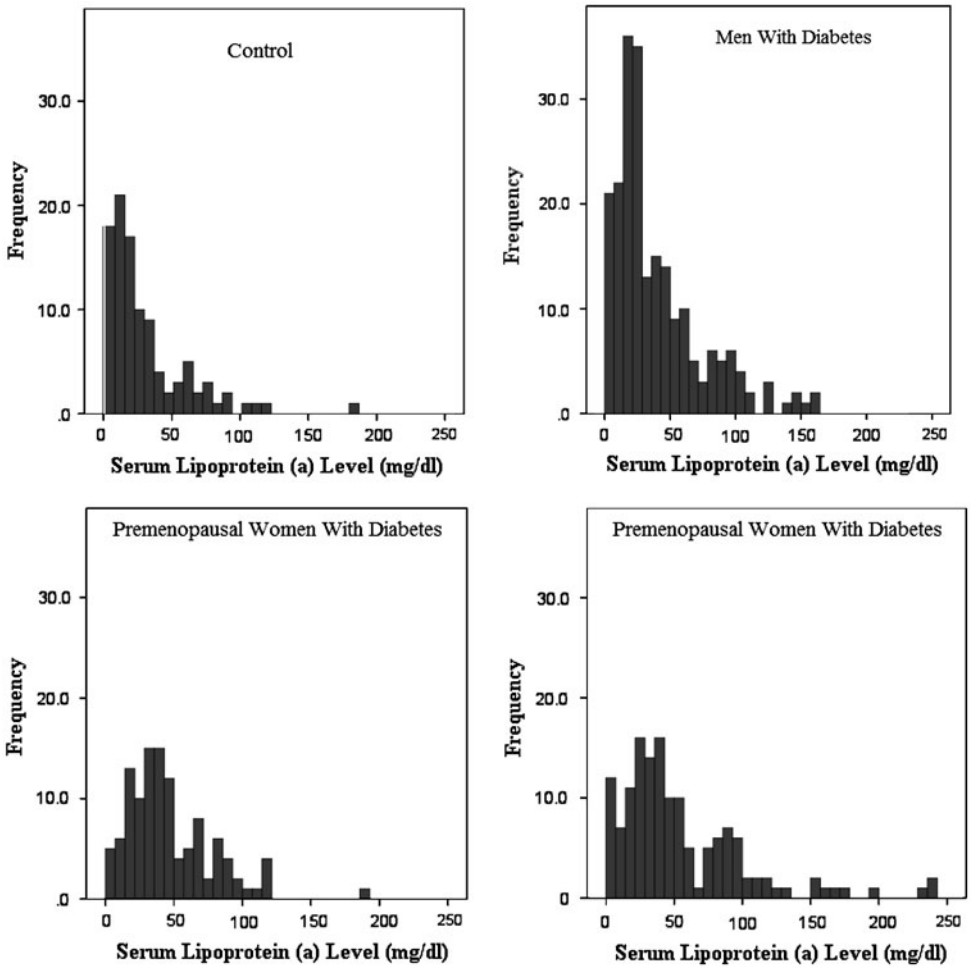

Fig. 1 The distribution of serum lipoprotein(a) level in control subjects, men with diabetes, premenopausal and postmenopausal women with diabetes

Table 2 Characteristics of women with diabetes according to menopausal status

	Premenopausal ($n = 115$)	Postmenopausal ($n = 144$)
Age (years)	42.7 ± 5.7	59.7 ± 7.19**
Body mass index (kg/m^2)	28 [28.2–35.5]	28.1 [27.3–29.5]*
Duration of diabetes (years)	6.7 ± 5.38	9.8 ± 7.8**
Lp(a) (mg/dl)	42 [41.3–54.6]	41 [47.4–63.1]
Apo (B) (mg/dl)	112.8 ± 18.2	120.4 ± 30.6*
Cholesterol (mg/dl)	203 ± 44.7	241 ± 65.5**
Triglyceride (mg/dl)	186 [179–222]	184 [185–215]
HDL-C (mg/dl)	46.5 ± 14.4	47.7 ± 15.09
LDL-C (mg/dl)	132 ± 38.36	147 ± 48.37*
HbA1c (%)	9.0 [8.4–9.8]	9.6 [9.0–10.1]
FBS (mg/dl)	180 [179.15–207.8]	200 [193.7–217.7]
Creatinine (mg/dl)	0.88 ± 0.15	0.93 ± 0.13
Systolic blood pressure (mmHg)	120 [120.8–129.1]	130 [133.4–140.2]**
Diastolic blood pressure (mmHg)	78.4 [76.2–81.8]	80 [80.3–84.32]

Variables distributed normally are expressed as means ± SD, otherwise the median [interquartile range]

* $P < 0.05$, ** $P < 0.01$, *** $P < 0.001$ when comparing premenopausal with postmenopausal women

group, 41% of men with diabetes, 58% of premenopausal women and 58% of postmenopausal women (Fig. 2). Logistic regression analysis was employed to predict the odds ratio of patients having a serum Lp(a) level higher than 35 mg/dl in each group, when adjusted for age and BMI. The odds ratio of having a serum Lp(a) level higher

Table 3 Partial correlation coefficients of lipoprotein(a) and apolipoprotein (B) with other studied variables after adjustments for age and BMI

	Control women		Control men		Premenopausal women with diabetes		Postmenopausal women with diabetes		Men with diabetes	
	Lp(a)	Apo (B)	Lp(a)	Apo (B)	Lp(a)	Apo (B)	Lp(a)	Apo (B)	Lp(a)	Apo(B)
Lp(a) (mg/dl)		0.1		0.27		0.20		0.06		0.13
Apo (B) (mg/dl)	−0.01		0.27		0.20		0.07		0.12	
FBS (mg/dl)	−0.54*	−0.26	−0.84*	−0.56	−0.04	0.11	0.00	0.01	0.07	0.13
HbA1c (%)	−0.31	0.34	−0.38	0.08	0.18	0.15	0.129	0.07	−0.06	0.00
Cholesterol (mg/dl)	−0.04	0.77**	−0.61	0.60	0.13	0.86***	0.13	0.91***	0.09	0.73***
HDL-C (mg/dl)	0.36	0.02	0.17	−0.27	0.10	0.39	0.13	0.46***	−0.03	0.08
LDL-C (mg/dl)	−0.09	0.73**	−0.26	0.66	0.04	0.81	0.15	0.88***	0.11	0.71***
Triglyceride (mg/dl)	−0.41	0.42	−0.62	−0.70	0.24	0.39	−0.01	0.55***	0.01	0.31***
Diastolic blood pressure (mmHg)	0.36	0.57*	0.44	0.51	−0.06	0.01	0.11	0.04	−0.01	0.02
Systolic blood pressure (mmHg)	−0.29	0.37	0.80	0.05	−0.06	0.07	0.05	0.08	0.04	0.08

* $P < 0.05$, ** $P < 0.01$, *** $P < 0.001$

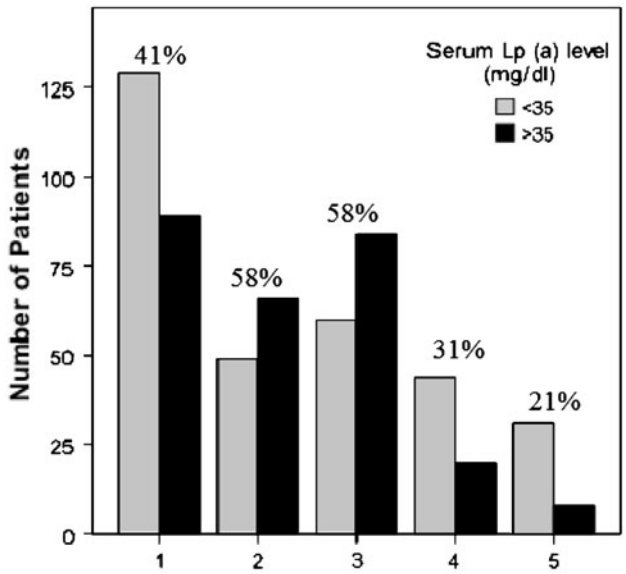

Fig. 2 Frequency of patients according to lipoprotein(a) level in *1* men with diabetes, *2* premenopausal women with diabetes, *3* postmenopausal women with diabetes, *4* women in the control group, *5* men in the control group. The *numbers* above the *bars* represent the percentage of participants with a high serum level of lipoprotein(a)

than 35 was 5.85 in premenopausal women with diabetes, 5.08 in postmenopausal women with diabetes, 2.41 in men with diabetes and 1.9 in women of the control group compared to men of the control group, when adjusting for age and BMI (Table 4).

Discussion

In this observational study, we present results that clearly indicate that the frequency distribution of Lp(a) levels in our studied population was highly skewed and ranged from very low toward high levels, which was more notable in patients with diabetes (Fig. 1). Patients with diabetes had higher serum Lp(a) levels than the controls. We showed that serum Lp(a) levels were higher in women with diabetes than men with diabetes. There was no gender difference in serum Lp(a) levels in the control group. Serum Lp(a) levels were higher in men with diabetes than men and women in the control group. The risk of having a serum Lp(a) levels above 35 (mg/dl) did not change according to menopausal status.

There are controversial reports on the effect of diabetes on serum Lp(a) levels. In agreement with our findings, some studies have shown increased levels of serum Lp(a) in patients with diabetes [28–30]. Koschinsky et al. [28] demonstrated higher levels of serum Lp(a) in patients with diabetes. Similarly, Labudovic et al. [29] showed increased serum Lp(a) levels in patients with diabetes which predicted the risk of atherosclerosis in these patients. Serum Lp(a) concentration also decreased by insulin treatment in non-obese patients with type 2 diabetes [30]. Some earlier case control studies found no difference in serum Lp(a) levels between patients with diabetes and controls [31–33]. Rainwater et al. [34] demonstrated lower serum Lp(a) levels in patients with type 2 diabetes. A recent meta-analysis, showed a lower serum Lp(a) level in patients with diabetes compared to controls [35]. They analyzed the results of 35 studies of which none were specifically focused on the populations with type 2 diabetes. The reference value of Lp(a) levels was determined to be 12.6 (4.9–32.1) which is in line with Lp(a) levels in our control group. They approximated that patients with diabetes have about 11% (4–17%) lower serum Lp(a) levels compared to the reference values. However, this result is not in line with most of the studies which have directly measured serum Lp(a) levels in patients with diabetes [28–30], including the present study.

Table 4 The odds ratio of having a serum lipoprotein(a) level higher than 35 (mg/dl) in different groups in comparison with normal men, after adjustment for age and BMI

	P value	Odds ratio	95% confidence interval	
			Lower	Upper
Men with diabetes	0.040	2.412	1.040	5.593
Premenopausal women with diabetes	<0.001	5.857	2.432	14.107
Postmenopausal women with diabetes	<0.001	5.085	2.103	12.293
Women in control group	<0.169	1.953	0.752	5.075

High serum Lp(a) levels are a powerful risk factor for coronary artery disease both in the general population and patients with diabetes [14, 36–39]. Since women with diabetes have a higher rate of mortality from cardiovascular disorders than men [7], it could be hypothesized that increased levels of serum Lp(a) in women with diabetes, may be one of the mechanisms for this observation. On the other hand, one could think that these results are affected by the gender effect on serum Lp(a) levels which is demonstrated by population based studies [40]. We showed that the odds ratio of having a serum Lp(a) level higher than 35 was 5.85 in premenopausal women with diabetes, 5.08 in postmenopausal women with diabetes, 2.41 in men with diabetes and 1.9 in women of the control group compared to men of the control group, when adjusting for age and BMI. Therefore, if our findings are confirmed by large longitudinal studies, serum Lp(a) levels could be considered as a powerful marker of coronary artery disease in men and especially in women with diabetes.

Previous studies have suggested that the postmenopausal state in women is associated with higher plasma LDL-C, VLDL, TG, apo (B) and lower HDL-C concentrations than premenopausal women of comparable age [41, 42]. However, we did not found any study addressing the question whether menopausal status has any effect on serum Lp(a) levels in patients with diabetes or not. In the current study, we clearly demonstrated that, irrespective of other lipid measures, serum Lp(a) levels do not differ between pre- and postmenopausal women, even after adjusting for duration of diabetes, age and BMI. This is notable because some experimental studies have shown an effective role for estrogen in lowering serum Lp(a) levels [43]. Nakagani et al. showed that ovariectomy increases serum Lp(a) levels in transgenic mice, whereas a continued replacement of 17 beta estradiol reverses the changes. They suggested that estrogen negatively regulates both plasma Lp(a) levels and Lp(a)-induced vascular remodeling [43]. In a large prospective study conducted by Shilpack et al. [44] Lp(a) was an independent risk factor for recurrent coronary heart disease in postmenopausal women and treatment with estrogen and progestin lowered its serum levels. Similar studies have also shown that estrogen therapy improves serum Lp(a) levels in the postmenopausal state [45–47]. Whether these findings are caused by the impact of diabetes or other confounding factors such as accelerated aging in premenopausal women with diabetes [48], has to be studied in the future.

In conclusion, we have shown a profound increase of serum Lp(a) levels in women with type 2 diabetes, irrespective of menopausal state. This may add to the understanding of the lipid metabolism in patients with diabetes. The limitations of the study are those inherent in a cross-sectional analysis which precludes the determination of the direction of causality. Nonetheless, this study took the advantage of a relatively large sample size and close similarity between groups in most of the affecting variables. Evaluating the association of the serum Lp(a) level with microalbuminuria in patients with diabetes may be an interesting topic for future studies.

Acknowledgment This study was not funded and was designed based on the questions we encountered during clinical practice.

Conflict of interest The authors declare they did not have any conflicts of interest.

References

1. Gu K, Cowie CC, Harris MI (1999) Diabetes and decline in heart disease mortality in US adults. JAMA 281:1291–1297
2. Kragelund C, Kober L, Faber J, Steffensen R, Hildebrandt P (2007) Metabolic syndrome and mortality in stable coronary heart disease: relation to gender. Int J Cardiol 121:62–67
3. Szmuilowicz ED, Stuenkel CA, Seely EW (2009) Influence of menopause on diabetes and diabetes risk. Nat Rev Endocrinol 5:553–558
4. Mooradian AD (2009) Dyslipidemia in type 2 diabetes mellitus. Nat Clin Pract Endocrinol Metab 5:150–159
5. Djindjic B, Rankovic G, Zivic M, Savic T, Spasic M, Bubanj M (2009) Gender difference in hypolipemic and anti-inflammatory effects of statins in diabetics with coronary artery disease. Vojnosanit Pregl 66:966–972
6. Njelekela MA, Mpembeni R, Muhihi A, Mligiliche NL, Spiegelman D, Hertzmark E, Liu E, Finkelstein JL, Fawzi WW, Willett WC, Mtabaji J (2009) Gender-related differences in the prevalence of cardiovascular disease risk factors and their correlates in urban Tanzania. BMC Cardiovasc Disord 9:30
7. Legato MJ, Gelzer A, Goland R, Ebner SA, Rajan S, Villagra V, Kosowski M (2006) Gender-specific care of the patient with diabetes: review and recommendations. Gend Med 3:131–158
8. Ariyo AA, Thach C, Tracy R (2003) Lp(a) lipoprotein, vascular disease, and mortality in the elderly. N Engl J Med 349: 2108–2115

9. Clarke R, Peden JF, Hopewell JC, Kyriakou T, Goel A, Heath SC, Parish S, Barlera S, Franzosi MG, Rust S, Bennett D, Silveira A, Malarstig A, Green FR, Lathrop M, Gigante B, Leander K, de Faire U, Seedorf U, Hamsten A, Collins R, Watkins H, Farrall M (2009) Genetic variants associated with Lp(a) lipoprotein level and coronary disease. N Engl J Med 361:2518–2528
10. Tian H, Han L, Ren Y, Li X, Liang J (2003) Lipoprotein(a) level and lipids in type 2 diabetic patients and their normoglycemic first-degree relatives in type 2 diabetic pedigrees. Diabetes Res Clin Pract 59:63–69
11. Murase T, Okubo M, Amemiya-Kudo M, Hiraga T, Oka J, Shimada M, Igarashi T (2007) Impact of markedly elevated serum lipoprotein(a) levels (> or = 100 mg/dL) on the risk of coronary heart disease. Metabolism 56:1187–1191
12. Chien KL, Hsu HC, Su TC, Sung FC, Chen MF, Lee YT (2008) Lipoprotein(a) and cardiovascular disease in ethnic Chinese: the Chin-Shan Community Cardiovascular Cohort Study. Clin Chem 54:285–291
13. Murase T, Okubo M, Amemiya-Kudo M, Ebara T, Mori Y (2008) Impact of elevated serum lipoprotein(a) concentrations on the risk of coronary heart disease in patients with type 2 diabetes mellitus. Metabolism 57:791–795
14. Nasri H (2008) Association of serum lipoprotein(a) with hypertension in diabetic patients. Saudi J Kidney Dis Transpl 19: 420–427
15. Wassef N, Sidhom G, Zakareya el K, Mohamed el K (1997) Lipoprotein(a) in android obesity and NIDDM. Diabetes Care 20:1693–1696
16. Khan MA, Baseer A (1998) Magnitude of lipoprotein(a) in diabetes mellitus. J Pak Med Assoc 48:11–13
17. Alsaeid M, Qabazard M, Shaltout A, Sharma PN (2001) Impact of glycemic control on serum lipoprotein(a) in Arab children with type 1 diabetes. Pediatr Int 43:246–250
18. Habib SS, Aslam M (2003) High risk levels of lipoprotein(a) in Pakistani patients with type 2 diabetes mellitus. Saudi Med J 24:647–651
19. Funatsu H, Shimizu E, Noma H, Mimura T, Hori S (2009) Association between serum lipoprotein(a) level and progression of non-proliferative diabetic retinopathy in type 2 diabetes. Acta Ophthalmol 87:501–505
20. Chen XF, Tang LJ, Jiang JJ, Jiang J, Hu XY, Yu WF, Wang JA (2008) Increased levels of lipoprotein(a) in non-smoking aortic dissection patients. Clin Exp Med 8:123–127
21. Drobny M, Svalekova A, Koskova E, Hazlingerova M, Celec S (1996) Selected parameters of lipoprotein metabolism in cerebrovascular diseases. Bratisl Lek Listy 97:267–272
22. Fukunaga N, Anan F, Kaneda K, Nawata T, Saikawa T, Yoshimatsu H (2008) Lipoprotein(a) as a risk factor for silent cerebral infarction in hemodialysis patients. Metabolism 57:1323–1327
23. Bennet A, Di Angelantonio E, Erqou S, Eiriksdottir G, Sigurdsson G, Woodward M, Rumley A, Lowe GD, Danesh J, Gudnason V (2008) Lipoprotein(a) levels and risk of future coronary heart disease: large-scale prospective data. Arch Intern Med 168:598–608
24. Okosun IS, Dever GE, Choi ST (2002) Low birth weight is associated with elevated serum lipoprotein(a) in white and black American children ages 5–11 y. Public Health 116:33–38
25. Kwiterovich PO Jr, Virgil DG, Garrett ES, Otvos J, Driggers R, Blakemore K, Cockrill SL, Macfarlane RD (2004) Lipoprotein heterogeneity at birth: influence of gestational age and race on lipoprotein subclasses and Lp(a) lipoprotein. Ethn Dis 14:351–359
26. Aasvee K, Jauhiainen M, Kurvinen E, Jordania R, Sundvall J, Ehnholm C (1999) Lipoprotein(a), apolipoprotein A-I and B serum levels in young families from Tallinn, Estonia. Relationships with other cardiovascular risk factors and nationality. Scand J Clin Lab Invest 59:179–189
27. Preis SR, Pencina MJ, Hwang SJ, D'Agostino RB, Savage PJ, Levy D, Fox CS (2009) Trends in cardiovascular disease risk factors in individuals with and without diabetes mellitus in the Framingham heart study. Circulation 120:212–220
28. Koschinsky ML, Marcovina SM (2003) The relationship between lipoprotein(a) and the complications of diabetes mellitus. Acta Diabetol 40:65–76
29. Labudovic DD, Toseska KN, Alabakovska SB, B Todorova B (2003) Apoprotein(a) phenotypes and plasma lipoprotein(a) concentration in patients with diabetes mellitus. Clin Biochem 36:545–551
30. Alagozlu H, Gultekin F, Candan F (2000) Lipid and lipoprotein patterns in type 2 non-obese diabetic patients. Do Lp(a) levels decrease with improved glycemic control in these patients? Nutr Metab Cardiovasc Dis 10:204–208
31. Chang CJ, Kao JT, Wu TJ, Lu FH, Tai TY (1995) Serum lipids and lipoprotein(a) concentrations in Chinese NIDDM patients. Relation to metabolic control. Diabetes Care 18:1191–1194
32. Csaszar A, Dieplinger H, Sandholzer C, Karadi I, Juhasz E, Drexel H, Halmos T, Romics L, Patsch JR, Utermann G (1993) Plasma lipoprotein(a) concentration and phenotypes in diabetes mellitus. Diabetologia 36:47–51
33. Klausen IC, Schmidt EB, Lervang HH, Gerdes LU, Ditzel J, Faergeman O (1992) Normal lipoprotein(a) concentrations and apolipoprotein(a) isoforms in patients with insulin-dependent diabetes mellitus. Eur J Clin Invest 22:538–541
34. Rainwater DL, MacCluer JW, Stern MP, VandeBerg JL, Haffner SM (1994) Effects of NIDDM on lipoprotein(a) concentration and apolipoprotein(a) size. Diabetes 43:942–946
35. Erqou S, Kaptoge S, Perry PL, Di Angelantonio E, Thompson A, White IR, Marcovina SM, Collins R, Thompson SG, Danesh J (2009) Lipoprotein(a) concentration and the risk of coronary heart disease, stroke, and nonvascular mortality. JAMA 302:412–423
36. Zlatohlavek L, Zidkova K, Vrablik M, Haas T, Prusikova M, Svobodova H, Ceska R (2008) Lipoprotein(a) and its position among other risk factors of atherosclerosis. Physiol Res 57: 777–783
37. Agoston-Coldea L, Rusu LD, Zdrenghea D, Rusu ML, Pop D, Craciun A, Poanta L, Gatfosse M, Rosenstingl S, Mocan T (2008) Lipoprotein(a) and lipid and non-lipid risk factors in coronaries risk assessment. Rom J Intern Med 46:137–144
38. Tselmin S, Julius U, Muller G, Fischer S, Bornstein SR (2009) Cardiovascular events in patients with increased lipoprotein(a)—retrospective data analysis in an outpatient department of lipid disorders. Atheroscler Suppl 10:79–84
39. Sawabe M, Tanaka N, Nakahara K, Hamamatsu A, Chida K, Arai T, Harada K, Inamatsu T, Ozawa T, Naka MM, Matsushita S (2009) High lipoprotein(a) level promotes both coronary atherosclerosis and myocardial infarction: a path analysis using a large number of autopsy cases. Heart 95:1997–2002
40. Katulanda GW, Katulanda P, Adler AI, Peiris SR, Draisey I, Wijeratne S, Sheriff R, Matthews DR, Shine B (2010) Apolipoproteins in diabetes dyslipidaemia in South Asians with young adult-onset diabetes: distribution, associations and patterns. Ann Clin Biochem 47:29–34
41. Eshtiaghi R, Esteghamati A, Nakhjavani M Menopause is an independent predictor of metabolic syndrome in Iranian women. Maturitas 65:262–266
42. Matthan NR, Jalbert SM, Barrett PH, Dolnikowski GG, Schaefer EJ, Lichtenstein AH (2008) Gender-specific differences in the kinetics of nonfasting TRL, IDL, and LDL apolipoprotein B-100 in men and premenopausal women. Arterioscler Thromb Vasc Biol 28:1838–1843
43. Nakagami F, Nakagami H, Osako MK, Iwabayashi M, Taniyama Y, Doi T, Shimizu H, Shimamura M, Rakugi H, Morishita R

(2010) Estrogen attenuates vascular remodeling in Lp(a) transgenic mice. Atherosclerosis 211(1):41–47
44. Shlipak MG, Simon JA, Vittinghoff E, Lin F, Barrett-Connor E, Knopp RH, Levy RI, Hulley SB (2000) Estrogen and progestin, lipoprotein(a), and the risk of recurrent coronary heart disease events after menopause. JAMA 283:1845–1852
45. Hemelaar M, van der Mooren MJ, Mijatovic V, Bouman AA, Schijf CP, Kroeks MV, Franke HR, Kenemans P (2003) Oral, more than transdermal, estrogen therapy improves lipids and lipoprotein(a) in postmenopausal women: a randomized, placebo-controlled study. Menopause 10:550–558
46. Suk Danik J, Rifai N, Buring JE, Ridker PM (2008) Lipoprotein(a), hormone replacement therapy, and risk of future cardiovascular events. J Am Coll Cardiol 52:124–131
47. Rosenson RS, Tangney CC, Mosca LJ (1998) Hormone replacement therapy improves cardiovascular risk by lowering plasma viscosity in postmenopausal women. Arterioscler Thromb Vasc Biol 18:1902–1905
48. White RE, Gerrity R, Barman SA, Han G (2010) Estrogen and oxidative stress: a novel mechanism that may increase the risk for cardiovascular disease in women. Steroids 75(11):788–793

Lipids (2011) 46:357–363
DOI 10.1007/s11745-011-3533-5

ORIGINAL ARTICLE

Glucokinase Regulatory Protein (GCKR) Gene rs4425043 Polymorphism is Associated with Overweight and Obesity in Chinese Women

Feifei Cao · Xiaofeng Wang · Ming Lu · Yajun Yang · Yu An · Juan Zhang · Xingdong Chen · Lei Li · Shuyuan Li · Jie Jiang · Weimin Ye · Li Jin

Received: 1 September 2010 / Accepted: 22 January 2011 / Published online: 13 February 2011

Abstract The aim of this study was to investigate the effects of *GCKR* polymorphism on the prevalence of overweight and obesity in Chinese female subjects using a gene-wide tagging- single nucleotide polymorphism (tSNP) strategy. We conducted a genetic association study in the Taizhou Retiree Women Cohort, a sub-cohort of the Taizhou longitudinal study. We genotyped four tSNPs (rs4425043, rs780094, rs814295, and rs8179206) of the *GCKR* gene using the Taqman assay in 2,851 female subjects and investigated their associations with overweight and obesity. Odds ratios and their 95% confidence intervals (CIs) were derived from ordered logistic regression model. We observed significant association between rs4425043 and body-mass-index-defined overweight and obesity. The frequencies of A allele of the rs4425043 exhibited a significant increasing trend from normal weight (13.20%), overweight (15.08%), to obese subjects (17.10%) ($P = 0.006$). Individuals with the GA or AA genotypes showed a 31% excessive risk to develop overweight or obesity (95% CI: 1.12–1.52, $P = 0.001$). In addition, we observed significantly increased levels of fasting plasma glucose associated with variations of both rs780094 and rs814295 (5.03, 5.09, and 5.15 mmol/L for rs780094 AA, GA and GG genotypes, respectively, and 5.03, 5.11, and 5.20 mmol/L for rs814295 AA, GA and GG genotypes, respectively). In conclusion, a novel polymorphism (rs4425043) in the *GCKR* gene increases the risk of overweight and obesity in Chinese women. Previous report that other polymorphisms in the *GCKR* gene are associated with glucose levels have also been confirmed.

Keywords Chinese Han · GCKR · Overweight · Obesity · Polymorphism · Women

Abbreviations

CVD	Cardiovascular disease
GCK	Glucokinase
GCKR	Glucokinase regulatory protein
TZL	The Taizhou longitudinal study
WC	Waist circumference
TG	Triglycerides
FPG	Fasting plasma glucose
ORs	Odds ratios
BMI	Body mass index
LD	Linkage disequilibrium
SNP	Single nucleotide polymorphism

F. Cao and X. Wang contributed equally to this work.

F. Cao · M. Lu (✉)
Clinical Epidemiology Unit, Qilu Hospital of Shandong University, Jinan 250012, Shandong, People's Republic of China
e-mail: lvming@sdu.edu.cn

X. Wang · M. Lu · Y. Yang · Y. An · X. Chen · L. Li · S. Li · J. Jiang · W. Ye · L. Jin (✉)
State Key Laboratory of Genetic Engineering and MOE Key Laboratory of Contemporary Anthropology, School of Life Sciences and Institutes of Biomedical Sciences, Fudan University, 220 Handan Rd, Shanghai 200433, People's Republic of China
e-mail: lijin.fudan@gmail.com

X. Wang · Y. Yang · J. Zhang · W. Ye · L. Jin
CMC Institute of Health Sciences, Taizhou 225300, Jiangsu, People's Republic of China

W. Ye
Department of Medical Epidemiology and Biostatistics, Karolinska Institutet, 171 77 Stockholm, Sweden

Introduction

Overweight and obesity are important modifiable risk factors for cardiovascular disease and associated conditions, including type 2 diabetes, hypertension, hypercholesterolemia, coronary heart disease, and stroke [1]. Excessive body weight is also associated with an increased risk for other health consequences, such as osteoarthritis, gall bladder disease, and some cancers [2, 3]. In Europe, the prevalence of obesity in women varies from 6.2 to 36.5% [4]. In recent decades, with the rapid economical growth in China, the prevalence of overweight and obesity has been increasing [2, 5]. In 2006, the prevalence of obesity was 7.2%, representing a 3.6-fold increase from 1996 [6].

Obesity demarcates an imbalance between energy intake and energy expenditure, and excess energy has been stored in fat cells that enlarge and increase in number resulting in elevated secretion of free fatty acids and numerous peptides [7]. Glucokinase (GCK) is a key regulatory enzyme in the pancreatic-cells, and it plays a crucial role in determining the threshold for glucose-stimulated insulin secretion [8]. GCK activity, at least in the liver, is closely regulated by the glucokinase regulatory protein (GCKR) [9]. The *GCKR* gene is localized on chromosome 2p23.2–3 [10], a genomic region previously linked to metabolic traits like fat mass and circulating lipid concentrations [11]. Animal studies indicated that *GCKR*-knockout mice show a parallel loss of GCK protein levels and activity in the liver, leading to altered glucose metabolism and impaired glycemic control [12].

Recently, a single nucleotide polymorphism (SNP) rs780094 in the *GCKR* gene was found to be associated with metabolic phenotypes in Caucasians or Japanese [13–18]. To appraise systematically the effect of *GCKR* genetic variation on these phenotypes, we conducted a genetic association study using a gene-wide tagging-SNP (tSNP) strategy. This method might save cost since only a small proportion of tSNPs of the studied gene give sufficient information to capture most of the haplotype structures in the high linkage disequilibrium (LD) regions [19].

Subjects and Methods

Study Subjects

The Taizhou longitudinal study (TZL), which was initiated in July 2007, was an open-ended prospective study with very broad research aims. The design and baseline characteristics of the study have been described previously [20]. The Taizhou Retiree Women Cohort is a sub-cohort of the TZL. This sub-cohort includes women who were born between 1944 and 1958 (aged 50–64 years). After baseline survey, 7,786 retired women without a history of cancer, stroke, and myocardial infarction were recruited for long-term followed up includes Taizhou is a prefecture of Jiangsu province in China. From the perspective of population size and economic development, Taizhou is a mid-sized city in China. The women in Taizhou retire at least 5 years earlier in age than men. Like women living in other mid-sized cities of China, the retired women in Taizhou are subject to much lower stress in life than their male counterparts. The Taizhou Retiree Women Cohort survey aims to investigate the relationship between the women's lifestyle and the incidence of metabolic and cardiovascular diseases.

A random sample of 2,851 women from the above-mentioned Taizhou Retiree Women Cohort was drawn for this genetic association study. Subjects who reported a history of autoimmune diseases, tuberculosis, and abnormal thyroid function, were excluded from this study since these conditions may affect the level of metabolic phenotypes. The study was approved by the Human Ethics Committee of Fudan University. Written informed consent was obtained from all participants.

Protocol and Measurements

All participants had a face-to-face interview and a physical examination. Body weight and height were measured to calculate the BMI (the ratio of weight in kg to the square of height in m). The waist circumference (WC) was measured midway between the caudal point of the costal arch as palpated laterally and the iliac crest. A blood specimen was drawn after overnight fasting and subjected to centrifugation within 3 h and analyzed within 8 h for measuring triglycerides (TG) and fasting plasma glucose (FPG). The normal weight group, overweight group, obesity group were defined as 18.5 up to 23.9, from 24 to 27.9, and greater than 28 kg/m^2, respectively, according to the Chinese criteria [21]. Hypertriglyceridemia was defined as TG $\geq$ 1.7 mmol/l. Type 2 diabetes mellitus was defined as FPG $\geq$ 7.0 mmol/l.

Selection of tSNPs

Haplotype-tagging SNPs of the *GCKR* gene were selected using the Chinese Han sample in Beijing, China, available from the International HapMap databank (public data release 21 a/phase II, Jan. 2007; http://www.hapmap.org/cgi-perl/gbrowse/hapmap_B35/). To identify common haplotype tSNPs, eligible SNPs were entered into the tagger program that has been implemented in Haploview version 3.32 [22]. We defined the common variants as those with a heterozygosity of >5% and set a threshold of

0.8 for the LD analysis r^2. In total, four tSNPs (rs4425043, rs780094, rs814295, rs8179206) in the *GCKR* gene capturing 13 genotyped alleles were selected.

Genotyping

Blood samples were collected in EDTA-containing receptacles and genomic DNA was extracted using a standard method. Genotyping of the selected tSNPs was conducted using the Taqman assay (Applied Biosystems, Foster City). Sample DNA (10 ng) were amplified by PCR following the recommendations of the manufacturer. Fluorescence was detected using an ABI 7900HT and the alleles were scored using sequence detection software (Applied Biosystems, Foster City, CA, USA). Allele-specific probes used in the TaqMan assay were designed for each of the polymorphic sites. The genotyping success rates for *GCKR* rs4425043, rs780094, rs814295, rs8179206 were 97.9, 99.7, 99.2 and 98.1%, respectively. Sequencing was implemented to test the validity of genotyping.

Statistical Analysis

The deviation from the Hardy–Weinberg expectation for the variants was tested by a Chi-square statistic. Differences of mean BMI, WC, FPG, TG across genotype groups were tested using an ANOVA method. Allelic and genotypic frequencies were compared among the normal weight, overweight, and obesity groups using the Chi-square test or Fisher's exact test. The odds ratios (ORs) and the corresponding confidence intervals (95% CIs) were estimated by ordered logistic regression models under the dominant genetic model assumption, to test the association between SNPs and BMI-defined overweight/obesity where appropriate due to the low frequency of a minor allele. The three categories of dependent variable were treated as ordered values (normal weight as 0, overweight as 1, and obesity as 2), and probabilities modeled were cumulated over the lower ordered values. A score test was used for testing the proportional odds assumption. For haplotype construction, the genotype data were used to estimate inter-marker linkage disequilibrium by measuring pairwise D' and r^2 and by defining LD blocks. Haplotype inferring and haplotype association testing were conducted using the Haploview software [22]. All analyses were performed using SAS statistical software (release 8.2, SAS Institute Inc, Cary, NC, USA).

Results

The clinical and metabolic characteristics of the studied subjects by BMI categories are summarized in Table 1. Compared with normal weight subjects, the overweight and obesity subjects had significantly higher WC, FPG, and TG. Genotypes at all loci were consistent with Hardy–Weinberg expectation. Allelic and genotypic frequencies of the four tSNPs for the overweight, obesity and normal weight subjects are shown in Table 2. The allelic and genotypic frequencies at rs780094, rs814295 and rs8179206 did not differ significantly among overweight, obesity, normal weight subjects. However, the rs4425043 was significantly associated with body mass indices (BMI) defined as overweight/obese. The frequency of the A allele of the rs4425043 increased from normal weight subjects (13.20%), overweight (15.08%) subjects, to obese subjects (17.10%). Individuals with the GA or AA genotypes had a 31% excessive risk (95% CI: 1.12–1.52, $P = 0.001$) of developing overweight or obesity (normal weight subjects as controls) or developing obesity (subjects of normal weight or overweight as controls) in a dominant model of A allele. The significance remained after adjusting for age, or further adjusting for FPG, and TG (Table 3).

We further explored whether the tSNPs affect the level of metabolic phenotypes in the subjects who had a BMI less than 28 kg/m^2. We further excluded those subjects whose TG $\geq$ 1.7 mmol/l and/or FPG $\geq$ 7.0 mmol/l. As shown in Table 4, rs780094 and rs814295 variations were significantly associated with increased FPG levels ($P = 0.034$ and $P = 0.002$, respectively). The level of

Table 1 Clinical characteristics of the studied subjects

Variables	Body mass index			$P^{\#}$
	18.5–23.9	24–27.9	≥28	
Number of subjects	1,115	1,019	717	–
Age (year, mean ± SD[a])	57.65 ± 3.99	57.77 ± 3.99	57.81 ± 3.96	0.673
Waist circumference (cm, mean ± SD)	76.30 ± 5.70	84.54 ± 5.30	93.55 ± 6.49	<0.001
Fasting plasma glucose (mmol/L, mean ± SD)	5.13 ± 0.91	5.35 ± 1.03	5.48 ± 1.80	<0.001
Triglycerides (mmol/L, mean ± SD)	1.53 ± 1.00	1.80 ± 1.02	1.82 ± 1.08	<0.001

[a] *SD* standard deviation

[#] *P* values were inferred from the ANOVA test

FPG increased with the copy of the minor G allele for both variants (the FPG levels were 5.03, 5.09, and 5.15 mmol/L for AA, GA and GG genotypes of rs780094 and 5.03, 5.11, and 5.20 mmol/L for AA, GA and GG genotypes of rs814295, respectively).

Table 2 The distribution of genotype and allele frequency of *GCKR* in studied subjects

Polymorphisms	Body mass index			$P^{\dagger}$
	18.5–23.9	24–27.9	≥28	
rs4425043				
GG	822 (75.34)	717 (71.63)	475 (67.95)	0.018
GA	250 (22.91)	266 (26.57)	209 (29.90)	–
AA	19 (1.74)	18 (1.80)	15 (2.15)	–
G	1,894 (86.80)	1,700 (84.92)	1,159 (82.90)	0.006
A	288 (13.20)	302 (15.08)	239 (17.10)	–
rs780094				
AA	336 (30.19)	275 (27.12)	188 (26.29)	0.191
GA	537 (48.25)	530 (52.27)	382 (53.43)	–
GG	240 (21.56)	209 (20.61)	145 (20.28)	–
A	1,209 (54.31)	1,080 (53.25)	758 (53.01)	0.686
G	1,017 (45.69)	948 (46.75)	672 (47.00)	–
rs814295				
AA	506 (45.75)	474 (46.88)	343 (48.31)	0.664
GA	483 (43.67)	446 (44.11)	300 (42.25)	–
GG	117 (10.58)	91 (9.00)	67 (9.44)	–
A	1,495 (67.59)	1,394 (68.94)	986 (69.44)	0.446
G	717 (32.41)	628 (31.06)	434 (30.56)	–
rs8179206				
AA	1020 (93.32)	936 (92.31)	653 (94.50)	0.344
GA	72 (6.59)	75 (7.40)	36 (5.21)	–
GG	1 (0.09)	3 (0.30)	2 (0.29)	–
A	2,112 (96.61)	1,947 (96.01)	1,342 (97.11)	0.216
G	74 (3.39)	81 (3.99)	40 (2.89)	–

Due to missing values of genotyping data, the numbers in the columns did not add up to the total numbers of subjects in each phenotype category

† *P* values were inferred from the Chi-square test or Fisher's exact test

LD analysis of rs4425043, rs780094, rs814295, rs8179206 revealed that the SNP rs780094 was in moderate LD with rs814295 which were about 2 kb apart ($D' = 0.97$, $r^2 = 0.51$). Haplotype analysis of rs780094 and rs814295 did not find major haplotypes conferring the risk of overweight/obesity (data not shown).

Discussion

In this study, we explored the relationship between four tSNPs in the *GCKR* gene and the risk of overweight/obesity defined by BMI in the Taizhou Retiree Women Cohort. We observed a dose–response effect of A allele in rs4425043 conferring an increased risk for overweight or obesity. To the best of our knowledge, this is the first study to correlate *GCKR*-rs4425043 with the risk of overweight and obesity in Chinese females.

GCKR, including 19 coding exons, spans 26.8 kb on chromosome 2. SNP rs4425043 is located at the 16th intron of the *GCKR* gene. The functional significance of rs4425043 is still unknown. As can be calculated from the data of Han Chinese (CHB) in the International Hapmap database, rs4425043 tags five SNPs located in a region from the 5th to the 11th intron. This positive SNP is likely a genetic marker which is in LD with a casual variant located within this region. It is noteworthy that we did not find significant association of this polymorphism with BMI levels in the non-obese female subjects. Different modifying effects of this polymorphism on the pathological status of obesity and physiologic level of BMI may be the explanation. Since only 1,356 non-obesity subjects were included in the association analysis for quantitative traits, false-negative association of rs4425043 with BMI levels may also be an alternative explanation due to insufficient statistical power.

Recently, two important SNPs in the *GCKR* gene were reported to be associated with specific metabolic phenotypes. SNP rs780094, located at intron 16 of the *GCKR* gene, is in strong LD with a non-synonymous SNP rs1260326 (P446L) located at exon 15 [13]. In two genome

Table 3 Odds ratios for overweight or obesity associated with *GCKR* rs4425043 polymorphism

rs4425043	BMI			OR (95% CI)	Adj-OR (95%CI)[a]	Adj-OR (95%CI)[b]
	18.5–23.9	24–27.9	≥28			
GG	822 (75.34)	717 (71.63)	475 (67.95)	1.0 (ref)	1.0 (ref)	1.0 (ref)
GA/AA	269 (24.66)	284 (28.37)	224 (32.05)	1.31 (1.12–1.52)	1.30 (1.12–1.52)	1.30 (1.12–1.52)

Odds ratios were derived from ordered logistic regression models. Due to missing values of genotyping data, the numbers in the columns did not add up to the total numbers of subjects in each phenotype category

[a] Adjusted for age

[b] Further adjusted for age, fasting plasma glucose, and triglycerides

Table 4 Clinical phenotypes according to *GCKR* genotypes in 1,356 subjects without obesity, diabetes (fasting plasma glucose ≥7.0 mmol/L), and hypertriglyceridemia (triglyceride ≥1.7 mmol/L)

Phenotype	Genotype			$P^{\dagger}$
	Major homozygote	Heterozygote	Minor homozygote	
rs4425043	GG	GA/AA	–	–
N^{a}	984	345	–	–
BMI (kg/m^2)	23.38 ± 2.27	23.49 ± 2.38	–	0.435
Waist circumference (cm)	79.02 ± 6.77	79.53 ± 7.07	–	0.237
Fasting plasma glucose (mmol/L)	5.09 ± 0.59	5.07 ± 0.56	–	0.597
Triglycerides (mmol/L)	1.16 ± 0.31	1.17 ± 0.29	–	0.667
rs780094	AA	GA	GG	–
N^{a}	373	677	300	–
BMI (kg/m^2)	23.26 ± 2.25	23.51 ± 2.31	23.26 ± 2.30	0.128
Waist circumference (cm)	78.84 ± 6.66	79.39 ± 7.04	78.94 ± 6.61	0.396
Fasting plasma glucose (mmol/L)	5.03 ± 0.56	5.09 ± 0.57	5.15 ± 0.67	0.034
Triglycerides (mmol/L)	1.18 ± 0.31	1.16 ± 0.31	1.17 ± 0.29	0.799
rs814295	AA	GA	GG	–
N^{a}	598	598	148	–
BMI (kg/m^2)	25.41 ± 2.31	25.41 ± 2.31	25.25 ± 2.16	0.721
Waist circumference (cm)	79.19 ± 6.97	79.10 ± 6.81	79.23 ± 6.54	0.966
Fasting plasma glucose (mmol/L)	5.03 ± 0.56	5.11 ± 0.58	5.20 ± 0.65	0.002
Triglycerides (mmol/L)	1.17 ± 0.31	1.16 ± 0.31	1.16 ± 0.29	0.833

[a] Due to missing values of genotyping data, the numbers in the row did not add up to the total number of 1,356 subjects

[†] *P* values were derived from *t* test or ANOVA test

wide association studies, the A allele of rs780094 was found in association with decreased concentration of plasma glucose and increased TG in Caucasians [14, 15]. Later, the A allele of rs780094 was found to be linked to decreased risk of type 2 diabetes in Japanese [16]. In 12 independent cohorts comprising 45,000 individuals of Caucasians, Asians, and African Americans, SNP rs780094 was found to be associated with decreased concentration of plasma glucose but increased TG level [17]. Sparsø et al. observed that the A allele of rs780094 polymorphism is associated with elevated fasting serum triacylglycerol, reduced fasting and OGTT-related insulinemia, and a reduced risk of type 2 diabetes. More recently Qi et al. [23] observed that the A allele of rs780094 is associated with a reduced risk of diabetes, and a decreased risk of BMI related obesity in Chinese subjects. Further, it was also associated with increased TG levels and decreased BMI and WC in this study [23]. A potential explanation of the different effects on glucose and TG observed in these studies is the opposite and overriding effects of increased glucose utilization and glycolytic flux on liver glucose and lipid metabolism [17]. Similar to these studies, we observed that the A allele of rs780094 decreased the level of plasma glucose (FPG was 5.15, 5.09, and, 5.03 for GG, GA, and AA, respectively). However, we did not observe that the rs780094-A allele increases the level of TG, as the aforementioned studies did [19–23]. We also did not observe that the rs780094-A allele increases the BMI and WC, as Qi et al. observed [23]. Genetic and phenotypic heterogeneity of these traits may be a reason for the lack of significant associations in our study. The lack of statistical power due to insufficient sample size, differences in gender (our sample comprised only women) and age (the ages of our sample ranged from 50 to 64 years) from other studies may also be other possible reasons.

In this study, we observed another SNP, rs814295, to be associated with the FPG level (FPG was 5.03, 5.11, and, 5.20 for AA, GA, and GG of rs814295, respectively). This SNP is located at the 17th intron of the *GCKR* gene and is in moderate LD with rs780094 ($r^2 = 0.50$), which is located at intron16. We could not exclude the possibility that the glucose decreasing effect of both the A allele of rs814295 and the A allele of rs780094 results from the effect of rs1260326 (P446L), which is in strong LD with rs814295. However, since there were only 69 diabetes subjects in the study, we did not have the statistical power to explore the effect of rs780094 and rs81429 on the prevalence of diabetes. Fortunately, Taizhou Retiree Women Cohort is an ongoing prospective study of old women which will be used to validate the genotype–phenotype association discovered in the baseline cross-sectional studies. The present study had other

limitations. For example, we did not consider the effects of dietary intake or physical activity on the studied metabolic phenotypes since we did not include measurement of these factors in this Retiree Women Subcohort. Fortunately, we did include these exposures in the community based sub-cohort of TZL, which can be analyzed in future studies.

In summary, we have reported a novel polymorphism (rs4425043) in the *GCKR* gene linked to the risk of overweight or obesity in Chinese women. We also confirmed the previous finding that polymorphisms in the *GCKR* gene are associated with the glucose level in a Chinese women cohort. Since our cross-sectional case–control design was based only on a baseline stage of an ongoing prospective study, our exploratory results need to be validated in future prospective studies.

Acknowledgments This study is supported by grant from the National Science Fund (30973595, 81072358), a grant from Independent Innovation Foundation of Shandong University, IIFSDU. We also thank the members of the survey teams and the participants for their contribution to this study.

References

1. Krauss RM, Winston M, Fletcher RN, Grundy SM (1998) Obesity: impact of cardiovascular disease. Circulation 98: 1472–1476
2. (2000) Obesity: preventing and managing the global epidemic. Report of a WHO consultation. World Health Organ Tech Rep Ser 894:i–xii, 1–253
3. (2000) Overweight, obesity, and health risk. National Task Force on the prevention and treatment of obesity. Arch Intern Med 160:898–904
4. Berghofer A, Pischon T, Reinhold T, Apovian CM, Sharma AM, Willich SN (2008) Obesity prevalence from a European perspective: a systematic review. BMC Public Health 8:200
5. Saw SM, Rajan U (1997) The epidemiology of obesity: a review. Ann Acad Med Singapore 26:489–493
6. Ding ZY (2008) National epidemiological survey on childhood obesity, 2006. Zhonghua Er Ke Za Zhi 46:179–184
7. Bray GA (2004) Medical consequences of obesity. J Clin Endocrinol Metab 89:2583–2589
8. Rose CS, Ek J, Urhammer SA, Glumer C, Borch-Johnsen K, Jorgensen T, Pedersen O, Hansen T (2005) A -30G>a polymorphism of the beta-cell-specific glucokinase promoter associates with hyperglycemia in the general population of whites. Diabetes 54:3026–3031
9. Chu CA, Fujimoto Y, Igawa K, Grimsby J, Grippo JF, Magnuson MA, Cherrington AD, Shiota M (2004) Rapid translocation of hepatic glucokinase in response to intraduodenal glucose infusion and changes in plasma glucose and insulin in conscious rats. Am J Physiol Gastrointest Liver Physiol 286:G627–G634
10. Hayward BE, Fantes JA, Warner JP, Intody S, Leek JP, Markham AF, Bonthron DT (1996) Co-localization of the ketohexokinase and glucokinase regulator genes to a 500-kb region of chromosome 2p23. Mamm Genome 7:454–458
11. Comuzzie AG, Hixson JE, Almasy L, Mitchell BD, Mahaney MC, Dyer TD, Stern MP, MacCluer JW, Blangero J (1997) A major quantitative trait locus determining serum leptin levels and fat mass is located on human chromosome 2. Nat Genet 15:273–276
12. Farrelly D, Brown KS, Tieman A, Ren J, Lira SA, Hagan D, Gregg R, Mookhtiar KA, Hariharan N (1999) Mice mutant for glucokinase regulatory protein exhibit decreased liver glucokinase: a sequestration mechanism in metabolic regulation. Proc Natl Acad Sci USA 96:14511–14516
13. Vaxillaire M, Cavalcanti-Proenca C, Dechaume A, Tichet J, Marre M, Balkau B, Froguel P (2008) The common P446L polymorphism in GCKR inversely modulates fasting glucose and triglyceride levels and reduces type 2 diabetes risk in the DESIR prospective general French population. Diabetes 57:2253–2257
14. Saxena R, Voight BF, Lyssenko V, Burtt NP, de Bakker PI, Chen H, Roix JJ, Kathiresan S, Hirschhorn JN, Daly MJ, Hughes TE, Groop L, Altshuler D, Almgren P, Florez JC, Meyer J, Ardlie K, Bengtsson Bostrom K, Isomaa B, Lettre G, Lindblad U, Lyon HN, Melander O, Newton-Cheh C, Nilsson P, Orho-Melander M, Rastam L, Speliotes EK, Taskinen MR, Tuomi T, Guiducci C, Berglund A, Carlson J, Gianniny L, Hackett R, Hall L, Holmkvist J, Laurila E, Sjogren M, Sterner M, Surti A, Svensson M, Svensson M, Tewhey R, Blumenstiel B, Parkin M, Defelice M, Barry R, Brodeur W, Camarata J, Chia N, Fava M, Gibbons J, Handsaker B, Healy C, Nguyen K, Gates C, Sougnez C, Gage D, Nizzari M, Gabriel SB, Chirn GW, Ma Q, Parikh H, Richardson D, Ricke D, Purcell S (2007) Genome-wide association analysis identifies loci for type 2 diabetes and triglyceride levels. Science 316:1331–1336
15. Willer CJ, Sanna S, Jackson AU, Scuteri A, Bonnycastle LL, Clarke R, Heath SC, Timpson NJ, Najjar SS, Stringham HM, Strait J, Duren WL, Maschio A, Busonero F, Mulas A, Albai G, Swift AJ, Morken MA, Narisu N, Bennett D, Parish S, Shen H, Galan P, Meneton P, Hercberg S, Zelenika D, Chen WM, Li Y, Scott LJ, Scheet PA, Sundvall J, Watanabe RM, Nagaraja R, Ebrahim S, Lawlor DA, Ben-Shlomo Y, Davey-Smith G, Shuldiner AR, Collins R, Bergman RN, Uda M, Tuomilehto J, Cao A, Collins FS, Lakatta E, Lathrop GM, Boehnke M, Schlessinger D, Mohlke KL, Abecasis GR (2008) Newly identified loci that influence lipid concentrations and risk of coronary artery disease. Nat Genet 40:161–169
16. Horikawa Y, Miyake K, Yasuda K, Enya M, Hirota Y, Yamagata K, Hinokio Y, Oka Y, Iwasaki N, Iwamoto Y, Yamada Y, Seino Y, Maegawa H, Kashiwagi A, Yamamoto K, Tokunaga K, Takeda J, Kasuga M (2008) Replication of genome-wide association studies of type 2 diabetes susceptibility in Japan. J Clin Endocrinol Metab 93:3136–3141
17. Orho-Melander M, Melander O, Guiducci C, Perez-Martinez P, Corella D, Roos C, Tewhey R, Rieder MJ, Hall J, Abecasis G, Tai ES, Welch C, Arnett DK, Lyssenko V, Lindholm E, Saxena R, de Bakker PI, Burtt N, Voight BF, Hirschhorn JN, Tucker KL, Hedner T, Tuomi T, Isomaa B, Eriksson KF, Taskinen MR, Wahlstrand B, Hughes TE, Parnell LD, Lai CQ, Berglund G, Peltonen L, Vartiainen E, Jousilahti P, Havulinna AS, Salomaa V, Nilsson P, Groop L, Altshuler D, Ordovas JM, Kathiresan S (2008) Common missense variant in the glucokinase regulatory protein gene is associated with increased plasma triglyceride and C-reactive protein but lower fasting glucose concentrations. Diabetes 57:3112–3121
18. Sparso T, Andersen G, Nielsen T, Burgdorf KS, Gjesing AP, Nielsen AL, Albrechtsen A, Rasmussen SS, Jorgensen T, Borch-Johnsen K, Sandbaek A, Lauritzen T, Madsbad S, Hansen T, Pedersen O (2008) The GCKR rs780094 polymorphism is associated with elevated fasting serum triacylglycerol, reduced fasting and OGTT-related insulinaemia, and reduced risk of type 2 diabetes. Diabetologia 51:70–75
19. Johnson GC, Esposito L, Barratt BJ, Smith AN, Heward J, Di Genova G, Ueda H, Cordell HJ, Eaves IA, Dudbridge F,

Twells RC, Payne F, Hughes W, Nutland S, Stevens H, Carr P, Tuomilehto-Wolf E, Tuomilehto J, Gough SC, Clayton DG, Todd JA (2001) Haplotype tagging for the identification of common disease genes. Nat Genet 29:233–237

20. Wang X, Lu M, Qian J, Yang Y, Li S, Lu D, Yu S, Meng W, Ye W, Jin L (2009) Rationales, design and recruitment of the Taizhou longitudinal study. BMC Public Health 9:223
21. Bei-Fan Z (2002) Predictive values of body mass index and waist circumference for risk factors of certain related diseases in Chinese adults: study on optimal cut-off points of body mass index and waist circumference in Chinese adults. Asia Pac J Clin Nutr 11(Suppl 8):S685–S693
22. Barrett JC, Fry B, Maller J, Daly MJ (2005) Haploview: analysis and visualization of LD and haplotype maps. Bioinformatics 21:263–265
23. Qi Q, Wu Y, Li H, Loos RJ, Hu FB, Sun L, Lu L, Pan A, Liu C, Wu H, Chen L, Yu Z, Lin X (2009) Association of GCKR rs780094, alone or in combination with GCK rs1799884, with type 2 diabetes and related traits in a Han Chinese population. Diabetologia 52:834–843

Lipids (2011) 46:365–370
DOI 10.1007/s11745-011-3526-4

ORIGINAL ARTICLE

Dietary Cocoa Butter or Refined Olive Oil Does Not Alter Postprandial hsCRP and IL-6 Concentrations in Healthy Women

Tine Tholstrup · Kim-Tiu Teng · Marianne Raff

Received: 25 August 2010 / Accepted: 27 December 2010 / Published online: 2 February 2011

Abstract Contrary to other long chain saturated fatty acids (SFA), fats high in stearic acid do not raise plasma cholesterol concentrations, however, a slight elevation in inflammatory markers, plasma fibrinogen and interleukin-6 (IL-6), has been observed in the fasting state. The effect of stearic acid on inflammation in the postprandial state has not yet been reported. We conducted a single blind cross-over, randomized, postprandial study to compare the effects of a fat load of cocoa butter high in stearic acid and olive oil in ten healthy women. The test meals contained 1 g of fat per kg body weight (mean 62 g). Blood samples were collected at 0 (fasting), 4 and 6 h. Both diets resulted in a significant increase in serum triacylglycerol (TAG) concentration over time ($P = 0.003$) and a decrease in serum IL-6 concentration after 4 h followed by an increase to post absorptive values after 6 h ($P < 0.001$); whereas serum high sensitivity C-reactive protein (hsCRP) concentration was not affected. There was no difference between diets in effects on serum TAG, hsCRP and IL-6 concentrations and no association between postprandial lipemia and inflammatory markers. High intake of dietary fats increase postprandial serum TAG, however, may not affect inflammatory markers postprandially. Thus, fat rich in stearic acid does not seem to increase postprandial inflammation.

T. Tholstrup (✉) · M. Raff
Department of Human Nutrition, Faculty of Life Sciences, Copenhagen University, 1958 Frederiksberg, Denmark
e-mail: tth@life.ku.dk

K.-T. Teng
Department of Physiology, Faculty of Medicine, University of Malaya, 50603 Kuala Lumpur, Malaysia
e-mail: kt.teng@gmail.com

Keywords Postprandial lipemia · C-reactive protein · Interleukin-6 · Stearic acid · Triacylglycerol

Abbreviations

hsCRP	High-sensitivity C-reactive protein
IL-6	Interleukin-6
OL	Olive oil
CB	Cocoa butter
%E	Percentage of energy
TAG	Triacylglycerol
TNF-α	Tumor necrosis factor-α
SFA	Saturated fatty acids
MUFA	Monounsaturated fatty acids
PUFA	Polyunsaturated fatty acids
BMI	Body mass index
CAM	Cellular adhesion molecules

Introduction

It is recognized that fats high in stearic acid are considered more beneficial than other long chain saturated fatty acids (SFA), as they do not raise plasma cholesterol concentration [1–3]. In addition, earlier studies from our group and others demonstrated that stearic acid given as a synthetic, interesterified fat resulted in a lower postprandial lipemia and factor VII coagulant activity than test fats high in unsaturated fatty acids [4, 5]. However, stearic acid may lead to a slight but consistent increase in fasting plasma fibrinogen, a marker of inflammation [6, 7]. A single study demonstrated a slight increasing effect of stearic acid compared to carbohydrate on fibrinogen, as well [8]. The main regulator of hepatic synthesis of acute phase reactants

such as C-reactive protein (CRP) is associated with future cardiovascular disease in apparently healthy individuals [9–12]. In the postprandial state, as well as in the fasting state, inflammatory events may increase atherogenesis. It was reported that an increase in plasma IL-6 was observed in response to postprandial lipemia in humans, however, no changes could be detected in plasma cell adhesion molecules (CAM) concentrations after a high fat meal [13].

Specific dietary fats may influence the expression of inflammatory markers in postprandial state differently. Results from a study investigating influence of postprandial TAG-rich lipoprotein on lipid mediated gene expression demonstrated that intake of butter compared to refined olive oil increased postprandial mRNA expression of tumor necrosis factor-α (TNF-α) in smooth muscle cell of the human coronary artery [14]. This is in agreement with a decrease in postprandial IL-6 and TNF-α concentrations in mononuclear cells after consuming olive oil and walnut meals compared to butter meal [15]. A recent study in healthy men, however, concluded that acute changes in the dietary content of saturated and unsaturated fatty acids had no adverse effect on postprandial circulation of the adipose-related factors such as adiponectin, IL-6, TNF-α, or hsCRP [16], although a transient increase in IL-6 after 6 h was observed after both type of fats.

The detrimental effects of hydrogenated fats to health have been confirmed by extensive epidemiological and clinical studies. The mandatory '*trans* fatty acids' labelling on packaged food products effective on 2006 has driven the food manufacturers to look for alternatives for hydrogenated vegetable oils. Hence, fats high in stearic acid may be used as a suitable replacement for hydrogenated vegetable oils with similar functionality by proving its health effects. To the best of our knowledge, no study has been conducted to examine the effect of a high stearic acid fat, cocoa butter (CB) as SFA source compared to olive oil (OL) on serum hsCRP and IL-6. Thus, we performed a pilot study to investigate the postprandial effect of olive oil and cocoa butter on serum TAG, hsCRP and IL-6 in healthy women.

Materials and Methods

Study Design

We conducted a randomized, crossover, postprandial study with refined OL and CB. The study participants ($n = 10$) were given two test meals separated by a minimum of 3 days. After an overnight fast, participants reported to the study center at 8:00 a.m. A venous blood sample was taken and the participants consumed test meals within 15 min. Blood samples were drawn at 4 and 6 h after the meal had begun. The participants were instructed to maintain same level of physical activity throughout the study period. They were allowed to consume water ad libitum. The Scientific Ethics Committee of the City of Copenhagen and Frederiksberg Municipality approved the research protocol (protocol no. HB-2008-056 additional protocol). All participants gave informed consent before the study was commenced.

Subjects

We recruited ten female participants from Department of Human Nutrition, Faculty of Life Sciences, University of Copenhagen, Denmark by advertisement. The participants were apparently healthy as indicated by interview, non-smoking, not taking medication and without history of cardiovascular diseases. Baseline characteristics of study participants are presented in Table 1. The study participants were advised to consume low fat diet and refrained from alcohol intake the day proceeding the study day. All participants recorded their food intake the evening before blood samples were drawn. To ensure the participants consume the same meals for dinner the evening before each intervention day, they were instructed to record all foods eaten for dinner the night before the first test meal, and to eat the same the evening before the second meal.

Test Diet

The test meals contained 1 g of fat per kg body weight (mean 62 g). The study participants consumed a high fat meal which consisted of OL or CB with the following %E: fat 76, carbohydrate 21 and protein 3, respectively. The nutrient composition of both test meals is shown in Table 2. OL consisted mainly of oleic acid (73.3% wt), whereas both oleic acid (34.1% wt) and stearic acid (34.7% wt) were the major fatty acids composition in CB. The high-fat meals were prepared using instant mashed potatoes (Coop Danmark, Hadsten, Denmark). Each test

Table 1 Baseline characteristics of study participants ($n = 10$)

Variable	Value
Age (years)	38.2 ± 10.7 (25.0–64.0)
Body weight (kg)	61.8 ± 5.5 (55.1–73.0)
BMI (kg/m^2)	20.9 ± 1.3 (19.5–23.8)
Triacylglycerols (mmol/L)	0.70 ± 0.20 (0.33–0.89)
hsCRP (mg/L)	0.95 ± 0.24 (0.05–3.10)
IL-6 (mg/L)	0.81 ± 0.57 (0.29–1.43)

Values are means ± SD (range)

BMI body mass index, *hsCRP* high-sensitivity C-reactive protein, *IL-6* interleukin-6

Table 2 Nutrient composition of test diets

Nutrient	OL	CB
Calorie (MJ/100 g)	2.6	2.6
Carbohydrates (%E)	21.3	21.3
Protein (%E)	2.6	2.6
Fat (%E)	76.1	76.1
SFA	11.8	47.7
C16:0	9.0	20.2
C18:0	2.1	26.4
MUFA	56.5	26.1
C18:1	55.8	26.0
PUFA	7.8	2.3
C18:2	7.3	2.2
C18:3	0.5	0.1

OL olive oil, *CB* cocoa butter, *SFA* saturated fatty acids, *MUFA* monounsaturated fatty acids, *PUFA* polyunsaturated fatty acids

meal consisted of 1 g test fat and 1 g mashed potato powder per kg body weight of the participant and was mixed with 3 ml of boiling water per g of mashed potato powder. The average energy intake per test meal was 2.6 MJ with 76% E fat. For OL refined olive oil was provided by Karlshamns BV, Zaandijk, The Netherlands whereas for CB cacao butter was provided by Urtekram A/S International, Mariager, Denmark.

Blood Collection

We collected venous fasting blood into plain tubes in the morning at 8:00 a.m. and after 4 and 6 h after the test meal. The tubes were clotted for 30 min and centrifuged at 2,200×*g* for 15 min at 4 °C. Aliquots of serum were harvested and stored at −80 °C until analyses.

TAG, hsCRP

Serum TAG was analyzed using enzymatic procedure (ABX Pentra Triglycerides CP kit) on an ABX Pentra autoanalyzer, Horiba Group, France. We measured serum hsCRP concentrations according to the procedure of a high sensitivity latex-enhanced immunoturbidimetric assay (ABX Pentra CRP CP kit) using ABX Pentra autoanalyzer, Horiba Group, France. The intra assay CV for TAG was 3.1% ($n = 6$) and 5.0% ($n = 6$) for hsCRP.

IL-6

We measured IL-6 using an enzyme-linked immunosorbent assay (ELISA) kit (Quantikine HS6000, R&D System Europe). All samples were assayed in duplicate within a plate. A standard procedure of ELISA was performed according to manufacturers' instruction. Intra assay value was 5.3% ($n = 31$).

Statistics

Outcome variables were analyzed using mixed model ANCOVA and baseline values were used as covariates. Variables were set as fixed effect and participant ID was random effect. Data was log-transformed to obtain variance homogeneity. Descriptive data of baseline characteristics of study participants are presented as means ± SD (range), and other data are presented as mean ± SEM. All analyses were conducted using SAS 9.0, SAS Institute, Cary, NC, USA. Age, BMI and the order in which the participants received the test meals were tested for influence on the results, and were found to have no influence. hsCRP measurements from one participant after one test meal (cocoa butter) were excluded from the analyses due to increased hsCRP values which reflected a cold; this exclusion did not influence the results. Two values from one test meal (cocoa butter, 4 and 6 h) were not detectable. In regard to IL-6 data were log-transformed to obtain variance homogeneity. One observation was excluded from the analysis (6 h, olive oil) to obtain variance homogeneity; this exclusion did not change the results.

Results

No drop-out or non-compliance was reported. There was a significant increase in plasma TAG over time for both test meals ($P = 0.003$), but there was no difference in response between the two test meals ($P = 0.41$) (Fig. 1a). There was no significant difference between the effects of the two test meals ($P = 0.53$) on the postprandial hsCRP response (Fig. 1b). A significant difference in plasma IL-6 was found over time after both meals ($P < 0.001$), but there was no difference between the two test meals ($P = 0.19$) for IL-6 (Fig. 1c). Likewise, it was necessary to exclude one very high observation from the analysis (OL, 6 h) to obtain variance homogeneity. This did not change the overall results.

Discussion

Although the fatty meals induced a considerable increase in postprandial lipemia the pro-inflammatory marker hsCRP was not activated after either of the two test fats in our study. This agrees with findings by others, a single study with a mixture of SFA, MUFA and PUFA [17], with the effects in healthy participants in trials including fat loads either low or high in SFA [16, 18], together with a study

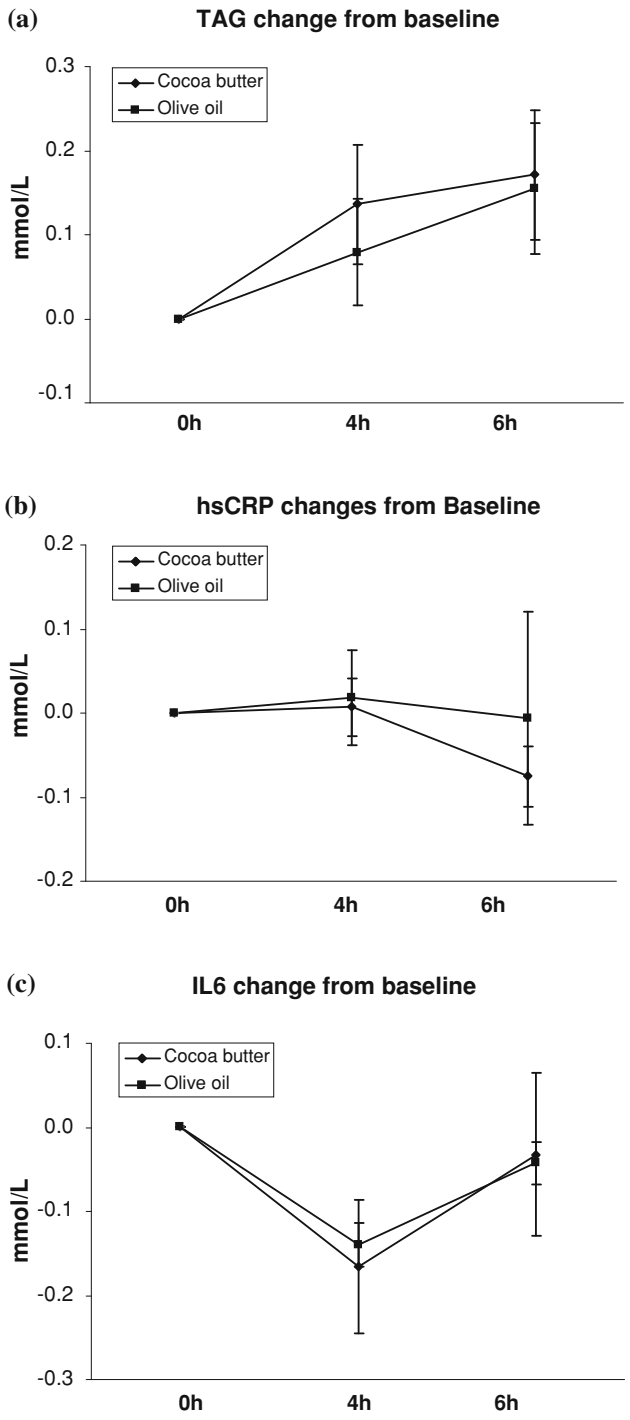

Fig. 1 Mean change of serum. **a** TAG, **b** hsCRP and **c** IL-6 from baseline ± SEM. Baseline values were included as covariates. **a** There was no difference in the effect of the test meals (Mixed model ANCOVA), but a significant increase was found over time for both test meals ($P = 0.003$), but there were difference between the two test meals ($P = 0.41$). **b** There were no significant difference between the effect of the two test meals ($P = 0.53$) on the postprandial hsCRP response. **c** A significant difference was found over time for both test meals ($P < 0.001$), but there were no difference between the two test meals ($P = 0.19$)

including participants with the metabolic syndrome in which ratio n-6/n-9 was modified [19]. Taken together results from these studies indicate that high fat meals irrespective of fatty acid composition do not increase postprandial hsCRP values.

With regard to IL-6 we observed a transient decrease after 4 h followed by an increase to postabsorptive values. The response pattern with a lack of increase in IL-6 over the day in our study is not in agreement with observations from other studies on fat load, which reported a postprandial increase in IL-6 in healthy individuals [13, 16, 18, 20–22]. It is noteworthy that also intake of carbohydrate was shown to increase IL-6 [21] and specifically potatoes raised IL-6 more compared to all bran meal [20]. In addition, there were no differences in the rate at which IL-6 concentrations increased after fatty meals compared with water [19]. Haack et al. [23] reported that diurnal variations of IL-6 levels may be confounded by blood drawing procedures. It is unknown why the postprandial response in IL-6 differed between our study and studies by others. We speculate, if the postprandial increase in IL-6 reported in more studies is due to diurnal variation, and that oleic acid (and stearic acid), the two dominating fatty acids of the test fats in our study, may have had a more neutral or even an attenuating role in regard to plasma IL-6. The cocoa butter meal contained 26.4% E as stearic acid, but also 20% E palmitic acid and 26% E oleic acid (Table 1). Since cocoa butter contains as much oleic acid as stearic acid, there is no objective reason to suppose that stearic acid in the cocoa butter meal could play the same neutral or attenuating role as that of oleic acid in the olive oil meal. Accordingly, it may be supposed that oleic acid at 26% E in the cocoa butter meal (only twice less compared to the olive oil meal) was sufficient by itself to prevent postprandial increases of inflammation markers. The two meals essentially differed by their ratio of total SFA to MUFA. A rationale for this idea is finding from in vitro studies. Thus, contrary to results from human intervention studies a different gene expression in pro-inflammatory markers after consumption of different dietary fat types was reported. Butter compared to olive oil and walnut increased postprandial mRNA expression of TNF-α and IL-6, in human coronary artery cells [15]. Another study reported an increased expression of inflammatory genes, TNF-α after butter compared to olive oil and vegetable/fish oil [14]. A recent in vitro study demonstrated that presence of as little as 1/10 ratio of oleic acid to that of stearic acid attenuates stearic acid-included pro-inflammatory responses in endothelial cells by reducing cellular stearic acid incorporation and NF-κB activation [24]. It is therefore, possible that a lack of differences between cocoa butter and refined olive oil on serum TG, IL-6 and hsCRP is mainly due to attenuation of stearic

acid-induced responses by the presence of substantial amounts of oleic acid in the cocoa butter. However, there is no previous evidence suggests that fatty acid quality affects postprandial IL-6 response or other inflammatory markers in human studies. In addition, although dietary fatty acid composition may regulate gene regulation to some extend, observed differences from in vitro studies may not be applicable to the in vivo situation.

We hypothesized that there would be an association between the postprandial lipemia and inflammatory markers, as suggested by others [21], however, we were not able to confirm this relation. This lack of association agrees with the results in healthy individuals [13], which did not demonstrate significant correlations between postprandial plasma TAG and IL-6, and CAMs. Based on our results and the results by others who included inflammatory markers as CAMs and TNF-α, we suggest that postprandial increase in plasma TAG may not be the only player during postprandial activation. Interestingly, the increased inflammatory activity reported induced by high fat meals was partly inhibited by antioxidant vitamins in one study [21], which may be due to some involvement of oxidative mechanism. Although there may be some affiliation the role of increased postprandial lipemia on pro-inflammatory activation is at the present not fully elucidated and lipemia may not be the main player in regard to inflammatory markers as agreed by others [16, 19].Taken together there are rather few studies on acute effect of dietary fatty acid composition on pro-inflammatory markers in humans, and although available data suggest that there may be some activation of fat load, this is not always the case. Moreover, this activation is not demonstrated to be dependent on fat quality in humans. More human intervention studies are needed to clarify a possible relation.

Conclusion

In our study, fat loads with cocoa butter high in stearic acid did not increase hsCRP and IL-6, both markers of inflammation compared to olive oil postprandially. There was no difference in postprandial response in plasma TAG and inflammatory markers after intake of cocoa butter and olive oil. In addition, we were not able to confirm any association between postprandial lipemia and markers of inflammation in healthy women. Overall, the study is an explorative pilot study which may inspire others to perform a larger study within this important research field. A larger sample size study may be warranted to observe a significant change in postprandial lipemia

Acknowledgments We thank our technician, Hanne Lysdal Petersen, from the Department of Human Nutrition, Faculty of Life Sciences, University of Copenhagen for technical assistance. The study was supported by Moth-Lunds Foundation, Denmark.

Conflict of interest The authors have declared no conflict of interest.

References

1. Bonanome A, Grundy SM (1988) Effect of dietary stearic acid on plasma cholesterol and lipoprotein levels. N Engl J Med 318(19):1244–1248
2. Mensink RP, Katan MB (1992) Effect of dietary fatty acids on serum lipids and lipoproteins. A meta-analysis of 27 trials. Arterioscler Thromb 12(8):911–919
3. Tholstrup T, Marckmann P, Jespersen J, Sandstrom B (1994) Fat high in stearic acid favorably affects blood lipids and factor VII coagulant activity in comparison with fats high in palmitic acid or high in myristic and lauric acids. Am J Clin Nutr 59(2):371–377
4. Tholstrup T, Miller GJ, Bysted A, Sandstrom B (2003) Effect of individual dietary fatty acids on postprandial activation of blood coagulation factor VII and fibrinolysis in healthy young men. Am J Clin Nutr 77(5):1125–1132
5. Tholstrup T, Sandstrom B, Bysted A, Holmer G (2001) Effect of 6 dietary fatty acids on the postprandial lipid profile, plasma fatty acids, lipoprotein lipase, and cholesterol ester transfer activities in healthy young men. Am J Clin Nutr 73(2):198–208
6. Aro A, Jauhiainen M, Partanen R, Salminen I, Mutanen M (1997) Stearic acid, trans fatty acids, and dairy fat: effects on serum and lipoprotein lipids, apolipoproteins, lipoprotein(a), and lipid transfer proteins in healthy subjects. Am J Clin Nutr 65(5):1419–1426
7. Bladbjerg EM, Marckmann P, Sandstrom B, Jespersen J (1994) Non-fasting factor VII coagulant activity (FVII:C) increased by high-fat diet. Thromb Haemost 71(6):755–758
8. Baer DJ, Judd JT, Clevidence BA, Tracy RP (2004) Dietary fatty acids affect plasma markers of inflammation in healthy men fed controlled diets: a randomized crossover study. Am J Clin Nutr 79(6):969–973
9. Danesh J, Collins R, Appleby P, Peto R (1998) Association of fibrinogen, C-reactive protein, albumin, or leukocyte count with coronary heart disease: meta-analyses of prospective studies. JAMA 279(18):1477–1482
10. Danesh J, Whincup P, Walker M, Lennon L, Thomson A, Appleby P et al (2000) Low grade inflammation and coronary heart disease: prospective study and updated meta-analyses. BMJ 321(7255):199–204
11. Libby P, Ridker PM (2004) Inflammation and atherosclerosis: role of C-reactive protein in risk assessment. Am J Med 116(Suppl 6A):9S–16S
12. Ridker PM, MacFadyen JG, Fonseca FA, Genest J, Gotto AM, Kastelein JJ et al (2009) Number needed to treat with rosuvastatin to prevent first cardiovascular events and death among men and women with low low-density lipoprotein cholesterol and elevated high-sensitivity C-reactive protein: justification for the use of statins in prevention: an intervention trial evaluating rosuvastatin (JUPITER). Circ Cardiovasc Qual Outcomes 2(6):616–623
13. Lundman P, Boquist S, Samnegard A, Bennermo M, Held C, Ericsson CG et al (2007) A high-fat meal is accompanied by increased plasma interleukin-6 concentrations. Nutr Metab Cardiovasc Dis 17(3):195–202
14. Bermudez B, Lopez S, Pacheco YM, Villar J, Muriana FJ, Hoheisel JD et al (2008) Influence of postprandial triglyceride-rich

lipoproteins on lipid-mediated gene expression in smooth muscle cells of the human coronary artery. Cardiovasc Res 79(2):294–303
15. Jimenez-Gomez Y, Lopez-Miranda J, Blanco-Colio LM, Marin C, Perez-Martinez P, Ruano J et al (2009) Olive oil and walnut breakfasts reduce the postprandial inflammatory response in mononuclear cells compared with a butter breakfast in healthy men. Atherosclerosis 204(2):e70–e76
16. Poppitt SD, Keogh GF, Lithander FE, Wang Y, Mulvey TB, Chan YK et al (2008) Postprandial response of adiponectin, interleukin-6, tumor necrosis factor-alpha, and C-reactive protein to a high-fat dietary load. Nutrition 24(4):322–329
17. Zahedi RG, Summers LK, Lumb P, Chik G, Crook MA (2001) The response of serum sialic acid and other acute phase reactants to an oral fat load in healthy humans. Eur J Intern Med 12(6):510–514
18. Dekker MJ, Wright AJ, Mazurak VC, Marangoni AG, Rush JW, Graham TE et al (2009) Fasting triacylglycerol status, but not polyunsaturated/saturated fatty acid ratio, influences the postprandial response to a series of oral fat tolerance tests. J Nutr Biochem 20(9):694–704
19. Tulk HM, Robinson LE (2009) Modifying the n-6/n-3 polyunsaturated fatty acid ratio of a high-saturated fat challenge does not acutely attenuate postprandial changes in inflammatory markers in men with metabolic syndrome. Metabolism 58(12):1709–1716
20. Manning PJ, Sutherland WH, McGrath MM, de Jong SA, Walker RJ, Williams MJ (2008) Postprandial cytokine concentrations and meal composition in obese and lean women. Obesity (Silver Spring) 16(9):2046–2052
21. Nappo F, Esposito K, Cioffi M, Giugliano G, Molinari AM, Paolisso G et al (2002) Postprandial endothelial activation in healthy subjects and in type 2 diabetic patients: role of fat and carbohydrate meals. J Am Coll Cardiol 39(7):1145–1150
22. Payette C, Blackburn P, Lamarche B, Tremblay A, Bergeron J, Lemieux I et al (2009) Sex differences in postprandial plasma tumor necrosis factor-alpha, interleukin-6, and C-reactive protein concentrations. Metabolism 58(11):1593–1601
23. Haack M, Kraus T, Schuld A, Dalal M, Koethe D, Pollmacher T (2002) Diurnal variations of interleukin-6 plasma levels are confounded by blood drawing procedures. Psychoneuroendocrinology 27(8):921–931
24. Harvey KA, Walker CL, Xu Z, Whitley P, Pavlina TM, Hise M et al (2010) Oleic acid inhibits stearic acid-induced inhibition of cell growth and pro-inflammatory responses in human aortic endothelial cells. J Lipid Res 51(12):3470–3480

Lipids (2011) 46:371–380
DOI 10.1007/s11745-011-3528-2

ORIGINAL ARTICLE

Modulation of Macrophage Fatty Acid Content and Composition by Exposure to Dyslipidemic Serum in Vitro

Bruce X. W. Wong · Reece A. Kyle · Kevin D. Croft · Carmel M. Quinn · Wendy Jessup · Bu B. Yeap

Received: 23 July 2010 / Accepted: 14 November 2010 / Published online: 1 February 2011

Abstract Macrophages in arterial walls accumulate lipids leading to the development of atherosclerotic plaques. However, mechanisms underlying macrophage lipid accumulation and foam cell formation are often studied without accounting for risk factors such as dyslipidemia. We investigated the effect of varying concentrations of triglyceride (TG) within physiological range on macrophage fatty acid (FA) accumulation and expression of cholesterol efflux proteins. Human monocytes were cultured in media supplemented with 10% sera containing low (0.7 mmol/L) to high (1.4 mmol/L) TG. The resulting macrophages were harvested after 10 days for analysis of FA content and composition and expression of genes involved in lipid metabolism. Exposure to higher TG and lower HDL concentrations in media increased macrophage lipid content. Macrophages exposed to higher TG had increased total FA content compared with controls (876 μg/mg protein vs. 652 μg/mg protein) and greater proportions of C16:0, C18:1 and C18:2. Macrophage expression of both ABCA1 and ABCG1 cholesterol efflux proteins were reduced when higher TG concentrations were present in the media. Expression of scavenger receptor CD36, involved in lipoprotein uptake, was also downregulated in macrophages exposed to higher TG. Culturing macrophages in conditions of higher versus lower TG influenced macrophage FA content and composition, and levels of regulatory proteins. Replicating in vitro levels of dyslipidemia encountered in vivo may provide an informative model for investigation of atherogenesis.

Keywords Dyslipidemia · Triglyceride · Macrophage · Fatty acids · Unsaturated fatty acids · Atherogenesis

Abbreviations

ABCA1	ATP-binding cassette transporter A1
ABCG1	ATP-binding cassette transporter G1
CD36	Cluster of differentiation 36
CLRP	Chylomicron remnant-like particles
CVD	Cardiovascular disease
FA	Fatty acid
FFP	Fresh frozen plasma
HDL	High density lipoprotein
hMDM	Human monocyte-derived macrophage
LDL	Low density lipoprotein
LPL	Lipoprotein lipase
LXR	Liver X receptor
PPARγ	Peroxisome proliferator-activated receptor gamma
SCD	Stearoyl-CoA desaturase
SR-A	Scavenger receptor A
TG	Triglyceride
VLDL	Very low density lipoprotein

B. X. W. Wong · R. A. Kyle · K. D. Croft · B. B. Yeap
School of Medicine and Pharmacology,
Fremantle and Royal Perth Hospitals,
University of Western Australia,
Perth, WA, Australia

C. M. Quinn · W. Jessup
Centre for Vascular Research, University of New South Wales,
Sydney, NSW, Australia

B. B. Yeap
Department of Endocrinology and Diabetes,
Fremantle Hospital, Fremantle, WA, Australia

B. B. Yeap (✉)
School of Medicine and Pharmacology, Fremantle Hospital,
Level 2, T-Block, Alma Street, Fremantle WA 6160, Australia
e-mail: byeap@cyllene.uwa.edu.au

Introduction

Atherosclerosis is the pathology underlying cardiovascular disease (CVD) and accounts for up to 50% of deaths in those with CVD [1]. A central step in atherogenesis occurs when monocytes adhere to endothelium and transmigrate into the subendothelial space where they differentiate into macrophages and express scavenger receptors CD36 and scavenger receptor-A (SR-A). These scavenger receptors take up lipids in the form of modified low-density lipoprotein (LDL) [2] and also regulate the uptake of free fatty acids (FA) [3]. Macrophage lipoprotein uptake is balanced by cholesterol efflux regulated by members of the ATP-binding cassette transporter family A1 and G1 (ABCA1 and ABCG1) [4]. Progression of foam cell formation to fatty streak and atherosclerotic plaque development reflects the cumulative effects of cholesterol and fatty acid accumulation from very low density lipoprotein (VLDL) and LDL uptake, balanced against anti-atherogenic cholesterol efflux into the reverse cholesterol pathway via apolipoprotein A-1 (apoA-1) and high-density lipoprotein (HDL) [4]. Hyperlipidemia especially hypercholesterolemia coupled with low HDL is a major risk factor for CVD [5]. Accumulating evidence suggests that elevated triglyceride (TG) levels are an independent risk factor for CVD [6]. However, the mechanisms by which hypertriglyceridemia increases development or progression of atherosclerosis are not fully understood.

Monocytic cell lines such as THP-1 and U937 which are differentiated into macrophages by the addition of phorbol 12-myristate 13-acetate provide a model of foam cell formation and lipid metabolism. However, they are not necessarily representative of the processes occurring in vivo [7, 8]. Human-derived macrophages (hMDMs) are more representative models, however, they tend to be cultured under generic conditions or with supplementation of modified LDL to supraphysiological levels to create a model of the diseased/pathological state [9, 10]. Data are lacking to demonstrate the effects of variation in lipid concentrations particularly TGs within the physiological range on mechanisms of macrophage lipid accumulation. To better understand how hypertriglyceridemia occurring might modulate macrophage lipid accumulation, we examined hMDMs grown in an environment which reflected varying degrees of hypertriglyceridemia encountered in vivo. We sought to test the hypothesis that subtle changes in TG levels would increase macrophage lipid accumulation altering FA content and composition and regulating proteins involved in both lipid uptake and cholesterol efflux.

Materials and Methods

Reagents

Chemicals and reagents used are listed below with the supplier. All solvents were high performance liquid chromatography grade (Mallinckrodt). Enhanced chemiluminescence (ECL) reagent; Full range Rainbow Molecular Weight Marker (GE healthcare, formerly Amersham Biosciences). RPMI 1640; L-glutamine; penicillin/streptomycin; phosphate buffered saline (PBS) (Invitrogen). Heptadecanoic acid and Nile red (SIGMA). Peroxisome proliferator-activated receptor γ (PPARγ) rabbit polyclonal antibody; SR-A; stearoyl-CoA desaturase (SCD) and beta-actin (goat polyclonal antibodies); RIPA lysis buffer (Santa Cruz). ABCA1; ABCG1; and CD36 (rabbit polyclonal antibody) (Novus Biologicals). Bio-Rad Protein Assay; bisacrylamide 30%; bovine serum albumin (BSA) (Bio-Rad). Aprotinin; Phenylmethylsulfonyl fluoride; FastStart SYBR Green Master mix (Roche Diagnostic). Glutaraldehyde; and analytical- or HPLC-grade solvents (Merck, formally BDH). TRIsure (Bioline).

Cell Culture and Serum Preparation

Human-derived macrophages were grown at 37 °C in a 5% CO_2 atmosphere. hMDMs were prepared from white buffy coat concentrates from healthy donors as described [11]. Briefly buffy coats obtained from the Australian Red Cross Blood Service (ARCBS) were diluted with PBS, layered over Ficoll-Paque and centrifuged for 30 min at 1,000×g at room temperature. The white blood cell layer was collected, pelleted at 700×g for 10 min at 4 °C, washed and re-suspended in RPMI media to allow purification of monocytes by adhesion. Monocytes at a concentration of 1.5×10^6 cells/mL were cultured in RPMI-1640 medium containing 10% (v/v) heat-inactivated whole human serum from healthy volunteers for 2 days. The cells were washed and incubated for a further 8 days in RPMI 1640 containing 10% (v/v) heat-inactivated pooled serum supplemented with penicillin/streptomycin 100 U/100 μg/mL and L-glutamine (2 mM) with replacement of media every 3 days. For experiments, serum was prepared using heat-inactivated pooled fresh frozen plasma (FFP) which was stood for 30 min and centrifuged at 16,000×g for 10 min before collection of the serum supernatant. The sera were pooled into four groups (A, B, C and D) according to varying TG, HDL and total cholesterol concentrations (Table 1). FFP was kindly provided by Transfusion Medicine, Fremantle Hospital. The protocol was approved by the South Metropolitan Area Health Service Human Research Ethics Committee.

Table 1 Biochemical analysis of pooled-sera with varying TG, HDL and cholesterol concentrations, termed A, B, C and D

	A	B	C	D
Triglyceride (mmol/L)	0.75	0.85	1.05	1.4
Cholesterol (mmol/L)	4.8	4.3	3.35	3.15
HDL (mmol/L)	1.2	0.9	1.15	0.8
LDL (mmol/L)	3.26	3.02	1.72	1.71

Monocytes were differentiated into macrophages in culture media containing 10% normal human sera for 2 days followed by culturing in media containing 10% sera of either A, B, C and D for a further 8 days. Pooled-sera A represented a control lipid profile, B, C and D represented profiles with higher TG and lower HDL levels

Nile Red Staining and Visualization of Lipids

Nile red stains neutral lipids such as TG and cholesterol esters and can be visualized with fluorescence microscopy. After 8 days incubation in experimental media, hMDMs were washed with PBS. Glutaraldehyde (1.5%) was added to each well and left to incubate at 4 °C for 5 min to fix cells. The wells were washed several times with PBS before Nile red in PBS (100 ng/mL) was added to each well and left to incubate at room temperature for 5 min. The cells were washed with PBS before visualization under fluorescence microscopy at yellow gold fluorescence (excitation 450–500 nm, emission >528 nm).

Fatty Acid Extraction and Gas Chromatography

On day 10 of culture, total FA content and FA composition for both media and hMDMs were extracted and measured by gas chromatography (GC) as previously described [11]. Samples were analyzed in a gas chromatograph (Hewlett Packard 5890) using a 25 cm BPX70 capillary column (SGE Scientific) of 0.35 mm internal diameter. The FA quantified were C16:0, C18:0, C18:1, C18:2 and C20:4. As SCD converts stearic acid (C18:0) to oleic acid (C18:1), the ratio of C18:1 to C18:0, known as the desaturation index, was calculated as an indicator of macrophage SCD activity where an increased ratio would indicate increased activity [12].

Biochemical Analysis

Fasting glucose, serum total cholesterol (TC), HDL-cholesterol and TGs were measured using the Cobas Integra 800 analyser (Roche Diagnostics, Australia) following assay methodologies previously described [11]. LDL-cholesterol levels were calculated using the formula LDL = TC – HDL − (TG/2.22) [13].

Macrophage RNA Extraction

Total RNA was isolated on day 10 of culture using TRIsure reagent, according to the manufacture's instructions. RNA samples were treated with DNase I (DNA-*free*™ Kit; Ambion, Inc.) and stored at −80 °C. The quantity and quality of RNA was determined on a NanoDrop 1000 Spectrophotometer (Thermo Fisher Scientific).

Reverse Transcription and Quantitative Real Time-PCR

First strand cDNA was synthesised from 1 μg of total RNA using oligo(dT)$_{20}$ primers with the SuperScript™ III First-Strand Synthesis System for RT-PCR (Invitrogen). Quantitative real time-PCR was performed on the Corbette Rotorgene system (Rotorgene Research, Australia). Each 20 μl PCR reaction amplified 1 μl of cDNA using FastStart SYBR Green Master mix and gene-specific primers. The sequences of the primers used were as follows: ABCA1: 5′-AGACGC AACACAAA AGTGG-3′ and 5′-TGG GTAGCTCAGCCGAACAG-3′, ABCG1: 5′-GAGGGATT TGGGTCTGAAC-3′ and 5′-GCAGCCTTCCATGGAC GA-3′, SCD: 5′-ATGCCG GCCCACTTGCTG-3′ and 5′-CGAATGTCGTCTTCCAAG-3′, CD36: 5′-CTGGGG CTGTCATTGGTG-3′ and 5′-TGTGGATTTTGCACAT CA-3′, LPL: 5′-GAGCCAA AAGAAGCAGCAAAA-3′ and 5′-CCACGGTGCCATACAGA G-3′, LXRα: 5′-CC CTGTGCCTGACATTCC-3′ and 5′-AGCAGGGCTGTG GGCTCT-3′, PPARγ: 5′-TCT CTCCGTAATGGAAGA CC-3′ and 5′-GCATTATGAGACAT CCCCAC-3′ and β-actin: 5′-CTGGCACCACA CCTTCTA-3′, and 5′-GGT GGT G AAGCTGTAGCC-3′. Standard curves were created using serial dilutions of reference plasmids containing full-length cDNA transcripts of ABCG1 (pcDNA4/*myc*-His.hABCG1 kindly provided by Dr. I Gelissen, University of New South Wales, Australia), PPARγ (pCR3.1.hPPARγ1 kindly provided by Prof. B Spiegelman, Dana-Farber Cancer Institute, Boston) and β-actin (pMET-mβ-actin kindly provided by Dr. S Busfield, University of Western Australia, Australia) or partial cDNA transcripts of ABCA1, SCD, CD36 (cloned into the pCRII-TOPO vector, Invitrogen) and LPL mRNAs (cloned into the pGEM—T Easy vector, Promega). Melting point analysis and ethidium bromide-stained gel electrophoresis were performed to confirm PCR product purity and size.

Western Analysis

On day 10 hMDMs were lysed in a buffer containing 50 mM Tris pH 7.4, 2% SDS, 5 mM EDTA, 1 mM DTT, 2 μg/ml aprotinin and 0.5 mM phenylmethylsulfonyl-fluoride, incubated on ice for 1 h, centrifuged at 14,000 rpm

for 10 min at 4 °C and stored in aliquots at −80 °C. Protein concentration was quantified using BCA protein assay kit (Pierce) and measuring absorbance at 580 nm. SDS-PAGE was performed using 50 μg of protein lysate per lane followed by semi-dry blot transfer. Membranes were blocked with 5% skim milk powder in TBS-T (20 mM Tris pH 7.4, 150 mM NaCl, 0.1% Tween-20) before sequential incubations with antibodies to detect CD36, SCD, ABCA1 and ABCG1. Actin was used as a loading control. ECL was performed with GE Healthcare ECL Western blotting detection reagents according to the manufacturer's protocol.

Statistical Analysis

Data are presented as either means ± standard deviation (SD) or means ± standard error of the means (SEM) of means from multiple independent experiments. Analysis was performed using one-way ANOVA. A two-tailed p value of <0.05 was considered significant.

Results

Lipid Content and Composition of Sera and Media

Eight units of FFP were processed and pooled into four sera conditions (A, B, C and D) with varying TG, HDL and cholesterol levels (Table 1). Conditions A to D were arranged according to increasing concentrations of TG (0.74–1.39 mmol/L), decreasing levels of HDL (1.2–0.8 mmol/L) and decreasing levels of cholesterol (4.79–3.14 mmol/L). The media used to culture hMDMs was supplemented with 10% of the pooled sera for each condition A–D. There were no significant differences in total FA content of the media between each of the conditions A–D (Fig. 1i). The media contained more saturated FAs than monounsaturated, and polyunsaturated FAs (Fig. 1ii). Media from condition D had less palmitic acid (C16:0) than media from condition A (117 ± 10 vs. 131 ± 5 ng/μg media, $p = 0.008$) (Fig. 1ii). Media from condition B had more stearic acid (C18:0) than media from condition A (109 ± 11 vs. 94 ± 8 ng/μg media,

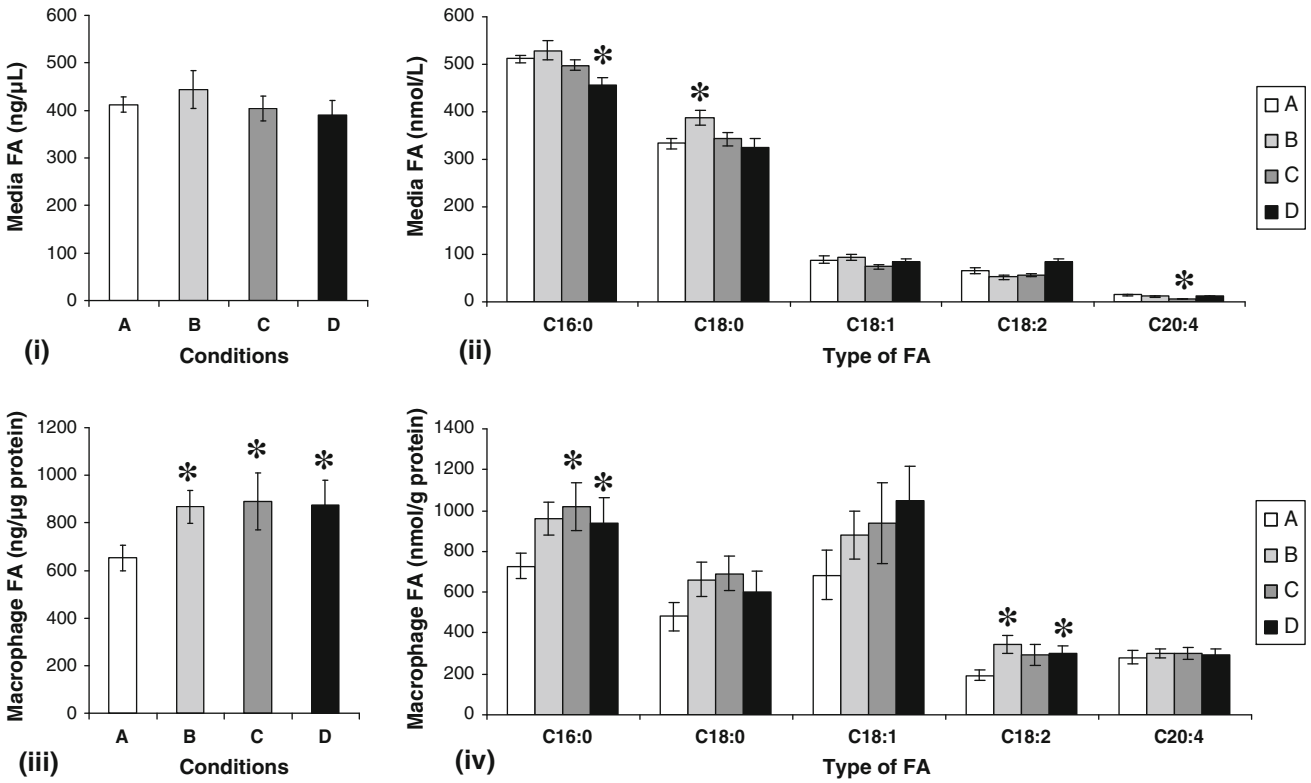

Fig. 1 Macrophages were cultured in media with 10% of sera A (*white bar*), B (*light grey bar*), C (*dark grey bar*) and D (*black bar*) and FA extraction performed on day 10. **i** and **iii**; total fatty acid content of media and cells, respectively. **ii** and **iv**; specific fatty acid composition of media and cells, respectively. Results for media are expressed in ng total FA content/μL media or nmol/L of individual FA and shown as mean ± SD of three independent experiments done in duplicates. Results for hMDM are expressed in ng total FA content/μg protein or nmol of individual FA/μg protein and shown as mean ± SE of five independent experiments done in triplicates. FA, fatty acids; C16:0, palmitic acid; C18:0, stearic acid; C18:1, oleic acid, C18:2; linoleic acid; C20:4, arachidonic acid. One-way ANOVA versus condition A; *$p < 0.05$

$p = 0.017$) (Fig. 1ii). Media from condition C had less arachidonic acid (C20:4) than media from condition A (2.2 ± 0.4 vs. 4.3 ± 0.9 ng/μg media, $p = 0.003$) (Fig. 1ii).

Effect of Dyslipidemia on Macrophage Lipid and Fatty Acid Content

During the period of culture in vitro, monocytes became adherent, increased in size and changed shape from being spheroid to being flatter with some macrophages being round and some being spindle-shaped in tissue culture. To test monocyte differentiation into macrophages, cells were incubated with latex bead particles and phagocytosis of latex beads occurred consistent with macrophage function (Fig. 2i). Macrophages also consistently showed strong CD68 immunostaining after 10–14 days of culture (Fig. 2ii, iii). Macrophages were cultured with the four pooled sera (A–D) with varying TG, HDL and cholesterol levels, and stained with nile red on day 10 or after 8 days in experimental media. Macrophages cultured in conditions B, C and D stained more intensely than controls A indicating more lipid accumulation (Fig. 2a–d). Macrophages grown in the four conditions were harvested and total FA content assayed via GC for quantitative analysis (Fig. 1iii, iv). Total fatty acid content was increased in macrophages grown in conditions B, C, D compared to A with D containing significantly more FAs compared to A (876 ± 102 vs. 652 ± 55 ng/μg protein, $p = 0.02$, respectively) (Fig. 1iii).

Effect of Dyslipidemia on Macrophage Fatty Acid Composition

Human-derived macrophages had a different FA profile to the media in which they were cultured in. Compared to the media, hMDMs had proportionately more monounsaturated and polyunsaturated FAs (Fig. 1ii vs.iv). The increase in total FA content in hMDMs cultured in conditions B, C and D was evident in the increase of individual FA C16:0, C18:0, oleic (C18:1) and C18:2 compared to hMDMs cultured in condition A (Fig. 1iv). The amount of C16:0 in hMDMs cultured in conditions C and D was significantly higher than hMDMs cultured in condition A (261 ± 30 and 240 ± 33 vs. 186 ± 16 ng/μg protein, $p = 0.04$ and 0.03,

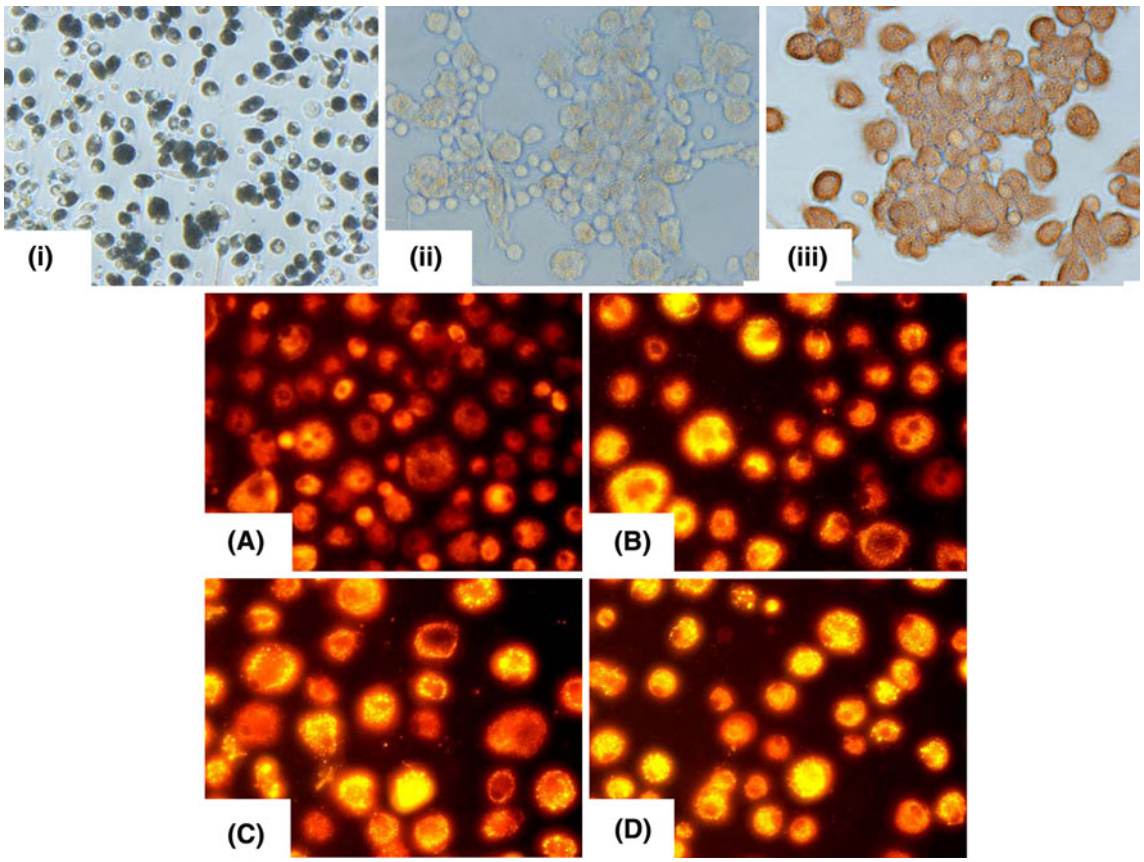

Fig. 2 Macrophages exhibited phagocytosis of latex beads (**i**) and immunostaining for negative control (**ii**) or the macrophage marker CD68 (**iii**). Macrophages were grown in media conditions A, B, C and D with varying concentrations of TG and HDL, and were stained with Nile red on day 10 to demonstrate differences lipid content (**a–d**)

respectively) (Fig. 1iv). There was a trend for the amounts of C18:0 and C18:1 in hMDMs grown in conditions B, C, and D to be higher than A (Fig. 1iv). The amount of C18:2 in macrophages grown in conditions B, C and D were higher than A, however, only conditions B and D were significantly increased compared to A (97 ± 12 and 83 ± 11 vs. 53 ± 7 ng/μg protein, $p = 0.03$ and 0.005, respectively) (Fig. 1iv). All conditions contained similar amounts of C20:4 (arachidonic acid) (Fig. 1iv).

Increased Ratio of C18:1 to C 18:0 FAs in Macrophages Exposed to Elevated TG

As SCD converts stearic acid (C18:0) to oleic acid (C18:1), the ratio of C18:1 to C18:0 was calculated as an indicator of macrophage SCD activity where an increased ratio would suggest increased activity [12]. There was no significant change in the ratio of C18:1/18:0 in media, however, the ratio of C18:1/18:0 was significantly increased in macrophages grown in condition D compared to A (0.74 ± 0.11 vs. 0.60 ± 0.10, $p = 0.004$).

Gene Expression in Macrophages Exposed to Varying TG Levels

RNA extracted from hMDMs cultured in conditions A–D was analysed using reverse transcription and real-time PCR (Table 2). mRNA levels were normalized to β-actin and expressed as a ratio relative to condition A. ABCA1, ABCG1, SCD and CD36 mRNA levels in hMDMs cultured in conditions B, C and D were found to be significantly reduced compared to condition A (Table 2). LXRα and PPARγ mRNA levels in hMDMs cultured in conditions C and D were significantly reduced compared to condition A (Table 2). There were no significant changes in LPL mRNA levels in hMDMs cultured in conditions A–D (Table 2).

Table 2 Expression ABCA1, ABCG1, SCD, CD36 LXRα, PPARγ and LPL in hMDMs cultured for 2 days in media with 10% normal human sera and a further 8 days in media supplemented with 10% sera A–D

	A	B	C	D
ABCA1	1.00 ± 0.06	0.73 ± 0.04*	0.48 ± 0.02*	0.44 ± 0.04*
ABCG1	1.00 ± 0.09	0.37 ± 0.04*	0.13 ± 0.01*	0.21 ± 0.02*
SCD	1.00 ± 0.04	0.60 ± 0.08*	0.48 ± 0.09*	0.63 ± 0.13*
CD36	1.00 ± 0.04	0.73 ± 0.03*	0.73 ± 0.02*	0.71 ± 0.01*
LXRα	1.00 ± 0.05	0.97 ± 0.04	0.76 ± 0.04*	0.78 ± 0.02*
PPARγ	1.00 ± 0.02	0.93 ± 0.08	0.75 ± 0.03*	0.78 ± 0.03*
LPL	1.00 ± 0.03	0.98 ± 0.08	1.01 ± 0.03	0.95 ± 0.05

mRNA expression was analysed by reverse transcription and real-time PCR. β-actin was used as a loading control and results were normalized to control A = 1.0. Results are expressed as mean ± SE of 2 independent experiments performed in triplicates. One-way ANOVA versus condition A; *$p < 0.05$

Protein extracted from macrophages cultured in conditions A to D were analyzed using Western analysis. Both representative blots as well as quantitative data from replicate experiments of ABCA1, ABCG1, SCD and CD36 proteins are shown in Fig. 3. Protein levels were normalized to actin and expressed as a ratio relative to condition A. ABCA1 protein was significantly decreased in conditions B and C compared to conditions A (0.45 ± 0.07 and 0.35 ± 0.12 vs. 1.0 ± 0.23, $p = 0.04$ and 0.03, respectively) (Fig. 3). Protein levels of ABCG1 were reduced in conditions B, C and D compared to A (0.60 ± 0.10; 0.42 ± 0.05 and 0.55 ± 0.12 vs. 1.0 ± 0.04, $p = 0.004$; <0.001 and 0.005, respectively) (Fig. 3). There were no significant changes in macrophage SCD protein levels (Fig. 3). Protein levels of CD36 were significantly decreased in conditions B and C compared to A (0.54 ± 0.08 and 0.65 ± 0.07 vs. 1.0 ± 0.03, $p = 0.0002$ and 0.001, respectively).

Discussion

Cultured macrophages are an accepted model for elucidating cellular mechanisms relevant to atherosclerosis [9, 10], however, these models have not been used previously to evaluate contributions of subtle dyslipidemia to modulate foam cell formation. Our study addresses an important issue of whether or not exposure to varying levels of TG in culture media would alter the phenotype of macrophages in relation to lipid accumulation. We found that macrophages exposed to sera with higher levels of TG had increased lipid content and altered expression of regulatory proteins, both plausible mechanisms which could contribute to foam cell formation and hence atherogenesis and CVD in patients with hypertriglyceridemia. Of note, these phenotypic differences were observed in macrophages grown in media containing varying concentrations of TG. Levels of TG in the sera (A–D) were within the physiological range and were further diluted 1:10 in the culture media.

Higher TG concentrations in the experimental media resulted in macrophages with greater intracellular lipid content compared with macrophages exposed to lower levels of TG. We have previously shown that macrophages cultured in autologous serum from patients with type 2 diabetes and controls, had significant differences in FA composition [11]. In that study, serum levels of TC and HDL between control and diabetic men and women were comparable whereas TG concentrations of subjects with diabetes had almost twice that of controls. However, the limited amount of blood sampled from each individual restricted the number of macrophages that could be grown

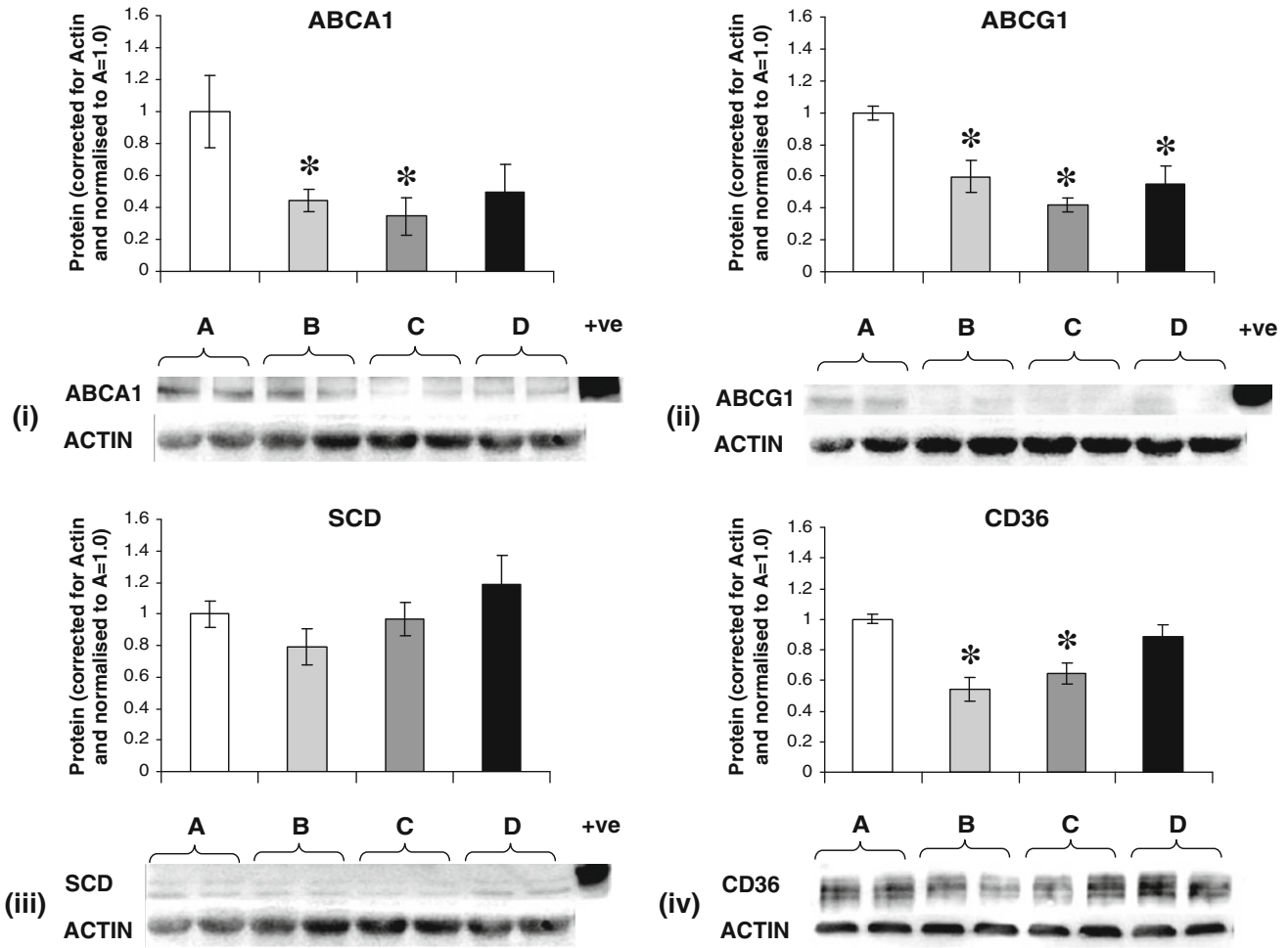

Fig. 3 Macrophages were grown for 2 days in 10% normal human serum 8 days in media supplemented with conditions A (*white bar*), B (*light grey bar*), C (*dark grey bar*) and D (*black bar*) before analysis. Protein lysates were analysed by Western blot and protein expression of ABCA1 (**i**), ABCG1 (**ii**), SCD (**iii**) and CD36 (**iv**) measured. hMDM treated with T0901317, which increases expression of ABCA1, ABCG1 and SCD was used as positive control. Results are shown as a representative blot from one experiment done in duplicates. β-actin was used as a loading control and results were normalized to control $A = 1.0$. Results were expressed as mean $\pm$ SD of three independent experiments performed in duplicates. One-way ANOVA versus condition A; $^{*}p < 0.05$

and hence the experimental work possible in that study. Furthermore, it was unclear whether the differences in macrophage FA composition were due to the origin of the macrophages from patients with and without diabetes or resulted from the differences in TG concentration in serum. By using a common source of monocytes, differentiating these cells over 2 days in the presence of normal human serum and exposing them to experimental sera from days 2 to 10, we found that relatively modest differences in TG concentrations in culture media resulted in significant changes in macrophage fatty acid composition and reduced expression of genes involved in lipid metabolism. Therefore, while the present study utilised pooled sera (A–D) for experiments rather than serum samples from multiple donors, advantages of this approach were that experimental conditions were constant, results were confirmed in multiple independent experiments each performed with replicates and characterization of the macrophage phenotype was more extensive, extending to analysis of FA content and composition, mRNA levels and protein levels via Western analysis. While the results are attributable to exposure to the different experimental sera, additional studies would be needed to confirm that sera from different individuals would yield similar results.

The role TG in CVD has been debated but higher TG is now accepted as a risk factor for coronary heart disease [6]. Increased plasma TG levels appear to increase risk of cardiovascular events independently of LDL concentrations [6, 14]. The effect of varying TG within serum in culture media to promote FA accumulation provides a mechanistic link between higher TG levels and atherosclerosis. The predominant class of lipoproteins in hypertriglyceridaemic serum is chylomicrons and VLDL which contains chylomicron remnant-like particles (CRLP).

CRLP are pro-atherogenic being able to induce macrophage to form foam cells without prior oxidation [15]. Therefore, our work is consistent with previous studies in which CRLP enriched with saturated and monounsaturated FA are taken up more rapidly by macrophages, resulting in greater lipid accumulation of saturated FA [16]. The findings that ABCA1 as well as ABCG1 mRNA and protein levels decreased are consistent with the observation of Moore et al. [17] in which lipid accumulated after exposure of macrophages to CRLP is resistant to efflux. Of note, total FA content in the various media was stable even though the TG levels varied. This is likely due to the fact that cholesterol level (mainly cholesterol esters) was lower in the group with higher TG as was HDL which contains substantial amounts of FA in the form of phospholipids and diacylglycerol.

Compositional analysis of FA revealed that hMDMs cultured in the presence of sera with higher TG had more C16:0 and to a certain extent more C18:0 than those with low TG. These differences are of interest given the range of cellular and metabolic functions which are influenced by saturated FA (for review, see [18]). Reverse cholesterol transport (RCT) is believed to be the primary mechanism by which HDL and its major protein apoA-I protect against atherosclerosis [4]. While all cells are capable of effluxing cholesterol, cholesterol efflux from macrophages critical step of RCT [4]. ABCA1 and ABCG1 mediate the transport of cholesterol and phospholipids from macrophages to apoA-1 and eventually HDL in the reverse cholesterol pathway. Unsaturated FA palmitoleate, oleate, linoleate, and arachidonate but not the saturated FA palmitate and stearate decrease ABCA1 expression in cells by increasing its protein degradation rate [19]. Furthermore, these unsaturated FA were shown to accelerate ABCA1 protein turnover through phospholipase D2 pathway, increased protein kinase C activity and the phosphorylation of ABCA1 serine residues [20]. We found that exposure to media with higher TG decreased macrophage ABCA1 and ABCG1 at both mRNA and protein levels. Therefore, destabilization of macrophage ABCA1 or ABCG1 protein by FA is not the sole mechanism by which cholesterol efflux pathways are downregulated.

CD36 belongs to the class B scavenger receptor family and is an integral membrane protein found on the surface of macrophages. In macrophages, CD36 binds oxidized LDL, native lipoproteins, oxidized phospholipids [21] and long-chain FA [3]. CD36 expression on macrophages is regulated by different molecules in vivo and in vitro. It is positively regulated by transcriptional factors such as PPARγ ligands [22], cytokines such as macrophage stimulating factor [23] and interleukin 4 [23], as well as lipid and lipid components such as cellular cholesterol, oxidized and modified LDL [24], and unsaturated FA (oleic, linoleic, eicosapentaenoic and docosahexaenoic acids) [25]. It is negatively regulated in response to cholesterol efflux [26], interferon-γ [27], transforming growth factor-β1 (TGF-β1) and TGF-β2 [28]. CD36 mRNA levels were lower in macrophages in B, C and D. In line with this CD36 protein levels were lower in B and C. These findings suggest that moderate variations in TG levels in culture media may affect macrophage expression of receptors involved in lipoprotein uptake as well as proteins involved in cholesterol efflux. Therefore, the observed increase in macrophage lipid content and composition could be due to reduced efflux or to uptake by other scavenger receptors [29].

Stearoyl-CoA desaturase catalyzes the critical committed step in the biosynthesis of monounsaturated FA from saturated FA [18]. This reaction involves the introduction of the cis- double bond in between carbons 9 and 10 of palmitoyl-CoA and stearoyl-CoA, which are converted into palmitoleoyl-CoA and oleoyl-CoA, respectively [30]. The roles of monounsaturated FA are diverse and crucial in living organisms. Oleic acid is found to be the major monounsaturated FA of membrane phospholipids, TG, cholesterol esters, wax esters and alkyl-1,2-diacylglycerol. A proper ratio of saturated to monounsaturated FAs contributes to membrane fluidity, while changes in cholesterol esters and TG affect lipoprotein metabolism [31]. Wang et al. [19] have shown that increasing SCD through LXR ligands destabilized ABCA1. We wanted to explore the possibility that with subtle variations in TG concentrations in the media would lead to increased SCD activity in our model of macrophage foam cell development leading to destabilization of ABCA1. We found that macrophages exposed to sera with the highest concentration of TG exhibited an elevated desaturation index suggesting an increase in SCD activity. However, protein quantification of SCD through Western analysis did not show any significant change in SCD protein levels. Therefore, as C16:0, C18:0 and C18:2 are increased, in addition to C18:1 in macrophages cultured in B, C and D, it appears that there is generalized increase in both saturated and unsaturated FA rather than a specific increase in conversion via SCD.

Whilst FA profiles were analysed for sera and macrophages, we did not analyse the FA composition of TG separately. The roles of saturated and polyunsaturated FA to influence phenotypes could be further explored, for instance they differentially modulate inflammatory responses in macrophages [32].

In our study, macrophages from the same source were cultured in media containing the various pooled sera, therefore the changes in FA accumulation and gene expression are attributable to the differences in the serum to which the macrophages were exposed during culture. We used pooled sera, instead of generic sera supplemented with chemically modified or supraphysiological levels of

lipoproteins. This approach provides an experimental model more closely reflecting physiological differences occurring in vivo. A limitation of this study is the fixed amount of pooled-serum A-D collected, all of which was used up during experimentation. While cholesterol content and efflux might have been informative, we did not have additional sera for further experiments. Macrophage cholesterol loading increases cholesterol efflux, partly via accumulation of oxysterols, which in turn activate LXR to increase expression of ABCA1 and ABCG1 [33, 34]. The reduced ABCA1 and ABCG1 mRNA and protein levels in macrophages under conditions C and D with lower LDL levels compared with A might reflect reduced macrophage cholesterol loading. However, macrophages in A and B were exposed to similar LDL levels but those in B had altered gene expression and increased lipid accumulation as a possible consequence of exposure to higher TG or lower HDL levels.

Compared with macrophages grown in A, those exposed to B, C and D had comparably increased lipid and FA accumulation and similar alterations in gene expression. Therefore, the altered macrophage phenotype appears to correspond more closely to higher TG and lower HDL-cholesterol levels rather than differences in total and LDL-cholesterol levels. Higher TG and lower HDL-cholesterol levels in the absence of grossly elevated LDL-cholesterol is characteristic of the metabolic syndrome or diabetic dyslipidemia [35]. In the Multi-Ethnic Study of Atherosclerosis, subjects with reduced HDL ($\leq$1.0 mmol/L in men, $\leq$1.3 mmol/L in women), LDL $<$4.1 mmol/L and TG $\geq$1.7 mmol/L represented 15% of the study population and had increased risk of prevalent coronary artery calcification [36]. Our results link dyslipidemia with altered macrophage phenotype favouring foam cell formation. However, further investigation is needed to clarify whether increased TG or reduced HDL is the primary factor underlying this association, and to clarify whether qualitative rather than quantitative alterations in LDL or HDL might play a role in this context [37].

Conclusions

Moderate variations in TG and cholesterol levels in culture media result in altered macrophage FA content and composition, and changes in the expression of proteins involved in cholesterol efflux and lipoprotein uptake. Hypertriglyceridemia may increase the risk of CVD via direct actions on macrophages favoring foam cell formation, thus leading to the development of atherosclerotic plaque. These findings indicate that replicating in vitro degrees of dyslipidemia encountered in vivo provides an informative model for investigation of atherogenesis.

Acknowledgments We thank Dr. Paul Chubb, Mary Anne Townsend and the staff of the Biochemistry Department and Specimen Reception Area, Fremantle Hospital and the staff of transfusion medicine, Fremantle Hospital for their assistance with this project. We thank the Australian Red Cross Blood Service for providing buffy coats for our experiments. This work was supported by research grants from the National Heart Foundation of Australia (G 07 P 3159), the Raine Medical Foundation of Western Australia, the University of Western Australia and the Fremantle Hospital Medical Research Foundation.

Conflicts of interest The authors have no conflicts of interest to disclose in relation to this work.

References

1. De Backer G, Ambrosioni E, Borch-Johnsen K, Brotons C, Cifkova R, Dallongeville J, Ebrahim S, Faergeman O, Graham I, Mancia G, Cats VM, Orth-Gomer K, Perk J, Pyorala K, Rodicio JL, Sans S, Sansoy V, Sechtem U, Silber S, Thomsen T, Wood D (2004) European guidelines on cardiovascular disease prevention in clinical practice. Atherosclerosis 173:381–391
2. Manning-Tobin JJ, Moore KJ, Seimon TA, Bell SA, Sharuk M, Alvarez-Leite JI, de Winther MP, Tabas I, Freeman MW (2009) Loss of SR-A and CD36 activity reduces atherosclerotic lesion complexity without abrogating foam cell formation in hyperlipidemic mice. Arterioscler Thromb Vasc Biol 29:19–26
3. Baillie AG, Coburn CT, Abumrad NA (1996) Reversible binding of long-chain fatty acids to purified FAT, the adipose CD36 homolog. J Membr Biol 153:75–81
4. Jessup W, Gelissen IC, Gaus K, Kritharides L (2006) Roles of ATP binding cassette transporters A1 and G1, scavenger receptor BI and membrane lipid domains in cholesterol export from macrophages. Curr Opin Lipidol 17:247–257
5. Ebrahim S, Papacosta O, Whincup P, Wannamethee G, Walker M, Nicolaides AN, Dhanjil S, Griffin M, Belcaro G, Rumley A, Lowe GD (1999) Carotid plaque, intima media thickness, cardiovascular risk factors, and prevalent cardiovascular disease in men and women: the British Regional Heart Study. Stroke 30: 841–850
6. Jacobson TA, Miller M, Schaefer EJ (2007) Hypertriglyceridemia and cardiovascular risk reduction. Clin Ther 29:763–777
7. Assmann A, Mohlig M, Osterhoff M, Pfeiffer AF, Spranger J (2008) Fatty acids differentially modify the expression of urokinase type plasminogen activator receptor in monocytes. Biochem Biophys Res Commun 376:196–199
8. Baird SK, Reid L, Hampton MB, Gieseg SP (2005) OxLDL induced cell death is inhibited by the macrophage synthesised pterin, 7,8-dihydroneopterin, in U937 cells but not THP-1 cells. Biochim Biophys Acta 1745:361–369
9. Gleissner CA, Sanders JM, Nadler J, Ley K (2008) Upregulation of aldose reductase during foam cell formation as possible link among diabetes, hyperlipidemia, and atherosclerosis. Arterioscler Thromb Vasc Biol 28:1137–1143
10. Sarov-Blat L, Kiss RS, Haidar B, Kavaslar N, Jaye M, Bertiaux M, Steplewski K, Hurle MR, Sprecher D, McPherson R, Marcel YL (2007) Predominance of a proinflammatory phenotype in monocyte-derived macrophages from subjects with low plasma HDL-cholesterol. Arterioscler Thromb Vasc Biol 27:1115–1122
11. Senanayake S, Brownrigg LM, Panicker V, Croft KD, Joyce DA, Steer JH, Puddey IB, Yeap BB (2007) Monocyte-derived macrophages from men and women with type 2 diabetes mellitus differ in fatty acid composition compared with non-diabetic controls. Diabetes Res Clin Pract 75:292–300

12. Attie AD, Krauss RM, Gray-Keller MP, Brownlie A, Miyazaki M, Kastelein JJ, Lusis AJ, Stalenhoef AF, Stoehr JP, Hayden MR, Ntambi JM (2002) Relationship between stearoyl-CoA desaturase activity and plasma triglycerides in human and mouse hypertriglyceridemia. J Lipid Res 43:1899–1907
13. Rifai N, Warnick GR (2006) Lipids, lipoproteins, apolipoproteins, and other cardiovascular risk factors. In: Burtis CA, Ashwood ER, Bruns DE (eds) Tietz Textbook of Clinical Chemistry and Molecular Diagnostics, 4th edn. Elsevier Saunders, St Louis, pp 903–981
14. Botham KM, Moore EH, De Pascale C, Bejta F (2007) The induction of macrophage foam cell formation by chylomicron remnants. Biochem Soc Trans 35:454–458
15. Batt KV, Patel L, Botham KM, Suckling KE (2004) Chylomicron remnants and oxidised low density lipoprotein have differential effects on the expression of mRNA for genes involved in human macrophage foam cell formation. J Mol Med 82:449–458
16. De Pascale C, Avella M, Perona JS, Ruiz-Gutierrez V, Wheeler-Jones CP, Botham KM (2006) Fatty acid composition of chylomicron remnant-like particles influences their uptake and induction of lipid accumulation in macrophages. FEBS J 273:5632–5640
17. Moore EH, Bejta F, Avella M, Suckling KE, Botham KM (2005) Efflux of lipid from macrophages after induction of lipid accumulation by chylomicron remnants. Biochim Biophys Acta 1735:20–29
18. Legrand P, Rioux V (2010) The complex and important cellular and metabolic functions of saturated fatty acids. Lipids 45:941–946
19. Wang Y, Kurdi-Haidar B, Oram JF (2004) LXR-mediated activation of macrophage stearoyl-CoA desaturase generates unsaturated fatty acids that destabilize ABCA1. J Lipid Res 45:972–980
20. Wang Y, Oram JF (2007) Unsaturated fatty acids phosphorylate and destabilize ABCA1 through a protein kinase C delta pathway. J Lipid Res 48:1062–1068
21. Podrez EA, Poliakov E, Shen Z, Zhang R, Deng Y, Sun M, Finton PJ, Shan L, Gugiu B, Fox PL, Hoff HF, Salomon RG, Hazen SL (2002) Identification of a novel family of oxidized phospholipids that serve as ligands for the macrophage scavenger receptor CD36. J Biol Chem 277:38503–38516
22. Tontonoz P, Nagy L, Alvarez JG, Thomazy VA, Evans RM (1998) PPARgamma promotes monocyte/macrophage differentiation and uptake of oxidized LDL. Cell 93:241–252
23. Yesner LM, Huh HY, Pearce SF, Silverstein RL (1996) Regulation of monocyte CD36 and thrombospondin-1 expression by soluble mediators. Arterioscler Thromb Vasc Biol 16:1019–1025
24. Han J, Hajjar DP, Febbraio M, Nicholson AC (1997) Native and modified low density lipoproteins increase the functional expression of the macrophage class B scavenger receptor, CD36. J Biol Chem 272:21654–21659
25. Vallve JC, Uliaque K, Girona J, Cabre A, Ribalta J, Heras M, Masana L (2002) Unsaturated fatty acids and their oxidation products stimulate CD36 gene expression in human macrophages. Atherosclerosis 164:45–56
26. Han J, Hajjar DP, Tauras JM, Nicholson AC (1999) Cellular cholesterol regulates expression of the macrophage type B scavenger receptor, CD36. J Lipid Res 40:830–838
27. Nakagawa T, Nozaki S, Nishida M, Yakub JM, Tomiyama Y, Nakata A, Matsumoto K, Funahashi T, Kameda-Takemura K, Kurata Y, Yamashita S, Matsuzawa Y (1998) Oxidized LDL increases and interferon-gamma decreases expression of CD36 in human monocyte-derived macrophages. Arterioscler Thromb Vasc Biol 18:1350–1357
28. Han J, Hajjar DP, Tauras JM, Feng J, Gotto AM Jr, Nicholson AC (2000) Transforming growth factor-beta1 (TGF-beta1) and TGF-beta2 decrease expression of CD36, the type B scavenger receptor, through mitogen-activated protein kinase phosphorylation of peroxisome proliferator-activated receptor-gamma. J Biol Chem 275:1241–1246
29. Kunjathoor VV, Febbraio M, Podrez EA, Moore KJ, Andersson L, Koehn S, Rhee JS, Silverstein R, Hoff HF, Freeman MW (2002) Scavenger receptors class A-I/II and CD36 are the principal receptors responsible for the uptake of modified low density lipoprotein leading to lipid loading in macrophages. J Biol Chem 277:49982–49988
30. Ntambi JM, Miyazaki M (2003) Recent insights into stearoyl-CoA desaturase-1. Curr Opin Lipidol 14:255–261
31. Graham A, Zammit VA, Brindley DN (1998) Fatty acid specificity for the synthesis of triacylglycerol and phosphatidylcholine and for the secretion of very-low-density lipoproteins and lysophosphatidylcholine by cultures of rat hepatocytes. Biochem J 249:727–733
32. de Lima-Salgado TM, Alba-Loureiro TC, do Nascimento CS, Nunes MT, Cuir R (2010) Molecular mechanisms by which saturated fatty acids modulate TNF-α expression in mouse macrophage lineage. Cell Biochem Biophys doi:10.1007/s12013-010-9117-9
33. Sankaranarayanan S, de la Llera-Moya M, Drazul-Schrader D, Asztalos BF, Weibel GL, Rothblat GH (2010) Importance of macrophage cholesterol content on the flux of cholesterol mass. J Lipid Res 51:3243–3249
34. Xu M, Zhou H, Tan KCB, Guo R, Shiu SWM, Wong Y (2009) ABCG1 mediated oxidised LDL-derived oxysterol efflux from macrophages. Biochm Biophys Res Commun 390:1349–1354
35. Mooradian AD (2009) Dyslipidemia in type 2 diabetes mellitus. Nat Clin Pract Endocrinol Metab 5:150–159
36. Paramsothy P, Knopp RH, Bertoni AG, Blumenthal RS, Wasserman BA, Tsai MY, Rue T, Wong ND, Heckbert SR (2010) Association of combinations of lipid parameters with carotid intima-media thickness and coronary artery calcium in the MESA (Multi-Ethnic Study of Atherosclerosis). J Am Coll Cardiol 56:1034–1041
37. Lagos KG, Filippatos TD, Tsimihodimos V, Gazi IF, Rizos C, Tselepis AD, Mikhailidis DP, Elisaf MS (2009) Alterations in the high density lipoprotein phenotype and HDL-associated enzymes in subjects with metabolic syndrome. Lipids 44:9–16

Lipids (2011) 46:381–388
DOI 10.1007/s11745-010-3516-y

ORIGINAL ARTICLE

Palm Olein and Olive Oil Cause a Higher Increase in Postprandial Lipemia Compared with Lard but Had No Effect on Plasma Glucose, Insulin and Adipocytokines

Kim-Tiu Teng · Gowri Nagapan · Hwee Ming Cheng · Kalanithi Nesaretnam

Received: 26 October 2010 / Accepted: 7 December 2010 / Published online: 1 January 2011

Abstract Postprandial lipemia impairs insulin sensitivity and triggers the pro-inflammatory state which may lead to the progression of cardiovascular diseases. A randomized, crossover single-blind study ($n = 10$ healthy men) was designed to compare the effects of a high-fat load (50 g fat), rich in palmitic acid from both plant (palm olein) or animal source (lard) versus an oleic acid-rich fat (virgin olive oil) on lipemia, plasma glucose, insulin and adipocytokines. Serum triacylglycerol (TAG) concentrations were significantly lower after the lard meal than after the olive oil and palm olein meals (meal effect $P = 0.003$; time effect $P < 0.001$). The greater reduction in the plasma non-esterified free fatty acids levels in the lard group compared to the olive oil meal was mirrored by the changes observed for serum TAG levels ($P < 0.05$). The magnitude of response for plasma glucose, insulin and adipocytokines [interleukin-6 (IL-6), tumor necrosis factor-α (TNF-α), interleukin-1β (IL-1β) and leptin] were not altered by the type of dietary fats. A significant difference in plasma IL-1β was found over time following the three high fat loads (time effect $P = 0.036$). The physical characteristics and changes in TAG structure of lard may contribute to the smaller increase in postprandial lipemia compared with palm olein. A high fat load but not the type of fats influences concentrations of plasma IL-1β over time but had no effect on other pro-inflammatory markers tested in the postprandial state.

Keywords Postprandial lipemia · Adipocytokines · Free fatty acids · Palmitic acid

Abbreviations

IL-1β	Interleukin-1β
IL-6	Interleukin-6
MUFA	Monounsaturated fatty acids
NEFA	Non-esterified free fatty acids
PUFA	Polyunsaturated fatty acids
SFA	Saturated fatty acids
TAG	Triacylglycerol
TNF-α	Tumor necrosis factor-α

Introduction

Extensive studies have demonstrated the effects of different types of dietary fats on postprandial lipemia [1–4]. The positional distribution of fatty acids in the triacylglycerol (TAG) structure is believed to affect lipid metabolism [5–7]. Fats from plant origin such as palm oil have palmitic acid distributed in the outer positions of the TAG molecule, namely *sn*-1 and *sn*-3 positions and oleic acid in the *sn*-2 position [8]. However, palmitic acid is found abundantly in the *sn*-2 position in fats with an animal origin, such as lard and human breast milk. Evidence from animal and human infant studies suggests that palmitic acid is better absorbed when found in the *sn*-2 position compared with the *sn*-1 and *sn*-3 positions and hence affects the metabolism of lipids [9]. Hence, it is noteworthy that dietary fats with similar

Supported by Malaysian Palm Oil Board, Malaysia.

K.-T. Teng (✉) · G. Nagapan · K. Nesaretnam
Food Technology and Nutrition Unit, Product Development and Advisory Services, Malaysian Palm Oil Board, 6 Persiaran Institusi, Bandar Baru Bangi, 43000 Kajang, Selangor, Malaysia
e-mail: kt.teng@gmail.com

K.-T. Teng · H. M. Cheng
Department of Physiology, Faculty of Medicine, University of Malaya, 50603 Kuala Lumpur, Malaysia

fatty acid composition may have different biochemical and physical characteristics dependent on their TAG structure which may influence the metabolism of lipids [9]. It has been well established that dietary oleic acid may be neutral to cardiovascular heart disease with regard to its plasma total cholesterol and LDL cholesterol-reducing effects. However, saturated fatty acids (SFA) such as palmitic acid are thought to be cholesterol-raising [10]. Palm olein with oleic acid almost exclusively in the *sn*-2 position may be less cholesterolemic compared to animal fat like lard.

A prolonged and elevated postprandial lipemic response is associated with an increased risk of cardiovascular diseases by a variety of mechanisms such as endothelial function [11], inflammation [12], insulin resistance [13] and oxidative stress [14]. A high fat load with different dietary fats acutely impairs plasma glucose and insulin levels in both healthy and diabetic subjects [13, 15]. Human clinical studies have demonstrated an inverse association between activation of pro-inflammatory cytokines and plasma insulin levels [16, 17]. Increased levels of adipocytokines such as interleukin-6 (IL-6), tumor necrosis factor-α (TNF-α), interleukin-1β (IL-1β) and leptin were reported in obese [18] and type 2 diabetes patients [19] after consuming a high fat meal. Earlier studies by our group [20] and others [21] reported that specific dietary fats with different fatty acid compositions alter plasma IL-6, TNF-α, E-selectin, and high sensitivity C-reactive protein (hsCRP) but the effect was not seen in the postprandial state [22].

Hence, given the fact that palm olein and lard have similar proportion of SFA and monounsaturated fatty acids (MUFA) content but differ in the structure of TAG and physical properties of fats, we hypothesized that these physical characteristics may determine the extent to which lard and palm olein affect postprandial lipemia. The current study sought to investigate the effects of two palmitic acid-rich fats, one from a plant source (palm olein) and one from an animal fat (lard) with similar SFA content but differing in physical characteristics and TAG structure versus oleic acid-rich fat (virgin olive oil) on postprandial changes in lipemia, plasma glucose, insulin and certain adipocytokines (IL-6, TNF-α, IL-1β and leptin). To the best of our knowledge, no study has been conducted to investigate the effect of a meal rich in palmitic acid from palm olein or lard compared to oleic acid on the pro-inflammatory cytokines and leptin in the postprandial state.

Methods

Subjects

Ten healthy male subjects aged 21.9 ± 0.7 years were recruited from the University Putra Malaysia student population. Exclusion criteria included history of cardiovascular disease, diabetes, body mass index (BMI) <18.5 or >30 kg/m^2, plasma cholesterol >5.2 mmol/L, TAG >1.7 mmol/L, hypertension, current use of medication and smoking. Fasting plasma lipid profile, body weight, blood pressure, blood cell count, liver function were confirmed to be within the prescribed limit as assessed by a physician. Baseline characteristics of study subjects are presented in Table 1.

Table 1 Baseline characteristics of study participants

Variables	Values
Male (*n*)	10
Age (years)	21.9 ± 0.7
BMI (kg/m^2)	21.0 ± 1.6
Systolic BP (mmHg)	126.8 ± 8.6
Diastolic BP (mmHg)	71.3 ± 4.9
Waist (cm)	79.5 ± 6.2
Total cholesterol (mmol/L)	4.8 ± 0.7
TAG (mmol/L)	0.9 ± 0.7
LDL cholesterol (mmol/L)	2.6 ± 0.8
HDL cholesterol (mmol/L)	1.6 ± 0.4
Glucose (mmol/L)	5.2 ± 0.5
Insulin (μIU/mL)	3.6 ± 1.6

Values are means with SD

BP blood pressure

Study Design

A randomized, single-blind, crossover postprandial study was conducted. Each study subject received three experimental meals separated by a minimum of 3-day wash out. Study subjects were provided with a standardized low fat dinner (mee soup, containing <10 g of fat) to consume as their evening meal the day preceding their postprandial day. The subjects were advised to refrain from consuming high fat foods, caffeinated drinks and alcohol. The subjects were asked to refrain from strenuous exercise before the study day. After an overnight fast, subjects reported to the study center at 07:30 morning. A venous blood sample was taken and the subjects consumed the test meals within 15 min. Further venous blood samples were obtained at 30 min, 1, 2, 3 and 4 h. During the postprandial period, subjects were asked to consume water at a regular interval throughout. The Medical Ethics Committee, University Malaya Medical Centre approved the study (Reference number 732.22). The study was conducted according to the guidelines laid down in the Declaration of Helsinki. The study was registered at ClinicalTrial.gov (NCT01124487). All subjects gave written informed consent before the study was commenced.

Test Meals

The test meal consisted of 60 g of mashed potatoes, 180 g of baked beans, 50 mL of skimmed milk, 200 mL of orange juice and 50 g of the test fat (virgin olive oil, palm olein or lard). The test meal was formulated to provide 683 kcal of which 7% of energy was protein, 33% of energy was carbohydrate and 60% of energy was fat. The nutrient composition of test meals is presented in Table 2. The olive oil-enriched diet consisted of 45% energy as MUFA, supplied by Unilever Bestfoods Italia s.r.l, Italy. Palm olein consisted of 24% of energy as SFA with 21% of energy from palmitic acid as provided by Wilmar International Limited, Singapore. Lard consisted of 29% of energy as SFA with 15% of energy from palmitic acid and 10% of energy from stearic acid (purchased from Sainsbury's, UK).

Blood Collection

Fasting venous blood samples of 20 mL were collected in vacutainers (Beckton Dickinson, UK). Serum samples for lipid analysis (TAG and total cholesterol) were collected in 10-mL plain tubes. Blood sample was allowed to clot for 30 min and centrifuged at 1,300*g* for 15 min at 4 °C. For plasma NEFA and pro-inflammatory markers, blood sample was collected into EDTA containing vacutainers and separated by centrifugation at 1,300*g* for 15 min at 4 °C. Blood sample for glucose analysis was collected into 4 mL fluoride oxalate tubes, and blood sample for insulin analysis was collected into 2 mL lithium heparin tubes, both were centrifuged at 1,300*g* for 15 min at 4 °C. Samples for all analyses were collected at hourly intervals. Samples for glucose and insulin were collected at 30 min, and then at hourly intervals after subjects had consumed the high fat meal. Aliquots of blood samples were harvested and stored at −80 °C until analysis.

Table 2 Nutrient composition of meals

	Olive oil	Palm olein	Lard
Calorie (kcal)	754	754	754
Energy (%)			
Carbohydrates	33	33	33
Protein	7	7	7
Fat	60	60	60
SFAs	9.2	23.5	28.5
C16:0	7.1	20.5	15.2
C18:0	1.7	2.2	10.2
MUFAs	44.6	27.7	27.8
C18:1	44.0	27.6	25.3
PUFAs	6.2	8.6	5.9
C18:2	5.6	8.4	5.5

Values are means of double determinations

TAG and Total Cholesterol

Serum TAG and total cholesterol were measured using enzymatic procedures (triglycerides GPO-PAP and cholesterol CHOD-PAP kits; Roche Diagnostics GmbH, Mannheim, USA). Both assays were analyzed using a Hitachi 902 analyzer, Roche Diagnostics GmbH, Germany. The intra-assay CV for TAG was 2.2% ($n = 5$) and 1.7% ($n = 5$) for total cholesterol.

Non-esterified Fatty Acids

Plasma NEFA were measured using non-esterified fatty acids detection 500 Point kit (Zen-Bio Inc., Research Triangle Park, NC, USA) according to standard procedures provided by manufacturer. All samples were assayed in duplicate within a plate. The intra-assay value was 2.8% ($n = 20$).

Plasma Glucose and Insulin

Plasma glucose (glucose GOD-PAP kit; Roche Diagnostics GmbH, Mannheim, USA) was analyzed using an enzymatic colorimetric assay procedure (Hitachi 902 analyzer, Roche Diagnostics GmbH, Germany). Insulin levels were measured using Immulite 1000 ver. 5.16, US (Immulite 1000 Insulin kit; Siemens Healthcare Diagnostics, Deerfield, USA). The intra-assay CV for glucose and insulin were 2.5% ($n = 8$) and 4.1% ($n = 9$), respectively.

IL-6, TNF-α, IL-1β and Leptin

Serum adipocytokines were analyzed using Procarta® Cytokine Assay kit, Panomics Inc., USA. The assays used the xMAP® technology with multi-analyte profiling beads to detect and quantify multiple protein targets simultaneously. The intra-assay values were 6.6% for IL-6 ($n = 20$), 3.0% for TNF-α ($n = 15$), 5.3% for IL-1β ($n = 20$) and 6.6% for leptin ($n = 20$).

Statistics

A sample size of ten subjects will have 80% power at $P = 0.05$ to detect a change of 0.28 mmol/L in plasma TAG concentrations from the baseline between groups. Outcome variables were analyzed using repeated measures ANOVA corrected with the baseline values. Descriptive data of baseline characteristics of study subjects are presented as means ± SD, and other data are presented as means ± 95% confidence interval. All analyses were

conducted using PASW statistics 18.0, Chicago, IL, USA and GraphPad Prism 5.03 for WINDOWS (GraphPad Software, San Diego, CA, USA). Incremental area under the curves (iAUC) were calculated using GraphPad Prism 5.03 using the trapezoid rule. Treatment and time were within-subject factors and age, BMI and the order in which the subjects received the test meals were between subject factors. Bonferroni adjustment was used for multiple comparisons.

Results

A total of 18 subjects were screened and 10 subjects fulfilled the inclusion criteria. All ten subjects completed the study. No drop-out or non-compliance was reported.

Postprandial Lipemia

Serum TAG concentrations were significantly lower after the lard-enriched meal than after the olive oil and palm olein meals (meal effect $P = 0.003$, Fig. 1a). The iAUC for serum TAG was 56 and 49% higher after the olive oil and palm olein meals than after the lard, respectively ($P < 0.05$, $P < 0.01$, respectively). Concentrations of TAG peaked at 3 h after the olive oil and palm olein meals but at 2 h after the lard-enriched meal (time effect $P < 0.001$). Plasma NEFA decreased after meal and displayed a transient increase after 1 h (time effect $P < 0.001$, Fig. 1b). Lard elicited a smaller increase in plasma NEFA at 2 h and 3 h (meal × time interaction, $P = 0.003$) as compared to olive oil ($P < 0.05$).

Postprandial Plasma Glucose and Insulin

There was a significant change in plasma glucose and insulin over time for the three meals ($P < 0.001$, for both meals; Fig. 2a, b, respectively), but there was no difference in response between the three meals. No differences in iAUC plasma insulin values were observed between the diets.

IL-6, TNF-α, IL-1β and Leptin

There was no significant difference between the effects of the three test meals on the postprandial plasma IL-6, TNF-α and leptin (Fig. 3a, b, d, respectively). There were also no significant changes over time for the markers measured. A significant difference in plasma IL-1β was found over time after the three meals ($P = 0.036$), but there was no difference between the meals (Fig. 3c).

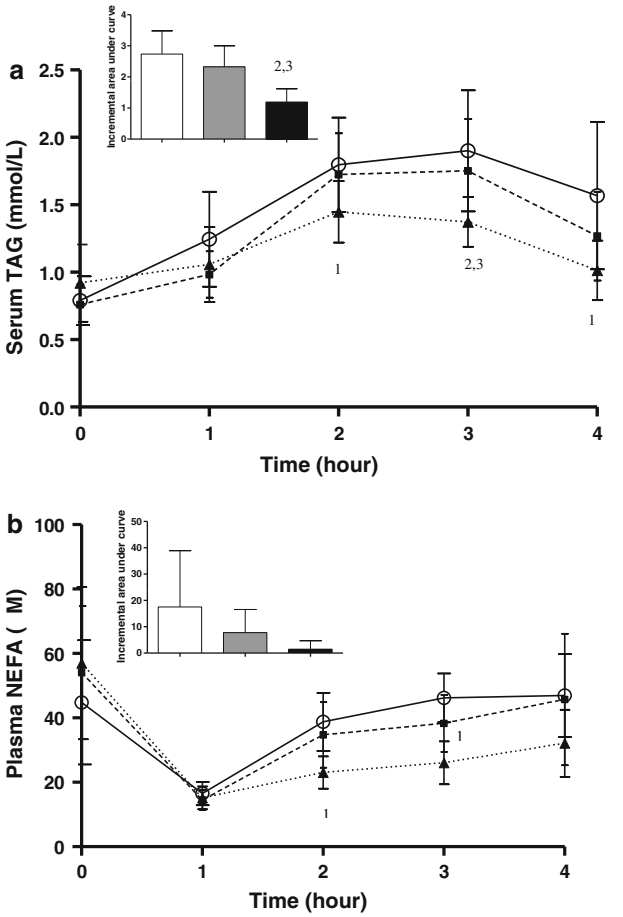

Fig. 1 Mean plasma **a** TAG and **b** NEFA concentrations and 95% CIs in healthy men ($n = 10$) after test meals containing 50 g test fat. Olive oil (*open circles*), palm olein (*filled squares*) and lard (*filled triangles*). Deviations from fasting values were analyzed by repeated measure ANOVA, with the three meals and time (0–4 h) as factors: **a** meal effect ($P = 0.003$), time effect ($P = 0.000$), and meal × time interaction ($P = 0.212$); **b** meal effect ($P = 0.072$), time effect ($P = 0.001$), and meal × time interaction ($P = 0.003$). Incremental area under the curve (0–4 h) values are inset and presented as mean and 95% CIs ($n = 10$) for olive oil (*open squares*), palm olein (*brackets*) and lard (*filled squares*). **a** *1* $P < 0.05$, significantly different from olive oil; *2* $P < 0.01$, significantly different from olive oil; *3* $P < 0.05$, significantly different from palm olein **b** *1* $P < 0.05$, significantly different from olive oil (Bonferroni multiple comparison test)

Discussion

The present study demonstrated that lard resulted in a lower postprandial TAG response in comparison with olive oil and palm olein. The lower postprandial level of lipemia following lard in the present study is in agreement with results reported from a previous study [23] comparing interesterified palm olein versus native palm olein but is not in accordance with other studies [5, 7]. The similar trend of increase over time for palm olein and olive oil concurs with findings from other studies [24, 25]. Rate of lipolysis and

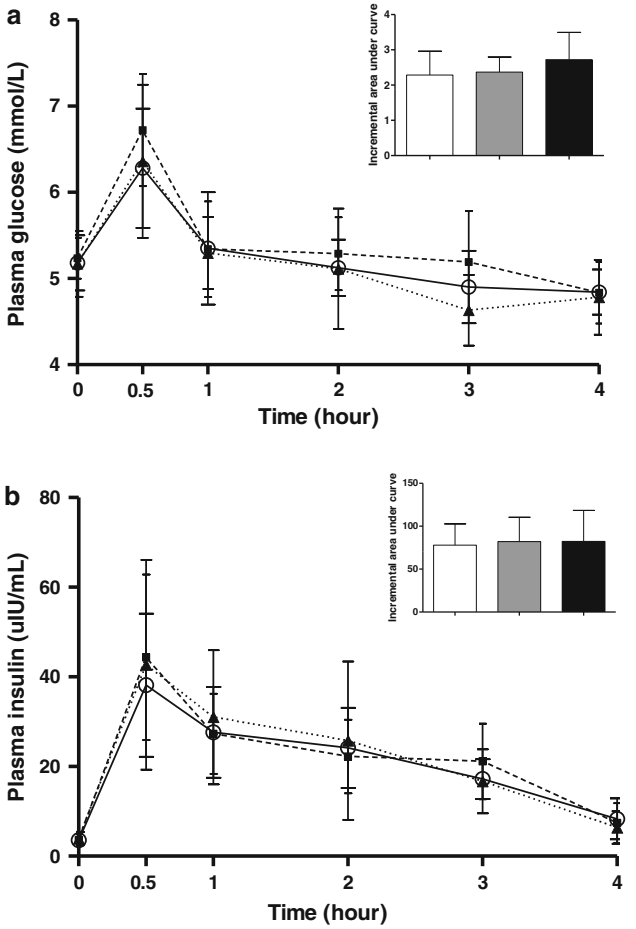

Fig. 2 Mean plasma **a** glucose and **b** insulin concentrations and 95% CIs in healthy men ($n = 10$) after test meals containing 50 g test fat. Olive oil (*open circles*), palm olein (*filled squares*) and lard (*filled triangles*). Deviations from fasting values were analyzed by repeated measure ANOVA, with the three meals and time (0–4 h) as factors: **a** meal effect ($P = 0.475$), time effect ($P = 0.000$), and meal × time interaction ($P = 0.719$); **b** meal effect ($P = 0.740$), time effect ($P = 0.000$), and meal × time interaction ($P = 0.711$). Incremental area under the curve (0–4 h) values are inset and presented as means and 95% CIs ($n = 10$) for olive oil (*open squares*), palm olein (*brackets*) and lard (*filled squares*); **a**, **b** no significant differences were observed

clearance of chylomicrons are unlikely contributed to the markedly lower response of lipemia after lard intake as a study has reported that lipoprotein lipase activity is similar following high fat loads with different types of fatty acid composition [25]. Although lard and palm olein have almost similar SFA content (24% in palm olein, 29% in lard), they differ significantly in the positional distribution of the fatty acids in the TAG molecule. Almost all of the palmitic acid in lard is present in the *sn*-2 position of TAG. Palm olein contains only 7–11% of palmitic acid in the *sn*-2 position, the predominant fatty acid in the *sn*-2 position is oleic acid (~70%). The position of fatty acids in the TAG molecule determines the physical properties of fat. Hence, it is probable that differences in the physical characteristics of fats and changes in TAG structure (for both lard and palm olein) may influence the level of postprandial lipaemia [9]. Lard which contains a higher proportion of solid fat at 37°C compared with olive oil and palm olein may be emulsified less readily and is less absorbed due to its higher melting point, resulting in a slower increase in serum TAG levels [1, 23].This finding would suggest that lard containing SFA in the *sn*-2 position might be cleared from the circulation slower than dietary fat containing SFA in the *sn*-1, 3 positions. This may lead to a more prolonged postprandial lipemia.

The greater reduction in the plasma NEFA levels after the lard meal compared to olive oil and palm olein was mirrored by the changes observed in serum TAG levels. In contrast with the current finding, previous studies have demonstrated that MUFA and polyunsaturated fatty acids (PUFA) suppressed plasma NEFA more than SFA [26, 27] and the increase in plasma NEFA following the initial suppression after a meal was markedly higher following a SFA-rich meal than MUFA, n-6 and n-3 PUFA [15]. However, a study reported that palmitic + myristic acid displayed higher and stearic acid lower in plasma NEFA levels in comparison with palmitic acid, MUFA and PUFA-rich high fat loads [25]. Taken together the results suggest that fatty acid composition per se influences plasma NEFA response in a different manner.

Several studies have demonstrated that dietary SFA impair postprandial glucose and insulin levels but the results are not consistent [13, 15, 23, 28]. The current study did not demonstrate any differences between the three meals on insulin and glucose levels over time. Direct examination in muscle cells in vitro indicates that SFA cause insulin resistance whereas unsaturated fatty acids improve insulin sensitivity [29]. However, observed differences from in vitro studies may not be applicable to the in vivo situation. The lack of significant response between meals could be partly explained by the relatively young and healthy individuals recruited in the present study. Obese subjects demonstrated exaggerated insulin responses compared with normal weight healthy individuals [30]. The single high fat load may not affect the changes in plasma glucose and insulin levels. Hence, a longer exposure of feeding may be needed to induce the changes by consuming high fat meals with different fatty acid composition. However, our results are in agreement with a large scale chronic study (RISCK study) comparing the consumption of SFA and MUFA which shows that SFA and MUFA show similar in insulin response [31]. Although the dietary fats in our study altered postprandial lipemia markedly, the magnitude of response in the pro-inflammatory cytokines, IL-6, TNF-α and IL-1β was not altered. This is in agreement with findings reported by other

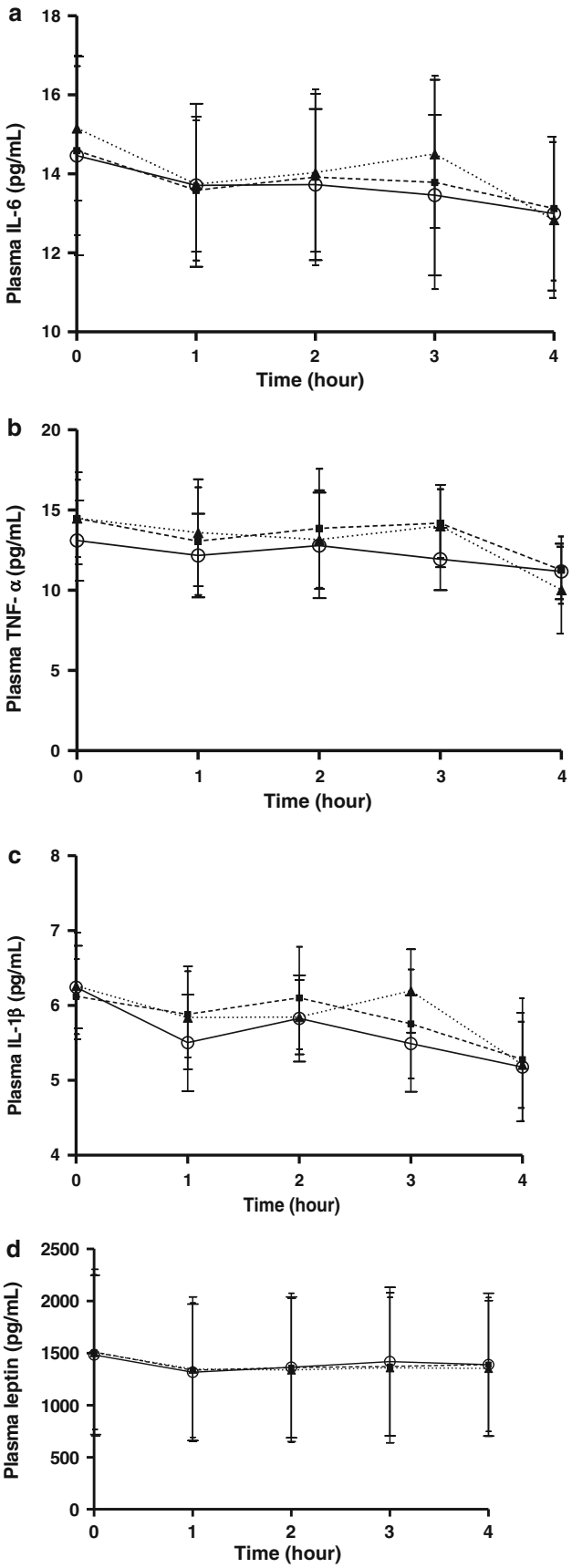

Fig. 3 Mean plasma **a** IL-6, **b** TNF-α, **c** IL-1β and **d** leptin ▶ concentrations and 95% CIs in healthy men ($n = 10$) after test meals containing 50 g test fat. Olive oil (*open circles*), palm olein (*filled squares*) and lard (*filled triangles*). Deviations from fasting values were analyzed by repeated measure ANOVA, with the three meals and time (0–4 h) as factors. **a**, **b**, **d** No significant differences were observed for meal, time and meal × time effects. **c** no significant differences were observed for meal and meal × time effects, but a significant time effect was observed ($P = 0.036$). Mean incremental area under the curve (0–4 h) values and 95% CIs were as follows: **a** olive oil (0.83; −0.14, 1.81), palm olein (0.47; −0.21, 1.14) and lard (0.23; −0.08, 0.53); **b** olive oil (12.6; −10.1, 35.2), palm olein (0.95; −0.40, 2.30) and lard (25.5; −29.8, 80.8); **c** olive oil (0.37; 0.05, 0.69), palm olein (0.65; 0.09, 1.20) and lard (0.57; 0.03, 1.11); **d** olive oil (175.0; −163.1, 513.2), palm olein (53.1; −4.98, 111.1) and lard (43.4; −7.69, 94.5); **a**–**d** no significant differences were observed

studies. In contrast with the present study, long term dietary intervention studies reported an increase in IL-6, E-selectin [21], hsCRP and IL-8 in healthy subjects after consuming a meal enriched with trans fatty acids in comparison with an oleic acid-enriched meal [20]. These findings suggest that a prolonged stimulation of an inflammatory state may be required in order to trigger a pro-inflammatory response in the body. Hence, repeated exposure to high fat diets may induce inflammatory activity in the body with regard to fatty acid composition per se. In regard to plasma IL-6 and TNF-α, the lack of increase over time in the present study is not in agreement with findings reported by other studies [18, 19, 32]. The lack of response might also be due to the relatively young and lean subjects who were recruited in the present study which may not trigger a significant response over time for plasma IL-6 and TNF-α. Overweight or obese subjects with increased adipose tissue are more vulnerable to enhanced pro-inflammatory cytokines increase after meals rich in fat load [18]. Excess adipose tissue may contribute to a substantially higher secretion of IL-6 and TNF-α as shown by other studies [18]. It is to be noted that the relatively small sample size may not produce significant differences between diets after a high fat load. The sample size was calculated based on the true difference of serum TAG on dietary treatments. A further study with a larger population may be needed to observe a significant change in plasma pro-inflammatory markers.

IL-1β, however, showed a significant change over time following the three high fat loads. The novel observation of a transient decrease at 1 h of plasma IL-1β concentrations in the present study is in accordance with an increase in the plasma insulin level at 1 h after the three meals. One likely explanation for this observation is that insulin activity is reported to possess anti-inflammatory and antioxidant properties [33] which may attenuate the pro-inflammatory response. The release of insulin is stimulated by IL-1β with the activation of protein kinase C and production of

diacylglycerol in an in vivo study [17]. With regard to this, IL-6 was also reported to enhance insulin-mediated glucose uptake [16]. IL-6 may directly affect insulin signalling by the induction of a suppressor of cytokine signalling-3 which inhibits insulin-dependent insulin receptor autophosphorylation.

The present study did not demonstrate that the activity of leptin is altered by high fat loads differing in fatty acid composition. This observation is in agreement with earlier findings [30, 34]. However, it is noteworthy that the postprandial leptin response is lower after a carbohydrate meal in obese women than in lean subjects, suggesting an impairment of postprandial leptin regulation in obese but not in lean subjects [30, 34]. This may explain the non-activated leptin levels in the present study. The evidence suggests that leptin, together with other adipocytokines (IL-6, TNF-α, IL-1β and other pro-inflammatory markers secreted from adipose tissue) and NEFA, displays a positive relationship with insulin resistance [35]. Leptin is thought to promote fatty acid oxidation and reduce ectopic fat accumulation in non-adipose tissues, thereby increasing insulin sensitivity which is probably mediated by the activation of 5′-AMP-activated protein kinase [36].

In conclusion, this study demonstrated that lard behaves differently from palm olein although both contain similar proportions of SFA in comparison with oleic acid-rich fat in postprandial lipemia. Positional distribution of fatty acids in the *sn*-2 position may play a role in postprandial lipemia. Palm olein and olive oil displayed similar effects on postprandial lipemia. There were no differences in plasma glucose, insulin and pro-inflammatory markers between the three meals suggesting that a high fat load but not fatty acid per se influences the trend of response of pro-inflammatory markers.

Acknowledgments We thank our colleagues, Fatmawati, Wong Weng Yew and Che Hui Ling from the Malaysian Palm Oil Board for technical assistance.

Conflict of interest There is no conflict of interest.

References

1. Berry SE, Miller GJ, Sanders TA (2007) The solid fat content of stearic acid-rich fats determines their postprandial effects. Am J Clin Nutr 85(6):1486–1494
2. Sanders TA, Berry SE, Miller GJ (2003) Influence of triacylglycerol structure on the postprandial response of factor VII to stearic acid-rich fats. Am J Clin Nutr 77(4):777–782
3. Tholstrup T, Marckmann P, Jespersen J, Vessby B, Jart A, Sandstrom B (1994) Effect on blood lipids, coagulation, and fibrinolysis of a fat high in myristic acid and a fat high in palmitic acid. Am J Clin Nutr 60(6):919–925
4. Tholstrup T, Miller GJ, Bysted A, Sandstrom B (2003) Effect of individual dietary fatty acids on postprandial activation of blood coagulation factor VII and fibrinolysis in healthy young men. Am J Clin Nutr 77(5):1125–1132
5. Yli-Jokipii KM, Schwab US, Tahvonen RL, Kurvinen JP, Mykkanen HM, Kallio HP (2002) Triacylglycerol molecular weight and to a lesser extent, fatty acid positional distribution, affect chylomicron triacylglycerol composition in women. J Nutr 132(5):924–929
6. Yli-Jokipii K, Kallio H, Schwab U, Mykkanen H, Kurvinen JP, Savolainen MJ et al (2001) Effects of palm oil and transesterified palm oil on chylomicron and VLDL triacylglycerol structures and postprandial lipid response. J Lipid Res 42(10):1618–1625
7. Cantwell MM, Flynn MA, Gibney MJ (2006) Acute postprandial effect of hydrogenated fish oil, palm oil and lard on plasma cholesterol, triacylglycerol and non-esterified fatty acid metabolism in normocholesterolaemic males. Br J Nutr 95(4):787–794
8. Renaud SC, Ruf JC, Petithory D (1995) The positional distribution of fatty acids in palm oil and lard influences their biologic effects in rats. J Nutr 125(2):229–237
9. Berry SE (2009) Triacylglycerol structure and interesterification of palmitic and stearic acid-rich fats: an overview and implications for cardiovascular disease. Nutr Res Rev 22(1):3–17
10. Mensink RP, Zock PL, Kester AD, Katan MB (2003) Effects of dietary fatty acids and carbohydrates on the ratio of serum total to HDL cholesterol and on serum lipids and apolipoproteins: a meta-analysis of 60 controlled trials. Am J Clin Nutr 77(5):1146–1155
11. Cortes B, Nunez I, Cofan M, Gilabert R, Perez-Heras A, Casals E et al (2006) Acute effects of high-fat meals enriched with walnuts or olive oil on postprandial endothelial function. J Am Coll Cardiol 48(8):1666–1671
12. Alipour A, Elte JW, van Zaanen HC, Rietveld AP, Castro Cabezas M (2008) Novel aspects of postprandial lipemia in relation to atherosclerosis. Atheroscler Suppl 9(2):39–44
13. Lopez S, Bermudez B, Pacheco YM, Villar J, Abia R, Muriana FJ (2008) Distinctive postprandial modulation of beta cell function and insulin sensitivity by dietary fats: monounsaturated compared with saturated fatty acids. Am J Clin Nutr 88(3):638–644
14. Aljada A, Ghanim H, Mohanty P, Kapur N, Dandona P (2002) Insulin inhibits the pro-inflammatory transcription factor early growth response gene-1 (Egr)-1 expression in mononuclear cells (MNC) and reduces plasma tissue factor (TF) and plasminogen activator inhibitor-1 (PAI-1) concentrations. J Clin Endocrinol Metab 87(3):1419–1422
15. Robertson MD, Jackson KG, Fielding BA, Williams CM, Frayn KN (2002) Acute effects of meal fatty acid composition on insulin sensitivity in healthy post-menopausal women. Br J Nutr 88(6):635–640
16. Carey AL, Steinberg GR, Macaulay SL, Thomas WG, Holmes AG, Ramm G et al (2006) Interleukin-6 increases insulin-stimulated glucose disposal in humans and glucose uptake and fatty acid oxidation in vitro via AMP-activated protein kinase. Diabetes 55(10):2688–2697
17. Eizirik DL, Sandler S, Welsh N, Juntti-Berggren L, Berggren PO (1995) Interleukin-1 beta-induced stimulation of insulin release in mouse pancreatic islets is related to diacylglycerol production and protein kinase C activation. Mol Cell Endocrinol 111(2):159–165
18. Manning PJ, Sutherland WH, McGrath MM, de Jong SA, Walker RJ, Williams MJ (2008) Postprandial cytokine concentrations and meal composition in obese and lean women. Obesity (Silver Spring) 16(9):2046–2052
19. Nappo F, Esposito K, Cioffi M, Giugliano G, Molinari AM, Paolisso G et al (2002) Postprandial endothelial activation in healthy subjects and in type 2 diabetic patients: role of fat and carbohydrate meals. J Am Coll Cardiol 39(7):1145–1150

20. Teng KT, Voon PT, Cheng HM, Nesaretnam K (2010) Effects of partially hydrogenated, semi-saturated, and high oleate vegetable oils on inflammatory markers and lipids. Lipids 45(5):385–392
21. Baer DJ, Judd JT, Clevidence BA, Tracy RP (2004) Dietary fatty acids affect plasma markers of inflammation in healthy men fed controlled diets: a randomized crossover study. Am J Clin Nutr 79(6):969–973
22. Poppitt SD, Keogh GF, Lithander FE, Wang Y, Mulvey TB, Chan YK et al (2008) Postprandial response of adiponectin, interleukin-6, tumor necrosis factor-alpha, and C-reactive protein to a high-fat dietary load. Nutrition 24(4):322–329
23. Berry SE, Woodward R, Yeoh C, Miller GJ, Sanders TA (2007) Effect of interesterification of palmitic acid-rich triacylglycerol on postprandial lipid and factor VII response. Lipids 42(4): 315–323
24. Sanders TA, de Grassi T, Miller GJ, Morrissey JH (2000) Influence of fatty acid chain length and cis/trans isomerization on postprandial lipemia and factor VII in healthy subjects (postprandial lipids and factor VII). Atherosclerosis 149(2):413–420
25. Tholstrup T, Sandstrom B, Bysted A, Holmer G (2001) Effect of 6 dietary fatty acids on the postprandial lipid profile, plasma fatty acids, lipoprotein lipase, and cholesterol ester transfer activities in healthy young men. Am J Clin Nutr 73(2):198–208
26. Roche HM, Zampelas A, Jackson KG, Williams CM, Gibney MJ (1998) The effect of test meal monounsaturated fatty acid: saturated fatty acid ratio on postprandial lipid metabolism. Br J Nutr 79(5):419–424
27. Jackson KG, Wolstencroft EJ, Bateman PA, Yaqoob P, Williams CM (2005) Acute effects of meal fatty acids on postprandial NEFA, glucose and apo E response: implications for insulin sensitivity and lipoprotein regulation? Br J Nutr 93(5):693–700
28. Paniagua JA, de la Sacristana AG, Sanchez E, Romero I, Vidal-Puig A, FJ Berral et al (2007) A MUFA-rich diet improves postprandial glucose, lipid and GLP-1 responses in insulin-resistant subjects. J Am Coll Nutr 26(5):434–444
29. Lee JS, Pinnamaneni SK, Eo SJ, Cho IH, Pyo JH, Kim CK et al (2006) Saturated, but not n-6 polyunsaturated, fatty acids induce insulin resistance: role of intramuscular accumulation of lipid metabolites. J Appl Physiol 100(5):1467–1474
30. Jensen J, Bysted A, Dawids S, Hermansen K, Holmer G (1999) The effect of palm oil, lard, and puff-pastry margarine on postprandial lipid and hormone responses in normal-weight and obese young women. Br J Nutr 82(6):469–479
31. Jebb SA, Lovegrove JA, Griffin BA, Frost GS, Moore CS, Chatfield MD et al (2010) Effect of changing the amount and type of fat and carbohydrate on insulin sensitivity and cardiovascular risk: the RISCK (Reading, Imperial, Surrey, Cambridge, and Kings) trial. Am J Clin Nutr 92(4):748–758
32. Payette C, Blackburn P, Lamarche B, Tremblay A, Bergeron J, Lemieux I et al (2009) Sex differences in postprandial plasma tumor necrosis factor-alpha, interleukin-6, and C-reactive protein concentrations. Metabolism 58(11):1593–1601
33. Dandona P, Aljada A, Mohanty P (2002) The anti-inflammatory and potential anti-atherogenic effect of insulin: a new paradigm. Diabetologia 45(6):924–930
34. Romon M, Lebel P, Fruchart JC, Dallongeville J (2003) Postprandial leptin response to carbohydrate and fat meals in obese women. J Am Coll Nutr 22(3):247–251
35. Peti A, Juhasz A, Kenyeres P, Varga Z, Seres I, Kovacs GL et al (2010) Relationship of adipokines and non-esterified fatty acid to the insulin resistance in nondiabetic individuals. J Endocrinol Invest (in press)
36. Vettor R, Milan G, Rossato M, Federspil G (2005) Review article: adipocytokines and insulin resistance. Aliment Pharmacol Ther 22(Suppl 2):3–10

Lipids (2011) 46:389–390
DOI 10.1007/s11745-011-3544-2

LETTER TO THE EDITOR

Supplementation of Monounsaturated and Polyunsaturated Fatty Acids in Non-Alcoholic Fatty Liver Disease and Metabolic Syndrome

Anna Alisi · Carlo Agostoni · Valerio Nobili

Received: 21 February 2011 / Accepted: 21 February 2011 / Published online: 16 March 2011

To the Editor

Metabolic syndrome is the result of a combination of risk factors, including abdominal obesity, hyperlipidemia, hypertension, and insulin resistance. Dietary fat intake may play a critical role in the development of the metabolic syndrome. It is now clear that it is not so much the amount of lipids introduced by the diet, but rather the type of fatty acid that is able to interfere with the development of the disease [1]. In fact, in a recent review published in this journal [2], the authors provided a critical evaluation of the evidence supporting the impact of dietary monounsaturated fatty acids (MUFA) on plasma lipidome. Furthermore, several studies highlight the efficacy of MUFA in improving insulin sensitivity and regulating glucose levels, thus reducing the risk of metabolic syndrome and cardiovascular disease [2].

Recently, metabolic syndrome has been also associated with non-alcoholic fatty liver disease (NAFLD) [3]. NAFLD is a multifactorial disease ranging from simple fatty liver to non-alcoholic steatohepatitis (NASH), with or without fibrosis [4]. The coexistence of metabolic syndrome and NAFLD represents an increased risk factor for type-2 diabetes and cardiovascular disease [3, 4]. There are currently no available therapies for NAFLD and NASH. Recently, lipotoxicity and plasma lipidome have emerged as novel targets for potential therapeutic strategies [5, 6]. Furthermore, several authors showed that n-3 polyunsaturated fatty acids (PUFA) may have beneficial effects in preventing the complications of lipotoxicity [6]. PUFA dietary intake has positive effects on intra-hepatic fat accumulation in patients with NAFLD [7]. In a recent study conducted on 60 children with biopsy-proven NAFLD, we demonstrated that docosahexaenoic acid (DHA), an n-3 long-chain PUFA, is able to decrease liver fat content, change the lipidomic profile, reduce insulin resistance, thus improving some of the metabolic signatures of obesity [8].

It is noteworthy that all these findings support the role of highly saturated fatty acids, and the n-6/n-3 ratio as modulators of these metabolic parameters, and suggest that early markers of developing metabolic syndrome may be ameliorated by the administration of n-3 long-chain PUFA and MUFA even if controversy still exists on the different effects of n-6 and n-3 PUFA, as well as on the interacting effect of dietary saturated and monounsaturated fat.

National dietary guidelines are increasingly recommending dietary MUFA, primarily at the expense of saturated fatty acids (SFA), the so-called Mediterranean diet.

As the debate on the beneficial dietary fatty acid combination continues, the mechanisms involved in the effects of MUFA and PUFA on metabolic syndrome and NAFLD, deserves considerable attention and further human studies. Nevertheless, we believe that the take home message is that if therapeutic MUFA-based strategies are effective in prevention of metabolic syndrome and are also applicable to NAFLD; and vice versa, then there is a good hope with regard to the possibility of successful implementation of PUFA as a therapy for both diseases. Finally, the inclusion of MUFA and PUFA supplements in the diet of individuals with metabolic syndrome and NAFLD should be warranted, in view of their potential to reduce the risk of cardiovascular disease.

A. Alisi · V. Nobili (✉)
Liver Research Unit, Bambino Gesù Children's Hospital, IRCCS, P.le S. Onofrio 4, 00165 Rome, Italy
e-mail: nobili66@yahoo.it

C. Agostoni
Department of Pediatrics, Fondazione IRCCS Cà Granda, Ospedale Maggiore Policlinico, University of Milan, Milan, Italy

References

1. Melanson EL, Astrup A, Donahoo WT (2009) The relationship between dietary fat and fatty acid intake and body weight, diabetes, and the metabolic syndrome. Ann Nutr Metab 55:229–243
2. Gillingham LG, Harris-Janz S, Jones PJ (2010) Dietary monounsaturated fatty acids are protective against metabolic syndrome and cardiovascular disease risk factors. Lipids. doi:10.1007/s11745-010-3524-y
3. Vanni E, Bugianesi E, Kotronen A, De Minicis S, Yki-Järvinen H, Svegliati-Baroni G (2010) From the metabolic syndrome to NAFLD or vice versa? Dig Liver Dis 42:320–330
4. Brunt EM (2010) Pathology of nonalcoholic fatty liver disease. Nat Rev Gastroenterol Hepatol 7:195–203
5. Puri P, Wiest MM, Cheung O, Mirshahi F, Sargeant C, Min HK, Contos MJ, Sterling RK, Fuchs M, Zhou H, Watkins SM, Sanyal AJ (2009) The plasma lipidomic signature of nonalcoholic steatohepatitis. Hepatology 50:1827–1838
6. Perez-Martinez P, Perez-Jimenez F, Lopez-Miranda J (2010) n-3 PUFA and lipotoxicity. Biochim Biophys Acta 1801:362–366
7. Masterton GS, Plevris JN, Hayes PC (2010) Review article: omega-3 fatty acids—a promising novel therapy for non-alcoholic fatty liver disease. Aliment Pharmacol Ther Aliment Pharmacol Ther 31:679–692
8. Nobili V, Bedogni G, Alisi A, Pietrobattista A, Risé P, Galli C, Agostoni C (2011) Docosahexaenoic acid supplementation decreases liver fat content in children with non-alcoholic fatty liver disease: double-blind randomised controlled clinical trial. Arch Dis Child. doi:10.1136/adc.2010.192401

Lipids (2011) 46:391–397
DOI 10.1007/s11745-011-3554-0

ORIGINAL ARTICLE

PGE_2 Release from Tryptase-Stimulated Rabbit Ventricular Myocytes is Mediated by Calcium-Independent Phospholipase $A_2\gamma$

Janhavi Sharma · Jane McHowat

Received: 16 February 2011 / Accepted: 16 March 2011 / Published online: 2 April 2011

Abstract Inflammation is associated with cardiovascular disease, including myocardial infarction, atherosclerosis, myocarditis and congestive heart failure. Mast cells have been implicated in inflammation, but their precise role in cardiac inflammation remains unclear. Mast cells contain a variety of pre-formed granule-associated mediators, including tryptase. We have previously demonstrated that the majority of the phospholipase A_2 (PLA_2) activity in isolated rabbit ventricular myocytes is membrane-associated, calcium-independent and selective for plasmalogen phospholipids. We hypothesized that tryptase stimulation of rabbit ventricular myocytes would increase $iPLA_2$ activity, leading to increased arachidonic acid and prostaglandin E_2 (PGE_2) release. Isolated rabbit ventricular myocytes were stimulated with tryptase and $iPLA_2$ activity, arachidonic acid and PGE_2 release were measured. Tryptase stimulation increased $iPLA_2$ activity after 5 min. Activation of $iPLA_2$ was accompanied by increased arachidonic acid and PGE_2 release in tryptase-stimulated myocytes. However no increase in platelet activating factor was observed with tryptase stimulation. To distinguish between different $iPLA_2$ isoforms in the myocardium, we pretreated ventricular myocytes with the (*R*)- and (*S*)-enantiomers of bromoenol lactone (BEL) to selectively inhibit $iPLA_2\gamma$ and β respectively. Pretreatment with (*R*)-BEL resulted in complete inhibition of tryptase-stimulated $iPLA_2$ activity, arachidonic acid and PGE_2 release, suggesting the $iPLA_2\gamma$ is the predominant myocardial isoform activated by tryptase. These studies demonstrate that PGE_2 release from tryptase stimulated rabbit ventricular myocytes is mediated primarily by $iPLA_2\gamma$.

Keywords Heart · Mast cell · Inflammation

Abbreviations

BEL	Bromoenol lactone
COX	Cyclooxygenase
ECM	Extracellular matrix
$iPLA_2$	Calcium-independent phospholipase A_2
MMP	Matrix metalloprotease
PAF	Platelet activating factor
PGE_2	Prostaglandin E_2
PMA	Phorbol 12-myristate 13-acetate

Introduction

It is estimated that one in three American adults has one or more types of cardiovascular disease [1], the leading cause of mortality and morbidity in the US. The pathology of many cardiovascular diseases, including myocardial infarction, atherosclerosis, congestive heart failure and myocarditis, are associated with myocardial inflammation [2]. Mast cells are normally present in heart tissue, and lie in close proximity to blood vessels and in between myocytes in the myocardium [3]. Previous studies have demonstrated a pathological role for mast cells in the heart, whereby following degranulation they cause myocardial tissue injury, contractile dysfunction and are proarrhythmic [4, 5]. Mast cell degranulation releases many harmful mediators such as histamine, chymase, tryptase and eicosanoids that can contribute to inflammation [5]. Mast cells

J. Sharma · J. McHowat (✉)
Department of Pathology, Saint Louis University School of Medicine, 1402 S. Grand Blvd., St Louis, MO 63104, USA
e-mail: mchowaj@slu.edu

have also been shown to contribute to fibrosis via the release of various profibrotic cytokines. Additionally, tryptase has been shown to stimulate fibroblast proliferation and collagen deposition [6, 7]. Tryptase is known to degrade denatured collagen and activate matrix metalloproteases (MMPs) that are responsible for extracellular matrix integrity. It also degrades a number of bioactive peptides and lipoproteins [8].

Previous studies from our laboratory have demonstrated that mast cell tryptase activates calcium-independent phospholipase A_2 ($iPLA_2$) in endothelial and epithelial cells, resulting in increased inflammatory phospholipid metabolite accumulation and propagating the inflammatory process [9, 10]. PLA_2 are a large family of esterases responsible for the hydrolysis of *sn*-2 esterified fatty acids from membrane phospholipids, resulting in the production of free fatty acid, including arachidonic acid and a lysophospholipid. These can serve as important precursors for metabolites that have been shown to initiate or propagate inflammation. For example, arachidonic acid can be converted to prostaglandins by the action of cyclooxygenases (COX). The liberated accompanying lysophospholipid can be acetylated at the *sn*-2 position to produce platelet-activating factor (PAF). Both, arachidonic acid metabolites and PAF have a well established role in the inflammatory process [11].

Several PLA_2 isoforms have been identified in the myocardium. Secretory phospholipase A_2 require millimolar amounts of calcium for their catalytic activity and act extracellularly. Intracellular phospholipases are divided into two groups- cytosolic PLA_2 ($cPLA_2$) and $iPLA_2$. All known $cPLA_2$, except for $cPLA_2\gamma$, require micromolar concentrations of Ca^{2+} for their translocation from the cytosol to intracellular membranes. They do not, however, require Ca^{2+} for their catalytic activity. As their name suggests, $iPLA_2$ do not require Ca^{2+} for their activity or substrate binding. Even though all three groups of PLA_2 have been identified in the myocardium, several studies show that the majority of myocardial PLA_2 activity is Ca^{2+}-independent [12].

The $iPLA_2$ family of enzymes contains at least seven members amongst which, $iPLA_2\gamma$ and $iPLA_2\beta$ are the most abundant in mammalian tissue and have been shown to be important for regulating myocardial function [13]. An inhibitor selective for $iPLA_2$, bromoenol lactone (BEL), has been useful in demonstrating the role of this enzyme in various settings. The separation of BEL into its enantiomers, (*R*)-BEL and (*S*)-BEL has further allowed us to discriminate between the major isoforms of $iPLA_2$, since they are ten fold selective for $iPLA_2\gamma$ and $iPLA_2\beta$ respectively [14].

In this study we examined the effect of tryptase stimulation on rabbit ventricular myocyte $iPLA_2$ activity, and the subsequent production of arachidonic acid, PGE_2 and PAF.

Methods

Rabbit Ventricular Myocyte Isolation and Culture

All studies using vertebrate animals were carried out under the approval of the Animal Care and Use Committee at Saint Louis University as outlined in protocol # 1207. Adult rabbits of either sex weighing 2–3 kg were anesthetized with intravenous pentobarbitone sodium (50 mg/kg) and the heart rapidly removed. The heart was mounted on a Langendorff perfusion apparatus and perfused for 5 min with a Tyrode solution containing (mmol/L) NaCl 118, KCl 4.8, $CaCl_2$ 1.2, and glucose 11; the Tyrode solution was saturated with $95\%O_2/5\%CO_2$ to yield a pH of 7.4. This was followed by a 4-min perfusion with a Ca-free Tyrode solution containing EGTA (100 μM) and a final perfusion for 20 min with the Tyrode solution containing 100 μM Ca^{2+} and 0.033% collagenase. The heart was removed from the perfusion apparatus, the atria were removed and the remaining ventricles were cut into small pieces and incubated in fresh 0.033% collagenase solution at 37 °C in a shaking water bath for 4 successive harvests of 20 min. Individual myocytes were washed with HEPES buffer containing (mmol/L): NaCl 133.5, KCl 4.8, $MgCl_2$, $CaCl_2$ 0.3, KH_2PO_4 1.2, glucose 10 and HEPES 10 (pH 7.4). Extracellular Ca^{2+} was increased to 1.2 mM in three stages at intervals of 20 min. Myocytes were incubated overnight in M199 medium with 10% fetal calf serum at 37 °C and then washed three times with 1.2 mM Ca^{2+} HEPES solution.

Phospholipase A_2 Activity

Myocytes were suspended in 1 mL buffer containing (mmol/L): sucrose 250, KCL 10, imidazole 10, EDTA 5, dithiothreitol (DTT) 2 with 10% glycerol, pH 7.8 (activity buffer). The suspension was sonicated on ice six times for 10 s (using microtip probe at 20% power output, 500 Sonic Dismembrator, Fisher Scientific) and the sonicate centrifuged at $20{,}000\times g$ for 20 min to remove cellular debris and nuclei. The supernatant was then centrifuged at $100{,}000\times g$ for 60 min to separate the membrane fraction from the cytosolic fraction. The membrane fraction was washed twice to minimize contamination with cytosolic protein by resuspending in activity buffer, and centrifuging at $100{,}000\times g$ for 60 min. The final membrane fraction was resuspended in activity buffer. Purity of the membrane fraction for sarcolemma and sarcoplasmic reticulum membranes was verified by verifying the presence of K^+-*p*-nitrophenyl phosphatase and NADPH-cytochrome *c* reductase and the absence of glucose 6-phosphate dehydrogenase and cytochrome *c* oxidase. PLA_2 activity in membrane fractions was assessed by incubating enzyme (8 μg

membrane protein) with 100 μM (16:0, [^{3}H]18:1) plasmenylcholine substrate in assay buffer containing (mmol/L): Tris 10, EGTA 4, 10% glycerol, pH 7.0 at 37 °C for 5 min in a total volume of 200 μL. The radiolabeled phospholipid substrate was introduced into the incubation mixture by injection in 5 μL ethanol to initiate the assay. Reactions were terminated by the addition of 100 μL butanol and released radiolabeled fatty acid was isolated by the application of 25 μL of the butanol phase to channeled Silica Gel G plates, development in the petroleum ether/diethyl ether/acetic acid (70/30/1, v/v) and subsequent quantification by liquid scintillation spectrometry. Protein content of each sample was determined by the Lowry method utilizing freeze dried bovine serum albumin as the protein standard.

Measurement of Total Arachidonic Acid Release

Arachidonic acid release was determined by measuring [^{3}H] arachidonic acid released into the surrounding medium from ventricular myocyte suspensions labeled previously with [^{3}H] arachidonic acid. Briefly, myocyte suspensions (10^6 myocytes in 10 mL culture media) were incubated at 37 °C with 3 μCi [^{3}H] arachidonic acid for 18 h. This incubation resulted in >70% incorporation of radioactivity into the myocytes. After incubation, myocyte suspensions were washed three times with Tyrode solution containing 0.36% bovine serum albumin to remove unincorporated [^{3}H] arachidonic acid. Myocytes were incubated at 37 °C for 15 min before being subjected to experimental conditions. At the end of the stimulation period, myocyte suspensions were centrifuged, and the supernatant was removed. Myocyte pellets were solubilized in 10% sodium dodecyl sulfate, and radioactivity in both supernatant and pellet was quantified by liquid scintillation spectrometry.

Measurement of PGE_2 Release

Rabbit myocytes were washed twice with Hanks balanced salt solution (HBSS) containing, in mmol/L, 135 NaCl, 0.8 $MgSO_4$, 10 HEPES (pH 7.6, 1.2 $CaCl_2$, 5.4 KCl, 0.4 KH_2PO_4 and 6.6 glucose. After washing, 0.5 mL of HBSS with 0.36% BSA was added to each culture well. Myocytes were then stimulated with the appropriate tryptase concentrations. The surrounding buffer was removed from the cells after selected time intervals, and PGE_2 release was measured immediately using an immunoassay kit (R&D Systems, Minneapolis, MN).

PAF Assay

Isolated rabbit ventricular myocytes were washed twice with Hanks' balanced salts solution containing NaCl 135 mM, $MgSO_4$ 0.8 mM, HEPES (pH = 7.4) 10 mM, $CaCl_2$ 1.2 mM, KCl 5.4 mM, KH_2PO_4 0.4 mM, Na_2HPO_4 0.3 mM and glucose 6.6 mM and incubated with 50 μCi [^{3}H] acetic acid for 20 min. After the selected time interval for incubation with the appropriate agents, lipids were extracted from the cells by the method of Bligh and Dyer. The chloroform layer was concentrated by evaporation under N_2, applied to a silica gel 60 TLC plate, and developed in chloroform/methanol/acetic acid/water (50/25/8/4 vol/vol). The region corresponding to PAF was scraped and radioactivity quantified using liquid scintillation spectrometry. Loss of PAF during extraction and chromatography was corrected for by adding a known amount of [^{14}C] PAF as an internal standard. [^{14}C] PAF is synthesized by acetylating the *sn*-2 position of lyso-PAF with [^{14}C] acetic anhydride using 0.33 M dimethylaminopyridine as a catalyst. The synthesized [^{14}C] PAF is purified by HPLC.

Statistical Analysis

Statistical comparison of values was performed by Student's *t* test or one way analysis of variance with post hoc analysis performed using Dunnett's test. All results are expressed as means ± SEM. Statistical significance was considered to be $P < 0.05$.

Results

Effect of Tryptase on PLA_2 Activity

To determine the contribution of $iPLA_2\beta$ and $iPLA_2\gamma$ to total $iPLA_2$ activity in rabbit ventricular myocytes, membrane protein was incubated with increasing concentrations of (*R*)-BEL or (*S*)-BEL and PLA_2 activity was measured in the absence of calcium (4 mM EGTA) using (16:0, [^{3}H]18:1) plasmenylcholine as substrate. Incubation with concentrations of (*R*)-BEL greater than 0.1 μM resulted in a significant inhibition of membrane-associated $iPLA_2$ activity (Fig. 1). Incubation of membrane protein with (*S*)-BEL resulted in a significant inhibition of $iPLA_2$ activity at concentrations greater than 1 μM (Fig. 1). Incubation with (*R*)-BEL inhibited $iPLA_2$ activity to a greater extent than incubation with (*S*)-BEL at all concentrations examined, suggesting that the majority of ventricular myocyte $iPLA_2$ activity is $iPLA_2\gamma$.

Isolated rabbit ventricular myocytes stimulated with tryptase (20 ng/mL) demonstrated a significant increase in $iPLA_2$ activity 5 min after stimulation, which returned to basal level after 10 min (Fig. 2). Ventricular myocytes pretreated with (*R*)-BEL (2 μM, 10 min) resulted in complete inhibition of tryptase-stimulated $iPLA_2$ activity (Fig. 2). However, pretreatment with (*S*)-BEL (2 μM,

10 min) did not significantly affect tryptase-stimulated iPLA$_2$ activity (Fig. 2). These data suggest that tryptase stimulation caused an increase in iPLA$_2$ activity in myocytes, most likely due to activation of iPLA$_2\gamma$.

Effect of Tryptase on Arachidonic Acid Release

Since iPLA$_2$ mediated membrane hydrolysis results in the production of free fatty acid from the *sn*-2 position, rabbit ventricular myocytes were stimulated with tryptase (20 ng/mL) and arachidonic acid release was measured. Tryptase stimulation resulted in a significant increase in arachidonic acid release after 2 min. Stimulation for a longer period resulted in a five-fold increase in arachidonic acid (Fig. 3). Pretreatment of ventricular myocytes with (*R*)-BEL (2 μM, 10 min) completely inhibited tryptase-stimulated arachidonic acid release whereas pretreatment with (*S*)-BEL (2 μM, 10 min) inhibited arachidonic acid release by approximately 40% (Fig. 3). This suggests that iPLA$_2\gamma$ is primarily responsible for arachidonic acid release in response to tryptase stimulation in rabbit ventricular myocytes.

Effect of Tryptase on PGE$_2$ Release

Free arachidonic acid can be metabolized to PGE$_2$ by the sequential actions of cyclooxygenase (COX-1 or COX-2) and prostaglandin E synthase. An increase in PGE$_2$ release was observed when rabbit ventricular myocytes were stimulated with tryptase (20 ng/mL, Fig. 4). In agreement

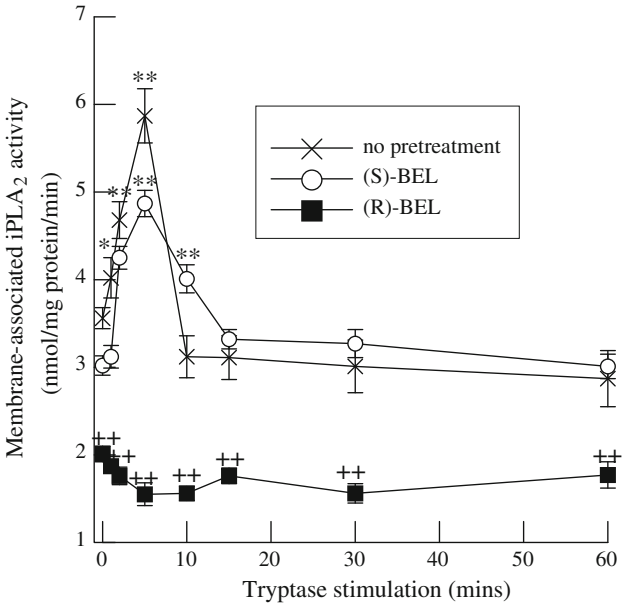

Fig. 2 Calcium-independent phospholipase A$_2$ (iPLA$_2$) activity in rabbit ventricular myocytes stimulated with tryptase (20 ng/mL) with or without pretreatment with (*R*)- or (*S*)-BEL (2 μM, 10 min). $^{*}p < 0.05$, $^{**}p < 0.01$ when compared to untreated controls. $^{++}p < 0.01$ when comparing tryptase stimulated results in the presence or absence of (*R*)-BEL. $N = 6$

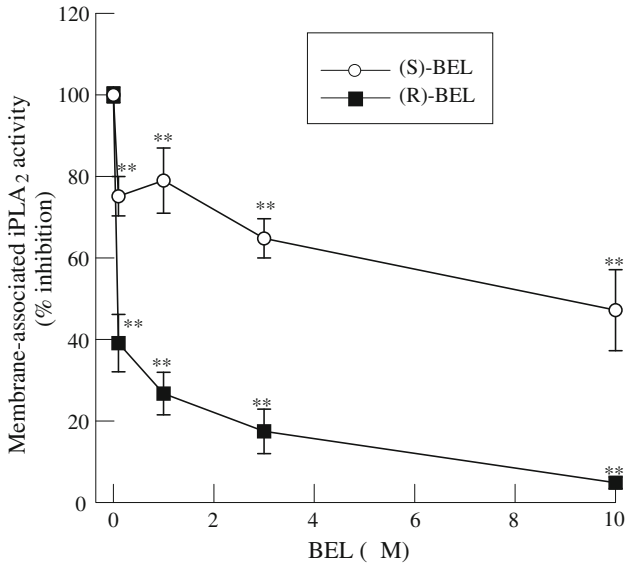

Fig. 1 Inhibition of calcium-independent phospholipase A$_2$ (iPLA$_2$) activity in rabbit ventricular myocytes treated with (*R*)- or (*S*)-BEL. Isolated membrane fractions were incubated with bromoenol lactone (BEL, 10 min) prior to assay of PLA$_2$ activity, measured using 100 μM (16:0, [^{3}H]18:1) plasmenylcholine in the presence of 4 mM EGTA. Untreated iPLA$_2$ activity was 6.1 ± 0.1 nmol/mg protein/min, $N = 9$. $^{*}p < 0.05$, $^{**}p < 0.01$ when compared to activity measured in the absence of BEL

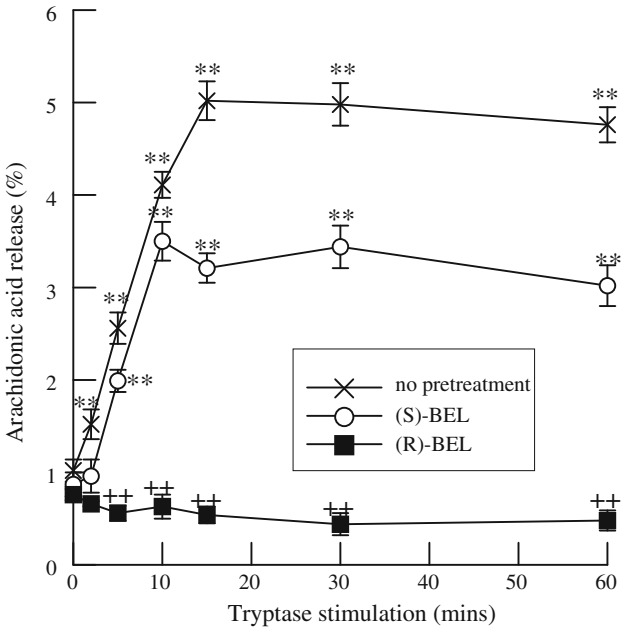

Fig. 3 Increase in arachidonic acid release from tryptase-stimulated (20 ng/mL) rabbit ventricular myocytes with or without pretreatment with (*R*)- or (*S*)-BEL (2 μM, 10 min). $^{**}p < 0.01$ when compared to unstimulated release. $^{++}p < 0.01$ when comparing tryptase stimulated results in the presence or absence of (*R*)-BEL. $N = 6$

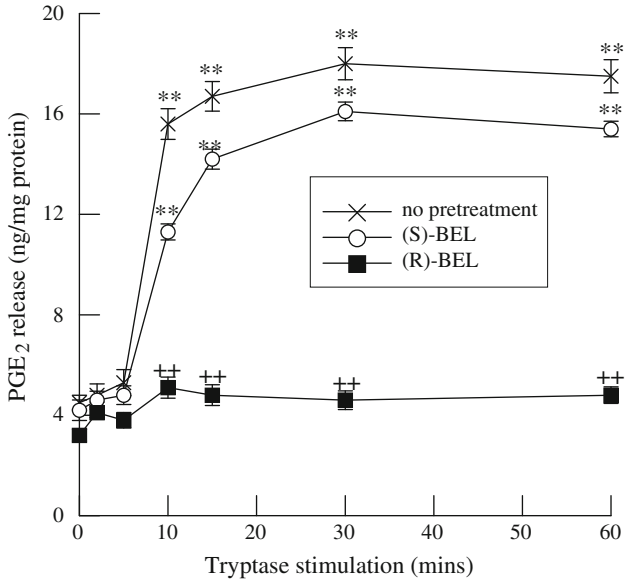

Fig. 4 Increase in prostaglandin E_2 (PGE_2) release from tryptase-stimulated (20 ng/mL) rabbit ventricular myocytes with or without pretreatment with (*R*)- or (*S*)-BEL (2 μM, 10 min). $^{**}p < 0.01$ when compared to unstimulated release. $^{++}p < 0.01$ when comparing tryptase stimulated results in the presence or absence of (*R*)-BEL. $N = 6$

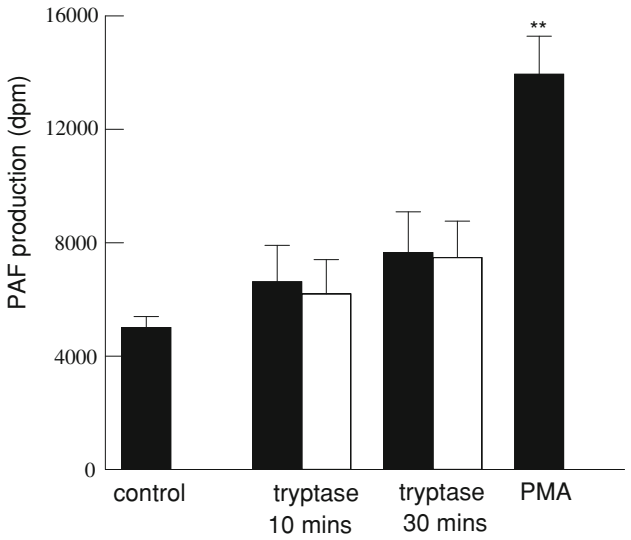

Fig. 5 Platelet-activating factor (PAF) production in rabbit ventricular myocytes stimulated with tryptase (20 ng/mL) or PMA (100 nm, 10 min) with (*open bars*) or without (*filled bars*) BEL pretreatment (2 μM, 10 min). $^{**}p < 0.01$ when compared with unstimulated values. $N = 8$

with our previous findings, PGE_2 release was inhibited completely with (*R*)-BEL, indicating that $iPLA_2\gamma$ activation is mostly responsible for PGE_2 production in tryptase stimulated rabbit ventricular myocytes (Fig. 4).

Effect of Tryptase on PAF Production

Previous studies from our laboratory have demonstrated an increase in PAF production in epithelial and endothelial cells in response to tryptase-stimulated $iPLA_2$ activity. We measured PAF production in rabbit ventricular myocytes following tryptase stimulation and observed no increase after 10 or 30 min stimulation (Fig. 5). However, treatment with PMA (100 nM, 10 min), caused a significant increase in PAF production (Fig. 5). Thus, though capable of producing PAF, tryptase-mediated stimulation of $iPLA_2$ does not appear to increase PAF production in ventricular myocytes.

Discussion

Prostaglandins are synthesized from membrane phospholipids by the sequential action of phospholipase A_2, COX and PG synthase enzymes. They are biologically active mediators which regulate heart rate, coronary blood flow, coronary microvascular permeability and left ventricular contractility [15]. In cardiac myocytes, PGE_2 production exceeds the production of all other PGs [16]. The production of arachidonic acid, a polyunsaturated fatty acid residing in cell membranes, is the rate limiting step for prostaglandin synthesis. Arachidonic acid is liberated from membrane phospholipids via the hydrolysis of the *sn*-2 bond by phospholipase A_2 enzymes and is acted upon by the cyclooxygenases to form PGG_2 and PGH_2, and subsequently converted to PGE_2 by PGE synthase Since PLA_2 determines the amount of arachidonic acid released from cell membranes, it also determines the amount of eicosanoids produced [17].

All major human organ systems, such as gastrointestinal, reproductive, neuroendocrine and immune systems, require PGE_2 to regulate their function [18]. Depending on their site of action, the effects of PGE_2 could be homeostatic, inflammatory or even anti-inflammatory [17]. PGE_2 has diverse actions in inflammation, such as having vasodilatory or vasoconstrictive effects based on various conditions [18]. These conflicting functions and effects make it challenging to elucidate the role of this eicosanoid in physiology and pathology. The receptors via which PGE_2 exerts its action are the prostaglandin E receptors (EP1-4), which are a set of G-protein-coupled receptors that differ in their tissue distribution, structure and signaling pathways [19]. It is suggested that this family of receptors is most likely responsible for the differing actions of PGE_2.

Previous studies from our laboratory have shown that mast cell tryptase activates $iPLA_2$, leading to the upregulation of arachidonic acid and prostaglandin production in epithelial [10] and endothelial cells [9, 11]. Mast cells are known to have a crucial role in a variety of disorders,

however their exact contribution to cardiovascular pathology is still unclear. One of the most distinctive morphological features of mast cells is the presence of numerous electron-dense secretory granules containing various preformed mediators [20]. In humans, mast cells are generally classified according to the type of protease enzymes they contain: tryptase (MC_T), chymase (MC_C) or both tryptase and chymase (MC_{TC}) [21]. It has been reported that the human heart contains 90% MC_{TC} type mast cells [22]. In the heart, mast cell tryptase is known to promote cardiac remodeling by altering the extracellular matrix (ECM) and increasing fibroblast proliferation [4]. Tryptase activates MMPs known to be associated with plaque destabilization and rupture in atherosclerosis and fibrosis associated with myocarditis [2, 23]. In cardiovascular inflammation tryptase levels are known to be elevated [24, 25], thus it is likely that mast cell tryptase directly affects cardiac myocytes following degranulation.

In rabbit ventricular myocytes, we have shown that majority of the PLA_2 activity is calcium-independent, membrane associated and selective for arachidonylated plasmalogen phospholipids [26]. Further, full length sequences of rabbit iPLA$_2\beta$ and γ were determined and found to be 91 and 88% identical to the corresponding human isoforms. We have previously demonstrated the presence of iPLA$_2\gamma$ in microsomes isolated from rabbit heart and ventricular myocytes [27]. Multiple iPLA$_2\gamma$ protein products are localized to intracellular compartments, including the plasma membrane, mitochondria and peroxisomes [28]. Rabbit microsomal iPLA$_2\gamma$ is approximately 88 kDa, which is the long form of iPLA$_2\gamma$ [26, 27]. We determined activation of iPLA$_2\gamma$ in the membrane fraction of ventricular myocytes, which contains sarcolemma and sarcoplasmic reticulum membranes. $iPLA_2$ activity measured in the cytosolic and mitochondrial fractions isolated from ventricular myocytes was not significantly increased by tryptase stimulation (data not shown). Thus, we hypothesize that tryptase stimulation of ventricular myocytes likely activates iPLA$_2\gamma$ localized in the sarcolemma at short intervals of stimulation.

Rabbit myocyte $iPLA_2$ is activated by thrombin in a similar time course to that observed here with tryptase [28]. We have previously observed comparable time courses of $iPLA_2$ activation in response to thrombin and tryptase in human coronary artery endothelial cells [11]. As with endothelial cells, thrombin activation of cardiac myocyte $iPLA_2$ is quicker than with tryptase, suggesting that cell signaling events between $iPLA_2$ activation and protease activated receptor-1 (PAR-1, cleaved and activated by thrombin) or PAR-2 (cleaved and activated by tryptase) are different. We have demonstrated that $iPLA_2$ activation by thrombin is mediated by protein kinase C, possibly via phosphorylation of the enzyme [29]. Pretreatment of tryptase-stimulated ventricular myocytes with GF 109203X (100 nM, 10 min) to inhibit protein kinase C resulted in inhibition of membrane-associated $iPLA_2$ activation (4.2 ± 0.3 nmol/mg protein/min vs. 3.8 ± 0.4 nmol/mg protein, $N = 6$). These data suggest that thrombin or tryptase stimulation results in similar increases in $iPLA_2$ activation and membrane phospholipid hydrolysis and that the presence of PAR-1 and PAR-2 increases the range of proteases to which ventricular myocytes can respond.

In the present study, (*R*)- and (*S*)-BEL were used to ascertain the specific contributions of iPLA$_2\beta$ and γ in ventricular myocytes in response to tryptase stimulation. The majority of membrane associated $iPLA_2$ activity in rabbit ventricular myocytes was inhibited by (*R*)-BEL, indicating that iPLA$_2\gamma$ was responsible. Membrane fractions of ventricular myocytes pretreated with (*R*)-BEL did not show an increase in $iPLA_2$ activity in response to tryptase stimulation. However, pretreatment with (*S*)-BEL did not inhibit tryptase-stimulated $iPLA_2$ activity. Tryptase-stimulated increases in arachidonic acid and PGE_2 release were completely inhibited by pretreatment of ventricular myocytes by (*R*)-BEL, indicating the dependence of these responses on iPLA$_2\gamma$ activation. While it has been determined that PLA_2 is a key enzyme in PGE_2 production, the exact contribution of $iPLA_2$ to this biosynthetic process in cardiac myocytes had not been illustrated. It is of particular interest to know the role of $iPLA_2$ in these settings since majority of the PLA_2 activity in cardiac myocytes is attributable to membrane associated $iPLA_2$. The lysophospholipid produced when arachidonic acid is released from membrane phospholipids by $iPLA_2$ can be acetylated to form platelet activating factor (PAF). PAF has various effects in the cardiovascular system where it is known to decrease cardiac output and affect vascular tone in addition to its direct influence on cardiac myocytes [30]. Previous studies from our laboratory have shown an increase in PAF production in endothelial cells following $iPLA_2$ activation [31, 32]. However, tryptase stimulation of myocytes for up to 30 min did not affect PAF production even though stimulation with PMA resulted in a significant increase in PAF in these cells. This suggests that while cardiac myocytes are able to produce PAF, this process is most likely independent of tryptase stimulation. In a previous study we have determined that thrombin stimulation of rabbit ventricular myocytes failed to increase PAF production [33]. Taken together, these data suggest that thrombin and tryptase activate ventricular myocytes $iPLA_2$ to release arachidonic acid from membrane phospholipids, but the accompanying lysophospholipid is not acetylated to form PAF.

In conclusion, our data suggest that in response to tryptase stimulation, majority of the $iPLA_2$ activity in rabbit ventricular myocytes is due to iPLA$_2\gamma$. This results in increased arachidonic acid and PGE_2 production, but does not affect PAF production in tryptase-stimulated myocytes.

References

1. Writing Group Members, Roger VL, Go AS, Lloyd-Jones DM, Adams RJ, Berry JD, Brown TM, Carnethon MR, Dai S, de Simone G, Ford ES, Fox CS, Fullerton HJ, Gillespie C, Greenlund KJ, Hailpern SM, Heit JA, Ho PM, Howard VJ, Kissela BM, Kittner SJ, Lackland DT, Lichtman JH, Lisabeth LD, Makuc DM, Marcus GM, Marelli A, Matchar DB, McDermott MM, Meigs JB, Moy CS, Mozaffarian D, Mussolino ME, Nichol G, Paynter NP, Rosamond WD, Sorlie PD, Stafford RS, Turan TN, Turner MB, Wong ND, Wylie-Rosett J, on behalf of the American Heart Association Statistics Committee and Stroke Statistics Subcommittee, Roger VL, Turner MB, On behalf of the American Heart Association Heart Disease and Stroke Statistics Writing Group (2011) Executive summary: heart disease and stroke statistics—2011 update: a report from the American Heart Association. Circulation 123:459–463
2. Fairweather D, Frisancho-Kiss S (2008) Mast cells and inflammatory heart disease: potential drug targets. Cardiovasc Hematol Disord Drug Targets 8:80–90
3. Marone G, Patella V, de Crescenzo G, Genovese A, Adt M (1995) Human heart mast cells in anaphylaxis and cardiovascular disease. Int Arch Allergy Immunol 107:72–75
4. Levick SP, McLarty JL, Murray DB, Freeman RM, Carver WE, Brower GL (2009) Cardiac mast cells mediate left ventricular fibrosis in the hypertensive rat heart. Hypertension 53:1041–1047
5. Walsh SK, Kane KA, Wainwright CL (2009) Mast cells, peptides and cardioprotection—an unlikely marriage? Auton Autacoid Pharmacol 29:73–84
6. Garbuzenko E, Nagler A, Pickholtz D, Gillery P, Reich R, Maquart FX, Levi-Schaffer F (2002) Human mast cells stimulate fibroblast proliferation, collagen synthesis and lattice contraction: a direct role for mast cells in skin fibrosis. Clin Exp Allergy 32:237–246
7. Albrecht M, Frungieri MB, Kunz L, Rämsch R, Meineke V, Köhn FM, Mayerhofer A (2005) Divergent effects of the major mast cell products histamine, tryptase and TNF-alpha on human fibroblast behaviour. Cell Mol Life Sci 62:2867–2876
8. Pejler G, Abrink M, Ringvall M, Wernersson S (2007) Mast cell proteases. Adv Immunol 95:167–255
9. Rickard A, Portell C, Kell PJ, Vinson SM, McHowat J (2005) Protease-activated receptor stimulation activates a Ca^{2+}-independent phospholipase A_2 in bladder microvascular endothelial cells. Am J Physiol Renal Physiol 288:F714–F721
10. Rastogi P, Young DM, McHowat J (2008) Tryptase activates calcium-independent phospholipase A_2 and releases PGE_2 in airway epithelial cells. Am J Physiol Lung Cell Mol Physiol 295:L925–L932
11. White MC, McHowat J (2007) Protease activation of calcium-independent phospholipase A_2 leads to neutrophil recruitment to coronary artery endothelial cells. Thromb Res 120:597–605
12. McHowat J, Creer MH (1998) Calcium-independent phospholipase A_2 in isolated rabbit ventricular myocytes. Lipids 33:1203–1212
13. Cedars A, Jenkins CM, Mancuso DJ, Gross RW (2009) Calcium-independent phospholipases in the heart: mediators of cellular signaling, bioenergetics, and ischemia-induced electrophysiologic dysfunction. J Cardiovasc Pharmacol 53:277–289
14. Jenkins CM, Han X, Mancuso DJ, Gross RW (2002) Identification of calcium-independent phospholipase A2 (iPLA2) beta, and not iPLA2 gamma, as the mediator of arginine vasopressin-induced arachidonic acid release in A-10 smooth muscle cells. Enantioselective mechanism-based discrimination of mammalian iPLA2s. J Biol Chem 277:32807–32814
15. Degousee N, Fazel S, Angoulvant D, Stefanski E, Pawelzik SC, Korotkova M, Arab S, Liu P, Lindsay TF, Zhuo S, Butany J, Li RK, Audoly L, Schmidt R, Angioni C, Geisslinger G, Jakobsson PJ, Rubin BB (2008) Microsomal prostaglandin E_2 synthase-1 deletion leads to adverse left ventricular remodeling after myocardial infarction. Circulation 117:1701–1710
16. Mendez M, LaPointe MC (2002) Trophic effects of the cyclooxygenase-2 product prostaglandin E_2 in cardiac myocytes. Hypertension 39:382–388
17. Park JY, Pillinger MH, Abramson SB (2006) Prostaglandin E_2 synthesis and secretion: the role of PGE_2 synthases. Clin Immunol 119:229–240
18. Miller SB (2006) Prostaglandins in health and disease: an overview. Semin Arthritis Rheum 36:37–49
19. Narumiya S, Sugimoto Y, Ushikubi F (1999) Prostanoid receptors: structures, properties, and functions. Physiol Rev 79:1193–1226
20. Pejler G, Rönnberg E, Waern I, Wernersson S (2010) Mast cell proteases: multifaceted regulators of inflammatory disease. Blood 115:4981–4990
21. Balakumar P, Singh AP, Ganti SS, Krishan P, Ramasamy S, Singh M (2008) Resident cardiac mast cells: are they the major culprit in the pathogenesis of cardiac hypertrophy? Basic Clin Pharmacol Toxicol 102:5–9
22. Weidner N, Austen KF (1993) Heterogeneity of mast cells at multiple body sites. Fluorescent determination of avidin binding and immunofluorescent determination of chymase, tryptase, and carboxypeptidase content. Pathol Res Pract 189:156–162
23. Kaartinen M, Penttilä A, Kovanen PT (1994) Accumulation of activated mast cells in the shoulder region of human coronary atheroma, the predilection site of atheromatous rupture. Circulation 90:1669–1678
24. Filipiak KJ, Tarchalska-Krynska B, Opolski G, Rdzanek A, Kochman J, Kosior DA, Czlonkowski A (2003) Tryptase levels in patients after acute coronary syndromes: the potential new marker of an unstable plaque? Clin Cardiol 26:366–372
25. Deliargyris EN, Upadhya B, Sane DC, Dehmer GJ, Pye J, Smith SC Jr, Boucher WS, Theoharides TC (2005) Mast cell tryptase: a new biomarker in patients with stable coronary artery disease. Atherosclerosis 178:381–386
26. Beckett CS, McHowat J (2008) Calcium-independent phospholipase A_2 in rabbit ventricular myocytes. Lipids 43:775–782
27. Kinsey GR, Cummings BS, Beckett CS, Saavedra G, Zhang W, McHowat J, Schnellman RG (2005) Identification and distribution of endoplasmic reticulum $iPLA_2$. Biochem Biophys Res Comm 327:287–293
28. McHowat J, Creer MH (1998) Thrombin activates a membrane-associated calcium-independent PLA_2 in ventricular myocytes. Am J Physiol 274:C1727–C1737
29. Steer SA, Wirsig KC, Creer MH, Ford DA, McHowat J (2002) Regulation of membrane-associated $iPLA_2$ activity by a novel PKC in ventricular myocytes. Am J Physiol 283:C1621–C1626
30. Montrucchio G, Alloatti G, Camussi G (2000) Role of platelet-activating factor in cardiovascular pathophysiology. Physiol Rev 80(4):1669–1699
31. McHowat J, Kell PJ, O'Neill HB, Creer MH (2001) Endothelial cell PAF synthesis following thrombin stimulation utilizes Ca^{2+}-independent phospholipase A_2. Biochemistry 40:14921–14931
32. Rastogi P, McHowat J (2009) Inhibition of calcium-independent phospholipase A_2 prevents inflammatory mediator production in pulmonary microvascular endothelium. Respir Physiol Neurobiol 165:167–174
33. McHowat J, Creer MH (2000) Selective plasmalogen substrate utilization by thrombin-stimulated Ca^{2+}-independent PLA_2 in cardiomyocytes. Am J Physiol Heart Circ Physiol 278:H1933–H1940

Lipids (2011) 46:399–407
DOI 10.1007/s11745-011-3535-3

ORIGINAL ARTICLE

Oral Docosapentaenoic Acid (22:5n-3) Is Differentially Incorporated into Phospholipid Pools and Differentially Metabolized to Eicosapentaenoic Acid in Tissues from Young Rats

Bruce J. Holub · Patricia Swidinsky · Eek Park

Received: 30 August 2010 / Accepted: 13 January 2011 / Published online: 6 March 2011

Abstract The present study assessed the effect of oral supplementation with docosapentaenoic acid (DPA, 22:5n-3) on the levels of serum and tissue lipid classes and their fatty acid compositions including individual phospholipid types in rat liver, heart, and kidney. Sprague–Dawley rats received daily oral gavage over 10 days as corn oil without (controls) or with purified DPA in free fatty acid form (21.2 mg/day). The DPA group exhibited significantly lower serum lipid concentrations. The concentrations in μmol/100 g serum or μmol/g tissue of DPA in the total lipid (TL) were higher by 2.3-, 2.4-, 10.9-, and 5.1-fold in the DPA group of serum, liver, heart, and kidney, respectively, with the phospholipids (PL) being the major DPA reservoir (45.2–52.1% of the DPA in the TL). No significant differences in DHA (22:6n-3) amounts in TL appeared. The highest relative mol% values as DPA were in heart tissue (means of 11.1% in PL and 16.2% in phosphatidylinositol) and lowest in kidney. The EPA (20:5n-3) concentrations were markedly higher in the DPA group and most pronounced in the kidney (5.1 times higher in the TL as compared to controls) relative to liver and heart yielding an estimated apparent % conversion of DPA to EPA of 67% and EPA:DPA ratios reaching 5.74 in kidney phosphatidylethanolamine. The serum lipid-lowering potential of dietary DPA and its impact in the kidney with the derived EPA warrants investigation.

Keywords Docosapentaenoic acid (DPA 22:5n-3) · Rat serum · Cholesteryl esters · Triacylglycerol(s) · Liver · Heart · Kidney · Apparent retroconversion · Eicosapentaenoic acid (EPA 20:5n-3) · Individual phospholipids

B. J. Holub (✉) · P. Swidinsky · E. Park
Department of Human Biology and Nutritional Sciences, Animal Science and Nutrition Building, University of Guelph, Guelph, ON N1G 2W1, Canada
e-mail: bholub@uoguelph.ca

Abbreviations

ARA	Arachidonic acid 20:4n-6
ACAT	Acyl-CoA:cholesterol acyltransferase
CE	Cholesteryl esters
CerPCho	Sphingomyelin
DHA	Docosahexaenoic acid 22:6n-3
DPA	Docosapentaenoic acid 22:5n-3
EPA	Eicosapentaenoic acid 20:5n-3
LCAT	Lecithin:cholesterol acyltransferase
NEFA	Non-esterified fatty acids
PL	Phospholipid(s)
PtdCho	Phosphatidylcholine
PtdEtn	Phosphatidylethanolamine
PtdIns	Phosphatidylinositol
PtdSer	Phosphatidylserine
PUFA	Polyunsaturated fatty acid
TAG	Triacylglycerol(s)
TC	Total cholesterol
TL	Total lipid(s)
TLC	Thin-layer chromatography

Introduction

Docosapentaenoic acid (DPA, 22:5n-3) as present in seal meat, whale meat/blubber, plus some fish/fish oils to a lesser extent is a significant component of the long-chain omega-3 fatty acids found in the Inuit diet [1]. While eicosapentaenoic acid (EPA, 20:5n-3) plus docosahexaenoic acid (DHA, 22:6n-3) are credited for the apparent cardioprotective effects of diets rich in marine fats [2],

higher levels of DPA in the circulation have been associated with a lower risk for coronary heart disease in population studies [3]. Furthermore, DPA has shown the ability to inhibit human platelet aggregation in vitro and to suppress thromboxane formation [4]. Intervention trials using seal oil containing DPA in addition to EPA/DHA have exhibited beneficial effects on selected cardiovascular disease risk factors in healthy volunteers [5, 6]. The much lower intakes of DPA in the diets of populations who consume small amounts of fish are derived mostly from meat plus poultry [7].

Very recently, supplementation with DPA in rats has indicated that it is both elevated and partly retroconverted to EPA in liver, adipose, heart, and skeletal muscle based on total lipid analyses along with data suggesting that dietary DPA can be converted to DHA in the liver [8]. We have extended the previous work herein by measuring the effect of DPA-supplementation in the rat on the levels of various serum and tissue lipids and their fatty acid profiles as well as the fatty acid compositions of various lipid fractions including individual phospholipids in liver, heart, and kidney. This present study differs from previous work [8] which was restricted to total lipid analyses only in selected tissues and excluded the serum and kidney. The present findings reveal dramatic differences in the resulting fatty acid compositions between individual lipid/phospholipid classes upon DPA supplementation and indicate a particularly high capacity for the retroconversion of DPA to EPA in the kidney.

Experimental Procedure

Animals and Study Design

This study was approved by Animal Care Services, Office of Research, University of Guelph (Animal Utilization Protocol No. 96R093). Seventeen male Sprague–Dawley weanling rats (Charles River Canada, St. Constant, P.Q.) having an average body weight of 49.6 ± 0.6 g and approximately 21 days of age were randomly housed in stainless steel cages with 12 h light–dark cycle and a constant room temperature of 25 °C. All animals were fed (ad libitum) Purina Laboratory Chow (Purina Mills Inc., St. Louis, MO), devoid of long-chain n-3 fatty acids including DPA, and given either 500 μL per day of corn oil alone (control group; Mazola Corn Oil, Corn Products Inc., St. Louis, MO) or an equal volume of corn oil containing a small amount of purified DPA [Nu-Chek Prep Inc., Elysian, MN, U-101-A (free fatty acid form), >99% DPA devoid of 20:5n-3 and 22:6n-3] via oral gavage. The fatty acid composition of the two oral gavages, namely corn oil versus corn oil-DPA, contained mostly oleic acid (28.9 and 26.5 wt%) and linoleic acid (55.0 and 53.4 wt%) with DPA representing 0 and 4.24 wt%, respectively, of total fatty acids. The oral gavages were administered for a period of 10 days after which time the animals were sacrificed and various tissues (plus serum via blood centrifugation) were taken for analyses. The dietary conditions and compositions (including oral gavage) for the DPA group (DPA-supplemented rats) were estimated to provide approximately 2.5% of the total fat intake (oral gavage plus dietary chow) as DPA which is in the general range as reported historically for the Greenland Inuit population [9]. In absolute amounts, the DPA dose was 21.2 mg/day which is higher than Inuit intakes on a body weight basis.

Lipid and Fatty Acid Analyses

Total serum cholesterol levels were determined by a microcolorimetric method [10]. The individual lipid classes were separated by thin-layer chromatographic (TLC) procedures following lipid extraction using methods similar to those described [11, 12]. The TLC plate developed in the neutral lipid system provided for the separation of triacylglycerols (TAG), total phospholipids (PL), non-esterified fatty acids (NEFA), and cholesteryl esters (CE) whereas development in the polar lipid system provided isolations of the individual phospholipids including phosphatidylcholine (PtdCho), phosphatidylethanolamine (PtdEtn), phosphatidylinositol (PtdIns), phosphatidylserine (PtdSer), and sphingomyelin (CerPCho) as described [11, 12]. The addition of known amounts of an internal standard (odd-carbon fatty acid) to the total lipid (TL) extracts and the isolated lipid fractions provided for determination of both the individual and total fatty acid amounts plus the relative wt% of total fatty acids following transmethylation and gas–liquid chromatographic analyses [11, 12].

Statistical Analyses

The experimental data were analyzed for statistical significance by Student's t-test [13].

Results

The initial and final body weights (following 10 days of oral gavage treatment) for all animals ($n = 17$) were 49.4 ± 0.4 (mean ± SE) and 102.2 ± 2.4 g, respectively. Weights of liver, heart, and kidney were 5.13 ± 0.17, 0.47 ± 0.01, and 0.57 ± 0.02 g, respectively. Total serum fatty acid amounts in the TL of the DPA-supplemented rats were significantly lower (by 15.7% overall) relative to controls (Table 1). Moderately lower levels were also found for the PL (by 13.4%) and the CE (by 15.9%)

Table 1 Concentrations (μmol/g serum) of total fatty acids in serum lipids from control and DPA-supplemented rats

Lipid class	Control	DPA
Total lipid (TL)	4.71 ± 0.25	3.97 ± 0.13[a]
Total phospholipids (PL)	2.02 ± 0.05	1.75 ± 0.05[b]
Triacylglycerols (TAG)	0.93 ± 0.13	0.73 ± 0.12
Non-esterified fatty acids (NEFA)	0.24 ± 0.02	0.27 ± 0.02
Cholesteryl esters (CE)	1.13 ± 0.06	0.95 ± 0.06[a]
Total cholesterol (TC), μmol sterol/g serum	2.17 ± 0.07	1.91 ± 0.04[b]

Data are mean values ± SE for 8 rats from each group

Statistical significance (DPA vs. control): [a]$P < 0.05$, [b]$P < 0.01$

whereas this was not statistically significant in the case of the TAG where the mean level was 21.5% lower as compared to the controls. Total serum cholesterol levels were moderately lower (by 12.0%) and statistically significant ($P < 0.01$) for the DPA group relative to controls (Table 1). The absolute amount of DPA in TL (μmol/100 g serum) increased by 2.28-fold in the DPA-supplemented rats relative to controls (Fig. 1) with considerable increases apparent in all the individual lipid classes. The single major reservoir of DPA following DPA supplementation was in the PL at a mean of 3.66 μmol/100 g serum (49.2% of DPA in TL) with the TAG, NEFA, and CE contributing 32.0, 13.1, and 5.3%, respectively. The corresponding concentrations (μmol/100 g serum) for EPA in the TL of the control versus DPA groups were 5.65 ± 0.50 and 12.13 ± 0.69, respectively, with a P value of <0.001. Interestingly, the single major reservoir of EPA was in the serum CE at 6.55 ± 0.46 μmol/100 g serum which represented 54.0% of the EPA in the TL for the DPA group. The absolute levels (μmol/100 g serum) of DHA in serum TL (Fig. 2) were not significantly different with values of

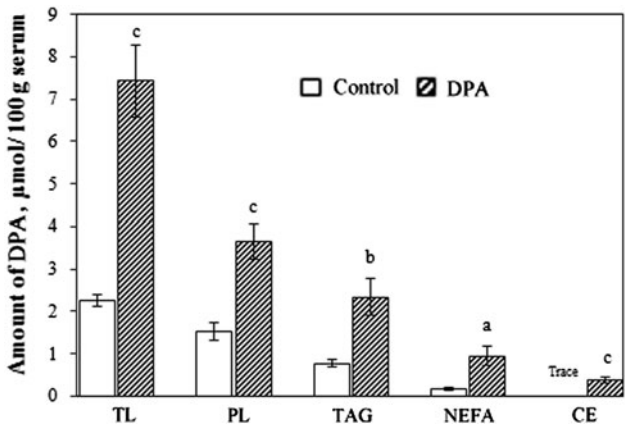

Fig. 1 Concentrations of DPA (22:5n-3) in serum lipids from control and DPA-supplemented rats. Statistical significance (DPA vs. control): [a]$P < 0.05$, [b]$P < 0.01$, [c]$P < 0.001$

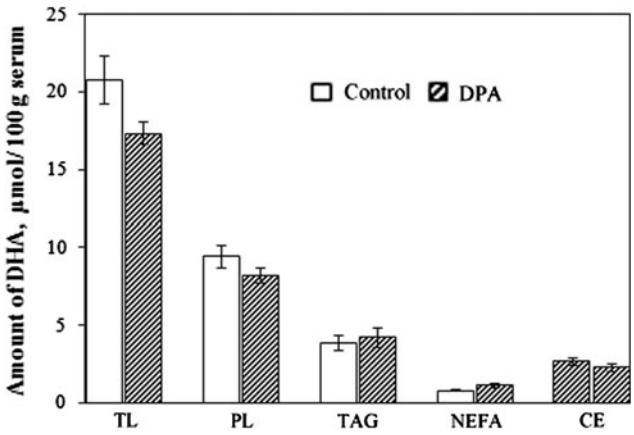

Fig. 2 Concentrations of DHA (22:6n-3) in serum lipids from control and DPA-supplemented rats. No statistically significant differences were found between the DPA versus control group

20.79 ± 1.55 and 17.38 ± 0.76 for the control and DPA groups, respectively. Significantly lower concentrations ($P < 0.001$) of ARA but not 18:2n-6 were found in the TL of the DPA group (48.70 ± 4.70) relative to the controls (87.88 ± 3.74).

The relative mol% of total fatty acids as DPA following supplementation was moderately higher in the TAG fraction as compared to the serum PL with the lowest level being in the CE (Table 2). A moderately higher level of DHA ($P < 0.05$) was found only in the TG upon DPA supplementation although the absolute amounts of DHA (in μmol/g serum) were not significantly different between the control and DPA group for any of the lipid fractions (data not shown). Significantly higher levels of EPA (Table 2) were found in the DPA group—particularly in the TAG and CE fractions. Markedly lower levels of arachidonic acid (ARA, 20:4n-6) but not linoleic acid (18:2n-6) were found in the TAG, PL, and CE within the DPA group relative to controls.

The total fatty acid amounts in TAG were considerably lower in the liver TAG of the DPA group relative to control (1.49 ± 0.28 vs. 4.07 ± 0.94, μmol/g tissue) and in the kidney TAG (2.30 ± 0.25 vs. 4.93 ± 0.56) whereas no statistically significant differences were found in the heart TAG or in the PL for any of the three tissues. The absolute concentrations of DPA in the total lipids of liver, heart, and kidney were dramatically higher (by 2.4-, 10.8-, and 5.1-fold, respectively) in the DPA group relative to controls without any statistically significant differences in the DHA contents (Table 3). The tissue concentrations of DPA in the PL fraction for the DPA group contributed 1.26 ± 0.11 (mean ± SE), 1.17 ± 0.05, and 0.54 ± 0.03 μmol/g tissue which represented 52.1, 45.2, and 51.9% of the DPA amounts in TL for liver, heart, and kidney, respectively. EPA levels were higher in the DPA group by 3.9-, 2.2-, and 4.1-fold, respectively. Considerably lower levels of ARA

Table 2 Fatty acid compositions of serum lipids from control and DPA-supplemented rats (mol% of total fatty acids)

Fatty acids	TAG		Total PL		NEFA		CE	
	Control	DPA	Control	DPA	Control	DPA	Control	DPA
16:0	25.50 ± 0.59	25.34 ± 1.32	25.64 ± 0.43	27.40 ± 0.45	26.69 ± 1.01	25.31 ± 1.05	9.00 ± 1.10	10.12 ± 1.75
18:0	5.83 ± 0.60	6.21 ± 0.60	24.53 ± 0.63	23.46 ± 0.51	9.06 ± 0.42	11.45 ± 0.84	0.21 ± 0.14	0.55 ± 0.24
18:1	36.23 ± 0.66	31.51 ± 2.28	7.86 ± 0.14	8.03 ± 0.31	27.63 ± 1.23	23.09 ± 1.31	8.48 ± 0.45	13.55 ± 0.75[c]
18:2n-6	20.59 ± 0.46	20.06 ± 0.51	20.61 ± 0.75	23.01 ± 1.17	21.37 ± 0.52	22.81 ± 1.13	27.03 ± 0.82	32.56 ± 1.50[b]
18:3n-3	0.83 ± 0.05	0.76 ± 0.08	0.01 ± 0.01	0.02 ± 0.02	0.96 ± 0.06	0.75 ± 0.14	0.02 ± 0.02	0.08 ± 0.04
20:4n-6 (ARA)	3.51 ± 0.38	2.02 ± 0.36[a]	14.47 ± 0.40	9.48 ± 0.42[c]	8.89 ± 0.56	6.83 ± 1.82	50.22 ± 1.22	32.57 ± 1.64[c]
20:5n-3 (EPA)	1.29 ± 0.13	3.85 ± 1.01[a]	0.66 ± 0.26	1.10 ± 0.10	0.63 ± 0.06	2.08 ± 0.25[c]	2.60 ± 0.21	6.96 ± 0.53[c]
22:4n-6	0.39 ± 0.04	0.03 ± 0.02[c]	0.47 ± 0.03	0.39 ± 0.04	0.45 ± 0.05	Trace[c]	Trace	Trace
22:5n-6	0.34 ± 0.02	0.01 ± 0.01[c]	0.30 ± 0.02	0.03 ± 0.02[c]	0.46 ± 0.05	Trace[c]	Trace	Trace
22:5n-3 (DPA)	0.93 ± 0.10	3.78 ± 0.82[a]	0.83 ± 0.13	2.18 ± 0.22[c]	0.58 ± 0.09	3.41 ± 0.63[b]	Trace	0.41 ± 0.07[c]
22:6n-3 (DHA)	4.57 ± 0.42	6.43 ± 0.64[a]	4.63 ± 0.48	4.90 ± 0.30	3.28 ± 0.27	4.28 ± 0.38	2.43 ± 0.16	3.20 ± 0.48

Data are mean values ± SE for each group

Statistical significance (DPA vs. control): [a]$P < 0.05$, [b]$P < 0.01$, [c]$P < 0.001$

Table 3 Concentrations (μmol/g) selected fatty acids in total lipids of liver, heart, and kidney from control and DPA-supplemented rats

Fatty acids	Liver		Heart		Kidney	
	Control	DPA	Control	DPA	Control	DPA
DPA (22:5n-3)	0.72 ± 0.08	2.42 ± 0.30[a]	0.22 ± 0.02	2.59 ± 0.20[b]	0.17 ± 0.03	1.04 ± 0.09[b]
DHA (22:6n-3)	7.01 ± 0.57	6.69 ± 0.63	2.01 ± 0.21	1.92 ± 0.09	1.21 ± 0.10	1.18 ± 0.06
EPA (20:5n-3)	0.31 ± 0.06	1.51 ± 0.19[a]	0.06 ± 0.00	0.19 ± 0.02[b]	0.43 ± 0.02	2.20 ± 0.08[b]
ARA (20:4n-6)	12.80 ± 1.00	7.83 ± 0.30[a]	3.13 ± 0.23	3.00 ± 0.22	8.01 ± 0.44	5.43 ± 0.24[a]

Data are mean values ± SE for each group

Statistical significance (DPA vs. control): [a]$P < 0.01$, [b]$P < 0.001$

were found in the liver and kidney upon DPA supplementation relative to controls with no significant differences appearing in heart tissue. No significant differences in the absolute amounts of 18:2n-6 were found in any tissue between the DPA and control groups (data not shown). The relative mol% of total fatty acids as DPA was found to be significantly higher in the TL, PL, and TAG for all three tissues in the DPA group (Tables 4, 5, 6). The DPA rose to similar levels (mean values of 2.93–3.62 mol%) in liver TL, PL, and TAG upon DPA supplementation with the highest level by far of DPA in the PL of all tissues being in the heart (11.09 mol%). In the case of TAG, the highest level of DPA following DPA-supplementation was in the kidney (5.33 mol%) followed by the heart and liver. The DHA levels as mol% were significantly higher in the DPA group relative to controls in the TAG but not the PL of all three tissues. In heart tissue, the DHA level was actually significantly lower in the PL fraction of the DPA group. Following DPA supplementation, the mol% of EPA was considerably higher in the PL as compared to the TAG fraction for all tissues and, in the case of the kidney, the mol% as DPA markedly surpassed that of DPA itself. In all three tissues, the PL exhibited a significant lowering of the mol% as ARA in the DPA group which was even more pronounced in the case of 22:5n-6.

The relative mass distribution (based on μmol/g tissue) for the esterified DPA (DPA group) found in association with the individual phospholipid types in the three tissues (Fig. 3 a–c) indicates that the major reservoir of DPA was almost equally distributed between PtdCho (39.3–46.4% of total) and PtdEtn (38.0–44.7% of total). The highest mol% of fatty acids as DPA for each individual phospholipid (Table 7) was found in heart tissue (relative to liver and kidney). In contrast, the levels of EPA for all individual phospholipids were considerably higher in kidney compared to the corresponding phospholipids in the other

Table 4 Fatty acid compositions of lipid classes from livers of control and DPA-supplemented rats (mol% of total fatty acids)

Fatty acids	TL		Total PL		TAG	
	Control	DPA	Control	DPA	Control	DPA
16:0	23.97 ± 0.75	23.80 ± 0.68	19.99 ± 0.40	21.16 ± 0.80	37.09 ± 0.85	38.13 ± 1.04
18:0	17.51 ± 0.28	18.94 ± 0.90	26.27 ± 0.43	24.61 ± 0.52[a]	2.01 ± 0.21	3.03 ± 0.89
18:1	19.33 ± 0.99	15.15 ± 1.44[a]	7.01 ± 0.06	7.67 ± 0.44	43.45 ± 0.71	37.63 ± 3.05
18:2n-6	12.83 ± 0.30	13.95 ± 0.41	9.20 ± 0.30	12.44 ± 0.26[c]	14.11 ± 0.51	13.85 ± 1.20
18:3n-3	0.12 ± 0.02	0.06 ± 0.02	0.01 ± 0.01	0.01 ± 0.01	0.14 ± 0.06	0.14 ± 0.06
20:4n-6 (ARA)	15.64 ± 0.40	11.99 ± 0.77[b]	23.94 ± 0.25	16.62 ± 0.51[c]	0.60 ± 0.12	0.55 ± 0.12
20:5n-3 (EPA)	0.38 ± 0.06	2.24 ± 0.19[c]	0.38 ± 0.05	2.40 ± 0.21[c]	0.27 ± 0.18	0.69 ± 0.32
22:4n-6	0.46 ± 0.02	0.26 ± 0.04[b]	0.36 ± 0.05	0.33 ± 0.07	0.40 ± 0.06	0.03 ± 0.02[b]
22:5n-6	0.33 ± 0.03	Trace[c]	0.28 ± 0.06	Trace[b]	0.23 ± 0.06	Trace[a]
22:5n-3 (DPA)	0.88 ± 0.06	3.62 ± 0.32[c]	0.11 ± 0.11	3.10 ± 0.25[c]	0.32 ± 0.04	2.93 ± 0.52[b]
22:6n-3 (DHA)	8.56 ± 0.29	9.98 ± 0.31[a]	12.44 ± 0.38	11.66 ± 0.33	1.37 ± 0.19	3.02 ± 0.54[a]

Data are mean values ± SE for each group

Statistical significance (DPA vs. control): [a]$P < 0.05$, [b]$P < 0.01$, [c]$P < 0.001$

Table 5 Fatty acid compositions of lipid classes from hearts of control and DPA-supplemented rats (mol% of total fatty acids)

Fatty acids	TL		Total PL		TAG		NEFA	
	Control	DPA	Control	DPA	Control	DPA	Control	DPA
16:0	18.41 ± 0.87	18.26 ± 0.35	14.77 ± 0.33	15.06 ± 0.45	28.70 ± 0.44	32.44 ± 1.01[a]	20.74 ± 0.51	22.42 ± 1.46
18:0	22.48 ± 0.21	21.87 ± 0.53	24 .66 ± 0.12	25.41 ± 0.22[a]	7.72 ± 0.46	7.97 ± 0.32	15.03 ± 0.23	15.15 ± 0.64
18:1	12.63 ± 0.39	11.66 ± 0.50	8.11 ± 0.22	7.86 ± 0.27	36.04 ± 0.53	30.67 ± 0.43[c]	19.62 ± 0.57	17.20 ± 0.65[a]
18:2 n-6	19.25 ± 0.49	16.47 ± 0.40[b]	18.52 ± 0.60	15.44 ± 0.55[b]	24.92 ± 0.38	21.56 ± 0.57[c]	21.38 ± 0.44	18.90 ± 0.59[b]
18:3n-3	0.19 ± 0.03	0.17 ± 0.02	0.01 ± 0.00	Trace	0.81 ± 0.06	0.82 ± 0.03	0.42 ± 0.04	0.32 ± 0.04
20:4n-6 (ARA)	15.04 ± 0.68	12.14 ± 0.60[b]	17.82 ± 0.33	14.45 ± 0.41[c]	0.71 ± 0.02	0.38 ± 0.02[c]	12.21 ± 0.49	8.46 ± 0.31[c]
20:5n-3 (EPA)	0.29 ± 0.01	0.77 ± 0.04[c]	0.29 ± 0.01	0.78 ± 0.04[c]	0.12 ± 0.01	0.46 ± 0.04[c]	0.39 ± 0.01	1.03 ± 0.04[c]
22:4n-6	0.61 ± 0.03	0.30 ± 0.04[c]	0.75 ± 0.03	0.35 ± 0.01[c]	0.11 ± 0.03	0.04 ± 0.02	0.53 ± 0.02	0.16 ± 0.02[c]
22:5n-6	0.34 ± 0.03	0.13 ± 0.02[c]	0.38 ± 0.03	0.15 ± 0.01[c]	0.04 ± 0.02	0.02 ± 0.01	0.26 ± 0.02	0.08 ± 0.00[c]
22:5n-3 (DPA)	1.05 ± 0.07	10.40 ± 0.28[c]	1.18 ± 0.05	11.09 ± 0.05[c]	0.14 ± 0.01	4.74 ± 0.50[c]	1.03 ± 0.07	9.98 ± 0.96[c]
22:6n-3 (DHA)	9.70 ± 0.94	7.83 ± 0.29	13.51 ± 0.56	9.41 ± 0.34[c]	0.69 ± 0.03	0.90 ± 0.05[b]	8.40 ± 0.58	6.29 ± 0.38[a]

Data are mean values ± SE for each group

Statistical significance (DPA vs. control): [a]$P < 0.05$, [b]$P < 0.01$, [c]$P < 0.001$

tissues (Table 7). The highest EPA:DPA molar ratios for all individual phospholipids were found in the kidney ranging from 1.03 in PtdIns to 5.74 in PtdEtn. The corresponding ratios across individual phospholipids were lowest in heart tissue (0.03–0.08) with intermediary ratios being found in the liver (0.15–0.91).

Discussion

Previous studies involving the feeding of dietary seal oil to human subjects have demonstrated a significant elevation in the level of DPA in the circulating lipid fractions [5, 6] as well as a significant rise in DPA concentrations in tissue lipid in animal studies [14]. Such effects cannot be directly attributed to the consumption of DPA since it represents approximately 5% of the fatty acids in seal oil with the higher level of EPA having the capacity to generate considerable amounts of DPA via chain elongation [15, 16]. In addition, previous studies in humans on the effects of dietary seal on circulating lipids [5, 6] cannot be attributed to the effects of DPA specifically since EPA plus DHA are more predominant components of such oils. In their newly released review, Kaur et al. [17] have updated the current knowledge available on the metabolism and the biological effects of DPA. The recently published study by Kaur et al. [8] evaluated the effect of purified dietary DPA directly in rats on the fatty acid compositions of liver, adipose, heart, skeletal muscle, and brain. The present study has measured changes in plasma and tissue lipid levels and fatty acid

Table 6 Fatty acid compositions of lipid classes from kidneys of control and DPA-supplemented rats (mol% of total fatty acids)

Fatty acids	TL		Total PL		TAG	
	Control	DPA	Control	DPA	Control	DPA
16:0	26.78 ± 0.72	25.61 ± 0.34	24.26 ± 0.62	24.62 ± 0.60	32.35 ± 1.44	29.15 ± 1.03
18:0	17.10 ± 0.09	17.90 ± 0.09[b]	20.19 ± 0.49	19.98 ± 0.33	8.12 ± 1.00	7.92 ± 0.89
18:1	15.19 ± 0.39	13.52 ± 0.35[b]	11.14 ± 0.15	11.19 ± 0.09	32.81 ± 0.63	31.16 ± 0.82
18:2n-6	16.93 ± 0.23	17.30 ± 0.23	16.34 ± 0.33	17.34 ± 0.45	24.51 ± 0.75	23.32 ± 0.79
18:3n-3	0.03 ± 0.01	0.24 ± 0.20	0.01 ± 0.01	0.01 ± 0.01	0.64 ± 0.05	0.66 ± 0.11
20:4n-6 (ARA)	18.98 ± 0.44	13.88 ± 0.30[c]	23.01 ± 0.42	15.87 ± 0.46[c]	0.62 ± 0.08	0.60 ± 0.12
20:5n-3 (EPA)	1.02 ± 0.04	5.64 ± 0.25[c]	1.17 ± 0.04	6.05 ± 0.30[c]	0.06 ± 0.03	0.40 ± 0.04[c]
22:4n-6	0.59 ± 0.04	0.26 ± 0.05[c]	0.55 ± 0.08	0.24 ± 0.04[a]	0.22 ± 0.04	0.13 ± 0.04
22:5n-6	0.10 ± 0.04	Trace[a]	0.05 ± 0.05	Trace	0.01 ± 0.01	Trace
22:5n-3 (DPA)	0.38 ± 0.06	2.64 ± 0.18[c]	0.28 ± 0.06	1.78 ± 0.06[c]	0.11 ± 0.02	5.33 ± 0.50[c]
22:6n-3 (DHA)	2.88 ± 0.19	3.02 ± 0.12	3.00 ± 0.13	2.92 ± 0.15	0.55 ± 0.04	1.31 ± 0.12[c]

Data are mean values ± SE for each group

Statistical significance (DPA vs. control): [a]$P < 0.05$, [b]$P < 0.01$, [c]$P < 0.001$

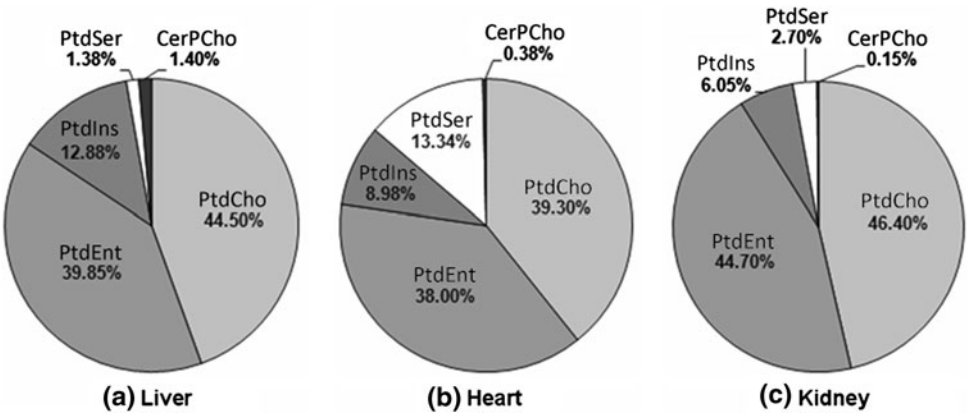

Fig. 3 The relative % distribution (based on μmol/g tissue) for the esterified DPA (DPA group) found in association with the individual phospholipid types in the liver, heart, and kidney

compositions resulting from DPA ingestion including an extensive analyses of the resulting fatty acid alterations in the liver, heart, and the kidney and individual phospholipid types therein.

The moderately lower levels of total lipid (based on total fatty acid concentrations) in the serum lipid of the DPA group (Table 1) was accounted for by significantly lower levels of the summed fatty acid as PL and CE while the lower levels as TAG did not reach statistical significance. Such measurements of circulating lipids were not reported in the recent publication by Kaur et al. [8]. Moderately lower levels of total serum cholesterol were also found in the present study as was found for plasma cholesterol levels in rats following dietary treatment with concentrated DHA [16]. In the circulation, serum PL was the single predominant reservoir of esterified DPA whereas the TAG fraction showed a moderately greater enrichment (as mol% of total fatty acids) in DPA as compared to PL (Table 2). Interestingly, the very low level of accumulation of DPA in serum CE (0.41%) upon supplementation (Table 2) resulted in the DPA:ARA molar ratio in serum CE to be only a small fraction of that in the corresponding PL (0.012 vs. 0.23). Since serum CE is derived from LCAT (lecithin:cholesterol acyltransferase) activity [18, 19] and tissue (liver) ACAT (acyl-CoA:cholesterol acyltransferase) activity [20], such esterification reactions appear to discriminate against substrates containing DPA. Previous human studies on plasma LCAT have suggested a preferential utilization of EPA-containing species of phospholipid (lecithin) relative to DHA species [21] which appears in keeping with the much higher levels of EPA (relative to DHA) in the serum CE relative to the PL of the DPA supplemented rats (Table 2). It is not yet known if the relative participation of DPA species in the LCAT reaction may influence its apparent role in reducing atherosclerosis [19]. It is noted that higher intakes of DPA in humans and higher levels of DPA in the circulation have been associated with protection against carotid atherosclerosis [22] and coronary heart disease [3].

Table 7 Long-chain polyunsaturated fatty acid compositions (mol% of total fatty acids) and EPA:DPA ratios of individual phospholipids from tissues of DPA-supplemented rats

Fatty acid	20:4n-6 (ARA)	20:5n-3 (EPA)	22:4n-6	22:5n-6	22:5n-3 (DPA)	22:6n-3 (DHA)	EPA:DPA Ratio
Liver							
PtdCho	14.41 ± 0.70	2.44 ± 0.24	0.02 ± 0.01	0.02 ± 0.01	2.69 ± 0.21	10.55 ± 0.45	0.91
PtdEtn	17.17 ± 0.61	3.41 ± 0.29	0.09 ± 0.02	0.01 ± 0.01	4.48 ± 0.35	18.24 ± 0.65	0.76
PtdIns	34.49 ± 0.51	0.68 ± 0.08	0.33 ± 0.03	0.12 ± 0.03	4.41 ± 0.48	5.10 ± 0.11	0.15
PtdSer	14.87 ± 0.75	2.37 ± 0.27	0.30 ± 0.09	Trace	3.49 ± 0.38	12.97 ± 0.78	0.68
Heart							
PtdCho	17.31 ± 0.56	0.76 ± 0.04	0.07 ± 0.03	0.03 ± 0.01	10.49 ± 0.43	6.07 ± 0.31	0.07
PtdEtn	15.13 ± 0.24	1.17 ± 0.06	0.23 ± 0.02	0.17 ± 0.01	14.11 ± 0.47	19.80 ± 0.52	0.08
PtdIns	23.60 ± 0.65	0.73 ± 0.06	0.08 ± 0.02	0.01 ± 0.01	16.23 ± 0.33	3.81 ± 0.44	0.04
PtdSer	4.43 ± 0.20	0.40 ± 0.02	0.93 ± 0.06	0.38 ± 0.03	13.32 ± 0.32	12.36 ± 0.43	0.03
Kidney							
PtdCho	8.25 ± 0.24	3.77 ± 0.28	0.03 ± 0.01	0.01 ± 0.00	1.73 ± 0.15	3.94 ± 0.13	2.18
PtdEtn	25.90 ± 0.83	10.84 ± 0.40	0.17 ± 0.01	Trace	1.89 ± 0.09	3.46 ± 0.13	5.74
PtdIns	31.64 ± 0.48	2.61 ± 0.22	0.25 ± 0.04	0.08 ± 0.01	2.54 ± 0.15	3.54 ± 0.27	1.03
PtdSer	19.18 ± 0.45	8.86 ± 0.38	0.45 ± 0.03	0.45 ± 0.03	3.20 ± 0.07	1.45 ± 0.06	2.77

Data are mean values ± SE for each group or mean values only (EPA:DPA ratio)

The considerably lower concentrations of TAG in the liver (by 64%) and kidney (by 53%) in the DPA-supplemented rats as found herein are consistent with the TAG-lowering effect of fish oils containing EPA plus DHA in these same tissues as reported [11, 23]. Potential mechanisms for such a suppression in tissue TAG levels with dietary DPA likely involve a diminution in lipogenic enzyme activities and corresponding gene expression, a significant suppression in 1,2-diacylglycerol conversion to TAG via CoA:1,2-diacylglycerol acyltransferase, and/or increased fatty acid oxidation [11].

In addition to the markedly higher concentrations of DPA in the TL and individual lipid types relative to controls in the DPA group, considerably higher levels of EPA were also found in the TL of serum, liver, heart, and kidney along with considerable heterogeneity in the magnitude of such elevations across the various lipid classes (Fig. 1; Tables 3, 4, 5, 6). The DPA concentration in liver averaged 2.42 μmol/g tissue (Table 3) which was approximately 20% lower than that reported upon DPA supplementation in the recent paper by Kaur et al. [8] which likely reflects the lower dose in our study (21.2 vs. 50 mg/day) and differences in animal body weights. We found a moderately higher rise in concentration of DPA in heart as compared to liver as observed by others [8] which may reflect a preferential uptake of DPA by cardiac tissue. In their study, Kaur et al. [8] observed increased concentrations of EPA, in addition to DPA, in liver, heart, and skeletal muscle which they attributed to the process of DPA retroconversion into EPA in vivo as described by others and attributed to involve the peroxisomal acyl-CoA oxidation [24, 25]. The former authors [8] estimated the extent of apparent retroconversion of DPA to EPA as [ΔEPA × 100/Δ(DPA + EPA)] and reported such to be 28% in liver and 4% in heart. Using such an approach from our data (Table 3), our corresponding estimates are generally similar to the aforementioned and amount to 41 and 5%, respectively. The moderately higher estimated percentages from our data may be due in part to the longer (10 day) supplementation regimen in our research as compared to 7 days by the other group [8]. It is particularly interesting that the estimated % conversion of DPA to EPA based on our kidney data (Table 3) is 67% and dramatically higher than that reported for all other tissues by us herein plus the previous work [8]. It is possible that the kidney may have an unique affinity for the uptake of EPA; however, this appears unlikely since it has been observed that the feeding of purified EPA to rats resulted in a lower mean EPA % in the kidney as compared to liver lipids [16]. It is likely that the kidney has a particularly high capacity for the retroconversion of DPA to EPA which accounts for the predominance of EPA over DPA following DPA supplementation in the total lipid, total phospholipid, and major phospholipid fractions (Tables 3, 6, 7).

The significantly lower percentages of fatty acids as ARA in the PL of all tissues with DPA supplementation (Tables 4, 5, 6), and as DHA in heart PL, likely represents competition from DPA and the derived EPA for esterification via acyltransferase activities. The relative cellular availability and preferential utilization of DPA versus other long-chain n-3 and n-6 fatty acids plus its enzymic competition with such for entry into individual phospholipid

types via various de novo biosynthetic, deacylation-reacylation, and transacylation reactions [26, 27] likely contribute to the fatty acid profiles in PtdCho, PtdEtn, PtdIns, and PtdSer following DPA ingestion (Table 7). The particularly high enrichment of heart PtdIns, PtdEtn, and PtdSer with DPA upon supplementation (Table 7) may possibly arise from a preferential utilization of DPA-CoA by the corresponding acyltransferase reactions and/or other reactions in the biosynthetic pathways. The marked differences in such compositions indicate that much heterogeneity exists in the regulation of DPA levels along with other long-chain polyunsaturates (PUFA) between individual phospholipid types and tissues. The extent to which these compositions influence the formation and functioning of bioactive products resulting from DPA such as hydroxylated derivatives via lipoxygenase activities [28] including cellular mediators from ARA, EPA, and DHA [29] upon their enzymic release from these PL reservoirs remains to be studied.

The observed serum lipid-lowering potential of DPA and other physiological effects will need evaluation in human trials as concentrates of DPA (devoid of EPA/DHA) become available in bulk amounts. Our current results strongly suggest a particularly high capacity for the apparent retroconversion of DPA to EPA in the kidney which is worthy of further investigation with respect to mechanisms and potential significance to renal functioning in health and disease.

Acknowledgments This research was supported by a research grant from the Medical Research Council of Canada (Grant 829–88). The authors extend their appreciation to Emily Sicilia for her assistance in preparation of the manuscript.

References

1. Dyerberg J (1989) Coronary heart disease in Greenland Inuit: a paradox. Implications for western diet patterns. Arctic Med Res 48:47–54
2. Manerba A, Vizzardi E, Metra M, Dei Cas L (2010) n-3 PUFAs and cardiovascular disease prevention. Future Cardiol 6:343–350
3. Simon JA, Hodgkins ML, Browner WS, Neuhaus JM, Bernert JT Jr, Hulley SB (1995) Serum fatty acids and the risk of coronary heart disease. Am J Epidemiol 142:469–476
4. Cheryk LA, Conquer JA, Holub BJ, Gentry PA (1999) Docosahexaenoic acid and docosapentaenoic acid incorporation into human platelets after 24 and 72 h: inhibitory effects on platelet reactivity. Platelets 10:203–211
5. Conquer JA, Cheryk LA, Chan E, Gentry PA, Holub BJ (1999) Effect of supplementation with dietary seal oil on selected cardiovascular risk factors and hemostatic variables in healthy male subjects. Thromb Res 96:239–250
6. Meyer BJ, Lane AE, Mann NJ (2009) Comparison of seal oil to tuna oil on plasma lipid levels and blood pressure in hypertriglyceridaemic subjects. Lipids 44:827–835
7. Howe P, Meyer B, Record S, Baghurst K (2006) Dietary intake of long-chain ω-3 polyunsaturated fatty acids: contribution of meat sources. Nutrition 22:47–53
8. Kaur G, Begg DP, Barr B, Garg M, Cameron-Smith D, Sinclair AJ (2009) Short-term docosapentaenoic acid (22:5n–3) supplementation increases tissue docosapentaenoic acid, DHA and EPA concentrations in rats. Br J Nutr 103:32–37
9. Bang HO, Dyerberg J, Sinclair HM (1980) The composition of the Eskimo food in north western Greenland. Am J Clin Nutr 33:2657–2661
10. Mercer NJ, Holub BJ (1981) Measurement of hepatic sterol synthesis in the Mongolian gerbil in vivo using [3H] water: diurnal variation and effect of type of dietary fat. J Lipids Res 22:792–799
11. Yeo YK, Holub BJ (1990) Influence of dietary fish oil on the relative synthesis of triacylglycerol and phospholipids in rat liver in vivo. Lipids 25:811–814
12. Skeaff CM, Holub BJ (1987) Nutritional regulation of cellular phosphatidylinositol. Meth Enzymol 141:234–244
13. Steel RGD, Torrie JH (1980) Principles and procedures of statistics, 2nd edn. Mcgraw-Hill, New York
14. Murphy MG, Wright V, Ackman RG, Horackova M (1997) Diets enriched in menhaden fish oil, seal oil, or shark liver oil have distinct effects on the lipid and fatty-acid composition of guinea pig heart. Mol Cell Biochem 177:257–269
15. von Schacky C, Weber PC (1985) Metabolism and effects on platelet function of the purified eicosapentaenoic and docosahexaenoic acids in humans. J Clin Invest 76:2446–2450
16. Froyland L, Vaagenes H, Asiedu DK, Garras A, Lie O, Berge RK (1996) Chronic administration of eicosapentaenoic acid and docosahexaenoic acid as ethyl esters reduced plasma cholesterol and changed the fatty acid composition in rat blood and organs. Lipids 31:169–178
17. Kaur G, Cameron-Smith D, Garg M, Sinclair AJ (2011) Docosapentaenoic acid (22:5n-3): a review of its biological effects. Prog Lipid Res 50:28–34
18. Ng DS (2004) Insight into the role of LCAT from mouse models. Rev Endocr Metabol Dis 5:311–318
19. Rouset X, Vaisman B, Amar M, Sethi AA, Remaley AT (2009) Lecithin: cholesterol acyltransferase—from biochemistry to role in cardiovascular disease. Curr Opin Endocrinol Diabetes Obes 16:163–171
20. Chang C, Dong R, Miyazaki A, Sakashita N, Zhang Y, Liu J, Guo M, Li BL, Chang TY (2006) Human acyl-CoA:cholesterol acyltransferase (ACAT) and its potential as a target for pharmaceutical intervention against atherosclerosis. Acta Biochim Biophys Sin 38:151–156
21. Holub BJ, Bakker DJ, Skeaff CM (1987) Alterations in molecular species of cholesterol esters formed via plasma lecithin–cholesterol acyltransferase in human subjects consuming fish oil. Atherosclerosis 66:11–18
22. Hino A, Adachi H, Toyomasu K, Yoshida N, Enomoto M, Hirastuka A, Hirai Y, Satoh A, Imaizumi T (2004) Very long chain n-3 fatty acids intake and carotid atherosclerosis: an epidemiological study evaluated by ultrasonography. Atherosclerosis 176:145–149
23. Yeo YK, Philbrick DJ, Holub BJ (1989) Effects of dietary n-3 fatty acids on mass changes and [3H] glycerol incorporation in various glycerolipid classes of rat kidney in vivo. Biochem Biophys Acta 1006:9–14
24. Stoffel W, Eker AssadH (1970) Enzymatic studies on the mechanism of the retroconversion of C22-polyenoic fatty acids to their C20-homologues. Hoppe Seylers Z Physiol Chem 351:1545–1554

25. Reddy JK, Hashimoto T (2001) Peroxisomal beta-oxidation and peroxisome proliferator-activated receptor alpha: an adaptive metabolic system. Annu Rev Nutr 21:193–230
26. Holub BJ, Kuksis A (1978) Metabolism of molecular species of diacylglycerophospholipids. Adv Lipid Res 16:1–125
27. Yamashita A, Sugiura T, Waku K (1997) Acyltransferases and transacylases involved in fatty acid remodeling of phospholipid and metabolism of bioactive lipids in mammalian cells. J Biochem 122:1–16
28. Careaga MM, Sprecher H (1984) Synthesis of two hydroxyl fatty acids from 7, 10, 13, 16, 19-docosapentaenoic acid by human platelets. J Biol Chem 259:14413–14417
29. Serhan CN, Chiang N (2008) Endogenous pro-resolving and anti-inflammatory lipid mediators: a new pharmacologic genus. Br J Pharmacol 153(Suppl 1):S200–S215

Lipids (2011) 46:409–416
DOI 10.1007/s11745-010-3523-z

ORIGINAL ARTICLE

Dietary n-3 Fatty Acid Deficiency in Mice Enhances Anxiety Induced by Chronic Mild Stress

Akiko Harauma · Toru Moriguchi

Received: 8 September 2010 / Accepted: 21 December 2010 / Published online: 7 February 2011

Abstract Docosahexaenoic acid (DHA), is the major polyunsaturated fatty acid in the brain and is important for both the structure and the function of the nervous system. Mice were fed either an n-3 fatty acid deficient (n-3 Def) or adequate (n-3 Adq) diet for two generations. The mice were housed under two conditions, as a group or in isolation and the major point of the study was to determine whether n-3 fatty acid deficiency would enhance isolation-induced anxiety. Isolation stress was assessed using the novelty suppressed feeding paradigm (NSF) after a 3-week period and the test lasted a maximal duration of 10 min. The number of successful mice consuming food pellets within 5 min in the n-3 Def diet group was low in both housing conditions (group housing, 33% and isolated, 30%), but was 92% in the group housed and 50% in the isolated group when fed the n-3 Adq diet. In the subsequent 5 min period, the isolated housing group consuming the n-3 Adq diet increased up to 79% and the group housed animals fed the n-3 Def diet increased to 67%. However, those that consumed the n-3 deficient diet combined with isolation stress exhibited no increase. These results suggested that the n-3 deficient mice had increased anxiety that was enhanced by the chronic mild stress of social isolation.

A. Harauma · T. Moriguchi
Healthcare Research Institute,
Wakunaga Pharmaceutical Co. Ltd, 1624 Shimokoutachi,
Akitakata, Hiroshima 739-1195, Japan

A. Harauma · T. Moriguchi (✉)
Laboratory of Food and Nutritional Science, Department of Food and Life Science, School of Life and Environmental Science,
Azabu University, 1-17-71, Fuchinobe, Chuou, Sagamihara,
Kanagawa 252-5201, Japan
e-mail: moriguchi@azabu-u.ac.jp

Keywords n-3 Fatty acid · Anxiety · Stress · Novelty suppressed feeding paradigm · Mice

Abbreviations

DHA	Docosahexaenoic acid, 22:6n-3
PUFA	Polyunsaturated fatty acid(s)

Introduction

The n-3 fatty acids, α-linolenic acid (ALA, 18:3n-3), eicosapentaenoic acid (EPA, 20:5n-3) and docosahexaenoic acid (DHA, 22:6n-3) are nutritionally essential polyunsaturated fatty acids and cannot be synthesized de novo in mammals. These fatty acids, particularly DHA, exist mainly in the form of membrane phospholipids which are known to be crucial for maintaining normal brain structure and function [1]. It has been well documented that animal model of dietary n-3 fatty acids deprivation produces a loss of brain function. Several rodent studies have reported that lower DHA levels in the brain led to poorer performance on a variety of cognitive and learning tasks [2–5]. There have recently been several reports concerning various mental functions including mood variations and underlying mechanisms. For example, epidemiological studies of healthy people and postpartum women indicate a negative correlation between dietary n-3 PUFA intake and mental illness including serious mood disorders, aggression, depression, and bipolar disorder [6–9]. These findings suggest that mental illness may be associated with reduced dietary intake of n-3 fatty acids. In animal studies, Delion et al. [10] indicated that an n-3 fatty acid deficient diet specifically affects the monoaminergic system in brain.

Kodas et al. [11] showed that dietary n-3 deficiency induced changes in the synaptic levels of 5-HT. On the other hand, it has been known that monoamine level in the brain are altered by chronic mild stress which may be induced by such animal housing conditions as lack of bedding, wet bedding, a tilted cage etc. [12, 13]. These lines of inquiry together suggest that n-3 fatty acid deficiency and stress are both factors that can modulate aspects of mental illness such as depression and anxiety.

In this study, the effects of n-3 fatty acid deficiency and social isolation stress were tested in mice using the novelty suppressed feeding paradigm (NSF) with the hypothesis that the combination of these factors would lead to the highest level of anxiety [14]. The NSF test has been considered useful for assessment of anxiety as it has lower sensitivity to changes in cognitive factors and thus has been used to evaluate anti-anxiety and anti-depressant drugs [15–17].

Materials and Methods

Animals and Study Design

Female CD-1 (ICR) mice were obtained at 3 weeks of age from Charles River Japan, Inc. and fed an n-3 deficient (n-3 Def) or n-3 adequate (n-3 Adq) diet (see experimental diet, Table 1). They were maintained within our animal facility under conventional conditions with controlled temperature (23 ± 3 °C), humidity (55 ± 10%), and illumination (12 h; 0700–1900). At 7 weeks of age, they were mated with 8-week-old males of the same strain (experimental scheme presented in Fig. 1). Their litters were culled to ten pups and the pups were weaned onto the same diet as their mothers. Each individual in a cage of five mice was from a different litter. When the male offspring (second generation) were 8 weeks old, half of them in the each diet group were maintained in a cage containing five mice (group housed), the other half were housed individually for 3 weeks (isolation group). Behavioral experiments were conducted when the male mice were 11 weeks of age. Spontaneous motor activity was first measured for each mouse and after following a 15-h fast, each animal was given the NSF test [15–17].

After the behavioral experiments, they were killed by decapitation and the brain and blood were collected. Blood was spun in a refrigerated centrifuge at 2,300×*g* for 15 min at 4 °C. An aliquot of the upper plasma phase was transferred to another tube. The plasma and brain samples were frozen at −80 °C prior to lipid extraction and measurement of fatty acid composition. This experimental protocol was approved by the Animal Care and Use Committee of the Wakunaga Pharmaceutical Co. in Japan.

Table 1 Composition of experimental diets

Ingredient	Amount (g/100 g diet)	
	n-3 Def.	n-3 Adq.
Casein, vitamin free	20	20
Carbohydrate	60	60
Cornstarch	15	15
Sucrose	10	10
Dextrose	19.9	19.9
Maltose-dextrin	15	15
Cellulose	5	5
Mineral-salt mix	3.5	3.5
Vitamin mix	1	1
L-cystine	0.3	0.3
Choline bitartrate	0.25	0.25
TBHQ	0.002	0.002
Fat	10	10
Hydrogenated coconut oil	8.1	7.75
Safflower oil	1.9	1.77
Flaxseed oil	None	0.48
Fatty acid composition[a]		
Saturates	80.3	76.7
Monounsaturates	3.8	5.2
18:2n-6	15.7	15.0
18:3n-3	0.14	2.5
n-6/n-3	112	5.9

The two experimental diets, an n-3 fatty acid adequate diet (n-3 Adq) and an n-3 fatty acid deficient diet (n-3 Def), were based on the AIN-93 formulation with several modifications to obtain the extremely low basal level of n-3 fatty acid required in this study

[a] The 20:4n-6, 20:5n-3 and 22:6n-3 fatty acids were less than 0.01%

Experimental Diet

The two experimental (n-3 Def and n-3 Adq) diets used were based on the AIN-93G diet recommendations for rodents (Table 1). The fat sources were altered to provide for the low n-3 fatty acid content required. The only difference between the n-3 Def and the n-3 Adq diets was the amount of n-3 fatty acids. This was achieved by adding a small amount of flaxseed oil to the n-3 Adq diet. The basal fat ingredients used were hydrogenated coconut and safflower oils for the n-3 Def diet. The fat content in both diets was 10/100 g diet and the amount of n-3 fatty acids as ALA in the n-3 Def and the n-3 Adq diets were 0.14 and 2.5% of total fatty acids, respectively. There was no difference in the total n-6 fatty acids between the two diets (n-3 Def, 15.7%; n-3 Adq, 15.0%). This diet was custom prepared and pelleted using low heat conditions (about 65 °C), then stored at 4 °C to prevent lipid oxidation (Oriental Yeast, Chiba, Japan) and the fatty acid distributions of the entire diet was quality assured within our own laboratory.

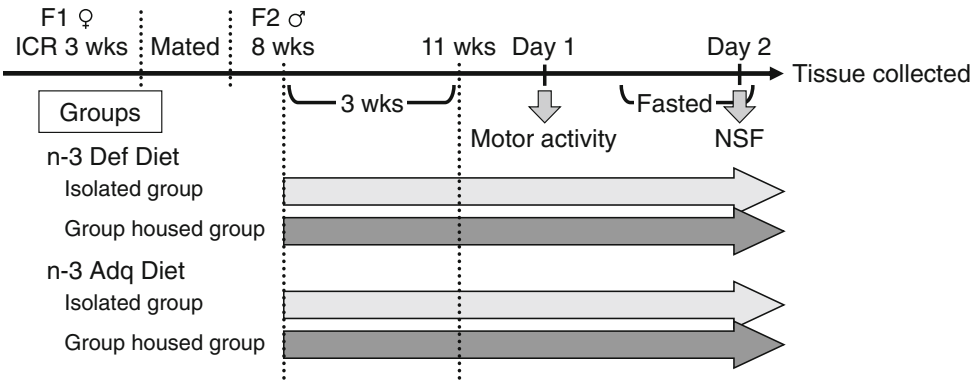

Fig. 1 Schematic diagram illustrates study design. Half of the mice in the each diet group were switched to the isolated housing condition from 8 weeks of age for 3 weeks. NSF was conducted the day following measurement of motor activity at 11 weeks of age. After NSF, the mice were killed by decapitation and plasma and brain collected and the tissues analyzed for fatty acid composition

Behavioral Experiment

The behavioral experiments including motor activity and NSF were performed in the morning (0900–1200 hours). Motor activity was measured using an activity sensor (Model NS-AS01, Neuroscience, Inc., Tokyo Japan). Each mouse was individually placed into a cage (22 × 34 × 14 cm), and the ambulatory time was measured during spontaneous motor activity for 30 min. After the measurement of motor activity, each mouse was returned to its home cage. The NSF was conducted the day following measurement of motor activity. All diet in the home cage was removed for 15 h prior to NSF testing. The NSF procedure was modified from that previously reported [15–17]. The test chamber was composed of an acrylic box (50 × 50 × 20 cm), and the floor was covered with approximately 2 cm of wooden bedding. At the time of testing, a single pellet of diet (n-3 Def or n-3 Adq diet) was placed on a platform positioned in the center of the box. A mouse was placed in a corner of the chamber and the session was recorded by video camera (HDR-SR1, SONY, Tokyo, Japan) until the mouse began to eat the pellet. The measurement time was set for 5 min and was extended to 10 min if eating behavior did not occur within the first 5 min. The parameters measured were the time to initially touch the food pellet, the latency of beginning to eat the pellet (defined as the mouse sitting on its haunches and biting the pellet with the use of forepaws) and the number of mice that were successful in eating (they ate within the measurement period). When the mouse failed to eat the pellet within 5 or 10 min, the latency was calculated as, 300 or 600 s, respectively. After starting to eat the pellet, the mouse was immediately transferred to a new cage in order to control for the time spent in the testing cage. The amount of food consumed over the 5 min period was measured. The feeding drive of each mouse was assessed by returning it to the familiar environment of its home cage immediately after the NSF test and measuring the amount of food subsequently consumed over a 5 min period.

Lipid Extraction, Transmethylation and Gas Chromatography

Tissue samples were thawed, weighed, and homogenized in methanol–hexane and methylated in acetyl chloride according to the modified method of Lepage and Roy [18]. Varying amounts of the internal standards methyl docosatrienoate (22:3n-3 for brain) or methyl tricosanoic (23:0 for plasma) were added to each sample to compensate for differences in tissue weight and lipid concentration (70 μg/250 mg brain, 20 μg/100 μl plasma). As an aid in preventing lipid oxidation during the procedures, 50 μg/ml of butylated hydroxytoluene was added in the methanol. The hexane extracts were concentrated into micro vials for gas chromatographic (GC) injection.

Fatty acid methyl esters were analyzed with a GC-2010 Network Gas Chromatograph (Shimadzu CO.LTD, Kyoto, Japan) equipped with a split injector, an AOC-20i automatic liquid sampler and an FID detector. The instrument was controlled and data was collected with GC solution (Shimadzu Co. Ltd, Kyoto, Japan). The GC column was a DB-FFAP 15 m × 0.10 mm i.d. × 0.10 μm film thickness (J&W Scientific from Agilent Technologies, California, US). The detector temperature was set at 260 °C and the injector at 250 °C. The oven temperature program began at 150 °C with a 0.25 min hold, and then ramped at 35 °C/min to 200 °C, then 3 °C/min to 225 °C with a 2.0 min hold, and finally ramped at 80 °C/min to 245 °C with a 25 min hold. Helium was used as carrier gas at a linear velocity of 56 cm/s [19]. A custom-mixed, 28-component, quantitative methyl ester standard containing 10–24 carbons and 0–6 double bonds was used for assignment of retention times and to ensure accurate quantification (Nu Chek Prep 462, Elysian, MN). The amount of each fatty acid was

expressed as the mole percentage (mol%) of total fatty acid content.

Statistical Analysis

All data are expressed as the mean ± the standard error of the mean (SEM). First touch time, food consumption and lipid composition in the plasma and brain were analyzed by Tukey test after one-way ANOVA. Latencies until eating the diet were evaluated using the Mann–Whitney *U* test, the number of successful mice were evaluated by Fisher's exact probability test (Statistica, Statsoft Japan, Tokyo, Japan).

Results

In this study, two types of diets were used including an n-3 Adq diet containing both n-6 (about 15% linoleic acid) and n-3 fatty acids (about 2.5% ALA) and an n-3 Def diet with the same level of linoleic acid but nearly devoid in n-3 fatty acids (0.14%). These diets produced no significant differences in body weight gain between dietary groups during the testing period (Table 2). Prior to starting the NSF measurements, mice were subjected to a single 30 min motor activity trial in which their moving time was recorded. There were no significant differences between any of the dietary groups in spontaneous motor activity (data not shown).

In the time of first touch of the food pellet in the NSF experiment, there was no significant difference between the n-3 Def and n-3 Adq groups in either housing condition (Table 2). The latency to eat diet in the n-3 Adq-group housed group in the first 5 min was 179.9 ± 20.7 (sec) and was significantly shorter than that of the other three groups (the n-3 Def-isolated group, 264.0 ± 24.0, $P < 0.05$; the n-3 Def-group housed, 248.8 ± 22.1, $P < 0.05$; the n-3 Adq-isolated group, 250.3 ± 19.9, $P < 0.05$). Also, these differences continued to be evident when measured after 5 min (Table 2).

The proportion of successful mice, those eating a food pellet within the first 5 min, was 30% (3/10 animal) in the n-3 Def-isolated housing group, 33% (5/15) in the n-3 Def-group housed, 50% (7/14) in the n-3 Adq-isolated group and 92% (12/13) in the n-3 Adq-group housed group, respectively (Fig. 2a). Most mice in the n-3 Def-isolated group were not able to perform the task, but the n-3 Adq-group housed animals were very successful. These proportions indicated a significant difference ($P < 0.01$) between the n-3 Def and n-3 Adq diet groups in the control breeding condition, i.e., group housed animals, but there was no significant difference between dietary groups in the isolated housing groups. Also, there was a significant difference between the isolated and group housed animals who consumed the n-3 Adq diet ($P < 0.05$), but this difference was not detected between the groups consuming the n-3 Def diet.

When the analysis of the measurement time was extended to its maximum of 10 min, the proportion of successful mice in each group increased to 67% (10/15) in the n-3 Def-group housed and to 79% (11/14) in the n-3 Adq-isolated, thus increasing to a level similar to that of the n-3 Adq-group housed animals (Fig. 2b). It was of importance that only the n-3 Def-isolated group remained at the same low level of success (30%) even when the trial was extended to 10 min. There was a significant difference between the n-3 Def and n-3 Adq diet groups in the isolated housing groups ($P < 0.01$). The significant difference between dietary groups in the group housed condition which was detected in the 5 min evaluation disappeared during the extended period. Also, there was the tendency for a difference between housing conditions in the n-3 Def diet group, although this was not observed in the 5 min evaluation. There was no appreciable difference between any of the groups in food consumption at the 5 min time point during NSF testing (data not shown).

The mice were killed and plasma and brain collected after the behavioral testing was completed. The lipid composition in these tissues was analyzed in order to

Table 2 Enhancement of the level of anxiety by n-3 fatty acid deficiency and mild stress on the novelty suppressed feeding paradigm

Group	No. of mice	Body weight (g)	First touch (s)	First 5 min latency 1 (s)	Max. 10 min latency 2 (s)
n-3 Def					
Isolated	10	47.5 ± 2.0	99.7 ± 23.0	264.0 ± 24.0[#]	474.0 ± 66.0[#]
Group housed	15	45.5 ± 1.3	61.6 ± 10.9	248.8 ± 22.1[#]	403.1 ± 53.0[#]
n-3 Adq					
Isolated	14	47.6 ± 1.0	63.7 ± 11.1	250.3 ± 19.9[#]	360.0 ± 49.1[#]
Group housed	13	48.5 ± 1.0	76.7 ± 12.8	179.9 ± 20.7	203.0 ± 37.7

Each parameter is presented as the mean ± SEM

[#] $P < 0.05$, vs. n-3 Adq group housed (Mann–Whitney *U*-test)

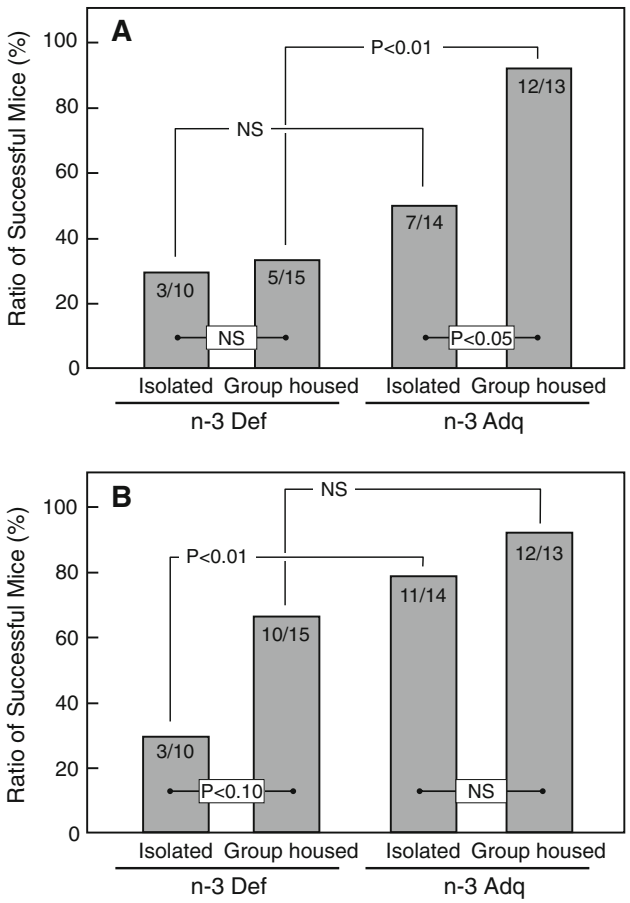

Fig. 2 The influence of the n-3 fatty acid deficiency and isolated housing on the anxiety level of mice. The measurement time was set initially for 5 min (**a**) and was extended to 10 min (**b**), if mice could not eat the food pellet within the first 5 min. The ratio of successful mice (mice who found the food and began to eat it) was calculated for each group. Significant differences between groups were analyzed by Fisher's exact probability test ($n = 10$–15 animals per group)

confirm the expected effects of the dietary fatty acid (Tables 3, 4). In both plasma and brain, there were no striking differences within the families of saturated or monounsaturated fatty acids nor the amount of total fatty acids between the n-3 Def and n-3 Adq groups in either housing condition. However, the n-3 Def group showed a marked increase in three n-6 fatty acids, 20:4n-6, 22:4n-6, 22:5n-6, and a decrease in two n-3 fatty acids, 22:5n-3 and 22:6n-3, in both tissues when compared to the n-3 Adq group and in both housing conditions. As expected, the ratio of n-6/n-3 fatty acids in the n-3 Def group markedly increased with a concomitant change in the level of n-6 and n-3 fatty acids. When animals in the two different housing conditions were compared, there were no significant differences in brain, although there were rather small differences in some plasma saturated, monounsaturated and n-6 fatty acids.

Discussion

In this study, effects of n-3 fatty acid deficiency and isolation stress on anxiety were studied. In all four groups, there was no significant difference in motor activity and the time of first touch on the NSF task, important controls for motor function, general level of arousal and motivation. However, the latency of eating the diet in the n-3 Adq group housed animals was significantly shorter than that of the other three groups in both evaluation periods ($P < 0.05$). In the first 5 min, the ratio of successful mice in the n-3 Def group was clearly lower than that of the n-3 Adq group in the group housed case ($P < 0.01$). Also, in the 10 min evaluation, the ratio of successful mice in the n-3 Adq group was greater than that of the n-3 Def group in the isolation stressed groups ($P < 0.01$). These results suggested that the n-3 Def mice had a higher anxiety level than the n-3 Adq mice. The proportion of successful mice was a better indicator than the latency to consume diet when comparing experimental diets or housing conditions.

The evaluations using two different periods (5 and 10 min) in the NSF test produce a change in the level of difficulty or what may be considered the sensitivity of the test since 10 min is long enough to allow for eating behavior in most mice. In the longer evaluation period only, the number of successful mice in the n-3 Def-group housing condition was increased and there was a tendency for a difference according to housing condition for the proportions of successful mice ($P < 0.10$). These results indicated that the anxiety level of the n-3 Def mice was increased in the isolated housing case.

Fedorova and Salem studied the anxiety level of n-3 fatty acid deficient mice exposed to sound stress using elevated plus maze performance [5]. In both n-3 fatty acid adequate and deficient dietary groups, the number of entries into the open arms and the time spent in the open arm decreased in the high-stress condition (a loud noise of 120 dB) but there was no difference between dietary groups under low-stress conditions. However, these parameters were markedly decreased in the n-3 deficient group relative to the n-3 adequate group [5, 20]. This result suggests that the n-3 fatty acid deficient animals exhibit an enhanced vulnerability to acute stressors. Nakashima et al. [21] demonstrated that n-3 fatty acid deficient mice (supplemented with safflower oil) tended to spend more time in the open arm relative to an n-3 adequate group (perilla oil) in the elevated plus maze task. However, in this task, a decline in cognitive function in the n-3 deficient animals may be an important factor rather than solely an increase in anxiety. Also the safflower oil group exhibited no change in drug sensitivities to scopolamine and pentobarbital, drugs known to alter behavior. From these considerations, it may be surmised that n-3 Def animals have a decrease

Table 3 Effects of n-3 fatty acid deficiency on fatty acid composition of mouse plasma (mol% of total fatty acids)

Fatty acid	n-3 Def		n-3 Adq	
	Isolated ($n = 10$)	Group housed ($n = 15$)	Isolated ($n = 14$)	Group housed ($n = 13$)
10:0	0.15 ± 0.04	0.17 ± 0.04	0.18 ± 0.03	0.21 ± 0.04
12:0	3.03 ± 0.43	3.50 ± 0.32	3.14 ± 0.39	4.08 ± 0.41
14:0	2.29 ± 0.18	2.60 ± 0.15	2.45 ± 0.15	2.82 ± 0.19
16:0 DMA	0.40 ± 0.03	0.34 ± 0.02	0.38 ± 0.03	0.37 ± 0.03
16:0	20.61 ± 0.25	22.30 ± 0.35**	21.90 ± 0.32	23.03 ± 0.22
18:0 DMA	0.12 ± 0.02	0.12 ± 0.01	0.13 ± 0.01	0.13 ± 0.02
18:0	11.48 ± 0.24	10.58 ± 0.31	11.37 ± 0.30	10.36 ± 0.14
20:0	0.20 ± 0.02	0.26 ± 0.02	0.21 ± 0.01	0.33 ± 0.02$^{*,\#\#}$
22:0	0.34 ± 0.03	0.37 ± 0.03	0.30 ± 0.02	0.41 ± 0.02$^{\#}$
24:0	0.10 ± 0.01	0.13 ± 0.01	0.12 ± 0.01	0.16 ± 0.01$^{\#}$
Total sat.	38.73 ± 0.69	40.37 ± 0.47	40.16 ± 0.52	41.90 ± 0.46
14:1	0.02 ± 0.02	0.08 ± 0.02	0.09 ± 0.02	0.04 ± 0.02
16:1n-7	3.29 ± 0.14	3.57 ± 0.15	3.35 ± 0.14	3.56 ± 0.17
18:1 DMA	0.25 ± 0.03	0.24 ± 0.02	0.24 ± 0.03	0.23 ± 0.02
18:1n-9	14.72 ± 0.51	14.89 ± 0.69	14.92 ± 0.55	13.32 ± 0.47
20:1n-9	0.28 ± 0.02	0.34 ± 0.02	0.29 ± 0.02	0.29 ± 0.01
24:1n-9	0.32 ± 0.02	0.29 ± 0.02	0.30 ± 0.02	0.23 ± 0.01$^{\#}$
Total mono.	18.88 ± 0.54	19.40 ± 0.81	19.19 ± 0.59	17.66 ± 0.60
18:2n-6	21.83 ± 0.69	22.84 ± 0.46	23.94 ± 0.49	25.78 ± 0.44$^{\#\#}$
18:3n-6	0.20 ± 0.03	0.22 ± 0.02	0.17 ± 0.01	0.24 ± 0.02
20:2n-6	0.19 ± 0.01	0.19 ± 0.01	0.21 ± 0.01	0.16 ± 0.01$^{\#\#}$
20:3n-6	1.62 ± 0.07	1.50 ± 0.04	1.32 ± 0.07**	1.39 ± 0.04
20:4n-6	15.90 ± 0.92	13.11 ± 0.80	9.52 ± 0.58**	7.97 ± 0.52**
22:4n-6	0.21 ± 0.04	0.18 ± 0.01	0.09 ± 0.01**	0.04 ± 0.01**
22:5n-6	1.81 ± 0.12	1.64 ± 0.08	0.31 ± 0.03**	0.19 ± 0.02**
Total n-6 PUFA	41.77 ± 0.81	39.68 ± 0.98	35.56 ± 0.71**	35.78 ± 0.68**
18:3n-3	nd	nd	0.53 ± 0.04**	0.63 ± 0.04**
22:5n-3	0.04 ± 0.02	0.02 ± 0.01	0.33 ± 0.03**	0.39 ± 0.02**
22:6n-3	0.58 ± 0.04	0.53 ± 0.04	4.23 ± 0.25**	3.64 ± 0.25**
Total n-3 PUFA	0.62 ± 0.04	0.54 ± 0.04	5.09 ± 0.22**	4.66 ± 0.23**
n-6/n-3	69.10 ± 4.38	75.83 ± 3.49	7.10 ± 0.22**	7.85 ± 0.32**
Total fatty acids (μg/μl)	5.92 ± 0.20	5.78 ± 0.20	6.23 ± 0.27	5.60 ± 0.25

Fatty acid methyl esters from 10:0 to 24:1n-9 were analyzed and 18:1n-7, 18:3n-3 and 20:5n-3 were not detected (nd, i.e. <0.01%). Each parameter is presented as the mean ± SEM

* $P < 0.05$, $^{**}P < 0.01$, compared between n-3 Def and n-3 Adq diet group in each breeding condition. $^{\#}P < 0.05$, $^{\#\#}P < 0.01$ compared between in the each diet group (one-way ANOVA and Tukey test)

in the threshold or an enhancement of vulnerability to stressors, a factor independent of any acute social stress induced by isolation. It is important to note here though that the balance of these factors likely depends upon the details of the conditions of each behavioral experiment as they determine the intensity of the stress.

The n-6 fatty acids increased and the n-3 fatty acids markedly decreased in the n-3 Def group compared with the n-3 Adq group in both brain and plasma. There was a marked decline in brain DHA with a concomitant increase in n-6 fatty acids including 22:5n-6, 22:4n-6 and 20:4n-6 as a result of the n-3 fatty acid dietary deficiency. However, there was no change in fatty acid composition between groups given different types of housing, even though we detected significant differences in the anxiety level between the isolated and group housed animals. Vancassel et al. [12] reported a change in monoamine content in the mouse brain when exposed to unpredictable chronic mild stress (UCMS) in various housing conditions including no-bedding, wet-bedding, a tilted cage, water in the home

Table 4 Effects of n-3 fatty acid deficiency on mouse brain fatty acid composition (mol% of total fatty acids)

Fatty acid	n-3Def		n-3 Adq	
	Isolated ($n = 10$)	Group housed ($n = 15$)	Isolated ($n = 14$)	Group housed ($n = 13$)
14:0	0.21 ± 0.01	0.22 ± 0.004	0.19 ± 0.01	0.20 ± 0.01
16:0 DMA	2.76 ± 0.02	2.65 ± 0.02	2.56 ± 0.02**	2.63 ± 0.02
16:0	21.15 ± 0.13	21.32 ± 0.10	20.23 ± 0.09**	20.16 ± 0.14**
18:0 DMA	4.00 ± 0.02	3.92 ± 0.03	4.16 ± 0.04*	4.18 ± 0.03**
18:0	20.03 ± 0.06	20.03 ± 0.08	20.24 ± 0.04	20.23 ± 0.05
20:0	0.48 ± 0.01	0.47 ± 0.01	0.48 ± 0.01	0.48 ± 0.01
22:0	0.67 ± 0.01	0.67 ± 0.01	0.69 ± 0.01	0.69 ± 0.01
23:0	0.16 ± 0.004	0.16 ± 0.004	0.16 ± 0.003	0.16 ± 0.004
24:0	0.81 ± 0.02	0.79 ± 0.02	0.81 ± 0.02	0.82 ± 0.03
Total sat.	50.27 ± 0.10	50.23 ± 0.12	49.52 ± 0.09**	49.55 ± 0.11**
16:1n-7	0.72 ± 0.07	0.82 ± 0.01	0.80 ± 0.02	0.77 ± 0.02
18:1 DMA	1.80 ± 0.03	1.78 ± 0.02	1.69 ± 0.02*	1.75 ± 0.02
18:1n-9	14.65 ± 0.10	14.71 ± 0.11	15.28 ± 0.07**	15.35 ± 0.12**
18:1n-7	4.39 ± 0.05	4.58 ± 0.05	4.27 ± 0.05	4.33 ± 0.09*
20:1n-9	1.81 ± 0.04	1.80 ± 0.03	1.93 ± 0.04	1.92 ± 0.04
22:1n-9	0.20 ± 0.01	0.20 ± 0.01	0.22 ± 0.01	0.22 ± 0.01
24:1	2.16 ± 0.04	2.09 ± 0.04	2.43 ± 0.05**	2.45 ± 0.04**
Total mono.	25.73 ± 0.19	25.98 ± 0.15	26.62 ± 0.16*	26.78 ± 0.22*
18:2n-6	0.42 ± 0.02	0.45 ± 0.02	0.49 ± 0.01	0.52 ± 0.02*
18:3n-6	0.06 ± 0.001	0.06 ± 0.001	0.06 ± 0.002	0.06 ± 0.002
20:2n-6	0.11 ± 0.003	0.11 ± 0.003	0.12 ± 0.004	0.13 ± 0.003**
20:3n-6	0.29 ± 0.01	0.27 ± 0.01	0.43 ± 0.02**	0.44 ± 0.02**
20:4n-6	8.31 ± 0.08	8.33 ± 0.07	7.35 ± 0.04**	7.38 ± 0.06**
22:4n-6	2.80 ± 0.04	2.75 ± 0.02	2.08 ± 0.03**	2.12 ± 0.01**
22:5n-6	5.51 ± 0.15	5.39 ± 0.10	0.30 ± 0.02**	0.28 ± 0.01**
Total n-6 PUFA	17.50 ± 0.23	17.36 ± 0.10	10.83 ± 0.06**	10.93 ± 0.07**
22:5n-3	0.01 ± 0.01	0.01 ± 0.004	0.16 ± 0.005**	0.17 ± 0.01**
22:6n-3	6.48 ± 0.13	6.42 ± 0.10	12.87 ± 0.07**	12.57 ± 0.10**
Total n-3 PUFA	6.49 ± 0.13	6.43 ± 0.10	13.02 ± 0.07**	12.74 ± 0.11**
n-6/n-3	2.71 ± 0.07	2.71 ± 0.05	0.83 ± 0.01**	0.86 ± 0.01**
Total fatty acids (μg/mg wet wt)	40.51 ± 0.70	41.07 ± 0.45	37.53 ± 0.29**	38.12 ± 0.87**

Fatty acid methyl esters from 14:0 to 24:1n-9 were analyzed. Each parameter is presented as the mean ± SEM. $^{*}P < 0.05$, $^{**}P < 0.01$ compared between n-3 Def and n-3 Adq diet groups in each housing condition. (one-way ANOVA and Tukey test)

cage, switching the light/dark cycle, etc. The UCMS induced a significant decrease of norepinephrine in the frontal cortex and striatum and tissue levels of serotonin. Moreover, Kodas et al. [11] demonstrated that chronic n-3 fatty acid dietary deficiency induced changes in the synaptic levels of 5-HT and subsequent provision of n-3 fatty acid was able to restore both biochemical and neurochemical factors altered by the n-3 deficient diet. Therefore, our results may be due in part to stress-induced alterations in brain monoamines that can alter emotional behavior. It is likely then that a decline in brain DHA and the level of stress are important factors modulating anxiety-related behavior.

In the present study, we demonstrated that the anxiety level of n-3 Def mice was greater than that of n-3 Adq mice and was enhanced by the social isolation stress of individual housing. These results suggest that n-3 fatty acid deficiency may decrease the threshold to stress and, conversely, that increased intake of dietary n-3 fatty acids may suppress the risk of emotional disorders. The relationship between various brain monoamines and behavioral performance in n-3 fatty acid deficient animals requires further investigation.

Acknowledgments The authors would like to thank Dr. Salem Norman, Jr. from Martek Biosciences Corp for his valuable comments.

References

1. Salem N Jr, Litman B, Kim HY, Gawrisch K (2001) Mechanisms of action of docosahexaenoic acid in the nervous system. Lipids 36:945–959
2. Moriguchi T, Greiner RS, Salem N Jr (2000) Behavioral deficits associated with dietary induction of decreased brain docosahexaenoic acid concentration. J Neurochem 75:2563–2573
3. Catalan JN, Moriguchi T, Slotnic BM, Murthy M, Greiner RS, Salem N Jr (2002) Cognitive deficits in docosahexaenoic acid deficient rats. Behav Neurosci 116:1022–1031
4. Moriguchi T, Salem N Jr (2003) Recovery of brain docosahexaenoate leads to recovery of spatial task performance. J Neurochem 87:297–309
5. Fedorova I, Salem N Jr (2006) Omega-3 fatty acids and rodent behavior. Prostaglandins Leukot Essent Fatty Acids 75:271–289
6. Hibbeln JR, Nieminen RGL, Blasbalg LT, Riggs AJ, Lands EMW (2006) Healthy intakes of n-3 and n-6 fatty acids: estimations considering worldwide diversity. Am J Clin Nutr 83(Suppl 6):1483S–1493S
7. Kiecolt GJK, Belury MA, Porter K, Beversdorf DQ, Lemeshow S, Glaser R (2007) Depressive symptoms, omega-6: omega-3 fatty acids, and inflammation in older adults. Psychosom Med 69:217–224
8. Hamazaki T, Sawazaki S, Itomura M, Asaoka E, Nagao Y, Nishimura N, Yazawa K, Kuwamori T, Kobayashi M (1996) The effect of docosahexaenoic acid on aggression in young adults. A placebo-controlled double-blind study. J Clin Invest 97:1129–1133
9. Hamazaki T, Thienprasert A, Kheovichai K, Samuhaseneetoo S, Nagasawa T, Watanabe S (2002) The effect of docosahexaenoic acid on aggression in elderly Thai. subjects-a placebo-controlled double-blind study. Nutr Neurosci 5:37–41
10. Delion S, Chalon S, Guilloteau D, Besnard JC, Durand G (1996) α-Linolenic acid dietary deficiency alters age-related changes of dopaminergic and serotoninergic neurotransmission in the rat frontal cortex. J Neurochem 66:1582–1591
11. Kodas E, Galineau L, Bodard S, Vancassel S, Guilloteau D, Besnard JC, Chalon S (2004) Serotoninergic neurotransmission is affected by n-3 polyunsaturated fatty acids in the rat. J Neurochem 89:695–702
12. Vancassel S, Leman S, Hanonick L, Denis S, Roger J, Nollet M, Bodard S, Kousignian I, Belzung C, Chalon S (2008) n-3 Polyunsaturated fatty acid supplementation reverses stress-induced modification on brain monoamine levels in mice. J Lipid Res 49:340–348
13. Willner P, Muscat R, Papp M (1992) Chronic mild stress-induced anhedonia: a realistic animal model of depression. Neurosci Biobehav Rev 16:525–534
14. Valzelli L (1973) The 'isolation syndrome' in mice. Psychopharmacologia (Berl.) 31:305–320
15. Bondnoff SR, Suranyi-Cadotte B, Quirion R, Meaney JM (1989) A comparison of the effects of diazepam versus several typical and atypical anti-depressant drugs in an animal model of anxiety. Psychopharmacology 97:277–279
16. Santarelli L, Gobbi G, Debs PC, Sibille EL, Hen R, Heath MJS (2001) Genetic and pharmacological disruption of neurokinin 1 receptor function decreases anxiety-related behaviors and increases serotonergic function. Proc Natl Acad Sci USA 98:1912–1917
17. David DJ, Klemenhagen KC, Holick AK, Saxe MD, Mendez I, Santarelli L, Craig DA, Zhong H, Swanson CJ, Hegde LG, Ping XI, Dong D (2007) Efficacy of the MCHR1 antagonist *N*-[3-(1-{[4-(3, 4-Difluorophenoxy) phenyl]methyl}(4-piperidyl))-4-methylphenyl]-2-methylpropanamide (SNAP 94847) in mouse models of anxiety and depression following acute and chronic administration is independent of hippocampal neurogenesis. J Pharmacol Exp Ther 321:237–248
18. Lepage G, Roy CC (1986) Direct transesterification of all classes of lipids in a one-step reaction. J Lipid Res 27:114–120
19. Masood A, Stark KD, Salem N Jr (2005) A simplified and efficient method for the analysis of fatty acid methyl esters suitable for large clinical studies. J Lipid Res 46:2299–2305
20. Bourre JM (2005) Dietary omega-3 fatty acids and psychiatry: mood, behavior, stress, depression, dementia and aging. J Nutr Health Aging 9:31–38
21. Nakashima Y, Yuasa S, Hukamizu Y, Okuyama H, Ohhara T, Kameyama T, Nabeshima T (1993) Effect of a high linoleate and a high α-linolenate diet on general behavior and drug sensitivity in mice. J Lipid Res 34:239–247

Lipids (2011) 46:417–423
DOI 10.1007/s11745-011-3551-3

ORIGINAL ARTICLE

Long-Term Administration of Cod Liver Oil Ameliorates Cognitive Impairment Induced by Chronic Stress in Rats

Emil Trofimiuk · Jan J. Braszko

Received: 30 June 2010 / Accepted: 4 March 2011 / Published online: 26 March 2011

Abstract Cod liver oil (CLO) is a rich source of omega-3 fatty acids (FA), especially eicosapentaenoic acid (EPA) and docosahexaenoic acid (DHA). The existing data suggest that EPA and DHA are the active agents of fish oil. In this study, we tested a hypothesis that the active constituents of CLO alleviate the negative impact of prolonged restraint stress on cognitive functions of male Wistar rats. Specifically, we attempted to characterize the preventive action of long-lasting treatment with CLO [0.375 ml/100 g body weight (equivalent to a dose of 300 mg/kg DHA and 225 mg/kg EPA), p.o. for 21 days] against an impairment caused by chronic restraint stress (2 h daily for 21 days) on recall as tested in a passive avoidance situation and on the spatial reference and working memory tested in a Barnes maze as well as on locomotor activity and anxiety behavior tested respectively in an open field and elevated plus-maze. We found that CLO administration statistically significantly ($p < 0.01$, both) prevented the deleterious effects of chronic restraint stress on recall and the spatial memory.

Keywords Cod liver oil · Stress · Open field · Elevated plus maze · Passive avoidance · Barnes maze · Spatial memory

Abbreviations

AD	Alzheimer's disease
ANOVA	One-way analysis of variance
BDNF	Brain-derived neurotrophic factor
BM	Barnes maze
CLO	Cod liver oil
CaMKII	Ca(2+)/calmodulin-dependent protein kinase II
DHA	Docosahexaenoic acid
EPA	Eicosapentaenoic acid
FA	Omega-3 fatty acids
LTP	Long-term potentiation
mPFC	Medial prefrontal cortex
MWM	Morris water maze
NMDA	*N*-methyl-D-aspartate
PA	Passive avoidance
PUFA	Polyunsaturated fatty acids
SEM	Standard error of mean

E. Trofimiuk (✉) · J. J. Braszko
Department of Clinical Pharmacology,
Medical University of Bialystok,
Waszyngtona 15A, 15-274 Bialystok, Poland
e-mail: e_trofim@umwb.edu.pl

Introduction

Neuropsychological dysfunctions, including learning and memory impairments, are the usual outcome of an exposition to prolonged stress [9, 31]. It is recognized that chronic stress is an important risk factor for the development of several cognitive deficits involving reference and working memory [10]. Although experimental studies identified many potentially effective neuroprotective agents, no clinically effective therapeutic strategy has yet been found to treat stress-induced cognitive impairment. Therefore, the search for substances that could be safe and effective in the prevention and treatment of the negative effects of stress on cognition is an urgent priority.

Docosahexaenoic acid (DHA, 22:6n-3) has been found to improve several brain functions including memory. DHA plays crucial role in maintaining structural and functional integrity of biological membranes [12, 13, 33]. In the brain and retina, DHA comprises, respectively, more

than 20 and 50%, of the membrane phospholipids [11]. DHA is essential for normal neurological function [18]. In the mammalian brain, lipids make up 10% of their fresh weight and 50% of dry weight, and DHA and arachidonic acid [20:4(n-6)] are the major polyunsaturated fatty acids (PUFA) in neuronal membranes [32]. Most DHA accumulation in the brain takes place during brain development from the beginning of the third trimester of gestation to 2 years after birth in humans and from prenatal day 7 to postnatal day 21 in rats [21, 26]. However, brain DHA levels decrease with age [14, 17] and are reduced in Alzheimer's disease (AD) [30]. Deficiency of brain DHA is associated with reduced learning ability and memory in rats [18] and with memory loss in AD patients [35]. Once incorporated into the phospholipids of the cell membrane, DHA modulates neurotransmitter release, membrane-bound enzymes and ion channel activity, gene expression, and synaptic plasticity [5, 23]. Numerous peripheral and central nervous system disorders have been associated with an imbalance in n-6 to n-3 PUFA, mainly arachidonic acid and DHA, respectively [12, 23, 33]. Dietary supplementation with fish oil containing standardized concentrations of EPA and DHA has been recommended by the American Heart Association for patients with documented chronic heart disease [13].

Whether oral administration of CLO, a principle dietary source of DHA and EPA, also could be effective in preventing the consequences of prolonged stress is not known. To our knowledge, no study has investigated the potential beneficial effects of fish oil in preventing stress-induced cognitive dysfunction. Therefore, the objective of the present study was to investigate whether prolonged treatment with a commercially available, standardized fish oil preparation is effective in alleviating the cognitive impairment and neurodegeneration caused by stress in rats. The specific hypothesis is that DHA treatment may protect brain cells from the stress-evoked damage, and the use of a standardized, high-grade DHA-containing fish oil formulation may be a safe, effective, and readily available means of preventing or even treating the negative consequences of stress on cognition. In this study, we tested this hypothesis in rats using a passive avoidance situation and Barnes maze paradigms. To control for unspecific influence of locomotor activity and anxiety we used open field and elevated plus-maze tests, respectively.

Materials and Methods

Animals

Seventy-five male, 6 week old Wistar rats, weighing 120–140 g at the beginning of the experiments, were used. The rats were kept in a temperature- (23°C) and humidity-(50–60%) controlled vivarium in groups of five under a constant 12/12 h light/dark schedule (lights switched on at 7:00 a.m.) with free access to standard lab chow and tap water.

Drugs

A standardized CLO formulation (Cod Liver Oil, Lysi HF, Island) was used. Each 5 ml contained 400 mg DHA, 300 mg EPA, and 4.6 mg vitamin E (artificial antioxidant), 0.23 mg vitamin A and 0.0046 mg vitamin D. CLO was administered by gavage in a volume of 0.375 mL/100 g body weight. Doses of DHA, EPA, and vitamins E, A and D contained in this volume of CLO were 300 [34], 225, 3.45, 0.175 and 0.00345 mg/kg, respectively. Control rats received 0.009% Cremophor (Sigma, Germany) as a vehicle [16].

Animals were divided into four groups treated daily as follows: (1) 20 rats received 0.009% Cremophor (Control); (2) 17 rats received 0.009% Cremophor followed by stress procedure described below (Stress); (3) 20 rats received 0.375 ml/100 g body weight CLO (CLO); (4) 18 rats received 0.375 ml/100 g body weight CLO followed by stress procedure (Stress + CLO).

The experimental procedures were carried out according to the European Council Directive of 24 November 1986 (6/609/EEC) and were approved by the Local Ethics Commission for Animal Experimentation.

Stress Procedure

Two groups of animals (19 rats and 16 rats) were subjected to chronic restraint stress [3], 2 h daily for 21 days. The restraint was imposed during the light phase from 0900 to 1100 hours. The restrainer was made of transparent perforated plastic tube, 20 cm long, and 7 cm in diameter. A rat was eased into the restrainer, head first, and once in the tube it was closed with a plexiglas lid. The animals fit tightly into the restrainers and it was not possible for them to move or turn around. Non-stressed control rats were at the same time briefly handled and returned to their home cages.

Behavioral Tests

Open Field

The next day after ending of the 3 week administration of CLO or vehicle animals were tested in an open field for assessment of their locomotor exploratory activity. Open field was a square 100 × 100 cm white floor divided by eight lines into 25 equal squares and surrounded by a

47 cm high wall [6]. Four plastic bars, 20 cm high, were designed as objects of possible animal's interest and fixed perpendicularly, parallel to each other, in four line crossings, in the central area of the floor. A rat was placed in the center of the floor and, following 1 min of adaptation, crossings, rearings and bar approaches were counted manually for 5 min.

Elevated 'Plus' Maze

Anxiety was evaluated in the same group of rats, next day after assessment of their open field performance. It was measured in an elevated plus-maze (made of gray colored wooden planks) consisted of four arms, 50 × 10 cm (length x width). Two arms (closed) had 40 cm high walls, covered with removable lid, and two remaining arms (opened) had no walls, such that the open or closed arms were opposite to each other. The maze was elevated to a height of 50 cm from the floor. Rats were placed for 5 min in a pretest arena (60 × 60 × 35 cm, constructed of the same material) prior to exposure to the maze. This step allowed facilitation of exploratory behavior. The experimental procedure was similar to that described by Pellow et al. [29]. Immediately after the pretest exposure rats were placed in the center of the elevated plus-maze facing one of the open arms. During the 5 min test period the following measures were taken: the number of entries into the open and closed arms and the time spent in the open and closed arms. An entry was defined as all four feet into one arm. An increase in open arms entries and increase in time spent in open arms were interpreted as indicative of potential anxiolytic activity.

Passive Avoidance

Passive avoidance (PA) behavior was studied in a one trial learning, step-trough situation [1], which utilizes the natural preference of rats for dark environments. The apparatus consisted of the platform (250 × 80 mm) connected to a dark compartment—a metal box (400 × 400 × 400 mm) with an opening (60 × 100 mm) in the middle of the front wall length. After a 2 min habituation to the dark compartment, the rat was placed on the illuminated platform and allowed to enter the dark compartment. Two more approach trials were given on the following day with a 2 min interval. At the end of the second trial unavoidable scrambled electric foot shock (0.25 mA, AC, 2 s) was delivered through the grid floor of the dark compartment (learning trial). Twenty-four hours later retention of the passive avoidance response was tested by placing the animal on the platform and measuring the latency to re-enter the dark compartment to a maximum of 300 s. Two rats were excluded from testing retention because they did not effectively learn the rules of the test.

Barnes Maze

On the first day of testing, the animals (40 rats, different from those used for PA) were brought in the testing suite and allowed to enter the goal box through one of the holes in the maze. Once the animal entered the hole, a black Plexiglas cover was positioned over the hole to prevent escape. A 4 min habituation in the goal box was given prior to the first training trial. Next, the animal was placed for 30 s in a 20 cm diameter by 30 cm high round non-transparent holding box that was positioned in the center of the maze. The holding box was then removed, a timer begun, and the experimenter moved behind the curtain.

An escape was counted when all four paws of the animal were in the goal box. Following successful location of the goal box, the animals were allowed to stay there for 60 s. A maximum of 4 min was allowed for each trial and if an animal did not locate in the goal box during this 4 min period it was removed from the maze and placed in the goal box for 60 s. During the 60 s period in the goal box, the maze was wiped with a paper towel to remove any feces or urine prior to the beginning of the next trial. The test paradigm consisted of two trials per day for 5 days. Prior to the start of the second trial the animal was returned to its home cage for 1 min and then placed again in the holding box in the center of the maze to start the second trial as described above. The maze was then rotated a random number of holes (between one and eight holes using a random numbers table) in order to prevent use of odor trails in solving the task. Following the rotation of the table, the procedure was repeated with the next animal.

Two measures were recorded on each trial. The first was the latency to find the goal box. The second was the number of errors committed by each animal. An error was defined as a head poke or exploration of any hole other than the hole above the goal box and including perseverative investigations of the same hole. At the end of each day the maze was cleaned using a 70% ethanol solution [4].

Statistical Analysis

Data were presented as means ± standard error of mean (SEM). One-way analysis of variance (ANOVA), followed by Bonferroni test for chosen group comparisons, was applied for mean performance of the rats in the open field, elevated plus-maze, passive avoidance; and two way analysis of variance (ANOVA II) (treatment × days) with repeated measures, followed by the post hoc Newman–Keuls test for multiple comparisons, was used for latencies to enter the escape hole and number of errors in the Barnes Maze (BM). The probability level less than 0.05 was accepted as significant.

Results

Effects of Stress and CLO on Locomotor Exploratory Activity of Rats in the Open Field

ANOVA of the results obtained in the open field (Fig. 1) yielded no statistically significant differences in the numbers of crossings $F(3,34) = 1.466$ ($p > 0.05$), rearings $F(3,34) = 1.681$ ($p > 0.05$) and bar approaches $F(3,34) = 1.107$ ($p > 0.05$). It indicates that stress and CLO administration did not affect musculo-skeletal aspects of the rats' psychomotor performance.

Effects of Stress and CLO Administration on Anxiety Behavior in the Elevated Plus-Maze

ANOVA of the results obtained in the elevated plus-maze test yielded no statistically significant differences in the times spent by rats in open arms $F(3,34) = 0.3771$ ($p > 0.05$) and in the numbers of open arms entries $F(3,34) = 0.2910$ ($p > 0.05$; Fig. 2). It means that stress and our treatments and procedures did not appreciably affect the emotional aspects of the rats' psychomotor performance.

Effects of Stress and CLO Administration on Passive Avoidance Behavior

ANOVA of the results obtained in the passive avoidance test yielded $F(3,35) = 13,167$ ($p < 0.001$) statistically significant differences between the groups in the re-entry latencies in the passive avoidance situation (Fig. 3). Post-hoc comparisons in preselected pairs with Bonferroni test revealed that stressed rats re-entered the dark part of the apparatus significantly earlier then all remaining groups: control ($p < 0.05$), treated with CLO ($p < 0.01$) pretreated with CLO and then stressed ($p < 0.001$) rats. This pattern showed that significant adverse effect of stress on retrieval of PA behavior was abolished by parallel CLO administration to the stressed animals.

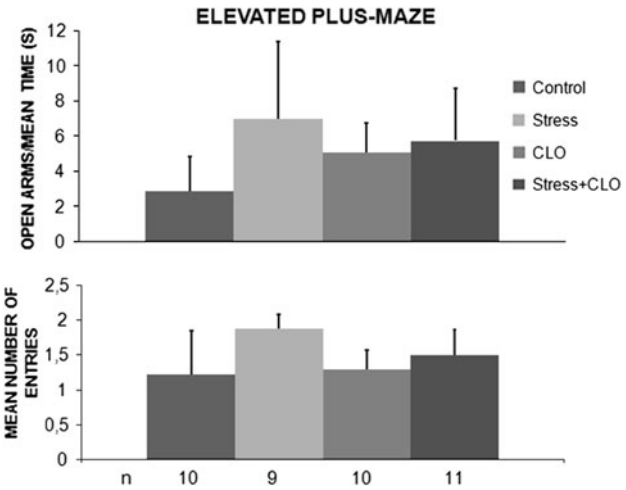

Fig. 2 Effects of stress and long-term CLO administration on the time spent by rats in, or the number of entries to the open arms of an elevated plus-maze. *Columns* represents means ± SEM of the values obtained from *n* rats indicated at the *bottom* of the figure

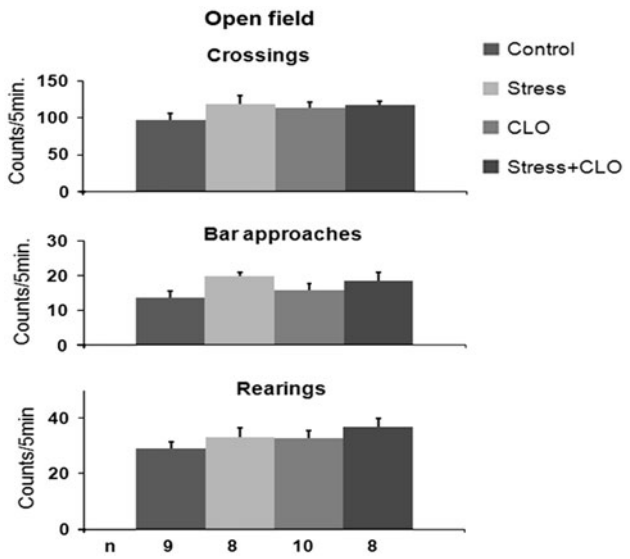

Fig. 1 Effects of stress and long-term CLO administration on the locomotor activity of rats in open field. *Columns* represent means ± SEM of the number of crossings, *rearings* or *bar* approaches obtained from *n* rats indicated at the *bottom* of the figure

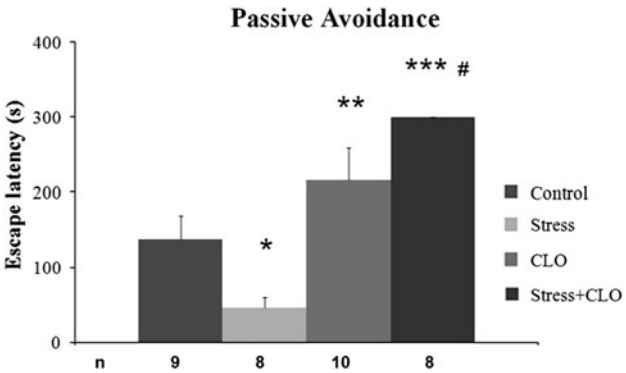

Fig. 3 Effects of chronic stress and CLO on the re-entry latencies in the passive avoidance situation. *Columns* represent means ± SEM of the values obtained from *n* rats indicated at the *bottom* of the figure. The two groups demonstrated significantly different results in re-entry latencies in comparison with Control: $*p < 0.05$ versus Stress, $\#p < 0.01$ versus Stress + CLO. The statistically significant differences were also in $**p < 0.01$ versus Stress, and $***p < 0.001$ versus Stress

Effects of Stress and CLO on Performance of Rats in the BM Test

ANOVA II of the mean numbers of errors made by rats in the BM revealed a significant treatment effect ($F(3,36) = 7.240$, $p < 0.001$), and also a significant day effect ($F(4,12) = 32.263$; $p < 0.001$) but no significant treatments × days interaction ($F(12,144) = 1.496$, $p > 0.05$) (Fig. 4). It means that all rats effectively learned the task over 5 days and specific treatment effect was detected. Further post hoc comparisons made with Bonferroni test revealed that the stressed rats made significantly more errors than the controls ($p < 0.05$), those treated with CLO ($p < 0.01$) and the rats pre-treated with CLO and subsequently stressed ($p < 0.001$).

ANOVA II of the mean latencies to enter the escape hole in the BM yielded a significant treatment effect ($F(3,35) = 5.495$; $p < 0.01$) and also a significant day effect ($F(4,12) = 51.299$; $p < 0.001$) and also a significant treatment × days effect ($F(12,144) = 2.796$; $p < 0.01$) (Fig. 5). It means that all rats effectively learned the task over 5 days and specific treatment effect and also treatment × days interaction were detected. Post hoc comparisons in preselected pairs with the Bonferroni test revealed that chronic stress ($p < 0.01$) significantly increased latency to finding the escape hole in comparison to control. Also, the animals treated with CLO ($p < 0.001$), pre-treated with CLO and subsequently stressed ($p < 0.001$) were faster in finding the escape hole in comparison with the stressed group.

Discussion

In this study we showed that CLO effectively restored examined cognitive functions impaired by stress. Specifically, CLO significantly reduced stress-related forgetting in

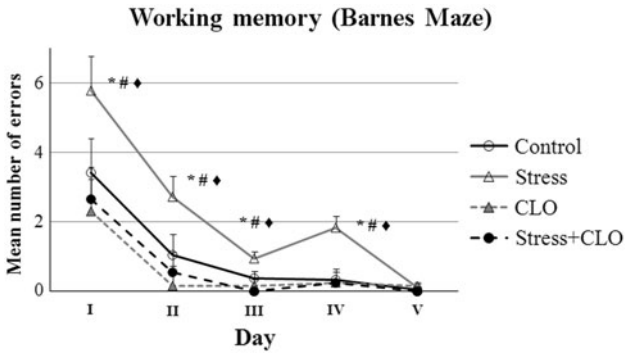

Fig. 4 Effects of chronic stress and CLO supplementation on performance in BM task. Each *graph* represent the mean ± SEM number of errors (two trials per day of 5 days) obtained from 9–11 rats per each group. The three group demonstrated significantly different results in making of errors in comparison with Stress: Control (*$p < 0.05$), CLO + Stress (#$p < 0.01$) and CLO (◆ $p < 0.001$)

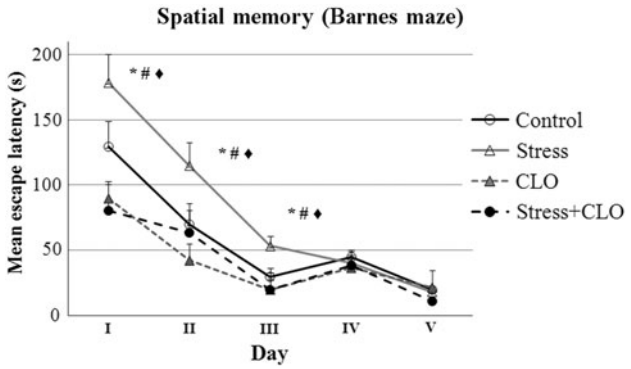

Fig. 5 Effects of chronic stress and CLO administration on performance in spatial memory test of BM. Each *graph* represent the mean escape latency ± SEM (two trials per day of 5 days) obtained from 9–11 rats per each group. The three group demonstrated significantly different results in making of errors in comparison with Stress: Control (*$p < 0.05$), CLO + Stress (#$p < 0.01$) and CLO (◆ $p < 0.001$)

rats and alleviated negative effects of stress on spatial memory.

In order to study the a possible influence of chronic stress related anxiety on the results of cognitive tests, the elevated plus-maze test was applied as it is known that cognitive processes may be impaired by anxiety [20]. Interestingly, in our study no influence of chronic mild stress or CLO treatment on anxiety as measured in the elevated plus-maze was seen.

Spontaneous open filed activity includes a variety of responses that could be interpreted as indices of exploration, arousal, locomotion, anxiety, and emotionality. In particular, increased locomotion (horizontal or forward or ambulatory activity) and vertical activity (rearing) characterize the rat's behavioral response to novelty. In this study we found that chronic stress and CLO administration is not associated with changes of locomotor activity in rats.

In studies employing DHA supplementation in a mouse model of Alzheimer's disease or in aged animals, learning and memory were improved by DHA [7, 22]. Reduced brain DHA levels are associated with poor spatial reference memory [24] which is restored by administration of exogenous DHA or docosapentaenoic acid [25].

Because most previous studies have examined memory in DHA-deficient animals [27], it was important to determine whether spatial reference memory or working memory can be enhanced in normal rats. Most previous studies have focused on whole brain DHA recovery and improved reference memory in DHA-deficient animals given a fish oil supplement. Chung et al. [8] examined the effects of fish oil administration to FA deficient rats. They found that recovery of brain DHA levels significantly improved both spatial reference and working memory. Moreover, comparison of escape latencies in Morris water maze (MWM)

test between control and control treated with fish oil groups showed that fish oil supplementation enhances spatial reference and working memory also in normal rats. In our study we did not observe nootropic effects of CLO administration in non-stressed rats. It is worth mentioning that in PA, an aversively motivated recall task, similarly as in the MWM used by Chung et al. [8], but not as in the Barnes maze (less stressful) we observed better performance in rats stressed and treated with CLO than in the control animals.

Admittedly, in some studies learning and memory improvement was observed in normal rats after repeated oral administration of DHA (300 mg/kg per day) when tested in the radial maze task [19, 34]. Their dose of DHA was the same as that used in our study, except for our DHA being not alone but as an ingredient of CLO.

Wu et al. [37] found that the DHA dietary supplementation increases activation of Akt in the hippocampus. Akt signaling is a crucial step by which BDNF exerts its action on synaptic plasticity, involving NMDA receptor stimulation [38]. In addition, Akt signaling is an important intermediate factor by which DHA influences neuroplasticity [2]. A DHA-enriched diet modulates hippocampal CaMKII activation and CaMKII is another signaling system whose action is critical for learning and memory [15], and plays a role in the DHA hippocampal-dependent cognitive enhancement [36].

Long-term potentiation (LTP) has long been recognized as a typical example of synaptic plasticity and is considered to represent a neuronal basis of learning and memory involving NMDA activation. Nishikawa et al. [28] reported that DHA potentiated the NMDA-induced response, suggesting a possible role of DHA in LTP formation. Furthermore, the beneficial effect of DHA (300 mg/kg per day for 12 weeks) on learning and memory measured in the radial maze was related to increased Fos expression in the hippocampus [34].

There are also few reports on the effects of pure EPA on cognition. Chronic administration of pure EPA attenuates memory impairment induced by interleukin 1β administration but does not enhance memory in control rats. Hashimoto et al. [22] suggests that EPA, as a precursor of DHA, ameliorates learning deficits associated with Alzheimer's disease and that these effects are modulated by the expression of proteins involved in neuronal plasticity.

In conclusion, the present study demonstrates that prolonged treatment with a standardized, high-concentration DHA- and EPA-containing fish oil reduces stress-induced retention deficit (amnesia) as measured in the PA task as well alleviates spatial reference and working memory impairments evoked by chronic stress. The present findings not only confirm the few to-date findings concerning the behavioral effects of DHA but also demonstrate for the first time that the use of a CLO facilitates functional recovery after stress evoked cognitive deficits.

Acknowledgments This study was supported by the Medical University of Bialystok (3-66775L).

References

1. Ader R, Weijnen JAWM, Moleman P (1972) Retention of passive avoidance response as function of the intensity and duration of electric shock. Psychon Sci 26:125–129
2. Akbar M, Calderon F, Wen Z, Kim HY (2005) Docosahexaenoic acid: a positive modulator of Akt signaling in neuronal survival. Proc Natl Acad Sci USA 102:10858–10863
3. Magariños AM, McEwen BS (1995) Stress-induced atrophy of apical dendrites of hippocampal CA3c neurons: Comparison of stressors. Neuroscience 69(1):83–88
4. Barnes CA (1979) Memory deficits associated with senescence: a neurophysiological and behavioral study in the rat. J Comparat Physiol Psychol 1:74–104
5. Bazan NG (2003) Synaptic lipid signaling: significance of polyunsaturated fatty acids and platelet-activating factor. J Lipid Res 44:2221–2233
6. Braszko JJ, Wiśniewski K, Kupryszewski G, Witczuk B (1987) Psychotropic affects of angiotensin II and III in rats: locomotor and exploratory vs cognitive behaviour. Behav Brain Res 25:195–203
7. Calon F, Lim GP, Yang F, Morihara T, Teter B, Ubeda O, Rostaing P, Triller A, Salem N Jr et al (2004) Docosahexaenoic acid protects from dendritic pathology in an Alzheimer's disease mouse model. Neuron 43:633–645
8. Chung WL, Chen JJ, Su HM (2008) Fish oil supplementation of control and (n-3) fatty acid-deficient male rats enhances reference and working memory performance and increases brain regional docosahexaenoic acid levels. J Nutr 138(6):1165–1171
9. Cook SC, Wellman CL (2004) Chronic stress alters dendritic morphology in rat medial prefrontal cortex. J Neurobiol 60: 236–248
10. Conrad CD. (2009) A critical review of chronic stress effects on spatial learning and memory. Prog Neuropsychopharmacol Biol Psychiatry. [Epub ahead of print]
11. Crawford MA, Golfetto I, Ghebremeskel K, Min Y, Moodley T, Poston L et al (2003) The potential role for arachidonic and docosahexaenoic acids in protection against some central nervous system injuries in preterm infants. Lipids 38:303–315
12. Das UN (2006) Essential fatty acids: a review. Curr Pharm Biotechnol 7:467–482
13. DeFilippis AP, Sperling LS (2006) Understanding omega-3's. Am Heart J 151:564–570
14. Delion S, Chalon S, Guilloteau D, Lejeune B, Besnard JC, Durand G (1997) Age-related changes in phospholipid fatty acid composition and monoaminergic neurotransmission in the hippocampus of rats fed a balanced or an n-3 polyunsaturated fatty acid-deficient diet. J Lipid Res 38:680–689
15. Elgersma Y, Sweatt JD, Giese KP (2004) Mouse genetic approaches to investigating calcium/calmodulin-dependent protein kinase II function in plasticity and cognition. J Neurosci 24:8410–8415
16. Ferrari D, Cysneiros RM, Scorza CA, Arida RM, Cavalheiro EA, de Almeida AC, Scorza FA (2008) Neuroprotective activity of omega-3 fatty acids against epilepsy-induced hippocampal damage: Quantification with immunohistochemical for calcium-binding proteins. Epilepsy Behav 13(1):36–42

17. Favrelere S, Stadelmann-Ingrand S, Huguet F, De Javel D, Piriou A, Tallineau C, Durand G (2000) Age-related changes in ethanolamine glycerophospholipid fatty acid levels in rat frontal cortex and hippocampus. Neurobiol Aging 21:653–660
18. Fedorova I, Salem N Jr (2006) Omega-3 fatty acids and rodent behavior. Prostaglandins Leukot Essent Fatty Acids 75:271–289
19. Gamoh S, Hashimoto M, Sugioka K, Shahdat Hossain M, Hata N, Misawa Y et al (1999) Chronic administration of docosahexaenoic acid improves reference memory-related learning ability in young rats. Neuroscience 93:237–241
20. Goswami M, Mund S, Ray A (1996) Effects of some psychotropic agents on cognitive functions in rats. Indian J Physiol Pharmacol 40(1):75–78
21. Green P, Glozman S, Kamensky B, Yavin E (1999) Developmental changes in rat brain membrane lipids and fatty acids. The preferential prenatal accumulation of docosahexaenoic acid. J Lipid Res 40:960–966
22. Hashimoto M, Hossain S, Tanabe Y, Kawashima A, Harada T, Yano T, Mizuguchi K, Shido O (2009) The protective effect of dietary eicosapentaenoic acid against impairment of spatial cognition learning ability in rats infused with amyloid β(1–40). J Nutr Biochem 20(12): 965–973
23. Horrocks LA, Farooqui AA (2004) Docosahexaenoic acid in the diet: its importance in maintenance and restoration of neural membrane function. Prostaglandins Leukot Essent Fatty Acids 70:361–372
24. Lim SY, Hoshiba J, Moriguchi T, Salem N Jr (2005) N-3 fatty acid deficiency induced by a modified artificial rearing method leads to poorer performance in spatial learning tasks. Pediatr Res 58:741–748
25. Lim SY, Hoshiba J, Salem N Jr (2005) An extraordinary degree of structural specificity is required in neural phospholipids for optimal brain function: n-6 docosapentaenoic acid substitution for docosahexaenoic acid leads to a loss in spatial task performance. J Neurochem 95:848–857
26. Martinez M (1992) Tissue levels of polyunsaturated fatty acids during early human development. J Pediatr 120:S129–S138
27. Moriguchi T, Salem N Jr (2003) Recovery of brain docosahexaenoate leads to recovery of spatial task performance. J Neurochem 87:297–309
28. Nishikawa M, Kimura S, Akaike N (1994) Facilitatory effect of docosahexaenoic acid on Nd-aspartate response in pyramidal neurons of rat cerebral cortex. J Physiol 475:83–93
29. Pellow S, File SE (1986) Anxiolytic and anxiogenic drug effects on exploratory activity in an elevated plus-maze: a novel test of anxiety in the rat. Pharmacol Biochem Behav 24:525–529
30. Prasad MR, Lovell MA, Yatin M, Dhillon H, Markesbery WR (1998) Regional membrane phospholipid alterations in Alzheimer's disease. Neurochem Res 23:81–88
31. Radley JJ, Sisti HM, Rocher AB, Hao J, McCall T, Hof PR, McEwen BS, Morrison JH (2004) Chronic behavioral stress induces apical dendritic reorganization in pyramidal neurons of the medial prefrontal cortex. Neuroscience 125:1–6
32. Sastry PS (1985) Lipids of nervous tissue: composition and metabolism. Prog Lipid Res 24:69–176
33. Simopoulos AP (2002) The importance of the ratio of omega-6/omega-3 essential fatty acids. Biomed Pharmacother 56:365–379
34. Tanabe Y, Hashimoto M, Sugioka K, Maruyama M, Fujii Y, Hagiwara R et al (2004) Improvement of spatial cognition with dietary docosahexaenoic acid is associated with an increase in Fos expression in rat CA1 hippocampus. Clin Exp Pharmacol Physiol 31:700–703
35. Tully AM, Roche HM, Doyle R, Fallon C, Bruce I, Lawlor B, Coakley D, Gibney MJ (2003) Low serum cholesteryl ester-docosahexaenoic acid levels in Alzheimer's disease: a case-control study. Br J Nutr 89:483–489
36. Vaynman S, Ying Z, Gomez-Pinilla F (2007) The select action of hippocampal calcium calmodulin protein kinase II in mediating exercise enhanced cognitive function. Neuroscience 144:825–833
37. Wu A, Ying Z, Gomez-Pinilla F (2008) Docosahexaenoic acid dietary supplementation enhances the effects of exercise on synaptic plasticity and cognition. Neuroscience 155(3):751–759
38. Yoshii A, Constantine-Paton M (2007) BDNF induces transport of PSD-95 to dendrites through PI3 K-AKT signaling after NMDA receptor activation. Nat Neurosci 10:702–711

Lipids (2011) 46:425–434
DOI 10.1007/s11745-011-3553-1

ORIGINAL ARTICLE

Dietary Saury Oil Reduces Hyperglycemia and Hyperlipidemia in Diabetic KKAy Mice and in Diet-Induced Obese C57BL/6J Mice by Altering Gene Expression

Zhi-Hong Yang · Hiroko Miyahara · Shuhei Takemura · Akimasa Hatanaka

Received: 20 December 2010 / Accepted: 15 March 2011 / Published online: 5 April 2011

Abstract We investigated the effect of saury oil on the alleviation of metabolic syndrome in mice. Saury oil contains 18% (w/w/) n-3 polyunsaturated fatty acids (n-3 PUFA) and 35% (w/w) monounsaturated fatty acids (MUFA). Diabetic KKAy mice were fed a 10% soybean oil diet (control) or a 10% saury oil diet for 4 weeks, and diet-induced obese C57BL/6J mice were fed a high-fat diet containing 32% lard (control) or 22% lard plus 10% saury oil for 6 weeks. After the intervention periods, the levels of glucose, insulin and lipids in plasma had decreased significantly for the saury oil diet group, and insulin sensitivity had improved. These favorable changes may be attributed to the increased adiponectin and decreased TNFα and resistin levels in plasma. The saury oil diet also resulted in downregulated expression of the lipogenic genes (*SREBP-1*, *SCD-1*, *FAS*, and *ACC*) as well as upregulation of the fatty acid oxidative gene, *CPT-1*, and the energy expenditure-related genes (*PGC1α* and *PGC1β*) in white adipose tissue for the diet-induced obese C57BL/6J mice. An increase in n-3 PUFA levels and the concomitant decrease in the n-6/n-3 PUFA level ratio in serum, white adipose tissue, and liver with a saury oil diet are likely to be involved in the beneficial changes to the metabolic indicators. MUFA may also play a positive role in remodeling lipid composition. Based on these mice models, our results suggest a potential use for saury oil for improving metabolic abnormalities.

Keywords Saury oil · n-3 PUFA · MUFA · Hypoglycemia · Hypolipidemia · Insulin resistance · Adipokine · Adipogenesis · Lipid composition

Abbreviations

ACC	Acetyl-CoA carboxylase
CPT-1	Carnitine palmitoyltransferase-1
FAS	Fatty acid synthase
HDL-C	High-density lipoprotein cholesterol
LDL-C	Low-density lipoprotein cholesterol
MetS	Metabolic syndrome
MUFA	Monounsaturated fatty acids
NEFA	Nonesterified fatty acids
PGC-1α	Peroxisome proliferator-activated receptor gamma coactivator 1-alpha
PGC-1β	Peroxisome proliferator-activated receptor gamma coactivator 1-beta
PUFA	Polyunsaturated fatty acids
RT-PCR	Reverse transcription polymerase chain reaction
SAF	Saturated fatty acids
SCD-1	Stearoyl CoA desaturase-1
SREBP-1	Sterol regulatory element binding protein-1
TAG	Triacylglycerol
TC	Total cholesterol
WAT	White adipose tissue

Z.-H. Yang (✉) · H. Miyahara · S. Takemura · A. Hatanaka
Central Research Laboratory,
Nippon Suisan Kaisha, Ltd.,
32-3 Nanakuni 1 Chome Hachioji,
Tokyo 192-0991, Japan
e-mail: yangzh@nissui.co.jp

Introduction

Metabolic syndrome (MetS) is a major and growing public health problem and is characterized by a group of metabolic risk factors for cardiovascular disease and diabetes

that includes hypertension, glucose intolerance, dyslipidemia and abdominal obesity [1]. The causes of MetS are unknown, although they are considered to involve both genetic and environmental factors, including diet [2].

Alteration of the type of dietary lipids is an important way of preventing and treating obesity-associated MetS. Studies have demonstrated that the health benefits of fish oil, which is rich in n-3 polyunsaturated fatty acids (n-3 PUFA) such as eicosapentaenoic acid (EPA) and docosahexaenoic acid (DHA), include its ability to prevent heart disease, inflammation, dyslipidemia and diabetes via multiple mechanisms [3]. Studies in rats and mice fed a high-fat or lipogenic, sucrose-rich diet have shown that n-3 PUFA have beneficial effects on obesity and insulin resistance [3, 4]. Several studies have also demonstrated a decrease in adiposity in obese humans and improved glucose metabolism in human subjects after n-3 PUFA supplementation [5, 6].

Fish lipids generally contain varying amounts of different types of fatty acids in addition to n-3 PUFA [7]. Consistently high levels of monounsaturated fatty acids (MUFA) are found in the lipids of some pelagic surface fish species, such as saury [8], capelin [9], sprats [10], and herring [11], whose lipids originate from their food source, such as zooplankton [12, 13]. It has been established that ingestion of fish oil rich in MUFA increases peroxisomal beta-oxidation [14] and promotes the synthesis of long-chain essential fatty acids [15]. Additionally, Osterude et al. [16] demonstrated that a seal/cod liver oil mixture and whale oil both increased high-density lipoprotein cholesterol (HDL-C) levels, and furthermore, cod liver oil reduced triacylglycerol (TAG) levels in healthy humans. Because all these fish oils contain a considerable amount of MUFA in addition to n-3 PUFA, some of these effects may be attributable to MUFA. All of these studies suggested a possible beneficial effect of MUFA for the treatment of MetS.

Saury, a seawater fish from the family Scomberesocidae, is one of the most highly consumed fish in Japan. Saury oil contains n-3 PUFA, such as EPA and DHA, as well as considerable amounts of MUFA (C20:1 and C22:1). Given the positive effects on glucose and lipid homeostasis by n-3 PUFA, and the findings that MUFA may have an impact on the treatment of MetS, we evaluated the effect of saury oil on glucose and lipid metabolism using diabetic KKAy mice and diet-induced obese C57BL/6J mice for our animal model. Our research revealed that saury oil intake reduced insulin resistance and plasma levels of glucose, insulin, and lipids. This effect may be attributable to favorable changes in the plasma adipokine profile and lipid metabolism-related gene expression. Our research constitutes the first investigation of the effect of saury oil ingestion on glucose and lipid metabolism, and our findings suggest that saury oil may have a favorable impact on MetS.

Materials and Methods

Animals and Diets

All animal experiments were conducted in complete compliance with the National Institutes of Health: Guide for the Care and Use of Laboratory Animals, and were approved by the Institutional Animal Care and Use Committee at Nihon Bioresearch Inc. (Gifu, Japan), where the animals were housed for the entire experimental period. Five-week-old spontaneously diabetic male KKAy mice were obtained from CLEA Japan Inc. (Shizuoka, Japan), and 5-week-old male C57BL/6J mice were from Charles River Laboratories Japan Inc. (Yokohama, Japan). Mice were housed 1/cage at 23 ± 1 °C with a 12-h light/dark cycle, and provided with free access to water and standard mouse chow CRF-1 (Oriental Yeast Co. Ltd., Tokyo, Japan) for an acclimatization period of 1 week.

The fatty acid composition of the dietary oils is shown in Table 1. Saury oil (Nippon Suisan Kaisya, Ltd., Tokyo, Japan) contained 34.7% MUFA (20:1 and 22:1 isomers) and 18% of EPA and DHA combined. Following the acclimatization period, the KKAy mice were randomly assigned into two groups for a 4-week feeding experiment. The control group ($n = 10$) was fed on AIN-93G growth diet (Oriental Yeast Co., Tokyo, Japan) containing 10% soybean oil, and the saury oil group ($n = 10$) was fed the same basal diet supplemented with 10% saury oil. The two groups were pair-fed throughout the experiment. The

Table 1 Fatty acid composition of dietary oils

Fatty acids (%)	Soybean oil	Lard	Saury oil
C14:0	0.06	1.49	5.68
C16:0	9.49	25.43	9.23
C16:1	0.10	2.35	2.99
C18:0	3.86	5.97	1.66
C18:1	22.8	40.64	5.83
C18:2n-6	55.14	10.81	1.60
C18:3n-3	7.55	1.00	1.22
C20:0	0.33	0.21	0.19
C20:1n-9	0.20	0.80	12.13
C20:1n-7	ND	ND	3.11
C20:4n-6	ND	0.20	0.63
C20:5n-3	ND	0.02	6.11
C22:1n-11	ND	ND	18.49
C22:1n-9	0.05	ND	1.02
C22:5n-3	0.00	0.10	1.56
C22:6n-3	ND	0.03	11.82

Values correspond to the means of three separate samples processed independently

ND not detected

C57BL/6J mice were randomly divided into two groups for a 6-week pair-feeding period. The control group was fed on a high-fat diet (D12492 Rodent Diet with 60 kcal% Fat; Research Diets, Inc., New Brunswick, NJ, USA) containing 32% lard (corresponding to 60% energy from fat; $n = 10$), and the saury oil group was fed a saury oil-supplemented diet (22% lard plus 10% saury oil, corresponding to 60% energy from fat; $n = 10$). The compositions of the experimental diets are shown in Table 2. All diet feeds were stored at −20 °C and were provided fresh daily to the mice. Body weight and food intake were monitored throughout the study.

At the end of the intervention periods, the KKAy mice and C57BL/6J mice were anesthetized with 4% sodium pentobarbital (Dainippon Sumitomo Pharma, Osaka, Japan) in the early light phase of the light–dark cycle (fed condition), and blood was collected by abdominal vein puncture. Plasma was obtained by centrifugation at 3,000 rpm for 15 min and stored at −80 °C pending further analysis. Liver and mesenteric adipose tissue (WAT) were snap-frozen in liquid nitrogen after weighing for further analysis.

Lipid Extraction and Fatty Acid Analysis

The fatty acid composition of plasma, WAT, and liver in the C57BL/6J mice was determined as described [17]. Lipids were extracted by homogenizing the tissue samples in a 4:1 (v/v) methanol/hexane solution supplemented with 50 μg/ml butylated hydroxytoluene (BHT) as an antioxidant. Fatty acids methyl esters were obtained by transmethylation of the lipids (500 μl) with acetyl chloride (200 μl) and heating at 80 °C for 1 h under a nitrogen atmosphere. Methyl docosatrienoate (22:3n-3) at a final concentration of 0.4 μg/mg for WAT and liver, and methyl tricosanoate (23:0) at a final concentration of 0.2 μg/μl for plasma were added to each sample as internal standards. Gas chromatographic analysis of fatty acid methyl esters was performed on an Agilent 6890N Network Gas Chromatograph System (Agilent Technologies Japan, Ltd., Japan) equipped with a split injector, FID detector and a fused silica capillary column (30 m × 0.25 mm ID × 0.25 μm film thickness, J & W Scientific, Agilent Technologies). Data were collected with GC Chemstation (Agilent Technologies). Fatty acid methyl esters were identified by co-chromatography with purified standard mixture (Nu-Chek Prep 462, Elysian, MN), and fatty acid data were expressed as the percentage peak area corresponding to the weight of individual fatty acids.

Table 2 Composition of the diets for the KKAy and C57BL/6J mice

Component (%)	KKAy mice		C57BL/6J mice	
	Soybean oil diet	Saury oil diet	Lard diet	Saury oil diet
Casein	20	20	25.8	25.8
L-Cysteine	0.3	0.3	0.4	0.4
Corn starch	49.9	49.9	–	–
Maltodextrin 10	–	–	16.2	16.2
Sucrose	10	10	8.9	8.9
Cellulose	5	5	6.5	6.5
Mineral mixture	3.5	3.5	1.3	1.3
Vitamin mixture	1	1	1.3	1.3
Choline bitartrate	0.3	0.3	0.3	0.3
Soybean oil	10	–	3.2	3.2
Lard	–	–	32	22
Saury oil	–	10	–	10

Insulin Tolerance Test

For the KKAy mice on the control diet and the saury oil diet, the insulin tolerance test was performed at the end of 3 weeks. Each mouse received an intraperitoneal injection of insulin (0.75 U/kg body weight, Humulin R U-100, Eli Lilly, Japan) after fasted for 6 h with free access to water. Blood samples were taken from the retro-orbital venous plexus prior to the insulin injection (0 min time point) and at indicated time points after the injection. The blood samples were centrifuged at 3,000 rpm for 15 min, and plasma glucose concentration was measured using a glucose test kit (Glucose CII-test, Wako Pure Chemicals Industries, Japan).

Biochemical Analysis of Plasma

The plasma concentrations of glucose, total cholesterol (TC), HDL-C, TAG, and nonesterified fatty acids (NEFA) were measured using a Glucose CII-Test, a Cholesterol E-Test, a HDL-Cholesterol E-Test, a TG E-Test and a NEFA C-Test, respectively (Wako), and low-density lipoprotein cholesterol (LDL-C) levels were calculated as TC−HDL-C−TGA × 0.2. Plasma insulin levels were determined using an Insulin ELISA kit (Morinaga Institute of Biological Science, Inc., Japan). Plasma concentrations of adipokines, including adiponectin, resistin, tumor necrosis factor-alpha (TNFα), and leptin, were measured using the following respective enzyme immunoassay kits: mouse adiponectin ELISA kit (Otsuka Pharmaceutical Co., Ltd., Japan), Mouse Resistin ELISA kit (Shibayagi Co. Ltd., Japan), Mouse TNF-α ELISA kit (Shibayagi) and Mouse Leptin ELISA kit (Morinaga).

Analysis of mRNA Expression Using Real-Time Reverse Transcription Polymerase Chain Reaction (RT-PCR)

For the C57BL/6J mice fed high-fat diets, total RNA was isolated from mesenteric WAT using TRIzol reagent (Qiagen, Tokyo, Japan) according to the manufacturer's protocol. The first strand of cDNA was generated from total RNA using a PrimeScript II 1st strand cDNA Synthesis kit (TaKaRa Bio, Otsu, Japan) using oligo dT-adaptor primers, and 1–2 μg of total RNA as the template. The resulting cDNA pool was used for real-time RT-PCR amplification and specific sequence detection on an Applied Biosystems 7300 Real-Time PCR System (Life Technologies Co., Japan). The forward and reverse PCR primers shown in Table 3 were used at final concentrations of 10 μM. SYBR Premix Ex Taq (TaKaRa Bio) was also used. The PCR cycling parameters were: 30 s at 95 °C; followed by 40 cycles of 5 s, 95 °C, 34 s at 60 °C; and a final melting curve of 15 s at 95 °C, 1 min at 60 °C, 15 s at 95 °C. Gene expression was scaled to the expression of the housekeeping gene encoding 18S ribosomal RNA.

Statistical Analysis

All data are expressed as means ± SE. Statistical differences between two groups were determined using Student's *t* test. The value was considered to be significantly different for values of $P < 0.05$.

Results

Fatty Acid Composition of Plasma, WAT and Liver

Plasma, mesenteric WAT, and liver fatty acid compositions in C57BL/6J mice fed the control diet (lard) or saury oil-supplemented diet are shown in Table 4. PUFA and MUFA percentages were significantly different in the saury oil group compared to the control group although there were no large differences in the levels of saturated fatty acids (SFA) between the two diet groups. The saury oil-supplemented diet resulted in reduced levels of arachidonic acid (C20:4 n-6) in plasma, WAT and liver by 33.8% ($P < 0.05$), 39.3% ($P < 0.01$), and 53.7% ($P < 0.001$) respectively, and reduced the total n-6 PUFA levels significantly in WAT and liver by 8% ($P < 0.05$) and 29.2% ($P < 0.05$), respectively. Ingestion of saury oil increased EPA levels significantly in both plasma and liver by 130% ($P < 0.05$) and 1118.5% ($P < 0.001$), respectively, and also increased DHA levels significantly in WAT and liver by 835.3% ($P < 0.001$) and 85% ($P < 0.001$), respectively. Compared to the control group, the total n-3 PUFA levels in the saury oil diet group increased significantly in plasma, WAT and liver by 35.9% ($P < 0.05$), 162.2% ($P < 0.001$), and 141.8% ($P < 0.001$), respectively. The decrease in n-6 PUFA and increase in n-3 PUFA with the saury oil diet resulted in significant decreases in n-6/n-3 PUFA ratios in plasma, WAT and liver by 39.7% ($P < 0.05$), 64.9% ($P < 0.001$), and 69% ($P < 0.001$), respectively. A different pattern of changes in lipid composition was observed for the MUFA levels with the saury oil diet. Compared to the control diet group, C22:1 levels in the saury oil group were significantly higher in plasma, WAT and liver by 110.3% ($P < 0.05$), 266.7% ($P < 0.001$), and 450% ($P < 0.01$), respectively. Also, C20:1 levels in WAT were significantly elevated (by 66.7%, $P < 0.001$) with the saury oil-supplemented diet. In contrast, saury oil intake decreased oleic acid (C18:1) levels markedly in WAT and liver, by 16.8% ($P < 0.01$) and 27.2% ($P < 0.05$), respectively.

Table 3 GenBank accession numbers and primer sequences used in real-time RT-PCR experiments

Gene	Primer sequences	Accession number
SREBP-1c	5′-GATGTGCGAACTGGACACAG-3′	NM_011480
	5′-CATAGGGGGCGTCAAACAG-3′	
SCD-1	5′-TTCTTGCGATACACTCTGGTGC-3′	NM_009127
	5′-CGGGATTGAATGTTCTTGTCGT-3′	
FAS	5′-GGAGGTGGTGATAGCCGGTAT-3′	NM_007988
	5′-TGGGTAATCCATAGAGCCCAG-3′	
ACC	5′-ATGGGCGGAATGGTCTCTTTC-3′	NM_133360
	5′-TGGGGACCTTGTCTTCATCAT-3′	
CPT-1	5′-CTCCGCCTGAGCCATGAAG-3′	NM_013495
	5′-CACCAGTGATGATGCCATTCT-3′	
PGC-1α	5′-GAAGTGGTGTAGCGACCAATC-3′	NM_008904
	5′-AATGAGGGCAATCCGTCTTCA-3′	
PGC-1β	5′-TCCTGTAAAAGCCCGGAGTAT-3′	NM_133249
	5′-GCTCTGGTAGGGGCAGTGA-3′	

SREBP-1 sterol regulatory element binding protein 1, *SCD-1* stearoyl CoA desaturase-1, *FAS* fatty acid synthase, *ACC* acetyl-CoA carboxylase, *CPT-1* carnitine palmitoyltransferase-1, *PGC-1α* peroxisome proliferator-activated receptor gamma coactivator 1-alpha, *PGC-1β* peroxisome proliferator-activated receptor gamma coactivator 1-beta

Table 4 Serum, mesenteric WAT and liver fatty acid composition (%) for diet-induced obese C57BL/6J mice

Fatty acid	Serum		Mesenteric WAT		Liver	
	Control	Saury oil	Control	Saury oil	Control	Saury oil
14:0	1.18 ± 0.2	2.2 ± 0.24	1.17 ± 0.02	2 ± 0.03*	0.72 ± 0.01	0.71 ± 0.01
16:0	15.81 ± 0.21	15.32 ± 0.26	22.47 ± 0.19	22.73 ± 0.23	18.96 ± 0.52	19.56 ± 0.24
18:0	29.34 ± 0.6	28.54 ± 0.48	4.29 ± 0.11	5.26 ± 0.17*	16.9 ± 0.52	16.86 ± 0.32
SAF	48.58 ± 1.42	47.7 ± 1.35	27.94 ± 1.42	30 ± 1.35	38.26 ± 1.17	38.39 ± 0.77
12:1	11.89 ± 1.5	10.27 ± 1.42	0.07 ± 0	0.07 ± 0	11.69 ± 0.6	13.41 ± 0.73
16:1	0.88 ± 0.05	0.85 ± 0.04	4.92 ± 0.16	3.85 ± 0.2*	1.34 ± 0.1	0.93 ± 0.05
18:1	23.31 ± 0.08	23.56 ± 0.19	47.84 ± 0.38	39.78 ± 0.58**	17.86 ± 1.24	13 ± 0.55*
20:1	0.21 ± 0.02	0.19 ± 0.01	0.69 ± 0.01	1.15 ± 0.03***	0.36 ± 0.03	0.35 ± 0.02
22:1	0.29 ± 0.03	0.61 ± 0.05*	0.03 ± 0	0.11 ± 0.01***	0.02 ± 0	0.11 ± 0.01**
MUFA	36.58 ± 1.4	35.48 ± 1.35	53.55 ± 0.36	44.96 ± 0.54**	31.26 ± 2.09	27.81 ± 1.42
18:2n-6	3.99 ± 0.27	3.75 ± 0.16	13.61 ± 0.18	12.72 ± 0.25*	10.05 ± 0.24	9.64 ± 0.21
18:3n-6	0.26 ± 0.07	0.21 ± 0.02	0.07 ± 0	0.03 ± 0	0.3 ± 0.01	0.18 ± 0*
20:2n-6	0.15 ± 0.01	0.16 ± 0.01	0.25 ± 0.01	0.23 ± 0	0.19 ± 0.01	0.14 ± 0
20:3n-6	0.29 ± 0.02	0.25 ± 0.02	0.13 ± 0.02	0.08 ± 0	0.81 ± 0.07	0.63 ± 0.04
20:4n-6	3.22 ± 0.5	2.13 ± 0.35*	0.28 ± 0.01	0.17 ± 0.01**	9.86 ± 0.24	4.57 ± 0.11***
22:4n-6	0.2 ± 0.03	0.16 ± 0.01	0.08 ± 0	0.04 ± 0	0.34 ± 0.01	0.09 ± 0.01**
n-6 PUFA	8.11 ± 0.86	6.66 ± 0.65	14.42 ± 0.19	13.27 ± 0.26*	21.55 ± 0.57	15.25 ± 0.4*
18:3n-3	0.16 ± 0.01	0.18 ± 0.01	0.77 ± 0.02	1.01 ± 0.02*	0.32 ± 0.02	0.43 ± 0.03*
20:5n-3	0.63 ± 0.22	1.45 ± 0.28*	0.16 ± 0.01	0.09 ± 0.01	0.27 ± 0.01	3.29 ± 0.1***
22:5n-3	2.25 ± 0.02	0.26 ± 0.01	0.09 ± 0	0.43 ± 0.01**	0.45 ± 0.02	1.36 ± 0.06***
22:6n-3	1.94 ± 0.19	2.16 ± 0.13	0.17 ± 0.01	1.59 ± 0.05***	6.47 ± 0.17	11.97 ± 1***
n-3 PUFA	2.98 ± 0.46	4.05 ± 0.54*	1.19 ± 0.03	3.12 ± 0.07***	7.51 ± 0.22	17.05 ± 1.2***
n-6/n-3	2.72 ± 0.42	1.64 ± 0.43*	12.11 ± 0.15	4.25 ± 0.08***	2.87 ± 0.04	0.89 ± 0.09***

Each value represents the mean ± SE ($n = 10$). C57BL/6J mice were fed a 32% lard diet (control) or a 32% lard plus 10% saury oil diet (saury oil group) for 6 weeks

SAF saturated fatty acids, *MUFA* monounsaturated fatty acids, *PUFA* polyunsaturated fatty acids

* $P < 0.05$, ** $P < 0.01$, *** $P < 0.001$ compared to controls

Effect of Saury Oil on Plasma Glucose Levels in an Insulin Tolerance Test

The plasma glucose concentrations in an insulin tolerance test are shown in Fig. 1 for KKAy mice fed a soybean oil (control) or saury oil diet. Plasma glucose levels in the saury oil group declined ($P = 0.14$) at 60 min, and then significantly decreased by 25.3% ($P < 0.05$) at 80 min after insulin injection, compared to the control group.

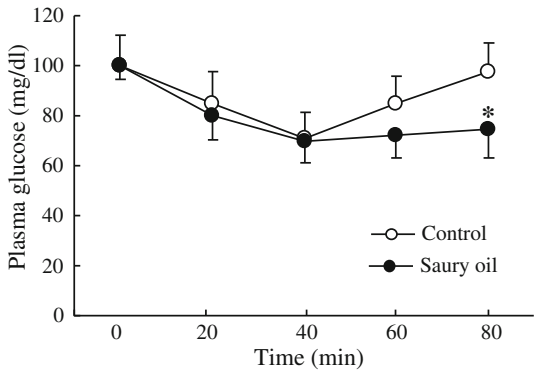

Fig. 1 The effect of saury oil on insulin sensitivity. An insulin tolerance test was performed at the end of 3 weeks to KKAy mice fed a 10% soybean oil diet (control) or 10% saury oil diet. Values are mean ± SE ($n = 10$) and are normalized relative to the control group. *$P < 0.05$ compared to controls

Effect of Saury Oil on Metabolic Variables in Plasma

The body weight, mesenteric WAT mass, and plasma concentrations of glucose, insulin, and lipids in KKAy mice and diet-induced obese C57BL/6J mice are shown in Table 5. After 4 weeks of feeding KKAy mice the saury oil diet, the mesenteric WAT mass in the saury oil group was 10.4% ($P < 0.05$), plasma concentrations of glucose were 13.7% ($P < 0.05$), insulin were 45.4% ($P < 0.01$), TC were 39.4% ($P < 0.001$), LDL-C were 76.4% ($P < 0.001$), and NEFA were 23.1% ($P < 0.01$) lower than in the control soybean oil group. Plasma TAG concentrations also tended to be lowered by the saury oil diet ($P = 0.14$).

Table 5 The effect of saury oil on body weight, mesenteric WAT mass, and plasma markers of glucose and lipid metabolism in KKAy and diet-induced obese C57BL/6J mice

	KKAy mice		C57BL/6J mice	
	Soybean oil diet (Control)	Saury oil diet	Lard diet (Control)	Saury oil diet
Body weight (g)	37.9 ± 0.6	36.9 ± 0.4	31.6 ± 1.3	32.1 ± 2.1
Body weight gain (g)	7.7 ± 0.4	6.9 ± 0.3	10.3 ± 0.9	9.8 ± 1.8
WAT mass (g)	2.4 ± 0.1	2.17 ± 0.1*	1.7 ± 0.09	1.7 ± 0.13
Glucose (mg/dl)	541.5 ± 20.1	467.3 ± 8.2*	301.4 ± 11.2	258.9 ± 19.8**
Insulin (ng/ml)	40.9 ± 4.4	22.3 ± 2.3**	4.7 ± 0.6	3.1 ± 0.4*
TC (mg/dl)	109.3 ± 3.7	65.9 ± 2.6***	134.7 ± 4.2	107.2 ± 5.1**
LDL-C (mg/dl)	45.9 ± 2.4	18.5 ± 1.2***	28.2 ± 6.4	20.5 ± 3.4*
TAG (mg/dl)	67.6 ± 9.1	54.1 ± 4.6	76.6 ± 5	60.5 ± 4.9***
NEFA (mequiv/l)	1.1 ± 0.07	0.8 ± 0.04**	0.5 ± 0.03	0.48 ± 0.06

Each value represents the mean ± SE ($n = 10$). KKAy mice were fed a 10% soybean oil diet (control) or a 10% saury oil diet for 4 weeks. C57BL/6J mice were fed a 32% lard diet (control) or a 22% lard plus 10% saury oil diet (saury oil diet) for 6 weeks

WAT white adipose tissue, *TC* total cholesterol, *LDL-C* low-density lipoprotein cholesterol, *TAG* triacylglycerol, *NEFA* nonesterified fatty acid

* $P < 0.05$, ** $P < 0.01$, *** $P < 0.001$ compared to controls

There was no difference in body weight between the saury oil group and the control group. Similarly, ingestion of saury oil also decreased the plasma concentrations of glucose in C57BL/6J mice by 13.6% ($P < 0.01$), of insulin by 35.2% ($P < 0.05$), of TC by 18.6% ($P < 0.01$), of LDL-C by 27.3% ($P < 0.05$), and of TAG by 19.4% ($P < 0.001$), although the mesenteric WAT mass did not differ between the saury oil group and the control group.

Effect of Saury Oil on Adipokine Levels in Plasma

Intake of saury oil increased the concentration of adiponectin in plasma by 28.7% ($P < 0.01$) in KKAy mice and by 23.6% ($P < 0.01$) in C57BL/6J mice (Fig. 2a). Plasma resistin concentrations were decreased by 28.5% ($P < 0.05$) and 9.5% ($P < 0.05$) with a saury oil diet in KKAy mice and C57BL/6J mice, respectively (Fig. 2b). Ingestion of saury oil also decreased plasma TNFα concentrations by 59.5% ($P < 0.01$) in KKAy mice (Fig. 2c) and plasma leptin concentrations by 66.9% ($P < 0.01$) in C57BL/6J mice (Fig. 2d).

Effect of Saury Oil on the Expression of mRNAs Related to Lipid Metabolism in WAT

The saury oil-supplemented diet downregulated the mRNA expression of lipogenic genes *SREBP-1* (sterol regulatory element binding protein 1), *SCD-1* (stearoyl-coenzyme A desaturase 1), *FAS* (Fatty acid synthase), and *ACC* (Acetyl-CoA carboxylase) by 65% ($P < 0.05$), 72% ($P < 0.01$), 70% ($P < 0.05$), and 74% ($P < 0.05$), respectively, compared to the control lard diet group (Fig. 3a), and upregulated expression of the oxidation-related gene *CPT-1* (Acetyl-CoA carboxylase Carnitine palmitoyltransferase-1), the energy consumption-related genes *PGC1α* (Peroxisome proliferator-activated receptor gamma coactivator 1-alpha) and *PGC1β* (Peroxisome proliferator-activated receptor gamma coactivator 1-beta) by 123% ($P < 0.05$), 171% ($P < 0.05$), and 176% ($P < 0.05$), respectively (Fig. 3b), in diet-induced obese C57BL/6J mice.

Discussion

The present study has demonstrated that ingestion of saury oil alleviates MetS in type II diabetic KKAy mice and diet-induced obese C57BL/6J mice by improving glycemic and lipid control. To understand the possible mechanisms of the hypoglycemic and hypolipidemic effects of saury oil, we investigated adipokine levels. As a key adipokine, adiponectin has received considerable attention due to its anti-inflammatory, antiatherogenic and antidiabetic properties [18, 19]. There is increasing evidence supporting the positive association of higher adipocyte-derived adiponectin with glycemic control, lipid profile, and inflammation [20]. By contrast, elevated levels of circulating NEFA and other adipokines such as TNFα, resistin, and leptin are associated with insulin resistance [21–26]. Therefore, the increase in plasma levels of adiponectin, as well as the decreases in plasma levels of NEFA, TNFα, resistin, and leptin with a saury oil diet are possibly associated with the improvement of hyperglycemia, hyperinsulinemia, and hyperlipidemia relative to insulin resistance.

Saury oil intake decreased mesenteric WAT mass significantly in KKAy mice, and several lines of evidence indicate that a lower content of WAT is associated with a

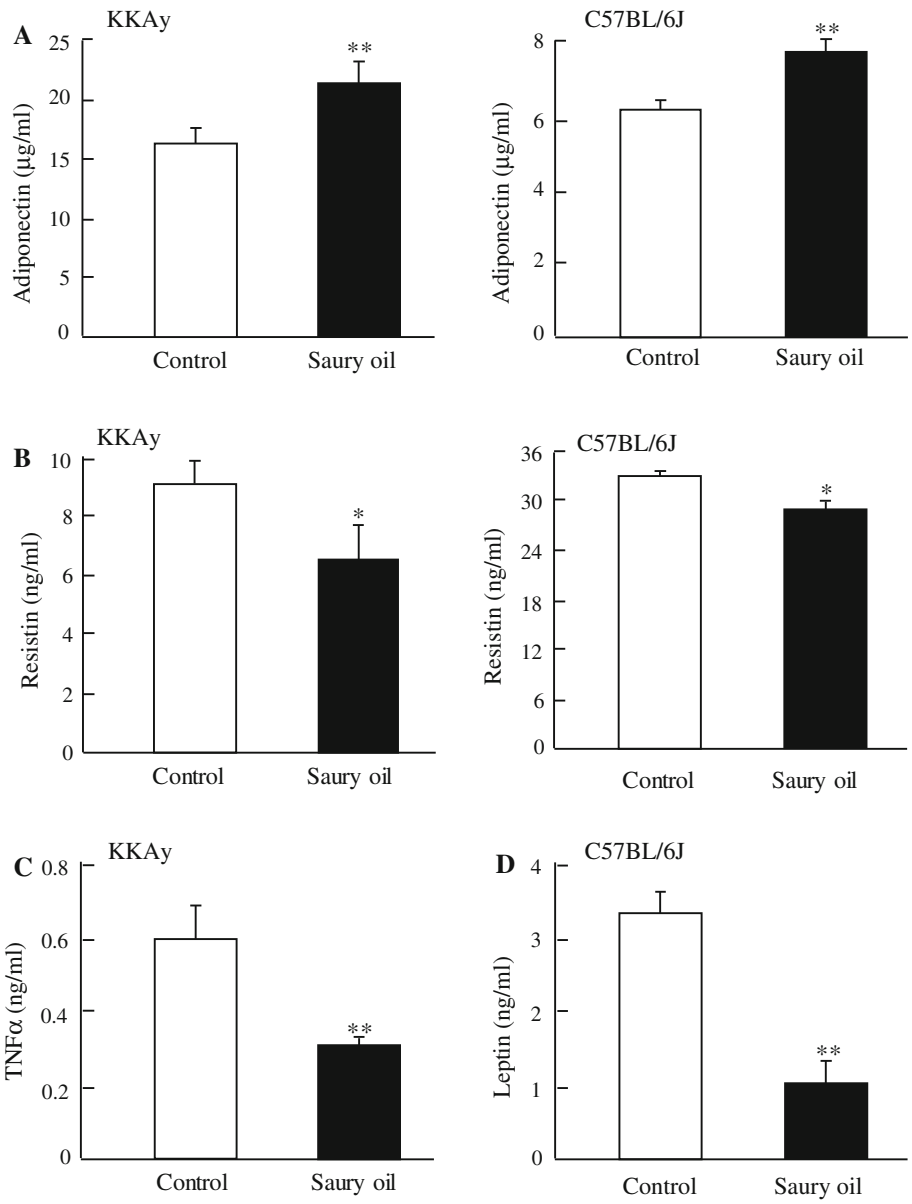

Fig. 2 The effect of saury oil on plasma adipokines. Plasma adipokine concentrations in KKAy mice (*left*) and in diet-induced obese C67BL/6 J mice (*right*) for: **a** adiponectin, **b** resistin, **c** TNFα, and **d** leptin. KKAy mice were fed a 10% soybean oil diet (control) or a 10% saury oil diet for 4 weeks. C57BL/6J mice were fed a 32% lard diet (control) or 22% lard plus 10% saury oil diet (saury oil group) for 6 weeks. After the feeding period, plasma adipokine levels were measured in duplicate by ELISA. Values are mean ± SE ($n = 10$). *$P < 0.05$, **$P < 0.01$ compared to controls

favorable profile of adipokines as well as a lower MetS risk [27]. Saury oil intake did not change WAT mass in diet-induced obese C67BL/6J mice, however, although there were favorable changes in plasma adipokines associated with a favorable metabolic profile. It is therefore suggested that adipose tissue mass loss is not the only essential factor for the improvement of metabolic disarrangement in diet-induced obese C57BL/6J mice fed a saury oil diet. Notably, Saraswathi et al. [28] demonstrated that by feeding fish oil to LDL receptor-deficient mice, WAT-specific inflammation and insulin sensitivity were improved and macrophage infiltration was reduced despite an increase in adipose tissue mass.

The n-3 PUFA levels in plasma, WAT and liver increased significantly in the saury oil group compared to the control group for C57Bl/6J mice. It has been demonstrated that EPA increases adiponectin secretion in rodent models of obesity and in human obese subjects, in part through TNFα downregulation in macrophages [29, 30]. n-3 fatty acids also decrease TNFα, resistin and leptin levels, all of which are implicated in insulin insensitivity [31–33]. The beneficial effect of saury oil in producing a more favorable adipokine profile and easing the onset of MetS may be partly attributed to the increase in n-3 PUFA.

SREBP-1 and its target genes *SCD-1*, *FAS* and *ACC* are involved in adipogenesis, and *SREBP-1* has a key role in regulating fatty acid synthesis [34]. Insulin-induced expression of *SREBP-1* mRNA can be prevented by the n-3 PUFA [35]. n-3 PUFA also prevented insulin induction of the downstream lipogenic enzyme targets *FAS* and *ACC*,

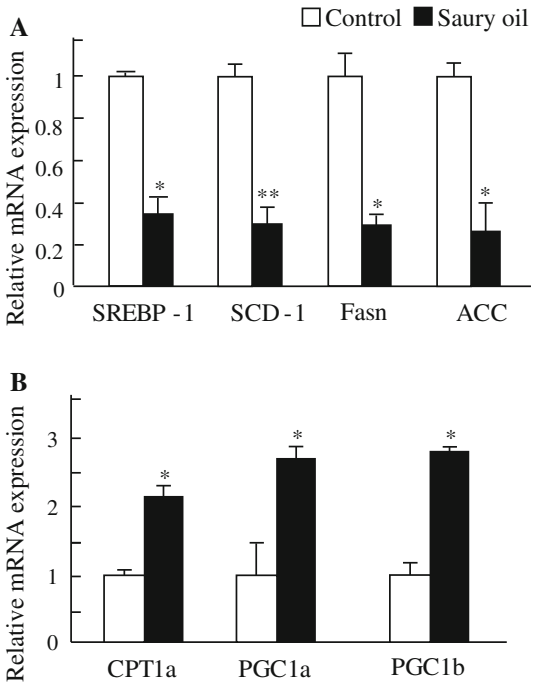

Fig. 3 The effect of saury oil on the mRNA expression levels of genes involved in lipid metabolism in mesenteric WAT. **a** mRNA expression of markers of lipogenesis (*SREBP1*, *SCD-1*, *FAS* and *ACC*). **b** mRNA expression of markers of lipid oxidation (*CPT1a*), and energy expenditure (*PGC1α* and *PGC1β*). C57BL/6J mice were fed a 32% lard diet (control) or a 22% lard plus 10% saury oil diet for 6 weeks. After the intervention period, mRNA levels in mesenteric WAT were measured by real-time RT-PCR. Values for expression levels were normalized to that of 18S ribosomal RNA and expressed relative to the control group. Values are means ± SE ($n = 10$). $^{*}P < 0.05$, $^{**}P < 0.01$ compared to controls

and reduced de novo lipogenesis [36]. Enzyme CPT-1 is rate limiting for fatty acid β-oxidation in mitochondria [37], and PGC1α is a molecular marker of energy expenditure via regulatory function for mitochondrial biogenesis and oxidative metabolism [38–40]. Flachs et al. [41] demonstrated that the antiadipogenic effect of an EPA/DHA concentrate (6% EPA and 51% DHA) may involve a metabolic switch in adipocytes that includes enhancement of β-oxidation with increase in mRNA expression of *CPT-1* and upregulation of mitochondrial biogenesis with an increase in the expression of genes encoding PGC1α and nuclear respiratory factor-1 (Nrf-1). Suppression of adipogenesis and promotion of fatty acid oxidation, as well as energy expenditure in mRNA levels with a saury oil diet are associated with improvement of glucose and lipid metabolism, and this is potentially derived from a significant increase in n-3 PUFA with an intake of saury oil.

In contrast to the increase in n-3 PUFA, there were marked reductions in n-6 PUFA including arachidonic acid, along with a corresponding decrease in the n-6/n-3 PUFA ratio, with the saury oil diet. n-6 PUFA, which compete with n-3 PUFA for several physiological processes, can increase inflammatory signals and have been associated with metabolic/cardiovascular disorders and cancer [42–44]. A decrease in the n-6/n-3 PUFA ratio can enhance glucose tolerance in healthy animals [45], and prolong survival of type I diabetes model non-obese diabetic mice by retaining the beta cell mass [46]. Thus, a decrease in n-6 PUFA, as well as in the n-6/n-3 PUFA ratio, contributes to the beneficial effects of saury oil on glucose and lipid metabolism in a saury oil diet.

In addition to n-3 PUFA, diets rich in MUFA are recommended for individuals with type 2 diabetes mellitus, and studies suggest the beneficial effect of dietary oleic acid on insulin sensitivity [47]. Levels of 18:1 in WAT and liver decreased significantly with a saury oil diet, however, suggesting a minor role for 18:1 in the improvement of MetS with saury oil treatment. Because a considerable fraction of the fatty acids in saury oil is comprised of MUFA (35% of C20:1 and C22:1), some of the beneficial effects of saury oil on metabolic control of hyperglycemia and hyperlipidemia observed in the present study may be associated with MUFA.

Whale oil is rich in MUFA—28% of it is comprised of C20:1 and C22:1 aliphatics—but contains only 54% of combined EPA/DHA found in cod liver oil and 68% of that found in seal oil. Despite this difference, Osterud et al. [16] demonstrated that the consumption of these three oils by healthy subjects increased the content of n-3 fatty acids in serum lipids significantly to a comparable degree and also reduced the arachidonic acid levels similarly for all three oils. Similarly, in another study by Halvorsen et al. [15] feeding rats fish oil fractions rich in MUFA (80% of C20:1 and C22:1), the level of EPA in the plasma lipids was increased while the content of arachidonic acid was reduced compared with that of rats fed lard. The increase in n-3 PUFA and the improved ratio of n-6 PUFA to n-3 PUFA, which contributes to the improvement of glycemic and lipid metabolism in diet-induced obese C57BL/6J mice fed a saury oil-supplemented diet, may therefore be partly attributable to MUFA. In addition, it has been demonstrated that MUFA-enriched whale oil supplementation reduces TNFα generation in lipopolysaccharide-stimulated blood [16]; this supports our finding that reduced blood TNFα levels correlated with improved insulin resistance in KKAy mice fed a saury oil diet. Taken together, these results are interesting and suggest a possible synergistic effect between n-3 PUFA and MUFA in the improvement of MetS.

Very limited data exist defining the health beneficial actions of saury oil, and the current study showed the beneficial effects of saury oil in reducing risk factors for metabolic syndrome in spontaneously diabetic mice and diet-induced obese mice. On the other hand, the mechanism by which MUFA boosts the effect of n-3 PUFA and whether

MUFA has a specific effect on metabolic disorders themselves still needs to be elucidated. This is of importance if the development of functional lipids from fish and MetS treatment with a diet rich in saury oil are to be pursued.

Acknowledgments The authors gratefully acknowledge the technical assistance of Dr. Toru Moriguchi (Azabu University), Ms. Akiko Harauma, Mr. Nobushige Doisaki and Ms. Kiyomi Furihata in Nippon Suisan Kaisya, Ltd.

References

1. Gupta A, Gupta V (2010) Metabolic syndrome: what are the risks for humans? Biosci Trends 4:204–212
2. Phillips C, Lopez-Miranda J, Perez-Jimenez F, McManus R, Roche HM (2006) Genetic and nutrient determinants of the metabolic syndrome. Curr Opin Cardiol 21:185–193
3. Ruxton CH, Reed SC, Simpson MJ, Millington KJ (2004) The health benefits of omega-3 polyunsaturated fatty acids: a review of the evidence. J Hum Nutr Diet 17:449–459
4. Perez-Matute P, Perez-Echarri N, Martinez JA, Marti A, Moreno-Aliaga MJ (2007) Eicosapentaenoic acid actions on adiposity and insulin resistance in control and high-fat-fed rats: role of apoptosis, adiponectin and tumour necrosis factor-alpha. Br J Nutr 97:389–398
5. Mori TA, Bao DQ, Burke V (1999) Dietary fish as a major component of a weight-loss diet: effect on serum lipids, glucose, and insulin metabolism in overweight hypertensive subjects. Am J Clin Nutr 70:817–825
6. Couet C, Delarue J, Ritz P (1997) Effect of dietary fish oil on body fat mass and basal fat oxidation in healthy adults. Int J Obes 21:637–643
7. Japan Aquatic Oil Association (ed) (1989) Fatty acid composition of fish and shellfish. Korin Press, Tokyo
8. Ota T, Takagi T, Kosaka S (1980) Changes in lipids of young and adult saury *Cololabis saira* (Pisces). Mar Ecol Prog Ser 3:11–17
9. Pascal JC, Ackman RG (1976) Long-chain monoethylenic alcohol and acid isomers in lipids of copepods and capelin. Chem Phys Lipids 16:219–223
10. Hardy R, Mackie P (1969) Seasonal variation in some of the lipid components of sprats (*Sprattus sprattus*). J Sci Food Agric 20:193–198
11. Ratnayake WN, Ackman RG (1979) Fatty alcohols in capelin, herring and mackerel oils and muscle lipids: I fatty alcohol details linking dietary copepod fat with certain fish depot fats. Lipids 14:795–803
12. Graeve M, Kattner G (1992) Species-specific differences in intact wax esters of *Calanus hyperboreus* and *C. finmarchicus* from Fram Strait-Greenland Sea. Mar Chem 39:269–281
13. Falk-Petersen S, Sargent JR, Tande KS (1987) Lipid composition of zooplankton in relation to the sub-arctic food web. Polar Biol 8:115–120
14. Flatmark T, Christiansen EN (1993) Modulation of peroxisomal biogenesis and lipid metabolizing enzymes by dietary factors. In: Gibson G, Lake B (eds) Peroxisomes: biology and importance in toxicology and medicine. Taylor & Francis Ltd, London, pp 247–275
15. Halvorsen B, Rustan AC, Christiansen EN (1995) Effect of long chain monounsaturated and n-3 polyunsaturated fatty acids on postprandial blood and liver lipids in rats. Scand J Clin Lab Invest 55:469–475
16. Osterud B, Elvevoll E, Barstad H, Brox J, Halvorsen H, Lia K, Olsen JO, Olsen RO, Sissener C, Rekdal O, Vogild E (1995) Effect of marine oils supplementation on coagulation and cellular activation in whole blood. Lipids 30:1111–1118
17. Lepage G, Roy CC (1986) Direct transesterification of all classes of lipids in a one-step reaction. J Lipid Res 27:114–120
18. Stefan N, Stumvoll M (2002) Adiponectin—its role in metabolism and beyond. Horm Metab Res 34:469–474
19. Kadowaki T, Yamauchi T, Kubota N, Hara K, Ueki K, Tobe K (2006) Adiponectin and adiponectin receptors in insulin resistance, diabetes, and the metabolic syndrome. J Clin Invest 116:1784–1792
20. Mantzoros CS, Li T, Manson JE, Meigs JB, Hu FB (2005) Circulating adiponectin levels are associated with better glycemic control, more favorable lipid profile, and reduced inflammation in women with type 2 diabetes. J Clin Endocrinol Metab 90:4542–4548
21. Shulman GI (2000) Cellular mechanisms of insulin resistance. J Clin Invest 106:171–176
22. Hotamisligil GS (1999) The role of TNF-alpha and TNF receptors in obesity and insulin resistance. J Intern Med 245:621–625
23. Das UN (1999) GLUT-4, tumor necrosis factor, essential fatty acids and daf-genes and their role in insulin resistance and non-insulin dependent diabetes mellitus. Prostaglandins Leukot Essent Fatty Acids 60:13–20
24. Savage DB, Sewter CP, Klenk ES, Segal DG, Vidal-Puig A, Considine RV, O'Rahilly S (2001) Resistin/Fizz3 expression in relation to obesity and peroxisome proliferator-activated receptor-gamma action in humans. Diabetes 50:2199–2202
25. Norata GD, Ongari M, Garlaschelli K, Raselli S, Grigore L, Catapano AL (2007) Plasma resistin levels correlate with determinants of the metabolic syndrome. Eur J Endocrinol 156:279–284
26. Munzberg H (2009) Leptin-signaling pathways and leptin resistance. Forum Nutr 63:123–132
27. Guerre-Millo M (2002) Adipose tissue hormones. J Endocrinol Invest 25:855–861
28. Saraswathi V, Gao L, Morrow JD, Chait A, Niswender KD, Hasty AH (2007) Fish oil increases cholesterol storage in white adipose tissue with concomitant decreases in inflammation, hepatic steatosis, and atherosclerosis in mice. J Nutr 137:1776–1782
29. Itoh M, Suganami T, Satoh N, Tanimoto-Koyama K, Yuan X, Tanaka M, Kawano H, Yano T, Aoe S, Takeya M, Shimatsu A, Kuzuya H, Kamei Y, Ogawa Y (2007) Increased adiponectin secretion by highly purified eicosapentaenoic acid in rodent models of obesity and human obese subjects. Arterioscler Thromb Vasc Biol 27:1918–1925
30. Krebs JD, Browning LM, McLean NK, Rothwell JL, Mishra GD, Moore CS, Jebb SA (2006) Additive benefits of long-chain n-3 polyunsaturated fatty acids and weight-loss in the management of cardiovascular disease risk in overweight hyperinsulinaemic women. Int J Obesity 30:1535–1544
31. Das UN (2005) A defect in the activity of Δ5 and Δ6 desaturases may be a factor in pre-disposing to the development of insulin resistance syndrome. Prostaglandins Leukot Essent Fatty Acids 72:343–350
32. Drevon CA (2005) Fatty acids and the expression of adipokines. Biochim Biophys Acta 1740:287–292
33. Reseland JE, Anderssen SA, Solvoll K, Hjermann I, Urdal P, Holme I, Drevon CA (2001) Effect of long-term changes in diet and exercise on plasma leptin concentrations. Am J Clin Nutr 73:240–245
34. Shimano H, Shimomura I, Hammer RE, Herz J, Goldstein JL, Brown MS, Horton JD (1997) Elevated levels of SREBP-2 and cholesterol synthesis in livers of mice homozygous for a targeted disruption of the SREBP-1 gene. J Clin Invest 100:2115–2124
35. Nakatani T, Kim HJ, Kaburagi Y, Yasuda K, Ezaki O (2003) A low fish oil inhibits SREBP-1 proteolytic cascade, while a

high-fish-oil feeding decreases SREBP-1 mRNA in mice liver: relationship to anti-obesity. J Lipid Res 44:369–379
36. Howell G 3rd, Deng X, Yellaturu C, Park EA, Wilcox HG, Raghow R, Elam MB (2009) N-3 polyunsaturated fatty acids suppress insulin-induced SREBP-1c transcription via reduced trans-activating capacity of LXRalpha. Biochim Biophys Acta 1791:1190–1196
37. McGarry JD, Brown NF (1997) The mitochondrial carnitine palmitoyltransferase system. From concept to molecular analysis. Eur J Biochem 244:1–14
38. Wu Z, Puigserver P, Andersson U, Zhang C, Adelmant G, Mootha V, Troy A, Cinti S, Lowell B, Scarpulla RC, Spiegelman BM (1999) Mechanisms controlling mitochondrial biogenesis and respiration through the thermogenic coactivator PGC-1. Cell 98:115–124
39. Puigserver P, Spiegelman BM (2003) Peroxisome proliferator-activated receptor-gamma coactivator 1 alpha (PGC-1 alpha): transcriptional coactivator and metabolic regulator. Endocr Rev 24:78–90
40. Uldry M, Yang W, St-Pierre J, Lin J, Seale P, Spiegelman BM (2006) Complementary action of the PGC-1 coactivators in mitochondrial biogenesis and brown fat differentiation. Cell Metab 3:333–341
41. Flachs P, Horakova O, Brauner P, Rossmeisl M, Pecina P, Franssen-van Hal N, Ruzickova J, Sponarova J, Drahota Z, Vlcek C, Keijer J, Houstek J, Kopecky J (2005) Polyunsaturated fatty acids of marine origin upregulate mitochondrial biogenesis and induce beta-oxidation in white fat. Diabetologia 48:2365–2375
42. Whelan J (1996) Antagonistic effects of dietary arachidonic acid and n-3 polyunsaturated fatty acids. J Nutr 126:1086S–1091S
43. Simopoulos AP (2002) The importance of the ratio of omega-6/omega-3 essential fatty acids. Biomed Pharmacother 56:365–379
44. Hibbeln JR, Nieminen LR, Blasbalg TL, Riggs JA, Lands WE (2006) Healthy intakes of n-3 and n-6 fatty acids: estimations considering worldwide diversity. Am J Clin Nutr 83:1483S–1493S
45. Smith BK, Holloway GP, Reza-Lopez S, Jeram SM, Kang JX, Ma DW (2010) A decreased n-6/n-3 ratio in the fat-1 mouse is associated with improved glucose tolerance. Appl Physiol Nutr Metab 35:699–706
46. Kris-Etherton P, Daniels SR, Eckel RH, Engler M, Howard BV, Krauss RM (2001) AHA scientific statement: summary of the Scientific Conference on Dietary Fatty Acids and Cardiovascular Health. Conference summary from the Nutrition Committee of the American Heart Association. J Nutr 131:1322–1326
47. Moon JH, Lee JY, Kang SB, Park JS, Lee BW, Kang ES, Ahn CW, Lee HC, Cha BS (2010) Dietary monounsaturated fatty acids but not saturated fatty acids preserve the insulin signaling pathway via IRS-1/PI3 K in rat skeletal muscle. Lipids 45:1109–1116

Lipids (2011) 46:435–441
DOI 10.1007/s11745-011-3545-1

ORIGINAL ARTICLE

Growth Temperature and Salinity Impact Fatty Acid Composition and Degree of Unsaturation in Peanut-Nodulating Rhizobia

Natalia S. Paulucci · Daniela B. Medeot · Marta S. Dardanelli · Mirta García de Lema

Received: 6 July 2010 / Accepted: 21 February 2011 / Published online: 10 March 2011

Abstract Growth and survival of bacteria depend on homeostasis of membrane lipids, and the capacity to adjust lipid composition to adapt to various environmental stresses. Membrane fluidity is regulated in part by the ratio of unsaturated to saturated fatty acids present in membrane lipids. Here, we studied the effects of high growth temperature and salinity (NaCl) stress, separately or in combination, on fatty acids composition and de novo synthesis in two peanut-nodulating *Bradyrhizobium* strains (fast-growing TAL1000 and slow-growing SEMIA6144). Both strains contained the fatty acids palmitic, stearic, and *cis*-vaccenic + oleic. TAL1000 also contained eicosatrienoic acid and cyclopropane fatty acid. The most striking change, in both strains, was a decreased percentage of *cis*-vaccenic + oleic (≥80% for TAL1000), and an associated increase in saturated fatty acids, under high growth temperature or combined conditions. Cyclopropane fatty acid was significantly increased in TAL1000 under the above conditions. De novo synthesis of fatty acids was shifted to the synthesis of a higher proportion of saturated fatty acids under all tested conditions, but to a lesser degree for SEMIA6144 compared to TAL1000. The major adaptive response of these rhizobial strains to increased temperature and salinity was an altered degree of fatty acid unsaturation, to maintain the normal physical state of membrane lipids.

N. S. Paulucci · D. B. Medeot · M. S. Dardanelli · M. G. de Lema (✉)
Departamento de Biología Molecular, Facultad de Ciencias Exactas, Físico-Químicas y Naturales, Universidad Nacional de Río Cuarto, CPX5804BYA Río Cuarto, Córdoba, Argentina
e-mail: mgarcia@exa.unrc.edu.ar

Keywords Fatty acid composition · Fatty acid synthesis · Adaptive response · Peanut-nodulating rhizobia

Abbreviations

CFU	Colony forming unit
FAME	Fatty acid methyl esters
FA	Fatty acids
GC	Gas chromatography
HPLC	High performance liquid chromatography
PL	Phospholipids
Ptd_2Gro	Cardiolipin
DMPtdEtn	Dimethyl phosphatidylethanolamine
LPtdEtn	Lysophosphatidylethanolamine
PtdCho	Phosphatidylcholine
PtdEtn	Phosphatidylethanolamine
PtdGro	Phosphatidylglycerol
SEM	Standard error of the mean
TLC	Thin layer chromatography
UFA	Unsaturated fatty acids
U/S	Ratio between sum of unsaturated to sum of saturated fatty acids
Z/A	Ratio of zwitterionic to anionic phospholipids

Introduction

Increased agricultural production plays a key role in enhancing food supply, economic growth, and the overall standard of living in developing countries. Bacteria termed "rhizobia", which have the ability to fix atmospheric nitrogen in symbiosis with roots of legumes, are economically important for increasing the yield of legume crops. Peanut is an important legume crop used for direct human

consumption and a variety of food products. It is a major agricultural crop in many countries such as China, United States and Argentina. Peanut is nodulated by the slow growing strain *Bradyrhizobium* sp. SEMIA6144 [1]. In addition, peanut is also nodulated by *Bradyrhizobium* sp. TAL1000 [2]. In peanut, the rhizobial infection mechanism differs from other legumes since rhizobia penetration into the root occurs without intracellular infection thread formation and involves intercellular penetration (crack entry) [3].

Environmental conditions, e.g., temperature and salinity, affect the symbiosis between rhizobia and host plant. Suboptimal temperatures reduce the competitiveness of rhizobia for nodulation [4], delay root infection and inhibit nodule development and nitrogenase activity [5]. Application of 100 mM NaCl to peanut plants completely inhibited nodule formation by *Bradyrhizobium* strains ATCC10317, TAL1000, and SEMIA6144 [6].

Survival of bacteria in stressful conditions is often determined by their capacity to adapt by altering the composition of the lipid bilayer of the cell surface membranes, which regulate or integrate many vital processes [7, 8]. The primary lipid components of the bilayer are phospholipids (PL). In bacterial membranes PL play key roles in energy transduction, signal transduction, solute transport, and cell–cell recognition [9]. Many microorganisms have been shown to modify lipid composition in order to maintain membrane fluidity within an optimal range [10]. In general, perturbation of membrane fluidity by extrinsic chemical agents or other factors initiates an active response based on intrinsic chemical changes such as the modification of existing lipids and the de novo synthesis that tend to counteract the perturbation [11, 12].

Previous studies of our laboratory demonstrated that, both PL composition and synthesis were modified by salt and temperature stresses in the peanut-nodulating *Bradyrhizobium* sp. SEMIA6144. The amount and the labeling of each individual PL was increased by NaCl, while they were decreased by temperature stress. The amount of PtdCho, PtdEtn, and PtdGro under the combined stresses decreased, as in the temperature effect [13]. Similar PL changes in response to salt and temperature stress have been observed in other microorganisms [8, 14]. Additional mechanisms to stabilize membrane fluidity in bacteria involve changes in fatty acids (FA), the major component of PL. Such mechanisms, which may occur in combination, involve changing the ratio of saturation to unsaturation; *cis* to *trans* unsaturation; branched to unbranched structures, type of branching; acyl chain length and formation of cyclopropane FA [15, 16].

Increased degree of unsaturation in response to reduced temperature has been described for many microorganisms [17, 18], and can be regarded as a universally conserved adaptation response [19]. In *Aeromonas*, alteration of growth temperature induced changes in unsaturation, branching, and chain length of the FA. At temperatures below 15 °C or above 25 °C, three species of *Aeromonas*, *A. caviae*, *A. hydrophila* and *A. sobria*, showed significant decrease of *cis*-vaccenic acid (*cis*-11-C18:1) content. In cells exposed to high NaCl concentration, maintenance of growth ability was related to a reduced ratio of unsaturated to saturated FA, reflecting membrane rigidification [20].

How the FA composition of membrane lipids is altered in response to change of growth temperature depends on the mechanism of unsaturated FA (UFA) synthesis [21]. In bacteria, UFA synthesis involves both anaerobic and aerobic mechanisms. UFA synthesis in response to low temperature was characterized in vivo for the gram-positive bacteria *Bacillus subtilis*, which desaturates palmitate to delta 5-hexadecenoate [22]. The molecular mechanism of UFA synthesis in response to temperature change has been well studied in the gram-negative bacteria *Escherichia coli*. Since membrane of *E. coli* lacks of PtdCho, its composition is quite different from that of the rhizobia [23]. However, little is known regarding the control of FA synthesis in legume-nodulating rhizobia under abiotic stress.

The FA composition profiles of *Bradyrhizobium* and *Rhizobium* are quite different, and have been used for chemotaxonomic purposes [24]. Effects of growth phase [25, 26] and low temperature [4, 27] on FA synthesis and composition in these genera have been studied, but not the effects of high temperature or high salinity.

While we have previously determined the composition of PL in SEMIA6144 [13], in this study we describe for the first time the composition of FA and the effect of high growth temperature and salinity on the FA composition and FA synthesis in this strain and in TAL1000, peanut-nodulating rhizobia. We also describe the composition of PL in TAL1000 and the effect of high growth temperature and salinity on this composition and on the survival of this strain. Our purpose was to clarify the role of cell membrane modifications in resistance and adaptation of these rhizobia to environmental stresses. The results may identify new strategies for increasing symbiotic efficiency between rhizobia and peanut.

Materials and Methods

Bacterial Strains and Culture Conditions

The fast-growing strain TAL1000 was kindly provided by NifTAL Microbiological Resource Center, Paia, HI (USA), and the slow-growing strain SEMIA6144 was provided by MIRCEN/FEPAGRO (Brazil). The strains were kept on yeast extract mannitol plates [2] at 28 °C, with the pH of

the medium adjusted to 7 before autoclaving. For the determination of bacterial growth, viability and biochemical parameters, the strains were grown in B^- medium [28] for 24 h (TAL1000) or 120 h (SEMIA6144) with an initial optical density of 0.1 (620 nm), in a shaking water bath at 28 °C or 37 °C for high growth temperature. Based on differential NaCl tolerance of each strain (data not shown), the medium was supplemented with 300 mM NaCl (TAL1000) or 50 mM NaCl (SEMIA6144) for saline stress experiments. Viable TAL1000 cells were counted (CFU) by removing samples at intervals, as described by da Silva [29].

Incorporation of Labelled Acetate

[1-^{14}C]acetate, sodium salt (43 mCi mmol^{-1}, New England Nuclear), sterilized, was added to the medium (1 μCi ml^{-1}) at the time of inoculation. Cells were harvested at the late exponential phase (24 h for TAL1000 and 96 h for SEMIA6144) by centrifugation at 6000×*g* for 10 min, in a Beckman Allegra 64R refrigerated centrifuge. Pellets were washed twice with 0.9% NaCl and used for further studies. The same procedures and conditions were used for unlabelled samples.

Lipid Extraction

Lipids were extracted from washed bacteria with chloroform/methanol/water [30]. The lower phase, containing lipids, was dried under N_2, and dissolved in appropriate volume of chloroform/methanol 2:1 (v/v).

Separation and Quantification of ^{14}C-labelled Phospholipids

Aliquots of total lipid extracts were analyzed by Analtech thin layer chromatography (TLC) plates (silica gel HLF, 250 μm) using chloroform/acetone/methanol/acetic acid/water (40:15:14:12:7, by vol) as solvent. All solvents were of analytical or HPLC grade. Lipids were detected by iodine vapors and separated lipids were identified by comparison with purified standards (Sigma Chemical Co., St. Louis, MO, USA). TLC bands were scraped, 3 mL Optiphase Hisafe 2 (PerkinElmer, USA) was added to each vial, and radioactivity was measured by liquid scintillation counter (Beckman LS 60001 C, USA) [31].

Separation and Quantification of ^{14}C-labelled Fatty Acids Based on the Degree of Unsaturation

Fatty acid methyl esters (FAME) were prepared from total lipid extracts with 10% BF_3 in methanol [32], and resolved according to number of double bonds on TLC plates impregnated with $AgNO_3$ (10%, w/v), using hexane/ethyl ether/acetic acid (94:4:2, by vol) as solvent. FAME bands were detected under UV light after spraying the plates with dichlorofluorescein, elution [33], and drying in counting vials as described above.

Analysis of Fatty Acids by GC-FID

FAME prepared as above were analyzed using a Hewlett Packard 5890 II gas chromatograph (GC) equipped with a methyl silicone column (length 50 m; inner diameter 0.2 mm; film thickness 0.33 μm) and a flame ionization detector (FID).

GC conditions: injector temperature 250 °C; detector temperature 300 °C; carrier gas nitrogen. Temperature program: 180 °C, 25 min isothermal; 3 °C min^{-1} to 250 °C. Peak areas of carboxylic acids in total ion were used to determine relative amounts.

Fatty acids were identified by comparison of retention times with commercial standards. (Sigma Chemical Co., St. Louis, MO, USA).

Statistical Analyses

Data were compared by one-way analysis of variance (ANOVA) test.

Results

Effects of High Growth Temperature (37 °C) and Salinity on TAL1000 Survival

Viability of TAL1000 (measured as CFU ml^{-1}) was reduced by NaCl stress alone, and by a combination of NaCl stress and high growth temperature (Fig. 1), although TAL1000 was able to survive in these conditions. Lowest CFU values were obtained with 300 mM NaCl. Viability at high growth temperature, 37 °C, was not significantly affected.

Effect of High Growth Temperature and Salinity on TAL1000 Phospholipid Metabolism

[1-^{14}C]acetate sodium salt was incorporated mostly (90–92%) into PL, and the rest into neutral lipid fraction. The predominant labeled PL was phosphatidylcholine (PtdCho), followed in descending order by phosphatidylglycerol (PtdGro), phosphatidylethanolamine (PtdEtn), dimethyl phosphatidylethanolamine (DMPtdEtn), cardiolipin (Ptd_2Gro), and lysophosphatidylethanolamine (LPtdEtn) (Table 1).

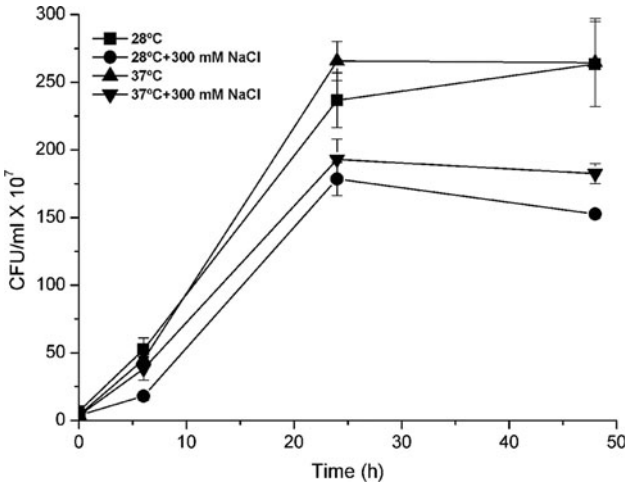

Fig. 1 Effect of NaCl and temperature on viability of fast-growing *Bradyrhizobium* strain TAL1000. Viability is expressed as CFU ml^{-1}. Values represent means ± SEM from three independent experiments

Table 1 Effect of temperature and salinity stress on the incorporation of [^{14}C]acetate into phospholipids of *Bradyrhizobium* TAL1000

PL (%)	Growth condition			
	28 °C	28 °C + NaCl	37 °C	37 °C + NaCl
PtdCho	44.5 ± 2.9	45.7 ± 2.2	49.4 ± 2.6*	54.0 ± 4.0*
DMPtdEtn	9.90 ± 1.5	9.70 ± 0.9	10.9 ± 1.4	10.8 ± 1.7
LPtdEtn	0.88 ± 0.3	2.50 ± 1.3	3.60 ± 0.9*	2.50 ± 0.9*
PtdEtn	13.7 ± 1.7	13.5 ± 2.0	7.60 ± 2.4*	8.10 ± 2.7*
Ptd_2Gro	4.20 ± 0.3	3.90 ± 0.1	3.00 ± 0.8*	4.10 ± 0.3
PtdGro	17.5 ± 1.1	15.4 ± 1.9	18.2 ± 1.5	12.4 ± 0.5*
NL	9.30 ± 3.5	9.60 ± 3.1	7.80 ± 3.0	9.00 ± 1.8

Values represent means ± SEM of three independent experiments

PL phospholipids, *PtdCho* phosphatidylcholine, *DMPtdEtn* Dimethyl phosphatidylethanolamine, *LPtdEtn* lysophosphatidylethanolamine, *PtdEtn* Phosphatidylethanolamine, *Ptd_2Gro* cardiolipin, *PtdGro* phosphatidylglycerol, *NL* neutral lipids

* Difference from control (28 °C) value statistically significant at $P < 0.05$ level

PL patterns for TAL1000 were qualitatively similar for all experimental conditions, but quantitative changes were observed for individual PL. High growth temperature caused an increase in PtdCho from 44 to 49.4% and combined conditions increased PtdCho from 44 to 54%. Compared to the control condition (28 °C), the amount of radiolabel in LPtdEtn (identity confirmed by ninhydrin spray reagent) increased about twofold in response to salt stress and increased about threefold in response to high growth temperature.

Decreased labeling was observed for PtdEtn under high growth temperature from 13.7 to 7.6% and combined conditions from 13.75 to 8.1%, for PtdGro under combined conditions from 17.5 to 12.4% and for Ptd_2Gro by high growth temperature from 4.2 to 3%. Under combined conditions, the ratio of zwitterionic to anionic PL (Z/A) increased (data not shown).

Fatty Acid Composition of TAL1000 and SEMIA6144

Major FA detected in TAL1000 and SEMIA6144 were *cis*-vaccenic (18:1n-7) + oleic (18:1n-9), stearic acid (18:0) and palmitic acid (16:0). Eicosatrienoic acid (20:3n-6) and cyclopropane fatty acid ($19:0_{cyclo}$) were only detected in TAL1000, while palmitoleic acid (16:1n-7) was only detected in SEMIA6144 (Table 2).

Effect of Growth Conditions on Fatty Acid Composition of TAL1000 and SEMIA6144

FA composition of the two strains under experimental conditions tested is shown in Table 2. In TAL1000 the FA showing greatest change in response to tested conditions was 18:1n-7 + 18:1n-9, whose percentage declined from 63.3 to 8.2% under high growth temperature, and to 4.3% under temperature plus NaCl stress. Conversely, 16:0 increased from 8.4 to 20% at 37 °C, and to 16.1% under the combined conditions. The other saturated FA, 18:0, increased from 12.6 to 24% at 37 °C, and to 29% under combined conditions. $19:0_{cyclo}$ increased from 3.4 to 10% at 37 °C and to 14.5% under combined conditions. The changes in FA percentages led to alteration of the ratio between unsaturated to saturated FA (U/S in Table 2), which decreased in all experimental conditions.

Of all the tested conditions, the growth temperature increase was the one causing the most significant changes in the level of FA in TAL1000.

Notably, in SEMIA6144, 18:1n-7 + 18:1n-9 decreased from 84 to 73.5% under temperature stress, and to 68.5% under combined stresses, while 16:0 increased from 11 to 18.6% under temperature stress, and to 19.7% under combined stresses. FA values under NaCl stress alone were not significantly different from control values. The U/S ratio for SEMIA6144 decreased under all experimental conditions, but not as markedly as in TAL1000.

Effect of Growth Conditions on Fatty Acid Metabolism of TAL1000 and SEMIA6144

[1-^{14}C]acetate sodium salt was used as precursor for study of FA metabolism. Radioactivity distribution of various FA in TAL1000, separated by TLC according to degree of unsaturation, is shown in Fig. 2. Under control conditions (28 °C), labeling in TAL1000 was found predominantly in monounsaturated FA, followed by triunsaturated, saturated, and diunsaturated fractions. Consistent with findings for

Table 2 Effects of temperature and salinity stress on fatty acid composition of two peanut-nodulating rhizobia

Fatty acid type (%)	Strain	Growth condition			
		28 °C	28 °C + NaCl	37 °C	37 °C + NaCl
Saturated					
Stearic acid (18:0)	TAL1000	12.6 ± 1.5	14.6 ± 1.6*	24.0 ± 2.7*	29.0 ± 0.9*
	SEMIA6144	1.40 ± 0.3	1.66 ± 0.3	2.00 ± 0.6	2.16 ± 0.9
Palmitic acid (16:0)	TAL1000	8.40 ± 1.7	9.30 ± 1.5	20.0 ± 2.3*	16.1 ± 1.8*
	SEMIA6144	11.0 ± 1.2	12.6 ± 2.7	18.6 ± 3.9*	19.7 ± 3.5*
Unsaturated					
Palmitoleic acid (16:1n-7)	TAL1000	ND	ND	ND	ND
	SEMIA6144	0.42 ± 0.0	0.90 ± 0.4	0.65 ± 0.2	0.56 ± 0.2
cis-vaccenic acid + oleic acid (18:1)	TAL1000	63.3 ± 5.4	55.8 ± 2.7	8.20 ± 0.4*	4.30 ± 0.0*
	SEMIA6144	84.0 ± 2.2	82.4 ± 2.9	73.5 ± 3.4*	68.5 ± 6.8*
Eicosatrienoic acid (20:3)	TAL1000	6.30 ± 1.9	9.20 ± 1.2	15.8 ± 1.6*	19.0 ± 4.7*
	SEMIA6144	ND	ND	ND	ND
Cyclopropane					
$19:0_{cyclo}$	TAL1000	3.40 ± 0.7	3.85 ± 0.3	10.0 ± 1.5*	14.5 ± 1.7*
	SEMIA6144	ND	ND	ND	ND
Others	TAL1000[a]	6.70 ± 1.6	7.10 ± 0.8	23.2 ± 2.6*	17.1 ± 1.9*
	SEMIA6144	1.10 ± 0.0	2.55 ± 0.7	5.00 ± 0.2	5.30 ± 1.3
U/S[b]	TAL1000	3.3	2.7	0.5	0.5
	SEMIA6144	7.0	6.1	3.6	3.1

Lipids were extracted, and fatty acids of total lipid were converted to methyl esters and analyzed by GC, as described in the text

Percentage of each fatty acid is relative to total fatty acids defined as 100%. Values represent means ± SEM of three independent experiments

ND not detected

[a] Correspond to two peaks of retention times of 36 min and 37.4 min. Such peaks could correspond to FA of more than 18 carbon atoms

[b] Ratio between sum of unsaturated and sum of saturated fatty acids

* Difference from control (28 °C) value statistically significant at $P < 0.05$ level

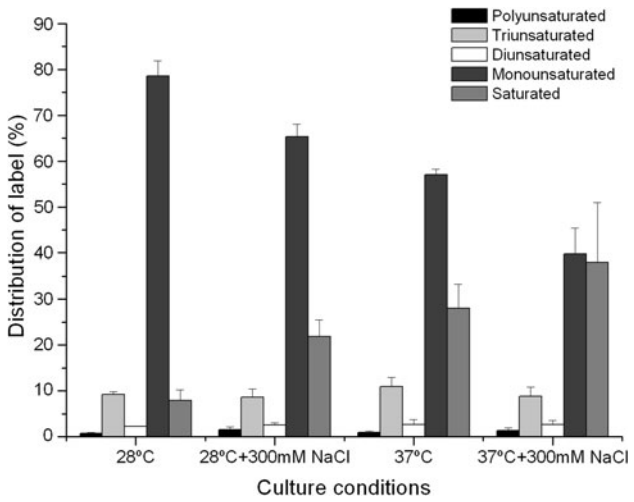

Fig. 2 Effect of NaCl and temperature on incorporation of [1-^{14}C]acetate in fatty acids of *Bradyrhizobium* TAL1000. FAMEs were prepared from total lipids, and separated according to unsaturation degree using TLC plates impregnated with 10% $AgNO_3$. Results are expressed as the percentage of total radioactivity incorporated in each FA fraction. Values represent means ± SEM from three independent experiments

FA composition (Table 2), high growth temperature and combined conditions decreased the [1-^{14}C]acetate incorporation in monounsaturated FA, 27.4 and 49.4% respectively. [1-^{14}C]acetate incorporation in saturated FA increased 3.5-fold by high growth temperature and 4.7-fold by combined conditions. [1-^{14}C]acetate incorporation in monounsaturated FA decreased from 78 to 65% and that of saturated FA increased from 8 to 22% by NaCl stress. Based on modified incorporation of labelled acetate, the U/S ratio decreased from 11.5 to 3.5 for NaCl stress, from 11.5 to 2.5 for high growth temperature, and from 11.5 to 1.6 for combined conditions.

Incorporation of [1-^{14}C]acetate in FA of SEMIA6144 was also tested. Labeling was observed primarily in monounsaturated FA, followed by saturated, diunsaturated, and triunsaturated FA. [1-^{14}C]acetate incorporation in saturated FA increased 28% under NaCl stress, 39% at 37 °C, and 45% under combined conditions. In contrast, radioactive incorporation in diunsaturated FA decreased 73% under NaCl stress, 66% at 37 °C, and 82% under combined conditions. As a consequence of these changes, the U/S

ratio decreased from 14.7 to 11.5 for NaCl stress, from 14.7 to 10.7 for high growth temperature, and from 14.7 to 10 for combined conditions.

Discussion

Our previous biochemical studies showed that *Bradyrhizobium* SEMIA6144, exhibited reduced viability and increased levels of PtdCho, when exposed to 37 °C, NaCl 50 mM and combined conditions [13]. In the present study we found that, viability of TAL1000 was reduced by NaCl 300 mM and by combined conditions (NaCl 300 mM plus 37 °C). Viability of salt-tolerant TAL1000 was unaffected by high temperature, consistent with studies that indicate a relationship between salt tolerance and temperature tolerance in rhizobial strains [34].

Adaptive mechanisms induced in cells in response to changes in environmental conditions, to maintain membrane fluidity involve modification of PL at the level of FA components and PL head groups [15, 35]. Behavior of SEMIA6144 PL labeling in response to stress [13] differed from those of TAL1000, resulting in different degree of modification in the Z/A ratio. We suggest that the two strains, although possessing similar PL composition, have different mechanisms for stabilizing membrane fluidity. The other adaptive mechanism developed by bacteria is alteration of membrane FA [36]. The FA composition of total lipids in the two strains was different, since TAL1000 contained 20:3n-6 and 19:0_{cyclo} FA, which were not present in SEMIA6144. Since the FA profile of TAL1000 is similar to that reported for *Rhizobium* [24], and both growth velocity and FA profile of TAL1000 differ from those of *Bradyrhizobium*, the taxonomic classification of TAL1000 may need to be reconsidered. High growth temperature and combined conditions caused significant reduction of 18:1 and increase of 18:0 and 16:0 (in TAL1000), or 16:0 (in SEMIA6144). These changes that were more pronounced in TAL1000, provoked modifications at the level of FA unsaturation degree coincident with results obtained for other rhizobia in which different environmental changes caused modifications in the U/S ratio [4, 26].

TAL1000 at 37 °C showed a decreased in the U/S ratio and enhanced formation of 19:0_{cyclo} (Table 2). Cyclic FA in the membranes of rhizobia could represent a mechanism to reduce membrane fluidity, similar to lactobacillus [37]. SEMIA6144, showed change in degree of FA unsaturation and increased 16:0/18:0 ratio under temperature stress, which may reflect decreased chain length and it may alter transition temperature for change from gel to liquid crystalline phase [19]. Results using [1-^{14}C]acetate labeling are consistent with FA composition studies and similar with studies in other gram-negative bacteria [38, 39] since showed synthesis of both saturated and monounsaturated FA. Tested experimental conditions altered incorporation of labeled acetate in FA of both rhizobial strains. We found no studies on effects of abiotic stress on FA synthesis in rhizobia, but a study showing increase of saturated FA synthesis at high temperature in *Bacillus subtilis* was consistent with our results [22].

We conclude that peanut-nodulating rhizobia strains are able to adapt to tested environmental conditions through FA modification, and that fast-growing TAL1000 is more efficient in this respect than slow-growing SEMIA6144. The most important mechanism for maintaining physical properties of the membrane is modification of the FA unsaturation degree. The ability of TAL1000 to alter its content of FA 19:0_{cyclo} may account for its tolerance of high temperature, while adaptation to environmental stresses in SEMIA6144 may involve shortening of the FA chain length [20].

The FA composition of strains of rhizobia used in commercial formulations should be considered as an indicator of whether or not an organism can adapt to changing environmental conditions, since differences in the capacity of rhizobia to adapt to environmental conditions may be related to differences in the FA composition.

Acknowledgments Financial assistance was provided by SECyT-UNRC/Argentina. N.S.P. is a fellow of CONICET-Argentina. D.B.M. was a fellow of CONICET-Argentina. M.S.D. is a member of the Research Career of CONICET-Argentina. The authors thank Dr. Laura Villasuso for her valuable assistance in the preparation of the figures and Dr. Ricardo Lema for his help with the language.

References

1. Gomes-Germano M, Menna P, Mostasso F, Hungria M (2006) RFLP analysis of the rRNA operon of a Brazilian collection of bradyrhizobial strains from 33 legume species. Int J Syst Evol Microbiol 56:217–229
2. Somasegaran P, Hoben H (1994) Handbook for Rhizobia: methods in legume-*Rhizobium* technology. Spring-Verlag, New York
3. Boogerd FC, van Rossum D (1997) Nodulation of groundnut by *Bradyrhizobium*: a simple infection process by crack entry. FEMS Microbiol Rev 21:5–27
4. Drouin P, Prevost D, Antoun H (2000) Physiological adaptation to low temperatures of strains of *Rhizobium leguminosarum* bv. viciae associated with *Lathyrus* spp. FEMS Microbiol Ecol 32:111–120
5. Zahran H (1999) Rhizobium-legume symbiosis and nitrogen fixation under severe conditions and in an arid climate. Microbiol Mol Biol Rev 63:968–989
6. Dardanelli M, González P, Medeot D, Paulucci N, Bueno M, Garcia M (2009) Effects of peanut rhizobia on the growth and symbiotic performance of *Arachis hypogaea* under abiotic stress. Symbiosis 47:175–180
7. Aricha B, Fishov I, Cohen Z, Sikron N, Pesakhov S, Khozin-Goldberg I, Ron Dagan R, Porat N (2004) Differences in membrane fluidity and fatty acid composition between phenotypic

variants of *Streptococcus pneumoniae*. J Bacteriol 186:4638–4644
8. Bakholdina S, Sanina N, Krasikova I, Popova O, Solov'eva T (2004) The impact of abiotic factors (temperature and glucose) on physicochemical properties of lipids from *Yersinia pseudotuberculosis*. Biochemistry 86:875–881
9. Dowhan W (1997) Molecular basis for membrane phospholipids diversity: why are there so many lipids? Annu Rev Biochem 66:199–232
10. Soltani M, Metzger P, Largeau C (2005) Fatty acid and hydroxy acid adaptation in three gram-negative hydrocarbon-degrading bacteria in relation to carbon source. Lipids 40:1263–1272
11. Beney L, Gervais P (2001) Influence of the fluidity of the membrane on the response of microorganisms to environmental stresses. Appl Microbiol Biotechnol 57:34–42
12. Denich T, Beaudette L, Lee H, Trevors J (2003) Effect of selected environmental and physico-chemical factors on bacterial cytoplasmic membranes. J Microbiol Methods 52:149–182
13. Medeot D, Bueno M, Dardanelli M, García de Lema M (2007) Adaptational changes in lipids of *Bradyrhizobium* SEMIA6144 nodulating peanut as a response to growth temperature and salinity. Curr Microbiol 54:31–35
14. Russell N (1992) In: Herber RA, Sharp RJ (eds) Psychrophilic Microorganisms. Molecular Biology and Biotechnology of Extremophiles. Blackie, Glasgow
15. Ramos J, Duques E, Rodriguez-Herva J, Godoy P, Haidour A, Reyes F, Fernandez-Barrero A (1997) Mechanisms for solvent tolerance in bacteria. J Biol Chem 272:3887–3890
16. Donato M, Jurado A, Antunes-Madeira M, Madeira V (2000) Membrane lipid composition of *Bacillus stearo-thermophilus* as affected by lipophilic environmental pollutants: an approach to membrane toxicity assessment. Arch Environ Contam Toxicol 39:145–153
17. Russell N, Fukunaga N (1990) A comparison of thermal adaptation of membrane lipids in psychrophilic and thermophilic bacteria. FEMS Microbiol 75:171–182
18. Suutari M, Liukkonen K, Laakso S (1990) Temperature adaptation in yeasts: the role of fatty acids. J Gen Microbiol 136:1469–1474
19. Suutari M, Laakso S (1994) Microbial fatty acid and thermal adaptation. Crit Rev Microbiol 20:285–328
20. Chihib N, Tierny Y, Mary P, Hornez J (2005) Adaptational changes in cellular fatty acid branching and unsaturation of *Aeromonas* species as a response to growth temperature and salinity. Int J Food Microbiol 102:113–119
21. Keweloh H, Heipieper H (1996) *Trans* unsaturated fatty acids in bacteria. Lipids 31:129–136
22. Aguilar P, Cronan J, de Mendoza D (1998) A *Bacillus subtilis* gene induced by cold shock encodes a membrane phospholipid desaturase. J Bacteriol 180:2194–2200
23. Sohlenkamp C, López-Lara IM, Geiger O (2003) Biosynthesis of phosphatidylcholine in bacteria. Prog Lipid Res 42:115–162
24. Tighe S, de Lajudie P, Dipietro K, Lindström K, Nick G, Jarvis B (2000) Analysis of cellular fatty acids and phenotypic relationships of *Agrobacterium, Bradyrhizobium, Mesorhizobium, Rhizobium* and *Sinorhizobium* species using the Sherlock Microbial Identification System. Int J Syst Evol Microbiol 50:787–801
25. Boumahdi M, Mary P, Hornez J (1999) Influence of growth phases and desiccation on the degrees of unsaturation of fatty acids and the survival rates of rhizobia. J Appl Microbiol 87:611–619
26. Boumahdi M, Mary P, Hornez J (2001) Changes in fatty acid composition and degree of unsaturation of (brady)rhizobia as a response to phases of growth, reduced water activities and mild desiccation. Antonie van Leeuwenhoek 79:73–79
27. Théberge M, Prévost D, Chalifour P (1996) The effect of different temperatures on the fatty acids composition of *Rhizobium leguminosarum* bv. viciae in the faba bean symbiosis. New Phytol 134:657–664
28. Spaink H, Aarts A, Stacey G, Bloemberg G, Lugtenberg B, Kennedy E (1992) Detection and separation of *Rhizobium* and *Bradyrhizobium* nod metabolites using thin-layer chromatography. Mol Plant Microbe Interact 5:72–80
29. da Silva R (1996) Técnica de Microgota para contagem de células bacterianas viáveis em uma suspensão, 1-7. Universidade Federal de Viçosa, Viçosa, Minas Gerais, Brazil
30. Bligh E, Dyer W (1959) A rapid method of total lipid extraction and purification. Can J Biochem Physiol 37:911–918
31. Kates M (1972) Radioisotopic techniques in lipidology. In: Work TS, Work E (eds) Techniques in lipidology. North Holland Amsterdam, Elsevier, New York
32. Morrison W, Smith L (1964) Preparation of fatty acid methyl esters and dimethylacetals from lipids with boron fluoride. J Lipid Res 5:600–608
33. Henderson R, Tocher D (1992) Thin layer chromatography. In: Hamilton R, Hamilton S (eds) Lipid analysis a practical approach. Oxford University Press, Oxford-New York-Tokyo
34. Lindstrom K, Lehtomaki S (1988) Metabolic properties, maximum growth temperature and phage sensitivity of *Rhizobium* sp. (Galea) compared with other fast growing rhizobia. FEMS Microbiol Lett 50:277–287
35. Härtig C, Loffhagen N, Harms H (2005) Formation of *trans* fatty acids is not involved in growth-linked membrane adaptation of *Pseudomonas putida*. Appl Environ Microbiol 71:1915–1922
36. Ramos J, Duque E, Gallegos M, Godoy P, Ramos-González M, Rojas A, Teran W, Segura A (2002) Mechanisms of solvent tolerant in gram negative bacteria. Ann Rev Microbiol 56:743–768
37. Guerzoni E, Lanciotti R, Cocconcelli S (2001) Alteration in cellular fatty acid composition as a response to salt, acid, oxidative and thermal stresses in *Lactobacillus helveticus*. Microbiology 147:2255–2264
38. Wada M, Fukunaga N, Sasaki S (1989) Mechanism of biosynthesis of unsaturated fatty acids in *Pseudomonas* sp. strain E-3, a psychotropic bacterium. J Bacteriol 171:4267–4271
39. Ghaneker A, Nair P (1973) Evidence for the existence of an aerobic pathway for synthesis of monounsaturated fatty acids by *Alcaligenes faecalis*. J Bacteriol 114:618–624

Lipids (2011) 46:443–454
DOI 10.1007/s11745-011-3527-3

ORIGINAL ARTICLE

Mild Testicular Hyperthermia Transiently Increases Lipid Droplet Accumulation and Modifies Sphingolipid and Glycerophospholipid Acyl Chains in the Rat Testis

Natalia E. Furland · Jessica M. Luquez · Gerardo M. Oresti · Marta I. Aveldaño

Received: 8 October 2010 / Accepted: 23 December 2010 / Published online: 13 February 2011

Abstract Spermatogenesis is known to be vulnerable to temperature. The aim of this study was to investigate the effects on testicular lipids of the transient germ cell loss that is induced by mild testicular hyperthermia. Adult rat testes were exposed once a day to 43 °C for 15 min for 5 days and the effects were followed for several weeks. Two week after the last heat exposure, spermatocytes and early spermatids had virtually disappeared and the seminiferous tubules were populated mostly by mature spermatids and spermatozoa. One week later, the latter were also absent and mostly Sertoli cells populated the tubules. During these 3 weeks, glycerophospholipids (Gpl) and triacylglycerols with long-chain polyunsaturated fatty acids (PUFA) (e.g., 22:5n-6) and species of sphingomyelin and ceramide with nonhydroxy and 2-hydroxy very long-chain (VLC) PUFA (e.g., 28:4n-6, 2-OH 30:5n-6) decreased alongside the germ cells. Concomitantly, the amounts of cholesteryl esters and ether-linked triglycerides increased, both lipids accumulating long-chain and very-long-chain polyenes. This concurred with a considerable buildup of lipid droplets in Sertoli cells, evidently containing these neutral lipids, apparently formed during germ cell-derived membrane lipid catabolism. Between week 4 and week 6, new cohorts of spermatocytes appeared, and by week 12 most cell changes were reversed. Accordingly, as germ cell differentiation proceeded, 22:5n-6-rich Gpl augmented and spermatocyte-associated sphingolipids with nonhydroxy VLCPUFA appeared before their 2-hydroxy counterparts. The unique fatty acids of rat testicular lipids after mild hyperthermia reveal lipid catabolic and biosynthetic reactions that occur in normal spermatogenesis.

Keywords Ceramide · Cholesteryl esters · Ether-linked glycerolipids · Germ cells · Glycerophospholipids · Lipid droplets · Sphingomyelin · Sertoli cells · Very-long-chain PUFA

Abbreviations

ADG	Ether-linked triglycerides (alkyl- plus alkenyl- diacylglycerols)
Cer	Ceramide
CE	Cholesteryl esters
ChoGpl	Choline glycerophospholipids
EtnGpl	Ethanolamine glycerophospholipids
FAME	Fatty acid methyl esters
Gpl	Glycerophospholipids
PUFA	Polyunsaturated fatty acids
TAG	Triacylglycerols
CerPCho	Sphingomyelin
VLCPUFA	Very long-chain polyunsaturated fatty acids (n- and 2-OH are used as prefixes to denote nonhydroxy and 2-hydroxy VLCPUFA, respectively)

Introduction

In mammals, increased testicular temperature is known to result in reduced fertility or sterility due to the loss of spermatogenic cells. Exposure of the testis to abdominal temperature in experimental cryptorchidism and transient

N. E. Furland (✉) · J. M. Luquez · G. M. Oresti · M. I. Aveldaño
Instituto de Investigaciones Bioquímicas de Bahía Blanca, Consejo Nacional de Investigaciones Científicas y Técnicas & Universidad Nacional del Sur, Centro Científico-Tecnológico Bahía Blanca, CONICET, 8000 Bahía Blanca, Argentina
e-mail: nfurland@criba.edu.ar

exposure of the testis to moderate hyperthermia (43 °C, 15 min) results in the activation, within a few hours, of apoptotic mechanisms in germ cells [1–6]. Primary spermatocytes and early spermatids are the cells most susceptible to temperature [1, 3, 7]. Thus, exposure to moderate heat induces the partial or total disappearance of cohorts of these early spermatogenic cells, which may be predicted to result, a few weeks later, in reduced numbers or total absence of their more differentiated cell descendants including spermatozoa. After returning the testis to its normal temperature, this germ cell nadir may be followed by the gradual repopulation of the seminiferous epithelium with new spermatogenic cell generations, originated in those stem spermatogonia that were not affected or had tolerated the heat episode. Whereas many studies have examined the causes and mechanisms of heat-induced germ cell death, research following its consequences for several weeks until they are reversed is relatively scarce.

In a previous study [8], the selective reduction in germ cell numbers from adult rat testes exposed to the corporal temperature by the surgical operation of placing the testis in the abdominal cavity was shown to concur with the virtual disappearance of sphingomyelin (CerPCho) species with very long chain (VLC) (C_{24}–C_{32}) polyunsaturated fatty acids (PUFA) and with an intensely reduced amount of glycerophospholipid (Gpl) species with 22:5n-6. Such selective reduction was an indication that these particular species of CerPCho and Gpl were originally specific membrane constituents of germ cells, a fact that was recently confirmed [9]. During cryptorchidism-induced germ cell loss, the concentration of testicular neutral lipids like triacylglycerols, triglycerides with an ether bond, and cholesteryl esters (TAG, ADG, and CE, respectively) increased markedly. The finding that CE accumulated 22:5n-6 and VLCPUFA suggested that this neutral lipid was formed in Sertoli cells, after phagocytosis of apoptotic bodies derived from former germ cells, with temporary esterification of membrane-derived free cholesterol with fatty acids arising from phospholipid catabolism [8]. Because spermatogonia and Sertoli cells stay alive under these conditions, all these temperature-dependent, cell-associated lipid changes were proposed to be potentially reversible, with spermatogenesis starting again provided that the testis could be returned in time to its normal position and temperature.

The purpose of the present study was to follow for some weeks the changes in testicular lipid classes as a consequence of applying a series of direct daily exposures of rat testes in vivo to transient mild heat episodes. This model was useful to follow the induction, and subsequent reversion, of the heat-associated effects on testicular cells and their main polar and neutral lipids with highly unsaturated long-chain and very-long-chain fatty acids, demonstrating the almost complete reversibility of the temperature-induced effects on lipids with germ cell recovery.

Materials and Methods

Animals and Study Design

Four-month-old male Wistar rats were housed in a standard animal facility under controlled temperature (22 °C) and photoperiod (12L:12D) with ad libitum access to food and water. Testicular warming was conducted as described previously [10], by immersing the rat scrota into a water bath at 43 °C for 15 min, with the modification that this procedure was performed once a day for five consecutive days in animals restrained with acepromazine (5 mg/kg) in order to obtain a more drastic and more reproducible germ cell depletion, in an attempt to mimic in part the effects of experimental cryptorchidism. Control rats were subjected to restraint and scrotal immersion in water at room temperature (22 °C). They showed no significant differences in subsequent cell or lipid analyses with untreated animals, and were used as zero-time controls in Figs. 1, 2, 3, 4, 5 and 6. The experimental animals were sacrificed 1, 2, 6, and 12 weeks after the last heat exposure and the testes were removed. Some of the testes were fixed in 10% formaldehyde, embedded in paraffin, and cut into 3 μm sections. The sections were stained with hematoxylin–eosin. The study protocol was approved by the Committee on the Care and Use of Research Animals at the University of the South.

Lipid Separation and Analysis

After weighing, capsules and visible vessels were removed from testes and lipids were extracted after homogenization in mixtures of chloroform–methanol [11]. All solvents used in this study were HPLC-grade (JT Baker, NJ, USA; UVE, Argentina), and most procedures were carried out under N_2.

Aliquots of lipid extracts were taken to determine total lipid phosphorus content and phospholipid composition, with quantification of main phospholipid classes and subclasses, and to isolate polar and neutral lipid classes for further analysis. For phospholipid quantification, aliquots were spotted on high performance TLC plates (Merck, Germany) along with commercial standards and resolved with chloroform/methanol/acetic acid/water (50:37.5:3.5:2, by vol.). The plates were exposed to iodine vapors, the spots scraped off, and the phospholipid classes quantified by phosphorus analysis [12].

Neutral lipids were separated from total phospholipids and resolved into classes in two steps. Chloroform/

methanol/aqueous ammonia (90:10:2 by vol.) was run up to the middle of the plates to separate the ceramide. After drying, a mixture of *n*-hexane/diethyl ether (80:20, by vol.) was run up to the top of the plates to resolve cholesteryl esters (CE), triacylglycerols (TAG), and triglycerides with an ether bond (abbreviated ADG to include 1-alkyl- and 1-alk-1′-enyl-diacylglycerols). After TLC, lipid bands were located under UV light by spraying with 2′,7′-dichlorofluorescein in methanol and scraped into tubes for elution. This involved thorough extraction (three successive times) of the scraped silica with a mixture of chloroform/methanol/water (5:5:1 by vol.). After collecting the eluates, they were partitioned with four volumes of water and centrifuged to recover the lipids.

The total phospholipid fraction that remained at the origin of the TLC plates was recovered and subjected to further separations. Aliquots were taken to study the total content and composition of Gpl fatty acids. The Gpl were resolved into classes by two-dimensional TLC [12] to isolate choline and ethanolamine glycerophospholipids (ChoGpl and EtnGpl). These were in turn separated into their two major (phosphatidyl- and plasmenyl-) subclasses by exposing the eluted, dried ChoGpl or EtnGpl for 1 min to a solution of 0.5 N HCl in acetonitrile [13] and immediately separating the products by TLC using chloroform/methanol/water (65:25:4, by vol.). The acid released the fatty aldehydes contained in the plasmalogen subclasses, allowing recovery of the corresponding 2-acyl-GPL, which were separated from the major 1,2-diacyl-Gpl (phosphatidylcholine, phosphatidylethanolamine) by TLC and both were subjected to fatty acid analysis.

Sphingomyelin (CerPCho) was resolved using chloroform/methanol/acetic acid/0.15 mol/L NaCl (50:25:8:2.5 by vol.) [14]. After isolation, CerPCho and Cer samples were subjected to mild alkali treatment to remove any potential lipid contaminant containing ester-bound fatty acids as previously described [8]. Briefly, both lipids were dried and treated (under N_2) with 0.5 N NaOH in anhydrous methanol at 50 °C for 10 min. This mild alkaline treatment was also used to obtain, as methyl esters, the fatty acids ester-bound to total Gpl, thus excluding from this fraction the fatty acids amide-bound to CerPCho.

Fatty Acid Analysis

For fatty acid quantification, methyl heneicosanoate and methyl 2-OH lignocerate were added as internal standards before methanolysis to the CerPCho and Cer samples, and just methyl heneicosanoate to the rest of the rat testicular lipids (which do not contain 2-OH fatty acids). Fatty acid methyl esters (FAME) were prepared from all lipid classes and subclasses by transesterification with 0.5 N H_2SO_4 in anhydrous methanol under N_2 [15] by keeping them overnight at 45 °C in Teflon®-lined, screw-capped tubes.

Before GC, all FAME were routinely purified by TLC using silica Gel G plates that had been pre-washed with methanol/ethyl ether (75:25, by vol.) and dried. The FAME from testicular lipids other than CerPCho and Cer were directly purified using hexane/ether (95:5, by vol.). The 2-hydroxy and non-hydroxy FAME from CerPCho and Cer were run with hexane/ether (80:20, by vol.) up to the middle of the plates, followed by hexane/ether (95:5, by vol.) up to near the top [16]. All FAME were eluted from the silica support by thoroughly mixing it with water, methanol and hexane (1:1:1, by vol.), centrifuging to recover the upper hexane layer, and repeating twice the hexane extractions.

Before GC, the 2-OH FAME from sphingomyelin and ceramide were converted into *O*-trimethylsilyl (O-TMS) derivatives [16]. A mixture of *N*,*O*-bis (trimethylsilyl)trifluoroacetamide (BSTFA) and 5% trimethylchlorosilane (TMCS) (Fluka reagent, Sigma-Aldrich) was added to the dried samples in small silanized glass tubes. After adding N_2 and capping the tubes, CerPCho and Cer samples were kept overnight at 45 °C with the reactants. The latter were evaporated and the TMS ethers, taken up into hexane, were subjected to GC. The VLCPUFA of CerPCho and Cer were identified by procedures and criteria described in detail in previous work [16–18].

For fatty acid quantification, a Varian 3700 Gas Chromatograph equipped with two (2 m × 2 mm) glass columns packed with 10% SP 2330 on Chromosorb WAW 100/120 (Supelco, Inc.) was used. Injector and detector temperatures were set at 220 and 230 °C, respectively, and N_2 (30 ml/min) was the carrier gas. For fatty acid detection and analysis, two flame ionization detectors, operated in the dual-differential mode, connected to a Varian Star Chromatography Workstation (version 4.51) were used. The column oven temperature was programmed from 150 to 230 °C at a rate of 5 °C/min for nonhydroxy fatty acids from all lipids and from 190 to 230 °C for 2-OH fatty acids from CerPCho and Cer, and then kept at the upper temperature long enough to elute FAME of different lengths.

Lipid Droplet Detection

Rat testes were fixed in 4% paraformaldehyde, rinsed in PBS containing 30% sucrose overnight at 4 °C, and placed in a small amount of optimal cutting temperature (OCT) compound (Crioplast®, Biopack) on plastic stubs. Preparations were frozen, cut into 5–7 μm sections using a cryostat, and processed for Nile Red staining as previously described [18]. All samples were observed in a laser scanning confocal microscope (Leica DMIRE2) with a 63 water objective. Images were collected and processed with LCS software (Leica) and Photoshop 8.0 (Adobe Systems, San Jose, CA).

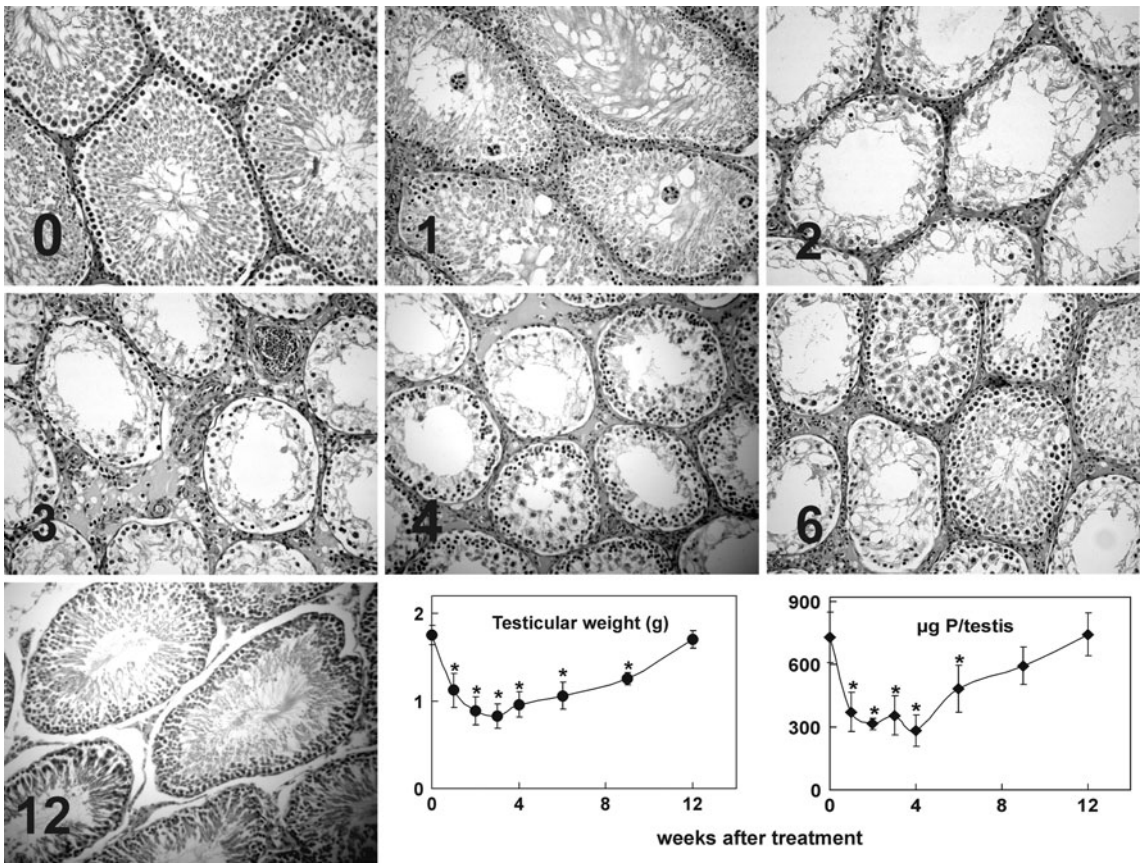

Fig. 1 Cellular changes in rat seminiferous tubules after mild hyperthermia. The micrographs depict hematoxylin-eosin stained sections prepared from rat testes that were subjected for 5 consecutive days to one daily exposure to 43 °C during 15 min, and were analyzed at the periods indicated (0, 1, 2, 3, 4, 6 and 12 weeks after the last day of exposure) (×200). On the *lower right panel*, the effect of these cell changes on the testicular weight and total lipid phosphorus are shown

Statistical Analyses

All data are presented as mean values ± SD, $n = 4$. In the figures, asterisks indicate statistically significant differences compared to non-treated testes at each time point ($p < 0.05$). Data analysis was done using one-way ANOVA followed by the Dunnett′s test.

Results

Testicular Histology and Weight

Episodes of mild hyperthermia applied to the rat testis as described here resulted in a significant reduction in the number of germ cells within seminiferous tubules (Fig. 1). One week after the last episode of heating (i.e., 12 days after the first one), the seminiferous epithelium had lost most of its pachytene spermatocytes and early spermatids, being still populated by remainders of the relatively more heat-tolerant elongated forms of spermatids and testicular spermatozoa, in reduced numbers with respect to controls. Interestingly, at this time point, giant multinucleated cells appeared in the epithelium of many tubules (Fig. 1). These cells are formed from developing round spermatids that are released together from their location around Sertoli cells (normally, there is cytoplasmic continuity between germ cells of a clone through small intercellular bridges, forming a so-called symplast) and are frequently found in the testis after any type of disturbance that destabilizes the cytoskeletal apparatus and leads to the opening of the intercellular bridges between round spermatids [19]. The reduced numbers of spermatids and spermatozoa that occupied the seminiferous tubules at week 1 were no longer present at weeks 2 and 3 post-treatment. At these time points, the cells populating the tubules were mostly Sertoli cells, exhibiting their intact typical nuclei (Fig. 1), plus some undifferentiated spermatogonia. At week 4, new cohorts of recently formed spermatocytes began to develop from the latter. At week 6 most tubules had increased in size with respect to the previous weeks to accommodate a new generation of pachytene spermatocytes and some, still relatively scarce, spermatids. By week 12 the tubules (although not yet the interstitium) looked similar to those

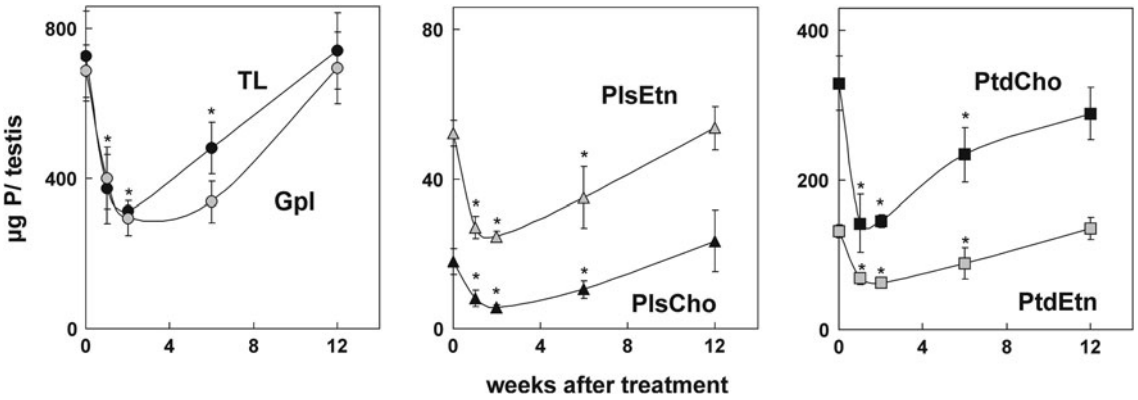

Fig. 2 Consequences of heat exposure on the phosphorus content of total lipids (*TL*) and glycerophospholipids (*Gpl*) of rat testis. The Gpl were resolved into classes to obtain the choline and ethanolamine GPL, and these were then resolved into phosphatidyl- and plasmenyl-subclasses. *Ptd-Cho* phosphatidylcholine, *Ptd-Etn* phosphatidylethanolamine, *Pls-Cho* plasmenylcholine, *PlsEt* plasmenylethanolamine

of untreated animals. In the first phase of germ cell number reduction, Sertoli cells apparently performed an efficient phagocytosis and elimination of the degenerating germ cells, whereas in the second phase of germ cell proliferation and differentiation Sertoli cells reassumed their main role as supporters and organizers of spermatogenesis. The described cellular changes were responsible for the rapid decrease of testicular weight that occurred in the first three weeks after heat treatment, and the gradual weight regain that occurred thereafter (Fig. 1). The total lipid phosphorus virtually paralleled these changes.

Total Phospholipids, Major Glycerophospholipid Classes and Their Fatty Acids

The heat-induced loss of germ cells within seminiferous tubules was accompanied by a 50 and a 57% drop in the total content of lipid phosphorus per testis at weeks 1 and 2 post-treatment, respectively (Fig. 2). Because testicular weight and lipid phosphorus decreased almost in parallel, the concentration of lipid phosphorus per gram of tissue did not change significantly.

The reduction in the amount per testis of total Gpl (Fig. 2) was mostly responsible for the decrease in total lipid (TL) phosphorus. In turn, the two major Gpl classes, ChoGpl and EtnGpl, were mostly responsible for the decrease in total Gpl phosphorus.

The diacyl- subclasses were mostly responsible for the decrease in ChoGpl and EtnGpl (Fig. 2), phosphatidylcholine decreasing more than phosphatidylethanolamine in relative and absolute terms. Although the plasmalogens of both Gpl also decreased, in this case plasmenyl ethanolamine decreased more than plasmenylcholine during the first two weeks following the heat treatment.

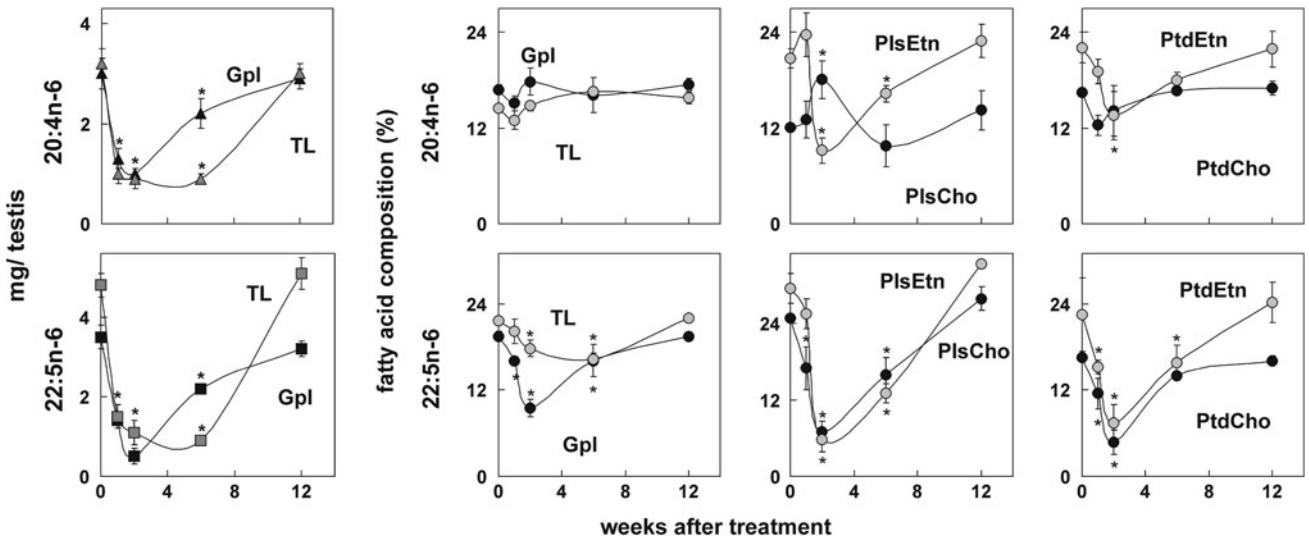

Fig. 3 Consequences of heat treatment on the amounts and percentages of arachidonic and docosahpentaenoic acids in testicular total lipids (*TL*), glycerophospholipids (*Gpl*), and the two major choline and ethanolamine glycerophospholipid subclasses

The decrease in lipid phosphorus was paralleled by a decrease in Gpl fatty acids. However, species with different types of fatty acids decreased at different rates, and there were even differences among species with the two major PUFA, as shown in the left panel of Fig. 3 for the amounts of 20:4n-6 and 22:5n-6. Although both fatty acids decreased dramatically, the amount of 20:4n-6 decreased less than that of 22:5n-6. The former reached its minimum at week 1, which was maintained for the next week, whereas the latter continued to decrease deeply between weeks 1 and 2 post-treatment. The amounts of Gpl species that contain both PUFA had started to recover at week 6, a period of intense new cell generation and concomitant membrane lipid biosynthesis, and were totally restored by week 12.

The *percentage* of 20:4n-6 and 22:5n-6 with respect to the total fatty acids (Fig. 3), show that the decrease of species containing these two PUFA was selective, considering that their proportions were significantly reduced in a decreasing mass of TL and Gpl, with their minima at week 1 and 2 post-treatment, respectively.

The fatty acid composition of phosphatidyl- and plasmenyl-subclasses of ChoGpl and EtnGpl (Fig. 3) shows this even more dramatically. The species of both lipids that contain 20:4n-6 decreased earlier than, and recovered before, the species containing 22:5n-6. Considering the quantitative data in Figs. 2 and 3, at week 2 post-treatment the amount of 20:4n-6 had decreased 3.5- and 4.6-fold, and that of 22:5n-6 10- and 8-fold, in phosphatidylcholine and phosphatidylethanolamine, respectively. Similarly, at week two, 20:4 had decreased 6- and 2-fold, and 22:5n-6 14- and 4-fold, in plasmenylethanolamine and plasmenylcholine, respectively.

Sphingomyelins, Ceramides and Their Fatty Acids

As did the major Gpl, the amount of total testicular CerP-Cho and Cer decreased concomitantly with the progressive loss of germ cells after heat exposure (Fig. 4). The species of these two lipids that contain VLCPUFA decreased up to their virtual disappearance between weeks 1 and 3 after the last heat exposure. The separation of the VLCPUFA of both lipids into nonhydroxy and 2-hydroxy VLCPUFA (n-V and HO-V in Fig. 4) allowed the additional observation that species of CerPCho and Cer with n-VLCPUFA decreased earlier than species with 2-OH VLCPUFA (their nadir occurred at weeks 1 and 2 post-treatment, respectively). This finds an explanation in the type of germ cell that is sequentially affected after heat treatment, considering that at week 1 pachytene spermatocytes had already disappeared from the testis, which still contained some elongated spermatids and spermatozoa (Fig. 1). Pachytene spermatocytes were recently shown to be rich in CerPCho and Cer with n-VLCPUFA, while the more differentiated spermatids and mature gametes are in turn much richer in CerPCho and Cer with 2-OH VLCPUFA [9].

The disappearance of germ cells during the first three weeks post-treatment resulted in a significant increase in the percentage of CerPCho as one of the remarkable changes in the phospholipid composition of the testis (from

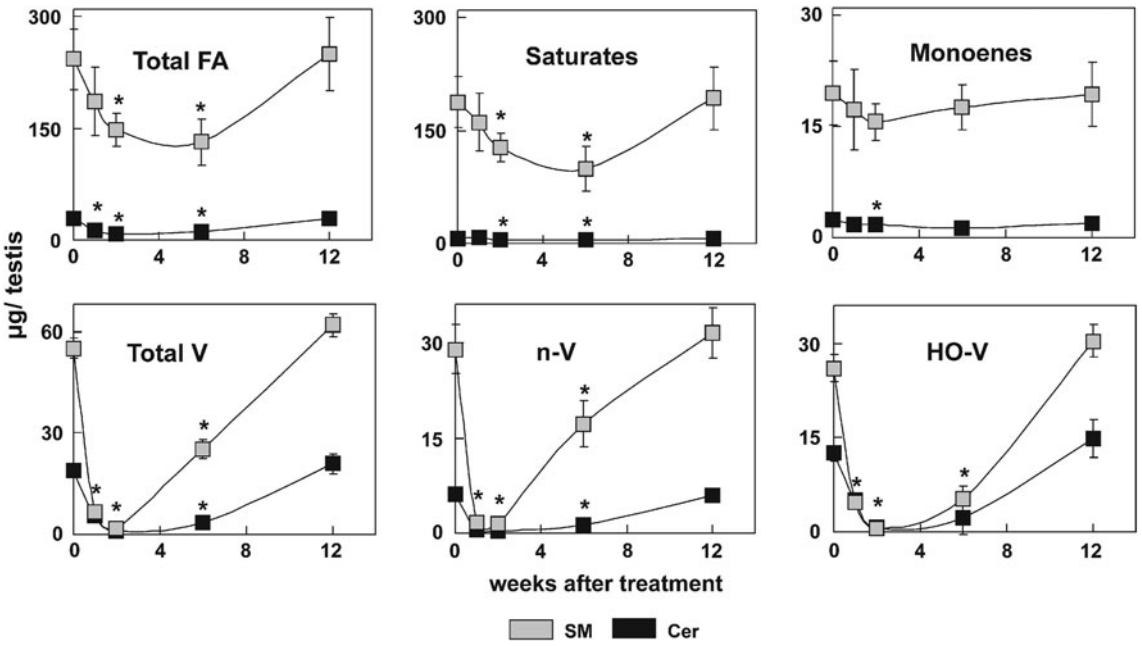

Fig. 4 Time-course of the in vivo changes after heat exposure in the amounts of rat testicular sphingomyelins and ceramides and their fatty acids. n-V, nonhydroxy VLCPUFA; 2-OH V, 2-OH VLCPUFA. Total V represents the sum of both types of VLCPUFA

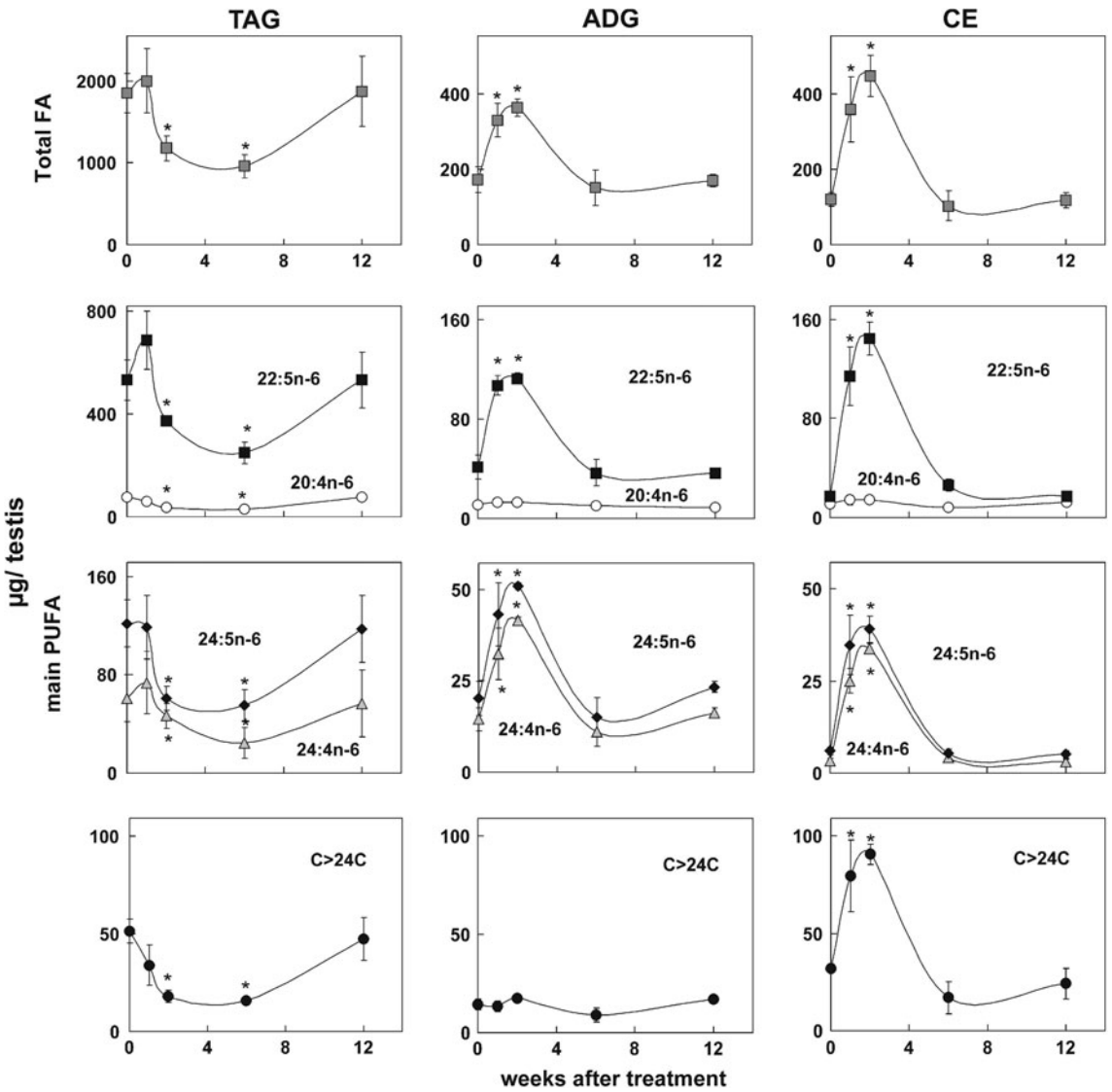

Fig. 5 Consequences of testicular heat exposure on the amount per testis of major neutral lipids and their polyenoic fatty acid constituents. *TAG*, *ADG* and *CE*: triacylglycerols, ether-linked triglycerides and cholesteryl esters, respectively. *Top panels* total fatty acids. *Bottom panels* main C_{20} to C_{32} carbon (n-6) tetraenoic and pentaenoic fatty acids in each lipid. Polyenoic fatty acids with chains longer than C24 are depicted as >24C

a 5 to a 10% of the total phospholipids at post-treatment weeks 1 and 2, not shown). This increase was associated, on the one hand, to the large decrease undergone by the major germ cell associated Gpl, and on the other, to the fact that Sertoli cells contain considerably more sphingomyelin than germ cells [9, 20]. On the basis of its total fatty acids (Fig. 4), 1 and 2 weeks after ending the treatment, the amount per testis of total CerPCho had decreased by 10 and 25%, respectively. Interestingly, at the same time as the sphingomyelins that contain saturated fatty acids were reduced by 12 and 24%, respectively, those that contain n-VLCPUFA were by reduced 90 and 100% and those that contain 2-OH VLCPUFA were reduced by 75 and 100%, respectively. These results agree with the fact that the sphingomyelins of Sertoli cells do not contain VLCPUFA but are instead rich in saturated, followed by monoenoic fatty acids [9], and explain the fact that these sphingomyelins decreased after heating much less than did the species that contain VLCPUFA (Fig. 4).

Neutral Lipids and Their Fatty Acids

The time course of the changes that occur after mild testicular hyperthermia in neutral lipids, focusing on species that contain PUFA of 20 to 32 carbon atoms, is shown in Fig. 5. This revealed a marked contrast between triacylglycerols (TAG) on the one hand and the other two neutral lipids of this study on the other, triglycerides with an ether

bond (abbreviated ADG to include alkyl- and alkenyl-diacylglycerols) and cholesteryl esters (CE) (Fig. 5).

In contrast to the marked reduction undergone by Gpl, the amount per testis of TAG remained unchanged during the first week after the last exposure to heat (Fig. 5). Interestingly, this lipid decreased abruptly (50%) between weeks 1 and 2, and remained at this low level for four additional weeks. Thus, only after post-treatment week 6 TAG started to increase, to return to control values by week 12. The quantitative importance of TAG is self-apparent from the data in Fig. 2, mostly explaining the post-treatment difference between the recovery of total Gpl and that of the total lipid in the testis.

The marked decrease undergone by the amounts of testicular TAG after week 1 in the heat-exposed testes involved predominantly their major species, i.e., those containing 22:5n-6 (Fig. 5), followed by species with 24:4n-6 and 24:5n-6 and also with longer polyenes. The time course of the changes, with persistence of TAG during the early germ cell loss phase, and with reappearance at a late period of the restoration phase, indicates that these TAG species bear an association with the most highly differentiated cells of the spermatogenic lineage.

In clear contrast with TAG, the ADG and CE exhibited an intense accumulation (twofold and fourfold, respectively) during the first two weeks after finishing the heat treatment (Fig. 5). By week 6, the amounts of both lipids had already returned to levels close to those of controls and continued at those relatively low levels for the next 6 weeks (Fig. 5).

Although ADG and CE collected an assortment of fatty acids (including saturates, 18:1 and 18:2, not shown), it was clearly apparent that they also accumulated tetraenoic and pentaenoic fatty acids (Fig. 5). Of these, 22:5n-6 was the single fatty acid that increased the most in quantitative terms in both neutral lipids during the first two weeks post-treatment. In ADG there was also a significant increase in that period of species that contain VLCPUFA with 24 carbon atoms (Fig. 5), but no changes in polyenoic fatty acids longer than C24. In contrast, VLCPUFA with 24 to 32 carbon atoms were collected in CE (Fig. 5).

Lipid Droplets

In histological sections of testicular tissue from untreated adult rats, where seminiferous tubules at different stages of the spermatogenic cycle can be observed, some of the tubules mostly contain spermatocytes at different stages, while others clearly contain mostly spermatids and spermatozoa in formation. In all of the tubules, the relatively minor and permanent population of Sertoli cells, located near the basement membrane of the tubules, can be observed. In control testis preparations, two types of lipid

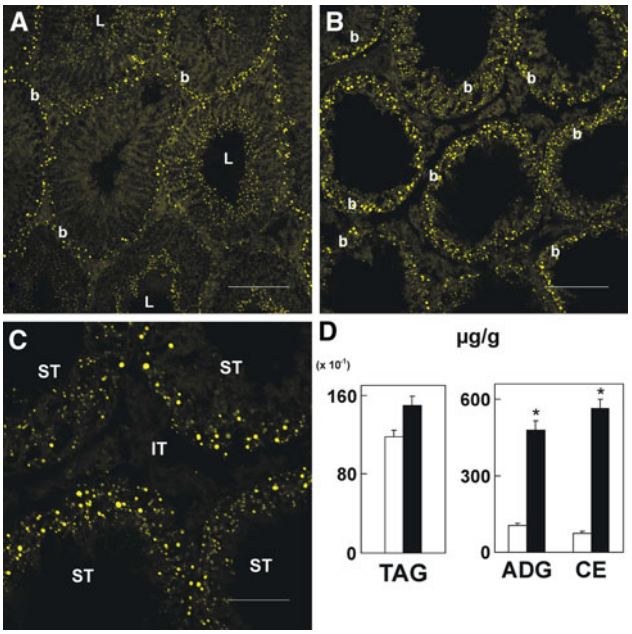

Fig. 6 Lipid droplets of rat testis, as revealed with Nile Red. **A** Control rat testis, showing the intense concentration of small lipid droplets near the lumen (*L*) in some seminiferous tubules and the more disperse and larger lipid droplets located near the basal (*b*) membrane in other tubules (*Bar* 150 µm); **B** Rat testis 2 weeks after the last heat exposure, showing large and abundant *L* and *S* lipid droplets near the (*b*) base of Sertoli cells (*Bar* 150 µm); **C** Enlarged field of another sample in the latter condition (*Bar* 50 µm) showing that lipid droplets were located within seminiferous tubules (*ST*) rather than in the interstitial tissue (*IT*). **D** Concentration (note that it is expressed as µg per gram of tissue) of the three neutral lipids surveyed in this study 2 weeks after daily transient exposures to 22 or to 43 °C (*white and black bars*, respectively)

inclusions were present, which were discriminated using Nile Red as previously described [18]. A population of small lipid droplets, located in the area of the epithelium facing the lumena of most of the tubules (i.e., mostly extracellular), was normally the most abundant (Fig. 6a). These droplets, recently shown to be TAG-rich [9], mostly correspond to the small but abundant lipid-laden "residual bodies" that are normally shed from elongated spermatids in differentiation to spermatozoa. The second type of lipid inclusion, a population of somewhat larger (but normally less numerous) lipid droplets, was observable near the peripheral basement membrane in some of the tubules (Fig. 6a), mainly included in Sertoli cells.

In the present study, 2 weeks after the last heat exposure (i.e., 3 weeks after the first), when virtually no germ cells but mostly Sertoli cells remained in the tubules, the small and the large type of lipid droplets were all concentrated in the latter cells (Fig. 6b). This extensive accumulation occurred exclusively within the seminiferous epithelium, not in the interstitium (Fig. 6c). The lipid profiles at this precise post-treatment time point, with maximum concentrations of TAG, ADG and EC (note that the results are

expressed as the amount per gram of tissue, not amount per testis in this case) (Fig. 6d) suggest that the small and the large lipid droplets observed in Sertoli cells contained these neutral lipids.

Discussion

The presented data demonstrate that repeated episodes of mild testicular hyperthermia applied to the rat testis result in virtually equivalent consequences as experimental cryptorchidism [8] on spermatogenic cells and their typical species of polar lipids, represented by their unique fatty acids, with drops to very low levels of Gpl species that contain 22:5n-6 and of CerPCho and Cer species that contain VLCPUFA. Similar decreases have been observed weeks after treatment with other germ cell apoptosis-inducing agents, such as administration of the antineoplastic agent doxorubicin [21] and X-ray irradiation [18]. In contrast with these two latter conditions, in which repopulation of the testis by new cohorts of germ cells does not occur, in the present experimental model it was possible to see these cells and their membrane lipids to spontaneously reappear in the testis by week 6 after the last heat exposure and reach their normal levels by week 12 post-treatment.

The observation that after heat-induced stress the sphingomyelins and ceramides that contain nonhydroxy-VLCPUFA disappeared *earlier* than the corresponding species of both lipids that contain 2-hydroxy VLCPUFA is consistent with the timed order of germ cell disappearance, considering the difference in fatty acid composition major germ cell types display in the rat testis [9]. Thus, the cells that in this study had vanished by week 1 post-heat treatment, pachytene spermatocytes, are exceedingly rich in sphingolipid species with n-VLCPUFA, in contrast to the more differentiated spermatids and spermatozoa, rich in species with 2-OH VLCPUFA. These cells were precisely the *last* to be lost from the heat-stressed seminiferous epithelium, in agreement with the fact that elongated spermatids are more resistant to thermal stress than primary spermatocytes and round spermatids [22]. The order of re-emergence of the two groups of species of both sphingolipids with time after reinitiating spermatogenesis was also consistent with (n-VLCPUFA-rich) spermatocytes reappearing before spermatids, their more mature (2-OH VLCPUFA-rich) counterparts.

The major Gpl are shown in the present study to loose most of their species with the major PUFA, 22:5n-6, in larger proportion than species with any other fatty acid, including the closely related 20:4n-6, during the first 2 weeks after the last heat exposure. Normally both fatty acids, in a nearly 1:1 proportion, are the main PUFA of the major Gpl of pachytene spermatocytes, while the 22:5n-6/20:4n-6 ratio is significantly higher in Gpl of spermatids and spermatozoa [9]. Thus, the marked decrease in the amount of both fatty acids observed here 7 days after the last heat exposure was associated with the virtual disappearance of spermatocytes, with elongated spermatids and spermatozoa still being present, in that period. The deep valley (in amount and percentage) of 22:5n-6-rich Gpl observed at week 2 post-heating concurs with a profound loss from the testis of virtually *all* germ cell types, and practically a "Sertoli cell only" seminiferous tubule system. Part of this drop at week 2 may be associated to the fact that the heat-tolerant spermatids that were still present at week 1 probably completed their differentiation to spermatozoa during this second week, and that these last gametes left the testis to be transported to the epididymis. This interpretation is consistent with the fact that heat impacts first the testis, then the epididymis. Thus, 7 days after a single episode of testicular heating (43 °C for 15 min), rat testicular weight declines to 70% of control, whereas epididymal weight does not decrease significantly until day 26 [7].

In contrast to the massive decrease of 22:5-rich Gpl observed during the first week after the last heat exposure, the amounts of 22:5n-6-rich TAG did not change significantly. These species of TAG are normally formed in elongating spermatids at the last stages of spermiogenesis and are highly concentrated in the particles known as "residual bodies" [9]. Taken together with the present results, this suggests that 22:5n-6-rich TAG continued to be produced throughout the period of heat exposure. This would explain that TAG levels per testis were still high during the first week after the last heat episode, in concomitance with the last round of spermiogenesis. The TAG concentration in the Sertoli-cell-rich testis at week 2 post-treatment, and the accumulation in these cells of the small lipid droplets representative of residual bodies (Fig. 6), suggests that this process apparently continued at its nearly normal pace by differentiation of pre-existing temperature-tolerant elongated spermatids. Eventually, the latter were also depleted, by transformation into spermatozoa, which left the testis normally in the course of the next week.

In its effects on neutral lipids, the period of two weeks of cell depopulation provoked by the five daily episodes of transient hyperthermia was comparable to the 10 days of unilateral experimental cryptorchidism previously reported [8]. Both had in common a significant buildup of CE species with specific PUFA (e.g., 22:5n-6) and VLCPUFA (e.g., 28:5n-6) in rat testes. Because this accumulation occurred concomitantly with vulnerable germ cell disappearance from, but sparing heat-tolerant Sertoli cells in, seminiferous tubules, it is clearly apparent that CE accumulation is a feature of the latter, not the former cells. The apoptotic bodies derived from heat-damaged germ cells

may be expected to have been phagocytosed by Sertoli cells, this being rapidly followed by hydrolysis and further processing of the ingested materials. Besides proteins and nucleic acids, these materials obviously comprised former germ cell membranes and their lipids (free cholesterol and phospholipids including Gpl and sphingomyelins). The temporary accumulation of 22:5- and VLCPUFA-rich species of CE is interpreted to occur mostly as a consequence of lipid catabolism in Sertoli cells.

One possible explanation for the heat-related CE accumulation, which we proposed in previous work [8], was biochemical, i.e., that this could in part be ascribed to reduced CE hydrolysis due to heat-induced inhibition or inactivation of HSL (*H*ormone *S*ensitive *L*ipase), or to increased CE synthesis due to activation of ACAT (acyl-CoA-cholesterol acyl transferase) in Sertoli cells. However, we now have more of a cellular conception, considering that Sertoli cells are active phagocytes, and that accumulation of 22:5n-6-rich CE in testis also occurs at physiological temperatures, as a consequence of diverse situations whose only common feature is that they are pro-apoptotic to germ cells while sparing Sertoli cells [doxorubicin treatment [21], X-ray irradiation [18], and ischemia-reperfusion (Zanetti SR and Aveldaño MI, unpublished observations)]. We favor the possibility that Sertoli cells habitually form CE, using ACAT as any phagocyte would do, after phagocytosing biological materials whose breakdown leads to an excess of free cholesterol and fatty acids.

The accumulation of 22:5-rich and VLCPUFA-rich species of CE is interpreted to reflect a phagocytic cell-typical activity of Sertoli cells that is always present, but that is markedly intensified in the presence of factors (like temperature) that increase the death of germ cells. This may include a lethal rapid destruction of some cells and the sublethal damage with survival but eventual degeneration of others. Thus, the buildup in Sertoli cells of an excess of germ-cell derived free cholesterol, and (after phospholipid hydrolysis) free fatty acids, may be naturally prevented in these cells by producing CoA esters of the latter and collecting them both in the form of innocuous CE. These CE may be temporarily set aside in their cytoplasm—in the form of lipid droplets—before their ultimate disposal, i.e., until all fatty acids can be oxidized to produce ATP [23] and/or until all that extra cholesterol can be effluxed, which requires ATP-driven transporters [24].

Almost in parallel to CE, the amounts per testis of ADG also increased significantly as a consequence of mild hyperthermia. Considering the reduced testicular weight, the concentration of both neutral lipids increased several fold in Sertoli cells during the first 2 weeks following heat exposures (Fig. 6). This also agreed with previous observations in the cryptorchid rat model [8], since in both temperature-induced situations significant accumulations of ADG with PUFA (largely 22:5n-6, and to a lesser extent 24:4n-5 and 24:5n-6), occurred in concomitance with the depletion of germ cells and the corresponding decrease of 22:5n-6 rich Gpl, including plasmalogens.

In physiological conditions, the ether linked triglycerides (mostly 1-*O*-alkyl, 2,3 diacyl-*sn*-glycerols) could somehow be related to the biosynthesis ether-linked lipids such as PAF or seminolipid, or be precursors of plasmalogens [25]. However, in pathological conditions like the present temperature-related massive germ cell loss, considering that ADG accumulate PUFA, their buildup during the first 2 weeks suggests a relation to catabolism rather than to biosynthesis of plasmalogens. By a similar self-defense reason as CE are accumulated in Sertoli cells, as a strategy to limit any excess of (cell toxic) free cholesterol and free fatty acids, ADG may represent a form of temporarily capturing potentially harmful or disturbing excesses of free PUFA and (diradyl) diglycerides derived from Gpl hydrolysis, in the form of innocuous (non-toxic, cell-signalling inactive) triglycerides. In other words, PUFA- and VLCPUFA-rich CE and ADG seem to be normal, transient by-products formed in Sertoli cells after they ingest and process apoptotic bodies derived from spermatogenic cells that die from *any* cause, whether pathological or physiological.

Physiologically, the same mechanisms operating during the normal spermatogenic cycle provide an explanation to the function of the PUFA- and VLCPUFA-rich CE and ADG previously reported to be present in seminiferous tubules of untreated rats [25]. Thus, Sertoli cells habitually perform phagocyte-typical activities at different stages of the spermatogenic cycle. Firstly, because they have a limited germ cell support capacity, they control the numbers of early germ cells (which are normally overproduced) by inducing their apoptosis [4] and then phagocytosing the resulting apoptotic bodies [26]. Secondly, although at a different stage of the spermatogenic cycle, Sertoli cells are also known to perform on a regular basis the phagocytosis of the myriad of residual bodies that are shed from spermatids during spermiogenesis. These particles were recently shown to be loaded with 22:5n-6-rich TAG, free cholesterol, 22:5n-6-rich Gpl and 2-OH VLCPUFA-rich sphingomyelins [9], lipids whose final destination is also Sertoli cells for eventual hydrolysis and disposal of their acyl chains.

The period that goes between weeks 4 and 6 post-treatment is an excellent phase in which to study biochemical aspects of germ cell development. From a germ cell deprived testis, there is a relatively long period in which pachytene spermatocytes predominate in seminiferous tubules, resembling in many aspects the onset of spermatogenesis at pubertal ages. This phase appears promising to study in vivo

aspects of the biosynthesis of PUFA and n-VLCPUFA, such as the expression and activity of fatty acid desaturases and elongases, and the pathways of incorporation of these fatty acids into the corresponding phospholipids and sphingolipids. The appearance of the first spermatids, with no interference from the presence of their more differentiated counterparts, may be useful to determine the cellular location and mechanism of the 2-hydroxylation that is responsible for the biosynthesis of the 2-OH VLCPUFA of rat testicular CerPCho and Cer. Lastly, the phase of fully restored spermiogenesis may allow the study of the 22:5n-6 rich TAG that is so actively synthesized by differentiating spermatids.

Concluding remarks

This study does not focus on those cells that were directly damaged by temperature: such cells were killed by apoptosis (a process that takes just 12–16 h) and disappeared from the testis in a day or two (the time required for Sertoli cells to phagocytize and completely eliminate apoptotic germ cells). These facts and the mechanisms involved have been comprehensively studied by other authors. It rather deals with those cells that, not having been lethally affected by temperature initially, or having succeeded to endure and overcome its damaging effects, managed to continue with their functions. During the first weeks, the marked decrease in the content of PUFA-rich species of Gpl and VLCPUFA-rich species of sphingolipids was caused mostly by the immediate death of vulnerable germ cell line *precursors* (e.g., pachytene spermatocytes), which led to the subsequent nonexistence of their whole progeny, but also by the eventual death of those cells that had been sublethally targeted by temperature but died at later stages of their differentiation. This phase seems to be a good period in which to study the biochemistry involved in many as yet unknown details of the catabolism of lipids with PUFA of diverse chain lengths and unsaturation (including 22:5n-6 and 2-OH VLCPUFA) in Sertoli cells. In turn, the phase of gradual germ cell repopulation after recovery from mild hyperthermia, with long-chain PUFA synthesized and incorporated into Gpl including plasmalogens, and with n-VLCPUFA restored before 2-OH VLCPUFA and both reappearing amide-bound to Cer and CerPCho, offers a good opportunity to study aspects of the expression of genes and activity of enzymes that take part in the biosynthesis of the unique lipid molecular species that germ cells contain in the adult rat testis.

Acknowledgments The authors gratefully thank Dr. Eduardo N. Maldonado for his helpful comments on the manuscript. This work was supported by grants from Agencia Nacional para la Promoción de la Ciencia y la Tecnología, Consejo Nacional de Investigaciones Científicas y Técnicas, and Secretaría General de Ciencia y Tecnología, Universidad Nacional del Sur, Argentina.

Conflict of interest The authors declare that there is no conflict of interests that could be perceived as prejudicing the impartiality of the research reported.

References

1. Hikim AP, Lue Y, Yamamoto CM, Vera Y, Rodriguez S, Yen PH, Soeng K, Wang C, Swerdloff RS (2003) Key apoptotic pathways for heat-induced programmed germ cell death in the testis. Endocrinology 144:3167–3175
2. Lue Y, Hikim AP, Wang C, Im M, Leung A, Swerdloff RS (2000) Testicular heat exposure enhances the suppression of spermatogenesis by testosterone in rats: the "two-hit" approach to male contraceptive development. Endocrinology 141:1414–1424
3. Lue YH, Hikim AP, Swerdloff RS, Im P, Taing KS, Bui T, Leung A, Wang C (1999) Single exposure to heat induces stage-specific germ cell apoptosis in rats: role of intratesticular testosterone on stage specificity. Endocrinology 140:1709–1717
4. Sinha Hikim AP, Swerdloff RS (1999) Hormonal and genetic control of germ cell apoptosis in the testis. Rev Reprod 4:38–47
5. Vera Y, Díaz-Romero M, Rodriguez S, Lue Y, Wang C, Swerdloff RS, Sinha Hikim AP (2004) Mitochondria-dependent pathway is involved in heat-induced male germ cell death: lessons from mutant mice. Biol Reprod 70:1534–1540
6. Yamamoto CM, Sinha Hikim AP, Huynh PN, Shapiro B, Lue Y, Salameh WA, Wang C, Swerdloff RS (2000) Redistribution of Bax is an early step in an apoptotic pathway leading to germ cell death in rats, triggered by mild testicular hyperthermia. Biol Reprod 63:1683–1690
7. Jegou B, Laws AO, de Kretser DM (1984) Changes in testicular function induced by short-term exposure of the rat testis to heat: further evidence for interaction of germ cells, Sertoli cells and Leydig cells. Int J Androl 7:244–257
8. Furland NE, Maldonado EN, Aresti PA, Aveldaño MI (2007) Changes in lipids containing long- and very long-chain polyunsaturated fatty acids in cryptorchid rat testes. Biol Reprod 77:181–188
9. Oresti GM, Reyes JG, Luquez JM, Osses N, Furland NE, Aveldaño MI (2010) Differentiation-related changes in lipid classes with long-chain and very long-chain polyenoic fatty acids in rat spermatogenic cells. J Lipid Res 51:2909–2921
10. Lue YH, Lasley BL, Laughlin LS, Swerdloff RS, Hikim AP, Leung A, Overstreet JW, Wang C (2002) Mild testicular hyperthermia induces profound transitional spermatogenic suppression through increased germ cell apoptosis in adult cynomolgus monkeys (Macaca fascicularis). J Androl 23:799–805
11. Bligh EG, Dyer WJ (1959) A rapid method of total lipid extraction and purification. Can J Biochem Physiol 37:911–917
12. Rouser G, Fkeischer S, Yamamoto A (1970) Two dimensional then layer chromatographic separation of polar lipids and determination of phospholipids by phosphorus analysis of spots. Lipids 5:494–496
13. Aveldaño MI, Rotstein NP, Vermouth NT (1992) Lipid remodelling during epididymal maturation of rat spermatozoa. Enrichment in plasmenylcholines containing long-chain polyenoic fatty acids of the n-9 series. Biochem J 283(Pt 1):235–241
14. Brown ER, Subbaiah PV (1994) Differential effects of eicosapentaenoic acid and docosahexaenoic acid on human skin fibroblasts. Lipids 29:825–829

15. Christie WW (1982). Lipid analysis: the preparation of derivates of lipids. Pergamon Press, Oxford
16. Zanetti SR, de Los Angeles MM, Rensetti DE, Fornes MW, Aveldaño MI (2010) Ceramides with 2-hydroxylated, very long-chain polyenoic fatty acids in rodents: from testis to fertilization-competent spermatozoa. Biochimie 92:1778–1786
17. Furland NE, Zanetti SR, Oresti GM, Maldonado EN, Aveldaño MI (2007) Ceramides and sphingomyelins with high proportions of very long-chain polyunsaturated fatty acids in mammalian germ cells. J Biol Chem 282:18141–18150
18. Oresti GM, Ayuza Aresti PL, Gigola G, Reyes LE, Aveldaño MI (2010) Sequential depletion of rat testicular lipids with long-chain and very long-chain polyenoic fatty acids after X-ray-induced interruption of spermatogenesis. J Lipid Res 51:2600–2610
19. Russell LD, Vogl AW, Weber JE (1987) Actin localization in male germ cell intercellular bridges in the rat and ground squirrel and disruption of bridges by cytochalasin D. Am J Anat 180:25–40
20. Beckman JK, Coniglio JG (1979) A comparative study of the lipid composition of isolated rat Sertoli and germinal cells. Lipids 14:262–267
21. Zanetti SR, Maldonado EN, Aveldaño MI (2007) Doxorubicin affects testicular lipids with long-chain (C18–C22) and very long-chain (C24–C32) polyunsaturated fatty acids. Cancer Res 67:6973–6980
22. Cataldo L, Mastrangelo MA, Kleene KC (1997) Differential effects of heat shock on translation of normal mRNAs in primary spermatocytes, elongated spermatids, and Sertoli cells in seminiferous tubule culture. Exp Cell Res 231:206–213
23. Xiong W, Wang H, Wu H, Chen Y, Han D (2009) Apoptotic spermatogenic cells can be energy sources for Sertoli cells. Reproduction 137:469–479
24. Selva DM, Hirsch-Reinshagen V, Burgess B, Zhou S, Chan J, McIsaac S, Hayden MR, Hammond GL, Vogl AW, Wellington CL (2004) The ATP-binding cassette transporter 1 mediates lipid efflux from Sertoli cells and influences male fertility. J Lipid Res 45:1040–1050
25. Furland NE, Maldonado EN, Aveldaño MI (2003) Very long chain PUFA in murine testicular triglycerides and cholesterol esters. Lipids 38:73–80
26. Shiratsuchi A, Umeda M, Ohba Y, Nakanishi Y (1997) Recognition of phosphatidylserine on the surface of apoptotic spermatogenic cells and subsequent phagocytosis by Sertoli cells of the rat. J Biol Chem 272:2354–2358

Lipids (2011) 46:455–461
DOI 10.1007/s11745-011-3541-5

METHODS

Efficient Synthesis of the Very-Long-Chain n-3 Fatty Acids, Tetracosahexaenoic Acid (C_{24}:6n-3) and Tricosahexaenoic Acid (C_{23}:6n-3)

Toshimasa Itoh · Ayako Tomiyasu · Keiko Yamamoto

Received: 8 January 2011 / Accepted: 4 February 2011 / Published online: 24 February 2011

Abstract Tetracosahexaenoic acid (C_{24}:6n-3, THA, **3**) is an essential biosynthetic precursor in mammals of docosahexaenoic acid (C_{22}:6n-3, DHA, **1**), the end-product of the metabolism of n-3 fatty acids. THA **3** is present in commercially valuable fishes, such as flathead flounder. Tricosahexaenoic acid (C_{23}:6n-3, TrHA, **2**), an odd-numbered-chain fatty acid, has been identified from marine organisms such as the dinoflagellate, *Amphidinium carterae*. To date, few studies have examined THA **3** and TrHA **2** due to difficulties in detecting and identifying these compounds, so their chemical and biological properties remain poorly characterized. Only one methodology for the chemical synthesis of THA **3** has been presented, and no method for the synthesis of TrHA **2** has been reported. We report here the efficient synthesis of THA **3** in four steps in 56% overall yield, and the synthesis of TrHA **2** in six steps in 48% overall yield. We also present the synthesis of Δ^2-THA **4**, an intermediate of β-oxidation of THA **3** to DHA **1**, in three steps in 73% overall yield.

Keywords Tetracosahexaenoic acid · Tricosahexaenoic acid · Docosahexaenoic acid · Chemical synthesis · Alzheimer's disease · β-oxidation · Biosynthetic precursor · Odd-numbered fatty acids · Fish oil · DHA metabolism

T. Itoh · A. Tomiyasu · K. Yamamoto (✉)
Laboratory of Drug Design and Medicinal Chemistry, Showa Pharmaceutical University, 3-3165 Higashi-Tamagawagakuen, Machida, Tokyo 194-8543, Japan
e-mail: yamamoto@ac.shoyaku.ac.jp

A. Tomiyasu
Institute of Biomaterials and Bioengineering, Tokyo Medical and Dental University, 2-3-10 Kanda-Surugadai, Chiyoda-ku, Tokyo 101-0062, Japan

Abbreviations

ALA	α-Linolenic acid
DHA	Docosahexaenoic acid
EPA	Eicosapentaenoic acid
THA	Tetracosahexaenoic acid
TrHA	Tricosahexaenoic acid
TAG	Triacyl-*sn*-glycerol

Introduction

The polyunsaturated fatty acid, docosahexaenoic acid (C_{22}:6n-3, DHA, **1**), is largely found in neuronal tissues such as brain and retina [1]. DHA **1** is an essential component of neuronal membranes, is a precursor of potent neuroprotective mediators, and is important in helping to prevent both cardiovascular disease and metabolic syndrome [2, 3]. Mammals obtain DHA **1** directly from dietary sources, especially fish, but can also generate DHA **1** in the liver from n-3 fatty acid precursors obtained from eating plants [4–6]. The capacity of the human liver to produce DHA **1** may become critical for maintaining normal levels of DHA **1** in the brain and retina [4, 6–8] if insufficient DHA **1** is available from the diet, as is often the case in modern societies [9].

The pathway for DHA biosynthesis in the liver is shown in Fig. 1. α-Linolenic acid (18:3n-3, ALA) is converted to eicosapentaenoic acid (20:5n-3, EPA), which is converted into docosapentaenoic acid (22:5n-3, DPA) and then into tetracosahexaenoic acid (24:6n-3, THA, **3**). Desaturase and elongase enzymes are localized in the endoplasmic reticulum of the hepatocyte and act on n-3 fatty acids. Desaturase progressively introduces double bonds, and elongase

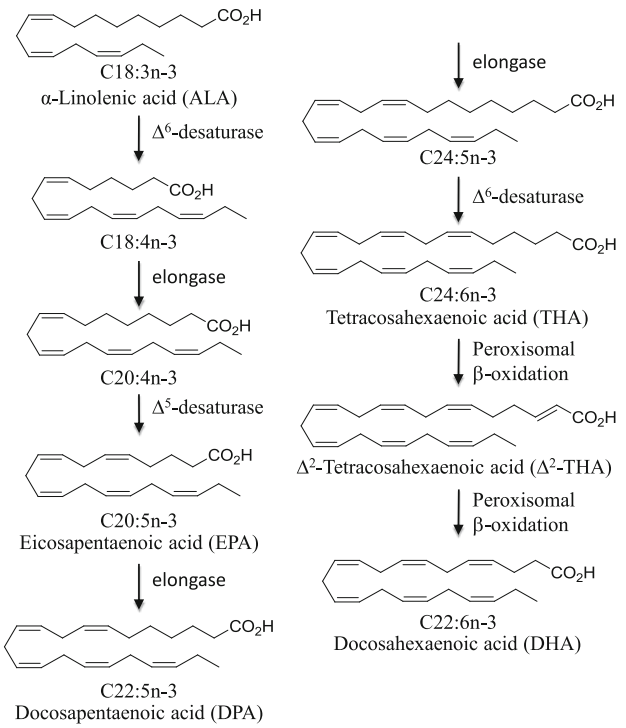

Fig. 1 Metabolic pathway of bioconversion of n-3 polyunsaturated fatty acids

extends shorter-chain n-3 fatty acids by two-carbon units, thereby generating very-long-chain THA **3** [10]. THA **3** is then transported into the peroxisomes and converted to DHA **1** by β-oxidation reactions that involve several specific enzymes: acyl-coenzyme A oxidase, D-bifunctional protein, and peroxisomal thiolases [11–14]. DHA **1**, the end-product of the metabolism of n-3 fatty acids, is delivered to the brain by the circulatory system and accumulates in the brain membranes. In contrast, THA **3** is not incorporated into the brain membranes but is an essential precursor of DHA **1**. Recently, Piomelli's group reported that levels of DHA precursors, particularly ALA and THA **3**, are elevated in the livers of patients with Alzheimer's disease, whereas expression of peroxisomal D-bifunctional protein, which catalyzes the conversion of THA **3** to DHA **1**, is reduced [15]. Piomelli et al. concluded that deficient liver biosynthesis of DHA **1** correlates with cognitive impairment in Alzheimer's patients. Thus, the critical importance of THA **3** in mammals is becoming clearer.

THA **3** is found in various marine organisms [16–18]. Nichols et al. [19] reported that THA **3** constitutes 9.3% of the total fatty acids in the jellyfish *Aurelia* sp. Recently, Tomita and Ando reported that THA **3** is found preferentially at the *sn*-2 position (1.6–23.3 mol%) of triacyl-*sn*-glycerols (TAG) from flathead flounder flesh [20]. Flathead flounder is extensively consumed by humans; therefore, we intake THA **3** in the form of TAG concentrating THA **3** at the *sn*-2 position. Odd-numbered very-long-chain

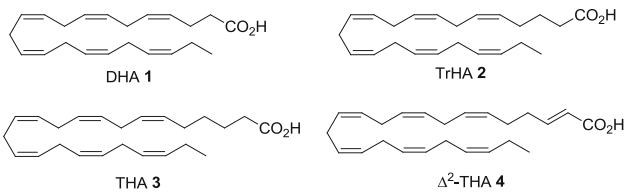

Fig. 2 Chemical structures of the fatty acids discussed in this paper. Docosahexaenoic acid (**1**), tricosahexaenoic acid (**2**), tetracosahexaenoic acid (**3**) and Δ^2-tetracosahexaenoic acid (**4**)

polyunsaturated fatty acids have also been identified from marine organisms [21]. Odd-chain fatty acids can be used in lipid metabolism [22]. The C_{23} fatty acid, tricosahexaenoic acid (C_{23}:6n-3, TrHA **2**), is found in the dinoflagellate, *Amphidinium carterae* [23]. To date, few studies have examined THA **3** and TrHA **2** due to difficulties in detecting and identifying these compounds, so their chemical and biological properties remain poorly characterized. To our knowledge, only one chemical synthesis method for THA **3** has been reported [24, 25], and none for TrHA **2**. In the course of our synthetic and structural biological studies of polyunsaturated fatty acids [26–30], we attempted to derive very-long-chain n-3 fatty acids from DHA ester. In this paper, we report the efficient chemical synthesis of THA **3**, TrHA **2**, and an intermediate of β-oxidation of THA **3** to DHA **1**, Δ^2-THA **4** (Fig. 2).

Materials and Methods

General Experimental Procedures

DHA ethyl ester **5** was a kind gift from the Maruha Nichiro holdings (Tsukuba, Japan). All the other reagents were purchased from commercial sources and used without further purification. Organic solvents used were dried by standard methods. All reactions were performed under a nitrogen atmosphere. Silica gel (wako gel C200) was used for column chromatography, and pre-coated silica gel $60F_{254}$ plates (0.25 mm, Merck) were used for TLC. ^{1}H NMR (300 MHz) and ^{13}C NMR (75 MHz) were recorded using a Bruker AV300 instrument in $CDCl_3$ solution with TMS as an internal standard and the chemical shifts are given in δ values. Splitting patterns are indicated as follows: s, singlet; d, doublet; t, triplet; q, quartet; quint, quintet; m, multiplet. Mass spectra were recorded on a JEOL MS700 spectrometer using NBA as positive-ion FAB matrix.

(4*Z*,7*Z*,10*Z*,13*Z*,16*Z*,19*Z*)-Docosa-4,7,10,13,16,19-Hexaenal (**6**)

To a stirred solution of DHA ethyl ester **5** (157 mg, 0.440 mmol) in CH_2Cl_2 (1 mL) was added 1.0 M

diisobutylaluminium hydride (DIBAL-H) in toluene (523 μL, 0.523 mmol) at −78 °C and the mixture was stirred for 1 h. The reaction was quenched with 1 N HCl aq. and the mixture was extracted with EtOAc. The organic layer was washed with brine, dried over $MgSO_4$ and evaporated. The residue was chromatographed on silica gel (9 g, 5% EtOAc–hexane) to give aldehyde **6** (117 mg, 85%). A large scale preparation of **6** was performed using 10.1 g of DHA ester **5** under the similar conditions and 7.45 g of pure compound **6** was obtained (84% yield).

^{1}H NMR ($CDCl_3$) δ: 9.78 (1 H, m, H-1), 5.33–5.44 (12 H, m, H-4, 5, 7, 8, 10, 11, 13, 14, 16, 17, 19, 20), 2.78–2.92 (10 H, m, H-6, 9, 12, 15, 18), 2.51 (2 H, m, H-2), 2.40 (2 H, m, H-3), 2.08 (2 H, quint, $J = 7.5$ Hz, H-21), 0.97 (3 H, t, $J = 7.5$ Hz, H-22); ^{13}C NMR ($CDCl_3$) δ: 201.9, 132.0, 129.4, 128.6, 128.4, 128.29, 128.27, 128.1 (2 carbons), 127.90, 127.86, 127.7, 127.0, 43.7, 25.64 (3 carbons), 25.59, 25.5, 20.6, 20.1, 14.3; HRMS (FAB): Calcd for $C_{22}H_{33}O$ $[M + H]^+$: 313.2531; found: 313.2537.

Methyl (2*E*,6*Z*,9*Z*,12*Z*,15*Z*,18*Z*,21*Z*)-Tetracosa-2,6,9,12,15,18,21-Heptaenoate (**7**)

To a stirred suspension of sodium hydride (0.71 g, 29.6 mmol) in THF (6 mL) was added trimethyl phosphonoacetate (4.25 mL, 29.6 mmol) at 0 °C and the mixture was stirred for 10 min. A solution of aldehyde **6** (4.63 g, 14.8 mmol) in THF (45 mL) was added to the mixture. The reaction mixture was stirred at 0 °C for 1 h, then quenched with water at 0 °C and extracted with EtOAc. The organic layer was washed with brine, dried over $MgSO_4$ and evaporated. The residue was chromatographed on silica gel (60 g, 0.5% EtOAc–hexane) to give 2*Z*-**7** (0.39 g, 7%) and 2*E*-**7** (4.71 g, 87%) in this order.

2*E*-**7** $R_f = 0.51$ (10% EtOAc-hexane). ^{1}H NMR ($CDCl_3$) δ: 6.96 (1 H, dt, $J = 15.6$, 6.6 Hz, H-3), 5.84 (1 H, d, $J = 15.6$ Hz, H-2), 5.28–5.46 (12 H, m, H-6, 7, 9, 10, 12, 13, 15, 16, 18, 19, 21, 22), 3.73 (3 H, s, H-CO_2Me), 2.78–2.91 (10 H, m, H-8, 11, 14, 17, 20), 2.25 (4 H, m, H-4, 5), 2.08 (2 H, quint, $J = 7.5$ Hz, H-23), 0.97 (3 H, t, $J = 7.5$ Hz, H-24); ^{13}C NMR ($CDCl_3$) δ: 167.0, 148.6, 132.0, 129.1, 128.6, 128.29, 128.26, 128.22 (2 carbons), 128.08, 128.06, 128.02, 127.9, 127.0, 121.3, 51.4, 32.1, 25.7, 25.6 (3 carbons), 25.5, 20.6, 14.3; HRMS (FAB): Calcd for $C_{25}H_{37}O_2$ $[M + H]^+$: 369.2794; found: 369.2780. 2*Z*-**7** $R_f = 0.65$ (10% EtOAc-hexane). ^{1}H NMR ($CDCl_3$) δ: 6.22 (1 H, dt, $J = 11.5$, 7.5 Hz, H-3), 5.79 (1 H, dt, $J = 11.5$, 1.7 Hz, H-2), 5.26–5.45 (12 H, m, H-6, 7, 9, 10, 12, 13, 15, 16, 18, 19, 21, 22), 3.70 (3 H, s, H-CO_2Me), 2.68–2.91 (12 H, m, H-4, 8, 11, 14, 17, 20), 2.22 (2 H, m, H-5), 2.07 (2 H, quint, $J = 7.5$ Hz, H-23), 0.97 (3 H, t, $J = 7.5$ Hz, H-24); ^{13}C NMR ($CDCl_3$) δ: 166.7, 149.8, 132.0, 128.8 (2 carbons), 128.6, 128.25, 128.23, 128.18, 128.16, 128.09 (2 carbons), 127.9, 127.0, 119.7, 51.0, 28.8, 26.6, 25.6 (4 carbons), 25.5, 20.6, 14.3; HRMS (FAB): Calcd for $C_{25}H_{37}O_2$ $[M + H]^+$: 369.2794; found: 369.2792.

Methyl (6*Z*,9*Z*,12*Z*,15*Z*,18*Z*,21*Z*)-Tetracosa-6,9,12,15,18,21-Hexaenoate (**8**)

To a solution of 2*E*/2*Z* mixture **7** (32 mg, 87 μmol) in MeOH (0.5 mL) was added Mg turnings (20 mg, 0.84 mmol) at 0 °C and the mixture was stirred for 3.5 h at room temperature. After addition of H_2O, the mixture was extracted with EtOAc. The organic layer was washed with brine, dried over $MgSO_4$ and evaporated. The residue was chromatographed on silica gel (10 g, 1% EtOAc–hexane) to give **8** (26 mg, 81%). A large scale preparation of **8** was performed using 1.07 g of 2*E*/2*Z* mixture **7** under the similar conditions and 820 mg of pure compound **8** was obtained (76% yield). ^{1}H NMR ($CDCl_3$) δ: 5.28–5.56 (12 H, m, H-6, 7, 9, 10, 12, 13, 15, 16, 18, 19, 21, 22), 3.67 (3 H, s, H-CO_2Me), 2.73–2.92 (10 H, m, H-8, 11, 14, 17, 20), 2.32 (2 H, m, H-2), 2.08 (4 H, m, H-5, 23), 1.65 (2 H, quint, $J = 7.7$ Hz, H-3), 1.40 (2 H, quint, $J = 7.7$ Hz H-4), 0.98 (3 H, t, $J = 7.5$ Hz, H-24); ^{13}C NMR ($CDCl_3$) δ: 174.1, 132.0, 129.7, 128.6, 128.4, 128.3, 128.19, 128.16, 128.12, 128.10, 128.0, 127.9, 127.0, 51.5, 34.0, 29.0, 26.9, 25.6 (4 carbons), 25.5, 24.6, 20.6, 14.3; HRMS (FAB): Calcd for $C_{25}H_{39}O_2$ $[M + H]^+$: 371.2950; found: 371.2954.

(6*Z*,9*Z*,12*Z*,15*Z*,18*Z*,21*Z*)-Tetracosa-6,9,12,15,18,21-Hexaenoic Acid (THA **3**)

A solution of **8** (1.19 g, 3.23 mmol) in 5% KOH/MeOH–H_2O (19:1, 16 mL) was stirred at 50 °C for 1 h. The reaction mixture was neutralized with 10% HCl aq. and extracted with EtOAc. The organic layer was washed with water, dried over $MgSO_4$, and evaporated. The residue was chromatographed on silica gel (110 g, 50% EtOAc–hexane) to give THA **3** (1.01 g, 87 %). ^{1}H NMR ($CDCl_3$) δ: 5.27–5.55 (12 H, m, H-6, 7, 9, 10, 12, 13, 15, 16, 18, 19, 21, 22), 2.74–2.91 (10 H, m, H-8, 11, 14, 17, 20), 2.36 (2 H, t, $J = 7.4$ Hz, H-2), 2.08 (4 H, m, H-5, 23), 1.66 (2 H, m, H-3), 1.42 (2 H, m, H-4), 0.98 (3 H, t, $J = 7.5$ Hz, H-24); ^{13}C NMR ($CDCl_3$) δ: 179.9, 132.0, 129.6, 128.6, 128.4, 128.3, 128.22, 128.18, 128.1, 128.03, 127.96, 128.9, 127.0, 33.9, 29.0, 26.8, 25.6 (4 carbons), 25.5, 24.3, 20.6, 14.3; HRMS (FAB): Calcd for $C_{24}H_{37}O_2$ $[M + H]^+$: 357.2794; found: 357.2790.

(2*E*,6*Z*,9*Z*,12*Z*,15*Z*,18*Z*,21*Z*)-Tetracosa-2,6,9,12,15,18,21-Heptaenoic Acid (Δ^2-THA **4**)

A solution of 2*E*-**7** (100 mg, 272 μmol) in 5% KOH/iPrOH–H_2O (19:1, 10 mL) was stirred at 50 °C for 3 h.

The reaction mixture was neutralized with 10% HCl aq. and extracted with EtOAc. The organic layer was washed with water, dried over $MgSO_4$, and evaporated. The residue was passed through a short silica gel column (1 g, 70% EtOAc–hexane) to give Δ^2-THA **4** (95 mg, 99 %). ^{1}H NMR ($CDCl_3$) δ: 7.07 (1 H, dt, $J = 15.6$, 6.6 Hz, H-3), 5.84 (1 H, d, $J = 15.6$ Hz, H-2), 5.28–5.46 (12 H, m, H-6, 7, 9, 10, 12, 13, 15, 16, 18, 19, 21, 22), 2.77–2.91 (10 H, m, H-8, 11, 14, 17, 20), 2.20–2.36 (4 H, m, H-4, 5), 2.08 (2 H, quint, $J = 7.5$ Hz, H-23), 0.97 (3 H, t, $J = 7.5$ Hz, H-24); ^{13}C NMR ($CDCl_3$) δ: 171.9, 151.3, 132.0, 129.2, 128.6, 128.3 (2 carbons), 128.2, 128.13, 128.08 (2 carbons), 128.0, 127.9, 127.0, 121.1, 32.2, 25.6 (4 carbons), 25.5, 20.5, 14.3; HRMS (FAB): Calcd for $C_{24}H_{35}O_2$ $[M + H]^+$: 355.2637; found: 355.2624.

(4*Z*,7*Z*,10*Z*,13*Z*,16*Z*,19*Z*)-Docosa-4,7,10,13,16,19-Hexaen-1-ol (**9**)

To a stirred solution of DHA ethyl ester **5** (6.17 g, 17.3 mmol) in CH_2Cl_2 (40 mL) was added 1.0 M DIBAL-H in toluene (51.5 mL, 51.5 mmol) at 0 °C and the mixture was stirred for 1.5 h. The mixture was quenched with 1 N HCl aq. at 0 °C and extracted with EtOAc. The organic layer was washed with brine, dried over $MgSO_4$ and evaporated. The residue was chromatographed on silica gel (100 g, 10% EtOAc–hexane) to give alcohol **9** (5.06 g, 93%). ^{1}H NMR ($CDCl_3$) δ: 5.28–5.47 (12 H, m, H-4, 5, 7, 8, 10, 11, 13, 14, 16, 17, 19, 20), 3.66 (2 H, t, $J = 6.4$ Hz, H-1), 2.85 (10 H, m, H-6, 9, 12, 15, 18), 2.16 (2 H, quint, $J = 6.4$ Hz, H-3), 2.08 (2 H, quint, $J = 7.5$ Hz, H-21), 1.65 (2 H, quint, $J = 6.4$ Hz, H-2), 0.98 (3 H, t, $J = 7.5$ Hz, H-22); ^{13}C NMR ($CDCl_3$) δ: 132.1, 129.4, 128.6, 128.5, 128.30, 128.27, 128.20, 128.16, 128.1 (2 carbons), 127.9, 127.0, 62.5, 32.5, 25.65 (2 carbons), 25.63, 25.60, 25.5, 23.6, 20.6, 14.3; HRMS (FAB): Calcd for $C_{22}H_{35}O$ $[M + H]^+$: 315.2688; found: 315.2686.

(4*Z*,7*Z*,10*Z*,13*Z*,16*Z*,19*Z*)-Docosa-4,7,10,13,16,19-Hexaen-1-yl 4-Methylbenzenesulfonate (**10**)

A mixture of alcohol **9** (5.06 g, 16.1 mmol) and *p*-toluenesulfonyl chloride (4.61 g, 24.2 mmol) in pyridine (25 mL) was stirred at 0 °C for 13 h. After addition of water, the mixture was extracted with EtOAc. The organic layer was washed with 1 N HCl aq., saturated $NaHCO_3$ aq. and brine, dried over $MgSO_4$ and evaporated. The residue was chromatographed on silica gel (110 g, 5% EtOAc–hexane) to give tosylate **10** (6.71 g, 89%). ^{1}H NMR ($CDCl_3$) δ: 7.79 (2 H, d, $J = 8.3$ Hz, H-Ar), 7.34 (2 H, d, $J = 8.3$ Hz, H-Ar), 5.29–5.42 (12 H, m, H-4, 5, 7, 8, 10, 11, 13, 14, 16, 17, 19, 20), 4.03 (2 H, t, $J = 6.5$ Hz, H-1), 2.75–2.87 (10 H, m, H-6, 9, 12, 15, 18), 2.44 (3 H, s, H-Ph-Me), 2.04–2.12 (4 H, m, H-3, 21), 1.71 (2 H, quint, $J = 6.5$ Hz, H-2), 0.97 (3 H, t, $J = 7.5$ Hz, H-22); ^{13}C NMR ($CDCl_3$) δ: 144.7, 133.2, 132.0, 129.8 (2 carbons), 129.4, 128.6, 128.29, 128.26 (2 carbons), 128.1 (2 carbons), 128.0, 127.9 (4 carbons), 127.0, 69.9, 28.8, 25.6 (3 carbons), 25.5 (2 carbons), 23.0, 21.6, 20.6, 14.3; HRMS (FAB): Calcd for $C_{29}H_{41}O_3S$ $[M + H]^+$: 469.2776; found: 469.2777.

(5*Z*,8*Z*,11*Z*,14*Z*,17*Z*,20*Z*)-Tricosa-5,8,11,14,17,20-Hexaenenitrile (**11**)

A mixture of tosylate **10** (6.71 g, 14.3 mmol) and KCN (1.31 g, 20.1 mmol) in DMSO (40 mL) was stirred at 70 °C for 2.5 h. After addition of H_2O at 0 °C, the mixture was extracted with EtOAc. The organic layer was washed with brine, dried over $MgSO_4$, and evaporated. The residue was chromatographed on silica gel (100 g, 5% EtOAc–hexane) to give cyanide **11** (4.51 g, 97%). ^{1}H NMR ($CDCl_3$) δ: 5.32–5.40 (12 H, m, H-5, 6, 8, 9, 11, 12, 14, 15, 17, 18, 20, 21), 2.78–2.87 (10 H, m, H-7, 10, 13, 16, 19), 2.34 (2 H, t, $J = 7.2$ Hz, H-2), 2.01–2.14 (4 H, m, H-4, 22), 1.66 (2 H, m, H-3), 1.42 (2 H, m, H-3), 0.98 (3 H, t, $J = 7.5$ Hz, H-23); ^{13}C NMR ($CDCl_3$) δ: 132.0, 130.3, 128.6, 128.4, 128.3 (2 carbons), 128.1, 128.0, 127.9, 127.8, 127.3, 127.0, 119.6, 26.0, 25.7 (4 carbons), 25.5, 25.3, 20.6, 16.5, 14.3; HRMS (FAB): Calcd for $C_{23}H_{34}N$ $[M + H]^+$: 324.2691; found: 324.2696.

(5*Z*,8*Z*,11*Z*,14*Z*,17*Z*,20*Z*)-Tricosa-5,8,11,14,17,20-Hexaenal (**12**)

To a stirred solution of cyanide **11** (2.53 g, 7.86 mmol) in CH_2Cl_2 (1 mL) was added 1.0 M DIBAL-H in toluene (10.1 mL, 10.1 mmol) at −20 °C and the mixture was stirred for 1 h. The mixture was quenched with 10% aqueous potassium sodium tartrate at 0 °C and the mixture was extracted with EtOAc. The organic layer was washed with brine, dried over $MgSO_4$ and evaporated. The residue was chromatographed on silica gel (55 g, 3% EtOAc–hexane) to give aldehyde **12** (1.93 g, 75%). ^{1}H NMR ($CDCl_3$) δ: 9.87 (1 H, t, $J = 1.6$ Hz, H-1), 5.23–5.48 (12 H, m, H-5, 6, 8, 9, 11, 12, 14, 15, 17, 18, 20, 21), 2.78–2.91 (10 H, m, H-7, 10, 13, 16, 19), 2.45 (2 H, td, $J = 7.3$ Hz, 1.6 Hz, H-2), 2.02–2.18 (4 H, m, H-4, 22), 1.71 (2 H, quint, $J = 7.3$ Hz, H-3), 0.97 (3 H, t, $J = 7.5$ Hz, H-23); ^{13}C NMR ($CDCl_3$) δ: 202.4, 132.0, 129.1, 128.8, 128.6, 128.3, 128.23, 128.19, 128.12 (2 carbons), 128.08, 127.9, 127.0, 43.8, 26.9, 25.7 (2 carbons), 25.6 (2 carbons), 25.5, 21.9, 20.6, 14.3; HRMS (FAB): Calcd for $C_{23}H_{35}O$ $[M + H]^+$: 327.2688; found: 327.2696.

Methyl (5*Z*,8*Z*,11*Z*,14*Z*,17*Z*,20*Z*)-Tricosa-5,8,11,14,17,20-Hexaenoate (**13**)

A mixture of aldehyde **12** (1.93 g, 5.92 mmol), KOH (864 mg, 15.4 mmol) and I_2 (1.95 g, 7.70 mmol) in MeOH (75 mL) was stirred at 0 °C for 1 h. After addition of 10% solution of aqueous $Na_2S_2O_3$, the mixture was extracted with EtOAc. The organic layer was washed with brine, dried over $MgSO_4$ and evaporated. The residue was chromatographed on silica gel (40 g, 2% EtOAc–hexane) to give methyl ester **13** (1.91 g, 91%). ^{1}H NMR ($CDCl_3$) δ: 5.28–5.44 (12 H, m, H-5, 6, 8, 9, 11, 12, 14, 15, 17, 18, 20, 21), 3.67 (3 H, s, H-CO_2Me), 2.76–2.90 (10 H, m, H-7, 10, 13, 16, 19), 2.32 (2 H, t, $J = 7.4$ Hz, H-2), 2.04–2.12 (4 H, m, H-4, 22), 1.70 (2 H, quint, $J = 7.4$ Hz, H-3), 0.98 (3 H, t, $J = 7.5$ Hz, H-23); ^{13}C NMR ($CDCl_3$) δ: 174.0, 132.0, 128.9, 128.8, 128.6, 128.25, 128.24, 128.19, 128.15, 128.09 (2 carbons), 127.9, 127.0, 51.5, 33.4, 26.5, 26.63 (4 carbons), 25.5, 24.8, 20.6, 14.3; HRMS (FAB): Calcd for $C_{24}H_{37}O_2$ $[M + H]^+$: 357.2794; found: 357.2790.

(5*Z*,8*Z*,11*Z*,14*Z*,17*Z*,20*Z*)-Tricosa-5,8,11,14,17,20-Hexaenoic Acid (TrHA **2**)

A solution of ester **13** (1.19 g, 3.34 mmol) in 5% KOH/MeOH–H_2O (19:1, 16 mL) was stirred at 50 °C for 1 h. The reaction mixture was neutralized with 10% HCl aq. and extracted with EtOAc. The organic layer was washed with water, dried over $MgSO_4$, and evaporated. The residue was chromatographed on silica gel (110 g, 50% EtOAc–hexane) to give TrHA **2** (1.01 g, 88 %). ^{1}H NMR ($CDCl_3$) δ: 5.27–5.44 (12 H, m, H-5, 6, 8, 9, 11, 12, 14, 15, 17, 18, 20, 21), 2.76–2.91 (10 H, m, H-7, 10, 13, 16, 19), 2.37 (2 H, t, $J = 7.4$ Hz, H-2), 2.02–2.17 (4 H, m, H-4, 22), 1.70 (2 H, quint, $J = 7.4$ Hz, H-3), 0.97 (3 H, t, $J = 7.5$ Hz, H-23); ^{13}C NMR ($CDCl_3$) δ: 179.9, 132.0, 129.0, 128.8, 128.6, 128.27, 128.20, 128.19, 128.15 (2 carbons), 128.09, 127.9, 127.0, 33.4, 26.5, 25.6 (4 carbons), 25.5, 24.5, 20.6, 14.3; HRMS (FAB): Calcd for $C_{23}H_{35}O_2$ $[M + H]^+$: 343.2637; found: 343.2643.

Results and Discussion

Two fatty acids, THA **3** and Δ^2-THA **4**, were synthesized using DHA ethyl ester **5** as the starting material as shown in Scheme 1. Ester **5** was reduced with 1.2 equivalents of diisobutylaluminium hydride (DIBAL-H) at −78 °C to afford aldehyde **6** in 85% yield. Aldehyde **6** was subjected to the Horner–Wadsworth–Emmons reaction using trimethyl phosphonoacetate [31] to give two-carbon elongated α,β-unsaturated ester **7** in 94% yield as a mixture of 2*E*-isomer (87%) and 2*Z*-isomer (7%). These two isomers were separated easily by silica gel column chromatography. Regioselective hydrogenation of α,β-unsaturated ester **7** was achieved by reduction using Mg turnings in MeOH to provide **8** in good yield (81%) [31–33]. Ester **8** was treated with 5% KOH/MeOH–H_2O (19:1) to provide desired compound THA **3** in 87% yield. On the other hand, Δ^2-THA **4** was obtained in 99% yield upon treatment of 2*E*-**7** with 5% KOH/iPrOH–H_2O (19:1). Thus, THA **3** was synthesized in four steps in 56% overall yield and Δ^2-THA **4** was synthesized in three steps in 73% overall yield. Kuklev et al. [24] reported the synthesis of THA **3** from DHA methyl ester, via a malonic ester derivative as a precursor of two-carbon-elongated fatty acid; he reported a 21% overall yield achieved in five steps. Thus, our synthetic route is more facile and efficient than the previously reported route.

TrHA **2** was synthesized from DHA ethyl ester **5** as shown in Scheme 2. Ester **5** was reduced with DIBAL-H at 0 °C to afford alcohol **9** in 93% yield. Alcohol **9** was then treated with TsCl to give tosylate **10** in 89% yield. Tosylate **10** was treated with KCN at 70 °C to afford one-carbon-elongated cyanide **11** in 97% yield. Cyanide **11** was reduced with DIBAL-H to afford aldehyde **12** in 75% yield. Aldehyde **12** was converted to ester **13** in 91% yield by alkaline-iodine oxidation, a reaction previously developed by our group [34]. Ester **13** was treated with 5% KOH/MeOH–H_2O (19:1) to provide desired compound TrHA **2** in 88% yield. Thus, TrHA **2** was synthesized in six steps in 48% overall yield. To our knowledge, this is the first report of the chemical synthesis of TrHA **2**.

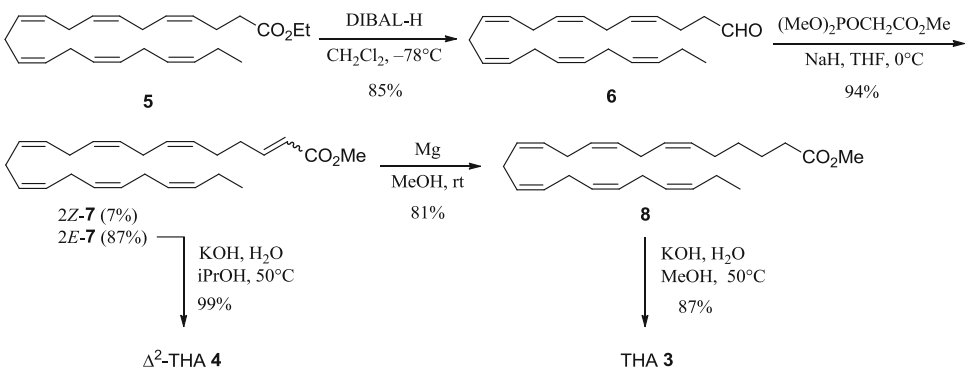

Scheme 1 Synthetic route from DHA ester to tetracosahexaenoic acid (**3**) and Δ^2-tetracosahexaenoic acid (**4**)

Scheme 2 Synthetic route from DHA ester to tricosahexaenoic acid (**2**)

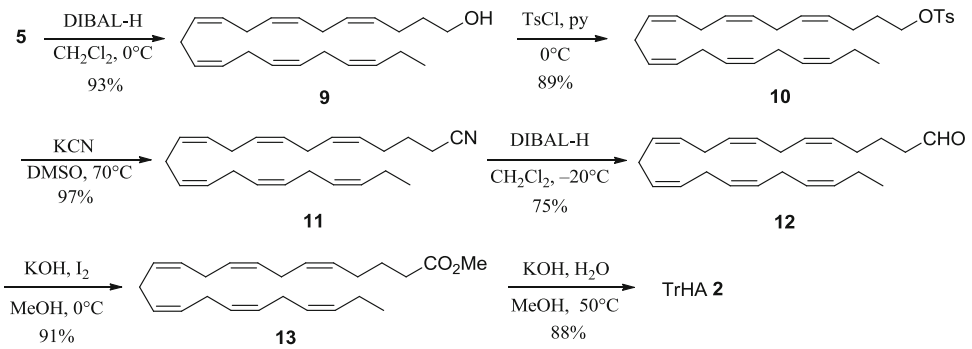

In conclusion, we have developed efficient chemical methods for the synthesis of the very-long-chain n-3 polyunsaturated fatty acids, THA **3**, Δ^2-THA **4** and TrHA **2**. Using these synthetic compounds, we are now investigating their biological activities and metabolism.

Acknowledgments We are grateful to Prof. Hirokazu Tamamura of Tokyo Medical and Dental University for support of this project. Part of this work was supported by a Grant-in-Aid for Young Scientist (no. 80536110) from the Ministry of Education, Culture, Sports, Science and Technology, Japan.

References

1. Alessandri JM, Guesnet P, Vancassel S, Astorg P, Denis I, Langelier B, Aïd S, Poumès-Ballihaut C, Champeil-Potokar G, Lavialle M (2004) Polyunsaturated fatty acids in the central nervous system: evolution of concepts and nutritional implications throughout life. Reprod Nutr Dev 44:509–538
2. Graham IA, Cirpus P, Rein D, Napier JA (2004) The use of very long chain polyunsaturated fatty acids to ameliorate metabolic syndrome: transgenic plants as an alternative sustainable source to fish oils. Nutr Bull 29:228–233
3. Nugent AP (2004) The metabolic syndrome. Nutr Bull 29:36–43
4. Scott B, Bazan N (1989) Membrane docosahexaenoate is supplied to the developing brain and retina by the liver. Proc Natl Acad Sci USA 86:2903–2907
5. Burdge G, Calder P (2005) Conversion of alpha-linolenic acid to longer-chain polyunsaturated fatty acids in human adults. Reprod Nutr Dev 45:581–597
6. Rapoport S, Rao J, Igarashi M (2007) Brain metabolism of nutritionally essential polyunsaturated fatty acids depends on both the diet and the liver. Prostaglandins Leukot Essent Fatty Acids 77:251–261
7. Rapoport SI, Igarashi M (2009) Can the rat liver maintain normal brain DHA metabolism in the absence of dietary DHA? Prostaglandins Leukot Essent Fatty Acids 81:119–123
8. Rapoport SI, Igarashi M, Gao F (2010) Quantitative contributions of diet and liver synthesis to docosahexaenoic acid homeostasis. Prostaglandins Leukot Essent Fatty Acids 82:273–276
9. Cordain L, Eaton SB, Sebastian A, Mann N, Lindeberg S, Watkins BA, O'Keefe JH, Brand-Miller J (2005) Origins and evolution of the Western diet: health implications for the 21st century. Am J Clin Nutr 81:341–354
10. Sprecher H (2000) Metabolism of highly unsaturated n-3 and n-6 fatty acids. Biochim Biophys Acta 1486:219–231
11. Voss A, Reinhart M, Sankarappa S, Sprecher H (1991) The metabolism of 7,10,13,16,9-docosapentaenoic acid to 4,7,10,13,16,19-docosahexaenoic acid in rat liver is independent of a 4-desaturase. J Biol Chem 266:19995–20000
12. Sprecher H, Luthria DL, Mohammed BS, Baykousheva SP (1995) Reevaluation of the pathways for the biosynthesis of polyunsaturated fatty acids. J Lipid Res 36:2471–2477
13. Moore SA, Hurt E, Yoder E, Sprecher H, Spector AA (1995) Docosahexaenoic acid synthesis in human skin fibroblasts involves peroxisomal retroconversion of tetracosahexaenoic acid. J Lipid Res 36:2433–2443
14. Su HM, Moser AB, Moser HW, Watkins PA (2001) Peroxisomal straight-chain Acyl-CoA oxidase and D-bifunctional protein are essential for the retroconversion step in docosahexaenoic acid synthesis. J Biol Chem 276:38115–38120
15. Astarita G, Jung KM, Berchtold NC, Nguyen VQ, Gillen DL, Head E, Cotman CW, Piomelli D (2010) Deficient liver biosynthesis of docosahexaenoic acid correlates with cognitive impairment in Alzheimer's disease. PLoS ONE 5:e12538
16. Kawasaki KI, Nabeshima YI, Ishihara K, Kaneniwa M, Ooizumi T (2000) High Level of 6,9,12,15,18,21-tetracosahexaenoic acid found in lipids of Ophiuroidea *Ophiura sarsi* Lutken. Fish Sci 66:614–615
17. Takagi T, Kaneniwa M, Itabashi Y (1986) Fatty Acids in Crinoidea and Ophiuroidea: occurrence of all-cis-6,9,12,15,18,21-tetracosahexaenoic acid. Lipids 21:430–433
18. Ota T, Chihara Y, Itabashi Y, Takagi T (1994) Occurrence of all-cis-6,9,12,15,18,21-tetracosahexaenoic acid in flatfish lipids. Fish Sci 60:171–175
19. Nichols PD, Danaher KT, Koslow JA (2003) Occurrence of high levels of tetracosahexaenoic acid in the jellyfish *Aurelia* sp. Lipids 38:1207–1210
20. Tomita Y, Ando Y (2009) Reinvestigation of positional distribution of tetracosahexaenoic acid in triacyl-*sn*-glycerols of flathead flounder flesh. Fish Sci 75:445–451
21. Rezanka T, Nedbalová L, Sigler K (2008) Odd-numbered very-long-chain polyunsaturated fatty acids from the dinoflagellate *Amphidinium carterae* identified by atmospheric pressure chemical ionization liquid chromatography–mass spectrometry. Phytochemistry 69:2849–2855
22. Rodríguez C, Henderson RJ, Porter AE, Dick JR (1997) Modification of odd-chain length unsaturated fatty acids by hepatocytes of rainbow trout (*Oncorhynchus mykiss*) fed diets containing fish oil or olive oil. Lipids 32:611–619
23. Rezanka T, Nedbalová L, Sigler K (2008) Identification of very-long-chain polyunsaturated fatty acids from *Amphidinium carterae* by atmospheric pressure chemical ionization liquid chromatography–mass spectroscopy. Phytochemistry 69:2391–2399
24. Kuklev DV, Popkov AA, Kas'yanov SP, Akulin VN, Bezuglov VV (1996) Synthesis of C2-elongated polyunsaturated fatty acids. Russ J Bioorg Chem 22:219–222
25. Baba N, Alam MK, Mori Y, Haider SS, Tanaka M, Nakajima S, Shimizu S (2001) A first synthesis of a phosphatidylcholine

bearing docosahexaenoic and tetracosahexaenoic acids. J Chem Soc Perkin Trans 1:221–223
26. Yamamoto K, Itoh T, Abe D, Shimizu M, Kanda T, Koyama T, Nishikawa M, Tamai T, Ooizumi H, Yamada S (2005) Identification of putative metabolites of docosahexaenoic acid as potent PPARγ agonists and antidiabetic agents. Bioorg Med Chem Lett 15:517–522
27. Itoh T, Murota I, Yoshikai K, Yamada S, Yamamoto K (2006) Synthesis of docosahexaenoic acid derivatives designed as novel PPARγ agonists and antidiabetic agents. Bioorg Med Chem 14:98–108
28. Itoh T, Yamamoto K (2008) Peroxisome proliferator activated receptorγ and oxidized docosahexaenoic acids as new class of ligand. Naunyn Schmiedebergs Arch Pharmacol 377:541–547
29. Itoh T, Fairall L, Amin K, Inaba Y, Szanto A, Balint BL, Nagy L, Yamamoto K, Schwabe JWR (2008) Structural basis for the activation of PPARγ by oxidized fatty acids. Nat Struct Mol Biol 15:924–931
30. Itoh T, Yoshimoto N, Yamamoto K (2010) Synthesis of oxidized fatty acid derivatives via an iodolactonization reaction. Heterocycles 80:689–695
31. Sakamaki Y, Inaba Y, Yoshimoto N, Yamamoto K (2010) Potent antagonist for the vitamin D receptor: vitamin D analogues with simple side chain structure. J Med Chem 53:5813–5826
32. Zarecki A, Wicha J (1996) Magnesium in methanol selective reduction of a conjugate double bond in an α,β-unsaturated ester related to pregnadiene. Synthesis 455–456
33. Youn IK, Yon GH, Pak CS (1986) Magnesium–methanol as a simple, convenient reducing agent for α,β-unsaturated esters. Tetrahedron Lett 27:2409–2410
34. Yamada S, Morizono D, Yamamoto K (1992) Mild oxidation of aldehydes to the corresponding carboxylic acids esters: alkaline iodine oxidation revised. Tetrahedron Lett 33:4329–4332

Lipids (2011) 46:463–467
DOI 10.1007/s11745-011-3550-4

METHODS

Mild Method for Preparation of 4,4-Dimethyloxazoline Derivatives of Polyunsaturated Fatty Acids for GC–MS

Vasily I. Svetashev

Received: 25 October 2010 / Accepted: 7 March 2011 / Published online: 3 April 2011

Abstract A mild and convenient method has been developed for preparing 4,4-dimethyloxazoline (DMOX) derivatives of fatty acids for GC–MS analysis. First, fatty acid methyl esters are converted to corresponding amides by incubation overnight at room temperature with 2-amino-2-methyl-1-propanol and a catalytic amount of sodium methoxide. The resulting 2-(methylpropanol) amides were isolated by partition between hexane–diethyl ether and water, and then converted to 4,4-dimethyloxazoline derivatives by treatment with trifluoroacetic anhydride under mild conditions (50 °C for 45 min). Structures of 2-methylpropanol amide and a DMOX derivative of oleic acid were confirmed by GC–MS. This method was applied to different FAME prepared from animal, plant or microbial lipids. The suggested method is most suitable for structure analysis of polyunsaturated fatty acids (PUFA) and for acids with double bonds in close to terminal positions. Application of the method is illustrated with spectra of the DMOX derivatives of 16:1(n-13), 24:5(n-6) and 24:6(n-3) acids.

Keywords GLC-MS · DMOX derivatives · Fatty acid structure analysis

Abbreviations

AMP	2-amino-2-methyl-1-propanol
DMOX	4,4-dimethyloxazoline
FAME	Fatty acid methyl ester(s)
FFA	Free fatty acid(s)
PUFA	Polyunsaturated fatty acid(s)
TFAA	Trifluoroacetic anhydride
TL	Total lipids
THA	Tetracosahexaenoic acid
TPA	Tetracosapentaenoic acid
GLC	Gas-liquid chromatography
MS	Mass spectrometry
TLC	Thin layer chromatography
NMR	Nuclear magnetic resonance
BSTFA	Bis(trimethylsilyl) trifluoroacetamide

V. I. Svetashev (✉)
A. V. Zhirmunsky Institute of Marine Biology, Russian Academy of the Sciences, Vladivostok 690041, Russia
e-mail: vsvetashev@mail.ru

Introduction

Fatty acid methyl esters (FAME) are generally accepted derivatives of fatty acids for analysis by GLC and GLC–MS. Methods for FAME preparation are now routine on a small scale and they have excellent chromatographic properties. FAME are most suitable for quantitative analysis, but have limited significance for structure analysis by mass spectrometry [1]. Methyl esters are useful for localization of some branching patterns (iso-, anteiso-), or oxygenated acid functions (2-OH, 3-OH) by MS. Polyenoic fatty acids often give a distinctive mass spectrometric fingerprint, which permits us to differentiate acids of n-3, n-6 and n-9 series, but does not prove the exact positions of double bonds. However, it is usually considered that methyl ester derivatives are not suitable for locating double bonds, especially in monoenoic fatty acids [1]. The main reason for this limitation is the bond migration in the unsaturated fatty acid alkyl chain during ionization. As a result, a number of nitrogen-containing derivatives have been suggested for GC–MS, because of the ability of nitrogen atom to stabilize the charge distribution, thus improving the information value of the spectra.

Of numerous nitrogen derivatives, mainly pyrrolidides [2, 3], DMOX [4, 5] and picolinyl esters [6] have found their use in GC–MS elucidation of fatty acid structure. Each derivative has advantages for GC–MS of fatty acids of a particular type; they are prepared by distinct methods, have different gas chromatographic properties and informativity of mass spectra. A recent review [1] provides comparative information for different derivatives useful in structure analysis of fatty acids.

There are several methods for the preparation of the respective derivatives; these methods have been thoroughly reviewed by Christie [7]. Preparation of acylpyrrolidides from FAME and glycerolipids is a relatively mild procedure [2]. At the same time, the usual direct one-step method for preparation of DMOX derivatives at 170–180 °C overnight [8] gives rise for concern about the risk of PUFA isomerization and/or degradation. This reaction is often incomplete, and on chromatograms some peaks were detected similar to target component mass spectra [9]. It has been also found that some FA can undergo isomerization upon such treatment. For example, *trans*-3-hexadecenoic acids, an essential component of plant phosphatidylglycerol, is mainly converted into *cis*-2-hexadecenoic acid [10]. Later, lengthier mild two-step methods for the preparation of oxazolines and DMOX derivatives [11, 12] have been developed. Methods based on the conversion of FAME or TL to free fatty acids and then to mixed anhydrides or acid chlorides with a subsequent reaction with ethanolamine or AMP. Resulting amides are cyclized by treatment with trifluoroacetic anhydride to target alkyl oxazolines or 4,4-dimethyloxazolines. Recently, a mild one pot-one step method for conversion carboxylic acids to range of amides and oxazolines has been reported [13]. In this method benzoxazoline, DMOX and 4-phenyloxazoline derivatives were prepared from FFA, a corresponding amine and fluorinating reagent Deoxo-Fluor at 0 °C. We present in this paper a mild and convenient method for preparation of DMOX derivatives starting from FAME.

Materials and Methods

Materials

Oleic acid, oleic acid methyl ester, methyl-2-hydroxytetradecanoate, trioleoylglycerol, (Sigma, USA), 2-amino-2-methyl-1-propanol, trifluoroacetic anhydride (Fluka, Germany) were used in the experiments. Chloroform, methanol, hexane, acetone, diethyl ether and benzene were redistilled. AMP was used as a 50%, (w/v) solution in benzene; it was stable at 5 °C for at least for 2 months. A 1% Na solution in methanol was prepared by careful dissolving sodium metal in cold methanol in a fume cupboard. The reagent is stable in tightly closed amber bottles for several months. Extracts of total lipids of the Alcyonaria *Gersemia rubiformis* and the fern *Polystichum subtripteron* were used in the experiments.

Extraction of Lipids and Preparation of FAME

Lipids were extracted from biological materials with chloroform/methanol [14]. FAME were prepared by the routine method [15] and purified by TLC in benzene or hexane/diethyl ether (9:1, by v/v).

Thin Layer Chromatography

Progress in the synthesis of the FA derivatives was controlled by TLC on aluminum sheets 10 × 10 cm with Silica gel 60 F_{254} Merck (Germany). The solvent system hexane/acetone (8:2, by v/v) was used for separation of FAME, FFA, acyl-2-methylpropanol amides, and DMOX derivatives. Spots on the chromatogram were visualized using iodine vapor or charring at 110 °C after spraying with 5% sulfuric acid in methanol.

Gas Chromatography and Gas Chromatography–Mass Spectrometry

GC and GC–MS analyses were performed on a GC 2010 chromatograph with a flame ionization detector and a gas chromatograph–mass spectrometer GCMS-QP5050, both Shimadzu (Japan). Fused silica capillary columns Supelcowax 10 and MDN-5S (both columns 30 m, 0.25 mm ID, 0.25 μm film, Supelco, USA) were used in the apparatus. FAME and DMOX derivatives were analyzed on Supelcowax 10 columns at 200 and 210 °C, respectively. On a nonpolar MDN-5S column, the temperature program started from 200 to 260 °C, 2 °C/min. Helium was used as the carrier gas at a linear velocity of 30 cm/sec. Mass spectra were recorded at 70 eV. Spectra were compared with the NIST library and internet fatty acid mass spectra archive site [7].

Preparation of DMOX Derivatives

To 1–3 mg of FAME or glycerolipids in a 2-ml vial with tightly fitting cap, were added 60 μl 50%, (w/v) AMP in benzene, this was mixed and 10 μl of $NaOCH_3$ reagent was added. After mixing, the vials were flushed with argon and incubated in the dark overnight at room temperature. Acyl-2-methylpropanol amides were isolated by partition between 0.5 ml hexane–diethyl ether 9:1, (v/v) and 0.5 ml water. Extraction was repeated with 0.5 ml hexane–ether. After solvent evaporation, acyl-2-methylpropanol amides were converted to DMOX by adding 150 μl TFAA and

incubated at 50 °C for 45 min. TFAA was evaporated under an argon stream. Derivatives were dissolved in hexane and washed with water to remove the residues of the reagents. Samples prepared from FAME were ready for GC or GC–MS. Samples prepared from total lipids, phospholipids or triacylglycerols needed additional purification by TLC or on a small silica gel column.

Results and Discussion

The current study presents a new method for the preparation of DMOX derivatives of fatty acids. The general plan of the synthesis is shown in Scheme 1. We used a modified method for the preparation of fatty amides or ethanolamides by low temperature aminolysis of FAME and laurel oil, catalyzed by sodium methoxide [16, 17]. The first experiments demonstrated that incubation of MEFA with AMP gives either no or very low yields of amides at room temperature or at 60 °C even after 24 h. An addition of a catalytic amount of $NaOCH_3$ resulted in conversion of FAME to the respective amides at room temperature overnight (Fig. 1). TLC analysis also demonstrated that FAME are more stable to catalytic amidation than triacylglycerols, TL and PL are, and therefore all experiments were conducted on methyl oleate. The use of methyl esters is especially convenient, since FAME are generally accepted derivatives in GC analysis. The proposed method has two main advantages. First, acyl-2-methylpropanol amides were prepared at room temperature and conversion to DMOX derivatives completed at 50 °C. Second, the method is simple, because it does not involve preparation of FFA and then acid halides or mixed anhydrides from TL or MEFA as the two-step method does [11–13]. The samples prepared for GC–MS contain only traces of MEFA.

The structure of oleoyl-2-methylpropanol amide was characterized by H^1NMR and after derivatization with BSTFA by GC–MS (data not shown). DMOX derivatives were characterized by TLC and GC–MS (see Figs. 1, 2). All spectra support the structures depicted in Scheme 1.

Figure 2a shows the spectrum of the DMOX derivative of the Δ3 isomer of hexadecenoic acid from the TL extract of the fern *Polystichum subtripteron*. The spectrum of this acid is very similar to those of Δ3-16:1 [10], and Δ3-18:1 [18] with the main characteristic peaks at *m/z* 152 (base) and 166. Since the peak with *m/z* 110 characteristic of acids

Fig. 1 TLC of starting materials, an intermediate (oleoyl-2-methylpropanol amide), and the final product (oleic acid DMOX). *Lane 1* standard FFA and ME of oleic acid, *Lane 2* oleoyl-2-methylpropanol amide, *Lane 3* DMOX derivative of oleic acid. Solvent system: chloroform/acetone (8:2, by v/v). Detection: charring at 110 °C after spraying with 5% H_2SO_4 in methanol

with a double bond at position 2 [18] was not observed, it seems, no isomerization took place during the DMOX preparation. The method described here has also been used successfully for PUFA of fish oil. Besides the usual acids of the n-3 series, we have also found an acid with a spectrum similar to the DMOX derivative of 16:4(n-1) (data not shown). Therefore, this method can be applied to fatty acids with a terminal position of the double bond.

Figures 2b and c show mass spectra of two tetracosapolyenoic acids, 24:5(n-6) and 24:6(n-3), that were prepared from total lipids of the Alcyonaria *Gersemia rubiformis*. Earlier, these very-long-chain PUFA were found in marine representatives of the phylum Cnidaria [19]. In both spectra, the double bond in position 6 was evident by the characteristic fingerprint of ions at *m/z* 126

Scheme 1 Preparation of DMOX derivatives from FAME

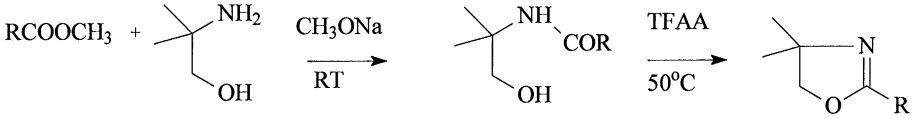

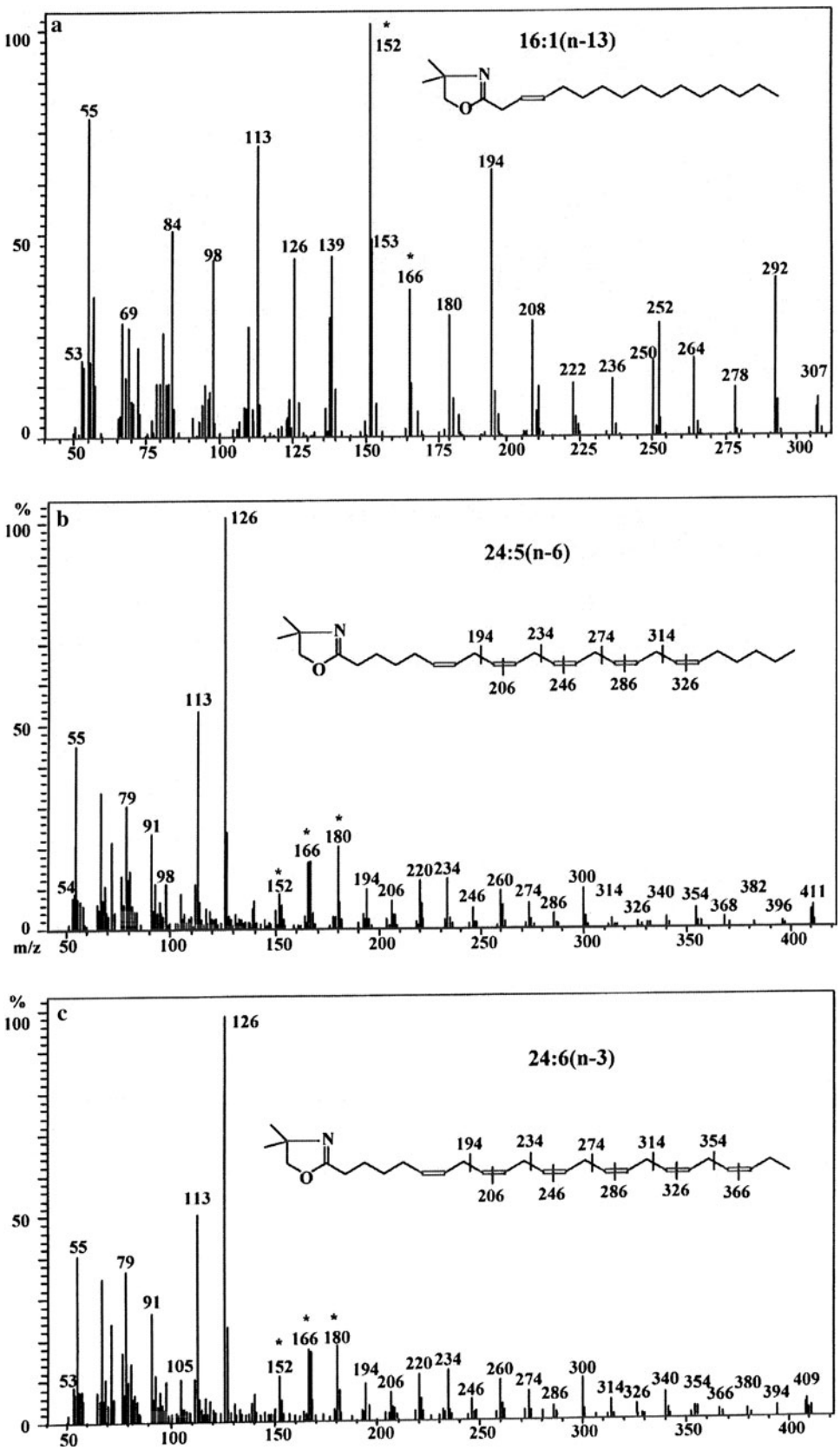

Fig. 2 Mass spectra of DMOX derivatives prepared from MEFA of total lipid extracts. **a** hexadecenoic acid from the fern *Polystichum subtripteron*; **b** and **c** tetracosapentaenoic 24:5(n-6) and tetracosahexaenoic 24:6(n-3) acids from the Alcyonaria *Gersemia rubiformis*

(base), 152, 166 and 180 [18]. The locations of the remaining double bonds were revealed by a gap of 12 amu, as shown on Figs. 2b and c.

Our attempt to prepare DMOX derivative from methyl-2-hydroxytetradecanoate by the suggested method was unsuccessful. A previous effort to synthesize DMOX derivatives of saturated 2-hydroxy fatty acids by the two-step method has also failed [7].

This method can probably be applied for the preparation of other nitrogen-containing derivatives of fatty acids suitable for GC–MS.

References

1. Dobson G, Christie WW (2002) Spectroscopy and spectrometry of lipids–Part 2 Mass spectrometry of fatty acid derivatives. Eur J Lipid Sci Technol 104:36–43
2. Andersson BA, Holman RT (1974) Pyrrolidides for mass spectrometric determination of the position of the double bond in monounsaturated fatty acids. Lipids 9:185–190
3. Andersson BA, Christie WW, Holman RT (1975) Mass spectrometric determination of positions of double bonds in polyunsaturated fatty acid pyrrolidides. Lipids 10:215–219
4. Yu QT, Liu BN, Zhang JY, Huang ZH (1989) Location of double bonds in fatty acids of fish oil and rat testis lipids. Gas chromatography–mass spectrometry of the oxazoline derivatives. Lipids 24:79–83
5. Spitzer V (1997) Structure analysis of fatty acids by gas chromatography–low resolution electron impact mass spectrometry of their 4, 4-dimethyloxazoline derivatives—a review. Prog Lipid Res 35:387–408
6. Harvey DJ (1992) Mass spectrometry of picolinyl and other nitrogen-containing derivatives of fatty acids. In: Christie WW (ed) Advances in lipid methodology. The Oily Press, Ayr, pp 19–80
7. Christie WW Mass spectrometry of fatty acid derivatives. www.lipidlibrary.aocs.org./ms/masspec.html. Accessed 4 August, 2010
8. Fay L, Richli U (1991) Location of double bonds in polyunsaturated fatty acids by gas chromatography–mass spectrometry after 4, 4-dimethyloxazoline derivatization. J Chromatogr 541:89–98
9. Christie WW (1998) Gas chromatography–mass spectrometry methods for structural analysis of fatty acids. Lipids 33:343–353
10. Lamberto M, Ackman RG (1995) Positional isomerization of *trans*-3-hexadecenoic acid employing 2-amino-2methyl-propanol as a derivatizing agent for ethylenic bond location by gas chromatography/mass spectrometry. Anal Biochem 230:224–228
11. Kuklev DV, Smith WL (2003) A procedure for preparing oxazolines of highly unsaturated fatty acids to determine double bond positions by mass spectrometry. J Lipid Res 44:1060–1066
12. Christie WW (1998) Mass spectrometry of fatty acids with methylene-interrupted ene-yne systems. Chem Phys Lipids 94:35–41
13. Kangani CO, Kelley DE, Evans RW (2007) Synthesis and mass spectrometry of benzoxazoline, dimethyloxazoline and 4-phenyloxazoline derivatives of polyunsaturated fatty acids. Rapid Commun Mass Spectrom 21:2129–2136
14. Bligh EG, Dyer WJ (1959) A rapid method of total lipid extraction and purification. Can J Biochem Physiol 37:911–917
15. Carreau JP, Dubacq JP (1978) Adaptation of macro-scale method to the micro-scale for fatty acid methyl transesterification of biological lipid extracts. J Chromatogr 151:384–390
16. Jordan EF, Port WS (1961) Low temperature aminolysis of methyl stearate catalyzed by sodium methoxide. JAOCS 38:600–605
17. Kolancilar H (2004) Preparation of laurel oil alkanolamide from laurel oil. JAOCS 81:597–598
18. Christie WW, Robertson GW, McRoberts WC, Hamilton JTG (2000) Mass spectrometry of the 4,4-dimethyloxazoline derivatives of isomeric octadecenoates (monoenes). Eur J Lipid Sci Technol 102:23–29
19. Vysotskii MV, Svetashev VI (1991) Identification, isolation and characterization of tetracosapolyenoic acids in lipids of marine coelenterates. Biochim Biophys Acta 1083:161–165

Lipids (2011) 46:469–477
DOI 10.1007/s11745-010-3493-1

METHODS

Quantitative Analysis of Phospholipids Using Nanostructured Laser Desorption Ionization Targets

Simona Colantonio · John T. Simpson · Robert J. Fisher · Amichai Yavlovich · Julie M. Belanger · Anu Puri · Robert Blumenthal

Received: 24 August 2010 / Accepted: 20 October 2010 / Published online: 15 February 2011

Abstract Since its introduction as an ionization technique in mass spectrometry, matrix-assisted laser desorption ionization (MALDI) has been applied to a wide range of applications. Quantitative small molecule analysis by MALDI, however, is limited due to the presence of intense signals from the matrix coupled with non-homogeneous surfaces. The surface used in nano-structured laser desorption ionization (NALDI) eliminates the need for a matrix and the resulting interferences, and allows for quantitative analysis of small molecules. This study was designed to analyze and quantitate phospholipid components of liposomes. Here we have developed an assay to quantitate the DPPC and $DC_{8,9}PC$ in liposomes by NALDI following various treatments. To test our method we chose to analyze a liposome system composed of DPPC (1,2-dipalmitoyl-*sn*-glycero-3-phosphocholine) and $DC_{8,9}PC$ (1,2-bis(tricosa-10,12-diynoyl)-*sn*-glycero-3-phosphocholine), as $DC_{8,9}PC$ is known to undergo cross-linking upon treatment with UV (254 nm) and this reaction converts the monomer into a polymer. First, calibration curves for pure lipids (DPPC and $DC_{8,9}PC$) were created using DMPC (1,2-dimyristoyl-*sn*-glycero-3-phosphocholine) as an internal standard. The calibration curve for both DPPC and $DC_{8,9}PC$ showed an R^2 of 0.992, obtained using the intensity ratio of analyte and internal standard. Next, DPPC:$DC_{8,9}PC$ liposomes were treated with UV radiation (254 nm). Following this treatment, lipids were extracted from the liposomes and analyzed. The analysis of the lipids before and after UV exposure confirmed a decrease in the signal of $DC_{8,9}PC$ of about 90%. In contrast, there was no reduction in DPPC signal.

Keywords NALDI · MALDI · Mass spectrometry · Lipids · Quantitation · Drug delivery

Abbreviations

9-AA	9-Aminoacridine
$DC_{8,9}PC$	(1,2-bis(tricosa-10,12-diynoyl)-*sn*-glycero-3-phosphocholine)
DHB	2,5-Dihydroxybenzoic acid
DIOS	Desorption ionization on silica
DMPC	1,2-Dimyristoyl-*sn*-glycero-3-phosphocholine
DPPC	1,2-Dipalmitoyl-*sn*-glycero-3-phosphocholine
ESI	Electrospray ionization
GALDI	Graphite-assisted laser desorption/ionization
GC	Gas chromatography
HPLC	High-performance liquid chromatography
LC	Liquid chromatography
LDI	Laser desorption ionization
MALDI	Matrix-assisted laser desorption/ionization
MS	Mass spectrometry
NALDI	Nano-assisted laser desorption/ionization
TOF	Time-of-flight

Electronic supplementary material The online version of this article (doi:10.1007/s11745-010-3493-1) contains supplementary material, which is available to authorized users.

S. Colantonio (✉) · J. T. Simpson · R. J. Fisher
Protein Chemistry Laboratory, Advanced Technology Program, SAIC-Frederick/NCI-Frederick, PO Box B, Bldg 469/Rm 237, Frederick, MD 21702, USA
e-mail: colantos@mail.nih.gov

A. Yavlovich · J. M. Belanger · A. Puri · R. Blumenthal
Membrane Structure and Function Section, Center for Cancer Research, Nanobiology Program, NCI-Frederick, NIH, Frederick, MD 21702, USA

Introduction

Chromatography has been the traditional technique of choice for the analysis of lipids. Thin-layer chromatography [1] and liquid chromatography [2] have been the most widely used methods in the field, especially in combination with UV detection [3]. Those techniques are well-established and robust but they are also time-consuming, because they often involve steps of derivatization and long separation times [4]. Spectroscopic methods, such as IR and NMR, have been applied in the lipid analysis field as well [3]. The first use of mass spectrometry for the analysis of lipids was reported by Gohlke in 1959 [5] using gas chromatography mass spectrometry (GC–MS). Mass spectrometry provides information on the molecular weight of the species of interest that can be useful for identification purposes. Since then GC–MS has been applied to many analytical questions regarding the biology and chemistry of lipids [6], however GC–MS may require derivatization when the analyte is not volatile and thermally stable [7]. While derivatization may help, in some cases it results in additional steps that can complicate the entire analysis [8].

In recent years with the introduction of the so-called "soft ionization" techniques, electrospray ionization (ESI) and matrix-assisted laser desorption ionization (MALDI), [9] that allow for the analysis of intact lipids [10], mass spectrometry has gained importance in the analysis of lipid mixtures [11] and in the rapidly growing field of mass spectrometry tissue imaging [12]. Electrospray ionization is the most frequently used mass spectrometry technique for lipid analysis, but MALDI represents a powerful tool in this field, because the time necessary for the analysis can be reduced to less than one minute per sample [10]. ESI mass spectrometry in association with liquid chromatography (LC) allows for separation and identification of molecular species, however analysis times can be long and the buffers used for LC/MS are often incompatible with lipid solubility.

In MALDI, the sample is mixed with a solution of matrix that absorbs the laser energy. The mixture is allowed to dry to form co-crystals on the surface of target. The homogeneity of the solid crystals on the plate is essential for the reproducibility of the analysis, therefore accurate sample preparation is necessary [10]. In most cases, the matrix is soluble in the same organic solvents as the lipid analytes, so very homogenous co-crystals are produced facilitating the analysis.

The choice of the most suitable matrix is often quite challenging. While water soluble analytes have a wide range of useful matrices [13], only a few matrices have been utilized for lipid analysis due to their lipophilic nature. Recently Teuber et al. [14] compared a series of matrices for lipids. Along with the most commonly used DHB (2,5-dihydroxybenzoic acid), other matrices showed interesting characteristics, especially a newly synthesized compound, α-cyano-2,4-difluorocinnamic acid, for analysis of charged phospholipids, and 9-aminoacridine (9-AA) for both positive [14, 15] and negative ion analysis [16–19]. In particular the interest in 9-AA, as a matrix for lipids analysis in MALDI, has recently been applied by Benaddellah et al., for lipid negative ion analysis in a tissue imaging study that compares MALDI-TOF and secondary ion mass spectrometry [20]. For small molecule analysis it is necessary to choose a matrix that does not generate polymers by photochemical reactions (e.g. sinapinic acid), because the polymerization products will saturate the detector [4] and suppress the signal from the analytes. In addition the presence of interfering peaks due to matrix adducts (e.g. DHB with Na^+), [21] in the lower *m/z* range is a crucial issue in the analysis of small molecules, therefore other approaches have been taken into consideration. Some studies suggested the use of high molecular weight matrices such as *meso*-tetrakis(pentafluorophenyl)porphyrin [22–24] for the analysis and quantification of fatty acids. In this case the signals due to molecular ions of the matrix or its impurities, adducts or clusters are in a higher mass range and do not overlap with the analyte signal.

Recently matrix-free laser desorption ionization (LDI) has become a promising approach in the field of small molecules. In this case the sample is applied onto a surface that absorbs the laser energy without the use of additional compounds. The direct deposition of the sample involves minimal sample preparation and practically no signal from the support surface [21]. Silicon has been one of the first materials to be used as a suitable support for matrix-free LDI [25]. Its surface can be easily oxidized and modified to trap the analyte and it has high absorptivity in the UV, therefore it can act like the matrix itself. This technique, termed desorption ionization on silica (DIOS), has been applied to a number of small molecule analytes [26]. The use of silicon as a LDI mass spectrometry support has evolved with the recent introduction of silicon nanowires [27]. Muck et al. [28] provided evidence of the superiority of this approach compared with other traditional techniques that use energy absorbing matrices of questionable purity and stability. Other nanostructures have interesting characteristics. Carbon nanotubes have shown low signal background and good capability to transfer energy to the analytes [29–31]. Carbon nanotubes often have solubility issues, however. Ren et al. [31] used oxidization to improve solubility and produced a more homogeneous phase with reproducible analysis.

Graphite, a polymorph of the element carbon, has been applied by several groups to MALDI analysis. Graphite-assisted laser desorption/ionization (GALDI) has been successfully used in different applications [32], in particular for protein and peptides [33] and small molecules such as triterpenes [34, 35]. More recently colloidal graphite has been introduced as a support for MALDI imaging studies of small metabolites from fruits and plants [36, 37] and cerebrosides from direct analysis of rat brain tissue [38].

An issue with the use of nano-structured materials is that they are produced by a random process [26] that cannot always guarantee a homogeneous surface where the sample should be applied. In contrast, ZnO nanowires can be selectively grown on a substrate, are easy to synthesize, and their orientation can be controlled, so that on a flat substrate they can be organized as vertical wire arrays with defined dimension and structure [39]. ZnO presents characteristics that are particularly suitable for many industrial applications [40, 41]. It is a semi-conductive material that can absorb energy from the laser in wavelengths typically used in MALDI and transfer it to the analyte. ZnO nanoparticles have been successfully applied to the desorption/ionization of several small molecules, from drugs to lipids [42]. Kang et al. [41] compared a suspension of analyte/ZnO nanowires and the direct deposition of the analyte onto the surface of a nanowire chip. The nanowire chip showed better performance and a potential applicability to quantitative analysis.

There are few examples in the literature of matrix-free LDI applications for lipids. Other small molecules, such as fatty acids, have been analysed by DIOS [43] and with silicon nano-wires in association with lithium hydroxide [28]. Diamond-like carbon matrix-free targets have been proven to be capable of absorbing laser energy and transferring it to a wide range of analytes, including lipids [44]. Another interesting application of a matrix-free approach for lipids analysis is the one proposed by Vidova et al. [45] for mice kidney tissue imaging experiments. This study makes use of a commercially available nanostructured surface (NALDI^{TM} chip, Bruker Daltonics) as a support in LDI MS and allows the identification of a slightly higher number of lipids species compared to analysis performed with alpha-cyano-4-hydroxy cinnamic acid as matrix in MALDI.

In this study we demonstrate how a NALDI^{TM} chip can be used as a support for desorption/ionization applied for small molecule quantitative analysis. We have examined two phospholipids, DPPC and $DC_{8,9}PC$, that have been recently used for development of photo-triggerable liposomes [46–48]. Our system represents a novel and elegant method to determinate the concentrations of the two phospholipids of interest in the liposomes. This methodology bears the potential for future applications for the analysis of molecules with similar chemical and physical properties.

Methods and Materials

Liposome Preparation and Treatment

Liposome Reagents

DPPC (1,2-dipalmitoyl-*sn*-glycero-3-phosphocholine) and DMPC (1,2-dimyristoyl-*sn*-glycero-3-phosphocholine) were purchased from Avanti Polar Lipids, Inc. (Alabaster, AL) as solutions in chloroform. $DC_{8,9}PC$ (1,2-bis(tricosa-10, 12-diynoyl)-*sn*-glycero-3-phosphocholine) was synthesized by Dr. Alok Singh at the Naval Research Laboratory (Washington, DC) using a previously published procedure [46]. Methanol HPLC grade was purchased from OmniSolv (EMD Chemicals, Inc., Gibbstown, NJ), while Chloroform ACS was from Fisher Scientific (Pittsburgh, PA).

Preparation of Liposomes

Liposomes were prepared using the probe sonication essentially as described [46]. Briefly, DPPC:$DC_{8,9}PC$ (80:20 mol%) lipid mixtures were mixed in a glass tube. The lipid film was formed by removing the solvent under nitrogen and any residual chloroform was removed by placing the film overnight in a vacuum desiccator. To encapsulate calcein, the lipid film was reconstituted in HEPES buffer (HBS, 10 mM HEPES, 140 mM NaCl, pH 7.5) containing self-quenched concentration of calcein (0.1 M at pH 7.2–7.6). Unilamellar vesicles were formed by sonication at 4 °C for 5–10 min (1 min pulses and 1 min rest) using a Probe Sonicator (W-375 Heat Systems-Ultrasonics, New York, USA). The samples were centrifuged to remove any titanium particles and larger aggregates. Solute-loaded liposomes were separated from unentrapped calcein using a size exclusion gel chromatography column (Bio Gel A0.5 m, 1 × 40 cm, 40 ml bed volume).

UV Treatment

Liposomes were placed in a 96-well plate (total volume of 0.2 ml) as described [47], and irradiated with a UV lamp (UVP, short wave assembly, 115 V, 60 Hz) at 254 nm in a distance of 1 inch for 45 min. We routinely examined calcein leakage and $DC_{8,9}PC$ photo-crosslinking to confirm the modification in our liposome preparations as previously described [46, 47]. For mass spectrometry analysis (see below) lipids were extracted according to the Bligh/Dyer method [49].

Mass Spectrometry Analysis

Reagents

Methanol was HPLC grade (OmniSolv, EMD Chemicals, Inc., Gibbstown, NJ). Chloroform was HPLC grade from Chromasolv (Sigma–Aldrich, St. Louis, MO). Water was LC–MS grade from J. T. Baker (Mallinckrodt Baker Inc., Phillipsburg, NJ). Cesium chloride (CsCl, 99.9%) was purchased from Sigma–Aldrich (St. Louis, MO).

Sample Preparation

Sample preparation used only glassware and Wiretrol disposable glass micropipettes (Drummond Scientific Company, Broomall, PA). The lipid films obtained from Bligh–Dyer extraction were reconstituted in 200 μL of chloroform, then diluted 1:10 in a mixture methanol/chloroform, 1/1, v/v. Standard solutions for each lipid were prepared in methanol/chloroform, 1/1, v/v. DMPC was used as an internal standard at a concentration of 25 ng/μL in methanol/chloroform, 1/1, v/v. A CsCl solution, 50 mM in methanol, was used as a matrix additive to promote formation of [M + Cs] pseudo molecular ions for the lipids studied. Calibration curves were created for the phospholipid combination by mixing $DC_{8,9}PC$ in equal volume (5 μL) with the corresponding dilution of DPPC, followed by addition of 5 μL of DMPC 25 ng/μL and 15 μL of CsCl 50 mM. Concentration ranges for DPPC and $DC_{8,9}PC$ were 10–200 and 2.5–100 ng/μL, respectively. We washed the NALDI target twice with HPLC grade chloroform and allowed to dry prior to use. The standard solutions were mixed and 3 μL spotted onto the surface of a NALDI chip (Bruker Daltonics, Billerica, MA). Standards were spotted in triplicate. In a similar fashion, 10 μL of the diluted sample solutions were mixed with DMPC 25 ng/μL (5 μL) and CsCl 50 mM (15 μL) and 3 μL of each solution spotted in triplicate onto the surface of the same target where the corresponding standard solutions were spotted.

Mass Spectrometry Analysis

All spectra were acquired on a Bruker Ultraflex III TOF/TOF mass spectrometer (Bruker Daltonics, Billerica, MA). Spectra of intact lipids were acquired in positive ion reflector mode, with no ion extraction delay. Ion source voltage 1 was 25 kV, ion source voltage 2 was 21.30 kV and lens voltage was 9.52 kV. Reflectron and reflectron 2 were 29.50 and 13.84 kV, respectively. Deflection was set at 600 Da. Monoisotopic masses were determined using FlexAnalysis 3.0 (Bruker Daltonics) with the SNAP peak picking algorithm. The instrument was calibrated in reflector mode using peptide standards of the Bruker peptide calibration kit (Bruker Daltonics, Billerica, MA). Data acquisition and peak analysis were completely automated with an accumulation of 1,200 shots using a random walk pattern. To create the calibration curves, intensity ratios of the analyte signal relative to the intensity of the internal standard were calculated and averaged from the three measurements at each concentration.

Results and Discussion

Phospholipids are the basis of cellular structures and because of their amphiphilic properties, they have the natural tendency to form a bilayers in an aqueous system [3]. These unique properties allowed A.D. Bangham to formulate the first preparation of liposomes with encapsulated materials in 1965 [50]. Since then, scientists have concentrated their efforts to take advantage of the characteristics of liposomes to understand the biophysical properties of membranes, study lipid interactions and to create efficient drug delivery systems [48, 51–54]. The evolution of this concept led Yavlovich et al. [46] to design an innovative liposome formulation for potential use as an efficient drug release system in appropriate organs and at the appropriate times. They were able to co-assemble several phospholipids (e.g. DPPC and EggPC) and $DC_{8,9}PC$ in the liposome bilayer. $DC_{8,9}PC$, a phospholipid with reactive diacetylenic groups, is known to undergo a photo cross-linking reaction when treated with UV radiation (254 nm) [55, 56]. Similar photo-crosslinking was observed when $DC_{8,9}PC$ was embedded in DPPC bilayers at mole ratios 1:9 and above leading to release of entrapped liposome contents [46]. It was hypothesized that photo cross-linking generates local defects in the liposome membrane that can promote drug release.

The detailed analysis of the individual lipids in these liposomes is critical to understand the nature of molecular interactions that result in photo-crosslinking and such information may improve design of these formulations. Initially, we set out to develop a quantitative method for the analysis of these lipids by MALDI mass spectrometry. MALDI-TOF MS has not been considered the first choice for quantitative analysis of lipids or other small molecular weight molecules for two main reasons: first the presence of matrix peaks and adducts in the low molecular range can interfere with analyte peak detection and second, inhomogeneity of the matrix/sample crystallization process reduces shot-to-shot reproducibility. Therefore, a matrix-free approach was chosen to avoid the disadvantages of the matrix and selected nanowire targets which had been

shown to be applicable to quantitative analysis of small molecules [41, 57].

In our initial method development we observed in the lipid spectra the presence of multiple peaks related to the analyte of interest—protonated and sodiated adducts—and realized this could present difficulties in data analysis and reproducibility of the assay. Considering the work of Schiller et al. [58], we decided to use CsCl as a cationization agent. Using CsCl, the MS signal of the phospholipids was shifted by 133 Da corresponding to the atomic mass of cesium. Other groups chose cesium acetate [24] and they were also able to obtain dominant cesiated adducts. Our analytes, dissolved in a mixture of chloroform/methanol, were mixed with a methanolic solution of cesium chloride prior to spotting on the NALDI target. Cesium chloride is soluble in water but not in chloroform/methanol; therefore we prepared a stock solution of 1 M cesium chloride in water and diluted to our working concentration—50 mM—in methanol, so it would be miscible with our analyte dilution buffer (chloroform/methanol, 50/50, v/v). We tried to use other, less volatile solvents to facilitate the sample dilution procedure, but a decrease in the quality of the spots was observed, and consequently of the analysis, probably due to solubility issues related to the lipophilic nature of the analytes.

The choice of organic solvents such as chloroform and methanol necessitated the use of glassware and glass micropipettes for the sample preparation. We observed an advantage in the use of volatile solvent systems: the rapid evaporation of the solvent mixture promoted an efficient co-crystallization of lipids and cesium chloride, resulting in homogeneous spots, as previously observed by other investigators [59]. Homogenous spots, along with triplicate analyses, allowed us to control variability issues, such as shot-to-shot, region-to-region and sample-to-sample [59, 60] variability. The possibility of bias acquisition was considered and therefore we opted for a completely automated acquisition of data collecting 1,200 shots, in a random walk pattern and with an intensity of laser between 15 and 60% in order to avoid saturation of the instrument. A better reproducibility was observed with the average of 1,200 spectra, rather than with a smaller number of acquisitions for each spot.

Release of contents from DPPC: $DC_{8,9}PC$ 4:1 liposomes occurs as a result of UV-triggered $DC_{8,9}PC$ polymerization in the bilayer [46]. Therefore the liposomes were loaded with 50 mM calcein and its release was monitored after treatment with UV (254 nm) for 45 min using a fluorescent micro plate reader (Methods section). Before and after UV treatment liposome lipids were extracted and analyzed by the NALDI mass spectrometry method.

MALDI signals for DPPC and $DC_{8,9}PC$ were linear over the selected ranges and the calibration curves resulted in coefficient of determinations (R^2) = 0.99, as shown in Fig. 1. Figure 2 shows two examples of spectra obtained from the lipids extracted and treated as described above. The decrease in intensity of the signal of the pseudo molecular ion for $DC_{8,9}PC$ after UV treatment is evident. We were able to determine the concentration for both DPPC and $DC_{8,9}PC$ using the equation from the linear regression for each compound. Figure 3 compares the concentration, expressed in μM, for both species before and after UV treatment. The concentration of DPPC remained constant (260 μM) while $DC_{8,9}PC$ decreased from 120 μM in the starting liposome to 12 μM in the liposome treated with 254 nm irradiation.

It is important to mention that the possibility of ion suppression and ionization efficiencies of the individual lipids we analyzed was considered. This is a common drawback in any mass spectrometry assay and we attempted to overcome this issue with the use of DMPC as the internal standard as it is structurally similar to the analytes of interest. The use of internal standards for quantitative analysis is standard practice [24, 61–63] and it is of crucial importance in any MALDI approach to these types of analyses. However in some cases a suitable internal standard may not be available, but reasonable quantitation may still be possible [64]. For optimal results, the use of a stable isotope analog of the analyte of interest would be the primary choice [63] for an internal standard, but in our case the available stable label analog of DPPC was not of sufficient purity for use as an internal standard so we chose a slightly smaller saturated PC as our internal standard.

By application of this novel MS method to the analysis of the phospholipids extracted from liposomes prepared and treated as described by Yavlovich et al. [46], we were

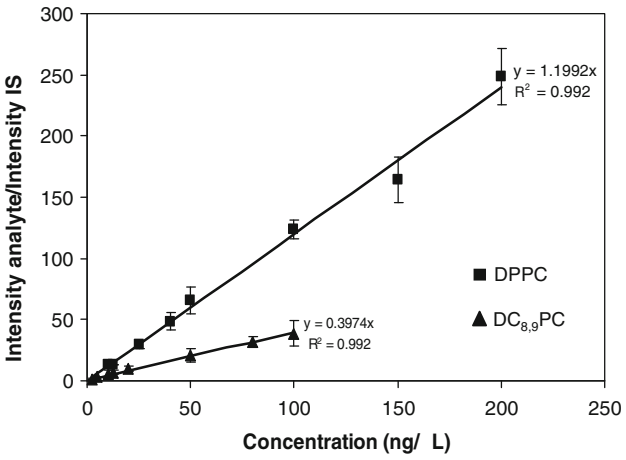

Fig. 1 Calibration curves for DPPC and $DC_{8,9}PC$. Concentration ranges for DPPC and $DC_{8,9}PC$ were respectively 10–200 ng/μL and 2.5–100 ng/μL

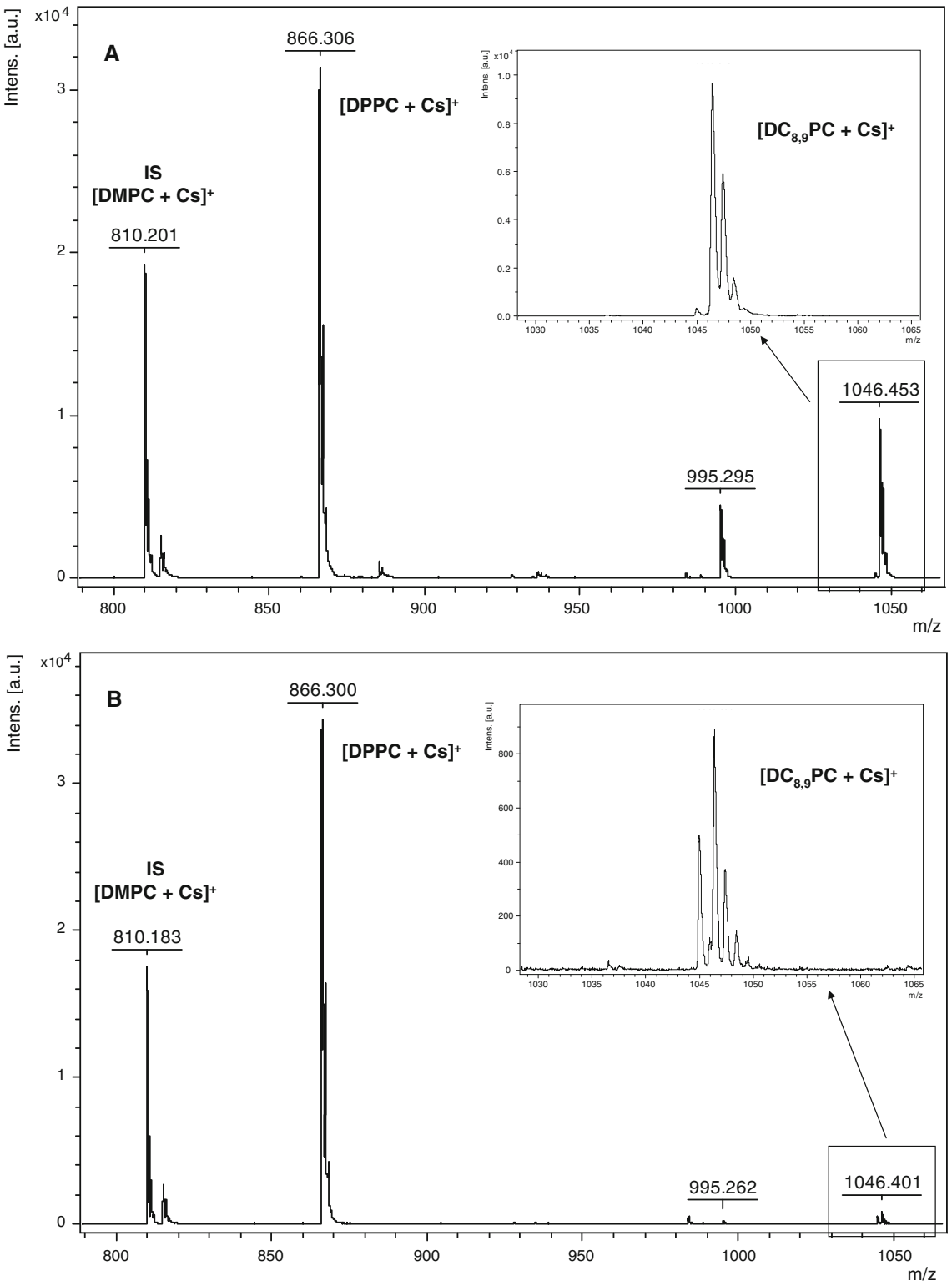

Fig. 2 Mass spectra of phospholipids from liposome before (**a**) and after (**b**) UV treatment (254 nm)

able to confirm the decrease of $DC_{8,9}PC$ from 120 μM to 12 μM, before and after the UV treatment (Fig. 3). As expected DPPC concentration did not change. It has been demonstrated that $DC_{8,9}PC$ liposomal photo-triggering by UV light occurs via direct photopolymerization mechanism [46].

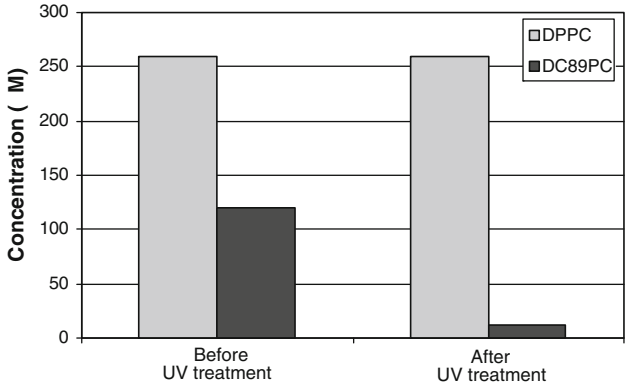

Fig. 3 Quantitative comparison of DPPC and $DC_{8,9}PC$ in liposome before and after UV treatment. A decrease of $DC_{8,9}PC$ from 120 μM to 12 μM, before and after the UV treatment, was observed, while the concentration of DPPC remained unchanged following exposure of the intact liposome at 254 nm irradiation

Conclusion

The NALDI-based analysis of the phospholipids presented here provides a fast and reproducible approach for the quantitative analysis of lipids in relatively complex mixtures. We have demonstrated that our method is sufficiently specific for the lipids of interest because it was not necessary to use tandem mass spectrometry as suggested by other investigators [21, 62, 65]. The use of the NALDI targets allows for greatly simplified sample preparation and eliminates the matrix-associated issues of inhomogeneous crystals and matrix adducts. This approach should also be possible to for a wide range of lipids and structurally similar molecules.

Acknowledgments This research was supported (in part) by federal funds from the Intramural Research Program of the NIH, National Cancer Institute, Center for Cancer Research. This project has been funded in part with federal funds from the National Cancer Institute, National Institutes of Health, under Contract No. HHSN261200800001E. The content of this publication does not necessarily reflect the views or policies of the Department of Health and Human Services, nor does mention of trade names, commercial products, or organizations imply endorsement by the US government.

References

1. Touchstone JC (1995) Thin-layer chromatographic procedures for lipid separation. J Chromatogr B Biomed Appl 671:169–195
2. McCluer RH, Ullman MD, Jungalwala FB (1986) HPLC of glycosphingolipids and phospholipids. Adv Chromatogr 25:309–353
3. Christie WW (2003) Lipid analysis. Oily Press, Bridgewater
4. Schiller J, Süß R, Arnhold J, Fuchs B et al (2004) Matrix-assisted laser desorption and ionization time-of-flight (MALDI-TOF) mass spectrometry in lipid and phospholipid research. Prog Lipid Res 43:449–488
5. Gohlke RS (1959) Time-of-flight mass spectrometry and gas–liquid partition chromatography. Anal Chem 31:535–541
6. Ryhage R (1993) The mass spectrometry laboratory at the Karolinska institute 1944–1987. Mass Spectrom Rev 12:1–49
7. Griffiths WJ (2003) Tandem mass spectrometry in the study of fatty acids, bile acids, and steroids. Mass Spectrom Rev 22: 81–152
8. Harvey DJ, Bateman BH, Bordoli RS, Tyldesley R (2000) Ionisation and fragmentation of complex glycans with a quadrupole time-of-flight mass spectrometer fitted with a matrix-assisted laser desorption/ionisation ion source. Rapid Commun Mass Spectrom 14:2135–2142
9. Siuzdak G (1994) The emergence of mass spectrometry in biochemical research. Proc Natl Acad Sci USA 91:11290–11297
10. Schiller J, Suss R, Fuchs B, Muller M et al (2007) MALDI-TOF MS in lipidomics. Front Biosci 12:2568–2579
11. Wolf C, Quinn PJ (2008) Lipidomics: practical aspects and applications. Prog Lipid Res 47:15–36
12. Isaac G, Jeannotte R, Esch SW, Welti R (2007) New mass-spectrometry-based strategies for lipids. Genet Eng (NY) 28: 129–157
13. Fitzgerald MC, Parr GR, Smith LM (1993) Basic matrices for the matrix-assisted laser desorption/ionization mass spectrometry of proteins and oligonucleotides. Anal Chem 65:3204–3211
14. Teuber K, Schiller J, Fuchs B, Karas M, Jaskolla TW (2010) Significant sensitivity improvements by matrix optimization: a MALDI-TOF mass spectrometric study of lipids from hen egg yolk. Chem Phys Lipids 163(6):552–560
15. Sun G, Yang K, Zhao Z, Guan S et al (2008) Matrix-assisted laser desorption/ionization time-of-flight mass spectrometric analysis of cellular glycerophospholipids enabled by multiplexed solvent dependent analyte-matrix interactions. Anal Chem 80:7576–7585
16. Fuchs B, Bischoff A, Suss R, Teuber K et al (2009) Phosphatidylcholines and -ethanolamines can be easily mistaken in phospholipid mixtures: a negative ion MALDI-TOF MS study with 9-aminoacridine as matrix and egg yolk as selected example. Anal Bioanal Chem 395:2479–2487
17. Dannenberger D, Suss R, Teuber K, Fuchs B et al (2010) The intact muscle lipid composition of bulls: an investigation by MALDI-TOF MS and 31P NMR. Chem Phys Lipids 163:157–164
18. Cheng H, Sun G, Yang K, Gross RW, Han X (2010) Selective desorption/ionization of sulfatides by MALDI-MS facilitated using 9-aminoacridine as matrix. J Lipid Res 51:1599–1609
19. Angelini R, Babudri F, Lobasso S, Corcelli A (2010) MALDI-TOF/MS analysis of archaebacterial lipids in lyophilized membranes dry-mixed with 9-aminoacridine. J Lipid Res 51:2818–2825
20. Benabdellah F, Seyer A, Quinton L, Touboul D et al (2010) Mass spectrometry imaging of rat brain sections: nanomolar sensitivity with MALDI versus nanometer resolution by TOF-SIMS. Anal Bioanal Chem 396:151–162
21. van Kampen JJ, Burgers PC, de Groot R, Gruters RA, Luider TM (2011) Biomedical application of MALDI mass spectrometry for small-molecule analysis. Mass Spectrom Rev 30(1):101–120
22. Ayorinde FO, Garvin K, Saeed K (2000) Determination of the fatty acid composition of saponified vegetable oils using matrix-assisted laser desorption/ionization time-of-flight mass spectrometry. Rapid Commun Mass Spectrom 14:608–615
23. Hlongwane C, Delves IG, Wan LW, Ayorinde FO (2001) Comparative quantitative fatty acid analysis of triacylglycerols using matrix-assisted laser desorption/ionization time-of-flight mass spectrometry and gas chromatography. Rapid Commun Mass Spectrom 15:2027–2034
24. Yu H, Lopez E, Young SW, Luo J et al (2006) Quantitative analysis of free fatty acids in rat plasma using matrix-assisted

laser desorption/ionization time-of-flight mass spectrometry with meso-tetrakis porphyrin as matrix. Anal Biochem 354:182–191
25. Wei J, Buriak JM, Siuzdak G (1999) Desorption-ionization mass spectrometry on porous silicon. Nature 399:243–246
26. Peterson DS (2007) Matrix-free methods for laser desorption/ionization mass spectrometry. Mass Spectrom Rev 26:19–34
27. Go EP, Apon JV, Luo G, Saghatelian A et al (2005) Desorption/ionization on silicon nanowires. Anal Chem 77:1641–1646
28. Muck A, Stelzner T, Hubner U, Christiansen S, Svatos A (2010) Lithographically patterned silicon nanowire arrays for matrix free LDI-TOF/MS analysis of lipids. Lab Chip 10:320–325
29. Xu S, Li Y, Zou H, Qiu J et al (2003) Carbon nanotubes as assisted matrix for laser desorption/ionization time-of-flight mass spectrometry. Anal Chem 75:6191–6195
30. Ren SF, Zhang L, Cheng ZH, Guo YL (2005) Immobilized carbon nanotubes as matrix for MALDI-TOF-MS analysis: applications to neutral small carbohydrates. J Am Soc Mass Spectrom 16:333–339
31. Ren SF, Guo YL (2005) Oxidized carbon nanotubes as matrix for matrix-assisted laser desorption/ionization time-of-flight mass spectrometric analysis of biomolecules. Rapid Commun Mass Spectrom 19:255–260
32. Najam-ul-Haq M, Rainer M, Szabo Z, Vallant R et al (2007) Role of carbon nano-materials in the analysis of biological materials by laser desorption/ionization-mass spectrometry. J Biochem Biophys Methods 70:319–328
33. Sunner J, Dratz E, Chen YC (1995) Graphite surface-assisted laser desorption/ionization time-of-flight mass spectrometry of peptides and proteins from liquid solutions. Anal Chem 67: 4335–4342
34. Zumbuhl S, Knochenmuss R, Wulfert S, Dubois F et al (1998) A graphite-assisted laser desorption/ionization study of light-induced aging in triterpene dammar and mastic varnishes. Anal Chem 70:707–715
35. Dietemann P, Edelmann M, Meisterhans C, Pfeiffer C et al (2000) Artificial photoaging of triterpenes studied by graphite-assisted laser desorption/ionization mass spectrometry. Helvetica Chimica Acta 83:1766–1777
36. Zhang H, Cha S, Yeung ES (6584) Colloidal graphite-assisted laser desorption/ionization MS and MS(n) of small molecules. 2. Direct profiling and MS imaging of small metabolites from fruits. Anal Chem 79:6575
37. Cha S, Zhang H, Ilarslan HI, Wurtele ES et al (2008) Direct profiling and imaging of plant metabolites in intact tissues by using colloidal graphite-assisted laser desorption ionization mass spectrometry. Plant J 55:348–360
38. Cha S, Yeung ES (2007) Colloidal graphite-assisted laser desorption/ionization mass spectrometry and MSn of small molecules. 1. Imaging of cerebrosides directly from rat brain tissue. Anal Chem 79:2373–2385
39. Greene LE, Yuhas BD, Law M, Zitoun D, Yang P (2006) Solution-grown zinc oxide nanowires. Inorganic Chemistry 45:7535–7543
40. Fan Z, Lu JG (2005) Zinc oxide nanostructures: synthesis and properties. J Nanosci Nanotechnol 5:1561–1573
41. Kang M-J, Pyun J-C, Lee J-C, Choi Y-J et al (2005) Nanowire-assisted laser desorption and ionization mass spectrometry for quantitative analysis of small molecules. Rapid Commun Mass Spectrom 19:3166–3170
42. Watanabe T, Kawasaki H, Yonezawa T, Arakawa R (2008) Surface-assisted laser desorption/ionization mass spectrometry (SALDI-MS) of low molecular weight organic compounds and synthetic polymers using zinc oxide (ZnO) nanoparticles. J Mass Spectrom 43:1063–1071
43. Budimir N, Blais JC, Fournier F, Tabet JC (2006) The use of desorption/ionization on porous silicon mass spectrometry for the detection of negative ions for fatty acids. Rapid Commun Mass Spectrom 20:680–684
44. Najam-ul-Haq M, Rainer M, Huck CW, Hausberger P et al (2008) Nanostructured diamond-like carbon on digital versatile disc as a matrix-free target for laser desorption/ionization mass spectrometry. Anal Chem 80:7467–7472
45. Vidova V, Novak P, Strohalm M, Pol J et al (2010) Laser desorption-ionization of lipid transfers: tissue mass spectrometry imaging without MALDI matrix. Anal Chem 82:4994–4997
46. Yavlovich A, Singh A, Tarasov S, Capala J et al (2009) Design of liposomes containing photopolymerizable phospholipids for triggered release of contents. J Therm Anal Calorim 98:97–104
47. Yavlovich A, Singh A, Blumenthal R, Puri A (2011) A novel class of photo-triggerable liposomes containing DPPC:DC(8,9)PC as vehicles for delivery of doxorubicin to cells. Biochim Biophys Acta 1808(1):117–126
48. Puri A, Loomis K, Smith B, Lee JH et al (2009) Lipid-based nanoparticles as pharmaceutical drug carriers: from concepts to clinic. Crit Rev Ther Drug Carrier Syst 26:523–580
49. Bligh EG, Dyer WJ (1959) A rapid method of total lipid extraction and purification. Can J Biochem Physiol 37:911–917
50. Bangham AD, Standish MM, Watkins JC (1965) Diffusion of univalent ions across the lamellae of swollen phospholipids. J Mol Biol 13:238–252
51. Gregoriadis G, Neerunjun ED (1975) Homing of liposomes to target cells. Biochem Biophys Res Commun 65:537–544
52. Chen H, Torchilin V, Langer R (1996) Lectin-bearing polymerized liposomes as potential oral vaccine carriers. Pharm Res 13:1378–1383
53. Allen TM (1997) Liposomes. Opportunities in drug delivery. Drugs 54(4):8–14
54. Allen TM, Cullis PR (2004) Drug delivery systems: entering the mainstream. Science 303:1818–1822
55. Johnston DS, McLean LR, Whittam MA, Clark AD, Chapman D (1983) Spectra and physical properties of liposomes and monolayers of polymerizable phospholipids containing diacetylene groups in one or both acyl chains. Biochemistry 22:3194–3202
56. Leaver J, Alonso A, Durrani AA, Chapman D (1983) The physical properties and photopolymerization of diacetylene-containing phospholipid liposomes. Biochim Biophys Acta (BBA)—Biomembranes 732:210–218
57. Shin WJ, Shin JH, Song JY, Han SY (2010) Effects of ZnO nanowire length on surface-assisted laser desorption/ionization of small molecules. J Am Soc Mass Spectrom 21:989–992
58. Schiller J, Süß R, Petkovic M, Hilbert N et al (2001) CsCl as an auxiliary reagent for the analysis of phosphatidylcholine mixtures by matrix-assisted laser desorption and ionization time-of-flight mass spectrometry (MALDI-TOF MS). Chem Phys Lipids 113:123–131
59. Duncan MW, Roder H, Hunsucker SW (2008) Quantitative matrix-assisted laser desorption/ionization mass spectrometry. Brief Funct Genomic Proteomic 7:355–370
60. Nicola AJ, Gusev AI, Proctor A, Jackson EK, Hercules DM (1995) Application of the fast-evaporation sample preparation method for improving quantification of angiotensin II by matrix-assisted laser desorption/ionization. Rapid Commun Mass Spectrom 9:1164–1171
61. Moskovets E, Chen H-S, Pashkova A, Rejtar T et al (2003) Closely spaced external standard: a universal method of achieving 5 ppm mass accuracy over the entire MALDI plate in axial matrix-assisted laser desorption/ionization time-of-flight mass spectrometry. Rapid Commun Mass Spectrom 17:2177–2187
62. Hatsis P, Brombacher S, Corr J, Kovarik P, Volmer DA (2003) Quantitative analysis of small pharmaceutical drugs using a high repetition rate laser matrix-assisted laser/desorption ionization source. Rapid Commun Mass Spectrom 17:2303–2309

63. Sleno L, Volmer DA (2006) Assessing the properties of internal standards for quantitative matrix-assisted laser desorption/ionization mass spectrometry of small molecules. Rapid Commun Mass Spectrom 20:1517–1524
64. Nimptsch A, Schibur S, Schnabelrauch M, Fuchs B et al (2009) Characterization of the quantitative relationship between signal-to-noise (S/N) ratio and sample amount on-target by MALDI-TOF MS: determination of chondroitin sulfate subsequent to enzymatic digestion. Anal Chim Acta 635:175–182
65. Corr JJ, Kovarik P, Schneider BB, Hendrikse J et al (2006) Design considerations for high speed quantitative mass spectrometry with MALDI ionization. J Am Soc Mass Spectrom 17:1129–1141

Lipids (2011) 46:479–486
DOI 10.1007/s11745-011-3542-4

ORIGINAL ARTICLE

Receptor Mediated Elevation in FABP4 Levels by Advanced Glycation End Products Induces Cholesterol and Triacylglycerol Accumulation in THP-1 Macrophages

Xiao Qun Wang · Ke Yang · Yu Song He · Lin Lu · Wei Feng Shen

Received: 6 August 2010 / Accepted: 8 February 2011 / Published online: 20 February 2011

Abstract Excessive formation of advanced glycation end products (AGE) and lipid accumulation in macrophages play a pivotal role in the progression of atherosclerosis in diabetes mellitus. This study aimed to determine the molecular link between AGE-induced fatty acid binding protein 4 (FABP4) expression and macrophage lipid accumulation. AGE–BSA markedly increased macrophage FABP4 expression via engagement of RAGE, a 35-kDa transmembrane receptor that is able to bind extracellular AGE and responsible for the corresponding signal transduction, whereas knockdown of RAGE significantly reversed the FABP4 up-regulation. This effect was further paralleled with elevated intracellular total cholesterol and triacylglycerol levels. Finally, administration of FABP4 inhibitor totally abolished the increased lipid contents in response to AGE–BSA. These results indicate that FABP4 up-regulation is responsible for the enhanced macrophage lipid accumulation by AGE, which may underlie the accelerated formation of foam cells and development of atherosclerotic cardiovascular diseases in diabetic patients.

Keywords Advanced glycation end products · Receptor for advanced glycation end products · Fatty acid binding protein 4 · Lipid accumulation

X. Q. Wang · L. Lu · W. F. Shen (✉)
Department of Cardiology, Rui Jin Hospital, Jiao Tong University School of Medicine, 197 Rui Jin Road II, Shanghai 200025, People's Republic of China
e-mail: rjshenweifeng@yahoo.com.cn

X. Q. Wang · K. Yang · Y. S. He · L. Lu · W. F. Shen
Institute of Cardiovascular Diseases, Jiao Tong University School of Medicine, Shanghai 200025, People's Republic of China

Abbreviations

AGE	Advanced glycation end products
aP2	Adipocyte protein 2
BSA	Bovine serum albumin
DMSO	Dimethyl sulfoxide
esRAGE	Endogenous secretary RAGE
FABP4	Fatty acid binding protein 4
FABP5	Fatty acid binding protein 5
FBS	Fetal bovine serum
LOX-1	Lectin-like oxidized low-density lipoprotein receptor 1
MSR	Macrophage scavenger receptor
OD	Optical density
ORO	Oil red O
oxLDL	Oxidized low-density lipoprotein
PBS	Phosphate-buffered saline
PMA	Phorbol 12-myristate 13-acetate
RAGE	Receptor for advanced glycation end products
sRAGE	Secretary RAGE
TAG	Triacylglycerol
TC	Total cholesterol

Introduction

Accelerated atherosclerosis accounts for about 80% of morbidity and mortality in patients with diabetes [1, 2]. Increased formation of advanced glycation end products (AGE) is recognized as an important player in diabetic vascular complications [3, 4]. After longstanding exposure to hyperglycemic milieu, proteins and lipids in blood and tissues undergo non-enzymatic Maillard reaction, and finally give rise to the irreversible formation of AGE [4].

AGE exert adverse effects largely through engagement of receptor for AGE (RAGE) on the cell membrane of vascular wall [5–7]. Postmortem studies have consistently shown that RAGE expression was mainly localized in macrophages within or around necrotic cores of atherosclerotic plaques, and was substantially increased in diabetic patients [8].

Macrophages actively participate in atherogenic processes, including formation of lipid-laden foam cells and atheromatous lipid cores [9]. FABP4, also known as adipocyte protein 2 (aP2), is highly expressed in macrophages [10]. It functions in cellular lipid metabolism, cholesterol trafficking and other biologic responses [11, 12]. Expression of FABP4 in THP-1 monocytes/macrophages was greatly increased upon treatment with phorbol 12-myristate 13-acetate (PMA) and oxidized low-density lipoprotein (oxLDL), while transformation of THP-1 monocytes into foam cells was significantly suppressed by FABP4 inhibitor, a small synthetic molecule designed to competitively prevent FABP4 from binding fatty acids [13, 14]. Likewise, inhibition of FABP4 expression either by macrophage-specific gene deficiency or administration of FABP4 inhibitor in vivo led to a protection from the development of atherosclerosis [15]. Iwashima et al. [6] observed that macrophage lipoprotein receptors, including CD36, macrophage scavenger receptor (MSR) class A and lectin-like oxLDL receptor 1 (LOX-1) were up-regulated in response to AGE stimulation, whereas key proteins localized on the cell membrane that mediate macrophage cholesterol efflux, including ABCA1 and ABCG1, were down-regulated or destabilized [16, 17].

It is still unclear, however, whether macrophage FABP4 remains, equally or to a greater extent, an active pro-atherogenic participator in the context of diabetes where AGE are greatly enriched. In this study, we tested the hypothesis that AGE-induced FABP4 expression in THP-1 macrophages was potentially associated with an increase in intracellular lipid levels. The assessment of lipid contents after FABP4 inhibitor administration was also performed.

Materials and Methods

Cell Culture

Human monocytic leukemia THP-1 cells were obtained from ATCC and cultured in Gibco RPMI 1640 medium supplemented with 10% heat-inactivated fetal bovine serum (FBS), 50 U/ml penicillin and 50U/ml streptomycin (Gibco, Auckland, New Zealand) at 37 °C in 5% CO_2. THP-1 monocytes were differentiated into macrophages by induction of 100nM phorbol 12-myristate 13-acetate (Sigma-Aldrich, MO) for 48 h. Cells were then incubated in the presence or absence of bovine serum albumin (BSA; fatty acid free, catalog no. 126575; Calbiochem, CA) or AGE–BSA (catalog no. 121800; Calbiochem, CA) for the indicated time intervals. FABP4 inhibitor (Calbiochem, CA) dissolved in dimethyl sulfoxide (DMSO) at the indicated concentrations was administrated for study purpose.

Transfection of RAGE-Specific siRNA

Transient transfection of THP-1 macrophages with RAGE-specific and negative control siRNA (Ambion CA) was scheduled as follows: Silencing RAGE expression was performed using human RAGE-specific siRNA and siRNA transfection reagent (Lipofectamine 2000, Invitrogen, CA) to macrophages. Macrophages grown in 6-well plates were transfected with various concentrations of siRNA according to the manufacturer's protocol. The RAGE-specific siRNA (100 pM) for reducing RAGE expression was added 48 h before AGE stimulation; macrophages were then exposed to BSA or AGE–BSA (Calbiochem CA) for 24 or 48 h for RNA or protein analysis and ORO-staining, respectively.

Assessment of Intracellular Lipid Contents

Cultured and transfected macrophages were washed twice in phosphate-buffered saline (PBS, Gibco, Auckland, New Zealand) and then fixed in 4% paraformaldehyde for 30 min. After rinsing with ddH2O, macrophages were incubated with filtered Oil Red O solution (0.6 g/L ORO in 60% isopropanol) (ORO, Sigma-Aldrich, MO) for 10 min and with 1 mL of Mayer's hemalum (Merck, Darmstadt) for 1 min. After rinsing with PBS four times, intracellular lipid droplets were evaluated under Olympus DP-71 microscope. Spectrophotometric quantification of the staining was performed as described previously [18]. Briefly, stained oil droplets were dissolved in 100% isopropanol for 10 min. Then optical density was measured at 500 nm and equalized with the cell numbers estimated by microscope. Quantifications of intracellular total cholesterol and triacylglycerol levels were performed following the protocols from the manufacture (Biovision, CA) and analyzed with a microtiter plate reader (Ex/Em = 538/587 nm). Total cholesterol and triacylglycerol concentrations were expressed as micrograms per milligram protein and nanomoles per milligram protein sample, respectively.

Quantitative Real-Time PCR Analysis

Total RNA was isolated using Trizol reagent (Invitrogen, CA). For reverse transcription, 1 μg of the total RNA was converted to first strand complementary DNA in 20-μl reactions using a reverse transcription kit (Promega, WI). Quantitative real-time PCR analysis was performed

(StepOne, Applied Biosystems) using SYBR Green (Takara, Dalian, China). The thermal cycling program was 10 s at 95 °C for enzyme activation and 40 cycles of denaturation for 5 s at 95 °C, 31 s 60 °C for annealing and extension. The comparative cycle threshold (CT) method was used to determine relative mRNA expression of genes as normalized by β-actin housekeeping gene. Primers used are as follows: 5′-TGGGATGGAAAATCAACC-3′ for FABP4-F, 5′-TCTCTCATAAACTCTCGTGG-3′ for FABP4-R, 5′-GGCAGAAAAACTCAGAC-3′ for FABP5-F, 5′-GACACACTCCACCACTAA-3′ for FABP5-R, 5′-GCTGGTGTTCCCAATAA-3′ for AGER-F, 5′-AGTGTGAAGAGCCCTGT-3′ for AGER-R, 5′-CGTGGACATCCGCAAAG-3′ for β-actin-F, and 5′-TGGAAGGTGGACAGCGA-3′ for β-actin-R.

Western Blot

Total proteins were prepared by standard procedures and assessed by microplate protein assay (BSA; Pierce, IL). Thirty micrograms of protein per sample and known molecular weight markers were loaded onto a 12% SDS-polyacrylamide gel. After SDS-polyacrylamide gel electrophoresis, proteins were transferred to PVDF membranes (Millipore, MA). The blocked membranes (5% nonfat milk in TBS buffer containing 0.1% Tween 20) were incubated with anti-FABP4 (1:1000; Santa Cruz Biotechnology, CA), anti-RAGE (1:1000; Abcam, MA) and anti-β-actin antibody (1:1000; Cell Signaling Technology, MA) for overnight at 4 °C. The membranes were then treated with horseradish peroxidase-conjugated rabbit anti-goat, goat anti-rabbit or goat anti-mouse antibodies (1:5000; Bio-Rad, Hercules, CA). After washing, immunodetection analysis was accomplished using the Immobilon Western Chemiluminescent HRP Substrate (Millipore, MA).

Statistical Analysis

Data are expressed as means ± SEM. The mean values for biochemical measurements from each group were compared using Student's t test. A $P < 0.05$ was considered statistically significant.

Results

AGE–BSA-Induced Up-Regulation of FABP4 Expression

After incubation with AGE–BSA for 24 h at various concentrations (from 25 to 200 μg/ml), FABP4 expression was substantially up-regulated, and reached the maximum level

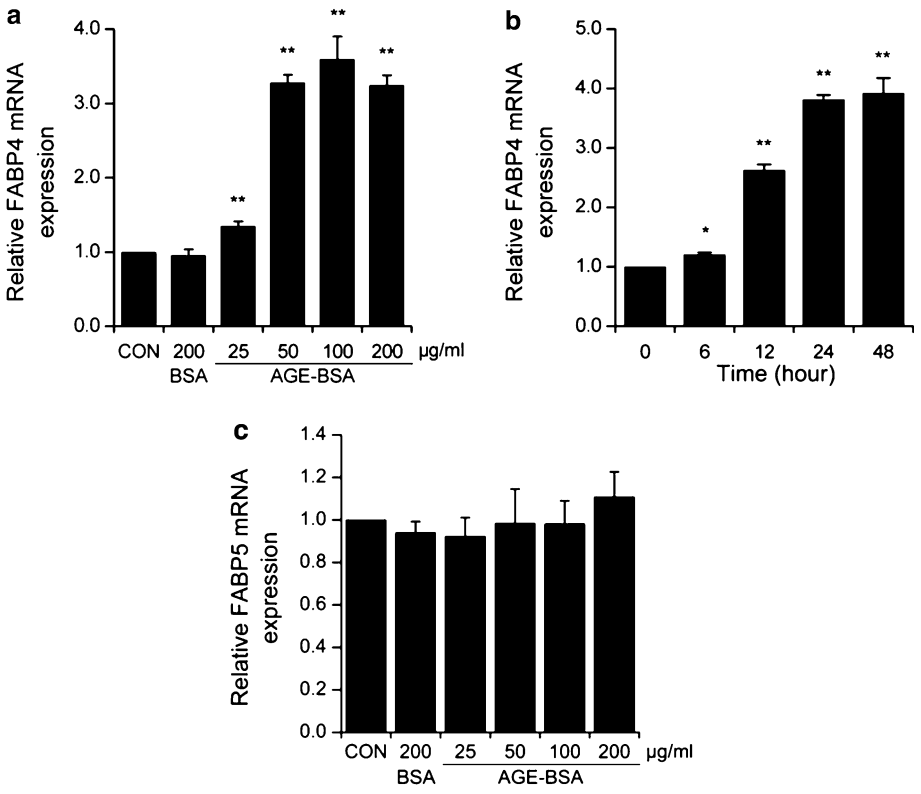

Fig. 1 Up-regulation of FABP4 mRNA expression by AGE–BSA. **a**, **c** THP-1 macrophages were treated with indicated doses of BSA or AGE–BSA for 24 h. **b** Macrophages were either untreated or treated with 100 μg/ml AGE–BSA for various time intervals. FABP4 and FABP5 mRNA levels were detected by quantitative real-time PCR; data are expressed relatively to untreated cells, arbitrarily set at the level of 1, and are the means ± SEM of at least three independent experiments. *$P < 0.05$ and **$P < 0.01$ when compared with untreated cells

at 100 μg/ml (3.59 ± 0.53-fold vs. con; $P = 0.001$), whereas BSA did not affect FABP4 expression significantly (0.95 ± 0.14-fold vs. con, $P = 0.577$; Fig. 1a). A 3.9-fold increase in FABP4 expression was observed by 48 h of incubation ($P = 0.0003$; Fig. 1b). FABP5, another fatty acid binding protein expressed in macrophages, was not affected by AGE (Fig. 1c).

RAGE Mediates AGE–BSA-Induced FABP4 Expression

AGE–BSA moderately increased RAGE expression by 1.2-fold in cells transfected with non-specific negative control siRNA ($P = 0.010$, Fig. 2a). After gene silencing of RAGE, AGE exposure no longer affected FAPB4 expression both at mRNA (1.38 ± 0.24-fold vs. BSA, $P = 0.069$; Fig. 2b) and protein (Fig. 2c) levels when compared with negative control-treated groups (2.78 ± 0.36-fold vs. BSA, $P = 0.001$).

AGE–BSA-Induced Macrophage Lipid Accumulation

Oil red O (ORO) staining of lipid droplets was most evident at 100 and 200 μg/ml of AGE–BSA (Fig. 3a, b). A similar trend was also obtained for intracellular TC (100 μg/ml AGE–BSA: 37.20 ± 2.52 μg/mg, $P = 0.0002$; 200 μg/ml AGE–BSA: 29.89 ± 4.67 μg/mg, $P = 0.0066$ vs. con: 15.10 ± 1.61 μg/mg; Fig. 3c) and TAG levels (100 μg/ml AGE–BSA: 4.35 ± 1.35 nmol/mg, $P = 0.0252$; 200 μg/ml AGE–BSA: 2.89 ± 0.75 nmol/mg, $P = 0.0463$ vs. con: 1.64 ± 0.08 nmol/mg; Fig. 3d). RAGE knockdown markedly reduced lipid contents in response to AGE exposure (TC, 21.92 ± 3.09 μg/mg vs. BSA: 17.23 ± 2.20 μg/mg, $P = 0.0980$; TAG, 5.64 ± 1.43 nmol/mg vs. BSA: 1.85 ± 1.10 nmol/mg, $P = 0.0220$) when compared with negative control-treated cells, as demonstrated by ORO staining (Fig. 3e, f), TC (Fig. 3g) and TAG (Fig. 3h) quantification.

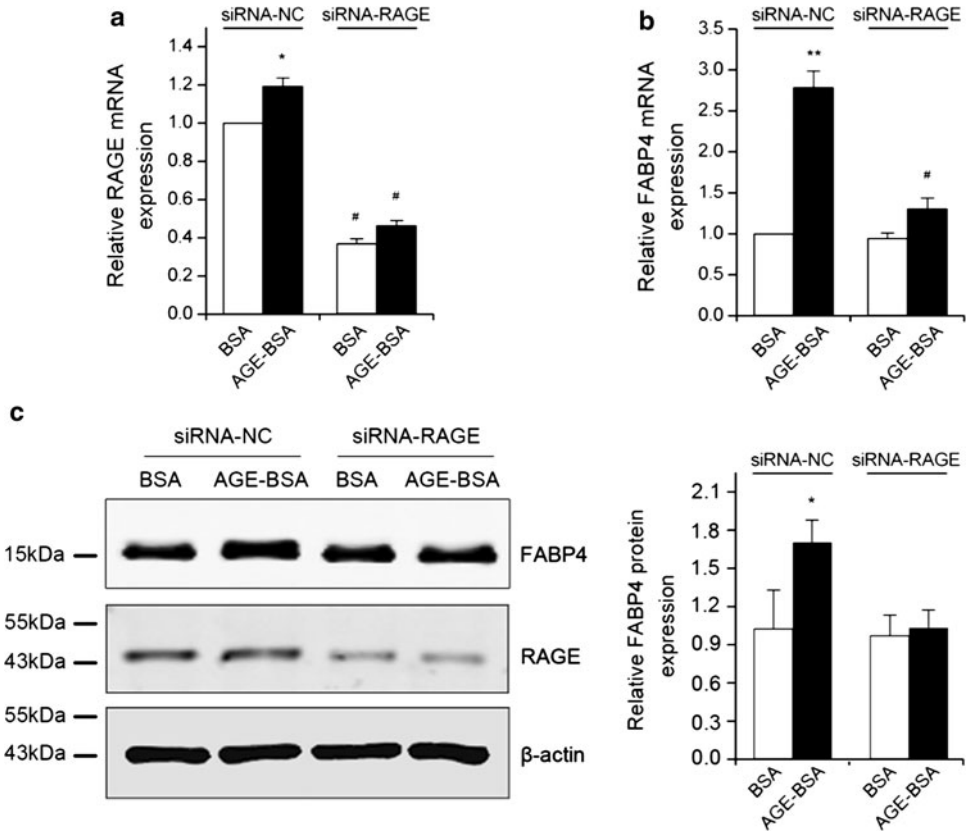

Fig. 2 Effect of RAGE knockdown by siRNA transfection on FABP4 expression. Macrophages were transfected with negative control or RAGE specific siRNA for 48 h and exposed to BSA or AGE–BSA, respectively, at the concentration of 100 μg/ml. Then mRNA expression levels of RAGE (**a**) and FABP4 (**b**) were determined using quantitative real-time PCR; data are expressed relatively to untreated cells, arbitrarily set at the level of 1, and are the means ± SEM of at least three independent experiments. **c** Protein expression levels of FABP4 and RAGE in each group were analyzed by Western blot. β-actin demonstrated equal loading. The right panel shows the average densitometric analysis of three independent experiments. Data are expressed in arbitrary units. $^{*}P < 0.05$ and $^{**}P < 0.01$ compared with BSA-treated cells in the same group. $^{\#}P < 0.01$ versus cells with the same BSA or AGE–BSA treatment in negative control group

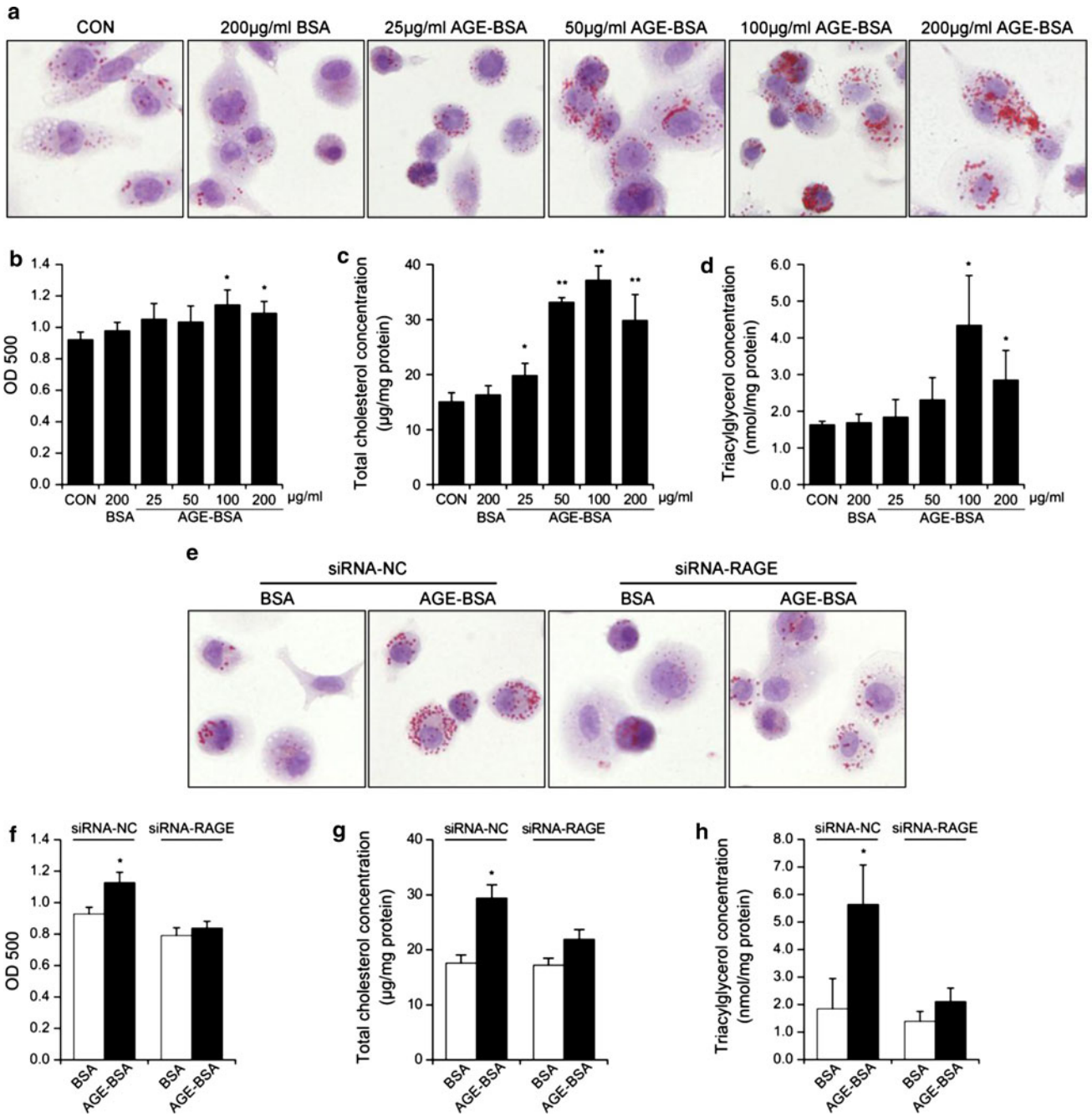

Fig. 3 Up-regulation of lipid contents by AGE–BSA via RAGE. **a**–**d** Macrophages were either untreated or treated with indicated doses of BSA and AGE–BSA for 48 h. **e**–**h** Macrophages were transfected with negative control or RAGE specific siRNA for 48 h and then exposed to BSA or AGE–BSA, respectively, at the concentration of 100 μg/ml. **a**, **e** Intracellular lipid droplets were observed through light microscope after ORO staining; pictures acquired at the magnification of 400× and processed using identical conditions are representative of three independent experiments. **b**, **f** Spectrophotometric quantifications of ORO staining by optical density at 500 nm were shown. Intracellular total cholesterol (**c**, **g**) and triacylglycerol (**d**, **h**) concentrations were determined using a fluorometric method; data are presented as micrograms of total cholesterol per milligrams of protein or nanomoles of triacylglycerol per milligrams of protein ± SEM of three independent experiments. $^{*}P < 0.05$ versus untreated cells (**b**, **c**, **d**) or BSA-treated cells in the same group (**f**, **g**, **h**). $^{**}P < 0.01$ versus untreated cells

Changes After Incubation with FABP4 Inhibitor

After incubation with FABP4 inhibitor for 48 h, AGE-induced lipid accumulation in macrophages was substantially suppressed and reached the maximum effect at 40 μM as demonstrated by ORO staining (Fig. 4a, b), TC (14.92 ± 1.54 μg/mg vs. BSA: 14.56 ± 0.81ug/mg, $P = 0.7356$; Fig. 4c) and TAG (0.79 ± 0.35 nmol/mg vs. BSA:

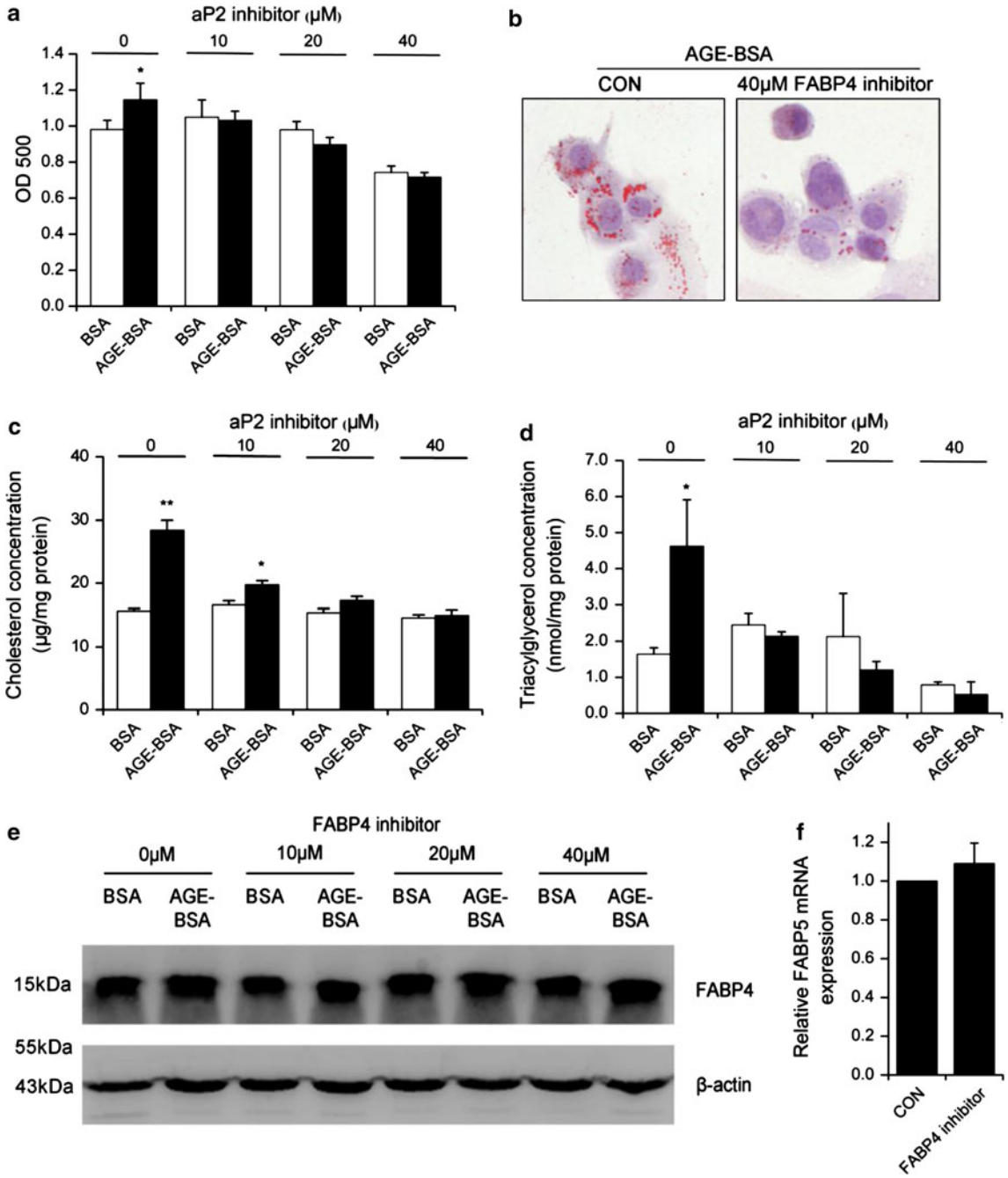

Fig. 4 Effect of FABP4 inhibitor on AGE–BSA-induced lipid accumulation. Macrophages were treated with 100 μg/ml BSA or AGE–BSA in the absence or presence of indicated doses of FABP4 inhibitor for 48 h. **a** Intracellular cellular lipid droplets were stained with ORO and quantified by optical density at 500 nm or **b** observed through light microscope; pictures acquired at the magnification of 400× and processed using identical conditions are representative of three independent experiments. Intracellular total cholesterol (**c**) and triacylglycerol (**d**) concentrations were determined using a fluorometric method; data are presented as micrograms of total cholesterol per milligrams of protein or nanomoles of triacylglycerol per milligrams of protein ± SEM of three independent experiments. **e** FABP4 protein expression levels in each group were analyzed by Western blot. *β*-actin demonstrated equal loading. **f** THP-1 macrophages were treated with or without 40 μM FABP4 inhibitor for 48 h. FABP5 mRNA levels were detected by quantitative real-time PCR; data are expressed relatively to untreated cells, arbitrarily set at the level of 1, and are the means ± SEM of at least three independent experiments. $*P < 0.05$; $**P < 0.01$ versus BSA-treated cells in the same group

0.52 ± 0.24 nmol/mg, $P = 0.2656$; Fig. 4d) quantification when compared with macrophages without FABP4 treatment. AGE–BSA up-regulated FABP4 protein levels irrespective of FABP4 inhibitor at each concentration (Fig. 4e). FABP5 expression was not affected by FABP4 inhibitor (Fig. 4f).

Discussion

In THP-1 macrophages, AGE-induced FABP4 expression via a RAGE-dependent signaling pathway resulted in increased intracellular lipid levels, which could be attenuated by FABP4 inhibitor.

AGE are increasingly regarded as an indispensable factor for severity and progression of atherosclerosis in patients with diabetes [8]. AGE-albumin, a further glycation modified protein derived from Amadori adduct exerts more severe pathogenic influence. Elevated serum AGE-albumin and decreased serum endogenous secretary RAGE (esRAGE) levels highly correlated with the extent of angiographic severity in patients with type 2 diabetes [19, 20]. In contrast, in vivo studies showed that administration of soluble RAGE (sRAGE), another truncated form of RAGE acting as a decoy for AGE, completely suppressed diabetic atherosclerosis in glycemia- and lipid-independent manners [21]. Other approaches utilizing inhibitors for AGE formation, including aminoguanidine and an AGE cross-link breaker ALT-711, also led to a striking reduction in atherosclerotic lesions in diabetic apoE-deficient mice [22].

Despite the important contribution of AGE to the accelerated atherosclerosis in diabetes, the specific molecular mechanisms in response to AGE within a macrophage (a central player in atherogenesis) remain unclear. In this study, we discovered that exposure of THP-1 macrophages to AGE was time-dependently associated with a significant elevation of FABP4 expression, reaching its maximum level when 100 μg/ml AGE–BSA was used. At the same time, the enhanced expression of FABP4 was paralleled with increases in intracellular TC and TAG levels. RAGE-specific gene silencing led to reversions both in FABP4 expression and lipid contents, suggesting that AGE-elicited atherogenic effects in macrophages were, at least partly, RAGE-dependent. Finally, this increase in lipid levels was totally abolished by simultaneous administration of FABP4 inhibitor.

Our study is the first to show that macrophage FABP4 expression, a critical participant in atherogenesis, is further enhanced in the context of diabetes. In an animal experiment, Gerrity et al. [2] observed that FABP4 deficiency protected against the development of insulin resistance, diabetes, and atherosclerotic cardiovascular disease. Recent population studies revealed that genetic variations at the FABP4 locus in humans led to lowered serum triglyceride levels, and a markedly reduced risk of coronary heart disease in type 2 diabetes [23]. These anti-atherosclerotic effects were mainly attributed to the improvement of glucose control, insulin resistance and dyslipidemia [24, 25]. In this study, we demonstrated that exposure of macrophages to AGE was capable of increasing intracellular FAPB4 levels and lipid contents, similar to that when transforming macrophages to foam cells in the presence of oxLDL stimulation [14]. These observations suggest that excessive formation of AGE could render diabetic patients under high risk of developing atherosclerosis like those with dyslipidemia. [26–28].

Furthermore, our results imply that FABP4 might be a potential therapeutic target for the treatment of diabetic patients with atherosclerosis. In this study, mild doses of FABP4 inhibitor (10–20 μM) greatly attenuated AGE–BSA elicited macrophage lipid accumulation, whereas lipid levels in the absence of AGE were not affected. These findings indicate that FABP4 inhibitor may not disturb physiological lipid metabolism in macrophages, but, on the contrary, suppresses exclusively pathological excessive lipid accumulation.

This study does not specify the mechanisms by which lipid contents and trafficking are affected by AGE besides the elevated FAPB4 level. Deficiency of FABP4 enhanced CD36-mediated lipoprotein entry and, at the same time, activated ABCA1-dependent lipid efflux to a greater extent, thereby lowering intracellular lipid contents [29]. Likewise, AGE stimulation on macrophages could increase SRA-1 and CD36 and decrease ABCG1 protein levels [6, 16, 17]. Thus, enhanced expression of FABP4 by AGE might extensively affect lipid influx and efflux, directly or indirectly, at the same time to increase lipid accumulation. Further studies including analysis of lipid trafficking in macrophages from FABP4-deficient mice and blocking lipoprotein transporters by their specific siRNA or antibodies, are needed to elucidate the mechanisms.

In conclusion, this study demonstrates a causal molecular link between AGE and FABP4 in macrophage lipid accumulation. FABP4 inhibitor may be useful for suppressing the atherosclerotic process in patients with diabetes.

Acknowledgments This work was supported by grant from Chinese National Nature Science Foundation (No. 30871084).

Conflict of interest All authors have no conflict of interest.

References

1. Kannel WB, McGee DL (1979) Diabetes and cardiovascular disease. The Framingham Study. JAMA 241:2035–2038
2. Gerrity RG, Natarajan R, Nadler JL, Kimsey T (2001) Diabetes-induced accelerated atherosclerosis in swine. Diabetes 50:1654–1665
3. Basta G, Schmidt AM, De Caterina R (2004) Advanced glycation end products and vascular inflammation: implications for accelerated atherosclerosis in diabetes. Cardiovasc Res 63:582–592
4. Goldin A, Beckman JA, Schmidt AM, Creager MA (2006) Advanced glycation end products: sparking the development of diabetic vascular injury. Circulation 114:597–605

5. Morigi M, Angioletti S, Imberti B, Donadelli R, Micheletti G, Figliuzzi M, Remuzzi A, Zoja C, Remuzzi G (1998) Leukocyte-endothelial interaction is augmented by high glucose concentrations and hyperglycemia in a NF-kB-dependent fashion. J Clin Invest 101:1905–1915
6. Iwashima Y, Eto M, Hata A, Kaku K, Horiuchi S, Ushikubi F, Sano H (2000) Advanced glycation end products-induced gene expression of scavenger receptors in cultured human monocyte-derived macrophages. Biochem Biophys Res Commun 277: 368–380
7. Lander HM, Tauras JM, Ogiste JS, Hori O, Moss RA, Schmidt AM (1997) Activation of the receptor for advanced glycation end products triggers a p21(ras)-dependent mitogen-activated protein kinase pathway regulated by oxidant stress. J Biol Chem 272:17810–17814
8. Burke AP, Kolodgie FD, Zieske A, Fowler DR, Weber DK, Varghese PJ, Farb A, Virmani R (2004) Morphologic findings of coronary atherosclerotic plaques in diabetics: a postmortem study. Arterioscler Thromb Vasc Biol 24:1266–1271
9. Luliano L (2001) Inflammation, atherosclerosis, and coronary artery disease. Lipids 352:S41–S44
10. Hotamisligil GS, Johnson RS, Distel RJ, Ellis R, Papaioannou VE, Spiegelman BM (1996) Uncoupling of obesity from insulin resistance through a targeted mutation in aP2, the adipocyte fatty acid binding protein. Science 274:1377–1379
11. Boord JB, Maeda K, Makowski L, Babaev VR, Fazio S, Linton MF, Hotamisligil GS (2002) Adipocyte fatty acid-binding protein, aP2, alters late atherosclerotic lesion formation in severe hypercholesterolemia. Arterioscler Thromb Vasc Biol 22:1686–1691
12. Fu Y, Luo N, Lopes-Virella MF, Garvey WT (2002) The adipocyte lipid binding protein (ALBP/aP2) gene facilitates foam cell formation in human THP-1 macrophages. Atherosclerosis 165:259–269
13. Pelton PD, Zhou L, Demarest KT, Burris TP (1999) PPARgamma activation induces the expression of the adipocyte fatty acid binding protein gene in human monocytes. Biochem Biophys Res Commun 261:456–458
14. Fu Y, Luo N, Lopes-Virella MF (2000) Oxidized LDL induces the expression of ALBP/aP2 mRNA and protein in human THP-1 macrophages. J Lipid Res 41:2017–2023
15. Furuhashi M, Tuncman G, Gorgun CZ, Makowski L, Atsumi G, Vaillancourt E, Kono K, Babaev VR, Fazio S, Linton MF, Sulsky R, Robl JA, Parker RA, Hotamisligil GS (2007) Treatment of diabetes and atherosclerosis by inhibiting fatty-acid-binding protein aP2. Nature 447:959–965
16. Passarelli M, Tang C, McDonald TO, O'Brien KD, Gerrity RG, Heinecke JW, Oram JF (2005) Advanced glycation end product precursors impair ABCA1-dependent cholesterol removal from cells. Diabetes 54:2198–2205
17. Isoda K, Folco EJ, Shimizu K, Libby P (2007) AGE–BSA decreases ABCG1 expression and reduces macrophage cholesterol efflux to HDL. Atherosclerosis 192:298–304
18. Kim KA, Kim JH, Wang Y, Sul HS (2007) Pref-1 (preadipocyte factor 1) activates the MEK/extracellular signal-regulated kinase pathway to inhibit adipocyte differentiation. Mol Cell Biol 27:2294–2308
19. Lu L, Pu LJ, Zhang Q, Wang LJ, Kang S, Zhang RY, Chen QJ, Wang JG, De Caterina R, Shen WF (2009) Increased glycated albumin and decreased esRAGE levels are related to angiographic severity and extent of coronary artery disease in patients with type 2 diabetes. Atherosclerosis 206:540–545
20. Pu LJ, Lu L, Shen WF, Zhang Q, Zhang RY, Zhang JS, Hu J, Yang ZK, Ding FH, Chen QJ, Shen J, Fang DH, Lou S (2007) Increased serum glycated albumin level is associated with the presence and severity of coronary artery disease in type 2 diabetic patients. Circ J 71:1067–1073
21. Bucciarelli LG, Wendt T, Qu W, Lu Y, Lalla E, Rong LL, Goova MT, Moser B, Kislinger T, Lee DC, Kashyap Y, Stern DM, Schmidt AM (2002) RAGE blockade stabilizes established atherosclerosis in diabetic apolipoprotein E-null mice. Circulation 106:2827–2835
22. Forbes JM, Yee LT, Thallas V, Lassila M, Candido R, Jandeleit-Dahm KA, Thomas MC, Burns WC, Deemer EK, Thorpe SR, Cooper ME, Allen TJ (2004) Advanced glycation end product interventions reduce diabetes-accelerated atherosclerosis. Diabetes 53:1813–1823
23. Tuncman G, Erbay E, Hom X, De Vivo I, Campos H, Rimm EB, Hotamisligil GS (2006) A genetic variant at the fatty acid-binding protein aP2 locus reduces the risk for hypertriglyceridemia, type 2 diabetes, and cardiovascular disease. Proc Natl Acad Sci USA 103:6970–6975
24. Furuhashi M, Fucho R, Görgün CZ, Tuncman G, Cao H, Hotamisligil GS (2008) Adipocyte/macrophage fatty acid-binding proteins contribute to metabolic deterioration through actions in both macrophages and adipocytes in mice. J Clin Invest 118:2640–2650
25. Shaughnessy S, Smith ER, Kodukula S, Storch J, Fried SK (2000) Adipocyte metabolism in adipocyte fatty acid binding protein knockout mice (aP2-/-) after short-term high-fat feeding: functional compensation by the keratinocyte fatty acid binding protein. Diabetes 49:904–911
26. Bahramian N, Ostergren-Lundén G, Bondjers G, Olsson U (2004) Fatty acids induce increased granulocyte macrophage-colony stimulating factor secretion through protein kinase C-activation in THP-1 macrophages. Lipids 39:243–249
27. Goff DC Jr, Bertoni AG, Kramer H, Bonds D, Blumenthal RS, Tsai MY, Psaty BM (2006) Dyslipidemia prevalence, treatment, and control in the Multi-Ethnic Study of Atherosclerosis (MESA): gender, ethnicity, and coronary artery calcium. Circulation 113:647–656
28. Nakhjavani M, Khalilzadeh O, Khajeali L, Esteghamati A, Morteza A, Jamali A, Dadkhahipour S (2010) Serum oxidized-LDL is associated with diabetes duration independent of maintaining optimized levels of LDL-cholesterol. Lipids 45:321–327
29. Makowski L, Brittingham KC, Reynolds JM, Suttles J, Hotamisligil GS (2005) The fatty acid-binding protein, aP2, coordinates macrophage cholesterol trafficking and inflammatory activity. Macrophage expression of aP2 impacts peroxisome proliferator-activated receptor gamma and IkappaB kinase activities. J Biol Chem 280:12888–12895

Lipids (2011) 46:487–494
DOI 10.1007/s11745-011-3525-5

ORIGINAL ARTICLE

Temporary Increase of PPAR-γ and Transient Expression of UCP-1 in Stromal Vascular Fraction Isolated Human Adipocyte Derived Stem Cells During Adipogenesis

Seong Jin Jo · Won Woo Choi · Eun Seong Lee · Jae Yong Lee · Hyun Sun Park · Dae Won Moon · Hee Chul Eun · Jin Ho Chung

Received: 14 July 2010 / Accepted: 20 December 2010 / Published online: 10 February 2011

Abstract In this study, cells from the stromal vascular fraction of human subcutaneous tissues were induced to differentiate toward adipose cells in vitro for 2 weeks. During adipogenic differentiation, we followed the chronological changes in their morphology with Coherent anti-Stokes Raman scattering (CARS) microscopy and checked the PPAR-γ and UCP-1 expression with RT-PCR. On day 4 after inducing adipogenic differentiation, CARS imaging showed multiple small lipid droplets (LD) distributed peripherally along the cellular membrane. PPAR-γ began to express at this time and increased until day 14 at a steady rate. On day 7, the cells appeared as brown adipocytes with numerous small LD throughout the cytoplasm, and the mRNA level of UCP-1 rose abruptly by 6- to 7-fold. After an additional 7 days, CARS imaging showed the development of a large LD, which is characteristic of white adipocytes, and the mRNA level of UCP-1 slumped significantly. These results demonstrate the possibility that ADSC pass through a brown adipocyte-like stage while differentiating into white adipocytes.

Keywords Adipogenesis · Adipose-derived stem cell · UCP-1

S. J. Jo · H. S. Park · H. C. Eun · J. H. Chung (✉)
Department of Dermatology, Seoul National University College of Medicine, Yongon-dong, Chongno-gu, Seoul, Korea
e-mail: jhchung@snu.ac.kr

W. W. Choi
Wells Dermatology Clinic, 584 Shinsa-dong, Kangnam-ku, Seoul, Korea

E. S. Lee · J. Y. Lee · D. W. Moon
Center for NanoBio Convergence, Korea Research Institute of Standards and Science, Doryong 1, Yusung, Daejeon, Korea

Abbreviations

ADSC	Adipose-derived stem cell
BAT	Brown adipose tissue
CARS	Coherent anti-Stokes Raman scattering
DMEM	Dulbecco's modified Eagle's medium
FBS	Fetal bovine serum
IBMX	Isobutyl-methylxanthine
LD	Lipid droplet
PBS	Phosphate-buffered saline
PPAR-γ	Peroxisome proliferator-activated receptor-γ
SVF	Stromal vascular fraction
UCP-1	Mitochondria-uncoupling protein-1
WAT	White adipose tissue

Introduction

Adipose tissue has been classified into two distinct types in mammals: WAT and BAT [1]. WAT is mainly involved in energy storage [2], while BAT forms heat using accumulated lipids [3] and the thermogenic capability depends on the presence of UCP-1 which is unique and specific to brown adipocytes [4, 5]. Although both of them are important to control the energy balance, they are regarded as distinct tissues and thought to develop independently for several reasons. One of the reasons is that white adipocytes do not express UCP-1 during adipogenesis, which was supported indirectly by an experiment using double transgenic mice [6].

Adipogenesis is a complicated process, which eventually results in the expression of various adipocyte-associated genes as well as an increased capacity of the cell for lipid-filling [7, 8]. For the past 20 years, many studies of adipogenesis have been conducted using preadipocyte clonal lines from rodents [8–10].

Although the results of studies using established cell lines have been invaluable, they are limited in their applicability to an in vivo human context because of their aneuploidy, unipotency, site-restriction and the species–species differences between humans and mice [9, 11]. Recently, a new era has started after the identification of human ADSC, mesenchymal stem cells isolated from adipose tissue. ADSC have a self-renewal capacity and multi-lineage potential toward adipocytes, osteoblast, chondrocytes, myoblasts and neuronal cells [12, 13]. Additionally, they are easily processed from lipoaspirated fat and can provide a significant quantity of multipotent stem cells [14]. Compared to clonal cell lines from mice, human ADSC may be much more appropriate for studies of adipocyte differentiation because they can offset the disadvantages of previous models and can better reflect the in vivo human context.

CARS microscopy is an advanced technique for the real-time imaging of live cells. It requires neither fixation nor a fluorescent probe. In the CARS process, a "pump" beam at a higher frequency (ω_p), a "Stokes" beam at a lower frequency (ω_s) and a "probe" beam (ω'_p) at the same frequency as the pump beam interact with a sample to generate an "anti-Stokes" beam, presented in the form of the equation $2\omega_p - \omega_s$. These signals are maximized by tuning the frequency difference ($\omega_p - \omega_s$) to the vibration of specific chemical bonds, which provides chemical selectivity in CARS microscopy [15]. In particular, CARS microscopy shows high sensitivity to the C–H vibration of lipid-rich molecules. Thus, CARS microscopy has been used to visualize lipids, axonal myelin sheaths and lipid-rich cells [16, 17]. Moreover, it was shown to be effective for imaging LD, in which the fatty acyl group is highly accumulated, in live cells without fixation [18].

In this study, we isolated the stromal-vascular fraction (SVF) cells from human subcutaneous tissue which contains ADSC and induced the cells to differentiate toward adipose tissue in vitro. To characterize the morphologic and molecular change of the cells during adipogenic differentiation, we serially imaged live cells with CARS microscopy and examined the PPAR-γ and UCP-1 expression with RT-PCR. On day 7 of adipogenesis, these cells transiently appeared multilocular with numerous small LD with an abrupt increase of UCP-1, thus suggesting that stem cells passes through a brown adipocytes-like stage while differentiating to white adipocytes.

Materials and Methods

Isolation and Culture of Human ADSC

Before the study, the protocols for fat collection were reviewed and approved by the institutional research board of the Seoul National University Hospital Clinical Research Institute, and informed consent was obtained from the human subjects. Liposuction aspirates from abdominal subcutaneous tissue were acquired from three healthy female donors undergoing elective procedures under tumescent anesthesia. The lipoaspirates were washed with PBS and were subsequently finely minced. The extracellular matrix was digested with 0.075% collagenase type I (Sigma-Aldrich, St. Louis, MO). Enzyme activity was neutralized with DMEM containing 10% FBS and the tissue was centrifuged for 10 min at 1,200g at room temperature. The supernatant, containing mature adipocytes, was aspirated. The pelleted SVF cells were collected and then plated in 175 cm^2 flasks (Becton–Dickinson AG, Basel. Switzerland) in a control medium which consisted of DMEM, 10% FBS, and 1% penicillin/streptomycin 5,000 U/ml (Invitrogen AG, Bagel, Switzerland). After that, they were incubated overnight at 37 °C in 5% CO_2. The resulting cell population includes human ADSC. [12, 13]. This initial passage was referred to as passage 0 (P0). After they achieved 90% confluence, the cells were passaged repeatedly until P8 by trypsin (0.05%, Invitrogen AG, Basel, Switzerland) in the same way.

Flow Cytometry

Cells at passage 4 were harvested and labeled with the following anti-human antibodies: anti-CD29-FITC (Santa Cruz Biotechnology, Santa Cruz, CA), anti-CD44-FITC (Dako, Carpinteria, CA), anti-CD31-FITC, and anti-CD34-FITC (Becton–Dickinson, San Diego, CA). Mouse isotype antibodies served as controls. Cells were analyzed using a FACS Calibur flow cytometer (Becton–Dickinson) [19].

Multilineage Differentiation of Human ADSC in Vitro

Human ADSC at passage 4 were analyzed to confirm their capacity to differentiate toward the adipogenic, osteogenic, and chondrogenic lineages. To induce the respective differentiations, ADSC were cultured with previously described lineage-specific induction media [12, 20, 21], as detailed in Table 1. To induce adipogenic and osteogenic differentiation, cultures in respective lineage-specific media were maintained at 37 °C in 5% CO_2 for 2 weeks. Chondrogenic differentiation was determined using a slight modification of a previously described pellet culture technique [22]. Briefly, ADSC were placed in 15 ml polypropylene conical tubes, centrifuged at 1,500 rpm for 5 min, and then cultured in chondrogenic medium (CM) at 37 °C in 5% CO_2 for 4 weeks. ADSC maintained in the control medium were analyzed as negative controls. During the culturing process, the medium was changed every 2 days.

Table 1 Media supplementation for lineage-specific differentiation

Medium	Media	Serum	Supplements
Adipogenic (AM)	DMEM	10% FBS	0.5 mM isobutyl-methylxanthine (IBMX), 1 μM dexamethasone, 10 μM insulin, 200 μM indomethacin, 1% antibiotic/antimycotic
Osteogenic (OM)	DMEM	10% FBS	0.1 μM dexamethasone, 50 μM ascorbate-2-phosphate, 10 mM β-glycerophosphate, 1% antibiotic/antimycotic
Chondrogenic (CM)	DMEM	10% FBS	1.08 μM insulin, 0.23 nMl TGF-β1, 50 nM ascorbate-2-phosphate, 1% antibiotic/antimycotic

Histological Analysis

Differentiated ADSC were confirmed using histological assays [12]. Oil red O stain was used for adipogenesis, alkaline phosphatase (AP) activity and von Kossa stain for osteogenesis, and Safranin O stain for chondrogenesis. For Oil red O stain, cells were fixed with a 3.7% solution of formaldehyde, washed with distilled water, and stained with Oil red O solution for 10 min. AP activity was detected by fixing the cells with a 3.7% solution of formaldehyde and staining with AP solution including 1% naphthol ABSI phosphate. For von Kossa staining, the cells were fixed with 1% paraformaldehyde for 15 min and overlaid for 15 min with a 5% silver nitrate solution in the dark at room temperature. Then, they were left under UV light for 20 min, followed by incubation with sodium thiosulfate for 2 min. For Safranin-O staining, the tissue sections were deparaffinized with xylene and ethanol. Then 1% aqueous Safranin-O was added for 30 min and 0.2% fast green was added for 3 min. After that, the sections were washed with distilled water and with serial concentrations of 70, 80, and 95% ethanol.

Coherent Anti-Stokes Raman Scattering (CARS) Microscopy

For the CARS image measurements, the pump and the Stokes beams were generated from two synchronized 76-MHz near-infrared mode-locked lasers. An Nd:Vanadate laser with a pulse duration of 7 ps (PicoTRAIN, High Q Laser Production GmbH, Hohenems, Austria) was used as the Stokes beam at 1,064 nm, and a pump beam with a duration of 6 ps at 776 nm was generated from an intracavity doubled optical parametric oscillator (Levante, APE GmbH, Berlin, Germany) that is synchronously pumped by the Nd:vanadate laser. The power levels of the pump and the Stokes beams were kept around 50 and 25 mW, respectively. A multiplexed pump beam of 30 nm bandwidth at 817.2 nm was produced from a femtosecond Ti:sapphire laser (Micra-10, Coherent Inc., Santa Clara, CA) with an average power of 900 mW, whose output pulse train was synchronized with that of the 1,064 nm picosecond laser by using an electronic cavity feedback module (SynchroLock-AP, Coherent Inc.). The Raman shift value set in the laser wavelengths was nearly in resonance with the CH-stretching vibrational modes of the sample. The synchronized three laser beams were then collinearly combined and sent to and inverted optical microscope (IX81, Olympus, Tokyo, Japan). The CARS excitation beams were then focused onto a sample by a 1.2-NA water immersion objective lens (UPLSAPO/IR 60X, Olympus). The forward CARS signal in the lipid window (644–683 nm) was collected by a 0.55-NA condenser lens and directed to the photomultiplier tube (R3896, Hamamatsu Photonics, Hamamatsu, Japan). The CARS images having a maximum field of view of 250 × 250 μm^2 were acquired by performing raster scans of the laser beams on the sample.

Reverse Transcription-Polymerase Chain Reaction (RT-PCR) Analysis

Adipogenic differentiated cells were collected at defined time points (day 1, 4, 7 and 14), and non-induced cells were also examined as a negative control. Total RNA from each cell group was extracted by TRIzol reagent (Invitrogen) and was reverse transcribed using the TaqMan Gold RT-PCR kit (Applied Biosystems, Foster City, CA, USA). All real-time PCR measurements were performed using an ABI 7000 real-time PCR system (Applied Biosystems) according to the standard temperature cycling protocol for the relative quantification assays. The expression of PPAR-γ and UCP-1 was quantitated and the primer pairs used were as follows: PPAR-γ: 5′-ATGACAGCGACTTGG CAA-3′ (forward primer) and 5′-AATGTTGGCAGTG GCTCA-3′ (reverse primer); UCP-1: 5′-AGAGCCATCT CCACGGAA-3′ (forward primer) and 5′-CCAGGATCCA AGTCGCAA-3′ (reverse primer). The expression of human glyceraldehyde-3-phosphate dehydrogenase (GAPDH) was used to normalize the gene expression levels.

Image Analysis

We used the IMT morphology program (iMT technology, Bucheon, Korea) to count the number of LD and to estimate the size of each LD.

Statistical Method

Statistical significance was determined using the Student's *t*-test and a p value of <0.05 was considered significant.

Statistical analysis was performed using SPSS version 17.0 (SPSS, Chicago, IL, USA).

Results

Primary Culture and Phenotypic Characterization of SVF Cells

SVF cells including ADSC extracted from the lipoaspirates adhered to the tissue culture dish and grew into spindle-shaped cells, while non-adherent cells such as red blood cells were removed by changing the media. SVF cells proliferated rapidly and exhibited a relatively consistent population doubling rate from passage 0–8 (data not shown). At passage 4, these cells appeared to have a fibroblast-like shape. To examine the immunophenotype of these cells, we characterized the cell population according to its CD marker profile using flow cytometry. The results demonstrated that cells at passage 4 expressed CD29 (99.5%) and CD44 (97.6%) but did not express hematopoietic lineage markers CD31 (6.1%) and CD34 (5.4%) (Fig. 1).

Multi-lineage Differentiation of ADSC

To verify the ADSC, we tested the multilineage capacity of the cultured cells. Cells were differentiated toward the adipogenic, osteogenic, and chondrogenic lineages using lineage-specific induction media, and the instances of differentiation were assessed by histology (Fig. 2). Our cells were cultured in AM for 2 weeks and developed lipid-containing droplets which were stained by Oil Red O, which is consistent with the phenotype of mature adipocytes. Cells treated with OM formed a dense and extensive network. They expressed the increased AP activity by which an osteoblast was characterized and calcification as detected by von Kossa staining. Finally, Safranin-O staining showed distinct proteoglycan production, which indicated chondrogenic differentiation, in cells cultured in CM by the pellet technique. These indicated that ADSC composed the SVF cells from human lipoaspirates.

Serial Observation of Human ADSC in Adipogenic Differentiation

SVF cells including ADSC were cultured in control medium and then switched to AM at passage 4. Using Oil red O stain and CARS microscopy, we observed the chronological change of morphology during the adipogenic differentiation of human ADSC on day 0, 1, 7, and 14 after induction. Treatment with AM generally resulted in enlarged cell morphology and a time-dependent increase in intracellular LD (Fig. 3). Details are as follows: on day 0, the cells were elongated and fibroblast-like. Oil red O staining was negative, and the CARS image showed a centered nucleus with low signal intensity and a ground glass-appearing cytoplasm with multiple medium signal intensity spots.

On Day 1, there appeared to be no significant changes in the morphology of the cells. Cells were still elongated and not stained with Oil red O. The CARS finding was somewhat similar to that on day 0. The characteristic changes began to be observed only after 4 days. The ADSC had become rounder, and Oil red O staining showed sparse positively stained LD. Additionally, multiple 1–3 μm sized high signal globules were distributed in a lace-like pattern peripherally along the cell border in the CARS image.

On day 7, slightly enlarged, rounder cells were observed. They had several enlarged and positively stained LD with Oil red O. The CARS image demonstrated a number of 4–6 μm high signal globules that filled the entire cytoplasm. The nucleus was spared and positioned in the center or on the slight periphery. These morphologic features in CARS image are similar to those of the brown adipocytes [1].

Treatment of AM for additional 7 days enlarged the cells much more. On day 14, Oil red O staining showed large and densely positive LD. On CARS microscopy, the ADSC resembled white adipocytes with a large globule approximately 10 μm in size that had been generated from aggregation of adjacent LD. The nucleus was distorted and leaned onto the cytoplasmic membrane. The number of LD per cell decreased compared to that on day 7.

Monitoring Adipogenesis with Real-Time qPCR

Real-time qPCR demonstrated that PPAR-γ was expressed at an essentially steady rate since it was detected initially on day 4 (Fig. 4a). The mRNA level of UCP-1, a specific marker of brown adipocytes, rose 6- to 7-fold abruptly on day 7 (Fig. 4b), however, slumped significantly on day 14.

Discussion

To reflect an in vivo human context better, we undertook this study using cells from human subcutaneous tissue. Before inducing these cells to differentiate toward adipose tissue, we showed that SVF cells exhibit a stable proliferation rate and a self-renewal capacity, and were positive for mesenchymal cell markers CD29, CD44 but negative for CD31, CD34. This indicates that our cells were not contaminated with progenitors from bone marrow or hematopoietic lineage cells from blood vessels. In addition, we demonstrated the multipotentiality of our cells at passage 4

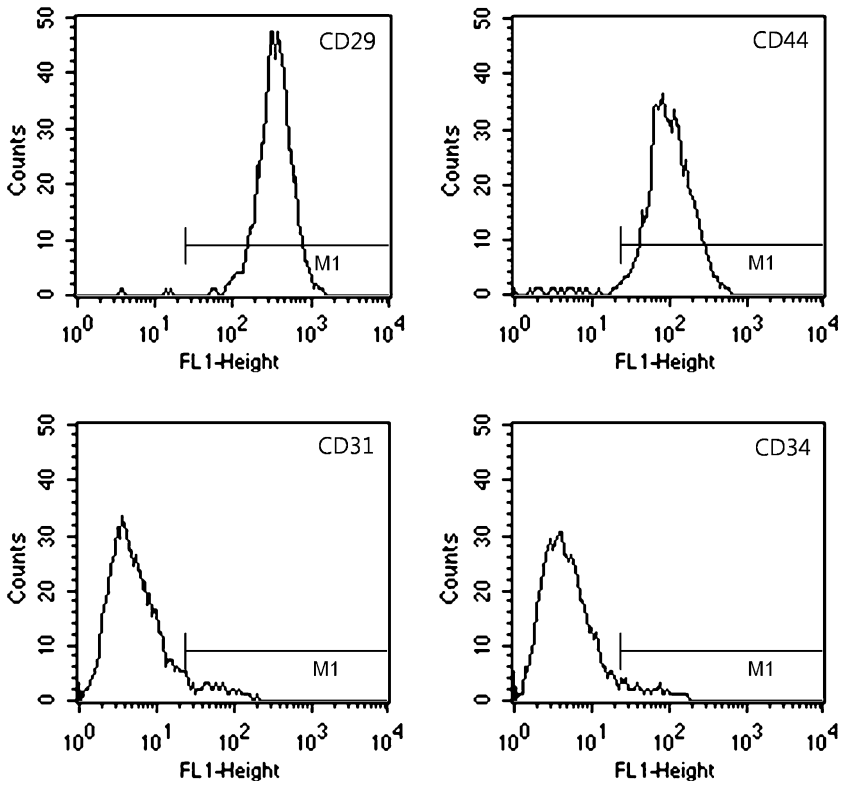

Fig. 1 Phenotypic characterization of human SVF cells. Cells at passage 4 were harvested and flow cytometric analyses of the expression of CD29, CD31, CD34 and CD44 were performed

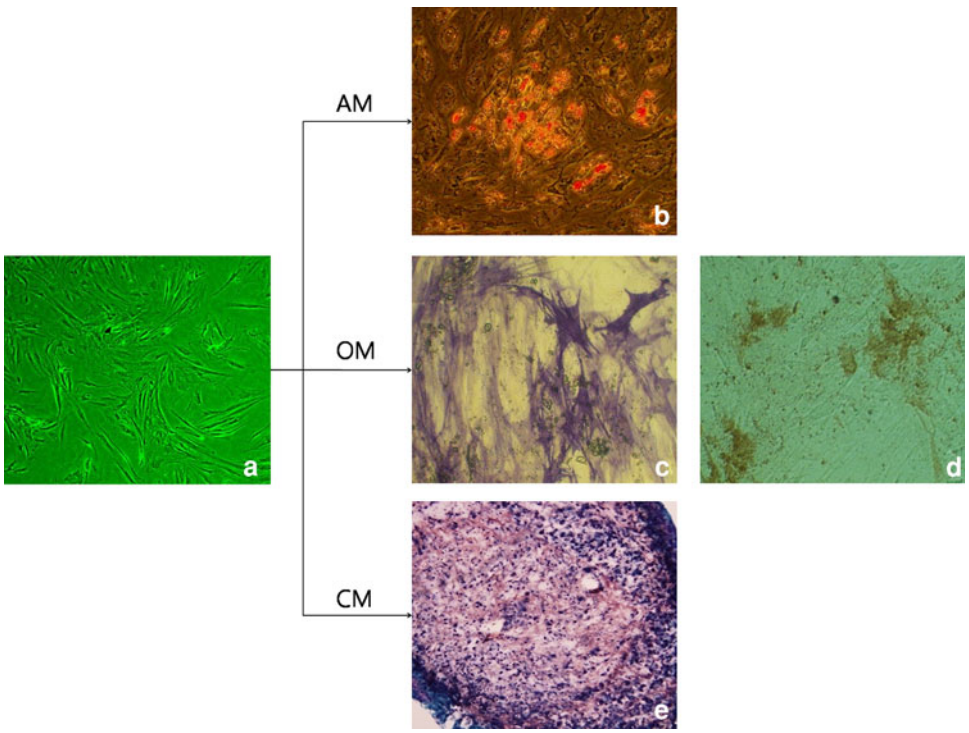

Fig. 2 Multi-lineage differentiation of SVF cells in vitro. SVF cells (**a**) were cultured in lineage-specific media respectively: adipogenic media (*AM*), osteogenic media (*OM*), and chondrogenic media (*CM*). Adipogenic differentiation was confirmed by Oil red O staining (**b**), osteogenic differentiation by alkaline phosphatase activity (**c**) and von Kossa staining (**d**), and chondrogenic differentiation by Safranin O staining (**e**). These indicated that the SVF cells contained ADSC

through differentiating them into osteoblasts, adipocytes, and chondrocytes using lineage-specific induction media. Thus, we concluded that the cultured cells included previously known ADSC. Afterward, the cells including ADSC were induced to differentiate into adipocytes as described previously [12, 20]. In the adipogenic media, IBMX and dexamethasone turn on the transcriptional factor PPAR-γ to direct the transcription of the lipid synthesis

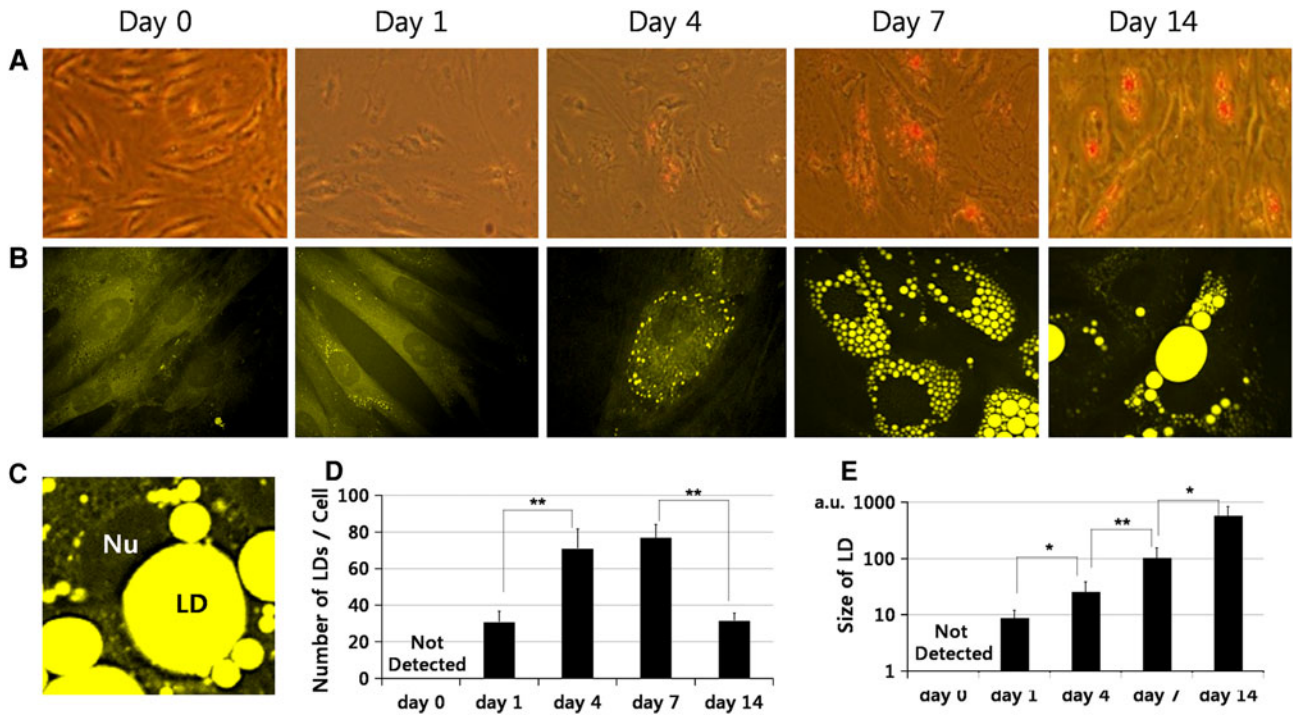

Fig. 3 Chronological observation of adipogenic differentiation with Oil red O staining (**a**) and CARS microscopy (**b**). Lipid droplets (LD) began to be stained sparsely on day 4 and showed a continuous increment of staining by Oil red O (**a**). CARS imaging also demonstrated that multiple 1–3 μm LD were distributed at the periphery of the cells on day 4, which then enlarged to 4–6 μm on day 7 with a centrally placed nucleus. On day 14, a few 10 μm LD pushing the nucleus to the periphery developed (**b**), and this was clearer in the magnified figure (**c**). The number of LD per cell decreased on day 14 compared to that on day 7 (**d**), while the mean size of LD increased (**e**). *LD* lipid droplet, *Nu* nucleus, *a.u.* arbitrary unit). $*p < 0.05$ and $**p < 0.01$

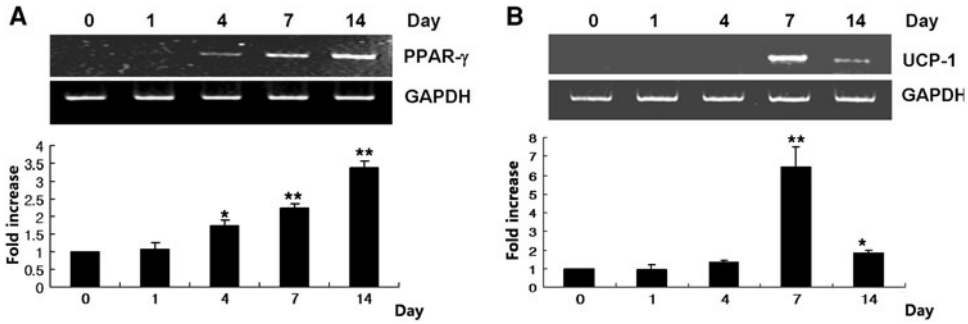

Fig. 4 Assessment of gene expression in adipogenesis. The mRNA level of PPAR-γ increased steadily since it was detected initially on day 4 (**a**). UCP-1 showed an abrupt six–sevenfold increment on day 7 though this regressed on day 14 (**b**). $*p < 0.05$ and $**p < 0.01$ versus day 0

gene, and insulin facilitates glucose uptake and promotes adipocyte differentiation of ADSC [23]. We continuously used this media for 2 weeks.

During adipogenic differentiation, we used CARS microscopy to image ADSC. Traditionally, LD, characteristic structures in adipocytes, can be labeled with Oil red O and imaged using fluorescent microscopy [24]. However, these methods are only applicable to a fixed sample; they disturb LD structures significantly when organic solvents such as ethanol and acetone are used for fixation [25]. Even with formalin fixation, aggregation, fusion, deformation and growth in size of LD arise [18, 26], preventing adipogenesis from being precisely evaluated. In contrast, CARS microscopy allows selective imaging of LD in unstained live cells with a very high contrast, as LD are aggregates of neutral lipids, mainly triglycerides rich in C–H bonds. Consequently, compared to conventional methods, we were able to observe adipogenic differentiation of live ADSC in real-time without fixing and without perturbing the cells.

In addition to the images of high-signal-intensity LD from day 4, CARS images on day 7 were reminiscent of brown adipocytes with numerous scattered small LD showing a multilocular appearance with a very recognizable nucleus, which was either central or somewhat displaced at the periphery of the cell in accordance with the

amount of LD. These features were strikingly similar to those of brown adipocytes in human newborns [27]. However, on day 14, a single large LD was eventually formed perhaps through the coalescence of numerous small LD, pushing the nucleus to the side, which is a typical morphology of mature white adipocytes. The result from the real-time qPCR of UCP-1, which is considered to be the single and best characterized means to distinguish clearly both cell types thus far [5, 6, 28], was consistent with the morphological change of ADSC in adipogenesis; UCP-1 showed a sudden peak on day 7 with a brown adipocyte-like appearance of ADSC, slumping on day 14 with a white adipocyte-like appearance.

As described previously, WAT and BAT has been thought to develop independently for several reasons. First, the developmental patterns of both adipose cells are different, as BAT occurs during late gestation and possesses all the features of mature tissue at birth whereas WAT development takes place mainly after birth [1]. Second, it has been assumed that functional BAT is absent in healthy adults. Third, in vitro precursor cells isolated from WAT or BAT are already committed and therefore differentiate primarily into white or brown adipocytes, respectively [29–31]. However, recent studies have shown that brown adipocytes are dispersed throughout human adipose tissue and are metabolically active [32]. It was also found that BAT activity occurs in healthy men during exposure to cold [33]. Additionally, large depots of BAT development were observed in a patient with a pheochromocytoma that secretes catecholamines [34], although it remains undetermined whether this was reactivation of remnant BAT from neonatal depots or conversion from WAT. Regarding the conversion of white adipocyte to brown adipocyte tissue, Tiraby et al. [35] suggested that it is possible to induce a metabolic shift in white fat cells with PPAR-γ coactivator 1α (PGC-1α) experimentally. Furthermore, upon chronic exposure to rosiglitazone, a specific PPAR-γ agonist, ADSC-derived white adipocytes are able to switch to brown adipocytes by expressing UCP-1 [28]. Our results also support that WAT and BAT do not develop independently, suggesting that white adipocytes undergo a momentary brown adipocyte-like stage during their development. Even if this is not the case, it remains possible that a certain association exists between the developmental processes of both adipocytes.

This study has some limitations. The SVF cells usually represent a very heterogeneous population, which means that every cell we dealt with was not a multipotent stem cell. However, ADSC seems to be mostly responsible for the changes during adipogenic differentiation including transient increase of UCP-1 because cells other than ADSC do not show adipogenic differentiation when cultured in AM. Another limitation is that the morphology of ADSC on day 14 during adipogenesis was not completely identical to that of mature lipid cells. There still remained several small LD although a distinctively large globule developed. However, we think that ADSC would show unilocular LD finally if observation were extended a few days more.

In summary, we observed and characterized the chronological stages of SVF cells including ADSC during adipogenic differentiation. On day 7 of adipogenesis, cells appeared multilocular with numerous small LD according to CARS imaging and the level of UCP-1 increased significantly. However, on day 14, they showed a unilocular appearance with a large single LD and the level of UCP-1 decreased markedly. Based on this morphological change and on the transient expression of UCP-1, we suggest that ADSC passes through a brown adipocyte-like stage while differentiating to white adipocytes.

Acknowledgments This work was supported by the Next-Generation New-Technology Development Program of MKE, and by the Bio-signal Analysis Technology Innovation Program (No. 2009-0084137) and the National Research Foundation of Korea grant (No. 2009-0092835) of MEST, Republic of Korea.

Conflict of Interest None.

References

1. Avram A, Avram M, James W (2005) Subcutaneous fat in normal and diseased states: 2. Anatomy and physiology of white and brown adipose tissue. J Am Acad Dermatol 53:671–683
2. Ramsay T (1996) Fat cells. Endocrinol Metab Clin North Am 25:847–870
3. Cannon B, Nedergaard J (2004) Brown adipose tissue: function and physiological significance. Physiol Rev 84:277–359
4. Jacobsson A, Stadler U, Glotzer MA, Kozak LP (1985) Mitochondrial uncoupling protein from mouse brown fat. Molecular cloning, genetic mapping, and mRNA expression. J Biol Chem 260:16250–16254
5. Ricquier D, Casteilla L, Bouillaud F (1991) Molecular studies of the uncoupling protein. FASEB J 5:2237–2242
6. Moulin K, Truel N, Andre M, Arnauld E, Nibbelink M, Cousin B et al (2001) Emergence during development of the white-adipocyte cell phenotype is independent of the brown-adipocyte cell phenotype. Biochem J 356:659
7. Lefterova M, Lazar M (2009) New developments in adipogenesis. Trends Endocrinol Metab 20:107–114
8. Gregoire F, Smas C, Sul H (1998) Understanding adipocyte differentiation. Physiol Rev 78:783–809
9. Avram M, Avram A, James W (2007) Subcutaneous fat in normal and diseased states: 3. Adipogenesis: from stem cell to fat cell. J Am Acad Dermatol 56:472–492
10. Ntambi J, Young-Cheul K (2000) Adipocyte differentiation and gene expression. J Nutr 130:S3122–S3126
11. Entenmann G, Hauner H (1996) Relationship between replication and differentiation in cultured human adipocyte precursor cells. Am J Physiol Cell Physiol 270:C1011–C1016
12. Zuk PA, Zhu M, Mizuno H, Huang J, Futrell JW, Katz AJ et al (2001) Multilineage cells from human adipose tissue: implications for cell-based therapies. Tissue Eng 7:211–228

13. Zuk P, Zhu M, Ashjian P, De Ugarte D, Huang J, Mizuno H et al (2002) Human adipose tissue is a source of multipotent stem cells. Mol Biol Cell 13:4279–4295
14. Gimble J, Guilak F (2003) Adipose-derived adult stem cells: isolation, characterization, and differentiation potential. Cytotherapy 5:362–369
15. Evans C, Xie X (2008) Coherent anti-Stokes Raman scattering microscopy: chemical imaging for biology and medicine. Annu Rev Anal Chem:883–909
16. Potma E, Xie X (2005) Direct visualization of lipid phase segregation in single lipid bilayers with coherent anti-Stokes Raman scattering microscopy. Chem Phys Chem 6:77–79
17. Wang H, Fu Y, Zickmund P, Shi R, Cheng J (2005) Coherent anti-Stokes Raman scattering imaging of axonal myelin in live spinal tissues. Biophys J 89:581–591
18. Nan X, Cheng J, Xie X (2003) Vibrational imaging of lipid droplets in live fibroblast cells with coherent anti-Stokes Raman scattering microscopy. J Lipid Res 44:2202
19. Strem B, Hicok K, Zhu M, Wulur I, Alfonso Z, Schreiber R et al (2005) Multipotential differentiation of adipose tissue-derived stem cells. Keio J Med 54:132–141
20. Pittenger M, Mackay A, Beck S, Jaiswal R, Douglas R, Mosca J et al (1999) Multilineage potential of adult human mesenchymal stem cells. Science 284:143–147
21. Grigoriadis A, Heersche J, Aubin J (1988) Differentiation of muscle, fat, cartilage, and bone from progenitor cells present in a bone-derived clonal cell population: effect of dexamethasone. J Cell Biol 106:2139
22. Johnstone B, Hering T, Caplan A, Goldberg V, Yoo J (1998) In vitro chondrogenesis of bone marrow-derived mesenchymal progenitor cells. Exp Cell Res 238:265–272
23. Saltiel A, Kahn C (2001) Insulin signalling and the regulation of glucose and lipid metabolism. Nature 414:799–806
24. Koopman R, Schaart G, Hesselink M (2001) Optimisation of oil red O staining permits combination with immunofluorescence and automated quantification of lipids. Histochem Cell Biol 116:63–68
25. DiDonato D, Brasaemle D (2003) Fixation methods for the study of lipid droplets by immunofluorescence microscopy. J Histochem Cytochem 51:773–780
26. Fukumoto S, Fujimoto T (2002) Deformation of lipid droplets in fixed samples. Histochem Cell Biol 118:423–428
27. Zancanaro C, Carnielli V, Moretti C, Benati D, Gamba P (1995) An ultrastructural study of brown adipose tissue in pre-term human new-borns. Tissue Cell 27:339–348
28. Elabd C, Chiellini C, Carmona M, Galitzky J, Cochet O, Petersen R et al (2009) Human multipotent adipose-derived stem cells differentiate into functional brown adipocytes. Stem Cells 27:2753–2760
29. Young P, Arch J, Ashwell M (1984) Brown adipose tissue in the parametrial fat pad of the mouse. FEBS Lett 167:10–14
30. Casteilla L, Nougues J, Reyne Y, Ricquier D (1991) Differentiation of ovine brown adipocyte precursor cells in a chemically defined serum-free medium. Importance of glucocorticoid and age of animals. Eur J Biochem 198:195–199
31. Klaus S (1997) Functional differentiation of white and brown adipocytes. Bioessays 19:215–223
32. Cypess A, Lehman S, Williams G, Tal I, Rodman D, Goldfine A et al (2009) Identification and importance of brown adipose tissue in adult humans. N Eng J Med 360:1509–1517
33. van Marken Lichtenbelt W, Vanhommerig J, Smulders N, Drossaerts J, Kemerink G, Bouvy N et al (2009) Cold-activated brown adipose tissue in healthy men. N Eng J Med 360:1500–1508
34. Lean M, James W, Jennings G, Trayhurn P (1986) Brown adipose tissue in patients with pheochromocytoma. Int J Obes 10:219–227
35. Tiraby C, Tavernier G, Lefort C, Larrouy D, Bouillaud F, Ricquier D et al (2003) Acquirement of brown fat cell features by human white adipocytes. J Biol Chem 278:33370–33376

Lipids (2011) 46:495–504
DOI 10.1007/s11745-011-3548-y

ORIGINAL ARTICLE

Growth Hormone Enhances Arachidonic Acid Metabolites in a Growth Hormone Transgenic Mouse

A. M. Oberbauer · J. B. German · J. D. Murray

Received: 16 August 2010 / Accepted: 4 March 2011 / Published online: 27 March 2011

Abstract In a transgenic growth hormone (GH) mouse model, highly elevated GH increases overall growth and decreases adipose depots while low or moderate circulating GH enhances adipose deposition with differential effects on body growth. Using this model, the effects of low, moderate, and high chronic GH on fatty acid composition were determined for adipose and hepatic tissue and the metabolites of 20:4n-6 (arachidonic acid) were characterized to identify metabolic targets of action of elevated GH. The products of Δ-9 desaturase in hepatic, but not adipose, tissue were reduced in response to elevated GH. Proportional to the level of circulating GH, the products of Δ-5 and Δ-6 were increased in both adipose and hepatic tissue for the omega-6 lipids (e.g., 20:4n-6), while only the hepatic tissues showed an increase for omega-3 lipids (e.g., 22:6n-3). The eicosanoids, PGE_2 and 12-HETE, were elevated with high GH but circulating thromboxane was not. Hepatic PTGS1 and 2 (COX1 and COX 2), SOD1, and FADS2 (Δ-6 desaturase) mRNAs were increased with elevated GH while FAS mRNA was reduced; SCD1 (stearoyl-coenzyme A desaturase) and SCD2 mRNA did not significantly differ. The present study showed that GH influences the net flux through various aspects of lipid metabolism and especially the desaturase metabolic processes. The combination of altered metabolism and tissue specificity suggest that the regulation of membrane composition and its effects on signaling pathways, including the production and actions of eicosanoids, can be mediated by the GH regulatory axis.

Keywords Growth hormone · Arachidonic acid · Fatty acid composition

Abbreviations

ARA	Arachidonic acid
cDNA	Complementary DNA
COX	Cyclooxygenase
DHA	Docosahexaenoic acid
ELISA	Enzyme-linked immunosorbent assay
FADS	Fatty acid desaturase
FAS	Fatty acid synthetase
GAPDH	Glyceraldehyde-3-phosphate dehydrogenase
GH	Growth hormone
HETE	Hydroxyeicosatetraenoic
HPLC	High-performance liquid chromatography
MMLV-RT	Moloney murine leukemia virus-reverse transcriptase
mRNA	Messenger ribonucleic acid
oMt1a-oGH	Ovine metallothionein 1a promoter driving ovine GH transgene construct
PCR	Polymerase chain reaction
PGE2	Prostaglandin $E_{2\alpha}$
PTGS	Prostaglandin H synthase
qPCR	Quantitative real time polymerase chain reaction
SCD	Stearoyl-coenzyme A desaturase
SOD	Superoxide dismutase
SREBP	Sterol regulatory element binding protein

A. M. Oberbauer (✉) · J. D. Murray
Department of Animal Science,
University of California, Davis, CA 95616, USA
e-mail: amoberbauer@ucdavis.edu

J. B. German
Food Science and Technology, University of California,
Davis, CA 95616, USA

J. D. Murray
Veterinary Health, Reproduction, and Population Biology,
University of California, Davis, CA 95616, USA

STAT	Signal transducers and activators of transcription
$ZnSO_4$	Zinc sulfate

Introduction

The fatty acid composition of membrane phospholipids plays an important role in the structural, functional, and signaling properties of biological membranes and has been implicated in regulation of immunologic, physiologic, reproductive and metabolic processes and the functions of tissues from liver to adipose [1]. Arachidonic acid (C20:4n-6, ARA), the most abundant long chain polyunsaturated fatty acid in membranes, appears to be the primary biologically active polyunsaturated species mediating signaling in a variety of peripheral tissues Similarly, the n-3 polyunsaturated fatty acid docosahexaenoic acid (C22:6n-3, DHA) has a role in neural and optical signaling [2].

The negative consequences of deficiencies or excesses of polyunsaturated fatty acids correlate with ARA levels [3–5]. For example, alteration in tissue arachidonate levels can quantitatively account for many of the effects of dietary fish oils due to the omega-3 fats replacing the omega-6 fats in the membranes [3, 6–8] and metabolic deficiencies of arachidonate affect the cardiovascular and immune systems [9]. Whereas all the metabolic, physiologic and immunologic roles of ARA are not yet known, the majority of recognized effects of ARA are thought to be mediated by its conversion to biologically active signal molecules, the eicosanoids [10]. ARA oxygenation by cyclooxygenases produce thromboxane and prostaglandins, while lipoxygenases produce the hydroxyeicosatetraenoic acids (HETE) and leukotrienes (reviewed in [11, 12]). ARA can be also metabolized by cytochrome P450 monooxygenases to yield the epoxyeicosatrienoic acids. These oxygenated derivatives of ARA function to maintain a variety of physiological systems, such as ion exchange in the kidney [13], gaseous exchange in the lung, vascular smooth muscle tone [14], immune cell recruitment and function [10, 15], and activation or inhibition of endocrine glands [16]. While important in specific roles of physiological functions, elevated eicosanoids are considered to be detrimental contributing to a variety of degenerative and inflammatory disease states. As a result of this link, minimizing eicosanoid synthesis is the basis for many therapeutics aimed at controlling inflammation, thrombosis, and pain. Eicosanoids are also a target for proliferative disorders including various cancers, vascular dysfunctions, and autoimmunity.

In vivo, the limiting step for eicosanoid synthesis is the availability of ARA. Although ARA levels are regulated highly within individuals, the absolute amounts vary significantly among a population. Nonetheless, little is known about the basic mechanisms that control the absolute and relative quantities of ARA within cellular membranes. While traditionally most attention has focused on diet, recent observations that polymorphisms of the various desaturase genes are associated with altered fatty acid composition of membranes and various health outcomes has redirected attention on the mechanisms by which fatty acids are metabolized, incorporated into membranes, and converted into bioactive signaling molecules [17]. The limiting steps to membrane composition are still not clear, with both diet and genotype appearing to be important [18, 19]. The importance of hormonal signaling to this interaction has not been defined.

Elevated circulating growth hormone (GH) in a growth hormone transgenic mouse model (the oMt1a-oGH transgenic mouse) reduced essential precursors of long chain polyunsaturated fatty acids (18:2n-6 and 18:3n-3) and increased desaturation and elongation products 20:4n-6 and 22:6n-3 indicating increased activity of the Δ-5 and Δ-6 desaturation enzymes [20]. These mice with chronically elevated circulating GH, relative to wild-type control mice, exhibit about a two-fold increase of ARA content in the phosphatidyl choline phospholipid pool of hepatic membranes. The phosphatidyl ethanolamine component of membrane phospholipids, while not as great a constituent of membrane phospholipids on a percentage basis as phosphatidyl choline pools, also show a modest though significant increase in ARA abundance in response to GH [20]. Arachidonate hydrolyzed from membrane phospholipids of the phosphatidyl choline compartment by phospholipase A2 can be metabolized to eicosanoids thereby serving as local or paracrine effectors [13]. A shift toward a greater proportion of ARA in membrane compartments that are the source of liberated ARA used for subsequent metabolism should correspond to an increase in ARA metabolites. The metabolites of ARA have a wide range of physiological, immunological, neurological and reproductive functions. Therefore, a GH-specific increase in ARA could alter many biological activities, even potentiating the various negative consequences associated with inappropriately elevated eicosanoids.

Dependent upon the degree of transgene induction in the oMT1a-oGH transgenic mouse model, differential adipose phenotypes can be generated: chronically highly expressed circulating GH generates a physically larger, leaner animal [21] while minimal expression of the transgene results in mice of normal in body weight but having enlarged fat depots [22] and moderate transgene stimulation induces an intermediate level of circulating oGH corresponding to a physically larger, yet obese animal [21]. These findings suggest that circulating GH affects growth and adipose

accretion profiles differentially, dependent upon the concentration of circulating GH. Because highly elevated GH induces a change in the fatty acid composition of membranes toward a more unsaturated profile [20, 23], we wanted to determine the extent of GH action on those membranes. Therefore, we asked if long-term different levels of circulating GH, known to alter body composition and fat mass, could change lipid characteristics, and alter the products derived from the arachidonate phosphatidyl pools. Further, we assessed whether genes predicted to respond to changes in the desaturation of tissue lipids were also affected.

Materials and Methods

Animals

Mice used in this study were produced by mating wild-type C57Bl/6 × CBA female mice with males hemizygous for the oMt1a-oGH transgene. This mating scheme produces an average of 50% hemizygous transgenic progeny and 50% homozygous wild-type (i.e., non-transgenic wild-type control) animals. A single copy of the transgene acts in an autosomal dominant fashion to elevate GH expression when stimulated by adding zinc sulfate to the drinking water [24]. Mice were toe-notched for identification and genotyping [25] at 10 days of age and weaned at 21 days of age. All mice were maintained in an AAALAC approved facility in accordance with NIH animal use guidelines under conditions of constant temperature (21°C), humidity (55%), and a 14:10 h light:dark cycle. The study protocol and all procedures were reviewed and approved by the Institutional Animal Care and Use Committee at the University of California, Davis.

Experiment 1

To characterize the role of GH on adipose and hepatic lipid profiles, five to six females were randomly assigned to each of three transgene stimulus groups within a genotype (wild-type or transgenic): 25, 15, or 0 mM $ZnSO_4$ in the drinking water to yield different circulating GH concentrations. Females were chosen to corroborate the lipid alterations observed in studies of male oMt1a-oGH mice [20, 23]. Mice were housed two per cage and provided food (Formulab Chow 5008, Purina Mills, St. Louis, MO) and drinking water ad libitum. Mice were weighed weekly until 10 weeks of age at which time the mice were killed by CO_2 narcosis and gonadal fat pads, blood, and livers collected. Plasma was isolated from blood samples collected at time of animal collection and plasma circulating ovine GH concentrations (resulting from transgene expression) were assayed in duplicate using a double-antibody radioimmunoassay; ovine somatotropin standards were used (NIADDK O-GH-I-3) and a rabbit anti-ovine GH antisera (NIDDK-anti oGH-2) [26].

Lipid Analyses

To determine the effect of GH on modifying the unsaturated lipid pool, the fatty acid class composition was quantified for the phosphatidyl choline fraction of adipose and hepatic tissue as previously described [20]. Briefly tissue lipids were extracted from 200 mg tissue with H_2O/SDS/EtOH/hexanm (1:1:2:2, v/v). Phospholipids were separated by high performance thin layer chromatography using a $CHCl_3$/MeOH/acetic acid/H_2O (50:37.5:3.5:2.0, v/v) solvent system. Samples and standards (Sigma Chemical Co., St. Louis, MO) were visualized and specific lipid-containing bands collected for methylation and gas chromatography separation. The analytical methods used [27] were the most appropriate to quantify the absolute amounts of lipid species present and were designed to be highly quantitative with a cocktail of internal standards and surrogates added quantitatively to each sample. The extractions, derivatizations, and analyses were conducted on platforms to minimize quantitation problems associated with ionization efficiency. Additional hepatic tissue was flash frozen and stored at −80 °C for mRNA analyses.

RNA Analyses

The mRNA levels of genes associated with fatty acid profiles were also assessed: FADS2 (Δ-6 desaturase), fatty acid synthetase (FAS), SCD1 (stearoyl-coenzyme A desaturase 1), and SCD2 (also named Δ-9 desaturase). Several enzymes regulate the production of ARA metabolites, therefore genes expected to change in response to alterations in the desaturation status of tissue lipids were also assessed: prostaglandin H synthase (PTGS) 1 and 2 (also known as cyclooxygenase (COX-1 and 2), and superoxide dismutase 1 (SOD1). RNA was analyzed by Northern blot analysis for SCD2, FAS, SOD1, and COX-1. All reagents, unless noted, were from Sigma Chemical Company (St. Louis, MO). The RNA probes were as follows: SCD2 was as described [28], FAS was a gift from S.D. Clarke [29], Cu–Zn SOD (SOD1) was from the American Type Tissue Collection, and a 1,257 bp fragment of the murine COX-1 (PTGS1) was synthesized using 5′-TTCCTGATTCAAAAGAAGTTCTGG-3′ as the forward primer and 5′-ATGGTGGCTGTTTTGGTAGGCTGT-3′ as the reverse primer on reverse transcribed RNA isolated from murine liver using published methodology [30]. Hepatic FADS2 (Δ-6 desaturase) and SCD 1 mRNA levels were assessed by quantitative real time PCR using

published primers [31, 32], respectively) and mouse specific primers for COX-2 (PTGS2, NM_011198.3) were designed using the NCBI Primer-blast tool: forward 5′-GGCTGTTGGAATTTACGCAT-3′ and reverse 5′-CAGGGCCTTCAAAATGTCTA-3′. The internal endogenous control was GAPDH and used published primers [33]. Primers were fluorescently labeled and the mRNA was transcribed to cDNA with the iScript cDNA synthesis kit (Bio-Rad, Hercules, CA) containing oligo d(t) and random-hexamer primers following the manufacturer's recommendations. All real-time qPCR reactions were run in 96-well plates using UDG-Supermix^{TM} (Invitrogen, Carlsbad, CA). Each reaction contained 10 μM of each primer (forward and reverse), and 5 μl diluted cDNA, in a final volume of 50 μl. The samples were amplified in an MJ Research Chromo 4TM Detector (BioRad, Hercules, CA) and fluorescence was collected during each plate read immediately following the annealing period at 60°C. All reactions were run in triplicate and average values used in quantifying the relative expression of the genes. Levels of mRNA for the genes evaluated were not different across zinc treatments in the wild-type animals ($p > 0.1$) and therefore the data were pooled and the relative quantification of the target genes was determined by the comparative Ct (ΔΔCT) method using the wild-type animal samples as the calibrator. Both the calibrator and samples from the transgenic animals were normalized to GAPDH.

Experiment 2

To explore the consequences of increased ARA levels in tissue, lungs which represent an excellent model to evaluate the production of lipoxygenase metabolites were collected from three adult male transgenic and three adult male wild-type mice maximally stimulated to express GH (25 mM $ZnSO_4$) for 7 days. Nakumura et al. [23] reported a 2.5-fold increase in liver and adipose Δ-6 desaturase activity within 7 days; therefore, this time frame was selected to evaluate the short term consequences on the products derived from the arachidonate phosphatidyl pools. Lungs were homogenized in four volumes of 0.05 M phosphate buffer (pH 7.4) and incubated for 10 min at 37°C. The lipoxygenase metabolite 12-hydroxyeicosatetraenoic acid (12-HETE) was extracted and analyzed by HPLC and diode array detection as described [34]. The effects of GH on circulating prostaglandin $E_{2\alpha}$ (PGE2) and thromboxane were determined for 15 adult male transgenic and 15 adult male wild-type mice supplemented with 25 mM $ZnSO_4$ for 3 weeks. An additional 15 adult male transgenic mice were supplemented with 0 mM $ZnSO_4$ for the same time period. The objective was to evaluate the effects of the transgenically derived GH and as such all wild-type mice received the transgene stimulus to control for any potential zinc effects on PGE2 or thromboxane. Male mice were used to avoid the confounding estrogen effects. Blood samples were collected by cardiac puncture immediately after sacrifice, plasma processed, derivatized and assayed using commercially available ELISA kits according to manufacturer's directions (Amersham, UK). Circulating GH was determined as described.

Statistical Analyses

Data were analyzed by least-squares analysis of variance procedures using PROC GLM of SAS (Version 9.1, 2004) with fixed effects of genotype, zinc stimulation level, and their interaction. Data are presented as means ± standard error of the mean. Post-hoc analysis was done using a *t* test with a Bonferroni adjustment. Significance was defined as $p < 0.05$.

Results

Experiment 1

Circulating ovine (transgene derived) GH in these transgenic mice was correlated directly with the concentration of zinc stimulus. Circulating ovine GH was 750.53 ± 43.83, 131.98 ± 40.40, and 49.22 ± 37.68 ng/ml for 25, 15, and 0 mM $ZnSO_4$, respectively. Zinc, regardless of the level (0, 15, or 25 mM), did not significantly alter body weight nor fat pad depots in the wild-type control mice used in the present study. The body weights associated with the circulating GH were 32.5 ± 0.4, 31.7 ± 0.6, and 22.2 ± 0.4 g for 25, 15, 0 mM $ZnSO_4$, respectively; wild-type mice across all zinc levels weighed 22.6 ± 0.4 g. This was reported in a previously published study of these mice [21].

Adipose Lipid Profiles

The composition of phosphatidyl choline esterified fatty acids was calculated as a mole percent for each lipid species. All three zinc treatments (0, 15, and 25 mM $ZnSO_4$) did not significant alter the adipose lipid profiles in the wild-type animal ($p > 0.1$); as such, the values for wild-type animals were pooled regardless of the zinc treatment given. The fatty acid composition of adipose lipids is presented in Table 1. In most cases, the profile for wild-type animals was generally equivalent to that for the transgenics without transgene stimulation (0 mM $ZnSO_4$) with some exceptions. In particular, the fatty acids typically associated with de novo lipogenesis, 14:1n-7 and 16:1n-7, were elevated significantly while 18:0 was reduced. These same fatty acids were also significantly

Table 1 Adipose lipid profile as mole percent for wild-type (WT) mice and transgenic (TG) mice supplemented with either 0, 15, or 25 mM $ZnSO_4$ to induce variable levels of chronic circulating GH

Fatty acid species	WT ($n = 9$)	TG + 0 mM $ZnSO_4$ ($n = 5$)	TG + 15 mM $ZnSO_4$ ($n = 4$)	TG + 25 mM $ZnSO_4$ ($n = 5$)	Model significance
14:0	2.27 ± 0.06	2.19 ± 0.09	2.22 ± 0.09	1.97 ± 0.08	$p < 0.13$
14:1n-7	0.21 ± 0.01^{ab}	0.23 ± 0.01^{bc}	0.25 ± 0.01^{c}	0.18 ± 0.01^{a}	$p < 0.003$
16:0	26.01 ± 0.46	25.93 ± 0.62	27.49 ± 0.68	25.25 ± 0.61	$p < 0.11$
16:1n-7	4.83 ± 0.22^{a}	5.69 ± 0.29^{a}	7.38 ± 0.32^{b}	4.67 ± 0.29^{a}	$p < 0.001$
18:0	5.03 ± 0.15^{bc}	4.59 ± 0.20^{ab}	4.07 ± 0.22^{a}	5.56 ± 0.22^{c}	$p < 0.001$
18:1n-9	33.4 ± 3.87	37.93 ± 5.20	35.72 ± 5.72	31.12 ± 5.07	$p < 0.836$
18:1n-7	6.80 ± 5.20	0.82 ± 10.41	2.48 ± 10.24	11.28 ± 7.18	$p < 0.841$
18:2	17.86 ± 0.22^{b}	19.14 ± 0.29^{c}	15.58 ± 0.32^{a}	16.40 ± 0.28^{a}	$p < 0.001$
18:3n-6	0.12 ± 0.00^{a}	0.13 ± 0.01^{ab}	0.14 ± 0.01^{bc}	0.15 ± 0.01^{c}	$p < 0.001$
18:3n-3	0.92 ± 0.31	1.07 ± 0.42	2.07 ± 0.46	0.70 ± 0.41	$p < 0.183$
20:0	0.11 ± 0.01^{b}	0.10 ± 0.01^{ab}	0.08 ± 0.01^{ab}	0.07 ± 0.01^{a}	$p < 0.011$
20:1	0.72 ± 0.07	0.45 ± 0.09	0.43 ± 0.10	0.42 ± 0.09	$p < 0.040$
20:2	0.18 ± 0.01^{a}	0.16 ± 0.01^{a}	0.18 ± 0.01^{a}	0.24 ± 0.01^{b}	$p < 0.001$
20:3	0.15 ± 0.00^{b}	0.13 ± 0.01^{a}	0.12 ± 0.01^{a}	0.13 ± 0.01^{a}	$p < 0.002$
20:4n-6	0.25 ± 0.01^{a}	0.32 ± 0.02^{b}	0.47 ± 0.02^{c}	0.60 ± 0.02^{d}	$p < 0.001$
20:5n-3	0.15 ± 0.01	0.18 ± 0.02	0.20 ± 0.02	0.21 ± 0.02	$p < 0.162$
22:0	0.02 ± 0.00	0.02 ± 0.00	0.02 ± 0.00	0.04 ± 0.00	$p < 0.196$
22:1	0.04 ± 0.00	0.03 ± 0.01	0.03 ± 0.01	0.02 ± 0.01	$p < 0.129$
22:4	0.05 ± 0.00^{a}	0.05 ± 0.01^{a}	0.07 ± 0.01^{a}	0.10 ± 0.01^{b}	$p < 0.001$
22:5n-3	0.20 ± 0.01	0.15 ± 0.02	0.19 ± 0.02	0.15 ± 0.02	$p < 0.118$
24:0	0.00 ± 0.00	0.00 ± 0.00	0.000 ± 0.00	0.16 ± 0.07	$p < 0.323$
22:6n-3	0.68 ± 0.06	0.68 ± 0.09	0.82 ± 0.09	0.56 ± 0.08	$p < 0.279$
24:1	0.01 ± 0.00	0.02 ± 0.00	0.01 ± 0.00	0.01 ± 0.00	$p < 0.621$
18:1n-9/18:0	6.65 ± 0.78	8.26 ± 1.04	8.779 ± 1.17	5.59 ± 1.26	$p < 0.133$
20:4n-6/18:2	0.01 ± 0.00^{a}	0.02 ± 0.00^{a}	0.03 ± 0.00^{b}	0.04 ± 0.00^{b}	$p < 0.001$
22:6n-3/18:3n-3	0.74 ± 0.08	0.63 ± 0.11	0.40 ± 0.07	0.80 ± 0.13	$p < 0.887$

Zinc treatment had no effect on lipid profiles in wild-type mice ($p > 0.1$) therefore the wild-type data represent values pooled over all three zinc treatments. Values are least square means ± sem; means carrying different superscripts within a row are significantly different ($p < 0.05$)

changed in mice receiving 15 mM $ZnSO_4$. In general, substrates of the Δ-5 and Δ-6 pathways were reduced in proportion to circulating GH ($p < 0.05$). Specifically, animals with the greatest circulating GH levels had reduced 18:2 and 20:3 (~10% reduction) with elevated 20:4n-6 (~2.4-fold increase); this pattern, though not the extent, was also true for the moderate level of GH (15 mM $ZnSO_4$). In contrast, animals exposed to the lowest level of chronic GH (transgenics receiving 0 mM $ZnSO_4$), while having significantly elevated 20:4n-6 (~1.2-fold increase), also had higher levels of 18:2 (~8%). The ratio of ARA to its 18:2 precursor was significantly elevated in animals exposed to high GH levels (~ 3- to 4-fold increase for the 15 and 25 mM $ZnSO_4$, respectively). Omega-3 lipids were not affected by the altered GH nor was the Δ-9 pathway ($p > 0.10$).

Hepatic Lipid Profiles

Similar to that found for adipose, dietary provision of zinc did not significantly alter any parameter evaluated for wild-type animals ($p > 0.2$), therefore values for wild-type animals were pooled across zinc treatments. The fatty acid composition of hepatic phosphatidyl choline esterified fatty acids, calculated as a mole percent for each lipid species, is presented in Table 2. For fatty acids associated with de novo lipogenesis, there was no affect of circulating GH levels on the proportion of the fatty acids within the hepatic tissue. In contrast, for all 18 carbon fatty acids other than 18:3n-6, elevated GH reduced their percentage in the membrane and did so in proportion to the level of transgene expression. A concomitant increase in 20:4n-6 (~1.8-fold increase) was seen also correlating with the level of GH

Table 2 Hepatic lipid profile as mole percent for wild-type (WT) mice and transgenic (TG) mice supplemented with either 0, 15, or 25 mM $ZnSO_4$ to induce variable levels of chronic circulating GH

Fatty acid species	WT ($n = 8$)	TG + 0 mM $ZnSO_4$ ($n = 4$)	TG + 15 mM $ZnSO_4$ ($n = 5$)	TG + 25 mM $ZnSO_4$ ($n = 4$)	Model significance
14:0	0.58 ± 0.05	0.51 ± 0.08	0.51 ± 0.07	0.32 ± 0.08	$p < 0.086$
14:1n-7	0.22 ± 0.01	0.01 ± 0.01	0.04 ± 0.01	0.01 ± 0.01	$p < 0.242$
16:0	23.68 ± 2.06	24.24 ± 3.00	25.36 ± 2.63	23.15 ± 2.93	$p < 0.881$
16:1n-7	4.27 ± 1.34	2.08 ± 1.96	2.44 ± 1.71	4.52 ± 1.91	$p < 0.665$
18:0	10.75 ± 0.63^{a}	14.25 ± 0.92^{b}	13.90 ± 0.81^{b}	14.84 ± 0.90^{b}	$p < 0.006$
18:1n-9	22.91 ± 1.16^{b}	17.33 ± 1.70^{a}	18.83 ± 1.48^{ab}	17.36 ± 1.66^{ab}	$p < 0.017$
18:1n-7	2.96 ± 0.24	1.90 ± 0.36	2.20 ± 0.31	1.87 ± 0.40	$p < 0.044$
18:2	14.44 ± 0.73^{b}	14.46 ± 1.07^{ab}	11.43 ± 0.93^{ab}	9.96 ± 1.04^{a}	$p < 0.007$
18:3n-6	0.19 ± 0.01^{a}	0.27 ± 0.02^{b}	0.26 ± 0.02^{b}	0.27 ± 0.02^{b}	$p < 0.007$
18:3n-3	0.33 ± 0.03^{b}	0.34 ± 0.04^{b}	0.29 ± 0.03^{ab}	0.18 ± 0.04^{a}	$p < 0.014$
20:0	0.05 ± 0.01	0.06 ± 0.01	0.06 ± 0.01	0.05 ± 0.01	$p < 0.913$
20:1	0.32 ± 0.02^{b}	0.18 ± 0.03^{a}	0.24 ± 0.02^{ab}	0.25 ± 0.03^{ab}	$p < 0.003$
20:2	0.42 ± 0.02	0.32 ± 0.03	0.37 ± 0.03	0.40 ± 0.03	$p < 0.107$
20:3	1.16 ± 0.04^{c}	0.92 ± 0.06^{b}	0.69 ± 0.05^{ab}	0.55 ± 0.06^{a}	$p < 0.001$
20:4n-6	7.00 ± 0.66^{a}	9.07 ± 0.96^{ab}	10.65 ± 0.84^{bc}	12.84 ± 0.94^{c}	$p < 0.001$
20:5n-3	0.95 ± 0.08^{b}	1.26 ± 0.11^{b}	0.94 ± 0.10^{b}	0.42 ± 0.11^{a}	$p < 0.001$
22:0	0.17 ± 0.01	0.19 ± 0.02	0.17 ± 0.02	0.20 ± 0.02	$p < 0.762$
22:1	0.01 ± 0.00	0.01 ± 0.01	0.02 ± 0.01	0.02 ± 0.01	$p < 0.232$
22:4n-6	0.16 ± 0.02^{a}	0.18 ± 0.03^{a}	0.22 ± 0.02^{a}	0.34 ± 0.03^{b}	$p < 0.001$
22:5n-3	0.48 ± 0.05	0.64 ± 0.08	0.47 ± 0.07	0.35 ± 0.08	$p < 0.139$
24:0	0.09 ± 0.02	0.12 ± 0.03	0.14 ± 0.03	0.17 ± 0.03	$p < 0.320$
22:6n-3	8.64 ± 0.54^{a}	11.35 ± 0.78^{ab}	10.42 ± 0.68^{ab}	11.53 ± 0.76^{b}	$p < 0.025$
24:1	0.31 ± 0.03	0.33 ± 0.05	0.33 ± 0.04	0.39 ± 0.05	$p < 0.494$
18:1n-9/18:0	2.13 ± 0.16^{b}	1.22 ± 0.24^{a}	1.35 ± 0.20^{ab}	1.17 ± 0.23^{a}	$p < 0.006$
20:4n-6/18:2	0.48 ± 0.08^{a}	0.63 ± 0.11^{ab}	0.93 ± 0.10^{bc}	1.29 ± 0.11^{c}	$p < 0.001$
22:6n-3/18:3n-3	26.25 ± 5.06^{a}	33.24 ± 7.04^{a}	35.53 ± 5.34^{ab}	64.77 ± 6.82^{b}	$p < 0.002$

Zinc treatment had no effect on lipid profiles in wild-type mice ($p < 0.1$) therefore the wild-type data represent values pooled over all three zinc treatments. Values are least square means ± sem; means carrying different superscripts within a row are significantly different ($p < 0.05$)

expressed from the transgene. Elevated GH reduced the 18:1/18:0 ratio by nearly 50% and the combined effects of GH raising ARA (20:4n-6) and decreasing alpha linoleic (18:2) resulted in a significantly elevated 20:4/18:2 (ARA: linoleic acid) ratio (~2.5-fold increase, $p < 0.001$). A similar result was detected for the 22:6/18:3n-3 (DHA: alpha linolenic acid) ratio ($p < 0.002$). The elevated ratios were proportional to the degree of elevated GH in circulation: the 25 mM $ZnSO_4$ treated transgenic animals had the greatest ratios followed by the 15 mM $ZnSO_4$ treated transgenics which were in turn greater than the 0 mM $ZnSO_4$; with the last group's ratios statistically equivalent to those of the wild-type controls.

Hepatic RNA

Wild-type control animals given 0, 15, and 25 mM $ZnSO_4$ supplementation did not exhibit significant differences in mRNA levels for any of the genes evaluated ($p > 0.1$) due to zinc treatment and were therefore pooled for analyses. Stearyl-CoA desaturase 1 hepatic mRNA levels were unaffected by alterations in circulating GH ($p > 0.5$) and SCD 2 levels were not significantly reduced in proportion to the level of circulating GH (Fig. 1; $p < 0.1$). Animals experiencing the highest levels of circulating GH had significantly reduced FAS mRNA compared to wild-type control animals ($p < 0.01$). The animals with low, but chronic GH had intermediate FAS mRNA values that were not significantly different than the wild-type animals that had the highest FAS mRNA levels. In contrast, SOD1 mRNA was elevated in animals expressing the highest levels of GH while animals with the low and moderately elevated GH levels had SOD1 levels equivalent to wild-type expression ($p < 0.001$). Levels of COX-1 mRNA were significantly elevated for the animals with moderate to highly elevated GH (transgenics supplemented with 15

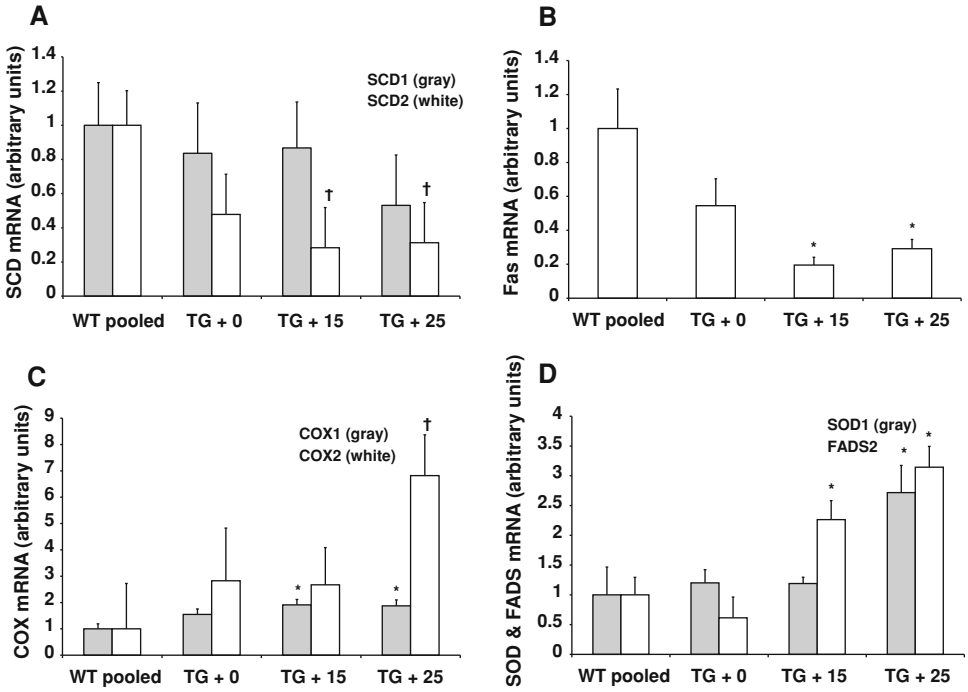

Fig. 1 Hepatic mRNA levels in oMT1a-oGH transgenic (TG) mice exposed to 0, 15, and 25 mM $ZnSO_4$ transgene stimulus used to vary the level of circulating GH as compared to wild-type control (WT) mice, pooled across all zinc treatment levels. Values are expressed as means + sem, $n = 5$–6 mice per group, and means with an *asterisk* differ from control mice $p < 0.05$; means denoted with a† differ from control mice $p < 0.1$. **a** Stearyl-CoA desaturase (SCD) 1 (*gray bars*) and 2 (*white bars*), **b** Fatty acid synthase (FAS), **c** Cyclooxygenase (COX) 1 (*gray bars*) and 2 (*white bars*), **d** Superoxide dismutase 1 (SOD1, *gray bars*) and FADS2 (*white bars*)

and 25 mM $ZnSO_4$, respectively) when compared to the wild-type animals ($p < 0.01$). Transgenic mice not given any zinc stimulus therefore having low chronic GH in circulation, had intermediate levels of COX-1 mRNA (Fig. 1). A similar trend was seen for the COX-2 mRNA levels ($p < 0.1$) with the highest mRNA levels showing a nearly a seven-fold increase, detected in the animals experiencing the greatest circulating GH. The mRNA levels of FADS2 paralleled the changes in hepatic lipid membranes: the highest GH exposure resulted in the greatest level of FADS2 mRNA ($p < 0.001$).

Experiment 2

Arachidonic Acid Metabolites

Because the transgene had not been stimulated during the growth phase of the adult males used in this experiment, body weights did not significantly differ: 42.5 ± 1.7 and 42.4 ± 0.9 g for the transgenic and wild-type mice, respectively. Upon activation of the transgene, circulating ovine GH levels in the adult transgenics were 332.0 ± 23.8 ng/ml. The arachidonic metabolite 12-HETE was significantly elevated in mice after 1 week of exposure to elevated GH ($p < 0.05$). Transgenic mice supplemented with 25 mM $ZnSO_4$ had over twice the quantity of 12-HETE in their lungs than wild-type mice also supplemented with 25 mM $ZnSO_4$ (Fig. 2). Similarly, plasma PGE2 was significantly elevated in response to high circulating GH. In contrast, the unstimulated transgenic mice

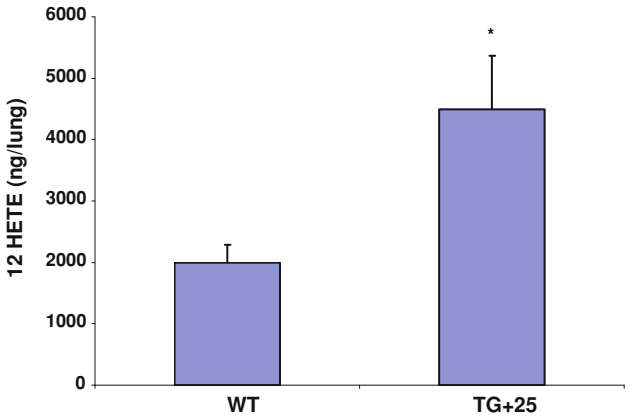

Fig. 2 Production of the 12 lipoxygenase product 12 HETE in lungs of wild-type control (WT) and oMT1a-oGH transgenic (TG) mice exposed to the transgene stimulus (25 mM zinc). Data are expressed as means + sem (ng/lung) and are significantly different ($n = 3$ per group)

with low chronic GH (0 mM $ZnSO_4$) did not exhibit any changes in PGE2 relative to the wild-type mice given 25 mM $ZnSO_4$ (Table 3). Circulating thromboxane was not significantly affected by elevated GH (Table 3).

Discussion

The effects of elevated circulating GH on the regulation of lipid profiles, specifically metabolites of the long chain saturated and polyunsaturated fatty acid desaturases, were

Table 3 Plasma arachidonic acid metabolites as a consequence of circulating growth hormone

Treatment	PGE2 (pg/ml)	Thromboxane (ng/ml)
WT + 25 mM $ZnSO_4$	13.54 ± 11.19[a] ($n = 8$)	224.8 ± 97.6 ($n = 8$)
TG + 0 mM $ZnSO_4$	13.23 ± 11.19[a] ($n = 8$)	385.3 ± 83.3 ($n = 11$)
TG + 25 mM $ZnSO_4$	49.84 ± 10.50[b] ($n = 9$)	237.1 ± 71.3 ($n = 15$)

Values are least square means ± sem; means carrying different superscripts within a column are significantly different ($p < 0.05$)

studied. In this GH transgenic model, mice exposed to moderate but chronically increased circulating GH become obese whereas highly elevated circulating GH reduces adipose stores [21] and alters hepatic membrane lipid profiles in a rapid and sustained manner [20, 23]. Although elevated GH is frequently associated with reduced adipose mass, in this model development of obesity in the presence of moderately elevated GH is thought to be mediated by greater expression of GH receptor binding protein [21] or through increased leptin and insulin secretion as seen in the moderately obese GHRH transgenic mouse that also has elevated GH levels [35].

In hepatic tissues, the activity of the Δ-9 desaturase as indicated by the lipid products was decreased in response to high circulating GH whereas the Δ-5 and Δ-6 enzymatic activities appeared to be increased in both adipose and hepatic tissues as evidenced by a greater percentage of ARA. Elevated DHA in response to GH was only detected in hepatic but not adipose tissue indicating that GH exerts tissue specificity in the processing of fatty acids. These findings corroborate previous studies evaluating hepatic lipid profiles [20, 23] although there were some discrepancies likely due to duration of GH exposure and downstream effects of the elevated GH. Specifically, short term elevated GH significantly depressed DHA and ARA in adipose, whereas the present study with long-term GH exposure did not significantly depress DHA and elevated ARA. Additionally, the data demonstrate that the GH induced change to lipid profiles occurs in both males and females. The latter is important in that women have lower Δ-6 enzymatic activities than men [36]; the finding that both male and female mice responded similarly with enhanced activity to GH suggests that GH may be a key endogenous regulator of the net flux through the desaturase pathway. The higher the circulating GH, the greater the Δ-5 and Δ-6 desaturase activity as evidenced by changes in the lipid profile and greater FADS expression. However, in this mouse model high GH is associated with elevated insulin; insulin levels decline following GH withdrawal [26] indicating that the transgenically derived GH impairs insulin signaling causing a mild diabetic state. Insulin is known to induce the expression of the Δ-5, Δ-6, and Δ-9 desaturases in rats [37] suggesting that long-term GH action observed in the present study may be mediated through elevated insulin.

An increased proportion of ARA in tissues would be expected to elevate ARA metabolites and that was the case for circulating PGE2 and lung produced 12-HETE. Similarly, the constitutively active COX1 mRNA as well as COX2 mRNA were increased in response to elevated circulating GH suggesting coordinated regulation of this pathway. In contrast, the most pro-thrombotic eicosanoid, thromboxane was unchanged despite the dramatic increase in the level of ARA, its precursor. Thromboxane has been shown to be associated directly with membrane arachidonate; specifically thromboxane is lower in animals fed alpha linolenic acid (18:3n-3) which correlates to higher levels of 18:3n-3 in the liver membranes [39] that replace 18:2 lowering overall arachidonate, a precursor of thromboxane [38]. Levels of circulating thromboxane in the current study did not significantly change with exposure to GH even though arachidonate was increased appreciably. The GH induced increase of ARA may not have been within the specific precursor pools for the thromboxane production.

Elevated highly unsaturated fatty acid species within membranes could serve as targets for reactive oxygen species and could increase the opportunities for oxidative modification and damage. As tissue membranes became more unsaturated in response to high GH, SOD1 mRNA was significantly elevated. Generally SOD1 is constitutively expressed although ARA can upregulate SOD1 gene transcription in vitro (39). High circulating GH with its shift toward unsaturated fatty acid species increased expression of SOD1 indicating that only supraphysiological arachidonic levels pose an oxidative risk and increase SOD1 expression in vivo.

Fatty acid synthetase, a key regulator of de novo long chain fatty acid biosynthesis, promotes adipose storage; inhibition of FAS in vivo results in weight loss [40]. FAS activity is regulated at the level of gene expression rather than enzymatic activation and FAS can be transcriptionally regulated by STAT5A, a GH signal transducer [41]. GH activation of STAT5 plays a defined role in adipogenesis [42] and by activating STAT5, GH can block the transcriptional activation of FAS in adipocytes [41] thereby reducing lipid accrual. GH also reduces glucose uptake thereby further reducing de novo long chain fatty acid biosynthesis and the substrates available for desaturation.

Hogan and Stephens [41] showed that GH inhibition of FAS is rapidly reversible, consistent with the observation that chronic exposure to GH produces a lean phenotype but withdrawal of GH results in the rapid accumulation of

adipose [25]. FAS mRNA was reduced in the presence of all levels of GH, even those known to promote adipogenesis and adipose accrual in these animals [21]. The increase in adipose deposition observed in these transgenic animals upon withdrawal of high GH or in response to moderate levels of GH occurs regardless of feed restriction [24] indicating that GH overrides the expected composition of gain observed for normal rodents [42] and the expectation of reduced adipose deposition associated with lowered FAS expression. Therefore, FAS expression alone is insufficient to account for adipose deposition in animals that become obese while experiencing moderately high GH levels. Although alterations in mRNA levels may not necessarily imply changes in protein activity, clearly this is an area that requires further exploration. Metabolic end-products of FAS, in particular 16:1n-7 have recently been identified as participating in tissue to tissue communication and the overall regulation of systemic energy [27]. In the present GH manipulated animals 16:1n-7 was elevated in the adipose of overweight animals and lowered in GH stimulated mice implying that an additional level of regulation by GH may be through this form of metabolic end product, i.e. lipokine signaling.

Exposure to GH did not significantly decrease hepatic SCD2 mRNA. In a study where only SCD1 mRNA was evaluated, lactating cows given recombinant bovine GH [43] had reduced SCD1 mRNA in adipose but not mammary tissue implying tissue specificity in GH modulation of SCD expression. SCD1 null mice have lowered body adiposity, depressed hepatic expression of fatty acid synthesis genes, and increased expression of fatty acid oxidation genes [44]. In response to elevated GH in the present study, SCD expression was reduced although not significantly so. FAS and fatty acid oxidation gene expression followed an expression pattern similar to that seen for the SCD1 null mouse indicating a potential mechanism of action for GH.

The interplay between circulating GH and adipose cannot be accounted for by changes in membrane lipids and their potential signaling metabolites. It is curious that GH stimulated the desaturase pathways in membrane lipids in a tissue specific manner between adipose and hepatic membranes with particular reference to the omega-3 lipids. Similarly, GH altered ARA metabolites differentially with PGE2 and 12-HETE elevated but with no effect on thromboxane. This mouse model, especially by targeting adipose tissue, may be useful in elucidating the mechanism behind the differential tissue and eicosanoid response. Particularly as the finding that the desaturase process responds to different GH levels is intriguing and suggests the possibility of modifying the pathway to minimize the negative aspects of inappropriately elevated eicosanoids.

Acknowledgments This research was supported by NIEHS-UCD Superfund Basic Research Program, and the NIEHS CHARGE Study R01 ES02710 and P42 ES04699 and NIEHS 1 P01 ES11269-01. The authors also acknowledge the animal care provided by Ms. Cyndi Stiglich and the technical assistance of Elaine Hoye, Susan Cushwa, Kelly Regan, and Janelle Belanger.

References

1. Nakamura MT, Nara TY (2004) Structure, function, and dietary regulation of Δ6, Δ5, and Δ9 desaturases. Annu Rev Nutr 24:345–376
2. Uauy R, Hoffman, Peirano P et al (2001) Essential fatty acids in visual and brain development. Lipids 36:685–695
3. Flower RJ, Perretti M (2005) Controlling inflammation: a fat chance? J Exp Med 201:671–674
4. Kaiser E, Chiba P, Zaky K (1990) Phospholipases in biology and medicine. Clin Biochem 23:349–370
5. Makheja AN (1992) Atherosclerosis: the eicosanoid connection. Mol Cell Biochem 111:137–142
6. Biscione F, Pignalberi C, Totteri A, Messina F, Altamura G (2007) Cardiovascular effects of omega-3 free fatty acids. Curr Vasc Pharmacol 5:163–172
7. Kinsella JE (1990) Lipids, membrane receptors, and enzymes: effects of dietary fatty acids. J Parenteral Enteral Nutr 14:200s–217s
8. Simopoulos AP (2006) Evolutionary aspects of diet, the omega-6/omega-3 ratio and genetic variation: nutritional implications for chronic diseases. Biomed Pharmacother 60:502–507
9. Lefkowith JB (1990) Essential fatty acid deficiency: probing the role of arachidonate in biology. Adv Prostaglandin Thromboxane Leukotriene Res 20:224–231
10. Bogatcheva NV, Sergeeva MG, Dudek SM, Verin AD (2005) Arachidonic acid cascade in endothelial pathobiology. Microvasc Res 69:107–127
11. Smith WL, DeWitt DL, Garavito RM (2000) Cyclooxygenases: structural, cellular, and molecular biology. Annu Rev Biochem 69:145–182
12. Yamamoto S, Suzuki H, Ueda N (1997) Arachidonate 12-lipoxygenases. Prog Lipid Res 36:23–41
13. Smith WL (1992) Prostanoid biosynthesis and mechanisms of action. Am J Physiol 263:F181–F191
14. Leaf A, Weber PC (1988) Cardiovascular effects of n-3 fatty acids. N Eng J Med 318:549–557
15. Gerrard JM (1985) Prostaglandins and leukotrienes. Marcel Dekker, New York
16. Persaud SJ, Muller D, Belin VD, Kitsou-Mylona I, Asare-Anane H, Papadimitriou A, Burns CJ, Huang GC, Amiel SA, Jones PM (2007) The role of arachidonic acid and its metabolites in insulin secretion from human islets of langerhans. Diabetes 56:197–203
17. Glaser C, Heinrich J, Koletzko B (2010) Role of FADS1 and FADS2 polymorphisms in polyunsaturated fatty acid metabolism. Metabolism 59:993–999
18. Mathias RA, Vergara C, Gao L, Rafaels N, Hand T, Campbell M, Bickel C, Ivester P, Sergeant S, Barnes KC, Chilton FH (2010) FADS genetic variants and omega-6 polyunsaturated fatty acid metabolism in a homogeneous island population. J Lipid Res 51:2766–2774
19. Tu WC, Cook-Johnson RJ, James MJ, Mühlhäusler BS, Gibson RA (2010) Omega-3 long chain fatty acid synthesis is regulated more by substrate levels than gene expression. Prostaglandins Leukot Essent Fatty Acids 83:61–68

20. Murray JD, Oberbauer AM, Sharp KR, German JB (1994) Expression of an ovine growth hormone transgene in mice increases arachidonic acid in cellular membranes. Transgenic Res 3:241–248
21. Oberbauer AM, Stiglich C, Murray JD, Keen CL, Fong DL, Smith LB, Cushwa S (2004) Dissociation of body growth and adipose deposition effects of growth hormone in oMt1a-oGH transgenic mice. Growth Dev Aging 68:33–45
22. Oberbauer AM, Murray JD (1998) Consequences of limited exposure to elevated growth hormone in the mature oMt1a-oGH transgenic mouse. Growth Dev Aging 62:87–93
23. Nakamura MT, Phinney SD, Tang AB, Oberbauer AM, German JB, Murray JD (1996) Increased hepatic delta 6-desaturase activity with growth hormone expression in the MG101 transgenic mouse. Lipids 31:139–143
24. Shanahan CM, Rigby NW, Murray JD, Marshall JT, Townrow CA, Nancarrow CD, Ward KA (1989) Regulation of expression of a sheep metallothionein 1a-sheep growth hormone fusion gene in transgenic mice. Mol Cell Biol 9:5473–5479
25. Pomp D, Oberbauer AM, Murray JD (1996) Development of obesity following inactivation of a growth hormone transgene in mice. Transgenic Res 5:13–23
26. Oberbauer AM, Stern JS, Johnson PR, Horwitz BA, German JB, Phinney SD, Beermann DH, Pomp D, Murray JD (1997) Body composition of inactivated growth hormone (oMt1a-oGH) transgenic mice: generation of an obese phenotype. Growth Dev Aging 61:169–179
27. Cao H, Gerhold K, Mayers JR, Wiest MM, Watkins SM, Hotamisligil GS (2008) Identification of a lipokine, a lipid hormone linking adipose tissue to systemic metabolism. Cell 134:933–944
28. Thiede MA, Strittmatter P (1985) The induction and characterization of rat liver stearyl-CoA desaturase mRNA. J Biol Chem 260:14459–14463
29. Mildner AM, Clarke SD (1991) Porcine fatty acid synthase: cloning of a complementary DNA, tissue distribution of its mRNA and suppression of expression by somatotropin and dietary protein. J Nutr 121:900–907
30. Tordjman C, Coge F, Andre N, Rique H, Spedding M, Bonnet J (1995) Characterization of cyclooxygenase 1 and 2 expression in mouse resident peritoneal macrophages in vitro; interactions of non steroidal anti-inflammatory drugs with COX2. Biochim Biophys Acta 1256:249–256
31. Xu Z, Le K, Moghadasian MH (2008) Long-term phytosterol treatment alters gene expression in the liver of apo E-deficient mice. J. Nutr Biochem 19(8):545–554
32. Lefrere I, De Coppet P, Camelin JC, Le Lay S, Mercier N, Elshourbagy N, Bril A, Berrebi-Bertrand I, Feve B, Krief S (2002) Neuropeptide AF and FF modulation of adipocyte metabolism. Primary insights from functional genomics and effects on beta-adrenergic responsiveness. J Biol Chem 277(42):39169–39178
33. Wong ML, Islas-Trejo A, Medrano JF (2002) Structural characterization of the mouse high growth deletion and discovery of a novel fusion transcript between suppressor of cytokine signaling-2 (Socs-2) and viral encoded semaphoring receptor (Plexin C1). Gene 299:153–163
34. German JB, Hu ML (1990) Oxidant stress inhibits the endogenous production of lipoxygenase metabolites in rat lungs and fish gills. Free Radic Biol Med 8:441–448
35. Cai A, Hyde JF (1999) The human growth hormone-releasing hormone transgenic mouse as a model of modest obesity: differential changes in leptin receptor (OBR) gene expression in the anterior pituitary and hypothalamus after fasting and OBR localization in somatotrophs. Endocrinology 140:3609–3614
36. Warensjő E, Ohrvall M, Vessby B (2006) Fatty acid composition and estimated desaturase activities are associated with obesity and lifestyle variables in men and women. Nutr Metab Cardiovasc Dis 16:128–136
37. Saether T, Tran TN, Rootwelt H, Christophersen BO, Haugen TB (2003) Expression and regulation of delta5-desaturase, delta6-desaturase, stearoyl-coenzyme A (CoA) desaturase 1, and stearoyl-CoA desaturase 2 in rat testis. Biol Reprod 69:117–124
38. Ikeda I, Mitsui K, Imaizumi K (1996) Effect of dietary linoleic, alpha-linolenic and arachidonic acids on lipid metabolism, tissue fatty acid composition and eicosanoid production in rats. J Nutr Sci Vitaminol (Tokyo) 42:541–551
39. Zelko IN, Mariani TJ, Folz RJ (2002) Superoxide dismutase multigene family: a comparison of the CuZn-SOD (SOD1), Mn-SOD (SOD2), and EC-SOD (SOD3) gene structures, evolution, and expression. Free Radic Biol Med 33:337–349
40. Ronnett GV, Kleman AM, Kim EK, Landree LE, Tu Y (2006) Fatty acid metabolism, the central nervous system, and feeding. Obesity (Silver Spring) 14(Suppl 5):201S–207S
41. Hogan JC, Stephens JM (2005) The regulation of fatty acid synthase by STAT5A. Diabetes 54:1968–1975
42. Thonney ML, Oberbauer AM, Duhaime DJ, Jenkins TC, Firth NL (1984) Empty body component gain of rats grown at different rates to a range of final weights. J Nutr 114(10):1777–1786
43. Beswick NS, Kennelly JJ (2000) Influence of bovine growth hormone and growth hormone-releasing factor on messenger RNA abundance of lipoprotein lipase and stearoyl-CoA desaturase in the bovine mammary gland and adipose tissue. J Anim Sci 78:412–419
44. Ntambi JM, Miyazaki M, Stoehr JP, Lan H, Kendziorski CM, Yandell BS, Song Y, Cohen P, Friedman JM, Attie AD (2002) Loss of stearoyl-CoA desaturase-1 function protects mice against adiposity. Proc Natl Acad Sci 99:11482–11486

Lipids (2011) 46:505–512
DOI 10.1007/s11745-010-3518-9

ORIGINAL ARTICLE

Oral Glucosylceramide Reduces 2,4-Dinitrofluorobenzene Induced Inflammatory Response in Mice by Reducing TNF-Alpha Levels and Leukocyte Infiltration

Jingjing Duan · Tatsuya Sugawara · Shota Sakai · Kazuhiko Aida · Takashi Hirata

Received: 17 August 2010 / Accepted: 13 December 2010 / Published online: 11 January 2011

Abstract Sphingolipids are constituents of cellular membranes and play important roles as second messengers mediating cell functions. As significant components in foods, sphingolipids have been proven to be critical for human health. Moreover, diverse metabolic intermediates of sphingolipids are known to play key roles both in proinflammatory and in anti-inflammatory effects. However, the effect of dietary sphingolipids on inflammation is a complicated field that needs to be further assessed. Our study evaluated the effects of orally administered maize glucosylceramide (GluCer), one of the most conventional dietary sphingolipids, on inflammation using the 2,4-dinitro-1-fluorobenzene-treated BALB/c murine model. Oral administration of GluCer inhibited ear swelling and leukocyte infiltration to the inflammatory site, suggesting that dietary GluCer has anti-inflammatory properties. ELISA analyses revealed that oral administration of GluCer for 6 days had not modified the Th1/Th2 balance, but significantly down-regulated the activation of TNF-α at the inflammatory site. Based on these results, the down-regulation of TNF-α by dietary GluCer may suppress vascular permeability and reduce the migration of inflammatory cells. Our findings increase understanding of the actions of dietary sphingolipids on the balance of the immune response.

J. Duan · T. Sugawara (✉) · S. Sakai · T. Hirata
Division of Applied Biosciences,
Graduate School of Agriculture, Kyoto University,
Kitashirakawaoiwakecho, Sakyo-ku, Kyoto 606-8502, Japan
e-mail: sugawara@kais.kyoto-u.ac.jp

K. Aida
Central Laboratory, Nippon Flour Mills Co., Ltd,
Atsugi, Kanagawa 243-0041, Japan

Keywords Sphingolipids · Dietary supplements · Glucosylceramide · Anti-inflammatory agents · DNFB · BALB/c mice · TNF-α · Immune response

Abbreviations

DNFB	2,4-Dinitro-1-fluorobenzene
GluCer	Glucosylceramide
IFN-γ	Interferon-gamma
IgE	Immunoglobulin E
IL-1β	Interleukin-1beta
IL-4	Interleukin-4
IL-6	Interleukin-6
NF-κB	Receptor activator of nuclear factor-kappa B
Th1	T-helper 1
Th2	T-helper 2
TNF-α	Tumor necrosis factor-alpha

Introduction

Sphingolipids are commonly believed to protect the cell surface against harmful environmental factors by forming the mechanically stable and chemically resistant outer leaflet of the plasma membrane lipid bilayer [1–4]. Sphingolipids generate diverse metabolic intermediates, notably ceramide, sphingosine, sphingosine-1-phosphate, and ceramide-1-phosphate, which serve as important mediators in the signaling cascades involved in apoptosis, proliferation, and stress responses [5–8]. Although we have already demonstrated that dietary sphingolipids are poorly absorbed by the intestine [9], sphingolipids that are significant components of foods have gained considerable attention for their potential and essential roles in human health

[10–14]. It has been reported that dietary supplementation with sphingolipids has diverse physiological effects, such as lowering plasma lipids [15], improving the skin barrier function [16], preventing melanin formation [17], contributing to central nervous system myelination [18] as well as protecting the colon against inflammation [19–25]. However, the functional, regulatory, and physiological significance of the immune regulating effects of dietary sphingolipids is an appreciably complicated field that is not well understood.

One hypothesis of immune regulation involves the balance between T-helper 1 (Th1) and T-helper 2 (Th2) cells, which direct different immune response pathways. Th1 cells drive the "cellular immunity" pathway to fight viruses and other intracellular pathogens, eliminate cancer cells, and stimulate delayed-type hypersensitivity skin reactions. Th2 cells are involved in "humoral immunity" and up-regulate antibody production to fight extracellular organisms. Either pathway can down-regulate the other. Disruption of the Th1/Th2 balance can cause immunological diseases [26, 27]. Via the actions of sphingolipid degrading enzymes, such as sphingomyelinase, glycoceramidases, and ceramidase, dietary sphingolipids are hydrolyzed to various kinds of metabolic intermediates which are critical for the activation and mediation of various types of immune cells. Metabolites of sphingolipids initiate and maintain diverse aspects of immune cell balance and functional responses by regulating cell migration and inflammatory pathways [8, 20, 28–31]. For instance, sphingolipid hydrolysis products regulate cyclooxygenase-2, interleukin 1β (IL-1β), interleukin 6 (IL-6), tumor necrosis factor α (TNF-α) and nuclear factor kappa B (NF-κB) via the sphingosine kinase 1/sphingosine-1-phosphate and ceramide kinase 1/ceramide-1-phosphate pathways, and thus cause the activation of mast cells, control thymocyte maturation and regulate the balance of lymphocyte subpopulations [32–37].

The goal of this study was to evaluate the effects of orally administered glucosylceramide (GluCer), one of the most important dietary sphingolipids, against DNFB-induced ear swelling in the BALB/c murine model, to provide further understanding of how dietary sphingolipids act on the balance between proinflammatory and anti-inflammatory responses.

Materials and Methods

Maize GluCer Preparation

GluCer from maize was kindly donated by Nippon Flour Mills Co. Ltd. (Atsugi, Japan). The purity of this GluCer was 96%, which was determined by HPLC equipped with an evaporative light-scattering detector, as described previously [12].

Animals

Female BALB/c mice (6 weeks old, 15–20 g body weight) were purchased from Japan SLC Inc. (Shizuoka, Japan). Animals were group-housed at six mice per cage, and were bred at the Institute's animal facilities at 25 °C with a 12-h light/dark cycle. Pure water and AIN-93G diet (Oriental Yeast Co., Ltd., Tokyo, Japan) were available ad libitum. All experiments were performed according to the guidelines of Kyoto University for the use and care of laboratory animals.

Contact Hypersensitivity Induced by DNFB

After a 2-week acclimatization period, allergic contact dermatitis was induced by DNFB in BALB/c mice according to a previously published method with minor modifications [38]. Briefly, mice were sensitized on day 0 by application of 100 µl 0.5% DNFB in acetone–soybean oil (4:1, v/v) on their shaved dorsal skin. The mice were divided into control, low dose (5 mg) and high dose (50 mg) groups ($n = 12$ in each group). An identifying mark was made on the tail of each mouse.

The maize GluCer was suspended in 0.5% carboxymethyl cellulose (CMC) (Nacalai Tesque Co. Ltd., Kyoto, Japan) solution and was orally administered at 5 or 50 mg to each mouse daily for 6 days. One hour after the final treatment, mice were challenged with 20 µL 0.5% DNFB in acetone–soybean oil (4:1) on both ears. The thickness of the right ear of each mouse was measured with a Dial Thickness Gauge (Mitutoyo Co., Kanagawa, Japan) at 0, 6 and 24 h after the DNFB challenge. Ear swelling was calculated as the difference in thickness before and after challenge [39].

Six hours ($n = 6$) and 24 h ($n = 6$) after DNFB treatment, blood was collected and mice were sacrificed under anesthesia. The right ear and spleen of each mouse was immediately excised and frozen in liquid nitrogen, then stored at −80 °C until use.

Morphological Analysis

The left ear of each mouse was fixed in 10% neutral buffered formalin solution and was then processed routinely into paraffin wax. Formalin fixed paraffin sections were stained with hematoxylin and eosin (H&E) to observe morphological changes using a microscope (Keyence Co., Osaka, Japan).

Measurement of Cytokine Production and Serum Immunoglobulin E

Amounts of IFN-γ, interleukin-4 (IL-4), TNF-α and interleukin-10 (IL-10) in homogenates of tissues were quantified using Murine IL-4 (Diaclone Research, Besancon, France), Murine IFN-γ (Diaclone Research), Mouse TNF-α (Pierce Biotechnology Inc., Rockford, IL, USA), and Murine IL-10 (Diaclone Research) ELISA kits, respectively, according to the manufacturer's instructions. Levels of those cytokines in each supernatant were normalized to total protein content, which was determined using a DC Protein assay kit (Bio-Rad Laboratories, Hercules, CA, USA). Total serum IgE levels of DNFB-challenged mice were quantified using a Mouse IgE ELISA kit (Immunology Consultants Laboratory, Newberg, ON, USA) according to the manufacturer's instructions.

Statistical Analysis

Data are reported as means ± SD. Statistical analyses were performed using one-way analysis of variance (ANOVA) with Fisher's PLSD method to identify levels of significance between the groups.

Results

GluCer Suppresses DNFB-Induced Ear Swelling of BALB/c Mice

After challenge with DNFB, typical allergic contact dermatitis was provoked in the ears of BALB/c mice, which was characterized by an initial increase in ear thickness and visible congestion of blood vessels. Oral treatment with maize GluCer suppressed DNFB-induced inflammatory symptom (redness and thickness) of ears. As shown in Fig. 1a significant depression of ear thickness was observed at 6 h in both low (5 mg/day) and high dose (50 mg/day) GluCer treated groups ($p < 0.05$). At 24 h, the average value of ear thickness was also reduced by GluCer, but there were no statistical differences among the three groups, which may due to large individual differences. The reduction of DNFB-induced ear swelling implies dietary GluCer has anti-inflammatory property.

GluCer Inhibits Inflammatory Infiltrates in the Ears of BALB/c Mice

Histological specimens of ears were prepared at 6 and 24 h after topical application of DNFB in BALB/c mice. In the control group, typical allergic contact dermatitis with congested blood vessels and apparent edema could be observed by H&E staining. As shown in Fig. 2a, b, microvascular dilations and dense leukocytes infiltrating the connective tissue, which are characteristics of inflammatory reactions, were clearly observed in the control group. At higher magnification, various kinds of migrated inflammatory cells could also be observed, including fibrocytes, mononuclear cells, degranulated mast cells and other leukocytes. These results confirm that DNFB induces severe inflammation in the ears of BALB/c mice and that a variety of lymphocytes migrated out from blood vessels during this contact sensitivity procedure. In both the low (5 mg/day) and the high (50 mg/day) dose GluCer-treated groups, microvascular dilation and leukocytes in inflammatory infiltrates were inhibited at 6 h (Fig. 2b, c) and 24 h groups (Fig. 2e, f). These results show that dietary GluCer inhibits microvascular dilation and inflammatory infiltration of DNFB-induced BALB/c mice.

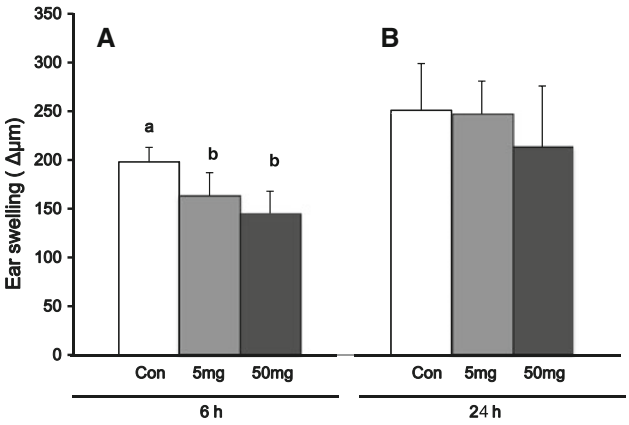

Fig. 1 Effect of orally administered GluCer on DNFB-induced ear swelling in BALB/c mice. The thickness of the left ear of each mouse was measured both before and after the DNFB challenge. Ear swelling values are presented as the *difference* in *thickness* at 6 h (**a**) and at 24 h (**b**). Ear swelling = ear thickness after challenge (6/24 h) − ear thickness before challenge (0 h). Con, 6 days 0.5% CMC (vehicle) orally administered; low, 6 days low dose (5 mg/day) maize GluCer orally administered; high, 6 days high dose (50 mg/day) maize GluCer orally administered. Values are means ± SD, $n = 6$. Values with different *superscript letters* are significantly different ($p < 0.05$)

GluCer Inhibits Inflammation by Reducing TNF-α Production in the Ear

To clarify the effect of GluCer on DNFB-induced inflammation, especially on Th1/Th2 balance, levels of IFN-γ as an indicator of Th1 cells and IL-4 as an indicator of Th2 cells were measured by ELISA assay. IFN-γ and IL-4 levels of GluCer-treated group were not significantly altered (Table 1). In other words, Th1/Th2 balance was not modified by oral administration of GluCer for 6 days.

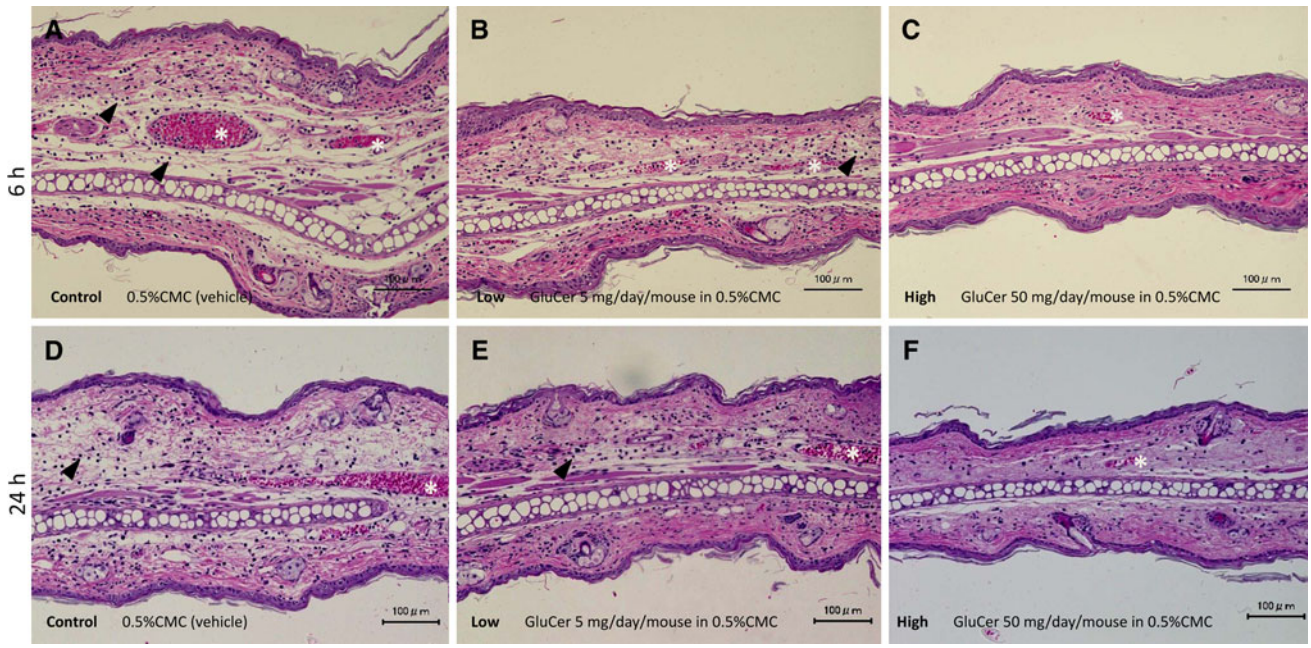

Fig. 2 Histopathological analysis of orally administered maize GluCer on DNFB-induced ear swelling in BALB/c mice. Morphological changes in the left ear of 6 and 24 h after DNFB-challenged BALB/c mice were observed. Ear sections from control mice (**a**), low dose (5 mg/day) maize GluCer administered mice (**b**) and high dose (50 mg/day) maize GluCer administered mice (**c**) were stained with hematoxylin and eosin (H&E). Microvascular (*asterisk* marks) and leukocyte (*arrowheads*) were pointed out in the histological sections. Sections are representatives of more than five observations

Table 1 IFN-γ, IL-4 and IL-10 levels in ears and spleens of DNFB-challenged BALB/c mice

GluCer Dose (mg/day)	Cytokines	Ear (pg/mg protein)		Spleen (pg/mg protein)	
		6 h	24 h	6 h	24 h
0	IFN-γ	482.4 ± 106.3	85.9 ± 16.7	7.6 ± 4.9	6.8 ± 1.7
5		362.0 ± 089.4	89.1 ± 18.3	7.5 ± 4.1	8.5 ± 2.7
50		373.2 ± 107.1	92.1 ± 13.1	5.9 ± 2.2	6.0 ± 2.9
0	IL-4	25.3 ± 4.4	10.3 ± 2.5	2.8 ± 0.9	1.9 ± 0.4
5		30.6 ± 6.5	10.7 ± 2.3	4.0 ± 1.0	1.8 ± 0.2
50		29.8 ± 8.4	09.0 ± 2.1	3.2 ± 0.7	1.5 ± 0.2
0	IL-10	3137.7 ± 881.3^{a}	698.7 ± 212.5	105.5 ± 23.5	56.3 ± 07.8^{a}
5		1326.7 ± 297.7^{a,b}	543.0 ± 158.9	131.0 ± 37.9	72.0 ± 33.1^{a,b}
50		1578.5 ± 352.3^{b}	618.0 ± 264.9	170.2 ± 47.6	110.4 ± 48.7^{b}

These data represent the means ± SD for groups of six mice. Values with different superscript letters in the same series differ significantly ($p < 0.05$)

For further evaluating the effect of GluCer on DNFB-induced inflammation, IL-10 was determined. In ear, IL-10 was significantly decreased at 6 h both low and high dose groups, whereas this effect did not prolong to 24 h (Table 1). However, in spleen, IL-10 was increased by GluCer treatment at 24 h, but not reached a statistical significance in 6 h because of the relatively large individual differences (Table 1).

TNF-α as the most important proinflammatory cytokine and IgE as the most important antibody in the serum were also measured. As shown in Fig. 3a, the TNF-α level in the ear was significantly suppressed both in the low and high dose GluCer groups ($p < 0.05$). Moreover, TNF-α level was also significantly down-regulated at 24 h by the effect of high dose GluCer (Fig. 3b). In contrast, IgE in the serum was almost at the same level among the control, low and high GluCer dose groups (Fig. 3c, d). The anti-inflammatory effect of dietary GluCer on contact dermatitis in DNFB-induced BALB/c mice is via regulation of the level of TNF-α secreted by inflammatory cells in the ear.

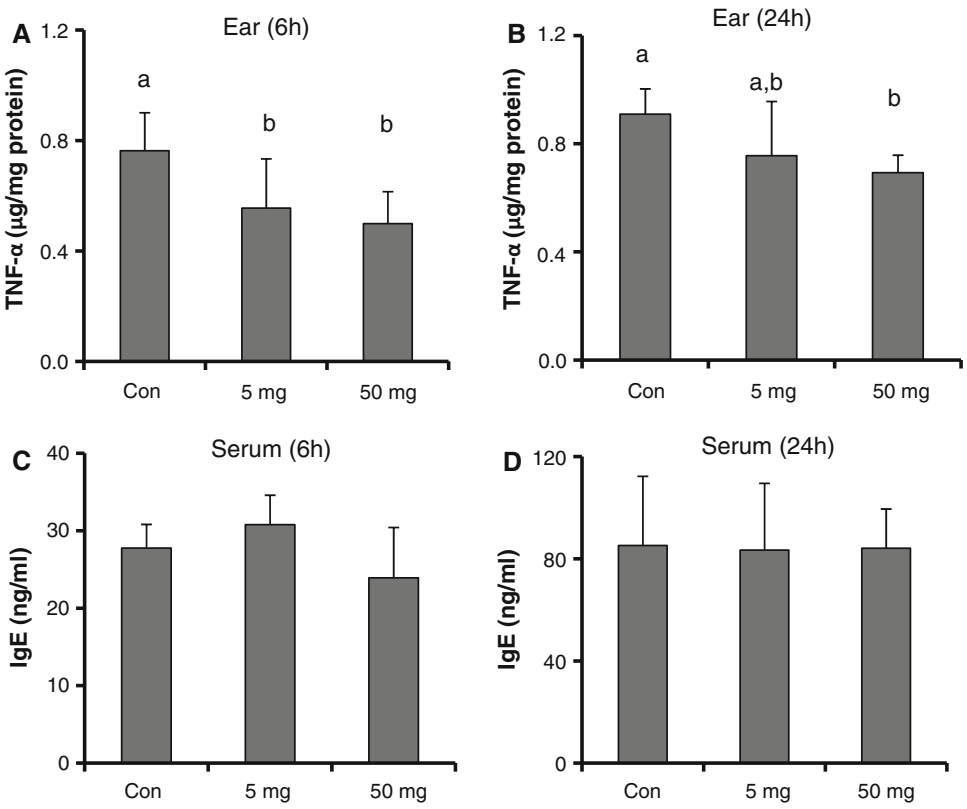

Fig. 3 TNF-α levels in the ears and IgE levels in the serum of DNFB-challenged BALB/c mice. TNF-α (**a**, **b**) levels in the right ear homogenates and IgE levels in the serum (**c**, **d**) of control, low dose (5 mg/day) and high dose (50 mg/day) maize GluCer administered mice were measured both 6 h (**a**, **b**) and 24 h (**b**, **d**) after the DNFB challenge. These data represent the means ± SD for groups of six mice. Values with *different letters* differ significantly ($p < 0.05$)

Discussion

The findings presented here indicate that dietary plant GluCer, one of the most important and abundant sphingolipids in food [12], suppresses the DNFB-induced ear swelling of BALB/c mice, and inhibits the microvascular dilation and inflammatory infiltration response via down-regulating levels of TNF-α, but not modifying the balance of Th1/Th2. Meanwhile, over-expressed IL-10 in inflammatory ear skin was suppressed by dietary GluCer. This anti-inflammatory effect of dietary GluCer increases our understanding of biofunctional sphingolipids.

Dietary GluCer is known to be hydrolyzed to ceramide, sphingosine and free fatty acids in the intestinal lumen. In mucosal cells, exogenous free sphingosine and dihydrosphingosine are rapidly absorbed and metabolized to palmitic acid [40]. A smaller portion of the sphingoid bases is reincorporated into ceramide and more complex sphingolipids. Our recent findings revealed that dietary GluCer originating from higher plants can be hydrolyzed in the intestine and that the intact plant form of sphingoid bases is barely absorbed by the tissues [9, 41]. Ono et al. [42] reported that dietary maize and yeast GluCer did not alter the sphingoid base composition in the skin of NC mice. We speculate that dietary maize GluCer accomplishes its anti-inflammatory effect, not only by producing bio-active metabolic intermediates through the sphingolipid metabolic pathways, but also via the activation of sphingolipid metabolic enzymes that affect endogenous sphingolipids at the inflammatory site, because diverse metabolic intermediates of sphingolipids, including ceramide, sphingosine, sphingosine-1-phosphate and ceramide-1-phosphate are well known important and highly bioactive endogenous regulators, which are involved in a complex metabolism network and play critical roles in inflammation [43–46].

In the case of our study, dietary maize GluCer accomplishes its inhibition of inflammation via the down-regulation of TNF-α level at the inflammatory site. TNF-α, produced by mononuclear phagocytes and other inflammatory cells (neutrophils, lymphocytes, natural killer cells, and mast cells) or non-inflammatory cells (endothelial cells), is known to be one of the most important inflammatory mediators [47, 48]. TNF-α facilitates the formation of adhesion molecules, vascular permeability and migration of leukocytes to sites of inflammation by affecting endothelial cells [49–51]. Our results reveal that dietary maize GluCer down-regulates levels of TNF-α in inflammatory ears. This down-regulation of TNF-α may affect endothelial cells and inflammatory cells, and also can inhibit vascular permeability at the site of inflammation. As a result, leukocyte migration is reduced. In the inflammatory cells, DNFB activates NF-κB by depredating the inhibitor of NF-κB (IκB) [52]. In addition, it has been reported that sphingolipids down regulated TNF-α via inactivating of NF-κB in

histamine-induced mouse skin tissues [53]. Thus, dietary GluCer seems to inhibit the DNFB activated NF-κB and down-modulate TNF-α expression in this study.

Moreover, IL-10 levels were increased in spleens but suppressed in ears by dietary GluCer. This well known anti-inflammatory cytokine, IL-10, has been reported over-expressed during the antigen-specific type of skin inflammation [54] and DNFB-challenged ear [55, 56]. IL-10 is released by CD4+ T helper 2 (Th2) cell clones and a variety of other cells, including keratinocytes, macrophages, B lymphocytes, and mast cells [56]. The suppressive effect of dietary GluCer on IL-10 expression in DNFB-challenged ears might be caused by the inhibition of leukocytes infiltrating to inflammatory site.

Ono et al. [42] demonstrated that supplementation of 0.1% GluCer diet for 7-week prevented atopic dermatitis-like symptoms in a mouse model by regulating the Th1/Th2 balance. However, IFN-γ, IL-4 and IgE levels, the markers of Th1/Th2 balance, were not notably affected by GluCer administration for 6 days in the present study. It appears that the period of treatment is important for immunological response of dietary GluCer.

Furthermore, allergic inflammatory skin disease is associated with a loss of ceramide in the extracellular lamellar membranes which causes an abnormal barrier function of the stratum corneum [57]. Application of ceramide on diseased skin could significantly reduce allergic inflammatory reactions by improving the severity score, stratum corneum cohesion and hydration [58–60]. Dietary GluCer might also improve the stratum corneum cohesion and hydration of ear skin to reduce the skin inflammation.

In summary, our data provide evidence that maize GluCer has anti-inflammatory effects on the DNFB-induced inflammation of BALB/c mice. We confirmed that dietary GluCer inhibits ear swelling and leukocyte infiltration. Furthermore, our results indicate that this effect is accomplished mainly by down-regulating TNF-α, but does not significantly affect Th1/Th2 balance or IgE levels in the serum. We hypothesize that dietary GluCer accomplishes its anti-inflammatory effect by down-regulating TNF-α to suppress vascular permeability. This reduces the migration of inflammatory cells, affects endogenous sphingolipids through metabolic pathways by activating sphingolipid-related enzymes, and moreover, by hydrolysis to ceramide to improve skin barrier function at the dermatitis site. Our findings increase the comprehensive understanding of the actions of dietary sphingolipids on the balance of immune responses.

Acknowledgments This work was supported by the Program for Promotion of Basic and Applied Researches for Innovations in Bio-oriented Industry (BRAIN).

References

1. Lingwood D, Simons K (2010) Lipid rafts as a membrane-organizing principle. Science 327:46–50
2. Bartke N, Hannun YA (2009) Bioactive sphingolipids: metabolism and function. J Lipid Res 50:91–96
3. Prabuddha S, Barbara B, David H (2007) Lipid rafts, fluid/fluid phase separation, and their relevance to plasma membrane structure and function. Semin Cell Dev Biol 18:583–590
4. Merrill AH Jr, Schmelz EM, Dillehay DL, Spiegel S, Shayman JA, Schroeder JJ, Riley RT, Voss KA, Wang E (1997) Sphingolipids—the enigmatic lipid class: biochemistry, physiology, and pathophysiology. Toxicol Appl Pharmacol 142:208–225
5. Spiegel S, Merrill AH Jr (1996) Sphingolipid metabolism and cell growth regulation. FASEB J 10:1388–1397
6. Zheng W, Kollmeyer J, Symolon H, Momin A, Munter E, Wang E, Kelly S, Allegood JC, Liu Y, Peng Q, Ramaraju H, Sullards MC, Cabot M, Merrill AH Jr (2006) Ceramides and other bioactive sphingolipid backbones in health and disease: lipidomic analysis, metabolism and roles in membrane structure, dynamics, signaling and autophagy. Biochim Biophys Acta 1758:1864–1884
7. Nixon GF (2009) Sphingolipids in inflammation: pathological implications and potential therapeutic targets. Br J Pharmacol 158:982–993
8. El Alwani M, Wu BX, Obeid LM, Hannun YA (2006) Bioactive sphingolipids in the modulation of the inflammatory response. Pharmacol Ther 112:171–183
9. Sugawara T, Tsuduki T, Yano S, Hirose M, Duan J, Aida K, Ikeda I, Hirata T (2010) Intestinal absorption of dietary maize glucosylceramide in lymphatic duct cannulated rats. J Lipid Res 51:1761–1769
10. Yunoki K, Ogawa T, Ono J, Miyashita R, Aida K, Oda Y, Ohnishi M (2008) Analysis of sphingolipid classes and their contents in meals. Biosci Biotechnol Biochem 72:222–225
11. Duan J, Sugawara T, Hirata T (2010) Sphingolipids in seafood using HPLC with evaporative light-scattering detection: its application in tissue distribution of sphingolipids in fish. J Oleo Sci 59:509–513
12. Sugawara T, Miyazawa T (1999) Separation and determination of glycolipids from edible plant sources by high performance liquid chromatography and evaporative light scattering detection. Lipids 34:1231–1237
13. Nyberg L, Duan RD, Nilsson Å (1998) Sphingomyelin—a dietary component with structural and biological function. Prog Colloid Polym Sci 108:119–128
14. Vesper H, Schmelz EM, Nikolova-Karakashian MN, Dillehay DL, Lynch DV, Merrill AH Jr (1999) Sphingolipids in food and the emerging importance of sphingolipids to nutrition. J Nutr 129:1239–1250
15. Duivenvoorden I, Voshol PJ, Rensen PC, van Duyvenvoorde W, Romijn JA, Emeis JJ, Havekes LM, Nieuwenhuizen WF (2006) Dietary sphingolipids lower plasma cholesterol and triacylglycerol and prevent liver steatosis in APOE*3Leiden mice. Am J Clin Nutr 84:312–321
16. Tsuji K, Mitsutake S, Ishikawa J, Takagi Y, Akiyama M, Shimizu H, Tomiyama T, Igarashi Y (2006) Dietary glucosylceramide improves skin barrier function in hairless mice. J Dermatol Sci 44:101–107
17. Kinoshita M, Hori N, Aida K, Sugawara T, Ohnishi M (2007) Prevention of melanin formation by yeast cerebroside in B16 mouse melanoma cells. J Oleo Sci 56:645–648
18. Oshida K, Shimizu T, Takase M, Tamura Y, Shimizu T, Yamashiro Y (2003) Effects of dietary sphingomyelin on central nervous system myelination in developing rats. Pediatr Res 53:589–593

19. Schmelz EM (2000) Dietary sphingomyelin and other sphingolipids in health and disease. Nutr Bull 25:135–139
20. Duan RD, Nilsson Å (2009) Metabolism of sphingolipids in the gut and its relation to inflammation and cancer development. Prog Lipid Res 48:62–72
21. Merrill AH Jr, Schmelz EM, Wang E, Schroeder JJ, Dillehay DL, Riley RT (1995) Role of dietary sphingolipids and inhibitors of sphingolipid metabolism in cancer and other diseases. J Nutr 125:1677–1682
22. Aida K, Kinoshita M, Tanji M, Sugawara T, Tamura M, Ono J, Ueno N, Ohnishi M (2005) Prevention of aberrant crypt foci formation by dietary maize and yeast cerebrosides in 1,2-dimethylhydrazine-treated mice. J Oleo Sci 54:45–49
23. Berra B, Colombo I, Sottocornola E, Giacosa A (2002) Dietary sphingolipids in colorectal cancer prevention. Eur J Cancer Prev 11:193–197
24. Sugawara T, Kinoshita M, Ohnishi M, Miyazawa T (2002) Apoptosis induction by wheat-flour sphingoid bases in DLD-1 human colon cancer cells. Biosci Biotechnol Biochem 66:2228–2231
25. Kinoshita M, Aida K, Tokuji Y, Sugawara T, Ohnishi M (2009) Effects of dietary plant cerebroside on gene expression in the large intestine of 1,2-dimethylhydrazine (DMH)-treated mice determined by DNA microarray analysis. J Food Lipids 16:200–208
26. Kidd P (2003) Th1/Th2 balance: the hypothesis, its limitations, and implications for health and disease. Altern Med Rev 8:223–246
27. Hernández-Pando R, Orozcoe H, Sampieri A, Pavón L, Velasquillo C, Larriva-Sahd J, Alcocer JM, Madrid MV (1996) Correlation between the kinetics of Th1, Th2 cells and pathology in a murine model of experimental pulmonary tuberculosis. Immunology 89:26–33
28. Dinarello CA (1997) Proinflammatory and anti-inflammatory cytokines as mediators in the pathogenesis of septic shock. Chest 112:321–329
29. Lahiri S, Futerman AH (2007) The metabolism and function of sphingolipids and glycosphingolipids. Cell Mol Life Sci 64:2270–2284
30. Yopp AC, Randolph GJ, Bromberg JS (2003) Leukotrienes, sphingolipids, and leukocyte trafficking. J Immunol 171:5–10
31. Melendez AJ, Khaw AK (2002) Dichotomy of Ca^{2+} signals triggered by different phospholipid pathways in antigen stimulation of human mast cells. J Biol Chem 277:17255–17262
32. Jolly PS, Bektas M, Olivera A, Gonzalez-Espinosa C, Proia RL, Rivera J, Milstien S, Spiegel S (2004) Transactivation of sphingosine-1-phosphate receptors by FcepsilonRI triggering is required for normal mast cell degranulation and chemotaxis. J Exp Med 199:959–970
33. Snider AJ, Orr Gandy KA, Obeid LM (2010) Sphingosine kinase: role in regulation of bioactive sphingolipid mediators in inflammation. Biochimie 92:707–715
34. Gilfillan AM, Tkaczyk C (2006) Integrated signalling pathways for mast-cell activation. Nat Rev Immunol 6:218–230
35. Allende ML, Dreier JL, Mandala S, Proia RL (2004) Expression of the sphingosine 1-phosphate receptor, S1P1, on T-cells controls thymic emigration. J Biol Chem 279:15396–15401
36. Wei SH, Rosen H, Matheu MP, Sanna MG, Wang SK, Jo E, Wong CH, Parker I, Cahalan MD (2005) Sphingosine 1-phosphate type 1 receptor agonism inhibits transendothelial migration of medullary T cells to lymphatic sinuses. Nat Immunol 6:1228–1235
37. Olivera A, Rivera J (2005) Sphingolipids and the balancing of immune cell function: lessons from the mast cell. J Immunol 174:1153–1158
38. Sakai S, Sugawara T, Kishi T, Yanagimoto K, Hirata T (2010) Effect of glucosamine and related compounds on the degranulation of mast cells and ear swelling induced by dinitrofluorobenzene in mice. Life Sci 86:337–343
39. Tomobe YI, Morizawa K, Tsuchida M, Hibino H, Nakano Y, Tanaka Y (2000) Dietary docosahexaenoic acid suppresses inflammation and immune responses in contact hypersensitivity reaction in mice. Lipids 35:61–69
40. Nilsson Å (1968) Metabolism of sphingomyelin in the intestinal tract of the rat. Biochim Biophys Acta 164:575–584
41. Sugawara T, Kinoshita M, Ohnishi M, Nagata J, Saito M (2003) Digestion of maize sphingolipids in rats and uptake of sphingadienine by Caco-2 cells. J Nutr 133:2777–2782
42. Ono J, Kinoshita M, Aida K, Tamura M, Ohnishi M (2010) Effects of dietary glucosylceramide on dermatitis in atopic dermatitis model mice. Eur J Lipid Sci Tech 112:708–711
43. Oskeritzian CA, Milstien S, Spiegel S (2007) Sphingosine-1-phosphate in allergic responses, asthma and anaphylaxis. Pharmacol Ther 115:390–399
44. Ma Y, Pitson S, Hercus T, Murphy J, Lopez A, Woodcock J (2005) Sphingosine activates protein kinase A type II by a novel cAMP-independent mechanism. J Biol Chem 280:26011–26017
45. Spiegel S, Milstien S (2003) Sphingosine-1-phosphate: an enigmatic signalling lipid. Nat Rev Mol Cell Biol 4:397–407
46. Pettus BJ, Kitatani K, Chalfant CE, Taha TA, Kawamori T, Bielawski J, Obeid LM, Hannun YA (2005) The coordination of prostaglandin E2 production by sphingosine-1-phosphate and ceramide-1-phosphate. Mol Pharmacol 68:330–335
47. Aggarwal BB (2003) Signalling pathways of the TNF superfamily: a double-edged sword. Nat Rev Immunol 3:745–756
48. Tartaglia LA, Goeddel DV (1992) Two TNF receptors. Immunol Today 13:151–153
49. Oppenheim JJ (2001) Cytokines: past, present, and future. Int J Hematol 74:3–8
50. Borish LC, Steinke JW (2003) Cytokines and chemokines. J Allergy Clin Immunol 111:460–475
51. Snider AJ, Orr Gandy KA, Obeid LM (2010) Sphingosine kinase: role in regulation of bioactive sphingolipid mediators in inflammation. Biochimie 92:707–715
52. Cruz MT, Duarte CB, Gonçalo M, Figueiredo A, Carvalho AP, Lopes MC (2002) Differential activation of nuclear factor kappa B subunits in a skin dendritic cell line in response to the strong sensitizer 2,4-dinitrofluorobenzene. Arch Dermatol Res 294:419–425
53. Ryu KR, Lee B, Lee IA, Oh S, Kim DH (2010) Anti-scratching behavioral effects of *N*-stearoyl-phytosphingosine and 4-hydroxysphinganine in mice. Lipids 45:613–618
54. Inoue R, Otsuka M, Nishio A, Ushida K (2007) Primary administration of *Lactobacillus johnsonii* NCC533 in weaning period suppresses the elevation of proinflammatory cytokines and CD86 gene expressions in skin lesions in NC/Nga mice. FEMS Immunol Med Microbiol 50:67–76
55. Fujiwara R, Sasajima N, Takemura N, Ozawa K, Nagasaka Y, Okubo T, Sahasakul Y, Watanabe J, Sonoyama K (2010) 2,4-Dinitrofluorobenzene-induced contact hypersensitivity response in NC/Nga mice fed fructo-oligosaccharide. J Nutr Sci Vitaminol 56:260–265
56. Wang M, Qin X, Mudgett JS, Ferguson TA, Senior RM, Welgus HG (1999) Matrix metalloproteinase deficiencies affect contact hypersensitivity: stromelysin-1 deficiency prevents the response and gelatinase B deficiency prolongs the response. PANS 96:6885–6889
57. Snider AJ, Orr Gandy KA, Obeid LM (2010) Sphingosine kinase: role in regulation of bioactive sphingolipid mediators in inflammation. Biochimie 92:707–715

58. Ishikawa J, Takada S, Hashizume K, Takagi Y, Hotta M, Masukawa Y, Kitahara T, Mizutani Y, Igarashi Y (2009) Dietary glucosylceramide is absorbed into the lymph and increases levels of epidermal sphingolipids. J Dermatol Sci 56:220–222
59. Proksch E, Fölster-Holst R, Jensen JM (2006) Skin barrier function, epidermal proliferation and differentiation in eczema. J Dermatol Sci 43:159–169
60. Piekutowska A, Pin D, Rème CA, Gatto H, Haftek M (2008) Effects of a topically applied preparation of epidermal lipids on the stratum corneum barrier of atopic dogs. J Comp Pathol 138:197–203

Lipids (2011) 46:513–520
DOI 10.1007/s11745-011-3537-1

ORIGINAL ARTICLE

The Acyl CoenzymeA:Monoacylglycerol Acyltransferase 3 (MGAT3) Gene is a Pseudogene in Mice but Encodes a Functional Enzyme in Rats

Yong Gang Yue · Yan Qun Chen · Youyan Zhang · He Wang · Yue-Wei Qian · Jeffrey S. Arnold · John N. Calley · Shuyu D. Li · William L. Perry III · Hong Y. Zhang · Robert J. Konrad · Guoqing Cao

Received: 29 November 2010 / Accepted: 25 January 2011 / Published online: 11 February 2011

Abstract Triglyceride (TAG) absorption involves its initial hydrolysis to fatty acids and monoacylglycerol (MAG), which are resynthesized back to diacylglycerol (DAG) and TAG within enterocytes. The resynthesis of DAG is facilitated by fatty acyl-CoA dependent monoacylglycerol acyltransferases (MGATs). Three MGAT enzymes have been isolated in humans and the expression of MGAT2 and MGAT3 in the intestines suggests their functional role in the TAG absorption. In this paper, we report that the Mogat3 gene appears to be a pseudogene in mice while it is a functional gene in rats. Examination of the mouse genomic Mogat3 sequence revealed multiple changes that would result in a translational stop codon or frameshifts. The rat Mogat3 gene, however, is predicted to encode a functional enzyme of 362 amino acids. Expression of rat MGAT3 in human embryonic kidney 293 (HEK293) cells led to the formation of a 36-kDa protein that displayed significant MGAT but not DGAT activity. Tissue expression analysis of rat MGAT3 by real-time PCR analysis indicated that rat MGAT3 has a high level of expression in intestines and pancreas. Our results thus provide the molecular basis to understand the relative functional role of MGAT2 and MGAT3 and also for future exploration of MGAT3 function in animal models.

Keywords Monoacylglycerol (MAG) · Diacylglycerol (DAG) · Triacylglycerol (TAG) · Acyl coenzymeA:monoacylglycerol acyltransferase (MGAT) · Acyl coenzymeA:diacylglycerol acyltransferase (DGAT)

Abbreviations

TAG	Triacylglycerol
DAG	Diacylglycerol
MAG	Monoacylglycerol
MGAT	Monoacylglycerol acyltransferase
DGAT	Diacylglycerol acyltransferase

Introduction

The pandemic of obesity is caused by the imbalance of energy absorption and energy expenditure. Nutrients are processed and absorbed primarily within the gastro-intestinal tract. The most energy-rich form of the nutrients, triacylglycerols (TAG), is first hydrolyzed primarily by pancreatic lipase into monoacylglycerols (MAG) and fatty acids. After absorption into the enterocytes within the intestinal tract, MAG and fatty acids are synthesized sequentially back to diacylglyceol (DAG) and TAG, which is subsequently assembled into chylomicrons and secreted into the lymph [1–4]. The critical role of TAG absorption

Y. G. Yue and Y. Q. Chen contributed equally to this work.

Electronic supplementary material The online version of this article (doi:10.1007/s11745-011-3537-1) contains supplementary material, which is available to authorized users.

Y. G. Yue · Y. Q. Chen · Y. Zhang · H. Wang · Y.-W. Qian · J. S. Arnold · J. N. Calley · S. D. Li · W. L. Perry III · H. Y. Zhang · R. J. Konrad · G. Cao (✉)
Lilly Research Laboratories, Eli Lilly & Company, Indianapolis, IN 46285, USA
e-mail: Guoqing_cao@lilly.com

Present Address:
W. L. Perry III
Intrexon Corporation, Germantown, MD, USA

in energy homeostasis has triggered substantial interest in developing therapies against this pathway and this is highlighted by the success of Orlistat, which is a pancreatic lipase inhibitor that inhibits TAG absorption and accordingly reduces body weight [5, 6].

Fatty acyl-CoA dependent monoacylglycerol acyltransferases (MGAT) and diacylglycerol acyltransferases (DGAT) are responsible for the sequential re-esterification of MAG [7]. Breakthroughs were made in recent years when these enzymes were cloned and studied. DGAT1 was the first enzyme that was isolated in the family with a high level of expression in the intestines [8]. DGAT1 deficient mice were resistant to diet-induced obesity and developed significant improvement in insulin sensitivity and hepatic steatosis [9, 10]. While the mechanisms of metabolic benefits from DGAT1 deficiency were not entirely understood, it was found that DGAT1 deficiency did not alter the balance of intestinal lipid absorption while the rate of TG absorption was significantly reduced [11]. Interestingly, DGAT1 also displayed MGAT activity in vitro [12, 13].

The first MGAT gene cloned was MGAT1 with low expression in intestines [14]. This led to the discovery of MGAT2 and MGAT3, which have a high level of expression in the intestines. MGAT2 is largely expressed in the proximal intestines while MGAT3 appears to have a high level of expression in the distal intestines [15–18]. Both enzymes have demonstrated significant enzymatic activity in vitro in catalyzing the formation of DAG from MAG and fatty acyl-CoA substrates [16–18]. Interestingly, MGAT2/3 displayed DGAT activity as well [19, 20]. The physiological role of MGAT2 was studied recently by Farese and colleagues via Mogat2 deficient mice. Similar to DGAT1 mice, Mogat2 deficient mice were resistant to diet-induced obesity, and had significant improvement in insulin sensitivity, dislipidemia, and hepatic steatosis. These mice exhibited increased energy expenditure and reduced body weight that could potentially explain the metabolic benefits of these mice. Again, the total lipid absorption was not different in Mogat2 deficient mice compared to that of the wild type animals, but significant temperal and spatial delays in TG absorption were observed [21]. These studies convincingly established MGAT2 as a critical enzyme in the intestinal TAG absorption process and whole body energy homeostasis.

A relevant question is the physiological role of MGAT3 in the intestinal TAG absorption process because of its high expression in intestines. In this study, we report that the Mogat3 gene in mice appears to be a pseudogene while the gene in rats is functional. Our studies thus provide the molecular basis for future exploration of MGAT3 function in vivo.

Materials and Methods

cDNA Cloning and the Expression Construct

Rat Mogat3 cDNA was isolated by PCR from rat small intestine mRNA (BioChain Co.) based on sequence prediction of rat Mogat3 in rat genomic database using the following primers: 5′ primer, 5′-TTGCTAGTGTGTGACT CCCCTCTAAAG-3′; and 3′ primer, 5′-GTCTCTCAGGA AGGCCAGGACATG-3′. Multiple independent PCR clones were sequenced to eliminate PCR-induced mutations. The nucleotide sequences encoding full-length rat Mogat3 were inserted into a mammalian expression vector pcDNA3.1(+) (Invitrogen) with an N-terminal FLAG tag. The resulting construct was used in transfection and functional assays. Human MGAT2 and DGAT1 cDNA were cloned from human intestinal tissues and the proteins were expressed in insect sf9 cells via a baculoviral expression system.

Cell Culture

HEK293 cells were purchased from American Type Culture Collection (Manassas, VA) and cultured in Dulbecco's modified Eagle's/F-12 (3:1) medium supplemented with 5% fetal bovine serum in a humidified air atmosphere containing 5% CO_2. For transfections, 5×10^5 HEK293 cells were seeded into 6-well plates (Falcon, Corning, NY). One μg of DNA was transfected using FuGENE 6 (Roche Diagnostics, Indianapolis, IN) according to the manufacturer's instructions. Expression of FLAG-tagged rat MGAT3 was verified by Western blotting analysis with a mouse anti-FLAG monoclonal antibody (Sigma, St. Louis, MO).

Rat cDNA Panel, Reverse Transcription and Real Time PCR

The total RNA was isolated from Sprague Dawley rat tissues using TRIzol reagent (Invitrogen, Carlsbad, CA). The cDNA was synthesized from 1 μg of total RNA utilizing the SuperScript™ III First-strand Synthesis System (Invitrogen) with random hexamers for reverse transcriptase-PCR. The SYBR Green PCR Master Mix for the TaqMan gene expression assay was ordered from Applied Biosystems (Foster City, CA). The rat Mogat2 and Mogat3 primers were designed by Primer Express following the amplicon design guidelines defined by the software and the primers were tested and optimized for PCR. The sequences of the primers for rat Mogat2 and Mogat3 are as follows: rat Mogat2; 5′GGTGAGTGCTGATCACATTCTGA-3′ (forward) and 5′-AAGGGAGATGCCCATGATCT-3′ (reverse), rat Mogat3; 5′-AGCCTGGAACAGTGAGTTTGC-3′ (forward)

and 5′GGCTTCGCTGCACTGGAA-3′ (reverse). Real-Time PCR was performed on 7900HT Fast Real-time PCR System (Applied Biosystems) using TaqMan® SYBR Green PCR Master Mix. Cycle threshold (Ct) values were obtained using Applied Biosystems SDS2.3 software, with 18S rRNA used as a reference gene. The data were normalized by setting the average brain expression value to 1.

In Vitro MGAT Activity Assay

Cell pellets were homogenized with three short 10-s pulses from a Brinkmann Polytron homogenizer in 20 mM NaCl containing a protease inhibitor mixture (Roche Diagnostics). The resultant homogenates were used to assess the relative acyltransferase activity. Protein concentrations were determined using a commercially prepared protein assay kit (Pierce, Rockford, IL) with bovine serum albumin used as a standard. MGAT activity was determined at room temperature in a final volume of 100 µl. Briefly, MGAT or DGAT activity was determined by measuring the incorporation of [^{14}C]oleoyl-CoA (American Radiolabeled Chemical Inc., St. Louis, MO) into the acyl acceptor monooleoylglycerol or dioleoylglycerol. The acyl acceptors were introduced into the reaction mixture by liposomes. The acyl acceptor and dioleoylphosphatidylcholine (molar ratio 1:5) were dissolved in chloroform and dried by vacuum. Liposomes were formed by adding water and sonicating for 5 min. The reaction mixture contained 100 mM Tris/HCl, pH 7.4, 5 mM $MgCl_2$, 1 mg/ml fatty acid free bovine serum albumin (Sigma), 200 mM sucrose, 10 µM [^{14}C]oleoyl-CoA (50 mCi/mmol; American Radiolabeled Chemicals), 100 µM acyl acceptors in liposomes, and various amounts of cellular homogenates. The reaction was initiated by adding protein homogenate, incubated for 20 min at room temperature and was stopped by adding 1 ml of chloroform/methanol (2:1, v/v). Lipids were extracted with chloroform/methanol (2:1, v/v) by vortexing for 30 s. After centrifugation to remove debris, aliquots of the organic phase containing lipids were dried under a N_2 stream and separated by the Linear-K Preadsorbent TLC plate (Waterman Inc., Clifton, NJ) with hexane/ethyl ether/acetic acid (80:20:1, v/v/v). The TLC plates were exposed to a Phosphor-Imager screen to assess the incorporation of ^{14}C-labeled acyl moieties into dioleoylglycerol or trioleoylglycerol products. Phosphorimaging signals were visualized using a Storm 860 PhosphorImager (Amersham Biosciences).

Comparative Genomic DNA Sequence Analysis

The analysis was carried out using the Artemis comparison tool (ACT) [22]. Mouse, rat and human genomic sequences in the target gene cluster, corresponding to the human sequences between ZHHIT1 and VGF genes, were downloaded from NCBI using the Entrez Gene functions. Both FASTA and "GenBank_Full" files were downloaded for each sequence. The source genomic sequence (e.g., the human FASTA file) to be used as the source database was first formatted using the "formatdb" tool. The comparator files were then generated for ACT by running the blastall alignment program between target genomic (e.g., mouse) and database (e.g., human): blastall -m 8 -i mouse_genomic.fasta -d human_genomic.fasta -p blastn -o mouse.human.blastn. Another copy of FASTA file, without being formatted by the "formatdb" program, is needed for ACT. In the file, all features from GenBank file are copied to the top of the FASTA sequence. The ACT program was run according to its user manual.

Phylogenetic Analysis

The Clustal multiple sequence alignment of DGAT2 and MGAT2/3 protein sequences of mouse, rat and human was carried out, using default parameters, with the integrated tools in JalView [23]. The construction of the phylogenetic tree was based on the percent identity of the protein sequences.

Results

The DGAT2 and MGAT2 tandem gene pair is located within a gene cluster that is conserved among mouse, rat and human (Supplemental Figure 1A). We reasoned that a similar syntenic relationship may also exist between human MGAT3 and its rodent homologues. Indeed, there is extensive orthology between human and rodent gene clusters that contain Mogat3. All of the five human genes (RABL5, FIS1, CLDN15, ZNHIT1, and PLOD3, excluding pseudogenes) upsteam of Mogat3 were found in mouse and rat in the same order, except that Zhhit1 was absent in the rat. Downstream of Mogat3, the orthology between human and mouse further extends to at least three other genes (VGF, AP1S1, and Serpine1). This human-rodent orthology around Mogat3 (Fig. 1a) suggests the likely chromosomal location of rodent Mogat3. In support of this hypothesis, TBLASTN search of translated mouse and rat genomes using human MGAT3 protein sequence resulted in hits within this cluster. In the mouse genome, one of the hits was LOC639992 (Mm7284), a predicted gene immediately downstream of Plod3. The top hit in rat genome was LOC68550, a predicted gene known as "similar to monoacylglycerol O-acyltransferase 2", also located at the expected locus of Mogat3. Based on the orthology and the predicted coding sequence similarity, we reasoned that

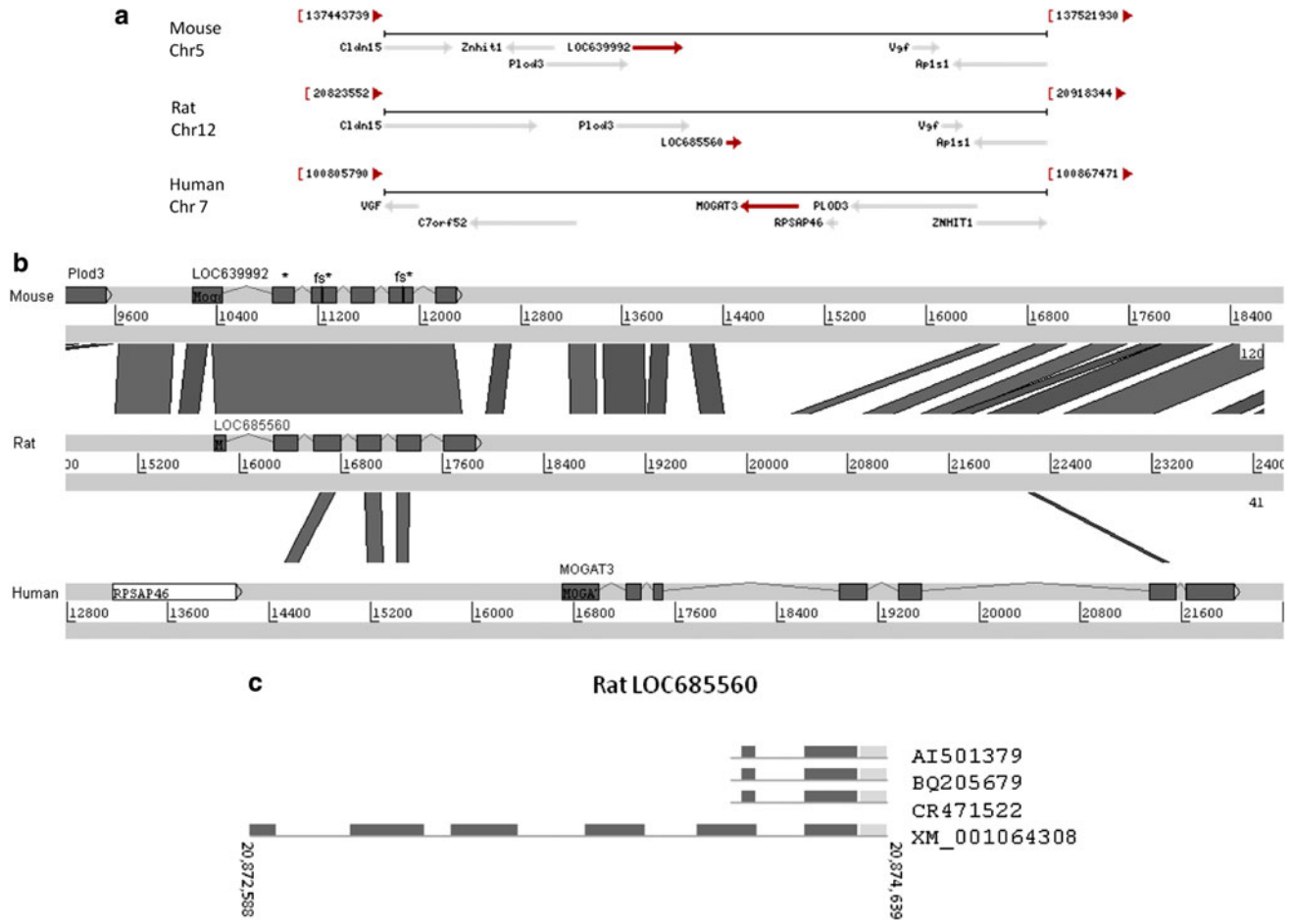

Fig. 1 **a** Conservation of the human chromosome 7 gene cluster surrounding Mogat3 in mouse chromosome 5 and rat chromosome 12. The human gene cluster is shown in opposite orientation to those of mouse and rat ones. Mogat3 and its suspected rodent homologues are marked with black *arrow*. Only the Cldn15-Zhhit1(mouse only)-Plod3 interval upstream of Mogat3, and Vgf-Ap1s1 interval downstream are shown. **b** Genomic sequence similarity between human MOGAT3 and suspected mouse and rat homologues. The predicted mouse and rat Mogat3 genomic sequences are highly homologous with each other throughout the entire gene, but only three exons (3, 4, and 5) showed similarity to human genomic sequences, and these are upstream of the Mogat3 locus. The predicted coding sequence of mouse Mogat3 is interrupted by one termination codon in exon 2 (marked with*) and two frameshifts in exon 3 (marked with Fs*). See supplemental Figure 2 for details. **c** Rat EST clone numbers and the relative locations within the rat Mogat3 gene

LOC639992 and LOC68550 could be MGAT3 candidate genes in mouse and rat, respectively.

Comparative genomic sequence analysis at the presumed Mogat3 locus showed a high degree of conservation between the mouse LOC639992 and the rat LOC68550 genomic DNA sequences (Fig. 1b). The putative rodent Mogat3 gene contains 6 exons and 5 introns (Fig. 1b). However, the mouse and rat genes exhibited low genomic sequence similarity to the human MGAT3 genomic sequence. Subsequent examination of the putative mouse Mogat3 gene revealed sequences that would result in an in-frame stop codon and frameshifts. Specifically, in the putative mouse Mogat3 gene, there is an in-frame stop codon in exon 2 and two deletions that would result in frameshifts within exon 3 (Supplemental Figure 2). Examination of the mouse Mogat3 genomic sequences of 12 different mouse strains from Perlegen revealed that the stop codons that interrupted exon 3 were present in all strains, thus precluding mutations or sequencing errors (data not shown). In addition, there was no Mogat3 EST discovered in the mouse expression sequence tag (EST) database. Our effort to amplify a potential Mogat3 cDNA did not yield any products either. Taken together, these data suggest that the mouse putative Mogat3 gene sequence does not appear to encode a functional gene and we conclude that the mouse Mogat3 is a pseudogene.

A similar analysis was performed in the rat genome, which revealed a potential functional gene product. Searches in the rat EST database revealed three EST clones at the 3′ end of the gene (Fig. 1c). Using sequences derived from the ESTs and the predicted rat cDNA sequence based on rat genomic sequences, a rat Mogat3 cDNA was cloned

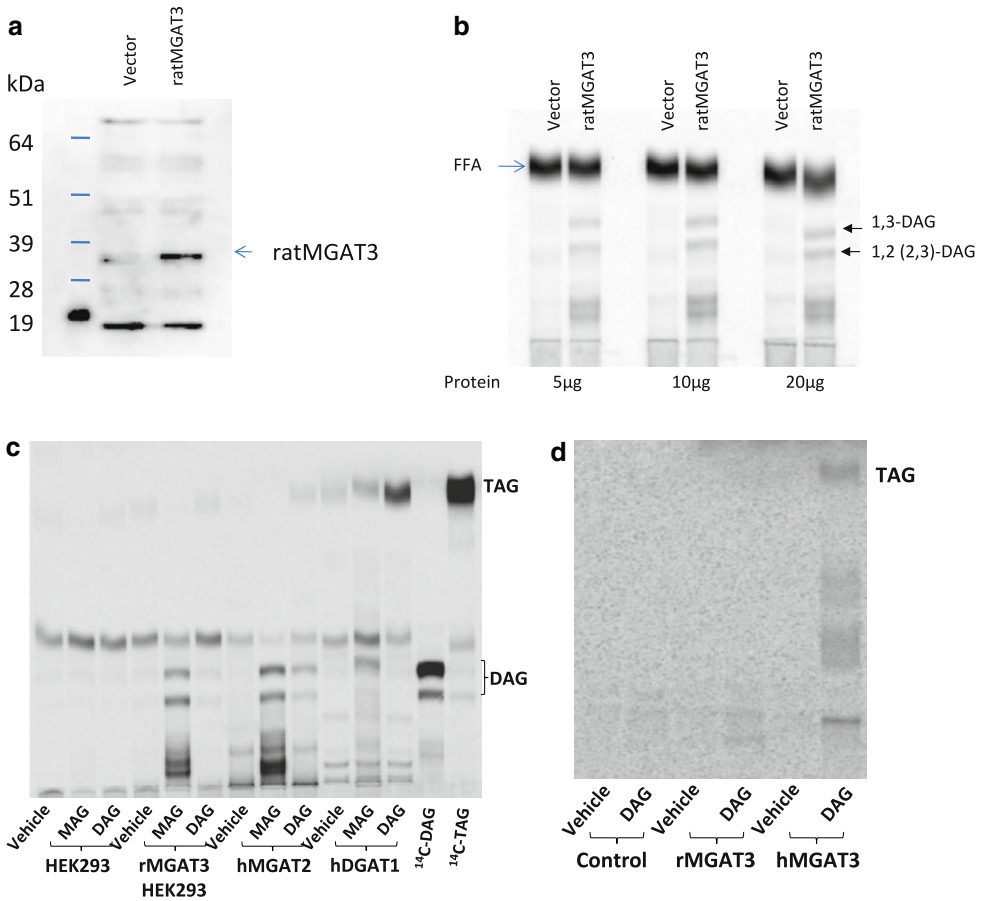

Fig. 2 **a** Rat MGAT3 protein expression in HEK 293 cells. Rat MGAT3 cDNA was cloned as described in the "Methods" section. The subcloning of rat MGAT3 cDNA into the expression vector and transfection to HEK293 cells were described in "Methods" section. Western blotting analysis was performed with a mouse anti-FLAG monoclonal antibody as described in the "Methods" section. **b** Rat MGAT3 protein displayed MGAT activity. The expression of rat MGAT3 in HEK293 cells, the preparation of cellular extracts for MGAT activity analysis and the details for MGAT activity assessment were described in the "Methods" section. Rat MGAT3 enzyme activity was compared to the vector control. **c** Rat MGAT3 protein has MGAT but not DGAT activity. Similar activity studies were carried out using either MAG or DAG as an acyl acceptor to assess potential MGAT or DGAT activity rat MGAT3 may have. Human MGAT2 and DGAT1 were used as controls. **d** Rat MGAT3 protein does not have DGAT activity. Rat MGAT3 and human MGAT3 were compared in the same experiment on their respective DGAT activity

from rat intestines and was subsequently subcloned into a mammalian expression vector. The predicted amino acid sequence and the alignment with human MGAT3; rat, mouse and human MGAT2 and DGAT2 are shown in Supplemental Figure 3. Rat MGAT3 protein contains 326 amino acids and shares 47% identity with human MGAT3 and is 56% identical compared to rat MGAT2 (Supplemental Table 1). To facilitate the expression analysis, a FLAG tag was inserted at the amino-terminus of the enzyme. When the expression vector was transfected into the human embryonic kidney (HEK) 293 cells and the cellular extracts were analyzed by Western blotting analysis against the FLAG tag, a protein of 36 kD was readily detectable compared to the vector control (Fig. 2a). To assess whether rat MGAT3 protein possesses MGAT activity, cellular extracts from HEK293 cells transfected with rat MGAT3 expression vector were incubated with substrates of MAG and radio-labeled oleoyl-CoA and the formation of DAG was analyzed by thin layer chromatography. Compared to the vector control, significant MGAT activity was detected using extracts from cells expressing rat MGAT3 (Fig. 2b). To further characterize the rat MGAT3 acyltransferease activity, we compared its relative MGAT and DGAT activities using either MAG or DAG as substrates. Human MGAT2 and DGAT1 proteins demonstrated significant MGAT or DGAT activities as controls (Fig. 2c). While rat MGAT3 displayed MGAT activity, no DGAT activity was detected. In the head-to-head experiment to compare human and rat MGAT3 activities, MGAT activity appeared comparable (data not shown) while only human MGAT3 displayed DGAT activities (Fig. 2d). Thus, the rat gene encodes a functional MGAT3 enzyme that displays only MGAT activity.

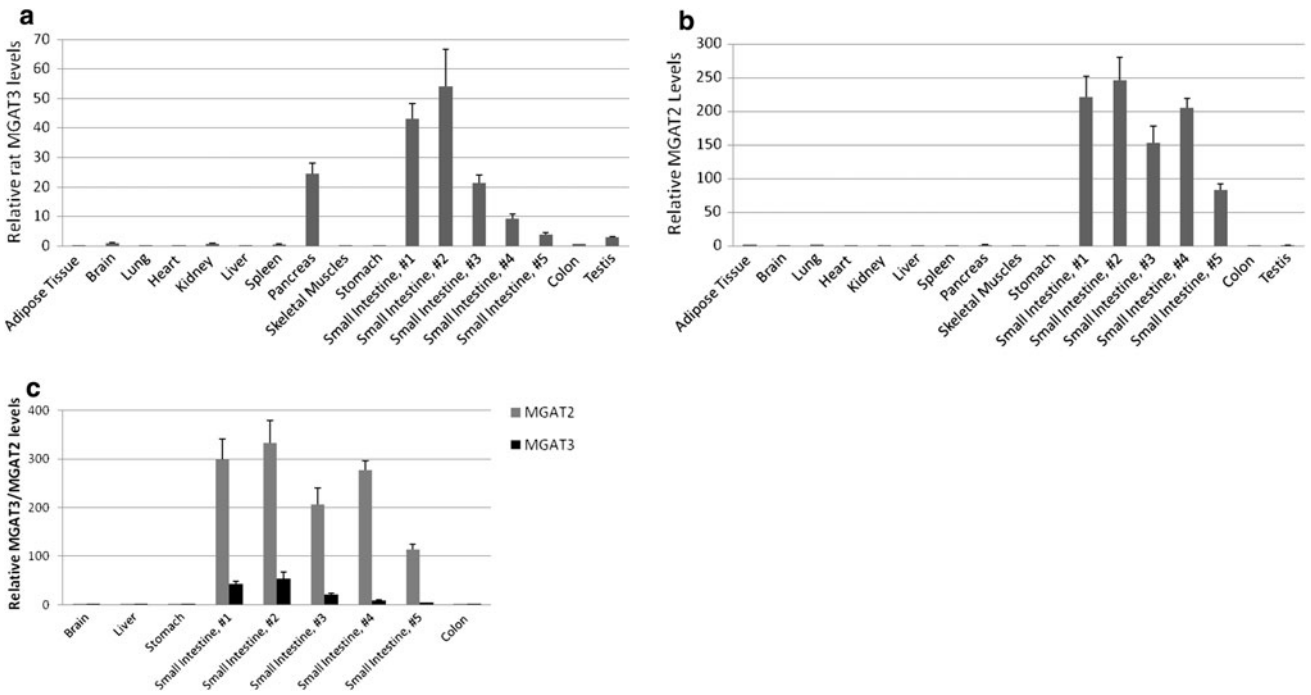

Fig. 3 **a** Tissue distribution of rat Mogat3. The Mogat3 mRNA level was quantified by real-time PCR and normalized by 18 s RNA. The small intestines were separated into 5 different parts from proximal to distal intestines. RNAs were prepared and analyzed as described in the "Methods" section. Data were normalized by setting the average brain expression value to 1. **b** Tissue distribution of rat Mogat2. The Mogat2 mRNA level was quantified by real-time PCR and normalized by 18 s RNA. The data were normalized by setting the average brain expression value to 1. **c** Relative expression levels of rat Mogat3 and Mogat2. The rat Mogat2 and Mogat3 mRNA levels were normalized by 18 s RNA level. Data were normalized by setting brain Mogat3 as 1

The rat Mogat3 mRNA expression pattern was examined in a rat tissue panel by real-time RT-PCR. As expected, rat Mogat3 was highly expressed within the intestines, and the expression was low in the majority of other tissues examined including the colon (Fig. 3a). Interestingly, rat Mogat3 had a fairly high level of mRNA expression in the pancreas as well (Fig. 3a). Rat Mogat2 expression was high in the intestines and low in all the other tissues examined as expected (Fig. 3b). On the relative scale as assessed by real-time PCR analysis, Mogat3 expression was much lower compared to rat Mogat3 although both genes had overlapping expression within the intestinal tract (Fig. 3c).

Because of its functional presence in rat but not in mouse, we searched for Mogat3 ESTs in other rodent species. There were two rodent EST hits, GH463792 and GH463793, belonging to oldfield mice (*Peromyscus polionotus subgrisieus*). A full-length oldfield mouse Mogat3 cDNA sequence was generated (Supplemental Figure 3), the function of which is yet to be tested.

A phylogenetic tree analysis (Fig. 4) was carried out on DGAT2/MGAT2/3 family proteins that suggested evolutionary branching of DGAT2 family genes including DGAT2 and MGAT2, while MGAT3 formed a distinct

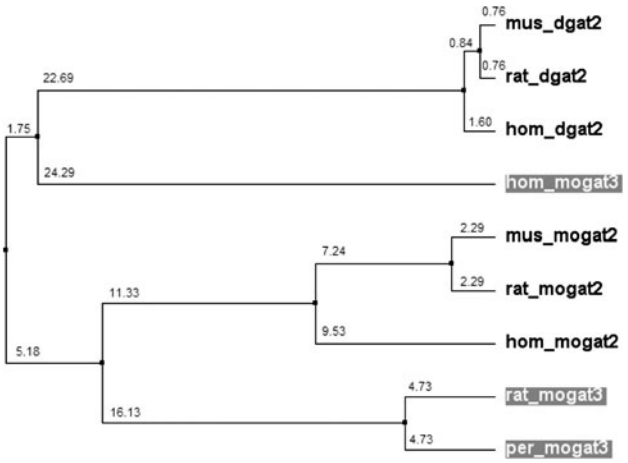

Fig. 4 Phylogenetic tree analysis of MGAT2/DGAT2/MGAT3 proteins based on sequence identity (See supplemental Figure 2 for sequence alignment). Evolutionary distances between different nodes are shown (as generated by JalView). mus_mogat2: NP_803231.1 (*Mus musculus*), hom_mogat2: NP_079374.2 (*Homo sapiens*), rat_mogat2: XP_001060766.1 (*Rattus norvegicus*), mus_dgat2: NP_080660.1 (*Mus musculus*), rat_dgat2: NP_001012345.1 (*Rattus norvegicus*), hom_mogat3: NP_835470.1 (*Homo sapiens*), rat_mogat3: Mogat3 sequence from this study (*Rattus norvegicus*), per_mogat3: Mogat3 sequence identified in this study (*Peromyscus polionotus*)

member of the family. Based on the percent identity assessment, rodent MGAT3 is closest evolutionarily to the MGAT2 gene, and human MGAT3 is most likely derived from gene duplication of DGAT2.

Discussion

The intestinal TAG absorption process is an important component of energy homeostasis. While it has been known for years that TAG is hydrolyzed to fatty acids and MAG, which are subsequently resynthesized back to TAG in enterocytes, it was only recently that the molecules responsible for sequential acylation of MAG to DAG and TAG were cloned and characterized. Specifically, the initial cloning of DGAT1, generation and characterization of DGAT1 deficient mice greatly improved the understanding in the field and also highlighted the importance of the pathway in the whole body energy balance. In addition, the metabolic benefits observed from the DGAT1 deficient mice triggered an industry-wide pursuit of DGAT1 inhibitors for metabolic disorders.

While MGAT1 does not have a high level of expression in intestines [14], successful cloning of both human and mouse MGAT2 revealed its tissue specific expression in intestines that implied a significant role of MGAT2 in the intestinal TAG absorption process [17, 18]. Not surprisingly, characterization of Mogat2 deficient mice indicated similar metabolic phenotypes to those of DGAT1 deficient mice [21]. A hypothesis was put forward suggesting that modulation of the dynamic intestinal TAG absorption process may trigger enteroendocrine and/or enteroneuronal signals that might control whole body energy homeostasis [21].

An interesting finding was made by Cheng and coworkers when the human MGAT3 gene was isolated and reported [16]. While the intestinal expression of MGAT3 also suggested its role in the intestinal TG absorption, its physiological role in this process is yet to be defined. In the case of Mogat2 deficient mice, a natural question arises as to whether MGAT3 and MGAT2 play complementary or overlapping roles in the intestinal TAG absorption process. We found that in mice, Mogat3 is likely a pseudogene and thus there is no other intestinal MGAT enzyme that would compensate for MGAT2 function in the Mogat2 deficient mice. In other words, Mogat2 deficient mice are actually Mogat2 and Mogat3 dual deficient mice. The finding of Mogat3 as a mouse pseudogene is supported by multiple changes in corresponding genomic regions that result in an in-frame stop codon and two frameshifts. The lack of mouse Mogat3 ESTs also supported this conclusion. More conclusively, we found that similar changes in nucleotide sequences within the Mogat3 gene exist in 12 different mouse strains.

We found in rats, however, the Mogat3 gene encodes a functional enzyme. First, the cDNA sequence predicted a functional MGAT3 orthologue in rats. Secondly, the presence of multiple ESTs in rat EST database and the successful cloning of a rat Mogat3 cDNA clearly indicated a possible functional MGAT3 enzyme. The expression of MGAT3 in mammalian cells resulted in the production of a protein of 36 kD, which is similar to the size of human MGAT3. In activity studies, expression of this enzyme in HEK293 cells produced robust MGAT activity. Taken together, we conclude that rat Mogat3 is a functional gene.

The expression pattern of Mogat3 in rats is similar to what was reported for human MGAT3. The quantitative assessment of rat MGAT2 against MGAT3 expression indicated that at the messenger RNA level, MGAT2 appears to be the predominant enzyme expressed in the intestinal tract. It is not known at the moment whether there is posttranslational regulation of MGAT2/3 expression, and thus our results do not necessarily prove that MGAT2 is the major enzyme responsible for intestinal TG absorption. While MGAT3 has overlapping expression with MGAT2, it is not clear whether MGAT3 can compensate for MGAT2 function when the MGAT2 gene is rendered deficient. The relative importance of MGAT2 versus MGAT3 in rats, humans or other species will need to be explored in future studies.

In summary, we report the functional cloning and biochemical characterization of a rat Mogat3 gene. In addition, we provide evidence that the mouse Mogat3 gene is a pseudogene. Our results provide an important molecular basis for understanding the relative roles of MGAT2 and MGAT3 in the intestinal TAG absorption and whole body energy homeostasis.

Acknowledgments The authors wish to thank Haihong Guo for technical assistance.

References

1. Lykidis A et al (1995) Kinetics of the two-step hydrolysis of triacylglycerol by pancreatic lipases. Eur J Biochem 230:892–898
2. Bell RM, Coleman RA (1980) Enzymes of glycerolipid synthesis in eukaryotes. Annu Rev Biochem 49:459–487
3. Levy E (1992) The 1991 Borden Award Lecture. Selected aspects of intraluminal and intracellular phases of intestinal fat absorption. Can J Physiol Pharmacol 70:413–419
4. Lehner R, Kuksis A (1996) Biosynthesis of triacylglycerols. Prog Lipid Res 35:169–201
5. Zhi J et al (1995) Review of limited systemic absorption of orlistat, a lipase inhibitor, in healthy human volunteers. J Clin Pharmacol 35:1103–1108

6. Lucas KH, Kaplan-Machlis B (2001) Orlistat—a novel weight loss therapy. Ann Pharmacother 35:314–328
7. Shi Y, Cheng D (2009) Beyond triglyceride synthesis: the dynamic functional roles of MGAT and DGAT enzymes in energy metabolism. Am J Physiol Endocrinol Metab 297:E10–E18
8. Cases S et al (1998) Identification of a gene encoding an acyl CoA:diacylglycerol acyltransferase, a key enzyme in triacylglycerol synthesis. Proc Natl Acad Sci USA 95:13018–13023
9. Chen HC et al (2002) Increased insulin and leptin sensitivity in mice lacking acyl CoA:diacylglycerol acyltransferase 1. J Clin Invest 109:1049–1055
10. Smith SJ et al (2000) Obesity resistance and multiple mechanisms of triglyceride synthesis in mice lacking Dgat. Nat Genet 25:87–90
11. Buhman KK et al (2002) DGAT1 is not essential for intestinal triacylglycerol absorption or chylomicron synthesis. J Biol Chem 277:25474–25479
12. Yen CL et al (2005) The triacylglycerol synthesis enzyme DGAT1 also catalyzes the synthesis of diacylglycerols, waxes, and retinyl esters. J Lipid Res 46:1502–1511
13. Cheng D et al (2008) Acylation of acylglycerols by acyl coenzyme A:diacylglycerol acyltransferase 1 (DGAT1). Functional importance of DGAT1 in the intestinal fat absorption. J Biol Chem 283:29802–29811
14. Yen CL et al (2002) Identification of a gene encoding MGAT1, a monoacylglycerol acyltransferase. Proc Natl Acad Sci USA 99:8512–8517
15. Cao J et al (2004) A predominant role of acyl-CoA:monoacylglycerol acyltransferase-2 in dietary fat absorption implicated by tissue distribution, subcellular localization, and up-regulation by high fat diet. J Biol Chem 279:18878–18886
16. Cheng D et al (2003) Identification of acyl coenzyme A:monoacylglycerol acyltransferase 3, an intestinal specific enzyme implicated in dietary fat absorption. J Biol Chem 278:13611–13614
17. Cao J et al (2003) Cloning and functional characterization of a mouse intestinal acyl-CoA:monoacylglycerol acyltransferase, MGAT2. J Biol Chem 278:13860–13866
18. Yen CL, Farese RV Jr (2003) MGAT2, a monoacylglycerol acyltransferase expressed in the small intestine. J Biol Chem 278:18532–18537
19. Cao J et al (2003) Properties of the mouse intestinal acyl-CoA:monoacylglycerol acyltransferase, MGAT2. J Biol Chem 278:25657–25663
20. Cao J et al (2007) Catalytic properties of MGAT3, a putative triacylgycerol synthase. J Lipid Res 48:583–591
21. Yen CL et al (2009) Deficiency of the intestinal enzyme acyl CoA:monoacylglycerol acyltransferase-2 protects mice from metabolic disorders induced by high-fat feeding. Nat Med 15:442–446
22. Carver TJ et al (2005) ACT: the Artemis comparison tool. Bioinformatics 21:3422–3423
23. Waterhouse AM et al (2009) Jalview Version 2—a multiple sequence alignment editor and analysis workbench. Bioinformatics 25:1189–1191

Lipids (2011) 46:521–528
DOI 10.1007/s11745-011-3538-0

ORIGINAL ARTICLE

High Doses of Rosuvastatin are Superior to Low Doses of Rosuvastatin Plus Fenofibrate or n-3 Fatty Acids in Mixed Dyslipidemia

A. P. Agouridis · V. Tsimihodimos · T. D. Filippatos · A. D. Tselepis · M. S. Elisaf

Received: 15 October 2010 / Accepted: 7 December 2010 / Published online: 15 February 2011

Abstract The aim of the study was to compare the efficacy of high-dose rosuvastatin, low-dose rosuvastatin plus fenofibrate and low-dose rosuvastatin plus omega-3 fatty acids with regard to the lipid profile in patients with mixed hyperlipidemia. The primary endpoint was changes in non-high density lipoprotein-cholesterol (non-HDL-C) levels. Study participants were randomly allocated to receive rosuvastatin 40 mg ($n = 30$, R group), rosuvastatin 10 mg plus fenofibrate 200 mg ($n = 30$, RF group) or rosuvastatin 10 mg plus n-3 fatty acids 2 g ($n = 30$, RN group). Non-HDL-C levels were reduced in all groups: in R group by 54%, in RF group by 42% and in RN group by 42%. Significant reductions in total cholesterol (TC), low density lipoprotein (LDL)-C and triglyceride levels were observed in all groups. The reductions in total and LDL-C were greatest in the R group while a more pronounced reduction of triglycerides in the RF group compared with that in the R and the RN group was observed. HDL-C levels were significantly increased only in the RF group. In conclusion, high doses of rosuvastatin and small doses of rosuvastatin plus either fenofibrate or n-3 fatty acids exhibit favorable effects on both LDL-C and non-HDL-C levels. However, rosuvastatin monotherapy more potently reduces these parameters. The combination of rosuvastatin plus fenofibrate leads to a greater decrease in triglyceride levels and a greater increase in HDL-C levels compared with the other two treatments. While awaiting the results of ongoing trials high doses of rosuvastatin may represent the treatment of choice in individuals with mixed dyslipidemia.

Keywords Mixed hyperlipidemia · Rosuvastatin · Fenofibrate · n-3 Fatty acids · Metabolic parameters · Non high-density lipoprotein · Triglycerides · High-density lipoprotein

Abbreviations

ApoA-1	Apolipoprotein A-1
apoB	Apolipoprotein B
ALT	Alanine aminotransferase
AST	Aspartate aminotransferase
DHA	Docosahexaenoic acid
EPA	Eicosapentaenoic acid
HDL	High density lipoprotein
HOMA	Homeostasis model assessment
IDL	Intermediate density lipoprotein
LDL	Low density lipoprotein
R group	Rosuvastatin group
RF group	Rosuvastatin-fenofibrate combination group
RN group	Rosuvastatin-n-3 fatty acids combination group
TC	Total cholesterol
TG	Triglycerides
TSH	Thyroid stimulating protein

Introduction

Mixed or combined hyperlipidemia is a common metabolic disorder characterized by elevated concentrations of both

A. P. Agouridis · V. Tsimihodimos · T. D. Filippatos · M. S. Elisaf (✉)
Department of Internal Medicine, Medical School, University of Ioannina, 45110 Ioannina, Greece
e-mail: egepi@cc.uoi.gr

A. D. Tselepis
Laboratory of Biochemistry, Department of Chemistry, University of Ioannina, Ioannina, Greece

cholesterol and triglycerides [1]. More specifically, patients with mixed hyperlipidemia have elevated low density lipoprotein-cholesterol (LDL-C) and triglyceride (TG) levels, a preponderance of small, dense LDL particles, and reduced concentrations of high density lipoprotein-cholesterol (HDL-C) [1]. Mixed hyperlipidemia usually results from the hepatic overproduction of apolipoprotein B that enters the circulation in the form of very low density lipoproteins (VLDLs) [1]. Although the term mixed dyslipidemia is used to describe a heterogeneous group of disorders with divergent metabolic causes that simply share a common clinical phenotype, it is widely accepted that this condition is associated with an increased cardiovascular risk [1]. Thus, this disorder should be promptly treated with lifestyle changes, dietary counseling, lipid-lowering drugs or combinations of these interventions. It is well known that monotherapy with conventional doses of statins or fibrates is usually sufficient to treat simple lipid disorders such as hypercholesterolemia or hypertriglyceridemia, respectively. On the other hand mixed hyperlipidemia represents an important therapeutic challenge since in this case monotherapies only partially correct the underlying metabolic defects.

Statins represent the cornerstone of hypolipidemic therapy. These compounds have shown enormous efficiency in reducing the incidence of cardiovascular disease, a phenomenon that is mainly related to the reductions in LDL-C concentrations. On the other hand, the use of older statins in individuals with mixed dyslipidemia usually results in residual hypertriglyceridemia and low HDL-C levels [2]. However, although the conventional doses of older statins do not markedly alter triglyceride or HDL-C levels, high doses of the newer statins such as rosuvastatin or atorvastatin may favorably affect these parameters. Thus, rosuvastatin (10 or 20 mg) and atorvastatin (20 or 40 mg) have been shown to reduce triglycerides by almost 30% in patients with primary hyperlipidemia [3]. In addition, rosuvastatin in high doses (40 mg) seems to be the most potent statin for HDL-C elevation demonstrating increases in HDL-C levels by 8–15% in large clinical trials [4–6]. Thus, the use of high doses of these potent statins represents a promising therapeutic option in patients with mixed dyslipidemia. An alternative approach to the treatment of mixed dyslipidemia is the combination of a statin with agents that reduce triglycerides and/or increase HDL-C values. Fibric acid derivatives (fibrates) and n-3 fatty acids represent ideal candidates for this kind of combination treatment. Fenofibrate belongs to a class of drugs that activate specific transcription factors known as peroxisome proliferator activated receptors α (PPAR-α) [7]. These drugs reduce the concentration of plasma TG by 30–50% and raise the level of HDL-C by 2–20%. Fenofibrate's effect on LDL-C is variable, ranging from a small decrease in hypercholesterolemic patients to no change or even a slight increase in individuals with combined dyslipidemia or hypertriglyceridemia [7]. Furthermore, the effects of fenofibrate on HDL-C are largely dependent on baseline HDL-C levels. In several clinical studies combined statin/fibrate therapy resulted in pronounced decreases in LDL-C, triglycerides and non-HDL-C as well as increases in HDL-C compared with either monotherapy [8]. However, the elevated risk for muscle side effects limits the widespread use of this combination [9]. The n-3 fatty acids mainly reduce TG concentration, but they exert many other anti-atherosclerotic properties [10]. Numerous prospective and retrospective trials from many countries have shown that moderate fish consumption lowers the risk of major cardiovascular events, such as myocardial infarction, sudden cardiac death, coronary heart disease, atrial fibrillation, and most recently, death in patients with heart failure [10, 11]. Adding n-3 fatty acids to statins reduces triglycerides and non-HDL-C to a greater extent than statin monotherapy [12]. It is currently unknown what would be the best treatment option for patients with mixed hyperlipidemia, i.e. high-dose statin therapy or low-dose statin plus fenofibrate (the only fibrate that can be coadministered with a statin) or low-dose statin plus n-3 fatty acids. The primary end-point of the present open-label randomized study was the lowering effect of high dose of rosuvastatin alone, low dose of rosuvastatin plus fenofibrate and low dose of rosuvastatin plus n-3 fatty acids treatment on non-HDL-C levels in patients with primary mixed hyperlipidemia. Secondary end-points were the treatment effects on LDL-C values, the percentage of patients that achieved their pre-specified LDL and non-HDL-C targets, the effects of these treatments on anthropometric variables (such as body weight and body mass index), lipid profile (triglycerides, HDL-C and apolipoprotein values), carbohydrate metabolism indices (fasting glucose and insulin concentrations, Homeostasis Model Assessment (HOMA)-index values) and serum uric acid (SUA) levels. To the best of our knowledge, this is the first time that these combinations have been compared directly.

Materials and Methods

Participants

Patients attending the Outpatient Obesity and Lipid Clinic of the University Hospital of Ioannina, Greece were recruited for the study. Patients were considered eligible if they had LDL-C >160 mg/dL and triglycerides >200 mg/dL at baseline. Exclusion criteria were known coronary heart disease or other atherosclerotic diseases, triglyceride values >500 mg/dL, renal disease (serum creatinine levels

>1.6 mg/dL or proteinuria of nephrotic range), diabetes mellitus (fasting blood glucose >126 mg/dL or ongoing treatment with oral hypoglycaemic agents), hypothyroidism [thyroid stimulating hormone (TSH) >5 IU/ml] and liver disease (ALT and/or AST levels > threefold upper limit of normal in more than two consecutive measurements). Patients with any medical conditions that might preclude successful completion of the study protocol were excluded. Patients with hypertension were included in the study but they were on stable medication for at least 3 months before study entry and their blood pressure was adequately controlled (no change in their treatment was be made during the study period). Patients currently taking lipid lowering drugs or having stopped them less than 4 weeks before study entry were excluded. After the initial screening all study participants gave a written informed consent. All subjects were given individualized dietary instructions by a clinical nutritionist, based on each one's basal energy requirements and on an estimation of the subject's typical activity level, according to NCEP-ATP III guidelines [13]. The treatment groups did not differ in their nutrient intake at baseline [regarding dietary cholesterol, total calories, percentage of calories from saturated, unsaturated, and monounsaturated fats, and percentage of calories from carbohydrates and alcohol (analyses not shown)]. There were no differences in diet composition between study groups. All patients were asked to attend the clinic monthly during the treatment in order to assess diet compliance. Patients who remained hyperlipidemic (LDL-C >160 mg/dL and triglycerides >200 mg/dL) on two consecutive measurements after a dietary intervention period of approximately 3 months were considered eligible for randomization. We followed a simple randomization method using a table of random numbers as previously described [14]. With this method patients were allocated to open-label rosuvastatin 40 mg ($n = 30$, group R), rosuvastatin 10 mg plus fenofibrate 200 mg ($n = 30$, group RF) or rosuvastatin 10 mg plus 2 gr of n-3 fatty acids [each gr of the preparation contained approximately 465 mg of eicosapentaenoic acid (EPA) and 375 mg of docosahexaenoic acid (DHA)] ($n = 30$, group RN) daily. Anthropometric variables and serum metabolic parameters were assessed at baseline and after 3 months of treatment. Non-HDL-C and LDL-C targets for each patient were determined according to NCEP-ATP III guidelines [13]. No external sponsor was involved in the study which was approved by the ethics committee of the University Hospital of Ioannina.

Biochemical Parameters

All laboratory determinations were carried out after an overnight fast. Non-HDL-C was calculated by the equation: non-HDL-C = TC − HDL-C. LDL-C was calculated using the Friedewald formula (provided that triglycerides were <400 mg/dL). Serum concentrations of fasting glucose, total cholesterol and triglycerides were determined enzymatically on an Olympus AU600 clinical chemistry analyzer (Olympus Diagnostica, Hamburg, Germany). HDL-C was determined in the supernatant, after precipitation of the apolipoprotein B-containing lipoproteins with dextran sulphate-Mg^{++} (Sigma Diagnostics, St. Louis, MO, USA). Serum apolipoproteins (Apo) A-I and B were measured by immunonephelometry on a BN ProSpec nephelometer (Dade-Behring, Lieberbach, Germany). Serum creatinine was measured using the Jaffé method. SUA was calculated with an enzymatic colorimetric test (uricase). Fasting serum insulin levels were measured by an AxSYM insulin assay microparticle enzyme immunoassay on an AzSYM analyzer (Abbott Diagnostics, Illinois, USA). Finally, HOMA index was calculated using the equation proposed by Matthews as follows: fasting insulin (mU/L) * fasting glucose (mg/dL)/405 [15].

Statistical Analyses

Values are given as means ± standard deviation (SD) and median (range) for parametric and non-parametric data, respectively. The chi-square test was used to access differences in proportions. Continuous variables were tested for lack of normality by the Kolmogorov–Smirnov test and logarithmic transformations were accordingly performed for triglycerides, insulin and HOMA index. The paired-samples t-test was used for assessing the effect of treatment in each group. Analysis of covariance (ANCOVA), adjusted for baseline values, was used for comparisons between treatment groups. Significance was defined as $p < 0.05$. Analyses were performed using the SPSS 15.0 statistical package for Windows (SPSS Inc., 1989–2004).

Results

We enrolled 90 patients (45 men and 45 women) with a mean age of 55 ± 10 years (Table 1). More than 75% of the study participants fulfilled the criteria for the diagnosis of metabolic syndrome [16]. On the other hand only exceptionally did study subjects have a positive family history of dyslipidemia and/or premature cardiovascular disease that could be consistent with the diagnosis of familial combined hyperlipidemia. There were no differences in age, sex distribution, body mass index values and proportion of smokers between study groups. The baseline values of TC, LDL-C, non-HDL-C and TG as well as the concentrations of apolipoproteins AI and B did not show any significant difference among the 3 treatment groups

Table 1 Baseline demographic characteristics of all study patients

Characteristic	Group R	Group RF	Group RN	*p*
n (males/females)	30 (11/19)	30 (16/14)	30 (18/12)	NS
Age (years)	58 ± 9	54 ± 12	54 ± 10	NS
Current smokers (%)	36	32	40	NS
Body weight (kg)	80 ± 14	85 ± 13	81 ± 13	NS
BMI (kg/m^2)	29 ± 4	30 ± 3	29 ± 3	NS
TC (mg/dL)	304 ± 69	300 ± 45	284 ± 42	NS
LDL-C (mg/dL)	204 ± 68	191 ± 44	183 ± 40	NS
TG (mg/dL)	239 (201–336)	268 (209–364)	259 (200–396)	NS
HDL-C (mg/dL)	50 ± 8	52 ± 10	48 ± 10	NS
Non-HDL-C (mg/dL)	253 ± 60	247 ± 38	235 ± 38	NS
Apo AI (mg/dL)	152 ± 20	163 ± 25	142 ± 25	NS
Apo B (mg/dL)	137 ± 38	142 ± 26	133 ± 20	NS

Values are expressed as means ± SD except for triglycerides that are expressed as median (range)

R rosuvastatin, *RF* rosuvastatin + fenofibrate, *RN* rosuvastatin + n-3 fatty acids, *BMI* body mass index, *Apo* apolipoprotein, *NS* non significant

(Table 1). There were no significant changes in blood pressure, BMI, waist circumference, and body weight at 3 months (data not shown). At the end of the 3-month treatment period, there was a significant reduction of non-HDL-C in all treatment groups ($p < 0.001$ compared to baseline values) with a greater decrease in the R group ($p < 0.05$ compared to RF and RN groups). More specifically non-HDL-C was reduced by 54% in the R group, by 42% in the RF group and by 42% in the RN group (Table 2). Twenty-seven patients out of 30 achieved the non-HDL-C target in R group (90%). The percentage of patients that achieved the non-HDL-C target was 70% in RF group (21 patients out of 30) and 76.6% in the RN group (23 patients out of 30). The proportion of patients that reached the non-HDL-C target was significantly higher in the R group compared to RF group ($p < 0.05$) but not to RN group. There were significant reductions in plasma levels of TC, LDL-C, and triglycerides in all study groups (Table 2). The reductions of TC and LDL-C levels were significantly greater in the R group (−46 and −59%, respectively) compared with the RF (−34 and −44%, respectively) and RN (−35 and −44%, respectively) groups. A greater proportion of patients in the R group achieved their LDL-C targets (87%) compared to those in RF and RN groups (70 and 83%, respectively). On the contrary, the reduction of triglyceride levels was significantly higher in the RF group (−50%) compared with the R (−33%) and the RN (−31%) group ($p < 0.01$ for both comparisons). In order to compare the overall lipid-lowering efficacy of the regimens tested we used the dual goal of non-HDL-C below 160 mg/dL and triglycerides lower than 150 mg/dL. A greater proportion of patients in the RF group achieved this dual target compared to the R and RN groups (Fig. 1). However, these differences did not reach statistical significance. In all groups smokers had

Table 2 Serum metabolic parameters at baseline and after 3 months of treatment

	Baseline	3 months	% change
TC (mg/dL)			
Group R	304 ± 69	164 ± 37	−46
Group RF	300 ± 45	197 ± 40	−34
Group RN	284 ± 42	185 ± 37	−35
LDL-C (mg/dL)			
Group R	204 ± 65	83 ± 33	−59
Group RF	191 ± 44	108 ± 49	−44
Group RN	183 ± 40	102 ± 31	−44
Triglycerides (mg/dL)			
Group R	239 (201–336)	160 (62–309)	−33
Group RF	268 (209–364)	134 (67–244)	−50
Group RN	259 (200–396)	174 (97–327)	−31
HDL-C (mg/dL)			
Group R	50 ± 8	52 ± 8	+4
Group RF	52 ± 10	56 ± 12	+8
Group RN	48 ± 10	50 ± 10	+4
Non HDL-C (mg/dL)			
Group R	253 ± 60	117 ± 32	−54
Group RF	247 ± 38	141 ± 39	−42
Group RN	235 ± 38	135 ± 33	−42
ApoA1 (mg/dL)			
Group R	152 ± 20	145 ± 22	−5
Group RF	163 ± 25	169 ± 28	+4
Group RN	142 ± 25	149 ± 29	+5
ApoB (mg/dL)			
Group R	137 ± 38	73 ± 23	−47
Group RF	142 ± 26	84 ± 26	−41
Group RN	133 ± 20	83 ± 22	−38
Serum creatinine (mg/dL)			
Group R	0.962 ± 0.162	0.971 ± 0.210	+1.1
Group RF	0.968 ± 0.164	1.086 ± 1.726	+12.8
Group RN	1.048 ± 0.231	0.996 ± 0.169	−3.7
Uric acid (mg/dL)			
Group R	5.5 ± 1.2	5.1 ± 1.5	−9
Group RF	6.2 ± 1.4	4.9 ± 1	−21
Group RN	6.3 ± 1.7	5.9 ± 1.5	−4

Values are expressed as means ± SD [except for triglycerides that are expressed as median (range)]

R rosuvastatin, *RF* rosuvastatin + fenofibrate, *RN* rosuvastatin + n-3 fatty acids, *TC* total cholesterol, *LDL-C* low density lipoprotein cholesterol, *HDL-C* high density lipoprotein cholesterol

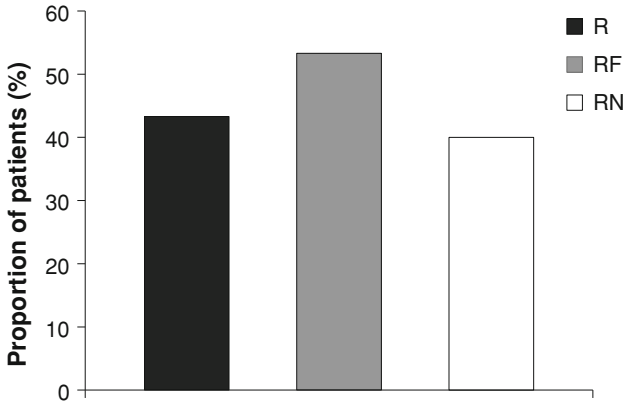

Fig. 1 Proportion of patients that reached the dual target of non-HDL-cholesterol <160 mg/dL and triglycerides <150 mg/dL. *R* rosuvastatin, *RF* rosuvastatin + fenofibrate, *RN* rosuvastatin + n-3 fatty acids

significantly lower HDL-C values compared to non-smokers (data not shown). HDL-C levels were significantly increased at 3 months in the RF group (+8%), while they were non-significantly increased in the R (+4%) and the RN (+4%) group (Table 2). Smoking status did not significantly affect the response of HDL-C levels to the therapeutic interventions (data not shown). After 3 months of treatment a more pronounced increase in ApoA-I levels was observed in the RF and RN groups (+4 and +5%, respectively) compared with changes in the R group (−5%). However this difference did not achieve statistical significance. ApoB levels were significantly reduced in all groups with a greater reduction in R compared with RN group. Serum uric acid levels decreased more in the RF group (−21%) compared with the R group (−9%) and with the RN group (−4%) (Table 2). Finally, serum creatinine significantly increased in the RF group (+12.8%) but it was not significantly altered in the R and RN groups (Table 2). Glucose in all groups was unaltered but insulin levels and HOMA index showed controversial results. HOMA index was significantly reduced in RF (−40%) group but it was increased in the R group (+55%, Table 3). The same results were observed as far as insulin levels were concerned. There were no significant changes in the HOMA index and insulin levels in the RN group.

Safety

Of the 90 patients enrolled 3 (3.3%) dropped out during the study: 1 man and 1 woman in the RF group due to adverse events (myalgia without elevated CK levels) and 1 woman in the RN group due to an asymptomatic abnormal liver function test (AST and ALT elevation >3 times the upper limit of normal). In the patients who completed the study rosuvastatin, fenofibrate and n-3 fatty acids were well tolerated.

Table 3 Glucose, insulin and HOMA index at baseline and after 3 months of treatment

	Baseline	3 months	% change
Glucose (mg/dL)			
Group R	95 ± 10	96 ± 11	+1
Group RF	94 ± 10	93 ± 7	−1
Group RN	96 ± 11	96 ± 10	0
Insulin (μU/mL)			
Group R	8 (2–17)	11 (2–26)	+55
Group RF	17 (2–82)	10 (2–28)	−41
Group RN	10 (5–18)	11 (2–26)	+10
HOMA index			
Group R	1.8 (0.4–4.5)	2.8 (0.4–6.9)	+55
Group RF	4.1 (0.5–22.6)	2.4 (0.5–6.8)	−40
Group RN	2.5 (1.1–4.1)	2.6 (0.5–6.4)	+4

Values are expressed as means ± SD for glucose and median (range) for insulin and HOMA

R rosuvastatin, *RF* rosuvastatin + fenofibrate, *RN* rosuvastatin + n-3 fatty acids, *HOMA* homeostasis model assessment

Discussion

In this open-label randomized study, we directly compared for the first time high doses of rosuvastatin with low doses of this statin plus fenofibrate or n-3 fatty acids in the treatment of mixed hyperlipidemia. The primary endpoint of the study was the lowering effect of these three different regimens on non-HDL-C. According to NCEP-ATP III the goal for non-HDL in our patients was set to 30 mg/dL higher than the corresponding LDL-C goal [13]. Since no study participant had a history of coronary heart disease or equivalents the non-HDL-C target for virtually all patients was 160 mg/dL. In our study, 3 months of treatment with the above regimens led to a significant reduction in non-HDL-C levels in all study groups. However, this reduction was significantly greater in the rosuvastatin monotherapy group compared with the combination treatment groups. Similar differences were also observed in the LDL-C-decreasing potency of the regimens tested.

Epidemiological studies have shown that LDLs represent the most atherogenic lipoproteins of human plasma and thus the levels of LDL-C should be considered as the primary target of preventive or therapeutic strategies in all individuals [17]. However, the utilization of LDL-cholesterol as a target for therapy in patients with mixed hyperlipidemia has several important limitations. It is well known that LDL-C is commonly determined by the Friedewald equation in specimens from fasting subjects and with triglyceride concentrations lower than 400 mg/dL. However, the equation is considerably inaccurate even at triglyceride concentrations of 200–400 mg/dL [18]. Thus, since mixed dyslipidemia is by definition

characterized by increased concentrations of triglycerides the use of Friedewald equation for the determination of LDL-cholesterol values in this patient population may result in important measurement errors. On the other hand, it is well known that mixed dyslipidemia is characterized by elevated concentrations of potentially atherogenic lipoprotein particles (such as VLDL, IDL and small, dense LDL particles) whose levels are not captured by conventional LDL measurement. As a result, NCEP ATPIII guidelines introduced non-HDL-C values as secondary targets of therapy in all patients with triglyceride values greater than 200 mg/dL [13]. The calculation of this parameter (which represents the sum of the concentrations of all apolipoprotein B-containing particles) overcomes the methodological limitations of LDL-cholesterol determination, does not require fasting specimens and, most importantly, in addition to LDL particles takes into account the concentrations of all apolipoprotein B-containing particles. Numerous studies in populations with different characteristics have shown that non-HDL-C levels represent a precise estimator of future cardiovascular risk whose accuracy may be even greater than that of conventional lipid parameters (such as total or LDL-C) [19, 20]. According to our results monotherapy with high doses of rosuvastatin represents the most plausible option for the treatment of patients with mixed hyperlipidemia since this regimen is more effective in reducing the concentrations of both non-HDL-C and LDL-C compared to combination treatment with low dose of rosuvastatin and either fenofibrate or n-3 fatty acids. Although the number of patients that concomitantly reached the non-HDL-C and TRG targets was (non significantly) greater in the RF group, to our knowledge there is no data suggesting that the achievement of this "dual" goal is clinically more beneficial than the achievement of the non-HDL-C target. Indeed, this marginal difference in the number of patients that reached the dual goal was mainly driven by the greater triglyceride-lowering efficiency of the RF combination; however, it is currently controversial if this higher TG-reducing potency can be translated into clinical benefit [21].

Since the regimens used in our study have never been directly compared in studies with hard clinical endpoints it is not known if the differences observed in the lipid-lowering potency of these drugs are reflective of differences in their ability to reduce the incidence of cardiovascular disease in individuals with mixed hyperlipidemia. In an elegant review Rubenfire et al. [22] summarized the currently available treatment options for individuals with mixed dyslipidemia and proposed a therapeutic algorithm suggesting that the first priority in these patients should be the maximally tolerated effective dose of a potent statin. This approached is based on results from clinical trials showing that the reduction in the incidence of cardiovascular disease is closely related to the dose of statins [23] as well as to the magnitude of LDL-C and non-HDL-C reduction [20, 23]. In addition, although the combination of a statin with a fibrate is pathophysiologically attractive the recently published The Action to Control Cardiovascular Risk in Diabetes (ACCORD) study showed that simvastatin-fenofibrate combination in patients with type 2 diabetes mellitus was not superior to simvastatin monotherapy in terms of cardiovascular risk reduction [24]. Although the study was not powered to assess efficacy on the basis of baseline lipids, there was a borderline significant reduction in major cardiovascular events in persons with a triglyceride level of 204 mg/dL or greater and an HDL cholesterol level of 34 mg/dL or less at baseline. We believe that our results are in line with the strategy proposed by Rubenfire et al. [22]; while awaiting the results of ongoing trials, monotherapy with high doses of potent statins seems to be the best therapeutic option in individuals with mixed dyslipidemia.

Although our study did not have sufficient power to assess differences in safety, our results indicate that the high doses of rosuvastatin as well as the combinations of low doses of this compound with fenofibrate or fish oils are extremely safe and very well tolerated. In agreement with previous studies we noticed a significant increase in serum creatinine levels after fenofibrate administration [25]. However, controversy exists as to whether this phenomenon represents a true deterioration in renal function or an increase in the rate of metabolic production of creatinine. On the other hand, the well-known uricosuric properties of fenofibrate possibly underlie the greater reduction in serum uric acid levels observed in the RF patient group [26]. In agreement with previous studies we found that the high doses of rosuvastatin (40 mg) may adversely affect glucose homeostasis leading to a worsening of insulin resistance indices [6, 27]. Indeed, in our patients rosuvastatin monotherapy resulted in a significant increase in HOMA index values by 55%, mirrored by a correspondent increase in serum insulin levels whereas fasting glucose values remained constant. These results seem to be in contrast with those reported in a recently published meta-analysis showing that statins, as a class, have no effect on insulin sensitivity [28]. However, when individual statins were analyzed separately a non significant trend towards insulin sensitivity deterioration was evident with rosuvastatin [28]. These changes were not of the same magnitude with those observed in our study; however, the differences in patients' selection criteria, in the duration of the study as well as in the dose of the drug may partially explain this discrepancy. The use of the inaccurate HOMA index as an indicator of insulin sensitivity in our study may also have played an important role. In the RN group the levels of HOMA index and insulin remained unaltered. This means either that the

lower doses of rosuvastatin and n-3 fatty acids do not exert any significant effect on carbohydrate metabolism or that the detrimental effect of the low doses of rosuvastatin on peripheral glucose uptake (that so far has been observed only in individuals with insulin resistance) [27] is milder and can be counterbalanced by the corresponding beneficial effect of fish oils [29, 30]. To make things more complicate other studies showed that n-3 fatty acids may exert an adverse effect on insulin sensitivity [31]. Finally, the significant reduction in the values of insulin resistance indices in the RF group can be attributed to the insulin sensitizing properties of the fibric acid derivatives [32]. It must be noted that the differential effects of the various treatments on insulin resistance indices (HOMA-IR and fasting insulin concentration) could have been influenced by the differences in the baseline values of these parameters. Although we tried to avoid this type of error by using ANCOVA and taking into account the baseline values of HOMA-IR and insulin as covariates we cannot fully exclude this possibility. Whether these differences are of potential clinical importance or not remains to be established.

In conclusion, in the present study mixed hyperlipidemic patients without diabetes responded generally well to rosuvastatin alone or in combination with fenofibrate or n-3 fatty acids. High doses of rosuvastatin, small doses of rosuvastatin plus fenofibrate and small doses of rosuvastatin plus n-3 fatty acids decreased significantly non-HDL-C with rosuvastatin monotherapy being more effective in reducing this parameter. On the contrary, the combination of rosuvastatin plus fenofibrate had a more potent effect in reducing triglyceride levels and increasing HDL-C values compared with the other two treatment groups. Larger, prospective clinical trials with a double blind design are needed to delineate whether these differences in biochemical efficiency can be translated into significant differences in clinical efficiency and more specifically in the ability of various regimens to reduce cardiovascular morbidity and mortality in patients with mixed dyslipidemia.

References

1. Durrington P (2003) Dyslipidaemia. Lancet 362:717–731
2. Fruchart JC, Sacks F, Hermans MP, Assmann G, Brown WV, Ceska R, Chapman MJ, Dodson PM, Fioretto P, Ginsberg HN, Kadowaki T, Lablanche JM, Marx N, Plutzky J, Reiner Z, Rosenson RS, Staels B, Stock JK, Sy R, Wanner C, Zambon A, Zimmet P (2008) The residual risk reduction initiative: a call to action to reduce residual vascular risk in patients with dyslipidemia. Am J Cardiol 102:1K–34K
3. McKenney JM, Jones PH, Adamczyk MA, Cain VA, Bryzinski BS, Blasetto JW (2003) Comparison of the efficacy of rosuvastatin versus atorvastatin, simvastatin, and pravastatin in achieving lipid goals: results from the STELLAR trial. Curr Med Res Opin 19:689–698
4. Nissen SE, Nicholls SJ, Sipahi I, Libby P, Raichlen JS, Ballantyne CM, Davignon J, Erbel R, Fruchart JC, Tardif JC, Schoenhagen P, Crowe T, Cain V, Wolski K, Goormastic M, Tuzcu EM (2006) Effect of very high-intensity statin therapy on regression of coronary atherosclerosis: the ASTEROID trial. JAMA 295:1556–1565
5. Milionis HJ, Rizos E, Kostapanos M, Filippatos TD, Gazi IF, Ganotakis ES, Goudevenos J, Mikhailidis DP, Elisaf MS (2006) Treating to target patients with primary hyperlipidaemia: comparison of the effects of ATOrvastatin and ROSuvastatin (the ATOROS study). Cur Med Res Opin 22:1123–1131
6. Ridker PM, Danielson E, Fonseca FA, Genest J, Gotto AM Jr, Kastelein JJ, Koenig W, Libby P, Lorenzatti AJ, MacFadyen JG, Nordestgaard BG, Shepherd J, Willerson JT, Glynn RJ (2008) Rosuvastatin to prevent vascular events in men and women with elevated C-reactive protein. N Engl J Med 359:2195–2207
7. Elisaf M (2002) Effects of fibrates on serum metabolic parameters. Curr Med Res Opin 18:269–276
8. Ginsberg HN, Elam MB, Lovato LC, Crouse JR, Leiter LA, Linz P, Friedewald WT, Buse JB, Gerstein HC, Probstfield J, Grimm RH, Ismail-Beigi F, Bigger JT, Goff DC Jr, Cushman WC, Simons-Morton DG, Byington RP (2010) Effects of combination lipid therapy in type 2 diabetes mellitus. N Engl J Med 362:1563–1574
9. Wierzbicki AS, Mikhailidis DP, Wray R, Schacter M, Cramb R, Simpson WG, Byrne CB (2003) Statin-fibrate combination: therapy for hyperlipidemia: a review. Curr Med Res Opin 19:155–168
10. Lavie CJ, Milani RV, Mehra MR, Ventura HO (2009) Omega-3 polyunsaturated fatty acids and cardiovascular diseases. J Am Coll Cardiol 54:585–594
11. Gazi I, Liberopoulos EN, Saougos VG, Elisaf M (2006) Beneficial effects of omega-3 fatty acids: the current evidence. Hellenic J Cardiol 47:223–231
12. Davidson MH, Stein EA, Bays HE, Maki KC, Doyle RT, Shalwitz RA, Ballantyne CM, Ginsberg HN (2007) Efficacy and tolerability of adding prescription omega-3 fatty acids 4 g/dl to simvastatin 40 mg/dL in hypertriglyceridemic patients: an 8-week, randomized, double-blind, placebo-controlled study. Clin Ther 29:1354–1367
13. Grundy SM, Cleeman JI, Merz CN, Brewer HB Jr, Clark LT, Hunninghake DB, Pasternak RC, Smith SC Jr, Stone NJ (2004) Implications of recent clinical trials for the national cholesterol education program adult treatment panel III guidelines. Circulation 110:227–239
14. Pocock SJ (1983) Clinical trials. A practical approach. Wiley, New York
15. Matthews DR, Hosker JP, Rudenski AS, Naylor BA, Treacher DF, Turner RC (1985) Homeostasis model assessment: insulin resistance and beta-cell function from fasting plasma glucose and insulin concentrations in man. Diabetologia 28:412–419
16. Grundy SM, Brewer HB Jr, Cleeman JI, Smith SC Jr, Lenfant C, American Heart Association, National Heart, Lung, Blood Institute (2004) Definition of metabolic syndrome: Report of the National Heart, Lung, and Blood Institute/American Heart Association conference on scientific issues related to definition. Circulation 109:433–438
17. Castelli WP, Garrison RJ, Wilson PW, Abbott RD, Kannel WB, Kalousdian S (1986) Incidence of coronary heart disease and lipoprotein cholesterol levels. The Framingham study. JAMA 256:2835–2838
18. Bairaktari ET, Seferiadis KI, Elisaf MS (2005) Evaluation of methods for the measurement of low-density lipoprotein cholesterol. J Cardiovasc Pharmacol Ther 10:45–54

19. Pischon T, Girman CJ, Sacks FM, Rifai N, Stampfer MJ, Rimm EB (2005) Non-high-density lipoprotein cholesterol and apolipoprotein B in the prediction of coronary heart disease in men. Circulation 112:3375–3383
20. Robinson JG, Wang S, Smith BJ, Jacobson TA (2009) Meta-analysis of the relationship between non-high-density lipoprotein cholesterol reduction and coronary heart disease risk. J Am Coll Cardiol 53:316–322
21. Robins SJ, Collins D, Wittes JT, Papademetriou V, Deedwania PC, Schaefer EJ, McNamara JR, Kashyap ML, Hershman JM, Wexler LF, Rubins HB, VA-HIT Study Group, Veterans Affairs High-Density Lipoprotein Intervention Trial (2001) Relation of gemfibrozil treatment and lipid levels with major coronary events: VA-HIT: a randomized controlled trial. JAMA 285:1585–1591
22. Rubenfire M, Brook RD, Rosenson RS (2010) Treating mixed hyperlipidemia and the atherogenic lipid phenotype for prevention of cardiovascular events. Am J Med 123:892–898
23. Cannon CP, Steinberg BA, Murphy SA, Mega JL, Braunwald E (2006) Meta-analysis of cardiovascular outcomes trials comparing intensive versus moderate statin therapy. J Am Coll Cardiol 48:438–445
24. ACCORD Study Group, Ginsberg HN, Elam MB, Lovato LC, Crouse JR 3rd, Leiter LA, Linz P, Friedewald WT, Buse JB, Gerstein HC, Probstfield J, Grimm RH, Ismail-Beigi F, Bigger JT, Goff DC Jr, Cushman WC, Simons-Morton DG, Byington RP (2010) Effects of combination lipid therapy in type 2 diabetes mellitus. N Engl J Med 362:1563–1574
25. Keech A, Simes RJ, Barter P, Best J, Scott R, Taskinen MR, Forder P, Pillai A, Davis T, Glasziou P, Drury P, Kesaniemi YA, Sullivan D, Hunt D, Colman P, d'Emden M, Whiting M, Ehnholm C, Laakso M (2005) Effects of long-term fenofibrate therapy on cardiovascular events in 9795 people with type 2 diabetes mellitus (the FIELD study): randomised controlled trial. Lancet 366:1849–1861
26. Tsimihodimos V, Miltiadous G, Daskalopoulou SS, Mikhailidis DP, Elisaf MS (2005) Fenofibrate: metabolic and pleiotropic effects. Curr Vasc Pharmacol 3:87–98
27. Kostapanos MS, Milionis HJ, Agouridis AD, Rizos CV, Elisaf MS (2009) Rosuvastatin treatment is associated with an increase in insulin resistance in hyperlipidaemic patients with impaired fasting glucose. Int J Clin Pract 63:1308–1313
28. Baker WL, Talati R, White CM, Coleman CI (2010) Differing effect of statins on insulin sensitivity in non-diabetics: a systematic review and meta-analysis. Diabetes Res Clin Pract 87:98–107
29. Lankinen M, Schwab U, Erkkila A, Seppanen-Laakso T, Hannila ML, Mussalo H, Lehto S, Uusitupa M, Gylling H, Oresic M (2009) Fatty fish intake decreases lipids related to inflammation and insulin signaling—a lipidomics approach. PLoS One 4:e5258
30. Kuda O, Jelenik T, Jilkova Z, Flachs P, Rossmeisl M, Hensler M, Kazdova L, Ogston N, Baranowski M, Gorski J, Janovska P, Kus V, Polak J, Mohamed-Ali V, Burcelin R, Cinti S, Bryhn M, Kopecky J (2009) n-3 fatty acids and rosiglitazone improve insulin sensitivity through additive stimulatory effects on muscle glycogen synthesis in mice fed a high-fat diet. Diabetologia 52:941–951
31. Mostad IL, Bjerve KS, Bjorgaas MR, Lydersen S, Grill V (2006) Effects of n-3 fatty acids in subjects with type 2 diabetes: reduction of insulin sensitivity and time-dependent alteration from carbohydrate to fat oxidation. Am J Clin Nutr 84:540–550
32. Tenenbaum H, Behar S, Boyko V, Adler Y, Fisman EZ, Tanne D, Lapidot M, Schwammenthal E, Feinberg M, Matas Z, Motro M, Tenenbaum A (2007) Long-term effect of bezafibrate on pancreatic beta-cell function and insulin resistance in patients with diabetes. Atherosclerosis 194:265–271

Lipids (2011) 46:529–535
DOI 10.1007/s11745-011-3546-0

ORIGINAL ARTICLE

Dietary Glucosylceramide Enhances Cornified Envelope Formation via Transglutaminase Expression and Involucrin Production

Tatsuya Hasegawa · Haruo Shimada · Taro Uchiyama · Osamu Ueda · Masaya Nakashima · Yasuhiro Matsuoka

Received: 31 January 2011 / Accepted: 28 February 2011 / Published online: 17 March 2011

Abstract In this study, we investigated whether dietary glucosylceramide (GlcCer) and its metabolite sphingoid bases, sphingosine (SS), phytosphingosine (PS), sphingadienine (SD) and 4-hydroxysphingenine (4HS), influence cornified envelope (CE) formation. CE is formed during terminal differentiation of the epidermis through cross-linking of specific precursor proteins by transglutaminases (TGases), and is essential for the skin's barrier function. Oral administration of GlcCer (0.25 mg/day) for 14 consecutive days dramatically reduced transepidermal water loss, an indicator of the skin barrier condition, in hairless mice with barrier perturbation induced by single-dose ultraviolet B (UVB) irradiation. The GlcCer treatment also increased the level of TGase-1 mRNA in UVB-irradiated murine epidermis approximately 1.6-fold compared with the control. Further, all four sphingoid bases at 1 μM concentration enhanced CE formation of cultured normal human keratinocyte cells. Among them, SS, PS and SD, but not 4HS, stimulated production of involucrin, one of the CE major precursor proteins. SD increased the expression of TGase-1 mRNA, while SS increased the expression of TGase-3 mRNA. These results indicate that the skin barrier improvement induced by oral GlcCer treatment might be at least partly due to a reinforcement of CE formation in the epidermis mediated by sphingoid bases metabolically derived from GlcCer.

T. Hasegawa (✉) · T. Uchiyama · O. Ueda · M. Nakashima · Y. Matsuoka
Shiseido Functional Food Research and Development Center, 2-12-1 Fukuura, Kanazawa-ku, Yokohama 236-8643, Japan
e-mail: tatsuya.hasegawa@to.shiseido.co.jp

H. Shimada
Shiseido Innovative Science Research Center, 2-12-1 Fukuura, Kanazawa-ku, Yokohama 236-8643, Japan

Keywords Glucosylceramide · Sphingoid base · Cornified envelope · Transglutaminase · Involucrin · Skin barrier

Abbreviations

AP-1	Activating protein 1
CE	Cornified envelope
CLE	Corneocyte lipid envelope
GlcCer	Glucosylceramide
4HS	4-Hydroxysphingenine
PS	Phytosphingosine
SC	Stratum corneum
SD	Sphingadienine
SS	Sphingosine
TEWL	Transepidermal water loss
TGase	Transglutaminase
UVB	Ultraviolet B

Introduction

The skin provides an effective barrier between the organism and the environment, preventing physical, chemical and microbial damage. The barrier function is mainly localized in the stratum corneum (SC), which is formed in the outmost layer of the epidermis, and consists of cornified envelope (CE) and intercellular multilamellar lipids.

The CE forms a highly durable and flexible barrier [1], consisting of a 15-nm thick structure composed of several insoluble proteins, such as involucrin, loricrin, small proline-rich proteins and other proteins, covalently cross-linked by transglutaminases (TGases) [2]. TGases are a family of calcium-dependent acyl-transfer enzymes. Some isozymes, TGase-1, -3 and -5, are expressed mainly in

human skin epidermis, and play roles in CE formation during keratinocyte differentiation [3]. TGase-1 and TGase-5 are present in the spinous and granular layers, and TGase-3 seems to be confined to the upper granular layer [4]. Several studies have shown that TGase-1 has an essential role in CE assembly for skin barrier formation. TGase-1 knockout mice show a phenotype with abnormal CE formation, and die within 4–5 h after birth due to dehydration [5]. TGase-1 function is also required for normal epidermal function in humans. Mutations of TGase-1 have been identified as a cause of lamellar ichthyosis (LI), and result in drastically reduced TGase-1 activity and deficiency of CE in the epidermis of patients with LI [6]. TGase-1 mutations are present in about 50% of autosomal recessive congenital ichthyosis patients [7]. In addition, cathepsin D, an aspartate protease, is involved in the activation of TGase-1 through cleaving the 150-kDa precursor of TGase-1 and producing its active 35-kDa form. Consequently, cathepsin D-deficient mice have a defective skin barrier, with reduced TGase-1 activity and impaired SC morphology [8]. These results suggest that CE formation by TGase-1 is crucial to maintain epidermal tissue homeostasis and a healthy skin surface.

Glucosylceramides (GlcCers), which are structurally constituted of sphingoid bases, long chain fatty acids, and sugar moieties, occur in plants, fungi and animals [9–11]. In animals, GlcCers are essential structural components of mammalian cell membranes and are mostly found at the cell surface; they participate in biological functions such as immunomodulation [12] and insulin resistance [13]. Likewise, GlcCers play vital roles in maintaining the skin barrier function, through their role as intracellular lipids [14]. Recently, it was reported that dietary GlcCer improves the skin barrier function, e.g., improving recovery of SC flexibility and reducing transepidermal water loss (TEWL) in acutely barrier-perturbed mice [15]. Furthermore, oral intake of GlcCer also improves TEWL in healthy human subjects [16]. However, the mechanism of improvement of the skin barrier function by oral GlcCer treatment remains unknown.

In this study, we initially examined the effect of dietary GlcCer, prepared from konjac tuber, on the improvement of skin barrier function and the level of TGase-1 gene expression in hairless mice following barrier perturbation by means of a single UVB exposure. Moreover, because sphingoid bases are generally known to be formed by digestion of GlcCer in the digestive tract [17–19] and are metabolites of ceramide in skin epidermis [20], we also investigated the effects of the four major sphingoid bases of konjac GlcCer on CE formation, TGase-1 and TGase-3 gene expression levels and involucrin production in normal human epidermal keratinocyte cells.

Materials and Methods

Materials

Normal human epidermal keratinocytes (NHEK) were obtained from Kurabo Co. Ltd. (Osaka, Japan). Serum-free keratinocyte growth medium (KGM) containing low calcium (0.06 mM), bovine pituitary extract (BPE) and epidermal growth factor (EGF), insulin, hydrocortisone and antibiotics (gentamycin/amphotericin) were purchased from GIBCO BRL (Montgomery County, USA). GlcCer, derived from konjac tubers, was kindly provided by Unitika Limited (Osaka, Japan). HPLC analysis indicated a purity of greater than 95%. Sphingadienine (SD) and 4-hydroxysphingenine (4HS) were isolated from konjac tubers by Unitika Limited, and the structures of these compounds were confirmed by spectroscopic analysis. Sphingosine (SS) and phytosphingosine (PS) were purchased from Avanti Polar Lipids, Inc. (Alabama, USA).

Animals

The present study was approved by the ethics committee of Shiseido Research Center in accordance with the guideline of the National Institute of Health. Hairless male mice (HR-1) were purchased from Hoshino Laboratory Animals, Inc. (Ibaraki, Japan). Five-week-old HR-1 mice were randomly allocated to two groups ($n = 6$ in each group), adjusted to be the same of weight average, and fed the AIN-93G (Oriental Yeast, Tokyo, Japan) rodent diet. GlcCer was prepared as an aqueous suspension in 1% tragacanth gum and was administered orally at 0.25 mg/day to each mouse in the dietary GlcCer group. The control group received an aqueous suspension in 1% tragacanth gum. After 2 weeks, each mouse was irradiated with a single dose of UVB (150 mJ/cm^2). TEWL was measured daily up to day 11 with a Tewameter (Courage + Khazaka, Cologne, Germany) to characterize the skin barrier function. In parallel, dorsal skin samples were obtained from each mouse at various time periods after UVB irradiation.

Cell Culture

NHEK were seeded at a density of 3–5 $\times$ 10^4 cells/cm^2 in 75-cm^2 cell culture flasks, and cultured in KGM with medium changes every other day at 37 °C under a 5% CO_2 atmosphere. Third passage cells were used for the experiments. Tested sphingoid bases were dissolved in ethanol and diluted with medium to obtain the appropriate concentrations, and the final volume of ethanol was adjusted to 0.05% (v/v). In some experiments, NHEK were cultured in KDM (KGM without BPE).

TGase-1 mRNA Expression Level in UVB-irradiated Mouse Skin

RNA was isolated from mouse skin epidermis as previously described [21]. Dorsal skin samples were obtained and the epidermis was separated from the dermis by heating. Epidermal sheets were placed in 1 ml of Isogen reagent (Nippon Gene, Toyama, Japan) and total RNA was isolated as recommended by the manufacturer. Total RNA was purified using a RNeasy® Mini Kit (Qiagen, California, USA) according to the instructions of the manufacturer. The total RNAs obtained (4 g) were used to produce cDNA and PCR using a LightCycler® TaqMan® Master kit (Roche Applied Science, Indianapolis, USA), following the manufacturer's protocols. The synthesized cDNAs were PCR-amplified with TGase-1 specific primer (Sigma-Aldrich Inc, Missouri, USA) and β-actin primer (Sigma-Aldrich Inc, Missouri, USA) as the internal control. Fluorograms are shown after 65 cycles of PCR for TGase-1 and β-actin. The sequences of the primer pairs, 5′ and 3′, were as follows. TGase-1: gtggtgccatcaccaaca and tccggtg acggtgttgta; β-actin: aaggccaaccgtgaaaagat and gtggtac gaccagaggcatac.

CE Formation Assay

CE content in NHEK cultures was determined as previously described [22]. NHEK suspended in KGM were seeded at 1.5×10^5 cells/well into 6-well plates and grown to confluence for 3 days. After confluence, NHEK were treated with test compounds for 8 days with medium changes every other day in KGM, then harvested with cell scrapers and homogenized in 2% sodium dodecylsulfate (SDS). After microcentrifugation at 12,000 rpm for 15 min, the obtained precipitates were boiled in 2% SDS and 20 mM dithiothreitol (DTT) for 1 h. Then, the amounts of soluble cross-linked envelopes were evaluated by measuring the absorbance (OD at 310 nm).

Involucrin Production Enhancement Assay

The amount of involucrin production in NHEK cultures was determined as previously described [22]. NHEK suspended in KGM were seeded at 7.5×10^4 cells/well into 12-well plates and grown to confluence for 3 days. The cultures were washed two times with KDM, grown in KDM for 1 day, and treated with test compounds for 4 days in KDM. After 4 days, cells were harvested and homogenized in 1 ml of TE buffer containing 10 mM Trs–HCl and 1 mM EDTA. After microcentrifugation at 12,000 rpm for 15 min, supernatants were collected and stored frozen at −80 °C until use. Supernatants were analyzed for protein production using an enzyme-linked immunosorbent assay (ELISA) kit (Biomedical Technologies Inc., Massachusetts, USA).

TGase-1 and -3 mRNA Expression Levels in Cultured NHEK Cells

NHEK suspended in KGM were seeded at 7.5×10^4 cells/well into 12-well plates and grown to confluence for 3 days. The cultures were washed two times with KDM, grown in KDM for 1 day, and treated with test compounds for 72 h in KDM. After treatment, cells were harvested and homogenized in lysis buffer. Total RNAs were extracted from harvested keratinocytes using a RNeasy® Mini Kit, according to the manufacturer's protocol. The total RNAs obtained (10 μg) were used for cDNA production with a LightCycler® TaqMan® Master Kit, following the manufacturer's protocols. The cDNAs were PCR-amplified with TGase-1 and -3 specific primers and β-actin primer as the internal control. Fluorograms are shown after 45 cycles of PCR for TGase-1 and -3 and β-actin. The sequences of the primer pairs, 5′ and 3′, were as follows. TGase-1: ccccaa gagactagcagtgg and agaccaggccattcttgatg; TGase-3: cagag gaagggcgaaacat and tctgtgtgatgcgcttgtc; β-actin: ccaacc gcgagaagatga and ccagaggcgtacagggatag.

Statistical Analysis

All data were expressed as the mean ± SD. Statistical significance of two-group comparisons was determined with Student's t test, while for multiple-group comparisons, we used Dunnett's multiple test or Steel's multiple test after Bartlett's multiple test, compared to a control group. Differences were considered significant at $P < 0.05$.

Results

Effect of Dietary GlcCer on Improvement of TEWL and TGase-1 mRNA Expression in HR-1 Mice with Barrier Perturbation Produced by a Single UVB Irradiation

A single dose of UVB irradiation perturbs the skin barrier in hairless mice, causing an increase in TEWL, which peaks at 2–4 days, and a simultaneous decrease in TGase-1 mRNA expression [23]. Here, we examined the effects of dietary GlcCer on the skin barrier improvement following damage caused by exposure to 150 mJ/cm^2 UVB irradiation. In control mice without oral GlcCer treatment, the TEWL dramatically increased within 3–4 days after irradiation, while the increase of TEWL of the oral GlcCer treatment mice group was significantly suppressed at 3–4 days, compared with the control group (Fig. 1).

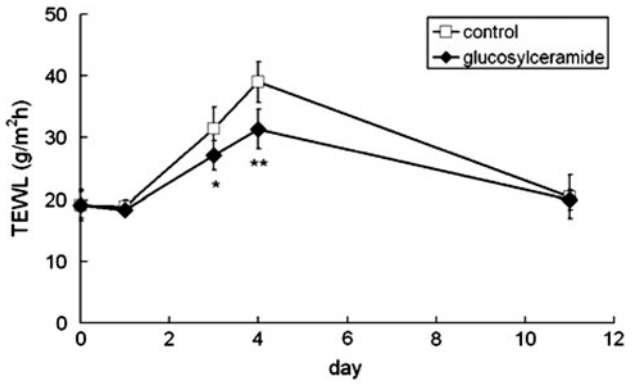

Fig. 1 Ameliorating effect of dietary GlcCer on the increase of TEWL in HR-1 mouse skin exposed to a single dose of UVB irradiation. HR-1 mice were fed either a control diet (without GlcCer) or a diet containing GlcCer for 2 weeks. Following a single UVB irradiation (150 mJ/cm^2), TEWL was measured up to day 11 in both groups. All data are expressed as means ± SD ($n = 6$). *$p < 0.05$ and **$p < 0.01$ compared with the control

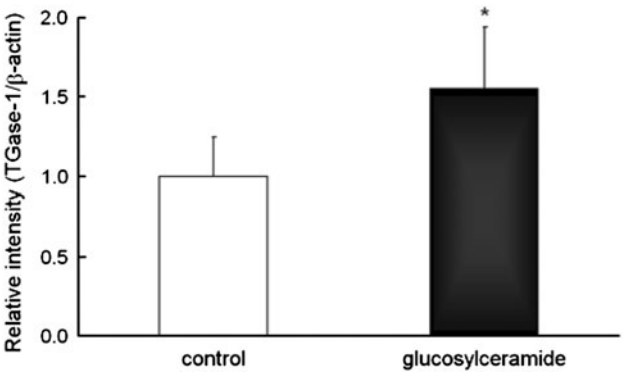

Fig. 2 Stimulatory effect of dietary GlcCer on TGase-1 mRNA expression in HR-1 mouse skin epidermis exposed to a single dose of UVB irradiation. HR-1 mice were fed either a control diet (without GlcCer) or a diet containing GlcCer for 2 weeks. Following a single UVB irradiation (150 mJ/cm^2), TGase-1 mRNA expression in the epidermis was analyzed by means of RT-PCR at day 3 in both groups. All data are expressed as means ± SD ($n = 5$). *$p < 0.05$ compared with the control

Finally, TEWL recovered completely in both the control group and oral GlcCer treatment group by day 11 (Fig. 1). Next, we determined the effect of dietary GlcCer on the decrease in expression of TGase-1 mRNA in epidermis of UVB-irradiated mice by means of RT-PCR. The oral GlcCer treatment group showed a significant increase in the level of TGase-1 mRNA expression in the epidermis on day 3, compared to the control group without GlcCer treatment (Fig. 2), and this coincided with the GlcCer-induced improvement of TEWL (Fig. 1).

Enhancement of CE Formation by Sphingoid Bases in Cultured NHEK Cells

It has been reported that ingested ceramide is metabolized to sphingoid bases, which are distributed into skin epidermis in mice [20]. Therefore, we investigated the effects of four sphingoid bases, which are metabolites of konjac GlcCer used in this study [24], on CE formation in cultured NHEK cells. NHEK cells were incubated in the presence or absence of each sphingoid base for 8 days, and CE formation was measured as described in Section Materials and Methods. As indicated in Fig. 3a, each sphingoid base enhanced CE formation at the concentration of 1 μM.

Increase of Involucrin Production by Sphingoid Bases in Cultured NHEK Cells

To determine whether the enhancement of CE formation by the four sphingoid bases is associated with increased production of CE precursors, the effects of the sphingoid bases on involucrin production were examined. Involucrin, a major early marker for terminal differentiation, is an important scaffold protein of CE, and is synthesized in the upper spinous layers of the epidermis [25]. Partly, involucrin forms ester-linkages with ω-hydroxyceramides at the outmost face of CE, catalyzed by TGase-1, and thus contributes to the barrier function of the epidermis [26]. As shown in Fig. 3b, in comparison with the control, involucrin production was increased by SS, PS or SD treatment of cultured NHEK cells at the concentration of 1 or 5 μM. In contrast, 4HS did not show any significant effect on involucrin production, even at 5 μM (data not shown).

Increase of TGase-1 and - 3 mRNA Expressions by Sphingoid Bases in Cultured NHEK Cells

Next, we examined whether the enhancement of CE formation by the four sphingoid bases was associated with an increase in gene expression of specific TGase isoforms, TGase-1 and -3, in cultured NHEK cells by means of RT-PCR. SD at 5 μM increased the TGase-1 mRNA level during 72 h incubation (Fig. 3c). In addition, SS increased the TGase-3 mRNA level at the same concentration (Fig. 3d).

Discussion

UVB irradiation causes a decline in the skin barrier function via down-regulation of TGase-1 gene [23], biophysical changes in the SC lipids [27], and perturbation of tight junction (TJ) function [28]. Further, TGase-1 is down-regulated in skin reconstructed in vitro after UVB exposure, and the expression levels of precursors of CE formation were also altered [29]. In UVB-exposed human skin, TGase-1 and involucrin expression levels were found

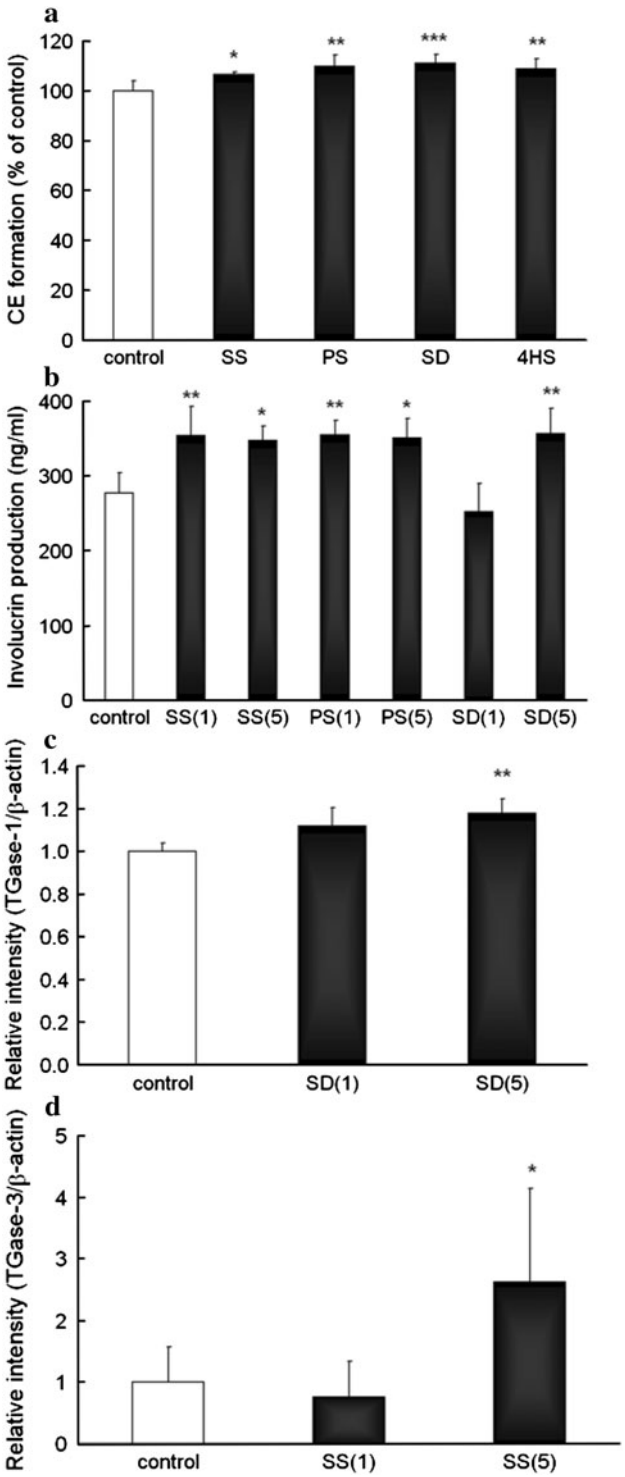

Fig. 3 Enhancing effects of sphingoid bases on CE formation via stimulation of TGase-1 and -3 gene expressions and involucrin production in cultured normal human epidermal keratinocyte cells. **a** Effects of sphingoid bases on CE formation. Normal human keratinocytes were treated with each sphingoid base (1 μM) in medium containing 0.06 mM Ca^{2+}. The cells were harvested 8 days thereafter and CE was assayed by means of spectrophotometry, measuring OD at 310 nm. **b** Effects of sphingoid bases on involucrin production. Normal human keratinocytes were treated with each sphingoid base (1 or 5 μM) in medium containing 0.06 mM Ca^{2+}. The cells were harvested after 96 h and involucrin levels were measured by means of ELISA. **c**, **d** Effects of sphingoid bases on the expression of TGase-1 and TGase-3 mRNAs. Normal human keratinocytes were treated with each sphingoid base (1 or 5 μM) in medium containing 0.06 mM Ca^{2+}. The cells were harvested after 72 h and TGase-1 (**c**) and TGase-3 (**d**) mRNA levels were measured by means of RT-PCR. All data are expressed as means ± SD ($n = 4$ or 6). $*p < 0.05$, $**p < 0.01$ and $***p < 0.001$ compared with the control

to decrease in histological and immunohistochemical studies [30]. Here, we used a single UVB-irradiated murine skin model to examine the effect of dietary GlcCer on skin barrier improvement and on the change of TGase-1 gene expression. We found that dietary GlcCer significantly suppressed the increase of TEWL and concomitantly stimulated the expression of TGase-1 mRNA in murine epidermis following UVB-induced barrier perturbation. These results suggested that one of the mechanisms of skin barrier improvement by dietary GlcCer is a reinforcement of CE formation mediated by increased TGase-1 gene expression in the epidermis. Further, the four sphingoid bases, SS, PS, SD and 4HS, which are metabolites of dietary konjac GlcCer [24], stimulated CE formation in cultured epidermal keratinocyte cells, and some of them significantly increased enhanced TGase-1 and TGase-3 mRNA expressions and involucrin production. Further, it is suggested that SD may participate in the enhancement effect of dietary GlcCer on TGase-1 gene expression, because SD stimulates TGase-1 mRNA expression in cultured epidermal keratinocyte cells, and accounts for about 40% of the total sphingoid bases constituting konjac GlcCer used this study [24]. However, further studies, such as investigation of the effect of oral SD treatment on TGase-1 gene expression in vivo, will be needed to confirm this. TGase-1 is known to catalyze the formation of ester bonds between specific glutaminyl residues of involucrin, localized the outmost face of CE and epidermal-specific ω-hydroxyceramides, forming the so-called corneocyte lipid envelope (CLE), and thus contributes to mature lamellar membrane formation in the SC and to skin barrier homeostasis [26, 31, 32]. Because UVB irradiation induces decreased levels of covalently bound ceramides in murine SC [23], and the tested sphingoid bases stimulated TGase-1 gene expression and involucrin production in cultured epidermal keratinocyte cells, it is possible that dietary GlcCer also contributes to changes in the levels of covalently bound ceramides in the SC.

Membrane-bound TGase-1 and cytosolic TGase-3 have proven themselves to play important roles in CE assembly during terminal differentiation of epidermal keratinocytes. TGase-1 is anchored on the inner surface of the plasma membrane, while TGase-3 is soluble and is localized in the

cytoplasm. Involucrin is cross-linked by TGase-1 in the presence of the plasma membrane as an early event [1, 2]. Some precursors, such as loricrin, are oligomerized by TGase-3 in cytosol, and then polymerized by TGase-1 to reinforce the insoluble structure of keratinocytes [33]. It is interesting that different sphingoid bases showed differential effects on TGase-1 and TGase-3 gene expressions. This suggests the existence of regulation at a specific transcriptional level, such as the activating protein 1 (AP-1) complex, which is involved in transcriptional regulation of epidermal genes, including TGase-1, TGase-3, involucrin and loricrin genes, during keratinocyte differentiation [34]. Although TGase-3 mRNA represents less than 2% of all TGase transcripts, the activated TGase-3 accounts for up to 75% of the total TGase activity in mammalian epidermis [35]. TGase activity in the SC also mediates the maturation of CE, and serves to maintain the water content in the SC, which has implications for the improvement of dry skin [36].

In conclusion, we have examined the mechanism of the skin barrier improvement induced by dietary GlcCer, and have shown that its metabolite sphingoid bases enhance CE formation via increased expression of TGase mRNAs and increased involucrin production in epidermis. These findings indicate that dietary GlcCer can play an important role in preserving a healthy skin barrier condition or in promoting recovery from skin barrier impairment, by enhancing CE formation. This information should help in the development of effective skin care through dietary supplements, i.e., internal skin care.

References

1. Candi E, Schmidt R, Melino G (2005) The cornified envelope: a model of cell death in the skin. Nat Rev Mol Cell Biol 6:328–340
2. Hitomi K (2005) Transglutaminases in skin epidermis. Eur J Dermatol 15:313–319
3. Eckert RL, Sturniolo MT, Broome AM, Ruse M, Rorke EA (2005) Transglutaminases in epidermis. Prog Exp Tum Res 38:115–124
4. Candi E, Oddi S, Paradisi A, Terrinoni A, Ranalli M, Teofoli P, Citro G, Scarpato S, Puddu P, Melino G (2002) Expression of transglutaminase 5 in normal and pathologic human epidermis. J Invest Dermatol 119:670–677
5. Matsuki M, Yamashita F, Ishida-Yamamoto A, Yamada K, Kinoshita C, Fushiki S, Ueda E, Morishima Y, Tabata K, Yasuno H, Hashida M, Iizuka H, Ikawa M, Okabe M, Kondoh G, Kinoshita T, Takeda J, Yamanishi K (1998) Defective SC and early neonatal death in mice lacking the gene for transglutaminase 1 (keratinocyte transglutaminase). Proc Natl Acad Sci USA 95:1044–1049
6. Huber M, Rettler I, Bernasconi K, Frenk E, Lavrijsen SP, Ponec M, Bon A, Lautenschlager S, Schorderet DF, Hohl D (1995) Mutations of keratinocyte transglutaminase in lamellar ichthyosis. Science 267:525–528
7. Farasat S, Wei MH, Herman M, Liewehr DJ, Steinberg SM, Bale SJ, Fleckman P, Toro JR (2009) Novel transglutaminase-1 mutations and genotype-phenotype investigations of 104 patients with autosomal recessive congenital ichthyosis in the USA. J Med Genet 46:103–111
8. Egberts F, Heinrich M, Jensen JM, Winoto-Morbach S, Pfeiffer S, Wickel M, Schunck M, Steude J, Saftig P, Proksch E, Schütze S (2004) Cathepsin D is involved in the regulation of transglutaminase 1 and epidermal differentiation. J Cell Sci 117:2295–2307
9. Oku H, Wongtangtintharn S, Iwasaki H, Inafuku M, Shimatani M, Toda T (2007) Tumor specific cytotoxicity of glucosylceramide. Cancer Chemother Pharmacol 60:767–775
10. Pinto MR, Rodrigues ML, Travassos LR, Haido RM, Wait R, Barreto-Bergter E (2002) Characterization of glucosylceramides in *Pseudallescheria boydii* and their involvement in fungal differentiation. Glycobiology 12:251–260
11. Madison KC (2003) Barrier function of the skin: "la raison d'être" of the epidermis. J Invest Dermatol 121:231–241
12. Kawano T, Cui J, Koezuka Y, Toura I, Kaneko Y, Motoki K, Ueno H, Nakagawa R, Sato H, Kondo E, Koseki H, Taniguchi M (1997) CD1d-restricted and TCR-mediated activation of valpha14 NKT cells by glycosylceramides. Science 278:1626–1629
13. Langeveld M, Aerts JM (2009) Glycosphingolipids and insulin resistance. Prog Lipid Res 48:196–205
14. Jennemann R, Sandhoff R, Langbein L, Kaden S, Rothermel U, Gallala H, Sandhoff K, Wiegandt H, Gröne HJ (2007) Integrity and barrier function of the epidermis critically depend on glucosylceramide synthesis. J Biol Chem 282:3083–3094
15. Tsuji K, Mitsutake S, Ishikawa J, Takagi Y, Akiyama M, Shimizu H, Tomiyama T, Igarashi Y (2006) Dietary glucosylceramide improves skin barrier function in hairless mice. J Dermatol Sci 44:101–107
16. Uchiyama T, Nakano Y, Ueda O, Mori H, Nakashima M, Noda A, Ishizaki C, Mizoguchi M (2008) Oral intake of glucosylceramide improves relatively higher level of transepidermal water loss in mice and healthy human subjects. J Health Sci 54:559–566
17. Sugawara T, Tsuduki T, Yano S, Hirose M, Duan J, Aida K, Ikeda I, Hirata T (2010) Intestinal absorption of dietary maize glucosylceramide in lymphatic duct cannulated rats. J Lipid Res 51:1761–1769
18. Nilsson Å (1969) Metabolism of cerebrosides in the intestinal tract of the rat. Biochim Biophys Acta 187:113–121
19. Schmelz EM, Crall KJ, Larocque R, Dillehay DL, Merrill AH Jr (1994) Uptake and metabolism of sphingolipids in isolated intestinal loops of mice. J Nutr 124:702–712
20. Fukami H, Tachimoto H, Kishi M, Kaga T, Waki H, Iwamoto M, Tanaka Y (2010) Preparation of ^{13}C-labeled ceramide by acetic acid bacteria and its incorporation in mice. J Lipid Res 51:3389–3395
21. Aoki H, Moro O (2005) Upregulation of the IFN-γ-stimulated genes in the development of delayed pigmented spots on the dorsal skin of F1 mice of HR-1 × HR/De. J Invest Dermatol 124:1053–1061
22. Kim S, Hong I, Hwang JS, Choi JK, Rho HS, Kim DH, Chang I, Lee SH, Lee MO, Hwang JS (2006) Phytosphingosine stimulates the differentiation of human keratinocytes and inhibits TPA-induced inflammatory epidermal hyperplasia in hairless mouse skin. Mol Med 12:17–24
23. Takagi Y, Nakagawa H, Kondo H, Takema Y, Imokawa G (2004) Decreased levels covalently bound ceramide are associated with ultraviolet B-induced perturbation of the skin barrier. J Invest Dermatol 123:1102–1109
24. Mukai K (2009) The possibility of glucosylceramide derived from konjac-tuber as the beauty materials. Cell (Japan) 41:206–208
25. Steinert PM, Marekov LM (1997) Direct evidence that involucrin is a major early isopeptide crosslinked component of the keratinocyte cornified cell envelope. J Biol Chem 272:2021–2030

26. Marekov LN, Steinert PM (1998) Ceramides are bound to structural proteins of the human foreskin epidermal cornified cell envelope. J Biol Chem 273:17763–17770
27. Jiang SJ, Chen JY, Lu ZF, Yao J, Che DF, Zhou XJ (2006) Biophysical and morphological changes in the SC lipids induced by UVB irradiation. J Dematol Sci 44:29–36
28. Yamamoto T, Kurasawa M, Hattori T, Maeda T, Nakano H, Sasaki H (2008) Relationship between expression of tight junction-related molecules and perturbed epidermal barrier function in UVB-irradiated hairless mice. Arch Dermatol Res 300:61–68
29. Bernerd F, Asselineau D (1997) Successive alteration and recovery of epidermal differentiation and morphogenesis after specific UVB-damages in skin reconstructed in vitro. Dev Biol 183:123–138
30. van der Vleuten CJ, Kroot EJ, de Jong EM, van de Kerkhof PC (1996) The immunohistochemical effects of a single challenge with an intermediate dose of ultraviolet B on normal human skin. Arch Dermatol Res 288:510–516
31. Nemes Z, Marekov LN, Fésüs L, Steinert PM (1999) A novel function for transglutaminase 1: attachment of long-chain omega-hydroxyceramides to involucrin by ester bond formation. Proc Natl Acad Sci USA 96:8402–8407
32. Behne M, Uchida Y, Seki T, de Montellano PO, Elias PM, Holleran WM (2000) Omega-hydroxyceramides are required for corneocyte lipid envelope (CLE) formation and normal epidermal permeability barrier function. J Invest Dermatol 114:185–192
33. Steinert PM, Marekov LN (1999) Initiation of assembly of the cell envelope barrier structure of stratified squamous epithelia. Mol Biol Cell 10:4247–4261
34. Rossi A, Catani MV, Candi E, Bernassola F, Puddu P, Melino G (2000) Nitric oxide inhibits cornified envelope formation in human keratinocytes by inactivating transglutaminases and activating protein 1. J Invest Dermatol 115:731–739
35. Kim SY, Chung SI, Steinert PM (1995) Highly active soluble processed forms of the transglutaminase 1 enzyme in epidermal keratinocytes. J Biol Chem 270:18026–18035
36. Hirao T (2003) Improvement of transglutaminase in *ex vivo* maturation of cornified envelopes in the SC. Int J Cosmet Sci 25:245–257

Lipids (2011) 46:537–543
DOI 10.1007/s11745-011-3547-z

ORIGINAL ARTICLE

Plasma Levels of *trans*-Fatty Acids are Low in Exclusively Breastfed Infants of Adolescent Mothers

Roseli de Souza Santos da Costa · Flavia da Silva Santos · Felipe Domingues da Conceição · Claudia Saunders · Fatima Lúcia de Carvalho Sardinha · Célia Regina Moutinho de Miranda Chaves · Maria da Graças Tavares do Carmo

Received: 23 August 2010 / Accepted: 15 February 2011 / Published online: 16 March 2011

Abstract The purpose of this study was to determine the levels of *trans*-octadecenoic acid (C18:1-*trans*) and *trans*-isomers of linoleic acid (18:2-*trans*), as well as long-chain polyunsaturated fatty acids (LC-PUFA), in the plasma from infants of adolescent mothers at 3 months of age, exclusively breastfed, and the relationship with the levels of the same isomers in plasma and milk of the mothers. Samples of blood and mature milk were obtained from 49 healthy adolescent mothers and their exclusively breastfed infants treated at the Instituto Fernandes Figueira-Fundação Oswaldo Cruz (IFF-FIOCRUZ) in Rio de Janeiro, Brazil. *trans*-Fatty acids (TFA) were analyzed by gas chromatography. The results of this study showed low levels of TFA in milk (1.53%), maternal plasma (0.50%), and plasma of infants (0.74%). The results show that, although TFA have been found in the plasma of the studied infants, the LC-PUFA levels are kept within normal limits. No association between TFA presence and parameters of nutritional status of the infants was observed, probably due to the low levels of these fatty acids found in this study.

R. de Souza Santos da Costa (✉) · F. da Silva Santos · F. D. da Conceição · C. Saunders · F. L. de Carvalho Sardinha · M. da Graças Tavares do Carmo
Instituto de Nutrição Josué de Castro, Universidade Federal do Rio de Janeiro, Rio de Janeiro, RJ, Brazil
e-mail: rsscosta@iff.fiocruz.br

R. de Souza Santos da Costa · F. da Silva Santos · F. D. da Conceição · C. Saunders · F. L. de Carvalho Sardinha · M. da Graças Tavares do Carmo
Centro de Ciências da Saúde, Universidade Federal do Rio de Janeiro, Rio de Janeiro, RJ, Brazil

R. de Souza Santos da Costa · C. R. M. de Miranda Chaves
Instituto Fernandes Figueira da Fundação Oswaldo Cruz, Rio de Janeiro, RJ, Brazil

Keywords Fatty acids · *trans*-Fatty acid · Mature milk · Plasma · Adolescents · Infants

Abbreviations

ALA	Alpha-linolenic acid (18:3n3)
ARA	Arachidonic acid (20:4n-6)
BMI/A	Body mass index for age
DHA	Docosahexaenoic acid (22:6n-3)
EFA	Essential fatty acid(s)
EPA	Eicosapentaenoic acid (20:5n-3)
FA	Fatty acid(s)
FIOCRUZ	Fundação Oswaldo Cruz
IFF	Instituto Fernandes Figueira
LC-PUFA	Long-chain polyunsaturated fatty acid(s)
LNA	Linoleic acid (18:2n-6)
LNBINJC/UFRJ	Laboratory of Nutritional Biochemistry, Institute of Nutrition Josué de Castro/Federal University of Rio de Janeiro
MUFA	Monounsaturated fatty acid(s)
PUFA	Polyunsaturated fatty acid(s)
SFA	Saturated fatty acid(s)
TFA	*trans*-Fatty acid(s)

Introduction

The importance of essential fatty acids (EFA), linoleic acid (n-6, LNA) and alpha-linolenic acid (n-3, ALA), in infant development has led to several studies about FA in women during pregnancy and lactation [1–7] because the supply of EFA to the infant depends almost exclusively on breast milk, which is the main source of long chain

polyunsaturated fatty acids (LC-PUFA). LC-PUFA are essential for normal development of neuronal tissue. Of the total lipid content in the brain, 60–65% are polyunsaturated fatty acids (PUFA), of which >85% are docosahexaenoic acid (DHA; 35–40%) and arachidonic acid (ARA; 40–50%) [8]. These fatty acids (FA) act as regulators of various cellular functions and are constituents of membranes, in addition to playing the role of ligands and nuclear transcription factors as substrates in the synthesis of prostanoids (prostaglandins and thromboxane) [9–11], especially during the first 6 months of life [12].

In recent years, investigations on the nutritional and biological control of *trans*-fatty acids (TFA) have grown extensively due to the realization of the importance of lipids on growth and infant development [13]. TFA are unsaturated FA with at least one double bond in the *trans* configuration. The maternal TFA can be transferred to the child through breastfeeding. The content of TFA in human milk is variable, reflecting maternal dietary intake [14, 15].

These FA compete with the n-6 (LNA and ARA) and n-3 (ALA and DHA) series in the reactions of desaturation and elongation of the chain, resulting in the formation of eicosanoids without biological activity, and can inhibit the enzymes, delta-6 and delta-5 desaturase, the blocking the metabolism of EFA [16, 17].

The dietary lipids reflect their composition in the plasma. They have a prominent role in infant growth and development, and when consumed by the mother, may be transferred to the infant in breast milk. For these reasons and because of the scarcity of research with adolescent mothers, specifically assessing levels of infant plasma TFA, this study aimed to investigate the relationship between the proportions of these FA in maternal plasma and mature milk and between the levels of those FA in plasma from the infants.

Methods

Forty-nine healthy young mothers between 15 and 19 years of age who were breastfeeding their infants who were being treated at the Instituto Fernandes Figueira (IFF), an agency of the Oswaldo Cruz Foundation (FIOCRUZ) located in Rio de Janeiro (RJ), Brazil, were selected for this study. All the adolescents and their parents gave written informed consent prior to the beginning of the research. The study was approved by the Ethics in Research Committee of the Instituto Fernandes Figueira.

Data from maternal dietary intake were obtained by two methods: qualitative food frequency questionnaire, which evaluated the number of times in the frequency category in which food or food group was consumed [18]; and the 24-h recall. Data from the food records were tabulated in Software NutWin®-Nutrition Support Program, version 1.5 [19]. We included information on the nutritional composition of food sources of TFA, obtained from the Brazilian Table of Food Composition [20].

Information on maternal food consumption and the collection of maternal blood and blood from the infants and mature milk were obtained in the third month postpartum. Anthropometric measurements of weight, length, and head circumference were obtained in the third month postpartum according to the recommendations of the Brazilian Ministry of Health [21].

The weights of unclothed infants (in grams) were recorded on calibrated digital-type scales (Filizola) with a sensitivity of 10 g. The length (expressed in centimeters) was measured with the baby supine using a wooden stadiometer from the crown to the heel. The head circumference (expressed in cm) was obtained using a tape measure positioned in the region of the supra-orbital ridges and the largest frontooccipital diameter. The nutritional status of infants was performed by the index weight for age and height for age. The criteria for classification were those recommended by the World Health Organization [22] and Brazil [23].

The anthropometric characteristics of maternal weight and height were measured according to the recommendations of the Brazilian Ministry of Health [24]. Teenage girls were measured while barefoot without excess clothing. Weight was obtained with a platform-type scale (Filizola) with 100-g subdivisions and a maximum load of 150 kg. The scale for measuring the height was fixed to the balance on a vertical shaft, with 0.5-cm subdivisions and an extension range of 95–195 cm.

Nutritional status was assessed by maternal body mass index for age (BMI/A) and the cutoff points established in *z* scores for adolescents, according to the recommendations of the World Heath Organization [25, 26] and adapted for Brazil [23].

Collection and Storage of Samples of Mature Milk, Maternal Blood, and Infant Blood

The milk samples from nursing mothers (1 mL) in the third month postpartum, were obtained by manual expression of the breast that had not been sucked in the last feeding in the morning. The blood of mothers and infants (about 2 mL) was collected in the morning 2–3 h after a feeding (between 8 and 10 a.m.) by venipuncture in tubes containing 1 g Na_2-EDTA/L. The nursing mothers had fasted overnight for approximately 12 h. Plasma was immediately separated by centrifugation (3,000*g* for 15 min) in the Laboratory of Hematology of the IFF/FIOCRUZ, stored in Eppendorf tubes, and properly identified.

All samples were stored in a freezer at −20 °C, then transported on ice to the Laboratory of Nutritional

Biochemistry of the Institute of Nutrition Josué de Castro/Federal University of Rio de Janeiro–LBNINJC/UFRJ, where they remained stored at −70 °C until the separation of lipids and relative quantification of FA.

Analysis of FA

Lipids in the plasma and milk samples were extracted and purified in a chloroform:methanol (2:1) [27] solution. Total lipid extracts were saponified and the fatty acids methylated following the method of Lepage and Roy [28], which determines treatment with 2 ml methanol:toluene 4:1 (v/v) solution and 200 µl of acetyl chloride added in the cold. The mixtures were subjected to methanolysis at 80 °C over a period of 2.5 h. Fatty acid methyl esters were separated and quantified on a Perkin Elmer Autosystem XL chromatograph equipped with a hydrogen flame ionization detector and the software Turbochrom. The fatty acids were separated on a 100 × 0.25 mm × 0.20 µm capillary column SP 2560 (biscyanopropyl-polysiloxane, 100 m × 0.25 mm ID, 0.20 µm film thickness; Supelco, Bellefonte, PA, USA, Supelco, USA). Hydrogen was used as the carrier gas at a pressure of 28 psi. Fatty acid methyl esters were identified by comparison of their retention times with authentic standards (Nu-Chek-Prep, Inc., Elysian, MN, USA, and Supelco, Inc., Bellefonte, PA, USA) and the relative levels of individual fatty acids were calculated as a percentage of all detected fatty acids with a chain length of 04–24 carbon atoms. The final results were expressed as free fatty acids, whereas the analytical data were expressed as FAME. Therefore, according to Craske e Bannon [29], the quantification of the relative levels of the free fatty acids required the use of theoretical correction factors—based on weight percent content of "active" carbon—due to the differences in the hydrogen flame ionization detector response. The theoretical correction factors calculated in the present study were 1.00068 (C18:1 *trans*), 1.00000 (C18:2 *trans*), 1.00000 (C18:2n6 (LNA) (ALA), 0.99315 (C18:3n3 ALA) 0.97341 (AA), 0.96725 (EPA), e 0.95167 (DHA).

Statistical Analysis

Data analysis was carried out using the Statistical Package Program for Social Sciences (version 15.0 for Windows; SPSS Inc., Chicago, USA). To determine the correlation between the study variables, the Spearman correlation coefficient was used. The differences between the concentrations of FA in mature milk, and maternal and infant plasma lipids were then compared using the Kruskal–Wallis test. A P value <0.05 was considered statistically significant. Results are presented as means and the standard errors of the means.

Results

Most women (63.3%) had a BMI/A within the normal range. Regarding the nutritional status of infants, relative to the weight/age and length/age, 86 and 90% had weight and length appropriate to age, respectively (Table 1).

According to the qualitative food frequency questionnaires answered by all of the mothers interviewed, the majority of teens (80%) reported consumption of fish less than once a month. Soybean oil was consumed daily by all nursing mothers in food preparation. Processed foods, sources of TFA consumed regularly, i.e., at least once per week, included cream cracker biscuits (60%), bread (65%), sweet bread (30%), sandwich cookies (65%), sweet biscuits (49%), cakes (26%), snacks (42%), creamy ice cream (33%), ice cream (42%), creamy candy (46%), instant noodles (37%), chocolate (46%), and margarine (83%).

According to the 24-h recall questionnaires conducted with the mothers, the intake of fat contributed to approximately 25% of the total daily energy intake of lactating women. The average daily maternal intake of FA was 3.11 ± 0.55 g of C18:1 TFA, 0.19 ± 0.05 g of C18:2 TFA, 8.90 ± 0.51% saturated fatty acids (SFA), 8.82 ± 0.41% of monounsaturated fatty acids (MUFA), 4.13 ± 0.34% of PUFA, 0.46 ± 0.09% of ALA, 3.46 ± 0.32% of LNA, 0.08 ± 0.02% ARA, 0.03 ± 0.02% DHA, and the ratio of LNA: ALA was 9.58 ± 0.74% (data not shown).

Table 1 General characteristics of mothers and infants studied ($n = 49$) in Rio de Janeiro, 2005–2008

Variables	*n*	%
Maternal age (years)		
15	12	24.5
16	09	18.4
17	15	30.6
18	06	12.2
19	07	14.3
Maternal nutritional status (BMI/A)		
Surveillance for low BMI/A	05	10.2
Appropriate BMI/A	31	63.3
Surveillance for BMI/A high	07	14.3
Overweight	06	12.2
Nutritional status of infants (weight/age)		
Surveillance for low weight for age	04	8.2
Appropriate weight for age	42	86.0
Surveillance for high weight for age	03	6.0
Nutritional status of infants (length/age)		
Low length for age	05	10.0
Appropriate length for age	44	90.0

BMI/A Body mass index for age

There was no association between the level of TFA in maternal plasma to nutritional status ($P = 0.61$) or between the concentrations of TFA in the plasma of infants with their nutritional status (weight/age; $P = 0.90$) and (length/age; $P = 0.46$) (data not shown).

Chromatographic analysis showed that C18:1 TFA accounted for $1.53 \pm 0.22\%$, $0.50 \pm 0.04\%$, and $0.74 \pm 0.16\%$ of FA in mature milk, maternal plasma, and infant plasma, respectively (Table 2).

C18:1 TFA and ALA levels were higher in mature milk than in maternal and infant plasma. Furthermore, the level of C18:2 TFA, LNA, ARA, EPA, and DHA was lower in mature milk than in maternal and infant plasma. C18:2 TFA and DHA levels were lower and the LNA level was higher in the maternal plasma than in infant plasma (Table 2).

As shown in Table 3, there was a negative correlation between the proportion of C18:1 TFA and the proportion of LNA in mature milk ($r = -0.44$, $P = 0.001$) and a positive correlation between the proportion of C18:1 TFA in mature milk and the proportion of FA in maternal plasma lipids ($r = 0.34$, $P = 0.016$). There was negative correlation between the proportion of ARA in the mature milk and the proportion of LNA in infant plasma lipids ($r = -0.43$, $P = 0.002$) and between the proportion of EPA in mature milk and the proportion of ARA ($r = -0$, 45, $P < 0.001$) and LNA in infant plasma lipids ($r = -0.51$, $P < 0.001$). A negative correlation was demonstrated between the proportion of C18:1 TFA and the proportion of LNA in infant plasma lipids ($r = -0.33$, $P = 0.020$) and a positive correlation was demonstrated between the proportion of LNA and the proportion of ARA in infant plasma lipids ($r = 0.45$, $P = 0.001$) and between the proportion of EPA and the proportion of ALA ($r = 0.77$, $P < 0.001$) in infant plasma lipids ($r = 0.45$, $P < 0.001$). Finally, a negative correlation was observed between the proportion of C18:1 TFA and the proportion of LNA in maternal blood lipids ($r = -0.58$, $P < 0.001$) and a positive correlation between the proportion of EPA and DHA ratio in maternal plasma lipids ($r = 0.51$, $P < 0.001$).

Discussion

The first important observation derived from this study is that TFA was found in plasma of infants exclusively breastfed, confirming the transfer of this kind of fat through breast milk [14, 15], although in smaller proportion to those found in milk, and suggests that like the placenta [30], the mammary gland must provide some degree of discrimination against these FA.

The concern about children's exposure to TFA is based on the negative effects of these FA on child growth and development [31] and the potential negative effects on the metabolism of EFA through inhibition of desaturation of LNA ARA and ALA to DHA [32, 33].

As the TFA derived from partially hydrogenated fats are not synthesized in the mother, it is believed that the TFA of milk and maternal blood come from dietary intake [14, 15]. Experimental studies with rats confirm a direct dose–response relationship between the intake of TFA and the incorporation of these in breast milk, but transferred to the pups through lactation, appear in the plasma [15].

References have been found in literature suggesting that the quality, not the quantity, of the lipid source in the mother's diet impacts the quality of the fatty acids in human milk [34, 35]. The present study showed low levels of TFA in milk and plasma of nursing mothers and infants, probably due to a lower proportion of TFA in processed products due to the current standards of the National Agency for Sanitary Surveillance (ANVISA) [36], which contains the mandatory declaration of TFA content on food

Table 2 Composition of free fatty acids (FAA%) of total lipids in samples of mature milk and plasma of nursing mothers and infants

Fatty acids	Mature milk FAA (area %)[a]	Maternal plasma FAA (area %)[a]	Infants plasma FAA (area %)[a]
C18:1 TFA	1.51 (0.22)	0.50 (0.04)[b]	0.70 (0.01)[b]
C18:2 TFA	0.08 (0.01)	0.40 (0.07)[b]	0.80 (0.02)[b,c]
C18:2n-6 (LNA)	19.80 (0.70)	37.0 (0.81)[b]	27.0 (1.0)[b,c]
C18:3n-3 (ALA)	0.49 (0.04)	0.11 (0.02)[b]	0.19 (0.14)[b]
C20:4n-6 (ARA)	0.38 (0.03)	4.08 (0.26)[b]	4.47 (0.3)[b]
C20:5n-3 (EPA)	0.02 (0.01)	0.49 (0.05)[b]	0.34 (0.09)[b]
C22:6n-3 (DHA)	0.161 (0.03)	0.57 (0.05)[b]	1.42 (0.3)[b,c]

Rio de Janeiro, 2005–2008 ($n = 49$). All values are means and standard errors of the means in parentheses

LNA, linoleic acid, *ALA*, alpha-linolenic acid, *ARA*, arachidonic acid, *EPA*, eicosapentaenoic acid, *DHA*, docosahexaenoic acid

[a] Corrected by a theoretical correction factor from FAME to FFA (see "Methods" section)

[b] Significantly different from the respective value in mature milk, $P < 0.05$ (Kruskal–Wallis)

[c] Significantly different from the respective value in maternal plasma, $P < 0.05$ (Kruskal–Wallis)

Table 3 Correlation between the proportions of FA in mature milk lipids, maternal plasma lipids, and infant plasma lipids

Variables		*r*	*P*
Mature milk lipids	Mature milk lipids		
C18:1 TFA	LNA	−0.44	0.001
Mature milk lipids	Maternal plasma lipids		
C18:1 TFA	C18:1 TFA	0.34	0.016
Mature milk lipids	Infants plasma lipids		
ARA	LNA	−0.43	0.002
EPA	ARA	−0.45	<0.001
EPA	LNA	−0.51	<0.001
Infants plasma lipids	Infants plasma lipids		
C18:1 TFA	LNA	−0.33	0.020
LNA	ARA	0.45	0.001
EPA	ALA	0.77	<0.001
EPA	DHA	0.38	0.006
Maternal plasma lipids	Maternal plasma lipids		
C18:1 TFA	LNA	−0.58	<0.001
EPA	DHA	0.51	<0.001

Rio de Janeiro, 2005–2008 ($n = 49$)

LNA, linoleic acid, *ALA*, alpha-linolenic acid, *ARA*, arachidonic acid, *EPA*, eicosapentaenoic acid, *DHA*, docosahexaenoic acid

labels, allowing the consumer to know which foods contain this type of fat and in what quantities, which caused many companies to formulate their products with lower levels of TFA.

It is known that the content of TFA consumed by a population is directly related to feeding patterns [37, 38]. Recent studies in Spanish prepubertal obese children have shown low plasma percentages of *trans*-fatty acids, confirming that the TFA intake in southern Spain is actually very low [39]. In the present study, the average intake of total TFA to adolescent mothers investigated was equal to 3.19 g, corresponding to approximately 1.4% of the total daily energy, exceeding slightly the maximum recommended intake (1% of total daily energy) [40]. However, the relative percentage of the total daily energy of this FA to the adolescent mothers being investigated, is still lower than that among non-pregnant adolescents living in the US (2.8%) and Costa Rica (4.35%) [41]. Therefore, another factor that may have contributed to this result is a possible change in the dietary habits of the mothers in this physiological period. In fact, this study showed that the majority of mothers reported not consuming many of these manufactured products.

In this study we observed significant correlations among the levels of TFA. The content of C18:1 TFA in milk correlated with the values of the same FA found in lipids of maternal plasma, indicating therefore that the fat in the diet can be incorporated into human fluids such as plasma and milk [42]. There was also an inverse correlation between the content of C18:1 TFA and content of LNA in mature milk. A similar inverse correlation between TFA and LNA in milk had been previously reported [43, 44]. With regard to maternal plasma lipids, there was a negative correlation between the proportion of C18:1 TFA and the proportion of LNA. One explanation for this fact is that mothers with a higher intake of foods containing TFA tend to consume less food containing LNA [43] or that the increase of TFA may occur at the expense of EFA, as foods with large amounts of TFA usually contain less EFA [44]. Moreover, a negative correlation was observed between the proportion of C18:1 TFA and the proportion of LNA in plasma lipids of infants.

From what has been stated above, one can see that the maternal consumption of TFA is a factor that influences the state of EFA. However, we found no associations between TFA with parameters of maternal nutritional status or infants, probably due to low levels of this FA found in this study.

Finally, we observed several significant correlations between several different FA in biological fluids. We observed a negative correlation between the proportion of ARA in the mature milk and the proportion of LNA in infant plasma lipids. This finding suggests the action of specific enzymes acting on the active conversion of LNA to ARA in plasma from infants, a nutrient essential for development at the expense of decreased ARA in milk.

Another negative correlation was observed between the proportion of EPA in mature milk and the proportion of ARA and LNA in plasma lipids of infants. The negative association between the FA of series *n*-3 and *n*-6 series was expected since there is competition between them for the metabolic pathways of elongation and desaturation, since they share the same enzymatic systems [45, 46].

There were also positive correlations between the proportion of LNA and the proportion of ARA in plasma lipids of infants between the proportion of EPA and the proportion of ALA also in the infant plasma lipids and between the proportion of EPA and DHA proportions of lipids in maternal plasma. This finding may be explained by the sharing of the enzymes, delta-6 desaturase and delta-5 fatty acid desaturase, as mentioned above [46] favoring its conversion or retro-conversion.

An interesting fact is that this is the first study in Brazil with adolescent mothers showing levels of TFA and PUFA in infant plasma. Note that the plasma levels of these FA in infants are similar to those in maternal plasma and milk, suggesting differences in the selective transfer of FA in preference to those that are of vital importance for growth and development as is the case of ARA and DHA showed higher levels (ARA, 4.65%; DHA, 1.52%) in infant plasma when compared with maternal plasma (ARA, 4.23%; DHA, 0 59%) and milk (ARA, 0.42%; DHA, 0.17%).

In conclusion, the results show that, although TFA have been found in the plasma of the studied infants, the LC-PUFA levels remain within normal limits. No association between TFA presence and parameters of nutritional status of the infants was observed, probably due to the low levels of these fatty acids found in this study. On the other hand, such an association may occur with higher *trans* levels, and this may be extremely relevant, once the use of hydrogenated or non-hydrogenated fats in foods can vary according to the processing costs involved and depends on the current availability of these ingredients in the country.

Acknowledgments The authors thank all the adolescent mothers who participated in this study. The present work was in part supported by Conselho Nacional de Desenvolvimento Científico e Tecnológico (CNPq)–Brazil and Fundação de Amparo a Pesquisa do Rio de Janeiro (FAPERJ), Brasil.

References

1. Al MD, van Houwelingen AC, Kester AD, Hasaart TH, de Jong AE, Hornstra G (1995) Maternal essential fatty acid patterns during normal pregnancy and their relationship to the neonatal essential fatty acid status. Br J Nutr 74:55–68
2. Matorras R, Ruiz JI, Perteagudo L, Barbazan MJ, Diaz A, Valladolid A, Sanjurjo P (2001) Longitudinal study of fatty acids in plasma and erythrocyte phospholipids during pregnancy. J Perinat Med 29:293–297
3. De Vriese SR, Matthys C, De Henauw S, De Backer G, Dhont M, Christophe AB (2002) Maternal and umbilical fatty acid status in relation to maternal diet. Prostaglandins Leukot Essent Fatty Acids 67:389–396. doi:10.1054/plef.2002.0446
4. Rump P, Hornstra G (2002) The n-3 and n-6 polyunsaturated fatty acid composition of plasma phospholipids in pregnant women and their infants. Relationship with maternal linoleic acid intake. Clin Chem Lab Med 40:32–39
5. Stark KD, Beblo S, Murthy M, Buda-Abela M, Janisse J, Rockett H, Whitty JE, Martier SS, Sokol RJ, Hannigan JH, Salem N Jr (2005) Comparison of bloodstream fatty acid composition from African-American women at gestation, delivery, and postpartum. J Lipid Res 46:516–525. doi:10.1194/jlr.M400394-JLR200
6. Meneses F, Torres AG, Trugo NM (2008) Essential and long-chain polyunsaturated fatty acid status and fatty acid composition of breast milk of lactating adolescents. Br J Nutr 100(5):1029–1037. doi:10.1017/S0007114508945177
7. Santos FS (2008) Avaliação das concentrações e distribuições relativas de ácidos graxos no sangue materno e no sangue do cordão umbilical de gestantes adolescentes [Evaluation of concentrations and distributions of fatty acid in maternal blood and cord blood of pregnant teens], MSc thesis. Universidade Federal do Rio de Janeiro. Available at http://teses2.ufrj.br/Teses/CCS_M/FlaviaDaSilvaSantos.pdf(Texto)
8. Valenzuela A, Nieto S (2001) Acido docosahexaenoico (DHA) en el desarrollo fetal y en la nutrición materno-infantil. Rev Med Chil 129:1203–1211. doi:10.4067/S0034-98872001001000015
9. Peng YM, Zhang TY, Wang Q, Zetterström R, Strandvik B (2007) Fatty acid composition in breast milk and serum phospholipids of healthy term Chinese infants during first 6 weeks of life. Acta Paediatr 96(11):1640–1645
10. Stubbs CF, Smith AD (1984) The modification of mammalian membrane polyunsaturated fatty acid composition in relation to membrane fluidity and function. Biochim Biophys Acta 779:89–137
11. de Urquiza, Liens S, Sjoberg M, Zetterstrom RH, Griffiths W, Sjovall J, Perlmann T et al (2000) Docosahexaenoic acid, a ligand to the retinal x-receptor. Science 290:2140–2144. doi:10.1126/science.290.5499.2140
12. VanderJagt DJ, Arndt CD, Okolo SN, Huang YS, Chuang LT, Glew RH (2000) Fatty acid composition of the milk lipids of Fulani women and the serum phospholipids of their exclusively breast-fed infants. Early Hum Dev 60(2):73–87
13. Tinoco SMB, Sichieri R, Moura AS, Santos FS, Carmo MGT (2007) The importance of essential fatty acids and the effect of *trans* fatty acids in human milk on fetal and neonatal development. Cad Saude Publica 23(3):525–534. doi:10.1590/S0102-311X2007000300011
14. Mojska H (2003) Influence of *trans* fatty acids on infant and fetus development. Acta Microbiol Pol 52(Suppl):67–74
15. Kummerow FA, Zhou Q, Mahfouz MM, Smiricky MR, Grieshop CM, Schaeffer DJ (2004) *Trans* fatty acids in hydrogenated fat inhibited the synthesis of the polyunsaturated fatty acids in the phospholipid of arterial cells. Life Sci 74:2707–2723
16. Mahfouz MM, Smith TL, Kummerow FA (1984) Effect of dietary fats on desaturase activities and the biosynthesis of fatty-acids in rat-liver microsomes. Lipids 19(3):214–222
17. Blond JP, Henchiri C, Precigou P, Grandgirar DA, Sebedio JL (1990) Effect of 18:3n-3 geometrical-isomers of heated linseed oil on the biosynthesis of arachidonic-acid in rat. Nutr Res 10(1):69–79. doi:10.1016/S0271-5317(05)80767-5
18. Chiara VL, Barros ME, Costa LP, Martins PD (2007) Redução de lista de alimentos para questionário de freqüência alimentar: questões metodológicas na construção. Rev Bras Epidemiol 10(3):410–420
19. Anção MS, Cuppari L, Draibe AS, Sigulem D (2002) Programa de apoio a Nutrição-NutWin-Versao 1, 5 [CD-ROM]. Departamento de Informática em Saúde, SPDM-UNIFESP/EPM, São Paulo
20. Núcleo de Estudos e Pesquisas em Alimentação. Universidade Estadual de Campinas versão 2. São Paulo: [NEPA/Unicamp] (2006) Tabela Brasileira de Composição de Alimentos—TACO (Brazilian food composition table—TACO). Campinas: UNICAMP/Ministério da Saúde
21. Ministério da Saúde, Brasil (2004) Vigilância Alimentar e Nutricional–SISVAN: orientações básicas para a coleta e análise de dados antropométricos em serviços de saúde. Série A. Normas e Manuais Técnicos. Ministério da Saúde, Brasília
22. WHO (2009) Anthro for personal computers, version 3: software for assessing growth and development of the world's children. Geneva: WHO. http://www.who.int/childgrowth/software/en/
23. Ministério da Saúde, Brasil. Secretaria de Atenção à Saúde. Departamento de Atenção Básica. Protocolos do Sistema de Vigilância Alimentar e Nutricional–SISVAN na assistência à saúde/Ministério da Saúde, Secretaria de Atenção à Saúde. Departamento de Atenção Básica–Brasília: Ministério da Saúde (2008). il.–(Série B. Textos Básicos de Saúde)
24. Ministério da Saúde. Departamento de Ações Programáticas Estratégicas. Área Técnica de Saúde da Mulher, Brasil (2005) Pré-natal e puerpério: atenção qualificada e humanizada: manual técnico. Brasília, DF. (Série A: Normas e Manuais técnicos)
25. World Health Organization (WHO) (2007) Growth reference data for 5–19 years. http://www.who.int/growthref/who2007_bmi_for_age_field/en/index.htmL
26. WHO (2009) AnthroPlus for personal computers Manual: Software for assessing growth of the world's children and adolescents. WHO, Geneva. http://www.who.int/growthref/tools/en/
27. Folch J, Lees M, Sloane-Stanley GH (1957) A simple method for the isolation and purification of total lipids from animal tissues. J Biol Chem 226:497–509

28. Lepage G, Roy CC (1986) Direct transesterification of all classes of lipids in a one-step reaction. J Lipid Res 27:114–120
29. Craske JD, Bannon CD (1988) Letter to the editor. JAOCS 65:1190–1191
30. Elias SL, Innis SM (2001) Infant plasma *trans*, n-6, and n-3 fatty acids and conjugated linoleic acids are related to maternal plasma fatty acids, length of gestation, and birth weight and length. Am J Clin Nutr 73:807–814
31. Koletzko B (1992) *Trans* fatty acids may impair biosynthesis on long-chain polyunsaturates and growth in man. Acta Paediatr 81:302–306
32. Carlson SE, Clandinin MT, Cook HW, Emken EA, Filer LJ Jr (1997) *trans* Fatty acids: infant and fetal development. Am J Clin Nutr 66:717S–736S
33. Larqué E, Zamora S, Gil A (2000) Dietary trans fatty acids affect the essential fatty-acid concentration of rat milk. J Nutr 130:847–851
34. Innis S (2007) Human milk: maternal dietary lipids and infant development. Proc Nutr Soc 66:397–404
35. Sauerwald U, Demmelmair H, Koletzko B (2001) Polyunsaturated fatty acid supply with human milk. Lipids 36:991–996
36. Agência Nacional de Vigilância Sanitária. Resolução RDC n. 360 de 23 de dezembro de, Brasil (2003) Regulamento técnico sobre rotulagem nutricional de alimentos embalados. Diário Oficial da União 2003
37. Bertolino CN, Castro TG, Sartorelli DS, Ferreira SRG, Cardoso MA (2006) Influência do consumo de ácidos graxos *trans* no perfil de lipídeos séricos em nipo-brasileiros de Bauru, São Paulo, Brasil. Cad Saude Publica 22(2):357–364
38. Vasconcelos Costa AG, Bressan J, Sabarense CM (2006) Ácidos Graxos *Trans*: Alimentos e Efeitos na Saúde. ALAN 56(1):12–21
39. Larqué E, Gil-Campos M, Ramírez-Tortosa MC, Linde J, Cañete R, Gil A (2006) Postprandial response of *trans* fatty acids in prepubertal obese children. Int J Obes 30:1488–1493
40. WHO/FAO Expert Consultation (2003) Diet nutrition, and the prevention of chronic diseases WHO Geneva, vol 916. WHO Technical Report Series, pp 89–90
41. Monge-Rojas R, Campos H, Rojas XF (2005) Saturated and *Cis*- and *Trans*-unsaturated fatty acids intake in rural and urban Costa Rican adolescents. J Am Coll Nutr 24(4):286–293
42. Larque E, Zamora S, Gil A (2001) Dietary *trans* fatty acids in early life: a review. Early Hum Dev 65(2):31S–41S
43. Innis SM, King DJ (1999) *trans* Fatty acids in human milk are inversely associated with concentrations of essential *all-cis* n-6 and n-3 fatty acids and determine *trans*, but not n-6 and n-3, fatty acids in plasma lipids of breast-fed infants. Am J Clin Nutr 70(3):383–390
44. Chen Z-Y, Pelletier G, Hollywood R, Ratnayke WMN (1995) *Trans* fatty acid isomers in Canadian human milk. Lipids 30:15–21
45. Calder PC (2001) n-3 polyunsaturated fatty acids, inflammation and Immunity: pouring oil on troubled waters or another fishy tale? Nutr Res 21:309–341
46. Barceló-Coblijn G, Murphy EJ (2009) Alpha-linolenic acid and its conversion to longer chain n-3 fatty acids: benefits for human health and a role in maintaining tissue n-3 fatty acid levels. Prog Lipid Res 48(6):355–374

Lipids (2011) 46:545–555
DOI 10.1007/s11745-010-3522-0

METHODS

The Development of Flow-through Bio-Catalyst Microreactors from Silica Micro Structured Fibers for Lipid Transformations

Sabiqah Tuan Anuar · Carla Villegas · Samuel M. Mugo · Jonathan M. Curtis

Received: 10 August 2010 / Accepted: 22 December 2010 / Published online: 13 February 2011

Abstract This study demonstrates the utility of a flow-through enzyme immobilized silica microreactor for lipid transformations. A silica micro structured fiber (MSF) consisting of 168 channels of internal diameter 4–5 μm provided a large surface area for the covalent immobilization of *Candida antartica* lipase. The specific activity of the immobilized lipase was determined by hydrolysis of *p*-nitrophenyl butyrate and calculated to be 0.81 U/mg. The catalytic performance of the lipase microreactor was demonstrated by the efficient ethanolysis of canola oil. The parameters affecting the performance of the MSF microreactor, including temperature and reaction flow rate, were investigated. Characterization of the lipid products exiting the microreactor was performed by non-aqueous reversed-phased liquid chromatography (NARP-LC) with evaporative light scattering detector (ELSD) and by comprehensive two-dimensional gas chromatography (GC × GC). Under optimized conditions of 1 μL/min flow rate of 5 mg/mL trioleoylglycerol (TO) in ethanol and 50 °C reaction temperature, 2-monooleoylglycerol was the main product at >90% reaction yield. The regioselectivity of the *Candida antartica* lipase immobilized MSF microreactor in the presence of ethanol was found to be comparable to that obtained under conventional conditions. The ability of these reusable flow-through microreactors to regioselectively form monoacylglycerides in high yield from triacylglycerides demonstrate their potential use in small-scale lipid transformations or analytical lipids profiling.

Keywords Microreactor · Micro structured fiber · Lipid transformation · Immobilized enzyme

Abbreviations

APTES	3-(Aminopropyl)triethoxysilane
DAG	Diacylglycerol
DO	Dioleoylglycerol
EE	Ethyl oleate/C18:1 ethyl ester
ELSD	Evaporative light scattering detector
FID	Flame ionization detector
GC × GC	Comprehensive two-dimensional gas chromatography
HPLC	High performance liquid chromatography
MAG	Monoacylglycerol
MO	Monooleoylglycerol
MSF	Micro structured fiber
NARP-LC	Non-aqueous reversed-phased liquid chromatography
PCF	Photonic crystal fibers
PDMS	Poly-dimethylsiloxane
PMMA	Poly(methyl-methacrylate)
*p*NP	*p*-Nitrophenol
*p*NPB	*p*-Nitrophenyl butyrate
SEM	Scanning electron microscope

S. Tuan Anuar · C. Villegas · J. M. Curtis (✉)
Lipid Chemistry Group, Department of Agricultural, Food and Nutritional Science (AFNS), University of Alberta, Edmonton, AB T6G 2P5, Canada
e-mail: jcurtis1@ualberta.ca

S. Tuan Anuar
Department of Chemistry, Universiti Malaysia Terengganu, 21030 Terengganu, Malaysia

S. M. Mugo
Department of Physical Sciences (Chemistry), Grant MacEwan University, Edmonton, AB T5J 4S2, Canada

J. M. Curtis
Lipid Chemistry Group and LiPRA, AFNS, University of Alberta, Edmonton, AB T6G 2P5, Canada

TAG	Triacylglycerol
TO	Trioleoylglycerol
U	Unit of lipase activity

Introduction

Recently, microreactor technologies have gained attention for their application in clinical diagnostics, analytical and synthetic chemistry [1–3]. For example, Kawaguchi et al. [4] have successfully demonstrated the use of a flow-system microreactor for the Moffatt–Swern oxidation of alcohols into carbonyl compounds. A microreactor integrates various chemical or analytical processes into a single platform made up of reaction channels in the micrometer (50–1,000 μm) range. In such systems, the chemical reaction takes place under conditions of continuous flow [1]. Whether for analytical or synthetic applications, microreactor technology offers several advantages including: reduced reaction time [2, 3] due to the large surface area to volume ratio in the microchannel; enhanced control over the reaction process [3]; it is less wasteful since only low volumes of reagent are used [3] and rapid optimization of reaction conditions can be achieved [2–5]. The microreactors are also ideally suited for continuous flow processes, a highly desired paradigm in processing.

The fabrication of commercially available microreactors (mainly made from glass, quartz, silica or polymers) is however, generally achieved via expensive photolithographic and wet-etching processes which are complicated and require specialized clean-room facilities [6]. Therefore, there is much interest in developing cheaper and more easily accessible approaches to the fabrication of microreactors for laboratory applications [1–10]. Amongst the attractive platforms used, are microreactors obtained by means of imprinting on polymers including poly-dimethylsiloxane (PDMS), poly(methyl-methacrylate) (PMMA) [11] or polyurethanes. However, the use of silica capillaries is possibly the easiest platform to employ as a flow through microreactor with potential for numerous chemical modifications for use in enzyme-, organo-, or metal-catalysts immobilization [8–10].

There is considerable interest in the use of enzymes for lipid transformations such as in the preparation of structured lipids [12] as well as in biodiesel production [13]. The interest is due to the high yields, minimal side products and mild reaction conditions that can be achieved with enzyme-catalyzed processes. A major impediment to the potential commercialization of enzyme-mediated processes is the cost of enzymes and their unstable nature. However, enzyme immobilized over the high surface area of the capillary walls will result in an efficient flow-through microreactor which is reusable for many process cycles after which the microreactors can be regenerated with new enzyme.

Micro structured fibers (MSF), also commonly known as photonic crystal fibers (PCF), are silica capillaries that consist of a micro structured arrangement of air channels within a flexible acrylate polymer-coated silica tube. They are widely used as radiation optical guides and in sensor applications [14]. Basically, these optical fibers are made up of three layers: the core, cladding and the coating. Both the core diameter (an individual air channel, usually in the 8–40 μm range) and the number of channels in the photonic fiber can vary depending on the design of the fiber. In addition, the coating diameter—outer diameter of the fiber—could range from 200 to 500 μm depending on the requirements of the application [14], such as in networking or bio-sensing.

Here, we propose that the presence and chemistry of silanol groups within MSFs could be exploited as a platform for enzyme immobilization, as has been widely reported for other silica supports [8]. MSF contain an array of microchannels and hence an enormous surface is available for enzyme immobilization, and may offer an excellent platform for a flow-through microreactor. In order to demonstrate the performance of such a microreactor in mediating lipid transformations, the lipase from *Candida antarctica* was selected, since it is one of the most widely used enzymes for catalysis in lipid transesterification reactions [13, 15]. Overall, the objective of this study was to demonstrate the feasibility of immobilizing enzymes onto MSF capillaries and utilizing the microreactors in lipid transformations. This will combine the advantages of microreactor technology with the green chemistry achievable via enzyme immobilization.

Materials and Methods

Materials

MSF capillary (F-SM20, ID: 4–5 μm, outer diameter: 340 μm, 168 holes) was obtained from Newport Corp. (Irvine CA, USA). Canola oil was obtained from a local grocery store (with ~50% trioleoylglycerol). Sodium hydroxide powder (reagent grade, 97%), sodium phosphate monobasic monohydrate, 3-(aminopropyl)triethoxysilane (APTES, 99%), di-sodium hydrogen phosphate (bioUltra, Fluka, >99%), glutaraldehyde solution (BioChemika, ~50% in H_2O), sodium cyanoborohydride ($NaCNBH_3$, reagent grade, 95%), lipase from *Candida antarctica* (EC 3.1.1.3, BioChemika) potassium sodium tartrate, copper sulfate, and Folin phenol reagent all were obtained from

Sigma-Aldrich Ltd (ON, Canada). Acetic acid (glacial, HPLC) was purchased from Fisher Scientific (New Jersey, USA). C18:1 ethyl ester (EE)and TLC 18-1-A [contains by weight 25% of each of trioleoylglycerol (TO), dioleoylglycerol (DO), monooleoylglycerol (MO), methyl oleate (ME)] standards were purchased from Nu-Chek (Elysian, MN, USA), while 1-monooleoylglycerol standard (98%) was obtained from Sigma-Aldrich (ON, Canada). All organic solvents were HPLC analytical grade from Sigma-Aldrich (ON, Canada). Water was purified by a Milli-Q system (Millipore; Bedford MA, USA).

MSF Activation

The MSF capillary (15 cm) was activated by flushing with 1 M NaOH solution for 2 h at a flow rate of 10 μL/min. The sodium hydroxide activated the inner surface (silanol groups) of the capillary wall. The residual alkali was flushed by 0.1 M HCl for 2 h at a flow rate of 10 μL/min. The activated MSF was then dried under N_2 gas before the lipase enzyme immobilization step.

Lipase Immobilization onto MSF Capillary Support

Candida antarctica lipase was immobilized by introduction of amine functional groups onto the silica wall by a silanization reaction; this was followed by the formation of an imide using glutaraldehyde as a bifunctional reagent; finally immobilization was achieved via a condensation reaction with the lipase. This procedure was adapted with some minor modifications from the method reported by Ma et al. [8]. Briefly, the activated MSF was filled with 20% (v/v) APTES (5:2:3 water: acetic acid: APTES) and left overnight with both capillary ends submerged in the 20% APTES solution to complete the reaction. The MSF was then flushed with 0.1 M sodium phosphate buffer (pH 7), followed by reaction with glutaraldehyde solution (5% glutaraldehyde dissolved in 0.1 M sodium phosphate buffer) and left for 4 h in the solution. The capillary was then flushed with buffer again before continuously infusing it with 8 mg/mL lipase from *Candida antarctica* in sodium phosphate buffer (0.1 M, pH 7 with 0.1% $NaCNBH_3$) for 24 h at room temperature. The sodium borohydride is used to reduce the Schiff base formation and to stabilize the binding of the enzyme to the support. The enzyme-loaded microreactor was finally flushed with the 0.1 M sodium phosphate buffer at which point it was ready for use.

Immobilized Lipase Assay

The amount of lipase immobilized on the MSF was determined using the standard Lowry protein assay [16]. This was achieved by determining the difference in protein concentration before and after passing the *Candida antarctica* lipase solution through the MSF during the immobilization process. The Lowry solution was prepared freshly by mixing solution A (4 mg/mL NaOH and 20 mg/mL Na_2CO_3 in water) and solution B (10 mg/mL potassium sodium tartrate and 50 mg/mL $CuSO_4$ in water), prior to use. Solutions of known protein concentration (calibration solutions containing 0, 2.5, 5, 7.5, 10, 12.5, 15, 17.5, 20, 25, 30, and 35 μg protein) and lipase solutions (2 μL) were made up to a total volume of 200 μL with deionized water. 1 mL of Lowry solution was added to each protein solution then after waiting for 15 min, 100 μL Folin phenol reagent was added. After a further 30 min, an aliquot was sampled in a UV-Vis cuvette (10 mm square cuvette) and their absorbance was measured at 750 nm. The concentration of the enzyme solution before and after passing through the microreactor was determined from the protein calibration curve in order to estimate the amount of enzyme immobilized in the microreactor.

Lipase Activity Assay

To determine the lipase (esterase) activity, a 3.5 mM solution of *p*-nitrophenyl butyrate (*p*NPB) was prepared in a 1:1 mixture of acetonitrile (ACN) and 0.1 mM sodium phosphate buffer). The *p*NPB solution was passed through a 15 cm MSF lipase immobilized microreactor at 1 μL/min for 1 h. The hydrolysis products were then collected, their volume measured and then diluted to 2.0 mL in mixture of ACN: sodium phosphate buffer (1:1). The absorbance of the resulting solution of products (absorbing molecule, *p*-nitrophenol) was measured at a wavelength of 410 nm. A calibration curve was obtained by measuring the absorbance of *p*-nitrophenol (*p*NP) standard solutions prepared in the same solvent mixture ACN: 0.1 mM sodium phosphate buffer at concentrations of 0. 5, 1, 3, 5 and 7 mM. The concentration of *p*NP hydrolyzed was determined and lipase enzyme activity calculated. The enzyme activity was expressed as amount of *p*NP formed on the microreactor under the condition used per minute, i.e., μg *p*NP/min. One enzyme unit (U) was the amount of protein liberating 1 μg of *p*NP per minute.

Specific Activity of Immobilized Lipase

Based on the amount of protein loaded and lipase activity, a specific activity of lipase immobilized in the MSF was calculated according to Dizge et al. [17].

Lipid Sample Preparation and Transformation

The reactant solution of 5 mg/mL canola oil was prepared in ethanol. The mixture was mixed vigorously using a

vortex mixer to dissolve the lipid in ethanol. The parameters affecting the performance of the microreactor including reaction flow rate and temperature were investigated and optimized as follows:

Temperature

Lipid transformation using the immobilized MSF was carried out at room temperature (24 °C), 30, 40, 50, and 60 °C. A schematic illustrating the experimental conditions is shown in Fig. 1. A syringe pump system (Harvard '11' Plus) was used to infuse reactant through the MSF microreactor. The products from the reaction were collected in a small capped vials with the microreactor poked through the septum of the vial. The temperature that produced highest yield was then used to optimize the flow rate for the reaction.

Reaction Flow Rate

The reactant solution was then pumped through the lipase-immobilized MSF microreactor held at the optimized temperature (50 °C) and using various flow rates (0.5, 1, 5 and 10 μL/min), each held for 3 h. The products were collected into vials for analysis, as described below.

In both the temperature and reaction flow optimization experiments, the reaction products collected from MSF microreactor were diluted 10–25 times in HPLC solvent A (methanol with 0.1% glacial acetic acid) before being analyzed. Standard calibration curves were prepared using 0.05, 0.1, 0.5 and 1.0 mg/mL of total TLC 18-A-1 and 0.05, 0.1, 0.2, 0.5, and 1.0 mg/mL of EE standards. The amount of each compound in the reaction products was determined from the standard calibration curve prepared.

For GC × GC analysis, samples were diluted in dichloromethane and quantified against a calibration curve covering the range of 0.01–1 mg/mL of each lipid component.

Instrumentation

(a) A Harvard Model '11' Plus syringe pump (Harvard Apparatus, Holliston MA) was used to pass all solutions through the MSF both during preparation of the microreactor and for lipid transformations.
(b) High-performance liquid chromatography (HPLC) analysis was performed using an Agilent 1200 HPLC system equipped with an evaporative light scattering detector (ELSD) model 1260 Infinity (Agilent Technologies, Santa Clara CA, USA).
(c) Either an Agilent Zorbax HT C18 column (4.6 × 50 mm, 1.8 μm) (Agilent Technologies; Santa Clara CA, USA) or a Supelco Ascentis Silica column (4.6 × 150 mm, 3 μm) (Sigma-Aldrich; ON, Canada) were used as described below.
(d) UV/Visible measurements were made using a Jenway spectrophotometer 6320D series (Bibby Scientific, Staffordshire, UK).
(e) A LECO comprehensive 2-dimensional GC × GC/FID system (LECO; St. Joseph, MI, USA) was used (Fig. 2). It consists of a dual oven GC equipped with flame ionization detector and cryogenic modulator (quadjet) cooled with liquid nitrogen and split–splitless injector. All data was collected by Leco ChromaTOF-GC software v 3.34 optimized for GC × GC/FID. The columns used for GCxGC were a DB5HT gas chromatography column (30 m × 0.32 mm × 0.1 μm, bonded and cross-linked 5% phenyl methylpolysiloxane, Agilent technologies; Santa Clara CA, USA) and an RXT65 column (1 m × 0.25 mm × 0.1 μm, crossbond 65% diphenyl-dimethyl polysiloxane, Restek; Bellefonte PA, USA).

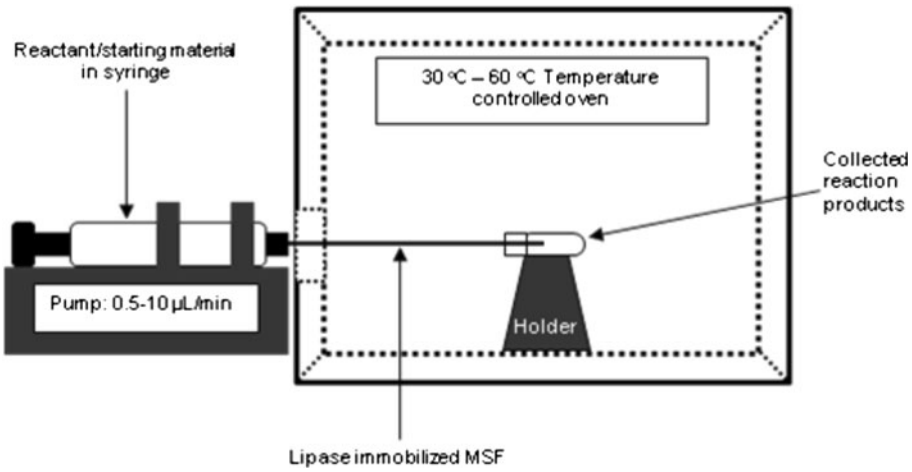

Fig. 1 Apparatus used with the fabricated MSF microreactor for small scale lipid reactions

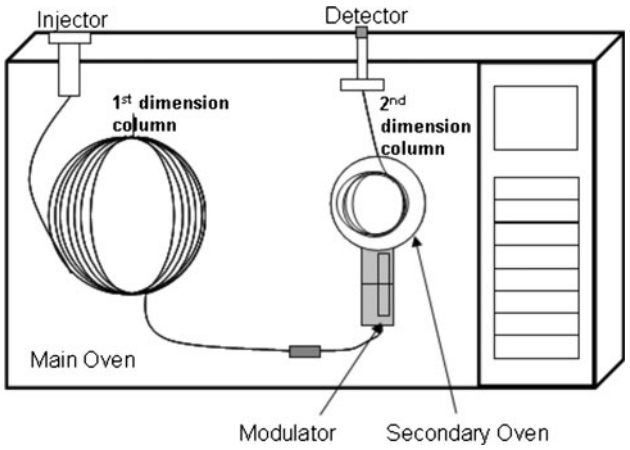

Fig. 2 Schematic diagram of GC × GC/FID used for analysis of lipid transformation products

NARP-LC/ELSD

Non-aqueous reversed phased (NARP) HPLC with a C18 column was used to speciate the lipid transformation products as well as the starting materials and lipid standards. The ELSD was set to 33 °C and the nitrogen gas flow rate was optimized. All samples were analysed using an injection volume of 10 μL and a mobile phase flow rate of 1 mL/min. A binary gradient of A, methanol with 0.1% glacial acetic acid; and B, isopropanol/hexane (5:4) was used. The starting condition was 0% B held for 5 min then increased to 66% B in 10 min, held at 66% B for 3.5 min before returning to 0% B (2.5 min) to equilibrate the column.

GC × GC

GC × GC was used as a second method to characterize the lipid classes produced by the MSF microreactor and to confirm the LC results. An aliquot of the product mixture was dissolved in dichloromethane prior to injection into the LECO GC × GC/FID system. The carrier gas was H_2 at a flow rate of 1.5 mL/min, injection volume 1 μL, split ratio of 15:1 and He FID make-up gas was used. The inlet and detector temperatures were set to 320 and 400 °C, respectively. The temperature program for the first oven was 45 °C (0.5 min) increased at 2 °C/min until 150 °C (0 min) then increased again at 3 °C/min until 375 °C (hold 10 min). The second oven tracked the first but at a temperature 25 °C higher at all times. The modulator offset was 15 °C.

Regiospecificity Determination Using Normal Phase-LC/ELSD

Normal phase HPLC with a silica column was used for the regiospecific separation of the MSF microreactor lipid products, following an AOCS standard method [18]. Aliquots of the products formed under the optimized conditions (50 °C, flow rate 1 μL/min) were analyzed by HPLC/ELSD along with a 1-monooleoylglycerol standard. The method used an injection volume of 10 μL, mobile phase flow rate of 0.5 mL/min, column temperature maintained at 40 °C and the ELSD operating at 90 °C. The mobile phase was a binary gradient of A hexane, and B hexane/isopropanol/ethyl acetate/10% formic acid (80:10:10:1, v/v) [18]. The gradient was 2% B, linear increase to 35% B in 15 min, then linearly increased to 98% in 1 min, and finally held for 10 min at 98% B. The column was allowed to equilibrate at the starting condition for 3 min. Note that all samples and standards were prepared in hexane/isopropanol (9:1, v/v) prior analysis.

Results and Discussion

Lipase-Immobilized Microreactor Fabrication

In this paper, we present the first demonstration of the use of a microreactor, fabricated by immobilizing lipase from *Candida antarctica* onto a silica MSF support, for the ethanolysis of canola oil triacylglycerols. The MSF morphology is shown in the scanning electron microscope image in Fig. 3.

Although the MSF have been mainly developed for use in light guiding optics, they contain numerous micrometer-sized pores (4–5 μm) and provide a very large surface area, which makes them ideally suited for immobilizing high amounts of catalysts. Furthermore, the fact that the MSF is made from silica makes it even more attractive for the enzyme immobilization by employing well-known

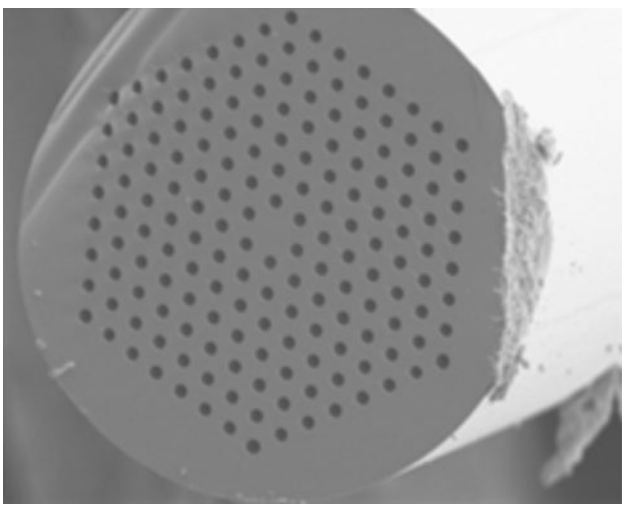

Fig. 3 Scanning electron microscope (SEM) image of a Lipase-Immobilized MSF (168 holes) at ×300 magnification

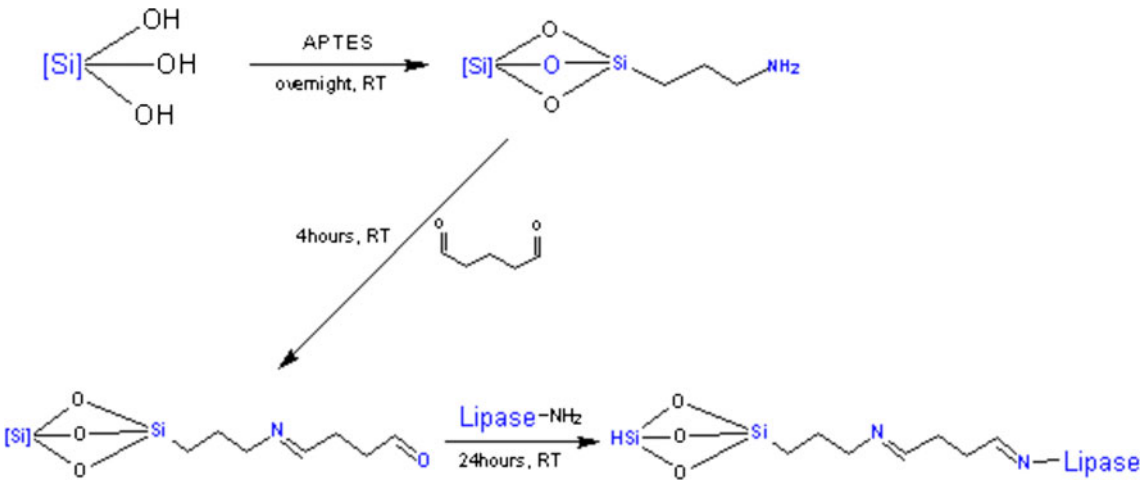

Fig. 4 The process of lipase-immobilization onto the silica support of a MSF

silanization chemistry. In order to ensure the maximum presence of silanol groups at the MSF surface, the use of alkali (NaOH) treatment has been shown to activate the silica wall by increasing hydrolysis of the silanol group [19]. The reaction sequence of the immobilization lipase from *Candida antarctica* onto the silica walls of the MSF is given in Fig. 4.

Immobilization onto the silica support was achieved by grafting aminopropyl triethoxysilane (APTES) onto the active silanol group (Si–OH) on the MSF wall [20]. The resultant pendant primary amine group provides a reactive functionality to form imines when reacted with the bifunctional reagent glutaraldehyde. This in turn results in a pendent carbonyl group from the grafted glutaraldehyde which further reacts with the amino groups of lipase forming a Schiff base, thus covalently attaching the enzyme to the MSF support [20, 21]. It is expected with such a strong covalent lipase attachment, the probability of enzyme leaching is low and hence the microreactor can potentially be reused multiple times. In contrast, using the simple, commonly used adsorption methods of immobilization, leaching is known to limit reusability [22, 23].

Enzyme Activity Assay

Before employing the lipase loaded MSF microreactor it was essential to determine the success of the immobilization method. The total free protein concentration was determined using the widely used Lowry protein assay [16]. The amount of protein bound to the MSF microreactor support was estimated by the difference between amount of protein in the lipase solution infused through the MSF and the effluent emerging from the MSF. Using this method, the amount of protein loaded on the MSF was determined to be 5.8 μg/μL (Table 1).

It is likely that not all lipase loaded in the MSF is active due to underlying physicochemical factors associated with the immobilization. As such, it was imperative to also determine the activity of the immobilized lipase. As described in detail in the Materials and Methods section, the lipase activity of immobilized MSF microreactor was determined by the enzymatic hydrolysis of p-nitrophenyl butyrate (*p*NBP) to *p*-nitrophenol which is quantified spectrophotometrically. Using this assay, a unit (U) of lipase activity is defined as the amount of enzyme that hydrolyses (liberates) 1 μg of *p*-nitrophenol (*p*NP) from *p*NPB as substrate. Table 1 summarizes of lipase activity assay yield. The enzymatic activity for the immobilized MSF microreactor was determined to be 4.7 μg *p*NP/min (U) for the 15 cm MSF microreactor. Hence, a specific activity of 0.81 U/mg was found for the immobilized lipase from *Candida antarctica* in the MSF microreactor. Data from the manufacturer indicates that the native lipase from *Candida antarctica* has specific activity of 1.06 U/mg

Table 1 Determination of the amount of lipase immobilized onto the MSF capillary

	Protein bound[a] from 1 mL lipase (mg/mL)	Protein bound yield (%)	Lipase activity[b] (μg *p*NP/min) (U)	Specific activity (U/mg) for 15 cm MSF microreactor	Specific activity for native enzyme (U/mg) before immobilization
Fabricated immobilized MSF	5.83	75.59	4.7	0.81	1.06

[a] 1 mL of 8 mg/mL lipase solution was immobilized onto the MSF capillary

[b] 1U = amount (mg) of enzyme to liberate 1 μg *p*NP/min under the assay condition

before immobilization (cf. Table 1). Therefore, only about 23.6% of the enzyme activity was found to have been lost using the proposed immobilization process. This result is comparable with that found in other studies, for example specific activities of 0.60–0.9 were found using similar methods for lipase immobilized onto styrene–divinylbenzene and styrene–divinylbenzene–polyglutaraldehyde copolymers for biodiesel production [17].

A goal in the development of the lipase immobilized MSF microreactor was to evaluate its performance in lipid transformations. This was done by transesterifying trioleoylglycerol (molecular weight 884, TO) in ethanol in the MSF microreactor. From this reaction, the major transesterified products which were obtained were monooleoylglycerol (MO) and ethyl oleate (EE). Since MO and EE results from the hydrolysis of two and three ester bonds/molecule, respectively, the theoretical conversion rates of trioleoylglycerol (TO) can be estimated from the measured lipase activity of 4.7 μg *p*NP/min (U) assuming that lipase catalysed hydrolysis of triacylglycerol (TAG) ester occurs at the same rate as the lipase catalysed hydrolysis of *p*NBP to give *p*NP. If this assumption is made, then the conversion rate of 5 mg/ml TO at 1 μL/min to MO and to EE would be predicted to be 10 and 6.7 μg/min (or 0.0115 and 0.0075 mol/min), respectively. It is apparent that notwithstanding the gross assumptions made, the observed conversion rate (TO–MO) is of the same order of magnitude as the rate predicted based on the measured enzyme activity. This implies that to a rough approximation, the enzyme activity assay is quite consistent with the measured results for TO conversion (described in the next section). It should also be pointed out that canola oil rather than TO was actually used in the experiments, but this does not change the general arguments used above.

Enzymatic-Catalyzed Ethanolysis Using the MSF Microreactor

The ethanolysis of canola oil was performed using the lipase-immobilized MSF microreactor at different temperatures and flow rates, in order to determine the optimal conditions. The selected temperature range was chosen based on the optimized lipase enzyme conditions of other researchers including Irimescu et al. [12] and Köse et al. [24] The former suggested optimal conditions at room temperature, while the latter indicated denaturation of enzyme at temperatures >50 °C, by decreasing the reaction yield. The products obtained were then analysed by NARP-LC/ELSD and Fig. 5a, b show the chromatograms obtained for both the starting material and pure standards. The conversion of TAG in canola oil was estimated by means of a calibration curve of a lipid standard consisting of TO, DO, MO and EE (Table 2).

The data in Table 2 show the relative concentrations of the reaction products obtained using a flow rate of 1 μL/min of canola oil triacylglycerols (TAG) in ethanol solution passing through the lipase immobilized MSF microreactor, conditioned at various temperatures. From the LC/ELSD analysis it was found that whilst EE and monoacylglycerols (MAG) products were formed under all conditions, diacylglycerols (DAG) were not observed above the limit of detection, possibly due to the microscale nature of our study. The predominant formation of MO relative to DO is consistent with results of others [12]. In Table 2 it is clear that at low temperatures, the conversion of TAG into other lipid forms was low, and a similar result was found at 60 °C. However, at around 50 °C virtually all of the TAG was consumed indicating a high efficiency of the immobilized lipase microreactor under these conditions.

The effect of the reaction flow rate on the lipid conversion was then investigated with the temperature fixed at 50 °C (cf. Fig. 5c–e). As indicated in Fig. 5c–e, the microreactor flow rates investigated included 1, 5 and 10 μL/min. The narrow flow rate range evaluated was due to the achievable linear force of the syringe pump utilized (Harvard '11' Plus). The results show that the optimal flow rate for the enzymatic MSF microreactor reaction is at 1 μL/min, where complete disappearance of the TAG starting material was evident along with the formation of MAG and EE. As the flow rate increased above 1 μL/min, a broad 'hump' is seen in the chromatogram, co-eluting with unreacted starting material (Fig. 5d, e). This is likely due to removal of oligomeric glutaraldehyde material from the walls of the microreactor attributable to the high pressures (~21 psi) that occur with higher flow rates through the small channels in the MSF reactor. However, since the flow rate of 1 μL/min (which corresponds to a residence time of 28.5 s in the 15 cm MSF) allows sufficient contact time between the starting material and the lipase immobilized in the microreactors, these destructive conditions can be avoided. As demonstrated in Fig. 5, the lipid transformation performance reduces as flow rate increases due to the lower contact time of the substrates with the immobilized lipase. At 10 μL/min the calculated MSF residence time was 3 s. Recently, there have been several reports describing how ethanolysis of TAG using immobilized lipase from *Candida antarctica* can, under certain conditions, become 1,3 regiospecific [12, 25]. Furthermore, the reaction in excess ethanol can also promote the formation of the 2-MAG, compared to other products [26]. For example, using an ethanol/TO molar ratio of 77:1 at 25 °C, Novozyme 435 beads and a reaction time of 4 h, Irimescu et al. [12] achieved an ~88% reaction yield of which >98% of the acylglycerol content was 2-monooleoylglycerol (2-MO). The actual molar ratio

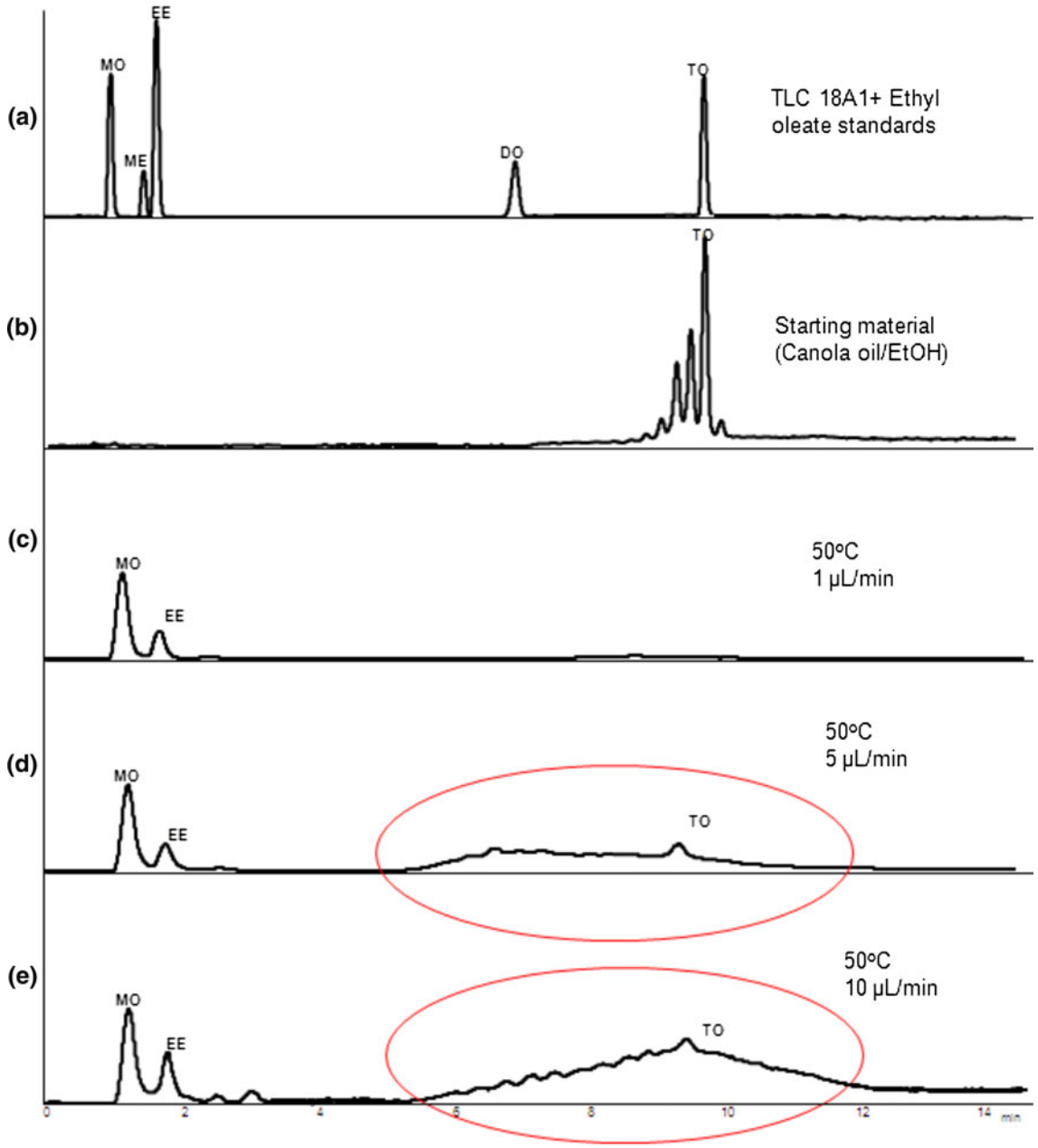

Fig. 5 NARP-LC/ELSD (nonaqueous reversed phase LC with evaporative light scattering detection (NARP-LC/ELSD) using a C18 column, ELSD temperature 33 °C, for gradient see "Materials and Methods") separation of **a** a lipid standard mixture containing *MO* monooleoylglycerol, *ME* methyl oleate, *EE* ethyl oleate, *DO* dioleoylglycerol, *TO* Trioleoylglycerol **b** canola oil/ethanol (the starting reactant mixture for the MSF microreactor), and **c**–**e** the effect of reaction flow rate for a canola oil solution in ethanol passing through the lipase immobilized MSF microreactor at: **c** 1 µL/min, **d** 5 µL/min; and, **e** 10 µL/min. All **c**–**e** reactions were carried out at 50 °C. The ellipse shows the MSF column carry-over around the TAG peak that could not be resolved

of ethanol:TAG has also been shown to be important in order to achieve regiospecificity and high reaction rates [27]. In systems where long reaction times are possible, it has been proposed [12, 25] that although 2-MAG is formed exclusively at low ethanolysis times, longer times (>7 h under the conditions used in that study) result in acyl migration forming some 1[3]-MAG. However, in the present experiment, reaction times range from seconds to a few minutes, so acyl migration is unlikely to occur.

To confirm the regiospecificity of the ethanolysis reaction in the microreactor, a sample of canola oil that passed through the reactor under the optimized conditions for maximum conversion of TAG to MAG (1 µL/min, 50 °C) was collected. The regiospecificity was then determined by

Table 2 Lipid products formed from canola oil using the lipase immobilized MSF microreactor at various temperatures using a reaction flow rate of 1 μL/min

Lipid classes	Reaction temperature																Starting material
	24 °C				30 °C				40 °C				50 °C				60 °C				
	EE	MAG	DAG	TAG	EE	MAG	DAG	TAG	EE	MAG	DAG	TAG	EE	MAG	DAG	TAG	EE	MAG	DAG	TAG	TAG
Analytical methods																					
LC/ELSD (mol%)	9%	9%	nd	82%	3%	14%	nd	84%	3%	24%	nd	73%	5%	95%	nd	nd	2%	3%	nd	96%	100%
GC × GC/FID (mol %)	22%	5%	21%	53%	nt	nt	nt	nt	nt	nt	nt	nt	37%	59%	n.d	3%	nt	nt	nt	nt	nt

Result of NARP-HPLC/ELSD analysis are compared to GC × GC/FID data for selected samples. Mole percentages were estimated based on the response of TO, DO, MO and EE standards

nd not detected

nt not tested

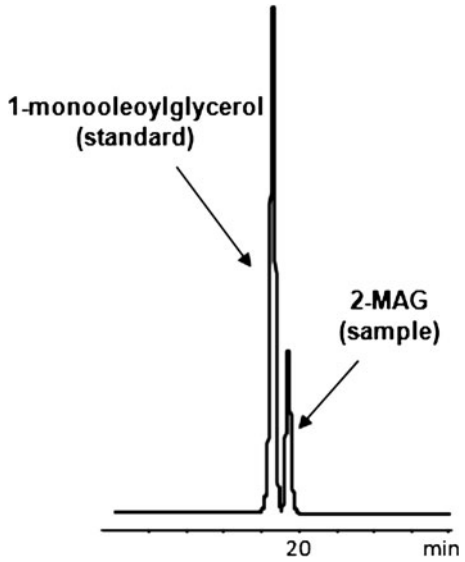

Fig. 6 Chromatograms (normal-phase-LC/ELSD separation. For gradients see "Materials and Methods") of a 1-monooleoylglycerol standard and the MAG product of passing canola oil through the microreactor

normal phase HPLC following AOCS official method Cd 11d-96 [18], as described in the Materials and Methods section. This confirmed that >96% of the MAG produced was indeed 2-MAG. Figure 6 illustrates that the addition of a 1-MO standard to the MAG product; before the addition there was no peak at the retention time of the 1-MO standard (data not presented) confirming that the product is the 2-MAG isomer.

It should be noted that Table 2 presents qualitative data which serves to illustrate the performance of the microreactor, rather than rigorous quantitative results. These shortcomings are in part due to the difficulties associated with collecting and manipulating small volumes of solution eluting from a prototype device. Also, there are several disadvantages of performing analysis using LC/ELSD, one which is that the ELSD response is not the same towards all compounds, being greatly affected by analyte volatility, and non-linearity. As a result, the measured EE concentration in particular, is less reliable. Another drawback of the LC/ELSD analysis is that it did not separate the microreactor column bleed from the DAG and TAG peaks, when operating at high reactant flow rates (Fig. 5d, e). Therefore, a second independent analytical method was carried out to support the findings of the LC/ELSD results. The method chosen uses comprehensive two-dimensional (GC × GC/FID) to separate neutral lipid microreactor products. GC × GC (cf. Fig. 2) is a multidimensional technique that consists of orthogonal hyphenation (via a cryogenic modulator) of two columns of different stationary phases, each housed in its own temperature programmable oven. On injection of the sample, chromatography

takes place conventionally on the first column but subsequently the modulator collects the effluent and periodically re-injects it into the second column for further separation [28, 29]. The sampling frequency is high enough that each peak eluting from first column is sampled at least multiple times, thus preserving the primary separation in addition to the separation on the second column phase[28–30]. Thus, GC × GC is essentially multiple sequential heart-cuts. The raw data has to be converted from the conventional linear form to a 2D representation using special software algorithms [29, 30]. The GC × GC results obtained for the MSF reaction products obtained at room temperature and 50 °C are presented in Fig. 7 and in Table 2. In both cases the optimal flow rate, 1 μL/min was used. Note that the tandem high temperature columns used in the GC × GC experiments preclude the need for the typical silylation derivatizations of lipids to increase their volatility in order to enable their GC analysis. Details of the development of this GC × GC method will be presented in a future report.

What is notable in Fig. 7 is the complete separation of EE, MAG, DAG and TAG along with the relatively higher response of EE compared to that seen by LC/ELSD. In addition, the presumably glutaraldehyde oligomeric material (carry-over) discharged from the microreactor especially at high flow rates does not interfere with the separation of lipid peaks (Fig. 7), further giving credence to the use of GC × GC. Using GC × GC method, the compounds with lower molecular weight (EE) elute first, followed by MAG, DAG and TAG. Also, the response for the volatile EE is higher than for the other lipid classes in contrast to the LC/ELSD method where the opposite is observed. This discrepancy in product yields (seen in Table 2) may be a consequence of the nonlinear nature of HPLC/ELSD, especially for compounds differing in volatility. In general, the GC × GC/FID results support the conclusions of the LC/ELSD data described above, but the estimated EE concentrations are considerably higher and likely much more realistic (Table 2).

In conclusion, these results clearly demonstrate the successful lipase immobilization on silica microstructure fibers and the use of the resulting microreactor for the ethanolysis of a vegetable oil under conditions of continuous flow. A high degree of regiospecificity was observed in the reaction under optimized conditions, with almost complete conversion to 2-MAG. This is consistent with earlier reports for ethanolysis using the same lipase [12, 25], although under quite different reaction conditions and at much lower reaction rates. Although not yet robust, the MSF microreactors have been reused several times, and future work will aim to produce microreactors with longer lifetimes. It is envisioned that on-line enzyme immobilized MSF microreactors will prove to be valuable in analytical lipid profiling applications.

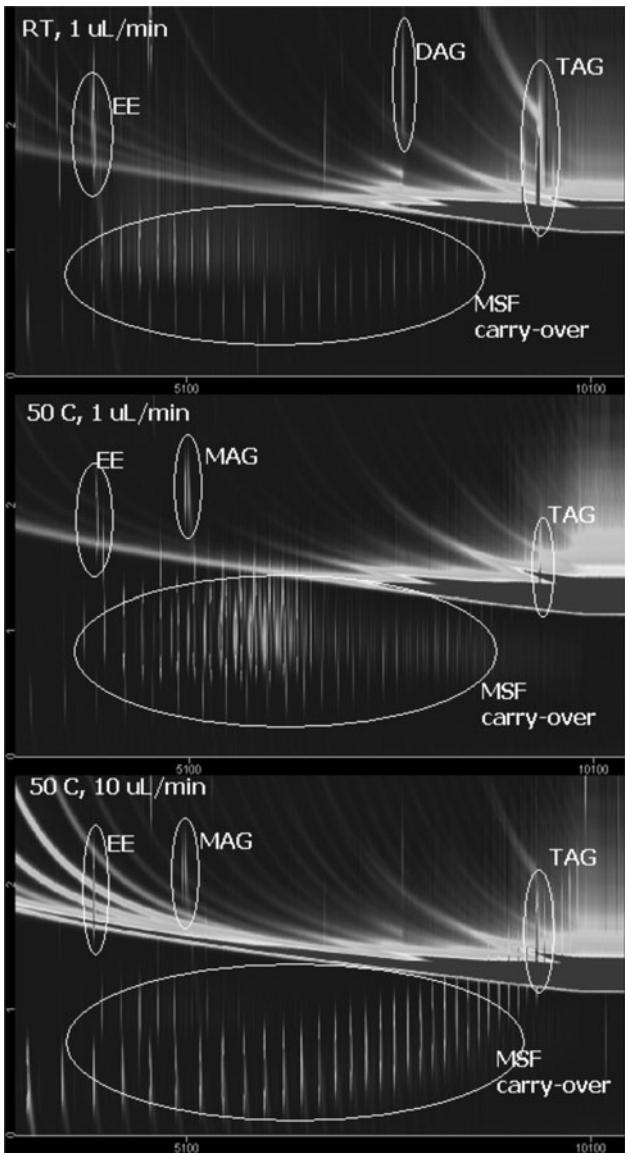

Fig. 7 GC × GC/FID chromatograms of products from ethanolysis of canola oil using the MSF microreactor. The microreactor bleed ("carry over") separates from the identified *circled* lipid products

Acknowledgments The authors acknowledge support from an NSERC Discovery grant (Dr. Jonathan Curtis) and from Grant MacEwan University Research Scholarly Activity (Dr. Samuel Mugo). The authors would also like to acknowledge Mr Olivier Niquette (LECO Canada; Mississauga, Ontario) for the generous loan of the GC × GC/FID system, Grant MacEwan Arts and Science faculty, and Ministry of Higher Education, Malaysia for providing graduate student funding (Sabiqah Tuan Anuar). The analytical assistance and support of Dr. Yuan Yuan Zhou and Karl Aryton (Grant MacEwan University, Physical Science department) and all Lipid Chemistry Group and LiPRA members is acknowledged.

References

1. Watts P, Wiles C (2007) Recent advances in synthetic micro reaction technology. Chem Commun 5:443–467
2. Watts P, Wiles C (2007) Micro reactors: a new tool for the synthetic chemist. Org Biomol Chem 5:727–732
3. Mason BP, Price KE, Steinbacher JL, Bogdan AR, McQuade DT (2007) Greener approaches to organic synthesis using microreactor technology. Chem Rev 107:2300–2318
4. Kawaguchi T, Miyata H, Ataka K, Mae K, Yoshida J (2005) Room-temperature Swern oxidations by using a microscale flow system. Angew Chem Int Ed 44:2413–2416
5. Lu SY, Watts P, Chin FT, Hong J, Musachio JL, Briard E, Pike VW (2004) Syntheses of ^{11}C- and ^{18}F-labeled carboxylic esters within a hydrodynamically driven micro-reactor. Lab Chip 4:523–525
6. McCreedy T (2000) Fabrication techniques and materials commonly used for the production of microreactors and micro total analysis systems. Trends Anal Chem 19:396–401
7. Carvalho AT, Lima RR, Silva LM, Simões EW, Silva MLP (2009) Three-dimensional microchannels as a simple microreactor. Sens Actuat B 137:393–402
8. Ma J, Liang Z, Qiao X, Deng Q, Tao D, Zhang L, Zhang Y (2008) Organic-inorganic hybrid silica monolith based immobilized trypsin reactor with high enzymatic activity. Anal Chem 80:2949–2956
9. Xie C, Ye M, Jiang X, Jin W, Zou H (2006) Octadecylated silica monolith capillary column with integrated nanoelectrospray ionization emitter for highly efficient proteome analysis. Molec Cell Proteom 5:454–461
10. Phan NTS, Brown DH, Styring P (2004) A facile method for catalyst immobilisation on silica: nickel-catalysed Kumada reactions in mini-continuous flow and batch reactors. Green Chem 6:526–532
11. Godino N, Campo FJ, Muñoz FX, Hansen MF, Kutter JP, Snakenborg D (2010) Integration of a zero dead-volume pdms rotary switch valve in a miniaturized (bio) electroanalytical system. Lab Chip 10:1841–1847
12. Irimescu R, Iwasaki Y, Hou CT (2002) Study of tag ethanolysis to 2-MAG by immobilzed *Candida antarctica* lipase and synthesis of symmetrically structured TAG. J Am Oil Chem Soc 79:879–883
13. Akoh CC, Chang SW, Lee GC, Shaw JF (2007) Enzymatic approach to biodiesel production. J Agric Food Chem 55:8995–9005
14. Holton C, Meissner K, Herz E, Kominsky D, Pickrell G (2004) Colloidal quantum dots entrained in micro-structured optical fiber In: Durvasula LN (ed) Fiber lasers: technology, systems, and applications, Proceedings of SPIE Bellingham 5335:258–265
15. Marchetti JM, Miguel VU, Errazu AF (2007) Possible methods for biodiesel production. Renew Sust Energy Rev 11:1300–1311
16. Lowry OH, Rosebrough NJ, Farr AL, Randall RJ (1951) Protein measurement with the Folin phenol reagent. J Biol Chem 193:265–275
17. Dizge N, Keskinler B, Tanriseven A (2009) Biodiesel production from canola oil by using lipase immobilized onto hydrophobic microporous styrene-divinylbenzene copolymer. Biochem Eng J 44:220–225
18. American Oil Chemists' Society (1998) Official method Cd 11d-96 mono- and diglycerides determination by HPLC-ELSD In: Firestone D (ed) Official methods and recommended practices of the AOCS, 5th edn. American Oil Chemists' Society, Champaign
19. Gibson GTT, Mugo SM, Oleschuk RD (2008) Surface mediated effects on porous polymer monolith formation within capillaries. Polymer 49:3084–3090
20. Lee DH, Park CH, Yeo JM, Kim SW (2006) Lipase immobilization on silica gel using a cross-linking method. J Ind Eng Chem 12:777–782
21. Cass T, Ligler FS (1998) Immobilized biomolecules in analysis: a practical approach, Oxford University Press, Oxford
22. Takahashi H, Li B, Sasaki T, Miyazaki C, Kajino T, Inagaki S (2000) Catalytic activity in organic solvents and stability of immobilized enzymes depend on the pore size and surface characteristics of mesoporous silica. Chem Mater 12:3301–3305
23. Kim MI, Kim J, Lee J, Jia H, Na HB, Youn JK, Kwak JH, Dohnalkova A, Grate JW, Wang P, Hyeon T, Park HG, Chang HN (2007) Crosslinked enzyme aggregates in hierarchically-ordered mesoporous silica: a simple and effective method for enzyme stabilization. Biotech Bioeng 96:210–218
24. Köse Ö, Tüter M, Ayşe Aksoy H (2001) Immobilized *Candida antarctica* lipase-catalyzed alcoholysis of cotton seed oil in a solvent-free medium. Biores Tech 83:125–129
25. Shimada Y, Ogawa J, Watanabe Y, Nagao T, Kawashima A, Kobayashi T, Shimizu S (2003) Regiospecific analysis by ethanolysis of oil with immobilized *Candida antarctica* lipase. Lipids 38:1281–1286
26. Watanabe Y, Nagao T, Shimada Y (2009) Control of the regiospecificity of *Candida antarctica* lipase by polarity. New Biotech 26:23–28
27. Muñío MM, Esteban L, Robles A, Hita E, Jiménez MJ, González PA, Camacho B, Molina E (2008) Synthesis of 2-monoacylglycerols rich in polyunsaturated fatty acids by ethanolysis of fish oil catalyzed by 1, 3 specific lipases. Process Biochem 43:1033–1039
28. Dalluge J, Beens J, Brinkman UAT (2003) Comprehensive two-dimensional gas chromatography: a powerful and versatile analytical tool. J Chrom A 1000:69–108
29. Górecki T, Harynuk J, Panic O (2004) The evolution of comprehensive two-dimensional gas chromatography. J Sep Sci 27:359–379
30. Semard G, Adahchour M, Focant JF (2009) Chapter 2 basic instrumentation for GC. Compr Anal Chem 55:15–48

Lipids (2011) 46:557–567
DOI 10.1007/s11745-011-3571-z

ORIGINAL ARTICLE

Dietary n-3 Fatty Acids Significantly Suppress Lipogenesis in Bovine Muscle and Adipose Tissue: A Functional Genomics Approach

Beate Hiller · Andrea Herdmann · Karin Nuernberg

Received: 21 February 2011 / Accepted: 12 May 2011 / Published online: 26 May 2011

Abstract Changes in fatty acid composition of longissimus muscle and subcutaneous adipose tissue of German Holstein bulls induced by a grass-silage/n-3 fatty acid based intervention diet versus a maize-silage/n-6 fatty acid based control diet were analyzed and related to shifts in lipogenic gene expression, protein expression, and enzyme activity patterns. Significantly higher amounts of n-3 fatty acids and by mean factors of 2.2–2.5 decreased n-6/n-3 fatty acid ratios in both tissues were obtained upon n-3 fatty acid intervention. In longissimus muscle, these changes of fatty acid profiles were associated with reduced SREBP1c ($p = 0.02$), ACC ($p = 0.00$), FAS ($p = 0.10$) and SCD ($p = 0.03$) gene expression, Δ6D ($p = 0.03$) and SCD ($p = 0.03$) protein expression as well as SCD enzyme activity ($p = 0.03$). In subcutaneous adipose tissue, significantly reduced ACC ($p = 0.00$) and FAS ($p = 0.01$) gene expression, SCD protein expression ($p = 0.02$) and SCD enzyme activity ($p = 0.03$) were detected upon n-3 fatty acid intervention, although lower degrees of correlation between gene and corresponding gene products were obtained in relation to longissimus muscle. The study elucidates tissue-specific functional genomic responses to dietary fatty acid manipulation in regard to fatty acid profile tailoring of animal tissues.

Keywords Lipogenesis · Fatty acid profile · Functional genomic approach · SREBP1c · SCD · ACC · FAS · Δ5D · Δ6D

Abbreviations

ACC	Acetyl-CoA carboxylase α
ACTB	β-actin
B2M	B2-microglobulin
CG	Control group
Δ5D	Δ5 Desaturase
Δ6D	Δ6 Desaturase
EEF1A2	Eukaryotic translation elongation factor 1α2
FAME	Fatty acid methyl ester(s)
FAS	Fatty acid synthase
GAPDH	Glyceraldehyde-3-phosphate dehydrogenase
IG	Intervention group
MUFA	Monounsaturated fatty acids
PUFA	Polyunsaturated fatty acids
RPS18	Ribosomal protein S18
SCD	Stearoyl-CoA desaturase
SFA	Saturated fatty acids
SF3A1	Splicing factor 3a, subunit 1
SREBP1c	Sterol regulatory element binding protein 1c

Introduction

In recent years, increasing interest has been directed towards altering the nutritional profile of food in regard to major public health concerns. Considering the continuously rising incidences of Western lifestyle diseases such as hyperlipidemia, hypertonus, obesity, type II diabetes and cardiovascular disorders, public health strategies primarily aim at

Electronic supplementary material The online version of this article (doi:10.1007/s11745-011-3571-z) contains supplementary material, which is available to authorized users.

B. Hiller (✉) · A. Herdmann · K. Nuernberg
Research Unit Muscle Biology and Growth, Leibniz Institute for Farm Animal Biology, Wilhelm-Stahl-Allee 2, 18196 Dummerstorf, Germany
e-mail: hiller@fbn-dummerstorf.de

reducing the overall dietary intake of saturated as well as n-6 unsaturated fatty acids and at increasing the intake of health-promoting n-3 unsaturated fatty acids [1–4].

Studies indicated that up to half of the average adult intake of n-3 fatty acids in industrial countries originates from meat [5], and that the n-6/n-3 fatty acid ratio of meat can further be improved by dietary intervention of ruminant and non-ruminant farm animals with exogenous n-3 fatty acid sources, stimulating either direct fatty acid incorporation into animal tissues or affecting in vivo fatty acid biosynthesis [1, 6–9]. Levels of long-chain n-3 polyunsaturated fatty acids in lamb, beef and pork meat were reported to be effectively elevated upon dietary supplementation with linseed/linseed oil, rapeseed cake/oil, algae, linolenic acid rich forages [10] as well as novel alimentary fatty acid sources such as hemp, camelina, and lupin [6]. Beneficially reduced n-6/n-3 fatty acid ratios in meat were also demonstrated to result from, e.g., pasture versus concentrate [11], red clover-silage versus grass-silage [12] as well as grass-silage versus maize-silage [13] feeding regimes.

The underlying mechanisms facilitating fatty acid profile tailoring of animal tissues have not been completely understood and been ascribed to a complex regulation network of genetically [14–17] and physiologically [7, 17] affected lipogenic gene expression, protein expression and enzyme activity levels in animal tissues [17–21]. The results of different studies as yet showed minor degrees of consistency, ranging from negligible [22] to high degrees [18] of correlation between expression levels of lipogenic genes/proteins and fatty acid profiles.

In this context, the present study aimed at a more in-depth elucidation of the effect of dietary n-3 fatty acid intervention on fatty acid profiles via a functional genomic approach, relating shifts in fatty acid composition of bovine muscle and adipose tissue observed during preliminary investigations [13, 23] with effects on lipogenic transcriptome and proteome, focusing on key-lipogenic transcription factors (SREBP1c) and enzymes involved in fatty acid de novo synthesis (ACC, FAS), monodesaturation (SCD) and polyunsaturation (Δ5D, Δ6D).

Materials and Methods

Animals, Study Design and Tissue Sampling

From an animal experiment ($n = 29$) [13, 23] conducted within the framework of EU Project FOOD-CT-36241, tissue samples from German Holstein bulls ($n = 27$) were obtained.

Animals had been assigned to a maize-silage based control diet (control group (CG); $n = 14$) or a grass-silage based intervention diet (intervention group (IG); $n = 13$) during a fattening period of 245 ± 40 days until a live weight of 625 ± 26 kg (CG) or 631 ± 23 kg (IG) at an age of 477 ± 40 days (CG) or 510 ± 37 days (IG) was reached.

Experimental diets were isoenergetically formulated; actual energy intake ranged between mean values of 112.5 MJ (CG) and 108.5 MJ (IG) metabolizable energy per day. Control diet consisted of 0.153 g crude protein, 0.03 g crude fat (22.9% SFA, 26.0% MUFA, 51.1% PUFA; 46.3% n-6 FA, 4.8% n-3 FA; n-6/n-3 FA ratio = 9.6) and 0.07 g crude ash per g dry matter, intervention diet of 0.149 g crude protein, 0.04 g crude fat (23.6% SFA, 17.6% MUFA, 58.8% PUFA; 22.3% n-6 FA, 36.5% n-3 FA; n-6/n-3 FA ratio = 0.6) and 0.12 g crude ash.

Immediately after slaughter and exsanguination of the experimental animals, subcutaneous adipose tissue as well as longissimus muscle samples were taken from the right side of the carcass (between the thirteenth and fourteenth rib) under RNase-free conditions, snap-frozen in liquid nitrogen and stored at −80 °C until further analysis.

Gene Expression Analysis

RNA Extraction

Frozen tissue samples of an approximate weight of 100 mg were homogenized in 1 mL Qiazol lysis reagent (Cat. No. 79306) (Qiagen GmbH, Hilden, Germany) with a gentleMACS™ dissociator in gentleMACS™ M Tubes (Cat. No. 130-093-458) (Miltenyi Biotec GmbH, Bergisch-Gladbach, Germany). RNA was extracted from 1 mL homogenate with the RNeasy Lipid Tissue Mini Kit (Cat. No. 74804) according to the manufacturer's protocol; optional DNase digestion was performed with the RNase-free DNase Set (Cat. No. 79254) (Qiagen GmbH, Hilden, Germany), incubating samples with DNase (80 µL DNase working solution/sample) for 15 min at 20 °C.

RNA extracts were immediately analyzed for RNA quantity (OD_{260nm}) and purity (OD_{260nm}/OD_{280nm}) (NanoDrop ND-1000, Peqlab GmbH, Erlangen, Germany); RNA integrity was checked with a Bio-Rad Experion™ System and StdSens Analysis Kit (Bio-Rad GmbH, Munich, Germany). RNA quantity ranged between 498.2 ± 43.5 µg ($OD_{260nm}/OD_{280nm} = 1.95–2.12$) (longissimus muscle) and 158.6 ± 27.3 µg ($OD_{260nm}/OD_{280nm} = 1.93–2.17$) (adipose tissue) per g tissue sample, RNA quality between RQI-values of 9.5 ± 0.2 (longissimus muscle) and 9.3 ± 0.1 (adipose tissue).

RNA aliquots were stored at −80 °C and further processed within 2 weeks.

Reverse Transcription

RNA was reverse transcribed with the iScript™ cDNA Synthesis Kit (Cat. No. 170-8890) (Bio-Rad GmbH,

Munich, Germany), incubating a reaction mix of 4 μL 5× iScript mix, 1 μL iScript reverse transcriptase, 5 μL nuclease-free water and 10 μL RNA template (10 ng/μL) at temperatures of 25 °C for 5 min, 42 °C for 30 min and 85 °C for 5 min. cDNA aliquots were stored at −20 °C and subjected to further analysis within 4 w.

qRT-PCR

qRT-PCR analysis was performed with a Bio-Rad iCycler with 96 × 0.2 mL reaction module (Cat. No. 170-8720) and iCycler iQ real-time PCR detection system (Cat. No. 170-8740) (Bio-Rad Laboratories GmbH, Munich, Germany) using SYBR® Green I chemistry. Gene-specific oligonucleotides were designed with Primer3 (Version 0.4.0.); specificity of primers and identity of predicted PCR products was checked in silico (NCBI Primer Blast, NCBI Sequence Blast). Primers were custom-synthesized and RP1-purified by Sigma-Aldrich GmbH (Steinheim, Germany); oligonucleotide sequences and specifications are listed in Table 1.

Reaction mixes of 5 μL iQ SYBR® Green Supermix (Cat. No. 170-8860), 4 μL forward/reverse primer solution (0.2 μmol/L) and 1 μL cDNA template (10 ng/μL) were pipetted into 96-well 0.2 mL thin-wall PCR plates (Cat. No. 223-9441) and sealed with optical-quality Microseal adhesive tape (Cat. No. MSB-1001) (Bio-Rad Laboratories GmbH, Munich, Germany). After an initial denaturation at

Table 1 Specifications of gene-specific oligonucleotides

Gene and accession	Primer sequence (5′–3′)	Location on template	Exon/exon junction	Amplicon length (bp)	Efficiency[a] of primer pair
ACC	Fwd: GAGCTGAACCAGCACTCCCGA	374–394	–	215	108.4%
NM_174224.2	Rev: TGCAAGCCAGACATGCTGGATCTCA	588–564	576/586		($R^2 = 0.990$)
ACTB	Fwd: GACACCGCAACCAGTTCGCCAT	73–94	–	194	102.2%
NM_173979.3	Rev: AGCCTCATCCCCCACGTACGA	266–246	–		($R^2 = 0.989$)
B2M	Fwd: TGGGTTCCATCCACCCCAGATTGA	181–204	–	237	108.9%
NM_173893.3	Rev: TGTTCAAATCTCGATGGTGCTGCT	417–394	408/409		($R^2 = 0.998$)
Δ5D	Fwd: AGTTCAGGCCCAGGCTGGCT	613–632	619/620	164	101.4%
XM_612398.5	Rev: TGGGCTTGGCATGGTGCTGG	776–757	–		($R^2 = 0.999$)
Δ6D	Fwd: TGCCAACTGGTGGAACCATCGC	654–675	–	189	106.0%
NM_001083444.1	Rev: GGCGGCCCGATCAGGAAGAAGTAC	842–819	832/833		($R^2 = 0.989$)
EEF1A2	Fwd: GCTCTGGACTCACTGCTCAGCTTCC	21–45	27/28	229	102.4%
NM_001037464.1	Rev: TCTCGGCCGCCTCCTTCTCAAA	249–228	–		($R^2 = 0.988$)
FAS	Fwd: GCCAGCGGGAAGCGTGTGAT	4,918–4,937	–	235	107.8%
NM_001012669.1	Rev: CGATGGCAGCCTGGCCTACG	5,152–5,133	–		($R^2 = 0.998$)
GAPDH	Fwd: CGCCTGGAGAAACCTGCCAAGTATG	808–832	–	234	98.3%
NM_001034034.1	Rev: CACCACCCTGTTGCTGTAGCCAA	1,041–1,019	822/823		($R^2 = 0.997$)
RPS18	Fwd: ACCAACATCGATGGGCGGCG	96–115	–	150	101.1%
NM_001033614.1	Rev: CACACGTTCCACCTCATCCTCGG	245–223	233/234		($R^2 = 1.000$)
SCD	Fwd: CTACAAAGCTCGGCTGCCTCTGC	525–547	–	202	100.5%
NM_173959.4	Rev: TTTGACAGCTGGGTGTTTGCGC	726–705	–		($R^2 = 0.990$)
SF3A1	Fwd: GCCCCCAACTCCAGACCAGGT	1,248–1,268	–	249	105.3%
NM_001081510.1	Rev: TCGATATCCAGACCTGGCGCGT	1,496–1,475	1,483/1,484		($R^2 = 0.990$)
SREBP1c	Fwd: TGGGCACCGAGGCCAAGTTGAAT	1,098–1,120	1,114/1,115	170	105.1%
NM_001113302	Rev: TCCACTGCCACAAGCCGACA	1,267–1,248	–		($R^2 = 0.996$)

ACC acetyl-CoA carboxylase α, *ACTB* β-actin, *B2M* β2-microglobulin, *Δ5D* Δ5 desaturase, *Δ6D* Δ6 desaturase, *EEF1A2* eukaryotic translation elongation factor 1α2, *FAS* fatty acid synthase, *GAPDH* glyceraldehyde-3-phosphate dehydrogenase, *RPS18* ribosomal protein S18, *SCD* stearoyl-CoA desaturase, *SF3A1* splicing factor 3a, subunit -1, *SREBP1c* sterol regulatory element binding protein 1c

[a] Determined by plotting the c_T-values of 10.0, 1.0, 0.5, 0.1 and 0.01 ng cDNA versus the logarithm of the corresponding cDNA amount

94 °C for 3 min, a thermocycling program of 10 s at 94 °C, 30 s at 60 °C and 45 s at 70 °C was applied (45 cycles); total fluorescence data and dynamic well factors were continuously collected to generate background subtracted amplification curves (iQ5 Software, Version 2.1.97.1001; Bio-Rad Laboratories GmbH, Munich, Germany). PCR analysis of cDNA samples was performed in triplicate; no-transcription and no-template samples were used as controls.

The specificity of the PCR amplification was confirmed by melt curve analysis (temperature range 60–94 °C), agarose gel electrophoresis of PCR products on 2% SYBR® Safe stained precast agarose gels (Cat. No. G5218-02) (Invitrogen GmbH, Darmstadt, Germany) as well as sequencing of PCR products. Accuracy, linearity and efficiency of the PCR reaction was checked by plotting the c_T-values of 10.0, 1.0, 0.5, 0.1 and 0.01 ng cDNA versus the logarithm of the corresponding cDNA amount. Accuracy was defined as the R^2 value of the standard curve, efficiency E was calculated as $E\,[\%] = (10^{-1/\text{slope of standard curve}} - 1) \times 100$.

Gene Expression Quantification and Statistical Evaluation

Relative gene expression of ACC [EC 6.4.1.2], FAS [EC 2.3.1.85], SCD [EC 1.14.19.1], Δ5D [EC 1.14.19.-], Δ6D [EC 1.14.19.3] and SREBP1c was calculated with the comparative, efficiency-corrected $\Delta\Delta C_T$ method. Based on preliminary investigations on tissue-specific reference genes, SF3A1, EEF1A2, RPS18 and B2M were selected for gene expression normalization of longissimus muscle and ACTB, GAPDH, RPS18 and B2M for gene expression normalization of subcutaneous adipose tissue. Differences in gene expression profiles between control and intervention group were tested for statistical significance using REST© algorithm (REST© 2009; Relative Expression Software Tool, Version V2.0.13) [24]; p values are given with the results.

Protein Expression and Enzyme Activity Analysis

Protein expression of ACC, SCD and Δ6D was determined by Western Blot analysis of cytosolic/microsomal tissue extracts as previously described [19].

Enzyme activity of SCD was assessed as time-dependent, enzyme-specific substrate-conversion rate (nmol substrate/mg microsomal protein/h) of ^{14}C-labeled palmitoyl-coenzyme A [23].

Data were analyzed for statistical significance by the least-squares method using the general linear model procedures of SAS® (2009) with the fixed factor feeding. $p \leq 0.05$ was considered as statistically significant.

Fatty Acid Analysis

Fatty acid analysis was performed by GC–FID analysis of fatty acid methyl esters (FAME), prepared by the isolation of fatty acids from homogenized tissue samples by chloroform/methanol extraction [25] and methylation as previously described [19, 26]. FAME were separated on a CP-Sil 88 fused-silica capillary column (100 m, 0.25 mm, 0.20 µm; Varian-Chrompack GmbH, Darmstadt, Germany) with a Perkin Elmer Autosystem XL gas chromatograph (Perkin Elmer, Watham, USA), applying a temperature gradient program [45 °C (4 min); to 150 °C (+13 °C/min); 150 °C (47 min); to 215 °C (+48 °C/min); 215 °C (35 min)] at a carrier gas flow rate of 1 mL hydrogen/min, and detected by flame ionization at 280 °C.

Analysis was performed in duplicate. FAME reference mixture (Cat. No. 18919-1; Sigma–Aldrich, Steinheim, Germany) plus *c*11-18:1, *c*9,*t*11-18:2, 18:4n-3, 22:5n-3 (Matreya, Biotrend, Cologne, Germany), *t*11-18:1 and 22:4n-6 FAME (Sigma-Aldrich, Deisenhofen, Germany) was used for calibration.

An unpaired, homoscedastic t test was applied to check fatty acid concentrations of both feeding groups for statistical significance, regarding p values of $p \leq 0.05$ as significant.

Results

Changes in fatty acid composition (Table 2) upon n-3 fatty acid supplementation of German Holstein bulls via a grass-silage based intervention diet versus a maize-silage based control diet were analyzed and related to corresponding shifts in lipogenesis-related gene expression (Fig. 1a, b, Table 3), protein expression (Table 3) and enzyme activity patterns (Table 3) of bovine muscle and adipose tissue.

Changes in Fatty Acid Composition

Table 2 summarizes the fatty acid composition of longissimus muscle and subcutaneous adipose tissue of control and intervention group. Significantly higher absolute concentrations (Table 2) as well as relative amounts (see Supplementary Table 1) of n-3 fatty acids were obtained in muscle (57.0 mg/100 g (IG) versus 27.5 mg/100 g (CG)) and adipose (472.9 mg/100 g (IG) versus 312.2 mg/100 g (CG)) tissue of intervention group animals. Furthermore, diminished amounts of n-6 fatty acids, saturated fatty acids and monounsaturated fatty acids as well as by factors of 2.5 (longissimus muscle) or 2.2 (adipose tissue) reduced n-6/n-3 fatty acid ratios were obtained upon n-3 fatty acid intervention (Table 2).

Table 2 Selected fatty acids in longissimus muscle and subcutaneous adipose tissue samples of control and intervention group

	Fatty acids[c] (mg/100 g tissue)			
	Longissimus muscle		Subcutaneous adipose tissue	
	Control group	Intervention group	Control group	Intervention group
12:0	1.5 ± 0.7[a]	1.1 ± 0.3[b]	82.0 ± 27.2	87.2 ± 34.5
14:0	64.9 ± 30.5[a]	43.8 ± 12.8[b]	2736.8 ± 521.0	2352.8 ± 550.4
14:1	16.9 ± 9.7	11.1 ± 3.9	677.5 ± 554.02	505.8 ± 421.0
16:0	635.7 ± 263.6[a]	460.2 ± 112.1[b]	18549.6 ± 1394.5	17215.1 ± 3408.1
16:1	91.9 ± 40.5[a]	59.4 ± 15.8[b]	4678.6 ± 862.8	4322.1 ± 988.7
18:0	342.4 ± 125.9	284.4 ± 64.4	7863.4 ± 928.1	7503.8 ± 2432.1
18:1n-9	907.8 ± 393.2[a]	629.6 ± 148.0[b]	25283.0 ± 2258.6[a]	22443.3 ± 3883.6[b]
*t*11-18:1	13.8 ± 5.2	14.2 ± 4.0	547.8 ± 83.3	593.8 ± 163 3
18:2n-6	113.6 ± 14.1[a]	95.5 ± 12.2[b]	1172.8 ± 126.1[a]	873.4 ± 226.8[b]
*c*9,*t*11-18:2	6.5 ± 3.4	5.5 ± 1.2	342.0 ± 79.2	344.9 ± 109.2
18:3n-3	13.0 ± 3.5[a]	33.6 ± 5.0[b]	277.1 ± 76.2[a]	428.7 ± 133.8[b]
18:3n-6	0.6 ± 0.1[a]	0.8 ± 0.1[b]	11.6 ± 5.8	12.8 ± 6.5
18:4n-3	1.3 ± 0.5[a]	0.9 ± 0.3[b]	25.5 ± 28.5	16.3 ± 15.6
20:0	2.4 ± 0.7	2.4 ± 0.6	63.9 ± 15.5	69.6 ± 26.5
20:4n-6	30.0 ± 3.8[a]	26.6 ± 3.8[b]	37.8 ± 9.4[a]	29.0 ± 11.8[b]
20:5n-3	3.8 ± 0.6[a]	8.9 ± 1.6[b]	3.1 ± 6.4[a]	10.3 ± 5.2[b]
22:5n-3	8.4 ± 0.7[a]	12.1 ± 1.5[b]	29.3 ± 15.4	31.1 ± 14.0
22:6n-3	1.0 ± 0.1[a]	1.4 ± 0.2[b]	2.7 ± 7.5	2.9 ± 10.5
Σ SFA	1088.1 ± 428.2[a]	826.7 ± 188.5[b]	30842.2 ± 2285.1	28797.2 ± 6346.4
Σ MUFA	1103.3 ± 474.1[a]	769.8 ± 176.5[b]	33474.4 ± 2041.1[a]	29874.8 ± 5179.1[b]
Σ PUFA	188.7 ± 22.0	193.0 ± 22.5	2154.3 ± 243.1	1965.9 ± 416.1
Σ n-3 FA	27.5 ± 4.1[a]	57.0 ± 6.4[b]	312.2 ± 95.2[a]	472.9 ± 148.3[b]
Σ n-6 FA	158.5 ± 18.3[a]	132.1 ± 15.4[b]	1309.2 ± 134.0[a]	963.3 ± 228.9[b]
n-6/n-3 FA ratio	5.8 ± 0.7[a]	2.3 ± 0.1[b]	4.6 ± 1.5[a]	2.1 ± 0.6[b]
Σ n-3 LCPUFA	13.2 ± 1.3[a]	22.4 ± 3.0[b]	35.2 ± 22.2	44.3 ± 24.5
Σ n-6 LCPUFA	34.8 ± 4.3[a]	29.3 ± 3.8[b]	61.6 ± 17.7[a]	40.5 ± 17.8[b]
Σ trFA	30.7 ± 14.2	25.9 ± 6.9	1290.0 ± 228.2	1175.1 ± 300.4
Σ TFA	2397.9 ± 932.0[a]	1805.7 ± 369.4[b]	66583.4 ± 3569.1	60733.1 ± 11065.2

FA fatty acids, *SFA* saturated fatty acids, *MUFA* monounsaturated fatty acids, *PUFA* polyunsaturated fatty acids, *LCPUFA* long-chain polyunsaturated fatty acids, *trFA* trans-fatty acids, *TFA* total fatty acids

Σ SFA, 10:0 + 11:0 + 12:0 + 13:0 + 14:0 + 15:0 + 16:0 + 17:0 + 18:0 + 20:0 + 21:0 + 22:0 + 23:0 + 24:0; Σ MUFA, 14:1 + 15:1 + 16:1 + 17:1 + 18:1n-9 + *c*11-18:1 + *t*9-18:1 + *t*10-18:1 + *t*11-18:1 + 22:1 + 24:1; Σ PUFA, Σ n-3 FA + Σ n-6 FA; Σ n-3 FA, 18:3n-3 + 18:4n-3 + 20:3n-3 + 20:5n-3 + 22:5n-3 + 22:6n-3; Σ n-6 FA, 18:2n-6 + 18:3n-6 + 20:2n-6 + 20:3n-6 + 20:4n-6 + 22:2n-6 + 22:4n-6; Σ n-3 LCPUFA, 20:3n-3 + 20:5n-3 + 22:5n-3 + 22:6n-3; Σ n-6 LCPUFA, 20:2n-6 + 20:3n-6 + 20:4n-6 + 22:2n-6 + 22:4n-6

[a,b] Significant difference ($p \leq 0.05$) between control and intervention group

[c] Mean ± standard deviation calculated for control ($n = 14$) and intervention ($n = 13$) group

Functional Genomic Effect of n-3 Intervention on Lipogenesis in Longissimus Muscle

Expression profiles of lipid metabolism associated genes (SREBP1c, ACC, FAS, Δ5D, Δ6D, SCD) in the longissimus muscle of control and intervention groups as assessed in relation to tissue-specific reference genes (SF3A1, EEF1A2, RPS18, B2M) are given in Fig. 1a. Significantly higher c_T-values ($p < 0.05$) and by factors of 0.59–1.02 (ACC) and 0.63–1.05 (SCD) diminished expression levels of ACC and SCD gene were obtained in longissimus muscle of the intervention group compared to the control group animals. Expression levels of FAS, SREBP1c, Δ5D and Δ6D gene did not significantly differ between both feeding groups (Fig. 1a), although FAS expression tended to be lower ($p = 0.10$) in intervention group tissue samples.

Relating diet-induced changes of gene expression with corresponding gene products, strongest association was obtained for SCD, considering decreased SCD gene

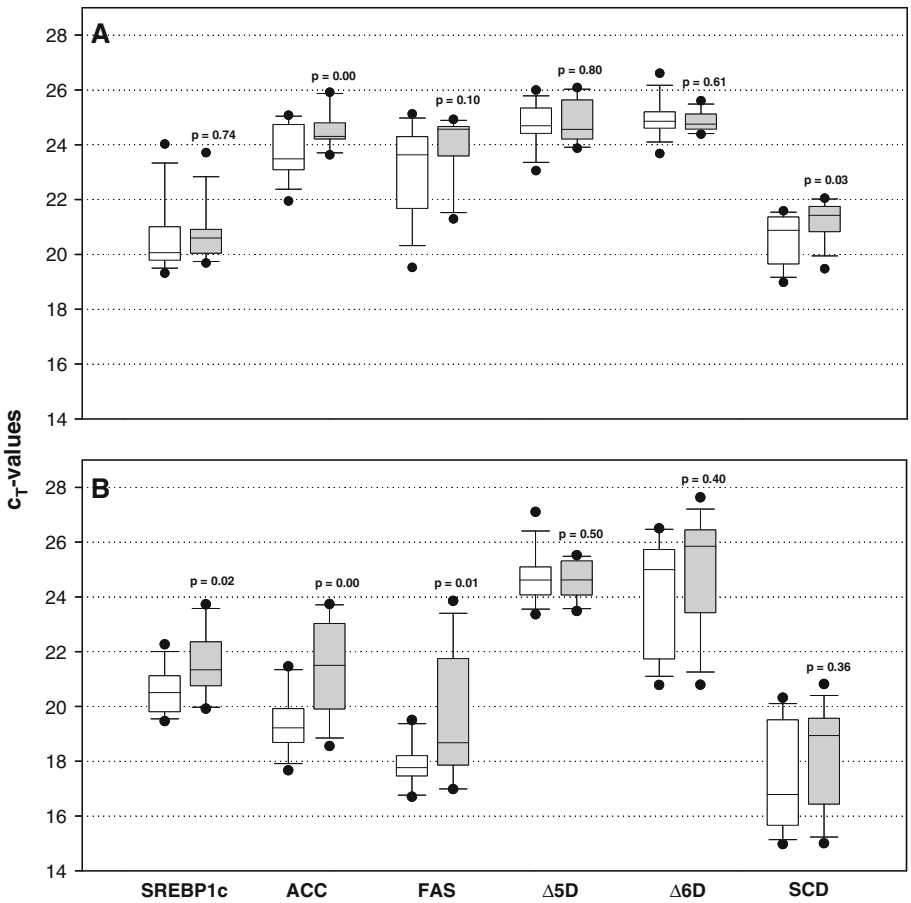

Fig. 1 Boxplots of c_T-values obtained by qRT-PCR gene expression analysis of longissimus muscle (**a**) and subcutaneous adipose tissue (**b**) of control (*squares*) ($n = 14$) and intervention (*filled squares*) ($n = 13$) group *SREBP1c* sterol regulatory element binding protein 1c, *ACC* acetyl-CoA carboxylase α, *FAS* fatty acid synthase, *Δ5D* Δ5 desaturase, *Δ6D* Δ6 desaturase, *SCD* stearoyl-CoA desaturase, *SF3A1* splicing factor 3a, subunit 1, *EEF1A2* eukaryotic translation elongation factor 1α2, *RPS18* ribosomal protein S18, *B2M* β2-microglobulin, *ACTB* β-actin, *GAPDH* glyceraldehyde 3-phosphate dehydrogenase *p* values represent significance levels of differences between control and intervention group, considering $p \leq 0.05$ as statistically significant; REST© hypothesis test; normalization via SF3A1, EEF1A2, RPS18 and B2M (longissimus muscle) or ACTB, GAPDH, RPS18 and B2M (subcutaneous adipose tissue)

expression ($p = 0.03$) (Fig. 1a), SCD protein expression ($p = 0.03$) (Table 3), SCD enzyme activity ($p = 0.03$) (Table 3) as well as amount of the SCD reaction products 14:1 ($p = 0.06$), 16:1 ($p = 0.01$) and 18:1n-9 ($p = 0.02$) (Tables 2 and 3) in intervention group than control group tissue samples. Similar interrelations were obtained for ACC and FAS, regarding their decreased levels of gene expression ($p = 0.00$, ACC; $p = 0.10$, FAS) (Fig. 1a) as well as minor amounts of their fatty acid reaction products 12:0 ($p = 0.03$), 14:0 ($p = 0.03$) and 16:0 ($p = 0.04$) (Tables 2 and 3) upon n-3 fatty acid intervention, although ACC protein expression ($p = 0.71$) (Table 3) was not found to be affected. Less consistent results were obtained for Δ5D and Δ6D: gene expression levels did not significantly differ between control and intervention group ($p = 0.80$, Δ5D; $p = 0.61$, Δ6D) (Fig. 1a), Δ6D protein expression was significantly lower ($p = 0.03$) (Table 2) in intervention group tissue samples, and the amounts of Δ5D and Δ6D reaction products were found to be significantly diminished in the intervention group in case of 20:4n-6 ($p = 0.03$) and 18:4n-3 ($p = 0.02$) and elevated in case of 20:5n-3 ($p = 0.00$) and 18:3n-6 ($p = 0.00$) (Tables 2 and 3).

Functional Genomic Effect of n-3 Intervention on Lipogenesis in Subcutaneous Adipose Tissue

Expression profiles of lipid metabolism associated genes (SREBP1c, ACC, FAS, Δ5D, Δ6D, SCD) as assessed in relation to tissue-specific reference genes (ACTB, GAPDH, RPS18, B2M) in subcutaneous adipose tissue samples are given in Fig. 1b. Comparing gene expression in adipose tissue of control and intervention group, significantly higher c_T-values ($p < 0.05$) and thus by factors of 0.36–1.01 (ACC), 0.35–1.13 (FAS) and 0.58–1.12 (SREBP1c) decreased expression levels of ACC, FAS and SREBP1c gene were obtained for intervention group tissue samples. Gene expression of Δ5D, Δ6D and SCD genes did not differ between the control and intervention group. Overall higher levels of ACC, FAS and SCD gene expression were detected in adipose (Fig. 1b) than in muscle tissue (Fig. 1a).

Relating genes and gene products, less consistent correlation was observed in adipose tissue than in muscle. Although ACC and FAS gene expression ($p = 0.00$, ACC; $p = 0.01$, FAS) (Fig. 1b) was significantly reduced upon n-3 fatty acid intervention, ACC protein expression

Table 3 Effect of n-3 fatty acid intervention on lipogenesis-related transcriptome, proteome and metabolome of longissimus muscle and subcutaneous adipose tissue

	Effects of dietary n-3 fatty acid intervention				
	Gene expression[a]	Protein expression[b]	Enzyme activity[c]	Fatty acid profile[a]	
Longissimus muscle					
ACC	↓↓↓ ($p = 0.00$)	↓↑ ($p = 0.71$)	n.a.	12:0	↓↓↓ ($p = 0.03$)
				14:0	↓↓↓ ($p = 0.03$)
				16:0	↓↓↓ ($p = 0.04$)
				Σ TFA	↓↓↓ ($p = 0.04$)
FAS	↓ ($p = 0.10$)	n.a.	n.a.	12:0	↓↓↓ ($p = 0.03$)
				14:0	↓↓↓ ($p = 0.03$)
				16:0	↓↓↓ ($p = 0.04$)
				Σ TFA	↓↓↓ ($p = 0.04$)
Δ5D	↓↑ ($p = 0.80$)	n.a.	n.a.	20:4n-6	↓↓↓ ($p = 0.03$)
				20:5n-3	↑↑↑ ($p = 0.00$)
Δ6D	↓↑ ($p = 0.61$)	↓↓↓ ($p = 0.03$)	n.a.	18:3n-6	↑↑↑ ($p = 0.00$)
				18:4n-3	↓↓↓ ($p = 0.02$)
SCD	↓↓↓ ($p = 0.03$)	↓↓↓ ($p = 0.03$)	↓↓↓ ($p = 0.03$)	14:1	↓ ($p = 0.06$)
				16:1	↓↓↓ ($p = 0.01$)
				18:1n-9	↓↓↓ ($p = 0.02$)
				*c*9,*t*11-18:2	↓↑ ($p = 0.34$)
Subcutaneous adipose tissue					
ACC	↓↓↓ ($p = 0.00$)	↓↑ ($p = 0.71$)	n.a.	12:0	↓↑ ($p = 0.67$)
				14:0	↓ ($p = 0.07$)
				16:0	↓↑ ($p = 0.19$)
				Σ TFA	↓ ($p = 0.07$)
FAS	↓↓↓ ($p = 0.01$)	n.a.	n.a.	12:0	↓↑ ($p = 0.67$)
				14:0	↓ ($p = 0.07$)
				16:0	↓↑ ($p = 0.19$)
				Σ TFA	↓ ($p = 0.07$)
Δ5D	↓↑ ($p = 0.50$)	n.a.	n.a.	20:4n-6	↓↓↓ ($p = 0.04$)
				20:5n-3	↑↑↑ ($p = 0.00$)
Δ6D	↓↑ ($p = 0.40$)	↓↑ ($p = 0.50$)	n.a.	18:3n-6	↓↑ ($p = 0.61$)
				18:4n-3	↓↑ ($p = 0.32$)
SCD	↓↑ ($p = 0.36$)	↓↓↓ ($p = 0.02$)	↓↓↓ ($p = 0.03$)	14:1	↓↑ ($p = 0.38$)
				16:1	↓↑ ($p = 0.33$)
				18:1n-9	↓↓↓ ($p = 0.03$)
				*c*9,*t*11-18:2	↓↑ ($p = 0.94$)

↓, in tendency reduced ($p \leq 0.10$); ↓↓↓, significantly reduced ($p \leq 0.05$); ↓↑, not affected; ↑, in tendency increased ($p \leq 0.10$); ↑↑↑, significantly increased ($p \leq 0.05$);

n.a. not assessed, *ACC* acetyl-CoA carboxylase α, *FAS* fatty acid synthase, *Δ5D* Δ5 desaturase, *Δ6D* Δ6 desaturase, *SCD* stearoyl-CoA desaturase, *TFA* total fatty acids

[a] $n = 27$

[b] $n = 14$, see [18]

[c] $n = 29$, see [22]

($p = 0.71$) (Table 3) as well as the amount of fatty acid reaction products 12:0 ($p = 0.67$) and 16:0 ($p = 0.19$) was not affected (Tables 2 and 3). SCD protein expression ($p = 0.02$) (Table 3), SCD enzyme activity ($p = 0.03$) (Table 3) and the amount of SCD product 18:1n-9 ($p = 0.03$) (Tables 2, 3) were significantly lower in intervention group than control group tissue samples, although SCD gene expression ($p = 0.36$) (Fig. 1b) as well as amount of SCD products 14:1 ($p = 0.38$), 16:1 ($p = 0.33$) and *c*9,*t*11-18:2 ($p = 0.94$) (Tables 2, 3) did not

substantially differ. Most consistent relationship was found for Δ6D which was neither affected in regard to gene expression ($p = 0.40$) (Fig. 1b), protein expression ($p = 0.50$) (Table 3) nor the amount of reaction products 18:3n-6 ($p = 0.61$) and 18:4n-3 ($p = 0.32$) (Tables 2, 3). Δ5D gene expression was found to be similar in both groups (Fig. 1b), but a significantly lower amount of Δ5D reaction product 20:4n-6 ($p = 0.04$) and a higher amount of 20:5n-3 ($p = 0.00$) was found in adipose tissue of the intervention group animals (Tables 2, 3).

Discussion

Strategies for improving the nutritional profile upon shifting the fatty acid composition of meat towards more beneficial ratios of n-6 to n-3 fatty acids have successfully exploited means of dietary intervention of farm animals with exogenous n-3 fatty acid sources [6, 10, 11, 27]. In this context, the present investigations revealed that n-3 fatty acid contents as well as n-6/n-3 fatty acid ratios in longissimus muscle and subcutaneous adipose tissue of German Holstein bulls were beneficially affected by a grass-silage based intervention diet versus a maize-silage based control diet, significantly reducing n-6/n-3 fatty acid ratios by mean factors of 2.5 in muscle and 2.2 in adipose tissue.

Considering an extensive biohydrogenation, isomerization and degradation of alimentary fatty acids by ruminal microbiota [7, 10], major mechanism underlying the obtained changes in fatty acid profiles seems to be an affected fatty acid biosynthesis in bovine tissues via shifted expression of lipogenic genes and gene products.

The present study applied a functional genomic approach to interrelate changes of fatty acid profiles with corresponding shifts in expression of lipogenic genes and gene products. Distinct functional genomic responses of muscle and adipose tissue to n-3 fatty acid intervention were obtained, indicating tissue-specific regulation networks between an initial induction of lipogenesis-related transcription factor SREBP1c, a subsequent expression of lipogenic ACC, FAS, Δ5D, Δ6D and SCD gene/protein, a regulation of lipogenic enzyme activities and an induction of feedback-mechanisms induced by fatty acid reaction products.

Lower total expression levels of the key-lipogenic genes ACC, FAS and SCD were found in longissimus muscle than in subcutaneous adipose tissue, probably due to the aspect that lipogenesis-related pathways play less fundamental metabolic roles in muscle than in adipose tissue, the primary site of energy storage via lipogenesis and lipid accumulation in ruminants [28]. In agreement with the present findings, higher expression in adipose tissue than in muscle was confirmed for the SCD gene [29] as well as the SCD protein [30] in cattle, and for SCD, ACC and FAS protein [31, 32] and enzyme activity [31] in pigs.

A comparatively more consistent relationship between the gene and associated gene products was obtained for muscle than for adipose tissue, supposedly due to the fact that the fatty acid profile of adipose tissue reflects rather long-term, cumulative anabolic developments, whereas more rapid lipid turnover [33] and thus a more real-time relation between gene, protein and metabolite can be found in muscle. Furthermore, the snap-shot approach of the present study addressed functional genomic relationships discontinuously, not dynamically during tissue development and maturation. Dynamic investigations performed in primary cell culture or animal experiments, for example, suggested that SCD gene expression and activity undergo marked dynamic fluctuations, considering peak among intermediate SCD gene expression levels at developmental stages of 24, 144 and 288 h of in vitro bovine preadipocyte differentiation [34] or of 7 and 20–28 months of in vivo bovine tissue development [35, 36]. In agreement with the present findings, more consistent effect of dietary manipulation via distinct feeding regimes was confirmed for SCD protein and activity levels in muscle than in adipose tissue [20, 31], an aspect which may also be explained by the occurrence of differentially regulated, tissue-specific isoenzyme forms [19, 30] as well as differences in cellular carbon precursor uptake [37].

Comparing distinct interrelations between genes and gene products, the most consistent correlation in both tissues was obtained for SCD. Reduced gene expression levels of transcription factor SREBP1c in adipose tissue, decreased SCD gene expression in muscle as well as significantly lower SCD protein expression, SCD enzyme activity and amount of major monounsaturated SCD fatty acid product 18:1n-9 in both tissues were detected upon n-3 fatty acid intervention

The results of the present study correspond to literature findings that SCD expression and activity in tissues positively relate to the levels of the SCD reaction products 14:1, 16:1, 18:1n-9 and *c*9,*t*11-18:2 [18, 21, 29, 30, 38–40]. For example, breed-specifically high levels of SCD expression were described as cause for increased intramuscular fat and monounsaturated fatty acid amounts in Japanese Black cattle muscle [29]. Effects of unsaturated fatty acid intervention on the SCD axis were discussed to relate to tissue- [41], gender- [41], breed- [30, 36, 42] and developmental stage- [35, 43] dependent decreases in SCD gene [36, 44–46] or protein expression [19], but also reduced expression of SCD transcription factor SREBP1c [18, 21, 38]. Reduced SCD gene expression was found to negatively correlate with the n-6/n-3 fatty acid ratio in bovine muscle tissue [18, 21], but no correlation between

SCD protein expression and its metabolites was observed in ovine muscle tissue [22]. Whereas no significant difference between intramuscular fat content of control (2.9 ± 1.3%) and intervention (2.2 ± 1.0%) group animals was found in the present investigations, some studies described SCD expression level as an indicator of intramuscular fat development [29, 32, 35, 39] and fat quality [47] in ruminants and non-ruminants, considering SCD as key-regulator of muscle metabolism by facilitating lipid biosynthesis and suppressing fatty acid degradation [48, 49]. The positive correlation between the amounts of SCD product 18:1n-9 and total fatty acids ($r = 0.984$) or saturated fatty acids ($r = 0.943$) in longissimus muscle obtained in this study strongly supports the lipogenic role of SCD in muscle metabolism.

Concerning enzymes involved in de novo fatty acid synthesis, the present study mainly suggested functional genomic correlations between gene and gene products in muscle tissue, relating decreased levels of ACC and FAS gene expression upon n-3 fatty acid intervention with significantly reduced amounts of their metabolites 12:0, 14:0 and 16:0. These results are in agreement with literature findings that supplementation with unsaturated fatty acids causes significantly down-regulated ACC and FAS gene expression in bovine muscle tissue [46] or reduced ACC and FAS enzyme activities and metabolite concentrations in bovine cell culture models [50].

Although intramuscular fat contents of both dietary groups did not differ in the present study, significantly minor total fatty acid amounts (1805.7 mg/100 g (IG) versus 2397.9 mg/100 g (CG)) in muscle tissue of intervention group animals correspond to postulations that FAS gene expression [35], FAS activity [51], ACC protein expression [37] or ACC activity [52] positively correlate with intramuscular fat deposition.

For enzymes involved in fatty acid polyunsaturation, inconsistent functional genomic effects were observed in the present study. Unaffected levels of Δ5D gene expression, but significantly higher amounts of Δ5D product 20:5n-3 and lower amounts of 20:4n-6 in muscle and adipose tissue were detected upon n-3 fatty acid intervention. Expression of Δ6D gene and its gene products was similar in adipose tissue samples of control and intervention group, whereas diminished Δ6D protein expression, increased amounts of Δ6D product 18:3n-6 and minor amounts of 18:4n-3 were obtained for muscle of intervention group animals.

Literature findings that Δ5D/Δ6D expression level positively correlates with tissue concentrations of n-6 unsaturated fatty acids [20] were only confirmed for Δ6D protein expression and n-6 fatty acid content in muscle. Anyhow, decreased levels of Δ5D product 20:4n-6 as well as Δ6D product 18:4n-3 in tissues of intervention group animals indicate that n-3 fatty acid supplementation indeed induced shifts in Δ5D/Δ6D expression and activity which probably occurred during tissue developmental stages preceding the chosen biological endpoints and finishing state.

Altogether, this study related shifts in fatty acid profiles upon n-3 fatty acid supplementation of farm animals with a broad spectrum of underlying functional genomic effects and thus expanded findings of previous cause-and-effect-studies. The aspect that an absolute functional genomic correlation between expression of genes and gene products was not obtained necessitates further investigations to address developmental stage dependencies [35], transcriptional, posttranscriptional, translational and posttranslational control mechanisms [17] as well as overlapping or conflicting effects of simultaneously proceeding, tissue-specific processes of substrate uptake, lipogenesis, lipolysis and lipid release [53].

The present study demonstrated that significantly higher amounts of n-3 fatty acids and by factors of 2.2–2.5 decreased n-6/n-3 fatty acid ratios were obtained in longissimus muscle and subcutaneous adipose tissue of German Holstein bulls upon n-3 fatty acid intervention by a grass-silage versus a maize-silage based diet.

Via a functional genomic approach, these beneficial changes in fatty acid profiles were related to reduced SREBP1c, ACC, FAS and SCD gene expression, Δ6D and SCD protein expression as well as SCD enzyme activity in longissimus muscle tissue, as well as to significantly reduced ACC and FAS gene expression, SCD protein expression and SCD enzyme activity in subcutaneous adipose tissue, although lower degrees of correlation between gene and corresponding gene products were observed for adipose tissue.

The study characterized a broad spectrum of functional genomic effects induced by dietary fatty acid manipulation, thus expanding findings of previous cause-and-effect-studies in regard to fatty acid profile tailoring of animal tissues.

Acknowledgments The study was conducted and financially supported within the framework of EU Project ProSafeBeef (Project No. FOOD-CT-2006-36241). The authors kindly thank B. Jentz and M. Dahm for their excellent technical assistance.

References

1. Givens DI, Kliem KE, Gibbs RA (2006) The role of meat as a source of n-3 polyunsaturated fatty acids in the human diet. Meat Sci 74:209–218
2. Carpentier YA, Portois L, Malaisse WY (2006) n-3 Fatty acids and the metabolic syndrome. Am J Clin Nutr 83:1499S–1504S
3. van Dijk SJ, Feskens EJM, Bos MB, Hoelen DWM, Heijligenberg R, Bromhaar MG, de Groot LCPGM, de Vries

JHM, Müller M, Afman LA (2009) A saturated fatty acid-rich diet induces an obesity-linked proinflammatory gene expression profile in adipose tissue of subjects at risk of metabolic syndrome. Am J Clin Nutr 90:1656–1664
4. Gebauer SK, Psota TL, Harris WS, Kris-Etherton PM (2006) n-3 Fatty acid dietary recommendations and food sources to achieve essentiality and cardiovascular benefits. Am J Clin Nutr 83:1526S–1535S
5. Howe P, Meyer B, Record S, Baghurst K (2006) Dietary intake of long-chain n-3 polyunsaturated fatty acids: contribution of meat sources. Nutr 22:47–53
6. Woods VB, Fearon AM (2009) Dietary sources of unsaturated fatty acids for animals and their transfer into meat, milk and eggs: a review. Livestock Sci 126:1–20
7. Scollan N, Hocquette J-F, Nuernberg K, Dannenberger D, Richardson I, Moloney A (2006) Innovations in beef production systems that enhance the nutritional and health value of beef lipids and their relationship with meat quality. Meat Sci 74:17–33
8. Wood JD, Richardson RI, Nute GR, Fisher AV, Campo MM, Kasapidou E, Sheard PR, Enser M (2003) Effects of fatty acids on meat quality: a review. Meat Sci 66:21–32
9. Wood JD, Enser M, Fisher AV, Nute GR, Sheard PR, Richardson RI, Hughes SI, Whittington FM (2008) Fat deposition, fatty acid composition and meat quality: A review. Meat Sci 78:343–358
10. Raes K, De Smet S, Demeyer D (2004) Effect of dietary fatty acids on incorporation of long chain polyunsaturated fatty acids and conjugated linoleic acid in lamb, beef and pork meat: a review. Anim Feed Sci Technol 113:199–221
11. Nuernberg K, Fischer A, Nuernberg G, Ender K, Dannenberger D (2008) Meat quality and fatty acid composition of lipids in muscle and fatty tissue of Skudde lambs fed grass versus concentrate. Small Ruminant Res 74:279–283
12. Lee MRF, Evans PR, Nute GR, Richardson RI, Scollan ND (2009) A comparison between red clover silage and grass silage feeding on fatty acid composition, meat stability and sensory quality of the M. longissimus muscle of dairy cull cows. Meat Sci 81:738–744
13. Machecha L, Dannenberger D, Nuernberg K, Nuernberg G, Hagemann E, Martin J (2010) Relationship between lipid peroxidation and antioxidant status in the muscle of German Holstein bulls fed n-3 and n-6 PUFA-enriched diets. J Agric Food Chem 58:8407–8413
14. Zhang S, Knight TJ, Reecy JM, Beitz DC (2008) DNA polymorphisms in bovine fatty acid synthase are associated with beef fatty acid composition. Anim Genet 39:62–70
15. Zhang S, Knight TJ, Reecy JM, Wheeler TL, Shackelford SD, Cundiff LV, Beitz DC (2010) Associations of polymorphisms in the promoter I of bovine acetyl-CoA carboxylase-alpha gene with beef fatty acid composition. Anim Genet 41:417–420
16. Orrù L, Cifuni GF, Piasentier E, Corazzin M, Bovolenta S, Moioli B (2011) Association analyses of single nucleotide polymorphisms in the LEP and SCD1 genes on the fatty acid profile of muscle fat in Simmental bulls. Meat Sci 87:344–348
17. Bernard L, Leroux C, Chilliard Y (2008) Expression and nutritional regulation of lipogenic genes in the ruminant lactating mammary gland. Adv Exp Med Biol 606:67–108
18. Dervishi E, Serrano C, Joy M, Serrano M, Rodellar C, Calvo JH (2010) Effect of the feeding system on the fatty acid composition, expression of the Δ9-desaturase, peroxisome proliferator-activated receptor alpha, gamma, and sterol regulatory element binding protein 1 genes in the semitendinosus muscle of light lambs of the Rasa Aragonesa breed. BMC Vet Res 6:1–11
19. Herdmann A, Nuernberg K, Martin J, Nuernberg G, Doran O (2010) Effect of dietary fatty acids on expression of lipogenic enzymes and fatty acid profile in tissues of bulls. Anim 4:755–762
20. Ward RE, Woodward B, Otter N, Doran O (2010) Relationship between the expression of key lipogenic enzymes, fatty acid composition, and intramuscular fat content of Limousin and Aberdeen Angus cattle. Livestock Sci 127:22–29
21. Waters SM, Kelly JP, O'Boyle P, Moloney AP, Kenny DA (2009) Effect of level and duration of dietary n-3 polyunsaturated fatty acid supplementation on the transcriptional regulation of {Delta}9-desaturase in muscle of beef cattle. J Anim Sci 87:244–252
22. Vasta V, Priolo A, Scerra M, Hallett KG, Wood JD, Doran O (2009) Δ9 desaturase protein expression and fatty acid composition of longissimus muscle in lambs fed green herbage or concentrate with or without added tannins. Meat Sci 82:357–364
23. Herdmann A, Martin J, Nuernberg G, Dannenberger D, Nuernberg K (2010) Effect of dietary n-3 and n-6 PUFA on lipid composition of different tissues of German Holstein bulls and the fate of bioactive fatty acids during processing. J Agric Food Chem 58:8314–8321
24. Pfaffl MW, Horgan GW, Dempfle L (2002) Relative expression software tool (REST©) for group-wise comparison and statistical analysis of relative expression results in real-time PCR. Nucleic Acids Res 30:1–10
25. Folch J, Lees M, Stanley GHS (1957) A simple method for the isolation and purification of total lipids from animal tissues. J Biol Chem 226:497–509
26. Dannenberger D, Nuernberg G, Scollan N, Schabbel W, Steinhart H, Ender K, Nuernberg K (2004) Effect of diet on the deposition of n-3 fatty acids conjugated linoleic- and C18:1 trans fatty acid isomers in muscle lipids of German Holstein bulls. J Agric Food Chem 52:6607–6615
27. Enser M, Richardson RI, Wood JD, Gill BP, Sheard PR (2000) Feeding linseed to increase the n-3 PUFA of pork: fatty acid composition of muscle, adipose tissue, liver and sausages. Meat Sci 55:201–212
28. Kim S, Moustaid-Moussa N (2000) Secretory, endocrine and autocrine/paracrine function of the adipocyte. J Nutr 130:3110S–3115S
29. Taniguchi M, Mannen H, Oyama K, Shimakura Y, Oka A, Watanabe H, Kojima T, Komatsu M, Harper GS, Tsuji S (2004) Differences in stearoyl-CoA desaturase mRNA levels between Japanese Black and Holstein cattle. Livestock Prod Sci 87:215–220
30. Dance LJE, Matthews KR, Doran O (2009) Effect of breed on fatty acid composition and stearoyl-CoA desaturase protein expression in the semimembranosus muscle and subcutaneous adipose tissue of cattle. Livestock Sci 125:291–297
31. Doran O, Moule SK, Teye GA, Whittington FM, Hallett KG, Wood JD (2006) A reduced protein diet induces stearoyl-CoA desaturase protein expression in pig muscle but not in subcutaneous adipose tissue: relationship with intramuscular lipid formation. Br J Nutr 95:609–617
32. Cánovas A, Estany J, Tor M, Pena RN, Doran O (2009) Acetyl-CoA carboxylase and stearoyl-CoA desaturase protein expression in subcutaneous adipose tissue is reduced in pigs selected for decreased backfat thickness at constant intramuscular fat content. J Anim Sci 87:3905–3914
33. Kokta TA, Dodsonb MV, Gertler A, Hill RA (2004) Intercellular signalling between adipose tissue and muscle tissue. Dom Anim Endocrinol 27:303–331
34. Ohsaki H, Sawa T, Sasazaki S, Kano K, Taniguchi M, Mukai F, Mannen H (2007) Stearoyl-CoA desaturase mRNA expression during bovine adipocyte differentiation in primary culture derived from Japanese Black and Holstein cattle. Comp Biochem Physiol A 148:629–634
35. Wang YH, Bower NI, Reverter A, Tan SH, De Jager N, Wang R, McWilliam SM, Café LM, Greenwood PL, Lehnert SA (2009)

Gene expression patterns during intramuscular fat development in cattle. J Anim Sci 87:119–130
36. Chung KY, Lunt DK, Kawachi H, Yano H, Smith SB (2007) Lipogenesis and stearoyl-CoA desaturase gene expression and enzyme activity in adipose tissue of short- and long-fed Angus and Wagyu steers fed corn- or hay-based diets. J Anim Sci 85:380–387
37. Guixuan Zhou G, Wang S, Wang Z, Zhu X, Shu G, Liao W, Yu K, Gao P, Xi Q, Wang X, Zhang Y, Yuan L, Jiang Q (2010) Global comparison of gene expression profiles between intramuscular and subcutaneous adipocytes of neonatal landrace pig using microarray. Meat Sci 86:440–450
38. Bartoň L, Kott T, Bureš D, Řehák D, Zahrádková R, Kottová B (2010) The polymorphisms of stearoyl-CoA desaturase (SCD1) and sterol regulatory element binding protein-1 (SREBP-1) genes and their association with the fatty acid profile of muscle and subcutaneous fat in Fleckvieh bulls. Meat Sci 85:15–20
39. Smith SB, Kawachi H, Choi CB, Choi CW, Wu G, Sawyer JE (2009) Cellular regulation of bovine intramuscular adipose tissue development and composition. J Anim Sci 87:E72–E82
40. Pavan E, Duckett SK (2007) Corn oil supplementation to steers grazing endophyte-free tall fescue. II. Effects on longissimus muscle and subcutaneous adipose fatty acid composition and stearoyl-CoA desaturase activity and expression. J Anim Sci 85:1731–1740
41. Dridi S, Taouis M, Gertler A, Decuypere E, Buyse J (2007) The regulation of stearoyl-CoA desaturase gene expression is tissue specific in chickens. J Endocrinol 192:229–236
42. Matsuhashi T, Maruyama S, Uemoto Y, Kobayashi N, Mannen H, Abe T, Sakaguchi S, Kobayashi E (2011) Effects of bovine fatty acid synthase, stearoyl-coenzyme A desaturase, sterol regulatory element-binding protein 1, and growth hormone gene polymorphisms on fatty acid composition and carcass traits in Japanese Black cattle. J Anim Sci 89:12–22
43. Serra A, Mele M, La Comba F, Conte G, Buccioni A, Secchiari P (2009) Conjugated linoleic acid (CLA) content of meat from three muscles of Massese suckling lambs slaughtered at different weights. Meat Sci 81:396–404
44. Daniel ZC, Wynn RJ, Salter AM, Buttery PJ (2004) Differing effects of forage and concentrate diets on the oleic acid and conjugated linoleic acid content of sheep tissues: the role of stearoyl-CoA desaturase. J Anim Sci 82:747–758
45. Deiuliis J, Shin J, Murphy E, Kronberg SL, Eastridge ML, Suh Y, Yoon JT, Lee K (2010) Bovine adipose triglyceride lipase is not altered and adipocyte fatty acid-binding protein is increased by dietary flaxseed. Lipids 45:963–973
46. Joseph SJ, Robbins KR, Pavan E, Pratt SL, Duckett SK, Rekaya R (2010) Effect of diet supplementation on the expression of bovine genes associated with fatty acid synthesis and metabolism. Bioinform Biol Insights 4:19–31
47. Lee S-H, Cho Y-M, Lee S-H, Kim B-S, Kim N-K, Choy Y-H, Kim K-H, Yoon D, Im S-K, Oh S-J, Park E-W (2008) Identification of marbling-related candidate genes in M. *longissimus dorsi* of high- and low marbled Hanwoo (Korean Native Cattle) steers. BMB reports 41:846–851
48. Dobrzyn A, Dobrzyn P (2006) Stearoyl-CoA desaturase—a new player in skeletal muscle metabolism regulation. J Physiol Pharmacol 57(S10):31–42
49. Sampath H, Miyazaki M, Dobrzyn A, Ntambi JM (2007) Stearoyl-CoA desaturase-1 mediates the pro-lipogenic effects of dietary saturated fat. J Biol Chem 282:2483–2493
50. Geetha CJ, Herbein JH (2000) Healthier dairy fat using transvaccenic acid. Nutr Food Sci 30:304–309
51. Bonnet M, Faulconnier Y, Leroux C, Jurie C, Cassar-Malek I, Bauchart D, Boulesteix P, Pethick D, Hocquette JF, Chilliard Y (2007) Glucose-6-phosphate dehydrogenase and leptin are related to marbling differences among Limousin and Angus or Japanese Black × Angus steers. J Anim Sci 85:2882–2894
52. Underwood KR, Tong J, Zhu MJ, Shen QW, Means WJ, Ford SP, Paisley SI, Hess BW, Du M (2007) Relationship between kinase phosphorylation, muscle fiber typing, and glycogen accumulation in longissimus muscle of beef cattle with high and low intramuscular fat. J Agric Food Chem 55:9698–9703
53. Wells T (2009) Ghrelin—defender of fat. Prog Lipid Res 48:257–274

Lipids (2011) 46:569–576
DOI 10.1007/s11745-011-3530-8

ORIGINAL ARTICLE

Branched Chain Fatty Acid Content of United States Retail Cow's Milk and Implications for Dietary Intake

R. R. Ran-Ressler · D. Sim · A. M. O'Donnell-Megaro · D. E. Bauman · D. M. Barbano · J. T. Brenna

Received: 30 September 2010 / Accepted: 14 January 2011 / Published online: 4 February 2011

Abstract Branched chain fatty acids (BCFA) have recently been shown to be a major component of the normal human newborn gastrointestinal tract and have long been known to be a component of human milk. Ruminant food products are major sources of fat in the American diet, but there are no studies of milkfat BCFA content in retail milk. We report here the profile and concentrations of BCFA in a representative sampling of retail milk in the 48 contiguous United States (US), and their estimated intake in the American diet. Conventionally produced whole fluid milk samples were obtained from 56 processing plants across the contiguous 48 states. Retail milk samples contain exclusively *iso*- and *anteiso*-BCFA with 14–18 carbons. BCFA were 2.05 ± 0.14%, w/w of milkfat fatty acids (mean ± SD), and *anteiso*-BCFA comprised more than half this total. Based on these data and USDA food availability data, the average per capita BCFA intake of Americans is estimated to be about 220 mg/d from dairy; if current dietary recommendations were followed, BCFA intake would be about 400 mg/d. Adding intake from beef consumption, these estimates rise to approximately 400 and 575 mg/d, respectively. These results indicate that BCFA intake is a substantial fraction of daily fat intake, in amounts exceeding those of many bioactive fatty acids.

Keywords Branched chain fatty acids · Retail milk · Dietary intake · Milkfat

Abbreviations

BCFA	Branched chain fatty acids
CACI-MS	Covalent adduct chemical ionization mass spectrometry
DHA	Docosahexaenoic acid
EPA	Eicosapentaenoic acid
FA	Fatty acids
FAME	Fatty acid methyl esters
FID	Flame ionization detector
GC	Gas chromatograph
MS	Mass spectrometry
NEC	Necrotizing enterocolitis
PUFA	Polyunsaturated fatty acids
SFA	Saturated fatty acids

Introduction

Milk and dairy products are major contributors to fat intake in the American diet. Cow's milkfat is characterized by high proportions of fatty acids (FA) with 16 carbons or less. Individual FA, such as conjugated linoleic acids (CLA), may have a beneficial effect on health maintenance and prevention of acute and chronic disease [1, 2]. The FA profile of milk in all species, including cow's milk, is sensitive to dietary fat intake, for instance, concentrate versus pasture versus fish oil supplementation [3–6], thus

R. R. Ran-Ressler · D. Sim · J. T. Brenna (✉)
Division of Nutritional Sciences, Cornell University, Savage Hall, Ithaca, NY 14853-6301, USA
e-mail: jtb4@cornell.edu

A. M. O'Donnell-Megaro · D. E. Bauman
Department of Animal Science, Cornell University, Morrison Hall, Ithaca, NY 14853-4801, USA

D. M. Barbano
Department of Food Science, Cornell University, Stocking Hall, Ithaca, NY 14853-7201, USA

milk composition may differ depending on production practices. O'Donnell-Megaro et al. [7] recently reported the composition of major FA retail milk in the United States (US). About 3.1% of FA were unidentified and listed as a group under "Other"; branched chain fatty acids (BCFA) are included in this group.

BCFA are primarily saturated FA (SFA) with one or more methyl branches. In human metabolism, they are best studied as components of skin lipids. Overall, several dozen specific BCFA, are found in milk and tissue of ruminants including sheep and goats, presumably synthesized by ruminal organisms that rely on them for membrane lipids [8, 9]. BCFA are conveniently categorized as mono- and di-/multi-methyl BCFA; in monomethyl BCFA, the predominant branching is at the terminal methyl (*iso*) or next to the terminal methyl (*anteiso*), as shown in Fig. 1. *iso*- and *anteiso*-BCFA are the main BCFA reported in cow's milk [3, 4, 6, 10, 11]. Terpenoid BCFA, exemplified by internal periodic poly-methyl branching such as phytanic acid (3,7,11,14 tetra-methyl hexadecanoic acid) and its alpha oxidation product pristanic acid (2,6,10,14 tetra-methyl pentadecanoic acid) are also reported in cow's milk [11, 12].

Information on human intake and metabolism of BCFA is scant, and there are no recommendations for or against dietary intake of BCFA. Ran-Ressler et al. [13] recently showed that BCFA are a major component of the late term fetal and newborn gut contents. They comprise almost one third of the FA in vernix [13], the white fatty film that covers the fetus in utero. Vernix suspended in amniotic fluid is normally swallowed by the fetus, increasingly so as parturition approaches [14], exposing the fetal gut to BCFA from an early age. Moreover, BCFA are also found in human milk [15, 16] where they reportedly comprise 1.5%, w/w. A 1981 report put the concentrations of *anteiso*-17:0 in colostrum at 0.45%, w/w, higher than the concentrations of docosahexaenoic acid (DHA; 22:6n-3; 0.32%, w/w) and arachidonic acid (20:4n-6; 0.4%, w/w) [16]. A study in rat pups shows that BCFA reduce the incidence of necrotizing enterocolitis (NEC), a devastating intestinal disease affecting premature infants (Ran-Ressler et al. unpublished data). Thus, BCFA are a major component in perinatal nutrition, and although they may have a beneficial role in human health, their presence in the US food chain has been almost completely neglected.

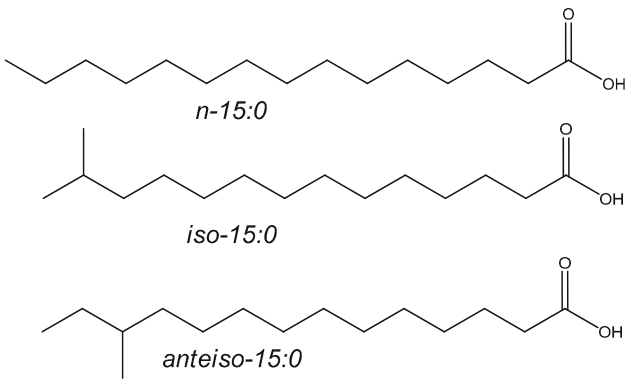

Fig. 1 Structures of *iso*- and *anteiso*-branched chain fatty acids (BCFA). *n*-(*normal*) hydrocarbon chains without branching. *iso*-BCFA have a bifurcated methyl branch (*iso*-15:0 is 13-methyl tetradecanoic acid). *anteiso*-BCFA have a methyl branch on the antepenultimate carbon. *anteiso*-15:0 is 12-methyl tetradecanoic acid

The objective of the present study is to analyze the levels and distribution of BCFA in US retail milk and to estimate the contribution of BCFA to the nutrition of Americans based on estimated intake of milk and other foods produced by ruminant animals such as cheese and beef. In a 1994 survey, dairy products contributed 7.5% of the protein, 4.2% of the total fat, and approximately 8% of the total saturated fat in the diet of adults [17]. Based on NHANES 1999–2004 [18] fluid milk, mostly whole milk, provided 7.5, and 6.4% of energy intake in children age 2–4 and 5–10, respectively. We hypothesized that BCFA are found in retail milk and dairy products in the US and thus are consumed in substantial amounts in the American diet. We report here the first data on the structure and quantitative analysis of BCFA in a representative samples of the US retail milk supply and we show that BCFA intake, per capita, is in excess than that of many bioactive FA.

Experimental Procedures

Sampling

Conventionally produced whole fluid milk samples were obtained from 56 US milk processing plants across the contiguous 48 states. All samples were whole milk obtained in December, 2008. They had been homogenized, pasteurized and packaged for transport to retail stores. Processing plants were selected based on the criteria that they represented at least 50% of the volume of milk produced in that area. Milk was shipped on ice overnight to Cornell University and immediately processed for the analysis of FA composition.

Fatty Acid Analysis

Milk fat extraction was based on the Mojonnier method (AOAC 995.19) as modified by Barbano [19]. Briefly, milkfat was obtained from 10 ml whole fluid milk by a sequence of 3 successive extractions. Ten milliliters of

95% alcohol and 25 ml ethyl ether plus milk was followed by vigorous mixing, then 25 ml petroleum ether was added and followed by vigorous mixing, and decanting of the ether layer. The second and third extractions were similar, except the volume of solvents was reduced to 5 ml of 95% alcohol and 15 ml each of ethyl and petroleum ethers, and the third extraction omitted the 95% alcohol. Ether solutions from the 3 extractions were combined, dried and resuspended in hexane. Methyl esters of the extracted fat were prepared using sodium methoxide as the methylation reagent, according to Christie [20] as modified by Chouinard [21].

Fatty acid methyl ester (FAME) analyses were performed using a Hewlett Packard 5890 Gas Chromatograph (GC) equipped with a split/splitless injector run in splitless mode at 250 °C, and with the flame ionization detector (FID) at 270 °C. A BPX-70 column (25 m × 0.22 mm × 0.25 μm, SGE, Austin, TX) was used for the analysis with H_2 as the carrier gas. The oven temperature program was initially 80 °C for one minute, increased by 30 °C per minute to 170 °C and held for 2 min, then increased by 10 °C per minute until a final temperature of 240 °C which was held for 1 min. An equal weight FAME mixture (68A; Nu-Chek Prep, Elysian, MN) was used to calculate response factors. Several pure BCFA were also used as reference standards: *iso*-14:0, *anteiso*-15:0; *iso*-16:0, *anteiso*-17:0, *iso*-18:0 and *iso*-20:0 (Larodan Fine Chemicals AB, Malmo, Sweden).

FAME identities were determined by electron impact ionization mass spectrometry (EI-MS), using a Varian Star 3400 GC coupled to a Varian Saturn 2000 ion trap MS, based on GC retention times and EI mass spectra. The GC–MS column was a BPX-70 (60 m × 0.32 mm × 0.25 μm, SGE, Austin, TX). The following primary characteristic ions were used for saturated and BCFA methyl ester identification: Molecular ion [M], 74 *m/z* (McLafferty rearrangement), and 87 *m/z* (formed by cleavage at the fourth carbon). Ions at 88 *m/z* and 101 *m/z* were used for the presence of a methyl branch in the second and third carbon, as in the multibranched FA pristanic and phytanic acid, respectively. In addition, the presence, in higher intensities compared to their normal homologues, of the fragments $[M\text{-}15]^+$ or $[M\text{-}43]^+$ or both indicated the presence of iso-BCFA; while the fragments $[M\text{-}29]^+$ or $[M\text{-}57]^+$ or both indicated the presence of *anteiso*-BCFA. The MS spectra of the BCFA were compared to the pure BCFA mixture described above and to an online spectra archive http://www.lipidlibrary.aocs.org/ms/arch_me/index.htm#branch.

Under the GC-FID conditions described above, two pairs of FAME coelute, *iso*-15:0/14:1 and *iso*-17:0/16:1. Coelutions of monoenic and BCFA are unavoidable even on long columns such as CP-Sil-88 [22]. The use of a semipolar column such as the CP-Sil 19 was reported recently to effectively separate BCFA from monounsaturated FA (MUFA) in cheese and fish samples [23]. In the present study, GC with covalent adduct chemical ionization mass spectrometry (CACI-MS) was used to resolve the two sets of overlapping peaks [24]. Solutions of pure 14:1, 15:0, 16:1, and 17:0 FAME (0.5 μg/μl, Nu-Chek Prep Inc., Elysian, MN) were used to determine response factors for ions characteristic of the respective FAME. Selected characteristic ions were plotted to resolve and quantify coeluting FAME. A plot for MH^+ was used for the *iso*-FAME in the milk sample, and a plot of $[MH\text{-}32]^+$, MH^+, and $[M + 54]^+$ intensities were used for the monounsaturated FAME. An example of GC-CACI-MS selected ion plots used for the resolution and quantification of *iso*-15:0 and 14:1 is shown in Fig. 2. An area to weight ratio [A/W, arbitrary units/(ug/ul)] was calculated for each of the pure FAME by dividing the area from the corresponding characteristic ions to the known concentrations of the pure FAME. The concentrations (ug/ul) of the sample *iso*- or the monounsaturated-FAME were then calculated using the ratio between the area under the characteristic ions of the sample FAME and the A/W of the pure corresponding FAME.

The relative percent contribution of the two interfering FAME was applied to the coeluting peaks to produce yield pure intensities. The percentages of the iso-15:0 and *iso*-17:0 that were obtained using this method fell within the range reported previously [10, 25].

Results and Discussion

BCFA in Retail Milk

Figure 3 presents in summary form the major classes of FA found in the present retail milk samples. The sum of palmitic acid (16:0) and all other SFA with shorter chain lengths comprised about 51%, w/w (mean). SFA with 17 or more carbons were 12%, MUFA were about 30%, and polyunsaturated FA (PUFA) were 4.7%. These values are similar to those previously found for our similar comprehensive retail milk sampling [7].

BCFA comprised a total of 2.05 ± 0.14% of FA, or most of the 3% of FA listed previously as "other" [7]. The mean BCFA levels reported in the present study fall within the range previously reported in studies that measured cow's milk FA in response to various diets in small scale experimental studies [3–5, 8, 10].

Table 1 presents the mean proportions of BCFA in retail milk as %, w/w of total FA and as a % of total BCFA (mean ± SD). BCFA with 14–18 carbons and *iso*- or *anteiso*-configuration were detected, and no BCFA with

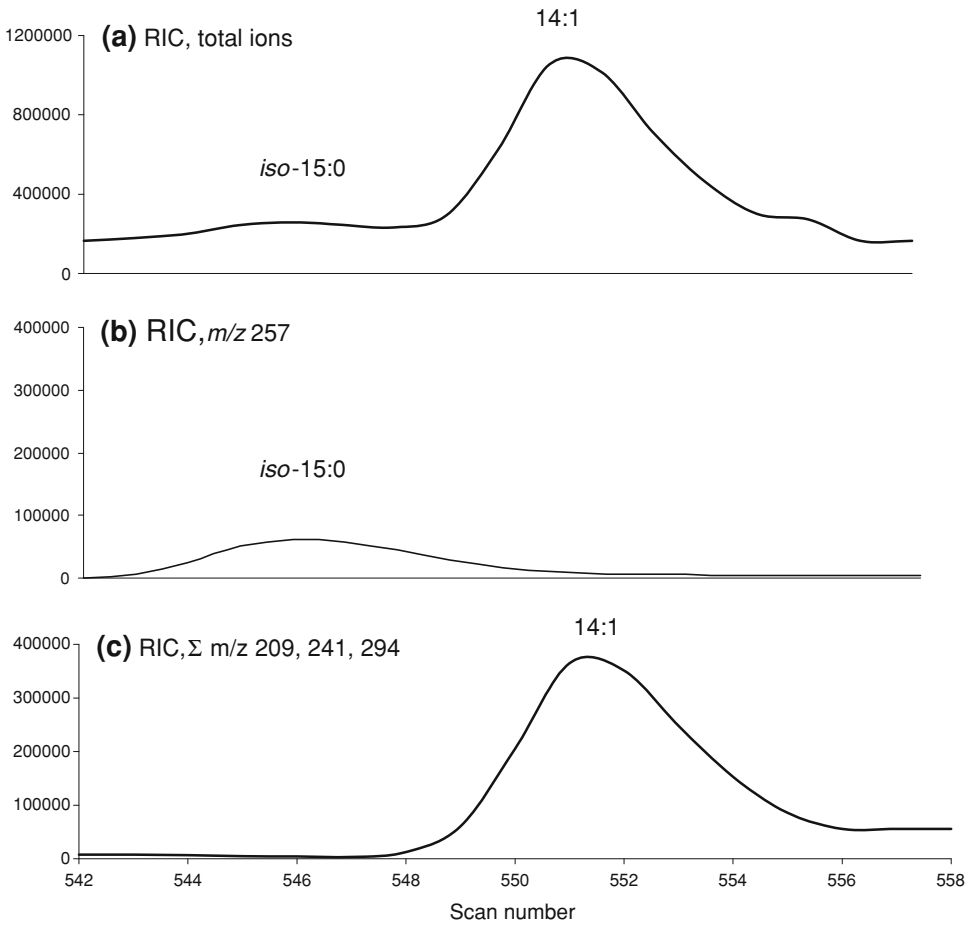

Fig. 2 Resolution of overlapping peaks using GC-CACI-MS. **a** A total reconstructed ion chromatogram (*RIC*) showing coelution of *iso*-15:0 with 14:1. **b** An RIC of the *m/z* 257 MH^+ used for *iso*-15:0. **c** An RIC plot of the sum of signals for *m/z* 209 $[MH-32]^+$, *m/z* 241 MH^+, and *m/z* 294 $[M + 54]^+$ for 14:1. See "Experimental Procedures" for further details on quantification

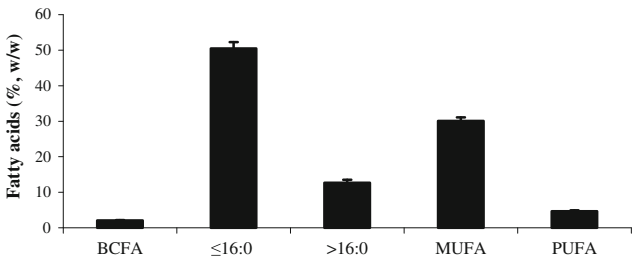

Fig. 3 Fatty acid (*FA*) composition (%, w/w; mean ± SD) of conventional whole milk samples. FA were grouped as follow: Branched chain fatty acids (*BCFA*); de novo synthesized saturated fatty acids (*SFA*), including 16:0 (≤16:0); SFA longer than 16:0 (>16:0); monounsaturated fatty acids (*MUFA*); polyunsaturated fatty acids (*PUFA*)

Table 1 Branched chain fatty acids (BCFA) in retail milk expressed as %, w/w of total fatty acids and as %, w/w of BCFA ($n = 56$; mean ± SD)

BCFA[a]	Total FA[b] (%, w/w)	BCFA[a] (%, w/w)
iso-14:0	0.13 ± 0.04	6.4 ± 1.4
iso-15:0	0.13 ± 0.01	6.6 ± 0.4
anteiso-15:0	0.56 ± 0.03	27.5 ± 1.3
iso-16:0	0.31 ± 0.03	14.9 ± 0.9
iso-17:0	0.26 ± 0.02	12.7 ± 0.7
anteiso-17:0	0.61 ± 0.06	29.9 ± 2.0
iso-18:0	0.04 ± 0.02	1.9 ± 0.9

[a] *BCFA* branched chain fatty acids

[b] *FA* fatty acids

multiple branching were found. Four *iso*-BCFA (*iso*-C14:0 to *iso*-C17:0) were detected in all samples; low levels of *iso*-18:0 were also detected in most but not all of the samples. *anteiso*-15:0 and *anteiso*-17:0 were the only *anteiso*-BCFA found. They were in comparable concentration and constituted more than half of the total BCFA detected.

BCFA with fewer than 14 carbons, such as *iso*- and *anteiso*-13:0, were not detected in any of the samples. Both *iso*- and *anteiso*-13:0 BCFA in cow's milk have been reported by some [3, 5, 8, 11] but not by others [4, 6, 26]. In the present study, retail milk samples were obtained from processing plants and represent pooled milk from many farms; use of specific feeds on some farms that may support small amounts of ruminal C13 BCFA could be diluted to below detection limits by the milk from other farms [10, 27].

Neither phytanic acid, a product of released phytol from chlorophyll by rumen bacteria [28], nor its peroxisomal oxidation product pristanic acid [29], were detected in the retail milk. As with C13 BCFA, these terpenoid BCFA were reported to be present in bovine milk by some [11, 12] but not by others [3–6]. When reported, the variance of these BCFA was high, and it was suggested [12] that differing feed compositions are responsible for variable terpenoid metabolizing ruminal bacteria. As with the case of *iso*- and *anteiso*-13:0, it is possible that minor amounts of phytanic and pristanic acid were present in milk from some farms, but diluted to below detection limits when pooled with milk from many farms in the processing plant.

For comparison with bioactive FA found primarily in dairy products, rumenic acid (*cis*-9, *trans*-11–18:2), the most concentrated conjugated linoleic acid (CLA) in cow's milk, was 0.55%, in conventionally produced retail milk. Vaccenic acid (*trans*-11–18:1), the most concentrated *trans* monoene in cow's milk, was 1.48% in US retail milk, and the sum of all *trans* FA was about 3.1% [7]. Thus, both *anteiso*- BCFA are at the same levels in milkfat as rumenic acid, and total BCFA are more than half the concentration of total *trans*-FA.

Estimated Human BCFA Intake from Retail Milk

Based on these data, we can estimate the contribution of BCFA to the nutrition of Americans, using measured and estimated milk intake. One cup (244 g = 8 oz) of whole milk (3.25% milkfat) contains 7.9 g fat [30]. Two percent of 7.9 g yields a total of 158 mg BCFA per cup whole milk. For comparison to intake of bioactive FA in the American diet, this value is greater than the 100 mg average *daily* consumption of the DHA and eicosapentaenoic acid (EPA) reported in a survey of 8604 Americans between 1999 and 2000 [31] and by women of child bearing age based on NHANES III data [32].

In some population groups, such as small children, milk consumption can be higher. Consumption by small children of 2.6 servings of milk was reported recently, mostly consumed as whole milk [33]. This consumption would thus represent 412 mg BCFA daily, which would provide almost 1% of the total fat intake of children age 2–5 [34]. It thus appears that the absolute daily intake of BCFA from milk—even more so, the amount of BCFA consumed per kilogram body weight—will be higher in some populations, such as in small children.

Apart from milk, other foods produced by ruminant animals, specifically cheese and beef, are expected to be other primary contributors of BCFA to the diet. US cheese BCFA can be estimated from the present measures of milkfat BCFA of about 2% of FA. BCFA averaged about 2%, w/w in Canadian retail beef [35], and similar to Malaysia beef tallow with C13-C20 BCFA with mean concentration 2.3% (mutton tallow had 4.0% BCFA) [36]. We assume American beef has the same BCFA levels as in Canada, and an average 28 and 18% fat content in cheese and in beef, respectively [30]. According to economic disappearance data adjusted for loss, American's average per capita consumption of cheese is 30 g (1.1 oz), at about 28% fat on average and at about 2% BCFA, cheese contributes 168 mg of BCFA. Similarly, Americans consume 50 g (1.8 oz) of cooked beef per day [37]; at about 18% fat and about 2% BCFA, beef contributes about 180 mg of BCFA per day. Table 2 presents these values summed to estimate total current per capita intake of BCFA of about 400 mg per day from the most common ruminant foods.

We also consider the implications of dietary guidelines on BCFA consumption [38]. Americans are advised to consume three servings from the milk group, where a serving, for example, is equal to 1 cup of milk or yogurt and 1.5 oz (42 g, 2 slices) of cheese. For simplicity we assume this to be represented by the present average dietary pattern of milk intake in the US, which is 31% whole milk, 39% low fat (2%) milk, 14% lower fat (1%) milk, with the balance nonfat milk [37]. Using these values we estimate a weighted sum of the total BCFA intake from three servings of milk and cheese to be about 400 mg.

Table 2 Estimated mean daily branched chain fatty acids (BCFA) consumption per capita in the US, based on actual and recommended[a] consumption of milk, cheese, and beef

Food	Actual[a]		Recommended[a]	
	Portion (g)	BCFA[b] (mg)	Portion (g)	BCFA[b] (mg)
Milk[c]	119	54	215	98
Cheese[d]	30	168	53	297
Beef[e]	50	180	50	180
Total	199	402	318	575

Intake data estimation based on reference [37]

[a] Actual consumption reflects the current consumption from milk, cheese and beef by Americans, which falls below recommended levels from the milk food group. Recommended consumption represents the levels of BCFA consumption that would obtain if Americans were to consume recommended amounts from the milk food group, keeping the same existing patterns as the actual consumption. For beef, the actual consumption was considered as the recommended one. Thus, the same value for beef was used for both

[b] *BCFA* branched chain fatty acids

[c] Mean, per capita, milk consumption, based on the proportions currently consumed by Americans of 3.25, 2, and 1% milk

[d] Cheese types included in the analysis are the main cheeses consumed by Americans. An average of 28% fat was used for estimation [30]. Amounts are based on patterns of current consumption of cheese

[e] For cooked beef, an average of 18% fat was used for estimation [30]. Americans consume enough from the meat food group, thus the actual and the recommended consumption were the same

Beef, cheese and milk together account for an average estimated recommended intake of about 575 mg BCFA per capita per day (Table 2).

Use of 2 cups of whole milk in place of reduced or no fat milks and consuming 1 serving of cheese (42 g, 1.5 oz) while consuming the same amount of beef would bring total BCFA to 731 mg/day (316 mg from milk + 235 mg from cheese + 180 mg from beef). These consumption levels, then, would be higher than the 500 mg/d intake for DHA and EPA for the general population recommended by the American Dietetic Association [39], and more than double the 300 mg/d of DHA and EPA recommended by the World Health Organization in pregnancy and lactation [32].

These estimates show that daily BCFA intake is substantial and that current recommendations promote an increase in present intake, considerably higher than other bioactive FA. Unlike DHA and EPA, for instance, BCFA sources include a greater variety of common food items, principally products of ruminants, regularly consumed by non-vegans. The low level of interest in BCFA nutrition is remarkable considering their long-standing intake.

The American dietary guidelines recommend consumption of low fat dairy products, however studies provide no convincing evidence that increased whole milk consumption is harmful with respect to ischemic heart disease and ischemic strokes [40], or vascular disease and diabetes [41]. Some studies provide evidence that higher consumption of whole fat compared to reduced fat milk was associated with lower body mass index in preschool- and elementary school-age children and less weight gain in adults [33, 42, 43] and with lower incidences of anovulatory infertility [44]. Thus, the emergence of potential benefits of whole milk consumption may have a significant effect on BCFA intake in the US population, increasing BCFA consumption even more.

BCFA are synthesized in large amounts by human skin [45], comprise 29%, w/w, of the FA in vernix and are normal constituents of the healthy newborn gut [13]. A systematic shift in BCFA profile was observed between vernix and meconium of the same infant, implying that the fetal alimentary canal selectively metabolizes BCFA. In very recent work, feeding anoxic rat pups rat milk substitute containing a mixture similar to most BCFA found in the retail milk samples (*iso*-14:0, *anteiso*-15:0, *iso*-16:0, *anteiso*-17:0, *iso*-18:0, and *iso*-20:0) reduced the incidence of NEC compared to a control group (Ran-Ressler et al. unpublished data) and elevated mRNA levels of the intestinal, anti-inflammatory cytokine IL-10. BCFA are selectively incorporated into phospholipids of rat pup ileum and into human Caco-2 cells [46]. The risk reduction in NEC development may be linked to these observations.

BCFA function in the membranes is similar to *cis* unsaturated double bonds; both interfere with the ability of saturated hydrocarbon chains to pack tightly forming rigid extended structures. Old data show that an *E. coli* strain that lost the ability to desaturate saturated FA was restored to wild-type growth rates by the addition of BCFA [47]. Apoptotic properties of BCFA on human breast cancer cells are structure-specific, with *iso*-16:0 having the highest activity among BCFA of C12-C20 [48]. *iso*-15:0 inhibited tumor growth in cultured cells and in an in vivo (mouse) models with no obvious deleterious effects [49]. Thus, BCFA of the type found in US retail milk may have a beneficial effect on proper tissue function and on gut development and function.

In conclusion, we document for the first time the profile and amounts of BCFA in retail whole milk in the US. Milk BCFA have chain lengths of 14–18 carbons and include both *iso*- and *anteiso*-BCFA. BCFA comprise 2.05%, w/w of the FA in retail whole milk. Estimated BCFA levels in beef and data on per capita milk, cheese, and beef intakes indicate that BCFA intake on average is in excess than that of many bioactive FA. Their importance in the US food supply and bioactivity suggest that they should be more carefully studied for their biological effects.

Acknowledgments R.R. Ran-Ressler thanks Dr. William Harris Ressler and Peter Lawrence for their valuable comments on the manuscript. Supported by NIH grant R21 HD064604 from the Eunice Kennedy Shriver National Institute Of Child Health & Human Development (NICHD). The content is solely the responsibility of the authors and does not necessarily represent the official views of the NICHD or the NIH. It was also supported by the Cornell Agricultural Experimental Station and Smith Lever funds from the Cooperative State Research, Education, and Extension Service, U.S. Department of Agriculture, under Agreement No. NYC-127437. RRR acknowledges support of NIH training grant HD007331, which includes funding from the NICHD and the Office of Dietary Supplements (ODS).

References

1. Lock AL, Bauman DE (2004) Modifying milk fat composition of dairy cows to enhance fatty acids beneficial to human health. Lipids 39:1197–1206
2. Bauman DE, Lock AL, Corl BA, Ip C, Salter AM, Parodi PW (2006) Milk fatty acids and human health: potential role of conjugated linoleic acid and trans fatty acids. In: Sejrsen K, Hvelplund T, Nielson MO (eds) Ruminant physiology: digestion, metabolism, and impact of nutrition on gene expression, immunology, and stress. Wageningen Academic Publishers, Wageningen, pp 529–561
3. Boeckaert C, Vlaeminck B, Dijkstra J, Issa-Zacharia A, Van Nespen T, Van Straalen W, Fievez V (2008) Effect of dietary starch or micro algae supplementation on rumen fermentation and milk fatty acid composition of dairy cows. J Dairy Sci 91:4714–4727

4. Craninx M, Steen A, Van Laar H, Van Nespen T, Martin-Tereso J, De Baets B, Fievez V (2008) Effect of lactation stage on the odd- and branched-chain milk fatty acids of dairy cattle under grazing and indoor conditions. J Dairy Sci 91:2662–2677
5. Osborne VR, Radhakrishnan S, Odongo NE, Hill AR, McBride BW (2008) Effects of supplementing fish oil in the drinking water of dairy cows on production performance and milk fatty acid composition. J Anim Sci 86:720–729
6. Chilliard Y, Martin C, Rouel J, Doreau M (2009) Milk fatty acids in dairy cows fed whole crude linseed, extruded linseed, or linseed oil, and their relationship with methane output. J Dairy Sci 92:5199–5211
7. O'Donnell-Megaro AM, Barbano DM, Bauman DE (2011) Survey of the fatty acid composition of retail milk in the united states including regional and seasonal variations. J Dairy Sci 94:59–65
8. Massart-Leen AM, DePooter H, Decloedt M, Schamp N (1981) Composition and variability of the branched-chain fatty acid fraction in the milk of goats and cows. Lipids 16:286–292
9. Duncan WR, Garton GA (1978) Differences in the proportions of branched-chain fatty acids in subcutaneous triacylglycerols of barley-fed ruminants. Br J Nutr 40:29–33
10. Vlaeminck B, Fievez V, Cabrita ARJ, Fonseca AJM, Dewhurst RJ (2006) Factors affecting odd- and branched-chain fatty acids in milk: A review. Animal Feed Science and Technology 131:389–417
11. Vlaeminck B, Lourenco M, Bruinenberg M, Demeyer D, Fievez V (2004) Odd and branched chain fatty acids in rumen contents and milk of dairy cows fed forages from semi-natural grasslands. Commun Agric Appl Biol Sci 69:337–340
12. Lough AK (1973) The chemistry and biochemistry of phytanic, pristanic and related acids. Prog Chem Fats Other Lipids 14:1–48
13. Ran-Ressler RR, Devapatla S, Lawrence P, Brenna JT (2008) Branched chain fatty acids are constituents of the normal healthy newborn gastrointestinal tract. Pediatr Res 64:605–609
14. Narendran V, Wickett RR, Pickens WL, Hoath SB (2000) Interaction between pulmonary surfactant and vernix: A potential mechanism for induction of amniotic fluid turbidity. Pediatr Res 48:120–124
15. Egge H, Murawski U, Ryhage R, Gyorgy P, Chatranon W, Zilliken F (1972) Minor constituents of human milk. Iv. Analysis of the branched chain fatty acids. Chem Phys Lipids 8:42–55
16. Gibson RA, Kneebone GM (1981) Fatty acid composition of human colostrum and mature breast milk. Am J Clin Nutr 34:252–257
17. Cotton PA, Subar AF, Friday JE, Cook A (2004) Dietary sources of nutrients among us adults, 1994 to 1996. J Am Diet Assoc 104:921–930
18. Wiley AS (2010) Dairy and milk consumption and child growth: Is BMI involved? An analysis of NHANES 1999–2004. Am J Hum Biol 22:517–525
19. Barbano DM, Clark JL, Dunham CE (1988) Comparison of Babcock and ether extraction methods for determination of fat content of milk: collaborative study. J Assoc Off Anal Chem 71:898–914
20. Christie WW (1982) A simple procedure for rapid transmethylation of glycerolipids and cholesteryl esters. J Lipid Res 23:1072–1075
21. Chouinard PY, Corneau L, Barbano DM, Metzger LE, Bauman DE (1999) Conjugated linoleic acids alter milk fatty acid composition and inhibit milk fat secretion in dairy cows. J Nutr 129:1579–1584
22. Dewhurst RJ, Moorby JM, Vlaeminck B, Fievez V (2007) Apparent recovery of duodenal odd- and branched-chain fatty acids in milk of dairy cows. J Dairy Sci 90:1775–1780
23. Hauff S, Vetter W (2010) Quantification of branched chain fatty acids in polar and neutral lipids of cheese and fish samples. J Agric Food Chem 58:707–712
24. Van Pelt CK, Brenna JT (1999) Acetonitrile chemical ionization tandem mass spectrometry to locate double bonds in polyunsaturated fatty acid methyl esters. Anal Chem 71:1981–1989
25. Vlaeminck B, Fievez V, Tamminga S, Dewhurst RJ, van Vuuren A, De Brabander D, Demeyer D (2006) Milk odd- and branched-chain fatty acids in relation to the rumen fermentation pattern. J Dairy Sci 89:3954–3964
26. Vlaeminck B, Fievez V, van Laar H, Demeyer D (2004) Rumen odd and branched chain fatty acids in relation to in vitro rumen volatile fatty acid productions and dietary characteristics of incubated substrates. J Anim Physiol Anim Nutr (Berl) 88:401–411
27. Keeney M, Katz I, Allison MJ (1962) On probable origin of some milk fat acids in rumen microbial lipids. J Am Oil Chem Soc 39:198–201
28. Patton S, Benson AA (1966) Phytol metabolism in the bovine. Biochim Biophys Acta 125:22–32
29. Verhoeven NM, Wanders RJA, Poll-The BT, Saudubray JM, Jakobs C (1998) The metabolism of phytanic acid and pristanic acid in man: a review. J Inherit Metab Dis 21:697–728
30. USDA ARS (2009) National nutrient database for standard reference, release 22. Nutrient data laboratory home page. USDA, Washington, DC [updated 2009; cited 2010 22 July]; Updated date: February 1, 2010 [Available from http://www.ars.usda.gov/ba/bhnrc/ndl
31. Ervin RB, Wright JD, Wang CY, Kennedy-Stephenson J (2004) Dietary intake of fats and fatty acids for the United States population: 1999–2000. Adv Data 348:1–6
32. Brenna JT, Lapillonne A (2009) Background paper on fat and fatty acid requirements during pregnancy and lactation. Ann Nutr Metab 55:97–122
33. Huh SY, Rifas-Shiman SL, Rich-Edwards JW, Taveras EM, Gillman MW (2010) Prospective association between milk intake and adiposity in preschool-aged children. J Am Diet Assoc 110:563–570
34. USDA ARS (2010) Nutrient intakes from food: Mean amounts consumed per individual, by gender and age, what we eat in America. NHANES (National Health and Nutrition Examination Survey), 2007–2008. USDA, Washington, DC [updated 2010 30 July 2010; cited 2010 4 August]; Available from http://www.ars.usda.gov/ba/bhnrc.fsrg
35. Aldai N, Dugan MER, Kramer JKG (2010) Can the trans-18:1 and conjugated linoleic acid profiles in retail ground beef be healthier than steak? Journal of Food Composition and Analysis 23:326–332
36. Chin ST, Man YBC, Tan CP, Hashim DM (2009) Rapid profiling of animal-derived fatty acids using fast gc × gc coupled to time-of-flight mass spectrometry. Journal of the American Oil Chemists Society 86:949–958
37. USDA_Economic_Research_Service_(ERS) (2008) Food availability (per capita) data system. USDA, Washington, DC [updated 2008; cited 2010 22 July]; Updated date: February 1, 2010 [Available from http://www.ers.usda.gov/Data/FoodConsumption
38. USDA (2005) Mypyramid.Gov. USDA, Washington, DC [updated 2005; cited 2010 22 July]; Available from http://www.mypyramid.gov/pyramid/index.html
39. Kris-Etherton PM, Innis S, American Dietetic Association, Dietitians of Canada (2007) Position of the American Dietetic Association and Dietitians of Canada: dietary fatty acids. J Am Diet Assoc 107:1599–1611
40. Elwood PC, Pickering JE, Hughes J, Fehily AM, Ness AR (2004) Milk drinking, ischaemic heart disease and ischaemic stroke ii. Evidence from cohort studies. Eur J Clin Nutr 58:718–724
41. Elwood PC, Pickering JE, Givens DI, Gallacher JE (2010) The consumption of milk and dairy foods and the incidence of vascular disease and diabetes: an overview of the evidence. Lipids 45:925–939

42. Barba G, Troiano E, Russo P, Venezia A, Siani A (2005) Inverse association between body mass and frequency of milk consumption in children. Br J Nutr 93:15–19
43. Rosell M, Hakansson NN, Wolk A (2006) Association between dairy food consumption and weight change over 9 y in 19,352 perimenopausal women. Am J Clin Nutr 84:1481–1488
44. Chavarro JE, Rich-Edwards JW, Rosner B, Willett WC (2007) A prospective study of dairy foods intake and anovulatory infertility. Hum Reprod 22:1340–1347
45. Nicolaides N, Ray T (1965) Skin lipids. 3. Fatty chains in skin lipids. The use of vernix caseosa to differentiate between endogenous and exogenous components in human skin surface lipid. J Am Oil Chem Soc 42:702–707
46. Ran-Ressler RR, Kothapalli KS, Glahn R, Brenna JT (eds) (2010) Branched chain fatty acids are taken up and metabolized by cultured human intestinal cells (caco-2). Exp Biol (Anahein, Ca)
47. Silbert DF, Ladenson RC, Honegger JL (1973) The unsaturated fatty acid requirement in *Escherichia coli*. Temperature dependence and total replacement by branched-chain fatty acids. Biochim Biophys Acta 311:349–361
48. Wongtangtintharn S, Oku H, Iwasaki H, Toda T (2004) Effect of branched-chain fatty acids on fatty acid biosynthesis of human breast cancer cells. J Nutr Sci Vitaminol (Tokyo) 50:137–143
49. Yang Z, Liu S, Chen X, Chen H, Huang M, Zheng J (2000) Induction of apoptotic cell death and in vivo growth inhibition of human cancer cells by a saturated branched-chain fatty acid, 13-methyltetradecanoic acid. Cancer Res 60:505–509

Lipids (2011) 46:577–585
DOI 10.1007/s11745-011-3534-4

ORIGINAL ARTICLE

Inclusion of Flaxseed in Hay- and Barley Silage Diets Increases Alpha-Linolenic Acid in Cow Plasma Independent of Forage Type

M. L. He · Y.-H. Chung · T. A. McAllister · K. A. Beauchemin · P. S. Mir · J. L. Aalhus · M. E. R. Dugan

Received: 15 September 2010 / Accepted: 12 January 2011 / Published online: 20 February 2011

Abstract Feeding flaxseed to cattle may be a means of increasing omega-3 fatty acid levels in ruminant products, but possible interactions with conserved forages have not been investigated. Twelve Holstein cows were used in a replicated 4 × 4 Latin Square experiment. Cows were fed one of four 50:50 forage:concentrate diets (DM basis): hay (hay control, HC), hay plus 15% ground flaxseed (hay-flaxseed, HF), barley silage (silage control, SC), and barley silage plus 15% ground flaxseed (silage-flaxseed, SF). Plasma concentrations of alpha-linolenic acid (ALA) did not differ between SC and HC diets. Flaxseed increased ALA ($P < 0.05$), but levels were not influenced by forage type. Flaxseed slightly increased 18:2n-6 ($P < 0.05$) and some n-6 and n-3 elongation and desaturation products, particularly arachidonic acid (ARA) and eicosapentaenoic acid (EPA). Flaxseed also increased C18:0 ($P < 0.05$) with this increase being greater ($P < 0.01$) for cows fed SF than HF. Feeding flaxseed also increased plasma C18:1-*trans* isomers ($P < 0.01$), predominantly vaccenic acid (VAA, 18:1-*t*11), with this increase being greater ($P < 0.05$) in cows fed HF than SF. Although conjugated linoleic acid (CLA) was increased ($P < 0.001$) with flaxseed it was not influenced by forage type ($P = 0.06$). Overall, feeding flaxseed increased plasma ALA, EPA, ARA and CLA independently of forage type. Feeding flaxseed with silage, however, resulted in more 18:0, while feeding flaxseed with hay resulted in greater accumulations of plasma 18:1-*trans* isomers mainly in the form of VAA.

Keywords Cow · Flaxseed · Omega-3 fatty acids · Conjugated linoleic acid

Abbreviations

ARA	Arachidonic acid
ADF	Acid detergent fiber
ALA	Alpha-linolenic acid
BD	Becton–Dickinson
CLA	Conjugated linoleic acid
CP	Crude protein
DHA	Decosahexaenoic acid
DM	Dry matter
DPA	Docosapen
EPA	Eicosapentaenoic acid
FAME	Fatty acid methyl esters
HC	Hay control
HF	Hay-flaxseed
LNA	Linoleic acid
MUFA	Monounsaturated fatty acids
NDF	Neutral detergent fiber
NE	Net energy
RUA	Rumenic acid
SC	Silage control
SF	Silage-flaxseed
VAA	Vaccenic acid

M. L. He · Y.-H. Chung · T. A. McAllister (✉) · K. A. Beauchemin · P. S. Mir
Agriculture and Agri-Food Canada, Research Centre, Lethbridge, AB, Canada
e-mail: tim.mcallister@agr.gc.ca

J. L. Aalhus · M. E. R. Dugan
Agriculture and Agri-Food Canada, Research Centre, Lacombe, AB, Canada

M. L. He
Department of Animal and Poultry Science, University of Saskatchewan, Saskatoon, SK, Canada

Introduction

Previous studies in cattle suggest that including flaxseed in diets increases plasma alpha-linolenic acid (ALA, 18:3n-3) levels [1–3] and its levels in beef [4, 5]. Health-promoting omega-3 (or n-3) fatty acids [6, 7] and conjugated linoleic acids (CLA) including rumenic acid (RUA, 18:2-*c*9,*t*11) [8] have been shown to increase in the fat of ruminants supplemented with flaxseed. Levels of ALA and CLA have also been shown to be increased by providing grass forage to ruminants [9], but it is less clear if this same response is achieved if the forage is conserved as silage [10]. Only a few studies have investigated the effect of dietary forage type on the fatty acid composition of ruminant products [11, 12], and evidence of an interaction between forage type and supplemental oil source has arisen with regard to their impact on the fatty acid composition of goats milk [13, 14].

In western Canada, silage and hay are the two most common forage sources available for feeding. It is possible that the epiphytic microbial populations associated with these forages as well as alterations in endogenous ruminal microbes could alter ruminal biohydrogenation of fatty acids, but studies that directly compare the effects of method of forage conservation on plasma fatty acids profiles in ruminants have not been conducted. In a recent study, differences in rumen microbial communities were found between cull cows fed a hay-based diet and those fed a silage-based diet [15]. Additionally, as compared to hay, ensiling may degrade antioxidants and alter plant secondary compounds in the forage, a factor that could also alter the biohydrogenation activity of rumen bacteria [16].

Plasma levels of functional fatty acids could serve as predictors of their accumulation in body tissues [17–19], a tool that could prove useful in the production of fatty acid enriched ruminant products. In Canada, forage finishing of beef is not common and mature, breeding cattle typically receive the greatest proportion of forage in their diet. Among the Canadian beef grades, cull cows are known to have the highest levels of CLA and omega-3 fatty acids and may present an economically viable opportunity to produce beef with enhanced levels of beneficial fatty acids [20]. Including flaxseed in cattle diets has generally not been that successful at increasing ALA or its partial hydrogenation products in beef due to the high efficiency of bacterial hydrogenation in the rumen [21]. Therefore, in the present experiment we hypothesized that the levels of 18:1-*trans*, CLA and omega-3 fatty acids in blood plasma of cull cows fed flaxseed would be lower in cows fed barley silage as compared to grass hay.

Materials and Method

Animals

The study was approved by the Animal Care Committee at Lethbridge Research Centre of Agriculture and Agri-food Canada with ACC#0837. Twelve non-lactating, non-pregnant Holstein dairy cows 849 ± 156 kg were used in a replicated 4 × 4 Latin Square design with four experimental diets and four 21-day experimental periods. Cows were housed in individual tie stalls. Cows were fed once daily (13:00 h) their total daily feed intake (DM basis). During each 21-days feeding period, days 1–4 was a diet transition period when the cows were fed mixed diets that gradually substituted ingredients to obtain the final diet composition for the next period by day 5. Ad libitum intake was estimated in the first week (days 1–7) and confirmed in the following 3 days. The intake was subsequently restricted to 90% of this estimate for the remainder of the period (days 11–21) to ensure complete consumption of diets.

Diets

Four experimental diets were arranged as a 2 × 2 factorial using either chopped grass hay or barley silage as the forage source with or without ground flaxseed which was substituted for steam-rolled barley grain (Table 1). Experimental diets were designated as hay control (HC), hay + flaxseed (HF), silage control (SC) or silage + flaxseed (SF). The diets were formulated at a 50:50 forage to concentrate ratio and fed as a total mixed ration (TMR). Flaxseed was fed at 15% of ration DM, so that total oil content of the diet accounted for approximately 6.5% of ration DM. It has been recommended that total dietary fat should not exceed 6–7% of dietary DM as a higher concentration of fat may reduce intake [22].

Flaxseed was premixed with barley in a ratio of 7:3 and subsequently ground through a 4-mm screen in a hammer mill. The ground material was screened, and whole flaxseeds recovered were estimated to account for approximately 2% of the flaxseed that was originally added to the diet. The distribution of hay particles as fed were 200 g/kg fine (0-mm), 290 g/kg short (1.19-mm), 250 g/kg medium (8-mm), and 260 g/kg long (19-mm). The experimental diets were supplemented with minerals and vitamins to meet nutrient requirements as described in NRC [22, 23]. The ingredient and nutrient compositions of diets are shown on Table 1. Levels of net energy (NE), neutral detergent fiber (NDF) and acid detergent fiber (ADF) in DM were similar among diets. The crude protein (CP) % in DM met or exceeded requirements [22, 23].

Table 1 Composition and nutrient content of experimental diets

	Treatment			
	Hay	Hay-flax	Silage	Silage-flax
Ingredient (%)				
Barley	47.37	32.74	29.28	20.17
Barley silage	0.00	0.00	67.80	68.20
Grass hay	47.91	48.36	0.00	0.00
Flaxseed	0.00	14.13	0.00	8.71
Supplement[a]	4.72	4.76	2.92	2.93
Nutrient				
Dry Matter (%)	87.76	88.58	54.24	54.56
Protein (% of DM)	13.65	15.39	12.64	14.37
NEm (Mcal/kg DM)	1.69	1.73	1.77	1.81
NEg (Mcal/kg DM)	1.06	1.08	1.15	1.17
NDF (% of DM)	33.09	30.39	33.32	30.63
ADF (% of DM)	19.66	19.96	18.39	18.69
Lipids (% of DM)	1.63	6.68	1.95	6.34

[a] The supplement was composed of: 56.5% barley, 10% canola meal, 2% urea, 25% limestone, 3% salt, 0.066% VIT E 500, 1% premix, 0.05% flavor and 2.5% molasses, which provided to diets in 5% (in DM) and supply to 1 kg diet (in DM) with additional: 14.67 mg copper, 58.32 mg zinc, 26.73 mg manganese, 0.66 mg iodine, 0.23 mg cobalt, 0.29 mg selenium, 4,825 IU vitamin A, 478 IU vitamin D and 32 IU vitamin E

Blood Sampling

One set of blood samples was collected before the start of the experiment. Blood samples were collected on day 14 and day 21 during each period (i.e., days 0, 14, 21, 35, 42, 56, 63, 77 and 84 days of the experiment) at 15:00 h, i.e. 2 h after the feeding. Blood samples were collected from the jugular vein using Becton–Dickinson (BD) evacuated tubes (NJ, USA) containing Na_2-EDTA. The tubes containing blood samples were kept in a cooler and transferred to the laboratory within 30 min. The blood samples were centrifuged at 2,000×*g* at 5 °C for 15 min. The upper layer of plasma was then collected and 1 mL was taken for extraction of lipids with the remainder stored in the freezer at −40 °C until analyzed.

Lipid Extraction

Plasma lipids were extracted using the procedures described previously [4, 24] with minor modifications. On occasions where the suppliers are not designated, chemicals were purchased from Sigma–Aldrich Canada. Plasma (1 mL) was transferred into a test tube and mixed with 4 mL of isopropanol. Tubes were vortexed each time after the addition of 4 mL hexane and 4 mL aqueous sodium sulfate (66.8 g/L) and the final mixture was centrifuged at 2,000×*g* at 5 °C for 5 min. The upper hexane layer was aspirated into a new tube and the extraction was repeated through adding hexane (4 mL). The hexane extraction was evaporated under nitrogen at 38 °C in a water bath. The remaining residue was stored in a freezer at −80 °C until further analysis.

Methylation and Determination of Fatty Acids

Nonadecanoic acid (19:0) methyl ester (100 μL, 5.96 mg/mL hexane Nu-Chek Prep, Inc., MN, USA) was added to the residues to serve as an internal standard. Fatty acids were methylated using the combined base/acid methylation procedure [25]. Sodium methoxide (2 mL, 0.5 mmol/L in methanol) was added as each tube was flushed with nitrogen and mixed. Tubes were placed in a 50 °C water bath for 10 min. Subsequently, boron trifluoride (1 mL; 14% in methanol) was added and tubes were placed in a water bath at 50 °C for 10 min. After cooling, 5 mL of water and 5 mL of hexane were added and the solution was thoroughly mixed. Samples were allowed to stand for 10 min and the upper layer (hexane) was transferred to a gas chromatography ampoule that was flushed with nitrogen for fatty acid determination. Fatty acid methyl esters (FAME) were quantified using a gas chromatograph (Hewlett Packard GC System 6890; Mississauga, ON, Canada) equipped with a flame ionization detector and SP-2560 fused silica capillary column (100 m × 0.25 mm × 0.2 μm, Supelco Inc., Oakville, ON, Canada). Samples were loaded onto the column via 1-μL splitless injections. The initial oven temperature (55 °C) was held for 0.5 min and then the following program was used: increased at 32 °C/min to 120 °C and held for 15 min, increased at 6 °C/min to 160 °C and held for 10 min, increased at 3 °C/min to 170 °C and held for 45 min, and increased at 7 °C/min to 240 °C and held for 33 min. The helium carrier gas flow rate through the column was 1.7 mL/min. Hydrogen flow to the detector was 34 mL/min, air flow was 320 mL/min and helium make-up gas flow rate was 29 mL/min. Peaks in the chromatograms were identified and quantified using pure methyl ester standards (Sigma–Aldrich Inc., Oakville, ON, Canada). The identification of unknown FAME of some *trans* 18:1 and combined CLA peaks were based on the references reported previously [26–28]. The amount of fatty acids was calculated based on the fatty acid standards and expressed as μmol/L of plasma.

Statistical Analysis

The MIXED procedure of SAS [29] was applied for comparison of diet effects on FAME plasma concentration and the dietary intake. Fixed effects included diets (flaxseed supplementation and forage type), sampling time

(i.e., day 14 and 21 of each period) and all interactions. Random effects included square and cow × square. The plasma concentration of FAME was the average of two sampling days (day 14 and 21) during each sampling period. There were no significant differences ($P > 0.05$) in plasma fatty acids level between these designated sampling days (data not shown). The correlation analysis was done with CORR procedure of SAS [29] on concentration of FAME between diet (mmol/kg DM) and plasma (μmol/L), or between FAME intake (mmol/day) and plasma concentration (μmol/L).

Results

Dietary Lipids and Fatty Acid Concentration

Dietary lipid content of HF and SF were 6.68 and 6.34% (wt%/DM), respectively, which was considerably higher than that in HC and SC diets which averaged 1.63 and 1.95%, respectively (Table 1). In HC and SC, linoleic acid (LNA, 18:2n-6) was the most abundant fatty acid accounting for 39.44 and 42.84 mol% of total FAME followed by ALA, palmitic acid (16:0) and oleic acid (18:1-*c*9), respectively (Table 2). Supplementation with flaxseed in HF and SF diets resulted in ALA accounting for 53.53 and 50.00 mol%, respectively, of total FAME while mol% of ALA in HC and SC diets were 19.76 and 14.43%, respectively.

Intake of Feed and Dietary Fatty Acids

Comparison of the DM and fatty acid intake of cows among treatments are shown in Table 3. No difference in DM intake was found among treatments, however, fatty acid intake did differ with flaxseed supplementation and forage type. Flax supplementation of hay- or silage-based diets (HF and SF) increased ($P < 0.001$) the intake of total and individual fatty acids as compared to the control diets (HC and SC).

In treatments supplemented with flaxseed (HF and SF), ALA accounted for more than half of the total fatty acid intake with 1,221.7 mmol/day in HF and 1,062.7 mmol/day in SF. In comparison, ALA intake in HC and SC groups was far lower ($P < 0.05$) at only 80.0 and 72.6 mmol/day, respectively (Table 3). Few differences in fatty acid intake were observed between HC and SC, with only minor ($P < 0.05$) differences being observed for palmitoleic (16:1-*c*9) and ARA.

Plasma Fatty Acid Concentrations

The plasma concentration of total FAME was higher ($P < 0.001$) in cows consuming diets supplemented with flaxseed (Table 4), resulting in a 1.39- and 1.49-fold increase in the HF and SF treatments, respectively. This response was also more pronounced ($P = 0.03$) in silage- than hay-based diets.

LNA and stearic acid (18:0) accounted for the majority of plasma fatty acids. LNA increased ($P < 0.01$) when cows were fed flaxseed and this was accompanied by increases in its elongation and desaturation product (20:4n-6; $P < 0.001$). A flaxseed level by forage type interaction ($P < 0.01$) was observed for C18:0. Flaxseed increased C18:0 when fed with hay, but the magnitude of this increase was even greater when it was fed in combination with barley silage. Interactions of a similar nature were also found for total SFA ($P < 0.01$).

Plasma concentrations of total polyunsaturated fatty acids (PUFA) and n-3 fatty acids were also greatly increased ($P < 0.001$) as a result of flaxseed supplementation, a response that was not affected by forage type ($P = 0.67$). The majority of the increase in n-3 was due to higher plasma concentrations of ALA ($P < 0.001$). Dietary effects on elongation and desaturation products of ALA were mixed. Plasma concentrations of EPA were higher ($P < 0.001$) when feeding flaxseed irrespective of forage type. Overall, flaxseed and forage type had very little affect on levels of DPA and EPA, although minor interactions were found for DPA ($P < 0.06$) and DHA ($P < 0.04$) with

Table 2 Fatty acid profile of experimental diets

FA mol% of total FAME	Treatment			
	Hay	Hay-flax	Silage	Silage-flax
14:0	0.46	0.10	1.15	0.31
15:0	0.10	0.03	0.14	0.04
16:0	20.07	8.17	21.04	9.17
16:1-*c*9	0.14	0.07	0.17	0.08
17:0	0.04	0.05	0.12	0.06
18:0	2.33	2.51	1.90	2.48
18:1-*c*9	15.72	14.30	16.34	14.52
18:1-*c*11	0.52	0.48	0.69	0.53
18:2n-6 (LNA)	39.44	20.29	42.84	22.31
18:3n-3 (ALA)	19.76	53.53	14.43	50.00
20:0	0.34	0.11	0.30	0.11
20:1-*c*9	0.66	0.21	0.60	0.23
20:4n-6 (ARA)	0.13	0.03	0.07	0.03
22:0	0.29	0.11	0.22	0.11
SFA	23.64	11.09	24.87	12.30
UFA	76.36	88.91	75.13	87.70
MUFA	17.04	15.06	17.80	15.36
PUFA	59.32	73.85	57.33	72.34

HC Hay control, *HF* Hay + flaxseed, *SC* Silage control, *SF* Silage + flaxseed

Table 3 Comparison of daily FAME intake among cows fed hay- or silage-based diets with or without 15% flaxseed

	Treatment				SEM	*P*-value		
	Hay	Hay-flax	Silage	Silage-flax		Flax	Forage	Flax × forage
Feed intake (kg DM)	10.3	10.3	11.0	10.6	0.4	0.52	0.08	0.64
FAME intake (mmol/day)								
14:0	1.9	2.3	5.8	6.6	0.6	<0.001	<0.001	0.17
16:0	81.3	186.4	105.9	195.0	15.5	<0.001	<0.001	0.08
16:1-*c*9	0.58[a]	1.57[c]	0.85[b]	1.62[c]	0.1	<0.001	<0.001	0.01
18:0	9.4	57.3	9.5	52.7	6.6	<0.001	0.10	0.08
18:1-*c*9	63.7[a]	326.4[b]	82.2[a]	308.6[b]	35.9	<0.001	0.95	0.03
18:1-*c*11	2.1	11.0	3.5	11.3	1.2	<0.001	<0.01	0.06
18:2-*c*9,*c*12 (LNA)	159.7	463.0	215.6	474.1	3.6	<0.001	<0.01	0.06
18:3 (ALA)	80.0[a]	1221.7[c]	72.6[a]	1062.7[b]	6.6	<0.001	0.01	0.02
20:0	1.4[a]	2.6[b]	1.5[a]	2.4[b]	0.2	<0.001	0.93	0.02
22:0	1.3	2.9	1.2	2.7	0.2	<0.001	0.02	0.40
20:4n-6 (ARA)	0.5[b]	0.7[c]	0.3[a]	0.6[c]	0.1	<0.001	<0.001	<0.001
Total	405.0[a]	2282.4[c]	503.3[a]	2125.6[b]	256.2	<0.001	0.55	0.03
SFA	95.9	253.3	125.3	261.7	22.8	<0.001	<0.01	0.09
UFA	309.1[a]	2029.0[c]	378.1[a]	1863.9[b]	234.0	<0.001	0.32	0.02
MUFA	69.0[a]	343.7[b]	89.6[a]	326.5[b]	37.6	<0.001	0.83	0.03
PUFA	240.2[a]	1685.3[c]	288.5[a]	1537.4[b]	196.5	<0.001	0.21	0.02

[a,b,c] Treatment means within rows without a common letter differ significantly $P < 0.05$

the addition of flaxseed to the hay diet resulting in minor increases in the plasma concentration of these fatty acids relative to silage.

Total plasma monounsaturated fatty acids (MUFA) were higher ($P < 0.001$) in cows fed flaxseed. Feeding silage resulted in lower MUFA in plasma as compared to the hay diet ($P = 0.05$). A flaxseed level by forage type interaction was found for total *trans* FA (CLA + 18:1-*trans*; $P < 0.03$), with flaxseed causing an increase in total *trans* FA, and this increase being even more magnified with hay as compared to the silage diet. Similar interactions were found for total 18:1-*trans* ($P = 0.03$) and all individual C18:1-*trans* isomers ($P < 0.05$ for *t*6-*t*8, *t*9, VAA and $P = 0.07$ for *t*10). Feeding flaxseed increased plasma concentrations of CLA (combined 18:2 *c*9,*t*11 and 18:2 *t*7,*c*9), but a flaxseed level by forage type interaction was not observed ($P > 0.05$).

Correlations Between Dietary and Plasma Fatty Acids

There was very strong correlation ($P < 0.001$) between dietary concentrations (Correlation 1) or the daily intake (Correlation 2) of SFA, USFA, MUFA and PUFA in the diet (mmol/kg DM) and the plasma concentrations (μmol/L) of these fatty acids with coefficients ranging from 0.51 to 0.75 (Table 5). Among individual fatty acids, these two correlations were the highest with plasma concentrations of ALA ($r = 0.93$ or 0.91, respectively; $P < 0.0001$). There were also strong correlations ($P < 0.01$) between diet or daily intake and plasma concentrations of palmitoleic (16:1 *c*-9), stearic (18:0), oleic (18:1 *c*-9), *cis*-vaccenic (18:1 *c*-11) and LNA. No correlations between plasma concentration and dietary intake of palmitic (16:0, $P = 0.28$), arachidic (20:0, $P = 0.52$) and behenic (22:0, $P = 0.32$) and arachidonic (20:4, $P = 0.37$) acids were observed.

Discussion

Consumption of high omega-3 fatty acid containing foods is recommended as result of their potential benefits for cardiovascular health [30]. Dietary strategies have been employed to enrich the omega-3 content of poultry, pork and dairy products, but attempts to significantly increase the omega-3 fatty acid of beef have been largely unsuccessful. Generally the transfer of dietary omega-3 fatty acids to animal tissues in non-ruminants is more efficient than ruminants due to hydrogenation of unsaturated fatty acids by rumen microorganisms. Even horse adipose tissues contain much higher concentrations of omega-3 fatty acids than beef cattle when these herbivores are fed similar diets [31].

In the present study, dietary flaxseed increased total plasma concentrations of omega-3 fatty acids. This result

Table 4 Comparison of plasma FAME concentrations among cows fed hay- or silage-based diets with or without 15% flaxseed

FAME (μmol/L)	Treatment				SEM	*P*-value		
	Hay	Hay-flax	Silage	Silage-flax		Flax	Forage	Flax × forage
14:0	60.6	60.9	68.0	69.7	4.3	0.34	<0.001	0.48
14:1-*c*9	22.6	23.0	24.0	22.3	1.9	0.42	0.68	0.23
16:0	326.4	333.4	349.3	389.1	16.3	0.01	<0.0001	0.06
16:1-*c*9	22.6	27.0	24.2	34.9	2.4	<0.001	0.01	0.09
18:0	771.5[a]	1069.4[b]	848.3[a]	1423.9[c]	23.88	<0.001	<0.001	<0.01
18:1-*t*6-*t*8	7.1[ab]	15.7[c]	4.1[a]	8.1[b]	1.1	<0.001	<0.001	0.05
18:1-*t*9	4.8[a]	10.2[b]	4.1[a]	5.4[a]	0.7	<0.001	<0.01	0.02
18:1-*t*10	10.7	44.1	4.4	9.9	4.9	0.01	<0.01	0.07
18:1-*t*11 (VAA)	28.3[a]	82.2[b]	14.2[a]	33.8[a]	6.0	<0.001	<0.001	0.02
18:1-*c*9	195.8	290.5	193.9	306.8	14.2	<0.001	0.42	0.31
18:1-*c*11	22.0	34.0	21.3	32.8	0.87	<0.001	0.66	0.91
18:2n-6 (LNA)	1288.2	1434.2	1346.6	1531.8	81.3	<0.01	0.14	0.71
18:2 *c*9,*t*11 + *t*7,*c*9 (CLA)	3.7	8.1	4.4	6.5	0.9	<0.001	0.62	0.22
18:3n-3 (ALA)	212.2	820.4	172.8	829.7	31.4	<0.001	0.62	0.43
20:0	39.4	31.4	40.0	37.9	4.1	<0.01	0.05	0.10
22:0	82.4[b]	72.3[a]	80.0[b]	82.5[b]	5.4	0.06	0.06	<0.01
20:4 n-6 (ARA)	115.0	124.8	116.5	134.3	9.2	<0.001	0.12	0.25
20:5n-3 (EPA)	21.9	32.2	19.8	34.7	2.6	<0.001	0.91	0.23
22:5n-3 (DPA)	24.7	23.5	24.0	25.9	1.8	0.64	0.27	0.06
22:6n-3 (DHA)	4.1[ab]	3.8[a]	4.1[ab]	4.2[b]	0.4	0.57	0.13	0.04
Total FAME	3264.1	4541.1	3363.8	5024.1	186.0	<0.001	0.03	0.15
SFA	1280.4[a]	1567.4[b]	1385.5[a]	2003.0[c]	86.3	<0.001	<0.001	<0.01
UFA	1983.7	2973.8	1978.4	3021.1	129.7	<0.001	0.82	0.77
MUFA	313.9	526.8	290.2	454.0	27.7	<0.001	0.05	0.32
PUFA	1669.8	2447.0	1688.1	2567.1	117.0	<0.001	0.38	0.52
trans FA	54.6[a]	160.3[b]	31.2[a]	63.7[a]	11.5	<0.001	<0.001	0.03
trans FA –CLA&VAA	22.6[a]	70.1[b]	12.7[a]	23.4[a]	6.1	<0.01	<0.01	0.05
18:1-*trans*	50.9[a]	152.3[b]	26.8[a]	57.2[a]	11.3	<0.001	<0.001	0.03
CLA + VAA	32.1[a]	90.3[b]	18.5[a]	40.3[a]	6.2	<0.001	<0.001	0.03
n-3 FA	262.9	879.9	220.6	894.5	32.5	<0.001	0.67	0.37

The data is the average value of plasma samples collected on day 14 and 21 or each sampling period

[a,b,c] Treatment means within rows without a common letter differ significantly $P < 0.05$

reflects the ability of some dietary ALA in flaxseed to escape hydrogenation in the rumen and be absorbed into the blood with potential delivery to tissues. These findings are consistent with earlier studies [2, 32, 33] in which the composition of omega-3 fatty acids were doubled when flaxseed or flax oil was added to cattle diets. In a study by Farran et al. [3], supplementation of crossbred heifers with 13% dietary flaxseed resulted in a plasma ALA concentration of 262.7 μg/mL plasma, a concentration that is comparable to that observed in our study. However, Doreau et al. [34] examined the effect of supplementing 7.5% flaxseed or flaxseed oil on dry cow plasma fatty acid profiles and found no increase in plasma omega-3 fatty acids.

The hydrogenation of ALA by rumen bacteria can be affected by the forage to concentrate ratio in the diet. The study of Doreau et al. [34] found the extent of ruminal hydrogenation of dietary ALA was 95% in the rumen of dry cows fed a 70% forage (60% silage and 10% hay) diet and up to 97% if the diet was supplemented with 7.5% flaxseed. In an in vitro study, Kronberg et al. [35] found that the 43% of ALA in flaxseed was hydrogenated, but protection with tannins reduced this to 13%. However, no significant differences were found in plasma LNA in steers consuming forage or grain based diets containing flaxseed when tannins were either included or excluded from the diet [34]. In the present experiment, feeding flaxseed

Table 5 Correlation analysis between FAME concentration in the plasma and that in the diets or that of daily fatty acids intake

Fatty acid	Correlation-1		Correlation-2	
	Coefficient 1	*P*-value	Coefficient 2	*P*-value
14:0	0.26	0.08	0.35	0.02
16:0	0.27	0.07	0.16	0.28
16:1-*c*9	0.38	<0.01	0.34	0.02
18:0	0.62	<0.001	0.57	<0.001
18:1-*c*9	0.72	<0.001	0.65	<0.001
18:1-*c*11	0.53	<0.001	0.45	<0.01
18:2n-6 (LNA)	0.30	0.04	0.27	0.05
18:3n-3 (ALA)	0.93	<0.001	0.91	<0.001
20:0	−0.15	0.29	−0.09	0.52
22:0	−0.09	0.54	−0.15	0.32
20:4n-6 (ARA)	0.11	0.45	0.13	0.37
SFA	0.60	<0.001	0.51	<0.001
UFA	0.75	<0.001	0.71	<0.001
MUFA	0.65	<0.001	0.60	<0.001
PUFA	0.71	<0.001	0.68	<0.001

Correlation 1 between dietary fatty acids concentration (mmol/kg DM) and that of plasma concentration (μmol/L). *Correlation 2* between calculated daily fatty acids intake (mmol/day) and that of plasma concentration (μmol/L)

increased plasma levels of ALA, but forage type did not influence ALA levels (mean value 1,142 μmol/L). Consequently, the forages in our study appear to have a similar impact on fatty acid biohydrogenation, even though ensiling may alter the activity of some plant secondary compounds that could alter this process [21].

Among the long chain omega-3-fatty acids, the plasma concentration of EPA was the only fatty acid that was increased as a result of the addition of flaxseed to diet. This result may reflect the high plasma concentrations of ALA as it is the precursor for the formation of EPA via elongation and desaturation. Others have previously found that feeding flaxseed to steers increased levels of EPA and DPA in bovine muscle without altering levels of DHA [6]. High levels of ALA may reduce formation of DHA as both ALA and the precursor for DHA synthesis compete for desaturation via Δ6 desaturase [36].

Feeding flaxseed to monogastric and ruminant animals has the potential benefit of increasing omega-3 fatty acids in meat, and for ruminants this is also accompanied by increased levels of ALA hydrogenation products, some of which have reported effects on human health. RUA is typically the most abundant CLA isomer in beef and it has many purported beneficial health effects [8]. RUA is a product of hydrogenation of PUFAs in the rumen and in the body arises mainly from endogenous synthesis via dehydrogenation of 18:1-*trans* fatty acids including VAA [37]. Overall, feeding flax increased plasma CLA, but levels were not influenced by forage type. Feeding flaxseed combined with silage, however, promoted more complete hydrogenation of ALA (i.e., 18:0) while feeding flaxseed combined with hay resulted in greater accumulations of plasma 18:1-*trans*, mainly in the form of VAA.

With the Latin square design used in the present study, it was possible to track the plasma ALA changes of the same animal during the overall experiment when the four different diets were fed. The plasma ALA concentration reached the highest level on day 14 and thereafter reached a plateau for the remaining time that flaxseed was supplemented. When changed to the control diet, without flaxseed, plasma ALA levels declined to pre-supplementation levels within 14 days (data not shown). These results suggest that the plasma ALA level was directly influenced by dietary flaxseed supplementation. Plasma fatty acid levels may be affected not only by absorption, but also by endogenous lipid metabolism including incorporation of fatty acids into tissues and lipolysis releasing fatty acids from adipose tissue. In a study using lactating dairy cows [1], it was found that inclusion of formaldehyde-treated (11%) or untreated flaxseed (13%) in silage diets resulted in a similar increase in plasma omega-3 fatty acid levels with ALA accounting for about 15% of the total fatty acids in plasma. Based on the current and previous studies [1–3, 33] it is suggested that including flaxseed in the diet at levels that result in 6% total lipid in the diet will result in significant levels of ALA escaping the rumen.

In fattening animals, plasma fatty acids may be directly used for incorporation into adipose tissue. A strong positive correlation has been reported for wt% of ALA between plasma and fat tissue with a coefficient (r) of 0.88 ($P < 0.0001$), while no correlation was observed for LNA ($r = 0.13$, $P = 0.33$) [38]. These results were based on 64 cull cows (16 per treatment) fed hay- or silage-based diet supplemented with or without ground flaxseed for 12 weeks. Plasma levels of ALA could have value as predictors for accretion of this fatty acid in adipose tissue, likely because this fatty acid is considered essential in mammals.

In conclusion, the results from this study indicated that flaxseed supplementation in cattle diets can be used to increase plasma levels of beneficial fatty acids including ALA, EPA, VAA and CLA (combined RUA and 18:2-*t*7,c9), but there is no difference in ALA, EPA or RA when flaxseed is included in a barley silage versus a hay-based diet. Feeding flaxseed combined with hay, however, can lead to preferential accumulations of plasma VAA which is a precursor for CLA synthesis [37]. Elevated plasma levels of this fatty acid could increase its availability for incorporation into tissues resulting in a more desirable fatty acid profile in beef.

References

1. Petit HV (2003) Digestion, milk production, milk composition, and blood composition of dairy cows fed formaldehyde treated flaxseed or sunflower seed. J.Dairy Sci 86:2637–2646
2. Scislowski V, Bauchart D, Gruffat D, Laplaud PM, Durand D (2005) Effect of dietary n-6 or n-3 polyunsaturated fatty acids protected or not against ruminal hydrogenation on plasma lipids and their susceptibility to peroxidation in fattening steers. J Anim Sci 83:2162–2174
3. Farran TB, Reinhardt CD, Blasi DA, Minton JE, Elsasser TH, Higgins JJ, Drouillard JS (2008) Source of dietary lipid may modify the immune response in stressed feeder cattle. J Anim Sci 86:1382–1394
4. Kronberg SL, Barceló-Coblijn G, Shin J, Lee K, Murphy EJ (2006) Bovine muscle n-3 fatty acid content is increased with flaxseed feeding. Lipids 41:1059–1068
5. Montgomery SP, Drouillard JS, Nagaraja TG, Titgemeyer EC, Sindt JJ (2008) Effects of supplemental fat source on nutrient digestion and ruminal fermentation in steers. J Anim Sci 86:640–650
6. Jump DB (2002) The Biochemistry of n-3 polyunsaturated fatty acids. J Biol Chem 277:8755–8758
7. Simopoulos AP (1991) Omega-3 fatty acids in health and disease and in growth and development. Am J Clin Nutr 54:438–463
8. Azain MJ (2003) Conjugated linoleic acid and its effect on animal products and health in single-stomached animals. Proc Nutr Soc 62:319–328
9. French P, Stanton C, Lawless F, O'Riordan EG, Monaham FJ, Caffrey PJ, Moloney AP (2000) Fatty acid composition, including conjugated linoleic acid, of intramuscular fat from steers offered grazed grass, grass silage, or concentrate-based diets. J Anim Sci 78:2849–2855
10. Lee MRF, Tweed JKS, Dewhurst RJ, Scollan ND (2006) Effect of forage: concentration ratio on ruminal metabolism and duodenal flow of fatty acids in beef steers. Anim Sci 82:31–40
11. Chilliard Y, Ferlay A, Doreau M (2001) Effect of different types of forages, animal fat or marine oils in cow's diet on milk fat secretion and composition, especially conjugated linoleic acid (CLA) and polyunsaturated fatty acids. Livestock Prod Sci 70:31–48
12. Dierking RM, Kallenbach RL, Grün IU (2010) Effect of forage species on fatty acid content and performance of pasture-finished steers. Meat Sci 85:597–605
13. Chilliard Y, Ferlay A (2004) Dietary lipids and forages interactions on cow and goat milk fatty acid composition and sensory properties. Reprod Nutr Dev 44:467–492
14. Bernard L, Shingfield KJ, Rouel J, Ferlay A, Chilliard Y (2009) Effect of plant oils in the diet on performance and milk fatty acid composition in goats fed diets based on grass hay or maize silage. Brit J Nutr 101:213–224
15. Kong YH, He ML, McAlister TA, Seviour R, Forster R (2010) Quantitative fluorescence in situ hybridization of microbial communities in the rumen of cattle fed different diets. Appl Environ Microbiol 76:6933–6938
16. Bagheripour E, Rouzbehan Y, Alipour D (2008) Effects of ensiling, air-drying and addition of polyethylene glycol on in vitro gas production of pistachio by-products. Anim Feed Sci Technol 146:327–336
17. Hultin M, Savonen R, Olivecronal M (1996) Chylomicron metabolism in rats: lipolysis, recirculation of triglyceride-derived fatty acids in plasma FFA, and fate of core lipids as analyzed by compartmental modeling. J Lipid Res 37:1022–1036
18. Koutsari C, Dumesic DA, Patterson BW, Votruba SB, Jensen MD (2008) Plasma free fatty acid storage in subcutaneous and visceral adipose tissue in post absorptive women. Diabetes 57:1186–1194
19. Brazle AE, Johnson BJ, Webel SK, Rathbun TJ, Davis DL (2009) Omega-3 fatty acids in the gravid pig uterus as affected by maternal supplementation with omega-3 fatty acids. J Anim Sci 87:994–1002
20. Dugan MER, Rolland DC, Aalhus JL, Aldai N, Kramer JKG (2008) Subcutaneous fat composition of youthful and mature Canadian beef: emphasis on individual conjugated linoleic acid and trans-18:1 isomers. Can J Anim Sci 88:591–599
21. Raes K, De Smet S, Demeyer D (2004) Effect of dietary fatty acids on incorporation of long chain polyunsaturated fatty acids and conjugated linoleic acid in lamb, beef and pork meat: a review. Anim Feed Sci Technol 113:199–221
22. NRC (2001) Nutrient requirements of dairy cattle: Seventh revised edn. National Academy Press, Washington DC
23. NRC (1996) Nutrient requirements of beef cattle: Seventh revised edn. update 2000. National Academy Press, Washington DC
24. Radin NS (1981) Extraction of tissue lipids with a solvent of low toxicity. Methods Enzymol 72:5–7
25. Lock AL, Garnsworthy PC (2002) Independent effects of dietary linoleic and linolenic fatty acids on the conjugated linoleic acid content of cows' milk. Anim Sci 74:163–176
26. Kramer JKG, Fellner V, Dugan MER, Sauer FD, Mossob MM, Yurawecz MP (1997) Evaluating acid and base catalysts in the methylation of milk and rumen fatty acids with special emphasis on conjugated dienes and total trans fatty acids. Lipids 32: 1219–1228
27. Ratnayake WMN (2004) Overview of methods for the determination of *trans* fatty acids by gas chromatography, silver-ion thin-layer chromatography, silver-ion liquid chromatography, and gas chromatography/mass spectrometry. J AOAC Int 87:523–539
28. Cruz-Hernandez C, Deng Z, Zhou J, Hill AR, Yurawecz MP, Dugan MER, Kramer JKG (2004) Methods for analysis of conjugated linoleic acids and trans-18:1 isomers in dairy fats by using a combination of gas chromatography, silver-ion thin-layer chromatography/gas chromatography, and silver-ion liquid chromatography. J AOAC Int 87:545–562
29. SAS Institute (2007) SAS/STAT Users Guide. SAS Inst., Inc., Cary, NC
30. Krauss RM, Eckel RH, Howard B, Appel LJ, Daniels SR, Deckelbaum RJ, Erdman JW Jr, Kris-Etherton P, Goldberg IJ, Kotchen TA, Lichtenstein AH, Mitch WE, Mullis R, Robinson K, Wylie-Rosett J, St Jeor S, Suttie J, Tribble DL, Bazzarre TL (2000) Revision 2000: a statement for healthcare professionals from the nutrition committee of the American Heart Association. J Nutr 131:132–146
31. He ML, Ishikawa S, Hidari H (2005) Fatty acid profiles of various muscles and adipose tissues from fattening horses in comparison with beef cattle and pigs. Asian-Aust J Anim Sci 18:1655–1661
32. Petit HV (2003) Digestion, milk production, milk composition, and blood composition of dairy cows fed formaldehyde treated flaxseed or sunflower seed. J Dairy Sci 86:2637–2646
33. Loor JJ, Ueda K, Ferlay A, Chilliard Y, Doreau M (2004) Biohydrogenation, duodenal flow, and intestinal digestibility of trans fatty acids and conjugated linoleic acids (CLA) in response to dietary forage: concentrate ratio and linseed oil in dairy cows. J Dairy Sci 87:2472–2485
34. Doreau M, Laverroux S, Normand J, Chesneau G, Glasser F (2009) Effect of linseed fed as rolled seeds, extruded seeds or oil on fatty acid rumen metabolism and intestinal digestibility in cows. Lipids 44:53–62
35. Kronberg SL, Scholljegerdes EJ, Barceló-Coblijin G, Murphy EJ (2007) Flaxseed treatment to reduce biohydrogenation of α-Linolenic acid by rumen microbes in cattle. Lipids 42:1105–1111
36. Cameron ND, Wood JD, Enser M, Whittington FM, Penman JC, Robinson AM (2000) Sensitivity of pig genotypes to short-term

manipulation of plasma fatty acids by feeding linseed. Meat Sci 56:379–386
37. Corl BA, Baumgard LH, Dwyer DA, Griinari JM, Phillips BS, Bauman DE (2001) The role of Δ9-desaturase in the production of cis-9, trans-11 CLA. J Nutr Biochem 12:622–630
38. He ML, McAllister TA, Kastelic JP, Chung YH, Beauchemin KA, Mir PS, Aalhus JL, Dugan MER, Aldai N (2010) Feeding flaxseed to beef cows increases concentrations of omega-3 fatty acids and linolenic acid biohydrogenation intermediates in subcutaneous fat. J Anim Sci 88(2):67–67

Lipids (2011) 46:587–606
DOI 10.1007/s11745-011-3561-1

ORIGINAL ARTICLE

Identification and Ruminal Outflow of Long-Chain Fatty Acid Biohydrogenation Intermediates in Cows Fed Diets Containing Fish Oil

Piia Kairenius · Vesa Toivonen · Kevin J. Shingfield

Received: 20 May 2010 / Accepted: 7 April 2011 / Published online: 12 May 2011

Abstract The abundance of 20- to 24-carbon fatty acids in omasal digesta of cows fed grass silage-based diets supplemented with 0 (Control) and 250 g/day of fish oil (FO) was examined to investigate the fate of long-chain unsaturated fatty acids in the rumen. Complimentary argentation thin-layer chromatography and gas-chromatography mass-spectrometry analysis of fatty acid methyl esters and corresponding 4,4-dimethyloxazoline derivatives prepared from fish oil and omasal digesta enabled the structure of novel 20- to 22-carbon fatty acids to be elucidated. Compared with the Control, the FO treatment resulted in the formation and accumulation of 27 novel 20- and 22-carbon biohydrogenation intermediates containing at least one *trans* double bond and the appearance of *cis*-14 20:1, 20:2n-3, 21:4n-3 and 22:3n-6 not contained in fish oil. No conjugated ≥20-carbon fatty acids were detected in Control or FO digesta. In conclusion, fish oil in the diet results in the formation of numerous long-chain biohydrogenation intermediates in the rumen of lactating cows. Comparison of the intake and flow of 20-, 21- and 22-carbon fatty acids at the omasum in cows fed the Control and FO treatments suggests that the first committed steps of 20:5n-3, 21:5n-3 and 22:6n-3 hydrogenation in the rumen involve the reduction and/or isomerisation of double bonds closest to the carboxyl group.

Keywords Biohydrogenation · Fish oil · Lactating cow · Gas-chromatography mass-spectrometry · Silver-ion thin-layer chromatography

P. Kairenius · V. Toivonen · K. J. Shingfield (✉)
Animal Production Research, MTT Agrifood Research Finland, 31600 Jokioinen, Finland
e-mail: kevin.shingfield@mtt.fi

Abbreviations

DMOX	4,4-Dimethyloxazoline
FAME	Fatty acid methyl ester
GC	Gas chromatography
GC–MS	Gas chromatography–mass spectrometry
HPLC	High-performance liquid chromatography
TLC	Thin-layer chromatography

Introduction

Clinical studies in human subjects have established that eicosapentaenoic acid (20:5n-3) and docosahexaenoic acid (22:6n-3) exert anti-thrombotic and anti-arrhythmic properties, with evidence that long-chain n-3 fatty acids decrease cardiovascular disease risk and the incidence of myocardial infarction [1–3]. Ruminant-derived foods are a major source of lipid in the human diet [4], and therefore a number of studies have examined the use of fish oil in the diet of growing and lactating cattle to enhance the concentrations of 20:5n-3 and 22:6n-3 in meat [5] and milk [4, 6] to improve long-term human health. However, the potential to enrich 20:5n-3 and 22:6n-3 in milk fat and tissue lipids is limited due to extensive metabolism of long-chain n-3 fatty acids in the rumen. It is well established that 20:5n-3 and 22:6n-3 are hydrogenated extensively in the rumen in vivo [7–9] and disappear during incubations with rumen fluid in vitro [10–12], but the metabolic pathways involved and the intermediates formed are not known. Characterizing the fatty acids formed during the metabolism of long-chain n-3 fatty acids in the rumen is important to providing a more fundamental understanding of the mechanisms involved in the hydrogenation of long-chain

unsaturated fatty acids in the rumen and also offering an explanation for the decreases in tissue adipogenesis and mammary lipogenesis in ruminants fed diets containing fish oil.

Several techniques have been developed for the determination of lipid composition in ruminal digesta [13, 14]. No single method in isolation can provide a comprehensive assessment of the occurrence of fatty acids in biological samples and therefore a combination of techniques are required [14–16]. Previous studies examining the effect of fish oil on ruminal biohydrogenation have been based on the determination of lipid composition in digesta using a combination of gas chromatography (GC), gas-chromatography mass-spectrometry (GC–MS) and silver-ion high-performance liquid-chromatography (Ag^+-HPLC) analysis of fatty acid methyl esters (FAME) [7–9]. However, these techniques provide only limited information on the structure of fatty acids formed during ruminal biohydrogenation of long-chain unsaturated fatty acids. In order to characterise the intermediates formed during ruminal biohydrogenation of long-chain fatty acids in fish oil, the structure and composition of 20- to 24-carbon fatty acids in fish oil and the omasal digesta of cows fed grass-silage-based diets supplemented with 0 or 250 g/day of fish oil was determined. Fatty acids were identified based on the fractionation of FAME by Ag^+-TLC and GC–MS analysis of FAME and corresponding 4,4-dimethyloxazoline (DMOX) derivatives. Detailed analysis of fish oil and omasal digesta fatty acid composition combined with measurements of nutrient flow at the omasum provided the first quantitative estimates of ruminal long-chain fatty acid biohydrogenation intermediate outflow in lactating cows.

Materials and Methods

Materials

Samples of freeze-dried omasal digesta reconstituted from individual liquid, small and large particulate fractions according to indigestible marker concentrations to represent true digesta at the omasal canal were obtained from following the completion of an experiment with five cows fed grass-silage-based diets supplemented with 0 (Control) or 250 g/day of refined fish oil (FO; EPAX 3000 TG, Pronova Biocare, Aalesund, Norway) fed over consecutive 14-day experimental periods [7]. Reconstituted omasal digesta of cows fed the Control and FO treatments were stored at −80 °C under nitrogen until analysed for non-esterified fatty acids [7] or subjected to more extensive analysis of total lipid composition as described in the present paper. All chemicals and solvents were of analytical grade. Authentic reference FAME standards were purchased from Nu-Chek Prep (GLC #463; 21:0, #N-21-M; 23:0, #N-23-M; 24:0, #N-24-M; *trans*-11 20:1, #U-64-M; *cis*-12-21:1, #U-85-M; *cis*-14 23:1, #U-87-M; Elysian, MN), Larodan Fine Chemicals (18:4n-3, #10-1840; *cis*-9 20:1, #20-2001-1-4; 20:4n-3, #20-2024-1; 21:3n-3, #20-2103-1-4; 21:5n-3, #20-2105-1-4; *trans*-13 22:1, #20-2210-9; 22:5n-6, #20-2265-7; 23:5n-3, #20-2305-1-4; 24:5n-3, #20-2405-4; 25:0, #20-2500-7; 29:0, #20-2900-7; 9-O-18:0, #14-1800-5-4; 12-O-18:0, #14-1800-6-4; 13-O-18:0, #14-1800-7-4; 16-O-18:0, #14-1800-8-39; Malmö, Sweden) and Sigma-Aldrich (26:0, #H-6389; 27:0, #H-6639; 28:0, #O-4129; 30:0 #T-1902; mixture of 18:2n-6 isomers, #L-8404; mixture of conjugated 18:2 isomers, #O-5632; mixture of 18:3n-3 isomers, #L-6031; St. Louis, MO).

Lipid Extraction and Preparation of Fatty Acid Methyl Esters

Samples (200 mg) of freeze-dried reconstituted omasal digesta were transferred into 10 mL glass tubes. Following the addition of 0.5 mL distilled water and 1 mL of internal standard (tridecanoic acid, #13-A, Nu-Check Prep) dissolved in ethanol (0.1%, w/v), the pH was adjusted to 2.0 with 2 M hydrochloric acid. After mixing for 5 min, lipid was extracted in duplicate with a mixture of hexane and isopropanol (3:2, v/v) [17]. After rinsing with 2 mL of deionized water, organic extracts were combined, dried over 1 g anhydrous sodium sulphate and dried at 45 °C under a steady stream of nitrogen. FAME were prepared using a two-step base-acid catalysed procedure. Extracted lipid was dissolved in 2 mL of hexane and transesterified using sodium methoxide in methanol [18]. After drying over 1 g calcium chloride for 30 min, the organic soluble phase was transferred to a clean test tube, evaporated to dryness under a stream of nitrogen at 30 °C and incubated at 50 °C for 30 min with 1.5 mL of 1% (v/v) sulphuric acid in methanol [7]. After rinsing according to standard procedures, [7] FAME were dissolved in hexane prior to GC analysis and Ag^+-TLC.

Argentation Silver Ion Thin Layer Chromatography

Argentation-TLC of FAME prepared from total lipid in digesta was performed using Silica gel G plates (200 × 200 mm and 0.50 mm thickness, No. 1.13894; Merck, Darmstadt, Germany) impregnated with 5% (w/v) silver nitrate in acetonitrile for 20 min and activated at 110 °C for 45 min just before sample application. Plates were developed with a solvent comprised of hexane and diethyl ether (90:10 v/v) and the separated bands were visualized under UV light after spraying with a 0.2% (w/v) solution of 2′,7′-dichlorofluorescein in methanol [14, 19, 20]. Five bands separated according to the degree of

unsaturation and corresponding to methyl esters of saturated, *cis*-, and *trans*-monoenoic, dienoic and polyenoic fatty acids containing three or more double bonds were removed individually from the plate and transferred to clean test tubes. Fractionated FAME were recovered from the silica after addition of 1 mL methanol, 2 mL of hexane and 1 mL of 6% (w/v) aqueous sodium chloride [21] and the hexane soluble phase was dried over anhydrous sodium sulphate. Each FAME fraction was submitted for GC and GC–MS analysis and converted to DMOX derivatives.

Preparation of 4,4-Dimethyloxazoline Derivatives

Samples of total and fractionated FAME were converted to DMOX derivatives by incubation overnight with 250 μL of 2-amino, 2-methyl, 1-propanol under a nitrogen atmosphere [22] at 170 °C. Once cooled, the reaction mixture was dissolved with 5 mL of a mixture of diethyl ether and hexane (1:1 v/v) and rinsed with 5 mL of distilled water. The organic phase was recovered, transferred to a clean tube and the extraction was repeated using 2 mL of the diethyl ether and hexane solvent mixture. Both organic extracts were combined, washed with 3 mL of distilled water, dried over anhydrous sodium sulphate, centrifuged and evaporated to dryness under nitrogen at 30 °C (http://lipidlibrary.aocs.org/ms/ms02/index.htm). Once prepared, DMOX derivatives were dissolved in hexane and analysed by GC–MS.

GC and GC–MS Analysis

Total FAME profile in a 2 μL sample at a split ratio of 1:50 was determined with a gas chromatograph (6890, Hewlett-Packard, Wilmington, DE) equipped with a flame ionization detector and a 100-m CP-Sil 88 fused silica capillary column (Chrompack, Middelburg, The Netherlands) using a temperature gradient program and hydrogen as the carrier gas operated at constant pressure (137.9 kPa) at a flow rate of 0.5 mL/min [7].

Mass spectra of FAME and DMOX derivatives were obtained using the same type of gas chromatograph and column used for analysis of FAME composition equipped with a selective quadrupole mass detector (model 5973 N, Agilent Technologies, Wilmington, DE) connected to a dedicated computer with ChemStation software installed. The mass spectrometer was operated at 230 °C in the electron impact ionization mode, and mass spectra were recorded under an ionization energy of 70 eV. The injector (split ratio of 1:50) and interface temperatures were maintained at 255 and 240 °C, respectively. Total DMOX profiles in a 4 μL sample volume were determined using helium as a carrier gas operated at constant pressure (142.6 kPa) at a flow rate of 0.6 mL/min and the same temperature gradient program applied for the analysis of FAME by GC.

Interpretation of mass spectra were performed according to established guidelines [23, 24]. Electron impact ionization spectra of DMOX derivatives were used to locate double bonds based on atomic mass unit distances (amu), with an interval of 12 amu between the most intense peaks of clusters of ions containing n and n − 1 carbon atoms being interpreted as cleavage of the double bond between carbon n and n + 1 in the fatty acid moiety. In addition, odd numbered fragments at *m*/*z* 139, 153 and 167 accompanied by even mass ions at *m*/*z* 138, 152 and 166 were used as diagnostic ions to locate double bonds at Δ4, Δ5 and Δ6, respectively [25–27]. When available, deduced fatty acid structure was verified by comparison with the mass spectrum of DMOX derivatives prepared from authentic FAME standards, reports in the literature [22, 25–27], and cross-referencing with an online reference spectra library (http://lipidlibrary.aocs.org/ms/masspec.html). Since GC–MS analysis of DMOX derivatives does not discriminate between geometric isomers, double bond geometry of monoenoic fatty acids was confirmed based on the appearance of FAME in bands separated by Ag^+-TLC. Fractionation of FAME by Ag^+-TLC did not resolve dienoic, trienoic, tetraenoic, pentaenoic and hexaenoic fatty acids, and therefore a *cis* or *trans* double bond configuration for fatty acids containing two or more double bonds was inferred based on comparisons of retention times of methyl esters in samples with authentic FAME standards and the known elution order of geometric isomers of 18:2n-6 and 18:3n-3 methyl esters (L-8404 and L-6031, Sigma-Aldrich) on a 100 m CP Sil 88 capillary column [28, 29].

Statistical Analysis

Differences in fatty acid flow at the omasum and ruminal fatty acid balance between the control and FO treatments were evaluated statistically by a paired *t* test (SAS® Systems, Release 9.2, SAS Institute, Cary, NC). A 95% confidence interval was used as the default for the hypothesis test and assumptions of data normality were validated using the univariate procedure (SAS® Systems). Differences at $P < 0.05$ were considered significant.

Results

Analysis of FAME by GC revealed the occurrence of a complex mixture of 20- to 22-carbon fatty acids in fish oil and omasal digesta of cows on the FO treatment eluting between 42.5 and 53.9 min (Figs. 1, 2, 3, 4). Relative abundance of long-chain methyl esters prepared from total

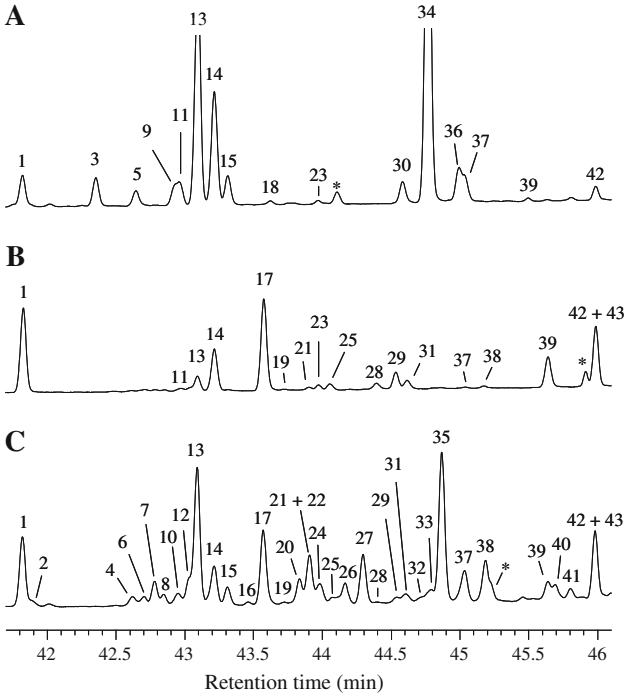

Fig. 1 Partial gas chromatogram indicating the separation of fatty acid methyl esters (FAME) prepared from total lipids in **a** refined fish oil and **b**,**c** omasal digesta of cows fed grass silage-based diets supplemented with 0 (**b**) or 250 g/day (**c**) of refined fish oil. Peaks were identified based on gas-chromatography mass-spectrometry (GC–MS) analysis of 4,4-dimethyloxaline derivatives prepared from FAME fractionated by silver-ion thin-layer chromatography (Ag^+-TLC). Molecular ions and key diagnostic ion fragments recorded during GC–MS analysis used to identify carbon chain length and locate the position of double bonds of unsaturated fatty acids are listed in Table 1. Parenthesis indicate tentative geometry of double bonds as inferred based on retention times and elution order of FAME during GC analysis relative to authentic methyl ester standards. Peak identification: *1*, 20:0; *2*, Δ7,9-17:2; *3*, *cis*-6, *cis*-9, *cis*-12 18:3; *4*, unresolved *trans*-9 20:1 and *trans*-10 20:1; *5*, *cis*-5 20:1; 6, *trans*-11 20:1; *7*, *trans*-12 20:1; *8*, *trans*-13 20:1; *9*, *cis*-8 20:1; *10*, *trans*-14 20:1; *11, cis*-9 20:1; *12*, *trans*-15 20:1; *13*, *cis*-11 20:1; *14*, *cis*-9, *cis*-12, *cis*-15 18:3; *15*, *cis*-13 20:1; *16*, *cis*-14 20:1; *17*, *cis*-9, *trans*-11 18:2; *18*, *cis*-15 20:1; *19*, *trans*-9, *cis*-11 18:2; *20*, unresolved *cis*-11, *trans*-13 18:2 and *trans*-11, *trans*-15 20:2; *21*, *cis*-16 20:1; *22*, unresolved *trans*-10, *cis*-12 18:2 and *trans*-9, *trans*-15 20:2; *23*, 21:0; *24*, *trans*-10, *trans*-16 20:2; *25*, *trans*-11, *cis*-13 18:2; *26*, *trans*-13, *trans*-17 20:2; *27*, *trans*-11, *cis*-15 20:2; *28*, *trans*-12, *trans*-14 18:2; *29*, *trans*-11, *trans*-13 18:2; *30*, *cis*-8, *cis*-11 20:2; *31*, unresolved *trans*-7, *trans*-9 18:2, *trans*-8, *trans*-10 18:2 and *trans*-9, *trans*-11 18:2; *32*, *cis*-10, *trans*-15 20:2; *33*, *trans*-11, *cis*-17 20:2; *34*, *cis*-6, *cis*-9, *cis*-12, *cis*-15 18:4; *35*, *trans*-13, *cis*-17 20:2; *36*, *cis*-8, *cis*-11, *cis*-14, *cis*-17 18:4; *37*, *cis*-11, *cis*-14 20:2; *38*, *trans*-14, *cis*-17 20:2; *39*, *cis*-9, *trans*-11, *cis*-15 18:3; *40*, *cis*-14, *cis*-17 20:2; *41*, (*trans*)-9, (*trans*)-14, (*trans*)-17 20:3; *42*, 22:0; *43*, (*trans*)-10, (*trans*)-14, (*trans*)-17 20:3; *asterisks*, unidentified peaks

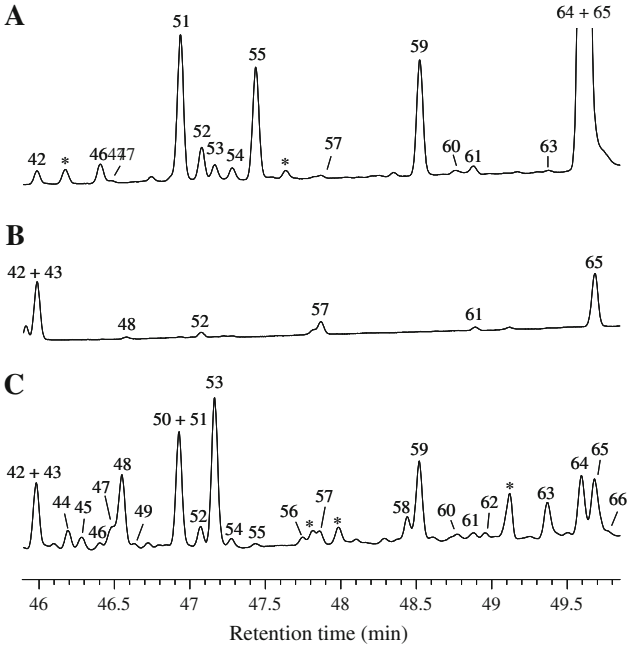

Fig. 2 Partial gas chromatogram indicating the separation of FAME prepared from total lipids in **a** refined fish oil and **b**,**c** omasal digesta of cows fed grass silage-based diets supplemented with 0 (**b**) or 250 g/day (**c**) of refined fish oil. Peaks were identified based on GC–MS analysis of 4,4-dimethyloxaline derivatives prepared from FAME fractionated by Ag^+-TLC. Molecular ions and key diagnostic ion fragments recorded during GC–MS analysis used to identify carbon chain length and locate the position of double bonds of unsaturated fatty acids are listed in Table 1. Parenthesis indicate tentative geometry of double bonds as inferred based on retention times and elution order of FAME during GC analysis relative to authentic methyl ester standards. Peak identification: *42*, 22:0; *43*, (*trans*)-10, (*trans*)-14, (*trans*)-17 20:3; *44*, (*cis*)-10, (*trans*)-14, (*trans*)-17 20:3 or (*trans*)-10, (*cis*)-14, (*trans*)-17 20:3; *45*, (*cis*)-11, (*trans*)-14, (*trans*)-17 20:3 or (*trans*)-11, (*cis*)-14, (*trans*)-17 20:3; *46*, *cis*-8, *cis*-11, *cis*-14 20:3; *47*, (*cis*)-11, (*cis*)-14, (*trans*)-17 20:3; *48*, (*trans*)-10, (*trans*)-14, (*cis*)-17 20:3; *49*, Δ11,14,18-20:3; *50*, (*trans*)-11, (*cis*)-14, (*cis*)-17 20:3; *51*, *cis*-11 22:1; *52*, *cis*-13 22:1; *53*, *cis*-11, *cis*-14, *cis*-17 20:3; *54*, *cis*-15 22:1; *55*, *cis*-5, *cis*-8, *cis*-11, *cis*-14 20:4; *56*, *trans*-12, *trans*-17 22:2; *57*, 23:0; *58*, (*trans*)-7, (*cis*)-11, (*cis*)-14, (*cis*)-17 20:4; *59*, *cis*-8, *cis*-11, *cis*-14, *cis*-17 20:4; *60*, *cis*-13, *cis*-16 22:2; *61*, *cis*-14 23:1; *62*, *cis*-12, *cis*-15, *cis*-18 21:3; *63*, Δ10,13,17-22:3; *64*, *cis*-5, *cis*-8, *cis*-11, *cis*-14, *cis*-17 20:5; *65*, 24:0; *66*, (*cis*)-10, (*trans*)-14, (*cis*)-19 22:3; *asterisk*, unidentified peaks

lipid in omasal digesta of cows on the FO diet was almost identical to the profile of FAME in the non-esterifed fatty acid fraction [7] (data not presented).

Development of TLC plates with hexane and diethyl ether allowed 18-, 20-, and 22-carbon *cis*-monoenoic isomers to be resolved from *trans*-monoenoic methyl esters, but did not result in the complete separation of methyl esters of long-chain dienoic and trienoic fatty acids. In total, five distinct bands comprised of saturated, *trans*- and *cis*-monoenoic, di- and trienoic species were recovered, while methyl esters of ≥18-carbon polyenoic fatty acids containing four or more double bonds remained at or near the origin (data not presented).

Initial identification of fatty acid carbon chain length and number of double bonds in fish oil and omasal digesta was based on GC–MS analysis of FAME. Appearance of 20:1, 20:2, 20:3, 20:4, 20:5, 21:3, 21:4, 21:5, 22:1, 22:2,

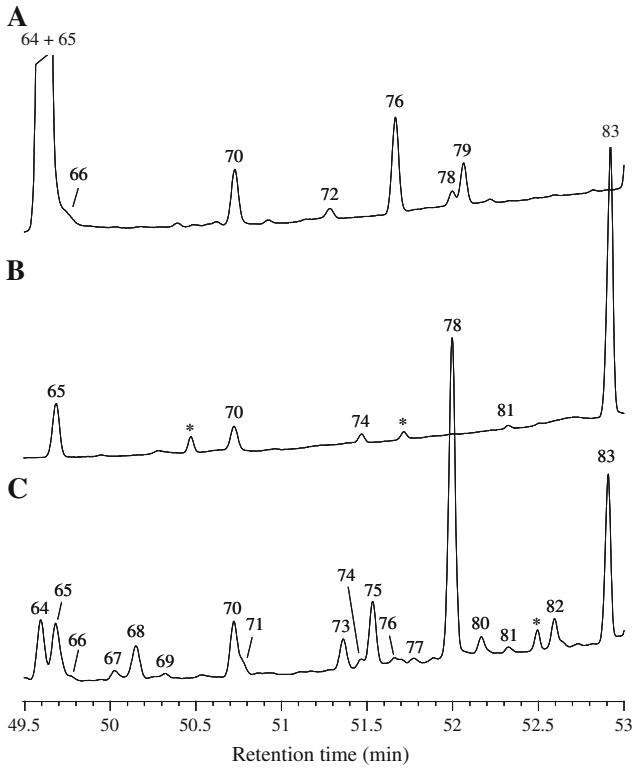

Fig. 3 Partial gas chromatogram indicating the separation of FAME prepared from total lipids in **a** refined fish oil and **b**,**c** omasal digesta of cows fed grass silage-based diets supplemented with 0 (**b**) or 250 g/day (**c**) of refined fish oil. Peaks were identified based on GC–MS analysis of 4,4-dimethyloxaline derivatives prepared from FAME fractionated by Ag^{+}-TLC. Molecular ions and key diagnostic ion fragments recorded during GC–MS analysis used to identify carbon chain length and locate the position of double bonds of unsaturated fatty acids are listed in Table 1. Parenthesis indicate tentative geometry of double bonds as inferred based on retention times and elution order of FAME during GC analysis relative to authentic methyl ester standards. Peak identification: *64*, *cis*-5, *cis*-8, *cis*-11, *cis*-14, *cis*-17 20:5; *65*, 24:0; *66*, (*cis*)-10, (*trans*)-14, (*cis*)-19 22:3; *67*, *cis*-10, *cis*-13, *cis*-16 22:3; *68*, (*trans*)-12, (*cis*)-16, (*cis*)-19 22:3; *69*, unresolved *cis*-9, *cis*-12, *cis*-15, *cis*-18 21:4 and *cis*-11 24:1; *70*, *cis*-15 24:1; *71*, *cis*-13, *cis*-16, *cis*-19 22:3; *72*, *cis*-7, *cis*-10, *cis*-13, *cis*-16 22:4; *73*, (*trans*)-10, (*trans*)-13, (*cis*)-16, (*cis*)-19 22:4; *74*, 25:0; *75*, (*trans*)-8, (*cis*)-13, (*cis*)-16, (*cis*)-19 22:4; *76*, *cis*-6, *cis*-9, *cis*-12, *cis*-15, *cis*-18 21:5; *77*, (*cis*)-7, (*trans*)-13, (*cis*)-16, (*cis*)-19 22:4; *78*, *cis*-10, *cis*-13, *cis*-16, *cis*-19 22:4; *79*, *cis*-4, *cis*-7, *cis*-10, *cis*-13, *cis*-16 22:5; *80*, 10-O-16:0; *81*, *cis*-16 25:1; *82*, (*trans*)-5, (*cis*)-10, (*cis*)-13, (*cis*)-16, (*cis*)-19 22:5; *83*, 26:0; *asteriks*, unidentified peaks

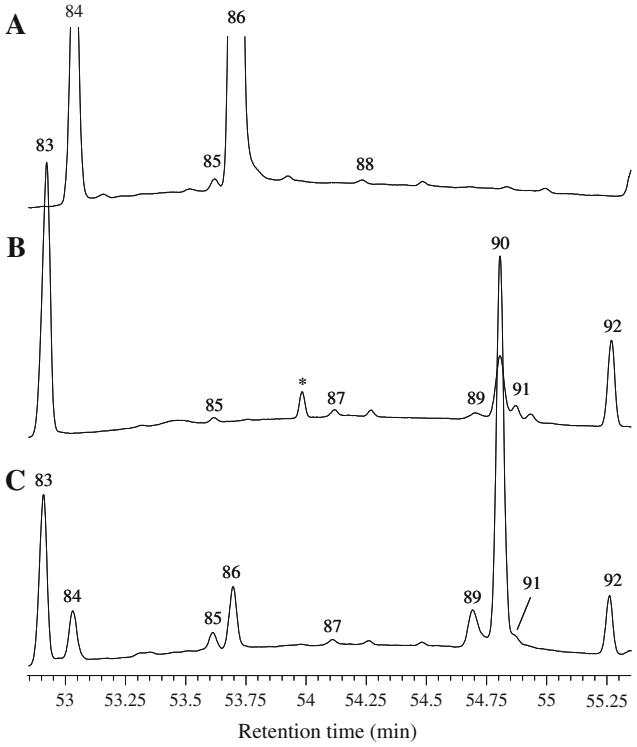

Fig. 4 Partial gas chromatogram indicating the separation of FAME prepared from total lipids in **a** refined fish oil and **b**,**c** omasal digesta of cows fed grass silage-based diets supplemented with 0 (**b**) or 250 g/day (**c**) of refined fish oil. Peaks were identified based on GC–MS analysis of 4,4-dimethyloxaline derivatives prepared from FAME fractionated by Ag^{+}-TLC. Molecular ions and key diagnostic ion fragments recorded during GC–MS analysis used to identify carbon chain length and locate the position of double bonds of unsaturated fatty acids are listed in Table 1. Parenthesis indicate tentative geometry of double bonds as inferred based on retention times and elution order of FAME during GC analysis relative to authentic methyl ester standards. Peak identification: *83*, 26:0; *84*, *cis*-7, *cis*-10, *cis*-13, *cis*-16, *cis*-19 22:5; *85*, *cis*-17 26:1; *86*, *cis*-4, *cis*-7, *cis*-10, *cis*-13, *cis*-16, *cis*-19 22:6; *87*, 27:0; *88*, *cis*-8, *cis*-11, *cis*-14, *cis*-17, *cis*-20 23:5; *89*, unresolved 10-OH-18:0 and 9-O-18:0; *90*, 10-O-18:0; *91*, 13-O-18:0; *92*, 28:0; *asterisks*, unidentified peaks

22:3, 22:4, 22:5, 22:6, 23:5, 24:5 and 24:6 methyl esters was confirmed based on molecular ions at *m*/*z* 324, 322, 320, 318, 316, 334, 332, 330, 352, 350, 348, 346, 344, 342, 358, 372 and 370, respectively. However, the mass spectra of FAME did not contain sufficient characteristic ion fragments to allow the position of double bonds to be located. Therefore, the structure of long-chain fatty acids contained in fish oil and omasal digesta were formally identified based on GC–MS analysis of DMOX derivatives. Selected regions of the total ion chromatogram for DMOX derivatives prepared from total lipid in omasal digesta of cows fed the FO treatment are shown in Figs. 5 and 6. Separation and relative retention of DMOX derivatives during GC–MS analysis was comparable to that obtained for FAME by GC analysis, but the elution order of certain peaks differed. For example, during the analysis of DMOX derivatives 18:3n-3 eluted after *cis*-13 20:1 and 22:0 eluted before *cis*-9, *trans*-11, *cis*-15 18:3, *cis*-14, *cis*-17 20:2 and *trans*-9, *trans*-14, *trans*-17 20:3 (Fig. 5), whereas the reverse was true during the analysis of methyl esters (Fig. 1). Relative retention times of *trans*-11, *cis*-14, *cis*-17 20:3, 20:3n-3, 20:5n-3, *cis*-11 22:1, *cis*-13 22:1, *cis*-15 22:1, *trans*-12, *trans*-17 22:2, Δ10,13,17 22:3, *trans*-10, *trans*-13, *cis*-16, *cis*-19 22:4, 22:4n-3, *trans*-5, *cis*-10, *cis*-13, *cis*-16, *cis*-19 22:5, 23:0, 24:0, *cis*-16 25:1 and 26:0

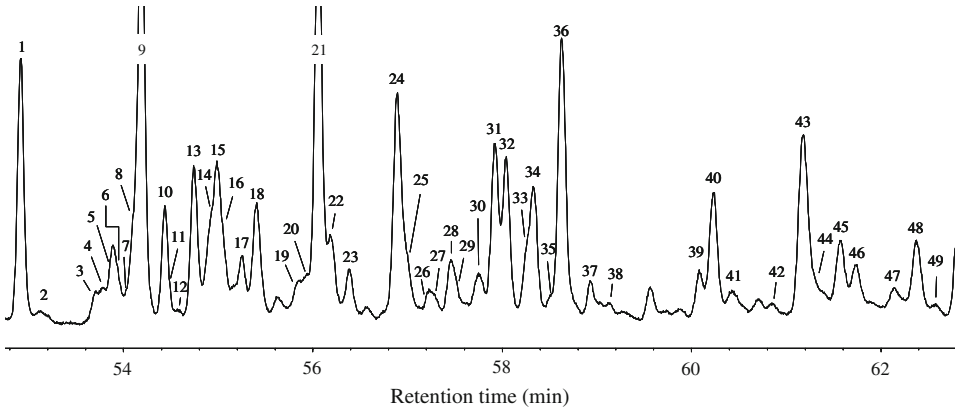

Fig. 5 Partial total ion mass chromatogram of 4,4-dimethyloxaline derivatives prepared from total lipids in omasal digesta of cows fed grass silage-based diets supplemented with 250 g/day of refined fish oil. Molecular ions and key diagnostic ion fragments recorded during GC–MS analysis used to identify unknown peaks are listed in Table 1. Parenthesis indicate tentative geometry of double bonds as inferred based on retention times and elution order of FAME during GC analysis relative to authentic methyl ester standards. Corresponding peaks in the partial gas chromatograms for FAME (Figs. 1–3) are indicated in parenthesis. Peak identification: *1*, 20:0 (#1); *2*, Δ7,9-17:2 (#2); 3, unresolved *trans*-9 20:1 and *trans*-10 20:1 (#4); *4*, *trans*-11 20:1 (#6); *5*, *trans*-12 20:1 (#7); *6*, *trans*-13 20:1 (#8); *7*, *trans*-14 20:1 (#10); *8*, *trans*-15 20:1 (#12); *9*, *cis*-11 20:1 (#13); *10*, *cis*-13 20:1 (#15); *11*, *cis*-9, *cis*-12, *cis*-15 18:3 (#14); *12*, *cis*-14 20:1 (#16); *13*, *cis*-9, *trans*-11 18:2 (#17); *14*, unresolved *cis*-11, *trans*-13 18:2 and *trans*-11, *trans*-15 20:2 (#20); *15*, unresolved *trans*-10, *cis*-12 18:2, *cis*-16 20:1 and *trans*-9, *trans*-15 20:2 (#21 and #22); *16*, *trans*-10, *trans*-16 20:2 (#24); *17*, *trans*-13, *trans*-17 20:2 (#26); *18*, *trans*-11, *cis*-15 20:2 (#27); *19*, unresolved conjugated 18:2 isomers and *trans*-11, *cis*-17 20:2 (#31 and #33); *20*, *cis*-10, *trans*-15 20:2 (#32); *21*, *trans*-13, *cis*-17 20:2 (#35); *22*, *cis*-11, *cis*-14 20:2 (#37); *23*, *trans*-14, *cis*-17 20:2 (#38); *24*, 22:0 (#42); *25*, unresolved *cis*-9, *trans*-11, *cis*-15 18:3 and *cis*-14, *cis*-17 20:2 (#39 and #40); *26*, (*trans*)-9, (*trans*)-14, (*trans*)-17 20:3 (#41); *27*, (*trans*)-10, (*trans*)-14, (*trans*)-17 20:3 (#43); *28*, (*cis*)-10, (*trans*)-14, (*trans*)-17 20:3 or (*trans*)-10, (*cis*)-14, (*trans*)-17 20:3 (#44); *29*, (*cis*)-11, (*trans*)-14, (*trans*)-17 20:3 or (*trans*)-11, (*cis*)-14, (*trans*)-17 20:3 (#45); *30*, (*cis*)-11, (*cis*)-14, (*trans*)-17 20:3 (#47); *31*, unresolved (*trans*)-10, (*trans*)-14, (*cis*)-17 20:3 and Δ11,14,18-20:3 (#48 and #49); *32*, *cis*-11 22:1 (#51); *33*, *cis*-13 22:1 (#52); *34*, (*trans*)-11, (*cis*)-14, (*cis*)-17 20:3 (#50); *35*, *cis*-15 22:1 (#54); *36*, *cis*-11, *cis*-14, *cis*-17 20:3 (#53); *37*, 23:0 (#57); *38*, *trans*-12, *trans*-17 22:2 (#56); *39*, (*trans*)-7, (*cis*)-11, (*cis*)-14, (*cis*)-17 20:4 (#58); *40*, *cis*-8, *cis*-11, *cis*-14, *cis*-17 20:4 (#59); *41*, unresolved *cis*-13, *cis*-16 22:2 and *cis*-14 23:1 (#60 and #61); *42*, *cis*-12, *cis*-15, *cis*-18 21:3 (#62); *43*, 24:0 (#65); *44*, Δ10,13,17-22:3 (#63); *45*, *cis*-5, *cis*-8, *cis*-11, *cis*-14, *cis*-17 20:5 (#64); *46*, (*cis*)-10, (*trans*)-14, (*cis*)-19 22:3 (#66); *47*, *cis*-10, *cis*-13, *cis*-16 22:3 (#67); *48*, (*trans*)-12, (*cis*)-16, (*cis*)-19 22:3 (#68); *49*, unresolved *cis*-9, *cis*-12, *cis*-15, *cis*-18 21:4 and *cis*-11 24:1 (#69)

were also found to differ when analysed as a methyl ester or DMOX derivative.

Characteristic ion fragments in the mass spectrum of DMOX derivatives used to locate the position of double bonds of 20-, 21- and 22-carbon unsaturated fatty acids in Control and FO omasal digesta are listed in Table 1. Spectra of all DMOX derivatives contained prominent ions at *m*/*z* at 113 and 126 (Table 1). A prominent fragment at *m*/*z* at 113 arises from a McLafferty rearrangement ion formed by the migration of the γ-hydrogen followed by cleavage between carbon atoms 2 and 3, while the abundant ion at *m*/*z* at 126 is thought to be formed due to cyclization-displacement reaction and cleavage between carbon atoms 4 and 5 [25]. Molecular ions of DMOX derivatives at *m*/*z* 363, 361, 359, 357, 355, 373, 371, 369, 391, 389, 387, 385, 383 and 381 confirmed a 20:1, 20:2, 20:3, 20:4, 20:5, 21:3, 21:4, 21:5, 22:1, 22:2, 22:3, 22:4, 22:5 and 22:6 structure, respectively. GC–MS analysis of DMOX derivatives revealed the appearance of several 20-carbon unsaturated fatty acids in FO omasal digesta not contained in fish oil or Control digesta (Table 2). Comparisons of 20-carbon unsaturated fatty acids in fish oil with Control and FO omasal digesta indicated that fish oil in the diet of lactating cows was associated with the formation of *cis*-14 20:1, several position and geometric 20:2 ($n = 10$) and 20:3 ($n = 8$) isomers and an unusual 20:4 isomer (Table 2).

The mass spectrum of the DMOX derivative of the unusual 20:4 intermediate in FO digesta contained four ions separated by 12 amu gaps at *m*/*z* 168 and 180; 222 and 234; 262 and 274; 302 and 314 (Fig. 7a) locating double bonds at positions Δ7, Δ11, Δ14 and Δ17, respectively. A prominent ion at *m*/*z* 208 that represents cleavage between carbon atoms at the 8 and 9 position corroborated a di-methylene-interupted ethylenic bond system [30], and confirmed the position of the first double bond between carbon atom 6 and 7 and the Δ7,11,14,17 20:4 structure. During GC analysis Δ7,11,14,17 20:4 eluted before 20:4n-3 (Fig. 2) indicating that this intermediate contains at least one *trans* double bond. Furthermore, the occurrence of a double bond between carbon atom 7 and 8 rather between carbon 8 and 9 as for 20:4n-3 and 20:5n-3, which share an all *cis* methylene-interrupted (homo-allylic) molecular structure provided further evidence to support the identification of *trans*-7, *cis*-11, *cis*-14, *cis*-17 20:4.

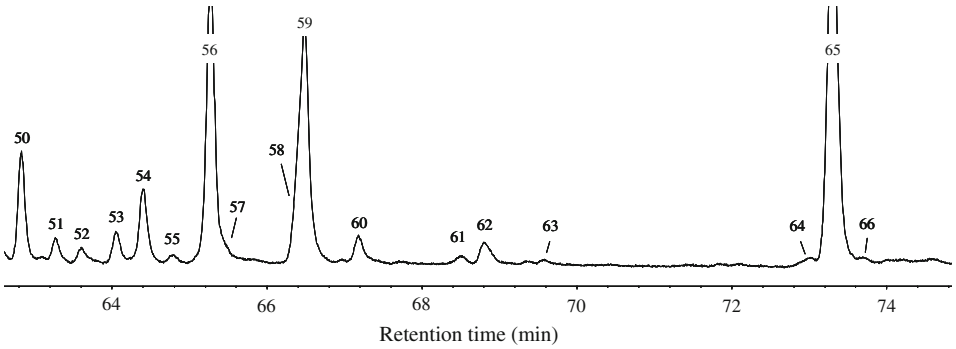

Fig. 6 Partial total ion mass chromatogram of 4,4-dimethyloxaline derivatives prepared from total lipids in omasal digesta of cows fed grass silage-based diets supplemented with 250 g/day of refined fish oil. Molecular ions and key diagnostic ion fragments recorded during GC–MS analysis used to identify unknown peaks are listed in Table 1. Parenthesis indicate tentative geometry of double bonds as inferred based on retention times and elution order of FAME during GC analysis relative to authentic methyl ester standards. Corresponding peaks in the partial gas chromatograms for FAME (Figs. 3, 4) are indicated in parenthesis. Peak identification: *50*, *cis*-15 24:1 (#70); *51*, *cis*-13, *cis*-16, *cis*-19 22:3 (#71); *52*, 25:0 (#74); *53*, (*trans*)-10, (*trans*)-13, (*cis*)-16, (*cis*)-19 22:4 (#73); *54*, unresolved (*trans*)-8, (*cis*)-13, (*cis*)-16, (*cis*)-19 22:4 and *cis*-6, *cis*-9, *cis*-12, *cis*-15, *cis*-18 21:5 (#75 and #76); *55*, (*cis*)-7, (*trans*)-13, (*cis*)-16, (*cis*)-19 22:4 (#77); *56*, *cis*-10, *cis*-13, *cis*-16, *cis*-19 22:4 (#78); *57*, *cis*-16 25:1 (#81); *58*, unresolved 10-O-16:0 and (*trans*)-5, (*cis*)-10, (*cis*)-13, (*cis*)-16, (*cis*)-19 22:5 (#80 and #82); *59*, 26:0 (#83), *60*, *cis*-7, *cis*-10, *cis*-13, *cis*-16, *cis*-19 22:5 (#84); *61*, *cis*-17 26:1 (#85); *62*, *cis*-4, *cis*-7, *cis*-10, *cis*-13, *cis*-16, *cis*-19 22:6 (#86); *63*, 27:0 (#87); *64*, unresolved 10-OH-18:0 and 9-O-18:0 (#89); *65*, 10-O-18:0 (#90) and *66*, 13-O-18:0 (#91)

Eight 20:3 isomers were detected in FO omasal digesta (Table 2). Recorded mass spectra of DMOX derivatives of all detected 20:3 isomers enabled the basic structure of these intermediates to be characterized. The mass spectrum of the DMOX derivative of Δ9, 14, 17, 20:3 (Fig. 7b) contained ions at *m*/*z* 196, 208, 264, 276, 304 and 316, separated by a series of ions 14 amu apart (Table 1) defining the position of double bonds in the fatty acid moiety at Δ9, Δ14 and Δ17. For isomers of Δ10,14,17 20:3, double bonds were located based on 12 amu intervals between ion fragments at *m*/*z* 210, 222, 264, 276, 304 and 316 (Table 1). The position of the first double bond at Δ10 was corroborated by an abundant ion at *m*/*z* 250 formed by cleavage between carbon 12 and 13 (Fig. 7c). Double bonds in geometric isomers of Δ11,14,17 20:3 were located based on 12 amu gaps at *m*/*z* 224, 236, 264, 276, 304 and 316 (Table 1) and a molecular ion at *m*/*z* 359 (Fig. 7d). A Δ11,14,17 20:3 structure was verified by comparison with published spectra [22]. Omasal digesta of cows fed fish oil also contained Δ11,14,18 20:3 (Table 2). Double bonds at Δ11, Δ14 and Δ18 were located based on ion fragments at *m*/*z* 224, 236, 264, 276, 318 and 330 (Table 1), while an abundant ion at *m*/*z* 304 attributable to cleavage between carbon atom 15 and 16 confirmed the occurrence of a bis-methylene-interrupted double bond system. During GC analysis of FAME two Δ10,14,17 20:3 and a Δ11,14,17 20:3 intermediate were found to elute before 20:3n-6, while other geometric Δ11,14,17 20:3 isomers, and a Δ10,14,17 20:3 and Δ11,14,18 20:3 intermediate eluted after 20:3n-6 but before 20:3n-3 (Fig. 2), indicating that all unique 20:3 isomers in FO omasal digesta contained at least one *trans* double bond. Relative retention and elution order of geometric 18:3n-3 methyl esters (*trans*-9, *trans*-12, *trans*-15 18:3 unresolved *trans*-9, *cis*-12, *trans*-15 and *cis*-9, *trans*-12, *trans*-15 18:3, unresolved *trans*-9, *trans*-12, *cis*-15 and *cis*-9, *cis*-12, *trans*-15 18:3, *cis*-9, *trans*-12, *cis*-15 18:3 and *trans*-9, *cis*-12, *cis*-15 18:3) [28, 29] enabled the tentative identification of *trans*-9, *trans*-14, *trans*-17 20:3, *trans*-10, *trans*-14, *trans*-17 20:3, *cis*-11, *cis*-14, *trans*-17 20:3, *trans*-10, *trans*-14, *cis*-17 20:3 and *trans*-11, *cis*-14, *cis*-17 20:3 in FO omasal digesta.

Inclusion of fish oil in the diet was also associated with the appearance of several 20:2 biohydrogenation intermediates in omasal digesta (Table 2). Mass spectrum of DMOX derivatives enabled the structure of Δ9,15 20:2, Δ10,15 20:2, Δ10,16 20:2, Δ11,15 20:2, Δ13,17 20:2 (Fig. 7e) and Δ14,17 20:2 to be identified. Double bonds were located based on 12 amu intervals between ions at *m*/*z* 196, 208, 278 and 290; 210, 222, 278 and 290; 210, 222, 292 and 304; 224, 236, 278 and 290; 252, 264, 306 and 318; 266, 278, 306 and 318, respectively (Table 1). Abundant ions at *m*/*z* 264 and 292 that represent the cleavage between carbon atom 12 and 13 and between carbon atom 14 and 15, respectively, confirmed the Δ11,15 20:2 (Table 1) and Δ13,17 20:2 structure (Fig. 7e). Elution order of 20:2 intermediates relative to 20:2n-6 and 20:2n-3 during GC analysis in combination with the relative retention of geometric 18:2n-6 methyl esters (*trans*-9, *trans*-12 18:2, *cis*-9, *trans*-12 18:2, *trans*-9, *cis*-12 18:2 and *cis*-9, *cis*-12 18:2 [28, 29]) enabled *trans*-9, *trans*-15 20:2, *trans*-10, *trans*-16 20:2, *trans*-13, *trans*-17 20:2, *trans*-11, *cis*-15 20:2, *cis*-10, *trans*-15 20:2, *trans*-11, *cis*-17 20:2, *trans*-13, *cis*-17 20:2 and *trans*-14, *cis*-17 20:2 to be identified.

Table 1 Characteristic ion fragments recorded during gas-chromatography mass-spectrometry (GC–MS) analysis of 4,4-dimethyloxazoline derivatives of selected 20- and 22-carbon unsaturated fatty acids in omasal digesta of cows fed grass silage-based diets supplemented with 250 g/day of refined fish oil

Fatty acid	RT[a] (min)	RT[b] (min)	Characteristic ion fragments (*m/z*, relative intensity)
trans-9 20:1	42.62	53.72	113 (100), 126 (98), 182 (25), 196 (8), 208 (7), 363 (M^+, 24)
trans-11 20:1	42.70	53.78	113 (100), 126 (82), 210 (12), 224 (4), 236 (6), 363 (M^+, 20)
trans-12 20:1	42.78	53.86	113 (100), 126 (82), 224 (13), 238 (5), 250 (4), 363 (M^+, 23)
trans-13 20:1	42.85	53.95	113 (100), 126 (90), 238 (12), 252 (3), 264 (4), 363 (M^+, 26)
trans-14 20:1	42.95	54.03	113 (100), 126 (67), 252 (7), 266 (5), 278 (3), 363 (M^+, 19)
trans-15 20:1	43.04	54.10	113 (100), 126 (62), 266 (9), 280 (3), 292 (2), 363 (M^+, 22)
Δ11,15 20:2	43.84	54.90	113 (76), 126 (89), 224 (8), 236 (4), 264 (69), 278 (12), 290 (4), 318 (17), 361 (M^+, 13)
Δ9,15 20:2	43.91	54.99	113 (90), 126 (100), 182 (18), 196 (6), 208 (5), 278 (9), 290 (3), 318 (16), 361 (M^+, 9)
Δ10,16 20:2	43.98	55.07	113 (100), 126 (89), 210 (9), 222 (12), 264 (41), 278 (41), 292 (12), 304 (13), 361 (M^+, 16)
Δ13,17 20:2	44.17	55.25	113 (100), 126 (91), 252 (5), 264 (6), 292 (96), 306 (<1), 318 (11), 361 (M^+, 20)
Δ11,15 20:2	44.30	55.40	113 (76), 126 (98), 224 (17) 236 (8), 264 (100), 278 (2), 290 (6), 318 (33), 361 (M^+, 30)
Δ10,15 20:2	44.74	55.46	113 (100), 126 (87), 210 (11), 222 (7), 250 (18), 264 (13), 278 (7), 290 (8), 304 (14), 361 (M^+, 15)
Δ13,17 20:2	44.87	56.03	113 (71), 126 (63), 252 (3), 264 (3), 292 (100), 306 (2), 318 (5), 361 (M^+, 14)
Δ14,17 20:2	45.19	56.40	113 (100), 126 (81), 252 (7), 266 (4), 278 (4), 292 (9), 306 (8), 318 (5), 346 (18), 361 (M^+, 15)
Δ9,14,17 20:3	45.80	57.24	113 (92), 126 (100), 196 (7), 208 (4), 250 (33), 264 (6), 276 (5), 290 (32), 304 (8), 316 (3), 359 (M^+, 8)
Δ10,14,17 20:3	46.19	57.46	113 (72), 126 (100), 196 (7), 210 (3), 222 (3), 236 (10), 250 (63), 264 (2), 276 (4), 290 (16), 304 (4), 316 (4), 359 (M^+, 7)
Δ10,14,17 20:3	46.55	57.93	113 (76), 126 (100), 196 (7), 210 (4), 222 (4), 236 (11), 250 (62), 264 (3), 276 (6), 290 (21), 304 (6), 316 (5), 359 (M^+, 12)
Δ11,14,17 20:3	46.51	57.75	113 (100), 126 (92), 224 (5), 236 (2), 250 (5), 264 (8), 276 (4), 290 (19), 304 (12), 316 (6), 359 (M^+, 20)
Δ11,14,17 20:3	46.93	57.90	113 (100), 126 (96), 224 (9), 236 (4), 250 (5), 264 (15), 276 (7), 290 (18), 304 (19), 316 (9), 359 (M^+, 25)
all-cis Δ11,14,17 20:3	47.16	58.64	113 (90), 126 (100), 224 (4), 236 (2), 250 (5), 264 (11), 276 (4), 290 (17), 304 (13), 316 (5), 359 (M^+, 18)
Δ11,14,18 20:3	46.63	57.93	113 (58), 126 (72), 210 (6), 224 (1), 236 (1), 250 (11), 264 (12), 276 (1), 290 (2), 304 (100), 318 (1), 330 (<1), 359 (M^+, 1)
Δ7,11,14,17 20:4	48.44	60.10	113 (44), 126 (70), 168 (9), 180 (11), 208 (100), 222 (4), 234 (4), 248 (6), 262 (8), 274 (1), 302 (4), 314 (4), 357 (M^+, 8)
all-cis Δ8,11,14,17 20:4	48.52	60.23	113 (49), 126 (100), 182 (10), 194 (3), 208 (15), 222 (12), 234 (6), 248 (12), 262 (17), 274 (7), 302 (5), 314 (4), 357 (M^+, 12)
all-cis Δ5,8,11,14,17 20:5	49.55	61.56	113 (100), 126 (31), 153 (21), 180 (5), 192 (4), 220 (6), 232 (3), 246 (5), 260 (3), 272 (1), 286 (6), 300 (1), 312 (<1), 355 (M^+, <1)
all-cis Δ12,15,18 21:3	48.96	60.86	113 (100), 126 (92), 224 (2), 238 (2), 250 (20), 264 (15), 278 (3), 290 (15), 304 (3), 318 (9), 330 (3), 373 (M^+, 1)
all-cis Δ9,12,15,18 21:4	50.32	62.63	113 (92), 126 (100), 182 (21), 196 (6), 208 (5), 222 (19), 236 (13), 248 (6), 262 (9), 276 (11), 288 (6), 302 (12), 316 (2), 328 (2), 371 (M^+, 9)

Table 1 continued

Fatty acid	RT[a] (min)	RT[b] (min)	Characteristic ion fragments (*m/z*, relative intensity)
all-cis Δ6,9,12,15,18 21:5	51.66	64.54	113 (62), 126 (100), 167 (12), 194 (8), 206 (6), 220 (10), 234 (9), 246 (3), 260 (6), 274 (4), 286 (1), 300 (7), 314 (1), 326 (1), 369 (M^+, 2)
cis-11 22:1	46.93	58.04	113 (100), 126 (76), 210 (17), 224 (4), 236 (1), 391 (M^+, 19)
cis-13 22:1	47.07	58.25	113 (100), 126 (76), 238 (17), 252 (4), 264 (5), 391 (M^+, 22)
cis-15 22:1	47.28	58.52	113 (100), 126 (67), 266 (17), 280 (4), 292 (3), 391 (M^+, 27)
Δ12,17 22:2	47.75	59.16	113 (100), 126 (70), 224 (6), 238 (3), 250 (7), 292 (14), 306 (3), 318 (2), 389 (M^+, 3)
Δ10,13,17 22:3	49.37	61.32	113 (23), 126 (4), 210 (2), 222 (3), 236 (6), 250 (10), 262 (1), 276 (4), 290 (100), 304 (1), 316 (3), 387 (M^+, 11)
Δ10,14,19 22:3	49.76	61.74	113 (100), 126 (82), 196 (14), 210 (8), 222 (3), 250 (62), 264 (7), 276 (12), 318 (49), 332 (3), 344 (2), 387 (M^+, 3)
Δ12,16,19 22:3	50.15	62.37	113 (93), 126 (100), 224 (10), 238 (6), 250 (1), 278 (98), 292 (3), 304 (10), 318 (27), 332 (9), 344 (8), 387 (M^+, 21)
Δ8,13,16,19 22:4	51.53	64.42	113 (56), 126 (100), 168 (20), 182 (8), 194 (3), 236 (37), 250 (2), 262 (6), 276 (15), 290 (7), 302 (4), 330 (5), 342 (2), 385 (M^+, 3)
Δ7,13,16,19 22:4	51.77	64.79	113 (89), 126 (100), 168 (10), 180 (12), 208 (12), 236 (14), 250 (7), 262 (3), 276 (12), 290 (18), 302 (3), 316 (15), 330 (7), 342 (3), 385 (M^+, 12)
all-cis Δ10,13,16,19 22:4	51.36	65.29	113 (81), 126 (100), 210 (3), 222 (8), 250 (12), 262 (1), 290 (36), 302 (8), 330 (8), 342 (5), 385 (M^+, 22)
Δ5,10,13,16,19 22:5	52.60	66.40	113 (100), 126 (21), 153 (18), 180 (14), 208 (1), 220 (4), 234 (9), 248 (3), 260 (1), 274 (4), 288 (3), 300 (1), 314 (5), 328 (1), 340 (<1), 383 (M^+, <1)
all-cis Δ4,7,10,13,16,19 22:6	53.71	68.83	113 (100), 126 (10), 139 (11), 152 (52), 166 (6), 178 (5), 192 (13), 206 (6), 218 (5), 232 (7), 246 (5), 258 (4), 272 (7), 286 (1), 298 (1), 312 (6), 326 (<1), 338 (<1), 381 (M^+, 2)

Parenthesis indicate tentative geometry of double bonds as inferred based on retention times and elution order of fatty acid methyl esters (FAME) during GC analysis relative to authentic methyl ester standards

[a] Retention time of FAME on a 100 m CP-Sil 88 fused silica capillary column using a temperature gradient program [7] and hydrogen as the carrier gas operated at constant pressure (137.9 kPa) at a flow rate of 0.5 mL/min

[b] Retention time of 4,4-dimethyloxazoline derivatives of fatty acids on a 100 m CP-Sil 88 fused silica capillary column using a temperature gradient program [7] and helium as the carrier gas operated at constant pressure (142.6 kPa) at a flow rate of 0.6 mL/min

Omasal digesta from cows fed both the Control and FO treatments contained several positional isomers of 20:1 (Table 2). Mass spectra of DMOX derivatives of 20:1 isomers allowed the position of double bonds at Δ9, Δ10, Δ11, Δ12, Δ13, Δ14 and Δ15 to be localized readily by ions at *m/z* 196, 208; 210, 222; 224, 236; 238, 250; 252, 264; 266, 278; 280 and 292, respectively (Table 1). Separation of FAME by Ag^+-TLC along with retention times during GC analysis (Fig. 1) confirmed that all 20:1 isomers unique to omasal digesta contained a *trans* double bond. Inclusion of fish oil in the diet also resulted in the appearance of *cis*-11, -13, -14 and -15 20:1 in FO omasal digesta (Table 2).

Characterization of 22-carbon unsaturated fatty acids in fish oil and omasal digesta of cows fed the control and FO treatment revealed that the inclusion of 22-carbon unsaturated fatty acids from fish oil was associated with the formation of several novel 22:2 ($n = 1$), 22:3 ($n = 3$), 22:4 ($n = 3$) and 22:5 ($n = 1$) intermediates in the rumen (Table 3).

The spectrum of the DMOX derivative of the 22:5 intermediate contained ion fragments with a mass interval of 12 amu at *m/z* 208, 220, 234, 248, 260, 274, 288, 300, 314, 328 and 340 that were separated by gaps of 14 amu (Fig. 8a), which enabled four of the five double bonds to be located at Δ10, Δ13, Δ16, and Δ19, respectively [25, 26]. The position of the final double bond between carbon atoms 4 and 5 was discerned based on the presence of ions at *m/z* 153, 166 and 180 (Table 1), and an even ion at *m/z* 152 (Fig. 8a) in the mass spectrum that served as characteristic fragments of a double bond in the Δ5 position [22, 26, 27] allowing the Δ5,10,13,16,19 22:5 structure to be elucidated. During GC analysis of FAME Δ5,10,13,16,19 22:5 eluted after 22:5n-6 but before 22:5n-3, which combined with considerations on the methylene-interrupted

Table 2 Mean concentration of 20- and 21-carbon fatty acids in refined fish oil and omasal digesta of lactating cows fed grass silage-based diets supplemented with 0 (Control) or 250 g/day of refined fish oil (FO)

Concentration (g/100 g fatty acids)	Fish oil[a]	Digesta[b]	
		Control	FO
20:0	0.27 ± 0.012	0.81 ± 0.040	0.54 ± 0.093
cis-5 20:1	0.13 ± 0.003	ND	ND
cis-8 20:1	0.15 ± 0.001	ND	ND
cis-9 20:1	0.17 ± 0.003	ND	ND
cis-11 20:1	1.79 ± 0.009	0.10 ± 0.026	0.43 ± 0.098
cis-12 20:1	ND[d]	0.02 ± 0.006	ND
cis-13 20:1	0.24 ± 0.002	ND	0.09 ± 0.012
cis-14 20:1	ND	ND	0.03 ± 0.017
cis-15 20:1	0.03 ± 0.002	ND	0.02 ± 0.008
trans-9 + *trans*-10 20:1	ND	0.01 ± 0.008	0.04 ± 0.012
trans-11 20:1	ND	0.02 ± 0.008	0.07 ± 0.036
trans-12 20:1	ND	0.01 ± 0.004	0.08 ± 0.043
trans-13 20:1	ND	0.02 ± 0.008	0.11 ± 0.066
trans-14 20:1	ND	0.02 ± 0.004	0.09 ± 0.060
trans-15 20:1	ND	0.03 ± 0.007	0.25 ± 0.236
cis-8, *cis*-11 20:2	0.18 ± 0.001	ND	ND
cis-11, *cis*-14 20:2	0.18 ± 0.002	0.03 ± 0.010	0.11 ± 0.023
cis-14, *cis*-17 20:2	ND	ND	0.04 ± 0.011
cis-10, *trans*-15 20:2	ND	ND	0.04 ± 0.017
trans-11, *cis*-15 20:2	ND	ND	0.16 ± 0.044
trans-11, *cis*-17 20:2	ND	ND	0.08 ± 0.017
trans-13, *cis*-17 20:2	ND	ND	0.36 ± 0.184
trans-14, *cis*-17 20:2	ND	ND	0.18 ± 0.061
trans-9, *trans*-15 20:2	ND	ND	0.24 ± 0.056
trans-10, *trans*-16 20:2	ND	ND	0.21 ± 0.028
trans-11, *trans*-15 20:2	ND	ND	0.15 ± 0.038
trans-13, *trans*-17 20:2	ND	ND	0.07 ± 0.024
cis-8, *cis*-11, *cis*-14 20:3	0.15 ± 0.001	ND	0.06 ± 0.016
cis-11, *cis*-14, *cis*-17 20:3	0.11 ± 0.002	ND	0.26 ± 0.110
(*cis*)-11, (*cis*)-14, (*trans*)-17 20:3	ND	ND	0.07 ± 0.019
Δ10,14,17 20:3[c]	ND	ND	0.05 ± 0.022
Δ11,14,17 20:3[c]	ND	ND	0.03 ± 0.008
(*trans*)-11, (*cis*)-14, (*cis*)-17 20:3	ND	ND	0.14 ± 0.015
(*trans*)-10, (*trans*)-14, (*cis*)-17 20:3	ND	ND	0.13 ± 0.077
(*trans*)-9, (*trans*)-14, (*trans*)-17 20:3	ND	ND	0.03 ± 0.001
(*trans*)-10, (*trans*)-14 (*trans*)-17 20:3	ND	ND	0.05 ± 0.022
Δ11,14,18 20:3	ND	ND	0.01 ± 0.009
cis-5, *cis*-8, *cis*-11, *cis*-14 20:4	0.89 ± 0.018	ND	0.02 ± 0.002
cis-8, *cis*-11, *cis*-14, *cis*-17 20:4	0.89 ± 0.018	ND	0.20 ± 0.022
(*trans*)-7, (*cis*)-11, (*cis*)-14, (*cis*)-17 20:4	ND	ND	0.02 ± 0.008
cis-5, *cis*-8, *cis*-11, *cis*-14, *cis*-17 20:5	15.9 ± 0.398	ND	0.18 ± 0.034
cis-12, *cis*-15, *cis*-18 21:3	0.01 ± 0.001	ND	0.01 ± 0.005
cis-9, *cis*-12, *cis*-15, *cis*-18 21:4	ND	ND	0.01 ± 0.002
cis-6, *cis*-9, *cis*-12, *cis*-15, *cis*-18 21:5	0.68 ± 0.021	ND	0.05 ± 0.016

Parenthesis indicate tentative geometry of double bonds as inferred based on retention times and elution order of FAME during GC analysis relative to authentic methyl ester standards

[a] Values are expressed as mean ± SE ($n = 3$)

[b] Values are expressed as mean ± SE ($n = 5$)

[c] Retention time comparisons inferred a *cis*, *trans*, *trans* or *trans*, *cis*, *trans* double bond configuration

[d] Not detected

(homo-allylic) molecular structure of 22:5n-3 and 22:6n-3 were used to infer a *trans*-5, *cis*-10, *cis*-13, *cis*-16, *cis*-19 22:5 structure.

Mass spectra of the DMOX derivatives of 22:4 isomers enabled the position of double bonds to be identified (Table 1). Ion fragments separated by 12 amu intervals at

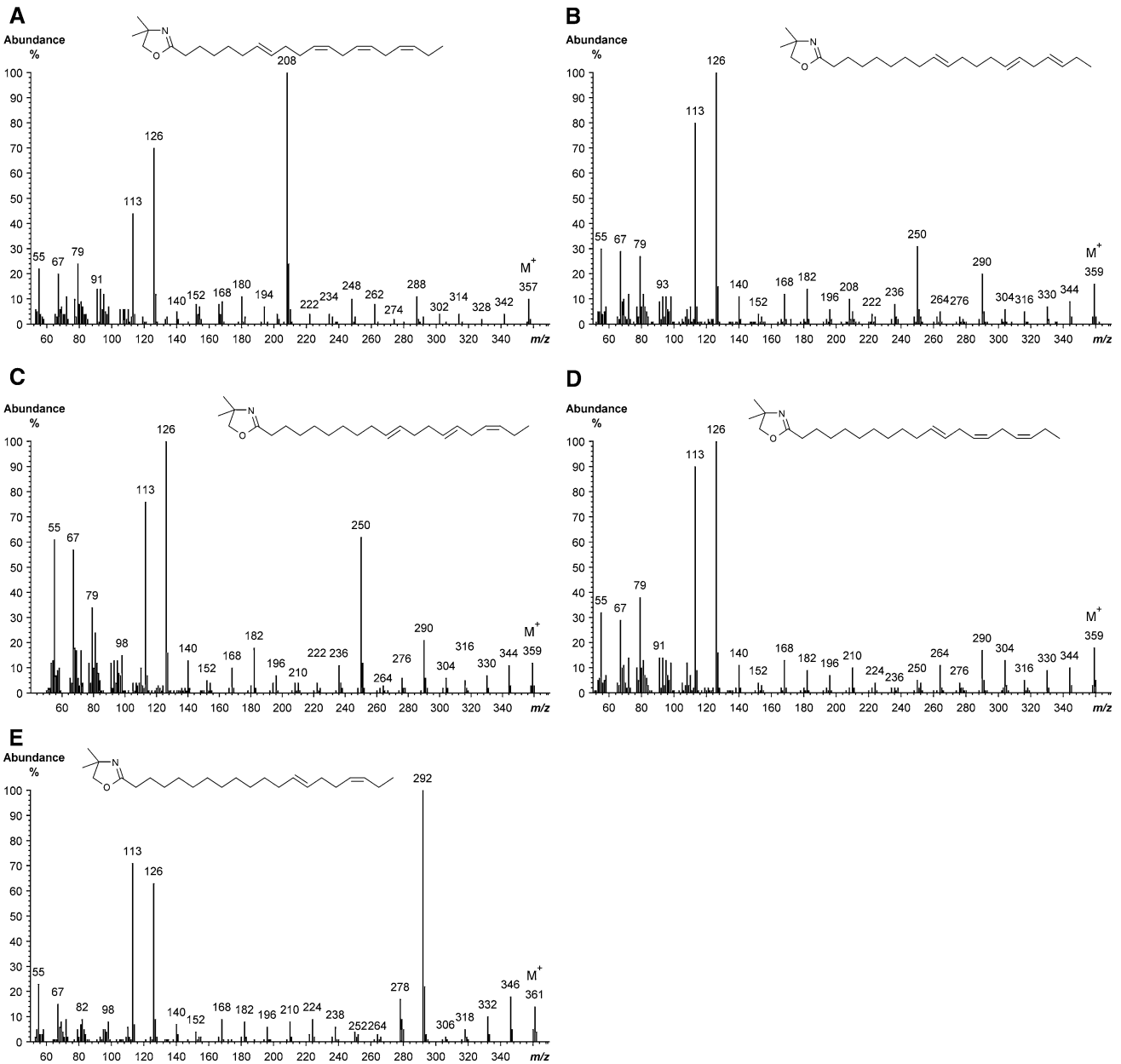

Fig. 7 Gas chromatography-electron-impact mass spectrum of the 4,4-dimethyloxaline (DMOX) derivative of (**a**) *trans*-7, *cis*-11, *cis*-14, *cis*-17 20:4, (**b**) *trans*-9, *trans*-14, *trans*-17 20:3, (**c**) *trans*-10, *trans*-14, *cis*-17 20:3, (**d**) *trans*-11, *cis*-14, *cis*-17 20:3 and (**e**) *trans*-13, *cis*-17 20:2 detected in omasal digesta of cows fed grass silage-based diets containing fish oil. The mass spectrum of DMOX derivatives in Fig. 7a–e corresponds to peaks #58, #41, #48, #50 and #35, respectively, in the GC chromatogram of methyl esters

m/*z* 182, 194, 250, 262, 290, 302, 330 and 342 (Fig. 8b) confirmed a Δ8,13,16,19 22:4 structure [22, 26, 27]. Similarly, readily discernible 12 amu gaps in the mass spectrum of DMOX derivatives also enabled Δ7,13,16,19 22:4 and Δ10,13,16,19 22:4 in FO omasal digesta to be identified (Table 1). Retention time comparisons with authentic FAME standards and the elution order of geometric isomers of 18:3 methyl esters during GC analysis was used in combination with the recorded mass spectra of DMOX derivatives to identify *trans*-8, *cis*-13, *cis*-16, *cis*-19 22:4, *cis*-7, *trans*-13, *cis*-16, *cis*-19 22:4 and *trans*-10, *trans*-13, *cis*-16, *cis*-19 22:4.

Four 22:3 intermediates were detected in variable concentrations in FO omasal digesta (Table 3). The DMOX derivative of Δ12,16,19 22:3 included ion fragments separated by 12 amu gaps at *m*/*z* 238, 250, 292, 304, 332 and 344 (Fig. 8c) that located double bonds at Δ12, Δ16 and Δ19, respectively [22, 25, 26]. A prominent ion at *m*/*z* 278 (Fig. 8c) confirmed the presence of allylic bonds at Δ12 and Δ16. A putative *trans*-12, *cis*-16, *cis*-19 22:3 structure

was deduced based on retention time during GC analysis of FAME. Trace amounts of Δ10,13,17 22:3 in fish oil and FO omasal digesta (Table 3) were able to be identified based on ions at *m/z* 210, 222, 250, 262, 292, 304 and 316 in the DMOX mass spectrum (Table 1), but it was not possible to establish or speculate on double bond geometry.

Inclusion of fish oil in the diet resulted in the appearance of 22:2n-6 and Δ12,17 22:2 in omasal digesta (Table 3). GC–MS analysis of DMOX derivatives confirmed the 22:2 structure based on a molecular ion at *m/z* 389, while ion fragments at *m/z* 252, 264, 292 and 304 located the position of double bonds at Δ13 and Δ16 (Table 1) and ions separated by 12 amu intervals at *m/z* 238, 250, 306 and 318 indicated double bonds at Δ12 and Δ17 (Fig. 8d). Differences in the retention time during GC analysis between an authentic 22:2n-6 methyl ester standard and the Δ12,17 22:2 biohydrogenation intermediate corroborated the identification of *trans*-12, *trans*-17 22:2.

Both fish oil and FO omasal digesta contained *cis*-11, -13 and -15 22:1 while trace amounts of *cis*-13 22:1 were also detected in the digesta of cows fed the Control diet (Table 3).

Detailed analysis of DMOX prepared from total lipid of omasal digesta provided no evidence of 20-, 21- or 22-carbon conjugated intermediates (Fig. 5). During GC analysis of FAME, several peaks in omasal digesta but absent in fish oil were found to elute towards the end of chromatogram between 54.6 and 54.9 min (Fig. 4). Retention time comparisons with authentic standards were consistent with the occurrence of one or more oxygenated 18-carbon fatty acids. GC–MS analysis of FAME and DMOX derivatives prepared from experimental samples

Table 3 Mean concentration of 22-, 23- and 24-carbon fatty acids in refined fish oil and omasal digesta of lactating cows fed grass silage-based diets supplemented with 0 (Control) or 250 g/day of refined fish oil (FO)

Concentration (g/100 g fatty acids)	Fish oil[a]	Digesta[b]	
		Control	FO
22:0	0.11 ± 0.003	0.61 ± 0.036	0.56 ± 0.026
cis-11 22:1	1.18 ± 0.009	ND	0.12 ± 0.062
cis-13 22:1	0.27 ± 0.003	0.03 ± 0.006	0.10 ± 0.006
cis-15 22:1	0.10 ± 0.002	ND	0.06 ± 0.008
cis-13, *cis*-16 22:2	0.03 ± 0.012	ND	0.02 ± 0.004
trans-12, *trans*-17 22:2	ND[c]	ND	0.03 ± 0.011
cis-10, *cis*-13, *cis*-16 22:3	ND	ND	0.02 ± 0.012
(*cis*)-10, (*trans*)-14, (*cis*)-19 22:3	ND	ND	0.08 ± 0.004
(*trans*)-12, (*cis*)-16, (*cis*)-19 22:3	ND	ND	0.14 ± 0.070
Δ10,13,17 22:3	0.02 ± 0.003	ND	0.19 ± 0.014
cis-7, *cis*-10, *cis*-13, *cis*-16 22:4	0.08 ± 0.003	ND	ND
cis-10, *cis*-13, *cis*-16, *cis*-19 22:4	0.09 ± 0.007	ND	0.35 ± 0.136
(*cis*)-7, (*trans*)-13, (*cis*)-16, (*cis*)-19 22:4	ND	ND	0.05 ± 0.010
(*trans*)-8, (*cis*)-13, (*cis*)-16, (*cis*)-19 22:4	ND	ND	0.13 ± 0.027
(*trans*)-10, (*trans*)-13, (*cis*)-16, (*cis*)-19 22:4	ND	ND	0.03 ± 0.007
cis-4, *cis*-7, *cis*-10, *cis*-13, *cis*-16 22:5	0.26 ± 0.008	ND	ND
cis-7, *cis*-10, *cis*-13, *cis*-16, *cis*-19 22:5	1.87 ± 0.059	ND	0.13 ± 0.047
(*trans*)-5, (*cis*)-10, (*cis*)-13, (*cis*)-16, (*cis*)-19 22:5	ND	ND	0.05 ± 0.022
cis-4, *cis*-7, *cis*-10, *cis*-13, *cis*-16, *cis*-19 22:6	10.3 ± 0.342	ND	0.09 ± 0.026
23:0	0.02 ± 0.003	0.11 ± 0.008	0.12 ± 0.014
cis-8, *cis*-11, *cis*-14, *cis*-17, *cis*-20 23:5	0.03 ± 0.009	ND	ND
24:0	0.30 ± 0.015	0.57 ± 0.036	0.18 ± 0.034
cis-9, *cis*-12, *cis*-15, *cis*-18, *cis*-21 24:5	0.15 ± 0.004	ND	0.01 ± 0.003
cis-6, *cis*-9, *cis*-12, *cis*-15, *cis*-18, *cis*-21 24:6	0.16 ± 0.006	ND	ND

Parenthesis indicate tentative geometry of double bonds as inferred based on retention times and elution order of fatty acid methyl esters during GC analysis relative to authentic methyl ester standards

[a] Values are expressed as mean ± SE ($n = 3$)

[b] Values are expressed as mean ± SE ($n = 5$)

[c] Not detected

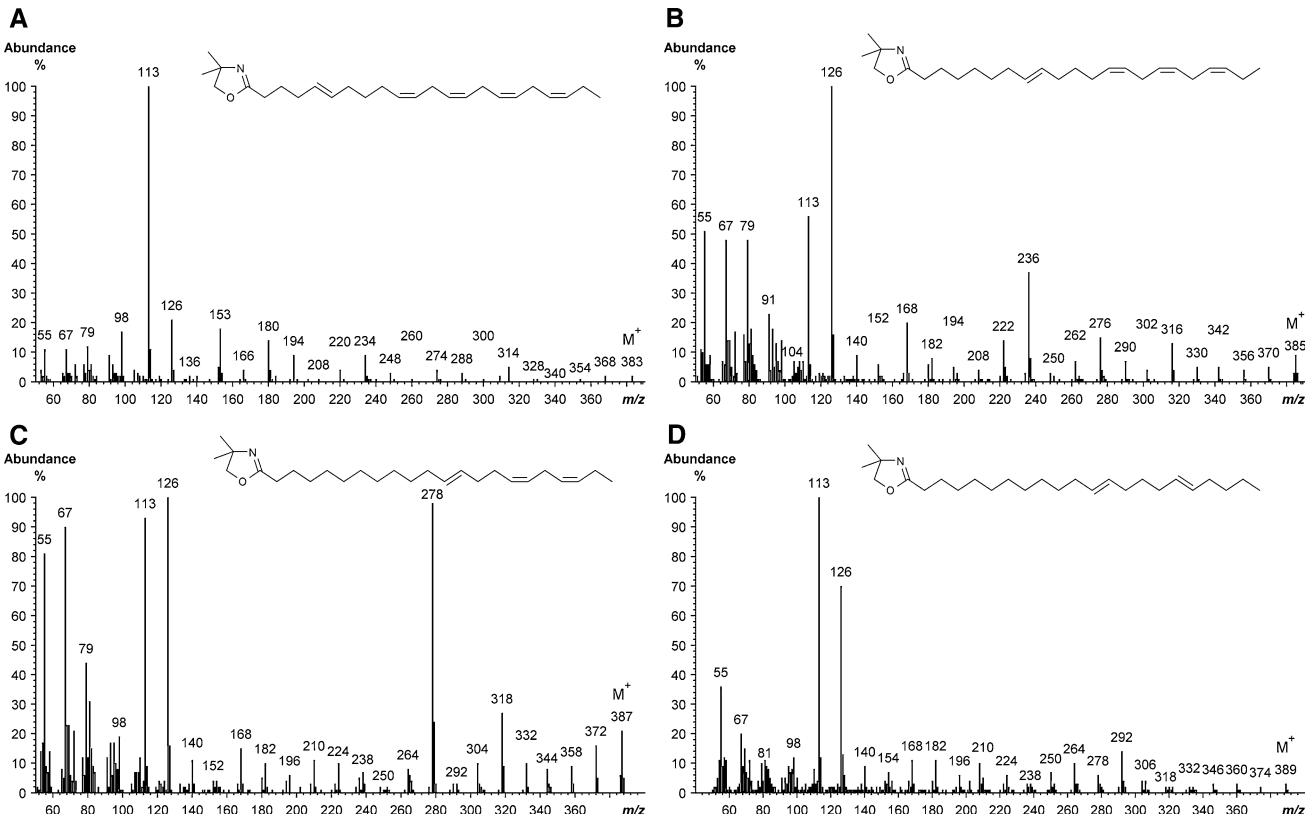

Fig. 8 Gas chromatography-electron-impact mass spectrum of the DMOX derivative of *trans*-5, *cis*-10, *cis*-13, *cis*-16, *cis*-19 22:5 (**a**), *trans*-8, *cis*-13, *cis*-16, *cis*-19 22:4 (**b**), *trans*-12, *cis*-16, *cis*-19 22:3 (**c**) and *trans*-12, *cis*-17 22:2 (**d**) detected in omasal digesta in cows fed grass silage-based diets containing refined fish oil. The mass spectrum of DMOX derivatives in Fig. 8a–d corresponds to peaks #82, #75, #68 and #56, respectively in the GC chromatogram of methyl esters

and available authentic standards, combined with reference to published mass spectra [31–34], enabled the appearance of 9-O-18:0, 10-O-18:0 and 13-O-18:0 in omasal digesta to be determined. Fish oil in the diet also resulted in the appearance of 10-O-16:0 in omasal digesta (Fig. 3).

The mass spectrum of the methyl ester of 10-O-18:0 indicated a molecular ion at *m/z* 312 and a characteristic fragmentation pattern with abundant ions at *m/z* 141, 171 and 199 arising from alpha cleavage with respect to the oxo group and ions at *m/z* 156 (155 + H) and 214 (213 + H) corresponding to beta cleavage (Fig. 9a) enabling the position of the oxo group to be located at the Δ10 position [31, 34]. GC–MS analysis of the corresponding DMOX derivative confirmed the appearance of 10-O-18:0 in omasal digesta based on a molecular ion at *m/z* 351, fragments at *m/z* 196 and 210 due to cleavages alpha and beta to the oxo group on the side of the oxiran ring and less abundant ions at *m/z* 238, 253 and 266 arising from cleavages on the other side of the oxo group (Fig. 9b) [33]. The mass spectrum of the methyl ester of 13-O-18:0 contained several diagnostic ions at *m/z* 99, 114, 167, 199, 241 and 256 (Fig. 9c) locating the position of the oxo group at the Δ13 position [31]. An expected molecular ion at *m/z* 312 was not detected (Fig. 9c) but could be deduced from the ion at *m/z* 281 (M-31). An inferred 13-O-18:0 structure was confirmed based on characteristic ion fragments in the mass spectrum of the corresponding DMOX derivative at *m/z* 238, 252, 280, 295 and 308 and a molecular ion at *m/z* 351 (Fig. 9d) [33].

Analysis of lipid in omasal digesta of cows fed grass-silage-based diets supplemented with 0 or 250 g/day of refined fish oil along with measurements of nutrient flow at the omasum [7] provided the first quantitative estimates of the ruminal outflow of long-chain fatty acid biohydrogenation intermediates in cattle (Table 4). Fish oil in the diet enhanced ($P < 0.05$) the flow of 20:5n-3, 22:5n-3, 22:6n-3 and 24:5n-3, but the increases were marginal relative to intake (Table 4). Ruminal long-chain fatty acid balance determined as the difference between flow at the omasum and intake confirmed that 20:4n-6, 20:5n-3, 22:4n-6, 22:5n-3, 22:6n-3, 23:5n-3, 24:5n-3 and 24:6n-3 were extensively hydrogenated in the rumen (95.6, 97.6, 100.0, 88.1, 98.2, 100.0, 87.4 and 100%, respectively), but also indicated a lower apparent disappearance of 20:2n-6 and 20:4n-3 in the rumen (3.0 and 66.9%, respectively). Inclusion of fish oil in the diet increased ($P < 0.05$) the flow of 20- and 22-carbon

intermediates containing at least one *trans* double bond from between 0.08–2.00 and 0.14-1.09 g/day, respectively (Table 4). Furthermore, measurements of ruminal fatty acid balance also indicated that fish oil in the diet was associated with the net synthesis of several all *cis* 20- (20:2n-3, 20:3n-3 and 20:3n-6), 21- (21:3n-3, 21:4n-3) and 22- (22:2n-6, 22:3n-6 and 22:4n-3) carbon fatty acids (Table 4). Even though fish oil in the diet increased the intake of 20- and 22-carbon unsaturated fatty acids, ruminal 20:0 and 22:0 balance was lower ($P < 0.05$) in cows fed the control than the FO treatment (Table 4). Fish oil in the diet also enhanced ($P < 0.05$) the flow of 10-O-16:0, 9-O-18:0 + 10-OH-18:0 and 10-O-18:0 at the omasum from 0.0, 0.12 and 2.00 to 1.91, 1.20 and 19.4 g/day, but had no effect ($P > 0.05$) on ruminal outflow of 13-O-18:0 (0.61 and 0.46 g/day for the Control and FO, respectively).

Discussion

The present report documents the re-analysis of omasal digesta collected from cows fed 0 or 250 g/day of refined fish oil. A more detailed analysis was initiated due to the relatively high number of unknown peaks in the GC chromatogram of methyl esters prepared from the non-esterified fatty acid fraction that could not be identified due to the lack of authentic standards. However, elucidating the structure of unknown intermediates in order to understand the fate of long-chain unsaturated fatty acids in the rumen relies on the assumption that no substantial changes in lipid composition occurred during the storage of digesta. Comparable flows of 20:4n-3, 20:5n-3, 22:4n-3, 22:5n-3 and 22:6n-3 at the omasum of cows on the Control and FO treatments based on the analysis of non-esterified fatty acids [7] or total lipid confirm that there were no substantial changes in the abundance of 20- and 22- carbon polyenoic fatty acids in samples used in this and earlier analysis. Furthermore, analysis of total lipid in omasal digesta also revealed that 10-O-16:0 in the non-esterified fatty acid fraction of FO omasal digesta was erroneously identified as 22:5n-6 [7].

Comparisons of the profile of FAME in fish oil and omasal digesta revealed the occurrence of numerous novel 20-, 21- and 22-carbon fatty acids in fish oil digesta, indicating that these isomers must originate from the incomplete hydrogenation of fish oil fatty acids in the

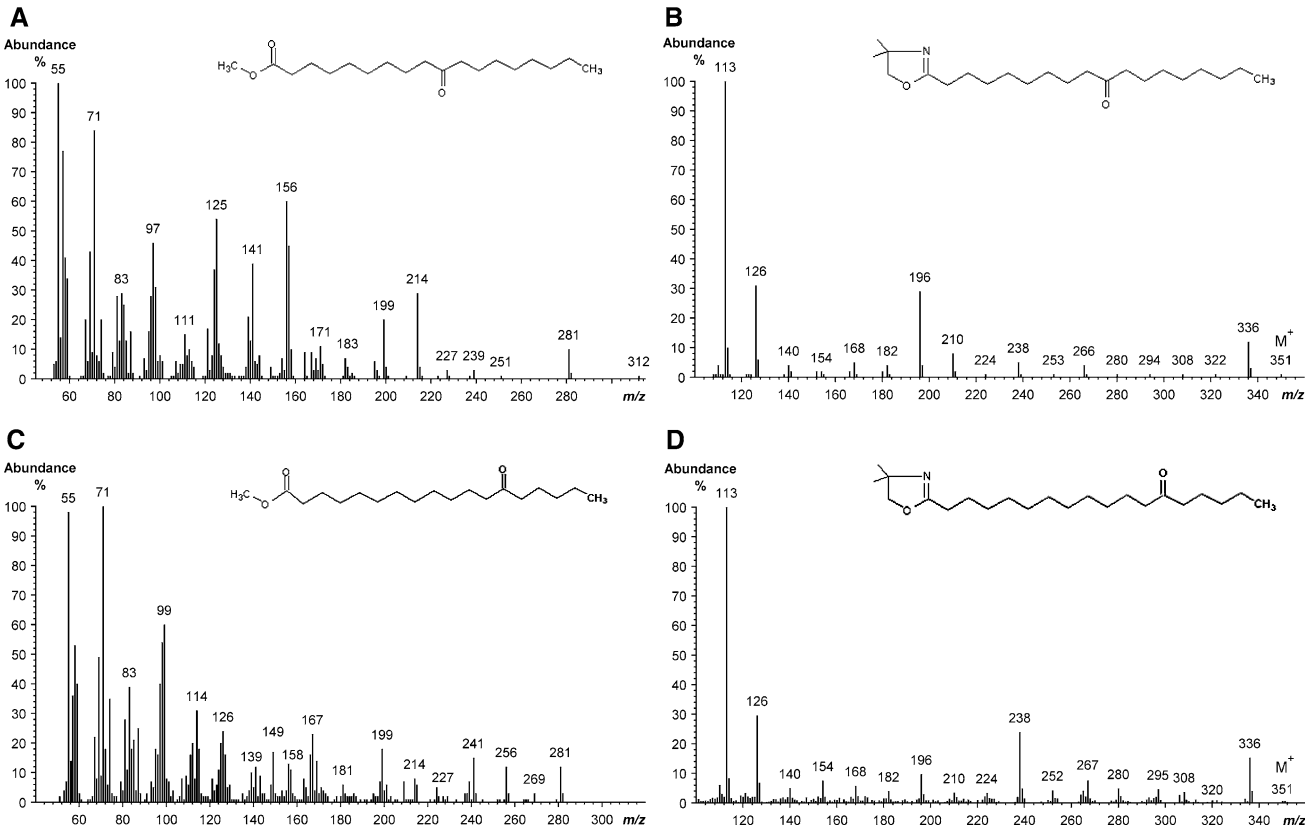

Fig. 9 Gas chromatography-electron-impact mass spectrum of **a** the methyl ester of 10-O-18:0, **b** DMOX derivative of 10-O-18:0, **c** methyl ester of 13-O-18:0, and **d** 4,4-dimethyloxaline derivative of 13-O-18:0 detected in omasal digesta in cows fed grass silage-based diets containing refined fish oil

Table 4 Mean flow at the omasum and ruminal balance of long-chain fatty acids in lactating cows fed grass silage-based diets supplemented with 0 (Control) or 250 g/day of refined fish oil (FO)

Fatty acid	Flow at the omasum (g/day)				Ruminal balance (g/day)[a]			
	Control	FO	SEM	*P* value	Control	FO	SEM	*P* value
20:0	4.33	3.14	0.349	0.074	3.50	1.87	0.255	0.011
cis-8 20:1	0.0	0.0	–	–	0.00	−0.32	<0.01	<0.001
cis-9 20:1	0.0	0.0	–	–	0.00	−0.37	<0.01	<0.001
cis-11 20:1	0.51	2.37	0.117	<0.001	−0.82	−0.85	0.098	0.831
cis-12 20:1	0.13	0.00	0.01	0.001	0.13	0.00	0.010	0.001
cis-13 20:1	0.0	0.53	0.018	<0.001	0.00	0.01	0.018	0.845
cis-14 20:1	0.0	0.17	0.042	0.050	0.00	0.17	0.042	0.049
cis-15 20:1	0.0	0.11	0.021	0.022	0.00	0.05	0.021	0.156
trans-9 20:1	0.03	0.25	0.039	0.017	0.03	0.25	0.040	0.017
trans-11 20:1	0.12	0.43	0.102	0.095	0.12	0.43	0.102	0.094
trans-12 20:1	0.06	0.46	0.107	0.059	0.06	0.46	0.107	0.059
trans-13 20:1	0.08	0.66	0.177	0.665	0.01	0.66	0.177	0.084
trans-14 20:1	0.09	0.58	0.159	0.095	0.09	0.57	0.158	0.010
trans-15 20:1	0.16	1.58	0.571	0.155	0.16	1.58	0.571	0.155
cis-8, *cis*-11 20:2	0.0	0.0	–	–	0.00	−0.39	<0.01	<0.001
cis-11, *cis*-14 20:2	0.14	0.64	0.083	0.013	−0.17	−0.01	0.074	0.212
cis-14, *cis*-17 20:2	0.0	0.20	0.011	<0.001	0.00	0.20	0.012	<0.001
cis-10, *trans*-15 20:2	0.0	0.26	0.046	0.016	0.00	0.26	0.046	0.016
trans-11, *cis*-15 20:2	0.0	0.89	0.055	<0.001	0.00	0.89	0.055	<0.001
trans-11, *cis*-17 20:2	0.0	0.47	0.045	0.002	0.00	0.47	0.043	0.002
trans-13, *cis*-17 20:2	0.0	2.00	0.285	0.008	0.00	2.00	0.286	0.008
trans-14, *cis*-17 20:2	0.0	1.07	0.163	0.010	0.00	1.07	0.163	0.010
trans-9, *trans*-15 20:2	0.0	1.38	0.153	0.003	0.00	1.38	0.154	0.003
trans-10, *trans*-16 20:2	0.0	1.19	0.110	0.002	0.00	1.19	0.110	0.002
trans-11, *trans*-15 20:2	0.0	0.89	0.099	0.003	0.00	0.88	0.099	0.003
trans-13, *trans*-17 20:2	0.0	0.39	0.040	0.003	0.00	0.39	0.040	0.003
cis-8, *cis*-11, *cis*-14 20:3	0.0	0.33	0.022	<0.001	0.00	0.01	0.021	0.829
cis-11, *cis*-14, *cis*-17 20:3	0.0	1.45	0.140	0.002	0.00	1.21	0.141	0.004
(*cis*)-11, (*cis*)-14, (*trans*)-17 20:3	0.0	0.39	0.035	0.002	0.00	0.39	0.035	0.001
Δ10,14,17 20:3[b]	0.0	0.26	0.031	0.004	0.00	0.27	0.031	0.004
Δ11,14,17 20:3[b]	0.0	0.16	0.011	0.001	0.00	0.16	0.012	0.001
(*trans*)-11, (*cis*)-14, (*cis*)-17 20:3	0.0	0.77	0.025	<0.001	0.00	0.77	0.024	<0.001
(*trans*)-10, (*trans*)-14, (*cis*)-17 20:3	0.0	0.69	0.104	0.009	0.00	0.69	0.104	0.009
(*trans*)-9, (*trans*)-14, (*trans*)-17 20:3	0.0	0.17	0.009	<0.001	0.00	0.17	0.008	<0.001
(*trans*)-10, (*trans*)-14, (*trans*)-17 20:3	0.0	0.27	0.147	<0.001	0.00	0.27	<0.01	<0.001
Δ11,14,18 20:3	0.0	0.08	0.021	0.060	0.00	0.08	0.022	0.060
cis-5, *cis*-8, *cis*-11, *cis*-14 20:4	0.0	0.10	0.009	0.002	0.00	−2.16	0.009	<0.001
cis-8, *cis*-11, *cis*-14, *cis*-17 20:4	0.0	1.11	0.052	<0.001	−1.99	−2.25	0.058	0.033
(*trans*)-7, (*cis*)-11, (*cis*)-14, (*cis*)-17 20:4	0.0	0.11	0.014	0.006	0.00	0.11	0.013	0.004
cis-5, *cis*-8, *cis*-11, *cis*-14, *cis*-17 20:5	0.0	1.05	0.082	0.001	0.00	−42.5	0.082	<0.001
cis-12, *cis*-15, *cis*-18 21:3	0.0	0.04	0.008	0.027	0.00	0.02	0.008	0.115
cis-9, *cis*-12, *cis*-15, *cis*-18 21:4	0.0	0.07	0.003	<0.001	0.00	0.07	0.003	<0.001
cis-6, *cis*-9, *cis*-12, *cis*-15, *cis*-18 21:5	0.0	0.33	0.109	<0.001	0.00	−1.42	<0.01	<0.001
22:0	3.24	2.95	0.092	0.091	−0.49	−0.28	0.117	0.280
cis-11 22:1	0.0	0.63	0.089	0.007	0.00	−1.90	0.089	<0.001
cis-13 22:1	0.17	0.59	0.044	0.002	0.17	0.00	0.044	0.054

Table 4 continued

Fatty acid	Flow at the omasum (g/day)				Ruminal balance (g/day)[a]			
	Control	FO	SEM	*P* value	Control	FO	SEM	*P* value
cis-15 22:1	0.0	0.32	0.008	<0.001	0.00	0.11	0.007	<0.001
cis-13, *cis*-16 22:2	0.0	0.10	0.008	0.001	0.00	0.03	0.009	0.057
trans-12, *trans*-17 22:2	0.0	0.19	0.032	0.014	0.00	0.19	0.031	0.014
cis-10, *cis*-13, *cis*-16 22:3	0.0	0.14	0.030	0.028	0.00	0.15	0.029	0.026
(*cis*)-10 (*trans*)-14, (*cis*)-19 22:3	0.0	0.46	0.092	<0.001	0.00	0.46	<0.01	<0.001
(*trans*)-12, (*cis*)-16 (*cis*)-19 22:3	0.0	0.84	0.154	0.019	0.00	0.84	0.154	0.019
Δ10,13,17 22:3	0.0	1.09	0.055	<0.001	0.00	1.04	0.055	<0.001
cis-7, *cis*-10, *cis*-13, *cis*-16 22:4	0.0	0.0	–	–	0.00	−1.17	<0.01	<0.001
cis-10, *cis*-13, *cis*-16, *cis*-19 22:4	0.0	1.92	0.175	0.002	0.00	1.72	0.177	0.002
(*cis*)-7, (*trans*)-13, (*cis*)-16, (*cis*)-19 22:4	0.0	0.30	0.008	<0.001	0.00	0.30	0.009	<0.001
(*trans*)-8, (*cis*)-13, (*cis*)-16, (*cis*)-19 22:4	0.0	0.74	0.040	<0.001	0.00	0.74	0.040	<0.001
(*trans*)-10, (*trans*)-13, (*cis*)-16, (*cis*)-19 22:4	0.0	0.14	0.010	0.001	0.00	0.14	0.011	0.001
cis-4, *cis*-7, *cis*-10, *cis*-13, *cis*-16 22:5	0.0	0.0	–	–	0.00	−0.86	<0.01	<0.001
cis-7, *cis*-10, *cis*-13, *cis*-16, *cis*-19 22:5	0.0	0.71	0.076	0.001	0.00	−5.23	0.076	<0.001
(*trans*)-5, (*cis*)-10, (*cis*)-13, (*cis*)-16, (*cis*)-19 22:5	0.0	0.30	0.030	0.002	0.00	0.30	0.031	0.002
cis-4, *cis*-7, *cis*-10, *cis*-13, *cis*-16, *cis*-19 22:6	0.0	0.49	0.045	0.002	0.00	−27.2	0.045	<0.001
23:0	0.61	0.70	0.071	0.404	0.61	0.65	0.071	0.720
cis-8, *cis*-11, *cis*-14, *cis*-17, *cis*-20 23:5	0.0	0.0	–	–	0.00	−0.07	<0.01	<0.001
24:0	3.04	2.88	0.207	0.611	−0.74	−1.27	0.055	0.003
cis-9, *cis*-12, *cis*-15, *cis*-18, *cis*-21 24:5	0.0	0.042	0.004	0.002	0.00	−0.29	0.004	<0.001
cis-6, *cis*-9, *cis*-12, *cis*-15, *cis*-18, *cis*-21 24:6	0.0	0.0	–	–	0.00	−0.35	<0.01	<0.001

Parenthesis indicate tentative geometry of double bonds as inferred based on retention times and elution order of FAME during GC analysis relative to authentic FAME standards

[a] Calculated as [mean flow at the omasum (g/day) − intake (g/day)] for cows fed grass-silage-based diets supplemented with 0 (Control) or 250 g/day of refined fish oil (FO)

[b] Retention time comparisons inferred a *cis*, *trans*, *trans* or *trans*, *cis*, *trans* double bond configuration

rumen. In total, 27 novel 20-, 21- and 22-carbon fatty acids containing at least one *trans* double bond and several unique all *cis* long-chain polyunsaturated fatty acids were detected in variable concentrations in omasal digesta of cows fed fish oil, with the implication that the hydrogenation of long-chain unsaturated fatty acids in the rumen involves a complicated series of metabolic reactions and the formation of numerous intermediates. GC–MS analysis of FAME confirmed chain length and degree of unsaturation of 20- to 24-carbon fatty acids in fish oil and omasal digesta but did not yield sufficient information enabling the position of double bonds to be located, which can be attributed to the high sensitivity of the carboxyl group to fragmentation and the propensity of double bonds in unsaturated methyl esters to migrate along the carbon chain [24].

During analysis of FAME by GC and GC–MS, the relative retention times of FAME, especially those of saturated compared with unsaturated methyl esters, were found to differ between CP-Sil 88 columns obtained from the same supplier, causing, for instance, the elution order of 20:5n-3 and 24:0 to vary, which is consistent with previous reports [35]. Furthermore, the use of helium as a carrier gas during GC–MS analysis was found to alter the relative retention times of certain FAME compared with hydrogen used for GC analysis. Differences in chromatography between columns, carrier gases and also the molecular weight of analysed fatty acid derivatives served to complicate the cross-referencing of peaks between GC and GC–MS analysis and the identification of minor fatty acids in analysed samples. Pinpointing unknown peaks resolved during GC analysis of FAME in the total ion chromatogram during GC–MS analysis of FAME and DMOX derivatives was achieved based on the relative abundance of specific isomers in omasal digesta and repeated injection and analysis of fatty acid derivatives over an extended period enabling variations in relative retention time and elution order of FAME and DMOX to be taken into account. While it is generally accepted that DMOX derivatives exhibit chromatographic properties comparable to those of FAME [23, 24], the current investigation highlighted that even subtle variations in the relative

retention and elution order of FAME and DMOX derivatives can introduce major challenges in attempts to identify the structure of minor components in samples containing a highly complex mixture of fatty acids.

Identification of the structure of unknown fatty acids was based on GC–MS analysis of DMOX derivatives since these can be prepared from FAME and purified without substantial losses of polyenoic fatty acids and are highly volatile, allowing the recording of mass spectra even for isomers at very low concentrations in complex samples under the same chromatographic conditions applied to FAME [23]. However, some reports have indicated that, in certain circumstances, fatty acid derivatization may cause the isomerization of double bonds and formation of artefacts [36–38]. Prior to the preparation of DMOX from FAME of fish oil and omasal digesta, a wide range of authentic FAME standards containing between one and six double bonds were converted to DMOX derivatives and analysed by GC–MS. There was no evidence based on the chromatography, order of elution of DMOX derivatives relative to parent FAME, or from the recorded mass spectrum to indicate that heating at 170 °C overnight altered the composition of fatty acids in the analysed samples.

Fractionation of FAME according to the degree of unsaturation and double bond geometry by Ag^+-TLC allowed *cis* and *trans* monoenoic fatty acids to be completely resolved, confirming the configuration of double bonds for 20:1 and 22:1 isomers. Despite the fractionation of FAME prior to the conversion of DMOX derivatives, it was not possible to elucidate the structure of all 20- and 22- carbon fatty acids due to a very low abundance and/or co-elution with other components. A mixture of hexane and diethyl ether was used to develop TLC plates based on reports that this solvent system resolves *trans* and *cis* 18:1 isomers in bovine milk fat [14, 19, 20], and therefore applied in the analysis of omasal digesta due to the occurrence of *cis* and *trans* 20:1 and *cis* 22:1 isomers. Previous investigations have reported the separation of methyl esters of *cis* 20:1, *cis* 22:1, *trans* 20:1, *trans* 22:1 and geometric isomers of 20:5n-3 and 22:6n-3 by Ag^+-TLC using plates developed with a mixture (50:50, v/v) of toluene and hexane [39] or a mixture (85:15, v/v) of toluene and methanol [40, 41], but the use of alternative solvents was not explored further in the current analysis. Methyl esters of 22-carbon fatty acids containing four or more double bonds were not resolved by Ag^+-TLC, which, combined with the inability of GC–MS analysis of DMOX derivatives to distinguish between geometric isomers, meant that inferences on double geometry of specific biohydrogenation intermediates in omasal digesta of cows fed fish oil had to be drawn on the basis of retention times and order of elution relative to authentic standards during GC analysis.

Fish oil in the diet is known to alter the hydrogenation of unsaturated fatty acids in the rumen, causing an increase in the flow of 16:1, 18:1, and 18:2 intermediates at the omasum or duodenum in cattle [7–9]. Studies in sheep have demonstrated that the inhibitory effects of fish oil fatty acids on the reduction of *trans* 18:1–18:0 is also associated with the accumulation of 10-OH-18:0 [42] and 10-O-18:0 [43] in the rumen. Identification of oxygenated 18-carbon fatty acids in Control and FO digesta confirmed that fish oil in the diet causes an increase in ruminal outflow of 10-O-16:0, 9-0-18:0, 10-OH-18:0 and 10-O-18:0 in cattle but has no effect on 13-O-18:0 at the omasum. Incubations of fatty acid substrates with rumen fluid or pure cultures of rumen bacteria have established that *cis*-9 18:1 [44–46] and *trans*-10 18:1 [46] can be hydrated to yield 10-OH-18:0, which is further oxidized to 10-O-18:0. Rumen bacteria are also known to be capable of converting 18:2n-6 to *cis*-9, 13-OH 18:1 [47]. It remains uncertain if one or more fatty acids in fish oil promote the hydration of unsaturated fatty acids or alternatively inhibit further transformations of 18-carbon oxo fatty acids in the rumen.

The inhibitory effects of fish oil in the diet on the complete reduction of 18-carbon unsaturated fatty acids to 18:0 in the rumen are thought to be related to the toxic effects of 20:5n-3 and 22:6n-3 on the growth and metabolic activity of ruminal bacteria capable of biohydrogenation [12, 48, 49]. Even though it is well established that 20:5n-3 and 22:6n-3 are extensively hydrogenated in the rumen [7–9], the intermediates formed and metabolic pathways responsible are not known.

Fish oil in the diet enhanced the flow of 20:5n-3, 22:5n-3 and 22:6n-3 at the omasum, with the increases determined from the analysis of total lipid in omasal digesta being almost identical to those based on the flow of non-esterified fatty acids at the omasum [7], indicating that the small amounts of long-chain fatty acids that escape the rumen are in free fatty acid form. Measurements of ruminal fatty acid balance indicated that fish oil in the diet resulted in the net synthesis of *cis*-14 20:1, 20:2n-3, 20:3n-3, 21:3n-3, 21:4n-3, 22:2n-6, 22:3n-6 and 22:4n-3. Extensive investigations have not yielded any substantive evidence that the carbon chain of unsaturated fatty acids is elongated or shortened during biohydrogenation in the rumen [50, 51]. Therefore, the occurrence of 21:3n-3 and 21:4n-3 in FO digesta must arise from the hydrogenation of 21:5n-3 in fish oil by a series of reactions that result in the sequential reduction of *cis* double bonds at Δ6 and Δ9. A serial reduction of double bonds closest to the carboxyl group also appears to represent one of the main pathways explaining the disappearance of 20:5n-3 and 22:6n-3 in the rumen. Hydrogenation of 20:5n-3 involving the reduction of *cis* double bonds at Δ5, Δ8 and Δ11 offers an explanation for the formation and accumulation of 20:2n-3 and 20:3n-3 and the lower extent

of hydrogenation of 20:4n-3 than 20:5n-3 in the rumen. Similarly, the lower ruminal hydrogenation of 22:5n-3 compared with 22:6n-3, along with the net synthesis of 22:4n-3 provides further evidence that one of the main transformations of 22:6n-3 in the rumen involves the initial removal of the double bond between carbon atoms 4 and 5 followed by the reduction of the double bond at Δ7. Measurements of ruminal fatty acid balance in cows fed fish oil also suggest that hydrogenation of 20:4n-6 may proceed via the reduction of double bonds at Δ5 and Δ8 to yield 20:2n-6, and that hydrogenation of 22:5n-6 involves the formation of 22:4n-6, 22:3n-6 and 22:2n-6 via sequential reduction of double bonds at Δ4, Δ7 and Δ10.

Inclusion of fish oil in the diet also resulted in the accumulation of numerous polyenoic 20- and 22-carbon intermediates containing at least one *trans* double bond, indicating that hydrogenation of long-chain unsaturated fatty acids also involves the isomerisation of *cis* double bonds. Owing to the complex composition of fish oil it is not possible to establish the metabolic origins of many of these biohydrogenation intermediates. However, the position of double bonds in *trans*-5, *cis*-10, *cis*-13, *cis*-16, *cis*-19 22:5 identified in FO omasal digesta indicate that this intermediate must originate from metabolism of 22:6n-3 in the rumen by a series of reactions involving isomerization of the *cis*-4 double bond and reduction of the *cis*-7 double bond. Furthermore, isomerisation of the *cis* bond between carbon atoms 8 and 9 in 20:4n-3 would also account for the formation of *trans*-7, *cis*-11, *cis*-14, *cis*-17 20:4 in the rumen but it remains unclear if this intermediate arises from 20:4n-3 in fish oil or from 20:4n-3 liberated from 20:5n-3 following the reduction of the *cis*-5 double bond. Since fish oil contained 18-fold more 20:5n-3 than 20:4n-3, it seems more likely that *trans*-7, *cis*-11, *cis*-14, *cis*-17 20:4 originates from 20:5n-3 in the diet.

By analogy with the known pathways of 18-carbon unsaturated fatty acid metabolism in the rumen it has been speculated that ruminal hydrogenation of 20:5n-3 and 22:6n-3 yields intermediates with 5 or 6 double bonds, containing at least one *trans* double bond [51]. Omasal digesta of cows on the FO treatment was devoid of 20:5 or 22:6 biohydrogenation intermediates, and no 20- and 22-carbon fatty acids containing a conjugated double bond were detected. Several studies have reported the occurrence of geometric and position isomers of conjugated 18:2 in omasal or duodenal digesta of cattle [7–9], and the appearance of *cis*-9, *trans*-11, *cis*-15 18:3 in omasal digesta of cows fed grass-silage-based diets [52]. Even though intermediates produced during the initial stages of biohydrogenation are known to be transient and rapidly hydrogenated [50, 51], it has been possible to isolate and identify conjugated intermediates formed during incubations of 18:2n-6 and 18:3n-3 with ruminal fluid [12, 53, 54]. An absence of conjugated 20- or 22- fatty acids in digesta of cows fed fish oil requires further corroboration based on reverse-phase HPLC analysis of FAME [55], but evidence from this investigation suggests that the first committed steps of 20:5n-3, 21:5n-3, 22:5n-3 and 22:6n-3 hydrogenation in the rumen do not appear to involve the formation of a conjugated bond system.

Fish oil in the diet enhanced the flow of *trans* 20:1 and *trans* 22:1 isomers at the omasum consistent with recent reports on temporal changes in fatty acid composition of ruminal digesta of sheep fed high concentrate diets containing fish oil and sunflower oil [43]. Increases in ruminal outflow of *trans* 20:1 and *trans* 22:1 were not accompanied by higher amounts of 20:0 and 22:0 leaving the rumen, indicating that one or more fatty acids in fish oil inhibit the complete hydrogenation of 20- and 22-carbon unsaturated fatty acids in the rumen. Studies in growing cattle have also shown that incremental amounts of fish oil in the diet do not increase 20:0 and 22:0 at the duodenum [8, 9].

Incubations with rumen fluid have established that 20:5n-3 and 22:6n-3 inhibit the complete hydrogenation of 18-carbon unsaturated fatty acids causing *trans* 18:1 isomers to accumulate [11]. Changes in the flow of *trans* 20:1 biohydrogenation intermediates were also accompanied by an increase in the amount of *cis*-11, -13, -14 and *cis*-15 20:1 at the omasum that may reflect ruminal escape of these fatty acids contained in fish oil, or formation of these isomers during the hydrogenation of 20-carbon polyunsaturated fatty acids in the rumen. Ruminal escape of fish oil fatty acids may also account for the increase in *cis*-11, -13 and -15 22:1 in FO omasal digesta, but the possibility that one or more of these isomers is formed during the penultimate step of 22-carbon polyunsaturated fatty acid hydrogenation in the rumen cannot be excluded.

Detailed analysis of lipid in omasal digesta of cows fed FO suggests that hydrogenation of long-chain polyenoic fatty acids in the rumen may proceed via two distinct mechanisms that involve sequential reduction and/or isomerization of *cis* double bonds closest to the carboxyl group. Further studies examining the fate of C^{13} labeled 20:5n-3 and 22:6n-3 administered in the rumen in vivo or incubations of pure fatty acid substrates with mixed rumen bacteria in the presence of deuterium oxide [46, 54] are required to verify these considerations. Techniques applied to the analysis of fatty acid composition allowed carbon chain length and double bond position for most of the 20- and 22-carbon biohydrogenation intermediates in omasal digesta to be identified, but the structure of several minor fatty acids remains unknown. Furthermore, double bond geometry of most polyenoic biohydrogenation intermediates had to be inferred rather than determined. Additional investigations based on GC–MS analysis of other FA derivatives including picolinyl esters [24], or analysis of

FAME by covalent adduct chemical ionization tandem MS [56, 57], two-dimensional GC analysis [58], GC-Fourier infrared spectroscopy-MS [59], reverse-phase HPLC [55] and Ag + HPLC [41] are required to verify the double bond geometry of polyenoic biohydrogenation intermediates and characterize other minor fatty acids formed during the hydrogenation of long-chain unsaturated fatty acids in the rumen.

The biological significance of the formation and accumulation of numerous 20- and 22-carbon fatty acids containing one or more *trans* double bonds in the rumen of cows fed fish oil remains uncertain. Ruminal outflow of specific 20- and 22-carbon biohydrogenation intermediates was of the same magnitude as the amount of 20:5n-3, 22:5n-3 and 22:6n-3 and it is probable that most of these intermediates are also incorporated into milk fat triacylglycerides and tissue lipids, albeit at low concentrations. A higher consumption of *trans* fatty acids in the human diet is known to be associated with an increase in cardiovascular disease risk, with recent evidence from clinical trials implicating 18-carbon fatty acids containing more than one double bond as being particularly harmful [60]. It is possible that increases in polyenoic *trans* fatty acids may offset some of the expected benefits to human health from the enrichment of 20:5n-3 and 22:6n-3 in ruminant derived foods.

Acknowledgments Financial support from the Finnish Ministry of Agriculture and Forestry is gratefully acknowledged and appreciated.

References

1. World Health Organization (2003) Diet, nutrition and the prevention of chronic diseases. World Health Organ Tech Rep Ser 916:1–148
2. Wang C, Harris WS, Chung M, Lichtenstein AH, Balk EM, Kupelnick B, Jordan HS, Lau J (2006) n-3 Fatty acids from fish or fish-oil supplements, but not α-linolenic acid, benefit cardiovascular disease outcomes in primary- and secondary-prevention studies: a systematic review. Am J Clin Nutr 84:5–17
3. Harris WS, Mozaffarian D, Lefevre M, Toner CD, Colombo J, Cunnane SC, Holden JM, Klurfeld DM, Morris MC, Whelan J (2009) Towards establishing dietary reference intakes for eicosapentaenoic and docosahexaenoic acids. J Nutr 139:804S–819S
4. Givens DI, Shingfield KJ (2006) Optimising dairy milk fatty acid composition. In: Williams C, Buttriss J (eds) Improving the fat content of foods. Woodhead, Cambridge, pp 252–280
5. Scollan N, Hocquette J-F, Nuernberg K, Dannenberger D, Richardson I, Moloney A (2006) Innovations in beef production systems that enhance the nutritional and health value of beef lipids and their relationship with meat quality. Meat Sci 74:17–33
6. Chilliard Y, Glasser F, Ferlay A (2007) Diet, rumen biohydrogenation and nutritional quality of cow and goat milk fat. Eur J Lipid Sci Technol 109:828–855
7. Shingfield KJ, Ahvenjärvi S, Toivonen V, Ärölä A, Nurmela KVV, Huhtanen P, Griinari JM (2003) Effect of dietary fish oil on biohydrogenation of fatty acids and milk fatty acid content in cows. Anim Sci 77:165–179
8. Lee MRF, Shingfield KJ, Tweed JKS, Toivonen V, Huws SA, Scollan ND (2008) Effect of fish oil on ruminal biohydrogenation of C18 unsaturated fatty acids in steers fed grass or red clover silages. Animal 2:1859–1869
9. Shingfield KJ, Lee MRF, Humphries DJ, Scollan ND, Toivonen V, Reynolds CK, Beever DE (2010) Effect of incremental amounts of fish oil in the diet on ruminal lipid metabolism in growing steers. Br J Nutr 104:56–66
10. Dohme F, Fievez K, Raes K, Demeyer DI (2003) Increasing levels of two different fish oils lower ruminal biohydrogenation of eicosapentaenoic and docosahexaenoic acid in vitro. Anim Res 52:309–320
11. AbuGhazaleh AA, Jenkins TC (2004) Disappearance of docosahexaenoic and eicosapentaenoic acids from cultures of mixed ruminal microorganisms. J Dairy Sci 87:645–651
12. Wąsowska I, Maia MRG, Niedźwiedzka KM, Czauderna M, Ribeiro JM, Ramalho C, Devillard E, Shingfield KJ, Wallace RJ (2006) Influence of fish oil on ruminal biohydrogenation of C18 unsaturated fatty acids. Br J Nutr 95:1199–1211
13. Kramer JKG, Fellner V, Dugan MER, Sauer FD, Mossoba MM, Yurawecz MP (1997) Evaluating acid and base catalysts in the methylation of milk and rumen fatty acids with special emphasis on conjugated dienes and total *trans* fatty acids. Lipids 32:1219–1228
14. Cruz-Hernandez C, Deng Z, Zhou J, Hill AR, Yurawecz MP, Delmonte P, Mossoba MM, Dugan MER, Kramer JKG (2004) Methods for analysis of conjugated linoleic acids and *trans*-18:1 isomers in dairy fats by using a combination of gas chromatography, silver-ion thin-layer chromatography/gas chromatography, and silver-ion liquid chromatography. JAOAC Int 87:545–562
15. Ratnayake WMN (2004) Overview of methods for the determination of *trans* fatty acids by gas chromatography, silver-ion thin-layer chromatography, silver-ion liquid chromatography, and gas chromatography/mass spectrometry. JAOAC Int 87:523–539
16. Kramer JKG, Hernandez M, Cruz-Hernandez C, Kraft J, Dugan MER (2008) Combining results of two GC separations partly achieves determination of all *cis* and *trans* 16:1, 18:1, 18:2 and 18:3 except CLA isomers of milk fat as demonstrated using Ag-ion SPE fractionation. Lipids 43:259–273
17. Radin NS (1981) Extraction of tissue lipids with a solvent of low toxicity. Methods Enzymol 72:5–8
18. Christie WW (1982) A simple procedure for rapid transmethylation of glycerolipids and cholesteryl esters. J Lipid Res 23:1072–1075
19. Precht D, Molkentin J (1996) Rapid analysis of the isomers of *trans*-octadecenoic acid in milk fat. Int Dairy J 6:791–809
20. Cruz-Hernandez C, Kramer JKG, Kraft J, Santercole V, Or-Rashid M, Deng Z, Dugan MER, Delmonte P, Yurawecz M (2006) Systematic analysis of *trans* and conjugated linoleic acids in the milk and meat of ruminants. In: Yurawecz MP, Kramer JKG, Gudmundsen O, Pariza MW, Banni S (eds) Advances in conjugated linoleic acid research, 3rd edn. AOAC, Urbana, pp 45–93
21. Kawashima H, Ohnishi M (2004) Identification of minor fatty acids and various non-methylene-interrupted diene isomers in mantle, muscle, and viscera of the marine bivalve *Megangulus zyonoensis*. Lipids 39:265–271
22. Fay L, Richli U (1991) Location of double bonds in polyunsaturated fatty acids by gas chromatography-mass spectrometry after 4,4-dimethyloxazoline derivatization. J Chromatogr 541:89–98
23. Spitzer V (1997) Structure analysis of fatty acids by gas chromatography–low resolution electron impact spectrometry of their 4,4-dimethyloxazoline derivatives–a review. Prog Lipid Res 35:387–408

24. Christie WW (1998) Gas chromatography-mass spectrometry methods for structural analysis of fatty acids. Lipids 33:343–353
25. Zhang JY, Yu QT, Liu BN, Huang ZH (1988) Chemical modification in mass spectrometry IV: 2-alkenyl-4, 4-dimethyloxazolines as derivatives for the double bond location of long-chain olefinic acids. Biomed Environ Mass Spectrom 15:33–44
26. Yu QT, Liu BN, Zhang JY, Huang ZH (1989) Location of double bonds in fatty acids of fish oil and rat testis lipids. Gas chromatography-mass spectrometry of the oxazoline derivatives. Lipids 24:79–83
27. Luthria DL, Sprecher H (1993) 2-Alkenyl-4, 4-dimethyloxazolines as derivatives for the structural elucidation of isomeric unsaturated fatty acids. Lipids 28:561–564
28. Kramer JKG, Blackadar CB, Zhou J (2002) Evaluation of two GC columns (60-m SUPELCOWAX 10 and 100-m CP Sil 88) for analysis of milk fat with emphasis on CLA, 18:1, 18:2 and 18:3 isomers, and short- and long-chain FA. Lipids 37:823–835
29. Alves SP, Bessa RJB (2009) Comparison of two gas–liquid chromatograph columns for the analysis of fatty acids in ruminant meat. J Chromatogr A 1216:5130–5139
30. Destaillats F, Wolff RL, Angers P (2001) A new Δ7-polyunsaturated fatty acid in Taxus spp. Seed lipids, dihomotaxoleic (7, 11–20:2) acid. Lipids 36:319–321
31. Ryhage R, Stenhagen E (1960) Mass spectrometric studies. VI. Methyl esters of normal chain oxo-, hydroxy-, methoxy- and epoxy-acids. Arkiv Kemi 15:545–574
32. Zhang JY, Yu QT, Yang YM, Huang ZH (1988) Chemical modification in mass spectrometry. 11. A study on the mass spectra of 4,4-dimethyloxazoline derivatives of hydroxy fatty acids. Chem Scripta 28:357–363
33. Classen E, Marx F, Fabricius H (1994) Mass spectra of 4,4-dimethyloxazoline derivatives of oxooctadecanoic acids. Fat Sci Technol 96:331–332
34. Hou CT (1994) Production of 10-ketostearic acid from oleic acid by *Flavobacterium sp*. strain DS5 (NRRL B-14859). Appl Environ Microbiol 60:3760–3763
35. Kramer JKG, Cruz-Hernandez C, Deng Z, Zhou J, Jahreis G, Dugan MER (2004) Analysis of conjugated linoleic acid and *trans* 18:1 isomers in synthetic and animal products. Am J Clin Nutr 79:1137S–1145S
36. Lamberto M, Ackman RG (1995) Positional isomerisation of *trans*-3-hexadecenoic acid employing 2-amino-2-methyl-propanol as a derivatizing agent for ethylenic bond location by gas chromatography/mass spectrometry. Anal Biochem 230:224–228
37. Christie WW (1998) Mass spectrometry of fatty acids with methylene-interrupted ene-yne systems. Chem Phys Lipids 94:35–41
38. Garrido JL, Medina I (2002) Identification of minor fatty acids in mussels (*Mytilus galloprovincialis*) by GC–MS of their 2-alkenyl-4,4-dimethyloxazoline derivatives. Anal Chim Acta 465: 409–416
39. Wilson R, Lyall K, Payne JA, Riemersma RA (2000) Quantitative analysis of long-chain *trans*-monoenes originating from hydrogenated marine oil. Lipids 35:681–687
40. Fournier V, Destaillats F, Juanéda P, Dionisi F, Lambelet P, Sébédio J-L, Berdeaux O (2006) Thermal degradation of long-chain polyunsaturated fatty acids during deodorization of fish oil. Eur J Lipid Sci Technol 108:33–42
41. Fournier V, Juanéda P, Destaillats F, Dionisi F, Lambelet P, Sébédio J-L, Berdeaux O (2006) Analysis of eicosapentaenoic and docosahexaenoic acid geometrical isomers formed during fish oil deodorization. J Chromatogr A 1129:21–28
42. Kitessa SM, Gulati SK, Ashes JR, Fleck E, Scott TW, Nichols PD (2001) Utilisation of fish oil in ruminants—I. Fish oil metabolism in sheep. Anim Feed Sci Technol 89:189–199
43. Toral PG, Shingfield KJ, Hervás G, Toivonen V, Frutos P (2010) Effect of fish oil and sunflower oil on rumen fermentation characteristics and fatty acid composition of digesta in ewes fed a high concentrate diet. J Dairy Sci 93:4804–4817
44. Hudson JA, MacKenzie CA, Joblin KN (1995) Conversion of oleic acid to 10-hydroxystearic acid by two species of ruminal bacteria. Appl Microbiol Biotechnol 44:1–6
45. Jenkins TC, AbuGhazaleh AA, Freeman S, Thies EJ (2006) The production of 10-hydroxystearic and 10-ketostearic acids is an alternative route of oleic acid transformation by the ruminal microbiota in cattle. J Nutr 136:926–931
46. McKain N, Shingfield KJ, Wallace RJ (2010) Metabolism of conjugated linoleic acids and 18:1 fatty acids by ruminal bacteria: products and mechanisms. Microbiology 156:579–588
47. Hudson JA, Morvan B, Joblin KN (1998) Hydration of linoleic acid by bacteria isolated from ruminants. FEMS Microbiol Lett 169:277–282
48. Maia MRG, Chaudhary LC, Figueres L, Wallace RJ (2007) Metabolism of polyunsaturated fatty acids and their toxicity to the microflora of the rumen. Antonie van Leeuwenhoek 91:303–314
49. Maia MRG, Chaudhary LC, Bestwick CS, Richardson AJ, McKain N, Larson TR, Graham IA, Wallace RJ (2010) Toxicity of unsaturated fatty acids to the biohydrogenating ruminal bacterium, *Butyrivibrio fibrisolvens*. BMC Microbiol 10:52
50. Harfoot CG, Hazlewood GP (1988) Lipid metabolism in the rumen. In: Hobson PN (ed) The rumen microbial ecosystem. Elsevier, London, pp 285–322
51. Jenkins TC, Wallace RJ, Moate PJ, Mosley EE (2008) BOARD-INVITED REVIEW: recent advances in biohydrogenation of unsaturated fatty acids within the rumen microbial ecosystem. J Anim Sci 86:397–412
52. Shingfield KJ, Ahvenjärvi S, Toivonen V, Vanhatalo A, Huhtanen P, Griinari JM (2008) Effect of incremental levels of sunflower-seed oil in the diet on ruminal lipid metabolism in lactating cows. Br J Nutr 99:971–983
53. Jouany J-P, Lassalas B, Doreau M, Glasser F (2007) Dynamic features of the rumen metabolism of linoleic acid, linolenic acid and linseed oil measured in vitro. Lipids 42:351–360
54. Wallace RJ, McKain N, Shingfield KJ, Devillard E (2007) Isomers of conjugated linoleic acids are synthesized via different mechanisms in ruminal digesta and bacteria. J Lipid Res 48:2247–2254
55. Banni S, Carta G, Contini MS, Angioni E, Deiana M, Dessi MA, Melis MP, Corongiu FP (1996) Characterization of conjugated diene fatty acids in milk, dairy products, and lamb tissues. J Nutr Biochem 7:150–155
56. Michaud AL, Yurawecz MP, Delmonte P, Corl BA, Bauman DE, Brenna T (2003) Identification and characterization of conjugated fatty acid methyl esters of mixed double bond geometry by acetonitrile chemical ionization tandem mass spectrometry. Anal Chem 75:4925–4930
57. Gómez-Córtes P, Tyburczy C, Brenna JT, Juárez M, Angel de la Fuente M (2009) Characterization of *cis*-9 *trans*-11 *trans*-15 C18:3 in milk fat by GC and covalent adduct chemical ionization tandem MS. J Lipid Res 50:2412–2420
58. Vlaeminck B, Harynuk J, Fievez V, Marriott P (2007) Comprehensive two-dimensional gas chromatography for the separation of fatty acids in milk. Eur J Lipid Sci Technol 109:757–766
59. Wahl HG, Habel S-Y, Schmieder N, Liebich HM (1994) Identification of *cis*/*trans* isomers of methyl ester and oxazoline derivatives of unsaturated fatty acids using GC-FTIR-MS. J High Resolut Chromatogr 17:543–548
60. Lemaitre RN, King IB, Mozaffarian D, Sotoodehnia N, Rea TD, Kuller LH, Tracy RP, Siscovick DS (2006) Plasma phospholipid *trans* fatty acids, fatal ischemic heart disease, and sudden cardiac death in older adults. Circulation 114:209–215

Lipids (2011) 46:607–616
DOI 10.1007/s11745-011-3552-2

ORIGINAL ARTICLE

Structure and Function of Cholesteryl Ester Transfer Protein in the Tree Shrew

Huirong Liu · Gang Wu · Bing Zhou · Baosheng Chen

Received: 13 October 2010 / Accepted: 15 March 2011 / Published online: 1 April 2011

Abstract Cholesteryl ester transfer protein (CETP) plays an important role in reverse cholesterol transport (RCT). To study on the structure and function of CETP in the tree shrew, a kind of animal resistant to atherosclerosis, we completed the cloning of the full-length tree-shrew CETP cDNA sequence based on the reported partial sequence. The full-length cDNA of tree shrew CETP was 1,704 bp and the deduced protein of the cDNA showed a sequence identity of 81, 80 and 74%, respectively, with the human, monkey and rabbit CETP. The level of CETP mRNA in the liver was much more abundant than that in the other tissues. A mutant protein with a substitution of Asn at position 110 by Gln was found to possess an impaired secretion property compared with the wild-type tree shrew CETP. The mutant proteins, respectively, with a substitution of Pro at position 344 by Ser and a substitution of Gln at position 452 by Arg displayed similar secretion ability, but a decreased cholesteryl ester transfer capability compared with the wild type (48 and 26% lower, respectively). These findings demonstrate that liver is the main tissue synthesizing CETP in the tree shrew. Asn at position 110 plays an important role in the secretion of tree shrew CETP. The residues at position 344 and 452 play essential roles in cholesteryl ester transferring process.

Keywords Tree shrew · Cholesteryl ester transfer protein · Structure · Function

Abbreviations

apoB	Apolipoprotein B
AS	Atherosclerosis
CE	Cholesteryl ester
CETP	Cholesteryl ester transfer protein
CHD	Coronary heart disease
HDL	High density lipoprotein
HDL-C	High density lipoprotein cholesterol
LDL	Low density lipoprotein
LDL-C	Low density lipoprotein cholesterol
RCT	Reverse cholesterol transport
VLDL	Very low density lipoprotein

Introduction

Tree shrews are animals belonging to the Class Mammalia, Order Scandentia, Family Tupaiidae, Genus *Tupaia* and supposed to be more closely related to humans than the rodents [1, 2]. It is documented that there is a very high plasma level of high density lipoprotein (HDL) in the tree shrew which accounts for about 70% of the total plasma lipoprotein levels [3]. Moreover, when the tree shrews are put on a high cholesterol diet, the plasma HDL still remains a similar high level to that prior to the diet and no typical atherosclerotic plaques are found in the artery wall though the gallstones are observed in 70% of the tested tree shrews. All of these data point out a high resistance of the tree shrew to atherosclerosis (AS).

H. Liu (✉)
College of Life Sciences, Inner Mongolia Agricultural University, Hohhot 010018, China
e-mail: lhz17@yahoo.com.cn

G. Wu · B. Chen (✉)
National Laboratory of Medical Molecular Biology, Institute of Basic Medical Sciences, Chinese Academy of Medical Sciences, Peking Union Medical College, Dong-Dan-San-Tiao 5, Beijing 100005, China
e-mail: bschen@ibms.pumc.edu.cn

B. Zhou
Beijing Center for ADR Monitoring, Beijing 100011, China

Cholesteryl ester transfer protein (CETP) is a hydrophobic plasma glycoprotein, possessing the ability to promote the transfer of cholesteryl ester (CE) from HDL to apolipoprotein B (apoB)-containing particles [i.e., very low density lipoprotein (VLDL) and LDL] in exchange for triacylglycerols in reverse cholesterol transport (RCT) [4–6]. Thus, CETP is a key protein in RCT because of its involvement in the regulation of plasma lipoprotein cholesterol levels and the remodeling of lipoprotein particles. Although the overall role of CETP in atherosclerosis is still unclear, numerous studies show that deficiency and decrease of CETP activity can lead to an increase in high density lipoprotein cholesterol (HDL-C) as well as a decrease in low density lipoprotein cholesterol (LDL-C) and finally a lower incidence of stroke and coronary heart disease (CHD) [7–9]. However, an increase in CETP activity decreases HDL-C, increases LDL-C, and finally increases atherosclerosis [10–12]. Recent comparative studies show that plasma CETP activity is significantly lower but the HDL-C/LDL-C ratio is higher in the tree shrew than in human and in the two species the CETP activities are negatively related with the HDL-C/LDL-C ratios, suggesting that the low CETP activity could lead to the high HDL-C level and resistance to AS in the tree shrew [13].

In 2001, Zeng et al. [14, 15] cloned the partial sequence of tree shrew CETP cDNA (AF334033). However, up until now, the full-length cDNA of tree shrew CETP had still not been discovered. In this study, we completed the molecular cloning of the full-length CETP cDNA in the tree shrew based on the reported partial sequence and revealed the distribution of CETP mRNA in 12 tissues. We also expressed tree shrew CETP in COS-7 cells and studied on the structure and function of tree shrew CETP by site-directed mutations.

Experimental Procedures

Materials and Reagents

TRIZOL reagent, SuperScript™ First-Strand Synthesis System for RT-PCR, culture media and reagents, and pcDNA3.1/myc-His(−)A were purchased from Invitrogen (Carlsbad, CA, USA). The SMART™ RACE cDNA Amplification Kit and Advantage® 2 PCR Kit were purchased from BD Clontech (Palo Alto, CA, USA). The fluorescein isothiocyanate (FITC) conjugated goat anti-rabbit secondary antibody, horseradish peroxidase-conjugated mouse anti-rabbit IgG, and the Enhanced Chemiluminescence (ECL) Western Blotting System were purchased from SantaCruz Biotechnology, Inc. (Santa Cruz, CA, USA). The CETP activity assay kit was purchased from BioVision, Inc. (Mountain View, CA, USA). The high performed transfection kit was purchased from Vigorous Instruments (Beijing) Co., Ltd. (Beijing, China). The QuikChange™ site-directed mutagenesis kit was purchased from Stratagene (La Jolla, CA, USA). Pyrobest DNA polymerase, *Taq* DNA polymerase, *Eco*RI, and *Xba*I, were purchased from TaKaRa Biotechnology (Dalian) Co., Ltd. (Dalian, China). The SYBR Green I was purchased from Molecular Probes (Eugene, OR, USA). The pGEM-T Easy Vector was purchased from Promega Corporation (Madison, WI, USA). The COS-7 cell line was purchased from the American Type Culture Collection (Manassas, VA, USA). All other reagents were from Sigma-Aldrich Chemical Co (St. Louis, MO, USA) unless stated otherwise.

Samples

All tissue samples were taken from 6-month-old male tree shrews (provided by Kunming Institute of Zoology, Chinese Academy of Science) and frozen in liquid nitrogen until use. The study protocol was approved by the Animal Research Ethical Committees at the Inner Mongolia Agricultural University and Peking Union Medical College.

Cloning of the 5′ Terminal Sequence of Tree Shrew CETP cDNA

Total RNA from tree shrew liver was prepared using TRIZOL reagent and checked by agarose gel electrophoresis. The liver RNA was reverse transcribed to the first strand cDNA using SMART™ RACE cDNA Amplification Kit. Based on the reported partial sequence of tree shrew CETP cDNA [14], a specific primer (5′-GGTAG-CAGTTGGGGGCGTTGGTCCG-3′) was synthesized for 5′ RACE. The RACE procedure was carried out using Advantage® 2 PCR Kit according to the manufacturer's instructions. The PCR products were cloned into pGEM-T Easy Vector for sequencing.

mRNA Quantitation

The relative expression of CETP mRNA in 12 tissues from tree shrews was measured by real-time RT PCR using β-actin as an internal control. Total RNA samples from the different tree shrew tissues were extracted by TRIZOL reagent. The RNA was reverse transcribed to the first strand cDNA using SuperScript™ First-Strand Synthesis System for RT-PCR. 1 μg of total RNA, 1 μl of 10 mM dNTP mix, 1 μl of oligo(dT)$_{12–18}$ (0.5 μg/μl), and some diethylpyrocarbonate (DEPC)-treated water were added into a tube to a final volume of 10 μl, mixed, and incubated at 65 °C for 5 min, then cooled on ice for at least 1 min. In a separate tube, 2 μl of 10× RT buffer, 4 μl of 25 mM

Table 1 The mutant tree shrew CETP

Mutants	Amino acid change	Mutagenic primers
N110Q	Asn110 to Gln110	5′-GGGGATTGAGCATTCAGCAGTCTGTCGACTTCG-3′
		5′-CGAAGTCGACAGACTGCTGAATGCTCAATCCCC-3′
P344S	Pro344 to Ser344	5′-GTGTCGTGGTCAACTCTTCTGTGGTCGTGAAATTCC-3′
		5′-GGAATTTCACGACCACAGAAGAGTTGACCACGACAC-3′
Q452R	Gln452 to Arg452	5′-CCTGAGATTATCACTCGGGATGGCTTCCTGCTGC-3′
		5′-GCAGCAGGAAGCCATCCCGAGTGATAATCTCAGG-3′

$MgCl_2$, 2 μl of 0.1 M DTT, and 1 μl of RNaseOUT™ (40 U/μl) were added and mixed with the first mixture. The mixture was incubated at 42 °C for 2 min. 1 μl of Super-Script™ II RT was added, mixed, and incubated at 42 °C for 50 min. The reaction was terminated at 70 °C for 15 min and chilled on ice. 1 μl of RNase H was added and incubated for 20 min at 37 °C. The sample was stored at −20 °C until use.

The primers for the amplification of tree shrew CETP cDNA were TC1 (5′-CAGTGGACGGTTACTTGGGC-3′) and TC2 (5′-GCAGTGTGCGGACCAACG-3′). The primers for the amplification of tree shrew *β*-actin cDNA were TA1 (5′-TCAGAAGGACTCCTATAGTGG-3′) and TA2 (5′-TCTCTTTGATGTCACGCACG-3′), which were designed according to the conserved sequences of the reported mouse, human, and other animal's *β*-actin cDNA. All Real-Time PCR reactions were performed in a 20 μl mixture containing 25 ng of the cDNA template, 0.6 μl of 1× SYBR Green buffer, 2 μl of 10× PCR buffer, 0.25 μM of each primers, 0.5 mM dNTPs mix and 1 Unit of *Taq* DNA polymerase. The cycling conditions comprised one cycle at 95 °C for 5 min, 35 cycles at 94 °C for 30 s, 56 °C for 30 s and 72 °C for 1 min and 30 s, and one cycle at 72 °C for 10 min. The real-time PCR was performed on the Opticon Continuous Fluorescence Detection System (MJ Research Inc., Boston, USA) and the fluorescence threshold value was calculated using the Opticon Continuous Fluorescence Detection System software. The data was analyzed by the comparative Ct method ($2^{-\Delta Ct}$ method) [16]. Assay was triplicate.

Construction of the Eukaryotic Expression Vector of the Wild-Type Tree Shrew CETP Gene

The coding region of the tree shrew CETP cDNA was amplified by PCR using 5′-Forward and 3′-Reverse oligonucleotides with desired restriction sites (5′ *Xba*I, 3′ *EcoR*I) as primers and tree shrew liver cDNA as template. The primers were TC5 (5′-GCTCTAGAGCCATGCTTGCCAC CACAC-3′) and TC3 (5′-CGGAATTCCTAACTCAAGCT CTGGAGG-3′). The PCR system was constructed as shown below: 25 ng of the cDNA template, 2 μl of 10× PCR buffer, 0.25 μM of each primer, 0.5 mM dNTPs mix and 1 Unit of Pyrobest DNA polymerase (TaKaRa).Thermal cycling was done using the following program: 1 cycle at 94 °C for 3 min, 30 cycles at 94 °C for 1 min, 63 °C for 1 min, 72 °C f or 3 min and 1 cycle at 72 °C for 10 min. The PCR product was restriction-cleaved and ligated into the mammalian expression vector pcDNA3.1/myc-His(−)A and was checked for mutations by DNA sequencing.

Site-Directed Mutagenesis and Transfection

Starting with the wild-type tree shrew CETP cDNA cloned into pcDNA3.1/myc-His(−)A, we conducted site-directed mutagenesis using a QuikChange™ site-directed mutagenesis kit according to the manufacturer's instructions. The mutagenic primers were designed according to the desired mutations (Table 1). 2.5 μl of 10× reaction buffer, 50 ng of dsDNA template, 2 μl of dNTP Mix (2.5 mM), 0.5 μl of each primer (10 μM), 0.5 U Pfu DNA polymerase, some PCR-Grade Water were added to a final volume of 25 μl and mixed. The cycling conditions were as follows: 1 cycle at 95 °C for 30 s, 14 cycles at 95 °C for 30 s, 55 °C for 1 min, and 68 °C for 14 min, 1 cycle at 68 °C for 14 min. The reaction was placed on ice for 2 min. Then, 1 μl of the *Dpn* I restriction enzyme (10 U/μl) was added directly to each amplification reaction, mixed, and incubated at 37 °C for 1 h. 1 μl of the *Dpn* I-treated DNA from each sample reaction was transformed to the supercompetent cells of *E. coli* DH5α. The mutants were verified by DNA sequencing.

COS-7 cells seeded on the culture dishes 1 day before transfection were transfected with the constructs using the high performed transfection kit according to the manufacturer's instructions. The cells were thereafter incubated in serum-free Dulbecco's modified Eagle's medium (DMEM) for expression.

Western Blot Analysis

After incubating for 72 h, the transfected cells and their culture medium were harvested, respectively. The medium was concentrated to 200× by ultrafilter centrifugation. The

transfected cells were washed with 1× PBS buffer and then were treated with 500 µl of 1× sample buffer (1% SDS, 10% glycerol, 25 mM Tris-HCl pH 6.8, 1 mM EDTA, 0.7 M mercaptoethanol). Aliquots of cell medium and lysates were submitted to SDS-PAGE using 12% gels. The resulting protein bands were transferred to a PVDF membrane and incubated in rabbit anti-CETP serum (1:1,000) raised in rabbit against the recombinant human CETP produced in *E. coli* [17]. Finally, the membrane was incubated with horseradish peroxidase-conjugated mouse anti-rabbit IgG (1:5,000) and the immunoreactive bands were visualized using the Enhanced Chemiluminescence (ECL) Western Blotting System according to the manufacturer's instructions. The cells transfected with the plain vector pcDNA3.1/myc-His(−)A were used as controls.

Immunofluorescence Microscopy

After incubating, respectively, for 24, 48, and 72 h, the transfected COS-7 cells were fixed for 10 min in 4% paraformaldehyde, 1× PBS, pH 7.4 and permeabilized with 0.1% Triton X-100 for 30 min at 4 °C. After blocking nonspecific binding of antibodies with 2% BSA/PBS, incubation was continued for about 12 h at 4 °C in the presence of the polyclonal rabbit anti-CETP serum diluted in 2% BSA/PBS (1:500). The bound antibody was detected with fluorescein isothiocyanate (FITC) conjugated goat anti-rabbit secondary antibody (1:5,000), and the cells were viewed with a Nikon fluorescence microscope (magnification, ×400) (Nikon, Tokyo, Japan). The cells transfected with the plain vector pcDNA3.1/myc-His(−)A were used as controls.

Cholesteryl Ester Transfer Activity

The medium was concentrated 200× by ultrafilter centrifugation. The cholesteryl ester transfer activity in the culture supernatants was determined by incubating aliquots of the concentrated medium together with the reagents from a CETP activity assay kit according to the manufacturer's instructions. Briefly, 3 µl of the supernatant sample (as the source of CETP) was added to the reaction mixture containing a fluorescent self-quenched neutral lipid as the donor molecule and an acceptor molecule. A CETP-mediated transfer of the fluorescent neutral lipid to the acceptor molecule resulted in an increase in fluorescence, which was read in a fluorescence plate reader at excitation 465 nm and emission 535 nm. CETP activity was expressed as picamole of neutral lipid transferred per microlitre plasma per hour. The cells transfected with the plain vector pcDNA3.1/myc-His(−)A were used as controls. Assay was triplicate. All CETP analyses were conducted in the same day to decrease variability. The relative mass of CETP mutants secreted in the culture supernatants was determined by Western blotting and quantitated with the UVIpro system (UVItec Ltd., Cambridge, UK). The specific activity of the mutants was expressed relative to that of the wild-type tree shrew CETP.

Statistical Analysis

Data were analyzed using SPSS for Windows XP. All descriptive data collected were expressed as mean values (±SEM) and the Student '*t*' test was used for analysis. Values of $P < 0.05$ were regarded as statistically significant.

Results

Sequence Analysis of the Full-Length Tree Shrew CETP cDNA

In 2001, Zeng et al. [14, 15] cloned the partial sequence of tree shrew CETP cDNA (AF334033). The sequence was 1,636 bp, including 178 bp at the 3′ end of the untranslated region and a 1,458 bp fragment in a coding region, which comprises the complete coding sequence of mature tree shrew CETP and partial coding sequence of signal peptide. According to the partial cDNA sequence [14], we cloned the 5′ terminal sequence of the tree shrew CETP cDNA. The 5′ terminal sequence was 68 bp long, including the putative initiation codon ATG (GenBank accession number: HQ589337). Combining the 5′ terminal sequence with the reported partial sequence, we obtained the full-length cDNA sequence of tree shrew CETP. The full-length cDNA was 1,704 bp, comprising of a 41 bp 5′-noncoding region, a 1,485 bp coding region, and a 178 bp 3′-noncoding region (excluding poly(A)-tail) (Fig. 1). The predicted protein comprised of 494 amino acids (including a predicted 17 amino acid signal peptide) and the calculated molecular mass of the protein was 54,888 Da (pI5.86). The predicted protein showed a sequence identity of 81, 80 and 74%, respectively, with the human, monkey and rabbit CETP (data not shown). The cysteine residues important for synthesis, secretion, and specific activity of CETP [18, 19] were all conserved in human, monkey, rabbit and tree shrew CETP. Moreover, more than half of the predicted glycosylation sites in these proteins were also conservative (PROSITE motif search, http://cubic.bioc.columbia.edu/predictprotein/). Interestingly, tree shrew CETP showed a characteristic proline insertion (amino acid 317 in the mature protein) which was absent in human and monkey CETP but corresponded to a threonine insertion in rabbit CETP. Same as human and monkey CETP, tree shrew

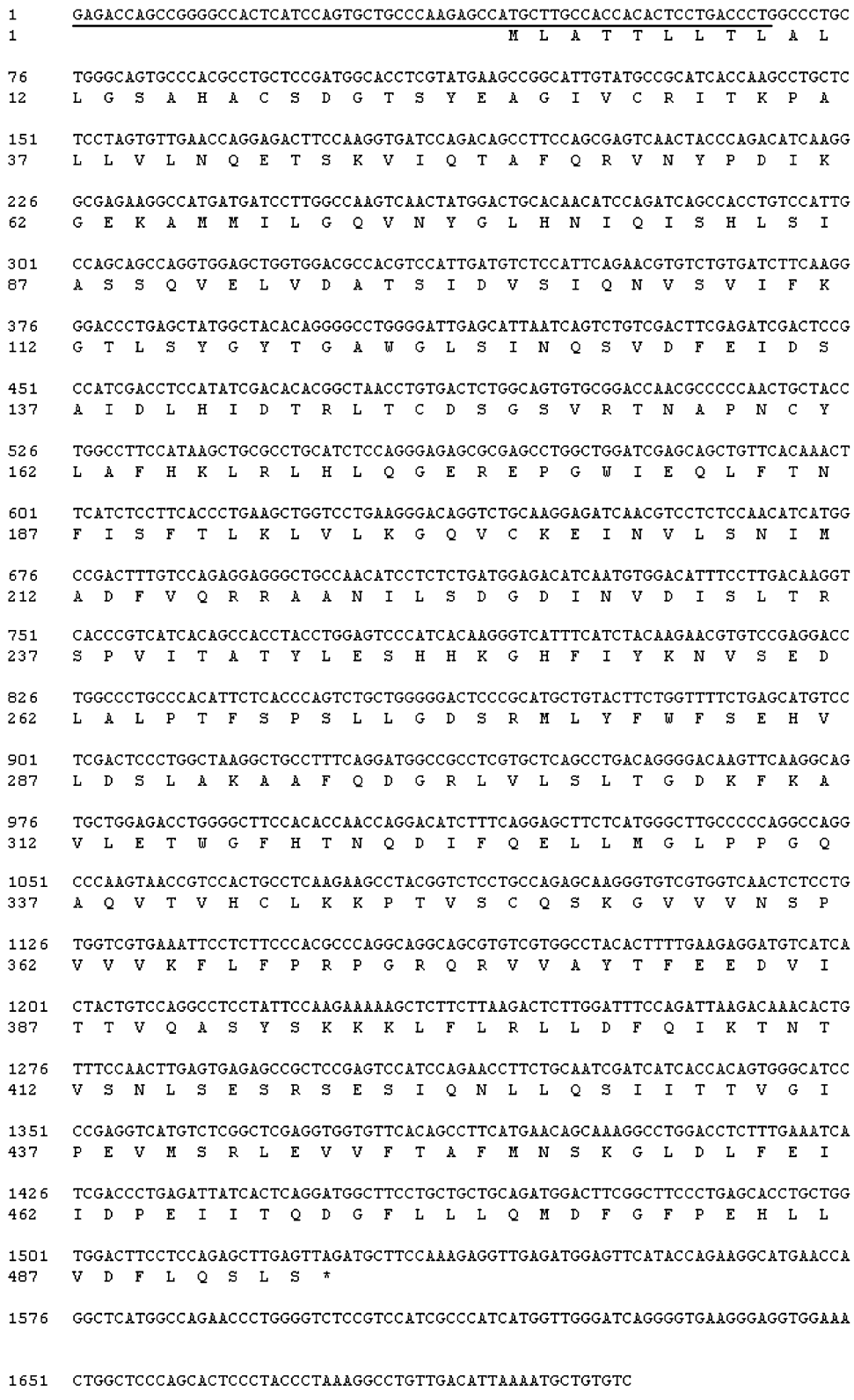

Fig. 1 Nucleotide and amino acid sequences of tree shrew CETP. The 5′ terminal sequence cloned in this study is *underlined*

CETP also did not have 19 amino acids insertion compared with rabbit CETP. However, due to the conservative character of most amino acids, prediction of the secondary structures (PROF predictions, http://cubic.bioc.columbia.edu/predictprotein/) revealed no significant differences between tree shrew CETP and the CETPs of other species.

Tissue Distribution of Tree Shrew CETP mRNA

To gain some information regarding which tissues synthesized CETP mRNA in tree shrews, total RNA was isolated from 12 tissues of tree shrews, and the levels of CETP mRNA were assessed by real-time RT PCR analysis. In 12 tissues investigated (Fig. 2), the relative quantitation of tree shrew CETP mRNA in the liver was much more abundant than that in the other tissues. Adipose and thoracic aorta also synthesized some CETP mRNA. Spleen, lung, and gallbladder had low levels of CETP mRNA, whereas brain, testicle, intestine, heart, kidney and muscle had almost undetectable levels. The tissue distribution profile that tree shrew CETP exhibited here was different from that of monkey [20], human [21], and rabbit CETP [22]. In monkeys, the levels of CETP mRNA in the liver and thoracic aorta were much higher than that in the other tissues, while the mesenteric fat, adrenal gland, spleen, and abdominal aorta had low but detectable levels of the mRNA. In humans, CETP mRNA was synthesized predominantly in adipose tissue, liver, and spleen, with lower levels of expression in the small intestine, adrenal gland, kidney, skeletal muscle, and heart. In rabbits, CETP mRNA was mainly synthesized in liver, adrenal gland and kidney. These data indicate a species-specific transcription control of CETP gene in tree shrews.

Expression and Secretion of Wild-Type and Mutant Tree Shrew CETP in COS-7 Cells

The sequence identity between human [21] and tree shrew CETP was analyzed in detail (data not shown). Three sites

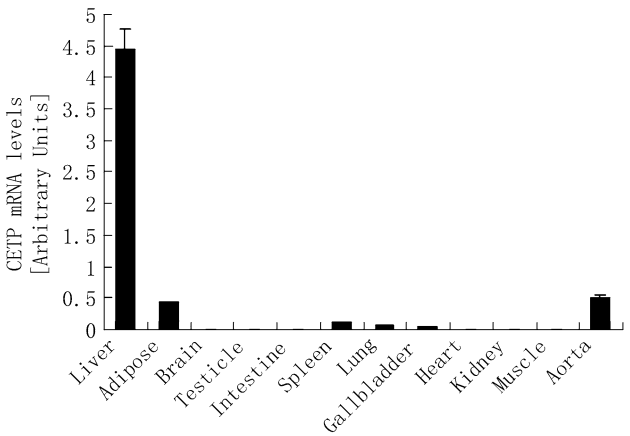

Fig. 2 Relative quantity of CETP mRNA in 12 tissues from tree shrews. The relative expression of CETP mRNA in 12 tissues from tree shrews was measured by the real-time RT PCR using β-actin as an internal control. Total RNA samples from the different tree shrew tissues were extracted and reverse transcribed to the first strand cDNA. The Real-Time PCR reactions were performed and the data was analyzed by the comparative Ct method ($2^{-\Delta Ct}$ method). Assay was triplicate

of tree shrew CETP, N110, N342 and Q452, were remarkable. N110 was a potential N-glycosylation sites in tree shrew CETP (PROSITE motif search, http://cubic.bioc.columbia.edu/predictprotein/), whereas the corresponding amino acid in human CETP was glutamine, a non-N-glycosylation site. It was reported that glycosylation was the crucial step for the secretion of human CETP [23]. So, N110 could be very important to the secretion of tree shrew CETP. In order to study the function of N110, we mutated it into Gln, a non-glycosylation site. N-glycosylation generally occurs at the β-amide of the asparagine of the Asn-Xaa-Ser/Thr sequon [24–26]. N342 in tree shrew CETP was a non-N-glycosylation site, corresponding to a variable glycosylation site at position 341 in human CETP [23]. It was suggested that the non-glycosylated form of human CETP at Asn_{341}-X-Ser was well secreted and displayed moderately increased cholesteryl ester transfer activity [23]. In order to study the function of N342 in tree shrew CETP (Asn_{342}-X-Pro, a non-glycosylation site), Pro344 was mutated into Ser, which made Asn342 become a potential N-glycosylation site. In tree shrew CETP, the amino acid Q452 corresponded to the R451Q polymorphism in human CETP. It was reported that the Q451 allele was associated with higher CETP activity [27–29]. Therefore, Q452 could be crucial to the activity of tree shrew CETP. To analyze the function of this site, we mutated it into R452. The above mutants were, respectively, named as N110Q, P344S and Q452R (Table 1).

The wild-type tree shrew CETP and the mutants were transiently expressed in COS-7 cells for 72 h. The culture medium and the cells were collected, respectively, for Western blot analysis. The results showed that the wild type protein was detectable in the culture medium and the cell lysates and had a molecular mass of approximately 68 kDa. The molecular mass of N110Q ($\sim$66 kDa) was about 2,000 lower than that of the wild type. Moreover, N110Q was only detectable in the cell lysates, but undetectable in the culture medium. These results indicated that the mutation at the amino acid N110 could affect the modification and secretion of the mutant protein. However, except N110Q, the other two mutant proteins (P344S and Q452R) were all detected in the culture medium and the cell lysates, and the mutant protein bands had similar molecular mass ($\sim$68 kDa) and strength compared with the wild type protein band either in the culture medium or in the cell lysates, suggesting that the mutation at the amino acid Q452 or P344 could not affected the modification and secretion property of the mutant protein (Fig. 3).

The secretion properties of the mutants were also showed in the immunofluorescence microscopic analysis (Fig. 4). At 24 h, all of the expressed proteins were localized around the cell nucleus. At 72 h, with the exception of N110Q, which was still localized around the cell nucleus, the other expressed proteins including the wild

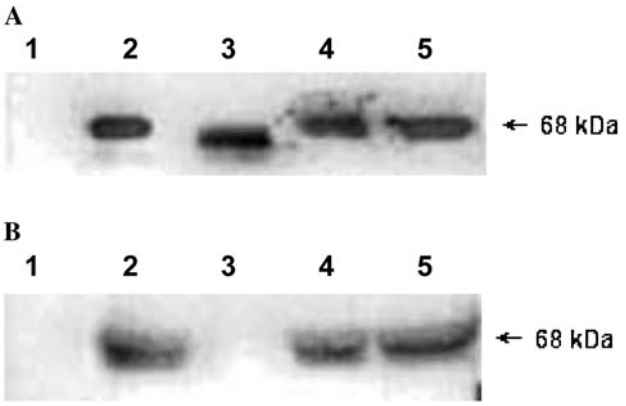

Fig. 3 Western blot analysis of the wild-type and mutant tree shrew CETP expressed in the COS-7 cells. COS-7 cells were transfected with the wild-type and mutant tree shrew CETP expressing vectors. After incubating for 72 h, the transfected cells and their culture medium concentrated to 200× were used to do the western blot analysis. **a** Western blot analysis of the cell lysates. **b** Western blot analysis of the cell culture medium. *Lane 1*, control (samples from the COS-7 cells transfected with plain vector plasmid); *lane 2*, samples from the COS-7 cells transfected with the expression vector of the wild-type tree shrew CETP gene; *lane 3*, samples from the COS-7 cells transfected with the expression vector of the N110Q mutant tree shrew CETP gene; *lane 4*, samples from the COS-7 cells transfected with the expression vector of the P344S mutant tree shrew CETP gene; *lane 5*, samples from the COS-7 cells transfected with the expression vector of the Q452R mutant tree shrew CETP gene

type were situated on one side near the cell nucleus. It appeared that the wild type, P344S, and Q452R were transferred gradually to one side near the cell nucleus from 24 to 72 h after expressed. The data suggested that the secretion property of N110Q was different from that of the others.

Cholesteryl Ester Transfer Activity of Tree Shrew CETP Mutants

The culture medium of the transfected cells was collected, concentrated, and then used to measure the cholesteryl ester transfer activity (Fig. 5). The results showed that the mutations at P344 and Q452 in tree shrew CETP impaired the activities of the mutant proteins, respectively, resulting in 48 and 26% reduction of cholesteryl ester transfer compared with the wild type protein, indicating that P344 and Q452 played an important role in tree shrew CETP-mediated cholesteryl ester transfer. However, the culture medium from the cells expressing N110Q did not show the cholesteryl ester transfer activity, providing further evidence that this mutant protein could not be secreted into the medium.

Discussion

In our study, tree shrew CETP showed a high sequence identity to human (81% identical), monkey (80% identical) and rabbit (74% identical) CETP, suggesting that tree shrew CETP might have similar structure and function with these proteins. However, there were also some significant differences on the amino acid sequences between tree shrew CETP and the other species' CETPs, which might cause some differences on the structure and function of the proteins.

In 12 tissues investigated (Fig. 2), the relative quantitation of tree shrew CETP mRNA in the liver was much more abundant than that in the other tissues, suggesting that the liver could be the main tissue synthesized CETP. The liver is a key organ in controlling systemic lipid metabolism. Its functions include lipoprotein clearance, intracellular lipid metabolism, synthesis and secretion of lipoproteins, and remodeling of circulating lipoproteins [30]. Therefore, high level of CETP in the liver could not only be the main source of the circulating CETP mass but also play an important role in the local uptake or removal of lipid in the liver [31]. In tree shrews, adipose tissue also synthesized some CETP mRNA. Radeau et al. [32] reported that adipocyte size was inversely correlated with CETP mRNA abundance in fresh human adipose tissue. In mice, adipose tissue-specific CETP expression led to decreased cholesterol and triglyceride contents and reduced adipocyte size [33]. CETP expressed in adipose could be involved in the local lipid metabolism by promoting HDL remodeling and then cholesterol efflux. The aorta also synthesized some CETP mRNA in the tree shrew. CETP synthesized in the aorta could participate in the removal of excessive cholesteryl ester from the arterial wall.

Glycosylation was crucial for the secretion of human CETP [23]. When the N-linked glycosylation was absent, the mutant proteins were poorly secreted, and the Mr of the mutants showed about 2,000 lower than that of the wild type protein. In our study, after analyzed, four potential glycosylation sits were found in the tree shrew CETP, of which three sites were the same as that in human CETP, but only one site, N110, corresponding to a non-N-glycosylation site Q110 in human CETP. Therefore, we mutated it into Gln, a non-glycosylation site, for studying its function. The results showed that the mutant protein in the cell lysates had about 2,000 lower molecular mass than the wild-type tree shrew CETP and was not able to be detected in the culture medium by the western blot analysis and the activity test (Figs. 3, 5), indicating that the mutant protein could not be secreted out of the cells because of the deficiency of the glycosylation at the amino acid 110. The immunofluorescence microscopic analysis also supported this conclusion (Fig. 4). It's well known that most of the secreted proteins are synthesized and glycosylated in the endoplasmic reticulum (ER) [34, 35]. The proteins are then delivered into the Golgi apparatus for further modification and finally secreted out of the cell. In our study, N110Q

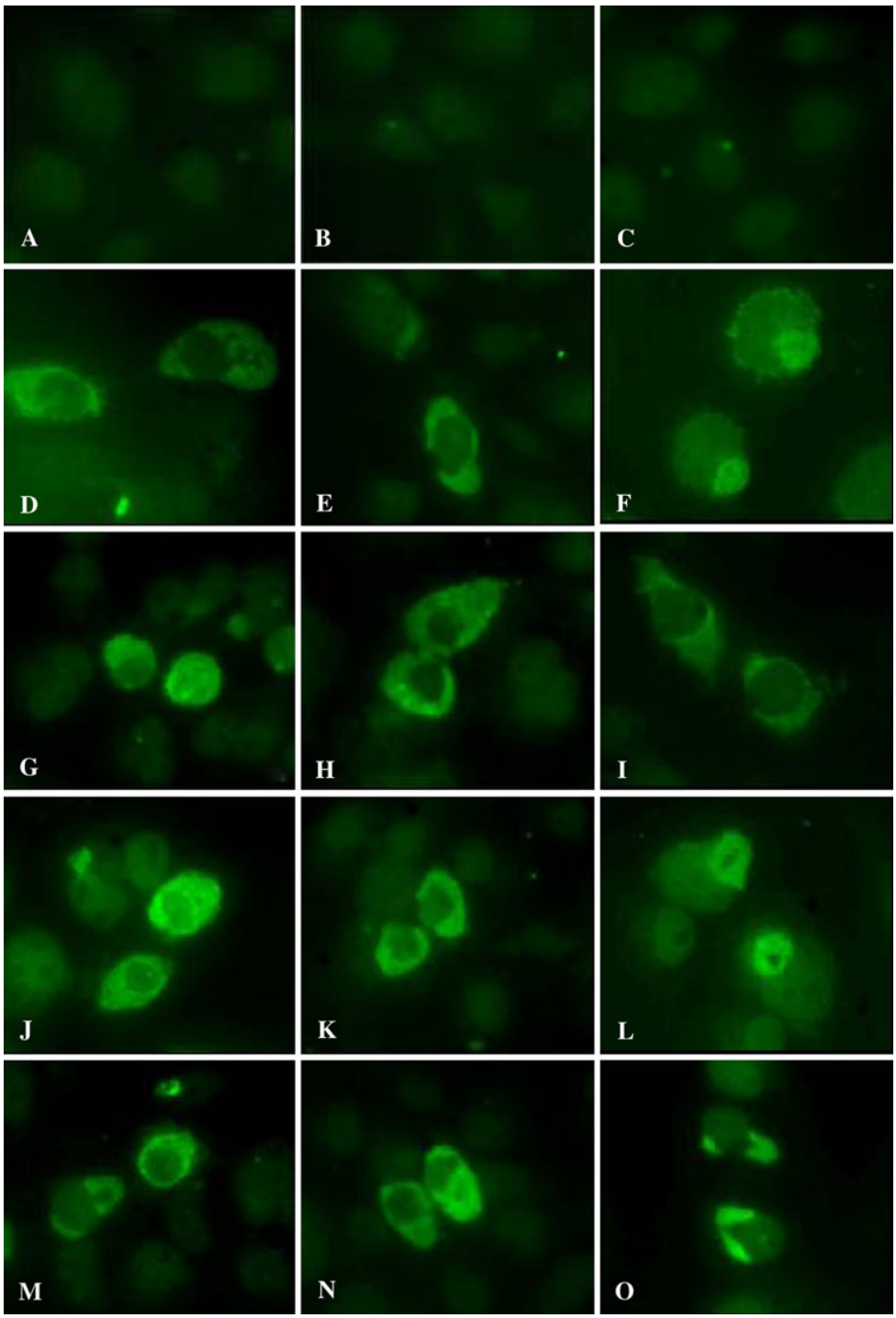

Fig. 4 Immunofluorescence microscopy analysis of the transfected COS-7 cells. COS-7 cells were transfected with the wild-type and mutant tree shrew CETP expressing vectors. After incubating, respectively, for 24, 48, and 72 h, the transfected COS-7 cells were used for immunofluorescence microscopy analysis. **a–c** the cells transfected with the plain vector plasmid; **d–f** the cells transfected with the expression vector of the wild-type tree shrew CETP gene; **g–i** the cells transfected with the expression vector of the N110Q mutant tree shrew CETP gene; **j–l** the cells transfected with the expression vector of the P344S mutant tree shrew CETP gene; **m–o** the cells transfected with the expression vector of the Q452R mutant tree shrew CETP gene. Expression time: **a–m**, 24 h; **b–n**, 48 h; **c–o**, 72 h

appeared to be always localized around the nucleus (possibly in the ER) from 24 to 72 h after expressed, whereas the other proteins including the wild type were localized around the cell nucleus (possibly in the ER) at 24 h and situated on one side near the cell nucleus (possibly associated with the Golgi apparatus) at 72 h, suggesting that N110Q could be remained in the ER instead of being delivered into the Golgi apparatus for the secretion because of deficiency of the glycosylation at the amino acid 110. Of cause, this hypothesis need to be proved further. In brief, these results suggested that the Glutamine at position 110 in tree shrew CETP could be a N-glycosylation site and the glycosylation of this site could be crucial for the secretion of the protein.

N342 in tree shrew CETP, a non-N-glycosylation site (Asn_{342}-X-Pro), correspond to a variable glycosylation site at position 341 in human CETP [23]. The non-glycosylated form of human CETP at Asn_{341}-X-Ser was well secreted

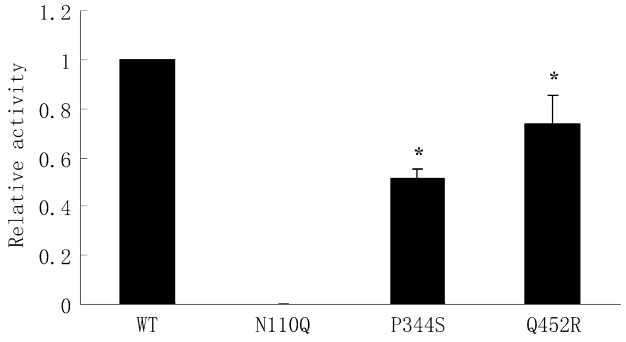

Fig. 5 Cholesteryl ester transfer activity of the wild-type and mutant tree shrew CETP. COS-7 cells were transfected with the wild-type and mutant tree shrew CETP expressing vectors. After incubating for 72 h, the culture medium was harvested and concentrated to 200×. The cholesteryl ester transfer activity in the culture supernatants was determined using a CETP activity assay kit according to the manufacturer's instructions. The results are mean values (±SEM) of three independent experiments, and are expressed relative to the activity of the wild-type tree shrew CETP (set at 1.0). The *asterisks* indicate a statistically significant difference (*t* test; $*P < 0.05$) from the wild-type tree shrew CETP

and displayed moderately increased cholesteryl ester transfer activity. To analyze the function of N342 in tree shrew CETP, we carried out mutagenesis study on the site. A Ser substitution for Pro at position 344 made N324 become a potential N-glycosylation site. From the western blot and immunoflouresence analysis (Figs. 3, 4), the secretion property of P344S was similar to that of the wild-type tree shrew CETP. Furthermore, the molecular mass of the mutant was also the same as that of the wild type, implying that the mutant could not be glycosylated at N342. In the case of NXS sequon, it was reported that the hydrophobic residues at positions 9th to 17th upstream of the sequons as well as the positively charged residues at positions 5th and 7th downstream of the sequons are crucial to the domains flanking glycosylated sequons [36]. The amino acid Lysine at position 13th upstream of the N-glycosylation site (Asn_{342}) in P344S was positively charged and significantly different from the amino acid Methionine at the corresponding position in human CETP. This could lead to the deficiency of N-glycosylation at N342 in the mutant. However, the activity of P344S was about 48% lower than that of the wild-type tree shrew CETP (Fig. 5), indicating that P344 plays an important role in the activity of tree shrew CETP. It has been observed [37–39] that Pro restricts the conformation of the residue preceding it in a protein sequence and can potentially increase protein stability. Therefore, Pro is usually conserved in proteins and often plays an important role in protein structure and function [38, 40, 41]. In our study, a Ser substitution for Pro could cause changes in the structure conformation of the mutant and lead to the decreased activity eventually.

Q452 in tree shrew CETP corresponded to the R451Q polymorphism in human CETP. The Q451 allele in human CETP was associated with higher CETP activity [27–29]. To analyze the function of this site in the tree shrew CETP, we mutated Q452 into R452. The results showed that the molecular mass and secretion of Q452R was similar to that of the wild-type tree shrew CETP (Figs. 3, 4). However, the activity of the mutant decreased by 26% (Fig. 5), indicating that Q452 was very important to the activity of tree shrew CETP. It is reported that human CETP has an elongated 'boomerang' shape with two similar domains connected by a linker, residues 240–259 in CETP [42]. The structure of CETP reveals four bound lipid molecules, which can be two neutral lipids and two phospholipids. The four lipids occupy a continuous tunnel that traverses the core of the protein and has two distinct openings. The two cholesteryl esters are buried in the middle of the tunnel called 'neck' and two phospholipids plug the tunnel, one at each end. Tunnel mutation experiments suggested that in CETP, I443, L457, and M459 are located at the neck. The neck of the tunnel makes marginal contacts with the flexible parts of bound cholesteryl ester and lipid passage through the neck is required for transfer activity. R451 is between I443 and L457 and could be involved in the formation of the neck of the tunnel. The Q451 allele in human CETP has higher CETP activity because Q451 could be more suitable to the formation of the neck of the tunnel and the binding of neutral lipid to CETP. Tree shrew CETP shared a high sequence identity with human CETP, about 81%, suggesting that the proteins might also have similar structure. So, a Arg substitution for Gln at position 452 in tree shrew CETP could affect the formation of the neck of the tunnel and the binding of neutral lipid to CETP and so the cholesteryl ester transfer activity at last. Of course, this hypothesis need to be confirmed in the future.

Taken together, our data demonstrate that tree threw CETP shares a high sequence identity with human, monkey and rabbit CETP. The liver is the major tissue synthesizing CETP mRNA. In tree shrew CETP, residues 344 (Pro) and 452 (Gln) play an important role in maintenance of high cholesteryl ester transfer activity and residue 110 (Asn) is crucial to the secretion of the protein.

Acknowledgments We are grateful to Dr. Xue-wei Zhu and Myngan Doung from Department of Pathology/Lipid Sciences, Wake Forest University School of Medicine, USA, for correcting English. This work was supported by the National Natural Science Foundation of China (No. 39770168) and the Doctor Research Fund from Inner Mongolia Agricultural University (No. BJ05-34).

References

1. Cao J, Yang EB, Su JJ et al (2003) The tree shrews: adjuncts and alternatives to primates as models for biomedical research. J Med Primatol 32:123–130

2. Yang EB, Cao J, Su JJ, Chow P (2005) The tree shrews: useful animal models for the viral hepatitis and hepatocellular carcinoma. Hepatogastroenterology 52:613–616
3. She MP, Lu YZ, Xia RY et al (1982) The role of α-lipoprotein in preventing atheromatous plaques developed in tree shrew associating with induced hypercholesterinemia. Zhong Hua Yao Li Xue Za Zhi 11:23–28
4. Barter PJ (2002) Hugh sinclair lecture: the regulation and remodelling of HDL by plasma factors. Atheroscler Suppl 3:39–47
5. Stein O, Stein Y (2005) Lipid transfer proteins (LTP) and atherosclerosis. Atherosclerosis 178:217–230
6. Masson D, Jiang XC, Lagrost L, Tall AR (2009) The role of plasma lipid transfer proteins in lipoprotein metabolism and atherogenesis. J Lipid Res 50:201–206
7. Brown ML, Inazu A, Hesler CB et al (1989) Molecular basis of lipid transfer protein deficiency in a family with increased high-density lipoproteins. Nature 342:448–451
8. Inazu A, Brown ML, Hesler CB et al (1990) Increased high-density lipoprotein levels caused by a common cholesteryl-ester transfer protein gene mutation. N Engl J Med 323:1234–1238
9. Thompson A, Di Angelantonio E, Sarwar N et al (2008) Association of cholesteryl ester transfer protein genotypes with CETP mass and activity, lipid levels, and coronary risk. JAMA 299:2777–2788
10. Plump AS, Masucci-Magoulas L, Bruce C et al (1999) Increased atherosclerosis in ApoE and LDL receptor gene knock-out mice as a result of human cholesteryl ester transfer protein transgene expression. Arterioscler Thromb Vasc Biol 19:1105–1110
11. Westerterp M, van der Hoogt CC, de Haan W et al (2006) Cholesteryl ester transfer protein decreases high-density lipoprotein and severely aggravates atherosclerosis in APOE*3-Leiden mice. Arterioscler Thromb Vasc Biol 26:2552–2559
12. Tsai MY, Johnson C, Kao WH et al (2008) Cholesteryl ester transfer protein genetic polymorphisms, HDL cholesterol, and subclinical cardiovascular disease in the multi-ethnic study of atherosclerosis. Atherosclerosis 200:359–367
13. Liu HR, Wu G, Zhou B, Chen BS (2010) Low cholesteryl ester transfer protein and phospholipid transfer protein activities are the factors making tree shrew and Beijing duck resistant to atherosclerosis. Lipids Health Dis 9:114
14. Zeng WW, Zhang J, Chen B (2001) Analysis of cDNA and protein structure of tree shrew cholesterol ester transfer protein. Zhong Hua Yi Xue Za Zhi 81:1316–1320
15. Zeng W, Zhang J, Chen B et al (2003) Cloning and characterization of cholesteryl ester transfer protein isolated from the tree shrew. Chin Med J 116:928–931
16. Schmittgen TD, Livak KJ (2008) Analyzing real-time PCR data by the comparative C(T) method. Nat Protoc 3:1101–1108
17. Liu HR, Zeng WW, Zhou B et al (2008) cDNA cloning and prokaryotic expression of human cholesteryl ester transfer protein and preparation of its antiserum. Xi Bao Yu Fen Zi Mian Yi Xue Za Zhi 24:471–474
18. Kotake H, Agellon LB, Yokoyama S (1997) Modification of the N-terminal cysteine of plasma cholesteryl ester transfer protein selectively inhibits triglyceride transfer activity. Biochim Biophys Acta 1347:69–74
19. Hope HR, Heuvelman D, Duffin K et al (2000) Inhibition of cholesteryl ester transfer protein by substituted dithiobisnicotinic acid dimethyl ester: involvement of a critical cysteine. J Lipid Res 41:1604–1614
20. Pape ME, Rehberg EF, Marotti KR, Melchior GW (1991) Molecular cloning, sequence, and expression of cynomolgus monkey cholesteryl ester transfer protein. Inverse correlation between hepatic cholesteryl ester transfer protein mRNA levels and plasma high density lipoprotein levels. Arterioscler Thromb 11:1759–1771
21. Drayna D, Jarnagin AS, Mclean J et al (1987) Cloning and sequencing of human cholesteryl ester transfer protein cDNA. Nature 327:632–634
22. Nagashima M, Mclean JW, Lawn RM (1988) Cloning and mRNA tissue distribution of rabbit cholesteryl ester transfer protein. J Lipid Res 29:1643–1649
23. Stevenson SC, Wang S, Deng L, Tall AR (1993) Human plasma cholesteryl ester transfer protein consists of a mixture of two forms reflecting variable glycosylation at asparagines 341. Biochemistry 32:5121–5126
24. Apweiler R, Hermjakob H, Sharon N (1999) On the frequency of protein glycosylation, as deduced from analysis of the SWISS-PROT database. Biochim Biophys Acta 1473:4–8
25. Marshall R (1972) Glycoproteins. Annu Rev Biochem 41:673–702
26. Spiro RG (2002) Protein glycosylation: nature, distribution, enzymatic formation, and disease implications of glycopeptide bonds. Glycobiology 12:43R–56R
27. Kakko S, Tamminen M, Paivansalo M et al (2000) Cholesteryl ester transfer protein gene polymorphisms are associated with carotid atherosclerosis in men. Eur J Clin Invest 30:18–25
28. Kakko S, Tamminen M, Kesaniemi YA, Savolainen MJ (1998) R451Q mutation in the cholesteryl ester transfer protein(CETP) gene is associated with high plasma CETP activity. Atherosclerosis 136:233–240
29. Agerholm-Larsen B, Tybjaerg-Hansen A, Schnohr P et al (2000) Common cholesteryl ester transfer protein mutations decreased HDL cholesterol, and possible decreased risk of ischemic heart disease. Circulation 102:2197–2203
30. Kaplowitz N (2006) Liver biology and pathobiology. Hepatology 43:S235–S238
31. Zhou H, Li Z, Silver DL, Jiang XC (2006) Cholesteryl ester transfer protein (CETP) expression enhances HDL cholesteryl ester liver delivery, which is independent of scavenger receptor BI, LDL receptor related protein and possibly LDL receptor. Biochim Biophys Acta 1761:1482–1488
32. Radeau T, Lau P, Robb M et al (1995) Cholesteryl ester transfer protein (CETP) mRNA abundance in human adipose tissue: relationship to cell size and membrane cholesterol content. J Lipid Res 36:2552–2561
33. Zhou H, Li Z, Hojjati MR et al (2006) Adipose tissue-specific CETP expression in mice: impact on plasma lipoprotein metabolism. J Lipid Res 47:2011–2019
34. Welply JK, Shenbagamurthi P, Lennarz WJ, Naider F (1983) Substrate recognition by oligosaccharyl transferase. Studies on glycosylation of modified Asn-X-Thr/Ser tripeptides. J Biol Chem 258:11856–11863
35. Yan A, Lennarz WJ (2005) Unraveling the mechanism of protein N-glycosylation. J Biol Chem 280:3121–3124
36. Ben-Dor S, Esterman N, Rubin E, Sharon N (2004) Biases and complex patterns in the residues flanking protein N-glycosylation sites. Glycobiology 14:95–101
37. Schimmel PR, Flory PJ (1968) Conformational energies and configurational statistics of copolypeptides containing L-proline. J Mol Biol 34:105–120
38. Macarthur MW, Thornton JM (1991) Influence of proline residues on protein conformation. J Mol Biol 218:397–412
39. Ho BK, Brasseur R (2005) The Ramachandran plots of glycine and pre-proline. BMC Struct Biol 5:14
40. Barlow DJ, Thornton JM (1988) Helix geometry in proteins. J Mol Biol 201:601–619
41. Brandl CJ, Deber CM (1986) Hypothesis about the function of membrane-buried proline residues in transport proteins. Proc Natl Acad Sci USA 83:917–921
42. Qiu X, Mistry A, Ammirati MJ et al (2007) Crystal structure of cholesteryl ester transfer protein reveals a long tunnel and four bound lipid molecules. Nat Struct Mol Biol 14:106–113

Lipids (2011) 46:617–625
DOI 10.1007/s11745-011-3555-z

ORIGINAL ARTICLE

Aerobic Exercise Improves Reverse Cholesterol Transport in Cholesteryl Ester Transfer Protein Transgenic Mice

D. D. F. M. Rocco · L. S. Okuda · R. S. Pinto · F. D. Ferreira · S. K. Kubo · E. R. Nakandakare · E. C. R. Quintão · S. Catanozi · M. Passarelli

Received: 12 October 2010 / Accepted: 14 March 2011 / Published online: 9 April 2011

Abstract We analyzed the effect of a 6-week aerobic exercise training program on the in vivo macrophage reverse cholesterol transport (RCT) in human cholesteryl ester transfer protein (CETP) transgenic (CETP-tg) mice. Male CETP-tg mice were randomly assigned to a sedentary group or a carefully supervised exercise training group (treadmill 15 m/min, 30 min sessions, five sessions per week). The levels of plasma lipids were determined by enzymatic methods, and the lipoprotein profile was determined by fast protein liquid chromatography (FPLC). CETP activity was determined by measuring the transfer rate of ^{14}C-cholesterol from HDL to apo-B containing lipoproteins, using plasma from CETP-tg mice as a source of CETP. The reverse cholesterol transport was determined in vivo by measuring the [^{3}H]-cholesterol recovery in plasma and feces (24 and 48 h) and in the liver (48 h) following a peritoneal injection of [^{3}H]-cholesterol labeled J774-macrophages into both sedentary and exercise trained mice. The protein levels of liver receptors were determined by immunoblot, and the mRNA levels for liver enzymes were measured using RT-PCR. Exercise training did not significantly affect the levels of plasma lipids or CETP activity. The HDL fraction assessed by FPLC was higher in exercise-trained compared to sedentary mice. In comparison to the sedentary group, a greater recovery of [^{3}H]-cholesterol from the injected macrophages was found in the plasma, liver and feces of exercise-trained animals. The latter occurred even with a reduction in the liver CYP7A1 mRNA level in exercised trained animals. Exercise training increased the liver LDL receptor and ABCA-1 protein levels, although the SR-BI protein content was unchanged. The RCT benefit in CETP-tg mice elicited by exercise training helps to elucidate the role of exercise in the prevention of atherosclerosis in humans.

Keywords Atherosclerosis · CETP · HDL · Physical exercise · Cholesterol

Abbreviations

ABC	Transporters ABCA-1 and ABCG-1
AcLDL	Acetylated LDL
Apo AI	Apolipoprotein AI
Apo E	Apolipoprotein E
B-E	Low density lipoprotein receptor
CETP	Cholesteryl ester transfer protein
CYP7A1	7 alpha hydroxylase
CYP27A	27 alpha hydroxylase
EC	Esterified cholesterol
EDTA-PBS	Ethylene diamine tetra acetic phosphate-buffered saline
FPLC	Fast protein liquid chromatography
HDL	High density lipoprotein
LCAT	Lecithin cholesterol acyltransferase
LDL	Low density lipoprotein
LRP	LDL-receptor related protein
LXR	Liver X receptor
LP	Lipoprotein
RCT	Reverse cholesterol transport

D. D. F. M. Rocco · L. S. Okuda · R. S. Pinto · F. D. Ferreira · E. R. Nakandakare · E. C. R. Quintão · S. Catanozi · M. Passarelli (✉)
Lipids Laboratory (LIM-10), Faculty of Medical Sciences, University of Sao Paulo, Av. Dr. Arnaldo 455, room 3305, Sao Paulo, SP CEP 01246000, Brazil
e-mail: mpassere@usp.br; lipideq@usp.br

S. K. Kubo
Emergency Care Research Unit (LIM-51), Faculty of Medical Sciences, University of Sao Paulo, Sao Paulo, Brazil

SR-BI Scavenger receptor class B type I
VLDL Very low density lipoprotein

Introduction

Regular exercise is independently associated with a reduced incidence of coronary heart disease and mortality by improving the cardiovascular risk profile [1]. In fact, a negative correlation between physical activity level and the carotid intima media thickness has been shown in aerobically exercised individuals [2].

Ramachandran et al. [3] demonstrated that regular, aerobic exercise reduces pre-existing atherosclerotic lesions in low density lipoprotein (LDL) receptor knockout mice, and more recently, Matsumoto et al. [4] showed that in low-density lipoprotein-receptor-deficient mice, regular exercise training prevents aortic valve sclerosis by numerous mechanisms, including preservation of endothelial integrity, reduced inflammation and oxidative stress, and inhibition of the osteogenic pathway. It has also been reported that a progressive aerobic exercise training protocol improves the apo E knockout mouse survival rate, an effect that was ascribed to the stabilization of atherosclerotic lesions and prevention of plaque rupture [5]. These events are most likely related to the role of aerobic exercise in improving high density lipoprotein (HDL) plasma levels, as well as antioxidant and anti-inflammatory defenses in the arterial wall [6].

Through the reverse cholesterol transport (RCT) process, HDL mediates the cholesterol removal from macrophages and peripheral cells and its delivery to the liver, where it is secreted into the bile and feces. The cholesteryl ester transfer protein (CETP) transfers esterified cholesterol from HDL to apo B-containing lipoproteins (LP) that are ultimately removed by the hepatic LDL receptor (B-E), LRP and E receptors. There are no consistent data in the literature regarding the effect of aerobic exercise training on the RCT, and most of the results were drawn from in vitro analyses that may not reflect the whole animal system in vivo. In this regard, an interplay of actions involving CETP, lecithin cholesterol acyltransferase (LCAT), ABC transporters (ABCA-1 and ABCG-1) and scavenger receptor class B, type I (SR-BI) could dictate the flow of cholesterol to the liver [7].

In the present study, we tested the hypothesis that aerobic exercise training can improve the in vivo RCT by modulating proteins and enzymes involved in the cholesterol flow to the liver. For this purpose, we used CETP transgenic C57BL/6 mice (CETP-tg), an animal model that simulates the RCT in humans. We assessed the effect of a 6 week aerobic training program on the redistribution of radiolabeled cholesterol into the plasma, liver and feces following the intraperitoneal injection of macrophages enriched with [^{3}H] cholesterol. We also investigated the hepatic protein levels of receptors involved in lipid metabolism, such as SR-BI, ATP-binding cassette transporter A-1 (ABCA-1), liver X receptor (LXR) and LDL receptor, and the mRNA of enzymes that convert cholesterol in bile acids (CYP7A1 and CYP27A). We found that aerobic exercise training improves the macrophage RCT. Exercise-trained mice had higher levels of macrophage-derived ^{3}H-cholesterol in their plasma, liver and feces. The enhanced protein levels of hepatic ABCA-1 and LDL receptor contributed to greater HDL plasma concentration and cholesterol flow into the liver, respectively. The RCT benefit seen in exercise-trained CETP-tg mice helps to elucidate the role of exercise in the prevention of atherosclerosis in humans.

Materials and Methods

Animals and Aerobic Exercise Protocol

Two-month-old male transgenic mice homozygous for human CETP (human natural promoter-driven CETP transgenic mice, CETP-tg; line 5203; back-crossed on a C57BL/6 background for 10 generations) that originated in Dr. AR Tall′s laboratory and were kindly provided by Dr. HCF Oliveira (University of Campinas, São Paulo, Brazil) were fed a pelleted commercial chow ad libitum (Nuvilab-Nuvital, São Paulo, Brazil) with free access to water. Animals were housed in conventional housing at 22 ± 2 °C with a 12 h light/dark cycle. Protocols were approved by the Institutional Animal Care and Research Advisory Committee (Hospital das Clinicas of the Faculty of Medical Sciences, University of São Paulo-CAPPesq # 773/06) according to the US National Institutes of Health Guidelines. Animal care was provided in accordance with the procedures outlined in the Guide for the Care and Use of Laboratory Animals [8], and experiments were performed under adherence to the American College of Sports Medicine (ACSM) animal care standards. CETP-tg animals were subjected to a 6 week monitored aerobic exercise training protocol performed on a treadmill (WEG CFW-08, São Carlos, Brazil) at 15 m/min during 30 min sessions five times a week. A control group was kept sedentary for the same amount of time. Exercise sessions were carried out in the late afternoon and were supervised by the same investigator (DDFM Rocco).

LDL Isolation and Acetylation

Procedures with humans conformed to the Declaration of Helsinki and all participants signed an informed written

consent form previously approved by The Ethical Committee for Human Research Protocols of the Hospital of the Faculty of Medical Sciences, University of São Paulo (CAPPesq # 773/06). Low density lipoprotein (LDL) was isolated from healthy plasma donors by sequential ultracentrifugation ($d = 1.019-1.063$ g/mL) and was further purified by discontinuous gradient ultracentrifugation. After dialysis against PBS, the protein content was determined using the Lowry procedure [9], and acetylation was performed with acetic anhydride according to Basu et al. [10]. After extensive dialysis against ethylene diamine tetra acetic phosphate-buffered saline (EDTA–PBS), acetylated LDL (AcLDL) was kept sterile at 4 °C under nitrogen atmosphere and was used within a month.

Measurement of the In Vivo RCT

J-774 macrophages were grown in an RPMI 1640 culture medium supplemented with 10% fetal bovine serum (FBS), labeled with 5 μ Ci/mL [^{3}H]-cholesterol and enriched with 50 μg/mL of AcLDL for 48 h, as previously described [11]. Cells were then removed from plaques by trypsin treatment followed by inactivation of the enzyme by adding RPMI plus FBS. The cells were then spun down by centrifugation at 4 °C at 1,500 rpm and rediluted in a small volume of PBS. Cell viability, assessed by exclusion with Trypan blue, was greater than 98%, and an aliquot was placed in a beta counter (Beckman model; Palo Alto, USA) to determine the radioactivity. The intracellular distribution of cholesterol fractions was determined by thin-layer chromatography and consisted of 96 and 4% in the free and esterified forms, respectively.

Forty-eight hours after the last bout of exercise, [^{3}H]-cholesterol-labeled J-774 foam cells (3.5×10^6 cells; ~80,000 dpm in 100 μL of PBS) were intraperitoneally injected into the exercise-trained and sedentary mice, which were individually housed in metabolic cages with free access to food and water. Samples of blood from the tail vein and feces were taken after 24 and 48 h. Plasma radioactivity was immediately determined after spinning the blood at 1,500 rpm for 20 min at 4 °C. The mice were euthanized 48 h after the injection. Their organs (liver, spleen, lung, heart, kidneys and adrenal glands) were subsequently removed, carefully washed with cold 0.9% NaCl solution, gently dried with filter paper and weighed.

The feces and organs were stored at −70 °C until further analyses. Total feces and organs or liver aliquots were homogenized with a 2:1 (v/v) mixture of chloroform/methanol [12] and stored at 4 °C overnight for lipid extraction. The lipid layer was drawn and evaporated under nitrogen flow, and the radioactivity was determined. Results are expressed as percentages of total dose (dpm) injected per gram of sample (liver or feces) or plasma volume (mL). The radioactivity recovery in heart, lung, spleen, kidney and adrenal glands was too low and represented less than 1% of the total radioactivity injected (data not shown).

Measurement of Hepatic Cholesterol Content

Lipids were extracted from the liver, and total cholesterol was determined from a supernatant aliquot using the enzymatic method (Roche Diagnóstica, SP, Brazil), and the protein concentration by using the Lowry technique [9].

Plasma Lipid Analysis

Plasma (100 μL) from each mouse was analyzed by fast protein liquid chromatography (FPLC) gel filtration on two Superose-6 columns. The cholesterol concentration in all LP fractions was measured with a Cobas Mira using an enzymatic colorimetric kit (Roche Diagnostic, Brazil).

CETP Activity Determination

CETP activity was measured as the transfer of [^{14}C]-cholesteryl oleate from HDL to VLDL and LDL using LP isolated from pools of human normolipidemic individuals and plasma from CETP-tg mice as a source of CETP as previously described [13].

Western Blotting Analysis

Protein lysates were obtained from frozen hepatic tissue from exercise-trained and sedentary CETP-tg mice. Tissue was homogenized in a Polytron (MA099 Potter Unit, Marcone Equip., Sao Paulo, Brazil) with a buffer containing 20 mM Hepes, 150 mM NaCl, 10% glycerol, 1% triton, 1 mM EDTA, 1.5 mM $MgCl_2$ and protease inhibitors. The supernatant was obtained after centrifugation, and an aliquot was dissolved in SDS-glycerol. Equal amounts of sample protein were applied to a polyacrylamide gel. SR-BI, ABCA-1, LXR and the LDL receptor protein levels were determined using anti-SR-BI (1:1,000), anti-ABCA-1 (1:1,000), anti-LXRα/β (1:1,000) (Novus Biologicals, Inc., Littleton, CO, USA), and anti-LDL receptor (M-20):sc-11826, (1:1,000) (Santa Cruz Biotechnology Inc, USA) followed by incubation with HRP-conjugated antibody and ECL reaction (Super Signal West Pico Chemiluminescent substrate, Pierce, Rockford, IL, EUA). Protein membrane stripping was performed by rinsing with 0.8 mM NaOH. The difference between the bands was analyzed in pixels using the JX-330 Color Image Scanner (Sharp®) and ImageMaster software (Pharmacia Biotech). The results are

expressed as arbitrary units. β-actin protein levels (anti β-actin 1:1,000, Fitzgerald Industries International, Inc., Concord, MA) were used as a control, and Ponceau staining of nitrocellulose membranes was implemented to assure equal protein loading.

CYP7A1 and CYP27A mRNA Expression in the Liver

At the final period of the study, the liver was removed and immediately frozen in liquid nitrogen. mRNA from liver samples (~50 mg) was extracted with 1 mL of Trizol (Invitrogen Life Technologies, Carlsbad, CA, USA). Reverse transcription reactions were performed with 2 μg of RNA using TaqMan Reverse Transcription Reagents (Applied Biosystems, Foster City, CA). Real time-PCR was performed on an Mx3000P QPCR System (Stratagene, La Jolla, CA) using the Brilliant SYBR Green QPCR Master Mix (Stratagene, catalogue no. 600548). The following primers were used: β actin sense 5′-TGG AGAGCACCAAGACAGACA-3′ and antisense 5′-TGC CGGAGTCGACAATGAT-3′; CYP7A1 sense 5′-AGCA ACTAAACAACCTGCCAGTACTA-3′ and antisense 5′-GTCCGGATATTCAAGGATGCA-3′; CYP27A sense 5′-GGAGGGCAAGTACCCAATAAGA-3′ and antisense 5′-TGCGATGAAGATCCCATAGGT-3′.

Determination of Apo A-I in the Peritoneal Fluid

Mouse peritoneal cavities were rinsed with PBS, and the fluid was collected in order to measure the apo A-I content. The sample volume was reduced using Amicon filters (Millipore, USA), and the same amount of protein was submitted to immunoblot analysis as described above using anti apo A-I Ab 1:1,000 (Santa Cruz Diag, USA).

Statistical Analysis

Statistical analyses were performed using GraphPad Prism 4.0 software (GraphPad Prism, Inc., San Diego, CA). A non-paired Student's *t* test was used to compare differences between groups. Summary data are reported as mean values ± standard error or mean values ± standard deviation as indicated. A p value <0.05 was considered statistically significant.

Results

CETP-tg C57BL/6 male mice were submitted to a 6 week period of supervised aerobic exercise training. Body weight, total plasma cholesterol and triacylglycerols were not modified by exercise training (Table 1). As shown in Fig. 1, the VLDL-cholesterol and LDL-cholesterol plasma profile was not modified by the aerobic exercise training, although the HDL-cholesterol fraction área was higher in the trained animals compared to the sedentary animals in the final period of the protocol. Plasma CETP activity was similar in sedentary and trained mice at the beginning of the protocol and did not change after the exercise training period. Moreover, CETP plasma activity was not different between the sedentary and trained groups when the initial and final periods were compared (Table 1).

Table 1 Body weight, plasma lipid profile and CETP activity in exercise trained and sedentary CETP-tg mice

	Trained ($n = 10$)		Sedentary ($n = 11$)	
	Basal	Final	Basal	Final
Weight (g)	19.4 ± 1.2	20.3 ± 1.3	20.0 ± 1.0	19.2 ± 1.0
TC (mg/dL)	52 ± 6	48 ± 5	64 ± 15	58 ± 11
TAG (mg/dL)	56 ± 19	55 ± 19	41 ± 13	46 ± 14
CETP activity (%)	29 ± 5	32 ± 8	28 ± 5	34 ± 11

TC total cholesterol, *TAG* triacylglycerols

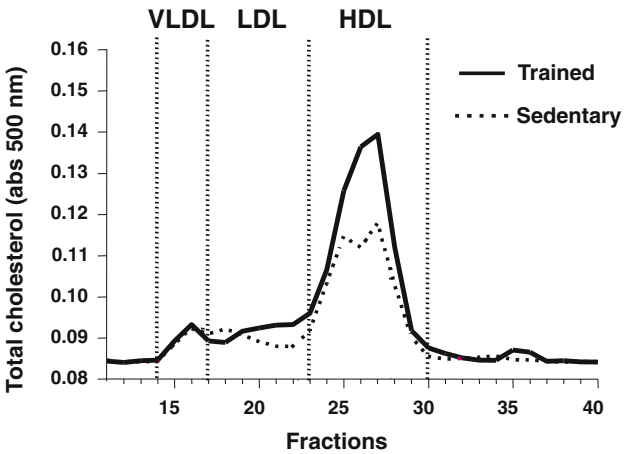

Fig. 1 Plasma lipoprotein profile of aerobically trained and sedentary CETP-tg mice. Plasma lipoproteins were isolated by fast protein liquid chromatography (FPLC), and total cholesterol was determined in all fractions using an enzymatic colorimetric kit. Sedentary (*dashed line*) and trained (*filled line*) CETP-tg mice

The [^{3}H]-cholesterol content was analyzed in plasma and feces at 24 and 48 h and in the liver at 48 h following the intraperitoneal injection of J774 macrophages enriched with AcLDL and radiolabeled cholesterol. A higher percentage of [^{3}H]-cholesterol was recovered from the plasma (Fig. 2a), liver (Fig. 2b) and feces (Fig. 2c) of the trained mice when compared to the sedentary animals.

As compared to the sedentary group, the increase in radiolabeled cholesterol in the liver of exercise-trained mice was accompanied by a 50% increase in protein levels of the hepatic LDL receptor (Fig. 3). In contrast, exercise

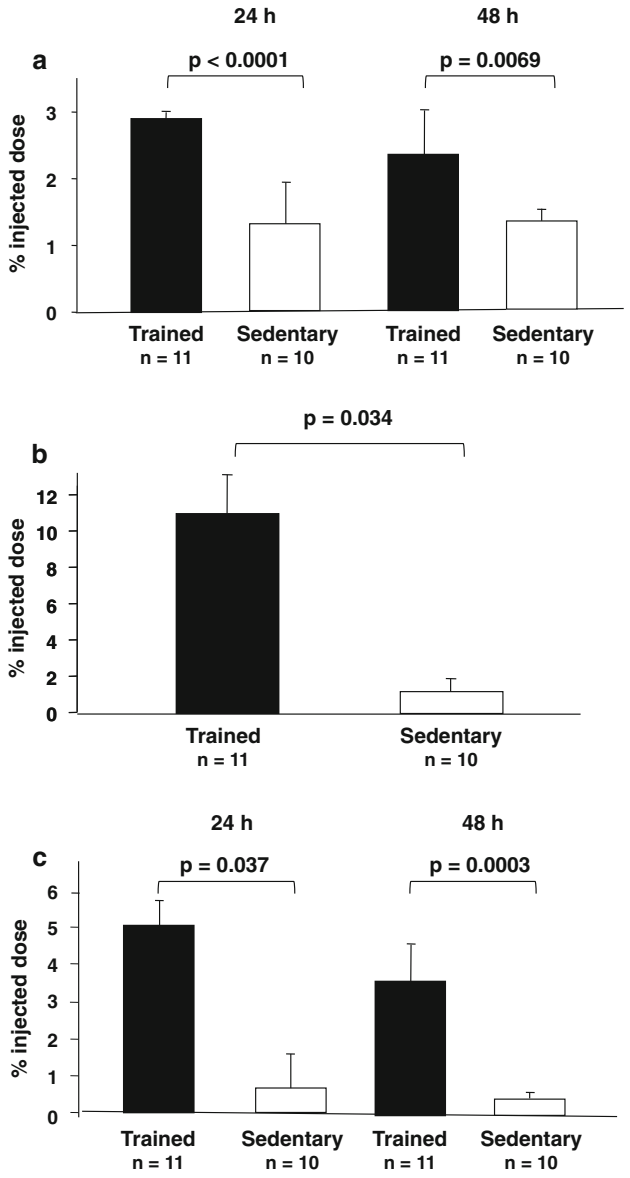

Fig. 2 Macrophage-derived [^{3}H]-cholesterol recovery in **a** plasma, **b** liver and **c** feces from aerobically trained and sedentary CETP-tg mice. J774 macrophages enriched with acetylated LDL and [^{3}H]-cholesterol were injected into the peritoneal cavities of sedentary and trained CETP-tg mice. **a** Plasma and **c** feces were collected after 24 and 48 h of the injection, and **b** the liver was removed after 48 h. After lipid extraction, the radioactivity was determined, and the recovery of [^{3}H]-cholesterol is expressed as the percentage of injected dose/mL of plasma or percentage of injected dose/mg of tissue or feces. Data are expressed as mean values ± standard error

training did not raise the SR-BI hepatic level (Fig. 3a). No changes were observed in the protein levels of LXR in the liver of exercise-trained animals (Fig. 3a). The hepatic ABCA-1 protein level was increased 100% in exercise-trained animals (Fig. 3a). CYP7A1 mRNA levels were reduced in exercise-trained CETP-tg mice, whereas their CYP27A mRNA levels were not influenced by exercise training (Fig. 3b). Total cholesterol content in the liver (mg of cholesterol/g of organ; mean ± SE) was not different between trained (43.3 ± 9.9; $n = 6$) and sedentary (40.4 ± 1.38; $n = 6$) animals.

The apo A-I content in peritoneal fluid as assessed by immunoblot was similar before and after exercise training (Fig. 4). Thus, the increase in the RCT after exercise training could not be ascribed to changes in apo A-I content.

Discussion

The importance of regular exercise for the prevention and treatment of chronic diseases is widely acknowledged [1]. Aerobic exercise improves LP metabolism and prevents the development of cardiovascular disease. Apart from the well-documented favorable effects of regular exercise on cardiovascular risk factors, it has been suggested that physical training may involve additional mechanisms that ameliorate atherosclerosis.

HDL is known for its anti-atherogenic properties that rely on its ability to support the cholesterol efflux from cholesterol-loaded arterial macrophages. Previous investigations focused on the benefits of exercise on lipoprotein lipase activity, including the mediation of triacylglycerol-rich LP metabolism and the increased levels of plasma HDL cholesterol [14, 15]. Nonetheless, it is unclear whether exercise plays a role in the RCT system in vivo. In this study, we used an experimental model designed to evaluate in vivo RCT and found that a 6 week carefully controlled aerobic exercise training program accelerates the RCT in CETP-tg mice.

CETP-tg mice are a useful tool for investigating the contribution of CETP to RCT. CETP is known to play a major role in RCT in humans. In huCETP-tg mice, the uptake of apo B-containing LP by the LDL receptor offers an additional route for the delivery of plasma esterified cholesterol to the liver. Accordingly, the increased RCT observed in the exercise-trained mice in this study may be ascribed to the enhanced protein levels of the LDL receptor in the liver. Elevated levels of hepatic LDL receptor mRNA have previously been shown in aerobic trained mice [16, 17], although the protein content has never been reported. In our investigation, exercise in the presence of CETP increased the uptake of LDL cholesterol by the liver and ABCA-1 protein levels, which may have prevented to liver cholesterol content from increasing by enhancing the export of cholesterol. In addition, by increasing the HDLc fraction as assessed by FPLC, exercise training may have contributed to a greater removal of cell cholesterol, despite a slight reduction in CYP7A1 mRNA levels.

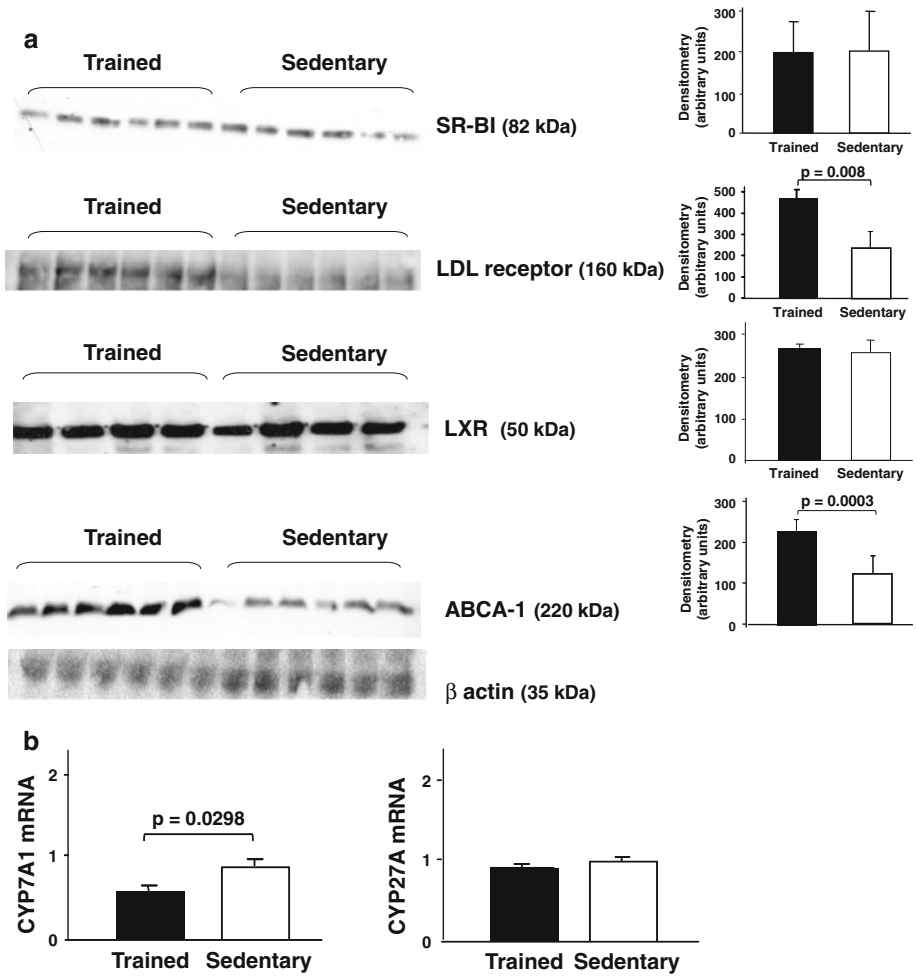

Fig. 3 LDL receptor, scavenger receptor class B type 1 (SR-BI), liver X receptor (LXR) and ATP binding cassette transporter (ABCA-1) protein levels and CYP7A1 and CYP27A mRNA in the livers of aerobically trained and sedentary CETP-tg mice. **a** liver samples from aerobically trained and sedentary CETP-tg mice were homogenized and dissolved in SDS-buffer. Equal amounts of protein lysates were applied to a 10% polyacrylamide gel and submitted to electrophoresis and immunoblotting with anti-LDL receptor Ab (1:1,000), anti-SR-BI Ab (1:1,000), anti-LXR Ab (1:1,000) and anti-ABCA-1 Ab (1:1,000). Following incubation with secondary Ab conjugated with HRP, bands were visualized after ECL reaction. Each *lane* represents one animal sample. Data are expressed as mean values ± standard deviation. **b** CYP7A1 and CYP27A mRNA was determined by RT-PCR as described in Material and Methods

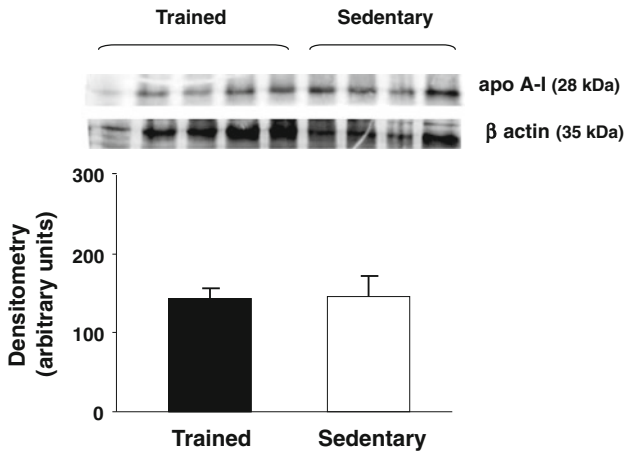

Fig. 4 Content of apo A-I in peritoneal fluid from aerobically trained and sedentary CETP-tg mice. Mouse peritoneal cavities were rinsed with PBS, and the fluid was collected. Protein was submitted to immunoblot analysis with anti apo A-I Ab 1:1,000

SR-BI plays a major role in the final step of the RCT system. Although macrophage SR-BI could not be related to an improvement in RCT efficiency [18], SR-BI protein levels in the liver are a positive regulator of macrophage RCT [19]. In fact, hepatic SR-BI is directly related to the secretion of cholesterol into the bile and to the reduction of atherosclerosis in animal models with low levels of HDL in plasma [20, 21]. Wei et al. [16] have described an enhancement of the hepatic SR-BI mRNA levels in wild-type C57BL/6 mice submitted to a 2 week aerobic training program. Surprisingly, the liver SR-BI protein levels did not change after aerobic exercise training in our study. This is likely due to a greater cholesterol influx mediated by the LDL receptor.

In huCETP-tg mice, a direct role of CETP in accelerating the tissue uptake of esterified cholesterol (EC) was demonstrated [22, 23]. Although improved HDL-EC removal and increased cholesterol content in the liver have been seen in CETP-tg mice, the excretion of biliary lipids and fecal bile acid have not been consistently found in these animals when compared to wild-type mice [24]. In CETP-tg mice, the in vivo RCT from macrophage to feces was not modified [25]. Nonetheless, the hypothesis that CETP facilitates RCT is strengthened by evidences related to mice expressing CETP alone [26] or combined with

knock-outs of LDL or SR-BI receptors. In these animals, CETP elicited macrophage RCT despite a reduction in HDL [27], and SR-BI-deficient mice were protected against diet-induced atherosclerosis [28]. On the other hand, the treatment of hamsters with torcetrapib, a drug that suppresses the CETP activity, increased the appearance of cholesterol originating from peritoneally injected macrophages in plasma and feces [26].

Increased levels of CYP27A mRNA have been described by Wilund et al. [17] in mice submitted to a 12 week aerobic exercise training program. In addition, voluntary wheel running increased fecal bile acid and cholesterol output and reduced intestinal cholesterol absorption in mice [29]. In our study, the CYP7A1 mRNA levels were reduced but CYP27A mRNA was not modified by exercise training, suggesting that the greater amount of radiolabeled cholesterol found in feces could be attributed to the increased excretion of cholesterol instead of bile acids. A recent paper from Yasuda et al. [30] showed that the activation of RCT resulted in a higher excretion of cholesterol, but not bile acids, in the feces of LXR agonist-treated mice. A limitation of our study was the fact that we did not measure the intestinal cholesterol absorption that could affect RCT in vivo as occurred in mice treated with ezetimibe [31]. Also, Temel et al. [32] used genetic and surgical models of biliary cholesterol insufficiency to demonstrate that a non-classical hepatobiliary pathway can contribute to RCT independently of biliary sterol secretion.

While this manuscript was under preparation, Meissner et al. [33] published a paper showing that the in vivo RCT, assessed by the same methodology used here, was not modified by voluntary wheel running in wild-type C57BL-6 mice compared to sedentary animals. Differences between their report and our results are likely ascribed to: (1) the presence of CETP in our model and its role in the alternative pathway of cholesterol disposal via the LDL receptor; (2) their results were obtained in free running wheel mice, which cannot assure equal training intensities along the protocol period, as opposed to the regular and carefully supervised exercise training protocol that was utilized in our study.

Although CETP activity was not changed after exercise training in our study, we should bear in mind that the CETP-mediated HDL-EC uptake by the liver is independent of the plasma activity responsible for the exchange of EC and TAG between LP [22]. Nonetheless, divergent data have been published regarding the role of CETP inhibitors like torcetrapib on this process [26]. Zhou et al. [34] suggested that the hepatic acquisition of EC from HDL mediated by CETP occurs independently of SR-BI, LDL-receptor related protein (LRP) and possibly the LDL receptor.

Controversial results have been published regarding the effect of exercise on the CETP mass and activity, which could be ascribed to the different methodologies used to measure CETP, as well as to variations in exercise intensity and frequency and the measurement of acute or chronic effects of exercise [14, 15]. Moreover, the efficiency of aerobic exercise in modulating the lipid profile is related to gender, age, insulin resistance, weight loss and genetic polymorphisms of CETP, apo E and apo A-I [36–38].

Exercise training did not modify the protein levels of LXR in CETP-tg mice. On the other hand, ABCA-1 was greatly enhanced following training, and this could have contributed to the higher levels of HDLc observed in exercise-trained CETP-tg mice in the final period of the study. ABCA-1 in the liver is known to contribute to HDL formation and plasma HDL cholesterol levels. Adenovirus-targeted protein levels of ABCA-1 in the liver increased HDL plasma levels in mice [39, 40]. On the other hand, an 80% reduction in plasma HDL cholesterol levels was observed in mice with a targeted inactivation of hepatic ABCA-1 [41], and ABCA-1 has been shown to play a critical role in HDL catabolism by the liver [42].

Systemic and macrophage ABCA-1 are positive regulators of macrophage RCT in vivo [18, 35]. This is consistent with our findings. An enhancement in ABCA-1 mRNA levels in the livers isolated from exercise-trained rats has also been described [43]. Furthermore, Butcher et al. [44] reported an increased expression of ABCA-1 and ABCG-1 mRNA in leukocytes isolated from trained subjects compared to sedentary ones.

In conclusion, aerobic exercise training improves RCT from macrophages in CETP-tg mice by increasing the concentration of HDL in plasma and by distinctly modulating the protein levels of liver receptors involved in the uptake of EC, which may contribute to the prevention and regression of atherosclerosis as previously reported by others [3, 5, 45]. With regards to the role of CETP in lipid metabolism in humans, the findings of our study shed light on an important effect of exercise on the RCT system. Taking into account that exercise has many effects on lipid and LP metabolism, the exact mechanisms by which exercise favorably modulates the lipid transport should be further investigated.

Acknowledgments This work was supported by Fundação de Amparo à Pesquisa do Estado de Sao Paulo—FAPESP [07/50387-8 to MP, 06/52702-5 to DDFM Rocco, 07/56654-8 to LS Okuda and 09/53412-9 to RS Pinto] and by Conselho Nacional de Desenvolvimento Científico e Tecnológico-CNPq [870248/1197-9 to DDFMR]. The authors are indebted to Dr. Marisa Dolhnikoff and Ana L B Silveira from the Pathology Museum, Faculty of Medical Sciences, University of Sao Paulo for helping with microscope analysis, and to Walter Campestre (LIM-16) and Antonio dos Santos Filho (LIM-17) for caring for the animals. The authors are thankful to Fundação Faculdade de Medicina and Laboratórios de Investigação Médica

(LIM). Results of the present study do not constitute endorsement by ACSM.

Conflict of interest None.

References

1. Lee IM, Hsieh CC, Paffenbarger RS Jr (1995) Exercise intensity and longevity in men. The Harvard Alumni Study. JAMA 273:1179–1184
2. Nordstrom CK, Dwyer KM, Merz NB, Shircore A, Dwyer JH (2003) Leisure time physical activity and early atherosclerosis: the Los Angeles atherosclerosis study. Am J Med 115:19–25
3. Ramachandran S, Penumetcha M, Merchant NK, Santanam N, Rong R, Parthasarathy S (2005) Exercise reduces preexisting atherosclerotic lesions in LDL receptor knock out mice. Atherosclerosis 178:33–38
4. Matsumoto Y, Adams V, Jacob S, Mangner N, Schuler G, Linke A (2010) Regular exercise training prevents aortic valve disease in low-density lipoprotein-receptor-deficient mice. Circulation 21:759–767
5. Napoli C, Williams-Ignarro S, Nigris F, Lerman LO, D'Armiento FP, Crimi E, Byrns RE, Casamassimi A, Lanza A, Gombos F, Sica V (2006) Physical training and metabolic supplementation reduce spontaneous atherosclerotic plaque rupture and prolong survival in hypercholesterolemic mice. PNAS 13:10479–10484
6. Meilhac O, Ramachandran S, Chiang K, Santanam N, Parthasarathy S (2001) Role of arterial wall antioxidant defense in beneficial effects of exercise on atherosclerosis in mice. Arterioscler Thromb Vasc Biol 21:1681–1688
7. Wang X, Rader DJ (2007) Molecular regulation of macrophage reverse cholesterol transport. Curr Opin Cardiol 22:368–372
8. Institute of Laboratory Animal Research CoLS (1996) National Research Council guide for the care and use of laboratory animals. In: Council NR (ed). National Academy Press, Washington (DC), p 124
9. Lowry OH, Rosebrough NJ, Farr Al, Randall RJ (1951) Protein measurement with folin phenol reagent. J Biol Chem 193:265–275
10. Basu SK, Goldstein JL, Anderson RGW, Brown MS (1976) Degradation of cationized low density lipoprotein and regulation of cholesterol metabolism in homozygous hypercholesterolemia fibroblasts. Proc Natl Acad Sci 73:3178–3182
11. Zhang Y, Zanotti I, Reilly MP, Glick JM, Rothblat GH, Rader DJ (2003) Overexpression of apolipoprotein A-1 promotes reverse transport of cholesterol from macrophages to feces in vivo. Circulation 108:661–663
12. Folch J, Lees M, Stanley S (1957) A simple method for the isolation and purification of total lipids from animal's tissues. J Biol Chem 226:497–509
13. Escolà-Gil JC, Julve J, Marzal-Casacuberta A, Ordóñez-Llanos J, González-Sastre F, Blanco-Vaca F (2001) ApoA-II expression in CETP transgenic mice increases VLDL production and impairs VLDL clearance. J Lipid Res 42:241–248
14. Gupta AK, Ross EA, Myers JN, Kashyap ML (1993) Increased reverse cholesterol transport in athletes. Metabolism 42:684–690
15. Olchawa B, Kingwell BA, Hoang A, Schneider L, Miyazaki O, Nestel P, Sviridov D (2004) Physical fitness and reverse cholesterol transport. Arterioscler Thromb Vasc Biol 24:1087–1091
16. Wei C, Penumetcha M, Santanam N, Liu GY, Garelnabi M, Parthasarathy S (2005) Exercise might favor reverse cholesterol transport and lipoprotein clearance: potential mechanism for its anti-atherosclerotic effects. Biochim Biophys Acta 1723:124–127
17. Wilund KR, Feeney LA, Tomayko EJ, Chung HR, Kim K (2008) Endurance exercise training reduces gallstone development in mice. J Appl Physiol 104:761–765
18. Wang X, Collins HL, Ranalletta M, Fuki IV, Billheimer JT, Rothblat GH, Tall AR, Rader DJ (2007) Macrophage ABCA1 and ABCG1, but not SR-BI, promote reverse cholesterol transport in vivo. J Clin Invest 117:2216–2224
19. Zhang Y, Da Silva JR, Reilly M, Billheimer JT, Rothblat GH, Rader DJ (2005) Hepatic expression of scavenger receptor class B type I (SR-BI) is a positive regulator of macrophage reverse cholesterol transport in vivo. J Clin Invest 115:2870–2874
20. Mardones P, Quiñones V, Amigo L, Moreno M, Miquel JF, Schwarz M, Miettinen HE, Trigatti B, Krieger M, VanPatten S, Cohen DE, Rigotti A (2001) Hepatic cholesterol and bile acid metabolism and intestinal cholesterol absorption in scavenger receptor class B type I-deficient mice. J Lipid Res 42:170–180
21. Kozarsky KF, Donahee MH, Glick JM, Krieger M, Rader DJ (2000) Gene transfer and hepatic overexpression of the HDL receptor SR-BI reduces atherosclerosis in the cholesterol-fed LDL receptor-deficient mouse. Arterioscler Thromb Vasc Biol 20:721–727
22. Gauthier A, Lau P, Zha X, Milne R, McPherson R (2005) Cholesteryl ester transfer protein directly mediates selective uptake of high density lipoprotein cholesteryl esters by the liver. Arterioscler Thromb Vasc Biol 25:2177–2184
23. Vassiliou G, McPherson R (2004) Role of cholesteryl ester transfer protein in selective uptake of high density lipoprotein cholesteryl esters by adipocytes. J Lipid Res 5:1683–1693
24. Harada LM, Amigo L, Cazita PM, Salerno AG, Rigotti AA, Quintão EC, Oliveira HC (2007) CETP expression enhances liver HDL-cholesteryl ester uptake but does not alter VLDL and biliary lipid secretion. Atherosclerosis 191:313–318
25. Rotllan N, Calpe-Berdiel L, Guillaumet-Adkins A, Süren-Castillo S, Blanco-Vaca F, Escolà-Gil JC (2008) CETP activity variation in mice does not affect two major HDL antiatherogenic properties: macrophage-specific reverse cholesterol transport and LDL antioxidant protection. Atherosclerosis 196:505–513
26. Tchoua U, D'Souza W, Mukhamedova N, Blum D, Niesor E, Mizrahi J, Maugeais C, Sviridov D (2008) The effect of cholesteryl ester transfer protein overexpression and inhibition on reverse cholesterol transport. Cardiovascular Res 77:732–739
27. Tanigawa H, Billheimer JT, Tohyama J, Zhang Y, Rothblat G, Rader DJ (2007) Expression of cholesteryl ester transfer protein in mice promotes macrophage reverse cholesterol transport. Circulation 116:1267–1273
28. Harder C, Lau P, Meng A, Whitman SC, McPherson R (2007) Cholesteryl ester transfer protein (CETP) expression protects against diet induced atherosclerosis in SR-BI deficient mice. Arterioscler Thromb Vasc Biol 27:858–864
29. Meissner M, Havinga R, Boverhof R, Kema I, Groen AK, Kuipers F (2010) Exercise enhances whole-body cholesterol turnover in mice. Med Sci Sports Exerc 42:1460–1468
30. Yasuda T, Grillot D, Bilheimer JT, Briand F, Delerive P, Huet S, Rader DJ (2010) Tissue-specific liver X receptor activation promotes macrophage reverse cholesterol transport in vivo. Arterioscler Thromb Vasc Biol 30(4):781–786
31. Sehayek E, Hazen SL (2008) Cholesterol absorption from the intestine is a major determinant of reverse cholesterol transport from peripheral tissue macrophages. Arterioscler Thromb Vasc Biol 28:1296–1297
32. Temel RE, Sawyer JK, Yu L, Lord C, Degirolamo C, McDaniel A, Marshall S, Wang N, Shah R, Rudel LL, Brown JM (2010) Biliary sterol secretion is not required for macrophage reverse cholesterol transport. Cell Metab 12:96–102
33. Meissner M, Nijstad N, Kuipers F, Tietge UJ (2010) Voluntary exercise increases cholesterol efflux but not macrophage reverse cholesterol transport in vivo in mice. Nutr Metab 1:54

34. Zhou H, Li Z, Silver DL, Jiang XC (2006) Cholesteryl ester transfer protein (CETP) expression enhances HDL cholesteryl ester liver delivery, which is independently of scavenger receptor BI, LDL receptor related protein and possibly LDL receptor. Biochim Biophys Acta 1761:1482–1488
35. Calpe-Berdiel L, Rotllan N, Palomer X, Ribas V, Blanco-Vaca F, Escolà-Gil JC (2005) Direct evidence in vivo of impaired macrophage-specific reverse cholesterol transport in ATP-binding cassette transporter A1-deficient mice. Biochim Biophys Acta 1738:6–9
36. Couillard C, Després JP, Lamarche B, Bergeron J, Gagnon J, Leon AS, Rao DC, Skinner JS, Wilmore JH, Bouchard C (2001) Effects of endurance exercise training on plasma HDL cholesterol levels depend on levels of triglycerides: evidence from men of the Health, Risk Factors, Exercise Training and Genetics (HERITAGE) Family Study. Arterioscler Thromb Vasc Biol 21:1226–1232
37. Mukherjee M, Shetty KR (2004) Variations in high-density lipoprotein cholesterol in relation to physical activity and Taq 1B polymorphism of the cholesteryl ester transfer protein gene. Clin Genet 65:412–418
38. Sorlí JV, Corella D, Francés F, Ramírez JB, González JI, Guillén M, Portolés O (2006) The effect of the APOE polymorphism on HDL-C concentrations depends on the cholesterol ester transfer protein gene variation in a Southern European population. Clin Chim Acta 366:196–203
39. Basso F, Freeman L, Knapper CL, Remaley A, Stonik J, Neufeld EB, Tansey T, Amar MJ, Fruchart-Najib J, Duverger N, Santamarina-Fojo S, Brewer HB Jr (2003) J Role of the hepatic ABCA1 transporter in modulating intrahepatic cholesterol and plasma HDL cholesterol concentrations. J Lipid Res 44(2):296–302
40. Wellington CL, Brunham LR, Zhou S, Singaraja RR, Visscher H, Gelfer A, Ross C, James E, Liu G, Huber MT, Yang YZ, Parks RJ, Groen A, Fruchart-Najib J, Hayden MR (2003) Alterations of plasma lipids in mice via adenoviral-mediated hepatic overexpression of human ABCA1. J Lipid Res 44(2):1470–1480
41. Timmins JM, Lee JY, Boudyguina E, Kluckman KD, Brunham LR, Mulya A, Gebre AK, Coutinho JM, Colvin PL, Smith TL, Hayden MR, Maeda N, Parks JS (2005) Targeted inactivation of hepatic Abca1 causes profound hypoalphalipoproteinemia and kidney hypercatabolism of apoA-I. J Clin Invest 115(5): 1333–1342
42. Singaraja RR, Stahmer B, Brundert M, Merkel M, Heeren J, Bissada N, Kang M, Timmins JM, Ramakrishnan R, Parks JS, Hayden MR, Rinninger F (2006) Hepatic ATP-binding cassette transporter A1 is a key molecule in high-density proprotein cholesteryl ester metabolism in mice. Arterioscler Thromb Vasc Biol 26(8):1821–1827
43. Ghanbari-Niaki A, Khabazian BM, Hossaini-Kakhak SA, Rahbarizadeh F, Hedayati M (2007) Treadmill exercise enhances ABCA1 expression in rat liver. Biochem Biophys Res Commun 361:841–846
44. Butcher LR, Thomas A, Backx K, Roberts A, Webb R, Morris K (2008) Low-intensity exercise exerts beneficial effects on plasma lipids via PPARgamma. Med Sci Sports Exerc 40:1263–1270
45. Okabe TA, Shimada K, Hattori M, Murayama T, Yokode M, Kita T, Kishimoto C (2007) Swimming reduces the severity of atherosclerosis in apolipoprotein E deficient mice by antioxidant effects. Cardiovasc Res 74:537–545

Lipids (2011) 46:627–636
DOI 10.1007/s11745-011-3562-0

ORIGINAL ARTICLE

EPA or DHA Supplementation Increases Triacylglycerol, but not Phospholipid, Levels in Isolated Rat Cardiomyocytes

Valeria Righi · Mattia Di Nunzio · Francesca Danesi · Luisa Schenetti · Adele Mucci · Elisa Boschetti · Pierluigi Biagi · Sergio Bonora · Vitaliano Tugnoli · Alessandra Bordoni

Received: 11 November 2010 / Accepted: 16 February 2011 / Published online: 5 May 2011

Abstract It is well recognized that a high dietary intake of long-chain polyunsaturated fatty acids (LC-PUFA) has profound benefits on health and prevention of chronic diseases. In particular, in recent years there has been a dramatic surge of interest in the health effects of n-3 LC-PUFA derived from fish, eicosapentaenoic (EPA) and docosahexaenoic (DHA) acids. Notwithstanding, the metabolic fate and the effects of these fatty acids once inside the cell has seldom been comprehensively investigated. Using cultured neonatal rat cardiomyocytes as model system we have investigated for the first time, by means of high-resolution magic-angle spinning nuclear magnetic resonance (HR-MAS NMR) spectroscopy in combination with gas chromatography (GC), the modification occurring in the cell lipid environment after EPA and DHA supplementation. The most important difference between control and n-3 LC-PUFA-supplemented cardiomyocytes highlighted by HR-MAS NMR spectroscopy is the increase of signals from mobile lipids, identified as triacylglycerols (TAG). The observed increase of mobile TAG is a metabolic response to n-3 LC-PUFA supplementation, which leads to an increased lipid storage. The sequestration of mobile lipids in lipid bodies provides a deposit of stored energy that can be accessed in a regulated fashion according to metabolic need. Interestingly, while n-3 LC-PUFA supplementation to neonatal rat cardiomyocytes causes a huge variation in the cell lipid environment, it does not induce detectable modifications in water-soluble metabolites, suggesting negligible interference with normal metabolic processes.

Keywords HR-MAS NMR · GC · Rat cardiomyocytes · Docosahexaenoic acid · Eicosapentaenoic acid · Lipids

Abbreviations

1D	Monodimensional
2D	Bidimensional
α-CH	α-CH of aminoacids
Ac	Acetate
Ala	Alanine
ARA	Arachidonic acid
C	Cholesterol
CE	Cholesteryl esters
Cho	Choline
ChoCC	Choline-containing compounds
COSY	Correlation spectroscopy
CPMG	Carr–Purcell–Meiboom–Gill
Cr	Creatine
DHA	Docosahexaenoic acid
DPAn-3	Docosapentaenoic acid
EPA	Eicosapentaenoic acid
Etn	Ethanolamine
FA	Fatty acid(s)

V. Righi · M. Di Nunzio · E. Boschetti · P. Biagi · S. Bonora · V. Tugnoli
Department of Biochemistry "G. Moruzzi", University of Bologna, Via Irnerio, 48, 40126 Bologna, BO, Italy

V. Righi · L. Schenetti · A. Mucci
Department of Chemistry, University of Modena and Reggio Emilia, Via Campi, 183, 41125 Modena, MO, Italy

F. Danesi · A. Bordoni
Department of Food Sciences, University of Bologna, Piazza Goidanich, 60, 47521 Cesena, FC, Italy

V. Tugnoli (✉)
Dipartimento di Biochimica "G. Moruzzi", University of Bologna, Via Belmeloro 8/2, 40126 Bologna, Italy
e-mail: vitaliano.tugnoli@unibo.it

FCS	Fetal calf serum
FFA	Unesterified fatty acids
GC	Gas chromatography
Gln	Glutamine
Glu	Glutamate
Gly	Glycine
GPC	Glycerophosphocholine
HR-MAS	High-resolution magic-angle spinning
HS	Horse serum
Lac	Lactate
LB	Lipid body(ies)
LC-PUFA	Long chain polyunsaturated fatty acid(s)
Lys	Lysine
MUFA	Monounsaturated fatty acid(s)
Myo	*Myo*-inositol
NMR	Nuclear magnetic resonance
PCho	Phosphocholine
PEtn	Phosphoethanolamine
PL	Phospholipid(s)
PtdCho	Phosphatidylcholine
PUFA	Polyunsaturated fatty acid(s)
Scy	*Scyllo*-inositol
TAG	Triacylglycerol(s)
Tau	Taurine
TLC	Thin-layer chromatography
TOCSY	Total correlation spectroscopy
UDP	Uridine diphosphate

Introduction

Cardiovascular diseases are responsible for significant morbidity and mortality throughout the world. It is well recognized that a significant dietary intake of polyunsaturated fatty acids (PUFA) has profound benefits on health and on prevention of chronic disease states, although the overall responsible mechanism remains partially unclear [1, 2].

Supplementation with the main n-3 long-chain polyunsaturated fatty acids (LC-PUFA), eicosapentaenoic acid (20:5n-3, EPA) and docosahexaenoic acid (22:6n-3, DHA), has been widely reported as protective for cardiovascular health, and fish oil feeding has been associated with reduced mortality in several studies [3–5]. Notwithstanding, the effects of these fatty acids (FA) on the cardiac cell lipid environment are almost unknown.

In this study we have coupled gas chromatographic (GC) analysis and high-resolution magic-angle spinning (HR-MAS) nuclear magnetic resonance (NMR) spectroscopy to obtain evidence of modifications occurring in the lipid environment and in the metabolic profile of cultured cardiomyocytes supplemented with n-3 PUFA. Chromatographic methods have become the standard for analyzing FA composition [6]. In particular, GC is sensitive and specific for FA analysis, and HR-MAS NMR spectroscopy takes a picture of the whole metabolic profile detecting lipids, macromolecules, and small metabolites. Using MAS NMR the sample can be analyzed directly with minimal manipulation, and many different compounds, for example macromolecules, lipids, and small metabolites, can be detected simultaneously [7–10]. Study of cellular metabolism in cell extracts solution, either hydrophilic or lipophilic, has been successfully carried out for years by use of NMR spectroscopy. More recently, the development of HR-MAS techniques has made the direct analysis of cells increasingly preferred for metabolomic studies [11]. HR-MAS NMR spectroscopy is currently used for analysis of the biochemical profile of complex systems such as biofluids, biological tissues, or cells. In fact, it can detect many different metabolites, and furnish information about the metabolic changes occurring in response to external stimuli, e.g. drug exposure, or disease [10]. As far as we are aware, HR-MAS NMR investigations, alone or combined with GC analysis, involving cardiomyocytes are still virtually non-existent. In our opinion, they could furnish baseline data for future investigation of the effects on mammalian cells of FA supplementation.

Materials and Methods

Materials

FA, Ham F10 media, fetal calf serum (FCS), horse serum (HS), gentamicin, amphotericin B, and 2′,7′-dichlorofluorescein were from Sigma (St Louis, MO, USA). Hexane, diethyl ether, and formic acid were purchased from Carlo Erba (Milan, Italy). All other chemicals and solvents were of the highest analytical grade.

Cardiomyocytes Cell Cultures

Primary cultures of neonatal rat cardiomyocytes were obtained from the ventricles of two to four-day old Wistar rats according to Yagev et al. [12]. Cells were seeded at a density of 1.5×10^6 cells/ml in 100-mm i.d. Petri dishes in Ham F10 nutrient mixture supplemented with 10% (*v*/*v*) FCS, 10% (*v*/*v*) HS, gentamicin (1%), amphotericin B (1%), and grown at 37 °C, 5% CO_2, and 95% humidity. The study protocol was approved by the Animal Care Committee of the University of Bologna (Italy) (prot. n. 58897-X/10). Forty-eight hours after seeding, cardiomyocytes were randomly divided into control and FA supplemented groups. EPA and DHA were dissolved in ethanol,

added to FCS to enable binding to albumin, and supplemented at 60 μM concentration. Control medium was added with the same volume of ethanol (≤0.1% *v*/*v*) to avoid interference from vehicle. Media were changed every 48 h, and cardiomyocytes were grown till complete confluence in a monolayer (day 8 from seeding).

Cardiomyocytes FA Composition

At confluence cardiomyocytes were washed three times with ice-cold phosphate-buffered saline, scraped off, and cell total lipids were extracted according to Folch et al. [13]. Washings were analyzed by GC to ensure that supplemented FA had been completely removed and did not interfere with subsequent analyses. Total cell lipids were separated by thin-layer chromatography (TLC) using plates coated with silica gel G. Plates were developed in hexane–diethyl ether–formic acid (8:2:0.1 *v*/*v*). Spots were made visible under ultraviolet light by spraying with 2′,7′-dichlorofluorescein (0.2% *w*/*v* in ethanol), and identified by comparison with authentic co-chromatographed standards. Spots corresponding to the phospholipid (PL) and triacylglycerol (TAG) fractions were scraped off, extracted with methanol or diethyl ether, respectively, and methylated according to Stoffel et al. [14]. Before methylation, pentadecanoic acid was added as internal standard. FA composition (as methyl esters) was determined by GC (GC 8000; Fisons, Milan, Italy) using a capillary column (SP 2340, 0.2 μm film thickness) with a programmed temperature gradient (160–210 °C, 8 °C/min), as previously reported [15]. The gas chromatographic peaks were identified on the basis of their retention time ratios relative to methyl stearate and predetermined by use of authentic samples. Gas chromatographic traces and quantitative evaluations were obtained using a Chrom Card Software computing integrator (Thermo Electron Scientific, Milan, Italy).

Nuclear Magnetic Resonance Spectroscopy

At confluence, after washing with ice-cold phosphate-buffered saline, cells were scraped off in deuterated water. Cell suspension (50 μl) was placed in a 50-μl MAS zirconia rotor (4 mm OD), closed with a cylindrical insert to increase sample homogeneity, then transferred to the probe cooled to 4 °C. ^{1}H and ^{13}C HR-MAS NMR spectra were recorded with a BrukerAvance 400 spectrometer operating at 400.13 and 100.61 MHz, respectively. The instrument was equipped with a ^{1}H,^{13}C HR-MAS probe, the temperature of which was controlled by a Bruker Cooling Unit. All experiments were performed at 4 °C to prevent cell degradation processes [16]. Samples were spun at 4,000 Hz. After set up for approximately 20 min, three different types of monodimensional (1D) proton spectra were acquired by using:

1. a composite pulse sequence (zgcppr) [17], with 1.5 s water-presaturation during relaxation delay, 8 kHz spectral width, 32 k data points, 32-64 scans;
2. a water-suppressed spin–echo Carr–Purcell–Meiboom–Gill (CPMG) sequence (cpmgpr) [18], with 1.5 s water presaturation during relaxation delay, 1 ms echo time (τ), and 360 ms total spin–spin relaxation delay ($2n\tau$), 8 kHz spectral width, 32 k data points, 128 scans; and
3. a sequence for diffusion measurements based on stimulated echo and bipolar-gradient pulses (ledbpgp2s1d) [19] with big delta 200 ms, eddy current delay T_e 5 ms, little delta 2 × 2 ms, sine-shaped gradient with 32 G/cm followed by a 200 μs delay for gradient recovery, 8 kHz spectral width, 8 k data points, 256 scans.

Two-dimensional (2D) ^{1}H,^{1}H-correlation spectroscopy (COSY) spectra [20, 21] were acquired using a standard pulse sequence (cosygpprqf) and 0.5 s water presaturation during relaxation delay, 8 kHz spectral width, 4 k data points, 32 scans per increment, 256 increments. 2D ^{1}H,^{1}H-total correlation spectroscopy (TOCSY) spectra [22, 23] were acquired using a standard pulse sequence (mlevphpr) and 0.5 s water-presaturation during relaxation delay, 100 ms mixing (spin-lock) time, 4 kHz spectral width, 4 k data points, 32 scans per increment, 128 increments. NMR spectra of specimens were analyzed using MestReC software (Mestrelab Research, Santiago de Compostela, Spain). A line-broadening apodization function of 5 Hz was applied to lead diffusion-edited HR-MAS ^{1}H FIDs before Fourier transformation. NMR spectra were referenced to the FA terminal $-CH_3$ signal at δ 0.89 ppm, manually phased, and a Whittaker baseline estimator was applied to subtract the broad components of the baseline.

Statistical Analysis

Three batches for each type of sample (control, EPA-supplemented, and DHA-supplemented cardiomyocytes) derived from three independent cell cultures were analyzed. Statistical analysis was performed by one-way ANOVA with Tukey as post test.

Results

HR-MAS NMR

The metabolic pattern of unsupplemented, control cardiomyocytes can be derived by analysis of the spectra shown in Fig. 1. The first spectrum (Fig. 1a) is a conventional

presaturated 1D spectrum detecting lipids, macromolecules, and small metabolite contribution. Figure 1b shows the spectrum obtained using a CPMG spin–echo sequence. This enables separation of signals according to their different T_2, and enhancement of the resonance of small metabolites relative to that of macromolecules. The small metabolites are labeled in Fig. 1b: alanine (Ala), choline-containing compounds (ChoCC), creatine (Cr), glutamate (Glu), glycine (Gly), *myo*-inositol (Myo), phosphoethanolamine (PEtn), *scyllo*-inositol (Scy), taurine (Tau), α-CH of aminoacids (α-CH). The diffusion-edited spectrum (Fig. 1c) displays broad resonances arising from macromolecules. In particular, mobile FA chains (signals at 0.89 ppm (–C**H**$_3$), 1.33 ppm (C**H**$_2$)$_n$, and 2.03 ppm C**H**$_2$C=C) and phosphatidylcholine (PtdCho) (signal at 3.26 ppm N(C**H**$_3$)$_3^+$) are clearly detectable. Membrane PL do not contribute significantly to the NMR signals because of their low mobility and short relaxation times. Control cardiomyocytes ^{1}H HR-MAS NMR spectra were used for the comparison with spectra obtained from cells supplemented with EPA and DHA.

In Fig. 2 the conventional water-presaturated ^{1}H spectra obtained from control (Fig. 2a), EPA-supplemented (Fig. 2b), and DHA-supplemented (Fig. 2c) cardiomyocytes are reported. In the spectra of n-3 LC-PUFA-supplemented cardiomyocytes it is possible to recognize the characteristic signals from unsaturated FA. The resonances of FA chains are identified as: 1, methyls (–C**H**$_3$) at 0.89 ppm (saturated FA chains), and 2, –C**H**$_3$ at 0.96 ppm (n-3 EPA, and DHA); 3, acyl chain methylenes (C**H**$_2$)$_n$ (1.33 ppm); 4, C**H**$_2$–C–CO (1.58 ppm); 5, C**H**$_2$C=C (2.02 ppm); 6, C**H**$_2$CO other than DHA (2.25 ppm) and 7, C**H**$_2$CO of DHA, (2.33 ppm); 8, =C–C**H**$_2$-C= (2.78 ppm); 9, –C**H**=C**H**-(5.33 ppm) [24–26]. Signals at 2.02 ppm are assigned to methylene protons of the C**H**$_2$–CH=CH moiety of both monounsaturated FA (MUFA) and PUFA, and the signal at 2.78 ppm is characteristic of PUFA [24, 25]. Both MUFA and PUFA are also identified by the signals at 5.33 ppm, because of the protons of the –C**H**=C**H**– moiety.

Comparison of ^{1}H NMR spectra of supplemented and control samples shows that the PUFA signals are dominant in EPA and DHA-supplemented cardiomyocyte spectra, whereas they are almost absent in those of control cells. Moreover, the signal at 2.33 ppm, characteristic of DHA

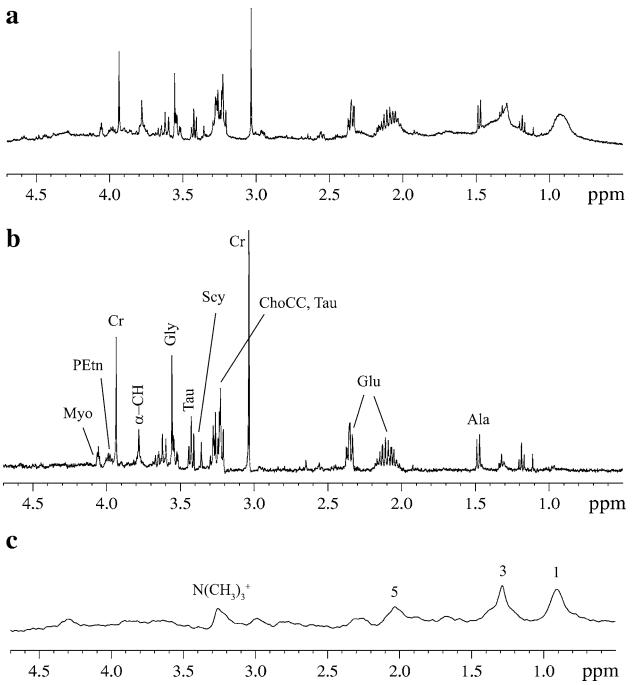

Fig. 1 Representative ex-vivo HR-MAS ^{1}H NMR spectra of neonatal rat cardiomyocytes: water-presaturated pulse sequence with composite pulse (**a**), CPMG spectrum (**b**), and diffusion-edited spectrum (**c**). The major metabolites are labeled: *Ala* alanine, *ChoCC* choline-containing compounds, *Cr* creatine, *Glu* glutamate, *Gly* glycine, *PEtn* phosphoethanolamine, *Scy scyllo*-inositol, *Myo myo*-inositol, *Tau* taurine, *α-CH* α-CH of aminoacids. Lipid components are labeled: *1*, –CH$_3$; *3*, acyl chain methylene (CH$_2$)$_n$; *5*, CH$_2$C=C; *N(CH$_3$)$_3^+$*, signal for PL components

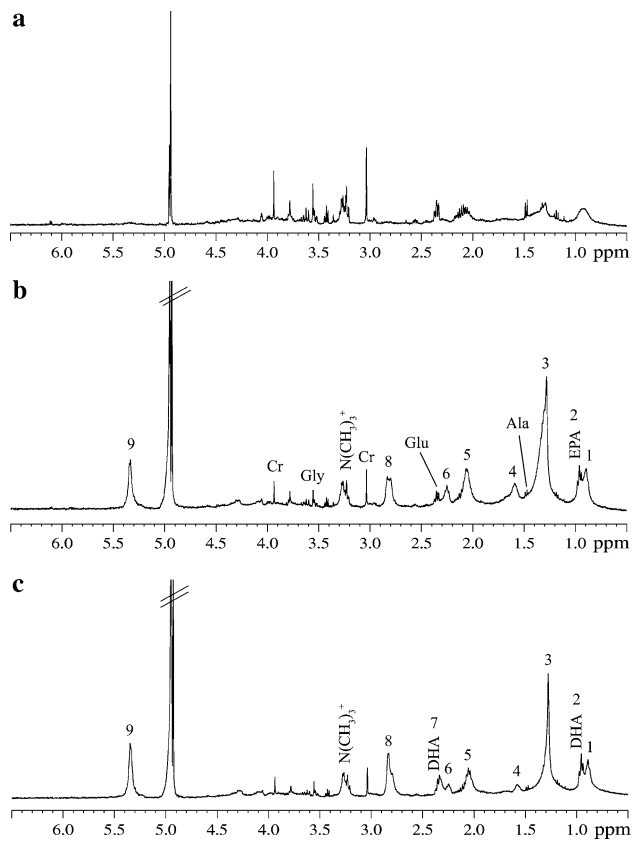

Fig. 2 Water-presaturated ex-vivo HR-MAS ^{1}H NMR spectra of control (**a**), EPA-supplemented (**b**), and DHA-supplemented (**c**) cardiomyocytes. Lipid components are labeled as in the previous figure and: *2*, DHA and EPA –CH$_3$; *4*, CH$_2$–C–CO; *6*, CH$_2$CO other than DHA; *7*, CH$_2$CO and CH$_2$–C–CO of DHA; *8*, =C–CH$_2$–C=; *9*, CH=CH

$C\underline{H_2}$–CO and $C\underline{H_2}$–C–CO protons, enables distinction between DHA and EPA-supplemented samples.

In Fig. 3 the ^{1}H HR-MAS NMR diffusion-edited spectra of control (Fig. 3a), EPA-supplemented (Fig. 3b), and DHA-supplemented (Fig. 3c) cardiomyocytes are reported. In accordance with the literature, lipid components are identified as above. Signals 10 and 11, from bonded glycerol (4.10 and 4.30 ppm) are clearly detected, especially for the DHA-supplemented cells.

These spectra show an increase of signals from mobile lipids in PUFA-supplemented cells compared with the unsupplemented cells. Low PL signals (in particular that of $N(CH_3)_3^+$ at 3.26 ppm) are present, together with broad peaks from the macromolecules, in the control cell spectrum (Fig. 3a). In supplemented cells, these signals are obscured by the high intensity of signals from PUFA, mainly bonded to glycerol in TAG. Signals from CH_2 of bonded glycerol in TAG are clearly seen at 4.30 and 4.10 ppm (Fig. 3, signals 10, 11), whereas the CH resonance at 5.26 ppm is overlapped by the CH=CH protons of FA chains. Signals attributable to cholesterol (C) or cholesteryl esters (CE), the most characteristic of which is that of 18-CH_3, at approximately 0.7 ppm, are not detected.

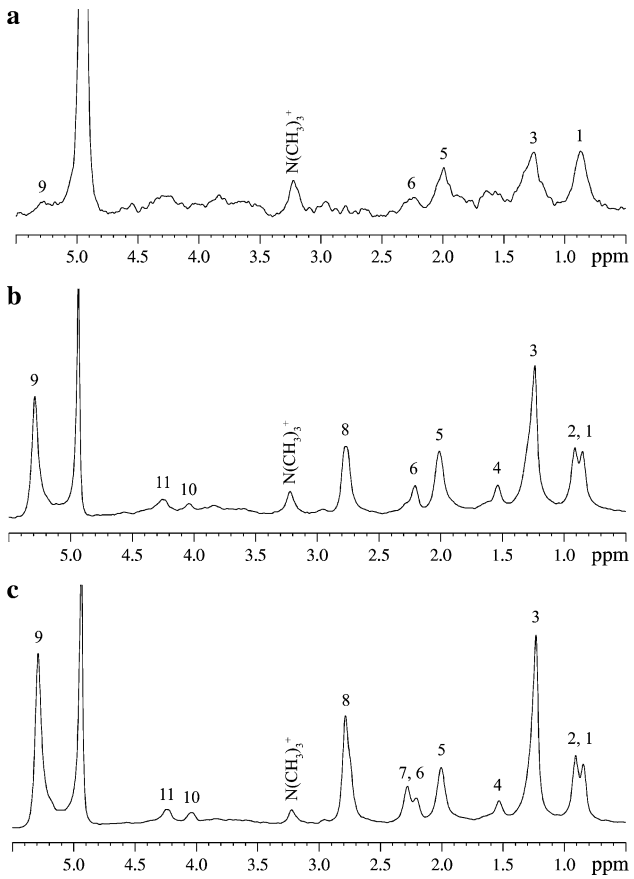

Fig. 3 ^{1}H HR-MAS NMR diffusion-edited spectra from control (**a**), EPA-supplemented (**b**), and DHA-supplemented (**c**) cardiomyocytes. Lipid components are labeled as in previous figures and: 10 and 11, bonded glycerol

Variation of the mobile lipid components can be evaluated by integration of the resonances present in HR-MAS led diffusion-edited spectra (Fig. 4). Supplemented cardiomyocytes furnish a general increase of lipid signals, particularly unsaturated FA, which are almost absent in control cells (lack of signals at 2.78 ppm and 5.33 ppm). Instead, the PL fraction ($N(CH_3)_3^+$ signal at 3.26 ppm) does not seem significantly affected by supplementation (Fig. 3). In EPA and DHA-supplemented cardiomyocytes glycerol bonded signals (at 4.10 and 4.30 ppm), absent in control cells, are detected, indicating that NMR-visible FA are involved in TAG. Comparison of the theoretical (6:4) and experimental (7.4:4) TAG integral ratio between the CH_2CO (2.25 ppm) and glycerol (4.30 and 4.10 ppm) signals in EPA-supplemented cell spectra points to the presence of almost completely glycerol-esterified FA chains, and a slight excess of unesterified FA (FFA). The same approach, if applied to DHA samples, is less straightforward. In this case two signals, at 2.33 and 2.25 ppm, are derived from CH_2CO protons (DHA and other FA, respectively), and the former also receives a contribution from CH_2–C–CO protons of DHA. Moreover, the signal at 2.25 ppm accounts for approximately 25–30% of the total integral (2.25 + 2.33). The theoretical ratio between the integrals of the signals at 2.25 + 2.33 ppm and that of glycerol (4.30 and 4.10 ppm) is 12:4 for glycerol-triesterified with DHA (signal at 2.25 ppm absent) and 6:4 for glycerol-triesterified with FA other than DHA (signal at 2.33 ppm absent). On this basis, for DHA-supplemented cells we calculate a [DHA/(FA other than DHA)] ratio of approximately 3:2 and a theoretical ratio of $(12 \times 0.6 + 6 \times 0.4) = 9.6{:}4$ for FA involved in TAG. This compares well with the experimental value of 10.1:4, and indicates that the NMR-visible lipid signals arise from almost completely glycerol-esterified FA chains in DHA-supplemented cells also.

Figure 5 reports the CPMG HR-MAS ^{1}H NMR spectra of control (Fig. 5a), EPA-supplemented (Fig. 5b), and DHA-supplemented (Fig. 5c) cardiomyocytes. In the spectra some residual signals from EPA and DHA are present, indicating that some protons in PUFA chains are characterized by long transverse relaxation times T_2. Hence the chains are not only slowly diffusing (as is apparent from diffusion edited spectra) but also free to rotate. This situation is usually indicative of the presence of lipid bodies (LB) in the cell [24, 25, 27]. As reported above, the NMR data show that these lipids are essentially constituted by mobile TAG.

Analysis of the CPMG spectra shows that supplementation has no relevant effects on the profile of the small

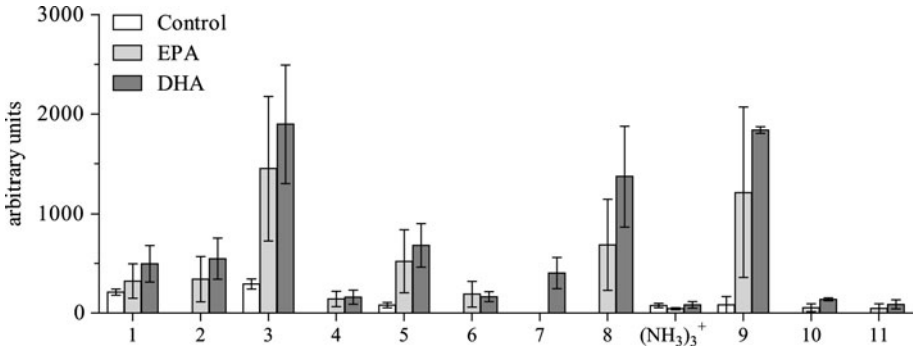

Fig. 4 Relative amount of lipid components from control, EPA and DHA-supplemented cardiomyocytes, as derived from integration of HR-MAS diffusion-edited spectra. The data are scaled relative to $-CH_3$, and reported as means ± SEM. Lipid components are labeled: *1*, $-CH_3$ (0.89 + 0.96 ppm); *2*, $-CH_3$ from EPA and DHA (0.96 ppm); *3*, acyl chain methylene- $(CH_2)_n$; *4*, CH_2–C–CO; *5*, CH_2C=C; *6*, CH_2CO (2.25 ppm); *7*, CH_2CO and CH_2–C–CO from DHA (2.33 ppm); *8*, =C–CH_2–C=; *9*, CH=CH; *10* and *11*, bonded glycerol (4.10 and 4.30 ppm)

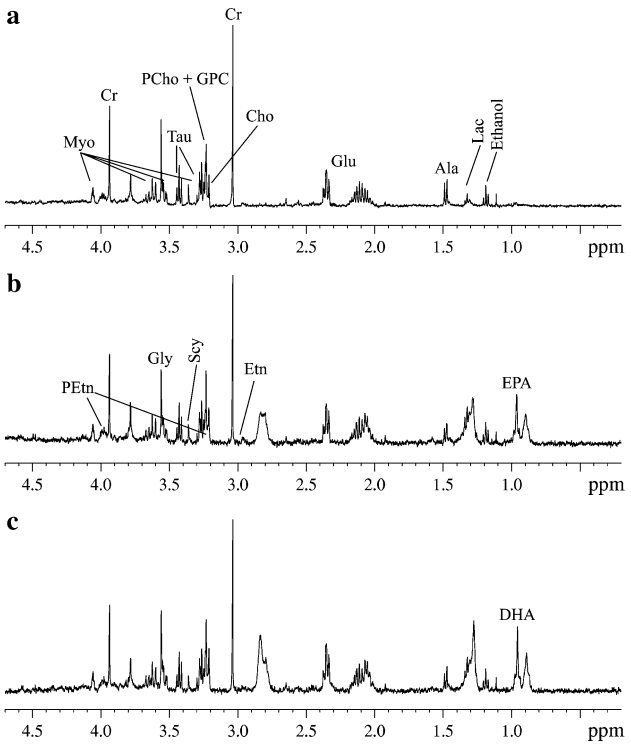

Fig. 5 CPMG ex-vivo HR-MAS ^{1}H NMR spectra of control (**a**), EPA-supplemented (**b**), and DHA-supplemented (**c**) cardiomyocytes. The major metabolites are labeled as in previous figures and: *Cho* choline, *Etn* ethanolamine, *GPC* glycerophosphocholine, *Lac* lactate, *PCho* phosphocholine

metabolites (polyols, osmolytes, and aminoacids). They were assigned by direct inspection of 1D and 2D spectra (COSY and TOCSY spectra, here not reported), and by comparison with literature data [28, 29]. The main metabolites detected by HR-MAS NMR in cardiomyocytes are ethanol, lactate (Lac), Ala, acetate (Ac), Glu, Cr, Tau, Gly, choline (Cho), ethanolamine (Etn), phosphocholine (PCho), glycerophosphocholine (GPC), Scy and Myo, PEtn, uridine-diphosphate (UDP), adenine, a trace of glutamine (Gln), and lysine (Lys).

GC

In the PL fraction (Fig. 6a), EPA supplementation of cardiomyocytes leads to enhancement of the relative molar content of both EPA itself and its metabolic elongation derivative docosapentaenoic acid (22:5n-3, DPA) [30]. No further conversion of n-3 DPA to DHA is detected. After DHA supplementation, the relative molar content of this FA increases, without any appreciable retroconversion to DPA or EPA. The increased incorporation of n-3 PUFA is accompanied by a decrease in the relative molar contents of palmitoleic (16:1n-7), oleic (18:1n-9), and arachidonic (20:4n-6, ARA) acids.

In the TAG fraction (Fig. 6b), EPA is not incorporated as itself but after conversion to its derivative DPA [30], whereas DHA is incorporated without any further metabolism. In both cases, a concomitant decrease in the relative molar content of saturated FA and ARA is detected.

The total amount of FA esterified in the PL fraction is lower in DHA-supplemented cells than in controls (Fig. 7a). In contrast, the small amount of FA esterified in the TAG fraction of control cells increases substantially after EPA and DHA supplementation, as shown in Fig. 7b.

Discussion

Cells contain a substantial amount of polar lipids, PL and C, and neutral lipids, for example TAG and CE. Taken together, these account for approximately 4–16% of total cell mass and approximately 20–50% of dry cell mass [31]. Although NMR is regarded as a universal detector, lipid ^{1}H NMR resonances are not always observed in tissues that

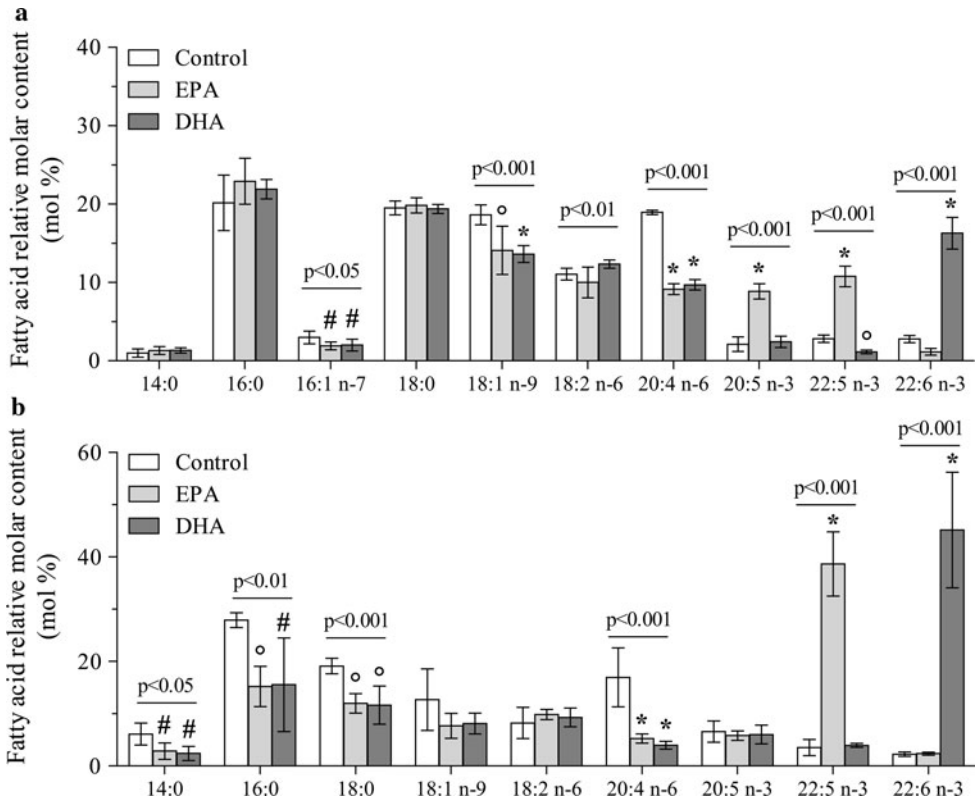

Fig. 6 Fatty acids composition of PL (**a**) and TAG (**b**) derived from control, EPA, and DHA-supplemented cardiomyocytes. Data are expressed as mol % and are means ± SD from at least three independent cell cultures. Statistical analysis was performed by one-way ANOVA (p values are shown above bars) with Tukey as post test comparing control and n-3 LC-PUFA-supplemented cells ($^{\#}p < 0.05$; $^{\circ}p < 0.01$; $^{*}p < 0.001$)

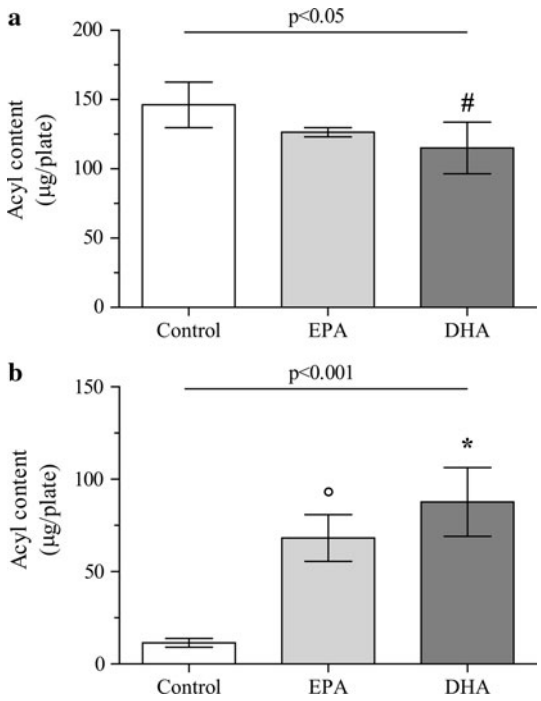

Fig. 7 Acyl content of PL (**a**) and TAG (**b**) derived from control, EPA, and DHA-supplemented cells. Data are expressed as µg/plate and are means ± SD from at least three independent cell cultures. Statistical analysis was performed by one way ANOVA (p values are shown above bars) with Tukey as post test comparing control and n-3 LC-PUFA-supplemented cells ($^{\#}p < 0.05$; $^{\circ}p < 0.01$; $^{*}p < 0.001$)

are rich in C and PL. This directly implies that ^{1}H NMR-visible lipids must have unique structural and biochemical properties that set them apart from the bulk of tissue lipids. This apparent paradox is resolved by considering the physical basis of NMR, which emphasizes the importance of sufficient molecular mobility in the immediate chemical environment for a given molecule to become detectable by NMR [27]. The first explanation of the contributions of mobile and non-mobile components to the NMR spectra of biological samples was reported in the key work on C-13 NMR by William et al. [32]. Much later, the important applications of MAS NMR to biological systems by the Oldfield [33] and Hamilton groups [34, 35] meticulously discriminated phase and molecules with different mobilities. Lipid resonances must arise from molecules with high molecular mobility. Because it is known that LC-PUFA is mainly incorporated into membrane PL, which do not significantly contribute to the NMR signal because of their rigid environment, we coupled GC analysis to NMR. As expected, the signal from PL is very weak in NMR analysis, irrespective of the experimental conditions, whereas GC analysis, besides detecting PL, shows that EPA and DHA supplementation causes substantial modification of PL FA composition. In several studies, the biological effects of n-3 LC-PUFA have been ascribed to the incorporation of these FA into PL into cellular membranes, where they may alter membrane fluidity and functionality,

and may affect cellular eicosanoid synthesis [36–39]. According to GC data, EPA and DHA are actively incorporated in the PL fraction, displacing ARA, the relative molar content of which is reduced by more than 50%. It is conceivable that the modifications occurring in PL after EPA and DHA supplementation could cause important changes not only in membrane structure, but also in membrane and cell functionality. The total amount of FA esterified in PL is reduced in DHA-supplemented cardiomyocytes (Fig. 7a). The larger packing free volume associated with LC-PUFA-rich membranes could explain in part the reduction of the acyl content in the PL fraction. In fact, in saturated or monounsaturated membranes the acyl chains pack quite uniformly whereas in membranes containing DHA the packing is distorted by the steric restrictions associated with a higher surface area of the FA [40]. As an alternative, DHA could have triggered a remodeling mechanism causing an increase in lyso-PL. Actually, DHA has been shown to alter cell membranes increasing the activation of phospholipase A2 [41].

The most important difference between control and n-3 LC-PUFA-supplemented cardiomyocytes highlighted by HR-MAS NMR spectroscopy is the increase of signals from mobile lipids, identified as TAG. Regarding TAG, two alternative sources of ^{1}H NMR-visible mobile lipid resonances have been proposed, i.e. membrane-associated globular microdomains [42, 43] and intracellular LB [44, 45]. Many in-vitro cell studies and in-vivo diffusion measurements have suggested the importance of LB as contributors to ^{1}H NMR-detectable lipid resonances [27, 44–46]. It is therefore conceivable that the observed increase of NMR-visible TAG in supplemented cells is associated with an enhanced presence of LB, as already reported for human cardiomyocytes [47]. The observed increase of mobile TAG could be a metabolic response to n-3 LC-PUFA supplementation, which leads to increased lipid storage. The increase in the total amount of FA incorporated in TAG, and the higher relative molar content of n-3 LC-PUFA in this fraction after supplementation, is confirmed by GC. Our results are in agreement with those of Finstad et al. [48], who observed an increase in the TAG content of monocytic U937-1 cells after treatment with 60 μM EPA. This TAG increase was accompanied by accumulation of LB.

The second hypothesis has been considered the more probable in recent years [49, 50]. The sequestration of mobile lipids in LB provides a deposit of stored energy that can be accessed in a regulated fashion according to metabolic need [51]. In particular, the myocardium stores FA, the major energy substrate for normal heart function, as TAG in LB [52].

Incorporation of n-3 LC-PUFA into TAG-rich LB could also be the basis for a yet unknown mechanism important for cell regulation. First, storage of FA in LB may function to protect the cells from exposure to high concentrations of FFA. Second, a TAG pool rich in LC-PUFA may be an important reservoir for signal molecules. Finstad et al. [48] suggested that EPA, DPA, and DHA, when liberated from an intracellular storage pool, affect intracellular signal transduction systems differently from when released from cellular PL. Furthermore, LC-PUFA stored as TAG in LB could be used for membrane PL synthesis. In the heart, the synthesis of PL to ensure membrane homeostasis is a priority that warrants the membrane depolarization that triggers cardiac contraction [52]. It is also possible that n-3 LC-PUFA stored in TAG may affect cardiomyocytes gene expression via PPAR-dependent signal pathways. We have already demonstrated that incubation of with 60 μM EPA and DHA alters the expression of different genes [53].

The accumulation of LB has been correlated with the reduction in cell number, inhibition of proliferation, and induction of apoptosis in monocytic U937-1 cells [48]. In a previous study in which neonatal rat cardiomyocytes were supplemented with the same EPA and DHA concentrations, we observed a modest increase in cell growth and no significant alteration in cell cycle distribution. Furthermore, n-3 LC-PUFA supplementation significantly protected cardiomyocytes from apoptosis [53]. The different cell type used in these studies might explain the different results, emphasizing that cell response to LC-PUFA supplementation can be very different.

The signals from C and, even more so, from CE are not detected in cardiomyocyte NMR spectra, probably because of their low mobility [54, 55]. Similarly, the TLC spot corresponding to CE was hardly detectable, irrespective of the supplementation. This is in agreement with Finstad et al. [56] who, supplementing different cell lines with labeled EPA, found only 1% of the FA was recovered in the CE fraction.

Regarding the small molecules, HR-MAS NMR metabolic characterization of cardiomyocytes reveals only negligible variations of the metabolic profile among differently treated cells. Indeed, the metabolome of unsupplemented and supplemented cells is characterized by the same small metabolites (mainly Ala, Lac, Ac, Glu, Cr, Tau, Gly, Cho, PCho, GPC, Scy, Myo, PEtn, Gln, UDP, adenine, and Lys) in almost the same relative ratios. N-3 LC-PUFA supplementation of neonatal rat cardiomyocytes causes a huge variation in the cell lipid environment, but negligible variation of the metabolome.

In conclusion, simultaneous use of ^{1}H HR-MAS NMR spectroscopy and GC furnishes information on the cell lipidome and metabolome. This work shows the complementary potential of these techniques. Furthermore, as far as we are aware this is the first report on changes in the lipid components of cardiomyocytes after n-3 LC-PUFA

supplementation. Understanding of the modification of the lipid environment is a further step toward clarification of the involvement of n-3 LC-PUFA in the prevention of cardiovascular disease.

Acknowledgments This study was supported by a grant of MIUR ex 60% to VT, SB and AB.

Conflict of interest The authors declare that there are no conflicts of interest.

References

1. Siddiqui RA, Shaikh SR, Sech LA, Yount HR, Stillwell W, Zaloga GP (2004) Omega 3-fatty acids: health benefits and cellular mechanisms of action. Mini Rev Med Chem 4:859–871
2. Jump DB (2002) Dietary polyunsaturated fatty acids and regulation of gene transcription. Curr Opin Lipidol 13:155–164. doi:10.1097/00041433-200204000-00007
3. Marik PE, Varon J (2009) Omega-3 dietary supplements and the risk of cardiovascular events: a systematic review. Clin Cardiol 32:365–372. doi:10.1002/clc.20604
4. von Schacky C (2003) The role of omega-3 fatty acids in cardiovascular disease. Curr Atheroscler Rep 5:139–145. doi:10.1007/s11883-003-0086-y
5. Engler MM, Engler MB (2006) Omega-3 fatty acids: role in cardiovascular health and disease. J Cardiovasc Nurs 21:17–24
6. Christie WW, Brechany EY, Shukla VK (1989) Analysis of seed oils containing cyclopentenyl fatty acids by combined chromatographic procedures. Lipids 24:116–120. doi:10.1007/BF02535247
7. Guo W, Hamilton JA (1996) 13C MAS NMR studies of crystalline cholesterol and lipid mixtures modeling atherosclerotic plaques. Biophys J 71:2857–2868. doi:10.1016/S0006-3495(96)79482-1
8. Forbes J, Husted C, Oldfield E (1988) High-field, high-resolution proton "magic-angle" sample-spinning nuclear magnetic resonance spectroscopic studies of gel and liquid crystalline lipid bilayers and the effects of cholesterol. J Am Oil Chem Soc 110:1059–1065. doi:10.1021/ja00212a010
9. Wishart DS (2005) Metabolomics: the principles and potential applications to transplantation. Am J Transplant 5:2814–2820. doi:10.1111/j.1600-6143.2005.01119.x
10. Nicholson JK, Lindon JC (2008) Systems biology: metabonomics. Nature 455:1054–1056. doi:10.1038/4551054a
11. Duarte IF, Marques J, Ladeirinha AF, Rocha C, Lamego I, Calheiros R, Silva TM, Marques MP, Melo JB, Carreira IM, Gil AM (2009) Analytical approaches toward successful human cell metabolome studies by NMR spectroscopy. Anal Chem 81:5023–5032. doi:10.1021/ac900545q
12. Yagev S, Heller M, Pinson A (1984) Changes in cytoplasmic and lysosomal enzyme activities in cultured rat heart cells: the relationship to cell differentiation and cell population in culture. In Vitro 20:893–898. doi:10.1007/BF02619662
13. Folch J, Lees M, Sloane Stanley GH (1957) A simple method for the isolation and purification of total lipids from animal tissues. J Biol Chem 226:497–509
14. Stoffel W, Chu F, Ahrens EH (1959) Analysis of long-chain fatty acids by gas–liquid chromatography. Micromethod for preparation of methyl esters. Anal Chem 31:307–308. doi:10.1021/ac60146a047
15. Bordoni A, Angeloni C, Leoncini E, Danesi F, Maranesi M, Biagi PL, Hrelia S (2005) Hypoxia/reoxygenation alters essential fatty acids metabolism in cultured rat cardiomyocytes: protection by antioxidants. Nutr Metab Cardiovasc Dis 15:166–173. doi:10.1016/j.numecd.2004.04.003
16. Schenetti L, Mucci A, Parenti F, Cagnoli R, Righi V, Tosi MR, Tugnoli V (2006) HR-MAS NMR spectroscopy in the characterization of human tissues: application to healthy gastric mucosa. Concepts Magn Reson Part A Bridg Educ Res 28A:430–443. doi:10.1002/cmr.a.20068
17. Price WS, Hayamizu K, Ide H, Arata Y (1999) Strategies for diagnosing and alleviating artifactual attenuation associated with large gradient pulses in PGSE NMR diffusion measurements. J Magn Reson 139:205–212. doi:10.1006/jmre.1999.1789
18. Meiboom S, Gill D (1958) Modified spin-echo method for measuring nuclear relaxation times. Rev Sci Instrum 29:688–691. doi:10.1063/1.1716296
19. Wu DH, Chen AD, Johnson CS (1995) An improved diffusion-ordered spectroscopy experiment incorporating bipolar-gradient pulses. J Magn Reson A 115:260–264. doi:10.1006/jmra.1995.1176
20. Jeener J (1971) Pulse pair techniques in high resolution NMR. Ampère International Summer School, Basko Polje
21. Aue WP, Bartholdi E, Ernst RR (1976) Two-dimensional spectroscopy. Application to nuclear magnetic resonance. J Chem Phys 64:2229–2246. doi:10.1063/1.432450
22. Bax A, Davis DG (1985) MLEV-17-based two-dimensional homonuclear magnetization transfer spectroscopy. J Magn Reson 65:355–360. doi 10.1016/0022-2364(85)90018-6
23. Braunschweiler L, Ernst RR (1983) Coherence transfer by isotropic mixing: Application to proton correlation spectroscopy. J Magn Reson 53:521–528. doi 10.1016/0022-2364(83)90226-3
24. Tugnoli V, Mucci A, Schenetti L, Righi V, Calabrese C, Fabbri A, Di Febo G, Tosi MR (2006) Ex vivo HR-MAS Magnetic Resonance Spectroscopy of human gastric adenocarcinomas: a comparison with healthy gastric mucosa. Oncol Rep 16:543–553
25. Subramanian A, Shankar Joshi B, Roy AD, Roy R, Gupta V, Dang RS (2008) NMR spectroscopic identification of cholesterol esters, plasmalogen and phenolic glycolipids as fingerprint markers of human intracranial tuberculomas. NMR Biomed 21:272–288. doi:10.1002/nbm.1191
26. Tugnoli V, Tosi MR, Tinti A, Trinchero A, Bottura G, Fini G (2001) Characterization of lipids from human brain tissues by multinuclear magnetic resonance spectroscopy. Biopolymers 62:297–306. doi:10.1002/bip.10005
27. Hakumaki JM, Kauppinen RA (2000) ^{1}H NMR visible lipids in the life and death of cells. Trends Biochem Sci 25:357–362. doi:10.1016/S0968-0004(00)01614-5
28. Fan TWM (1996) Metabolite profiling by one- and two-dimensional NMR analysis of complex mixtures. Prog Nucl Magn Reson Spectrosc 28:161–219. doi:10.1016/0079-6565(95)01017-3
29. Tugnoli V, Schenetti L, Mucci A, Parenti F, Cagnoli R, Righi V, Trinchero A, Nocetti L, Toraci C, Mavilla L, Trentini G, Zunarelli E, Tosi MR (2006) Ex vivo HR-MAS MRS of human meningiomas: a comparison with in vivo ^{1}H MR spectra. Int J Mol Med 18:859–869
30. Leonard AE, Pereira SL, Sprecher H, Huang YS (2004) Elongation of long-chain fatty acids. Prog Lipid Res 43:36–54. doi:10.1016/S0163-7827(03)00040-7
31. Bangham AD (1975) Cell membranes: biochemistry, cell biology and pathology. In: Weissmann G, Claiborne R (eds) Models of cell membranes, hospital practice. HP Publishing, New York, pp 24–34
32. Williams E, Hamilton JA, Jain MK, Allerhand A, Cordes EH, Ochs S (1973) Natural abundance carbon-13 nuclear magnetic resonance spectra of the canine sciatic nerve. Science 181:869–871. doi:10.1126/science.181.4102.869

33. Montez B, Oldfield E, Urbina JA, Pekerar S, Husted C, Patterson J (1993) Editing 13C-NMR spectra of membranes. Biochim Biophys Acta 1152:314–318. doi:10.1016/0005-2736(93)90263-Y
34. Peng S, Guo W, Morrisett JD, Johnstone MT, Hamilton JA (2000) Quantification of cholesteryl esters in human and rabbit atherosclerotic plaques by magic-angle spinning (13)C-NMR. Arterioscler Thromb Vasc Biol 20:2682–2688
35. Ruberg FL, Viereck J, Phinikaridou A, Qiao Y, Loscalzo J, Hamilton JA (2006) Identification of cholesteryl esters in human carotid atherosclerosis by ex vivo image-guided proton MRS. J Lipid Res 47:310–317. doi:10.1194/jlr.M500431-JLR200
36. Bruno MJ, Koeppe RE II, Andersen OS (2007) Docosahexaenoic acid alters bilayer elastic properties. Proc Natl Acad Sci USA 104:9638–9643. doi:10.1073/pnas.0701015104
37. Schmitz G, Ecker J (2008) The opposing effects of n-3 and n-6 fatty acids. Prog Lipid Res 47:147–155. doi:10.1016/j.plipres.2007.12.004
38. Catalá A (2009) Lipid peroxidation of membrane phospholipids generates hydroxy-alkenals and oxidized phospholipids active in physiological and/or pathological conditions. Chem Phys Lipids 157:1–11. doi:10.1016/j.chemphyslip.2008.09.004
39. Siener R, Alteheld B, Terjung B, Junghans B, Bitterlich N, Stehle P, Metzner C (2010) Change in the fatty acid pattern of erythrocyte membrane phospholipids after oral supplementation of specific fatty acids in patients with gastrointestinal diseases. Eur J Clin Nutr 64:410–418. doi:10.1038/ejcn.2009.151
40. Stillwell W, Wassall SR (2003) Docosahexaenoic acid: membrane properties of a unique fatty acid. Chem Phys Lipids 126:1–27. doi:10.1016/S0009-3084(03)00101-4
41. Bate C, Marshall V, Colombo L, Diomede L, Salmona M, Williams A (2008) Docosahexaenoic and eicosapentaenoic acids increase neuronal death in response to HuPrP82–146 and Abeta 1–42. Neuropharmacology 54:934–943. doi:10.1016/j.neuropharm.2008.02.003
42. Mountford CE, Wright LC (1988) Organization of lipids in the plasma membranes of malignant and stimulated cells: a new model. Trends Biochem Sci 13:172–177. doi:10.1016/0968-0004(88)90145-4
43. Mackinnon WB, May GL, Mountford CE (1992) Esterified cholesterol and triglyceride are present in plasma membranes of Chinese hamster ovary cells. Eur J Biochem 205:827–839. doi:10.1111/j.1432-1033.1992.tb16847.x
44. Barba I, Cabañas ME, Arús C (1999) The relationship between nuclear magnetic resonance-visible lipids, lipid droplets, and cell proliferation in cultured C6 cells. Cancer Res 59:1861–1868
45. Iorio E, Di Vito M, Spadaro F, Ramoni C, Lococo E, Carnevale R, Lenti L, Strom R, Podo F (2003) Triacsin C inhibits the formation of ^{1}H NMR-visible mobile lipids and lipid bodies in HuT 78 apoptotic cells. Biochim Biophys Acta 1634:1–14. doi:10.1016/j.bbalip.2003.07.001
46. Ferretti A, Knijn A, Iorio E, Pulciani S, Giambenedetti M, Molinari A, Meschini S, Stringaro A, Calcabrini A, Freitas I, Strom R, Arancia G, Podo F (1999) Biophysical and structural characterization of ^{1}H-NMR-detectable mobile lipid domains in NIH-3T3 fibroblasts. Biochim Biophys Acta 1438:329–348. doi:10.1016/S1388-1981(99)00071-2
47. Paul A, Chan L, Bickel PE (2008) The PAT family of lipid droplet proteins in heart and vascular cells. Curr Hypertens Rep 10:461–466. doi:10.1007/s11906-008-0086-y
48. Finstad HS, Drevon CA, Kulseth MA, Synstad AV, Knudsen E, Kolset SO (1998) Cell proliferation, apoptosis and accumulation of lipid droplets in U937–1 cells incubated with eicosapentaenoic acid. Biochem J 336(Pt 2):451–459
49. Quintero M, Cabañas ME, Arús C (2007) A possible cellular explanation for the NMR-visible mobile lipid (ML) changes in cultured C6 glioma cells with growth. Biochim Biophys Acta 1771:31–44. doi:10.1016/j.bbalip.2006.10.003
50. Luciani AM, Grande S, Palma A, Rosi A, Giovannini C, Sapora O, Viti V, Guidoni L (2009) Characterization of ^{1}H NMR detectable mobile lipids in cells from human adenocarcinomas. FEBS J 276:1333–1346. doi:10.1111/j.1742-4658.2009.06869.x
51. Martin S, Parton RG (2006) Lipid droplets: a unified view of a dynamic organelle. Nat Rev Mol Cell Biol 7:373–378. doi:10.1038/nrm1912
52. Gambert S, Helies-Toussaint C, Grynberg A (2005) Regulation of intermediary metabolism in rat cardiac myocyte by extracellular glycerol. Biochim Biophys Acta 1736:152–162. doi:10.1016/j.bbalip.2005.08.004
53. Bordoni A, Astolfi A, Morandi L, Pession A, Danesi F, Di Nunzio M, Franzoni M, Biagi P (2007) N-3 PUFAs modulate global gene expression profile in cultured rat cardiomyocytes. Implications in cardiac hypertrophy and heart failure. FEBS Lett 581:923–929. doi:10.1016/j.febslet.2007.01.070
54. Guo W, Kurze V, Huber T, Afdhal NH, Beyer K, Hamilton JA (2002) A solid-state NMR study of phospholipid-cholesterol interactions: sphingomyelin-cholesterol binary systems. Biophys J 83:1465–1478. doi:10.1016/S0006-3495(02)73917-9
55. Husted C, Montez B, Le C, Moscarello MA, Oldfield E (1993) Carbon-13 "magic-angle" sample-spinning nuclear magnetic resonance studies of human myelin, and model membrane systems. Magn Reson Med 29:168–178. doi:10.1002/mrm.1910290204
56. Finstad HS, Dyrendal H, Myhrstad MC, Heimli H, Drevon CA (2000) Uptake and activation of eicosapentaenoic acid are related to accumulation of triacylglycerol in Ramos cells dying from apoptosis. J Lipid Res 41:554–563

Lipids (2011) 46:637–645
DOI 10.1007/s11745-011-3557-x

ORIGINAL ARTICLE

Fish Oil Supplementation During Lactation: Effects on Cognition and Behavior at 7 Years of Age

Carol L. Cheatham · Anne Sofie Nerhammer · Marie Asserhøj · Kim F. Michaelsen · Lotte Lauritzen

Received: 4 March 2011 / Accepted: 23 March 2011 / Published online: 22 April 2011

Abstract Early accumulation of n-3 long-chain PUFA (LCPUFA) in the brain may contribute to differences in later cognitive abilities. In this study, our objective was to examine whether fish oil (FO) supplementation during lactation affects processing speed, working memory, inhibitory control, and socioemotional development at 7 years. Danish mothers ($n = 122$) were randomized to FO [1.5 g/d n-3 LCPUFA] or olive oil (OO) supplementation during the first 4 months of lactation. The trial also included a high-fish intake (HFI) reference group ($n = 53$). Ninety-eight children were followed-up with an assessment of processing speed, an age-appropriate Stroop task, and the Strength and Difficulties Questionnaire at 7 year. A group effect of the intervention (FO vs. OO) was found in prosocial behavior scores; this negative effect was carried by the boys. Exploratory analyses including all participants revealed the speed of processing scores were predicted by maternal n-3 LCPUFA intake during the intervention period (negative relation) and maternal education (positive relation). Stroop scores indicative of working memory and inhibitory control were predicted by infant erythrocyte DHA status at 4 months of age (negative relation). Early fish oil supplementation may have a negative effect on later cognitive abilities. Speed of processing and inhibitory control/working memory are differentially affected, with speed of processing showing effects of fish oil intake as a whole, whereas inhibitory control/working memory was related more specifically to DHA status.

Keywords n-3 Polyunsaturated fatty acids · Intervention · Cognition · Executive function · Programming

Abbreviations

EPA	Eicosapentaenoic acid
DHA	Docosahexaenoic acid
LCPUFA	Long-chain polyunsaturated fatty acids
RBC	Red blood cell
RCT	Randomized control trial
SDQ	Strength and Difficulties Questionnaire

Introduction

Long-chain n-3 polyunsaturated fatty acids (n-3 LCPUFA) are accumulated in the central nervous system during early life and are thought to play an important role in the proper function and development of the brain and retina [1, 2]. Early intake of n-3 LCPUFA has been shown to affect the development of visual acuity in both preterm and term infants [3, 4], but its effect on mental function is less well established [5]. Recent reviews of randomized controlled trials (RCT) conclude that further studies are needed to determine if early intake of n-3 LCPUFA is associated with changes in cognitive or behavioral performance [6, 7]. Moreover, the optimal intake of n-3 LCPUFA during early life is not yet known [2].

Breastfeeding has been shown to confer a long-term advantage in cognitive performance in meta-analyses [8],

C. L. Cheatham
Department of Psychology, University of North Carolina at Chapel Hill, Chapel Hill, NC, USA

A. S. Nerhammer · M. Asserhøj · K. F. Michaelsen · L. Lauritzen (✉)
Department of Human Nutrition of Life Sciences, University of Copenhagen, Rolighedsvej 30, 1958 Frederiksberg, Denmark
e-mail: ll@life.ku.dk

and studies has shown that the advantage is dependent on both maternal and infant genotypes at certain single nucleotide polymorphisms on the fatty acid desaturase gene complex (FADS1/FADS2) indicating that this is at least partly due to LCPUFA [9, 10]. Maternal supplementation studies have been performed to examine if variations in maternal n-3 LCPUFA intake can affect functional outcomes in the infants. Researchers observed improved mental processing scores at 4 years of age in children of mothers who were supplemented with fish oil during pregnancy and lactation [11]. Sequential processing at 7 years of age was related to alpha-linolenic acid (18:3n-3) and docosahexaenoic acid (DHA, 22:6n-3) levels in maternal plasma during pregnancy [12]. Perinatal plasma DHA status as measured in cord blood has also been found to be significantly negatively correlated with internalizing problem behavior at 7 years of age [13]. Moreover, scientists who conducted a large cohort study found positive associations between maternal intake of marine foods and verbal IQ measured at 8 years of age [14]. Thus, maternal fatty acid status may have long-lasting effects on the cognitive abilities of the offspring.

Conceptually, fish oil supplementation during pregnancy and lactation, which are critical periods for brain development, should affect subsequent cognitive development as DHA is implicated in many neural processes. DHA is involved in synaptogenesis and maturation of the synapses [15] and neuronal membrane structure and function [16]. Importantly, there is direct evidence that the presence of DHA increases processing speed at the membrane [17]. Speed of processing, a basic cognitive process which underlies all cognitive functioning, can be defined as the time required to move information from one neuron to the next, and it is reasonable to hypothesize that DHA will have an effect on speed of processing.

Higher, more complex, cognitive processes are subserved by the frontal lobes, which have a high concentration of DHA [18]. The frontal lobes and the cognitive functions that they support show a protracted development reaching functional maturity at 12–15 months of age and continuing to develop into adolescence [19]. Moreover, dopamine, an important modulator of higher-order cognitive functions [20], has been shown to be low in the frontal lobes when DHA is low [21]. Thus, it is reasonable to posit that DHA status will be related to the higher-order functions subserved by the frontal lobes. Cognitive abilities thought to be early precursors of the higher-order functions, such as means-end problem solving, begin to emerge at the end of the first year of life and have been shown to be related to DHA levels [22]. However, higher-order cognitive functions such as working memory and inhibitory control cannot be reliably tested until children reach 3–5 years of age.

Socioemotional behaviors related to higher-order cognition such as hyperactivity and inattention have been studied in relation to differences in LCPUFA status [23]. Treatment with n-3 LCPUFA has been found to ameliorate the symptoms of attention deficit hyperactivity disorder [24]. It is not known whether improved LCPUFA status early on is related to the differences in socioemotional behavior in typically developing children. In one study, scientists reported that higher n-3 LCPUFA status in children was related positively to prosocial behavior and negatively to inattention, emotional difficulties, and hyperactivity [25]. However, it is not known whether maternal n-3 LCPUFA status is similarly related.

Here we report the results of a follow-up of an RCT in which lactating mothers were supplemented with either fish oil or olive oil for the first 4 months of their infants' lives [26, 27]. The aim was to investigate whether maternal n-3 LCPUFA intake during lactation had an effect on socioemotional functioning, as assessed by the Strength and Difficulties Questionnaire (SDQ), and cognition, specifically speed of processing, working memory, and inhibitory control, when the children were 7 years of age. The results indicated no group effects of the early intervention on cognitive scores at 7 years of age, but exploratory model building using continuous biochemical markers revealed that maternal n-3 LCPUFA intake was negatively related to speed of processing, and the DHA content of infant erythrocytes was negatively related to working memory/inhibitory control scores. Regarding the socioemotional scores, there was a group effect of the intervention on the prosocial score. Post hoc analyses revealed this negative relation was carried by the boys.

Methods

Participants and Intervention

The trial and its follow-up studies at 2.5 and 7 years were approved by the Scientific-Ethical Committees for Copenhagen and Frederiksberg (KF 01-300/98, KF 01-183/01 and KF 11321572, respectively). The RCT was by design double-blinded throughout the intervention period and the researches were blinded at both the 2.5 and 7 year follow-ups, but the participants and their parents were not. Both parents of the child gave written consent to participate in the 7 year follow-up after the study had been explained to at least one of them orally, as well as in writing.

The participating mothers were recruited during pregnancy from the Danish National Birth Cohort during December 1998–November 1999. The dietary intake of the mothers in the Danish National Birth Cohort was determined in the 25th week of pregnancy using a food

frequency questionnaire as described by Olsen and colleagues [28]. Women in the 36th week of pregnancy living in the greater Copenhagen area and having a fish intake below population median (fish intake of 12.3 ± 8.2 g/d and less than 0.40 g/d of n-3 LCPUFA) were asked to participate in the trial as a low fish group. Women with a fish intake in the highest quartile of the population (fish intake of 55.2 ± 26.7 g/d or 0.82 g/d of n-3 LCPUFA) were also asked to participate in the trial as a high fish intake reference group (HFI group). One hundred and twenty-two women with a low fish intake and 53 with a high fish intake were accepted to participate in the trial. The trial is described in detail elsewhere [26].

After the birth of their children, the women in the low fish intake group were randomly assigned to one of two supplementation groups with stratification according to mean parental education: an experimental group receiving fish oil (FO) supplement and a control group receiving an equal amount of olive oil (OO) supplement as described previously [26]. Both supplements were given as microencapsulated oils (from BASF Health and Nutrition A/S, Ballerup, Denmark) incorporated and concealed in müsli bars (produced by Halo Foods Ltd., Tywyn Gwynedd, Wales, United Kingdom) or home baked cakes (ordinary capsules were given as an alternative if the women disliked the dishes). The supplement levels in the FO group were intended to match the intake of the HFI reference group. The FO supplement supplied the women with 4.5 g/d fish oil containing 1.5 g/d of *n*-3 LCPUFA, of which 0.62 g was eicosapentaenoic acid (EPA, 20:5n-3) and 0.79 g was DHA. Throughout the 4 month intervention, the mean self-reported compliance, expressed as the percentage of oil consumed relative to the intended dose was in both groups 88% (SD = 9%, $n = 99$). Of the 150 women who completed the supplementation period, 107 mothers fulfilled the criterion of exclusive breastfeeding during the 4 months. The children who were partially breastfed were not excluded from the study, but the degree of breastfeeding was taken into account in the analysis of the results [26].

The n-3 LCPUFA intakes of the mothers were determined at recruitment and at the 2, 4, and 9 month visit by food frequency questionnaires of fish intake [26] and the diet of the children was determined at 2.5 [29] and 7 years of age [30]. Breastmilk was collected at 9 days and 2, 4, and 9 months of age. Additionally, a blood sample was collected from the mother at recruitment and at the end of the intervention and from the infant at 4 months of age in order to measure the biochemical effect of the intervention by analyzing the fatty acid composition of the red blood cells [26].

All the children who participated in the 9 month follow-up visit ($n = 149$) were invited to participate in the 7 year follow-up study. Nine of the children were lost to follow-up due to lack of contact. Ten participants were excluded because they were living outside Zealand, one child was excluded due to a broken leg, and 31 did not wish to participate. Thus, 98 children participated in the 7 year follow-up study. The characteristics of these children are given in Table 1.

Cognitive and Socioemotional Assessments

Means-End Problem Solving at 9 Months

The effects of the intervention on the mental development of the infants were tested with a means-end problem solving task at 9 months of age (36.6–40.6 weeks) as previously reported [27]. In short, the means-end problem solving ability was assessed with The Infant Planning Test

Table 1 Characteristics of the participants

	High fish	Olive oil	Fish oil
Children included *(n)*	34	28	36
Sex ratio in group (M:F)[b]	18:16	12:16	24:12
Age at follow-up (years)[c]	7.3, 6.9–7.6 (34)	7.3, 6.8–7.7 (28)	7.4, 6.9–7.8 (36)
Birth weight (kg)[a]	3.7 ± 0.5 (34)	3.6 ± 0.4 (28)	3.7 ± 0.4 (36)
Birth length (cm)[c]	52.5, 50.0–55.5 (34)	52.0, 49.9–55.1 (28)	52.0, 50.0–55.3 (36)
Head circumference at birth (cm)[a]	36.1 ± 1.6 (33)	35.7 ± 1.3 (25)	36.0 ± 1.2 (33)
Degree of breastfeeding during the 4-month intervention *(%)*[c]	100, 86–100 (34)	100, 97–100 (28)	100, 35–100 (26)

[a] Values are given as means ± SD (*n*). Differences between groups are tested with a Student *t* test when comparing the two randomized groups and with an ANOVA when comparing all three groups

[b] Values are given as a ratio. Differences between groups are tested with a χ^2 test

[c] Data are not normally distributed. Values are given as median, 10th–90th percentile (*n*). Differences between the two randomized groups were tested with the Mann–Whitney *U* test and differences between all three groups were tested with a Kruskall–Wallis test

designed by Willatts [31] by one trained tester (72.5%) or in her absence, by one of two trained tester stand-ins (17.2 and 10.3%). The infant was presented with the same two-step problem multiple times (3.7 ± 1.8 presentations; equal in the three groups). All trials were recorded on videotape, and two trained observers scored the behavior independently. Two outcome measures were coded: scores on individual problems (0–6 points) and percent of intentional solutions (defined as problems solved with a score of at least one in all single score parameters or a minimum score of 6). Successful results on the problem-solving test were obtained for 89% of the tested children ($n = 122$ of 138; 14 refused, 2 video malfunctions).

Speed of Information Processing Test at 7 Years

Speed of processing was assessed using a subtest of the Woodcock Johnson Tests of Cognitive Abilities III® [32]. Participants were presented with a page of pictures of puppies, balls, and cups in random order. They were instructed to work as quickly as possible and to circle all instances where the picture of the ball was followed immediately by a picture of a puppy. They were given 3 min to complete the task: there were 69 possible pairs. Scoring was a simple count of correct pairs divided by the expected number of correct pairs for the specific age of the participant.

Higher-Order Cognitive Functioning Test at 7 Years of Age

Working memory and inhibitory control were tested using an age-appropriate day/night Stroop task as described in Archibald and Kerns [33]. The Stroop task requires the participant to inhibit a prepotent response and respond according to a rule held in working memory. Participants were presented with a booklet of pages populated with pictures of suns and moons. For the first phase, they were instructed to quickly say "sun" when they saw a picture of a sun and "moon" when they saw a picture of a moon. After 45 s, the administrator said to stop. For the second phase, they were instructed to say "moon" when they saw a picture of a sun and "sun" when they saw a picture of a moon. The Stroop score was computed as an interference score (difference between # correct in Phase 2 and # correct in Phase 1 divided by the # correct in Phase 1).

Strengths and Difficulties Questionnaire (SDQ) at 7 Years of Age

Caregivers completed the SDQ revised for Danish speakers [34]. The SDQ elicits ratings of 25 behaviors on a 3-point scale (not true, somewhat true, or certainly true). Behaviors include things such as "Considerate of other people's feelings" and "Often loses temper". Items were combined to yield sub-scale scores for Emotional Symptoms, Conduct Problems, Hyperactivity, Peer Problems, and Prosocial Behavior. All sub-scale scores except Prosocial Behavior were added together to yield the Total Difficulties Score.

Statistics

All cognitive data were normally distributed and met all assumptions for analyses. To assess the validity of the measures (i.e. continuity in cognitive abilities), 7 year speed of processing scores, 7 year Stroop scores, 9 month means-end problem solving, and 9 month means-end intentional solutions were entered into a bivariate correlation analysis. In addition, correlations between cognitive measures and socioemotional behavior (SDQ scores) were evaluated.

To test the efficacy of the intervention on cognitive abilities at 7 years of age, speed of processing scores and Stroop scores were entered in a multivariate analysis of variance (MANOVA) by RCT groups (FO and OO). The SDQ data were analyzed by non-parametric tests (Mann–Whitney U test) as these variables tended to be limited to a few distinct values. The HFI group was not included in these analyses in accordance with the trial design.

To explore individual differences in the cognitive outcomes as they related to the continuous biochemical data, we undertook model-building analyses subsequent to the trial analyses that included all the participants (HFI, FO, and OO). First, each independent variable was regressed onto the set of remaining independent variables to test for multicollinearity issues as described by Lewis-Beck [35]. Using the criterion of $r^2 < 0.80$, it was determined that maternal RBC–DHA and breastmilk DHA accounted for significant variance in the other independent variables. Thus, maternal RBC–DHA and breastmilk DHA were not considered in further analyses. Variables determined to be independent variables and thus, utilized in the model-building analyses were infant RBC–DHA (FA%) at 4 months, weighted infant DHA intake (breastmilk DHA content x% of total nutrition that was from breastmilk), and mean maternal intake of DHA during intervention period (g/d; includes intake from intervention supplement plus daily intake related to lifestyle). Maternal education was used as a proxy for socio-economic factors. Data were entered into regression analyses using backward elimination. Using the same independent variables (infant RBC–DHA at 4 months, weighted infant DHA intake, and mean maternal intake of n-3 LCPUFA), backward elimination was used to predict the individual sub-scale and total scores from the SDQ.

Results

Randomized Controlled Trial Analyses (Only FO and OO Groups)

The cognitive scores at 7 years of age in the two randomized groups (OO and FO) and the HFI-reference group are shown in Table 2. There were no group differences between the randomized groups with respect to the speed of processing score [$F(1, 62) = 0.777$, ns] or the Stroop score [$F(1, 61) = 0.302$, ns]. Given that degree of breastfeeding was not controlled, we repeated the analyses controlling for the weighted infant intake. The results did not change. There were also no significant group differences (between FO and OO) in the socioemotional behavior data from the SDQ (see Table 3) although the Prosocial score tended to be higher in the control group [$Z(62) = -1.796$, $p < 0.10$]. Post hoc analyses revealed this effect was carried by the boys and in fact, was significant when analyses included only the boys [$Z(35) = -2.264$, $p < 0.05$].

Correlations Between Cognitive and Behavioral Scores Across and Within Ages (FO and OO Groups)

Across ages, the 9 month means-end intentional solution scores were correlated with the 7 year speed of processing scores [$r(56) = 0.281$, $p = 0.03$]. No relation was found between means-end intentional solutions at 9 months and working memory/inhibitory control, as measured by the Stroop score at 7 years of age [$r(55) = -0.02$, ns]. However, intentional solution scores were related to the aspect of the Stroop task that relies directly on speed of processing (number of correct responses when asked to say sun when the picture was a sun) [$r(56) = 0.335$, $p = 0.01$]. Because degree and length of breastfeeding were not controlled in the intervention, analyses were repeated partialling out the weighted infant intake variable. The same pattern of significance was found. Means-end scores were also positively related to the Prosocial score [$r(54) = 0.261$, $p < 0.05$], but not to any other SDQ scores.

Within ages, speed of processing scores were not related to the Stroop interference score, but as one would expect, were related to the individual aspects of the Stroop task (i.e. sun = sun and sun = moon) [$r(63) = 0.285$, $p = 0.02$ and $r(62) = 0.309$, $p = 0.01$, respectively]. Also as expected, processing speed was negatively related to the Emotional score [$r(61) = -0.247$, $p = 0.05$] and Total Difficulties score [$r(61) = -0.272$, $p = 0.03$], whereas the Stroop scores were negatively related to the Hyperactivity score [$r(61) = -0.343$, $p = 0.007$], Conduct score [$r(61) = -0.392$, $p = 0.002$], and Total Difficulties score [$r(61) = -0.357$, $p = 0.005$]. When analyses were repeated partialling out weighted infant DHA intake, the relations remained.

Exploratory Analyses of Prediction by the Continuous Biomarkers (FO, OO, and HFI groups)

Bivariate correlations between the variables used in the exploratory analyses are provided in Table 4. When predicting the speed of processing scores, one multiple regression model was significant: predictors were total maternal n-3 LCPUFA intake [$t(72) = -1.98$, $p = 0.05$], and maternal education [$t(72) = 2.13$, $p = 0.04$]. This model accounted for 9% of the variance in the speed of processing scores. For the Stroop interference scores, the best model included only infant RBC–DHA [$t(72) = -2.23$, $p = 0.05$]. This model accounted for 7% of the variance in the Stroop interference scores. In the model-building undertaken to explore the effects of the biological markers on socioemotional behavior as measured by the SDQ, no variable predicted the Prosocial, Emotional, Hyperactivity, or Conduct sub-scores. However, maternal education predicted the Peer Problems sub-score [$t(72) = -2.04$, $p = 0.04$], and Total Difficulties [$t(72) = -2.32$, $p = 0.02$], accounting for 6% and 7% of the variance, respectively.

Table 2 Description of the cognitive test scores at 7½ years and biological markers in the two randomized groups (OO and FO) and the reference group (HFI)

Mean ± SD (*n*)	High fish	Olive oil	Fish oil
Standardized speed of processing	1.08 ± 0.27 (32)	1.02 ± 0.26 (27)	0.96 ± 0.26 (36)
Stroop scores	−0.19 ± 0.13 (32)	−0.21 ± 0.10 (28)	−0.23 ± 0.14 (35)
Maternal education[a]	5.34 ± 1.26 (32)	5.43 ± 1.17 (28)	5.39 ± 1.10 (36)
Maternal n-3 LCPUFA intake (g/dg)	0.93 ± 0.48 (32)	0.26 ± 0.19 (28)	1.59 ± 0.32 (35)
Infant DHA intake (FA%)	0.74 ± 0.34 (32)	0.42 ± 0.23 (28)	1.22 ± 0.52 (33)
Infant RBC–DHA at 4 months (FA%)	7.30 ± 1.60 (29)	6.49 ± 1.52 (25)	9.04 ± 1.79 (23)

[a] Official Danish Classification of Educations from 1994 (1 = primary school and 8 = Ph.D. from university). The rank of 5 is equivalent to a category of parental education ≥14 years, the rank of 4 to 12–13 years, the rank of 3 to 11 years, the rank of 2 to 9–10 years and the rank of 1 to ≤8 years of education

Table 3 Description of the SDQ scores at 7½ years in the two randomized groups (OO and FO) and the reference group (HFI) (Panel A) and scores by gender (Panel B)

Panel A mean ± SD (min–max)	High fish $n = 30$	Olive oil $n = 28$	Fish oil $n = 34$	Fish oil versus olive oil[a] p
Prosocial score	8.7 ± 1.2 (6.0–10.0)	8.3 ± 1.7 (4.0–10.0)	7.6 ± 1.7 (3.0–10.0)	0.072
Hyperactivity score	2.3 ± 2.0 (0.0–8.0)	1.9 ± 2.1 (0.0–8.0)	2.6 ± 2.0 (0.0–8.0)	0.126
Emotional score	1.7 ± 1.6 (0.0–6.0)	1.0 ± 1.2 (0.0–5.0)	1.4 ± 1.3 (0.0–5.0)	0.202
Conduct score	0.8 ± 1.0 (0.0–4.0)	1.0 ± 1.0 (0.0–3.0)	1.1 ± 1.0 (0.0–4.0)	0.608
Peer problems score	0.4 ± 0.9 (0.0–4.0)	0.8 ± 1.1 (0.0–3.0)	0.0 ± 1.3 (0.0–5.0)	0.922
Total difficulties	5.1 ± 3.7 (1.0–17.0)	4.6 ± 3.7 (0.0–15.0)	5.9 ± 3.3 (0.0–13.0)	0.111

Panel B median (10th–90th %ile)	High fish		Olive oil		Fish oil		Fish oil versus Olive oil[a]		Girls versus boys[a]
	Girls	Boys	Girls	Boys	Girls	Boys	p_{girls}	p_{boys}	p
Prosocial score	9.0 (7.0–10.0)	9.0 (6.6–10.0)	8.5 (4.7–10.0)	9.0 (4.9–10.0)	9.0 (6.0–10.0)	7.0 (5.0–9.0)	0.761	0.024	0.108
Hyperactivity score	1.0 (0.0–3.4)	2.0 (0.0–7.4)	1.5 (0.0–4.3)	1.5 (0.0–7.4)	1.0 (0.0–4.8)	2.0 (0.4–6.0)	0.960	0.133	0.011
Emotional score	1.0 (0.0–3.0)	2.0 (0.0–5.4)	1.0 (0.0–3.0)	1.0 (0.0–4.1)	2.0 (0.0–4.6)	1.0 (0.0–3.0)	0.104	0.742	0.910
Conduct score	0.0 (0.0–2.0)	1.0 (0.0–2.8)	1.0 (0.0–2.3)	1.0 (0.0–3.0)	1.0 (0.0–2.0)	1.0 (0.0–2.6)	0.236	0.637	0.119
Peer problems score	0.0 (0.0–2.8)	0.0 (0.0–1.0)	0.5 (0.0–3.0)	0.0 (0.0–2.7)	0.0 (0.0–2.8)	0.0 (0.0–3.0)	0.706	0.553	0.222
Total difficulties	4.0 (1.0–7.4)	5.0 (2.0–15.8)	4.0 (0.0–10.0)	4.0 (1.0–13.5)	5.0 (0.6–9.8)	5.0 (2.0–11.8)	0.427	0.256	0.150

[a] Comparisons by Mann–Whitney U test

Discussion

To our knowledge, this is the first report of a direct assessment of executive functions in 7-year-olds from an early intervention RCT. No group effect of the intervention was evident in the speed of processing, inhibitory control, and working memory abilities of 7-year-olds whose mothers were supplemented with DHA during the first 4 months of breastfeeding. However, there was a trend in the behavioral data for the group whose mothers consumed fish oil to have lower prosocial scores relative to the OO group; this effect was carried by the boys. These results are consistent with the reported results at 9 months and at 1–2 years in this sample. No differences were found between groups on the means-end task at 9 months of age [27]. Importantly, lower language comprehension scores found in the FO group relative to the OO group at one year of age were also found to be specific to the boys. This decrement in language comprehension at 1 year by the boys in the FO group may account for the lower Prosocial scores in the same boys: perceived pro-sociality is related to language abilities [36]. It is not clear from these data why early maternal fish oil intake would have a negative effect on prosocial development in boys.

Exploratory analyses revealed a negative relation between total maternal n-3 LCPUFA intake (intervention supplement plus background diet) during the intervention period and speed of processing scores: the higher the early intake, the lower the speed of processing scores. Level of maternal education was a positive predictor of speed of processing scores. Stroop scores, which are indicative of working memory and inhibitory control, were negatively related to infant RBC–DHA levels. The differential prediction of cognitive abilities by maternal and infant biomarkers may be attributed to the differences between the predictors themselves: maternal intake is a measure of whole food fatty acid intake (fish and fish oil), whereas the infant status reflects only DHA. Therefore, it is possible that speed of processing relies on more than just DHA for optimal functioning. Conceptually, it is feasible as speed of processing is a ubiquitous function occurring in whole brain; working memory and inhibitory control may be more specific to frontal lobe function where DHA levels are reported the highest in the brain. Moreover, a study of the effect of fish consumption on breastmilk revealed that maternal intake results in significant differences in EPA and docosapentaenoic acid (22:5n-3) as well as DHA [37]. Further research is needed to explore the potential effects of these n-3 LCPUFA on speed of processing.

Our data indicate continuity in some of the tested cognitive abilities, as the scores of the means-end task administered at 9 months of age in this sample were correlated with the speed of processing scores obtained at

Table 4 Bivariate correlations between variables used in exploratory analyses

	Speed of processing	Stroop	Peer problems	Conduct	Emotional	Hyper-activity	Prosocial	Total difficulties
Maternal education								
r[a]	0.210[b]	−0.059	−0.196[c]	−0.074	−0.059	−0.199[c]	−0.056	−0.200[c]
p	0.041	ns	0.058	ns	ns	0.055	ns	0.054
n	95	95	94	94	94	94	94	94
Infant RBC–DHA at 4 months (FA%)								
r	−0.099	−0.226[b]	−0.029	−0.001	0.077	−0.69	−0.123	0.057
p	ns	0.050	ns	ns	ns	ns	ns	ns
n	76	76	76	76	76	76	76	76
Maternal n-3 LCPUFA intake 0–4 months (g/d)								
r	−0.127	−0.074	−0.044	−0.088	0.195	−0.001	−0.112	0.068
p	ns	ns	ns	ns	ns	ns	ns	ns
n	94	94	91	91	91	91	91	94
Weighted infant DHA intake								
r	−0.077	−0.013	0.092	−0.181[c]	0.032	−0.093	−0.055	−0.017
p	ns	ns	ns	0.086	ns	ns	ns	ns
n	92	92	91	91	91	91	91	91

[a] Pearson for the Gauss distributed variables and Spearman for the SDQ-data

[b] Significant at the 0.05 level (2-tailed)

[c] Significant at the 0.10 level (2-tailed)

7 years of age. The means-end task is a problem-solving assessment that has been considered by some to be an early indication of executive function abilities [38]. However, we found that the 9 month scores were not related to the 7 year executive functions working memory and inhibitory control, but rather were related only to 7 year speed of processing. Working memory and inhibitory control are late-emerging abilities. It is possible that the precursor abilities related to working memory and inhibitory control that are present at 9 months of age are not necessary in the successful completion of a means-end problem. Nonetheless, the relation between means-end problem solving at 9 months of age and speed of processing at 7 years of age is evidence that the children's general underlying cognitive abilities were continuous throughout the follow-up years. Thus, our outcome measures are valid.

Importantly, the 9 month cognitive scores were not significantly related to the continuous n-3 LCPUFA intervention variables. Thus, the negative relation between the early RBC–DHA levels and cognitive abilities was not evident in this sample previous to the 7 year assessment. One could speculate that early intervention with DHA presents an environmental "mismatch" between prenatal and postnatal life that may be detrimental to the organism [39, 40] over time. However, given the small effect size (0.06–0.09), it is premature to speculate from these data. Conclusions regarding these negative relations between early intake/status and later cognitive functions (specifically speed of processing, working memory, and inhibitory control) cannot be confidently drawn from these data alone and certainly, replication will be necessary.

The intervention in the first 4 months of life did not have an effect on cognitive abilities at 7 years of age. There is much discussion in the literature as to the optimal timing of n-3 LCPUFA supplementation. Importantly, DHA should be present during critical periods of brain development to exact a measurable effect [41]. Thus, it is possible that an intervention during the first 4 months of life was not appropriate timing given the outcomes assessed. Indeed, the period of most rapid frontal lobe development is toward the end of the first year of life [42]. An n-3 LCPUFA intervention during this period might have a more measurable effect on executive functions.

The reported study has many strengths including randomization and the inclusion of a high fish intake reference group. However, there are a few potential weaknesses. First, the sample size may not have been sufficient. When all three groups were included in a MANOVA controlling for infant intake, a group difference began to emerge [$F(2, 82) = 2.74$, $p = 0.07$]. This could be taken as evidence that the sample size was too small to detect the small effect size. Second, the generalizability of these results may be limited. The Danish people have a high intake of n-3 LCPUFA compared to samples from other studies exploring the relationship between n-3 LCPUFA intake/status and cognitive functions. Third, the study was not designed to evaluate whether the results suggest an inverted-U effect of fish oil supplementation. The negative relations detected

may indicate that DHA has an optimum level below and above which may be detrimental to the developing brain.

In summary, the results of this intervention were not as hypothesized. Boys whose mothers consumed fish oil had lower prosocial scores relative to the OO group. Moreover, speed of processing scores and inhibitory control/working memory scores were differentially negatively predicted by maternal n-3 LCPUFA intake and infant RBC–DHA status. Continuity in outcome measures lends confidence, but the study was not without limitations. However, this study is the first of its kind. The results presented here provide important information for the design of future studies to elucidate these long-term effects from which we will be able to draw more firm conclusions.

Acknowledgments LL planned and designed the RCT in collaboration with KFM. CLC designed the 7 year cognitive follow-up and trained SN and MA who completed all the data collection. LL and CLC were responsible for data management, statistical analysis, interpretation, and writing of the manuscript. All authors approved the paper in its final version. None of the authors has any financial or personal relationships with the company or organization sponsoring the research. This trial was funded by the Food Technology Research and Development Programme, Denmark (FØTEK).

References

1. Cheatham CL, Colombo J, Carlson SE (2006) n-3 Fatty acids and cognitive and visual acuity development: methodologic and conceptual considerations. Am J Clin Nutr 83:1458S–1466S
2. Lauritzen L, Hansen HS, Jorgensen MH, Michaelsen KF (2001) The essentiality of long chain n-3 fatty acids in relation to development and function of the brain and retina. Prog Lipid Res 40:1–94
3. SanGiovanni JP, Berkey CS, Dwyer JT, Colditz GA (2000) Dietary essential fatty acids, long-chain polyunsaturated fatty acids, and visual resolution acuity in healthy full-term infants: a systematic review. Early Hum Dev 57:165–188
4. Uauy R, Calderon F (2003) Long-chain polyunsaturated fatty acids in visual and neural development: cellular and molecular mechanisms. Forum Nutr 56:71–73
5. Cheatham CL (2008) Omega-3 fatty acids and the development of cognitive abilities: a review of DHA supplementation studies. CAB Reviews: Perspectives in Agriculture, Veterinary Science, Nutrition and Natural Resources 3:1–15
6. Eilander A, Hundscheid DC, Osendarp SJ, Transler C, Zock PL (2007) Effects of n-3 long chain polyunsaturated fatty acid supplementation on visual and cognitive development throughout childhood: a review of human studies. Prostaglandins Leukot Essent Fatty Acids 76:189–203
7. McCann JC, Ames BN (2005) Is docosahexaenoic acid, an n-3 long-chain polyunsaturated fatty acid, required for development of normal brain function? An overview of evidence from cognitive and behavioral tests in humans and animals. Am J Clin Nutr 82:281–295
8. Anderson JW, Johnstone BM, Remley DT (1999) Breast-feeding and cognitive development: a meta-analysis. Am J Clin Nutr 70:525–535
9. Caspi A et al (2007) Moderation of breastfeeding effects on the IQ by genetic variation in fatty acid metabolism. Proc Natl Acad Sci USA 104:18860–18865. doi:10.1073/pnas.0704292104
10. Xie L, Innis SM (2008) Genetic variants of the FADS1 FADS2 gene cluster are associated with altered (n-6) and (n-3) essential fatty acids in plasma and erythrocyte phospholipids in women during pregnancy and in breast milk during lactation. J Nutr 138:2222–2228. doi:10.3945/jn.108.096156
11. Helland IB et al (2003) Maternal supplementation with very-long-chain n-3 fatty acids during pregnancy and lactation augments children's IQ at 4 years of age. Pediatrics 111:e39–e44
12. Helland IB et al (2008) Effect of supplementing pregnant and lactating mothers with n-3 very-long-chain fatty acids on children's IQ and body mass index at 7 years of age. Pediatrics 122:e472–e479
13. Krabbendam L et al (2007) Relationship between DHA status at birth and child problem behaviour at 7 years of age. Prostaglandins Leukot Essent Fatty Acids 76:29–34
14. Hibbeln JR et al (2007) Maternal seafood consumption in pregnancy and neurodevelopmental outcomes in childhood (ALSPAC study): an observational cohort study. Lancet 369:578–585. doi:10.1016/S0140-6736(07)60277-3
15. Martin RE, Bazan NG (1992) Changing fatty acid content of growth cone lipids prior to synaptogenesis. J Neurochem 59:318–325
16. Bourre JM et al (1993) Function of dietary polyunsaturated fatty acids in the nervous system. Prostaglandins Leukot Essent Fatty Acids 48:5–15
17. Stillwell W, Wassall SR (2003) Docosahexaenoic acid: membrane properties of a unique fatty acid. Chem Phys Lipids 126:1–27
18. Martinez M (1992) Tissue levels of polyunsaturated fatty acids during early human development. J Ped 120:S129–S138
19. Casey BJ, Giedd JN, Thomas KM (2000) Structural and functional brain development and its relation to cognitive development. Biol Psychol 54:241–257. doi:S0301051100000582
20. Nieoullon A (2002) Dopamine and the regulation of cognition and attention. Prog Neurobiol 67:53–83
21. Delion S et al (1994) Chronic dietary alpha-linolenic acid deficiency alters dopaminergic and serotoninergic neurotransmission in rats. J Nutr 124:2466–2476
22. Willatts P, Forsyth JS, DiModugno MK, Varma S, Colvin M (1998) Effect of long-chain polyunsaturated fatty acids in infant formula on problem solving at 10 months of age. Lancet 352:688–691
23. Milte CM, Sinn N, Howe PR (2009) Polyunsaturated fatty acid status in attention deficit hyperactivity disorder, depression, and Alzheimer's disease: towards an omega-3 index for mental health? Nutr Rev 67:573–590. doi:10.1111/j.1753-4887.2009.00229.x
24. Sinn N, Bryan J (2007) Effect of supplementation with polyunsaturated fatty acids and micronutrients on learning and behavior problems associated with child ADHD. J Development Behav Ped 28:82–91
25. Kirby A, Woodward A, Jackson S, Wang Y, Crawford MA (2010) Children's learning and behaviour and the association with cheek cell polyunsaturated fatty acid levels. Res Dev Disabil 31:731–742. doi:10.1016/j.ridd.2010.01.015
26. Lauritzen L et al (2004) Maternal fish oil supplementation in lactation: effect on visual acuity and n-3 fatty acid content of infant erythrocytes. Lipids 39:195–206
27. Lauritzen L, Jorgensen MH, Olsen SF, Straarup EM, Michaelsen KF (2005) Maternal fish oil supplementation in lactation: effect on developmental outcome in breast-fed infants. Reprod Nutr Dev 45:535–547

28. Olsen J et al (2001) The Danish National Birth Cohort—its background, structure and aim. Scand J Public Health 29:300–307
29. Ulbak J, Lauritzen L, Hansen HS, Michaelsen KF (2004) Diet and blood pressure in 2.5-y-old Danish children. Am J Clin Nutr 79:1095–1102
30. Asserhoj M, Nehammer S, Matthiessen J, Michaelsen KF, Lauritzen L (2009) Maternal fish oil supplementation during lactation may adversely affect long-term blood pressure, energy intake, and physical activity of 7-year-old boys. J Nutr 139:298–304. doi:10.3945/jn.108.095745
31. Willatts P (1999) Development of means-end behavior in young infants: pulling a support to retrieve a distant object. Dev Psychol 35:651–667
32. Woodcock RW (1997) In: Flanagan DP, Genshaft JL, Harrison PL (eds) Contemporary intellectual assessment: theories, tests, and issues. Guilford Press, New York, pp 230–246
33. Archibald SJ, Kerns KA (1999) Identification and description of new tests of executive functioning in children. Child Neuropsychol 5:115–129
34. Muris P, Meesters C, van den Berg F (2003) The Strengths and Difficulties Questionnaire (SDQ)—further evidence for its reliability and validity in a community sample of Dutch children and adolescents. Eur Child Adolesc Psychiatry 12:1–8. doi:10.1007/s00787-003-0298-2
35. Lewis-Beck MS (1980) Applied regression: an introduction. Sage University Paper Series on quantitative applications in the social sciences, 07-022
36. Bouchard C, Cloutier R, Gravel F, Sutton A (2008) The role of language skills in perceived prosociality in kindergarten boys and girls. Eur J Dev Psychol 5:338–357. doi:10.1080/17405620600823744
37. Lauritzen L, Jorgensen MH, Hansen HS, Michaelsen KF (2002) Fluctuations in human milk long-chain PUFA levels in relation to dietary fish intake. Lipids 37:237–244
38. Sun J, Mohay H, O'Callaghan M (2009) A comparison of executive function in very preterm and term infants at 8 months corrected age. Early Hum Dev 85:225–230. doi:10.1016/j.earlhumdev.2008.10.005
39. Wells JC (2007) The thrifty phenotype as an adaptive maternal effect. Biol Rev Camb Philos Soc 82:143–172. doi:10.1111/j.1469-185X.2006.00007.x
40. Wong-Goodrich SJE et al (2008) Spatial memory and hippocampal plasticity are differentially sensitive to the availability of choline in adulthood as a function of choline supply in utero. Brain Res 1237:153–166
41. Nelson CA (2000) In: Shonkoff JP, Meisels SJ (eds) Handbook of early childhood intervention (2nd edn). Cambridge University Press, pp 204–227
42. Chugani HT (1998) A critical period of brain development: studies of cerebral glucose utilization with PET. Prev Med 27:184–188. doi:10.1006/pmed.1998.0274

Lipids (2011) 46:647–657
DOI 10.1007/s11745-011-3569-6

ORIGINAL ARTICLE

Vaccenic and Elaidic Acid Equally Esterify into Triacylglycerols, but Differently into Phospholipids of Fed Rat Liver Cells

Zhen-Yu Du · Pascal Degrace · Joseph Gresti · Olivier Loreau · Pierre Clouet

Received: 20 December 2010 / Accepted: 2 May 2011 / Published online: 26 May 2011

Abstract Elaidic acid (*trans*-9-$C_{18:1}$ or *trans*-9) is assumed to exert atherogenic effects due to its double bond configuration. The possibility that *trans*-9 and vaccenic acid (*trans*-11-$C_{18:1}$ or *trans*-11), its positional isomer, were biochemically equivalent and interchangeable compounds, was investigated by reference to their *cis*-isomers through esterification-related activities using rat liver cells and subcellular fractions. In hepatocytes, both *trans*-$C_{18:1}$ were incorporated to the same extent in triacylglycerols, but *trans*-9 was more esterified than *trans*-11 into phospholipids ($P < 0.05$). Glycerol-3-phosphate acyltransferase activity in microsomes was lower with *trans*-11 than with *trans*-9, while this activity in mitochondria was ~40% greater with *trans*-11 than with *trans*-9 ($P < 0.05$). Activity of 2-lysophosphatidic acid acyltransferase in microsomes was of comparable extent with both *trans* isomers, but activity of 2-lysophosphatidylcholine acyltransferase was significantly greater with *trans*-9 than with *trans*-11 at $P < 0.01$. Lipoproteins secreted by hepatocytes reached equivalent levels in the presence of any isomers, but triacylglycerol production was more elevated with *trans*-11 than with *trans*-9 at $P < 0.05$. Cholesterol efflux from previously labelled hepatocytes was lower with *trans*-11 than with *trans*-9. When these cells were exposed to either *trans*-$C_{18:1}$, the gene expression of proteins involved in fatty acid esterification and lipoprotein synthesis was unaffected, which indicates that the biochemical differences essentially depended on enzyme/substrate affinities. On the whole, vaccenic and elaidic acid were shown to incorporate cell phospholipids unequally, at least in vitro, which suggests they can differently affect lipid metabolic pathways in normal cells.

Keywords Vaccenic and elaidic acid · Esterification · Phospholipid · Cholesterol efflux · Gene expression

Abbreviations

ACC	Acetyl-CoA carboxylase
cis-9	*cis*-9-$C_{18:1}$, oleic acid
cis-11	*cis*-11-$C_{18:1}$
CLA	Conjugated linoleic acid
DGAT	Diacylglycerol acyltransferase
FA	Fatty acid
GPAT	Glycerol-3-phosphate acyltransferase
HMG-Red	Hydroxymethylglutaryl-CoA reductase
LDL-R	Low-density lipoprotein-receptor
mtGPAT	Mitochondrial GPAT
trans-9	*trans*-9-$C_{18:1}$, elaidic acid
trans-11	*trans*-11-$C_{18:1}$, vaccenic acid

Introduction

The consumption of fats containing *trans*-fatty acids (FA) has been correlated with an increased risk of coronary

Z.-Y. Du · P. Degrace · J. Gresti · P. Clouet
Faculté des Sciences Gabriel, UMR 866, INSERM-UB, 21000 Dijon, France

Z.-Y. Du
National Institute of Nutrition and Seafood Research, 5817 Bergen, Norway

O. Loreau
iBiTecS, Service Chimie Bioorganique et Marquage, CEA, 91191 Gif sur Yvette, France

P. Clouet (✉)
Pierre Clouet, UMR 866, INSERM-UB, Equipe Physiopathologie des dyslipidémies, Faculté des Sciences Gabriel, Université de Bourgogne, 21000 Dijon, France
e-mail: pclouet@u-bourgogne.fr

heart disease, principally through elevated levels of plasma total cholesterol, LDL cholesterol, apolipoprotein B and increased LDL/HDL ratios [1, 2]. The partial hydrogenation of vegetable oils for margarine production [3, 4] gave rise to by-products as *trans*-FA whose levels may reach 60% of total FA [5]. Among these, elaidic acid (*trans*-9) could represent 30–40% and vaccenic acid (*trans*-11) 10% [6, 7]. *trans*-9 was assumed to exert atherogenic effects because its concentration in margarines was associated with abnormal plasma lipid concentrations [2, 8]. Some *trans*-$C_{18:1}$ are also produced in the digestive system of ruminants through the microbial hydrogenation of vegetable oils and are consequently recovered in related products as milk and meat. In dairy fats, *trans*-11 was found to represent more than 80% of all the identified *trans*-$C_{18:1}$ isomers [9, 10]. Epidemiological surveys suggested that *trans*-9 increases more the cardiovascular risk than *trans*-11 [11–13]. However with hamsters, plasma LDL/HDL-cholesterol ratios were more elevated with diets enriched in *trans*-11 than in *trans*-9 [14]. Yet with the same animal model, the hypercholesterolemic effects of partially hydrogenated vegetable oils was demonstrated not to directly depend on the presence of *trans*-9 or *trans*-11 [15]. In the whole, the use of versatile experimental models, atherosclerosis markers and dietary fat blends provide inconsistent results, which suggests that *trans*-9 and *trans*-11 exert similar effects, but whose amplitude would depend in humans on particular parameters as specific dietary lipid levels [16] or hormonal status [6].

Geometrical isomers exhibit comparable fates as regards their hydrolysis from triacylglycerols and their absorption in the intestinal tract [17], as well as their distribution among lymph lipids [18]. Thus the specific effects of *trans* isomers would occur beyond the intestinal step and then affect most organs with possible interrelations. This prompted us to limit the whole issue to the comparison of actions of pure *trans*-$C_{18:1}$ isomers by using only one tissue model. Liver was chosen because of its pivotal role in the re-distribution of ingested lipids to other organs via lipoprotein secretion. *trans*-9 and *trans*-11 were all the more recovered in lipoproteins because they were shown to be weakly oxidised in liver mitochondria [19, 20] and were then available for the esterification reactions. Besides, the incorporation of FA into membrane lipids is associated with cholesterol efflux, which should increase plasma cholesterol levels [1, 2]. The present study was designed to compare first the esterification capacities of *trans*-9 and *trans*-11, relative to their respective *cis*-isomers, in rat liver extracts, second the effects of the four $C_{18:1}$ isomers on membrane cholesterol efflux and esterification-related gene expression in isolated hepatocytes. Rats were fed a standard diet, instead of diets enriched in the tested isomers, to prevent alterations of enzyme activities induced by these isomers within membranes [21].

Experimental Procedure

Chemicals

Oleic (*cis*-9-$C_{18:1}$), elaidic (*trans*-9-$C_{18:1}$), *cis*-11-octadecenoic (*cis*-11-$C_{18:1}$) and vaccenic (*trans*-11-$C_{18:1}$) acids, abbreviated *cis*-9, *trans*-9, *cis*-11 and *trans*-11, respectively, were purchased from Sigma Chemical Co. (St. Louis, MO). [1-^{14}C] oleic acid and [4-^{14}C] cholesterol were obtained from Amersham Biosciences Europe (Saclay, France). The other [1-^{14}C] isomers were specifically prepared by CEA (Gif sur Yvette, France) from commercial unlabelled FA and $^{14}CO_2$ using procedures described in [22]. Radiochemical purity (>98%) of [1-^{14}C] labelled compounds was determined by RP-HPLC (Zorbax SB C18; acetone/(methanol/water/acetic acid, 50:50:1, by vol), 60:40, by vol) and TLC (Silicagel Merck 60F254, pentane/diethylether/acetic acid, 80:20:0.1, by vol). They were all stored in chloroform/ethyl alcohol (50:50, by vol) at −30 °C. Evaporation of solvents under nitrogen was followed by the saponification of FA with NaOH or KOH for assays with whole cells or intracellular organelles, respectively, and their binding to essentially FA-free bovine serum albumin (BSA). These preparations were added to the other components of media immediately prior to incubations. [U-^{14}C]Glycerol-3-phosphate was obtained from NEN Life Science Products (NEN, Paris, France). BSA, cholesterol, collagenase (type I) and other biochemicals were from Sigma. Methylene chloride, 2,4,6-collidine, ethyl chloroformate and tetrahydrofuran, supplied by Aldrich Chemical Co. (Milwaukee, WI), were used for acyl-CoA synthesis [23]. Concentrations of synthesised acyl-CoAs were determined through their respective molar extinction coefficients at 260 nm and corrections based on their 232/260 nm ratios, relative to those with pure products [24–26].

Animals

Official French regulations (No. 87848) for the use and care of laboratory animals were followed throughout and the experimental protocol was approved by the local ethics committee for animal experimentation (No. BL0612). Male Wistar rats were purchased from Janvier (Le Genest St Isle, France). They were kept at 23 °C in a light-controlled room (light period fixed between 08:00 a.m. and 08:00 p.m.). They had free access to tap water and were fed a standard laboratory chow (ref AO4 from UAR, Epinay-sur-Orge, France) containing 58.7% carbohydrate, 17% protein, and 3% fat (palmitic, stearic, oleic and linoleic acids

representing 8.7, 1.7, 26.7 and 48.3%, respectively, of the total FA mass). When rats were 7–8 weeks old (250–300 g), they were anaesthetised with isoflurane and killed by exsanguination at 08:00 a.m.

Activity Rate Measurements

All the biochemical activity measurements were performed with increasing substrate concentrations, but the concentration retained for each experimental presentation was selected among those giving rise to the increasing part of activity curves.

FA Esterification by Isolated Hepatocytes and Liver Slices (Intact Cells)

Hepatocytes were isolated through a two-step collagenase perfusion as in [27]. Cell viability was assessed by trypan blue exclusion and suspensions with viability lower than 85% were discarded. Immediately after isolation, cells were preincubated in William's Medium E (WME) from PAN-Biotech GmbH (Aidenbach, Germany) containing 10% (v/v) fetal bovine serum and 1% (v/v) antibiotic antimycotic solution (Sigma Chemical, Co.) in water-saturated atmosphere (5% CO_2, 95% air) for ~3 h at 37 °C, in dishes of 60-mm diameter (~3×10^6 cells per dish). The attached cell monolayer was gently washed with 3 mL of fresh WME that was replaced by 2.5 mL of Krebs-Henseleit buffer (KHB) containing 118 mM NaCl, 4.7 mM KCl, 1 mM KH_2PO_4, 1.2 mM $MgSO_4$, 0.5 mM $CaCl_2$, and 25 mM $NaHCO_3$, pH 7.4. The reaction was started by addition of 1 mL of [1-^{14}C] FA (2.25 Ci/mol) with BSA (0.4 and 0.1 mM of final concentration, respectively) under 95% O_2 and 5% CO_2 atmosphere. Liver slices were also prepared using the procedure detailed in [19] and were incubated (0.2 g per assay) in 2.5 mL of KHB. The reaction was initiated by addition of 1 mL of labelled FA with BSA, as above for the cell monolayers. After 2 h of incubation at 37 °C, the supernatants were decanted, and the cell monolayers or tissue stripes were washed two times with KHB containing 2% FA-free BSA at 37 °C. Total lipids of both liver extracts were obtained using the Folch procedure [28] and were separated by TLC in hexane/ethyl ether/acetic acid/methanol (90:20:2:3, by vol). The radioactivity of triacylglycerol (TAG) and phospholipid (PL) spots was measured by AR-2000 TLC Imaging Scanner (Bioscan, Inc., Washington DC).

FA Esterification by Liver Homogenates (Disrupted or Disorganised Cells)

Liver pieces were homogenised by manual rotation of a Teflon pestle in an ice-cooled Potter–Elvehjem apparatus and diluted (1:40, w/v) in a chilled mixture of 0.25 M sucrose, 2 mM EGTA and 10 mM Tris/HCl, pH 7.4 [29]. The reaction was initiated by the injection of 0.1 mL homogenate into 1.5 mL of a mixture containing 2 mM ATP, 50 μM CoA, 4 mM $MgCl_2$, 1% glucose and 120 μM [1-^{14}C] FA (3.7 Ci/mol). Incubations were performed at 37 °C for 30 min and total lipids were extracted and separated as above for whole cells.

Microsomal and Mitochondrial Esterification onto the *sn*-1 Position of Glycerol-3-phosphate

The isolation of mitochondrial fractions was performed as in [29], using a medium containing 1% FA-free BSA to bind free FA released during and after the cell disruption. Microsomal fractions were isolated after mitochondria pelleting as in [30]. The protein content of these fractions cleared from BSA was measured using the bicinchoninic acid procedure [31] and their purity was checked through activity of enzymes specific to mitochondria, peroxisomes and microsomes, as detailed in [30]. Glycerol-3-phosphate acyltransferase (GPAT) activity was measured in 1 mL of medium buffered at pH 7.4 and containing 75 mM KCl, 0.2 mM EGTA, 4 mM $MgCl_2$, 80 mM mannitol, 25 mM HEPES, 2 mM KCN, 2 mM ATP, 50 μM CoA, 0.5 mM L-[H^3] glycerol-3-phosphate (0.72 mCi/mol), 0.1 mM of each $C_{18:1}$ isomer and 50 μM BSA, at 37 °C. The reaction was initiated by addition of 0.3 mg of microsomal or mitochondrial protein, or of 0.1 mL of liver homogenate (2.5 mg liver). After 7 min, 3 mL of 0.1 M HCl containing 10 mM DL-glycerol-3-phosphate (Prolabo, Paris, France) was added and the radioactivity of 1-monoacyl-[H^3] glycerol phosphate extracted with butan-1-ol [32] was determined after mixing with Ultima Gold XR (Packard, Meriden, CT).

Microsomal Esterification onto the *sn*-2 Position of Monoacylglycerolipids

2-lysophosphatidic acid acyltransferase and 2-lysophosphatidylcholine acyltransferase activities were measured according to the method described in [33]. Briefly, a preincubation time of 2 min was performed at 25 °C by addition of 0.2 mg of microsomal protein to 2 mL of a medium containing 10 mM 5,5′-dithiobis-(2-nitrobenzoic acid) (DTNB), 5 mM Tris–boric acid and 5 μM of $C_{18:1}$-CoA, at pH 7.4. The specific reactions of esterification were recorded over 4 min after addition of 50 mM 1-palmitoyl-2-hydroxy-*sn*-glycero-3-phosphate or 150 mM 1-palmitoyl-2-hydroxy-*sn*-glycero-3-phosphocholine (Avanti Polar Lipids, Alabaster, AL). The change in absorption at 413 nm results from the binding to DTNB of thiol groups released by acyl-CoA hydrolysis during the esterification reactions.

Results were corrected from control values obtained in the absence of $C_{18:1}$-CoA.

Components of Lipoprotein Secreted by Hepatocytes Exposed to $C_{18:1}$ Isomers

Hepatocytes prepared as already described were incubated in 4 mL of WME containing 100 μM of each $C_{18:1}$ isomer bound to 50 μM BSA, 100 nM insulin and 1% antibiotic antimycotic solution, under a water-saturated atmosphere (5% CO_2, 95% air) at 37 °C. Control assays were performed in the same way, but in the absence of exogenous $C_{18:1}$ isomer. After 24 h, the media were centrifuged at 2,000×*g* for 5 min and the supernatants containing the cell lipid secretions were assayed with commercial kits from Orion Diagnostica (Espoo, Finland) for apolipoproteins A1 and B100, and from BioMérieux (Marcy l'Etoile, France) for triacylglycerols (TG PAP 150) and cholesterol (Cholesterol RTU). The efflux of cholesterol originating from all the cell structures was measured as follows: Hepatocytes prepared as above were cultured until the attachment step (∼4 h), then were added with 4 mL of WME containing 10% BSA, 4 μCi [4-^{14}C] cholesterol and 75 μL of fresh rat plasma. In this medium, the final amounts of cholesterol and LDL, expressed per mL, were 65 nmol and 50 μg, respectively. After 24 h of incubation at 37 °C in water-saturated atmosphere (5% CO_2, 95% air), radioactive and unlabelled forms of cholesterol in cells were assumed to balance each other. The supernatants were decanted and cells were washed once with KHB containing 1% BSA. Hepatocytes were then incubated in 4 mL of WME in the presence of 0.2 mM $C_{18:1}$ isomer and 70 μM BSA, with control assays performed in the absence of isomer. After 5 h, the supernatants were centrifuged to discard cells detached from the ground monolayer and the radioactivity of clarified samples, mixed with Ultima Gold XR, was measured in a scintillation spectrometer.

Gene Expression in Hepatocytes Exposed to $C_{18:1}$ Isomers

Hepatocytes prepared as above were incubated in 4 mL of WME containing 100 μM of $C_{18:1}$ isomer, 50 μM BSA, 100 nM insulin and 1% antibiotic antimycotic solution, in water-saturated atmosphere (5% CO_2, 95% air) at 37 °C. After 24 h, total mRNA of hepatocyte monolayers was extracted using Tri-Reagent (Euromedex, Souffelweyersheim, France) as described in [34]. Total mRNA was reverse-transcripted using Iscript cDNA kit (Bio-Rad, Marnes-La-Coquette, France). Real-time quantitative PCR was performed in 96-well plate using an iCycler iQ (Bio-Rad). Each well contains: 12.5 μL of iQ Sybr Green Supermix (Bio-Rad), 2.5 μL of forward primer (0.3 μM), 2.5 μL of reverse primer (0.3 μM), 5 μL of cDNA (25, 2.5, 0.25 and 0.025 ng for standards and 2.5 ng for samples) and 2.5 μL of water. Primer pairs were designed using 'Primers!' software and were synthesised by MWG-Biotech AG (Ebersberg, Germany). The sequences of the forward and reverse primers used were, respectively, as follows: 5′-caccggctgaaggacatac-3′ and 5′-gctcaaaggggtct caaaaga-3′ for acetyl-CoA carboxylase 2 (ACC 2); 5′-tt caaccccagtatcccatct-3′ and 5′-ggtgccttgtgtgagtttca-3′ for mitochondrial glycerol-3-phosphate acyltransferase (mtG-PAT); 5′-tcctaccgggatgtcaatct-3′ and 5′-ctcggtaggtcagg ttgtcc-3′ for diacylglycerol acyltransferase (DGAT); 5′-tgagcttagcgttgcttttg-3′ and 5′-agctttctttggggtcacg-3′ for HMG-CoA reductase; 5′-tgggttccatagggtttctg-3′ and 5′-ttg gggatcaggctggtat-3′ for LDL-receptor (LDL-R); and 5′-aat cgtgcgtgacatcaaag-3′ and 5′-gaaaagagcctcagggcat-3′ for *β*-actin. The relative expression of each gene was calculated with cDNA standard curves and normalised with actin cDNA.

Statistics

Differences between groups were determined performing repeated measures of ANOVA followed by the Tukey–Kramer multiple comparison post-hoc test using GraphPad Instat 3.1 software. Difference were considered significant at $P < 0.05$.

Results

Esterification of $C_{18:1}$ Isomers in Intact Cells

In hepatocytes (Fig. 1a) and liver slices (data not presented), the results were qualitatively comparable and showed that all the isomers were ∼2 times as much esterified into TAG as into PL. In TAG, *trans*-$C_{18:1}$ were ∼2-fold less incorporated than the *cis*-ones, while in PL, the amount of *trans*-9 was 25% greater than that of *trans*-11, and 3 times as elevated as that of *cis*-9 at $P < 0.05$. In liver homogenates, i.e. in disrupted cells, all the isomers were ∼2 times more incorporated into PL than into TAG (Fig. 1b). In TAG, the *trans*-$C_{18:1}$ were 40% less abundant than the *cis*-forms, while in PL, both *trans*-$C_{18:1}$ and *cis*-11 amounted to ∼50% more than *cis*-9 at $P < 0.05$.

Esterification onto the *sn*-1 Position of Glycerophosphate in Microsomes and Mitochondria

GPAT, through the esterification of acyl groups in *sn*-1 position of glycero-3-phosphate, initiates the synthesis of glycerolipids. In liver homogenates (Fig. 2a), GPAT activity was maximum with *cis*-9 and minimum with *trans*-11,

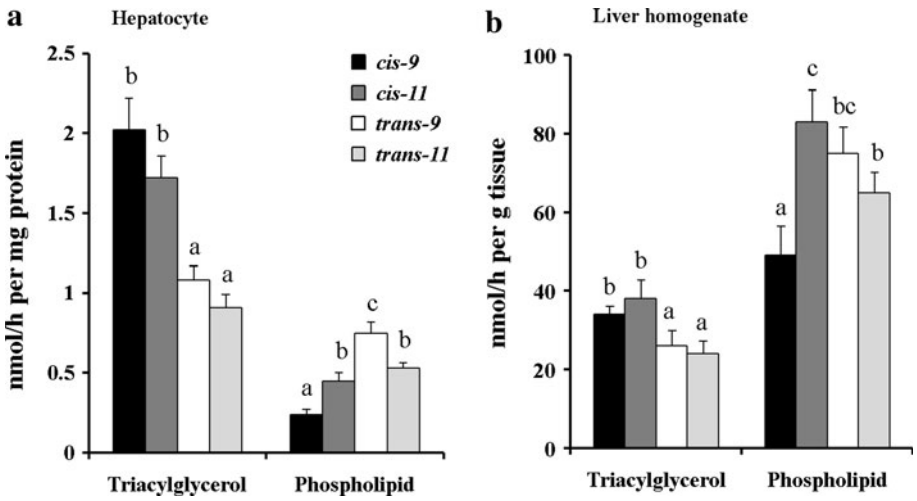

Fig. 1 Incorporation of $C_{18:1}$ isomers into TAG and PL of intact (**a**) and disrupted (**b**) liver cells. Concentrations of [1-^{14}C] isomer substrates in the final media were 0.4 and 0.12 mM with hepatocytes and liver homogenates, respectively. All results are expressed as nmol of $C_{18:1}$ isomers esterified per hour per mg hepatocyte protein or g wet liver. *T-bars* show SEM ($n = 3$). For each series and lipid class, values with different *letters* on columns statistically differ at $P < 0.05$

this latter exhibiting activity values lower than those of *trans*-9 at $P < 0.05$. The same pattern was observed in microsomes (Fig. 2b) except that the enzyme activity was comparable with *cis*-9 and *cis*-11. In mitochondria (Fig. 2c), GPAT (mtGPAT) was shown to exert activities of different extents as the considered $C_{18:1}$ isomer, in the following order: *cis*-11 > *cis*-9 > *trans*-11 > *trans*-9 ($P < 0.05$).

Esterification onto the *sn*-2 Position of Monoacylglycerolipids in Microsomes

The acylation in *sn*-2 position of 1-palmitoyl-2-hydroxyl-*sn*-glycero-3-phosphate is catalysed by 2-lysophosphatidic acid acyltransferase and regards as a step of the synthesis of glycerolipids as TAG and PL. Fig. 3a indicates that both *trans*-isomers were 40% less esterified in the *sn*-2 position than their *cis*-isomers ($P < 0.05$). The acylation at the same position of 1-palmitoyl-2-hydroxy-*sn*-3-phosphocholine is carried out by 2-lysophosphatidylcholine acyltransferase and reflects the renewing of cellular PL. This reaction was shown to be highly sensitive to the position of the double bond in the acyl chain, both Δ-11 isomers being ~4.5 times less esterified than both Δ-9-$C_{18:1}$ (Fig. 3b).

Lipid Secretion by Hepatocytes Exposed to $C_{18:1}$ Isomers

Total apolipoprotein A1 secretion was, compared to the control assay performed in the absence of FA, unaffected after 24 h-exposure of hepatocytes to any $C_{18:1}$ isomers, except that this production was decreased with *cis*-11 by reference to the control and *trans*-9 assays (Fig. 4a). Secretion of apolipoprotein B100 and total cholesterol was also unchanged after the same time of exposure to $C_{18:1}$ isomers (Fig. 4b, d). The TAG secretion was greater with *cis*-9 and *trans*-11 than with the control and *trans*-9 assays (Fig. 4c). When the efflux of cholesterol was studied with hepatocytes in which labelled cholesterol was previously balanced with the unlabelled cholesterol of cell structures (Fig. 5), values obtained after 5 h of incubation with the

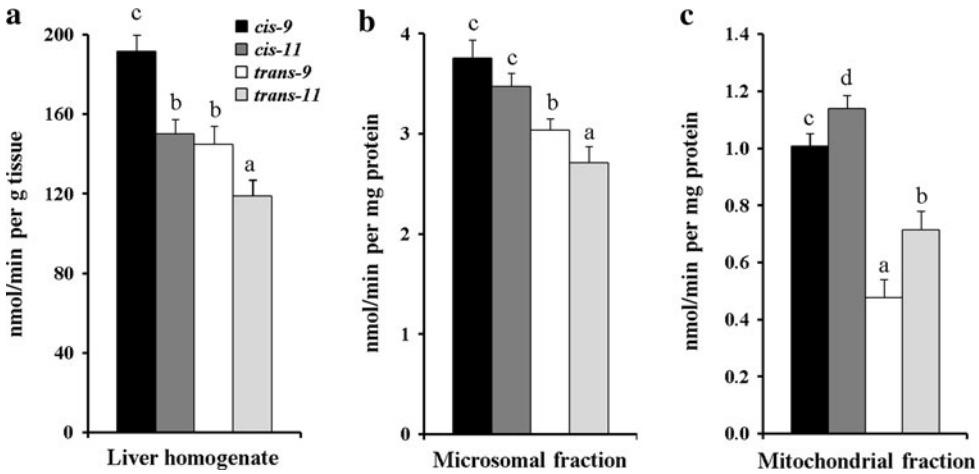

Fig. 2 Activity of glycerol-3-phosphate acyltransferase in the presence of 0.1 mM $C_{18:1}$ isomers with liver homogenates (2.5 mg wet liver) and 0.3 mg of microsomal or mitochondrial protein. All results are expressed as nmol of $C_{18:1}$ bound to glycerol-3-phosphate per min per g wet liver or mg microsomal protein. *T-bars* show SEM ($n = 3$). For each series, values with different *letters* on columns statistically differ at $P < 0.05$

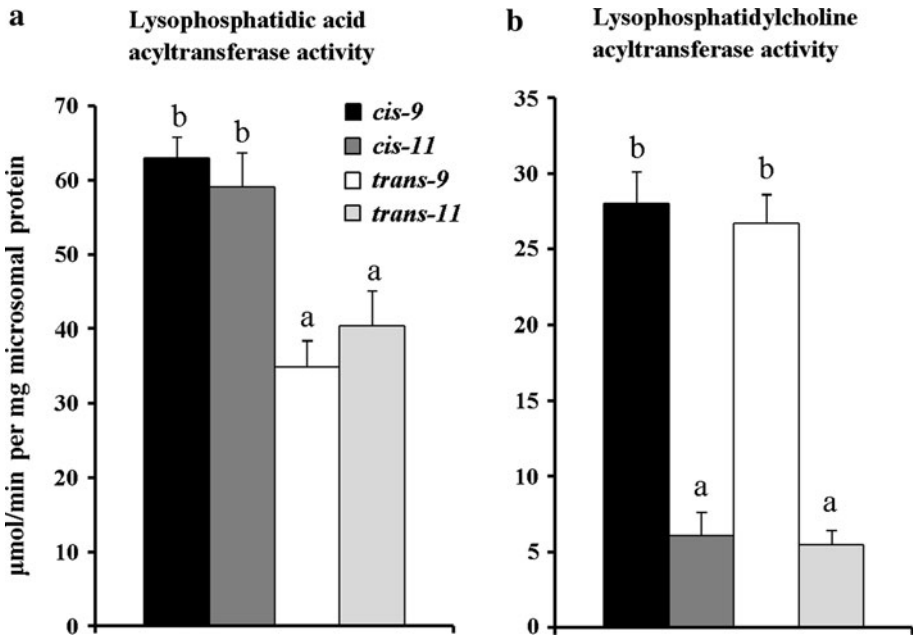

Fig. 3 Activity of 2-lysophosphatidic acid or 2-lysophosphatidylcholine acyltransferase in the presence of 5 µM $C_{18:1}$ isomers as CoA-esters with 1-palmitoyl-2-hydroxy-*sn*-glycero-3-phosphate (**a**) or 1-palmitoyl-2-hydroxy-*sn*-glycero-3-phosphocholine (**b**), respectively, in liver microsomes. Enzyme activities were measured by following the absorbance at 413 nm of the binding of CoA (released from CoA-esters) to DTNB. Results are expressed as µmol of $C_{18:1}$ esterified per min per mg microsomal protein. *T-bars* show SEM ($n = 3$). For each activity, values with different *letters* on columns statistically differ at $P < 0.05$

isomers were all greater than in their absence, but were ~30% lower with *cis*-11 and *trans*-11 than with *cis*-9 and *trans*-9 at $P < 0.05$.

Esterification-Related Gene Expression

In hepatocytes cultured over 24 h with each $C_{18:1}$ isomer, the levels of gene expression for mtGPAT, DGAT and LDL-R were comparable to those obtained in the absence of FA (Fig. 6). A decrease in expression levels was observed only for ACC-2 with the *cis*-11 isomer and for HMG-CoA reductase with *trans*-11 at $P < 0.05$.

Discussion

The aim of the study was to determine whether the small difference in the double bond position of *trans*-11 versus *trans*-9 gave rise to comparable effects on FA esterification-related parameters. In this goal, rats were used in the fed state because this nutritional condition was shown to depress FA oxidation in liver and most other organs [35], which made all unbound FA available for TAG and PL synthesis. This ex vivo study shows that *trans*-11 and *trans*-9 were not interchangeable substrates for the esterification reactions in intact or disrupted liver cells, as well

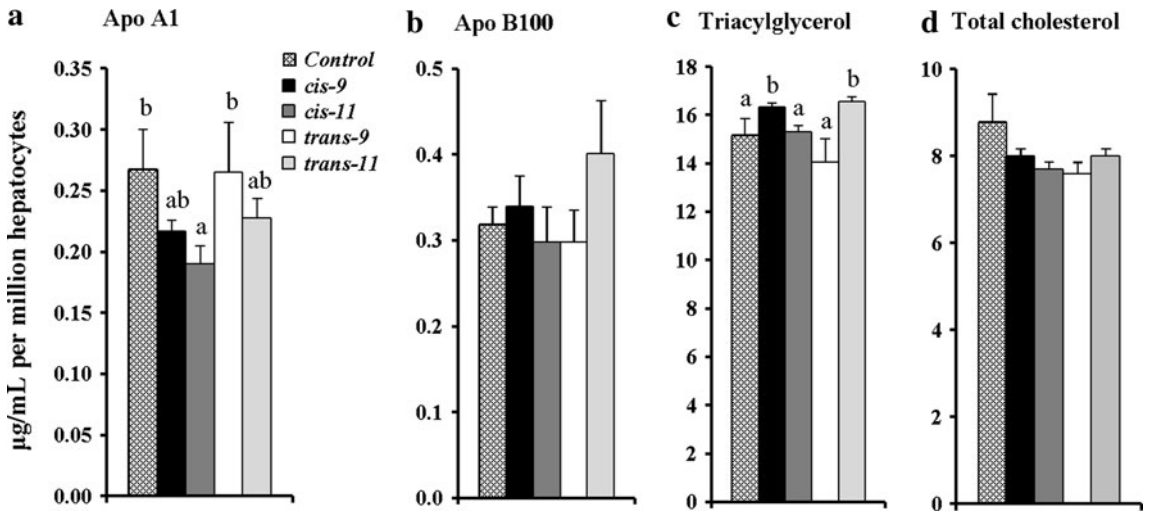

Fig. 4 Components of lipoproteins secreted by hepatocytes cultured for 24 h in the absence (*control assay*) or presence of 0.1 mM $C_{18:1}$ isomers. Results are expressed as µg of each component per mL of incubation medium per million hepatocytes. *T-bars* show SEM ($n = 3$). For each measurement, values with different *letters* on columns statistically differ at $P < 0.05$

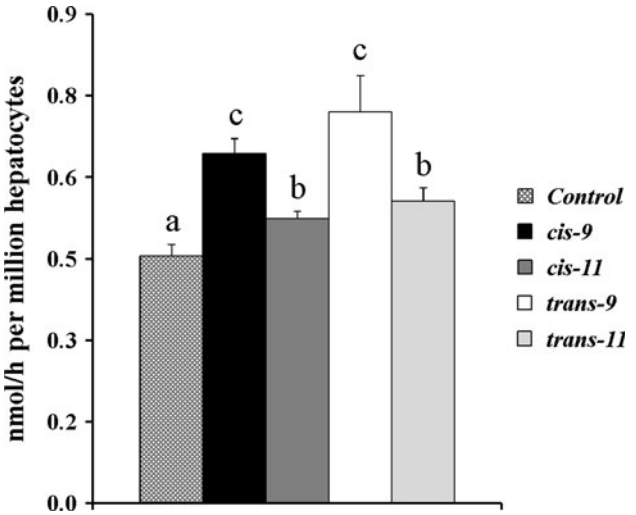

Fig. 5 Efflux of cholesterol from cholesterol-prelabelled hepatocytes in the presence of 0.2 mM $C_{18:1}$ isomers. After 5 h of incubation, the media were centrifuged and the radioactivity of their supernatants was determined as indicated in the "Experimental procedure" section. Results are expressed as nmol labelled cholesterol released per hour per million hepatocytes. *T-bars* show SEM ($n = 3$). Efflux values with different *letters* on columns statistically differ at $P < 0.05$

as in isolated microsomes and mitochondria. Yet the *trans* configuration of the single double bond gives both *trans*-11 and *trans*-9 a common linear aspect as for saturated FA [36–38]. Enzyme activities mainly depend on specific protein synthesis regulated by genes and on affinity of enzymes for their substrates. The genic expression of enzymes related to lipogenesis (FA and cholesterol synthesis) and FA esterification was about of the same range in the assays performed in the presence or not of isomers. These data may indicate that the expression levels of genes were increased with insulin, but without additional effects of isomers. Indeed, after various treatments, weakly higher or lower expression levels of the involved genes were found in fed animals [39–42]. Consequently, under this nutritional condition, the study of biochemical reactions related to TAG and PL synthesis appeared to be convenient to test the possible similarity of both *trans*-isomers through activity levels only depending on enzyme/substrate affinities.

Esterification of Isomers into TAG and PL of Liver Cells

In liver slices and isolated hepatocytes, i.e. in intact cells, the esterification of isomers into TAG and PL implied that some of their OH groups were available from pre-existent TAG and PL after specific hydrolysis [43–45]. In each of our assays, the labelled isomers, once within cells, were expected to compete for the esterification reactions with the endogenous FA present in the surroundings of partially hydrolysed TAG and PL. This competition also depended on the position of available OH groups in these lipids and the amounts of compatible FA. For instance, as regards a convenient position of esterification, the labelled isomers were recovered on TAG and PL to a greater extent when these lipids were previously weakly hydrolysed.

In perfused liver, *trans*-9 and *trans*-11, as well as stearic acid ($C_{18:0}$), were principally recovered on the 1- and 3-positions of TAG, while *cis*-9 and -11 isomers were mainly present on the 2-position [36]. With this specific information, our results show that, in intact and disrupted cells, the affinities of either *trans*-$C_{18:1}$ for the external 2 positions of TAG were equivalent and always at a

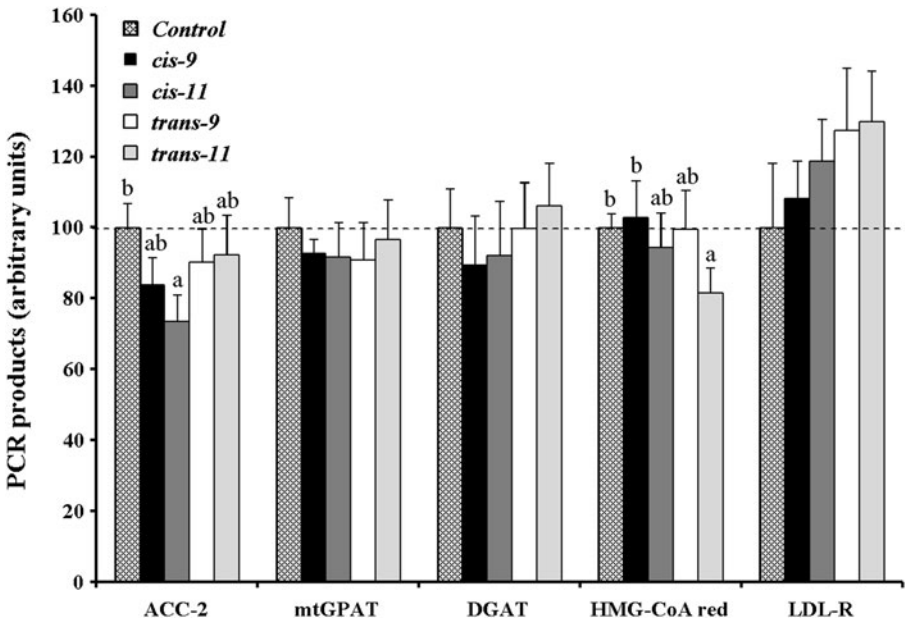

Fig. 6 mRNA levels of FA synthesis- and esterification-related proteins after incubation of fed rat hepatocytes with 0.1 mM of each $C_{18:1}$ isomer for 24 h. Arbitrary units ± SEM with $n = 3$ (different hepatocyte culture dishes) are percentages expressed by reference to control assays (*dotted line*) performed in the absence of any $C_{18:1}$ isomer (=100 for each gene). Different *letters* on columns denote statistically different results at $P < 0.05$

significantly less extent than those of either *cis*-$C_{18:1}$ for the internal position alone. The inversion of the rough distribution of the labelling between TAG and PL in intact and disrupted cells (Fig. 1a vs. b) could originate, as mentioned above, from a weak rate of TAG hydrolysis in intact cells and, after cell disruption, from increased hydrolysis of both TAG [44, 46] and PL through phospholipase activation [46, 47].

In PL, as the *sn*-2 position was preferentially occupied by *cis*-unsaturated FA [36–38], the low level of esterification of labelled *cis*-9 (see Fig. 1a) could result from the dilution of this exogenous isomer with endogenous *cis*-9 and other unsaturated FA, as linoleic acid representing ~50% of total FA of dietary lipids (see "Experimental procedure" section). The incorporation of *cis*-11 also occurred onto the *sn*-2 position, but was significantly greater than that of *cis*-9 both in intact and disrupted cells. This may be due to the fact that, contrary to oleic acid, *cis*-11 is not present in the natural lipids and its labelled form, once within cells, had not to compete with any endogenous equivalent, allowing it to be better incorporated than *cis*-9 into PL. In spite of the presence of endogenous *cis*-unsaturated FA, the notable incorporation of both *trans*-$C_{18:1}$ into PL suggests that these isomers, like saturated FA, were more convenient substrates for the *sn*-1 position, as has already been shown [36–38]. In this context, *trans*-9 was esterified significantly more than *trans*-11 in hepatocytes and marginally more in disrupted cells, which could result from greater or lower cell concentrations of unesterified *trans*-9 or *trans*-11, respectively. In this line, *trans*-9 that is less oxidised than *trans*-11 in liver mitochondria from fasted rats [19], should be present in concentration greater than that of *trans*-11 within cells. However in fed rat livers, the FA-oxidation pathway is strongly inhibited [48], which should normally maintain labelled *trans*-9 and *trans*-11 concentrations to equivalent levels in cells. A possibility was that either *trans*-isomer was transformed into another compound exhibiting distinct affinities for the available OH groups of PL. Indeed, *trans*-11 was found to give rise to *cis*-9, *trans*-11-$C_{18:2}$ (as a conjugated linoleic acid, CLA) through Δ-9 desaturation in liver microsomes, while under the same experimental conditions *trans*-9 stayed unchanged [49]. In whole rats, dietary *trans*-11 was also transformed into *cis*-9, *trans*-11-$C_{18:2}$ in most organs [50]. This CLA added to the diet of pigs was abundantly recovered in liver PL [51]. The gain of a *cis*-9 double bond could be thought to confer to the resulting CLA a high affinity for the *sn*-2 position of PL, but being then in competition, as labelled *cis*-9, with endogenous FA for this position, which would decrease its incorporation into PL via the initial labelling of its precursor. This hypothesis however was not relevant under our experimental conditions because the Δ-9 desaturation of *trans*-11 into CLA has been shown to be very weak in liver and to take place exclusively in peripheral tissues [52]. Further, contrary to what could be expected, *cis*-9, *trans*-11-CLA preferentially esterified as *trans*-11 onto the *sn*-1 position of PL [53].

Esterification-Related Enzyme Activities

As previously mentioned, the esterification of isomers in intact and disrupted cells could be distorted because of the competition with endogenous FA and the fact that this reaction was connected or not to lipoprotein formation and membrane remodeling. By contrast, the measurement of biochemical activities with isolated subcellular particles in appropriate medium strongly limited the mentioned interferences and allowed exogenous *trans*-11 and *trans*-9 to be strictly compared as substrates in the chosen activities. GPAT activity represents an early step common to TAG and PL synthesis with the esterification of acyl groups onto the *sn*-1 position of glycerol-3-phosphate. The about same decreasing order of activities with all the isomers in liver homogenates and microsomal fractions suggests that the whole cell GPAT activity was mainly supported by endoplasmic reticulum. The differences of activities found between both *trans*-$C_{18:1}$ could result from a preferential channeling of *trans*-9 towards the PL synthesis pathway in hepatocytes (Fig. 1a). Unexpectedly, these differences did not concomitantly give rise to comparable effects on the incorporation of both *trans*-$C_{18:1}$ into TAG. GPAT activities in mitochondria (mtGPAT) were qualitatively inversed with these isomers, compared to those in microsomes, but were likely of too low amplitude to affect the distribution of these labelled isomers in TAG and PL of intact or disrupted cells (Fig. 1a, b). This effect could however influence the FA esterification/oxidation balance in mitochondria, since mtGPAT and carnitine palmitoyltransferase I activities have been shown to interfere negatively each other in fasted rats [54].

With glycerol-derived compounds whose *sn*-1 and *sn*-3 positions are already occupied, the esterification activity in microsomes was comparable with both *trans*-isomers when the *sn*-3 position was bound to phosphate, but totally different when this position was bound to phosphocholine. The latter activity was much more greater with *cis*-9 and *trans*-9 isomers than with their *cis*-11 and *trans*-11 counterparts, which indicates that the position of the double bond in the acyl chain was then more important than its geometric configuration. This reaction, catalysed by 2-lysophosphatidylcholine acyltransferase, was shown to possess lysophospholipase and transacylase activities [55], and was believed to take part in the permanent remodeling of membrane PL [56]. Further the purified enzyme exhibited much affinity for arachidonoyl-CoA and to a lesser extent for linoleoyl- and oleoyl-CoA [57, 58]. The comparable

enzyme activity in our assays with oleoyl- and elaidoyl-CoA suggests that *trans*-9 could participate much more actively than *trans*-11 in the PL remodeling. The higher GPAT and 2-lysophosphatidylcholine acyltransferase activities exhibited by isolated microsomes could explain, at least partly, that *trans*-9 was incorporated to a greater extent than *trans*-11 into PL of hepatocytes (Fig. 1a). This point was supported by other studies carried out in hamsters fed diets containing both *trans*-isomers and showing that *trans*-9 was recovered more abundantly than *trans*-11 in *sn*-2 position of platelet PL [14].

Lipoprotein Secretion by Hepatocytes

Measurements of apolipoproteins, TAG and total cholesterol did not reveal any manifest effect of the exposure of hepatocytes to isomers, relative to control assays. Indeed similar experiments performed in the presence of insulin demonstrated that TAG synthesis and secretion were stimulated [59, 60], but that apolipoprotein secretions were equivalent [59] or decreased [60, 61], depending on the time of incubation. When oleic acid was added to incubation medium [59], TAG synthesis and secretion were increased, which meets our results (Fig. 4c). The same effect was observed with *trans*-11, but not with *trans*-9 that could be used preferentially for PL synthesis/remodeling as already suggested. The same amounts of cholesterol secreted by hepatocytes exposed to *trans*-11 versus *trans*-9 (Fig. 4d) appeared to disagree with the different levels of labelled cholesterol released from cells previously incubated with [^{14}C] cholesterol after exposure to both *trans*-$C_{18:1}$ (Fig. 5). In fact during the preincubation time of this latter experiment, exogenous cholesterol was expected to settle down between membrane PL. The collected data suggest that the greater incorporation of *trans*-9 versus *trans*-11 into whole PL of hepatocytes (Fig. 1a) allowed more cholesterol molecules to be shifted from their unsteady positions into the surrounding medium for lipoprotein formation. This would not be the case for *trans*-11 that, contrary to *trans*-9, was associated with lower blood total and LDL-cholesterol in rats [62].

This study carried out with intact cells and cell subfractions demonstrates that vaccenic and elaidic acids, in spite of their chemical resemblance, differ as substrates in esterification-related activities, particularly for PL synthesis and remodeling. It could be assumed that the differences observed would be modified by the fasting period, known to be associated with increased FA oxidation [48], reduced mitochondrial GPAT activity [54] and greater oxidability of vaccenic versus elaidic acid [19]. All these differences found in ex vivo and in vitro assays with liver extracts could be modulated in whole animals, for instance because *cis*-9, *trans*-11-CLA mainly synthesised from *trans*-11 in extrahepatic organs might interfere in the liver lipid metabolism. In the same way, hormonal specificities could differently affect FA oxidation and esterification pathways in humans ingesting both *trans*-$C_{18:1}$ [6]. These data support the fact that vaccenic and elaidic acids are dissimilar substrates for crucial steps of the PL synthesis pathway in liver.

Acknowledgments We thank Mr Jean-Michel Chardigny DR INRA, Mr Koenraad Duhem, Mrs Corinne Marmonier for helpful discussions, and Mrs Monique Baudoin for figure construction and typing of the manuscript. This work was supported by Grants from the CNIEL (Paris) and the Région Bourgogne (Dijon), France.

References

1. Ascherio A, Katan MB, Zock PL, Stampfer MJ, Willett WC (1999) *Trans* fatty acids and coronary heart disease. N Engl J Med 340:1994–1998
2. Nelson GJ (1998) Dietary fat, *trans* fatty acids, and risk of coronary heart disease. Nutr Rev 56:250–252
3. Constant J (2004) The role of eggs, margarines and fish oils in the nutritional management of coronary artery disease and strokes. Keio J Med 53:131–136
4. Schwandt P (1995) *Trans*-fatty acids and atherosclerosis. Med Monatsschr Pharm 18:78–79
5. Ackman RG, Mag TK (1998) *Trans* fatty acids and the potential for less in technical products. In: Sébédio JL, Christie WW (eds) *Trans* fatty acids in human nutrition. The Oily Press, Dundee
6. Chardigny JM, Destaillats F, Malpuech-Brugere C, Moulin J, Bauman DE, Lock AL, Barbano DM, Mensink RP, Bezelgues JB, Chaumont P, Combe N, Cristiani I, Joffre F, German JB, Dionisi F, Boirie Y, Sebedio JL (2008) Do *trans* fatty acids from industrially produced sources and from natural sources have the same effect on cardiovascular disease risk factors in healthy subjects? Results of the *trans* fatty acids collaboration (Transfact) study. Am J Clin Nutr 87:558–566
7. Wolff RL, Combe NA, Destaillats F, Boue C, Precht D, Molkentin J, Entressangles B (2000) Follow-up of the Δ4 to Δ16 trans-18:1 isomer profile and content in french processed foods containing partially hydrogenated vegetable oils during the period 1995–1999. Analytical and nutritional implications. Lipids 35:815–825
8. Whayne TF, Alaupovic P, Curry MD, Lee ET, Anderson PS, Schechter E (1981) Plasma apolipoprotein B and VLDL-, LDL-, and HDL-cholesterol as risk factors in the development of coronary artery disease in male patients examined by angiography. Atherosclerosis 39:411–424
9. Ledoux M, Rouzeau A, Bas P, Sauvant D (2002) Occurrence of *trans*-C18:1 fatty acid isomers in goat milk: effect of two dietary regimens. J Dairy Sci 85:190–197
10. Precht D, Molkentin J (1997) Effect of feeding on *trans* positional isomers of octadecenoic acid in milk fats. Milchwissenschaft 52:564–568
11. Ascherio A, Hennekens CH, Buring JE, Master C, Stampfer MJ, Willett WC (1994) *Trans*-fatty acids intake and risk of myocardial infarction. Circulation 89:94–101
12. Bolton-Smith C, Woodward M, Fenton S, Brown CA (1996) Does dietary *trans* fatty acid intake relate to the prevalence of coronary heart disease in Scotland ? Eur Heart J 17:837–845
13. Willett WC, Stampfer MJ, Manson JE, Colditz GA, Speizer FE, Rosner BA, Sampson LA, Hennekens CH (1993) Intake of *trans*

fatty acids and risk of coronary heart disease among women. Lancet 341:581–585
14. Meijer GW, van Tol A, van Berkel TJ, Weststrate JA (2001) Effect of dietary elaidic versus vaccenic acid on blood and liver lipids in the Hamster. Atherosclerosis 157:31–40
15. Tyburczy C, Major C, Lock AL, Destaillats F, Lawrence P, Brenna JT, Salter AM, Bauman DE (2009) Individual *trans* octadecenoic acids and partially hydrogenated vegetable oil differentially affect hepatic lipid and lipoprotein metabolism in Golden Syrian Hamsters. J Nutr 139:257–263
16. Motard-Belanger A, Charest A, Grenier G, Paquin P, Chouinard Y, Lemieux S, Couture P, Lamarche B (2008) Study of the effect of trans fatty acids from ruminants on blood lipids and other risk factors for cardiovascular disease. Am J Clin Nutr 87:593–599
17. Jensen RG, Sampugna J, Pereira RL (1964) Pancreatic lipase. Lipolysis of synthetic triglycerides containing a *trans* fatty acid. Biochim Biophys Acta 84:481–483
18. Coots RH (1964) A comparison of the metabolism of elaidic, oleic, palmitic, and stearic acids in the rat. J Lipid Res 5:468–472
19. Du ZY, Degrace P, Gresti J, Loreau O, Clouet P (2010) Dissimilar properties of vaccenic versus elaidic acid in beta-oxidation activities and gene regulation in rat liver cells. Lipids 45:581–591
20. Yu W, Liang X, Ensenauer RE, Vockley J, Sweetman L, Schulz H (2004) Leaky beta-oxidation of a *trans*-fatty acid: incomplete beta-oxidation of elaidic acid is due to the accumulation of 5-*trans*-tetradecenoyl-CoA and its hydrolysis and conversion to 5-*trans*-tetradecenoylcarnitine in the matrix of rat mitochondria. J Biol Chem 279:52160–52167
21. Høy CE, Hølmer G (1979) Incorporation of *cis*- and *trans*-octadecenoic acids into the membranes of rat liver mitochondria. Lipids 14:727–733
22. Channing MA, Simpson N (1993) Radiosynthesis of [1–^{11}C] polyhomoallylic fatty acids. J Label Compd Radiopharm 33: 541–546
23. Goldman P, Vagelos PR (1961) The Specificity of triglyceride synthesis from diglycerides in chicken adipose tissue. J Biol Chem 236:2620–2623
24. Korsrud GO, Conacher HB, Jarvis GA, Beare-Rogers JL (1977) Studies on long chain *cis*- and *trans*-acyl-CoA esters and acyl-CoA dehydrogenase from rat heart mitochondria. Lipids 12:177–181
25. Lawson LD, Kummerow FA (1979) Beta-oxidation of the coenzyme A esters of elaidic, oleic, and stearic acids and their full-cycle intermediates by rat heart mitochondria. Biochim Biophys Acta 573:245–254
26. Lawson LD, Kummerow FA (1979) Beta-oxidation of the coenzyme A esters of vaccenic, elaidic, and petroselaidic acids by rat heart mitochondria. Lipids 14:501–503
27. Seglen PO (1973) Preparation of rat liver cells. 3. Enzymatic requirements for tissue dispersion. Exp Cell Res 82:391–398
28. Folch J, Lees M, Sloane Stanley GH (1957) A simple method for the isolation and purification of total lipids from animal tissues. J Biol Chem 226:497–509
29. Demizieux L, Degrace P, Gresti J, Loreau O, Noel JP, Chardigny JM, Sebedio JL, Clouet P (2002) Conjugated linoleic acid isomers in mitochondria: evidence for an alteration of fatty acid oxidation. J Lipid Res 43:2112–2122
30. Niot I, Pacot F, Bouchard P, Gresti J, Bernard A, Bezard J, Clouet P (1994) Involvement of microsomal vesicles in part of the sensitivity of carnitine palmitoyltransferase I to malonyl-CoA inhibition in mitochondrial fractions of rat liver. Biochem J 304:577–584
31. Smith PK, Krohn RI, Hermanson GT, Mallia AK, Gartner FH, Provenzano MD, Fujimoto EK, Goeke NM, Olson BJ, Klenk DC (1985) Measurement of protein using bicinchoninic acid. Anal Biochem 150:76–85
32. Bates EJ, Saggerson D (1977) A selective decrease in mitochondrial glycerol phosphate acyltransferase activity in livers from streptozotocin-diabetic rats. FEBS Lett 84:229–232
33. Okuyama H, Eibl H, Lands WE (1971) Acyl coenzyme A:2-acyl-*sn*-glycerol-3-phosphate acyltransferase activity in rat liver microsomes. Biochim Biophys Acta 248:263–273
34. Chomczynski P, Sacchi N (1987) Single-step method of RNA isolation by acid guanidinium thiocyanate–phenol–chloroform extraction. Anal Biochem 162:156–159
35. McGarry JD, Woeltje KF, Kuwajima M, Foster DW (1989) Regulation of ketogenesis and the renaissance of carnitine palmitoyltransferase. Diabetes Metab Rev 5:271–284
36. Bickerstaffe R, Annison EF (1970) Lipid metabolism in the perfused chicken liver. The uptake and metabolism of oleic acid, elaidic acid, *cis*-vaccenic acid, *trans*-vaccenic acid and stearic acid. Biochem J 118:433–442
37. Wolff RL, Entressangles B (1994) Steady-state fluorescence polarization study of structurally defined phospholipids from liver mitochondria of rats fed elaidic acid. Biochim Biophys Acta 1211:198–206
38. Woldseth B, Retterstol K, Christophersen BO (1998) Monounsaturated *trans* fatty acids, elaidic acid and *trans*-vaccenic acid, metabolism and incorporation in phospholipid molecular species in hepatocytes. Scand J Clin Lab Invest 58:635–645
39. Casaschi A, Maiyoh GK, Adeli K, Theriault AG (2005) Increased diacylglycerol acyltransferase activity is associated with triglyceride accumulation in tissues of diet-induced insulin-resistant hyperlipidemic Hamsters. Metabolism 54:403–409
40. Degrace P, Demizieux L, Du ZY, Gresti J, Caverot L, Djaouti L, Jourdan T, Moindrot B, Guilland JC, Hocquette JF, Clouet P (2007) Regulation of lipid flux between liver and adipose tissue during transient hepatic steatosis in carnitine-depleted rats. J Biol Chem 282:20816–20826
41. Sul HS, Wang D (1998) Nutritional and hormonal regulation of enzymes in fat synthesis: studies of fatty acid synthase and mitochondrial glycerol-3-phosphate acyltransferase gene transcription. Annu Rev Nutr 18:331–351
42. Takeuchi K, Reue K (2009) Biochemistry, physiology, and genetics of GPAT, AGPAT, and lipin enzymes in triglyceride synthesis. Am J Physiol Endocrinol Metab 296:E1195–E1209
43. Hornick CA, Thouron C, DeLamatre JG, Huang J (1992) Triacylglycerol hydrolysis in isolated hepatic endosomes. J Biol Chem 267:3396–3401
44. Malewiak MI, Rozen R, Le Liepvre X, Griglio S (1988) Oleate metabolism and endogenous triacylglycerol hydrolysis in isolated hepatocytes from rats fed a high-fat diet. Diabete Metab 14: 270–276
45. Newkirk JD, Waite M (1973) Phospholipid hydrolysis by phospholipase A 1 and A 2 in plasma membranes and microsomes of rat liver. Biochim Biophys Acta 298:562–576
46. Pykalisto OJ, Vogel WC, Bierman EL (1974) The tissue distribution of triacylglycerol lipase, monoacylglycerol lipase and phospholipase A in fed and fasted rats. Biochim Biophys Acta 369:254–263
47. Franson R, Waite M, LaVia M (1971) Identification of phospholipase A 1 and A 2 in the soluble fraction of rat liver lysosomes. Biochemistry 10:1942–1946
48. McGarry JD, Meier JM, Foster DW (1973) The effects of starvation and refeeding on carbohydrate and lipid metabolism in vivo and in the perfused rat liver. The relationship between fatty acid oxidation and esterification in the regulation of ketogenesis. J Biol Chem 248:270–278
49. Mahfouz MM, Valicenti AJ, Holman RT (1980) Desaturation of isomeric *trans*-octadecenoic acids by rat liver microsomes. Biochim Biophys Acta 618:1–12

50. Kraft J, Hanske L, Möckel P, Zimmermann S, Härtl A, Kramer JK, Jahreis G (2006) The conversion efficiency of *trans*-11 and *trans*-12 18:1 by delta9-desaturation differs in rats. J Nutr 136:1209–1214
51. Kramer JK, Sehat N, Dugan ME, Mossoba MM, Yurawecz MP, Roach JA, Eulitz K, Aalhus JL, Schaefer AL, Ku Y (1998) Distributions of conjugated linoleic acid (CLA) isomers in lipid tissue classes of pigs fed a commercial CLA mixture determined by gas chromatography and silver ion-high-performance liquid chromatography. Lipids 33:549–558
52. Gruffat D, De La Torre A, Chardigny JM, Durand D, Loreau O, Bauchart D (2005) Vaccenic acid metabolism in the liver of rat and bovine. Lipids 40:295–301
53. Subbaiah PV, Gould IG, Lal S, Aizezi B (2011) Incorporation profiles of conjugated linoleic acid isomers in cell membranes and their positional distribution in phospholipids. Biochim Biophys Acta 1811:17–24
54. Beauseigneur F, Tsoko M, Gresti J, Clouet P (1999) Reciprocal enzymatic interference of carnitine palmitoyltransferase I and glycerol-3-phosphate acyltransferase in purified liver mitochondria. Adv Exp Med Biol 466:69–78
55. Sugimoto H, Yamashita S (1994) Purification, characterization, and inhibition by phosphatidic acid of lysophospholipase transacylase from rat liver. J Biol Chem 269:6252–6258
56. Yamashita A, Sugiura T, Waku K (1997) Acyltransferases and transacylases involved in fatty acid remodeling of phospholipids and metabolism of bioactive lipids in mammalian cells. J Biochem 122:1–16
57. Colard O, Bard D, Bereziat G, Polonovski J (1980) Acylation of endogenous phospholipids and added lyso derivatives by rat liver plasma membranes. Biochim Biophys Acta 618:88–97
58. Hasegawa-Sasaki H, Ohno K (1980) Extraction and partial purification of acyl-CoA:1-acyl-*sn*-glycero-3-phosphocholine acyltransferase from rat liver microsomes. Biochim Biophys Acta 617:205–217
59. Patsch W, Tamai T, Schonfeld G (1983) Effect of fatty acids on lipid and apoprotein secretion and association in hepatocyte cultures. J Clin Invest 72:371–378
60. Sparks CE, Sparks JD, Bolognino M, Salhanick A, Strumph PS, Amatruda JM (1986) Insulin effects on apolipoprotein B lipoprotein synthesis and secretion by primary cultures of rat hepatocytes. Metabolism 35:1128–1136
61. Kalopissis AD, Griglio S, Malewiak MI, Rozen R, Liepvre XL (1981) Very-low-density-lipoprotein secretion by isolated hepatocytes of fat-fed rats. Biochem J 198:373–377
62. Wang Y, Jacome-Sosa MM, Ruth MR, Goruk SD, Reaney MJ, Glimm DR, Wright DC, Vine DF, Field CJ, Proctor SD (2009) *trans*-11 vaccenic acid reduces hepatic lipogenesis and chylomicron secretion in JCR:LA-cp rats. J Nutr 139:2049–2054

Lipids (2011) 46:659–667
DOI 10.1007/s11745-011-3567-8

METHODS

Fast and Minimally Invasive Determination of the Unsaturation Index of White Fat Depots by Micro-Raman Spectroscopy

M. Giarola · B. Rossi · E. Mosconi · M. Fontanella · P. Marzola · I. Scambi · A. Sbarbati · G. Mariotto

Received: 23 September 2010 / Accepted: 19 April 2011 / Published online: 15 May 2011

Abstract In the last 20 years increasing interest has been devoted to the investigation of white adipose tissue (WAT) because hypo- or hyperfunction of WAT is involved in the pathogenesis of obesity and other pathologies. The investigation and discrimination of different characteristics in adipose tissues by means of spectroscopic techniques appears as a topic of current interest, also in view of possible medical–technological applications. The aim of this work was to establish micro-Raman spectroscopy as a tool for the characterization of mammals fat tissue. After preliminary tests aimed at defining a suitable sample preparation protocol, Raman spectra of WAT specimens excised from mice of different ages were recorded in the energy range 750–3,350 cm^{-1}. Quantitative values of the unsaturation index were obtained through the calibration with HR-NMR spectra of lipid extracts. Raman spectroscopy detected a sharp increase in the unsaturation index between 22 and 30 days of age in close correspondence with the weaning of mice (21 days). The present results show that Raman spectroscopy is an inexpensive, fast and robust technique to analyze the unsaturation index of mammals fat tissues that could be routinely used in bioptic samples.

Keywords White adipose tissue · Unsaturation index · Micro-Raman spectroscopy · High-resolution nuclear magnetic resonance

M. Giarola · B. Rossi · P. Marzola · G. Mariotto (✉)
Dipartimento di Informatica, Università di Verona, Verona, Italy
e-mail: gino.mariotto@univr.it

E. Mosconi · M. Fontanella · I. Scambi · A. Sbarbati
Dipartimento di Scienze Neurologiche, Neuropsicologiche, Morfologiche e Motorie, Università di Verona, Verona, Italy

Abbreviations

BAT	Brown adipose tissue
CCD	Charge coupled device
EEC	European Community Council
FA	Fatty acid(s)
FAME	Fatty acids methyl ester(s)
FVB/NHsd	Friend virus B/derived from breeding nucleus obtained from National Institutes of Health, Bethesda in 1988
HR-NMR	High-resolution nuclear magnetic resonance
LCModel	Linear combination of model
MCL	Mean chain length
μl	Micro-liters
mRNA	Messenger ribonucleic acid
MRS	Magnetic resonance spectroscopy
NA	Normalized area
NEX	Number of excitations
NIH	National Institute of Health
NMR	Nuclear magnetic resonance
PI	Polyunsaturation index
ppm	Part per million
PRESS	Point resolved spectroscopy
TE	Time echo
TG	Triglyceride(s)
TR	Time repetition
TXI	Triple-resonance inverse
UI	Unsaturation index
VOI	Volume-of-interest
WAT	White adipose tissue

Introduction

The adipose tissue exists in two morphologically and functionally distinct forms, i.e. white adipose tissue

(WAT) and brown adipose tissue (BAT). These two forms of adipose tissue have, in fact, different cell structure, location, vascularization, morphology and biological functions [1, 2]. The characterization of WAT is very important due to its role in well defined metabolic dysfunctions leading to several diseases, like obesity [3], heart disease, diabetes, hypertension and atherosclerosis [4]. Three main functions of this adipose tissue in mammals are nowadays well recognized. The first one is the storage of triglycerides, i.e. the uppermost energy reserve. The second one is the catabolization of triglycerides which results in the release of glycerol and fatty acids participating in glucose metabolism in liver and in other organs and tissues. Finally, its adipocytes secrete the adipokines, which include hormones and other proteins with specific biological functions [5]. In addition, recent studies have shown a strong correlation between age of the living organisms and specific changes of the fat characteristics in obese individuals [6, 7]. Some results indicate that during the first three months of rat life there are distinct phases of the metabolic evolution in WAT related to leptin mRNA and serum leptin concentration changes regulating the amount of body fat [6, 7].

In the past years, several studies, mainly based on invasive approaches, have investigated the release process of fatty acids [8–15] but only few of them have considered their mobilization [8, 9, 14, 15]. On the other hand, this last property is related to their degree of unsaturation [9, 14, 15], a very important feature because differential mobilization could greatly influence the storage and the subsequent utilization of the individual fatty acids. The mobilization also determines the type of fatty acids supplied by adipose tissue to other tissues and organs, notably in conditions of negative energy balance.

In more recent years there has been an increasing interest in spectroscopic techniques for fast, non destructive and minimally invasive characterization of adipose tissue [16, 17]. To this aim vibrational spectroscopy, dealing with Raman scattering, has been extensively used for the analysis of fats with specific concern for its classification, in terms of its composition and constituents [18–26]. Part of these Raman investigations were focused on fatty acids [18, 20, 22–24, 26] while some of them were specifically addressed to the assessment of their molar unsaturation [20, 23, 24, 26].

Fat composition assessment by high resolution proton NMR spectra (HR-NMR) of tissue extracts is a relatively simple matter since signals from protons adjacent to double bonds are easily resolved [27]. Nevertheless, NMR analysis of fat requires an extraction procedure that is time consuming and destructive for the sample. Recently, we have demonstrated that micro Raman spectroscopy performed in freshly excised and unprocessed fat tissues allows the determination of the unsaturation index (UI), with results in good agreement with the literature [28].

In the present work we further validate the usefulness of Raman spectroscopy by a quantitative comparison with proton HR-NMR and demonstrate that both techniques are able to detect the substantial increase in the unsaturation index occurring in mice WAT after weaning. Since HR-NMR spectra are acquired in lipid extracts while Raman spectra are recorded in unprocessed tissue, localized Magnetic Resonance Spectroscopy (MRS) of in vivo WAT tissue was also exploited in order to detect the possible effect of the extraction procedure. Hereafter, the experimental results will be presented and discussed in terms of lipid mobilization and of the related physiological aspects.

Materials and Methods

Animals and Tissue Extraction

Male young (10, 15, 22 days), adult (1, 3, 6 months) and old (12 months) mice of FVB/NHsd strain (Harlan, Italy) were used for the study. They were maintained in a colony at 25 °C with an alternating 12 h dark and light schedule and had free access to standard mice feed and drinking water. Experimental protocols were approved by the animal ethical committee of the University of Verona and followed the NIH Guide for the Use Care of Laboratory Animals and the European Community Council (86/609/EEC) directive. For each age, $n = 4$ mice were used, except for the 12 months group ($n = 3$). After in vivo MRS experiments, animals were killed by cervical dislocation and inguinal adipose tissue was removed for ex vivo Raman and HR-NMR measurement.

Raman measurements were run on the tissue immediately after its removal. For HR-NMR, the lipidic fraction of adipose WAT was extracted in a chloroform–ethanol mixtures (2:1 v/v) according to Folch et al. [29]. The procedure yielded an aqueous fraction containing water-soluble molecules and an organic fraction containing lipids. The latter phase was dried under a stream of anhydrous nitrogen gas, lyophilized in a freeze-drying apparatus (Freeze-Dryer Modulyo) and dissolved in 600 µl deuterated chloroform for HR-NMR measurements. A similar extraction procedure was applied to standard mice feed. After a short period of suckling, two pups were killed by cervical dislocation and a few drops of milk samples obtained by manual squeezing of the stomach. Raman spectra were recorded on mother milk without any treatment.

Raman Measurements

Micro-Raman spectra were carried out in backscattering geometry at room temperature using a triple-monochromator (Horiba-Jobin Yvon, model T64000), set in double-subtractive/single configuration, and equipped with holographic gratings having 1,800 lines mm^{-1}. The scattered radiation was detected at the spectrograph output by a charge coupled device (CCD) detector, with 1,024 × 256 pixels, cooled by liquid nitrogen. The spectra were excited by the 514.5 nm line of a mixed Ar–Kr ion gas laser and laser power on the sample surface was kept below 5 ± 0.1 mW, and was focused with a spot of 2 μm in diameter through the lens of an objective 80× (numerical aperture 0.75). The spectral resolution was better than 0.6 cm^{-1} pixel while the spectral linearity of the system was calibrated using a 50:50 (v/v) acetonitrile/toluene mixture and comparing to frequency standards from the American Standard Testing Method ASTM E 1840 (1996). Repeated micro-Raman measurements were carried out under the same experimental conditions from several regions of the same sample, obtaining very reproducible spectra for WAT tissue. The spectra collected from morphologically similar regions showed good reproducibility (the mean error of peak intensity was of the order of 3%). The recorded spectra were processed to remove artifacts due to cosmic rays, while the luminescence background, consisting of a flat and structureless background of very weak intensity spread over the whole Raman spectrum, was removed by comparing replicate spectra of each sample over the whole sampled spectral range.

MRS and HR-NMR Measurements

In vivo MRS experiments were carried out using a Biospec System (Bruker Biospin, Germany) equipped with a 4.7 T horizontal Oxford Magnet, 33-cm bore size. A 72-mm internal diameter bird-cage coil and a flat surface receiver coil were used. Animals were pre-anesthetized with 5% of isofluorane, and maintained during acquisitions with 1–1.5% of isofluorane in a mixture of O_2 and air. The surface coil was carefully positioned in the inguinal part of the mice. After acquisition of reference images for localization of inguinal fat deposits, localized proton spectra were acquired from a volume-of-interest (VOI) of 1 mm^3. The dimensions of the inguinal fat deposits in young animals were too small to reliably position the 1 mm^3 Voxel. In vivo spectra were consequently acquired only in adult and old mice. Spectra were acquired using a Point Resolved Spectroscopy (PRESS) sequence with TR = 4,000 ms, TE = 22 ms, 256 number of excitations (NEX), 1,024 points, without water suppression. PRESS sequence uses a combination of magnetic fields gradients and r.f. pulses (90°–180°–180°) to select a three dimensional voxels of a well defined size. In vivo spectra were then analyzed with LCModel [30].

HR-NMR was performed using a Bruker DRX-500 spectrometer operating at 500.13 MHz proton Larmor frequency, and equipped with a 5 mm TXI probe head. The sample temperature in the probe was 25 °C. Pulse programs from the standard Bruker library (Topspin 1.3) were used. Proton NMR spectra were acquired with an acquisition time of 1.6 s, flip angle of 45°, 2 s of relaxation delays, spectral width of 5 kHz, 16 K acquired points, and total number of scans equal to 128. Data were processed with 32 K points, baseline corrections and phase adjustments. No line broadening was applied in data processing. The chloroform proton signal at 7.27 ppm was used as chemical shift reference. Resonances were identified based on available chemical shift data. Mean lipid acyl chain unsaturation and polyunsaturation indexes were calculated from proton spectra according to the methods reported in literature [31], exploiting the areas of the peaks of the different chemical groups in the lipid chains.

Peak assignment and the procedures followed for extraction of triglyceride (TG) parameters, both for HR-NMR and MRS spectra, are reported hereafter.

Peak Assignment and Calculation of TG Parameters

White adipose tissue is mainly constituted by TG molecules and NMR spectra reflect its composition. Figure 1a, b shows representative ex vivo and in vivo spectra of inguinal adipose tissue, respectively. The proton resonance peaks are labelled according to the different chemical groups constituting TG molecules (see Fig. 1c). The two spectra show the same number of peaks at the same chemical shifts, with the exception of a small water (W) signal that is present in the in vivo experiments (Fig. 1b).

The chemical properties of TG molecules namely unsaturation (UI) and polyunsaturation (PI) indexes and mean chain length (MCL) were determined by applying the following formulas according to Zancanaro et al. [31].

$$\mathrm{UI} = (L + M)/(2/3A)$$

$$\mathrm{PI} = G/(2/3A)$$

$$\mathrm{MCL} = (2/3A + B + C + D + E + F + G + 2(L + M))/(2/3A)$$

where, each letter represents the area under the corresponding peak. The index UI is equivalent to the number of vinilyc protons ratioed to the terminal methyl group and is a molar measurement of unsaturation. The index PI is equivalent to the number of protons attached to the diallylic methylene of conjugated double bonds ratioed

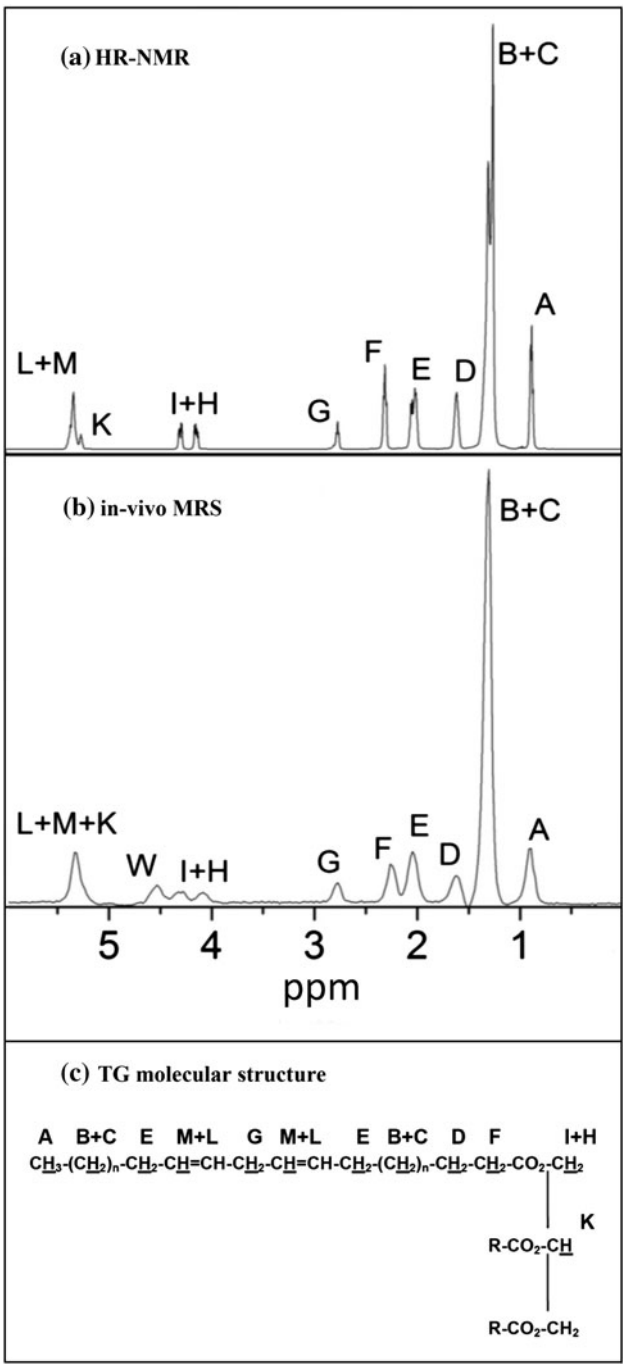

Fig. 1 The representative ex vivo (**a**) and in vivo (**b**) spectra of inguinal adipose tissue. The areas under a peaks (*A*, *B*, *C*…) are proportional to the number of protons in a given chemical environment within a TG molecular structure (**c**)

to the methyl group and provides a measurement of molar poly-unsaturation. In agreement with Zancanaro et al. [31], relevant presence of mono- and diglycerides in WAT samples was excluded by verifying that the two following relationships were in good agreement with experimental data:

$$A/(I+H) = 9/4$$

$$F/(I+H) = 6/4$$

The two relationships represent, respectively, the ratio between the number of protons bound to the methyl (*A*) or acetalyc (*F*) groups and the glyceril esterified methylene ones ($I + H$).

Thanks to high resolution and good separation of the signals, the areas under the peaks could be calculated by simple integration in HR-NMR spectra. This procedure could not be applied to in vivo MRS experiments, because of the low resolution and partial overlapping of the peaks [27] as clearly apparent in Fig. 1b. MRS spectra were consequently analyzed by using the LCModel software [30]. Since LCModel does not distinguish peak *K* from ($L + M$), the integral of the peak *K* was obtained from the peak *A* according to the theoretical value $K = A/9$ which holds for TG molecules, i.e. the number of methynic esterified glycerol protons (*K*) is assumed to be 1/9 of that of methyl group (*A*). In agreement with the fact that WAT consists mainly of TG molecules, ex vivo HR-NMR spectra confirmed that the ratio between *A* and *K* is in agreement with the above mentioned theoretical value. Then the ($L + M$) peak was obtained using the following formula:

$$(L+M) = (L+M+K) - A/9$$

Results and Discussion

A typical micro-Raman spectrum of WAT, after subtraction of the luminescence background, in the extended wave number range 750–3,350 cm^{-1} is reported in Fig. 2 (full panel). It consists of several bands and some sharp peaks of different intensity occurring in the spectral region between 800 and 1,800 cm^{-1}, but is dominated by some very strong bands in the region 2,800–3,100 cm^{-1}.

In order to identify the origin of the different spectral features of adipose tissue we can refer to some reference database of Raman spectra of bio-molecules, either in form of text-book [32] or full-length paper [17]. Table 1 lists both the position, in terms of wave numbers, and the assignment of main bands observed in the 800–3,050 cm^{-1} spectral region of Raman spectrum of WAT, according the some available literature reports [17, 25, 33–43].

According to the assignments of this Table we can claims that the overall structure of the observed spectrum is that of TG molecules, which indeed constitute the main component of WAT [30]. Therefore, a finer spectral analysis of the Raman features of TG component of WAT will allow us to gain further insights into the white adipose tissue, especially into its unsaturation index, which is related to the number of double C=C bonds present in each

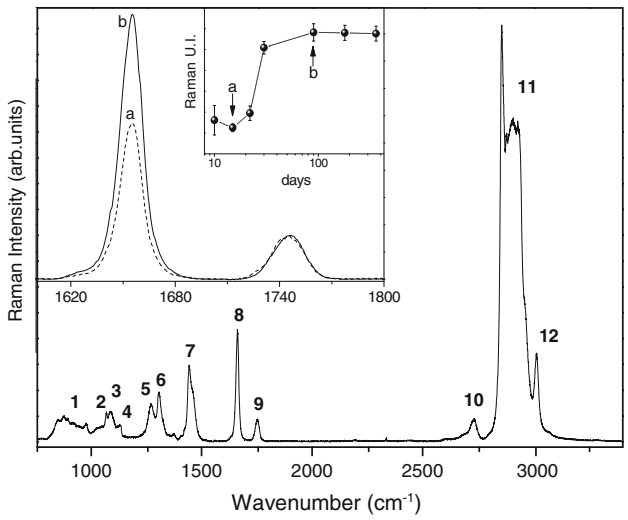

Fig. 2 Typical Raman spectrum of WAT recorded at room temperature in the wave number range 750–3,350 cm^{-1} (*full panel*); partial Raman spectra of WAT in the region of C=C and C=O symmetric stretching modes (*internal panel*). Representative spectra acquired at 15 (**a**) and 90 days (**b**) are compared. The *inset* of the *internal panel* shows the dependence of the normalized intensity of the 1,655 cm^{-1} peak as a function of the mice age is reported. *Points* labelled by "*a*" and "*b*" refer to the UI obtained from spectra plotted in the figure

TG chain. To this aim, the key spectral feature is the peak at 1,655 cm^{-1}, which is attributed to the symmetric stretching mode of the double C=C bonds of the TG component [17, 39]. Obviously, the spectral intensity of this peak is expected to depend on the number of C=C bands in TG, and therefore, the intensity of Raman peak at 1,655 cm^{-1} can be straightforwardly related to unsaturation index of lipid component in WAT. Therefore, white adipose tissues characterized by different unsaturation index will show different spectral intensity of the 1,655 cm^{-1} peak.

Representative, partial Raman spectra, acquired in the spectral region between 1,600 and 1,800 cm^{-1}, from two WAT specimens, excised from 15-day (spectrum a) old and 90-day (spectrum b) old mice, respectively, are also shown in Fig. 2 (internal panel). Before the plot, the spectra were normalized to the area of the peak centred at about 1,745 cm^{-1}, which is attributed to the stretching vibration of the C=O group [17, 38]. The Raman peak due to the vibrational of C=O groups is assumed to be an internal reference because the number of carbonyl groups for each TG is constant independent of the unsaturation index of their hydrocarbon chains. This assumption is justified because the presence of mono- and diglycerides in WAT is negligible [31].

We have taken the intensity of the peak at 1,745 cm^{-1} as the reference, instead of that of the band at 1,440 cm^{-1}, because this one constitutes, in our opinion, a much less reliable standard, since it clearly consists of some overlapping spectral components (see, for instance, the spectrum of Fig. 2, full panel, or ref. [17]), the position of which turns out to depend on the length of the fatty acid (FA) chains. In fact, it has been proved that the intensity of this 1,440 cm^{-1} band turns out to depend on the number of carbons within the FA chain [20, 44], which, on the other hand, is not constant in TGs chains forming WAT. In alternative, in the case of adipose tissue, the peak at 1,745 cm^{-1} seem to provides a much more reliable standard for evaluating the UI of WAT, being specifically related to number of carbonyl groups in TGs, i.e. the paramount component of WAT, as revealed by the NMR measurements, which also were not able to detect any

Table 1 Assignment of bands observed in the Raman spectra of white adipose tissue

Band regions	Band position (cm^{-1})	Band assignment [refs.]
1	800–920	ν (C–C), $CH_{3\ rk}$ mixture of stretch and rock modes at acyl and methyl terminals in solid state [33]
2	1,060–1,065	ν_{op} (C–C) out-of-phase aliphatic C–C stretch all *trans* [34]
3	1,080–1,090	ν_g (C–C) liquid: aliphatic C–C stretch in *gauche* [35]
4	1,100–1,135	ν_{ip} (C–C) in-phase aliphatic C–C stretch all *trans* [36]
5	1,250–1,280	δ_{ip} (=CH) in-plane *cis* olefinic hydrogen bend [37]
6	1,295–1,305	δ_{tw} (CH_2) methylene twist deformation [37]
7	1,400–1,500	δ_{sc} (CH_2) methylene scissor deformation [17] and asymmetric bending CH_3 [32]
8	1,650–1,680	ν (C=C) *cis* and *trans* olefinic stretch [17, 39]
9	1,730–1,750	ν (C=O) carbonyl stretch [17, 38]
10	2,720–2,730	ν (CH) olefinic stretching mode [40] or combination of δ_{sc} ($-CH_2$) + ρ_w ($-CH_2$) methylene modes [41, 42]
11	2,800–2,950	ν_s (CH_2), ν_{as} (CH_2) symmetric and anti-symmetric methylene stretch and ν_s (CH_3), ν_{as} (CH_3) symmetric and anti-symmetric methyl stretch [42, 43]
12	3,010–3,040	ν_{as} (=C–H) anti-symmetric =C–H stretch [25]

The band regions are defined in Fig. 2 (full panel)

ν stretching modes, δ deformation modes, ρ_w wagging mode

appreciable component of free fatty acids in it [31]. By the way, it is worth to mention that the intensity of the peak at 1,745 cm^{-1} is is taken as the reference to evaluate the molar parameters of fatty acids methyl esthers (FAME) by some authors [20, 43–45]. On the other hand, the intensity of this peaks cannot be properly adopted as the reference for the assessment of the UI of free fatty acids, for which the situation is much more complex due to the spectral intermixing of C=C and C=O stretching modes. In fact, in the case of oleic acid, a well-known free FA, Muik et al. [24] did not observe any peak at about 1,740 cm^{-1} associated with C=O stretching mode since the wave number of the C=O stretching vibration in the free FA chains at room temperature occurs near the C=C stretching vibration peak at 1,650 cm^{-1} as it can be clearly inferred from Ref. [25]. On the other hand, Tandon et al. [25] show that the peak wave number of C=O stretching in free FA shifts from about 1,638 to 1,643 cm^{-1} when the temperature varies from −20 to +12 °C. Therefore, this finding clearly shows that, in the case of free FA, it is improper to refer to the intensity of the band peaked at 1,650 cm^{-1} at room temperature in order to evaluate the molar unsaturation parameter of free FA, since this peak intensity could be affected by the contribution of the C=O stretching mode, which is nearly degenerate with the C=C mode. Therefore, on the basis of the above considerations it should be inferred that the unsaturation parameter of FA, assessed according to this procedure, is affected by a systematic error, e.g., overestimated, due to the spurious contribution of the C=O stretching.

In conclusion, taking the above discussed considerations into account, in the case of WAT a quantitative evaluation of the unsaturation index of TG chains can be obtained simply by measuring the area of the 1,655 cm^{-1} peak normalized to the intensity of the 1,745 cm^{-1} peak, in the following referred to as the normalized area (NA). The NA of the peak at 1,655 cm^{-1} versus animals age (in days) is reported in the internal panel inset of Fig. 2. This plot suggests a remarkable change of the unsaturation index of lipid component of WAT between 21 and 30 days of age.

The chemical properties extracted from HR-NMR and MRS spectra at different mice age are summarized in Table 2. Mice younger than 1 month were not examined by MRS due to small size (<1 mm^3) of inguinal deposits. Mean values of UI obtained by the two techniques are very close. PI values could not be calculated by MRS spectra due to the low signal/noise of peak *G*. MCL values evaluated by HR-NMR differ substantially from those evaluated by MRS. The reasons for this discrepancy are currently under evaluation. However, the results of HR-NMR, obtained on mice older than 21 days, correlate with the literature data [18, 19]. In fact, UI and MCL values obtained by us on WAT samples of mice older that 21 days are quite close to those observed by Beattie et al. [19] on pork and kitchen fat. This fact seems to confirm that a strong correlation exists between the adipose tissue composition and the presence of mono and poly-unsaturated fatty acids in the diet of different species of mono-gastric animals [46, 47].

Table 2 Chemical properties of TGs (UI, PI and MCL) calculated from HR-NMR spectra

Mice age (days)	UI	PI	MCL
HR-NMR			
10	0.64 ± 0.06	0.19 ± 0.01	16.23 ± 0.25
15	0.61 ± 0.01	0.18 ± 0.00	16.13 ± 0.24
22	0.65 ± 0.01	0.18 ± 0.00	16.30 ± 0.22
30	0.99 ± 0.01	0.34 ± 0.01	17.26 ± 0.21
90	1.02 ± 0.03	0.32 ± 0.01	17.08 ± 0.09
180	1.08 ± 0.01	0.33 ± 0.01	17.25 ± 0.12
360	1.03 ± 0.05	0.30 ± 0.02	16.96 ± 0.16
MRS			
30	0.98 ± 0.06	–	15.19 ± 0.21
90	1.06 ± 0.12	–	13.45 ± 0.28
180	1.05 ± 0.10	–	14.19 ± 0.46
360	1.07 ± 0.24	–	12.45 ± 0.20

Figure 3 shows the behaviour of the value of NA versus the unsaturation index obtained by HR-NMR in the WAT samples of the animals investigated. The plot shows a good linear correlation between the Raman normalized intensity and the unsaturation index, as determined by HR-NMR. By using the extrapolated linear relationship, quantitative values of the unsaturation index can be straightforwardly obtained from Raman spectra of WAT.

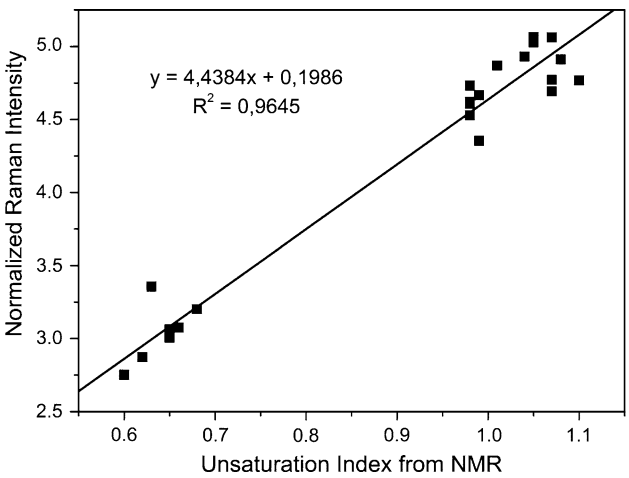

Fig. 3 Correlation between UI, as determined by HR-NMR, and the intensity of the Raman 1,650 cm^{-1} peak (normalized to that of the peak at 1,745 cm^{-1}, see text)

Figure 4 shows the dependence of the UI, determined either by Raman or HR-NMR versus mice age in days. Here the data are plotted in the form of mean values with related standard deviations. Values obtained by MRS are additionally reported in the inset, but only for animals older than 22 days. Both in Raman and HR-NMR data, a sudden increase in the unsaturation index between 22 and 30 days is clearly evident in close correspondence with the weaning of mice (21 days). A similar trend was observed also for the PI. Moreover, MRS and HR-NMR provide results in good agreement, indicating that the extraction procedure does not affect the determination of the UI. The substantially higher standard deviation in MRS determinations compared to either HR-NMR or Raman data is due to errors introduced in the in vivo measurement by imperfect shimming, mouse movements and relatively low signal-to-noise ratio.

The physiological aspects of the observed experimental results need to be discussed. In principle, the dietary FA could have a profound influence on both the quantity and quality of the FA of adipose tissue, which in turn determines the kinds and amounts of FA available to meet metabolic requirements. In fact, a direct correlation between the amount of FA present in the diet and their deposition into the adipose tissue was observed, although the degree of FA deposition varied with the unsaturation, saturation and structure of the FA of the diet [48]. In our case, the sudden increase of the UI up to about 160% of its starting value, observed soon after weaning of animals, correlates, at least qualitatively, with the dietary change. In fact, the ratio between the Raman Index for the unsaturation index, namely the NA of the peak at 1,655 cm^{-1}, was estimated to increase by a factor of about 1.5 when the spectra of the mother milk and of the standard mice feed are considered. It is noteworthy that UI starts increasing immediately after weaning and its increase seems to be almost complete within approximately 1 week after the diet change. To the best of our knowledge, such a sudden increase in the UI in correspondence to mice weaning has not been reported previously. It is reasonable to expect that similar changes, although slower than in mice because of the different metabolism, may occur in other mammals, including humans. Our data show that, soon after the weaning, the mice body builds up a reservoir of TG composed of unsaturated fatty acids, which are easily mobilized from fat tissue toward organs and tissues for the energetic needs. In fact, mobilization of fatty acids from cells and tissues has been investigated in mammals, including humans, and more recently, in migratory birds [9, 12, 14].

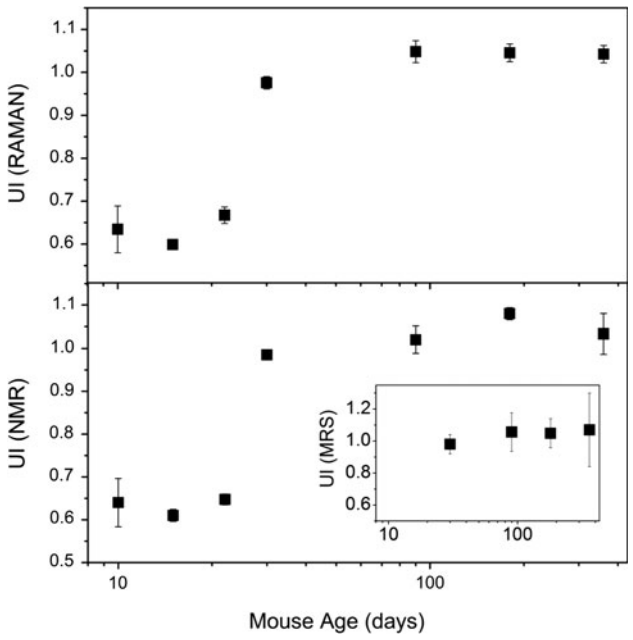

Fig. 4 Dependence of UI on the mouse age (days) as determined by Raman (*top panel*) and HR-NMR (*bottom panel*). The values of UI determined in vivo by MRS are shown in the *inset* of the *bottom panel*

It appears that fatty acids are not mobilized in direct proportion to TG contents of cells but differentially depending on their unsaturation. Specifically, polyunsaturated rather than saturated fatty acids are preferentially mobilized from adipose tissue [12]. Our results thus show that after weaning mice body possesses a reservoir of TGs more easily mobilized than before weaning. This is probably related to changes in energy metabolism. During the first days of ectopic life, shivering thermogenesis is not active. Heat production occurs mainly through not-shivering thermogenesis in brown adipose tissue (BAT) the last tissue being strongly developed and active in pups. At weaning, a substantial change in energetic metabolism does occur: BAT, which posses its own lipid depots, decreases its activity while muscle increases its motor activity and shivering thermogenesis. Differently from BAT, muscle does not have its own lipid reserve. This fact determines the organism request of the need of a lipid reservoir of easy mobilization. On the bases of the above considerations, our results shows that, after weaning, fat depots are composed by unsaturated (i.e. easily mobilized) fatty acids which, likely, can meet the growing energy demands of mature muscle tissue.

Conclusions

In the present paper Raman spectroscopy has been used to quantitatively determine the unsaturation index of mammal fat tissues. The UI value have been quantitatively assessed through calibration with HR-NMR data. Both Raman and HR-NMR require animal sacrifice and tissue resection. Differently from HR-NMR, Raman spectroscopy does not

need chemical extraction of the lipid component that is time consuming and destructive for the sample. Raman spectra can be acquired from a few milligrams of fat tissue in a few seconds with a good signal-to-noise ratio. In fact, they were carried out in a systematic way from WAT specimens of mice of different ages, ranging between a few days and 12 months. Our Raman results turns out to be very reliable in monitoring, in a very simple way, the sudden changes occurring in the fat composition after the mice were weaned, through the evaluation of the intensity changes of the C=C stretch mode peaked at 1,655 cm^{-1}, normalized to the C=O group stretching mode intensity.

In conclusion, Raman spectroscopy could provide an inexpensive, fast and robust approach to analyze important characteristics of the fat tissues of mammals for routine use in bioptic samples. The present results demonstrate that the method is useful for monitoring diet-induced changes of the unsaturation index of fat deposits. Moreover, they show that, soon after weaning, the organisms build up adipose tissue depots rich in unsaturated TG, easily mobilized from the tissue itself. On one side this process is correlated to dietary changes, but, on the other side, it is probably also related to the switch from non-shivering to shivering thermogenesis.

Acknowledgments The authors are grateful to G. Guella for the useful discussions and the critical reading of the manuscript. One of the authors (E. M.) is a Ph.D. student supported by Veneto Nanotech S.C.p.A., Italy. This research was partially funded by the Fondazione Cariverona, Italy, under contract with the University of Verona.

References

1. Bartnessand TJ, Bamshad M (1998) Innervation of mammalian white adipose tissue: implications for the regulation of total body fat. Am J Physiol 275:1399–1411
2. Nnodimand JO, Lever JD (1988) Neural and vascular provisions of rat interscapular brown adipose tissue. Am J Anat 182:283–293
3. Vázquez-Vela MEF, Torres N, Tovar AR (2008) White adipose tissue as endocrine organ and its role in obesity. Arch Med Res 39:715–728
4. Cinti S (1999) The adipose organ, Kurtis, Milan
5. Morrison RF, Farmer SR (2000) Hormonal signaling and transcriptional control of adipocyte differentiation. J Nutr 130:3116S–3121S
6. Rousseau V, Becker DJ, Ongemba LN, Rahier J, Henquin JC, Brichard SM (1997) Developmental and nutritional changes of ob and PPAR gamma 2 gene expression in rat white adipose tissue. Biochem J 321:451–456
7. Nogalska A, Swierczynski J (2001) The age-related differences in obese and fatty acid synthase gene expression in white adipose tissue of rat. Biochim Biophys Acta 1533:73–80
8. Hunter JD, Buchanan H, Nye ER (1970) The mobilization of free fatty acids in relation to adipose tissue triglyceride fatty acids in the rat. J Lipid Res 11:259–265
9. Raclot T, Groscolas R (1993) Differential mobilization of white adipose tissue fatty acids according to chain length, unsaturation, and positional isomerism. J Lipid Res 34:1515–1526
10. Sanderson P, Thies F, Calder PC (2000) Extracellular release of free fatty acids by rat T lymphocytes is stimulus-dependent and is affected by dietary lipid manipulation. Cell Biochem Funct 18:47–58
11. Raclot T, Oudart H (2000) Net release of individual fatty acids from white adipose tissue during lipolysis in vitro: evidence for selective fatty acid re-uptake. Biochem J 348:129–136
12. Hailiwell KJ, Fielding BA, Samra JS, Humphreys SM, Frayn KN (1996) Release of individual fatty acids from human adipose tissue in vivo after an overnight fast. J Lipid Res 37:1842–1848
13. Lin DS, Connor WE (1990) Are the n-3 fatty acids from dietary fish oil deposited in the triglyceride stores of adipose tissue? Am J Clin Nutrition 51:535–539
14. Price ER, Krokfors A, Guglielmo CG (2008) Selective mobilization of fatty acids from adipose tissue in migratory birds. J Exp Biol 211:29–34
15. Yli-Jama P, Haugen TS, Rebnord HM, Ringstad J, Pedersen JI (2001) Selective mobilisation of fatty acids from human adipose tissue. Eur J Intern Med 12:107–115
16. Notingher I, Hench LL (2006) Raman microspectroscopy: a noninvasive tool for studies of individual living cells in vitro. Expert Rev Med Devices 3:215–234
17. De Gelder J, De Gussem K, Vandenabeele P, Moens L (2007) Reference database of Raman spectra of biological molecules. J Raman Spectrosc 38:1133–1147
18. Beattie JR, Bell SEJ, Borgaard C, Fearon A, Moss BW (2006) Prediction of adipose tissue composition using Raman spectroscopy: average properties and individual fatty acids. Lipids 41:287–294
19. Beattie JR, Bell SEJ, Borggaard C, Fearon AM, Moss BW (2007) Classification of adipose tissue species using Raman spectroscopy. Lipids 42:679–685
20. Beattie JR, Bell SJ, Moss BW (2004) A critical evaluation of Raman spectroscopy for the analysis of lipids: fatty acid methyl esters. Lipids 39:407–419
21. Olsen EF, Baustad C, Egelandsdal B, Rukke EO, Isaksson T (2010) Long-term stability of a Raman instrument determining iodine value in pork adipose tissue. Meat Sci 85:1–6
22. Olsen EF, Rukke EO, Flatten A, Isaksson T (2007) Quantitative determination of saturated-, monounsaturated- and polyunsaturated fatty acids in pork adipose tissue with non-destructive Raman spectroscopy. Meat Sci 76:628–634
23. Farhad SFU, Abedin KM, Islam MR, Talukder AI, Haider AFMY (2009) Determination of ratio of unsaturated to total fatty acids in edible oils by laser Raman spectroscopy. J Appl Sci 9:1538–1543
24. Muik B, Lendl B, Molina-Dìaz A, Ayora-Cañada MJ (2003) Direct, reagent-free determination of free fatty acid content in olive oil and olives by Fourier transform Raman spectrometry. Anal Chim Acta 487:211–220
25. Tandon P, Förster G, Neubert R, Wartewig S (2000) Phase transitions in oleic acid as studied by X-ray diffraction and FT-Raman spectroscopy. J Mol Struct 524:201–215
26. Afseth NK, Wold JP, Segtan VH (2006) The potential use of Raman spectroscopy for characterisation of the fatty acid unsaturation of salmon. Anal Chim Acta 572:85–92
27. Strobel K, van den Hoff J, Pietzsch J (2008) Localized proton magnetic resonance spectroscopy of lipids in adipose tissue at high spatial resolution in mice in vivo. J Lipid Res 49:473–480
28. Giarola M, Guella G, Mariotto G, Monti F, Rossi B, Sanson A, Sbarbati A (2008) Vibrational and structural investigations on adipose tissues. Phil Mag 88:3953–3959
29. Folch J, Ascoli I, Lees M, Meath JA, LeBaron FN (1951) Preparation of lipid extracts from brain tissue. J Biol Chem 191:833–841
30. Provencher SW (2001) Automatic quantitation of localized in vivo 1H spectra with LCModel. NMR Biomed 14:260–264

31. Zancanaro C, Nano R, Marchioro C, Sbarbati A, Boicelli A, Osculati F (1994) Magnetic resonance spectroscopy investigations of brown adipose tissue and isolated brown adipocytes. J Lipid Res 35:2191–2199
32. Socrates G (2001) Infrared and Raman characteristic group frequencies. J Wiley and Sons, NY
33. Brown KG, Bicknell-Brown E, Ladjadj M (1987) Raman active bands sensitive to motion and conformation at the chain termini and backbones of alkalenes and lipids. J Phys Chem 91:3436–3442
34. Susi H, Sampugna J, Hampson JW, Ard JS (1979) Laser-Raman investigation of phospholipid-polypeptide interactions in model membranes. Biochemistry 18:297–301
35. Lawson EE, Anigbogu ANC, Williams AC, Barry BW, Edwards HGM (1998) Thermally induced molecular disorder in human stratum corneum lipids compared with a model phospholipid system; FT-Raman spectroscopy. Spectrochim. Acta A: Mol Biomol Spectros 54:543–558
36. Snyder RG, Cameron DG, Casal HL, Compton DAC, Mantsch HH (1982) Studies on determining conformational order in n-alkanes and phospholipids from the 1,130 cm^{-1} Raman band. Biochim Biophys Acta 684:111–116
37. Butler M, Salem N, Hoss W, Spoonhower J (1979) Raman spectral analysis of the 1,300 cm^{-1} region for lipid and membrane studies. Chem Phys Lipids 29:99–102
38. Sadeghi-Jorabchi H, Hendra PJ, Wilson RH, Belton PS (1990) Determination of the total unsaturation in oils and fats by Fourier transform Raman spectroscopy. J Am Oil Chem Soc 67:483–486
39. Chmielarz B, Bajdor K, Labudzinska A, Klukowska-Majewska Z (1995) Studies on the double-bond positional isomerization process in linseed oil by UV, IR and Raman-spectroscopy. J Mol Struct 348:313–316
40. da Silva CE, Vandenabeele P, Edwuards HGM, de Oliveir LFC (2008) NIR-FT-Raman spectroscopic analitica characterization of the fruits, seeds, and phytotherapeutic oils from roseships. Anal Bioanal Chem 392:1489–1496
41. Capelle F, Lhert F, Blaudez D, Kellay H, Turlet HL (2000) Thickness and organization of black films using confocal microraman spectroscopy. Colloids Surf A: Physicochem Eng Asp 171:199–205
42. Antipolphan R, Rades T, Strachan CJ, Gordon KC, Medlicott NJ (2006) Analysis of lecithin-choelsterol mixtures using Raman spectroscopy. J Pharma Biomed Anal 41:476–484
43. Muik B, Lendl B, Molina-Dìaz A, Ayora-Canada MJ (2005) Direct monitoring of lipid oxidation in edible oils by Fourier transform Raman spectroscopy. Chem Phys Lipids 134:173–182
44. Oakes RE, Beattie JR, Moss BW, Bell SEJ (2003) DFT studies of long-chain FAMEs: theoretical justification for determining chain length and unsaturation from experimental Raman spectra. J Mol Structure Theochem 626:27–45
45. Beattie JR, Bell SEJ, Borgaard C, Fearon AM, Moss BW (2004) Multivariate prediction of clarified butter composition using Raman spectroscopy. Lipids 39:897–906
46. Wood JD, Enser M, Fisher AV, Nute GR, Richardson RI, Sheard PR (1999) Manipulating meat quality and composition. Proc Nutr Soc 58:363–370
47. Hebean V, Habeanu M, Neagu M (2005) Influence of teh unsaturation fatty acids from different sources on pig meat quality. Arch Zootech 8:79–86
48. Lin DS, Connor WE, Spenler CW (1993) Are dietary saturated, monounsaturated, and polyunsaturated fatty acids deposited to the same extent in adipose tissue of rabbits? Am J Clin Nutr 58:174–179

Lipids (2011) 46:669–677
DOI 10.1007/s11745-011-3563-z

ORIGINAL ARTICLE

Increased Elongase 6 and Δ9-Desaturase Activity are Associated with n-7 and n-9 Fatty Acid Changes in Cystic Fibrosis

Kelly F. Thomsen · Michael Laposata · Sarah W. Njoroge · Obi C. Umunakwe · Waddah Katrangi · Adam C. Seegmiller

Received: 17 December 2010 / Accepted: 12 April 2011 / Published online: 5 May 2011

Abstract Patients with cystic fibrosis, caused by mutations in CFTR, exhibit specific and consistent alterations in the levels of particular unsaturated fatty acids compared with healthy controls. Evidence suggests that these changes may play a role in the pathogenesis of this disease. Among these abnormalities are increases in the levels of n-7 and n-9 fatty acids, particularly palmitoleate (16:1n-7), oleate (18:1n-9), and eicosatrienoate or mead acid (20:3n-9). The underlying mechanisms of these particular changes are unknown, but similar changes in the n-3 and n-6 fatty acid families have been correlated with increased expression of fatty acid metabolic enzymes. This study demonstrated that cystic fibrosis cells in culture exhibit increased metabolism along the metabolic pathways leading to 16:1n-7, 18:1n-9, and 20:3n-9 compared with wild-type cells. Furthermore, these changes are accompanied by increased expression of the enzymes that produce these fatty acids, namely Δ5, Δ6, and Δ9 desaturases and elongases 5 and 6. Taken together, these findings suggest that fatty acid abnormalities of the n-7 and n-9 series in cystic fibrosis are as a result, at least in part, of increased expression and activity of these metabolic enzymes in CFTR-mutated cells.

K. F. Thomsen
Department of Pediatrics,
Vanderbilt University Medical Center,
Nashville, TN, USA

M. Laposata · S. W. Njoroge · O. C. Umunakwe · W. Katrangi · A. C. Seegmiller (✉)
Department of Pathology,
Vanderbilt University Medical Center,
Nashville, TN, USA
e-mail: adam.seegmiller@vanderbilt.edu

Keywords Fatty acid metabolism · Gene expression · Elongases · Desaturases · Monounsaturated fatty acids · Cystic fibrosis

Abbreviations

CF	Cystic fibrosis
CFTR	Cystic fibrosis transmembrane regulator
FAME	Fatty acid methyl ester
HPLC	High-performance liquid chromatography
GC	Gas chromatography

Introduction

Cystic fibrosis (CF) is the most common life-threatening genetic disease in the Caucasian population, affecting 1 in every 3,000 newborns [1]. CF is caused by mutations in the cystic fibrosis transmembrane regulator (CFTR) gene [2]. The protein product of this gene is a cAMP-regulated chloride channel that belongs to the ATP binding cassette family. This protein also transports bicarbonate and indirectly regulates sodium flux. The mutations in CFTR cause accumulation of viscous secretions in the body, ultimately leading to pancreatic insufficiency, intestinal malabsorption, chronic airway infection, inflammation, and progressive lung disease [1].

In addition to the classic clinical findings in CF, specific fatty acid abnormalities have been consistently identified in the plasma and tissues of CF animal models, human patients, and cultured cell models compared with wild-type controls (reviewed in Refs. [3, 4]). The most noted of these are decreases in linoleate (18:2n-6) and docosahexaenoate (22:6n-3), and, in most cases, elevation of arachidonate

(20:4n-6). Studies in mice suggest that these abnormalities are involved in the pathophysiology of CF [5].

Less attention has been paid to important fatty acid changes outside of the n-6 and n-3 pathway. These include increased concentrations of palmitoleate (16:1n-7), oleate (18:1n-9), and eicosatrienoate or mead acid (20:3n-9) in the cells and plasma of CF patients. In some studies, these changes were present along with pancreatic insufficiency and intestinal malabsorption [6, 7], and elevations of these fatty acids are a known marker of essential fatty acid deficiency [8, 9]. However, similar observations have been made in well-nourished CF patients [10–12] and some cultured CF cells [13], suggesting additional underlying causes exist to explain these alterations. Importantly, DHA therapy, which is known to reverse the n-3 and n-6 fatty acid abnormalities in CF patients and correct CF pathology in mice, also reduces 20:3n-9 levels [14].

These fatty acids are of particular interest in CF pathophysiology because of their functional properties outside cell membranes. A recent study revealed that 16:1n-7 acts as a lipid hormone, a so-called lipokine, providing communication between adipose tissue and distant organs to regulate systemic metabolic homeostasis [15]. Furthermore, there is evidence suggesting that products of Δ9-desaturase, which include 16:1n-7 and 18:1n-9, are involved in modulating inflammation [16–18], as are oxygenated products of 20:3n-9 [19].

Unlike the n-3 and n-6 series fatty acids, 16:1n-7, 18:1n-9, and 20:3n-9 can be synthesized de novo. Palmitate (16:0; PAM), synthesized from acetyl CoA, can be converted to these fatty acids via the pathways indicated in Fig. 1. Our group has shown that alterations in n-3 and n-6 fatty acids in CF cells are associated with increased expression and activity of Δ6 and Δ5 desaturases compared with wild-type cells [20]. The objective if this study was to test whether the above-described changes in n-7 and n-9 fatty acids are also a result of altered activity of fatty acid metabolizing enzymes.

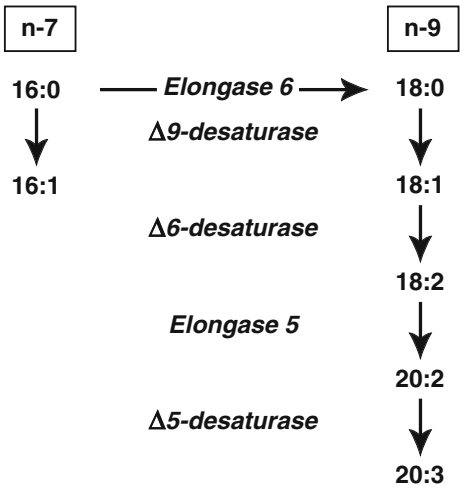

Fig. 1 Fatty acid metabolism through the n-7 (*left*) and n-9 (*right*) pathways

This hypothesis was tested in two cell culture models of CF with similar fatty acid abnormalities to those present in humans [13, 21]. To investigate the relative activities of fatty acid-metabolizing enzymes, the conversion of radiolabeled palmitate (16:0), stearate (18:0), and 18:1n-9 to downstream fatty acid products was measured and correlated with the expression of desaturase and elongase enzymes in CF cells. The results show increased metabolism of these fatty acids to 16:1n-7, 18:1n-9, and 20:3n-9 in CF compared with wild-type cells. There was also increased expression of Δ9, Δ6, and Δ5 desaturases and elongase 6. These findings suggest that increases in the expression and activity of these fatty acid metabolic enzymes are at least in part responsible for changes in the levels of these fatty acids observed in CF.

Materials and Methods

Materials

Radiolabeled fatty acids, [1-^{14}C]16:0 (55 mCi/mmol), [1-^{14}C]18:0 (55 mCi/mmol), and [1-^{14}C]18:1n-9 (55 mCi/mmol) were obtained from American Radiolabeled Chemicals (St Louis, MO, USA). Fatty acid methyl ester (FAME) standards were purchased from NuChek Prep (Elysian, MN, USA). HPLC-grade solvents were purchased from Fisher Scientific (Pittsburgh, PA, USA) and liquid scintillation cocktail (IN-flow 2:1) was purchased from IN/US Systems (Tampa, FL, USA).

Cell Culture

16HBEo^{-} sense and antisense cells were a gift from Dr Pamela Davis (Case Western Reserve University School of Medicine, Cleveland, OH, USA). These are human bronchial epithelial cells stably transfected with plasmids expressing the first 131 nucleotides of human CFTR in the sense or antisense orientation such that sense cells express wild-type CFTR and antisense cells lack CFTR expression [22]. IB3 and C38 cells were obtained from ATCC (Manassas, VA, USA). IB3 cells are compound heterozygotes which contain one ΔF508 allele and one nonsense mutation, W1282X, with a premature termination signal [23]. The CF phenotype present in the IB3-1 cells has been corrected in the C38 cell line by transfection with wild-type CFTR [24]. Cell culture techniques were performed as previously described [13, 21]. Cells were grown in

tissue-culture flasks coated with LHC basal media (Invitrogen, Carlsbad, CA, USA) containing 0.1 mg/mL BSA (Sigma–Aldrich, St Louis, MO, USA), 10 μg/mL human fibronectin (Sigma–Aldrich), and 3 μg/mL vitrogen (Angiotech Biomaterials, Palo Alto, CA, USA). Complete culture medium comprised minimum essential medium + glutamax (Invitrogen) supplemented with 100 μg/mL streptomycin, 100 U/mL penicillin, and 10% horse serum (Atlanta Biologicals, Lawrenceville, GA, USA). Cells were grown at 37 °C in a 5% CO_2 humidified incubator. Medium was changed three times weekly.

For experiments, cells were seeded in six-well experimental plates. Sense cells were seeded at 3×10^5 cells/well and antisense cells were seeded at 1×10^5 cells/well. This enables the sense cells, which are smaller in size, to reach confluence at approximately the same time as antisense cells. C38 and IB3 cells were seeded at 1×10^5 cells/well. All cells were allowed to grow until two days post-confluence (7–8 days) before being used for experiments. This time point was chosen because it is the point at which the fatty acid abnormalities are most distinct [13].

Fatty Acid Composition Analysis

Sense and antisense cells were cultured as above until two days post-confluence, after which they were washed twice in ice-cold PBS, scraped, and transferred to a glass tube. The saturated fatty acid 17:0 (10 μg) was added as an internal standard. Lipids were extracted using a modification of the method of Folch et al. [25]. Cells were harvested by rinsing twice with ice-cold phosphate-buffered saline (Invitrogen), then scraping on ice with a rubber policeman. The cells were pelleted by centrifugation (100×*g* for 8 min). The cell pellet was resuspended in 0.5 mL cold phosphate-buffered saline, and lipids were extracted by adding six volumes of chloroform–methanol (2:1, *v*/*v*). These samples were incubated on ice for 10 min, vortex mixed, and centrifuged (1,100×*g* for 10 min). The lower, organic, phase was transferred to a new glass tube and dried down completely under a stream of nitrogen. Fatty acids were methylated using boron trifluoride (BF_3; 14% in methanol; Sigma–Aldrich) and a methanolic-base reagent [26] as follows: 0.5 mL 0.5 M methanolic NaOH (Acros Organics, Geel, Belgium) was added to the sample, vortex mixed, and heated at 100 °C for 3 min, followed by addition of 0.5 mL BF_3 at 100 °C for 1 min. To extract the fatty-acid methyl esters (FAMEs), 1 mL hexane was added to the mixture which was then incubated at 100 °C for 1 min, followed by addition of 6.5 mL saturated NaCl solution. The sample was then vortex mixed and centrifuged (500×*g* for 4 min) to separate the liquid phases. The upper, hexane, layer was used for quantification of FAMEs by gas chromatography (GC) using an Agilent 7980A GC system (Agilent Technologies, Santa Clara, CA, USA) equipped with a Supelcowax SP-10 capillary column (Supelco, Bellefonte, PA, USA) coupled to a mass spectrometer (model 5975c, Agilent Technologies). FAME mass was determined by comparing areas of unknown FAMEs with that of a fixed concentration of the 17:0 internal standard. Results were expressed as the molar percentage (mol%) of each FAME relative to the total FAME mass of the sample.

Fatty Acid Metabolism Experiments

For fatty acid metabolism experiments, medium containing radiolabeled fatty acids was prepared by drying the fatty acids dissolved in ethanol under a continuous stream of nitrogen gas. Reduced-lipid medium was added to the tube and sonicated three times for 5 s each. At two days post-confluence, each well was incubated for 4 h with media supplemented with reduced-lipid fetal bovine serum (Hyclone, Logan, UT, USA) and containing 0.5 μCi/well radiolabeled 16:0, 18:0, or 18:1n-9 and either harvested (4 h samples) or washed with PBS and incubated in complete medium for an additional 20 h before harvest (24 h samples). Lipids were then extracted and methylated as above. After methylation, the samples were dried under nitrogen, reconstituted in 200 μL methanol, then dried to a volume of approximately 50 μL. The mixture was vortex mixed, and 20 μL was injected for HPLC analysis (Agilent Technologies 1200 series instrument) on a 4.6 × 250 mm, 5 μm, Agilent Zorbax Eclipse XDB-C18 column. A 4.6 × 12.5 mm, 5 μm, guard column was used in conjunction with the analytical column. The fatty acids were separated using a binary mobile phase with a constant flow rate of 1 mL per minute. The solvent program began with 90% solvent A (100% HPLC-grade methanol) and 10% solvent B (HPLC-grade H_2O) for 40 min, followed by 100% solvent A for 20 min. Peaks were detected using ultraviolet detection at 205 nm and identified by comparing retention times with those of unlabeled FAME standards. Quantification of the radiolabeled peaks was performed by use of a scintillation detector (β-RAM Model 4, IN/US Systems) coupled to the HPLC. Data are reported as percentage of total counts.

Quantitative Real-Time PCR

Specific primers for each gene of interest were designed using Beacon Designer software (Premier Biosoft International, Palo Alto, CA, USA), the sequences of which are listed in Table 1. To prevent amplification of genomic DNA, forward and reverse primers were designed from adjacent exons. Primer fidelity and efficiency were tested using an iCycler iQ system (Bio-Rad Laboratories,

Table 1 Primer sequences used for quantitative real-time PCR

Gene name	Product	Sequence of forward and reverse primers (5′–3′)	Genbank accession no.
RPLP0	Ribosomal protein, large, P0	ATGGCAGCATCTACAACCC GACAGACACTGGCAACATTG	NM_001002
SCD	Δ9- (stearoyl-CoA) desaturase	CCCAAGCCCCAAGGTTGAATATG CCCCAAAGCCAGGTGTAGAAC	NM_005063
ELOVL6	Fatty acid elongase 6	CAACGAGAATGAAGCCATC GCAGCATACAGAGCAGAA	NM_024090

Hercules, CA, USA) using iQ5 software (Bio-Rad). Each primer pair produced a single product on melt curve analysis and had amplification efficiencies >94%.

At two days post-confluence, total RNA was prepared from cells using TRIzol reagent (Invitrogen) according to the manufacturer's instructions. Residual DNA was removed by treatment with DNase I (DNA-free kit; Ambion, Austin, TX, USA). First-strand cDNA was synthesized from 2 μg total RNA using TaqMan reverse transcription reagents with random hexamer primers (Applied Biosystems, Foster City, CA, USA).

Quantitative real-time PCR was performed in a 20 μL reaction containing 50 ng reverse-transcribed total RNA, 156 nM forward and reverse primers, and 10 μL 2× SYBR green PCR Master Mix (Applied Biosystems). PCR reactions were performed in triplicate in 96-well plates using the iCycler iQ or CFX96 system (Bio-Rad). Results were analyzed using iQ5 or CFX Manager software (Bio-Rad). The relative amount of mRNAs was calculated using the comparative C_T method [27]. RPLP0 mRNA was used as an invariant control.

Statistical Analysis

Data are presented as mean ± standard error of the mean (SEM). Statistically significant differences between groups were evaluated by use of Student's *t* test to compare means in the sense and antisense groups using Excel (Microsoft, Redmond, WA, USA). $P < 0.05$ was interpreted as statistically significant.

Results

The metabolic pathways leading to the formation of 16:1n-7, 18:1n-9, and 20:3n-9 are shown in Fig. 1. These pathways were evaluated first in 16HBEo$^-$ human bronchial epithelial cells stably transfected with plasmids expressing the first 131 nucleotides of the *cftr* gene in either the sense or antisense orientation [22]. Consequently, the sense cells express CFTR protein whereas the antisense cells show nearly complete loss of both CFTR expression and activity [13, 22].

The relative fatty acid composition of sense and antisense cells is shown in Table 2. A small, but statistically significant increase in the saturated fatty acids 16:0 and 18:0 was observed for antisense cells (3.2 and 4.1% increase, respectively, compared with sense cells). Larger increases are seen in the monounsaturated derivatives of these fatty acids, 16:1n-7 and 18:1n-9 (13 and 15% increase, respectively). The largest relative increase in antisense cells was for 20:3n-9, which was 80% higher in antisense than sense cells. Of note, the 20:3n-9/20:4n-6 ratio, a marker of EFA deficiency [28], is significantly increased in antisense versus sense cells (0.09 vs. 0.05; $P < 0.001$).

To determine if these fatty acid changes in antisense cells were a result of alterations in enzymatic metabolism, sense and antisense cells were incubated with radiolabeled 16:0, 18:0, and 18:1n-9, and conversion to downstream metabolites was measured. The results of labeling experiments with [1-^{14}C]16:0 are shown in Fig. 2. After 4 h incubation, there was significant diminution of 16:0 with increased conversion to 16:1n-7, 18:0, and 18:1n-9 in antisense cells compared with sense cells (Fig. 2a). This effect persisted for all but 18:0 at 24 h (Fig. 2b), perhaps because of subsequent conversion to 18:1n-9.

Similar results were observed when cells were incubated with [1-^{14}C]18:0. Metabolism of 18:0 to 18:1n-9 was increased in antisense versus sense cells at both time points (Fig. 3a, b), although these differences were statistically significant at 24 h only. Further metabolism to 20:3n-9 was significantly increased in antisense cells at both time points.

Increased production of 20:3n-9 is, in part, because of increased metabolism of 18:1n-9. When incubated with [1-^{14}C]18:1n-9, antisense cells showed increased conversion of this substrate to 20:3n-9 at both time points, with difference reaching statistical significance at 24 h (Fig. 4a, b).

Taken together, these fatty acid metabolism results indicate that antisense cells exhibit increased enzymatic activity catalyzing the conversion of 16:0 to 16:1n-7 and from 16:0 through 18:0 to 18:1n-9. The enzymes responsible for these metabolic conversions are Δ9-desaturase

Table 2 Fatty acid composition (mol %[a]) of sense and antisense cells

Acid	Sense	Antisense	Acid	Sense	Antisense
14:0	2.04 ± 0.04	1.60 ± 0.01[d]	18:3n-3	0.20 ± 0.09	0.09 ± 0.01
15:0	1.11 ± 0.02	0.51 ± 0.01[d]	20:3n-3	0.12 ± 0.01	0.04 ± 0.00[b]
16:0	**16.45 ± 0.10**	**16.97 ± 0.07[b]**	20:5n-3	0.34 ± 0.01	3.20 ± 0.02[d]
18:0	**16.06 ± 0.11**	**16.72 ± 0.04[c]**	22:5n-3	4.40 ± 0.05	5.15 ± 0.03[d]
20:0	0.21 ± 0.07	0.30 ± 0.01	22:6n-3	1.00 ± 0.02	0.58 ± 0.01[d]
22:0	0.18 ± 0.01	0.26 ± 0.01[c]	18:2n-6	14.37 ± 0.24	11.88 ± 0.08[d]
24:0	0.19 ± 0.01	0.26 ± 0.02	20:2n-6	1.17 ± 0.06	0.40 ± 0.07[c]
16:1n-7	**2.47 ± 0.05**	**2.79 ± 0.05[c]**	18:3n-6	0.38 ± 0.00	0.69 ± 0.01[d]
18:1n-7	3.65 ± 0.07	2.79 ± 0.04[d]	20:3n-6	1.50 ± 0.05	2.27 ± 0.02[d]
18:1n-9	**17.83 ± 0.07**	**20.43 ± 0.12[d]**	20:4n-6	10.73 ± 0.24	10.71 ± 0.06
20:1n-9	0.59 ± 0.13	0.32 ± 0.01	22:4n-6	2.61 ± 0.05	0.48 ± 0.01[d]
20:3n-9	**0.53 ± 0.02**	**0.96 ± 0.02[d]**	22:5n-6	1.68 ± 0.08	0.11 ± 0.01[d]
22:1n-9	0.12 ± 0.00	0.29 ± 0.01[d]			
24:1n-9	0.06 ± 0.01	0.19 ± 0.00[d]			

Data are given as mean ± SEM of three replicates. Fatty acids of interest to this study are in bold

[a] Molar percentage of total fatty acids

[b] $P < 0.05$

[c] $P < 0.01$

[d] $P < 0.001$

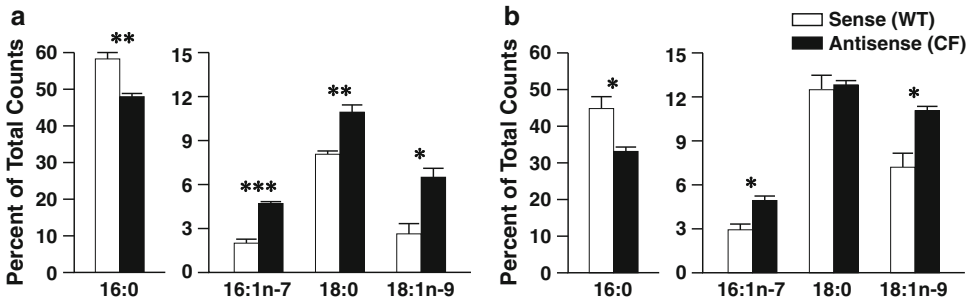

Fig. 2 Palmitate (16:0) metabolism through the n-7 and n-9 pathways in 16HBE cells. Sense (wildtype, WT) and antisense (cystic fibrosis, CF) cells were cultured in complete medium for seven days and then incubated with 4.1 μM [1-^{14}C]16:0 in reduced-lipid cell culture medium for 4 h and harvested (**a**) or washed twice in PBS and incubated for an additional 20 h in serum-containing medium (**b**). Levels of labeled 16:0, 16:1n-7, 18:0, and 18:1n-9 were determined by HPLC as described in "Materials and Methods". Data are expressed as percentages of total counts and *bars* represent mean ± SEM ($n = 3$). The findings are representative of at least two independent experiments. *$P < 0.05$, **$P < 0.01$, ***$P < 0.001$ for sense versus antisense cells

and elongase 6, which are regulated almost entirely at the transcriptional level [29, 30]. To test potential changes in the expression of these enzymes, quantitative RT-PCR was performed on total RNA extracted from sense and antisense cells using primers specific to these two enzymes. As predicted, there was a significant increase in the relative mRNA levels corresponding to both elongase 6 and Δ9-desaturase (Fig. 5a).

To confirm these findings, expression of these enzymes was measured in a second cell-culture system. The IB3 cell line consists of immortalized bronchial epithelial cells from an actual CF patient that carried a compound heterozygous genotype (ΔF508/W1282X) [23]. C38 cells are IB3 cells stably transfected with a wild-type *cftr* gene, restoring normal CFTR function [24]. They were used as controls. Similar to the sense and antisense cells, the IB3 cells exhibit increased expression of both elongase 6 and Δ9-desaturase compared with C38 cells (Fig. 5b).

Further metabolism of 18:1n-9 is catalyzed by Δ6-desaturase, elongase 5, and Δ5-desaturase (Fig. 1). Previous studies [20] in these cell culture systems demonstrated that expression of the two desaturase enzymes is significantly increased in antisense versus sense cells. All three enzymes show increased expression in IB3 versus C38 cells.

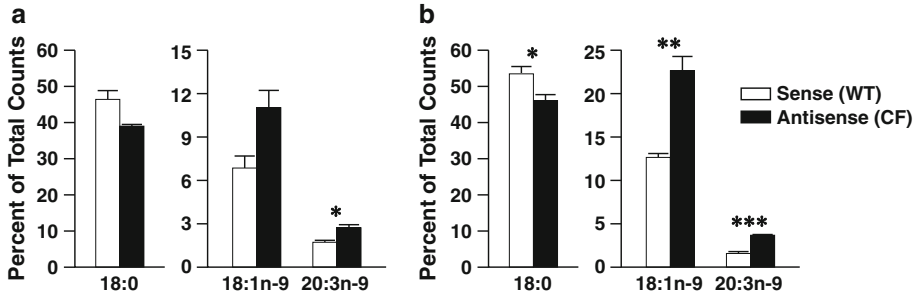

Fig. 3 Stearate (18:0) metabolism through the n-9 pathway in 16HBE cells. Sense (WT) and antisense (CF) cells were cultured in complete medium for seven days and then incubated with 4.1 μM [1-^{14}C]18:0 in reduced-lipid cell culture medium for 4 h and harvested (**a**) or washed twice in PBS and incubated for an additional 20 h in serum-containing medium (**b**). Levels of labeled 18:0, 18:1n-9, and 20:3n-9 were determined by HPLC as described in "Materials and Methods". Data are expressed as percentages of total counts and *bars* represent mean ± SEM ($n = 3$). The findings are representative of at least two independent experiments. *$P < 0.05$, **$P < 0.01$, ***$P < 0.001$ for sense versus antisense cells

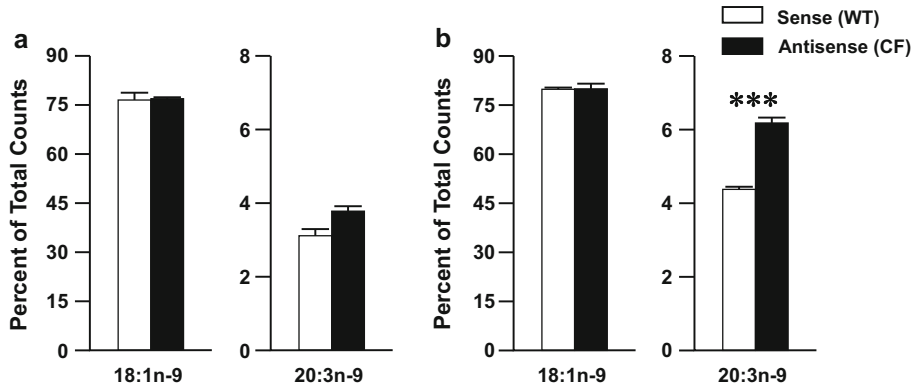

Fig. 4 Oleate (18:1n-9) metabolism through the n-9 pathway in 16HBE cells. Sense (WT) and antisense (CF) cells were cultured in complete medium for seven days and then incubated with 4.1 μM [1-^{14}C]18:1n-9 in reduced-lipid cell culture medium for 4 h and harvested (**a**) or washed twice in PBS and incubated for an additional 20 h in serum-containing medium (**b**). Levels of labeled 18:1n-9 and 20:3n-9 were determined by HPLC as described in "Materials and Methods". Data are expressed as percentages of total counts and *bars* represent mean ± SEM ($n = 3$). The findings are representative of at least two independent experiments. *$P < 0.05$, **$P < 0.01$, ***$P < 0.001$ for sense versus antisense cells

Discussion

Changes in fatty acid levels are a consistent feature of CF and there is increasing evidence that they are involved in the pathogenesis of the disease. For example, studies have shown that fatty acid alterations are more pronounced in patients carrying genotypes associated with more severe disease [12, 31]. Accordingly, the degree of fatty acid alteration correlates with the severity of CF-associated clinical data [32–34]. Furthermore, correction of fatty acid alterations by docosahexaenoate (22:6n-3) in a mouse model of CF also corrects CF-associated respiratory and gastrointestinal tract pathology [5].

If fatty acid imbalances play a role in CF pathogenesis, it is important to understand their underlying molecular mechanisms. A recent study demonstrated that changes in n-3 and n-6 polyunsaturated fatty acids in CF cells are a result of increased expression of fatty acid metabolic enzymes, specifically the Δ5 and Δ6 desaturases [20]. Our study extends this analysis to alterations observed in n-7 and n-9 fatty acids. It demonstrates increased metabolism of 16:0 to 16:1n-7 and of 16:0 through 18:0 to 18:1n-9 and 20:3n-9 in antisense cells. These changes are associated with increased expression of fatty acid metabolic enzymes, including Δ5, Δ6, and Δ9 desaturases and elongase 6 both in antisense cells and in IB3 cells. Combined, the findings of these two studies strongly support the notion that induction of metabolic enzymes underlies alterations of fatty acid composition in CF. Furthermore, the detection of these changes in an isolated, homogenous cell culture system confirms that the alterations are a result of intrinsic alterations in the CFTR-mutated cells, and not caused by malabsorption or other physiologic abnormalities of CF patients.

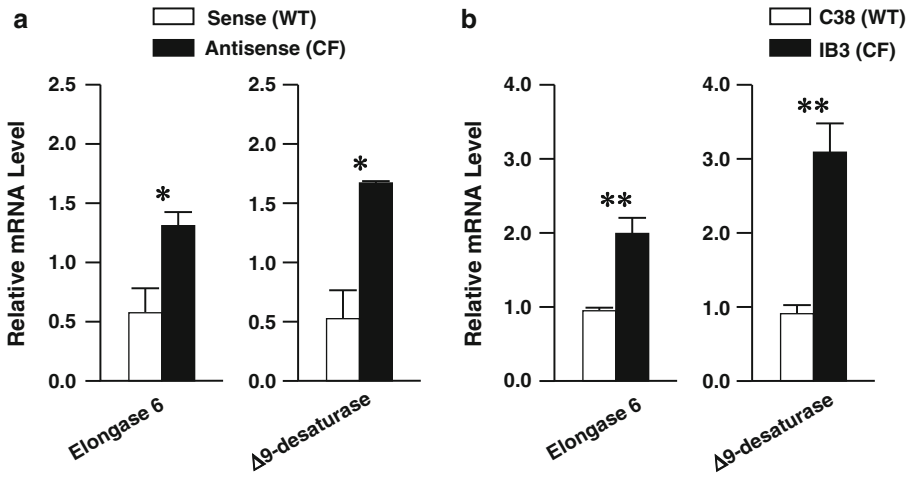

Fig. 5 Relative mRNA expression of metabolic enzymes in the n-7 and n-9 pathways. Sense (WT) and antisense (CF) cells (**a**) or C38 (WT) and IB3 (CF) cells (**b**) were incubated in complete medium for seven days, after which RNA was extracted and cDNA synthesized as described in "Materials and Methods". qRT-PCR was performed using primers for the mRNA sequences of elongase 6 (*ELOVL6*) and Δ9-desaturase (*SCD*). Relative expression was determined by the $\Delta\Delta C_T$ method using ribosomal protein *RPLP0* as a control. *Bars* represent mean ± SEM ($n = 3$). The findings are representative of at least two independent experiments. $^*P < 0.05$, $^{**}P < 0.01$, $^{***}P < 0.001$ for sense versus antisense or IB3 versus C38 cells

Although this study begins to unravel the mechanisms of fatty acid changes in CF, the relationship between CFTR mutations and these alterations remains unclear. While CFTR, functions primarily as a chloride channel, it interacts with other proteins and is involved in several other physiologic processes [35]. Thus, changes in fatty acid metabolism could result from a number of different molecular and physiologic alterations caused by CFTR mutation. Consequently, it may be most sensible to begin with the fatty acid metabolic changes and work backwards, establishing this connection step by step. Our work contributes to early first steps in that process.

Others have described similar changes in fatty acid metabolism. Mailhot et al. [36], using a different cell type, a model of Caco-2/15 cells deficient in CFTR, showed altered regulation of lipid metabolism in the CFTR deficient cells. These cells had higher cellular fatty acid content and an elevated proportion of saturated and n-7 fatty acids. These changes were felt to be a result of increased de-novo lipogenesis, enhanced fatty acid uptake, and suppression of transcription factors PPAR-α, RXR-α, LXR-α, and LXR-β mRNA, which are involved in the regulation of lipid metabolism. Altered Δ9-desaturase expression in CF is also supported by the findings of Xu et al. [37], who examined the expression of selected lipid metabolizing enzymes in bone marrow-derived dendritic cells from wild-type and *cftr*$^{-/-}$ knockout mice. They did not detect a difference in Δ9-desaturase mRNA levels between wild-type and CF cells at baseline. However, when exposed to *Pseudomonas* infection, Δ9-desaturase expression was down-regulated in wild-type, but not CF cells. The net result was significantly increased expression of this enzyme in infected CF versus wild-type cells.

Some have speculated that abnormalities in n-3 and n-6 fatty acid levels contribute to CF pathogenesis by increasing production of oxygenated fatty acid species, notably the eicosanoids. The specific role that increased n-7 and n-9 fatty acids, for example 16:1n-7, 18:1n-9, and 20:3n-9, might play in the pathophysiology of CF is less obvious. However, there is a growing recognition that these lipids are important in mammalian physiology and disease. For example, several recent studies have demonstrated that 16:1n-7 increases the insulin sensitivity of peripheral tissues, particularly muscle and liver [15, 38]. In this "lipokine" role, it may also partially mediate the effect of insulin-sensitizing drugs, for example thiazolidinediones [39]. These findings may partially explain the described role of Δ9-desaturase in obesity and insulin resistance [40] and emphasize the role of 16:1n-7 as a signaling molecule.

The other major product of Δ9-desaturase metabolism, 18:1n-9, has been shown to be involved in inflammation, a process particularly germane to CF pathophysiology. Liu et al. [17] showed that decreased 18:1n-9 in Δ9-desaturase-deficient mice attenuated inflammation in adipocytes, macrophages, and endothelial cells. In contrast, Harvey et al. [41] showed that 18:1n-9 blocks 18:0-induced cell growth inhibition and inflammatory signaling. Other studies [16, 18] have found that decreased 18:1n-9 levels because of Δ9-desaturase inhibition or deletion exacerbate inflammation in mouse models of acute colitis and atherosclerosis. Thus, 18:1n-9 may have cell-specific effects in inflammation. In addition, Patel et al. [19] demonstrated that 20:3n-9 may mediate inflammation via oxygenated

derivatives. This study found that the major product of 20:3n-9 metabolism was 5-hydroxy-20:3, a potent pro-inflammatory mediator and activator of neutrophils and eosinophils.

It should be noted that a high-fat diet is recommended for patients with CF, with no suggestion that the fat be of a specific type and therefore provide the patient with higher concentrations of specific fatty acids. Understanding the metabolic mechanisms responsible for the specific fatty acid alterations observed in CF may lead to better informed and more specific dietary and therapeutic recommendations that may be beneficial for patients.

Acknowledgments The authors thank Jesse Gilliam for technical assistance and Eva Henderson and the Vanderbilt Molecular Cell Biology Core Laboratory for primer design and testing and qRT-PCR support. This work was funded in part by Clinical Translational Science Award 1UL-1RR024975 from the National Center for Research Resources and Training Grant in Gastroenterology 5T32DK007673-18 from the National Institutes of Health to K.F.T., the Edward and Nancy Fody Endowed Chair in Pathology (M.L.), and the Vanderbilt Physician Scientist Training Program (A.C.S.).

References

1. O'Sullivan BP, Freedman SD (2009) Cystic fibrosis. Lancet 373:1891–1904
2. Kerem B, Rommens JM, Buchanan JA, Markiewicz D, Cox TK et al (1989) Identification of the cystic fibrosis gene: genetic analysis. Science 245:1073–1080
3. Al-Turkmani MR, Freedman SD, Laposata M (2007) Fatty acid alterations and n-3 fatty acid supplementation in cystic fibrosis. Prostaglandins Leukot Essent Fatty Acids 77:309–318
4. Strandvik B (2010) Fatty acid metabolism in cystic fibrosis. Prostaglandins Leukot Essent Fatty Acids 83:121–129
5. Freedman SD, Katz MH, Parker EM, Laposata M, Urman MY et al (1999) A membrane lipid imbalance plays a role in the phenotypic expression of cystic fibrosis in cftr(−/−) mice. Proc Natl Acad Sci USA 96:13995–14000
6. Hubbard VS, Dunn GD (1980) Fatty acid composition of erythrocyte phospholipids from patients with cystic fibrosis. Clin Chim Acta 102:115–118
7. Lepage G, Levy E, Ronco N, Smith L, Galeano N et al (1989) Direct transesterification of plasma fatty acids for the diagnosis of essential fatty acid deficiency in cystic fibrosis. J Lipid Res 30:1483–1490
8. Fokkema MR, Smit EN, Martini IA, Woltil HA, Boersma ER et al (2002) Assessment of essential fatty acid and omega3-fatty acid status by measurement of erythrocyte 20:3omega9 (mead acid), 22:5omega6/20:4omega6 and 22:5omega6/22:6omega3. Prostaglandins Leukot Essent Fatty Acids 67:345–356
9. Siguel EN, Chee KM, Gong JX, Schaefer EJ (1987) Criteria for essential fatty acid deficiency in plasma as assessed by capillary column gas-liquid chromatography. Clin Chem 33:1869–1873
10. Aldamiz-Echevarria L, Prieto JA, Andrade F, Elorz J, Sojo A et al (2009) Persistence of essential fatty acid deficiency in cystic fibrosis despite nutritional therapy. Pediatr Res 66:585–589
11. Roulet M, Frascarolo P, Rappaz I, Pilet M (1997) Essential fatty acid deficiency in well nourished young cystic fibrosis patients. Eur J Pediatr 156:952–956
12. Van Biervliet S, Vanbillemont G, Van Biervliet JP, Declercq D, Robberecht E et al (2007) Relation between fatty acid composition and clinical status or genotype in cystic fibrosis patients. Ann Nutr Metab 51:541–549
13. Andersson C, Al-Turkmani MR, Savaille JE, Alturkmani R, Katrangi W et al (2008) Cell culture models demonstrate that CFTR dysfunction leads to defective fatty acid composition and metabolism. J Lipid Res 49:1692–1700
14. Van Biervliet S, Devos M, Delhaye T, Van Biervliet JP, Robberecht E et al (2008) Oral DHA supplementation in DeltaF508 homozygous cystic fibrosis patients. Prostaglandins Leukot Essent Fatty Acids 78:109–115
15. Cao H, Gerhold K, Mayers JR, Wiest MM, Watkins SM et al (2008) Identification of a lipokine, a lipid hormone linking adipose tissue to systemic metabolism. Cell 134:933–944
16. Chen C, Shah YM, Morimura K, Krausz KW, Miyazaki M et al (2008) Metabolomics reveals that hepatic stearoyl-CoA desaturase 1 downregulation exacerbates inflammation and acute colitis. Cell Metab 7:135–147
17. Liu X, Miyazaki M, Flowers MT, Sampath H, Zhao M et al (2010) Loss of Stearoyl-CoA desaturase-1 attenuates adipocyte inflammation: effects of adipocyte-derived oleate. Arterioscler Thromb Vasc Biol 30:31–38
18. MacDonald ML, van Eck M, Hildebrand RB, Wong BW, Bissada N et al (2009) Despite antiatherogenic metabolic characteristics, SCD1-deficient mice have increased inflammation and atherosclerosis. Arterioscler Thromb Vasc Biol 29:341–347
19. Patel P, Cossette C, Anumolu JR, Gravel S, Lesimple A et al (2008) Structural requirements for activation of the 5-oxo-6E, 8Z, 11Z, 14Z-eicosatetraenoic acid (5-oxo-ETE) receptor: identification of a mead acid metabolite with potent agonist activity. J Pharmacol Exp Ther 325:698–707
20. Njoroge SW, Seegmiller AC, Laposata M (2010) Fatty acid changes in cultured cystic fibrosis cells result from increased expression of Δ5- and Δ6-desaturases and eicosanoid forming enzymes. Pediatr Pulmonol 45:279
21. Al-Turkmani MR, Andersson C, Alturkmani R, Katrangi W, Cluette-Brown JE et al (2008) A mechanism accounting for the low cellular level of linoleic acid in cystic fibrosis and its reversal by DHA. J Lipid Res 49:1946–1954
22. Rajan S, Cacalano G, Bryan R, Ratner AJ, Sontich CU et al (2000) *Pseudomonas aeruginosa* induction of apoptosis in respiratory epithelial cells: analysis of the effects of cystic fibrosis transmembrane conductance regulator dysfunction and bacterial virulence factors. Am J Respir Cell Mol Biol 23:304–312
23. Zeitlin PL, Lu L, Rhim J, Cutting G, Stetten G et al (1991) A cystic fibrosis bronchial epithelial cell line: immortalization by adeno-12-SV40 infection. Am J Respir Cell Mol Biol 4:313–319
24. Egan M, Flotte T, Afione S, Solow R, Zeitlin PL et al (1992) Defective regulation of outwardly rectifying Cl- channels by protein kinase A corrected by insertion of CFTR. Nature 358:581–584
25. Folch J, Lees M, Sloane Stanley GH (1957) A simple method for the isolation and purification of total lipides from animal tissues. J Biol Chem 226:497–509
26. Alvarez JG, Storey BT (1995) Differential incorporation of fatty acids into and peroxidative loss of fatty acids from phospholipids of human spermatozoa. Mol Reprod Dev 42:334–346
27. Applied-Biosystems (2001) User bulletin No. 2, Rev. B. Applied Biosystems, Forster City
28. Holman RT (1960) The ratio of trienoic: tetraenoic acids in tissue lipids as a measure of essential fatty acid requirement. J Nutr 70:405–410
29. Nakamura MT, Nara TY (2002) Gene regulation of mammalian desaturases. Biochem Soc Trans 30:1076–1079
30. Jakobsson A, Westerberg R, Jacobsson A (2006) Fatty acid elongases in mammals: their regulation and roles in metabolism. Prog Lipid Res 45:237–249

31. Strandvik B, Gronowitz E, Enlund F, Martinsson T, Wahlstrom J (2001) Essential fatty acid deficiency in relation to genotype in patients with cystic fibrosis. J Pediatr 139:650–655
32. Guilbault C, Wojewodka G, Saeed Z, Hajduch M, Matouk E et al (2009) Cystic fibrosis fatty acid imbalance is linked to ceramide deficiency and corrected by fenretinide. Am J Respir Cell Mol Biol 41:100–106
33. Maqbool A, Schall JI, Garcia-Espana JF, Zemel BS, Strandvik B et al (2008) Serum linoleic acid status as a clinical indicator of essential fatty acid status in children with cystic fibrosis. J Pediatr Gastroenterol Nutr 47:635–644
34. Olveira G, Dorado A, Olveira C, Padilla A, Rojo-Martinez G et al (2006) Serum phospholipid fatty acid profile and dietary intake in an adult Mediterranean population with cystic fibrosis. Br J Nutr 96:343–349
35. Vankeerberghen A, Cuppens H, Cassiman JJ (2002) The cystic fibrosis transmembrane conductance regulator: an intriguing protein with pleiotropic functions. J Cyst Fibros 1:13–29
36. Mailhot G, Rabasa-Lhoret R, Moreau A, Berthiaume Y, Levy E (2010) CFTR depletion results in changes in fatty acid composition and promotes lipogenesis in intestinal Caco 2/15 cells. PLoS One 5:e10446
37. Xu Y, Tertilt C, Krause A, Quadri LE, Crystal RG et al (2009) Influence of the cystic fibrosis transmembrane conductance regulator on expression of lipid metabolism-related genes in dendritic cells. Respir Res 10:26
38. Stefan N, Kantartzis K, Celebi N, Staiger H, Machann J et al (2010) Circulating palmitoleate strongly and independently predicts insulin sensitivity in humans. Diabetes Care 33:405–407
39. Kuda O, Stankova B, Tvrzicka E, Hensler M, Jelenik T et al (2009) Prominent role of liver in elevated plasma palmitoleate levels in response to rosiglitazone in mice fed high-fat diet. J Physiol Pharmacol 60:135–140
40. Flowers MT, Ntambi JM (2008) Role of stearoyl-coenzyme A desaturase in regulating lipid metabolism. Curr Opin Lipidol 19:248–256
41. Harvey KA, Walker CL, Xu Z, Whitley P, Pavlina TM et al (2010) Oleic acid inhibits stearic acid-induced inhibition of cell growth and pro-inflammatory responses in human aortic endothelial cells. J Lipid Res 51:3470–3480

Lipids (2011) 46:679–689
DOI 10.1007/s11745-011-3536-2

ORIGINAL ARTICLE

Tetradecylthioacetic Acid Increases Hepatic Mitochondrial β-Oxidation and Alters Fatty Acid Composition in a Mouse Model of Chronic Inflammation

Lena Burri · Bodil Bjørndal · Hege Wergedahl · Kjetil Berge · Pavol Bohov · Asbjørn Svardal · Rolf K. Berge

Received: 5 October 2010 / Accepted: 10 January 2011 / Published online: 9 April 2011

Abstract The administration of tetradecylthioacetic acid (TTA), a hypolipidemic and anti-inflammatory modified bioactive fatty acid, has in several experiments based on high fat diets been shown to improve lipid transport and utilization. It was suggested that increased mitochondrial and peroxisomal fatty acid oxidation in the liver of Wistar rats results in reduced plasma triacylglycerol (TAG) levels. Here we assessed the potential of TTA to prevent tumor necrosis factor (TNF) α-induced lipid modifications in human TNFα (hTNFα) transgenic mice. These mice are characterized by reduced β-oxidation and changed fatty acid composition in the liver. The effect of dietary treatment with TTA on persistent, low-grade hTNFα overexpression in mice showed a beneficial effect through decreasing TAG plasma concentrations and positively affecting saturated and monounsaturated fatty acid proportions in the liver, leading to an increased anti-inflammatory fatty acid index in this group. We also observed an increase of mitochondrial β-oxidation in the livers of TTA treated mice. Concomitantly, there were enhanced plasma levels of carnitine, acetyl carnitine, propionyl carnitine, and octanoyl carnitine, no changed levels in trimethyllysine and palmitoyl carnitine, and a decreased level of the precursor for carnitine, called γ-butyrobetaine. Nevertheless, TTA administration led to increased hepatic TAG levels that warrant further investigations to ascertain that TTA may be a promising candidate for use in the amelioration of inflammatory disorders characterized by changed lipid metabolism due to raised TNFα levels.

Keywords Tetradecylthioacetic acid · hTNFα transgenic mice · Low-grade inflammation · Dietary treatment · Plasma · Liver

Abbreviations

ACC	Acetyl-CoA carboxylase
ACS	Acyl-CoA synthetase
CPT-I and -II	Carnitine palmitoyltransferase-I and -II
FAO	Fatty acyl-CoA oxidase
FAS	Fatty acid synthase
HDL	High-density lipoprotein
HMG-CoA synthase	3-Hydroxy-3-methylglutaryl-coenzyme A synthase
HPLC	High-performance liquid chromatography
MUFA	Monounsaturated fatty acid(s)
PPAR	Peroxisome proliferator-activated receptor(s)
PUFA	Polyunsaturated fatty acid(s)
SFA	Saturated fatty acid(s)
TAG	Triacylglycerol
TCA	Tricarboxylic acid cycle (Krebs cycle)
hTNFα	Human tumor necrosis factor α
TTA	Tetradecylthioacetic acid
VLDL	Very low density lipoprotein

L. Burri (✉) · B. Bjørndal · K. Berge · P. Bohov · A. Svardal · R. K. Berge
Section of Medical Biochemistry, Institute of Medicine, Haukeland University Hospital, University of Bergen, N-5021 Bergen, Norway
e-mail: lena.burri@med.uib.no

H. Wergedahl
Faculty of Education, Bergen University College, Bergen, Norway

R. K. Berge
Department of Heart Disease, Haukeland University Hospital, Bergen, Norway

Introduction

Chronic low-grade inflammation accompanies the development of metabolic syndrome features, like abdominal obesity, dyslipidemia, hypertension, and insulin resistance, known risk factors for cardiovascular disease affecting millions of people worldwide. The first indication that there is a connection between obesity, diabetes and chronic inflammation came from the observation that the pro-inflammatory cytokine tumor necrosis factor (TNF) α is overexpressed in adipose tissues of obese mice and humans [1, 2]. Moreover, its inactivation with anti-TNFα antibodies improved insulin resistance in obese mice [2], whereas TNFα null mice would not develop insulin resistance after diet-induced obesity [3]. The multifunctional cytokine TNFα was shown thereafter to perturb lipid metabolism by increasing free fatty acid production [4, 5], promoting lipolysis [6–9], affecting lipid-metabolism-related gene expression [10, 11], controlling cholesterol metabolism [12, 13], and influencing expression and secretion of other adipokines [14–17].

Used as a model for persistent low-grade TNFα exposure, we have found previously that hTNFα transgenic mice show a down-regulation of peroxisome proliferator-activated receptor (PPAR) α target genes [18]. The mitochondrial enzymes involved in hepatic lipid metabolism were influenced, leading to changes in fatty acid synthesis and oxidation [18]. In particular, not only carnitine palmitoyltransferase-I and -II (CPT-I and -II), proteins important for the β-oxidation of long-chain fatty acids in mitochondria, but also fatty acyl-CoA oxidase (FAO), which is important for peroxisomal β-oxidation, proved to have decreased hepatic activity in the hTNFα transgenic mice [18]. In addition, TNFα overexpression was associated with a significant reduction of hepatic mRNA levels of mitochondrial HMG-CoA synthase, the rate-limiting enzyme in ketogenesis [18]. Moreover, lipogenesis is affected by TNFα. Namely, the two important enzymes in lipogenesis, acetyl-CoA carboxylase (ACC), which produces malonyl-CoA for fatty acid synthesis, showed a tendency for lowered activity, whereas fatty acid synthase (FAS), an enzyme involved in long-term regulation of fatty acid synthesis, displayed a significantly decreased activity [18].

As lipids have the ability to modulate metabolic, inflammatory and innate immune processes [19], we investigated in the present study, whether the fatty acid analogue tetradecylthioacetic acid (TTA) could counteract the health risks as a consequence of TNFα-overexpression. To be able to investigate inflammation in relation to lipid accumulation as seen in the nutritional disorder of obesity, we chose to administer a high-fat diet. TTA is a saturated fatty acid containing 16 carbons and one sulfur atom at position three of the carbon chain from the alpha end, a characteristic that results in its increased metabolic stability [20]. TTA is known to act, at least partly, through the activation of PPAR [21–23], and influence plasma lipids by increasing hepatic β-oxidation [24, 25]. Moreover, we have reported that TTA has antioxidant and antiinflammatory properties [26].

In the present work, we show that the administration of TTA to hTNFα transgenic mice fed a high-fat diet showed beneficial effects on serum cholesterol and triacylglycerol (TAG) levels, hepatic fatty acid composition and cholesterol levels, with a concurrent increase in hepatic β-oxidation and fatty inflammatory index.

Experimental Procedure

Transgenic Mice

The study was performed on female transgenic mice expressing low levels of human TNFα (hTNFα) mice from Taconic (Germantown, USA). The transgenic mouse line was generated in strain C57Bl/6 [27]. The experiments were performed in accordance with, and under the approval of, the Norwegian State Board for Biological Experiments, the Guide for the Care and Use of Laboratory Animals, and the Guidelines of the Animal Welfare Act. The mice were between 6 and 8 weeks of age at the start of the experimental feeding and were divided into two experimental groups of five animals each with comparable mean body weight. They were housed in cages with constant temperature (22 ± 2 °C) and humidity (55 ± 5%), where they were exposed to a 12 h light-dark cycle (light from 07.00 to 19.00) and had unrestricted access to tap water and food. The mice were acclimatized to these conditions before the start of the experiment.

Protein and fat of the feeding diets were from casein sodium salt from bovine milk, 20% (Sigma-Aldrich Norway AS, Oslo, Norway) and lard, 23% (Ten Kate Vetten BV, Musselkanaal, Netherlands) plus soy oil, 2% (Dyets Inc., Bethlehem, PA, USA). In addition, in the TTA group 0.6% of the lard was substituted by TTA. The TTA was synthesized as described earlier [28]. There were no significant differences in fatty acid composition between control and TTA diets, except the TTA content (SFA 43.9 vs. 42.8 wt%, MUFA 38.8 vs. 37.8 wt%, PUFAn-3 1.51 vs. 1.48 wt%, PUFAn-6 15.6 vs. 15.3 wt%, TTA 0.0 vs 2.5 wt%).

The mice were anaesthetized under fasting conditions by inhalation of 2% isoflurane (Schering-Plough, Kent, UK) after two weeks of feeding. Blood was collected by aortic

puncture with 7.5% EDTA and immediately chilled on ice. Plasma was prepared and stored at −80 °C prior to analysis. Parts of the liver were used for β-oxidation analysis and chilled on ice, and the rest was freeze-clamped and stored at −80 °C until the analysis of fatty acids, triacylglycerols, cholesterol, and enzyme activities.

Plasma and Hepatic Lipids

Liver lipids were extracted according to Bligh and Dyer [29], evaporated under nitrogen, and redissolved in isopropanol before analysis. Lipids were subsequently measured enzymatically on a Hitachi 917 system (Roche Diagnostics GmbH, Mannheim, Germany) using the triacylglycerol (GPO-PAP) and cholesterol kit (CHOD-PAP) from Roche Diagnostics (Mannheim, Germany) and the phospholipid kit from bioMérieux SA (Marcy l'Etoile, France).

Hepatic Fatty Acid and Plasma Carnitine Compositions

Total hepatic fatty acid composition was analyzed as described previously [18]. The anti-inflammatory fatty acid index was calculated as (docosapentaenoic acid + docosahexaenoic acid + dihomo-γ-linolenic acid + eicosapentaenoic acid)x100/arachidonic acid. Slightly different indexes have been used by [30, 31]. Free carnitine, short-, medium-, and long-chain acylcarnitines, and the precursors for carnitine, trimethyllysine and γ-butyrobetaine, respectively, were analysed in plasma using HPLC/MS/MS as described previously [32] with some modifications (Svardal et al., in preparation).

Hepatic Enzyme Activities

The livers were homogenized and fractionated as described earlier [33]. Palmitoyl-CoA oxidation was measured in a mitochondria-enriched extract from liver as acid-soluble products [34]. The activities of carnitine palmitoyltransferase (CPT)-I [35] and acyl-CoA synthetase (ACS) [35] were measured in the mitochondrial fraction. Fatty acid synthase (FAS) was measured in the post-nuclear fraction as described by Skorve et al. [36].

Statistical Analysis

Data sets were analyzed using Prism Software (Graph-Pad Software, San Diego, CA) to generate the figures and determine statistical significance. The results are shown as means with their standard deviations (S.D.). A *t*-test was used to determine significant differences between the control and the TTA treatment group. *P*-values < 0.05 were considered significant.

Results

Body/Liver Weights and Feed Intake

We found that TTA supplementation for two weeks to hTNFα-overexpressing mice promoted a significant decrease in body weights (−0.8 ± 0.8 g) as compared to high-fat-fed control animals (1.4 ± 0.6 g) (Table 1). Whereas liver weights and liver index were significantly increased in the TTA supplemented group (1.4 ± 0.09 and 7.2 ± 0.43) in comparison to the control group (0.9 ± 0.08 and 4.3 ± 0.3). The TTA group displayed a reduced total feed intake, 30 g versus 34 g of diet per TTA- or control-fed mouse, respectively. Thus, the TTA group seems more efficient in converting feed into increased body mass, as shown by a lower total feed efficiency (−0.03) in comparison to the control group (0.04).

Serum and Hepatic Lipids

In previous studies, comparing transgenic hTNFα-overexpressing with wildtype mice, TNFα interfered with lipid metabolism, leading to increased hepatic TAG and total cholesterol levels. Serum cholesterol concentrations were decreased, whereas serum TAG levels were unchanged [18].

In this study, two weeks of 0.6% TTA administration promoted positive effects on plasma parameters in hTNFα-overexpressing mice fed a high fat diet. The transgenic mice showed increased levels of total cholesterol due to a 39% increase in HDL-cholesterol in the TTA treated group (Fig. 1a) as compared to the high fat-fed controls. With regard to plasma TAG, a drastic reduction of 54% was observed after TTA treatment (Fig. 1b) as compared to the control. Plasma phospholipids (Fig. 1c) and free fatty acids (data not shown) were not significantly changed. The hepatic levels of total cholesterol showed a non-significant tendency to decrease in the TTA-treated group (Fig. 1d), and the already high TAG amounts in transgenic mice

Table 1 Body and liver weights, liver index [100 × (liver weight in g/body weight in g)], total feed intake, and feed efficiency (weight gain in g/food intake in g)

	Control	TTA
Initial body weight (g)	19.2 ± 1.1	20.2 ± 1.3
Final body weight (g)	20.6 ± 1.5	19.4 ± 1.3
Body weight gain (g)	1.4 ± 0.6	−0.8 ± 0.8
Liver weight (g)	0.9 ± 0.08	1.4 ± 0.09
Liver index	4.3 ± 0.3	7.2 ± 0.43
Total feed intake (g)	34.2	30
Total feed efficiency	0.04	−0.03

Values are mean ± S.D. ($n = 5$)

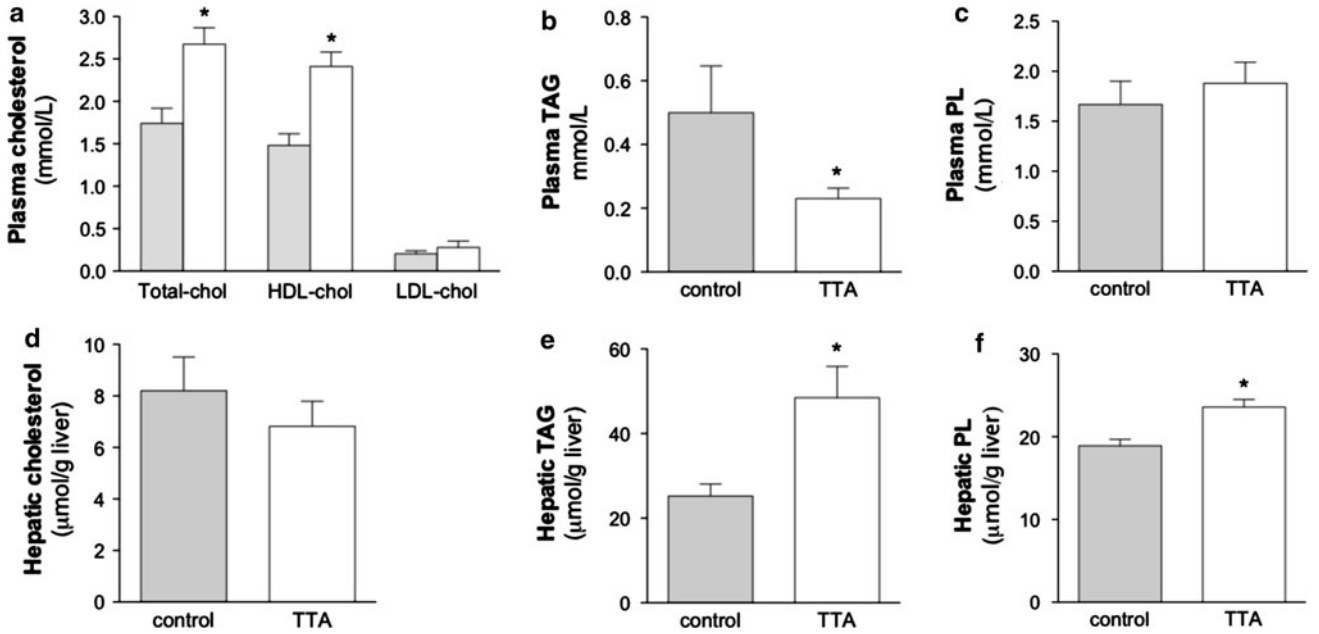

Fig. 1 TTA treatment induces a significant increase in plasma HDL-cholesterol levels in hTNFα transgenic mice (**a**) and a decrease in plasma TAG levels (**b**), whereas phospholipids showed no change (**c**). Hepatic cholesterol showed no significant change (**d**), but a TAG and phospholipid-increasing effect in the liver was found after treatment with TTA (**e**, **f**). Data are means ± S.D. ($n = 5$). * denotes statistical significant differences by Student's *t*-test between control (*grey bars*) and TTA (*white bars*) ($P < 0.05$). *chol*, cholesterol; *HDL*, high-density lipoprotein; *LDL*, low density lipoprotein; *PL*, phospholipid; *AG*, triacylglycerol; *TTA*, tetradecylthioacetic acid

further increased after TTA treatment (Fig. 1e). The hepatic phospholipid level was also elevated after TTA administration in comparison to control mice (Fig. 1f).

Fatty Acid Composition in Liver

In order to investigate if the results obtained for hepatic lipids were specific for cholesterol and TAG or if fatty acids were also affected significantly, we performed an analysis of the total hepatic fatty acid composition. We have previously demonstrated an increased weight % of saturated fatty acids (SFAs) in TNFα-overexpressing mice on a chow diet [18].

Here we observed a comparable level of SFAs in TNFα-overexpressing mice (in spite of higher dietary SFA content in the high-fat diet used- see Discussion). TTA treatment lead to decreased weight % in saturated fatty acid levels (Fig. 2a). The most significant individual decreases could be found in the fatty acids C15:0, C17:0, C18:0, C22:0, C23:0, and C24:0 (Table 2). The most impact on decreasing total SFAs had C18:0.

The relative amounts of monounsaturated fatty acids (MUFA) that were shown to be decreased in hTNFα transgenic in comparison to wildtype mice [18], were significantly increased by TTA in the diet (Fig. 2b). This was mainly due to the increased amount of oleic acid (C18:1n-9) that was to some extent induced by increased Δ9 desaturase activity as the index Δ9 desaturase activity suggests (Table 2).

A significant decrease in weight % of n-3 and n-6 polyunsaturated fatty acids (PUFA) was observed in the transgenic mice treated with TTA (Fig. 2c and d) when compared to control animals. This was reflected in decreased amounts of the n-3 PUFA alpha-linolenic acid (18:3n-3), stearidonic acid (C18:4n-3) and docosahexaenoic acid (C22:6n-3), along with linoleic acid (C18:2n-6) and arachidonic acid (C20:4n-6) that can mainly be attributed to lowered levels of n-6 PUFA (Table 1). The sums result in a decreased ratio of n-3 to n-6 PUFA (Table 1). TTA seems to counteract the increased PUFA levels seen in transgenic mice in contrast to wildtype mice that were due to increased weight % of n-3, with unchanged n-6 levels, giving an increased n-3 to n-6 ratio [18].

In addition, after TTA administration, there was a strong decrease in the C20:4n-6/C20:3n-6 ratio as an indirect measure of the n-6 Δ5 desaturase activity, an enzyme important for the production of arachidonic acid (Table 2). This indicates that TTA might decrease the hepatic desaturation of dihomo-γ-linolenic acid (20:3n-6) to arachidonic acid (20:4n-6) in hTNFα transgenic mice. Whereas beforehand, we observed increased ratios pointing towards increased activities of Δ6 and Δ5 desaturases in transgenic mice in comparison to control animals [18].

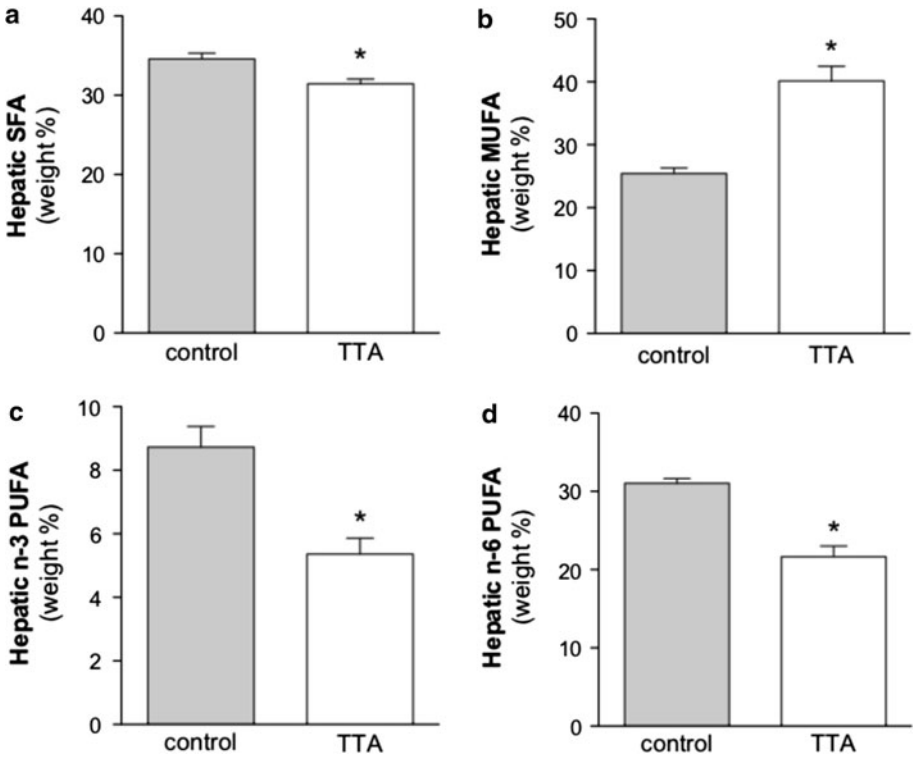

Fig. 2 Dietary treatment for 2 weeks with TTA affects hepatic fatty acid composition and changes saturated fatty acids (**a**), monounsaturated fatty acids (**b**), n-3 polyunsaturated fatty acids (**c**), and n-6 polyunsaturated fatty acids (**d**) levels significantly. The data is given as weight % of total fatty acid ± S.D. ($n = 5$). * denotes statistical significant differences to the control by Student's t test ($P < 0.05$). *SFA* saturated fatty acids, *MUFA* monounsaturated fatty acids, *PUFA* polyunsaturated fatty acids, *TTA* tetradecylthioacetic acid

The anti-inflammatory fatty acid index, calculated as (docosapentaenoic acid + docosahexaenoic acid + dihomo-γ-linolenic acid + eicosapentaenoic acid) × 100/arachidonic acid [30], increased after TTA treatment.

Hepatic β-Oxidation of Fatty Acids

The TAG-lowering effect observed in plasma of hTNAα transgenic mice after TTA treatment, could be due to an enhanced mitochondrial and peroxisomal β-oxidation that is responsible for the shortening of long-chain fatty acyl-CoAs. Indeed, β-oxidation increased by 48% in the TTA treated mice, when using ^{14}C-palmitoyl-CoA as substrate (Fig. 3a), counterbalancing the decreased β-oxidation values from transgenic mice [18]. In the previous study, the sensitivity towards malonyl-CoA, an inhibitor of CPT-I, was unaffected by TNFα [18]. However, in the TTA treated group we detected a lowering of the inhibition capacity of malonyl-CoA from 35% to 14% inhibition (Fig. 3b) and the transport of fatty acids across the mitochondrial outer membrane is facilitated even in the presence of malonyl-CoA.

Activities of Enzymes Involved in Degradation and Biosynthesis of Fatty Acids

In order to explain the mechanisms of TTA in more detail, enzyme activities were measured in the post-nuclear fraction of the liver. The enzymatic activity of CPT-I, the rate-limiting enzyme of mitochondrial β-oxidation, involved in acyl group transport into the matrix, was increased after TTA treatment (Fig. 4a). Likewise, the mitochondrial enzyme acyl-CoA synthetase (ACS) that activates fatty acids prior to oxidation, showed increased activity (Fig. 4b). On the other hand, a major cytosolic, multifunctional enzyme involved in the biosynthesis of fatty acids, called fatty acid synthase (FAS), showed reduced activity (Fig. 4c).

Oxidation of fatty acids can be facilitated not only by the up-regulation of CPT-I, but also by an increased concentration of its substrate carnitine, to ensure efficient transport of fatty acids into mitochondria. Carnitine can be taken up from dietary sources or is endogenously synthesized primarily in the liver and kidney [37, 38]. All other tissues have to take carnitine actively up from the blood. We found that in plasma, free carnitine concentrations have increased during TTA treatment by 36% in comparison to control animals (Fig. 5a). The precursors for carnitine, were either unchanged (trimethyllysine, Fig. 5b) or reduced (γ-butyrobetaine, Fig. 5c). The two quantitatively most important acyl-esters, acetyl carnitine (Fig. 5d) and propionyl carnitine (Fig. 5e) were significantly increased by TTA compared to high fat-fed controls. The plasma medium-chain acylcarnitine, octanoyl carnitine, was significantly increased (Fig. 5f) and the long-chain acylcarnitine, palmitoyl carnitine, remained unchanged by TTA treatment (Fig. 5g).

Table 2 Comparison of hepatic fatty acid composition in control and TTA treated hTNFα transgenic mice

Fatty acid	control	TTA	Level of significance
SFA			
C15:0	0.07 ± 0.002	0.03 ± 0.001	$P < 0.0001$
C16:0	21.42 ± 0.35	24.3 ± 0.204	$P < 0.0001$
C17:0	0.19 ± 0.012	0.10 ± 0.009	$P < 0.0001$
C18:0	12.02 ± 0.554	6.42 ± 0.585	$P < 0.0001$
C22:0	0.15 ± 0.017	0.07 ± 0.016	$P < 0.0001$
C23:0	0.08 ± 0.004	0.03 ± 0.004	$P < 0.0001$
C24:0	0.11 ± 0.009	0.05 ± 0.006	$P < 0.0001$
MUFA			
C16:1	0.02 ± 0.003	0.01 ± 0.001	$P < 0.002$
C16:1n-7	1.03 ± 0.127	1.44 ± 0.291	$P < 0.03$
C18:1n-7	1.6 ± 0.079	1.72 ± 0.23	NS
C18:1n-9	21.77 ± 0.748	35.22 ± 1.796	$P < 0.0001$
C20:1n-9	0.26 ± 0.022	0.49 ± 0.064	$P < 0.0001$
n-6 PUFA			
C18:2n-6	16 ± 0.540	9.90 ± 0.743	$P < 0.0001$
C20:4n-6	12.96 ± 0.788	8.61 ± 0.628	$P < 0.0001$
C20:3n-6	0.9 ± 0.059	2.51 ± 0.291	$P < 0.0001$
n-3 PUFA			
C18:3n-3	0.42 ± 0.027	0.13 ± 0.010	$P < 0.0001$
C18:4n-3	0.04 ± 0.005	0.01 ± 0.002	$P < 0.0001$
C22:6n-3	7.60 ± 0.646	4.49 ± 0.431	$P < 0.0001$
C20:5n-3	0.29 ± 0.028	0.27 ± 0.043	NS
Anti-inflammatory index	70.12 ± 2.883	88.94 ± 4.551	$P < 0.0002$
C20:4n-6/C20:3n-6	14.41 ± 1.429	3.46 ± 0.380	$P < 0.0001$
C18:1n-9/C18:0	1.81 ± 0.117	5.54 ± 0.752	$P < 0.0001$

The anti-inflammatory index is calculated as described in Experimental Procedure. The ratio of C20:4n-6 to C20:3n-6 gives an indirect index of the n-6 Δ5 desaturase activity. The data are given as weight % ± S.D. ($n = 5$). A two sample, two-tailed *t*-test assuming equal variance was calculated. NS means not significant

Discussion

Obesity-related metabolic disorders are associated with a state of chronic low-intensity inflammation. Inflammation induces a wide array of metabolic changes in the body and affects expression of many proteins involved in lipid metabolism. The different subtypes of the nuclear ligand-dependent transcription factors, PPAR, play key roles in lipid homeostasis. They are involved in the regulation of lipoprotein metabolism, fatty acid oxidation, glucose and carnitine homeostasis and also seem to be involved in inflammatory processes [39]. TNFα is one of the factors that mediate alterations in lipid metabolism, including decreased PPARα mRNA and protein levels [40]. With the knowledge in mind that previous studies have shown that the biological response to TTA treatment is at least partly a result of PPAR activation, and that this bioactive fatty acid analogue has the ability to activate all three isoforms of PPAR [21, 23, 41], as well as increase the mRNA level of PPARα [42], we wanted to test if TTA was able to counteract TNFα-induced metabolic aberrations.

In the present study we demonstrated that TTA, in addition to its health-promoting effects in previous in vivo [43] and in vitro experiments [26, 44], could also ameliorate several parameters in a mouse model of chronic inflammation. TNFα might induce hypertriglyceridemia, characterized by the accumulation of very low density lipoprotein (VLDL) in the plasma, due to impaired removal of VLDL [45] and increased hepatic lipogenesis [46]. TAG-rich lipoproteins were shown to be important for the acute phase response by binding to endotoxins to reduce their harmful action [47]. However, systemic low-grade inflammation with elevated circulating levels of TNFα seen in obese subjects is typically associated with high plasma TAG levels that will increase the risk for metabolic and cardiovascular complications [48]. It is therefore of importance to note that TTA has the capability to strongly reduce plasma TAG levels in a chronic inflammatory state with persistently high TNFα levels.

The observation of decreased TAG in the plasma is compatible with the hypothesis that there is a higher flux of fatty acids from the plasma to the liver, with a

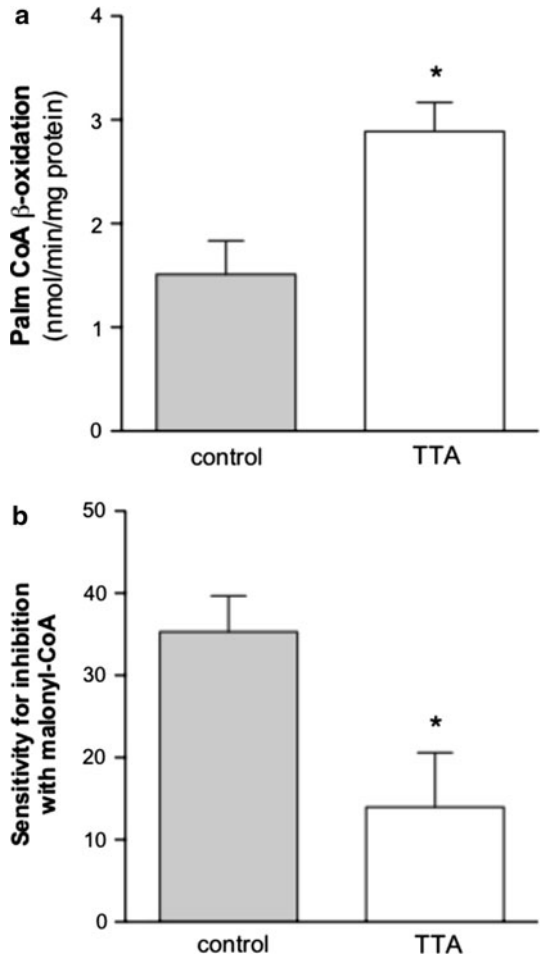

Fig. 3 Palmitoyl-CoA β-oxidation is increased in liver mitochondria of TTA-treated mice (**a**) and the sensitivity for inhibition of oxidation of palmitoyl-CoA with malonyl-CoA (given in % inhibition) is lower in the TTA group compared to high fat-fed controls (**b**). Oxidation of palmitoyl-CoA was measured in purified mitochondria as acid-soluble products. *Bars* indicate $\pm$ S.D. ($n = 5$). * $P < 0.05$ different from the control. *Palm-CoA*, palmitoyl-CoA; *TTA*, tetradecylthioacetic acid

simultaneous reduction in fatty acid biosynthesis. But even though TTA up-regulates hepatic mitochondrial CPT-I and ACS activities, accompanied by an increase in hepatic β-oxidation and plasma carnitine levels, it is not sufficient to deal with the already existing high TAG levels in the transgenic mice. It is noteworthy that TTA has the capability to downregulate the hepatic biosynthesis of fatty acids, since the FAS activity is reduced by 27% in the TTA treated animals. Reduced lipogenesis and increased fatty acid oxidation after TTA treatment seem to be the reason for decreased plasma TAG levels by 54% after TTA treatment. Yet, the exact reasons why hepatic TAG were not affected similarly by TTA are not yet elucidated at the molecular level and will require further detailed studies. It might be that a higher dose of TTA is required to get a more pronounced effect on lipogenesis, thereby influencing hepatic TAG levels. Previously, we have found indications that the effect on hepatic TAG metabolism may be dose dependent and that the amount of hepatic TAG is decreased with increasing doses of TTA [49]. It could also be that a longer feeding period than the two weeks applied is needed to overcome hepatic TAG accumulation. Noteworthy is that we have never detected a TTA-induced liver steatosis in any of the mouse or rat models used previously. It is however of importance to verify in future studies if increasing amounts of TTA could counteract this effect in the mouse model used and if this finding is of significance for humans.

The increased hepatic phospholipid level that we measure in the TTA treated group, is probably a consequence of increased membrane production due to mitochondrial and peroxisomal proliferation as seen after TTA treatment previously [50–52]. Moreover, administration of PPARα ligands has been described to lead to hepatic hypertrophy and hyperplasia leading to increased liver weights as seen in our study. The liver enlargement is however restricted to rodents and has never been described in humans [53–58].

By measuring plasma free carnitine and its acyl-esters, in particular the two most abundant species, acetyl carnitine and propionyl carnitine, we looked at overall changes in the β-oxidation process. We found that plasma free carnitine levels were increased due to TTA administration, as well as the short- and medium-chain carnitine esters, but not long-chain fatty acyl carnitines. It is important to note that in addition to being essential for transport of fatty acids into mitochondria, carnitine is crucial to increase acyl and acetyl group export out of mitochondria into the blood [59]. By increasing carnitine levels through TTA administration, lipotoxicity of β-oxidation metabolites is reduced and mitochondrial capacity is improved. The excess short-chain acyl-esters, that cannot be used by the TCA cycle, will be secreted in urine. The formation of trimethyllysine and its conversion to γ-butyrobetaine is reported to occur in most tissues, but the last step in carnitine biosynthesis, the hydroxylation of γ-butyrobetaine to carnitine, occurs only in liver and kidney in mice. Therefore interorgan transport of γ-butyrobetaine and carnitine are of importance. It was of interest that plasma γ-butyrobetaine levels were decreased, whereas carnitine levels were increased. This may be due to increased consumption of γ-butyrobetaine for carnitine biosynthesis and increased mitochondrial oxidation of long-chain fatty acids.

TTA affects the capacity for insertion of double bonds and counteracts the abnormal hepatic fatty acid composition levels under the influence of TNFα. Correct proportions of fatty acids are crucial to maintain cellular

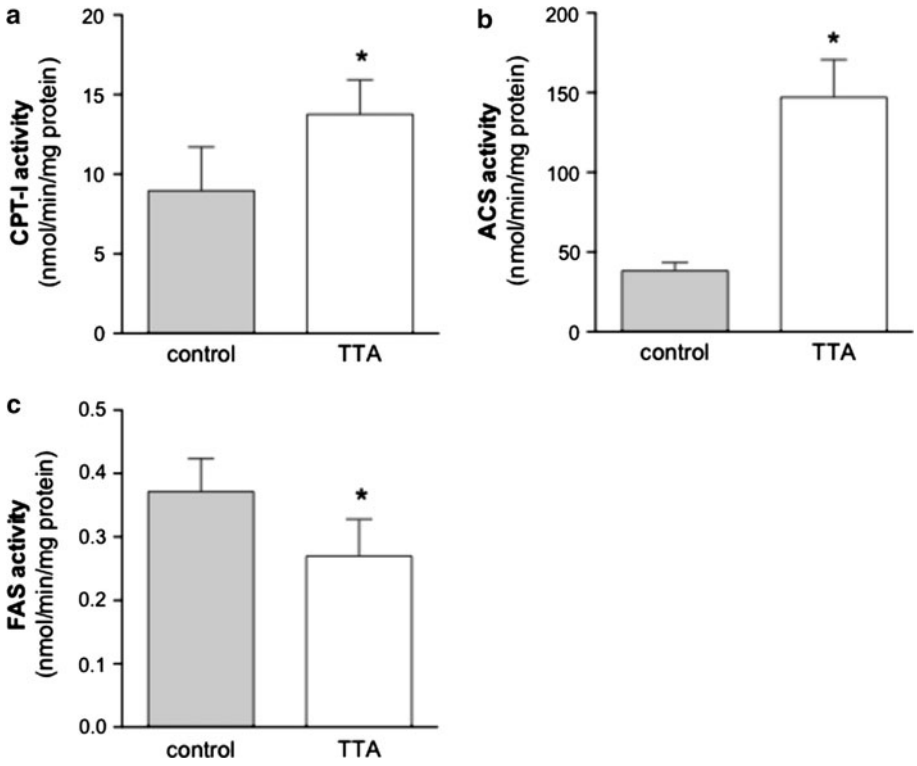

Fig. 4 Enzyme activities of the mitochondrial enzymes CPT-I (**a**) and ACS (**b**) involved in β-oxidation are increased in the liver of hTNFα transgenic mice treated with TTA, whereas the cytosolic FAS activity involved in biosynthesis of fatty acids shows reduced activity after two weeks of treatment (**c**). Values are means ± S.D. ($n = 5$) and * shows a $P < 0.05$ difference from the control. *CPT-I*, carnitine palmitoyl transferase I; *ACS*, acyl-CoA synthetase; *FAS*, fatty acid synthase; *TTA*, tetradecylthioacetic acid

functions, a balance that was disturbed in the TNFα transgenic mice. hTNFα overexpression was accompanied by increased saturated and polyunsaturated fatty acids, but decreased levels of monounsaturated fatty acids in liver [18]. The basic values of these fatty acid families in hTNFα control group in our high fat diet experiment compared to the previous study were less pronounced, which could be partially attributed to a different diet in [18] (low fat standard mouse chow with 26 % SFA, 25 % MUFA, 4 % PUFAn-3 and 45 % PUFAn-6). Nevertheless, it did not affect the trends of fatty acid changes inside the dietary groups (high fat diet and standard chow diet, respectively). Moreover, TTA reduced the n-6 Δ5 desaturase activity index in transgenic mice as fatty acid saturation was increased. This was accompanied by decreases of n-3 and n-6 polyunsaturated fatty acids including stearidonic acid (C18:4n-3) and docosahexaenoic acid (C22:6n-3), as well as linoleic acid (C18:2n-6) and arachidonic acid (C20:4n-6). The amount of arachidonic acid is of importance for the calculation of the anti-inflammatory fatty acid index, and decreased amounts after TTA treatment increased the fatty anti-inflammatory index in this group. Saturated fatty acids, that have pro-inflammatory and insulin-antagonizing properties [60], were decreased by TTA, thereby lowering the risk for the development of metabolic syndrome. On the other hand, monounsaturated fatty acids were increased after TTA treatment. This is potentially beneficial, as high levels were associated with low rates of cardiovascular disease [61]. Another risk factor for cardiovascular disease in humans is low HDL-cholesterol due to its important function in reverse cholesterol transport to the liver [62]. We found elevated plasma HDL-cholesterol levels with an increase of 63% in TTA treated TNFα transgenic mice. However, in a study including a small group of HIV-infected patients, we found that TTA in combination with dietary intervention can reduce total cholesterol, LDL-cholesterol, and LDL/HDL cholesterol, but no increase in HDL-cholesterol could be observed [63]. It has been shown previously that apolipoprotein compositions and responses to PPARα activation are different between humans and rodents [64, 65]. The result of increased HDL-cholesterol in hTNFα overexpressed mice in our study might therefore be rodent-specific. However, effects of PPARα activation on other pathways of lipid metabolism including FA uptake and activation, β-oxidation, and lipogenesis support similarities between mice and humans [39]. This suggests similar responses upon TTA treatment in humans as seen in our mice study.

In summary, given the ability of TTA to increase β-oxidation, reduce plasma TAG, and positively affect hepatic saturated and monounsaturated fatty acid compositions

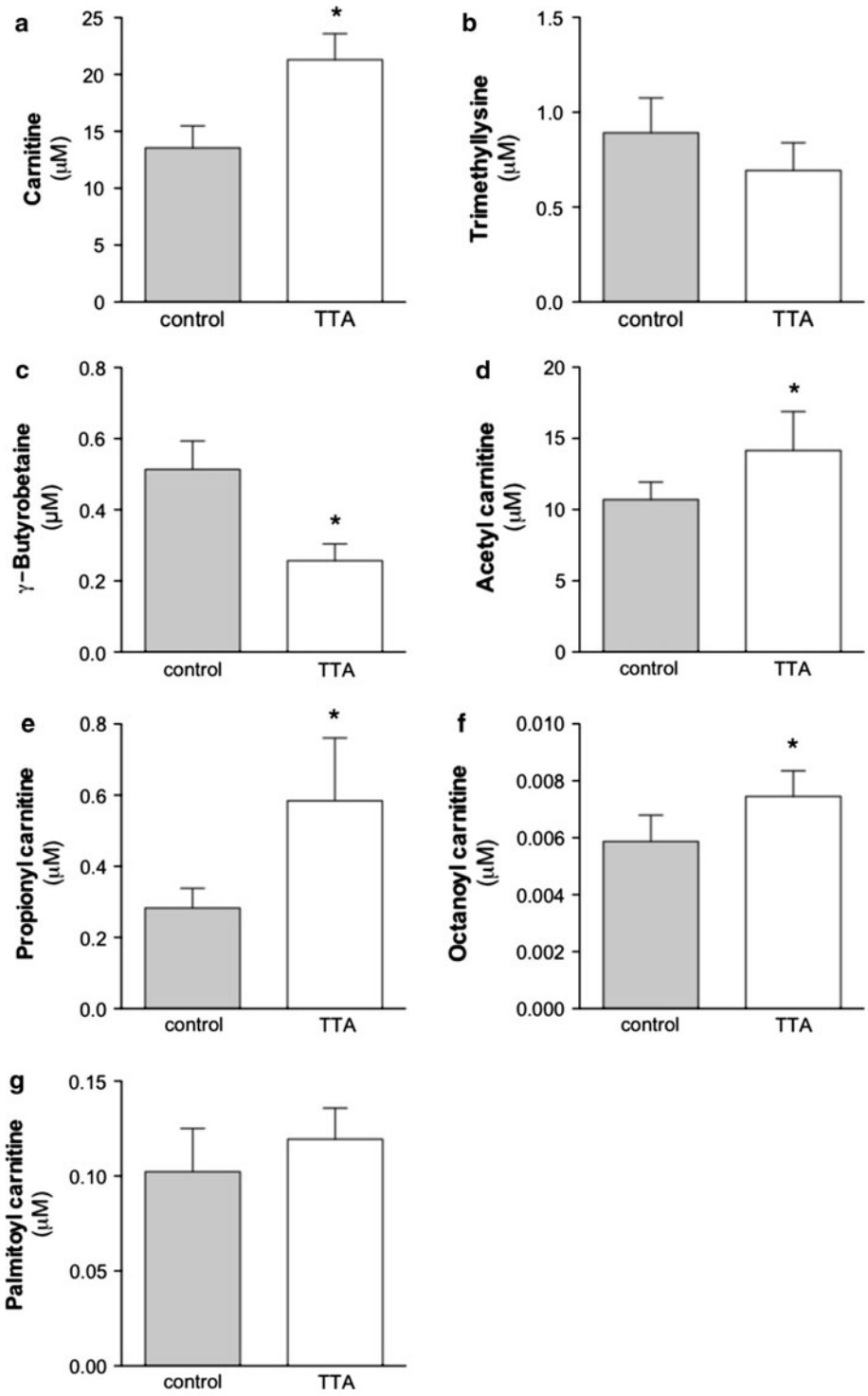

Fig. 5 A change in plasma levels of free carnitine (**a**), trimethyllysine (**b**), γ-butyrobetaine (**c**), acetyl carnitine (**d**), propionyl carnitine (**e**), octanoyl carnitine (**f**), and palmitoyl carnitine (**g**) could be detected after TTA treatment. * denotes statistical significant differences by Student's *t*-test between control (*grey bars*) and TTA (*white bars*) ($P < 0.05$) and *bars* indicate ± S.D. ($n = 5$)

leading to an increase in the anti-inflammatory fatty acid index, indicates that TTA has a high potential to ameliorate chronic inflammation such as with obesity, arthritis or atherosclerosis.

Acknowledgments We thank Kari Williams, Liv Kristine Øysæd, Randi Sandvik, Svein Krüger, and Torunn Eide for excellent technical assistance. This work was supported by grants from NordForsk, grant no. 070010, MitoHealth; EEA Polish-Norwegian Research Fund, grant no. PNRF-104-Al-1/07; the Research Council of Norway, grant no. 190287/110; and the European Community's Seventh Framework Programme (FP7/2007-2013), grant no. 201668, AtheroRemo.

References

1. Hotamisligil GS, Arner P, Caro JF, Atkinson RL, Spiegelman BM (1995) Increased adipose tissue expression of tumor necrosis factor-alpha in human obesity and insulin resistance. J Clin Invest 95:2409–2415
2. Hotamisligil GS, Shargill NS, Spiegelman BM (1993) Adipose expression of tumor necrosis factor-alpha: direct role in obesity-linked insulin resistance. Science 259:87–91
3. Uysal KT, Wiesbrock SM, Marino MW, Hotamisligil GS (1997) Protection from obesity-induced insulin resistance in mice lacking TNF-alpha function. Nature 389:610–614
4. Beier K, Volkl A, Fahimi HD (1992) Suppression of peroxisomal lipid beta-oxidation enzymes of TNF-alpha. FEBS Lett 310:273–276
5. Grunfeld C, Verdier JA, Neese R, Moser AH, Feingold KR (1988) Mechanisms by which tumor necrosis factor stimulates hepatic fatty acid synthesis in vivo. J Lipid Res 29:1327–1335
6. Gasic S, Tian B, Green A (1999) Tumor necrosis factor alpha stimulates lipolysis in adipocytes by decreasing Gi protein concentrations. J Biol Chem 274:6770–6775
7. Ogawa H, Nielsen S, Kawakami M (1989) Cachectin/tumor necrosis factor and interleukin-1 show different modes of combined effect on lipoprotein lipase activity and intracellular lipolysis in 3T3–L1 cells. Biochim Biophys Acta 1003:131–135
8. Plomgaard P, Fischer CP, Ibfelt T, Pedersen BK, van Hall G (2008) Tumor necrosis factor-alpha modulates human in vivo lipolysis. J Clin Endocrinol Metab 93:543–549
9. Ryden M, Dicker A, van Harmelen V, Hauner H, Brunnberg M, Perbeck L, Lonnqvist F, Arner P (2002) Mapping of early signaling events in tumor necrosis factor-alpha-mediated lipolysis in human fat cells. J Biol Chem 277:1085–1091
10. Pape ME, Kim KH (1988) Effect of tumor necrosis factor on acetyl-coenzyme A carboxylase gene expression and preadipocyte differentiation. Mol Endocrinol 2:395–403
11. Sumida M, Sekiya K, Okuda H, Tanaka Y, Shiosaka T (1990) Inhibitory effect of tumor necrosis factor on gene expression of hormone sensitive lipase in 3T3–L1 adipocytes. J Biochem 107:1–2
12. Memon RA, Grunfeld C, Moser AH, Feingold KR (1993) Tumor necrosis factor mediates the effects of endotoxin on cholesterol and triglyceride metabolism in mice. Endocrinology 132:2246–2253
13. Memon RA, Moser AH, Shigenaga JK, Grunfeld C, Feingold KR (2001) In vivo and in vitro regulation of sterol 27-hydroxylase in the liver during the acute phase response. potential role of hepatocyte nuclear factor-1. J Biol Chem 276:30118–30126
14. Hector J, Schwarzloh B, Goehring J, Strate TG, Hess UF, Deuretzbacher G, Hansen-Algenstaedt N, Beil FU, Algenstaedt P (2007) TNF-alpha alters visfatin and adiponectin levels in human fat. Horm Metab Res 39:250–255
15. Komai N, Morita Y, Sakuta T, Kuwabara A, Kashihara N (2007) Anti-tumor necrosis factor therapy increases serum adiponectin levels with the improvement of endothelial dysfunction in patients with rheumatoid arthritis. Mod Rheumatol 17:385–390
16. Li L, Yang G, Shi S, Yang M, Liu H, Boden G (2009) The adipose triglyceride lipase, adiponectin and visfatin are down-regulated by tumor necrosis factor-alpha (TNF-alpha) in vivo. Cytokine 45:12–19
17. Chen X, Xun K, Chen L, Wang Y (2009) TNF-alpha, a potent lipid metabolism regulator. Cell Biochem Funct 27:407–416
18. Glosli H, Gudbrandsen OA, Mullen AJ, Halvorsen B, Rost TH, Wergedahl H, Prydz H, Aukrust P, Berge RK (2005) Down-regulated expression of PPARalpha target genes, reduced fatty acid oxidation and altered fatty acid composition in the liver of mice transgenic for hTNFalpha. Biochim Biophys Acta 1734: 235–246
19. Yu C, Chen Y, Cline GW, Zhang D, Zong H, Wang Y, Bergeron R, Kim JK, Cushman SW, Cooney GJ, Atcheson B, White MF, Kraegen EW, Shulman GI (2002) Mechanism by which fatty acids inhibit insulin activation of insulin receptor substrate-1 (IRS-1)-associated phosphatidylinositol 3-kinase activity in muscle. J Biol Chem 277:50230–50236
20. Lau SM, Brantley RK, Thorpe C (1988) The reductive half-reaction in Acyl-CoA dehydrogenase from pig kidney: studies with thiaoctanoyl-CoA and oxaoctanoyl-CoA analogues. Biochemistry 27:5089–5095
21. Berge K, Tronstad KJ, Flindt EN, Rasmussen TH, Madsen L, Kristiansen K, Berge RK (2001) Tetradecylthioacetic acid inhibits growth of rat glioma cells ex vivo and in vivo via PPAR-dependent and PPAR-independent pathways. Carcinogenesis 22:1747–1755
22. Raspe E, Madsen L, Lefebvre AM, Leitersdorf I, Gelman L, Peinado-Onsurbe J, Dallongeville J, Fruchart JC, Berge R, Staels B (1999) Modulation of rat liver apolipoprotein gene expression and serum lipid levels by tetradecylthioacetic acid (TTA) via PPARalpha activation. J Lipid Res 40:2099–2110
23. Westergaard M, Henningsen J, Svendsen ML, Johansen C, Jensen UB, Schroder HD, Kratchmarova I, Berge RK, Iversen L, Bolund L, Kragballe K, Kristiansen K (2001) Modulation of keratinocyte gene expression and differentiation by PPAR-selective ligands and tetradecylthioacetic acid. J Invest Dermatol 116:702–712
24. Berge RK, Tronstad KJ, Berge K, Rost TH, Wergedahl H, Gudbrandsen OA, Skorve J (2005) The metabolic syndrome and the hepatic fatty acid drainage hypothesis. Biochimie 87:15–20
25. Lovas K, Rost TH, Skorve J, Ulvik RJ, Gudbrandsen OA, Bohov P, Wensaas AJ, Rustan AC, Berge RK, Husebye ES (2009) Tetradecylthioacetic acid attenuates dyslipidaemia in male patients with type 2 diabetes mellitus, possibly by dual PPAR-alpha/delta activation and increased mitochondrial fatty acid oxidation. Diabetes Obes Metab 11:304–314
26. Dyroy E, Yndestad A, Ueland T, Halvorsen B, Damas JK, Aukrust P, Berge RK (2005) Antiinflammatory effects of tetradecylthioacetic acid involve both peroxisome proliferator-activated receptor alpha-dependent and -independent pathways. Arterioscler Thromb Vasc Biol 25:1364–1369
27. Hayward MD, Jones BK, Saparov A, Hain HS, Trillat AC, Bunzel MM, Corona A, Li-Wang B, Strenkowski B, Giordano C, Shen H, Arcamone E, Weidlick J, Vilensky M, Tugusheva M, Felkner RH, Campbell W, Rao Y, Grass DS, Buiakova O (2007) An extensive phenotypic characterization of the hTNFalpha transgenic mice. BMC Physiol 7:13
28. Spydevold O, Bremer J (1989) Induction of peroxisomal beta-oxidation in 7800 C1 Morris hepatoma cells in steady state by fatty acids and fatty acid analogues. Biochim Biophys Acta 1003:72–79
29. Bligh EG, Dyer WJ (1959) A rapid method of total lipid extraction and purification. Can J Biochem Physiol 37:911–917
30. Chavali SR, Zhong WW, Utsunomiya T, Forse RA (1997) Decreased production of interleukin-1-beta, prostaglandin-E2 and thromboxane-B2, and elevated levels of interleukin-6 and -10 are associated with increased survival during endotoxic shock in mice consuming diets enriched with sesame seed oil supplemented with Quil-A saponin. Int Arch Allergy Immunol 114:153–160
31. Utsunomiya T, Chavali SR, Zhong WW, Forse RA (2000) Effects of sesamin-supplemented dietary fat emulsions on the ex vivo production of lipopolysaccharide-induced prostanoids and tumor necrosis factor alpha in rats. Am J Clin Nutr 72:804–808
32. Vernez L, Wenk M, Krahenbuhl S (2004) Determination of carnitine and acylcarnitines in plasma by high-performance liquid chromatography/electrospray ionization ion trap tandem mass spectrometry. Rapid Commun Mass Spectrom 18:1233–1238

33. Berge RK, Flatmark T, Osmundsen H (1984) Enhancement of long-chain acyl-CoA hydrolase activity in peroxisomes and mitochondria of rat liver by peroxisomal proliferators. Eur J Biochem 141:637–644
34. Madsen L, Garras A, Asins G, Serra D, Hegardt FG, Berge RK (1999) Mitochondrial 3-hydroxy-3-methylglutaryl coenzyme A synthase and carnitine palmitoyltransferase II as potential control sites for ketogenesis during mitochondrion and peroxisome proliferation. Biochem Pharmacol 57:1011–1019
35. Madsen L, Froyland L, Dyroy E, Helland K, Berge RK (1998) Docosahexaenoic and eicosapentaenoic acids are differently metabolized in rat liver during mitochondria and peroxisome proliferation. J Lipid Res 39:583–593
36. Skorve J, al-Shurbaji A, Asiedu D, Bjorkhem I, Berglund L, Berge RK (1993) On the mechanism of the hypolipidemic effect of sulfur-substituted hexadecanedioic acid (3-thiadicarboxylic acid) in normolipidemic rats. J Lipid Res 34:1177–1185
37. Rebouche CJ, Seim H (1998) Carnitine metabolism and its regulation in microorganisms and mammals. Annu Rev Nutr 18:39–61
38. Vaz FM, Wanders RJ (2002) Carnitine biosynthesis in mammals. Biochem J 361:417–429
39. Burri L, Thoresen GH, Berge RK (2010) The role of PPARalpha activation in liver and muscle. PPAR Res 2010 pii: 542359
40. Beier K, Volkl A, Fahimi HD (1997) TNF-alpha downregulates the peroxisome proliferator activated receptor-alpha and the mRNAs encoding peroxisomal proteins in rat liver. FEBS Lett 412:385–387
41. Forman BM, Chen J, Evans RM (1997) Hypolipidemic drugs, polyunsaturated fatty acids, and eicosanoids are ligands for peroxisome proliferator-activated receptors alpha and delta. Proc Natl Acad Sci U S A 94:4312–4317
42. Gudbrandsen OA, Rost TH, Berge RK (2006) Causes and prevention of tamoxifen-induced accumulation of triacylglycerol in rat liver. J Lipid Res 47:2223–2232
43. Berge RK, Skorve J, Tronstad KJ, Berge K, Gudbrandsen OA, Grav H (2002) Metabolic effects of thia fatty acids. Curr Opin Lipidol 13:295–304
44. Aukrust P, Wergedahl H, Muller F, Ueland T, Dyroy E, Damas JK, Froland SS, Berge RK (2003) Immunomodulating effects of 3-thia fatty acids in activated peripheral blood mononuclear cells. Eur J Clin Invest 33:426–433
45. Kaufmann RL, Matson CF, Beisel WR (1976) Hypertriglyceridemia produced by endotoxin: role of impaired triglyceride disposal mechanisms. J Infect Dis 133:548–555
46. Feingold KR, Grunfeld C (1987) Tumor necrosis factor-alpha stimulates hepatic lipogenesis in the rat in vivo. J Clin Invest 80:184–190
47. Harris HW, Grunfeld C, Feingold KR, Read TE, Kane JP, Jones AL, Eichbaum EB, Bland GF, Rapp JH (1993) Chylomicrons alter the fate of endotoxin, decreasing tumor necrosis factor release and preventing death. J Clin Invest 91:1028–1034
48. Hardman AE (1999) Physical activity, obesity and blood lipids. Int J Obes Relat Metab Disord 23(Suppl 3):S64–S71
49. Skorve J, Berge RK (1993) The hypocholesterolemic effect of sulfur-substituted fatty acid analogues in rats fed a high carbohydrate diet. Biochim Biophys Acta 1167:175–181
50. Berge RK, Aarsland A, Kryvi H, Bremer J, Aarsaether N (1989) Alkylthio acetic acids (3-thia fatty acids)–a new group of non-beta-oxidizable peroxisome-inducing fatty acid analogues–II. Dose-response studies on hepatic peroxisomal- and mitochondrial changes and long-chain fatty acid metabolizing enzymes in rats. Biochem Pharmacol 38:3969–3979
51. Froyland L, Helland K, Totland GK, Kryvi H, Berge RK (1996) A hypolipidemic peroxisome proliferating fatty acid induces polydispersity of rat liver mitochondria. Biol Cell 87:105–112
52. Totland GK, Madsen L, Klementsen B, Vaagenes H, Kryvi H, Froyland L, Hexeberg S, Berge RK (2000) Proliferation of mitochondria and gene expression of carnitine palmitoyltransferase and fatty acyl-CoA oxidase in rat skeletal muscle, heart and liver by hypolipidemic fatty acids. Biol Cell 92:317–329
53. Ashby J, Brady A, Elcombe CR, Elliott BM, Ishmael J, Odum J, Tugwood JD, Kettle S, Purchase IF (1994) Mechanistically-based human hazard assessment of peroxisome proliferator-induced hepatocarcinogenesis. Hum Exp Toxicol 13(Suppl 2):S1–S117
54. Bentley P, Calder I, Elcombe C, Grasso P, Stringer D, Wiegand HJ (1993) Hepatic peroxisome proliferation in rodents and its significance for humans. Food Chem Toxicol 31:857–907
55. Hays T, Rusyn I, Burns AM, Kennett MJ, Ward JM, Gonzalez FJ, Peters JM (2005) Role of peroxisome proliferator-activated receptor-alpha (PPARalpha) in bezafibrate-induced hepatocarcinogenesis and cholestasis. Carcinogenesis 26:219–227
56. Peters JM, Cheung C, Gonzalez FJ (2005) Peroxisome proliferator-activated receptor-alpha and liver cancer: where do we stand? J Mol Med 83:774–785
57. Rao MS, Reddy JK (1991) An overview of peroxisome proliferator-induced hepatocarcinogenesis. Environ Health Perspect 93:205–209
58. Reddy JK, Rao MS (1977) Malignant tumors in rats fed nafenopin, a hepatic peroxisome proliferator. J Natl Cancer Inst 59:1645–1650
59. Mynatt RL (2009) Carnitine and type 2 diabetes. Diabetes Metab Res Rev 25(Suppl 1):S45–S49
60. Baer DJ, Judd JT, Clevidence BA, Tracy RP (2004) Dietary fatty acids affect plasma markers of inflammation in healthy men fed controlled diets: a randomized crossover study. Am J Clin Nutr 79:969–973
61. Willett WC, Sacks F, Trichopoulou A, Drescher G, Ferro-Luzzi A, Helsing E, Trichopoulos D (1995) Mediterranean diet pyramid: a cultural model for healthy eating. Am J Clin Nutr 61:1402S–1406S
62. Yaari S, Goldbourt, Even-Zohar S, Neufeld HN (1981) Associations of serum high density lipoprotein and total cholesterol with total, cardiovascular, and cancer mortality in a 7-year prospective study of 10 000 men. Lancet 1:1011-1015
63. Fredriksen J, Ueland T, Dyroy E, Halvorsen B, Melby K, Melbye L, Skalhegg BS, Bohov P, Skorve J, Berge RK, Aukrust P, Froland SS (2004) Lipid-lowering and anti-inflammatory effects of tetradecylthioacetic acid in HIV-infected patients on highly active antiretroviral therapy. Eur J Clin Invest 34:709–715
64. Rakhshandehroo M, Hooiveld G, Muller M, Kersten S (2009) Comparative analysis of gene regulation by the transcription factor PPARalpha between mouse and human. PLoS One 4:e6796
65. Ramaswamy M, Wallace TL, Cossum PA, Wasan KM (1999) Species differences in the proportion of plasma lipoprotein lipid carried by high-density lipoproteins influence the distribution of free and liposomal nystatin in human, dog, and rat plasma. Antimicrob Agents Chemother 43:1424–1428

Lipids (2011) 46:691–700
DOI 10.1007/s11745-011-3559-8

ORIGINAL ARTICLE

Identification of Diacylglycerol Acyltransferase Inhibitors from *Rosa centifolia* Petals

Hidehiko Kondo · Kohjiro Hashizume · Yusuke Shibuya · Tadashi Hase · Takatoshi Murase

Received: 2 September 2010 / Accepted: 14 March 2011 / Published online: 3 May 2011

Abstract Diacylglycerol acyltransferase (DGAT) catalyzes the final step of triacylglycerol (TAG) synthesis, and is considered as a potential target to control hypertriglyceridemia or other metabolic disorders. In this study, we found that the extract of rose petals suppressed TAG synthesis in cultured cells, and that the extract showed DGAT inhibitory action in a dose-dependent manner. Fractionation of the rose extract revealed that the DGAT inhibitory substances in the extract were ellagitannins; among them rugosin B, and D, and eusupinin A inhibited DGAT activity by 96, 82, and 84% respectively, at 10 μM. These substances did not inhibit the activities of other hepatic microsomal enzymes, glucose-6-phosphatase and HMG-CoA reductase, or pancreatic lipase, suggesting that ellagitannins inhibit DGAT preferentially. In an oral fat load test using mice, postprandial plasma TAG increase was suppressed by rose extract; TAG levels 2 h after the fat load were significantly lower in mice administered a fat emulsion containing rose extract than in control mice (446.3 ± 33.1 vs 345.3 ± 25.0 mg/dL, control vs rose extract group; $P < 0.05$). These results suggest that rose ellagitannins or rose extract could be beneficial in controlling lipid metabolism and used to improve metabolic disorders.

Keywords Diacylglycerol acyltransferase · Postprandial hypertriglyceridemia · Rose petal · Ellagitannin

H. Kondo (✉) · K. Hashizume · Y. Shibuya · T. Hase · T. Murase
Biological Science Laboratories, Kao Corporation, 2606 Akabane, Ichikai-machi, Haga-gun, Tochigi 321-3497, Japan
e-mail: kondo.hidehiko@kao.co.jp

Abbreviations

AUC	Area under the curve
ACAT	Acyl coenzyme A:cholesterol acyltransferase
BALB	Dimercaptopropanol tributyrate
DGAT	Diacylglycerol acyltransferase
DMEM	Dulbecco's modified Eagle's medium
DTNB	5,5′-dithiobis(2-nitrobenzoic acid)
EGCG	Epigallocatechin gallate
G6Pase	Glucose-6-phosphatase
MFI	Mean fluorescent intensity
TAG	Triacylglycerol

Introduction

Epidemiologic studies have indicated that hypertriglyceridemia is associated with obesity, diabetes, and coronary heart disease [1–4]. Carlson et al. [2] have reported that fasting levels of plasma triacylglycerol (TAG) act as an independent risk factor for death by myocardial infarction. Additionally, a postprandial increase in serum TAG levels is also reported to be a risk marker for ischemic heart diseases [5–8]. TAG-rich lipoproteins are thought to decrease endothelial dysfunction and increase oxidative stress, contributing to the development of metabolic disorders [9, 10].

Diayclglycerol acyltransferase (DGAT) catalyzes the final step of TAG synthesis [11, 12], and thereby plays an important role as one of the key enzymes responsible for the incorporation of TAG into the body. DGAT also plays essential roles in the synthesis and secretion of very-low-density lipoprotein (VLDL) in the liver, and TAG accumulation in adipose tissue. Several studies have shown that

DGAT is a potential target to control hypertriglyceridemia or other metabolic disorders [13–16]. It has been reported that mice genetically lacking DGAT1—one of two known DGAT isozymes—showed substantially decreased levels of chylomicron-derived plasma TAG following oral fat load [13, 14]. The DGAT1-deficient mice showed resistance to obesity, and increased insulin and leptin sensitivity [15]. In addition, Liu et al. [16] have demonstrated that knockdown of DGAT2—another DGAT isozyme—using antisense oligonucleotide resulted in the reduction of VLDL-TAG and apoB secretion in mice.

So far, several natural DGAT inhibitors have been reported [17–20]. Tabata et al. [18] found that xanthohumols from *Humulus lupulus* showed DGAT inhibitory action, and TAG formation in cultured cells. Recently, Casaschi et al. [19] reported that taxifolin, a plant flavonoid, reduced DGAT activity as well as microsomal triglyceride transfer protein in HepG2 cells; however, few reports have demonstrated that DGAT inhibitors showed a beneficial effect in vivo.

On the other hand, by screening hundreds of plant extracts, we found that an extract of petals of *Rosa centifolia* showed inhibitory action against TAG synthesis in IEC-6 cells. Rose petals are rich in polyphenols and free gallic acid, and have been demonstrated to have antioxidant [21] and antibacterial activities [22], but there are no reports on the inhibition of TAG synthesis. In this study, we investigated the biological activity of rose extract, and the causative substances inhibiting TAG synthesis contained in rose petals.

Experimental Procedure

Materials

Pink rose petals (*Rosa centifolia*) were purchased from Tochimoto Tenkaido (Osaka, Japan). Epigallocatechin gallate (EGCG) was obtained from Tokyo Chemical Industry (Tokyo, Japan).

Flow Cytometry Analysis of Lipid Accumulation

The rat small intestinal epithelial cell line IEC-6 (American Type Culture Collection, Rockville, MD) was cultured in Dulbecco's modified Eagle's medium (DMEM) (Invitrogen, Paisley, UK) supplemented with 5% FBS and 100 units/mL penicillin and 100 μg/mL streptomycin (complete medium) at 37 °C in air and 5% CO_2. Cells were seeded with 1×10^5 cells/well in 6-well plates. After overnight incubation, the culture medium was changed to complete medium containing 500 μM oleic acid (Cayman Chemical, Ann Arbor, MI) complexed with 250 μM fatty acid-free BSA (Wako Chemical, Osaka, Japan) and 0.01% rose extract. After incubation for 6 h, the culture medium was removed and the remaining cells were rinsed twice with PBS and detached from plates with 0.25% trypsin and 1 mM EDTA in PBS. Cells were collected with 1 mL complete medium, precipitated by centrifugation, and suspended in PBS containing 100 ng/mL Nile Red (Acros Organics, Geel, Belgium). The suspension was then incubated at room temperature for 5 min, and analyzed by FACSCalibur (Becton-Dickinson Bioscience, San Jose, CA). Fluorescence-activated cell scan excitation was 488 nm, and emission was monitored through band-pass filters at 530 ± 15 nm (FL1) to detect the yellow-gold fluorescence of neutral lipids [23]. Effects of samples on lipid accumulation were judged by suppression of the increase of mean fluorescent intensity by incubation with 500 μM oleic acid.

Analysis of TAG Synthesis and Secretion in Cultured Cells

The hepatoma cell line HepG2 (American Type Culture Collection) was seeded with 1×10^5 cells/well in 6-well plates and cultured at 37 °C in air and 5% CO_2 in complete medium. After 3 days, the medium was changed and incubated with or without 0.01% rose extract. After 24 h, the medium was changed to serum-free medium containing 250 μM [1-^{14}C] oleic acid (3.7 MBq/mmol; PerkinElmer Life Science, Boston, MA) complexed with 125 μM fatty acid-free BSA, supplemented or not with 0.01% rose extract. After incubation for 6 h, the medium was removed and the remaining cells were rinsed twice with PBS, and lysed with 0.1M NaOH. The cell lysate was collected after neutralization by addition of 1/30 volume 3M HCl. Lipids in the cell lysate and the medium were extracted following the method of Bligh-Dyer [24]. The organic phase was dried under a stream of nitrogen at 30 °C. Radioactivity was measured using a liquid scintillation counter TriCarb 1500 (Packard Instrument, Meriden, CT). The extracted lipids were separated by TLC using a Silica gel 60 F 254 plate (Merck, Darmstadt, Germany) and hexane/diethyl ether/acetic acid (80/20/1, by vol) as the development solvent. The TLC plates were exposed to a Fuji Imaging Plate (Fuji Photo Film, Tokyo, Japan) for 2 days, and the obtained fluorograms were analyzed with a BAS2500 system (Fuji Photo Film) to quantitate the amount of radiolabeled TAG.

Fractionation of Rose Extract

Pink rose petals were extracted by soaking in 10 volumes of 50% ethanol at room temperature for 1 week. The insoluble substances were filtrated, and the obtained 50% ethanol extract was concentrated in vacuum and

resuspended in water. After liquid–liquid separation with an equal volume of hexane, the water phase was extracted by an equal volume of *n*-butanol. The resultant *n*-butanol extract was concentrated in vacuum, resuspended in 20% ethanol, and then fractionated by column chromatography using a Diaion HP-20 column (Mitsubishi Chemical, Tokyo, Japan). The column was washed and eluted with 20, 40, 60, and 99.5% ethanol. The fractions containing DGAT inhibitory substances were separated by column chromatography using a Sephadex LH-20 column (GE Healthcare, Tokyo, Japan). The column was washed and eluted with 50% methanol, 99.5% ethanol, and ethanol/acetone (1:1, by vol), and then the fractions containing DGAT inhibitory substances were separated by HPLC using an Intersil ODS-3 column (20 × 250 mm; Metachem Technologies, Torrance, CA). The column was eluted with 0.5% trifluoroacetic acid/acetonitrile (87:13, by vol) for 30 min, and then 0.5% trifluoroacetic acid/acetonitrile (1:1, by vol) for 20 min. Separated fractions were analyzed by HPLC using an Inertsil ODS-3 column (4.6 × 250 mm) under the following conditions: a 30-min gradient from 0.1% acetic acid to 100% methanol; 1.0 ml/min; 40 °C. UV spectra were obtained using a UV–VIS Detector L-7420 (Hitachi, Tokyo, Japan).

Oral Fat Load Test

C57BL/6J mice were obtained from Charles River Japan (Yokohama, Japan) at 7 weeks of age, and maintained at 23 ± 2 °C under a 12-h light–dark cycle (lights on from 7:00 a.m. to 7:00 p.m.). The mice were fed laboratory chow for 1 week to stabilize their metabolic conditions, and divided into two groups so that the average plasma TAG level and body weight could be equalized between the groups. Following an overnight fast, 40 μL/g body weight of fat emulsion with or without 1% rose extract was administered orally. The fat emulsion contained 10% (w/v) edible oil, 1% (w/v) egg yolk lecithin (Wako), and 4% (w/v) BSA. The edible oil was composed of 98.1% TAG and 1.9% diacylglycerol with the fatty acid composition of 5.5% C16:0; 2.2% C18:0; 37.2% C18:1; 46.1% C18:2; 8.0% C18:3; 0.5% C20:0; 0.3% C20:1; 0.1% C22:0; 0.1% C22:1. Blood samples were collected from mice via the tail vein at the times indicated, and the plasma was isolated. Plasma TAG and FFA concentrations were determined using enzyme assay kits: L-type Wako TG-H, NEFA-HA test Wako, (Wako), respectively. This study was approved by the Animal Care Committee of Kao Tochigi Institute.

Measurement of Enzyme Activities

The liver was homogenized on ice with 8 volumes (w/v) of 250 mM sucrose buffer containing 0.1 mM EDTA and 2 mM HEPES (pH 7.3). Subcellular fractionation was performed according to the methods described by de Duve et al. [25]. After centrifugation of the homogenate of the intestinal mucosa at 12,500 *g* for 20 min, the supernatant was centrifuged at 100,000 *g* for 60 min. The resultant precipitate was resuspended and used as a microsomal protein. Protein concentrations were determined using a Micro BCA protein assay kit (Pierce, Rockford, IL).

DGAT activity was determined according to the method described by Luan et al. [26]. Microsomal protein (50 μg) was incubated at 37 °C for 20 min in 200 μL of a reaction mixture in the presence or absence of test samples. EGCG, a major polyphenol present in green tea, which has an anti-obesity effect [27, 28], was used as a control.

The reaction mixture contained 250 mM sucrose, 10 mM Tris–HCl (pH 7.5), 10 mM $MgCl_2$, 0.8 mM EDTA, 0.1% BSA, 100 μM oleoyl-CoA (55 mCi/mmol), and 1.2 mM 1,2-diolein. Incubation was terminated by the addition of 1.5 mL chloroform/methanol (1:1, by vol). Lipids were extracted by the Folch method [29]. Radioactivity was measured using a liquid scintillation counter, TriCarb 1500. The extracted lipids were separated by TLC using a Silica gel 60 F 254 plate (Merck) and hexane/diethyl ether/acetic acid (80:20:1, by vol) as the development solvent. The TLC plates were exposed to a Fuji Imaging Plate (Fuji) for 1 or 2 days, and the obtained fluorograms were analyzed with a BAS2500 system (Fuji Photo Film). DGAT activity was calculated based on the radioactivity of the extracted lipid and the ratio of labeled TAG to labeled lipid.

In addition, acyl coenzyme A:cholesterol acyltransferase (ACAT) activity, cholesteryl ester formation from endogenous cholesterol was also calculated based on the radioactivity of the extracted lipid and the ratio of labeled cholesteryl ester.

Glucose-6-phosphatase (G6Pase) activity was measured according to the method described by Tang et al. [30]. Microsomal protein (50 μg) was incubated in reaction mixture [50 mM HEPES (pH 7.2), 100 mM KCl, 2.5 mM EDTA, 2.5 mM $MgCl_2$, 1 mM DTT, 10 mM glucose-6-phosphate, 2 mM EDTA] at 37 °C for 30 min. The reaction was stopped by the addition of 4 volumes of stop solution (6:2:1, by vol, mixture of 0.42% ammonium molybdate tetrahydrate in 1 *N* H_2SO_4, 10% SDS, and 10% ascorbic acid), and then incubated at 50 °C for 30 min. Absorbance (OD_{820}) was measured using a microplate absorbance plate reader Viento XS (DS Pharma Biomedical, Osaka, Japan). A standard curve was obtained using inorganic phosphorus solution (Wako).

3-Hydroxy-3-methylglutaryl-coenzyme A (HMG-CoA) reductase activity was measured according to the method described by Sumiyoshi et al. [31]. Microsomal protein (50 μg) was incubated in reaction mixture [0.128 mM

^{14}C-HMG-CoA (72 MBq/mmol), 1 mM NADPH, 10 mM DTT, 10 mM EDTA, 0.12 mM phosphate buffer (pH 7.2)] at 37 °C for 20 min. The reaction was stopped by the addition of 1/10 volume of 5 *N* HCl, and further incubated for 30 min. After the addition of 4-^{14}C-testosterone (0.08 nCi) as an internal standard, mevalonolactone generated from mevalonic acid by HMG-CoA reductase was extracted by ethyl acetate. Part of the extract was separated by TLC using benzene/acetone (1:1, by vol) as a developing solvent.

Lipase activity was measured using lipase kit S (DS Pharma Biomedical) according to the improved dimercaptopropanol tributyrate (BALB) method [32]. Two units/reaction of porcine pancreas lipase (Sigma, St. Louis, MO) were used as the enzyme source. Absorbance (OD_{412}) of the products formed by reaction of the SH groups formed from lipase cleavage of BALB with 5,5′-dithiobis(2-nitrobenzoic acid) (DTNB) was measured at 412 nm using the microplate absorbance plate reader Viento XS.

NMR

^{1}H- and ^{13}C-NMR spectra were recorded on a JNM-α500 spectrometer (JEOL Ltd., Tokyo, Japan; 500 MHz for ^{1}H-NMR and 125.7 MHz for ^{13}C-NMR). Chemical shifts are given in δ (ppm), based on those of the ^{1}H and ^{13}C signals of acetone-d_6 (δ_H 2.04; δ_C 29.8).

Statistical Analysis

All values are presented as the means ± SEM. Statistical analyses between two groups were performed with an unpaired *t* test. In the analysis of enzyme inhibition by serial concentration of rose extract, ellagitannins, or EGCG, one-way analysis of variance (ANOVA) followed by Dunnett's test was performed. $P < 0.05$ was considered statistically significant.

Results

Effect of Rose Extract on TAG Accumulation in IEC-6 Cells

Firstly, screening of plant extracts that inhibit TAG accumulation was conducted against hundreds of plant extracts, using fluorescent flow cytometry analysis on IEC-6 cells cultured with oleic acid in the presence or absence of the plant extracts. As a result, we found that 50% ethanol extract of rose petals exhibited an inhibitory action against TAG accumulation as shown in Fig. 1. Incubation of IEC-6 cells with 500 μM oleic acid increased the fluorescent intensity of TAG stained by Nile Red compared with incubation without oleic acid (Fig. 1a). Mean fluorescent intensity (MFI) was significantly different between groups ($P < 0.01$); MFI was 75.8 ± 0.8 in the absence of oleic acid, whereas MFI in the presence of oleic acid was 119.3 ± 3.4. When IEC-6 cells were pre-incubated in the presence of the rose extract at final 0.01%, the FFA-induced increase of MFI was significantly suppressed ($P < 0.05$) (Fig. 1a). MFI (106.1 ± 2.9) was decreased by 30.4 ± 6.6%.

Furthermore, in the analysis of TAG synthesis and secretion using HepG2 cells, incubation in the presence of

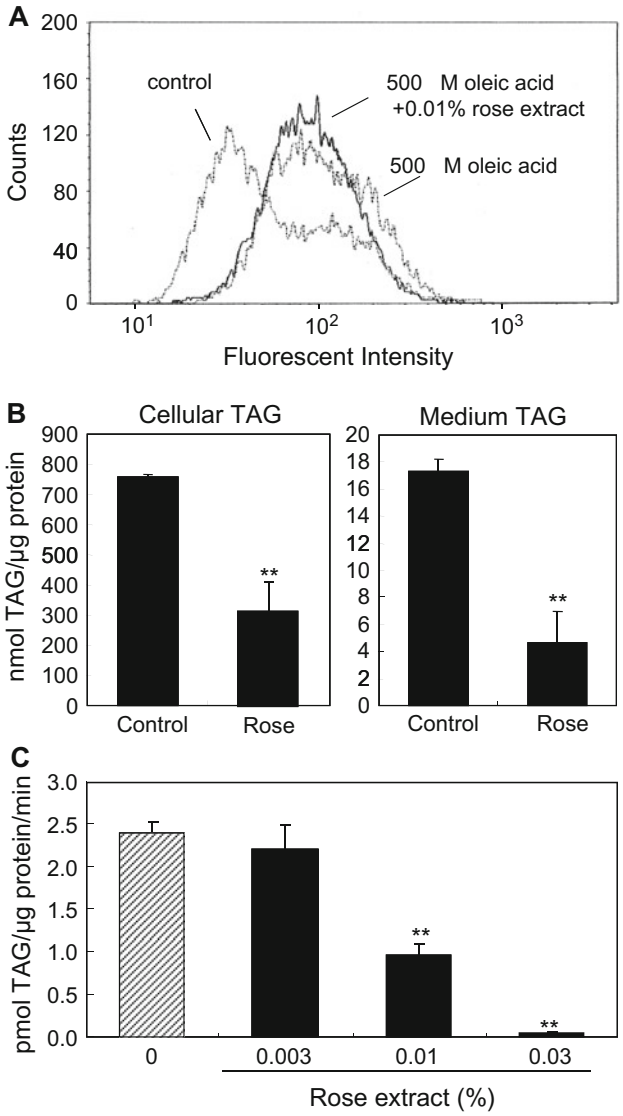

Fig. 1a–c Effect of rose extract on triacylglyceraol (TAG) synthesis and diayclglycerol acyltransferase (DGAT) activities. **a** Flow cytometric analysis of IEC-6 cells stained with Nile Red. Flow cytometric histograms show the relative fluorescence intensities of 10^4 cells. **b** Analysis of TAG synthesis and secretion in HepG2 cells. Cells were treated and analyzed as described in Materials and Methods. **c** Effect of rose extract on microsomal DGAT activities. Values are shown as the mean ± SEM ($n = 3$). $^{**}P < 0.01$

0.01% rose extract reduced cellular TAG synthesis from radio-labeled oleic acid, and TAG secretion into the medium by 58.5 ± 6.7%, and 73.4 ± 15.0%, respectively ($P < 0.01$) (Fig. 1b). These results indicate that the rose extract inhibits TAG synthesis from FFA.

In the measurement of DGAT activity using microsomal protein, the addition of rose extract to the reaction mixture reduced DGAT activity in a dose-dependent manner; microsomal DGAT activity was reduced by 60.0 ± 5.8% at a concentration of 0.01%. This result suggests that rose extract suppresses TAG synthesis via the inhibition of DGAT activity (Fig. 1c).

Fractionation of Rose Extract

First, 50% ethanol extract (solid content: 260 g) obtained from 600 g pink rose petals was extracted by hexane/water partition, and then the water phase was extracted by *n*-butanol (liquid–liquid partition; Fig. 2a). Next, the *n*-butanol extract was fractionated using a Diaion HP-20 column. Fractions containing DGAT inhibitory substances were determined by measurement of DGAT activity using microsomal protein in the presence of one of the fractions supplemented at the original weight ratio in the rose extract. Measurement of DGAT activity revealed that most of the DGAT inhibitory substances were eluted by 20% ethanol. In subsequent fractionation using a Sephadex LH-20 column of the 20% ethanol fraction, DGAT inhibition was found in the ethanol elution fraction (fraction RO-Bu-a5) and acetone/ethanol elution fraction (fraction RO-Bu-a6).

In further separation of part of the fraction RO-Bu-a5 by reversed phase HPLC, two fractions (RO-Bu-a5A and -a5B) showed DGAT inhibition (Fig. 2b). NMR analysis of fraction RO-Bu-a5A, which was composed of a single component (>99% pure), revealed that the chemical shift was coincident with the actual measurement value and the reported value of an ellagitannin, tellimagrandin I [33]. In addition, further separation by HPLC and NMR analysis of fraction RO-Bu-a5B revealed that the fractions contained tellimagrandin I (RO-Bu-a5B1) and another ellagitannin (RO-Bu-a5B2); the chemical shift of the latter (>99% pure) was coincident with the reported value of rugosin B [34, 35]. Fraction RO-Bu-a5B3 was a mixture of tellimagrandin I and rugosin B, which were likely separated as anomers of the ellagitannins.

On the other hand, further separation of part of fraction RO-Bu-a6 by HPLC revealed that the fraction was composed of at least three >99% pure components (Fig. 2c). Structure determination by NMR of the components isolated in fractions RO-Bu-a6D, -a6E, and -a6F revealed that their chemical shifts were coincident with the values of rugosin A [34, 35], rugosin D [36, 37], and eusupinin A

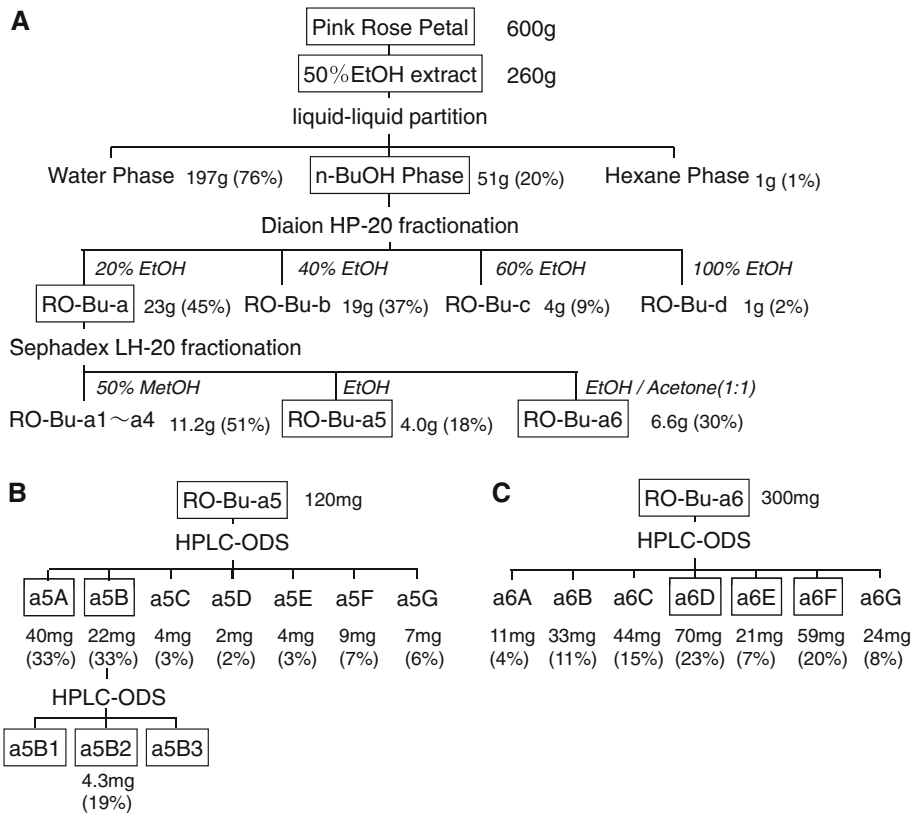

Fig. 2a–c Fractionation of DGAT inhibitory substances from rose petals. **a** Early steps of fractionation from rose petals. **b** Fractionation of fraction RO-Bu-a5. **c** Fractionation of fraction RO-Bu-a6. *BuOH* butanol, *EtOH* ethanol, *MetOH* methanol

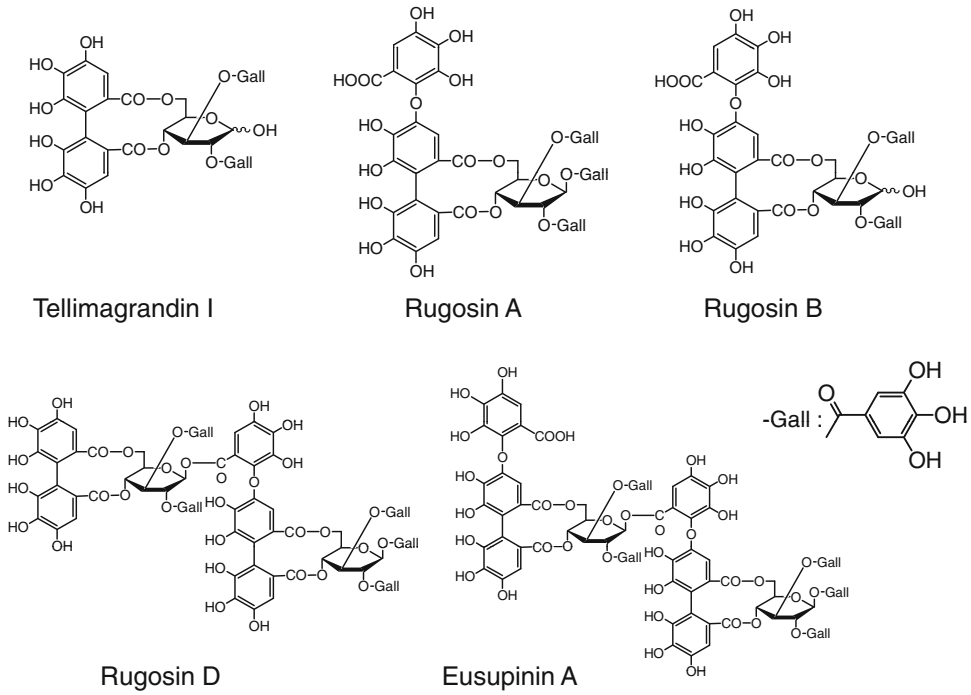

Fig. 3 Chemical structure of DGAT inhibitory ellagitannins identified from rose petals

[38], respectively. The chemical structures of these ellagitannins isolated from rose petals are shown in Fig. 3.

Effects of Rose Ellagitannins on Enzyme Activities

The ellagitannins isolated from rose petals inhibited DGAT activity in a dose-dependent manner (Fig. 4a). In particular, rugosin B, rugosin D, and eusupinin A strongly inhibited activity; these ellagitannins inhibited activity by 96, 82, and 84%, respectively, at 10 μM. Ellagic acid, a constituent of ellagitanin, did not affect activity even when used at 20 and 60 μM (data not shown). EGCG, a major polyphenol present in green tea, also did not affect DGAT activity (Fig. 4a).

In order to examine the selectivity of the enzyme-inhibitory action of ellagitannins, their effects on other hepatic microsomal enzymes were investigated. Since, in measurement of DGAT activity, substantial amount of label added as ^{14}C oleoyl-CoA was incorporated into cholesteryl ester (10.4 ± 1.0% of labeled lipid) as well as TAG (27.1 ± 0.9% of labeled lipid), the effect of rose ellagitannins on formation of cholesteryl ester (i.e., ACAT activity) was also evaluated. While the ellagitannins showed substantial inhibition of ACAT activity, the degree of inhibition of ACAT activity by ellagitannins was less than that of DGAT activity.

On the other hand, none of the five ellagitannins isolated from rose petals inhibited G6Pase activity (Fig. 4c). These ellagitannins had little effect on HMG-CoA reductase activity at 5 and 10 μM, although rugosin B, rugosin D, and eusupinin A significantly suppressed activity at 20 μM (Fig. 4d); however, the degree of inhibition of HMG-CoA reductase activity by ellagitannins was also less than that of DGAT activity.

In addition, the inhibitory action of ellagitannins against a pancreatic lipase, a major lipid degradation enzyme, was examined. As a result, the five rose ellagitannins had little effect on lipase activity at 5–20 μM, whereas EGCG inhibited lipase activity by more than 20% at 20 μM (Fig. 4e). Thus, the rose ellagitannins showed preferable DGAT inhibitory action.

Reduction by Rose Extract of Postprandial Increase in Plasma TAG

An oral fat load causes an increase in plasma TAG levels with a peak at 2 h. Administration of a fat emulsion containing 1% rose extract resulted in suppression of the postprandial plasma TAG increase (Fig. 5a); TAG levels 2 h after loading were significantly lower than in mice administered the fat emulsion without rose extract (446.3 ± 33.1 vs 345.3 ± 25.0 mg/dL, control vs rose extract group; $P < 0.05$). The total area under the curve (AUC) for the plasma TAG increase was also significantly reduced in mice administered rose extract (Fig. 5b; $P < 0.05$). In addition, plasma FFA levels of mice administered the fat emulsion containing rose extract showed a reducing trend compared with those given emulsion without the extract (Fig. 5c,d).

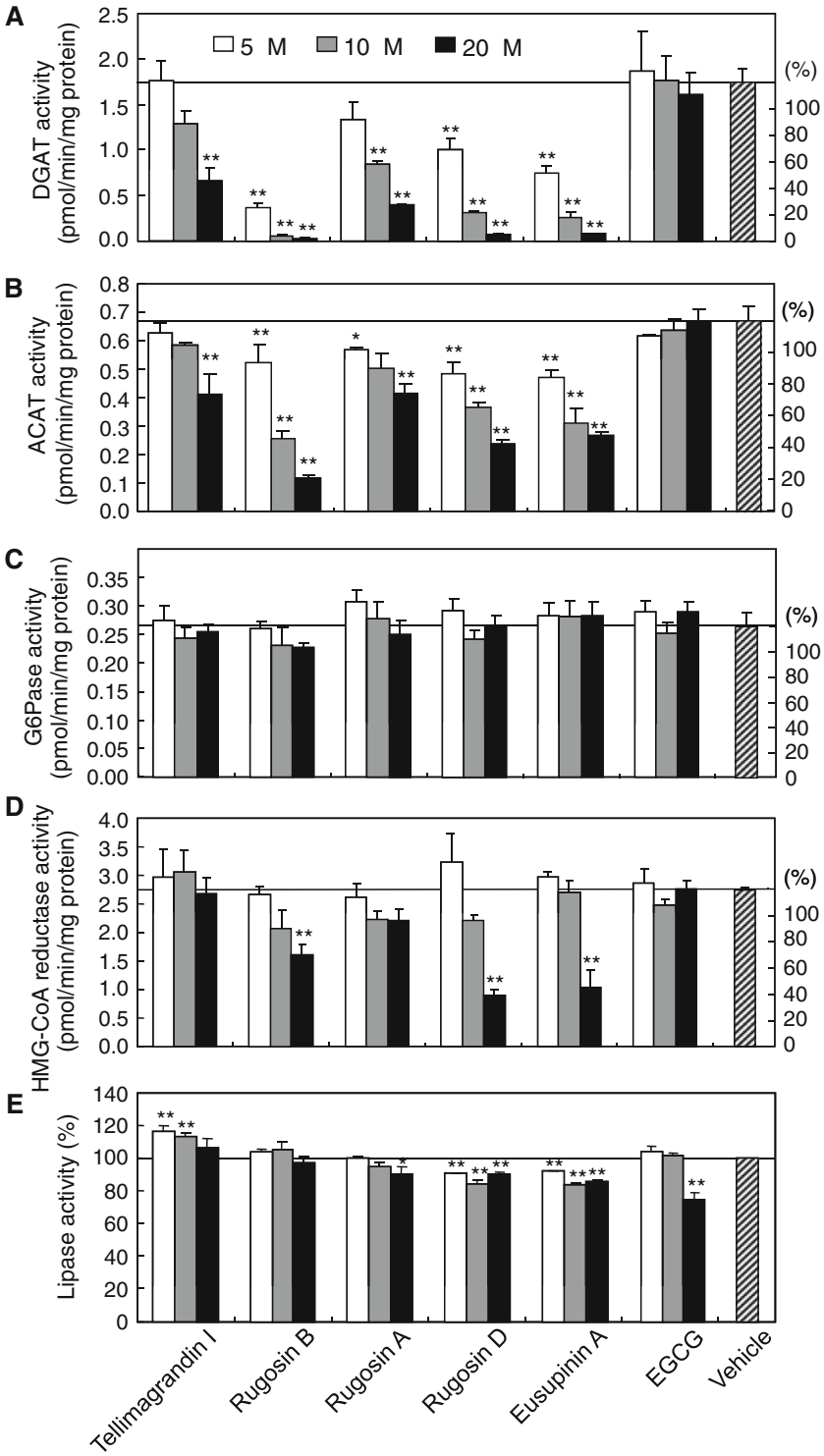

Fig. 4a–e Effect of rose ellagitannins on hepatic microsomal enzyme and lipase activities. **a** DGAT, **b** acyl coenzyme A:cholesterol acyltransferase (ACAT), **c** glucose-6-phosphatase (G6Pase), and **d** 3-hydroxy-3-methylglutaryl-coenzyme A (HMG-CoA) reductase activities in the hepatic microsomal fraction, and **e** pancreatic lipase activity were measured in the presence of rose ellagitannins or rose extract, as described in Materials and Methods. Values are the mean ± SEM ($n = 3$). $^{*}P < 0.05$; $^{**}P < 0.01$, vs vehicle control

Discussion

In this study, we found that ellagitannins present in rose petals, i.e., tellimagrandin I, rugosins A, B, and D, and eusupinin A, showed DGAT inhibitory action. Several studies have demonstrated that ellagitannins have diverse biological activities [39–43]; rugosin D and tellimagrandin II show antibacterial activities against intestinal bacteria [39]; several ellagitannins, including rugosin A, have anti-tumor activity and induce interleukin-1 [40]; however, no report has demonstrated that ellagitannins have DGAT inhibitory actions. This study therefore revealed a novel

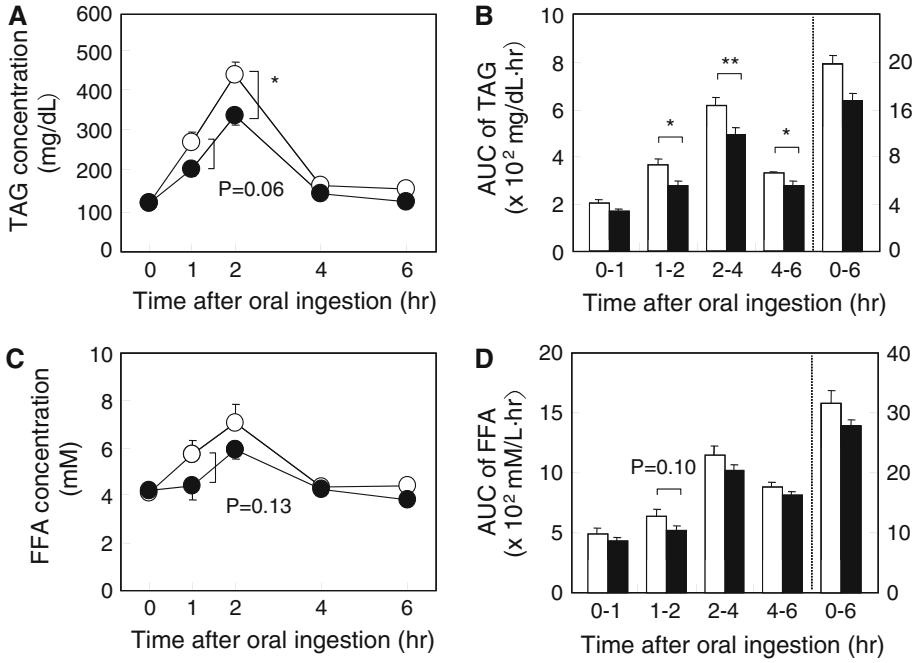

Fig. 5a–d Effect of rose extract on plasma TAG and free fatty acid (FFA) increase in mice after oral fat loading. **a** At 8 weeks of age, C57BL/6J mice were administered orally fat emulsions with or without 1% rose extract. At the times indicated, blood samples were collected and plasma TAG levels were determined. Increases in plasma TAG levels from before oral fat loading. **b** Areas under the curve (AUC) of plasma TAG levels. **c** Plasma FFA levels. **d** AUC of plasma FFA levels. *Open circles* or *bars* control fat emulsion without rose extract, *closed circles* or *bars* fat emulsion containing rose extract. Values are mean ± SEM ($n = 9$). *$P < 0.05$

feature of rose ellagitannins; DGAT inhibitory action was not observed in EGCG, a major polyphenol present in green tea, which has an anti-obesity effect [28, 44].

So far, several DGAT inhibitory substances derived from plants and fungi have been reported [17–20]. Quinolone alkaloids isolated from the fruits of *Evodia rutaecarpa* have been demonstrated to inhibit DGAT activity with IC_{50} values of 13–70 μM [45]. Prenylflavonoids isolated from the roots of *Sophora flavescens* have been reported to inhibit DGAT activity with IC_{50} values of 9–250 μM [46]. Ganji et al. have shown that niacin, widely distributed among plants and animals and used as a lipid-regulating agent in dyslipidemic patients, inhibited DGAT activity with IC_{50} values of 0.1 mM [47]. In this study, ellagitannins inhibited DGAT activity with comparable or somewhat higher efficiency than these naturally occurring DGAT inhibitory compounds; IC_{50} of rugosin B and eusupinin A was less than 5 μM.

Rugosin D and eusupinin A, which inhibit DGAT more than rugosin A, are dimeric hydrolyzable tannins, including the rugosin A moiety. Rugosin B, which showed the highest DGAT inhibitory activity among the examined ellagitannin, differ from rugosin A by the presence of the galloyl group at the anomeric position in the former. Further detailed analysis using ellagitannin derivatives, however, are needed to clarify the relation between the DGAT inhibitory action and the structures of ellagitannins.

In this study, we demonstrated that rose ellagitannins inhibit DGAT activity preferentially. The ellagitannins had little effect on hepatic enzymes (i.e., G6Pase and HMG-CoA reductase) or pancreatic lipase. So far, it has been reported that tea catechins with a galloyl moiety, which showed lipase inhibitory action at much higher concentration (1–2 mM), suppressed postprandial hypertriglyceridemia, suggesting the hypolipidemica action of tea catechins through lipase inhibition [48]; however, since the ellagitannis intensely inhibited DGAT activity at concentrations that had little effect on lipase activity, it is plausible that the hypolipidemic action of rose extract could be attributed to the DGAT inhibitory action of ellagitannins.

The structures of these ellagitannins possess at least a superficial similarity to the structures of the phorbol esters, which have been demonstrated to activate protein kinase C via interaction with the binding domain common to diacylglycerol, an obligatory substrate of DGAT [49]. This suggests that ellagitannins inhibit DGAT activity through the competitive interaction with a binding domain common to diacylglycerol. In addition, it is also possible that rose extract and rose ellagitannins affect the expression of DGAT. So far, it has been demonstrated that expression of DGAT is regulated not only transcriptionally but also post-transcriptionally; the expression of DGAT1 is reportedly regulated mainly at the translational level [50]. In all cases, the detailed mechanisms of the inhibitory action of rose extract and rose ellagitannins should be clarified by future intensive studies.

It is well known that DGAT plays an important role in the synthesis of TAG in the small intestine [51]. Dietary TAG is hydrolyzed to 2-monoacylglycerol and FFA in the intestinal lumen. Most of the digestive products are absorbed by the intestinal mucosa and re-synthesized into TAG by monoacylglycerol acyltransferase (MGAT) and

DGAT. Subsequently, the re-synthesized TAG is assembled into chylomicron and released into the bloodstream; therefore, it is assumed that inhibition of DGAT activities in the small intestine results in a reduction of the rate of TAG synthesis and secretion in the intestine. Consistent with this assumption, in this study, we found that the extract of rose petals suppressed the postprandial increase of plasma TAG levels.

It has been demonstrated that elevations of serum FFA cause insulin resistance [52, 53]. Since most of the FFA generated from chylomicron TAG has been shown to mix in the same metabolic compartments as does plasma FFA [54], it is likely that the reduction in plasma TAG mass after fat loading results in FFA reduction. In this study, however, the administration of rose extract did not significantly affect the plasma FFA increase after fat loading, regardless of the suppression of plasma TAG increase by the administration of rose extract. It is likely that the efficient utilization of FFA by peripheral tissues, such as skeletal muscles after fat loading [55], reduced the difference in FFA levels in normal mice.

In conclusion, we demonstrated that ellagitannins isolated from rose petals have DGAT inhibitory action, and that rose extract rich in ellagitannins reduced postprandial increase of the plasma TAG level. These results suggest that rose ellagitannins or rose extract can be beneficial in controlling lipid metabolism and could be used to improve metabolic disorders.

References

1. Ford S Jr, Bozian RC, Knowles HC Jr (1968) Interactions of obesity, and glucose and insulin levels in hypertriglyceridemia. Am J Clin Nutr 21:904–910
2. Carlson LA, Bottiger LE (1985) Risk factors for heart disease in men and women. Results of the 19-year follow-up of the Stockholm Prospective Study. Acta Med Scand 218:207–211
3. Castelli WP (1986) The triglyceride issue: a view from Framingham. Am Heart J 112:432–437
4. Krentz AJ (2003) Lipoprotein abnormalities and their consequences for patients with type 2 diabetes. Diabetes Obes Metab 5:19–27
5. Boquist S, Ruotolo G, Tang R, Björkegren J, Bond MG, de Faire U, Karpe F, Hamsten A (1999) Alimentary lipemia, postprandial triglyceride-rich lipoproteins, and common carotid intima-media thickness in healthy, middle-aged men. Circulation 100:723–728
6. Karpe F, Steiner G, Uffelman K, Olivecrona T, Hamsten A (1994) Postprandial lipoproteins and progression of coronary atherosclerosis. Atherosclerosis 106:83–97
7. Kugiyamaj K, Doi H, Motoyama T, Soejima H, Misumi K, Kawano H, Nakagawa O, Yoshimura M, Ogawa H, Matsumura T, Sugiyama S, Nakano T, Nakajima K, Yasue H (1998) Association of remnant lipoprotein levels with impairment of endothelium-dependent vasomotor function in human coronary arteries. Circulation 97:2519–2526
8. Mero N, Malmström R, Steiner G, Taskinen MR, Syvänne M (2000) Postprandial metabolism of apolipoprotein B-48- and B-100-containing particles in type 2 diabetes mellitus: relations to angiographically verified severity of coronary artery disease. Atherosclerosis 150:167–177
9. Ceriello A, Taboga C, Tonutti L, Quagliaro L, Piconi L, Bais B, Da Ros R, Motz E (2002) Evidence for an independent and cumulative effect of postprandial hypertriglyceridemia and hyperglycemia on endothelial dysfunction and oxidative stress generation: effects of short- and long-term simvastatin treatment. Circulation 106:1211–1218
10. Tolman KG, Fonseca V, Tan MH, Dalpiaz A (2004) Narrative review: hepatobiliary disease in type 2 diabetes mellitus. Ann Intern Med 141:946–956
11. Bell RM, Coleman RA (1989) Enzymes of glycerolipid synthesis in eukaryotes. Annu Rev Biochem 49:459–487
12. Lehner R, Kuksis A (1996) Biosynthesis of triacylglycerols. Prog Lipid Res 35:169–201
13. Buhman KK, Smith SJ, Stone SJ, Repa JJ, Wong JS, Knapp FF Jr, Burri BJ, Hamilton RL, Abumrad NA, Farese RV Jr (2002) DGAT1 is not essential for intestinal triacylglycerol absorption or chylomicron synthesis. J Biol Chem 277:25474–25479
14. Smith SJ, Cases S, Jensen DR, Chen HC, Sande E, Tow B, Sanan DA, Raber J, Eckel RH, Farese RV Jr (2000) Obesity resistance and multiple mechanisms of triglyceride synthesis in mice lacking DGAT. Nat Genet 25:87–90
15. Chen HC, Smith SJ, Ladha Z, Jensen DR, Ferreira LD, Pulawa LK, McGuire JG, Pitas RE, Eckel RH, Farese RV Jr (2002) Increased insulin and leptin sensitivity in mice lacking acyl CoA:diacylglycerol acyltransferase 1. J Clin Invest 109: 1049–1055
16. Liu Y, Millar JS, Cromley DA, Graham M, Crooke R, Billheimer JT, Rader DJ (2008) Knockdown of acyl-CoA:diacylglycerol acyltransferase 2 with antisense oligonucleotide reduces VLDL TG and ApoB secretion in mice. Biochim Biophys Acta 1781:97–104
17. Tomoda H, Tabata N, Ito M, Omura S (1995) Amidepsines, inhibitors of diacylglycerol acyltransferase produced by Humicola sp. FO-2942. II. Structure elucidation of amidepsines A, B and C. J Antibiot 48:942–947
18. Tabata N, Ito M, Tomoda H, Omura S (1997) Xanthohumols, diacylglycerol acyltransferase inhibitors, from *Humulus lupulus*. Phytochemistry 46:683–687
19. Casaschi A, Rubio BK, Maiyoh GK, Theriault AG (2004) Inhibitory activity of diacylglycerol acyltransferase (DGAT) and microsomal triglyceride transfer protein (MTP) by the flavonoid, taxifolin, in HepG2 cells: potential role in the regulation of apolipoprotein B secretion. Atherosclerosis 176:247–253
20. Lee SW, Kim K, Rho M-C, Chung MY, Kim YH, Lee S, Lee HS, Kim YK (2004) New polyacetylenes, DGAT inhibitors from the roots of *Panax ginseng*. Planta Med 70:197–200
21. Vinokur Y, Rodov V, Reznick N, Goldman G, Horev B, Umiel N, Friedman H (2006) Rose petal tea as an antioxidant-rich beverage: cultivar effects. J Food Sci 71:S42–S47
22. Darokar MP, Khanuja SPS, Bagchi GD, Kumar S (1999) Spectrum of antibacterial activity possessed by petals of rose varieties. Curr Sci 77:123–1241
23. Greenspan P, Mayer EP, Fowler SD (1985) Nile red: a selective fluorescent stain for intracellular lipid droplets. J Cell Biol 100:965–973
24. Bligh EG, Dyer WJ (1959) A rapid method of total lipid extraction and purification. Can J Biochem Physiol 37:911–917
25. de Duve C, Pressman BC, Gianetto R, Wattiaux R, Appelmans F (1955) Tissue fractionation studies. 6. Intracellular distribution patterns of enzymes in rat-liver tissue. Biochem J 60:604–617

26. Luan Y, Hirashima T, Man ZW, Wang MW, Kawano K, Sumida T (2002) Pathogenesis of obesity by food restriction in OLETF rats-increased intestinal monoacylglycerol acyltransferase activities may be a crucial factor. Diabetes Res Clin Pract 57:75–82
27. Nagao T, Komine Y, Soga S, Meguro S, Hase T, Tanaka Y, Tokimitsu I (2005) Ingestion of a tea rich in catechins leads to a reduction in body fat and malondialdehyde-modified LDL in men. Am J Clin Nutr 81:122–129
28. Murase T, Nagasawa A, Suzuki J, Hase T, Tokimitsu I (2002) Beneficial effects of tea catechins on diet-induced obesity: stimulation of lipid catabolism in the liver. Int J Obes 26:1459–1464
29. Folch J, Lees M, Sloane Stanley GH (1957) A simple method for the isolation and purification of total lipides from animal tissues. J Biol Chem 226:497–509
30. Tang Y, Lee TS, Khosla C (2004) Engineered biosynthesis of regioselectively modified aromatic polyketides using bimodular polyketide synthases. PLoS Biol 2:E31
31. Sumiyoshi M, Sakanaka M, Kimura Y (2006) Chronic intake of high-fat and high-sucrose diets differentially affects glucose intolerance in mice. J Nutr 136:582–587
32. Furukawa I, Kurooka S, Arisue K, Kohda K, Hayashi C (1982) Assays of serum lipase by the "BALB-DTNB method" mechanized for use with discrete and continuous-flow analyzers. Clin Chem 28:110–113
33. Wilkins CK, Bohm BA (1976) Ellagitannins from *Tellima grandiflora*. Phytochemistry 15:211–214
34. Okuda T, Hatano T, Yazaki K, Ogawa N (1982) Rugosin A, B, C, and praecoxin A, tannins having a valoneoyl group. Chem Pharm Bull 30:4230–4233
35. Hatano T, Ogawa N, Yasuhara T, Okuda T (1990) Tannins of rosaceous plants VIII. Hydrolyzable tannin monomers having a valoneoyl group from flower petals of Rosa rugosa THUNB. Chem Pharm Bull 38:3308–3313
36. Okuda T, Hatano T, Ogawa N (1982) Rugosin D, E, F and G, dimeric and trimeric hydrolyzable tannins. Chem Pharm Bull 30:4234–4237
37. Hatano T, Ogawa N, Shingu T, Okuda T (1990) Tannins of rosaceous plants IX. Rugosins D, E, F and G, dimeric and trimeric hydrolyzable tannins with valoneoyl group(s), from flower petals of *Rosa rugosa* THUNB. Chem Pharm Bull 38:3341–3346
38. Agata I, Hatano T, Nakaya Y, Sugaya T, Nishibe S, Yoshida T, Okuda T (1991) Tannins and related polyphenols of Euphorbiaceous plants.VIII. Eumaculin A and Eusupinin A, and accompanying polyphenols from *Euphorbia maculate* L. and *E. supine* RAFIN. Chem Pharm Bull 39:881–883
39. Kamijo M, Kanazawa T, Funaki M, Nishizawa M, Yamagishi T (2008) Effects of *Rosa rugosa* petals on intestinal bacteria. Biosci Biotechnol Biochem 72:773–777
40. Miyamoto K, Murayama T, Nomura M, Hatano T, Yoshida T, Furukawa T, Koshiura R, Okuda T (1993) Antitumor activity and interleukin-1 induction by tannins. Anticancer Res 13:37–42
41. Kuo PL, Hsu YL, Lin TC, Tzeng WS, Chen YY, Lin CC, Rugosin E et al (2007) An ellagitannin, inhibits MDA-MB-231 human breast cancer cell proliferation and induces apoptosis by inhibiting nuclear factor-κB signaling pathway. Cancer Lett 248:280–291
42. Toda M, Kawabata J, Kasai T (2001) Inhibitory effects of ellagi- and gallotannins on rat intestinal alpha-glucosidase complexes. Biosci Biotechnol Biochem 65:542–547
43. Funatogawa K, Hayashi S, Shimomura H, Yoshida T, Hatano T, Ito H, Hirai Y (2004) Antibacterial activity of hydrolyzable tannins derived from medicinal plants against *Helicobacter pylori*. Microbiol Immunol 48:251–261
44. Klaus S, Pültz S, Thöne-Reineke C, Wolfram S (2005) Epigallocatechin gallate attenuates diet-induced obesity in mice by decreasing energy absorption and increasing fat oxidation. Int J Obes 29:615–623
45. Ko JS, Rho MC, Chung MY, Song HY, Kang JS, Kim K, Lee HS, Kim YK (2002) Quinolone alkaloids, diacylglycerol acyltransferase inhibitors from the fruits of *Evodia rutaecarpa*. Planta Med 68:1131–1133
46. Chung MY, Rho MC, Ko JS, Ryu SY, Jeune KH, Kim K, Lee HS, Kim YK (2004) In vitro inhibition of diacylglycerol acyltransferase by prenylflavonoids from *Sophora flavescens*. Planta Med 702:258–260
47. Ganji SH, Tavintharan S, Zhu D, Xing Y, Kamanna VS, Kashyap ML (2004) Niacin noncompetitively inhibits DGAT2 but not DGAT1 activity in HepG2 cells. J Lipid Res 45:1835–1845
48. Ikeda I, Tsuda K, Suzuki Y, Kobayashi M, Unno T, Tomoyori H, Goto H, Kawata Y, Imaizumi K, Nozawa A, Kakuda T (2005) Tea catechins with a galloyl moiety suppress postprandial hypertriacylglycerolemia by delaying lymphatic transport of dietary fat in rats. J Nutr 135:155–159
49. Yu YH, Zhang Y, Oelkers P, Sturley SL, Rader DJ, Ginsberg HN (2002) Posttranscriptional control of the expression and function of diacylglycerol acyltransferase-1 in mouse adipocytes. J Biol Chem 277:50876–50884
50. Nacro K, Bienfait B, Lee J, Han KC, Kang JH, Benzaria S, Lewin NE, Bhattacharyya DK, Blumberg PM, Marquez VE (2000) Conformationally constrained analogues of diacylglycerol (DAG). 16. How much structural complexity is necessary for recognition and high binding affinity to protein kinase C? J Med Chem 43:921–944
51. Friedman HI, Nylund B (1980) Intestinal fat digestion, absorption, and transport. A review. Am J Clin Nutr 33:1108–1139
52. Boden G (1997) Role of fatty acids in the pathogenesis of insulin resistance and NIDDM. Diabetes 46:3–10
53. Roden M, Price TB, Perseghin G, Petersen KF, Rothman DL, Cline GW, Shulman GI (1996) Mechanism of free fatty acid-induced insulin resistance in humans. J Clin Invest 97:2859–2865
54. Hultin M, Savonen R, Olivecrona T (1996) Chylomicron metabolism in rats: lipolysis, recirculation of triglyceride-derived fatty acids in plasma FFA, and fate of core lipids as analyzed by compartmental modeling. J Lipid Res 37:1022–1036
55. Evans K, Clark ML, Frayn KN (1999) Effects of an oral and intravenous fat load on adipose tissue and forearm lipid metabolism. Am J Physiol 276:E241–E248

Lipids (2011) 46:701–708
DOI 10.1007/s11745-011-3560-2

ORIGINAL ARTICLE

Glycosidic Bond Cleavage is Not Required for Phytosteryl Glycoside-Induced Reduction of Cholesterol Absorption in Mice

Xiaobo Lin · Lina Ma · Robert A. Moreau · Richard E. Ostlund Jr.

Received: 11 February 2011 / Accepted: 15 April 2011 / Published online: 3 May 2011

Abstract Phytosteryl glycosides occur in natural foods but little is known about their metabolism and bioactivity. Purified acylated steryl glycosides (ASG) were compared with phytosteryl esters (PSE) in mice. Animals on a phytosterol-free diet received ASG or PSE by gavage in purified soybean oil along with tracers cholesterol-d_7 and sitostanol-d_4. In a three-day fecal recovery study, ASG reduced cholesterol absorption efficiency by $45 \pm 6\%$ compared with $40 \pm 6\%$ observed with PSE. Four hours after gavage, plasma and liver cholesterol-d_7 levels were reduced 86% or more when ASG was present. Liver total phytosterols were unchanged after ASG administration but were significantly increased after PSE. After ASG treatment both ASG and deacylated steryl glycosides (SG) were found in the gut mucosa and lumen. ASG was quantitatively recovered from stool samples as SG. These results demonstrate that ASG reduces cholesterol absorption in mice as efficiently as PSE while having little systemic absorption itself. Cleavage of the glycosidic linkage is not required for biological activity of ASG. Phytosteryl glycosides should be included in measurements of bioactive phytosterols.

Keywords Stable isotopes · Plant sterols · Mass spectrometry · Lipid absorption

X. Lin · L. Ma · R. E. Ostlund Jr. (✉)
Division of Endocrinology, Metabolism and Lipid Research, Department of Medicine, Washington University School of Medicine, Campus Box 8127, 660 South Euclid Ave., St. Louis, MO 63110, USA
e-mail: Rostlund@dom.wustl.edu

R. A. Moreau
USDA Agricultural Research Service, Eastern Regional Research Center, Wyndmoor, PA, USA

Abbreviations

ASG	Acylated steryl glycosides
SG	Steryl glycosides
PSE	Phytosteryl esters
GC–MS	Gas chromatography/mass spectrometry

Introduction

Phytosterols are structurally similar to cholesterol, occur naturally in plant-derived foods, and reduce cholesterol absorption [1–4] and plasma LDL-cholesterol [5, 6]. Because of these potentially beneficial health effects, the US National Cholesterol Education Program Adult Treatment Panel III has recommended adding 2.0 g/day phytosterols to the diet of adults to reduce LDL-cholesterol and coronary heart disease risk [7, 8].

To reach the 2.0 g/day of phytosterols, pure phytosterols (free or esters) have been routinely added to various functional foods. The chemical or physical form of the phytosterol is potentially important for bioactivity because crystalline phytosterols are not readily soluble in bile and do not reduce cholesterol absorption [9]. When properly formulated with lecithin or other emulsifiers, free phytosterols do reduce cholesterol absorption and plasma LDL cholesterol [10]. Phytosteryl esters solubilized in the triglyceride phase of margarines are also bioactive [11, 12].

Phytosterols are conjugated to various components in food matrices and not all have been tested for bioactivity [13]. Recently, we have demonstrated that pure phytosteryl esters supplemented at an amount achievable from a diet (459 mg phytosterols/day) reduce cholesterol absorption and increase fecal cholesterol excretion in humans [14].

Furthermore, phytosterols present in natural food matrices (449 mg/day) are also bioactive in reducing cholesterol absorption and enhancing fecal cholesterol excretion [15]. Because phytosteryl glycosides comprise a significant proportion of naturally occurring phytosterols in some foods [16–18], we have studied them and demonstrated that phytosteryl glycosides (mostly acylated steryl glycosides, ASG) purified from soybean-derived lecithin reduce cholesterol absorption efficiency in humans [19]. However, several questions remain unanswered regarding their mechanisms of action. Phytosteryl glycosides could act intact, as glycosides (with the fatty acid cleaved), or as free phytosterols (with both fatty acid and glucose cleaved).

ASG consist of a fatty acid and a glucose moiety in addition to the phytosterol [19]. Previous work has shown that fatty acids are cleaved from glycosylated phytosterols in vitro by pancreatin and cholesterol esterase but the sugar moiety itself is not removed [20]. Acetylated ^{14}C-sitosteryl glucoside was not absorbed in the stomach or small bowel of rats after intragastric administration [21]. However, the ^{14}C label was located in the phytosterol moiety, which did not enable the authors to answer whether or not any cleavage had occurred in vivo.

In this study we prepared purified ASG and tested the hypotheses that ASG is active in reducing cholesterol absorption efficiency in mice and that it is cleaved to SG or free phytosterols in mice consuming a cholesterol and phytosterol-free diet.

Materials and Methods

Materials

[25,26,26,26,27,27,27-$^{2}H_7$]Cholesterol (cholesterol-d_7) was purchased from CDN Isotopes (Pointe-Claire, QC, Canada). Soybean oil (Bakers & Chefs, Sam's Club) was purified as described elsewhere [3] to reduce the content of phytosterols. [5,6,22,23-$^{2}H_4$]sitostanol (sitostanol-d_4) was obtained from Medical Isotopes (Pelham, NH, USA). The phytosteryl glycosides were partially purified from lecithin granules (Vitamin Shoppe, North Bergen, NJ, USA) as previously described [19]. Crude phytosteryl glycosides were then dissolved in hexane and applied to a Supelclean LC-Si SPE column (Sigma, St Louis, MO, USA) that had been conditioned with hexane. The column was eluted with 30% ethyl acetate in hexane, followed by 50% ethyl acetate in hexane. The material in the second elution was ASG without free phytosterols, phytosteryl esters, or phospholipids. ASG contained 48.5% phytosterols by weight. Phytosteryl esters (PSE) were derived from soy and 60.6% of the mass was the phytosteryl moiety. ASG and SG for HPLC standards were obtained from Matreya (Pleasant Gap, PA, USA).

Mice

Male C57BL/6J mice (5 weeks old) were purchased from Jackson Laboratory (Bar Harbor, ME, USA). Mice were housed in a room maintained at 24°C with a 12:12 h light–dark cycle (6:00 a.m.–6:00 p.m.). All mice were fed first on Purina mouse chow 5053 containing 4.5% fat, 20.0% protein, and 54.8% carbohydrate (LabDiet) for one week before switching to the sterol-free diet. All animal procedures were performed in accordance with guidelines of Washington University's Animal Studies Committee and approved by the Institutional Animal Care and Use Committee of Washington University (study protocol: 20070024).

Effect of a Single-Dose ASG/PSE on Cholesterol Absorption Over a Three-Day Period

Mice (5 each for control, PSE, or ASG) were fed a special cholesterol and phytosterol-free diet [22] for two weeks to minimize the effects of dietary sterols. Each mouse was gavaged with 0.5 mL purified soybean oil containing 40 μg cholesterol-d_7 and 10 μg sitostanol-d_4. The oil also contained 1.0 mg phytosterols delivered as either phytosteryl esters or glycosides or no addition (control). Stool samples from each mouse was collected individually in a cage with wire floor for three days. Mice were approximately eight weeks old at the time of experimentation.

Single-Time-Point Oral Study

Male C57BL/6J mice were equilibrated on the sterol-free diet and then fasted for 2 h before gavage of 0.5 mL purified soybean oil with 40 μg cholesterol-d_7 containing 6.1 mg phytosterols given as either phytosteryl esters (PSE, $n = 5$) or phytosteryl glycosides (ASG, $n = 5$), or oil only (control, $n = 5$). Mice were sacrificed 4 h after gavage. Blood was obtained by heart puncture and centrifuged at 8,000 rpm for 5 min to obtain serum. The liver and small intestine were removed and the small intestine was divided into four equal segments, lumenal contents were washed out and collected with ice-cold PBS. After the small bowel was opened longitudinally, the mucosa was extruded from the bowel wall by exerting pressure using a microscopic slide.

Gas Chromatography–Mass Spectrometry (GC–MS)

For the cholesterol absorption study, lipids were extracted from stool samples by the Bligh and Dyer method [23], hydrolyzed in alkali, and the neutral sterols were extracted

into petroleum ether, dried, and converted to pentafluorobenzoyl esters [24]. The derivatized material was analyzed for cholesterol-d_7, coprostanol-d_7, and sitostanol-d_4 by negative-ion chemical ionization gas chromatography–mass spectrometry (GC–MS) [14]. For the single-time-point oral study, 40 μg sitostanol-d_4 was added as an internal recovery standard and lipids were extracted [23] from liver, lumen washings, and mucosa; aliquots of extracted lipids were processed by both acid and alkaline hydrolysis as described elsewhere [25] and analyzed by GC–MS [26]. Plasma was analyzed as described for liver, lumen washings, and mucosa without undergoing lipid extraction. Acid hydrolysis liberates free phytosterols from ASG and SG whereas alkaline hydrolysis does not.

ASG/SG Analysis

The ASG/SG contents of lumenal and mucosal samples and stool samples were analyzed by HPLC with an evaporative light scattering detector, exactly as described elsewhere [27]. A standard curve using ASG and SG standards was constructed and used to calculate the amount of ASG and SG in the samples.

Statistical Analysis

Data are reported as means ± SEM. All statistical analyses were performed with SAS (version 9.2; Cary, NC, USA). The Proc Mixed procedure was used to analyze treatment effects on cholesterol absorption and cholesterol-d_7 levels in liver and plasma with Tukey adjustment for multiple comparisons. Proc Mixed was also used to analyze the independent effect of treatments and quarters and their interactions. Statistical significance was accepted if $P < 0.05$, or otherwise as indicated.

Results

Purity of Phytosteryl Glycosides

Phytosteryl glycosides were obtained from lecithin granules by removing most of the phospholipids and neutral sterols [19]. To further increase purity the material was passed through a Supelclean LC-Si SPE column. Thin layer chromatographic analysis showed no detectable sterols or phospholipids (data not shown). The purified phytosteryl glycosides contained mostly ASG (92.5%) and a smaller fraction of SG (7.5%) by HPLC. Campesterol, stigmasterol, and sitosterol accounted for 27.3 ± 0.5, 21.4 ± 0.2, and 51.6 ± 0.8% of total phytosterols, respectively, for the phytosteryl esters; corresponding values for the phytosteryl glycosides were 21.3 ± 0.8, 17.5 ± 0.5, and 53.9 ± 1.2%.

Effect of ASG on Percent Cholesterol Absorption in Mice

To determine whether phytosteryl glycosides were bioactive in reducing cholesterol absorption efficiency [19], we gavaged mice with ASG (1.0 mg phytosterols) solubilized in purified soybean oil. PSE (1.0 mg phytosterols) was administered in the same way as an experimental positive control and purified soybean oil alone was given to another group as a negative control. As expected, relative to control, PSE reduced cholesterol absorption by 40 ± 6% in a three-day fecal recovery experiment (Fig. 1). ASG reduced cholesterol absorption by 45 ± 6% when compared with control. The difference between ASG and PSE treatment groups was not statistically significant.

Single-Time-Point Oral Study

To explore the site where ASG reduced cholesterol absorption efficiency, groups of mice were gavaged with soybean oil containing ASG (6.1 mg phytosterols), PSE (6.1 mg phytosterols), or no addition and sacrificed 4 h later. Figures 2 and 3 report the levels of phytosterols, ASG, and SG found in the gut, lumen, and mucosa by quarter of small intestine. When no phytosterols were included in the gavage the measured phytosterol levels were very low, demonstrating the effectiveness of the prior two-week low-phytosterol baseline diet in reducing background. When either ASG or PSE was given, the total phytosterols found in the lumen (which included those

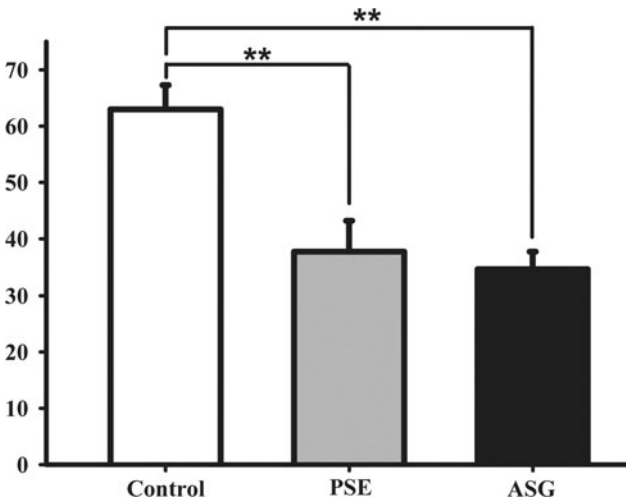

Fig. 1 Three-day study: effect of ASG on percent cholesterol absorption in mice. Mice were gavaged with purified soybean oil containing ASG (1.0 mg phytosterols), PSE (1.0 mg phytosterols), or no addition ($n = 5$ for each group). Percent cholesterol absorption was determined as described in "Materials and Methods". *Bars* represent means ± SE. Significance of differences between treatments is indicated by **($P < 0.01$)

present in the form of ASG and SG) were elevated and there was a significant treatment effect on total lumenal phytosterols ($P = 0.0088$, Fig. 2a). There was no significant relation of intestinal quarter to lumenal phytosterols ($P = 0.54$). Figure 2b shows that phytosterols accumulated in the mucosa after both ASG and PSE gavage. Total phytosterol content was largest in quarters 3 and 4 and was similar for the two phytosterol forms. There were statistically significant and independent effects of quarter ($P = 0.012$) and treatment ($P = 0.0039$) on total mucosal phytosterols.

Further studies were performed to determine the chemical form of phytosterols present in lumen and mucosa after ASG treatment. Differential hydrolysis strongly suggested that they were present as glycosides. While combined acid + alkaline hydrolysis enables total phytosterols to be measured, alkaline hydrolysis alone does not liberate free phytosterols from glycosides to be measured by GC–MS. Phytosterols from lumen and mucosa after ASG treatment determined after alkaline-only hydrolysis were very low and similar to those in the control group (data not shown), suggesting that the total phytosterols reported in Fig. 2 after ASG treatment were derived from glycosylated phytosterols. This was confirmed by direct HPLC measurement of ASG and SG in intestinal fractions (Fig. 3; Table 1). As expected, after PSE or control gavage there was no detectable ASG or SG in the lumen or mucosa. However, after ASG gavage both ASG and SG were present in lumen and mucosa. The amount of SG exceeded that of ASG in all quarters, showing active but incomplete hydrolysis of the fatty acid of ASG to yield the deacylated product SG. In other experiments in which stools were collected for three days and analyzed by HPLC, the biological hydrolysis of ASG to SG was complete (Table 1). Recovery of SG in stool samples was 95.3 ± 1.9% of the ASG given. No detectable SG was found in stool samples from control or PSE groups.

ASG administration was associated with less systemic absorption of total phytosterols than PSE (Fig. 4). Four hours after gavage, total liver phytosterols were increased 34.0 ± 8.5% (SEM) over control with PSE but only 2.7 ± 4.7% with ASG. Plasma phytosterol levels did not change significantly with either treatment.

ASG had a large inhibitory effect on absorption of cholesterol-d_7 into plasma and liver at 4 h (Fig. 5). Compared with control, ASG reduced plasma cholesterol-d_7 by 90 ± 3.7% (SEM) and liver cholesterol-d_7 by 86.2 ± 3.8%. Reductions by PSE of 51.4 ± 19.4% in plasma and 45.9 ± 25.7% in liver were more variable and not statistically significant.

Discussion

Extensive research has demonstrated that pure phytosterols, when properly formulated, reduce cholesterol absorption efficiency and plasma LDL cholesterol in animals and in humans. On the other hand, there is little published research on the physiological effects of phytosteryl glycosides. Recently we have demonstrated that ASG reduced cholesterol absorption efficiency in humans [19]. In the current study, ASG obtained from soybean-derived lecithin, was further purified and used to determine effects on cholesterol absorption and on uptake and cleavage of ASG

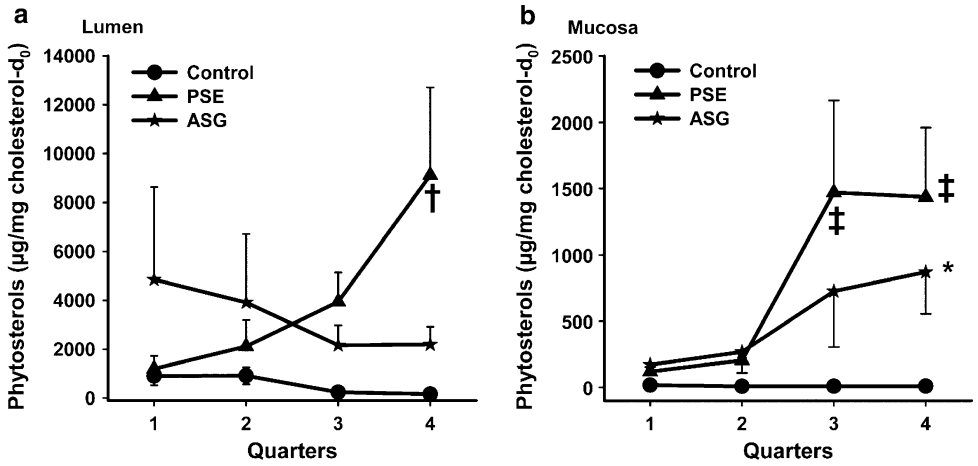

Fig. 2 Single-time-point study: total phytosterols in lumen (panel **a**) and mucosa (**b**). Mice ($n = 5$ for each group) were fasted for 2 h before gavage of purified soybean oil with cholesterol-d_7 containing ASG (6.1 mg phytosterols), PSE (6.1 mg phytosterols), or no addition. Mice were sacrificed 4 h later, the small intestine was cut into four equal quarters (quarter 1: proximal, quarter 4: distal), and mucosa was scraped after removal of lumenal contents. Levels of total phytosterols relative to natural cholesterol in the lumen and mucosa were determined by GC–MS as described in "Materials and Methods". Values are means ± SE. Statistical significance is indicated by $^{\dagger}(P < 0.05)$ or $^{\ddagger}(P < 0.01)$ (between control and PSE) and by $^{*}(P < 0.05)$ (between control and ASG)

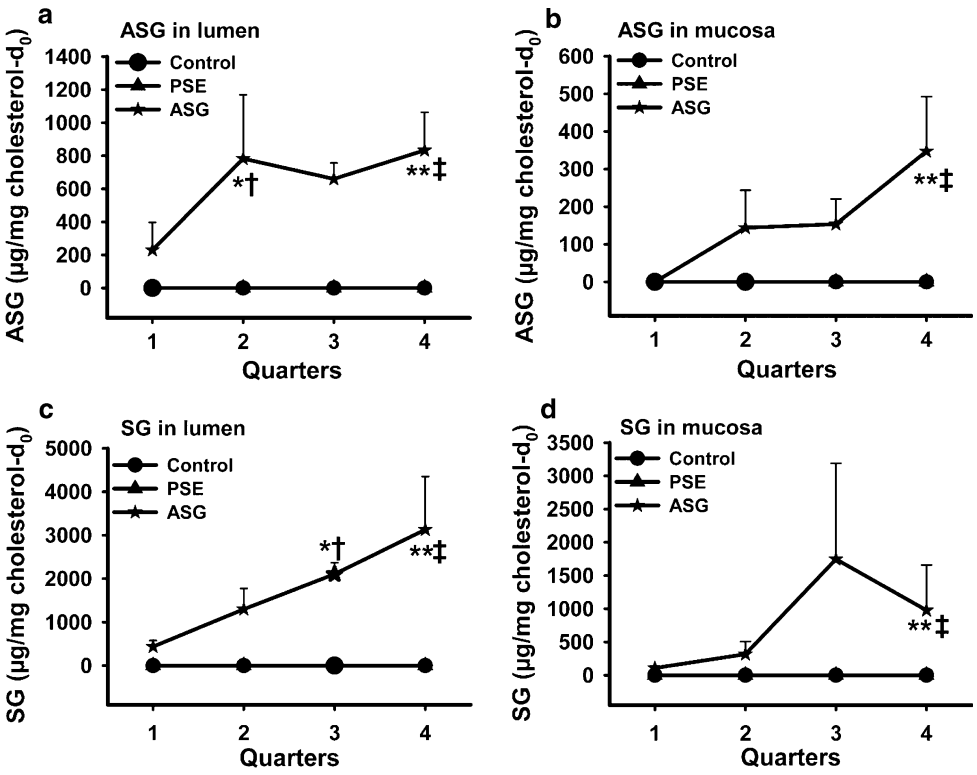

Fig. 3 Single-time-point study: ASG and SG in lumen and mucosa. Mice ($n = 5$ for each group) were fasted for 2 h before gavage of purified soybean oil with cholesterol-d_7 containing ASG (6.1 mg phytosterols), PSE (6.1 mg phytosterols), or no addition. Mice were sacrificed 4 h later, the small intestine was cut into four equal quarters (quarter 1: proximal, quarter 4: distal), and mucosa was scraped after removal of lumenal contents. The levels of directly measured ASG and SG relative to natural cholesterol in lumen and mucosa were determined as described in "Materials and Methods". Values are means ± SE. Significance is indicated by *($P < 0.05$) or **($P < 0.01$) (between control and ASG) and by †($P < 0.05$) or ‡($P < 0.01$) (between PSE and ASG). Symbols for control and PSE overlap near zero

Table 1 Phytosterol recovery in the form of steryl glycosides from stool samples three days after gavage

	Control ($n = 5$)	PSE ($n = 5$)	ASG ($n = 5$)
Total phytosterol gavaged (μg)	27.9 ± 0.6	1034.2 ± 37.3	852.1 ± 19.7
Phytosterols contained in SG (μg)	ND	ND	810.8 ± 11.7
Recovery rate in the form of SG (%)	NA	NA	95.3 ± 1.9

C57BL/6J male mice (nine weeks old) were gavaged with 0.5 mL soybean oil alone (control, $n = 5$), 0.5 mL soybean oil with phytosteryl esters (PSE, $n = 5$) containing 1.0 mg phytosterols, and 0.5 mL soybean oil with phytosteryl glycosides (ASG, $n = 5$) with 1.0 mg phytosterol equivalents. SG was determined as described in "Materials and Methods"

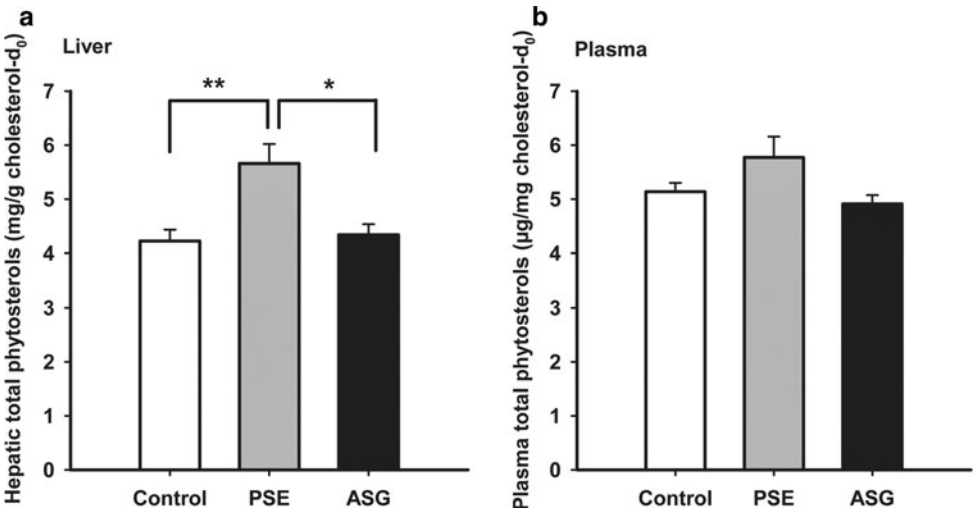

Fig. 4 Single-time-point study: total phytosterols in liver (**a**) and plasma (**b**). Mice ($n = 5$ for each group) were fasted for 2 h before gavage of purified soybean oil with cholesterol-d_7 containing ASG (6.1 mg phytosterols), PSE (6.1 mg phytosterols), or no addition and were sacrificed 4 h later. Levels of total phytosterols in liver and plasma expressed relative to natural cholesterol were determined as described in the "Materials and Methods". Values are means ± SE. Significance is indicated by *($P < 0.05$) or **($P < 0.01$)

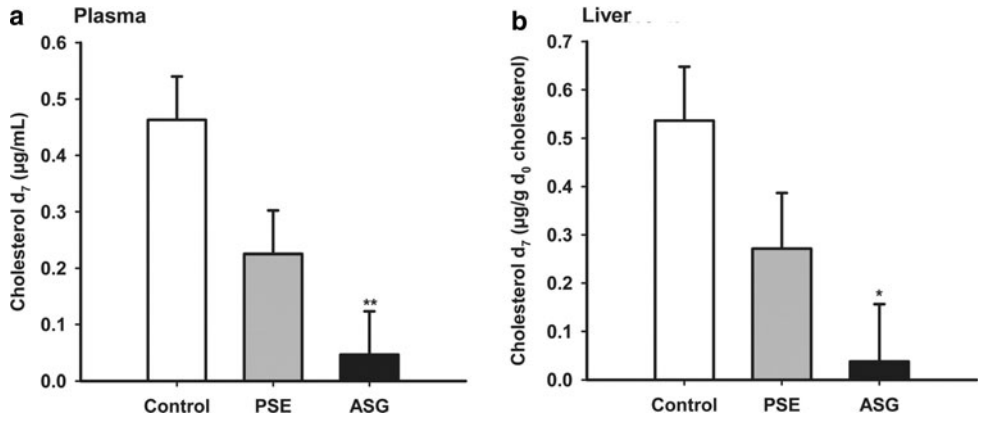

Fig. 5 Single-time-point study: cholesterol-d_7 in plasma (**a**) and liver (**b**). Mice ($n = 5$ for each group) were fasted for 2 h before gavage of purified soybean oil with cholesterol-d_7 containing ASG (6.1 mg phytosterols), PSE (6.1 mg phytosterols), or no addition. Mice were sacrificed 4 h later and levels of cholesterol d_7 in plasma and liver were determined as described in "Materials and Methods". Values are means ± SEM. Significance is indicated by **($P < 0.01$)

in mouse intestine. Consistently, ASG reduced cholesterol absorption in vivo in mice, as observed in humans. ASG seemed to act locally in the gut lumen and mucosa with very little absorption into the systemic circulation. Furthermore, cleavage of glycosidic bonds was not required for biological activity of ASG. Most of the fatty acid moieties of ASG were removed, converting them to SG whereas the glycosidic bond remained intact.

Consistent with the known reduction in cholesterol absorption in humans, ASG reduced cholesterol absorption by 45% as determined by a three-day procedure when compared with the negative control (Fig. 1), indicating that ASG was bioactive in mice. PSE, the experimental positive control, reduced cholesterol absorption by 40% (Fig. 1). In a shorter time frame of 4 h, cholesterol d_7, gavaged together with ASG in purified soybean oil, was subsequently found to be significantly reduced in liver and plasma compared with control (Fig. 5). These results show that ASG acts rapidly to reduce both the rate of cholesterol transport and the overall extent of cholesterol absorption.

Because standard rodent chow diets are rich in phytosterols, we used a novel cholesterol and phytosterol-free diet to enable better assessment of phytosterol absorption. Total phytosterols in the liver of mice given PSE were significantly higher than in those of control or ASG mice (Fig. 4a). In contrast, total phytosterols in the liver or plasma of mice gavaged with ASG were similar to those of the control (Fig. 4a, b), indicating that ASG was not absorbed into the systemic circulation. Our finding agrees with results from a study in which [4-^{14}C]sitosteryl β-D-glucoside administered intragastrically to rats was not found after 3 h in liver, kidney, heart, lungs, spleen, muscle, brain, adipose tissue, or blood [21]. The same study fed unlabeled sitosteryl β-D-glucoside at 0.5 g/kg body weight to rats for four weeks and neither sitosteryl β-D-glucoside nor sitosterol or sitosteryl esters were found in significant amounts in tissues outside the alimentary canal during the entire feeding period. It is therefore unlikely that ASG enters the systemic circulation.

ASG seemed to act locally in the lumen or in the mucosa or both. After PSE treatment total phytosterols seemed to accumulate in the lumen across the quarters (Fig. 2a), consistent with the established mechanism of action of interfering with micellar cholesterol formation in the lumen. Total phytosterols in the mucosa from the PSE group increased rapidly from the second quarter onward, indicating uptake of phytosterols into mucosa and possible action of phytosterols inside the mucosa (Fig. 2b), albeit present at a much lower level compared with lumenal total phytosterols. After ASG treatment, total phytosterols in the mucosa increased from the second quarter onward (Fig. 2), similar to the pattern with PSE. Direct HPLC measurement confirmed that the accumulated phytosterols were in the form of ASG and SG (Fig. 3).

Our results strongly suggest that the bioactive components reducing cholesterol absorption are ASG or SG, but not the free phytosterols. Most of the phytosterol glycosides (92.5%) administered were in the form of ASG. Yet both ASG and SG were abundant in the lumen and mucosa in 4 h, indicating that ASG was hydrolyzed to SG in these locations. Consistent with the previous report that ASG was cleaved to SG in vitro by pancreatin and cholesterol esterase [20], most of the ASG was recovered as SG in stool samples three days after gavage, indicating that cleavage of ASG to SG was complete in three days. The complete recovery of ASG as fecal SG also indicates that SG were not hydrolyzed to free phytosterols. Furthermore, total phytosterol levels in the liver or plasma were similar to the respective levels in the control. This also is in agreement with the finding that only a small fraction of

[4-^{14}C]sitosteryl β-D-glucoside (<0.5%) was detected in the form of sitosterol and sitosteryl esters in the duodenum, jejunum, ileum, and stomach [21]. Therefore, cleavage of the glycosidic bond seems to not be required for the biological activity of ASG in mice.

In summary, the results of this study have demonstrated that ASG is bioactive in mice. ASG was taken up rapidly into the mucosa 4 h after oral gavage. ASG was cleaved to SG so that most of the ASG given was present in the form of SG in the lumen and mucosa. ASG administered was recovered quantitatively from stool samples as SG. There was little systemic absorption of ASG into the plasma or liver and ASG/SG seemed to act locally in both the lumen and mucosa without being significantly absorbed into the systemic circulation. Bioactive in reducing cholesterol absorption in mice and humans, phytosteryl glycosides from either natural or synthetic sources could potentially be used for the treatment of hypercholesterolemia. Phytosteryl glycosides must be measured and taken into account when assessing the effects of phytosterols in the diet and for treatment of hypercholesterolemia.

Acknowledgments This work was supported by National Institutes of Health Grant R01 50420 and the Washington University Mass Spectrometry Resource (P41 RR00954). We appreciate Mrs. Robin Fitzgerald for her excellent technical assistance.

Conflict of interest Dr. Ostlund and Washington University have a financial interest in Lifeline Technologies, a biotechnology company developing bioactive phytosterols. Lifeline products were not used in this study, and Lifeline and the authors have no financial interest in phytosteryl glycosides.

References

1. Ostlund RE Jr (2002) Phytosterols in human nutrition. Ann Rev Nutr 22:533–549
2. Ostlund RE Jr, Racette SB, Okeke A, Stenson WF (2002) Phytosterols that are naturally present in commercial corn oil significantly reduce cholesterol absorption in humans. Am J Clin Nutr 75(6):1000–1004
3. Ostlund RE Jr, Racette SB, Stenson WF (2003) Inhibition of cholesterol absorption by phytosterol-replete wheat germ compared with phytosterol-depleted wheat germ. Am J Clin Nutr 77(6):1385–1389
4. Nestel P, Cehun M, Pomeroy S, Abbey M, Weldon G (2001) Cholesterol-lowering effects of plant sterol esters and non-esterified stanols in margarine, butter and low-fat foods. Eur J Clin Nutr 55(12):1084–1090
5. Law MR (2000) Plant sterol and stanol margarines and health. West J Med 173(1):43–47
6. Nguyen TT (1999) The cholesterol-lowering action of plant stanol esters. J Nutr 129(12):2109–2112
7. Aronow WS (2001) Cholesterol 2001. Rationale for lipid-lowering in older patients with or without CAD. Geriatrics 56(9): 22–30
8. Expert Panel on Detection (2001) Executive summary of the third report of the national cholesterol education program (NCEP) Expert panel on detection, evaluation, and treatment of high blood cholesterol in adults (Adult Treatment Panel III). JAMA 285(19):2486–2497
9. Ostlund RE Jr, Spilburg CA, Stenson WF (1999) Sitostanol administered in lecithin micelles potently reduces cholesterol absorption in humans. Am J Clin Nutr 70(5):826–831
10. Gremaud G, Dalan E, Piguet C, Baumgartner M, Ballabeni P, Decarli B, Leser ME, Berger A, Fay LB (2002) Effects of non-esterified stanols in a liquid emulsion on cholesterol absorption and synthesis in hypercholesterolemic men. Eur J Nutr 41(2): 54–60
11. Spilburg CA, Goldberg AC, McGill JB, Stenson WF, Racette SB, Bateman J, McPherson TB, Ostlund RE Jr (2003) Fat-free foods supplemented with soy stanol-lecithin powder reduce cholesterol absorption and LDL cholesterol. J Am Diet Assoc 103(5): 577–581
12. Katan MB, Grundy SM, Jones P, Law M, Miettinen T, Paoletti R (2003) Efficacy and safety of plant stanols and sterols in the management of blood cholesterol levels. Mayo Clin Proc 78(8):965–978
13. Moreau RA, Whitaker BD, Hicks KB (2002) Phytosterols, phytostanols, and their conjugates in foods: structural diversity, quantitative analysis, and health-promoting uses. Prog Lipid Res 41(6):457–500
14. Racette SB, Lin X, Lefevre M, Spearie CA, Most MM, Ma L, Ostlund RE Jr (2010) Dose effects of dietary phytosterols on cholesterol metabolism: a controlled feeding study. Am J Clin Nutr 91(1):32–38
15. Lin X, Racette SB, Lefevre M, Spearie CA, Most M, Ma L, Ostlund RE Jr (2010) The effects of phytosterols present in natural food matrices on cholesterol metabolism and LDL-cholesterol: a controlled feeding trial. Eur J Clin Nutr 64(12): 1481–1487
16. Jonker D, van der Hoek GD, Glatz JFC, Homan C, Posthumus MA, Katan MB (1985) Combined determination of free, esterified and glycosylated plant sterols in foods. Nutr Rep Int 32:943–951
17. Normén L, Bryngelsson S, Johnsson M, Evheden J, Ellegard LBH, Brants H, Andersson H, Dutta P (2002) The phytosterol content of some cereal foods commonly consumed in Sweden and in the Netherlands. J Food Comp Anal 15(6):693–704
18. Normen L, Johnsson M, Andersson H, van Gameren Y, Dutta P (1999) Plant sterols in vegetables and fruits commonly consumed in Sweden. Eur J Clin Nutr 38:84–89
19. Lin X, Ma L, Racette SB, Anderson Spearie CL, Ostlund RE Jr (2009) Phytosterol glycosides reduce cholesterol absorption in humans. Am J Physiol Gastrointest Liver Physiol 296(4):G931–G935
20. Moreau RA, Hicks KB (2004) The in vitro hydrolysis of phytosterol conjugates in food matrices by mammalian digestive enzymes. Lipids 39(8):769–776
21. Weber N (1988) Metabolism of sitosteryl beta-D-glucoside and its nutritional effects in rats. Lipids 23(1):42–47
22. Lin X, Ma L, Gopalan C, Ostlund RE (2009) D-chiro-Inositol is absorbed but not synthesised in rodents. Br J Nutr 102(10): 1426–1434
23. Bligh EG, Dyer WJ (1959) A rapid method of total lipid extraction and purification. Can J Biochem Physiol 37(8): 911–917
24. Ostlund RE Jr, Hsu FF, Bosner MS, Stenson WF, Hachey DL (1996) Quantification of cholesterol tracers by gas chromatography–negative ion chemical ionization mass spectrometry. J Mass Spectrom 31(11):1291–1296

25. Racette SB, Spearie CA, Phillips KM, Lin X, Ma L, Ostlund RE Jr (2009) Phytosterol-deficient and high-phytosterol diets developed for controlled feeding studies. J Am Diet Assoc 109:2043–2051
26. Ostlund RE Jr, McGill JB, Zeng CM, Covey DF, Stearns J, Stenson WF, Spilburg CA (2002) Gastrointestinal absorption and plasma kinetics of soy Delta(5)-phytosterols and phytostanols in humans. Am J Physiol Endocrinol Metab 282(4):E911–E916
27. Moreau RAS KM, Haas MJ (2008) The identification and quantification of steryl glucosides in precipitates from commercial biodiesel. J Am Oil Chem Soc 85:761–770

Lipids (2011) 46:709–721
DOI 10.1007/s11745-011-3566-9

ORIGINAL ARTICLE

Is the Fatty Acid Composition of Freshwater Zoobenthic Invertebrates Controlled by Phylogenetic or Trophic Factors?

Olesia N. Makhutova · Nadezhda N. Sushchik · Michail I. Gladyshev · Alexander V. Ageev · Ekaterina G. Pryanichnikova · Galina S. Kalachova

Received: 25 May 2010 / Accepted: 1 April 2011 / Published online: 13 May 2011

Abstract We studied the fatty acid (FA) content and composition of ten zoobenthic species of several taxonomic groups from different freshwater bodies. Special attention was paid to essential polyunsaturated fatty acids, eicosapentaenoic acid (EPA, 20:5n-3), docosahexaenoic acid (DHA, 22:6n-3), and arachidonic acid (ARA, 20:4n-6); and the n-3/n-6 and DHA/ARA ratios, which are important for consumers of higher trophic levels, i.e., fish. The content and ratios of these FA varied significantly in the studied zoobenthic species, consequently, the invertebrates were of different nutritional quality for fish. *Eulimnogammarus viridis* (Crustacea) and *Dendrocoelopsis* sp. (Turbellaria) had the highest nutrition value for fish concerning the content of EPA and DHA and n-3/n-6 and DHA/ARA ratios. Using canonical correspondence analysis we compared the FA profiles of species of the studied taxa taking into account their feeding strategies and habitats. We gained evidence that feeding strategy is of importance to determine fatty acid profiles of zoobenthic species. However, the phylogenetic position of the zoobenthic species is also responsible and may result in a similar fatty acid composition even if species or populations inhabit different water bodies or have different feeding strategies.

Keywords Benthic invertebrates · Fish · Feeding strategy · Phylogeny · Polyunsaturated fatty acids

Abbreviation

ALA	α-Linolenic acid, 18:3n-3
ARA	Arachidonic acid, 20:4n-6
BFA	Branched fatty acids
DHA	Docosahexaenoic acid, 22:6n-3
DPA	Docosapentaenoic acid, 22:5n-3
EPA	Eicosapentaenoic acid, 20:5n-3
FA	Fatty acid(s)
FAME	Fatty acid methyl ester(s)
LNA	Linoleic acid, 18:2n-6
MUFA	Monounsaturated fatty acid(s)
NMI	Nonmethylene interrupted
PUFA	Polyunsaturated fatty acid(s)
SFA	Saturated fatty acid(s)

O. N. Makhutova (✉) · N. N. Sushchik · M. I. Gladyshev · G. S. Kalachova
Institute of Biophysics of the Siberian Branch of the Russian Academy of Science, Akademgorodok, 660036 Krasnoyarsk, Russia
e-mail: makhutova@ibp.krasn.ru

N. N. Sushchik · M. I. Gladyshev · A. V. Ageev
Siberian Federal University, Svobodny av 79, 660041 Krasnoyarsk, Russia

E. G. Pryanichnikova
Institute for Biology of Inland Waters of the Russian Academy of Science, 152742 Borok, Russia

Introduction

The fatty acid composition and FA ratios of different taxonomic groups are widely used as biochemical markers of trophic interactions in aquatic ecosystems [1, 2]. FA markers have been used to trace the transfer of the organic matter through aquatic food webs and to evaluate diet patterns of the aquatic animals [3–5]. Some polyunsaturated fatty acids (PUFA), namely eicosapentaenoic and docosahexaenoic acids are essential components in the nutrition of aquatic invertebrates and fish [6, 7]. It should

be noted that the essential PUFA are of large physiological importance for animals of different taxonomic levels, including humans [8–10]. Besides the PUFA content, the n-3/n-6 and DHA/ARA ratios are very important. These ratios are quite species-specific and their dietary levels must be optimal to sustain normal growth and development of organisms [11].

Benthic invertebrates (zoobenthos) are one of the most important components of riverine ecosystems and a major food source for fish. The most data on fatty acid content and the composition of benthic invertebrates come primarily from the aquaculture of marine economically important food species [12–16]. In contrast, data on the fatty acid composition of freshwater zoobenthos in rivers are scarce.

As it is known, the FA profiles of aquatic animals can be affected both by their food sources and by genetically predetermined metabolism [17]. The relative importance of these factors is continuously discussed, especially for zooplankton species. On the one hand, there is experimental evidence that some zooplankton species, e.g. *Daphnia*, have quite variable FA profiles that are strongly influenced by diet [18–21]. Variations in FA composition of natural zooplankton were also determined primarily by seasonal changes in the FA composition of their food, seston [22]. On the other hand, some zooplankton species are believed to selectively accumulate and metabolically alter dietary essential fatty acids [23–26].

In contrast to the comparatively well-studied zooplankton, there are sparse data on factors determining FA profiles of freshwater benthic invertebrates. Though there are several studies that demonstrate a capacity of zoobenthic species to synthesize long-chain PUFA from short-chain precursors. For instance, the free-living nematode *Caenorhabditis elegans* evidently has a unique pathway of PUFA synthesis from oleic acid to linoleic (LNA, 18:2n-6) and α-linolenic (ALA, 18:3n-3) acids and then to ARA and EPA, and, as a result, FA composition of *C. elegans* does not reflect the FA composition of its food [27]. Larvae of chironomids, *Chironomus riparius* are able to synthesize a large enough quantity of ARA and EPA from dietary LNA and ALA to support normal larval growth and development [28]. However, the above-mentioned zoobenthic species neither synthesized DHA nor accumulated this acid from their food [28]. We have previously demonstrated using fatty acids as trophic markers that benthic *Chironomus plumosus* selectively consumed food particles originating from green algae and cyanobacteria and contained little EPA and no DHA [4]. Riverine larvae of chironomids were shown to contain only traces of DHA [29, 30]. In contrast to the nematode and chironomids mentioned, larvae of caddisfly, *Hydropsyche* sp., have been shown to have a very limited ability to elongate and desaturate C18 PUFA to C20 PUFA [31]. There is evidence that the PUFA composition in gammarids depends on both diet and the inherent capacity of the animals to desaturate and elongate linoleic and linolenic acids to long-chain PUFA [32].

Kraffe and coauthors [33] have revealed a striking relationship between cardiolipin FA composition and phylogenetic groups of bivalve mollusks. They have suggested that cardiolipin FA profiles in bivalves are likely similar in species of the same phylogenetic group.

The majority of the above cited studies were focused on rather narrow phylogenetic groups of zoobenthos or did not consider the effect of phylogenetic factors. Therefore, a notion still occurs that trophic factors are key determinants of FA composition including essential PUFA in most aquatic invertebrates. We considered that studies covering a wider range of taxa and habitats were necessary to elucidate the true role of trophic and phylogenetic factors as determinants of FA profiles in zoobenthic invertebrates.

The aim of the present work was to compare the FA composition of freshwater benthic invertebrates of diverse taxonomic groups, potentially important for fish feeding, from different aquatic ecosystems. We addressed the following questions: (1) Whether phylogenetically close species inhabiting the same water body have different fatty acid spectra? (2) Can the populations of the same species inhabiting different water bodies with variable food sources, have a similar fatty acid composition? (3) Do phylogenetic factors are important determinants of essential EPA and DHA contents in benthic invertebrates?

Materials and Methods

Sampling and Fatty Acid Analysis

We included ten zoobenthic species in the study; most of them were taken from one water body, and only one species, *C. plumosus*, was sampled from two water bodies. Invertebrates were collected from the Yenisei River, Rybinskoe reservoir, Bugach reservoir and Chistoe lake (Table 1). The total number of samples was 100. Samples were collected in different periods of the year due to the seasonal occurrence and dominance of the species. The list of species, number of samples, and sampling periods are shown in Table 1. Each sample consisted of 2–20 individuals of various sizes, most of them were adults or premature larval stages. Whole bodies of the animals were taken for the analyses, except dreissenids, from which the closing muscle was removed and used for the following analysis.

Organisms from the river littoral were sampled using a Surber-type kick-bottom sampler by disturbing an area in a frame 40 × 35 cm upstream of an attached net (mouth

Table 1 Sampling protocol of studied invertebrates

Species	Number of samples	Sampling period	Water body
Dendrocoelopsis sp.	7	2005 April, October 2006 January, October, December 2007 January, September	The Yenisei River (Siberia, Russia, 55°58′ N and 92°43′ E)
Lumbriculus variegatus O.F. Muller	4	2004 June, August, November, December	The Yenisei River
Tubifex tubifex O.F. Muller	3	2005 February, April 2006 December	The Yenisei River
Eulimnogammarus viridis Dybowsky	6	2004 March, June, July 2005 March 2006 July 2008 March	The Yenisei River
Apatania crymophila MacLachlan	18	2004 September, November 2005 February, April, July–November 2006 January, February, September–December, 2007 January, February, September	The Yenisei River
Ephemerella setigera Bajkova	3	2006 September, December 2007 January	The Yenisei River
Prodiamesa olivacea Meigen	3	2006 October–December	The Yenisei River
Chironomus plumosus Linnaeus 'B'*	19	2007 May–September 2008 May–September	Bugach reservoir (Siberia, Russia, 56°03′ N and 92°43′ E)
Chironomus plumosus Linnaeus 'C'*	6	2008 June–August	Chistoe lake (Volga River basin, Russia, 57°43′ N and 40°33′ E)
Dreissena polymorpha Pallas	15	2007 June–September 2008 June–September	Rybinskoe reservoir (Volga River basin, 58°03′ N and 38°17′ E)
Dreissena bugensis Andrusov	16	2007 June–September 2008 June–September	Rybinskoe reservoir

* The designations of two populations of *Chironomus plumosus* are the same in the text

40 × 40 cm, mesh size 0.25 mm). Organisms from the reservoirs and the lake were sampled using Petersen-type bottom samplers. Immediately after sorting, the live animals were placed in beakers with tap water for 24 h to empty their guts. Then the animal's body surfaces were gently wiped with filter paper and the animals were weighed and placed in chloroform:methanol mixture (2:1, v/v) and kept until further analysis at −20 °C.

Laboratory FA analyses and the comprehensive identification of fatty acids are described in detail elsewhere [29, 34]. Briefly, lipids from the samples were extracted with chloroform:methanol (2:1, v/v) 3 times simultaneously with mechanical homogenization of the tissues with glass beads. Before the extraction, a fixed volume of an internal standard solution (19:0) was added to the samples. The combined lipid extracts were filtered, dried by passing through anhydrous Na_2SO_4 layer and evaporated at 35 °C. The lipid extract was subjected to acidic methanolysis as described previously [5]. Fatty acid methyl esters (FAME) were analyzed on a gas chromatograph equipped with a mass spectrometer detector (GCD Plus, Hewlett-Packard, USA) and a 30-m long × 0.32-mm internal diameter capillary column HP-FFAP. The column temperature programming was as follows: from 100 to 190 °C at 3 °C/min, 5 min isothermally, to 230 °C at 10 °C/min, and 20 min isothermally. Other instrumental conditions were as described elsewhere [5]. Peaks of FAME were identified by their mass spectra compared to those in the database (Hewlett-Packard, USA) and to those of available authentic standards (Sigma, USA). Positions of double bonds in monoenoic acids were determined by GC–MS of FAME dimethyl disulfide adducts prepared as described elsewhere [35]. To determine double bond positions in polyenoic acids, GC–MS of dimethyloxazoline derivatives of FA was used [29].

Statistical Analysis

Means, standard errors (SE) and Fisher LSD tests were calculated conventionally [36]. To check differences among taxa and the seasonal effect, the data matrix was formed which included all samples of the animals. Mollusk

samples were averaged for each date and used in the analysis. The data matrix included percentages of total FA of the most prominent FA and those of high marker significance, in the total eighteen FA. Canonical correspondence analysis of the data matrix was carried out using STATISTICA software (version 9; StatSoft Inc., Tulsa, OK, USA). To test differences among phylogenetic groups, such as classes Insecta, Oligochaeta, Crustacea, Turbellaria, Bivalvia, the data matrix was formed in similar manner as for the canonical correspondence analysis. Taxa groups comprised: Insecta—*A. crymophila*, *E. setigera*, *P. olivacea*, *C. plumosus*; Oligochaeta—*L. variegates* and *T. tubifex*; Crustacea—*E. viridis*; Turbellaria—*Dendrocoelopsis sp.*; Bivalvia—*D. polymorpha* and *D. bugensis*. The data matrix included percentages (mol% of the total) of essential FA, such as LNA, ALA, EPA, DPA, and DHA, and 16:0 and 18:1n-9 which is the most significant as energy sources. Tukey HSD test of the data matrix was carried out using STATISTICA software (version 9; StatSoft Inc., Tulsa, OK, USA).

Results

Fatty acid content and composition of zoobenthos from four phyla were studied. Taxonomy position and phylogenetic relationships between the studied species are shown in Fig. 1 [37].

More than fifty FA species were identified in samples (Tables 2, 3).

The levels of saturated fatty acids (SFA) in the studied species varied from 26.3 to 41.4% (mol% of the total) (Tables 2, 3). Levels of SFA were low in *E. viridis* and *Dendrocoelopsis* sp. and high in mollusks. Among SFA, 16:0, 18:0 and 14:0 dominated in most of the invertebrates, although their ratios significantly differed among the species (Tables 2, 3).

Branched fatty acids (BFA) comprised mostly i15:0, ai15:0, i17:0 and ai17:0 and their levels varied from 1.0 to 9.2% of the total (Tables 2, 3). The distribution of 15:0 BFA differed from that of 17:0 BFA. The levels of i15:0 and ai15:0 were significantly higher in *C. plumosus* 'C' in comparison with other species (Tables 2, 3). The levels of i17:0 and ai17:0 were high in mollusks and oligochaetes, especially in *L. variegatus*.

Monoenoic acids (MUFA) varied from 17.8 to 36.5% of the total and were primarily represented by 16:1n-7, 18:1n-7, 18:1n-9, 20:1n-7, 20:1n-9 and 20:1n-11 (Tables 2, 3). However, MUFA profiles differed among the species studied. *Dendrocoelopsis* sp. and *E. viridis* showed significant levels of 18:1n-9, while mollusks had the highest level of 20:1n-9. It should be noted that 20:1n-11 was found in all studied species in traces, except mollusks and oligochaetes, which had this acid dominant among MUFA. Monoenoic C22 acids were found mainly in worms and mollusks (Table 2).

The levels of polyunsaturated fatty acids varied from 25.1 to 39.3% of the total. The lowest value of PUFA was found in larvae of Chironomidae and the highest value was in *E. viridis* and *D. bugensis.* Dominant PUFA patterns in the studied invertebrates were evidently species-specific (Tables 2, 3).

In samples of *Dendrocoelopsis* sp. 20:5n-3, 22:5n-3, ALA, LNA and 22:6n-3 dominated. Note that the studied planarian was characterized by a very high content of 22:5n-3 (Tables 2, 4).

In both mollusk species, 22:6n-3, 20:5n-3, 22:5n-3, 22:5n-6, 20:4n-6 dominated, while their levels of C16 and C18 PUFA were negligible. The levels of 22:6n-3 in mollusks were significantly higher in comparison with other species (Tables 2, 3).

In oligochaetes the following acids dominated: 20:5n-3, LNA, ALA, 20:4n-6, and 22:6n-3. The per cent levels of 20:5n-3 in both Oligochaeta species were high and

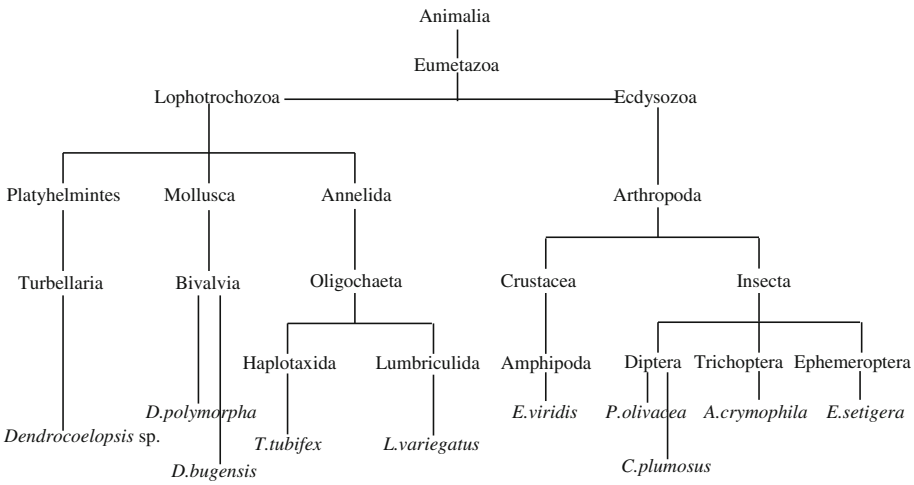

Fig. 1 The scheme of phylogenetic tree of benthic invertebrates, *Dendrocoelopsis sp.*, *D. polymorpha*, *D. bugensis*, *T. tubifex*, *L. variegatus*, *E. viridis*, *C. plumosus*, *P. olivacea*, *A. crymophila*, and *E. setigera* [by 37]

Table 2 Mean levels of FA (mol% of the total) of *Dendrocoelopsis sp*., *L. variegatus*, *T. tubifex* from the Yenisei River, *D. polymorpha* and *D. bugensis* from Rybinskoe reservoir

Fatty acids	*Dendrocoelopsis* sp.	*Dreissena polymorpha*	*Dreissena bugensis*	*Lumbriculus variegatus*	*Tubifex tubifex*
12:0	0.3 ± 0.15	0.2 ± 0.08	0.1 ± 0.03	0.4 ± 0.12	0.7 ± 0.30
14:0	**2.8 ± 0.42^{f}**	**1.6 ± 0.16^{c}**	**1.4 ± 0.15^{c}**	**4.0 ± 0.91^{be}**	**3.8 ± 0.45^{be}**
15:0	0.5 ± 0.13	0.9 ± 0.05	0.7 ± 0.06	0.5 ± 0.07	0.8 ± 0.17
16:0	**17.7 ± 1.20^{bc}**	**32.4 ± 1.95^{a}**	**31.2 ± 1.74^{a}**	**15.2 ± 4.78^{c}**	**13.5 ± 2.61^{c}**
17:0	0.6 ± 0.08	1.6 ± 0.11	1.7 ± 0.08	1.2 ± 0.22	1.5 ± 0.03
18:0	**4.5 ± 0.51^{e}**	**4.4 ± 0.20^{e}**	**4.3 ± 0.25^{e}**	**8.1 ± 0.93^{bc}**	**9.7 ± 1.02^{b}**
20:0	0.3 ± 0.03	0.2 ± 0.05	0.2 ± 0.02	0.4 ± 0.19	0.5 ± 0.04
22:0	0.4 ± 0.03	0.1 ± 0.02	0.1 ± 0.01	0.6 ± 0.19	0.8 ± 0.20
SFA	27.3 ± 1.60	41.4 ± 1.86	39.7 ± 1.94	30.8 ± 4.74	31.9 ± 2.97
i-14:0	0.1 ± 0.02	tr.	tr.	0.5 ± 0.31	0.6 ± 0.05
***ai*-15:0**	**0.4 ± 0.05^{cd}**	**0.1 ± 0.02^{d}**	**0.1 ± 0.03^{d}**	**1.7 ± 0.76^{b}**	**1.6 ± 0.14^{b}**
***i*-15:0**	**0.2 ± 0.06^{a}**	**0.1 ± 0.02^{a}**	**tr.^{a}**	**0.6 ± 0.15^{a}**	**0.9 ± 0.11^{a}**
i-15:1n-6	0.1 ± 0.01	tr.	tr.	0.5 ± 0.30	0.7 ± 0.16
i-16:0	0.1 ± 0.02	0.2 ± 0.01	0.2 ± 0.02	0.4 ± 0.08	0.5 ± 0.25
***ai*-17:0**	**0.2 ± 0.01^{a}**	**1.0 ± 0.10^{cd}**	**1.0 ± 0.04^{cd}**	**0.9 ± 0.24^{d}**	**1.2 ± 0.21^{c}**
***i*-17:0**	**tr.^{a}**	**0.4 ± 0.06^{b}**	**0.5 ± 0.06^{c}**	**0.7 ± 0.25^{c}**	**1.6 ± 0.44^{d}**
BFA	1.1 ± 0.14	1.8 ± 0.18	1.9 ± 0.13	5.2 ± 1.78	7.1 ± 0.78
14:1n-7	0.2 ± 0.06	0.1 ± 0.02	tr.	0.8 ± 0.44	0.3 ± 0.17
16:1n-7 + n-9	9.3 ± 0.94	4.1 ± 0.21	4.0 ± 0.21	11.0 ± 0.74	7.1 ± 2.48
16:1n-5	0.2 ± 0.05	0.2 ± 0.07	0.2 ± 0.03	0.1 ± 0.11	0.2 ± 0.25
18:1n-9	**16.8 ± 1.50^{a}**	**3.2 ± 0.16^{bc}**	**2.3 ± 0.14^{b}**	**6.4 ± 1.57^{f}**	**5.7 ± 1.49^{cf}**
18:1n-7	**7.7 ± 0.80^{b}**	**2.0 ± 0.12^{ae}**	**1.8 ± 0.04^{a}**	**3.7 ± 1.03^{c}**	**6.8 ± 0.29^{bd}**
18:1n-5	0.1 ± 0.03	tr.	tr.	0.4 ± 0.24	0.7 ± 0.09
20:1n-11	**n.d.^{d}**	**6.1 ± 0.38^{a}**	**5.5 ± 0.37^{ac}**	**3.3 ± 0.76^{b}**	**4.3 ± 1.57^{bc}**
20:1n-9	**0.5 ± 0.14^{cdf}**	**3.0 ± 0.15^{a}**	**1.7 ± 0.10^{b}**	**0.2 ± 0.11^{ce}**	**0.3 ± 0.03^{ed}**
20:1n-7	0.3 ± 0.12	1.2 ± 0.14	1.9 ± 0.13	0.1 ± 0.13	0.1 ± 0.09
22:1n-11	0.1 ± 0.02	0.2 ± 0.03	0.1 ± 0.01	n.d.	n.d.
22:1n-9	tr.	1.0 ± 0.49	0.2 ± 0.09	tr.	0.6 ± 0.11
MUFA	35.4 ± 1.24	21.3 ± 0.35	17.8 ± 0.50	26.5 ± 2.01	26.4 ± 3.26
16:2n-4	**1.3 ± 0.19^{df}**	**tr.^{c}**	**0.1 ± 0.01^{c}**	**1.2 ± 0.57^{def}**	**0.2 ± 0.23^{ce}**
16:3n-4	**0.9 ± 0.13^{df}**	**n.d.^{a}**	**n.d.^{a}**	**0.8 ± 0.55^{bde}**	**0.8 ± 0.29^{bcf}**
16:3n-3	**0.9 ± 0.28^{b}**	**n.d.^{c}**	**n.d.^{c}**	**0.4 ± 0.20^{bd}**	**0.4 ± 0.18^{bd}**
16:4n-3	**0.5 ± 0.17^{b}**	**n.d.^{b}**	**n.d.^{b}**	**0.5 ± 0.30^{b}**	**0.5 ± 0.21^{b}**
16:4n-1	**0.8 ± 0.24^{bc}**	**n.d.^{a}**	**n.d.^{a}**	**1.0 ± 1.01^{bc}**	**0.6 ± 0.48^{ab}**
LNA	**2.4 ± 0.04^{ef}**	**1.1 ± 0.13^{ce}**	**0.9 ± 0.08^{c}**	**5.4 ± 2.60^{d}**	**2.4 ± 0.90^{cfi}**
18:2n-4	0.4 ± 0.05	tr.	tr.	0.6 ± 0.31	0.4 ± 0.41
18:3n-6	0.4 ± 0.04	tr.	tr.	0.3 ± 0.06	0.1 ± 0.02
ALA	**4.6 ± 0.79^{b}**	**1.2 ± 0.22^{d}**	**1.5 ± 0.13^{d}**	**3.3 ± 1.12^{bd}**	**2.4 ± 0.86^{bd}**
18:4n-3	**1.4 ± 0.13^{befg}**	**0.6 ± 0.13^{c}**	**0.6 ± 0.12^{ce}**	**0.9 ± 0.47^{cdg}**	**0.9 ± 0.33^{cdg}**
20:2n-6	**0.4 ± 0.04^{a}**	**0.5 ± 0.07^{ac}**	**0.6 ± 0.05^{c}**	**1.0 ± 0.31^{b}**	**1.3 ± 0.55^{b}**
20:3n-6	0.1 ± 0.01	0.4 ± 0.04	0.4 ± 0.03	0.6 ± 0.10	0.2 ± 0.03
20:4n-6	**0.6 ± 0.09^{be}**	**5.1 ± 0.26^{a}**	**5.1 ± 0.23^{a}**	**2.0 ± 0.26^{cd}**	**2.7 ± 0.51^{c}**
20:3n-3	0.3 ± 0.03	tr.	0.1 ± 0.01	0.2 ± 0.10	0.4 ± 0.10
20:4n-3	0.3 ± 0.02	0.3 ± 0.06	0.3 ± 0.03	0.7 ± 0.22	0.4 ± 0.15
20:5n-3	**9.8 ± 1.03^{bd}**	**5.0 ± 0.18^{a}**	**8.3 ± 0.32^{bc}**	**15.0 ± 3.86^{fg}**	**15.4 ± 3.18^{fg}**
22:2n-6	n.d.	2.2 ± 0.15	1.5 ± 0.16	n.d.	n.d.
21:5n-3	0.3 ± 0.03	0.2 ± 0.03	0.5 ± 0.07	0.2 ± 0.12	0.4 ± 0.22
22:4n-6	0.8 ± 0.13	1.1 ± 0.11	1.7 ± 0.18	0.5 ± 0.08	0.6 ± 0.31

Table 2 continued

Fatty acids	*Dendrocoelopsis* sp.	*Dreissena polymorpha*	*Dreissena bugensis*	*Lumbriculus variegatus*	*Tubifex tubifex*
22:5n-6	0.1 ± 0.01	5.0 ± 0.33	3.9 ± 0.23	0.2 ± 0.04	0.1 ± 0.14
22:5n-3	**8.0 ± 1.10^{a}**	**4.8 ± 0.26^{b}**	**6.4 ± 0.39^{c}**	**1.3 ± 0.36^{ef}**	**1.9 ± 0.39^{fg}**
22:6n-3	**1.8 ± 0.37^{ce}**	**7.2 ± 0.32^{a}**	**7.6 ± 0.47^{a}**	**1.1 ± 0.29^{cd}**	**2.2 ± 2.06^{c}**
PUFA	36.3 ± 2.25	34.7 ± 1.55	39.3 ± 1.78	37.4 ± 5.59	34.7 ± 4.03
NMI 20:2	n.d.	tr.	tr.	n.d.	n.d.
NMI 20:2	n.d.	0.3 ± 0.03	0.3 ± 0.04	n.d.	n.d.
NMI 20:2	n.d.	tr.	0.1 ± 0.02	n.d.	n.d.
NMI 22:2	n.d.	0.5 ± 0.06	0.9 ± 0.10	n.d.	n.d.

Fisher LSD tests were calculated for FA indicated in bold for data of both Tables 2 and 3. Values labeled with the same letter are not significantly different at $p < 0.05$ according to the Fisher LSD test

n.d. not detected; *tr.* trace; *NMI* nonmethylene interrupted

Table 3 Mean levels of FA (mol% of total) of *P. olivacea*, A. *crymophila*, *E. setigera*, *E. viridis* from the Yenisei River, *C. plumosus* 'B' from Bugach reservoir and *C. plumosus* 'C' from Chistoe lake

Fatty acids	*Prodiamesa olivacea*	*Chironomus plumosus* 'B'	*Chironomus plumosus* 'C'	*Apatania crymophila*	*Ephemerella setigera*	*Eulimnogammarus viridis*
12:0	0.6 ± 0.09	0.6 ± 0.04	0.8 ± 0.18	0.2 ± 0.04	0.6 ± 0.06	0.3 ± 0.04
14:0	**7.7 ± 0.46^{a}**	**6.4 ± 0.29^{a}**	**5.2 ± 0.87^{e}**	**3.6 ± 0.23^{b}**	**4.4 ± 0.54^{be}**	**3.8 ± 0.55^{f}**
15:0	0.4 ± 0.04	1.2 ± 0.10	0.9 ± 0.22	0.4 ± 0.05	0.5 ± 0.04	0.3 ± 0.05
16:0	**18.1 ± 0.18^{bc}**	**18.1 ± 0.29^{bc}**	**17.6 ± 1.19^{bc}**	**21.1 ± 0.51^{b}**	**22.7 ± 1.19^{b}**	**19.0 ± 0.80^{bc}**
17:0	0.2 ± 0.00	1.1 ± 0.07	1.9 ± 0.23	0.6 ± 0.09	0.8 ± 0.02	0.6 ± 0.15
18:0	**2.9 ± 0.08^{ae}**	**6.3 ± 0.33^{d}**	**6.6 ± 0.63^{cd}**	**4.1 ± 0.40^{e}**	**5.1 ± 1.69^{de}**	**2.0 ± 0.20^{a}**
20:0	0.3 ± 0.05	0.8 ± 0.05	0.9 ± 0.10	0.5 ± 0.08	0.5 ± 0.15	0.1 ± 0.02
22:0	0.1 ± 0.02	0.2 ± 0.02	0.2 ± 0.07	0.3 ± 0.04	0.5 ± 0.24	0.1 ± 0.04
SFA	30.3 ± 0.53	35.0 ± 0.44	34.5 ± 1.54	30.8 ± 0.90	35.2 ± 2.03	26.3 ± 1.05
i-14:0	0.2 ± 0.00	0.2 ± 0.03	0.8 ± 0.19	0.1 ± 0.04	0.1 ± 0.01	0.1 ± 0.01
***ai*-15:0**	**0.6 ± 0.01^{bd}**	**1.0 ± 0.06^{bc}**	**3.7 ± 1.40^{a}**	**0.3 ± 0.04^{d}**	**0.6 ± 0.05^{bd}**	**0.3 ± 0.04^{cd}**
***i*-15:0**	**0.2 ± 0.04^{a}**	**0.3 ± 0.02^{a}**	**3.3 ± 1.32^{b}**	**0.1 ± 0.03^{a}**	**0.1 ± 0.01^{a}**	**0.1 ± 0.02^{a}**
i-15:1n-6	0.1 ± 0.02	0.2 ± 0.02	0.2 ± 0.05	0.1 ± 0.02	tr.	0.1 ± 0.03
i-16:0	0.1 ± 0.02	0.2 ± 0.01	0.4 ± 0.09	0.1 ± 0.01	0.1 ± 0.01	0.1 ± 0.01
***ai*-17:0**	**0.2 ± 0.03^{ab}**	**0.3 ± 0.02^{ab}**	**0.5 ± 0.08^{b}**	**0.4 ± 0.04^{ab}**	**0.4 ± 0.02^{ab}**	**0.3 ± 0.04^{ab}**
***i*-17:0**	**0.1 ± 0.01^{ab}**	**0.1 ± 0.01^{ae}**	**0.3 ± 0.07^{be}**	**0.1 ± 0.01^{a}**	**0.1 ± 0.02^{ae}**	**0.1 ± 0.03^{ae}**
BFA	1.5 ± 0.03	2.3 ± 0.15	9.2 ± 2.86	1.1 ± 0.13	1.4 ± 0.08	1.0 ± 0.15
14:1n-7	0.5 ± 0.12	0.3 ± 0.03	0.8 ± 0.21	0.9 ± 0.23	0.1 ± 0.04	0.1 ± 0.02
16:1n-7 + n-9	22.5 ± 0.36	14.3 ± 0.94	14.4 ± 1.70	15.1 ± 1.05	11.2 ± 0.34	10.7 ± 0.65
16:1n-5	0.4 ± 0.04	0.9 ± 0.10	0.9 ± 0.27	0.2 ± 0.03	0.3 ± 0.03	0.2 ± 0.02
17:1	0.1 ± 0.02	0.4 ± 0.07	0.9 ± 0.06	0.1 ± 0.02	0.2 ± 0.03	0.2 ± 0.05
18:1n-9	**8.7 ± 0.97^{egf}**	**6.6 ± 0.24^{fg}**	**7.3 ± 0.53^{fg}**	**10.6 ± 0.73^{e}**	**13.3 ± 1.85^{d}**	**17.8 ± 0.97^{a}**
18:1n-7	**3.6 ± 0.23^{c}**	**6.5 ± 0.43^{d}**	**6.4 ± 0.63^{bd}**	**1.3 ± 0.20^{a}**	**3.6 ± 0.33^{c}**	**3.2 ± 0.18^{ce}**
20:1n-11	**0.2 ± 0.03^{d}**	**tr.^{d}**	**n.d.^{d}**	**n.d.^{d}**	**n.d.^{d}**	**n.d.^{d}**
20:1n-9	**0.3 ± 0.05^{de}**	**0.2 ± 0.02^{e}**	**0.1 ± 0.01^{ef}**	**0.1 ± 0.02^{e}**	**tr.^{e}**	**0.6 ± 0.14^{d}**
20:1n-7	0.1 ± 0.02	0.1 ± 0.01	tr.	0.1 ± 0.02	n.d.	0.4 ± 0.11
MUFA	36.5 ± 0.68	29.3 ± 1.13	31.3 ± 2.36	29.4 ± 1.02	29.8 ± 1.55	33.4 ± 1.11
16:2n-7	0.1 ± 0.02	0.2 ± 0.02	n.d.	0.1 ± 0.04	0.1 ± 0.01	0.1 ± 0.03
16:2n-6	0.2 ± 0.03	0.1 ± 0.02	0.2 ± 0.05	0.8 ± 0.11	0.1 ± 0.02	tr.
16:2n-4	**3.8 ± 0.14^{a}**	**2.4 ± 0.24^{b}**	**0.6 ± 0.25^{cd}**	**2.2 ± 0.18^{b}**	**2.0 ± 0.10^{bf}**	**1.3 ± 0.26^{df}**

Table 3 continued

Fatty acids	*Prodiamesa olivacea*	*Chironomus plumosus* 'B'	*Chironomus plumosus* 'C'	*Apatania crymophila*	*Ephemerella setigera*	*Eulimnogammarus viridis*
16:3n-6	n.d.	0.1 ± 0.01	n.d.	0.3 ± 0.06	n.d.	n.d.
16:3n-4	**0.7 ± 0.15^{bcf}**	**1.3 ± 0.20^{cd}**	**0.2 ± 0.07^{ab}**	**1.4 ± 0.18^{c}**	**1.2 ± 0.15^{cef}**	**1.1 ± 0.20^{cef}**
16:3n-3	**0.8 ± 0.03^{d}**	**0.1 ± 0.04^{d}**	**0.3 ± 0.06^{d}**	**1.7 ± 0.26^{a}**	**0.7 ± 0.19^{bd}**	**0.4 ± 0.11^{bd}**
16:4n-3	**0.2 ± 0.04^{b}**	**0.3 ± 0.03^{b}**	**tr.^{b}**	**4.0 ± 0.35^{a}**	**0.5 ± 0.21^{b}**	**0.4 ± 0.12^{b}**
16:4n-1	**0.3 ± 0.18^{ac}**	**0.9 ± 0.12^{bc}**	**n.d.^{a}**	**1.2 ± 0.13^{b}**	**0.6 ± 0.12^{ab}**	**1.3 ± 0.34^{b}**
LNA	**4.4 ± 0.76^{dfi}**	**10.9 ± 0.55^{a}**	**9.4 ± 0.27^{b}**	**3.4 ± 0.27^{fg}**	**3.2 ± 0.66^{dfi}**	**2.5 ± 0.30^{egi}**
18:2n-4	0.5 ± 0.25	n.d.	0.2 ± 0.05	tr.	0.4 ± 0.04	0.3 ± 0.04
18:3n-6	0.8 ± 0.11	0.3 ± 0.01	0.3 ± 0.04	0.3 ± 0.04	0.5 ± 0.04	0.3 ± 0.02
ALA	**3.1 ± 0.45^{bd}**	**4.7 ± 0.50^{b}**	**8.5 ± 1.64^{a}**	**10.4 ± 0.75^{a}**	**10.0 ± 1.38^{a}**	**2.8 ± 0.40^{bd}**
18:4n-3	**1.4 ± 0.07^{bc}**	**2.8 ± 0.24^{a}**	**0.5 ± 0.07^{cf}**	**2.1 ± 0.31^{b}**	**0.9 ± 0.13^{cdg}**	**1.7 ± 0.46^{bd}**
20:2n-6	**tr.^{d}**	**tr.^{d}**	**tr.^{d}**	**tr.^{d}**	**n.d.^{d}**	**0.7 ± 0.06^{c}**
20:3n-6	0.1 ± 0.01	tr.	n.d.	0.1 ± 0.01	0.2 ± 0.05	0.2 ± 0.03
20:4n-6	**0.6 ± 0.03^{beg}**	**1.0 ± 0.07^{ef}**	**1.4 ± 0.14^{dfg}**	**0.6 ± 0.05^{b}**	**1.3 ± 0.12^{bde}**	**1.5 ± 0.25^{df}**
20:3n-3	0.1 ± 0.01	tr.	n.d.	0.1 ± 0.01	0.1 ± 0.03	0.6 ± 0.06
20:4n-3	0.3 ± 0.12	0.2 ± 0.01	n.d.	0.2 ± 0.02	0.1 ± 0.01	0.4 ± 0.05
20:5n-3	**13.7 ± 1.10^{fg}**	**8.0 ± 0.63^{b}**	**3.5 ± 0.54^{a}**	**8.7 ± 0.57^{bc}**	**11.3 ± 1.38^{cdf}**	**16.5 ± 1.03^{g}**
22:5n-6	n.d.	n.d.	n.d.	tr.	tr.	0.3 ± 0.10
22:5n-3	**0.3 ± 0.12^{deg}**	**tr.^{d}**	**n.d.^{de}**	**0.1 ± 0.04^{de}**	**0.1 ± 0.03^{deh}**	**1.5 ± 0.21^{fgh}**
22:6n-3	**0.1 ± 0.08^{de}**	**0.1 ± 0.04^{d}**	**n.d.^{d}**	**0.2 ± 0.04^{d}**	**0.1 ± 0.07^{de}**	**4.9 ± 1.11^{b}**
PUFA	31.7 ± 0.86	33.5 ± 1.13	25.1 ± 2.21	38.7 ± 1.18	33.7 ± 2.33	39.3 ± 0.91

Designations are the same as in Table 2

comparable with those in some arthropod species, *E. setigera*, *E. viridis*, and *P. olivacea* (Tables 2, 3).

All chironomids had similar dominant PUFA: 20:5n-3, LNA, ALA, with their levels being markedly different. Both populations of *C. plumosus*, 'B' and 'C', contained significant levels of LNA (Table 3). In contrast, *P. olivacea* was rich in 20:5n-3. In addition, *P. olivacea* had the highest level of 16:2n-4; and *C. plumosus* 'B' had the highest level of 18:4n-3. Studied chironomids were lacking in DHA, moreover in *C. plumosus* 'C' DHA was not detected at all (Table 3).

Like in Chironomidae, the dominant PUFA of *A. crymophila*, *E. setigera* and *E. viridis* also comprised 20:5n-3, ALA and LNA. In addition, these invertebrates had significant percentage levels of 18:4n-3 and C16 PUFA, especially 16:2n-4, 16:3n-4, 16:4n-1. In contrast to most of the invertebrates, *A. crymophila* had the highest values of 16:4n-3 and 16:3n-3 (Table 3).

In the invertebrates studied the highest values of n-3/n-6 and DHA/ARA ratios were found in *E. viridis* and *Dendrocoelopsis* sp. (Table 4). *A. crymophila* and *T. tubifex* had comparatively high values of n-3/n-6 ratio and low values of DHA/ARA. High n-3/n-6 ratios were found in *E. setigera* and *P. olivacea* however, DHA/ARA ratios were very low in these species (Table 4). In both mollusks, n-3/n-6 ratios were similar to DHA/ARA ratios. In samples of *C. plumosus* 'B' and 'C' both ratios were very low (Table 4).

Using correspondence analysis, the zoobenthic invertebrates studied were represented in a two-dimensional space according to their levels (mol% of the total) of prominent fatty acids (Fig. 2). The first dimension explained 51.65% of inertia (of total Chi-square value) of the data set, and the second dimension reproduced 13.34%. Chi-square values for both dimensions and the total Chi-square were significant ($p < 0.0001$). The first dimension (Fig. 2) demonstrated large differences between mollusks on the one hand and larvae of insects on the other. *E. viridis* and worms had an intermediate position. These positions of invertebrates in the first dimension were provided mostly by difference in their levels of 22:5n-6 and 20:1n-11 on the one hand and 16:4n-3, 16:2n-4, LNA and ALA on the other. The second dimension, although comparatively less substantial was also significant, indicating that the largest differences between *C. plumosus* and *A. crymophila* with *E. setigera* is primary due to LNA and 16:4n-3. *P. olivacea* had an intermediate position. Besides, the second dimension demonstrated differences between *T. tubifex*, *L. variegatus* and *E. viridis*, *Dendrocoelopsis* sp. provided mostly by the difference in their levels of 15:0 and 18:1n-9 (Fig. 2). Note, none of each studied species showed evident seasonal tendencies in the two-dimensional space. For example,

Table 4 Content of FA in total lipids (mg/g wet weight) of zoobenthic species from the Yenisei River, Bugach Reservoir, Rybinskoe reservoir and Chistoe lake

Fatty acids	*Dendrocoelopsis* sp.	*Dreissena polymorpha*	*Dreissena bugensis*	*Lumbriculus variegatus*	*Tubifex tubifex*	*Prodiamesa olivacea*	*Chironomus plumosus* 'B'	*Chironomus plumosus* 'C'	*Apatania crymophila*	*Ephemerella setigera*	*Eulimnogammarus viridis*
ALA	1.1 ± 0.28	0.03 ± 0.01	0.03 ± 0.003	0.3 ± 0.06	0.2 ± 0.10	0.8 ± 0.05	0.6 ± 0.11	0.6 ± 0.13	2.6 ± 0.31	2.1 ± 0.67	0.5 ± 0.12
ARA	0.2 ± 0.04	0.1 ± 0.01	0.1 ± 0.005	0.2 ± 0.05	0.2 ± 0.03	0.2 ± 0.01	0.1 ± 0.02	0.1 ± 0.02	0.1 ± 0.01	0.3 ± 0.06	0.3 ± 0.06
EPA	2.6 ± 0.65	0.1 ± 0.01	0.2 ± 0.01	1.8 ± 0.80	1.2 ± 0.09	3.6 ± 0.09	1.0 ± 0.10	0.3 ± 0.04	2.3 ± 0.28	3.1 ± 0.54	3.8 ± 1.02
DPA n-3	2.1 ± 0.21	0.1 ± 0.01	0.1 ± 0.01	0.2 ± 0.06	0.2 ± 0.01	0.1 ± 0.07	0.004 ± 0.001	n.d.	0.0 ± 0.01	0.01 ± 0.003	0.4 ± 0.06
DHA	0.5 ± 0.13	0.2 ± 0.01	0.2 ± 0.01	0.1 ± 0.06	0.2 ± 0.17	0.03 ± 0.02	0.01 ± 0.004	n.d.	0.1 ± 0.01	0.03 ± 0.02	1.1 ± 0.22
n-3 18–22 PUFA	6.9 ± 1.17	0.5 ± 0.03	0.5 ± 0.03	2.6 ± 1.05	1.9 ± 0.10	5.0 ± 0.01	1.9 ± 0.20	0.9 ± 0.17	5.6 ± 0.58	5.5 ± 1.22	6.5 ± 1.47
n-6 18–22 PUFA	1.2 ± 0.21	0.4 ± 0.03	0.3 ± 0.01	1.0 ± 0.21	0.6 ± 0.13	1.5 ± 0.29	1.3 ± 0.12	0.8 ± 0.09	1.1 ± 0.12	1.1 ± 0.16	1.1 ± 0.31
n-3/n-6	5.9 ± 0.40	1.3 ± 0.03	1.8 ± 0.05	2.8 ± 0.99	3.5 ± 0.87	3.6 ± 0.78	1.4 ± 0.09	1.12 ± 0.18	5.5 ± 0.54	4.9 ± 0.60	6.2 ± 1.07
DHA/ARA	3.3 ± 0.45	1.6 ± 0.05	1.6 ± 0.07	0.6 ± 0.11	1.2 ± 1.10	0.2 ± 0.15	0.2 ± 0.05	n.c.	0.5 ± 0.11	0.1 ± 0.04	3.7 ± 0.38
SFA	6.1 ± 0.97	0.9 ± 0.12	0.7 ± 0.07	2.6 ± 0.34	2.4 ± 0.36	6.8 ± 0.53	3.6 ± 0.31	2.2 ± 0.31	7.2 ± 0.81	6.6 ± 1.22	5.0 ± 0.99
MUFA	8.3 ± 1.35	0.5 ± 0.04	0.3 ± 0.02	2.4 ± 0.30	2.2 ± 0.59	8.7 ± 0.77	3.1 ± 0.24	2.2 ± 0.41	7.0 ± 0.75	6.3 ± 1.38	6.6 ± 1.20
PUFA	9.2 ± 1.59	0.9 ± 0.04	0.8 ± 0.05	4.3 ± 1.58	2.8 ± 0.11	8.1 ± 0.36	3.9 ± 0.38	1.8 ± 0.26	9.9 ± 1.01	8.2 ± 1.66	8.8 ± 2.01
Total	24.0 ± 3.82	2.3 ± 0.17	1.9 ± 0.10	9.8 ± 2.10	7.9 ± 1.08	24.0 ± 1.66	10.5 ± 0.88	6.8 ± 0.90	24.4 ± 2.48	21.7 ± 4.17	20.7 ± 4.19

n-3 18–22 PUFA sum of polyunsaturated FA of n-3 family with 18–22 carbon atoms; *n-6 18–22 PUFA* sum of polyunsaturated FA of n-6 family with 18–22 carbon atoms

Total total content of fatty acids, *n.c.* not calculated

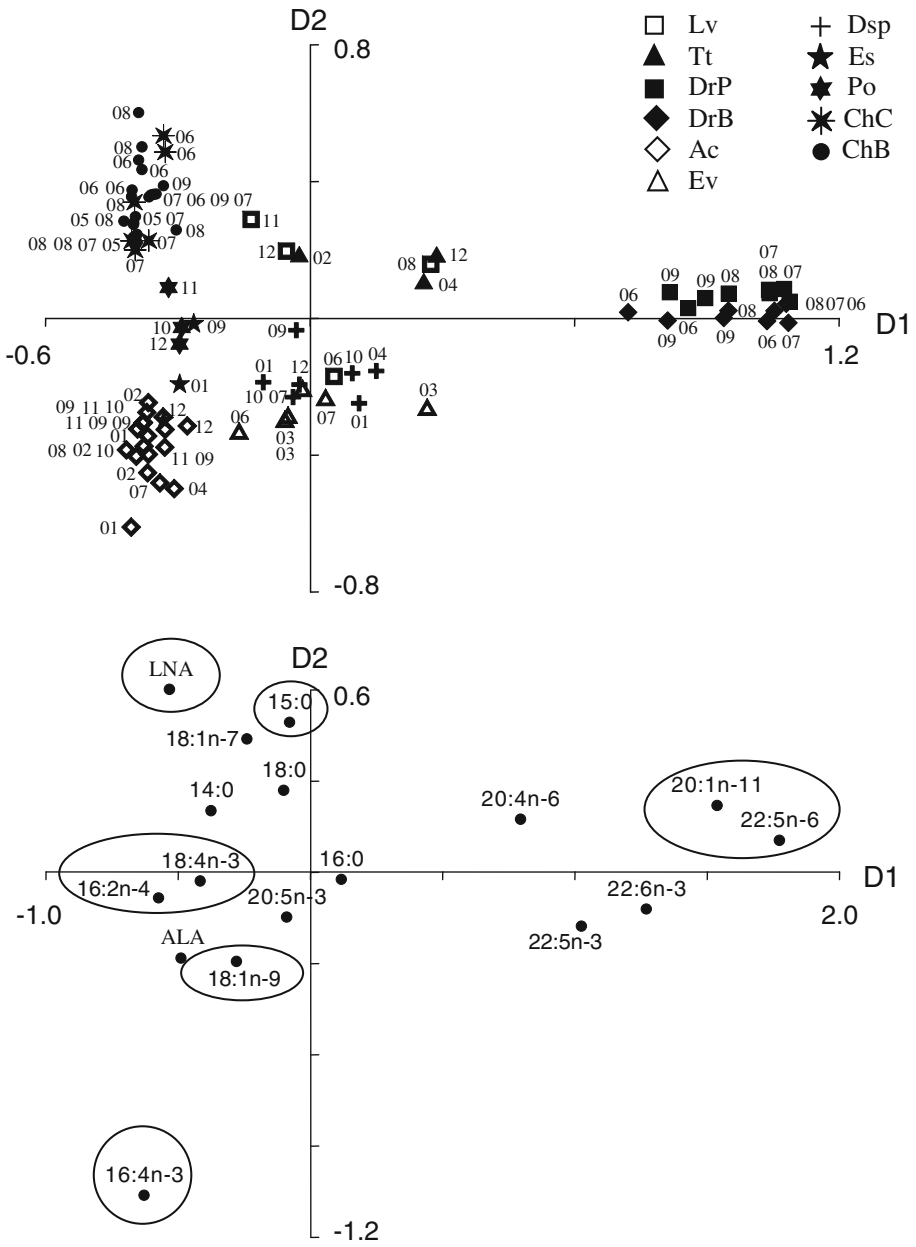

Fig. 2 Results of correspondence analysis of zoobenthic invertebrates and fatty acids (mol% of the total) represented in a two-dimensional space reproduced 65% of total inertia. *Lv*: *L. variegatus*, *Tt*: *T. tubifex*, *DrP*: *D. polymorpha*, *DrB*: *D. bugensis*, *Ac*: *A. crymophila*, *Ev*: *E. viridis*, *Dsp*: *Dendrocoelopsis sp*., *Es*: *E. setigera*, *Po*: *P. olivacea*, *ChC*: *C. plumosus* from Chistoe lake, *ChB*: *C. plumosus* from Bugach reservoir. The *numbers* indicate the months of sampling dates, e.g. 05 May, 08 August, 11 November. The FA which provided the major part of total inertia for axes D1 and D2 are *circled*

samples of *C. plumosus* collected in May, July and August were close to each other, while all samples of *C. plumosus* collected in August, were distant. The samples of *A. crymophila* collected in different seasons, such as February, August and November, were closer than the samples of winter months (Fig. 2).

To find differences in percentages of the essential and quantitatively valuable FA between large phylogenetic groups, such as Classes, we performed Tukey HSD test (Table 5). The mean levels of all eight tested FA were different among the groups. Bivalvia were markedly high in 16:0, while Crustacea and Turbellaria showed the significantly high levels of 18:1n-9. The highest level of LNA and ALA was found in Insecta. Oligochaeta and Bivalvia were rich in ARA, while the former group and Crustacea were rich in EPA. C22 n-3 PUFA were highly variable, being the most prominent in Bivalvia, Turbellaria and Crustacea (Table 5).

Discussion

We found that the FA content and composition of the studied benthic invertebrates differed significantly. Levels of essential PUFA, EPA and DHA, in the species varied by more than an order of magnitude (Tables 2, 3). Some

Table 5 Tukey HSD test on mean FA levels (mol% of the total) in groups of zoobenthic invertebrates combined as described in the text ("Materials and Methods", "Statistical Analysis")

Taxa	16:0	18:1n-9	LNA	ALA	20:4n-6	20:5n-3	22:5n-3	22:6n-3	N
Insecta	19.4 ± 0.69^{a}	8.7 ± 0.37^{a}	7.1 ± 0.43^{a}	7.5 ± 0.41^{a}	0.9 ± 0.09^{a}	8.3 ± 0.45^{a}	0.1 ± 0.17^{a}	0.1 ± 0.18^{a}	49
Oligochaeta	14.5 ± 1.84^{a}	6.1 ± 0.97^{a}	4.1 ± 1.14^{ab}	2.9 ± 1.09^{b}	2.3 ± 0.24^{b}	15.2 ± 1.19^{b}	1.6 ± 0.44^{b}	1.6 ± 0.47^{b}	7
Crustacea	19.0 ± 1.98^{a}	17.8 ± 1.05^{b}	2.5 ± 1.23^{b}	2.8 ± 1.18^{b}	1.5 ± 0.26^{ab}	16.5 ± 1.29^{b}	1.5 ± 0.47^{b}	4.9 ± 0.51^{c}	6
Turbellaria	17.7 ± 1.84^{a}	16.8 ± 0.97^{b}	2.4 ± 1.14^{b}	4.6 ± 1.09^{ab}	0.6 ± 0.24^{a}	9.8 ± 1.19^{a}	8.0 ± 0.44^{c}	1.8 ± 0.47^{b}	7
Bivalvia	31.7 ± 0.87^{b}	2.8 ± 0.46^{c}	1.0 ± 0.54^{b}	1.4 ± 0.52^{b}	5.1 ± 0.11^{c}	6.7 ± 0.57^{a}	5.6 ± 0.21^{d}	7.4 ± 0.23^{d}	16

Cells in a row labeled with the same letter are not significantly different at $p < 0.05$

authors emphasized the importance of n-3/n-6 and DHA/ARA ratios in zoobenthos because higher aquatic consumers, fish, need food with optimal FA ratios to achieve high rates of growth and reproduction and to optimize immune functioning [11, 38]. Some data collected from the literature showed that n-3/n-6 and DHA/ARA ratios in the fish food should be at least 2–3 and >0, respectively, i.e. some ARA are also needed to give good growth and reproduction [11]. In addition, the ratio values depend on trophic positions of fish, e.g., n-3/n-6 and DHA/ARA ratios in the carnivorous-benthivorous freshwater fish were 3.8 and 4.8, respectively, while for carnivorous-piscivorous fish the ratios were 2.6 and 2.7, respectively [11]. In the Yenisei River, the habitat for seven of the studied invertebrates, one of the most abundant fish species is Siberian grayling *Thymallus arcticus* (Pallas) which is benthivorous during most of its life stages. The ratios of n-3/n-6 and DHA/ARA in *Thymallus arcticus* are 9.4 and 5.5, respectively [39]. These ratios in *Thymallus arcticus* are markedly higher in comparison with those in other carnivorous-benthivorous freshwater fish species described by Ahlgren and colleagues [11].

Considering the food quality for the dominant fish *Thymallus arcticus*, the ratios in *E. viridis* and *Dendrocoelopsis* sp. are the most optimal. The larvae of *A. crymophila*, *E. setigera*, *P. olivacea* and oligochaete *T. tubifex* are of good nutritional quality in respect to the n-3/n-6 ratio, but their DHA/ARA ratios are lower than required (Table 4). Thus, the zoobenthic species from the Yenisei River are of variable food quality in respect to the fatty acid ratios.

In the Bugach reservoir, the habitat for *C. plumosus*, the most abundant benthivorous fish is *Carassius auratus gibelio* (Bloch). The mean ratios in *C. auratus* are 3.3 and 3.9, respectively (Sushchik and Makhutova, unpublished data). In contrast to the fish, *C. plumosus* had very low ratios, as a result, it was of low food quality for the population of crucian carp. Note that crucian carp of the Bugach reservoir had comparatively lower FA ratios than found in other benthivorous species [11] probably due to the food being of low biochemical quality.

We compared n-3/n-6 and DHA/ARA ratios of the studied invertebrates with available data. On average, n-3/n-6 ratios of chironomids were reported to vary from 1 to 3 [29, 30, 40]. Three chironomids studied in the present work were from different water bodies and showed differences in n-3/n-6 ratio. Both populations of *C. plumosus* inhabited black silts and had a relatively low n-3/n-6 ratio, within 1–2, while the population of *P. olivacea*, inhabited a river site rich in epilithic biofilms, had significantly higher value, >3. Hence, *C. plumosus* showed an n-3/n-6 ratio close to the range reported in the literature, while riverine *P. olivacea* was enriched in n-3 PUFA.

The studied oligochaetes and larvae of Trichoptera and Ephemeroptera had ratios very similar to the literature data [29, 30, 40–42].

Many researchers reported n-3/n-6 and DHA/ARA ratios in Gammaridae as 1–3 and ≤1, respectively [29, 32, 34, 41, 43, 44]. These values were significantly lower than those for the gammarids in the present study (Table 4). It is noteworthy that the studied *E. viridis* had n-3/n-6 and DHA/ARA ratios similar to those of predatory *Mysis relicta* [45].

There are many data on the FA composition of various taxa of mollusks, except for the dreissenids. The FA composition of mollusks is highly variable. Some representatives of mollusks, especially bivalves, have high levels of EPA and DHA [46–49], while others, especially gastropods, have high values of n-6 PUFA, 22:4n-6, 20:4n-6 and LNA [50, 51]. The mussels of *D. polymorpha* and *D. bugensis* in the present study were rich both in n-3 and n-6 C20-22 PUFA (Table 2). The bivalve mollusk *Potamocorbula amurensis* had the ratios similar to those in the studied dreissenids, n-3/n-6 ca. 2.5 and DHA/ARA ca. 2 [46].

The data on the FA composition of planarians are scarce. The only paper that describes the FA composition of phospholipids in the planarian *Dugesia anceps* is Ref.[52]. Both planarians, *D. anceps* studied by Politi and colleagues [52], and *Dendrocoelopsis* sp., studied in the present work, were characterized by unusually high levels of 22:5n-3. The level of this acid in the studied

Dendrocoelopsis sp. was close to 20:5n-3, and it was 2–10 times higher than that of 22:6n-3 (Table 2). In contrast to the species studied in the present work, *D. anceps* had significant levels of n-6 PUFA, 20:4n-6, LNA and 22:5n-6 [52]. Ratios of n-3/n-6 and DHA/ARA in phospholipids of *D. anceps* were much lower than those in *Dendrocoelopsis* sp.

We used FA trophic markers to elucidate nutritional preferences of the studied invertebrates. We considered increased levels of C16 PUFA of n-1, n-4, n-7 family and 20:5n-3 in biomass of the animals as markers of consumption of diatoms. *P. olivacea*, *A. crymophila*, *E. setigera*, *C. plumosus* 'B' and *E. viridis* accumulated C16 PUFA of n-1, n-4, n-7 family and 20:5n-3, therefore, a significant part of their diet probably comprises diatoms. Diatoms were also present in diets of *Dendrocoelopsis* sp. and *L. variegatus*, but in comparatively lower proportions. High levels of C16 and C18 PUFA of n-3 and n-6 family in *A. crymophila*, both *C. plumosus* populations and *E. setigera* indicated that green algae and cyanobacteria were probably abundant in their diets. Hence, *A. crymophila*, *E. setigera* and *C. plumosus* 'B' probably had a mixed diet. High levels of bacterial FA and C18–22 SFA was found in deposit-feeding *C. plumosus* 'C', *T. tubifex* and *L. variegatus*, indicating that detritus composed a significant part of their diets. Content of DHA and ratios of 18:1n-9/18:1n-7 and PUFA/SFA were reported to be high in carnivorous species [53–55]. Thus, *E. viridis*, which contained the highest value of DHA and the highest 18:1n-9/18:1n-7 and PUFA/SFA ratios among the studied benthic invertebrates, seemed to be partly a carnivore. In spite of the above-mentioned ratios in *Dendrocoelopsis* sp. being moderate, planarians are known to be carnivores [56, 57].

We suppose that benthic organisms have variable requirements in dietary FA, essentially determined by genetic and metabolic factors. To meet such requirements, most zoobenthic species need to feed selectively and to have the capacity to selectively retain and (or) convert dietary FA, which is reflected in the FA composition of their bodies.

Some authors have discussed different feeding strategies of zoobenthic species, as detritivorous, omnivorous, carnivorous [e.g. 33, 54]. Using the canonical correspondence analysis we obtained evidence that feeding strategy can be of importance to predetermine the fatty acid profile of a zoobenthic species, however, the phylogenetic position of a species is a more powerful factor which results in close FA composition even if taxonomically close species or populations inhabit different places. We initially suggested that a seasonal variation within each invertebrate's species composition is a very important factor. However, most species formed distinct groups in the two-dimensional space of the multivariate analysis. Note that these groups comprised samples of the same species taken in various seasonal periods (Table 1). One can easily see that phylogenetic differences were much larger than seasonal ones (Fig. 2). Thus, the seasonal variations in the FA composition of the zoobenthos were obviously a factor of secondary importance.

In correspondence analysis of the FA composition, we found large differences among mollusks, larvae of insects, and worms. However, samples of the crustacean *E. viridis* and the planarian *Dendrocoelopsis* sp. are very close to each other (Fig. 2). Although these species are very phylogenetically distant (Fig. 1), they both feed like carnivores, at least partly.

D. polymorpha and *D. bugensis* differ from other species by feeding strategy (filter feeders) and taxonomic position (particular phylum), and they were sampled from another water body. As a result, all samples of dreissenids formed the group that was the most distant from others (Fig. 2). *A. crymophila* and *E. setigera*, which formed a joint group, belonged to the same class Insecta (Figs. 1, 2). In addition, they inhabited the same site (Table 1). Note that samples of the two populations of the chironomid *C. plumosus*, although taken in waters from geographically very distant regions, formed a joint group, too. Obviously, populations of the same species have the close metabolic processes including FA biosynthesis and conversion capacity of dietary FA. Alternatively, *C. plumosus* has selective feeding [4] and thereby might have the same feeding spectrum even in different water bodies. Nevertheless, we consider the phylogenetic proximity as a factor that mostly determines similarity in FA profiles of the two different populations of *C. plumosus*. Another species of chironomids, *P. olivacea*, inhabitant of the river, formed a small separate group (Fig. 2).

Oligochaetes, *L. variegatus* and *T. tubifex,* showed variable levels of most FA, therefore, they were the only phylogenetic group that did not show a clear trend in the multidimensional analysis (Fig. 2). This finding is probably explained by the feeding strategy of the Oligochaetes. Due to detritivorous feeding, their diet might change strongly during the studied period, and FA profiles of their bodies reflected this variation in the diet.

It is important to note that positions of *C. plumosus*, *P. olivacea*, and *A. crymophila* with *E. setigera* were rather close to each other in the first dimension, which explained the major part of the total inertia (Fig. 2). All of these species are of the same class, Insecta, but were sampled from different water bodies (the Yenisei River, the Chistoe lake and the Bugach reservoir). Moreover, their feeding strategies are variable. Therefore, the FA profiles of the studied species of Insecta were likely primarily dependent on the genetically predetermined FA metabolism rather than on the biochemical composition of their diet.

Besides the differences in FA profiles between the particular species studied, we revealed significant variation in the mean levels of essential PUFA for large taxa which joined several species (Table 5). It is interesting to remark that C22 n-3 PUFA are depleted in the phylogenetically advanced group, Insecta, compared to that in worms, mollusks and crustaceans. It is well known that DHA is crucial for nervous system functioning [9] and enriched in neural tissues of highly organized animals. It is surprising that the larvae of Insecta which have a rather well-developed nervous system and complicated behavior do not evidently possess a mechanism for accumulating C22 n-3 PUFA.

In general, the fatty acid content and composition of the studied zoobenthic species significantly differed, including the essential PUFA and the FA ratios which are important factors of biochemical food quality for fish. *E. viridis* (Crustacea, Gammaridae) and *Dendrocoelopsis* sp. (Turbellaria) were of the highest nutritional value for carnivorous-benthivorous fish. Answering the initially formulated questions we can conclude that: (1) most phylogenetically close species inhabiting the same water body have similar fatty acid spectra; (2) the populations of the same species inhabiting different water bodies, e.g., the populations of *C. plumosus*, may have similar fatty acid composition; (3) just as trophic strategies, phylogenetic factors seem to be the important determinants of fatty acid profiles in benthic invertebrates.

Acknowledgments The work was supported by grants from the Russian Foundation for Basic Research (RFBR) No. 09-04-01085 and No. 08-05-00095, by "Thematic plan programs" from the Ministry of Education and Sciences of Russian Federation (Theme B-4 of Siberian Federal University).

References

1. Desvilettes Ch, Bourdier G, Amblard C, Barth B (1997) Use of fatty acids for the assessment of zooplankton grazing on bacteria, protozoans and microalgae. Freshw Biol 38:629–637
2. Leveille JC, Amblard C, Bourdier G (1997) Fatty acids as specific algal markers in a natural lacustrian phytoplankton. J Plankton Res 19:469–490
3. Ederington M, McManus GB, Harvey R (1995) Trophic transfer of fatty acids, sterols, and a triterpenoid alcohol between bacteria, a ciliate, and the copepod *Acartia tonsa*. Limnol Oceanogr 40:860–867
4. Gladyshev MI, Sushchik NN, Skoptsova GN, Parfentsova LS, Kalachova GS (1999) Use of biochemical markers provides evidence of selective feeding in zoobenthic omnivorous organisms of a fish-rearing pond. Doklady Biol Sci 364:67–69
5. Gladyshev MI, Emelianova AY, Kalachova GS, Zotina TA, Gaevsky NA, Zhilenkov MD (2000) Gut content analysis of *Gammarus lacustris* from Siberian lake using biochemical and biophysical methods. Hydrobiologia 431:155–163
6. Brett MT, Muller-Navarra DC (1997) The role of highly unsaturated fatty acids in aquatic foodweb processes. Freshw Biol 38:483–499
7. Muller-Navarra DC, Brett MT, Liston AM, Goldman CR (2000) A highly unsaturated fatty acid predicts carbon transfer between primary producers and consumers. Nature 403:74–77
8. Arts MT, Ackman RG, Holub BJ (2001) 'Essential fatty acids' in aquatic ecosystems: a crucial link between diet and human health and evolution. Can J Fish Aquat Sci 58:122–137
9. Lauritzen L, Hansen HS, Jorgensen MH, Michaelsen KF (2001) The essentiality of long chain n-3 fatty acids in relation to development and function of the brain and retina. Prog Lipid Res 40:1–94
10. Broadhurst CL, Wang Y, Crawford MA, Cunnane SC, Parkington JE, Schmidt WF (2002) Brain-specific lipids from marine, lacustrine, or terrestrial food resources: potential impact on early African *Homo sapiens*. Comp Biochem Physiol B 131:653–673
11. Ahlgren G, Vrede T, Goedkoop W (2009) Fatty acid ratios in freshwater fish, zooplankton and zoobenthos—are there specific optima? In: Arts MT, Brett MT, Kainz MJ (ed) Lipids in aquatic ecosystems, Springer, Dordrecht
12. Lim C, Ako H, Brown CL, Hahn K (1997) Growth response and fatty acid composition of juvenile *Penaeus uannamei* fed different sources of dietary lipid. Aquaculture 151:143–153
13. Deerign MJ, Fielder DR, Hewitt DR (1997) Growth and fatty acid composition of juvenile leader prawns, *Penaeus monodon*, fed different lipids. Aquaculture 151:131–141
14. Milke LM, Bricelj VM, Parrish CC (2004) Growth of postlarval sea scallops, *Placopecten magellanicus*, on microalgal diets, with emphasis on the nutritional role of lipids and fatty acids. Aquaculture 234:293–317
15. Özyurt G, Duysak Ö, Akamca E, Tureli C (2006) Seasonal changes of fatty acids of cuttlefish *Sepia officinalis* L. (Mollusca: Cephalopoda) in the north eastern Mediterranean sea. Food Chem 95:382–385
16. Sinanoglou VJ, Meimaroglou D, Miniadis-Meimaroglou S (2008) Triacylglycerols and their fatty acid composition in edible Mediterranean molluscs and crustacean. Food Chem 110:406–413
17. Napolitano GE (1998) Fatty acids as trophic and chemical markers in freshwater ecosystems. In: Arts MT, Wainman BC (eds) Lipids in freshwater ecosystems. Springer, New York
18. Brett MT, Muller-Navarra DC, Ballantyne AP, Ravet JL, Goldman CR (2006) *Daphnia* fatty acid composition reflects that of their diet. Limnol Oceanogr 51:2428–2437
19. Muller-Navarra DC (2006) The nutritional importance of polyunsaturated fatty acids and their use as trophic markers for herbivorous zooplankton: does it contradict? Arch Hydrobiol 164:501–513
20. Weers PMM, Siewertsen K, Gulati RD (1997) Is the fatty acid composition of *Daphnia galeata* determined by the fatty acid composition of the ingested diet? Freshw Biol 48:731–738
21. Von Elert E (2002) Determination of limiting polyunsaturated fatty acids in *Daphnia galeata* using a new method to enrich food algae with single fatty acids. Limnol Oceanogr 47:1764–1773
22. Gladyshev MI, Sushchik NN, Makhutova ON, Dubovskaya OP, Kravchuk ES, Kalachova GS, Khromechek EB (2010) Correlations between fatty acid composition of seston and zooplankton and effects of environmental parameters in a eutrophic Siberian reservoir. Limnologica 40:343–357
23. Graeve M, Albers C, Kattner G (2005) Assimilation and biosynthesis of lipids in arctic *Calanus* species based on feeding experiments with a ^{13}C labelled diatom. J Exp Mar Biol Ecol 317:109–125
24. Veloza AJ, Chu F-LE, Tang KW (2006) Trophic modification of essential fatty acids by heterotrophic protists and its effects on the fatty acid composition of the copepod *Acartia tonsa*. Mar Biol 148:779–788
25. Smyntek PM, Teece MA, Schulz KL, Storch AJ (2008) Taxonomic differences in the essential fatty acid composition of

groups of freshwater zooplankton relate to reproductive demands and generation time. Freshw Biol 53:1768–1782
26. Ravet JL, Brett MT, Arhonditsis GB (2010) The effects of seston lipids on zooplankton fatty acid composition in Lake Washington, Washington, USA. Ecology 91:180–190
27. Wallis JG, Watts JL, Browse J (2002) Polyunsaturated fatty acid synthesis: what will they think of next? Trends Biochem Sci 27: 467–473
28. Goedkoop W, Demandt M, Ahlgren G (2007) Interactions between food quantity and quality (long-chain polyunsaturated fatty acids concentrations) effects on growth and development of *Chironomus riparius*. Can J Fish Aquat Sci 64:425–436
29. Sushchik NN, Gladyshev MI, Moskvicheva AV, Makhutova ON, Kalachova GS (2003) Comparison of fatty acid composition in major lipid classes of the dominant benthic invertebrates of the Yenisei river. Comp Biochem Physiol B 134:111–122
30. Bell JG, Ghioni C, Sargent JR (1994) Fatty acid composition of 10 freshwater invertebrates which are natural food organisms of Atlantic salmon parr (*Salmo salar*); a comparison with commercial diet. Aquaculture 128:301–313
31. Torres-Ruiz M, Wehr JD, Perrone AA (2010) Are net-spinning caddisflies what they eat? An investigation using controlled diets and fatty acids. J N Am Benthol Soc 29:803–813
32. Maazouzi C, Masson G, Izquierdo MS, Pihan J-C (2007) Fatty acid composition of the amphipod *Dikerogammarus villosus*: Feeding strategies and trophic links. Comp Biochem Physiol A 147:868–875
33. Kraffe E, Grall J, Le Duff M, Soudant P, Marty Y (2008) A striking parallel between cardiolipin fatty acid composition and phylogenetic belonging in marine bivalves: a possible adaptative evolution? Lipids 43:961–970
34. Makhutova ON, Sushchik NN, Kalachova GS, Ageev AV (2009) Fatty acid content and composition of freshwater planaria *Dendrocoelopsis* sp. (Planariidae, Turbellaria, Platyhelminthes) from the Yenisei River. J Sib Fed Univ Biol 2:135–144
35. Christie WW (1989) Gas Chromatography and Lipids. A Practical Guide. The Oily Press, England
36. Campbell RC (1967) Statistics for Biologists, University Press, Cambridge
37. Halanych KM (2004) The new view of animal phylogeny. Annu Rev Ecol Evol Syst 35:229–256
38. Arts MT, Kohler CC (2009) Health and condition in fish: the influence of lipids on membrane competency and immune response. In: Arts MT, Brett MT, Kainz MJ (eds) Lipids in aquatic ecosystems, Springer, Dordrecht
39. Sushchik NN, Gladyshev MI, Kalachova GS, Makhutova ON, Ageev AV (2006) Comparison of seasonal dynamics of the essential PUFA contents in benthic invertebrates and grayling *Thymallus arcticus* in the Yenisei river. Comp Biochem Physiol B 145:278–287
40. Goedkoop W, Sonesten L, Ahlgren G, Boberg M (2000) Fatty acids in profundal benthic invertebrates and their major food resources in Lake Erken, Sweden: seasonal variation and trophic indications. Can J Fish Aquat Sci 57:2267–2279
41. Sushchik NN, Gladyshev MI, Kravchuk ES, Ivanova EA, Ageev AV, Kalachova GS (2007) Seasonal dynamics of long-chain polyunsaturated fatty acids in littoral benthos in the upper Yenisei River. Aquat Ecol 41:349–365
42. Torres-Ruiz M, Wehr JD, Perrone AA (2007) Trophic relations in a stream food web: importance of fatty acids for macroinvertebrate consumers. J N Am Benthol Soc 26:509–522
43. Biandolino F, Prato E (2006) A preliminary investigation of the lipids and fatty acids composition of *Gammarus aequicauda* (Crustacea: Amphipoda) and its main food source. J Mar Biol Ass 86:345–348
44. Kolanowski W, Stolyhwo A, Grabowski M (2007) Fatty acid composition of selected fresh water gammarids (Amphipoda, Crustacea): a potentially innovative source of omega-3 LC PUFA. J Am Oil Chem Soc 84:827–833
45. Schlechtriem Ch, Arts MT, Johannsson OE (2008) Effect of long-term fasting on the use of fatty acids as trophic markers in the opossum shrimp *Mysis relicta*—a laboratory study. J Great Lakes Res 34:143–152
46. Canuel EA, Cloern JE, Ringelberg DB, Guckert JB, Rau GH (1995) Molecular and isotopic tracers used to examine sources of organic matter and its incorporation into the food webs of San Francisco Bay. Limnol Oceanogr 40:67–81
47. Murphy KJ, Mooney BD, Mann NJ, Nichols PD, Sinclair AJ (2002) Lipid, FA, and sterol composition of New Zealand green lipped mussel *(Perna canaliculus)* and Tasmanian blue mussel *(Mytilus edulis)*. Lipids 37:587–595
48. Berge J-P, Barnathan G (2005) Fatty acids from lipids of marine organisms: molecular biodiversity, roles as biomarkers, biologically active compounds, and economical aspects. Adv Biochem Eng Biotechnol 96:49–125
49. Pernet F, Tremblay R, Comeau L, Guderley H (2007) Temperature adaptation in two bivalve species from different thermal habitats: energetics and remodelling of membrane lipids. J Exp Biol 210:2999–3014
50. Fried B, Rao KS, Sherma J, Huffman JE (1993) Fatty acid composition of *Goniobasis virginica*, *Physa* sp. and *Viviparus malleatus* (Mollusca: Gastropoda) from lake Musconetcong, New Jersey. Biochem Syst Ecol 21:809–812
51. Zhukova N (2007) Lipid classes and fatty acid composition of the tropical Nudibranch mollusks *Chromodoris* sp. and *Phyllidia coelestis*. Lipids 42:1169–1175
52. Politi LE, De Santos SV, De Linares LV (1992) Phospholipids and fatty acids in intact and regenerating *Dugesia anceps*, a fresh water planaria. Zool Sci 9:671–674
53. Cripps GC, Atkinson A (2000) Fatty acid composition as an indicator of carnivory in Antarctic krill, *Euphausia superba*. Can J Fish Aquat Sci 57:31–37
54. Falk-Petersen S, Hagen W, Kattner G, Clarke A, Sargent J (2000) Lipids, trophic relationships, and biodiversity in Arctic and Antarctic krill. Can J Fish Aquat Sci 57:178–191
55. Stevens CJ, Deibel D, Parrish CC (2004) Species-specific differences in lipid composition and omnivory indices in Arctic copepods collected in deep water during autumn (North Water Polynya). Mar Biol 144:905–915
56. Cazzaniga NJ, Tamburi N, Carrizo M, Ponce GF (2002) Feeding *Girardia anceps* (Platyhelminthes: Tricladida) in the laboratory. J Freshw Ecol 17:93–98
57. Tranchida MC, Macia A, Brusa F, Micieli MV, Garcia JJ (2009) Predation potential of three flatworm species (Platyhelminthes: Turbellaria) on mosquitoes (Diptera: Culicidae). Biol Control 49:270–276

Lipids (2011) 46:723–740
DOI 10.1007/s11745-011-3549-x

ORIGINAL ARTICLE

Characteristics of Fatty Acid Composition of the Deep-Sea Vent Crab, *Shinkaia crosnieri* Baba and Williams

Hiroaki Saito

Received: 1 November 2010 / Accepted: 19 January 2011 / Published online: 12 April 2011

Abstract The neutral and polar lipids of the Galatheidae vent crab, *Shinkaia crosnieri*, with its eggs were studied to assess its lipid physiology and trophic relationship at hydrothermal vents. The vent crab obtained many of its lipids from *Bathymodiolus* mussels and chemosynthetic microorganisms which live on a mat of long, silky setae on the crab body as exosymbionts. In all lipid classes, the major monounsaturated fatty acids were 16:1n-7 and 18:1n-7, which originate from bacteria. The major polyunsaturated fatty acids (PUFA) in the triacylglycerols were 16:2n-4, 18:2n-4, 18:2n-7, 18:3n-4,7,10, and 16:2n-3, while those of the crab polar lipids were 16:2n-4, 18:2n-4, 18:3n-4,7,10, 20:4n-6 (arachidonic acid), 20:5n-3 (icosapentaenoic acid), and 22:6n-3 (docosahexaenoic acid) in the phosphatidylethanolamine, and 16:2n-4, 18:2n-4, and 18:3n-4,7,10, with noticeable levels of 20:4n-6, 20:5n-3, and 22:6n-3 in the phosphatidylcholine. In the crab and its eggs, TAG and phospholipid PUFA consisted primarily of n-4 family (n-4 and n-7) methylene-interrupted PUFA with n-3 and n-6 PUFA. The unique fatty acid composition mix of n-3, n-4, and n-6 PUFA in *S. crosnieri* lipids suggests the vent crab utilizing chemosynthetic bacteria, which produce both unusual n-4 and normal n-3 and n-6 PUFA. Such unique fatty acid composition differs from that reported for other common marine animals, which depend on organic matter derived from phytoplankton lipids.

Keywords Chemoecology · Chemosynthesis · Food chain · Geothermal energy · Hydrothermal vents · Polyunsaturated fatty acids · Symbiotic microorganisms

H. Saito (✉)
National Research Institute of Fisheries Science,
2-12-4 Fuku-ura, Kanazawa-ku, Yokohama 236-8648, Japan
e-mail: hiroakis@affrc.go.jp

Abbreviations

ARA	Arachidonic acid
DHA	Docosahexaenoic acid
DMA	Dimethylacetals
DMOX	4,4-Dimethyloxazoline
EPA	(E)icosapentaenoic acid
GC–MS	Gas chromatography–mass spectrometry
MUFA	Monounsaturated fatty acid
NMR	Nuclear magnetic resonance
PC	Phosphatidylcholine
PE	Phosphatidylethanolamine
PUFA	Polyunsaturated fatty acids
TAG	Triacylglycerols
TFA	Total fatty acids

Introduction

All marine animals contain n-3 polyunsaturated fatty acids (PUFA), which originate from both phytoplankton and symbiotic microorganisms, depending on solar energy [1], and from unique deep-sea barophilic bacteria [2, 3]. In particular, marine animals contain high levels of long-chain n-3 PUFA, such as docosahexaenoic acid (DHA, 22:6n-3) and icosapentaenoic acid (EPA, 20:5n-3), in both their depot and tissue lipids [1, 4]. Similarly, n-6 PUFA, such as linoleic acid (LA, 18:2n-6) and arachidonic acid (ARA, 20:4n-6), are generally vital for terrestrial animals [5, 6]. Either n-3 or n-6 PUFA usually dominate in marine or terrestrial animals, especially in their cell membrane phospholipids.

In the deep sea, many nutritional constituents are provided by the fall of organic matter from the surface (the detrital food chain) and vertical migrations of both

zooplankton and micronekton (the grazing food chain) [7]. Not only do all marine animals in the upper water layers gain nutrition through the marine grazing food chain, but also benthic animals involved in the detrital food chain on or near the ocean bottom in some communities are indirectly supported by surface phytoplankton [1, 8].

However, in previous papers [9, 10], several novel unusual n-4 family PUFA (n-1, n-4, and n-7 non-methylene-interrupted PUFA and n-4 and n-7 methylene-interrupted PUFA) were observed in the lipids of vent bivalves (*Calyptogena* clams and *Bathymodiolus* mussels). Both vent Vesicomyidae clams (Bivalvia, Veneroida, genera *Vesicomya* and *Calyptogena*) and *Bathymodiolus* mussels (Bivalvia, Mytiloida, Mytilidae) are important members of the community that are supported by chemosynthetic bacteria [11–13]. Their major PUFA consist of only the n-4 family PUFA and were completely lacking in n-3 and n-6 PUFA [9, 10]. They assimilate the products and energy from chemosynthetic symbionts [14–16], which use only geothermal energy and minerals from the vents. The chemosynthetic bacteria essential for these communities must use geothermal energy and nutrients originating from the vents, and be independent of food sources originating from photosynthesis [9, 11, 17].

In deep-sea hydrothermal vents, crustaceans were also found as other important members of the community (Figs. 1, 2, 3). Vent Galatheidae crab, *Shinkaia crosnieri* Baba and Williams [18], is a typical member and feeds on polychaetes and "culture" filamentous bacteria on their abdominal surface [19, 20]. Its phylogeny has begun to be studied [21], but there is no information on the chemical components and trophic relationship between the crab and its symbionts. Although isolation and cultivation of symbiotic marine microorganisms from their hosts is very difficult, particularly in vent organisms, we are able to know their lipid physiology by studying the host lipids, which reflect those of the symbionts. In the present paper, the fatty acids of the lipids in the crab, which were sampled near hydrothermal vents on the Iheya Ridge, Mid-Okinawa Trough (at a depth of 1,005 m), were analyzed to determine trophic relationships at hydrothermal vents.

Fig. 1 *Shinkaia crosnieri* Baba and Williams, 1998, sampled by the submersible *Shinkai 2000*, 115 mm, dorsal view. It bears *Beggiatoa*-type filamentous bacteria on abdominal surface. After measurements of body length and weight of *S. crosnieri*, the body (whole body with filamentous epibiotic bacteria) and eggs were separated

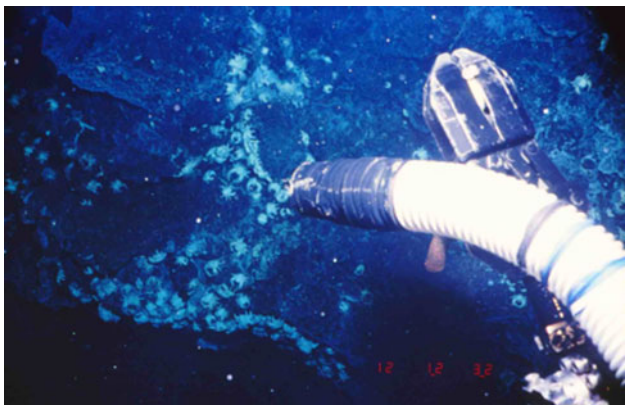

Fig. 2 The sampling site of *S. crosnieri*. The deep-sea crab was caught at the hydrothermal vents at the depth of 1,047 m at 27°47′N and 126°54′E on the Iheya Ridge, Mid Okinawa Trough in the East China Sea on May 12, 1999 (No. 1097 dive for the submersible "*Shinkai 2000*" belonging to the Japan Marine Science and Technology Center)

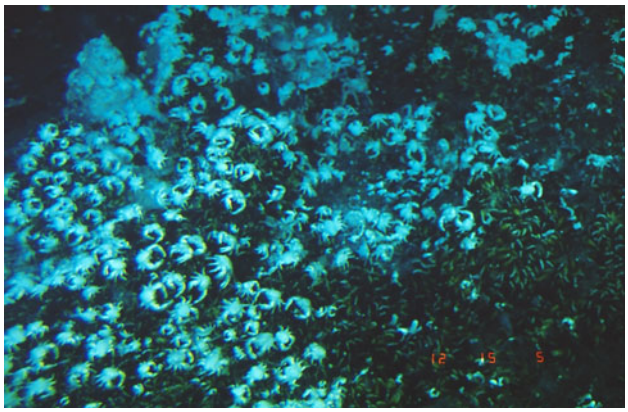

Fig. 3 The swarm of the vent crab on the colony of the mussel *B. platifrons* at the hydrothermal vents on the Iheya Ridge

Materials and Methods

Materials

Specimens of the crab *Shinkaia crosnieri*, were collected during a survey by the submersible *Shinkai 2000*, which belongs to the Japan Marine Science and Technology Center, at a depth of 1,005 m at 27°47′N and 126°54′E on

Table 1 Biological data of the *Shinkaia crosnieri*

Scientific name	Sample no.	Sex	Date	Locality		Depth (m)	Temperature (°C)	Length (mm)	Width (mm)	Weight (g)
Shinkaia crosnieri										
	1	–	May 12, 1999	Iheya Ridge	East China Sea	27°47.18′N 126°53.96′E	1,019	4.6	41	31	22.8
	1	–	May 12, 1999	Iheya Ridge	East China Sea	27°47.18′N 126°53.96′E	1,019	4.6	41	30	22.0
	1	–	May 12, 1999	Iheya Ridge	East China Sea	27°47.18′N 126°53.96′E	1,019	4.6	45	30	23.8
	1	–	May 12, 1999	Iheya Ridge	East China Sea	27°47.18′N 126°53.96′E	1,019	4.6	38	28	18.1
	1	–	May 12, 1999	Iheya Ridge	East China Sea	27°47.18′N 126°53.96′E	1,019	4.6	50	40	41.4
	1	–	May 12, 1999	Iheya Ridge	East China Sea	27°47.18′N 126°53.96′E	1,019	4.6	43	32	24.8
	1	–	May 12, 1999	Iheya Ridge	East China Sea	27°47.18′N 126°53.96′E	1,019	4.6	45	32	20.5
	1	–	May 12, 1999	Iheya Ridge	East China Sea	27°47.18′N 126°53.96′E	1,019	4.6	44	31	22.6
	1	–	May 12, 1999	Iheya Ridge	East China Sea	27°47.18′N 126°53.96′E	1,019	4.6	40	28	16.1
	1	–	May 12, 1999	Iheya Ridge	East China Sea	27°47.18′N 126°53.96′E	1,019	4.6	58	43	49.1
	1	–	May 12, 1999	Iheya Ridge	East China Sea	27°47.18′N 126°53.96′E	1,019	4.6	59	43	54.2
	1	–	May 12, 1999	Iheya Ridge	East China Sea	27°47.18′N 126°53.96′E	1,019	4.6	61	44	71.5
	1	–	May 12, 1999	Iheya Ridge	East China Sea	27°47.18′N 126°53.96′E	1,019	4.6	62	43	53.5
	1	–	May 12, 1999	Iheya Ridge	East China Sea	27°47.18′N 126°53.96′E	1,019	4.6	58	40	59.6
	1	–	May 12, 1999	Iheya Ridge	East China Sea	27°47.18′N 126°53.96′E	1,019	4.6	59	42	59.0
		–							35.8 ± 1.6	49.6 ± 2.3	37.3 ± 4.9
	2	Female	May 12, 1999	Iheya Ridge	East China Sea	27°47.18′N 126°53.96′E	1,019	4.6	42	28	19.59
	2	Female	May 12, 1999	Iheya Ridge	East China Sea	27°47.18′N 126°53.96′E	1,019	4.6	43	31	19.87
		Female							29.5 ± 1.5	42.5 ± 0.5	19.7 ± 0.1

Results are expressed as mean ± standard error ($n = 2$–15). *S. crosnieri* were collected by #1097 dive of *Shinkai 2000*

Two females holded eggs, and the body (whole body with filamentous epibiotic bacteria) and eggs were separated

the Iheya Ridge of the East China Sea. The specimens are described in detail in Table 1 (Figs. 1, 2, 3). The morphological data of the specimens are presented in Fig. 1. A total of 32 specimens (mean weight: 23.4 ± 1.4 g) was collected, out of which 15 randomly selected specimens (sample No. 1; mean length: 35.8 ± 1.6 cm, mean width: 49.6 ± 2.3 cm, mean weight: 37.3 ± 4.9 g in Table 1) were considered for lipid analysis. Two female specimens (sample No. 2; mean length: 29.5 ± 1.5 cm, mean width: 42.5 ± 0.5 cm, mean weight: 19.7 ± 0.1 g in Table 1) laden with eggs were also analyzed. After measurements of body length and weight of *S. crosnieri*, the eggs were separated from the bodies.

Lipid Extraction and Analysis of Lipid Classes

Each specimen (whole body with filamentous epibiotic bacteria) was immersed in a reagent mixture containing chloroform and methanol (2:1, v/v) after the biological data were measured. The lipids of the specimens were individually analyzed. Briefly, each sample (samples No. 1 and 2 in Tables 1, 2) was homogenized in the same reagent mixture as described above, and the crude lipid of each homogenized sample was extracted according to the Folch extraction procedure [22]. The eggs (sample No. 3 in Table 2), which were carried outside by the two female crabs, were also individually extracted by the same kinds of solvents.

The extracted crude lipids were individually separated into classes on silicic acid columns (Merck and Co. Ltd., Kieselgel 60, 70–230 mesh) and a quantitative analysis of the lipid constituents was performed using gravimetric analysis of the fractions collected from column chromatography [23]. The first eluate (dichloromethane/*n*-hexane, 2:3, v/v: first fraction) was collected as steryl ester, wax ester, and diacylglyceryl ether fractions. This was followed by dichloromethane (second fraction) which eluted the triacylglycerols (TAG) and dichloromethane/ether (35:1, v/v: third fraction) which eluted the sterols. Dichloromethane/ether (9:1, v/v: fourth fraction) eluted the diacylglycerols; dichloromethane/methanol (9:1, v/v: fifth fraction) eluted the free fatty acids; dichloromethane/methanol (1:5, v/v: sixth fraction) eluted the phosphatidylethanolamine (PE); dichloromethane/methanol (1:20,v/v: seventh fraction) eluted the ceramide aminoethyl phosphonate with other minor phospholipids; and dichloromethane/methanol (1:50, v/v: eighth fraction) eluted phosphatidylcholine (PC).

The lipid classes from each lipid fraction were identified by comparison of the retention (R_f) values of standards using plate thin-layer chromatography (Merck & Co. Ltd., Kieselgel 60, thickness of silica gel: 0.25 mm) for analysis. All lipids were dried under argon at room temperature and stored at −40 °C.

Table 2 The lipid classes of *Shinkaia crosnier*

Scientific name	Sample no.	Organs	Sex	Replications for lipid extraction	Lipid contents[a]	Replications for separation	WE[b, c]	SE[b, c]	DAGE[b, c]	TAG[b, c]	ST[b, c]	DG[b, c]	FFA[b, c]	PE[b, c]	PL[b, c]	PC[b, c]
Shinkaia crosnieri																
	1	Body	–	15	0.8 ± 0.1	15	2.2 ± 0.6	4.2 ± 1.1	1.8 ± 0.3	46.1 ± 4.7	5.9 ± 0.6	3.7 ± 0.4	8.3 ± 0.8	12.2 ± 1.1	4.1 ± 1.1	11.5 ± 1.0
	2	Body	Female	2	1.3 ± 0.7	2	1.1 ± 0.5	2.8 ± 1.6	1.0 ± 0.3	58.9 ± 8.7	3.7 ± 0.9	4.6 ± 0.3	9.5 ± 2.1	7.6 ± 1.2	0.9 ± 0.4	9.8 ± 2.3
	3	Eggs	–	2	53.4 ± 0.2	2	0.2 ± 0.2	0.7 ± 0.4	0.1 ± 0.0	94.4 ± 0.2	0.6 ± 0.1	0.5 ± 0.0	0.7 ± 0.1	1.0 ± 0.1	0.2 ± 0.0	1.7 ± 0.8

Data are mean ± standard errors (n = 2–20)

[a] Results are expressed as weight percent of wet tissues

[b] Results are expressed as weight percent of total lipids

[c] WE, SE, DAGE, TAG, ST, DG, and FFA means wax esters, steryl esters, diacylglyceryl ethers, triacylglycerols, sterols, diacylglycerols, and free fatty acids, respectively. PE, PL, and PC means phosphatidylethanolamine, other phospholipids, and phosphatidylcholine, respectively

Nuclear Magnetic Resonance Spectrometry and Determination of Lipid Classes

Spectra were recorded on a GSX-270 nuclear magnetic resonance (NMR) spectrometer (JEOL Co. Ltd., Tokyo, Japan) in pulsed Fourier transform mode at 270 MHz in a deuterochloroform solution using tetramethylsilane as the internal standard. Some fractions often contained several classes. For example, the first fraction contained wax esters, diacylglyceryl ethers, and steryl esters. The molar ratios of these classes were determined by quantitative analysis of the NMR results using characteristic peaks [9]. In NMR, the amount of wax esters was obtained by the total amount of combined integrations of the triplet peaks (from 3.90 to 4.20 ppm) as the two protons at the ester alcohol, that of diacylglyceryl ethers was obtained by that of the singlet peak (3.50–3.80 ppm) as the two ether protons linked with glycerol carbons, and that of steryl esters was obtained by that of multiplet peaks (4.30–4.80 ppm) as one proton at the carbon linked esterified C-3 alcohol of the sterols. The actual ratios of the wax esters, diacylglyceryl ethers, and steryl esters in the first fraction were determined as the respective integration divided by the sum of total integrations of the three combined peaks from 3.50 to 4.80 ppm. The actual weight of each class was obtained by calculating the ratio and multiplying by the total weight of the first fraction. Similarly, the third fraction sometimes contained TAG and sterols, which have two characteristic peaks: for TAG (3.90–4.40 ppm), an octet-like peak for four protons, and for sterols (3.40–3.60 ppm), a multiplet peak for one proton. The actual weight of the TAG and sterols in the third fraction was obtained by calculating the integration of the divided respective peak and multiplying it by the total weight of the third fraction [9].

Preparation of Methyl Esters and Gas–Liquid Chromatography Analysis

Individual components of TAG, PE, and PC fractions were converted into fatty acid methyl esters by direct transesterification with methanol containing 1% concentrated hydrochloric acid under reflux for 1.5 h. The methyl esters were purified using silica gel column chromatography by elution with dichloromethane/*n*-hexane (2/1, v/v) [23].

The compositions of the fatty acid methyl esters were determined by gas–liquid chromatography. Analysis was performed on a Shimadzu GC-8A (Shimadzu Seisakusho Co. Ltd., Kyoto, Japan) and HP-5890 series II (Hewlett Packard Co. Ltd., Yokogawa Electric Corporation, Tokyo, Japan) using gas chromatographs equipped with an Omegawax 250 fused silica capillary column (30 m × 0.25 mm i.d.; 0.25-μm film, Supelco Japan Co. Ltd., Tokyo, Japan). The temperatures of the injector and the column were held at 230 and 215 °C, respectively, and the split ratio was 1:76. Helium was used as the carrier gas at a constant inlet rate of 0.7 mL/min. PE contained noticeable levels of plasmalogen-type PE [23, 24] and significant levels of dimethylacetals (DMA), such as DMA 18:0, were included in the fatty acid composition of PE (Fig. 4). The theoretical values of the fatty acid composition were obtained by deleting the DMA from the total fatty acids (TFA) of PE. After this treatment, we expressed the PE so as to provide a more correctable form in Table 3.

Quantitation of the components was performed by Shimadzu Model C-R3A (Shimadzu Seisakusho Co. Ltd., Kyoto, Japan) and HP ChemStation System (A. 06 revision, Hewlett Packard Co. Ltd., Yokogawa Electric Corporation, Tokyo, Japan) electronic integrators.

Preparation of 4,4-Dimethyloxazoline Derivatives (DMOX) and Analysis of DMOX by Gas Chromatography–Mass Spectrometry

DMOX derivatives were prepared by adding an excess amount of 2-amino-2-methyl propanol (1 mL) to a small amount of fatty acid methyl esters (10.0 mg) in a test tube under an argon atmosphere. The mixture was heated at 180 °C for 18 h. The reaction mixture was cooled and poured into saturated brine and extracted with *n*-hexane (3 times). The pooled *n*-hexane extract was washed with saturated brine and dried over anhydrous sodium sulfate. The solvent was removed under reduced pressure and the samples were again dissolved in *n*-hexane for analysis by gas chromatography–mass spectrometry (GC–MS) [23, 25].

Analysis of the DMOX derivatives was performed on a HP G1800C GCD Series II (Hewlett Packard Co. Ltd., Yokogawa Electric Corporation, Tokyo, Japan) GC–MS equipped with the same capillary column for determining the respective fatty acids with the HP WS (HP Kayak XA, G1701BA version, PC workstation). The temperatures of the injector and the column were held at 230 and 215 °C, respectively. The split ratio was 1:75, and the ionization voltage was 70 eV. Helium was used as the carrier gas at a constant inlet rate of 0.7 mL/min. Fatty acid methyl esters were simultaneously analyzed by GC–MS and identified by comparison to the mass spectral data obtained by GC–MS. The author did not check the quantification of the fatty acid methyl esters by the internal standards.

Structural Elucidation of the DMOX Derivatives of the Fatty Acids in *S. crosnieri* Lipids

Representative chromatograms of the DMOX derivatives of the *S. crosnieri* lipids and the MS charts of the major fatty acids are displayed in Figs. 4, 5, 6, 7, 8, 9. Each MS

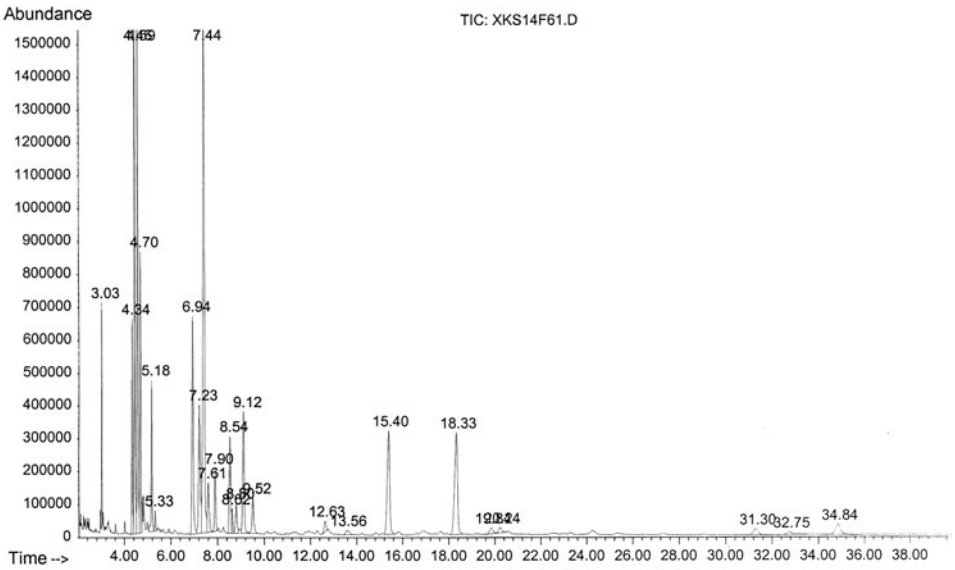

Retention time (min)	Fatty acids	Area % (total ion chromatogram)
3.03	16:0 DMA	2.46
4.34	16:0	4.00
4.46	18:0 DMA	12.01
4.59	16:1n-7	10.40
4.70	18:1 DMA	5.10
5.18	16:2n-4,7	3.10
5.33	16:2n-3,6	0.40
6.94	18:0	6.84
7.23	18:1n-9	4.85
7.44	18:1n-7	19.51
7.61	20:1 DMA	1.97
7.90	18:2n-7,10	1.81
8.54	18:2n-4,7	3.09
8.62	DBPh[a]	0.65
8.80	18:2n-3,6	1.10
9.12	18:3n-4,7,10	4.21
9.52	18:4n-4,7,10,13	1.49
12.63	20:1n-7	0.47
13.56	20:2n-7,10	0.38
15.40	20:4n-6	5.96
18.33	20:5n-3	6.95
19.84	21:4n-7	0.49
20.24	unknown	0.41
31.30	DOPh[a]	0.71
32.75	22:5n-3	0.39
34.84	22:6n-3	1.27
		100.00

a DBPh and DOPh means dibutyl phthalate and dioctyl phthalate as an impurity, respectively.

Fig. 4 The chromatogram of the DMOX derivatives of the fatty acids in *S. crosnieri* lipids. Analysis of the DMOX derivatives was performed on a HP G1800C GCD Series II gas chromatograph mass spectrometer equipped with an Omegawax-250 fused silica capillary column with the HP WS (HP Kayak XA, G1701BA version, personal computer workstations). The temperatures of the injector and the column were held at 230 and 215 °C, respectively. The split ratio was 1:75, and the ionization voltage was 70 eV, respectively. Helium was used as the carrier gas at a constant inlet rate of 0.7 mL/min. Each MS spectrum was obtained by every 0.009 min

spectrum was obtained every 0.009 min (Figs. 4, 5, 6, 7, 8, 9). For example, a spectrum at 18.283 min (Scan No. 1814 in Fig. 10) is one of the representative spectra of 20:5n-3 (Δ5,8,11,14,17–20:5) because 20:5n-3 was detected near 18.33 min as one peak in the chromatogram (Fig. 4) of DMOX derivatives of the crab lipids; more than 35 spectra (M^+-355) were obtained by scanning the peak (18.15–18.50 min).

In Fig. 5 (5.185 min, Scan No. 352), MS peaks of a DMOX derivative of 16:2n-4,7 are M^+-305, 290, 276, 262, 248, 236, 222, 208, 196, 182, 168, 154, 140, 126, 113 (base peak) and two pairs of the peaks (M-248/M-236 and M-208/M-196) are, respectively, reflected by two double bonds: Δ-12 (n-4) and Δ-9 (n-7). In Fig. 6 (8.509 min, Scan No. 723), MS peaks of a DMOX derivative of 18:2n-4,7 are M^+-333, 318, 304, 290, 276, 264, 250, 236, 224, 210, 196, 182, 168, 154, 140, 126, 113 (base peak) and two pairs of the peaks (M-276/M-264 and M-236/M-224) are, respectively, reflected by two double bonds: Δ-14 (n-4) and Δ-11 (n-7). In Fig. 7 (9.055 min, Scan No. 784), MS peaks of a DMOX derivative of 18:3n-4,7,10 are M^+-331, 316, 302, 288, 274, 262, 248, 234, 222, 208, 194, 182, 168, 154, 140, 126, 113 (base peak) and three pairs of the peaks (M-274/M-262, M-234/M-222, and M-194/M-182) are, respectively, reflected by three double bonds: Δ-14 (n-4), Δ-11 (n-7) and Δ-8 (n-10). In Fig. 8 (5.355 min, Scan No. 371), MS peaks of a DMOX derivative of 16:2n-3,6 are M^+-305, 290, 276, 262, 250, 236, 222, 210, 196, 182, 168,

Table 3 Fatty acid composition of the *S. crosnieri* lipids examined

Sample no.	1TAG Mean ± SE	1PE Mean ± SE	1PE revised Mean ± SE	1PC Mean ± SE	2TAG Mean ± SE	2PE Mean ± SE	2PE revised Mean ± SE	2PC Mean ± SE	3TAG Mean ± SE	3PE Mean ± SE	3PE revised Mean ± SE	3PC Mean ± SE
Total saturated	17.2 ± 0.9	8.4 ± 0.1	9.4 ± 0.1	16.3 ± 0.2	13.0 ± 1.7	8.0 ± 0.2	7.9 ± 0.1	11.4 ± 0.1	10.7 ± 0.6	7.5 ± 0.9	8.5 ± 0.8	9.5 ± 0.2
12:0	2.5 ± 0.3	0.2 ± 0.0	0.3 ± 0.0	0.0 ± 0.0	1.0 ± 0.5	0.2 ± 0.0	0.1 ± 0.0	0.0 ± 0.0	0.1 ± 0.0	0.2 ± 0.0	0.2 ± 0.1	0.0 ± 0.0
13:0	2.3 ± 0.6	0.0 ± 0.0	0.0 ± 0.0	0.0 ± 0.0	0.7 ± 0.4	0.0 ± 0.0	0.0 ± 0.0	0.0 ± 0.0	0.0 ± 0.0	0.3 ± 0.1	0.3 ± 0.1	0.2 ± 0.1
14:0	3.5 ± 0.2	0.6 ± 0.1	0.7 ± 0.1	1.2 ± 0.1	2.6 ± 0.8	0.5 ± 0.1	0.3 ± 0.0	0.4 ± 0.0	1.1 ± 0.1	0.6 ± 0.0	0.7 ± 0.1	0.4 ± 0.0
15:0	0.2 ± 0.0	0.0 ± 0.0	0.0 ± 0.0	0.2 ± 0.0	0.1 ± 0.0	0.0 ± 0.0	0.1 ± 0.0	0.1 ± 0.0	0.1 ± 0.0	0.6 ± 0.2	0.6 ± 0.3	0.1 ± 0.0
16:0	6.6 ± 0.2	2.8 ± 0.1	3.2 ± 0.1	10.5 ± 0.2	7.3 ± 0.2	2.6 ± 0.1	2.5 ± 0.1	7.3 ± 0.1	7.9 ± 0.4	3.7 ± 0.5	4.2 ± 0.5	5.1 ± 0.1
18:0	1.4 ± 0.1	4.2 ± 0.1	4.7 ± 0.1	3.5 ± 0.1	0.9 ± 0.2	4.1 ± 0.1	4.4 ± 0.1	3.0 ± 0.0	0.9 ± 0.3	1.7 ± 0.1	1.9 ± 0.1	2.8 ± 0.3
20:0	0.1 ± 0.0	0.2 ± 0.0	0.2 ± 0.0	0.1 ± 0.0	0.0 ± 0.0	0.2 ± 0.0	0.2 ± 0.1	0.2 ± 0.0	0.1 ± 0.0	0.1 ± 0.0	0.2 ± 0.0	0.4 ± 0.1
Total monoenoic	50.1 ± 0.7	34.3 ± 0.3	38.5 ± 0.3	52.3 ± 0.4	55.2 ± 2.1	34.1 ± 0.9	39.9 ± 0.1	58.2 ± 0.1	60.4 ± 2.3	36.6 ± 0.7	42.5 ± 1.0	62.9 ± 0.3
12:1n-7	2.7 ± 0.5	0.1 ± 0.0	0.1 ± 0.0	0.0 ± 0.0	0.7 ± 0.4	0.1 ± 0.0	0.0 ± 0.0	0.0 ± 0.0	0.1 ± 0.0	0.1 ± 0.0	0.1 ± 0.0	0.0 ± 0.0
14:1n-9	5.1 ± 0.4	0.3 ± 0.0	0.3 ± 0.1	0.2 ± 0.0	3.1 ± 1.1	0.3 ± 0.0	0.2 ± 0.0	0.3 ± 0.1	1.0 ± 0.1	0.4 ± 0.1	0.5 ± 0.1	0.4 ± 0.0
14:1n-5	0.5 ± 0.0	0.1 ± 0.0	0.1 ± 0.0	0.1 ± 0.0	0.6 ± 0.0	0.1 ± 0.0	0.1 ± 0.0	0.1 ± 0.0	0.5 ± 0.1	0.3 ± 0.1	0.4 ± 0.1	0.1 ± 0.0
16:1n-7	22.5 ± 0.8	11.7 ± 0.2	13.1 ± 0.3	21.8 ± 0.5	28.8 ± 2.8	11.3 ± 0.3	13.5 ± 0.3	17.2 ± 0.5	28.9 ± 2.6	14.5 ± 0.5	16.9 ± 0.8	15.5 ± 1.1
16:1n-5	0.8 ± 0.0	0.3 ± 0.0	0.3 ± 0.0	0.6 ± 0.0	0.8 ± 0.1	0.2 ± 0.0	0.1 ± 0.0	0.4 ± 0.0	0.7 ± 0.0	0.2 ± 0.0	0.2 ± 0.0	0.4 ± 0.0
18:1n-9	4.0 ± 0.6	3.6 ± 0.5	4.0 ± 0.6	8.4 ± 0.6	7.4 ± 1.8	4.4 ± 0.5	7.3 ± 0.3	16.6 ± 0.6	14.6 ± 3.8	7.9 ± 0.3	9.3 ± 0.6	19.6 ± 1.0
18:1n-7	12.0 ± 0.6	16.0 ± 0.4	18.0 ± 0.5	18.1 ± 0.3	11.8 ± 0.8	15.3 ± 0.6	15.6 ± 0.2	17.7 ± 0.2	12.2 ± 0.9	10.6 ± 0.5	12.2 ± 0.2	17.6 ± 0.4
18:1n-5	0.5 ± 0.0	0.4 ± 0.0	0.4 ± 0.0	0.7 ± 0.0	0.4 ± 0.1	0.4 ± 0.0	0.6 ± 0.2	0.8 ± 0.1	0.6 ± 0.0	0.2 ± 0.0	0.3 ± 0.0	0.7 ± 0.0
20:1n-9	0.2 ± 0.0	0.2 ± 0.0	0.2 ± 0.0	0.4 ± 0.0	0.2 ± 0.1	0.3 ± 0.0	0.5 ± 0.0	1.2 ± 0.2	0.6 ± 0.2	0.5 ± 0.1	0.6 ± 0.1	2.2 ± 0.2
20:1n-7	1.3 ± 0.1	0.6 ± 0.0	0.7 ± 0.0	1.0 ± 0.1	0.9 ± 0.2	0.6 ± 0.0	0.7 ± 0.0	1.9 ± 0.1	0.9 ± 0.2	0.8 ± 0.1	0.9 ± 0.1	3.4 ± 0.2
22:1n-7	0.2 ± 0.0	0.6 ± 0.0	0.6 ± 0.0	0.6 ± 0.1	0.2 ± 0.1	0.5 ± 0.0	0.5 ± 0.0	1.2 ± 0.1	0.2 ± 0.1	0.2 ± 0.0	0.2 ± 0.0	2.5 ± 0.4
Total PUFA	30.2 ± 0.5	42.5 ± 0.3	47.7 ± 0.3	28.6 ± 0.5	30.0 ± 0.3	41.7 ± 1.1	47.5 ± 0.4	27.8 ± 0.1	27.8 ± 2.7	38.2 ± 1.0	44.3 ± 0.8	25.0 ± 0.2
Ttotal n-4 PUFA	23.7 ± 1.1	15.4 ± 0.6	17.2 ± 0.7	20.3 ± 0.7	25.6 ± 0.9	15.5 ± 0.7	20.0 ± 0.9	21.4 ± 0.9	23.5 ± 1.4	26.0 ± 1.0	30.5 ± 2.1	22.1 ± 0.6
16:2n-4,7	7.2 ± 0.2	3.1 ± 0.1	3.5 ± 0.2	5.1 ± 0.2	9.4 ± 0.5	2.9 ± 0.2	3.3 ± 0.2	4.8 ± 0.4	8.5 ± 1.2	4.1 ± 0.5	4.9 ± 0.7	4.8 ± 0.3
18:2n-7,10	3.6 ± 0.2	1.9 ± 0.0	2.2 ± 0.0	2.9 ± 0.0	3.1 ± 0.4	1.8 ± 0.1	2.0 ± 0.1	2.8 ± 0.0	2.5 ± 0.1	2.1 ± 0.1	2.4 ± 0.1	2.6 ± 0.1
18:2n-4,7	6.7 ± 0.4	2.9 ± 0.1	3.3 ± 0.2	5.4 ± 0.3	7.5 ± 0.4	2.8 ± 0.1	3.0 ± 0.2	6.2 ± 0.4	7.3 ± 0.1	3.0 ± 0.1	3.5 ± 0.1	7.2 ± 0.2
18:3n-4,7,10	5.0 ± 0.3	3.3 ± 0.2	3.7 ± 0.3	4.6 ± 0.2	4.4 ± 0.5	4.0 ± 0.3	7.1 ± 0.7	5.3 ± 0.3	3.8 ± 0.0	14.5 ± 0.9	17.1 ± 1.6	4.5 ± 0.3
18:4n-4,7,10,13	0.1 ± 0.0	1.5 ± 0.1	1.7 ± 0.1	0.5 ± 0.0	0.2 ± 0.1	1.5 ± 0.1	1.8 ± 0.1	0.3 ± 0.0	0.3 ± 0.0	0.8 ± 0.1	1.0 ± 0.1	0.4 ± 0.1
20:2n-7,10	0.2 ± 0.0	0.3 ± 0.0	0.4 ± 0.0	0.3 ± 0.0	0.2 ± 0.0	0.3 ± 0.0	0.2 ± 0.1	0.3 ± 0.0	0.1 ± 0.0	0.2 ± 0.1	0.2 ± 0.1	0.3 ± 0.0
20:2n-4,7	0.8 ± 0.1	0.4 ± 0.0	0.4 ± 0.0	0.6 ± 0.1	0.8 ± 0.1	0.4 ± 0.0	0.5 ± 0.0	0.9 ± 0.0	0.8 ± 0.1	0.3 ± 0.0	0.4 ± 0.0	1.6 ± 0.1
20:3n-4,7,10	0.1 ± 0.0	0.3 ± 0.0	0.3 ± 0.0	0.3 ± 0.0	0.1 ± 0.0	0.3 ± 0.0	0.5 ± 0.0	0.4 ± 0.1	0.2 ± 0.1	0.5 ± 0.1	0.6 ± 0.1	0.3 ± 0.0
21:4n-7,10,13,16	0.0 ± 0.0	1.0 ± 0.1	1.1 ± 0.1	0.3 ± 0.0	0.0 ± 0.0	0.9 ± 0.1	1.0 ± 0.2	0.3 ± 0.0	0.0 ± 0.0	0.3 ± 0.1	0.3 ± 0.1	0.3 ± 0.1
22:2n-4,7	0.0 ± 0.0	0.6 ± 0.0	0.7 ± 0.1	0.3 ± 0.0	0.0 ± 0.0	0.5 ± 0.0	0.5 ± 0.1	0.1 ± 0.0	0.0 ± 0.0	0.2 ± 0.1	0.3 ± 0.1	0.0 ± 0.0
Total n-6 PUFA	0.5 ± 0.0	8.5 ± 0.3	9.5 ± 0.3	2.6 ± 0.1	0.4 ± 0.1	8.6 ± 0.3	9.4 ± 0.2	2.2 ± 0.1	0.6 ± 0.3	2.5 ± 0.4	2.8 ± 0.3	0.8 ± 0.1
18:2n-6,9	0.1 ± 0.0	0.2 ± 0.0	0.2 ± 0.0	0.3 ± 0.0	0.0 ± 0.0	0.2 ± 0.0	0.3 ± 0.1	0.2 ± 0.0	0.1 ± 0.0	0.1 ± 0.0	0.2 ± 0.0	0.1 ± 0.1
20:4n-6,9,12,15	0.4 ± 0.0	8.1 ± 0.3	9.1 ± 0.3	2.3 ± 0.1	0.4 ± 0.1	8.2 ± 0.3	8.9 ± 0.3	1.9 ± 0.1	0.5 ± 0.2	2.3 ± 0.3	2.6 ± 0.3	0.6 ± 0.1

Table 3 continued

Sample no.	1TAG Mean ± SE	1PE Mean ± SE	1PE revised Mean ± SE	1PC Mean ± SE	2TAG Mean ± SE	2PE Mean ± SE	2PE revised Mean ± SE	2PC Mean ± SE	3TAG Mean ± SE	3PE Mean ± SE	3PE revised Mean ± SE	3PC Mean ± SE
22:4n-6,9,12,15	0.0 ± 0.0	0.2 ± 0.0	0.2 ± 0.0	0.0 ± 0.0	0.0 ± 0.0	0.2 ± 0.0	0.3 ± 0.0	0.0 ± 0.0	0.0 ± 0.0	0.1 ± 0.0	0.1 ± 0.0	0.0 ± 0.0
Total n-3	6.1 ± 0.8	18.6 ± 0.5	21.0 ± 0.6	5.7 ± 0.4	4.0 ± 0.8	17.6 ± 0.7	18.1 ± 0.8	4.2 ± 0.7	3.7 ± 1.6	9.7 ± 1.4	10.9 ± 1.3	2.1 ± 0.5
16:2n-3,6	5.5 ± 0.8	0.5 ± 0.1	0.6 ± 0.1	1.5 ± 0.2	3.6 ± 0.7	0.5 ± 0.1	1.0 ± 0.2	1.4 ± 0.4	3.2 ± 1.4	1.0 ± 0.3	1.1 ± 0.3	1.3 ± 0.4
18:2n-3,6	0.3 ± 0.1	0.2 ± 0.0	0.3 ± 0.0	0.4 ± 0.1	0.3 ± 0.1	0.2 ± 0.0	0.2 ± 0.1	0.3 ± 0.1	0.3 ± 0.1	0.0 ± 0.0	0.0 ± 0.0	0.2 ± 0.1
20:5n-3	0.2 ± 0.0	12.8 ± 0.3	14.4 ± 0.4	2.7 ± 0.2	0.2 ± 0.0	12.2 ± 0.5	12.6 ± 0.5	1.8 ± 0.2	0.2 ± 0.0	4.8 ± 0.5	5.4 ± 0.5	0.4 ± 0.0
22:5n-3	0.0 ± 0.0	0.8 ± 0.0	0.9 ± 0.0	0.2 ± 0.0	0.0 ± 0.0	0.8 ± 0.0	0.8 ± 0.0	0.2 ± 0.0	0.0 ± 0.0	0.3 ± 0.1	0.4 ± 0.1	0.0 ± 0.0
22:6n-3	0.0 ± 0.0	4.2 ± 0.1	4.8 ± 0.2	0.8 ± 0.1	0.0 ± 0.0	3.9 ± 0.2	3.5 ± 0.2	0.6 ± 0.1	0.0 ± 0.0	3.5 ± 0.5	4.0 ± 0.5	0.1 ± 0.1
Total fatty acids	97.5 ± 0.2	85.2 ± 0.3	95.7 ± 0.1	97.2 ± 0.2	98.3 ± 0.3	83.8 ± 2.1	95.3 ± 0.3	97.4 ± 0.2	98.9 ± 0.2	82.2 ± 2.1	95.2 ± 0.7	97.3 ± 0.4
DMA 15:0		0.3 ± 0.0				0.2 ± 0.0				0.4 ± 0.2		
DMA 16:0		1.6 ± 0.1				1.5 ± 0.1				1.6 ± 0.3		
DMA 18:0		5.1 ± 0.2				4.8 ± 0.2				8.0 ± 1.9		
DMA 18:0 i		0.2 ± 0.1				0.0 ± 0.0				0.0 ± 0.0		
DMA 20:0		0.8 ± 0.0				0.7 ± 0.0				0.7 ± 0.1		
DMA 18:1		3.0 ± 0.1				2.6 ± 0.1				2.3 ± 0.4		
DMA 20:1		0.0 ± 0.0				0.0 ± 0.0				0.5 ± 0.2		
Total DMA		11.0 ± 0.2				9.9 ± 0.4				13.6 ± 2.8		

Results are expressed as weight per cent of total fatty acids. The average data are mean ± standard errors of 3–28 replications. In Table 3, the major fatty acids are selected if at least one mean datum was detected at a level of about 0.3% or more of total fatty acids

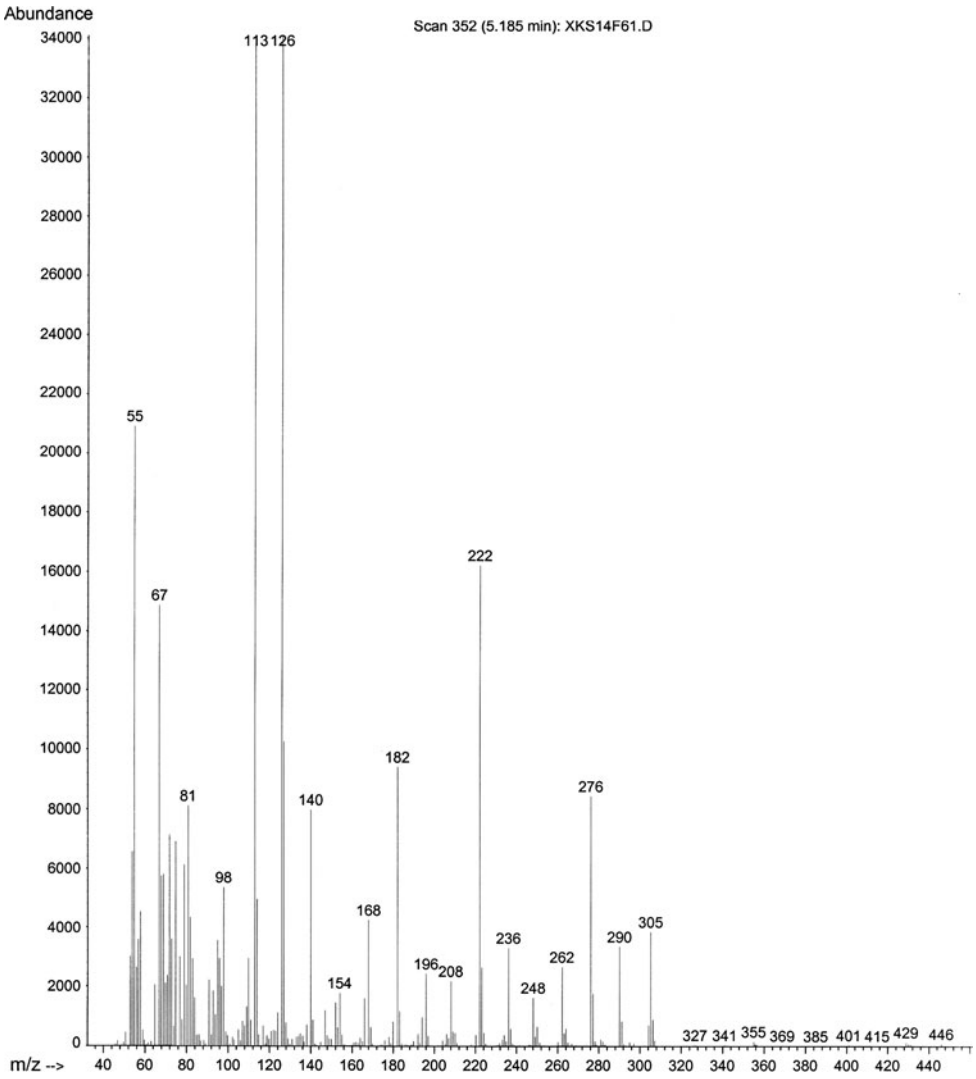

Fig. 5 The MS peaks (5.185 min, Scan No. 352) of the DMOX derivative of 16:2n-4,7 are M^+-305, 290, 276, 262, 248, 236, 222, 208, 196, 182, 168, 154, 140, 126, 113 (*base peak*), and two pairs of peaks (M-248/M-236 and M-208/M-196) are, respectively, reflected by two double bonds; Δ-12 (n-4) and Δ-9 (n-7)

154, 140, 126, 113 (base peak) and two pairs of peaks (M-262/M-250 and M-222/M-210) are, respectively, reflected by two double bonds: Δ-13 (n-3) and Δ-10 (n-6). In Fig. 9 (9.494 min, Scan No. 833), the MS peaks of a DMOX derivative of 18:4n-4,7,10,13 are M^+-329, 314, 300, 286, 272, 260, 246, 232, 220, 206, 192, 180, 166, 153, 136, 126, 113 (base peak) and three pairs of the peaks (M-272/M-260, M-232/M-220, and M-192/M-180) are, respectively, reflected by three double bonds: Δ-14 (n-4), Δ-11 (n-7) and Δ-8 (n-10): a pair of the peak (M-153/M-136) shows a Δ-5 (n-13) double bond. This is the same as the authentic n-3 PUFA in Christie's home page [26] and n-4 PUFA [10].

Statistical Analyses

Two to 15 experimental replications were completed for each lipid class. For all samples of fatty acids analyzed by GLC, four to 39 replications were completed. Significant mean differences were determined using Student's *t* test at a significance level of $p < 0.05$.

Results

Lipid Content and Classes of *S. crosnieri*

The lipid content of female *S. crosnieri*, which was laden with eggs, was relatively high (sample No. 2, 1.3 ± 0.7%, Table 2) in comparison to those of both sexes (sample No. 1, 0.8 ± 0.1%, Table 2). Furthermore, the lipid content of *S. crosnieri* eggs was very high (sample No. 3, 53.4 ± 0.2%, Table 2). The lipids of the bodies and eggs (samples No. 1–3) contained a high level of neutral lipids (mainly TAG, 46.1–58.9%) with noticeable levels of polar lipids (PE and PC). All PE

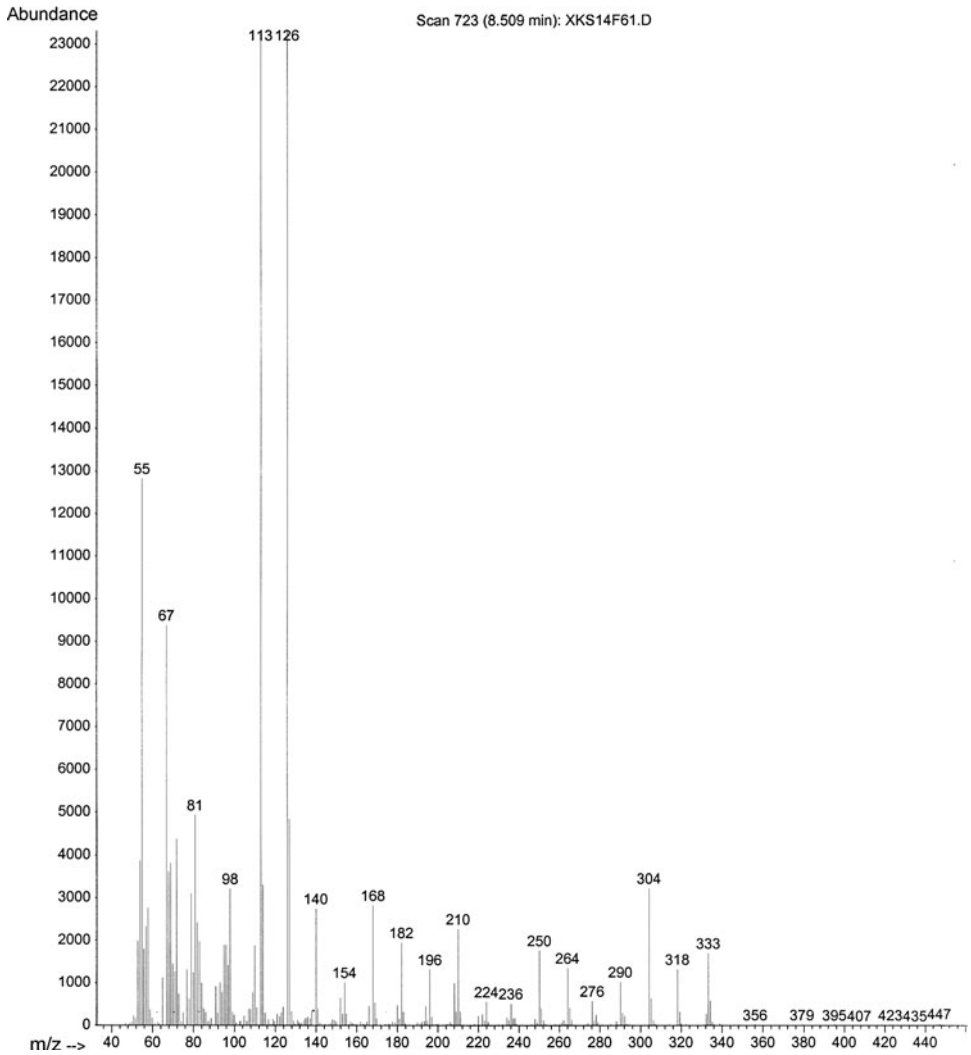

Fig. 6 The MS peaks (8.509 min, Scan No. 723) of the DMOX derivative of 18:2n-4,7 are M^+-333, 318, 304, 290, 276, 264, 250, 236, 224, 210, 196, 182, 168, 154, 140, 126, 113 (*base peak*), and two pairs of the peaks (M-276/M-264 and M-236/M-224) are, respectively, reflected by two double bonds; Δ-14 (n-4) and Δ-11 (n-7)

contained noticeable levels of plasmalogen-type PE (Fig. 4) and the fatty acid composition of PE contained significant levels of DMA [23, 24].

Fatty Acid Composition in Depot TAG of *S. crosnieri* Lipids

More than 50 kinds of fatty acids from C_{12} to C_{22} were determined in *S. crosnieri* lipids. The fatty acids in the body TAG (more than 0.3% of TFA) are listed in Table 3. In its body TAG (samples No. 1–2), 11 dominant fatty acids (each accounted for more than about 3% of TFA) were detected: 14:0 and 16:0 as saturated fatty acids; 14:1n-9, 16:1n-7, 18:1n-7, and 18:1n-9 as monounsaturated fatty acids (MUFA); 16:2n-4 (Fig. 5), 18:2n-4 (Fig. 6), 18:2n-7, and 18:3n-4 (Fig. 7) as n-4 family PUFA; and 16:2n-3 (Fig. 8) as n-3 dienoic acid with noticeable levels (more than about 1% of TFA) of 5 other minor fatty acids: 12:0, 12:1n-8, 13:0, 18:0, and 20:1n-7. Similarly, the same major fatty acids were observed in its egg TAG (sample No. 3). Nine dominant fatty acids were detected: 16:0, 16:1n-7, 18:1n-7, 18:1n-9, 16:2n-4, 18:2n-4, 18:2n-7, 18:3n-4, and 16:2n-3 as n-3 with noticeable levels of the same four minor fatty acids: 14:0, 14:1n-5, 18:0, and 20:1n-7.

High levels of total MUFA (sample No. 1, 50.1 ± 0.7% for 15 specimens; sample No. 2, 55.2 ± 2.1% for 2 female specimens; sample No. 3, 60.4 ± 2.3% for 2 eggs) were observed in *S. crosnieri* TAG, while it had comparatively low levels of saturated fatty acids (sample No. 1, total saturated fatty acids: 17.2 ± 0.9% for 15 specimens; sample No. 2, 13.0 ± 1.7% for 2 female specimens; sample No. 3, 10.7 ± 0.6% for 2 eggs). For example, palmitoleic acid 16:1n-7 (22.5–28.8% for the whole body of samples No. 1–2; 28.9% for the eggs of sample No. 3) and vaccenic acid 18:1n-7 (11.8–12.0% for the whole body of samples No. 1–2; 12.2% for the eggs of sample No. 3) were determined as major MUFA in *S. crosnieri* body TAG.

In all *S. crosnieri* TAG (samples No. 1–3), the four n-4 methylene-interrupted PUFA (16:2n-4, 18:2n-4, 18:2n-7, and 18:3n-4) were observed as major PUFA (Table 3).

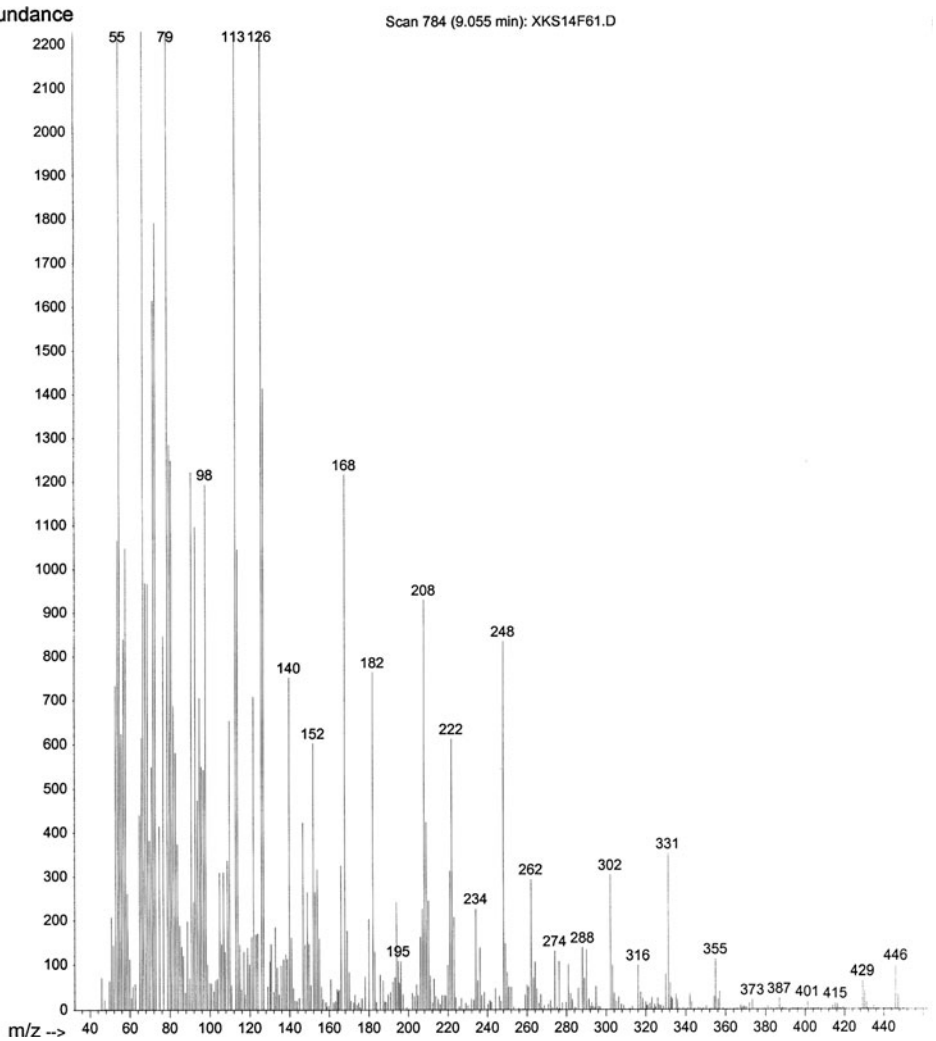

Fig. 7 The MS peaks (9.055 min, Scan No. 784) of the DMOX derivative of 18:3n-4,7,10 are M^{+}-331, 316, 302, 288, 274, 262, 248, 234, 222, 208, 194, 182, 168, 154, 140, 126, 113 (*base peak*), and three pairs of the peaks (M-274/M-262, M-234/M-222, and M-194/M-182) are, respectively, reflected by three double bonds; Δ-14 (n-4), Δ-11 (n-7) and Δ-8 (n-10)

With the four major n-4 PUFA, various other n-4 methylene-interrupted PUFA and n-7 MUFA were found in all crab TAG. Furthermore, significant levels of unusual n-3 PUFA 16:2n-3, with trace levels of normal n-3 and n-6 PUFA were found in the *S. crosnieri* body TAG (samples No. 1–2). In the egg TAG (sample No. 3), the same n-3, n-4, and n-6 PUFA were also observed at a similar level and the high levels of n-7 MUFA were observed in both body and egg lipids (Table 3).

Fatty Acid Composition in Tissue Phospholipids of *S. crosnieri* Lipids

Compared with the fatty acid composition in the TAG (Table 3), similar saturated fatty acids and MUFA were determined as dominant in the two major *S. crosnieri* body phospholipids (PE and PC): 16:0, 18:0, 16:1n-7, 18:1n-7, and 18:1n-9. In both PE and PC, 16:0 and 18:0 were major saturated fatty acids while 14:0, which was a major acid in the *S. crosnieri* body TAG, was a minor acid. As for MUFA in the phospholipids, the same trends between PE and PC were found. For example, low levels of 14:1n-9 with slightly higher levels of 18:1n-7 and 18:1n-9 with noticeable levels of 20-carbon n-7 and n-9 MUFA were found in the phospholipids.

Similar to the major PUFA in the *S. crosnieri* body TAG, the same four n-4 methylene-interrupted PUFA (16:2n-4, 18:2n-4, 18:2n-7, and 18:3n-4) were also observed as major PUFA in the phospholipids (Table 3). Furthermore, a tetraenoic fatty acid, 18:4n-4 (Fig. 9) was found at noticeable levels in the body PE, with small levels of other various n-4 family PUFA.

In contrast, the levels of n-3 and n-6 PUFA in the *S. crosnieri* polar lipids markedly differed from those in its TAG. In particular, significantly high levels of n-3 and n-6 long-chain PUFA were contained in PE: 20:4n-6 (ARA, 8.7–9.1% in the body PE), 20:5n-3 (EPA, 12.2–14.4% in the body PE), and 22:6n-3 (DHA, 3.4–4.8% in the body PE). Furthermore, different from the medium levels of 16:2n-3 in the TAG (4.7–5.3%) without DHA, significant

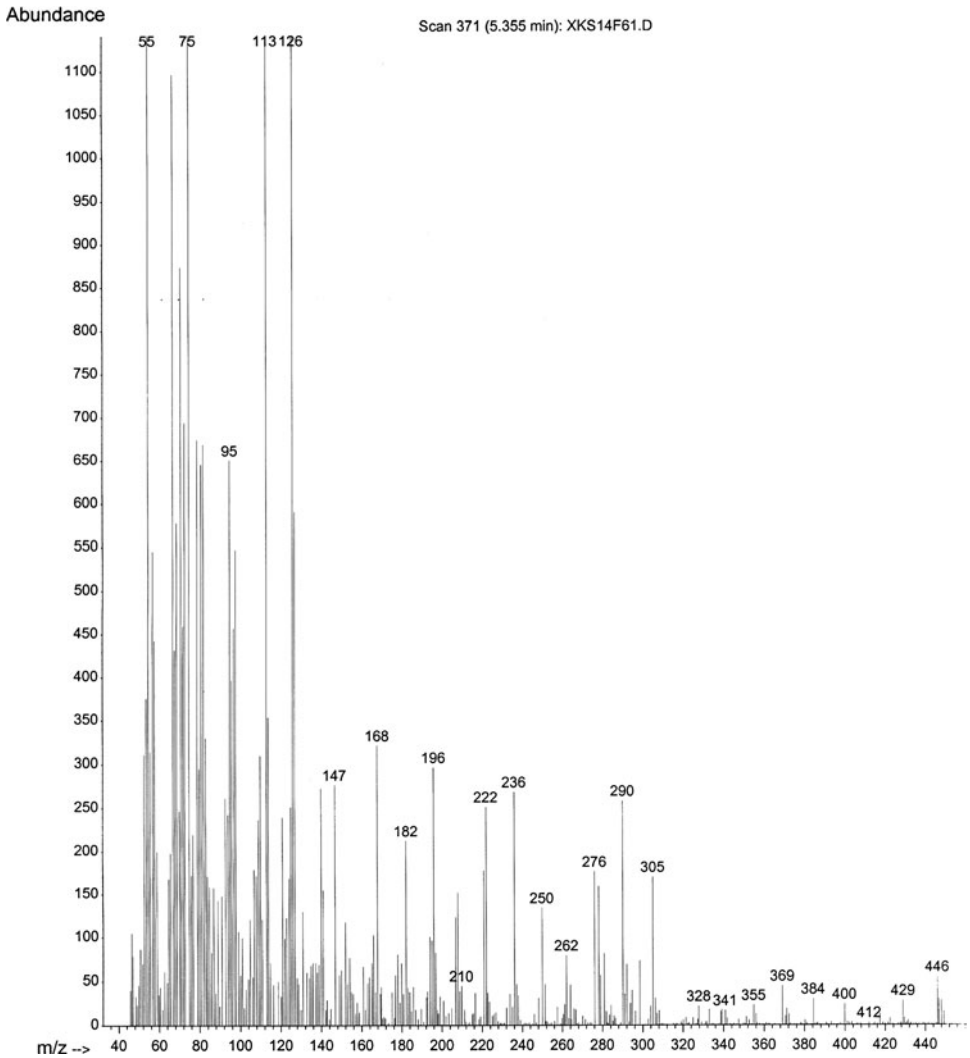

Fig. 8 The MS peaks (5.355 min, Scan No. 371) of the DMOX derivative of 16:2n-3,6 are M^{+}-305, 290, 276, 262, 250, 236, 222, 210, 196, 182, 168, 154, 140, 126, 113 (*base peak*), and two pairs of peaks (M-262/M-250 and M-222/M-210) are, respectively, reflected by two double bonds; Δ-13 (n-3) and Δ-10 (n-6)

levels of ARA, EPA, and DHA were characteristically detected in both phospholipids (Table 3).

In egg PE, the same n-4, n-3, and n-6 PUFA (2.6% for ARA, 5.4% for EPA, and 4.0% for DHA) were observed. However, the total n-4 and n-7 PUFA levels in the egg phospholipids were higher than those in body phospholipids, while the levels of n-3 and n-6 PUFA in the egg polar lipids were lower than those in the body polar lipids.

Discussion

Lipid Content and Classes of *S. crosnieri*

The slightly high lipid content of female *S. crosnieri* suggests that females at spawning season need good nutritional conditions, and transfer lipids to their eggs (sample No. 3, 53.4 ± 0.2%, Table 2) in a manner similar to marine common crustaceans [27–29]. The lipid classes of *S. crosnieri*, whose body lipids contain a high level of neutral TAG lipids (sample No. 1–2, Table 2), differed from those of other vent crustaceans, such as shrimps *Microcaris fortunata* and *Rimicaris exoculata*, which have high levels of wax esters as depot lipids [30, 31]. In spite of the difference between crab TAG and shrimp wax esters, the consistently high levels of both their depot neutral lipids is a common feature of vent crustaceans, and this finding suggests similar high nutritional levels, which imply abundant food resources in the vent habitat. Similar to other reports about invertebrate PE [32, 33], the *S. crosnieri* PE also contained noticeable levels of plasmalogen-type PE. This trend was similar to those in crustacean lipids whose PE contained comparatively high levels of plasmalogens (37.5–69.4%) [32].

High Levels of n-7 MUFA in Depot TAG of *S. crosnieri* Lipids

Similar to some bacterial fatty acids [34, 35], high levels of n-7 MUFA were observed in all *S. crosnieri* TAG. In

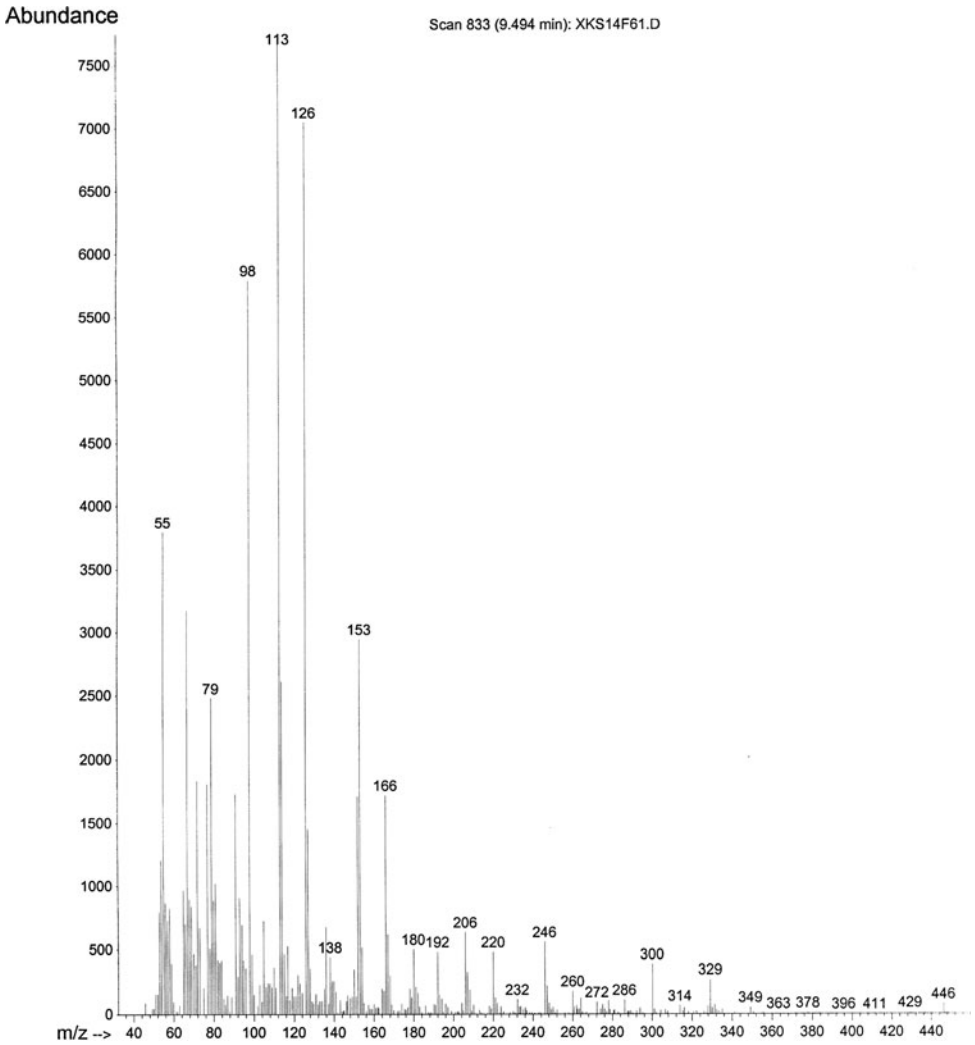

Fig. 9 The MS peaks (9.494 min, Scan No. 833) of the DMOX derivative of 18:4n-4,7,10,13 are M^+-329, 314, 300, 286, 272, 260, 246, 232, 220, 206, 192, 180, 166, 153, 136, 126, 113 (*base peak*), and three pairs of the peaks (M-272/M-260, M-232/M-220, and M-192/M-180) are, respectively, reflected by three double bonds; Δ-14 (n-4), Δ-11 (n-7) and Δ-8 (n-10), and a pair of the peak (M-153/M-136) shows a Δ-5 (n-13) double bond

particular, two short-chain n-7 MUFA (16:1n-7 and 18:1n-7: both more than 10% of TFA) were determined as major MUFA in *S. crosnieri* body TAG, similar to those in various vent animal lipids (neutral lipids for shrimp, *R. exoculata* [31]; for a clams, *Calyptogena* spp. [9, 36]; for mussels, *Bathymodiolus* spp. [10, 36, 37]; and for gastropods, *Ifremeria nautilei* [23] and *Alviniconcha hessleri* [38]). Similar trends are also found in total lipids of vent animals (total lipids for crabs, *Munidopsis subsquamosa* [39] and *Bythograea thermydron* [39]; for shrimp, *M. fortunata* [30]; for worms, *Ridgea piscesae*, *Protis hydrothermica* [40], and *Riftia pachyptila* [39]; for clam, *Calyptogena pacifica* [41]; and for mussels, *Bathymodiolus* spp. [42]). For adaptation to deep-sea low temperatures (4.6 °C, Table 1), high levels of MUFA are more advantageous than are those of saturated fatty acids [43]. 18:1n-7, which might be directly derived from C_2 elongations of 16:1n-7 as a parent acid [1] or by an exceptional anaerobic pathway of bacteria [34], was determined as a major MUFA in *S. crosnieri*, while stearic acid (18:0) was detected at a low level (0.9–1.4%). In general, two n-9 MUFA (18:1n-9 and 20:1n-9) are observed as major MUFA in marine deep-sea animal lipids [8, 44–46] because almost all animals biosynthesize long-chain MUFA mainly by derivation from 18:0 with a reaction of the same Δ-9 desaturase through a normal oxygen-dependent pathway [34, 35]. In contrast, some species of bacteria, such as *Thiobacillus* A2 [47] and *Paracoccus versutus* [48], mainly produce 18:1n-7 in their lipids. The similarity to the n-7 MUFA in the bacteria, as well as the significant presence of 18:1n-7 in *S. crosnieri* TAG (Table 3), indicate that this crab depends on the above types of bacterial lipids. It is known that the crab assimilates several species of sulfur-oxidizing bacteria [19–21] that inhabit the mat of long, silky setae on the crab body as exosymbionts. Both ecological and chemical aspects suggest that one main food source of the crab is these vent bacteria [19–21].

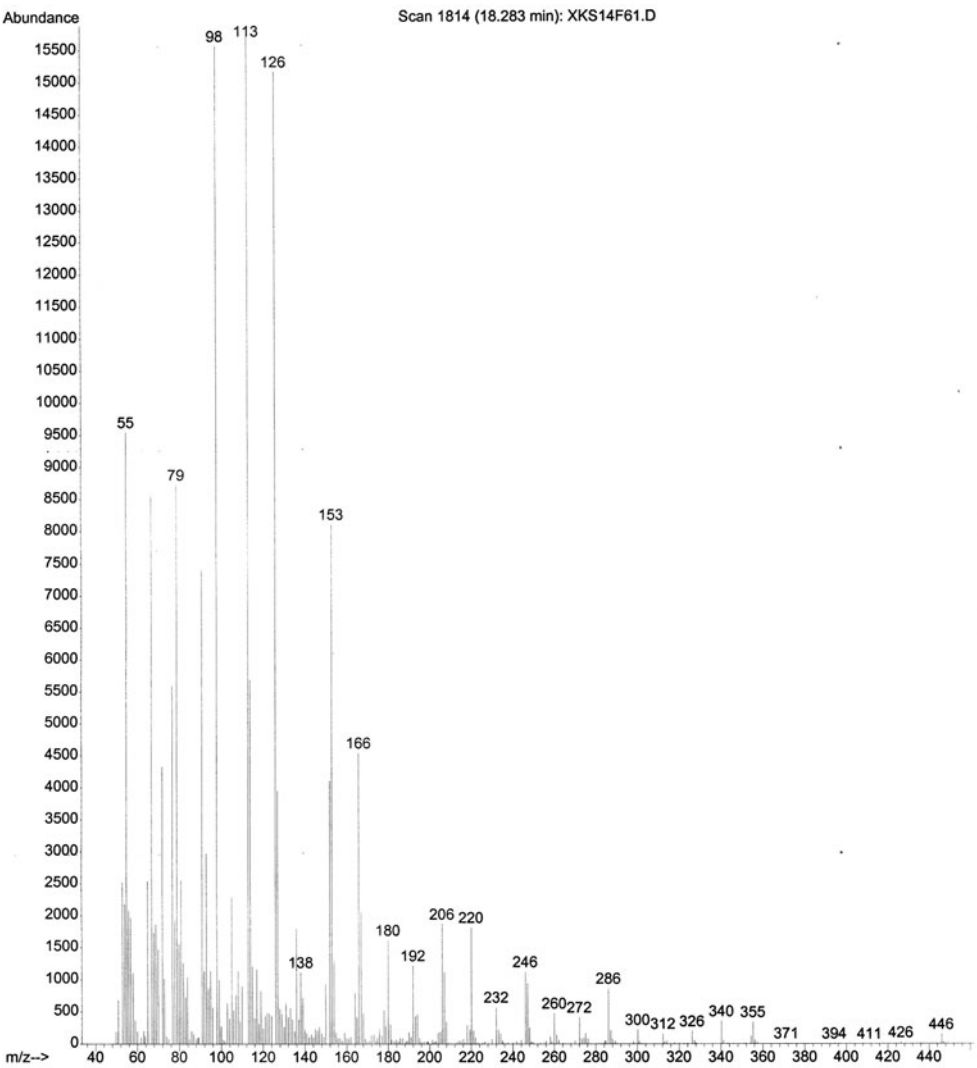

Fig. 10 The MS peaks (18.283 min, Scan No. 1814) of the DMOX derivative of 20:5n-6, 9,12,15,18 are M^+-355, 340, 326, 312, 300, 286, 272, 260, 246, 232, 220, 206, 192, 180, 166, 153, 136, 126, 113 (*base peak*), and four pairs of the peaks (M-312/M-300, M-272/M-260, M-232/M-220, and M-192/M-180) are, respectively, reflected by four double bonds; Δ-17 (n-3), Δ-14 (n-6), Δ-11 (n-9) and Δ-8 (n-12), and a pair of the peak (M-153/M-136) shows a Δ-5 (n-15) double bond

High Levels of Various n-4 PUFA in *S. crosnieri* Depot TAG

Marine animals at the higher trophic levels in the marine food chain generally contain significant levels of DHA and EPA even in their TAG [1, 4] because they have a chance to take these long-chain n-3 PUFA and accumulate them as needed. Different from the high levels of the n-3 PUFA in common marine animal TAG, the main PUFA in the *S. crosnieri* TAG only consist of short-chain (C_{14}–C_{18}) low unsaturated (mono, di, and tri) n-4 family methylene-interrupted PUFA, with trace levels of EPA, 22:5n-3 (docosapentaenoic acid), and DHA. This indicates that the food source of the crab is primarily bacterial and that the symbionts supplying nutrition to the crab are able to make simple MUFA, dienoic acids, and short-chain PUFA.

Four major PUFA in the crab TAG (Table 3) were 16:2n-4 (Fig. 5), 18:2n-4 (Fig. 6), 18:2n-7, and 18:3n-4 (Fig. 7) and these unusual n-4 family PUFA have already been found in vent shrimps and mussels [10, 30, 31]. For example, *Bathymodiolus* mussels, bresilioid shrimp, and vent worms have the same n-4 and n-7 methylene-interrupted PUFA (16:2n-4, 18:2n-4, 18:2n-7, 18:3n-4, 18:3n-7, and 20:3n-7) at small levels [10, 31, 40, 42]. As for the unique n-4 family PUFA in vent crustacean lipids, Pond et al. [31] found small levels of 18:2n-4 and 18:3n-7 in bresilioid shrimp and 18:2n-4 in another vent shrimp [30]. All four major n-4 family PUFA with various other n-4 family PUFA and n-7 MUFA were common in some *Bathymodiolus* mussels previously reported [10, 42]. Similarly, some vent bivalves have many unknown PUFA [36–38, 41] whose double bond positions were undetermined. These might correspond to n-4 family PUFA [9, 10].

In particular, two *Bathymodiolus* mussels (*Bathymodiolus japonicus* and *Bathymodiolus platifrons*) have the same n-4 and n-7 methylene-interrupted PUFA as *S. crosnieri* TAG [10]. The similarity of all major fatty

acids in TAG between the crab and these mussels suggests the similarity of their symbionts or a strong trophic relationship between them. High levels of n-4 PUFA in crab TAG also suggest that methanotrophic bacterial lipids, which pass through vent *Bathymodiolus* mussels, are a primary source of key nutrition for the crab. If the crab can prey on polychaetes [20], it can also take parasitic polychaetes from the mussels. Otherwise, *S. crosnieri* may directly prey on mussel carcasses or indirectly use nutrition originating from mussels and their symbionts because many crabs are regularly observed on *B. platifrons* beds (Fig. 3). If not, the lipid characteristics of the chemosynthetic exosymbionts (*Beggiatoa*-type filamentous bacteria of the crab) may be implausibly close to those of the *Bathymodiolus* endosymbionts [16].

Significant Levels of Unusual n-3 Short-Chain PUFA, 16:2n-3 in *S. crosnieri* Depot TAG

Different from that of all other marine animals, the fatty acid composition of *S. crosnieri* TAG contained significant levels of unusual short-chain n-3 PUFA (16:2n-3, Fig. 8) with trace levels of normal n-3 and n-6 PUFA. The exosymbiotic bacteria probably biosynthesize the 16 carbon n-3 fatty acid because in all other organisms have it is at non-detectable levels and no sufficient sources for the acid have been reported in the literature. Some vent chemosynthetic bacteria produce noticeable levels of various short-chain n-4 and n-6 fatty acids, such as 16:1n-6, 16:2n-4, 16:3n-3, 18:1n-6, 18:2n-4, and 18:2n-6 [30, 31, 38]. Therefore, it is thought that the symbionts of *S. crosnieri* might be able to make 16:2n-3.

The same n-3 and n-4 PUFA in *S. crosnieri* egg TAG observed at a level similar to its body TAG suggests that the crab transfers various PUFA of the body depot lipids to its ovary TAG as is (Table 3). However, higher levels of MUFA (16:1n-7, 18:1n-7, and 18:1n-9) in egg TAG were found compared with those lower levels of short-chain fatty acids (12:0, 13:0, 14:0, 12:1n-8, and 14:1n-9) in the body TAG. This suggests that MUFA are the most important energy source for the larvae, and that *S. crosnieri* selectively accumulates the MUFA, similar to those in other ordinary deep-sea organisms [27, 28, 44–46].

High Levels of n-4 PUFA in Tissue Phospholipids of *S. crosnieri*

Compared with noticeable levels of short-chain fatty acids (12:0, 13:0, and 14:0) in the TAG, 16:0 and 18:0 were the major saturated fatty acids in both body PE and PC. This fact indicates that the crab is able to elongate fatty chains in its tissues by using C_2 elongase.

Similar to *S. crosnieri* depot TAG, the same four n-4 family PUFA (16:2n-4, 18:2n-4, 18:2n-7, and 18:3n-4) were observed as major acids in its phospholipids (Table 3). Furthermore, n-4 tetraenoic PUFA,18:4n-4 (Fig. 9), which had already been found in the *B. platifrons* lipids [10], were observed at noticeable levels in the *S. crosnieri* body PE (Table 3). Similar to the high levels of various n-4 family PUFA in the *Bathymodiolus* mussel lipids, the crab has high levels of the same n-4 PUFA both in its depot and tissue lipids. The crabs inhabit mussel beds, and both the crabs and mussels accumulate n-4 PUFA in their phospholipids.

High Levels of n-3 and n-6 PUFA in *S. crosnieri* Tissue Phospholipids

The n-4 family PUFA, which were found in *S. crosnieri* lipids, have been characteristically found in some vent bivalve lipids [9, 10, 42], entirely different from various n-3 and n-6 PUFA found in the lipids of common crustaceans in normal marine food webs [27–29]. Contrary to the lipid profiles of these specific vent bivalves [9, 10, 42], significant levels of long-chain PUFA (ARA, EPA, and DHA) were simultaneously found as major PUFA in *S. crosnieri* PE (Table 3), which is similar to that in vent crustaceans [30, 31, 39]. Although high levels of n-3 and n-6 PUFA were found in *S. crosnieri* polar lipids, its fatty acid composition differed from those in pelagic marine animals, which have the same n-3 and n-6 PUFA without n-4 PUFA. Deep-sea animals require sufficient levels of PUFA in their plasma membrane lipids to maintain fluidity [40], either because of the low seawater temperature of the habitat [49, 50] or due to close packing in membranes under high pressure [2, 51]. *S. crosnieri* uses both n-4 family PUFA and n-3 and n-6 PUFA in its cellular membrane phospholipids for its plasma membrane fluidity. It is different from vent bivalves [9, 10, 36, 37, 41, 42], which have small or non-detectable levels of these n-3 and n-6 PUFA. High levels of total PUFA in crab phospholipids (44.3–47.7% for PE and 25.0–28.6% for PC) suggest its adaptation to extremely high pressure and low seawater temperature (Table 1) because measured seawater temperatures and depths around the colonies were about 4.5–4.7 °C and more than 950 m, respectively [43, 51]. Furthermore, significantly high levels of ARA, EPA, and DHA contained in *S. crosnieri* PE were markedly different from those in its TAG, which contained only 16:2n-3 without DHA. Some other vent crustaceans also have significant levels of these n-3 and n-6 PUFA in their polar lipids (for vent crabs [39] and for vent shrimps [30, 31]) and these findings suggest that both high n-3 and n-6 PUFA levels in their polar lipids is common for vent crustaceans. Although tubeworms and vent gastropods also contain high levels of n-3 and n-6 PUFA in their lipids similar to those in the lipids of vent crustaceans, their n-3 PUFA generally consist of only

ARA and EPA without DHA [23, 38–40]. These phenomena imply that crustaceans with their symbionts are able to produce various n-3 PUFA, while vent mollusks and tubeworms with their symbionts are unable to biosynthesize DHA, which is not essential for them.

Biosynthesis of DHA in *S. crosnieri* tissue Levels

Long-chain n-3 PUFA are often found in the cells of deep-sea barophilic prokaryotes with high levels of n-7 MUFA [2, 51]. These barophilic bacteria heterotrophically biosynthesize DHA and EPA by using organic matter from surface or intestinal matter of deep-sea animals. Compared with the negligible levels of long-chain n-3 and n-6 PUFA in *S. crosnieri* depot TAG, high ARA, EPA, and DHA levels were found in its polar lipids. This suggests that enzymatic biosynthesis and chemical modification of these PUFA occurs at the crab tissue level. Actually, high levels of EPA and DHA with low levels of 16:2n-3 in PE (12.2-14.4% for EPA and 3.4-4.8% for DHA) and PC (1.6–2.7% for EPA and 0.5–0.8% for DHA, Table 3) differed markedly from non-detectable levels of these PUFA (for EPA 0.2–0.2% and for DHA 0.0–0.2%) with significant levels of 16:2n-3 (4.7–5.3%) in the crab body TAG. This points to active accumulation or biosynthesis of ARA, EPA, and DHA in crab polar lipids after intake of short-chain n-3 PUFA, such as 16:2n-3. Otherwise, similar to deep-sea barophilic bacteria, some of the exosymbiotic bacteria might biosynthesize n-3 and n-6 PUFA in polar lipids for their plasma membrane fluidity [2, 3, 43, 51, 52]. Similar to pelagic crustaceans [53], *S. crosnieri* may biosynthesize DHA, in contrast with low n-3 PUFA essentiality for vent bivalves, which exclusively depend on symbiotic organisms making only n-4 family PUFA [9, 10]. Similarly, this trend is found in significant DHA levels in other vent crabs [39] and mixotrophic polychaeta [40, 54]. Different from strong trophic linkages between some vent bivalves and their symbionts through n-4 family PUFA, *S. crosnieri* utilize nutrition from both symbiotic n-3 and n-6 PUFA and n-4 family PUFA of the prey mussels. This finding suggests similarity of the filamentous symbionts and chemosynthetic bacteria in vent gastropods (*I. nautilei* and *A. hessleri*) [23, 38] or vent crabs (*M. subsquamosa* and *B. thermydron*) [39], whose lipids contained high levels of both n-3 and n-6 PUFA. The unique fatty acid composition of mixed n-3, n-4, and n-6 PUFA in *S. crosnieri* lipids indicates the existence of a specific vent crustacean utilizing both filamentous symbionts and outside mussel beds. Compared with high levels of n-3, n-4, and n-6 PUFA in *S. crosnieri* body phospholipids, slightly higher levels of n-4 family PUFA with lower levels of n-3 and n-6 PUFA in egg PE were found. These findings suggest that the n-3 and n-6 PUFA were biosynthesized or concentrated in the crab tissues concerned with PE and the body polar lipids were transferred to the ovary, similar to its depot lipids. It is thought that both these normal n-3 and n-6 PUFA with unusual n-4 family PUFA are important cell membrane lipids for the crab and its larvae (Table 3).

Acknowledgments The author thanks Mikiko Tanaka and Akihito Takashima for their skilled technical assistance. The author also thanks the captains and crews of the Research Vessel "*Natsushima*" and the submersible "*Shinkai 2000*" operation teams for their cooperation and enthusiasm throughout the work. He also recognizes the Japan Marine Science and Technology Center for providing us with the opportunity to use their submersible.

References

1. Ackman RG (1989) Fatty acids. In: Ackman RG (ed) Marine Biogenic Lipids, Fats, and Oils, vol I. CRC Press Inc, Boca Raton, pp 103–137
2. DeLong EF, Yayanos AA (1986) Biochemical function and ecological significance of novel bacterial lipids in deep-sea procaryotes. Appl Environ Microbiol 51:730–737
3. Yano Y, Nakayama A, Saito H, Ishihara K (1994) Production of docosahexaenoic acid by marine bacteria isolated from deep sea fish. Lipids 29:527–528
4. Saito H, Seike Y, Ioka H, Osako K, Tanaka M, Takashima A, Keriko J, Kose S, Souza JCR (2005) High docosahexaenoic acid levels in both neutral and polar lipids of a highly migratory fish: *Thunnus tonggol* Bleeker. Lipids 40:941–953
5. Ackman RG (2000) Fatty acids in fish and shellfish. In: Chow CK (ed) Fatty acids in food and their health implications, 2nd edn. Marcel Dekker, New York, pp 47–65
6. Arts MT, Ackman RG, Holub BJ (2001) "Essential fatty acids" in aquatic ecosystems: a crucial link between diet and human health and evolution. Can J Fish Aquat Sci 58: 122–137
7. Raymont JEG (1983) Vertical migration of zooplankton. In: Raymont JEG (ed) Plankton and productivity in the oceans, vol 2, 2nd edn. Pergamon Press Ltd, Elmsford, pp 489–524
8. Dalsgaard J, St John M, Kattner G, Müller-Navarra D, Hagen W (2003) Fatty trophic markers in the pelagic marine environment. Adv Mar Biol 46:225–340
9. Saito H (2007) Identification of novel n-4 series polyunsaturated fatty acids in a deep-sea clam, *Calyptogena phaseoliformis*. J Chromatogr A 1163:247–259
10. Saito H (2008) Unusual novel n-4 polyunsaturated fatty acids in cold-seep mussels (*Bathymodiolus japonicus* and *Bathymodiolus platifrons*), originating from symbiotic methanotrophic bacteria. J Chromatogr A 1200:242–254
11. Childress JJ, Fisher CR (1992) The biology of hydrothermal vent animals: physiology, biochemistry, and autotrophic symbioses. Oceanogr Mar Biol Ann Rev 30:337–441
12. Luts RA, Kennish MJ (1993) Ecology of deep-sea hydrothermal vent communities: a review. Rev Geophys 31:211–242
13. Sibuet M, Olu K (1998) Biogeography, biodiversity and fluid dependence of deep-sea cold-seep communities at active and passive margins. Deep-sea Res II 45:517–567
14. Nelson DC, Fisher CR (1995) Chemoautotrophic and methanotrophic endosymbiotic bacteria at deep-sea vents and seeps. In: Karl DM (ed) The microbiology of deep-sea hydrothermal vents, CRC Press Inc, Boca Raton, pp 125–167
15. Van Dover CL (2000) The ecology of deep-sea hydrothermal vents. In: Van Dover CL (ed) Princeton University Press, Chichester, West Susssex

16. Cavanaugh CM, Mckiness ZP, Newton ILG, Stewart FJ (2006) Marine chemosynthetic symbioses. Prokaryotes 1:475–507
17. Tunnicliff V, McArthur AG, McHugh D (1998) A biogeographical perspective of the deep-sea hydrothermal vent fauna. Adv Mar Biol 34:353–442
18. Baba K, Williams AB (1998) New Galatheoidea (Crustacea, Decapoda, Anomura) from hydrothermal systems in the west Pacific Ocean: Bismarck Archipelago and Okinawa Trough. Zoosystema 20:143–156
19. Chan T-Y, Lee D-A, Lee C-S (2000) The first deep-sea hydrothermal animals reported from Taiwan: *Shinkaia crosnieri* Baba and Williams, 1998 (Crustacea: Decapoda: Galatheidae). Bull Mar Sci 67:799–804
20. Ohta S, Kim D (2001) Submersible observations of the hydrothermal vent communities on the Iheya Ridge, Mid Okinawa Trough, Japan. J Oceanogr 57:663–677
21. Yang J-S, Yang WJ (2008) The complete mitochondrial genome sequence of the hydrothermal vent galatheid crab *Shinkaia crosnieri* (Crustacea: Decapoda: Anomura): a novel arrangement and incomplete tRNA suite. BMC Genomics 9:479–485
22. Folch J, Lees M, Sloan-Stanley GH (1957) A simple method for the isolation and purification of total lipids from animal tissues. J Biol Chem 226:497–509
23. Saito H, Hashimoto J (2010) Characteristics of the fatty acid composition of a deep-sea vent gastropod, *Ifremeria nautilei*. Lipids 45:537–548
24. Kraffe E, Soudant P, Marty M (2004) Fatty acids of serine, ethanolamine, and choline plasmalogens in some marine bivalves. Lipids 39:59–66
25. Yu QT, Liu BN, Zhang JY, Huang ZH (1989) Location of double bonds in fatty acids of fish oil and rat testis lipids. Gas chromatography-mass spectrometry of the oxazoline derivatives. Lipids 24:79–83
26. Christie WW (2010) Dimethyloxazoline (DMOX) derivatives of fatty acids in mass spectra, the lipid library. The Scottish Crop Research Institute, Dundee. http://www.lipidlibrary.co.uk/
27. Kattner G, Graeve M, Calcagno JA, Lovrich GA, Thatje S, Anger K (2003) Lipid, fatty acid and protein utilization during lecithotrophic larval development of *Lithodes santolla* (Molina) and *Paralomis granulose* (Jacquinot). J Exp Mar Biol Ecol 292:61–74
28. Graeve M, Wehrtmann IS (2003) Lipid and fatty acid composition of Antarctic shrimp eggs (Decapoda: Caridea). Polar Biol 26:55–61
29. Garcia-Guerrero M, Racotta IS, Villarreal H (2003) Variation in lipid, protein, and carbohydrate content during the embryonic development of the crayfish *Xherax quadricarinatus* (Decapoda: Parastacidae). J Crustacean Biol 23:1–6
30. Pond DW, Segonzac M, Bell MV, Dixon DR, Fallick AE, Sargent JR (1997) Lipid and lipid carbon stable isotope composition of the hydrothermal vent shrimp *Mirocaris fortunata*: evidence for nutritional dependence on photosynthetically fixed carbon. Mar Ecol Prog Ser 157:221–231
31. Pond DW, Gebruk A, Southward EC, Southward AJ, Fallick AE, Bell MV, Sargent JR (2000) Unusual fatty acid composition of storage lipids in the bresilioid shrimp *Rimcaris exoculata* couples the photic zone with MAR hydrothermal vent sites. Mar Ecol Prog Ser 198:171–179
32. Sargent, JR (1989) Ether-linked glycerides in marine animals. In: Ackman RG (ed) Marine biogenic lipids, fats, and oils, CRC Press, Boca Raton, pp 176–193
33. Joseph JD (1982) Lipid composition of marine and estuarine invertebrates. Part II: Mollusca. Prog Lipid Res 21:109–153
34. Fulco AJ (1983) Fatty acid metabolism in bacteria. Prog Lipid Res 22:133–160
35. Cook HW (1991) Fatty acid desaturation and chain elongation in Eucaryotes. In: Vance DE, Vance J (eds) Biochemistry of lipids, lipoproteins, and membranes. Elsevier Science Publishers, London, pp 141–169
36. Ben-Mlih F, Marty J-C, Fiala-Médioni A (1992) Fatty acid composition in deep hydrothermal vent symbiontic bivalves. J Lipid Res 33:1797–1806
37. Pranal V, Fiala-Médioni A, Guezennec J (1997) Fatty acid characteristics in two symbiot-bearing mussels from deep-sea hydrothermal vents of the south-western Pacific. J Mar Biol Ass UK 77:473–492
38. Pranal V, Fiala-Médioni A, Guezennec J (1996) Fatty acid characteristics in two symbiotic gastropods from a deep hydrothermal vent of the West Pacific. Mar Ecol Prog Ser 142:175–184
39. Phleger CF, Nelson MM, Groce AM, Cary SC, Coyne KJ, Nichols PD (2005) Lipid composition of deep-sea hydrothermal vent tubeworm *Riftia pachyptila*, crabs *Munidopsis subsquamosa* and *Bythograea thermydron*, mussels *Bathymodiolus* sp. and limpets *Lepetodrilus* spp. Comp Biochem Physiol B 141:196–210
40. Pond DW, Allen CE, Bell MV, Van Dover CL, Fallick AE, Dixon DR, Sargent JR (2002) Origins of long-chain polyunsaturated fatty acids in the hydrothermal vent worms *Ridgea piscesae* and *Protis hydrothermica*. Mar Ecol Prog Ser 225: 219–226
41. Allen CE, Tyler PA, Van Dover CL (2001) Lipid composition of the hydrothermal vent clam *Calyptogena pacifica* (Mollusca: Bivalvia) as a trophic indicator. J Mar Biol Ass UK 81:817–821
42. Pond DW, Bell MV, Dixon DR, Fallick AE, Segonzac M, Sargent JR (1998) Stable-carbon-isotope composition of fatty acids in hydrothermal vent mussels containing methanotrophic and thiotrophic bacterial endosymbionts. Appl Environ Microbiol 64:370–375
43. DeLong EF, Yayanos AA (1985) Adaptation of the membrane lipids of a deep-sea bacteria to changes in hydrostatic pressure. Science 228:1101–1103
44. Falk-Petersen S, Mayzaud P, Kattner G, Sargent JR (2009) Lipids and life of Calanus. Mar Biol Res 5:18–39
45. Saito H, Murata M (1998) Origin of the monoene fats in the lipid of midwater fishes: relationship between the lipids of myctophids and those of their prey. Mar Ecol Prog Ser 168:21–33
46. Drazen JC, Phleger CF, Guest MA, Nichols PD (2008) Lipid, sterols and fatty acids of abyssal polychaetes, crustaceans, and a cnidarian from the northeast Pacific Ocean: food web implications. Mar Ecol Prog Ser 372:157–167
47. Thiele OW, Oulevey J, Hunneman DH (1984) Ornithine-containing lipids in *Thiobacillus* A2 and *Achromobacter* sp. Euro J Biochem 139:131–135
48. Knief C, Altendorf K, Lipski A (2003) Linking autotrophic activity in environmental samples with specific bacterial taxa by detection of 13C-labelled fatty acids. Environ Microbiol 5:1155–1167
49. Nichols DS, Nichols PD, McMeekin TA (1993) Polyunsaturated fatty acids in Antarctic bacteria. Antarctic Sci 5:149–160
50. Jøstensen J-P, Landfald B (1997) High prevalence of polyunsaturated-fatty-acid producing bacteria in arctic invertebrates. FEMS Microbiol Lett 151:95–101
51. Yano Y, Nakayama A, Ishihara K, Saito H (1998) Adaptive changes in membrane lipids of barophilic bacteria in response to changes in growth pressure. Appl Environ Microbiol 64: 479–485
52. Metz JG, Roessler P, Facciotti D, Levering C, Dittrich F, Lassner M, Valentine R, Lardizabal K, Domergue F, Yamada A, Yazawa K, Knauf V, Browse J (2001) Production of polyunsaturated fatty acids by polyketide synthases in both prokaryotes and eukaryotes. Science 293:290–293

53. Nanton DA, Castell JD (1999) The effects of temperature and dietary fatty acids on the fatty acid composition of harpacticoid copepods, for use as a live food for marine fish larvae. Aquaculture 175:167–181

54. ten Hove HA, Ztbrowius H (1986) *Laminatubus alvini* gen. et sp.n. and *Protis hydrothermica* sp. n. (Polychaeta, Serpulidae) from the bathyal hydrothermal vent communities in the eastern Pacific. Zoologica Scripta 15:21–31

Lipids (2011) 46:741–751
DOI 10.1007/s11745-011-3565-x

ORIGINAL ARTICLE

Dietary Fish Oil Supplements Increase Tissue n-3 Fatty Acid Composition and Expression of Delta-6 Desaturase and Elongase-2 in Jade Tiger Hybrid Abalone

Hintsa T. Mateos · Paul A. Lewandowski · Xiao Q. Su

Received: 20 January 2011 / Accepted: 20 April 2011 / Published online: 7 May 2011

Abstract This study was conducted to investigate the effects of fish oil (FO) supplements on fatty acid composition and the expression of Δ6 desaturase and elongase 2 genes in Jade Tiger abalone. Five test diets were formulated to contain 0.5, 1.0, 1.5, 2.0 and 2.5% of FO respectively, and the control diet was the normal commercial abalone diet with no additional FO supplement. The muscle, gonad and digestive glands (DG) of abalone fed with all of the five test diets showed significantly high levels of total n-3 polyunsaturated fatty acid (PUFA), eicosapentaenoic acid (EPA), docosapentaenoic acid n-3 (DPAn-3), and docosahexaenoic acid (DHA) than the control group. In all three types of tissue, abalone fed diet supplemented with 1.5% FO showed the highest level of these fatty acids ($P < 0.05$). For DPAn-3 the higher level was also found in muscle and gonad of abalone fed diet supplemented with 2% FO ($P < 0.05$). Elongase 2 expression was markedly higher in the muscle of abalone fed diet supplemented with 1.5% FO ($P < 0.05$), followed by the diet containing 2% FO supplement. For Δ6 desaturase, significantly higher expression was observed in muscle of abalone fed with diet containing 0.5% FO supplement ($P < 0.05$). Supplementation with FO in the normal commercial diet can significantly improve long chain n-3 PUFA level in cultured abalone, with 1.5% being the most effective supplementation level.

Keywords Abalone · Muscle · Gonad · Digestive gland · Fish oil · Fatty acid composition · n-3 Fatty acids · Gas–liquid chromatography · Gene expression · Desaturase · Elongase

Abbreviations

FO	Fish oil
DG	Digestive gland
PUFA	Polyunsaturated fatty acid(s)
EPA	Eicosapentaenoic acid
DHA	Docosahexaenoic acid
DPAn-3	Docosapentaenoic acid, n-3
ALA	Alpha-linolenic acid
LA	Linoleic acid
ARA	Arachidonic acid
MUFA	Monounsaturated fatty acid(s)
SFA	Saturated fatty acid(s)
FAME	Fatty acid methyl ester(s)
RT-PCR	Real-time polymerase chain reaction

A portion of this study was presented in abstract form at 101st AOCS Annual Meeting & Expo, May 16–19, 2010, Phoenix, Arizona, USA.

H. T. Mateos · X. Q. Su (✉)
School of Biomedical and Health Sciences,
Victoria University, P.O. Box 14428, MCMC,
Melbourne, VIC 8001, Australia
e-mail: xiao.su@vu.edu.au

P. A. Lewandowski
Molecular Nutrition Unit, School of Medicine,
Deakin University, Geelong, VIC 3217, Australia

Introduction

The long chain n-3 polyunsaturated fatty acids (PUFA) particularly, eicosapentaenoic acid (EPA) and docosahexaenoic acid (DHA) are associated with a broad range of health benefits including reducing the risk of coronary

heart disease [1], lowering blood pressure [2] and plasma triacylglycerol level [3], reducing the risk of colorectal cancer [4] and breast cancer [5]. In addition, they have also been found to play a role in reducing the risk of Alzheimer's disease [6], depression and schizophrenia [7]. A more recent study also suggested that long chain n-3 PUFA have the potential to improve calcium absorption in the intestine, reduce bone demineralization and inflammatory factors [8].

Blacklip abalone (*Haliotis rubra*), greenlip abalone (*H. laevigata*) and hybrid abalone (*H. laevigata x H. rubra*) are the three main types of abalone farmed in Australia [9], and like other seafood, they are a good source of long chain n-3 PUFA [10–12]. However, a previous study reported that cultured Australian blacklip abalone fed an artificial diet showed lower concentrations and compositions of total n-3 PUFA, EPA, docosapentaenoic acid (DPAn-3) and alpha linolenic acid (ALA) than wild abalone [12]. Dunstan et al. [9, 10] found that the muscle of wild adult greenlip abalone fed a natural diet of macroalgae contained higher EPA, DPAn-3 and total n-3 PUFA proportion compared to juvenile cultured hybrid abalone fed artificial diets. Similarly wild adult blacklip abalone fed a natural diet of macroalgae contained a higher proportion of DPAn-3 compared to hybrid abalone fed artificial diets. In addition Dunstan et al. [10] reported that muscle of juvenile cultured greenlip and hybrid abalone fed an artificial diet showed lower levels of EPA, DPAn-3 and total n-3 PUFA than those fed green algae. Lower level of ALA was also recorded in juvenile hybrid abalone fed an artificial diet compared to the juvenile cultured greenlip abalone fed green algae.

Fatty acid biosynthesis in fish has been well studied and it has been found that the overall conversion of ALA to highly unsaturated fatty acids (HUFA) occurs poorly in the marine species [13, 14]. For abalone, however, there is no direct evidence on the pathways of fatty acid biosynthesis. Available information suggested that *H. discus hannai* may have the capacity to synthesize EPA and DHA from ALA through elongation and desaturation [15]. Another study also suggested that *H. fulgens* is capable of desaturation and elongation of ALA to EPA [16]. Fatty acid desaturases and fatty acid elongases were found to be critical in the biosynthetic pathways of highly unsaturated fatty acids from shorter chain PUFA [17]. Desaturases genes have been cloned and characterized from a number of fish, including Δ6 desaturase from rainbow trout [18], and Δ5 and Δ6 desaturase from Atlantic salmon [19]. Genes coding for proteins specifically involved in the elongation of HUFA biosynthesis have been cloned from a number of fish including fresh water zebra fish, carp and tilapia, the salmonoids, rainbow trout and Atlantic salmon, and marine fish, including cod, turbot and sea bream [20–22].

This study investigated the effects of feed supplemented with fish oil on fatty acid composition in muscle, gonad and digestive gland (DG) of cultured adult female jade tiger hybrid abalone. In addition the effects of FO supplementation on fatty acid Δ6 desaturase and elongase 2 gene expressions in muscle tissue of this animal were also studied. These data will provide useful information for seafood and abalone aquaculture industries. To the best of our knowledge, there is no information available on desaturase and elongase gene expression in abalone.

Materials and Methods

Experimental Diets

A commercial diet (Adam and Amos Pty Ltd) of Australian abalone was used in the formulation of experimental diets. Diet 1 (control diet) was the normal commercial abalone diet with no additional fish oil (FO) supplement. Diets 2–6 were supplemented with 0.5, 1, 1.5, 2, and 2.5% FO respectively. Fatty acid composition and total lipid content of the experimental diets are shown in Table 1. The control diet contained 57.6% total saturated fatty acid (SFA), 5.6% monounsaturated fatty acid (MUFA) and 36.8% polyunsaturated fatty acid (PUFA). The diets with FO supplements (diets 2–6) contained 21–24.7% total SFA, 18.6–22.9% total MUFA, and 52.3–60.3% total PUFA. The composition of EPA, DPAn-3, DHA and total n-3 PUFA of the diets with FO supplement were gradually increased in the experimental diets. The control diet contained 0.42 g/100 g total lipids while other diets contained lipids ranging from 1.10 to 2.72 g/100 g. All of these experimental diets were stored at 4 °C until use.

Abalone and Experimental Conditions

Ninety cultured adult Jade Tiger abalone with an average body weight of 44.0 ± 0.3 g were obtained from Great Southern Waters abalone farm, Victoria, Australia. Abalone were acclimatized to laboratory conditions and fed a normal commercial diet for a week before initiation of the feeding experiments. Each individual abalone was gently blotted dry on a paper towel, tagged, measured and weighed, and then five abalone were placed into a 30 L plastic aquarium supplied with filtered seawater via a flow through system, and assigned one of the six experimental diets. There were three replicates for each of the six dietary treatments. All animals were maintained under a 24 h dark photoperiod. Temperature was maintained at 16 °C throughout the feeding trial. Salinity (31–35 ppt), dissolved oxygen (no less than 6 mg/L), nitrite, ammonia and pH (7–8) were monitored daily. Aquaria were cleaned three

Table 1 Fatty acid composition (mol %) and total lipid content (g/100 g) of experimental diets

Fatty acid	Diet					
	1	2	3	4	5	6
14:0	0.8	2.4	3.5	4.7	4.6	4.5
16:0	55.4	15.7	16.4	15.0	13.0	12.8
17:0	0.3	0.1	0.3	0.3	0.4	0.2
18:0	0.8	2.4	3.5	4.3	4.6	4.9
20:0	0.1	0.2	0.1	0.1	0.1	0.1
24:0	0.2	0.2	0.1	0.3	0.1	0.1
Total SFA	57.6	21.0	23.8	24.7	22.6	22.6
16:1	0.6	3.2	4.3	5.4	5.9	6.3
17:1	0.4	0.9	1.4	1.3	1.4	1.7
18:1n9	3.6	12.0	12.4	12.6	11.1	9.7
18:1n7	0.5	1.2	1.1	1.2	1.1	1.0
20:1	0.5	1.3	2.3	2.4	3.0	3.6
Total MUFA	5.6	18.6	21.5	22.9	22.5	22.3
18:2n6	16.5	36.0	30.4	22.0	20.5	17.6
18:3n3	1.4	3.2	2.9	2.5	3.1	2.8
20:2n6	0.6	0.2	0.2	0.2	0.2	0.2
20:3n6	0.4	0.2	0.2	0.2	0.2	0.2
20:4n6	0.5	1.6	0.6	0.7	0.8	0.9
20:5n3	9.2	9.6	10.2	14.7	16.1	18.2
22:4n6	0.6	0.4	0.6	0.3	0.8	1.0
22:5n6	0.4	0.5	0.6	0.5	0.5	0.5
22:5n3	1.2	1.5	1.5	1.6	2.0	2.1
22:6n3	6.0	7.1	7.5	9.6	10.7	11.6
Total n-3	17.8	21.4	22.1	28.4	31.9	34.7
Total n-6	19.0	38.9	32.6	23.9	23.0	20.4
Total PUFA	36.8	60.3	54.7	52.3	54.9	55.1
n-3/n-6 PUFA	0.9	0.6	0.7	1.2	1.4	1.7
Total lipid (g/100 g)	0.42	1.10	1.59	1.92	2.23	2.72

SFA saturated fatty acids, *MUFA* monounsaturated fatty acids, *PUFA* polyunsaturated fatty acids

times a week. The experimental diets were hand-fed every day in the evening at a rate of 2% of body weight. At the end of the experiment, abalone were fasted for 1 day and collected from their aquaria. They were then measured and weighed. Fourteen abalone per treatment were sampled to obtain muscle, gonad and DG tissues for lipid and fatty acid analyses. Four samples from each treatment group were used for investigation of gene expression. This feeding trial was conducted for 90 days.

Analyses of Lipid and Fatty Acids

Five grams of fresh muscle, gonad and digestive gland (DG) were cut finely and left in chloroform to extract the lipids overnight in the dark: methanol (2:1, v/v) which contained 10 mg/L butylated hydroxytoluene was an antioxidant. The lipid extracts were washed according to the Folch procedure [23]. The solvent containing lipids were evaporated under vacuum in a rotary evaporator (Heidolph Standard evaporator, VV2000). The lipid content was determined gravimetrically [24].

Fatty acid methyl esters (FAME) were prepared by saponification of approximately 10 mg of lipid, using KOH (0.68 mol/L in methanol), followed by esterification with 14% boron trifluoride in methanol, with 0.25 mg of tricosanoic acid (23:0) added as an internal standard. FAME were separated by a capillary gas liquid chromatograph (Varian 3400) equipped with an auto sampler and a flame ionization detector (FID) using a 50 m × 0.32 mm (I.D) fused silica bonded phase capillary column (BPX70, SGE, Melbourne, Australia). The column oven was programmed from 140 to 220 °C at 5 °C/min and held for 3 min. The oven temperature was then increased to 260 °C at a rate of 8 °C/min and held for 8 min. Helium was used as the carrier gas at a flow rate of 1.6 mL/min and a linear velocity 43 cm/s. The injector and detector were maintained at 250 and 300 °C respectively. Fatty acids were identified by comparison of retention times with those of standard mixtures of fatty acid methyl esters (GLC reference standard 403) and the results were calculated using response factors derived from chromatograph standards of known composition (Nu-Chek-Prep, Elysian, MN, USA).

RNA Extraction and Quantitative Polymerase Reaction

After the completion of the feeding trial, muscle samples of four abalone were randomly selected from each treatment group. They were then frozen immediately in liquid nitrogen and stored at −80 °C prior to RNA extraction. Total RNA was extracted from 50 mg of muscle tissue using TRI reagent (Molecular Research Center, USA) according to the manufacturer's specification. The total RNA concentration was determined by A260/A280 measurement. One microgram of total RNA was reverse transcribed into cDNA using AMV reverse transcriptase first strand cDNA synthesis kit (Marligen Biosciences, USA). The expression of Δ-6 desaturase and elongase 2 genes in muscle tissue from abalone fed with the different experimental diets were studied by real-time polymerase chain reaction (RT-PCR). PCR primers known to be specific for, Δ6 desaturase (F 5′-ACCTAGTGGCTCCTCTGGTC-3′ and R 5′-CAGATCCCCTGACTTCTTCA-3′, AF301910) and elongase 2 (F 5′-GAACAGCTTCATCCATGTCC-3′ and R 5′-TGACTGCACATATCGTCTGG-3′, AY605100) were used for PCR amplification of cDNA. ß-actin (F 5′-CAAGCAGGAGTACGACGAGT-3′ and R 5′-CTGAAG TGGTAGTCGGGTGT-3′, AJ438158) was used as a housekeeping gene for normalizing mRNA levels of the

target genes. The amplification of cDNA samples was carried out using the SYBR green PCR kit. Fluorescent emission data were captured and mRNA levels were analyzed using the critical threshold (CT) value [25]. Thermal cycling and fluorescence detection were conducted using the Biorad IQ50 sequence detection system (Biorad USA).

Statistical Analyses

Results are presented as means ± SD. The data were tested for homogeneity of variances using a Levene test. All data were analysed by one-way analysis of variance (ANOVA) to determine significance of differences among total lipid content, fatty acid composition and gene expression of abalone fed the different experimental diets. Tukey HSD tests were used for post hoc comparison. P values of less than 0.05 were considered statistically different. Statistical analysis was performed using the SPSS package (version 17.0).

Results

The fatty acid composition of muscle, gonad and DG of Jade Tiger hybrid abalone fed different experimental diets are given in Tables 2, 3 and 4. In general, fatty acid profiles

Table 2 Fatty acid composition (mol %) and total lipid content (g/100 g wet tissue) of muscle in Jade Tiger abalone fed different experimental diets for 12 weeks ($n = 10$)

Fatty acid	Diet					
	1	2	3	4	5	6
14:0	1.3 ± 0.1a	0.9 ± 0.1b	1.3 ± 0.1a	0.8 ± 0.1b	1.3 ± 0.2a	1.3 ± 0.1a
16:0	23.8 ± 1.0a	18.1 ± 0.6b	17.0 ± 0.4bc	16.0 ± 0.4c	18.1 ± 0.4b	17.9 ± 0.4b
17:0	1.3 ± 0.1a	1.8 ± 0.1b	1.0 ± 0.1a	1.0 ± 0.1a	1.0 ± 0.2a	1.0 ± 0.1a
18:0	7.0 ± 0.5a	7.5 ± 0.7a	6.5 ± 0.2b	5.3 ± 0.4c	5.7 ± 0.6c	5.9 ± 0.6bc
20:0	0.2 ± 0.0a	0.2 ± 0.0a	0.2 ± 0.0a	0.2 ± 0.0a	0.2 ± 0.0a	0.1 ± 0.0a
24:0	0.1 ± 0.0a	0.1 ± 0.0a	0.1 ± 0.0a	0.1 ± 0.0a	0.1 ± 0.0a	0.1 ± 0.0a
Total SFA	33.7 ± 1.7a	28.6 ± 1.5b	26.1 ± 0.8c	23.4 ± 1.1d	26.4 ± 1.4c	26.3 ± 1.2c
16:1	1.5 ± 0.1a	1.5 ± 0.2a	1.6 ± 0.1a	1.9 ± 0.2b	1.5 ± 0.1a	1.6 ± 0.1a
17:1	8.0 ± 0.4ac	5.0 ± 0.3b	8.7 ± 0.4ac	4.3 ± 0.3b	7.2 ± 0.3a	8.9 ± 0.5c
18:1n9	6.2 ± 0.4a	6.2 ± 0.4a	5.7 ± 0.3a	6.0 ± 0.4a	5.7 ± 0.2a	5.7 ± 0.2a
18:1n7	4.8 ± 0.4ab	5.1 ± 0.4b	4.4 ± 0.5ab	5.0 ± 0.3b	4.6 ± 0.4ab	4.8 ± 0.2ab
20:1	3.4 ± 0.4a	5.0 ± 0.5b	4.0 ± 0.3a	4.9 ± 0.2b	3.7 ± 0.2a	3.3 ± 0.6a
Total MUFA	23.9 ± 1.7a	22.8 ± 1.8a	24.4 ± 1.6a	22.1 ± 1.4a	22.7 ± 1.2a	24.3 ± 1.6a
18:2n6	6.5 ± 0.3a	6.7 ± 0.8a	7.2 ± 0.6ab	8.3 ± 0.8b	7.7 ± 0.5ab	7.1 ± 0.4ab
18:3n3	0.7 ± 0.1a	0.8 ± 0.1a	1.1 ± 0.1b	1.3 ± 0.1bc	1.1 ± 0.2b	0.8 ± 0.1a
20:2NMI	0.9 ± 0.1a	0.9 ± 0.1a	0.9 ± 0.1a	0.8 ± 0.1a	0.8 ± 0.2a	0.9 ± 0.1a
20:2n6	1.4 ± 0.1a	1.4 ± 0.1a	1.5 ± 0.1ab	1.8 ± 0.2b	1.7 ± 0.2ab	1.3 ± 0.1a
20:3n6	0.6 ± 0.1a	0.7 ± 0.1a	0.7 ± 0.1a	0.8 ± 0.1a	0.8 ± 0.1a	0.6 ± 0.1a
20:4n6	5.3 ± 0.4a	5.2 ± 0.5a	5.2 ± 0.2a	5.7 ± 0.3a	4.5 ± 0.3b	5.3 ± 0.5a
20:5n3	6.9 ± 0.5a	8.6 ± 0.1b	8.9 ± 0.2b	10.4 ± 0.4c	9.5 ± 0.7b	9.3 ± 0.5b
22:2NMI	6.0 ± 0.5a	6.6 ± 0.5b	6.6 ± 0.5b	5.1 ± 0.7c	6.3 ± 0.9ab	6.3 ± 0.9ab
22:4n6	0.4 ± 0.2a	0.4 ± 0.1a	0.3 ± 0.1a	0.3 ± 0.1a	0.4 ± 0.1a	0.3 ± 0.1a
22:5n6	0.9 ± 0.1a	0.9 ± 0.1a	0.8 ± 0.1a	0.8 ± 0.1a	0.9 ± 0.1a	0.9 ± 0.1a
22:5n3	9.8 ± 0.1a	12.0 ± 0.7b	11.9 ± 0.6b	14.3 ± 0.9c	13.3 ± 0.7 cd	12.3 ± 0.5b
22:6n3	2.0 ± 0.2a	3.5 ± 0.3b	3.5 ± 0.2b	4.9 ± 0.1c	4.0 ± 0.3b	3.1 ± 0.4b
Total n-3	19.4 ± 1.0a	25.1 ± 1.3b	25.3 ± 1.1b	30.8 ± 1.5c	27.9 ± 2.1d	25.5 ± 1.5b
Total n-6	15.1 ± 1.3a	15.3 ± 1.5a	15.7 ± 0.9a	17.7 ± 1.7b	16.0 ± 1.4a	15.5 ± 1.3a
Total PUFA	34.5 ± 2.3a	40.4 ± 2.8b	41.0 ± 2.0b	48.5 ± 3.2c	43.9 ± 3.5d	41.0 ± 2.8b
n-3/n-6	1.3 ± 0.1a	1.6 ± 0.1b	1.6 ± 0.1b	1.7 ± 0.1b	1.7 ± 0.1b	1.6 ± 0.1b
Lipid (g/100 g)	1.24 ± 0.02a	1.31 ± 0.02b	1.32 ± 0.03b	1.40 ± 0.05c	1.36 ± 0.04bc	1.34 ± 0.03bc

Values are expressed as means ± SD. Values in the same row with different letters indicate significant differences ($P < 0.05$)

SFA saturated fatty acids; *MUFA* monounsaturated fatty acids; *PUFA* polyunsaturated fatty acids; *NMI* non-methylene-interrupted fatty acids

Table 3 Fatty acid composition (mol %) and total lipid content (g/100 g wet tissue) of gonad in Jade Tiger abalone fed the different experimental diets for 12 weeks ($n = 10$)

Fatty acid	Diet					
	1	2	3	4	5	6
14:0	6.3 ± 0.3a	4.1 ± 0.4b	4.3 ± 0.3b	2.0 ± 0.2c	4.1 ± 0.4b	2.0 ± 0.3c
16:0	25.1 ± 2.2a	17.3 ± 1.2bc	19.0 ± 1.5c	12.4 ± 1.3d	20.0 ± 2.0c	15.0 ± 1.3bd
17:0	1.2 ± 0.2a	0.8 ± 0.2b	0.7 ± 0.1b	0.8 ± 0.1b	0.8 ± 0.1b	0.7 ± 0.1b
18:0	3.7 ± 0.4a	3.4 ± 0.3a	3.3 ± 0.2a	3.3 ± 0.2a	3.4 ± 0.3a	3.3 ± 0.5a
20:0	0.2 ± 0.0a	0.2 ± 0.0a	0.3 ± 0.0a	0.2 ± 0.0a	0.2 ± 0.0a	0.2 ± 0.0a
24:0	0.1 ± 0.0a	0.1 ± 0.0a	0.1 ± 0.0a	0.1 ± 0.0a	0.1 ± 0.0a	0.1 ± 0.0a
Total SFA	36.6 ± 3.1a	25.9 ± 2.1b	27.5 ± 2.1b	18.9 ± 1.8c	28.4 ± 2.8b	21.5 ± 2.2c
16:1	1.3 ± 0.1a	3.6 ± 0.2b	3.4 ± 0.2b	2.9 ± 0.2bc	1.9 ± 0.2ac	3.8 ± 0.5b
17:1	1.2 ± 0.0a	2.1 ± 0.3b	2.6 ± 0.2c	2.9 ± 0.1c	1.1 ± 0.0a	3.7 ± 0.1d
18:1n9	14.1 ± 0.9a	10.5 ± 0.7b	4.2 ± 0.2c	6.1 ± 0.5d	9.3 ± 0.8e	9.8 ± 0.8be
18:1n7	10.8 ± 0.7a	7.8 ± 0.5b	15.2 ± 1.2c	5.3 ± 0.3d	7.8 ± 0.4b	8.4 ± 0.4b
20:1	4.0 ± 0.4a	7.4 ± 0.5b	3.9 ± 0.3a	6.9 ± 0.5b	3.5 ± 0.2a	7.2 ± 0.4b
Total MUFA	31.4 ± 2.2a	31.4 ± 2.2a	29.2 ± 2.1ab	24.0 ± 1.6c	23.5 ± 1.5c	33.1 ± 2.2d
18:2n6	7.6 ± 0.7a	12.7 ± 1.0b	12.8 ± 1.0b	20.0 ± 1.8c	18.3 ± 1.2c	14.7 ± 1.4b
18:3n3	0.7 ± 0.2a	1.0 ± 0.1ab	0.8 ± 0.2a	1.7 ± 0.2c	1.3 ± 0.2b	1.2 ± 0.1b
20:2NMI	1.8 ± 0.1a	2.4 ± 0.2b	1.6 ± 0.1a	2.0 ± 0.3ab	1.7 ± 0.1a	1.6 ± 0.1a
20:2n6	2.0 ± 0.2a	2.5 ± 0.2b	2.5 ± 0.1b	2.5 ± 0.1b	2.1 ± 0.1a	2.5 ± 0.1b
20:3n6	0.3 ± 0.0a	0.3 ± 0.0a	0.7 ± 0.1b	0.6 ± 0.1b	0.4 ± 0.0a	0.4 ± 0.0a
20:4n6	2.1 ± 0.2a	2.2 ± 0.2a	1.9 ± 0.2a	2.9 ± 0.4b	2.4 ± 0.2ab	2.7 ± 0.2b
20:5n3	4.5 ± 0.3a	6.5 ± 0.4b	7.3 ± 0.2bd	9.9 ± 0.8c	7.1 ± 0.2b	7.7 ± 0.5d
22:2NMi	5.7 ± 0.3a	5.6 ± 0.5a	6.4 ± 0.4b	6.4 ± 0.5b	5.0 ± 0.4c	5.6 ± 0.7a
22:4n6	0.4 ± 0.0a	0.8 ± 0.1b	0.4 ± 0.1a	0.4 ± 0.1a	0.4 ± 0.0a	0.4 ± 0.0a
22:5n6	2.0 ± 0.3a	1.7 ± 0.3a	1.0 ± 0.1b	1.1 ± 0.1b	0.5 ± 0.1b	1.9 ± 0.2a
22:5n3	2.2 ± 0.2a	4.0 ± 0.2b	3.6 ± 0.4b	5.3 ± 0.3c	5.0 ± 0.3 cd	4.4 ± 0.2bd
22:6n3	1.7 ± 0.1a	2.7 ± 0.2b	2.8 ± 0.2b	4.5 ± 0.3c	3.5 ± 0.2d	3.0 ± 0.2bd
Total n-3	9.2 ± 0.7a	14.4 ± 0.8b	14.5 ± 1.0b	21.1 ± 1.6c	16.9 ± 1.0d	15.7 ± 1.4bd
Total n-6	14.4 ± 1.7a	20.1 ± 1.8b	19.3 ± 1.6b	27.5 ± 2.8c	24.5 ± 1.9d	22.5 ± 2.3de
Total PUFA	23.6 ± 2.4a	34.6 ± 2.6b	33.8 ± 2.6b	48.6 ± 3.4c	41.4 ± 2.9d	38.2 ± 3.6e
n-3/n-6	0.6 ± 0.0a	0.7 ± 0.0a	0.8 ± 0.1a	0.8 ± 0.1a	0.7 ± 0.0a	0.7 ± 0.1a
Lipid (g/100 g)	3.88 ± 0.17a	3.92 ± 0.11a	3.95 ± 0.14a	6.64 ± 0.21b	6.08 ± 0.28c	4.25 ± 0.19a

Values are expressed as means ± SD. Values in the same row with different letters indicate significant differences ($P < 0.05$)

SFA saturated fatty acids, *MUFA* monounsaturated fatty acids, *PUFA* polyunsaturated fatty acids, *NMI* non-methylene-interrupted fatty acids

of abalone tissue reflected the fatty acid profiles of experimental diets (Table 1). Feed supplemented with FO at levels between 0.5 and 2.5% (diets 2–6) showed significant effects on n-3 PUFA composition in all three types of tissues (Tables 2–4). Higher levels of total PUFA, n-3 PUFA, EPA, DPAn-3, and DHA ($P < 0.05$) were observed in all the groups fed with diets supplemented with FO, with the most significant improvement being recorded from the group fed the diet containing 1.5% FO supplement (diet 4). For DPAn-3 the higher level was also found in muscle and gonad of abalone fed diet supplemented with 2% FO (diet 5) ($P < 0.05$). The higher ALA level was found in the muscle of abalone fed diets containing 1–2% FO (diets 3, 4 & 5). In gonad and DG, higher ALA was recorded in abalone fed diet containing 1.5% FO (diet 4).

FO supplementation also improved the n-3/n-6 PUFA ratio in all three types of tissue. In muscle tissue all of the five treatment groups fed the diets with FO supplement showed a significantly higher ratio ($P < 0.05$) than the control group (Table 2). For gonad, no marked differences were recorded between the control group and the five treatment groups fed FO supplement (Table 3). The significantly higher ratio of n-3/n-6 PUFA in DG (Table 4) was found in abalone fed diets containing 1.0–2.5% FO supplements (diets 3–6).

There were no significant differences in the total MUFA composition between the six treatment groups in the

Table 4 Fatty acid composition (mol %) and total lipid content (g/100 g wet tissue) of digestive gland in Jade Tiger abalone fed the different experimental diets for 12 weeks ($n = 10$)

Fatty acid	Diet					
	1	2	3	4	5	6
14:0	3.3 ± 0.3a	3.0 ± 0.2a	3.0 ± 0.2a	2.5 ± 0.2b	3.8 ± 0.2c	3.1 ± 0.2a
16:0	20.9 ± 1.0a	15.0 ± 1.1b	15.3 ± 0.8b	11.3 ± 1.7c	16.6 ± 2.0bd	18.7 ± 0.5ad
17:0	0.5 ± 0.1a	1.3 ± 0.1b	0.6 ± 0.1a	0.6 ± 0.1a	1.2 ± 0.1b	0.6 ± 0.0a
18:0	3.4 ± 0.2a	3.3 ± 0.2a	4.3 ± 0.4b	3.7 ± 0.2ab	4.1 ± 0.3b	3.4 ± 0.2a
20:0	0.2 ± 0.0a	0.2 ± 0.0a	0.2 ± 0.0a	0.2 ± 0.0a	0.2 ± 0.0a	0.2 ± 0.0a
24:0	0.1 ± 0.0a	0.1 ± 0.0a	0.1 ± 0.0a	0.1 ± 0.0a	0.1 ± 0.0a	0.1 ± 0.0a
Total SFA	28.5 ± 1.8a	23.0 ± 1.1b	23.6 ± 0.5b	18.4 ± 1.6c	26.0 ± 2.1d	26.1 ± 1.8d
16:1	2.2 ± 0.2a	2.5 ± 0.3a	2.2 ± 0.3a	1.5 ± 0.1b	1.5 ± 0.1b	2.4 ± 0.1a
17:1	2.4 ± 0.2a	2.0 ± 0.2a	3.6 ± 0.2b	3.0 ± 0.2c	3.6 ± 0.2b	3.8 ± 0.2b
18:1n9	13.0 ± 0.8a	8.5 ± 0.9b	8.1 ± 0.6b	6.4 ± 0.3c	8.2 ± 0.5b	11.9 ± 0.8d
18:1n7	8.6 ± 0.7a	5.3 ± 0.4b	6.8 ± 0.2c	4.3 ± 0.2d	6.4 ± 0.4c	8.5 ± 0.3a
20:1	7.1 ± 2.8a	11.0 ± 0.9b	8.0 ± 0.6a	7.0 ± 0.2a	7.0 ± 0.2a	7.8 ± 0.2a
Total MUFA	33.3 ± 0.4a	29.4 ± 1.7b	28.6 ± 1.0bc	22.1 ± 1.1d	26.7 ± 1.9c	34.4 ± 1.3f
18:2n6	11.0 ± 0.9ac	16.8 ± 0.3b	11.9 ± 1.0ce	19.0 ± 1.4d	13.0 ± 0.9e	10.0 ± 1.1a
18:3n3	1.1 ± 0.1a	1.5 ± 0.1b	1.5 ± 0.1b	1.7 ± 0.2c	1.5 ± 0.1b	0.9 ± 0.1a
20:2NMI	1.9 ± 0.1a	1.9 ± 0.1a	1.7 ± 0.1a	1.8 ± 0.1a	1.7 ± 0.1a	1.6 ± 1.3a
20:2n6	2.2 ± 0.2a	2.2 ± 0.2a	2.8 ± 0.2b	2.4 ± 0.1a	2.4 ± 0.1a	2.2 ± 0.1a
20:3n6	0.3 ± 0.1a	0.3 ± 0.0a	0.7 ± 0.1b	0.7 ± 0.1b	0.3 ± 0.1a	0.4 ± 0.0a
20:4n6	2.2 ± 0.2a	2.2 ± 0.2a	3.2 ± 0.3b	2.9 ± 0.2ab	3.0 ± 0.2b	3.0 ± 0.1b
20:5n3	5.1 ± 0.4a	7.0 ± 0.5bd	7.0 ± 0.3bd	8.8 ± 0.6c	7.8 ± 0.5d	6.3 ± 0.4b
22:2NMI	6.0 ± 0.3a	5.6 ± 0.1ab	5.7 ± 0.3ab	6.4 ± 0.2a	4.9 ± 0.2b	4.8 ± 0.2b
22:4n6	0.4 ± 0.0a	0.5 ± 0.1a	0.4 ± 0.0a	0.4 ± 0.0a	0.4 ± 0.0a	0.4 ± 0.0a
22:5n6	2.2 ± 0.3a	1.3 ± 0.2b	2.7 ± 0.2c	1.5 ± 0.1b	1.3 ± 0.1b	1.0 ± 0.1b
22:5n3	2.9 ± 0.2a	4.4 ± 0.3b	5.4 ± 0.3c	7.8 ± 0.4d	5.6 ± 0.3c	4.4 ± 0.1b
22:6n3	2.2 ± 0.2a	3.7 ± 0.2b	4.8 ± 0.4c	6.2 ± 0.2d	5.0 ± 0.2c	5.9 ± 0.1c
Total n-3	11.4 ± 1.1a	16.8 ± 0.7b	18.7 ± 1.4bd	24.5 ±1.6c	19.8 ± 1.0d	16.3 ± 0.3b
Total n-6	18.4 ± 1.8a	23.3 ± 0.9b	21.4 ± 1.2c	26.8 ± 1.6d	20.9 ± 1.2bc	17.2 ± 0.3a
Total PUFA	29.8 ± 2.6a	40.1 ± 1.4b	40.1 ± 1.7b	51.3 ± 2.6c	40.7 ± 1.2b	33.5 ± 1.2d
n-3/n-6	0.6 ± 0.0a	0.7 ± 0.0a	0.9 ± 0.0b	0.9 ± 0.1b	0.9 ± 0.1b	0.9 ± 0.1b
Lipid (g/100 g)	3.44 ± 0.09a	3.45 ± 0.10a	3.68 ± 0.16ab	6.05 ± 0.14c	4.07 ± 0.11d	3.83 ± 0.1bd

Values are expressed as means ± SD. Values in the same row with different letters indicate significant differences ($P < 0.05$)

SFA saturated fatty acids, *MUFA* monounsaturated fatty acids, *PUFA* polyunsaturated fatty acids, *NMI* non-methylene-interrupted fatty acids

muscle. However, for gonad and DG higher MUFA level was recorded in abalone fed diet with 2.5% FO supplement (diet 6) ($P < 0.01$). In all three types of tissue, abalone fed the diets with FO supplements (diets 2–6) showed significantly lower SFA than the control group (diet 1) ($P < 0.05$) with diet containing 1.5% FO supplement (diet 4) being the most effective.

The total lipid content in muscle, gonad and DG are also shown in Tables 2–4. Muscle of abalone fed the five diets supplemented with FO contained significantly higher contents of total lipid than the control group ($P < 0.05$). The highest total lipid content was recorded in abalone fed diet containing 1.5% FO supplement (diet 4) with 1.40 g/100 g, 5.64 g/100 g and 6.05/100 g being recorded in muscle, gonad and DG respectively while the control group (diet 1) showed 1.24 g/100 g total lipid in muscle, 3.88 g/100 g in gonad and 3.44 g/100 g in DG ($P < 0.01$).

The expression of fatty acid elongase 2 and Δ6 desaturase genes in muscle tissue from abalone fed diets 1–6 are shown in Figs. 1 and 2. Values are expressed as arbitrary units of elongase and desaturase normalized against the expression levels of β-actin. For Δ6 desaturase, significantly higher expression was observed in the muscle of abalone fed diet 2 (with 0.5% FO supplement, $P < 0.05$). There were no significant differences between other treatment groups (Fig. 2). Elongase 2 expression was

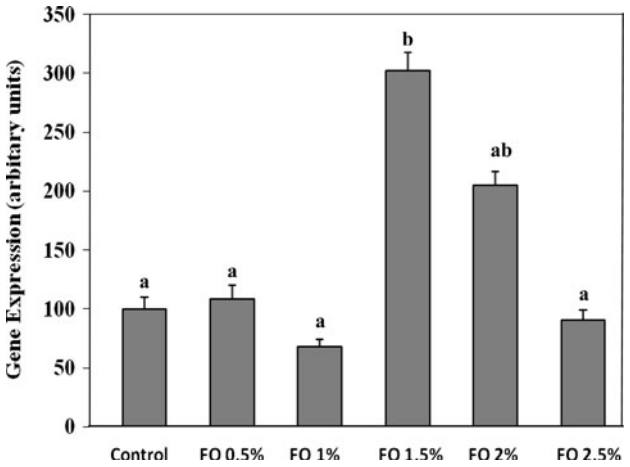

Fig. 1 Effect of experimental diets on expression of fatty acid elongase 2 gene in the muscle of Jade Tiger abalone. Data are presented as means ± SME ($n = 4$). *Different letters* above the *bars* indicate significant differences ($P < 0.05$)

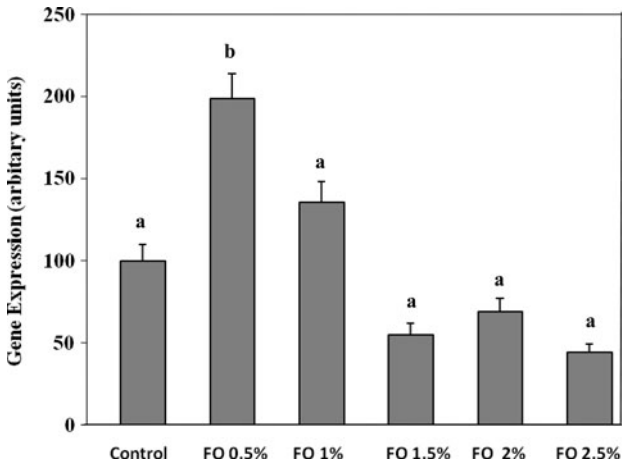

Fig. 2 Effect of experimental diets on expression of fatty acid Δ6 desaturase gene in the muscle of Jade Tiger abalone. Data are presented as means ± SME ($n = 4$). *Different letters* above the *bars* indicate significant differences ($P < 0.05$)

significantly higher in muscle of abalone fed 1.5% FO (diet 4), followed by 2.0% FO (diet 5). No marked differences were recorded between the treatment groups fed diets containing 0.5, 1.0 and 2.5% FO (diets 2, 3 & 6) ($P > 0.05$) (Fig. 1).

Discussion

Abalone fed diets with fish oil supplement significantly improved the levels of total n-3 PUFA, EPA, DPAn-3 and DHA in Jade Tiger hybrid abalone. These results are consistent with previous reports on other abalone species, such as greenlip abalone (*Haliotis laevigata*) [9], green abalone (*Haliotis fulgens*) [16], Donkey ear abalone (*Haliotis asinine* Linne) [26] and *Haliotis discus hannai* Ino [15]. The present study showed that muscle, gonad and digestive gland (DG) of Jade Tiger abalone fed diet supplemented with 1.5% FO (diet 4) contained the highest levels of total n-3 PUFA, EPA, DPAn-3 and DHA. This might be attributed to the efficiency in utilization of dietary lipids by abalone. Abalone are herbivores and previous study showed that their lipid requirement is very low as they are highly efficient in utilizing lipids [31]. An optimal increase of FO in the diet has resulted in a higher n-3 PUFA profiles and growth rate. It has been reported that greenlip abalone showed an improved composition of long chain n-3 PUFA and optimal growth when fish oil levels are at 1.0–2.5% in the diets. Juvenile abalone, *Haliotis discus hannai* Ino also showed higher levels of EPA and DHA when diet supplemented with 2% FO [15].

In general the lipid level of balanced diets developed for abalone ranges from 1.5 to 5.0% [30]. Abalone showed a poor response to elevated lipid levels due to the lower capacity of dealing with high dietary oil and this might be attributed to the low digestibility of lipids in this animal [9, 16, 27–31]. This probably explains why at higher FO levels (2 & 2.5% as in diets 5 & 6) in the present study, the long chain n-3 PUFA, EPA and DHA tended to decrease in comparison with the effect of diet containing 1.5% FO. The similar results have also been reported from other herbivorous marine species [33, 34]. In addition a decreased utilization of dietary fat in juvenile cod (*Hexagrammos otakii* Jordan et Starks) with excessive dietary level of long chain n-3 PUFA has been reported [32]. In green abalone (*Haliotis fulgens*), maximum growth rates were obtained when they were fed a formulated feed containing 1.5% lipids [16]. The Japanese feed Nihon Kogyo contained only 1.5% lipid but produced significantly increased growth rates in abalone relative to those with 3% lipid [9]. In contrast, some species showed an improved growth rate at the higher lipid levels. In greenlip abalone, growth rates were improved when abalone fed diets containing 2.6 and 4.2% total lipids. Other diet with total lipid content of 3.8% also increased growth rates [9]. The dietary lipid level of 3.5% has been considered to be optimum level for Juvenile *Haliotis discus hannai* Ino [29]. It appears that the lipid requirements of abalone might be species specific although the overall range is lower in comparison with other animals. In our study the total dietary lipid contents ranged from 0.42 to 2.92% dry wt. The diet supplemented with 1.5% FO had 1.92% of total lipid and this probably is the optimal lipid level for Jade Tiger hybrid abalone and thus achieved the best outcome.

Study also showed that, addition of marine or vegetable oils to commercial abalone diets should be limited to 3% in order to maintain the optimal digestibility of nitrogen and

amino acids, and gross energy [34]. Formulated abalone diets from around the world contain a wide range of total lipid content (1–11% wet wt) [9]. In these diets, a large variation in fatty acid composition was evident. The diets containing high lipid level and no fish products are not recommended [9].

Abalone require n-3 and n-6 PUFA as essential fatty acids [46] with the n-3/n-6 ratio providing a broad indication of fatty acid utilization within the tissues. The foot muscle contained a high proportion of n-3 PUFA; whereas n-6 PUFA were more prominent in the gonad and DG. One of the abundant fatty acids in the diet, LA only formed a moderate component of the fatty acid fraction in the muscle but was more common in the gonad and DG. In the muscle, arachidonic acid (ARA, 20:4n-6) composition was higher but a lower level was found in the gonad and DG. In all three tissues the proportion of EPA was present in similar abundance, resulting in a relatively high EPA: ARA ratios in the gonad and DG. Dunstan et al. [9] reported that most of the tissue ARA originated from dietary linoleic acid (LA). Our results showed a similar trend. Although a high level of ARA may not be required for muscle growth, it may be required for oogenesis and embryogenesis. In agreement with our present results, Nelson et al. [45] also observed a higher ARA level in the muscle of *Haliotis fulgens* than in the gonad and DG. One of the less abundant n-3 PUFA in the diet, DPAn-3 formed a major component of n-3 PUFA fraction in the muscle but was less prominent in the gonad and DG. These results suggest that abalone may require less DPAn-3 in the gonad and DG to meet their physiological needs in comparison with muscle. Other possible explanation is that DPAn-3 in the gonad and DG may be converted to DHA through desaturase and elongase at a higher rate than in the muscle tissue. However further study is required to compare the level of gene expression in different tissues. Lower composition of DPAn-3 in the gonad and DG has also been reported for female green abalone [45], greenlip and blacklip abalone [47]. In general, the variation in LA, ARA, and DPAn-3 were largely responsible for the differences in n-3/n-6 ratio in tissues of Jade Tiger abalone. This may explain the differential proportion of n-3/n-6 ratio between the tissues in the present study. In our study all the five diets supplemented with FO have improved the n-3/n-6 PUFA ratio in the muscle. This is in agreement with the reports that muscle n-3/n-6 ratio is affected by dietary n-3 levels [9, 16, 35–44]. As muscle is widely used for human consumption, the higher n-3/n-6 PUFA ratio will improve the nutritional value of cultured abalone.

Previous studies showed that cultured abalone contained less long chain n-3 PUFA than wild abalone. The results of our study demonstrated that the muscle of abalone fed with diet containing 1.5% FO supplement can reach similar amounts of EPA, DPAn-3 and total n-3 PUFA as those in wild abalone [10, 12]. Dunstan et al. [10] reported that the muscle of wild greenlip abalone contained 0.2% DHA, 14.1% DPAn-3, 9.9% EPA, and 25.1% total n-3 PUFA, while wild blacklip abalone contained 0.3% DHA, 13.5% DPAn-3, 6.8% EPA, and 22.2% total n-3 PUFA. The study by Su et al. [12] also showed the similar composition of fatty acids in the muscle of wild blacklip abalone with DHA, DPAn-3, EPA, and total n-3 PUFA at 0.4, 10.1, 8.8 and 20.5% of total fatty acids, respectively. As shown in Table 2, we found that DHA, DPAn-3, EPA and total n-3 PUFA levels were at 4.9, 14.3, 10.4 and 30.8% of total fatty acids respectively in the muscle of abalone fed a diet with a 1.5% FO supplement. These results are comparable with the published data on wild abalone. In addition a higher DHA level was observed in all three types of tissue from our study. Thongrod et al. [26] showed that cultured abalone (*H. asinina,* Linne) fed a diet supplemented with FO contained similar long chain n-3 PUFA to wild-caught abalone. The higher DHA level recorded in the present study might be attributed to the higher DHA levels in the experimental diets than in the natural macroalgae diets reported in the previous studies [10, 12, 45]. The macroalgae diet of the adult wild greenlip and blacklip abalone contained 0.7% DHA and produced only 0.2% to 0.4% DHA in the muscle tissue [9, 10, 12]. Uki et al. [27] found that the level of DHA in abalone tissue increased when abalone were fed a diet containing more DHA although DPAn-3 remained the most abundant long chain n-3 PUFA [46]. The higher DHA level in our study also implicates that Jade Tiger abalone can accumulate DHA directly from dietary sources and may also have the ability to bio-convert 18-carbon n-3 PUFA, such as ALA, to EPA and DHA to a certain extent. The low level of ALA in abalone tissue at the present study supports this possibility. Wei et al. [15] suggested that *H. discus hannai* has the capability to synthesize EPA and DHA from ALA through elongation and desaturation. A similar study by Durazo-Beltran et al. [16] with *H. fulgens* also suggested that abalone is capable of desaturation and elongation of ALA to EPA.

Data presented here represent new information on the Δ6 desaturase and elongase 2 gene expression in abalone. The expression of Δ6 desaturase and elongase 2 involved in the highly unsaturated fatty acid biosynthetic pathway varied in muscle of abalone fed with the different experimental diets (Figs. 1, 2). Elongase 2 gene expression was significantly increased in abalone fed 1.5% FO. The increase in elongase 2 gene expression positively coincides with the highest EPA, DPAn-3 and DHA levels in muscle of abalone fed with this diet. This may indicate the metabolism of ALA and further suggests that abalone have the ability to convert ALA to EPA, DPAn-3 and DHA to a certain extent. The highest level of elongase gene

expression in the abalone fed with 1.5% FO diet may also relate to the direct conversion of EPA to DPAn-3 and then DHA. Dietary EPA bypass the initial rate limiting Δ6 desaturase step in the n-3 long chain PUFA biosynthetic pathway and this may lead to DPAn-3 and DHA being synthesized. Abalone fed the diet with the highest level of FO supplement (2.5%) did not produce the highest level of elongase 2 expression. This may suggest that abalone have a limited capacity to utilize and/or a limited requirement for long chain n-3 PUFA [9] and an elevated level of these fatty acids in the diet may decrease elongase 2 expression. Conflicting results have been reported on fatty acid elongase gene expression in salmon liver with the replacement of dietary FO with vegetable oil [17, 52]. Fatty acid elongase gene expression increased in liver with graded replacement of linseed oil [17]. However, in a more recent trial, a high level of elongase gene expression in salmon fed FO compared to salmon fed with vegetable oil has been reported [52]. This is in agreement with our findings that, FO inclusion in abalone increased elongase 2 expression.

Gene expression of Δ6 desaturase showed a significant increase in muscle of abalone fed the diet containing the 0.5% FO supplement. This result does not coincide with the highest EPA, DPAn-3 and DHA levels in abalone muscle. Previous studies demonstrated that dietary concentrations of substrates such as ALA had a positive correlation with the expression of the fatty acid desaturase gene [17, 48]. The reason that the diet containing 0.5% FO (diet 2) increased expression of desaturase compared to the control diet in the present study may also relate to the high level of ALA in the diet. The high level of dietary n-6 PUFA relative to n-3 PUFA in the diet containing 0.5% FO, contributed to a high n-6/n-3 ratio, particularly LA to ALA ratio in the diet. This may have resulted in a smaller rise in EPA, DPAn-3 and DHA levels in tissue due to the competitive inhibitory effect of n-6 and n-3 at the level of initial desaturation reaction. Miller et al. [48] also suggested that increased n-6 PUFA in fish fed a diet containing a high level of n-6 PUFA is probably associated with the markedly higher n-6/n-3 fatty acid ratio in the white muscle and liver of fish and increased competition between n-6 and n-3 PUFA for desaturase enzymes. It is also known that the conversion rate of ALA to long chain n-3 PUFA is affected by the fatty acid composition of the diet. In particular the presence of LA has been demonstrated to compete with the ALA for the desaturase and elongase enzymes [14, 49]. Our results suggest that essential fatty acids such as ALA can be metabolized into EPA, DPAn-3 and DHA. Also, EPA may be converted to DPAn-3 and DPAn-3 to DHA to certain extent. This process involves sequential desaturase (adding double bonds) and chain elongase (adding carbon atoms to the hydrocarbon backbone [50]. The enzymatic competition between n-6 and n-3 PUFA require dietary balance in the precursor fatty acids, as an overabundance in one will lead to a relative deficiency in the metabolites of the other and vice versa [14, 49].

Studies also showed that dietary fatty acids, environmental factors, and the life cycle can affect elongase and desaturase activity [17, 51, 52]. Each step along the long chain n-3 PUFA pathway depends on the amount of substrate. Therefore, increased elongase 2 and Δ6 desaturase gene expression could be influenced by increased dietary concentrations of substrate ALA. The elongase and desaturase genes also act upon the n-6 pathway. However, fatty acid profiles and the Δ6 desaturase and elongase 2 gene expression of this study indicate that there is a preference for the n-3 pathway. Available information suggested that abalone have the capacity to synthesize EPA and DHA from ALA through elongation and desaturation [15, 16]. These few studies were all based on the feeding trial which involved only dietary lipid sources. Our results on the Δ6 desaturase and elongase 2 gene expression in abalone provide further evidence on biosynthesis pathway of long chain n-3 PUFA. Although actual enzymatic activities of both genes were not measured, studies on several fish species have shown that expression of Δ6 desaturase and elongase mRNA correlated with their enzymatic activities [53–55]. To the best of our knowledge, this is the first study on abalone gene expression. Future studies on the gene expression in other tissues/organs such as the DG as well as the analysis of actual enzymatic activities of both Δ6 desaturase and elongase 2 are required to further support the suggestion of HUFA biosynthesis activities within the muscle.

In conclusion, the present study demonstrated that supplementation with FO in the normal commercial diet of abalone can increase the level of long chain n-3 PUFA in cultured abalone. FO supplementation at a concentration of 1.5% appears to achieve the best outcome. The study also found that Jade Tiger abalone fed a diet containing 1.5% FO supplement contained similar amounts of EPA, DPAn-3 and total n-3 PUFA, and even higher DHA than in wild-caught abalone. In addition, the expression of Δ6 desaturase and elongase 2 genes in muscle of Jade Tiger abalone could be enhanced with FO supplementation. Elongase 2 expression in the muscle of abalone fed with the diet containing 1.5% FO supplement coincided with the level of long chain n-3 PUFA in the tissue. Overall, these findings suggest that abalone have the ability to synthesize the highly unsaturated fatty acids in their tissues and further studies to detail the activity of elongation/desaturation pathway is warranted.

Acknowledgments This project was funded by a postgraduate scholarship at Victoria University, Australia. We thank the Great Southern Waters abalone farm, Victoria, Australia for suppling

abalone samples and ADAM and AMOS Pty Ltd, SA, Australia for their assistance in formulating the experimental diets. The authors also thank Melrose Laboratories Pty Ltd, Victoria, Australia for the supply of fish oil, and Assoc. Prof. David Cameron-Smith, Deakin University, Victoria, Australia for providing the PCR primers.

References

1. Breslow JL (2006) n-3 Fatty acids and cardiovascular disease. Am J Clin Nutr 83:1477S–1482S
2. Rasmussen B, Vessby B, Uusitupa M, Berglund L, Pedersen E, Riccardi G, Rivellese AA, Tapsell L, Hermansen K (2006) Effects of dietary saturated, monounsaturated and n-3 fatty acids, on blood pressure in healthy subjects. Am J Clin Nutr 83: 221–226
3. Schwellenbach LJ, Olson KL, McConnell KJ, Stolcpart RS, Nash JD, Merenich JA, Clinical Pharmacy Cardiac Risk Service Study Group (2006) The triglyceride-lowering effects of a modest dose of docosahexaenoic acid alone vs in combination with low dose eicosapentaenoic acid alone versus in combination with low dose eicosapentaenoic acid in patients with coronary artery disease and elevated triglycerides. J Am Coll Nutr 25:480–485
4. Kimura Y, Kono S, Toyomura K, Nagano J, Mizoue T, Moore MA, Mibu R, Tanaka M, Kakeji Y, Maehara Y, Okamura T, Ikejiri K, Futami K, Yasunami Y, Maekawa T, Takemaka K, Ichimiya H, Imaizumi N (2007) Meat, fish and fat intake in relation to subsite-specific risk colorectal cancer: The Fukuoka Colorectal Cancer Study. Cancer Sci 98:590–597
5. Kuriki K, Hirose K, Wakai K, Ito H, Suzuki T, Hiraki A, Saito T, Iwata H, Tatematsu M, Tajima K (2007) Breast cancer risk and erythrocyte compositions of n-3 highly unsaturated fatty acids in Japanese. Int J Cancer 121:377–385
6. Morris MC, Evans DA, Tangney CC, Bienias JL, Wilson RS (2005) Fish consumption and cognitive decline with age in a large community study. Arch Neurol 62:1849–1853
7. Su KP, Huang SY, Chiu TH, Huang KC, Huang CL, Chang HC, Pariante CM (2008) Omega-3 fatty acids for major depressive disorder during pregnancy: results from a randomized, double-blind, placebo-controlled trial. J Clin Psychiatry 69: 644–651
8. Hogstrom M, Nordstrom P, Nordstrom A (2007) n-3 Fatty acids are positively associated with peak bone mineral density and bone accrual in healthy men: the NO_2 study. Am J Clin Nutr 85:803–807
9. Dunstan GA, Valkman JK, Maguire GB (1999) Optimisation of essential lipids in artificial feeds for Australian abalone. Fisheries Research and Development Corporation Final Report. CSIRO marine research project no 94/85, 68
10. Dunstan GA, Baillie HJ, Barrett SM, Volkman JK (1996) Effect of diet on the lipid composition of wild and cultured abalone. Aquaculture 140:115–127
11. Nichols PD, Virtue P, Mooney BD, Elliott NG, Yearsley GK (1998) Seafood the good food: the oil (fat) content and composition of Australian commercial fisheries, shellfish and crustaceans. CSRO Marine Research
12. Su XQ, Antonas KN, Li D (2004) Comparison of n-3 polyunsaturated fatty acid contents of wild and cultured Australian abalone. Int J Food Sci Nutr 55:148–154
13. D'Abramo LR, Conklin DE, Akiyama DE (1997) Triacylglycerols and fatty acids. Crustacean nutrition. Advances in world aquaculture. The World Aquaculture Society 6:71–84
14. Sargent JR, Tocher DR, Bell JG (2002) The lipids. Fish nutrition. Academic Press, San Diego, pp 181–257
15. Wei X, Kangsen M, Wenbing Z, Zhiguo L, Beping T, Hongming MA, Qinghui A (2004) Influence of dietary lipid sources on growth and fatty acid composition of juvenile abalone, *Haliotis discus hannai* Ino. J Shellfish Res 127:29–40
16. Durazo-Beltran, D'Abramo ELR, Toro-Vazquezc JF, Vasquez-Pelaezd C, Viana MT (2003) Effect of triacylglycerols in formulated diets on growth and fatty acid composition in tissue of green abalone (*Haliotis fulgens*). Aquaculture 224:257–270
17. Zheng X, Tocher DR, Dickson CA, Bell JG, Teale AJ (2004) Effects of diets containing vegetable oil on expression of genes involved in highly unsaturated fatty acid biosynthesis in liver of Atlantic salmon (*Salmo salar*). Aquaculture 236:467–483
18. Seiliez I, Panseat S, Kaushik S, Bergot P (2001) Cloning, tissue distribution and nutritional regulation of a Δ6-desaturase-like enzyme in rainbow trout. Comp Biochem Physiol 130B:83–93
19. Hastings N, Agaba M, Tocher DR, Leaver MJ, Dick JR, Sargent JR, Teale AJ (2001) A vertebrate fatty acid desaturase with Δ5 and Δ6 activities. Proc Natl Acad Sci USA 98:14304–14309
20. Hastings N, Agaba MK, Zheng X, Tocher DR, Dick JR, Dickson C, Teale AJ (2004) Molecular cloning and functional characterization of fatty acyl desaturase and elongase cDNAs involved in the production of eicosapentaenoic and docosahexanoic acids from α-linolenic acid in Atlantic salmon (*Salmo salar*). Mar Biotechnol 6:463–474
21. Agaba M, Tocher DR, Dickson CA, Dick JR, Teale AJ (2004) Zebra fish cDNA encoding multifunctional fatty acid elongase involved in production of eicosapentaenoic (20:5n–3) and docosahexaenoic (22:6n-3) acids. Mar Biotechnol 6:251–261
22. Agaba MK, Tocher DR, Zheng X, Dickson CA, Dick JR, Teale AJ (2005) Cloning and functional characterisation of polyunsaturated fatty acid elongases of marine and freshwater teleost fish. Comp Biochem Physiol B 142:342–352
23. Folch J, Lees M, Sloane Stanley GH (1957) A simple method for the isolation and purification of total lipids from animal tissues. J Biol Chem 226:497–509
24. Sinclair AJ, O'Dea K, Naughton JM (1983) Elevated levels of arachidonic acid in fish from Northern Australian coastal waters. Lipids 18:877–881
25. Schmittgen TD, Zakrajsek BA, Mills AG, Gorn V, Singer MJ, Reed MW (2000) Quantitative reverse transcription-polymerase chain reaction to study mRNA decay comparison of endpoint and real-time methods. Anal Biochem 285:194–204
26. Thongrod S, Tamtin M, Chairat C, Boonyaratpalin M (2003) Lipid to carbohydrate ratio in donkey's ear abalone (*Haliotis asinina*, Linne) diets. Aquaculture 225:165–174
27. Uki N, Kemuyama A, Watanabe T (1985) Development of semipurified test diets for abalone. Bull Jpn Soc Sci Fish 51: 1825–1833
28. Delaunay F, Marty Y, Moal J, Cochard JC, Samain JF (1991) Fatty acid requirements of *Pecten maximus* larvae. Oceanus 17:287–288
29. Mai K, Mercer JP, Donlon J (1995) Comparative studies on the nutrition of two species of abalone, *Haliotis tuberculata* L and *Haliotis discus hannai* Ino III. The role of polyunsaturated fatty acids of macroalgae in abalone nutrition. Aquaculture 134:65–80
30. Fleming AE, Van Bernevald RJ, Hone PW (1996) The development of artificial diets for abalone: a review and future directions. Aquaculture 140:5–53
31. Castanos M (1997) Abalone R and D at AQD. SEAFDEC Asian Aquaculture 19:18–23
32. Lee SM, Cho SH (2009) Influences of dietary fatty acid profile on growth, body composition and blood chemistry in juvenile fat cod (*Hexagrammos otakii* Jordan et Starks). Aqua Nutr 15:19–28
33. Lee SM, Park HG (1998) Evaluation of dietary lipid sources for juvenile abalone (*Haliotis discus hannai*). J Aquacult 11:381–390
34. Van Barneveld RJ, Fleming AE, Vandepeer ME, Kruk JA, Hone PW (1998) Influence of dietary oil type and oil inclusion level in

manufactured feeds on the digestibility of nutrients by juvenile greenlip abalone (*Haliotis laevigata*). J Shellfish Res 17:649–655
35. Boggio SM, Hard R, Babbitt JK, Brannon EL (1985) The influence of dietary lipid source and alpha-tocopheryl acetate level on product quality of rainbow trout (*Salmo gairdneri*). Aquaculture 51:13–24
36. Waagbo R, Sandnes K, Torrissen OJ, Sandvin A, Lie Ø (1993) Chemical and sensory evaluation of fillets from Atlantic salmon (*Salmo salar*) fed three levels of n-3 polyunsaturated fatty acids at two levels of vitamin E. Food Chem 46:361–366
37. Bell JG, McEvoy J, Tocher DR, McGhee F, Campbell PJ, Sargent JR (2001) Replacement of fish oil with rapeseed oil in diets of Atlantic salmon (*Salmo salar*) affects tissue lipid compositions and hepatocyte fatty acid metabolism. J Nutr 131:1535–1543
38. Bell JG, Henderson RJ, Tocher DR, McGhee F, Dick JR, Porter A, Smullen RP, Sargent JR (2002) Substituting fish oil with crude palm oil in the diet of Atlantic salmon (*Salmo salar*) affects muscle fatty acid composition and hepatic fatty acid metabolism. J Nutr 132:222–230
39. Turchini GM, Mentasti T, Froyland L, Orban E, Caprino F, Moretti VM, Valfre F (2003) Effects of alternative dietary lipid sources on performance, tissue chemical composition, mitochondrial fatty acid oxidation capabilities and sensory characteristics in brown trout (*Salmo trutta* L.). Aquaculture 225:251–267
40. Fonseca-Madrigal J, Karalazos V, Campbell PJ, Bell JG, Tocher DR (2005) Influence of dietary palm oil on growth, tissue fatty acid compositions, and fatty acid metabolism in liver and intestine in rainbow trout (*Oncorhynchus mykiss*). Aqua Nutr 11:241–250
41. Higgs DA, Balfry SK, Oakes JD, Rowshandeli M, Skura BJ, Deacon G (2006) Efficacy of an equal blend of canola oil and poultry fat as an alternate dietary lipid source for Atlantic salmon (*Salmo salar* L.) in sea water. I: effects on growth performance, and whole body and fillet proximate and lipid composition. Aquac Res 37:180–191
42. Ng WK, Sigholt T, Bell JG (2004) The influence of environmental temperature on the apparent nutrient and fatty acid digestibility in Atlantic salmon (*Salmo salar L.*) fed finishing diets containing different blends of fish oil, rapeseed oil and palm oil. Aquac Res 35:1228–1237
43. Rosenlund G, Obach A, Sandberg MG, Standal H, Tveit K (2001) Effect of alternative lipid sources on long-term growth performance and quality of Atlantic salmon (*Salmo salar* L.). Aquac Res 32:323–328
44. Tortensen BE, Lie O, Froyland L (2000) Lipid metabolism and tissue composition in Atlantic salmon (*Salmo salar* L.)—effects of capelin oil, palm oil and oleic acid-enriched sunflower oil as dietary lipid sources. Lipids 35:653–664
45. Nelson MM, Leighton DL, Phleger CH, Nichols PD (2002) Comparison of growth & lipid composition in the green abalone, *Haliotis fulgens*, provided specific macroalgal diets. Comp Biochem Physiol 131B:695–712
46. Uki N, Kemuyama A, Watanake T (1986) Requirement of essential fatty acid in the abalone *Haliotis discus hannai*. Bull Jpn Soc Sci Fish 52:1013–1023
47. Grubert MA, Dunstan GA, Rita AJ (2004) Lipid and fatty acid composition of pre- and post-spawning blacklip (*Haliotis rubra*) and greenlip (*Haliotis laevigata*) abalone conditioned at two temperatures on a formulated feed. Aquaculture 242:297–311
48. Miller MR, Bridle AR, Nichols PD, Carter CG (2008) Increased elongase and desaturase gene expression with stearidonic acid enriched diet does not enhance long-chain (n-3) content of seawater Atlantic salmon (*Salmo salar* L.). J Nutr Nutrient Physiol Metab Nutr-Nutr Interact 138:2179–2185
49. Turchini GM, Francis DS, De Silva SS (2006) Fatty acid metabolism in the freshwater fish Murray cod (*Maccullochella peelii peelii*) deduced by the whole-body fatty acid balance method. Comp Biochem Physiol B 144:110–118
50. Rawn JD (1989) Biochemistry. Neil Patterson Publishers, Burlington
51. Jump DB, Clarke SD, Thelen A, Liimatta M, Ren B, Badin M (1996) Dietary polyunsaturated fatty acid regulation of gene transcription. Prog Lipid Res 35:227–241
52. Zheng X, Torstensen BE, Tocher DR, Dick JR, Henderson RJ, Bell JG (2005) Environmental and dietary influences on highly unsaturated fatty acid biosynthesis and expression of fatty acyl desaturase and elongase genes in liver of Atlantic salmon (*Salmo salar*). Biochim Biophys Acta 1734:13–24
53. Ling S, Kuah M-K, Tengku Muhammad TS, Kolkovski S, Shu-Chien A (C2006) Effect of dietary HUFA on reproductive performance, tissue fatty acid profile and desaturase and elongase mRNAs in female swordtail *Xiphophorus helleri*. Aquaculture 26:204–214
54. Jaya-Ram A, Kuah M-K, Lim P-S, Kolkovski S, Shu-Chien AC (2008) Influence of dietary HUFA levels on reproductive performance, tissue fatty acid profile and desaturase and elongase mRNAs expression in female zebrafish *Danio rerio*. Aquaculture 277:275–281
55. Kennedy SR, Leaver MJ, Campbell PJ, Zheng X, Dick JR, Tocher DR (2006) Influence of dietary oil content and conjugated linoleic acid (CLA) on lipid metabolism enzyme activities and gene expression in tissues of Atlantic Salmon (*Salmo salar* L.). Lipids 41:423–436

Lipids (2011) 46:753–764
DOI 10.1007/s11745-011-3558-9

ORIGINAL ARTICLE

Development of a Fish Cell Culture Model to Investigate the Impact of Fish Oil Replacement on Lipid Peroxidation

Melissa K. Gregory · Hamish W. King · Peter A. Bain · Robert A. Gibson · Douglas R. Tocher · Kathryn A. Schuller

Received: 28 February 2011 / Accepted: 5 April 2011 / Published online: 29 April 2011

Abstract Fish oils are rich in omega-3 long-chain polyunsaturated fatty acids (n-3 LC-PUFA), predominantly 20:5n-3 and 22:6n-3, whereas vegetable oils contain abundant C_{18}-PUFA, predominantly 18:3n-3 or 18:2n-6. We hypothesized that replacement of fish oils with vegetable oils would increase the oxidative stability of fish lipids. Here we have used the long established and easily cultivated FHM cell line derived from the freshwater fish species fathead minnow (*Pimephales promelas*) to test this hypothesis. The FHM cells were readily able to synthesize 20:5n-3 and 24:6n-3 from 18:3n-3 but 22:6n-3 synthesis was negligible. Also, they were readily able to synthesize 20:3n-6 from 18:2n-6 but 20:4n-6 synthesis was negligible. Mitochondrial β-oxidation was greatest for 18:3n-3 and 20:5n-3 and the rates for 16:0, 18:2n-6, 22:6n-3 and 18:1n-9 were significantly lower. Fatty acid incorporation was predominantly into phospholipids (79–97%) with very little incorporation into neutral lipids. Increasing the fatty acid concentration in the growth medium substantially increased the concentrations of 18:3n-3 and 18:2n-6 in the cell phospholipids but this was not the case for 20:5n-3 or 22:6n-3. When they were subjected to oxidative stress, the FHM cells supplemented with either 20:5n-3 or 22:6n-3 (as compared with 18:3n-3 or saturated fatty acids) exhibited significantly higher levels of thiobarbituric reactive substances (TBARS) indicating higher levels of lipid peroxidation. The results are discussed in relation to the effects of fatty acid unsaturation on the oxidative stability of cellular lipids and the implications for sustainable aquaculture.

Keywords Aquaculture · β-oxidation · Cell culture · Fish oil replacement · Lipid peroxidation · Phospholipids · Polyunsaturated fatty acids

Abbreviations

ALA	α-Linolenic acid
ARA	Arachidonic acid
BHT	Butylated hydroxytoluene
CerPCho	Sphingomyelin
DHA	Docosahexaenoic acid
EDTA	Ethylenediamine tetraacetic acid
EPA	Eicosapentaenoic acid
FAF-BSA	Fatty acid free-bovine serum albumin
FAME	Fatty acid methyl esters
FBS	Foetal bovine serum
FHM	Fathead minnow
HP-TLC	High performance-thin layer chromatography
LC-PUFA	Long-chain polyunsaturated fatty acids (carbon chain length $\geq C_{20}$ with ≥ 3 double bonds)
LNA	Linoleic acid
NR	Neutral red
OLA	Oleic acid
PAM	Palmitic acid
PBS	Phosphate buffered saline
PBSA	Phosphate buffered saline without Ca^{2+} or Mg^{2+}
PCR	Polymerase chain reaction
PtdCho	Phosphatidylcholine

M. K. Gregory · H. W. King · P. A. Bain · K. A. Schuller (✉)
School of Biological Sciences, Flinders University,
GPO Box 2100, Adelaide, SA 5001, Australia
e-mail: kathy.schuller@flinders.edu.au

R. A. Gibson
School of Agriculture, Food and Wine, University of Adelaide,
Adelaide, Australia

D. R. Tocher
Institute of Aquaculture, University of Stirling,
Stirling FK9 4LA, UK

PtdEtn	Phosphatidylethanolamine
Ptd_2Gro	Cardiolipin
PtdIns	Phosphatidylinositol
PtdOH	Phosphatidic acid
PtdSer	Phosphatidylserine
PUFA	Polyunsaturated fatty acids
SDS	Sodium dodecyl sulphate
STA	Stearic acid
TBA	Thiobarbituric acid
TBARS	Thiobarbituric acid reactive substances
TLC	Thin-layer chromatography
TN	Total neutral lipids
T/V	Trypsin/versene

Introduction

Fisheries and aquaculture are major contributors to world food security with ≥15% of animal protein for human consumption being derived from these sources in recent years [1]. Traditionally, feeds for farmed fish have contained high proportions of fish oil derived from wild-catch fisheries. However, in the 10 years prior to 2007, wild-catch fisheries production has remained static whereas aquaculture production has almost doubled [1]. Thus, there has been considerable interest in the replacement of fish oils with more sustainable oils [2, 3]. The preferred candidates have been vegetable oils from oilseed plants. However, while these are rich in C_{18} polyunsaturated fatty acids (PUFA), they are completely lacking in the omega-3 long-chain PUFA (n-3 LC-PUFA) that are abundant in fish oils. These n-3 LC-PUFA give seafood its reputation as a health food. In particular, eicosapentaenoic acid (EPA, 20:5n-3) and docosahexaenoic acid (DHA, 22:6n-3) have been shown to be beneficial in the prevention of cardiovascular disease, rheumatoid arthritis, inflammatory bowel disease, childhood learning and behavior disorders and adult psychiatric and neurodegenerative illnesses [4].

The fatty acid profile of fish flesh generally reflects the fatty acid profile of their diet [5]. Therefore, the dietary substitution of fish oils with vegetable oils reduces the n-3 LC-PUFA content of fish flesh thereby reducing its human health value [6–10]. In freshwater fish and salmonids (e.g. trout and salmon), this may be partially offset by their varying ability to synthesize LC-PUFA from C_{18} PUFA but in marine fish this is not the case [11–14]. Marine fish appear to be poorly able to synthesize LC-PUFA from C_{18} PUFA and this may reflect the relative abundance of preformed LC-PUFA, particularly 22:6n-3, in the marine food web [5]. Although freshwater fish and salmonids have some capacity to synthesize LC-PUFA from C_{18} PUFA, this is insufficient to compensate for a decreased dietary intake of LC-PUFA.

The generally accepted pathway for the synthesis of LC-PUFA from C_{18} PUFA in fish, as in mammals, is a series of desaturation and elongation steps in the endoplasmic reticulum followed by chain shortening in the peroxisomes (Fig. 1). In particular, the synthesis of 22:6n-3 from 18:3n-3 involves a Δ6 desaturation step followed by a chain elongation step, a Δ5 desaturation step and two consecutive chain elongation steps before a second Δ6 desaturation step and the final chain shortening step. Recent studies indicate that the C_{18} and C_{20} elongation steps are catalysed by an ELOVL5-like elongase whereas the C_{22} elongation step is catalysed by an ELOVL2-like elongase [15, 16]. Studies with fish cell lines indicate that freshwater fish and salmonids have substantial activities of the desaturase and elongase enzymes required to synthesize 20:5n-3 from 18:3n-3 whereas for marine fish there is an apparent limitation at either the C_{18} elongation or the Δ5 desaturation step [11–14]. In contrast, synthesis of 22:6n-3 appears to be limited in all fish species.

Fish lipids are highly susceptible to peroxidative deterioration because of the high proportions of LC-PUFA they contain and this explains the shorter shelf life of fish flesh products as compared with terrestrial animal meat products [17]. The C_{18} PUFA abundant in vegetable oils, 18:2n-6 and 18:3n-3, contain 2 and 3 double bonds, respectively, whereas the LC-PUFA abundant in fish oils, 20:5n-3 and 22:6n-3, contain 5 and 6 double bonds, respectively. Lipid peroxidation occurs when reactive oxygen species (ROS) attack PUFA at their double bonds setting off a chain reaction of hydrogen abstraction and lipid radical formation. This is particularly damaging to cell membranes because of the close proximity of fatty acids in the phospholipid bilayer [17]. Thus, a cell culture model would be useful to precisely define the effects of fish oil replacement at the cellular level.

The abundance of individual fatty acids in cellular lipids, particularly phospholipids, is affected by their uptake and esterification into the different lipid classes as well as by their mitochondrial β-oxidation for energy generation and their possible desaturation and/or elongation to form LC-PUFA [5]. Thus, all of these factors need to be considered when developing a cell culture model. Here we have used the long established and easily cultivated FHM cell line derived from the freshwater fish species fathead minnow (*Pimephales promelas*). In particular we have investigated the capacity of the cell line to synthesize LC-PUFA from C_{18} PUFA, to metabolize various fatty acids by β-oxidation and to incorporate various fatty acids into cellular lipids. Finally, we have investigated the impact of fatty acid unsaturation on the susceptibility of the cells to lipid peroxidation.

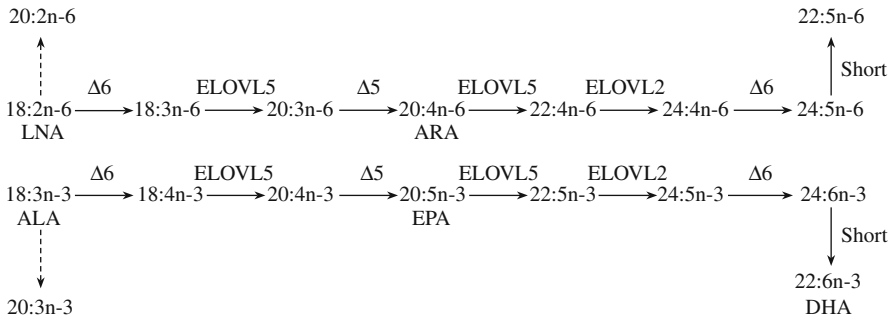

Fig. 1 The generally accepted pathway for the synthesis n-3 and n-6 LC-PUFA from their C_{18} fatty acid precursors in fish (adapted from Miller et al. [2]) showing the alternative reactions when Δ6 fatty acyl desaturase activity is limiting (*broken lines*). *Δ5* Δ5 fatty acyl desaturase, *Δ6* Δ6 fatty acyl desaturase, *ARA* arachidonic acid, *ALA* α-linolenic acid, *DHA* docosahexaenoic acid, *ELOVL2* fatty acyl elongase 2, *ELOVL5* fatty acyl elongase 5, *EPA* eicosapentaenoic acid, *LNA* linoleic acid, *short* peroxisomal shortening of LC-PUFA

Materials and Methods

Cells, Media and Standard Culture Conditions

A stock culture of the FHM cell line derived from fathead minnow (*Pimephales promelas*) was obtained from the Australian Animal Health Laboratory (CSIRO Livestock Industries, Geelong, Victoria, Australia) and the species of origin was confirmed by polymerase chain reaction (PCR) using the mitochondrial cytochrome oxidase subunit I (*cox1*) primers of Ward et al. [18]. For routine culture, the FHM cells were maintained in 75 cm^2 flasks containing 20 ml Leibovitz's L-15 medium supplemented with antibiotics (100 IU ml^{-1} penicillin, 100 μg ml^{-1} streptomycin) and 10% (v/v) foetal bovine serum (FBS). To subculture or harvest the cells, the medium was decanted, the cell monolayer was rinsed with phosphate buffered saline without Ca^{2+} or Mg^{2+} (PBSA) and the cells were detached with T/V solution containing 0.05% (w/v) trypsin and 0.02% (w/v) ethylenediamine tetraacetic acid (EDTA) in PBSA. For the experiments with [1-^{14}C]-labelled fatty acids, the cells were cultured to 80% confluence in 75 cm^2 flasks containing 20 ml L-15 medium supplemented with 5% (v/v) FBS. The medium was then replaced with 10 ml of fresh medium containing no FBS and the [1-^{14}C]-labelled fatty acids as complexes with fatty acid free-bovine serum albumin (FAF-BSA). The complexes were prepared as described by Ghioni et al. [19]. For the experiments with unlabelled fatty acids, the cells were cultured to 80% confluence in 75 cm^2 flasks containing 20 ml L-15 medium supplemented with 10% (v/v) FBS and then they were subcultured (at a split ratio of 1 to 12) into 25 cm^2 flasks containing 10 ml L-15 medium supplemented with 2% (v/v) FBS and the unlabelled fatty acids as complexes with FAF-BSA. The complexes were prepared as described by Best et al. [20] with a molar ratio of fatty acid to BSA of 4:1. For all experiments, the culture temperature was 25 °C and the incubation period with either the [1-^{14}C]-labelled or the unlabelled fatty acids was 24 h.

LC-PUFA Synthesis Assay Using [1-^{14}C]-labelled Fatty Acids

The FHM cells were incubated for 24 h in 75 cm^2 flasks containing 1 μCi (2 μM) [1-^{14}C]-labelled 18:2n-6, 18:3n-3 or 20:5n-3 in 10 ml L-15 medium containing no FBS. At the end of the 24-h incubation, the cells were detached with T/V solution and washed with FAF-BSA to remove any residual labelled fatty acid. Total lipids were extracted from the cell pellets by the addition of 5 ml ice-cold chloroform/methanol (2:1, v/v) containing 0.01% (v/v) butylated hydroxytoluene (BHT) followed by 1 ml 0.88% (w/v) KCl. The method was essentially that of Folch et al. [21] with the modifications described by Tocher et al. [22]. Fatty acid methyl esters (FAME) were prepared by incubating the lipid extract overnight at 50 °C with 1 ml of toluene and 2.5 ml of 1% (v/v) H_2SO_4 in methanol. The method was essentially that of Christie [23]. At the end of the incubation, the FAME were extracted by the addition of 2 ml of 2% (w/v) $KHCO_3$ followed by 5 ml isohexane/diethyl ether (1:1, v/v) containing 0.01% (v/v) BHT. The mixture was centrifuged at 500*g* and the upper layer was re-extracted with 5 ml isohexane/diethyl ether (1:1, v/v) containing no BHT. The upper layers were combined and the solvent was evaporated under a stream of N_2. The dried FAME were dissolved in 100 μl isohexane containing 0.01% (w/v) BHT and separated by thin-layer chromatography (TLC) on 20 × 20 cm TLC plates which had been impregnated with 2 g $AgNO_3$ in 20 ml acetonitrile before being dried/activated at 110 °C for 30 min. The TLC plates were developed in toluene/acetonitrile (95:5, v/v). The method was essentially as described by Wilson and Sargent [24]. Autoradiography was performed and the areas of silica containing the individual PUFA were scraped into

scintillation vials and radioactivity determined using a scintillation counter as previously described [25].

β-Oxidation Assay Using [1-^{14}C]-labelled Fatty Acids

The FHM cells were incubated for 24 h in 75-cm^2 flasks containing 0.5 μCi (1 μM) [1-^{14}C]-labelled 16:0, 18:1n-9, 18:2n-6, 18:3n-3, 20:5n-3 or 22:6n-3 in 10 ml L-15 medium containing no FBS. At the end of the incubation, 0.5 ml of the medium was removed for scintillation counting and the cells were detached with T/V solution and washed as described above. The washed cell pellets were resuspended in 1 ml PBS and homogenized to disrupt the cells. Acid soluble products were obtained by adding 100 μl of 6% (w/v) FAF-BSA and 1.0 ml ice-cold 4 M $HClO_4$ to 500 μl each of the growth medium and the cell homogenate and then centrifuging to remove the precipitated material. An aliquot of the supernatant (500 μl) was mixed with 4 ml scintillation fluid and radioactivity determined using a scintillation counter as previously described [25].

Incorporation of [1-^{14}C]-labelled Fatty Acids into Various Lipid Classes

The FHM cells were incubated for 24 h in 75 cm^2 flask containing 1.0 μCi (2 μM) [1-^{14}C]-labelled 16:0, 18:1n-9, 18:2n-6, 18:3n-3, 20:5n-3 or 22:6n-3 in 10 ml L-15 medium containing no FBS. At the end of the 24-h incubation, the cells were harvested and total lipid was extracted as described above. To separate the various lipid classes, the total lipid was dissolved in 100 μl chloroform/methanol (2:1, v/v) and applied to a high performance-thin layer chromatography (HPTLC) plate. The plate was developed in methyl acetate/isopropanol/chloroform/methanol/0.25% (w/v) aqueous KCl (25/25/25/10/9, by volume) as described by Vitiello and Zanetta [26]. The separated lipids were stained with iodine and the corresponding bands of silica were scraped into scintillation vials. Scintillation fluid (2.5 ml) was added and radioactivity determined using a scintillation counter as above.

Incorporation of Unlabelled Fatty Acids into the FHM Cell Phospholipids

The FHM cells were incubated for 24 h in 25-cm^2 flasks containing 10 ml L-15 medium supplemented with 2% (v/v) FBS and various concentrations of unlabelled 18:3n-3, 18:2n-6, 20:5n-3, 20:4n-6 or 22:6n-3. At the end of the incubation, the cells were harvested and total lipid was extracted from approximately 10^6 cells according to the method of Folch et al. [21]. The phospholipids were separated from the neutral lipids by TLC with petroleum ether/glacial acetic acid (3:1, v/v) and then they were transmethylated by incubation with 1% (v/v) H_2SO_4 in methanol for 3 h at 70 °C. The resulting FAME were extracted in heptane and analyzed by gas chromatography using a Hewlett-Packard 6890 gas chromatograph (Hewlett Packard, Palo Alto, CA, USA) fitted with a flame ionisation detector and a BPX-70 50 m capillary column coated with 70% (v/v) cyanopropyl polysilphenylene-siloxane (0.25 mm film thickness and 0.32 mm internal diameter, SGE, Australia). The carrier gas was helium at a flow rate of 2.0 ml min^{-1} and the split-ratio was 20:1. The injection port temperature was 250 °C and the detector temperature was 300 °C. The column temperature was increased from 140 to 220 °C at a rate of 4 °C min^{-1} and then held at 220 °C for up to 3 min. The identity of each fatty acid peak in the chromatogram was ascertained by comparison with an authentic lipid standard (Nu-Chek Prep, Inc., MN, USA). The amount of each fatty acid was quantified by comparing its peak area with the peak area of a heptadecaenoic acid (17:0) internal standard added prior to lipid extraction.

Effect of Fatty Acid Unsaturation on Cell Viability and Lipid Peroxidation

The FHM cells were seeded into 6-well plates at a density of 5×10^5 cells per well in L-15 medium containing 2% (v/v) FBS. The cells were allowed to attach overnight and then they were incubated for 24 h with fresh medium containing 2% (v/v) FBS and 20 μM 16:0, 18:0, 18:3n-3, 20:5n-3 or 22:6n-3 coupled with FAF-BSA in a 4:1 fatty acid to BSA ratio. At the end of the incubation period, the cell monolayer was rinsed twice with PBSA and then lipid peroxidation was induced by treating the cells for 1 h with 500 μM cumene hydroperoxide plus 100 nM hemin in PBSA. Following this treatment, the cell monolayer was rinsed twice with PBSA and the cells were subjected to either the Neutral Red (NR) cell viability assay [27] or the thiobarbituric acid reactive substances (TBARS) assay for lipid peroxidation [28]. Briefly, the NR cell viability assay involved incubating the cells for 3 h in NR dye diluted in L-15 containing 10% (v/v) FBS and then fixing them in 10% (w/v) $CaCl_2$:4% (v/v) formaldehyde before solubilizing the incorporated dye with 50% (v/v) ethanol:1% (v/v) acetic acid and reading the absorbance at 550 nm. Viable cells take up the dye whereas non-viable cells do not. For the TBARS assay, the cells were lysed with 1% (w/v) sodium dodecyl sulphate (SDS), the cell lysates were mixed 1:1 with the TBARS reagent and the mixture was incubated for 2 h at 75 °C before removing any insoluble material by centrifugation and reading the fluorescence

using excitation/emission wavelengths of 540/590 nm. The TBARS reagent contained 25 mM thiobarbituric acid (TBA), 15% (w/v) trichloroacetic acid and 0.005% (w/v) BHT dissolved in 1 M HCl.

Statistical Analyses

Statistical analyses were performed using SPSS software. The Levene statistic was calculated to test for homogeneity of variances and means were compared using one-way ANOVA followed by Tukey's post-hoc test. Differences where the P value was >0.05 were considered to be significant.

Results

Effect of the FBS Concentration in the Growth Medium on the Fatty Acid Composition of the FHM Cell Phospholipids

The fatty acid composition of the FHM cell phospholipids closely resembled that of the FBS in the growth medium, with the exceptions that 16:0 and 18:0 were less abundant and 18:1n-9 was more abundant (Table 1). Increasing the concentration of FBS in the growth medium from 2 to 20% (v/v) significantly increased the concentrations of 22:5n-3, 22:6n-3 and 20:4n-6 in the cell phospholipids (Fig. 2).

Metabolism of [1-^{14}C]-labelled Fatty Acids by the FHM Cells

Radioactivity from [1-^{14}C]18:3n-3 was readily recovered in 20:4n-3, 20:5n-3, 22:5n-3 and 24:6n-3 but there was relatively little recovery in 22:6n-3 (Table 2). Thus, the cells expressed considerable desaturase and elongase activity but only limited peroxisomal chain shortening activity. This was confirmed by supplying the cells with [1-^{14}C]20:5n-3. A somewhat different pattern was observed when the cells were supplied with [1-^{14}C]18:2n-6. In this case, the label was incorporated predominantly into 20:3n-6. This indicated considerable Δ6 desaturase activity to yield 18:3n-6 followed by elongase activity to yield 20:3n-6 but limited Δ5 desaturase activity to yield 20:4n-6. Thus, the FHM Δ5 desaturase apparently preferred the n-3 over the n-6 substrate.

The capacity of the FHM cells to metabolise fatty acids by mitochondrial β-oxidation was also investigated (Fig. 3). This showed that 18:3n-3 and 20:5n-3 were more readily oxidized than 16:0, 18:2n-6 or 22:6n-3 which in turn were more readily oxidized than 18:1n-9. This result was consistent with the high retention levels for 18:1n-9 in the cell phospholipids (Table 1).

Table 1 Fatty acid composition of foetal bovine serum (FBS) and the phospholipids of FHM cells maintained in L-15 medium containing 10% (v/v) FBS

Fatty acid	Fatty acid composition (% of total fatty acids)	
	FBS	FHM cells in L-15 + 10% FBS
14:0	0.8	1.3
16:0 (PAM)	23.0	17.8
18:0 (STA)	18.8	9.0
Total saturates[a]	45.3	32.0
16:1n-9	0.9	2.0
16:1n-7	1.3	2.2
18:1n-9 (OLA)	15.3	24.1
18:1n-7	2.0	7.9
Total monounsaturates[b]	23.5	42.4
18:2n-6 (LNA)	7.6	1.8
18:3n-6	0.3	0.4
20:2n-6	0.2	0.4
20:3n-6	3.4	3.0
20:4n-6 (ARA)	9.9	8.4
Total n-6 PUFA[c]	23.3	15.3
18:3n-3 (ALA)	0	0.2
20:5n-3 (EPA)	0.3	0.2
22:5n-3 (DPA)	3.7	1.5
22:6n-3 (DHA)	4.0	2.9
Total n-3 PUFA[d]	8.1	4.9
Total PUFA	31.4	20.2
n-3/n-6	0.35	0.32

Data are expressed as % of total fatty acids. For FBS, the data are the means of 3 separate batches. For the FHM cells, the data are the mean of 3 replicate flasks; [a] also includes 15:0, 17:0, 20:0, 22:0 and 24:0; [b] also includes 20:1, 22:1 and 24:1; [c] also includes 22:4n-6; [d] also includes 18:4n-3 and 20:4n-3

PAM palmitic acid, *STA* stearic acid, *OLA* oleic acid, *LNA* linoleic acid, *ARA* arachidonic acid, *ALA* α-linolenic acid, *EPA* eicosapentaenoic acid, *DHA* docosahexaenoic acid,

Incorporation of [1-^{14}C]-labelled Fatty Acids into Lipid Classes in the FHM Cells

Total incorporation into all lipid classes was similar for 18:1n-9, 18:2n-6 and 20:5n-3 but significantly greater for 18:3n-3 and significantly less for 16:0 and 22:6n-3 (Table 3). The lower incorporation rate for 16:0 was consistent with its lower steady state level in the FHM cell phospholipids as compared with FBS (Table 1). This contrasts with the higher steady state level for 18:1n-9 which was apparently due to a lower rate of β-oxidation. For all of the fatty acids tested, the majority of the label (79–97%) was incorporated into phospholipids with very little incorporation into neutral lipids. For 16:0, 18:1n-9

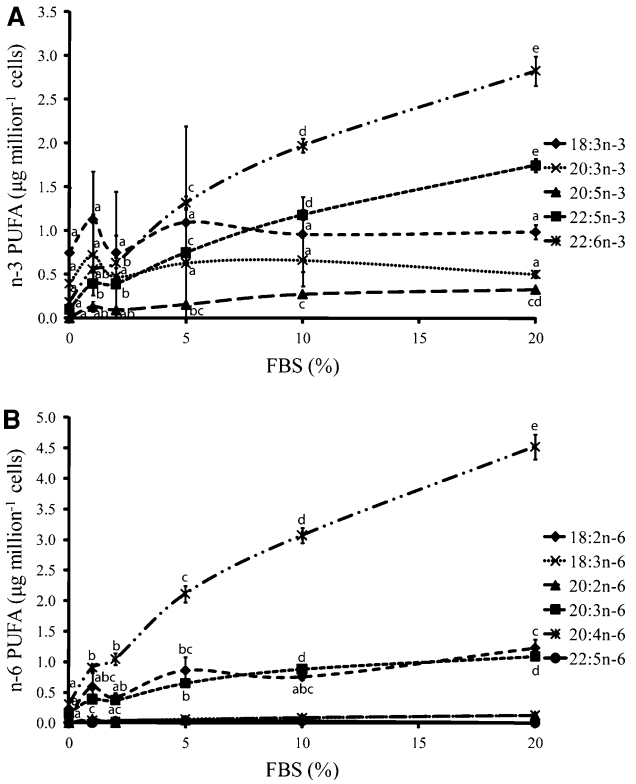

Fig. 2 The effect of increasing FBS concentration in the growth medium on the PUFA content of the FHM cell phospholipids. The growth medium contained 2% (v/v) BSA, 2 μM 18:3n-3 and increasing concentrations of FBS and the cells were cultured for 24 h at 25 °C. Each data point represents the mean of 3 flasks and the *vertical bars* represent the standard error of the mean. For each fatty acid, data points with *different letters* represent values that are significantly different from one another at the $P = 0.05$ level

and 18:2n-6, most of the label (44–50%) was incorporated into phosphatidylcholine (PtdCho) with phosphatidylethanolamine (PtdEtn) ranked second. For 18:3n-3 and 20:5n-3, the ranking was reversed with the greatest incorporation into PtdEtn followed by PtdCho. For 22:6n-3, the pattern was different again with the greatest incorporation into PtdEtn followed by phosphatidylserine (PtdSer) and then PtdCho. Thus, the lower overall incorporation of 22:6n-3 into total lipids was associated with lower incorporation into PtdCho and higher incorporation into PtdSer. In addition, as the unsaturation of the fatty acids increased, there was a trend away from incorporation into PtdCho.

Effect of Concentration on the Accumulation of Unlabelled Fatty Acids in the FHM Cell Phospholipids

Figure 4 shows the effects of increasing concentrations of 18:3n-3 or 18:2n-6 in the growth medium on their accumulation in the cell phospholipids. In both cases, accumulation in the cell phospholipids paralleled the increase in concentration in the growth medium up to a concentration of 5 μM but above this concentration an incorporation threshold was reached. The accumulation of 18:3n-3 was roughly paralleled by an accumulation of 20:3n-3, the direct elongation product of 18:3n-3. Thus, Δ6 desaturase activity, which would have produced 18:4n-3, appeared to be limiting. In contrast, 18:2n-6 was a poor substrate for direct elongation as evidenced by limited accumulation of 20:2n-6. However, 20:3n-6 accumulation was significant and this is consistent with the earlier observation of limited Δ5 desaturase activity towards 20:3n-6 in the [1-^{14}C]-labelling experiment (Table 2).

Further metabolism of 18:3n-3 to produce 20:5n-3 and 22:6n-3 or of 18:2n-6 to produce 20:4n-6 was negligible. This was surprising given the results of the [1-^{14}C]-labelling experiment which showed significant synthesis of 20:5n-3 from 18:3n-3 (Table 2). To determine whether this apparent anomaly was due to limited incorporation of higher concentrations of LC-PUFA into the cellular phospholipids, the FHM cells were supplied with various concentrations of either 20:5n-3, 20:4n-6 or 22:6n-3 (Figs. 5, 6). Incorporation of 20:5n-3 into the cell phospholipids increased approximately linearly with the increase in the concentration in the growth medium up to a concentration of 5 μM whereas at higher concentrations it reached a plateau. The accumulation of 20:5n-3 was paralleled by an accumulation of 22:5n-3, the direct elongation product of 20:5n-3. Further metabolism of

Table 2 Metabolism of [1-^{14}C]-labelled 18:3n-3, 20:5n-3 and 18:2n-6 by desaturation and elongation in FHM cells

Fatty acid	Substrate		
	[1-^{14}C]18:3n-3	[1-^{14}C]20:5n-3	[1-^{14}C]18:2n-6
18:3n-3	14.5 ± 0.7	–	–
20:3n-3	7.7 ± 0.3	–	–
18:4n-3/24:5n-3	9.9 ± 0.5	–	–
20:4n-3	18.3 ± 0.3	–	–
22:4n-3	1.9 ± 0.2	–	–
20:5n-3	22.1 ± 0.8	42.7 ± 1.6	–
22:5n-3	15.2 ± 0.5	26.9 ± 0.7	–
24:5n-3	–[a]	8.3 ± 1.3	
22:6n-3	1.0 ± 0.1	3.2 ± 0.7	–
24:6n-3	9.4 ± 0.6	18.9 ± 0.5	
18:2n-6	–	–	53.4 ± 1.4
20:2n-6	–	–	6.7 ± 0.3
18:3n-6	–	–	7.1 ± 1.0
20:3n-6	–	–	26.8 ± 1.0
22:3n-6	–	–	1.6 ± 0.2
20:4n-6	–	–	4.5 ± 0.3

[a] Indicates not applicable. Data are expressed as percentage of total radioactivity recovered in total lipid and are means ± SD ($n = 4$)

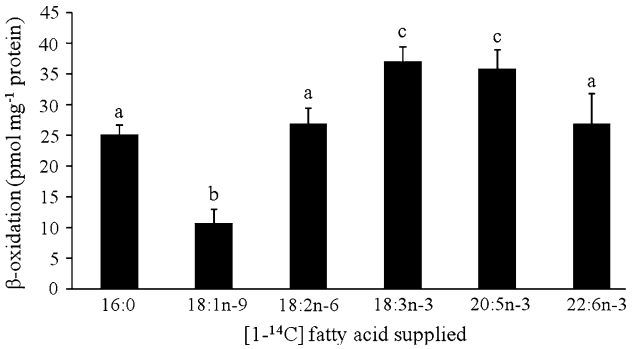

Fig. 3 *β*-oxidation activity of the FHM cell line with various fatty acids. The cells were incubated for 24 h at 25 °C with 1 μCi (2 μM) of the [1-^{14}C]-labelled fatty acids in L-15 medium containing no FBS. Data points with *different letters* represent values that are significantly different from one another at the $P = 0.05$ level

20:5n-3 to produce 22:6n-3 by chain shortening was negligible.

Incorporation of 20:4n-6 was less straightforward (Fig. 5). At lower concentrations up to 5 μM, there was some evidence of increasing incorporation with increasing concentration in the medium. However, at higher concentrations in the medium (5–20 μM) there was no increase in incorporation of 20:4n-6 into the cells. This was not unexpected given that the cells were cultured in the presence of 2% (v/v) FBS which is relatively rich in 20:4n-6 and therefore the capacity of the cell phospholipids to incorporate 20:4n-6 may already have reached its maximum level.

Incorporation of 22:6n-3 into the cell phospholipids reached its maximum level at a very low concentration of only 2 μM in the growth medium (Fig. 6). This was lower than the concentration of approximately 5 μM observed for 20:5n-3. This was consistent with the ^{14}C-labelling data which showed significantly lower incorporation of 22:6n-3 into total lipid (Table 3). Interestingly, there was also some evidence for retro-conversion of 22:6n-3 to 20:5n-3 (Fig. 6).

Effect of Fatty Acid Unsaturation on Cell Viability and Lipid Peroxidation

There was no significant difference in cell viability between any of the fatty acid treatments except for the treatment with 18:0 which showed significantly higher cell viability (Fig. 7). For TBARS, the concentration was significantly greater in the cells supplemented with either 20:5n-3 or 22:6n-3 as compared with the cells supplemented with either 16:0, 18:0 or 18:3n-3. Thus, increasing fatty acid unsaturation increased the susceptibility of the cells to lipid peroxidation but did not decrease cell viability.

Discussion

The aim of this study was to develop a cell culture model for the impact of fish oil replacement with vegetable oils on the oxidative stability of fish lipids. Fish oils are rich in LC-PUFA with 5 or 6 double bonds whereas vegetable oils are rich in C_{18} PUFA with only 2 or 3 double bonds [3] and since the fatty acid composition of fish lipids reflects the fatty acid composition of their diet and fatty acid susceptibility to peroxidation increases with increasing unsaturation, we hypothesized that replacing LC-PUFA with C_{18} PUFA would increase the oxidative stability of fish lipids. Previous studies had shown that fish cells in culture have decreased proportions of n-3 LC-PUFA in their lipids as compared with whole fish or fish fillets and this was

Table 3 Incorporation of [1-^{14}C]-labelled fatty acids into total lipid and lipid classes in FHM cells

	Substrate					
	[1-^{14}C]16:0	[1-^{14}C]18:1n-9	[1-^{14}C]18:2n-6	[1-^{14}C]18:3n-3	[1-^{14}C]20:5n-3	[1-^{14}C]22:6n-3
Total incorporation (pmol mg^{-1} protein)	315 ± 12^{a}	382 ± 37^{b}	432 ± 36^{b}	561 ± 13^{c}	430 ± 13^{b}	239 ± 24^{d}
Incorporation into lipid classes (% of total)						
PtdCho	48.7 ± 3.5^{ab}	50.2 ± 3.0^{a}	43.8 ± 1.7^{b}	38.8 ± 0.4^{c}	31.8 ± 2.2^{d}	18.8 ± 0.3^{e}
PtdEtn	16.2 ± 1.6^{a}	21.5 ± 0.5^{b}	18.2 ± 0.2^{a}	40.3 ± 0.8^{c}	52.9 ± 1.9^{d}	49.7 ± 0.7^{e}
PtdSer	5.3 ± 0.1^{a}	6.1 ± 0.8^{ab}	6.8 ± 0.3^{b}	6.9 ± 0.3^{b}	7.0 ± 0.4^{b}	23.5 ± 0.7^{c}
PtdIns	5.7 ± 0.2^{a}	8.3 ± 0.9^{b}	12.2 ± 1.9^{c}	2.7 ± 0.1^{d}	3.7 ± 0.2^{ad}	3.3 ± 0.2^{d}
PtdOH/Ptd$_2$Gro	2.9 ± 1.4^{a}	2.0 ± 0.3^{a}	10.7 ± 0.3^{b}	7.1 ± 0.8^{c}	1.5 ± 0.1^{a}	1.5 ± 0.1^{a}
CerPCho	13.4 ± 3.4^{a}	5.2 ± 3.0^{b}	2.9 ± 1.0^{bc}	1.0 ± 0.3^{bc}	0.5 ± 0.2^{c}	0.5 ± 0.1^{c}
TN	7.7 ± 0.2^{a}	6.7 ± 0.2^{b}	5.4 ± 0.3^{c}	3.3 ± 0.0^{d}	2.7 ± 0.2^{e}	2.7 ± 0.1^{e}

Data are the means ± SD ($n = 4$). Within each row, values sharing the same superscript are not significantly different at the $P = 0.05$ level

CerPCho sphingomyelin, *PtdCho* phosphatidylcholine, *PtdEtn* phosphatidylethanolamine, *PtdIns* phosphatidylinositol, *PtdOH* phosphatidic acid, *PtdSer* phosphatidylserine, *Ptd$_2$Gro* cardiolipin, *TN* total neutral lipids

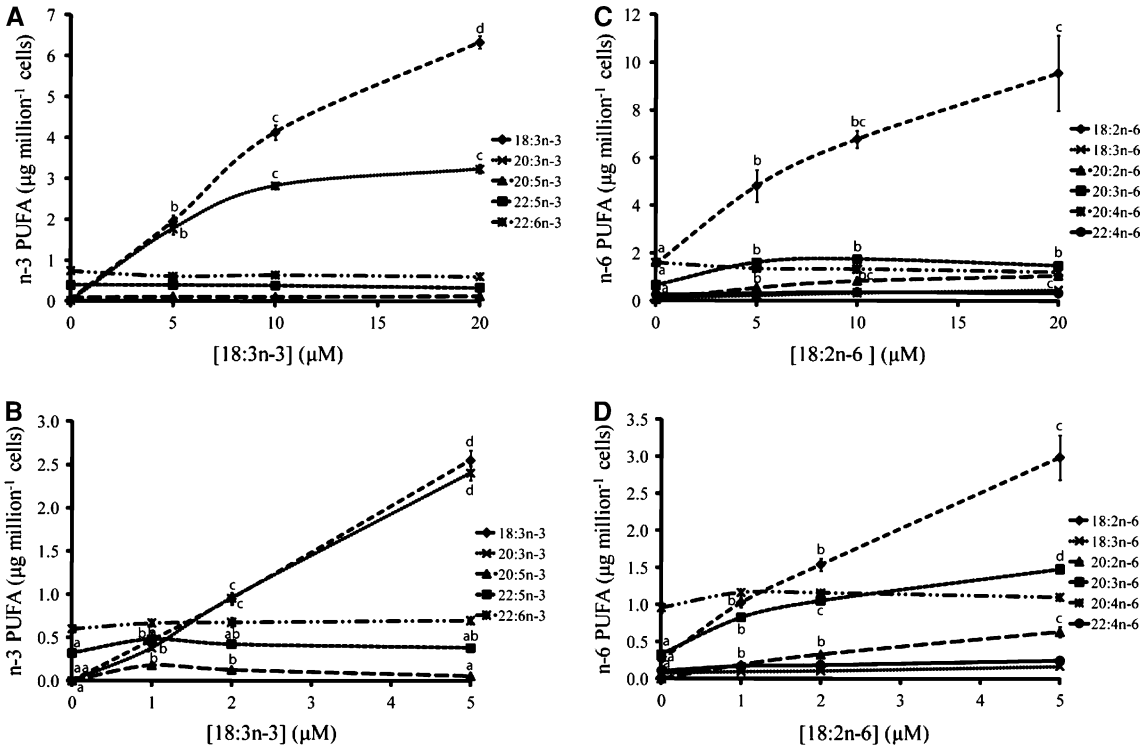

Fig. 4 The effect of increasing 18:3n-3 or 18:2n-6 concentration in the growth medium on the PUFA content of the FHM cell phospholipids. The growth medium contained 2% (v/v) BSA and increasing concentrations of either 18:3n-3 or 18:2n-6 and the cells were cultured for 24 h at 25 °C. Each data point represents the mean of 3 flasks and the *vertical bars* represent the standard error of the mean. For each fatty acid, data points with *different letters* represent values that are significantly different from one another at the $P = 0.05$ level

attributed to the low concentrations of n-3 LC-PUFA in the mammalian serum which is the usual source of fatty acids for cells in culture [13, 22, 29]. The present study confirmed this and in particular we found that the proportions of the beneficial n-3 LC-PUFA, 20:5n-3 and 22:6n-3, were much lower in the FHM cells in culture than in fish tissues in general.

The effects of fish oil replacement on the fatty acid profile of fish flesh are determined by fatty acid metabolism and incorporation into cellular lipids. Previous studies had shown that cell lines derived from fresh water or anadromous fish species (Atlantic salmon, rainbow trout and common carp) were readily able to synthesize 20:5n-3 from 18:3n-3 whereas cell lines derived from carnivorous marine fish species (turbot and gilthead sea bream) were not [11–14]. In turbot this was attributed to low C_{18} to C_{20} elongase activity whereas in gilthead sea bream it was attributed to low Δ5 desaturase activity. Importantly, none of these cell lines could synthesize significant quantities of 22:6n-3. In the present study, the FHM cell line was readily able to synthesize 20:5n-3, 22:5n-3 and 24:6n-3 from 18:3n-3 and/or 20:5n-3 but 22:6n-3 synthesis was negligible. Thus, the FHM cell line expressed substantial Δ5 and Δ6 desaturase activities as well as $C_{18\text{-}20}$, $C_{20\text{-}22}$ and $C_{22\text{-}24}$ elongase activities but negligible peroxisomal chain shortening activity. This was similar to cell lines from other freshwater fish species.

The FHM cells were also readily able to desaturate 18:2n-6 to 18:3n-6 and further elongate this to 20:3n-6 but they synthesized little 20:4n-6. This suggested limited Δ5 desaturase activity towards n-6 fatty acids, which was in contrast to the results obtained with the n-3 substrates. Thus, the Δ5 desaturase of the FHM cell line appeared to prefer n-3 over n-6 fatty acids. Previous studies with cell lines from Atlantic salmon, rainbow trout, turbot and gilthead sea bream also showed limited Δ5 desaturase activity towards 20:3n-6 [11–13]. Thus, this appears to be a general phenomenon for fish cell lines regardless of whether they originate from freshwater, anadromous or marine fish species.

Fatty acid utilization via *β*-oxidation in the FHM cells was investigated by supplying them with [1-^{14}C]-labelled 16:0, 18:1n-9 18:2n-6, 18:3n-3, 20:5n-3 or 22:6n-3. The *β*-oxidation rates were similar for 16:0, 18:2n-6 and 22:6n-3 but significantly lower for 18:1n-9 and significantly higher for 18:3n-3 and 20:5n-3. In a previous study with Atlantic salmon hepatocytes isolated from fish fed a fish oil-based diet, *β*-oxidation rates were similar for 16:0 and 18:2n-6,

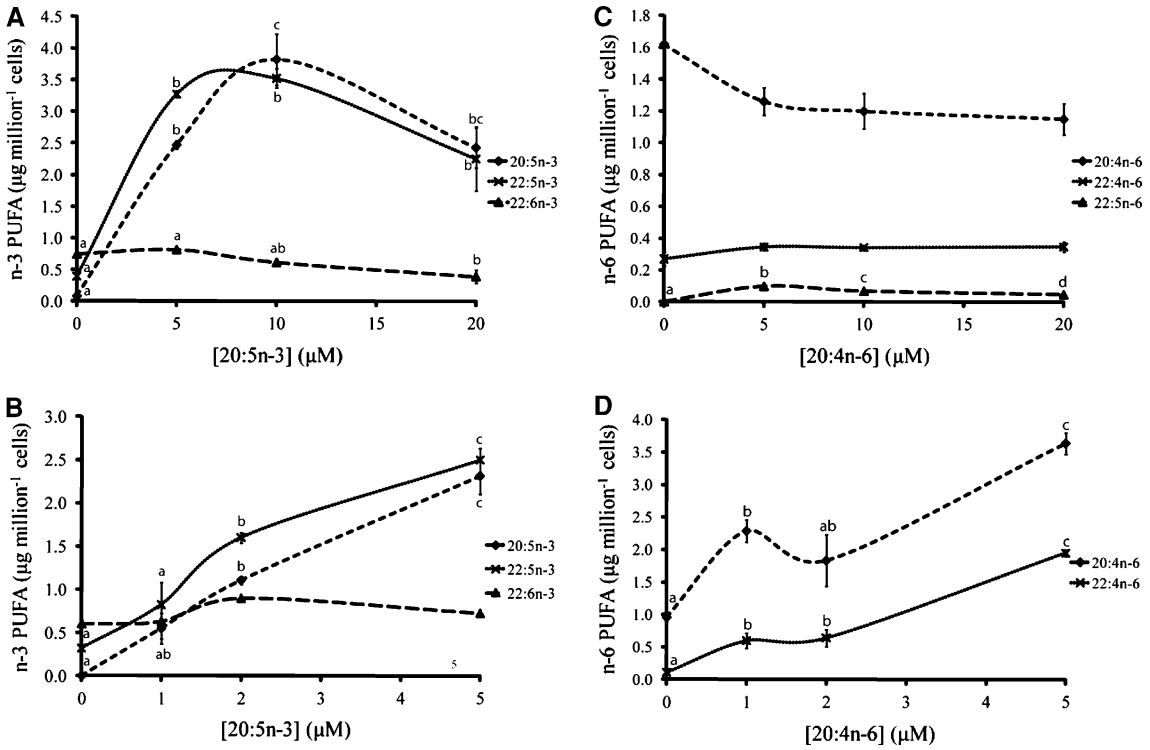

Fig. 5 The effect of increasing 20:5n-3 or 20:4n-6 concentration in the growth medium on the PUFA content of the FHM cell phospholipids. The growth medium contained 2% (v/v) BSA and increasing concentrations of either 20:5n-3 or 20:4n-6 and the cells were cultured for 24 h at 25 °C. Each data point represents the mean of 3 flasks and the *vertical bars* represent the standard error of the mean. For each fatty acid, data points with *different letters* represent values that are significantly different from one another at the $P = 0.05$ level

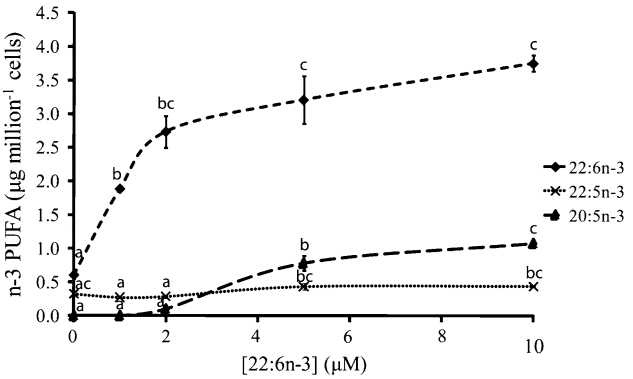

Fig. 6 The effect of increasing 22:6n-3 concentration in the growth medium on the PUFA content of the FHM cell phospholipids. The growth medium contained 2% (v/v) BSA and increasing concentrations of 22:6n-3 and the cells were cultured for 24 h at 25 °C. Each data point represents the mean of 3 flasks and the *vertical bars* represent the standard error of the mean. For each fatty acid, data points with *different letters* represent values that are significantly different from one another at the $P = 0.05$ level

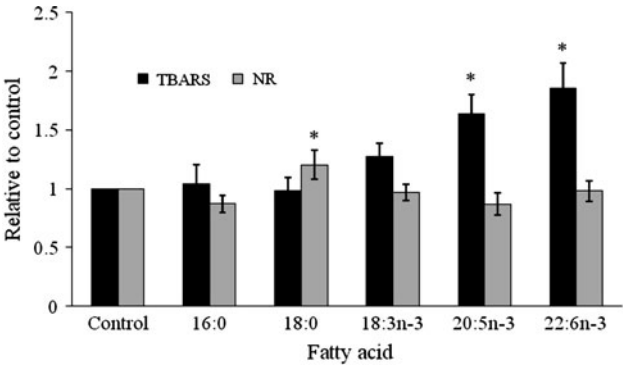

Fig. 7 The effect of increasing fatty acid unsaturation on cell viability and lipid peroxidation in the FHM cells. The cells were supplied with the various fatty acids at a concentration of 20 μM in L-15 medium containing 2% (v/v) FBS. The control contained ethanol at the concentration present in the fatty acid supplements. Three separate flasks of cells were analyzed for each data point and the columns represent the mean while the *vertical bars* represent the standard deviation. For the TBARS assay, * indicates a significant difference (at the $P = 0.05$ level) between the results for 20:5n-3 and 22:6n-3 and the results for the other fatty acids. For the NR assay * indicates a significant difference (at the $P = 0.05$ level) between the results for 18:0 and the results for the other fatty acids

slightly lower for 18:1n-9 and much lower for 18:3n-3, 20:5n-3 and 22:6n-3 [30]. Feeding the fish a predominantly vegetable oil-based diet significantly increased the β-oxidation of 18:1n-9, 18:2n-6, 18:3n-3 and 20:5n-3 but the rank order was still similar. Clearly the metabolism of primary hepatocytes is likely to be different to that of cells maintained in culture for long periods of time and therefore more work needs to be done to understand β-oxidation in fish cell lines. In particular, the rates measured using

radiolabelled substrates may be affected by the pool sizes of unlabelled substrates in the cells due to dilution of the label. The FHM cell phospholipids were particularly rich in 16:0 and 18:1n-9, with moderate levels of 18:2n-6 and 22:6n-3 and low levels of 18:3n-3 and 20:5n-3. Thus, the β-oxidation rates for 16:0 and 18:1n-9, in particular, may have been underestimated. In addition, the incorporation of 22:6n-3 into total cellular lipids was significantly lower compared with the other fatty acids and this may have resulted in an underestimation of the β-oxidation rate for this fatty acid as well. Overall, therefore, the FHM cells were readily able to oxidize all six of the different fatty acids supplied to them.

The incorporation of fatty acids into cellular lipids in the FHM cells was studied in two different ways, firstly using a trace (2 μM) concentration of [1-^{14}C]-labelled fatty acids and secondly using increasing concentrations of unlabelled fatty acids in the range 1–20 μM. Previous studies with fish cell lines and trace concentrations of [1-^{14}C]-labelled 18:2n-6, 18:3n-3 and 20:5n-3 had shown that the label was incorporated predominantly (mostly >90%) into phospholipids, especially PtdCho and PtdEtn, with very little incorporation into neutral lipids [11, 13, 14]. The FHM cell line behaved the same way. In addition, we found that [1-^{14}C]-labelled 16:0, 18:1n-9 and 22:6n-3 were also incorporated predominantly into phospholipids. Interestingly, there was substantial incorporation of [1-^{14}C]-labelled 22:6n-3 into PtdSer and less incorporation into PtdCho than for the other fatty acids. This has also been observed for cell lines from rainbow trout, Atlantic salmon and turbot [31–33]. PtdSer is less abundant than PtdCho in fish cell lines in general [13, 14] and this may explain the lower level of incorporation of [1-^{14}C]-labelled 22:6n-3 into total lipid observed in the present study.

Increasing the concentration of unlabelled 18:3n-3 in the culture medium from 1 to 20 μM resulted in a roughly corresponding increase in the concentration of this fatty acid in the FHM cell phospholipids but there was no corresponding increase in the conventional desaturation/elongation products 20:5n-3, 22:5n-3 or 24:6n-3. Instead, there was an accumulation of 20:3n-3. This fatty acid is produced by the direct elongation of 18:3n-3. Thus, Δ6 desaturase activity apparently limited the flux through the conventional pathway as the 18:3n-3 concentration was increased above the trace concentration used in the [1-^{14}C]-labelling experiments. This was in contrast to the results of previous studies with rainbow trout and Atlantic salmon cell lines supplied increasing concentrations of unlabelled fatty acids [34, 35]. In those studies, increasing the concentration of unlabelled 18:3n-3 from 5 to 50 μM resulted in a greater increase in 20:5n-3 than 20:3n-3. The main difference between the present and the previous studies is that the previous studies analyzed total lipid whereas in the present study we analyzed phospholipids. Thus, there may have been incorporation into neutral lipids which was not detected in the present study. Tocher et al. [34] noted that there were no large increases in neutral lipids in either rainbow trout or turbot cell lines supplied fatty acids at concentrations up to 20 μM however lipid droplets did appear when the concentration was increased above 50 μM. Thus, in the future, it will be interesting to investigate the incorporation of fatty acids into neutral lipids in the FHM cells and compare this with their incorporation into phospholipids to determine the relative distributions as fatty acid concentrations are increased.

Incorporation of 18:2n-6 into the FHM cell phospholipids with increasing concentrations of this fatty acid in the growth medium showed a similar pattern to that observed with 18:3n-3 except that 20:3n-6 was the major desaturation/elongation product incorporated. This is produced by the conventional Δ6 desaturation of 18:2n-6 to yield 18:3n-6 followed by the conventional elongation of 18:3n-6 to yield 20:3n-6. Thus, the result obtained with unlabelled 18:2n-6 was similar to that obtained with labelled 18:2n-6 and this confirmed that Δ5 desaturase was the limiting step in n-6 LC-PUFA synthesis in the FHM cell line. This was consistent with the results of previous work with other freshwater and anadromous fish cell lines [34, 35]. Taking the results with 18:3n-3 and 18:2n-6 together, it suggests that fish cells in culture are suitable for the study of the effects of increasing concentrations of C_{18} PUFA derived from vegetable oils. However, in order to have a control representative of a fish oil-based diet, it will be necessary to supply the cultured cells with either 20:5n-3 or 22:6n-3 to significantly raise the levels of these fatty acids in the cellular lipids. Thus, this was also investigated.

When the FHM cells were supplied with increasing concentrations of 20:5n-3, there was a corresponding increase in the concentration of this fatty acid in their phospholipids but only up to a culture medium concentration of 10 μM. Above this concentration, the incorporation of 20:5n-3 into the cell phospholipids did not change significantly. Thus, incorporation of 20:5n-3 reached a plateau at a lower concentration than incorporation of either of the C_{18} fatty acids. This was in contrast to the results obtained with a cell line from turbot, a marine fish species [34]. In that case 20:5n-3 incorporation continued increasing up to a culture medium concentration of at least 50 μM. Perhaps this reflects a greater capacity for incorporation of 20:5n-3 in marine fish than in freshwater fish but it should also be noted that total lipid was analyzed in the previous study whereas only phospholipids were analyzed in the present study. The direct incorporation of 22:6n-3 into the FHM cell phospholipids was also investigated. This reached a plateau at a very low concentration

of only 2 μM in the culture medium. This has not been studied before and it clearly warrants further investigation.

In general fish flesh products (i.e. seafood) have a shorter shelf life than terrestrial animal meat products and this is due to the greater susceptibility of fish flesh to lipid peroxidation as a result of the higher proportions of LC-PUFA in fish lipids [17]. Thus, it can be hypothesized that feeding farmed fish vegetable oils with their abundance of either 18:3n-3 or 18:2n-6 as opposed to fish oils with their abundance of 20:5n-3 and 22:6n-3 will result in extended shelf life. To test this hypothesis in our in vitro system, we enriched the FHM cells with either saturated fatty acids (16:0 or 18:0), PUFA (18:3n-3) or LC-PUFA (20:5n-3 or 22:6n-3) and then subjected them to oxidative stress to stimulate lipid peroxidation. The cells enriched with 20:5n-3 or 22:6n-3 had significantly higher concentrations of TBARS than the cells enriched with 16:0, 18:0 or 18:3n-3. TBARS is a commonly used indicator of lipid peroxidation in fish [17]. Thus, increasing the unsaturation of the FHM lipids increased the susceptibility of the cells to lipid peroxidation. Therefore in this respect, the cells are a good model for the effects of dietary fish oil replacement on the flesh quality of farmed fish. Previous studies with Atlantic salmon fed diets containing either fish oil, vegetable oil or oils enriched with either 20:5n-3 or 22:6n-3 showed that increasing dietary unsaturation increased indicators of oxidative stress and apoptosis in liver and white adipose tissue [36, 37]. In particular, fish fed diets enriched with either 20:5n-3 or 22:6n-3 had greater activities of the antioxidant enzyme superoxide dismutase and the apoptosis marker caspase 3 as well as reduced integrity of their mitochondria as evidenced by almost undetectable levels of β-oxidation of ^{14}C-palmitoyl CoA. More direct evidence for the effect of dietary fatty acid unsaturation on the oxidative stability of fish lipids comes from a study with grass carp fed diets containing either lard, plant oil or fish oil [38]. In that study, TBARS concentration in the plasma of the fish increased with increasing dietary lipid content and also with increasing unsaturation of the dietary oil. It has also been shown that supplementing the growth medium with the antioxidant α-tocopherol (vitamin E) decreased the longer term inhibitory effect of 20:5n-3 supplementation on the growth of a turbot cell line [39].

In conclusion, the FHM cells had substantial capacity to synthesize 20:5n-3 from 18:3n-3 but only limited capacity to synthesize 22:6n-3. In addition they had substantial capacity to synthesize 20:3n-6 from 18:2n-6 but only limited capacity to synthesize 20:4n-6. Together the data indicated limited chain shortening activity in the peroxisomes and limited Δ5 desaturase activity especially towards 20:3n-6 but also towards 20:4n-3. At a trace (2 μM) concentration, fatty acid incorporation into total lipid was greatest for 18:3n-3 followed closely by 18:2n-6 and 20:5n-3 with incorporation of 22:6n-3 being substantially less. Fatty acid incorporation into phospholipids reached a plateau at much lower concentrations for 20:5n-3 and 22:6n-3 than for 18:3n-3 and 18:2n-6 indicating that the cell membranes had limited capacity for incorporation of 20:5n-3 and 22:6n-3 presumably because of the need to maintain appropriate levels of fluidity. Thus, dietary fish oil replacement with vegetable oils may result in substantial displacement of LC-PUFA by C_{18} PUFA in fish cell membranes. Despite the limited capacity of the cell membranes to incorporate either 20:5n-3 or 22:6n-3, the FHM cells still showed greater susceptibility to lipid peroxidation when the culture medium was supplemented with LC-PUFA as compared with either 18:3n-3 or saturated fatty acids. Thus, the FHM cell line can be a useful model for the effects of dietary fish oil replacement on lipid stability and shelf life in farmed fish.

Acknowledgments MKG was the recipient of a Flinders University Postgraduate Research Scholarship and KAS received funding from the Flinders University Outside Studies Program.

References

1. Food and Agriculture Organization of the United Nations (FAO) (2009) The state of world fisheries and aquaculture 2008, Rome
2. Miller MM, Nichols PD, Carter CG (2008) n-3 Oil sources for use in aquaculture—alternatives to the unsustainable harvest of wild fish. Nutr Res Rev 21:85–96
3. Turchini GM, Torstensen BE, Ng W-K (2009) Fish oil replacement in finfish nutrition. Rev Aquac 1:10–57
4. Calder PC, Yaqoob P (2009) Omega-3 polyunsaturated fatty acids and human health outcomes. BioFactors 35:266–272
5. Tocher DR (2003) Metabolism and functions of lipids and fatty acids in teleost fish. Rev Fish Sci 11:107–184
6. Torstensen BE, Bell JG, Rosenlund G, Henderson RJ, Graff IE, Tochers DR, Lie Ø, Sargent JR (2005) Tailoring of Atlantic salmon (*Salmo salar* L.) flesh lipid composition and sensory quality by replacing fish oil with a vegetable oil blend. J Agric Food Chem 53:10166–10178
7. Zheng X, Torstensen BE, Tocher DR, Dick JR, Henderson RJ, Bell JG (2005) Environmental and dietary influences on highly unsaturated fatty acid biosynthesis and expression of fatty acyl desaturase and elongase genes in liver of Atlantic salmon (*Salmo salar*). Biochim Biophys Acta 1734:13–24
8. Leaver MJ, Villeneuve LAN, Obach A, Jensen L, Bron JE, Tocher DR, Taggart JB (2008) Functional genomics reveals increases in cholesterol biosynthetic genes and highly unsaturated fatty acid biosynthesis after dietary substitution of fish oil with vegetable oils in Atlantic salmon (*Salmo salar*). BMC Genomics 9:299
9. Pratoomyot J, Bendiksen EÅ, Bell JG, Tocher DR (2008) Comparison of effects of vegetable oils blended with southern hemisphere fish oil and decontaminated northern hemisphere fish oil on growth performance, composition and gene expression in Atlantic salmon (*Salmo salar* L.). Aquaculture 280:170–178
10. Trushenski JT, Boesenberg J (2009) Influence of dietary fish oil concentration and finishing duration on beneficial fatty acid profile restoration in sunshine bass *Morone chrysops* ♀ × *M. Saxatilis* ♂. Aquaculture 296:277–283

11. Tocher DR, Sargent JR (1990) Effect of temperature on the incorporation into phospholipid classes and metabolism via desaturation and elongation of n-3 and n-6 polyunsaturated fatty acids in fish cells in culture. Lipids 25:435–442
12. Ghioni C, Tocher DR, Bell MV, Dick JR, Sargent JR (1999) Low C_{18} to C_{20} fatty acid elongase activity and limited conversion of stearidonic acid, 18:4(*n*-3), to eicosapentaenoic acid, 20:5(*n*-3), in a cell line from the turbot, *Scophthalmus maximus*. Biochim Biophys Acta 1437:170–181
13. Tocher DR, Dick JR (1999) Polyunsaturated fatty acid metabolism in a cell culture model of essential fatty acid deficiency in a freshwater fish, carp (*Cyprinus carpio*). Fish Physiol Biochem 21:257–267
14. Tocher DR, Ghioni C (1999) Fatty acid metabolism in marine fish: low activity of fatty acyl Δ5 desaturation in gilthead sea bream (*Sparus aurata*) cells. Lipids 34:433–440
15. Morais S, Monroig O, Zheng X, Leaver MJ, Tocher DR (2009) Highly unsaturated fatty acid synthesis in Atlantic salmon: characterization of ELOVL5- and ELOVL2-like elongases. Mar Biotechnol 11:627–639
16. Gregory MK, See VHL, Gibson RA, Schuller KA (2010) Cloning and functional characterisation of a fatty acyl elongase from southern bluefin tuna (*Thunnus maccoyii*). Comp Biochem Physiol 155:178–185
17. Mourente G, Bell JG, Tocher DR (2007) Does dietary tocopherol level affect fatty acid metabolism in fish? Fish Physiol Biochem 33:269–280
18. Ward RD, Zemlak TS, Innes BH, Last PR, Hebert PDN (2005) DNA barcoding Australia's fish species. Philos Trans Royal Soc Lond Ser B Biol Sci 360:1847–1857
19. Ghioni C, Tocher DR, Sargent JR (1997) The effect of culture on morphology, lipid and fatty acid composition, and polyunsaturated fatty acid metabolism of rainbow trout (*Oncorhynchus mykiss*) skin cells. Fish Physiol Biochem 16:499–513
20. Best CA, Laposata M, Proios VG, Szczepiorkowski ZM (2006) Method to assess fatty acid ethyl ester binding to albumin. Alcohol Alcohol 41:240–246
21. Folch J, Lees M, Sloane Stanley GH (1957) A simple method for the isolation and purification of total lipids from animal tissues. J Biol Chem 226:497–509
22. Tocher DR, Sargent JR, Frerichs GN (1988) The fatty acid compositions of established fish cell lines after long-term culture in mammalian sera. Fish Physiol Biochem 5:219–227
23. Christie WW (1982) Lipid analysis, 2nd edn. Pergamon Press, Oxford
24. Wilson R, Sargent JR (1992) High resolution separation of polyunsaturated fatty acids by argentation thin-layer chromatography. J Chromatogr 623:403–407
25. Tocher DR, Fonseca-Madrigal J, Dick JR, Ng W-K, Bell JG, Campbell PJ (2004) Effects of water temperature and diets containing palm oil on fatty acid desaturation and oxidation in hepatocytes and intestinal enterocytes of rainbow trout (*Oncorhynchus mykiss*). Comp Biochem Physiol Part B 137:49–63
26. Vitiello F, Zanetta J-P (1978) Thin-layer chromatography of phospholipids. J Chromatogr 166:637–640
27. Repetto G, del Peso A, Zurita JL (2008) Neutral red uptake assay for the estimation of cell viability/cytotoxicity. Nat Protocols 3:1125–1131
28. Hoyland DV, Taylor AJ (1991) A review of the methodology of the 2-thiobarbituric acid test. Food Chem 40:271–291
29. Tocher DR, Dick JR, Sargent JR (1995) Development of an in vitro model of essential fatty acid deficiency in fish cells. Prostaglandins Leukotrienes Essent Fat Acids 53:365–375
30. Stubhaug I, Tocher DR, Bell JG, Dick JR, Torstensen BE (2005) Fatty acid metabolism in Atlantic salmon (*Salmo salar* L.) hepatocytes and influence of dietary vegetable oil. Biochim Biophys Acta 1734:277–288
31. Tocher DR (1990) Incorporation and metabolism of (n-3) and (n-6) polyunsaturated fatty acids in phospholipid classes in cultured rainbow trout (*Salmo gairdneri*) cells. Fish Physiol Biochem 8:239–249
32. Tocher DR, Dick JR (1990) Incorporation and metabolism of (*n*-3) and (*n*-6) polyunsaturated fatty acids in phospholipid classes in cultured Atlantic salmon (*Salmo salar*) cells. Comp Biochem Physiol Part B 96:73–79
33. Tocher DR, Mackinlay EE (1990) Incorporation and metabolism of (n-3) and (n-6) polyunsaturated fatty acids in phospholipid classes in turbot (*Scophthalmus maximus*) cells. Fish Physiol Biochem 8:251–260
34. Tocher DR, Carr J, Sargent JR (1989) Polyunsaturated fatty acid metabolism in fish cells: differential metabolism of (n-3) and (n-6) series acids by cultured cells originating from a freshwater teleost fish and from a marine teleost fish. Comp Biochem Physiol Part B 94:367–374
35. Tocher DR, Dick JR (1990) Polyunsaturated fatty acid metabolism in cultured fish cells: incorporation and metabolism of (n-3) and (n-6) series acids by Atlantic salmon (*Salmo salar*) cells. Fish Physiol Biochem 8:311–319
36. Kjær MA, Todorčević M, Torstensen BE, Vegusdal A, Ruyter B (2008) Dietary n-3 HUFA affects mitochondrial fatty acid β-oxidation capacity and susceptibility to oxidative stress in Atlantic salmon. Lipids 43:813–827
37. Todorčević M, Kjær MA, Djaković N, Vegusdal A, Torstensen BE, Ruyter B (2009) N-3 HUFAs affect fat deposition, susceptibility to oxidative stress, and apoptosis in Atlantic salmon visceral adipose tissue. Comp Biochem Physiol Part B 152:135–143
38. Du ZY, Clouet P, Huang LM, Degrace P, Zheng WH, He JG, Tian LX, Liu YJ (2008) Utilization of different dietary lipid sources at high level in herbivorous grass carp (*Ctenopharyngodon idella*): mechanism related to hepatic fatty acid oxidation. Aquac Nutr 14:77–92
39. Tocher DR, Dick JR (1991) Effect of polyunsaturated fatty acids on the growth of fish cells in culture. Comp Biochem Physiol Part A 100:461–466

Lipids (2011) 46:765–780
DOI 10.1007/s11745-011-3556-y

ORIGINAL ARTICLE

Hydrophilic Interaction Liquid Chromatography: ESI–MS/MS of Plasmalogen Phospholipids from *Pectinatus* Bacterium

Tomáš Řezanka · Lucie Siristova · Dagmar Matoulková · Karel Sigler

Received: 3 February 2011 / Accepted: 3 March 2011 / Published online: 11 April 2011

Abstract Liquid chromatography–electrospray tandem mass spectrometry (LC/ESI–MS/MS) was used to analyze phospholipids from three species of the anaerobic beer-spoilage bacterial genus *Pectinatus*. Analysis of total lipids by HILIC (Hydrophilic Interaction Liquid Chromatography) column succeeded in separating diacyl- and plasmalogen phospholipids. Plasmalogens were then analyzed by means of the ESI–MS/MS and more than 220 molecular species of four classes of plasmalogens (PlsCho (choline plasmalogen), PlsEtn (ethanolamine plasmalogen), PlsGro (glycerol plasmalogen), and PlsSer (serine plasmalogen)) were identified. Major molecular species were c-p19:0/15:0 PlsEtn and PlsSer, which accounted for more than 4% of the total lipids.

Keywords *Pectinatus* · Plasmalogens · Liquid chromatography–electrospray tandem mass spectrometry · HILIC column

Electronic supplementary material The online version of this article (doi:10.1007/s11745-011-3556-y) contains supplementary material, which is available to authorized users.

T. Řezanka (✉) · K. Sigler
Institute of Microbiology, Academy of Sciences of the Czech Republic, Vídeňská 1083, 142 20 Prague, Czech Republic
e-mail: rezanka@biomed.cas.cz

L. Siristova
Department of Fermentation Chemistry and Bioengineering, Institute of Chemical Technology Prague, Technická 5, 166 28 Prague, Czech Republic

D. Matoulková
Research Institute of Brewing and Malting, Lípová 511/15, 120 44 Prague, Czech Republic

Abbreviations

CID	Collision-induced dissociation
DMSZ	Deutsche Sammlung von Mikroorganismen und Zellkulturen (German Collection of Microorganisms and Cell Cultures)
ECL	Equivalent chain length
FA	Fatty acid(s)
FAME	Fatty acid methyl ester(s)
GC-MS	Gas chromatography–mass spectrometry
HILIC	Hydrophilic Interaction Liquid Chromatography
LC/ESI–MS/MS	Liquid chromatography–electrospray ionization tandem mass spectrometry
PtdOH	Phosphatidic acid
PtdIns	Phosphatidylinositol
PlsCho	Choline plasmalogen
PlsEtn	Ethanolamine plasmalogen
PlsGro	Glycerol plasmalogen
PlsSer	Serine plasmalogen
RIBM	Research Institute of Brewing and Malting
RSD	Relative standard deviation
TLC	Thin layer chromatography

Introduction

Microbial contamination that can occur during the brewing process can negatively affect the process of beer production and the quality of the final product. The contaminants can include, besides the so-called wild yeasts and molds, a

number of bacterial genera [1–3]. Improvements in beer handling and bottling technology have resulted in a significant reduction in the oxygen content during the process and in packaged beer, which has permitted the growth of anaerobic beer-spoilage bacteria such as *Pectinatus*, *Megasphaera*, *Selenomonas* and *Zymophilus* [1–5].

These anaerobic beer-spoilage bacteria belong to the class *Clostridia* and the family Veillonellacea; despite their phylogenetic affiliation to Gram-positive bacteria the cells stain Gram-negative or Gram-variable [6, 7]. The bacteria *Pectinatus* and *Zymophilus* have been isolated only from breweries, and their natural environment is still unknown [5, 6, 8].

The anaerobic beer-spoilage bacterium *Pectinatus* has become a serious problem in the brewing industry because it can cause strong turbidity and sediment in beer and produces unpleasant volatile compounds, mostly acids, e.g. acetic, propionic, succinic, butyric, valeric and caproic acid and also acetoin and hydrogen sulfide [1–3]. As a result, bacterial spoilage activity can completely damage the beer taste and quality and thus cause serious financial problems to the brewery.

Detection of these spoilage bacteria in breweries is still based on traditional incubation on special diagnostic/selective media [2, 3], which is very time-consuming. For example, development of turbidity in beer forcing tests takes 4–6 weeks [5, 6]. Using the SMMP-medium (a selective medium for *Megasphaera* and *Pectinatus*) the incubation takes up to 14 days [5]. Further alternatives are fatty acids or *O*-alk-1′-enyl chains analysis [3], epifluorescence microscopy, immunofluorescence [6] or modern genetic methods such as PCR [5], fluorescence in situ hybridization [6] or oligonucleotide microarrays [9].

Plasmalogen is any derivative of *sn*-glycero-3-phosphoric acid that contains an *O*-alk-1′-enyl residue (sometimes named vinyl ether moiety or enol ether moiety, see Fig. 1) attached to the glycerol moiety at *sn*-1 position and a polar head made of a nitrogenous base, a glycerol, inositol, etc. moiety.

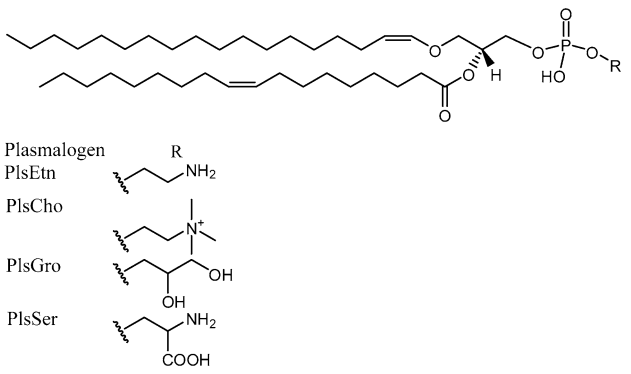

Fig. 1 The structures of plasmalogens. The explanation is in the abbreviations, the structures of the major ions is in Tables 2, 3, 4 and 5

Plasmalogens are among the most specific lipids since their occurrence is limited to strictly anaerobic bacteria [10] and they are not present in aerobic or facultatively anaerobic bacteria. They have been exceptionally found also in fungi [11] while their presence in higher plants is a matter of contention [12, 13]. By contrast, they are common constituents of animal lipids from invertebrates to humans [14]. They are found mostly as PlsCho (choline plasmalogen), PlsEtn (ethanolamine plasmalogen), PlsGro (glycerol plasmalogen), and PlsSer (serine plasmalogen), etc. (Fig. 1).

Analysis of plasmalogens makes use of their vinyl ether bond at the *sn*-1 position, which is liable to acid-catalyzed hydrolysis. The presence of mere traces of an acid causes hydrolysis resulting in a lysophospholipid and a fatty aldehyde. Following their separation by, e.g., TLC, fatty aldehydes can be determined by GC–MS. Another possibility is the removal of the polar moiety of the molecule by phospholipase C and identification of alkyl-acyl, alkenyl-acyl and diacyl-glycerols by HPLC or, after derivatization of the free hydroxyl group, by GC [15]. All these methods are time- and labor-demanding. Another possibility, which has rather rarely been mentioned in the literature, is the separation of intact plasmalogens from diacylphospholipids by HPLC on diol columns [15]. The authors [16–18] have always used an HPLC column with a diol bonded stationary phase and a highly complex organic phase consisting of up to six solvents [17] and, in addition, elution with a nonlinear gradient. The mobile phase also contained a buffer composed of an organic acid (acetic or formic) and base (ammonia, ammonium acetate or triethylamine). The elution order of individual phospholipids was different but, fortunately, plasmalogen was always eluted ahead of the corresponding diacyl-derivative.

Amphiphilic molecules such as phospholipids can be separated on a HILIC (Hydrophilic Interaction Liquid Chromatography) column, although it has more often been used for separating water-soluble analytes [19]. Separation of phospholipids on a HILIC column is described in only a few papers, with relatively controversial results concerning especially the elution of individual phospholipid classes. Thus Schwalbe-Herrmann has described an elution order of PtdGro, PtdEtn and PtdCho [20], whereas Kamleh reported on the order PtdCh, PtdSer and PtdGro [21] and Scherer obtained the sequence PtdGro and PtdOH [22]. To our knowledge, our paper is the first to describe gradient HILIC separation of at least five phospholipid classes including plasmalogens.

Identification of intact plasmalogens has already been described by, e.g., Hsu et al. [23–26] who reported on ESI–MS or ESI–MS/MS identification as lithiated adducts, e.g.

$[M + Li]^+$ molecular ions and their cleavage to give characteristic fragments that allow identification of individual molecular species. The CID spectra of $[M + H]^+$ and $[M + Na]^+$ ions of PtdCho and PtdEtn are rather uninformative regarding the nature and position of the fatty acyl substituents in lipids [27]. In the presence of lithium salts, PtdCho and PtdEtn form $[M + Li]^+$ ions which, upon CID, produce product ion spectra that contain diagnostic fragment ions for both the polar head group and the fatty acyl groups.

This report is part of our investigation of analysis bacterial lipids within the framework of a comprehensive program on the analysis and biosynthesis of lipids [28, 29].

In this article, we present for the first time separation of intact plasmalogen phospholipids from diacyl phospholipids of anaerobic bacteria, and identification and quantitation of individual molecular species of four plasmalogens, i.e. PtdEtn, PtdGro, PtdSer, and PtdCho by LC-ESI/MS^2 from the three strains of bacterium *Pectinatus*.

Experimental

Bacterial Strains

Pectinatus frisingensis DSM 20465 and *P. cerevisiiphilus* DSM 20467 were purchased from the DSMZ Collection (Deutsche Sammlung von Mikroorganismen und Zellkulturen, Braunschweig, Germany). *P. frisingensis* RIBM 2-86 was obtained from the RIBM Collection (Research Institute of Brewing and Malting, Prague, Czech Republic). All strains originated from brewery environment.

Cultivation and Extraction of Bacterium Strains

Pectinatus strains were grown in a modified MRS broth (medium according to de Man, Rogosa, and Sharpe, Merck, Darmstadt, Germany) supplemented with cysteine hydrochloride (0.5 g/L) and sodium thioglycollate (0.5 g/L), pH 5.6–5.7, for 48 h at 28 °C. Cultivation was performed under aerobic conditions (300 mL of modified MRS broth in 500-mL Erlenmeyer flasks, the surface of the medium was covered with sterile mineral oil to ensure anaerobiosis). No anaerobic atmosphere is needed if the medium is freshly prepared, is not stirred, the transfer of culture by pipette is quick and the inoculum is placed in the bottom of the test tube. After cultivation, the biomass was transferred to new tubes, chilled on ice and harvested immediately by centrifugation (10 min/6,000 rpm/0 °C). The tubes with pellets were placed on dry ice and stored frozen until freeze-dried. The yields of biomass and their lipid components are given in Table 1.

The extraction procedure was based on the method of Bligh and Dyer [30], except that 2-propanol was substituted for methanol, since 2-propanol does not serve as a substrate for phospholipases [31]. The alcohol–water mixture was cooled and one part chloroform was added and the lipids were extracted for 30 min. Insoluble material was sedimented by centrifugation and the supernatant was separated into two phases. The aqueous phase was aspirated off and the chloroform phase was washed three times with two parts 1 M KCl each. The resulting chloroform phase was evaporated to dryness under reduced pressure.

Table 1 Yields of biomass, total lipids and phospholipids of *Pectinatus frisingensis* DSM 20465, *P. cerevisiiphilus* DSM 20467, and *P. frisingensis* RIBM 2-86

	RIBM 2-86	DSM 20465	DSM 20467
Biomass in mg	306.0	407.0	469.0
Total lipids in mg	12.3	13.7	14.1
Total lipids in %	4.0	3.4	3.0
Phospholipids in mg	5.9	7.1	7.5
Phospholipids in % of total lipids	48.0	52.0	23.0

Data were obtained by weighing and by means of a Sep-Pak Cartridge with an aminopropylsilica-based polar bonded phase

First, total lipid extracts were applied to the Sep-Pak Cartridge Vac 35 cc (Waters; with 10 g of aminopropylsilica-based polar bonded phase), and from the cartridge were subsequently eluted nonacidic lipids with 40 mL of chloroform–methanol (7:3), and acidic lipids with 30 mL of chloroform–methanol-concentrated aqueous ammonia (70:30:2) containing 0.4% (w/v) ammonium acetate. The eluate was reduced in volume and subjected to semipreparative HILIC or LC–MS. No alkyl acyl species were present.

LC–MS Analysis and Semipreparative HILIC

The HPLC equipment consisted of a 1090 Win system, a PV5 ternary pump and an automatic injector (HP 1090 series, Hewlett Packard, USA). Gradient chromatographic separation was performed on a Merck ZIC®-HILIC HPLC column, with 3.5 µm 100 Å and 2.1 × 250 mm. The injection volume was 5 µL, and the column was maintained at 50 °C. The mobile phase consisted of (a) acetonitrile/water (8:2) with buffer (10 mM ammonium formate, 0.5 mM LiOH and 0.5 mM AcOLi) and (b) acetonitrile/water (5:5) with buffer (20 mM ammonium formate, 0.5 mM LiOH and 0.5 mM AcOLi). A gradient elution was performed with 100% A for 1 min, a step to 75% A until 5 min, a linear decrease to 50% A until 25 min, 50% A up to 10 min, and re-equilibration to 100% A for less than 5 min. The flow rate was set to 180 µL/min. The efficiency of the column was approximately 25,000 plates/250 mm.

The detector was an Applied Biosystems Sciex API 4000 mass spectrometer (Applied Biosystems Sciex, Ontario, Canada) using electrospray mass spectra. The ionization mode was positive, the nebulizing gas (N_2) pressure was 345 kPa and the drying gas (N_2) flow and temperature were 9 L/min and 300 °C, respectively. The electrospray needle was at ground potential, whereas the capillary tension was held at 3,900 V. The cone voltage was kept at 240 V. The mass resolution was 0.1 Da and the peak width was set to 6 s. For an analysis, total ion currents (full scan) were acquired from 200 to 1,100 Da.

CID ions mass spectra were acquired by colliding the Q1 selected precursor ions with Ar gas as a collision target gas and applying a collision energy of 50 eV in Q2. The scanning range of Q3 was *m*/*z* 150–1,100 with a step size of *m*/*z* 0.3 and a dwell time of 1 ms. A peak threshold of 0.3% intensity was applied to the mass spectra. The instrument was interfaced to a computer running Applied Biosystems Analyst version 1.4.1 software.

The liquid chromatograph was the semipreparative Gradient LC System G-1 (Shimadzu, Kyoto, Japan) with two LC-6A pumps (0.5 mL/min), an SCL-6A system controller, an SPD ultraviolet detector, an SIL-1A sample injector and a C-R3A data processor, with semipreparative normal phase HPLC ZIC®-HILIC 250 × 10 mm, 5 μm, 200 Å column. The gradient was as described above, with a flow rate of 4.5 mL/min, and was monitored by a variable wavelength detector at 210 nm (HP 1040 M Diode Array Detector).

Isolation of Aldehydes and Fatty Acids from Plasmalogens

In order to hydrolyze plasmalogens, the eluted compounds from semipreparative HILIC (∼ 10–100 μg) were treated with 90% acetic acid at 37 °C for 18 h and dried under reduced pressure. The products were dissolved in a small volume of chloroform and subjected to thin-layer chromatography on silica gel G, eluted by chloroform–methanol–7 M ammonia 60:35:5 (v/v/v) mixture and spots were located by spraying with water. The aldehydes, derived from the alk-l-enyl groups, and lysophospholipids were extracted from the plates with chloroform–methanol 1:2 (v/v). The fatty aldehydes were stored in hexane at −20 °C until analyzed. The lysophospholipid was heated at 75 °C in the presence of 10% NaOH and 50% methanol (1 mL) for 3 h. The hydrolysate was cooled, extracted twice with petroleum ether, and then adjusted to pH 3 with concentrated HCl. The acidified solution was extracted three times with diethyl ether (1 mL) and the combined extracts were then washed with water, and the sample was concentrated under nitrogen. The fatty acids were then methylated with diazomethane [32].

GC–MS

Gas chromatography–mass spectrometry of FAME and free aldehydes was done on a GC–MS system consisting of a Varian 450-GC, a Varian 240-MS ion trap detector with electron impact ionization, and a CombiPal autosampler (CTC, USA). The sample was injected onto a 25 m × 0.25 mm × 0.1 μm Ultra-1 capillary column (Supelco, Czech Republic) under a temperature program: 5 min at 50 °C, increasing at 10 °C/min to 280 °C and 15 min at 280 °C. Helium was the carrier gas at a flow of 0.52 °C/min. All spectra were scanned within the range *m*/*z* 50–500.

Results

Cells of three strains of genus *Pectinatus* were cultivated as described in Experimental and were harvested in log phase when the optical density of the culture was maximal. The time of cultivation was 48 h. The yield of lyophilized cells is shown in Table 1, which also gives the yield of lipids obtained by the Bligh–Dyer [30] extraction of lyophilized cells. Part of total lipids was fractionated by means of cartridges with aminopropyl silica-based polar bonded phase, which were rinsed in a chloroform–methanol mixture and phospholipids were further eluted by a mixture of chloroform–methanol–concentrated aqueous ammonia.

The HILIC employing a column with sulfobetaine group (3-(trimethylammonio)propane-1-sulfonate) with a zwitterionic character phase is suitable for separating phospholipids as well as their plasmalogen forms thanks to the use of an appropriate mobile phase, i.e. a buffer containing ammonium formate. This prevents acid hydrolysis of the enol bonds. Baseline resolution was achieved between all identified lipid classes, with partial resolution between alkenylacyl and diacyl phospholipids (Fig. 2) and Fig. 1 in Supplemental, describing the separation of five standards (16:0–18:1 PtdCho, 16:0–18:1 PtdEtn, 16:0–18:1 PtdSer, 16:0–18:1 PtdOH, and 16:0–18:1 PtdGro). The identities of alkenylacyl- and diacyl-phospholipid peaks were confirmed after HILIC separation followed by ESI–MS/MS, see below.

Baseline was stable and retention times of all identified classes of phospholipids were well reproducible, with standard deviations ± 0.05 min for the commercially obtained standards 1-*O*-1′-(*Z*)-octadecenyl-2-(9*Z*-octadecenoyl)-*sn*-glycero-3-phosphoethanolamine (p18:0/9*Z*-18:1-PtdEtn) and ± 0.07 min for 1-*O*-1′-(*Z*)-octadecenyl-2-(9*Z*-octadecenoyl)-*sn*-glycero-3-phosphocholine (p18:0/9*Z*-18:1-PtdCho).

Under these conditions, the main phospholipid classes were separated well. PtdGro was eluted first, followed by

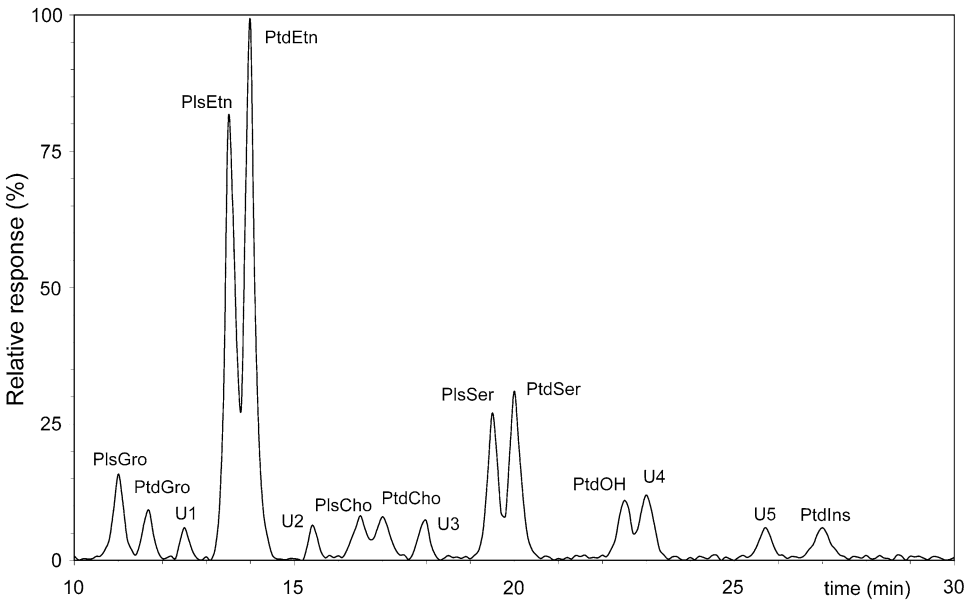

Fig. 2 HILIC/APCI-MS chromatogram of the phospholipids from *Pectinatus frisingensis* DSM 20465, analyzed by a linear gradient semipreparative normal phase HPLC ZIC®-HILIC 250 × 10 mm, 5 µm, 200-Å column, with a flow rate of 4.5 mL/min, and monitored by a variable wavelength detector at 210 nm

PtdEtn, PtdCho, PtdSer, PtdOH, and PtdIns (Fig. 2). Because different molecular species within a class have the same polar head, their retention times in HILIC are very similar. The differences in retention times for compounds within one class are less than that between two different classes. The different molecular species can be determined by MS/MS.

As mentioned in the Introduction, mass spectrometry fragmentation of diacylphospholipids has already been described but the situation with plasmalogen phospholipids is different. ESI tandem mass spectra of phospholipids as monolithiated $[M + Li]^+$ adduct molecular ions, arising at about 1 mM lithium salt concentrations in the mobile phase, show rich fragmentation, i.e. loss of some different neutral moieties, chiefly substituents at *sn*-3 or *sn*-2 position, exceptionally *sn*-1 (1-*O*-alk-1′-enyl) of plasmalogen. The corresponding ions are given in Tables 2, 3, 4 and 5. Apart from these ions that occur regularly in all four plasmalogens, some plasmalogens give rise to specific ions that can serve for direct identification of the given plasmalogen. Fast and exact identification was based on the separation by HILIC column and identification of phospholipids as monolithiated adducts, which allows for a ready identification of plasmalogens even in very low concentrations of about ~0.7 ng/µl.

The most abundant phospholipid was PtdEtn (29.7% total lipids) including its plasmalogen form (PlsEtn; 24.2%). Structural characterization of PlsEtn is complicated by numerous homologues that consist of various isomers (Fig. 3). Identification of individual molecular species was based on tandem MS. For example, the MS/MS spectrum of ion at *m/z* 678 of lithiated molecular species c-p17:0/15:1 PlsEtn showed the most abundant ion at *m/z* 635 ($[M + Li\text{-}43]^+$), i.e. ion with the structure shown in Fig. 4 and Table 2. Other ions present in the spectrum are formed by cleavage of neutral molecules, see e.g. ions at *m/z* 555 $[M + Li\text{-}123]^+$, *m/z* 549 $[M + Li\text{-}129]^+$, *m/z* 532 $[M + Li\text{-}141]^+$ and *m/z* 531 $[M + Li\text{-}147]^+$, arising from neutral losses; for structures see Table 2.

Two ions with moderate abundance at *m/z* 383, representing combined losses of aziridine and the *sn-1* alk-1′-enyl as an alcohol, i.e. $C_{15}H_{29}CH = CHOH$ and ion at *m/z* 291, representing the combined losses of lithium 2-aminoethyl hydrogenphosphate (for the structure see Table 2) and the *sn-2* fatty acid, i.e. pentadecenoic acid, were identified. The nature of the fatty acid at *sn*-2 was further verified by the presence of the acylium ion at *m/z* 240. Based on the above ions it is thus possible to determine in this plasmalogen the bond of the alkenyl ether at *sn-1* as well as the fatty acid at *sn-2*. The mass spectrum displays, below *m/z* 200, a dominant ion at *m/z* 148, which, though it does not provide information about the pPE structure, is nevertheless characteristic for PlsEtn and naturally also PtdEtn. This ion is not shown in the spectrum.

Identification of molecular species with the same molecular mass, i.e. isobaric species, was more complicated but not unfeasible, see Fig. 5. This can be best illustrated on two cases. First the mixture of two molecular species, i.e. c-p17:0/c-19:0 (5.5% of total PlsEtn) and c-p19:0/c-17:0 (4.8% of total PlsEtn), exhibits ions $[M + Li\text{-neutral molecules}]^+$, i.e. ions at *m/z* 691, 673, 611, 605, 593, and 587, which only confirm the structure of both molecular species and do not permit an even semi-quantitative estimate of their abundances. This estimate was only possible based on the cluster of cluster of four ions, i.e. two pairs (losses of aziridine with the *sn-1*

Table 2 Some important ions observed in the product ion spectrum of the $[M + Li]^+$ of molecular species c-p17:0/15:1-PlsEtn at *m/z* 678

PlsEtn	*m/z* for c-p17:0/15:1-PlsEtn
$[M+Li]^+$- 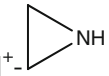	678 − 43 = 635
$[M+Li]^+$- 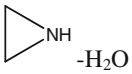 -H_2O	678 − 43 − 18 = 617
*$[M+Li]^+$- 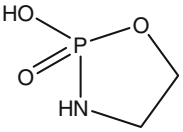	678 − 123 = 555
*$[M+Li]^+$- 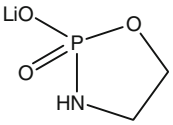	678 − 129 = 549
$[M+Li]^+$- 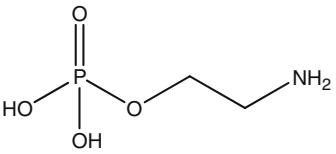	678 − 141 = 537
$[M+Li]^+$- 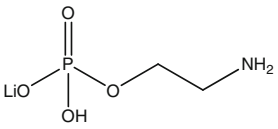	678 − 147 = 531
$[M+Li]^+$- 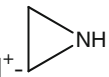 -$R_1CH{=}CHOH$	678 − 43 − 252 = 383
$[M+Li]^+$- 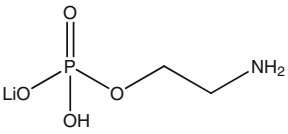 -R_2COOH	678 − 147 − 240 = 291
R_2CO^+	223

Though Hsu and Turk [24] describe a linear structure of neutral fragments, i.e. $(HO)P(O)(OCH_2CH_2NH_2)$, a cyclic structure gives a better fit (see the neutral loss products in the paper by Zemski Berry and Murphy [50])

Data were obtained by RP-HPLC/ESI-tandem MS/MS operated in positive ionization mode

alk-1′-enyl and combined losses of lithium 2-aminoethyl hydrogen phosphate with the *sn-2* fatty acid. The abundance of ions at *m/z* 439 and 409, or those at *m/z* 319 and 291, enabled us to determine the semiquantitative abundances of individual molecular species.

The same holds for four molecular species, i.e. a most complex mixture of positional isomers containing these four molecular species, i.e. p15:0/c-17:0, p17:0/15:1, c-p17:0/15:0, and c-p19:0/13:0. Based on losses of aziridine with the *sn-1* alk-1′-enyl and combined losses of lithium 2-aminoethyl hydrogen phosphate with the *sn-2* fatty acid we could again determine the percent abundances. Further molecular species of next plasmalogens were identified similarly.

Like with the PlsEtn, also the tandem MS/MS spectrum of p17:0/15:0-PlsSer having $[M + Li]^+$ ion at *m/z* 726 contains prominent ions at *m/z* 541 and at *m/z* 535 arising from loss of phosphoserine as free acid and as a lithium salt, respectively (see Table 3). ESI spectrum of PlsGro is shown in Fig. 2 in Supplemental. The ion at *m/z* 639 (726-aziridine carboxylic acid) having medium abundance, and ions at *m/z* 397 (639-R_2COOH) and at *m/z* 415 (639-$R_2'CH = CO$) resulting from loss of the 15:0-fatty acid moiety and the corresponding loss of fatty acyl ketene, respectively, provide information needed for assignment of the *sn*-2 position of the fatty acyl substituents on the glycerol backbone. The ion at *m/z* 628 corresponding to loss of the phosphoric acid originated by rearrangement in which the anionic site of the serine head group makes a nucleophilic attack on C-3 of the glycerol backbone, followed by expulsion of the phosphoric acid. The mass spectrum also features an ion at *m/z* 484 arising from $[M + Li]^+$ loss of the fatty acid group. The presence of ion at *m/z* 281 confirms the position of the alkenyl ether at *sn*-1. The structure of fatty acid bonded to glycerol backbone was again confirmed by the presence of ion $[R_2CO]^+$

Table 3 Some important ions observed in the product ion spectrum of the $[M + Li]^+$ of molecular species p17:0/15:0 PlsSer at *m/z* 726

PlsSer	*m/z* for p17:0/15:0 PlsSer
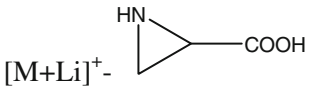 $[M+Li]^+$-	726 − 87 = 639
$[M + Li]^+$-H_3PO_4	726 − 98 = 628
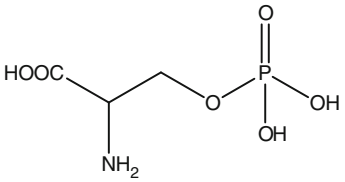 $[M+Li]^+$-	726 − 185 = 541
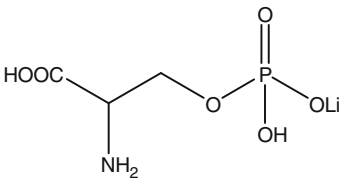 $[M+Li]^+$-	726 − 191 = 535
$[M + Li]^+$-R_2COOH	726 − 242 = 484
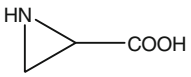 $[M+Li]^+$- -R´$_2$CH=C=O	726 − 87 − 224 = 415
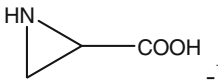 $[M+Li]^+$- -R_2COOH	726 − 87 − 242 = 397
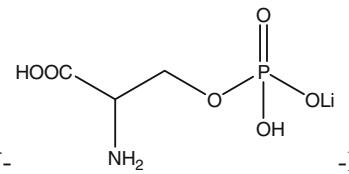 $[M+Li]^+$- -R´$_1$CH=CHOH	726 − 191 − 214 = 321
R_2CO^+	225

Data were obtained by RP-HPLC/ESI-tandem MS/MS operated in positive ionization mode

at *m/z* 225. Further, the spectrum displayed an ion at *m/z* 192 corresponding to a lithiated phosphoserine ion via cleavage of the C_3-OP bond. This ion (not shown in our spectrum) is characteristic only for PtdSer and therefore also for PlsSer.

The qualitative and quantitative abundance of molecular species having the same summary formula and thus the same molecular weight, i.e. c-p19:0/18:1 and p18:1/c-19:0, was analyzed as described with PlsEtn. Hence we can determine the abundance of two ions at *m/z* 423 and at *m/z* 409, i.e. ion with structure [M-aziridine carboxylic acid-fatty acid]$^+$ and two appropriate ions at *m/z* 335 and at *m/z* 321 with structure [M-phosphoserine as lithium salt-$R_1'CH = CHOH]^+$. Semiquantitative abundance of three or four molecular species with the same summary formula, e.g. c-p19:0/15:0, p18:1/16:1, c-p17:0/17:0, and p17:0/c-17:0, was estimated as described above with PlsEtn.

The c-p17:0/15:1 PlsCho molecular species having $[M + Li]^+$ ion at *m/z* 720 yields a prominent product ion at *m/z* 661 caused by loss of $N(CH_3)_3$ (Table 4). For the ESI spectrum of PlsCho from *Pectinatus frisingensis* see Fig. 3 in the Supplemental Material. This *m/z* 661 $[M + Li-59]^+$ ion yields ions of *m/z* 537 $[M + Li-183]^+$ and *m/z* 531 $[M + Li-189]^+$ resulting from losses of ethylene phosphate and lithium ethylene phosphate, respectively. Identification of the fatty acid substituent at *sn*-2 is based on the occurrence of the *m/z* 472 ion $[M + Li-R_2COOLi]^+$ that is produced by loss of lithium pentadecanoate from *m/z* 720, and a prominent ion of *m/z* 291 $[531-C_{16}H_{31}COOH]^+$ caused by loss of pentadecenoic acid from *m/z* 531. The pentadecanoate moiety is clearly identified by the presence of the acylium ion at *m/z* 223 $[C_{16}H_{31}CO]^+$. Weak ions at *m/z* 468 and 409, which identify the 1-*O*-heptadecenyl moiety, arise by loss of the 1-alkenyl moiety as an alcohol ($C_{13}H_{27}CH = CHOH$) from *m/z* 720 and 661, respectively, and further dissociation of the latter ion yields a weak ion at *m/z* 395.

The last plasmalogen was identified as PlsGro; its ESI spectrum is shown in Fig. 4 in Supplemental. The tandem MS/MS spectrum of an ion $[M + Li]^+$ at *m/z* 793 indicates

Table 4 Some important ions observed in the product ion spectrum of the $[M + Li]^+$ of molecular species c-p17:0/15:1-PlsCho at *m/z* 720

PlsCho	*m/z* for c-p17:0/15:1-PlsCho
$[M + Li]^+$-NMe_3	720 − 59 = 661
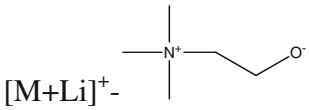	720 − 103 = 617
$[M+Li]^+$-	
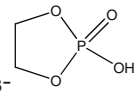	720 – 59 − 124 = 537
$[M+Li]^+$-NMe_3-	
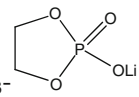	720 – 59 − 130 = 531
$[M+Li]^+$-NMe_3-	
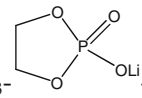	720 – 59 − 130 − 18 = 513
$[M+Li]^+$-NMe_3- -H_2O	
$[M + Li]^+$- $R'_1CH = CHOH$	720 − 252 = 468
$[M + Li]^+$-R_2COOLi	720 − 248 = 472
$[M + Li]^+$-NMe_3- $R'_1CH = CHOH$	720 − 59 − 252 = 409
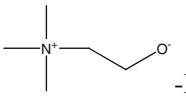	720 − 103 − 222 = 395
$[M+Li]^+$- -$R'_2CH=C=O$	
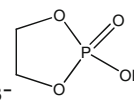	720 − 59 − 130 − 240 = 291
$[M+Li]^+$-NMe_3- -R_2COOH	
R_2CO^+	223

Data were obtained by RP-HPLC/ESI-tandem MS/MS operated in positive ionization mode

the structure of p19:0/c-19:0 PlsGro. Loss of dihydroxycyclopropane from this $[M + Li]^+$ ion gives rise to a prominent ion at *m/z* 719, see Table 4. Loss of fatty acid from this ion yields in turn an ion at *m/z* 423, which is important for the diagnostics of the structure of fatty acid at *sn*-2. Also the ion at *m/z* 497, arising by a mere loss of fatty acid from the $[M + Li]^+$, determines the structure of fatty acid at *sn*-2. Like PtdSer, also PtdGro molecule undergoes a rearrangement with a concomitant expulsion of phosphoric acid, giving rise to the ion $[M + Li\text{-}H_3PO_4]^+$ at *m/z* 695. As mentioned in the Introduction, many ions are common for all phospholipids; in the case of PtdGro these are the ions arising by splitting of the polar part of molecule form *sn*-3 of glycerol backbone, i.e. ions at *m/z* 621 and at *m/z* 615. These ions arise by the splitting of glycerophosphoric acid (systematic name is 2,3-dihydroxypropyl dihydrogen phosphate) or its lithium salt $[M + Li\text{-}172]^+$ and $[M + Li\text{-}178]^+$, respectively. For structure of both ions see Table 5.

The remaining two phospholipids, i.e. PtdOH and PtdIns, in which no plasmalogens have been found, were identified based on literature data, see below. After identifying all four plasmalogens we performed quantitation of fatty acids and phospholipids in the three strains of genus *Pectinatus*.

Phospholipids were further separated by semipreparative HILIC, see Experimental. The major phospholipids were PtdGro, PtdEtn, PtdCho, and PtdSer, including their plasmalogens; PtdIns was present in minor amounts. Five peaks were not identified, see Fig. 3.

The content of fatty acids determined by GC–MS in the three species of *Pectinatus* is given in Table 6. The fatty acids included saturated ones from C11 to C18, as well as monoenoic ones and also two acids having a cyclopropane ring in the midchain position. The quantitative proportion of FA in different phospholipids of one species, as well as in individual strains did not substantially differ.

A similar situation was found in the case of aldehydes arising by mild acidic hydrolysis; an interesting feature was the minor proportion of octadecenal in all three PlsEtn.

Discussion

The comparison of our results with the literature data is difficult or nearly impossible. As was found already in the

Table 5 Some important ions observed in the product ion spectrum of the $[M + Li]^+$ of molecular species p19:0/c-19:0-PlsGro at *m/z* 793

PlsGro	*m/z* for p19:0/c-19:0-PlsGro
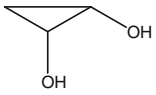 $[M+Li]^+$-	793 − 74 = 719
$[M + Li]^+$-H_3PO_4	793 − 98 = 695
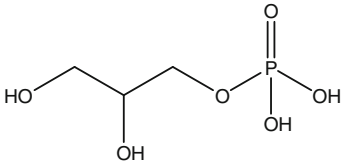 $[M+Li]^+$-	793 − 172 = 621
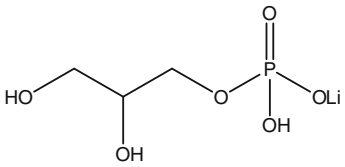 $[M+Li]^+$-	793 − 178 = 615
$[M + Li]^+$-R_2COOH	793 − 296 = 497
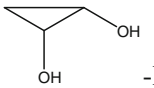 $[M+Li]^+$- -R_2COOH	793 − 74 − 296 = 423
R_2CO^+	279

Data were obtained by RP-HPLC/ESI-tandem MS/MS operated in positive ionization mode

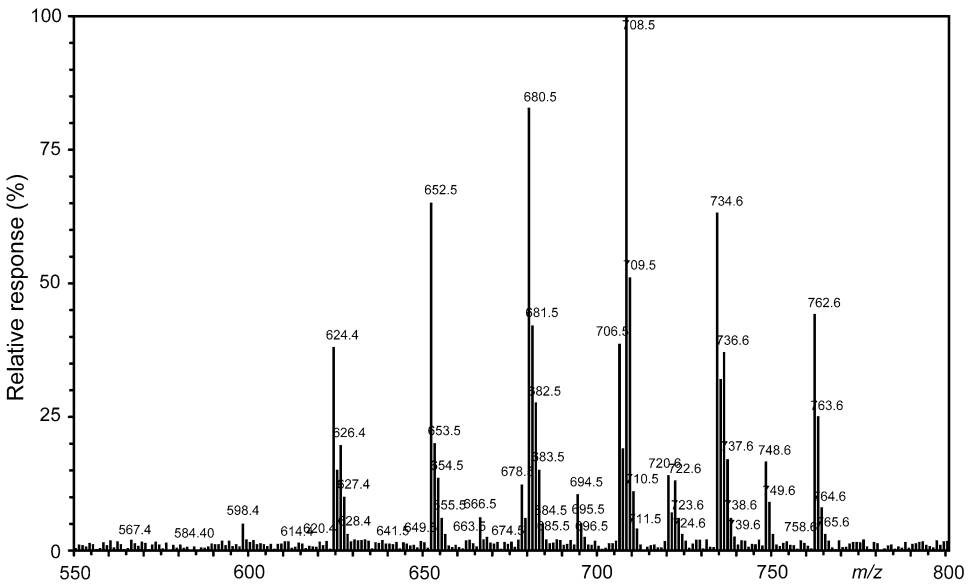

Fig. 3 ESI spectrum of PlsEtn from *Pectinatus frisingensis* DSM 20465. MS was run by using the electrospray mode and set to scan from 200 to 1,100 kDa. Only the most relevant part of the mass spectrum is shown (550–800 kDa). Adduct ions in the form of $[M + Li]^+$ are seen throughout the spectrum

1960s, fatty acids with a cyclopropane ring are very susceptible to acidic conditions that cause cleavage of the ring. This was documented in 1965 by Nesbitt and Lennarz [33] who therefore saponified cells of the genus *Proteus* by 10% NaOH and methylated free FA by diazomethane. This approach, which was used also by other authors [34], avoided the cleavage of the cyclopropane ring. As noted in 1989 by Christie in his book, "Cyclopropane fatty acids of bacterial origin are more susceptible to chemical attack, e.g. cyclopropane ring is disrupted by acidic conditions, and lipid samples containing such acids are best transesterified with basic reagents; the free fatty acids can be methylated safely with diazomethane" [35]. The dramatic drop in the content of cyclopropane FA under acidic conditions when preparing FAME was recently amply documented by Basconcillo and McCarry [36]. The table published in their paper shows that basic hydrolysis and acid esterification of FA from the bacterium *Sinorhizobium meliloti* brings about a drop of cis-11,12-C19:0_{cyclo} from 31 to 2.5% total FA, i.e. by more than one order of magnitude.

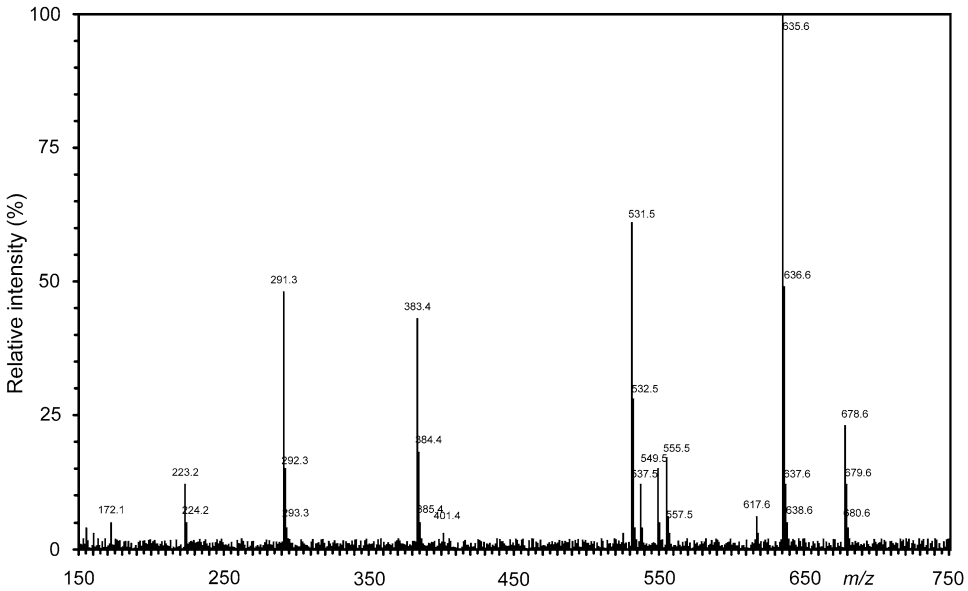

Fig. 4 The MS/MS spectrum of lithiated molecular species c-p17:0/15:1 PlsEtn obtained in ESI. The ion at *m/z* 678.6 was selected for fragmentation. This ion was further fragmented with CID resulting in the presented spectrum. Fragment identities and their structures are explained in Table 2

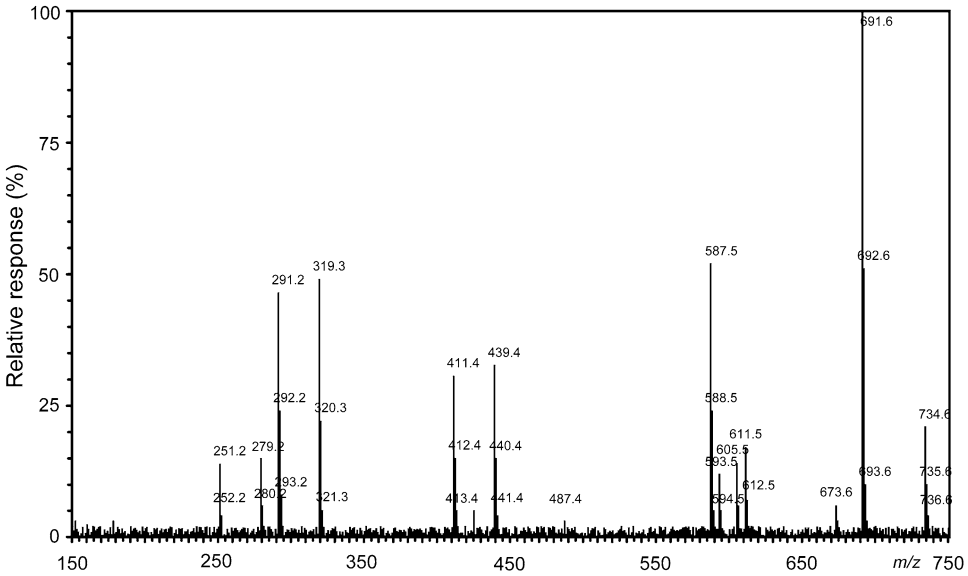

Fig. 5 Tandem MS/MS of the mixture of two molecular species—c-p17:0/c-19:0 and c-p19:0/c-17:0 PlsEtn. Quantification of isobaric species of plasmalogens was based on six ions, i.e. ions at *m/z* 251 and 279 $[RCO]^+$, *m/z* 291.3 and 319.3 $[M + Li\text{-}147\text{-}R'2COOH]^+$, and *m/z* 411.4 and 439.4 $[M + Li\text{-}43\text{-}R'1CH = CHOH]^+$

Accordingly, Moore et al. [37], who used basic hydrolysis and acid-catalyzed esterification, found no cyclopropane FA in *Pectinatus*. Gonzalez et al. [38], who erroneously identified the species *P. portalensis*, also failed to find any cyclo-FA, not even in the previously described *P. frisingensis* or *P. cerevisiiphilus*. Moreover, their data showed completely baffling differences between the contents of FA in individual species. Johnston and Goldfine [39], who analyzed the related genus *Megasphaera*, realized that the chromatographic peak of monoenoic FAME could contain cyclopropane FAME and found that, following catalytic reduction that disrupts the cyclopropane ring, major c-17:0 acyl chain peak decreased from 60.5 to 2.9% of total FA. This means that it was in fact a mixture of two FA, i.e. cyclo-17:0 and 17:1 in a ratio of about 20:1, not a pure 17:1.

Unusual ions arising from 9-methoxy acids and found in the MS spectrum by Helander and Haikara [3] led to the conclusion that these acids were artificially created during methanolysis from cyclopropane acids. The substantial differences between FAME prepared by methanolysis and those prepared by saponification can thus be explained by the degradation of cyclopropanoic acids.

Even when using reaction conditions preventing degradation of cyclopropane FA, the experimenter is faced with two other problems. As has been known for several decades [35], the ECL values of C18 cyclopropane FAME and corresponding C18 monoenoic methyl esters are approximately equal, see, e.g., Fig. 2 in the paper by Helander and Haikara [3]. Moreover, cyclopropanoid FAME are not readily distinguished by MS from monoenoic FAME with a

Table 6 Fatty acid content of the three strains of *Pectinatus frisingensis* DSM 20465, *P. cerevisiiphilus* DSM 20467, and *P. frisingensis* RIBM 2-86

	P. frisingensis RIBM 2-86				*P. cerevisiiphilus* DSM 20467				*P. frisingensis* DSM 20465			
	PlsEtn	PlsSer	PlsGro	PlsCho	PlsEtn	PlsSer	PlsGro	PlsCho	PlsEtn	PlsSer	PlsGro	PlsCho
11:0	18.1	16.4	16.5	22.6	17.4	16.8	17.1	21.1	14.7	12.2	14.2	13.8
12:0	0.8	0.3	0.4	0.8	1.2	0.0	0.0	1.5	0.8	0.3	0.8	0.4
13:0	6.2	6.8	5.3	8.6	6.3	6.7	5.1	8.5	6.5	6.9	8.2	5.6
14:0	1.7	0.6	1.0	1.6	2.1	0.2	0.5	2.2	1.8	0.6	1.5	1.1
15:0	27.1	26.2	17.6	15.1	25.9	27.2	18.3	14.3	26.3	31.4	27.5	28.6
16:0	1.8	0.3	2.2	1.5	2.2	0.0	1.8	2.2	1.9	0.3	1.4	2.3
17:0	5.0	3.9	4.7	2.0	5.2	3.7	4.5	2.6	5.3	4.0	1.9	5.0
18:0	1.2	2.0	1.6	1.7	1.6	1.6	1.1	2.3	1.3	2.0	1.6	1.7
15:1	5.9	3.0	5.8	7.4	6.0	2.7	5.7	7.4	6.2	3.0	7.1	6.1
16:1	0.8	1.1	1.3	4.0	1.2	0.7	0.8	4.4	0.8	1.1	3.8	1.4
c-17:0	10.6	16.0	14.9	16.6	10.4	16.5	15.4	15.7	10.5	12.2	11.4	11.6
18:1	4.8	8.7	6.2	5.7	5.0	8.8	6.1	5.9	5.0	8.8	5.4	6.6
c-19:0	16.0	14.7	22.5	12.4	15.5	15.1	23.6	11.9	18.9	17.2	15.2	15.8
p15:0	4.6	0.0	5.3	2.3	3.2	2.1	7.2	2.4	4.9	0.0	2.4	5.5
p17:0	16.0	11.2	18.7	12.4	14.8	18.6	6.8	10.6	27.8	11.4	12.8	22.7
c-p17:0	34.2	33.2	20.9	23.8	25.9	25.8	29.7	30.1	27.6	25.4	24.6	21.6
p18:1	0.0	20.2	3.6	19.4	4.9	10.2	12.6	6.3	0.2	20.5	20.0	3.7
c-p19:0	45.2	35.4	51.5	42.1	51.2	43.3	43.7	50.6	39.5	42.7	40.2	46.5

0.0 = less than 0.1%

Data were obtained by GC–MS of fatty acid methyl esters, the structure of unsaturated fatty acids was determined by the mass spectra of picolinyl esters

similar total number of carbon atoms, apparently because on ionisation the cyclopropane ring opens up to form some degradation products [40, 41]. Much better results are obtained with picolinyl ester derivatives (see Harvey [42] and also our two mass spectra given in Figs. 5 and 6 of Supplemental).

Most authors analyzing the *Pectinatus* FA failed to employ optimum conditions and the reliability of their data is therefore questionable. The same holds for monoenoic and cyclopropanoic aldehydes.

Quantification of individual classes of phospholipids including plasmalogens is based on the total ion current of commercially available standards. The calibration curves of four standards, i.e. PtdCho, PlsCho, PtdEt and PlsEtn (9*Z*-18:1/9*Z*-18:1-PtdCho, p18:0/9*Z*-18:1-PlsCho, 9*Z*-18:1/9*Z*-18:1-PtdEtn, and p18:0/9*Z*-18:1-PlsEtn) showed that these molecular species have a linear response in the range of nearly four orders of magnitude, i.e. from 1 μmol/mL to 10 mmol/mL (i.e. ~0.7 μg/mL to ~7 mg/mL). The worst values of % RSD (relative standard deviation) were obtained for the lowest and the highest chromatographic peaks. This could be due to the signal being too weak (a low signal to noise ratio) or to a charge space phenomenon caused by the accumulation of too many ions in the mass spectrometer (in the case of the highest chromatographic peak, i.e. at a high concentration of the compound). The samples were therefore appropriately diluted to an optimal concentration (100 μmol/mL) to avoid the loss of signal from the lowest chromatographic peak and limit the charge space phenomenon for the highest chromatographic peak. This compromise maximizes reproducibility. Unfortunately, PlsGro and PlsSer are not commercially available but both these plasmalogens can be assumed to have a very similar mechanism of ionization (see above) allowing thus also the same quantification by means of the total ion current. Comparison of relative concentrations of individual FAME calculated from GC/MS and from HPLC/MS-APCI of TAGs is given in Table 1 in Supplemental.

The quantification of single ion molecular species was much more complicated. Based on the measurements of commercially available standards PlsCho and PlsEtn and the corresponding homologs PtdCho and PtdEtn (i.e. 9*Z*-18:1/9*Z*-18:1-PtdCho and 9*Z*-18:1/9*Z*-18:1-PtdEtn, respectively) we found that the abundant ions at *m/z* 425 $[M + Li\text{-}43\text{-}R'_1CH = CHOH]^+$ and at *m/z* 305 $[M + Li\text{-}147\text{-}R'_2COOH]^+$ in PlsEtn and ions at *m/z* $[M + Li\text{-}43\text{-}R_1COOH]^+$ and $[M + Li\text{-}43\text{-}R_2COOH]^+$ in PtdEtn, and also ions $[M + Li\text{-}59\text{-}R_1COOH]^+$ and $[M + Li\text{-}59\text{-}R_2COOH]^+$ in PtdCho and ions at *m/z* 465 ($[M + Li\text{-}59\text{-}R'_1CH = CHOH]^+$) and at *m/z* 395 ($[M + Li\text{-}103\text{-}R'_2$

$CH = C{=}O]^+$) in PlsCho show a linear response in an interval of more than three orders of magnitude, i.e. from 5 to 10 mmol/mL. Individual molecular species of plasmalogens were therefore quantified based on the above ion. Because of the lack of commercial standards of PlsGro and PlsSer we again used the assumption of a very similar mechanism of ionization. More exact quantification would require either the use of two-dimensional HPLC (normal and reversed phase HPLC) or acquisition (synthesis) of appropriate standards, i.e. different molecular species of PlsSer and PlsGro.

As already mentioned in the Introduction and in the paragraph describing the occurrence of fatty acids in *Pectinatus* and related bacteria, the determination of both qualitative and quantitative proportions of FA is highly questionable. To our knowledge, no paper devoted to identification and quantitation of molecular species of plasmalogens in *Pectinatus* has as yet been published. The results of our analyses of these molecular species are shown in Table 7. Although the molecular species of individual classes of phospholipids have been described in bacteria such as *Escherichia coli* [43] or *Corynebacterium* [44], these bacteria are taxonomically relatively distant from *Pectinatus*. The taxonomically nearest bacterial genus that has been described in the literature is *Clostridium*, which also belongs to anaerobes and is taxonomically classed to the same order (Clostridiales), although to a different family (Clostridiaceae) [45].

Both our literature survey and a recent review [15] point to the scarcity of data on the analysis of molecular species of phospholipids, especially of plasmalogens in bacteria. Only a single study by Hsu and Turk [43] reported on the analysis of cardiolipin from *E. coli* using modern techniques, identified cardiolipin and described the quantitative analysis of isobaric molecular species.

Only six molecular species of *O*-alanylphosphatidylglycerol and six molecular species of phosphatidylethanolamine were identified in the genus *Clostridium*, which

Table 7 The content of molecular species of plasmalogens in the three strains of *Pectinatus frisingensis* DSM 20465, *P. cerevisiiphilus* DSM 20467, and *P. frisingensis* RIBM 2-86

Molecular species		*P. frisingensis* RIBM 2-86				*P. cerevisiiphilus* DSM 20467				*P. frisingensis* DSM 20465			
		PlsEtn	PlsSer	PlsGro	PlsCho	PlsEtn	PlsSer	PlsGro	PlsCho	PlsEtn	PlsSer	PlsGro	PlsCho
p15:0	/11:0	0.8	0.0	0.0	0.5	0.0	0.7	0.3	0.8	0.6	0.4	1.2	0.5
p17:0	/11:0	2.9	1.8	1.8	2.8	1.4	4.1	1.8	3.1	2.6	3.1	1.2	2.2
c-p17:0	/11:0	6.2	5.4	5.4	5.4	3.1	4.1	3.5	3.0	4.5	4.3	5.1	6.4
p18:1	/11:0	0.0	3.3	3.3	4.4	2.5	0.0	2.8	0.5	0.9	1.7	2.2	1.3
c-p19:0	/11:0	8.2	5.8	5.8	9.5	5.2	5.8	5.7	6.4	8.9	7.3	7.5	10.7
p15:0	/12:0	0.0	0.0	0.0	0.0	0.0	0.0	0.0	0.0	0.0	0.0	0.0	0.0
p17:0	/12:0	0.1	0.0	0.0	0.1	0.0	0.2	0.1	0.1	0.2	0.0	0.0	0.2
c-p17:0	/12:0	0.3	0.1	0.1	0.2	0.1	0.2	0.2	0.1	0.3	0.0	0.0	0.5
p18:1	/12:0	0.0	0.1	0.1	0.2	0.1	0.0	0.2	0.0	0.1	0.0	0.0	0.1
c-p19:0	/12:0	0.4	0.1	0.1	0.3	0.1	0.3	0.3	0.2	0.6	0.0	0.0	0.8
p15:0	/12:0	0.3	0.0	0.0	0.2	0.0	0.3	0.2	0.3	0.2	0.1	0.4	0.2
p17:0	/13:0	1.0	0.8	0.8	1.1	0.8	1.8	1.0	1.3	0.9	1.2	0.3	0.9
c-p17:0	/13:0	2.1	2.3	2.3	2.0	1.8	1.8	2.0	1.2	1.6	1.7	1.5	2.6
p18:1	/13:0	0.0	1.4	1.4	1.7	1.4	0.0	1.6	0.2	0.3	0.7	0.6	0.5
c-p19:0	/13:0	2.8	2.4	2.4	3.6	2.9	2.6	3.3	2.6	3.2	2.9	2.2	4.3
p15:0	/14:0	0.1	0.0	0.0	0.0	0.0	0.1	0.0	0.1	0.1	0.0	0.0	0.1
p17:0	/14:0	0.3	0.1	0.1	0.2	0.1	0.5	0.2	0.2	0.3	0.0	0.0	0.2
c-p17:0	/14:0	0.6	0.2	0.2	0.4	0.2	0.5	0.4	0.2	0.5	0.1	0.1	0.7
p18:1	/14:0	0.0	0.1	0.1	0.3	0.1	0.0	0.3	0.0	0.1	0.0	0.1	0.1
c-p19:0	/14:0	0.8	0.2	0.2	0.7	0.3	0.7	0.6	0.5	1.1	0.1	0.2	1.1
p15:0	/15:0	1.2	0.0	0.0	0.3	0.0	1.3	0.7	1.6	0.8	0.6	1.3	0.3
p17:0	/15:0	4.3	2.9	2.9	1.9	3.6	7.3	3.5	6.5	3.8	5.1	1.2	1.5
c-p17:0	/15:0	9.3	8.7	8.7	3.6	8.0	7.3	6.8	6.2	6.7	7.0	5.4	4.3
p18:1	/15:0	0.0	5.3	5.3	2.9	6.4	0.1	5.5	1.1	1.3	2.8	2.3	0.9
c-p19:0	/15:0	12.2	9.3	9.3	6.4	13.4	10.4	11.1	13.3	13.3	11.8	8.4	7.2
p15:0	/16:0	0.1	0.0	0.0	0.0	0.0	0.1	0.0	0.1	0.1	0.0	0.1	0.1

Table 7 continued

Molecular species		*P. frisingensis* RIBM 2-86				*P. cerevisiiphilus* DSM 20467				*P. frisingensis* DSM 20465			
		PlsEtn	PlsSer	PlsGro	PlsCho	PlsEtn	PlsSer	PlsGro	PlsCho	PlsEtn	PlsSer	PlsGro	PlsCho
p17:0	/16:0	0.3	0.0	0.0	0.2	0.0	0.5	0.2	0.5	0.3	0.0	0.1	0.2
c-p17:0	/16:0	0.6	0.1	0.1	0.4	0.1	0.5	0.3	0.5	0.6	0.0	0.5	0.7
p18:1	/16:0	0.0	0.1	0.1	0.3	0.1	0.0	0.3	0.1	0.1	0.0	0.2	0.1
c-p19:0	/16:0	0.8	0.1	0.1	0.6	0.1	0.8	0.6	1.1	1.1	0.0	0.8	1.1
p15:0	/17:0	0.2	0.0	0.0	0.0	0.0	0.3	0.0	0.3	0.2	0.1	0.3	0.1
p17:0	/17:0	0.8	0.4	0.4	0.2	0.5	1.5	0.2	1.1	0.8	0.7	0.3	0.3
c-p17:0	/17:0	1.7	1.3	1.3	0.5	1.0	1.5	0.5	1.1	1.3	1.0	1.3	0.8
p18:1	/17:0	0.0	0.8	0.8	0.4	0.8	0.0	0.4	0.2	0.3	0.4	0.6	0.2
c-p19:0	/17:0	2.3	1.4	1.4	0.8	1.7	2.1	0.8	2.3	2.7	1.6	2.0	1.3
p15:0	/18:0	0.1	0.0	0.0	0.0	0.0	0.1	0.0	0.1	0.1	0.0	0.1	0.1
p17:0	/18:0	0.2	0.2	0.2	0.2	0.2	0.4	0.2	0.4	0.2	0.3	0.1	0.2
c-p17:0	/18:0	0.4	0.7	0.7	0.4	0.5	0.4	0.4	0.4	0.4	0.4	0.3	0.7
p18:1	/18:0	0.0	0.4	0.4	0.3	0.4	0.0	0.3	0.1	0.1	0.2	0.1	0.1
c-p19:0	/18:0	0.5	0.7	0.7	0.7	0.9	0.5	0.6	0.8	0.8	0.7	0.5	1.2
p15:0	/15:1	0.3	0.0	0.0	0.2	0.0	0.3	0.2	0.3	0.2	0.1	0.4	0.2
p17:0	/15:1	0.9	0.3	0.3	0.9	0.3	1.7	0.9	1.4	0.9	0.5	0.4	0.8
c-p17:0	/15:1	2.0	1.0	1.0	1.8	0.8	1.7	1.7	1.3	1.6	0.7	1.7	2.2
p18:1	/15:1	0.0	0.6	0.6	1.4	0.6	0.0	1.4	0.2	0.3	0.3	0.7	0.5
c-p19:0	/15:1	2.7	1.1	1.1	3.1	1.3	2.4	2.9	2.8	3.1	1.2	2.5	3.7
p15:0	/16:1	0.0	0.0	0.0	0.1	0.0	0.0	0.1	0.1	0.0	0.0	0.1	0.1
p17:0	/16:1	0.1	0.1	0.1	0.5	0.1	0.2	0.5	0.3	0.2	0.1	0.1	0.5
c-p17:0	/16:1	0.3	0.4	0.4	1.0	0.3	0.2	0.9	0.3	0.3	0.2	0.2	1.3
p18:1	/16:1	0.0	0.2	0.2	0.8	0.2	0.0	0.8	0.1	0.1	0.1	0.1	0.3
c-p19:0	/16:1	0.4	0.4	0.4	1.7	0.5	0.3	1.5	0.7	0.6	0.3	0.3	2.2
p15:0	/c-17:0	0.5	0.0	0.0	0.4	0.0	0.5	0.3	0.6	0.3	0.3	1.1	0.4
p17:0	/c-17:0	1.7	1.8	1.8	2.1	1.4	2.9	1.5	2.6	1.5	3.1	1.0	1.7
c-p17:0	/c-17:0	3.6	5.3	5.3	4.0	3.1	2.9	2.8	2.5	2.7	4.3	4.6	4.7
p18:1	/c-17:0	0.0	3.2	3.2	3.2	2.5	0.0	2.3	0.4	0.5	1.7	1.9	1.0
c-p19:0	/c-17:0	4.8	5.7	5.7	7.0	5.2	4.1	4.6	5.4	5.3	7.1	6.7	7.9
p15:0	/18:1	0.2	0.0	0.0	0.1	0.0	0.2	0.1	0.4	0.2	0.2	0.4	0.1
p17:0	/18:1	0.8	1.0	1.0	0.7	1.0	1.4	0.7	1.5	0.7	1.6	0.4	0.6
c-p17:0	/18:1	1.6	2.9	2.9	1.4	2.2	1.4	1.3	1.4	1.3	2.3	1.8	1.8
p18:1	/18:1	0.0	1.8	1.8	1.1	1.8	0.0	1.1	0.2	0.2	0.9	0.8	0.4
c-p19:0	/18:1	2.2	3.1	3.1	2.4	3.8	2.0	2.2	3.1	2.6	3.8	2.7	2.9
p15:0	/c-19:0	0.7	0.0	0.0	0.3	0.0	0.9	0.4	0.9	0.5	0.3	1.7	0.3
p17:0	/c-19:0	2.6	1.6	1.6	1.5	2.0	5.3	1.9	3.6	2.3	2.8	1.6	1.3
c-p17:0	/c-19:0	5.5	4.9	4.9	3.0	4.4	5.2	3.7	3.4	3.9	3.9	7.0	3.6
p18:1	/c-19:0	0.0	3.0	3.0	2.4	3.5	0.0	3.0	0.6	0.8	1.4	3.0	0.7
c-p19:0	/c-19:0	7.2	5.2	5.2	5.2	7.3	7.5	6.1	7.3	7.9	6.5	10.3	6.0

Data were obtained from ESI spectra

belongs to the same order as the genus *Pectinatus*, although the polar lipids of *C. perfringens* were analyzed by LC/MS with electrospray ionization. The assumed presence of plasmalogens was based only on a TLC plate treated with HCl vapors, lyso-phosphatidylethanolamine being derived by acid hydrolysis of the plasmalogens of PtdEtn [46].

A later work on *C. tetani* identified phospholipids such as PtdEtn, PtdGro, cardiolipin and EtnPGlcNAcdiradylglycerol. FA on *sn*-1/*sn*-2 were determined only in

seven out of 35 molecular species of PE and PG, no data on their quantitative proportions being given [47].

The high variability of bacteria can be illustrated in the paper [48] in which plasmalogens were identified in *C. tetani* ATCC 454 but not in strain ATCC 10779. The authors again identified plasmalogen forms of PtdEtn, PtdGro, cardiolipin, etc., but acyls at the *sn*-1 and *sn*-2 positions were determined in only 7 of them, again with no quantification.

An excellent paper on phospholipids and also plasmalogens of lower organisms was published in Parasitology [49]. Many hundreds of molecular species of phospholipids were identified in parasitic protist species *Trypanosoma brucei*, which included, e.g., 128 molecular species of PtdEtn, out of which 15 were plasmalogens.

Conclusion

The HILIC/ESI-MS^n method used here efficiently separated plasmalogens and all other phospholipids usually found in anaerobic bacteria by a single chromatographic run. We determined more than 200 lipid molecular species from four lipid classes with one injection on an HILIC column, which is nearly ideal for separating amphiphilic compounds such as phospholipids with excellent reproducibility, high sensitivity (from 1 μmol/mL) and dynamic range (4 orders of magnitude). This column was used for both analytical determination and semipreparative isolation of alkenyl-acyl- and diacyl-phospholipids. Irrespective of the class of phospholipids, plasmalogen is eluted first and this is followed by a nearly baseline-separated corresponding diacyl-phospholipid. The elution can be performed conveniently by an aqueous phase with a buffer compatible with ESI.

Simultaneous detection of intact plasmalogens together with other phospholipid classes (odd-chains fatty acids, aldehydes) offers a valuable tool for the study of phospholipids. The fragmentation processes observed by tandem MS of plasmalogens generate unique determinants of the identities of the 1-*O*-alk-1-enyl chains at the *sn*-1 position and the fatty acid esterified at the *sn*-2 position of the glycerol backbone.

Tandem MS of plasmalogen molecules as lithiated adduct ions offers an optimum means for structural characterization. The structure of plasmalogen molecules can be easily determined from the positive ESI showing abundant fragment ions with different polar head groups, fatty acid constituents and regiospecificity. The $[M + Li]^+$ ions of plasmalogens that have undergone consecutive losses of the fatty acid substituent at *sn*-2 and the polar head group, i.e. the $[M + Li–R_2COOH–polar\ head\ group]^+$ ions greatly aid in the differentiation of the plasmenyl- and diacyl-phospholipid subclasses, including PtdEtn, PtdCho, PtdGro and PtdSer. Thus, structures of plasmalogens with isobaric isomers in mixtures can be unambiguously unveiled.

We believe that the method will be valuable for studying phospholipid profiles in different biological samples.

Acknowledgments This work was supported by the Ministry of Education, Youth and Sports of the Czech Republic (Project MSM2B08022 and MSM6046137305), Institutional Research Concept AV0Z50200510 and Research Centre 1M0570).

References

1. Jespersen L, Jakobsen M (1996) Specific spoilage organisms in breweries and laboratory media for their detection. Food Microbiol 33:139–155
2. Sakamoto K, Konings WN (2003) Beer spoilage bacteria and hop resistance. Int J Food Microbiol 89:105–124
3. Basařová G, Šavel J, Basař P, Lejsek T (2010) Brewing, theory and practice of beer production (Pivovarství, teorie a praxe výroby piva). Vydavatelství VŠCHT Praha, Prague, pp 310–348
4. Helander IM, Haikara A (1995) Cellular fatty acyl and alkenyl residues in *Megasphaera* and *Pectinatus* species: contrasting profiles and detection of beer spoilage. Microbiology 141:1131–1137
5. Satokari R, Juvonen R, Mallison K, von Wright A, Haikara A (1998) Detection of beer spoilage bacteria *Megasphaera* and *Pectinatus* by polymerase chain reaction and colorimetric microplate hybridization. Int J Food Microbiol 45:119–127
6. Juvonen R, Koivula T, Haikara A (2008) Group-specific PCR-RFLP and real-time PCR methods for detection and tentative discrimination of strictly anaerobic beer-spoilage bacteria of the class *Clostridia*. Int J Food Microbiol 125:162–169
7. Schleifer KH, Leuteritz M, Weiss N, Ludwig W, Kirchhof G, Sedel-Rüfer H (1990) Taxonomic study of anaerobic, gram-negative, rod-shaped bacteria from breweries: Emended description of *Pectinatus cerevisiiphilus* and description of *Pectinatus frisingensis* sp. nov., *Selenomonas lacticifex* sp. nov., *Zymophilus raffinosivorans* gen. nov., sp. nov., and *Zymophilus paucivorans* sp. nov. Int J Syst Bacteriol 40:19–27
8. Matoulková D (2008) Strictly anaerobic bacteria in beer and in breweries. Kvasny Prum 54:338–343
9. Weber DG, Sahm K, Polen T, Wendisch VF, Antranikian G (2008) Oligonucleotide microarrays for the detection and identification of viable beer spoilage bacteria. J Appl Microbiol 105:951–962
10. Takatsuka Y, Kamio Y (2004) Molecular dissection of the *Selenomonas ruminantium* cell envelope and lysine decarboxylase involved in the biosynthesis of a polyamine covalently linked to the cell wall peptidoglycan layer. Biosci Biotechnol Biochem 68:1–19
11. Horrocks LA, Sharma M (1982) Plasmalogens and O-alkyl glycerophospholipids. In: Hawthorne JN, Ansell GB (eds) Phospholipids. Elsevier, Amsterdam, pp 51–93
12. Felde R, Spiteller G (1994) Search for plasmalogens in plants. Chem Phys Lipids 71:109–113
13. Mangold HK (1972) The search for alkoxylipids in plants. In: Snyder F (ed) Ether lipids: chemistry and biology. Academic Press, New York, pp 399–405
14. Goldfine H (2010) The appearance, disappearance and reappearance of plasmalogens in evolution. Prog Lipid Res 49:493–498

15. Christie WW, Han X (2010) Lipid analysis, 4th edn. The Oily Press, Bridgwater
16. Uran S, Larsen A, Jacobsen PB, Skotland T (2001) Analysis of phospholipid species in human blood using normal-phase liquid chromatography coupled with electrospray ionization ion-trap tandem mass spectrometry. J Chromatogr B 758:265–275
17. Olsson NU, Harding AJ, Harper C, Salem N (1996) High-performance liquid chromatography method with light scattering detection for measurements of lipid class composition: analysis of brains from alcoholics. J Chromatogr B 681:213–218
18. Mawatari S, Okuma Y, Fujino T (2007) Separation of intact plasmalogens and all other phospholipids by a single run of high-performance liquid chromatography. Anal Biochem 370:54–59
19. Nguyen HP, Schug KA (2008) The advantages of ESI-MS detection in conjunction with HILIC mode separations: fundamentals and applications. J Sep Sci 31:1465–1480
20. Schwalbe-Herrmann M, Willmann J, Leibfritz D (2010) Separation of phospholipid classes by hydrophilic interaction chromatography detected by electrospray ionization mass spectrometry. J Chromatogr A 1217:5179–5183
21. Kamleh A, Barrett MP, Wildridge D, Burchmore RJS, Scheltema RA, Watson DG (2008) Metabolomic profiling using Orbitrap Fourier transform mass spectrometry with hydrophilic interaction chromatography: a method with wide applicability to analysis of biomolecules. Rapid Commun Mass Spectrom 22:912–1918
22. Scherer M, Schmitz G, Liebisch G (2010) Simultaneous quantification of cardiolipin, bis(monoacylglycero)phosphate and their precursors by hydrophilic interaction LC-MS/MS including correction of isotopic overlap. Anal Chem 82:8794–8799
23. Hsu FF, Turk J (2009) Electrospray ionization with low-energy collisionally activated dissociation tandem mass spectrometry of glycerophospholipids: mechanisms of fragmentation and structural characterization. J Chromatogr B 877:2673–2695
24. Hsu FF, Turk J (2000) Characterization of phosphatidylethanolamine as a lithiated adduct by triple quadrupole, tandem mass spectrometry with electrospray ionization. J Mass Spectrom 35:596–606
25. Hsu FF, Turk J (2005) Studies on phosphatidylserine by tandem quadrupole and multiple stage quadrupole ion-trap mass spectrometry with electrospray ionization: Structural characterization and the fragmentation processes. J Am Soc Mass Spectr 16:1510–1522
26. Hsu FF, Turk J, Thukkani AK, Messner MC, Wildsmith KR, Ford DA (2003) Characterization of alkylacyl, alk-1-enylacyl and lyso subclasses of glycerophosphocholine by tandem quadrupole mass spectrometry with electrospray ionization. J Mass Spectrom 38:752–763
27. Hsu FF, Turk J (2005) Electrospray ionization with low-energy collisionally activated dissociation tandem mass spectrometry of complex lipids: structural characterization and mechanisms of fragmentation. In: Byrdwell WC (ed) Modern methods for lipid analysis by liquid chromatography/mass spectrometry and related techniques. AOCS Press, Champaign, pp 61–178
28. Lisa M, Holcapek M, Rezanka T, Kabatova N (2007) High-performance liquid chromatography-atmospheric pressure chemical ionization mass spectrometry and gas chromatography-flame ionization detection characterization of delta 5-polyenoic fatty acids in triacylglycerols from conifer seed oils. J Chromatogr A 1146:67–77
29. Rezanka T, Mares P, Husek P, Podojil M (1986) Gas-chromatography mass-spectrometry and desorption chemical ionization mass-spectrometry of triacylglycerols from the green-alga *Chlorella kessleri*. J Chromatogr 355:265–271
30. Bligh EG, Dyer WJ (1959) A rapid method of total lipid extraction and purification. Can J Biochem Physiol 37:911–917
31. Kates M (1986) Techniques of lipidology: isolation, analysis and identification of lipids. In: Work TS, Work E (eds) Laboratory techniques in biochemistry and molecular biology, 2nd edn. Elsevier, Amsterdam, pp 220–223
32. Khuller GK, Goldfine H (1974) Phospholipids of *Clostridium butyricum*. V. Effects of growth temperature on fatty alk-1-enyl ether group, and phospholipid. J Lip Res 15:500–507
33. Nesbitt JA, Lennarz WJ (1965) Comparison of lipids and lipopolysaccharide from the bacillary and L forms of *Proteus* P18. J Bacteriol 89:1020–1025
34. Khuller GK, Goldfine H (1974) Phospholipids of *Clostridium butyricum*. V. Effects of growth temperature on fatty acid, 1-alkenyl ether group, and phospholipid composition. J Lipid Res 15:500–507
35. Christie WW (1989) Gas chromatography and lipids. A practical guide, Oily Press Ltd
36. Basconcillo LS, McCarry BE (2008) Comparison of three GC/MS methodologies for the analysis of fatty acids in *Sinorhizobium meliloti*: development of a micro-scale, one-vial method. J Chromatogr B 871:22–31
37. Moore LVH, Bourne DM, Moore WEC (1994) Comparative distribution and taxonomic value of cellular fatty acids in thirty-three genera of anaerobic Gram-negative bacilli. Int J Syst Bact 44:338–347
38. Gonzalez JM, Jurado V, Laiz L, Zimmermann J, Hermosin B, Saiz-Jimenez C (2004) *Pectinatus portalensis* nov sp., a relatively fast-growing, coccoidal, novel *Pectinatus* species isolated from a wastewater treatment plant. Antonie van Leeuwenhoek 86:241–248
39. Johnston NC, Goldfine H (1982) Effects of growth temperature on fatty acid and alk-1-enyl group compositions of *Veillonella parvula* and *Megasphaera elsdenii* phospholipids. J Bacteriol 149:567–575
40. Christie WW, Holman RT (1966) Mass spectrometry of lipids. I. Cyclopropane fatty acid esters. Lipids 1:176–182
41. Wood R, Reiser R (1965) Cyclopropane fatty acid metabolism; physical and chemical identification of propane ring metabolic products in the adipose tissue. J Am Oil Chem Soc 42:315–320
42. Harvey DJ (1984) Picolinyl derivatives for the characterization of cyclopropane fatty acids by mass spectrometry. Biomed Mass Spectrom 11:187–192
43. Hsu FF, Turk J (2006) Characterization of cardiolipin from *Escherichia coli* by electrospray ionization with multiple stage quadrupole ion-trap mass spectrometric analysis of [M–2H + Na]-ions. J Am Soc Mass Spectr 17:420–429
44. Mazzella N, Molinet J, Syakti AD, Barriol A, Dodi A, Bertrand JC, Doumenq P (2005) Effects of pure n-alkanes and crude oil on bacterial phospholipid classes and molecular species determined by electrospray ionization mass spectrometry. J Chromatogr B 822:40–53
45. de Vos P, Garrity G, Jones D, Krieg NR, Ludwig W, Rainey FA, Schleifer KH, Whitman WB (eds) (2009) Bergey's manual of systematic bacteriology. Vol 3: The Firmicutes, Springer
46. Johnston NC, Baker JK, Goldfine H (2004) Phospholipids of *Clostridium perfringens*: a reexamination. FEMS Microbiol Lett 233:65–68
47. Mazzella N, Molinet J, Syakti AD, Dodi A, Doumenq P, Artaud J, Bertrand JC (2004) Bacterial phospholipid molecular species analysis by ion-pair reversed-phase HPLC/ESI/MS. J Lipid Res 45:1355–1363
48. Johnston NC, Aygun-Sunar S, Guan Z, Ribeiro AA, Daldal F, Raetz CRH, Goldfine H (2010) A phosphoethanolamine-modified glycosyl diradylglycerol in the polar lipids of *Clostridium tetani*. J Lipid Res 51:1953–1961
49. Richmond GS, Gibellini F, Young SA, Major L, Denton H, Lilley A, Smith TK (2010) Lipidomic analysis of bloodstream and procyclic form *Trypanosoma brucei*. Parasitology 137:1357–1392

50. Zemski Berry KA, Murphy RC (2004) Electrospray ionization tandem mass spectrometry of glycerophosphoethanolamine plasmalogen phospholipids. J Am Soc Mass Spectr 15:1499–1508
51. Holčapek M, Lísa M, Jandera P, Kabátová N (2005) Quantitation of triacylglycerols in plant oils using HPLC with APCI-MS, evaporative light-scattering, and UV detection. J Sep Sci 28:1315–1333 (this paper is cited in Supplementary material 1)
52. Rezanka T (1990) Identification of very long polyenoic acids as picolinyl esters by Ag+ ion-exchange high-performance liquid-chromatography, reversed-phase high-performance liquid-chromatography and gas-chromatography mass-spectrometry. J Chromatogr 513:344–348 (this paper is cited in Supplementary material 1)

Lipids (2011) 46:781–788
DOI 10.1007/s11745-011-3564-y

ORIGINAL ARTICLE

Non-Polar Lipid Components of Human Cerumen

Karel Stránský · Irena Valterová · Edita Kofroňová · Klára Urbanová · Marie Zarevúcka · Zdeněk Wimmer

Received: 21 January 2011 / Accepted: 19 April 2011 / Published online: 6 May 2011

Abstract Human cerumen was separated by column chromatography into the following groups of compounds: hydrocarbons, squalene, wax esters and cholesterol esters, triacylglycerols, free fatty acids, free fatty alcohols, monoacylglycerols, free cholesterol, free sterols, and free hydroxy acids. The groups of compounds obtained were examined in detail by gas chromatography and gas chromatography–mass spectrometry. In total, about one thousand compounds have been identified.

Keywords Cerumen · Ear wax · Lipids · ECL values · ACL values

Abbreviations

ACL	Alcohol chain length
APCI	Atmospheric pressure chemical ionization
CC	Column chromatography
DMDS	Dimethyl disulfide
ECL	Equivalent chain length
FAME	Fatty acid methyl ester
GC–MS	Gas chromatography/mass spectrometry
HPLC	High performance liquid chromatography
I	Kováts index
PTLC	Preparative thin layer chromatography
R_F	Retention factor
TAG	Triacylglycerol(s)
TLC	Thin layer chromatography
UV	Ultra violet

Electronic supplementary material The online version of this article (doi:10.1007/s11745-011-3564-y) contains supplementary material, which is available to authorized users.

K. Stránský · I. Valterová · E. Kofroňová · K. Urbanová · M. Zarevúcka
Institute of Organic Chemistry and Biochemistry AS CR, v.v.i., Flemingovo náměstí 2, 16610 Prague 6, Czech Republic

E. Kofroňová · Z. Wimmer (✉)
Institute of Chemical Technology in Prague, Technická 5, 16628 Prague 6, Czech Republic
e-mail: wimmer@biomed.cas.cz; Zdenek.Wimmer@vscht.cz

Z. Wimmer
Institute of Experimental Botany AS CR, v.v.i., Isotope Laboratory, Vídeňská 1083, 14220 Prague 4, Czech Republic

Introduction

Cerumen is the secretory product of the sebaceous and ceruminal glands in the outer third of external auditory canal and it is the main component of earwax. Other components of earwax are sheets of desquamated keratin squames, sweat, sebum, and various foreign substances (hair spray, shampoo, shaving cream, bath oil, cosmetics, dirt, etc. [1, 2]. A number of scientists have dealt with its chemical composition. Several papers have been focused on investigation of proteins [3–6], amino acids [3, 7–9], and other nitrogen-containing compounds [3, 10], sugars [9, 11], and glycopeptides [12–14]. Several elements (Na, K, Ca, Mg, P and Cu) were identified and the presence of volatile products was mentioned as well [15]. A majority of papers have been focused on the investigation of lipids, which represent major components of ear wax (up to 64%) [4, 16]. Nakamichi [17] described the presence of a large quantity of glycerol esters and cholesterol esters, and Nakashima [3] identified several fatty acids, triacylglycerols, and cholesterol. Nitta and Ikai [18] found short chain fatty acids (C_4–C_6). Wheatley [19] was the first one who identified squalene in human cerumen, but he also

described [20] the presence of hydrocarbons, wax alcohols, cholesterol, and sterol-like substances. Akobjanoff et al. [21] found cholesterol and fatty acids. For the first time, gas chromatography was used by Haahti et al. [22, 23] for identification of fatty acids, squalene, cholesterol, alcohols, and esters. Sumiko and Akikatsu [8] used fractionation into different solvent systems for separation the cerumen components, and described the presence of free cholesterol and its esters, triacylglycerols and phospholipids. Kataura [24] used column chromatography on silica gel for isolation of several groups of compounds (cholesterol, triacylglycerols, fatty acids and unidentified lipids). Kataura and Kataura [25] isolated cholesterol esters, triacylglycerols, diacylglycerols, monoacylglycerols, free fatty acids, and unidentified polar lipids by column chromatography on silica gel. Aitzetmüller and Koch [26] found by HPLC of methylated and non-methylated chloroform extracts that cerumen contains lipid classes similar to sebum. Gershbein et al. [27] used alumina for fractionation of the groups of compounds. Saponified part of human cerumen was separated into hydrocarbons (with squalene as the main component), cholesterol, alcohols, and fatty acids. Lipid composition of earwax in connection to hircismus (strong odor) was studied by Inaba et al. [28]. Bortz et al. [29] also studied the hydrocarbon content in cerumen. However, Harvey [30] published so far the most detailed analysis of cerumen by application of a GC–MS analysis. Human cerumen was saponified, and the compounds were analyzed by GC-MS after derivatization. Nearly 200 compounds were found in a chromatogram, and nearly one half of them were identified. In view of the fact that a majority compounds were present both free and bonded, it has not been possible to characterize their "origin". Bortz et al. [1] solved this handicap: They separated the human cerumen into the individual groups of compounds (squalene, cholesterol esters, wax esters, triacylglycerols, fatty acids, cholesterol, ceramides, and cholesterol sulfate) using preparative chromatography, however, they did not perform a more detailed analysis of these product groups.

For quantitative evaluation of sebum lipid components, nuclear magnetic resonance was also used [31]. The composition of cerumen was also investigated by using flash pyrolysis–gas chromatography–mass spectrometry analysis [32]. Simple aromatic hydrocarbons were found together with non-branched chain aliphatic hydrocarbons, several diterpenoids and steroid compounds including cholesterol. Due to the destructive character, this method may be only used for fingerprinting of cerumens from different origin.

Besides the human cerumen, lipids in cow's cerumen [33], in dog's cerumen [34–36], and complex carbohydrates in the ceruminous glands of the goats [37] were studied. Cerumen was also studied from a microbiology point of view [38–40]). Its bacteriostatic and fungistatic properties were described in the 1960s [22, 35, 36, 41–48]. A considerable number of people suffer from cerumen secretion, which may result in serious health problems. Absence of cerumen may lead to infection, in that, cerumen plays an antibacterial role through physically protecting the external auditory canal skin, establishing a low pH and an inhospitable environment for pathogens and producing antimicrobial compounds such as lysozyme, so that its absence leaves the canal vulnerable to infection [48].

Cerumen represents a complex mixture of at least one thousand compounds the systematic analysis of which has not been done yet. In this paper, we present a detail analysis of non-polar lipids of human cerumen achieved by current analytical methodology.

Experimental

Collection of Materials

Ear wax (1.323 g) was collected twice a week from both ears of a healthy individual (a male, 65 years old) by means of a small wooden spatula (approx. 200 doses collected throughout 1 year, each approx. 6.6 mg), and it was kept at −18 °C up to the work-up. One of the authors of this work was the volunteer to have ear wax collected and, therefore, no special regulations for including humans in this research were needed.

Column Chromatography (CC)

Ear wax (1.323 g) was adsorbed on silica gel (6.5 g, 60–120 μm) and chromatographed on a column (2.5 × 31 cm) containing silica gel Pitra (Technical support laboratories of IOCB, Czech Republic; 80 g, 60–120 μm, water content 12%). Preparation of silica gel for chromatography was made by its 48-h extraction of silica gel with methanol/chloroform (1:1, v/v) in a Soxhlet apparatus, followed by drying, activating at 120 °C for 24 h, and finally by controlled deactivating the purified silica gel by adding water (12%, w/w). The components were eluted with a mixture of light petroleum-diethyl ether (concentration of diethyl ether increased continuously from 0 to 100%, v/v), and then with a mixture of chloroform–methanol (1:1 v/v). All solvents were distilled before using. The mixture was separated into 35 fraction [(25–100 ml, total solvent volume 1,750 ml (light petroleum-diethyl ether), and 1,000 ml (chloroform–methanol)]. Eluted compounds were monitored using thin-layer chromatography (TLC) and fractions containing compounds with the same R_F were combined.

Thin-layer Chromatography (TLC)

Analytical TLC was carried out on glass plates (36 × 76 mm) coated with Adsorbosil-Plus, layer thickness 0.2 mm (Applied Science Laboratories, USA) with gypsum (12%, w/w). Visualization of the spots was achieved by heating the plates sprayed with conc. sulfuric acid.

Preparative TLC (PTLC) was carried out on glass plates (20 × 20 cm) coated with the same silica gel as in analytical TLC. Visualization of the bands were achieved by spraying with Rhodamine 6G (Merck, Germany, 0.05% in ethanol), UV 235 nm. The chromatographic bands consisting of group of compounds were scraped off and transferred into small columns (8 mm i.d.) filled with silica gel (0.3 g, 25–50 μm), eluted with freshly distilled dry diethyl ether (15 ml), and evaporated to dryness.

Gas Chromatography (GC)

GC was performed on a 5890A gas chromatograph (Hewlett-Packard, USA) equipped with a flame ionization detector and split/splitless injector, the carrier gas was hydrogen. The following programs (a)–(f) were used for the columns DB-1 and DB-WAX (J&W Scientific, USA, length 30 m, I.D. 0.25 mm, film thickness 0.25 μm):

DB-1: (a) injector and detector temperatures 250 °C, oven temperature 140 °C (0 min), then increased at a rate of 5 °C min^{-1} to 320 °C (20 min or more), 90 kPa, $\bar{u}$ 45 cm s^{-1} (at 150 °C), split ratio 39:1; (b) injector and detector temperatures 250 °C, oven temperature 200 °C, 86 kPa, $\bar{u}$ 40 cm s^{-1}, split ratio 35:1; (c) injector temperature 280 °C, detector and oven temperatures 270 °C, 83 kPa, $\bar{u}$ 35.6 cm s^{-1}, split ratio 25:1.

DB-1 ms: (d) injector and detector temperatures 260 °C, oven temperature 240 °C (0 min), then increased at a rate of 1 °C min^{-1} to 340 °C (15 min), $\bar{u}$ 61 cm s^{-1} at 260 °C, split ratio 29:1.

DB-WAX: (e) injector temperature 220 °C, detector temperature 250 °C, oven temperature 140 °C (0 min), then increased at a rate of 5 °C min^{-1} to 230 °C (20 min or more), 90 kPa, $\bar{u}$ 46.2 cm s^{-1} (at 150 °C), split ratio 36:1; (f) injector and detector temperatures 250 °C, oven temperatures 200 °C, $\bar{u}$ 40 cm s^{-1}, split ratio 35:1.

Gas Chromatography–Mass Spectrometry

Gas Chromatography–Mass Spectrometry (GC–MS) was performed on a gas chromatograph (CE 8000 series, Fisons, Milan, Italy) coupled with a mass detector (Fisons MD 800 VG Masslab, Manchester, UK) working in electron ionization mode. DB-5 ms and DB-WAX columns (30 m × 0.25 mm × 0.25 μm, J & W Scientific) with helium flow 0.95 ml min^{-1} (at 140 °C) were used. Chromatographic conditions: injector temperature 250 °C, interface temperature 200 °C, oven temperature 140 °C (0 min), then increased at a rate of 5 °C min^{-1} to 320 °C (30 min or more for DB-5 ms) and to 230 °C (50 min for DB-WAX), split ratio 50:1. The National Institute of Standards and Technology (NIST) Library was used for identification of some compounds.

High Performance Liquid Chromatography

High Performance Liquid Chromatography (HPLC) was performed on a liquid chromatograph (Thermo Separation Products, San Jose, USA), which consisted of a SCM 1000 vacuum membrane degasser, a P 4000 quaternary gradient pump, an AS 3000 autosampler) and an LCQ classic ion trap mass spectrometer (Thermo Finnigan, San Jose, USA). The system was controlled by an SN 4000 control unit (Thermo Separation Products, San Jose, USA) and a PC using Xcalibur Software (Thermo Finnigan). TAG were separated on two Nova-Pack C18 stainless steel columns (length 300 mm, i.d. 3.9 mm, film thickness 4 μm (Waters, USA) connected in series. The mobile phase was a mixture of acetonitrile (A) and 2-propanol (B). The linear gradient from 0 to 70% of B in 108 min (1 mL min^{-1}) was followed by a linear gradient to 80% of B (130 min, 0.7 mL min^{-1}). The columns were kept at 30 °C during analysis. The mobile phase was mixed post-column in a low dead-volume T-piece with 100 mM ammonium acetate prepared in 2-propanol/water (1:1, v/v), flow rate 10 μL min^{-1}. The full scan mass spectra were recorded in the range of *m/z* 75–1,300. The temperatures of the vaporizer and heated capillary were set to 400 and 200 °C, respectively. The corona discharged current was 4.5 μA, capillary voltage and tube lens offset were 3 and 10 V, respectively. TAG were quantified from reconstructed chromatograms calculated for $[M + H]^+$ and $[M + NH_4]^+$ ions [49].The mass spectra (MS) were interpreted by software program TriglyAPCI developed specially for interpretation of APCI mass spectra of TAG isolated from various natural sources [50].

Transesterification

A mixture of TAG (1.5 mg) was dissolved in a mixture of chloroform/methanol (2:3 (v/v), 250 μl) in a sealed glass vial. Acetyl chloride (29.4 μl) was added and the vial was sealed and heated in a water bath at 70 °C for 90 min. The reaction mixture was neutralized with silver carbonate (57.1 mg). This procedure prevents the loss of volatile fatty acid methyl esters (FAME). After centrifugation, the supernatant was directly analyzed by GC or GC–MS. Using this method, fatty acid methyl esters were more easily prepared also from the free fatty acids and from free hydroxy acids [51, 52].

Calculation of Kováts Retention Indexes (I), Equivalent Chain Length Values and Alcohol Chain Length Values

Calculation of the I, equivalent chain lengths (ECL) and alcohol chain lengths (ACL) values was made by using the method described earlier [53, 54], using the reference compounds (*n*-alkanes, fatty acids methyl esters, 1-alkanols) co-injected with a sample. The number of experimental points (n) was a minimum of 5, remote experimental points were automatically excluded using the Dixon test (significance level $p = 0.01$).

Results

By means of gradient CC on silica gel, cerumen was separated into the following well-defined groups of compounds: aliphatic hydrocarbons, squalene, wax esters and cholesterol esters, triacylglycerols, free fatty acids, free fatty alcohols, monoacylglycerols, free cholesterol, free sterols, and free hydroxy acids (Table S1). These groups of compounds were then analyzed separately, and identified by GC and GC–MS techniques. The composition of these fractions is described below in the Discussion section, and the quantitative data are summarized in Tables S1–S8, located in the supplements.

Discussion

Hydrocarbons

The fractions 1–4 appeared as one spot at TLC (hexane, $R_F = 0.98$). The main part is formed by a homologous series of *n*-alkanes (C_{14}–C_{47}) with almost identical quantity of odd and even homologs (1.18:1). The branched and unsaturated hydrocarbons were present in small quantities (Fig. S1) and were not analyzed in details. Wheatley [20] mentioned hydrocarbons in cerumen for the first time in 1954. Due to the fact that the content of the minor quantity of alkanes could not be analyzed at that time, it has been supposed that he detected squalene [19], the content of which is much higher. Later, Bortz et al. [29] investigated the content of alkanes in a human skin surface lipid layer and in the ear wax. Although the composition of these alkanes strongly resembles petroleum waxes, it has been proposed that they are biosynthetic products of human skin. Hydrocarbons found in human cerumen are not environmental contaminants [29]. The presence of hydrocarbons had been reported by Harvey [30], however, without analytical details.

Squalene

The fractions 5–11 appeared as one spot at TLC (hexane, $R_F = 0.28$). The R_F value of this fraction was identical with that of squalene (2,6,10,15,19,23-hexamethyl-2,6,10,14,18,22-tetracosahexaene). Gas chromatography analysis resulted in finding one main peak (98.3%), the Kováts retention index ($I = 2819.03$) of which was found identical with that of the reference compound ($I = 2819.09$) [DB-1, program (**c**)]. The mass spectra were also found to be identical. Squalene forms almost 1% of the cerumen (Table S1).

Wax Esters and Cholesterol Esters

The fractions 14 and 15 appeared as one spot at TLC (hexane/diethyl ether 93:7, $R_F = 0.78$). Their R_F value was identical with that of stearyl palmitate. The chromatogram (DB-1, program (a) and DB-1 ms column, program (d) showed approximately 135 peaks, of which about 100 peaks (84 area %) represented the wax esters, 36 peaks (16 area %) represented cholesterol esters. Wax esters were analyzed by GC–MS. They formed a homologous series of the saturated and unsaturated, even and odd higher esters in the range from C_{23} to C_{41} with a maximum $C_{36:1}$. Based on a detailed analysis of the mass spectra [55, 56], one single GC peak of aliphatic esters always represents at least three isomers. The position of the ester functionality in the molecule has a low influence on the retention behavior at the GC, and a majority of the isomers could not be separated [57]. In total, about 550 esters (Table S2) were identified; their relative content has not been given because it rarely exceeded an area of 1%.

After transesterification of an aliquot part of the esters, three groups of compounds were found: methyl esters of acids ($R_F = 0.62$), aliphatic alcohols ($R_F = 0.15$) and cholesterol ($R_F = 0.09$) (TLC in hexane/diethyl ether 93:7). Each of the identified groups of compounds was isolated by PTLC and subsequently analyzed by GC and GC–MS.

The acid fraction (as methyl esters) consisted of a homologous series of saturated and unsaturated fatty acids (Table S3). Their identification was performed both by measurement of ECL values [53, 54] and by mass spectrometry of dimethyl disulfide (DMDS) adducts [58, 59]. Saturated acids formed a homologous series (C_{12}–C_{34}; 33.2%) with prevalent hexadecanoid acid (16:0, 9.0%). To a lesser extent, *n*-acids with odd C-atoms are present (4.2%), predominant 15:0 (3.0%) and branched *iso*-acids (7.9%) and *anteiso*-acids (5.2%). Monoenic fatty acids (C_{13}–C_{32}, 64.1%) form more than one half of all the acids. Based on retention times and mass spectra, one can deduce

that some unsaturated homologs are branched (9.4%, shown in the Tables with the prefix *br*-). A small quantity of dienoic acid 18:2 n-6 acid (2.4%) was also identified. Several unidentified minor peaks (0.3%) were also present in the chromatogram.

The alcohol fraction consisted of a homologous series of saturated and unsaturated 1-alkanols and 1-alkenols (Table S4). Their identification was performed both by measurement of the ACL values, and by mass spectrometry of underived alcohols and their DMDS adducts [60]. The ACL values were introduced for easier identification of unknown alcohols. The ACL value is analogous to the equivalent chain length value (ECL). Saturated non-branched chains of 1-alkanols were used in the measurement and calculation of the ACL values instead of methyl esters of saturated fatty acids used in the measurement and calculation of the ECL values. It was found that the ACL values for *iso*- and *anteiso*- alcohols are identical with the ECL values of the corresponding fatty acids methyl esters. As an example, several pairs of ECL values for methyl esters and ACL values for the corresponding alcohols are given: *i*-14:0 (13.6470; 13.6508), *i*-15:0 (14.6447; 14.6475), *a*-15:0 (14.7296; 14.7310), *i*-16:0 (15.6437, 15.6450); *i*-18:0 (17.6411; 17.6412), *i*-20:0 (19.6397; 19.6417), *i*-22 (21.6376; 21.6404), and *a*-22 (21.7238; 21.7197). It should be noted that the ECL values were measured in 1996 [54] while the ACL values were calculated only recently (2009) from another column [DB-1, program (**b**)].

Saturated alkanols form a homologous series (C_{12}–C_{30}, 73.2%) with prevailing 1-octadecanol (18:0, 8.8%). It is worth mentioning that there are high proportions of alkanols with odd C-atoms (8.4%) and branched *iso*-alkanols (17.3%) and *anteiso*- alkanols (17.2%). Unsaturated alcohols form a homologous series (C_{18}–C_{31}, 24.3%) with prevalent 1-icosenols (20:1, 8.9%). Some of them are branched (5.6%). Several minor peaks were not identified (2.6%).

In the case of alcohols, the DMDS derivatization under conditions described in the literature [58] was not quantitative and the unreacted alcohols made the identification of products difficult. Therefore, the procedure was modified (70 °C, 5 h in a sealed vial), and under those conditions the yield was almost 100%.

Cholesterol was represented by one peak by GC and its Kováts retention index ($I = 3093.45$) was identical with that of standard cholesterol [$I = 3093.43$; DB-1, program (**c**)]. Both the R_F value at TLC ($R_F = 0.30$, hexane/diethyl ether 7:3) and the mass spectrum were identical with those of the reference.

Triacylglycerols

The fractions 19 and 20 gave one spot at TLC, its R_F value was identical with that of tripalmitin (TLC in hexane/diethyl ether, 93:7, $R_F = 0.34$). A more detailed analysis was done by HPLC. 95 peaks were found in the chromatogram, but only 19 peaks represented individual triacylglycerols. The remaining 76 peaks were mixtures of two or more compounds. The applied method enabled assigning positions of fatty acids in TAG [49, 50] (Table S5). More than 200 TAG were identified in total with over 120 present in significant amounts (printed in bold).

The *acids* were determined by means of the ECL values of their methyl esters and by GC–MS after transesterification of the original TAG. Acids formed a homologous series of saturated and unsaturated fatty acids (Table S6). Saturated acids (C_{12}–C_{30}, 62.1%) with prevalent 16:0 (26.9%) contain considerable part of *n*-acid with odd C-atoms (12.1%), and branched *iso*-acids (5.2%) and *anteiso*-acids (3.5%). Monounsaturated acids (C_{12}–C_{22}) were found at a level of 28.5% and the 18:2n-6 and 2-hydroxyhexadecanoic acids were found in quantities of 0.33 and 1.29%, respectively. Several minor peaks remained unidentified (4.8%).

Free Fatty Acids, Free Alcohols and Monoacylglycerols

Fractions 23–26 contained a mixture of free fatty acids and free alcohols together with a small quantity of *monoacylglycerols*. PTLC enabled separation of monoacylglycerols (hexane/diethyl ether mixture, 80:20, $R_F = 0.05$). A GC chromatogram [DB-1 program (**a**)] showed 2 peaks in a 1:1 ratio, which were determined as 2-monopalmitin (2-hexadecanoylglycerol) and 2-monostearin (2-octadecanoylglycerol).

To enable separation of free fatty acids from free alcohols, the mixture was esterified, and the fatty acid methyl esters were separated from the free alcohols subsequently by means of PTLC. Each fraction was then analyzed by GC, GC–MS and GC–MS of DMDS derivatives.

Free fatty acids form a series of odd and even homologs ($C_{12:0}$ to $C_{34:0}$, 58.6%) (Table S7) with two maxima at $C_{16:0}$ (19.0%) and at $C_{24:0}$ (5.3%), but *iso*- and *anteiso*-fatty acid content was 4.1 and 3.0%, respectively. A smaller content was formed by the monounsaturated acids, namely 37.8%, with some of them being branched. The 18:2n-6 fatty acid formed only 1.2%. Several minor peaks were not identified (2.5%).

Free alcohols form a homologous series of saturated (75.4%) and unsaturated (14.9%) alcohols in the range of C_{12}–C_{31} (Table S8). A high content of *iso*- and *anteiso*-fatty acids (19.4 and 16.0%, respectively) was found analogously as already mentioned in the fraction of alcohols originating from the wax esters. The content of unsaturated alcohols (15.0%) is lower than the content of alcohols from wax esters. Identification of the peaks was made by GC–MS analysis of free and derived alcohols in combination with the ACL values.

Free cholesterol

Fractions 27 and 28 were characterized as a single spot in the TLC (hexane/diethyl ether 7:3). The R_F value = 0.30 was identical with that of cholesterol used as a reference. The main peak (97.4%, Kováts retention index $I = 3093.59$) was identical with that of the standard [$I = 3093.43$; DB-1, program (**c**)] and it was confirmed by its mass spectrum. A minor peak (2.6%) was identified as 3β-cholest-7-en-3-ol, which was the main peak in fractions 29 and 30.

Free Sterols

Fractions 29 and 30 were characterized by the R_F value identical with the R_F value of β-sitosterol (3β-stigmast-5-en-3ol; TLC in hexane/diethyl ether 7:3). The GC analysis showed two peaks: the first (minor) peak was identified as cholesterol (3β-cholest-5-en-3-ol; $I = 3094.14$), the second one (main peak) was identified as 3β-cholest-7-en-3-ol ($I = 3138.78$).

Free Hydroxy Acids

Based on a GC analysis (Fig. S2), fraction 31 contained mainly two peaks in a 8.4 : 1 ratio, which were characterized by their Kováts indexes ($I_1 = 2080.79$ and $I_2 = 2091.24$, [DB-1, program (**b**)]. Their mass spectra indicated two isomeric C_{17} hydroxy acids bearing a single double bond. The structures of both hydroxy acids were suggested on the basis of molecular peaks of free acids ($m/z = 284$) and their methyl esters ($m/z = 298$). The hydroxy acids were eluted from the silica gel column after the free fatty acid fraction, which indicates higher polarity of these products in comparison with free fatty acids. Their longer retention time in comparison with that of free fatty acid fraction supports the suggested structures of unsaturated hydroxy acids over saturated epoxy acids with identical molecular peaks. The yield of hydroxy acids was low, which fact prevented their derivatization for assigning the double bond location, and hydroxyl group location in the acid chains.

Conclusion

The data presented show that cerumen is a very complex mixture of compounds. Non-polar lipids (11%) were separated into ten groups of compounds by column chromatography and by PTLC on silica gel. Polar lipids form about 30% of the cerumen. The remaining compounds (60%) represent a highly polar fraction that could not be eluted from the column even by a mixture of chloroform–methanol.

Among the cited papers, only Harvey [30] analyzed a broad spectrum of compounds in cerumen systematically. However, that analysis was performed after saponification of the cerumen extract. Therefore, wax esters, cholesterol esters, and mono- and triacylglycerols could not be identified in the mixture. Our results are in agreement with those of Harvey [30], but we added new information on the content of wax esters and mono- and triacylglycerols. We found that the main part of the long-chain unsaturated fatty acids is formed by those bearing a Δ6 double bond. In turn, most of the unsaturated fatty alcohols bear Δ10 unsaturation.

In the analyses of some groups of compounds (wax esters, fatty acids, fatty alcohols), we were faced with the following problems: (a) in many peaks of the chromatogram several isomers were overlapping, causing shifts of the retention values; (b) the retention values (ECL, ACL) of many compounds could not be compared with those of unavailable reference compounds; (c) coelution of peaks of non-derived compounds with the formed adducts (retention times of DMDS adducts are shifted by 6 carbon atoms approx.); (d) mass spectra of methyl-branched compounds (*iso-, anteiso-*) are very similar to those of straight-chain compounds. To avoid misinterpretation of the mass spectra, it is always necessary to consider the retention data (RT, ECL values, ACL values).

Supplements

We have very large amounts of experimental data, and all of them cannot be placed in the text of the paper. We therefore decided to make the supplements available on the web page of the journal, where they can be found. The data summarize the composition of cerumen, and the lists of fatty acid derivatives found in the cerumen (Tables S1–S8), and the chromatograms of the selected compounds (Figs. S1–S2).

Acknowledgments The authors thank the Czech Science Foundation (grant No. 502/10/1734), and the Ministry of Education, Youth and Sports of the Czech Republic (grants Nos. 2B06024, 2B06007, and OC10001 and research program MSM6046137305) for the financial support. The authors also thank Ms. Helena Ernyeiová and Ms. Anna Nekolová for their skillful technical assistance.

References

1. Bortz JT, Wertz PW, Downing DT (1990) Composition of cerumen lipids. J Am Acad Dermatol 23:845–849
2. Hawke M (2002) Update on cerumen and ceruminolytics. ENT-Ear Nose Throat J Suppl, pp 4 (www.entjournal.com/html/article_11_0208.html)

3. Nakashima S (1933) The chemical composition of cerumen. Z Physiol Chem 216:105–109
4. Chiang SP, Lowry OH, Senturia BH (1957) Micro-chemical studies on normal cerumen, II. The percentage of lipid and protein in casual and fresh cerumen. J Invest Dermatol 28:63–68
5. Schenkels LCPM, Rathman WM, Veerman ECI, Amerongen AVN (1991) Detection of proteins related to a salivary glycoprotein (EP/GP): concentrations in human secretions (saliva, sweat, tears, nasal mucus, cerumen, seminal plasma). Biol Chem Hoppe-Seyler 372:325–329
6. Schwaab M, Hansen S, Gurr A, Schwaab T, Minovi A, Sudhoff H, Dazert S (2009) Protein isolation from ear wax made easy. Eur Arch Otorhinolaryngol 266:1699–1702
7. Chiang SP, Lowry OH, Senturia BH (1955) Microchemical studies on normal cerumen. I. The lipid and protein content of normal cerumen as affected by age and sex. Laryngoscope 65:927–934
8. Ueda S, Kataura A, Matsunaga E (1962) Chemical composition of human normal cerumen. I. Preliminary studies on solvent fractionation of dry and wet cerumen. Sapporo Igaku Zashi 22:1–4 Chem Abstr (1965) 62:9535
9. Burkhart CN, Burkhart CG, Williams S, Andrews PC, Adappa V, Arbogast J (2000) In pursuit of ceruminolytic agents: a study of earwax composition. Am J Otol 21:157–160
10. Suzuki M, Suzuki A, Yamakawa T, Matsunaga E (1985) Characterization of 2,7-anhydro-*N*-acetylneuraminic acid in human wet cerumen. J Biochem (Tokyo) 97:509–515
11. Bailnatova GD, Khasanov SA, Babadzhanova SY, Popova IA (1989) Detecting disturbances in carbohydrate metabolism in obese children by determination of glucose in earwax. Med Zh Uzb 1989:36–37 Chem. Abstr. (1989) 111:228238
12. Masuda H, Shichijo S, Goya T, Takeuchi M (1978) Isolation and partial characterization of glycopeptide from cerumen. Kurume Med J 25:203–205 Chem Abstr (1979) 90:50010
13. Shichijo S, Masuda H, Takeuchi M (1979) Carbohydrate composition of glycopeptides from the human cerumen. Biochem Med 22:256–263
14. Masuda H, Shichijo S, Takeuchi M (1979) Glycopeptide from cerumen. Seibutsu Butsuri Kagaku 22:267–271 Chem Abstr (1979) 91:85800
15. de Jorge FB, de Ulhoa AB, Cintra LJ, Paiva LJ, Correa AP, Nova R (1964) The chemistry of the cerumen: ash, volatile substances, Na, K, Ca, Mg, P, and Cu. Ann Otol Rhinol Laryngol 73:218–221 Chem Abstr (1964) 61:9846
16. Hamsík A, Šantavý F (1962) Biochemie. Státní zdravotnické nakladatelství Praha, p 372
17. Nakamichi K (1925) The occurrence of fatty substances in the human ear. Japan J Med Sci 2:141–142 Chem Abstr 20:1656
18. Nitta H, Ikai K (1953) Body odor. I. Separation of the lower fatty acids of cutaneous excretion by paper chromatography. Nagoya Med J 1:217–224 Chem Abstr (1954) 48:6531
19. Wheatley VR (1953) Studies of sebum. IV. Estimation of squalene in sebum and sebum-like materials. Biochem J 55:637–640
20. Wheatley VR (1954) Studies of sebum. 5. The composition of some sebum like materials of human origin. Biochem J 58:167–172
21. Akobjanoff L, Carruthers C, Senturia BH (1954) The chemistry of cerumen: a preliminary report. J Invest Dermatol 23:43–50
22. Haahti E, Nikkari T, Koskinen O (1960) Fatty acids composition of human cerumen (earwax). Scand J Clin Lab Invest 12:249–250
23. Haahti E, Horning EC, Castren O (1962) Microanalysis of sebum and sebum like materials by temperature-programmed gas chromatography. Scand J Clin Lab Invest 14:368–372
24. Kataura K (1965) Chemical composition of human normal cerumen. IV. Separation of the lipid fraction by silicic acid column. Sapporo Igaku Zasshi 28:315–319 Chem Abstr (1968) 69:94222
25. Kataura A, Kataura K (1967) The comparison of lipids between dry and wet types of cerumen. Tohoku J Exp Med 91:227–237 Chem Abstr (1967) 67:1289
26. Aitzetmüller K, Koch J (1978) Liquid chromatographic analysis of sebum lipids and other lipids of medical interest. J Chromatogr 145:195–202
27. Gersbein LL, Broder AI, Sheladia K (1980) Lipids of cerumen from elderly human adults. J Appl Biochem 2:489–494
28. Inaba M, Chung TH, Kim JC, Choi YC, Kim JH (1987) Lipid composition of ear wax in hircismus. Yonsei Med J 28:49–51 J Am Acad Dermatol (1990) 23:845–849
29. Bortz JT, Wertz PW, Downing DT (1989) The origin of alkanes found in human skin surface lipids. J Invest Dermatol 93:723–727
30. Harvey DJ (1989) Identification of long-chain fatty acids and alcohols from human cerumen by the use of picolinyl and nicotinate esters. Biomed Environ Mass Spectrom 18:719–723
31. Robosky LC, Wade K, Woolson D, Baker JD, Manning ML, Gage DA, Reily MD (2008) Quantitative evaluation of sebum lipid components with nuclear magnetic resonance. J Lipid Res 49:686–692
32. Burkhart CN, Kruge MA, Burkhart CG, Black C (2001) Cerumen composition by flash pyrolysis–gas chromatography/mass spectrometry. Otol Neurotol 22:715–722
33. Taishin VA, Rudneva NA, Mikhailova LA (1985) Fat content in cow's cerumen in relation to the fat content in milk. S—kh Biol 1985:25–26 Chem Abstr (1986) 104:49258
34. Huang HP, Fixter LM, Little CJL (1994) Lipid-content of cerumen from normal dogs and otitic canine ears. Vet Rec 134:380–381
35. Huang HP, Fixter LM, Little CJL (1995) Canine cerumen faty acid composition. Guoli Taiwan Daxue Nongxueyuan Yanjiu Baogao 35:375–392 Chem Abstr (1996) 125:54215
36. Masuda A, Sukegawa T, Mizumoto N, Tani H, Miyamoto T, Sasai K, Baba E (2000) Study of lipid in the ear canal in canine otitis externa with Malassezia pachydermatis. J Vet Med Sci 62:1177–1182 Chem Abstr (2000) 134:308887
37. Yasui T, Tsukise A, Habata I, Nara T, Meyer W (2004) Histochemistry of complex carbohydrates in the ceruminous glands of the goat. Arch Dermatol Res 296:12–20
38. Campos A, Arias A, Betancor L, Rodriguez C, Hernandez AM, Aquado DL, Sierra A (1998) Study of common aerobic flora of human cerumen. J Laryngol Otol 112:613–616
39. Burkhart CN, Arbogast J, Gunning WT, Adappa V, Burkhart CG (2000) *Aspergillus flavus* isolated in cerumen by scanning electron microscopy. Infect Med 17:624–626
40. Stroman DW, Roland PS, Dohar J, Burt W (2001) Microbiology of normal external auditory canal. Laryngoscope 111:2054–2059
41. Chai TJ, Chai TC (1980) Bactericidal activity of cerumen. Antimicrob Agents Chemother 18:638–641 Chem Abstr (1980) 93:231610
42. Stone M, Fulghum RS (1984) Bactericidal activity of wet cerumen. Ann Otol Rhinol Laryngol 93:183–186
43. Jankowski A, Kapusta E, Nowacka B (1992) Concerning the bacteriostatic or bactericidal function of the secretion of ceruminous glands. Otolaryngol Pol 46:557–560
44. Dibb WL (1993) The microbial etiology of otitis-externa—a review. Saudi Med J 14:181–185
45. Sokolov VE, Ushakova NA, Chernova OF, Shubkina AV, Alimharova LM, Barinskii IF (1995) On antiinfectional properties of cerumen in mammals. Izv Akad Nauk Ser Biol 1995:579–585
46. Campos A, Betancor L, Arias A, Rodriguez C, Hernandez AM, Aguado DL, Sierra A (1999) The influence of human wet cerumen on *Candida albicans* growth. J Mycol Med 9:36–38
47. Campos A, Betancor L, Arias A, Rodríguez C, Hernández AM, Aguado DL, Sierra A (2000) The influence of human wet

cerumen on the growth of common and pathogenic bacteria of the ear. J Laryngol Otol 114:925–929
48. Pata YS, Ozturk C, Akbas Y, Gorur K, Unal M, Ozcan C (2003) Has cerumen a protective role in recurrent external otitis? Am J Otolaryngol 24:209–212
49. Cvačka J, Hovorka O, Jiroš P, Kindl J, Stránský K, Valterová I (2006) Analysis of triacylglycerols in fat body of bumblebees by chromatographic methods. J Chromatogr A 1101:226–237
50. Cvačka J, Krafková E, Jiroš P, Valterová I (2006) Computer-assisted interpretation of atmospheric pressure chemical ionization mass spectra of triacylglycerols. Rapid Commun Mass Spetrom 20:3586–3594
51. Stránský K, Jursík T (1996) Simple quantitative transesterification of lipids. 1. Introduction. Fett/Lipid 98:65–71
52. Stránský K, Jursík T (1996) Simple quantitative transesterification of lipids. 2. Applications. Fett/Lipid 98:71–77
53. Stránský K, Jursík T, Vítek A, Skořepa J (1992) An improved method of characterizing fatty acids by Equivalent Chain Length values. J High Resolut Chromatogr 15:730–740
54. Stránský K, Jursík T, Vítek A (1997) Standard Equivalent Chain Length values of monoenic and polyenic (methylene interrupted) fatty acids. J High Resolut Chromatogr 20:143–158
55. Sun KK, Holman RT (1968) Mass spectrometry of lipid molecules. J Am Oil Chem Soc 45:810–817
56. Aasen AJ, Hofstetter HH, Iyengar BTR, Holman RT (1971) Identification and analysis of wax esters by mass spectrometry. Lipids 6:502–507
57. Stránský K, Zarevúcka M, Valterová I, Wimmer Z (2006) Gas chromatographic retention data of wax esters. J Chromatogr A 1128:208–219
58. Dunkelblum E, Tan SH, Silk PJ (1985) Double-bond location in monounsaturated fatty acids by dimethyl disulfide derivatization and mass spectrometry: application to analysis of fatty acids in pheromone glands of four lepidoptera. J Chem Ecol 11:265–277
59. Christie WW (1997) Dimethyl disulphide derivatives in fatty acid analysis. Lipid Technol 1997:17–19
60. Leonhardt BA, DeVilbiss ED (1985) Separation and double bond determination on nanogram quantities of aliphatic monounsaturated alcohols, aldehydes and carboxylic acid methyl esters. J Chromatogr 322:484–490

Lipids (2011) 46:789–793
DOI 10.1007/s11745-011-3570-0

COMMUNICATION

Dietary Guar Gum Reduces Lymph Flow and Diminishes Lipid Transport in Thoracic Duct-Cannulated Rats

Bungo Shirouchi · Sayaka Kawamura · Ryosuke Matsuoka · Sanae Baba · Kazuko Nagata · Sawako Shiratake · Hiroko Tomoyori · Katsumi Imaizumi · Masao Sato

Received: 18 January 2011 / Accepted: 9 May 2011 / Published online: 25 May 2011

Abstract Guar gum has a well-recognized hypolipidemic effect. This effect is thought to be due to the physicochemical properties of guar gum, which may cause changes in adsorption of lipids or the viscosity of the intestinal contents. Guar gum is a non-specific absorption inhibitor of any type of lipid-soluble compound. Permanent lymph duct cannulation was performed on rats to investigate the effects of dietary guar gum on lymph flow and lipid transport. Rats fed a 5% guar gum diet were compared with those fed a 5% cellulose diet, and lymph was collected after feeding. The water-holding capacity (WHC), settling volume in water (SV), and viscosity of guar gum were compared with those of cellulose. Rats fed with the guar gum diet had significantly lower lymph flow and lymphatic lipid transport than did rats fed with the cellulose diet. The WHC, SV, and viscosity of guar gum were significantly higher than those of cellulose. We propose that dietary guar gum reduces lymph flow and thereby diminishes lipid transport by means of its physicochemical properties related to water behavior in the intestine.

B. Shirouchi · S. Kawamura · R. Matsuoka · S. Baba · K. Nagata · S. Shiratake · K. Imaizumi · M. Sato (✉)
Laboratory of Nutrition Chemistry, Department of Bioscience and Biotechnology, Faculty of Agriculture, Graduate School, Kyushu University, 6-10-1 Hakozaki, Higashi-ku, Fukuoka 812-8581, Japan
e-mail: masaos@agr.kyushu-u.ac.jp

R. Matsuoka
R&D Division, Kewpie Corporation, 403-2 Motokurihashi, Goka-machi, Sashima-gum, Ibaraki 306-0313, Japan

H. Tomoyori
Department of Food and Health Sciences, Faculty of Environmental and Symbiotic Sciences, Prefectural University of Kumamoto, 3-1-100 Tsukide, Kumamoto 862-8502, Japan

Keywords Guar gum · Lymph flow · Permanent thoracic lymph duct cannulation · Lipid transport · Water-soluble dietary fiber · Cellulose

Abbreviations

WHC	Water-holding capacity
SV	Settling volume in water

Introduction

Many previous studies have shown that water-soluble fibers, such as β-glucan, psyllium, pectin, and guar gum, are more effective in preventing cardiovascular disease than are water-insoluble fibers [1]. Several studies on men have demonstrated that consumption of water-soluble dietary fibers may produce a hypocholesterolemic effect [1, 2]. This effect is exerted in the intestine. The hypocholesterolemic effect may be attributed to the adsorption of cholesterol and bile acids by the dietary fibers in the intestine [1], the fermentability of these fibers in the colon, and the physicochemical properties of the dietary fibers, such as viscosity [3].

Guar gum consists of a (1 → 4)-linked-β-D-mannopyranose backbone with (1 → 6)-linked-α-D-galactose side chains, with the overall ratio of mannose to galactose being around 2:1 (Fig. 1). Numerous studies suggest that dietary guar gum inhibits absorption of lipid-soluble compounds such as cholesterol [1–3], lutein [4], canthaxanthin [4], α-tocopherol [4], 1,1,2-trichloroethylene [5], and 2,3,7,8-tetrachlorodibenzo-*p*-dioxin [6]. One of the characteristics of guar gum is that it is a non-specific absorption inhibitor of any type of lipid-soluble compound.

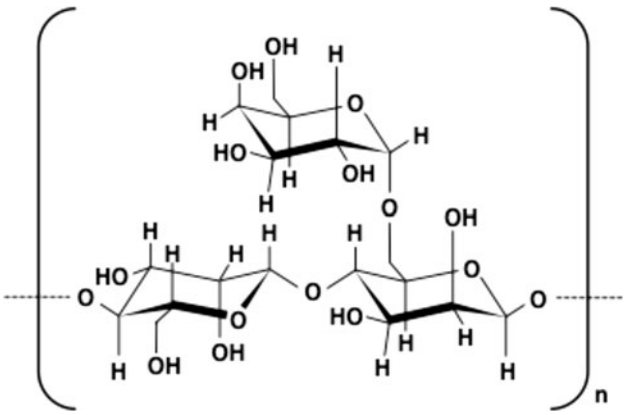

Fig. 1 The chemical structure of guar gum

The lymphatic transport of dietary lipids in rats has often been measured by infusing a lipid emulsion into the stomach or duodenum for quantitative measurement [7, 8]. However, the methods used have failed to take into account the interaction of the lipid emulsion with other dietary components, particularly proteins and carbohydrates, which is necessary to investigate the interaction between the respective dietary fibers and food components [9]. In this study, we used permanent cannulation of the thoracic duct to measure the lymphatic transport of dietary lipids in rats under near-physiological conditions. This method has the advantage of evaluating the lymphatic transport of dietary lipids during actual dietary fat absorption, using "actual" diets without restraint stress [10–12].

In this study, rats were fed a diet containing guar gum or cellulose (a water-insoluble dietary fiber). The lymphatic transport of cholesterol, triacylglycerols, and phospholipids in the rats was measured using permanent cannulation of the thoracic duct. Additionally, we compared the water-holding capacity (WHC), settling volume in water (SV), and viscosity of guar gum with those of cellulose.

Materials and Methods

Materials

Crystalline guar gum powder (MW, approximately 20,000) containing 80% fiber, 5% protein, and 1% ash was purchased from Wako Pure Chemical Industries Ltd. (Osaka, Japan). Crystalline cellulose powder containing 96.4% fiber, 4.6% moisture, and 0.1% protein was purchased from Oriental Yeast Co. Ltd. (Tokyo, Japan).

Animals, Diets, and Permanent Thoracic Lymph Duct Cannulation

Male Sprague–Dawley rats (Kud:SD), 7 weeks old, were obtained from Kyudo (Kumamoto, Japan) and maintained in a temperature-controlled room (23 °C). Experimental diets were prepared according to recommendations of the AIN-93G [13] and contained the following ingredients (in weight %): cellulose or guar gum, 5; casein, 20; α-cornstarch, 13.2; sucrose, 10; mineral mixture, 3.5; vitamin mixture, 1; choline bitartrate, 0.25; soybean oil, 7; cholesterol, 0.5; cholic acid, 0.125; *tert*-butylhydroquinone, 0.0014; and *β*-cornstarch, 39.4236. The rats were trained to consume the cellulose diet as a basal diet twice a day from 10:00–11:00 to 16:00–17:00, respectively, for 5 days. On day 6, all the rats were anesthetized using Nembutal prior to permanent cannulation of the thoracic duct lymph, as described previously [12]. In brief, a cannula (SH silicon tube, 0.5 mm i.d. and 1.0 mm o.d.; Kaneka Medics, Osaka, Japan) filled with heparinized saline was inserted into the thoracic duct and secured within the abdominal cavity. The rats were returned to their cages and provided glucose isocratic liquid (139 mM glucose and 85 mM NaCl in distilled water) alone. On days 7 and 8, the rats were provided with the cellulose diet twice a day, as described. On day 9, the rats were attached to a long polyethylene cannula (0.58 mm i.d. and 0.97 mm o.d.; Becton–Dickinson and Company, MD, USA) to collect the lymph. The end of the cannula was located 5–10 cm below the bottom of the cage to allow the lymph to drain into the cannula. The lymph was collected for 20 min, and the rats were then given free access to the cellulose diet or the guar gum diet for 30 min from 10:00 to 10:30 hours. Therefore, the fasting period from 17:00 to 10:00 hours was between meals. At this time, the lymph was collected every hour for 7 h. The collected lymph was kept at 4 °C overnight, after which the fibrin was removed. The lymph was stored at −30 °C until lipid analysis.

The rats had free access to deionized water throughout the feeding periods and during lymph collection. This experiment was carried out following the Guidelines for Animal Experiments of Kyushu University (Fukuoka, Japan) and the Law (No. 105) and Notification (No. 6) of the Government of Japan. The authorization number was A19-195-0.

Measurement of Lymphatic Lipids

Lymphatic cholesterol levels were measured using a commercial enzyme assay kit (T-CHO Kainos kit; Kainos Laboratories Inc., Tokyo, Japan). Lymphatic triacylglycerol and phospholipid levels were measured using commercial enzyme assay kits (Triglyceride *E* test Wako and Phospholipid *C* test Wako, respectively; Wako Pure Chemicals, Tokyo, Japan,).

Water-Holding Capacities of Guar Gum and Cellulose

The WHC of guar gum and cellulose were measured according to the method reported by Takeda and Kiriyama

[14]. Samples (0.1 g) were placed on 2 filter papers fitted in a stainless steel container (hole diameter, 2.5 cm; diameter, 5 cm; and height, 1.5 cm) with a polypropylene net. This weight was measured as dry weight. After being placed in a case with distilled water for 24 h at room temperature, the container was removed and weighed. The WHC of guar gum and cellulose were evaluated by measuring the difference between the wet and dry weights.

Settling Volumes in Water of Guar Gum and Cellulose

The SV of guar gum and cellulose were measured according to the method described by Takeda and Kiriyama [14]. Samples (17.5 mg) were blended with 7 ml of distilled water in 10-ml graduated cylinders. The cylinders were left to stand for 24 h at room temperature. The SV of guar gum and cellulose were evaluated on the basis of precipitation volume.

Viscosities of Guar Gum and Cellulose

The viscosities of guar gum and cellulose were measured using an Ostwald viscometer with a 0.75-mm capillary diameter. Samples (0.1 g) were blended with distilled water. After being stored for 24 h at room temperature, 0.1% (w/v) suspending solutions were prepared in 100-ml volumetric flasks. The solutions were preheated at 37 °C for 15 min, and then the flow times were determined. Each measurement was repeated three times. The viscosities of guar gum and cellulose were calculated relative to the viscosity of distilled water, and therefore, they had no units.

Statistical Analysis

All values are expressed as means ± SEM. The significance of differences between means for two groups was determined by Student's *t* test. Differences were considered significant at $P < 0.05$.

Results and Discussion

There was no significant difference between the consumption of the cellulose and guar gum diets for 30 min (4.64 ± 0.15 and 3.94 ± 0.55 g, respectively, $n = 5$). Therefore, the input levels of cellulose and guar gum were identical. However, as shown in Fig. 2a, rats fed the guar gum diet had significantly lower lymph flow than did rats fed the cellulose diet (3.88 ± 1.31 and 11.9 ± 1.1 ml, respectively, for 7 h; $P < 0.005$). In comparison with the cellulose diet, the guar gum diet also significantly reduced

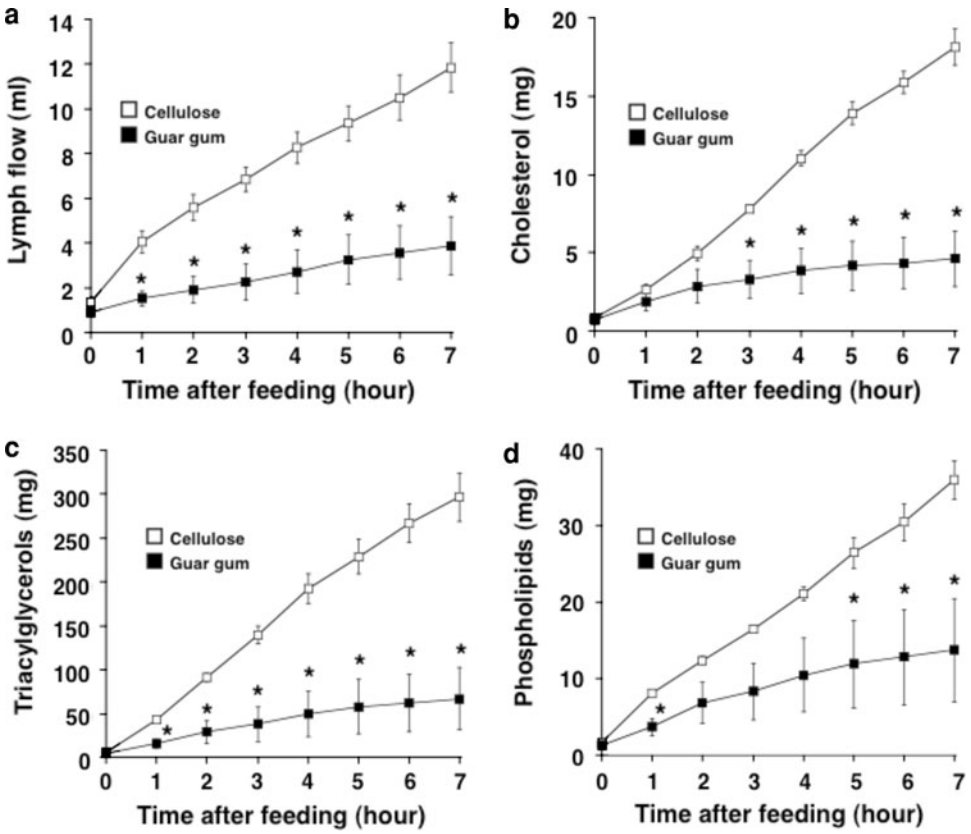

Fig. 2 Cumulative lymph flow (**a**), lymphatic transport of cholesterol (**b**), triacylglycerols (**c**), and phospholipids (**d**) in rats fed a cellulose or guar gum diet. Values are expressed as mean ± SEM ($n = 5$). *Asterisk* shows a significant difference at $P < 0.05$

Table 1 Water-holding capacities, settling volumes in water, and viscosities of the cellulose and the guar gum

	Cellulose	Guar gum
Water-holding capacity (g wet fiber per g dry fiber)	3.33 ± 0.13	44.5 ± 1.9*
Settling volume in water (ml per g fiber)	3.37 ± 0.03	72.3 ± 4.3*
Viscosity	1.00 ± 0.00	3.33 ± 0.00*

Values are expressed as mean ± SEM ($n = 3$)

* Significant difference at $P < 0.05$

the transport of cholesterol (4.60 ± 1.77 and 18.1 ± 1.1 mg, respectively, for 7 h; $P < 0.0005$) (Fig. 2b), triacylglycerols (66.8 ± 35.3 and 297 ± 27 mg, respectively, for 7 h; $P < 0.001$) (Fig. 2c), and phospholipids (13.7 ± 6.7 and 36.0 ± 2.5 mg, respectively, for 7 h; $P < 0.05$) (Fig. 2d). The apparent lymphatic recovery rates of cholesterol and triacylglycerols were calculated on the basis of their consumption. The guar gum diet as compared to the cellulose diet significantly reduced the apparent lymphatic recovery rates of cholesterol (78.3 ± 4.4 and 24.8 ± 10.1%, respectively; $P < 0.005$) and triacylglycerols (91.0 ± 7.0 and 27.9 ± 15.4%, respectively; $P < 0.01$) for a 7-h period. We did not calculate the apparent lymphatic recovery rate of phospholipids. The lymphatic phospholipids may be derived from bile, intestinal mucosa exfoliation, bacterial flora, etc., but not from the diet. The reduction pattern of phospholipid absorption by the guar gum diet was similar to that of lymph flow at around 35% lower than the cellulose diet. However, the reduction in the absorption of cholesterol and triacylglycerols were accelerated by the guar gum diet. This accelerated suppression of the absorption of cholesterol and triacylglycerols by the guar gum diet may be due to the reduction of lymph flow as well as other mechanisms. For example, guar gum might form a stable thick unstirred water layer that acts as a physical barrier in the intestinal lumen [1]. In contrast to our results, Ikeda et al. [15] showed that the thoracic duct lymph flow of rats administered cellulose or guar gum were identical. This discrepancy may be due to differences between the administration protocols and the quantities of dietary fiber infused. Ikeda et al. [15] employed forced administration with an indwelling stomach catheter to feed emulsions containing 25 mg of [^{14}C] cholesterol, 50 mg of either cellulose or guar gum, and 200 mg of either safflower, high-oleic safflower, or palm oil prior to continuous infusion of physiological saline—5% glucose solution for 24 h. The forced administration of saline–glucose solution resulted in a higher lymph flow rate (approximately 100 ml/24 h) compared with that in our experiment. The main purpose of Ikeda's study was to acquire knowledge about the interaction of dietary fibers and fats. Therefore, our results may provide a novel understanding about the inhibition of lipid absorption by dietary fiber via a change in lymph flow.

Although there was a previous study about WHC of guar gum and cellulose [16], our study also indicated clear differences between the WHC of guar gum and cellulose (Table 1). The WHC of guar gum was approximately 13 times higher than that of cellulose. The SV of guar gum was approximately 22-fold higher than that of cellulose (Table 1). Moreover, the viscosity of guar gum was approximately 3 times higher than that of cellulose (Table 1). Rainbird et al. [17] showed that guar gum decreases water absorption in isolated loops of the jejunum obtained from conscious growing pigs. The addition of guar gum to the intestine reduced the percentage of water absorption to approximately 25%. They suggested that this effect is related to the WHC of guar gum. Furthermore, Phillips reported a reduction in the rate of diffusion of cholesterol mixed micelles with an increase in guar gum concentration [18]. He also demonstrated that this reduction in rate was related to the viscosity of guar gum. These physicochemical properties of the water-soluble fiber are thought to exert their effects in the gut, thereby reducing the lymph flow. The WHC and viscosity of dietary fibers have been shown to affect intestinal transit time [19]. A fiber with a higher WHC and viscosity, such as guar gum, can delay gastric emptying and slow transit through the gut, thereby reducing the rate of dietary lipid absorption [20]. Moreover, the inhibition of absorption of various lipid-soluble compounds may rely almost entirely on these physicochemical properties. The hypolipidemic mechanism of guar gum has been shown to occur because of the adsorption of bile acids and cholesterol by this fiber in the intestine [1]. Therefore, further studies are necessary to evaluate the effects of dietary guar gum on time courses of the change of bile acid levels in feces and portal blood.

In conclusion, dietary guar gum (a water-soluble fiber) decreased the absorption of dietary cholesterol, triacylglycerols, and endogenous phospholipids through a reduction in the lymph flow. These effects may be due to the physicochemical properties of guar gum.

References

1. Theuwissen E, Mensink RP (2008) Water-soluble dietary fibers and cardiovascular disease. Physiol Behav 94:285–292
2. Brown L, Rosner B, Willett WW, Sacks FM (1999) Cholesterol-lowering effects of dietary fiber: a meta-analysis. Am J Clin Nutr 69:30–42

3. Dikeman CL, Fahey GC (2006) Viscosity as related to dietary fiber: a review. Crit Rev Food Sci Nutr 46:649–663
4. Hoffmann J, Linseisen J, Riedl J, Wolfram G (1999) Dietary fiber reduces the antioxidative effect of a carotenoid and alpha-tocopherol mixture on LDL oxidation ex vivo in humans. Eur J Nutr 38:278–285
5. Nakashima Y, Ikegami S (2001) Guar gum reduces trichloroethylene accumulation in the body by reducing TCE absorption and fat tissue mass. J Agric Food Chem 49:3499–3505
6. Aozasa O, Ohta S, Nakao T, Miyata H, Nomura T (2001) Enhancement in fecal excretion of dioxin isomer in mice by several dietary fibers. Chemosphere 45:195–200
7. Imaizumi K, Havel RJ, Fainaru M, Vigne JL (1978) Origin and transport of the A-I and arginine-rich apolipoproteins in mesenteric lymph of rats. J Lipid Res 19:1038–1046
8. Tso P (1985) Gastrointestinal digestion and absorption of lipid. Adv Lipid Res 21:143–186
9. Carey MC, Hernell O (1992) Digestion and absorption of fat. Semin Gastrointest Dis 3:189–208
10. Tomoyori H, Carvajal O, Nakayama M, Kishi T, Sato M, Ikeda I, Imaizumi K (2002) Lymphatic transport of dietary cholesterol oxidation products, cholesterol and triacylglycerols in rats. Biosci Biotechnol Biochem 66:828–834
11. Tomoyori H, Kawata Y, Higuchi T, Ichi I, Sato H, Sato M, Ikeda I, Imaizumi K (2004) Phytosterol oxidation products are absorbed in the intestinal lymphatics in rats but do not accelerate atherosclerosis in apolipoprotein E-deficient mice. J Nutr 134:1690–1696
12. Sato M, Kawata Y, Erami K, Ikeda I, Imaizumi K (2008) LXR agonist increases the lymph HDL transport in rats by promoting reciprocally intestinal ABCA1 and apo A-I mRNA levels. Lipids 43:125–131
13. Reeves PG, Nielsen FH, Fahey GC Jr (1993) AIN-93 purified diets for laboratory rodents: final report of the American Institute of Nutrition ad hoc writing committee on the reformulation of the AIN-76A rodent diet. J Nutr 123:1939–1951
14. Takeda H, Kiriyama S (1979) Correlation between the physical properties of dietary fibers and their protective activity against amaranth toxicity in rats. J Nutr 109:388–396
15. Ikeda I, Tomari Y, Sugano M (1989) Interrelated effects of dietary fiber and fat on lymphatic cholesterol and triglyceride absorption in rats. J Nutr 119:1383–1387
16. Stephen AM, Cummings JH (1979) Water-holding by dietary fibre in vitro and its relationship to faecal output in man. Gut 20:722–729
17. Rainbird AL, Low AG, Zebrowska T (1984) Effect of guar gum on glucose and water absorption from isolated loops of jejunum in conscious growing pigs. Br J Nutr 52:489–498
18. Phillips DR (1986) The effect of guar gum in solution on diffusion of cholesterol mixed micelles. J Sci Food Agric 37:548–552
19. Blackwood AD, Salter J, Dettmar PW, Chaplin MF (2000) Dietary fibre, physicochemical properties and their relationship to health. J R Soc Promot Health 120:242–247
20. Rainbird AL, Low AG (1986) Effect of guar gum on gastric emptying in growing pigs. Br J Nutr 55:87–98

Lipids (2011) 46:795–804
DOI 10.1007/s11745-011-3582-9

ORIGINAL ARTICLE

Mifepristone Treatment Results in Differential Regulation of Glycerolipid Biosynthesis in Baby Hamster Kidney Cells Expressing a Mifepristone-Inducible ABCA1

Kristin D. Hauff · Ryan W. Mitchell · Fred Y. Xu · Thomas Dembinski · David Mymin · Xiaohui Zha · Patrick C. Choy · Grant M. Hatch

Received: 2 March 2011 / Accepted: 9 June 2011 / Published online: 28 June 2011

Abstract ATP binding cassette A1 (ABCA1) transports cholesterol, phospholipids and lipophilic molecules to and across cellular membranes. We examined if ABCA1 expression altered cellular de novo glycerolipid biosynthesis in growing Baby hamster kidney (BHK) cells. Mock BHK cells or cells expressing a mifepristone-inducible ABCA1 (ABCA1) were incubated plus or minus mifepristone and then with [^{3}H]serine or [^{3}H]inositol or [^{3}H]ethanolamine or [*methyl*-^{3}H]choline or [^{3}H]glycerol or [^{14}C]oleate and radioactivity incorporated into glycerolipids determined. Mifepristone did not affect [1,3-^{3}H]glycerol or [^{14}C]oleate or [^{3}H]ethanolamine or [*methyl*-^{3}H]choline uptake in BHK cells. In contrast, [^{3}H]glycerol and [^{14}C]oleate incorporated into phosphatidylserine (PtdSer) were elevated 2.4-fold ($p < 0.05$) and 54% ($p < 0.05$), respectively, upon ABCA1 induction confirming increased PtdSer biosynthesis from these precursors. However, mifepristone inhibited [^{3}H]serine uptake and incorporation into PtdSer indicating that PtdSer synthesis from serine in BHK cells is dependent on serine uptake. Mifepristone stimulated [^{3}H]inositol uptake in mock and ABCA1 cells but not its incorporation into phosphatidylinositol indicating that its synthesis from inositol is independent of inositol uptake in BHK cells. [^{3}H]glycerol and [^{14}C]oleate incorporated into triacylglycerol were reduced and into diacylglycerol elevated only in mifepristone-induced ABCA1 expressing cells due to a decrease in diacylglycerol acyltransferase-1 (DGAT-1) activity. The presence of trichostatin A, a class I and II histone deacetylase inhibitor, reversed the ABCA1-mediated reduction in DGAT-1 activity but did not affect DGAT-1 mRNA expression. Thus, mifepristone has diverse effects on de novo glycerolipid synthesis. We suggest that caution should be exercised when using mifepristone-inducible systems for studies of glycerolipid metabolism in cells expressing glucocorticoid responsive receptors.

Keywords Phospholipid synthesis · Cholesterol transport · Triacylglycerol · ATP binding cassette-1 · ABCA1 · Diacylglycerol acyltransferase · BHK cells · Mifepristone · Amino acid · Inositol · Serine

Abbreviations

ABCA1	ATP binding cassette A1
BHK	Baby hamster kidney
DAG	Diacylglycerol
DGAT	Diacylglycerol acyltransferase
TAG	Triacylglycerol
PtdCho	Phosphatidylcholine
PtdEth	Phosphatidylethanolamine
PtdGro	Phosphatidylglycerol
Ptd_2Gro	Cardiolipin
PtdIns	Phosphatidylinositol
PtdSer	Phosphatidylserine
PLA_2	Phospholipase A_2
PtdOH	Phosphatidic acid

K. D. Hauff · R. W. Mitchell · F. Y. Xu · G. M. Hatch (✉)
Department of Pharmacology and Therapeutics,
Manitoba Institute of Child Health, Faculty of Medicine,
University of Manitoba, 715 McDermot Avenue,
Winnipeg, MB R3E 0T6, Canada
e-mail: hatchgm@ms.umanitoba.ca

T. Dembinski · P. C. Choy · G. M. Hatch
Biochemistry and Medical Genetics, Center for Research
and Treatment of Atherosclerosis, Winnipeg, Canada

D. Mymin
Internal Medicine, University of Manitoba,
Winnipeg, MB R3E 0T6, Canada

X. Zha
Ottawa Health Institute, University of Ottawa,
Ottawa, Ontario, Canada

Introduction

Phospholipids and cholesterol are the principal lipid components in mammalian cellular membranes [1]. Phospholipids provide a protective barrier for selective permeability, define organelles and are key components of various metabolic and cellular reactions. For example, phosphatidylserine (PtdSer) is present in significant quantities in mammalian tissues and is required for surface recognition of apoptotic cells by phagocytes [2]. Cholesterol regulates the fluidity of cell membranes and is found in plasma membrane lipid rafts where it anchors cell signaling proteins [3]. Alteration of intracellular lipid transport within and between membranes may affect eukaryotic glycerolipid biosynthesis. For example, mitochondrial phosphatidylethanolamine (PtdEtn) de novo biosynthesis in yeast was regulated by control of PtdSer import into the mitochondria [4]. Sphingomyelin (CerPCho) de novo biosynthesis in hepatocytes was regulated by control of phosphatidylcholine (PtdCho) transport from the endoplasmic reticulum to the Golgi [5]. Expression of phospholipid scramblase-3 in Hela cells which altered movement of cardiolipin (Ptd_2Gro) between inner and outer mitochondrial membranes stimulated de novo Ptd_2Gro biosynthesis [6]. In contrast, there is little information on the role that altered plasma membrane lipid transport plays in regulating glycerolipid de novo biosynthesis.

ATP binding cassette A1 (ABCA1) is a 2261 amino acid integral membrane protein and member of the ATP binding cassette transporter family of transporters [reviewed in 7]. ABCA1 functions to transport cholesterol, phospholipids and other lipophilic molecules to and across the cellular membranes where they can be removed by lipid-poor high density lipoprotein apolipoproteins. Induction of ABCA1 in baby hamster kidney (BHK) cells was shown to increase PtdSer levels in the plasma membrane exofacial leaflet [8]. However, it was unknown if this increase in PtdSer level in the plasma membrane exofacial leaflet was associated with altered PtdSer de novo biosynthesis.

Mifepristone or 17β-hydroxy-11β-(4-dimethyl-aminophenyl 1)-17α-(prop-1-ynyl)-estra-4,9-dien-3-one (RU 486) is a potent abortifactant in clinical use [9]. It acts during the luteal phase in the endometrium, provoking bleeding, and also decreases luteinizing hormone secretion which results in luteolysis. In addition to its role as an abortifactant, mifepristone is used for expression of proteins in the mifepristone-inducible gene regulatory system. The mifepristone-inducible gene regulatory system allows for the control of spatiotemporal expression of transgenes in vivo in a ligand-dependent manner [reviewed in 10]. The regulatory system is composed of two components: (1) a chimeric transactivator protein that activates transgene transcription only in the presence of mifepristone, and (2) a target transgene placed in the context of a promoter which is responsive only to the mifepristone-bound chimeric transactivator.

In this study, we examined if increased expression of ABCA1, mediated by the mifepristone-inducible gene regulatory system altered cellular glycerolipid de novo biosynthesis. We show that expression of ABCA1 using the mifepristone-inducible gene system stimulates PtdSer de novo biosynthesis from glycerol and oleic acid (OLA) precursors in growing BHK cells. In addition, expression of ABCA1 decreases triacylglycerol (TAG) de novo biosynthesis by reducing the activity of diacylglycerol acyltransferase-1 (DGAT-1). Moreover, we show that the glucocorticoid antagonist mifepristone, at concentrations (10 nM) widely used for the mifepristone-inducible gene system, inhibits serine uptake and stimulates *myo*-inositol uptake in BHK cells. Our findings indicate that mifepristone has diverse effects on de novo glycerolipid synthesis and thus caution should be exercised when using mifepristone-inducible systems for the study of cellular glycerolipid metabolism.

Materials and Methods

Materials

[1,3-^{3}H]Glycerol, [1-^{14}C]OLA, *myo*-[^{3}H]inositol, [1-^{14}C] palmitate (PAM), [*methyl*-^{3}H]choline, [^{3}H]ethanolamine, [^{3}H]serine and Ptd[^{14}C]Cho were obtained from either Dupont, Mississauga, Ontario, or Amersham, Oakville, Ontario, Canada. DMEM and fetal bovine serum were products of Canadian Life Technologies (GIBCO), Burlington, Ontario, Canada. Lipid standards were obtained from Serdary Research Laboratories, Englewood Cliffs, New Jersey, USA. Thin layer chromatographic plates (silica gel G, 0.25 mm thickness) were obtained from Fisher Scientific, Winnipeg, Canada. Ecolite scintillant was obtained from ICN Biochemicals, Montreal, Quebec, Canada. BHK cells expressing mifepristone-inducible ABCA1 were a generous gift from Dr. John F. Oram, University of Washington, Seattle, WA, USA [11]. The rate of growth of mock and ABCA1 cells were similar. Primary ABCA1 and heat shock protein-70 (HSP-70) antibodies and secondary antibodies were obtained from Novus Biological Inc. Littleton, CO, USA. All other chemicals were certified ACS grade or better and obtained from Sigma Chemical Company, St. Louis, USA or Fisher Scientific, Winnipeg, Manitoba, Canada.

Cell Culture and Radiolabeling Experiments

Cells (mock, BHK control; ABCA1, BHK cells containing mifepristone-inducible ABCA1) were grown in DMEM

containing 10% fetal bovine serum until 70% confluence. Cells were then incubated for 24 h in the absence or presence of 10 nM mifepristone and then for 4 h with DMEM medium in the presence of 0.1 μM [^{3}H]serine (5 μCi/dish) or *myo*-[^{3}H]inositol (2 μCi/dish). Phospholipids were separated by two-dimensional thin-layer chromatography and radioactivity incorporated into phospholipids determined as described [12]. Essentially, the medium was removed and the cells washed twice with ice cold saline and then harvested from the dish with 2 mL methanol:water (1:1, v/v). The mixture was vortexed, and a 25 μL aliquot was taken for protein analysis and a 25 μL aliquot taken for determination of total radioactivity. Appropriate volumes of chloroform, 0.9% NaCl and methanol were added to the tubes in a 4:3:2 ratio to initiate phase separation. The tubes were vortexed and then centrifuged at 2,000 rpm for 10 min in a bench top centrifuge) and the aqueous phase was removed and 2 mL of chloroform/methanol/NaCl (3:48:47, by vol) was added to wash the organic phase. The tubes were vortexed and centrifuged as described above and the aqueous phase removed. The organic phase was dried under a stream of N_2 gas and resuspended in 100 μL chloroform. A 50-μL aliquot of organic phase was placed onto a thin-layer plate along with phospholipid standards and phospholipids were separated by two-dimensional thin-layer chromatography. In the first dimension, the plate was developed in a solvent system containing chloroform/methanol/NH_4OH/water (70:30:2:3, by vol). The second dimension, at 90° to the first separation, was performed in a solvent system containing chloroform/methanol/water (65:55:5, by vol). Plates were allowed to dry overnight and the separated phospholipids were visualized by exposing the plate to iodine vapor. Corresponding radioactive phospholipids of interest were removed and placed in 6-mL scintillation vials containing 5 mL Ecolite scintillation cocktail. The radioactivity was determined in a Beckman Model LS3801 liquid scintillation counter. For phospholipid pool size analysis, the organic phase was separated on thin-layer chromatographic plates as above in the absence phospholipid standards.

In other experiments, cells were incubated for 24 h in the absence or presence of 10 nM mifepristone and then for 4 h with 0.1 mM [1,3-^{3}H]glycerol (10 μCi/dish) or 0.1 mM [1-^{14}C]OLA (bound to albumin 1:1 molar ratio) (1 μCi/dish) or 0.1 mM [1-^{14}C]PAM (bound to albumin 1:1 molar ratio) (1 μCi/dish) and radioactivity incorporated into phospholipids determined as described above. For neutral lipid analysis, the organic phase was isolated as described above and dried under a stream of N_2 gas and resuspended in 100 μL chloroform [13]. A 50-μL aliquot of organic phase was placed onto a thin-layer plate along with neutral lipid standards and DAG and TAG were separated by one-dimensional thin-layer chromatography in a solvent system containing benzene/diethylether/absolute ethanol/acetic acid (50:45:2:0.2, by vol). Plates were allowed to dry overnight and the separated DAG and TAG were visualized by exposing the plate to iodine vapor. Corresponding radioactive DAG and TAG were removed and placed in 6-mL scintillation vials containing 5 mL Ecolite scintillation cocktail and radioactivity incorporated determined as described above.

Subcellular Fractionation and Assay of Enzyme Activities

Cells were incubated for 24 h in the absence or presence of 10–100 nM mifepristone washed twice with ice cold saline and harvested with 2 mL lysis buffer (10 mM Tris–HCL, pH 7.4, 0.25 M sucrose). Cells were homogenized with 30 strokes of a Dounce A homogenizer. The homogenate was centrifuged at 1,000×*g* for 5 min to remove debris. The pellet was resuspended in 0.5 mL homogenization buffer and used for assay of enzyme activities. 1,2-Diacylglycerol acyltransferase (DGAT) was determined in membrane fractions prepared from BHK cells in the absence or presence of 100 mM $MgCl_2$ to distinguish between DGAT-1 and DGAT-2 isoforms as previously described [14]. Essentially, the assay measured the incorporation of [^{14}C]oleoyl-CoA (specific activity: 20,000 dpm/nmol) into TAG in a 5 min assay using 50 μg protein, 0.4 mM DAG and 25 μM oleoyl-CoA plus or minus 100 mM $MgCl_2$ in 0.25 M sucrose, 1 mM EDTA, 100 mM Tris–HCl buffer pH 7.5. The reaction was terminated by the addition of chloroform:methanol (2:1 v:v). Tubes were vortexed and the organic phase removed and separated by thin-layer chromatorgraphy as described above for neutral lipid synthesis. Prior to chromatography TAG standard was added to the plate. The TAG band was identified by iodine vapor and radioactivity in TAG measured by liquid scintillation counting as described above. PS synthase activity was determined as described [15]. Essentially, the assay measured the incorporation of 0.5 mM L-[^{3}H]serine (10,000 dpm/nmol) into PtdSer in 50 mM Tris–HCl buffer (pH 8.0) with 0.6 mM $MnCl_2$, 0.2 mM CDP-diacylglycerol. 4 mM Triton X-100 and 25 μg enzyme protein in a total volume of 0.1 mL assayed a 30 °C for 10 min. The reaction was terminated by addition of 0.1 N HCl followed by phase separation with 1 mL chloroform and 1.5 mL 1 M $MgCl_2$. A 0.5-mL aliquot of the organic phase was removed, dried and radioactivity determined. Phospholipase A_2 (PLA_2) activity was determined as described [16]. Essentially, the assay measured the hydrolysis of 0.2 mM Ptd[^{14}C]Cho (1,000 dpm/nmol) to lysoPtD[^{14}C]Cho in 0.25 M Tris–HCl, pH 8.5, 25 mM $CaCl_2$ and 0.1 mg protein in a total volume of 0.5 mL at 37 °C for 30 min. The reaction was terminated by addition of 2 mL of chloroform

followed by 1 mL of 0.1 M HCl in methanol and 1 mL of 0.73% NaCl. The mixture was vortexed and the organic phase removed, dried and separated on a thin layer plate as described above for phospholipids with lysoPtdCho standard. The lysoPtdCho spot was visualized by iodine vapor, removed and radioactivity determined by liquid scintillation counting as described above. In other experiments, ABCA1 cells were incubated for 24 h in the absence or presence of 10 nM mifepristone or 100 μM trichostatin A or both and DGAT-1 activity determined as above.

Real Time-PCR Analysis of DGAT-1

ABCA1 cells were incubated for 24 h in the absence or presence of 10 nM mifepristone or 100 μM trichostatin A or both. Total RNAs from cells were isolated using the TRIZOL Reagent according to the manufactures instructions. The RNA pellets were suspended in autoclaved, double-distilled water and quantitated by absorbance at 260 nm using the 260:280 nm ratio as an index of purity. The integrity of the RNA was confirmed by denaturing agarose gel electrophoresis of the isolated RNA. Primers were synthesized by Invitrogen™ Life Technologies. The primers for DGAT-1 were Forward 5′-GTA GAA GAG GAC GAG GTG CGA GAC -3′; Reverse 5′-GGG CTT CAT GGA GTT CTG GAT AGT -3′. The primers for β-actin were Forward 5′-GTG GGG CGC CCC AGG CAC CA-3′; Reverse 5′-CTC CTT AAT GTC ACG CAC GAT TTG-3′. DGAT-1 mRNA expression relative to the constitutive expression of β-actin was determined under the conditions described [17].

Western Blot Analysis of ABCA1

Mock and ABCA1 cells were incubated with 10 nM mifepristone for 24 h. Cells were placed on ice, media was aspirated, and cells washed twice with cold 1X PBS. Cells were lysed with 1× SDS buffer (50 mM Tris–Cl pH 6.8, 100 mM dithiothreitol, 2% SDS, 10% glycerol, and 1 tablet PhosSTOP per 10 mL buffer). Cells were immediately scraped off plates and transferred to microcentrifuge tubes on ice. Lysates were sonicated for 10–15 s (to shear DNA) and then heated to 72 °C for 5 min. Lysates were centrifuged for 2 min at 9000×*g* and protein levels determined as described below. 4× SDS loading buffer (200 mM Tris HCl pH 6.8, 400 mM dithiothreitol, 8% SDS, 40% glycerol, 0.4% bromophenol blue) was added to 30–45 μg of cell lysates. Samples were loaded onto 10% acrylamide resolving gels (10% acrylamide mix (9.67% acrylamide, 0.33% bis), 375 mM Tris–HCl, pH 8.8, 1% SDS, 1% ammonium persulfate, 0.04% TEMED) and subjected to SDS-PAGE at 180 V for 90 min. Separated proteins were electro-transferred to PVDF membranes at 70 V for 150 min. PVDF membranes were blocked with TBS-T (50 mM Tris HCl, (pH 7.4) 150 mM NaCl, 0.1% Tween-20) containing 2.5% BSA for 30 min. Membranes were incubated with primary ABCA1 antibody (1:1,000), or primary HSP-70 antibody as protein loading control, with gentle agitation overnight at 4 °C. Membranes were then washed with TBS-T three times for 5 min. Membranes were then incubated and gently agitated for 2 h in secondary antibody (1:2,000) diluted in TBS-T with 5% BSA. Once again, membranes were washed three times for 5 min each with TBS-T. PVDF membranes were incubated for 1 min with 1–2 mL chemiluminescent substrate, excess substrate was drained, and membranes were covered in plastic wrap. In a dark room, membranes were exposed to X-ray film for appropriate exposure time and then processed using Raytech Medical Film Processor SRX-101A.

Other Determinations

The pool size of the major phospholipids were determined as described [18]. Protein was determined as described [19]. Dunnet's *t* test for multiple comparisons with a single mean was used for determination of statistical significance. The level of significance was defined as $p < 0.05$.

Results

Expression of ABCA1 Does not Alter Glycerophospholipid Pool Size

Expression of the ABCA1 cholesterol transporter was shown to increase PtdSer levels in the plasma membrane exofacial leaflet [8]. However, it was unknown if this was associated with elevated biosynthesis. BHK cells expressing a mifepristone-inducible ABCA1 (ABCA1 cells) were incubated in the absence or presence of 10 nM mifepristone for 24 h and western blot analysis performed. Mifepristone-treatment of ABCA1 cells resulted in a marked increase in the expression of ABCA1 (Fig. 1). To examine if expression of ABCA1 would alter the glycerophospholipid pool size BHK cells (mock) and ABCA1 cells were incubated in the absence or presence of 10 nM mifepristone for 24 h and the pool size of glycerophospholipids determined. Mifepristone-treatment did not alter the pool size of the major glycerophospholipids in mock or ABCA1 cells (Table 1). Thus, total PtdSer levels in ABCA1 expressing cells were unaltered.

Mifepristone Alters Serine and *myo*-Inositol Uptake

To examine if expression of ABCA1 would alter glycerophospholipid de novo biosynthesis, mock and ABCA1 cells

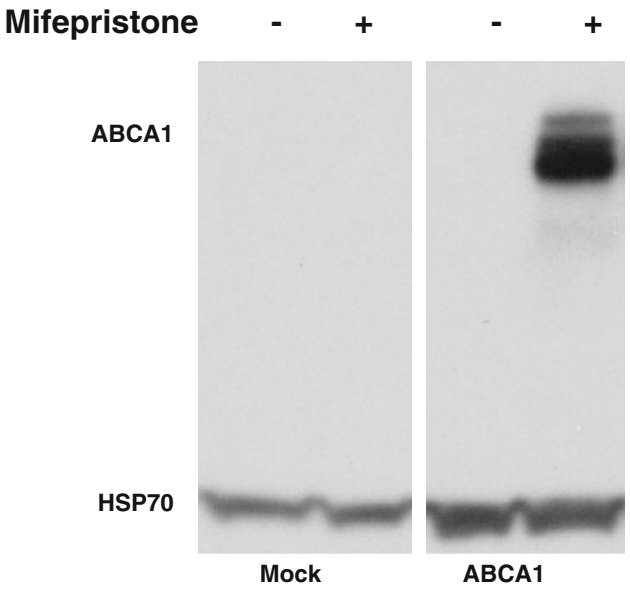

Fig. 1 Western blot analysis of Mock and ABCA1 cells treated with mifepristone. Mock and ABCA1 cells were incubated for 24 h in the absence (−) or presence (+) of 10 nM mifepristone and western blot analysis performed as described in "Materials and Methods". A representative blot is depicted

were incubated for 24 h in the absence or presence of 10 nM mifepristone and then for 4 h with [^{3}H]serine or *myo*-[^{3}H]inositol or [*methyl*-^{3}H]choline or [^{3}H]ethanolamine and radioactivity incorporated into glycerophospholipids was determined. [^{3}H]Serine incorporated into PtdSer was reduced 41 and 38% in mock and ABCA1 cells treated with mifepristone, respectively, compared to untreated cells (Table 2). However, this reduction of [^{3}H]serine incorporated into PtdSer was likely due to a mifepristone-mediated inhibition of serine uptake since mifepristone inhibited [^{3}H]serine uptake 38 and 25% in mock and ABCA1 cells, respectively, compared to untreated cells. These data indicate that de novo PtdSer synthesis from serine is dependent upon serine uptake in BHK cells and that mifepristone attenuates serine uptake in these cells. Mifepristone-treatment of mock and ABCA1 cells resulted in a 3.5- to 4.8-fold increase in *myo*-[^{3}H]inositol uptake, respectively, but this had no effect on *myo*-[^{3}H]inositol incorporation into phosphatidylinositol (PtdIns) (Table 2). These data indicate that mifepristone increased *myo*-inositol uptake but that de novo synthesis of PtdIns in BHK cells is independent of *myo*-inositol uptake. Mifepristone-treatment did not affect [*methyl*-^{3}H]choline into phosphatidylcholine (PtdCho) or [^{3}H]ethanolamine incorporation into phosphatidylethanolamine (PtdEth) in mock or ABCA1 cells (data not shown), indicating that the de novo biosynthesis of these phospholipids were not altered by mifepristone or the expression of ABCA1 in BHK cells.

Expression of ABCA1 Stimulates PS Synthesis from Glycerol and OLA Precursors and Inhibits TAG Synthesis

Since glycerol and fatty acids form the diacylglycerol (DAG) backbone for all glycerophospholipids we examined glycerophospholipid and neutral lipid synthesis from glycerol and OLA precursors in mock and ABCA1 expressing cells treated with mifepristone. Cells were incubated for 24 h in the absence or presence of 10 nM mifepristone and then for 4 h with [1,3-^{3}H]glycerol or [^{14}C]OLA and radioactivity incorporated into the major glycerophospholipids and neutral lipids determined. [1,3-^{3}H]Glycerol incorporated into PtdSer was elevated 75% in ABCA1 cells treated with mifepristone compared to untreated ABCA1 cells (Table 3). In contrast, mifepristone-treatment did not affect [1,3-^{3}H]glycerol incorporated into PtdSer in mock cells compared to untreated cells. In addition, mifepristone did not alter the uptake of [1,3-^{3}H]glycerol into mock or ABCA1 BHK cells. These data indicated that PtdSer de novo biosynthesis from [1,3-^{3}H]glycerol was elevated by ABCA1 induction. Interestingly, mifepristone-treatment resulted in a 42% reduction in [1,3-^{3}H]glycerol incorporated into TAG and a 55% increase in [1,3-^{3}H]glycerol incorporated into DAG in ABCA1 cells but did not affect [1,3-^{3}H]glycerol

Table 1 Pool size of major glycerophospholipids in Mock and ABCA1 cells treated with mifepristone

Phospholipid (nmol/mg protein)	Mock (−)	Mock (+)	ABCA1 (−)	ABCA1 (+)
PtdCho	38.8 ± 3.0	39.1 ± 3.1	39.8 ± 3.5	37.0 ± 3.7
PtdEtn	13.8 ± 2.0	14.3 ± 2.0	14.4 ± 2.0	13.3 ± 2.1
PtdSer	2.9 ± 0.3	2.7 ± 0.2	2.9 ± 0.2	3.1 ± 0.3
PtdIns	6.5 ± 0.5	6.6 ± 0.5	6.8 ± 0.6	6.6 ± 1.2
Ptd_2Gro	4.9 ± 0.6	5.0 ± 0.6	6.1 ± 0.5	6.1 ± 1.2

Mock or ABCA1 cells were incubated for 24 h in the absence (−) or presence (+) of 10 nM mifepristone and the pool size of the major phospholipids determined as described in "Materials and Methods". Data represent the mean ± standard deviation of three dishes assayed in duplicate. The pool size of PtdGro and PtdOH were too low to be accurately determined

Table 2 PtdSer synthesis from [^{3}H]serine and PtdIns synthesis from *myo*[^{3}H]inositol in Mock and ABCA1 cells

	Mock (−)	Mock (+)	ABCA1 (−)	ABCA1 (+)
PtdSer (dpm/mg protein $\times 10^3$)	2.7 ± 0.5	1.5 ± 0.4*	2.1 ± 0.4	1.3 ± 0.1*
Total (dpm/mg protein $\times 10^5$)	5.5 ± 0.3	3.4 ± 0.2*	5.1 ± 0.5	3.8 ± 0.2*
PtdIns (dpm/mg protein $\times 10^3$)	13.8 ± 1.8	13.7 ± 2.5	16.0 ± 1.5	19.2 ± 2.1
Total (dpm/mg protein $\times 10^5$)	2.2 ± 0.3	7.8 ± 1.1*	2.7 ± 0.5	12.9 ± 0.2*

Mock or ABCA1 cells were incubated for 24 h in the absence (−) or presence (+) of 10 nM mifepristone and then incubated for 4 h with [^{3}H]serine or *myo*[^{3}H]inositol and radioactivity incorporated into PtdSer (*upper panel*) or PtdIns (*lower panel*) and total radioactivity incorporated into cells determined as described in "Materials and Methods". Data represent the mean ± standard deviation of three dishes assayed in duplicate

* $p < 0.05$

Table 3 Glycerolipid and neutral lipid synthesis from [1,3-^{3}H]glycerol in Mock and ABCA1 cells

Phospholipid (dpm/mg protein $\times 10^3$)	Mock (−)	Mock (+)	ABCA1 (−)	ABCA1 (+)
PtdCho	22.3 ± 2.5	21.9 ± 2.9	24.7 ± 2.7	23.9 ± 1.5
PtdEtn	2.7 ± 0.2	2.6 ± 0.1	2.9 ± 0.3	2.6 ± 0.3
PtdSer	0.4 ± 0.1	0.4 ± 0.1	0.4 ± 0.1	0.7 ± 0.1*
PtdIns	0.4 ± 0.1	0.4 ± 0.1	0.4 ± 0.1	0.5 ± 0.1
PtdGro	0.9 ± 0.1	0.9 ± 0.2	0.9 ± 0.1	0.8 ± 0.1
Ptd_2Gro	1.1 ± 0.1	0.8 ± 0.2	1.0 ± 0.1	0.9 ± 0.1
DAG	4.9 ± 1.1	4.8 ± 1.0	4.9 ± 0.7	7.6 ± 0.7*
TAG	3.2 ± 0.2	3.2 ± 0.3	4.5 ± 0.7	2.6 ± 0.2*
Total (dpm/mg protein $\times 10^4$)	6.1 ± 0.3	5.8 ± 0.2	6.6 ± 0.4	6.7 ± 1.0

Mock or ABCA1 cells were incubated for 24 h in the absence (−) or presence (+) of 10 nM mifepristone then incubated with [1,3-^{3}H]glycerol for 4 h and radioactivity incorporated into the major glycerophospholipids and neutral lipids and total incorporation into cells determined as described in "Materials and Methods". Data represent the mean ± standard deviation of three dishes assayed in duplicate

* $p < 0.05$

incorporated into TAG or DAG in mifepristone-treated mock cells compared to untreated cells. These data indicated that TAG de novo biosynthesis from glycerol was reduced by expression of ABCA1 in BHK cells.

[1-^{14}C]OLA incorporated into PtdSer was elevated 32% in ABCA1 cells treated with mifepristone compared to untreated cells (Table 4). Mifepristone-treatment did not affect [1-^{14}C]OLA incorporated into PtdSer in mock cells compared to untreated cells. In addition, mifepristone did not alter the uptake of [^{14}C]OLA into mock or ABCA1 BHK cells. These data indicate that PtdSer synthesis from [1-^{14}C]OLA was stimulated by ABCA1 expression in BHK cells. Mifepristone-treatment of ABCA1 cells resulted in a 21% reduction in [1-^{14}C]oleate incorporated into TAG and a 21% increase in [1-^{14}C]OLA incorporated into DAG. In contrast, mifepristone-treatment did not affect [1-^{14}C]OLA incorporation into DAG or TAG in mock cells. These data confirmed that TAG de novo biosynthesis from OLA was reduced by expression of ABCA1 in BHK cells. A previous study had shown that 10 nM mifepristone did not alter PtdEth, PtdCho and PtdSer synthesis from [1-^{14}C]PAM in a murine fibroblast cell line [20]. We confirmed this observation in BHK cells using [1-^{14}C]PAM (Table 5). This indicates that the mifepristone-mediated effects on phospholipid metabolism involved unsaturated fatty acids.

The reason for the increase in PtdSer synthesis from glycerol and OLA precursors was examined in mifepristone-treated ABCA1 cells. Cells were incubated for 24 h in the absence or presence of 10 nM mifepristone then harvested and cell lysates prepared and PtdSer synthase activity determined. PtdSer synthase activity was 39 ± 2 pmol/min/mg protein in ABCA1 cells and was unaltered (38 ± 2 pmol/min/mg protein) in mifepristone-treated ABCA1 cells. These data indicate that de novo PtdSer biosynthesis from glycerol and OLA precursors was increased but not via an increase in PtdSer synthase activity. Interestingly, the increase in de novo PtdSer synthesis from [1,3-^{3}H]glycerol or [1-^{14}C]OLA precursors seen with induction of ABCA1 did not correlate with an accumulation of PtdSer mass nor changes in PtdSer synthase activity. This may have been due to an increase in PLA_2 activity towards newly synthesized PtdSer in ABCA1 cells treated with mifepristone (Fig. 2).

Table 4 Glycerolipid synthesis from [1-^{14}C]OLA in Mock and ABCA1 cells

Phospholipid (dpm/mg protein $\times 10^3$)	Mock (−)	Mock (+)	ABCA1 (−)	ABCA1 (+)
PtdCho	36.5 ± 1.5	35.2 ± 1.4	42.6 ± 1.6	41.0 ± 1.0
PtdEtn	53.0 ± 2.4	53.1 ± 2.0	60.1 ± 4.1	57.7 ± 3.9
PtdSer	1.4 ± 0.2	1.5 ± 0.1	1.9 ± 0.1	2.5 ± 0.2*
PtdIns	6.3 ± 0.3	6.5 ± 0.2	7.6 ± 0.3	7.6 ± 0.8
Ptd_2Gro	2.3 ± 0.1	2.0 ± 0.2	2.6 ± 0.3	2.9 ± 0.2
DAG	21.2 ± 1.1	21.3 ± 1.0	24.1 ± 0.7	29.2 ± 1.7*
TAG	84.8 ± 4.0	88.0 ± 6.9	98.7 ± 7.6	77.7 ± 1.9*
Total (dpm/mg protein $\times 10^5$)	11.9 ± 1.0	11.4 ± 1.4	13.1 ± 0.7	12.2 ± 0.7

Mock or ABCA1 cells were incubated for 24 h in the absence (−) or presence (+) of 10 nM mifepristone and then incubated for 4 h with [1-^{14}C]OLA and radioactivity incorporated into the major glycerophospholipids and neutral lipids and total incorporation into cells determined as described in "Materials and Methods". Data represent the mean ± standard deviation of three dishes assayed in duplicate

* $p < 0.05$

Table 5 PtdCho, PtdEtn and PtdSer synthesis from [1-^{14}C]PAM in Mock and ABCA1 cells incubated with mifepristone

Phospholipid (dpm/mg protein $\times 10^3$)	Mock (−)	Mock (+)	ABCA1 (−)	ABCA1 (+)
PtdCho	32.0 ± 2.4	30.9 ± 1.4	35.6 ± 3.7	32.5 ± 1.9
PtdEtn	47.7 ± 3.0	49.8 ± 1.8	51.4 ± 2.5	52.1 ± 1.3
PtdSer	1.3 ± 0.1	1.3 ± 0.1	1.7 ± 0.1	1.8 ± 0.1

Mock or ABCA1 cells were incubated for 24 h in the absence (−) or presence (+) of 10 nM mifepristone and then incubated for 4 h with [1-^{14}C] and radioactivity incorporated into PtdCho, PtdEtn and PtdSer determined. Data represent the mean ± standard deviation of three dishes assayed in duplicate

Expression of ABCA1 Reduces DGAT-1 Activity

The reason for the reduction in [1,3-^{3}H]glycerol and [1-^{14}C]oleate incorporation into TAG in ABCA1 cells was examined. Mock and ABCA1 cells were incubated for 24 h in the absence or presence of various concentrations of mifepristone and then membrane fractions prepared and DGAT activity determined in the absence or presence of 100 mM $MgCl_2$ in the assay incubation mixture. The presence of 100 mM $MgCl_2$ in the incubations will inhibit DGAT-2 enzyme activity [14]. Mifepristone-treatment (10–100 nM) resulted in a 34–39% ($p < 0.05$) reduction in DGAT-1 activity in ABCA1 cells but not in mock cells (Fig. 3a). In contrast, mifepristone-treatment did not affect DGAT-2 activity in either ABCA1 cells or mock BHK cells (Fig. 3b). The decrease in DGAT-1 enzyme activity was maximum with ABCA1 expression using 10 nM mifepristone.

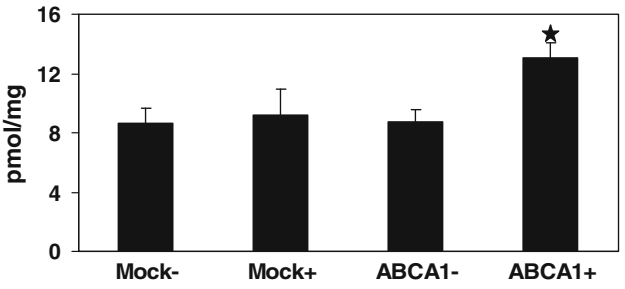

Fig. 2 PLA_2 activities in Mock and ABCA1 cells. Mock or ABCA1 cells were incubated for 24 h in the absence (Mock − or ABCA1 −) or presence (Mock + or ABCA1 +) of 10 nM mifepristone and PLA_2 activities determined as described in "Materials and Methods". Data represent the means ± standard deviation of three dishes assayed in duplicate *$p < 0.05$

Membrane fractions from ABCA1 cells were then prepared and DGAT-1 activity determined in the absence or presence of 10–100 nM exogenous mifepristone in the assay. The presence of exogenous mifepristone added to the assay incubation mixture did not affect DGAT-1 in vitro enzyme activity in membrane fractions prepared from ABCA1 cells indicating that mifepristone did not directly affect in vitro DGAT-1 activity (data not shown). We next examined if DGAT-1 activity and its mRNA expression were regulated by ABCA1 expression in ABCA1 cells. ABCA1 cells were incubated for 24 h in the absence or presence of 10 nM mifepristone and DGAT-1 enzyme activity determined. In addition, total mRNA was isolated and DGAT-1 mRNA expression examined by real

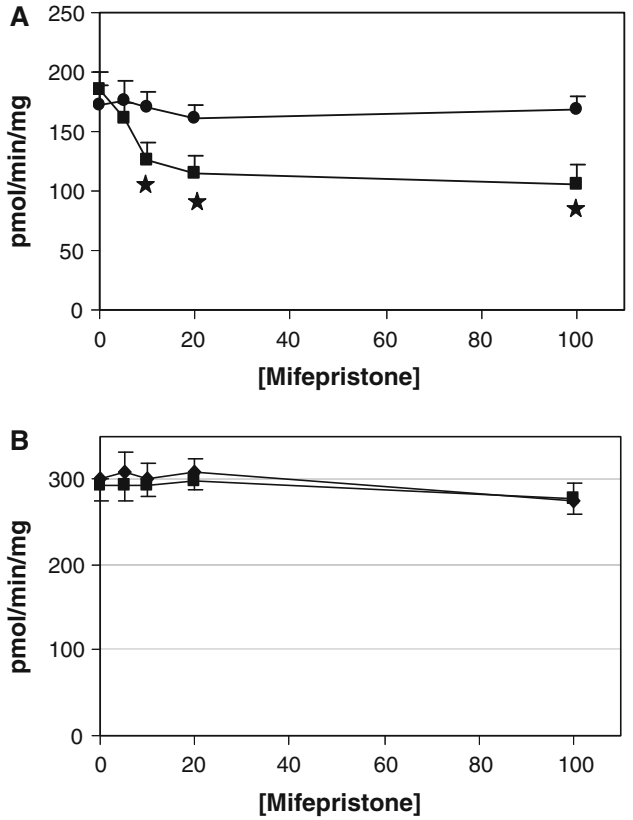

Fig. 3 Concentration-dependent effect of mifepristone on DGAT activities in mock BHK and ABCA1 cells. Mock cells (*circles*) or ABCA1 cells (*squares*) were incubated for 24 h in the absence or presence of 5–100 nM mifepristone and DGAT-1 (**a**) and DGAT-2 (**b**) activities determined as described in "Materials and Methods". Data represent the means ± standard deviation of three dishes assayed in duplicate $*p < 0.05$

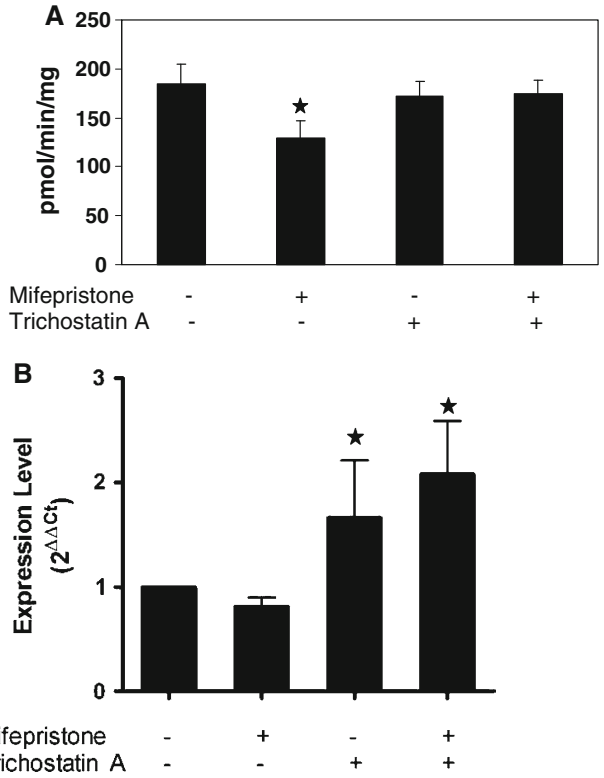

Fig. 4 DGAT-1 activity and mRNA expression in ABCA1 cells treated with mifepristone or trichostatin A or both. **a** ABCA1 cells were incubated for 24 h in the absence (−) or presence (+) of 10 nM mifepristone or 100 μM trichostatin A or both and DGAT-1 enzyme activity determined as in Fig. 2. **b** ABCA1 cells were incubated for 24 h in the absence (−) or presence (+) of 10 nM mifepristone or 100 μM trichostatin A or both and DGAT-1 mRNA expression determined by real time-PCR as described in "Materials and Methods". Data represent the means ± standard deviation of three dishes assayed in duplicate $*p < 0.05$

time-PCR. As expected DGAT-1 activity was reduced by mifepristone treatment (Fig. 4a). In contrast, DGAT-1 mRNA expression relative to the constitutive expression of β-actin was unaltered (Fig. 4b). Histone deacetylation increases the charge density on the N-termini of the core histones and thus strengthens histone tail-DNA interactions and blocks access of transcriptional machinery to the DNA template [21]. ABCA1 cells were then incubated for 24 h with 10 nM mifepristone in the absence or presence of 100 μM trichostatin A, a class I and II histone deacetylase inhibitor, and DGAT-1 activity and mRNA expression determined. Trichostatin A-treatment reversed the ABCA1-mediated reduction in DGAT-1 activity (Fig. 4a). In addition, trichostatin A-treatment increased the mRNA expression of DGAT-1 in both mock and ABCA1 cells but did not alter DGAT-1 mRNA expression in cells incubated in the absence or presence of mifepristone (Fig. 4b). These data indicate that the expression of ABCA1 reduces DGAT-1 enzyme activity but not DGAT-1 mRNA expression.

Discussion

The objective of this study was to examine if expression of ABCA1 altered cellular glycerolipid de novo biosynthesis in BHK cells. The main findings of this study are; (1) mifepristone inhibits serine uptake and its incorporation into PtdSer and stimulates *myo*-inositol uptake but does not affect PtdIns de novo biosynthesis, (2) expression of ABCA1 stimulates PtdSer de novo biosynthesis from glycerol and OLA precursors, (3) expression of ABCA1 inhibits TAG de novo biosynthesis and this is due to a decrease in DGAT-1 activity and, (4) caution should be exercised when using the mifepristone-inducible gene system for the study of cellular glycerolipid de novo biosynthesis.

Treatment of both mock and ABCA1 cells for 24 h with 10 nM mifepristone resulted in a dramatic increase in *myo*-[^{3}H]inositol uptake but had no effect on *myo*-[^{3}H]inositol incorporation into PtdIns compared to untreated cells

indicating that de novo synthesis of PtdIns from *myo*-[^{3}H]inositol in BHK cells is independent of *myo*-[^{3}H]inositol uptake. This was confirmed in mock and ABCA1 cells incubated with [1-^{14}C]OLA and [1,3-^{3}H]glycerol in which PtdIns synthesis from these precursors was unaltered. On the other hand, 10 nM mifepristone inhibited [^{3}H]serine uptake and its incorporation into PtdSer in both mock and ABCA1 cells indicating that de novo PtdSer synthesis from serine is dependent upon serine uptake in BHK cells. In contrast, PtdSer synthesis from OLA and glycerol precursors was increased possibly as a compensatory mechanism to maintain PtdSer levels. It is possible that the increase in [^{3}H]serine incorporation into PtdSer upon ABCA1 expression in [1-^{14}C]OLA and [1,3-^{3}H]glycerol incubated cells was due to altered movement of newly synthesized PtdSer to the plasma membrane and/or efflux from the cells. However, in the [1,3-^{3}H]glycerol radiolabeling experiments, no protein acceptor (albumin) was present in the medium to bind phospholipid. The fact that the PtdSer content did not change might have been due to an increase in PLA_2 activity towards newly synthesized PtdSer in ABCA1 cells treated with mifepristone. Alternatively, it is possible that the change in PtdSer localization due to ABCA1 expression makes the phospholipid more accessible to PLA_2. To our knowledge this is the first demonstration that *myo*-inositol and serine uptake may be regulated by inhibition of glucocorticoid responsive receptors. In addition, the above findings indicate that caution with the use of the mifepristone-inducible gene system should be exercised when studying cellular processes which may be influenced by uptake of glycerolipid precursor molecules. The level of mifepristone used for ABCA1 induction in our study (10 nM) and incubation time (24 h) are typical of that used for the mifepristone-inducible gene system [22].

Mifepristone (RU486) is a Type I high affinity glucocorticoid antagonist that is known to induce a glucocorticoid receptor conformation capable of binding to DNA [23]. In addition, mifepristone (at 1–1,000 nM) treatment of COS cells transfected with human glucocorticoid receptor α exhibited an increased receptor translocation rate to the nucleus compared to the potent glucocorticoid receptor agonist dexamethasone [24]. These authors hypothesized that upon ligand binding the glucocorticoid receptor undergoes a conformational change, of which the degree correlates with the affinity of the ligand. This conformational change enables the receptor to transiently bind nuclear structures or domains that are immobile or moving slowly, which is reflected in a decrease in the average mobility of the receptors in the nucleus. Previous studies had shown that injection of the glucocorticoid agonist dexamethasone into rats stimulated hepatic TAG synthesis [25] and stimulated hepatic microsomal DGAT activity 22% and the mRNA expression of both DGAT-1 and DGAT-2 [26]. Since BHK cells contain glucocorticoid responsive receptors [27], it is logical to surmise that mifepristone might have had an opposing effect on DGAT activity. A previous study had shown that mifepristone treatment of human amnion cells inhibited [^{14}C]ARA release in either untreated or dexamethasone-treated cells indicating an independent effect of mifepristone from that of dexamethasone [28]. However, in our study in BHK cells mifepristone did not alter DGAT-1 activity in the absence of ABCA1 expression.

DGAT-1 was previously shown to be regulated mainly at the posttranscriptional level in differentiated 3T3-L1 preadipocytes [29]. In addition, protein stability is not a significant factor in the control of DGAT-1 expression. In the current study, expression of ABCA1 in BHK cells resulted in a reduction in de novo biosynthesis of TAG from OLA and glycerol precursors. This reduction in TAG de novo biosynthesis was mediated by a reduction in the enzyme activity of DGAT-1. The histone deacetylase inhibitor trichostatin A blocked the ABCA1-mediated reduction in DGAT-1 enzyme activity but did not affect DGAT-1 mRNA expression indicating that DGAT-1 mRNA expression was not regulated by ABCA1 expression.

Previous studies in murine macrophages and ABCA1-transfected BHK cells indicated that unsaturated fatty acid, but not saturated fatty acid, increased the rate of ABCA1 degradation via destabilization of ABCA1 by increasing the phosphorylation of serine residues of ABCA1 and this was mediated via activation of PKCδ [30, 31]. In the current study, the destabilizing effect of OLA on ABCA1 did not appear to alter PtdSer, DAG or TAG biosynthesis since the changes in biosynthesis of these lipids were similar in ABCA1 cells incubated with [1,3-^{3}H]glycerol in the absence of OLA. A previous study had shown that although the cellular contents of most phospholipids were not significantly altered in cells from Tangier Disease patients, in which ABCA1 is defective, Ptd_2Gro levels were elevated three- to five-fold [32]. In the present corollary study, expression of ABCA1 did not alter Ptd_2Gro levels or the mass of any other major glycerophospholipid.

We observed a markedly elevated expression of ABCA1 protein in BHK ABCA1 cells incubated with mifepritone for 24 h. A previous study had demonstrated over a 60-fold increase in ABCA1 protein expression in BHK ABCA1 cells after an 18 h treatment with mifepritone [11]. This large elevation in ABCA1 protein was associated with a dramatic efflux of cholesterol in the ABCA1 overexpressing cells. It is difficult to interpret the direct physiological effects of ABCA1 overexpression versus the effects of ABCA1 alone on lipid metabolism when the model may vastly and rapidly change various lipid pathways as a compensatory effect resulting in changes in cholesterol and

other biosynthetic pathways. The mechanism of how ABCA1 expression alters DGAT-1 activity is intriguing. Is it due to a particular lipid transport activity of ABCA1 or changes in plasma membrane lipid composition or a direct signaling event that leads to repression of DGAT-1 activity? These questions will form the basis for future studies on how ABCA1 expression regulates DGAT-1 activity. In summary, mifepristone has diverse effects on cellular de novo glycerolipid synthesis in BHK cells. Thus, caution should be exercised when using mifepristone-inducible systems for studies of cellular glycerolipid metabolism in cells which express glucocorticoid responsive receptors.

Acknowledgments This work was supported by Grants from the Canadian Institutes of Health Research (X.Z. and G.M.H.) and from the Heart and Stroke Foundation of Manitoba (G.M.H.). K.H. was the recipient of a Manitoba Institute of Child Health (MICH) Studentship. G.M.H. is a Canada Research Chair in Molecular Cardiolipin Metabolism and a MICH Scientist.

References

1. Vance DE (2002) Glycerolipid biosynthesis in eukaryotes. In: Vance DE, Vance JE (eds) Biochemistry of lipids, lipoproteins and membranes. Elsevier, Amsterdam
2. Fadok WA, Voelker DR, Campbell PA, Cohen JJ, Bratten DL, Henson PM (1992) Exposure of phosphatidylserine on the surface of apoptotic lymphocytes triggers specific recognition and removal by macrophages. J Immunol 148:2207–2216
3. Michel V, Bakovic M (2007) Lipid rafts in health and disease. Biol Cell 99:129–140
4. Voelker DR (1991) Adriamycin disrupts phosphatidylserine import into the mitochondria of permeabilized CHO-K1 cells. J Biol Chem 266:12185–12188
5. Hatch GM, Vance DE (1992) Stimulation of sphingomyelin biosynthesis by brefeldin A and sphingomyelin breakdown by okadaic acid treatment of rat hepatocytes. J Biol Chem 267:12443–12451
6. Van Q, Liu J, Lu B, Feingold K, Shi Y, Lee RM, Hatch GM (2007) Phospholipid scramblase-3 regulates cardiolipin de novo biosynthesis and its resynthesis in growing HeLa cells. Biochem J 401:103–109
7. Oram JF, Vaughan AM (2006) ATP-Binding cassette cholesterol transporters and cardiovascular disease. Circ Res 99:1031–1043
8. Smith JD, Waelde C, Horwitz A, Zheng P (2002) Evaluation of the role of phosphatidylserine translocase activity in ABCA1-mediated lipid efflux. J Biol Chem 277:17797–17803
9. Baulieu EE, Ulmann A, Philibert D (1987) Contragestion by antiprogestin RU 486: a review. Arch Gynecol Obstet 241:73–85
10. Ngan ES, Schillinger K, DeMayo F, Tsai SY (2002) The mifepristone-inducible gene regulatory system in mouse models of disease and gene therapy. Semin Cell Dev Biol 13:143–149
11. Vaughan AN, Oram JF (2003) ABCA1 redistributes membrane cholesterol independent of apolipoprotein interactions. J Lipid Res 44:1373–1380
12. Hatch GM, McClarty G (1996) Regulation of cardiolipin biosynthesis in H9c2 cardiac myoblasts by cytidine 5′-triphosphate. J Biol Chem 271:25810–25816
13. Hatch GM, Smith AJ, Xu FY, Hall AM, Bernlohr DA (2002) FATP1 channels exogenous FA into 1,2,3-triacyl-sn-glycerol and down-regulates sphingomyelin and cholesterol metabolism in growing 293 cells. J Lipid Res 43:1380–1389
14. Cases S, Stone S, Zhou P, Yen E, Tow B, Lardizabal KD, Voelker T, Farese RV (2001) Cloning of DGAT2, a second mammalian diacylglycerol acyltransferase, and related family members. J Biol Chem 276:38870–38876
15. Carman GM, Bae-Lee M (1992) Phosphatidylserine synthase from yeast. Methods Enzymol 209:298–305
16. Hatch GM, Cao SG, Angel A (1995) Decrease in cardiac phosphatidylglycerol in streptozotocin-induced diabetic rats does not affect cardiolipin biosynthesis: evidence for distinct pools of phosphatidylglycerol in the heart. Biochem J 306:759–764
17. Taylor WA, Hatch GM (2009) Identification of the human mitochondrial linoleoyl-Coenzyme A monolysocardiolipin acyltransferase (MLCL AT-1). J Biol Chem 284:30360–30371
18. Rouser G, Fleischer S, Yamamoto A (1970) Two dimensional then layer chromatographic separation of polar lipids and determination of phospholipids by phosphorus analysis of spots. Lipids 5:494–496
19. Lowry OH, Rosebrough NJ, Farr AL, Randall RJ (1951) Protein measurement with the folin phenol reagent. J Biol Chem 193:265–275
20. Takagi M, Yamakawa H, Watanabe T, Suga T, Yamada J (2003) Inducible expression of long-chain acyl-CoA hydrolase gene in cell cultures. Mol Cell Biochem 252:379–385
21. Gallinari P, Di Marco S, Jones P, Pallaora M, Steinkuhler C (2007) HDACs, histone deacetylation and gene transcription: from molecular biology to cancer therapeutics. Cell Res 17:195–211
22. Wang Y, O'Malley BW Jr, Tsai SY, O'Malley B (1994) A regulatory system for use in gene transfer. Proc Natl Acad Sci 91:8180–8184
23. Cadepond F, Ulmann A, Baulieu EE (1997) RU486 (mifepristone): mechanisms of action and clinical uses. Annu Rev Med 48:129–156
24. Schaaf MJM, Cidlowski JA (2003) Molecular determinants of glucocorticoid receptor mobility in living cells: the importance of ligand affinity. Mol Biol Cell 23:1922–1934
25. Lau DC, Roncari DA (1983) Effects of glucocorticoid hormones on lipid-synthetic enzymes from different adipose tissue regions and from liver. Can J Biochem Cell Biol 61:1245–1250
26. Dolinsky VW, Douglas DN, Lehner R, Vance DE (2004) Regulation of the enzymes of hepatic microsomal triacylglycerol lipolysis and re-esterification by the glucocorticoid dexamethasone. Biochem J 378:967–974
27. Johnson TS, Scholfield CI, Parry J, Griffin M (1998) Induction of tissue transglutaminase by dexamethasone: its correlation to receptor number and transglutaminase-mediated cell death in a series of malignant hamster fibrosarcomas. Biochem J 331: 105–112
28. Potestio FA, Olson DM (1990) Arachidonic acid release from cultured human amnion cells: the effect of dexamethasone. J Clin Endocrinol Met 70:647–654
29. Yu YH, Zhang Y, Oelkers P, Sturley SL, Rader DJ, Ginsberg HN (2002) Posttranscriptional control of the expression and function of diacylglycerol acyltransferase-1 in mouse adipocytes. J Biol Chem 277:50876–50884
30. Wang Y, Oram JF (2005) Unsaturated fatty acids phosphorylate and destabilize ABCA1 through a phospholipase D2 pathway. J Biol Chem 280:35896–35903
31. Wang Y, Oram JF (2007) Unsaturated fatty acids phosphorylate and destabilize ABCA1 through a protein kinase C delta pathway. J Lipid Res 48:1062–1068
32. Fobker M, Voss R, Reineke H, Crone C, Assman G, Walter M (2001) Accumulation of cardiolipin and lysocardiolipin in fibroblasts from Tangier disease subjects. FEBS Lett 500:157–162

Lipids (2011) 46:805–811
DOI 10.1007/s11745-011-3568-7

ORIGINAL ARTICLE

Ethanolic Extract of Propolis Promotes Reverse Cholesterol Transport and the Expression of ATP-Binding Cassette Transporter A1 and G1 in Mice

Yang Yu · Yanhong Si · Guohua Song · Tian Luo · Jiafu Wang · Shucun Qin

Received: 10 September 2010 / Accepted: 27 April 2011 / Published online: 3 June 2011

Abstract The ethanolic extract of propolis (EEP) is beneficial in increasing high density lipoprotein (HDL) cholesterol (HDL-C) and diminishing risks of atherosclerosis. In this study, we examined the effects of EEP on reverse cholesterol transport in mice. ^{3}H -cholesterol laden macrophage was injected intraperitoneally into mice fed by gastric gavage with EEP. Plasma lipid level was determined and ^{3}H-cholesterol was traced in plasma, liver and feces. The effects of EEP on ATP-binding cassette transporter A1 and G1 (ABCA1 and ABCG1) and scavenger receptor BI (SR-BI) in mice liver and in cultured cells were also investigated. EEP administration led to a significant increase in HDL-C and peritoneal macrophage-original ^{3}H-cholesterol in plasma, liver and feces. Liver protein expressions of ABCA1 and ABCG1 were increased but SR-B1 was not. In vitro experiments with HepG2 and Raw264.7 cell lines confirmed the above results. The finding of these studies shows that EEP-enhanced reverse cholesterol transport may have resulted from EEP stimulated plasma HDL level and hepatic ABCA1 and ABCG1 expression.

Keywords Ethanolic extract of propolis · Reverse cholesterol transport · High density lipoprotein · ATP-binding cassette transporters A1 · ATP-binding cassette transporters G1 · Scavenger receptor BI

Abbreviations

ABCA1	ATP-binding cassette transporter A1
ABCG1	ATP-binding cassette transporter G1
Ac-LDL	Acetylated low density lipoprotein
ANOVA	Analysis of variance
CPM	Count/min
DMEM	Dulbecco's modified eagle medium
DMSO	Dimethyl sulfoxide
EEP	Ethanolic extract of propolis
FBS	Fetal bovine serum
HDL	High density lipoprotein
HDL-C	High density lipoprotein cholesterol
LDL	Low density lipoprotein
LDL-C	Low density lipoprotein cholesterol
PVDF	Polyvinylidene fluoride
RCT	Reverse cholesterol transport
SDS-PAGE	Sodium dodecyl sulfate polyacrylamide gel electrophoresis
SR-BI	Scavenger receptor BI
TC	Total cholesterol
TG	Triglyceride(s)

Y. Yu · G. Song · T. Luo · S. Qin (✉)
Institute of Atherosclerosis, Taishan Medical University, 2# Yingsheng E Road, Taian 271000, Shandong, People's Republic of China
e-mail: shucunqin@hotmail.com

Y. Si · J. Wang · S. Qin
Department of Basic Medicine, Taishan Medical University, Taian 271000, Shandong, People's Republic of China

Introduction

Atherosclerosis is the principle cause of coronary artery disease and stroke. There is a strong inverse relation between plasma high density lipoprotein cholesterol (HDL-C) levels and the incidence of atherosclerotic cardiovascular diseases. The primary function of high density lipoprotein (HDL) is to mediate reverse cholesterol transport

(RCT), a vital transport fashion of cholesterol metabolism [1]. Excess cholesterol from peripheral tissue is transferred to the liver by HDL for bile acid synthesis and excretion to the feces. Cholesterol efflux from peripheral tissues to HDL is mediated by ATP-binding cassette transporter A1 and G1 (ABCA1 and ABCG1) [1, 2]. Afterward, cholesterol in HDL is transported into hepatocytes through the scavenger receptor BI (SR-BI) [3]. Cholesterol efflux is the initial step of RCT and has become one of the therapeutic targets for atherosclerotic disease [4].

Propolis is a sticky, resinous substance collected by honey bees (*Apis mellifera*) and has been used as a folk medicine from ancient times in South America, Asia and Eastern Europe. The chemical composition of the ethanolic extract of propolis (EEP) is extremely complex and its flavonoid derivatives have been widely cited as its biologically active compounds [5].

Recent studies have indicated that EEP and its subfractions are beneficial in increasing plasma HDL-C level as well as diminishing the risk of atherosclerosis in the rabbit [6–9]. It is therefore conceivable that propolis might play a positive role in RCT. In this study, we examined the effects of EEP on RCT in mice and investigated the change of certain transporters involved in RCT. The results showed that EEP enhances cholesterol transport to the feces, which might be related to an increased plasma HDL-C level and ABCA1 and ABCG1 expression stimulated by EEP.

Materials and Methods

Materials

EEP was obtained from the Taishan bee yard in China. Beeswax was removed and refined. EEP was extracted as described previously [10]. EEP used in this study contained 6.8 mg/mL of flavonoids. Acetylated low density lipoprotein (Ac-LDL) was prepared following a previous study with partial modification [11]. Raw264.7 and HepG2 cell lines were obtained from the American Type Culture Collection (USA). [1,2-^{3}H]-cholesterol was obtained from Perkin-Elmer (USA). Assay kits for triglycerides (TG), high density lipoprotein (HDL)-cholesterol (HDL-C) and low density lipoprotein (LDL)-cholesterol (LDL-C) were from Biosino Bio-technology and Science Inc. Antibodies of ABCA1 and ABCG1 were obtained from Abcam (Cambridge, UK). Antibodies of SR-BI and β-actin were obtained from Novus (USA) and Cell Signaling Technology (USA), respectively.

Animals

Twenty-week old C57BL/6 mice were obtained from the experimental animal center of Peking University, and fed a chow diet and water ad libitum. The mice were kept in a temperature- and humidity-controlled room with a 12/12 h light–dark cycle. This study was approved by the Laboratory Animal Care Committee of Taishan Medical University, and all animal experiments were conducted in accordance with the Guidelines of Care and Use of Laboratory Animals at the Taishan Medical University.

Preparation of ^{3}H-Cholesterol-Laden Cells

Raw264.7 cells were grown in RPMI/HEPES supplemented with 10% FBS. Cells were cultured in Teflon flasks and radiolabeled with 5 μCi/mL ^{3}H-cholesterol and cholesterol loaded with 50 μg/mL acetylated LDL (acLDL). Forty-eight hours later, cells were washed with RPMI/HEPES and equilibrated for 4 h in fresh RPMI/HEPES supplemented with 0.2% BSA, then harvested for mice intraperitoneal injection. Ratio of intracellular ^{3}H-cholesterol and total ^{3}H-cholesterol in cell suspension were determined by liquid scintillation counter (LSC).

In Vivo Experiments

Twelve mice were divided into two groups. The EEP group was dosed with 150 mg/kg EEP once a day for 4 weeks using oral gavage. The control group received only the vehicle (20% pure honey in distilled water) of 10 mL/kg mouse weight. Before injection of Raw264.7 cells, all animals were bled to measure plasma lipid levels (total cholesterol, TC; triglyceride, TG; HDL-C; LDL-cholesterol; LDL-C). On the day of injection, animals were caged individually with access to food and water ad libitum. ^{3}H-Cholesterol-labeled and acLDL-loaded Raw264.7 cells (typically 6.6×10^6 cells containing 1.86×10^6 counts/min [cpm] in 6.2 mL RPMI1640 medium, 0.5 mL/mouse) were injected intraperitoneally as described previously [12]. Both vehicle-treated and EEP-treated mice were injected. Blood was collected at 6, 24, and 48 h after injection, and plasma were used for LSC. Feces were collected continuously at 24 and 48 h and stored at 4 °C before extraction of cholesterol and bile acid. Animals continued to receive vehicle or drug during the 48-h RCT study. At study termination (48 h after injection), mice were exsanguinated and perfused with cold PBS, and portions of the liver were removed and flash-frozen for lipid extraction and protein expression analysis.

Liver ^{3}H-Cholesterol Extraction

Tissue lipids were extracted according to the procedure described previously [13] Results for liver were expressed as percentages of CPM injected (whole organ). Briefly, a 10-mg piece of tissue was homogenized in water, and then lipids were extracted with a mixture of hexane/isopropanol

3:2 (v/v). The lipid layer was collected, evaporated, resuspended in toluene, and counted in a LSC.

Fecal ^{3}H-Tracer Extraction

Feces were weighed and soaked in Millipore water (1 mL water/100 mg feces) overnight at 4 °C. The next day, an equal volume of ethanol was added, and the samples were homogenized. A 200-μL aliquot of each homogenized fecal sample was counted in a LSC to calculate the ^{3}H-total sterols [13].

In Vitro Experiments

Raw264.7 or HepG2 cells were cultured in Dulbecco's Modified Eagle Medium (DMEM) supplemented with 10% fetal bovine serum (FBS). Cultured media was refreshed by DMEM with 1% FBS, 0.1% dimethyl sulfoxide (DMSO) containing various concentrations of EEP (0, 0.2, 1.0, 5.0 μg/mL) for another 48 h incubation. Cells were harvested and stored at −70 °C for Western blot analysis.

Western Blot

Total protein extracted from liver tissue or cultured cell was separated by sodium dodecyl sulfate polyacrylamide gel electrophoresis (SDS-PAGE). The proteins were transferred on polyvinylidene fluoride (PVDF) membranes. Protein levels of ABCA1, ABCG1 and SR-BI were evaluated and referenced with β-actin by Western blot. The target bands were quantified using Image-Pro Plus software ver. 6.0 (Media Cybernetics Corp., USA).

Statistics

Data were reported as means ± standard deviations (SD) and subjected to ANOVA analysis. F test and the Student–Neuman–Keuls post test analyses were performed on these data to analyze the variances and significances between groups. Probability values <0.05 were considered significant.

Results

Effects of EEP on Plasma Cholesterol

Figure 1 shows the effects of EEP on plasma lipid. HDL-C increased significantly by 10% in EEP group compared with the control (74.24 vs. 81.76 mg/dL). Plasma TC also increased significantly in the EEP group by 17% compared with the control (90.28 vs. 106.56 mg/dL). Yet no significant change was observed in either LDL-C or TG levels between the control and EEP group.

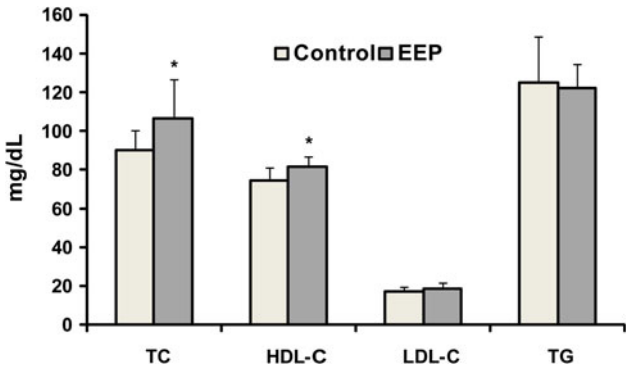

Fig. 1 Plasma HDL-C increased in the EEP Group. Plasma total cholesterol (TC), triglycerides (TG), high density lipoprotein cholesterol (HDL-C) and low density lipoprotein cholesterol (LDL-C) were determined by enzyme methods, respectively. Data (means ± SD, $n = 6$) are expressed as microgram per deciliter. *$P < 0.05$ versus control

Effects of EEP on Reverse Cholesterol Transport

To evaluate the role of EEP in cholesterol transport from peripheral tissue to feces, a classic isotope-labeled cholesterol tracing assay was employed. As shown in Fig. 2a, plasma ^{3}H-labelled cholesterol had increased significantly by 118 and 99% in EEP group at 6 and 24 h, respectively, after injection compared with the control, but there was no significant difference in the ^{3}H-tracer at 48 h. This time course of ^{3}H-cholesterol distribution in plasma suggests that in the first 24 h, EEP enhances cholesterol transport from the macrophages to plasma at the first 24 h. Tritium-labeled cholesterol also increased significantly by 130% in liver from the EEP group compared with the control group (Fig. 2b). The fecal ^{3}H-tracer level was augmented significantly by 49 and 20% in the EEP group at 0–24 h and at 24–48 h, respectively (Fig. 2c).

Effects of EEP on ABCA1, ABCG1 and SR-BI Expression in Mice Liver

Liver protein levels of ABCA1, ABCG1, and SR-BI may involve both HDL formation and RCT. As shown in Fig. 3, ABCA1 and ABCG1 in liver increased significantly (by 28.9 and 140.5%, respectively) in the EEP group compared with the control. No significant change in SR-BI was observed between the EEP and control group.

Effects of EEP on ABCA1, ABCG1 and SR-BI Expression in Cultured Cells

To further elucidate the effect of EEP on ABCA1, ABCG1 and SR-BI, we treated cultured HepG2 and Raw264.7 with EEP in different dosage. When treated with 0.2–5 μg/mL EEP, HepG2 cell showed that both ABCA1 and ABCG1 protein levels increased significantly compared with the

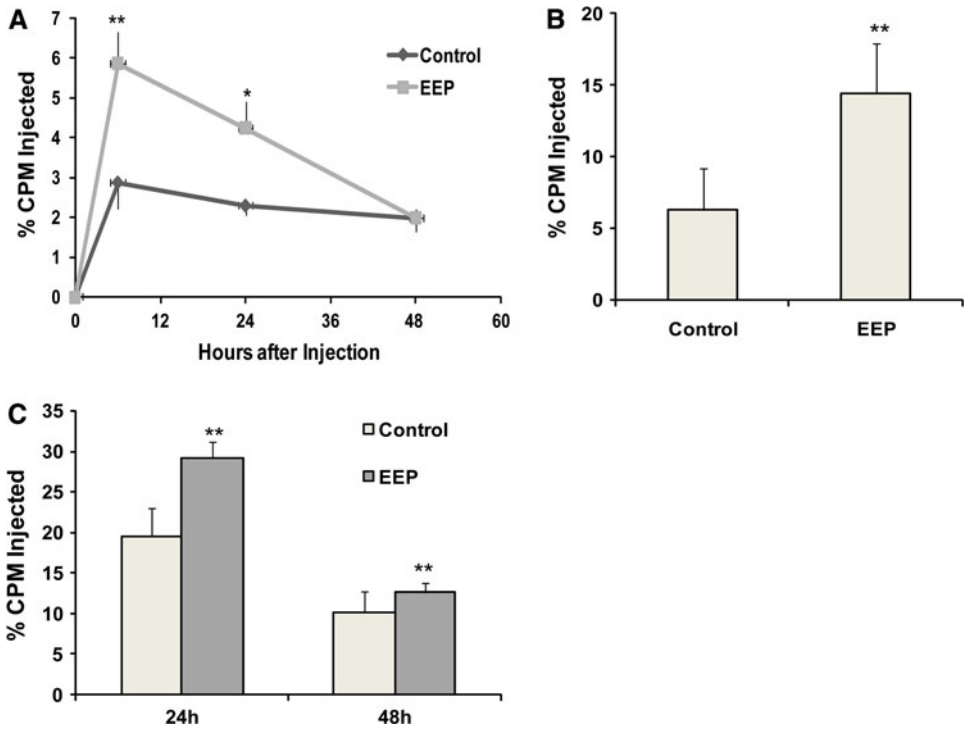

Fig. 2 EEP promoted reverse cholesterol transport in mice. **a** Time course of ^{3}H-cholesterol distribution in plasma. C57BL/6 mice were treated with either vehicle alone or with EEP for 4 weeks. ^{3}H-Cholesterol-labeled and acLDL-loaded Raw264.7 cells (typically 6.6×10^{6} cells containing 1.86×10^{6} counts/min [cpm] in 6.2 mL RPMI1640 medium, 0.5 mL per mouse) were injected intraperitoneally. Plasma was collected at 0, 6, 24, and 48 h after injection for liquid scintillation counting and the levels were expressed as the percentage of total counts per minute (means ± SD, $n = 6$). $^{*}P < 0.05$; $^{**}P < 0.01$ versus control. **b** Liver ^{3}H-cholesterol distribution in mice. C57BL/6 mice were treated with either vehicle alone or with EEP for 4 weeks. ^{3}H-cholesterol-labeled and acLDL-loaded Raw264.7 cells (typically 6.6×10^{6} cells containing 1.86×10^{6} counts/min [cpm] in 6.2 mL RPMI1640 medium, 0.5 mL per mouse) were injected intraperitoneally. At the end of the study (48 h after injection), mice were exsanguinated and perfused with cold PBS, and portions of the liver were removed and flash-frozen for ^{3}H-tracer analysis. The levels were expressed as the percentages of the total counts per minute (means ± SD, $n = 6$). $^{*}P < 0.05$; $^{**}P < 0.01$ versus control. **c** Fecal ^{3}H-tracer distribution in mice. C57BL/6 mice were treated with either vehicle alone or with EEP for 4 weeks. ^{3}H-cholesterol-labeled and acLDL-loaded Raw264.7 cells (typically 6.6×10^{6} cells containing 1.86×10^{6} counts/min [cpm] in 6.2 mL RPMI1640 medium, 0.5 mL per mouse) were injected intraperitoneally. Feces were collected continuously at 24 and 48 h and stored at 4 °C before analysis of ^{3}H-tracer. The levels were expressed as the percentages of the total counts per minute (means ± SD, $n = 6$). $^{*}P < 0.05$; $^{**}P < 0.01$ versus control

control regardless of dosage amount (Fig. 4a). In addition, no significant change of SR-BI expression was observed between EEP and control groups.

In the Raw264.7 cell experiment (Fig. 4b), partially similar to the HepG2 setting, ABCG1 protein levels increased significantly in each EEP group compared with the control, whereas no dose-dependent manner of ABCG1 expression was observed in the groups of higher EEP concentrations (1–5 μg/mL). The ABCA1 expression level was improved significantly in 1 and 5 μg/mL EEP groups only. Additionally, no significant change of SR-BI expression was observed between the EEP and control groups.

Discussion

In this study, we found that EEP promoted the reverse cholesterol transport from intraperitoneal macrophages to feces. This result suggests that EEP plays a positive role in cholesterol transport from peripheral tissue to the liver and secreted into the feces. It is well known that the RCT pathway includes a series of steps beginning in peripheral tissues with the efflux of cholesterol to lipid-poor HDL and ending in the liver and gastrointestinal tract with the secretion of cholesterol into the bile and their removal through the feces. Among this series of steps, HDL and its related cholesterol transporters play a crucial role. In this study our novel findings also indicate that EEP increases plasma HDL-C level and enhances liver ABCA1 and ABCG1 protein expression. The results suggest that EEP may involve increased nascent HDL particle formation, thus leading to an increased plasma HDL concentration and promoting RCT.

Our previous studies in the rabbit [6, 9] reported that EEP could diminish atherogenesis by improving the plasma lipid profile and endothelial function. However,

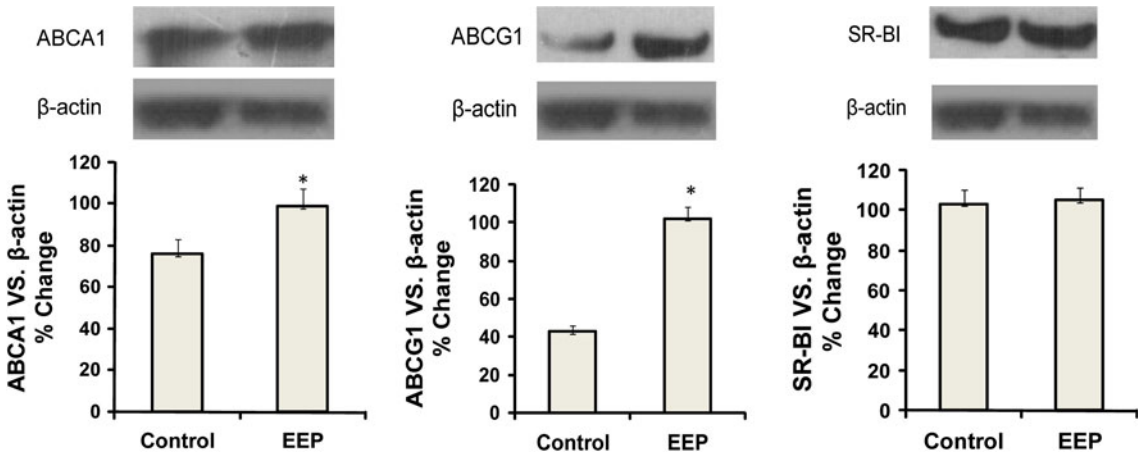

Fig. 3 EEP increased the liver expression of ABCA1 and ABCG1 in mice. Liver protein levels of ABCA1, ABCG1, and SR-BI in mice fed with EEP (EEP) and vehicle (control) group. 20 μg protein of liver tissue from EEP or control were conducted to SDS-PAGE and the proteins were transferred on PVDF membranes for Western blot analysis and quantified by densitometry (see details in "Materials and Methods"). A representative Western blot result from four independent experiments is shown in the (*upper panel*) and the quantification of these proteins is shown in the *down panel*. All values are presented as means ± SD of four independent experiments. $^{*}P < 0.01$ versus control

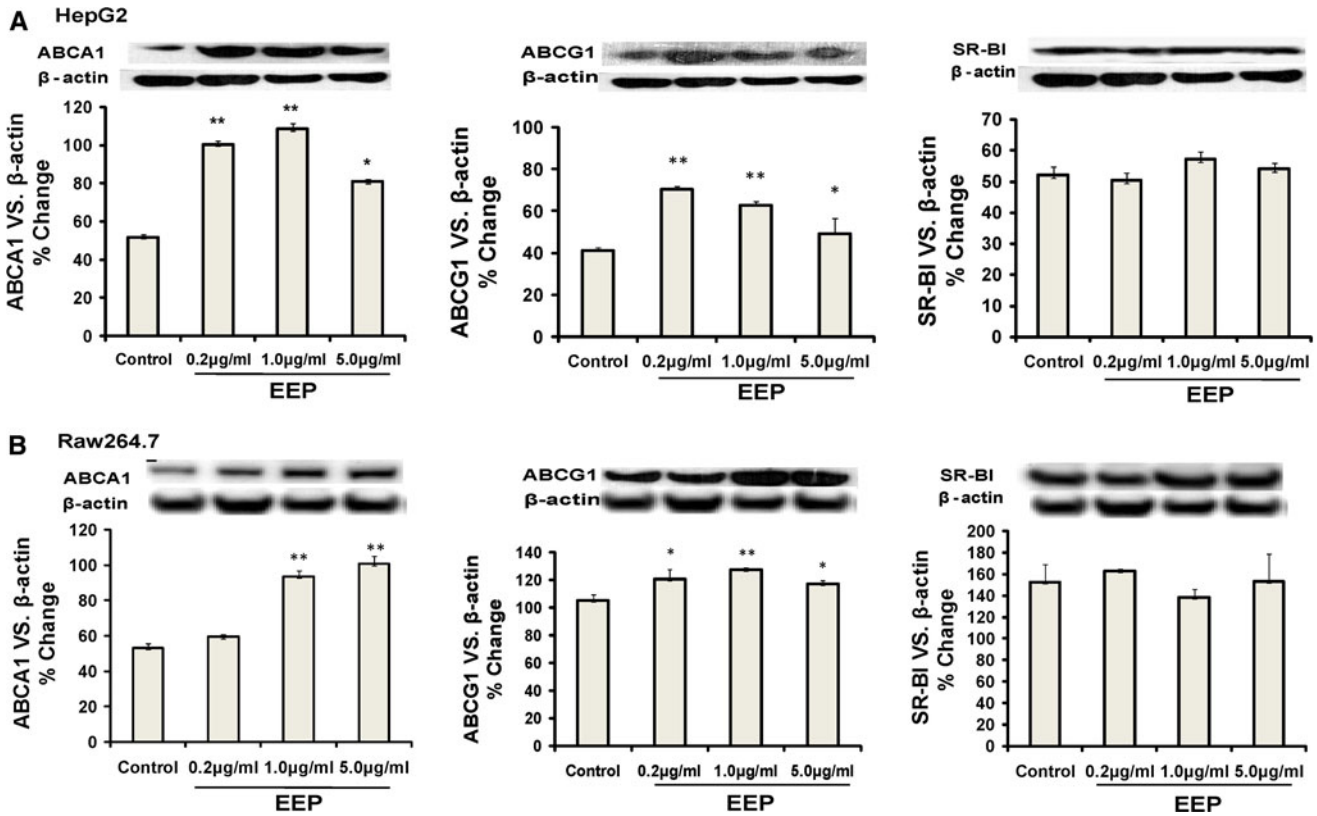

Fig. 4 EEP stimulated the expression of ABCA1, ABCG1 in HepG2 and Raw264.7. Protein levels of ABCA1 and ABCG1 and SR-BI in HepG2 and Raw264.7 were determined with the treatment of EEP in various concentrations (control, 0.2, 1.0, 5.0 μg/mL). Then 20 μg protein of the cells from each group was conducted to SDS-PAGE and the proteins were transferred on PVDF membranes for Western blot analysis and quantified by densitometry (see details in "Materials and Methods"). **a** ABCA1 and ABCG1 and SR-BI expression in HepG2 cell line. **b** ABCA1 and ABCG1 and SR-BI expression in Raw264.7 cell line. A representative Western blot result from four independent experiments is shown in the (*upper panel*) and the quantification of these proteins is shown in the *down panel*. All values are presented as means ± SD of four independent experiments. $^{*}P < 0.05$; $^{**}P < 0.01$ versus control

whether propolis or EEP is beneficial to RCT in the animal model remains unsolved. In this study, our result provides evidence for the first time that EEP can promote reverse cholesterol transport in the murine model for the first time.

ABCA1 and ABCG1 are members of the ABC family of transporters. Many studies have shown that macrophage ABCA1 and ABCG1 play important roles in cholesterol efflux from peripheral tissues to plasma [14]. The main bioactive component of EEP in this study is the phenolic compounds named flavonoids. One in vitro study indicated that a flavonoids pigment, anthocyanins induced cholesterol efflux from mouse peritoneal macrophages and macrophage-derived foam cells by activating liver X receptor α—ABCA1 signaling pathway [15]. Another flavonoids derivates study also demonstrated that procyanidins could attenuate the development of foam cell formation via reducing CD36 expression and enhancing ABCA1 expression [16]. All the studies showed us a phenomenon that flavonoids could stimulate the expression of ABCA1 in macrophages. In the present study, we found EEP not only increased the expression of macrophage ABCA1, but also ABCG1, which might play a role, at least in part, in promoting the first step of RCT by EEP. In addition, the plasma LDL-C level was not affected by EEP treatment, but the HDL-C level was increased by EEP which might also contribute to the enhancement of reverse cholesterol transport by EEP. The elevated TC level by EEP might be attributable to the increased HDL-C level, not LDL-C.

Besides macrophage ABC transporters, previous studies support hepatic ABCA1 exerted anti-atherogenic effect via its contribution to HDL formation [12] and hepatic ABCG1 might mediate hepatocyte cholesterol efflux towards plasma from a pool accessible for biliary secretion [17]. Our results showed that the expression of hepatic ABCA1 and ABCG1 was increased by EEP treatment in vitro and in vivo, these data gave us a clue that the elevated plasma HDL-C level by EEP in this study might be closely associated with the enhanced hepatic ABCA1 and ABCG1 expression stimulated by EEP. Additionally, our unpublished data showed ABCA1 and ABCG1 expressions in endothelial cell were not affected by EEP, which indicated that no other cell types but hepatocyte might be the target contributing to the enhancement of hepatic ABCA1 and ABCG1 expression treated by EEP.

Distribution and regulation of SR-BI are more complex than those of ABCA1 or ABCG1. For instance, hepatic expression of SR-BI is modulated by many factors including farnesoid X receptor, liver X receptors, the liver receptor homolog 1, peroxisome proliferator-activated receptor γ and hepatocyte nuclear factor 4 α. As a result, strong activators or specific stimulatory factors might be effective in promoting SR-BI expression. A recent report has shown that two flavonoids acids in coffee could increase SR-BI and ABCG1 expression and enhance HDL-mediated cholesterol efflux from the macrophages [18]. However, in the present study, no SR-BI change was observed, which probably indicates that EEP employed in this study might be deficient in a component that stimulates SR-BI expression.

Additionally, in the present in vitro experiment we did not observe a dose-dependent manner of enhancement of ABCG1 expression stimulated by EEP. The multi-step regulatory mechanism of ABCA1 and ABCG1 might be the possible reason and the stimulation of EEP (0.2–5 μg/mL) in this study could be attenuated through liver X receptor—ABCA1/ABCG1 signalling pathways. As mentioned above, Uto-Kondo found that dose-dependent manner of ABCG1 and SR-BI expression was observed neither when macrophage was treated with 0.25–0.5 μM caffeic acid nor in ferulic acid [18]. Therefore, the results from this study and from other team's suggest that the effective range of the effect of EEP and flavonoids on the expression of ABCA1 and ABCG1 still needs further investigation.

To summarize, our study showed that EEP promoted cholesterol transport to the plasma and increased expression of ABCA1 and ABCG1 in both in vitro and in vivo experiments. These findings suggest that EEP is an effective substance in improving RCT, one of the contributors to the inhibition of atherosclerosis. The present study adds to the accumulating evidence for bioactive components in cholesterol metabolism. To further understand the promotion of EEP on cholesterol efflux in mice, investigations are required to focus on its isolated bioactive components and signalling pathways involved in RCT. In this study, EEP showed a significant increasing HDL-C effect without affecting LDL-C in plasma, which suggests that EEP and its flavonoids contents may be beneficial in developing medications on atherosclerotic diseases.

Acknowledgments This study was supported by a grant from the "Tai Shan Scholars" foundation of Shandong province (ZD056, ZD057), and by a special foundation of Tai Shan Medical College (1065). We would like to thank Guanghai Zhou and Xinnong Wang for expert technical assistance.

References

1. Lewis GF, Rader DJ (2005) New insights into the regulation of HDL metabolism and reverse cholesterol transport. Circ Res 96(12):1221–1232
2. Oram JF, Vaughan AM (2006) ATP-binding cassette cholesterol transporters and cardiovascular disease. Circ Res 99(10):1031–1043
3. Wang X et al (2007) Macrophage ABCA1 and ABCG1, but not SR-BI, promote macrophage reverse cholesterol transport in vivo. J Clin Invest 117(8):2216–2224

4. Cavelier C, Lorenzi I, Rohrer L, von Eckardstein A (2006) Lipid efflux by the ATP-binding cassette transporters ABCA1 and ABCG1. Biochim Biophys Acta 1761(7):655–666
5. Volpert R, Elstner EF (1993) Biochemical activities of propolis extracts I Standardization and antioxidative properties of ethanolic and aqueous derivatives. Z Naturforsch C 48(11–12): 851–857
6. Nader MA, el-Agamy DS, Suddek GM (2010) Protective effects of propolis and thymoquinone on development of atherosclerosis in cholesterol-fed rabbits. Arch Pharm Res 33(4):637–643
7. Newairy AS, Salama AF, Hussien HM, Yousef MI (2009) Propolis alleviates aluminium-induced lipid peroxidation and biochemical parameters in male rats. Food Chem Toxicol 47(6):1093–1098
8. El-Sayed el SM, Abo-Salem OM, Aly HA, Mansour AM (2009) Potential antidiabetic and hypolipidemic effects of propolis extract in streptozotocin-induced diabetic rats. Pak J Pharm Sci 22(2):168–174
9. Si Y-H et al (2005) Interventional effect of propolis on atherosclerosis induced by hyperlipid in rabbits. Chin J Clin Rehabil 9(35):82–84
10. Koya-Miyata S et al (2009) Propolis prevents diet-induced hyperlipidemia and mitigates weight gain in diet-induced obesity in mice. Biol Pharm Bull 32(12):2022–2028
11. Miyazaki A et al (1994) Acetylated low density lipoprotein reduces its ligand activity for the scavenger receptor after interaction with reconstituted high density lipoprotein. J Biol Chem 269(7):5264–5269
12. Moore RE et al (2005) Increased atherosclerosis in mice lacking apolipoprotein A-I attributable to both impaired reverse cholesterol transport and increased inflammation. Circ Res 97(8):763–771
13. Naik SU et al (2006) Pharmacological activation of liver X receptors promotes reverse cholesterol transport in vivo. Circulation 113(1):5–8
14. Owen JS, Mulcahy JV (2002) ATP-binding cassette A1 protein and HDL homeostasis. Atheroscler Suppl 3(4):13–22
15. Xia M et al (2005) Anthocyanins induce cholesterol efflux from mouse peritoneal macrophages: the role of the peroxisome proliferator-activated receptor {gamma}-liver X receptor {alpha}-ABCA1 pathway. J Biol Chem 280(44):36792–36801
16. Terra X et al (2009) Inhibitory effects of grape seed procyanidins on foam cell formation in vitro. J Agric Food Chem 57(6):2588–2594
17. Wiersma H et al (2009) Lack of Abcg1 results in decreased plasma HDL cholesterol levels and increased biliary cholesterol secretion in mice fed a high cholesterol diet. Atherosclerosis 206(1):141–147
18. Uto-Kondo H et al (2010) Coffee consumption enhances high-density lipoprotein-mediated cholesterol efflux in macrophages. Circ Res 106(4):779–787

Lipids (2011) 46:813–820
DOI 10.1007/s11745-011-3583-8

ORIGINAL ARTICLE

Acute Up-Regulation of Adipose Triglyceride Lipase and Release of Non-Esterified Fatty Acids by Dexamethasone in Chicken Adipose Tissue

Julie Serr · Yeunsu Suh · Shin-Ae Oh · Sangsu Shin · Minseok Kim · J. David Latshaw · Kichoon Lee

Received: 2 May 2011 / Accepted: 8 June 2011 / Published online: 3 July 2011

Abstract The mechanism of adipose tissue lipolysis has not been fully elucidated. Greater understanding of this process could allow for increased feed efficiency and reduced fat in poultry. Studies in avian species may provide important insight in developing therapies for human obesity, as lipolytic pathways are highly conserved. Adipose triglyceride lipase (ATGL) cleaves triacylglycols, releasing non-esterified fatty acids (NEFA) into the bloodstream. Glucocorticoids have been shown to elevate circulating NEFA. To determine the regulation of ATGL and regulator proteins comparative gene identification-58 (CGI-58) and G(0)/G(1) switch gene 2 (G0S2) by glucocorticoid, 36 chickens received an injection of dexamethasone (4 mg/kg). Saline was administered to an additional 12 birds to determine any effect of stress during handling. Dexamethasone-injected birds were harvested at 0, 0.5, 1, 2, 4, and 6 h after treatment; saline-treated birds were collected at 4 and 6 h. Abdominal and subcutaneous adipose tissue and blood were collected. Gene and protein expression were analyzed via quantitative real-time PCR and western blot. Compared with the saline group, ATGL expression increased in birds injected with dexamethasone. When dexamethasone response was compared to the untreated group up to 6 h following injection, an increase in ATGL protein was observed as quickly as 0.5 h and increased further from 1 to 6 h. Plasma NEFA and glucose increased gradually from 0 to 6 h, reaching statistical significance at 4 h. These data show that ATGL expression is stimulated by glucocorticoid in a time-dependent manner.

J. Serr · Y. Suh · S.-A. Oh · S. Shin · M. Kim · J. D. Latshaw · K. Lee (✉)
Department of Animal Science, The Ohio State University, 2029 Fyffe Ct, Columbus, OH 43210, USA
e-mail: lee.2626@osu.edu

Keywords Adipose triglyceride lipase · Chicken · Comparative gene identification-58 · G(0)/G(1) switch gene 2 · Glucocorticoid · Lipolysis

Abbreviations

ATGL	Adipose triglyceride lipase
CGI-58	Comparative gene identification-58
DEX	Dexamethasone
G0S2	G(0)/G(1) switch gene 2
GC	Glucocorticoid(s)
NEFA	Non-esterified fatty acid(s)
qRT-PCR	Quantitative real-time PCR

Introduction

Lipolysis is an important process in animal adipose tissue. Adipose depots are highly adapted to provide energy as glycerol and fatty acids in times of stress, nutrient deprivation, or high activity or to store excess energy as triacylglycerides in a postprandial state. The ability to switch quickly and efficiently between catabolic and anabolic states in adipose is important for survival; therefore, proteins involved in lipolytic and lipogenic processes are highly regulated at multiple levels.

Understanding the mechanisms of adipose tissue lipolysis is of great importance in animal agriculture. The maximization of feed efficiency is a chief concern to producers, decreasing the energy stored in fat and increasing the energy directed toward lean muscle growth is a key concept in providing lean meat at a low cost. Additionally, as the lipolytic pathways are highly conserved across species, enhancing our knowledge of the regulation of lipolysis may be beneficial in developing new therapies for

human obesity. Adipose triglyceride lipase (ATGL) is the rate-limiting enzyme in triacylglycerol hydrolysis [1, 2]. The regulation of ATGL is not yet fully understood.

Recently, studies in mice have shown that ATGL is stimulated by the synthetic glucocorticoid, dexamethasone [3]. Glucocorticoids (GC) are an end product of the hypothalamic-pituitary-adrenal axis and have a variety of metabolic effects to maintain energy homeostasis during stress [4]. Glucocorticoids regulate adipose differentiation, function, and distribution and in excess, promote hyperlipidemia [5]. Daily GC exposure has been shown to decrease body weight and feed intake in broiler chickens after 2 weeks, however, no significant long-term changes in ATGL expression were observed at the conclusion of the study [6]. It is the hypothesis of this study that injection of dexamethasone may acutely increase ATGL expression and increase plasma fatty acids in broiler chickens.

Materials and Methods

Experimental Animals

Animal care and experimental procedures were approved by the OSU Institutional Animal Care and Use Committee. Experimental animals were allowed ad libitum access to food and water throughout the experiment. To investigate the effect of glucocorticoid administration in vivo, 30 Ross 308 broiler chickens, 25 days old, were injected with a synthetic glucocorticoid, dexamethasone (DEX; 4 mg/kg). At 0.5, 1, 2, 4, and 6 h following injection, six birds were euthanized via CO_2 inhalation. Six additional chickens were euthanized without receiving a DEX injection to be used as a negative control; an additional 12 chickens received saline injections as a placebo and were harvested 4 and 6 h after injection. Tissue samples were collected from abdominal and subcutaneous adipose depots and snap frozen in liquid nitrogen. Prior to euthanasia, blood samples were collected via cardiac puncture and cooled on ice. Tissues were kept at −80 °C for analysis by western blot, RNA isolation, and quantitative real-time PCR (qRT-PCR). Blood samples were centrifuged at 1,700×*g* at 4 °C for 10 min to obtain plasma for glucose, insulin, and non-esterified fatty acid (NEFA) assays.

Primary Cell Culture and In Vitro Treatments

Abdominal adipose tissue was obtained from an adult broiler chicken. Primary cells were cultured by a procedure which has been previously described [7]. Adipose tissue was washed in PBS, finely minced and incubated, shaking, at 37 °C in a digestion buffer containing 2 mg/mL collagenase I (5 mL per gram of tissue). After 45 min, the tissue was passed through nylon strainers with 100 μm openings. The filtered cells were centrifuged to separate floating adipocytes from pelleted stromal-vascular cells. The pellet was washed in fresh DMEM, centrifuged, and re-suspended in DMEM medium containing 5% chicken serum to a concentration of 6×10^6 cells/mL. Cells were seeded in 12-well plates at a density 3×10^6 cells/mL and maintained in a humidified incubator at 37 °C, 5% CO_2. When the cells reached 50% confluence, the cell media was altered to contain 5% chicken serum and 50 mm linoleic and oleic acids in DMEM to induce adipocyte differentiation. Cells were maintained in this media for 2 days, at which point there was visible lipid accumulation in the cells. All cells were serum-starved for 3 h prior to treatment by incubation in DMEM alone. The cells were then treated at the indicated time-points by removing the media and replacing it with fresh DMEM for control cells, or 1,000 nM DEX in DMEM. Cells were treated at −12, −6, −3 and 0 h prior to collection of cells in Trizol reagent for RNA isolation.

RNA Isolation and Quantitative Real-Time PCR

Tissue samples were homogenized in Trizol reagent (Invitrogen, Carlsbad, CA) using a Tissuemiser homogenizer (Fischer Scientific, Pittsburgh, PA). Total RNA was isolated according to the manufacturer's protocol. The quality and relative quantity of RNA was assessed via gel electrophoresis. To investigate mRNA expression of ATGL, comparative gene identification-58 (CGI-58) and G(0)/G(1) switch gene 2 (G0S2), cDNA was generated by reverse transcription using 1 μg total RNA and M-MLV RT (Moloney murine leukemia virus reverse transcriptase, Invitrogen) according to the manufacturer's protocol using OligoDT as the primer. Reverse transcription conditions for cDNA amplification were as follows: 65 °C for 5 min, 37 °C for 52 min, and 70 °C for 15 min. Relative gene expression was quantified by SYBR green real-time PCR on an ABI 7300 real-time PCR Instrument (Applied Biosystems, Foster City, CA). Primer sequences for the ATGL, G0S2, and β-actin genes have been described in our previous reports [7, 8]. Primer sequences for the chicken CGI-58 gene are forward primer 5′-ACC GTG GTT TAT GGA GCA CG-3′ and reverse primer 5′- GAA ACA GTG TGC AAA CAG AGC C-3′. Forward and reverse primers were designed to span genomic introns (> 1 Kb) to avoid the amplification of genomic DNA that may have been present. PCR was performed using AmpliTaq Gold polymerase (Applied Biosystems) with SYBR green as a detection dye. Reactions were performed in duplicate 25 μL reactions. Conditions for qRT-PCR were 95 °C for 10 min, 40 cycles of 94 °C 15 s, 60 °C 40 s, 72 °C 30 s, and 82 °C 33 s. The comparative $2^{-\Delta\Delta Ct}$ method for relative quantification [9]

was used to calculate the relative gene expression (as determined by ABI software). Beta-actin was used as the housekeeping gene to normalize the qRT-PCR calculation.

Protein Isolation and Western Blot Analysis

For protein analysis, adipose samples were homogenized in ice-cold 1X lysis buffer (62.5 mM Tris, 5% SDS) with a tissuemiser and combined with 2× Laemmli buffer (Bio-Rad Laboratories, Hercules, CA) containing 62.5 m*M* Tris, 1% SDS, 5% 2-mercaptoethanol, 12.5% glycerol, 0.05% bromophenol blue. Proteins were separated by SDS-PAGE and wet-transferred to a 0.45 μm pore polyvinylidine fluoride membrane (GE Biosciences, Piscataway, NJ). Membranes were blocked in 5% nonfat dry milk in Tris-buffered saline-Tween (TBST; 20 mM Tris, 150 mM NaCl, pH 7.4, plus 0.15% Tween 20) for 1 h at room temperature. Membranes were incubated overnight at 4 °C in primary antibodies ATGL (1:1,000 dilution; Cell Signaling Technology, Inc., Danvers, MA) or α-tubulin (1:7,000 dilution; Developmental Studies Hybridoma Bank, The University of Iowa, Iowa City, Iowa). The specificity of the ATGL antibody to avian ATGL has been demonstrated previously [8]. Membranes were then washed in TBST for 1 h and incubated with horseradish peroxidase-conjugated secondary antibodies (Santa Cruz Biotechnology Inc., Santa Cruz, CA) for 2 h at room temperature. Membranes were washed again for 1 h in TBST followed by detection with ECL Plus (GE Biosciences). The membranes were exposed to Bio-Max X-ray film (GE Biosciences) for visualization of the ATGL and α-tubulin proteins.

Plasma Parameter Analysis

Blood samples were collected in tubes containing sodium heparin (BD Medical, Franklin Lakes, New Jersey), cooled on ice, and centrifuged at 1,700×*g* for 10 min at 4 °C to separate plasma. Glucose was measured by glucose oxidase method using Autokit Glucose Enzymatic Method (Mutarotase-GOD) (Wako Pure Chemical Industries Ltd., Osaka, Japan). Non-esterified fatty acid (NEFA) concentration was measured with the HR Series NEFA-HR (2) ACS-ACOD kit (Wako Pure Chemical Industries Ltd.) at the Laboratory of Veterinary Diagnostic Medicine at the University of Illinois. Plasma insulin determination was performed using an Insulin RIA kit (Diagnostic Systems Laboratories, Inc, Webster, TX) at the Michigan State University Diagnostic Center for Population and Animal Health.

Gene Promoter Analysis

Transcription factor binding sites on the promoter region of the ATGL gene were identified by entering the nucleic acid sequence into the MatInspector program version 8.0 (Genomatrix software).

Statistical Analysis

Comparison of gene expression and plasma metabolites between saline- and DEX-treated chickens was done by a Student's *t* test. Time-dependent plasma parameters and qRT-PCR data were analyzed by the PROC GLM procedure of the SAS software system (version 9.1, SAS Institute Inc., Cary, NC). Individual comparisons between groups are by one-way ANOVA followed by Tukey's test.

Results

To ensure any changes in gene expression were not due to the stress of handling, DEX treated birds were compared with birds injected with saline as a placebo. When compared with saline-injected birds, qRT-PCR data reveal a significant increase of ATGL mRNA expression in DEX-injected birds in both the abdominal and subcutaneous adipose depots (Fig. 1a, b). Western blot analysis shows that ATGL protein responds similarly, with greater expression in the DEX treatment group over the placebo group (Fig. 1c, d). Plasma measurements of NEFA and glucose were compared between saline- and DEX- injected birds. In the DEX group, NEFA was greater 4 and 6 h after treatment ($P < 0.05$) than that of the saline group; plasma glucose was clearly elevated at in the DEX-treated birds (Fig. 2).

Quantitative RT-PCR was performed to investigate the mRNA expression of ATGL and regulatory proteins, comparative gene identification-58 (CGI-58) and G(0)/G(1) switch gene 2 (G0S2) following DEX treatment. In subcutaneous fat, ATGL expression begins increasing incrementally at 1 h post-injection, and is significantly elevated from basal expression at 4 and 6 h ($P < 0.05$; Fig. 3a). The mRNA expression of CGI-58 is not significantly altered with treatment, though G0S2 is decreased slightly from control levels at 1 h, and it increases significantly thereafter, reaching peak expression at 6 h (Fig. 3b, c). In abdominal fat, ATGL expression increased starting 2 h following DEX injection, reaching its highest expression at 6 h, a 12-fold increase ($P < 0.05$; Fig. 4a). Similar to the pattern seen in subcutaneous fat, changes in CGI-58 expression were negligible and G0S2 decreased slightly following injection (0.5–1 h) and increased about 5-fold at 4 h ($P < 0.05$; Fig. 4b, c).

To evaluate acute changes in ATGL protein following glucocorticoid exposure, Western blot analysis was performed for 0, 0.5, 1, and 2 h after treatment. Subcutaneous and abdominal fat both showed increases in ATGL protein following DEX injections (Fig. 5). The subcutaneous fat

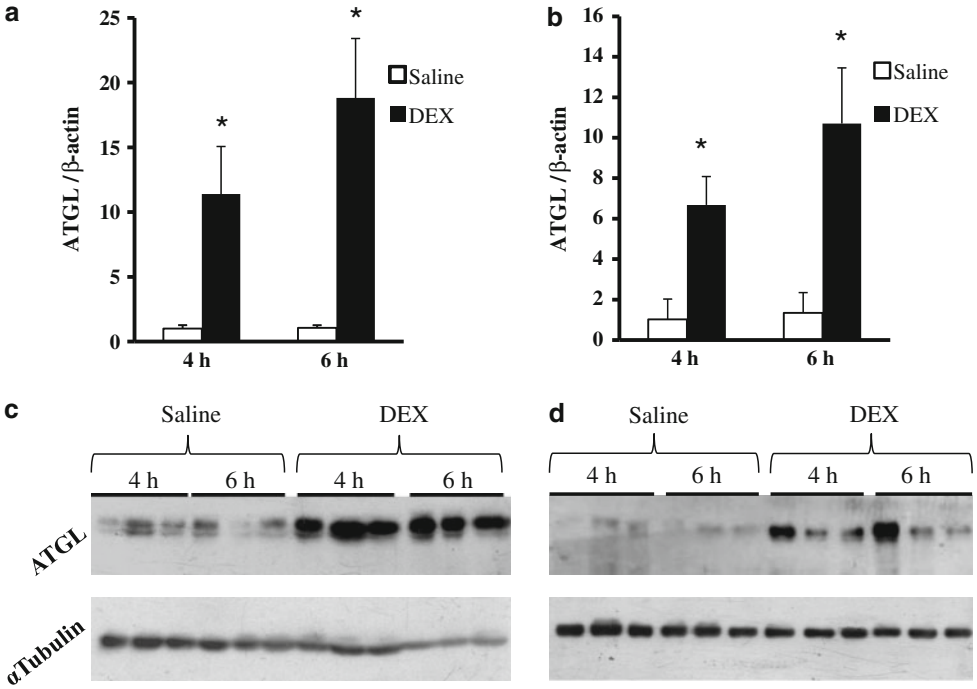

Fig. 1 Expression of adipose triglyceride lipase (ATGL) in chickens following saline or dexamethasone (DEX) injection. The mRNA expression of ATGL was measured by quantitative Real-Time PCR in **a** abdominal and **b** subcutaneous adipose tissue of chickens injected with saline or DEX (4 mg/kg). *β*-actin was used as a housekeeping gene. Unfilled and filled bars represent samples collected 4 h and 6 h post-injection, respectively. *Bars* represent mean ± SEM, with * indicating ($P < 0.05$) between treatments. Expression of ATGL protein was visualized by Western blot analysis of cell lysates from **c** abdominal **d** abdominal fat of chickens injected with saline or DEX. α-Tubulin was used to normalize loading

exhibits increased ATGL at 0.5 h; abdominal expression is apparently greater at 1 h. The slightly delayed ATGL protein expression in abdominal fat compared to subcutaneous fat is concordant with mRNA expression in these depots.

To evaluate the effect of DEX on fatty acid release, plasma NEFA was measured (Fig. 6a). Plasma NEFA increased gradually following DEX-injection reaching its greatest levels at 4 and 6 h ($P < 0.05$), concurrent with peak ATGL mRNA expression. Daily treatment with dietary glucocorticoid has been associated with hyperinsulemia and hyperglycemia in chickens [10]. We measured plasma insulin and glucose to determine if there is an acute response to dexamethasone. Glucose increases steadily from 0.5 to 6 h following treatment, whereas insulin increases up to 2 h (Fig. 6b, c). At 4 h post-injection, insulin levels return to those seen in control birds.

In a whole-body system, there are numerous factors that may alter gene expression in response to exogenous chemicals. To test whether ATGL expression is altered directly by dexamethasone or through indirect mechanisms, we treated cultured chicken adipocytes with DEX for 0, 3, 6, and 12 h. In DEX-treated adult chicken adipocytes, mRNA expression of ATGL is increased by 13-fold at 3 h ($P < 0.05$; Fig. 7). We also measured the expression of CGI-58 and G0S2, which were largely unchanged.

Discussion

Glucocorticoids, primarily corticosterone in chickens, are the final effectors of the hypothalamic–pituitary–adrenal axis [6]. Synthesis of GC occurs in the adrenal cortex and has a wide array of metabolic effects to maintain homeostasis during times of stress [4], including the elevation of circulating free fatty acids and hepatic glucose [3, 10]. Multiple mechanisms for GC-enhanced lipolysis have been suggested, including through the activation of cAMP-dependent hormone sensitive lipase [11], "permissive" effects through disrupted insulin signaling, and direct action on ATGL [3]. The primary objective in this study is to determine the acute regulation of ATGL by glucocorticoid in broiler chickens.

Handling is a known stressor to broiler chickens. To ensure any responses observed were not due to handling during injection, a saline injection was administered to two groups of chickens as a placebo and compared with the DEX groups. The marked increase in ATGL expression and plasma NEFA in the DEX groups over saline groups support that there is a physiological response specifically to the dose of DEX administered. Over the course of 6 h, ATGL mRNA and protein expression increases in abdominal and subcutaneous fat, concurrent with a gradual increase in plasma NEFA. These changes occur quickly after injection (about 1 h); we suspect such an early onset of this response is unlikely to be through an indirect mechanism involving other hormones, but may occur at the cellular level within adipose tissue.

To provide further support for CG regulation of ATGL at the cellular level, we treated cultured chicken adipocytes with DEX over a period of 12 h. After 3 h incubation with DEX, ATGL expression increased dramatically (13-fold). Interestingly, at 6 h, when in vivo ATGL expression is

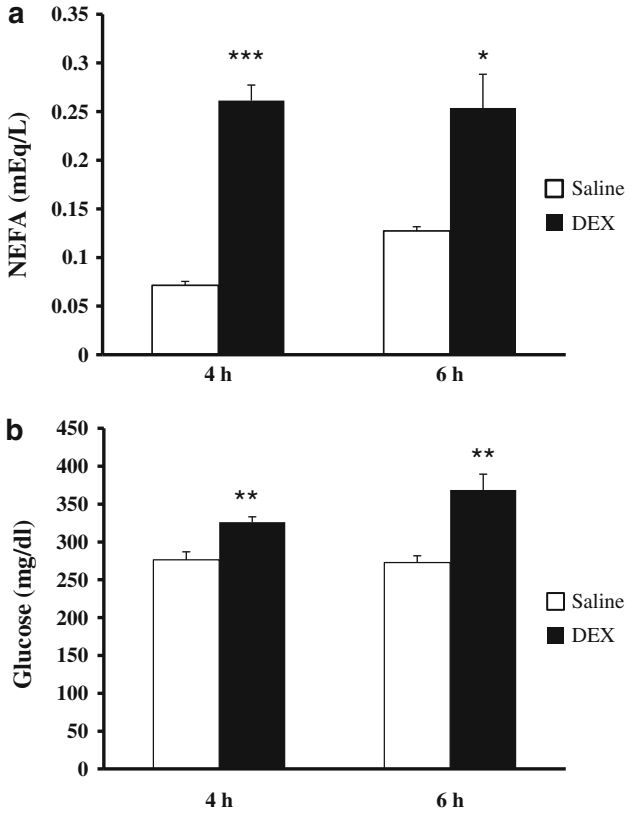

Fig. 2 Plasma parameters of chickens following injection of saline or dexamethasone (DEX). **a** Non-esterified fatty acids (NEFA) measured in mequiv/l. **b** Plasma glucose measured in mg/dl. *Unfilled bars* represent samples collected 4 h after injection; *filled bars* represent collection 6 h following injection. *Bars* represent means ± SEM, with * indicating ($P < 0.05$), ** is ($P < 0.01$) and *** is ($P < 0.001$) by *t* test between treatments

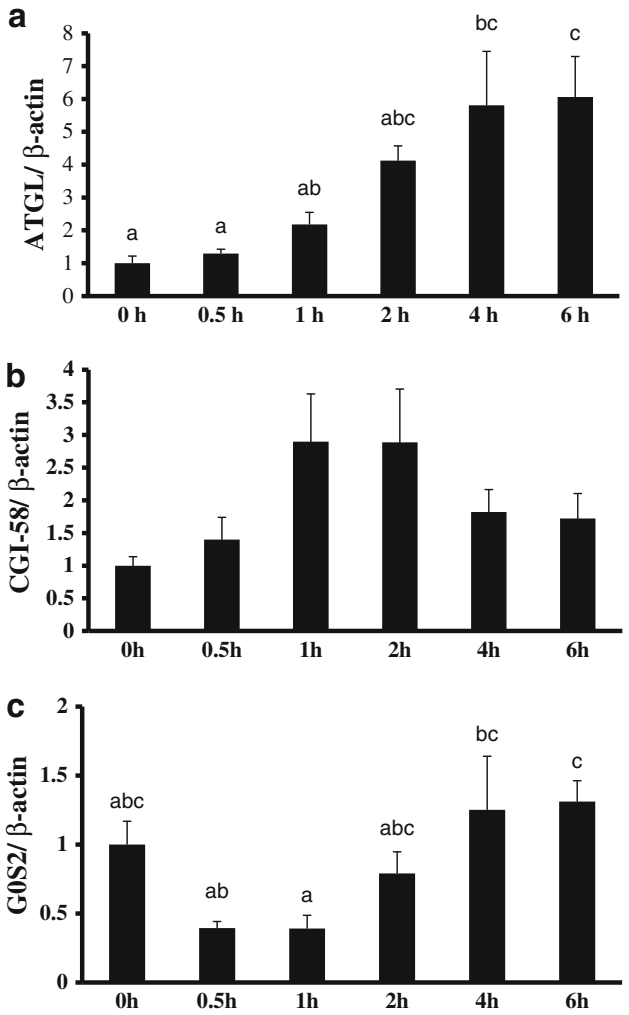

Fig. 3 Relative mRNA expression of **a** adipose triglyceride lipase (ATGL) **b** comparative gene identification-58 (CGI-58), and **c** G(0)/G(1) switch gene 2 (G0S2) in subcutaneous adipose tissue of dexamethasone-injected broiler chickens. Treated birds were collected 0.5–6 h following injection ($n = 6$). Untreated control birds are indicated as 0 h. Quantitative Real-Time PCR was performed to determine relative gene expression. *Bars* represent means ± SEM, with differing letters indicating statistical significance ($P < 0.05$) by one-way ANOVA followed by Tukey's test

greatest, the in vitro expression has decreased by more than half of its peak expression. This observation has led us to postulate that the regulation of ATGL by dexamethasone may occur in two waves: (1) transcriptional regulation in the very short-term, and (2) through reduced insulin signaling within several hours. Immediate transcriptional regulation by steroid hormones can occur through hormone response elements present on the 5' flanking region of the target gene [12]. Using the MatInspector program version 8.0 (Genomatrix software), transcription factor binding sites were analyzed in the nucleic acid sequence of the ATGL. Five glucocorticoid response elements were identified at −4602 {ctgGGACagagcgtcctaa (−)}, −3787 (aaaGAACagttaattcttt (−)), −3334 {agaGAACatccagttacca (−)}, −2044 {aggGAACaaaaggtcccat (+)}, and −907 {gtaGCACatgtggtgatgt (+)} bp upstream of the transcription start site. The presence of these response elements, combined with the observed increase in ATGL expression in an insulin-free in vitro system, suggests direct transcriptional regulation by GC. Insulin promotes triacylglycerol storage in adipose tissue, and is reported to downregulate ATGL expression [13]. In addition, insulin introduced in cultured rat adipose cells is capable of blocking DEX-stimulated fatty acids release [14]. Our plasma analysis revealed that insulin concentration increases 0.5–2 h after DEX injection, and begins to taper to basal levels at 4 h. Interestingly, glucose and NEFA continue to elevate concurrent with increased insulin following injection, demonstrating some insensitivity. We believe that decreased insulin sensitivity and secretion may permit increased ATGL expression and fatty acid release through the absence of insulin-mediated suppression, though future research should be conducted to confirm this hypothesis.

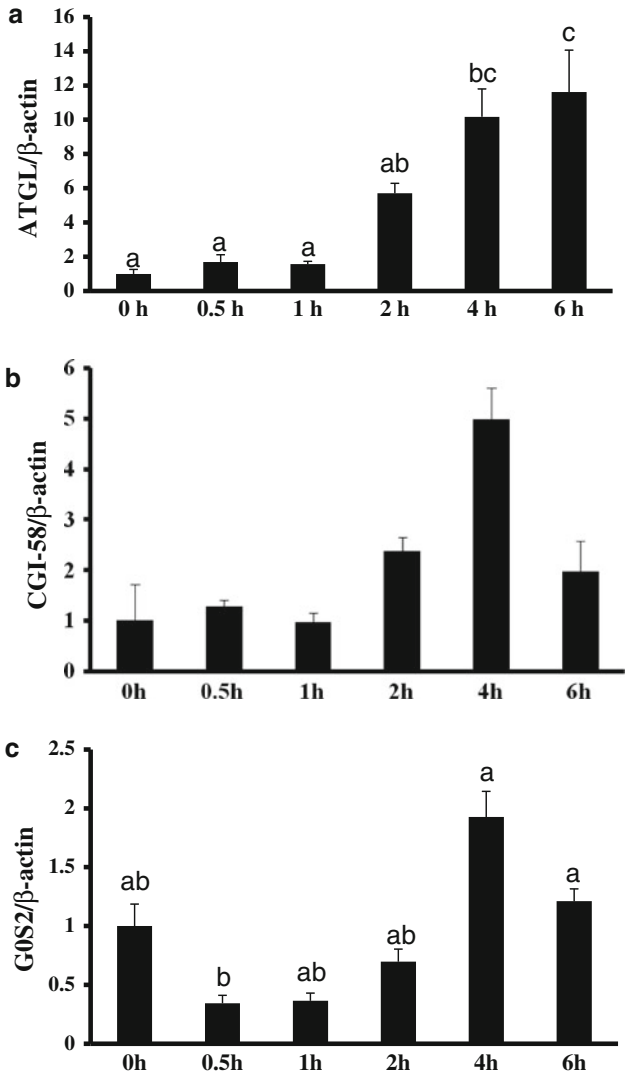

Fig. 4 Relative mRNA expression in abdominal adipose tissue of dexamethasone-injected broiler chickens. Total RNA was isolated from abdominal fat of treated birds collected 0.5–6 h following injection ($n = 6$). Untreated control birds are indicated as 0 h. Quantitative Real-Time PCR was done to determine relative expression of **a** adipose triglyceride lipase (ATGL), **b** comparative gene identification-58 (CGI-58), **c** G(0)/G(1) switch gene 2 (G0S2). *Bars* are means ± SEM. Letters represent a significant difference ($P < 0.05$) among groups at various time points

Recent studies have reported that ATGL activity may be regulated through interactions with activator protein CGI-58 and inhibitor protein G0S2. Upon stimulated lipolysis, mammalian CGI-58 co-localizes with ATGL on the lipid droplet surface. Disruption of this interaction results in complete inability of CGI-58 to activate ATGL-mediated triacylglyceride hydrolysis [15]. Conversely, G0S2 interaction with ATGL inhibits its activity as a lipase [16]. We have recently observed that upregulation of ATGL during fasting in chickens occurs simultaneously with increased CGI-58 expression [17, 18] and decreased expression of

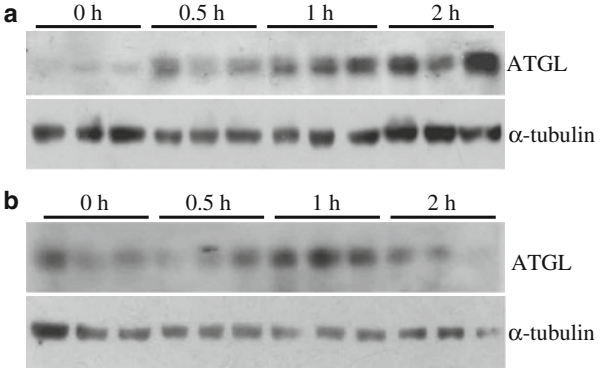

Fig. 5 Western blot analysis of adipose triglyceride lipase (ATGL) protein following dexamethasone injection. Protein lysates of **a** subcutaneous and **b** abdominal adipose tissue were separated by SDS-PAGE. α-Tubulin was used as a loading control. ATGL protein was determined at 0.5, 1, and 2 h following treatment, 0 h indicates control birds receiving no treatment

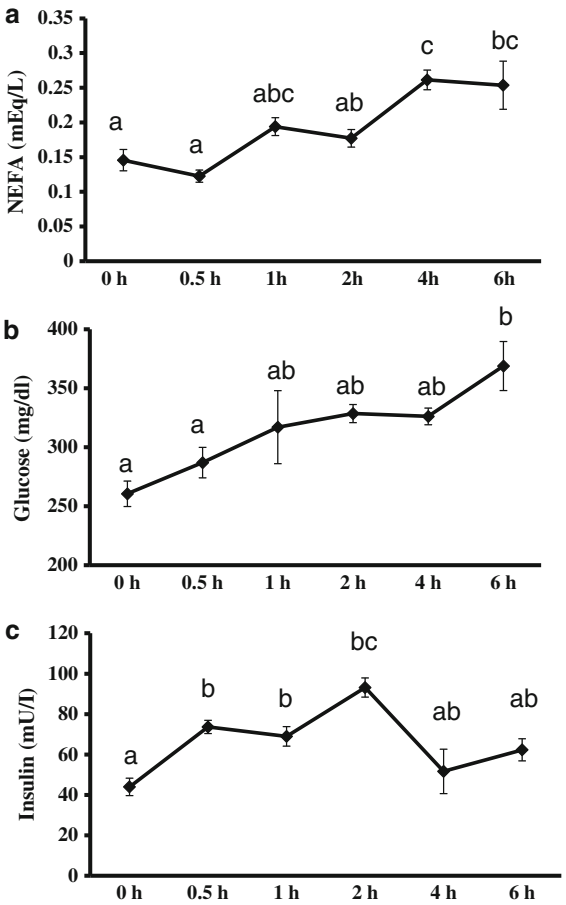

Fig. 6 Plasma parameters obtained from chickens injected with dexamethasone. Blood samples were collected via cardiac puncture at 0.5–6 h following dexamethasone (4 mg/kg) injection. A no-treatment control group is indicated by 0 h. **a** Plasma non-esterified fatty acids (NEFA) reported in mequiv/l. **b** Plasma glucose measured in mg/dl. **c** Plasma insulin concentrations measured in mU/I. Data points represent means ± SEM, with differing letters indicating statistical significance ($P < 0.05$)

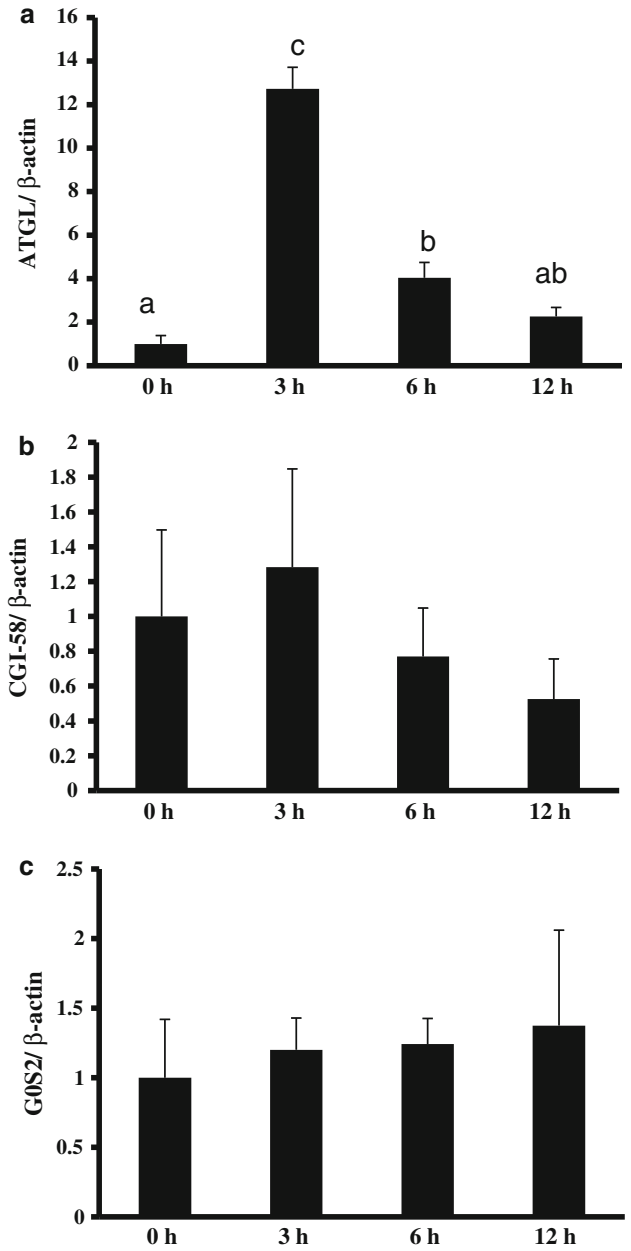

Fig. 7 Relative mRNA expression in dexamethasone (DEX)-treated cultured chicken adipocytes. Quantitative Real-Time PCR was performed to determine relative gene expression in cultured chicken adipocytes in DMEM (0 h) or DMEM containing 1000 nM DEX (incubated from 3–12 h). Relative expression of **a** adipose triglyceride lipase (ATGL); **b** comparative gene identification-58 (CGI-58); (C) G(0)/G(1) switch gene 2 (G0S2). *Bars* represent means ± SEM, Different letters indicating statistical significance ($P < 0.05$) between groups

G0S2 [7], suspecting that changes in regulator protein expression contributes to NEFA release during nutrient deprivation. To evaluate whether regulatory proteins are involved in GC-stimulated lipolysis, we measured the expression of CGI-58 and G0S2 during our in vivo and in vitro DEX treatments. Only negligible changes in CGI-58 expression were observed in both experiments. Interestingly, G0S2 expression decreased slightly immediately following DEX injections in vivo. It has been reported by Lu and colleagues that overexpression of ATGL in G0S2-expressing HeLa cells failed to enhance lipolytic activity as it did in non-G0S2 control cells [19]. We therefore suspect that downregulation of G0S2 may be necessary at some point in stimulated lipolysis. It is possible that GC may directly regulate G0S2 within 1 h of exposure; however, additional research is needed to support this hypothesis. Further study is needed, also, to determine if GC may regulate ATGL-mediated lipolysis through changes in physical interaction between ATGL, CGI-58, and G0S2.

In summary, we investigated the effect of exogenous glucocorticoids on the expression of ATGL in chickens. Our analyses show that ATGL mRNA and protein are stimulated by DEX in vitro and in vivo, contributing to increased plasma NEFA. The increased ATGL expression following DEX treatment may result from a combination of direct transcriptional regulation at hormone response elements and disrupted insulin signaling. A known activator of ATGL, CGI-58, does not appear to respond to DEX stimulation. The ATGL-inhibitor G0S2 may have some immediate transcriptional response, though further research is needed to confirm this.

Acknowledgments This work was supported by the Edna Jaap Poultry Endowment Fund (K. Lee).

References

1. Zimmermann RJ, Strauss JG, Haemmerle G, Schoiswohl G, Birner-Gruenberger R, Riederer M, Lass A, Neuberger G, Eisenhaber F, Hermetter A, Zecher R (2004) Fat mobilization in adipose tissue is promoted by adipose triglyceride lipase. Science 306:1383–1386
2. Haemmerle G, Lass A, Zimmermann R, Gorkiewicz G, Meyer C, Rozman J, Heldmaier G, Maier R, Theussl C, Eder S, Kratky D, Wagner EF, Klingenspor M, Hoefler G, Zechner R (2006) Defective lipolysis and altered energy metabolism in mice lacking adipose triglyceride lipase. Science 312:734–737
3. Xu C, Jinhan H, Jiang H, Zu L, Zhai W, Pu S, Xu G (2009) Direct effect of glucocorticoids on lipolysis in adipocytes. Mol Endocrinol 23:1161–1170
4. Matteri RL, Carroll JA, Dyer CJ (2000) Neuroendocrine responses to stress. In: Moberg GP, Mench JA (eds) The biology of animal stress, CAB International, Wallingford
5. Masuzaki H, Paterson J, Shinyama H, Morton NM, Mullins JJ, Seckl JR, Flier JS (2001) A transgenic model of visceral obesity and the metabolic syndrome. Science 294:2166–2170
6. Cai Y, Song Z, Zhang X, Wang X, Jiao H, Lin H (2009) Increased de novo lipogenesis in liver contributes to the augmented fat deposition in dexamethasone exposed broiler chickens (Gallus gallus domesticus). Comp Biochem Physiol C 150:164–169
7. Oh SA, Suh Y, Pang MG, Lee K (2010) Cloning of avian G(0)/G(1) switch gene 2 (G0S2) genes and developmental and nutritional regulation of G0S2 in chicken adipose tissue. J Anim Sci 89:367–375

8. Lee K, Shin J, Latshaw JD, Suh Y, Serr J (2009) Cloning of adipose triglyceride lipase in poultry and expression of adipose triglyceride lipase during development of adipose in chickens. Poult Sci 88:620–630
9. Livak KJ, Schmittgen TD (2001) Analysis of relative gene expression data using real-time quantitative PCR and the 2 (–Delta Delta C(T)). Methods 25:402–408
10. Dupont J, Derouet M, Simon J, Taouis M (1999) Corticosterone alters insulin signaling in chicken muscle and liver at different steps. J Endocrinol 162:67–76
11. Cahill GF Jr (1971) Action of adrenal cortex steroids on carbohydrate metabolism. In: Christy NP (ed) The human adrenal cortex, Harper and Row, New York
12. Aranda A, Pascual A (2001) Nuclear hormone receptors and gene expression. Physiol Rev 81:1269–1304
13. Kim JY, Tillison K, Lee JH, Rearick DA, Smas CM (2006) The adipose tissue triglyceride lipase ATGL/PNPLA2 is downregulated by insulin and TNF-alpha in 3T3-L1 adipocytes and is a target for transactivation by PPARgamma. Am J Physiol Endocrinol Metab 291:E115–E127
14. Fain JN, Kovacev VP, Scow RO (1965) Effect of growth hormone and dexamethasone on lipolysis and metabolism in isolated fat cells of the rat. J Biol Chem 240:3522–3529
15. Gruber A, Cornaciu I, Lass A, Schweiger M, Poeschl M, Eder C, Kumari M, Schoiswohl G, Wolinski H, Kohlwein SD, Zechner R, Zimmerman R, Oberer M (2010) The N-terminal region of comparative gene identification-58 (CGI-58) is important for lipid droplet binding and activation of adipose triglyceride lipase. J Biol Chem 285:12289–12298
16. Yang X, Lu X, Lombès M, Rha GB, Chi YI, Guerin TM, Smart EJ, Liu J (2010) The G(0)/G(1) switch gene 2 regulates adipose lipolysis through association with adipose triglyceride lipase. Cell Metab 11:194–205
17. Serr J, Suh Y, Lee K (2009) Regulation of adipose triglyceride lipase by fasting and refeeding in avian species. Poult Sci 88:2585–2591
18. Serr J, Suh Y, Lee K (2011) Cloning of comparative gene identification-58 gene in avian species and investigation of its developmental and nutritional regulation in chicken adipose tissue. J Anim Sci. doi:10.2527/jas.2011-3897
19. Lu X, Yang X, Liu J (2010) Differential control of ATGL-mediated lipid droplet degradation by CGI-58 and G0S2. Cell Cycle 9:2719–2725

Lipids (2011) 46:821–830
DOI 10.1007/s11745-011-3574-9

ORIGINAL ARTICLE

Dietary Conjugated Linoleic Acid Induces Lipolysis in Adipose Tissue of Coconut Oil-Fed Mice but not Soy Oil-Fed Mice

S. Ippagunta · T. J. Hadenfeldt · J. L. Miner · K. M. Hargrave-Barnes

Received: 2 August 2010 / Accepted: 10 May 2011 / Published online: 4 June 2011

Abstract Mice fed diets containing conjugated linoleic acid (CLA) are leaner than mice not fed CLA. This anti-obesity effect is amplified in mice fed coconut oil-containing or fat free diets, compared to soy oil diets. The present objective was to determine if CLA alters lipolysis in mice fed different base oils. Mice were fed diets containing soy oil (SO), coconut oil (CO), or fat free (FF) for 6 weeks, followed by 10 or 12 days of CLA or no CLA supplementation. Body fat, tissue weights, and ex vivo lipolysis were determined. Relative protein abundance and activation of perilipin, hormone sensitive lipase (HSL), adipose triglyceride lipase (ATGL), and adipose differentiation related protein (ADRP) were determined by western blotting. CLA feeding caused mice to have less ($P < 0.05$) body fat than non-CLA fed mice. This was enhanced in CO and FF-fed mice (CLA × oil source, $P < 0.05$). There was also a CLA × oil source interaction on lipolysis as CO + CLA and FF + CLA-fed mice had increased ($P < 0.05$) rates of lipolysis but SO + CLA-fed mice did not. However, after 12 days of CLA consumption, activated perilipin was increased ($P < 0.05$) only in SO + CLA-fed mice and total HSL and ATGL were decreased ($P < 0.05$) in CO + CLA-fed mice. Therefore, the enhanced CLA-induced body fat loss in CO and FF-fed mice appears to involve increased lipolysis but this effect may be decreasing by 12 days of CLA consumption.

Keywords Conjugated linoleic acid (CLA) · Specific Lipids · Dietary fat · Nutrition · Hormone sensitive lipase · Lipases

Abbreviations

ADRP	Adipose differentiation related protein
ATGL	Adipose triglyceride lipase
CGI-58	Comparative gene identification-58
CLA	Conjugated linoleic acid (18:2)
CO	Coconut oil
FF	Fat free
HSL	Hormone sensitive lipase
LNA	Linoleic acid
LD	Lipid droplets
NEFA	Non esterified fatty acids
PKA	Protein kinase A
SO	Soy oil
TNF-α	Tumor necrosis factor α

This study was presented in part at the Midwest Section of the American Society of Animal Science, American Dairy Science Association Meetings 2005, Des Moines, IA [Hadenfeldt TJ, KM Hargrave, and JL Miner. J. Anim. Sci. 2005; 83(Suppl. 2):279.] and at Experimental Biology 2009, New Orleans, LA [Ippagunta S, and KM Barnes. FASEB J. 23:Abst #722.14.]. This work is published with the approval of the Director of West Virginia Agriculture and forestry experiment station as scientific paper no. 3103.

S. Ippagunta · K. M. Hargrave-Barnes (✉)
Division of Animal and Nutritional Sciences,
West Virginia University, Morgantown, WV 26506, 6108, USA
e-mail: KMBarnes@mail.wvu.edu

T. J. Hadenfeldt · J. L. Miner
Department of Animal Science, University of Nebraska,
Lincoln, NE 68583, USA

Introduction

Conjugated linoleic acid (CLA) refers to a group of positional and geometric isomers of linoleic acid. A biological function of CLA was first discovered in ground beef as it

was found to have anti-carcinogenic properties [1]. Since then, dietary CLA has been found to have anti-inflammatory [2], anti-atherogenic [3–5], anti-carcinogenic [1, 6, 7], and anti-obesity effects [8, 9]. The 18:2 c9, t11 and t10, c12 isomers are the two biologically active isomers known to date. The t10, c12 isomer is solely responsible for the induction of body fat loss [6, 10].

The loss of body fat induced by dietary CLA can be enhanced when mice are fed a coconut oil (CO)-containing diet compared to mice fed a soybean oil (SO)-containing diet [11]. CO is composed of a higher concentration of short (8–10 carbons) and medium chain saturated fatty acids (12–16 carbons) and is deficient in the essential fatty acids linoleic acid and α-linolenic acid, compared to SO which has mostly saturated and unsaturated 18 carbon fatty acids and an abundant supply of linoleic acid. We have also reported increased sensitivity to CLA-induced body fat loss in mice consuming fat free diets [12], indicating that something in SO, and not in CO, interferes with the full effect of CLA. The mechanism behind the enhanced response with CO feeding is not yet known. However, several cell culture studies have reported that CLA supplementation causes an increase in lipolysis [13, 14]. Coconut oil is composed mainly of medium chain saturated fatty acids hence it is likely that they would undergo oxidation more rapidly as compared to the longer chain and unsaturated fatty acids present in soy oil diets [15, 16]. Hence when CLA is supplemented to these diets we hypothesize that there will be an enhanced turnover of fatty acids, leading to an increased lipolysis.

Mature adipocytes have unilocular lipid droplets (LD) surrounded by the protein perilipin. In the basal state of lipolysis, perilipin and comparative gene identification-58 (CGI-58) form a complex on the LD, adipose triglyceride lipase (ATGL) is localized partially to the LD, and hormone sensitive lipase (HSL) is localized to the cytoplasm [17]. When lipolysis is stimulated, cAMP-dependent protein kinase (PKA) activation results in phosphorylation of HSL and perilipin. Phosphorylated perilipin (p-perilipin) releases CGI-58, which binds and activates ATGL and initiates lipolysis. Phosphorylated HSL (p-HSL) translocates to the LD, interacts with p-perilipin, and degrades diacylglycerol (DAG) [18]. CLA has caused an increase in cytosolic perilipin (activated form of perilipin) followed by a decrease in HSL and total perilipin expression in human adipocyte cultures [13]. It was observed that the expression of cytosolic perilipin increases with CLA exposure for 12 h, while treatment with CLA for 24 h caused a decrease in perilipin expression. Thus the effects of CLA on lipolysis appear to vary with the duration of exposure to CLA.

In addition to perilipin, adipocyte differentiation related protein (ADRP), is known to surround the multilocular lipid droplets of immature adipocytes [19]. CLA has been reported to suppress perilipin expression while enhancing ADRP expression in human adipocyte cultures [13], this could indicate reduced lipolytic potential in these cells and possible de-differentiation of the mature adipocytes. In the current study, we determined the effect of base oil and CLA on lipolysis and the expression and activation of perilipin, associated lipases, and ADRP in vivo.

Methods and Procedures

Animal Protocol

Study 1: All animal procedures were approved by the University of Nebraska Institutional Animal Care and Use Committee. Male mice ($n = 48$) used were from a control line four-way composite developed at the University of Nebraska [20, 21] which was maintained without genetic selection and were housed in a temperature-controlled room (22 °C) with a 12 h light:dark cycle. Mice were fed a purified base diet (Dyets Inc., Bethlehem, PA), identical to those fed previously ([11, 12]; Table 1). A modification of the purified AIN-93G diet with soy protein instead of casein was used so as to avoid possible intake of CLA from the casein. For the coconut oil (CO) diet, soybean oil was replaced by fully hydrogenated coconut oil (wt/wt); Dyets Inc. For the fat free (FF) diet, oil was replaced completely by cornstarch (wt/wt). CLA replaced the base oil or cornstarch (wt/wt) and was added in the diets to provide 0.5% CLA isomers in the diet. The CLA mixture contained an equal amount of c9, t11 and t10, c12 (60% pure, LUTA-CLA, Catalog #56746397, BASF, Offenbach/Quiech, Germany). It has been previously shown that the mixture of CLA isomers (50:50) cause a lowering of the fat pad weight or triacylglycerol content to the same extent as that caused by t10, c12 isomer alone in mouse adipose tissue and in 3T3-L1 cells [10, 22]. All diets were stored at 4 °C. Mice were fed ad libitum throughout the study and fresh feed was added every 2 days.

Weanling male mice were housed individually. Animals were blocked by body weight and litter and assigned to base diets: SO (soy oil) or CO (coconut oil) or FF (fat free). After 6 weeks, half of each group were fed a 0.5% CLA diet for 10 days. Body weight and feed intake were measured weekly. At the end of the study, the mice were killed by carbon dioxide asphyxiation. Epididymal and retroperitoneal fat pads were collected and tissues were weighed. Epididymal fat pads were utilized for lipolysis analysis. A body fat index was calculated as: [(epididymal + retroperitoneal fat pad weights)/total body weight]*100.

Study 2: A second study to allow for the analysis of lipolysis-associated protein in adipose tissue was conducted with all animal procedures approved by the West Virginia

Table 1 Ingredient composition of experimental diets

Ingredient[a] (g/kg)	SO	SO + CLA	CO	CO + CLA	FF	FF + CLA
Isolated soy protein	200	200	200	200	200	200
L-cystine	2.54	2.54	2.54	2.54	2.54	2.54
L-methionine	2.54	2.54	2.54	2.54	2.54	2.54
Cornstarch	395.406	395.406	395.406	395.406	465.406	457.106
Maltodextrin	132	132	132	132	132	132
Sucrose	100	100	100	100	100	100
Cellulose	50	50	50	50	50	50
AIN-93G mineral mix	35	35	35	35	35	35
AIN-93G vitamin mix	10	10	10	10	10	10
Choline bitartrate	2.5	2.5	2.5	2.5	2.5	2.5
Soybean oil	70	61.7	–	–	–	–
Coconut oil	–	–	70	61.7	–	–
CLA[b]	–	8.3	–	8.3	–	8.3
TBHQ[c]	0.014	0.014	0.014	0.014	0.014	0.014

[a] Study 1, all ingredients obtained from Dyets, Inc. Study 2, diets were prepared by Harlan

[b] The purity of CLA used in study 1 and study 2 was different. Hence the actual amount of CLA added was different to include 0.5% CLA in the diet. Values shown are for study 1; study 2 included 5.3 g/kg CLA and 64.7 g/kg soybean or coconut oil

[c] TBHQ (*tert*-butylhydroquinone)

University Animal Care and Use Committee. Weanling male mice [$n = 80$; 3 weeks old; ICR (Imprinting Control Region)] were obtained from Harlan Inc. (Madison, WI) and housed in a temperature-controlled animal room (25 °C) with a 12:12 h light:dark cycle. The composite strain was not available at West Virginia University; therefore the ICR strain was selected as it was one of the strains in the four-way composite used in study 1, and has been previously reported to respond to dietary CLA with reduced body fat [6, 8]. Diets were formulated to match study 1 (Table 1) except only SO and CO were used and were obtained from Harlan Teklad (Madison, WI). The FF diet was not used as based on previous results [12] it was expected to yield similar results to CO. The CLA mixture (95% purity, methyl esters of CLA, catalog # UC-59-MX) was obtained from Nu-Check-Prep (Elysian, MN). All diets were stored at 4 °C. Mice were fed ad libitum throughout the study and fresh feed was added every 2 days.

Mice were housed four per cage for weeks 1–5 and then were individually caged during weeks 6–8. Animals were randomly assigned to base diets: SO or CO. After 6 weeks, half of each group were fed 0.5% CLA, replacing base oil w/w, for 12 days. Previous reports studying CO–CLA interaction consisted of 14 days of CLA consumption, by the end of which the CO + CLA mice have extremely small fat pads [12], thus in order to have adequate lipid stores to study lipolysis we chose a 10 day feeding period for study 1. However, we were unable to detect the oil × CLA interaction on body fat index. So we subsequently chose a 12 day feeding period for study 2, with the goal of being able to detect both lipolysis and the oil × CLA interaction on body fat.

At the end of the 54 days, the mice were killed by carbon dioxide asphyxiation. One fat pad pool, consisting of one epididymal and one retroperitoneal fat pad (~3:1 based on weight), for each of eight mice per diet was utilized for lipolysis analysis and the remaining tissues were flash frozen in liquid nitrogen and stored at −80 °C until further analysis was performed. The pooling of two abdominal fat pads per mouse was used to allow for lipolysis and protein expression to be analyzed in the same depots. No differences in the response to CLA by the two depots were expected, based on a recent report [23] of no differences in epinephrine-induced lipolysis between epididymal and retroperitoneal adipocytes. All measurements of body weight, feed intake, and body fat index were done as in study 1.

Lipolysis

The lipolysis assay was performed as described previously [24, 25] with slight modifications. Briefly, tissue pieces (~50 to 100 mg) were incubated in 0.8 ml of DMEM (containing 250 mU/ml adenosine deaminase (Sigma-Aldrich Inc., St Louis, MO) without serum) for 3 h at 37 °C in a shaking water bath. This was done in triplicate for both baseline and stimulated lipolysis (10 μM isoproterenol (Sigma-Aldrich Inc.). Media samples were collected and analyzed for non-esterified fatty acids (NEFA- HR kit, Wako Chemicals, Richmond, VA) and glycerol (free glycerol reagent, Sigma-Aldrich Inc., St Louis, MO) by colorimetry, following the manufacturer's instructions. NEFA and glycerol concentrations were corrected for tissue weight and reported as μmol released per gram tissue.

Blood was collected at the time of euthanasia approximately 2 h after the start of the light cycle and maintained on ice until centrifugation at 2,000×*g* for 20 min at 4 °C was performed. The serum was collected and stored at −20 °C until analysis. Mice had free access to feed up until euthanasia. The concentration of serum NEFA was

analyzed similar to the method above ($n = 20$/diet). Samples were run in triplicate for the assay.

Western Blotting

The additional fat pad pool per mouse from study 2 ($n = 12$/diet) which was flash frozen at the time of sample collection and stored at −80 °C until next day, was homogenized in 1 ml of lysis buffer [25 mM HEPES, 5 mM EDTA, 5 mM $MgCl_2$, 10 µl/ml of protease and phosphatase inhibitor mix (Thermo Scientific, Rockford, IL)] and centrifuged at 14,000×*g* for 20 min at 4 °C within 24 h of freezing. These samples represent the in vivo basal state. Protein content of the supernatant was analyzed by the BCA method (BCA kit, Thermo Scientific, Rockford, IL). Polyacrylamide gels (12.5%) were prepared and equal amounts of protein (2 µg for ADRP, ATGL or 5 µg for perilipin, HSL) were resolved at 75 V and transferred to a nitrocellulose membrane (Bio-Rad, Hercules, CA) at 100 V for 45 min on ice. The membranes were blocked with tris-buffered saline containing 0.05% Tween and 5% skimmed milk powder overnight at 4 °C, then probed with antibodies for perilipin (1:500, Santa Cruz Biotechnology, Santa Cruz, CA), ATGL (1:1,000, Santa Cruz Biotechnology), ADRP (1:500, Santa Cruz Biotechnology), phosphorylated-PKA (p-PKA) substrate (1:1,000 for p-perilipin, Cell Signaling Technology, Danvers, MA), HSL (1:1,000, Cell Signaling Technology), and p-HSL (1:500, Cell Signaling Technology) for 2 h at room temperature. The membranes were then probed with a HRP-conjugated secondary antibody (1:10,000, Santa Cruz Biotechnology) for 1 h at room temperature. Membranes were stripped and re-probed for β-actin (1:1,000, Santa Cruz Biotechnology). All antibodies were diluted in 1× PBS with 5% non fat dry milk. Chemiluminescence was produced using Super Signal West Pico chemiluminescent substrate (Thermo Scientific). Band density was analyzed by densitometry (Fluor Chem 8000 imaging system). Blot to blot variability was corrected for by running a pooled sample on each blot and adjusting the blots based on the relative expression of the pooled sample. The results are presented as the protein of interest/β-actin or in case of the phosphorylated proteins the results are presented as phospho-protein/total protein. The specificity of the p-PKA antibody was determined by performing an immunoprecipitation with the perilipin antibody and then probing the membrane with the p-PKA antibody. The immunoprecipitation determined that the band at 57 KDa was specific to p-perilipin (Fig. 1).

Statistical Analysis

All data were analyzed by two-way analysis of variance (ANOVA) using a fixed model testing the main effects of oil source (SO, CO, FF) and CLA, and the interaction of oil source × CLA. Body weight and feed intake measurements were analyzed by day. *F* tests, least-squares means, and standard errors of means (SEMs) were calculated using the mixed procedure of SAS (SAS Institute Inc., Cary, NC). For all tests $P < 0.05$ was considered significant, $0.05 > P < 0.1$ was considered a trend.

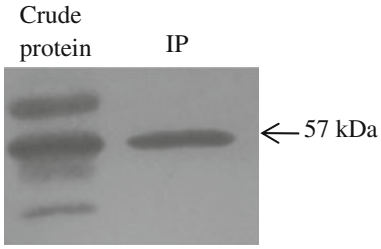

Fig. 1 Immunoprecipitation with anti-perilipin antibody and then probing with p-PKA antibody. Perilipin was identified at 57 kDa, indicated by the *arrow*

Results

Body Weight, Feed Intake, and Body Composition

Body weight was not affected by diet in study 1 (Table 2). In study 1, CLA inhibited feed intake ($P < 0.01$). Also, CLA caused a decrease in body fat index which was more pronounced in the CO and FF-fed mice (Fig. 2a).

In study 2, body weight was also not affected except in the last week when an oil source × CLA interaction was detected ($P < 0.05$). CLA caused a 6% increase in weight in SO-fed mice while causing a 5% decrease in CO-fed mice (Table 2). In study 2, feed intake was not affected by oil source until week 6, but during the last 2 weeks there was a main effect of oil source ($P < 0.05$) when CO-fed mice consumed 5% more feed than SO-fed mice. An oil source × CLA interaction ($P < 0.05$) indicated that CLA caused a decrease in feed intake, but only in CO-fed mice. When total feed intake for the 12 day period of CLA consumption was analyzed there was a main effect of oil source ($P < 0.05$) where SO-fed mice consumed less than CO-fed mice, but we did not observe a main effect of CLA (data not shown). Both CO ($P < 0.001$) and CLA ($P < 0.05$) caused decreases in the body fat index (Fig. 2b). CO caused a 32% decrease in the body fat index while CLA caused a 20% decrease in body fat index.

Lipolysis

In study 1, there was an interaction of oil source × CLA ($P < 0.05$) on the amount of NEFA released under basal conditions (Fig. 3a); CLA caused an increase in NEFA

Table 2 Effect of oil source and/or CLA on feed intake and body weight

	Diets[1]							*P* values		
	SO	SO + CLA	CO	CO + CLA	FF	FF + CLA	SEM	Oil	CLA	Oil × CLA
Study 1										
Body weight (g)										
Initial[2]	16.05	15.77	15.89	15.77	15.39	15.83	0.5	0.85	0.97	0.74
Before CLA[2]	34.70	34.25	34.97	35.16	33.41	34.28	1.27	0.63	0.83	0.85
Final[2]	35.94	35.44	36.54	34.11	34.26	34.84	1.32	0.72	0.44	0.53
Feed intake (g/d)										
Initial[3]	3.57	3.37	3.82	3.52	3.12	3.55	0.18	0.21	0.86	0.11
Before CLA[3]	5.07	4.84	4.87	4.69	5.17	4.78	0.22	0.64	0.13	0.89
Final[3]	5.15	4.39	5.18	4.73	4.84	4.36	0.23	0.34	**0.004**	0.75
Study 2										
Body weight (g)										
Initial[2]	9.62	9.42	9.58	9.53			0.07	0.65	0.09	0.33
Before CLA[2]	31.73	32.8	32.75	31.65			0.76	0.46	0.53	0.06
Final[2]	33.60[ab]	35.88[a]	35.05[ab]	33.31[b]			0.86	0.51	0.75	**0.02**
Feed intake (g/d)										
Initial[3]	2.85	2.82	2.83	2.87			0.02	0.59	0.70	0.13
Before CLA[3]	4.05	4.21	4.33	4.41			0.11	**0.03**	0.27	0.67
Final[3]	2.88[b]	3.04[ab]	3.25[a]	2.99[b]			0.09	0.09	0.61	**0.04**

[1] *Diets* SO (7% Soy oil); SO + CLA (6.5% soy oil + 0.5% CLA); CO (7% coconut oil); CO + CLA (6.5% coconut oil + 0.5% CLA); FF (fat free); FF + CLA (0.5% CLA)

[2] *Initial* Day 0, *Before CLA* day 42, *Final* day 52 (study 1) or 54 (study 2)

[3] *Initial* is feed intake measured from day 0–7, *Before CLA* day 35–42, *Final* day 43–52 (study 1) or 43–54 (study 2)

[ab] Different letters within a row indicate significant differences, $P < 0.05$

Bold values are statistically significant

release in CO and FF-fed mice, but not in SO-fed mice. There was also an interaction of oil source × CLA ($P < 0.05$) on the amount of glycerol released (Fig. 3b) where CLA caused an increase in CO and FF-fed mice but not SO-fed mice. There were no differences in either NEFA or glycerol release under stimulated conditions.

The effect on NEFA release was confirmed in study 2 where there was an interaction of oil source × CLA ($P < 0.05$), where CLA caused an increase in NEFA release in CO-fed mice but not in SO-fed mice (Fig. 3c). In study 2, there was no significant effect on the amount of glycerol released (Fig. 3d), although it followed the same numeric trend as NEFA release. Similar to study 1 there were no differences under stimulated conditions. Furthermore, the serum NEFA concentration did not differ between mice fed any of the dietary treatments, although CO-fed mice tended ($P < 0.1$) to have higher serum NEFA levels compared to the SO-fed mice (Fig. 3e).

Protein Expression

The lipolysis data indicated an effect of diet on NEFA release, so we also determined the effect of diets on the expression of proteins involved in lipolysis. The western blots indicated that the total protein concentration of perilipin was reduced ($P < 0.05$) in CO-fed mice compared to SO-fed mice (Fig. 4a). The activation of perilipin (concentration of p-perilipin) had a tendency toward an interaction of oil source × CLA ($P < 0.1$), as CLA tended to increase the amount of p-perilipin but only in SO-fed mice (Fig. 4b). SO + CLA-fed mice had 255% of the p-perilipin expression found in SO-fed mice, while CO + CLA-fed mice had only 76% of the p-perilipin expression found in CO-fed mice. HSL expression and activation weren't altered by CLA (Fig. 4c, d), but there was a decrease in total HSL expression in CO-fed mice ($P < 0.05$; Fig. 4c). ATGL expression was also decreased in CO-fed mice ($P < 0.01$) but there was no effect of CLA (Fig. 4e). ADRP expression was not altered (Fig. 4f).

Discussion

We have previously reported that feeding coconut oil enhances the CLA-induced body fat loss in mice [11, 12]. This effect was again observed in the present study. Based on the results presented here, it appears to involve CLA-induced lipolysis in CO-fed mice. Previously, some studies have reported that CLA enhances lipolysis in adipocyte cultures [13]. In our study we observed an enhanced lipolysis in response to dietary CLA but only in CO-or FF-fed mice.

We did not detect a significant interaction of oil source × CLA on body fat. This is likely due to the fact that in the current study a body fat index was calculated, which may not be as sensitive to changes in body fat as direct measurements using DEXA (Dual-emission X-ray absorptiometry) or whole carcass ether extractions as have been

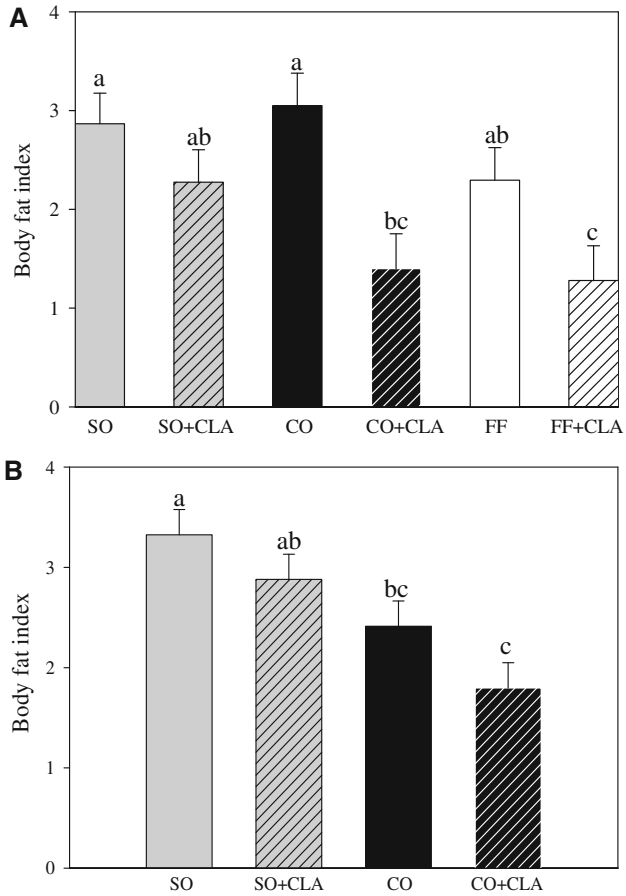

Fig. 2 Effect of dietary CLA and oil source on body composition. *Body fat index* [(Retroperitoneal + Epididymal fat pad weights)/body weight] × 100; study 1, $n = 7$/diet; study 2, $n = 20$/diet. *Diets* SO (7% soy oil), SO + CLA (6.5% soy oil + 0.5% CLA), CO (7% coconut oil), CO + CLA (6.5% coconut oil + 0.5% CLA), FF (0% oil), FF + CLA (0.5% CLA). **a** Study 1, CLA, $P < 0.001$. **b** Study 2, oil source, $P < 0.001$; CLA, $P < 0.05$. Data are shown as means ± SEM. *Different letters* indicate significant differences between treatments

used previously [11, 12]. Additionally in study 1, the mice fed the FF diet had less body fat and hence the reduction due to CLA supplementation in these mice was not as pronounced. In study 2, we observed that CO diets caused a decrease in body fat even without CLA supplementation, which is in contrast to the previous reports [11, 12] and to study 1 results. These mice didn't consume as much feed or gain as much as weight as in previous experiments [12], which could have led to the differing results. Although, a previous study has shown that reduction in feed intake alone is not sufficient to explain the CLA-induced body fat loss as mice pair-fed a control diet to the intake level of CLA-fed mice didn't differ in body fat compared to ad libitum fed controls, while the CLA-fed mice were leaner [10].

Similar to the body fat index, there was an effect of CO itself on the expression of perilipin, HSL, and ATGL. The reason for this effect of CO is not known but perhaps may be related to mouse strain (ICR vs. a four strain composite of ICR, C57BL/6, NIH Swiss, and CF-1). Although, others have reported anti-obesity actions of coconut oil; Dulloo et al. [26] fed mice different fat sources after a period of energy restriction and reported that the coconut oil-fed group had a lower body fat compared to groups fed other high fat diets. In fact, the level of body fat and serum cholesterol were similar to mice fed low fat diets. Others have found that coconut oil feeding causes an increase in uncoupling protein-1 (UCP1) expression in energy restricted mice [27]. Therefore, the lower body fat in coconut oil-fed mice may be due to diet-induced thermogenesis. The mice on study 1 and study 2 were housed under different temperatures (22 vs 25 °C), this small difference potentially could cause a difference in UCP expression, but a previous study has shown that UCP expression was not significantly different between mice housed at 20 versus 25 °C [28]. Hence we concluded that the different effects seen in the two studies was not likely to be attributed to differences in housing temperature. More likely, coconut oil has a higher content of medium chain saturated fatty acids that would undergo oxidation at a greater rate as compared to the fatty acids present in SO diets [16].

We observed a CLA-induced increase in basal lipolysis in CO-fed mice, but not SO-fed mice. This differential effect of CLA likely contributes to the overall enhanced body fat loss, although we cannot rule out an effect on lipogenesis or fatty acid oxidation at this time. Although, we have not observed any difference in total CPT activity between CLA supplemented SO and CO-fed mice in the muscle (unpublished data). Hence we hypothesize that there is no difference in transport of fatty acids into the mitochondria. There is difference in nutrient partitioning as we have previously observed an increase in muscle mass in CLA-fed animals [12]. The CLA-supplemented CO diets caused an increase in NEFA release but a significant effect on the amount of glycerol released was only detected in study 1. This is not unexpected given that 2–5 times more NEFA were released in study 1 and glycerol:NEFA exists in a 1:3 ratio, so the amount of glycerol released was small in study 2. This is likely an effect of feeding CLA for 12 versus 10 days, but could also be impacted by mouse strain. Additionally, we used only epididymal fat pads in study 1 and combined the two depots in study 2, but no differences in the response to CLA by the two depots were expected, based on a recent report [23] of no differences in epinephrine-induced lipolysis between epididymal and retroperitoneal adipocytes. Also it has been shown in previous studies that dietary CLA causes a reduction in both epididymal and retroperitoneal fat pad weights [10].

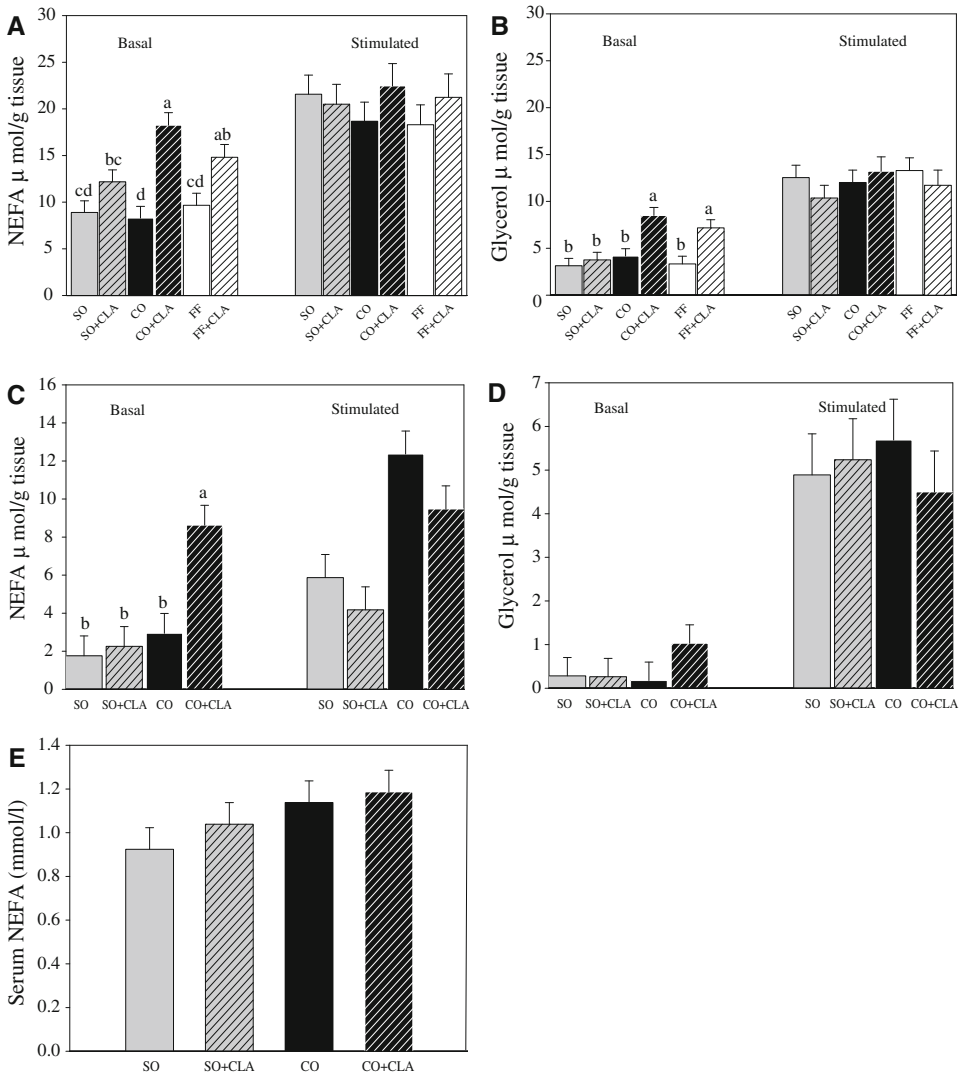

Fig. 3 Effect of dietary CLA and oil source on lipolysis. Fat pads were cultured for 3 h ex vivo. *Basal* 0 and *Stimulated* 10 μM Isoproterenol; study 1, $n = 7$/diet; study 2, $n = 8$/diet. *Diets* SO (7% soy oil); SO + CLA (6.5% soy oil + 0.5% CLA); CO (7% coconut oil); CO + CLA (6.5% coconut oil + 0.5% CLA); FF (0% oil); FF + CLA (0.5% CLA). **a** Study 1, NEFA release, expressed as μmol/g tissue, *Basal* oil × CLA, $P < 0.05$. **b** Study 1, Glycerol release, expressed as μmol/g tissue, *Basal* oil × CLA, $P < 0.05$. **c** Study 2, NEFA release, expressed as μmol/g tissue, Basal: oil × CLA, $P < 0.05$. **d** Study 2, Glycerol release, expressed as μmol/g tissue. **e** Study 2, Serum NEFA, expressed as mmol/l. Data are shown as means ± SEM. *Different letters* indicate significant differences between treatments

Several studies have shown that CLA causes an increase in lipolysis [13, 14], while others have reported no effect of CLA on lipolysis [29–31]. The responses to CLA tended to be observed in cells that had been cultured in serum-free media [13, 14]. Serum starving makes the cultures devoid of fatty acids that could potentially interfere with CLA. Explant cultures of WAT from CLA-fed pigs didn't exhibit enhanced lipolysis in response to CLA [29]; similar to our SO + CLA-fed mice, as both the pig and mouse diets were rich in linoleic acid. Coconut oil is deficient in essential fatty acids. Although this may be the reason for the increased CLA interaction, we found no change in the CLA interaction after supplementing essential fatty acids to CO diets [12]. The CO × CLA interaction thus does not appear to depend on a nutritional deficiency of essential fatty acids. SO, however, contains large amounts of linoleic acid (LNA), well in excess of the dietary requirement, that perhaps interferes with the actions of CLA. LNA is converted to arachidonic acid (AA) via desaturation and elongation; AA can then be converted to PGE_2 (prostaglandin E2) via cyclooxygenase. PGE_2 has 4 cognate receptors (EP (E-prostanoid) 1, EP2, EP3, and EP4), G_i-coupled EP3 is expressed at >10-fold higher levels than the other EP receptors in adipose tissue. The binding of PGE_2 to this receptor causes an inhibition of lipolysis [32]. CLA can undergo the same desaturation and elongation forming a conjugated AA [33, 34]. The formation of conjugated isomers of AA from CLA could reduce the EP3 signaling, as PGE_2 synthesis has been shown to be reduced [35] and cause an increase in cAMP levels which could stimulate lipolysis. The lack of LNA in the CO diet could result in a greater amount of CLA being converted to conjugated AA, which could lead to the enhancement in CLA-induced lipolysis in CO-fed mice. This hypothesis can be supported by our study, which showed that the inhibition of delta 6-desaturase prevented CLA from inducing a body fat loss [36]. Further research is needed to identify and quantify the conjugated AA isomers formed in

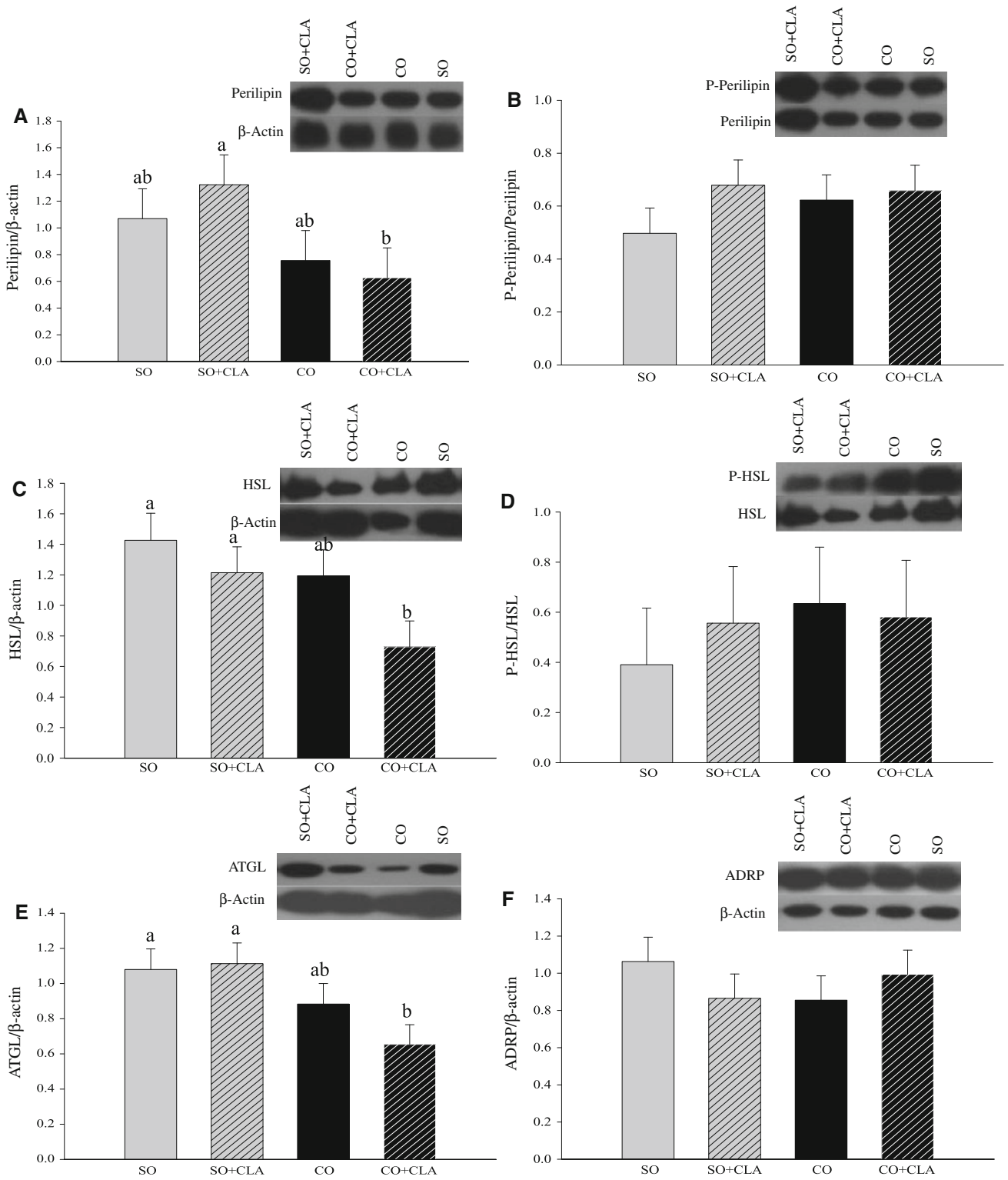

Fig. 4 Effect of dietary CLA and oil source on adipose tissue protein expression, study 2. Densitometry analysis of each protein, relative to β-actin or total protein was performed; A representative blot and the quantification of $n = 12$/diet are shown. *Diets* SO (7% soy oil); SO + CLA (6.5% soy oil + 0.5% CLA); CO (7% coconut oil); CO + CLA (6.5% coconut oil + 0.5% CLA). **a** Total perilipin expression, oil source, $P < 0.05$. **b** P-Perilipin expression, oil source × CLA, $P = 0.08$. **c** Total HSL expression, oil source, $P < 0.05$; CLA $P = 0.05$. **d** P-HSL expression. **e** ATGL expression, oil source, $P < 0.01$. **f** ADRP expression. Data are shown as means ± SEM. *Different letters* indicate significant differences between treatments

SO versus CO-fed mice supplemented with CLA, and to determine their potential role in CLA-induced lipolysis.

We detected no differences in stimulated lipolysis, indicating that there were no differences in the total amount of lipases present in the cell. When lipolysis is stimulated perilipin is phosphorylated by PKA. Phosphorylated perilipin releases CGI-58, which then binds to ATGL, activating it [17]. ATGL is a major lipase which is known to catalyze the first step of triacylglycerol (TAG) hydrolysis [37]. Also, when lipolysis is stimulated HSL is phosphorylated by PKA, and activated. The p-HSL then rapidly and specifically translocates from the cytosol to the surface of the lipid droplets. This translocation is dependent on presence of p-perilipin [17]. Based on the lipolysis data we expected an increase in the relative expression of p-perilipin and p-HSL. However, we found that CLA did not increase lipolysis-associated protein expression in CO-fed mice. Rather, CLA caused an increase in expression of p-perilipin but only in SO-fed mice. There was no effect of CLA on any of the other proteins. We hypothesize that the effect of CLA is time-dependent and feeding CLA first causes an increase in lipase activation, followed by a decrease in the expression or activation, as this has been reported in a cell culture study [13]. CLA supplemented to human adipocytes caused an increase in lipolysis and in cytosolic perilipin, indicating activation, after 12 h of CLA supplementation. This was followed by a decrease in the expression of perilipin and HSL at 24 h of supplementation. It is possible that after 12 days of CLA consumption our mice were experiencing a decline in perilipin and lipase expression. This might have also contributed to the lowered degree of lipolysis in study 2, compared to study 1, when the mice were fed CLA for only 10 days. In this study we didn't observe any effect of CLA on ADRP expression.

The body fat lowering effect of CLA in mice has not been fully reciprocated in humans. The exact reasons for this are not known. One possibility maybe that the large quantity of various PUFA in a typical human diet could have an antagonist effect on the body-fat lowering effect of CLA. The adequate intake levels of PUFA as determined by the Institute of Medicine's Food and Nutrition Board (DRI report for energy and macronutrients (2002/2005)) is 17 g/day for males and 12 g/day for females. In support of this, we have reported previously [11, 12] and in the current study that the CLA-induced body fat reduction is enhanced in CO and fat-free fed mice as compared to SO-fed mice which have a much higher content of PUFA.

In conclusion, coconut oil enhances the anti-obesity effect of CLA and this effect, at least in part, appears to be due to enhanced lipolysis. The effect of CLA on the expression and activation of lipases and other lipolysis-related proteins may be time-dependent and therefore, were not clear in the current experiment. Further studies evaluating the effect of different feeding durations of CLA will be helpful in determining the mechanism of CLA action on lipolysis.

References

1. Pariza MW, Hargraves WA (1985) A beef-derived mutagenesis modulator inhibits initiation of mouse epidermal tumors by 7, 12-dimethylbenz[a]anthracene. Carcinogenesis 6:591–593
2. Cook ME, Miller CC, Park Y, Pariza M (1993) Immune modulation by altered nutrient metabolism: nutritional control of immune-induced growth depression. Poult Sci 72:1301–1305
3. Lee KN, Kritchevsky D, Pariza MW (1994) Conjugated linoleic acid and atherosclerosis in rabbits. Atherosclerosis 108:19–25
4. Munday JS, Thompson KG, James KA (1999) Dietary conjugated linoleic acids promote fatty streak formation in the C57BL/6 mouse atherosclerosis model. Br J Nutr 81:251–255
5. Nicolosi RJ, Rogers EJ, Kritchevsky D, Scimeca JA, Huth PJ (1997) Dietary conjugated linoleic acid reduces plasma lipoproteins and early aortic atherosclerosis in hypercholesterolemic hamsters. Artery 22:266–277
6. Park Y, Storkson JM, Albright KJ, Liu W, Pariza MW (1999) Evidence that the *trans*-10,*cis*-12 isomer of conjugated linoleic acid induces body composition changes in mice. Lipids 34:235–241
7. Ip C, Banni S, Angioni E et al (1999) Conjugated linoleic acid-enriched butter fat alters mammary gland morphogenesis and reduces cancer risk in rats. J Nutr 129:2135–2142
8. Park Y, Albright KJ, Liu W, Storkson JM, Cook ME, Pariza MW et al (1997) Effect of conjugated linoleic acid on body composition in mice. Lipids 32:853–858
9. West DB, Delany JP, Camet PM, Blohm F, Truett AA, Scimeca J (1998) Effects of conjugated linoleic acid on body fat and energy metabolism in the mouse. Am J Physiol 275:R667–R672
10. Hargrave KM, Li C, Meyer BJ et al (2002) Adipose depletion and apoptosis induced by *trans*-10, *cis*-12 conjugated linoleic acid in mice. Obes Res 10:1284–1290
11. Hargrave KM, Meyer BJ, Li C, Azain MJ, Baile CA, Miner JL (2004) Influence of dietary conjugated linoleic acid and fat source on body fat and apoptosis in mice. Obes Res 12:1435–1444
12. Hargrave KM, Azain MJ, Miner JL (2005) Dietary coconut oil increases conjugated linoleic acid-induced body fat loss in mice independent of essential fatty acid deficiency. Biochim Biophys Acta 1737:52–60
13. Chung S, Brown JM, Sandberg MB, McIntosh M (2005) *trans*-10,*cis*-12 CLA increases adipocyte lipolysis and alters lipid droplet-associated proteins: role of mTOR and ERK signaling. J Lipid Res 46:885–895
14. Moon HS, Lee HG, Seo JH et al (2008) Lipolysis is stimulated by PEGylated conjugated linoleic acid through the cyclic adenosine monophosphate-independent signaling pathway in 3T3-L1 cells: activation of MEK/ERK MAPK signaling pathway and hypersecretion of adipo-cytokines. J Cell Physiol 214:283–294
15. DeLany JP, Windhauser MM, Champagne CM, Bray GA (2000) Differential oxidation of individual dietary fatty acids in humans. Am J Clin Nutr 72:905–911
16. Papamandjaris AA, White MD, Raeini-Sarjaz M, Jones PJ (2000) Endogenous fat oxidation during medium chain versus long chain triglyceride feeding in healthy women. Int J Obes Relat Metab Disord 24:1158–1166

17. Granneman JG, Moore HP, Granneman RL, Greenberg AS, Obin MS, Zhu Z (2007) Analysis of lipolytic protein trafficking and interactions in adipocytes. J Biol Chem 282:5726–5735
18. Jaworski K, Sarkadi-Nagy E, Duncan RE, Ahmadian M, Sul HS (2007) Regulation of triglyceride metabolism. IV. Hormonal regulation of lipolysis in adipose tissue. Am J Physiol Gastrointest Liver Physiol 293:G1–G4
19. Brasaemle DL, Barber T, Wolins NE, Serrero G, Blanchette-Mackie EJ, Londos C (1997) Adipose differentiation-related protein is an ubiquitously expressed lipid storage droplet-associated protein. J Lipid Res 38:2249–2263
20. Jones LD, Nielsen MK, Britton RA (1992) Genetic variation in liver mass, body mass, and liver:body mass in mice. J Anim Sci 70:2999–3006
21. Nielsen MK, Jones LD, Freking BA, DeShazer JA (1997) Divergent selection for heat loss in mice: I. Selection applied and direct response through fifteen generations. J Anim Sci 75:1461–1468
22. Evans M, Geigerman C, Cook J, Curtis L, Kuebler B, McIntosh M (2000) Conjugated linoleic acid suppresses triglyceride accumulation and induces apoptosis in 3T3-L1 preadipocytes. Lipids 35:899–910
23. Anthony NM, Gaidhu MP, Ceddia RB (2009) Regulation of visceral and subcutaneous adipocyte lipolysis by acute AICAR-induced AMPK activation. Obesity (Silver Spring) 17:1312–1317
24. Lanna DP, Bauman DE (1999) Effect of somatotropin, insulin, and glucocorticoid on lipolysis in chronic cultures of adipose tissue from lactating cows. J Dairy Sci 82:60–68
25. Kershaw EE, Hamm JK, Verhagen LA, Peroni O, Katic M, Flier JS (2006) Adipose triglyceride lipase: function, regulation by insulin, and comparison with adiponutrin. Diabetes 55:148–157
26. Dulloo AG, Mensi N, Seydoux J, Girardier L (1995) Differential effects of high-fat diets varying in fatty acid composition on the efficiency of lean and fat tissue deposition during weight recovery after low food intake. Metabolism 44:273–279
27. Portillo MP, Serra F, Simon E, del Barrio AS, Palou A (1998) Energy restriction with high-fat diet enriched with coconut oil gives higher UCP1 and lower white fat in rats. Int J Obes Relat Metab Disord 22:974–979
28. Uchida K, Shiuchi T, Inada H, Minokoshi Y, Tominaga M (2010) Metabolic adaptation of mice in a cool environment. Pflugers Arch 459:765–774
29. Jose AA, Gama MA, Lanna DD (2008) Effects of *trans*-10, *cis*-12 conjugated linoleic acid on gene expression and lipid metabolism of adipose tissue of growing pigs. Genet Mol Res 7:284–294
30. Perfield JW 2nd, Bernal-Santos G, Overton TR, Bauman DE (2002) Effects of dietary supplementation of rumen-protected conjugated linoleic acid in dairy cows during established lactation. J Dairy Sci 85:2609–2617
31. Xu X, Storkson J, Kim S, Sugimoto K, Park Y, Pariza MW (2003) Short-term intake of conjugated linoleic acid inhibits lipoprotein lipase and glucose metabolism but does not enhance lipolysis in mouse adipose tissue. J Nutr 133:663–667
32. Cohen-Luria R, Rimon G (1992) Prostaglandin E2 can bimodally inhibit and stimulate the epididymal adipocyte adenylyl cyclase activity. Cell Signal 4:331–335
33. Sebedio JL, Juaneda P, Dobson G et al (1997) Metabolites of conjugated isomers of linoleic acid (CLA) in the rat. Biochim Biophys Acta 1345:5–10
34. Banni S (2002) Conjugated linoleic acid metabolism. Curr Opin Lipidol 13:261–266
35. Stachowska E, Dolegowska B, Dziedziejko V et al (2009) Prostaglandin E2 (PGE2) and thromboxane A2 (TXA2) synthesis is regulated by conjugated linoleic acids (CLA) in human macrophages. J Physiol Pharmacol 60:77–85
36. Hargrave-Barnes KM, Azain MJ, Miner JL (2008) Conjugated linoleic acid-induced fat loss dependence on delta6-desaturase or cyclooxygenase. Obesity (Silver Spring) 16:2245–2252
37. Zimmermann R, Strauss JG, Haemmerle G et al (2004) Fat mobilization in adipose tissue is promoted by adipose triglyceride lipase. Science 306:1383–1386

Lipids (2011) 46:831–841
DOI 10.1007/s11745-011-3586-5

ORIGINAL ARTICLE

Trans-18:1 and CLA Isomers in Rumen and Duodenal Digesta of Bulls Fed n-3 and n-6 PUFA-Based Diets

Xiangzhen Shen · Dirk Dannenberger · Karin Nuernberg · Gerd Nuernberg · Ruqian Zhao

Received: 6 December 2010 / Accepted: 20 June 2011 / Published online: 8 July 2011

Abstract The aim of the study was to investigate the effect of n-6 PUFA (maize silage/grass silage, soybean meal and soybean oil, control) and n-3 PUFA (grass silage, rapeseed cake and rapeseed oil, experiment) based diets on the occurrence of rumen- and duodenal digesta *trans*-C18:1 and CLA isomers of German Simmental bulls. The results based on rumen and duodenal digesta samples immediately taken from the bulls just after slaughter. The diet affected the occurrence of individual *trans*-C18:1 and CLA isomers in the rumen and duodenal digesta in different ways. The isomer *trans*-11,*cis*-13 CLA was detected as the most abundant isomer in the rumen of n-3 PUFA based diet fed bulls compared to n-6 PUFA based diet fed bulls. The *trans*-7,*cis*-9 CLA isomer was not detected in the rumen samples of bulls fed both diets, however abundant *trans*-7,*cis*-9 CLA was identified and quantified in the duodenum digesta. Both the concentration of the sum of *trans*-18:1 fatty acids and individual isomers in the rumen were not affected by the diet, except *trans*-16-18:1. The concentration of *trans*-16-18:1 was significantly decreased in the rumen of n-3 PUFA supplemented-fed bulls compared to n-6 PUFA supplemented-fed bulls.

Keywords Rumen · Digesta · CLA isomers · *Trans*-18:1 isomers · Bulls

Abbreviations

CLA	Conjugated linoleic acids
DM	Dry matter
PUFA	Polyunsaturated fatty acid(s)
SCD	Stearoyl-CoA desaturase
MFD	Milk fat depression
FAME	Fatty acid methyl ester(s)
HRGC	High resolution gas chromatography
FID	Flame ionization detector
Ag^{+}-ion HPLC	Silver ion high performance liquid chromatography
SEM	Standard error of mean
LSM	Least square mean
TMR	Total mixed ratio
VA	Vaccenic acid
GC	Gas chromatography
PDA	Photodiode array

Introduction

During the biohydrogenation in the rumen microbial ecosystem, a broad range of intermediates are formed, such as monounsaturated *cis*- and *trans*-fatty acids and conjugated linoleic acid (CLA) isomers. It is widely recognized that diet plays a major role in modulating fatty acid composition in ruminant meat and milk. Understanding the mechanisms underlying the biosynthesis of individual *trans*-18:1 and CLA isomers in the rumen are important because the ruminal outflow affects the availability of these bioactive

X. Shen · R. Zhao
Key Laboratory of Animal Physiology and Biochemistry, Nanjing Agricultural University, Nanjing 210095, People's Republic of China

D. Dannenberger (✉) · K. Nuernberg · G. Nuernberg
Leibniz Institute for Farm Animal Biology, Research Units Muscle Biology and Growth, and Genetics and Biometry, Wilhelm-Stahl-Allee 2, 18196 Dummerstorf, Germany
e-mail: dannenberger@fbn-dummerstorf.de

fatty acid isomers for incorporation into muscle and milk [1–3]. CLA is a term used to describe a mixture including a range of positional and geometric isomers of conjugated octadecadienoic acids. The predominant isomer in ruminant muscle is *cis*-9,*trans*-11 CLA accounting for more than 80% of the total CLA, yet *trans*-10,*cis*-12 CLA comprises 3–5% of the total CLA, however the occurrence of these bioactive fatty acid isomers is also diet dependent [4, 5]. Until now, predominantly two CLA isomers, *cis*-9,*trans*-11 CLA and *trans*-10,*cis*-12 CLA, have been shown to have biological activity including prevention of different types of cancer, cardiovascular health and improved immune response predominantly in animal models; however, in recent human studies inconsistent effects have been reported [6, 7]. Very recently, it has also been shown that *trans,trans* CLA isomers (*trans*-9,*trans*-11 CLA, *trans*-10,*trans*-12 CLA) inhibit rat mammary tumorigenesis through the induction of apoptosis in conjunction with the reduction of arachidonic acid metabolites [8]. There is much evidence that the physiological properties of CLA are isomer specific with partly opposing effects [6–8]. Ruminant meat, milk and their products are the major source of CLA in human diet [9, 10]. The monounsaturated *cis*- and *trans*-fatty acids and CLA isomers are formed either directly in the rumen or from precursors formed in the rumen during the biohydrogenation of dietary PUFA. Over 10 years ago, ruminal fatty acid metabolism was described in a classic review [11] and the intensive research was more recently summarized [12]. Most dietary fatty acids are esterified, and they are almost completely metabolized to free fatty acids in the rumen. Until now not all biohydrogenation processes and pathways are fully understood [1–3]. It is well known that the main CLA isomer, *cis*-9, *trans*-11 CLA, is formed from different sources. This bioactive compound can be produced in the rumen via biohydrogenation by *Butyrivibrio fibrisolvens* and other microbes, with consequent transport into tissues and endogenous synthesized in the mammary gland of dairy cows and ruminant adipose tissues by the conversion of *trans*-11-18:1 (VA) catalysed by stearoyl-CoA desaturase (SCD, EC 1.14.19.1) [13, 14]. So, VA is a major precursor in the formation of *cis*-9,*trans*-11 CLA in tissues. The diet is the most important factor affecting the *cis*- and *trans*-18:1 and CLA isomers profiles in different tissues and milk of cattle. Dietary fatty acid biohydrogenation in the rumen has a major influence on fatty acid composition of ruminant meat and milk. The phenomenon of diet-induced milk fat depression (MFD) has been of extensive research interest over many years and is also actually under investigation [1, 2, 15, 16]. MFD is associated with an increase in the content of *trans*-10-18:1, and the *trans*-10,*cis*-12 CLA is also responsible for reduced milk fat synthesis, whereas *cis*-9,*trans*-11 CLA has no effect [1, 2, 14]. Recently, the role of protozoa in the biosynthesis of *trans*-18:1 fatty acids and CLA isomers in the rumen contents of fistulated cows was investigated [2, 17]. The rumen protozoa are capable for synthesizing CLA isomers from 18*:*2n-6, however they are incapable of metabolizing CLA isomers further. In vitro batch incubations showed the dynamic feature of rumen metabolism of pure 18:3n-3 and 18*:*2n-6 in comparison to linseed oil [18]. Investigations of ruminal bacteria cultures revealed that the reduction of 9,11 geometric CLA isomers occurs via different mechanisms compared to other unsaturated fatty acids [19].

However, until now there has been a lack of results from in vivo studies of animals fed n-3 and n-6 PUFA-based diets on *trans*-18:1 and CLA isomers occurrence in the rumen and duodenum digesta in cattle using different GC and additional Silver ion-HPLC (Ag^{+}-ion HPLC) methods [20]. A study with 25 German Simmental bulls fed n-3 and n-6 PUFA-based diets was carried out to investigate dietary effects on the lipid metabolism in different tissues [21, 22]. The objective of the present paper is focused on the occurrence of *trans*-18:1 and CLA isomers in the rumen and duodenal digesta by feeding diets based on n-3 PUFA (grass silage and a concentrate containing rapeseed cake and rapeseed oil) and n-6 PUFA (maize silage/grass silage and a concentrate containing soybean meal and soybean oil) of German Simmental bulls after slaughter.

Experimental Materials and Methods

Animals, Diet Treatments and Experimental Design

Twenty-five German Simmental bulls (9–10 months old, approximately 290 kg initial weight) were assigned to three groups in the experiment with different feeding regimes, the control group and two experimental groups. All the animals were housed in individual tie stalls and offered three different dietary treatments. The details of the experiment were recently reported [21, 22]. One experimental group was fed a diet restricted to 1 kg of concentrate (50%) per day during the first 112 days of the fattening period [21]. However, the main objective of the present paper is the effect of n-3 and n-6 PUFA based diets on rumen digesta and duodenal digesta lipids. A diet restriction in the fattening period approximately 250 days before slaughter not affects the rumen digesta and duodenal digesta lipids after slaughter. Because of that the animals of restricted experimental group were excluded. In this paper the results of the control group ($n = 9$) and the experimental group ($n = 7$) are presented (Table 1). The control group ($n = 9$) were daily fed maize silage/

Table 1 Experimental design and fatty acid composition of the diets, part of the experiment [21, 22]

	Control group ($n = 9$)	Experimental group ($n = 7$)
Initial age (d)	$283.7_{3.41}$	$277.1_{3.41}$
Initial weight (kg)	$295.1_{9.54}$	$284.0_{9.54}$
Diet	Maize silage/grass silage (70%/30%, ad libitum), sugar beet pulp, concentrate containing 20% soybean meal and 2% soybean oil	Grass silage (ad libitum), sugar beet pulp, concentrate containing 32% rapeseed cake and 2% rapeseed oil
Chemical composition[a]	Maize silage/grass silage (70%/30%)	Grass silage
Crude protein	11.3	20.1
Crude fat	3.9	3.6
Crude ash	7.8	14.1
ADF	20.2	22.3
Fatty acids[b]		
14:0	0.36	0.62
16:0	15.7	18.9
18:0	2.2	1.7
18:1*cis*-9	19.8	3.4
18:2n-6	47.1	22.5
18:3n-3	8.3	43.6
PUFA	56.8	68.8
n-3 FA	8.7	44.7
n-6-FA	48.0	24.0
Ratio n-6/n-3 FA	5.5	0.54

[a] Expressed on dry matter basis

[b] Percentage of total fatty acids

grass silage (70/30, ad libitum), 1 kg of molasses, 1 kg of hay and concentrate including soybean meal (2 kg the first 112 days, 2.5 kg the next 110 days and 3 kg until slaughter). The experimental group I ($n = 7$) were fed grass silage (ad libitum), 1 kg of molasses, 1 kg of hay and concentrate (39% triticale, 22% barley, 32% rape cake, 5% minerals, 2% rapeseed oil). Both groups have got the same amount of hay and straw. In Table 1 fatty acid composition of the main diet components (maize silage/grass silage (70%/30%) and grass silage) is presented. The main fatty acids in the fat of the total mixed ratio (TMR, control group) were 18:2n-6 (46.6%), 18:1*cis*-9 (23.1%), 16:0 (12.1%), 18:3n-3 (7.2%) and 18:0 (3.0%). The main fatty acids in the fat of the TMR (experimental group) were 18:1*cis*-9 (35.6%), 18:2n-6 (27.0%), 18:3n-3 (8.1%), 16:0 (7.9%), and 18:0 (1.5%). All animals were fasted with fixed time before slaughter. The morning meal at the day before slaughter was the last meal. The animals were slaughtered next midmorning at approximately 620 kg live weight in the abattoir of the Leibniz Institute for Farm Animal Biology in Dummerstorf, Germany. The slaughter and dressing procedures were in accordance with European Union (EU) specifications. Approximately 50 g rumen content (representative mix of whole rumen content) and 50 g duodenal digesta (1 m after pylorus, representative mix of duodenal digesta content) samples were taken immediately after slaughter, and were stored frozen at –20 °C and freeze-dried until lipid extraction.

Extraction and Methylation of Lipids

Approximately 1.5 g freeze-dried rumen and 2.0 g freeze-dried duodenal digesta samples were taken for total lipid extraction (triplicates). A modified direct fatty acid methylation method was used [23]. The samples were treated with 3.5 mL toluene (containing 19:0 fatty acid methyl ester as internal standard) and 5.25 mL of 5% methanolic hydrochloric acid. The mixture was shaken in water bath at 70 °C for 2 h. After cooling down to room temperature, methyl esters of total fatty acids (FAME) were extracted with 3.5 mL *n*-hexane in the presence of 8.75 mL 6% K_2CO_3 solution and mixed with a vortex mixer. After centrifugation (1230*g* for 5 min at 4 °C), toluene phase was separated and transferred to a new tube. Then, 1 g Na_2SO_4 and activated charcoal were added and stored at 4 °C overnight until disappearance of the yellow color in the extracts. Samples were centrifuged at 800*g* for 2 min at 4 °C, filtered and evaporated with a gentle N_2 stream to dryness. For high resolution gas chromatography (HRGC) analysis, rumen samples were resolved with 500 µL *n*-heptane and duodenal digesta samples with 200 µL *n*-heptane.

For Ag^+-HPLC analysis, both rumen and digesta samples were resolved with 200 μL *n*-heptane.

Separation of Total Fatty Acid and Trans-18:1 Isomers by HRGC

A Perkin Elmer gas chromatograph Autosys XL was used and equipped with a flame ionization detector (FID), split injection and TotalChrom software (Perkin Elmer Instruments, Shelton, USA). The fatty acid composition of the FAME extract samples was determined on a CP SIL 88 100 m × 0.25 mm × 0.25 μm capillary column (Chrompack-Varian, USA). The initial oven temperature was 150 °C, held for 5 min, subsequently increased to 175 °C at a rate of 2 °C min^{-1} to 200 °C, held for 10 min, then at 1.5 °C min^{-1} to 225 °C and held for 25 min. Hydrogen was used as the carrier gas at a flow rate of 1 ml min^{-1}. The split ratio was 1:20; the injector was set at 260 °C and the detector at 280 °C [24]. A combination of two HRGC temperature programs with the above-mentioned capillary column was used for the separation and identification of *trans*-18:1 isomers in rumen and digesta extracts as recently described for milk fat [25]. By the use of only one GC time program the problem of overlapping of some *trans*- and *cis*-18:1 isomers remains and the correct identification and quantification of individual isomers cannot be achieved [25]. The details of first temperature program: initial oven temperature was 45 °C, held for 4 min, then increased to 150 °C at a rate of 13 °C min^{-1}, held for 47 min, then to 215 °C at a rate of 4 °C min^{-1}, held for 35 min. The use of the time program with the plateau at 150 °C permits the correct identification of *trans*-4-18:1, *trans*-5-18:1, *trans*-6/7/8-18:1, *trans*-10-18:1 and *trans*-11-18:1 isomers. The second temperature program: initial oven temperature was 45 °C, held for 4 min, then increased to 175 °C at a rate of 13 °C min^{-1}, held for 27 min, then to 215 °C at a rate of 4 °C min^{-1}, held for 35 min. The use of the time program with the plateau at 175 °C permits the correct identification of *trans*-12-18:1, *trans*-13/14-18:1, *trans*-15-18:1 and *trans*-16-18:1 isomers. Injector temperature was kept at 260 °C, and detector at 280 °C. Hydrogen was used as carrier gas at a flow rate of 1 mL min^{-1}. The injection volume was 1 μL for rumen samples and 2 μL for digesta samples. The split ratio was 1:19.2. The concentrations were calculated by internal standard method and 19:0 was used as internal standard.

Separation and Identification of CLA Isomers by Ag^+-HPLC

Identification and quantification analysis of the CLA isomers in rumen and digesta extracts was performed by Ag^+-ion HPLC involved an HPLC system (LC 10A, Shimadzu, Japan) equipped with a pump (LC-10AD VP), auto sampler (SIL-10AF), 50 μL injection loop, a photodiode array detector (SPD-M 10Avp, Shimadzu, Japan), and a Shimadzu CLASS-VP software system (Version 6.12 SP4). Four ChromSpher 5 Lipids analytical silver ion-impregnated columns (4.6 mm i.d. × 250 mm stainless steel; 5 μm particle size; Chrompack-Varian, USA) were used in series. The mobile phase (0.1% acetonitrile in *n*-hexane) was prepared fresh daily and pumped at a flow rate of 1.0 mL/min as described in detail before [4, 20]. The injection volume was 50 μL, since the content of minor CLA isomers in rumen and duodenal digesta was low. The detector was operated at 233 nm to identify CLA isomers based the measurement of integrated area under the 233 nm peaks attributed to conjugated dienes. The identification of CLA isomers was made by the retention time of individual CLA methyl esters (*cis*-9,*trans*-11 CLA, *trans*-9,*trans*-11 CLA, *trans*-10,*cis*-12 CLA, *cis*-9,*trans*-11 CLA, *cis*-9,*cis*-11 CLA and *cis*-11,*trans*-13 CLA). The external calibration plots of the standard solutions were adapted to different concentration levels of individual CLA isomers in the lipid extracts, recently in detail described [4].

Reagents

A reference standard 'Sigma-FAME mixture' was obtained from Sigma-Aldrich (Deisenhofen, Germany). Additionally, individual methyl esters of 18:4n-3, 22:4n-6, 22:5n-3 and the individual isomers of CLA methyl esters (CLA-ME), *cis*-9,*trans*-11 CLA, *trans*-9,*trans*-11 CLA, *trans*-10,*cis*-12 CLA, *cis*-9,*cis*-11 CLA and *cis*-11,*trans*-13 CLA (as a free fatty acid) were purchased from Matreya (Pleasnet Gap, United States). Methyl esters of *trans*-11-18:1 and *cis*-11-18:1 were purchased from Larodan Fine Chemicals (Malmö, Sweden). Additional, *trans*-6 and *trans*-13-18:1 FAME was purchased from Nu-Check Prep (MN, USA). All solvents used for GC and Ag^+-HPLC were HPLC grade from Lab-Scan (Dublin, Ireland). The derivatization reagents, sodium methylate and boron trifluoride/methanol (14% w:v), were respectively obtained from Fluka (Buchs, Switzerland) and from Sigma-Aldrich (Deisenhofen, Germany).

Statistical Analysis

Statistical data analysis was conducted by one-way analysis of variance with fixed factor feed (three feeding groups) using the GLM procedure of SAS®/STAT software (Version 9.2, SAS Inst. Inc.,Cary, NC, 2008). All data were expressed as least squares means (LSM) and the standard error (SEM) of the LSM. Statistical significance was considered at $P < 0.05$.

Results

Trans-18:1 and CLA Isomer Concentrations in the Rumen and Duodenal Digesta of Bulls Fed n-3 and n-6 PUFA-Based Diets

Generally, the sum of *trans*-18:1 isomer concentrations were up to approximately 60 times higher compared to sum CLA isomer concentrations in the rumen and duodenal digesta of differently fed German Simmental bulls. The *trans*-18:1 isomer concentration in Tables 2 and 3 based on mg/100 g dry matter (DM) and CLA isomers concentration based on μg/100 g DM. The most abundant isomer was *trans*-11-18:1 (VA), however, no dietary effect was detected. The concentration of the sum and individual *trans*-18:1 isomers in the rumen was not affected by the diet, except only one individual *trans* isomer, *trans*-16-18:1. The concentration of *trans*-16-18:1 was significantly decreased in the rumen of the experimental group compared to control group. There was a tendency for increasing concentrations of *trans*-6/7/8-18:1, *trans*-10-18:1, *trans*-11-18:1 from control group to experimental group, however without statistical significance. There was a large variation of *trans*-18:1 data in the duodenal digesta and the sum of *trans*-18:1 fatty acids was significantly lower, compared to the rumen (Tables 2, 3). The individual and sum of *trans*-18:1 isomers showed no dietary effects. *Trans*-4,-5- and *trans*-13/14-18:1 was not detected in duodenal digesta samples according to the used sample preparation method.

Up to eleven individual CLA isomers were detected and quantified in rumen and duodenal digesta samples of the different diet groups (Table 2, 3). The isomers, *trans*-8,*cis*-10 CLA and *trans*-7,*cis*-9 CLA were not detected in the rumen whether in animal of the control or the experimental group (Table 2). The minor isomer *trans*-7,*trans*-9 CLA was below the detection limit (<1 μg/100 g DM) in the rumen of control animals (Table 2). The CLA isomer distribution pattern in the rumen of German Simmental bulls fed n-3 and n-6 PUFA-based diets was significantly affected. The main isomer in the rumen content was *trans*-11,*cis*-13 CLA, and it was significantly increased in the experimental group compared with control group. The second abundant CLA isomer was *cis*-9,*trans*-11 CLA showing no dietary effect, however in tendency higher concentrations in the experimental group. The third abundant CLA isomer was *trans*-11,*trans*-13 CLA, and compared to the control group, the concentration of this isomer increased significantly in the experiment diet group. *Trans*-10,*cis*-12 CLA was decreased by experimental feeding, however not reached statistical significance because of a high data variation (Table 2). The sum of CLA concentrations in the duodenal digesta of all animals was significantly lower compared to the rumen sum CLA concentrations. However, also the CLA isomer distribution pattern in duodenal digesta was affected by different diet systems. Contrary to that in the rumen, the main isomer in duodenal digesta samples was *cis*-9, *trans*-11 CLA, and the experiment diet resulted in a significant increase in this isomer compared to the control group (Table 3). The second most abundant CLA isomers in duodenal digesta samples were *trans*-11,*trans*-13 CLA, *trans*-9,*trans*-11 CLA and *trans*-11,*cis*-13 CLA. The concentration of *trans*-11,*cis*-13 CLA was significantly higher in the duodenal digesta of the experimental group. The isomers *cis*-11,*trans*-13 CLA and *trans*-7,*cis*-9 CLA were in tendency decreased in experimental group compared to control group, however the values did not reach statistical significance. No dietary effects were detected for all identified *trans*,*trans* CLA isomers. *Trans*-7,*trans*-9 CLA and *cis*-12,*trans*-14 CLA were below the detection limit (<1 μg/100 g DM) in digesta samples of both feeding groups (Table 3).

Total Fatty Acid Concentration in the Rumen and Digesta of Bulls Fed n-3 and n-6 PUFA-Based Diets

The total fatty acid composition (mg/100 g DM) in the rumen and duodenal digesta contents of differently fed German Simmental bulls after slaughter is given in Tables 4 and 5. The concentration of the saturated fatty acids (12:0, 14:0, 16:0 and 16:0) in the rumen of the bulls of the experimental group had a tendency to decrease compared to the corresponding concentration of SFA in the control group, however, without statistical significance. Only, the content of 20:5n-3 in the rumen of the experimental group increased significantly compared to control group (Table 4). There was no significant dietary effect on concentration of other fatty acids in the rumen digesta. There was a large individual data variation, and the total concentration of fatty acids in the duodenal digesta was much lower compared to the rumen (Table 5). The content of 22:5n-3 in duodenal digesta of the animals of the experimental group increased significantly, compared to the control group. There was a declining tendency of n-6/n-3 fatty acid ratio from control group to the experimental group without significant relevance.

Discussion

Bioactive fatty acids that escape the rumen via the duodenal digesta, either in unmodified forms or intermediates

Table 2 *Trans*-18:1 fatty acids and CLA isomers concentration in the rumen of German Simmental bulls fed n-3 and n-6 PUFA-based diets (*trans*-18:1 isomers in mg/100 g DM, CLA isomers in μg/100 g DM)

Fatty acid	Control group ($n = 9$)		Experimental group ($n = 7$)		Significance
	LSM	SEM	LSM	SEM	
trans-18:1 isomers					
trans-4-18:1	n.d.		n.d.		
trans-5-18:1	n.d.		n.d.		
trans-6/7/8-18:1	2.64	1.00	4.07	1.07	0.3443
trans-9-18:1	3.74	0.68	3.88	0.73	0.8936
trans-10-18:1	3.68	0.95	4.55	1.02	0.5441
trans-11-18:1	26.61	3.20	29.56	3.43	0.5400
trans-12-18:1	5.33	1.18	4.09	1.26	0.4826
trans-13/14-18:1	12.42	2.61	12.13	2.78	0.9401
trans-15-18:1	5.29	0.88	4.75	0.93	0.6817
trans-16-18:1	5.05[a]	0.78	1.52[b]	0.82	0.0008
Σ *trans*-18:1 isomers	64.78	9.93	64.55	10.62	0.9883
tr,tr isomers					
trans-12,*trans*-14 CLA	43.44	11.44	38.26	12.23	0.7621
trans-11,*trans*-13 CLA	124.33[a]	27.64	209.46[b]	29.55	0.0455
trans-10,*trans*-12 CLA	35.45	10.54	47.01	11.26	0.4669
trans-9,*trans*-11 CLA	47.21	15.16	64.75	16.20	0.4437
trans-8,*trans*-10 CLA	19.93	3.98	13.64	4.26	0.2999
trans-7,*trans*-9 CLA	n.d.		5.78	2.33	
tr,cis; *cis,tr* isomers					
cis-12,*trans*-14 CLA	13.56[a]	3.89	29.82[b]	4.17	0.0137
trans-11,*cis*-13 CLA	388.92[a]	102.40	731.28[b]	109.48	0.0400
cis-11,*trans*-13 CLA	4.16	0.88	6.59	1.02	0.0978
trans-10,*cis*-12 CLA	144.77	75.91	45.13	81.15	0.3862
cis-9,*trans*-11 CLA	273.01	50.46	316.54	53.94	0.5658
trans-8,*cis*-10 CLA	n.d.		n.d.		
trans-7,*cis*-9 CLA	n.d.		n.d.		
Σ CLA	1094.80	225.65	1505.69	241.24	0.2355
VA[A]/*cis*-9,*trans*-11 CLA ratio	82.05	14.41	105.30	16.74	0.2480

Different small letters denote significant differences between groups ($P < 0.05$)

DM dry matter, *LSM* least square means, *SEM* standard error of mean, *n.d.* not detectable

[A] *trans*-11-18:1

of incomplete ruminal biohydrogenation of dietary lipids, have a significant potential to improve the nutritional value of ruminant foods. Investigation of metabolic pathways for the formation of *trans*-18:1 and CLA isomers in the rumen and duodenal digesta could help to explain the endogenous synthesis and post ruminal deposition of these bioactive fatty acids in muscle tissues and milk. Research on mechanisms of ruminal biohydrogenation of 18:2n-6 or 18:3n-3 has been most focused with regard to milk fat synthesis in dairy cows [1, 15, 26, 27]. However, investigations into the occurrence of *trans*-18:1 and CLA isomers in the rumen and duodenum digesta of bulls fed 18:2n-6 or 18:3n-3 PUFA-based diets were only sparsely described. The occurrence of CLA isomers in the rumen and digesta of German Holstein bulls compared pasture with indoor feeding has been recently described by Dannenberger et al. [20], however, not with regard to *trans*-18:1 isomers. It has to take into account in the following discussion that the rumen and duodenal digesta samples of the present study with German Simmental bulls were taken at slaughter only. The *trans*-18:1 and CLA isomer contribution in the rumen and duodenal digesta is a reflection of the diet of the last few days prior to slaughter.

The major pathway of 18:2n-6 metabolism in the rumen involves the formation of *cis*-9,*trans*-11 CLA as the initial intermediate by isomerization, then this isomer is subsequently reduced via VA to 18:0 [11]. The dynamic feature of rumen metabolism of pure 18:2n-6 and in in vitro batch incubations showed the predominantly formation of *trans*-10-18:1, *cis*-12-18:1, *cis*-9,*trans*-11 CLA, *trans*-10,*cis*-12 CLA, *cis*-10,*trans*-12 CLA, *trans*-9,*trans*-11 CLA [18]. The sum of the two main *trans*-18:1 isomers (*trans*-10 and VA) accounted for approximately 50% of the total 18:1 isomers. The sum of the two main CLA isomers in the in vitro investigations (*cis*-9,*trans*-11 CLA and *trans*-10,*cis*-12 CLA) accounted for about 50% of the total 18:2

Table 3 *Trans*-18:1 and CLA isomers concentration in the duodenal digesta of German Simmental bulls fed n-3 and n-6 PUFA-based diets (*trans*-18:1 isomers in mg/100 g DM, CLA isomers in μg/100 g DM)

Fatty acid	Control group ($n = 9$)		Experimental group ($n = 7$)		Significance
	LSM	SEM	LSM	SEM	
trans-18:1 isomers					
trans-4-18:1	n.d.		n.d.		
trans-5-18:1	n.d.		n.d.		
trans-6/7/8-18:1	0.15	0.09	0.24	0.10	0.5083
trans-9-18:1	0.22	0.11	0.25	0.13	0.8417
trans-10-18:1	0.31	0.13	0.29	0.15	0.9214
trans-11-18:1	1.11	0.71	1.29	0.81	0.8684
trans-12-18:1	0.43	0.18	0.26	0.22	0.5595
trans-13/14-18:1	n.d.		n.d.		
trans-15-18:1	0.21	0.12	0.18	0.13	0.8976
trans-16-18:1	0.45	0.20	0.47	0.23	0.9454
Σ *trans* FA	2.88	1.46	2.95	1.66	0.9730
tr,tr isomers					
trans-12,*trans*-14 CLA	2.02	0.59	3.26	0.67	0.1827
trans-11,*trans*-13 CLA	11.42	1.77	11.13	2.00	0.9148
trans-10,*trans*-12 CLA	2.57	1.10	4.55	1.25	0.2570
trans-9,*trans*-11 CLA	4.65	4.13	16.20	5.06	0.1000
trans-8,*trans*-10 CLA	2.08	0.64	2.17	0.72	0.9250
trans-7,*trans*-9 CLA	n.d.		n.d.		
tr,cis; *cis,tr* isomers					
cis-12,*trans*-14 CLA	n.d.		n.d.		
trans-11,*cis*-13 CLA	4.01[a]	1.78	10.41[b]	2.02	0.0323
cis-11,*trans*-13 CLA	6.36	1.53	3.96	1.74	0.3187
trans-10,*cis*-12 CLA	3.05	1.21	3.53	1.38	0.7974
cis-9,*trans*-11 CLA	12.69[a]	4.26	28.75[b]	4.83	0.0257
trans-8,*cis*-10 CLA	1.69	0.58	2.58	0.66	0.3233
trans-7,*cis*-9 CLA	2.26	0.59	1.68	0.67	0.5320
Σ CLA	52.80	12.27	85.92	13.91	0.0960
VA[A]/*cis*-9,*trans*-11 CLA ratio	33.15	6.78	27.13	7.12	0.7608

Different small letter superscripts denote significant differences between groups ($P < 0.05$)

DM dry matter, LSM least square means, *SEM* standard error of mean, *n.d.* not detectable

[A] *trans*-11-18:1

intermediates [18]. Also, investigations of in vitro studies of ovine rumen samples and pure bacteria incubated with 18:2n-6 yield the main CLA isomers *cis*-9,*trans*-11 CLA, *trans*-10,*cis*-12 CLA, *trans*-9,*trans*-11 CLA with traces of *trans*-9,*cis*-11 CLA and *cis*-10,*cis*-12 CLA [28]. Further investigations of ruminal bacteria cultures revealed that the reduction of 9,11 geometric CLA isomers occurs via different mechanisms compared to other unsaturated fatty acids [19]. Recently, beside the bacterial metabolism the contribution of protozoa in the biosynthesis of *trans*-18:1 fatty acids and CLA isomers in the rumen was investigated [2, 17]. Protozoa only isomerizes 18:2n-6 to *cis*-9,*trans*-11 CLA, *trans*-9,*cis*-11 CLA, *trans*-10,*cis*-12 CLA, *trans*-9,*trans*-11 CLA, and *trans*-10,*trans*-12 CLA, however, these isomers were not further metabolized. Additionally, bacteria in the rumen produce two *cis,cis* CLA isomers (*cis*-10,*cis*-12 CLA, *cis*-9,*cis*-11 CLA) and these isomers are biohydrogenated to *trans*-18:1 isomers and 18:0 [2, 17].

The results of the present in vivo study with German Simmental bulls fed 18:2n-6 or 18:3n-3 PUFA-based diets confirmed the results of the occurrence of the predominantly formed *trans*-18:1 and CLA isomers from the in vitro studies mentioned above, except *cis,cis* CLA isomers. In contrast to the previous in vitro studies based only on GC investigations, the present study involved two different GC methods and an Ag^+-HPLC method for correct isomer identification of *trans*-18:1 and CLA isomers. By the use of the latter HPLC method the correct CLA isomer identification was achieved in rumen and duodenal digesta samples (Fig. 1).

Contrary to the in vitro studies based on GC measurements, the Ag^+-HPLC measurements in this study did not show the occurrence of *cis,cis* CLA isomers in the rumen samples. The peaks detected in the retention time region of the *cis,cis* CLA isomers in standard solution of the chromatograms did not show UV-spectra typical of *cis,cis* CLA

Table 4 Total fatty acid concentration in the rumen of German Simmental bulls fed n-3 and n-6 PUFA-based diets (mg/100 g DM)

Fatty acid	Control ($n = 9$)		Experiment ($n = 7$)		Significance
	LSM	SEM	LSM	SEM	
12:0	2.04	0.46	0.97	0.49	0.1332
14:0	24.43	6.68	9.46	7.14	0.1499
16:0	138.22	19.49	106.15	20.84	0.2814
16:1	3.85	0.68	2.14	0.73	0.1097
18:0	441.05	63.71	345.80	68.10	0.3257
cis-9-18:1	14.41	2.70	17.88	2.89	0.3974
cis-11-18:1	3.63	0.61	4.38	0.65	0.4129
18:2n-6	18.71	3.24	18.07	3.47	0.8945
18:3n-3	1.35	0.28	1.14	0.30	0.6282
20:4n-6	0.29	0.09	0.18	0.11	0.4865
20:5n-3	1.35[a]	0.31	2.88[b]	0.33	0.0048
22:4n-6	0.37	0.10	0.22	0.11	0.3644
22:5n-3	1.19	0.30	0.87	0.32	0.4883
22:6n-3	0.32	0.09	0.60	0.10	0.0633
Σ SFA[A]	657.20	96.81	508.33	103.49	0.3126
Σ UFA[B]	129.44	19.96	130.56	21.34	0.9700
Σ PUFA[C]	26.37	4.27	27.15	4.57	0.9030
n-3FA[D]	5.02	0.82	6.38	0.88	0.2827
n-6 FA[E]	19.77	3.37	18.95	3.60	0.8706
n-6/n-3 ratio	4.06	0.44	3.05	0.47	0.1432
Σ FA[F]	786.64	114.05	638.89	121.93	0.3922

Different letters denote significant differences between groups ($P < 0.05$)

DM dry matter, *LSM* least square means, *SEM* standard error of mean

[A] Sum of C10:0 + C11:0 + C12:0 + C13:0 + C14:0 + C15:0 + C16:0 + C17:0 + C18:0 + C20:0 + C21:0 + C22:0 + C23:0 + C24:0

[B] Sum of C14:1 + C15:1 + C16:1 + C17:1 + C18:1t + C18:1*c*9 + C18:1*c*11 + C18:2*t* + C18:2 n-6 + C18:3 n-3 + C18:4 n-3 + C20:3 n-6 + C20:4 n-6 + C20:5 n-3 + C22:1 + C22:4 n-6 + C22:5 n-3 + C22:6 n-3 + c9.tr11CLA + C18:3 n-6 + C20:2 n-6 + C20:3 n-3 + C22:2 n-6 + C24:1

[C] Sum of C18:2*t* + C18:2 n-6 + C18:3 n-3 + C18:4 n-3 + C20:3 n-6 + C20:4 n-6 + C20:5 n-3 + C22:1 + C22:4 n-6 + C22:5 n-3 + C22:6 n-3 + c9,tr11CLA + C18:3 n-6 + C20:2 n-6 + C20:3 n-3 + C22:2 n-6

[D] Sum of C20:3n-3 + C22:6n-3 + C22:5n-3 + C20:5n-3 + C18:4n-3 + C18:3n-3

[E] Sum of C22:2n-6 + C20:2n-6 + C18:3n-6 + C22:4n-6 + C20:3n-6 + C18:2n-6 + C20:4n-6

[F] Sum SFA + UFA

isomers using PDA detector and were not identified as *cis,cis* CLA isomers, also described in our earlier study with German Holstein bulls [20]. The rumen biohydrogenation of the CLA isomers to *trans*-10-18:1 and *trans*-11-18:1 yields between 47 and 53% of the total *trans*-18:1 isomers without significant differences between the different groups.

Ruminal biohydrogenation of 18:3n-3 is not fully understood compared to that of 18:2n-6 [2, 28]. In vitro incubations with 18:3n-3 resulted predominantly in VA, *trans*-13/14-18:1, *trans*-11,*cis*-13 CLA, *trans*-11,*trans*-13 CLA, *cis*-11,*trans*-13 CLA and conjugated linolenic isomers compared to 18:2n-6 incubations [2, 18]. After 24 h incubation of 18:3n-3 the biohydrogenation yielded mainly in *trans*-18:1 isomers and lower in the final product (18:0) of this process [18]. Also, these findings based on GC measurements correspond to the results of our feeding experiment with German Simmental bulls. *N*-3 PUFA based diet (experimental group) resulted in significant higher concentration of predominantly *trans*-11,*cis*-13 CLA and *trans*-11,*trans*-13 CLA determined by the use of Ag^{+}-HPLC in the rumen of bulls compared to bulls of the control group. It was shown that *cis*-9,*trans*-11 CLA is rapidly metabolized, while VA accumulates during biohydrogenation of PUFA in the rumen as shown by Piperova et al. [29]. The ratio of VA to *cis*-9,*trans*-11 CLA in the rumen of the present study was high and ranged between 82-105:1, however, not diet dependent (Table 2). This high ratio of VA to *cis*-9,*trans*-11 CLA in the rumen is supported by other studies [20, 29]. The complete biohydrogenation in the rumen of the diet groups seems not affected by the diet,

Table 5 Total fatty acid concentration in the duodenal digesta of German Simmental bulls fed n-3 and n-6 PUFA-based diets (mg/100 g DM)

Fatty acid	Control ($n = 9$)		Experiment II ($n = 7$)		Significance
	LSM	SEM	LSM	SEM	
12:0	0.39	0.19	0.61	0.21	0.4606
14:0	3.91	1.83	5.83	2.07	0.4984
16:0	11.77	6.74	12.39	7.65	0.9520
16:1	0.64	0.26	0.40	0.29	0.5468
18:0	25.54	13.62	20.91	15.44	0.8257
cis-9-18:1	8.18	3.74	8.10	4.24	0.9876
cis-11-18:1	0.76	0.38	0.76	0.43	0.9988
18:2n-6	21.19	11.47	15.48	13.01	0.7470
18:3n-3	2.60	1.60	3.70	1.81	0.6557
20:4n-6	3.32	1.43	2.06	1.65	0.5743
20:5n-3	0.48	0.35	1.14	0.40	0.2378
22:4n-6	0.44	0.18	0.79	0.19	0.2061
22:5n-3	0.44[a]	0.37	1.88[b]	0.42	0.0220
22:6n-3	0.70	0.22	0.73	0.26	0.9183
Σ SFA[A]	48.85	22.98	48.94	26.05	0.9978
Σ UFA[B]	47.85	23.43	46.78	26.57	0.9763
Σ PUFA[C]	30.33	15.58	27.34	17.67	0.9009
n-3FA[D]	17.52	7.92	19.43	8.298	0.8751
n-6 FA[E]	26.07	13.54	19.83	15.36	0.7650
n-6/n-3 ratio	0.94	0.15	0.76	0.18	0.4600
Σ FA[F]	96.70	46.23	95.73	52.42	0.9890

For footnotes see Table 4

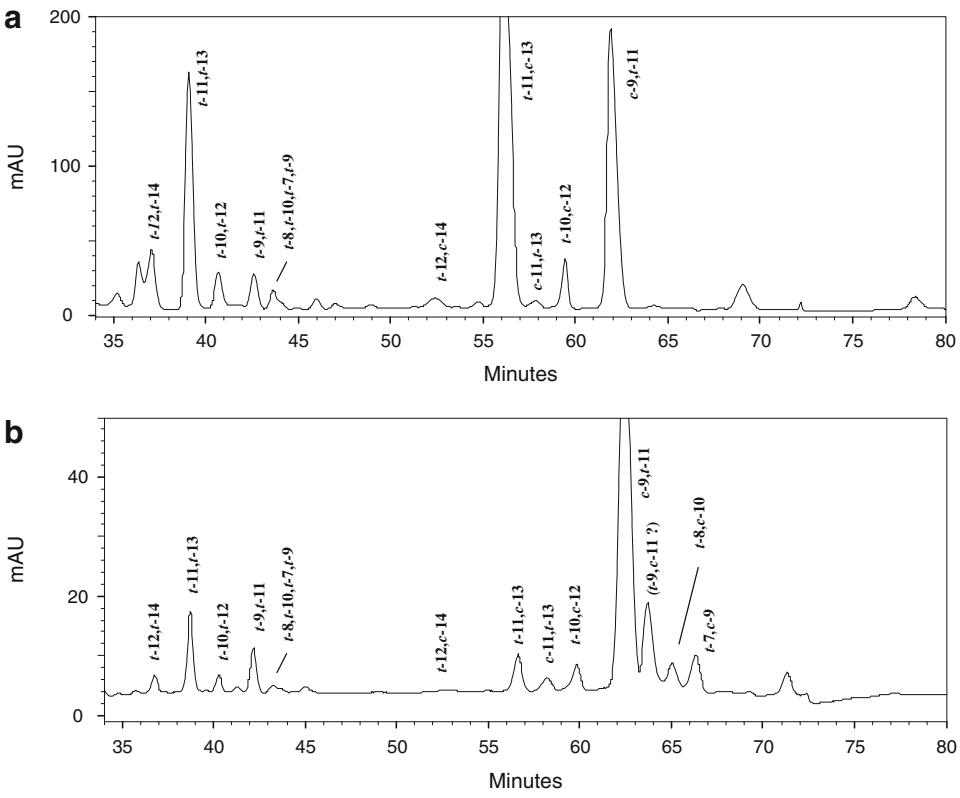

Fig. 1 CLA isomers in rumen content (**a**) and duodenal digesta (**b**) of German Simmental bulls of an experimental group (partial Ag^{+}-HPLC/DAD chromatograms, detected at 233 nm)

because the concentrations of the final product of rumen biohydrogenation 18:0 showed no significant differences between both groups (Table 4). The total *trans*-18:1 and CLA isomers concentrations in the duodenal digesta of slaughtered bulls were approximately 22 and 19 times lower, respectively, compared to the corresponding concentrations in the rumen. This is not in agreement with another bull experiment where approximately 1.4-fold higher CLA isomer concentration was measured in the duodenal digesta compared to the rumen [20]. In contrast, the total *trans*-18:1 concentration was up to 3.9 times higher in the rumen compared to duodenal digesta [20]. A more detailed discussion was complicated by a lack of available data in the literature using complimentary GC techniques and an additional Ag^{+}-HPLC method. Furthermore, the CLA isomer distribution pattern in duodenal digesta was totally different compared to the rumen. In the duodenal digesta, *cis*-9,*trans*-11 CLA, the second most abundant isomer in the rumen, occurred as the main CLA isomer in the duodenal digesta with significant higher concentrations in the experimental group. The comparison of VA/*cis*-9,*trans*-11 CLA ratio in the rumen and duodenal digesta pointed to a predominantly production of VA in the rumen (82-105:1, Table 2). In contrast, the VA/*cis*-9,*trans*-11 CLA ratio in the duodenum digesta revealed higher amounts of *cis*-9,*trans*-11 CLA resulting in lower ratio compared to the rumen (27-33:1, Table 3). The study of Piperova et al. [29] investigated the duodenal *trans*-18:1 and CLA isomers in lactating dairy cows found similar VA/*cis*-9,*trans*-11 CLA ratio. However, no comparable investigation has been conducted in the rumen of lactating dairy cows. One probably explanation for the higher *cis*-9,*trans*-11 CLA concentration in the duodenal digesta could be that the collected samples include bile and pancreatic juice because the sample-taking was 1 m after the pylorus and both the bile and the pancreatic duct open less than 1 m after the pylorus. Another explanation could be the conversion of VA to *cis*-9,*trans*-11 CLA catalyzed by the SCD enzyme in the duodenal digesta. Archibeque et al. [30] found a high SCD enzyme activity in duodenal mucosal tissue of beef steers fed with different grains [30]. However, until now it remains unclear if the SCD enzyme in the duodenal mucosal tissue is involved in the conversion of VA to *cis*-9,*trans*-11 CLA. Generally, *cis*-9,*trans*-11 CLA, known as the main isomer in beef muscle, resulting most likely from the endogenous biosynthesis via SCD enzyme activity of ruminally formed VA [13, 15]. Furthermore, the isomers *trans*-7,*cis*-9 CLA and *trans*-8,*cis*-10 CLA including their geometrical isomers occurred in the duodenal digesta samples, but were not detected in the rumen (Fig 1). Consistent with this result, the *trans*-7,*cis*-9 CLA and *trans*-8,*cis*-10 CLA isomers were not present in the fatty acids isolated from the rumen fluid of lactating dairy cows [29]. To our knowledge, it seems unclear if the formation of these CLA isomers from the corresponding *trans*-18:1 isomers is based on the activity of SCD enzyme in the duodenal mucosal tissue [30] or other mechanisms in the duodenal digesta. The present results were supported by other studies investigating the reduction of *trans*-7,*cis*-9 CLA concentrations in milk by the use of SCD inhibitors [29, 31]. Taking into account that the inhibition of SCD is not complete, the authors measured endogenous synthesis rates of *trans*-7,*cis*-9 CLA between 85 and 100% in milk fat and concluded that this CLA isomer is biosynthesized almost exclusively from endogenous synthesis via SCD [31].

The results indicated that the diet-dependent occurrence of predominantly CLA isomers in rumen and duodenal digesta gives us the opportunity to regulate the post ruminal deposition of bioactive fatty acids in tissue lipids.

Acknowledgments This study was supported by the Federal Ministry of Food, Agriculture and Consumer Protection of Germany and the Ministry of Agriculture of China (Grant No. 30/2008-2009 "Biosynthesis of CLA in beef"), and the National Natural Science Foundation of China (No. 30371040) funding to Xiangzhen Shen. The authors gratefully appreciate B. Jentz and H. Rooch of the Research Unit Muscle Biology and Growth for excellent technical assistance in sample preparation and fatty acid isomer analysis. All the authors have contributed to the preparation of the paper and agree with the submitted manuscript content. There are no conflicts of interest.

References

1. Lourenco M, Ramos-Morales E, Wallace RJ (2010) The role of microbes in rumen lipolysis and biohydrogenation and their manipulation. Animal 4:1008–1023
2. Or-Rashid MM, Wright TC, McBride BW (2009) Microbial fatty acid conversion within the rumen and the subsequent utilization of these fatty acids to improve the healthfulness of ruminant food products. Appl Microbiol Biotechnol 84:1033–1043
3. Chillard Y, Glasser F, Ferlay A, Bernard L, Rouel J, Doreau M (2007) Diet, rumen biohydrogenation and nutritional quality of cow and goat milk fat. Eur J Lipid Sci Technol 109:828–855
4. Dannenberger D, Nuernberg K, Nuernberg G, Scollan ND, Ender K (2005) Effect of pasture vs. concentrate diet on CLA isomer distribution in different tissue lipids of beef cattle. Lipids 40:589–598
5. Cruz-Hernandez C, Kramer JKG, Kraft J, Santercole V, Or-Rashid M, Deng Z, Dugan MER, Delmonte P, Yurawecz MP (2006) Systematic analysis of *trans* and conjugated linoleic acids in the milk and meat of ruminants. In: Yurawecs MP, Kramer JKG, Gudmundsen O, Pariza MW, Banni S (eds) Advances in conjugated linoleic acid research, vol 3. AOCS Press, Champaign, USA, pp 45–93
6. Kennedy A, Martinez K, Schmidt S, Mandrup S, LaPoint K, McIntosh M (2010) Antiobesity mechanisms of action of conjugated linoleic acid. J Nutr Biochem 21:171–179
7. Benjamin S, Spener F (2009) Conjugated linoleic acids as functional food: an insight into their health benefits. Nutr Metab 6:13
8. Islam MA, Kim YS, Oh TW, Kim GS, Won CK, Kim HG, Choi MS, Kim JO, Ha YL (2010) Superior anticarcinogenic activity of trans, trans conjugated linoleic acid in *N*-methyl-*N*-nitrosourea-induced rat mammary tumorigenesis. J Agric Food Chem 58:5670–5678

9. Scollan ND, Hocquette J, Nuernberg K, Dannenberger D, Richardson RI, Moloney A (2006) Innovations in beef production systems that enhance the nutritional and health value of beef lipids and their relationship with meat quality. Meat Sci 74:17–33
10. Cruz-Hernandez C, Kramer JKG, Kennelly JJ, Glimm DR, Sorensen BM, Okine EK, Goonewardene LA, Weselake RJ (2007) Evaluating the conjugated linoleic acid and *trans* 18:1 isomers in milk fat of dairy cows fed increasing amounts of sunflower oil and a constant level of fish oil. J Dairy Sci 90:3786–3801
11. Harfoot CG, Hazlewood GP (1997) The rumen microbial ecosystem. In: Hobson PN, Stewart SC (eds) Lipid metabolism in the rumen.. Blackie Academic & Professional, London, UK, pp 382–426
12. Jenkins TC, Wallace RJ, Moate PJ, Mosley EE (2008) Board-invited review: recent advances in biohydrogenation of unsaturated fatty acids within the rumen microbial ecosystem. J Anim Sci 86:397–412
13. Griinari JM, Corl BA, Lacy SH, Chouinard PY, Nurmela KV, Bauman DE (2000) Conjugated linoleic acid is synthesized endogenously in lactating dairy cows by delta(9)-desaturase. J Nutr 130:2285–2291
14. Gruffat D, Remond C, Durand D, Loreau O, Bauchart D (2008) 9cis,11trans conjugated linoleic acid (CLA) is synthesised and desaturated into conjugated 18:3 in bovine adipose tissues. Animal 2:645–652
15. Bauman DE, Perfield JW, Harvatine KJ, Baumgard LH (2008) Regulation of fat synthesis by conjugated linoleic acid: lactation and the ruminant model. J Nutr 138:403–409
16. Glasser F, Ferlay A, Dourau M, Loor JJ, Chillard Y (2010) t10,c12–18:2-induced milk fat depression is less pronounced in cows fed high-concentrate diets. Lipids 45:877–887
17. Or-Rashid MM, Alzahal O, McBride BW (2008) Studies on the production of conjugated linoleic acid from linoleic and vaccenic acid by mixed rumen protozoa. Appl Microbiol Biotechnol 81:533–541
18. Jouany JB, Lassalas B, Doreau M, Glasser F (2007) Dynamic features of the rumen metabolism of linoleic, linolenic acid and linseed oil measured in vitro. Lipids 42:351–360
19. McKain N, Shingfield KJ, Wallace RJ (2010) Metabolism of conjugated linoleic acids and 18:1 fatty acids by ruminal bacteria: products and mechanisms. Microbiology 156:579–588
20. Dannenberger D, Nuernberg K, Nuernberg G (2009) Diet-dependent occurrence of CLA isomers in rumen and duodenal digesta of slaughtered bulls. Eur J Lipid Sci Technol 111: 553–562
21. Mahecha L, Nuernberg K, Nuernberg G, Ender K, Hagemann E, Dannenberger D (2009) Effects of diet and storage on fatty acid profile, micronutrients and quality of muscle from German Simmental bulls. Meat Sci 82:365–371
22. Herdmann A, Martin J, Nuernberg G, Wegner J, Dannenberger D, Nuernberg K (2010) How does n-3 fatty acid (short time restricted *vs* unrestricted) and n-6 fatty acid enriched diets affect the fatty acid profile in different tissues of German Simmental bulls? Meat Sci 86:712–719
23. Sukhija PS, Palmquist DL (1988) Rapid method for determination of total fatty acid content and composition of feedstuffs and feces. J Agric Food Chem 36:1202–1206
24. Dannenberger D, Nuernberg G, Scollan ND, Schabbel W, Steinhart H, Ender K, Nuernberg K (2004) Effect of diet on the deposition of n-3 fatty acids, conjugated linoleic and C18:1*trans* fatty acid isomers in muscle lipids of German Holstein bulls. J Agric Food Chem 52:6607–6615
25. Kramer JKG, Hernandez M, Cruz-Hernandez C, Kraft J, Dugan MER (2008) Combining results of two GC separations partly achieves determination of all *cis* and *trans* 16:1, 18:1, 18:2 and 18:3 except CLA isomers of milk fat as demonstrated using Ag-Ion SPE fractionation. Lipids 43:259–273
26. Shingfield KJ, Chillard Y, Toivonen V, Kairenius P, Givens DI (2008) Trans fatty acids and bioactive lipids in ruminant milk. In: Bioactive components of milk, advances in experimental medicine and biology, vol 606. Springer, New York, pp 3–65
27. Destaillats F, Trottier JP, Galvez JM, Angers P (2005) Analysis of a-linolenic acid biohydrogenation intermediates in milk fat with emphasis on conjugated linoleic acids. J Dairy Sci 88:3231–3239
28. Wallace RJ, McKain N, Shingfield KJ, Devillard E (2007) Isomers of conjugated linoleic acids are synthesized via different mechanisms in ruminal digesta and bacteria. J Lipid Res 48:2247–2254
29. Piperova LS, Sampugna J, Teter BB, Kalscheur KF, Yurawecz MP, Ku Y, Morehouse KM, Erdman RA (2002) Duodenal and milk *trans* octadecenoic acid and conjugated linoleic acid (CLA) isomers indicate that post absorptive synthesis is the predominant source of *cis*-9-containing CLA in lactating dairy cows. J Nutr 132:1235–1241
30. Archibeque SL, Lunt DK, Gilbert CD, Tume RK, Smith SB (2005) Fatty acid indices of stearoyl-CoA desaturase do not reflect actual stearoyl-CoA desaturase activities in adipose tissues of beef steers finished with corn-, flaxseed-, or sorghum-based diets. J Anim Sci 83:1153–1166
31. Corl BA, Baumgard LH, Griinari JM, Delmonte P, Morehouse KM, Yurawecz ME, Bauman DE (2002) *Trans*-7,*cis*-9 CLA is synthesized endogenously by Δ^9-desaturase in dairy cows. Lipids 37:681–688

Lipids (2011) 46:843–850
DOI 10.1007/s11745-011-3584-7

ORIGINAL ARTICLE

Isomerization of Vaccenic Acid to *cis* and *trans* C18:1 Isomers During Biohydrogenation by Rumen Microbes

S. Laverroux · F. Glasser · M. Gillet · C. Joly · M. Doreau

Received: 10 September 2010 / Accepted: 7 June 2011 / Published online: 26 June 2011

Abstract In ruminants, *cis* and *trans* C18:1 isomers are intermediates of fatty acid transformations in the rumen and their relative amounts shape the nutritional quality of ruminant products. However, their exact synthetic pathways are unclear and their proportions change with the forage:concentrate ratio in ruminant diets. This study traced the metabolism of vaccenic acid, the main *trans* C18:1 isomer found in the rumen, through the incubation of labeled vaccenic acid with mixed ruminal microbes adapted to different diets. [1-^{13}C]*trans*-11 C18:1 was added to in vitro cultures with ruminal fluids of sheep fed either a forage or a concentrate diet. ^{13}C enrichment in fatty acids was analyzed by gas-chromatography-mass spectrometry after 0, 5 and 24 h of incubation. ^{13}C enrichment was found in stearic acid and in all *cis* and *trans* C18:1 isomers. Amounts of ^{13}C found in fatty acids showed that 95% of vaccenic acid was saturated to stearic acid after 5 h of incubation with the concentrate diet, against 78% with the forage diet. We conclude that most vaccenic acid is saturated to stearic acid, but some is isomerized to all *cis* and *trans* C18:1 isomers, with probably more isomerization in sheep fed a forage diet.

S. Laverroux (✉) · F. Glasser · M. Doreau
INRA, UR1213 Herbivores, Site de Theix,
63122 Saint-Genès-Champanelle, France
e-mail: Sophie.Laverroux@clermont.inra.fr

M. Gillet
CEA, IBiTecS, Service de Chimie Bioorganique et de Marquage,
91191 Gif-sur-Yvette, France

C. Joly
INRA, Plateforme métabolisme et spectrométrie de masse,
Site de Theix, 63122 Saint-Genès-Champanelle, France

Keywords Vaccenic acid · Isomerization · C18:1 isomers · Biohydrogenation · Rumen microbes · Fatty acids · Forage:concentrate ratio

Abbreviations

DMDS	Dimethyl disulfide
FA	Fatty acid(s)
FAME	Fatty acid methyl ester(s)
GC–FID	Gas chromatography–flame ionization detection
GC–MS	Gas chromatography–mass spectrometry

Introduction

In ruminants, dietary fatty acids (FA) are extensively hydrogenated and isomerized by rumen microbes. These transformations directly determine milk and meat FA composition, which is a criterion of the nutritional quality of the products [1]. Ruminal contents contain numerous C18:1 isomers (from *cis*-6 to *cis*-15 and from *trans*-6 to *trans*-16), which relative proportions depend on diet composition [2]. However, the detailed production pathways of all the C18:1 isomers found in the rumen are unclear. Recently Shingfield [3] reviewed studies on ruminal biohydrogenation and advanced some hypotheses on the production of many C18:1 isomers from the biohydrogenation of oleic, linoleic and linolenic acids. More specifically, Mosley et al. [4] and Proell et al. [5] found that *cis*-9 and *trans*-9 C18:1 were not only hydrogenated to stearic acid, but were also isomerized to several positional and geometric isomers. However, little is known about the metabolization of other C18:1 isomers in ruminants or about the share of these metabolized FA between stearic acid and C18:1 isomers. As vaccenic acid

(*trans*-11 C18:1) is the main *trans* C18:1 isomer present in the rumen [6], we undertook to study its isomerization and biohydrogenation pathways. As the forage:concentrate ratio of the diet modifies the ruminal FA profile and biohydrogenation [7, 8], as well as the rumen microbial community [9], we also examined whether this ratio modified the isomerization and biohydrogenation pathways of vaccenic acid. For this purpose, rumen fluid from sheep fed two contrasting diets was incubated with [1-^{13}C]*trans*-11 C18:1 during 24 h and the appearance of ^{13}C was traced in stearic acid and in the C18:1 isomers.

Materials and Methods

Experimental Design

Four adult sheep at maintenance, weighing on average 62 kg and fitted with ruminal cannulas were used as donors of ruminal contents. Animal surgery and care complied with the Guide for the Care and Use of Laboratory Animals [10]. Two sheep received a forage diet (F) composed of 100% meadow hay. The other two sheep were progressively switched to a concentrate diet (C) composed of 40% meadow hay and 60% barley pellets. The sheep were fed 1,200 g dry matter per day in two equal meals. The ruminal contents were collected after 2 weeks of adaptation to the diets. On 3 days (three replicates), 250 mL of ruminal contents were collected before the morning meal, pooled by diet and immediately transferred to the laboratory for in vitro incubation.

In Vitro Incubations

For each of the three replicates, two series of incubators (F and C) were prepared for the ruminal contents of sheep fed the F and C diets. Each series contained three control incubators (without labeled vaccenic acid) and three experimental incubators (with labeled vaccenic acid), corresponding to the three incubation times (0, 5 and 24 h). Each incubator was a 120-mL bottle containing 500 mg of substrate (50% meadow hay, 50% barley pellets) and 25 mL of Simplex buffer [11] prewarmed to 39 °C. The control incubators received 250 µL of pure ethanol. The experimental incubators received 5 mg of [1-^{13}C]*trans*-11 C18:1 in 250 µL of pure ethanol [4]. [1-^{13}C]*trans*-11 C18:1 (chemical purity >95%, isotopic enrichment >99%) was synthesized by the Commissariat à l'Énergie Atomique (CEA, Gif-sur-Yvette, France) according to well-established procedures [12, 13]. The ruminal contents were strained through a 250-µm nylon cloth and 15 mL of ruminal fluid were added to the corresponding incubators previously gassed with CO_2 for 10 min. The incubators were sealed to ensure anaerobic conditions and placed in a shaking water bath at 39 °C and 100 shakes/min. One control incubator and one experimental incubator from each series (F and C) were taken just before incubation (t_0) or removed after 5 or 24 h of incubation. The pressure was measured with a pressure sensor to calculate gas production, gases were sampled with a syringe to analyze the gas composition as described by Broudiscou et al. [14], pH was measured and the whole content of each incubator was immediately frozen. The contents were then freeze-dried and weighed to determine the total dry matter content. The contents were ground in a micro hammer mill through a 1-mm sieve before FA analysis.

Fatty Acid Analysis

Fatty acids were directly transmethylated, essentially as described by Sukhija and Palmquist [15] with modifications according to Loor et al. [16]. In addition, recovered methyl esters were purified through a florisil column (Florisil®, Sigma-Aldrich, St Louis, USA). Methyl tricosanoate (0.2 mg, Sigma-Aldrich, St Louis, USA) was used as internal standard. Fatty acid methyl esters (FAME) were divided into three fractions. A first fraction was used for FA quantification. For this purpose, 1 µl of FAME at a 30:1 split ratio was injected by auto-sampler into a Varian CP-3800 gas chromatograph (GC) equipped with a flame ionization detector (FID) and a 100 m × 0.25 mm i.d. CP-Sil 88 fused silica capillary column (ChromPack—Varian Inc., Lake Forest, USA). Chromatographic conditions followed the procedure of Loor et al. [16] except that the detector temperature was 300 °C. Pure methyl ester standards purchased from Supelco (Bellefonte, USA), Sigma (St Louis, USA), Nu-chek Prep (Elysian, USA), and Biovalley (Conches, France) were used to identify FA peaks, except for some *trans* and *cis* C18:1 isomers that were identified by order of elution according to Kramer et al. [17]. Some C18:1 isomers were coeluted (as stated in Tables 1, 2).

^{13}C Enrichment of Palmitic, Stearic, Linoleic and Linolenic Acids

A second fraction of the FAME was used to measure ^{13}C enrichment in C16:0, C18:0, C18:2 n-6 and C18:3 n-3. Analysis was performed by GC (Agilent model 7890A) equipped with a mass spectrometer (MS) (Agilent model 5975C inert XL EI/CI) and a 100 m × 0.25 mm i.d. CP-Sil 88 fused silica capillary column (ChromPack—Varian Inc., Lake Forest, USA). GC–MS conditions were as follows: 1 µL was injected in splitless mode; the injector temperature was maintained at 250 °C; the carrier gas was helium at

Table 1 Fatty acid amount and composition in the control incubators at t_0 according to the diet of the ruminal fluid donor (diet F: 100% hay; diet C: 60% barley and 40% hay)

	F	C	SEM	Diet effect *P* value
Total fatty acids (mg/incubator)	9.72	31.21	2.369	0.012
Fatty acids (g/100 g total FA)				
C16:0	23.49	22.88	0.342	0.136
C18:0	16.99	43.69	0.895	<0.001
C18:1				
trans-6 + 7 + 8	0.05	0.13	0.011	0.024
trans-9	0.06	0.09	0.008	0.086
trans-10	0.06	0.19	0.022	0.045
trans-11	1.24	2.27	0.149	0.003
trans-12	0.06	0.33	0.006	0.001
trans-13 + 14	0.12	0.34	0.021	0.017
cis-9	7.78	4.52	0.230	0.003
cis-10	0.12	0.18	0.018	0.011
cis-11	0.71	0.41	0.046	0.030
cis-12	0.01	0.10	0.006	0.056
cis-13	ND	ND	–	–
cis-14 + *trans*-16	0.05	0.21	0.014	0.002
cis-15	0.01	0.01	0.006	–[a]
C18:2				
trans-11, *cis*-15	0.07	0.06	0.021	0.786
cis-9, *cis*-12	25.88	11.77	0.402	0.001
Conjugated	0.45	0.18	0.055	0.045
C18:3 n-3	8.00	2.97	0.214	0.004

Values are LS means of three replicates

ND not detectable

[a] Detected in 3 samples for C and 1 sample for F, no *P* value

a constant injector pressure of 30 psi; the oven temperature was started at 60 °C, ramped to 165 °C at 15 °C/min (held for 1 min) and then to 225 °C at 2 °C/min (held for 5 min); the mass spectrometer was operated under positive chemical ionization with ammonia reagent gas at 20 mL/min.

^{13}C Enrichment of C18:1 Isomers

To analyze ^{13}C enrichment of each *cis* and *trans* C18:1 isomers, a third fraction of the FAME was separated into *cis* and *trans* C18:1 fractions, which were converted into DMDS adducts and analyzed by GC–MS. More precisely, this third fraction of the FAME was evaporated under N_2 and dissolved in acetone for HPLC separation of *cis* and *trans* C18:1. The HPLC analysis was performed as described by Juaneda [18], except that the detector was a photodiode spectrophotometer at 194 nm (Beckman 168 Detector, Brea, CA). The fractions containing the *cis* and *trans* C18:1 isomers were collected and converted into DMDS adducts using the procedure of Bernard et al. [19]. The DMDS adducts were analyzed by GC (Agilent model 7890A) with mass spectrometry detection (Agilent model 5975C inert XL EI/CI mass detector) using a 30 m × 0.25 mm i.d. with 0.25 μm film HP5MS (Agilent Technologies, Santa Clara, USA). Injection volume was 1 μL in splitless mode. Injector temperature was maintained at 250 °C. The carrier gas was helium at a constant flow rate of 1 mL/min. The oven temperature was started at 70 °C, ramped to 195 °C at 20 °C/min, then to 225 °C at 1 °C/min (held for 5 min), and finally to 290 °C at 10 °C/min (held for 5 min). The transfer line heater was set at 300 °C. The mass spectrometer was operated under electron impact ionization conditions (electron energy 70 eV, source temperature 200 °C). Data were collected in single reaction monitoring mode.

Calculations and Statistics

Biohydrogenation rates were calculated for oleic, linoleic and linolenic acids as follows: $(\%FA_{t0} - \%FA_{5\ or\ 24h})/\%FA_{t0} \times 100$. A statistical analysis of biohydrogenation rates and fermentation data (pH, gas production and composition) was performed using the Mixed procedure of SAS with diet and vaccenic acid addition as fixed effects, replicate as random effect and incubation time as repeated measure.

For C16:0, C18:0, C18:2 n-6 and C18:3 n-3 methyl esters, the atom percent excess (APE) was calculated from the mass abundance of the labeled and unlabeled molecular ions using the equation $APE = (^{13}C)/(^{12}C + {}^{13}C)$. The DMDS adducts produce two distinct spectral fragments

Table 2 Evolution of the fatty acid amount and composition in the experimental incubators, according to the diet of the ruminal fluid donor (diet F: 100% hay; diet C: 60% barley and 40% hay)

Diet	F			C			SEM	Diet effect *P* value
Time (h)	0	5	24	0	5	24		
Total fatty acids (mg/incubator)	15.35	14.96	16.72	33.54	31.97	37.42	2.978	<0.001
Fatty acids (g/100 g total FA)								
C16:0	16.09	15.42	15.87	19.33	19.61	19.83	0.384	<0.001
C18:0	11.71	19.83	37.38	38.32	45.37	53.86	1.127	<0.001
C18:1								
trans-6 + 7 + 8	0.04	1.11	0.44	0.11	0.29	0.22	0.048	<0.001
trans-9	0.04	0.44	0.22	0.06	0.16	0.12	0.021	<0.001
trans-10	0.02	0.56	0.38	–[a]	0.25	0.41	0.255	0.621
trans-11	32.56	31.95	24.07	16.02	12.80	9.48	0.620	<0.001
trans-12	0.32	0.98	0.55	0.43	0.54	0.43	0.031	<0.001
trans-13 + 14	0.24	1.53	0.74	0.36	0.60	0.49	0.037	<0.001
cis-9	5.25	4.23	2.10	3.88	3.35	1.82	0.158	<0.001
cis-10	0.10	0.44	0.29	0.14	0.24	0.24	0.028	0.011
cis-11	0.58	0.75	0.59	0.38	0.42	0.24	0.023	<0.001
cis-12	0.02	0.17	0.08	0.09	0.13	0.07	0.012	0.312
cis-13	ND	0.06	0.01	0.00	0.01	0.01	0.010	0.311
cis-14 + *trans*-16	0.03	0.38	0.30	0.18	0.31	0.20	0.036	0.890
cis-15	ND	0.06	0.03	0.01	0.03	0.02	0.010	0.171
C18:2								
trans-11, *cis*-15	0.06	0.23	0.11	0.05	0.07	0.03	0.014	<0.001
cis-9, *cis*-12	17.10	8.30	2.22	9.83	5.76	2.20	0.388	<0.001
Conjugated	0.31	0.28	0.10	0.16	0.09	0.03	0.032	<0.001
C18:3 n-3	5.44	2.76	1.02	2.50	1.23	0.46	0.089	<0.001
Biohydrogenation (%)[b]								
cis-9 C18:1		19.6	60.0		13.3	52.9	2.86	0.071
cis-9, *cis*-12 C18:2		51.5	87.0		41.0	77.5	1.73	0.004
cis-9, *cis*-12, *cis*-15 C18:3		49.2	81.2		50.8	81.4	1.50	0.439

Values are LS means of three replicates

ND not detectable

[a] *trans*-10 C18:1 of C incubators was coeluted with *trans*-11 C18:1 at t_0

[b] Biohydrogenation (%) = $(\%FA_{t0} - \%FA_{5 \text{ or } 24 \text{ h}})/\%FA_{t0} \times 100$

that are indicative of the double bond position when analyzed by mass spectrometry. The F fragment is the methyl thio adduct of the methyl end of the FAME, and the G fragment is the methyl thio adduct of the carboxyl end. Thus for DMDS adducts of C18:1 isomers, APE was calculated from the mass abundance of G and G + 1 fragments using the equation APE = (G + 1)/[G + (G + 1)]. To eliminate the natural levels of ^{13}C, ^{13}C enrichment (%E) of each FA was calculated as $(APE_{experimental} - APE_{control}) \times 100$ for each incubation time. Data of total FA content, FA percentages, and ^{13}C enrichments (all on experimental incubators) were analyzed using the Mixed procedure of SAS with diet as fixed effect, replicate as random effect and incubation time as repeated measure.

We estimated the fraction of vaccenic acid that was saturated to C18:0 or isomerized to the other C18:1 isomers. To this end, we calculated the amounts of ^{13}C-labeled FA that appeared between 0 and 5 h in C18:0 and in all C18:1 isomers. For the isomers that were strongly metabolized (*cis*-6, *cis*-7 and *cis*-9), these amounts were corrected for their metabolization rates. The amounts of ^{13}C that appeared in C18:0 and in each C18:1 isomer were expressed as a percentage of the ^{13}C-labeled vaccenic acid that disappeared. This calculation was made after 5 h of incubation, which corresponds to the beginning of biohydrogenation, whereas after 24 h of incubation most FA were saturated and isomerization could not be accurately assessed. These data were analyzed using the Mixed procedure of SAS with diet as fixed effect and replicate as random effect.

Results

Fermentation Parameters

Addition of 5 mg of vaccenic acid to the incubators did not modify the fermentations, as no modification of the fermentation parameters (pH, gas production and composition) was observed between the control and experimental incubators (data not shown).

The pH of the ruminal fluid did not vary between diets (7.00 vs. 6.81 for F donors and C donors, respectively). However, the diet of the ruminal fluid donors induced some modifications of in vitro fermentations: pH at 24 h was not significantly different for C control incubators and for F control incubators (6.05 vs. 6.12) but gas production was higher in C control incubators (3.2 vs. 2.6 mmol after 24 h; $P < 0.001$) with a higher percentage of CH_4 (20.6 vs. 17.1% at 24 h; $P < 0.001$).

Fatty Acid Composition and Kinetics

The amounts and composition of the FA in the whole contents of the control incubators at t_0 are in Table 1. The diet of the ruminal fluid donor modified the amounts and composition of the FA in the incubators: at t_0 the C incubators contained more FA and had higher percentages of C18:0 and *trans* C18:1, and lower percentages of *cis* C18:1, C18:2 and C18:3 n-3 than the F incubators.

The amounts and composition of the FA in the experimental incubators during the incubations are presented in Table 2. Linolenic, linoleic and oleic acid percentages declined with time, stearic acid percentage increased and percentages of the intermediates of biohydrogenation increased for the first 5 h of incubation, and decreased thereafter. The amounts of vaccenic acid decreased over time in the experimental incubators.

Across control and experimental incubators, the biohydrogenation of linolenic acid was not modified by the diet (82.2% for C incubators, and 83.7% for F incubators after 24 h of incubation). The biohydrogenation of oleic and linoleic acids were lower in C incubators than in F incubators (54.2 vs. 65.8% for oleic acid and 79.0 vs. 89.2% for linoleic acid after 24 h of incubation).

Vaccenic Acid Metabolism

No ^{13}C enrichment was found in palmitic, linoleic or linolenic acids (data not shown).

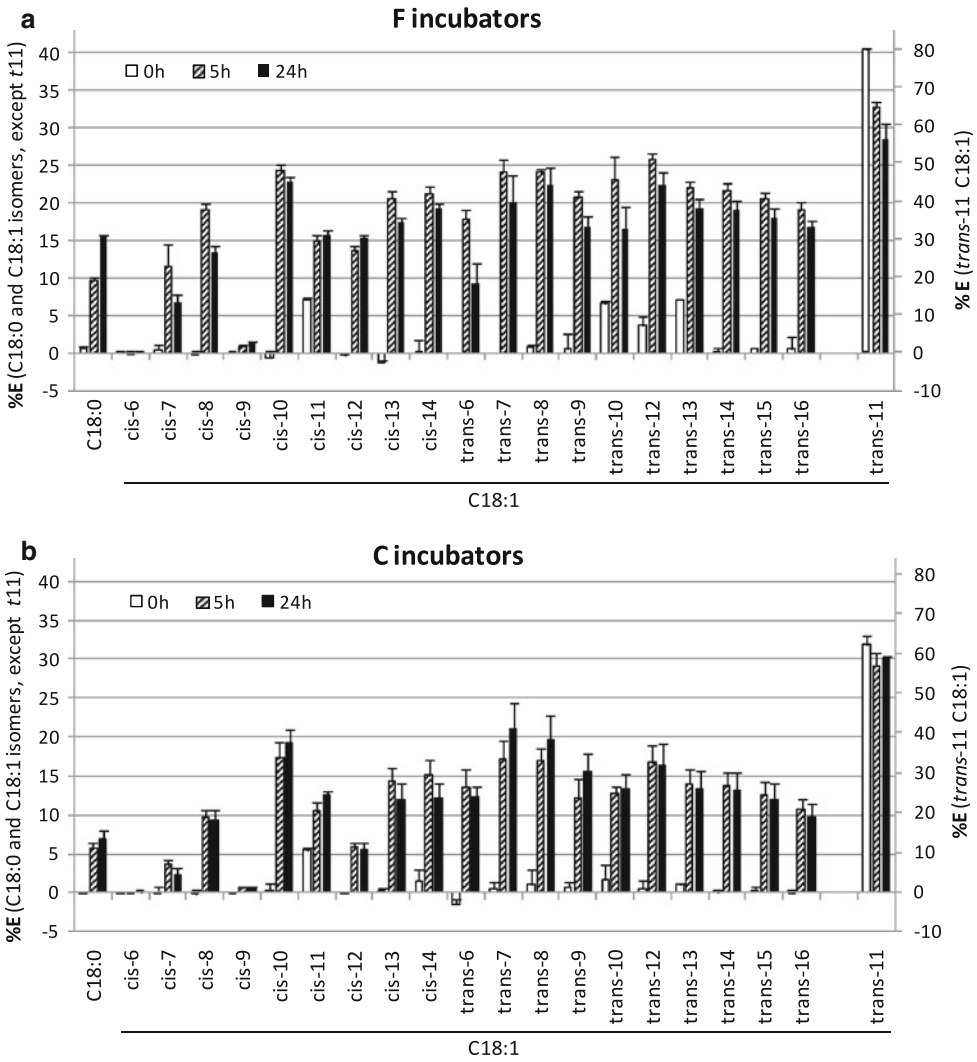

Fig. 1 ^{13}C enrichment of C18:0 and C18:1 isomers after 0 (*white bars*), 5 (*hatched bars*) and 24 h (*black bars*) of incubation of [1-^{13}C]*trans*-11 C18:1 with ruminal fluid of sheep fed a forage diet (**a**) or a concentrate diet (**b**). Each bar is the mean of three replicates. *Error bars* are SE

Following the introduction of labeled vaccenic acid into the experimental incubators, ^{13}C enrichment was significant in C18:0 and in all the *cis* and *trans* C18:1 isomers after 5 and 24 h of incubation, except in *cis*-6 C18:1 at 5 h (Fig. 1). *cis*-6 and *cis*-9 C18:1 were strongly metabolized compared with the other isomers, as shown by the decrease in their amounts between t_0 and 5 h or 24 h (data not shown), which could explain their lower ^{13}C enrichment.

We observed some ^{13}C enrichment of *cis*-11 C18:1 at t_0. This might be due to an analytical bias with some contamination between *cis* and *trans* C18:1 isomers, or possibly to a very rapid isomerization of vaccenic acid to its geometric isomer. We also observed ^{13}C enrichment of *trans*-10, *trans*-12 and *trans*-13 C18:1 at t_0 in F incubators. This might also be due to an analytical bias (the large amount of vaccenic acid did not allow complete separation of isomers by GC–MS), or to a rapid isomerization to neighboring positional isomers (during the freezing time just after vaccenic acid addition) that was more marked in the F incubators. Indeed, isomerization of vaccenic acid to these isomers is confirmed by the fact that the ^{13}C enrichment of these isomers increased between t_0 and 5 h.

In general, ^{13}C enrichment of all FA was higher in the F incubators (diet effect was significant ($P < 0.05$) for C18:0, *cis*-7 to *cis*-14 C18:1 and *trans*-11 to *trans*-16 C18:1). The ^{13}C enrichment of vaccenic acid in the F incubators decreased as early as 5 h of incubation, but the total amount of vaccenic acid was stable. In the C incubators, ^{13}C enrichment of C18:0 and the C18:1 isomers markedly increased between t_0 and 5 h and then remained stable between 5 and 24 h. In contrast, in the F incubators, ^{13}C enrichment of C18:0 and the C18:1 isomers increased between t_0 and 5 h, and then ^{13}C enrichment of the C18:1 isomers decreased while ^{13}C enrichment of C18:0 markedly increased between 5 and 24 h.

The ^{13}C enrichments were different between the C18:1 isomers but the amounts of these isomers also differed. ^{13}C enrichment data could thus not be used directly to estimate the fraction of labeled vaccenic acid converted to C18:0 or C18:1 isomers. For this reason, we calculated the percentage of disappeared ^{13}C-labeled vaccenic acid that appeared in C18:0 and in each of the C18:1 isomers (Fig. 2). Most vaccenic acid was saturated to stearic acid. Saturation tended to be higher in the C incubators than in the F incubators (95 vs. 78%, $P = 0.06$), and conversely the isomerization into other C18:1 isomers was (or tended to be) higher in the F incubators. Figure 2 shows a preferential isomerization of vaccenic acid to *trans*-12, *trans*-13, *trans*-14, *trans*-15 and *cis*-11 C18:1, and then to *cis*-9, *cis*-10 ans *cis*-12 C18:1. The isomerization to the other isomers was markedly lower. These isomerization preferences were the same for F and C incubators.

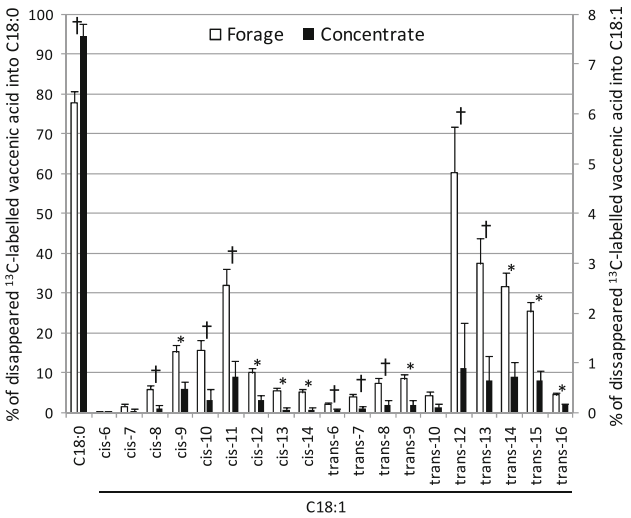

Fig. 2 Distribution of disappeared ^{13}C-labeled vaccenic acid into C18:0 (*left scale*) and C18:1 isomers (*right scale*) after 5 h of incubation with ruminal fluid of sheep fed a forage diet (*white bars*) or a concentrate diet (*black bars*). Each bar is the mean of three replicates. *Error bars* are SEM. † diet effect, $P < 0.10$; * diet effect, $P < 0.05$

Discussion

As the substrate was the same between incubators, the differences between diets in the fermentation parameters were probably due to a difference between the ruminal fluids. As the pH of the ruminal fluids was the same between diets and as the pH of C incubators was not significantly different from that of the F incubators, we can infer that the differences were mainly due to differences in metabolic activity of the microbial communities [20, 21] rather than pH.

Differences in the amounts of FA at t_0 in control incubators show that the ruminal fluid of sheep fed the F diet contained less FA than the ruminal fluid of sheep fed the C diet, probably because of a low quality hay that was very poor in lipids. As the ruminal fluid of sheep fed the F diet contained small amounts of FA, the proportion of FA provided by the substrate was higher in the F incubators than in the C incubators. This explains the differences in FA percentages between incubators at t_0: the FA profile of the F incubators was closer to the FA profile of a feedstuff (lower in C18:0 and higher in polyunsaturated FA).

The kinetics of the FA were consistent with the literature [6], with a decrease in C18 unsaturated FA and an increase in C18:0 over time. In the control incubators, vaccenic acid concentration increased during the first 5 h and decreased thereafter, like all intermediates of biohydrogenation. In the experimental incubators, vaccenic acid decreased over time, which can be explained by the biohydrogenation of the exogenous vaccenic acid that was

higher than the synthesis of vaccenic acid from the polyunsaturated FA.

A lower biohydrogenation is generally observed with high concentrate diets compared with forage diets [7, 16]. Our data are consistent with the literature and show that our in vitro study was representative of FA metabolism in the rumen.

The ^{13}C enrichment of C18:0 reflects the saturation of vaccenic acid and the ^{13}C enrichment of the *cis* and *trans* C18:1 isomers reflects its isomerization. Some authors have shown isomerization of *cis* C18:1 isomers [4, 22] but few have studied the isomerization of *trans* isomers. Kemp et al. [23] reported the isomerization of some *trans* C18:1 isomers but only to the adjacent positional isomers and to the isomer with the opposite geometric configuration. Proell et al. [5] showed isomerization of *trans*-9 C18:1 but only to other *trans* C18:1 and to *cis*-9 and *cis*-11 C18:1.

The larger ^{13}C enrichment of FA in the F incubators was probably due to a higher initial ^{13}C enrichment of vaccenic acid in these incubators as less vaccenic acid was naturally present in the incubators. The decrease in ^{13}C enrichment of vaccenic acid while its amount did not vary shows a synthesis of unlabeled vaccenic acid, most probably from the partial biohydrogenation of the linoleic and linolenic acids present in the incubators. The initial percentages of linoleic and linolenic acids and their biohydrogenation were higher in the F incubators and so induced a higher synthesis of unlabeled vaccenic acid.

The kinetics of ^{13}C enrichment of C18:0 and the C18:1 isomers show that the microbial community of sheep fed the C diet metabolized vaccenic acid rapidly (saturation and isomerization) during the first 5 h and was less active thereafter. By contrast, in F incubators there seemed to be either a promotion of saturation after 5 h or an increased synthesis of the intermediates (C18:1) from biohydrogenation of polyunsaturated FA present in the F incubators.

Figure 2 shows a slightly lower isomerization of vaccenic acid in the C incubators than in the F incubators. Abughazaleh et al. [24] studied labeled *cis*-9 C18:1 in continuous cultures of ruminal content and showed that a low pH decreased the conversion of *cis*-9 C18:1 to *trans* C18:1. He advanced the hypotheses of a diminution of bacterial growth, a diminution of microbial attachment to feed particles, a change in microbial community, or an altered enzyme activity. Several authors have shown that isomerization and saturation can be altered by the composition of the diet, especially fish oil supplementation [25] or by pH and polyunsaturated FA present in the rumen [26]. In our study, the pH were similar between conditions; the differences between C and F incubators could thus arise from differences in initial polyunsaturated FA contents or differences in microbial community or activity [25]. Our study show that a diet rich in forage tends to stimulate isomerization at the expense of saturation of vaccenic acid; however our study cannot show whether the difference between diets was due to an increase in isomerization or to a decrease in saturation, because the amounts of FA at t_0 were very different.

Conclusion

In conclusion, vaccenic acid was preferentially saturated to stearic acid by rumen microbes in vitro but was also isomerized to all C18:1 isomers, though in variable proportion. A higher forage:concentrate ratio tended to increase isomerization of vaccenic acid at the expense of saturation but did not modify the profile of the isomers synthesized.

Acknowledgments This work was carried out with the financial support of the The French National Research Agency (ANR) under the Programme National de Recherche en Alimentation et Nutrition Humaine, project ANR-05-PNRA-017-04, Transqual (*trans* fatty acids from dairy sources: a comparison of the biological effect compared to *trans* fatty acids of technological origin).

References

1. Chilliard Y, Glasser F, Ferlay A, Bernard L, Rouel J, Doreau M (2007) Diet, rumen biohydrogenation and nutritional quality of cow and goat milk fat. Eur J Lipid Sci Technol 109:828–855
2. Glasser F, Schmidely P, Sauvant D, Doreau M (2008) Digestion of fatty acids in ruminants: a meta-analysis of flows and variation factors: 2. C18 fatty acids. Animal 2:691–704
3. Shingfield KJ, Bernard L, Leroux C, Chilliard Y (2010) Role of *trans* fatty acids in the nutritional regulation of mammary lipogenesis in ruminants. Animal 4:1140–1166
4. Mosley EE, Powell GL, Riley MB, Jenkins TC (2002) Microbial biohydrogenation of oleic acid to *trans* isomers in vitro. J Lipid Res 43:290–296
5. Proell JM, Mosley EE, Powell GL, Jenkins TC (2002) Isomerization of stable isotopically labeled elaidic acid to *cis* and *trans* monoenes by ruminal microbes. J Lipid Res 43:2072–2076
6. Harfoot C, Hazlewood G (1988) Lipid metabolism in the rumen. In: Hobson P (ed) The rumen microbial ecosystem. Elsevier, Amsterdam, pp 285–322
7. Kalscheur KF, Teter BB, Piperova LS, Erdman RA (1997) Effect of dietary forage concentration and buffer addition on duodenal flow of *trans*-C18:1 fatty acids and milk fat production in dairy cows. J Dairy Sci 80:2104–2114
8. Doreau M, Ferlay A (1994) Digestion and utilisation of fatty acids by ruminants. Anim Feed Sci Technol 45:379–396
9. Sadet S, Martin C, Meunier B, Morgavi DP (2007) PCR-DGGE analysis reveals a distinct diversity in the bacterial population attached to the rumen epithelium. Animal 1:939–944
10. Institute of Laboratory Animal Resources (1996) Guide for the care and use of laboratory animals. National Academy Press, Washington D.C
11. Williams A, Coleman G (1992) The rumen protozoa. Springer-Verlag, New York, pp 145–156
12. Channing MA, Simpson N (1993) Radiosynthesis of 1-[^{11}C] polyhomoallylic fatty acids. J Label Comp Radiopharm 33: 541–546

13. Loreau O, Maret A, Poullain D, Chardigny JM, Sébédio JL, Beaufrère B, Noël JP (2000) Large-scale preparation of (9Z,12E)-[1–13C]-octadeca-9, 12-dienoic acid, (9Z,12Z,15E)-[1–13C]-octadeca-9,12,15-trienoic acid and their [1–13C] all-*cis* isomers. Chem Phys Lipids 106:65–78
14. Broudiscou LP, Papon Y, Broudiscou A (1999) Effects of inorganic nitrogen and amino acids on the degradation of ammonia-treated barley straw and proteosynthesis in a continuous culture of rumen microbes. Anim Feed Sci Technol 77:149–162
15. Sukhija PS, Palmquist DL (1988) Rapid method for determination of total fatty acid content and composition of feedstuffs and feces. J Agric Food Chem 36:1202–1206
16. Loor JJ, Ueda K, Ferlay A, Chilliard Y, Doreau M (2004) Biohydrogenation, duodenal flow, and intestinal digestibility of *trans* fatty acids and conjugated linoleic acids in response to dietary forage:concentrate ratio and linseed oil in dairy cows. J Dairy Sci 87:2472–2485
17. Kramer J, Blackadar C, Zhou J (2002) Evaluation of two GC columns (60-m supelcowax 10 and 100-m CP sil 88) for analysis of milkfat with emphasis on CLA, 18:1, 18:2 and 18:3 isomers, and short- and long-chain FA. Lipids 37:823–835
18. Juanéda P (2002) Utilisation of reversed-phase high-performance liquid chromatography as an alternative to silver-ion chromatography for the separation of *cis*- and *trans*-C18:1 fatty acid isomers. J Chromatogr A 954:285–289
19. Bernard L, Mouriot J, Rouel J, Glasser F, Capitan P, Pujos-Guillot E, Chardigny J, Chilliard Y (2010) Effects of fish oil and starch added to a diet containing sunflower-seed oil on dairy goat performance, milk fatty acid composition and in vivo Δ9-desaturation of ^{13}C-vaccenic acid. Br J Nutr 104:346–354
20. Mackie RI, Gilchrist FMC, Robberts AM, Hannah PE, Schwartz HM (1978) Microbiological and chemical changes in the rumen during the stepwise adaptation of sheep to high concentrate diets. J Agric Sci 90:241–254
21. Martin SA, Jenkins TC (2002) Factors affecting conjugated linoleic acid and *trans*-C18:1 fatty acid production by mixed ruminal bacteria. J Anim Sci 80:3347–3352
22. Van de Vossenberg JLCM, Joblin KN (2003) Biohydrogenation of C18 unsaturated fatty acids to stearic acid by a strain of *Butyrivibrio hungatei* from the bovine rumen. Lett Appl Microbiol 37:424–428
23. Kemp P, Lander DJ, Gunstone FD (1984) The hydrogenation of some *cis*- and *trans*-octadecenoic acids to stearic acid by a rumen *Fusocillus* sp. Br J Nutr 52:165–170
24. AbuGhazaleh AA, Riley MB, Thies EE, Jenkins TC (2005) Dilution rate and pH effects on the conversion of oleic acid to *trans* C18:1 positional isomers in continuous culture. J Dairy Sci 88:4334–4341
25. Lourenço M, Ramos-Morales E, Wallace R (2010) The role of microbes in rumen lipolysis and biohydrogenation and their manipulation. Animal 4:1008–1023
26. Troegeler-Meynadier A, Bret-Bennis L, Enjalbert F (2006) Rates and efficiencies of reactions of ruminal biohydrogenation of linoleic acid according to pH and polyunsaturated fatty acids concentrations. Reprod Nutr Dev 46:713–724

Lipids (2011) 46:851–861
DOI 10.1007/s11745-011-3579-4

ORIGINAL ARTICLE

Isolation of a Novel Oil Globule Protein from the Green Alga *Haematococcus pluvialis* (Chlorophyceae)

Ehud Peled · Stefan Leu · Aliza Zarka · Meira Weiss · Uri Pick · Inna Khozin-Goldberg · Sammy Boussiba

Received: 23 December 2010 / Accepted: 1 June 2011 / Published online: 6 July 2011

Abstract Cytoplasmic oil globules of *Haematococcus pluvialis* (Chlorophyceae) were isolated and analyzed for pigments, lipids and proteins. Astaxanthin appeared to be the only pigment deposited in the globules. Triacyglycerols were the main lipids (more than 90% of total fatty acids) in both the cell-free extract and in the oil globules. Lipid profile analysis of the oil globules showed that relative to the cell-free extract, they were enriched with extraplastidial lipids. A fatty acids profile revealed that the major fatty acids in the isolated globules were oleic acid (18:1) and linoleic acid (18:2). Protein extracts from the globules revealed seven enriched protein bands, all of which were possible globule-associated proteins. A major 33-kDa globule protein was partially sequenced by MS/MS analysis, and degenerate DNA primers were prepared and utilized to clone its encoding gene from cDNA extracted from cells grown in a nitrogen depleted medium under high light. The sequence of this 275-amino acid protein, termed the *Haematococcus* Oil Globule Protein (HOGP), revealed partial homology with a *Chlamydomonas reinhardtii* oil globule protein and with undefined proteins from other green algae. The HOGP transcript was barely detectable in vegetative cells, but its level increased by more than 100 fold within 12 h of exposure to nitrogen depletion/high light conditions, which induced oil accumulation. HOGP is the first oil-globule-associated protein to be identified in *H. pluvialis*, and it is a member of a novel gene family that may be unique to green microalgae.

Keywords Astaxanthin · *Haematococcus* · Oil globules · Oil globule protein · Triacylglycerols

Abbreviations

CFE	Cell-free extract
CGP	Carotene globule protein
DGDG	Digalactosyldiacylgycerol
DGTS	Diacylglyceroltrimethylhomoserine
EDA	Eicosadienoic acid
HOGP	*Haematococcus* oil globule protein
IEF	Isoelectric focusing
LHCP	Light-harvesting complex proteins
MGDG	Monogalactosyldiacylglycerol
ORF	Open reading frame
SQDG	Sulfoquinovosyldiacylglycerol
TFA	Total fatty acids

Introduction

Oil globules are discrete, sub-cellular organelles surrounded by a monolayer of polar phospholipids, glycolipids or sterols that encircle a hydrophobic core of neutral lipids [1]. These oil globules are ubiquitous in animals, plants, and microorganisms. In many microorganisms, such as yeasts, microalgae and bacteria, the accumulation of oil globules appears to be induced specifically in response to environmental stresses, such as nutrient limitation, high

E. Peled · S. Leu · A. Zarka · I. Khozin-Goldberg · S. Boussiba (✉)
Microalgal Biotechnology Laboratory, French Associates Institute for Agriculture and Biotechnology of Drylands, Jacob Blaustein Institutes for Desert Research, Ben-Gurion University of the Negev, 84990 Sede boker campus, Israel
e-mail: sammy@bgu.ac.il

M. Weiss · U. Pick
Biological Chemistry, Weizmann Institute of Science, Rehovot, Israel

irradiance or osmotic stress [1, 2]. Although a variety of oil globule biogenesis models have been postulated, the actual process remains to be elucidated. Nonetheless, it is commonly accepted that globules are formed by vesiculation from the endoplasmic reticulum (ER) [3].

Two major groups of surface-associated proteins, oleosins and caleosins, are contained in the oil globules of plants. Oleosins comprise the most abundant family of oil–body-associated proteins identified in plants, but to date they have not been found in algae [4]. Caleosin, a calcium binding lipid-body protein that has also been found to be associated with ER membranes [5–7], is ubiquitous among higher plants, and a database search by the authors has revealed putative caleosin super-family proteins in green microalgae (unpublished data). A number of studies have attributed different roles to globule proteins, including globule formation, degradation, stabilization, and involvement in globule–globule or globule-other organelle interactions [1, 4, 7, 8]. Drosophila, yeast, and mammalian globules have also been shown to house refugee proteins that are not directly linked to lipid metabolism [9, 10].

It is known that some unicellular algae contain very large amounts of oil sequestered in oil globules. In some species, oil can amount to as much as 60% of the cell dry mass, with oil accumulation usually being accompanied by the cessation of cell growth [11–13]. However, little is known about the protein composition and functional roles of algal oil globules.

Of particular interest is the high-oil-producing unicellular green alga *Haematococcus pluvialis*. This alga is regarded as the best natural source of the high-value red pigment astaxanthin, a carotenoid that accumulates in algal cytoplasmic oil globules under various stress conditions [14]. The accumulation of astaxanthin in *H. pluvialis* is positively correlated with lipid accumulation, with the former depending on the latter but not vice versa [15]. Lipid accumulation, in turn, depends on de novo fatty acid synthesis [2, 15, 16]. Under nitrate deprivation, astaxanthin and fatty acids may comprise up to 4 and 40%, respectively, of cell dry mass [16]. As is the case for other organisms, oil globule formation in *Haematococcus* was suggested to be structurally related to ER membranes [17].

H. pluvialis is a unique organism for studying oil globule formation, since it accumulates both lipids and carotenoids in the same compartment. Analyses of lipid class distribution in isolated globules have previously been reported by Grunewald et al. [18], whose studies indicated the cytoplasmic origin of globule polar lipids. Zhekisheva et al. [2] found 16:0, 18:1 and 18:2 fatty acids to be the major fatty acids in TAG and astaxanthin esters. To deepen the current understanding of oil globule biogenesis and function, we isolated astaxanthin-rich oil globules from *H. pluvialis* to characterize and identify oil globule proteins.

Seven distinct protein bands associated with globules were identified. The mRNA for one 33-kDa protein was isolated and sequenced. The resulting sequence was found to encode a novel, hydrophobic protein that may have a specific function in green algae, since homologous sequences were found only in other species of green algae.

Materials and Methods

Haematococcus pluvialis Strain

H. pluvialis Flotow 1,844 em. Wille K-0084 (Chlorophyceae, order Volvocales) was obtained from the Scandinavia Culture Center for Algae and Protozoa (SCCAP) at the University of Copenhagen, Denmark.

Growth Conditions for Algal Cultures

H. pluvialis algal cultures were cultivated as previously described [2]. To induce the accumulation of astaxanthin-rich oil globules, cultures were inoculated into nitrate-free mBG-11 medium to a final cell concentration of 2×10^5 cell mL^{-1} and subjected to 350 µmol photon m^{-2} s^{-1} (designated high light). After 7 days, red cells were harvested for globule isolation.

For RNA isolation, axenic cultures were grown up to a cell concentration of 2×10^5 cell mL^{-1} in 250-mL flasks, each containing 100 mL of mBG-11; the flasks were held in a shaker (150 rpm) and exposed to light of 90 µmol photon m^{-2} s^{-1}. Cells were then transferred to 250-mL flasks, each containing 50 mL of nitrogen-depleted mBG-11 medium and exposed to a light intensity of 200 µmol photon $m^{-2}s^{-1}$ to induce astaxanthin accumulation. For each sample, a separate flask was harvested at 0, 12, 24, 48, and 72 h.

Growth Parameter Measurements and Pigment Extraction and Quantification

Culture cell concentration, chlorophyll quantification and total carotenoid quantification were evaluated as previously described [16].

Isolation of Globules

An *H. pluvialis* culture was harvested by centrifugation (1,500×*g*, 10 min), suspended in breakage buffer comprising 0.2 M sucrose (10 mM MOPS, pH 7.0; 10 mM KCl; 5 mM Na EDTA; 1 mM DTT; 1 mM PMSF; 1 mM benzamidine; and 0.5 mg/mL leupeptin), and ruptured with a Mini Beadbeater (BioSpec Products Inc., OK, USA) using 2.5-mm glass beads for 4 min. The resulting

homogenate was centrifuged (1,500×g, 10 min), and the cell-free extract obtained was fractionated by centrifugation (25,000×g, 60 min, Sorvall RC 5C plus) on a discontinuous sucrose flotation gradient (0.6, 0.4, 0.2, 0 M sucrose in breakage buffer). The upper layer of the sucrose gradient containing the oil globules was collected and centrifuged in an ultracentrifuge (100,000×g, 120 min, Sorvall Combi plus). The floating oily layer was collected in 0.3-mL aliquots and kept frozen (−20 °C) until analyzed. The microsomal fraction comprised the ultracentrifuge (100,000×g, 120 min) pellet of the sucrose gradient supernatant minus the oil globules.

High-Performance Liquid Chromatography Pigment Analysis

The pigment profile was determined by high-performance liquid chromatography (HPLC) as described in Zhekisheva et al. [2]. The chromatogram was recorded at 450 nm, but the quantification of pigments (in % based on pigment weights) was performed at 478 nm for xanthophylls, 655 nm for chlorophyll a and 645 nm for chlorophyll b. Astaxanthin and chlorophylls were identified by comparison to their standards, and astaxanthin isomers were identified from their UV–VIS absorbance spectra, according to Yuan and Chen [19]. Xanthophylls other than astaxanthin were identified by their absorbance spectra and calculated peak III/II ratios, according to Briton et al. [20].

Lipid Analysis

Lipids were extracted from the cell-free extract and oil globules by the method of Bligh and Dyer [21]. Total lipid extract was separated into neutral and polar lipids by silica Bond-Elute cartridges (Varian, CA) using 1.5% methanol in chloroform (v/v) and methanol to elute neutral and polar lipids, respectively.

Polar lipids were separated into individual lipids by two dimensional TLC on Silica Gel 60 glass plates (10 × 10 cm, 0.25 mm thickness [Merck, Darmstadt, Germany]) according to Khozin et al. [22]. Neutral lipids were resolved with petroleum ether:diethyl ether:acetic acid (70:30:1, v/v/v). Lipid spots on TLC plates were visualized with 0.05% 8-anilino-4-naphthosulphonic acid in methanol (w/v) and UV light exposure and then scraped from the plates and transmethylated for fatty acid analysis.

Fatty Acid Analysis

Fatty acid methyl esters (FAME) were obtained by transmethylation of the lipid extracts or individual lipids with dry methanol containing 2% H_2SO_4 (v/v) and heating at 80 °C for 1.5 h while stirring under an argon atmosphere. Gas chromatographic analysis of FAME was performed on a Thermo Ultra Gas chromatograph (Thermo Scientific, Italy) equipped with PTV injector, FID detector, and a fused silica capillary column (30 m × 0.32 mm; ZB WAXplus, Phenomenex). FAME were identified by co-chromatography with authentic standards (Sigma Chemical Co., St. Louis, MO; Larodan Fine Chemicals, Malmö, Sweden) and FAME of fish oil (Larodan Fine Chemicals). Each sample was analyzed in duplicates of three independent experiments.

Protein Analysis

Protein samples were prepared as described in Wang et al. [23], and the BCA method was used for protein determination [24]. Separation of isolated protein fractions was performed by SDS PAGE (12%) according to Laemmli [25] with minor changes. Sample preparation entailed 1 h of incubation at room temperature in sample buffer containing 80 mM DTT. Bio Rad Precision Plus protein unstained standards were used as molecular weight markers.

Two-dimensional gels were prepared as described [26] with minor changes. Samples of 130 µl, each containing 50 µg of protein, were loaded on 7-cm isoelectric focusing (IEF) dry strips, pH 3–10 nonlinear (Amersham Biosciences AB, Uppsala). Protein spots of about 33 kDa were selected for analysis by mass spectrometry (MS).

Partial Amino Acid Sequencing

Protein spots were manually excised from 2D gels and digested in-gel with trypsin.

The peptide mixtures were subjected to solid phase extraction with a C18 resin filled tip (ZipTip Milipore, Billerica, MA USA) and nanosprayed into the Orbi-trap MS system in a 50% CH_3CN/1% CHOOH solution. MS was carried out with an Orbi-trap (Thermo Finnigen) using a nanospray attachment [27]. Data analysis was done using the Bioworks 3.3 package, and database searches were performed against the NCBInr database with the Sequest and Mascot software packages (Matrix Science, England). De novo sequencing was performed using the Biolynx package (Micromass, England).

Isolation of Total RNA

Total RNA was isolated with an SV Total RNA Isolation Kit (Promega USA). From 40 ml of medium containing 2 × 10^5 cells mL^{-1}, cells were harvested, resuspended in the kit lysis buffer and broken in Mini Beadbeater (Bio-Spec Products Inc., OK, USA) using 2.5-mm glass beads for 4 min. RNA samples were quantified with a Nano Drop

(ND-1000, Thermo Scientific, USA) spectrophotometer and stored at −80 °C.

cDNA Preparation, PCR and Sequencing

The Reverse iT 1st Strand Synthesis Kit (ABgene, UK) was used according to the manufacturer's instructions to synthesize cDNA from total RNA. The synthesized cDNA was used as the template in PCR amplification (with the degenerate primers listed in Table 3) using touch down PCR at 56 to 46 °C. The PCR product was extracted and subcloned, and specific primers for 3′ and 5′ RACE were designed. Full-length cDNA was synthesized according to the protocol described in the manufacturer's instructions (BD SMART RACE, Clontech). Searches for homologues sequences were performed in the NCBI database using the BLAST program [28].

Results

Globule Isolation

Oil globule accumulation was induced by exposing exponentially growing cells (chlorophyll and astaxanthin were 5 and 1 μg mL^{-1}, respectively) to high light and to nitrogen deprivation. Chlorophyll and astaxanthin contents in red cells harvested after seven days were 5 and 168 μg mL^{-1}, respectively.

The isolation of pure oil globules from *H. pluvialis* was hampered by the need to first rupture the robust algal cell wall. In light of this problem, earlier studies have explored the rupture process, examining the methods available for cell breakage (including grinding, French press or freeze thaw cycles), algal strains with different cell wall morphologies, and the treatments for purifying the isolated globules, including high ionic strength washes, chaotropic agents and detergents [29]. Although it was found that the different procedures produced similar results in terms of the pigment, fatty acid, and protein compositions of the isolated globules, all preparations also contained some contaminating membranes and proteins that were probably introduced into the globules during cell breakage. We found that breaking the cells with a Mini Beadbeater was an efficient and reproducible method for producing a high oil globule yield. Light microscopy of our preparations showed a mixed-sized population of yellow–red globules ranging in diameter from about 200 nm to 4 μm (Fig. 1).

Pigment Analyses

Eight different astaxanthin esters, amounting to about 70% of the total pigments, were found in the cell-free extract (CFE), while in the oil globules astaxanthin esters amounted to about 86% of the total pigments. The three major peaks on the HPLC chromatogram were attributed to astaxanthin esters 3, 5 and 6 (peaks 7, 8 and 9, respectively, in Fig. 2). UV–VIS absorbance spectra (not shown) indicated that peaks 8 and 9 were those of the *trans* isomer. In addition to the astaxanthin esters, minor amounts of chlorophyll and the chloroplast-derived xanthophylls—antheraxanthin, lutein and zeaxanthin—were also detected (Fig. 2). The retention time of zeaxanthin differed from the typical retention time previously reported by our group [2], and zeaxanthin may thus have been present in ester form. The relative chlorophyll content was higher in the CFE than in the oil globules—12.7% versus 4.5% (Table 1). The relative amounts of the other three xanthophylls were also higher in the CFE than in the oil globule fraction.

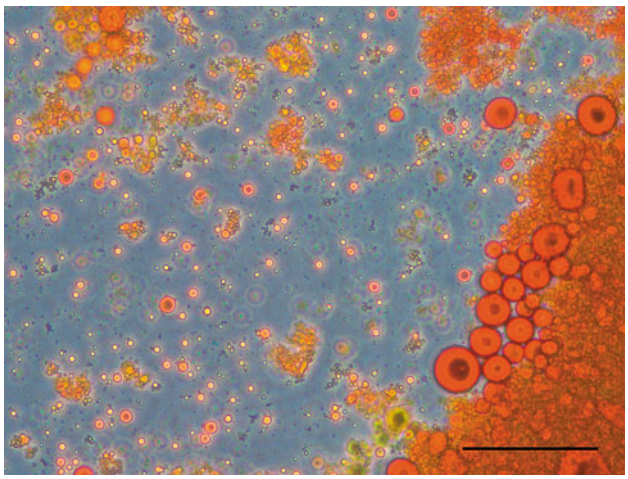

Fig. 1 Oil globules isolated from *H. pluvialis*. The oil globules were fractionated on a sucrose flotation gradient. *Bar* 20 μm

Fatty Acid and Lipid Analyses

Fatty acid composition of the total homogenate was similar to that of the oil globules and was characterized by the four major fatty acids: 16:0, 18:1, 18:2 and 18:3n-3 (not shown). To further analyze fatty acid composition and estimate the distributions of polar and neutral lipids in the oil globule enriched fraction, we performed a detailed lipid analysis of the representative sample of oil globules fractionation by two-dimensional TLC followed by GC analysis of fatty acid composition and content. About 70% of the total fatty acids (TFA) in CFE were recovered in the oil globule fraction, but polar membrane glycerolipids (PL), which constituted only 3.5% of the TFA in CFE, were reduced to 1.5% in the oil globules. Accordingly, neutral lipid TAG was a major component of both fractions (Table 2), accounting for more than 70% of the TFA in neutral lipids (NL). Diacylglycerol (DAG) and free fatty acids (FFA)

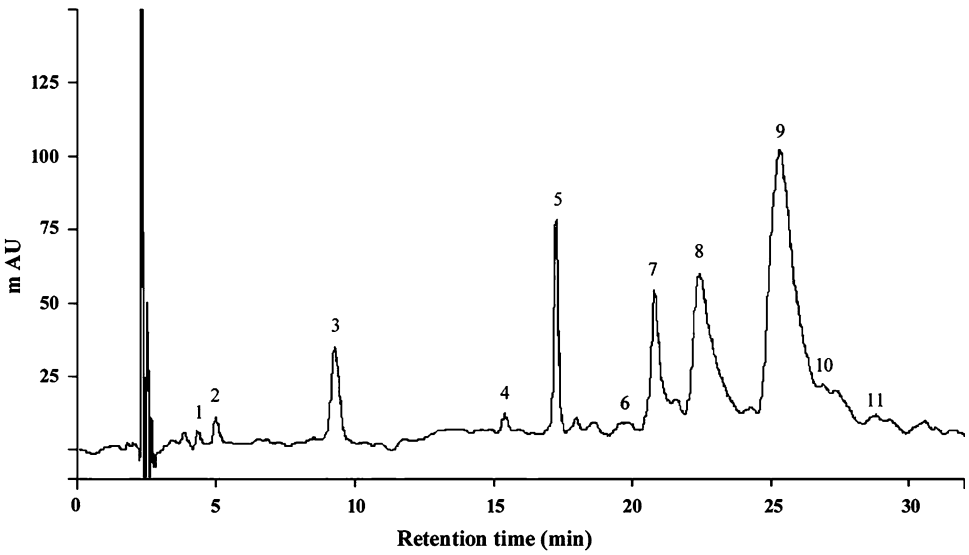

Fig. 2 HPLC chromatogram (recorded at 450 nm) of the pigment extract from *H. pluvialis* oil globules. Peaks: 1, antheraxanthin; 2, lutein; 3, zeaxanthin; 4, astaxanthin ester 1; 5, chlorophyll b; 6, astaxanthin ester 2; 7, chlorophyll a + astaxanthin ester 3; 8–11, astaxanthin esters 5, 6, 7 and 8

Table 1 Pigment composition[a] of cell free extract and of isolated oil globules

Rt (min)	Ant *4.10*	Lut *4.70*	Zea *8.50*	Ast 1 *14.90*	Chl b *16.90*	Ast 2 *19.20*	Chl a *20.40*	Ast 3 *20.50*	Ast 4 *20.90*	Ast 5 *22.00*	Ast 6 *24.60*	Ast 7 *26.40*	Ast 8 *27.80*
Cell free extract	2.6	4.0	13.9	0.0	6.4	0.0	6.3	**7.6**	1.5	**17.4**	**36.7**	2.0	1.7
Oil globules	1.5	1.7	5.8	1.9	1.9	1.1	2.7	**10.5**	3.0	**23.5**	**42.9**	3.7	0.0

Samples containing 10 μg of total pigments were injected into the HPLC. Bold values indicate three major peaks

Ant antheraxanthin, *Lut* lutein, *Zea* zeaxanthin, *Ast* astaxanthin ester, *Chl* chlorophyll, *Rt* retention time

[a] Values are expressed as the percentages of total pigment weight

constituted 7% each of the TFA in NL. FFA were also included in the calculation due both to their relatively high proportion and to their potential involvement in NL turnover. A relatively large percentage of the fatty acids in the NL fraction were esterified to astaxanthin in its mono- and diester forms, with the majority existing as monoesters.

The most salient difference between the oil globules and the CFE was the decreased proportion of the major thylakoid and inner chloroplast membrane lipid [30] monogalactosyldiacylglycerol (MGDG) in the oil globules. The ratio of two galactolipids, MGDG to digalactosyldiacylglycerol (DGDG), decreased from 1.3 to 0.4 during oil globule purification. Consequently, the relative proportions of the polar lipids—DGDG, sulfoquinovosyldiacylglycerol (SQDG) and diacylglyceroltrimethylhomoserine (DGTS)—increased, while that of phosphatidylcholine (PtdCho) remained unchanged.

There were no substantial differences between the fatty acid compositions of individual lipids in the CFE (not shown) and in the oil globule fraction. Despite tiny amounts of PL, a characteristic fatty acid signature was evident for each lipid class (Table 2). The galactolipids MGDG and DGDG were typically enriched with chloroplast PUFA, specifically linoleic acid (LNA, 18:2n-6) and α-linolenic acid (ALA, 18:3n-3), and with C16 PUFA 16:3n-3 and 16:4n-3. Another chloroplast-associated lipid, SQDG, contained less PUFA but was rich in saturated palmitic acid, 16:0. Phosphatidylglycerol (PtdGro) contained about 3% 16:1Δ3-*trans*—a distinctive feature of this class of chloroplast lipids (not shown). It appeared that *H. pluvialis* oil globules contained the phospholipid PtdCho and the betaine lipid DGTS as major extraplastidial polar lipids. PtdCho and DGTS featured similar fatty acid compositions, namely, the highest percentages of γ-linolenic acid (GLA; $18{:}3^{\Delta6,9,12}$, n-6) and stearidonic acid (SDA; $18{:}4^{\Delta6,9,12,15}$, n-3), indicating their possible involvement in the Δ6 lipid-linked desaturation of LNA ($18{:}2^{\Delta9,12}$, n-6) and of ALA ($18{:}3^{\Delta9,12,15}$, n-3), respectively. Phosphatidylethanolamine (PtdEth), the minor component of the PL fraction, contained the highest proportions of C20 long-chain PUFA, particularly, of arachidonic acid (AA; $20{:}4^{\Delta5,8,11,14}$, n-6) at 16%. In addition eicosadienoic acid (EDA; $20{:}2^{11,14}$, n-6) and eicosapentaenoic acid (EPA; $20{:}5^{\Delta5,8,11,14,17}$, n-3) comprised for about 4% each of TFA in this lipid class. This characteristic fatty acid composition allows speculation on the involvement of PtdEth in the Δ8 desaturation of 20:2n-6 and Δ17 (n-3) desaturation of AA. In this context, although it is worth

Table 2 Fatty acid profiles[a] of individual lipids from cell free extract (CFE) and isolated oil globules (OG)

	16:0	16:2 n-6	16:3 n-3	16:4 n-3	18:0	18:1 n-9	18:1 n-7	18:2 n-6	18:3 n-6	18:3 n-3	18:4 n-3	20:2 n-6	20:3 n-6	20:4 n-6	20:5 n-3	Others[b]	OG	CFE
Polar lipids																	% PL	% PL
MGDG	18.3	1.9	9.2	12.7	1.9	4.8	0.7	12.4	0.7	30.4	0.7	0.3	0.3	0.8	0.3	4.5	9	24
DGDG	29.5	1.7	12.1	1.6	0.9	2.9	0.2	13.9	0.2	34.2	0.3	0.1	0.0	0.1	0.0	2.2	23	19
SQDG	54.8	0.0	0.3	0.1	0.8	4.3	0.4	21.8	0.6	13.5	0.6	0.1	0.4	0.3	0.1	1.8	14	10
PtdGro	42.6	1.8	1.2	0.3	2.2	6.0	6.8	19.5	0.2	8.4	0.9	1.8	0.3	1.6	0.4	6.2	6	3
DGTS	26.9	0.3	0.9	0.6	1.3	1.5	1.0	30.1	7.1	19.0	7.8	0.3	0.1	1.3	0.6	1.3	25	21
PtdCho	34.6	0.3	0.9	0.5	1.4	1.4	1.1	23.2	8.3	15.7	9.1	0.2	0.2	0.8	0.8	1.5	16	16
PtdEtn	26.4	0.3	1.6	0.5	1.9	2.7	9.5	14.3	1.9	6.8	2.1	4.3	0.2	16.2	3.6	7.7	1	2
PtdIns	43.5	0.0	0.4	0.4	2.5	1.8	6.4	31.6	0.5	3.9	0.5	0.4	1.4	1.1	0.3	5.1	6	4
Neutral lipids																	% NL	% NL
TAG	19.8	0.9	3.1	4.3	1.2	26.9	0.7	26.4	1.0	9.9	0.9	0.8	0.5	0.6	0.5	2.4	76	73
FFA	3.7	0.3	0.3	0.4	1.4	33.0	0.6	26.3	0.2	7.2	0.3	24.8	0.2	0.3	0.0	1.0	6	7
DAG	4.2	0.0	0.3	0.2	1.8	44.1	0.8	35.7	0.2	8.3	0.2	0.7	0.5	0.5	0.3	2.1	7	7
Astaxanthin monoester	13.5	0.4	1.9	2.4	2.3	23.3	1.4	25.9	1.3	18.7	2.0	1.0	0.5	1.2	0.5	3.7	9	10
Astaxanthin diester	12.4	0.3	0.9	0.7	3.0	37.3	1.5	23.5	1.1	10.8	1.6	2.1	0.5	0.8	0.2	3.5	2	3

Data are presented as the means of replicated representative samples of oil globules and CFE

[a] Fatty acid composition (% of total fatty acids)

[b] Includes 14:0, isomers of 16:1, 20:0, 20:1, and 22:0

noting the abundance of EDA in the FFA pool, we realize that more thorough studies of PUFA biosynthesis in *H. pluvialis* are obviously needed to confirm the predictions made in the present work.

The neutral acyl lipids TAG and DAG and astaxanthin esters were enriched with oleic acid (OA, 18:1n-9) and LNA. The astaxanthin monoesters contained the highest relative proportions of ALA, and the percentage of palmitic acid was lowest in DAG and FFA.

Protein Analysis

Four major protein bands with estimated molecular weights of 20–30 kDa (Fig. 3 lane 8) that appeared in the isolated globule preparation were also evident in the total homogenate fraction of both green (astaxanthin and oil free) and red (astaxanthin and oil rich) cells (Fig. 3, lanes 1 and 7). These proteins were identified as chloroplast light-harvesting proteins on the basis of their positive cross-reactivity with anti light-harvesting complex protein (LHCP) antibodies (not shown). To reveal the native proteins of the globules, we followed the changes in protein profile during 14 days of exposure to nitrate depletion and high light. During this period, astaxanthin accumulated and chlorophyll levels decreased (Fig. 4).

As the globules accumulated, the relative abundances of only a few protein bands seemed to increase while the total protein content decreased. Of the proteins that did increase, we could distinguish seven different protein bands that appeared in the globule fraction but not in the microsomal fraction. These proteins were thus all considered to be globule-associated proteins (Fig. 3).

Globule proteins were also analyzed by 2D gel electrophoresis. Two major protein spots, both of about 33 kDa but with different PI values (Fig. 5), were cleaved with trypsin and analyzed by MS/MS. Identical partial sequences comprising 12 peptides were obtained for the two 2D protein spots, and these were designated *Haematococcus* oil globule protein (HOGP). Based on the sequences of five peptides, forward and reverse degenerate nucleotide primers were designed and used in different combinations for PCR amplification on cDNA from induced cells. The three peptides whose primers produced PCR amplification products are shown in Table 3, and the five peptides identified in the final amino acid sequence are indicated in bold letters in Fig. 6. A PCR product was initially cloned, and the sequencing was completed by 3′-RACE and 5′-RACE extensions (see Table 3 for the primers). A DNA product of 910 bp was obtained with an open reading frame (ORF) of 825 bp (accession number HQ213938) that encoded for a protein of 275 amino acids. An NCBI search with the protein query produced significant hits only from green microalgae. Multiple sequence alignment of HOGP with putative green algal orthologs revealed identities of 40, 38, and 36% with

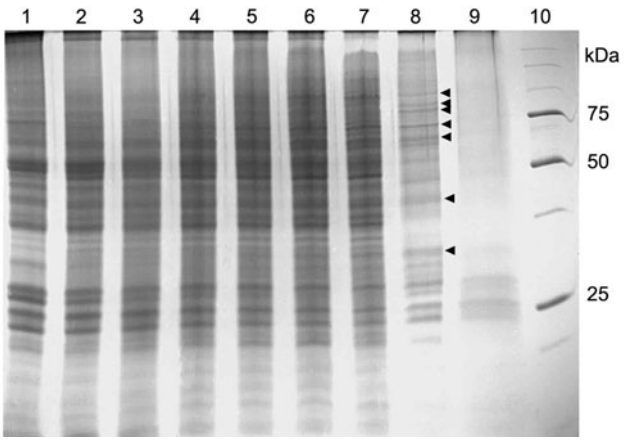

Fig. 3 Protein analysis of *H. pluvialis* total cells and oil globules by SDS–PAGE: (1-7) protein extracts of total cell homogenates during stress induction on days 0, 2, 4, 6, 8, 10, and 12; (8), oil globules; (9), microsomes; (10), molecular weight markers. *Arrows* between lanes 8 and 9 indicate the proteins thought to be globule-associated

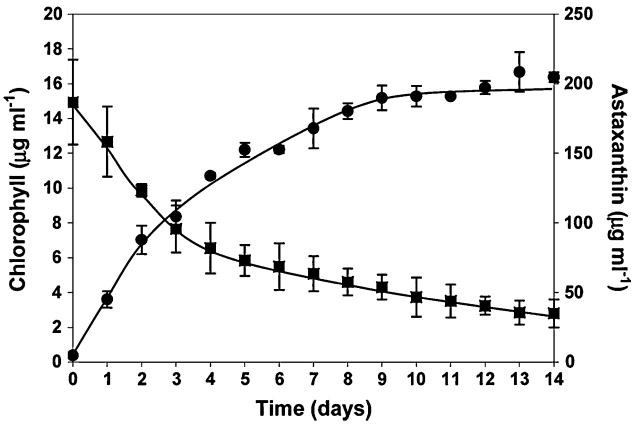

Fig. 4 Changes in chlorophyll (*filled square*) and astaxanthin (*filled circle*) contents during 14 days of cultivation in a column under high light and nitrogen starvation to induce the accumulation of oil globules for protein extraction

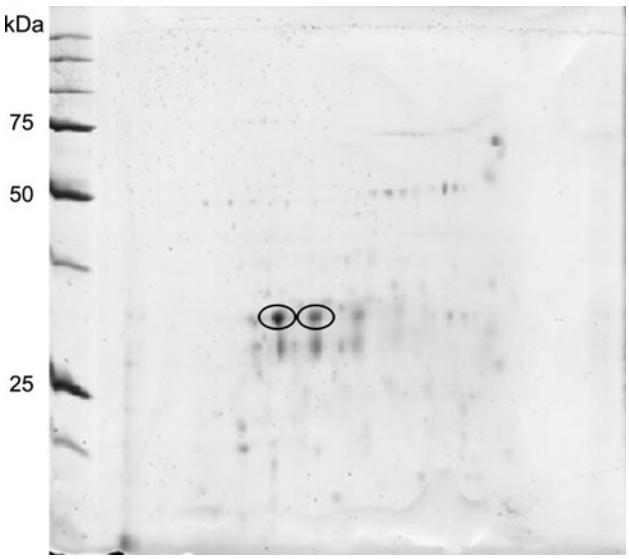

Fig. 5 2D gel electrophoresis of *H. pluvialis* oil globule proteins. The marked bands were excised and subjected to MS analysis

Volvox carteri f. nagariensis, *Polytomella parva*, and *Chlamydomonas reinhardtii*, respectively (Fig. 6). A significant but smaller homology of 27% identity was also found with *Coccomyxa* sp., accession number GW230985 (not shown).

A comparison of the secondary structure of HOGP with its *C. reinhardtii* ortholog, which is the only full-length published sequence, was performed by hydrophobicity plot analyses [31]. The two proteins showed very similar patterns, with the majority of their hydrophobic regions situated between amino acids 55–65 and 170–190 of HOGP (Fig. 7). A short hydrophilic region that is evident in HOGP at amino acids 105–113 also appeared in the *P. parva* sequence but is absent in the *C. reinhardtii* and *V. carteri f. nagariensis* sequences (Figs. 6, 7).

To characterize the induction of the *Hogp* gene, cultures were induced to accumulate astaxanthin (see above) for a period of 72 h, during which RNA was isolated at different time intervals. Specific primers were designed from our cDNA sequence, while actin control primers were adopted from Huang et al. [32]. Astaxanthin accumulation could be detected spectrophotometrically in a total pigment extract after as short a time as 12 h, and after three days astaxanthin increased by more than tenfold (Fig. 8). Transcript levels of the *Hogp* gene, which were almost undetected in green non-stressed cells, increased by >100-fold after 12 h of induction. They remained almost constant for 48 h and started to decrease after 72 h (Fig. 9).

Discussion

The ability of plant or algal cells to accumulate secondary carotenoids depends on the availability of a sink for carotenoid deposition [33, 34]. It is likely that deposition of carotenoids in a lipid sink will prevent end product inhibition of the biosynthetic pathway [35]. In yeasts, for example, the expression of carotenogenic genes leads only to minor astaxanthin accumulation [36–38], supposedly as a consequence of the lack of sinks for the carotenoid end product. This "sink hypothesis" is supported by our earlier studies with the carotene globule protein (Cgp), a protein that is associated with plastidic β-carotene oil globules in *Dunaliella bardawil* and that functions in globule stabilization [8]. The "sink hypothesis" may also be applicable to TAG biosynthesis, where the availability of oil globules or the enhanced ability to produce them should facilitate the parallel synthesis and accumulation of storage lipids. Identifying the main globule-associated enzymes and

Table 3 Primers used in this work

Degenerative
Peptide no. 1: NDAWNMCAS
1FOR: 5′ GAY GCN TGG AAY ATG TG 3′
1REV: 5′ CA CAT RTTCCA NGC RTC 3′
Peptide no. 2: TADPVTQTGDDGF
2FOR: 5′ ACN GCN GAY CCN GTN AC 3′
2REV: 5′ TC NCC NGT YTG NGT NAC 3′
Peptide no. 3: TAPVVAQAQDL
3FOR: 5′ CCN GTN GTN GCN CAR GC 3′
3REV: 5′ GCY TGN GCN CAN CAN GG 3′
Differential expression of *Hogp*
For 5′ AGCGGGAGATAGTGCGGGACA 3′
Rev 5′ ATGCCCACCGCCTCCATGC 3′ (actin control primers)
For 5′ CAGCACGCCCTGGACACCCTGAAC 3′
Rev 5′ GGTTTGGGTGACTGGGTCGGCTGT 3′ (specific primers)
RACE
GSP3 5′ ACAAGGCGGTGGCAGACGGGAAG 3′
NGSP3 5′ CAGCACGCCCTGGACACCCTGAAC 3′
5 ukII 5′ ATCAACTACGCCCTTCTTCCCGTCTG 3′
5 ukIII 5′ AAAGTAGCTGTTGCTCGTGGCGATG 3′

proteins taking part in the assembly of oil globules can therefore be a key to future biotechnological manipulation of microalgae for the high yield production of oil and carotenoids. Indeed, carotenoid biosynthetic enzymes have already been shown to be localized in oil globules [18, 39].

The lack of sufficient molecular information and sequence data for *H. pluvialis* limits the use of bioinformatics to identify specific protein genes. We therefore applied proteomics approaches to identify possible globule-associated proteins, an approach requiring enriched and contaminant-free oil globule preparations. This approach poses a major challenge when organelles have to be isolated from cells with a rigid cell wall, as is the case for *Haematococcus*, which necessitates aggressive cell breakage. This is particularly true for the isolation of hydrophobic organelles such as oil globules, which can easily adsorb hydrophobic proteins or pigments released from the chloroplast during aggressive lysis in apparatuses such as a French press or a bead beater [40]. Indeed, the chlorophylls, xanthophylls and some of the plastid lipids in our preparations undoubtedly originated in chloroplast membranes, and the consistent detection of LHCPs as the major proteins in isolated globules (also verified by MS analysis), even after purification, may be an artifact of isolation. A possible solution may lie in the production of spheroplasts by enzymatic treatment, followed by gentle lysis via osmotic shock. Although previous studies have reported the successful application of this approach in *H. pluvialis* [41, 42], our group has never succeeded in reproducing their results, even after successful removal of the cellulose layer from the cell wall [43]. As an alternative, we tried to use flagellated (motile) cells with reduced cell walls. Our attempts to isolate oil globules using different breakage methods and/or motile cells, however, resulted in almost the same globule composition as that presented in Fig. 1 and Tables 1 and 2.

The globule preparations obtained were rich in astaxanthin and in the fatty acids that are characteristic of TAG in microalgae as compared to the CFE. Moreover, some chloroplast lipids (MGDG) were substantially reduced in globule fraction (Table 2). We are therefore confident that our preparations are largely representative of oil globules composition in vivo, with the exception of some contaminating pigments, lipids and proteins, as mentioned above.

Based on the pigment content of the globules, we concluded that astaxanthin is the only carotenoid accumulating in the globule fraction. This conclusion is supported by earlier findings of Grunewald and Hagen [44]. Three astaxanthin esters comprise the majority of astaxanthin contributing to the absorbance maximum at 476.6–480 nm. None of the intermediates of the astaxanthin biosynthesis pathway or free astaxanthin or β-carotene was detected in globules, although minor amounts of these pigments were reported in the total homogenate of red *H. lacustris* cells [19]. The fatty acids content of oil globule resembled that of the CFE, which is to be expected, since oil globule TAG comprise the vast majority of lipids [16] (Table 2). These results are in agreement with the findings of Zhekisheva et al. [2], who induced astaxanthin accumulation in *H. pluvialis* only by high light exposure, and those of Wang et al. [45] for *C. reinhardtii* cytosolic isolated oil globules.

The results of oil globule individual lipid analysis are largely in agreement with the data of Grunewald et al. [18], who estimated the proportions of different lipid classes in oil globules of vegetative cells of *H. pluvialis* by densitometry of charred lipid spots on TLC plates. In the course of their preparations, the authors also detected lipids of plastid origin—DGDG, SQDG, and PG—but they reported the complete absence of MGDG. We were able to detect a relatively low proportion of MGDG in our oil globule preparations; however, this lipid class was substantially reduced in oil globules compared to in CFE, indicating enrichment of oil globules with other oil globule-specific lipid classes. The betaine lipid DGTS and the phospholipid PtdCho constituted the major portion of extraplastidial lipids in oil globules (about 40% of PL). It appears that DGTS contributed significantly to the formation of an oil globule polar lipid monolayer in green algae [18, 46] in contrast to higher plants whose oil globule phospholipid monolayer is enriched in PtdCho and PtdEtn. DGTS shares some properties with PtdCho, and is abundant in some algal groups and low plants,

```
Polytomella     ------------------------------------------------------------
Haematococcus   MSE---KQLKRLGFVHQGASYAYSYTGTAEKLYKTARSFAPTFVEPTLAQVEDRVVAITA 57
Chlamydomonas   MAESAGKPLKHLEFVHTYAHKFASGAAYVEGGYQKAKTYVPAVAQPYIAKAEETCLAYAA 60
Volvox          MAD--DRKLKRLGFVDAYTHKLANGAAYVEGAYKKVKPLVPQQVQPFLAKVEDAVLAYTA 58
                *::   : **:* **.  :    . :. .*  *:..:. .*  .:* :*:.*:  :* :*

Polytomella     ----NAQDKAEKILKKADDQVDKVVSNAHNIYQAGRSTVDTAVNNIMEIHQNNIETYQQT 56
Haematococcus   PVVAQAQDLSEKALHIADDQVECIVNTTDKAVADGKKGVIDCMNGVKEMHEKNMQTYIAT 117
Chlamydomonas   PLATKATDHAEKILRSTDAQLDALYAASASWLSSSQK-----------LADSNIAAFRGA 109
Volvox          PVVAKASDQAEKFLRITDEQVDYLYVETAAYLTQTRK-----------LTQSNIDTFRSA 107
                *::::* * :** *: :* *:: :   :       :. *   :* : *: :.*: ::  :

Polytomella     THKYFQLVSSTAEWVAARVAPTQAFQKAHEILRLSLNKAQECADPDKAVKIVYDSWVVFS 116
Haematococcus   SNRYFEYIKGMSEWAKDKMNPIKGGQHALDTLNAAIAKAQEATDPDVAAKMALDAWNSFA 177
Chlamydomonas   ADKYYDLVKSTAQHVTSKLPTDLSVAKARELLSASLEQAKALADPDAAVAAALDAWTKFA 169
Volvox          ADKYYQMVKSTADYLASKLSYDISVQAARDFISKSVEKAKELSDPDAAVRIVYDSWQQFA 167
                :.:*:: :.. ::    ::    .   * : :  :: :*:  :*** *.  . *:*  *:

Polytomella     SVPVVASVLPYLEPAAARAFQNFRSIHDSLVVSPHYKQGYDMASATLQWATTTSPFRLGA 176
Haematococcus   SVPVVAKVLETADPVTQTGLSSFYKLHDTLVSWPLYSKVVSTGVSTLSWATTTMPYKLGA 237
Chlamydomonas   AIPAVAKVLSAASPLTGKGVAAFTAAHDLLVHSALYRYGVSVGASTLGWATSTTPYKLSA 229
Volvox          AIPAVAKTLEKTAPVTRKGFETFIAAHDALVSSLVYKRSVSLGATTLGWATTTTPYKLGA 227
                ::*.**..*    * :  ..  *   ** **    *    . . :** ***:* *::*.*

Polytomella     NVM---------------------------------- 179
Haematococcus   QYMYPLVQPVADPALAKITNSKVINGTLSYWKPTASAA- 275
Chlamydomonas   AYLYPLVQPVADPALDKVSKSTYVNAAIKYWAPAPVAAA 268
Volvox          QYLYPMVQSVADPAL----------------------- 242

                  :**:**.****** *::.:  :*.::.** *:  **
```

Fig. 6 Multiple sequence alignment of *H. pluvialis* HOGP protein with putative green algal orthologs from *C. reinhardtii* (XP_001697668), *Volvox carteri f. nagariensis* (FD812477), and *Polytomella parva* (EC748417). The peptides identified in MS/MS are marked in *bold*. The insert is *shaded*. The region of misalignment in the hydropathy plot is *underlined*. Symbols: identical (*asterisk*), conserved (*colon*), semi-conserved (*dot*)

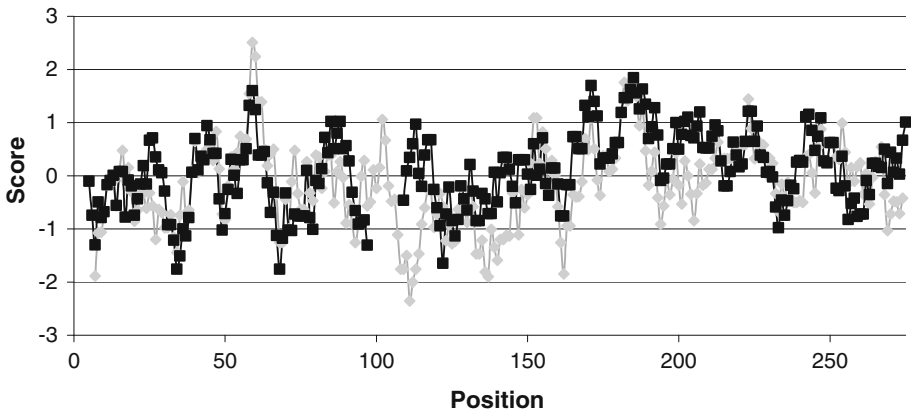

Fig. 7 Hydropathy plots for *H. pluvialis* HOGP (*filled diamond*) and for *C. reinhardtii* protein (*filled square*). Word = 9. The *C. reinhardtii* sequence was introduced with a gap from aa 98–108

but it is absent in higher plants. In *C. reinhardtii,* PtdCho is missing, and DGTS is present as a major polar lipid in the oil globule-enriched fraction [46].

Protein analysis of the isolated globule fraction by SDS PAGE identified at least seven protein bands that were not present in the microsomal fraction. The same proteins accumulated during astaxanthin accumulation, as can be seen in the protein pattern of total cell homogenates (Fig. 3). These findings support the notion that the bands are indeed authentic oil-globule-associated proteins (Fig. 3). One of the protein bands showed two major 33 kDa spots on 2D gel electrophoresis and was termed HOGP. The different PIs of the two HOGP spots could be due to protein phosphorylation. HOGP was analyzed by MS/MS, and the partial amino acid sequences were utilized to prepare degenerate DNA primers that were used to clone the gene encoding HOGP. A database search revealed that HOGP has orthologs only among green algae. One such ortholog was recently identified in *C. reinhardtii* oil globules and has been shown to affect globule size [46].

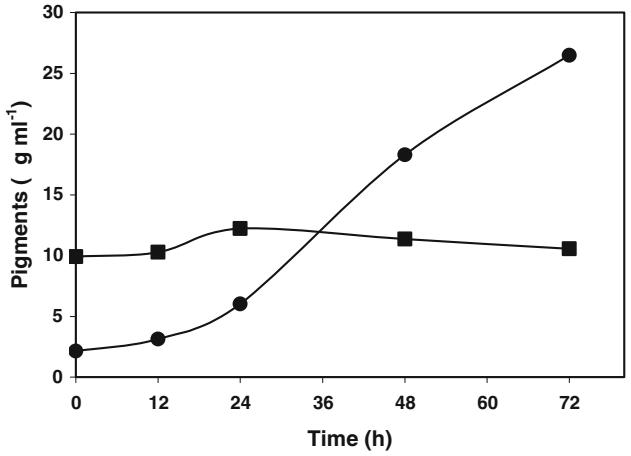

Fig. 8 Changes in chlorophyll (*filled squares*) and astaxanthin (*filled circles*) contents during 72 h of cultivation in an Erlenmeyer flask under nitrogen starvation and 200 μmol photon m^{-2} s^{-1} to induce the accumulation of oil globules for RNA extraction

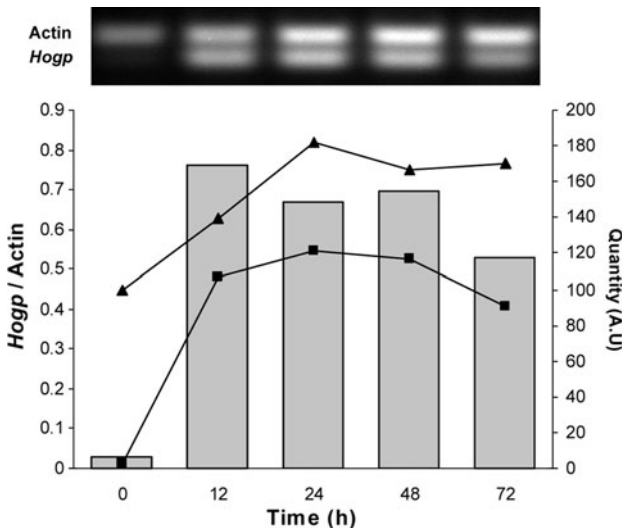

Fig. 9 Transcript levels of actin (*filled triangles*) and *Hogp* gene (*filled squares*) during 72 h of cultivation under nitrogen starvation and 200 μmol photon m^{-2} s^{-1} to induce the accumulation of oil globules for RNA extraction. PCR product on agarose gel and densitometric representation. *Bars* refer to left axis

The novel family of globule-associated proteins differs completely in sequence and in secondary structure from plant oleosins and caleosins, suggesting that green algae evolved these unique globule-associated proteins, which may or may not share similar functions with plant oleosins. A comparison of the orthologous amino acid sequences from four microalgal species showed that the *H. pluvialis* and *P. parva* sequences each have an insert of 11 amino acids (Fig. 6) that is not found in *C. reinhardtii* or *V. carteri f. nagariensis*. The hydropathy plot comparison between the *H. pluvialis* and *C. reinhardtii* proteins revealed another significant difference between the two proteins, i.e., a highly hydrophilic 9-amino-acid domain following the 11-amino-acid insertion in *H. pluvialis* (and *Polytomella*) that is hydrophobic in *C. reinhardtii* and *Volvox*. Both differences may account for the divergent functions of the two proteins. The induction pattern of HOGP is consistent with its predicted localization in oil globules: the appearance of the 33-kDa protein in nitrate depletion/high light inductive conditions is roughly correlated with astaxanthin induction (Figs. 3, 4). The transcript of the *Hogp* gene is hardly detectable in green cells but is highly induced upon exposure of the cells to astaxanthin-inducing conditions, preceding the appearance of the protein as expected. The findings presented in this paper thus indicate that the HOGP protein is a promising candidate for involvement in globule biogenesis and the stress response in *Haematococcus* and related species of green algae.

Acknowledgments The authors would like to thank Mrs. Shoshana Didi-Cohen for the help in lipid and fatty acid analysis. This work was supported in part by the FP 7 project GIAVAP.

References

1. Murphy D (2001) The biogenesis and functions of lipid bodies in animals, plants and microorganisms. Prog Lipid Res 40:325–438
2. Zhekisheva M, Zarka A, Khozin-Goldberg I, Cohen Z, Boussiba S (2005) Inhibition of astaxanthin synthesis under high irradiance does not abolish triacylglycerol accumulation in the green alga *Haematococcus pluvialis* (Chlorophyceae). J Phycol 41:819–826
3. Walther TC, Farese RV Jr (2008) The life of lipid droplets. Biochim Biophys Acta Mol Cell Biol Lipids 1791:459–466
4. Frandsen GI, Mundy J, Tzen JTC (2001) Oil bodies and their associated proteins, oleosin and caleosin. Physiol Plantarum 112:301–307
5. Frandsen G, Muller-Uri F, Nielsen M, Mundy J, Skriver K (1996) Novel plant Ca (2+)-binding protein expressed in response to abscisic acid and osmotic stress. J Biol Chem 271:343–348
6. Naested H, Frandsen G, Jauh G, Hernandez-Pinzon I, Nielsen H, Murphy D, Rogers J, Mundy J (2000) Caleosins: Ca2+ -binding proteins associated with lipid bodies. Plant Molec Biol 44:463–476
7. Murphy DJ (2004) The roles of lipid bodies and lipid-body proteins in the assembly and trafficking of lipids in plant cells. In: 16th international plant lipid symposium, Budapest, June 2004
8. Katz A, Jimenez C, Pick U (1995) Isolation and characterization of a protein associated with carotene globules in the alga *Dunaliella bardawil*. Plant Physiol 108:1657–1664
9. Cermelli S, Guo Y, Gross SP, Welte MA (2006) The lipid-droplet proteome reveals that droplets are a protein-storage depot. Curr Biol 16:1783–1795
10. Hodges BDM, Wu CC (2010) Proteomic insights into an expanded cellular role for cytoplasmic lipid droplets. J Lipid Res 51:262–273
11. Borowitzka MA (1988) Fats, oils and hydrocarbons. In: Borowitzka MA, Borowitzka LJ (eds) Micro-algal biotechnology, Cambridge: Cambridge University Press, pp 257–287
12. Chisti Y (2007) Biodiesel from microalgae. Biotechnol Adv 25:294–306
13. Rodolfi L, Chini Zittelli G, Bassi N, Padovani G, Biondi N, Bonini G, Tredici M (2009) Microalgae for oil: Strain selection,

induction of lipid synthesis and outdoor mass cultivation in a low-cost photobioreactor. Biotechnol Bioeng 102:100–112
14. Boussiba S (2000) Carotenogenesis in the green alga *Haematococcus pluvialis*: cellular physiology and stress response. Physiol Plantarum 108:111–117
15. Schoefs B, Rmiki N-E, Rachadi J, Lemoine Y (2001) Astaxanthin accumulation in *Haematococcus* requires a cytochrome P450 hydroxylase and an active synthesis of fatty acids. FEBS Lett 500:125–128
16. Zhekisheva M, Boussiba S, Khozin-Goldberg I, Zarka A, Cohen Z (2002) Accumulation of oleic acid in *Haematococcus pluvialis* (Chlorophyceae) under nitrogen starvation or high light is correlated with that of astaxanthin esters. J Phycol 38:325–331
17. Santos M, Mesquita J (1984) Ultrastructural study of *Haematococcus lacustris* (Girod.) rostafinski (Volvocales) 1. Some aspects of carotenogenesis. Cytologia 49:215–228
18. Grunewald K, Hirschbeg J, Hagen C (2001) Ketocarotenoid biosynthesis outside of plastids in the unicellular green alga *Haematococcus pluvialis*. JBC 276:6023–6029
19. Yuan J, Chen F (1997) Identification of astaxanthin isomers in *Haematococcus lacustris* by HPLC-photodiode array detection. Biotechnol Tech 11(7):455–459
20. Britton G, Liaaen-Jensen S, Pfander H (2004) Carotenoids handbook. Birkhauser, Basel, Switzerland
21. Bligh EG, Dyer WJ (1959) A rapid method of total lipid extraction and purification. Can J Biochem Physiol 37:911–917
22. Khozin I, Adlerstein D, Bigogno C, Heimer YM, Cohen Z (1997) Elucidation of the biosynthesis of eicosapentaenoic acid in the microalga *Porphyridium cruentum* (II. Studies with radiolabeled precursors). Plant Physiol 114:223–230
23. Wang W, Vignani R, Scali M, Sensi E, Tiberi P, Cresti M (2004) Removal of lipid contaminants by organic solvents from oilseed protein extract prior to electrophoresis. Anal Biochem 329: 139–141
24. Smith PK, Krohn RI, Hermanson GT, Mallia AK, Gartner FH, Provenzano MD, Fujimoto EK, Goeke NM, Olson BJ, Klenk DC (1985) Measurement of protein using bicinchoninic acid. Anal Biochem 150:76–85
25. Laemmli UK (1970) Cleavage of structural proteins during the assembly of the head of bacteriophage T4. Nature 227:680–685
26. Liska AJ, Shevchenko A, Pick U, Katz A (2004) Enhanced photosynthesis and redox energy production contribute to salinity tolerance in Dunaliella as revealed by homology-based proteomics. Plant Physiol 136:2806–2817
27. Wilm M, Mann M (1996) Analytical properties of the nanoelectrospray ion source. Anal Chem 68:1–8
28. Altschul SF, Gish W, Miller W, Myers EW, Lipman DJ (1990) Basic local alignment search tool. J Mol Biol 215:403–410
29. Tzen JTC (1997) A new method for seed oil body purification and examination of oil body integrity following germination. J Biochem 121:762–768
30. Joyard J, Teyssier E, Miège C, Berny-Seigneurin D, Maréchal E, Block MA, Dorne A-J, Rolland N, Ajlani G, Douce R (1998) The biochemical machinery of plastid envelope membranes. Plant Physiol 118:715–772
31. Kyte J, Doolittle RF (1982) A simple method for displaying the hydropathic character of a protein. J Mol Biol 157:105–132
32. Huang J-C, Chen F, Sandmann G (2006) Stress-related differential expression of multiple [beta]-carotene ketolase genes in the unicellular green alga *Haematococcus pluvialis*. J Biotechnol 122:176–185
33. Li L, Van Eck J (2007) Metabolic engineering of carotenoid accumulation by creating a metabolic sink. Transgenic Res 16:581–585
34. Cazzonelli CI, Pogson BJ (2010) Source to sink: regulation of carotenoid biosynthesis in plants. Trends Plant Sci 15:266–274
35. Rabbani S, Beyer P, Lintig JV, Hugueney P, Kleinig H (1998) Induced beta-carotene synthesis driven by triacylglycerol deposition in the unicellular alga *Dunaliella bardawil*. Plant Physiol 116:1239–1248
36. Misawa N, Shimada H (1998) Metabolic engineering for the production of carotenoids in non-carotenogenic bacteria and yeasts. J Biotechnol 159:169–181
37. Miura Y, Kondo K, Saito T, Shimada H, Fraser P, Misawa N (1998) Production of the carotenoids lycopene, β-carotene, and astaxanthin in the food yeast *Candida utilis*. Appl Environ Microb 64:1226–1229
38. Ukibe K, Hashida K, Yoshida N, Takagi H (2009) Metabolic engineering of *Saccharomyces cerevisiae* for astaxanthin production and oxidative stress tolerance. Appl Environ Microb 75:7205–7211
39. Suire C, Bouvier F, Backhaus RA, Begu D, Bonneu M, Camara B (2000) Cellular localization of isoprenoid biosynthetic enzymes in *Marchantia polymorpha* uncovering a new role of oil bodies. Plant Physiol 124:971–978
40. Digel M, Ehehalt R, Fullekrug J (2010) Lipid droplets lighting up: insights from live microscopy. FEBS Lett 584:2168–2175
41. Tjahjono AE, Kakizono T, Hayama Y, Nagai S (1993) Formation and regeneration of protoplast from a unicellular green alga *Haematococcus pluvialis*. J Ferment Bioeng 75:196–200
42. Triki A, Maillard P, Gudin C (1997) Protoplasts from zoospores and cysts of *Haematococcus pluvialis* alga (Chlorophyta, Volvocales). Russ J Plant Physiol 14:935–942
43. Montsant A, Zarka A, Boussiba S (2001) Presence of nonhydrolyzable biopolymer in the cell wall of vegetative cells and astaxanthin-rich cysts of *Haematococcus pluvialis*. Mar Biotechnol 3:515–521
44. Grunewald K, Hagen C (2001) β-Carotene is the intermediate exported from the chloroplast during accumulation of secondary carotenoids in *Haematococcus pluvialis*. J Appl Phycol 13:89–93
45. Wang ZT, Ullrich N, Joo S, Waffenschmidt S, Goodenough U (2009) Algal lipid bodies: stress induction, purification, and biochemical characterization in wild-type and starch-less *Chlamydomonas reinhardtii*. Eukaryot Cell 1856–1868
46. Moellering ER, Benning C (2010) RNA interference silencing of a major lipid droplet protein affects lipid droplet size in *Chlamydomonas reinhardtii*. Eukaryot Cell 9:97–106

Lipids (2011) 46:863–871
DOI 10.1007/s11745-011-3581-x

ORIGINAL ARTICLE

Changes in the Composition of Triacylglycerols in the Fat Bodies of Bumblebee Males During Their Lifetime

Pavel Jiroš · Josef Cvačka · Robert Hanus · Jiří Kindl · Edita Kofroňová · Irena Valterová

Received: 8 November 2010 / Accepted: 8 June 2011 / Published online: 1 July 2011

Abstract The age-dependent changes in the composition of triacylglycerols (TAG) in the fat bodies of bumblebee males were studied using HPLC/MS. Two related species (*Bombus terrestris* and *B. lucorum*) were compared, with the age of the males being 0–30 days. The total amount of TAG in *B. lucorum* was about 2.7 times higher than that in *B. terrestris* for all of the ages studied. One to three-day-old males had the highest content of TAG in their fat bodies (1.6–2.3 mg/individual in *B. terrestris* and 3.8–4.2 mg/individual in *B. lucorum*). The analytical data show different patterns in both species. The qualitative composition of fatty acids in TAG was similar, but the mean relative abundance between *B. terrestris* and *B. lucorum* differed: 14:0, 7 and 14%; 16:0, 20 and 44%; 18:3, 62 and 23%; 18:1, 3 and 8%, respectively (the data is based on a GC/MS integration). A statistical evaluation of the dynamic changes in the TAG composition revealed that in *B. terrestris* different age classes were well separated according to their TAG composition while in *B. lucorum* the TAG did not change substantially during the male's life. The TAG analyses provide more precise information on the differences between the classes studied than the FA composition alone.

Electronic supplementary material The online version of this article (doi:10.1007/s11745-011-3581-x) contains supplementary material, which is available to authorized users.

P. Jiroš · J. Cvačka · R. Hanus · J. Kindl · E. Kofroňová · I. Valterová (✉)
Institute of Organic Chemistry and Biochemistry, Academy of Sciences of the Czech Republic, Flemingovo nám. 2, 166 10 Prague 6, Czech Republic
e-mail: irena@uochb.cas.cz

P. Jiroš · E. Kofroňová
Institute of Chemical Technology in Prague, Technická 5, 166 28 Prague 6, Czech Republic

Keywords *Bombus terrestris* · *Bombus lucorum* · Fat body · Lipids · Triacylglycerols · Fatty acids · LC/APCI-MS

Abbreviations

TAG	Triacylglycerol(s)
FA	Fatty acid(s)
FAME	Fatty acid methyl ester(s)
La	Lauric acid (12:0)
M	Myristic acid (14:0)
Mo	Myristoleic acid (14:1)
P	Palmitic acid (16:0)
Po	Palmitoleic acid (16:1)
S	Stearic acid (18:0)
O	Oleic acid (18:1)
L	Linoleic acid (18:2)
Ln	Linolenic acid (18:3)
A	Arachidic acid (20:0)
Go	Gadoleic acid (20:1)
Ara	Arachidonic acid (20:4)
ECN	Equivalent carbon number
TIC	Total ion current
UPGMA	Unweighted pair-group method with arithmetic mean
PCA	Principal component analysis
DA	Discriminant analysis

Introduction

The metabolism and management of the nutrients in insects take place in the fat body [1]. It is a relatively large organ unique to insects, which is distributed throughout the insect body, preferentially underneath the integument, and

surrounding the gut as well as the reproductive organs [2, 3]. The fat body is composed of adipocytes containing lipid droplets. Most of the energy stores are triacylglycerols (TAG) and carbohydrates (mainly glycogen); the latter serves as a fast energy source. Long-term storage is covered by TAG because of a higher caloric content per weight unit than that of glycogen. TAG provide a useful source of water upon oxidation, yielding almost twice as much metabolic water as glycogen does. These considerations have direct implications on the energy metabolism of insects [4]. TAG originate either from dietary fats or de novo biosynthesis. Newly-formed fatty acids (FA) are bound to the glycerol backbone by acyl transferases. The composition of the TAG depends both on the acyl transferase specificity and on the pool of available FA [5].

Lipids supply energy for flight and reproduction; they are crucial during starvation and stress. When needed, lipases in the fat body hydrolyze TAG to 1,2-diacylglycerols, which are bound to lipophorins in the hemolymph and transported to target tissues. The target cells unload diacylglycerols, hydrolyze them, and liberate FA. The FA act as a source of metabolic energy to meet the energy requirements of the insect. They are also essential precursors in the biosynthesis of many important compounds, including eicosanoids acting in reproduction or hormone signal transduction, cuticular hydrocarbons that protect insects from desiccating, or pheromones and other semiochemicals [6, 7].

Recently, we have studied the TAG composition in male fat bodies of several bumblebee species [8, 9] and found that TAG are species-specific. Our results on lipids and male-marking pheromones in particular bumblebee species have led us to a hypothesis on pheromone formation from lipidic precursors [10, 11]. In several species, the chain length and double-bond positions in FA seem to correlate with those in the pheromonal components (*B. lapidarius, B. pratorum, B. ruderatus, B. confusus, B. campestris* and *B. bohemicus*). Statistical evaluation of our previous analytical results has revealed a great similarity in TAG composition between closely related species, *B. terrestris* and *B. lucorum* [8, 9]. On the other hand, the male-marking pheromone of these species differs in its main components and only medium or minor components are shared [12, 13]. Furthermore, the dynamics in the pheromone production differ greatly; in *B. terrestris*, the pheromone is formed only during the first 5 days and stored for the rest of the male's life, whereas in *B. lucorum* the biosynthesis goes on for the male's entire life [14, 15]. In connection with our hypothesis on pheromone formation from lipidic precursors, the different ontogeny of the pheromonal gland in these closely related species raised the question of whether the fat bodies will follow a similar pattern. The present study therefore focuses on the temporal dynamics in TAG compositions in the fat bodies of *B. terrestris* and *B. lucorum* males.

Materials and Methods

Insect Material

Colonies of *Bombus lucorum* (L.) and *Bombus terrestris* (L.) were established by the two-queen cascade method [16]. All of the mother queens were taken from their natural habitats during the nest-searching period in order to minimize the possible negative influence of artificial conditions on the progeny. Bumblebee colonies were kept in plastic boxes with a volume of 0.6–1 L and fed with honeybee pollen pellets and concentrated sugar solution (sucrose: fructose 1:1). When the colonies started to produce males, male cocoons were removed from the parental hives and left to mature separately under the care of several workers supplied with food [16]. The freshly emerged males were removed and kept according to age. Animals of the following age were studied: *Bombus terrestris*: shortly after eclosion, 1, 2, 3, 4, 5, 7, 10, 12, and 24 days after eclosion (5 individuals of each age); *B. lucorum*: shortly after eclosion, 1, 2, 3, 4, 5, 6, 7, 8, 9, 10, 15, 20, 25, and 30 days after eclosion (5 individuals of each age). The males were killed by freezing (−18 °C) and kept frozen prior to dissection. The abdomens were opened with fine scissors. The incision was made from the tip of the abdomen along the right side of the tergites and transversely back to the left side of the tergites at the upper end of the abdomen, so the cavity of the abdomen could be opened like a tin can. The digestive tract and genital organs including the accessory glands were removed. All of the other tissues (muscles, dorsal vessel, central nervous system) covered by peripheral fat body were removed with microsurgery forceps. The remaining fat was used for further analysis to minimize the loss of mass.

Chemicals

The TAG standards (99% purity) were purchased from Larodan Fine Chemicals (Malmö, Sweden) or Nu-Chek Prep (Elysian, MN, USA). Gradient grade methanol and hexane (Merck) were used as received; the other solvents (chloroform, diethyl ether, and 2-propanol) were distilled in glass from analytical-grade products. The 2,6-di-*tert*-butyl-4-methylphenol (butylated hydroxytoluene, BHT) and ammonium acetate were purchased from Fluka (Buchs, Switzerland).

Sample Preparation

The dissected fat bodies were transferred one by one into glass vials with 100 μL of a $CHCl_3/CH_3OH$ mixture (1:1, v/v) containing BHT (25 mg/mL). The samples were sonicated for 15 minutes and stored at −28 °C prior to TLC.

The isolation of the TAG from the fat body tissues using semipreparative TLC has been described previously [8]. Briefly, the tissue in the vial was crushed using a small glass stick, extracted several times with $CHCl_3$, and the combined total extracts were separated on TLC plates with hexane/diethyl ether/formic acid (80:20:1) as the mobile phase. The TAG zone was scraped off the plate and extracted with freshly distilled diethyl ether. The solvent was evaporated under an argon stream to dryness and the residues were weighed and reconstituted in chloroform to a concentration of 1%. The TAG samples were stored in sealed amber glass ampoules at −28 °C. For measuring the TAG age profile of the bumblebee males, we used five repetitions for each age class.

High Performance Liquid Chromatography/Mass Spectrometry

HPLC/MS analyses were performed on a system that consisted of a SMC 1000 vacuum membrane degasser, P 4000 gradient pump, SN 4000 control unit, LCQ classic ion-trap mass spectrometer (Thermo Finnigan, San Jose, CA, USA) (all of the instruments come from Thermo Separation Products, San Jose, CA, USA), and a personal computer with Xcalibur software (Thermo Finnigan). Manual injection was accomplished with a Rheodyne-type Model D injection valve (Ecom, Prague, Czech Republic) equipped with a 5 μL internal injection loop. A Labio RT 04 column thermostat (Labio, Prague, Czech Republic) served to maintain the column temperature at 30 °C. Two stainless-steel columns Nova-Pak C18 (300 × 3.9 mm, 150 × 3.9 mm, with a particle size of 4 μm; Waters, Milford, MA, USA) connected in a series were used. Non-aqueous reversed phase HPLC gradient separations were performed using acetonitrile (A) and 2-propanol (B) as the mobile phases. The gradient program was 0 min—100% A, with a flow rate of 1 mL/min; 108 min—30% A, 70% B, 1 mL/min; 122 min—20% A, 80% B, 0.7 mL/min; 127 min—100% A, 0.7 mL/min; 130 min—100% A, 1 mL/min. Ammonium acetate dissolved in 2-propanol/water (1:1) at a 100 mmol/L concentration was added post-column via a tee at a flow rate of 10 μL/min. These conditions are based on our previous work [17]. The atmospheric pressure chemical ionization (APCI) source was operated at 400 °C, where the heated capillary temperature was 200 °C and the corona discharge current was set to 4.5 μA. The full-scan mass spectra were recorded in the *m/z* range of 75–1,300. The mass spectra were interpreted with the aid of *TriglyAPCI* software [18]. Because of the different probabilities of FA loss during fragmentation, the relative intensities of the diacylglycerol ions provide regiospecific distribution information of the FA on the glycerol backbone. APCI-MS has not been demonstrated to be able to differentiate between diacylglycerol ions formed by the loss of *sn*-1 versus *sn*-3 FA. Therefore, one can distinguish FA bonded to the *sn*-2 position from those attached to the *sn*-1/*sn*-3 positions [19]. In this work, the FA in *sn*-2 positions are deduced from the diacylglycerol fragment with the least abundance. However, the intensity ratio depends also on the number and position of the double bonds in a particular FA. Therefore, if the TAG standards are not available, the positions of the FA on the glycerol backbone may be interpreted incorrectly [20]. The peak areas were calculated from reconstructed chromatograms for the $[M + H]^+$ and $[M + NH_4]^+$ ions (with the two added together).

Transesterification

The TAG fractions were transesterified using a method described earlier [21]. Briefly, the TAG were dissolved in $CHCl_3/CH_3OH$ (2:3, v/v) in a small glass ampoule. After adding acetyl chloride, the ampoule was sealed and placed in a water bath at 70 °C. This procedure prevents the loss of volatile FAME during transesterification. After 90 min, the ampoule was opened and the reaction mixture was neutralized with silver carbonate. After a brief centrifugation, the supernatant was directly analyzed by GC/MS.

Gas Chromatography/Mass Spectrometry

The FAME were analyzed to confirm the results of the TAG composition. The GC/MS analyses were performed using a Focus GC (Thermo) coupled with a MD800 quadrupole mass detector (Fisons). A non-polar DB-5 ms column (30 m × 0.25 mm i.d., with a film thickness of 0.25 μm; J&W Scientific, Folsom, CA, USA) was used. The injector was operated in the splitless mode at 220 °C. The detector temperature was set to 200 °C; the standard 70 eV spectra were recorded at 1 scan/s. The temperature of the GC oven was programmed as follows: 50 °C held for 1 min, 7 °C/min to 320 °C, held at 320 °C for 10 min. Helium was used as a carrier gas at 1 ml/min. The data were analyzed using the Xcalibur (ver. 2.0.7) program. The relative proportions of the FAME were estimated from the total ion current (TIC) integration.

Data Analysis

The data for both species were processed with multivariate exploratory tools to visualize and evaluate the chemical variability among the particular age classes. All of the analyses were performed in the Statistica 8 Package by Statsoft. The relative peak areas representing more than 1 relative percent (0.5% in the FAME analyses) in at least two individuals of at least one age group were selected and

standardized again to 100%. Then the relative percentages were subjected to an analysis of the principle components (PCA) to reduce the number of descriptive variables. The PCA allowed us to extract 7 factors explaining more than 92% of the variability in *B. terrestris* and 8 factors explaining more than 90% of the variability in *B. lucorum*. The factor scores for each individual and the selected factors were subsequently used to separate the age classes by means of discriminant analysis (DA) with the age class as a grouping variable. The dissimilarities between the age classes were evaluated using the matrix of the Mahalanobis distances, visualized using cluster analysis with the unweighted pair-group method with arithmetic mean (UPGMA).

Results

TAG Quantity

In both species, the amounts of TAG changed during the life with a high content in the first 5 days in *B. terrestris* and 7 days in *B. lucorum*, respectively (Fig. 1, Tables S1 and S2 in the Supplementary Material). The amount reached a maximum at 1–2 days in *B. terrestris* (2.3 mg/individual) and 2–3 days in *B. lucorum* (5.1 mg/individual). After that, a slowly decreasing trend was observed. In *B. terrestris*, the seven-day-old males contained around 50% of the highest amount. In very old males, approximately 10% of the highest values were left (Table S1). In *B. lucorum*, the observed trend was similar but with the amounts shifted to higher values and with higher age (Table S2). The amount of TAG in *B. lucorum* was about 2.2 times higher than that in *B. terrestris* for all of the ages studied. If we take into account the body weight, the *B. lucorum* males (an average weight of 222 mg) contained 2.7 times more TAG in the fat body than *B. terrestris* (with an average weight of 280 mg).

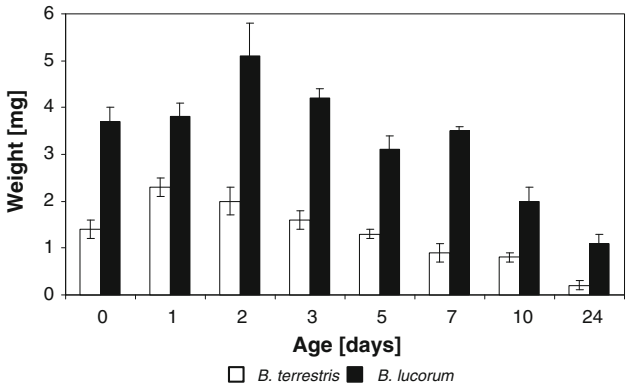

Fig. 1 The weight of the TAG (in milligrams) extracted from the fat bodies of males of different ages. The data represent the mean values of five specimens ± standard error

LC/MS Analysis of TAG

The main TAG in both species was POLn (10–20% in *B. terrestris* and 11–26% in *B. lucorum*; Tables S3 and S4 in the Supplementary Material). Other relatively abundant components differed. In *B. terrestris* these were OLnLn (3–14%) and LLL + OLLn (5–13%), whereas in *B. lucorum* POO (7–13%) and OOO (3–13%) were of relatively high abundance. A seemingly identical medium-abundant component turned out to be the isomeric TAG OLnO (12–19% in *B. terrestris*) and OOLn (9–18% in *B. lucorum*), based on the fragment intensities in mass spectra. A difference between the species was observed in the composition of the TAG with respect to the male's age. In *B. terrestris*, differences in TAG profiles were observed among young, mature, and old males (Fig. 2, left). The profiles of the old males were more complex than those of the younger ones. Interestingly, this was not the case in *B. lucorum*, where the TAG profiles were more or less stable during the male's entire life (Fig. 2, right). The variations within particular age classes were small in both species.

Regarding the particular compounds in the lipids of the specimens of different age (Tables S3 and S4 in Supplementary Material), all *B. lucorum* males as well as younger *B. terrestris* males differed only on a quantitative level. A statistical evaluation (PCA) led to the formation of data clusters separating several age classes in *B. terrestris* (Fig. 3). 1-, 2-, and 3-day-old males have very similar TAG profiles, 0-, 5-, and 10-day-old males are mixed together, and 7- and 12-day-old males are distinguished from other classes as well as from one another. The compounds responsible for the separation of the class of seven-day-old males were LLnLn, MoLnO, PLnLn, OLnLn, and LLL + OLLn. These components were significantly more abundant in TAG of seven-day-old males as compared to the other age classes. A clearly distinct class of old *B. terrestris* males (24 days) was characterized by the presence of several unique TAG: MoLL, LL20:4, XLLn, XLP, XOL, XOP, XOO, and XLnLn. The X moiety appears at a nominal mass of 15:2 FA, but its presence was not confirmed after transesterification and the FAME analysis. It is more likely that X belongs to an oxidation product. The fat body of old specimens is different from the younger ones. Its color is darker and the structure looks corrupted. Thus, some less stable FA may undergo oxidative processes in lipids of the old males [22].

No trend for grouping according to age classes was observed in *B. lucorum*. The TAG composition changes very little with age. The newborn class (0 days) is separated to some extent because of higher quantities of

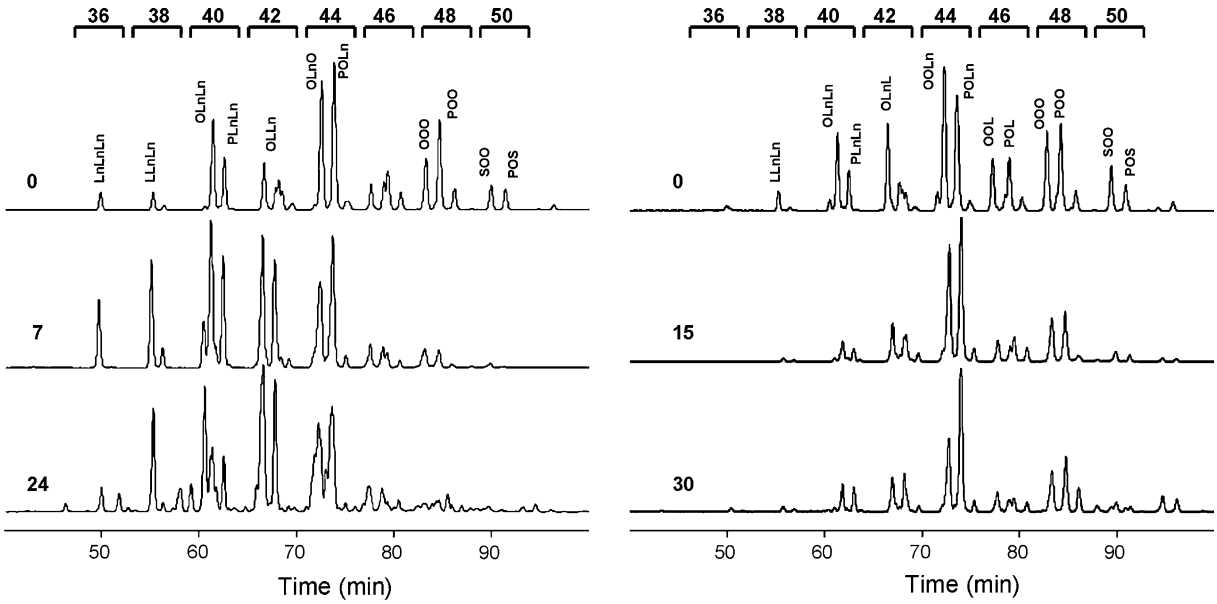

Fig. 2 The TIC chromatograms of the TAG of three age classes of *B. terrestris* males (0, 7 and 24 days, *left*) and *B. lucorum* males (0, 10 and 30 days, *right*). The numbers above chromatograms represent equivalent carbon numbers (ECN)

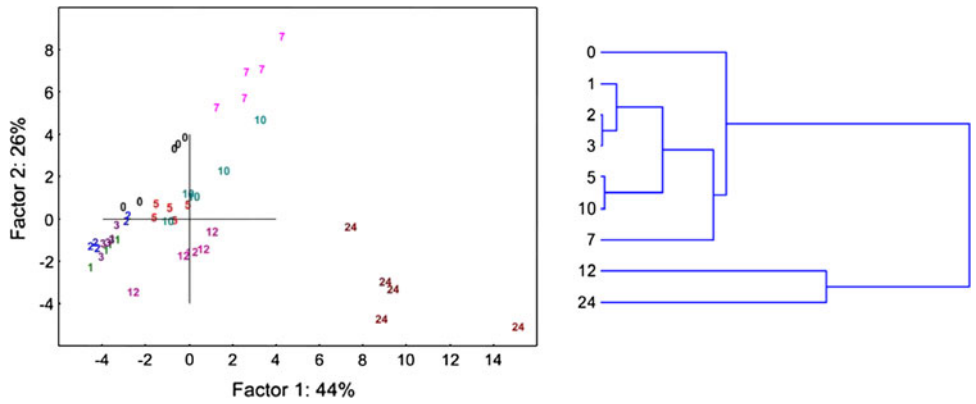

Fig. 3 A multivariate exploratory analysis of the data from the LC–MS analyses in *B. terrestris*. *Left* A graphic representation of the factor scores based on the first 2 principal components extracted from the PCA performed with the relative areas of the 43 most represented peaks. *Right* The patterns of the dissimilarities among the particular age classes inferred from the LC–MS analysis, visualized as a cluster tree based on the matrix of the Mahalanobis distances (UPGMA clustering)

LLnLn, PLnLn, SLnO, and POS in the TAG. At its developmental stage, the metabolism undergoes a lot of complex processes that may be responsible for a clear separation of this age class. A continuous shift from younger to older males (from right to left) can be seen in Fig. 4. However, in the cluster tree (Fig. 4, right), the age classes are distributed more or less randomly.

Our TAG quantifications are based on the integration of signal $[M + H]^+$ and $[M + NH_4]^+$ ions (summed together) from the MS detector. The post-column addition of ammonium acetate enabled us to visualize the TAG-bearing saturated FA (the $[M + H]^+$ fragment in these is very low or almost absent). The response factors (within a range of 0.4–2.8 according to the data published by Holčapek et al. [23]) were not taken into account. The aim of our study was a comparison of the TAG composition between insect species and age classes, not an absolute quantification that would have to be based on many standards and calibration curves. Even without an absolute quantification, we were able to compare the analyzed samples and see the differences.

GC/MS Analysis of Methyl Esters After Transesterification

At least three samples of each age class for both studied species were transesterified and the resulting FAME were

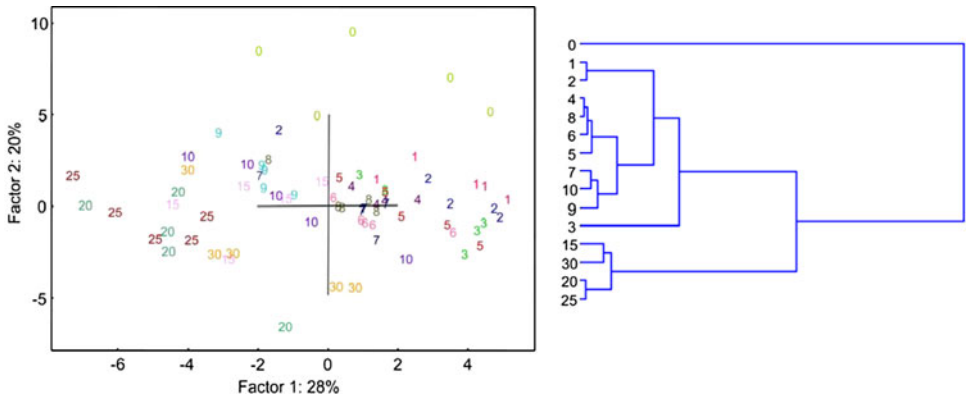

Fig. 4 A multivariate exploratory analysis of the data from the LC–MS analyses in *B. lucorum*. *Left* A graphic representation of the factor scores based on the first 2 principal components extracted from the PCA performed with the relative areas of the 34 most represented peaks. *Right* The patterns of the dissimilarities among the particular age classes inferred from the LC–MS analysis, visualized as a cluster tree based on the matrix of the Mahalanobis distances (UPGMA clustering)

analyzed using GC/MS. In both species, the FA with chain length of 16 and 18 carbon atoms dominate (Tables S5 and S6 in the Supplementary Material). The composition does not change much during the life of the males. For *B. lucorum,* lower amounts of unsaturated FA are characteristic; the *B. terrestris* samples contained up to twice as high amounts of unsaturated C18 FA than the *B. lucorum* ones.

The distribution of the FAME in the PCA plot (Fig. 5) in *B. terrestris* lipids shows only a slight tendency of grouping, much less pronounced than that with TAG (Fig. 3). The 24-day-old males are again far from the other samples. We can see from a comparison of Figs. 5 and 3 that an analysis of the TAG yields more information on species-specific lipids than an analysis of the FAME after transesterification. For *B. lucorum*, the PCA plot of FAME shows a similar distribution as the above-discussed TAG plot (Fig. 4). We can see small changes with increasing age. The FAME responsible for this trend are C16Me, C20:1Me, C20Me and C22Me. It corresponds to the LC/MS analyses, where the TAG containing these acids were present only in the old specimens. The species-specificity of the lipid composition can be seen in Fig. 5 as two well-separated groups, one for each species. The fine structure of the age classes is not so obvious in this plot.

Discussion

When we compare the results on TAG with our previous studies [8, 9] regardless of the *sn*-positions, we can see a high similarity. The small differences between the results may be caused by the use of another LC separation method [17]. The resolution of the peaks in this study is better than in the previous paper [8]. The overlapping peaks are thus resolved here and their integration differs. Furthermore, the insect specimens were different, and one has to take into account a natural variability of samples from living organisms. In addition, our threshold (1% for at least 2 samples per age group) can contribute to the difference. What differs more is the comparison of the *sn*-positions for each TAG. The abilities of reversed-phase chromatographic systems to separate regioisomers are limited. Although the general principles of the determination of *sn*-positions from mass spectra are known [19], the complexity of our biological samples prevents us from drawing unambiguous conclusions about the regioisomery of a particular molecular species. The use of silver-ion HPLC [24], particularly in the 2D arrangement [25], would certainly help, but such a detailed analysis of TAG is not required in this work. The TAG proportions in such a mixed peak can vary during the life of males. Therefore, significant conclusions should not be drawn from the *sn*-positions determined by this method.

During the life of the male, the TAG in the fat body undergo structural changes with some TAG dominating in young males and others in the older males despite the amounts of a particular FA remaining the same. According to the earlier literature, all insect lipids share the same FA composition based on 8 fatty acids, saturated, monounsaturated, and 2 polyunsaturated ones, 18:2 and 18:3 [26]. However, many exceptions from this rule have since been reported [27]. These exceptions may be the result of selective adaptations of different insect species. The two bumblebee species studied in this paper fall more or less into the pattern of the most common insect FA.

The polyunsaturated FA, 18:2 and 18:3, are highly abundant in both species; they dominate the FA of the *B. terrestris* fat body. It was generally accepted earlier that polyunsaturated FA (PUFA) are essential to animals and cannot be biosynthesized. Later, many authors demonstrated the ability of some insect orders to synthesize linoleic acid [27]. The literature data about the TAG

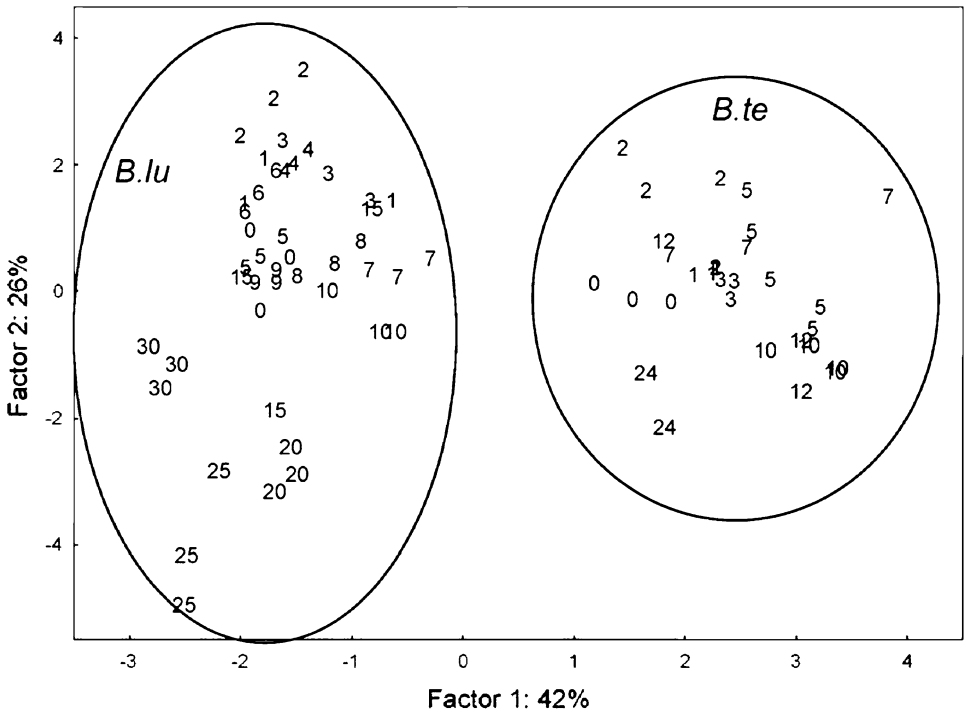

Fig. 5 A graphic representation of the factor scores based on the first two principal components extracted from the PCA performed with the relative areas of the FAME in *B. terrestris* and *B. lucorum* added together

composition in Hymenoptera are scarce. The TAG were studied on the prepupae of the leafcutting bee *Megachile rotundata* [28]. Their results show that about 76% of all of the FA are unsaturated, mainly 16:1 and 18:3. Such a high amount of unsaturated FA is probably connected to their adaptation for overwintering and a cold climate.

The composition of the TAG correlates with the FAME analysis except for the lauric acid. After transesterification, the proportion of this acid is not insignificant (0.7–3.5% in *B. terrestris* and 1.5–5.3% in *B. lucorum*). However, the amounts of those TAG containing La seem to be too low (LaOLn 1%; LaOP 1.2%, Table S3). These discrepancies arise from the fact that La is distributed in many small peaks that were cut off by the set threshold.

The fatty acids bound in the TAG are not only a pool of energy [2], but there is a great deal of evidence that they participate in the biosynthesis of the FA-derived sex pheromones in Lepidoptera and Diptera [29–31]. Lipophorin, the protein transporting diacylglycerols (DAG) in the hemolymph, is able to transport other molecules, too, such as TAG, free FA, sterols, carotenoids, and hydrocarbons [32]. Thus, the role of lipids as pheromone precursors has been demonstrated. In bumblebees, our recent results indicate that the male-marking pheromones, typically consisting of ethyl esters of fatty acids, may be formed from precursors bound in TAG in the fat body [10]. The original idea on the connection between a primary lipid metabolism and the patrolling male sex pheromone was based on an observation of the structural similarity of the lipids in the fat tissue and the labial gland extracts. The chain length, double-bond position, and geometry are the same, the putative lipid precursors only need to be transesterified or further modified to a labial-gland major component. Indeed, we have found lipase activity in the labial gland tissue in vitro trans-esterification (Jiroš et al., unpublished results). Assuming energy efficiency in nature, it seems to be unnecessary for bumblebees to invest in an enzymatic system producing the sex-pheromone component in the gland if a large pool of precursors has been produced already. The amounts of the pheromone stored in the gland are huge when compared to Lepidoptera (several milligrams per gland as reported by Žáček et al. [15]). Lepidopteran sex pheromones have double-bond positions, and their configuration is different from the fat lipids [33, 34]. The "trick" used by bumblebees is that the common fatty acid is esterified to uncommon ethyl esters, thus becoming a distinct pheromone signal.

In some species such as *B. pratorum, B. lapidarius, B. ruderatus, B. confusus, B. campestris,* or *B. bohemicus*, striking similarities were found in the chain length and double-bond positions of some FA in the TAG and the pheromonal components [10, 11]. We have shown in our previous study that the TAG compositions in fat bodies of bumblebee males are species-specific [9]. However, no attention has been paid to the influence of the age of the specimens studied on the TAG composition. Reports exist in unrelated insects (moths, beetles or fruit flies) on the changes of the FA pattern at various stages of development [35–37]. We have shown here that such changes exist in bumblebees even within one developmental stage (adult

males) depending on the age of the specimens. These changes must be based on the males' physiology, as their diet was a standard one, identical in both species and in all age classes.

B. terrestris and *B. lucorum* males differ in the temporal dynamics of the physiological activity of the pheromone gland and consequently in the time-related production of the marking pheromone [14, 15]. While in *B. terrestris* the pheromone is produced up to the fifth day of a male's life and then stored in the gland, in *B. lucorum* the pheromone biosynthesis goes on for the male's entire life. Our finding on the lipid composition as a result of the fat-body development correlates with the earlier published ontogeny of the pheromonal gland: it confirmed significant changes of the TAG composition with age in *B. terrestris* as opposed to *B. lucorum*, where the TAG did not significantly differ with the males' age.

It could still be possible that de novo synthesis is additionally involved, perhaps for a tighter regulation of its production. It has been shown in leaf beetles that different strategies for producing allomonal compounds are related to its evolution. The older species are sequestering the host plant-related compounds while the more evolved species produce those or similar compounds de novo. The insects can even switch between the two pathways according to the conditions and availability of precursors [38]. In bumblebees, we still do not have clear evidence disproving our original schemes of how the male-marking pheromones are produced. The analytical results on fat-body TAG do not support our above-mentioned hypothesis showing anticipated higher levels of particular TAG as possible precursors. Thus, the biosynthesis of the male-marking pheromone will be a more complex process than so far believed.

Acknowledgments The financial support of the Czech Science Foundation (Project 502/10/1734) is herewith acknowledged with appreciation. The research was also carried out as a part of Project No. Z4 055 0506 (Academy of Sciences of the Czech Republic). The authors are deeply indebted to Prof. Vladimír Ptáček for the insect material, Dr. Ales Svatoš for his valuable advice and Mr. Sean Mark Miller for language correction.

References

1. Law JH, Wells MA (1989) Insects as biochemical models. J Biol Chem 264:16335–16338
2. Arrese EL, Soulages JL (2010) Insect fat body: energy, metabolism, and regulation. Annu Rev Entomol 55:207–225. doi:10.1146/annurev-ento-112408-085356
3. Dean RL, Collins JV, Locke M (1985) Structure of the fat body. In: GA Kerkut, LI Gilbert (ed) Comprehensive insect physiology, biochemistry, and pharmacology, Pergamon, New York, pp 155–210
4. Downer RGH, Matthews JR (1976) Patterns of lipid distribution and utilization in insects. Am Zool 16:733–745
5. Canavoso LE, Jouni ZE, Karnas KJ, Pennington JE, Wells MA (2001) Fat metabolism in insects. Annu Rev Nutr 21:23–46
6. Stanley-Samuelson DW, Nelson DR (eds) (1993) Insect lipids: chemistry, biochemistry and biology. University of Nebraska Press, Lincoln, USA, pp 353–388
7. Blomquist GJ, Bagnères A (eds) (2010) Insect hydrocarbons: biology, biochemistry, and chemical ecology. Cambridge University Press, Cambridge, UK, pp 35–52, pp 75–99
8. Cvačka J, Hovorka O, Jiroš P, Kindl J, Stránský K, Valterová I (2006) Analysis of triacylglycerols in fat body of bumblebees by chromatographic methods. J Chromatogr A 1101:226–237. doi:10.1016/j.chroma.2005.10.001
9. Kofroňová E, Cvačka J, Vrkoslav V, Hanus R, Jiroš P, Kindl J, Hovorka O, Valterová I (2009) A comparison of HPLC/APCI-MS and MALDI-MS for characterising triacylglycerols in insects: species-specific composition of lipids in the fat bodies of bumblebee males. J Chromatogr B Biomed Appl 877:3878–3884. doi:10.1016/j.jchromb.2009.09.040
10. Luxová A, Valterová I, Stranský K, Hovorka O, Svatoš A (2003) Biosynthetic studies on marking pheromones of bumblebee males. Chemoecology 13:81–87. doi:10.1007/s00049-003-0230-8
11. Cvačka J, Kofroňová E, Vašíčková S, Stránský K, Jiroš P, Hovorka O, Kindl J, Valterová I (2008) Unusual fatty acids in the fat body of the early nesting bumblebee, *Bombus pratorum*. Lipids 43:441–450. doi:10.1007/s11745-008-3174-5
12. Urbanová K, Valterová I, Hovorka O, Kindl J (2001) Chemotaxonomical characterisation of males of *Bombus lucorum* (Hymenoptera : Apidae) collected in the Czech Republic. Eur J Entomol 98:111–115
13. Valterová I, Kunze J, Gumbert A, Luxová A, Liblikas I, Kalinová B, Borg-Karlson AK (2007) Male bumble bee pheromonal components in the scent of deceit pollinated orchids: unrecognized pollinator cues? Arthropod-Plant Interact 1:137–145. doi:10.1007/s11829-007-9019-y
14. Šobotník J, Kalinová B, Cahlíková L, Weyda F, Ptáček F, Valterová I (2008) Age-dependent changes in structure and function of the male labial gland in *Bombus terrestris*. J Insect Physiol 54:204–214. doi:10.1016/j.jinsphys.2007.09.003
15. Žáček P, Kalinová B, Šobotník J, Hovorka O, Ptáček V, Coppée A, Verheggen F, Valterová I (2009) Comparison of age-dependent quantitative changes in the male labial gland secretion of *Bombus terrestris* and *Bombus lucorum*. J Chem Ecol 35:698–705. doi:10.1007/s10886-009-9650-4
16. Ptáček V, Pernová E, Borovec R (2000) The two-queen cascade method as an alternative technique for starting bumble bee (Bombus, Hymenoptera, Apidae) colonies in laboratory (Preliminary study). Pszczel Zesz Nauk 44:305–309
17. Kofroňová E, Cvačka J, Jiroš P, Sýkora D, Valterová I (2009) Analysis of insect triacylglycerols using liquid chromatography-atmospheric pressure chemical ionization-mass spectrometry. Eur J Lipid Sci Technol 111:519–525. doi:10.1002/ejlt.200800228
18. Cvačka J, Krafková E, Jiroš P, Valterová I (2006) Computer-assisted interpretation of atmospheric pressure chemical ionization mass spectra of triacylglycerols. Rapid Commun Mass Spectrom 20:3586–3594. doi:10.1002/rcm.2770
19. Mottram HR, Woodbury SE, Evershed RP (1997) Identification of triacylglycerol positional isomers present in vegetable oils by high performance liquid chromatography/atmospheric pressure chemical ionization mass spectrometry. Rapid Commun Mass Spectrom 11:1240–1252
20. Laakso P (2002) Mass spectrometry of triacylglycerols. Eur J Lipid Sci Technol 104:43–49
21. Stránský K, Jursík T (1996) Simple quantitative transesterification of lipids. 1. Introduction. Fett-Lipid 98:65–71

22. Porter NA, Caldwell SE, Mills KA (1995) Mechanism of free-radical oxidation of unsaturated lipids. Lipids 30:277–290
23. Holčapek M, Lísa M, Jandera P, Kabátová N (2005) Quantitation of triacylglycerols in plant oils using HPLC with APCI-MS, evaporative light-scattering, and UV detection. J Sep Sci 28:1315–1333
24. Holčapek M, Dvořáková H, Lísa M, Girón AJ, Sandra P, Cvačka J (2010) Regioisomeric analysis of triacylglycerols using silver-ion liquid chromatography atmospheric pressure chemical ionization mass spectrometry: comparison of five different mass analyzers. J Chromatogr A 1217:8186–8194
25. Holčapek M, Velínská H, Lísa M, Česla P (2009) Orthogonality of silver-ion and non-aqueous reversed-phase HPLC/MS in the analysis of complex natural mixtures of triacylglycerols. J Sep Sci 32:3672–3680
26. Thompson SN (1973) A review and comparative characterization of the fatty acid compositions of seven insect orders. Comp. Biochem. Physiol. B 45:467–482
27. Stanley-Samuelson DW, Jurenka RA, Cripps C, Blomquist GJ, de Renobales M (1988) Fatty acids in insects: composition, metabolism, and biological significance. Arch Insect Biochem Physiol 9:1–33
28. Buckner JS, Kemp WP, Bosch J (2004) Characterization of triacylglycerols from overwintering prepupae of the alfalfa pollinator *Megachile rotundata* (Hymenoptera: megachilidae). Arch Insect Biochem Physiol 57:1–14. doi:10.1002/arch.20008
29. Jurenka RA, Roelofs W (1993) Biosynthesis and endocrine regulation of fatty acid derived sex pheromones in moths. In: Insect Lipids: chemistry, biochemistry and biology, University of Nebraska Press, Lincoln
30. Tumlinson JH, Teal PEA, Fang N (1996) The integral role of triacyl glycerols in the biosynthesis of the aldehydic sex pheromones of *Manduca sexta* (L). Bioorg Med Chem 4:451–460
31. Morgan ED (2004) Biosynthesis in insects. The Royal Society of Chemistry, Cambridge, UK
32. Arrese EL, Canavoso LE, Jouni ZE, Pennington JE, Tsuchida K, Wells MA (2001) Lipid storage and mobilization in insects: current status and future directions. Insect Biochem Mol Biol 31:7–17
33. Tillman JA, Seybold SJ, Jurenka RA, Blomquist GJ (1999) Insect pheromones—an overview of biosynthesis and endocrine regulation. Insect Biochem Mol Biol 29:481–514
34. Jurenka R (2004) Insect pheromone biosynthesis. In: Schulz S (ed) Topics in current chemistry, Springer, Berlin Heidelberg New York, pp 97–132
35. Hodges JD, Barras SJ (1974) Fatty-acid composition of *Dendroctonus frontalis* at various developmental stages. Ann Entomol Soc Am 67:51–54
36. Madariag MA, Mata F, Municio AM, Ribera A (1974) Changes in fatty-acid patterns of glycerolipids of *Dacus oleae* during metamorphosis and development. Insect Biochem 4:151–160
37. Janda V (1975) Synthesis and utilization of tissue proteins and lipids during the larval–pupal transformations of *Galleria mellonella* (Lepidoptera). Acta Entomol Bohemoslov 72:227–235
38. Matsuki M, Kay N, Serin J, Scott JK (2011) Variation in the ability of larvae of phytophagous insects to develop on evolutionarily unfamiliar plants: a study with gypsy moth *Lymantria dispar* and *Eucalyptus*. Agric Forest Entomol 13:1–13

Lipids (2011) 46:873–878
DOI 10.1007/s11745-011-3592-7

COMMUNICATION

Efficient and Specific Conversion of 9-Lipoxygenase Hydroperoxides in the Beetroot. Formation of Pinellic Acid

Mats Hamberg · Ulrika Olsson

Received: 31 May 2011 / Accepted: 24 June 2011 / Published online: 10 July 2011

Abstract The linoleate 9-lipoxygenase product 9(*S*)-hydroperoxy-10(*E*),12(*Z*)-octadecadienoic acid was stirred with a crude enzyme preparation from the beetroot (*Beta vulgaris* ssp. *vulgaris* var. *vulgaris*) to afford a product consisting of 95% of 9(*S*),12(*S*),13(*S*)-trihydroxy-10(*E*)-octadecenoic acid (pinellic acid). The linolenic acid-derived hydroperoxide 9(*S*)-hydroperoxy-10(*E*),12(*Z*),15(*Z*)-octadecatrienoic acid was converted in an analogous way into 9(*S*),12(*S*),13(*S*)-trihydroxy-10(*E*),15(*Z*)-octadecadienoic acid (fulgidic acid). On the other hand, the 13-lipoxygenase-generated hydroperoxides of linoleic or linolenic acids failed to produce significant amounts of trihydroxy acids. Short-time incubation of 9(*S*)-hydroperoxy-10(*E*),12(*Z*)-octadecadienoic acid afforded the epoxy alcohol 12(*R*),13(*S*)-epoxy-9(*S*)-hydroxy-10(*E*)-octadecenoic acid as the main product indicating the sequence 9-hydroperoxide → epoxy alcohol → trihydroxy acid catalyzed by epoxy alcohol synthase and epoxide hydrolase activities, respectively. The high capacity of the enzyme system detected in beetroot combined with a simple isolation protocol made possible by the low amounts of endogenous lipids in the enzyme preparation offered an easy access to pinellic and fulgidic acids for use in biological and medical studies.

Keywords Fatty acid hydroperoxide · Epoxy alcohol · Trihydroxy oxylipin · Pinellic acid

M. Hamberg (✉) · U. Olsson
Division of Physiological Chemistry II,
Department of Medical Biochemistry and Biophysics,
Karolinska Institutet, Stockholm, Sweden
e-mail: Mats.Hamberg@ki.se

Abbreviations

EAS	Epoxy alcohol synthase
GC-MS	Gas-liquid chromatography-mass spectrometry
GLC-FID	Gas-liquid chromatography with flame-ionization detection
HODE	Hydroxyoctadecadienoic acid
HPODE	Hydroperoxyoctadecadienoic acid
HPOTrE	Hydroperoxyoctadecatrienoic acid
MC	(–)-Menthoxycarbonyl
Me_3Si	Trimethylsilyl
NMR	Nuclear magnetic resonance
SP-HPLC	Straight-phase high-performance liquid chromatography
UV	Ultraviolet

Introduction

The first characterization of unsaturated trihydroxy oxylipins was published by Graveland in 1970 [1]. In this study, lipoxygenase-catalyzed oxygenation of linoleic acid in doughs and flour–water suspensions afforded hydroperoxides, hydroxides and epoxy alcohols as well as a fraction consisting of a mixture of 9,12,13-trihydroxy-10-octadecenoic and 9,10,13-trihydroxy-11-octadecenoic acids. Although separation of the regio- and stereoisomeric trihydroxyoctadecenoates was not achieved, it could be concluded that the 9,12,13-trihydroxy isomer was the dominating one and further be deduced that this compound originated in linoleic acid 9-hydroperoxide (9-HPODE). Eight stereoisomers (four pairs of enantiomers) of 9,12,13-trihydroxy-10-octadecenoic acid are possible because of the three chiral carbons at C-9, C-12 and C-13. In 1991, two studies demonstrated that naturally occurring 9,12,13-trihydroxy-10-octadecenoic acid has the

9(*S*),12(*S*),13(*S*) configuration [2, 3]. More recently, 9(*S*),12(*S*),13(*S*)-trihydroxy-10(*E*)-octadecenoic acid was isolated from tubers of *Pinellia ternata* (crow-dipper), and the trivial name *pinellic acid* was given to the compound [4]. The $\Delta^{15(Z)}$-unsaturated analog of pinellic acid, *i.e.* fulgidic acid, has also been described [5].

Biosynthesis of pinellic acid in plants can take place by lipoxygenase-catalyzed oxygenation of linoleic acid into 9(*S*)-HPODE, which can be further converted into the epoxy alcohol 12(*R*),13(*S*)-epoxy-9(*S*)-hydroxy-10(*E*)-octadecenoic acid in the presence of epoxy alcohol synthase (EAS) [6, 7] or peroxygenase [8]. Pinellic acid is formed from the epoxy alcohol by action of epoxide hydrolase activity, which catalyzes regio- and stereospecific opening at C-12 of the C-12/C-13 epoxide [7, 8]. Also linoleic acid 13-hydroperoxide (13-HPODE) can be converted to 9,12,13-trihydroxyoctadecenoates as shown in chemical model systems [9, 10].

Pinellic acid and other trihydroxyoctadecenoates are produced in plants during wounding and infection by fungal pathogens [11–13]. Interestingly, such trihydroxy oxylipins inhibit growth of fungi and germination of spores [12, 13] and may play a role in plants' defense against pathogenic fungi. Further interest in trihydroxyoctadecenoates stems from their presence in beer [3, 14, 15], in which beverage they may contribute a bitter taste [16]. More recent studies on pinellic acid are focussed on the use of this trihydroxy oxylipin as an oral adjuvant for nasal influenza vaccines [4, 17–19].

The present paper describes a new EAS-epoxide hydrolase pathway in the beetroot by which 9-lipoxygenase-generated fatty acid hydroperoxides are converted into specific trihydroxy acids. Based on the results, a procedure for easy preparation of pinellic acid of >99.5% stereochemical purity was elaborated. This enzymatic approach offers an alternative to earlier described preparations of pinellic acid by organic chemical synthesis [17, 20–23].

Experimental Procedures

Fatty Acid Hydroperoxides

9(*S*)-HPODE, 13(*S*)-HPODE, 9(*S*)-HPOTrE and 13(*S*)-HPOTrE were prepared by lipoxygenase-catalyzed oxygenation of linoleic or linolenic acids [7] followed by purification by straight-phase high-performance liquid chromatography (SP-HPLC). [1-^{14}C]9(*S*)-HPODE (specific radioactivity 15.1 kBq/μmol) was prepared in the same way starting with [1-^{14}C]linoleic acid (Perkin-Elmer, Boston, MA).

Reference Oxylipins

Regio- and stereoisomeric epoxy alcohols including methyl 12(*R*),13(*S*)-epoxy-9(*S*)-hydroxy-10(*E*)-octadecenoate were prepared by incubating fatty acid hydroperoxides with peroxygenase from broad bean or oat seeds followed by isolation by SP-HPLC [7]. 9(*S*),12(*S*),13(*S*)-Trihydroxy-10(*E*)-octadecenoic acid (pinellic acid), 9(*S*),12(*S*),13(*S*)-trihydroxy-10(*E*),15(*Z*)-octadecadienoic acid (fulgidic acid) and other isomeric trihydroxy oxylipins were prepared from linoleic and linolenic acids as described in detail [7].

Enzyme Preparation

Beetroots (red beets) obtained from a local market were peeled and the flesh portion finely diced in 6 volumes/weight of ice-cold 0.1 M phosphate buffer pH 6.7. The mixture was homogenized at 0 °C for 3 × 30 s using a Polytron and then filtered through gauze. The filtrate was used for all preparative incubations with fatty acid hydroperoxides. For ultraviolet (UV) spectrophotometric assay, the filtrate was diluted 1:7.7 (v/v) with 0.1 M phosphate buffer pH 6.7.

Incubations and Treatments

For generation of oxidation products for structural work, fatty acid hydroperoxides (300 μM) were stirred with enzyme preparation (5 mL) at 23 °C for 5 or 30 min. The mixtures were acidified to pH 5 and rapidly extracted with 75 mL of diethyl ether. Material obtained after evaporation of the solvent was methyl-esterified by treatment with diazomethane and either analyzed by SP-HPLC or trimethylsilylated and analyzed by gas–liquid chromatography-mass spectrometry (GC–MS) or gas–liquid chromatography with flame-ionization detection (GLC-FID).

Preparation of Pinellic Acid (free acid form of compound **II**)

A typical preparation of pinellic acid (batches of 15–20 mg) was carried out as follows. Beetroots were peeled and the flesh portion finely diced (40 g). Potassium phosphate buffer (240 mL) was added, and homogenization was performed at 0 °C using a Polytron. Following filtration through gauze, 179 mL of the filtrate was stirred with 500 μM 9(*S*)-HPODE (27.9 mg) at 23 °C for 1 h. The incubation mixture was acidified to pH 3 and extracted with ethyl acetate. The extracted product (53 mg) was dissolved in 3 mL of 2-propanol/chloroform 1:2 (v/v); this solution was divided and loaded on two 0.5-g aminopropyl cartridges (Supelco, Bellefonte, PA). Neutral lipids were eluted with 6 mL of the

same solvent mixture, whereas pinellic acid was obtained by elution with 15 mL of ethyl acetate/acetic acid 98:2 (v/v). The latter eluates from the two columns were combined and taken to dryness affording a white solid (23.6 mg; yield, 80%). Analysis of this material by GC–MS and GLC-FID revealed 97% trihydroxyoctadecenoate and 3% other materials (mainly 9-HODE). Regio- and stereochemical analysis of the trihydroxyoctadecenoate [24] showed 98% 9(*S*),12(*S*),13(*S*)-trihydroxy-10(*E*)-octadecenoic acid (pinellic acid) and 2% of other isomeric trihydroxyoctadecenoates. An aliquot of this material was crystallized from methanol/diethyl ether to provide pinellic acid, >99.5% pure according to GC–MS and GLC-FID, m.p. 105.5–106.5 °C (earlier reported, 104–106 °C [17, 21]).

Instrumental Methods

For SP-HPLC, a column of Nucleosil 50-5 (200 × 4.6 mm) purchased from Macherey–Nagel (Düren, Germany) was used. The column effluent was passed through serially connected detectors for measurement of UV absorbance (210 or 234 nm) and radioactivity. For isolation of methyl esters of epoxy alcohols and trihydroxy acids, solvent systems of 2-propanol/hexane (1.5:98.5, vol/vol) and 2-propanol/hexane (7:93, vol/vol), respectively, were used. The flow rate was 2 mL/min.

For GC–MS, a Hewlett-Packard model 5970B mass selective detector connected to a Hewlett-Packard model 5890 gas chromatograph equipped with a 12-m phenylmethylsilicone capillary column was used.

GLC-FID was carried out with a Hewlett-Packard model 5890 gas chromatograph equipped with a flame-ionization detector and a 25-m methyl silicone capillary column. Helium at a flow rate of 25 cm/s was used as the carrier gas. Retention times were converted into C-values as described [25].

UV spectra were recorded on a Hitachi (Tokyo, Japan) model U-2000 UV/VIS instrument. Assay of EAS activity was performed by continuous measurement of the absorbency at 235 nm.

^{1}H-NMR spectra were recorded on deuteriochloroform solutions using a Bruker 400 MHz instrument. Tetramethylsilane was used as internal chemical shift reference.

Chemical Methods for Structure Determination

Catalytic hydrogenation of epoxy alcohols and trihydroxyesters [26], oxidative ozonolysis [27], and acid-promoted hydrolysis of allylic epoxy alcohols [24] were performed as indicated. Steric analysis of epoxy alcohols and trihydroxyesters was carried out as described in detail [24].

Results and Discussion

Isolation of oxidation products

[1-^{14}C]9(*S*)-HPODE (300 μM) was stirred at 23 °C for 30 min with the enzyme preparation from beetroot, and the methyl-esterified product was subjected to SP-radio-HPLC. A major peak of radioactivity due to compound **II** appeared (95% of the chromatographed radioactivity) (Fig. 1b). Reducing the time of incubation to 5 min resulted in lower formation of compound **II**, and instead the less polar compound **I** was the main product (Fig. 1a).

Incubation of 9(*S*)-HPOTrE (300 μM) with enzyme preparation for 30 min followed by extraction, methyl-esterification and isolation by SP-HPLC afforded the trihydroxyester compound **III** (>90%). As described for 9(*S*)-HPODE, when the incubation time was reduced to 5 min, the yield of compound **III** was lowered, and instead an epoxy alcohol methyl ester was the main product; this however, was not further characterized.

Structure of Compound I

No absorption band in the range 210–300 nm was observed in the UV spectrum of compound **I** demonstrating the disappearance of the conjugated diene of the incubated 9(*S*)-HPODE. On SP-HPLC, compound **I** comigrated with methyl 12(*R*),13(*S*)-epoxy-9(*S*)-hydroxy-10(*E*)-octadecenoate, suggesting the identity of compound **I** with this epoxy alcohol or an isomer thereof. The mass spectrum of the Me_3Si derivative of compound **I** showed a molecular ion at *m/z* 398 (relative intensity, 2%) and further ions at *m/z* 383 (3; M^+—15; loss of $\cdot CH_3$), 259 [18; Me_3SiO^+=CH-$(CH_2)_7$-$COOCH_3$], 241 [87; M^+ - 157; loss of $\cdot(CH_2)_7$-$COOCH_3$], 225 (21), 99

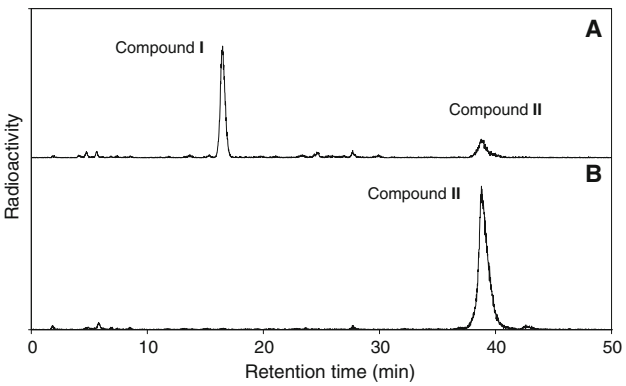

Fig. 1 SP-radio-HPLC analysis of methyl-esterified incubation products obtained after incubation of [1-^{14}C]9(*S*)-HPODE (300 μM) with enzyme preparation (5 mL) from beetroot. **a** Incubation at 23 °C for 5 min. **b** Incubation at 23 °C for 30 min. The column was eluted with 2-propanol/hexane (1.5:98.5, vol/vol) (0–20 min) followed by 2-propanol/hexane (7:93, vol/vol) (20–50 min) at a flow rate of 2 mL/min

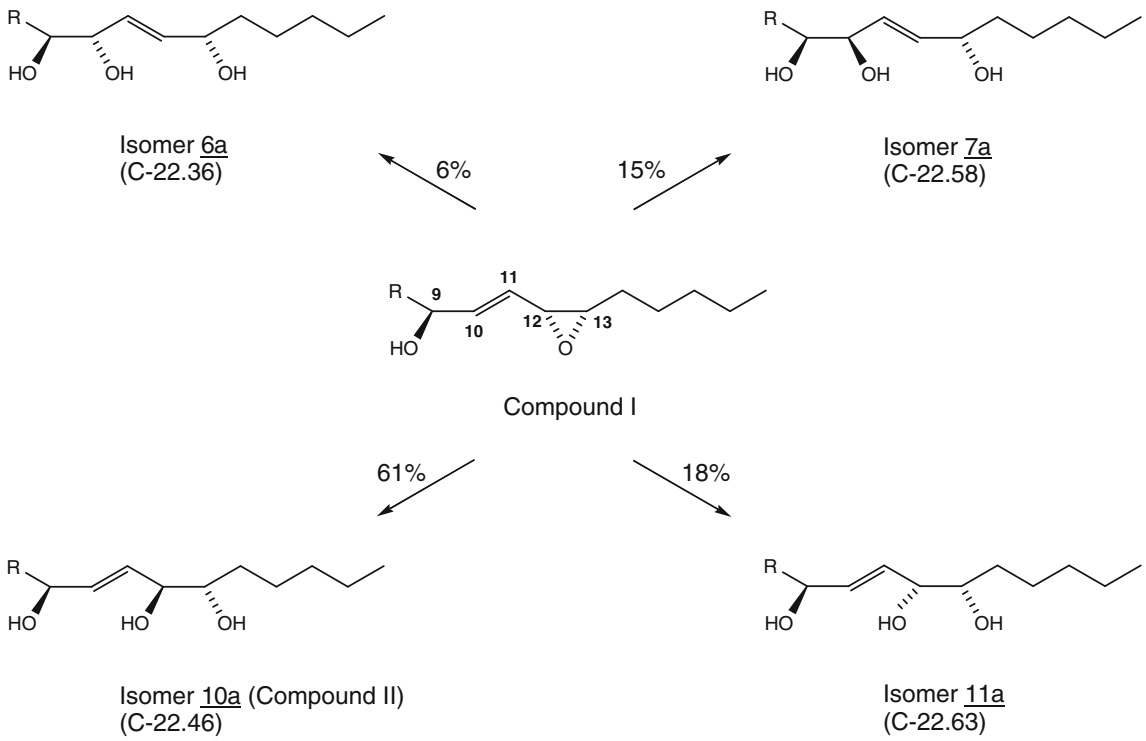

Scheme 1 Structures, percentages and C-values of isomeric trihydroxyesters produced upon acid-catalyzed hydrolysis of compound **I**. Numbering of trihydroxyesters corresponds to numbers used in Ref. [24]. R = $(CH_2)_7$-$COOCH_3$

[100; $^+O{\equiv}C$-$(CH_2)_4$-CH_3], and 73 (80; Me_3Si^+), thus indicating the presence of an epoxide group at C-12/C-13 and a hydroxyl group at C-9. The mass spectrum and C-value were identical to those of the Me_3Si derivative of authentic methyl 12(*R*),13(*S*)-epoxy-9(*S*)-hydroxy-10(*E*)-octadecenoate [7]. Oxidative ozonolysis performed on the (-)-menthoxycarbonyl (MC) derivative of compound **I** followed by methyl-esterification afforded the MC derivative of dimethyl 2(*S*)-hydroxy-1,10-decanedioate, in this way demonstrating the presence of a double bond in the Δ^{10} position and showing that the C-9 alcohol had the "*S*" configuration. Oxylipins possessing an allylic epoxy alcohol structure undergo facile hydrolysis into predictable patterns of trihydroxyesters under mildly acidic conditions [10, 24], and accordingly a sample of 1 mg of compound **I** was treated with methanol/1 mM hydrochloric acid (1:50, v/v) at 23 °C for 10 min. Regio- and stereochemical analysis [24] of the resulting trihydroxyesters (Me_3Si derivatives) by GC–MS and GLC-FID revealed the presence of the following compounds (abundance, C-value, numbering according to Ref. [24]): methyl 9(*S*),12(*S*),13(*S*)-trihydroxy-10(*E*)-octadecenoate (61%, C-22.46, isomer 10a), methyl 9(*S*),12(*R*),13(*S*)-trihydroxy-10(*E*)-octadecenoate (18%, C-22.63, isomer 11a), methyl 9(*S*),10(*R*),13(*S*)-trihydroxy-11(*E*)-octadecenoate (15%, C-22.58, isomer 7a), and methyl 9(*S*),10(*S*),13(*S*)-trihydroxy-11(*E*)-octadecenoate (6%, C-22.36, isomer 6a) (Scheme 1). Acid treatment of authentic methyl 12(*R*),13(*S*)-epoxy-9(*S*)-hydroxy-10(*E*)-octadecenoate produced an identical result, thus conclusively demonstrating the identity of compound **I** with this epoxy alcohol.

Structure of compound **II**

The mass spectrum of the Me_3Si derivative of compound **II** showed ions at *m/z* 545 (0.4%; M^+-15; loss of $\cdot CH_3$), 460 [15; M^+-100; rearrangement with loss of OHC-$(CH_2)_4$-CH_3], 439 [2; $M^+-(31+90)$; loss of $\cdot OCH_3$ plus Me_3SiOH], 387 (4; M^+ - 173; loss of $\cdot CH(OSiMe_3)$-$(CH_2)_4$-CH_3), 259 [16; Me_3SiO^+=CH-$(CH_2)_7$-$COOCH_3$], 230 [5; rearrangement with loss of OHC-CH = CH–$CH(OSiMe_3)$-$CH(OSiMe_3)$-$(CH_2)_4$-CH_3], 173 [100; Me_3SiO^+=CH-$(CH_2)_4$-CH_3], 147 (11; Me_3Si-O^+=$SiMe_2$), 103 (11; Me_3SiO^+=CH_2), and 73 (69; Me_3Si^+), thus indicating a 9,12,13-trihydroxyoctadecenoate. The C-value (22.46) was identical to that of the corresponding derivative of authentic methyl 9(*S*),12(*S*),13(*S*)-trihydroxy-10(*E*)-octadecenoate but differed from those of other possible trihydroxyoctadecenoate isomers (*cf.* Ref. [24]). Oxidative ozonolysis performed on the tris-MC derivative of compound **II** followed by methyl-esterification afforded the MC derivative of dimethyl 2(*S*)-hydroxy-1,10-decanedioate, thus locating the double bond to the Δ^{10} position and assigning the "*S*" configuration to C-9. ^{1}H-NMR spectral data of compound **II** are given in Table 1. The coupling constant observed for the

Table 1 ^{1}H-NMR data for compound **II**

Proton	δ (ppm)	Multiplicity	J (Hz)
2	2.31	t	7.4
3	1.62	m	
4–7,14–17	1.25–1.45	m	
8	1.53	m	
9	4.15	q	6.1, 12.2
10	5.83	dd	5.8, 15.5
11	5.72	dd	6.2, 15.5
12	3.95	dd	6.1
13	3.48	m	
18	0.90	t	6.9
OCH_3	3.67	s	
OH	2.29	s	

Recorded at 400 MHz in $CDCl_3$ with tetramethylsilane as internal chemical shift reference

olefinic protons at C-10 and C-11 (J = 15.5 Hz) confirmed that the Δ^{10} double bond had the "*E*" configuration. Final identification of compound **II** as methyl 9(*S*),12(*S*),13(*S*)-trihydroxy-10(*E*)-octadecenoate (methyl ester of pinellic acid) was provided by melting point data, *i.e.* 92.0–92.5 °C; earlier reported 92.5–93.0 °C [21].

Structure of Compound **III**

The trihydroxyester formed following incubation of 9(*S*)-HPOTrE gave analytical results identical to those previously recorded for methyl 9(*S*),12(*S*),13(*S*)-trihydroxy-10(*E*),15(*Z*)-octadecadienoate (methyl ester of fulgidic acid) with regard to C-value and mass spectrum [7]. Proof for the identity of compound **III** with this oxylipin, i.e., the $\Delta^{15(Z)}$-unsaturated analog of compound **II**, was provided by results of catalytic hydrogenation, which produced methyl 9(*S*),12(*S*),13(*S*)-trihydroxyoctadecanoate, and oxidative ozonolysis, which produced methyl hydrogen 2(*S*)-hydroxy-1,10-decanedioate (cf. Ref. [7]).

Substrate Specificity of the Beetroot EAS Activity

As described above, 9(*S*)-HPODE and 9(*S*)-HPOTrE were both rapidly converted when added to the enzyme preparation from beetroot. However, neither 13(*S*)-HPODE nor 13(*S*)-HPOTrE were similarly converted as judged by analysis of the incubation products by SP-HPLC or GC–MS. In order to further study this point, UV spectrophotometric assays of the rate of hydroperoxide consumption by the beetroot enzyme preparation were performed. As seen in Fig. 2, a rapid disappearance of the conjugated diene chromophore absorbing at 235 nm was noted for the two 9-hydroperoxides, whereas the two 13-hydroperoxides were essentially stable during the incubation period.

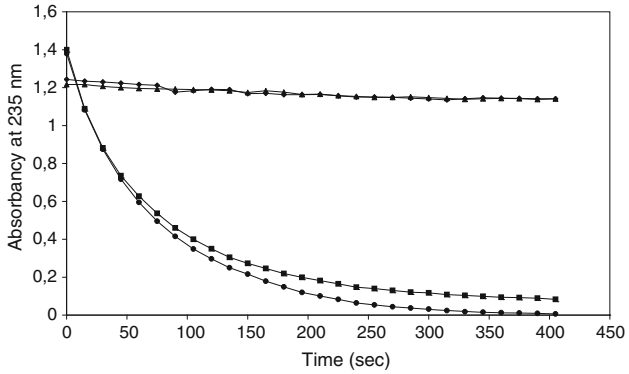

Fig. 2 UV-spectrophotometric assay of hydroperoxidase activity in the beetroot. Enzyme preparation diluted 1:7.7 (v/v) with potassium phosphate buffer pH 6.7 (2 mL) was treated at 23 °C with the following fatty acid hydroperoxides: 9(*S*)-HPODE (51 μM; *filled circles*), 9(*S*)-HPOTrE (52 μM; *filled squares*), 13(*S*)-HPODE (46 μM; *filled diamonds*), and 13(*S*)-HPOTrE (45 μM; *filled triangles*). The absorbance at 235 nm was monitored versus time

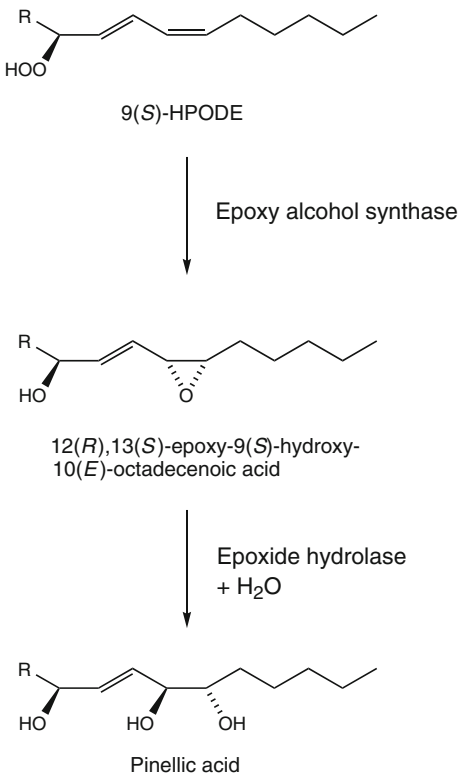

Scheme 2 Sequence of reactions in the conversion of 9(*S*)-HPODE into pinellic acid (free acid form of compound **II**). R = $(CH_2)_7$-COOH

Conclusion

Beetroot contains a strong EAS activity, which is active on linoleic and linolenic acid 9-hydroperoxides, as well as an epoxide hydrolase activity, which stereospecifically converts the epoxy alcohol produced into a trihydroxy acid

(Scheme 2). The former activity is reminiscent of the EAS enzymes earlier studied in the fungus *Saprolegnia parasitica* [6] and in potato leaves [7], however, whereas these enzymes produce two isomeric epoxy alcohols from each hydroperoxide, the beetroot EAS forms a single one. A related conversion has been studied using an enzyme preparation from oat seeds, in which case the EAS activity was due to a peroxygenase [8]. The epoxide hydrolase activity found in beetroot appears to be related to similar activities earlier found in potato leaves [7] and oat seeds [8].

The nature of the beetroot EAS and epoxide hydrolase is currently under investigation and the results will be reported shortly. Meanwhile, the high catalytic activities of the two enzymes, combined with an uncomplicated protocol for product isolation, offer a practical way to prepare considerable amounts of pinellic and fulgidic acids.

Acknowledgments The expert technical assistance of Mrs. G. Hamberg is gratefully acknowledged. This work was supported by a grant from the Swedish Research Council (project 2009-5078).

References

1. Graveland A (1970) Enzymatic oxidations of linoleic acid and glycerol-1-monolinoleate in doughs and flour-water suspensions. J Am Oil Chem Soc 47:352–361
2. Kato T, Yamaguchi Y, Hirukawa T, Hoshino N (1991) Structural elucidation of naturally occurring 9,12,13-trihydroxy fatty acids by a synthetic study. Agric Biol Chem 55:1349–1357
3. Hamberg M (1991) Trihydroxyoctadecenoic acids in beer: qualitative and quantitative analysis. J Agric Food Chem 39:1568–1572
4. Nagai T, Kiyohara H, Munakata K, Shirahata T, Sunazuka T, Harigaya Y, Yamada H (2002) Pinellic acid from the tuber of *Pinellia ternata* Breitenbach as an effective oral adjuvant for nasal influenza vaccine. Int Immunopharmacol 2:1183–1193
5. Herz W, Kulanthaivel P (1985) Trihydroxy-C_{18}-acids and a labdane from *Rudbeckia fulgida*. Phytochemistry 24:89–91
6. Hamberg M (1989) Fatty acid hydroperoxide isomerase in *Saprolegnia parasitica*: structural studies of epoxy alcohols formed from isomeric hydroperoxyoctadecadienoates. Lipids 24:249–255
7. Hamberg M (1999) An epoxy alcohol synthase pathway in higher plants: biosynthesis of antifungal trihydroxy oxylipins in leaves of potato. Lipids 34:1131–1142
8. Hamberg M, Hamberg G (1996) Peroxygenase-catalyzed fatty acid epoxidation in cereal seeds: sequential oxidation of linoleic acid into 9(*S*),12(*S*),13(*S*)-trihydroxy-10(*E*)-octadecenoic acid. Plant Physiol 110:807–815
9. Gardner HW, Nelson EC, Tjarks LW, England RE (1984) Acid-catalyzed transformation of 13(*S*)-hydroperoxylinoleic acid into epoxyhydroxyoctadecenoic and trihydroxyoctadecenoic acids. Chem Phys Lipids 35:87–101
10. Hamberg M (1987) Vanadium-catalyzed transformations of 13(*S*)-hydroperoxy-9(*Z*),11(*E*)-octadecadienoic acid: structural studies on epoxy alcohols and trihydroxy acids. Chem Phys Lipids 43:55–67
11. Kato T, Yamaguchi Y, Abe N, Uyehara T, Namai T, Kodama M, Shiobara Y (1985) Structure and synthesis of unsaturated trihydroxy C_{18} fatty acids in rice plant suffering from rice blast disease. Tet Lett 26:2357–2360
12. Masui H, Kondo T, Kojima M (1989) An antifungal compound, 9,12,13-trihydroxy-(*E*)-10-octadecenoic acid, from *Colocasia antiquorum* inoculated with *Ceratocystis fimbriata*. Phytochemistry 28:2613–2615
13. Walters DR, Cowley T, Weber H (2006) Rapid accumulation of trihydroxy oxylipins and resistance to the bean rust pathogen *Uromyces fabae* following wounding in *Vicia faba*. Ann Bot 97:779–784
14. Esterbauer H, Schauenstein E (1977) Isomeric trihydroxyoctadecenoic acids in beer - evidence for their presence and quantitative determination. Z Lebensm Unters Forsch 164:255–259
15. Kuroda H, Kobayashi N, Kaneda H, Watari J, Takashio M (2002) Characterization of factors that transform linoleic acid into di- and trihydroxyoctadecenoic acids in mash. J Biosci Bioengineering 93:73–77
16. Baur C, Grosch W (1977) Investigation about taste of dihydroxy, trihydroxy and tetrahydroxy fatty acids. Z Lebensm Unters Forsch 165:82–84
17. Shirahata T, Sunazuka T, Yoshida K, Yamamoto D, Harigaya Y, Kuwajima I, Nagai T, Kiyohara H, Yamada H, Omura S (2006) Total synthesis, elucidation of absolute stereochemistry, and adjuvant activity of trihydroxy fatty acids. Tetrahedron 62:9483–9496
18. Nagai T, Shimizu Y, Shirahata T, Sunazuka T, Kiyohara H, Omura S, Yamada H (2010) Oral adjuvant activity for nasal influenza vaccines caused by combination of two trihydroxy fatty acid stereoisomers from the tuber of *Pinellia ternata*. Int Immunopharmacol 10:655–661
19. Licciardi PV, Underwood JR (2011) Plant-derived medicines: a novel class of immunological adjuvants. Int Immunopharmacol 11:390–398
20. Naidu SV, Kumar P (2007) Enantioselective synthesis of (-)-pinellic acid. Tet Lett 48:2279–2282
21. Miura A, Kuwahara S (2009) A concise synthesis of pinellic acid using a cross-metathesis approach. Tetrahedron 65:3364–3368
22. Sharma A, Mahato S, Chattopadhyay S (2009) chemoenzymatic asymmetric synthesis of (9*S*,12*S*,13*S*)- and (9*S*, 12*RS*,13*S*)-pinellic acids. Tetrahedron Lett 50:4986–4988
23. Sabitha G, Bhikshapathi M, Reddy EV, Yadav JS (2009) Synthesis of (-)-pinellic acid and its (9*R*,12*S*,13*S*)-diastereomer. Helv Chim Acta 92:2052–2057
24. Hamberg M (1991) Regio- and stereochemical analysis of trihydroxyoctadecenoic acids derived from linoleic acid 9- and 13-hydroperoxides. Lipids 26:407–415
25. Hamberg M (1968) Metabolism of prostaglandins in rat liver mitochondria. Eur J Biochem 6:135–146
26. Hamberg M (1992) A method for determination of the absolute stereochemistry of α,β-epoxy alcohols derived from fatty acid hydroperoxides. Lipids 27:1042–1046
27. Hamberg M (1971) Steric analysis of hydroperoxides formed by lipoxygenase oxygenation of linoleic acid. Anal Biochem 43:515–526

Lipids (2011) 46:879–884
DOI 10.1007/s11745-011-3575-8

METHODS

LipidomeDB Data Calculation Environment: Online Processing of Direct-Infusion Mass Spectral Data for Lipid Profiles

Zhenguo Zhou · Shantan Reddy Marepally · Daya Sagar Nune · Prashanth Pallakollu · Gail Ragan · Mary R. Roth · Liangjiang Wang · Gerald H. Lushington · Mahesh Visvanathan · Ruth Welti

Received: 18 April 2011 / Accepted: 19 May 2011 / Published online: 7 June 2011

Abstract LipidomeDB Data Calculation Environment (DCE) is a web application to quantify complex lipids by processing data acquired after direct infusion of a lipid-containing biological extract, to which a cocktail of internal standards has been added, into an electrospray source of a triple quadrupole mass spectrometer. LipidomeDB DCE is located on the public Internet at http://lipidome.bcf.ku.edu:9000/Lipidomics. LipidomeDB DCE supports targeted analyses; analyte information can be entered, or preformulated lists of typical plant or animal polar lipid analytes can be selected. LipidomeDB DCE performs isotopic deconvolution and quantification in comparison to internal standard spectral peaks. Multiple precursor or neutral loss spectra from up to 35 samples may be processed simultaneously with data input as Excel files and output as tables viewable on the web and exportable in Excel. The preformulated compound lists and web access, used with direct-infusion mass spectrometry, provide a simple approach to lipidomic analysis, particularly for new users.

Keywords Triple quadrupole mass spectrometry · Precursor scan · Neutral loss scan · Direct infusion · Lipid quantification · Lipidomics

Abbreviations

DCE	Data Calculation Environment
m/z	Mass/charge
MS	Mass spectrometry
QqQ	Triple quadrupole

Introduction

Lipidomics is a developing strategy for functional genomics. Characterizing large numbers of mutants or the results of experimental manipulations applied to large numbers of samples is becoming increasingly feasible. Triple quadrupole (QqQ) mass spectrometers are robust and widely available instruments, and their ability to isolate a signal stemming from the subset of a sample's molecules that produce a specific pair of mass/charge (*m/z*) values provides detection specificity for lipidomic analysis. Direct-infusion QqQ mass spectrometry (MS), using precursor and neutral loss scans, as originally proposed by Brügger et al. [1], offers many advantages as a lipidomics platform. Direct infusion, in comparison to introducing samples through a liquid chromatography interface, is more easily implemented and allows for the rapid analysis of many samples. Another, less recognized advantage of

Z. Zhou and S. R. Marepally contributed equally.

Z. Zhou · S. R. Marepally · D. S. Nune · G. H. Lushington · M. Visvanathan (✉)
K-INBRE Bioinformatics Core Facility, University of Kansas, 2121 Simons Drive, Lawrence, KS 66047, USA
e-mail: mvisvanathan@ku.edu

P. Pallakollu · G. Ragan · M. R. Roth · R. Welti (✉)
Division of Biology, Kansas Lipidomics Research Center, Kansas State University, Ackert Hall, Manhattan, KS 66506-4901, USA
e-mail: welti@ksu.edu

L. Wang
Division of Biology, Kansas State University, Manhattan, KS 66506, USA

Present Address:
L. Wang
Department of Genetics and Biochemistry, Clemson University, Clemson, SC 29634, USA

direct-infusion is that the continuous influx of sample allows the user to adjust the scanning time to improve signal detection, without concern for elution time. However, a potential bottleneck in the implementation of any lipidomic strategy is the ability to process the data into quantitative lipid profiles. In particular, new users need a simple approach, and many users need to be able to process large data sets.

A number of tools for analysis of mass spectral data from lipids have been developed. Tools designed for direct-infusion QqQ MS analysis include the algorithm developed by Kurvinen et al. [2], LIMSA [3, 4], and the method developed by Ejsing et al. [5], LipidQA [6] and AMDMS-SL [7]. Each tool is capable of lipid quantification from direct infusion QqQ mass spectral data, and each has special features. Some have the ability to combine data from multiple spectra for identification and analysis of lipids at the true molecular species level [5–7]. Some provide for visualization and statistical analysis of the output data [2–5].

Here we describe a new tool for mass spectral data analysis for lipidomics. The strength of LipidomeDB Data Calculation Environment (DCE) is its ability to rapidly and simultaneously analyze multiple spectra from up to 35-sample input in one step. It differs from currently available tools in being on the web. It provides pre-formulated lists of target lipid analytes, including lists for plant lipids, and can accept user-defined target analyte lists.

Materials and Methods

Programming

LipidomeDB DCE has a web interface and a database backend (called LipidomeDB), and scripts to read and perform calculations on input data provided in Excel format. LipidomeDB is a MySQL database that stores the defined lipid species and formulas, and the users' experimental data. Much of the LipidomeDB DCE is coded in JSP. The user interface is implemented primarily in JSP with Javascript used to perform client-side computations, such as those related to isotopic abundances, and with Java used for server-side data analysis, such as searching the database for target lipid species matching uploaded data with the target species lists, and isotopic deconvolution.

Input Spectral Data

The input data are spectral peak lists acquired by precursor or neutral loss scanning, typically using a triple quadrupole mass spectrometer in the multiple channel analyzer (MCA) mode (a mode that averages or sums the signal from multiple scans to produce a spectrum). Data processing, i.e., baseline subtraction, smoothing and centroiding (or integration), are performed with the mass spectrometer's acquisition software. Spectra, each as a list of *m/z* versus signal, are exported from the acquisition program to Excel files for upload to LipidomeDB DCE. AB Sciex programmers have written a script, called "Multiple Period Processing," that exports data in the proper format; however, the format may be replicated manually or through other scripts. The format of the Excel spreadsheets for upload is specified in the documentation accompanying LipidomeDB DCE, and example files are provided.

Algorithms and Functions

Algorithms and functions are described briefly below. Full details are provided in the documentation (tutorial) for LipidomeDB DCE accessed from its home page: http://lipidome.bcf.ku.edu:9000/Lipidomics.

Target Lipid Information

The mass of target lipids and abundances of their isotopic variants are calculated from the chemical formula by adding the masses of the component atoms. The adduct formed by the target lipids is specified by the user. Possible adduct choices, in the negative mode, are $[M - H]^-$, $[M-CH_3]^-$, $[M + Cl]^-$ and $[M + C_2H_3O_2]^-$ (i.e., $[M +$ acetate$]^-$), and in the positive mode, $[M + H]^+$, $[M + NH_4]^+$, $[M + Li]^+$, $[M + Na]^+$ and $[M + K]^+$.

Lipid Search

The peaks corresponding to specified adduct ions of the internal standards and target lipids are located in the input data by *m/z*, and the value of each corresponding signal is collected. Any mass that is within the specified mass tolerance window (specified compound mass ± the mass tolerance) is considered a candidate mass for the specified target lipid or internal standard. The search algorithm provides three options, in case multiple masses are found within the mass tolerance window. The three options are: "Nearest Mass," which selects the *m/z* closest to the lipid ion's *m/z*, "Highest Signal," which selects the *m/z* having the highest corresponding signal value, and "Sum of Signals," which sums signals within the specified mass tolerance target window.

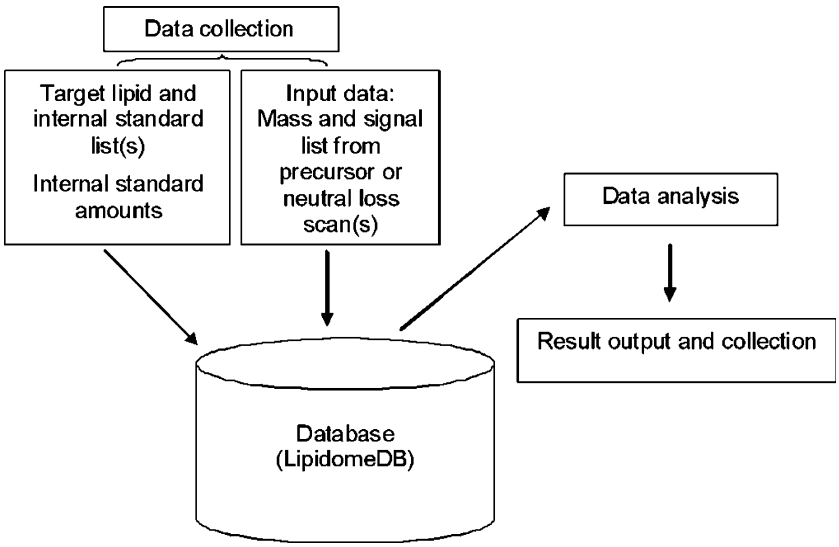

Fig. 1 Scheme indicating the workflow of the system and relationships of the three phases of LipidomeDB DCE: data collection, data analysis, and result output and collection

Isotopic Deconvolution (Correction) of Signal and Lipid Analyte Quantification

Quantification is essentially the method described by Brügger et al. [1] and used in the LIMSA analytical tool [3, 4]. Isotopic deconvolution to remove signals because of "A + 1" and "A + 2" isotopic variants (in LipidomeDB DCE, called a_1 and a_2), in order to detect the "A" peaks of other compounds at the same nominal mass, is performed in a manner similar to the "subtraction" method in the LIMSA analytical tool [3].

After the corrected signals are established by deconvolution, the amount of each target lipid is calculated. The amount is calculated from the corrected signals for the target lipids, the signals for 1–3 internal standards and the corresponding internal standard amounts specified by the user. A linear calibration curve (signal vs. *m/z*) fits the signals of the internal standards [3] and is used to correct for mass-dependent variation in instrument response. If any internal standard is not detected, an error message appears on an output page for the individual spectrum (i.e., the spectrum for one target list and one sample); if this error is present, the target analytes are not quantified in the sample with the missing standards. If the internal standards are detected, data calculations are shown on the output page for the individual spectrum.

Results and Discussion

The primary function of LipidomeDB DCE is to search for *m/z* and signal for entered target lipid species in integrated (centroided) mass spectra uploaded by the user, to isotopically deconvolute the signals, and to quantify the signals in comparison to internal standard signals and amounts, in order to calculate the amount of each target lipid species in the samples. LipidomeDB DCE has three phases, shown in Fig. 1, data collection, data analysis, and result output and collection.

Getting Started

To use LipidomeDB DCE, a login ID can be acquired by following instructions on the home page. A "tutorial" (i.e., documentation) accessible from the home page includes complete instructions for the use of LipidomeDB DCE. The instructions include brief directions for performing the lipidomic experiments, including suggestions for sample preparation, internal standards and their addition, acquisition of the mass spectral data and formatting of the mass spectral data for input into LipidomeDB DCE. The intent of this part of the tutorial is to simplify and describe the process of performing lipidomic analyses. Also available, on the home page and by following links in the tutorial, are example input data files, acquired on mouse intestinal lipid

Table 1 Categories of step-by-step directions in the LipidomeDB DCE tutorial

Step 1. Assemble the data to be entered
Step 2. User log-in
Step 3. Enter data about the samples
Step 4. Enter the first target compound set
a. Enter a target compound set from an existing (pre-formulated) list
b. Enter your own target compound set
Step 5. Enter any additional target compound sets
Step 6. Provide data about internal standard amounts
Step 7. Upload the input data generated from the experiments in Excel format
Step 8. Collect the results

Animal LPC

Internal Standards

Mass of Detected Ion	Chemical Formula of M	Compound Name	Adduct	a_1	a_2
454.28	C21H44O7PN	LPC(13:0)	[M + H]	0.242	0.022
538.37	C27H56O7PN	LPC(19:0)	[M + H]	0.309	0.036
Fragment Formula	C5H15O4PN	phosphocholine (184+)			

Target Compounds

Lipid No.	Mass of Detected Ion	Chemical Formula of M	Compound Name	Adduct	a_1	a_2
0	494.31	C24H48O7PN	LPC(16:1)	[M + H]	0.275	0.028
1	496.33	C24H50O7PN	LPC(16:0)	[M + H]	0.275	0.028
2	518.31	C26H48O7PN	LPC(18:3)	[M + H]	0.297	0.033
3	520.33	C26H50O7PN	LPC(18:2)	[M + H]	0.297	0.033
4	522.34	C26H52O7PN	LPC(18:1)	[M + H]	0.297	0.033
5	524.36	C26H54O7PN	LPC(18:0)	[M + H]	0.298	0.033
6	542.31	C28H48O7PN	LPC(20:5)	[M + H]	0.319	0.039
7	544.33	C28H50O7PN	LPC(20:4)	[M + H]	0.319	0.039

Fig. 2 Screenshot of target compound input sheet. The screenshot shows the pre-formulated list for "Animal LPC"

Fig. 3 Screenshot of spectral files upload sheet

Spectral Files Upload

Upload Target Compound Set: **Animal LPC** C:\Documents and Setti Browse...

Upload Target Compound Set: **Animal PC-ePC-SM** C:\Documents and Setti Browse...

Upload Target Compound Set: **Animal LPE** C:\Documents and Setti Browse...

Upload Target Compound Set: **Animal PE-ePE-PECer** C:\Documents and Setti Browse...

Upload Target Compound Set: **Animal PA** C:\Documents and Setti Browse...

Upload Target Compound Set: **Animal PG** C:\Documents and Setti Browse...

Upload Target Compound Set: **Animal PI** C:\Documents and Setti Browse...

Upload Target Compound Set: **Animal PS** C:\Documents and Setti Browse...

Continue Clear All

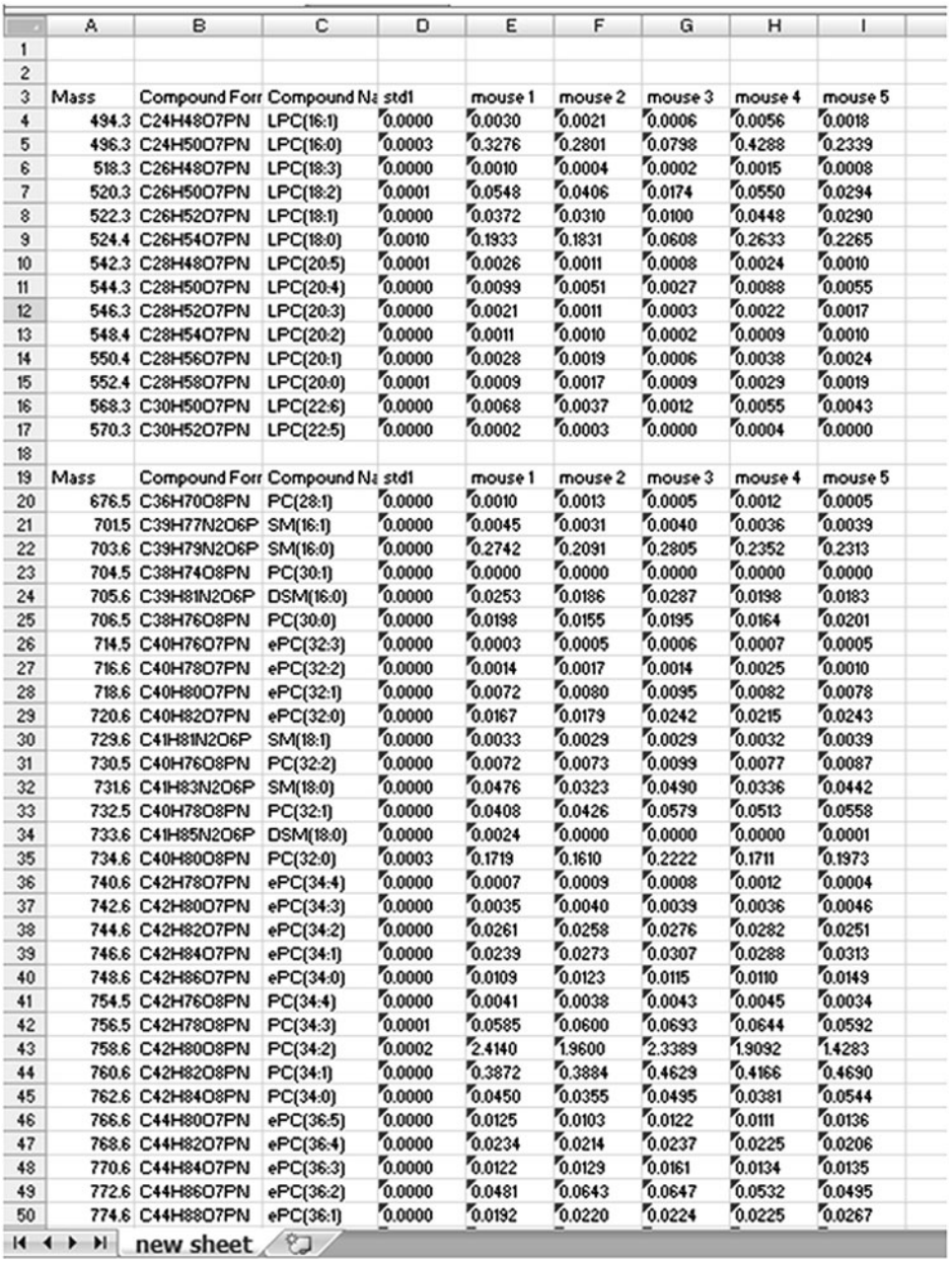

	A	B	C	D	E	F	G	H	I
1									
2									
3	Mass	Compound Forr	Compound Na	std1	mouse 1	mouse 2	mouse 3	mouse 4	mouse 5
4	494.3	C24H48O7PN	LPC(16:1)	0.0000	0.0030	0.0021	0.0006	0.0056	0.0018
5	496.3	C24H50O7PN	LPC(16:0)	0.0003	0.3276	0.2801	0.0798	0.4288	0.2339
6	518.3	C26H48O7PN	LPC(18:3)	0.0000	0.0010	0.0004	0.0002	0.0015	0.0008
7	520.3	C26H50O7PN	LPC(18:2)	0.0001	0.0548	0.0406	0.0174	0.0550	0.0294
8	522.3	C26H52O7PN	LPC(18:1)	0.0000	0.0372	0.0310	0.0100	0.0448	0.0290
9	524.4	C26H54O7PN	LPC(18:0)	0.0010	0.1933	0.1831	0.0608	0.2633	0.2265
10	542.3	C28H48O7PN	LPC(20:5)	0.0001	0.0026	0.0011	0.0008	0.0024	0.0010
11	544.3	C28H50O7PN	LPC(20:4)	0.0000	0.0099	0.0051	0.0027	0.0088	0.0055
12	546.3	C28H52O7PN	LPC(20:3)	0.0000	0.0021	0.0011	0.0003	0.0022	0.0017
13	548.4	C28H54O7PN	LPC(20:2)	0.0000	0.0011	0.0010	0.0002	0.0009	0.0010
14	550.4	C28H56O7PN	LPC(20:1)	0.0000	0.0028	0.0019	0.0006	0.0038	0.0024
15	552.4	C28H58O7PN	LPC(20:0)	0.0001	0.0009	0.0017	0.0009	0.0029	0.0019
16	568.3	C30H50O7PN	LPC(22:6)	0.0000	0.0068	0.0037	0.0012	0.0055	0.0043
17	570.3	C30H52O7PN	LPC(22:5)	0.0000	0.0002	0.0003	0.0000	0.0004	0.0000
18									
19	Mass	Compound Forr	Compound Na	std1	mouse 1	mouse 2	mouse 3	mouse 4	mouse 5
20	676.5	C36H70O8PN	PC(28:1)	0.0000	0.0010	0.0013	0.0005	0.0012	0.0005
21	701.5	C39H77N2O6P	SM(16:1)	0.0000	0.0045	0.0031	0.0040	0.0036	0.0039
22	703.6	C39H79N2O6P	SM(16:0)	0.0000	0.2742	0.2091	0.2805	0.2352	0.2313
23	704.5	C38H74O8PN	PC(30:1)	0.0000	0.0000	0.0000	0.0000	0.0000	0.0000
24	705.6	C39H81N2O6P	DSM(16:0)	0.0000	0.0253	0.0186	0.0287	0.0198	0.0183
25	706.5	C38H76O8PN	PC(30:0)	0.0000	0.0198	0.0155	0.0195	0.0164	0.0201
26	714.5	C40H76O7PN	ePC(32:3)	0.0000	0.0003	0.0005	0.0006	0.0007	0.0005
27	716.6	C40H78O7PN	ePC(32:2)	0.0000	0.0014	0.0017	0.0014	0.0025	0.0010
28	718.6	C40H80O7PN	ePC(32:1)	0.0000	0.0072	0.0080	0.0095	0.0082	0.0078
29	720.6	C40H82O7PN	ePC(32:0)	0.0000	0.0167	0.0179	0.0242	0.0215	0.0243
30	729.6	C41H81N2O6P	SM(18:1)	0.0000	0.0033	0.0029	0.0029	0.0032	0.0039
31	730.5	C40H76O8PN	PC(32:2)	0.0000	0.0072	0.0073	0.0099	0.0077	0.0087
32	731.6	C41H83N2O6P	SM(18:0)	0.0000	0.0476	0.0323	0.0490	0.0336	0.0442
33	732.5	C40H78O8PN	PC(32:1)	0.0000	0.0408	0.0426	0.0579	0.0513	0.0558
34	733.6	C41H85N2O6P	DSM(18:0)	0.0000	0.0024	0.0000	0.0000	0.0000	0.0001
35	734.6	C40H80O8PN	PC(32:0)	0.0003	0.1719	0.1610	0.2222	0.1711	0.1973
36	740.6	C42H78O7PN	ePC(34:4)	0.0000	0.0007	0.0009	0.0008	0.0012	0.0004
37	742.6	C42H80O7PN	ePC(34:3)	0.0000	0.0035	0.0040	0.0039	0.0036	0.0046
38	744.6	C42H82O7PN	ePC(34:2)	0.0000	0.0261	0.0258	0.0276	0.0282	0.0251
39	746.6	C42H84O7PN	ePC(34:1)	0.0000	0.0239	0.0273	0.0307	0.0288	0.0313
40	748.6	C42H86O7PN	ePC(34:0)	0.0000	0.0109	0.0123	0.0115	0.0110	0.0149
41	754.5	C42H76O8PN	PC(34:4)	0.0000	0.0041	0.0038	0.0043	0.0045	0.0034
42	756.5	C42H78O8PN	PC(34:3)	0.0001	0.0585	0.0600	0.0693	0.0644	0.0592
43	758.6	C42H80O8PN	PC(34:2)	0.0002	2.4140	1.9600	2.3389	1.9092	1.4283
44	760.6	C42H82O8PN	PC(34:1)	0.0000	0.3872	0.3884	0.4629	0.4166	0.4690
45	762.6	C42H84O8PN	PC(34:0)	0.0000	0.0450	0.0355	0.0495	0.0381	0.0544
46	766.6	C44H80O7PN	ePC(36:5)	0.0000	0.0125	0.0103	0.0122	0.0111	0.0136
47	768.6	C44H82O7PN	ePC(36:4)	0.0000	0.0234	0.0214	0.0237	0.0225	0.0206
48	770.6	C44H84O7PN	ePC(36:3)	0.0000	0.0122	0.0129	0.0161	0.0134	0.0135
49	772.6	C44H86O7PN	ePC(36:2)	0.0000	0.0481	0.0643	0.0647	0.0532	0.0495
50	774.6	C44H88O7PN	ePC(36:1)	0.0000	0.0192	0.0220	0.0224	0.0225	0.0267

new sheet

Fig. 4 Screenshot of summary. A summary of data for all targeted compound sets from all samples can be exported as an Excel file

extracts, and the output file that should be obtained when the data are processed according to the instructions, allowing users to test the interface function and verify correct usage. Step-by-step directions for using LipidomeDB DCE (as shown in Table 1) with screenshots are provided in the tutorial. Also in the tutorial are sections discussing normalization to tissue metrics and practical considerations about the limitations of the quantitative capabilities of direct-infusion electrospray ionization QqQ MS-based analysis.

Input Data

The input to LipidomeDB consists of lists of target lipids, i.e., lipid species being analyzed, lists of internal standards utilized, internal standard amounts, and the mass and signal lists from precursor or neutral loss scan(s) (Fig. 1). Either pre-formulated lipid species target lists, user-specified lipid target lists or a combination of the two types of lists can be used. If the user composes his own sheets, they can be saved for his later use. The pre-formulated target lists for "plants"

and "animals" are based on lipid species detected by the Kansas Lipidomics Research Center's analytical laboratory by electrospray ionization QqQ MS in a number of higher plant and mammalian species. Figure 2 is a screenshot of the interface for indicating the target lipids and the corresponding internal standards. Similar pages are used for each group of lipids to be analyzed (i.e., for each precursor or neutral loss scan). The pre-formulated lists provide a suitable and quick starting point for many users. Amounts of internal standards are entered, and mass spectral data are uploaded in Excel files. The interface for uploading the mass spectral data is shown in Fig. 3. LipidomeDB DCE searches the *m/z* of mass spectral data for the *m/z* values of lipids and internal standards in the target lists.

Data Calculation and Output

Data calculation is described briefly in the "Materials and Methods" section, and in more detail in the tutorial. The output of LipidomeDB DCE can be viewed on (1) a sheet showing calculations for one target list for one sample, (2) as a summary showing calculated data for one target compound set from all samples or (3) as a summary of data for all targeted compound sets from all samples (Fig. 4). The sheet showing calculations for one target list for one sample (i.e., data from one spectrum) allows the user to confirm detection of the internal standards, to view the corrections for isotopic variants (isotopic deconvolution results) and to view the results of the quantification. The summary sheets provide the data in several convenient forms. All sheets can be viewed on the web or exported in Excel format.

Summary

LipidomeDB DCE is a well-documented web application for analysis of direct infusion electrospray ionization QqQ mass spectral data, with the capability to analyze multiple scans from up to 35 samples simultaneously. The pre-formulated lists of plant and animal polar lipids provide a quick start for lipidomic data analysis that should provide for ease in performing lipidomics analyses. In the long term, the web-accessible lipidomics data calculation system and database can be developed for storage and retrieval of lipidomics data in the context of experimental metadata.

Acknowledgments The authors would like to thank Dr. Susan Brown for helping us start the LipidomeDB project and obtain financial support for it. We are also grateful to Dr. Youping Deng for his efforts to initiate a lipidomics database and to Drs. Todd Williams and Xuemin Wang for helping us initiate lipidomics work. We appreciate Emily Archer Slone, Byron Sparkes and Dr. Sherry Fleming for allowing us to use their data as example data. We also wish to thank members of the Welti and Visvanathan groups, who provided helpful suggestions. Funding for development of LipidomeDB Data Calculation Environment was from Kansas IDeA Networks of Biomedical Research Excellence (National Institutes of Health grant P20 RR16475 from the National Center for Research Resources). Mass spectrometer acquisition and mass spectrometry method development were supported by National Science Foundation grants MCB 0455318, MCB 0920663 and DBI 0521587, Kansas National Science Foundation EPSCoR grant EPS-0236913, Kansas Technology Enterprise Corp. and Kansas State University. Contribution no. 11-295-J from the Kansas Agricultural Experiment Station.

References

1. Brügger B, Erben G, Sandhoff R, Wieland FT, Lehmann WD (1997) Quantitative analysis of biological membrane lipids at the low picomole level by nano-electrospray ionization tandem mass spectrometry. Proc Natl Acad Sci USA 94:2339–2344
2. Kurvinen J-P, Aaltonen J, Kuksis A, Kallio H (2002) Software algorithm for automatic interpretation of mass spectra of glycerolipids. Rapid Commun Mass Spectrom 16:1812–1820
3. Haimi P, Uphoff A, Hermansson M, Somerharju P (2006) Software tools for analysis of mass spectrometric lipidome data. Anal Chem 78:8324–8331
4. Haimi P, Chaithanya K, Kainu V, Hermansson M, Somerharju P (2009) Instrument-independent software tools for the analysis of MS-MS and LC-MS lipidomics data. In: Armstrong D (ed) Lipidomics, methods in molecular biology, vol 580. Humana Press, Totowa, pp 285–294
5. Ejsing CS, Duchoslav E, Sampaio J, Simons K, Bonner R, Thiele C, Ekroos K, Shevchenko A (2006) Automated identification and quantification of glycerolipid molecular species by multiple precursor scanning. Anal Chem 76:6202–6214
6. Song H, Hsu F-F, Ladenson J, Turk J (2007) Algorithm for processing raw mass spectrometric data to identify and quantitate complex lipid molecular species in mixtures by data-dependent scanning and fragment ion database searching. J Am Soc Mass Spectrom 18:1848–1858
7. Yang K, Cheng H, Gross RW, Han X (2009) Automated lipid identification and quantification by multi-dimensional mass spectrometry-based shotgun lipidomics. Anal Chem 81:4356–4368

Lipids (2011) 46:885–892
DOI 10.1007/s11745-011-3587-4

ORIGINAL ARTICLE

JNK Inhibition by SP600125 Attenuates *trans*-10, *cis*-12 Conjugated Linoleic Acid-Mediated Regulation of Inflammatory and Lipogenic Gene Expression

Kristina Martinez · Arion Kennedy · Michael K. McIntosh

Received: 1 April 2011 / Accepted: 20 June 2011 / Published online: 10 July 2011

Abstract Supplementation with a mixture of *trans*-10, *cis*-12 (t10,c12) and *cis*-9, *trans*-11 (c9,t11) isomers of conjugated linoleic acid (CLA), or t10,c12 CLA alone, reduces body weight and fat deposition in animals and some humans. However, these anti-obesity actions of t10,c12 CLA are routinely accompanied by increased markers of inflammation and insulin resistance. Thus, we examined the extent to which blocking c-Jun NH2-terminal kinase (JNK) signaling using the JNK inhibitor SP600125 attenuated markers of inflammation and insulin resistance in primary human adipocytes treated with t10,c12 CLA. SP600125 attenuated t10,c12 CLA-mediated phosphorylation of cJun and increased protein levels of activating transcription factor (ATF) 3, two downstream targets of JNK. SP600125 attenuated t10,c12 CLA-mediated induction of inflammatory genes, including interleukin (IL)-6, IL-8, IL-1β, ATF3, monocyte chemoattractant protein (MCP)-1, and cyclooxygenase-2. Consistent with these data, SP600125 prevented t10,c12 CLA-mediated secretion of IL-8, IL-6, and MCP-1. SP600125 prevented t10,c12 CLA suppression of lipogenic genes including peroxisome proliferator activated receptor gamma, liver X receptor, sterol regulatory element binding protein, acetyl-CoA carboxylase, and stearoyl-CoA desaturase. Additionally, SP600125 blocked t10,c12 CLA-mediated induction of suppressor of cytokine synthesis-3 and suppression of adiponectin and insulin-dependent glucose transporter 4 mRNA levels. Collectively, these data suggest that JNK signaling plays an important role in t10,c12 CLA-mediated regulation of inflammatory and lipogenic gene expression in primary cultures of human adipocytes.

Keywords Conjugated linoleic acid · Adipocytes · JNK · cJun · Inflammation · Lipogenic genes

Abbreviations

ACC	Acetyl-CoA carboxylase
AP-1	Activator protein
apm-1	Adiponectin
ATF	Activating transcription factor 3
BMI	Body mass index
BSA	Bovine serum albumin
c9,t11 CLA	*Cis*-9, *trans*-11 conjugated linoleic acid
t10,c12 CLA	*Trans*-10, *cis*-12 conjugated linoleic acid
COX	Cyclooxygenase
DEX	Dexamethasone
ER	Endoplasmic reticulum
ERK	Extracellular signal-regulated kinase
FA	Fatty acid
GAPDH	Glyceraldehyde-3-phosphate dehydrogenase
GLUT4	Insulin-dependent glucose transporter 4
HBSS	Hanks balanced salt solution
IBMX	1-methyl-3-isobutylxanthine
IL	Interleukin
IRS	Insulin receptor substrate
ISR	Integrated stress response
JNK	c-Jun-NH2-terminal kinase
LXR	Liver X receptor

K. Martinez · M. K. McIntosh (✉)
Department of Nutrition, University of North Carolina, 318 Stone Building, PO Box 26170, Greensboro, NC 27402-6170, USA
e-mail: mkmcinto@uncg.edu

K. Martinez
e-mail: kbmarti2@uncg.edu

A. Kennedy
Department of Molecular Physiology, Vanderbilt University Medical Center, Nashville, TN 37232, USA
e-mail: arion.kennedy@vanderbilt.edu

MAPK	Mitogen-activated protein kinase
MCP	Monocyte chemoattractant protein
MEK	Mitogen-activated protein kinase kinase
NFκB	Nuclear factor kappa B
PPAR	Peroxisome proliferator activated receptor
SCD	Stearoyl-CoA desaturase
SOCS	Suppressor of cytokine synthesis
SREBP	Sterol regulatory element binding protein
SV	Stromal vascular
TG	Triglyceride
TZD	Thiazolidinedione

Introduction

Obesity is a global health issue with ~500 million people classified as obese and 1.5 billion overweight in 2008, including 43 million children under the age of five reported in 2010 [1]. One potential strategy for reducing adiposity is consumption of conjugated linoleic acid (CLA), unsaturated fatty acids found in ruminant meats and dairy products, or in dietary supplements and fortified foods. Conjugated linoleic acid refers to a group of conjugated octadecadienoic acid isomers derived from linoleic acid, a fatty acid that contains 18 carbons and 2 double bonds in *cis* configuration at the 9th and 12th carbons [i.e., *cis*-9, *cis*-12 octadecadienoic acid]. Microbes in the gastrointestinal tract of ruminant animals convert linoleic acid into different isoforms of CLA through biohydrogenation. This process changes the position and configuration of the double bonds, resulting in a single bond between one or both of the two double bonds (i.e., *cis*-9, *trans*-11 (c9,t11) or *trans*-10, *cis*-12 (t10,c12) octadecadienoic acid). Consuming a mixture of c9,t11 and t10,c12 CLA isomers, or t10,c12 CLA alone, reduces body fat mass in rodents, particularly mice, and some humans [reviewed in 2]. However, the isomer-specific mechanism by which CLA reduces adiposity is unclear. Furthermore, a number of clinical studies report potential side effects of CLA supplementation including increased levels of markers of inflammation (e.g., inflammatory cytokines, chemokines, or prostaglandins), insulin resistance, hyperlipidemia, and lipodystrophy [3–7]. These anti-obesity and adverse side effects of CLA appear to be due primarily to the t10,c12 isomer. In contrast, the c9,t11 isomer appears to have anti-inflammatory and anti-diabetic properties without reducing body weight [8].

We have demonstrated that t10,c12 CLA reduces glucose and fatty acid uptake and triglyceride content in cultures of human adipocytes, in part, by activating extracellular signal-related kinase (ERK) [9] and nuclear factor kappa B (NFκB) [10]. These in vitro data have been confirmed in vivo [11]. Activated NFκB [12–14] and ERK [15–17] induce markers of inflammation and antagonize peroxisome proliferator activated receptor (PPAR)γ activity, thereby causing insulin resistance. However, the extent to which t10,c12 CLA activates other kinases or transcription factors that impact inflammatory signaling, insulin sensitivity, and triglyceride content in human adipocytes, and their mechanism of action, are unclear.

We recently demonstrated that t10,c12 CLA increased the phosphorylation levels of c-Jun NH2-terminal kinase (JNK) and downstream targets cJun and activating transcription factor (ATF3), members of the redox-sensitive transcription factor activator protein-1 (AP-1), that induce inflammatory gene transcription [18, 19]. c-Jun NH2-terminal kinase activation is known to enhance inflammation and insulin resistance associated with obesity, and lack of JNK1 or JNK2 reduces body fat and improves insulin sensitivity in vivo [20, 21] and in vitro [22]. However, the role of JNK in activating cJun or ATF3 in CLA-treated cultures and the extent to which this activation regulates inflammatory and lipogenic gene expression has not been investigated.

Based on these data, we hypothesized that JNK plays an important role in t10,c12 CLA-mediated activation of AP-1 and induction of inflammatory genes and suppression of lipogenic genes. To test this hypothesis, we employed the chemical JNK1-3 inhibitor, SP600125. By using this inhibitor, we demonstrate that JNK is involved in the regulation of t10,c12 CLA-induced inflammatory signaling, and suppression of gene markers for adipogenesis, lipogenesis, and insulin signaling in cultures of newly-differentiated human adipocytes. Therefore, JNK may be an important target for preventing 10,12 CLA-mediated inflammation.

Materials and Methods

Materials

All cell culture ware were purchased from Fisher Scientific (Norcross, GA). Lightning Chemiluminescence Substrate was purchased from Perkin Elmer Life Science (Boston, MA). Immunoblotting buffers and precast gels were purchased from Invitrogen (Carlsbad, CA). Adipocyte media was purchased from Zen Bio (Research Triangle Park, NC). The Nuclear Extract Kit was purchased from Active Motif (Carlsbad, CA). Polyclonal antibodies for anti-glyceraldehyde-3-phosphate dehydrogenase (GAPDH) and ATF3 and monoclonal antibody for anti-PPARγ were obtained from Santa Cruz Biotechnology (Santa Cruz, CA). Anti-total and anti-phospho (P) JNK (Thr183/Try185) and P-cJun (Ser63) antibodies were purchased from Cell

Signaling Technologies (Beverly, MA). Anti-nucleoporin was purchased from BD transduction laboratories (San Jose, CA). HyClone fetal bovine serum was purchased from Fisher Scientific. Isomers of CLA (+98% pure) were purchased from Matreya (Pleasant Gap, PA). The cell permeable selective JNK1-3 inhibitor SP600125 (#420119; Anthra [1,9-*cd*]pyrazol-6(2*H*)-one, 1,9-pyrazoloanthrone; JNKII) was purchased from EMD Chemicals (Gibbstown, NJ). This inhibitor of JNK1-3 is competitive with respect to ATP, and has over a 300-fold greater selectivity for JNK compared to other mitogen-activated protein kinase (MAPK) including ERK and p38 [23], and specifically inhibits the phosphorylation of cJun serine residues 63 and 67 [24, 25]. All other reagents and chemicals were purchased from Sigma Chemical Co. (St. Louis, MO) unless otherwise stated.

Culturing of Human Primary Adipocytes

Abdominal white adipose tissue was obtained with consent from the Institutional Review Boards at the University of North Carolina at Greensboro and the Moses Cone Memorial Hospital, during elective abdominoplasty of non-diabetic Caucasian and African American females between the ages of 20–50 years old with a body mass index $\leq$32.0. These selection criteria allow for reduced variation in gender, age, and obesity status. Tissue was digested using collagenase; stromal vascular cells were isolated as previously described [9]. Stromal vascular cells were differentiated with adipocyte media (AM-1) containing 1 μM rosiglitazone and 250 μM 1-methyl-3-isobutylxanthine for 3 days, which yielded cultures containing $\sim$30–50% adipocytes. On days 6–12, cells were pretreated with 5, 20, or 80 μM SP600125 JNK inhibitor dissolved in DMSO for 30 min, and subsequently treated with 50 μM t10,c12 CLA or bovine serum albumin (BSA) vehicle control for 12–24 h depending on the experimental outcome measured. All cultures were normalized to contain the same amount of BSA and DMSO vehicles. Each independent experiment was repeated at least twice using a mixture of cells from three subjects, unless otherwise indicated.

Fatty Acid Preparation

t10,c12 CLA was delivered as a free acid complexed to 7.5% fatty acid-free BSA at a 4:1 molar ratio as previously described [9].

RNA Isolation and PCR

Total RNA was isolated from the cultures using Tri Reagent purchased from Molecular Research Center (Cincinnati, OH), according to manufacturer's protocol. For quantitative real time PCR, 2.0 μg total RNA was converted into first strand cDNA using Applied Biosystems High-Capacity cDNA Archive Kit (Foster City, CA). Real time PCR was performed in an Applied Biosystems 7500 FAST Real Time PCR System using Taqman Gene Expression Assays. To account for possible variation in cDNA input or the presence of PCR inhibitors, the endogenous reference gene GAPDH was simultaneously quantified for each sample, and these data normalized accordingly. The Relative Standard Curve Method using seven, two-fold dilutions ranging from 100–1.56 ng RNA was used to check primer efficiency and linearity of each transcript according to Applied Biosystem's Guide to Performing Relative Quantification of Gene Expression Using Real-Time Quantitative PCR.

Nuclear and Cytosolic Separation

Nuclear and cytosolic cellular fractions were prepared using a commercially available kit from Active Motif as previously described [10].

Immunoblotting

Immunoblotting using 20 μg of protein per lane was conducted using 4-12% NuPage precast gels (Invitrogen) as previously described [10]. Briefly, PVDF membranes were blocked with 5% milk in TBST for 1 h and washed 3 × in TBST for 5 min. Blots were incubated overnight at 4°C with primary antibodies targeting P-JNK, P-cJun, total cJun, and ATF3 at a dilution of 1:1,000, and subsequently incubated in the respective horseradish peroxidase-conjugated secondary antibody at a dilution of 1:5,000 at room temperature for 1 h. Primary and secondary antibodies targeting GAPDH were used at a 1:5,000 dilution. Primary and secondary antibodies targeting PPARγ were used at dilutions 1:200 and 1:2,000, respectively. After washing, blots were treated with chemiluminescence reagent for 1 min and film was exposed using a SRX-101A Konica Minolta flim developer. Densitometry was performed using a Kodak Image Station 440 CF by Perkin Elmer and Kodak Molecular Imaging Software Version 4.0.

Secretion of IL-6, IL-8, and Monocyte Chemoattractant Protein (MCP)-1

The concentrations of IL-6, IL-8, and MCP-1 were determined using the BioPlex® Suspension Array System from Bio-Rad (Hercules, CA) following the manufacturer's protocol. Briefly, media was collected from cultures that were pretreated with 5, 20, or 80 μM SP600125 for 30 min, and subsequently treated with 50 μM t10,c12 CLA or BSA for 24 h. The media was centrifuged at 13,200×*g* for

10 min at 4°C to clear the samples of any cell debris. Samples and standards were run in duplicate. Based on the manufacturer's report 'Bio-Plex Pro Human Cytokine, Chemokine, and Growth Factor Assays-Bulletin 5828,' the intra-assay % CVs for IL-6, IL-8, and MCP-1 are 7, 9, and 9%, respectively. The inter-assay % CVs are 11, 4, and 7%, respectively.

Statistical Analyses

Data are expressed as the means ± S.E. Data were analyzed using one-way analysis of variance followed by Tukey's-HSD tests for each pair for multiple comparisons. Differences were considered significant if $p < 0.05$. All analyses were performed using JMP IN, Version 9 Software (SAS Institute, Cary, NC).

Results

The JNK Inhibitor SP600125 Attenuates t10,c12 CLA-Mediated Activation of cJun and ATF3

We previously demonstrated that treatment of newly-differentiated human adipocytes with 50 μM t10,c12 CLA, but not c9,t11 CLA, for 6 h increased phosphorylation levels of JNK and cJun, which was sustained for 24 h when compared to vehicle (BSA)-treated cultures in total cell extract [18, 19]. However, a direct role for JNK in the activation of cJun and upregulation of inflammatory genes in response to t10,c12 CLA treatment has not been determined. In order to implicate a role for JNK in the activation of cJun, we examined JNK and cJun phosphorylation in cytosol and nuclear fractions after 6, 12, and 24 h of treatment with t10,c12 CLA. Phosphorylation of JNK was increased at 6 h and was sustained at 24 h in the cytosolic fraction, and increased in the nuclear fraction at 24 h with t10,c12 CLA. Consistently, cJun phosphorylation by t10,c12 CLA was detected almost exclusively in the nuclear fraction at all time points (Fig. 1a). Interestingly, t10,c12 CLA increased total cJun levels compared to the BSA control in the nuclear fraction at all time points. Based on the robust t10,c12 CLA-mediated activation of JNK and cJun, we investigated the extent to which pretreatment with the JNK inhibitor SP600125 blocked t10,c12 CLA-mediated phosphorylation of cJun after 12 h of treatment. Concentrations of SP600125 ranging between 5–80 μM were chosen based on studies using Jurkat T cells in which the IC_{50} for blocking cJun phosphorylation was 10 μM and using CD4 + cells isolated from human peripheral blood mononuclear cells in which the IC_{50} for blocking cyclooxygenase (COX)-2 and tumor necrosis factor alpha expression was 5 and 10 μM, respectively [23]. SP600125 suppressed t10,c12 CLA-mediated phosphorylation of cJun and increase in the protein levels of ATF3, an AP-1 family member, in total cell lysates (Fig. 1b). These data suggest that JNK is involved in t10,c12 CLA-mediated cJun activation.

SP600125 Attenuates t10,c12 CLA Induction of Inflammatory Genes

Next, we determined the extent to which SP600125 blocked t10,c12 CLA-induced inflammatory gene expression. Pretreatment of cultures with SP600125 attenuated t10,c12 CLA-induction of IL-8, IL-6, IL-1β, MCP-1, COX2, and ATF3 (Fig. 2a). Consistent with these data, SP600125 attenuated t10,c12 CLA-mediated secretion of IL-8, IL-6, and MCP-1 (Fig. 2b). Collectively, these data demonstrate that SP600125 suppresses t10,c12 CLA-mediated induction of inflammatory gene expression and protein secretion.

SP600125 Blocks t10,c12 CLA Suppression of Lipogenic Genes

Inflammatory transcription factors such as NFκB and AP-1 in concert with MAPKs like ERK have been shown to inhibit lipogenic gene expression, in part, by suppressing

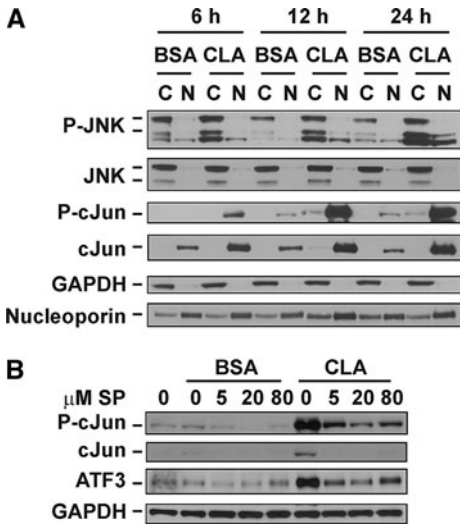

Fig. 1 **a** Cultures of newly-differentiated human adipocytes were treated with BSA vehicle or 50 μM t10,c12 CLA for 6, 12, or 24 h. Nuclear and cytosolic fractions were prepared using the Nuclear Extract Kit from Active Motif and analyzed for the determination of the protein levels of P-JNK, JNK, P-cJun, cJun, GAPDH, and nucleoporin. **b** Cultures were pretreated for 30 min with 5, 20, or 80 μM SP600125 (SP) followed by a 12 h treatment with BSA vehicle or 50 μM t10,c12 CLA. Subsequently, total cell lysates were harvested for the determination of the protein levels of P-cJun, cJun, ATF3, and GAPDH. Data are representative of two **a** or three **b** independent experiments

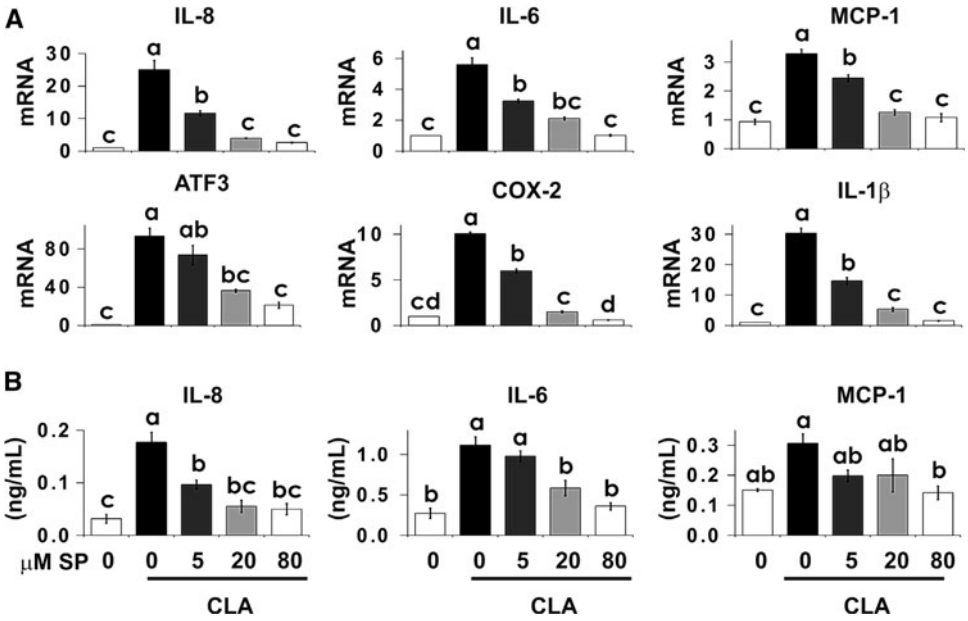

Fig. 2 **a** Cultures of newly-differentiated human adipocytes were pretreated with 5, 20, or 80 μM SP600125 (SP) for 30 min, followed by treatment with BSA vehicle or 50 μM t10,c12 CLA for 18 h **a** or 24 h **b**. Subsequently, RNA was harvested and the mRNA levels of IL-8, IL-6, IL-1β, MCP-1, ATF3, and COX-2 were measured by real time qPCR and normalized to GAPDH endogenous control. Means (+SE; $n = 2$–3 **a** or n = 4 **b**) not sharing a lower case letter differ significantly ($p < 0.05$). **(b).** Media were collected and analyzed for IL-8, IL-6, and MCP-1 levels using the BioRad Multiplex System. Data are representative of two **b** or three **a** independent experiments

PPARγ activity [12–17]. Due to the hypothesized role of JNK in regulating t10,c12 CLA-induced inflammation, we investigated the impact of SP600125 on t10,c12 CLA-mediated suppression of lipogenic gene expression and PPARγ protein levels. Consistent with our hypothesis, SP600125 blocked t10,c12 CLA-mediated suppression of the expression of transcription factors that regulate lipid metabolism (i.e., PPARγ/α, sterol regulatory element binding protein (SREBP)-1c, liver X receptor (LXR)α) and several of their downstream targets (i.e., acetyl-CoA carboxylase (ACC)-1, stearoyl-CoA desaturase (SCD)-1) in a concentration-dependent manner (Fig. 3a). Additionally, 20 μM SP600125 modestly prevented a CLA-mediated decrease in PPARγ protein levels (Fig. 3b). Taken together, these data suggest that JNK activity regulates t10,c12 CLA-mediated suppression of lipogenic genes, which may contribute to the ability of t10,c12 CLA to decrease the triglyceride levels in adipocytes.

SP600125 Prevents t10,c12 CLA-Mediated Regulation of Genes Involved in Insulin Signaling

We previously demonstrated that t10,c12 CLA-induced inflammation leads to a suppression of insulin signaling and sensitivity [9, 10, 18, 19]. Therefore, we determined the extent to which JNK impacted the expression of genes associated with insulin signaling. SP600125 attenuated t10,c12 CLA-mediated induction of suppressor of cytokine synthesis (SOCS)-3, a protein reported to cause insulin resistance (Fig. 4). Consistent with these data, t10,c12 CLA-mediated suppression of insulin-dependent glucose transporter (GLUT) 4 and adiponectin mRNA levels, which are positively associated with insulin sensitivity, was attenuated by SP600125 in a concentration-dependent manner (Fig. 4). Further studies are needed to confirm a role for JNK in CLA-mediated suppression of insulin-stimulated glucose uptake.

Discussion

Consistent with our hypothesis, t10,c12 CLA-mediated activation of cJun and ATF3 was attenuated by the chemical JNK inhibitor, SP600125. SP600125 also blocked t10,c12 CLA-induced inflammatory gene expression and cytokine secretion, and suppression of lipogenic genes and markers of insulin signaling. Taken together, these data suggest that JNK plays a role in t10,c12 CLA-mediated induction of markers of inflammation and insulin resistance in cultures of human adipocytes. However, due to the potential lack of specificity of chemical inhibitors (i.e., they can inhibit other kinases including ERK and p38, albeit at much lower selectivities [23]), JNK gene silencing experiments are needed to confirm these results. Knockdown experiments are also need to determine the extent to which JNK signaling impairs insulin-stimulated glucose uptake in t10,c12 CLA-treated cultures, because such longer-term studies were not possible with SP600125 (data not shown).

Treatment times differed based on the experimental outcome measured. Historically, we have shown in our primary cultures of newly-differentiated human adipocytes that t10,c12 CLA increases phosphorylation of MAPKs between 6–24 h, induces inflammatory gene expression and protein secretion between 12–48 h, decreases adipogenic gene expression from 18 to 72 h, and PPARγ protein

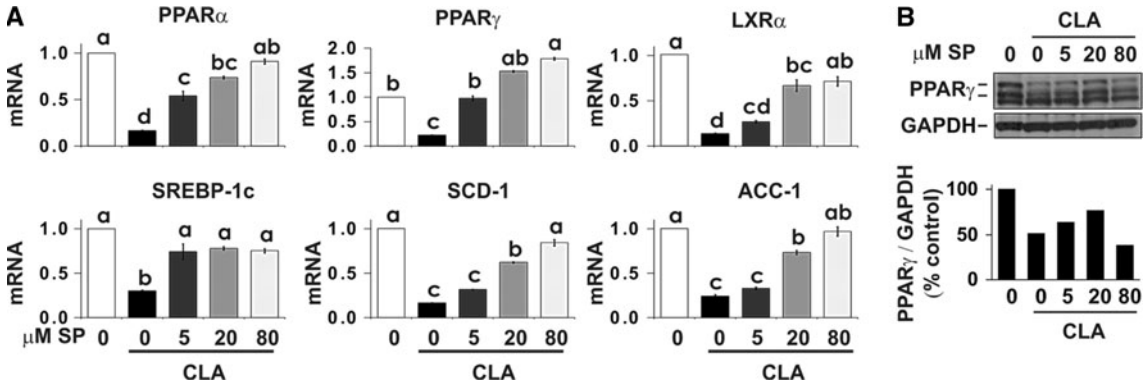

Fig. 3 Cultures of newly-differentiated human adipocytes were pretreated with 5, 20, or 80 μM SP600125 (SP) for 30 min, followed by treatment with BSA vehicle or 50 μM t10,c12 CLA for 24 h. **a** RNA was harvested and the mRNA levels of PPARγ, PPARα, LXRα, SREBP-1c, ACC-1, and SCD-1 were measured using real time qPCR and normalized to GAPDH endogenous control. Means (+SE; n = 2–3) not sharing a lower case letter differ significantly ($p < 0.05$). **b** Cultures were harvested for the determination of the protein levels of PPARγ and GAPDH. PPARγ levels were quantified by densitometry and normalized to the loading control, GAPDH. Densitometry values are expressed as % of BSA vehicle control. Data are representative of two **b** or three **a** independent experiments

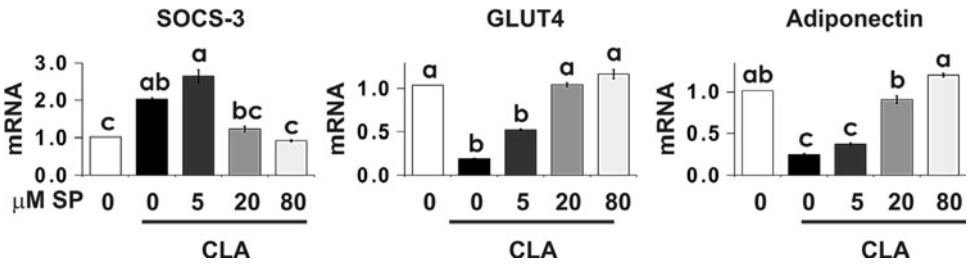

Fig. 4 Cultures of newly-differentiated human adipocytes were pretreated with 5, 20, or 80 μM SP600125 (SP) for 30 min, followed by treatment with BSA vehicle or 50 μM t10,c12 CLA for 24 h. Subsequently, RNA was harvested and the mRNA levels of SOCS-3, GLUT4, and apm1 were measured by real time qPCR and normalized to GAPDH endogenous control. Means (+SE; n = 2–3) not sharing a lower case letter differ significantly ($p < 0.05$)

from 24 to 48 h [9, 10, 18, 19, 32, 33]. Therefore, we chose a 12 h time point to examine JNK phosphorylation, 18 h for inflammatory gene expression, 24 h for cytokine/chemokine secretion, and 24 h for adipogenic, lipogenic, and insulin-sensitizing gene expression. The timing of these events fits our hypothesis that JNK phosphorylation occurs prior to t10,c12 CLA-mediated induction and secretion of inflammatory proteins, leading to the suppression of adipogenic/lipogenic gene and protein levels.

c-Jun NH2-terminal kinase-mediated activation of cJun results in induction of several inflammatory genes including IL-8, IL-6, and COX2, and also genes involved in cell death or apoptosis. For example, SP600125 or RNA interference of JNK in 3T3-L1 adipocytes prevented free fatty acid-induced MCP-1 expression [26]. Consistent with these data, we showed that inhibiting JNK with the chemical inhibitor SP600125 prevented t10,c12 CLA-mediated inflammatory gene expression and protein secretion (Fig. 2). This prevention was accompanied by an increase in the expression lipogenic and insulin sensitizing genes and PPARγ protein levels that promote lipogenesis or insulin signaling (Fig. 3).

One possible explanation for these data is that by inhibiting JNK activity, t10,c12 CLA was unable to decrease PPARγ activity, which drives the expression of genes that promote glucose and fatty acid uptake and triglyceride synthesis and deposition in adipocytes. Indeed, PPARγ2 activity is regulated by phosphorylation [27]. Notably, phosphorylation at serine residue 112 by ERK or JNK has been reported to decrease PPARγ activity by ubiquination and proteosome degradation [28], and by decreasing its ligand-dependent and ligand-independent transactivating functions [15, 29–31]. Consistent with this hypothesis, we have shown that t10,c12 CLA increases PPARγ phosphorylation prior to reducing PPARγ protein levels. Furthermore, supplementation with Rosiglitazone, a PPARγ agonist [32], or resveratrol, an anti-inflammatory polyphenol [33], attenuates delipidation by t10,c12 CLA. Thus, inhibiting t10,c12 CLA-mediated JNK signaling may increase PPARγ activity, thereby increasing the expression of lipogenic and insulin-signaling genes. Consistent with this hypothesis, SP600125 supplementation of t10,c12 CLA-treated cultures increased the expression of lipogenic and insulin-

signaling genes compared to cultures treated with t10,c12 CLA alone (Fig. 3).

We previously showed using the ERK inhibitor U0126 that ERK activation by t10,c12 CLA is one mechanism by which t10,c12 CLA suppresses lipogenic gene expression and insulin-stimulated glucose uptake [9]. Therefore, it is tempting to speculate that t10,c12 CLA antagonizes PPARγ activity via activation of MAPKs like ERK and JNK, thereby inhibiting PPARγ target genes. In support of this hypothesis, knockdown of JNK1, but not JNK2, increased basal and troglitazone-stimulated PPARγ reporter activity [34].

c-Jun NH2-terminal kinase deficiency in animals on a high-fat diet protects them from developing insulin resistance [20]. Similarly, mitochondrial dysfunction-induced insulin resistance in 3T3-L1 adipocytes is prevented by knockdown of JNK1 [35]. Several reports show that JNK directly phosphorylates insulin receptor substrate (IRS)-1 at serine 307, thus inactivating insulin receptor signaling. However, we did not observe any effects of t10,c12 CLA or SP600125 on IRS-1 ser 307 phosphorylation (data not shown), in spite of SP600125 blocking t10,c12 CLA induction of SOCS-3, a protein reported to phosphorylate ser 307 on IRS-1. Nevertheless, t10,c12 CLA-mediated suppression of the mRNA levels adiponectin and GLUT4, proteins associated with insulin sensitivity, was completely prevented by SP600125 (Fig. 4).

Taken together, these data suggest that JNK may be an important target for preventing t10,c12-CLA mediated inflammation. Further studies are needed to confirm a role for JNK in t10,c12 CLA-mediated insulin resistance. RNA interference studies targeting JNK are also needed to confirm these data. Future research will also focus on identifying upstream activators of JNK and ERK and potential mechanisms by which these MAPK pathways are linked to insulin resistance and suppression of lipogenesis in adipocytes.

Acknowledgments This work was supported by grants from the National Institute of Health (NIH) National Institute of Diabetes and Digestive and Kidney Diseases/Office of Dietary Supplements (NIDDK/ODS) (5R01-DK063070) to MM, the North Carolina Agriculture Research Service (NCARS 06520) to MM, the NIH 5F31DK076208 and United Negro College Fund (UNCF)-Merck fellowships to AK, and NIH F31DK084812 to KM.

References

1. World Health Organization (2011). Obesity and Overweight. http://www.who.int/mediacentre/factsheets/fs311/en/index.html Accessed 7 Mar 2011
2. Kennedy A, Martinez K, Schmidt S, Mandrup S, Lapoint K, McIntosh M (2010) Anti-obesity mechanisms of action of conjugated linoleic acid. J Nutr Biochem 21:171–179
3. Risérus U, Arner P, Brismar K, Vessby B (2002) Treatment with dietary trans10cis12 conjugated linoleic acid causes isomer-specific insulin resistance in obese men with the metabolic syndrome. Diabetes Care 25:1516–1521
4. Moloney F, Yeow TP, Mullen A, Nolan JJ, Roche HM (2004) Conjugated linoleic acid supplementation, insulin sensitivity, and lipoprotein metabolism in patients with type 2 diabetes mellitus. Am J Clin Nutr 80:887–895
5. Steck SE, Chalecki AM, Miller P, Conway J, Austin GL, Hardin JW, Albright CD, Thuillier P (2007) Conjugated linoleic acid supplementation for twelve weeks increases lean body mass in obese humans. J Nutr 137:1188–1193
6. Thrush AB, Chabowski A, Heigenhauser GJ, McBride BW, Or-Rashid M, Dyck DJ (2007) Conjugated linoleic acid increases skeletal muscle ceramide content and decreases insulin sensitivity in overweight, non-diabetic humans. Appl Physiol Nutr Metab 32:372–382
7. Tholstrup T, Raff M, Straarup EM, Lund P, Basu S, Bruun JM (2008) An oil mixture with trans-10, cis-12 conjugated linoleic acid increases markers of inflammation and in vivo lipid peroxidation compared with cis-9, trans-11 conjugated linoleic acid in postmenopausal women. J Nutr 138:1445–1451
8. Moloney F, Toomey S, Noone E, Nugent A, Allan B, Loscher C, Roche H (2007) Antidiabetic effects of cis-9, trans-11 conjugated linoleic acid may be mediated via anti-inflammatory effects in white adipose tissue. Diabetes 56:574–582
9. Brown JM, Boysen M, Chung S, Fabiyi O, Morrision R, Mandrup S, McIntosh M (2004) Conjugated linoleic acid (CLA) induces human adipocyte delipidation: autocrine/paracrine regulation of MEK/ERK signaling by adipocytokines. J Biol Chem 279:26735–26747
10. Chung S, Brown JM, Provo JN, Hopkins R, McIntosh M (2005) Conjugated linoleic acid promotes human adipocyte insulin resistance through NFkappaB-dependent cytokine production. J Biol Chem 280:38445–38456
11. Poirier H, Shapiro H, Kim R, Lazar M (2006) Nutritional supplementation with trans-10, cis-12 conjugated linoleic acid induces inflammation of white adipose tissue. Diabetes 55:1634–1641
12. Ruan H, Hacohen N, Golub T, Van Parijs L, Lodish H (2002) Profiling gene transcription in vivo reveals adipose tissue as an intermediate target for tumor necrosis alpha: implications for insulin resistance. Diabetes 51:1319–1336
13. Ruan H, Pownall H, Lodish H (2003) Troglitazone antagonizes tumor necrosis factor-a induced reprogramming of adipocyte gene expression by inhibiting the transcriptional regulatory functions of NFkB. J Biol Chem 278:28181–28192
14. Suzawa M, Takada I, Yanagisawa J, Ohtake F, Ogawa S, Yamauchi T, Kadowaki T, Takeuchi Y, Shibuya H, Gotoh Y, Matsumoto K, Kato S (2003) Cytokines suppress adipogenesis and PPAR-gamma function through the TAK1/TAB 1/NIK cascade. Nat Cell Biol 5:224–230
15. Adams M, Reginato M, Shao D, Lazar M, Chatterjee V (1997) Transcriptional activation by peroxisome proliferator activated receptor gamma is inhibited by phosphorylation at a consensus mitogen-activated protein kinase site. J Biol Chem 272:5128–5132
16. Camp H, Tafuri S (1997) Regulation of peroxisome proliferators-activated receptor γ activity by mitogen activated protein kinase. J Biol Chem 272:10811–10816
17. de Mora J, Porras A, Ahn N, Santos E (1997) Mitogen-activated protein kinase activation is not necessary for, but antagonizes, 3T3–L1 adipocytic differentiation. Mol Cell Biol 17:6068–6075
18. Kennedy A, Martinez K, Chung S, LaPoint K, West T, Hopkins R, Schmidt S, Andersen K, Mandrup S, McIntosh M (2010) Inflammation and insulin resistance induced by trans-10, cis-12

conjugated linoleic acid are dependent on intracellular calcium levels in primary cultures of human adipocytes. J Lipid Res 51:1906–1917
19. Martinez K, Kennedy A, West T, Milatovic D, Aschner M, McIntosh MK (2010) Trans-10, cis-12 conjugated linoleic acid promotes inflammation to a greater extent in human adipocytes compared to preadipocytes. J Biol Chem 285:17701–17712
20. Hirosumi J, Tuncman G, Chang G, Gorgun C, Uysal K, Maeda K, Karin M, Hotamisligil G (2002) A central role of JNK in obesity and insulin resistance. Nature 420:333–336
21. Tuncman G, Hirosumi H, Solinas G, Chang L, Karin M, Hotamisligil G (2006) Functional in vivo interactions between JNK1 and JNK2 isoforms in obesity and insulin resistance. Proc Natl Acad Sci USA 103:10741–10746
22. Davis J, Gabler N, Walker-Daniels J, Spurlock M (2009) The c-Jun N terminal kinase mediates the induction of oxidative stress and insulin resistance by palmitate and toll-like receptor 2 and 4 ligands in adipocytes. Horm Metab Res 41:523–530
23. Bennett BL, Sasaki DT, Murray BW, O'Leary EC, Sakata ST, Xu W, Leisten JC, Motiwala A, Pierce S, Satoh Y, Bhagwat SS, Manning AM, Anderson DW (2001) SP600125, an anthrapyrazolone inhibitor of Jun N-terminal kinase. Proc Natl Acad Sci USA 98:13681–13686
24. Gupta S, Barrett T, Whitmarsh A, Cavanagh J, Sluss H, Derijard B, Davis R (1996) Selective interaction of JNK protein kinase isoforms with transcription factors. EMBO J 15:2760–2770
25. Holzberg D, Knight G, Dittrich-Breiholz O, Schneider H, Dorrie A, Hoffman E, Resch K, Krach M (2003) Disruption of c-JUN-JNK complex by a cell permeable peptide containing the c-JUN g domain induces apoptosis and affects a distinct set of interleukin-1-induced inflammatory genes. J Biol Chem 41:40213–40223
26. Jiao P, Chen Q, Shah S, Du J, Tao J, Tzamelim I, Wan W, Xu G (2009) Obesity-related upregulation of monocyte chemotactic factors in adipocytes. Diabetes 58:104–115
27. Hu E, Kim JB, Sarraf P, Spiegelman BM (1996) Inhibition of adipogenesis through MAP kinase-mediated phosphorylation of PPARgamma. Science 274:2100–2103
28. Floyd ZE, Stephens JM (2002) Interferon-gamma-mediated activation and ubiquitin-proteasome-dependent degradation of PPARgamma in adipocytes. J Biol Chem 277:4062–4068
29. Shao DL, Rangwala SM, Bailey ST, Krakow SL, Reginato MJ, Lazar MA (1998) Interdomain communication regulating ligand binding by PPARgamma. Nature 396:377–380
30. Diradourian C, Girard J, Pégorier JP (2005) Phosphorylation of PPARs: from molecular characterization to physiological relevance. Biochimie 87:33–38
31. Burns KA, Vanden Heuvel JP (2007) Modulation of PPAR activity via phosphorylation. Biochim Biophys Acta 1771: 952–960
32. Kennedy A, Chung S, LaPoint K, Fabiyi O, McIntosh MK (2008) Trans-10, cis-12 conjugated linoleic acid antagonizes ligand-dependent PPARgamma activity in primary cultures of human adipocytes. J Nutr 138:455–461
33. Kennedy A, Overman A, Lapoint K, Hopkins R, West T, Chuang CC, Martinez K, Bell D, McIntosh MK (2009) Conjugated linoleic acid-mediated inflammation and insulin resistance in human adipocytes are attenuated by resveratrol. J Lipid Res 50:225–232
34. Rozo A, Vijayvargia R, Weiss H, Ruan H (2008) Silencing JNK1 and JNK2 accelerate basal lipolysis and promote fatty acid re-esterification in mouse adipocytes. Diabetologia 51:1493–1504
35. Kim T, Leitner J, Adochio R, Draznin B (2009) Knockdown of JNK rescues 3T3–L1 adipocytes from insulin resistance induced by mitochondrial dysfunction. Biochem Biophys Res Commun 378:772–776

Lipids (2011) 46:893–906
DOI 10.1007/s11745-011-3589-2

ORIGINAL ARTICLE

2-Polyunsaturated Acyl Lysophosphatidylethanolamine Attenuates Inflammatory Response in Zymosan A-Induced Peritonitis in Mice

Nguyen Dang Hung · Mee Ree Kim · Dai-Eun Sok

Received: 18 April 2011 / Accepted: 16 June 2011 / Published online: 10 July 2011

Abstract In the present study, the anti-inflammatory action of lysophosphatidylethanolamine (lysoPtdEtn), orally administered, in zymosan A-induced peritonitis was examined. Oral administration of 2-DHA-lysoPtdEtn (ED_{50}, ~111 μg/kg) or 2-ARA-lysoPtdEtn (ED_{50}, 221 μg/kg) was found to inhibit the plasma leakage in mice treated with zymosan A. In support of this, 2-polyunsaturated acyl-lysoPtdEtn diminished the formation of LTC_4, a lipid mediator responsible for vascular permeability. Next, 2-DHA-lysoPtdEtn (ED_{50}, 110 μg/kg) or 2-ARA-lysoPtdEtn (ED_{50}, 123 μg/kg) effectively inhibited the leukocyte extravasation into the peritoneum. Consistent with this, each polyunsaturated-lysoPtdEtn diminished the formation of LTB_4 and 12-HETE, potent chemotactic factors. Additionally, the level of pro-inflammatory mediator (IL-1 β, IL-6, TNF-α or NO) was lowered remarkably in contrast to the augmentation of anti-inflammatory interleukin IL-10. Furthermore, 2-(15-HETE)-lysoPtdEtn and 2-(17-HDHE)-lysoPtdEtn, 15-lipoxygenation product of 2-ARA-lysoPtdEtn and 2-DHA-lysoPtdEtn, respectively, were more potent than corresponding lysoPtdEtn, suggesting the action of 2-acyl-lysoPtdEtn might be expressed through 15-lipoxygenation. In support of this, the formation of 15-HETE and LXA_4 was upgraded in accordance with an increasing dose of 2-ARA-lysoPtdEtn. Separately, anti-inflammatory actions, 2-polyunsaturated acyl-lysoPtdEtns also drastically diminished leukocyte infiltration in a later phase of zymosan A-induced peritonitis, indicating that these lipids also possess pro-resolving activity. Taken together, it is suggested that polyunsaturated lysoPtdEtns and their lipoxygenation derivatives, could be classified as potent anti-inflammatory lipids.

Keywords Anti-inflammatory · 2-ARA-lysoPtdEtn · 2-DHA-lysoPtdEtn · 2-(15-HETE)-lysoPtdEtn · 2-(17-HDHE)-lysoPtdEtn · Zymosan A

Abbreviations

2-ARA-lysoPtdEtn	1-Lyso-2-arachidonoyl-*sn*-glycero-3-phosphoethanolamine
2-DHA-lysoPtdEtn	1-Lyso-2-docosahexaenoyl-*sn*-glycero-3-phosphoethanolamine
2-(15-HpETE)-lysoPtdEtn	1-Lyso-2-15(*S*)-hydroperoxy-5,8,11,13-eicosatetraenoyl-*sn*-glycero-3-phosphoethanolamine
2-(15-HETE)-lysoPtdEtn	1-Lyso-2-15(*S*)-hydroxy-5,8,11,13-eicosatetraenoyl-*sn*-glycero-3-phosphoethanolamine
2-(17-HDHE)-lysoPtdEtn	1-Lyso-2-17(*S*)-hydroxy-4,7,10,13,15,19-docosahexaenoyl-*sn*-glycero-3-phosphoethanolamine
2-(17-HpDHE)-lysoPtdEtn	1-Lyso-2-17-(*S*)-hydroperoxy-

N. D. Hung · D.-E. Sok (✉)
College of Pharmacy, Chungnam National University, Yuseoung-Gu, Daejeon 305-764, Republic of Korea
e-mail: daesok@cnu.ac.kr

N. D. Hung
e-mail: hung_hanoi_vietnam@yahoo.com

M. R. Kim
Department of Food and Nutrition, Chungnam National University, Yuseong-Gu, Daejeon 305-764, Republic of Korea
e-mail: mrkim@cnu.ac.kr

	4,7,10,13,15,19-docosahexaenoyl-*sn*-glycero-3-phosphoethanolamine
ARA	Arachidonic acid
DHA	Docosahexaenoic acid
15-HETE	15(*S*)-hydroxy-5,8,11,13-eicosatetraenoic acid
17-HDHE	17-(*S*)-hydroxy-4,7,10,13,15,19-docosahexaenoic acid
LTB_4	Leukotriene B_4
LTC_4	Leukotriene C_4
PGE_2	Prostaglandin E_2
LXA_4	Lipoxin A_4
ED_{50}	50% Effective dose
LOX	Lipoxygenase
TNF-α	Tumor necrosis factor alpha
IFN-γ	Interferon gamma
IL-1β	Interleukin 1-beta
IL-6	Interleukin-6

Introduction

Inflammation is defined as a part of complex biological responses of vascular tissue toward exogenous harmful stimuli [1]. It becomes apparent that inflammation, normally results from an excessive inflammatory response or failure of resolution [2], is recognized as a causative in various diseases such as atherosclerosis, cancer, or asthma, and some neuropathological disorders such as Alzheimer's disease or Parkinson's disease. Additionally, lipid-derived mediators have proved to actively participate in the inflammation process and cooperate with others components in regulating the biological response to inflammation [3]. During the time course of inflammation, the lipid mediator could switch from a pro-inflammatory class such as prostaglandins and leukotrienes in the initial phase to biosynthesis of an anti-inflammatory and pro-resolving class including resolvin D series, resolvin E series, protectin D [4], maresin [5] in the resolution phase.

Lysophospholipid is a bioactive lipid class that plays important roles in the physical function and pathological conditions in the human body [6, 7]. Whereas the biological function of lysophosphatidylcholine (lysoPtCho), an abundant lysophospholipid in vivo, in inflammation it has been extensively studied and proved to be dependent upon the length and unsaturation degree of fatty acyl group [8, 9], the biological action of lysoPtdEtn, presents in human serum at a level of about several hundred ng mL^{-1}, has been still unknown [10] except that the report that lysoPtdEtn expressed a potent anti-inflammatory activity in colitis induced by rectal administration of ethanol and trinitrobenzene sulfonic acid in rats [11]. Our recent works have proved that polyunsaturated-lysoPtCho, containing omega-3 or omega-6 fatty acid and its hydroxyl derivatives possess potent anti-inflammatory properties in vivo as well as in the in vitro model [8, 9, 12]. Anti-inflammatory activity of polyunsaturated lysoPtCho was suggested to be due to the combination effect of lysoPtCho itself and its metabolites. Moreover, 15-hydroxy derivative or 17-hydroxy derivative, derived from the sequential action of 15-LOX [13, 14] and GSH-peroxidase [15] on 1-ARA-lysoPtCho and 1-eicosapentaenoyl-lysoPtCho or 1-DHA-lysoPtCho, respectively, proved to possess more potent anti-inflammatory activity than their corresponding lysoPtCho suggesting that 15-lipoxygenase might be crucial for the anti-inflammatory effect of polyunsaturated lysoPtChos. However, the lysoPtCho form had been reported to be cytotoxic at relative small concentrations, in contrast to lysoPtdEtn which was less cytotoxic [16, 17]. Separately, it was reported that 18:0a/15S-HETE-PE potently inhibited cytokine generation in human monocytes, providing more evidence for anti-inflammatory activity of phosphatidylethanolamine (PtdEtn) in vitro [18]. However, it is still questionable whether polyunsaturated-lysoPtdEtn could express anti-inflammatory activity as observed with polyunsaturated acyl lysoPtCho. In this study we examined the anti-inflammatory actions of 2-ARA-lysoPtdEtn and 2-DHA-lysoPtdEtn, their corresponding oxygenation products, 2-(15-HETE)-lysoPtdEtn and 2-(17-HpDHE)-lysoPtdEtn, respectively, to elucidate the mechanism responsible for their anti-inflammatory actions.

Materials and Methods

C18 (plasm)-22:6 PtEtn and C18 (plasm)-20:4 PtEtn, arachidonic acid (ARA), docosahexaenoic acid (DHA) (purity, 99%) were procured from Avanti Polar Lipids Inc. (Alabaster, Alabama, USA). All the enzyme were from the Sigma Company, unless otherwise indicated. Soybean lipoxygenase-1 (Type I-B), zymosan A (Z4250-1G) (*Saccharomyces cerevisiae*) were purchased from Sigma-Aldrich Corp. (St. Louis, MO, USA). 12/15-lipoxygenase (porcine leukocyte, 135.6 units/ml), 15-lipoxygenase-2 (human recombinant, 250 units/ml), 15-LOX inhibitor (PD 146176), EIA assay kits for prostaglandin E_2 (PGE_2), 15-HETE, leukotriene B_4 (LTB_4), leukotriene C_4 (LTC_4), and the nitrate/nitrite colorimetric assay kit were from Cayman Chemical (Ann Arbor, MI, USA). Lipoxin A_4 (LXA_4) and 12-HETE were from Oxford Biochemical Research Corp. (Box 522, Oxford, MI, USA) and Assay Designs Corp., respectively. The EIA assay kit for

12-HETE was supplied by Assay Design Inc. (Ann Arbor MI, USA). ELISA assay kits for cytokines (TNF-α, IL-1β, IL-4, IL-6 and IL-10) were obtained from eBioscience, Inc. (Science Center Drive, San Diego, USA).

Preparation of 2-ARA-lysoPtdEtn and 2-DHA-lysoPtdEtn

2-DHA-lysoPtdEtn and 2-ARA-lysoPtdEtn were from the acidic hydrolysis of C18 (plasm)-22:6 PE and C18 (plasm)-20:4 PE, respectively according to a previous report with slight modification [19]. Briefly, PE was suspended in a mixture of 2.5 M HCl (0.8 ml), methanol (2 ml) and chloroform (1 ml) for 20 min at room temperature with vigorous stirring. Hydrolysis products were extracted from the reaction mixtures by the method of Bligh and Dyer and further purified by TLC on silica gel 60 plate, which was developed with a mobile solvent system (chloroform: methanol: H_2O; 65:25:4). Eventually, the band containing lysoPtdEtn was scraped off, extracted with methanol and kept at −80 °C until used.

Preparation of 2-(15-HETE)-lysoPtdEtn and 2-(17-HDHE)-lysoPtdEtn

2-ARA-lysoPtdEtn or 2-DHA-lysoPtdEtn (200 μM) was oxidized by soybean LOX-1B (4 KU/ml) in 5 ml of borax buffer (50 mM, pH 9.0) for 1 h. Then, hydroperoxide was subsequently reduced to the corresponding hydroxide by addition of $SnCl_2$ (1 mM) with vigorous stirring for 10 min at room temperature. The hydroxide derivative product was extracted using the Bligh and Dyer method [9, 20] and further purified by RP-HPLC using Zorbrax eclipse XDB C18 column (5 μm, 50 × 4.6 mm, Agilent Technologies, USA) with an isocratic solvent system (ACN: water: formic acid; 60:40:0.1) [21]. The amount of 1-(15-HEPE)-lysoPtdEtn or 2-(17-HDHE)-lysoPtdEtn was determined by measuring absorbance of purified lipid at 234 nm using $E_{1m,1cm} = 28{,}000$, and the lipids were stored at −80 °C until used [18]

Determination of Kinetic Values in LOXs-Catalyzed Oxygenation of 2-ARA-lysoPtdEtn or 2-DHA-lysoPtdEtn

Oxygenation of 2-ARA-lysoPtdEtn or 2-DHA-lysoPtdEtn by LOXs was monitored via the increase in absorbance at 234 nm according to the formation of conjugated diene. In the kinetic study, lysoPtdEtns (0–20 μM) were incubated with soybean LOX-1B (2.5 units/ml), porcine leukocyte 12/15 LOX (1 unit/ml), or human 15-LOX-2 (1 unit/ml) in 50 mM borax buffer (pH 9.0), 50 mM phosphate buffer (pH 7.4) containing 5 mM EDTA and 0.03% Tween 20, or 50 mM Tris–HCl buffer (pH 7.2) containing 0.003% Tween 20, respectively. The kinetic parameters, Km and Vm, were determined by Linwear–Burk plot analysis as previously reported [9]. One unit of LOX activity was defined as the amount of LOX that can produce one nanomole of conjugated diene per min.

Identification of Oxygenation of 2-docosahexaenoyl-lysoPtdEtn or 2-ARA-lysoPtdEtn by Soybean 15-LOX Using LC/ESI-MS

Soybean 15-LOX-1B (10 units/ml) was incubated with either 2-ARA-lysoPtdEtn or 2-DHA-lysoPtdEtn (100 μM) in 500 μl of 5 mM borax buffer (pH 9.0). After 30 min incubation at room temperature, the reaction products (30 μl) were directly analyzed by LC/ESI-MS which was performed using a MSDI spectrometer (HP 1100 series LC/MSA, Hewlett Packard, USA), equipped with a Zorbrax eclipse XDB C18 column (5 μm, 50 × 4.6 mm, Agilent Technologies, Washington, USA). The LC–MS solution was utilized for data collection and manipulation. The oxidized product was eluted (0.5 ml/min) with an isocratic solvent system of 60% solvent B [0.1% formic acid/acetonitrile in solvent A (0.1% formic acid/methanol], and the eluent was monitored at 234 nm, full-scan mass spectra were obtained within the range of m/z 400–700, and the data acquisition was conducted in both negative and positive modes. The condition for EIS–MS analysis of HPLC peak included a capillary voltage of 200 V, a drying gas flow of 1.5 mL/min, and a temperature of 200 °C.

Animal Experiment

ICR mice (4–6 weeks of age, 29–30 g body weight) were procured from Koatech Co., Korea, and housed in cages (10 mice per cage) under viral antibody-free conditions. Mice were fed with standard food (Sangyang Co., Korea) that containing no less than 4.5% total fat with 0.26% omega-3 fatty acid and <0.01% ARA acid. All animal experiments were conducted according to the Guide for Care and Use of Laboratory Animals of the National Research Council (NRC, 1996), which was approved by the Committee of Animal Care and Experiment of Chungnam National University, Korea.

Zymosan A-Induced Peritonitis in ICR Mice

Peritonitis was stimulated by i.p. administration of zymosan A (1 mg/mouse) as described previously [22–24]. For the measurement of plasma leakage, mice were treated orally with 200 μl of each lysoPtdEtn taken from

ethanol stock solution and diluted in PBS buffer (final ethanol concentration <0.5%), 60 min prior to i.p. administration (1 mg/mouse) of zymosan A, and 100 μl of 0.5% Evans Blue dye, dissolved in PBS, was intravenously injected just prior to zymosan A injection [25, 26]. Sixty minutes later, unless otherwise indicated, mice were killed using isoflurane inhalation, and peritoneal lavage was performed with 3 ml of ice cold PBS. Then, cells were centrifuged out of the lavage fluid. Finally, Evans blue dye extravasation amount was determined by measuring the absorbance of supernatants at 610 nm, and normalized with a standard curve [22, 23, 27]. Separately, in order to measure leukocyte infiltration, lipids were administered 60 min prior to i.p administration of zymosan A. Four hours after zymosan A injection, peritoneal lavage was taken, and total cells in the lavage fluid was enumerated using light microscopy with trypan blue staining [22, 28]. In an attempt to evaluate the effect of 15-LOX inhibitor (PD146176) [29] on the pharmacological activity of polyunsaturated lysoPtdEtns, mice were treated orally with 2-ARA-lysoPtdEtn or 2-docosahexaenoyl-lysoPtdEtn (50–150 μg/kg), followed by i.p. administration of PD146176, a specific 15-LOX inhibitor, 60 min prior to intra-peritoneal administration of zymosan A (1 mg/mice) and eventually, leukocyte infiltration was assessed as described above.

Determination of Inflammatory Lipid Mediators or Cytokine Level in Peritoneal Lavage Fluid

To determine the level of pro-inflammatory lipid mediators in exudates, 1 ml of peritoneal lavage fluid was transferred to micro-centrifuge tubes and centrifuged (15,000 rpm, 3 min). Supernatants were used directly for enzyme immunoassay (EIA) analysis of PGE_2, LTB_4, LTC_4, 12-HETE, 15-HETE, or LXA_4 level as described before [24, 30]. Whereas levels of pro-inflammatory (IL-1β, IL-6, TNF-α) or anti-inflammatory cytokines (IL-4, IL-10) were determined by ELISA assay according to the manufacturer's instructions. Additionally, the content of nitric oxide (NO) in the lavage fluid was quantitated by a nitrate/nitrite colorimetric assay kit supplied by Cayman Chemical Company (Ann Arbor, MI, USA).

Statistical Analysis

Data were calculated and displayed as means ± SEM. Group comparisons were performed using one-way analysis of variance (ANOVA) followed by Neuman Keuls multiple comparison test or Student's t test where appropriate; with P value ≤ 0.05 was considered as statistically significant (sufficient to reject the null hypothesis).

Results

Identification of Product from 15-LOX-catalyzed Oxygenation of 2-ARA-lysoPtdEtn or 2-DHA-lysoPtdEtn

The formation of 2-(15-HpETE)-lysoPtdEtn and 2-(17-HpDHE)-lysoPtdEtn, 15-LOX-catalyzed oxidation products of 2-ARA-lysoPtdEtn and 2-DHA-lysoPtdEtn, respectively, was analyzed by LC–ESI–MS using both the positive and negative mode. Figure 1 shows that a peak with a retention time of 1.6 min (Inset, Fig. 1a) appeared as a predominant product possessing the mass spectrum of a compound corresponding to hydroperoxy derivative of 2-ARA-lysoPtdEtn (Fig. 1a); mass-to-charge ratio (m/z) at 532 $(M–H)^-$ in negative scan mode, and 500 $(M + H–H_2O–O)^+$, 516 $(M + H–H_2O)^+$, 534 $(M + H)^+$, 556 $(M + Na)^+$, and 572 $(M + K)^+$ in positive scan mode (Fig. 1b). Likewise, as shown in Fig. 1c, d, the mass spectrum of the major peak (RT, 1.7 min) (Inset, Fig. 1c) including molecular ions indicative of hydroperoxy derivative of 2-DHA-lysoPtdEtn had been obtained; m/z at 556 $(M–H)^-$ in negative scan mode, and 524 $(M + H–H_2O–O)^+$, 540 $(M + H–H_2O)^+$, 558 $(M + H)^+$, 580 $(M + Na)^+$, and 596 $(M + K)^+$ in positive scan mode [31]. Therefore, it was suggested that soybean LOX effectively converted 2-ARA-lysoPtdEtn and 2-DHA-lysoPtdEtn into their corresponding 15-hydroperoxy derivative products.

Determination of Kinetic Values in Oxygenation of 2-ARA-lysoPtdEtn and 2-DHA-lysoPtdEtn by Various LOXs

As 15-lipoxygenation had been known to be required for anti-inflammatory action of polyunsaturated lysoPtCho [12], the oxygenation of 2-polyunsaturated acyl-lysoPtdEtn by different LOXs was examined. When 2-ARA-lysoPtdEtn or 2-DHA-lysoPtdEtn was incubated with 15-LOXs (soybean LOX-1, leukocyte 12/15-LOX or human recombinant 15-LOX-2), a time-dependent increase in absorbance at 234 nm was observed, indicating the formation of a conjugated diene (data not shown). Subsequently, the kinetic values for oxygenation of 2-ARA-lysoPtdEtn or 2-DHA-lysoPtdEtn by 15-LOX were determined from Lineweaver–Burk plot analysis, and compared to those for ARA or DHA. As displayed in Table 1, the most favorable substrate in case of soybean LOX-catalyzed oxygenation was found to be 2-DHA-lysoPtdEtn, showing catalytic efficacy (Vm/Km) value of 30.4 units/μg/μM, which was approximately ninefold higher than that of DHA (Vm/Km, 3.5 units/μg/μM). Meanwhile, 2-ARA-lysoPtdEtn demonstrated a Vm/Km value of 10.9 units/μg/μM, which was

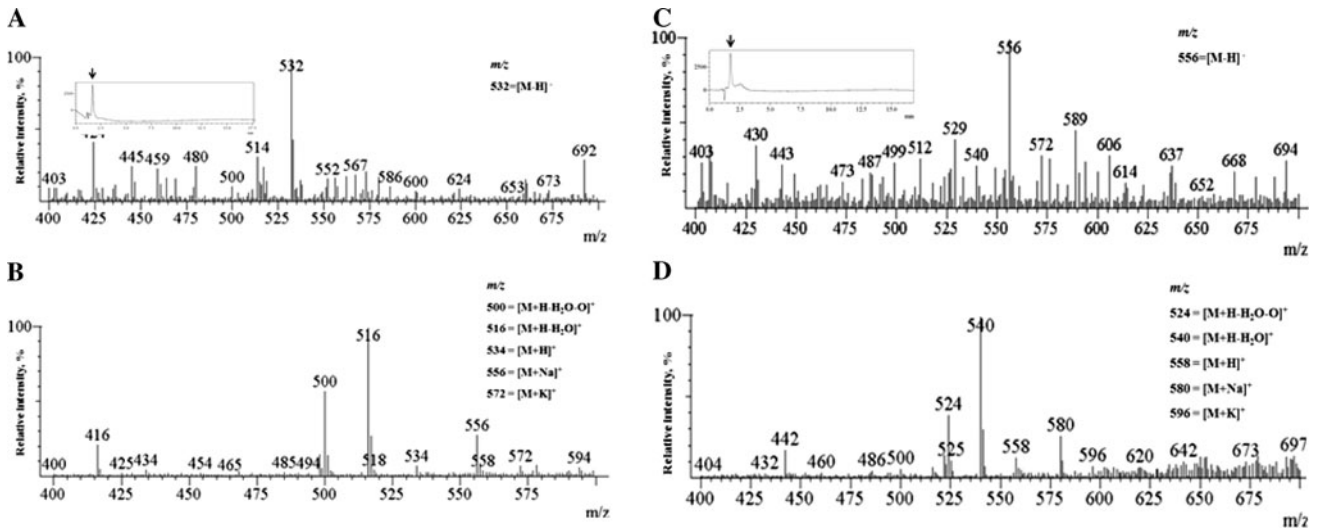

Fig. 1 LC/ESI–MS analysis of products from soybean 15-LOX catalyzed oxidation of 2-ARA-lysoPtdEtn (**a**, **b**) or 2-DHA-lysoPtdEtn (**c**, **d**). The hydroperoxide derivative obtained from 30 min-incubation of soybean 15-LOX with 2-ARA-lysoPtdEtn or 2-DHA-lysoPtdEtn (100 μM) in 500 μl of 5 mM borax buffer (pH 9.0) was directly analyzed by LC/ESI-MS as described in "Materials and Methods". The representative mass spectra of a major peak with retention time of 1.6 and 1.7 min (*inset* of **a** and **b**), respectively were obtained by the ESI–MS system using negative scan mode (**a**, **b**) and positive scan mode (**c**, **d**)

larger than that of ARA (Vm/Km, 7.4 units/μg/μM). Similarly, when the oxygenation of 2-ARA-lysoPtdEtn and 2-DHA-lysoPtdEtn by human 15-LOX-2 was analyzed, the Vm/Km values for 2-DHA-lysoPtdEtn and 2-ARA-lysoPtdEtn were estimated to be 48.2 and 14.8 units/μg/μM, respectively, which were about 8- and 1.5-fold higher than that of DHA and ARA, respectively. Thus, it was demonstrated that 2-DHA-lysoPtdEtn and 2-ARA-lysoPtdEtn were more effective substrates than DHA and ARA, respectively, for human recombinant 15-LOX-2. Finally, in the oxygenation by leukocyte 12-LOX, the Vm/Km value for 2-ARA-lysoPtdEtn was estimated to be 10.3 units/μg/μM, which was found to be two times larger than that of ARA (Vm/Km, 4.5 units/μg/μM). Taken all together, it was suggested that 2-polyunsaturated acyl-lysoPtdEtn is a more effective substrate than the acid form in 12-LOX or 15-LOX-catalyzed oxygenation. Nonetheless, 2-ARA-lysoPtdEtn and 2-DHA-lysoPtdEtn were not oxygenated significantly by murine recombinant 12-lipoxygenase from platelets (data not shown).

Table 1 Kinetic values in oxygenation of each lipid by soybean LOX-1, leukocyte 12/15-LOX, or human recombinant 15-LOX-2

Enzyme	Substrate	Km (μM)	Vmax (units/mg)	Vm/Km (units/mg/μM)
Soybean LOX-1	2-ARA-lysoPtdEtn	5.4 ± 0.9[a]	59.0 ± 8.6[a]	10.9 ± 0.2[a]
	2-DHA-lysoPtdEtn	2.7 ± 0.7[b]	80.6 ± 8.3[a]	30.4 ± 5.1[b]
	ARA	12.7 ± 0.4[c]	93.5 ± 6.5[a]	7.4 ± 1.5[a]
	DHA	24.2 ± 2.1[d]	84.4 ± 5.2[a]	3.5 ± 0.2[c]
Leukocyte 12-LOX	2-ARA-lysoPtdEtn	8.4 ± 0.5[a]	87.1 ± 3.9[a]	10.3 ± 1.0[a]
	2-DHA-lysoPtdEtn	6.1 ± 0.0[a]	60.2 ± 4.5[a]	9.9 ± 2.2[a]
	ARA	8.5 ± 0.6	30.9 ± 6.5	4.5 ± 1.0[b]
	DHA	11.6 ± 1.6[c]	95.8 ± 8.2[c]	8.2 ± 0.8[a]
Human 15-LOX-2	2-ARA-lysoPtdEtn	2.1 ± 0.4[a]	31.9 ± 3.7[a]	14.8 ± 0.9[a]
	2-DHA-lysoPtdEtn	1.4 ± 0.3[a]	68.8 ± 10.1[b]	48.2 ± 4.5[b]
	ARA	5.1 ± 1.2[b]	59.7 ± 7.6[b]	11.7 ± 0.4[a]
	DHA	8.1 ± 1.5[c]	50.2 ± 4.6[b]	6.2 ± 0.1[c]

Each lipid (0–20 μM) was incubated with soybean LOX-1B (2.5 units/ml), porcine leukocyte 12/15 LOX (1 unit/ml), and human 15-LOX-2 (1 unit/ml) in 50 mM borax buffer (500 μl, pH 9.0), 50 mM phosphate buffer (500 μl, pH 7.4) containing 5 mM EDTA and 0.03% Tween 20, and 50 mM Tris–HCl buffer (500 μl, pH 7.2) containing 0.003% Tween 20, respectively. Data were expressed as means ± SEM values of triplicates experiments. Means displayed with same letter are not significantly different

Prevention by 2-ARA-lysoPtdEtn or 2-DHA-lysoPtdEtn Against Zymosan A-Induced Plasma Leakage

Increased vascular permeability caused by reversible opening of endothelial cells tight junction, followed by the leak of protein and fluids from the vascular compartment into the extravascular compartment, is one predominant event in acute inflammation. In order to see anti-inflammatory actions of 2-ARA-lysoPtdEtn or 2-docosahexaneoyl-lysoPtdEtn in acute inflammation, we investigated the effect of lysoPtdEtn, orally administered, on zymosan A-induced vascular permeability based on the extravasation of Evans Blue dye as marker. As shown in Fig. 2, both 2-ARA-lysoPtdEtn and 2-DHA-lysoPtdEtn, orally administered, 60 min prior to zymosan A treatment (i.p., 1 mg/mouse) dose-dependently decreased zymosan A-induced plasma leakage in ICR mice. Oral intake of 2-ARA-lysoPtdEtn at doses of 50 and 150 μg/kg suppressed the plasma leakage by 17 and 36%, respectively, while that of 2-DHA-lysoPtdEtn at doses of 50 and 150 μg/kg caused ~42 and ~58% reduction of plasma leakage, respectively. The 50% effective dose (EC_{50}) for 2-ARA-lysoPtdEtn and 2-DHA-lysoPtdEtn was estimated to be about 221 and 111 μg/kg, respectively. By contrast, no remarkable inhibition of plasma was expressed by oral intake of DHA up to 150 μg/kg (data not shown), suggesting the structural importance of 2-ARA-lysoPtdEtn and 2-DHA-lysoPtdEtn.

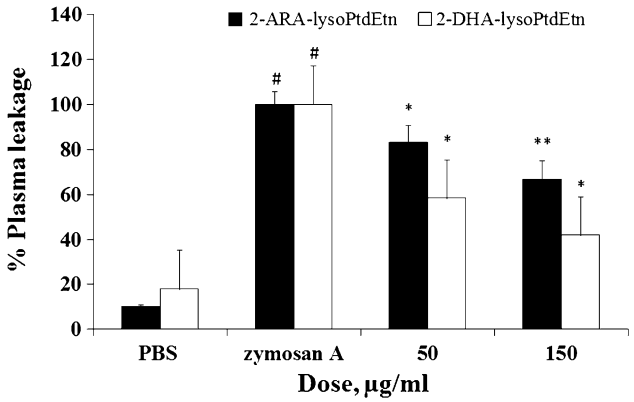

Fig. 2 Prevention by 2-ARA-lysoPtdEtn and 2-DHA-lysoPtdEtn against zymosan A-induced plasma leakage. 2-ARA-lysoPtdEtn (*filled*) or 2-DHA-lysoPtdEtn (*blank*) (50 or 150 μg/kg), diluted in ice cold PBS, was administered orally to mice, 1 h prior i.p. administration of zymosan A (1 mg/mouse), followed by intravenous injection of Evans blue (5% in PBS, 100 μl/mouse). Two hours later, plasma leakage was determined by measuring the absorbance of cell free-supernatant of lavages at 610 nm, and calculating the amount of Evans blue using a standard curve of known concentrations of the dye. The value was expressed as the percentage of the sample value of the value of the zymosan A-treated group. Result are presented as means ± SEM ($n = 5$). #, $P < 0.001$ when compared to PBS-treated group; *, $P < 0.05$ and; **, $P < 0.01$ when compared to zymosan A-treated group

Effect of the 15-LOX Inhibitor, administrated i.p., on Anti-inflammatory Action of 2-ARA-lysoPtdEtn and 2-DHA-lysoPtdEtn in Zymosan A-Induced Leukocyte Infiltration

Leukocyte extravasation is a subsequent event after the reversible opening of the endothelial cell tight junction at the onset of acute inflammation [32]. Therefore, in order to examine the ability of polyunsaturated lysoPtdEtn to regulate zymosan A-induced inflammation, the effect of 2-ARA-lysoPtdEtn or 2-DHA-lysoPtdEtn on zymosan A-induced leukocyte infiltration was investigated. As displayed in Fig. 3, 2-ARA-lysoPtdEtn and 2-DHA-lysoPtdEtn, orally administered, significantly ($P < 0.05$) prohibited the zymosan A-induced migration of leukocytes into the peritoneum in dose-dependent fashion; 2-ARA-lysoPtdEtn and 2-DHA at 150 μg/kg decreased total leukocyte infiltration by 56 and 60%, respectively, compared with the group challenged with zymosan A alone, suggesting that two lysoPtdEtn derivatives were potent inhibitors of leukocyte trafficking. The EC_{50} values for 2-ARA-lysoPtdEtn and 2-DHA-lysoPtdEtn were estimated to be about 123 and 110 μg/kg, respectively. However, such anti-inflammatory actions of 2-DHA-lysoPtdEtn or 2-ARA-lysoPtdEtn were completely reversed by concomitant treatment with PD146176, a specific 15-LOX inhibitor (Fig. 3), indicating that the action of 2-DHA-lysoPtdEtn or 2-ARA-lysoPtdEtn might be expressed mainly through the 15-LOX-induced oxygenation pathway.

Suppressive Effect of 2-ARA-lysoPtdEtn and 2-DHA-lysoPtdEtn on Zymosan A-Induced Formation of Pro-inflammatory Lipid Mediator in Peritoneum

In separate experiments, to investigate the mechanism responsible for the inhibitory effect of 2-ARA-lysoPtdEtn or 2-DHA-lysoPtdEtn on plasma leakage as well as leukocyte infiltration, the effect of 2-ARA-lysoPtdEtn or 2-DHA-lysoPtdEtn on zymosan A-induced formation of pro-inflammatory or anti-inflammatory lipid mediators was assessed. As displayed in Fig. 4a, oral administration of 2-ARA-lysoPtdEtn and 2-DHA-lysoPtdEtn significantly reduced zymosan A-induced formation of LTC_4 with EC_{50} values of about 132 and 84 μg/kg, respectively. Thus, 2-DHA-lysoPtdEtn was more potent than 2-ARA-lysoPtdEtn in suppressing the formation of LTC_4, an important vascular permeability inducer. Furthermore, Fig. 4b indicated that the formation of LTB_4, a potent chemoattractant lipid, was also diminished by 2-ARA-lysoPtdEtn

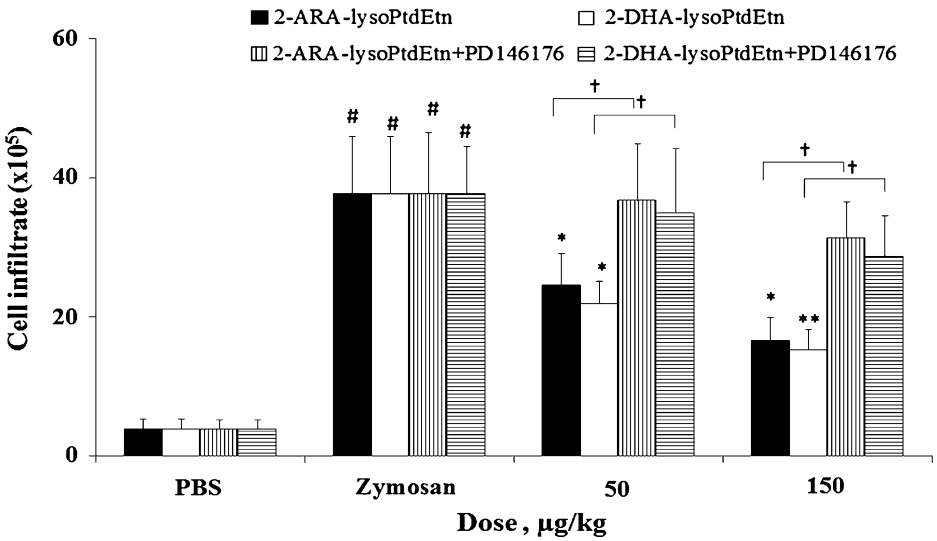

Fig. 3 Effect of 15-LOX inhibitor on anti-inflammatory action of 2-ARA-lysoPtdEtn or 2-DHA-lysoPtdEtn in zymosan A-induced leukocyte extravasation. Mice were orally given 2-ARA-lysoPtdEtn (*filled*) or 2-DHA-lysoPtdEtn (*blank*) (50 or 150 μg/kg) concurrently with or without PD146176 (i.p., 100 μg/mouse), 60 min prior i.p. administration of zymosan A (1 mg/mouse). Peritoneal lavages were collected after 4 h, and the total number of leukocyte was enumerated utilizing light microscopy after staining with trypan blue dye. Results are mean ± SEM. ($n = 5$). $^{\#}$, $P < 0.001$ when compared to PBS-treated group; *, $P < 0.05$; **, $P < 0.01$ when compared to zymosan A-treated group; †, $P < 0.05$, significant difference between treated groups

(EC_{50}, 139 μg/kg) and 2-DHA-lysoPtdEtn (EC_{50}, 211 μg/kg) in a dose-dependent manner, supporting the notion that the reduction of LTB_4 formation might be related to the suppressive effect of 2-polyunsaturated acyl-lysoPtdEtn on zymosan A-induced leukocyte extravasation. Additionally, the amount of 12-HETE, another chemo-attractant lipid mediator was also dose-dependently reduced by 2-ARA-lysoPtdEtn or 2-DHA-lysoPtdEtn (Fig. 4c), supporting the idea that the decrease of 12-HETE level might at least partially account for the suppressive effect of 2-polyunsaturated acyl-lysoPtdEtn on vascular permeability. Especially, 2-DHA-lysoPtdEtn almost completely inhibited 12-HETE formation at dose of 150 μg/kg. However, no significant alternation of PGE_2 level was observed after the treatment with 2-polyunsaturated acyl-lysoPtdEtn (not shown), suggesting that suppression of PGE_2 might not be responsible for the anti-inflammatory action of 2-polyunsaturated acyl-lysoPtdEtn.

Effect of 2-ARA-lysoPtdEtn and 2-DHA-lysoPtdEtn on Zymosan A-Induced Formation of Pro-inflammatory or Anti-inflammatory Cytokine

Production of both pro-inflammatory cytokines (e.g. IL-1, IL-6, TNF-α) and anti-inflammatory cytokines such as IL-10 is essential in the control of inflammation [1]. Here, we monitored a panel of cytokines in the exudate to assess whether 2-polyusaturated acyl-lysoPtdEtn could regulate their levels. Four hours after zymosan A treatment, most cytokine was dramatically up-regulated, compared to the control (Fig. 5). Of interest, 2-ARA-lysoPtdEtn and 2-docosahexaenoyl-lysoPtdEtn dose-dependently reduced the levels of pro-inflammatory cytokine including TNF-α, IL-1β or IL-6, while showing no significant effect on other pro-inflammatory cytokines such as IL-2 or IFN-γ (not shown). In the meantime, oral administration of 2-ARA-lysoPtdEtn and 2-DHA-lysoPtdEtn caused a dose-dependent elevation of anti-inflammatory cytokine, IL-10. Noticeably, 2-DHA-lysoPtdEtn and 2-ARA-lysoPtdEtn (150 μg/kg) increased the IL-10 level by approximately four- and five-fold, respectively, compared to the zymosan A-challenged group ($P < 0.05$).

Suppressive Effect of 2-polyunsaturated Acyl-lysoPtdEtn on Zymosan A-Induced NO Production in Plasma Leakage

Nitric oxide (NO) plays a key role in the inflammation process especially including regulation of inflammatory cell transmigration into the inflamed site and up-regulation of vascular permeability In zymosan A-induced peritonitis, NO is produced by activated macrophages and eventually be oxidized within few second to nitrite or nitrate [33]. Therefore, to examine whether 2-polyusaturated acyl-lysoPtdEtn could attenuate the level of NO, we determined the amount of NO formation in exudate. As expected, 2-DHA-lysoPtdEtn as well as 2-ARA-lysoPtdEtn, orally administered, drastically suppressed zymosan A-induced NO production in ICR mice (Fig. 6). Interestingly, 2-DHA-lysoPtdEtn (50 μg/kg) almost completely suppressed the

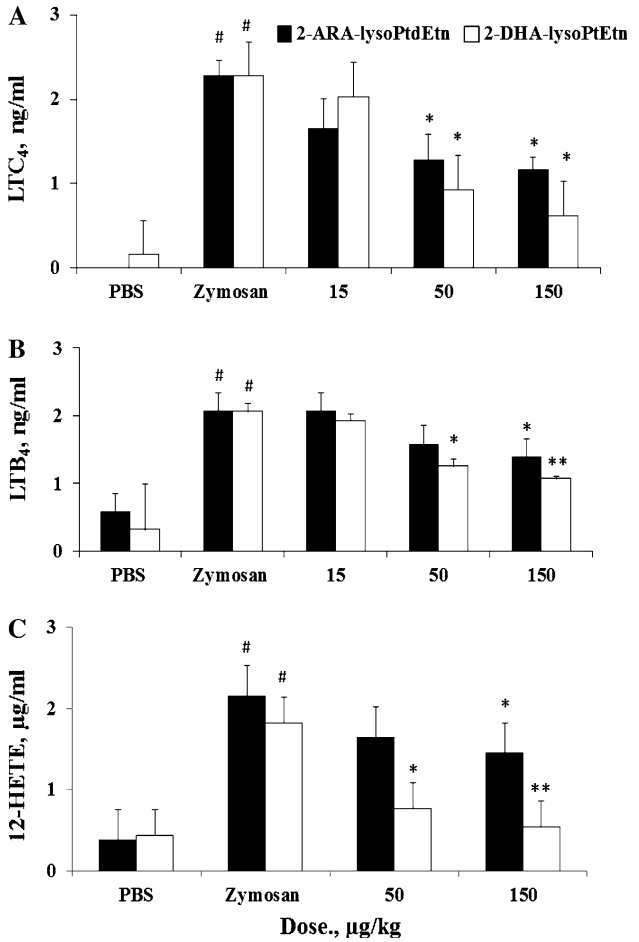

Fig. 4 Suppressive effect of 2-ARA-lysoPtdEtn or 2-docosahexaenoyl-lysoPtdEtn on zymosan A-induced pro-inflammatory lipid mediator formation in mice. Mice were orally given 2-ARA-lysoPtdEtn (*filled*) or 2-DHA-lysoPtdEtn (*blank*) (15–150 μg/kg) 60 min prior to administration of zymosan A (i.p., 1 mg/mouse). Peritoneal lavages were collected at 4 h and the level of pro-inflammatory lipid mediator in cell-free supernatant was assessed by an EIA kit according to the manual. Each sample was determined in duplicate. Results are means ± SEM ($n = 5$). #, $P < 0.001$ when compared to the PBS-treated group; *, $P < 0.05$; **, $P < 0.01$ when compared to zymosan A-treated group

NO formation caused by zymosan A stimulation; 2-ARA-lysoPtdEtn at 50 and 150 μg/kg diminished the NO level by 60 and 70%, respectively. Taken all together, it was suggested that at least some part of inflammatory action of 2-polyunsaturated lysoPtdEtn was ascribed to the inhibition of NO production.

Suppressive Effect of 2-(15-HETE)-lysoPtdEtn and 2-(17-HDHE)-lysoPtdEtn on Zymosan A-Induced Plasma Leakage and Leukocyte Infiltration

In a subsequent experiment, we elucidated which metabolic pathway is crucial for the anti-inflammatory action of 2-polyunsaturated acyl-lysoPtdEtn. Since 15-LOX activity, but not COX activity, was crucial for the anti-inflammatory action of 2-polyunsaturated lysoPtdEtn (Figs. 3, 4), we investigated the anti-inflammatory effect of 2-(15-HETE)-lysoPtdEtn and 2-(17-HDHE)-lysoPtdEtn, derived from 15-LOX-oxygenation of 2-ARA-lysoPtdEtn and 2-DHA-lysoPtdEtn, respectively, on zymosan A-induced peritonitis. As demonstrated in Fig. 7a, plasma leakage induced by zymosan A was suppressed by 2-(15-HETE)-lysoPtdEtn (EC_{50}, ~48 μg/kg) and 2-(17-HDHE)-lysoPtdEtn (EC_{50}, 42 μg/kg) in a dose-dependent manner. Of notice, Fig. 7b indicated that EC_{50} of 2-(15-HETE)-lysoPtdEtn and 2-(17-HDHE)-lysoPtdEtn was estimated to be about ~42 and 28 μg/kg, respectively. Especially, 2-(15-HETE)-lysoPtdEtn and 2-(17-HDHE)-lysoPtdEtn, orally administered at a dose as low as 50 μg/kg could almost completely suppress leukocyte infiltration. In comparison, it was found that the suppression effect of 2-(15-HETE)-lysoPtdEtn and 2-(17-HDHE)-lysoPtdEtn on leukocyte infiltration was more potent than that of 2-ARA-lysoPtdEtn (EC_{50}, ~123 μg/kg) and 2-DHA-lysoPtdEtn (EC_{50}, ~110 μg/kg), respectively ($P < 0.01$), indicating that oxidized derivatives were more potent than the corresponding polyunsaturated acyl lysoPtdEtn in expressing anti-inflammatory action in vivo. Taken together, these data indicate that 15-LOX oxygenation products of 2-polyunsaturated acyl-lysoPtdEtn could be active metabolites directly responsible for the anti-inflammatory action in vivo.

Effect of 2-ARA-lysoPtdEtn on the Formation of 15-HETE and LXA_4 in the Peritoneum of Mice

Previously, lysophospholipids administered to mice, were reported to be hydrolyzed by lipase activity [9] to release the hydrolysis product which in turn was converted to an active anti-inflammatory metabolite [12]. With this in mind, we examined the possible formation of 15-HETE and LXA_4 from 2-ARA-lysoPtdEtn in peritoneal exudate after oral administration of 2-ARA-lysoPtdEtn. Figure 8 indicates that oral administration of 2-ARA-lysoPtdEtn causes an increase in the level of 15-HETE (Fig. 8a) and LXA_4 (Fig. 8b) in the exudate; 2-ARA-lysoPtdEtn at 15, 50 and 150 μg/kg enhances 15-HETE level by approximately 3.5-, 5- and 9-fold, respectively, and the LXA_4 level by about 2-, 4- and 5.5-fold, respectively. However, the formation of 15-HETE was not significant in the exudate from mice administered with 2-ARA-lysoPtd in combination with PD146176 (100 μg/mouse) (data not shown). Separately, the 4 h hydrolysis of the exudate sample in 1 N NaOH was carried out to see the possible reincorporation of the 15-HETE product into the phospholipids. As illustrated in Fig. 8a, the amount of 15-HETE in hydrolyzed samples, obtained from alkaline hydrolysis of peritoneal exudates was apparently greater than that in the

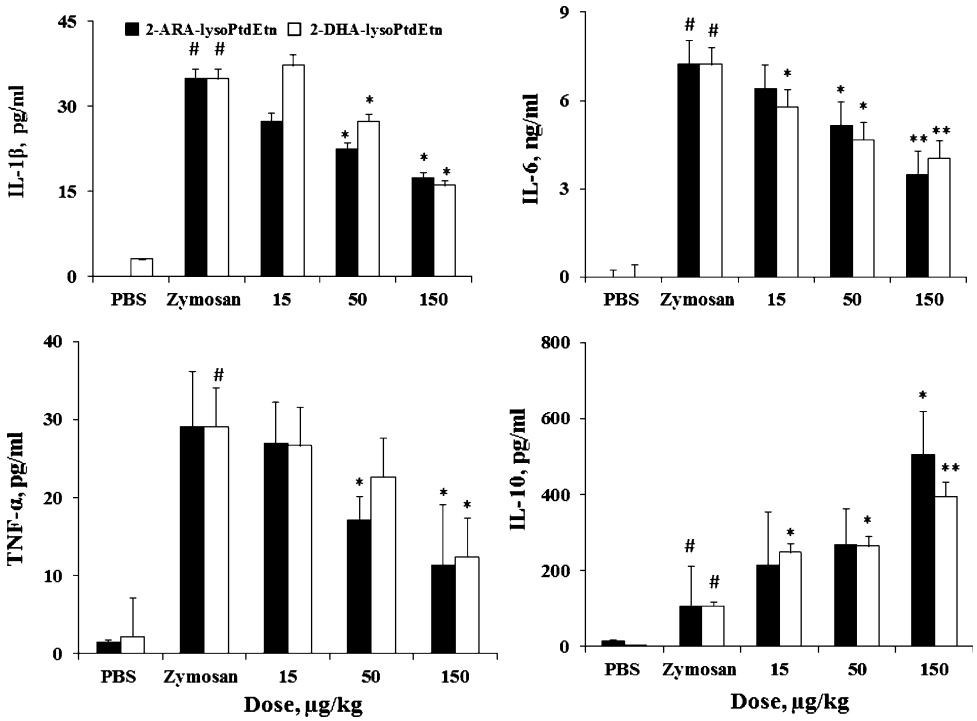

Fig. 5 Effect of 2-ARA-lysoPtdEtn or 2-docosahexaenoyl-lysoPtdEtn on zymosan A-induced pro-inflammatory and anti-inflammatory cytokine formation. Mice were orally given 2-ARA-lysoPtdEtn (*filled*) or 2-DHA-lysoPtdEtn (*blank*) (15–150 μg/kg) 60 min prior administration of zymosan A (i.p., 1 mg/mouse). Peritoneal lavages were collected at 4 h, and the cytokine level in cell-free supernatant was assessed by ELISA assay kit according to manufactures' protocol. Results are means ± SEM ($n = 5$). #, $P < 0.001$ when compared to PBS-treated group; *, $P < 0.05$; **, $P < 0.01$ when compared to the zymosan A-treated group

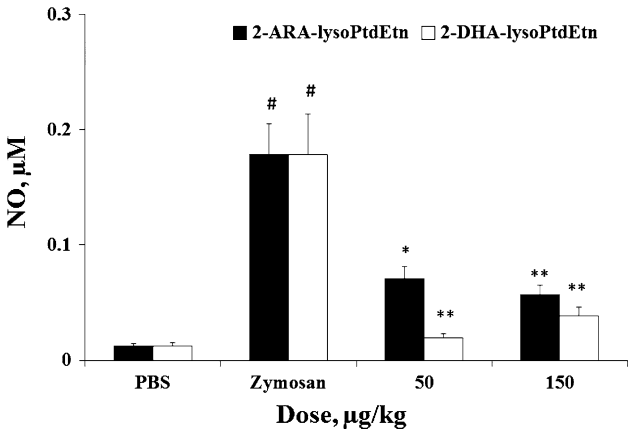

Fig. 6 Suppressive effects of 2-ARA-lysoPtdEtn and 2-docosahexaenoyl-lysoPtdEtn on zymosan A-induced formation of NO in mice. Mice were orally given 2-ARA-lysoPtdEtn (*filled*) or 2-DHA-lysoPtdEtn (*blank*) (15–150 μg/kg), 60 min prior to administration of zymosan A (i.p., 1 mg/mouse). Peritoneal lavages were collected at 4 h and the NO level in cell-free supernatant was measured by colorimetric assay according to the manufacturer's protocol. Results are means ± SEM ($n = 5$). #, $P < 0.001$ when compared to PBS-treated group; *, $P < 0.05$; **, $P < 0.01$ when compared to the zymosan A-treated group

corresponding non-hydrolyzed samples, suggesting that some part of 15-lipoxygenation products of 2-ARA-lysoPtdEtn, could exist as the lysophospholipid or phospholipid form. In contrast, there was no alteration of the 15-HETE level irrespective of alkaline hydrolysis in peritoneal samples from mice treated orally with 2-DHA-lysoPtdEtn up to 150 μg/kg (data not shown). From this, it was supposed that some part (<40%) of 15-HETE might be deposited in the lysophospholipid or phospholipid. The presence of lysophospholipid- and phospholipid-bound 15-HETE could provide a support for the 15-lipoxygenation of polyunsaturated acyl-lysoPtdEtn in vivo. Nonetheless, it is not excluded that free 15-HETE was reincorporated into the phospholipid.

Oral Administration of 2-Polyunsaturated Acyl-lysoPtdEtn Induced Resolution of Zymosan A Induced Peritonitis

In order to see whether 2-ARA-lysoPtdEtn and 2-DHA-lysoPtdEtn could attenuate the resolution of zymosan A-induced peritonitis, we examined the effect of 2-ARA-lysoPtdEtn and 2-DHA-lysoPtdEtn on zymosan A-induced leukocyte infiltration in ICR mice. In our previous data [9], it was observed that the total number of leukocytes infiltrated reached a maximum approximately 12 h after zymosan A treatment. Therefore, 2-ARA-lysoPtdEtn or 2-DHA-lysoPtdEtn was administered 12 h after zymosan A treatment to see their effect on the resolution phase in zymosan A-induced peritonitis. As shown in Fig. 9, 2-ARA-lysoPtdEtn or 2-DHA-lysoPtdEtn, orally administered at the peak of inflammation (12 h post-zymosan A treatment), effectively decreased the total leukocyte infiltration at the time points of 15, 20 and 24 h, whereas 2-ARA-lysoPtdEtn produced ~23, 21 and 33% reduction of total leukocyte number, respectively, 2-DHA-lysoPtdEtn gave approximate 29, 33 and 44% reduction. In summary,

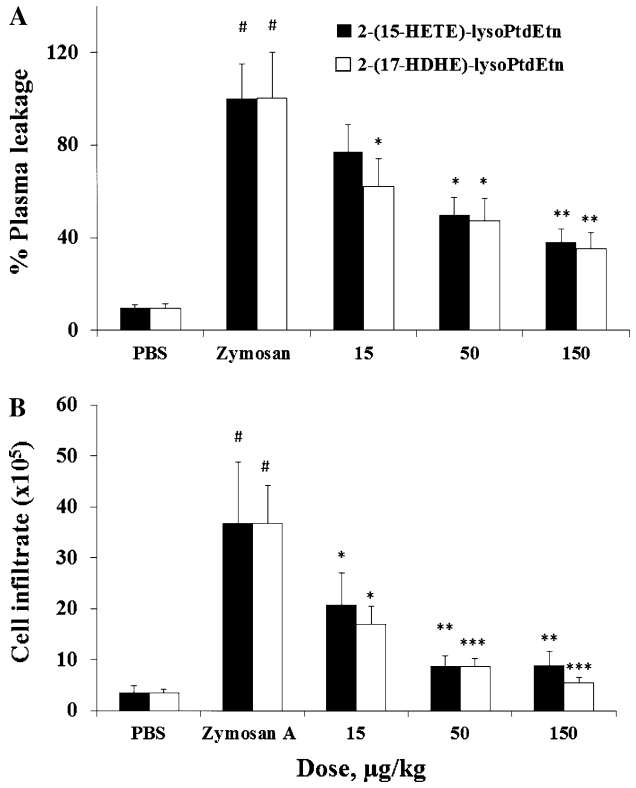

Fig. 7 Suppressive effect of hydroxyl derivatives of polyunsaturated acyl-lysoPtdEtn on zymosan A-induced plasma leakage or leukocyte infiltration. 2-(15-HETE)-lysoPtdEtn (*filled*) or 2-(17-HDHE)-lysoPtdEtn (*blank*) was orally administered to mice 60 min prior to the zymosan A challenge (1 mg/mouse; i.p.). Plasma leakage (**a**) and total leukocyte migration (**b**) was determined according to the methods described in Figs. 2 and 3, respectively. Results are means ± SEM ($n = 5$). #, $P < 0.001$ when compared to PBS-treated group; *, $P < 0.05$; **, $P < 0.01$, ***, $P < 0.001$ when compared to the zymosan A-treated group

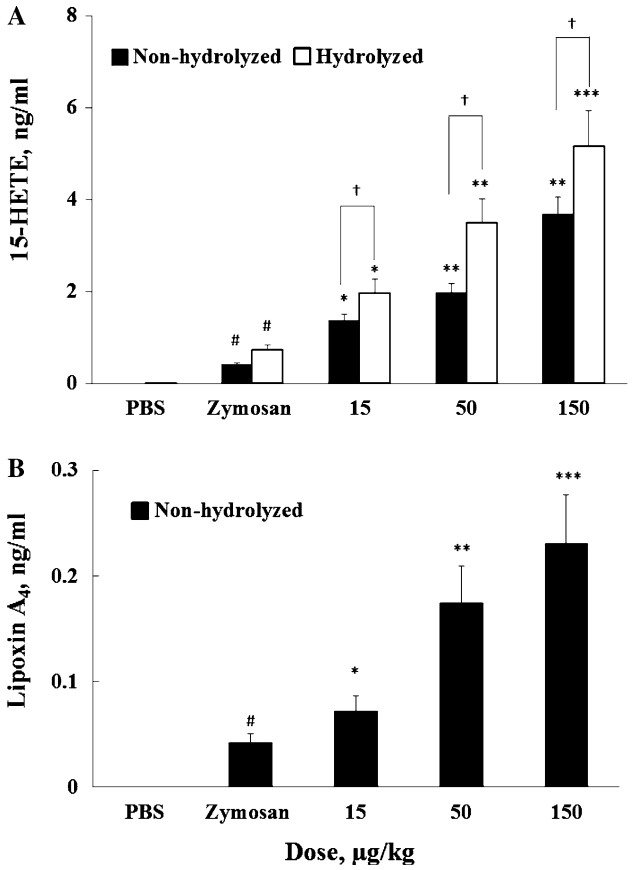

Fig. 8 Dose-dependent effect of 2-ARA-lysoPtdEtn on the level of 15-HETE or LXA_4 before or after alkaline hydrolysis of the exudate from mice. Mice were orally treated with 2-ARA-lysoPtdEtn, 60 min prior to administration of zymosan A (i.p., 1 mg/mouse). The exudate samples were collected at 120 min after zymosan A treatment, and then 15-HETE (**a**) or LXA_4 (**b**) in non-hydrolyzed (*filled*) or 1 N NaOH-hydrolyzed sample (*blank*) was extracted and determined by EIA kit according to manual. Results are means ± SEM ($n = 5$). #, $P < 0.01$ when compared to the PBS-treated group; *, $P < 0.05$; **, $P < 0.01$, ***, $P < 0.001$ when compared to the zymosan A-treated group; +, $P < 0.05$ was the significant difference between groups

it is suggested that 2-polyunsaturated acyl-lysoPtdEtn accelerates the resolution of zymosan A-induced peritonitis.

Discussion

Nowadays, inflammation has been recognized as the central component of many prevalent diseases such as atherosclerosis, cancer, asthma, autoimmune disease, stroke, Alzheimer's disease and Parkinson's disease [1]. Interestingly, it now become apparent that inflammation is a dynamic process with the participation of new family of endogenous anti-inflammatory and pro-resolving lipid mediators such as resolvins, maresin and protectin derived from omega 3-polyunsaturated fatty acids [4, 5, 34]. These lipid mediators, actively biosynthesized in the resolution phase of acute inflammation, control the duration and magnitude of inflammation [4]. Whereas anti-inflammatory actions of lipid mediators, derived from polyunsaturated fatty acids and polyunsaturated lysoPtCho, have been well-established [3, 4, 8, 9, 12, 35], the biological function of polyunsaturated lysoPtdEtn derivatives in inflammation has not been clarified yet. Very recently, we found that oral administration of 1-DHA-lysoPtCho prevented zymosan A-induced peritonitis [13]. In our present study, it is proposed that 2-polyunsaturated acyl lysoPtdEtns also effectively suppresses acute inflammation induced by zymosan A.

It has been known that induction of vascular permeability and leukocyte infiltration are important events of biological response at the onset of acute inflammation [36]. In the present work, the anti-inflammatory action of 2-ARA-lysoPtdEtn and 2-DHA-lysoPtdEtn was first substantiated by their effective prevention against zymosan A-induced plasma leakage with a potency similar to that of

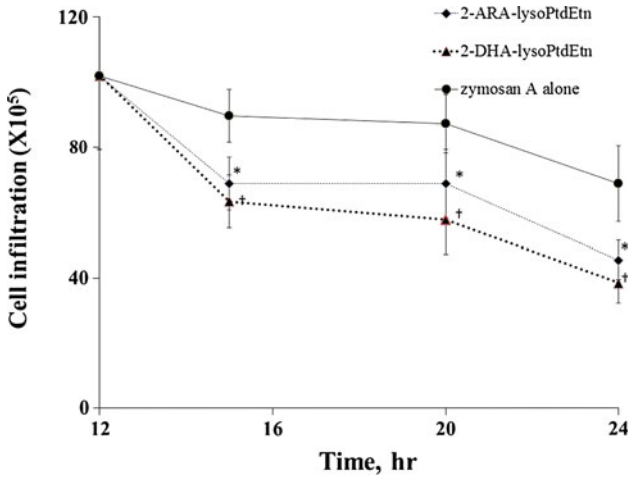

Fig. 9 Induction of resolving zymosan A-induced peritonitis by 2-ARA-lysoPtdEtn or 2-DHA-lysoPtdEtn. Mice were i.p. administered with zymosan A (1 mg/mouse) alone (*triangles*) or with either 2-ARA-lysoPtdEtn (*open circles*) or 2-DHA-lysoPtdEtn (*closed circles*) (12 h after zymosan A treatment). At the indicated periods, peritoneal lavage samples were collected and the total number of leukocyte infiltrated was enumerated according to the method described in Fig. 3. Results are means ± SEM ($n = 5$). *, $P < 0.05$; the 2-ARA-lysoPtdEtn-treated group vs. the zymosan A-treated group; †, $P < 0.05$, ††, $P < 0.01$, 2-DHA-lysoPtdEtn-treated group vs. zymosan A-treated group

polyunsaturated lysoPtCho [12]. Such a potent effect is possibly associated with the suppressive effect of 2-acyl-lysoPtdEtn on the formation of LTC_4 since early vascular permeability depends largely on cysteinyl-leukotriene (cysLT) released by resident peritoneal macrophages. Although vascular permeability is known to depend on PGE_2 from multiple cellular origins in zymosan A-induced peritonitis [26, 37], the level of PGE_2 was not altered by 2-polyunsaturated-lysoPtdEtn. Another mechanism possibly responsible for the anti-inflammatory action of polyunsaturated acyl lysoPtdEtns could be due to the decreased formation of NO, released from macrophages, which reversibly opens the endothelial cells tight junction leading to an enhancement of vascular permeability [33]. This might be partly supported by our present finding that the formation of NO in the peritoneum was reduced by 2-ARA-lysoPtdEtn and 2-DHA-lysoPtdEtn at relatively small doses.

In addition, the anti-inflammatory action of 2-polyunsaturated-lysoPtdEtn, represented by inhibition of leukocyte migration, could be related to the suppression of the formation of pro-inflammatory chemotactic lipid mediators. Support for this may come from the suppressive effect of 2-polyunsaturated-lysoPtdEtns on the formation of LTB_4 [4] and 12-HETE [38, 39], two potent arachidonate-derived chemo-attractants responsible for leukocyte infiltration in the initial process of the inflammatory phase. Moreover, the levels of representative pro-inflammatory cytokines (TNF-α, IL-1β, IL-6), possessing chemo-attractant properties [1, 40] were significantly diminished by 2-polyunsaturated-lysoPtdEtns. Noteworthy is that 2-polyunsaturated acyl-lysoPtdEtn up-regulated IL-10, a potent anti-inflammatory cytokine, secreted by macrophage in acute inflammation, which showed a tonic inhibitory effect on the leukocyte migration and the formation of pro-inflammatory cytokine (TNF-α, IL-1β, IL-6) as well as chemokines (MCP-1, MIP-1α and MIP-2) in zymosan A peritonitis [41]. Additionally, IL-10 could block NF-kB activation by stabilization of IkBα [42, 43], and in turn, inhibit the induction of inducible nitric oxide synthetase (iNOS), resulting in decreased formation of nitric oxide (NO). Furthermore, activation of human monocyte and monocyte-derived dendritic cells by cysteinylated leukotrienes was down-regulated by IL-10 [44]. Collectively, IL-10 could extensively regulate zymosan A-induced peritonitis through both direct and indirect manners.

In previous studies we proved that 15-lipoxygenase activity was necessary for the anti-inflammatory function of 2-polyunsaturated acyl-lysoPtCho in zymosan A-induced peritonitis [8, 9]. Our present study also indicated that 15-lipoxygenase activity was crucial for the anti-inflammatory function of 2-polyunsaturated acyl-lysoPtdEtn, since PD146176, a specific inhibitor of 15-LOX, suppressed the effect of 2-polyunsaturated acyl-lysoPtdEtn on leukocyte infiltration. In support of this, 2-(15-HETE)-lysoPtdEtn and 2-(17-HDHE)-lysoPtdEtn were more potent as anti-inflammatory lipids than 2-ARA-lysoPtdEtn and 2-DHA-lysoPtdEtn, respectively, supporting the assumption that the hydroxyl derivatives might be more direct precursors for active metabolites accounting for the anti-inflammatory action of 2-polyunsaturated acyl-lysoPtdEtn in vivo.

A pathway for further metabolism for 2-polyunsaturated acyl-lysoPtdEtn might be a hydrolytic process since a lipase activity capable of hydrolyzing polyunsaturated lysophospholipids had been reported to be available in an in vivo system [9]. In support of this notion, the formation of 15-HETE in the peritoneum was augmented in accordance with an increasing dose of 2-ARA-lysoPtdEtn, and diminished by PD146176, a specific inhibitor for 15-LOX. Therefore, 15-HETE-lysoPtdEtn metabolite, generated from the oxygenation of 2-ARA-lysoPtdEtn, orally administered, by 15-LOX, could serve as a source for the 15-HETE supplement in vivo. Noteworthy, the 15-HETE level of 1 N NaOH-hydrolyzed sample was significantly higher than that of non-hydrolyzed sample, suggesting two possibilities; some part of 2-(15-HETE)-lysoPtdEtn was still not hydrolyzed by lipase activity or 15-HETE, released from 2-(15-HETE)-lysoPtdEtn, could be re-incorporated into the lipid or lysophospholipid by the lysophospholipid acyltransferase activity [45] in the in vivo condition. It had

been previously reported that 15-HETE could be stored in the phospholipid, and the lipid after hydrolysis might be used as precursory substrate for LXA_4 formation [46]. In this regard, the dose-dependent increase of LXA_4 formation in the peritoneum after oral administration of 2-ARA-lysoPtdEtn may indicate that 15-HETE generated from 15-lipoxygenation of 2-ARA-lysoPtdEtn and subsequent enzymatic hydrolysis, was oxygenated by 5-LOX activity to produce 5-hydroperoxy, 15-hydroxyeicosatetraenoic acid, a direct precursor for LXA_4 and LXB_4 formation [47]. Likewise, it is quite possible that 2-DHA-lysoPtdEtn may be oxygenated to form 2-(17-hydroxyDHA)-lysoPtdEtn, which subsequently is hydrolyzed by a lipase activity to release 17-hydroxydocosahexaenoic acid (17-HDHE), a precursor for the formation of anti-inflammatory and proresolving lipid mediators such as protectin D [34] or resolvin D [32, 48]. Taken together, it is quite possible that the anti-inflammatory activity of 2-ARA-lysoPtdEtn and 2-DHA-lysoPtdEtn in zymosan A-induced peritonitis is the consequence of bioactive oxygenated lipid mediators. Besides, an additional mechanism for anti-inflammatory activity of 2-polyunsaturated acyl-lysoPtdEtn was reported to be related to the inhibition of 5-LOX activity by 15-HETE [49], resulting in the reduction of LTB_4 and LTC_4 level, as well as the suppression of LTB_4-evoked chemotaxis for leukocyte in acute inflammation [50]. Likewise, DHA [51] and 17-HDHE [52], generated from the metabolite of 2-DHA-lysoPtdEtn can indirectly or directly participate in the inhibition of 5-LOX activity, leading to the reduction of the leukotrienes level. As suggested from the present results, the anti-inflammatory action of 2-ARA-lysoPtdEtn in vivo might be at least partially ascribed to the effect of its oxygenated metabolites such as lipoxins (LXs). Previously, the anti-inflammatory activity of LXA_4 through various mechanistic routes has been well-established. For instance, LXs inhibit leukocytes activation, chemotaxis, adhesion, transmigration, and pro-inflammatory mediator generation [53, 54]. Additionally, it also inhibits the increase in vascular permeability triggered by activated leukocytes [55, 56]. Additionally, LXA_4 could diminish LTC_4-induced vascular permeability [56]. Noteworthy, LXA_4 formation could give an elevation of IL-10 level [57]. Meanwhile, the anti-inflammatory action of 2-DHA-lysoPtdEtn in vivo may be derived from the effect of its bioactive metabolites such as 17-HDHE or protectin D in vivo [27, 32]. 17-HDHE has been known to express the anti-inflammatory action through inhibition of the NF-κB pathway and down-regulation of 5-LOX expression in macrophages [52]. Besides, anti-inflammatory lipids such as protectin D1 or resolvin D [32, 48], presumably derived from the in vivo metabolism of 2-DHA-lysoPtdEtn, might be involved in its anti-inflammatory activity through suppression of leukocyte migration, down-regulation of pro-inflammatory cytokines, and inhibition of the NF-κB pathway. Since the anti-inflammatory effect of 2-DHA-lysoPtdEtn was almost completely reversed by a specific inhibitor of 15-LOX, it was suggested that maresin [5], formed via 12-LOX oxygenation pathway, might not be important for the anti-inflammatory action of 2-DHA-lysoPtdEtn [5]. Moreover, 2-DHA-lysoPtdEtn was not oxygenated by platelet 12-LOX (data not shown). Separately, the suppressive effects of 2-arachidonoyl-lysoPtdEtn and 2-DHA-lysoPtdEtn on leukocyte infiltration in the exudate in a later phase (12 h) of zymosan A-induced peritonitis may reflect their effects on pro-resolution through the removal of phagocytized cells [58]. Such a pro-resolving action of 2-polyunsaturated acyl-lysoPtdEtn may be related to the generation of bioactive metabolites such as LXA_4, resolving or protectin, responsible for resolution of acute inflammation [59].

An alternative mechanism accountable for the anti-inflammatory action of 2-ARA-lysoPtdEtn or 2-DHA-lysoPtdEtn could be re-acylation of the corresponding oxygenation product; 15-HETE or 17-HDHE into phospholipids [18, 60]. In an earlier study, 18:0/15-HETE-phosphatidylethanolamine derivatives, generated from the re-acylation of 15-HETE into lysophospholipid, was reported to inhibit the release of pro-inflammatory cytokine from lipopolysaccharide-stimulated monocytes [18]. Another plausible mechanism for the anti-inflammatory actions of 2-polyunsaturated acyl-lysoPtdEtn in vivo may be from the inhibitory effect 15-HETE and 17-HDHE on 12-LOX activity, responsible for 12-HETE formation, as suggested from a strong inhibition of 12/15 LOX by 15-HETE and 17-HDHE [61]. In agreement with this, the present study has shown that oral administration of 2-ARA-lysoPtdEtn and 2-DHA-lysoPtdEtn, precursors for formation of 15-HETE and 17-HDHE, respectively, diminished the level of 12-HETE in the peritoneum dose-dependently. In turn, the reduction of 12-HETE could result in abrogation of pro-inflammatory cytokine levels and monocyte chemoattractant protein (MCP-1) as had been reported previously [62–64]. Of note, the suppressive effect of 2-polyunsaturated acyl-lysoPtdEtns on zymosan A-induced 12-HETE formation in the present study was greater than that of 1-polyunsaturated acyl-lysoPtChos [9]. Taken together, the anti-inflammatory actions of 2-polyunsaturated acyl-lysoPtdEtn could be exerted through multiple mechanisms.

In conclusion, our present observations concerning the anti-inflammatory and pro-resolving activity of 2-polyunsaturated acyl-lysoPtdEtn may suggest that it can be a new anti-inflammatory lipid useful for the prevention as well as treatment of the zymosan A-induced peritonitis model. In future studies to expand its application, anti-inflammatory and pro-resolving activity of 2-polyunsaturated

acyl-lysoPtdEtn is to be studied using other inflammation models. Furthermore, the structural design to obtain more stable derivatives of 2-polyunsaturated acyl-lysoPtdEtn should be also considered to broaden the practical use of 2-polyunsaturated acyl-lysoPtdEtn as an anti-inflammatory lipid agent.

Acknowledgments This research was supported by the Basic Science Research Program through the National Research Foundation of Korea (NRF) funded by the Ministry of Education, Science and Technology (2010-0021372).

Conflict of interest There is no conflict of interest to declare.

References

1. Nathan C (2002) Points of control in inflammation. Nature 420:846–852
2. Gilroy DW, Lawrence T, Perretti M, Rossi AG (2004) Inflammatory resolution: new opportunities for drug discovery. Nat Rev Drug Discov 3:401–416
3. Serhan CN, Chiang N, Van Dyke TE (2008) Resolving inflammation: dual anti-inflammatory and pro-resolution lipid mediators. Nat Rev Immunol 8:349–361
4. Serhan CN, Savill J (2005) Resolution of inflammation: the beginning programs the end. Nat Immunol 6:1191–1197
5. Serhan CN, Yang R, Martinod K, Kasuga K, Pillai PS, Porter TF, Oh SF, Spite M (2009) Maresins: novel macrophage mediators with potent antiinflammatory and proresolving actions. J Exp Med 206:15–23
6. Schmitz G, Ruebsaamen K (2010) Metabolism and atherogenic disease association of lysophosphatidylcholine. Atherosclerosis 208:10–18
7. Ye XQ (2008) Lysophospholipid signaling in the function and pathology of the reproductive system. Hum Reprod Update 14:519–536
8. Huang LS, Hung ND, Sok DE, Kim MR (2010) Lysophosphatidylcholine containing docosahexaenoic acid at the *sn*-1 position is anti-inflammatory. Lipids 45:225–236
9. Hung ND, Kim MR, Sok DE (2011) Mechanisms for anti-inflammatory effects of 1-[15(S)-hydroxyeicosapentaenoyl] lysophosphatidylcholine, administered intraperitoneally, in zymosan A-induced peritonitis. Br J Pharmacol 162:1119–1135
10. Makide K, Kitamura H, Sato Y, Okutani M, Aoki J (2009) Emerging lysophospholipid mediators, lysophosphatidylserine, lysophosphatidylthreonine, lysophosphatidylethanolamine and lysophosphatidylglycerol. Prostaglandins Other Lipid Mediat 89:135–139
11. Sturm A, Zeeh J, Sudermann T, Rath H, Gerken G, Dignass AU (2002) Lisofylline and lysophospholipids ameliorate experimental colitis in rats. Digestion 66:23–29
12. Hung ND, Kim MR, Sok DE (2009) Anti-inflammatory action of arachidonoyl lysophosphatidylcholine or 15-hydroperoxy derivative in zymosan A-induced peritonitis. Prostaglandins Other Lipid Mediat 90:105–111
13. Huang LS, Kim MR, Sok DE (2007) Oxygenation of 1-docosahexaenoyl lysophosphatidylcholine by lipoxygenases; conjugated hydroperoxydiene and dihydroxytriene derivatives. Lipids 42:981–990
14. Huang LS, Kang JS, Kim MR, Sok DE (2008) Oxygenation of arachidonoyl lysophospholipids by lipoxygenases from soybean, porcine leukocyte, or rabbit reticulocyte. J Agric Food Chem 56:1224–1232
15. Huang LS, Kim MR, Sok DE (2009) Enzymatic reduction of polyunsaturated lysophosphatidylcholine hydroperoxides by glutathione peroxidase-1. Eur J Lipid Sci Tech 111:584–592
16. Olofsson KE, Andersson L, Nilsson J, Bjorkbacka H (2008) Nanomolar concentrations of lysophosphatidylcholine recruit monocytes and induce pro-inflammatory cytokine production in macrophages. Biochem Bioph Res Co 370:348–352
17. Wong JT, Tran K, Pierce GN, Chan ACOK, Choy PC (1998) Lysophosphatidylcholine stimulates the release of arachidonic acid in human endothelial cells. J Biol Chem 273:6830–6836
18. Morgan AH, Dioszeghy V, Maskrey BH, Thomas CP, Clark SR, Mathie SA, Lloyd CM, Kuhn H, Topley N, Coles BC, Taylor PR, Jones SA, O'Donnell VB (2009) Phosphatidylethanolamine-esterified eicosanoids in the mouse tissue localization and inflammation-dependent formation in th-2 disease. J Biol Chem 284:21185–21191
19. Tokumura A, Sinomiya J, Kishimoto S, Tanaka T, Kogure K, Sugiura T, Satouchi K, Waku K, Fukuzawa K (2002) Human platelets respond differentially to lysophosphatidic acids having a highly unsaturated fatty acyl group and alkyl ether-linked lysophosphatidic acids. Biochem J 365:617–628
20. Bligh EG, Dyer WJ (1959) A rapid method of total lipid extraction and purification. Can J Biochem Physiol 37:911–917
21. Yu S, Peng M, Ronis M, Badger T, Fang N (2010) Analysis of polar lipids in the serum from rats fed shiitake by liquid chromatography–mass spectrometry/mass spectrometry. J Agric Food Chem 58:12650–12656
22. Byrum RS, Goulet JL, Snouwaert JN, Griffiths RJ, Koller BH (1999) Determination of the contribution of cysteinyl leukotrienes and leukotriene b4 in acute inflammatory responses using 5-lipoxygenase- and leukotriene A4 hydrolase-deficient mice. J Immunol 163:6810–6819
23. Leite DFP, Echevarria-Lima J, Ferreira SC, Calixto JB, Rumjanek VM (2007) Abc transporter inhibition reduces zymosan-induced peritonitis. J Leukocyte Biol 82:630–637
24. Rao NL, Dunford PJ, Xue X, Jiang X, Lundeen KA, Coles F, Riley JP, Williams KN, Grice CA, Edwards JP, Karlsson L, Fourie AM (2007) Anti-inflammatory activity of a potent, selective leukotriene a4 hydrolase inhibitor in comparison with the 5-lipoxygenase inhibitor zileuton. J Pharmacol Exp Ther 321:1154–1160
25. Arita M, Bianchini F, Aliberti J, Sher A, Chiang N, Hong S, Yang R, Petasis NA, Serhan CN (2005) Stereochemical assignment, antiinflammatory properties, and receptor for the omega-3 lipid mediator resolvin E1. J Exp Med 201:713–722
26. Kolaczkowska E, Barteczko M, Plytycz B, Arnold B (2008) Role of lymphocytes in the course of murine zymosan-induced peritonitis. Inflamm Res 57:272–278
27. Sun YP, Oh SF, Uddin J, Yang R, Gotlinger K, Campbell E, Colgan SP, Petasis NA, Serhan CN (2007) Resolvin D1 and its aspirin-triggered 17r epimer. Stereochemical assignments, anti-inflammatory properties, and enzymatic inactivation. J Biol Chem 282:9323–9334
28. Bannenberg G, Moussignac RL, Gronert K, Devchand PR, Schmidt BA, Guilford WJ, Bauman JG, Subramanyam B, Perez HD, Parkinson JF, Serhan CN (2004) Lipoxins and novel 15-epi-lipoxin analogs display potent anti-inflammatory actions after oral administration. Brit J Pharmacol 143:43–52
29. Jeon SG, Moon HG, Kim YS, Choi JP, Shin TS, Hong SW, Tae YM, Kim SH, Zhu Z, Gho YS, Kim YK (2009) 15-lipoxygenase metabolites play an important role in the development of a T-helper type 1 allergic inflammation induced by double-stranded RNA. Clin Exp Allergy 39:908–917
30. Yuhki KI, Ushikubi F, Naraba H, Ueno A, Kato H, Kojima F, Narumiya S, Sugimoto Y, Matsushita M, Oh-Ishi S (2008)

Prostaglandin I-2 plays a key role in zymosan-induced mouse pleurisy. J Pharmacol Exp Ther 325:601–609
31. Hui SP, Chiba H, Jin S, Nagasaka H, Kurosawa T (2010) Analyses for phosphatidylcholine hydroperoxides by lc/ms. J Chromatogr B 878:1677–1682
32. Serhan CN, Hong S, Gronert K, Colgan SP, Devchand PR, Mirick G, Moussignac RL (2002) Resolvins: a family of bioactive products of omega-3 fatty acid transformation circuits initiated by aspirin treatment that counter proinflammation signals. J Exp Med 196:1025–1037
33. Guzik TJ, Korbut R, Adamek-Guzik T (2003) Nitric oxide and superoxide in inflammation and immune regulation. J Physiol Pharmacol 54:469–487
34. Bazan NG (2009) Neuroprotectin D1-mediated anti-inflammatory and survival signaling in stroke, retinal degenerations, and Alzheimer's disease. J Lipid Res 50(Suppl):S400–S405
35. Schwab JM, Chiang N, Arita M, Serhan CN (2007) Resolvin E1 and protectin D1 activate inflammation-resolution programmes. Nature 447:869–874
36. Medzhitov R (2008) Origin and physiological roles of inflammation. Nature 454:428–435
37. Kolaczkowska E, Shahzidi S, Seljelid R, van Rooijen N, Plytycz B (2002) Early vascular permeability in murine experimental peritonitis is co-mediated by resident peritoneal macrophages and mast cells: crucial involvement of macrophage-derived cysteinyl-leukotrienes. Inflammation 26:61–71
38. Goetzl EJ, Woods JM, Gorman RR (1977) Stimulation of human eosinophil and neutrophil polymorphonuclear leukocyte chemotaxis and random migration by 12-L-hydroxy-5,8,10,14-eicosatetraenoic acid. J Clin Invest 59:179–183
39. Kronke G, Katzenbeisser J, Uderhardt S, Zaiss MM, Scholtysek C, Schabbauer G, Zarbock A, Koenders MI, Axmann R, Zwerina J, Baenckler HW, van den Berg W, Voll RE, Kuhn H, Joosten LA, Schett G (2009) 12/15-lipoxygenase counteracts inflammation and tissue damage in arthritis. J Immunol 183(5):3383–3389
40. Van Assche G, Rutgeerts P (2005) Physiological basis for novel drug therapies used to treat the inflammatory bowel diseases—I. Immunology and therapeutic potential of antiadhesion molecule therapy in inflammatory bowel disease. Am J Physiol-Gastr L 288:G169–G174
41. Ajuebor MN, Das AM, Virag L, Flower RJ, Szabo C, Perretti M (1999) Role of resident peritoneal macrophages and mast cells in chemokine production and neutrophil migration in acute inflammation: Evidence for an inhibitory loop involving endogenous IL-10. J Immunol 162:1685–1691
42. Thelen M, Stein JV (2008) How chemokines invite leukocytes to dance. Nat Immunol 9:953–959
43. Malleo G, Mazzon E, Genovese T, Di Paola R, Caminiti R, Esposito E, Bramanti P, Cuzzocrea S (2008) Absence of endogenous interleukin-10 enhanced organ dysfunction and mortality associated to zymosan-induced multiple organ dysfunction syndrome. Cytokine 41:136–143
44. Woszczek G, Chen LY, Nagineni S, Shelhamer JH (2008) Il-10 inhibits cysteinyl leukotriene-induced activation of human monocytes and monocyte-derived dendritic cells. J Immunol 180:7597–7603
45. Brown WJ, Plutner H, Drecktrah D, Judson BL, Balch WE (2008) The lysophospholipid acyltransferase antagonist CI-976 inhibits a late step in copii vesicle budding. Traffic 9:786–797
46. Brezinski ME, Serhan CN (1990) Selective incorporation of (15s)-hydroxyeicosatetraenoic acid in phosphatidylinositol of human neutrophils—agonist-induced deacylation and transformation of stored hydroxyeicosanoids. Proc Natl Acad Sci USA 87:6248–6252
47. Schwab JM, Serhan CN (2006) Lipoxins and new lipid mediators in the resolution of inflammation. Curr Opin Pharmacol 6:414–420
48. Spite M, Norling LV, Summers L, Yang R, Cooper D, Petasis NA, Flower RJ, Perretti M, Serhan CN (2009) Resolvin D2 is a potent regulator of leukocytes and controls microbial sepsis. Nature 461(7268):1287–1291
49. Miller C, Yamaguchi RY, Ziboh VA (1989) Guinea pig epidermis generates putative anti-inflammatory metabolites from fish oil polyunsaturated fatty acids. Lipids 24:998–1003
50. Wu SH, Liao PY, Yin PL, Zhang YM, Dong L (2009) Elevated expressions of 15-lipoxygenase and lipoxin a(4) in children with acute poststreptococcal glomerulonephritis. Am J Pathol 174:115–122
51. Nauroth JM, Liu YC, Van Elswyk M, Bell R, Hall EB, Chung G, Arterburn LM (2010) Docosahexaenoic acid (DHA) and docosapentaenoic acid (DPAN-6) algal oils reduce inflammatory mediators in human peripheral mononuclear cells in vitro and paw edema in vivo. Lipids 45:375–384
52. Gonzalez-Periz A, Planaguma A, Gronert K, Miquel R, Lopez-Parra M, Titos E, Horrillo R, Ferre N, Deulofeu R, Arroyo V, Rodes J, Claria J (2006) Docosahexaenoic acid (DHA) blunts liver injury by conversion to protective lipid mediators: Protectin D1 and 17S-hydroxy-DHA. FASEB J 20:2537–2539
53. Maderna P, Godson C (2009) Lipoxins: revolutionary road. Br J Pharmacol 158:947–959
54. Filep JG, Zouki C, Petasis NA, Hachicha M, Serhan CN (1999) Anti-inflammatory actions of lipoxin A4 stable analogs are demonstrable in human whole blood: modulation of leukocyte adhesion molecules and inhibition of neutrophil-endothelial interactions. Blood 94:4132–4142
55. Takano T, Clish CB, Gronert K, Petasis N, Serhan CN (1998) Neutrophil-mediated changes in vascular permeability are inhibited by topical application of aspirin-triggered 15-epi-lipoxin A(4) and novel lipoxin B-4 stable analogues. J Clin Invest 101:819–826
56. Gronert K, Martinsson-Niskanen T, Ravasi S, Chiang N, Serhan CN (2001) Selectivity of recombinant human leukotriene D-4, leukotriene B-4, and lipoxin A(4) receptors with aspirin-triggered 15-epi-lxa(4) and regulation of vascular and inflammatory responses. Am J Pathol 158:3–9
57. Souza DG, Fagundes CT, Amaral FA, Cisalpino D, Sousa LP, Vieira AT, Pinho V, Nicoli JR, Vieira LQ, Fierro IM, Teixeira MM (2007) The required role of endogenously produced lipoxin A4 and annexin-1 for the production of IL-10 and inflammatory hyporesponsiveness in mice. J Immunol 179:8533–8543
58. Serhan CN (2008) Systems approach with inflammatory exudates uncovers novel anti-inflammatory and pro-resolving mediators. Prostag Leukotr Ess 79:157–163
59. Serhan CN (2007) Resolution phase of inflammation: novel endogenous anti-inflammatory and proresolving lipid mediators and pathways. Annu Rev Immunol 25:101–137
60. Matsumoto K, Morita I, Hibino H, Murota S (1993) Inhibitory effect of docosahexaenoic acid-containing phospholipids on 5-lipoxygenase in rat basophilic leukemia-cells. Prostag Leukotr Ess 49:861–866
61. Tsunomori M, Fujimoto Y, Muta E, Nishida H, Sakuma S, Fujita T (1996) 15-hydroperoxyeicosapentaenoic acid inhibits arachidonic acid metabolism in rabbit platelets more potently than eicosapentaenoic acid. Bba-Lipid Lipid Met 1300:171–176
62. Moreno JJ (2009) New aspects of the role of hydroxyeicosatetraenoic acids in cell growth and cancer development. Biochem Pharmacol 77:1–10
63. Chakrabarti SK, Cole BK, Wen YS, Keller SR, Nadler JL (2009) 12/15-Lipoxygenase products induce inflammation and impair insulin signaling in 3t3–l1 adipocytes. Obesity 17:1657–1663
64. Wen Y, Gu J, Chakrabarti SK, Aylor K, Marshall J, Takahashi Y, Yoshimoto T, Nadler JL (2007) The role of 12/15-lipoxygenase in the expression of interleukin-6 and tumor necrosis factor-alpha in macrophages. Endocrinology 148:1313–1322

Lipids (2011) 46:907–921
DOI 10.1007/s11745-011-3572-y

ORIGINAL ARTICLE

Pleiotropic Effects of a Schweinfurthin on Isoprenoid Homeostasis

Sarah A. Holstein · Craig H. Kuder · Huaxiang Tong · Raymond J. Hohl

Received: 20 January 2011 / Accepted: 12 May 2011 / Published online: 2 June 2011

Abstract The schweinfurthins, a family of natural products derived from the isoprenoid biosynthetic pathway (IBP), have marked growth inhibitory activity. However, the biochemical basis for the schweinfurthins cellular effects has remained ill-defined. Here, the effects of the synthetic schweinfurthin, 3-deoxyschweinfurthin (3dSB) on multiple aspects of isoprenoid homeostasis are explored. Cytotoxicity assays demonstrate a synergistic interaction between 3dSB and the HMG-CoA reductase inhibitor lovastatin but not with other IBP inhibitors in a variety of human cancer cell lines. The cytotoxic effects of 3dSB were enhanced in cells incubated in lipid-depleted serum. 3dSB was found to enhance the lovastatin-induced decrease in protein prenylation. In addition, 3dSB decreases intracellular farnesyl pyrophosphate and geranylgeranyl pyrophosphate levels in both established cell lines and primary cells. To determine whether 3dSB alters the regulation of expression of genes involved in isoprenoid homeostasis, real-time PCR studies were performed in human cell lines cultured in either lipid-replete or -deplete conditions. These studies demonstrate that 3dSB abrogates lovastatin-induced upregulation of sterol regulatory element-containing genes and lovastatin-induced downregulation of ABCA1. In aggregate, these studies are the first to demonstrate that a schweinfurthin exerts pleiotropic effects on isoprenoid homeostasis.

Keywords Isoprenoid · Schweinfurthin · Lovastatin · Farnesyl pyrophosphate · Geranylgeranyl pyrophosphate · Sterol · ABCA1 · Prenylation

Abbreviations

3dSB	3-Deoxyschweinfurthin B
ABCA1	ATP-binding cassette transporter 1
DGBP	Digeranyl bisphosphonate
ER	Endoplasmic reticulum
FCS	Fetal calf serum
FDPS	Farnesyl diphosphate synthase
FPP	Farnesyl pyrophosphate
FTase	Farnesyl transferase
GGDPS	Geranylgeranyl diphosphate synthase
GGPP	Geranylgeranyl pyrophosphate
GGTase	Geranylgeranyl transferase
GI_{50}	50% growth inhibition
HMGR	3-Hydroxy-3-methyl-glutaryl-CoA reductase
IBP	Isoprenoid biosynthetic pathway
LPDS	Lipoprotein deficient serum
LXR	Liver X receptor
MTT	3-(4,5-Dimethyl-2-thiazolyl)-2,5-diphenyl-2*H*-tetrazolium bromide
SRE	Sterol regulatory element
SREBP	Sterol regulatory element-binding protein
SS	Squalene synthase
ZA	Zoledronic acid
Zara	Zaragozic acid

Electronic supplementary material The online version of this article (doi:10.1007/s11745-011-3572-y) contains supplementary material, which is available to authorized users.

S. A. Holstein · C. H. Kuder · H. Tong · R. J. Hohl (✉)
Department of Internal Medicine, University of Iowa, Iowa City, IA 52242, USA
e-mail: raymond-hohl@uiowa.edu

R. J. Hohl
Department of Pharmacology, University of Iowa, 200 Hawkins Dr, SE 313 GH, Iowa City, IA 52242, USA

Introduction

Schweinfurthins are a family of natural compounds that were originally isolated from the leaves of the flowering tree *Macaranga schweinfurthii* in Western Cameroon [1]. The extracts from these leaves were noted to have potent growth inhibitory activity in the NCI 60-cell line cancer screen and subsequent isolation of the active components identified schweinfurthins A and B with mean GI_{50}'s of 0.36 and 0.81 μM, respectively [1]. Extensive structure–function analysis has provided insight into the key structural features which are necessary to retain schweinfurthin-like activity [2–7], but the mechanism of action has yet to be determined. Given the difficulty in isolating sufficient quantities of these compounds to allow for further biological exploration, a number of analogues have been prepared, including 3-deoxyschweinfurthin B (3dSB) (Fig. 1), which has a mean GI_{50} of 0.74 μM and has been shown to retain schweinfurthin-like activity [8].

The schweinfurthin family shares the common structural feature of having one or more prenyl side chains. The prenyl groups are derived from the isoprenoid biosynthetic pathway (IBP) which is responsible for the synthesis of all sterol and non-sterol isoprenoids (Fig. 1). In addition to the products displayed in Fig. 1, this pathway also leads to the synthesis of other biologically important molecules such as the ubiquinones, dolichols, and retinoids [9]. There is an extraordinary degree of complexity with regards to regulation of the IBP and sterol homeostasis [10]. The expression of the majority of the enzymes in the IBP are regulated through sterol regulatory element-binding protein (SREBP) transcription factors [11, 12]. In conditions of sterol depletion, SREBPs upregulate the expression of genes with SRE-containing promoters, leading to increased de novo synthesis of sterols and nonsterols as well as increased cellular uptake of sterols via the LDL receptor. Conversely, in conditions of sterol excess, SREBPs are sequestered in the endoplasmic reticulum (ER) via Insigs and there is upregulation of sterol efflux proteins such as ATP-binding cassette transporter 1 (ABCA1) via liver X receptor (LXR)-mediated regulation [13–15].

Sterols (including oxysterols, cholesterol, and lanosterol), nonsterols [e.g., farnesyl pyrophosphate (FPP) and geranylgeranyl pyrophosphate (GGPP)], and miRNA (MiR-33) have all been shown to be important regulators of isoprenoid homeostasis [16–21]. Furthermore, a multitude of natural products derived from the IBP have been demonstrated to affect IBP regulation and sterol homeostasis through a variety of mechanisms, including the diterpenes cafestol, Daphnetoxin and Gniditrin [22, 23], monoterpenes [24, 25], tocotrienols [26], and triterpenoids [27–29], further highlighting the extraordinarily complex relationship between the IBP and its products. Finally, select inhibitors of the IBP also alter regulation of the IBP and affect the expression of derivatives of the IBP [30–35]. Thus, given the extent to which IBP products and inhibitors can influence IBP regulation, we were interested in exploring the potential interaction between schweinfurthins

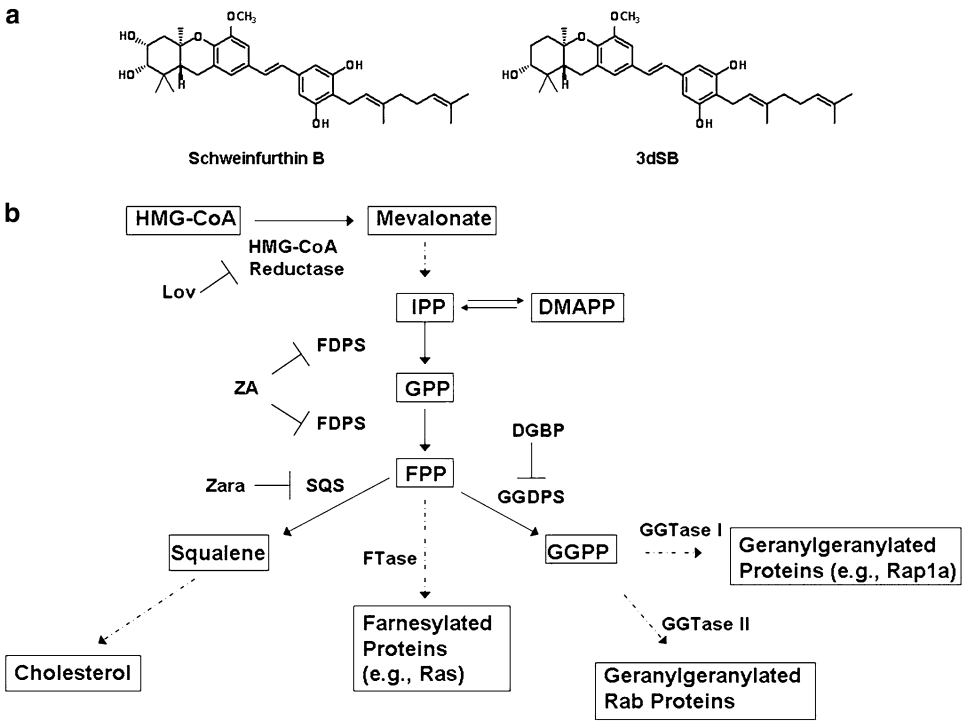

Fig. 1 **a** Structures of schweinfurthin B and 3-deoxyschweinfurthin B (3dSB). **b** The isoprenoid biosynthetic pathway (IBP) and pharmacological inhibitors. Abbreviations: *Lov* lovastatin, *ZA* zoledronic acid, *Zara* zaragozic acid, *DGBP* digeranyl bisphosphonate

and IBP inhibitors, determining the effects of schweinfurthins on isoprenoid homeostasis, and providing insight into the basis for schweinfurthins' biological activity. Here we demonstrate that the synthetic schweinfurthin 3dSB enhances inhibition of protein prenylation and induction of cytotoxicity in the setting of mevalonate depletion and reveal that 3dSB disrupts regulation of isoprenoid homeostasis.

Materials and Methods

Reagents

Lovastatin (converted to the dihydroxy-open acid form prior to use), DL-mevalonic acid lactone (converted to mevalonate prior to use), FPP, GGPP, and zaragozic acid were obtained from Sigma (St. Louis, MO). Zoledronic acid was purchased from Novartis (East Hanover, NJ). Digeranyl bisphosphonate (DGBP) [36] and 3-deoxy-schweinfurthin [5] were kindly supplied by Professor David Wiemer, Department of Chemistry, University of Iowa. 3dSB was dissolved in DMSO. Anti-pan-Ras was obtained from InterBiotechnology (Tokyo, Japan). Anti-β-tubulin, anti-Rap1a, anti-Rab6, and anti-goat IgG HRP antibodies were purchased from Santa Cruz Biotechnology (Santa Cruz, CA). Anti-mouse and anti-rabbit HRP-linked antibodies were obtained from Amersham (GE Healthcare, Piscataway, NJ). D*-GCVLS and D*-GCVLL (dansyl-labeled peptides) were obtained from Bio-Synthesis (Lewisville, TX). Rat recombinant FTase and GGTase I were purchased from Jena Biosciences (Jena, Germany). HPLC-grade water was prepared with a Milli-Q system (Millipore, Bedford, MA). All solvents were optima or HPLC grade. Lipoprotein deficient serum was obtained from Hyclone (Thermo Scientific, Logan, UT).

Cell Cultures

Human multiple myeloma (RPMI-8226 and U266) and human glioblastoma multiforme (SF-295) cell lines were purchased from American Type Culture Collection (Manassas, VA). A549 cells, a human non-small cell lung cancer cell line, were obtained from the NCI (Frederick, MD). Cells were grown in RPMI-1640 media with 10% (RPMI-8226, SF-295) or 15% (U266) heat-inactivated fetal calf serum supplemented with glutamine and penicillin–streptomycin at 37 °C and 5% CO_2. A549 cells were maintained in F-12 media supplemented with 10% fetal calf serum, glutamine, and penicillin–streptomycin. For the studies involving primary cells, after informed consent, peripheral blood samples were obtained from patients with acute leukemia. The protocol (IRB ID # 200610770) was approved by our Institutional Review Board for human subjects. Mononuclear cells were isolated from peripheral blood of patients with newly diagnosed acute leukemia and incubated ex vivo with 3dSB or lovastatin for 24 h. Formal pathological review of the bone marrow samples as well as cytogenetic analysis was performed by UIHC Hemato-pathology.

MTT Assay

For the suspension cell lines (RPMI-8226 and U266), cells were seeded (5×10^4/150 μL per well) in 96-well flat-bottom plates and incubated for 48 h at 37 °C and 5% CO_2 in the presence or absence of compounds. For the adherent cell lines (SF-295 and A549), cells were plated in 24-well plates, allowed to reach 65% confluency, and then incubated in the presence or absence of compounds for 48 h. MTT assays were performed as previously described [3, 43]. The absorbance for control untreated cells was defined as an MTT activity of 100%. DMSO treatment did not alter MTT activity by more than 5%.

Western Blot Analysis

Cells (5×10^6/5 mL) were incubated in the presence or absence of drugs. At the conclusion of the incubations, cells were collected, washed with PBS, and lysed in RIPA buffer (0.15 M NaCl, 1% sodium deoxycholate, 0.1% SDS, 1% Triton (v/v) X-100, 0.05 M Tris–HCl) containing protease and phosphatase inhibitors. Protein content was determined using the bicinchoninic acid method (Pierce Chemical, Rockford, IL). Equivalent amounts of cell lysate were resolved by SDS-PAGE, transferred to polyvinylidene difluoride membrane, probed with the appropriate primary antibodies, and detected using HRP-linked secondary antibodies and Amersham Pharmacia Biotech ECL Western blotting reagents per manufacturer's protocols.

Intracellular FPP and GGPP Measurements

Intracellular FPP and GGPP levels were measured using the previously reported reversed phase HPLC methodology [38]. Briefly, following incubation with drugs, cells were collected and counted using a hemocytometer. Isoprenoid pyrophosphates were extracted from cell pellets with extraction solvent (butanol/75 mM ammonium hydroxide/ethanol 1:1.25:2.75). Following drying down by nitrogen gas, the FPP and GGPP in the residue were incorporated into fluorescent GCVLS or GCVLL peptides by farnesyltransferase or geranylgeranyl transferase I, respectively. The prenylated fluorescent peptides were separated and quantified by reversed phase HPLC with fluorescence detection.

HMGR Activity Assay

The HMG-CoA reductase assay kit was purchased from Sigma (St. Louis, MO) and the assay was performed according to manufacturer's specifications. This assay detects the oxidation of NADPH by HMGR in the presence of HMG-CoA. The decrease in absorbance at 340 nm over time was measured using a Molecular Devices SpectraMax M2e microplate reader. Measurements were taken every 25 s. Pravastatin, which was included in the kit, was used as the positive control. The reaction mixture was incubated in the presence or absence of varying concentrations of 3dSB.

Real-Time PCR

RPMI-8226 or U266 cells were grown in the presence or absence of drugs in media containing either standard FCS or 10% LPDS for 24 h. Each condition was performed in triplicate. RNA was isolated using an RNeasy kit (Qiagen, Valencia, CA) and a BioRad (Hercules, CA) cDNA synthesis kit was used to prepare cDNA. Primers for HMGR, FDPS, SS, GGDPS, SREBP-2, Insig-1, LXRα, ABCA1 and β-actin (Supplementary Table 1) were designed using PrimerQuest. Real-time PCR was performed on an Applied Biosystems Model 7900HT using an Applied Biosystems (Carlsbad, CA) reaction kit with SYBR green. Data were analyzed using ABI SDS 2.3 software and normalized to β-actin RNA. Quantities were determined using the relative standard curve method. Each sample was run in triplicate.

Statistical Analysis

Two-tailed t testing was used to calculate statistical significance for the studies involving measurement of FPP and GGPP levels. An α of 0.05 was set as the level of significance. Isobologram analysis was used to evaluate the data from the MTT assays via CalcuSyn software (Biosoft). The software analyzes drug interactions based on the method of Chou and Talalay [26]. Combination indices (CI) <0.8 were deemed synergistic, CI >1.2 antagonistic, and CI >0.8 but less than 1.2 were deemed additive. ANOVA was used to compare changes in gene expression level following treatment with two drugs (lovastatin alone, 3dSB alone, and the two in combination) under four sets of conditions (two cell lines, two media conditions). The gene expression levels were compared separately for each of the four conditions. Expression levels were log-transformed to satisfy the ANOVA assumptions of normality and equal variances. Differences in expression levels were evaluated with the two-sided pair-wise comparisons of the treatment groups. The False Discovery Rate approach using q values was applied to adjust for multiple comparisons [39, 40] (Supplementary Table 2). Pair-wise comparisons for which the q values were less than 0.05 were declared to be statistically significant. This criterion ensures that the expected proportion of incorrectly rejected pair-wise comparisons is no greater than 5%. SAS version 9.2 and R 2.11.1 were used for the analysis.

Results

The Combination of 3dSB and Lovastatin Induces Synergistic Cytotoxic Effects in Human Malignant Cell Lines

The cytotoxic effects of 3dSB, both alone and in combination with the HMGR inhibitor lovastatin, in MTT assays were assessed in two human multiple myeloma cell lines (RPMI-8226 and U266), a human glioblastoma multiforme cell line (SF-295) and a human non-small cell lung cancer cell line (A549) (Fig. 2a). The RPMI-8226 and SF-295 cells have been previously noted to be particularly sensitive to schweinfurthins with mean GI_{50}'s for schweinfurthin B of 15 and 24 nM, respectively [1]. The A549 cells, on the other hand, represent a relatively more resistant cell line, with a mean GI_{50} of 0.34 μM [1]. The U266 cell line was not part of the NCI 60-cell line panel, but was chosen for these studies based on our prior work which demonstrated resistance to select IBP inhibitors as a consequence of markedly elevated basal isoprenoid levels [41]. Consistent with the NCI findings for schweinfurthin B, the RPMI-8226 cells were noted to be the most sensitive to 3dSB with an IC_{50} of $\sim$150 nM and the A549 cells the least sensitive with an IC_{50} of 5 μM at 48 h. The SF-295 and U266 cells displayed intermediate sensitivity to 3dSB alone with IC_{50} values of 0.5 and 1 μM, respectively. Interestingly, the addition of lovastatin to 3dSB resulted in enhanced cytotoxicity in all four cells. The nature of this interaction was evaluated by isobologram analysis and determined to be synergistic (Table 1). Furthermore, when RPMI-8226 or U266 cells were incubated in media containing lipoprotein deficient serum (LPDS), the cytotoxicity of 3dSB, both alone (3dSB IC_{50} of 80 nM for RPMI-8226 and 0.3 μM for U266) and in combination with lovastatin, was increased (Fig. 2b). This suggested a dependence on sterol availability for 3dSB cytotoxicity.

To determine whether the synergistic interaction was unique to lovastatin, or was observed with other IBP inhibitors, additional MTT assays were performed in which cells were treated with 3dSB in the presence or absence of the FDPS inhibitor zoledronic acid (ZA), the GGDPS inhibitor digeranyl bisphosphonate (DGBP), or the squalene synthase inhibitor zaragozic acid (Zara). As shown in Table 1, none of these agents displayed a synergistic

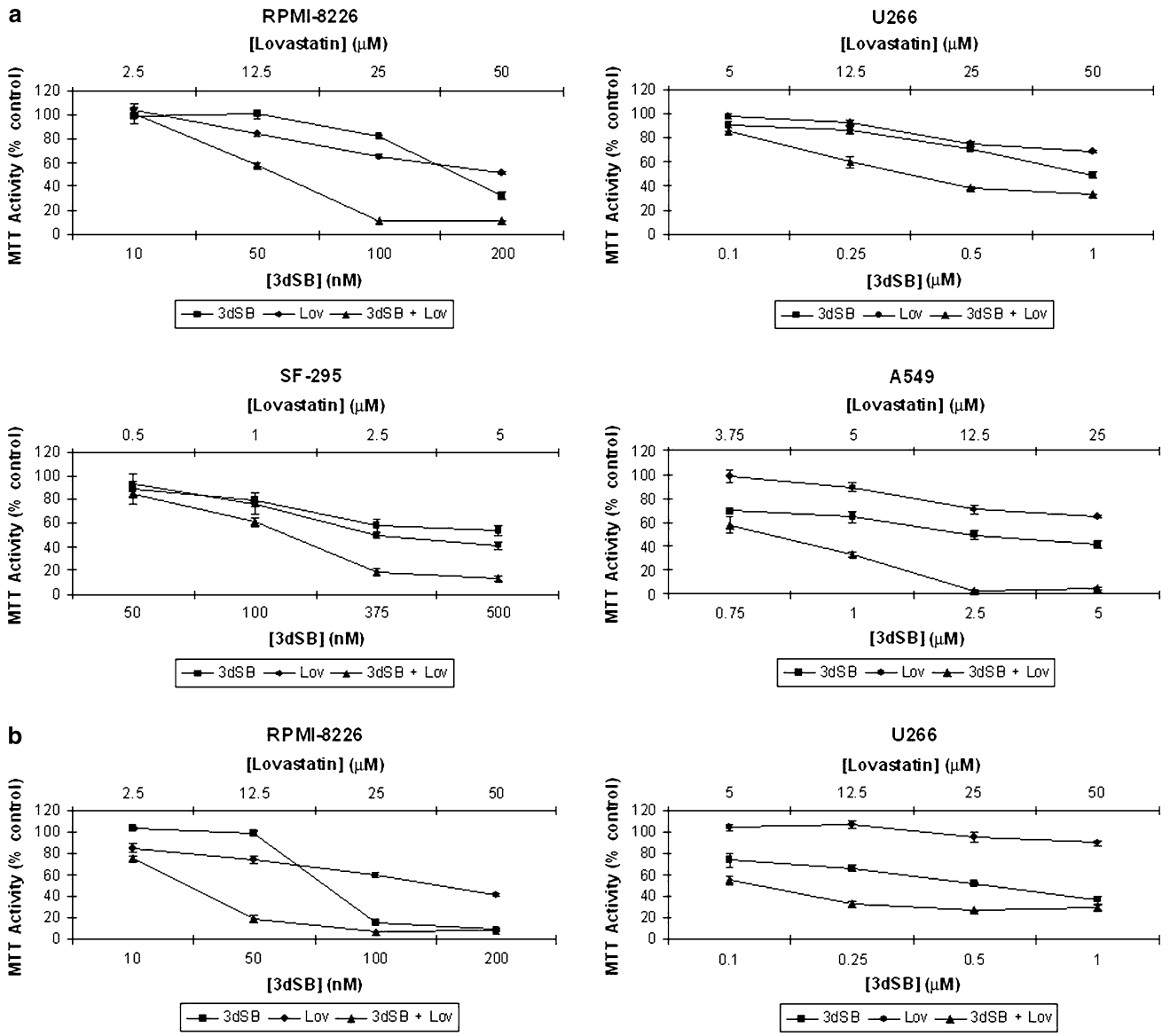

Fig. 2 The combination of lovastatin and 3dSB induces a synergistic cytotoxic effect in malignant cell lines. Cells were incubated for 48 h in the presence or absence of drugs and the MTT assay was performed as described in the "Materials and methods". **a** RPMI-8226, U266, SF-295, and A549 cells were incubated in standard FCS. **b** RPMI-8226 and U266 cells were incubated in LPDS. Data are expressed as a percentage of control (mean ± SD, $n = 4$) and are representative of at least two independent experiments

interaction with 3dSB. In particular, for the RPMI-8226 cells, both DGBP and ZA displayed an antagonistic interaction with 3dSB.

3dSB Enhances Lovastatin-Induced Decrease in Protein Prenylation

The pleiotropic effects of statins in malignant cells have generally been attributed to their ability to inhibit protein prenylation. To determine whether 3dSB, either alone or in combination with lovastatin, altered protein prenylation, immunoblot analysis was performed. Antibodies directed against Ras (substrate of FTase), Rap1a (substrate of GGTase I) and Rab6 (substrate of GGTase II) were utilized. For Ras and Rab6, the appearance of a more slowly migrating band represents unmodified protein, while for Rap1a, the antibody detects only unmodified protein. As shown in Fig. 3a, 3dSB alone has no effect on the prenylation status of the three proteins. As expected, lovastatin decreases both farnesylation and geranylgeranylation. Interestingly, 3dSB was noted to potentiate the effects of lovastatin in the RPMI-8226 cells as evidenced by the increase in the ratio of unmodified to modified protein for Ras and Rab6 and the increase in total unmodified protein

Table 1 Summary of 3dSB-IBP inhibitor interactions in MTT cytotoxicity assays

Combination	Cell line			
	RPMI-8226	U266	SF-295	A549
3dSB + Lov	Synergistic[a]	Synergistic[a]	Synergistic[a]	Synergistic[a]
3dSB + ZA	Additive[b]	Antagonistic[d]	Antagonistic/Additive[f]	ND
3dSB + DGBP	Antagonistic[c]	Antagonistic[d]	Additive[b]	ND
3dSB + Zara	Antagonistic[e]	Antagonistic[e]	ND	ND

Cells were incubated in standard FCS for 48 h in the presence of 3dSB and/or IBP inhibitors (*Lov* lovastatin, *ZA* zoledronic acid, *DGBP* digeranyl bisphosphonate, *Zara* zaragozic acid) prior to the addition of MTT salt. Combination indices (CI) for ED_{30} and ED_{50} (unless otherwise specified) were determined via isobologram analysis

ND Not determined

[a] CI < 0.8 as determined by isobologram analysis

[b] CI 0.8–1.2 as determined by isobologram analysis

[c] CI > 1.2 as determined by isobologram analysis

[d] MTT Activity of combination >3dSB alone as determined by two-tailed *t* testing

[e] CI's for ED_{20} and ED_{30} calculated

[f] CI antagonistic for ED_{30} and additive for ED_{50}

for Rap1a. This potentiation occurred in a concentration-dependent manner and was observed for all three prenylated proteins. This effect was particularly evident in cells incubated with LPDS; disruption of protein prenylation was not detected in cells treated with 2.5 μM lovastatin alone, but was detected when cells were co-incubated with ≥50 nM 3dSB. Minimal potentiation was noted when cells were incubated with 3dSB and either zoledronic acid or DGBP (Fig. 3a). 3dSB was also found to potentiate lovastatin's effects in U266 cells, particularly in cells treated with 2.5 μM lovastatin in either FCS or LPDS conditions (Fig. 3b). The effect of 10 μM lovastatin on disruption of protein prenylation in cells incubated with standard FCS was near maximal and the addition of 3dSB did not significantly alter the prenylation pattern.

To determine whether the induced changes in protein prenylation could be prevented by exogenous isoprenoid species, studies were performed in which RPMI-8226 or U266 cells incubated in media containing standard FCS were treated with 3dSB and/or lovastatin in the presence or absence of mevalonate or GGPP. As shown in Fig. 3c, addition of mevalonate or GGPP completely prevented the lovastatin- or lovastatin + 3dSB-induced decrease in Rap1a geranylgeranylation. Mevalonate completely prevented the disruption of Ras prenylation while GGPP only partially restored Ras prenylation, consistent with the ability of normally farnesylated N- and K-Ras isoforms to undergo geranylgeranylation when farnesylation is disrupted [42].

Effects of 3dSB on Intracellular FPP and GGPP Levels

As 3dSB alone did not appear to inhibit protein prenylation, but did potentiate lovastatin's effects, it was hypothesized that 3dSB could be altering isoprenoid availability. Therefore, the effects of 3dSB on intracellular FPP and GGPP levels were determined. Lovastatin, which depletes cells of both FPP and GGPP, was used as a positive control. As shown in Fig. 4a, 3dSB decreased both FPP and GGPP levels in a concentration-dependent manner in all tested cell lines, with the exception of the RPMI-8226 cells. In addition, 3dSB also variably decreased FPP and GGPP levels in primary human acute myeloid leukemia cells which were incubated with the drug in an ex vivo manner (Fig. 5).

The effects of 3dSB on FPP and GGPP levels were also evaluated in RPMI-8226 and U266 cells incubated with media containing LPDS. As shown in Fig. 4b, little effect was seen in the RPMI-8226 cells, but an enhanced depletion of FPP and GGPP levels was observed in the U266 cell line. As described previously [41], basal FPP levels are significantly higher in the U266 cell line compared with the RPMI-8226 line. Of note, incubation in LPDS-containing media significantly increased basal FPP (8.3-fold), but not GGPP levels in the U266 cells (Table 2), while basal levels of FPP and GGPP did not significantly change in RPMI-8226 cells. The LPDS-induced increase in FPP observed in the U266 cells could be overcome by either lovastatin or 3dSB (Fig. 4b). Incubation of SF-295 and A549 cells in LPDS resulted in an approximately 1.5-fold increase in FPP and GGPP levels compared with cells incubated in standard FCS (Table 2).

To investigate the effect of combining 3dSB on IBP inhibitor-induced changes in FPP and GGPP levels, studies were performed in which U266 cells were treated with 3dSB and/or lovastatin, ZA, or DGBP. Consistent with our prior studies, treatment with ZA or DGBP only partially

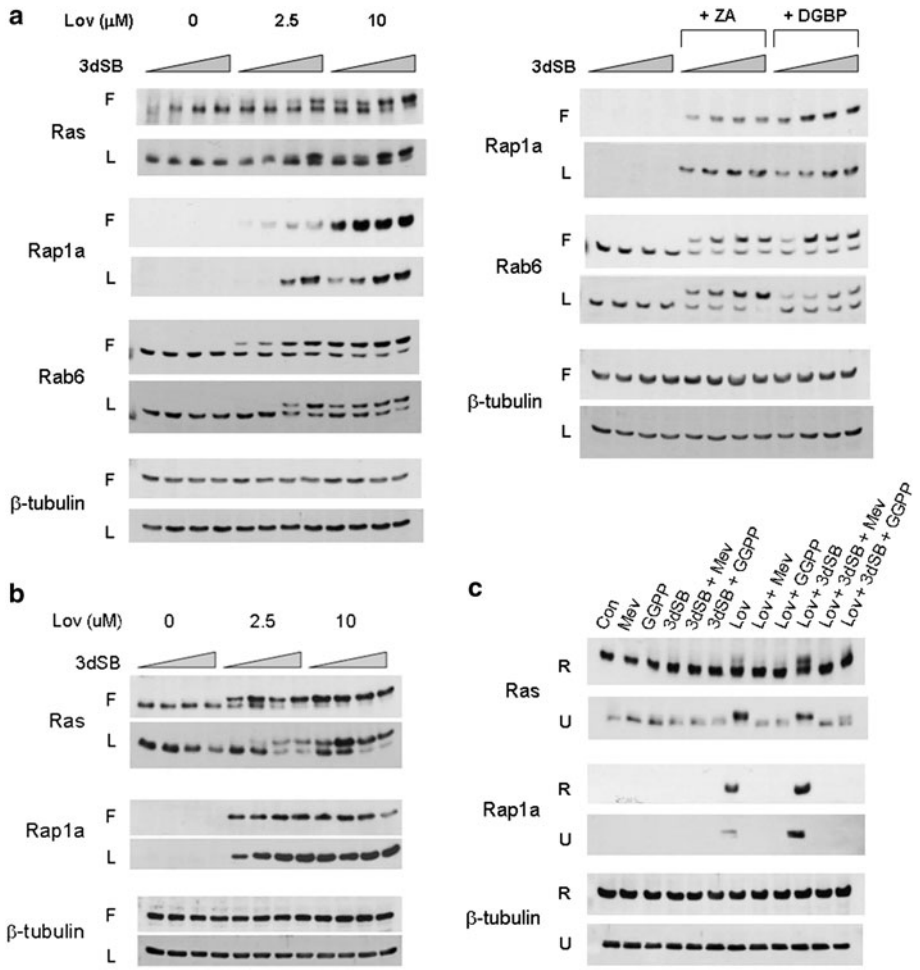

Fig. 3 3dSB potentiates lovastatin-induced decrease in protein prenylation. **a** RPMI-8226 or **b** U266 cells were incubated in the presence or absence of 3dSB ± IBP inhibitor (*Lov* lovastatin, *ZA* zoledronic acid (50 μM) or *DGBP* digeranyl bisphosphonate (2.5 μM)) in either standard FCS (F) or LPDS (L) for 24 h. The wedge indicates increasing concentrations of 3dSB (0, 10, 50, 100 nM for RPMI-8226 cells and 0, 0.1, 0.5, 1 μM for U266 cells). **c** Lovastatin- or lovastatin + 3dSB-induced decrease in protein prenylation is prevented by co-incubation with select isoprenoid intermediates. RPMI-8226 (*R*) and U266 (U) cells were incubated for 24 h in media containing standard FCS in the presence or absence of lovastatin (10 μM), 3dSB (50 nM for RPMI-8226 and 1 μM for U266), mevalonate (1 mM), or GGPP (10 μM). Western blot analysis of Ras (more slowly migrating band represents unmodified Ras), Rap1a (antibody detects only unmodified Rap1a), Rab6 (more slowly migrating band represents unmodified Rab6) and *β*-tubulin (as a loading control) was performed. Data are representative of at least two independent experiments

depletes FPP or GGPP levels, respectively, in U266 cells incubated in standard FCS [43]. Interestingly, however, the addition of 3dSB to either ZA or DGBP results in a significant decrease in both FPP and GGPP levels. Similar results were observed when cells were incubated in media containing LPDS (Fig. 6). The lovastatin-induced depletion of FPP and GGPP was near maximal in U266 cells incubated with standard FCS and the addition of 3dSB did not significantly alter FPP or GGPP levels. In contrast, when cells were incubated with LPDS, the addition of 3dSB to lovastatin resulted in a further decrease in GGPP levels. In aggregate these studies demonstrate the ability of 3dSB to lower intracellular FPP and GGPP levels irrespective of the presence of agents which disrupt the IBP. Finally, the ability of 3dSB to directly inhibit HMGR was evaluated in an in vitro enzyme assay and inhibitory activity was not observed (Fig. 7).

The Effects of Exogenous Isoprenoids on 3dSB-Induced Cytotoxicity and FPP and GGPP Levels

Lovastatin-induced cytotoxicity has previously been shown to be prevented by co-incubation with select isoprenoid species [43]. To determine whether 3dSB-induced cytotoxicity could be similarly prevented, MTT experiments were performed in which RPMI-8226 and U266 cells were treated with 3dSB and/or lovastatin in the presence or

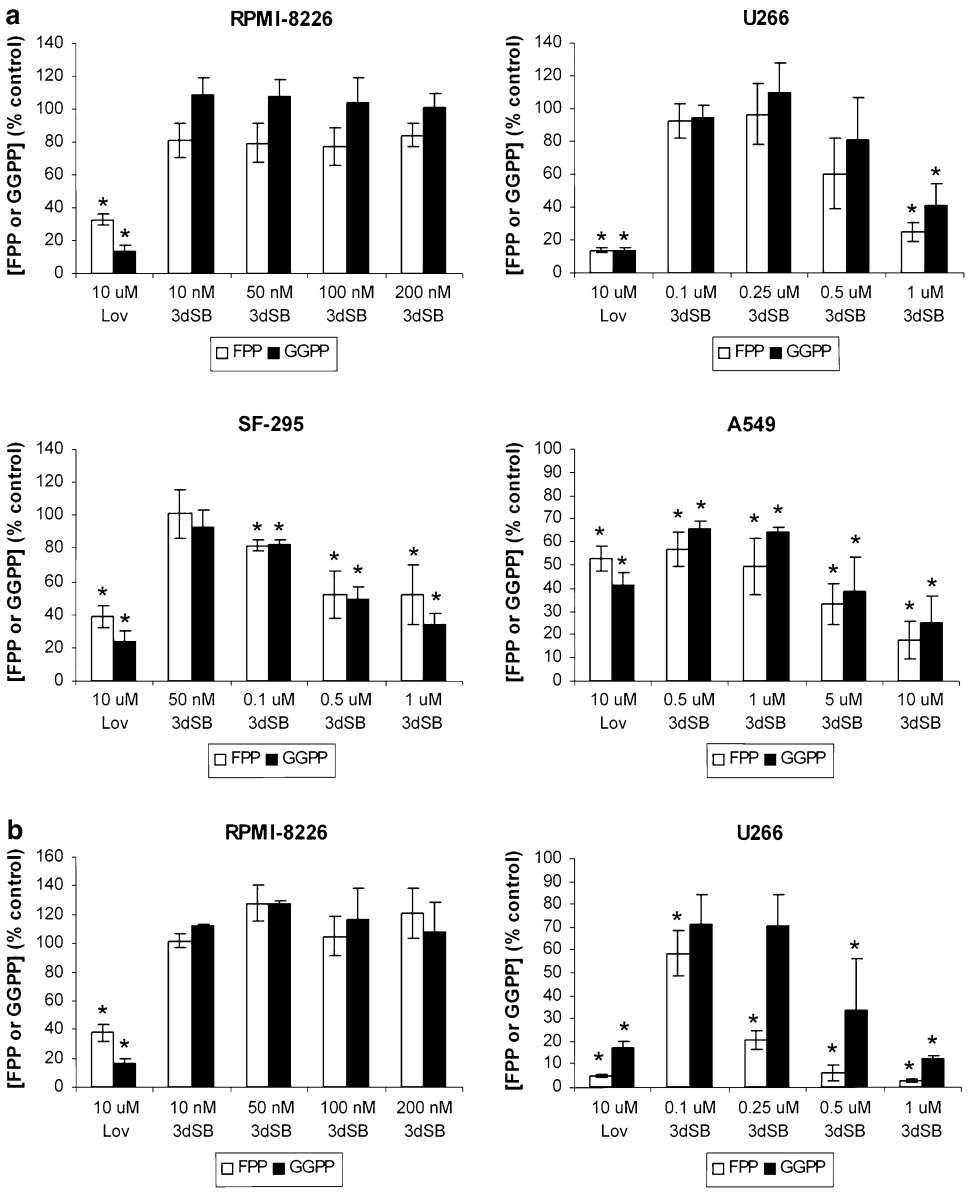

Fig. 4 Effects of 3dSB on intracellular FPP and GGPP levels. Cells were incubated in the presence of 3dSB or lovastatin (Lov) for 24 h in media containing either standard FCS (**a**) or LPDS (**b**). Intracellular FPP and GGPP levels were determined as described in the "Materials and methods" and are expressed as a percent of control (mean ± SD of three independent experiments). * Denotes $p < 0.05$ per unpaired two-tailed t test and compares the treated cells to the control untreated cells

absence of select isoprenoids (mevalonate, FPP, or GGPP). As shown in Fig. 8a, mevalonate or GGPP, and to a lesser extent FPP, could prevent lovastatin-induced cytotoxicity. However, none of the isoprenoid species prevented 3dSB-induced cytotoxicity. The enhanced cytotoxicity observed with the combination of 3dSB and lovastatin was only partially reversed by co-incubation with the isoprenoids. Co-incubation with either mevalonate or GGPP induced a level of cytotoxicity equivalent to 3dSB alone in the drug-combination treatment. To determine whether the add-back of isoprenoid species was effective in repleting FPP and GGPP levels in 3dSB and/or lovastatin-treated cells, levels of FPP and GGPP were measured in U266 cells. As shown in Fig. 8b, mevalonate most efficiently restored both FPP and GGPP levels in drug-treated cells. Incubation with exogenous FPP only partially restored FPP levels in drug-treated cells and had no effect on GGPP levels. Incubation with GGPP completely restored GGPP levels in either 3dSB- or lovastatin-treated cells and partially restored levels in 3dSB + lovastatin-treated cells. Thus, although incubation with exogenous isoprenoids (mevalonate/GGPP > FPP) restores isoprenoid levels in 3dSB-treated cells, this agent's cytotoxic effects are not significantly altered. In aggregate these data suggest that the mechanism underlying 3dSB's cytotoxic effects extends beyond this agent's ability to alter FPP and GGPP levels.

3dSB Disrupts Regulation of Isoprenoid Homeostasis

While lovastatin disrupts sterol homeostasis by targeting HMGR and inhibiting isoprenoid biosynthesis, it appeared that 3dSB might be more indirectly disrupting the IBP. To

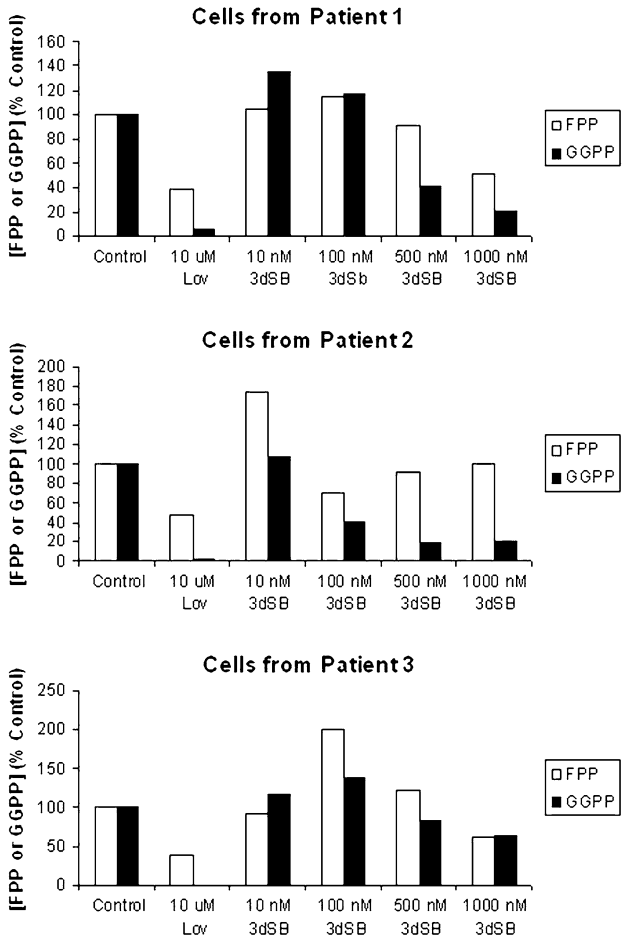

Fig. 5 Effect of 3dSB on FPP and GGPP levels in primary acute leukemia cells. Mononuclear cells were isolated from the peripheral blood of patients with newly diagnosed acute leukemia and incubated ex vivo with 3dSB or lovastatin for 24 h. All patients had greater than 40,000 K/mm^3 circulating blasts. Formal pathological review of the patient bone marrow samples revealed acute myelomonocytic leukemia for patient 1, acute myeloid leukemia with t(11;17) translocation for patient 2, and acute myeloid leukemia with aberrant CD7 expression for patient 3

address this hypothesis, real-time PCR was used to assess the effects of 3dSB, either alone or in combination with lovastatin, on the expression of key components of the IBP (HMGR, FDPS, SS, GGDPS) and regulators of sterol homeostasis (SREBP-2, Insig-1, LXRα, ABCA1). Treatment with lovastatin resulted in an increase in expression (1.5- to 4-fold) of the SRE-containing genes HMGR, FDPS, SS, SREBP-2, and Insig-1 in the RPMI-8226 and U266 cells under standard serum conditions while decreasing ABCA1 expression (Fig. 9). With the exception of HMGR (increase) and ABCA1 (decrease), 3dSB had little effect on any of the tested genes in the RPMI-8226 cell line, while in the U266 cells, statistically significant increases in HMGR, SS, SREBP-2, and Insig-1 levels were observed. Interestingly, 3dSB abrogated lovastatin-induced upregulation of HMGR,

Table 2 Effects of serum composition on basal FPP and GGPP levels

	FPP (pmol/10^6 cells) (Mean ± SD)	GGPP (pmol/10^6 cells) (Mean ± SD)
RPMI-8226, FCS	0.168 ± 0.030	0.273 ± 0.022
RPMI-8226, LPDS	0.122 ± 0.033	0.235 ± 0.096
U266, FCS	1.87 ± 0.271	0.682 ± 0.193
U266, LPDS	15.5 ± 1.25[a]	1.115 ± 0.223
SF-295, FCS	0.088 ± 0.002	0.367 ± 0.023
SF-295, LPDS	0.155 ± 0.005[a]	0.534 ± 0.032[a]
A549, FCS	0.146 ± 0.003	0.291 ± 0.031
A549, LPDS	0.242 ± 0.026[a]	0.460 ± 0.048[a]

Cells were incubated for 24 h in media containing either standard FCS or LPDS. FPP and GGPP levels were measured as described in the section "Materials and Methods". The means and standard deviations of the results of three independent experiments are shown

[a] $p < 0.05$ by two-tailed t testing comparing FCS to LPDS levels

FDPS, SS, and Insig-1 in the RPMI-8226 cell line while potentiating the upregulation of GGDPS. In contrast, in the U266 cell line, 3dSB minimally altered lovastatin-induced upregulation of HMGR, FDPS, SS, or SREBP-2 but enhanced the upregulation of GGDPS, LXR, and ABCA1 compared with either drug alone.

These studies were also performed with cells that had been incubated with LPDS (Fig. 9). Overall, there was little difference in effect on gene expression between the FCS- and LPDS-treated RPMI-8226 cells: lovastatin induced an increase in HMGR, FDPS, SS, SREBP-2, and Insig-1, had little effect on LXRα, and decreased ABCA1 expression. 3dSB induced minimal effects on HMGR and Insig-1levels. Likewise, as seen in the FCS-treated cells, the combination of lovastatin and 3dSB resulted in suppression of the lovastatin-induced increase in the SRE-dependent genes and an increase in GGDPS expression. While the effects of the drugs on the expression profile were concordant between FCS and LPDS conditions in the RPMI-8226 cells, there were profound differences noted between FCS and LPDS conditions in the U266 cell line. Notably, lovastatin failed to induce an increase in any of the tested SRE-containing genes. In addition, with the exception of SREBP-2, 3dSB markedly decreased the expression of the SRE-containing genes. Most striking was the greater than 60-fold increase in ABCA1 expression induced by 3dSB in the LPDS-treated U266 cells; an effect which was further enhanced by co-incubation with lovastatin.

Discussion

The basis for the schweinfurthins' potent cellular activities has thus far not been determined. In the studies presented

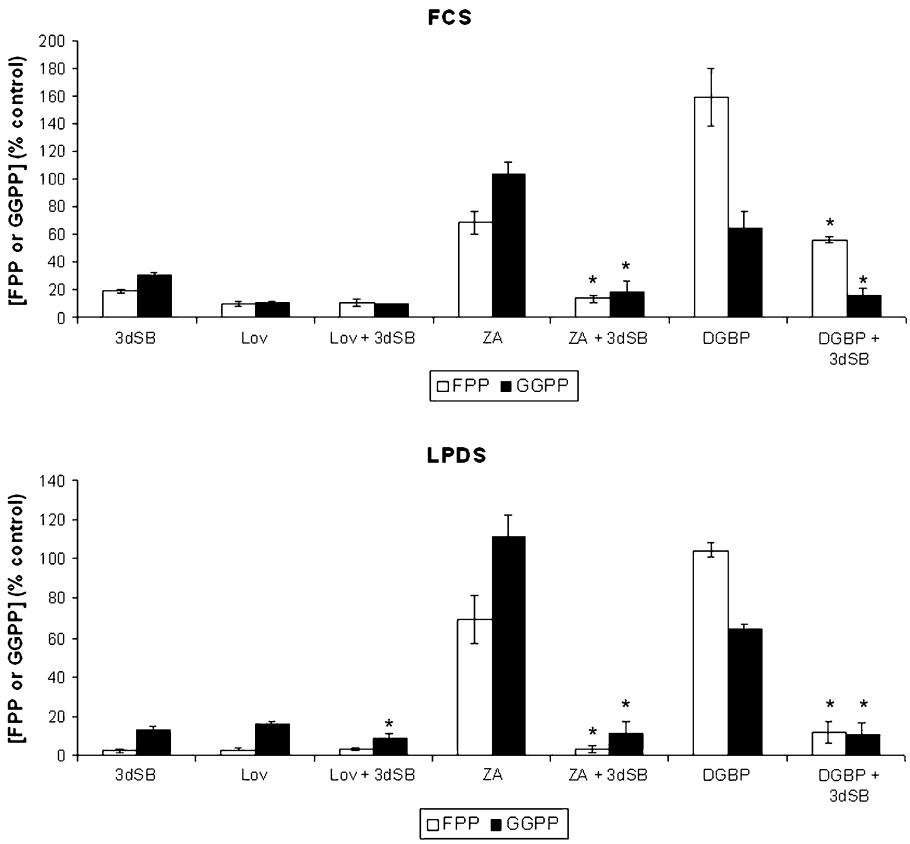

Fig. 6 Effects of 3dSB on IBP inhibitor-induced changes in FPP and GGPP levels in U266 cells. Cells were incubated in the presence or absence of 1 μM 3dSB and/or 10 μM lovastatin, 50 μM ZA, or 10 μM DGBP for 24 h in media containing either standard FCS or LPDS. Intracellular FPP and GGPP levels were determined as described in the section "Materials and Methods" and are expressed as a percentage of the control (mean ± SD of three independent experiments). The * denotes $p < 0.05$ per unpaired two-tailed t test and compares the IBP inhibitor + 3dSB combination to the IBP inhibitor alone

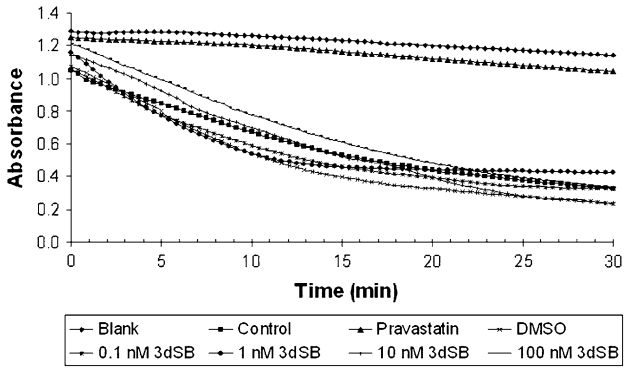

Fig. 7 3dSB does not inhibit HMGR in an in vitro enzyme assay. The enzyme assay was performed as described in the "Materials and methods" section. *Blank* represents reaction mixture lacking HMGR while *Control* represents the complete reaction mixture. Pravastatin was used as a positive control

herein we demonstrate that the synthetic schweinfurthin 3dSB has a very complex relationship with the IBP. In particular, 3dSB: (1) exerts a synergistic cytotoxic effect with the HMGR inhibitor lovastatin but additive or antagonistic effects with other IBP inhibitors, (2) enhances lovastatin-induced disruption of prenylation, (3) induces changes in intracellular FPP and GGPP levels, and (4) disrupts both SRE- and LXR-mediated regulation of genes involved in the IBP and sterol homeostasis. That these effects are enhanced under conditions of limited sterol availability, provides further evidence for the link between 3dSB and isoprenoid homeostasis.

The synergistic interaction between 3dSB and lovastatin is a consequence of lovastatin's ability to deplete cells of one or more down-stream isoprenoids such as FPP, GGPP, or sterols. Notably, an antagonistic interaction was observed between 3dSB and agents that increase FPP levels but have disparate effects on GGPP and sterol synthesis (the GGDPS inhibitor DGBP and the squalene synthase inhibitor Zara), suggesting that the lovastatin/3dSB interaction is dependent on depletion of both nonsterols and sterols down-stream of FPP. Furthermore, 3dSB-induced cytotoxicity is enhanced under conditions of sterol depletion, providing further evidence for a connection between 3dSB activity and isoprenoid levels. In fact, 3dSB was found to decrease cellular FPP/GGPP levels in a variety of cultured and primary cells (Figs. 4, 5, 6). It is interesting to note that although 3dSB decreased FPP and GGPP to levels equivalent to lovastatin in the U266 cell line (Fig. 4), 3dSB alone did not decrease protein prenylation (Fig. 3). In addition, while 3dSB did not significantly alter FPP and GGPP levels in the RPMI-8226 cells, this agent did enhance lovastatin-induced decrease of protein prenylation

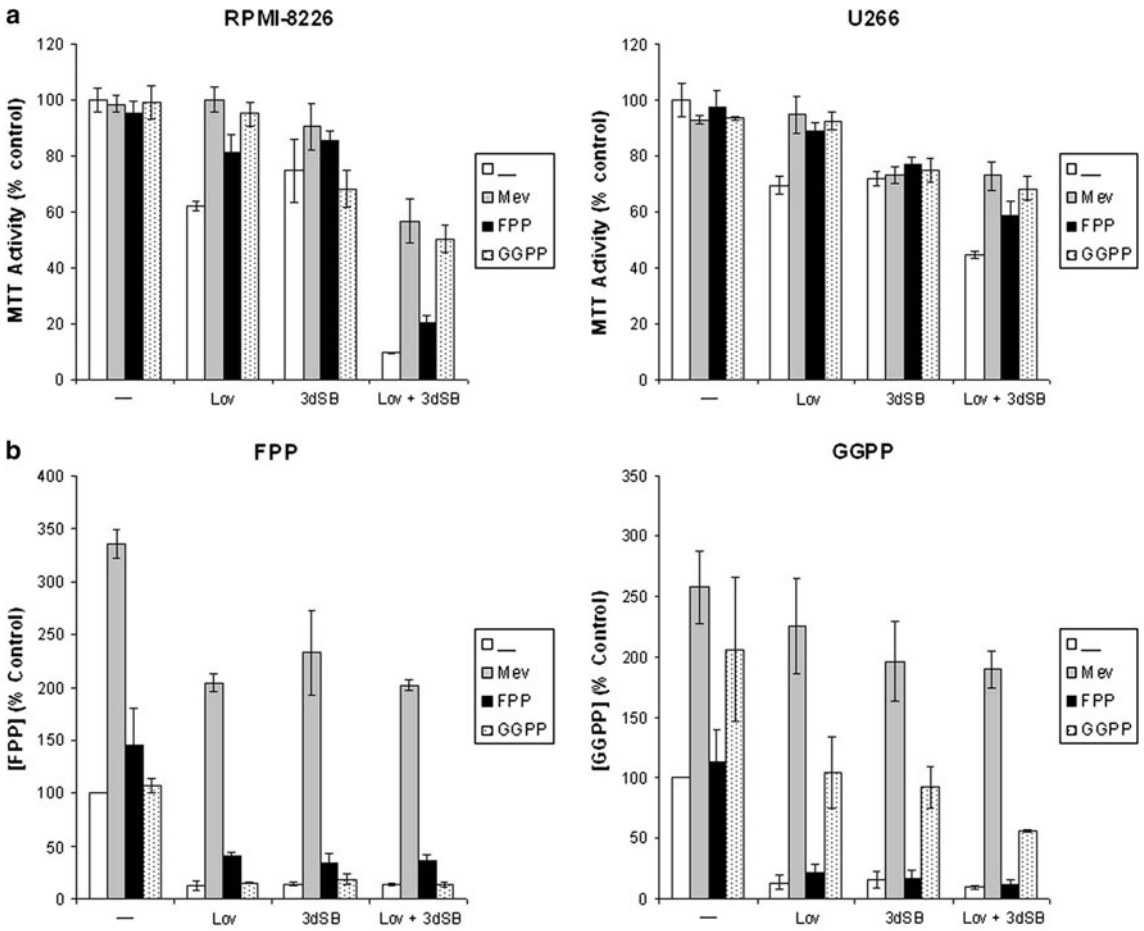

Fig. 8 **a** Add-back of select IBP intermediates prevents lovastatin-, but not 3dSB-induced cytotoxicity in RPMI-8226 and U266 cells. Cells were incubated for 48 h in the presence or absence of 25 μM lovastatin (Lov), 3dSB (0.1 μM for RPMI-8226 and 0.5 μM for U266), 1 mM mevalonate (Mev), 10 μM FPP or 10 μM GGPP. MTT assays were performed as described in the "Materials and methods". Data are expressed as a percent of control (mean ± SD, $n = 4$) and are representative of two independent experiments. **b** Effects of exogenous IBP intermediates on intracellular FPP and GGPP levels in U266 cells treated with 1 μM 3dSB and/or lovastatin for 24 h. Data are expressed as a percent of control (mean ± SD, $n = 3$ independent experiments)

(Fig. 3). These results, in conjunction with the finding that 3dSB-mediated enhancement of lovastatin-induced decrease of protein prenylation is further augmented in the presence of LPDS, suggests that these effects are not only due to changes in steady state levels of isoprenoids, but may also reflect alterations in flux through the pathway. The FPP/GGPP assay that was employed measures steady state total cellular FPP/GGPP levels. It remains to be determined whether shunting of isoprenoids to various branches of the IBP is altered in the presence of 3dSB. In addition, it is unknown whether there are discrete pools of these isoprenoid intermediates within the cell, and if so, whether 3dSB alters specific pools, thereby affecting substrate availability for disparate processes.

Further understanding of the mechanism(s) for 3dSB activity may be gained from the marked increase in FPP levels in U266 cells, but not in RPMI-8226 cells in response to incubation with LPDS. We have previously demonstrated that the U266 cell line is less sensitive than the RPMI-8226 cells to lovastatin and is resistant to downstream IBP inhibitors such as ZA and DGBP, likely a consequence of the markedly elevated basal FPP levels [43]. It has been noted that statin sensitivity in myeloma cell lines may be a consequence of altered HMGR regulation [44]. However, our work, which demonstrates a loss of lovastatin-induced upregulation of SRE-regulated genes in U266 cells incubated in LPDS-containing media suggests that statin-sensitivity is dependent on factors that extend beyond the level of HMGR regulation. In a similar manner, 3dSB-sensitivity may be a consequence of variation in isoprenoid pathway regulation.

In addition to revealing novel activities of 3dSB, these studies also provide insight into the regulation of isoprenoid levels. In our studies, GGDPS expression was minimally induced by either lovastatin or 3dSB alone, but was upregulated to a greater extent when the two agents were

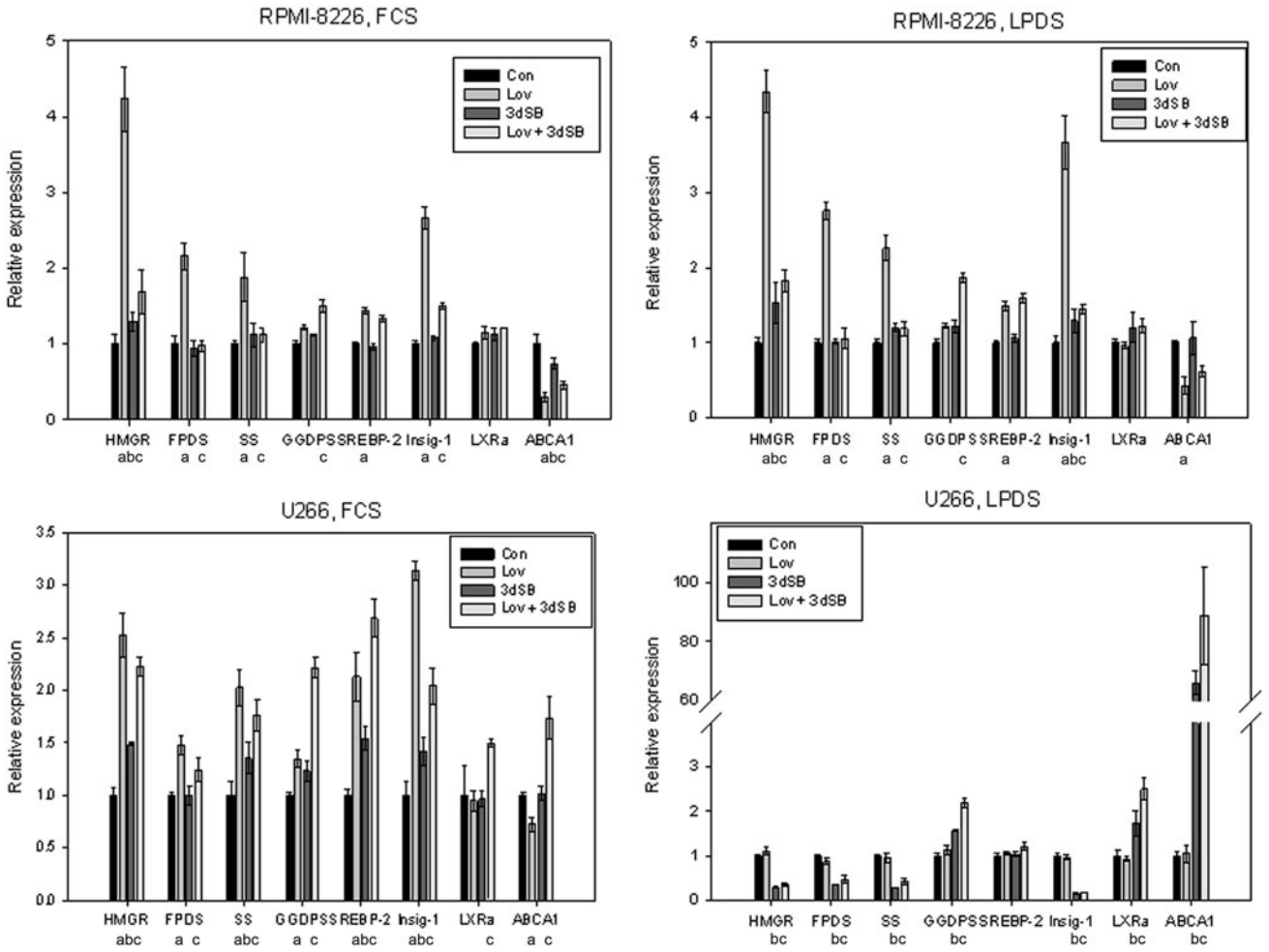

Fig. 9 3dSB induces alteration in expression of genes involved with isoprenoid homeostasis. RPMI-8226 or U266 cells were incubated for 24 h in the presence or absence of lovastatin (Lov, 10 μM) and/or 3dSB (0.1 μM for RPMI-8226 and 0.5 μM for U266) in either standard FCS or LPDS. Real-time PCR was performed using primers for HMG-CoA reductase (HMGR), farnesyl diphosphate synthase (FDPS), squalene synthase (SS), geranylgeranyl diphosphate synthase (GGDPS), SREBP-2, Insig-1, ABCA1 and LXRα. Data were normalized to β-actin levels and are expressed as relative to control untreated cells (mean ± SE, $n = 3$). Data are representative of two independent experiments. Statistical significance, as described in the "Materials and methods" (q value <0.05), is represented by "*a*" (lovastatin compared to control), "*b*" (3dSB compared to control), and "*c*" (3dSB + lovastatin compared to lovastatin)

used in combination (Fig. 9). This effect was particularly evident in the LPDS-treated cells. Analysis of FDPS has demonstrated that it is transcriptionally regulated by both SREBP and LXR [37, 45–47]. Less is known about the regulation of GGDPS. While one report in a transgenic system suggested that GGDPS is a target of SREBP, another demonstrated that GGDPS mRNA levels did not significantly change in HeLa cells incubated with either an HMGR inhibitor or with LPDS in the presence or absence of sterols [48, 49]. The product of this enzyme, GGPP, has been shown to serve as a negative regulator for LXR [21, 50]. Our results suggest that GGPP levels may in part regulate expression of GGDPS. Whether this is due to an effect on LXR activity or is via another mechanism remains to be determined.

The add-back experiments, which demonstrated that exogenous FPP/GGPP can restore isoprenoid levels in 3dSB-treated cells, but does not reverse the cytotoxic effects (Fig. 8), further suggest that 3dSB's effects extend beyond altering FPP and GGPP levels. In fact, we found that in RPMI-8226 cells, 3dSB abrogates statin-induced upregulation of SREBP-2-dependent genes as well as statin-induced downregulation of ABCA1 in both sterol replete (FCS) and deplete (LPDS) conditions (Fig. 9). In aggregate these data suggest that 3dSB shifts the cell's sterol regulatory pathways from a sterol-deficient state to a sterol-replete state. This hypothesis is further supported by the findings from the U266-LPDS studies. As noted in Table 2, U266 cells, in response to incubation with LPDS, markedly increase intracellular FPP levels, presumably in

an effort to compensate for the exogenous depletion of sterols. In this setting, 3dSB alone significantly downregulates SREBP-2-dependent genes while markedly upregulating ABCA1 (a LXRα-dependent gene). This pattern implies sterol excess. Possible mechanisms by which 3dSB could induce these changes include interference by 3dSB of the SRE-SREBP-2 interaction, disruption of SREBP-2 trafficking, direct activation of LXR, RXR or PPAR, or interference with the function of oxysterol binding proteins (OSBPs). A variety of oxysterols have been shown to be ligands for LXR and to induce LXR-target gene expression [51]. For example, the dietary plant sterol, stigmasterol, has been shown to induce ABCA1 expression and to suppress the SREBP pathway by promoting the formation of a Scap-SREBP-Insig-1 complex in the ER, thereby decreasing expression of SREBP target genes [16]. Whether 3dSB shares a similar mechanism of action, changes sterol levels, or alters the sterol-sensing machinery is of considerable interest and studies addressing these hypotheses are underway.

Schweinfurthin A has recently been shown to induce reorganization of the actin cytoskeleton and to inhibit EGF-induced Rho activation in serum-starved astrocytoma cells [52]. It is interesting to note that a variety of interactions have been described between OSBPs and elements of the cytoskeleton. For example, overexpression of ORP4S induced collapse of the vimentin network and inhibited LDL-cholesterol esterification while silencing of ORP3 resulted in reorganization of the actin cytoskeleton [53, 54]. It remains to be determined whether schweinfurthins, either directly or indirectly, interact with OSBPs, thereby impairing sterol sensing/trafficking and disrupting the cytoskeleton.

In conclusion, these studies are the first to demonstrate that the synthetic schweinfurthin 3dSB exerts pleiotropic effects on isoprenoid homeostasis. Specifically, 3dSB has a synergistic interaction with lovastatin, can alter steady state isoprenoid levels, and can disrupt multiple aspects of the regulatory elements controlling the IBP and sterol homeostasis. These studies, which advance understanding the basis for schweinfurthin activities, also indicate that there is a complexity to regulation of the isoprenoid pathway that is as yet unknown but may depend upon isoprenoid flux as compared to absolute isoprenoid levels.

Acknowledgments This project was supported by the Roy J. Carver Charitable Trust as a Research Program of Excellence and the Roland W. Holden Family Program for Experimental Cancer Therapeutics. S.A.Holstein was supported through a NIH T32 training [T32 HL07734] and a PhRMA Foundation Career Development Award. Brian Smith, PhD and Anna Button, MS from the University of Iowa Holden Comprehensive Cancer Center Biostatistics Core provided support with statistical analysis.

Conflict of interest Nothing to disclose.

References

1. Cuervo AM, Stefanis L, Fredenburg R, Lansbury PT, Sulzer D (2004) Impaired degradation of mutant alpha-synuclein by chaperone-mediated autophagy. Science 305:1292–1295
2. Ulrich NC, Kodet JG, Mente NR, Kuder CH, Beutler JA, Hohl RJ, Wiemer DF (2010) Structural analogues of schweinfurthin F: probing the steric, electronic, and hydrophobic properties of the D-ring substructure. Bioorg Med Chem 18:1676–1683
3. Kuder CH, Neighbors JD, Hohl RJ, Wiemer DF (2009) Synthesis and biological activity of a fluorescent schweinfurthin analogue. Bioorg Med Chem 17:4718–4723
4. Mente NR, Wiemer AJ, Neighbors JD, Beutler JA, Hohl RJ, Wiemer DF (2007)Total synthesis of (*R*,*R*,*R*)- and (*S*,*S*,*S*)-schweinfurthin F: differences of bioactivity in the enantiomeric series. Bioorg Med Chem Lett 17:911–915
5. Neighbors JD, Salnikova MS, Beutler JA, Wiemer DF (2006) Synthesis and structure-activity studies of schweinfurthin B analogs: Evidence for the importance of a D-ring hydrogen bond donor in expression of differential cytotoxicity. Bioorg Med Chem 14:1771–1784
6. Neighbors JD, Beutler JA, Wiemer DF (2005) Synthesis of nonracemic 3-deoxyschweinfurthin B. J Org Chem 70:925–931
7. Topczewski JJ, Kuder CH, Neighbors JD, Hohl RJ, Wiemer DF (2010) Fluorescent schweinfurthin B and F analogs with antiproliferative activity. Bioorg Med Chem 18:6734–6741
8. Hamadmad SN, Henry MK, Hohl RJ (2006) Erythropoietin receptor signal transduction requires protein geranylgeranylation. J Pharmacol Exp Ther 316:403–409
9. Holstein SA, Hohl RJ (2004) Isoprenoids: remarkable diversity of form and function. Lipids 39:293–309
10. Goldstein JL, Brown MS (1990) Regulation of the mevalonate pathway. Nature 343:425–430
11. Horton JD, Goldstein JL, Brown MS (2002) SREBPs: activators of the complete program of cholesterol and fatty acid synthesis in the liver. J Clin Invest 109:1125–1131
12. Brown MS, Goldstein JL (1997) The SREBP pathway: regulation of cholesterol metabolism by proteolysis of a membrane-bound transcription factor. Cell 89:331–340
13. Yang T, Espenshade PJ, Wright ME, Yabe D, Gong Y, Aebersold R, Goldstein JL, Brown MS (2002) Crucial step in cholesterol homeostasis: sterols promote binding of SCAP to INSIG-1, a membrane protein that facilitates retention of SREBPs in ER. Cell 110:489–500
14. Yabe D, Brown MS, Goldstein JL (2002) Insig-2, a second endoplasmic reticulum protein that binds SCAP and blocks export of sterol regulatory element-binding proteins. Proc Natl Acad Sci USA 99:12753–12758
15. Costet P, Luo Y, Wang N, Tall AR (2000) Sterol-dependent transactivation of the ABC1 promoter by the liver X receptor/retinoid X receptor. J Biol Chem 275:28240–28245
16. Yang C, McDonald JG, Patel A, Zhang Y, Umetani M, Xu F, Westover EJ, Covey DF, Mangelsdorf DJ, Cohen JC, Hobbs HH (2006) Sterol intermediates from cholesterol biosynthetic pathway as liver X receptor ligands. J Biol Chem 281:27816–27826
17. Marquart TJ, Allen RM, Ory DS, Baldan A (2010) miR-33 links SREBP-2 induction to repression of sterol transporters. Proc Natl Acad Sci USA 107:12228–12232
18. Rayner KJ, Suarez Y, Davalos A, Parathath S, Fitzgerald ML, Tamehiro N, Fisher EA, Moore KJ, Fernandez-Hernando C (2010) MiR-33 contributes to the regulation of cholesterol homeostasis. Science 328:1570–1573
19. Correll CC, Ng L, Edwards PA (1994) Identification of farnesol as the non-sterol derivative of mevalonic acid required for the

accelerated degradation of 3-hydroxy-3-methylglutaryl-coenzyme A reductase. J Biol Chem 269:17390–17393
20. Song BL, Javitt NB, DeBose-Boyd RA (2005) Insig-mediated degradation of HMG CoA reductase stimulated by lanosterol, an intermediate in the synthesis of cholesterol. Cell Metab 1:179–189
21. Gan X, Kaplan R, Menke JG, MacNaul K, Chen Y, Sparrow CP, Zhou G, Wright SD, Cai TQ (2001) Dual mechanisms of ABCA1 regulation by geranylgeranyl pyrophosphate. J Biol Chem 276:48702–48708
22. Zhang Y, Zhang H, Hua S, Ma L, Chen C, Liu X, Jiang L, Yang H, Zhang P, Yu D, Guo Y, Tan X, Liu J (2007) Identification of two herbal compounds with potential cholesterol-lowering activity. Biochem Pharmacol 74:940–947
23. Ricketts ML, Boekschoten MV, Kreeft AJ, Hooiveld GJ, Moen CJ, Muller M, Frants RR, Kasanmoentalib S, Post SM, Princen HM, Porter JG, Katan MB, Hofker MH, Moore DD (2007) The cholesterol-raising factor from coffee beans, cafestol, as an agonist ligand for the farnesoid and pregnane X receptors. Mol Endocrinol 21:1603–1616
24. Clegg RJ, Middleton B, Bell GD, White DA (1982) The mechanism of cyclic monoterpene inhibition of hepatic 3-hydroxy-3-methylglutaryl coenzyme A reductase in vivo in the rat. J Biol Chem 257:2294–2299
25. Clegg RJ, Middleton B, Bell GD, White DA (1980) Inhibition of hepatic cholesterol synthesis and S-3-hydroxy-3-methylglutaryl-CoA reductase by mono and bicyclic monoterpenes administered in vivo. Biochem Pharmacol 29:2125–2127
26. Chou TC, Talalay P (1984) Quantitative analysis of dose-effect relationships: the combined effects of multiple drugs or enzyme inhibitors. Adv Enzyme Regul 22:27–55
27. Einbond LS, Soffritti M, Esposti DD, Park T, Cruz E, Su T, Wu HA, Wang X, Zhang YJ, Ham J, Goldberg IJ, Kronenberg F, Vladimirova A (2009) Actein activates stress- and statin-associated responses and is bioavailable in Sprague-Dawley rats. Fundam Clin Pharmacol 23:311–321
28. Ondeyka JG, Jayasuriya H, Herath KB, Guan Z, Schulman M, Collado J, Dombrowski AW, Kwon SS, McCallum C, Sharma N, MacNaul K, Hayes N, Menke JG, Singh SB (2005) Steroidal and triterpenoidal fungal metabolites as ligands of liver X receptors. J Antibiot (Tokyo) 58:559–565
29. Jayasuriya H, Herath KB, Ondeyka JG, Guan Z, Borris RP, Tiwari S, de Jong W, Chavez F, Moss J, Stevenson DW, Beck HT, Slattery M, Zamora N, Schulman M, Ali A, Sharma N, MacNaul K, Hayes N, Menke JG, Singh SB (2005) Diterpenoid, steroid, and triterpenoid agonists of liver X receptors from diversified terrestrial plants and marine sources. J Nat Prod 68:1247–1252
30. Brown MS, Faust JR, Goldstein JL, Kaneko I, Endo A (1978) Induction of 3-hydroxy-3-methylglutaryl coenzyme A reductase activity in human fibroblasts incubated with compactin (ML-236B), a competitive inhibitor of the reductase. J Biol Chem 253:1121–1128
31. Sever N, Song BL, Yabe D, Goldstein JL, Brown MS, DeBose-Boyd RA (2003) Insig-dependent ubiquitination and degradation of mammalian 3-hydroxy-3-methylglutaryl-CoA reductase stimulated by sterols and geranylgeraniol. J Biol Chem 278:52479–52490
32. Wong J, Quinn CM, Brown AJ (2004) Statins inhibit synthesis of an oxysterol ligand for the liver X receptor in human macrophages with consequences for cholesterol flux. Arterioscler Thromb Vasc Biol 24:2365–2371
33. Holstein SA, Wohlford-Lenane CL, Hohl RJ (2002) Consequences of mevalonate depletion. Differential transcriptional, translational, and post-translational up-regulation of Ras, Rap1a, RhoA, and RhoB. J Biol Chem 277:10678–10682
34. Holstein SA, Wohlford-Lenane CL, Hohl RJ (2002) Isoprenoids influence expression of Ras and Ras-related proteins. Biochemistry 41:13698–13704
35. Ness GC, Zhao Z, Keller RK (1994) Effect of squalene synthase inhibition on the expression of hepatic cholesterol biosynthetic enzymes, LDL receptor, and cholesterol 7 alpha hydroxylase. Arch Biochem Biophys 311:277–285
36. Shull LW, Wiemer AJ, Hohl RJ, Wiemer DF (2006) Synthesis and biological activity of isoprenoid bisphosphonates. Bioorg Med Chem 14:4130–4136
37. Ericsson J, Jackson SM, Lee BC, Edwards PA (1996) Sterol regulatory element binding protein binds to a cis element in the promoter of the farnesyl diphosphate synthase gene. Proc Natl Acad Sci USA 93:945–950
38. Tong H, Holstein SA, Hohl RJ (2005) Simultaneous determination of farnesyl and geranylgeranyl pyrophosphate levels in cultured cells. Anal Biochem 336:51–59
39. Storey JD (2002) A direct approach to false discovery rates. J Roy Stat Soc B 64:479–498
40. Storey JD, Tibshirani R (2003) Statistical significance for genomewide studies. Proc Natl Acad Sci USA 100:9440–9445
41. Gutierrez MG, Munafo DB, Beron W, Colombo MI (2004) Rab7 is required for the normal progression of the autophagic pathway in mammalian cells. J Cell Sci 117:2687–2697
42. Whyte DB, Kirschmeier P, Hockenberry TN, Nunez-Oliva I, James L, Catino JJ, Bishop WR, Pai JK (1997) K- and N-Ras are geranylgeranylated in cells treated with farnesyl protein transferase inhibitors. J Biol Chem 272:14459–14464
43. Holstein SA, Tong H, Hohl RJ (2010) Differential activities of thalidomide and isoprenoid biosynthetic pathway inhibitors in multiple myeloma cells. Leuk Res 34:344–351
44. Clendening JW, Pandyra A, Li Z, Boutros PC, Martirosyan A, Lehner R, Jurisica I, Trudel S, Penn LZ (2010) Exploiting the mevalonate pathway to distinguish statin-sensitive multiple myeloma. Blood 115:4787–4797
45. Jackson SM, Ericsson J, Metherall JE, Edwards PA (1996) Role for sterol regulatory element binding protein in the regulation of farnesyl diphosphate synthase and in the control of cellular levels of cholesterol and triglyceride: evidence from sterol regulation-defective cells. J Lipid Res 37:1712–1721
46. Ericsson J, Jackson SM, Edwards PA (1996) Synergistic binding of sterol regulatory element-binding protein and NF-Y to the farnesyl diphosphate synthase promoter is critical for sterol-regulated expression of the gene. J Biol Chem 271:24359–24364
47. Fukuchi J, Song C, Ko AL, Liao S (2003) Transcriptional regulation of farnesyl pyrophosphate synthase by liver X receptors. Steroids 68:685–691
48. Sakakura Y, Shimano H, Sone H, Takahashi A, Inoue N, Toyoshima H, Suzuki S, Yamada N (2001) Sterol regulatory element-binding proteins induce an entire pathway of cholesterol synthesis. Biochem Biophys Res Commun 286:176–183
49. Ericsson J, Greene JM, Carter KC, Shell BK, Duan DR, Florence C, Edwards PA (1998) Human geranylgeranyl diphosphate synthase: isolation of the cDNA, chromosomal mapping and tissue expression. J Lipid Res 39:1731–1739
50. Forman BM, Ruan B, Chen J, Schroepfer GJ Jr, Evans RM (1997) The orphan nuclear receptor LXRalpha is positively and negatively regulated by distinct products of mevalonate metabolism. Proc Natl Acad Sci USA 94:10588–10593
51. Lehmann JM, Kliewer SA, Moore LB, Smith-Oliver TA, Oliver BB, Su JL, Sundseth SS, Winegar DA, Blanchard DE, Spencer TA, Willson TM (1997) Activation of the nuclear receptor LXR by oxysterols defines a new hormone response pathway. J Biol Chem 272:3137–3140
52. Turbyville TJ, Gursel DB, Tuskan RG, Walrath JC, Lipschultz CA, Lockett SJ, Wiemer DF, Beutler JA, Reilly KM (2010)

Schweinfurthin A selectively inhibits proliferation and Rho signaling in glioma and neurofibromatosis type 1 tumor cells in a NF1-GRD-dependent manner. Mol Cancer Ther 9:1234–1243

53. Wang C, JeBailey L, Ridgway ND (2002) Oxysterol-binding-protein (OSBP)-related protein 4 binds 25-hydroxycholesterol and interacts with vimentin intermediate filaments. Biochem J 361:461–472
54. Lehto M, Mayranpaa MI, Pellinen T, Ihalmo P, Lehtonen S, Kovanen PT, Groop PH, Ivaska J, Olkkonen VM (2008) The R-Ras interaction partner ORP3 regulates cell adhesion. J Cell Sci 121:695–705

Lipids (2011) 46:923–929
DOI 10.1007/s11745-011-3591-8

ORIGINAL ARTICLE

Modified-Policosanol Does Not Reduce Plasma Lipoproteins in Hyperlipidemic Patients When Used Alone or in Combination with Statin Therapy

James M. Backes · Cheryl A. Gibson · Janelle F. Ruisinger · Patrick M. Moriarty

Received: 25 January 2011 / Accepted: 22 June 2011 / Published online: 8 July 2011

Abstract Policosanol is a poorly absorbed nutritional supplement used primarily for cholesterol management. Findings from previous trials evaluating the effects of policosanol are mixed with early data reporting positive lipid effects while more recent studies indicate negligible efficacy. We hypothesized that re-formulating policosanol would result in an improvement in major lipoproteins and possibly provide some explanation for previously conflicting trial data. Our primary objectives were to assess the efficacy and safety of modified-policosanol (MP) on the major lipoproteins among hyperlipidemic subjects receiving background statin therapy or as monotherapy. This 8-week clinical trial consisted of 3 arms. Subjects receiving chronic statin therapy ($N = 36$) were randomized in a double-blind design to MP 20 mg daily or placebo. In the third arm, subjects not receiving statin therapy ($N = 18$) were assigned open-label MP 20 mg daily. The utilization of MP when added to background statin therapy or as monotherapy resulted in no significant changes in major lipoproteins (all $p > 0.05$). The MP therapy was well tolerated with no major adverse events reported. Consistent with recent clinical trial data, MP demonstrated an excellent safety profile but produced no significant effects on major lipoproteins when used as monotherapy or when given with concomitant statin therapy.

Keywords HMG reductase · Hyperlipidemia · Low-density lipoprotein · Policosanol · Plasma lipoproteins

Abbreviations

ANOVA	Analysis of variance
ATP-III	Adult Treatment Panel III
CHD	Coronary heart disease
HDL-C	High-density lipoprotein cholesterol
HMG CoA	Hydroxymethylglutaryl Coenzyme A
HRT	Hormone replacement therapy
LDL-C	Low-density lipoprotein cholesterol
Lp(a)	Lipoprotein a
MP	Modified policosanol
NCEP	National Cholesterol Education Program
SPSS	Statistical Package for the Social Sciences
VLDL	Very low-density lipoprotein cholesterol

Introduction

Elevated low-density lipoprotein cholesterol (LDL-C) is a major modifiable risk factor for coronary heart disease (CHD) [1]. The National Cholesterol Education Program (NCEP) Adult Treatment Panel's third report (ATP-III) and 2004 Update focus on LDL-C treatment to reduce CHD events [1, 2]. For most patients statins are the cornerstone for LDL-C reduction. However, because of aggressive LDL-C goals and dose-dependent side effects associated

J. M. Backes · J. F. Ruisinger
Schools of Pharmacy and Medicine,
The University of Kansas Medical Center, Kansas, USA

J. M. Backes (✉) · P. M. Moriarty
Atherosclerosis and LDL-Apheresis Center,
University of Kansas Medical Center,
3901 Rainbow Blvd., Kansas City, KS 66160-7231, USA
e-mail: jbackes@kumc.edu

C. A. Gibson
Department of Internal Medicine,
The University of Kansas Medical Center, Kansas, USA

P. M. Moriarty
Department of Internal Medicine, Division of Clinical Pharmacology, The University of Kansas Medical Center, Kansas, USA

with statin therapy, additional agents are often required to achieve optimal LDL-C levels [3]. Other lipoproteins also play key roles in the development of atherosclerosis. Lipoprotein (a) [Lp (a)] is an emerging risk factor that has recently demonstrated an independent association with CHD [4]. Effective therapies for treating Lp (a) are limited, therefore new treatment options are greatly needed.

Policosanol is a nutritional supplement used for the treatment of hypercholesterolemia. The agent consists of a natural mix of aliphatic alcohols that are derived primarily from sugar cane (*Saccharum officinarum* L) and/or rice wax. The formulation of policosanol can vary between products but the major components are octacosanol, triacontanol and hexacosanol [5]. The clinical pharmacology of policosanol is not fully understood but findings suggest suppression of hydroxymethylglutaryl Coenzyme A (HMG-CoA) reductase and increased LDL-C degradation via enhanced hepatic binding and internalization [6, 7]. The agent has been associated with a low rate of generally mild and transient adverse effects with no reports of increased hepatic transaminases [5, 8].

Early studies indicated policosanol, when used as monotherapy, significantly reduced LDL-C and raised high-density lipoprotein cholesterol (HDL-C) [9–16]. Another study indicated the agent produced significant reductions in Lp (a) [17]. However, more recent studies, including one evaluating policosanol in combination with statin therapy, have not replicated the beneficial findings seen from the early trials [18–27]. Despite the lack of proven benefit, policosanol use remains widespread. A recent internet search indicated many common retailers continue stocking the product.

The discrepant results from clinical trials are not well understood, however, limited absorption and subtle composition differences between products may be key variables. The mixture of very long chain aliphatic alcohols and very long chain fatty acids composing policosanol have limited bioavailability and varying composition, are highly hydrophobic, with very poor overall absorption [28]. Although data are limited, the plasma concentrations of very long chain fatty alcohols present in policosanol are increased in high fat dietary states (i.e. ketogenic diets) [29]. Other trials evaluating lipid-based delivery systems further support this data. Porter et al. [30] describe how exogenous lipids in the small intestine stimulate the secretion of factors (e.g. bile salt) aiding in the solubilization for both lipid products and drugs. Because of these findings and known properties of policosanol we formulated the product with a lipid-base to potentially enhance absorption and ultimately clinical efficacy. Lastly, most clinical trials utilized a similar policosanol mixture consistent with octacosanol (66%), triacontanol (12%) and hexacosanol (7%), despite each apparently possessing lipid-altering properties [18].

The inconsistent findings from previous trials with similarly composed alcohol mixtures, and data indicating improved absorption with increased fat intake, led us to perform a prospective clinical study designed to answer some of the lingering questions regarding policosanol. We hypothesized adjusting the aliphatic alcohol content and formulating the agent with a vehicle composed of a long chain fatty acid would enhance the lipid-altering effects, including Lp (a). Our findings add to the negligible results of recent studies but also demonstrate markedly altering the aliphatic alcohol content to the formulation utilized in the present study and adding long chain fatty acids do not provide lipid-altering effects.

Materials and Methods

Study Design and Protocol

This was an 8-week, single-site, three arm clinical trial. Subjects receiving chronic statin therapy ($N = 36$) were randomized, in a double-blind parallel design, to modified-policosanol (MP) 20 mg daily or matching placebo (arms 1 and 2). Subjects not receiving statin therapy ($N = 18$) were assigned to receive open-label MP 20 mg daily (arm 3). Prior to commencement, the study was approved by the institutional review board at the Kansas University Medical Center.

The policosanol doses and matching placebo capsules were compounded with long chain fatty acids by the University of Kansas Inpatient Pharmacy. The mixture consisted of 0.48 ml United States Pharmacopeia (USP) soybean oil, 0.05 ml beeswax, and 20 mg policosanol. Matching placebo capsules were formulated with 0.495 ml USP soybean oil and 0.05 ml beeswax. All doses for arms 1 and 2 were packaged in identical bottles and labeled by a non-investigator pharmacist according to the randomization table. The policosanol (Marcosanol)®, derived from rice bran wax, was provided by Marcor Development Corporation (Carlstadt, NJ) and the certificate of analysis indicated the composition consisted of 98.8% C22–C36 alcohols including 1-octacosanol 33.5%, 1-triacontanol 44.1%, 1-hexacosanol 13.3% and 1-dotriacontanol 7.9%.

Fasting blood samples were drawn for lipoprotein analysis and safety measures at visit 1 (baseline) and visit 2 (8-weeks). All subjects received counseling at visit 1 on the Adult Treatment Panel III Therapeutic Lifestyle Changes including dietary changes, weight reduction and increased physical activity. Demographic information was also collected and vitals were measured at each visit. Adherence was determined at the 8-week visit by pill count, subjects who had a >20% non-adherence rate were excluded from the final data analysis.

The primary outcome measures of the study were to determine the changes in lipoproteins [LDL-C, HDL-C,

triglycerides, total cholesterol, non-HDL, and Lp(a)] from baseline to 8-weeks, when MP was added to statin therapy (compared to placebo) or when administered as monotherapy. The evaluation of safety measures (i.e. hepatic transaminases) and reported adverse events among groups were also assessed.

Subjects

Adult hyperlipidemic subjects between the ages of 18 and 75 years with serum LDL-C levels >80 mg/dl were eligible for enrollment. For arms 1 and 2 participants were required to be on background statin therapy with intentions to continue the same dose throughout the course of the trial. Key exclusion criteria included patients with chronic renal or hepatic disease, dependence on alcohol or illicit drugs, previous sensitivity to policosanol, or currently receiving agents with potential to interact with policosanol (i.e. warfarin, high-dose aspirin). Female subjects were allowed to enroll if they were using a reliable form of contraception or surgically sterile, not pregnant or lactating, or postmenopausal and not on hormone replacement therapy (HRT) or using HRT with the intention of continuing the same agent and dose throughout the study.

Laboratory Analysis

The Vertical Auto Profile II method was used to assess the concentration of cholesterol carried in large, buoyant (LDL_1 and LDL_2) and small, dense (LDL_3 and LDL_4) LDL particles. The Vertical Auto Profile II method utilizes single vertical spin density gradient ultracentrifugation to separate the various plasma lipoprotein fractions. After centrifugation, the cholesterol content of the tube is continuously analyzed and digitized. A cholesterol absorbance curve profile is generated by plotting digitized absorbance units on the *Y* axis and the relative gradient position on the *X* axis. A deconvolution program is used to separate the different lipoprotein classes and subclasses [31].

Statistical Analysis

Sample size estimation was based on the percentage change in LDL-C levels from baseline to visit two (8-weeks). It was expected that the active treatment would result in a 24% reduction in LDL-C with a SD of 20 compared to placebo. To achieve a power of 80% and Type 1 error of 0.05, at least 12 subjects had to be enrolled in each treatment group.

Data analyses were performed using SPSS for Windows (Statistical Package for the Social Sciences) software (SPSS version 11.5, Chicago, IL). One way ANOVA was used to assess the change in lipid parameters from baseline to 8 weeks of supplementation among groups, followed by a post hoc analysis with a Bonferroni correction. Data are expressed as means ± SD, unless indicated otherwise. The level of significance was set at $p < 0.05$ for the primary analyses.

Results

A total of 54 subjects were enrolled, of whom all completed the study. Baseline characteristics were similar between groups with the exception of total cholesterol, LDL-C and non-HDL concentrations (Table 1). Subjects not receiving background statin therapy had significantly higher baseline total cholesterol and LDL-C levels compared to those receiving statins. Among the statin groups, participants receiving statin/MP also had higher baseline total cholesterol and LDL-C levels compared to those receiving statin/placebo.

The addition of MP 20 mg daily for 8-weeks to background statin therapy or when given as monotherapy did not significantly alter any major lipoproteins including total cholesterol, LDL-C, HDL-C or Lp (a) (Table 2). No differences were observed when comparing between background statin groups (arms 1 and 2) or when evaluating changes in lipoprotein levels from baseline to follow-up across all arms. Additionally, we examined LDL-C changes among those patients with higher and lower baseline LDL-C levels based on median value split. Only patients in Arm 2 (statin/placebo) with higher baseline levels demonstrated a modest reduction in LDL-C values (see Table 3) at 8 weeks.

Adverse events were collected throughout the study from subject reports and by a questionnaire at visit two. Overall, adverse events associated with the use of MP were minimal and considered mild to moderate with rates similar to placebo. Of those receiving MP, one subject reported an intermittent headache while another reported constipation. No patients withdrew from the study due to adverse events in any arm. The use of MP did not affect hepatic transaminases including aspartate aminotransferase or alanine aminotransferase levels. Adherence to therapy in all arms was excellent (>80%); no subject data was excluded from final analysis secondary to non-adherence.

Discussion

The results of the present study are consistent with findings from recent clinical trials performed in the United States and Germany. Earlier studies, performed primarily in Latin America, indicated policosanol was highly effective at lowering LDL-C and raising HDL-C. We theorized that

Table 1 Baseline patient characteristics of study groups

	Arm 1 Statin/ Policosanol ($N = 18$)	Arm 2 Statin/ Placebo ($N = 18$)	Arm 3 Policosanol ($N = 18$)
Age (y)	54 ± 12	54 ± 14	46 ± 13
Gender			
Female	12	10	9
Male	6	8	9
Race			
White	18	15	16
Black	0	3	1
Other	0	0	1
Weight (kg)	84.4 ± 21.6	87.8 ± 13.5	84.8 ± 16.8
Body mass index (kg/m^2)	29.9 ± 5.1	28.8 ± 4.1	28.4 ± 4.8
Waist Circumference (cm)	98.7 ± 18.1	102.4 ± 9.1	94.4 ± 9.8
Blood pressure (mmHg)			
Systolic	122 ± 13	121 ± 17	120 ± 19
Diastolic	76 ± 8	76 ± 11	78 ± 9
Plasma lipids (mg/dl)			
Total Cholesterol*	204 ± 32.5	190 ± 35.1	228 ± 24.6
LDL-C*	131 ± 27.9	114 ± 27.4	147 ± 19.1
HDL-C	51 ± 10.3	54 ± 14.2	60 ± 20.4
Triglycerides	148 ± 70.7	146 ± 77.7	120 ± 67.6
non-HDL*	153 ± 29.2	136 ± 32.0	168 ± 23.2
Lp (a)	7 ± 4.5	10 ± 6.6	8 ± 5.7
VLDL	23 ± 4.6	22 ± 8.4	21 ± 7.6

Values are means ± SD

LDL-C low-density lipoprotein cholesterol, *HDL-C* high-density lipoprotein cholesterol, *Lp (a)* lipoprotein (a), *VLDL* very low density lipoprotein cholesterol

* Statistically significant differences between groups at $p < 0.005$

these inconsistent results may have been due to the poor absorption and bioavailability of policosanol.

It was our goal to develop an MP agent which would significantly improve major lipoproteins when used as monotherapy or when given with a background statin, and provide some possible explanation for previously mixed clinical trial data. We evaluated this by designing a rigorous, randomized, placebo-controlled, parallel, and double-blind trial with an additional open-label arm. However our findings indicate that the addition of long chain fatty acids to a mixture of aliphatic alcohols (policosanol) does not offer any additional lipoprotein benefit when added to background statin therapy or produce significant changes in lipids when used as monotherapy. When evaluating safety measures and adverse events, our results are consistent with previous data demonstrating that policosanol is well tolerated with a safety profile similar to placebo.

The MP failed to provide any significant changes to the major lipoproteins including LDL-C, HDL-C, very low-density lipoprotein cholesterol (VLDL-C), triglycerides or Lp (a). It is plausible that the effects of policosanol may be dependent upon baseline LDL-C levels. We therefore grouped subjects into high or low baseline LDL-C values based on median value splits. However, similar to the overall findings MP was ineffective at reducing LDL-C regardless of baseline levels. Arm 2 (statin/placebo) did experience a modest reduction in LDL-C from baseline to end of study. However, with the Bonferroni adjustment, the LDL-C reduction was not considered statistically significant.

The vast majority of the positive trials evaluating policosanol were conducted in Cuba prior to 2004 [10, 11, 13–16]. In fact, a meta-analysis of these early trials published in 2005, indicating overall mean LDL-C reductions of 24% and HDL-C increases of 11% drew the attention of many practitioners [14]. However, subsequent studies performed outside of Cuba have failed to reproduce the same positive results. A randomized, placebo-controlled trial using policosanol derived from wheat germ conducted in the Netherlands found no lipid-alterations among its 58 participants [20]. A well-designed, placebo-controlled, multicenter trial evaluating the dose-dependent effects of policosanol (10–80 mg/day) further questioned the efficacy of the agent [19]. The German investigators utilized the same sugarcane policosanol product (Dalmer Laboratories; La Habana, Cuba) as the early Cuban studies, yet failed to produce any significant changes on the lipid profile among 143 subjects. A US study evaluating the effects of policosanol as monotherapy or when added to statin therapy yielded similar results; policosanol produced no significant

Table 2 Baseline and end of study mean lipid levels (±SEM)

Lipids (mg/dl)	Arm 1 (±SEM) Statin/Policosanol ($N = 18$)	Arm 2 (±SEM) Statin/Placebo ($N = 18$)	Arm 3 (±SEM) Policosanol ($N = 18$)	p value
Total Cholesterol				
Baseline	204 ± 7.68	190 ± 8.29	228 ± 5.97	0.606
End of study	199 ± 9.35	185 ± 7.37	230 ± 7.93	
LDL-C				
Baseline	131 ± 6.57	114 ± 6.45	147 ± 4.65	0.700
End of study	127 ± 8.51	110 ± 4.96	147 ± 4.99	
HDL-C				
Baseline	51 ± 2.44	54 ± 3.37	60 ± 4.95	0.981
End of Study	51 ± 2.61	53 ± 3.60	59 ± 5.34	
Triglycerides				
Baseline	148 ± 16.68	146 ± 18.32	120 ± 16.40	0.103
End of study	152 ± 18.20	144 ± 14.41	155 ± 20.40	
non-HDL				
Baseline	153 ± 6.89	136 ± 7.56	168 ± 5.65	0.534
End of study	149 ± 8.76	132 ± 6.11	171 ± 5.12	
Lp (a)				
Baseline	7 ± 1.06	10 ± 1.56	8 ± 1.40	0.312
End of study	7 ± 0.95	10 ± 6.25	9 ± 1.32	
VLDL				
Baseline	23 ± 1.08	22 ± 1.98	21 ± 1.85	0.160
End of study	22 ± 1.21	23 ± 1.81	24 ± 1.95	

Values are means ± SEM. No statistically significant differences among groups. The distribution of changes for lipid values is the same across treatment groups

LDL-C low-density lipoprotein cholesterol, *HDL-C* high-density lipoprotein cholesterol, *Lp (a)* lipoprotein (a), *VLDL* very low density lipoprotein cholesterol

Table 3 LDL-C changes among groups divided into low vs high levels at baseline based on median value splits (±SD)

	Low LDL-C group (mg/dL)		p value	High LDL-C group (mg/dL)		p value
Regimen	Baseline	8 weeks		Baseline	8 weeks	
Arm 1 ($N = 18$) Statin/policosanol	109 ± 14.5	103 ± 14.3	0.306	148 ± 23.7	146 ± 37.4	0.725
Arm 2 ($N = 18$) Statin/placebo	93 ± 17.7	100 ± 17.6	0.244	131 ± 13.8	117 ± 20.0	0.035
Arm 3 ($N = 18$) Policosanol	133 ± 5.8	145 ± 24.6	0.150	160 ± 17.5	151 ± 19.6	0.119

LDL-C low-density lipoprotein cholesterol

changes to major lipoproteins when used alone or in addition to statin therapy [18]. Since the publication of these trials additional studies have continued to corroborate their negative findings [21–27]. Conversely, the last positive trials demonstrating lipid alterations with policosanol were performed in Cuba and published in 2005 [9, 12].

An explanation for the inconsistent results among the clinical studies evaluating policosanol remains unclear. One potential factor is the variability in aliphatic alcohol content of the different policosanol mixtures used in studies. The formulation in the present study differed from Cuban-manufactured policosanol by having lower octacosanol and higher triacontanol and hexacosanol composition. However, each of these three major alcohols is proposed to be responsible for the apparent lipid-altering effects of policosanol [18]. Additionally, the recent clinical trials demonstrating a lack of response with policosanol utilized formulations comparable in composition to previous studies indicating lipid-altering benefits [18]. Therefore, we find it unlikely that the variable alcohol compositions played a major role in our findings or previous studies.

Additional factors that may account for the discrepancy in results include dosage and duration of study. Prior positive studies evaluated dosages ranging from 2 to 40 mg daily [14]. Dose-dependent improvements in most lipoproteins were observed with doses up to 20 mg/day. Trial duration for most studies ranged from 4 to 104 weeks with a mean of 30 weeks. The trials with shorter duration (4–8 weeks) still produced significant reductions in LDL-C ($\sim$17–40%). Because of these data, we find it doubtful that the dosage of policosanol utilized or duration of the present trial was sub-optimal.

There are perceivable limitations to our study. While two arms of the trial were randomized, double-blind and placebo controlled the third arm evaluating the efficacy of MP as monotherapy was open-label and without a control group. Additionally, significant differences in baseline total cholesterol, LDL-C and non-HDL values were present between the statin/placebo and the statin/MP arms. However, given the overall lack of response with MP, we do not feel that the absence of a placebo comparator group for the monotherapy arm or differences between groups at baseline impact our overall findings. Lastly, although we encouraged subjects to follow the guidelines set forth by ATPIII Therapeutic Lifestyle Changes we have no information on dietary patterns and we did not assess physical activity levels during the study. However, weight did not significantly change across the 3 groups at 8 weeks.

In summary, our study findings support the growing body of evidence published in the last 5 years indicating policosanol does not significantly improve any major lipoproteins including LDL-C, HDL-C and Lp (a). Our policosanol formulation was unique because of the added long chain fatty acids and differing composition of aliphatic alcohols compared to most products used in clinical trials. However, despite these factors, the MP formulation produced no lipid-altering benefits when added to background statin therapy or when used as a monotherapy. Lastly, the history of policosanol perfectly illustrates the dire need for more independent research in evaluating the safety and efficacy of nutritional supplements prior to mass utilization by consumers worldwide. Fortunately with policosanol we found a supplement that was safe but simply not effective.

Acknowledgments This study was supported by the University of Kansas General Research Fund allocation #23011083 and by Marcor Development Corporation (Carlstadt, NJ). We would also like to express our sincere gratitude to David Mueller, R.Ph., for his diligence and expertise in pharmaceutical compounding and Roger Rajewski Ph.D. for his expertise and assistance in product formulation.

Conflict of interest Drs. Backes, Gibson, Ruisinger and Moriarty—all report no conflicts of interest with submitted material.

References

1. National Cholesterol Education Program Expert Panel on Detection, Evaluation, and Treatment of High Blood Cholesterol in Adults: Third Report of the National Cholesterol Education Program (NCEP) (2002) Expert Panel on Detection, Evaluation, and Treatment of High Blood Cholesterol in Adults (Adult Treatment Panel III) final report (see comment). Circulation 106:3143-3421
2. Grundy SM, Cleeman JI, Merz CN, Brewer HB Jr, Clark LT, Hunninghake DB, Pasternak RC, Smith SC Jr, Stone NJ, National Heart LaBI et al (2004) Implications of recent clinical trials for the National Cholesterol Education Program Adult Treatment Panel III guidelines (erratum appears in Circulation. 2004 Aug 10;110(6):763). Circulation 110:227-239
3. Davidson MH (2002) Combination therapy for dyslipidemia: safety and regulatory considerations. Am J Cardiol 90:20
4. Kamstrup PR, Tybjaerg-Hansen A, Steffensen R (2009) Nordestgaard BG: Genetically elevated lipoprotein (a) and increased risk of myocardial infarction. JAMA 301:2331–2339
5. Janikula M (2002) Policosanol: a new treatment for cardiovascular disease? Altern Med Rev 7:203–217
6. Menendez R, Amor AM, Gonzalez RM, Fraga V, Mas R (1996) Effect of policosanol on the hepatic cholesterol biosynthesis of normocholesterolemic rats. Biol Res 29:253–257
7. Menendez R, Amor AM, Rodeiro I, Gonzalez RM, Gonzalez PC, Alfonso JL, Mas R (2001) Policosanol modulates HMG-CoA reductase activity in cultured fibroblasts. Arch Med Res 32:8–12
8. Gouni-Berthold I, Berthold HK (2002) Policosanol: clinical pharmacology and therapeutic significance of a new lipid-lowering agent. Am Heart J 143:356–365
9. Castano G, Fernandez L, Mas R, Illnait J, Fernandez J et al (2005) Effects of addition of policosanol to omega-3 fatty acid therapy on the lipid profile of patients with type II hypercholesterolaemia. Drugs R D 6:207–219
10. Castano G, Fernandez L, Mas R, Illnait J, Fernandez JC et al (2003) Comparison of the effects of policosanol and atorvastatin on lipid profile and platelet aggregation in patients with dyslipidaemia and type 2 diabetes mellitus. Clinic Drug Investig 23:639–650
11. Castano G, Mas R, Fernandez JC, Fernandez L, Alvarez E, Lezcay M (2000) Efficacy and tolerability of policosanol compared with lovastatin in patients with type II hypercholesterolemia and concomitant coronary risk factors. Curr Ther Res 61:137–146
12. Castano G, Mas R, Fernandez L, Illnait J, Mendoza S, Gamez R, Fernandez J, Mesa M (2005) A comparison of the effects of D-003 and policosanol (5 and 10 mg/day) in patients with type II hypercholesterolemia: a randomized, double-blinded study. Drugs Exp Clin Res 31(Suppl):31–44
13. Castano G, Mas R, Fernandez L, Illnait J, Mesa M, Alvarez E, Lezcay M (2003) Comparison of the efficacy and tolerability of policosanol with atorvastatin in elderly patients with type II hypercholesterolaemia. Drugs Aging 20:153–163
14. Chen JT, Wesley R, Shamburek RD, Pucino F, Csako G (2005) Meta-analysis of natural therapies for hyperlipidemia: Plant sterols and stanols versus policosanol. Pharmacotherapy 25: 171–183
15. Fernandez JC, Mas R, Castano G, Menendez R, Alvarez E et al (2001) Comparison of the efficacy, safety and tolerability of policosanol versus fluvastatin in elderly hypercholesterolemic women. Clinic Drug Invest 21:103–113
16. Marcello S, Gladstein J, Tesone P, Mas R (2000) Effects of bezafibrate plus policosanol or placebo in patients with combined dyslipidemia: a pilot study. Curr Ther Res 61:346–357

17. Alcocer LCA, Mas R, Fernandez L (1997) A comparative study of policosanol vs acipimox in patients with type II hypercholesterolemia. Data on File @ http://www.policosanol.com
18. Cubeddu LX, Cubeddu RJ, Heimowitz T, Restrepo B, Lamas GA, Weinberg GB (2006) Comparative lipid-lowering effects of policosanol and atorvastatin: a randomized, parallel, double-blind, placebo-controlled trial. Am Heart J 152:982.e1–982.e5
19. Berthold HK, Unverdorben S, Degenhardt R, Bulitta M, Gouni-Berthold I (2006) Effect of policosanol on lipid levels among patients with hypercholesterolemia or combined hyperlipidemia: a randomized controlled trial. JAMA 295:2262–2269
20. Lin Y, Rudrum M, van der Wielen RP, Trautwein EA, McNeill G, Sierksma A, Meijer GW (2004) Wheat germ policosanol failed to lower plasma cholesterol in subjects with normal to mildly elevated cholesterol concentrations. Metabolism 53:1309–1314
21. Dulin MF, Hatcher LF, Sasser HC, Barringer TA (2006) Policosanol is ineffective in the treatment of hypercholesterolemia: a randomized controlled trial. Am J Clin Nutr 84:1543–1548
22. Francini-Pesenti F, Beltramolli D, Dall'acqua S, Brocadello F (2008) Effect of sugar cane policosanol on lipid profile in primary hypercholesterolemia. Phytother Res 22:318–322
23. Francini-Pesenti F, Brocadello F, Beltramolli D, Nardi M, Caregaro L (2008) Sugar cane policosanol failed to lower plasma cholesterol in primitive, diet-resistant hypercholesterolaemia: a double blind, controlled study. Complement Ther Med 16:61–65
24. Greyling A, De Witt C, Oosthuizen W, Jerling JC (2006) Effects of a policosanol supplement on serum lipid concentrations in hypercholesterolaemic and heterozygous familial hypercholesterolaemic subjects. Br J Nutr 95:968–975
25. Kassis AN, Jones PJ (2006) Lack of cholesterol-lowering efficacy of Cuban sugar cane policosanols in hypercholesterolemic persons. Am J Clin Nutr 84:1003–1008
26. Kassis AN, Jones PJ (2008) Changes in cholesterol kinetics following sugar cane policosanol supplementation: a randomized control trial. Lipids Health Dis 7:17
27. Reiner Z, Tedeschi-Reiner E, Romic Z (2005) Effects of rice policosanol on serum lipoproteins, homocysteine, fibrinogen and C-reactive protein in hypercholesterolaemic patients. Clinic Drug Invest 25:701–707
28. Marinangeli CP, Kassis AN, Jain D, Ebine N, Cunnane SC, Jones PJ (2007) Comparison of composition and absorption of sugarcane policosanols. Br J Nutr 97:381–388
29. Hargrove JL, Greenspan P, Hartle DK (2004) Nutritional significance and metabolism of very long chain fatty alcohols and acids from dietary waxes. Exp Biol Med (Maywood) 229:215–226
30. Porter CJ, Pouton CW, Cuine JF, Charman WN (2008) Enhancing intestinal drug solubilisation using lipid-based delivery systems. Adv Drug Deliv Rev 60:673–691
31. Kulkarni KR (2006) Cholesterol profile measurement by vertical auto profile method. Clin Lab Med 26:787–802

Lipids (2011) 46:931–941
DOI 10.1007/s11745-011-3578-5

ORIGINAL ARTICLE

Dyslipidemic Diabetic Serum Increases Lipid Accumulation and Expression of Stearoyl-CoA Desaturase in Human Macrophages

Bruce X. W. Wong · Reece A. Kyle · Paul C. Myhill · Kevin D. Croft · Carmel M. Quinn · Wendy Jessup · Bu B. Yeap

Received: 23 March 2011 / Accepted: 25 May 2011 / Published online: 15 June 2011

Abstract Type 2 diabetes and dyslipidemia are risk factors for cardiovascular disease. However, mechanisms by which hypertriglyceridemia influences atherogenesis remain unclear. We examined effects of dyslipidemic diabetic serum on macrophage lipid accumulation as a model of foam cell formation. Normal human macrophages were cultured in media supplemented with 10% serum from non-diabetic normolipidemic or non-diabetic hypercholesterolemic adults versus adults with Type 2 diabetes; diabetes and hypertriglyceridemia; or diabetes and hypercholesterolemia. Exposure to diabetic sera resulted in increased macrophage fatty acids (2–3 fold higher, both saturated and unsaturated). Macrophage expression of CD36, scavenger receptor A (SR-A) and stearoyl-CoA desaturase (SCD) was increased, most prominently in macrophages exposed to hypertriglyceridemic diabetic serum (twofold increase in CD36 and fourfold increase in SCD, $p < 0.05$). In these conditions, RNA inhibition of CD36 reduced macrophage free cholesterol (163.9 ± 10.5 vs. 221.9 ± 26.2 mmol free cholesterol/g protein, $p = 0.04$). RNA inhibition of SCD decreased macrophage fatty acid content, increased ABCA1 level and enhanced cholesterol efflux (18.0 ± 3.9 vs. $8.0 \pm 0.8\%$ at 48 h, $p = 0.03$). Diabetic dyslipidemia may contribute to accelerated atherosclerosis via alterations in macrophage lipid metabolism favoring foam cell formation. Increased expression of CD36 and SR-A would facilitate macrophage lipid uptake, while increased expression of SCD could block compensatory upregulation of ABCA1 and cholesterol efflux. Further studies are needed to clarify whether modulation of macrophage lipid metabolism might reduce progression of diabetic atherosclerosis.

Keywords Type 2 diabetes · Dyslipidemia · Macrophage · Fatty acid · Cholesterol · CD36 · Stearoyl-CoA desaturase

Abbreviations

ABCA1	ATP-binding cassette transporter A1
ABCG1	ATP-binding cassette transporter G1
CD36	Cluster of differentiation 36
CE	Cholesterol ester
CVD	Cardiovascular disease
FA	Fatty acid(s)
FC	Free cholesterol
GC	Gas chromatography
GC–MS	Gas chromatography–mass spectrometry
HDL	High density lipoprotein
hMDM	Human monocyte-derived macrophage(s)
LDL	Low density lipoprotein
LXR	Liver X receptor
PPARγ	Peroxisome proliferator-activated receptor gamma
RNAi	RNA inhibition
SCD	Stearoyl-CoA desaturase

B. X. W. Wong · R. A. Kyle · K. D. Croft · B. B. Yeap
School of Medicine and Pharmacology, Fremantle and Royal Perth Hospitals, University of Western Australia, Perth, WA, Australia

P. C. Myhill · B. B. Yeap
Department of Endocrinology and Diabetes, Fremantle Hospital, Fremantle, WA, Australia

C. M. Quinn · W. Jessup
Centre for Vascular Research, University of New South Wales, Sydney, NSW, Australia

B. B. Yeap (✉)
School of Medicine and Pharmacology, Level 2, T-Block, Fremantle Hospital, Alma Street, Fremantle, WA 6160, Australia
e-mail: byeap@cyllene.uwa.edu.au

siRNA Small interfering RNA
SR-A Scavenger receptor A
TG Triglyceride

Introduction

Atherosclerosis is the underlying pathology behind cardiovascular disease (CVD) which is increased in patients with Type 2 diabetes mellitus [1]. Patients with Type 2 diabetes exhibit a characteristic dyslipidemia with increased TG and reduced HDL [2]. Concentrations of LDL cholesterol are typically not raised, with a predominance of small dense forms. However, specific pathways by which dyslipidemia accelerates development of atherosclerosis in patients with diabetes have not been fully elucidated.

In the process of atherogenesis macrophages within arterial walls express scavenger receptors such as CD36 which mediate uptake of excess oxidized LDL leading to foam cell development, fatty streaks and atheromatous plaque [3, 4]. Macrophage lipid accumulation is balanced by the function of ATP-binding cassette transporter family members ABCA1 and ABCG1 which mediate cholesterol efflux, thus facilitating reverse cholesterol transport to inhibit progression of atherosclerosis [5–7]. Macrophages from patients with Type 2 diabetes cultured in autologous serum exhibited altered fatty acid (FA) profiles with increased ratios of unsaturated to saturated FA [8], and reduced ABCG1 expression and cholesterol efflux [9]. Similar differences in fatty acid content and composition are found in macrophages exposed to serum containing moderately increased TG levels [10]. However, the wider applicability of these findings and other mechanisms by which diabetes might contribute to altered macrophage phenotypes remain unclear.

The enzyme stearoyl-CoA desaturase (SCD) represents a potential link between macrophage FA content and cholesterol efflux. Increased activity of SCD results in conversion of saturated FA to their monounsaturated equivalents and inhibits ABCA1-mediated cholesterol efflux [11, 12]. Recently there has been high interest in the putative role of SCD as a modulator of atherogenesis, based on experimental work in knockout mice [13–15]. However, these data are contradictory, with *SCD*−/− mice exhibiting increased inflammation and atherosclerosis in one study [13], but reduced inflammation and inhibition of atherosclerosis in others [14, 15]. Data which examine the role of SCD in human macrophages cultured in an environment representative of diabetic dyslipidemia could clarify the relevance of these experimental findings to human disease.

We examined the effects of the dyslipidemia encountered in patients with Type 2 diabetes on macrophage lipid accumulation, using macrophages from a common source to isolate the effects of diabetic serum on macrophage phenotype. By replicating in vitro the dyslipidemia seen in patients with diabetes in vivo we tested the hypothesis that diabetic serum with or without dyslipidemia modulates macrophage lipid content and composition reflecting differential expression of proteins involved in lipid uptake. We found that expression of macrophage CD36 and SCD was increased in the presence of diabetic sera and tested the effect of RNA inhibition (RNAi) of these genes on macrophage cholesterol efflux.

Materials and Methods

Study Protocol

Inclusion criteria were: age 35–60 years, non-smoker or ex-smoker, no history of CVD, not on lipid lowering therapy, consumption of <3 standard drinks alcohol/day (<30 g ethanol/day), body mass index <35, blood pressure <160/90. Additional criteria for participants with Type 2 diabetes were: known history of Type 2 diabetes (duration >6 months) and HbA1c <8.5%. Exclusion criteria were: major medical comorbidity or treatment with insulin or glitazones within the previous 6 months. A fasting blood sample (80 mL) was obtained from each study participant. The study was approved by the South Metropolitan Area Health Service Human Research Ethics Committee and participants provided written informed consent.

Serum Preparation

Blood from study participants was stood for 30 min and centrifuged at 16,000×*g* for 10 min before collection of the serum supernatant. Sera were pooled into 5 groups (A–E) and stored at −40 °C until use.

Biochemical Analysis

Fasting glucose, serum total cholesterol (TC), HDL-cholesterol and triglyceride (TG) were measured using the Cobas Integra 800 analyser (Roche Diagnostics) as previously described [8]. LDL-cholesterol levels were calculated using the formula LDL = TC − HDL − (TG/2.22) [16].

Cell Culture and Experimental Strategy

Buffy coats from healthy blood donors were obtained from the Australian Red Cross Blood Service and human monocyte-derived macrophages (hMDM) prepared from white

cell concentrates as previously described [8]. Briefly, monocytes were differentiated by plating at 1.5 × 10^6 cells/ml in RPMI-1640 containing 10% heat-inactivated normal human serum and re-fed at Day 2. For experiments, hMDM were washed at Day 5 and incubated for a further 8 days (to Day 13) in RPMI 1640 containing 10% heat-inactivated pooled human serum (A–E). Macrophages were re-fed every 3 days (Days 8 and 11) with the respective pooled human sera (A–E), and harvested on Day 13 for analyses.

RNA Inhibition of Macrophage CD36 and SCD

At Day 7, transfection of small interfering RNA (siRNA) targeting either CD36 or SCD, or a negative control siRNA was performed using Lipofectamine™ RNAiMAX according to the manufacturer's forward transfection procedure (Invitrogen). The cells were incubated for 24 h at 37 °C in a 5% CO_2 atmosphere. On Day 8, the transfected hMDM were washed with warm PBS and re-fed with experimental media containing 10% sera (A–E). Macrophages were re-fed on Day 10 and harvested on Day 12 for analyses.

Visualization of Lipids with Nile Red Stain

Nile Red (Invitrogen) stains neutral lipids and can be visualized with fluorescence microscopy. At Day 13, human monocyte-derived macrophages (hMDM) were washed with PBS, 1.5% glutaraldehyde added and cells fixed by incubation at 4 °C for 5 min. Cells were washed several times with PBS, Nile Red in PBS (100 ng/mL) was added and left to incubate at room temperature for 5 min. Cells were washed with PBS before visualization under fluorescence microscopy at yellow gold fluorescence (excitation 450–500 nm, emission >528 nm).

Lipid Extraction and Fatty Acid Analysis Through Gas Chromatography

Fatty acid (FA) content and composition for both media and hMDM was analysed using gas chromatography (GC) as previously described [8]. The ratios of C16:1/C16:0 and C18:1/C18:0 was calculated with higher ratios being consistent with increased SCD activity [17].

Cholesterol Analysis Using Gas Chromatography Mass Spectrometry

Cholesterol was extracted using $CHCl_3$/MeOH in the same way FA extraction was conducted as previously described [8]. For total cholesterol analysis, deuterated cholesterol ($^{13}C_2$)(Sigma) was added as an internal standard (10 nmol) to extracted samples and dried under N_2 before addition of 1 mL of KOH/MeOH (1 M) and overnight saponification. Samples were dried under N_2, derivatised by addition of pyridine (30 μL) (Sigma) and *N*,*O*-bis(trimethylsilyl) trifluoro acetamide (BSTFA) (30 μL) (Sigma) followed by heating at 60 °C for 20 min. Lastly, samples were dried under N_2 and reconstituted in iso-octane (200 μL) followed by analysis in a gas chromatograph (Hewlett Packard 6890) mass spectrometer (GC–MS) using a HP-1MS column (Agilent) (30 m × 0.25 mm internal diameter). Ions that were monitored were cholesterol (458.8) and $13C_2$ (460.8). For free cholesterol (FC) analysis, internal standard was added to samples and derivatisation was carried out in the same way. Samples were reconstituted in iso-octane (200 μL) followed by analysis via GCMS. Cholesterol ester (CE) was calculated by subtracting FC content in samples from total cholesterol content.

Western Analysis

hMDM were lysed in RIPA lysis buffer (Sigma) and lysates stored at −80 °C. Protein was quantified using BCA protein assay kit (Pierce) and absorbance measured at 580 nm. SDS-PAGE was performed using 20–50 μg of protein lysate per lane followed by semi-dry blot transfer. Membranes were blocked with 5% skim milk powder in TBS-T (20 mM Tris pH 7.4, 150 mM NaCl, 0.1% Tween-20) before sequential incubations with antibodies to detect CD36 (Novus), SRA (Santa Cruz), ABCA1 (Novus), ABCG1 (Novus), SCD (Sigma), PPARγ (Sigma) and LXRα. (Invitrogen). Actin (Sigma) was used as a loading control. ECL was performed with GE Healthcare ECL Western blotting detection reagents according to the manufacturer's protocol.

Cholesterol Efflux

hMDM were loaded by adding 2 μCi/mL [^{3}H]-cholesterol (PerkinElmer) in ethanol to the media for 24 h. Cells were subsequently washed and equilibrated overnight in RPMI 1640 containing 0.1% (v/v) fatty acid free BSA. [^{3}H]-cholesterol-enriched cells were washed with PBS and incubated in 1.0 mL of efflux medium comprising media with 0.1% (v/v) fatty acid free BSA and 25 μg/mL apoA-1. At 24 and 48 h, an aliquot of media (100 μL) were removed and spun for 5 min at 16,000×*g* to remove any detached cells. The cultures were washed twice with ice cold PBS and then scraped into cold PBS (500 μL). 60-μL media aliquots and 10-μL cell aliquots were analysed by scintillation counting to quantify efflux of [^{3}H]-cholesterol.

Statistical Analysis

Data are presented either as mean ± standard deviation (SD) or mean ± standard error of the means (SE) of means

from multiple independent experiments. Mean comparisons were made using one-way analysis of variance (ANOVA). A p value of <0.05 was considered significant.

Results

Lipid Content of Sera

Sera from participants were pooled into 5 conditions termed A–E. Sera A was from non-diabetic normolipidemic adults; B was from non-diabetic hypercholesterolemic adults; C was from adults with Type 2 diabetes; D was from adults with Type 2 diabetes and hypertriglyceridemia; and E was from adults with Type 2 diabetes and hypercholesterolemia (Table 1). Glucose concentrations in media were fixed at 10.4–11.2 mmol/L. Due to high TG levels in two of the participants from group D, calculated LDL values were not available for this condition.

Effect of Diabetic and Hyperlipidemic Sera on Macrophage Lipid and Fatty Acid Content

On Day 13, there was increased fluorescent staining of hMDM cultured in C, D and E versus A and B (Fig. 1). We performed quantitative analysis using GC which demonstrated increased total FA in hMDM cultured in diabetic, dyslipidemic and hypercholesterolemic conditions (C, D and E) compared with non-diabetic controls (A and B) (Fig. 2a). The increase in FA content in hMDM exposed to diabetic sera (two- threefold increase for C, D and E vs. A, B) was substantially larger than the difference in FA content in the respective media ($\sim$50% higher in D, E vs. A, B) (Fig. 2c). Of note, FA content of media containing A, B and C was similar (Fig. 2c), but hMDM cultured in C had increased macrophage FA content compared to B (Fig. 2a).

Effect of Diabetic and Hyperlipidemic Sera on Macrophage Fatty Acid Composition

hMDM cultured in diabetic conditions C, D and E exhibited increased levels of the individual FA, namely, palmitic (C16:0), palmitoleic (C16:1), stearic (C18:0), oleic (C18:1), linoleic (C18:2) and arachidonic (C20:4) acids compared to A and B (Fig. 2b). These differences in hMDM were greater than differences in FA levels in the respective media (Fig. 2d). hMDM cultured in C accumulated more C16:0, C16:1, C18:0, C18:1 and C18:2 than hMDM in control A or B (Fig. 2b) although FA composition in media C was similar to media A or B (Fig. 2d). hMDM cultured in D had higher levels of C16:0, C16:1, C18:1 and C18:2 compared with A (Fig. 2b). hMDM cultured in E had higher levels of C16:0, C18:0, C18:1, C18:2 and C20:4 compared to A (Fig. 2b).

Ratios of Unsaturated to Saturated Fatty Acid in Macrophages

The ratio of both C16:1/C16:0 and C18:1/C18:0 were significantly higher in hMDM cultured in condition D compared to A (D vs. A, C16:1/C16:0: 2.5 ± 0.4 vs. 1.0 ± 0.2, $p = 0.005$ and C18:1/C18:0: 2.2 ± 0.1 vs. 1.0 ± 0.2, $p < 0.001$).

Effect of Diabetic and Hyperlipidemic Sera on Macrophage Cholesterol Content and Composition

The amounts of free cholesterol (FC) and cholesterol ester (CE) in hMDM cultured under conditions A to E was measured via GC–MS. FC and CE in hMDM was normalized according to the quantity per number of cells, and compared with their concentrations in the respective media. hMDM contained a greater quantity of FC compared to CE (Fig. 3a, b), despite the concentration of CE in the media being higher than that of FC (Fig. 3c, d). There

Table 1 Biochemical analysis of sera from non-diabetic and diabetic study participants

	A ($n = 11$)	B ($n = 7$)	C ($n = 6$)	D ($n = 5$)	E ($n = 4$)
Age (years)	49.2	45.7	61.7	48.0	48.3
Diabetes	No	No	Yes	Yes	Yes
Duration (years)	N/A	N/A	9.2	6.3	7.8
Cholesterol (mmol/L)	4.81 ± 0.17	5.57 ± 0.19	3.50 ± 0.45	4.78 ± 0.34	6.13 ± 0.15
Triglycerides (mmol/L)	0.67 ± 0.05	0.77 ± 0.07	1.35 ± 0.18	3.46 ± 0.75	1.73 ± 0.19
HDL (mmol/L)	2.08 ± 0.12	1.58 ± 0.09	1.37 ± 0.25	1.50 ± 0.13	1.20 ± 0.17
ApoB 100 (g/L)	0.86 ± 0.04	1.18 ± 0.03	0.65 ± 0.09	0.95 ± 0.11	1.41 ± 0.03
LDL (mmol/L)	2.42 ± 0.13	3.64 ± 0.14	1.53 ± 0.34	N/A	4.10 ± 0.21

Sera from study participants were pooled into 5 conditions. *A* Normolipidemic non-diabetic adults, *B* hypercholesterolemic non-diabetic adults, *C* normolipidemic diabetic adults, *D* hypertriglyceridemic diabetic adults and *E* hypercholesterolemic diabetic adults

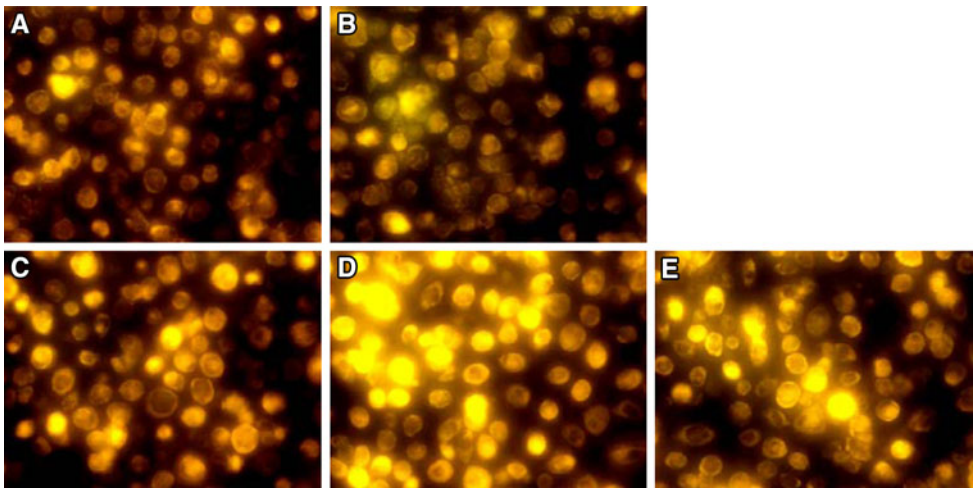

Fig. 1 Macrophages were exposed to sera from *A* normolipidemic non-diabetic adults, *B* hypercholesterolemic non-diabetic adults, *C* normolipidemic diabetic adults, *D* hypertriglyceridemic diabetic adults and *E* hypercholesterolemic diabetic adults, stained with Nile red and photomicrographs (X400) taken under yellow–gold fluorescence

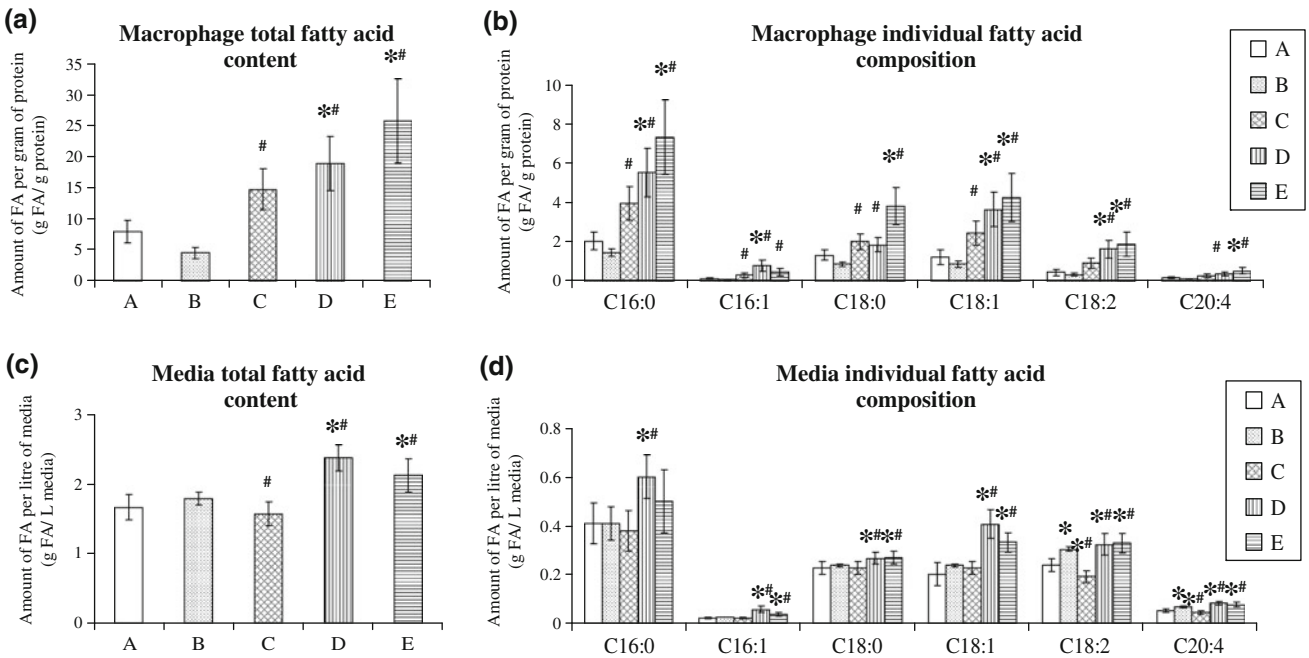

Fig. 2 Macrophage fatty acid (FA) content (**a**) and composition (**b**), and media FA content (**c**) and composition (**d**) following exposure to sera A–E. C16:0, palmitic acid; C18:0, stearic acid; C18:1, oleic acid; C18:2, linoleic acid; C20:4, arachidonic acid. Data are shown as mean ± SE of 3 independent experiments in triplicates. One-way ANOVA; $^{*}p < 0.05$ versus A; $^{\#}p < 0.05$ versus B

was a higher level of FC in media E (Fig. 3c). There was a trend for increased CE content in hMDM cultured across conditions A–E, but CE was increased significantly only in hMDM cultured in E (E vs. A: 2.3 ± 0.4 vs. 1.0 ± 0.2 nmol Chol/5 × 10^5 cells, $p = 0.01$) (Fig. 3b).

Western Analysis in Macrophages Cultured in Conditions A, B, C, D and E

CD36 protein was increased significantly in D compared to controls A or B (Fig. 4). SR-A protein were increased in hMDM cultured in C and D compared to A. ABCA1 protein levels did not vary appreciably between hMDM cultured in A–E. ABCG1 protein was not detected (data not shown). SCD protein level was increased in hMDM cultured in C, D and E compared to A (Fig. 4). PPARγ protein was decreased in hMDM cultured in C, D and E compared to A. LXRα protein levels were similar across conditions A–E.

RNA Inhibition of Macrophage CD36 and SCD

As upregulation of CD36 and SCD protein levels was greatest in hMDM in D, this condition was selected for functional studies using RNAi. hMDM were treated with

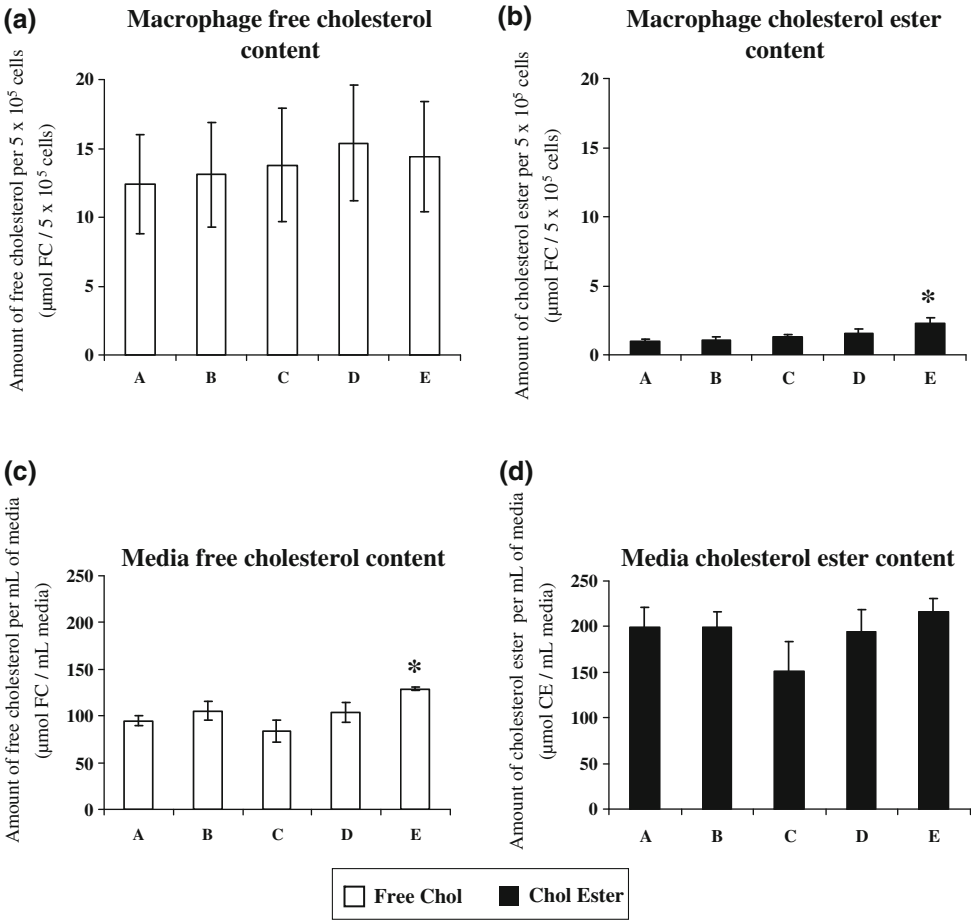

Fig. 3 Free cholesterol (FC, *white bars*) and cholesterol ester (CE, *black bars*) mass in macrophages (**a**), (**b**), and in media (**c**), (**d**). Data are shown as mean ± SE of three experiments in triplicates. One-way ANOVA; $*p < 0.05$ versus A

siRNA targeting CD36 or SCD followed by incubation in A or D. A random siRNA was used as a negative control. Treatment with the respective siRNA successfully reduced CD36 and SCD protein levels (Fig. 5a, e).

Results of siRNA Inhibition of Macrophage CD36 and SCD in Conditions A and D

As expected baseline FA content was higher in D than A (controls in Fig. 5b, d). CD36 siRNA treatment of hMDM cultured in D reduced the amount of macrophage C16:0 and C16:1 (Fig. 5c), and reduced macrophage FC content (D: CD36 siRNA vs. control: 163.9 ± 10.5 vs. 221.9 ± 26.2 mmol free cholesterol/g protein, $p = 0.04$) (Fig. 5d). Treatment with SCD siRNA significantly reduced FA content in hMDM cultured in either A or D (SCD siRNA vs. control: A, 2.1 ± 0.2 vs. 3.4 ± 0.4 g FA/g protein, $p = 0.01$; and D, 3.5 ± 0.3 vs. 4.8 ± 0.5 g FA/g protein, $p = 0.03$) (Fig. 5d). SCD siRNA reduced the amount of C16:0, C16:1, C18:1, C18:2 and C20:4 in A, and the amount of C16:0, C16:1 and C18:1 in D (Fig. 5g). SCD siRNA appeared to reduce macrophage FC content, with the difference in condition A being statistically significant (SCD siRNA vs. control: A, 168.6 ± 9.3 vs. 212.1 ± 23.2 mmol free cholesterol/g protein, $p = 0.04$) (Fig. 5h).

Effects of SCD Inhibition on Macrophage Cholesterol Efflux

Treatment of macrophages with CD36 siRNA did not alter ratios of C16:1/C16:0 or C18:1/C18:0 (Fig. 6a). By contrast, RNA inhibition of SCD decreased the ratios of C16:1/C16:0 and C18:1/C18:0 in macrophages cultured in media A and D (Fig. 6a). The amount of ABCA1 protein was increased consistently after SCD siRNA treatment compared to control siRNA in macrophages cultured in medium D (Fig. 6b). Cholesterol efflux was increased after SCD siRNA treatment in macrophages cultured in condition D (SCD siRNA vs. control siRNA: 18.0 ± 3.9% vs. 8.0 ± 0.8, $p = 0.03$) (Fig. 6c).

Discussion

We found that normal human macrophages exposed to diabetic sera had greater FA accumulation compared to

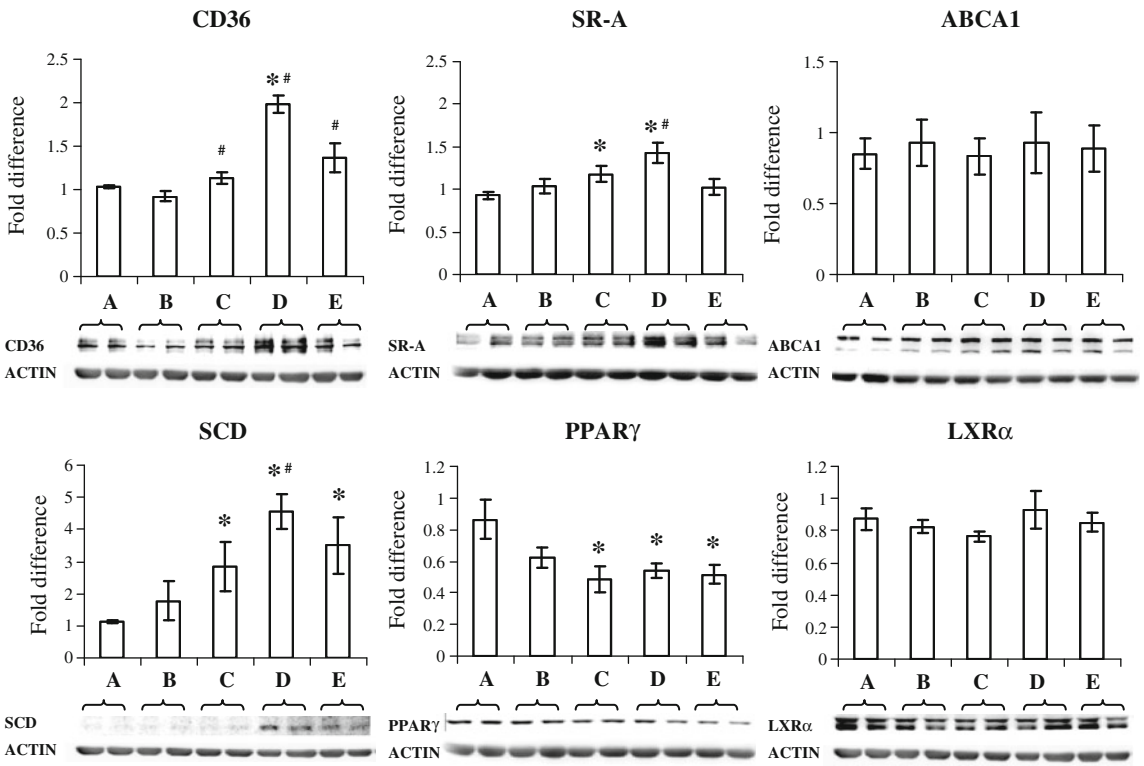

Fig. 4 Western analysis of protein lysates from macrophages cultured in conditions A–E. Data are shown as a representative blot from one experiment in duplicates. β-actin was used as a loading control. Quantitative data are mean ± SE of three independent experiments in duplicates, normalized to A = 1.0. One-way ANOVA; $^{*}p < 0.05$ versus A; $^{\#}p < 0.05$ versus B

non-diabetic sera. Exposure to hypertriglyceridemic diabetic serum resulted in even greater FA accumulation, while exposure to hypercholesterolemic diabetic serum resulted in the highest FA content and increased macrophage CE. Of note, both saturated and unsaturated FA was increased. Alterations in macrophage phenotype were accompanied by increased CD36, SR-A and SCD but reduced PPARγ protein level. A key finding was that in the dyslipidemic environment, RNA inhibition of macrophage SCD not only altered FA composition, but also increased ABCA1 protein level and enhanced cholesterol efflux.

We employed a common source of human monocytes from healthy blood donors thus allowing the specific effect of different diabetic sera to be evaluated. The media content of FC and CE approximately corresponded to total cholesterol levels in the original sera. There was a "dose–response" gradient with the lowest FA content present in macrophages exposed to A and B, intermediate FA content with C and the highest FA content with D and E, with macrophages exposed to E also having increased CE. Increases in saturated and unsaturated FA are potentially relevant to a range of cellular and metabolic functions (for review, see [18]). By contrast, previous studies have used murine macrophages, or loaded macrophages with supra-physiological levels of chemically oxidized lipoproteins [19–21]. Our findings are in keeping with a previous report in which lipoprotein constituents of hypertriglyceridemic sera including chylomicron remnant-like particles induced macrophages to form foam cells and were present in atherosclerotic lesions [22]. By using sera collected from study participants with diabetes, hypertriglyceridemia and hypercholesterolemia, we provided a series of culture environments which more closely replicated the pathophysiology of Type 2 diabetes.

Mauldin et al. [9] found that hMDM from patients with Type 2 diabetes cultured over a 4 day period in autologous serum had reduced cholesterol efflux. Loading macrophages with cholesterol would be expected to result in up-regulation of ABCA1 expression [23]. The degree of macrophage cholesterol loading induced under conditions D and E may be less than seen in experiments using pharmacological concentrations of lipoproteins, and thus could have been insufficient to up-regulate ABCA1. However, conditions B and more so E contained substantial concentrations of LDL thus providing adequate substrate for uptake and there was a trend for increasing macrophage CE content across A–E. It is possible that a particular diabetic milieu suffices to stimulate macrophage lipid accumulation without crossing a threshold needed to induce compensatory increases in cholesterol efflux. An

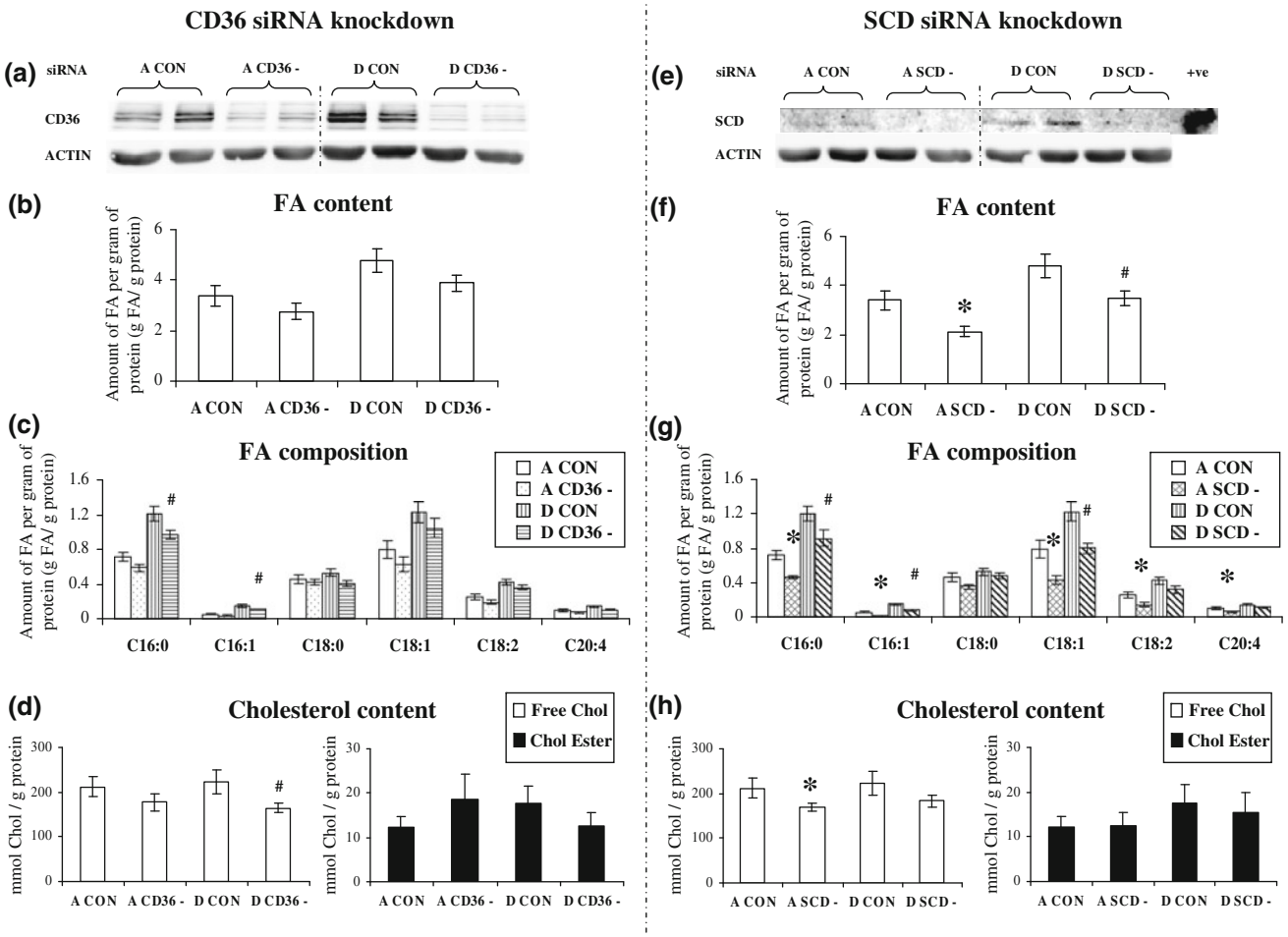

Fig. 5 Macrophages were treated with random siRNA as a negative control (CON) or with siRNA to inhibit CD36 (CD36−) or SCD expression (SCD−). This was followed by culture in conditions A or D. **a** Western blot of CD36 protein level in macrophages ± CD36 siRNA. **b** FA content, **c** FA composition and **d** cholesterol content of macrophages cultured in A or D following siRNA inhibition of CD36. **e** SCD protein level in macrophages ± SCD siRNA. **f** FA content, **g** FA composition and **h** cholesterol content of macrophages cultured in A or D following siRNA inhibition of SCD. Two experiments were done in duplicates for protein analysis and a representative blot is shown. Data are FA or cholesterol content/g protein and shown as mean ± SE of four independent experiments done in triplicates. One-way ANOVA; $^{*}p < 0.05$ versus A control; $^{\#}p < 0.05$ versus D control

alternative explanation is that increased macrophage SCD and unsaturated FA levels seen on exposure to dyslipidemic diabetic sera could blunt the expected upregulation of ABCA1 and cholesterol efflux. Greater SCD expression and activity would increase cellular content of monounsaturated FA such as oleic acid resulting in destabilization of ABCA1 [11, 12], thus inhibiting increases in ABCA1 protein level and cholesterol efflux on exposure to lipid-rich diabetic sera.

Since levels of CD36 and SCD protein were increased in macrophages exposed to dyslipidemic diabetic sera, we selected this condition for extended investigation using RNA inhibition. The experimental protocol was successful in reducing CD36 and SCD protein levels in macrophages cultured under control (A) and diabetic dyslipidemic (D) conditions. CD36 inhibition reduced C16:0 and C16:1 and FC levels in macrophages exposed to diabetic dyslipidemic sera. Therefore, this observation supports a role for elevated CD36 protein levels in macrophages exposed to diabetic and dyslipidemic diabetic sera to enhance FA and cholesterol accumulation.

A key finding was that SCD siRNA reduced unsaturated FA in hMDM exposed to both non-diabetic (A) and dyslipidemic diabetic serum (D). SCD inhibition in macrophages exposed to dyslipidemic diabetic serum consistently reduced macrophage FA levels and reduced the C16:1/C16:0 and C18:1/C18:0 ratios to levels comparable to non-diabetic normolipidemic controls. Furthermore, SCD inhibition in macrophages exposed to dyslipidemic diabetic serum resulted in increased ABCA1 protein levels

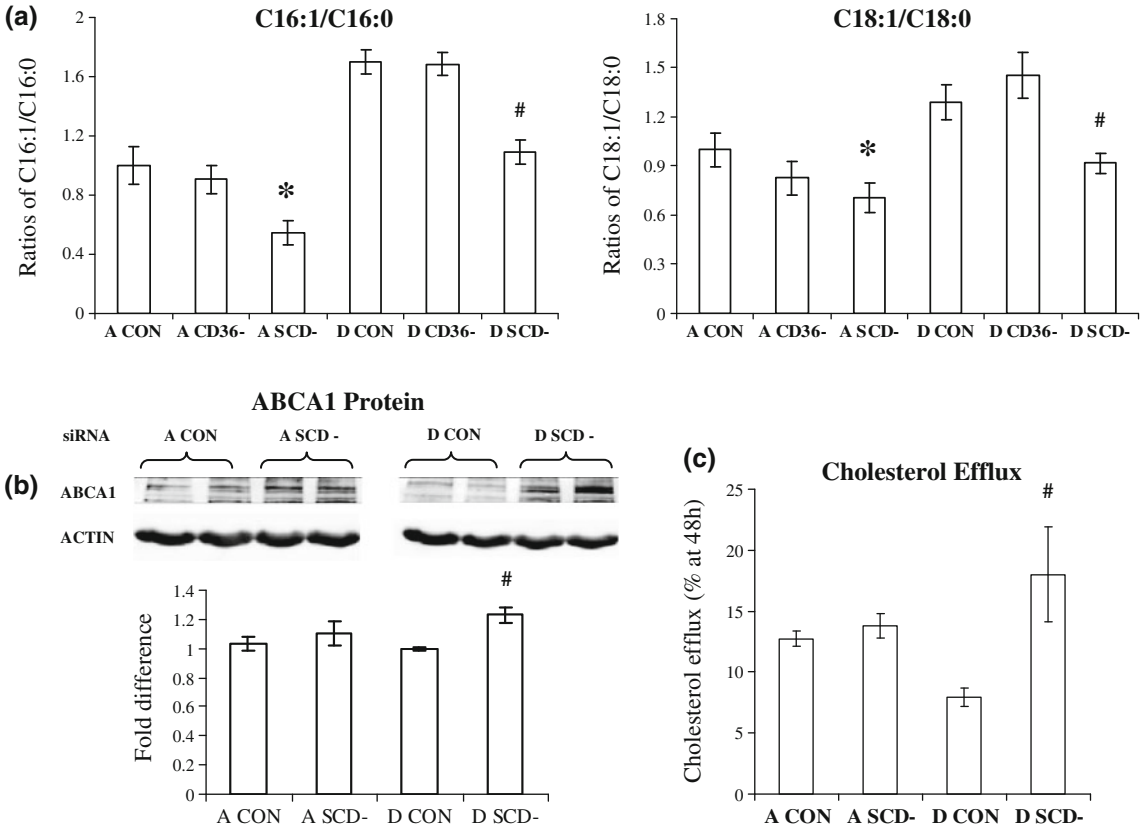

Fig. 6 Macrophages were treated with random siRNA as a negative control (CON) or with siRNA to inhibit CD36 (CD36−) or SCD expression (SCD−) followed by culture in conditions A or D. **a** Effect of CD36 or SCD siRNA on ratios of C16:1/C16:0 and C18:1/C18:0 in macrophages. Data for FA ratios are shown as mean ± SE of four independent experiments, each performed in triplicate. **b** Effect of SCD siRNA on ABCA1 protein level in macrophages. Data are from two independent experiments, each performed in duplicate. **c** Cholesterol efflux from macrophages treated with anti-SCD siRNA and cultured in conditions A and D for 48 h. Data (% efflux) are mean ± SE of four independent experiments, each performed in triplicate. One-way ANOVA; $^{*}p < 0.05$ versus A control; $^{\#}p < 0.05$ versus D control

and enhanced cholesterol efflux. These findings support the concept that increased SCD protein levels seen in macrophages exposed to dyslipidemic diabetic serum might prevent the anticipated compensatory increase in ABCA1 expression and cholesterol efflux, thus predisposing to foam cell formation. Further investigation is required to evaluate whether modulation of macrophage SCD might inhibit the development or progression of atherosclerosis in the context of Type 2 diabetes.

We observed reduced macrophage PPARγ protein levels on exposure to diabetic sera, while LXRα protein levels were stable. Previously activation of macrophage PPARγ has been reported to increase expression of CD36, reduce SR-A, and enhance expression of ABCA1 in part via activation of LXRα [5, 24]. Therefore, downregulation of PPARγ may contribute to a pro-atherogenic macrophage phenotype in the presence of diabetic dyslipidemia. Examining the effects of PPARγ and LXR ligands was beyond the scope of this project, and further investigation would be needed to assess whether LXR agonists might inhibit foam cell formation in the context of Type 2 diabetes [25].

Of note, a 10% serum supplement was used in each condition. The differences observed in the experiments might reflect variation in the amount of lipid added to macrophages, in addition to intrinsic differences in diabetic sera. Nevertheless, these conditions still provide a model for diabetes-related differences in circulating lipids. Sera were frozen promptly following collection which should have minimized in vitro oxidation of lipids. However we can not exclude the possibility that some differences in susceptibility of lipids within diabetic serum to oxidation may have contributed to increased uptake by the scavenger receptor pathway. It is possible that larger differences in the experimental results might have been seen had higher concentrations of serum been used, however 10% is the usual serum supplement for cell culture.

We acknowledge several limitations of this study. We were unable to recruit non-diabetic hypertriglyceridemic persons to provide an additional comparison which would

have been useful. HDL concentrations were highest in condition A, and we did not extend the analysis to differences in lipoprotein subclasses [26]. Therefore, additional investigation would be needed to clarify the role of HDL in this context. As a fixed volume of blood was sampled from each study participant, there was a finite supply of pooled sera for experiments. Consequently the analysis of proteins was not exhaustive, for example cellular lipid loss also involves mobilization of FC from macrophages to HDL via scavenger receptor class B Type 1 (SR-B1) [27]. Within a fixed number of experiments we could not extend the Western analyses to encompass SR-B1 or other proteins. Finally, availability of sera and the protocol for maintaining optimal macrophage growth placed constraints on the functional studies involving RNAi. These experiments were limited to conditions A and D representing a non-diabetic normolipidemic control and a diabetic dyslipidemic condition. Nevertheless, the significant alterations in macrophage phenotypes observed following RNAi of CD36 and particularly SCD were sufficient to demonstrate functional effects attributable to these proteins in human macrophages in the setting of diabetic dyslipidemia.

Our findings also provide an additional helpful context for considering the metabolic role of SCD. Mice with a targeted disruption in the SCD gene are resistant to diet-induced weight gain and have increased insulin sensitivity relative to the WT controls [28]. In another study, inhibition of *Scd* in severely hyperlipidemic LDL receptor-deficient mice challenged with a Western diet reduced plasma triglycerides and weight gain, and increased insulin sensitivity [29]. Despite favorable metabolic characteristics, SCD-deficient mice had increased skin inflammation and atherosclerosis [13], but reduced inflammation in adipocytes [14]. If SCD is inhibited rather than completely abrogated, and combined with dietary fish oil supplements this prevents atherosclerosis in mice [15]. Our results extend these previous reports and support a pro-atherogenic role for SCD in human macrophages in response to dyslipidemic diabetic serum. Further investigation is necessary to extend these findings and to evaluate whether inhibition of macrophage SCD might modulate development or progression of diabetic atherogenesis.

In summary, replicating in vitro diabetic dyslipidemia encountered in vivo provides an informative model to study macrophage phenotypes relevant to diabetic atherogenesis. Macrophages exposed to dyslipidemic diabetic sera exhibited a lipid-rich phenotype, increased expression of CD36 and SR-A, and higher levels of SCD. Inhibition of CD36 reduced macrophage free cholesterol, while inhibition of SCD decreased macrophage FA content, increased ABCA1 protein and enhanced cholesterol efflux. Additional research is needed to clarify whether abrogating the increased macrophage expression of CD36 and SCD that occurs on exposure to dyslipidemic diabetic sera might inhibit diabetic atherogenesis, thus reducing the burden of cardiovascular disease in persons with Type 2 diabetes.

Acknowledgments We thank staff from Biochemistry, Specimen Reception and Transfusion Medicine, Fremantle Hospital for their assistance with this project, and the Australian Red Cross Blood Service for providing buffy coats. This work was supported by research Grants from the National Heart Foundation of Australia (G07 P3159), the Raine Medical Foundation of Western Australia, the University of Western Australia and the Fremantle Hospital Medical Research Foundation, Western Australia.

Conflict of interest The authors have no conflicts of interest to declare.

References

1. Schramm TK, Gislason GH, Kober L, Rasmussen S, Rasmussen JN, Abildstrom SZ, Hansen ML, Folke F, Buch P, Madsen M, Vaag A, Torp-Pedersen C (2008) Diabetes patients requiring glucose-lowering therapy and non-diabetics with a prior myocardial infarction carry the same cardiovascular risk: a population study of 3.3 million people. Circulation 117:1945–1954
2. Mooradian AD (2009) Dyslipidemia in type 2 diabetes mellitus. Nat Clin Pract Endocrinol Metab 5:150–159
3. Osterud B, Bjorklid E (2003) Role of monocytes in atherogenesis. Physiol Rev 83:1069–1112
4. Manning-Tobin JJ, Moore KJ, Seimon TA, Bell SA, Sharuk M, Alvarez-Leite JI, de Winther MP, Tabas I, Freeman MW (2009) Loss of SR-A and CD36 activity reduces atherosclerotic lesion complexity without abrogating foam cell formation in hyperlipidemic mice. Arterioscler Thromb Vasc Biol 29:19–26
5. Chawla A, Boisvert WA, Lee CH, Laffitte BA, Barak Y, Joseph SB, Liao D, Nagy L, Edwards PA, Curtiss LK, Evans RM, Tontonoz P (2001) A PPAR gamma-LXR-ABCA1 pathway in macrophages is involved in cholesterol efflux and atherogenesis. Mol Cell 7:161–171
6. Vaughan AM, Oram JF (2006) ABCA1 and ABCG1 or ABCG4 act sequentially to remove cellular cholesterol and generate cholesterol-rich HDL. J Lipid Res 47:2433–2443
7. Jessup W, Gelissen IC, Gaus K, Kritharides L (2006) Roles of ATP binding cassette transporters A1 and G1, scavenger receptor BI and membrane lipid domains in cholesterol export from macrophages. Curr Opin Lipidol 17:247–257
8. Senanayake S, Brownrigg LM, Panicker V, Croft KD, Joyce DA, Steer JH, Puddey IB, Yeap BB (2007) Monocyte-derived macrophages from men and women with Type 2 diabetes mellitus differ in fatty acid composition compared with non-diabetic controls. Diabetes Res Clin Pract 75:292–300
9. Mauldin JP, Nagelin MH, Wojcik AJ, Srinivasan S, Skaflen MD, Ayers CR, McNamara CA, Hedrick CC (2008) Reduced expression of ATP-binding cassette transporter G1 increases cholesterol accumulation in macrophages of patients with type 2 diabetes mellitus. Circulation 117:2785–2792
10. Wong BXW, Kyle RA, Croft KD, Quinn CM, Jessup W, Yeap BB (2011) Modulation of macrophage fatty acid content and composition by exposure to dyslipidemic serum in vitro. Lipids 46:371–380
11. Wang Y, Oram JF (2002) Unsaturated fatty acids inhibit cholesterol efflux from macrophages by increasing degradation of ATP-binding cassette transporter A1. J Biol Chem 277:5692–5697

12. Wang Y, Kurdi-Haidar B, Oram JF (2004) LXR-mediated activation of macrophage stearoyl-CoA desaturase generates unsaturated fatty acids that destabilize ABCA1. J Lipid Res 45:972–980
13. MacDonald MLE, van Eck M, Hildebrand RB, Wong BWC, Bissada N, Ruddle P, Kontush A, Hussein H, Pouladi MA, Chapman MJ, Fievet C, van Berkel TJC, Staels B, McManus BM, Hayden MR (2009) Despite antiatherogenic metabolic characteristics, SCD1-deficient mice have increased inflammation and atherosclerosis. Arterioscler Thromb Vasc Biol 29:341–347
14. Liu X, Miyazaki M, Flowers MT, Sampath H, Zhao M, Chu K, Paton CM, Joo DS, Ntambi JM (2010) Loss of stearoyl-CoA desaturase-1 attenuates adipocyte inflammation: effects of adipocyte-derived oleate. Arterioscler Thromb Vasc Biol 30:31–38
15. Brown JM, Chung S, Sawyer JK, Degirolamo C, Alger HM, Nguyen TM, Zhu X, Duong M-N, Brown AL, Lord C, Shah R, Davis MA, Kelley K, Wilson MD, Madenspacher J, Fessler MB, Parks JS, Rudel LL (2010) Combined therapy of dietary fish oil and stearoyl-CoA desaturase 1 inhibition prevents the metabolic syndrome and atherosclerosis. Arterioscler Thromb Vasc Biol 30:24–30
16. Rifai N, Warnick GR (2006) Lipids, lipoproteins, apolipoproteins, and other cardiovascular risk factors. In: Burtis CA, Ashwood ER, Bruns DE (eds) Tietz textbook of clinical chemistry and molecular diagnostics, 4th edn edn. Elsevier Saunders, St Louis, pp 903–981
17. Attie AD, Krauss RM, Gray-Keller MP, Brownlie A, Miyazaki M, Kastelein JJ, Lusis AJ, Stalenhoef AF, Stoehr JP, Hayden MR, Ntambi JM (2002) Relationship between stearoyl-CoA desaturase activity and plasma triglycerides in human and mouse hypertriglyceridemia. J Lipid Res 43:1899–1907
18. Legrand P, Rioux V (2010) The complex and important cellular and metabolic functions of saturated fatty acids. Lipids 45: 941–946
19. Mertens A, Verhamme P, Bielicki JK, Phillips MC, Quarck R, Verreth W, Stengel D, Ninio E, Navab M, Mackness B, Mackness M, Holvoet P (2003) Increased low-density lipoprotein oxidation and impaired high-density lipoprotein antioxidant defense are associated with increased macrophage homing and atherosclerosis in dyslipidemic obese mice: LCAT gene transfer decreases atherosclerosis. Circulation 107:1640–1646
20. Liang CP, Han S, Okamoto H, Carnemolla R, Tabas I, Accili D, Tall AR (2004) Increased CD36 protein as a response to defective insulin signaling in macrophages. J Clin Invest 113:764–773
21. Mauldin JP, Srinivasan S, Mulya A, Gebre A, Parks JS, Daugherty A, Hedrick CC (2006) Reduction in ABCG1 in Type 2 diabetic mice increases macrophage foam cell formation. J Biol Chem 281:21216–21224
22. De Pascale C, Avella M, Perona JS, Ruiz-Gutierrez V, Wheeler-Jones CP, Botham KM (2006) Fatty acid composition of chylomicron remnant-like particles influences their uptake and induction of lipid accumulation in macrophages. FEBS J 273:5632–5640
23. Oram JF, Heinecke JW (2005) ATP-binding cassette transporter A1: a cell cholesterol exporter that protects against cardiovascular disease. Physiol Rev 85:1343–1372
24. Moore KJ, Rosen ED, Fitzgerald ML, Randow F, Andersson LP, Altshuler D, Milstone DS, Mortensen RM, Spiegelman BM, Freeman MW (2001) The role of PPAR-gamma in macrophage differentiation and cholesterol uptake. Nat Med 7:41–47
25. Larrede A, Quinn CM, Jessup W, Frisdal E, Olivier M, Hsieh V, Kim M-J, Van Eck M, Couvert P, Carrie A, Giral P, Chapman MJ, Guerin M, Le Goff W (2009) Stimulation of cholesterol efflux by LXR agonists in cholesterol-loaded human macrophages is ABCA1-dependent but ABCG1-independent. Arterioscler Thromb Vasc Biol 29:1930–1936
26. Lagos KG, Filippatos TD, Tsimihodimos V, Gazi IF, Rizos C, Tselepis AD, Mikhailidis DP, Elisaf MS (2009) Alterations in the high density lipoprotein phenotype and HDL-associated enzymes in subjects with metabolic syndrome. Lipids 44:9–16
27. Cuchel M, Lund-Katz S, de la Llera-Moya M, Millar JS, Chang D, Fuki I, Rothblat GH, Phillips MC, Rader DJ (2010) Pathways by which reconstituted high-density lipoprotein mobilizes free cholesterol from whole body and from macrophages. Arterioscler Thromb Vasc Biol 30:526–532
28. Rahman SM, Dobrzyn A, Dobrzyn P, Lee SH, Miyazaki M, Ntambi JM (2003) Stearoyl-CoA desaturase 1 deficiency elevates insulin-signaling components and down-regulates protein-tyrosine phosphatase 1B in muscle. Proc Natl Acad Sci USA 100: 11110–11115
29. MacDonald ML, Singaraja RR, Bissada N, Ruddle P, Watts R, Karasinska JM, Gibson WT, Fievet C, Vance JE, Staels B, Hayden MR (2008) Absence of stearoyl-CoA desaturase-1 ameliorates features of the metabolic syndrome in LDLR-deficient mice. J Lipid Res 49:217–229

Lipids (2011) 46:943–952
DOI 10.1007/s11745-011-3588-3

ORIGINAL ARTICLE

Amadori-Glycated Phosphatidylethanolamine, a Potential Marker for Hyperglycemia, in Streptozotocin-Induced Diabetic Rats

Phumon Sookwong · Kiyotaka Nakagawa · Ikuko Fujita · Naoki Shoji · Teruo Miyazawa

Received: 14 April 2011 / Accepted: 14 June 2011 / Published online: 6 July 2011

Abstract It has been demonstrated in vivo that lipid glycation products such as Amadori-glycated phosphatidylethanolamine (Amadori-PE) accumulate in the plasma of diabetic humans and animals, but how lipid glycation products are formed under hyperglycemic conditions are not clear. We sought to clarify the occurrence of lipid glycation and its relationships with lipid peroxidation and protein glycation during the development of hyperglycemia using the streptozotocin (STZ)-induced diabetic rat model. A significant increase in Amadori-PE was observed in STZ rats 7 days after STZ treatment, and Amadori-PE (especially 18:0–20:4 Amadori-PE) was found at high levels in the blood and in organs that are strongly affected by diabetes, such as the kidney. Significant changes in Amadori-PE appeared to occur prior to changes in levels of oxidized lipids, which increased after 21–28 days. In addition, accumulation of *N*ε-(carboxymethyl)lysine (CML), a protein glycation product, proceeded somewhat more slowly and moderately than that of Amadori-PE, suggesting that Amadori-PE and CML are early and advanced glycation products, respectively. Our results suggest that Amadori-PE may be a useful predictive marker for hyperglycemia, particularly in the early stages of diabetes. Similar speculations have been made from previous human studies, but this study provides a direct evidence to support the speculations in rat study.

Keywords Diabetes · Hyperglycemia · Lipid glycation · Oxidized lipids

Abbreviations

1,5-AG	1,5-Anhydroglucitol
ALT	Alanine aminotransferase
Amadori-PE	Amadori-glycated phosphatidylethanolamine
AST	Aspartate aminotransferase
CL	Chemiluminescence
CML	*N*ε-(carboxymethyl)lysine
Hb_{A1c}	Hemoglobin A1c
LC	Liquid chromatography
MRM	Multiple reaction monitoring
MS/MS	Tandem mass spectrometry
NFPA	Nonafluoropentanoic acid
NLS	Neutral loss scanning
PCOOH	Phosphatidylcholine hydroperoxide
PE	Phosphatidylethanolamine
PL	Phospholipid
RBC	Red blood cells
STZ	Streptozotocin
TBARS	Thiobarbituric acid reactive substances
T-cho	Total cholesterol
TAG	Triacylglycerol

Introduction

The clinical significance of non-enzymatic protein glycation in complications of diabetes has been studied

Electronic supplementary material The online version of this article (doi:10.1007/s11745-011-3588-3) contains supplementary material, which is available to authorized users.

P. Sookwong · K. Nakagawa · I. Fujita · T. Miyazawa (✉)
Food and Biodynamic Chemistry Laboratory,
Graduate School of Agricultural Science,
Tohoku University, Sendai 981-8555, Japan
e-mail: miyazawa@biochem.tohoku.ac.jp

N. Shoji
Industrial Technology Institute, Miyagi Prefectural Government,
Sendai 981-3206, Japan

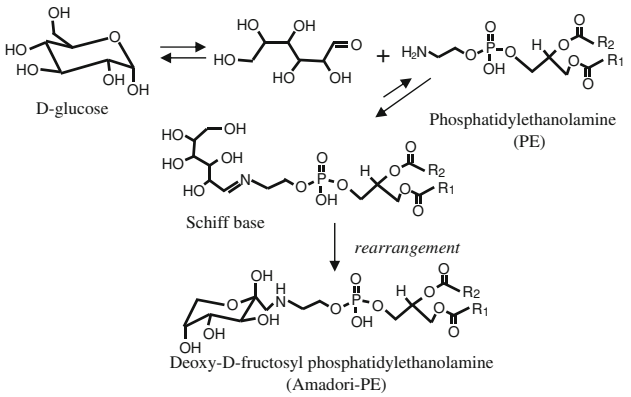

Fig. 1 Scheme for the glycation of phosphatidylethanolamine (PE). Glucose reacts with the amino group of PE to form a Schiff base, which undergoes an Amadori rearrangement to yield deoxy-D-fructosyl PE (Amadori-PE)

extensively [1]. In addition to protein glycation, our group and other researchers have found that glycation of lipids and glucose also occurs in vivo [2–4]. A previous study by our group demonstrated that Amadori-glycated phosphatidylethanolamine (Amadori-PE, Fig. 1) can accumulate in the plasma of diabetic rats [5]. Accumulation of Amadori-PE was also detected in the plasma of diabetic patients [6], and a positive correlation was found between Amadori-PE and lipid peroxides such as phosphatidylcholine hydroperoxide (PCOOH). This relationship between Amadori-PE and lipid peroxides suggests that lipid glycation may play an important role in diabetogenesis and the development of diabetic complications such as retinopathy, nephropathy, neuropathy, and atherosclerotic macrovascular disease [7, 8].

Although there is increasing evidence of the involvement of lipid glycation in diabetic complications, it is still unclear how lipid glycation products are formed during the development of hyperglycemia. Furthermore, since Amadori-PE is able to induce lipid peroxidation [9], it is of interest to determine whether levels of Amadori-PE and lipid peroxides change during the development of hyperglycemia. In addition, lipid and protein glycation are understood to be related to the pathogenesis of diabetes, but there have been no comparative studies of the prevalence of the two glycation products (glycated lipids and glycated proteins) during diabetes development. Such a comparative study would provide greater insight into the relationship between glycation and diabetogenesis, and could reveal whether glycation products can be used as indicators of diabetes.

Therefore, in the present study, we sought to confirm the occurrence of lipid glycation (Amadori-PE) during the development of hyperglycemia and to investigate the relationship between lipid glycation, lipid peroxidation, and protein glycation in streptozotocin (STZ)-induced diabetic rats. Since Amadori-PE is comprised of two fatty acids, several molecular species are possible due to the presence of different fatty acid structures. Accordingly, in this study, a recently developed liquid chromatography–tandem mass spectrometry (LC–MS/MS) technique was used to quantify eight molecular species of Amadori-PE [6, 10]. STZ rats were evaluated for biological and pathological changes (including formation of lipid glycation and protein glycation products) during the period of diabetes development. Based on the results of this study, we discuss the presence and significance of lipid and protein glycation products during diabetes development and the potential use of lipid glycation products as biomarkers for hyperglycemia.

Materials and Methods

Materials

All PE molecular species were purchased from Avanti Polar Lipids (Alabaster, AL). PE molecular species were identified by carbon chain length and degree of unsaturation of the *sn*-1,2 acyl chains; e.g., "18:0–18:1 PE" for 1-octadecanoyl-2-octadecenoyl-*sn*-glycero-3-phosphoethanolamine. Amadori-PE standards were synthesized using PE species as starting materials, as previously described [9] with minor modifications. In brief, PE (e.g., 18:0–18:1 PE; 15 μmol) and glucose (5 mmol) were dissolved in 50 ml of methanol, and incubated at 60 °C for 24 h. After incubation, lipid-soluble products were extracted using Folch's partition [11]. The extract was evaporated to dryness, and the residue was dissolved in 10 ml of chloroform–methanol (2:1, v/v). Amadori-PE was then isolated using a preparative reversed-phase column (5C-18-MS-II, 250 × 10 mm; Nacalai Tesque, Japan) with methanol-5 mM aqueous ammonium acetate (99:1, v/v) as the eluent. The structure and purity of each synthesized Amadori-PE was evaluated by LC–MS (Mariner, Applied Biosystems, Foster City, CA), high resolution fast atom bombardment MS (JEOL-JMS-700 mass station, JEOL, Tokyo, Japan), and NMR (Varian Unity 600 spectrometer, Varian, Palo Alto, CA). All other reagents were purchased from Wako (Osaka, Japan) using the highest grade available.

Animal Experiments

Male Sprague–Dawley rats (4 weeks of age) were purchased from Japan SLC (Hamamatsu, Japan). Rats were given free access to standard laboratory chow (MF pellet; Oriental Yeast, Tokyo, Japan) and water for 1 week before the experiment began. Rats were housed in a temperature- and humidity-controlled room with a 12 h light cycle. All animal experiments were conducted in accordance with the Animal Experimentation Guidelines of Tohoku University.

On day 0 (the first experimental day after acclimatization for 1 week), diabetes was induced in rats by a single intraperitoneal injection of 70 mg/kg streptozotocin (STZ; Sigma, St. Louis, MO) dissolved in citric acid buffer (50 mM, pH 4.5), whereas control rats received an injection of buffer only. Blood glucose was measured 3 days after STZ injection, and rats with blood glucose levels >250 mg/dl were considered diabetic.

On days 0, 7, 14, 21 and 28, diabetic and control rats ($n = 6$ for each time point) were anesthetized with Avertin and slaughtered. Blood (10 ml) was collected into a tube containing heparin as an anticoagulant, and was centrifuged at 1,000*g* for 10 min at 4 °C. After the plasma and buffy coat were removed, red blood cells (RBC) were washed three times with phosphate-buffered saline (pH 7.4) to prepare packed cells. Total lipids were extracted from 1 ml of the packed cells using 2-propanol and chloroform [12]. Plasma (0.5 ml) was subjected to total lipid extraction using Folch's partition [11]. For tissue analysis, liver, kidney, pancreas, cerebrum, and cerebellum were collected, and these samples (100 mg) were also subjected to Folch lipid extraction. Each lipid extract was evaporated to dryness, and the residue was dissolved in 0.5 ml of chloroform–methanol (2:1, v/v).

MS/MS Analysis of Amadori-PE

A 4000 QTRAP quadrupole/linear ion-trap tandem mass spectrometer (Applied Biosystems) was used for MS/MS analysis. MS/MS parameters (e.g., collision energy) were optimized using synthesized 18:0–18:1 Amadori-PE as a reference compound. After optimization, neutral loss scanning (NLS) was performed to profile Amadori-PE molecular species in blood samples. The MS/MS instrument was programmed to scan parent ions that yielded a neutral loss of 303 Da after fragmentation in the collision cell. Sample (lipid extract, 5 μl) was injected directly into MS/MS using methanol as a carrier solvent (0.2 ml/min). Electrospray ionization was used as an ion source with collision energy of 45 eV, transition dwell time of 100 ms, turbo gas temperature of 500 °C, and spray voltage of 5,500 V. Nitrogen pressure values for turbo, nebulizer, and curtain gases were set at 40, 60, and 20 pounds per square inch, respectively.

LC–MS/MS Analysis of Amadori-PE

For LC–MS/MS analysis, a Shimadzu liquid chromatography system (Shimadzu, Kyoto, Japan) was equipped with the 4000 QTRAP. Amadori-PE was analyzed using a silica column (Inertsil, 2.1 × 100 mm; GL Sciences, Tokyo, Japan) with a binary gradient consisting of solvent A [acetonitrile–methanol–1 M aqueous ammonium formate (pH 6.0) (78:20:2, v/v/v)] and solvent B [acetonitrile–methanol–1 M aqueous ammonium formate (pH 6.0) (49:49:2, v/v/v)]; [10]. The gradient profile was as follows: 0–1.25 min, 10% B; 1.25–2 min, 10–100% B linear gradient; 2–6 min, 100% B; 6–6.5 min, 100–10% B linear gradient; 6.5–8 min, 10% B. The flow rate was 0.4 ml/min, and the column temperature was 40 °C. Amadori-PE was detected in the postcolumn by MS/MS with multiple reaction monitoring (MRM) for the transition of parent ion to product ion.

For quantitation of Amadori-PE in blood and tissue samples, we focused on eight molecular species (16:0–18:1, 16:0–18:2, 16:0–20:4, 16:0–22:6, 18:0–18:1, 18:0–18:2, 18:0–20:4, and 18:0–22:6 Amadori-PE), because their presence in RBC was revealed by NLS by MS/MS analysis. Using synthesized Amadori-PE species, we prepared standard solutions at concentrations of 5–1,000 pmol/ml (a range expected to encompass concentrations encountered in vivo). Plasma extract, RBC extract, tissue extract, or standard solution (2 μl each) was then subjected to LC–MS/MS, and the Amadori-PE molecular species were individually detected using MRM. The concentrations of Amadori-PE in plasma, RBC, and tissues were calculated using calibration curves for the synthesized Amadori-PE molecules. The concentrations of PE in plasma, RBC, and tissues were similarly determined by LC–MS/MS with MRM [10].

Detection of Lipid Peroxides

To examine oxidative stress, PCOOH in total lipid extracts from plasma and liver was measured by HPLC with chemiluminescence (CL) detection [13, 14]. The column was a Finepak SIL NH2-5 (4.6 × 250 mm; Japan Spectroscopic Co., Tokyo, Japan), the eluent was 2-propanol–methanol–water (135:45:20, v/v/v), and the flow rate was 1 ml/min. Post-column CL detection was carried out using a CLD-100 detector (Tohoku Electronic Industries Co., Sendai, Japan). A mixture of luminol and cytochrome c in 50 mM borate buffer (pH 10.0) was used as a hydroperoxide-specific post-column CL reagent. Calibration was carried out using standard PCOOH. In addition to PCOOH, thiobarbituric acid reactive substances (TBARS) were measured as described previously [15].

*N*ε-(Carboxymethyl)lysine Analysis

*N*ε-(Carboxymethyl)lysine (CML) was measured by LC–MS/MS [16]. Blood and tissue samples were analyzed by reversed-phase HPLC on an Atlantis T3 column (2.1 × 100 mm, Waters, Milford, MA). Mobile phase A was 5 mM aqueous nonafluoropentanoic acid (NFPA) and mobile phase B was acetonitrile containing NFPA (5 mM).

The gradient profile was as follows: 0–8 min, 15–50% B linear gradient; 8–8.5 min, 50–90% B linear gradient; 8.5–9.5 min, 90% B; 9.5–11 min, 90–15% B linear gradient; 11–15 min, 15% B. Analyses were performed in positive-ion mode with the ion-spray voltage at 5,500 V. MRM pairs (parent ion/product ion) for CML and lysine were 205/84 and 147/84, respectively.

Other Biochemical Measurements

Blood glucose and insulin levels were measured using a Glucose C II test kit (Wako) and a Rat/Mouse Insulin ELISA Kit (EZRMI-13K, Linco Research, St. Charles, MO) according to the manufacturers' protocols. Blood parameters, including 1,5-anhydroglucitol (1,5-AG), hemoglobin A1c (Hb_{A1c}), aspartate aminotransferase (AST), alanine aminotransferase (ALT), triacylglycerol (TG), and total cholesterol (T-cho), were analyzed by Mitsubishi Chemical Medicine Corporation (Japan). Phospholipid (PL) content in plasma was measured using methods described by Bartlett [17]. Hepatic lipid parameters were analyzed using standard methods.

Statistical Analysis

Data are expressed as mean values ± SD. Statistical analyses in this study included the Student's t test and Mann–Whitney U test. Differences were considered significant at $P < 0.05$ and $P < 0.01$.

Results

General Characteristics of STZ Rats

During the 28-day experimental period, weight gain, plasma insulin, and 1,5-AG were suppressed in STZ rats, and blood glucose and Hb_{A1c} levels were consistently elevated in these animals (Fig. 2). Plasma levels of AST, ALT, TG, T-cho, and

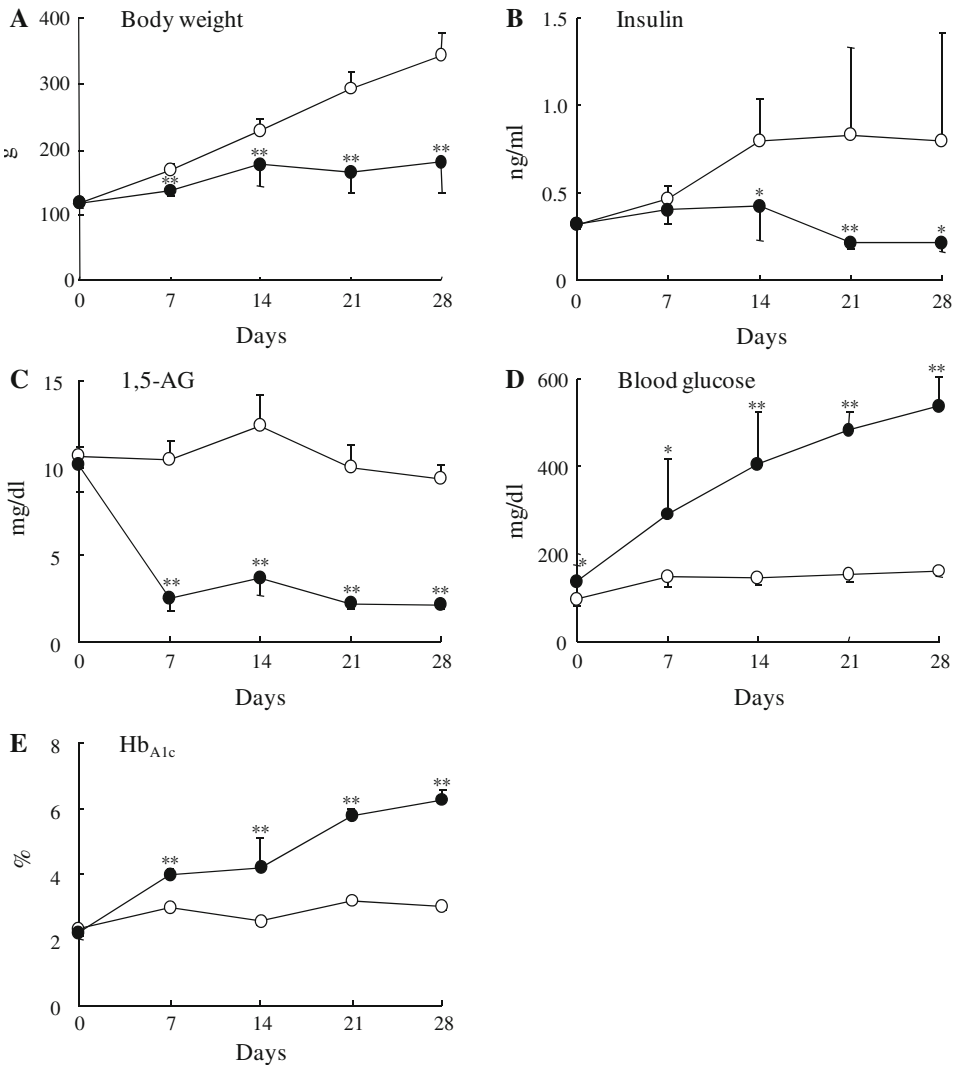

Fig. 2 Characteristic changes in **a** body weight, **b** insulin, **c** 1,5-AG, **d** blood glucose, and **e** Hb_{A1c}. Values are means ± SD ($n = 6$; $*P < 0.05$ and $**P < 0.01$). *White circles* represent control rats, and *black circles* represent STZ rats

Table 1 Time course of changes in plasma and liver parameters of STZ-induced diabetic rats

Determination	Group	Days				
		0	7	14	21	28
Plasma						
AST (IU/l)	Control	108 ± 10	106 ± 10	116 ± 41	77.0 ± 10.3	74.0 ± 10.4
	STZ	98.3 ± 4.6	261 ± 146*	360 ± 210*	236 ± 60**	221 ± 142**
ALT (IU/l)	Control	42.7 ± 3.0	43.3 ± 3.0	39.0 ± 8.3	35.7 ± 3.9	38.3 ± 4.3
	STZ	41.3 ± 3.3	142 ± 76**	180 ± 95*	169 ± 42**	150 ± 52**
TG (mg/dl)	Control	59.7 ± 16.1	31.0 ± 8.3	22.0 ± 10.3	31.0 ± 16.1	36.3 ± 24.4
	STZ	68.0 ± 36.9	102 ± 60*	332 ± 350**	396 ± 299*	387 ± 246**
T-Cho (mg/dl)	Control	79.3 ± 6.3	57.7 ± 5.3	58.0 ± 1.8	51.0 ± 4.5	55.0 ± 5.0
	STZ	76.7 ± 7.2	51.0 ± 8.9	113 ± 89*	153 ± 84**	121 ± 43**
PL (mg/dl)	Control	125 ± 14	95.2 ± 11.7	101 ± 13	93.3 ± 15.2	114 ± 16
	STZ	119 ± 24	76.6 ± 7.8**	159 ± 74*	204 ± 86*	235 ± 79**
Liver						
TG (mg/g)	Control	38.6 ± 14.7	36.9 ± 6.6	37.7 ± 5.1	37.7 ± 14.9	34.2 ± 12.5
	STZ	36.6 ± 13.5	38.9 ± 4.4	41.8 ± 10.5*	47.4 ± 5.6*	46.1 ± 9.3*
T-Cho (mg/g)	Control	3.3 ± 0.2	3.9 ± 0.2	3.8 ± 0.2	3.7 ± 0.5	3.7 ± 0.5
	STZ	3.6 ± 0.2	4.6 ± 0.2	5.7 ± 0.7*	6.0 ± 0.5*	5.9 ± 0.2*

Values are means ± SD ($n = 6$). Significantly different from counterpart control at *$P < 0.05$ and **$P < 0.01$

AST aspartate aminotransferase, *ALT* alanine aminotransferase, *TG* triacylglycerol, *T-Cho* total cholesterol, *PL* phospholipids

PL were higher in the STZ group (Table 1). Among hepatic lipid parameters, TG and T-cho were increased in the STZ group (Table 1). These data indicate that low insulin secretion in these STZ rats led to hyperglycemia and hyperlipidemia, and resulted in severe diabetes.

(LC)-MS/MS Profiling and Determination of Amadori-PE Molecular Species

MS/MS NLS is useful for analyzing PE glycation [6, 10], and Amadori-PE can be detected by searching for the loss of glycated group ($H_2PO_4CH_2CH_2NHC_6H_{11}O_5$, 303 Da) (refer to Fig. 3a). Using NLS, we profiled the molecular Amadori-PE species in STZ rats. For example, in neutral loss spectra of 303 Da of STZ rat RBC, a series of ion peaks was observed to correspond to Amadori-PE molecular species (16:0–18:1, 16:0–18:2, 16:0–20:4, 16:0–22:6, 18:0–18:1, 18:0–18:2, 18:0–20:4, and 18:0–22:6) (Fig. 3b). Based on the NLS data, the eight Amadori-PE species were individually quantified using LC–MS/MS with MRM (Fig. 3c).

PE Glycation During the Development of Hyperglycemia

Changes in accumulation of total Amadori-PE (as determined by LC–MS/MS with MRM) in plasma, RBC, liver, kidney, pancreas, cerebrum, and cerebellum over the study period are shown in Fig. 4. Amadori-PE content was significantly increased in blood and in most tissues of STZ rats compared with the control group after experimental day 7, and the difference between the two groups increased over time. The accumulation of Amadori-PE was greatest in liver, followed by kidney, cerebrum, cerebellum, and pancreas. Among Amadori-PE molecular species, 18:0–20:4 Amadori-PE and 18:0–18:2 Amadori-PE were predominant in the blood and tissues of STZ rats (Fig. 5). After 28 experimental days, STZ rats showed marked accumulation of 18:0–20:4 Amadori-PE, and the ratios of those species in the STZ and control groups were 20, 8, 3, 4, 35, 7, and 5 in plasma, RBC, liver, kidney, pancreas, cerebrum, and cerebellum, respectively. These results suggest that PE glycation actually proceeded and Amadori-PE concentration markedly increased under hyperglycemic conditions. Consistent with this hypothesis, glycation rates (mol % Amadori-PE vs. native PE), especially to 18:0–20:4 PE, were higher in STZ rats (Supplementary Figs. 1 and 2).

Lipid Peroxidation and Protein Glycation

Given our previous finding that Amadori-PE can cause lipid peroxidation [9], we also monitored changes in lipid peroxides during the experimental period. On day 28, PCOOH and TBARS were observed at high levels in the plasma and livers of STZ rats (Fig. 6). With respect to protein glycation, all blood and tissues analyzed showed higher CML accumulation

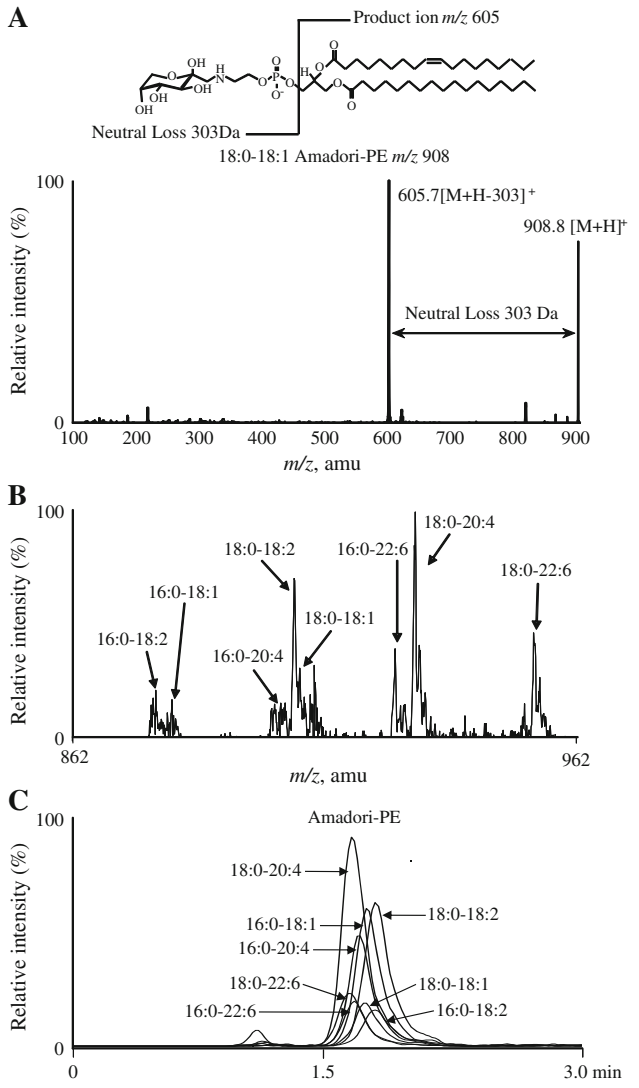

Fig. 3 MS/MS and LC–MS/MS analysis of Amadori-PE. **a** Product ion scan of synthesized 18:0–18:1 Amadori-PE. **b** Neutral loss scan spectrum of 303 Da allowing detection of predominant Amadori-PE species (16:0–18:1, 16:0–18:2, 16:0–20:4, 16:0–22:6, 18:0–18:1, 18:0–18:2, 18:0–20:4, and 18:0–22:6) in RBC of STZ rats. **c** MRM chromatograms of the eight Amadori-PE species in RBC of STZ rats

in STZ rats (Fig. 7). However, the accumulation of CML was somewhat slower and more moderate than that of Amadori-PE. These results suggest the importance of lipid glycation, and imply the potential involvement of lipid glycation and peroxidation in diabetogenesis.

Discussion

Like proteins, lipids (PE) can be modified by glycation during the development of hyperglycemia. PE glycation is likely to induce changes in the biosynthesis and turnover of membrane phospholipids, the physical properties of membranes, the activity of membrane-bound enzymes, and the susceptibility to oxidative stress [9, 18–20]. These changes may contribute to diabetogenesis and the development of diabetic complications. In the present study, we sought to characterize the occurrence of Amadori-PE and its relationship with lipid peroxidation and protein glycation during the development of hyperglycemia in STZ-induced diabetic rats.

In the present study, STZ rats showed significant decreases in weight, plasma insulin, and 1,5-AG (Fig. 2). High levels of blood glucose and Hb_{A1c} were also observed in these rats. Based on these characteristic features, it was presumed that these rats had undergone the irreversible necrosis of pancreatic β-cells that is characteristic of STZ treatment [21], resulting in lowered insulin secretion, and thereby inducing severe type-1 diabetes. Blood lipid levels were also increased in STZ rats (Table 1), probably due to increased free fatty acid release from adipose tissue [22] in response to low insulin levels. Low insulin secretion also decreases hepatic lipase activity [23], thereby increasing hepatic TG content (Table 1).

We used a recently developed (LC)-MS/MS method [6, 10] to analyze Amadori-PE in STZ rats in this study. With the advent of MS/MS, the product ion scan, NLS, and MRM can provide useful structural information about the analyte, even in the presence of major background contaminants from complex biological matrices [24]. Indeed, as shown in this study (LC)-MS/MS is particularly suitable for analysis of Amadori-PE. MS/MS NLS is highly effective at "fishing out" major Amadori-PE species in blood and tissue samples (Fig. 3a, b). LC–MS/MS with MRM also enables quantitative determination of individual Amadori-PE species (Fig. 3c). These techniques constitute a powerful tool to understand the pathophysiological consequences of in vivo lipid glycation.

As mentioned in the introduction, although there is increasing evidence for the involvement of lipid glycation in diabetic complications [2–10], it is still unclear how lipid glycation products are formed during the development of hyperglycemia. In this study, we used STZ rats to demonstrate that PE glycation occurs during the development of hyperglycemia and that Amadori-PE concentrations are markedly increased under hyperglycemic conditions (Fig. 4). To our knowledge, this is the first report documenting the occurrence of Amadori-PE species in various organs. Amadori-PE content in the kidneys of STZ rats appeared to be equivalent to that in liver. Furthermore, pancreatic Amadori-PE levels were 35 times higher in STZ rats than in control rats. These findings suggest that Amadori-PE is more likely to be generated in organs that are involved in the pathogenesis of diabetes. We measured eight Amadori-PE molecular species and

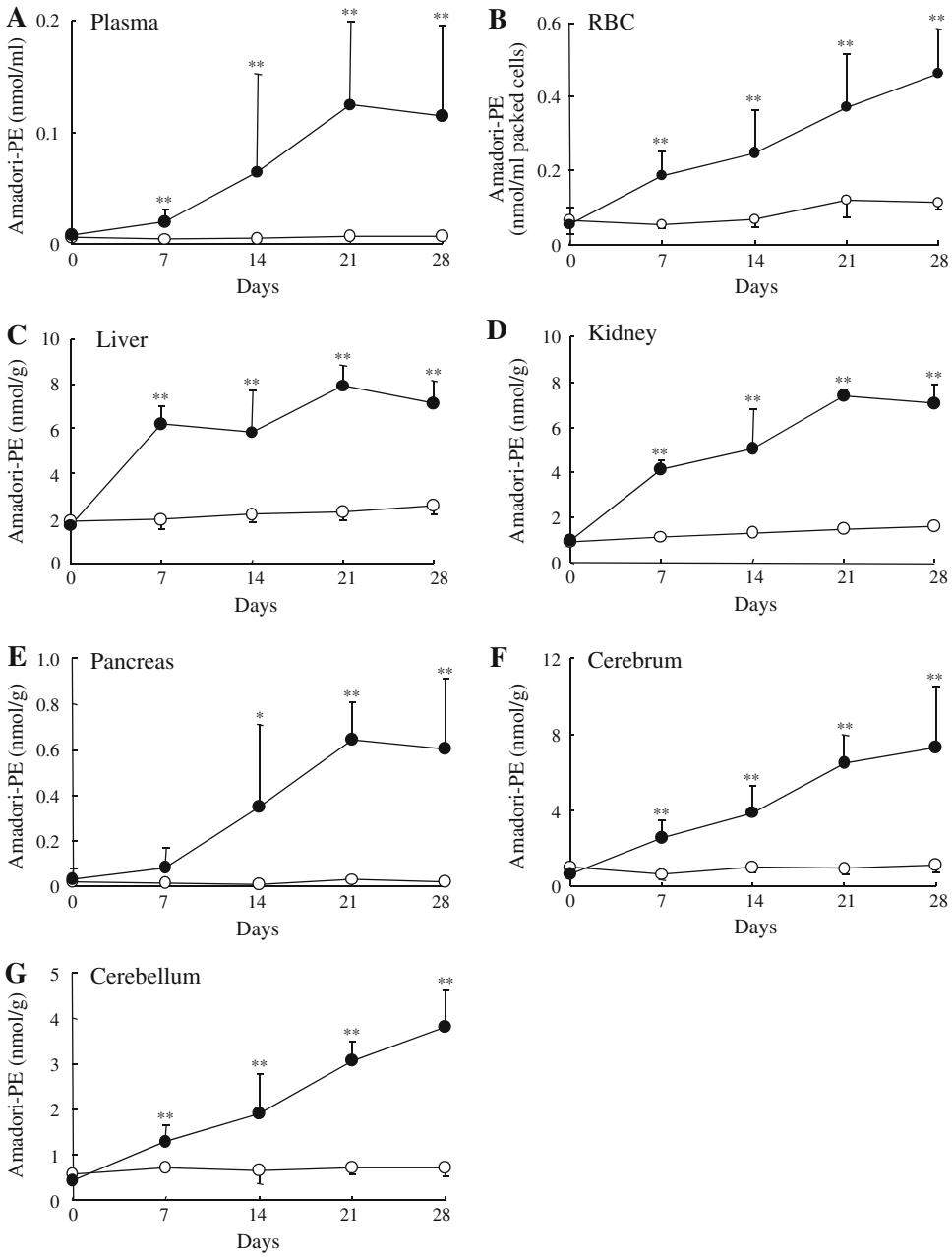

Fig. 4 Time course of changes in total Amadori-PE (sum of 8 species) in **a** plasma, **b** RBC, **c** liver, **d** kidney, **e** pancreas, **f** cerebrum, and **g** cerebellum. Values are means ± SD ($n = 6$; *$P < 0.05$ and **$P < 0.01$). *White circles* represent control rats, and *black circles* represent STZ rats

found that PE glycation did not simply occur in proportion to PE content in blood or tissues, but was influenced by differences in fatty acid structure in the PE bodies. In the first 7 days after STZ treatment, 18:0–20:4 PE was the first PE species to be glycated, and other PE species (e.g., 18:0–18:2 PE) were glycated subsequently (data not shown). Consequently, by day 28, 18:0–20:4 Amadori-PE and 18:0–18:2 Amadori-PE were the predominant species in blood and many tissues (Fig. 5). This finding suggests that these two Amadori-PE species are highly susceptible to glycation, probably due to relatively higher amount of 18:0–20:4 PE and 18:0–18:2 PE in blood and tissues. Another possibility is that these 18:0–20:4 Amadori-PE and 18:0–18:2 Amadori-PE might be more stable in the glycated state than other Amadori-PE species. Thus, these Amadori-PE species (18:0–20:4 Amadori-PE and 18:0–18:2 Amadori-PE) could potentially be utilized as a sensitive marker of the early stages of diabetes. However, further study is needed to clarify the relationship between PE fatty acid structure and glycation rate, since other factors may also influence PE glycation.

In the present study, significant increase in Amadori-PE was observed in STZ rats 7 days after STZ treatment, but meaningful changes in oxidized lipid levels (PCOOH and TBARS) were observed only after 21 or 28 days (Fig. 6). This suggests that Amadori-PE is pathologically formed

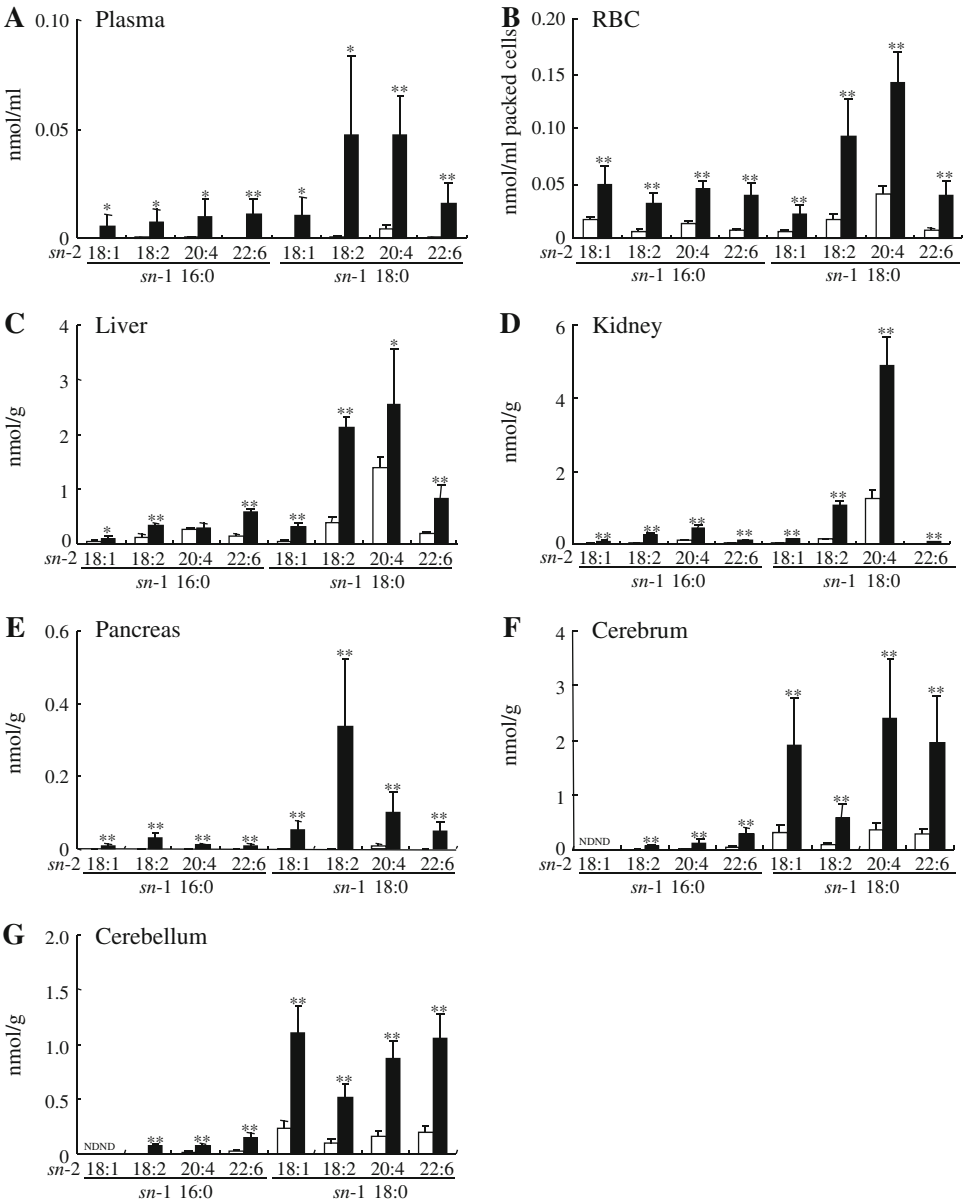

Fig. 5 Concentration of each Amadori-PE species 28 days after STZ injection. **a** Concentration in plasma, **b** RBC, **c** liver, **d** kidney, **e** pancreas, **f** cerebrum, and **g** cerebellum. Values are means ± SD ($n = 6$; $^{*}P < 0.05$ and $^{**}P < 0.01$). *White bars* represent control rats, and *black bars* represent STZ rats

prior to the induction of lipid peroxidation. Accordingly, the increased accumulation of oxidized lipids during diabetes pathogenesis may be partly due to the ability of Amadori-PE to induce oxidation of lipids [9, 20], which can worsen diabetes. On the other hand, accumulation of advanced protein glycation end products such as CML is also well-known to be related to diabetic complications [25, 26]. It has been reported that STZ treatment can increase levels of CML by up to 200% in plasma and up to 150–200% in the kidneys of diabetic animals [27, 28]. Our study showed similar effects of STZ treatment on CML levels (Fig. 7). However, CML accumulation was somewhat slower and more moderate than Amadori-PE accumulation. This may be due to the fact that Amadori-PE and CML are early and advanced glycation products, respectively. In addition, concentrations of Hb_{A1c} in STZ rats on days 7 and 28 were 180% and 300% of the initial values, respectively, whereas Amadori-PE levels in erythrocytes on days 7 and 28 were 330% and 800% of initial values, respectively (Figs. 2, 4). These findings support the idea that Amadori-PE can be used as a sensitive predictive marker for hyperglycemia development in the early stages of diabetes.

As for the involvement of Amadori-PE on the development of STZ-induced diabetes, Amadori-PE showed higher concentrations in blood and tissues immediately (7 days) after injection of STZ. It is therefore likely that formation and accumulation of Amadori-PE might be closely related with the progression and worsening of the STZ-induced diabetes. Now, we are preparing Amadori-PE

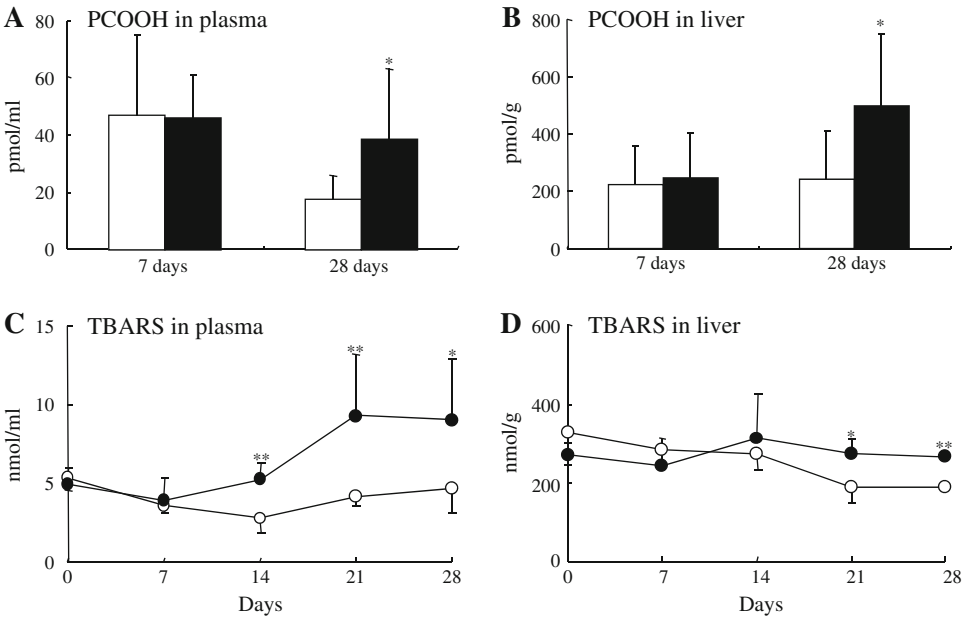

Fig. 6 Time course of changes in oxidative stress as indicated by phosphatidylcholine hydroperoxide (PCOOH) and thiobarbituric acid reactive substances (TBARS). **a** PCOOH in plasma, **b** PCOOH in liver, **c** TBARS in plasma, and **d** TBARS in liver. Values are means ± SD ($n = 6$; $^{*}P < 0.05$ and $^{**}P < 0.01$). *White bars* (**a**, **b**) and *white circles* (**c**, **d**) represent control rats, and *black bars* (**a**, **b**) and *black circles* (**c**, **d**) represent STZ rats

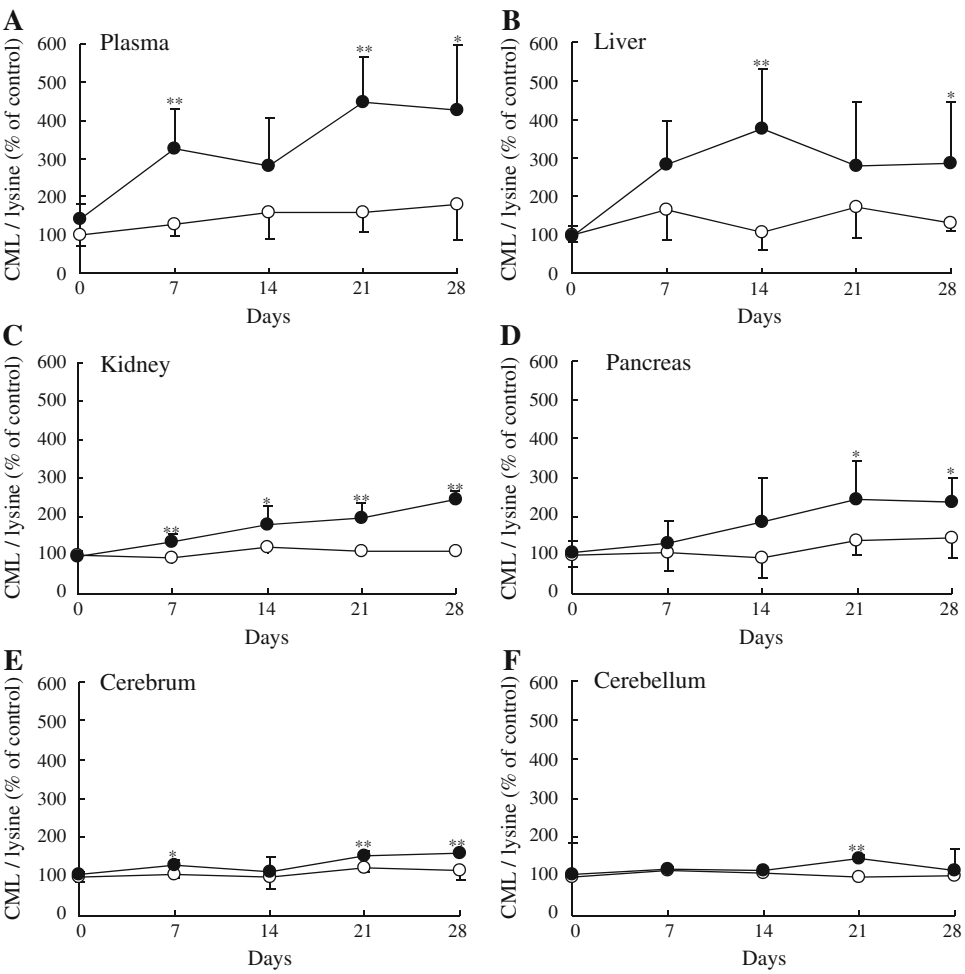

Fig. 7 Time course of changes in CML (% of control) in **a** plasma, **b** liver, **c** kidney, **d** pancreas, **e** cerebrum, and **f** cerebellum. Values are means ± SD ($n = 6$; $^{*}P < 0.05$ and $^{**}P < 0.01$). *White circles* represent control rats, and *black circles* represent STZ rats

antibody and clarify these points by using histological techniques.

In conclusion, we monitored the periodical change of Amadori-PE species during hyperglycemia development in STZ-induced diabetic rats and found that Amadori-PE tends to accumulate in blood and in organs that are involved in the pathogenesis of diabetes, such as the kidney. Certain molecular species of Amadori-PE, such as 18:0–20:4 Amadori-PE may be more sensitive indicators of early hyperglycemia than markers such as CML and Hb_{A1c}. Therefore, Amadori-PE should be considered for use as a predictive marker for hyperglycemia.

Acknowledgments A part of this study was supported by KAKENHI (S) (20228002, to T. M.) of JSPS, Japan.

References

1. Ahmed N, Thornalley PJ (2007) Advanced glycation end products: what is their relevance to diabetic complications? Diabetes Obes Metab 9:233–245
2. Bucala R, Makita Z, Koschinsky T, Cerami A, Vlassara H (1993) Lipid advanced glycosylation: pathway for lipid oxidation in vivo. Proc Natl Acad Sci USA 90:6434–6438
3. Ravandi A, Kuksis A, Marai L, Myher JJ, Steiner G, Lewisa G, Kamido H (1996) Isolation and identification of glycated aminophospholipids from red cells and plasma of diabetic blood. FEBS Lett 381:77–81
4. Lertsiri S, Shiraishi M, Miyazawa T (1998) Identification of deoxy-D-fructosyl phosphatidylethanolamine as a non-enzymic glycation product of phosphatidylethanolamine and its occurrence in human blood plasma and red blood cells. Biosci Biotechnol Biochem 62:893–901
5. Higuchi O, Nakagawa K, Tsuzuki T, Suzuki T, Oikawa S, Miyazawa T (2006) Aminophospholipid glycation and its inhibitor screening system: a new role of pyridoxal 5′-phosphate as the inhibitor. J Lipid Res 47:964–974
6. Nakagawa K, Oak JH, Higuchi O, Tsuzuki T, Oikawa S, Otani H, Mune M, Cai H, Miyazawa T (2005) Ion-trap tandem mass spectrometric analysis of Amadori-glycated phosphatidylethanolamine in human plasma with or without diabetes. J Lipid Res 46:2514–2524
7. Ravandi A, Kuksis A, Shaikh NA (1999) Glycated phosphatidylethanolamine promotes macrophage uptake of low density lipoprotein and accumulation of cholesteryl esters and triacylglycerols. J Biol Chem 274:16494–16500
8. Ravandi A, Kuksis A, Shaikh NA (2000) Glucosylated glycerophosphoethanolamines are the major LDL glycation products and increase LDL susceptibility to oxidation: evidence of their presence in atherosclerotic lesions. Arterioscler Thromb Vasc Biol 20:467–477
9. Oak JH, Nakagawa K, Miyazawa T (2000) Synthetically prepared Amadori-glycated phosphatidylethanolamine can trigger lipid peroxidation via free radical reactions. FEBS Lett 481:26–30
10. Shoji N, Nakagawa K, Asai A, Fujita I, Hashiura A, Nakajima Y, Oikawa S, Miyazawa T (2010) LC–MS/MS analysis of carboxymethylated and carboxyethylated phosphatidylethanolamines in human erythrocytes and blood plasma. J Lipid Res 51:2445–2453
11. Folch J, Lees M, Sloane-Stanley GH (1957) A simple method for the isolation and purification of total lipids from animal tissues. J Biol Chem 226:497–509
12. Rose HG, Oklander M (1965) Improved procedure for the extraction of lipids from human erythrocytes. J Lipid Res 6:428–434
13. Miyazawa T, Suzuki T, Fujimoto K, Yasuda K (1992) Chemiluminescent simultaneous determination of phosphatidylcholine hydroperoxide and phosphatidylethanolamine hydroperoxide in the liver and brain of the rat. J Lipid Res 33:1051–1059
14. Kinoshita M, Oikawa S, Hayasaka K, Sekikawa A, Nagashima T, Toyota T, Miyazawa T (2000) Age-related increase in plasma phosphatidylcholine hydroperoxide concentrations in normal subjects and patients with hyperlipidemia. Clin Chem 46:822–828
15. Ohkawa H, Ohishi N, Yagi K (1979) Assay for lipid peroxides in animal tissues by thiobarbituric acid reaction. Anal Biochem 95:351–358
16. Teerlink T, Barto R, Ten Brink HJ, Schalkwijk CG (2004) Measurement of Nepsilon-(carboxymethyl)lysine and Nepsilon-(carboxyethyl)lysine in human plasma protein by stable-isotope-dilution tandem mass spectrometry. Clin Chem 50:1222–1228
17. Bartlett GR (1957) Colorimetric assay methods for free and phosphorylated glyceric acids. J Biol Chem 226:497–509
18. Obsil T, Amler E, Obsilová V, Pavlícek Z (1999) Effect of aminophospholipid glycation on order parameter and hydration of phospholipid bilayer. Biophys Chem 80:165–177
19. Levi V, Villamil Giraldo AM, Castello PR, Rossi JP, González Flecha FL (2008) Effects of phosphatidylethanolamine glycation on lipid-protein interactions and membrane protein thermal stability. Biochem J 416:145–152
20. Simões C, Simões V, Reis A, Domingues P, Domingues MR (2010) Oxidation of glycated phosphatidylethanolamines: evidence of oxidation in glycated polar head identified by LC-MS/MS. Anal Bioanal Chem 397:2417–2427
21. Tourrel C, Bailbe D, Meile MJ, Kergoat M, Portha B (2001) Glucagon-like peptide-1 and exendin-4 stimulate beta-cell neogenesis in streptozotocin-treated newborn rats resulting in persistently improved glucose homeostasis at adult age. Diabetes 50:1562–1570
22. Ramesh B, Pugalendi KV (2005) Antihyperlipidemic and antidiabetic effects of umbelliferone in streptozotocin diabetic rats. Yale J Biol Med 78:189–196
23. Geethan PK, Prince PS (2008) Antihyperlipidemic effect of D-pinitol on streptozotocin-induced diabetic Wistar rats. J Biochem Mol Toxicol 22:220–224
24. King R, Fernandez-Metzler C (2006) The use of Qtrap technology in drug metabolism. Curr Drug Metab 7:541–545
25. Helen Vlassara H, Uribarri J (2004) Glycoxidation and diabetic complications: modern lessons and a warning? Rev Endocr Metab Dis 5:181–188
26. Nagai R, Fujiwara Y, Mera K, Motomura K, Iwao Y, Tsurushima K, Nagai M, Takeo K, Yoshitomi M, Otagiri M, Ikeda T (2008) Usefulness of antibodies for evaluating the biological significance of AGEs. Ann N Y Acad Sci 1126:38–41
27. Thornalley PJ, Battah S, Ahmed N, Karachalias N, Agalou S, Babaei-Jadidi R, Dawnay A (2003) Quantitative screening of advanced glycation endproducts in cellular and extracellular proteins by tandem mass spectrometry. Biochem J 375:581–592
28. Kang KS, Yamabe N, Kim HY, Yokozawa T (2008) Role of maltol in advanced glycation end products and free radicals: in vitro and in vivo studies. J Pharm Pharmacol 60:445–452

Lipids (2011) 46:953–960
DOI 10.1007/s11745-011-3580-y

ORIGINAL ARTICLE

Leptospirosis is Associated with Markedly Increased Triglycerides and Small Dense Low-Density Lipoprotein and Decreased High-Density Lipoprotein

Irene F. Gazi · Fotini A. Apostolou · Evangelos N. Liberopoulos · Theodosios D. Filippatos · Constantinos C. Tellis · Moses S. Elisaf · Alexandros D. Tselepis

Received: 7 April 2011 / Accepted: 1 June 2011 / Published online: 19 June 2011

Abstract The objective of the present study was to evaluate the effects of acute infection with *Leptospira interrogans* on lipids, lipoproteins and associated enzymes. Fasting serum levels of total cholesterol (TC), low-density lipoprotein cholesterol (LDL-C), high-density lipoprotein cholesterol (HDL-C), triglycerides (TG), apolipoproteins (apo) A-I, B, E, C-II, C-III and lipoprotein (a) [Lp(a)] were determined in patients with Leptospirosis on diagnosis and 4 months after recovery as well as in age- and sex-matched controls. Activities of cholesteryl-ester transfer protein (CETP) and lipoprotein-associated phospholipase A_2 (Lp-PLA_2) as well as paraoxonase 1 (PON1) hydrolysing activity and levels of cytokines were determined. LDL subclass analysis was performed with Lipoprint LDL System. Eleven patients (10 men, mean age 49.5 ± 8.4 years) and 11 controls were included. TC, HDL-C, LDL-C, apoA-I, apoB and Lp(a) levels were lower at baseline, whereas TG and apoE levels were elevated compared with 4 months later. At baseline, higher levels of cytokines and cholesterol concentration of small dense LDL particles (sdLDL-C) were noticed, whereas LDL particle size was lower compared with follow-up. Activities of plasma Lp-PLA_2 and HDL-associated Lp-PLA_2 were lower at baseline compared with post treatment values, whereas PON1 activity was similar at baseline and 4 months later. 4 months after recovery, the levels of all lipid parameters evaluated did not differ compared with controls, except for HDL-C which remained lower. PON1 activity both at baseline and 4 months later was lower in patients compared with controls. Leptospirosis is associated with atherogenic changes of lipids, lipoproteins and associated enzymes.

Keywords Leptospira · Lipids · Lipoproteins · Cytokines · sdLDL · LDL Particle size

Abbreviations

CMV	Cytomegalovirus
HSV	Herpes simplex virus
HIV	Human immunodeficiency virus
sdLDL	Small dense LDL
EBV	Epstein-Barr virus
sdLDL-C	sdLDL cholesterol
Lp-PLA_2	Lipoprotein-associated phospholipase A_2
PON1	Paraoxonase 1
CETP	Cholesteryl-ester transfer protein
HDL-C	HDL cholesterol
TSH	Thyroid-stimulating hormone
TC	Total cholesterol
TG	Triglycerides
LDL-C	LDL cholesterol
Apo	Apolipoprotein
Lp(a)	Lipoprotein (a)
IL	Interleukin
TNFα	Tumor necrosis factor α
CVs	Coefficient variates
VLDL-C	VLDL cholesterol
sdLDL%	Proportion of cholesterol on sdLDL particles
CRP	C-reactive protein
APR	Acute-phase response
SAA	Serum amyloid A

I. F. Gazi · F. A. Apostolou · E. N. Liberopoulos · T. D. Filippatos · M. S. Elisaf (✉)
Department of Internal Medicine, Medical School, University of Ioannina, 451 10 Ioannina, Greece
e-mail: egepi@cc.uoi.gr

C. C. Tellis · A. D. Tselepis
Laboratory of Biochemistry, School of Chemistry, University of Ioannina, Ioannina, Greece

LPL	Lipoprotein lipase
EL	Endothelial lipase
LCAT	Lecithin:cholesterol acyltranferase
ARF	Acute renal failure

Introduction

Leptospirosis is a zoonotic acute bacterial infection, caused by spirochetes of the genus *Leptospira*, with a worldwide distribution [1]. Human infection results from exposure to infected urine of carrier mammals, either directly or via contamination of soil or water [1]. Host infection produces a diverse array of clinical manifestations ranging from subclinical infection to undifferentiated febrile illness to jaundice, renal failure, and potentially lethal pulmonary haemorrhage [1]. Weil's disease represents the most severe form and can develop after the acute phase as the second phase of a biphasic illness or as a progressive illness. It is characterised by jaundice, renal failure, bleeding disorders and altered mental status [1].

Various infectious agents have been previously linked to an increased atherogenic potential and these include *Chlamydia pneumoniae*, CMV, HSV and *Helicobacter pylori* [2]. Moreover, regardless of the cause, infection is associated with alterations in lipid and lipoprotein concentrations [2]. Several studies have shown that sdLDL particles are more atherogenic compared with large buoyant ones [3]. Periodontitis, HIV infection as well as *Brucella melitensis* and EBV infections have been associated with increased levels of sdLDL-C [4–7].

Lp-PLA_2, a risk factor for vascular disease [8], is mainly distributed on LDL subclasses while the remaining is found on HDL (HDL-Lp-PLA_2) [9, 10]. Various changes in Lp-PLA_2 activity in response to infection have been reported among different animal species [11] and in human studies [4, 7, 12, 13]. PON1 is an esterase exclusively associated with HDL in plasma which plays an important role in HDL-mediated anti-atherogenic action [14]. During infection and inflammation serum PON1 activity may decrease and acute-phase HDL is unable to protect LDL against oxidation [15]. CETP, which plays a central role in the regulation of serum HDL-C levels, may exert higher activity during infection leading to decreased HDL-C levels [7].

We have previously shown that severe Leptospirosis was associated with altered lipid profile in a small number of patients ($n = 5$) [16]. However, there are no detailed data on the possible alterations in lipid and lipoprotein profile and associated enzymes in patients with Leptospirosis. We undertook the present study to evaluate the possible quantitative and qualitative effects of Leptospirosis on serum lipid parameters and associated enzymes.

Materials and Methods

Study Population

Eleven consecutive patients who were diagnosed with Leptospirosis at the 2nd Department of Internal Medicine, University Hospital of Ioannina, Greece, between January 2006 and September 2008 were included in the present study. The diagnosis of Leptospirosis was established by the presence of specific IgM antibodies against *L. interrogans* as determined by ELISA. No patient was receiving any hypolipidaemic agents or had any evidence of any disease known to affect lipid metabolism, such as neoplasia and hypo- (TSH $>$ 5 μU/mL) or hyperthyroidism (TSH $<$ 0.01 μU/mL). Moreover, patients with a known history of renal dysfunction (serum creatinine levels $>$1.5 mg/dL) were not included. All patients were examined on diagnosis and 4 months after recovery. No change in patients' dietary habits and body weight was recorded during follow-up. Eleven age- and sex-matched healthy volunteers (control population) were also included. These individuals visited the outpatient clinic of the 2nd Department of Internal Medicine for a regular check-up and were selected for the participation in the present study based on their age. All individuals signed a form giving their informed consent for the participation in the present study. This study was approved by the Ethics Committee of the University Hospital of Ioannina.

Laboratory Measurements

All laboratory parameters were blindly assessed with regard to each subject's group and sampling time.

Fasting serum levels of TC, HDL-C and TG were determined enzymatically on an Olympus AU600 Clinical Chemistry analyser (Olympus Diagnostica, Hamburg, Germany). LDL-C was calculated using the Friedewald formula (except for one patient whose TG levels exceeded the cut-off point of 400 mg/dL, for whom LDL-C concentration was not calculated). Apo A-I, B, E as well as Lp(a) levels were measured with a Behring Nephelometer BN100 using reagents from Date Behring Holding Gmbh (Liederbach, Germany). ApoC-II and apoC-III were determined by an immunoturbidimetric assay provided by Kamiya Biomedical Company (Seattle, WA).

LDL subclass analysis was performed electrophoretically using high-resolution 3% polyacrylamide gel tubes and the Lipoprint LDL System (Quantimetrix) according to the manufacturer's instructions [9].

Lp-PLA_2 and CETP activities as well as PON1 hydrolysing activities against paraoxon [PON1 (paraoxonase)] and phenyl acetate [PON1 (arylesterase)] were determined as previously described [7, 17].

Cytokines (IL-1b, IL-6 and TNFα) were determined by ELISA using a commercially available immunoassay kit (Quantikine; R&D Systems, Inc., Minneapolis, MN, USA). Each sample was measured in duplicate with appropriate sensitivities for IL-1b (<0.1 pg/mL), IL-6 (<0.7 pg/mL) and TNFα (<4.4 pg/mL). The median and mean intra-assay and inter-assay CVs were <10% for all the above measurements.

CRP levels were measured by an immunoturbidimetric assay (Roche Diagnostics).

Statistical Analysis

Preliminary analysis was performed to ensure no violation of the assumptions of normality and linearity. The Shapiro–Wilk test was used to evaluate whether each variable followed a Gaussian distribution. Data are expressed as means ± SD, except for parameters not following a Gaussian distribution which are expressed as median (range). Paired samples *t* test (or Wilcoxon's rank test, as appropriate) was used for the comparison of study parameters between baseline and 4 months later. Independent samples *t* test (or the Mann–Whitney *U* test, as appropriate) was used for the comparison of the study parameters between patients and controls. Analysis of covariance (ANCOVA) was used to assess whether the lipid profile of patients was impaired compared with the lipid profile of controls after adjusting for differences between the two groups regarding renal function as assessed by serum creatinine levels. The relationships between study parameters were investigated using Spearman correlation coefficient (ρ). In order to minimise the possibility of differences observed been a random effect due to multiple comparisons, a p value of <0.03 was considered as significant [18]. All analyses were carried out with SPSS 16.0 softpack (SPSS Inc., 2008, Chicago, IL, USA).

Results

Clinical Characteristics and Lipid Profile

The patients (10 male and 1 female, mean age 49.5 ± 8.4 years) presented with fever and myalgias, while 4 of them (36%) also presented with jaundice and acute renal failure. The clinical and biochemical characteristics of study participants are shown in Table 1. After confirmation of the diagnosis, patients were treated with ceftriaxone 1 g IV o.d. for 7 days.

Patients with Leptospirosis had decreased levels of TC, HDL-C, LDL-C, Lp(a) and apoA-I, whereas TG, apoE and VLDL-C levels as well as apoB/apoA-I ratio were elevated compared with 4 months after recovery (Table 1). On the other hand, apoC-II and apoC-III levels were not significantly different at baseline compared with 4 months later. Mean LDL particle size was decreased and sdLDL-C levels were increased at baseline compared with 4 months after recovery. Also, sdLDL-C% was markedly elevated at baseline compared with the values after recovery (Table 1).

We adjusted the baseline lipid and lipoprotein levels for serum creatinine concentration (data not shown). According to these results, the only parameters significantly affected by creatinine levels were LDL-C and large LDL-C levels ($p < 0.05$ for both). Moreover, we divided patients into two subgroups according to serum creatinine levels (<1.5 mg/dL, $n = 7$ vs. ≥1.5 mg/dL, $n = 4$). We found that the two subgroups differed in HDL-C (23 ± 5 mg/dL vs. 11 ± 2 mg/dL, $p < 0.01$), LDL-C (100 ± 25 mg/dL vs. 52 ± 21 mg/dL, $p < 0.05$) and large LDL-C (88 ± 18 mg/dL vs. 61 ± 21 mg/dL, $p < 0.05$) levels. However, all three parameters in the subgroup of patients with serum creatinine levels <1.5 mg/dL were still significantly lower compared with the corresponding values of the control population ($p < 0.03$ for all). We also found that the subgroup of Leptospirosis patients with impaired renal function had more severe infection defined as higher cytokine levels [IL-1b: 14.9 (4.6–16.9) pg/mL vs. 4.2 (3.7–5.5) pg/mL, $p < 0.03$, IL-6: 11.4 (2.5–58.2) pg/mL vs. 3.6 (3.4–58.4) pg/mL, $p < 0.03$ and TNFα: 24.4 (17.2–39.0) pg/mL vs. 12.0 (10.7–31.2) pg/mL, $p < 0.03$] as well as higher CRP levels [150 (38–224) mg/L vs. 31 (29–325) mg/L, $p < 0.01$].

With the exception of HDL-C and apoA-I levels, which remained low (Table 1), all other parameters had returned to levels similar to controls 4 months after recovery (Table 1).

CETP activity was similar in patients with acute Leptospirosis and 4 months after recovery, while no significant difference was observed in its activity between post-recovery and controls (Table 1).

Lp-PLA_2 and PON1 Activities

At baseline, total plasma Lp-PLA_2 and HDL-Lp-PLA_2 activity were decreased compared with 4 months after recovery from Leptospirosis (Table 2). No difference was observed in the activities of PON1 (paraoxonase) and PON1 (arylesterase) between baseline and 4 months after recovery.

Total plasma Lp-PLA_2 and HDL-Lp-PLA_2 activities were similar in patients 4 months after recovery and controls. However, both PON1 (paraoxonase) and PON1 (arylesterase) activities were lower in patients 4 months after recovery as compared with the control population.

Markers of Inflammation

Levels of inflammatory markers (CRP, IL-1β, IL-6, and TNFα) were increased at baseline compared with 4 months

Table 1 Clinical characteristics and lipid profile of patients with Leptospirosis at baseline (diagnosis of Leptospirosis) and 4 months after recovery as well as of the control population

	Baseline ($n = 11$)	4 months later ($n = 11$)	p*	Controls ($n = 11$)	p**
Age	49.5 ± 8.4	–	–	47.5 ± 9.6	NS
Sex (M/F)	10/1	–	–	10/1	
Smokers (Yes/no)	9/2	9/2	NS	7/4	NS
Creatinine (mg/dL)	2.4 ± 1.4	1.1 ± 0.1	0.01	1.0 ± 0.1	NS
AST (IU/L)	103 ± 54	28 ± 16	<0.001	23 ± 7	NS
ALT (IU/L)	91 ± 46	28 ± 11	<0.01	31 ± 15	NS
TBL (mg/dL)	5.4 ± 1.8	1.4 ± 0.6	<0.01	0.9 ± 0.1	NS
TC (mg/dL)	145 ± 49	211 ± 40	<0.01	223 ± 29	NS
HDL-C (mg/dL)	17 ± 7	44 ± 11	<0.001	57 ± 10	0.01
TGs (mg/dL)	259 (131–614)	122 (68–433)	<0.01	111 (45–209)	NS
LDL-C (mg/dL)	72 ± 45	140 ± 35	0.01	141 ± 25	NS
apoA-I (mg/dL)	59 ± 41	128 ± 50	<0.01	156 ± 16	<0.03
apoB (mg/dL)	118 ± 31	95 ± 26	NS	101 ± 20	NS
apoB/apoA-I	2.7 (0.6–14.1)	0.7 (0.4–2.4)	0.01	0.7 (0.4–0.9)	NS
apoE (mg/L)	103 (44–153)	49 (35–68)	0.01	35 (28–66)	NS
apoC-II (mg/dL)	4.2 (1.8–14.3)	3.4 (2.0–8.3)	NS	3.4 (0.7–4.7)	NS
apoC-III (mg/dL)	9.1 (3.3–14.1)	7.8 (6.3–12.3)	NS	8.7 (3.0–11.3)	NS
Lp(a) (mg/dL)	2.4 (2.4–34.8)	7.0 (2.4–78.6)	0.03	8.8 (2.4–70.0)	NS
VLDL-C (mg/dL)	45 (35–93)	29 (20–52)	0.03	33 (10–63)	NS
Large LDL-C (mg/dL)	79 ± 27	116 ± 31	0.01	124 ± 23	NS
sdLDL-C (mg/dL)	8 (0–33)	4 (0–14)	0.03	5 (0–23)	NS
sdLDL-C (%)	22 (0–33)	3 (0–11)	0.01	3 (0–13)	NS
LDL particle size (nm)	261 ± 5	267 ± 6	0.03	269 ± 3.6	NS
CETP activity (nmol/mL/h)	217 ± 98	234 ± 109	NS	169 ± 38	NS

Values are expressed as means ± SD or median (range)

To convert mg/dL to mmol/L multiply with 0.0259 for cholesterol and with 0.0113 for TG. To convert mg/dL to g/L for apoA-I and apoB multiply with 0.1

AST aspartate transaminase, *ALT* alanine transaminase, *TBL* total bilirubin, *TC* total cholesterol, *TGs* triglycerides, *HDL*-C high-density lipoprotein cholesterol, *LDL*-C low-density lipoprotein cholesterol, *apo* apolipoprotein, *Lp*(a) lipoprotein (a), *VLDL*-C very low density lipoprotein cholesterol, *sdLDL-C* small, dense LDL-C, *CETP* cholesteryl ester transfer protein, *NS* not significant

* p for the comparison of values between baseline and 4 months after recovery

** p for the comparison of values between patients 4 months after recovery and controls

Table 2 Lp-PLA_2, PON1 (paraoxonase) and PON1 (arylesterase) activities in patients with Leptospirosis at baseline (diagnosis of Leptospirosis) and 4 months after recovery as well as in the control population

	Baseline ($n = 11$)	4 months later ($n = 11$)	p*	Controls ($n = 11$)	p**
Total plasma Lp-PLA_2 (nmol/min/mL)	45 ± 16	59 ± 20	0.03	52 ± 10	NS
HDL-Lp-PLA_2 (nmol/min/mL)	1.4 ± 0.9	2.4 ± 1.0	0.03	2.3 ± 0.5	NS
PON1 (paraoxonase) (U/L)	47.2 (18.9–106.8)	48.2 (17.3–116.7)	NS	111.5 (43.6–240.7)	0.03
PON1 (arylesterase) (U/L)	20.8 ± 8.9	26.3 ± 7.3	NS	49.2 ± 11.5	<0.001

Values are expressed as mean ± SD or median (range)

Lp-PLA_2 lipoprotein-associated phospholipase A_2, *PON1* paraoxonase 1, *NS* not significant

* p for the comparison of values between baseline and 4 months after recovery

** p for the comparison of values between patients 4 months after recovery and controls

after recovery (Table 3). No difference in the levels of the inflammatory markers was observed between patients 4 months after the resolution of Leptospirosis and controls, with the exception of the concentration of TNFα, which remained elevated 4 months after recovery compared with the control population (Table 3).

Table 3 Markers of inflammation in patients with Leptospirosis at baseline (diagnosis of Leptospirosis infection) and 4 months after recovery as well as of the control population

	Baseline ($n = 11$)	4 months later ($n = 11$)	p*	Controls ($n = 11$)	p**
CRP (mg/L)	128 (29–325)	2 (1–18)	<0.001	1 (1–2)	NS
IL-1β (pg/mL)	6.7 (3.7–16.9)	3.7 (3.6–5.5)	0.01	3.6 (3.0–35.4)	NS
IL-6 (pg/mL)	8.8 (2.5–58.4)	2.7 (1.7–4.8)	0.01	1.1 (0.6–64.0)	NS
TNFα (pg/mL)	17.3 (10.0–39.0)	4.2 (1.4–24.0)	0.03	0.2 (0.1–17.5)	0.01
WBC (μL)	5,043 ± 432	6,440 ± 1,091	NS	5,680 ± 1,008	NS
NEUT (%WBC)	84 ± 6	54 ± 7	<0.001	59 ± 4	NS
LYMPH (%WBC)	10 ± 5	38 ± 5	<0.001	34 ± 4	NS
MONO (%WBC)	6 ± 1	5 ± 2	NS	4 ± 2	NS

Values are expressed as means ± SD or median (range)

CRP C-reactive protein, *IL* interleukin, *TNFα* tumor necrosis factor α, *WBC* white blood cells, *NEUT* neutrophil granulocytes, *LYMPH* lymphocytes, *MONO* monocytes, *NS* not significant

* p for the comparison of values between baseline and 4 months after recovery

** p for the comparison of values between patients 4 months after recovery and controls

Correlations Between Lipid and Lipoprotein Levels and Cytokine Concentrations

At baseline, HDL-C levels were inversely associated with IL-1b concentration (Table 4), while the increase in HDL-C levels 4 months after recovery was associated with the decrease in TNFα (ρ 0.47, $p < 0.05$) and CRP levels (ρ 0.65, $p < 0.05$) (data not shown). TG levels at baseline were positively associated with IL-6 and CRP levels (Table 4), and also the decrease in TGs after treatment was associated with the decrease in these inflammatory markers (ΔIL-6 ρ 0.75, $p < 0.01$ and ΔCRP ρ 0.66, $p < 0.05$). Baseline LDL-C levels were negatively associated with IL-6, TNFα and CRP concentration, while apoB levels were associated only with IL-6 and CRP levels (Table 4). While apoE concentration was not correlated with any inflammatory markers, its decrease post-recovery was associated with the fall in TNFα levels (ρ 0.75, $p < 0.05$). No correlation was established between Lp(a) levels or its increase following recovery and any inflammatory marker. At baseline, sdLDL-C levels were inversely associated with all inflammatory markers evaluated (Table 4), while LDL particle size was positively associated only with CRP levels (Table 4).

It should be noted that the increase in the activity of Lp-PLA$_2$ observed after recovery from Leptospirosis was marginally associated with the increase in LDL-C levels (ρ 0.45, p 0.04) while the elevation of HDL-Lp-PLA$_2$ activity was strongly associated with the increase in HDL-C concentration (ρ 0.65, p 0.03).

Table 4 Spearman's correlation coefficients (ρ) showing the association between lipid and lipoprotein levels at baseline and the concentration of inflammatory markers

	IL-1b	IL-6	TNFα	CRP
HDL-C	−0.90*	−0.09	−0.66*	−0.29
TGs	0.58	0.84***	0.21	0.68*
LDL-C	−0.52	−0.66*	−0.63*	−0.56*
apoA-I	−0.16	−0.23	−0.46	−0.14
apoB	−0.58	−0.73**	−0.26	−0.90***
apoE	0.33	0.23	0.33	0.11
Lp(a)	−0.23	−0.04	−0.22	−0.47
sdLDL-C	0.89*	0.60*	0.59*	0.55*
sdLDL-C%	0.33	0.02	0.32	0.08
LDL particle size	−0.55	−0.49	−0.28	−0.64*

IL interleukin, *TNFα* tumor necrosis factor α, *CRP* C-reactive protein, *HDL-C* high-density lipoprotein cholesterol, *TGs* triglycerides, *LDL-C* low-density lipoprotein cholesterol, *apo* apolipoprotein, *Lp(a)* lipoprotein (a), *sdLDL-C* small dense LDL-C

* $p < 0.05$, ** $p < 0.01$, *** $p < 0.001$

Discussion

In the present study, we showed for the first time that Leptospirosis is associated with an atherogenic lipid profile (i.e. increased TGs, apoB/apoA-I ratio, and sdLDL-C levels and decreased HDL-C concentration, LDL particle size and HDL-Lp-PLA$_2$ activity). This profile is restored 4 months after the recovery from Leptospirosis, with the exception of HDL-C levels and PON1 activities which remain lower compared with the control population.

Infection-induced alteration in lipid profile include increases in TG and apoE levels and decreases in the concentration of LDL-C, HDL-C, apoA-I, apoB and Lp(a) [2]. These changes are largely due to the actions of cytokines (IL-1b, IL-6 and TNFα) [19].

We have shown that acute brucellosis and EBV infection are associated with a reduction in LDL-C levels compared with values after recovery and controls [7] and these reductions were associated with IL-6 levels. IL-6 stimulates LDL receptor expression in hepatic cells and subsequently leads to increased uptake of LDL particles and decreased LDL-C levels [20]. In the present study, we found that baseline LDL-C levels were associated not only with IL-6 concentration, but also with TNFα and CRP levels. TNFα may increase LDL receptor activity [2]. Moreover, experimental data show that hepatic cells exposed to TNFα, IL-1b and IL-6 exhibit decreased synthesis of apos (such as apoB), leading to decreased LDL-C levels [21].

The markedly increased TG levels at the time of the diagnosis of Leptospirosis were associated with CRP and IL-6 levels, while the decrease in their concentration followed the fall in cytokine levels. TNFα, ILs and interferons can increase serum TG levels [2] by stimulating hepatic fatty acid synthesis, resulting in elevated VLDL production [19], consistent with our finding of increased VLDL-C levels at baseline. To further elucidate this hypothesis, we measured apoC-II and apoC-III which are critical determinants of the metabolism of TG-containing lipoproteins [22]. However, no change in the concentration or either apoC-II or apoC-III was established in the present study. ApoE has been shown to accelerate the secretion rate and decrease the efficiency of lipolysis of the TG-rich lipoproteins [23]. The elevated apoE levels at baseline, possibly due to increased apoE synthesis by the activated macrophages and/or the liver, might contribute to the observed hypertriglyceridaemia [16]. This finding is in agreement with our previous observations that apoE behaves as a positive acute-phase protein in patients with infection [16].

During infection, serum levels of HDL-C and apoA-I decrease [2]. Patients with Leptospirosis at baseline had markedly lower HDL-C and apoA-I levels compared with 4 months later. The exact mechanisms for the reduction in HDL-C levels during acute infection have not been firmly established. EL overexpression leads to reduced HDL-C levels, and this effect may be mediated by TNFα and IL-1b [24]. Accordingly, we have shown that HDL-C levels at baseline were negatively associated with IL-1b concentration, while 4 months after recovery the increase in HDL-C levels was associated with the decrease in TNFα levels. It is worth mentioning that TNFα attenuates the activity of LCAT [25], and a decrease in LCAT activity could decrease HDL-C concentration. Cytokines also stimulate the displacement of apoA-I by SAA, thus resulting in decreased HDL-C levels [26]. The altered HDL metabolism during infection may be mediated by the cytokine-induced changes in CETP activity. However, no change in CETP activity was established in patients with Leptospirosis at baseline compared with 4 months later or with controls. Of note, no measurements of EL and LCAT activity or SAA levels were performed in the present study.

Lp(a) behaves as a negative acute-phase reactant during major inflammatory response in humans [27]. Transforming growth factor-β1 and TNFα, which predominate in severe inflammation, inhibit the expression of the apo(a) gene in primary cultures of monkey hepatocytes [28], leading to decreased Lp(a) levels. However, no association between the low Lp(a) levels at baseline and TNFα concentration was established, possibly due to the small sample size.

Serum PON1 activity has been shown to be low in several infections such as hepatitis C [29], HIV [30] and helicobacter pylori [31, 32], primarily because of changes in synthesis and/or secretion of HDL and apoA-I particles. The activities of both PON1 (paraoxonase) and PON1 (arylesterase) were lower in patients 4 months after recovery compared with controls. This finding implies that the activities of PON1 may have not yet returned to normal 4 months later, as is the case for HDL-C. TNFα and IL-1 treatment of HEPG2 cells results in a decrease in PON1 mRNA levels [33]. No association between PON1 activity and cytokine levels was established at baseline. Therefore, the mechanisms for the decrease of PON1, other than the decrease in HDL-C, remain unknown.

An increase in plasma Lp-PLA_2 activity in patients with sepsis [34, 35] or HIV [13] has been reported, while other studies showed that total plasma Lp-PLA_2 activity is decreased in sepsis [12, 36–38]. Moreover, HDL-Lp-PLA_2 activity is acutely increased during acute infection and later decreased [11, 39, 40]. Serum Lp-PLA_2 activity may be a potential marker for *Leptospira*-induced pulmonary haemorrhage [41]. In our study, total plasma Lp-PLA_2 and HDL-Lp-PLA_2 activities were lower in patients on admission compared with 4 months after recovery. The changes in Lp-PLA_2 and HDL-Lp-PLA_2 activities can be explained by the parallel changes in the levels of LDL-C and HDL-C. Moreover, there was a slight -although not significant-association between low Lp-PLA_2 activity and elevated TNFα levels at baseline (ρ 0.44, $p = 0.07$). Indeed, TNFα is considered as one potent inhibitor of Lp-PLA_2 secretion [42]. Of note, the increase in HDL-Lp-PLA_2 activity was associated with the decrease in TNFα levels.

There was a shift in LDL subclass distribution toward smaller particles in patients with Leptospirosis compared with 4 months later. Studies have shown that advanced HIV infection and severe periodontitis are associated with a high prevalence of sdLDL particles [5, 6]. We have previously shown that patients with acute brucellosis and EBV infection have decreased mean LDL particle size

[4, 7]. Very recently it was shown that oligouric patients with *Hantaan virus* infection also exhibit a shift towards smaller LDL particles [43]. In the present study, the increased sdLDL particles and the decreased LDL particle size can be explained by the elevated TG concentration at baseline. The association between increased TG levels and the preponderance of sdLDL particles is well established [3]. Moreover, possibly through their actions on VLDL metabolism during infection, cytokines may affect the metabolic rate of LDL towards a more atherogenic profile, as implied by the association between the sdLDL-C at baseline and elevated levels of cytokines.

ARF is associated with increased TG and decreased LDL-C and HDL-C levels [44] due to impaired lipolysis, increased mobilisation of fat from adipose tissue and altered lipid clearance. In our study, Leptospirosis patients with ARF had lower HDL-C and LDL-C levels compared with the subgroup with normal kidney function, while no difference was observed in TG levels. However, this finding may be attributed to the more severe infection seen in the ARF subgroup as evidenced by the higher levels of cytokines compared with those with normal kidney function.

It must be noted that the lipid alterations found in patients with Leptospirosis seem more prominent than those observed in patients with brucellosis or EBV infection, especially in the case of TG and HDL-C levels and sdLDL-C concentration. However, the lipid profile of patients with Leptospirosis after recovery is almost fully restored while patients with brucellosis and EBV infection after recovery still exert alterations in the lipid profile compared with the control population.

Study Limitations

The number of study participants is small, since the prevalence of Leptospirosis is relatively low. We used a cross-over design to compare subjects with matched healthy controls. Despite the limitations of this design, a prospective study of lipid alterations in this setting is not possible. Although this study was open-label, laboratory data was blindly assessed with regard to the investigator who performed the measurements and the experiments.

Conclusion

Leptospirosis causes impressive alterations in the lipid profile that include markedly elevated TG and sdLDL-C concentration and low HDL-C and LDL-C levels. Most of these disturbances return to normal after recovery. However, HDL-C levels and the activities of PON1 remain lower than the control population 4 months after recovery.

Conflict of interest None declared.

References

1. Vijayachari P, Sugunan AP, Shriram AN (2008) Leptospirosis: an emerging global public health problem. J Biosci 33:557–569
2. Khovidhunkit W, Kim MS, Memon RA, Shigenaga JK, Moser AH, Feingold KR et al (2004) Effects of infection and inflammation on lipid and lipoprotein metabolism: mechanisms and consequences to the host. J Lipid Res 45:1169–1196
3. Gazi IF, Tsimihodimos V, Tselepis AD, Elisaf M, Mikhailidis DP (2007) Clinical importance and therapeutic modulation of small dense low-density lipoprotein particles. Expert Opin Biol Ther 7:53–72
4. Apostolou F, Gazi IF, Lagos K, Tellis CC, Tselepis AD, Liberopoulos EN et al (2010) Acute infection with Epstein-Barr virus is associated with atherogenic lipid changes. Atherosclerosis 212:607–613
5. Badiou S, Merle De Boever C, Dupuy AM, Baillat V, Cristol JP, Reynes J (2003) Decrease in LDL size in HIV-positive adults before and after lopinavir/ritonavir-containing regimen: an index of atherogenicity? Atherosclerosis 168:107–113
6. Rufail ML, Schenkein HA, Barbour SE, Tew JG, van Antwerpen R (2005) Altered lipoprotein subclass distribution and PAF-AH activity in subjects with generalized aggressive periodontitis. J Lipid Res 46:2752–2760
7. Apostolou F, Gazi IF, Kostoula A, Tellis CC, Tselepis AD, Elisaf M et al (2009) Persistence of an atherogenic lipid profile after treatment of acute infection with Brucella. J Lipid Res 50:2532–2539
8. Ikonomidis I, Michalakeas CA, Lekakis J, Parissis J, Anastasiou-Nana M (2011) The role of lipoprotein-associated phospholipase A2 (Lp-PLA2) in cardiovascular disease. Rev Recent Clin Trials 6:108–113
9. Gazi I, Lourida ES, Filippatos T, Tsimihodimos V, Elisaf M, Tselepis AD (2005) Lipoprotein-associated phospholipase A2 activity is a marker of small, dense LDL particles in human plasma. Clin Chem 51:2264–2273
10. Tellis CC, Tselepis AD (2009) The role of lipoprotein-associated phospholipase A2 in atherosclerosis may depend on its lipoprotein carrier in plasma. Biochim Biophys Acta 1791:327–338
11. Memon RA, Fuller J, Moser AH, Feingold KR, Grunfeld C (1999) In vivo regulation of plasma platelet-activating factor acetylhydrolase during the acute phase response. Am J Physiol 277:R94–R103
12. Trimoreau F, Francois B, Desachy A, Besse A, Vignon P, Denizot Y (2000) Platelet-activating factor acetylhydrolase and haemophagocytosis in the sepsis syndrome. Mediators Inflamm 9:197–200
13. Khovidhunkit W, Memon RA, Shigenaga JK, Pang M, Schambelan M, Mulligan K et al (1999) Plasma platelet-activating factor acetylhydrolase activity in human immunodeficiency virus infection and the acquired immunodeficiency syndrome. Metabolism 48:1524–1531
14. Mackness MI, Mackness B, Durrington PN (2002) Paraoxonase and coronary heart disease. Atheroscler Suppl 3:49–55
15. Cabana VG, Reardon CA, Feng N, Neath S, Lukens J, Getz GS (2003) Serum paraoxonase: effect of the apolipoprotein composition of HDL and the acute phase response. J Lipid Res 44:780–792

16. Liberopoulos E, Apostolou F, Elisaf M (2004) Serum lipid profile in patients with severe leptospirosis. Nephrol Dial Transpl 19:1328–1329
17. Georgiadis AN, Papavasiliou EC, Lourida ES, Alamanos Y, Kostara C, Tselepis AD et al (2006) Atherogenic lipid profile is a feature characteristic of patients with early rheumatoid arthritis: effect of early treatment—a prospective, controlled study. Arthritis Res Ther 8:R82
18. Kusuoka H, Hoffman JI (2002) Advice on statistical analysis for circulation research. Circ Res 91:662–671
19. Khovidhunkit W, Memon RA, Feingold KR, Grunfeld C (2000) Infection and inflammation-induced proatherogenic changes of lipoproteins. J Infect Dis 181(Suppl 3):S462–S472
20. Gierens H, Nauck M, Roth M, Schinker R, Schurmann C, Scharnagl H et al (2000) Interleukin-6 stimulates LDL receptor gene expression via activation of sterol-responsive and Sp1 binding elements. Arterioscler Thromb Vasc Biol 20:1777–1783
21. Ettinger WH, Varma VK, Sorci-Thomas M, Parks JS, Sigmon RC, Smith TK et al (1994) Cytokines decrease apolipoprotein accumulation in medium from Hep G2 cells. Arterioscler Thromb 14:8–13
22. Ribalta J, Vallve JC, Girona J, Masana L (2003) Apolipoprotein and apolipoprotein receptor genes, blood lipids and disease. Curr Opin Clin Nutr Metab Care 6:177–187
23. Mahley RW, Weisgraber KH, Huang Y (2009) Apolipoprotein E: structure determines function, from atherosclerosis to Alzheimer's disease to AIDS. J Lipid Res 50(Suppl):S183–S188
24. Jin W, Sun GS, Marchadier D, Octtaviani E, Glick JM, Rader DJ (2003) Endothelial cells secrete triglyceride lipase and phospholipase activities in response to cytokines as a result of endothelial lipase. Circ Res 92:644–650
25. Ly H, Francone OL, Fielding CJ, Shigenaga JK, Moser AH, Grunfeld C et al (1995) Endotoxin and TNF lead to reduced plasma LCAT activity and decreased hepatic LCAT mRNA levels in Syrian hamsters. J Lipid Res 36:1254–1263
26. van Leeuwen HJ, van Beek AP, Dallinga-Thie GM, van Strijp JA, Verhoef J, van Kessel KP (2001) The role of high density lipoprotein in sepsis. Neth J Med 59:102–110
27. Mooser V, Berger MM, Tappy L, Cayeux C, Marcovina SM, Darioli R et al (2000) Major reduction in plasma Lp(a) levels during sepsis and burns. Arterioscler Thromb Vasc Biol 20:1137–1142
28. Ramharack R, Barkalow D, Spahr MA (1998) Dominant negative effect of TGF-beta1 and TNF-alpha on basal and IL-6-induced lipoprotein(a) and apolipoprotein(a) mRNA expression in primary monkey hepatocyte cultures. Arterioscler Thromb Vasc Biol 18:984–990
29. Kilic SS, Aydin S, Kilic N, Erman F, Aydin S, Celik I (2005) Serum arylesterase and paraoxonase activity in patients with chronic hepatitis. World J Gastroenterol 11:7351–7354
30. Parra S, Alonso-Villaverde C, Coll B, Ferre N, Marsillach J, Aragones G et al (2007) Serum paraoxonase-1 activity and concentration are influenced by human immunodeficiency virus infection. Atherosclerosis 194:175–181
31. Aslan M, Nazligul Y, Horoz M, Bolukbas C, Bolukbas FF, Gur M et al (2008) Serum paraoxonase-1 activity in *Helicobacter pylori* infected subjects. Atherosclerosis 196:270–274
32. Akbas HS, Basyigit S, Suleymanlar I, Kemaloglu D, Koc S, Davran F et al (2010) The assessment of carotid intima media thickness and serum paraoxonase-1 activity in *Helicobacter pylori* positive subjects. Lipids Health Dis 9:92
33. Feingold KR, Hardardottir I, Grunfeld C (1998) Beneficial effects of cytokine induced hyperlipidemia. Z Ernährungswiss 37(Suppl 1):66-74
34. Endo S, Inada K, Yamashita H, Takakuwa T, Nakae H, Kasai T et al (1994) Platelet-activating factor (PAF) acetylhydrolase activity, type II phospholipase A2, and cytokine levels in patients with sepsis. Res Commun Chem Pathol Pharmacol 83:289–295
35. Takakuwa T, Endo S, Nakae H, Suzuki T, Inada K, Yoshida M et al (1994) Relationships between plasma levels of type-II phospholipase A2, PAF-acetylhydrolase, leukotriene B4, complements, endothelin-1, and thrombomodulin in patients with sepsis. Res Commun Chem Pathol Pharmacol 84:271–281
36. Karasawa K, Harada A, Satoh N, Inoue K, Setaka M (2003) Plasma platelet activating factor-acetylhydrolase (PAF-AH). Prog Lipid Res 42:93–114
37. Graham RM, Stephens CJ, Silvester W, Leong LL, Sturm MJ, Taylor RR (1994) Plasma degradation of platelet-activating factor in severely ill patients with clinical sepsis. Crit Care Med 22:204–212
38. Howard KM, Olson MS (2000) The expression and localization of plasma platelet-activating factor acetylhydrolase in endotoxemic rats. J Biol Chem 275:19891–19896
39. Van Lenten BJ, Hama SY, de Beer FC, Stafforini DM, McIntyre TM, Prescott SM et al (1995) Anti-inflammatory HDL becomes pro-inflammatory during the acute phase response Loss of protective effect of HDL against LDL oxidation in aortic wall cell cocultures. J Clin Invest 96:2758–2767
40. Van Lenten BJ, Wagner AC, Nayak DP, Hama S, Navab M, Fogelman AM (2001) High-density lipoprotein loses its anti-inflammatory properties during acute influenza a infection. Circulation 103:2283–2288
41. Yang J, Zhang Y, Xu J, Geng Y, Chen X, Yang H et al (2009) Serum activity of platelet-activating factor acetylhydrolase is a potential clinical marker for leptospirosis pulmonary hemorrhage. PLoS One 4:e4181
42. Narahara H, Johnston JM (1993) Effects of endotoxins and cytokines on the secretion of platelet-activating factor-acetylhydrolase by human decidual macrophages. Am J Obstet Gynecol 169:531–537
43. Kim J, Park HH, Choi I, Kim YO, Cho KH (2010) Severely modified lipoprotein properties without a change in cholesteryl ester transfer protein activity in patients with acute renal failure secondary to Hantaan virus infection. BMB Rep 43:535–540
44. Wiesen P, Van Overmeire L, Delanaye P, Dubois B, Preiser JC (2011) Nutrition disorders during acute renal failure and renal replacement therapy. JPEN J Parenter Enteral Nutr 35:217–222

Lipids (2011) 46:961–968
DOI 10.1007/s11745-011-3585-6

ORIGINAL ARTICLE

Trans–trans Conjugated Linoleic Acid Enriched Soybean Oil Reduces Fatty Liver and Lowers Serum Cholesterol in Obese Zucker Rats

William Gilbert · Vidya Gadang · Andrew Proctor · Vishal Jain · Latha Devareddy

Received: 2 February 2010 / Accepted: 13 June 2011 / Published online: 9 July 2011

Abstract Conjugated linoleic acid (CLA) is a collection of octadecadienoic fatty acids that have been shown to possess numerous health benefits. The CLA used in our study was produced by the photoisomerization of soybean oil and consists of about 20% CLA; this CLA consists of 75% *trans–trans* (a mixture of t8,t10; t9,t11; t10,t12) isomers. This method could be readily used to increase the CLA content of all soybean oil used as a food ingredient. The objective of this study was to determine the effects of *trans–trans* CLA-rich soy oil, fed as a dietary supplement, on body composition, dyslipidemia, hepatic steatosis, and markers of glucose control and liver function of obese *fa/fa* Zucker rats. The *trans–trans* CLA-rich soy oil lowered the serum cholesterol and low density lipoprotein–cholesterol levels by 41 and 50%, respectively, when compared to obese controls. *Trans–trans* CLA-rich soy oil supplementation also lowered the liver lipid content significantly ($P < 0.05$) with a concomitant decrease in the liver weight in the obese rats. In addition, glycated hemoglobin values were improved in the group receiving CLA-enriched soybean oil in comparison to the obese control. PPAR-γ expression in white adipose tissue was unchanged. In conclusion, *trans–trans* CLA-rich soy oil was effective in lowering total liver lipids and serum cholesterol.

Keywords Metabolic syndrome · *Trans–trans* CLA · CLA-rich soy oil · PPAR-γ

W. Gilbert · V. Gadang · A. Proctor · V. Jain · L. Devareddy (✉)
Department of Food Science, University of Arkansas, 2650 North Young Avenue, Fayetteville, AR 72704, USA
e-mail: ldevared@uark.edu

Abbreviations

AIN	American Institute of Nutrition
AST	Aspartate transaminase
BUN	Blood urea nitrogen
CLA	Conjugated linoleic acid
DXA	Dual-energy X-ray absorptiometry
HbA1C	Glycated hemoglobin
HDL-C	High density lipoprotein cholesterol
LDL-C	Low density lipoprotein cholesterol
NFκB	Nuclear factor κ B
PPAR	Peroxisome proliferator activator receptor
TC	Total cholesterol
TG	Triglycerides
VLDL	Very low density lipoprotein

Introduction

Obesity, cardiovascular disease, and type 2 diabetes are international health problems with their rates predicted to rise [1]. Research has shown that when human weight increases to the point of being classified as "obese," the risk of health problems such as hypertension, type 2 diabetes, coronary heart disease, stroke, cancer, gallbladder disease, osteoarthritis, sleep apnea, and respiratory problems increase [2–7].

Conjugated linoleic acid (CLA) is a collection of octadecadienoic fatty acid isomers that have been shown to positively affect health in human and animal models [8]. Some of the health benefits of CLA include reduced adiposity, antidiabetogenic, antiatherogenic, and anticarcinogenic effects [9–12]. The benefits have been seen primarily with the *cis*-9,*trans*-11 (c9,t11) and *trans*-10,*cis*-12 (t10,c12) isomers. At present, it is known that the effects of

CLA are dose-, time-, and species-dependent [13]. In addition, the activity of CLA is highly isomer specific; t10,c12 CLA isomer is antiadipogenic in differentiating human preadipocytes and the c9,t11 CLA isomer promotes adipogenesis [14]; therefore, it is important to identify isomer-specific responses.

Determination of the isomer-specific effects of CLA is necessary before CLA can be used in fortified foods or supplements. The major sources of CLA in the human diet are meat and dairy products derived from ruminants, and in these products the predominant CLA isomer (>90%) is c9,t11 [15]. However, to obtain the estimated optimum dietary CLA levels of about 3 g/d, from natural sources it would be necessary to increase the animal or dairy products which would increase saturated fat intake [16, 17]. Therefore, a concentrated source of dietary CLA that is low in saturated fat is desirable [18]. Jain and Proctor [18] showed that CLA isomers can be rapidly produced in large quantities in a pilot scale by efficient photoisomerization of soy oil. This reaction produces mainly *trans–trans* CLA isomers, the nutritional effects of which have not been studied. This CLA-rich soy oil produced by the pilot-scale system contained 180 times the total CLA isomers obtained from beef or dairy products [18]. Hence, the objectives of this study were to determine the effects of dietary supplementation of *trans–trans* CLA-rich soy oil on body composition, dyslipidemia, hepatic steatosis, and markers of glucose control and liver function of obese *fa/fa* Zucker rats.

Experimental Procedures

Study Design

This study was conducted using 3-month old female obese *fa/fa* Zucker rats (Harlan Laboratories, Indianapolis, IN), a commonly used model for studying obesity. Thirty-six rats were divided into the following treatment groups ($n = 12$): lean control (L-Ctrl), obese control (O-Ctrl), and obese CLA (O-CLA). The L-Ctrl and O-Ctrl groups were fed AIN-93M purified rodent diet. The O-CLA group was fed AIN-93M modified to contain ~0.5% *trans–trans* CLA isomers by diet mass. All animals were pair-fed to the mean intake of the L-Ctrl group and the food intake was measured three times a week. Although pair-feeding may cause stress in hyperphagic obese Zucker rats, in this study we did not observe any visual signs of stress. Pair-feeding was necessary to match the macronutrient intake of all the groups. The body weight of the animals was recorded once per week. The rats had free access to deionized water. After 100 days of treatment, the rats were fasted for 12 h before being sacrificed by exsanguination via cardiac puncture. University of Arkansas Institutional Animal Care and Use Committee guidelines for the treatment and care of the animals were followed throughout the study duration.

Diets

Animals in the control group were fed AIN-93M purified rodent diet formulated in accordance to the American Institute of Nutrition committee report [19]. Animals in the O-CLA group received AIN-93M containing 40 g/kg of *trans–trans* CLA-rich soybean oil substituted for regular soybean oil. The rat diet composition is given in Table 1. Refined, bleached deodorized soy oil was photo-irradiated in a pilot-plant regime using the optimal conditions discussed by Jain and Proctor [18]. The total CLA and isomer content of the oil was measured as fatty acid methyl esters (FAMES) by base-catalyzed conversion [20]. The CLA isomer composition of the CLA-rich soybean oil is presented in Table 2.

Table 1 Rat diet composition

Ingredients[a] (g/1,000 g)	Ctrl[b]	CLA[c]
Cornstarch	435.692	435.692
Maltodextrin	155	155
Sucrose	100	100
Casein	170	170
Soybean oil	40	0
trans-trans-CLA-rich soybean oil[d]	0	40
Cellulose	50	50
AIN-93-VX vitamin mix	10	10
AIN-93 M-MX mineral mix	35	35
TBHQ[e]	0.008	0.008
L-Cysteine	1.8	1.8
Choline bitartrate	2.5	2.5

[a] Diet ingredients were purchased from Harlan (Harlan Laboratories, Indianapolis, IN) unless otherwise noted

[b] *Ctrl* Control diet

[c] *CLA* CLA diet

[d] Produced by in-house using procedure referenced in methods

[e] ACROS organics (New Jersey, USA)

Table 2 Isomeric composition of soybean oil used in experimental diet

CLA Isomer	Average concentration (%)
c9, t11 CLA	1.25
t9, c11/c10, t12 CLA	2.26
t10, c12 CLA	1.19
t, t[a] CLA	13.73
Total CLA	18.43

[a] Consists of *trans*-8, *trans*-10 CLA, *trans*-9, *trans*-11 CLA, and *trans*-10, *trans*-12 CLA

Body Composition

Dual-energy X-ray Absorptiometry (DXA; GE Lunar DXA, Waukesha, WI) was used to analyze the body composition of the rats at baseline and immediately prior to sacrifice. The animals were anesthetized and placed stomach down on the scan bed of the DXA. The absorbance of two X-ray beams was measured and percent lean tissue and percent fat tissue were calculated by software (enCORE, GE Lunar, Waukesha, WI) appropriate for the body composition assessment of small animals.

Necropsy and Tissue Collection

Organs and tissues of interest were removed from the animal immediately after sacrifice. The liver and white adipose tissue were placed in cryogenic storage containers and flash-frozen in liquid nitrogen before being stored at −80 °C. Approximately 7 mL of blood collected from the animal via cardiac puncture during sacrifice was stored on ice before being centrifuged to separate serum from whole blood. Aliquots of serum were transferred to microcentrifuge tubes and stored at −80 °C until analysis. A small amount of blood collected from the heart during sacrifice was placed in a microtube containing K_2 EDTA (an anticoagulant) and stored at −80 °C.

Biochemical Analysis

Serum triglycerides (TG), total cholesterol (TC), high density lipoprotein–cholesterol (HDL–C), low density lipoprotein–cholesterol (LDL–C), aspartate transaminase (AST), blood urea nitrogen (BUN), glycated hemoglobin (HbA1c), and glucose concentrations were determined using commercially available kits from Alfa Wassermann Diagnostic Technologies (West Caldwell, NJ). An ACE Alera clinical chemistry system (Alfa Wassermann Diagnostic Technologies, West Caldwell, NJ) was used according to the manufacturer's instructions to perform these tests.

Insulin

Serum insulin was quantified using a commercially available ELISA kit (Alpco Immunoassays, Salem, NH). An aliquot of serum was thawed at 2–8 °C before use. A 96-well plate in the kit was prepared per manufacturer instructions to include duplicate standards, appropriate controls, and sample duplicates. Absorbance was measured using a BioTek ELx808 microplate reader (Winooski, VT) attached to a PC running BioTek Gen5 data analysis software (Winooski, VT).

Liver Lipids

One gram of liver was homogenized in a 20-fold volume of 2:1 chloroform–methanol (v/v) mixture. Following homogenization, 0.58% NaCl solution was added to achieve separation of the phases and centrifuged for 20 min at $500\times g$. Supernatant was discarded and the organic phase was filtered and washed with chloroform through fat free filter paper (3.2 cm Whatman, Whatman International Ltd, Maidstone, England). The filtered organic phase containing the tissue lipids was then transferred to a pre-weighed scintillation vial. Liver lipids were determined using the Folch gravimetric method [21]. Liver total cholesterol was determined using the method described by Searcy and Bergquist [22].

Gene Expression in White Adipose Tissue

RNA Extraction and cDNA Synthesis

RNA was extracted from approximately 100 mg of white adipose tissue by TRIzol Reagent method using RNeasy Lipid Tissue Mini Kit (Qiagen, USA) by following the supplier's instructions. The total amount of RNA present in each sample was quantitated using Nanodrop (Thermo Scientific, Wilmington, DE) and 1 μg/sample of total RNA was used for cDNA synthesis using a QuantiTect Rev. Transcription Kit (Qiagen, USA).

Quantitative Real-Time PCR

Following cDNA synthesis, qRT-PCR was performed using the Mastercycler ep realplex with SYBR Green system (Eppendorf, Hamburg, Germany). Concentrations of reagents were used per the manufacturer's instructions. Real-time PCR primers were designed using Primer3 primer design software and all primer sets were synthesized by Invitrogen (Invitrogen, Carlsbad, CA). Primer sequences used for this study are summarized in Table 3. The following experimental conditions were used for all target gene expression including generation of standard curves. The initial denaturation cycle was performed at 95 °C for 5 min. All subsequent denaturation and annealing cycles were repeated 45 times at 95 °C for 15 s and 60 °C (55 °C annealing for reference gene β-actin) for 45 s, respectively. The relative gene expression ratio by qRT-PCR was calculated using "REST" software.

Statistical Methods

The data analysis involved estimation of means and standard error (SE) using JMP 8 (2009 SAS Institute Inc. Cary, NC). The effects of treatment were analyzed by one-way

Table 3 Primers used in real time qPCR

Gene name	Gene bank accession no.	Primer sequence		BP size
β-Actin	BC138614	Forward	AGATCTGGCACCACACCTTC	139
		Reverse	GGGGTGTTGAAGGTCTCAAA	
PPAR-γ	NM_013124	Forward	GACCACTCCCATTCCTTTGA	109
		Reverse	CAACCATTGGGTCAGCTCTT	

PPAR-γ Peroxisome proliferator-activated receptor-γ, *NF-κB* nuclear factor-κB

ANOVA model followed by post hoc analysis using the Fisher's least squares means separation test when F values were significant. For all analyses, a P-value less than 0.05 was considered significant.

Results

Food Intake, Body Weight, Body Composition, and Organ Weights

There were no significant differences ($P > 0.05$) in the mean food intake between the three experimental groups, as the rats were pair-fed to the mean intake of the L-Ctrl group. The effects of treatment on body weights, body composition, and organ weights are shown in Table 4. There were no significant differences in the final body weights or body composition of O-Ctrl and O-CLA groups. A significant difference was found between the body weights and body composition of the L-Ctrl group when compared to the O-Ctrl and O-CLA group. The liver weights of the O-CLA group were significantly lower than those of the O-Ctrl, but were significantly higher than the liver weights for the L-Ctrl group ($P < 0.05$). These results provide evidence that *trans–trans* CLA enriched soybean oil reduces hepatomegaly in *fa/fa* obese Zucker rats.

Serum Lipid Profiles

The serum lipid profiles are presented in Table 5. The serum TC and LDL-C concentrations of the rats in the O-CLA group were significantly lower compared to the obese control, 41 and 50%, respectively. There was no difference in the TG and HDL-C levels in rats in the O-CLA and O-Ctrl group. This indicates that CLA was able to reduce the total cholesterol concentration without lowering the HDL-C. All serum lipid parameters measured (TC, LDL-C, HDL-C, and TG) were significantly lower in the L-Ctrl group when compared to the O-CLA and O-Ctrl groups ($P < 0.05$).

Liver Lipids

The liver lipid data is presented in Table 5. Percent total liver lipids were significantly different among the experimental groups. Percent liver lipids in the O-CLA group were significantly lower than the percent liver lipids in the O-Ctrl group. The reduced liver lipid content of the O-CLA group could explain the lower liver weights in the O-CLA group compared to the O-Ctrl group, and also support a claim that *trans–trans* CLA-rich soy oil supplementation lowers the accumulation of fat in the liver. The percentage of liver cholesterol was reported as the ratio of cholesterol to total liver lipids. No significant differences were found between the percent liver cholesterol in rats in the O-CLA and O-Ctrl group, and rats in the L-Ctrl group showed

Table 4 Effects of CLA enriched soybean oil on food consumption, body weight, body composition, and organ weights in obese zucker rats

	L-Ctrl		O-Ctrl		O-CLA	
	Mean	SE	Mean	SE	Mean	SE
Average food consumption (g/day)	17.0	2.4	18.00	1.4	18.1	1.4
Initial body weight (g)	179.2^{b}	4.1	329.9^{a}	9.4	330.3^{a}	6.7
Final body weight (g)	300^{b}	6.6	551.9^{a}	9.4	538.4^{a}	6.9
Initial body fat (%)	24^{b}	2	81^{a}	2	81^{a}	2
Final body fat (%)	36^{b}	3	82^{a}	2	85^{a}	2
Liver weight (g)	8.57^{c}	0.61	31.34^{a}	1.81	20.48^{b}	1.75
Liver weight (g/100 g bwt)	2.83^{c}	0.13	5.8^{a}	0.29	3.73^{b}	0.34

Data represents the mean values and standard error (SE; $n = 12$/group)

Values in a row without common superscripts are significantly different ($P < 0.05$)

L-Ctrl Lean + control diet, *O-Ctrl* obese + control diet, *O-CLA* obese + conjugated linoleic acid diet (0.5%), *bwt* body weight

Table 5 Effects of CLA enriched soybean oil on serum and liver lipids in obese Zucker Rats

	L-Ctrl		O-Ctrl		O-CLA	
	Mean	SE	Mean	SE	Mean	SE
Cholesterol (mmol/L)	2.16[c]	0.09	13.32[a]	1.53	7.86[b]	1.14
HDL-C (mmol/L)	0.58[b]	0.02	1.8[a]	0.1	1.7[a]	0.17
LDL-C (mmol/L)	0.13[c]	0.01	1.39[a]	0.18	0.7[b]	0.15
Triglycerides (mmol/L)	0.97[b]	0.09	1.95[a]	0.31	1.87[a]	0.23
Liver lipid (%)	9.7[c]	0.4	32.9[a]	1.3	20.1[b]	1.8
Liver cholesterol (%)	21.9[b]	0.4	23.7[a]	0.3	23.4[a]	0.6

Data represents the mean values and standard error (SE; $n = 12$/group)

Values in a row without common superscripts are significantly different ($P < 0.05$)

Cholesterol, HDL-C, LDL-C, and triglycerides were measured in serum. Liver lipid percentage and liver cholesterol percentage were measured in the liver. Liver lipid percentage refers to the percentage of total liver weight found to be lipid. Liver cholesterol percentage refers to the percentage of liver lipids found to be cholesterol

L-Ctrl Lean + control diet, *O-Ctrl* obese + control diet, *O-CLA* obese + conjugated linoleic acid diet (0.5%)

significantly ($P < 0.05$) lower liver cholesterol values than the O-Ctrl and O-CLA groups.

Serum Glucose, HbA1c, AST and Insulin

The serum and whole blood metabolite results are presented in Table 6. Glucose and AST levels in the L-Ctrl group were significantly lower than in the O-Ctrl and O-CLA groups. There was no significant difference in the AST level between the O-CLA and O-Ctrl group. Rats in the L-Ctrl group also had serum insulin values significantly lower than the O-Ctrl group. CLA supplementation had an intermediary effect in lowering the serum insulin levels as the values were not different from either L-Ctrl or O-Ctrl groups. The HbA1c levels of the rats in the O-CLA treatment were found to be significantly lower than the O-Ctrl group, indicating that CLA supplementation effectively regulates the blood sugar levels.

Expression of PPAR-γ in White Adipose Tissue in Zucker Rats

We measured the expression of PPAR-γ in white adipose tissue (WAT). We found no significant difference in the expression of PPAR-γ in the O-CLA group when compared to the O-Ctrl group (Figure 1). The expression of PPAR-γ mRNA in both O-Ctrl and O-CLA groups were significantly lower than the L-Ctrl group.

Discussion

Natural CLA sources, such as dairy fats, reportedly contain over twenty-five CLA isomers; chemical synthesis and modification of existing isomers are adding to this list [23]. Most studies examining the biological activities of CLA have used c9,t11 CLA and t10,c12 CLA which are primarily derived from an alkaline catalyzed reaction of

Table 6 Effects of CLA enriched soybean oil on serum and whole blood parameters in obese Zucker Rats

	L-Ctrl		O-Ctrl		O-CLA	
	Mean	SE	Mean	SE	Mean	SE
Aspartate transaminase (g/L)	9.58[b]	0.5	30.8[a]	3.4	23.4[a]	4.5
Total protein (g/L)	0.79	0.02	0.76	0.03	0.72	0.04
Blood urea nitrogen (mmol/L)	5.95	0.45	5	0.21	5.71	0.45
Glucose (mmol/L)	14.1[b]	0.6	26.1[a]	1.5	27.9[a]	1.4
Insulin (μg/L)	0.22[b]	0.03	2.11[a]	0.68	1.25[ab]	0.16
HbA1c (%)	3.51[c]	0.06	3.89[a]	0.07	3.71[b]	0.05

Data represents the mean values and standard error (SE; $n = 12$/group)

Values in a row without common superscripts are significantly different ($P < 0.05$)

L-Ctrl Lean + control diet, *O-Ctrl* Obese + control diet, *O-CLA* obese + conjugated linoleic acid diet (0.5%), *HbA1c* glycated hemoglobin

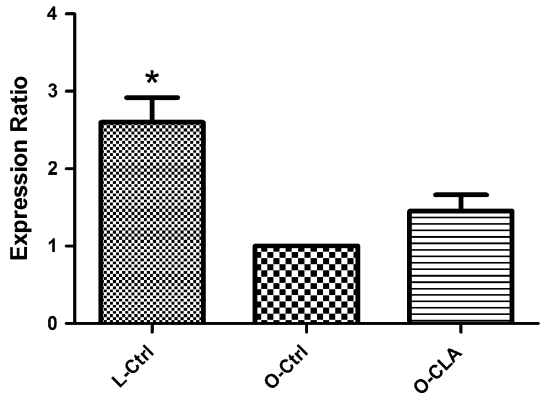

Fig. 1 Expression of PPAR-γ in Zucker rat adipose tissue treated with *trans–trans* CLA compared to obese control by qRT-PCR. The experiment was normalized to β-actin as an internal control and results were expressed as a percentage ratio of the control value. Values are means, standard errors represented by *vertical bars* ($n = 4$). * Represents significant difference ($P < 0.05$) compared to the obese control. *PPAR-γ* Peroxisome proliferator-activated receptor-γ, *L-Ctrl* lean + control diet, *O-Ctrl* obese + control diet, *O-CLA* obese + conjugated linoleic acid diet (0.5%)

linoleate [10]. To the authors' knowledge, no studies have been done to examine the effects of *trans–trans* CLA-enriched soybean oil on the body composition, cardiovascular risk factors, and diabetes risk factors in animal models or humans. Lack of knowledge on the health effects of dietary supplementation of *trans–trans* CLA isomers is due to fiscal impracticalities in obtaining enough *trans–trans* CLA isomers to conduct a feeding trial. The development of a new method of CLA production by the photoisomerization of soy oil that creates primarily *trans–trans* CLA isomers by Jain and Proctor [18, 24] allowed us to examine the possible in vivo health benefits of *trans–trans* CLA isomers. Unfortunately, at the time of study it was not possible to produce CLA-rich soybean oil containing only *trans–trans* CLA isomers. However, *trans–trans* CLA isomers make up 75% of the CLA isomers in the oil, and we think it unlikely that the small portion of the remaining *cis–trans* and *trans–cis* could have confounded our results. This study was designed to determine whether dietary supplementation of soybean oil rich with *trans–trans* CLA isomers is effective in improving body composition, dyslipidemia, hepatic steatosis, and markers of glucose control and liver function in obese *fa/fa* Zucker rats that are associated with an increased risk for type 2 diabetes and cardiovascular disease.

The present study demonstrated that *trans–trans* CLA rich soybean oil had no effect on the body composition, which is in agreement with the findings of Sanders and colleagues [25], who also reported that the body fat percentage of female obese Zucker rats treated with CLA (50:50 t9,c11:c10,t12 or t9,c11 or c10,t12) via intragastric gavage at 1.5 g CLA/kg bwt did not differ from those receiving the control corn oil vehicle. In contrast, Sisk and others [26] reported that supplementing with 0.5% CLA consisting of primarily c9,t11 and c10,t12 isomers caused an increase in adiposity in obese Zucker rats. Others have shown that dietary supplementation of CLA is effective in reducing the percentage of body fat and increasing the percentage of body protein [27, 28]. These contradictory results can be explained due to the sex of the rats and the type of CLA isomers used in the study. Poulos and others [29] demonstrated that dietary CLA can have sex-dependent effects on the body composition of rats. With dietary CLA supplementation of c9,t11 and c10,t12 isomers at 0.5% concentration, the CLA was found to have positive effects on male rats by increasing muscle mass and bone growth, but similar changes were not observed in the females [29]. Nonetheless, we observed that the *trans–trans* CLA isomers are effective in reducing hepatic steatosis which was in contrast to the results reported by Sanders and colleagues [25] who indicated that supplementation of c9,t11 CLA, t10,c12 CLA or a mixture of the two isomers did not lower hepatic steatosis. Our study shows that dietary supplementation of CLA rich soybean oil significantly ($P < 0.05$) reduced the total liver lipid content. This is in agreement with similar findings by Noto et al. [30] who reported a similar decrease ($\sim$60% Noto, $\sim$40% current study) in the liver lipid content of Zucker rats supplemented with a 1.5% (w/w) CLA. Although we saw no improvement in liver function like was reported by Noto et al., the lack of significant difference in the AST, BUN, or total protein, supports a claim that liver function was not adversely affected by CLA supplementation. The discrepancy in improved liver function and reduction in liver lipid percentage could be attributed to the higher CLA level used by Noto et al. and the fact that CLA intake in the present study was controlled by pair-feeding.

Excess accumulation of lipid in the liver is associated with insulin resistance [30]. Interestingly, our study showed that dietary supplementation of *trans–trans* CLA lowered the HbA1c, a long-term measure of glucose control and reduced the circulating insulin levels, moderately but not significantly, in the obese rats. However, we did not see any improvements in fasting blood glucose. We feel that the elevated glucose values were caused by both the anesthetic mixture, which is known to elevate fasting glucose values and the stress response of the animal model [31–33]. Similar insulin-sensitizing effects of CLA were reported by Houseknecht and coworkers in the ZDF rat [34]. The insulin-sensitizing effect of CLA is believed to be by activation of peroxisome proliferator-activated receptor-γ (PPAR-γ) [35]. Polyunsaturated fatty acids and their metabolites have been identified as PPAR-γ ligands [36]; hence, based on the data discussed above, insulin sensitizing effects of *trans–trans* CLA rich soy oil may be

due to prevention of hepatic steatosis and moderate upregulation of PPAR-γ. However, upregulation of PPAR-γ in white adipose tissue was not found to be significant (Fig. 1).

CLA rich soybean oil supplementation in obese rats also reduced the serum cholesterol and LDL-C levels. Our results are in agreement with other studies that have shown that dietary CLA can lower the serum cholesterol levels [30, 37]. This decreased serum cholesterol and LDL levels by CLA rich soybean oil can be due to a possible transcriptional activation of the LDL receptor gene which in turn enhances the uptake of VLDL and LDL cholesterol via hepatic LDL receptors [38]. Other possible cholesterol lowering effects of CLA could be due to inhibition of secretion of apolipoprotein B or by inhibiting cholesterol absorption by down-regulating the intestinal sterol O-acyltransferase activity [39, 40].

CLA has been reported to be a potent ligand activator of PPAR-α [41, 42], however, further studies are necessary to evaluate the role of *trans–trans* CLA in inducing hepatic fatty acid oxidation by ligand activation of PPAR-α. Increased fatty acid oxidation is associated with reduced LDL secretion rate [43], which is in agreement with our findings that show lower serum LDL levels in the obese rats supplemented with *trans–trans* CLA. In addition, it is plausible that hepatic fatty acid synthesis is strongly downregulated by *trans–trans* CLA, which is in agreement with others who reported that polyunsaturated fats strongly downregulated hepatic lipogenesis [44–46]. CLA also enhances the mRNA levels of lipogenic enzymes and their activity with concomitant reduction in the body fat content [47]. However, the *trans–trans* isomer in CLA enriched soy bean oil in our study did not lower the body fat percentage which further supports our hypothesis that *trans–trans* CLA prevents hepatomegaly, lowers the hepatic lipid content and improves the serum lipid profiles by increasing the hepatic fatty acid oxidation rather than compensatory increase in the hepatic lipogenesis.

Conclusion

In summary, dietary supplementation with soybean oil rich in *trans–trans* CLA isomers is effective in lowering serum cholesterol in obese Zucker rats. *Trans–trans* CLA-rich soy oil supplementation also lowered the liver lipid content. Glycated hemoglobin values for rats receiving *trans–trans* CLA were also significantly lower, indicating that *trans–trans* CLA may have a role in regulating blood sugar.

Acknowledgments This study was funded by the Arkansas Biosciences Institute.

References

1. Kopelman PG (2000) Obesity as a medical problem. Nature 404(6778):635–643
2. Kopelman P (2007) Health risks associated with overweight and obesity. Obes Rev 8(Suppl 1):13–17
3. Van Itallie TB (1985) Health implications of overweight and obesity in the United States. Ann Intern Med 103(6 (Pt 2)): 983–988
4. Giovannucci E, Michaud D (2007) The role of obesity and related metabolic disturbances in cancers of the colon prostate, and pancreas. Gastroenterology 132(6):2208–2225
5. Punjabi NM (2008) The epidemiology of adult obstructive sleep apnea. Proc Am Thorac Soc 5(2):136–143
6. Larsson B, Bjorntorp P, Tibblin G (1981) The health consequences of moderate obesity. Int J Obes 5(2):97–116
7. Bray GA (2003) Risks of obesity. Endocrinol Metab Clin North Am 32(4):787–804 viii
8. Scimeca JA, Miller GD (2000) Potential health benefits of conjugated linoleic acid. J Am Coll Nutr 19(4):470S–471S
9. Wang YW, Jones PJ (2004) Conjugated linoleic acid and obesity control: efficacy and mechanisms. Int J Obes Relat Metab Disord 28(8):941–955
10. Belury MA (2002) Dietary conjugated linoleic acid in health: physiological effects and mechanisms of action. Annu Rev Nutr 22:505–531
11. Brown JM, McIntosh MK (2003) Conjugated linoleic acid in humans: regulation of adiposity and insulin sensitivity. J Nutr 133(10):3041–3046
12. Churruca I, Fernandez-Quintela A, Portillo MP (2009) Conjugated linoleic acid isomers: differences in metabolism and biological effects. Biofactors 35(1):105–111
13. Evans M, Brown J, McIntosh M (2002) Isomer-specific effects of conjugated linoleic acid (CLA) on adiposity and lipid metabolism. J Nutr Biochem 13(9):508
14. Brown JM et al (2003) Isomer-specific regulation of metabolism and PPARgamma signaling by CLA in human preadipocytes. J Lipid Res 44(7):1287–1300
15. Ma DW et al (1999) Conjugated linoleic acid in Canadian dairy and beef products. J Agric Food Chem 47(5):1956–1960
16. Whigham LD, Watras AC, Schoeller DA (2007) Efficacy of conjugated linoleic acid for reducing fat mass: a meta-analysis in humans. Am J Clin Nutr 85(5):1203–1211
17. Ip C et al (1994) Conjugated linoleic acid suppresses mammary carcinogenesis and proliferative activity of the mammary gland in the rat. Cancer Res 54(5):1212–1215
18. Jain VP, Proctor A, Lall R (2008) Pilot-scale production of conjugated linoleic acid-rich soy oil by photoirradiation. J Food Sci 73(4):E183–E192
19. Reeves PG, Nielsen FH, Fahey GC Jr (1993) AIN-93 purified diets for laboratory rodents: final report of the American Institute of Nutrition ad hoc writing committee on the reformulation of the AIN-76A rodent diet. J Nutr 123(11):1939–1951
20. Christie WW, Dobson G, Adlof RO (2007) A practical guide to the isolation analysis and identification of conjugated linoleic acid. Lipids 42(12):1073–1084
21. Folch J, Lees M, Sloane Stanley GH et al (1957) A simple method for the isolation and purification of total lipids from animal tissues. J Biol Chem 226(1):497–509
22. Searcy RL, Bergquist LM (1960) A new color reaction for the quantitation of serum cholesterol. Clin Chim Acta 5:192–199
23. Benjamin S, Spener F (2009) Conjugated linoleic acids as functional food: an insight into their health benefits. Nutr Metab (Lond) 6:36

24. Jain VP, Proctor A (2006) Photocatalytic production and processing of conjugated linoleic acid-rich soy oil. J Agric Food Chem 54(15):5590–5596
25. Sanders SR et al (2004) Effects of specific conjugated linoleic acid isomers on growth characteristics in obese Zucker rats. Lipids 39(6):537–543
26. Sisk MB et al (2001) Dietary conjugated linoleic acid reduces adiposity in lean but not obese Zucker rats. J Nutr 131(6):1668–1674
27. Pariza MW, Park Y, Cook ME (2001) The biologically active isomers of conjugated linoleic acid. Prog Lipid Res 40(4):283–298
28. Whigham LD, Cook ME, Atkinson RL (2000) Conjugated linoleic acid: implications for human health. Pharmacol Res 42(6): 503–510
29. Poulos SP et al (2001) Pre- and postnatal dietary conjugated linoleic acid alters adipose development, body weight gain and body composition in Sprague-Dawley rats. J Nutr 131(10):2722–2731
30. Noto A et al (2006) Conjugated linoleic acid reduces hepatic steatosis, improves liver function, and favorably modifies lipid metabolism in obese insulin-resistant rats. Lipids 41(2):179–188
31. Fish R et al (2008) Anesthesia and Analgesia in Laboratory Animals. Academic Press, San Diego, CA
32. Sinert R et al (2005) The effect of non-insulin dependent diabetes mellitus on uncontrolled hemorrhage in a rodent model. Resuscitation 66(1):83–90
33. Saha JK et al (2005) Acute hyperglycemia induced by ketamine/xylazine anesthesia in rats: mechanisms and implications for preclinical models. Exp Biol Med (Maywood) 230(10):777–784
34. Houseknecht KL et al (1998) Dietary conjugated linoleic acid normalizes impaired glucose tolerance in the Zucker diabetic fatty fa/fa rat. Biochem Biophys Res Commun 244(3):678–682
35. Aminot-Gilchrist DV, Anderson HD (2004) Insulin resistance-associated cardiovascular disease: potential benefits of conjugated linoleic acid. Am J Clin Nutr 79(6 Suppl):1159S–1163S
36. Duan SZ et al (2008) PPAR-gamma in the cardiovascular system. PPAR Res 2008:745804
37. Miranda J et al (2009) A comparison between CLNA and CLA effects on body fat, serum parameters and liver composition. J Physiol Biochem 65(1):25–32
38. Ringseis R et al (2006) LDL receptor gene transcription is selectively induced by t10c12-CLA but not by c9t11-CLA in the human hepatoma cell line HepG2. Biochim Biophys Acta 1761(10):1235–1243
39. Yeung C, Yang L, Huang Y, Wang J, Chen Z (2000) Dietary conjugated linoleic acid mixture affects the activity of intestinal acyl coenzyme A: cholesterol acyltransferase in hamsters. Br J Nutr 84:935–941
40. Yotsumoto H, Hare E, Naka S, Adlof RO, Emken EA, Yanagita T et al (1999) *Trans*-10, *cis*-12-linoleic acid reduces apolipoprotein B secretion in HepG2 cells. Food Res Int 31:403–409
41. Peters JM et al (2001) Influence of conjugated linoleic acid on body composition and target gene expression in peroxisome proliferator-activated receptor alpha-null mice. Biochim Biophys Acta 1533(3):233–242
42. Moya-Camarena SY et al (1999) Conjugated linoleic acid is a potent naturally occurring ligand and activator of PPARalpha. J Lipid Res 40(8):1426–1433
43. Ide T, Ontko JA (1981) Increased secretion of very low density lipoprotein triglyceride following inhibition of long chain fatty acid oxidation in isolated rat liver. J Biol Chem 256(20):10247–10255
44. Yahagi N et al (1999) A crucial role of sterol regulatory element-binding protein-1 in the regulation of lipogenic gene expression by polyunsaturated fatty acids. J Biol Chem 274(50):35840–35844
45. Fukuda H, Katsurada A, Iritani N (1992) Nutritional and hormonal regulation of mRNA levels of lipogenic enzymes in primary cultures of rat hepatocytes. J Biochem 111(1):25–30
46. Ide T et al (2000) Comparative effects of perilla and fish oils on the activity and gene expression of fatty acid oxidation enzymes in rat liver. Biochim Biophys Acta 1485(1):23–35
47. Takahashi Y et al (2003) Activity and mRNA levels of enzymes involved in hepatic fatty acid synthesis and oxidation in mice fed conjugated linoleic acid. Biochim Biophys Acta 1631(3):265–273

Lipids (2011) 46:969–979
DOI 10.1007/s11745-011-3577-6

ORIGINAL ARTICLE

Regulation of Phosphatidic Acid Levels in *Trypanosoma cruzi*

Alba Marina Gimenez · Verónica S. Santander · Ana L. Villasuso · Susana J. Pasquaré · Norma M. Giusto · Estela E. Machado

Received: 5 November 2010 / Accepted: 9 May 2011 / Published online: 11 June 2011

Abstract Lipid kinases and phosphatases play essential roles in signal transduction processes involved in cytoskeletal rearrangement, membrane trafficking, and cellular differentiation. Phosphatidic acid (PtdOH) is an important mediator lipid in eukaryotic cells, but little is known regarding its regulation in the parasite *Trypanosoma cruzi*, an agent of Chagas disease. In order to clarify the relationship between PtdOH metabolism and developmental stages of *T. cruzi*, epimastigotes in culture were subjected to hyperosmotic stress (~1,000 mOsm/L), mimicking the environment in the rectum of vector triatomine bugs. These experimental conditions resulted in differentiation to an intermediate form between epimastigotes and trypomastigotes. Morphological changes of epimastigotes were correlated with an increase in PtdOH mass accomplished by increased enzyme activity of diacylglycerol kinase (DAGK, E.C. 2.7.1.107) and concomitant decreased activity of phosphatidate phosphatases type 1 and type 2 (PAP1, PAP2, E.C. 3.1.3.4). Our results indicate progressive increases of PtdOH levels during the differentiation process, and suggest that the regulation of PtdOH metabolism is an important mechanism in the transition from *T. cruzi* epimastigote to intermediate form.

Keywords *Trypanosoma cruzi* · Intermediate forms · Phosphatidate phosphatase · Phosphatidate kinase · Diacylglycerol kinase

Abbreviations

DAG	Diacylglycerol
DAGK	Diacylglycerol kinase
DGPP	Diacylglycerol pyrophosphate
$InsP_3$	Inositol 1,4,5-trisphosphate
InsPx	Total inositol phosphates
LPP	Lipid phosphate phosphatase
NEM	*N*-ethylmaleimide
PAK	Phosphatidate kinase
PAP	Phosphatidate phosphatase
PLC	Phospholipase C
PtdCho	Phosphatidylcholine
PtdIns	Phosphatidylinositol
PtdIns-4,5-P_2	Phosphatidylinositol 4,5-bisphosphate
PtdIns-4-P	Phosphatidylinositol 4-phosphate
PtdOH	Phosphatidic acid
TLC	Thin-layer chromatography

Introduction

The flagellate protozoan *Trypanosoma cruzi* is responsible for Chagas disease [1], a serious endemic illness and major public health problem in Latin America. The life cycle of this parasite comprises three different morphological and functional forms: amastigotes, epimastigotes, and trypomastigotes [2, 3]. The transformation of epimastigotes to metacyclic trypomastigotes (metacyclogenesis process), leading to forms that are eventually able to

V.S. Santander and A.L. Villasuso contributed equally to the work reported in this article.

A. M. Gimenez · V. S. Santander · A. L. Villasuso · E. E. Machado (✉)
Química Biológica, FCEFQN, Universidad Nacional de Río Cuarto, X5804BYA Río Cuarto, Córdoba, Argentina
e-mail: emachado@exa.unrc.edu.ar

S. J. Pasquaré · N. M. Giusto
INIBIBB (CONICET), Universidad Nacional del Sur, Bahía Blanca, Argentina

infect mammalian hosts, is of particular interest. In vivo and in vitro metacyclogenesis studies have demonstrated the presence of intermediate forms between epi- and trypomastigotes [3–9]. These intermediate forms were identified morphologically through the position of the kinetoplast relative to the nucleus, similar to the transitional stage described in the reduviid midgut [4, 7, 10, 11]. These forms are characterized by a lengthened flagellum, which is considered to be a pre-adaption for differentiation to the next life-cycle stage, i.e., metacyclic trypomastigote [12]. The biochemical characteristics of these intermediate forms are poorly known. Bourguignon et al. [9] demonstrated that they display electrophoretic mobility similar to that of trypomastigotes, indicating the presence of some specific trypomastigote proteins and surface carbohydrates. On the other hand, the intermediate forms were unable to infect either Vero or 3T3 cells, suggesting that their behavior is similar to that of epimastigotes rather than trypomastigotes [9]. No studies so far have addressed the lipid metabolism of the intermediate forms. Metacyclogenesis can be induced in vitro by incubating epimastigotes in TAU3AAG, a chemically defined medium that mimics the urine of triatomine bugs [13]. However, little is known regarding the exact environmental stimulus leading to intermediate and trypomastigote forms, or the metabolic changes that occur during this process.

Responses of parasites to environmental changes often involve changes in the phospholipid metabolism. Our previous studies have shown that *T. cruzi* epimastigotes respond to external stimuli by the modification of their phospholipid metabolism, in which phosphatidic acid (PtdOH) plays a central role [14–16]. In higher eukaryotic cells, PtdOH is well known as an important second messenger, rapidly produced in receptor-stimulated cells by phospholipase D (PLD, E.C. 3.1.4.4) and/or the combined action of phospholipase C (PLC, E.C. 3.1.4.11) and diacylglycerol kinase (DAGK, E.C. 2.7.1.107) activities [17]. Enzymes that switch off PtdOH signaling are important in the metabolism of this phospholipid. One pathway leading to PtdOH reduction is its degradation to diacylglycerol (DAG) by phosphatidate phosphatase (PAP, E.C. 3.1.3.4), a key enzyme in both lipid synthesis and the generation or degradation of lipid-signaling molecules. PAP enzymes are classified based on cofactor requirement for catalytic activity, i.e., as Mg^{2+}-dependent (termed PAP1, or lipins) or Mg^{2+}-independent (PAP2, or lipid phosphate phosphatases) [18]. In *T. cruzi*, no studies have yet addressed PAP activity, and the possible role of this enzyme in the regulation of PtdOH levels is, therefore, unknown. We previously demonstrated a functional mechanism of PtdOH reduction in epimastigotes in which PtdOH is converted to diacylglycerol pyrophosphate (DGPP) by a phosphatidate kinase (PAK) [15]. DGPP in plant cells appears to be involved in the regulation of cellular responses [19], and this compound may well have a similar function in *T. cruzi* [16].

The possible involvement of PtdOH metabolism in *T. cruzi* differentiation has not yet been studied. We did observe that the activation of both DAGK and PAK in epimastigotes is triggered by peptide 1–40 [16], which can also induce metacyclogenesis [20], suggesting that the regulation of PtdOH levels may play a role in the formation of intermediate forms.

In the present study, we found that lipid kinases (DAGK, PAK) and phosphatases (PAP1, PAP2) are regulated in opposite directions in *T. cruzi* epimastigotes versus intermediate forms. We describe for the first time PAP activity in membrane fractions of *T. cruzi*, and discuss the possible physiological involvement of PtdOH metabolism in the transition from epimastigote to intermediate forms.

Materials and Methods

Organisms and Growth Conditions

T. cruzi Tulahuen strain was used. Epimastigote forms were grown at 28°C in modified Warren medium [21], supplemented with 10% fetal bovine serum (FBS), as described previously [14]. Cells in logarithmic growth phase (day 6) were harvested by centrifugation at $1{,}000\times g$ for 10 min, and washed twice with 25 mM Tris–HCl, pH 7.35, 1.2 mM $MgSO_4$, 2.6 mM $CaCl_2$, 4.8 mM KCl, 120 mM NaCl, and 100 mM glucose [Krebs-Ringer-Tris (KRT) buffer]. To obtain intermediate forms, epimastigote forms were grown in the same culture medium but in the presence of 0.5 M NaCl or 1 M mannitol, and the cells were harvested at day 13 by centrifugation at $1{,}000\times g$ for 10 min and washed twice with KRT buffer.

Optical Microscopy Analysis

Cells were grown as described above and fresh parasite samples were taken at defined times and quantified using a Neubauer's hemocytometric chamber. For morphological studies, parasites were fixed with absolute methanol, stained with 10% Giemsa in 0.1 M sodium phosphate buffer, pH 7.2, and counted (at least 400 organisms per sample) in a Zeiss Axiolab Standard Fluorescence Microscope. Parasites were classified as epimastigotes, trypomastigotes, or intermediate forms based on cell shape, size, and Giemsa staining, as previously published [6, 8, 10].

Determination of Osmolarity

Aliquots of culture medium were taken at various stages of parasite growth, cells were removed by centrifugation, and osmolarity in the supernatant was measured using a Wescor 5500 vapor pressure osmometer.

Preparation of Membranes from Epimastigotes and Intermediate Forms

Washed cells were resuspended in five volumes of 50 mM HEPES (pH 7.4) containing 0.25 M sucrose, 5 mM KCl, 1 mM EDTA, and 4 μg/mL leupeptin. The suspension was frozen at −180°C in liquid nitrogen and thawed; this freeze/thaw cycle was performed three times. Membrane fractions were prepared as described previously [22]. Briefly, the homogenate was centrifuged at 100×*g* for 15 min to remove cell debris, and supernatant was centrifuged at 1,000×*g* for 15 min and at 105,000×*g* for 60 min. Pellets from the two centrifugations were washed, resuspended with 50 mM HEPES (pH 7.4), and used as a source of enzymatic activities.

Determination of Lipid Kinase Activity

Lipid Kinase Assay

PAK and DAGK were assayed simultaneously using endogenous lipids as substrates. The membrane fraction isolated (30–80 μg protein) was added to thermally equilibrated buffer 50 mM HEPES (pH 7.4) containing 0.1 mM EDTA, 0.5 mM DTE, 10 mM $MgCl_2$, 0.1 mM sodium o-vanadate, and 1 mM [γ-^{32}P]ATP (500 cpm/pmol). Endogenous lipid phosphorylation proceeded for 5 min at 30°C in a total volume of 100 μL, and was then terminated by the addition of 1.5 mL chloroform/methanol (1:2, by vol). The protein content of membrane samples was determined by the Bradford method [23], with bovine serum albumin as the standard.

Lipid Extraction and Separation

Lipids were extracted from membranes as described previously [15]. Samples were spotted on silica gel plates coated with potassium oxalate solution and heated at 110°C for 60 min just before use. Thin-layer chromatography (TLC) was developed with chloroform/methanol/acetone/acetic acid/water (40:14:15:12:7, by vol) for the first dimension, and chloroform/pyridine/formic acid (35:30:7, by vol) for the second dimension. The positions of radiolabeled lipids were determined by autoradiography on Kodak film. Spots were scraped off the plates and fractions counted in a liquid scintillation counter.

Determination of PtdOH Mass

Epimastigotes or intermediate forms were grown and harvested as described above. Total lipids were extracted from washed parasites as described previously [14] and aliquots were taken for the determination of total lipid phosphorus. Individual phospholipids were resolved using the TLC procedure described for labeled samples. PtdOH areas were scraped out and the fractions were quantified by phosphorus determination according to Fiske and Subbarow [24]. The experiments, carried out in duplicate, were conducted threefold.

Measurement of PLC Activity

Epimastigotes or intermediate forms were harvested by centrifugation at 1,000×*g* for 10 min and washed twice with KRT buffer. The cells were pre-incubated and gently agitated in a shaking water bath at 28°C for 12 h in KRT buffer plus 0.1% albumin, 10% FBS, 3 mM $MnCl_2$, and 4 μCi myo-[^{3}H]inositol/25 mg of cells. Total [^{3}H]inositol phosphates ([^{3}H]InsPx, the sum of cpm obtained for [^{3}H]InsP, [^{3}H]$InsP_2$, [^{3}H]$InsP_3$, and [^{3}H]$InsP_4$ column fractions) were separated by anion-exchange chromatography on Dowex AG 1-X8, as described previously [25].

Determination of PAP Activity

Preparation of Radiolabeled 1,2-Diacyl-sn-glycerol-3-phosphate

Radiolabeled PtdOH was obtained from [2-^{3}H]-phosphatidylcholine (PtdCho), which was synthesized from bovine retinas incubated with [2-^{3}H]glycerol (200 mCi/mmol), as described previously [26]. Lipids were extracted from tissues as described previously [27], and [2-^{3}H]PtdCho was isolated by TLC and eluted therefrom. [2-^{3}H]-PtdCho was hydrolyzed with PLD, and PtdOH was purified by TLC on silica gel H, developed with chloroform/methanol/acetic acid/acetone/water (9:3:3:12:1.5, by vol). The substrate was eluted from silica gel with neutral solvents to avoid the formation of lyso-PtdOH, and then converted to free acid by washing twice using an upper phase containing 0.1 M sulfuric acid. [2-^{3}H]PtdOH had a specific radioactivity of 0.1–0.2 μCi/μmol. For the determination of type 1 PAP (PAP1) activity, the substrate was prepared by sonicating 3.33 mM [2-^{3}H]-phosphatidate (0.1–0.2 μCi/μmol) and 2.22 mM dipalmitoyl PtdCho in 5.56 mM EGTA and 5.56 mM EDTA. For the determination of type 2 PAP (PAP2) activity, an emulsion was prepared as described above, except that PtdCho was omitted.

Isolation of Radiolabeled PtdOH

Lipids were extracted with chloroform/methanol (2:1, by vol) and washed with 0.2 volumes of 0.05% $CaCl_2$ [27]. Neutral lipids were separated by gradient-thickness TLC on silica gel G and developed with hexane/diethyl ether/acetic acid (35:65:1, by vol). When the chromatogram was developed, [2-^{3}H]-PtdOH and phospholipids were retained at the spotting site. Lipids were visualized by exposing the chromatogram to iodine vapor and scraped off for liquid scintillation counting, followed by the addition of 0.4 mL water and 10 mL 5% OmniFluor in toluene/Triton X-100 (4:1, by vol).

PAP Activity Assay

PAP activities were differentiated based on *N*-ethylmaleimide (NEM) sensitivity [28, 29]. NEM-insensitive PAP activity (PAP2) was determined using an assay mixture consisting of 50 mM Tris–maleate buffer, pH 6.5, 1 mM DTT, 1 mM EDTA plus 1 mM EGTA, 4.2 mM NEM, and 100 μg membrane protein in a volume of 100 μL, with the reaction started by adding 0.6 mM [2-^{3}H]-phosphatidate. NEM-sensitive PAP activity (PAP1) was determined using the same assay mixture but including 0.2 mM Mg^{2+}, with the reaction started by adding 0.6 mM [2-^{3}H]-PtdOH plus 0.4 mM PtdCho.

Parallel incubations were carried out after pre-incubating membrane fractions with 4.2 mM NEM for 10 min. The difference between the two types of activity was labeled as PAP1. All assays for the determination of PAP1 or PAP2 activity were performed for 30 min at 37°C, and were terminated by the addition of chloroform/methanol (2:1, by vol). PAP activity product 1,2-diacyl[^{3}H]glycerol was isolated and measured as described above. PAP activity was expressed as the sum (in nmol) of [^{3}H]diacylglycerol and [^{3}H]monoacylglycerol per h per mg protein.

Sequence Alignment and Phylogenetic Analysis

Sequence analysis was performed using tools provided by the National Center for Biotechnology Information (http://www.ncbi.nlm.nih.gov) and the ExPASy Molecular Biology Server (http://us.expasy.org). The *T. cruzi* genome database at GeneDB (http://www.genedb.org/genedb/tcruzi) was searched using Wu-Blast2. Sequence identity was analyzed using BlastP (http://www.ncbi.nlm.nih.gov/blast). Sequences were initially aligned using ClustalW (http://www.ebi.ac.uk/clustalw) with BioEdit Sequence Alignment Editor 4.8.8 [30, 31], and the alignment was then visually refined. Transmembrane segments were determined using TMPred (http://www.ch.embnet.org/software/TMPRED_form.html). Phylogenetic analysis was performed using the neighbor-joining method, with PAM distances computed on 118 reliably aligned sites [32].

Statistical Analysis

The results are shown as mean ± standard error of the mean (SEM) for three or more independent experiments. Statistical analysis of the data was performed using OriginPro 8 software.

Results

Generation of Intermediate Forms in Hyperosmotic Media

Experiments were performed to find out the stress conditions in the culture medium of growing *T. cruzi* epimastigotes similar to those found in the rectum of triatomine bugs, leading to the development of intermediate forms. For this purpose, we added 0.5 M NaCl or 1 M mannitol (which raises the osmolarity to ~1,000 mOsm/L) to medium, and monitored growth curves and morphologic changes of parasites for 13 days.

At day 0, the osmolarity values were 349 ± 27 mOsm/L in control medium, 1,207 ± 50 mOsm/L in NaCl-added medium, and 1,367 ± 68 mOsm/L in mannitol-added medium. In the hyperosmotic media, the proportion of intermediate forms increased steadily, reaching 87 ± 4% in NaCl-added medium at day 13 (Table 1). Morphologic changes observed in NaCl- and mannitol-added media were similar (Fig. 1a–c) and hyperosmolar media did not affect parasite viability. In the control culture, epimastigotes remained the predominant form.

The intermediate forms generated in hyperosmotic media showed increased flagellar length, a 96-h delay in the lag period of the growth curve, increased generation time (twofold), and a reduction in the maximal growth to ~50% of the control value (Fig. 1d).

DAGK and PLC Activities are Increased in the Membrane of Intermediate Forms

Changes in the membrane lipid composition of parasites are often reflected in morphological changes. We showed previously that various stimuli modified the PtdOH metabolism in membrane fractions of *T. cruzi* epimastigotes [15, 16, 22]. In the present study, we looked for correlations between observed morphological changes and PtdOH levels.

We measured the PtdOH mass in both epimastigotes and intermediate forms. The PtdOH amounts were 90.2 ± 1.5 pmol in epimastigotes versus 148.5 ± 2.5 pmol in

Table 1 Percentage of different forms of the parasite grown in different osmolarity conditions

Days	Epimastigote			Intermediate forms			Trypomastigote		
	Control	NaCl	Mannitol	Control	NaCl	Mannitol	Control	NaCl	Mannitol
0	93 ± 6	84 ± 6	86 ± 8	6 ± 3	16 ± 6	14 ± 7	1 ± 0.1	0 ± 0.0	0 ± 0.0
1	87 ± 4	76 ± 5	84 ± 5	11 ± 3	22 ± 6	12 ± 5	2 ± 0.5	2 ± 0.2	4 ± 0.3
3	86 ± 6	81 ± 6	82 ± 7	10 ± 3	17 ± 3	18 ± 5	4 ± 0.3	2 ± 0.1	0 ± 0.0
6	96 ± 6	85 ± 2	88 ± 6	3 ± 1	10 ± 2	8 ± 2	1 ± 0.3	5 ± 0.8	4 ± 0.1
9	84 ± 4	66 ± 7	63 ± 9	13 ± 4	34 ± 6	35 ± 3	3 ± 0.4	0 ± 0.0	2 ± 3.0
11	66 ± 2	45 ± 3	34 ± 10	31 ± 3	54 ± 5	62 ± 7	3 ± 0.6	1 ± 0.2	3 ± 0.2
13	61 ± 2	12 ± 2	10 ± 4	38 ± 6	87 ± 4	89 ± 5	1 ± 0.2	1 ± 0.1	1 ± 0.1

Epimastigotes were inoculated in an isosmotic medium (control) or in a hyperosmotic medium obtained by supplement with 0.5 M NaCl or 1 M mannitol. At the indicated times, aliquots were extracted in order to calculate the percent of each parasite stage. Parasites were colored by Giemsa staining and counting under an optical microscope. The data are the mean ± standard deviation (SD) of four experiments performed separately

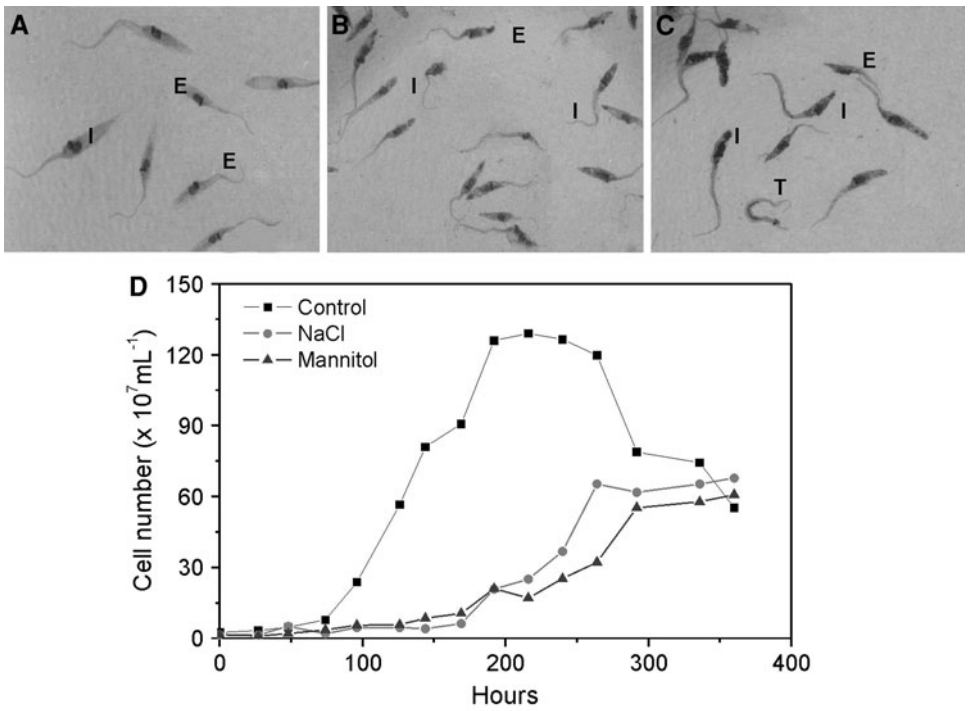

Fig. 1 Morphology and growth curve of *Trypanosoma cruzi* under various osmolarity conditions. Epimastigotes were grown in isosmotic medium (control) or hyperosmotic media (addition of 0.5 M NaCl or 1 M mannitol). An aliquot of each culture was extracted at day 13, subjected to Giemsa staining, and visualized by optical microscopy. **a** Control. **b** NaCl culture. **c** Mannitol culture. *E* epimastigote; *I* intermediate form; *T* trypomastigote. Growth curves were monitored over a period of 13 days (**d**). The parasite number was measured daily by counting in a Neubauer chamber. The data are from a representative experiment out of eight (control) and six (hyperosmotic media) independent experiments

intermediate forms, per nmol of total phospholipids ($n = 3$, $P < 0.05$). Thus, the PtdOH content increased by 64% in intermediate forms, whereas no significant variation in the total amount of phospholipids was detected.

In order to find the origin of the incremented PtdOH, we assayed lipid kinase activities in parasite membranes. [γ-^{32}P]ATP phosphorylation of membrane fractions from epimastigotes resulted in the rapid labeling of chloroform-soluble products. Enzymatic activities of lipid kinases DAGK and PAK were both higher (12.5 and 85%, respectively) in the 1,000×*g* membrane fraction than in the 105,000×*g* membrane fraction (Table 2). Activity values assayed in the 1,000×*g* fraction were 70 pmol/min/mg of protein for DAGK and 25 pmol/min/mg of protein for PAK.

The DAGK activity measured in the 1,000×*g* fraction of intermediate forms was 350 pmol/min/mg of protein, which is fivefold higher than for epimastigotes (Fig. 2a). The DAGK activity in the 105,000×*g* fraction was also roughly fivefold higher for intermediate forms. The difference in PAK activity between intermediate forms and epimastigotes was not significant (Fig. 2a). To elucidate the origin of increased DAGK activity in intermediate forms, we measured the activity of PtdIns-PLC, which yields DAG and inositol 1,4,5-trisphosphate ($InsP_3$) as

Table 2 Lipid kinase activities in 1,000×*g* and 105,000×*g* membrane fractions of *T. cruzi* epimastigotes

Enzyme	Membrane fraction	
	1,000×*g*	105,000×*g*
DAGK	63.10 ± 1.07*	56.40 ± 3.96
PAK	4.80 ± 1.00*	2.60 ± 0.27
Other kinases	32.26 ± 1.78	40.99 ± 2.78

Lipid kinase activities were determinated by phosphorylation with [γ-^{32}P]ATP of epimastigote membrane fractions. The results are expressed as the percentage of the total radioactivity of the organic phase ± standard error of the mean (SEM) ($n = 32$ for 1,000×*g* and $n = 17$ for 105,000×*g* fraction, respectively)

* Statistically significant differences ($P < 0.05$)

products. The accumulation of total inositol phosphates (InsPx) is summarized in Fig. 2b. The levels of these metabolites, representing 0.1–0.2% of cpm incorporated, showed a clear increase (25 ± 5%; $n = 3$, $P < 0.05$) in the intermediate forms compared to epimastigotes. $InsP_3$ levels were also increased (70 ± 5%; $n = 3$, $P < 0.05$), confirming the PtdIns-PLC activity change.

Decrease of PAP Activity in the Membrane of Intermediate Forms

In eukaryotic organisms that contain DGPP, the increase in PtdOH formation which occurs in response to various physiological stresses is often accompanied by increased DGPP [15, 16, 33]. Since PtdOH increase was not correlated with DGPP formation in intermediate forms (Fig. 2a), we considered the possibility that PtdOH might be metabolized by PAP. We differentiated PAP activities on the basis of sensitivity to NEM, a thiol-reactive compound that inhibits PAP1 activity but has no effect on the PAP2 activity. PAP activities were detected in both 1,000×*g* and 105,000×*g* membrane fractions from epimastigotes. In the 1,000×*g* fraction, the specific activity was 77 nmol/h/mg of protein for PAP2 and 25 nmol/h/mg of protein for PAP1. The PAP2 activity was reduced by ~50% in the 1,000×*g* fraction (but not in the 105,000×*g* fraction) of intermediate forms compared to epimastigotes (Fig. 3a). The PAP1 activity was reduced around fivefold in both 1,000×*g* and 105,000×*g* fractions of intermediate forms (Fig. 3b).

Lipid Phosphate Phosphatase Genes Encoded in the *T. cruzi* Genome

PAP2 enzymes are believed to be involved in signal transduction processes. These phosphatases belong to a phosphatase/phosphotransferase family and hydrolyze a

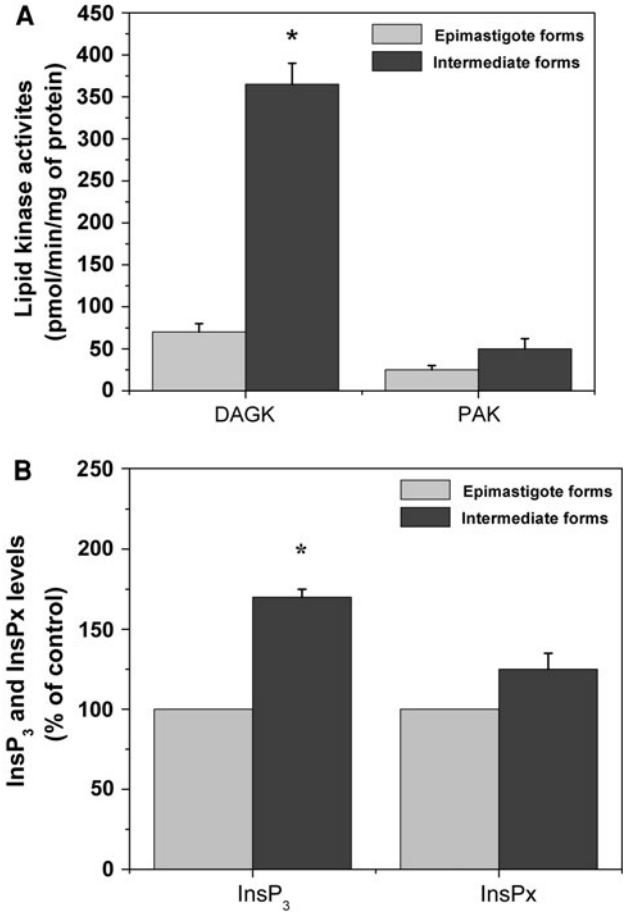

Fig. 2 Lipid kinase and phospholipase C activities. The enzymatic activities of phosphatidate kinase (PAK) and diacylglycerol kinase (DAGK) (**a**) were determined based on [γ-^{32}P] ATP phosphorylation of parasite membrane fractions. Values are mean ± standard error of the mean (SEM) from five independent experiments. [^{3}H] inositol-labeled cells were pre-incubated with 10 mM LiCl for 15 min. $InsP_3$ and InsPx levels (**b**) were analyzed as described in the "Materials and Methods" section. The results are expressed as the percentage of unstimulated control value (defined as 100%) ± SEM, $n = 4$. *$P < 0.05$

broad range of lipid phosphates, including PtdOH and DGPP. The PAP2 enzyme family was renamed "lipid phosphate phosphatases" (LPP) because of a lack of clear substrate preference in vitro and uncertainty regarding their function in vivo [18].

To try to clarify the function of parasite LPP, we conducted a search of *T. cruzi* databases (http://www.genedb.org/genedb/tcruzi) using *LPP* or *PAP* genes from human, plant, and yeast sources as query sequences. This resulted in the identification of three open reading frames, designated at GeneDB as Tc00.1047053511277.359, Tc00.1047053511277.370, and Tc00.1047053511355.30, which showed high similarity to *LPP* genes and were, therefore, termed *TcLPP1*, *TcLPP2*, and *TcLPP3*. The open reading frames of *TcLPP1* and *TcLPP2* are 948 and 879 bp in

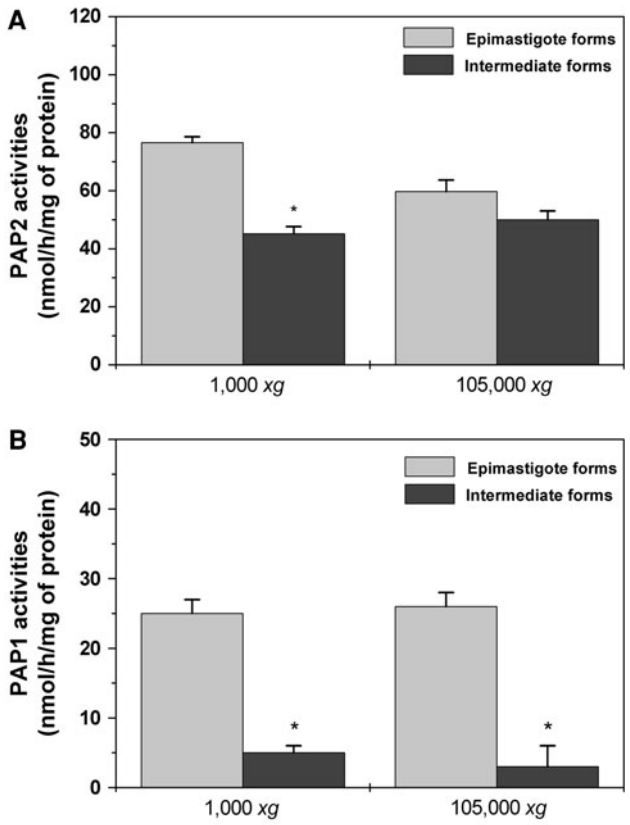

Fig. 3 The enzymatic activities of phosphatidate phosphatases type 2 (PAP2) (**a**) and phosphatidate phosphatases type 1 (PAP1) (**b**) were assayed using [^{3}H]-PtdOH (0.6 mM) plus dipalmitoyl PtdCho (0.4 mM) or [^{3}H]-PtdOH (0.6 mM) as substrates, respectively, and expressed as nmol [^{3}H]-DAG plus [^{3}H]-MAG/h/mg protein. Values are mean ± SEM, $n = 3$. *$P < 0.05$

length and code for putative proteins of 315 and 292 amino acids, here termed TcLpp1 and TcLpp2, respectively. TcLpp1 and TcLpp2 have a molecular mass of 35.3 and 32.2 kDa, respectively, and are both integral membrane proteins and contain six highly hydrophobic regions of sufficient length to be membrane-spanning, here termed TM1–6 (Fig. 4). *TcLPP3* is 954 bp in length and encodes a putative protein, here termed TcLpp3, having 317 amino acids (35.7 kDa) with seven predicted transmembrane helices (TM1–7).

Amino acid sequence analysis showed that TcLpp proteins have the highest identity with human PAP type 2 domain (HsLpp3) (Fig. 4), followed by orthologs of *Arabidopsis thaliana* (AtLpp3) and *Saccharomyces cerevisiae* (ScDpp1) (Table 3). Alignment analysis between TcLpp1, TcLpp2, and TcLpp3 revealed fairly high amino acid identity (33–40%). However, TcLpp3 had a signal peptide predicted in the N-terminal region 22 amino acids in length that did not align with sequences of TcLpp1 or TcLpp2. A phylogenetic tree was constructed for members of the LPP protein family, including TcLpp1, TcLpp2, and TcLpp3 (Fig. 5). The *T. cruzi* proteins were grouped with putative Lpp proteins belonging to other kinetoplastids, such as *T. brucei* (TbLpp) and *Leishmania* (LmLpp, LbLpp).

Discussion

In this study, the transition from *T. cruzi* epimastigotes to intermediate forms stimulated the activities of DAGK and PtdIns-PLC, while the activity of PAK, an enzyme absent in mammalian cells, was unchanged. PAP activity was reduced, suggesting that PtdOH metabolism is involved in this transition process. Intermediate forms generated when epimastigotes were incubated in high-osmolarity conditions were characterized as parasite forms, with nucleus-adjacent kinetoplasts. They also showed increased flagellar length, considered to be a pre-adaptation of epimastigotes for differentiation to trypomastigotes [12]. Carvalho-Moreira et al. [8] reported that epimastigotes incubated in saline solution failed to complete metacyclogenesis, which was interrupted in the intermediate stage, similar to our finding. We observed that NaCl and mannitol treatment evoked similar morphological changes, supporting the idea that increased osmolarity of culture medium, rather than ionic stress, was the factor promoting the formation of intermediate forms. During the course of parasite growth, such morphological alterations, reflected in the changes of membrane phospholipids, may help maintain biophysical properties for optimal membrane function, allowing the parasites to cope with environmental changes. In this sense, it is critical that the intracellular DAG level be tightly regulated, since the conversion of DAG to PtdOH by DAGK is the major route to terminate DAG signaling [22]. PtdOH itself has a broad array of signaling properties distinct from those of DAG. The ability of *T. cruzi* to generate PtdOH through DAGK in intermediate forms provides two ways of terminating the effects of DAG: breaking down DAG metabolically and producing PtdOH. Accordingly, the PtdOH amount was increased in intermediate forms (64%), indicating that the PtdOH metabolism is clearly an important part of the complex mechanism for transition from epimastigotes to intermediate forms in this species.

The presence of DAGK activity in both 1,000×*g* and 105,000×*g* membrane fractions indicates a complex distribution pattern similar to that observed in bacteria and higher eukaryotes [34]. Enzymatic activity in epimastigote 1,000×*g* fraction was comparable to previously reported values [15], but activity in intermediate forms was fivefold higher. This increase was not due to the higher availability of DAG, since the results from experiments with saturating concentrations of exogenous substrates were not significantly different from those in assays with endogenous substrates. Furthermore, the decreased PAP2 activity

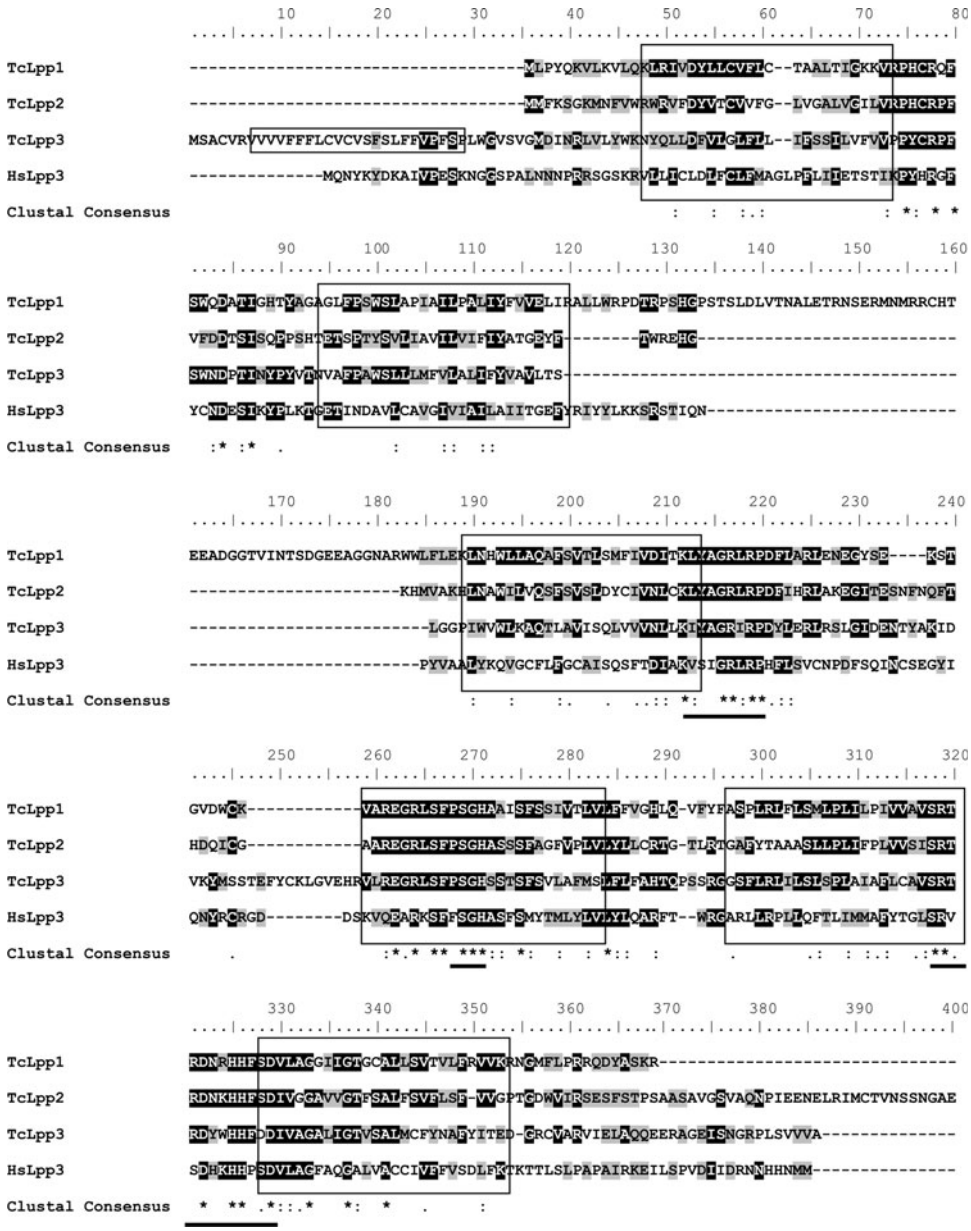

Fig. 4 Amino acid sequence comparison between the deduced sequences of TcLpp1, TcLpp2, TcLpp3, and human lipid phosphate phosphatase 3 (Lpp3). Invariant amino acids and conserved amino acids are indicated by *black* and *gray boxes*, respectively. *Open boxes* transmembrane regions. *Black bars* three domains of phosphatase sequence motif. *Conserved amino acid residues of all lipid phosphate phosphatase (Lpp) proteins

Table 3 Homology of *Trypanosoma cruzi* Lpp with human, plant, and yeast Lpp proteins

Putative proteins (I/S, %)	Lpp used for homology analysis		
	HsLpp3	AtLpp3	ScDpp1
TcLpp1	35/49	35/51	33/48
TcLpp2	40/54	36/47	28/43
TcLpp3	35/50	31/48	28/48

Percentages of identity (I) and similarity (S) values for *T. cruzi* protein sequences compared with Lpp isoforms from human (HsLpp3), *A. thaliana* (AtLpp3), and *S. cerevisiae* (ScDpp1) proteins, defined by BLAST2 sequence analysis, is shown

recorded in intermediate forms would indicate that DAGK substrate is produced by other pathways. Specific activity of DAGK was highest in the 1,000×*g* fraction of intermediate forms, which is enriched in flagellar membranes (data not shown), suggesting an important role of this enzyme and/or its substrate and product lipids in the self-function of flagellae. Tyler and Engman [12] proposed that epimastigotes react to some stimuli by extending their flagellae in order to adhere to the insect vector hindgut wall and undergo metacyclogenesis.

DAGK enzymes identified in unicellular organisms (bacteria) are structurally different from those in higher

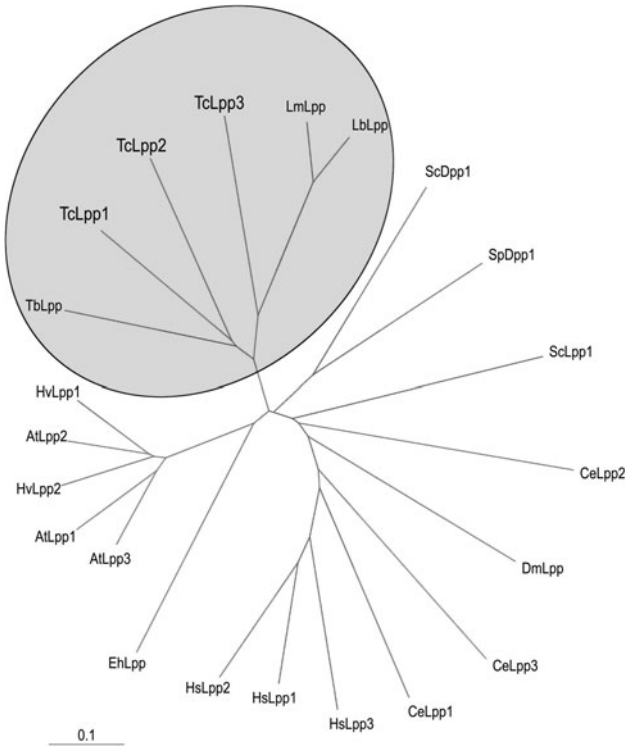

Fig. 5 Phylogenetic analysis of the Lpp protein family, including *T. cruzi* TcLpp1, TcLpp2, TcLpp3 proteins, human HsLpp1, HsLpp2, HsLpp3 proteins, *Arabidopsis thaliana* AtLpp1, AtLpp2, AtLpp3 proteins, and *Saccharomyces cerevisiae* Dpp1, Lpp1 proteins. Uncharacterized putative Lpp-like proteins identified in *T. brucei*, *Leishmania mayor*, *L. brazilensis*, *Entamoeba histolytica*, *Hordeum vulgare*, *Drosophila melanogaster*, *Caenorhabditis elegans*, and *Schizosaccharomyces pombe* genomes were used for comparison. The tree was constructed by the application of the neighbor-joining method to PAM distances computed for 118 reliably aligned sites. *Gray circle* grouping of flagellated protozoa from order Kinetoplastida (e.g., *Leishmania*, *T. brucei*, *T. cruzi*)

eukaryotes [34 and references therein]. Little is known about regulation of DAGK in parasites. Our search of *T. cruzi* databases (http://www.genedb.org/genedb/tcruzi) identified only a sequence noted as putative DAG kinase-like protein. Mammalian DAGK isoforms are classified into five subtypes based on structural motifs [34 and references therein]. In *T. cruzi*, the above sequence (accession number EAN 99355) showed the highest homology with mammalian DAGKε (data not shown). These isoforms are the only type III enzymes showing an unusual specificity toward acyl chains of DAG, i.e., they strongly prefer unsaturated fatty acids—particularly arachidonate—in the sn-2 (middle) position of the glycerol backbone [35]. Although arachidonic acid (20:4) is not a major component of *T. cruzi* lipids, linoleic acid (18:2) is the major fatty acid of DAG, as well as PtdIns-4,5-P_2 [36, 37]. We hypothesize that DAGK in the parasite plays a role equivalent to that of DAGKε, helping to enrich PtdIns, and, therefore, PtdIns-4-P and PtdIns-4,5-P_2 with unsaturated fatty acids, in membrane microdomains.

Our previous studies demonstrated that *T. cruzi* responds to external stimuli that induce changes in the inositol cycle and calcium signaling [14, 16, 22]. In this situation, DAGK activity causes a dynamic increase of PtdOH, with simultaneous DGPP formation through PAK activation [15, 16]. Since DGPP appears to regulate cellular responses, we considered that increased levels of PtdOH in *T. cruzi* might be metabolized immediately through this pathway. However, the fivefold increase of PtdOH levels by DAGK that we observed in the intermediate forms was not correlated with an increased DGPP level. This finding suggested the existence of another enzymatic activity that utilizes PtdOH as the substrate in order to reduce its signal, consistent with our previous hypothesis that the metabolism of both PtdOH and DGPP is coupled to LPP activity in this parasite [15, 16]. As a test, we determined the activities of two PAP isoforms, PAP1 and PAP2, in parasite membrane fractions, which were decreased in intermediate forms. This result, coupled with the increased PtdOH mass in intermediate forms, indicate a function of PtdOH in this transitional stage. It has been shown that trypanosoma subpellicular microtubules, extended during differentiation, are crosslinked to the plasma membrane through a microtubule-associated protein, p15, which can bind both tubulin and phospholipids in vitro [38], although the nature of the phospholipid participating in the binding is unknown. Since p15 is an amphipathic and positively charged protein, its counterpart in the membrane should be an acidic phospholipid, such as PdtOH. In *T. cruzi*, increased PtdOH mass during differentiation to intermediate forms makes PtdOH a good candidate for that binding and, therefore, an important mediator of microtubular rearrangement. This seems to occur in plant cells, where decreased level of PtdOH causes the release of microtubules from the plasma membrane [17]. Alternatively, PtdOH might be acting as the substrate for *T. cruzi* CDP-DAG synthase (E.C. 2.7.7.41), an enzyme coded in the parasite genome [39]. The latter explanation seems probable, since we found increased PtdIns-PLC activity in intermediate forms, and Tang et al. [35] showed that CDP-DAG is involved in the re-synthesis of PtdIns as a precursor of PtdIns-4,5-P_2. We can not rule out the possible presence of PtdCho-PLC (E.C. 3.1.4.3) activity, which also yields DAG through the hydrolysis of PtdCho, although this enzyme has not been detected so far in *T. cruzi*.

The finding of PAP activity in epimastigotes and intermediate forms of *T. cruzi* is the first biochemical evidence for the presence of LPP in parasitic protozoa. A bioinformatic search of the GeneDB *T. cruzi* database revealed the presence of three putative proteins structurally similar to

the PAP enzymes of yeast, mammalian cells, and plant cells [40]. The candidate proteins TcLpp1, TcLpp2, and TcLpp3 were grouped by phylogenetic analysis into a main branch with other putative PAP of protozoa. The three putative proteins of *T. cruzi* contain a three-domain phosphatase sequence motif that is conserved in Lpp from *S. cerevisiae*, *A. thaliana*, and mammalian cells [41]. TcLpp proteins also showed the presence of conserved amino acid residues important for phosphate phosphatase activity [42], suggesting that the putative proteins are functional. Follow-up studies are needed in order to determine whether the three proteins are expressed in parasites and to identify their substrate specificities.

Our findings help clarify novel aspects of the PtdOH metabolism in *T. cruzi*, the mechanism of phosphorylation/dephosphorylation, and a role of PtdOH in transduction pathways upstream of the trypomastigote stage.

Acknowledgments This work was supported by FONCyT (BID 1728 OC/AR PICT 2007-02212) Buenos Aires, Argentina and SECyT, UNRC, Río Cuarto, Córdoba, Argentina. A.M. Gimenez is a fellow of CONICET. V.S. Santander and A.L. Villasuso are Career Investigators of CONICET.

References

1. Chagas C (1909) Nova tripanozomiase humana. Estudos sobre a morfologia e o ciclo evolutivo do *Schizotrypanum cruzi*, n. gen., n. sp. agente etiológico de nova entidade mórbida do homem. Mem Inst Oswaldo Cruz 1:159–218
2. de Souza W (1984) Cell biology of *Trypanosoma cruzi*. Int Rev Cytol 86:197–283
3. Brener Z (1973) Biology of *Trypanosoma cruzi*. Ann Rev Microbiol 27:343–382
4. Dias E (1934) Estudos sobre o *Schizotrypanum cruzi*. Mem Inst Oswaldo Cruz 28:100–110
5. Schaub GA (1988) Metacyclogenesis of *Trypanosoma cruzi* in the vector *Triatoma infestans*. Mem Inst Oswaldo Cruz 83:563–570
6. Perlowagora-Szumlewicz A, Moreira CJC (1994) In vivo differentiation of *Trypanosoma cruzi*. I. Experimental evidence of the influence of vector species on metacyclogenesis. Mem Inst Oswaldo Cruz 89:603–618
7. Cortez MGR, Gonzalez MS, Cabral MMO, Garcia ES, Azambuja P (2002) Dynamic development of *Trypanosoma cruzi* in *Rhodnius prolixus*: role of decapitation and ecdysone therapy. Parasitol Res 88:697–703
8. Carvalho-Moreira CJ, Spata MCD, Coura JR, Garcia ES, Azambuja P, Gonzalez MS, Mello CB (2003) In vivo and in vitro metacyclogenesis tests of two strains of *Trypanosoma cruzi* in the triatomine vectors *Triatoma pseudomaculata* and *Rhodnius neglectus*: short/long-term and comparative study. Exp Parasitol 103:102–111
9. Bourguignon SC, Mello CB, Santos DO, Gonzalez MS, Souto-Padron T (2006) Biological aspects of the *Trypanosoma cruzi* (Dm28c clone) intermediate form, between epimastigote and trypomastigote, obtained in modified liver infusion tryptose (LIT) medium. Acta Trop 98:103–109
10. Schaub GA, Grünfelder CG, Zimmermann D, Peters W (1989) Binding of lectin–gold conjugates by two *Trypanosoma cruzi* strains in ampullae and rectum of *Triatoma infestans*. Acta Trop 46:291–301
11. Asin S, Catalá S (1995) Development of *Trypanosoma cruzi* in *Triatoma infestans*: influence of temperature and blood consumption. J Parasitol 81:1–7
12. Tyler KM, Engman DM (2000) Flagellar elongation induced by glucose limitation is preadaptive for *Trypanosoma cruzi* differentiation. Cell Motil Cytoskeleton 46:269–278
13. Contreras VT, Salles JM, Thomas N, Morel CM, Goldenberg S (1985) In vitro differentiation of *Trypanosoma cruzi* under chemically defined conditions. Mol Biochem Parasitol 16:315–327
14. Machado de Domenech EE, García M, Garrido MN, Racagni G (1992) Phospholipids of *Trypanosoma cruzi*: increase of polyphosphoinositides and phosphatidic acid after cholinergic stimulation. FEMS Microbiol Lett 95:267–270
15. Marchesini N, Santander V, Machado-Domenech E (1998) Diacylglycerol pyrophosphate: a novel metabolite in the *Trypanosoma cruzi* phosphatidic acid metabolism. FEBS Lett 436:377–381
16. Santander V, Bollo M, Machado-Domenech E (2002) Lipid kinases and Ca^{2+} signaling in *Trypanosoma cruzi* stimulated by a synthetic peptide. Biochem Biophys Res Commun 293:314–320
17. Wang X, Devaiah SP, Zhang W, Welti R (2006) Signaling functions of phosphatidic acid. Prog Lipid Res 45:250–278
18. Brindley DN, Pilquil C, Sariahmetoglu M, Reue K (2009) Phosphatidate degradation: phosphatidate phosphatases (lipins) and lipid phosphate phosphatases. Biochim Biophys Acta 1791:956–961
19. van Schooten B, Testerink C, Munnik T (2006) Signalling diacylglycerol pyrophosphate, a new phosphatidic acid metabolite. Biochim Biophys Acta 1761:151–159
20. Fraindenraich D, Peña C, Isola EL, Lammel EL, Coso O, Diaz Añel A, Pongors S, Baralle F, Torres H, Flawiá M (1993) Stimulation of *Trypanosoma cruzi* adenyl cyclase by an αD-globin fragment from *Triatoma* hindgut: effect on differentiation of epimastigote and trypomastigote forms. Proc Natl Acad Sci 90:10140–10144
21. Warren LG (1960) Metabolism of *Schizotrypanum cruzi* Chagas. I. Effect of culture age and substrate concentration on respiratory rate. J Parasitol 46:429–539
22. Marchesini N, Bollo M, Hernández G, Garrido MN, Machado-Domenech E (2002) Cellular signalling in *Trypanosoma cruzi*: biphasic behaviour of inositol phosphate cycle components evoked by carbachol. Mol Biochem Parasitol 120:83–91
23. Bradford MM (1976) A rapid and sensitive method for the quantitation of microgram quantities of protein utilizing the principle of protein-dye binding. Anal Biochem 72:248–254
24. Fiske CH, Subbarow Y (1925) The colorimetric determination of phosphorus. J Biol Chem 66:375–400
25. Garrido MN, Bollo MI, Machado-Domenech EE (1996) Biphasic and dose-dependent accumulation of $InsP_3$ in *Trypanosoma cruzi* stimulated by a synthetic peptide carrying a chicken αD-globin fragment. Cell Mol Biol 42:859–864
26. Pasquaré de García SJ, Giusto NM (1986) Phosphatidate phosphatase activity in isolated rod outer segment from bovine retina. Biochim Biophys Acta 875:195–202
27. Folch J, Lees M, Sloane Stanley GH (1957) A simple method for the isolation and purification of total lipides from animal tissues. J Biol Chem 226:497–509
28. Jamal Z, Martin A, Gomez-Muñoz A, Brindley DN (1991) Plasma membrane fractions from rat liver contain a phosphatidate phosphohydrolase distinct from that in the endoplasmic reticulum and cytosol. J Biol Chem 266:2988–2996
29. Hooks SB, Ragan SP, Lynch KR (1998) Identification of a novel human phosphatidic acid phosphatase type 2 isoform. FEBS Lett 427:188–192

30. Thompson JD, Higgins DG, Gibson TJ (1994) CLUSTAL W: improving the sensitivity of progressive multiple sequence alignment through sequence weighting, position-specific gap penalties and weight matrix choice. Nucleic Acids Res 22:4673–4680
31. Hall TA (1999) BioEdit: a user-friendly biological sequence alignment editor and analysis program for Windows 95/98/NT. Nucl Acids Symp Ser 41:95–98
32. Saitou N, Nei M (1997) The neighbor-joining method: a new method for reconstructing phylogenetic trees. Mol Biol Evol 4:406–425
33. Racagni G, Villasuso AL, Pasquaré SJ, Giusto NM, Machado E (2008) Diacylglycerol pyrophosphate inhibits the α-amylase secretion stimulated by gibberellic acid in barley aleurone. Physiol Plant 134:381–393
34. Cai J, Abramovici H, Gee SH, Topham MK (2009) Diacylglycerol kinases as sources of phosphatidic acid. Biochim Biophys Acta 1791:942–948
35. Tang W, Bunting M, Zimmerman GA, McIntyre TM, Prescott SM (1996) Molecular cloning of a novel human diacylglycerol kinase highly selective for arachidonate-containing substrates. J Biol Chem 271:10237–10241
36. Villasuso AL, Aveldaño M, Vicario A, Machado-Domenech EE, García de Lema M (2005) Culture age and carbamoylcholine increase the incorporation of endogenously synthesized linoleic acid in lipids of *Trypanosoma cruzi* epimastigotes. Biochim Biophys Acta 1735:185–191
37. Racagni G, García de Lema M, Domenech CE, Machado de Domenech EE (1992) Phospholipids in *Trypanosoma cruzi*: phosphoinositide composition and turnover. Lipids 27:275–278
38. Rasooly R, Balaban N (2002) Structure of p15 trypanosome microtubule associated protein. Parasitol Res 88:1034–1039
39. Smith TK, Bütikofer P (2010) Lipid metabolism in *Trypanosoma brucei*. Mol Biochem Parasitol 172:66–79
40. Stukey J, Carman GM (1997) Identification of a novel phosphatase sequence motif. Protein Sci 6:469–472
41. Toke DA, McClintick ML, Carman GM (1999) Mutagenesis of the phosphatase sequence motif in diacylglycerol pyrophosphate phosphatase from *Saccharomyces cerevisiae*. Biochemistry 38:14606–14613
42. Zhang QX, Pilquil CS, Dewald J, Berthiaume LG, Brindley DN (2000) Identification of structurally important domains of lipid phosphate phosphatase-1: implications for its sites of action. Biochem J 345:181–184

Lipids (2011) 46:981–990
DOI 10.1007/s11745-011-3576-7

METHODS

Fatty Acid Status Determination by Cheek Cell Sampling Combined with Methanol-Based Ultrasound Extraction of Glycerophospholipids

Mario Klingler · Hans Demmelmair · Berthold Koletzko · Claudia Glaser

Received: 4 January 2011 / Accepted: 19 May 2011 / Published online: 17 June 2011

Abstract Tissue and blood fatty acid compositions are used as biological markers of fatty acid intakes to improve dietary assessments. These approaches are invasive and not well accepted, particularly in infants and young children. We developed a sensitive method for the analysis of fatty acids in cheek cell glycerophospholipids, which includes significant improvements of cell sampling, non-chromatographic isolation of glycerophospholipids and base-catalyzed synthesis of fatty acid methyl esters. Sphingophospholipids are not detected by this method. This enables a highly accurate determination of cheek cell glycerophospholipid fatty acids, even if cell numbers are limited. Coefficients of variation for fatty acids contributing more than 0.3% to total glycerophospholipid fatty acids are below 10% in samples with more than 10^5 cells. Good correlations were shown between docosahexaenoic and eicosapentaenoic acid percentages in cheek cell and plasma glycerophospholipids ($r = 0.83$ and 0.64, respectively; $P < 0.001$) with a linear relationship over the whole concentration range observed in adult study participants ($n = 29$). Cheek cell sampling is non-invasive and can easily be applied in infants. The accuracy and reliability of this new method is comparable to conventional invasive methods for the determination of the n-3 fatty acid status in humans, and it is well applicable in interventional or epidemiological studies.

Keywords Cheek cells · Glycerophospholipids · Lipids · Fatty acid status · Docosahexaenoic acid · Gas chromatography

M. Klingler · H. Demmelmair · B. Koletzko (✉) · C. Glaser
Division of Metabolic and Nutritional Medicine, Dr. von Hauner Children's Hospital, University of Munich Medical Center, Lindwurmstr. 4, 80337 Munich, Germany
e-mail: office.koletzko@med.uni-muenchen.de

Abbreviations

ARA	Arachidonic acid
BHT	Butylated hydroxytoluene
CE	Cholesterol ester
CV	Coefficient of variation
DHA	Docosahexaenoic acid
EPA	Eicosapentaenoic acid
FA	Fatty acid
FAME	Fatty acid methyl ester
LC-PUFA	Long chain polyunsaturated fatty acid
PL	Phospholipid
SPE	Solid phase extraction
TAG	Triacylglycerols
TLC	Thin layer chromatography
PtdEtn	Phosphatidyletholamine
PtdCho	Phosphatidylcholine

Introduction

Docosahexaenoic acid (DHA) and other long chain polyunsaturated fatty acids (LC-PUFA) play import roles in human health. Increased intake of DHA has been associated with increased DHA content in blood lipids and lower risk for cardiovascular disease [1, 2]. Studies with infants and young children showed that DHA can affect their behavioral and mental development [3]. Studies on fatty acid (FA) intake often rely on food intake questionnaires, which provide information about the type of diet consumed, but they do not allow accurate estimation of the FA status [4]. Analysis of FAs in various body compartments, such as plasma, erythrocytes and adipose tissue, have been used to obtain information on FA status [5]. These

approaches are invasive and not well accepted in population studies, particularly in infants and young children.

McMurchie et al. [6] reported that changes in dietary FA compositions were reflected in cheek cell phospholipids and suggested those as an alternative marker for FA status. Later studies focusing on LC-PUFA uptake confirmed these findings. Diets rich in LC-PUFAs increased infantile DHA and eicosapentaenoic acid (EPA) levels in erythrocytes, plasma and cheek cell phospholipids [7–9]. DHA contents in all compartments were significantly correlated. This was also shown in a study with infants (age <12 months) who received DHA and arachidonic acid (ARA) with an infant formula [10]. Laitinen et al. [11] found differences in cheek cell phospholipid FA compositions associated with eczema in children. A large intervention study in school children showed a positive relationship of n-3 supplementation and cheek cell DHA levels in cheek cell total lipids [12].

The sampling and analytical methods applied in these studies differed widely, which limits the comparison of results [6, 7, 9–14]. Data about cell yield, analytical precision and reliability or storage stability are not available. Therefore, a validated analytical method is needed to utilize cheek cells as FA markers in future interventional or epidemiological studies.

Our group developed a high-throughput method for the determination of FA profiles in plasma glycerophospholipids, which avoids the chromatographic separation of lipid classes and excludes sphingophospholipids [15]. Glycerophospholipid FAMEs were obtained with two single steps. The method is highly selective for glycerophospholipids, and serum samples of more than 1,300 young children were analyzed to provide reference values for clinical practice [16].

This method was adapted for the analysis of glycerophospholipid FA profiles in cheek cells. This article describes the method development and explored factors that may influence the obtained results. Cheek cell and plasma glycerophospholipid FA contents of patients with inborn errors of metabolism were correlated to validate the use of cheek cells as FA status marker.

Materials and Methods

Subjects

Cheek cell samples for method development were obtained from healthy male and female adult volunteers employed at the Dr. von Hauner Children's Hospital, Munich. Cheek cell and plasma samples for correlation analyses were available from a quality of life study comparing adult patients with phenylketonuira and healthy controls. Complete sets of data were available from 17 healthy subjects (40.0 ± 8.5 years, mean ± SD) and 12 patients (37.5 ± 3.5 years). The Ethics Committee of the University of Munich Medical Center had reviewed the study protocol (project number 034-10). Written informed consent was obtained from all study participants prior to the study.

Chemicals and FA Standards

All solvents and chemicals were purchased in the highest available purity from Merck KGaA (Darmstadt, Germany). Sodium methoxide (25 wt% in methanol) and methanolic HCl (3 M) were obtained from Sigma-Aldrich (Taufkirchen, Germany). An internal standard A consisting of dipentadecanolyl-sn-glycero-phosphocholine (Sigma-Aldrich) dissolved in methanol was used for the quantification of glycerophospholipid FAs only. Pentadecanoic acid, cholesteryl pentadecanoate, tripentadecanoin and 1,2-dipentadecanoyl-sn-glycero-phosphocholine dissolved in methanol/chloroform (35:15 by vol.) was used as internal standard B to quantify FA concentrations of individual lipid fractions or total lipids. FA oxidation was minimized by adding 2 g/l 2,6-di-*tert*-butyl-*p*-cresol (butylated hydroxytoluene, BHT; Sigma-Aldrich) to all standard solutions.

Cheek Cell Sampling Procedure

Different methods were tested by a trained adult panel to test sampling procedures for adults and young children. The optimal adult sampling procedure comprised mouth cleaning with tap water three times prior to sampling, followed by rubbing of each inner cheek side with a Gynobrush Plus (Herenz, Hamburg, Germany). Subsequently, the mouth was rinsed with 10 ml pure water (Braun, Melsungen, Germany), and the rinsing solution containing cells washed off the inner cheeks was collected in a tube. The tube with the brush used for scraping inserted was centrifuged at 1,400×*g* for 10 min at 4 °C. The supernatant was discarded, the cell pellet resuspended with distilled water to a total volume of 1 ml, and 25 µl of this volume was used for cell counting. The remaining volume was centrifuged (1,400×*g*, 10 min, 4 °C), the supernatant discarded, and cheek cells either processed immediately or stored at −80 °C until analysis.

The cheek cell sampling procedure for infants <1 year of age was identical, but did not include mouth cleaning before or mouth rinsing after swabbing.

The average cell number obtained by both procedures was estimated by dividing the volunteers ($n = 10$) into two groups: group 1 executed the "children" procedure without mouth rinse, group 2 the "adult" procedure with repeated mouth rinse. After 1 week, sampling was repeated, but

group 1 executed the "adult" procedure and group 2 the "children" procedure. Cells were counted with a hemocytometer (dilution factor 50,000) after staining with trypan blue.

Pooled cheek cell samples were used for method development. Cell samples were collected from each volunteer separately at the same time. Samples were centrifuged at 1,400×*g* for 10 min at 4 °C, supernatants discarded, cell pellets redissolved in 500 µl distilled water and combined in a 15-ml plastic tube. Distilled water was added to a total volume of 10 ml, and the cell suspension shaken vigorously. A 50-µl aliquot was used for cell counting. Based on total cell count, aliquots were obtained with defined cell numbers. Cell sampling for each analysis was conducted at a different day, and numbers of volunteers varied depending on the need of cell numbers; thus, the composition of each cheek cell pool was different, and only the coefficient of variation (CV) can be compared between sample sizes.

The Analysis of Cheek Cell Glycerophospholipid FAs

Glycerophospholipid FAs determinations were based on the method of Glaser et al. [15]; 1.3 ml methanol and 100 µl standard A were added to the cheek cell pellet, the suspension was placed in an ultrasound water bath (120 W, 35 kHz) for 20 min, and precipitated proteins were separated by centrifugation (3,030×*g*, 20 min, 4 °C). Glycerophospholipid containing supernatant was transferred into a 4-ml brown glass vial. Glycerophospholipid FAs were transesterified into FAME after the addition of 50 µl sodium methoxide solution (25 wt% in methanol) at room temperature (21 °C). The reaction was stopped after 4 min with 150 µl 3 M methanolic HCl. FAMEs were extracted twice with 600 µl hexane, dried under a steady nitrogen flow and re-dissolved in 30 µl hexane (containing 2 g/l BHT) for gas chromatographic analysis.

Determination of Cheek Cell TAG and Total Phospholipids

TAG contents in the methanolic supernatant were determined to evaluate their contribution to the total phospholipid content. Briefly, the cell pellet was suspended in 1.4 ml methanol without standard and placed in an ultrasound water bath (120 W, 35 kHz) for 20 min. The precipitated proteins were separated by centrifugation (20 min, 3,030×*g*, 4 °C). After transfer, the methanolic supernatant was dried under nitrogen. The lipid residue was dissolved in 400 µl chloroform-methanol and separated by thin layer chromatography (TLC; SIL G-25, Macherey-Nagel, Düren, Germany) with a mixture of *n*-heptane, diisopropyl ether and acetic acid (60:40:3) as mobile phase [17]. After visualization of the components with 2′,7′-dichlorofluorescein under UV light, the PL and TAG bands were individually scraped off the plate and transferred into brown glass tubes. FAMEs were synthesized in 1.5 ml methanolic HCl at 85 °C for 45 min. Methyl esters were extracted twice with 1 ml hexane, dried under a nitrogen flow and redissolved in 30 µl hexane (containing 2 g/l BHT) for gas chromatographic analysis. Proportions of TAG contents in the PL fraction were calculated by peak area comparison of respective individual FA.

Analysis of Cheek Cell Total Lipids

Glycerophospholipid and total lipid FA concentrations of cheek cells were compared to estimate the glycerophospholipid proportion to total lipids. Briefly, cheek cells were lysed in 2 ml chloroform/methanol (2:1 by vol.) and 25 µl standard B. The solution was placed in an ultrasound water bath (120 W, 35 kHz) for 20 min and centrifuged at 3,030×*g* for 10 min at 4 °C. The supernatant containing total cheek cell lipids was transferred into a 4-ml brown glass vial and dried under a continuous nitrogen flow. The dried lipids were heated to 85 °C for 45 min in 1.5 ml 3 M methanolic HCl transesterifying FAs into their methyl esters. The FAMEs were extracted twice with 1 ml hexane, dried under nitrogen and re-dissolved in 50 µl hexane (containing 2 g/l BHT) for gas chromatographic analysis.

Determination of Plasma Glycerophospholipid FA

Glycerophospholipid contents of plasma and cheek cell FAs were compared in controls and patients with inborn errors of metabolism. Plasma glycerophospholipids were analyzed by the method of Glaser et al. [15].

Gas Chromatography

Individual FAMEs were quantified by gas chromatography with flame ionization detection (GC-FID) on a Agilent 5890 series II GC (Waldbronn, Germany), equipped with a BPX 70 column (25 m × 0.22 mm, 0.25-µm film, SGE, Weiterstadt, Germany).

FAMEs obtained from samples with more than 1.5×10^5 cells were injected at a temperature of 250 °C with a split ratio of 1/30. An optimized temperature program was used. Starting at 150 °C, the oven temperature was increased by 2.5 °C per minute to 180 °C, by 1.5 °C per minute to a final temperature of 200 °C, which was held for 1 min. Helium was used as carrier gas. The initial pressure was set to 0.9 bar, increasing by 0.02 bar per minute to 1.2 bar, 0.05 bar per minute to 1.5 bar, and 0.1 bar per minute to the final pressure of 2.0 bar. The final pressure was held until completion of the temperature program [15].

FAME obtained from samples with fewer than 1.5×10^5 cells were injected at a temperature of 300 °C in splitless mode. While pressure programs for split and splitless mode were identical, the temperature program was adjusted as follows: starting temperature 60 °C, temperature increase by 20 °C per minute without initial hold to 150 °C, 2.5 °C per minute to 185 °C, 0.5 °C per minute to 195 °C and final isothermal period of 2 min.

Data Quantitation

Individual FAMEs were identified by comparison with authentic standards (GLC-569B, Nu-Check Prep, Inc. Elysian, MN). A FAME mixture (GLC-85) was used as external standard, which was analyzed directly by GC and used to determine the response of each FAME relative to pentadecanoic acid methyl ester (internal standard). Peaks were integrated with EZChrom Elite version 3.1.7 (Agilent, Waldbronn, Germany).

Statistical Analysis

The results for FAs with chain lengths of 14–24 carbon atoms were expressed as absolute concentrations (nmol/cell) or percentages of total analyzed FAs (mole%). FA profiles of pooled cheek cell samples were presented as mean ± standard deviation (SD). Intra-assay was performed by measuring individual FA proportions in ten aliquots of three pooled cheek cell samples with different FA compositions and expressed as CV in percent. Inter-assay was done by measuring individual FA proportions in eight aliquots of three pooled cheek cell samples with different FA compositions over a period of 4 weeks and expressed as CV in percent. A linear regression model was used to determine the coefficients of determination to evaluate relationships between cheek cell numbers and FA concentrations. Correlation analysis of FA contents in cheek cells and plasma were performed according to Pearson for normally distributed variables. Differences between cheek cell sampling methods with and without mouth rinsing, and differences between plasma and cheek cell glycerophospholipid FAs were evaluated using paired *t* tests. PASW Statistics for Windows, version 17.0.2 (IBM SPSS), was used for all statistical calculations.

Results

Cheek Cell Sampling

The average cell yield (mean ± SD) with mouth rinsing was $8.3 \times 10^5 \pm 4.3 \times 10^5$ cells, which was significantly higher compared to $5.3 \times 10^5 \pm 2.4 \times 10^5$ cells without mouth rinsing ($n = 10$, $P < 0.001$). The minimal and maximal numbers of cells collected with mouth rinsing were 2.1×10^5 and 1.6×10^6 cells, and without 1.5×10^5 and 9.0×10^5 cells, respectively. Inclusion of mouth rinsing increased the cell yield by approximately 60%.

FA Composition of Cheek Cell Glycerophospholipids

Table 1 shows the FA composition of cheek cell glycerophospholipids present in cell amounts representative for sampling procedures without or with mouth rinsing (5.0×10^5 cells or 8.5×10^5 cells). Results of sample aliquots containing 10^5 cells are included, as this sample size was the smallest that could be analyzed with acceptable variations.

Samples from different subjects were combined for each tested cell number; thus, the FA composition of pooled cell samples varied, and only CV can be compared between sample sizes. CV ranged from 1.4 to 9.7% in samples with 10^5 cells, from 1.3 to 9.4% in samples containing 5.0×10^5 cells and from 0.7 to 8.2% in samples with 8.5×10^5 cells.

Oleic, palmitic, linoleic and stearic acid were the quantitatively dominant FAs, which together comprised approximately 77% of total FAs. Monounsaturated FAs were the largest FA group, followed by saturated FAs, n-6 and n-3 PUFAs (Table 1).

The inter-assay reproducibility was determined by analyzing eight aliquots of pooled cell samples with different cell numbers (10^5, 5.0×10^5 or 8.5×10^5 cells) over a period of 4 weeks (Table 2). The CV of 5.0×10^5 cell samples ranged from 2.6 to 9.1%, and for 8.5×10^5 cell samples from 1.1 to 9.8%, respectively. The CV of samples containing 10^5 cells ranged from 2.0 to 9.3%, except for FAs with a proportion of less than 0.5% of total FAs, the CV values of which were about 14%. Proportions of individual FAs were comparable to results of the intra-assay.

Samples with low cell numbers ($<1.5 \times 10^5$ cells) had to be analyzed in splitless mode because of the low concentrations of some FAs. Solvents and reagents for lipid extraction and FAME synthesis were reduced to half of the standard volume. This was necessary as chemicals were contaminated with traces of palmitic and stearic acid. The reduction in volume reduced the contamination by approximately 50–2.2% for palmitic acid and 3.7% for stearic acid, based on corresponding FA concentrations in 10^5 cheek cells. It was not possible to reduce the background of C14:0 and C20:2n-6; therefore, both FAs were excluded from the analysis.

Table 1 Intra-assay reproducibility of glycerophospholipid FA compositions in cheek cell samples of different size

Fatty acids	Cheek cell fatty acid composition[a]					
	100,000 cells ($n = 10$)		500,000 cells ($n = 10$)		850,000 cells ($n = 10$)	
	Mean	CV	Mean	CV	Mean	CV
Saturated fatty acids						
C14:0	n/a	n/a	1.68	7.8	1.15	4.2
C16:0	15.07	2.3	18.33	2.7	16.28	1.8
C17:0	1.10	4.2	1.12	1.9	0.87	4.8
C18:0	15.00	4.1	14.32	1.3	13.88	1.5
C20:0	0.73	5.3	0.57	3.1	0.63	3.1
C22:0	1.15	5.2	0.61	4.5	0.64	8.1
C24:0	n/d	n/d	n/d	n/d	n/d	n/d
Monounsaturated fatty acids						
C16:1n-7	6.58	1.7	7.00	2.0	7.60	2.6
C18:1n-7	4.35	6.0	4.63	1.3	4.97	1.7
C18:1n-9	32.43	1.6	30.03	1.3	31.06	1.4
C20:1n-9	n/d	n/d	0.33	9.0	0.50	4.8
C24:1n-9	n/d	n/d	0.13	8.1	0.13	5.8
n-6 Polyunsaturated fatty acids						
C18:2n-6	16.15	1.4	15.47	1.6	15.42	0.7
C18:3n-6	0.37	5.7	0.15	8.2	0.18	4.9
C20:2n-6	n/a	n/a	n/a	n/a	n/a	n/a
C20:3n-6	1.34	9.6	1.25	2.3	1.35	2.1
C20:4n-6	3.04	9.7	2.56	4.1	3.06	4.6
C22:5n-6	0.11	5.7	0.10	7.8	0.08	8.2
n-3 Polyunsaturated fatty acids						
C18:3n-3	0.25	5.7	0.26	9.4	0.25	2.7
C20:5n-3	0.46	5.7	0.13	8.2	0.22	8.0
C22:5n-3	0.50	8.1	0.32	8.3	0.41	7.6
C22:6n-3	1.07	8.9	0.64	6.2	0.87	5.2

Means ± SD and coefficients of variation (CV) are expressed in % of total glycerophospholipid-associated FA

n/d Not detected, *n/a* not analyzed

[a] Samples from different subjects were pooled for each assay with different cell numbers; thus, FA compositions vary

Table 2 Inter-assay reproducibility of glycerophospholipid FA compositions in cheek cell samples of different size

Fatty acids	Cheek cell fatty acid composition[a]					
	100,000 cells ($n = 8$)		500,000 cells ($n = 8$)		850,000 cells ($n = 8$)	
	Mean	CV	Mean	CV	Mean	CV
Saturated fatty acids						
C14:0	n/a	n/a	1.28	3.0	1.55	4.2
C16:0	16.26	5.1	16.52	4.8	17.19	1.8
C17:0	1.14	8.5	0.96	4.1	1.14	1.8
C18:0	14.62	3.0	14.45	3.9	14.22	1.7
C20:0	0.74	4.8	0.47	4.0	0.48	5.1
C22:0	1.16	6.3	0.37	6.1	0.41	5.9
C24:0	n/d	n/d	n/d	n/d	n/d	n/d
Monounsaturated fatty acids						
C16:1n-7	7.03	8.7	6.35	5.7	7.15	2.1
C18:1n-7	4.90	5.5	4.70	3.4	4.86	1.2
C18:1n-9	31.01	3.0	31.95	3.4	30.73	1.1
C20:1n-9	n/d	n/d	0.39	9.1	0.38	9.8
C24:1n-9	n/d	n/d	0.18	6.4	0.20	7.2
n-6 Polyunsaturated fatty acids						
C18:2n-6	15.81	2.0	16.65	4.9	15.48	1.2
C18:3n-6	0.26	14.1	0.10	8.0	0.19	5.6
C20:2n-6	n/a	n/a	n/a	n/a	n/a	n/a
C20:3n-6	1.41	5.4	1.13	2.6	1.30	7.3
C20:4n-6	3.16	5.3	2.40	4.9	2.70	6.4
C22:5n-6	0.11	14.1	0.07	7.6	0.07	5.7
n-3 Polyunsaturated fatty acids						
C18:3n-3	0.26	14.1	0.36	4.9	0.25	4.8
C20:5n-3	0.51	5.3	0.26	5.5	0.28	7.8
C22:5n-3	0.56	7.9	0.20	6.4	0.22	7.2
C22:6n-3	1.05	9.3	1.22	8.0	1.20	6.9

Means ± SD and coefficient of variation (CV) are expressed in % of total glycerophospholipid-associated FA

n/d Not detected, *n/a* not analyzed

[a] Samples from different subjects were pooled for each assay with different cell numbers; thus, FA compositions vary

Linear Relationship of Cell Numbers and FA Concentrations

Aliquots containing 10^5–10^6 cells of a pooled cheek cell sample were analyzed for the determination of the application range. Coefficients of determination were evaluated for absolute values in a linear regression model. The r values for all FAs were higher than 0.995, except for EPA ($r = 0.993$), C22:5n-6 ($r = 0.992$) and C22:0 ($r = 0.995$). CV values calculated for FA proportions were below 10%, with the exception of C22:5n-6 (16.7%). The concentrations of mead acid (C20:3n-9) and C20:3n-3 remained constant despite increasing cell numbers, indicating that the size of the evaluated peaks was compromised by contaminations, which prohibited quantification of these FAs.

Contamination of Phospholipid-Associated FAs by TAG-Derived FA

The total TAG FA content in the methanolic supernatant was determined to estimate its contribution to the total PL FA content ($n = 4$). The degree of contamination depended on centrifugation time. The total TAG FA content averaged 5.4 ± 1.2% of total PL, if the supernatant was centrifuged for 10 min at 3,030×g and 4 °C. Increasing the centrifugation time to 20 min resulted in a reduced total

TAG content of 2.3 ± 0.3% of PL. Individual FAs were affected differently by TAG contamination. Prolonged centrifugation reduced palmitic and stearic acid contaminations from 8.5 and 3.6% to 4.3 and 1.9%, respectively. These figures were 10.7 and 3.3% for C16:1n-7, 4.0 and 1.4% for oleic acid, and 7.9 and 2.0% for linoleic acid. TAG-bound n-3 PUFAs were below the detection limit.

Stability of Cheeks Cell Glycerophospholipid FA Composition at Ambient Temperature

A pooled cheek cell sample was split into equal volumes, centrifuged, and cells kept either in saline solution (NaCl, 0.9%) or distilled water over a period of 48 h at ambient temperatures. Nine aliquots were analyzed. Total glycerophospholipid FAs decreased by about 25% in saline and pure water (Fig. 1). FA patterns did not change over the storage period because the concentrations of individual FAs were evenly affected, as shown by a CV of less than 10% for all FA proportions, except for 22:5n-6 and 18:3n-3 in saline solution (10.6 and 12.9%, respectively), and 22:5n-6 (10.8%) in distilled water.

Comparison Between FA Compositions of Cheek Cell Glycerophospholipids and Total Lipids

Table 3 shows the absolute (nmol/5 × 10^5 cells) and relative (mole%) FA content of total lipids and glycerophospholipid FAs of a pooled cheek cell sample. Approximately 75% of FAs in total lipids were contributed by glycerophospholipids, but major differences were observed for some individual FAs. Proportions of stearic, palmitoleic, oleic, linoleic and γ-linolenic acids were significantly higher in glycerophospholipids compared to total lipids. On the contrary, the proportions of saturated FAs, with the exception of stearic acid, or most FAs with 20 and more carbon atoms were significantly reduced in glycerophospholipids compared to total lipids (paired t test, $P < 0.05$). In cheek cells glycerophospholipid ARA and DHA comprised approximately two-thirds of the total ARA and DHA content.

Comparison of Cheek Cell and Plasma Glycerophospholipid Patterns

Cheek cell and plasma glycerophospholipids were compared in participants of a quality of life study (Table 4). Cheek cells contained mainly monounsaturated FAs (39.1 ± 4.9 mol%), plasma mainly saturated FAs (45.0 ± 1.2 mol%). Oleic acid (29.9 ± 1.5 mol%) was the predominant FA in cheek cells, while palmitic acid (30.7 ± 2.1 mol%) showed the largest percentage in plasma. However, in both compartments the total amount of palmitic, stearic, oleic and linoleic acid

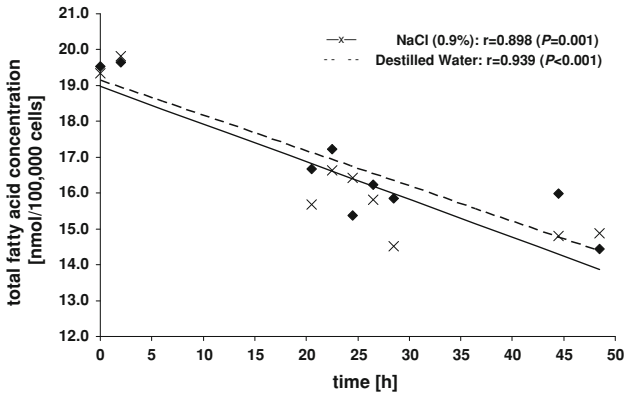

Fig. 1 Glycerophospholipid total FA content in cheek cells kept at ambient temperature in saline solution (NaCl, 0.9%) or distilled water over periods up to 48 h

comprised approximately 78% of the total FAs. ARA and DHA contents were approximately three times higher in plasma than in cheek cells (9.8 vs. 3.39 mol% and 3.12 vs. 0.88 mol%, respectively).

Numerous saturated and polyunsaturated FAs, but not the monounsaturated FAs were significantly correlated between cheek cell and plasma glycerophospholipids (Table 4). The correlation coefficients for DHA and EPA were $r = 0.83$ and 0.64 ($P < 0.001$), respectively; their sum showed a correlation of $r = 0.47$ ($P < 0.010$). The relationships of plasma and cheek cell DHA and EPA appeared linear over the entire concentration range observed (Fig. 2). The correlation coefficients for ARA and linoleic acid were $r = 0.44$ ($P = 0.017$) and $r = 0.58$ ($P = 0.001$), respectively.

Discussion

A strict sampling procedure is important to collect adequate amounts of cheek cell samples of high quality. Studies showed that cleaning the mouth prior to sampling did reduce possible food particle residues, although some cheek cells might get lost through this process [13]. Furthermore, using a brush instead of a cotton swab for cheek cell sampling was superior with respect to the overall cell yield [11], and rinsing the mouth after scraping the inner cheeks led to significantly higher cell yields [13]. We combined these procedures for cheek cell sampling and observed an increased cell yield of up to 60% by the additional mouth rinse after scraping.

Rinsing the mouth is not applicable when collecting cheek cells in infants or young children, which might limit the FA profiling. In a study with preterm infants cheek cells were collected with a cotton swab up to day 14 of life and at week 52 [9]. The average cell yield was

Table 3 FA concentrations (nmol/500,000 cells) and proportions (mole%) of cheek cell total lipids and glycerophospholipids ($n = 4$)

	Total lipids (TL)		Glycerophospholipids (GPL)		GPL in TL [%]
	nmol/5 × 10^5 cells Mean ± SD	Prop [%] Mean ± SD	nmol/5 × 10^5 cells Mean ± SD	Prop [%] Mean ± SD	
Saturated fatty acids					
C14:0	3.37 ± 0.04	1.61 ± 0.08[a]	2.24 ± 0.13	1.14 ± 0.06[b]	66.6
C16:0	44.02 ± 1.49	20.99 ± 0.47[a]	28.91 ± 1.03	18.22 ± 0.33[b]	65.7
C17:0	2.17 ± 0.06	1.04 ± 0.05[a]	1.62 ± 0.05	1.02 ± 0.01[a]	74.5
C18:0	27.86 ± 0.74	13.29 ± 0.45[a]	22.28 ± 0.63	14.04 ± 0.22[b]	80.0
C20:0	2.41 ± 0.19	1.15 ± 0.12[a]	0.88 ± 0.06	0.55 ± 0.04[b]	36.6
C22:0	1.94 ± 0.04	0.92 ± 0.04[a]	0.65 ± 0.04	0.41 ± 0.03[b]	33.7
C24:0	6.57 ± 0.28	3.14 ± 0.60	nd	nd	na
Monounsaturated fatty acids					
C16:1n-7	11.76 ± 0.78	5.60 ± 0.12[a]	10.00 ± 0.41	6.30 ± 0.13[b]	85.2
C18:1n-7	7.67 ± 0.55	3.65 ± 0.10[a]	4.19 ± 0.25	4.53 ± 0.03[b]	93.9
C18:1n-9	57.22 ± 4.00	27.25 ± 0.71[a]	47.85 ± 1.44	30.15 ± 0.29[b]	83.8
C20:1n-9	1.06 ± 0.09	0.51 ± 0.05[a]	0.66 ± 0.02	0.42 ± 0.01[b]	62.1
C24:1n-9	0.77 ± 0.17	0.37 ± 0.07[a]	0.20 ± 0.03	0.13 ± 0.02[b]	26.5
n-6 Polyunsaturated fatty acids					
C18:2n-6	29.21 ± 2.23	13.90 ± 0.47[a]	25.14 ± 1.03	15.84 ± 0.25[b]	86.3
C18:3n-6	0.25 ± 0.03	0.12 ± 0.01[a]	0.25 ± 0.03	0.16 ± 0.02[b]	100.0
C20:2n-6	0.38 ± 0.03	0.18 ± 0.01[a]	0.21 ± 0.02	0.13 ± 0.01[b]	55.3
C20:3n-6	2.55 ± 0.16	1.22 ± 0.02[a]	1.96 ± 0.07	1.23 ± 0.01[a]	76.8
C20:4n-6	6.59 ± 0.47	3.14 ± 0.09[a]	4.19 ± 0.09	2.64 ± 0.06[b]	63.7
C22:5n-6	0.16 ± 0.03	0.08 ± 0.01[a]	0.12 ± 0.00	0.08 ± 0.00[a]	70.0
n-3 Polyunsaturated fatty acids					
C18:3n-3	0.43 ± 0.05	0.20 ± 0.02[a]	0.37 ± 0.02	0.23 ± 0.01[a]	83.9
C20:5n-3	0.45 ± 0.02	0.21 ± 0.02[a]	0.23 ± 0.00	0.15 ± 0.00[b]	75.0
C22:5n-3	1.25 ± 0.11	0.60 ± 0.08[a]	0.58 ± 0.02	0.37 ± 0.01[a]	49.8
C22:6n-3	1.74 ± 0.09	0.83 ± 0.03[a]	1.16 ± 0.04	0.73 ± 0.01[b]	66.7
Total	209.8 ± 9.8		158.7 ± 4.7		75.6

Different letters indicate significant differences between FA proportions (paired t test; $P < 0.05$)

n/d Not detected, *n/a* not analyzed

$1.45 \times 10^5 \pm 0.77 \times 10^5$ cells without mouth rinsing. Our tests with adults showed that the average cell yield with a cotton swab is approximately two-thirds compared to the yield with a small endocervical brush (data not shown). The use of a brush might be crucial to collect a sufficient amount of cells ($>10^5$ cells) in young children for a reliable analysis of glycerophospholipid FAs with our method.

Preliminary tests showed that cheek cells are robust and hard to disrupt by isolated applications of detergents, ultrasound or polar solvents. Furthermore, some methods inherently include long processing times (freezing), the risk of contamination (grinding, ultrasound micro tip) or are unsuitable for the analytical procedure (water, detergents). Thus, a combination of methanol and ultrasound was used to disrupt cell membranes. The degree of disruption was >90% (data not shown).

Methanol was chosen as solvent, as it enables the direct transfer of the two-step procedure developed for the selective preparation of FAMEs from glycerophospholipid-bound FAs in plasma [15]. After centrifugation the supernatant contained the polar lipids and only minor amounts of TAG and cholesterol esters (CEs). CEs, non-esterified fatty acids and sphingomyelin do not contribute to synthesized FAMEs, as their FAs are not transesterified under the alkaline conditions applied [15]. However, small amounts of TAG remain in the cheek cell lipid extract, which accounted for 2.3 ± 0.3% of total PLs.

In this regard, it is notable that the centrifugation time affects the TAG content in the supernatant. Increasing the

Table 4 FA compositions (mole%) of plasma and cheek cell glycerophospholipids from adults participating in a quality of life study ($n = 29$)

Fatty acids	Cheek cells	Plasma	Correlation[§]	
	Mean ± SD	Mean ± SD	*R*	*P*
Saturated fatty acids				
C14:0	1.00 ± 0.49[a]	0.58 ± 0.24[b]	0.29	n/s
C16:0	16.15 ± 1.72[a]	30.70 ± 2.13[b]	0.38	0.045
C17:0	0.84 ± 0.24[a]	0.35 ± 0.07[b]	0.24	n/s
C18:0	15.10 ± 1.36[a]	12.88 ± 1.50[b]	0.54	0.002
C20:0	0.64 ± 0.08	n/d ± n/d	n/a	n/a
C22:0	0.61 ± 0.12	n/d ± n/d	n/a	n/a
Monounsaturated fatty acids				
C16:1n-7	5.64 ± 1.35[a]	0.90 ± 0.34[b]	0.10	n/s
C18:1n-7	4.60 ± 0.81[a]	1.61 ± 0.23[b]	0.32	n/s
C18:1n-9	29.85 ± 1.52[a]	11.92 ± 1.27[b]	0.03	n/s
C20:1n-9	0.27 ± 0.09[a]	0.15 ± 0.03[b]	−0.14	n/s
C24:1n-9	0.15 ± 0.04	n/d ± n/d	n/a	n/s
n-6 Polyunsaturated fatty acids				
C18:2n-6	18.09 ± 2.79[a]	22.17 ± 2.91[b]	0.58	0.001
C18:3n-6	0.15 ± 0.04[a]	0.13 ± 0.07[a]	0.13	n/s
C20:2n-6	0.28 ± 0.08[a]	0.32 ± 0.08[a]	0.01	n/s
C20:3n-6	1.46 ± 0.27[a]	3.04 ± 0.65[b]	0.63	<0.001
C20:4n-6	3.39 ± 0.67[a]	9.75 ± 1.58[b]	0.44	0.017
C22:5n-6	0.08 ± 0.06[a]	0.22 ± 0.11[b]	0.66	<0.001
n-3 Polyunsaturated fatty acids				
C18:3n-3	0.28 ± 0.15[a]	0.27 ± 0.12[a]	0.40	0.030
C20:5n-3	0.24 ± 0.13[a]	1.07 ± 0.80[b]	0.64	<0.001
C22:5n-3	0.29 ± 0.09[a]	0.82 ± 0.22[b]	0.64	<0.001
C22:6n-3	0.88 ± 0.29[a]	3.12 ± 0.98[b]	0.83	<0.001
Σ 20:5n-3, 20:6n-3	1.12 ± 0.39[a]	4.18 ± 1.57[b]	0.47	0.010

Different letters indicate significant differences between plasma and cheek cell FA contents (paired *t* test; $P < 0.05$)

n/d Not detected, *n/a* not analyzed, *n/s* not significant

[§] Pearson's correlation coefficient

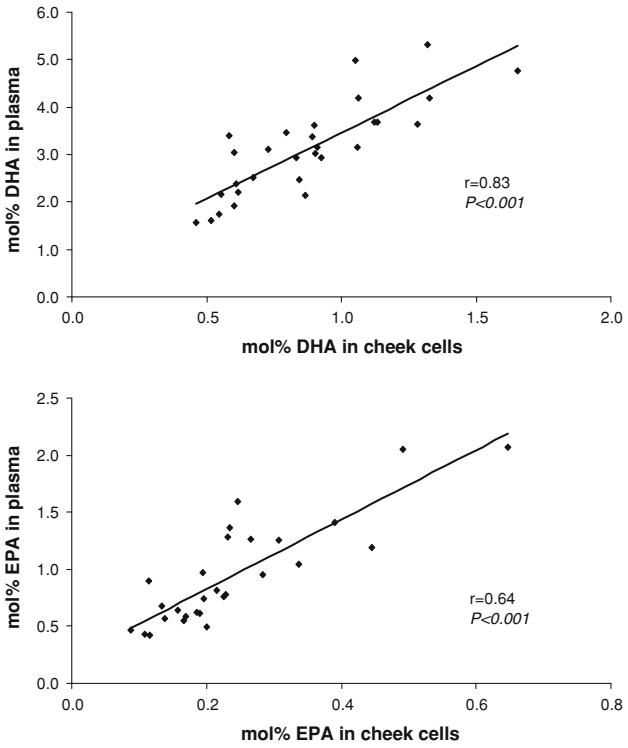

Fig. 2 Correlation between DHA and EPA in cheek cells and plasma glycerophospholipids

centrifugation time to 20 min reduced the TAG content of individual FAs by 50–80% compared to 10 min. No further improvements were observed for centrifugation times greater than 20 min. The underlying mechanism is not known, but TAGs are possibly bound to cell fragments with much higher molecular weights.

Methanol is a potent extraction solvent for polar lipids. The recovery rate of plasma phospholipids extracted with methanol compared to chloroform-methanol (2:1) is approximately 90% [15]. Furthermore, losses through the interaction of lipids with a stationary phase are excluded. This might be crucial for small sample volumes as losses of plasma PL separated by solid phase extraction (SPE) or TLC were reported to be 6.5–60% [18–20], although early studies showed recovery rates of almost 100% for PLs [21, 22]. The differences observed may relate to the samples analyzed; high recovery rates were reported for lipid standards only, but not for the complete extraction procedure of plasma PL [19]. Another aspect, which seems to limit the SPE separation of lipids in cheek cells, is the lipid to sorbent ratio, which should be greater than 2.5% [20]. The total PL concentration of cheek cell samples (5.0×10^5–8.0×10^5 cells) averages 60–110 µg; for an optimal PL recovery the sorbent weight needs to be less than 2.4–4.4 mg.

Data on the precision of glycerophospholipid FA analysis have only been published for plasma so far [15]. The described CV for glycerophospholipid FA determinations ranged from 1.0 to 10.5%, which is in accordance to our cheek cell data.

A minimum of 10^5 cheek cells is needed for a precise glycerophospholipid FA profiling. At this level some FA concentrations are below the detection limit, or CVs are greater than 10%. However, proportions of major FAs are equal to those in samples with higher cell numbers; thus, samples with 10^5 cells are still suitable for cheek cell FA profiling. For samples smaller than 10^5 cells, a reliable quantification seems not to be possible with our method. It does not reflect the actual FA profile as contaminations of solvents with palmitic and stearic acid significantly falsify the proportion of all FA.

The identification of false-positive peaks is important for an accurate qualification of FAs. This not only defines the lower limit of the method, it also excludes FAs from analysis. The systematic analysis of blanks gave information about contaminations derived from chemicals or consumables. Mainly palmitic and stearic acid traces were found in solvents, but also a smaller amount oleic acid. Splitless injection of blanks with BHT showed an additional peak, which co-eluted with C14:0. This was identified as a co-product of BHT. Small peaks caused by not identified sample-derived compounds can also cause false-positive peaks. They have been identified by the linear increase of cell numbers (10^5–10^6), i.e., peaks, which did not increase proportionally to the cell concentration were excluded, such as peaks co-eluting with mead acid (20:3n-9) and C20:2n-6. An increased mead acid level in plasma indicates a deficiency of essential FAs [23]. The inability to detect mead acid in cheek cells limits the use of this compartment as an essential FA deficiency marker.

Connor et al. [10] determined the cheek cell PL FA pattern of infants on various diets. The observed distribution of FAs is similar to our results, except for C18:1n-9 and C18:1n-7; both FAs combined contributed a 5–10% higher proportion in our study population. The observed differences might relate to higher dietary oleic acid intakes by our volunteers. Moreover, oleic acid is preferentially incorporated in glycerophospholipids, as shown by Glaser et al. [15]. Data presented by other authors are limited to PL PUFA contents only; saturated and monounsaturated FAs were summarized [7, 11]. Reported PUFA levels are comparable in all studies. However, the sum of saturated FAs tended to be lower in our study. Again, this might reflect dietary differences or the exclusion of sphingophospholipids, but could also be explained by a reduced palmitic and stearic acid contamination in our analyses compared to those previously reported. The average DHA content observed in our study cohort of 0.88 ± 0.29 mol% agrees with previous studies [7, 10, 11].

The concentration of the total PL fraction was reported to be 115 ± 35 μg/10^6 cells by comparison to a standard lipid mixture [13]. This is comparable to the glycerophospholipid total FA concentration of our study, which averaged 317.0 ± 9.4 nmol/10^6 cells (88.6 ± 2.6 μg). Our data suggest that most FAs in cheek cells originate from the glycerophospholipid fraction (75.6 ± 1.6%), which is much higher than the proportion reported by Devereux-Graminski and Sampugna for human buccal cheek cells (11–14%) [13]. They also described a free FA content of 14–23%, which seems to be unusually high. The observed results could relate to phospholipase A_2 activity, which catalyzes the hydrolysis of membrane glycerophospholipids into free FAs and lysophospholipids [24]. In agreement with our results, PLs were found to be the major fraction in cheek cells of pigs [25, 26]. These authors determined the distribution of lipid fractions by photodensitometry and lipid proportions was based on total molar amounts of lipids, including cholesterol. The differences in PL contents observed in comparison to our results might be explained by interspecies differences, but also by the applied analytical methods. The glycerophospholipid content in our study was based on the total FAME content analyzed by GC-FID.

In addition, proportions of ARA, EPA and DHA in glycerophospholipids are lower compared to these LC-PUFAs in total lipid FAs. This seems to be in contrast to erythrocytes where phosphatidyletholamine (PtdEtn) showed higher LC-PUFA proportions than total lipids [27]. On the other hand, the LC-PUFA proportion of phosphatidylcholine (PtdCho) is lower than that of total lipids. Thus, the lower LC-PUFA levels of glycerophospholipids may be related to the different distribution of PtdCho and PtdEtn, which is approximately 2:1 (PtdCho:PtdEtn) in cheek cells [13].

The impact of distilled water and saline solution (NaCl, 0.9%) on the quality of the cheek cell samples was tested over 48 h at room temperature. Interestingly, the total FA concentration decreased over time, but FA compositions did not change. Distilled water had no adverse effect on the stability of cheek cells or the FA concentration. This suggests that the addition of antioxidants to cheek cell samples is not required if only proportions are determined.

Previous studies reported that the cheek cell FA composition reflects the dietary FA intake as well as erythrocyte and plasma levels of essential PUFAs [7, 10–12]. Good correlations were shown for n-3 FAs in plasma and cheek cell PLs, and a trend to lower correlations for ARAs [7, 10, 11]. This is in accordance with our results for glycerophospholipid FAs. Proportions of ARA and DHA differ strongly in plasma and cheek cells, and may limit the latter as a FA status marker. The biological variances in plasma and cheek cells were comparable in our cohort; nevertheless, the precision of the cheek cell method is suitable to detect even small differences in cheek cell glycerophospholipid FA components.

We conclude that this non-invasive method for cheek cell FA analysis is reliable, even if cell numbers are limited. The applied modifications to sampling, non-chromatographic isolation of glycerophospholipids and synthesis of FAME result in a highly accurate determination of cheek cell glycerophospholipid FAs. The precision of this method is comparable to conventional invasive methods determining the n-3 FA status in humans, based on blood lipid FA analyses. Therefore, this novel technique could be used for interventional or epidemiological studies.

Acknowledgments We are truly grateful to the ten volunteers who donated their cheek cells for this work. We also acknowledge the

financial support by the Federal Ministry of Education and Research (project number: 0315680B). B. Koletzko is the recipient of a Freedom to Discover Award of the Bristol-Myers Squibb Foundation, New York, NY. The method for glycerophospholipid FA analysis in cheek cells and plasma described in this article is in patent pending status.

References

1. von Schacky C (2007) Omega-3 fatty acids and cardiovascular disease. Curr Opin Clin Nutr Metab Care 10:129–135
2. European-Food-Safety-Authority (2010) Panel on dietic products nutrition, and allergies (NDA): scientific opinion on dietary reference values for fats, including saturated fatty acids, polyunsaturated fatty acids, monounsaturated fatty acids, trans fatty acids, and cholesterol. EFSA J 8:1461–1568
3. Koletzko B, Uauy R, Palou A, Kok F, Hornstra G, Eilander A et al (2010) Dietary intake of eicosapentaenoic acid (EPA) and docosahexaenoic acid (DHA) in children—a workshop report. Br J Nutr 103:923–928
4. Hodson L, Skeaff CM, Fielding BA (2008) Fatty acid composition of adipose tissue and blood in humans and its use as a biomarker of dietary intake. Prog Lipid Res 47:348–380
5. Katan MB, Deslypere JP, van Birgelen AP, Penders M, Zegwaard M (1997) Kinetics of the incorporation of dietary fatty acids into serum cholesteryl esters, erythrocyte membranes, and adipose tissue: an 18-month controlled study. J Lipid Res 38:2012–2022
6. McMurchie EJ, Margetts BM, Beilin LJ, Croft KD, Vandongen R, Armstrong BK (1984) Dietary-induced changes in the fatty-acid composition of human cheek cell phospholipids—correlation with changes in the dietary poly-unsaturated saturated fat ratio. Am J Clin Nutr 39:975–980
7. Hoffman DR, Birch EE, Birch DG, Uauy R (1999) Fatty acid profile of buccal cheek cell phospholipids as an index for dietary intake of docosahexaenoic acid in preterm infants. Lipids 34:337–342
8. Hoffman DR, Uauy R (1992) Essentiality of dietary omega 3 fatty acids for premature infants: plasma and red blood cell fatty acid composition. Lipids 27:886–895
9. Koletzko B, Knoppke B, von Schenck U, Demmelmair H, Damli A (1999) Noninvasive assessment of essential fatty acid status in preterm infants by buccal mucosal cell phospholipid analysis. J Pediatr Gastroenterol Nutr 29:467–474
10. Connor SL, Zhu N, Anderson GJ, Hamill D, Jaffe E, Carlson J et al (2000) Cheek cell phospholipids in human infants: a marker of docosahexaenoic and arachidonic acids in the diet, plasma, and red blood cells. Am J Clin Nutr 71:21–27
11. Laitinen K, Sallinen J, Linderborg K, Isolauri E (2006) Serum, cheek cell and breast milk fatty acid compositions in infants with atopic and non-atopic eczema. Clin Exp Allergy 36:166–173
12. Kirby A, Woodward A, Jackson S, Wang Y, Crawford MA (2010) A double-blind, placebo-controlled study investigating the effects of omega-3 supplementation in children aged 8–10 years from a mainstream school population. Res Dev Disabil 31:718–730
13. Devereux-Graminski B, Sampugna J (1993) Variability in lipids isolated from human cheek cells. J Nutr Biochem 4:264–267
14. Sampugna J, Light L, Enig MG, Jones DY, Judd JT, Lanza E (1988) Cheek cell fatty acids as indicators of dietary lipids in humans. Lipids 23:131–136
15. Glaser C, Demmelmair H, Koletzko B (2010) High-throughput analysis of fatty acid composition of plasma glycerophospholipids. J Lipid Res 51:216–221
16. Glaser C, Demmelmair H, Sausenthaler S, Herbarth O, Heinrich J, Koletzko B (2010) Fatty acid composition of serum glycerophospholipids in children. J Pediatr 157(5):826–831 e821
17. Carnielli VP, Pederzini F, Vittorangeli R, Luijendijk IH, Boomaars WE, Pedrotti D et al (1996) Plasma and red blood cell fatty acid of very low birth weight infants fed exclusively with expressed preterm human milk. Pediatr Res 39:671–679
18. Bateman HG, Jenkins TC (1997) Method for extraction and separation by solid phase extraction of neutral lipid, free fatty acids, and polar lipid from mixed microbial cultures. J Agric Food Chem 45:132–134
19. Burdge GC, Wright P, Jones AE, Wootton SA (2000) A method for separation of phosphatidylcholine, triacylglycerol, non-esterified fatty acids and cholesterol esters from plasma by solid-phase extraction. Br J Nutr 84:781–787
20. Pernet F, Pelletier CJ, Milley J (2006) Comparison of three solid-phase extraction methods for fatty acid analysis of lipid fractions in tissues of marine bivalves. J Chromatogr A 1137:127–137
21. Kaluzny MA, Duncan LA, Merritt MV, Epps DE (1985) Rapid separation of lipid classes in high yield and purity using bonded phase columns. J Lipid Res 26:135–140
22. Kim HY, Salem N Jr (1990) Separation of lipid classes by solid phase extraction. J Lipid Res 31:2285–2289
23. Siguel EN, Chee KM, Gong JX, Schaefer EJ (1987) Criteria for essential fatty acid deficiency in plasma as assessed by capillary column gas-liquid chromatography. Clin Chem 33:1869–1873
24. Kudo I, Murakami M (2002) Phospholipase A2 enzymes. Prostaglandins Other Lipid Mediat 68–69:3–58
25. Wertz PW, Cox PS, Squier CA, Downing DT (1986) Lipids of epidermis and keratinized and non-keratinized oral epithelia. Comp Biochem Physiol B 83:529–531
26. Squier CA, Cox P, Wertz PW (1991) Lipid content and water permeability of skin and oral mucosa. J Investig Dermatol 96:123–126
27. Geppert J, Kraft V, Demmelmair H, Koletzko B (2005) Docosahexaenoic acid supplementation in vegetarians effectively increases omega-3 index: a randomized trial. Lipids 40:807–814

Lipids (2011) 46:991–1003
DOI 10.1007/s11745-011-3596-3

ORIGINAL ARTICLE

ApoB siRNA-induced Liver Steatosis is Resistant to Clearance by the Loss of Fatty Acid Transport Protein 5 (*Fatp5*)

Brandon Ason · Jose Castro-Perez · Samnang Tep · Alice Stefanni · Marija Tadin-Strapps · Thomas Roddy · Thomas Hankemeier · Brian Hubbard · Alan B. Sachs · W. Michael Flanagan · Nelly A. Kuklin · Lyndon J. Mitnaul

Received: 16 March 2011 / Accepted: 6 July 2011 / Published online: 9 August 2011

Abstract The association between hypercholesterolemia and elevated serum apolipoprotein B (APOB) has generated interest in APOB as a therapeutic target for patients at risk of developing cardiovascular disease. In the clinic, mipomersen, an antisense oligonucleotide (ASO) APOB inhibitor, was associated with a trend toward increased hepatic triglycerides, and liver steatosis remains a concern. We found that siRNA-mediated knockdown of *ApoB* led to elevated hepatic triglycerides and liver steatosis in mice engineered to exhibit a human-like lipid profile. Many genes required for fatty acid synthesis were reduced, suggesting that the observed elevation in hepatic triglycerides is maintained by the cell through fatty acid uptake as opposed to fatty acid synthesis. Fatty acid transport protein 5 (*Fatp5*/*Slc27a5*) is required for long chain fatty acid (LCFA) uptake and bile acid reconjugation by the liver. *Fatp5* knockout mice exhibited lower levels of hepatic triglycerides due to decreased fatty acid uptake, and shRNA-mediated knockdown of *Fatp5* protected mice from diet-induced liver steatosis. Here, we evaluated if siRNA-mediated knockdown of *Fatp5* was sufficient to alleviate *ApoB* knockdown-induced steatosis. We determined that, although *Fatp5* siRNA treatment was sufficient to increase the proportion of unconjugated bile acids 100-fold, consistent with FATP5's role in bile acid reconjugation, *Fatp5* knockdown failed to influence the degree, zonal distribution, or composition of the hepatic triglycerides that accumulated following *ApoB* siRNA treatment.

Keywords APOB · Liver steatosis · siRNA · FATP5 · Slc27a5 · siRNA combinations

Abbreviations

APOB	Apolipoprotein B
ASO	Antisense oligonucleotide
CLinDMA	2-{4-[(3b)-cholest-5-en-3-yloxy]-butoxy}-N,N-dimethyl-3-[(9Z,12Z)-octadeca-9,12-dien-1-yloxy]propan-1-amine
d	Deoxy
f	2′ fluoro
FATP5	Fatty acid transport protein 5
H & E	Hematoxylin and eosin
IHTG	Intra-hepatic triglyceride
LCFA	Long chain fatty acid uptake
LDL-c	LDL cholesterol
LNP	Lipid nanoparticle
MTP	Microsomal transfer protein
PEG-DMG	Monomethoxy(polyethyleneglycol)-1,2-dimyristoylglycerol

Brandon Ason and Jose Castro-Perez contributed equally.

Electronic supplementary material The online version of this article (doi:10.1007/s11745-011-3596-3) contains supplementary material, which is available to authorized users.

B. Ason · S. Tep · M. Tadin-Strapps · A. B. Sachs · W. Michael Flanagan · N. A. Kuklin
Sirna Therapeutics/Merck & Co. Inc., San Francisco, CA 94158, USA

B. Ason (✉)
Amgen Inc., 1120 Veterans Blvd, San Francisco, CA 94080, USA
e-mail: brandon.ason@amgen.com

J. Castro-Perez · A. Stefanni · T. Roddy · B. Hubbard · L. J. Mitnaul
Division of Cardiovascular Diseases and Atherosclerosis, Merck Research Laboratories, Rahway, NJ 07065, USA

J. Castro-Perez · T. Hankemeier
Division of Analytical Biosciences, LACDR, Leiden University, P.O. Box 9502, 2300 RA, Leiden, The Netherlands

siRNAs	Small interfering RNAs
TCA	Taurocholic acid
o	2′ O-methyl (o)
VLDL	Very low density lipoprotein

Introduction

Elevated LDL cholesterol (LDL-c) promotes atherosclerosis, and it is well established that reducing LDL-c helps to mitigate the risk of developing cardiovascular disease in patients with hypercholesterolemia [1–7]. LDL-c consists of a single apolipoprotein B-100 (APOB-100) molecule, cholesterol, cholesterol-esters and triacylglycerols that are comprised of various dietary and de novo synthesized fatty acids [8]. In the liver, APOB is required for very low density lipoprotein (VLDL) formation and serves as the scaffold to solubilize cholesterol and fatty acids (in the form of triglycerides) for secretion into the blood for circulation [8]. An association between hypercholesterolemia and increased APOB protein levels, together with the observation that reductions in *ApoB* synthesis reduce LDL-c and the incidence of atherosclerosis, has generated interest in APOB as a therapeutic target [9–13]. Both antisense oligonucleotides (ASOs) and small interfering RNAs (siRNAs) targeting *ApoB* reduce LDL-c in mice and in non-human primates [14–18]. In mice, *ApoB* ASOs reduced LDL-c without inducing hepatic steatosis, a liability of microsomal transfer protein (MTP) inhibitors that block triglyceride-rich lipoprotein assembly and secretion [19]. In patients, mipomersen, an *ApoB* targeting ASO, reduces both LDL-c and APOB, demonstrating the potential for an *ApoB*-targeted therapeutic [20–24]. Liver steatosis induced by inhibiting *ApoB*, however, remains an important concern. Recently, mipomersen administration at a sub-maximum efficacious dose was shown to be associated with a trend toward increased intra-hepatic triglyceride (IHTG) content for mipomersen-treated patients with one of the ten patients developing mild steatosis [20]. In addition, mice harboring a base-pair deletion in the coding region of *ApoB* (*ApoB-38.9*) exhibited hepatic triglyceride accumulation [25]. In order to attenuate the risk of liver steatosis associated with an *ApoB*-targeted therapeutic, one approach would be to combine an *ApoB* ASO or siRNA with another therapeutic that increases the clearance of hepatic triglycerides.

Fatty acid transport protein 5 (*Fatp5*/*Slc27a5*) mediates the uptake of long chain fatty acids (LCFAs) to the liver and is involved in bile acid reconjugation during enterohepatic recirculation [26, 27]. *Fatp5* knockout mice exhibit lower levels of hepatic triglycerides and free fatty acids due to decreased liver fatty acid uptake [27]. Furthermore, Doege et al. [25] recently showed that adenovirus-shRNA-mediated silencing of *Fatp5* mRNA not only protected mice from high fat diet-induced liver steatosis but also reversed steatosis once it was established. This suggested that a FATP5 inhibitor may be an attractive combination therapy with an APOB-targeted therapeutic.

Besides of its role in free fatty acid uptake, FATP5 also plays a critical role in reconjugation of bile acids during enterohepatic recirculation to the liver, and complete deletion of *Fatp5* resulted in a significant increase in unconjugated bile acids in both bile and serum [26]. Activation of FXR, a bile acid nuclear receptor, with bile acids or synthetic activators has been shown to reduce the secretion of triglyceride-rich VLDL from the liver in mice, which was associated with a decrease in *Srebp1* and *2* pathway genes [28]. The involvement of FATP5 in bile acid metabolism suggests that it too may play a role in hepatic triglyceride metabolism via FXR. However, the contributions of the bile acid reconjugation activity of FATP5 on hepatic steatosis or the contribution of FATP5 on APOB-induced steatosis are currently unknown. By utilizing two siRNAs specifically targeting *Fatp5* and *ApoB*, we evaluated the ability of *Fatp5* siRNA treatment to alleviate *ApoB* siRNA-induced liver steatosis.

Materials and Methods

siRNA Design

siRNAs were designed to the mRNA transcripts using a previously published design algorithm [34]. siRNA sequences contained the following chemical modifications added to the 2′ position of the ribose sugar when indicated: deoxy (d), 2′ fluoro (f), or 2′ O-methyl (o) [34]. Modification abbreviations are given immediately preceding the base to which they were applied. Passenger strands were capped with an inverted abasic nucleotide on the 5′ and 3′ ends. The control siRNA sequence (Cntrl siRNA) consists of:
iB;fluU;fluC;fluU;fluU;fluU;fluU;dA;dA;fluC;fluU;fluC;
fluU;fluC;fluU;fluU;fluC;dA;dG;dG;dT;dT;iB
passenger strand and
fluC;fluC;fluU;omeG;omeA;omeA;omeG;omeA;omeG;
omeA;omeG;fluU;fluU;omeA;omeA;omeA;rA;rG;rA;omeU;
omeU guide strand sequences.
The *Fatp5*(951) siRNA sequence consists of:
iB;fluC;fluU;dG;fluC;fluC;dA;fluU;dA;fluU;fluU;fluC;dA;
fluU;fluC;fluU;fluU;fluU;dA;fluC;dT;dT;iB
passenger strand and

rG;rU;rA;omeA;omeA;omeG;omeA;fluU;omeG;omeA;
omeA;fluU;omeA;fluU;omeG;omeG;fluC;omeA;omeG;
omeU;omeU guide strand sequences.
The *ApoB*(10168) siRNA sequence consists of:
iB;fluU;fluC;dA;fluU;fluC;dA;fluC;dA;fluC;fluU;dG;dA;
dA;fluU;dA;fluC;fluC;dA;dA;dT;dT;iB
passenger strand and
rU;rU;rG;omeG;fluU;omeA;fluU;fluU;fluC;omeA;omeG;
fluU;omeG;fluU;omeG;omeA;fluU;omeG;omeA;omeU;
omeU guide strand sequences.

siRNA Synthesis

siRNAs were synthesized by methods previously described [35]. For each siRNA, the two individual strands were synthesized separately using solid phase synthesis, and purified by ion-exchange chromatography. The complementary strands were annealed to form the duplex siRNA. The duplex was then ultrafiltered and lyophilized to form the dry siRNA. Duplex purity was monitored by LC/MS and tested for the presence of endotoxin by standard methods.

Preparation of siRNA-Lipid Nanoparticle (LNP) Complex

LNPs were made as described previously [36]. The encapsulation efficiency of the particles was determined using a SYBR Gold fluorescence assay in the absence and presence of triton, and the particle size measurements were performed using a Wyatt DynaPro plate reader. The siRNA and lipid concentrations in the LNP were quantified by a HPLC method, developed in house, using a PDA detector.

In Vivo siRNAs Treatments

All in vivo work was performed according to an approved animal protocol as set by the Institutional American Association for the Accreditation of Laboratory Animal Care. C57Bl/6 mice engineered to be hemizygous for a knockout of the LDL receptor and hemizygous for the overexpression of the human cholesterol ester transfer protein (CETP) driven by the endogenous apoA1 promoter within a C57Bl/6 background [B6-Ldlr<tm1>Tg(apoA1-CETP); Taconic] were used for these studies. Mice ~16–20 weeks of age were fed Lab Diets (5020 9F) starting 2 weeks prior to the start of the study. siRNAs were administered by intravenous (i.v.) injection. Animals were dosed on days 0 and 14 with either 3 mg/kg of a single LNP formulated siRNA or 1.5 mg/kg of two LNP formulated siRNAs for a 3 mg/kg total siRNA combination dose. For siRNA combinations, siRNA were formulated individually and hand-mixed immediately prior to injections. Animals were euthanized by CO_2 inhalation. Immediately after euthanasia, serum was collected using serum separator tubes and allowed to clot at room temperature for 30 min. Liver sections were excised, placed in either RNA Later (Qiagen) (right medial lobe), 10% buffered formalin (10% NBF, left medial lobe), or flash frozen (the remainder), and stored until further use.

RNA Isolation and qRT-PCR

RNA was isolated using an RNeasy96 Universal Tissue Kit (Qiagen) according to the supplied product protocol and as described previously [37]. TaqMan Gene Expression Assays (Applied Biosystems) were performed as described within the product protocol using the following primer probes, Mm00447768_m1 for *Fatp5*, Mm01545154_g1 for *ApoB*, and Cat# 4352339E for the reference, *Gapdh*. All reactions were performed in duplicate, and data were analyzed using the ddCt method with *Gapdh* serving as in [38]. Data represented as the $\log_2$-fold change (ddCt) relative to the control siRNA. For analysis of the selected *Srebp1c* and *Srebp2* pathway genes and *Scd1*, expression was normalized to an average of that of mouse *β-actin* (*Actb*), Glyceraldehyde 3-phosphate dehydrogenase (*Gapdh*), Beta-glucuronidase (*Gusb*), Hypoxanthine–guanine phosphoribosyltransferase (*Hprt1*), Peptidylprolyl isomerase A (*Cyclophilin A*/*Ppia*) and ribosomal protein 113a (*Rp113a*) in each sample. Expression levels of all genes analyzed were normalized to an average of the housekeeping genes (listed above) to obtain dCt. Fold regulation is calculated as: ddCt of gene in treatment group/dCt of gene in control group. Significance (p value) was calculated from a two-tailed t test between control and treatment groups. Accession numbers for the primer/probes used are listed in Supplemental Table 1.

Cholesterol and Triglyceride Analysis

Serum for cholesterol and triglyceride analysis was analyzed using Wako's total and HDL cholesterol kits according to the supplied product protocol and as described previously [37]. Non-HDL, which serves as an approximation for LDL, was calculated by subtracting HDL from total cholesterol measurements. The percent difference relative to the control siRNA was calculated using the following equation $\{100 \times [1-(\text{experimental/control})]\}$.

Histology and Hematology

Mouse livers were fixed with 10% neutral buffered formalin. One hepatic lobe was treated with osmium tetroxide solution, to visualize lipids, overnight at room temperature prior to paraffin embedding and processing. The other

hepatic lobe was embedded and processed in paraffin and hematoxylin and eosin (H&E) stained. Samples were sectioned at a thickness of 5 μm. The osmium-stained samples were digitalized using an Aperio ScanScope XT. Percent area (positive pixel count) was calculated using the positive pixel count algorithm (MAN-0024) supplied with the imaging software (Aperio). Samples were also reviewed by a board-certified veterinary pathologist and scored for inflammation and lipidosis using a semi-quantitative score.

Measurement of Serum APOB

The APOB levels in serum were measured by LC/MS as described previously [29]. The concentration of APOB peptide was calculated by dividing the area under the curve for the analyte by the area of its internal standard and multiplying by the internal standard concentration. The concentration of APOB was then converted to and reported as mg/dL.

LC/MS Sample Preparation and Analysis for Bile Acid Conjugation and Hepatic Triglycerides

Terminal bile samples from each group were collected using the stick and pull method. Samples were diluted 1:1,000 v/v in 50% acetonitrile + 0.1% formic acid/50% water + 0.1% formic acid, followed by the addition of 1 μM total internal standard solution (D_4-TCA, D_4-CA, D_4-GCA) (Sigma-Isotec, St. Louis, MO, USA). The mixture was vortexed for 10 s, centrifuged for 10 min at 15,000*g*, and then stored at −20 °C until LC/MS analysis. Supernatant was injected (10 μL) directly onto the LC/MS system.

A 50-mg slice of frozen liver from each animal was homogenized in 2-mL polypropylene tubes containing a 14-mm ceramic bead using a Precellys 24 homogenizer (Bertin Technologies, Montigny-le-Bretonneux, France). A non-naturally occurring internal standard solution (20 μL) containing TG 51:0 (Sigma Aldrich, St Louis, MO, USA) 0.8 mg/mL along with dichloromethane/methanol (2:1 v/v) was added to each sample prior to homogenization [39]. Samples were homogenized at 5,500 RPM, 2 × 30 s, with a 15 s pause between cycles. In order to generate a two layer liquid separation, 200 μL of distilled water was added, vortexed for 30 s, followed by centrifugation at 20,000*g* at 5 °C for 10 min. 10 μL of the lower layer, containing the lipids, was removed without disrupting the liver tissue homogenate disk. This was followed by dilution of the extracted lipid sample 1/50 in a solvent mixture (65% ACN, 30% IPA, 5% H_2O).

External endogenous calibration standards in buffer solution were used to cover the endogenous concentrations present in the bile and liver tissues. The inlet system was comprised of an Acquity UPLC (Waters, Milford, MA, USA). Bile and lipid extracts were injected (2 μL) onto a 1.8-μm particle 100 × 2.1 mm id Waters Acquity HSS T3 column (Waters). The column was maintained at 55 °C with a 0.4-mL/min flow rate for the lipid analysis and 65 °C with a 0.7-mL/min flow rate for the bile analysis. A binary gradient system was utilized for the analysis of both sample sets. Two different gradient conditions were used. For the lipid analysis, the same conditions were used as previously described [40]. For the bile acid analysis, water + 0.1% formic acid was used as eluent A. Eluent B consisted of acetonitrile + 0.1% formic acid (Burdick & Jackson, USA). A linear gradient (curve 6) was performed over a 13-min total run time. During the initial portion of the gradient, it was held at 80% A and 20% B. For the next 10 min, the gradient was ramped in a stepped linear fashion to 35% B (curve 5) in 4 min, 45% B in 7.5 min and 99% B in 9.5 min and held at this composition for 1.6 min. Hereafter, the system was switched back to 80% B and 20% A and equilibrated for an additional 2.9 min.

The inlet system described was directly coupled to a hybrid quadrupole orthogonal time of flight mass spectrometer (SYNAPT G2 HDMS; Waters MS Technologies, Manchester, UK). Electrospray (ESI) positive and negative ion ionization modes were used. In both ESI modes, a capillary voltage and cone voltage of ±2 kV and ±30 V, respectively, were used. The desolvation source conditions were as follows: for the desolvation gas 700 L/h was used and the desolvation temperature was kept at 450 °C. Data were acquired over the mass range of 50–1,200 Da.

The LC/MS data acquired was processed by the use of a quantitative data deconvolution package (Positive software by MassLynx; Waters, MA, USA). Data are presented as ± standard error of the mean (SEM). Differences between groups were computed by either Student's *t* test or by two-way ANOVA (GraphPad Prism, La Jolla, CA, USA). Post-test analysis for quantifiable variables was conducted using either Bonferroni or Mann–Whitney *U* non-parametric test with two-tailed *p* values. Values of $p < 0.05$ were considered statistically significant.

Lipid Nomenclature

The nomenclature utilized in this manuscript is in accordance with Lipidmaps (http://www.lipidmaps.org). In brief, a triglyceride described as TG 52:2 is interpreted as a triglyceride containing 52 carbons attached to the glycerol back-bone and two double bonds in the fatty acyl chain as described by Fahy et al. [41].

Results

Sustained Knockdown of Both ApoB and Fatp5 mRNA Transcripts was Achieved with siRNAs Administered Either Alone or in Combination

To investigate if we can simultaneously silence both *ApoB* and *Fatp5*, we administered siRNAs specifically targeting *ApoB* and *Fatp5*, alone and in combination, to CETP/LDLR hemizygous female mice (mice exhibiting a human-like lipid profile) fed a low-fat western diet. Changes to the lipid profile were obtained through a hemizygous mutation of the LDL receptor (±LDLR) and the hemizygous over-expression of a mouse apoA1 promoter-driven human CETP transgene (±apoA1-hCETP). This led to an elevation in LDL and a cholesterol profile that more closely resembled the HDL–LDL ratio observed in humans [29]. Female mice were fed a low-fat western diet ad libitum and treated with siRNAs formulated in a lipid nanoparticle (LNP) to achieve delivery to the liver [30]. Animals were dosed on days 0 and 14 with either 3 mg/kg of a single siRNA or 1.5 mg/kg of two siRNAs for a 3 mg/kg total siRNA combination dose. Efficacy was analyzed using qRT-PCR on liver samples collected on day 21. Analysis of mRNA expression levels revealed no appreciable difference in knockdown (KD) between *ApoB* siRNA treatments administered either alone or in combination with the *Fatp5* siRNA (Fig. 1a; ≥90% KD across all groups). Similar results were observed for the *Fatp5* siRNA, where ≥89% knockdown of *Fatp5* was observed (Fig. 1b).

Fatp5 Knockdown Impaired Bile Acid Reconjugation

The ratio of unconjugated/conjugated bile acid in the bile was used as a biological indicator for the loss of FATP5 activity following siRNA treatment to female mice fed a low-fat western diet ad libitum [26]. A significant increase in the proportion of unconjugated bile acids was observed for all *Fatp5* siRNA treatment groups, indicative of the loss of FATP5 activity (Fig. 2a; $p = 0.0003$, t test, Mann–Whitney post-test, cntrl siRNA groups vs. *Fatp5* siRNA groups). The unconjugated/conjugated ratio for the cntrl/cntrl siRNA group and the *Fatp5*/*Fatp5* siRNA group was 0.004 and 2.2, respectively. The ratio was lower for some of the *Fatp5* siRNA treatment groups when combined with the *ApoB* siRNA, but nevertheless exhibited a significant level of target engagement when compared with the control siRNA. Cholic acid in the *Fatp5* groups was the most predominant unconjugated bile acid found in bile (Fig. 2b), which showed a dramatic increase in concentration (0.77 mM in control siRNA vs. 77.95 mM in *Fatp5*) after knockdown of *Fatp5* ($p = 0.0003$, t test, Mann–Whitney post-test). Conjugated bile acids, specifically taurocholic acid (TCA), showed the reverse effect following *Fatp5* knockdown ($p = 0.1304$, t test, Mann–Whitney post-test). The levels of TCA decreased to 43.2 mM in comparison with the cntrl siRNA group 69.7 mM (data not shown). The ratio of unconjugated/conjugated bile acid in the serum reflected that of the bile, with a significant increase in the unconjugated levels (data not shown).

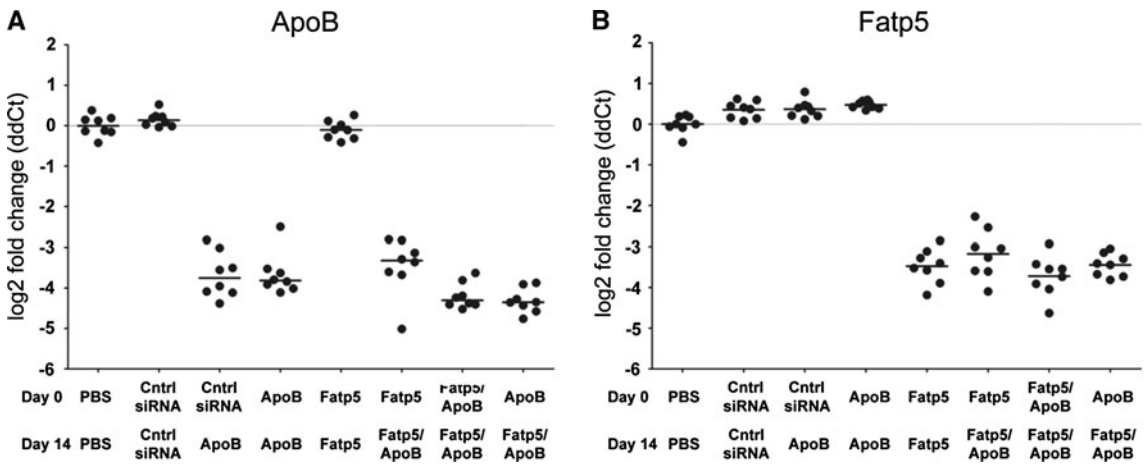

Fig. 1 Similar levels of *ApoB* and *Fatp5* mRNAs were observed for all groups containing siRNAs targeting these genes, either alone or in combination. Mice ($n = 8$/group) were treated with siRNAs targeting *ApoB* and *Fatp5* alone or in combination (*ApoB*, *Fatp5*, *Fatp5*/*ApoB*) at days 0 and 14. Gene expression was analyzed using qRT-PCR (TaqMan) on day 21 (**a**, **b**) post the initial dose. PBS and a control siRNA (*cntrl siRNA*) served as negative controls. Data represented as the log2 fold change (*ddCt*) relative to the cntrl siRNA treatment of individual animals (*circles*) and the group means (*bars*) are shown

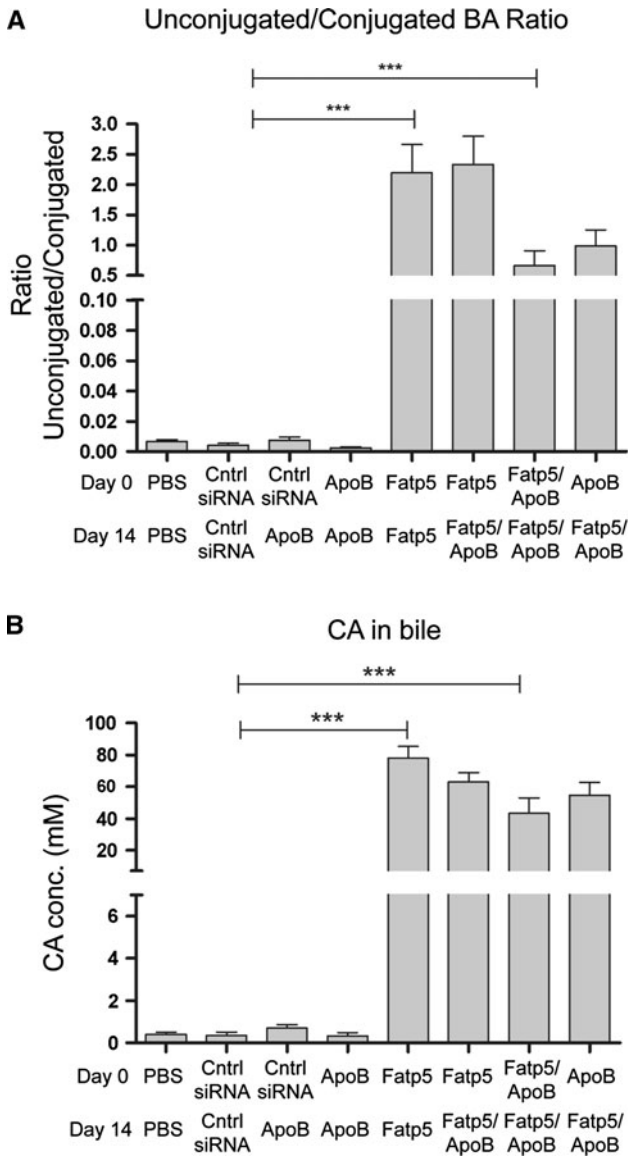

Fig. 2 *Fatp5* knockdown reduces bile acid (*BA*) reconjugation. **a** An increase in the level of unconjugated/conjugated bile acid ratio (***$p \leq 0.001$, *t* test, Mann–Whitney post-test) was observed following *Fatp5* knockdown. **b** Cholic acid (*CA*) concentrations exhibited an increase in the concentration measured (***$p \leq 0.001$, *t* test, Mann–Whitney post-test) by LC/MS after treatment with the *Fatp5* siRNA. Data represented as the group means (*bars*) ± SD ($n = 8$/group)

ApoB siRNA Treatment Led to Significant Reductions in Serum APOB Protein, Cholesterol and Triglyceride Levels Alone and in Combination with a Fatp5-Targeting siRNA

ApoB siRNA treatment, either alone or in combination with a siRNA targeting *Fatp5*, caused a significant reduction ($p \leq 0.001$) in serum APOB levels in female mice fed a low-fat western diet ad libitum (Fig. 3). APOB protein reductions were consistent with the reductions in hepatic

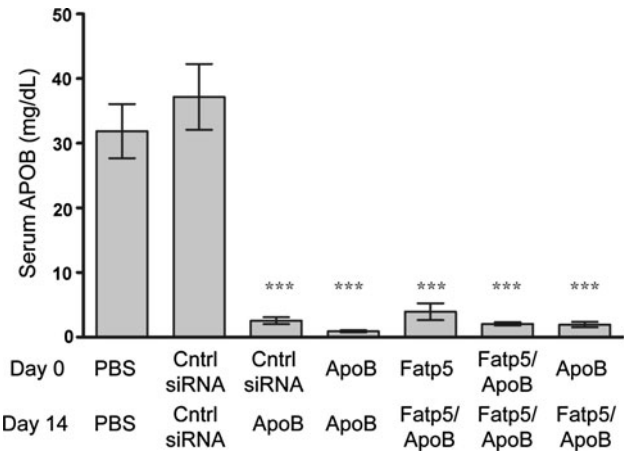

Fig. 3 Serum APOB protein levels were reduced following *ApoB* siRNA treatment. APOB levels in serum were measured by LC/MS on day 21 following days 0 and 14 doses as indicated on the *x*-axis. Data represented as the group means (*bars*) ± SD ($n = 8$/group). Significance (***$p \leq 0.0001$) relative to the siRNA control-treated group was calculated using a one-way ANOVA, Tukey post-test

ApoB mRNA levels (Fig 1a). This led to reductions in circulating cholesterol and triglyceride levels. On day 21, similar reductions in total (76–84%), HDL (67–78%), and non-HDL (79–90%) cholesterol were observed across all *ApoB* siRNA treatment groups (Fig. 4a–c). No significant decrease in cholesterol levels were observed for the *ApoB* + *Fatp5* siRNA combination group relative to the *ApoB* siRNA individual treatment group.

Serum triglycerides were also significantly reduced for *ApoB* siRNA treatments either alone or in combination on day 21 (Fig. 4d). Taken together, these data point to similar and significant changes in serum cholesterol across *ApoB* siRNA treatment groups that correlated with the observed reductions in *ApoB* mRNA and serum protein levels.

Fatp5 siRNA Treatment Failed to Alleviate ApoB siRNA-induced Liver Steatosis

To determine if *Fatp5* siRNA treatment was sufficient to alleviate *ApoB* siRNA-induced liver steatosis, liver sections were processed, sectioned, and stained with either osmium or H&E. Image analysis of the osmium stained slides revealed similar levels of significant lipid accumulation across all *ApoB* siRNA treatment groups relative to the PBS, *Fatp5*, or control siRNA groups (Fig. 5a, b). These data indicated that *Fatp5* siRNA treatment failed to alleviate *ApoB* siRNA-induced liver steatosis in female mice fed a low-fat western diet ad libitum. For the PBS, *Fatp5*, and control siRNA groups, there was some evidence of a periportal to midzonal (zones 1 and 2) distribution of lipid droplets within hepatocytes (Fig. 5b). This contrasted the lipid distribution following *ApoB* siRNA treatment,

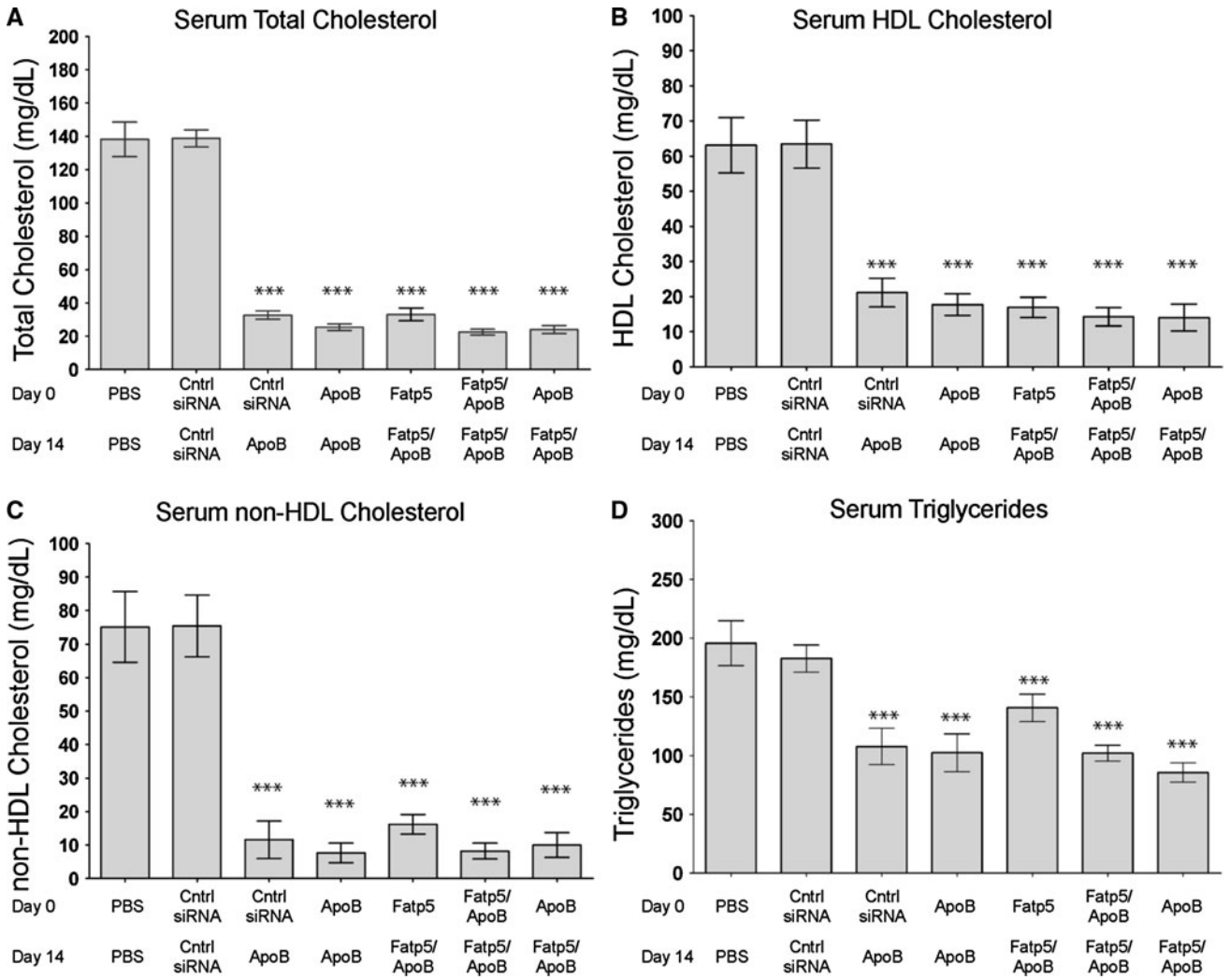

Fig. 4 Comparable levels of serum cholesterol and triglycerides were observed for *ApoB* siRNA treatments either alone or in combination with a siRNA-targeting *Fatp5*. Total cholesterol (**a**), HDL cholesterol (**b**), and triglycerides (**d**) were measured on day 21 following days 0 and 14 doses as indicated on the *x*-axis. Non-HDL cholesterol (**c**) was calculated by subtracting the HDL cholesterol value from the total cholesterol value. Data represented as group means (*bars*) ± SD ($n = 8$/group). The percent difference relative to the control siRNA is shown. Significance (***$p \leq 0.0001$) was calculated using a one-way ANOVA, Tukey post-test, and reported for treated groups relative to the siRNA control (*cntrl siRNA*) treatment

where diffuse infiltration (all zones) was observed (Fig. 5b). The *ApoB*-treated groups displayed lipid droplets that were smaller and more evenly distributed, while fewer but larger lipid droplets were observed for the remaining groups in many instances and as shown in Fig. 5b. By H&E staining, hepatocytes in the *ApoB* siRNA treatment groups appeared diffusely swollen, with granular to vacuolated cytoplasmic spaces (data not shown).

Fatp5 Knockdown Failed to Alter ApoB siRNA-induced Liver Triglyceride levels or Composition

Total triglyceride composition analysis by LC/MS revealed a significant increase in the level of triglycerides found in the liver following treatment with *ApoB* siRNA when compared with siRNA control (Fig. 6a; Cntrl siRNA 7.5 μg/mg of tissue vs. *ApoB* siRNA 35.5 μg/mg of tissue, $p = 0.0002$, *t* test with Mann–Whitney post-test). Comparative measurements between the *ApoB*/*ApoB* and the *Fatp5*/*Fatp5* + *ApoB* groups demonstrated that there was no protection from triglyceride accumulation in female mice fed a low-fat western diet ad libitum. LC/MS indicated that triglycerides 52:2 and 52:3 were significantly higher ($p \leq 0.0001$, two-way ANOVA with Bonferroni post-test) following *Fatp5*/*Fatp5* + *ApoB* treatment relative to *ApoB*/*ApoB* treatment (Fig. 6b). Triglycerides 52:4 and 54:3, although not statistically significant, also showed an increase in the *Fatp5*/*Fatp5* + *ApoB* cohort in

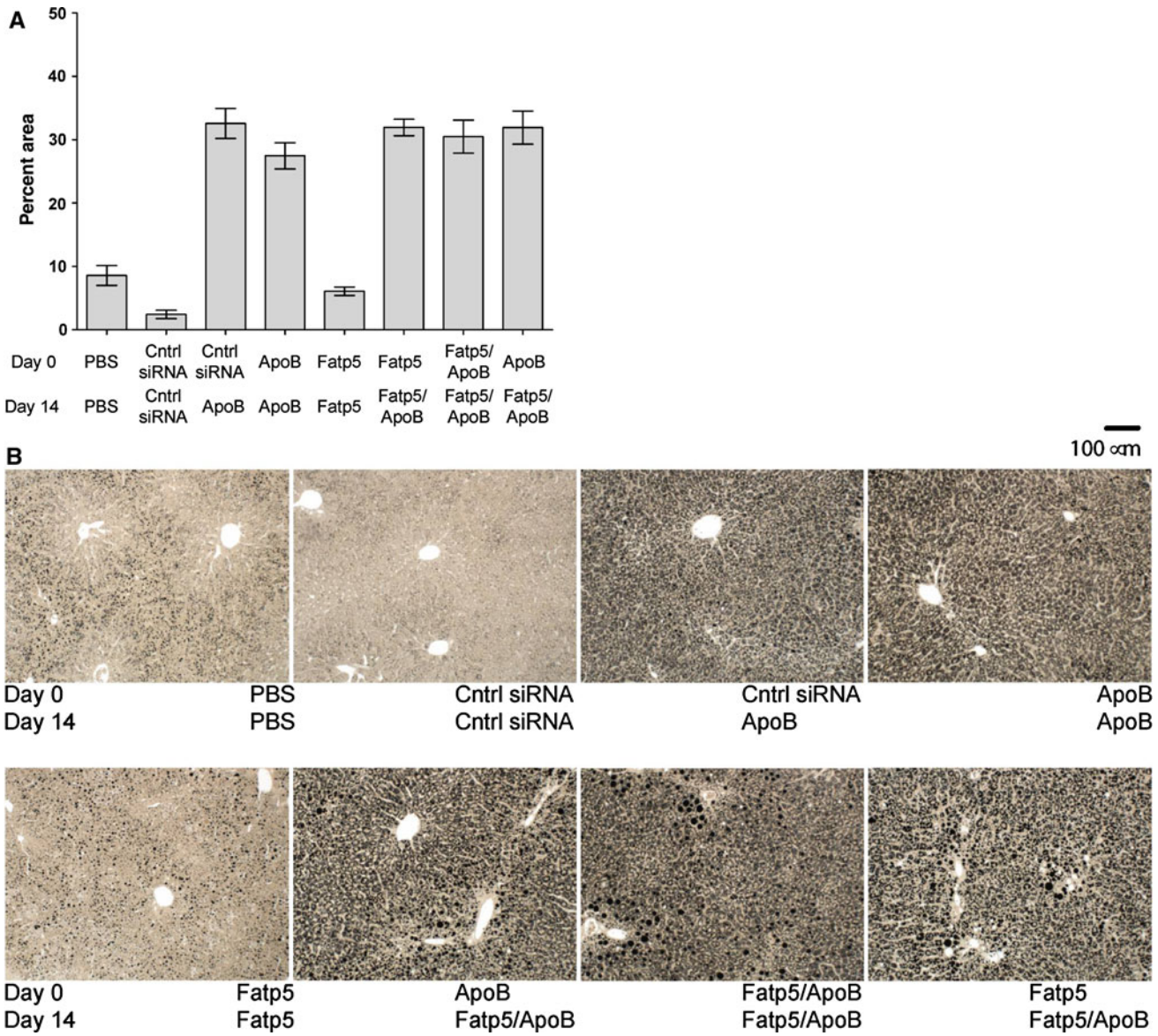

Fig. 5 Similar levels of liver steatosis were observed across all *ApoB* siRNA treatment groups. **a** Osmium-stained images were digitized and pixel intensities were quantitated for day 21. Data represented as the group mean ± SD ($n = 8$/group). **b** Images representative of each of the treatment groups are shown

comparison with the *ApoB*/*ApoB* cohort. Structure elucidation by collision-induced dissociation MS/MS provided information about the possible fatty acid composition for each triglyceride. Triglyceride 52:2 contained 16:0/18:1/18:1, triglyceride 52:3 contained 16:0/18:1/18:2, triglyceride 54:3 contained 18:1/18:1/18:1 and triglyceride 54:3 contained 18:1/18:2/18:1. These triglycerides were confirmed by accurate mass and the use of external standards (data not shown). All of these significantly relevant triglycerides have constituent fatty acids which are non-essential, suggesting that they may be derived from de novo synthesis.

The Hepatic Sterol Response Differed After ApoB and Fatp5 siRNA Treatments

To investigate the hepatic gene response to *ApoB*, *Fatp5* or combination treatments, we performed qRT-PCR analysis on genes involved in the sterol response element binding protein 1 and 2 pathways (*Srebp1* and *Srebp2*). Interestingly, although *ApoB* knockdown induced steatosis, it resulted in a significant decrease in many genes involved in both pathways (Table 1), including genes that are key regulators of fatty acid and triglyceride synthesis (*Fasn*, *Scd*, *Fads1/2*, *Acsl3/5*). As previously described, deletion

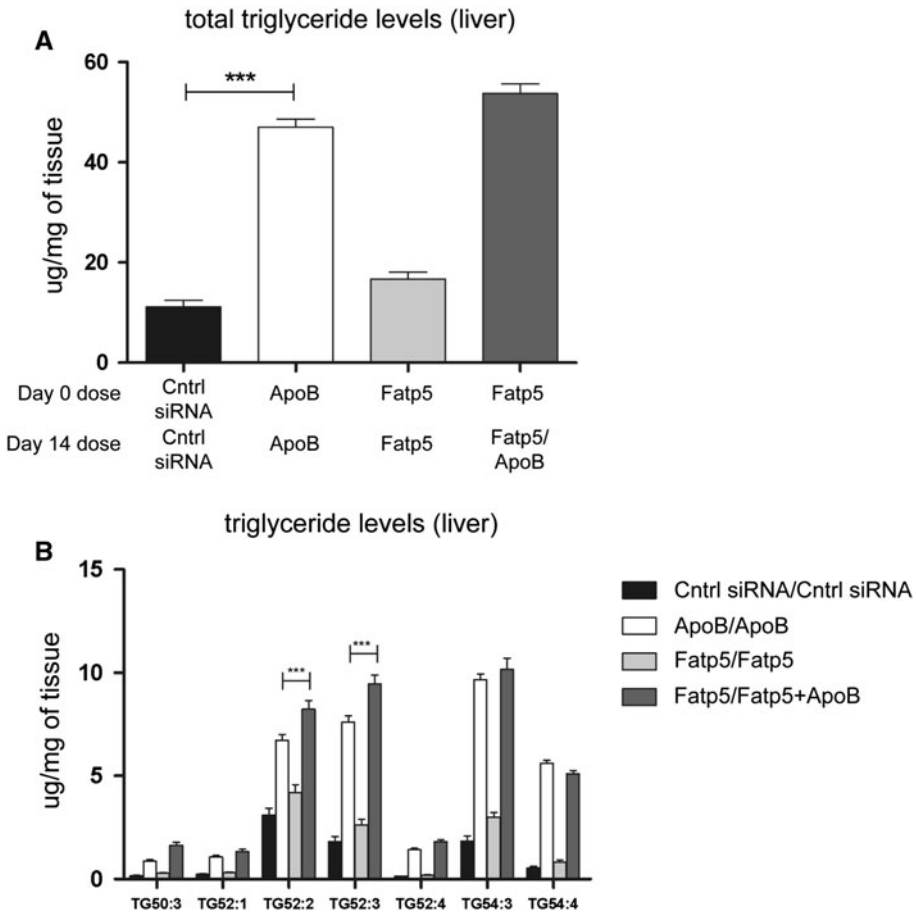

Fig. 6 *Fatp5* siRNA treatment fails to alter *ApoB* siRNA-induced liver triglyceride levels or composition. The total triglyceride pool size and composition was measured for different siRNA administrations (*Cntrl siRNA/Cntrl siRNA*, *ApoB/ApoB*, *Fatp5/Fatp5* and *Fatp5/Fatp5 + ApoB*). **a** A large increase in liver triglycerides was observed for the *ApoB/ApoB* group relative to the control siRNA (***$p = 0.0002$, *t* test with Mann–Whitney post-test). *Fatp5* siRNA treatment (*Fatp5/Fatp5 + ApoB*) did not show protection from *ApoB* siRNA-induced liver steatosis. **b** Specific triglycerides *TG 52:2* and *TG 52:3* showed an increase in their concentrations in both the *ApoB/ApoB* and *Fatp5/Fatp5 + ApoB* groups suggesting that *Fatp5* knockdown fails to alter the triglyceride composition induced by *ApoB* knockdown (***$p \leq 0.0001$, two-way ANOVA with Bonferroni post-test)

[31] or silencing [25] of *Fatp5* caused a reduced uptake of hepatic free fatty acids from serum, which caused a subsequent increase in genes involved in fatty acid synthesis. In contrast to *ApoB* siRNA treatment, Table 1 shows that *Fatp5* siRNA treatment resulted in a significant increase in both *Srebp1* and *Srebp2* pathways. Although bile acid conjugation levels changed and there was a significant increase in cholic acid in bile (Fig 3b), transcription of FXR or key regulators of FXR did not change (data not shown). *ApoB* siRNA treatment appeared to have a stronger effect on the *Srebp1/2* pathways than *Fatp5* siRNA since the simultaneous reductions of both resulted in a hepatic gene signature more similar to that of *ApoB* siRNA treatment alone.

Discussion

In this report, we found that siRNA-mediated knockdown of *ApoB* led to a significant reduction in serum lipids, including HDL, which was associated with an increase in hepatic triglycerides leading to liver steatosis in CETP/LDLR hemizygous mice (a mouse model having a human-like lipid profile). It is worth noting that similar results were observed on day 28 for all end points measured [mRNA knockdown, serum lipids, and histological analysis of hepatic lipid levels (data not shown)].

ApoB siRNA-mediated steatosis contrasts with results reported for ASO-mediated *ApoB* knockdown where only modest but not significant increases in hepatic triglycerides were observed following 6 weeks of biweekly (25 mg/kg) treatment that resolved by week 20 [14]. Crooke et al. reasoned that a compensatory mechanism, which included the activation of AMPK leading to increased fatty acid oxidation and the down-regulation of genes involved in fatty acid synthesis and transport, led to the resolution of hepatic triglyceride accumulation [14]. However, we also observed decreased gene expression within these pathways following the knockdown of *ApoB*. In addition, we observed increased serum ketone levels following *ApoB* siRNA treatment, which is indicative of increased fatty acid oxidation (data not shown). Furthermore, mice harboring a base-pair deletion in the coding region of *ApoB* (*ApoB-38.9*) also exhibited hepatic triglyceride accumulation and decreased expression of genes involved in fatty acid synthesis [25]. Taken together, these data suggest that an alternative mechanism may explain the lack of ASO-mediated steatosis and the discrepancy between *ApoB*

Table 1 *Srebp1c* and *Srebp2* gene expression changes observed following *ApoB*, *Fatp5,* and combination siRNA treatments

	Gene	ApoB		Fatp5		Fatp5/Fatp5 + ApoB	
		Fold regulation	*p* value	Fold regulation	*p* value	Fold regulation	*p* value
Srebp1c pathway	Acaca	–1.46	0.0705	1.78[a]	0.0156	–1.86[b]	0.0266
	Acacb	–1.69[b]	0.0084	1.61[a]	0.0070	–5.40[b]	0.0098
	Fasn	–2.99[b]	0.0026	2.05[a]	0.0203	–2.03	0.0830
	Scd	–3.62[b]	0.0009	1.95[a]	0.0007	–2.91[b]	0.0104
	Fads1	–2.18[b]	0.0000	1.13	0.0514	–2.18[b]	0.0000
	Fads2	–2.39[b]	0.0000	1.24	0.0705	–2.36[b]	0.0001
	Acsf2	1.36[a]	0.0075	1.12	0.0792	1.28[a]	0.0074
	Acsl1	1.19	0.1635	–1.18	0.3571	1.06	0.6852
	Acsl3	–2.16[b]	0.0002	1.05	0.8005	–1.76[b]	0.0202
	Acsl4	–1.24	0.1148	–1.10	0.3702	–1.25	0.0948
	Acsl5	–1.28[b]	0.0405	1.40[a]	0.0020	–1.40[b]	0.0475
Srebp2 pathway	Hmgcs1	–1.60[b]	0.0238	1.93[a]	0.0020	–1.24	0.3368
	Hmgcr	–2.23[b]	0.0034	1.72	0.0740	–1.30	0.5900
	Mvk	–1.11	0.3513	1.51[a]	0.0086	–1.02	0.8580
	Pmvk	–2.30[b]	0.0004	1.52[a]	0.0068	–2.33[b]	0.0033
	Mvd	–3.26[b]	0.0033	1.94[a]	0.0072	–1.98	0.0528
	Idi1	–1.63[b]	0.0212	1.99[a]	0.0017	–1.24	0.3330
	Fdps	–2.60[b]	0.0022	1.88[a]	0.0039	–2.20[b]	0.0237
	Fdft1	–1.43[b]	0.0095	1.72[a]	0.0011	–1.10	0.6770
	Cyp51a1	–1.75[b]	0.0058	1.81[a]	0.0010	–1.40	0.1238
	Dhcr7	–1.65[b]	0.0065	1.65[a]	0.0007	–1.54	0.1193

Selected *Srebp1* and *Srebp2* pathway genes were analyzed after siRNA treatments. Mice were treated with siRNAs targeting *ApoB* and *Fatp5* alone or in combination (*ApoB*, *Fatp5*, *Fatp5*/*ApoB*) at days 0 and 14. Gene expression was analyzed using qRT-PCR (TaqMan) on day 21. Fold regulation was calculated for the treatment group relative to the control siRNA group.

[a] Indicates a significant induction ($p \leq 0.05$) and [b]a significant reduction ($p \leq 0.05$) in expression relative to the control siRNA group. Significance (*p* value) was calculated using a two-tailed *t* test between control and treatment groups

siRNA and ASO treatments, which could be explained, at least in part, by the fact that we are observing slightly greater *ApoB* knockdown (~90 vs. ~75%) and cholesterol lowering [~80 (non-HDL) vs. 66% (LDL)] relative to the ASO-mediated changes.

From our results, HDL appears lower and serum triglycerides higher than one would initially expect for *ApoB* knockdown. While the cause of the decrease in HDL following *ApoB* siRNA treatment is unknown, it is likely that the HDL components provided by APOB-containing particles are reduced following *ApoB* knockdown leading to a reduction HDL levels, which is consistent with findings by Tadin-Strapps et al. [29, 31]. In addition, while serum triglycerides appear disproportionately higher relative to serum APOB for *ApoB* siRNA-treated groups (Fig. 3 relative to Fig. 4d), some of this apparent discrepancy could be due to the production of larger, more triglyceride-rich, non-HDL particles for the limited number of particles produced. It also remains likely that serum triglycerides are artificially elevated relative to other endpoints, since serum triglycerides are measured enzymatically and glycerol is a reaction intermediate. Thus, any glycerol within the serum would lead to a higher reading than would otherwise be expected.

Fatty acids are either transported into the liver or synthesized de novo. Since fatty acids are required for triglyceride synthesis and *ApoB* knockdown reduced the expression of many of the genes involved in de novo hepatic fatty acid synthesis, we rationalized that liver steatosis induced by *ApoB* knockdown could be maintained, at least in part, by the accumulation of fatty acids taken up by hepatocytes [29]. FATP5 is a transporter of long chain fatty acids (LCFAs) into hepatocytes [27, 32], and we reasoned that reducing LCFA uptake by knocking-down *Fatp5* would reduce hepatic triglyceride levels induced by *ApoB* knockdown. We found that *Fatp5* knockdown does not influence the size, composition, or zonal distribution of the hepatic triglyceride pool generated by *ApoB* siRNA treatment. Lipid levels for the *Fatp5* siRNA treatment alone were too low to reliably assess differences in the hepatic triglyceride population relative to the control siRNA group, although results reported by Doege et al. [27] would

suggest that reductions in FATP5 would disproportionately decrease the saturated and polyunsaturated fatty acid containing triglycerides relative to monounsaturated fatty acid containing triglycerides.

It remains possible that FATP5 may not function as a transporter of fatty acids under our conditions. In the studies reported here, animals were fed a chow diet containing 9% fat ad libitum, whereas *Fatp5* knockout mice fed a similar diet (a chow diet containing 5% fat) exhibited the most dramatic changes in hepatic lipid accumulation under prolonged fasting conditions [32]. One could also argue that *Fatp5* knockdown may induce the expression of other *Fatp* family members, which could compensate for the loss of FATP5 activity under our conditions. However, this is unlikely, since *Fatp5* knockout mice did not exhibit altered expression of *Fatp1-4* or *Fatp6* [32], and we did not observe a change in the expression of either of the two *Fatps* evaluated (*Fatp2* or *Fatp4*, data not shown). Alternatively, both *Fatp2* and *Fatp5* are highly expressed in liver, and *Fatp2* knockdown has also been reported to decrease hepatic fatty acid uptake in mice [33]. Therefore, it remains possible that FATP2 is sufficient to mediate hepatic fatty acid uptake in the absence of FATP5 under our conditions.

Even though *Fatp5* knockdown failed to influence the hepatic triglyceride pool generated following *ApoB* knockdown, it did lead to a 100-fold increase in ratio of unconjugated to conjugated bile acids. The magnitude of the shift within the bile acid pool, from predominately conjugated to predominately unconjugated bile acids, is consistent with FATP5 being required for the majority of bile acid reconjugation during enterohepatic recirculation. Our results are inline with the results reported for *Fatp5* knockout mice and suggest that *Fatp5* siRNA treatment is sufficient to influence FATP5 activity [26]. We expect these changes to have only a minor effect on fat absorption, since, consistent with Hubbard et al. [26], we observed that unconjugated bile acids are found within gall bladder bile. Thus, unconjugated bile acids can be efficiently secreted into bile following *Fatp5* knockdown and should therefore be available for fat absorption. *Fatp5* knockout mice also exhibited secondary metabolic changes leading to decreased food intake. Although, it is unclear if this is due to altered bile acid metabolism via the inhibition of bile acid reconjugation, altered lipid metabolism via the inhibition of fatty acid uptake, or both. While outside the scope of this work, it remains possible to use siRNAs targeting *Fatp5* to address this question, since we observed the inhibition of bile acid reconjugation but not fatty acid uptake under these conditions.

Finally, we have shown that *Fatp5* knockdown resulted in a significant increase in genes involved in hepatic cholesterol biosynthesis (*Srebp2* pathway) and fatty acid synthesis (*Srebp1* pathway). This is consistent with the increase in fatty acid synthase expression and defects in bile acid reconjugation reported for the loss of FATP5 activity [26, 27].

One could, therefore, speculate that changes in bile acid conjugation levels would result in an increase in de novo cholesterol synthesis, requiring more acetyl-CoA, which may promote fatty acid synthesis.

Acknowledgments We would like to thank Duncan Brown for siRNA design, Dipali Ruhela and her group for providing the LNP formulations, Jing Kang and Natalya Dubinina for their help with the 'in-life' portion of these studies, Carla S. Colon and David McLaren for their help with metabolite profiling, Wu Yin for help with the gene expression analysis, Kenny K. Wong, Steven R. Bartz, and Anthony K. Ogawa for helpful discussions, as well as Premier Laboratory for histological services and support with pathology review.

References

1. Steinberg D (2004) Thematic review series: the pathogenesis of atherosclerosis—an interpretive history of the cholesterol controversy: part I. J Lipid Res 45:1583–1593. doi:10.1194/jlr.R400003-JLR200
2. Steinberg D (2005) Thematic review series: the pathogenesis of atherosclerosis—an interpretive history of the cholesterol controversy: part II: the early evidence linking hypercholesterolemia to coronary disease in humans. J Lipid Res 46:179–190. doi:10.1194/jlr.R400012-JLR200
3. Steinberg D (2005) Thematic review series: the pathogenesis of atherosclerosis: an interpretive history of the cholesterol controversy, part III: mechanistically defining the role of hyperlipidemia. J Lipid Res 46:2037–2051
4. Steinberg D (2006) Thematic review series: The Pathogenesis of Atherosclerosis. An interpretive history of the cholesterol controversy, part V: The discovery of the statins and the end of the controversy. J Lipid Res 47:1339–1351. doi:10.1194/jlr.R600009-JLR200
5. Davis RA, Hui TY (2001) 2000 George Lyman Duff Memorial Lecture: atherosclerosis is a liver disease of the heart. Arterioscler Thromb Vasc Biol 21:887–898
6. Skalen K, Gustafsson M, Rydberg EK, Hulten LM, Wiklund O, Innerarity TL, Boren J (2002) Subendothelial retention of atherogenic lipoproteins in early atherosclerosis. Nature 417:750–754
7. Hulthe J, Fagerberg B (2002) Circulating oxidized LDL is associated with subclinical atherosclerosis development and inflammatory cytokines (AIR Study). Arterioscler Thromb Vasc Biol 22:1162–1167
8. Davidson NO, Shelness GS (2000) Apolipoprotein B: mRNA editing, lipoprotein assembly, and presecretory degradation. Annu Rev Nutr 20:169–193
9. Gaffney D, Forster L, Caslake MJ, Bedford D, Stewart JP, Stewart G, Wieringa G, Dominiczak M, Miller JP, Packard CJ (2002) Comparison of apolipoprotein B metabolism in familial defective apolipoprotein B and heterogeneous familial hypercholesterolemia. Atherosclerosis 162:33–43

10. Veerkamp MJ, de Graaf J, Bredie SJ, Hendriks JC, Demacker PN, Stalenhoef AF (2002) Diagnosis of familial combined hyperlipidemia based on lipid phenotype expression in 32 families: results of a 5-year follow-up study. Arterioscler Thromb Vasc Biol 22:274–282
11. Tybjaerg-Hansen A, Steffensen R, Meinertz H, Schnohr P, Nordestgaard BG (1998) Association of mutations in the apolipoprotein B gene with hypercholesterolemia and the risk of ischemic heart disease. N Engl J Med 338:1577–1584
12. Boren J, Lee I, Zhu W, Arnold K, Taylor S, Innerarity TL (1998) Identification of the low density lipoprotein receptor-binding site in apolipoprotein B100 and the modulation of its binding activity by the carboxyl terminus in familial defective apo-B100. J Clin Invest 101:1084–1093
13. Innerarity T, Mahley R, Weisgraber K, Bersot T, Krauss R, Vega G, Grundy S, Friedl W, Davignon J, McCarthy B (1990) Familial defective apolipoprotein B-100: a mutation of apolipoprotein B that causes hypercholesterolemia. J Lipid Res 31:1337–1349
14. Crooke RM, Graham MJ, Lemonidis KM, Whipple CP, Koo S, Perera RJ (2005) An apolipoprotein B antisense oligonucleotide lowers LDL cholesterol in hyperlipidemic mice without causing hepatic steatosis. J Lipid Res 46:872–884
15. Rozema DB, Lewis DL, Wakefield DH, Wong SC, Klein JJ, Roesch PL, Bertin SL, Reppen TW, Chu Q, Blokhin AV et al (2007) Dynamic PolyConjugates for targeted in vivo delivery of siRNA to hepatocytes. Proc Natl Acad Sci USA 104:12982–12987. doi:10.1073/pnas.0703778104
16. Zimmermann TS, Lee AC, Akinc A, Bramlage B, Bumcrot D, Fedoruk MN, Harborth J, Heyes JA, Jeffs LB, John M et al (2006) RNAi-mediated gene silencing in non-human primates. Nature 441:111–114
17. Soutschek J, Akinc A, Bramlage B, Charisse K, Constien R, Donoghue M, Elbashir S, Geick A, Hadwiger P, Harborth J et al (2004) Therapeutic silencing of an endogenous gene by systemic administration of modified siRNAs. Nature 432:173–178
18. Merki E, Graham MJ, Mullick AE, Miller ER, Crooke RM, Pitas RE, Witztum JL, Tsimikas S (2008) Antisense oligonucleotide directed to human apolipoprotein B-100 reduces lipoprotein(a) levels and oxidized phospholipids on human apolipoprotein B-100 particles in lipoprotein(a) transgenic mice. Circulation 118:743–753
19. Chandler CE, Wilder DE, Pettini JL, Savoy YE, Petras SF, Chang G, Vincent J, Harwood HJ Jr (2003) CP-346086: an MTP inhibitor that lowers plasma cholesterol and triglycerides in experimental animals and in humans. J Lipid Res 44:1887–1901
20. Visser ME, Akdim F, Tribble DL, Nederveen AJ, Kwoh TJ, Kastelein JJ, Trip MD, Stroes ES Effect of apolipoprotein-B synthesis inhibition on liver triglyceride content in patients with familial hypercholesterolemia. J Lipid Res 51:1057-1062
21. Akdim F, Visser ME, Tribble DL, Baker BF, Stroes ES, Yu R, Flaim JD, Su J, Stein EA, Kastelein JJ Effect of mipomersen, an apolipoprotein B synthesis inhibitor, on low-density lipoprotein cholesterol in patients with familial hypercholesterolemia. Am J Cardiol 105:1413-1419
22. Akdim F, Stroes ES, Sijbrands EJ, Tribble DL, Trip MD, Jukema JW, Flaim JD, Su J, Yu R, Baker BF et al (2010) Efficacy and safety of mipomersen, an antisense inhibitor of apolipoprotein B, in hypercholesterolemic subjects receiving stable statin therapy. J Am Coll Cardiol 55:1611–1618
23. Raal FJ, Santos RD, Blom DJ, Marais AD, Charng MJ, Cromwell WC, Lachmann RH, Gaudet D, Tan JL, Chasan-Taber S et al (2010) Mipomersen, an apolipoprotein B synthesis inhibitor, for lowering of LDL cholesterol concentrations in patients with homozygous familial hypercholesterolaemia: a randomised, double-blind, placebo-controlled trial. Lancet 375:998–1006
24. Kastelein JJ, Wedel MK, Baker BF, Su J, Bradley JD, Yu RZ, Chuang E, Graham MJ, Crooke RM (2006) Potent reduction of apolipoprotein B and low-density lipoprotein cholesterol by short-term administration of an antisense inhibitor of apolipoprotein B. Circulation 114:1729–1735
25. Lin X, Schonfeld G, Yue P, Chen Z (2002) Hepatic fatty acid synthesis is suppressed in mice with fatty livers due to targeted apolipoprotein B38.9 mutation. Arterioscler Thromb Vasc Biol 22:476–482
26. Hubbard B, Doege H, Punreddy S, Wu H, Huang X, Kaushik VK, Mozell RL, Byrnes JJ, Stricker-Krongrad A, Chou CJ et al (2006) Mice deleted for fatty acid transport protein 5 have defective bile acid conjugation and are protected from obesity. Gastroenterology 130:1259–1269
27. Doege H, Grimm D, Falcon A, Tsang B, Storm TA, Xu H, Ortegon AM, Kazantzis M, Kay MA, Stahl A (2008) Silencing of hepatic fatty acid transporter protein 5 in vivo reverses diet-induced non-alcoholic fatty liver disease and improves hyperglycemia. J Biol Chem 283:22186–22192
28. Mencarelli A, Renga B, Distrutti E, Fiorucci S (2009) Antiatherosclerotic effect of farnesoid X receptor. Am J Physiol Heart Circ Physiol 296:H272–H281
29. Tadin-Strapps M, Peterson LB, Cumiskey AM, Rosa RL, Mendoza VH, Castro-Perez J, Puig O, Zhang L, Strapps WR, Yendluri S et al. (2011) siRNA induced liver ApoB knockdown lowers serum LDL-cholesterol in a mouse model with human-like serum lipids. J Lipid Res 52:1084–1097
30. Morrissey DV, Lockridge JA, Shaw L, Blanchard K, Jensen K, Breen W, Hartsough K, Machemer L, Radka S, Jadhav V et al (2005) Potent and persistent in vivo anti-HBV activity of chemically modified siRNAs. Nat Biotechnol 23:1002–1007
31. Lieu HD, Withycombe SK, Walker Q, Rong JX, Walzem RL, Wong JS, Hamilton RL, Fisher EA, Young SG (2003) Eliminating atherogenesis in mice by switching off hepatic lipoprotein secretion. Circulation 107:1315–1321
32. Doege H, Baillie RA, Ortegon AM, Tsang B, Wu Q, Punreddy S, Hirsch D, Watson N, Gimeno RE, Stahl A (2006) Targeted deletion of FATP5 reveals multiple functions in liver metabolism: alterations in hepatic lipid homeostasis. Gastroenterology 130:1245–1258
33. Falcon A, Doege H, Fluitt A, Tsang B, Watson N, Kay MA, Stahl A (2010) FATP2 is a hepatic fatty acid transporter and peroxisomal very long-chain acyl-CoA synthetase. Am J Physiol Endocrinol Metab 299:E384–E393
34. Majercak J, Ray WJ, Espeseth A, Simon A, Shi XP, Wolffe C, Getty K, Marine S, Stec E, Ferrer M et al (2006) LRRTM3 promotes processing of amyloid-precursor protein by BACE1 and is a positional candidate gene for late-onset Alzheimer's disease. Proc Natl Acad Sci USA 103:17967–17972
35. Wincott F, DiRenzo A, Shaffer C, Grimm S, Tracz D, Workman C, Sweedler D, Gonzalez C, Scaringe S, Usman N (1995) Synthesis, deprotection, analysis and purification of RNA and ribozymes. Nucleic Acids Res 23:2677–2684
36. Abrams MT, Koser ML, Seitzer J, Williams SC, DiPietro MA, Wang W, Shaw AW, Mao X, Jadhav V, Davide JP et al (2010) Evaluation of efficacy, biodistribution, and inflammation for a potent siRNA nanoparticle: effect of dexamethasone co-treatment. Mol Ther 18:171–180
37. Ason B, Tep S, Davis HR Jr, Xu Y, Tetzloff G, Galinski B, Soriano F, Dubinina N, Zhu L, Stefanni A et al (2011) Improved efficacy for ezetimibe and rosuvastatin by attenuating the induction of PCSK9. J Lipid Res 52:679–687
38. Livak KJ, Schmittgen TD (2001) Analysis of relative gene expression data using real-time quantitative PCR and the 2(-delta delta C(T)) method. Methods 25:402–408

39. Bligh EG, Dyer WJ (1959) A rapid method of total lipid extraction and purification. Can J Biochem Physiol 37:911–917
40. Castro-Perez J, Previs SF, McLaren DG, Shah V, Herath K, Bhat G, Johns DG, Wang SP, Mitnaul L, Jensen K et al (2011) In vivo D_2O labeling to quantify static and dynamic changes in cholesterol and cholesterol esters by high resolution LC/MS. J Lipid Res 52:159–169
41. Fahy E, Subramaniam S, Murphy RC, Nishijima M, Raetz CR, Shimizu T, Spener F, van Meer G, Wakelam MJ, Dennis EA (2009) Update of the LIPID MAPS comprehensive classification system for lipids. J Lipid Res 50(Suppl):S9–S14

Lipids (2011) 46:1005–1012
DOI 10.1007/s11745-011-3615-4

ORIGINAL ARTICLE

cis-9,*trans*-11,*cis*-15 and *cis*-9,*trans*-13,*cis*-15 CLNA Mixture Activates PPARα in HEK293 and Reduces Triacylglycerols in 3T3-L1 cells

Jonatan Miranda · Arrate Lasa · Alfredo Fernández-Quintela · Cristina García-Marzo · Josune Ayo · Renaud Dentin · María P. Portillo

Received: 14 April 2011 / Accepted: 12 September 2011 / Published online: 9 October 2011

Abstract Scientific research is constantly working to find new molecules that are effective in preventing excessive accumulation of body fat. The aim of the present work was to assess the potential agonism on PPARα and PPARγ of a conjugated linolenic acid (CLNA) isomer mixture, consisting of two CLNA isomers (*cis*-9,*trans*-11,*cis*-15 and *cis*-9,*trans*-13,*cis*-15). Secondly, we aimed to analyze the effects of this mixture on triacylglycerol accumulation in 3T3-L1 mature adipocytes. Luciferase transactivation assay was used to analyze whether the CLNA mixture activated PPARs. The expression of several enzymes and transcriptional factors involved in the main metabolic pathways that control triacylglycerol accumulation in adipocytes was assessed by real time RT-PCR in 3T3-L1 adipocytes treated for 20 h with the CLNA mixture. The mixture activated PPRE in cells with PPARα receptor over-expression, but not those with PPARγ over-expression. Decreased triacylglycerol was found in treated adipocytes. The lowest dose (10 μM) increased HSL expression and the highest dose (100 μM) increased ATGL gene expression. The other genes analyzed remained unchanged. The hypothesis of an anti-obesity action of the analyzed CLNA mixture, based on increased lipid mobilization in adipose tissue, can be proposed.

Keywords PPARα · PPARγ · Conjugated linolenic acid · HSL · ATGL · 3T3-L1

Abbreviations

ACC1	Acetyl-CoA carboxylase1
ATGL	Adipose triglyceride lipase
CLA	Conjugated linoleic acid
CLNA	Conjugated linolenic acid
FASN	Fatty acid synthase
HSL	Hormone-sensitive lipase
IBMX	3-Isobutyl-1-methyl-xanthine
LPL	Lipoprotein lipase
PPAR	Peroxisome proliferator-activated receptor
PPRE	Peroxisome proliferator response element
SREBP-1c	Sterol regulatory element binding protein
TAG	Triacylglycerol

J. Miranda · A. Lasa · A. Fernández-Quintela · M. P. Portillo (✉)
Department of Nutrition and Food Sciences, Faculty of Pharmacy, University of the Basque Country, Paseo de la Universidad, 7, 01006 Vitoria, Spain
e-mail: mariapuy.portillo@ehu.es

C. García-Marzo · J. Ayo
Food Research Unit, AZTI-Tecnalia, Derio, Spain

R. Dentin
Institut Cochin, Département d'Endocrinologie, Métabolisme et Cancer, Université Paris Descartes, CNRS (UMR 8104), INSERM, U567, Paris, France

Introduction

Being overweight and obesity are a public health problem in developed societies because of their high prevalence, not only in adults but also in children. They generate numerous metabolic disturbances and other associated diseases, such as insulin resistance, diabetes, hypertension and dyslipemia [1]. Scientific research is constantly working to find new molecules, either drugs or dietary ingredients, which are

effective in preventing excessive accumulation of body fat and/or in reducing the fat previously stored.

In recent years a great deal of scientific work has been performed to analyze the anti-obesity effects of conjugated linoleic acid (CLA) and has shown that it strongly reduces body fat in rodents (mice, hamsters and rats) [2–5]. Despite these promising results, CLA testing on humans produced effects which were far less noticeable, and frequently highly controversial. Whereas CLA was not effective in several studies, in others it led to a very weak reduction in body fat [6–9]. Thus, the EFSA (European Food Safety Authority) Panel on Dietetic Products, Nutrition and Allergies, based on the results reported in human studies, concluded that a cause and effect relationship has not been established between the consumption of an equimolecular mixture of CLA isomers, *cis*-9,*trans*-11 and *trans*-10,*cis*-12, and contribution to the maintenance or achievement of a normal body weight [10].

This scientific scenario has directed researchers' attention towards conjugated linolenic acid isomers (CLNA), defined as octadecatrienoic fatty acid isomers with at least two conjugated double bonds. The literature shows that, although in general terms beneficial effects on health are induced by CLNA isomers, important differences exist in terms of anti-obesity action among *cis*-9,*trans*-11,*trans*-13 (α-eleostearic acid) [11], *trans*-9,*trans*-11,*cis*-13 (catalpic acid) [12], *cis*-9,*trans*-11,*cis*-13 (punicic acid) [13–15], *trans*-8,*trans*-10,*cis*-12 (calendic acid) [16] and *cis*-8,*trans*-10,*cis*-12 (jacaric acid) [17]. Based on published results, it has been proposed that punicic acid (*cis*-9,*trans*-11,*cis*-13) will be further developed for regulating blood sugar levels [18] and catalpic acid (*trans*-9,*trans*-11,*cis*-13) for lipid-lowering and anti-obesity applications. The interest in calendic acid (*trans*-8,*trans*-10,*cis*-12) is limited because its effectiveness on body-fat reduction is lower than that of conjugated linoleic acid (CLA) [16]. Jacaric acid (*cis*-8,*trans*-10,*cis*-12) seems not to be useful for these purposes [19].

Taking all these results into consideration, and in the line of searching new CLNA isomers with anti-obesity properties, the present study focused on a CLNA mixture consisting of two CLNA isomers (rumelenic acid *cis*-9,*trans*-11,*cis*-15 18:3 and *cis*-9,*trans*-13,*cis*-15 18:3; 50:50) not extensively investigated yet. In the first part of the present study the potential agonism of these CLNA isomers on PPARα and PPARγ was assessed. Secondly, the effects of this mixture on triacylglycerol (TAG) accumulation in 3T3-L1 mature adipocytes, as well as on the expression of enzymes and transcriptional factors involved in the main metabolic pathways that control TAG accumulation in adipocytes, such as de novo lipogenesis, fatty acid uptake from circulating TAG and lipolysis, were also evaluated. Our research revealed that the analyzed CLNA mixture was able to activate PPARα but not PPARγ. Moreover, it increased the expression of HSL and ATGL but not that of LPL, PPARγ, ACC1, FASN and SREBP-1c. Therefore, our findings suggest that analyzed CLNA mixture may have anti-obesity properties.

Methods and Procedures

Method for Obtaining the CLNA Mixture

The CLNA isomer mixture was prepared by alkali isomerization of hydrolyzed linseed oil using an adaptation of the procedure described by Galvez et al. [21]. The CLNA isomers were isolated from the isomerized product by silver ion thin layer chromatography, according to the method described by Destaillats et al. [22]. The two CLNA isomers were identified as rumelenic acid (*cis*-9,*trans*-11,*cis*-15) and *cis*-9,*trans*-13,*cis*-15 18:3 in a molar ratio of 50:50, previous derivatization with 4-methyl-1,2,4-triazoline-3,5-dione (Sigma, St. Louis, Mo, USA) following the procedure of Destaillats et al. [23].

Reporter Assay

Human Kidney Embryonic HEK293T cells were maintained and transfections were carried out as previously described [24]. HEK293T were transiently transfected with 25 ng of the reporter expression vector under study (PGL2-PPRE-Luc) and with 25 ng of the internal control vector (β-galactosidase), using Lipofectamin 2000® (Invitrogen, Carlsbad, CA, USA), according to the manufacturer's instructions. Cells were divided into two experimental groups: cells with over-expression of PPARα (transfected with 5 ng of PPARα) and cells with over-expression of PPARγ (transfected with 5 ng of PPARγ). WY-14643 (Calbiochem-Merck, Darmstadt, Germany) and rosiglitazone (Cayman Chemical, Michigan, USA) were used as the positive controls of PPARα and PPARγ receptors activation, respectively. After 24 h, cells were treated with the CLNA mixture at different doses (3, 15, 30 μM) during 18 h. CLNA, as well as PPAR ligands, were dissolved in 95% ethanol. At this point luciferase activity was measured. Luciferase activity was normalized for transfection efficiency using a β-galactosidase reporter (RSV β-gal) as an internal control. Experimental data are the mean of at least three independent experiments with luciferase activity normalized to β-galactosidase activity, conducted in triplicate.

β-Galactosidase assays for normalization of PPRE-luciferase activity were performed using 10 μl of cell lysate, 50 μl 2× buffer (1.33 mg/mL 2-nitrophenyl β-D-galactopyranoside, 100 mM 2-mercaptoethanol, 2 mM magnesium chloride, 200 mM sodium phosphate pH 7.5),

and 40 μL water in each well of a clear 96-well plate. All these were purchased from Sigma (St. Louis, MO, USA). The plate was covered and incubated for 30 min at 37 °C, and absorbance at 405 nm was determined with a BioRad Lumimark Plus plate reader. Lysate samples were assayed in triplicate. Lysates from untransfected cells were used as controls for background activity.

3T3-L1 Adipocyte Culture

The 3T3-L1 cells were maintained and cultured as previously described [25]. In brief, cells were cultured at 37 °C in a humidified atmosphere of 5% CO_2/95% air. 3T3-L1 pre-adipocytes were maintained in DMEM (Invitrogen, Carlsbad, CA, USA) containing 10% (v/v) fetal calf serum (FCS; Sigma, St. Louis, MO, USA) and antibiotics (penicillin/streptomycin). Differentiation of the cells was initiated 24 h after confluence by incubation for 2 days in FCS free medium containing 0.25 μM dexamethasone (Sigma, St. Louis, MO, USA), 500 μM 3-isobutyl-1-methyl-xanthine (IBMX; Sigma, St. Louis, MO, USA) and 10 nM insulin (Sigma, St. Louis, MO, USA). Differentiation into adipocytes was visualized under the microscope from the accumulation of lipid droplets. Until day 11 (adipogenic phase) the cells were maintained in a feeding medium (DMEM containing 10% (v/v) FCS and antibiotics, as well as insulin) that was renewed every 3 days.

On day 11 after differentiation, the cells were pre-incubated for 24 h with an insulin-free feeding medium in order to avoid the influence of insulin. On day 12 after differentiation, mature adipocytes, grown in 6-well plates, were incubated with either 0.1% ethanol (95%) (control group) or with the CLNA mixture (10 or 100 μM, diluted in 95% ethanol) for 20 h. Cells were harvested after the treatment and TAG content, normalized by protein content [26], were quantified by using AdipoRed® assay reagent (Lonza, Walkersville, USA). Gene expression was assessed by real time RT-PCR as described below.

Gene Expression Analysis by Reverse Transcription-Quantitative PCR (RT-PCR)

Total RNA was extracted from adipocytes with Trizol (Invitrogen, Carlsbad,CA, USA). RNA samples were then treated with a DNA-free kit (Ambion, Applied Biosystems, USA) according to the manufacturer's instructions, to remove any contamination with genomic DNA. The yield and quality of RNA were assessed by measuring absorbance at 260, 270, 280 and 310 nm and by electrophoresis on 1.3% agarose gels. Then, 1.5 μg of total RNA of each sample was reverse-transcribed to first-strand complementary DNA (cDNA) using iScript® cDNA Synthesis Kit (Bio-Rad, Hercules, CA, USA).

Relative PPARγ, LPL (lipoprotein lipase), ACC1 (acetyl-CoA carboxylase1), FASN (fatty acid synthase), SREBP-1c (sterol regulatory element binding protein), HSL (hormone-sensitive lipase) and ATGL (adipose triglyceride lipase) mRNA levels were quantified using real-time PCR with an iCycler® – MyiQ® Real Time PCR Detection System (BioRad, Hercules, CA, USA). β-Actin mRNA levels were similarly measured and served as the reference gene.

Then, 0.1 μL of each cDNA was added to the PCR reagent mixture (SYBR® Green Master Mix; Applied Biosystems, USA), with the upstream and downstream primers (300 nM each). The PCR parameters were as follows: initially 2 min at 50 °C, denaturation at 95 °C for 10 min followed by 40 cycles of denaturation at 95 °C for 15 s, annealing for 30 s and extension at 60 °C for 30 s. Information concerning specific sense/antisense primers and PCR annealing extension temperatures is described in Table 1.

Table 1 Primers and annealing temperature for PCR amplification of each gene studied

SYBR® Green RT-PCR			
Primers	Sense primer	Antisense primer	Annealing temperature
SREBP-1c	5′-GCGGACGCAGTCTGGG-3′	5′-ATGAGCTGGAGCATGTCTTCAAA-3′	60.9 °C [27]
FASN	5′-AGC CCC TCA AGT GCA CAG TG-3′	5′-TGCCAATGTGTTTTCCCTGA-3′	60.0 °C
ACC1	5′-GGACCACTGCATGGAATGTTAA-3′	5′-TGAGTGACTGCCGAAACATCTC-3′	60.0 °C
PPARγ	5′-ATTCTGGCCCACCAACTTCGG -3′	5′-TGGAAGCCTGATGCTTTATCCCCA -3′	63.9 °C
LPL	5′-CAGCTGGGCCTAACTTTGAG-3′	5′-CTCTCTGCAATCACACG-3′	60.0 °C
ATGL	5′-CACTTTAGCTCCAAGGATGA-3′	5′-TGGTTCAGTAGGCCATTCCT-3′	60.8 °C
HSL	5′-GGTGACACTCGCAGAAGACAATA-3′	5′-GCCGCCGTGCTGTCTCT-3′	60.0 °C
β-Actin	5′-ACGAGGCCCAGAGCAAGAG-3′	5′-GGTGTGGTGCCAGATCTTCTC-3′	60.0 °C

SREBP Sterol-regulatory element binding protein, *LPL* lipoprotein lipase, *PPAR* peroxisome proliferator-activated receptor, *ACC1* acetyl-CoA carboxylase1, *FASN* fatty acid synthase, *HSL* hormone-sensitive lipase and *ATGL* adipose tissue TAG lipase

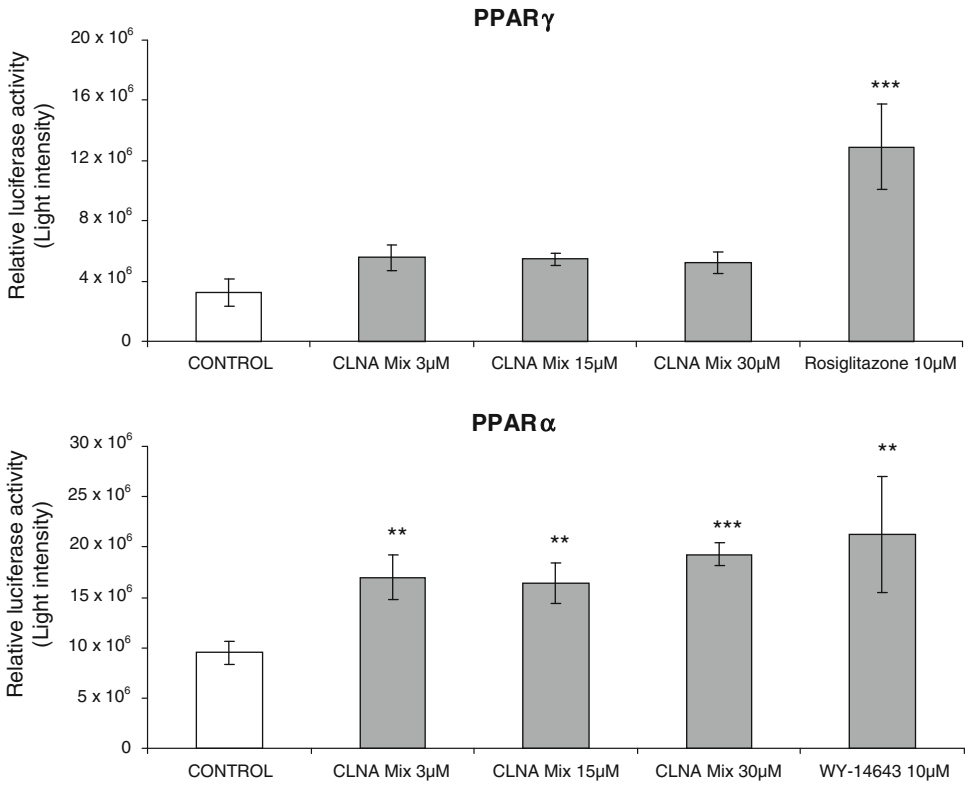

Fig. 1 Effects of 3, 15 and 30 μM CLNA mixture *cis*-9,*trans*-11,*cis*-15 and *cis*-9,*trans*-13,*cis*-15 on peroxisome proliferator response element (PPRE) reporter activity of HEK293T cells with PPARγ/PPARα receptors over-expressed. Values (luciferase activity normalized to β-galactosidase activity) are means with the standard error of the mean, shown by *vertical bars*. 10 μM Rosiglitazone and 10 μM WY-14643 were used as positive control of PPARγ and PPARα receptor activation respectively. Data were analyzed by one-way analysis of variance followed by the Tukey post hoc test. $^{**}P < 0.01$, $^{***}P < 0.001$

mRNA levels were normalized to the values of β-actin and the results expressed as fold changes of threshold cycle (Ct) value relative to controls using the 2-ΔΔCt method [28].

Statistical Analysis

Results are presented as means ± standard errors of the means. Statistical analysis was performed using SPSS 17.0 (SPSS Inc. Chicago, IL, USA). Data was analyzed by one-way analysis of variance followed by the Tukey post hoc test. Statistical significance was set-up at the $P < 0.05$ level.

Results

PPRE Activation on HEK293 Cells

The mixture of CLNA isomers activates peroxisome proliferator response element (PPRE) of cells with PPARα receptor over-expression, but not those with PPARγ over-expression. In the case of the PPARα transcriptional factor the activity increase was as evident as that shown with the positive control (10 μM of WY-14643). No dose-dependent effect among the doses was observed (Fig. 1).

Effect of the CLNA Mixture on Triacylglycerol Accumulation in Nature Adipocytes

The TAG content in the control group was not modified after 20 h of treatment. It was found that 10 and 100 μM of the CLNA mixture decreased TAG content in mature adipocytes (−49 and −39% respectively). As shown in Fig. 2, dose-dependent effects were not found, according to the percentage of reduction.

Effect of the CLNA Mixture on the Expression of Adipocyte-Specific Genes in Mature Adipocytes

With regard to the adipocyte-specific genes, LPL, PPARγ, ACC1, FASN and SREBP-1c remained unchanged (Fig. 3a, b). The expression of the main lipases, HSL and ATGL, was also analyzed. HSL expression was increased with the lower dose (10 μM) and ATGL expression was increased with the higher dose (100 μM) (Fig. 3a).

Discussion

Genes involved in lipid metabolism are controlled by several peroxisome proliferator-activated receptors (PPARs) [29–31]. PPARα, mainly expressed in oxidative tissues such

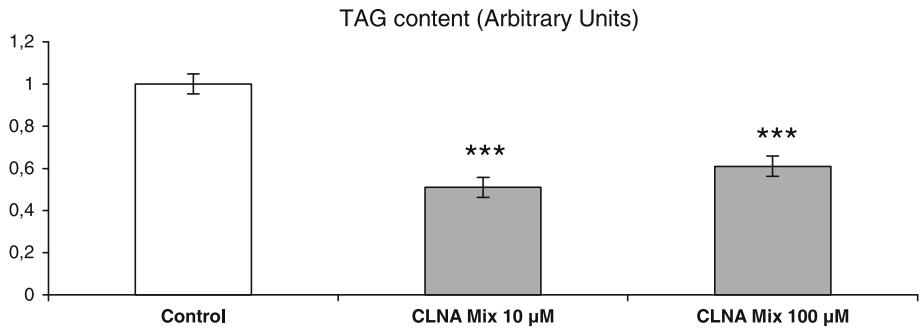

Fig. 2 Triacylglycerol content normalized by protein in mature adipocytes 3T3-L1 treated for 20 h with 10 and 100 µM of the CLNA mixture *cis*-9,*trans*-11,*cis*-15 and *cis*-9,*trans*-13,*cis*-15. Values are means with the standard error of the mean, shown by *vertical bars*. Data were analyzed by one-way analysis of variance followed by the Tukey post hoc test. ***$P < 0.001$

as liver, activates the expression of enzymes involved in fatty acid oxidation [31]. PPARγ, widely expressed in white adipose tissue, regulates genes related to adipogenesis, fatty acid storage as TAG, adipokine release and improves insulin sensitivity [31–33]. Thus, when the anti-obesity and/or anti-diabetic properties of new potential functional ingredients are analyzed it is important to know if they are able to activate these transcriptional factors.

It has been reported that conjugated linoleic acid isomers have the ability to bind PPARα [34, 35] and PPARγ [36, 37]. With regard to conjugated linolenic isomers, Hontecillas et al. [15] observed that punicic acid (*cis*-9,*trans*-11,*cis*-13) activated both PPARγ and PPARα in 3T3-L1 adipocytes transfected with PPAR-Luciferase plasmids. In another study Chuang et al. [11], found that α-eleostearic acid (*cis*-9,*trans*-11,*trans*-13) activated PPARα in a transactivation assay performed with a clone of CHOK1 cells. By contrast, in previous studies from our laboratory, jacaric acid (*cis*-8,*trans*-10,*cis*-12) a CLNA isomer that does not show the sequence *cis*-9,*trans*-11 observed in punicic and α-eleostearic acids, did not activate PPARγ or PPARα in a transactivation assay performed with HEK293T cells [19]. These results suggest that the ability of CLNA isomers for activating PPARs depends on their chemical structure.

In this context, in order to broaden the knowledge about CLNA isomers, the first aim of the present study was to evaluate the potential activation of PPARα and PPARγ by means of a CLNA mixture consisting of two CLNA isomers (rumelenic acid *cis*-9,*trans*-11,*cis*-15 18:3 and *cis*-9,*trans*-13,*cis*-15 18:3; 50:50). This process has not been extensively investigated before. In fact, as far as we know, there is only one paper addressing the effect of these two isomers on lipid synthesis, which specifically concerns their effect on milk fat synthesis in lactating dairy cows [20]. The results concerning the activation of PPARs by CLNA isomers will be very helpful in order to know if these molecules may be good candidates to be used as functional ingredients for obesity, diabetes and dyslipidemia prevention.

The mixture analyzed in the present study activated PPRE of cells with PPARα receptor over-expression, but not those with PPARγ over-expression. By comparing the present results with those published by other authors, by using other CLNA isomers, it can be observed that our mixture shares with punicic acid and α-eleostearic acids the ability for activating PPARα.

As previously explained in this discussion, the activation of PPARα leads to the activation of enzymes involved in mitochondrial and peroxisomal fatty acid oxidation [28, 38, 39]. Thus, the present results suggests that, when administered in vivo, this CLNA mixture could have the capability of reducing steatosis, hypertriglyceridemia, and even body fat accumulation (anti-obesity effect), by increasing fatty acid oxidation [40–45].

The CLNA mixture did not act as a PPARγ agonist; this is a difference from other CLNA isomers, such as punicic acid [15]. The lack of PPARγ activation means that this CLNA mixture is probably not useful for insulin resistance management and glycemic control. In contrast, it could be an interesting prospect for avoiding an increase in adipose tissue because, as explained before, PPARγ activation promotes lipid storage in adipose tissue. Other potential actions of the CLNA mixture on adipocyte metabolism cannot be discarded because changes in the expression of this transcriptional factor, as well as modifications in metabolic pathways that are not regulated by PPARγ, could take place.

In order to obtain more evidences concerning the effect of the CLNA mixture on adipose tissue metabolism, a second experiment devoted to analyze its effects on TAG accumulation in 3T3-L1, as well as on the expression of lipid-related genes, was carried out in the present study. The amount of accumulated TAG was lower in treated cells than in the controls, suggesting that the analyzed CLNA mixture may be of interest as a potential anti-obesity agent, not only by increasing liver fatty acid oxidation through the activation of PPARα, but also by acting directly on other molecular mechanisms in adipocytes.

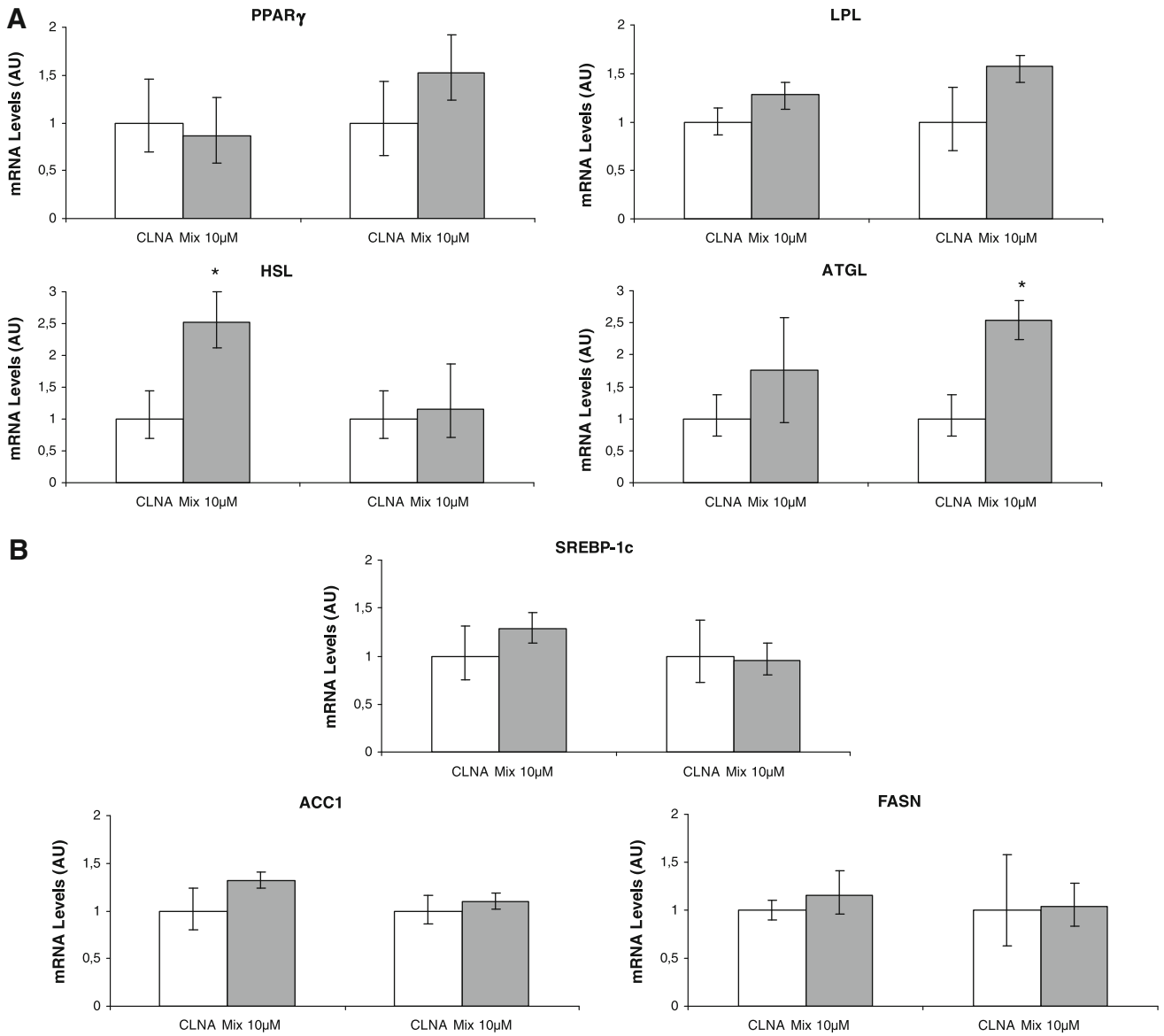

Fig. 3 mRNA levels were measured by Real Time RT-PCR in mature 3T3-L1 adipocytes treated for 20 h with 10 and 100 μM of the CLNA mixture *cis*-9,*trans*-11,*cis*-15 and *cis*-9,*trans*-13,*cis*-15. **a** Genes related to fatty acid uptake from circulating triacylglycerol and lipolysis (LPL, PPARγ, ATGL, HSL) and **b** genes related to lipogenesis (SREBP-1c, FASN, ACC1). Values are expressed relative to control group and results are given as means with the positive and negative error, shown by *vertical bars*. Data were analyzed by one-way analysis of variance followed by the Tukey post hoc test. *$P < 0.05$

In the present study, the effects of the CLNA mixture on the expression of enzymes and transcriptional factors involved in de novo lipogenesis, fatty acid uptake from circulating TAG and lipid mobilization were assessed. No changes were observed in the expression of LPL or PPARγ. These results, together with the absence of activation of this transcriptional factor, suggest that the CLNA mixture does not modify fatty acid uptake from circulating TAG in adipocytes.

The expression of ACC1 and FASN, as well as the transcriptional factor SREBP-1c, also remained unchanged, indicating that the reduction in the accumulation in TAG induced by the CLNA mixture is not due to decreased de novo lipogenesis. With regard to HSL and ATGL, two lipases controlling lipolysis, an increase in their expression was observed in adipocytes treated with the CLNA mixture. These data suggest that the reduction in TAG accumulation can result from increased lipid mobilization.

In summary, on the basis of the present in vitro delipidation effect, the hypothesis of an anti-obesity action of the CLNA mixture, consisting of *cis*-9,*trans*-11,*cis*-15 and *cis*-9,*trans*-13,*cis*-15 isomers, increased lipid mobilization in adipose tissue, can be proposed. These results open the way for further research. Obviously, checking whether this

CLNA mixture indeed induces a reduction in fat accumulation requires further studies performed in animal models as a first step, and later on in humans.

Acknowledgments This study was supported by grants from the Government of País Vasco (IT-386-10; CTP09/R5), Instituto de Salud Carlos III (RETIC PREDIMED) and CYTED (208RT0343). J. Miranda is a recipient of a doctoral fellowship from the Ministerio de Educación y Ciencia. PPAR response element (PPRE) luciferase reporter plasmid (pPPRE-Luc), as well as PPARα and γ receptors expression plasmids, were kind gifts from Dr. Renaud Dentin.

Conflict of interest There are no conflicts of interest to disclose.

References

1. Mutch D, Clément K (2006) Genetics of human obesity. Best Pract Res Clin Endocrinol Metab 20(4):647–664
2. Evans M, Brown J, McIntosh M (2002) Isomer-specific effects of conjugated linoleic acid (CLA) on adiposity and lipid metabolism. J Nutr Biochem 13(9):508
3. Martin JC, Valeille K (2002) Conjugated linoleic acids: all the same or to everyone its own function? Reprod Nutr Dev 42(6):525–536
4. Domeneghini C, Di Giancamillo A, Corino C (2006) Conjugated linoleic acids (CLAs) and white adipose tissue: how both in vitro and in vivo studies tell the story of a relationship. Histol Histopathol 21(6):663–672
5. Navarro V, Fernández-Quintela A, Churruca I, Portillo M (2006) The body fat-lowering effect of conjugated linoleic acid: a comparison between animal and human studies. J Physiol Biochem 62(2):137–147
6. Terpstra AH (2004) Effect of conjugated linoleic acid on body composition and plasma lipids in humans: an overview of the literature. Am J Clin Nutr 79(3):352–361
7. Larsen TM, Toubro S, Astrup A (2003) Efficacy and safety of dietary supplements containing CLA for the treatment of obesity: evidence from animal and human studies. J Lipid Res 44(12):2234–2241
8. Salas-Salvado J, Marquez-Sandoval F, Bullo M (2006) Conjugated linoleic acid intake in humans: a systematic review focusing on its effect on body composition, glucose, and lipid metabolism. Crit Rev Food Sci Nutr 46(6):479–488
9. Whigham L, Watras A, Schoeller D (2007) Efficacy of conjugated linoleic acid for reducing fat mass: a meta-analysis in humans. Am J Clin Nutr 85(5):1203–1211
10. EFSA Panel on Dietetic Products NaAN (2010) Scientific Opinion on the substantiation of health claims related to conjugated linoleic acid (CLA) isomers and contribution to the maintenance or achievement of a normal body weight (ID 686, 726, 1516, 1518, 2892, 3165), increase in lean body mass (ID 498, 731), increase in insulin sensitivity (ID 1517), protection of DNA, proteins and lipids from oxidative damage (ID 564, 1937), and contribution to immune defences by stimulation of production of protective antibodies in response to vaccination (ID 687, 1519) pursuant to Article 13(1) of Regulation (EC) No 1924/2006. EFSA J 8 (10): 26. doi:10.2903/j.efsa.2010.1794
11. Chuang C, Hsu C, Chao C, Wein Y, Kuo Y, Huang C (2006) Fractionation and identification of 9c,11t,13t-conjugated linolenic acid as an activator of PPARalpha in bitter gourd (Momordica charantia L.). J Biomed Sci 13(6):763–772
12. Hontecillas R, Diguardo M, Duran E, Orpi M, Bassaganya-Riera J (2008) Catalpic acid decreases abdominal fat deposition, improves glucose homeostasis and upregulates PPAR alpha expression in adipose tissue. Clin Nutr 27(5):764–772
13. Arao K, Yotsumoto H, Han S, Nagao K, Yanagita T (2004) The 9cis,11trans,13cis isomer of conjugated linolenic acid reduces apolipoprotein B100 secretion and triacylglycerol synthesis in HepG2 cells. Biosci Biotechnol Biochem 68(12):2643–2645
14. Koba K, Imamura J, Akashoshi A, Kohno-Murase J, Nishizono S, Iwabuchi M, Tanaka K, Sugano M (2007) Genetically modified rapeseed oil containing *cis*-9,*trans*-11,*cis*-13-octadecatrienoic acid affects body fat mass and lipid metabolism in mice. J Agric Food Chem 55(9):3741–3748
15. Hontecillas R, O'Shea M, Einerhand A, Diguardo M, Bassaganya-Riera J (2009) Activation of PPAR gamma and alpha by punicic acid ameliorates glucose tolerance and suppresses obesity-related inflammation. J Am Coll Nutr 28(2):184–195
16. Chardigny J, Hasselwander O, Genty M, Kraemer K, Ptock A, Sébédio J (2003) Effect of conjugated FA on feed intake, body composition, and liver FA in mice. Lipids 38(9):895–902
17. Miranda J, Fernández-Quintela A, Macarulla M, Churruca I, García C, Rodríguez V, Simón E, Portillo M (2009) A comparison between CLNA and CLA effects on body fat, serum parameters and liver composition. J Physiol Biochem 65(1):25–32
18. Bassaganya-Riera J, Guri AJ, Hontecillas R (2011) Treatment of obesity-related complications with novel classes of naturally occurring PPAR agonists. J Obes 2011:897894. doi:10.1155/2011/897894
19. Miranda J, Fernández-Quintela A, Churruca I, Ayo J, García-Marzo C, Dentin R, Portillo M (2011) The presence of the *trans*-10, *cis*-12 sequence does not have a body fat-lowering effect on jacaric acid, a conjugated linolenic acid isomer. Food Chem. doi:10.1016/j.foodchem.2011.01.037
20. Gervais R, Chouinard PY (2008) Effects of intravenous infusion of conjugated diene 18:3 isomers on milk fat synthesis in lactating dairy cows. J Dairy Sci 91(9):3568–3578
21. Galvez J, Paul A, Sandi B (2008) Conjugated linolenic acids and methods of preparation and purification and uses thereof. US Patent, Application 10/567, 419. Universite Laval, Quebec (Ca)
22. Destaillats F, Trottier J, Galvez J, Angers P (2005) Analysis of alpha-linolenic acid biohydrogenation intermediates in milk fat with emphasis on conjugated linolenic acids. J Dairy Sci 88(9):3231–3239
23. Destaillats F, Berdeaux O, Sébédio J, Juaneda P, Grégoire S, Chardigny J, Bretillon L, Angers P (2005) Metabolites of conjugated isomers of alpha-linolenic acid (CLnA) in the rat. J Agric Food Chem 53(5):1422–1427
24. Dentin R, Liu Y, Koo S, Hedrick S, Vargas T, Heredia J, Yates Jr, Montminy M (2007) Insulin modulates gluconeogenesis by inhibition of the coactivator TORC2. Nature 449(7160):366–369
25. Wabitsch M, Brenner R, Melzner I, Braun M, Möller P, Heinze E, Debatin K, Hauner H (2001) Characterization of a human preadipocyte cell strain with high capacity for adipose differentiation. Int J Obes Relat Metab Disord 25(1):8–15
26. Bradford MM (1976) A rapid and sensitive method for the quantitation of microgram quantities of protein utilizing the principle of protein-dye binding. Anal Biochem 72:248–254
27. Born Field FJ, Mathur SN E (2003) Fatty acid flux suppress fatty acid synthesis in hamster intestine independently of SREBP-1 expression. J Lipid Res 44(6):1199–1208
28. Livak K, Schmittgen T (2001) Analysis of relative gene expression data using real-time quantitative PCR and the 2(-Delta Delta C(T)) Method. Methods 25(4):402–408
29. Latruffe N, Vamecq J (1997) Peroxisome proliferators and peroxisome proliferator activated receptors (PPARs) as regulators of lipid metabolism. Biochimie 79(2–3):81–94
30. Kersten S (2002) Peroxisome proliferator activated receptors and obesity. Eur J Pharmacol 440(2–3):223–234

31. Ferré P (2004) The biology of peroxisome proliferator-activated receptors: relationship with lipid metabolism and insulin sensitivity. Diabetes 53(Suppl 1):S43–S50
32. Gurnell M (2005) Peroxisome proliferator-activated receptor gamma and the regulation of adipocyte function: lessons from human genetic studies. Best Pract Res Clin Endocrinol Metab 19(4):501–523
33. Hammarstedt A, Andersson CX, Rotter Sopasakis V, Smith U (2005) The effect of PPARgamma ligands on the adipose tissue in insulin resistance. Prostaglandins Leukot Essent Fatty Acids 73(1):65–75
34. Moya-Camarena S, Vanden Heuvel J, Blanchard S, Leesnitzer L, Belury M (1999) Conjugated linoleic acid is a potent naturally occurring ligand and activator of PPARalpha. J Lipid Res 40(8):1426–1433
35. Moya-Camarena S, Van den Heuvel J, Belury M (1999) Conjugated linoleic acid activates peroxisome proliferator-activated receptor alpha and beta subtypes but does not induce hepatic peroxisome proliferation in Sprague-Dawley rats. Biochim Biophys Acta 1436(3):331–342
36. Houseknecht K, Vanden Heuvel J, Moya-Camarena S, Portocarrero C, Peck L, Nickel K, Belury M (1998) Dietary conjugated linoleic acid normalizes impaired glucose tolerance in the Zucker diabetic fatty fa/fa rat. Biochem Biophys Res Commun 244(3):678–682
37. Belury M (2002) Dietary conjugated linoleic acid in health: physiological effects and mechanisms of action. Annu Rev Nutr 22:505–531
38. Leone TC, Weinheimer CJ, Kelly DP (1999) A critical role for the peroxisome proliferator-activated receptor alpha (PPARalpha) in the cellular fasting response: the PPARalpha-null mouse as a model of fatty acid oxidation disorders. Proc Natl Acad Sci USA 96(13):7473–7478
39. Khan SA, Vanden Heuvel JP (2003) Role of nuclear receptors in the regulation of gene expression by dietary fatty acids (review). J Nutr Biochem 14(10):554–567
40. Guerre-Millo M, Gervois P, Raspé E, Madsen L, Poulain P, Derudas B, Herbert JM, Winegar DA, Willson TM, Fruchart JC, Berge RK, Staels B (2000) Peroxisome proliferator-activated receptor alpha activators improve insulin sensitivity and reduce adiposity. J Biol Chem 275(22):16638–16642
41. Kamisoyama H, Honda K, Tominaga Y, Yokota S, Hasegawa S (2008) Investigation of the anti-obesity action of licorice flavonoid oil in diet-induced obese rats. Biosci Biotechnol Biochem 72(12):3225–3231
42. Honda K, Kamisoyama H, Tominaga Y, Yokota S, Hasegawa S (2009) The molecular mechanism underlying the reduction in abdominal fat accumulation by licorice flavonoid oil in high fat diet-induced obese rats. Anim Sci J 80(5):562–569
43. Motawi TM, Hashem RM, Rashed LA, El-Razek SM (2009) Comparative study between the effect of the peroxisome proliferator activated receptor-alpha ligands fenofibrate and n-3 polyunsaturated fatty acids on activation of 5′-AMP-activated protein kinase-alpha1 in high-fat fed rats. J Pharm Pharmacol 61(10): 1339–1346
44. Wensaas AJ, Rustan AC, Rokling-Andersen MH, Caesar R, Jensen J, Kaalhus O, Graff BA, Gudbrandsen OA, Berge RK, Drevon CA (2009) Dietary supplementation of tetradecylthioacetic acid increases feed intake but reduces body weight gain and adipose depot sizes in rats fed on high-fat diets. Diabetes Obes Metab 11(11):1034–1049
45. Cho KW, Kim YO, Andrade JE, Burgess JR, Kim YC (2011) Dietary naringenin increases hepatic peroxisome proliferators-activated receptor α protein expression and decreases plasma triglyceride and adiposity in rats. Eur J Nutr 50(2):81–88

Lipids (2011) 46:1013–1020
DOI 10.1007/s11745-011-3593-6

ORIGINAL ARTICLE

Effect of Synthetic Ligands of PPAR α, β/δ, γ, RAR, RXR and LXR on the Fatty Acid Composition of Phospholipids in Mice

Kathrin Weiss · Johanna Mihály · Gerhard Liebisch · Tamás Marosvölgyi · Gerd Schmitz · Tamás Decsi · Ralph Rühl

Received: 2 January 2011 / Accepted: 1 June 2011 / Published online: 27 July 2011

Abstract Nuclear hormone receptors are transcription factors that can be activated by nutrition-derived ligands and alter the expression of various specific target genes. Stearoyl-Coenzyme A desaturase (SCD1) converts palmitic acid (16:0) to palmitoleic acid (16:1n-7) as well as stearic acid (18:0) to oleic acid (18:1n-9). At the same time, elongase 6 (ELOVL6) elongates 16:1n-7 and 18:1n-9 to vaccenic acid (18:1n-7) and eicosenoic acid (20:1n-9). We examined how synthetic selective ligands of nuclear hormone receptors alter the gene expression of hepatic enzymes in mice. In addition, we examined how the regulation of these two enzymes influences fatty acid composition of phospholipids in liver and plasma. Mice were gavaged daily for 1 week with synthetic ligands of peroxisome proliferator-activated receptor (PPAR) α, β/δ, γ, liver X receptor (LXR), retinoic acid receptor (RAR) and retinoid-X receptor (RXR) for 1 week. Phospholipids from liver and plasma were analysed using ESI-MS/MS and GC after saponification. Hepatic gene expression of SCD1 and ELOVL6 was measured using QRT-PCR. SCD1 and ELOVL6 expression increased after the gavage of LXR and RXR ligands. The analysis of fatty acid composition of total phospholipids in plasma and liver showed increased percentage contributions of the SCD1 and ELOVL6 products 18:1n-9, 18:1n-7 and 20:1n-9 after LXR and RXR ligand application. Analysis of total phospholipids from plasma and liver revealed a significant increase in monounsaturated fatty acids bound in phosphatidylcholine (PtdCho) and lysophosphatidylcholine (PtdEtn) after LXR and RXR ligand administration. Increased hepatic gene expression of SCD1 and ELOVL6 after gavage of selective RXR or LXR ligands to mice resulted in increased concentrations of their metabolic products in phospholipids of liver and plasma.

Keywords Nuclear receptor · Monounsaturated fatty acids · Polyunsaturated fatty acid · Phospholipids · SCD1 · ELOVL6

Abbreviations

PPAR	Peroxisome proliferator-activated receptor
LXR	Liver X receptor
RXR	Retinoid X receptor
RAR	Retinoic acid receptor
MUFA	Monounsaturated fatty acid(s)
PUFA	Polyunsaturated fatty acid(s)
SFA	Saturated fatty acid(s)
SCD1	Steroyl-coenzyme A desaturase
ELOVL6	Elongase 6

Introduction

Nuclear hormone receptors which can be activated by nutritional derived ligands are transcription factors that

K. Weiss · J. Mihály · R. Rühl (✉)
Laboratory of Nutritional Bioactivation and Bioanalysis, Department of Biochemistry and Molecular Biology, University of Debrecen, Medical and Health Center, Nagyerdei Krt. 98, 4032 Debrecen, Hungary
e-mail: rruehl@dote.hu

G. Liebisch · G. Schmitz
Institute of Clinical Chemistry and Laboratory Medicine, University of Regensburg, Regensburg, Germany

T. Marosvölgyi · T. Decsi
Department of Paediatrics, University of Pécs, Pécs, Hungary

R. Rühl
Apoptosis and Genomics Research Group of the Hungarian Academy of Sciences, Debrecen, Hungary

modulate the expression of various specific target genes at the transcriptional level. Peroxisome proliferator-activated receptor α (PPARα) is mainly expressed in the liver, skeletal and heart muscle as well as in blood vessels and the pancreas. PPARα plays an important role in fatty acid uptake, liver steatosis, cardiac lipid accumulation, and is critical for the development of atherosclerosis [1, 2]. PPARβ/δ is ubiquitously expressed, and is involved in HDL-cholesterol metabolism in obese and non-obese mice [2]. PPARγ is mainly expressed in adipose tissue, in macrophages and in low levels in the liver. It is primarily involved in fatty acid uptake and inflammation control [3, 4]. Apart from the synthetic ligands used in our study for each PPAR isoform, mainly monounsaturated fatty acids (MUFA) and polyunsaturated fatty acids (PUFA) were also reported to be natural activators [5].

Liver X receptor (LXR) is highly expressed in the liver, and to a lesser extent in the adipose tissue and in macrophages. LXR is a key modulator of lipid metabolism, inflammatory signalling and regulation of cholesterol efflux in macrophages. Cholesterol and its metabolites are natural ligands that can activate LXR [6]. Retinoid-X receptor (RXR) and retinoic acid receptor (RAR) are activated by vitamin A derivates like all-*trans*-retinoic acid (ATRA) and its *cis*-isomer the 9-*cis*-retinoic acid (9CRA). This activation can also take place by specific synthetic ligands. Furthermore RXR forms heterodimers with various nuclear receptors including the LXR, RAR and PPARs [3, 7], which is crucial to induce a signal transduction. Alternatively besides natural ligands also synthetic, high specific ligands for LXR, RXR, RAR and PPARs have been developed.

SCD1 is an enzyme mainly expressed in adipogenic tissues including hepatic and adipose tissue [8, 9]. SCD1 desaturates 16:0 and 18:0 to 16:1n-7 and 18:1n-9, respectively. The regulation of SCD1 and its consequences on metabolic disease has been studied in several models. The depletion of SCD1 in SCD1-knock-out mouse models reduces triglyceride synthesis in the liver [10] and further protects against induced hepatic steatosis and adiposity [11]. Elongases extend fatty acids by two additional carbon atoms. The enzyme ELOVL6 extends 16:0, 16:1n-7 and 18:1n-9 to 18:0, 18:1n-7 and 20:1n-9, respectively [12, 13]. It is mainly expressed in brown and white adipose tissue, hepatic tissue and brain [12, 14]. The gene expression of both enzymes is suggested to be regulated by the SREBP1, a transcription factor inducible by the activated nuclear hormone receptors LXR and RXR but not by other hormone receptors like PPARα and PPARγ [15–17].

This study investigated how the nuclear hormone receptors RAR, RXR, PPARs and LXR alter the gene expression of the enzymes SCD1 and ELOVL6 by the application of their specific selective ligands. Due to this alteration of the gene expression the impact on the composition of various phospholipids and the contents of the metabolic products of SCD1 and ELOVL6 had been studied in plasma and liver of mice. The activation of the nuclear hormone receptors RAR, RXR, PPARs and LXR can also occur by various semi-stable and multi-potent endogenous/nutritional-relevant ligands. An induction of these receptors regulates various nutritional relevant pathways like in the present study - the metabolism of monounsaturated and saturated fatty acids. We postulate that an alteration of gene expression of SCD1 and ELOVL6 caused by the application of different nuclear hormone receptor ligands influences the content of MUFAs/saturated fatty acids (SFAs) and therefore indirectly effects the fatty acid composition of phospholipids and membranes.

Materials and Methods

Experimental Design

Animal experiments were performed at the Laboratory Animal Core Facility at the University of Debrecen in Hungary in accordance with Hungarian ethical guidelines. Six to eight week old female C57BL6 mice, purchased from Charles River (Budapest, H), were fed for 2 weeks with chow (VRF1, Altromin, D). After the acclimatization period, animals were gavaged daily for one week with specific synthetic ligands dissolved in 25% Cremophor EL (Sigma-Aldrich, Budapest, H)/water (v/v) (Table 1). The vehicle (cremophor EL) was applied at 5 ml/kg body weight (b.w.). Rosiglitazone a PPARγ ligand was bought at Biomol (Butler Pike, USA) [18] and LG268 an RXR ligand [19] was a gift from Ligand Pharmaceuticals (San Diego, CA, USA). AM580 (RAR ligand) [20], GW7647 (PPARα ligand) [21] and GW0742 (PPARβ/δ ligand) [22] were purchased from Biotrend Chem. GmbH (Cologne, D) and T0901317 (LXR ligand) [23] from the Cayman Chemical Company (Tallinn, EST).

Table 1 Amount of ligands applied to mice by oral gavage

Receptor	Specific ligand	Daily dose
Vehicle	Cremophor/EL	5 ml/kg b.w.
PPARα	GW7647	3 mg/kg b.w.
PPARβ/δ	GW0742	5 mg/kg b.w.
PPARγ	Rosiglitazone	3 mg/kg b.w.
LXR	T0901317	20 mg/kg b.w.
RAR	AM580	10 mg/kg b.w.
RXR	LG268	30 mg/kg b.w.

Ligands: GW7647, GW0742, Rosiglitazone, T0901317, AM580 and LG268 were dissolved in 25% Cremophor/water (v/v) and gavaged once a day

Animal Study

Mice had free access to water and food over the duration of the experiment. They were kept at 22 °C room temperature with a 12 h day/night cycle. All animals were killed by anaesthesia with halothane. Blood collection was carried out by cardiac puncture. The blood was centrifuged for 10 min and plasma was stored at −80 °C. The mice were dissected, and liver samples were weighed and immediately frozen in liquid nitrogen and later stored at −80 °C.

Analysis of Composition of Fatty Acid in Total Phospholipids in Plasma by Gas Chromatography (GC)

For the analysis of plasma fatty acids, frozen plasma samples were thawed and the dipentadecanoylphosphatidylcholine (Phosphatidylcholine Dipentadecanoyl, Sigma-Aldrich, Budapest, Hungary) internal standard was added. Lipids were extracted by the addition of 3 ml chloroform and 1 ml methanol according to the method of [24]. The mixture was vortexed at 3,000 rpm for 15 min. The lower layer was then aspirated into vials and evaporated under an N2 stream. Lipid extracts were reconstituted in 70 µl chloroform and lipid classes were separated by thin layer chromatography (TLC). The solvent-mix for TLC of plasma lipids was as follows: hexane:diethyl ether:chloroform:acetic acid (21:6:3:1, v/v). The bands were stained with dichlorofluorescein, removed by scraping and transesterified in 1 ml of 3 N-HCl-methanol solution (Methanolic HCl, 3 N, Supelco, Budapest, Hungary) at 84 °C for 45 min [25]. Fatty acids were analysed by high-resolution capillary GC using a Finnigan 9001 gas chromatograph (Finnigan/Tremetrics Inc., Austin, TX, USA) with split injection (ratio 1:25), automatic sampler (A200SE; CTC Analytic, Zwingen, CH, USA) and flame ionisation detector with a DB-23 cyanopropyl column of 40 m length (J & W Scientific, Folsom, CA, USA). The temperature program was set to the following parameters: temperature of injector at 80 °C/min up to 280 °C, temperature of detector at 280 °C, temperature of column area at 60 °C for 0.2 min, temperature increase by 40 °C/min up to 180 °C, 5 min isothermal period, temperature increase by 1.5 °C/min up to 200 °C, 8.5 min isothermal period, temperature increase by 40 °C/min up to 240 °C and 13 min isothermal period. The constant linear velocity was 0.3 m/s (referred to 100 °C). Peak identification was confirmed by comparison with authentic mixtures of weighed fatty acid (FA) methyl esters (GLC-463: Nu-Chek Prep, Elysian, MN, USA; and Supelco 37 FAME Mix: Supelco, Bellefonte, PA, USA). Individual FA response factors determined from these weighed standards were used to calculate the percentage by weight for individual FA between 12 and 24 carbon atoms from the percentage of area under the curve.

RNA Isolation from Liver and QRT-PCR

Total RNA was isolated from liver and quantified by QRT-PCR (quantitative real time-PCR). In brief, samples of liver tissue (50 mg) were homogenized in Trizol (10 mg tissue/100 µl Trizol, Sigma-Aldrich, Budapest, Hungary) and extracted with chloroform (20 µl/100 µl Trizol). The aqueous phase was mixed with 700 µl of ethanol (70% v/v) and loaded on the RNA isolation column (GenElute Mammalian Total RNA Miniprep Kit, Sigma-Aldrich, Budapest, Hungary). RNA was isolated from tissues according to the given protocol of Sigma-Aldrich and eluted in nuclease free water. Concentration and purity were measured by Nanodrop (Thermo, Budapest, Hungary), while the RNA quality was examined by agarose-gel-electrophoresis (1%, Sigma-Aldrich, Hungary). cDNA was obtained by reverse transcription (10 min 25 °C, 120 min 42 °C, 5 min 72 °C) and amplified via QRT-PCR (40 cycles: 12 s 94 °C, 45 s 60 °C, 60 s 94 °C). Primer and probe for expression analysis (Taq-Man-Gene Expression Assay) as well as quantitative real-time PCR detection system (ABI-PRISM, 7900HT Sequence Detection System) were purchased from Applied Biosystems (Budapest, Hungary). The expression of genes was normalized to cyclophilin A (house-keeping gene): primer 77"+" 5′-CG ATGACGAGCCCTTGG-3′, primer 142 "−" 5′-TCTGCT GTCTTTGGAACTTTGTC-3′, probe (69+, 96+): FAM-CGCGTCTCCTTCGAGCTGTTTGCA. The amplification signal was detected and analysed by the SDS2.1 program from Applied Biosystems, Budapest, Hungary. The expression of SCD1, ELOVL6 and cyclophilin A was determined in the liver.

Analysis of Lipid Species in Plasma and Liver by ESI-MS/MS

Liver homogenate and plasma were extracted according to the procedure described by Bligh and Dyer et al. [26] in the presence of non-naturally occurring lipid species as internal standards. Lipids were quantified by electrospray ionization tandem mass spectrometry (ESI-MS/MS) in positive ion mode as described previously by Brugger et al. and Liebisch et al. [27–29]. Samples were quantified by direct flow injection analysis using the analytical setup described by Liebisch et al. [28, 29]. A precursor ion scan of *m/z* 184 specific for phosphocholine containing lipids was used for phosphatidylcholine (PtdCho), sphingomyelin (CerPCho) [28] and lysophosphatidylcholine (LysoPtdCho) [30]. Neutral loss scans of 141 and 185 were used for phosphatidylethanolamine (PtdEtn) and phosphatidylserine

(PtdSer), respectively [27]. Ceramide was analyzed similarly to a previously described methodology [31] using *N*-heptadecanoyl-sphingosine as the internal standard. Quantification was achieved by standard addition calibration to liver homogenates or plasma using a number of naturally occurring lipid species for each lipid class. The following non-naturally occurring lipid species were used as internal standards: PtdCho 28:0, 44:0, LysoPtdCho 13:0, 19:0, PtdEtn 28:0, 40:0, PtdSer 28:0, 40:0. Quantification was performed by standard addition calibration to plasma and liver homogenates using several naturally occurring lipid species for each lipid class (PtdCho 34:1, 36:2, 38:4, 40:0; Sphingomyelin 16:0, 18:1, 18:0; LysoPtdCho 16:0, 18:1, 18:0; PtdEtn 34:1, 36:2, 38:4, 40:6 and PtdEtnp16:0/20:4; PtdSer 34:1, 36:2, 38:4, 40:6). All standards were purchased from Avanti Polar Lipids (Alabaster, AL, USA). Isotopic overlap corrections of lipid species as well as data analysis by self programmed Excel Macros were performed for all lipid classes according to the principles described previously [28].

Statistical Analysis

Results were displayed as mean with standard error and statistically analysed by ANOVA followed by the Bonferroni post hoc test using the program SPSS (15.0) (SPSS Inc., Chicago, USA). Statistically significant differences were displayed at a value of $P < 0.05$.

Results

Analysis of Fatty Acids Composition in Plasma Phospholipids

Plasma phospholipids fatty acids for substrates, products and product/substrate ratios of SCD1 and ELOVL6 enzymes in the treatment groups are compared to the vehicle group in Table 2. Palmitic acid (16:0) decreased significantly in treatment groups of LXR, RAR and RXR, whereas significantly increased in the PPARα group. Stearic acid (18:0) percentages decreased significantly in the RXR group and increased significantly in the RAR group. Percentages of palmitoleic acid (16:1n-7) did not differ, whereas vaccenic acid (18:1n-7), oleic acid (18:1n-9) and eicosenoic acid (20:1n-9) percentages increased significantly in the LXR and RXR groups. The product/substrate ratios exhibited significant increases following treatment (with the exception of the 20:1n-9/18:1n-9 ratio). Specifically, a significant increase of the 16:1n-7/16:0 ratio has been observed in the LXR group, of the 18:1n-9/18:0 ratio in the PPARα, LXR and RXR groups and of the 18:1n-7/16:1n-7 ratio in PPARγ and RXR groups.

Table 2 Analysis of fatty acid composition of phospholipids in plasma of mice

	Vehicle Mean ± SD	PPAR α Mean ± SD	PPAR δ/β Mean ± SD	PPAR γ Mean ± SD	LXR Mean ± SD	RAR Mean ± SD	RXR Mean ± SD
16:0	27.129 ± 0.722	31.030 ± 0.503*	28.233 ± 0.238	26.637 ± 0.463	20.793 ± 0.424*	23.278 ± 0.247*	24.394 ± 0.126*
16:1n-7	0.430 ± 0.051	0.505 ± 0.026	0.419 ± 0.048	0.381 ± 0.032	0.647 ± 0.120	0.206 ± 0.018	0.627 ± 0.049
18:0	22.376 ± 0.591	16.728 ± 0.395	20.603 ± 0.836	21.856 ± 0.458	20.638 ± 0.590	24.762 ± 0.330*	18.644 ± 0.972*
18:1n-7	1.509 ± 0.136	1.751 ± 0.131	1.829 ± 0.168	1.697 ± 0.141	4.576 ± 0.374*	1.231 ± 0.059	5.112 ± 0.239*
18:1n-9	5.209 ± 0.207	6.221 ± 0.120	6.173 ± 0.301	4.847 ± 0.072	8.356 ± 0.281*	4.812 ± 0.208	9.515 ± 0.295*
20:1n-9	0.209 ± 0.023	0.158 ± 0.010	0.206 ± 0.010	0.158 ± 0.028	0.351 ± 0.021*	0.205 ± 0.016	0.371 ± 0.020*
18:0/16:0	0.830 ± 0.043	0.539 ± 0.012*	0.730 ± 0.029	0.821 ± 0.013	1.065 ± 0.022*	0.993 ± 0.021*	0.765 ± 0.041
18:1n-9/18:0	0.234 ± 0.014	0.373 ± 0.013*	0.305 ± 0.025	0.222 ± 0.005	0.409 ± 0.027*	0.195 ± 0.011	0.518 ± 0.034*
16:1n-7/16:0	0.016 ± 0.002	0.016 ± 0.001	0.015 ± 0.002	0.014 ± 0.001	0.032 ± 0.007*	0.009 ± 0.001	0.026 ± 0.002
18:1n-7/16:1n-7	3.607 ± 0.285	3.460 ± 0.148	4.471 ± 0.213	4.500 ± 0.261	7.894 ± 1.098*	6.168 ± 0.519	8.377 ± 0.685*
20:1n-9/18:1n-9	0.041 ± 0.005	0.025 ± 0.002	0.034 ± 0.002	0.032 ± 0.005	0.042 ± 0.002	0.043 ± 0.004	0.039 ± 0.001

Substrates, products and product/substrate ratios for steroyl-coenzyme A desaturase and elongase 6 enzymes in plasma phospholipids in mice ($n = 6$). Data are given as means ± standard error of percentage of total fatty acid and statistically compared to vehicle, *$P < 0.05$

Hepatic Gene Expression of SCD1 and ELOVL6

Hepatic SCD1 and ELOVL6 expression significantly increased in animals gavaged with LXR and RXR ligands, while treatment with PPARα, PPARβ/δ and PPARγ ligand did not show any significant alteration. Application of an RAR ligand leads to a slight, non-significant suppression of hepatic SCD1 expression, while the expression of ELOVL6 was not effected (Fig. 1).

Analysis of Composition of Fatty Acids of PtdEtn, PtdCho and LysoPtdCho by ESI-MS/MS

Saturated and monounsaturated fatty acids of selected phospholipid classes phosphatidylcholine (PtdCho), phosphatidylethanolamine (PtdEtn) and lysophosphatidylcholine (LysoPtdCho) were determined in plasma and liver by ESI-MS/MS and displayed in mean of % of specific lipid class related to total lipid class (Fig. 2). The composition of phosphatidylethanolamine (PtdEtn) species containing one monounsaturated fatty acid (36:1 and 34:1) was mainly influenced by the application of RXR and LXR ligand leading to an increase of bound monounsaturated fatty acids in liver tissue and plasma (Fig. 2). The oral gavage of the RAR ligand, by contrast, decreased monounsaturated fatty acids (displayed by: 32:1, 34:1) in liver and plasma. As with PtdEtn, an increase of monounsaturated fatty acids (displayed by: 32:1, 34:1 and 36:1) in PtdCho was determined in the liver and plasma after the application of RXR and LXR agonists, while the activation of RAR, PPARα and PPARγ lead to a decrease of phosphatidylcholine (PtdCho) 36:1 in the liver and plasma. Furthermore, RAR activation reduced the content of PtdCho 32:1, 34:1 and 36:1 in liver and plasma. The activation of RXR and LXR by their synthetic ligands altered the composition of lysophosphatidylcholine (LysoPtdCho) in liver and plasma in which monounsaturated fatty acids (16:1 and 18:1) were increased. 16:1 in plasma and 18:1 in liver were additionally increased by application of ligands for RXR and PPARα, respectively. A reduction of 18:1 in liver tissue and 16:1 in plasma and liver was determined after the gavage of the RAR agonist. Additionally, the composition of ceramides and sphingomyelins were investigated and remained unchanged in 16:0, 18:0, 16:1 and 18:1 species. In summary, activation of RXR and LXR by their specific ligands was found to lead to an increase of bound MUFAs.

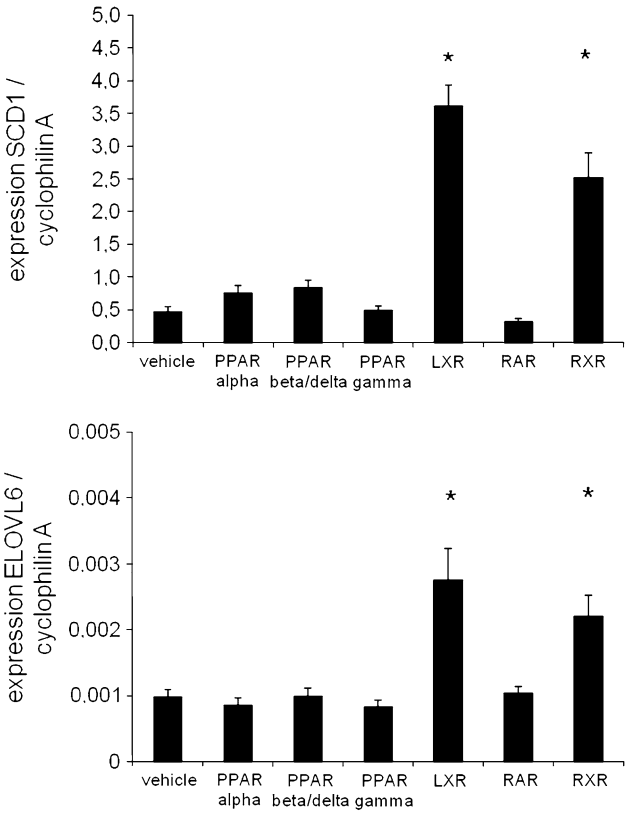

Fig. 1 Expression of SCD1 and ELOVL6 in liver of mice, $n = 6$, measured by QRT-PCR. Expression of SCD1 and ELOVL6 were normalized to cyclophilin A, mean ± standard error of gene expression were displayed and statistically analysed compared to the vehicle, $P < 0.05$(*)

Discussion

In this study, we investigated the influence of nuclear hormone receptor ligand treatment on hepatic SCD1 and ELOVL6 gene expression and the composition of SFA/MUFA bound to phospholipids in liver and plasma. We gavaged specific synthetic ligands of nuclear hormone receptors in concentrations that are able to activate these receptors regarding to previous published studies [18–23]. Our results revealed that the hepatic gene expression of SCD1 and ELOVL6 was significantly increased by LXR and RXR ligand treatment, while RAR and PPARα, β/δ and γ ligands did not significantly alter SCD1 and ELOVL6 gene expression. In addition, metabolic products of SCD1 and ELOVL6 such as 18:1n-7, 18:1n-9 and 20:1n-9 as well as product / substrate ratios 18:1n-9 / 18:0 and 18:1n-7 / 16:1n-7 was significantly increased by RXR and LXR ligand treatments, but not by PPARα, PPARβ/δ or PPARγ ligand treatment.

The nutritional impact of this study is how these nutrient-activated nuclear hormone receptors RXR, RAR, PPARs and LXR are regulating fatty acid metabolism and thereby membrane composition. The connection of food intake and nuclear hormone activations is not very deeply investigated [32, 33], so instead of semi-stable and multipotent natural ligands we used the synthetic ligands specific for these nuclear hormone receptors.

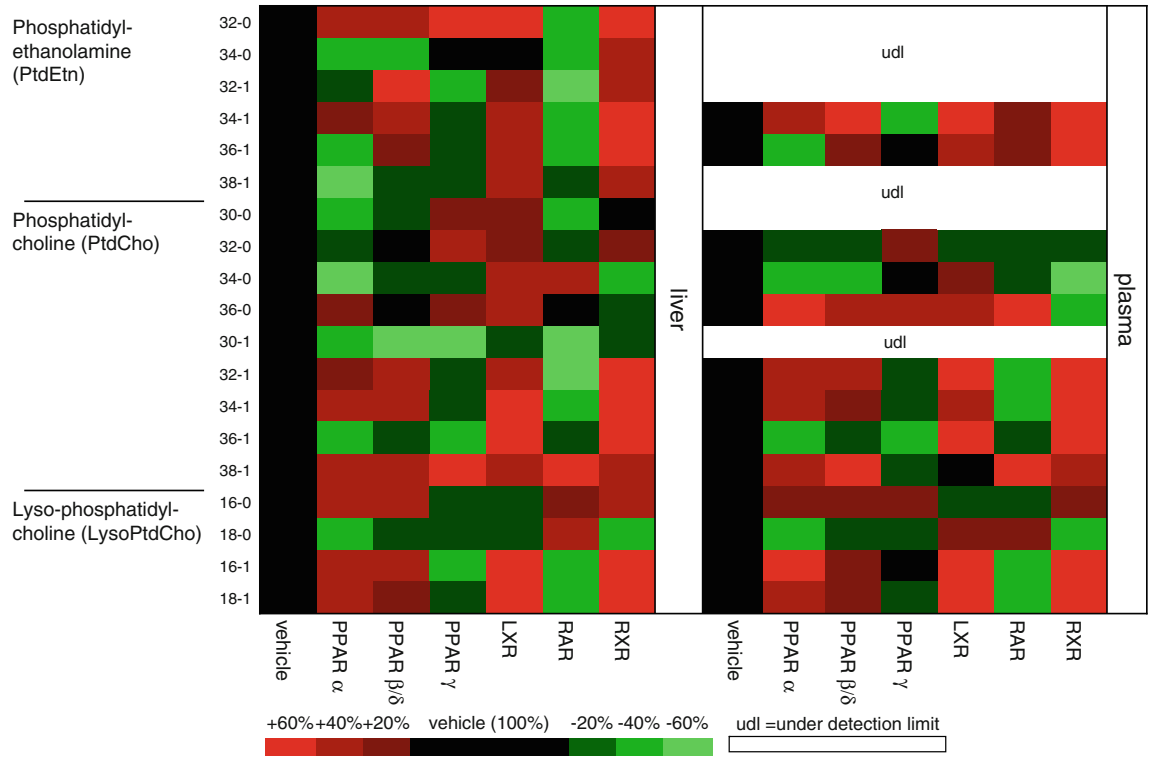

Fig. 2 Analysis of the fatty acids in PtdEtn (phosphatidylethanolamine), PtdCho (phosphatidylcholine) and LysoPtdCho (lysophosphatidylcholine) in liver and plasma of mice, $n = 6$. Percentage of total lipid class and fold change from the vehicle (=100%). *udl* under detection limit

Hepatic SCD1 expression has been extensively investigated and known to be an LXR target gene [10]. Our studies corroborate previous results in mice, namely, that the application of LXR and RXR ligands induces hepatic SCD1 expression. In these same studies, the gavage of PPARα ligands also resulted in an increased SCD1 gene expression, thereby increasing the plasma and hepatic ratios of 16:1n-7/16:0 and 18:1n-9/18:0 [34–37]. Both SCD1 and ELOVL6 are target genes of sterol regulatory element-binding protein 1 (SREBP1). It is a transcription factor inducible by the activation of LXR in hepatic tissue, adipose tissue and intestine [15, 16] and by a synthetic RXR ligand, but not by PPARα or PPARγ ligands [17]. An activation of this transcription factor pathways results in an induction of SCD1 and ELOVL6 [38]. As expected the PPARγ ligand rosiglitazone did not alter hepatic expression of ELOVL6 or SCD1 or phospholipid composition [37–39].

The role of vitamin A in the regulation of SCD1 expression remains controversial. Bioactive vitamin A metabolites like all-*trans*-retinoic acid and *9-cis*-retinoic acid are natural ligands for the activation of RAR, RXR as well as PPARβ/δ mediated pathways [40]. RXR induces SCD1 gene expression, while RAR displayed tendencies to reduce it. The previously reported induction of gene expression of SCD1 by vitamin A has not been specified regarding the responsible nuclear hormone receptor RXR and RAR. RXR can form heterodimers with several nuclear hormone receptors like LXR, which are activated by metabolites of cholesterol and specific synthetic ligands like T091317 [41]. This LXR-RXR heterodimer can also be activated by the synthetic RXR ligand LG268, the potential natural ligand of RXR 9-*cis*-retinoic acid or the selective ligands for LXR and result in an induced expression of LXR specific target genes [42, 43]. In summary, in our study, the activation of LXR by a synthetic LXR-ligand as well as by a synthetic RXR-ligand maybe responsible for the strong induction of the hepatic expression of SCD1 and we postulate that the RXR ligands induced effects are mediated via LXR–RXR pathways. This activation can be inhibited if other nuclear hormone receptors are activated by their ligands. PPARα and LXR are competitors to bind to RXR. This competition leads to a suppression of the SREBP-1c pathway (LXR activated) by the increased formation of PPARα/RXR and decreased availability of LXR/RXR [44].

Following LXR and RXR ligand application 18:1n-7 and 20:1n-9, metabolic products of ELOVL6, as well as product/substrate ratios of 18:1n-7/16:1n-7 but not 20:1n-9/18:1n-9 was significantly increased in plasma phospholipids. In contrast the ratio of 16:1/18:1 in liver of ELOVL6 knock-out mice increased, by reduced conversion of 16:1 to 18:1 compared to wild-type mice [13]. PtdCho, PtdEtn

and LysoPtdCho were analysed separately, and fatty acid composition was determined in order to investigate, which specific phospholipids are influenced by nuclear receptor ligand treatments. PtdEtn and PtdCho contain two esterified fatty acids, while in LysoPtdCho only one fatty acid is contained. In our analysis of the specific phospholipid classes PtdCho and PtdEtn the two bound fatty acids were detected and resulted in an increase of monounsaturated fatty acids incorporated in PtdEtn and PtdCho after the application of LXR and RXR ligands and a tendency to decrease in liver and in plasma by the treatment with an RAR ligand. The increase could be explained by the induction of SCD1 and ELOVL6 in the liver, while the tendency of decrease may be the result of the tendency of suppressed expression of SCD1 by RAR ligand treatment.

In summary, hepatic SCD1 and ELOVL6 expression and product formation was found to be strongly influenced by the activation of LXR–RXR pathways, while RAR and PPARα, PPARγ, and PPARβ/δ pathways exerted minor influence.

Studies directly connecting the activation of nuclear hormone receptors with the formation of phospholipids, reported that the activation of LXR reduced the biosynthesis of PtdEtn by inhibiting the phosphoethanolamine cytidylyltransferase [45]. However, in our study, LXR resulted in an increased total content of PtdCho and PtdEtn in liver and in plasma. Additionally, with the administration of rosiglitazone the synthetic PPARγ ligand is thought to inhibit the formation of PtdCho and PtdEtn in a dose-dependent manner [46]. This could not be confirmed in our studies.

In conclusion, hepatic expression of SCD1 and ELOVL6 was significantly induced by LXR and RXR ligand application, while RAR, PPARα, β/δ and γ ligands did not significantly alter their gene expression. The nutritional relevance of these findings must be examined using various nutritional supplementations [47, 48], which have been shown to activate specific nuclear hormone receptor pathways to elucidate nutritional activation of gene expression pathways. Unfortunately selective activations by nutrients have been reported as difficult [49]. The MUFA incorporated into phospholipids were increased suggesting that the phospholipid MUFA and SFA compositions in plasma and liver are mainly under the control of SCD1 and ELOVL6 pathways.

Acknowledgments This study was conducted with the support of Tamas Röszer and Eva Papp. Ralph Rühl and Johanna Mihály are members of the EU FP7 COST "Mitofood" project. GS and GL were supported by the seventh framework program of the EU-funded "LipidomicNet" (proposal number 202272).

References

1. Lefebvre P, Chinetti G, Fruchart JC, Staels B (2006) Sorting out the roles of PPAR alpha in energy metabolism and vascular homeostasis. J Clin Invest 116:571–580
2. Barish GD, Narkar VA, Evans RM (2006) PPAR delta: a dagger in the heart of the metabolic syndrome. J Clin Invest 116:590–597
3. Desvergne B, Michalik L, Wahli W (2006) Transcriptional regulation of metabolism. Physiol Rev 86:465–514
4. Lehrke M, Lazar MA (2005) The many faces of PPARgamma. Cell 123:993–999
5. Kliewer SA, Sundseth SS, Jones SA, Brown PJ, Wisely GB, Koble CS, Devchand P, Wahli W, Willson TM, Lenhard JM, Lehmann JM (1997) Fatty acids and eicosanoids regulate gene expression through direct interactions with peroxisome proliferator-activated receptors alpha and gamma. Proc Natl Acad Sci USA 94:4318–4323
6. Zelcer N, Tontonoz P (2006) Liver X receptors as integrators of metabolic and inflammatory signaling. J Clin Invest 116:607–614
7. Mangelsdorf DJ, Evans RM (1995) The RXR heterodimers and orphan receptors. Cell 83:841–850
8. Miyazaki M, Gomez FE, Ntambi JM (2002) Lack of stearoyl-CoA desaturase-1 function induces a palmitoyl-CoA Delta6 desaturase and represses the stearoyl-CoA desaturase-3 gene in the preputial glands of the mouse. J Lipid Res 43:2146–2154
9. Man WC, Miyazaki M, Chu K, Ntambi JM (2006) Membrane topology of mouse stearoyl-CoA desaturase 1. J Biol Chem 281:1251–1260
10. Chu K, Miyazaki M, Man WC, Ntambi JM (2006) Stearoyl-coenzyme A desaturase 1 deficiency protects against hypertriglyceridemia and increases plasma high-density lipoprotein cholesterol induced by liver X receptor activation. Mol Cell Biol 26:6786–6798
11. Miyazaki M, Dobrzyn A, Sampath H, Lee SH, Man WC, Chu K, Peters JM, Gonzalez FJ, Ntambi JM (2004) Reduced adiposity and liver steatosis by stearoyl-CoA desaturase deficiency are independent of peroxisome proliferator-activated receptor-alpha. J Biol Chem 279:35017–35024
12. Wang Y, Botolin D, Xu J, Christian B, Mitchell E, Jayaprakasam B, Nair MG, Peters JM, Busik JV, Olson LK, Jump DB (2006) Regulation of hepatic fatty acid elongase and desaturase expression in diabetes and obesity. J Lipid Res 47:2028–2041
13. Matsuzaka T, Shimano H, Yahagi N, Kato T, Atsumi A, Yamamoto T, Inoue N, Ishikawa M, Okada S, Ishigaki N, Iwasaki H, Iwasaki Y, Karasawa T, Kumadaki S, Matsui T, Sekiya M, Ohashi K, Hasty AH, Nakagawa Y, Takahashi A, Suzuki H, Yatoh S, Sone H, Toyoshima H, Osuga J, Yamada N (2007) Crucial role of a long-chain fatty acid elongase, Elovl6, in obesity-induced insulin resistance. Nat Med 13:1193–1202
14. Jakobsson A, Westerberg R, Jacobsson A (2006) Fatty acid elongases in mammals: their regulation and roles in metabolism. Prog Lipid Res 45:237–249
15. Kumadaki S, Matsuzaka T, Kato T, Yahagi N, Yamamoto T, Okada S, Kobayashi K, Takahashi A, Yatoh S, Suzuki H, Yamada N, Shimano H (2008) Mouse Elovl-6 promoter is an SREBP target. Biochem Biophys Res Commun 368:261–266
16. Sekiya M, Yahagi N, Matsuzaka T, Takeuchi Y, Nakagawa Y, Takahashi H, Okazaki H, Iizuka Y, Ohashi K, Gotoda T, Ishibashi S, Nagai R, Yamazaki T, Kadowaki T, Yamada N, Osuga J, Shimano H (2007) SREBP-1-independent regulation of lipogenic gene expression in adipocytes. J Lipid Res 48:1581–1591
17. Repa JJ, Liang G, Ou J, Bashmakov Y, Lobaccaro JM, Shimomura I, Shan B, Brown MS, Goldstein JL, Mangelsdorf DJ (2000) Regulation of mouse sterol regulatory element-binding protein-1c gene (SREBP-1c) by oxysterol receptors, LXRalpha and LXRbeta. Genes Dev 14:2819–2830
18. Muurling M, Mensink RP, Pijl H, Romijn JA, Havekes LM, Voshol PJ (2003) Rosiglitazone improves muscle insulin sensitivity, irrespective of increased triglyceride content, in ob/ob mice. Metabolism 52:1078–1083

19. Zhang Y, Repa JJ, Gauthier K, Mangelsdorf DJ (2001) Regulation of lipoprotein lipase by the oxysterol receptors, LXRalpha and LXRbeta. J Biol Chem 276:43018–43024
20. Elmazar MM, Ruhl R, Reichert U, Shroot B, Nau H (1997) RARalpha-mediated teratogenicity in mice is potentiated by an RXR agonist and reduced by an RAR antagonist: dissection of retinoid receptor-induced pathways. Toxicol Appl Pharmacol 146:21–28
21. Yue TL, Bao W, Jucker BM, Gu JL, Romanic AM, Brown PJ, Cui J, Thudium DT, Boyce R, Burns-Kurtis CL, Mirabile RC, Aravindhan K, Ohlstein EH (2003) Activation of peroxisome proliferator-activated receptor-alpha protects the heart from ischemia/reperfusion injury. Circulation 108:2393–2399
22. Li AC, Binder CJ, Gutierrez A, Brown KK, Plotkin CR, Pattison JW, Valledor AF, Davis RA, Willson TM, Witztum JL, Palinski W, Glass CK (2004) Differential inhibition of macrophage foam-cell formation and atherosclerosis in mice by PPARalpha, beta/delta, and gamma. J Clin Invest 114:1564–1576
23. Jakel H, Nowak M, Moitrot E, Dehondt H, Hum DW, Pennacchio LA, Fruchart-Najib J, Fruchart JC (2004) The liver X receptor ligand T0901317 down-regulates APOA5 gene expression through activation of SREBP-1c. J Biol Chem 279:45462–45469
24. Folch J, Lees M, Sloane Stanley GH (1957) A simple method for the isolation and purification of total lipides from animal tissues. J Biol Chem 226:497–509
25. Decsi T, Szabó E, Burus I, Marosvölgyi T, Kozári A, Erhardt E, Soltész G (2007) Low contribution of n-3 polyunsaturated fatty acids to plasma and erythrocyte membrane lipids in diabetic young adults. Prostaglandins Leukot Essent Fatty Acids 76:159–164
26. Bligh EG, Dyer WJ (1959) A rapid method of total lipid extraction and purification. Can J Biochem Physiol 37:911–917
27. Brugger B, Erben G, Sandhoff R, Wieland FT, Lehmann WD (1997) Quantitative analysis of biological membrane lipids at the low picomole level by nano-electrospray ionization tandem mass spectrometry. Proc Natl Acad Sci USA 94:2339–2344
28. Liebisch G, Lieser B, Rathenberg J, Drobnik W, Schmitz G (2004) High-throughput quantification of phosphatidylcholine and sphingomyelin by electrospray ionization tandem mass spectrometry coupled with isotope correction algorithm. Biochim Biophys Acta 1686:108–117
29. Liebisch G, Binder M, Schifferer R, Langmann T, Schulz B, Schmitz G (2006) High throughput quantification of cholesterol and cholesteryl ester by electrospray ionization tandem mass spectrometry (ESI-MS/MS). Biochim Biophys Acta 1761:121–128
30. Liebisch G, Drobnik W, Lieser B, Schmitz G (2002) High-throughput quantification of lysophosphatidylcholine by electrospray ionization tandem mass spectrometry. Clin Chem 48:2217–2224
31. Liebisch G, Drobnik W, Reil M, Trumbach B, Arnecke R, Olgemoller B, Roscher A, Schmitz G (1999) Quantitative measurement of different ceramide species from crude cellular extracts by electrospray ionization tandem mass spectrometry (ESI-MS/MS). J Lipid Res 40:1539–1546
32. Chawla A, Repa JJ, Evans RM, Mangelsdorf DJ (2001) Nuclear receptors and lipid physiology: opening the X-files. Science 294:1866–1870
33. Muller M, Kersten S (2003) Nutrigenomics: goals and strategies. Nat Rev Genet 4:315–322
34. Joseph SB, Laffitte BA, Patel PH, Watson MA, Matsukuma KE, Walczak R, Collins JL, Osborne TF, Tontonoz P (2002) Direct and indirect mechanisms for regulation of fatty acid synthase gene expression by liver X receptors. J Biol Chem 277:11019–11025
35. Miller CW, Waters KM, Ntambi JM (1997) Regulation of hepatic stearoyl-CoA desaturase gene 1 by vitamin A. Biochem Biophys Res Commun 231:206–210
36. Samuel W, Kutty RK, Nagineni S, Gordon JS, Prouty SM, Chandraratna RA, Wiggert B (2001) Regulation of stearoyl coenzyme A desaturase expression in human retinal pigment epithelial cells by retinoic acid. J Biol Chem 276:28744–28750
37. Singh Ahuja H, Liu S, Crombie DL, Boehm M, Leibowitz MD, Heyman RA, Depre C, Nagy L, Tontonoz P, Davies PJ (2001) Differential effects of rexinoids and thiazolidinediones on metabolic gene expression in diabetic rodents. Mol Pharmacol 59:765–773
38. Miyazaki M, Flowers MT, Sampath H, Chu K, Otzelberger C, Liu X, Ntambi JM (2007) Hepatic stearoyl-CoA desaturase-1 deficiency protects mice from carbohydrate-induced adiposity and hepatic steatosis. Cell Metab 6:484–496
39. Gavrilova O, Haluzik M, Matsusue K, Cutson JJ, Johnson L, Dietz KR, Nicol CJ, Vinson C, Gonzalez FJ, Reitman ML (2003) Liver peroxisome proliferator-activated receptor gamma contributes to hepatic steatosis, triglyceride clearance, and regulation of body fat mass. J Biol Chem 278:34268–34276
40. Michalik L, Wahli W (2007) Guiding ligands to nuclear receptors. Cell 129:649–651
41. Schultz JR, Tu H, Luk A, Repa JJ, Medina JC, Li L, Schwendner S, Wang S, Thoolen M, Mangelsdorf DJ, Lustig KD, Shan B (2000) Role of LXRs in control of lipogenesis. Genes Dev 14:2831–2838
42. Lehmann JM, Kliewer SA, Moore LB, Smith-Oliver TA, Oliver BB, Su JL, Sundseth SS, Winegar DA, Blanchard DE, Spencer TA, Willson TM (1997) Activation of the nuclear receptor LXR by oxysterols defines a new hormone response pathway. J Biol Chem 272:3137–3140
43. Willy PJ, Umesono K, Ong ES, Evans RM, Heyman RA, Mangelsdorf DJ (1995) LXR, a nuclear receptor that defines a distinct retinoid response pathway. Genes Dev 9:1033–1045
44. Yoshikawa T, Ide T, Shimano H, Yahagi N, Amemiya-Kudo M, Matsuzaka T, Yatoh S, Kitamine T, Okazaki H, Tamura Y, Sekiya M, Takahashi A, Hasty AH, Sato R, Sone H, Osuga J, Ishibashi S, Yamada N (2003) Cross-talk between peroxisome proliferator-activated receptor (PPAR) alpha and liver X receptor (LXR) in nutritional regulation of fatty acid metabolism. I. PPARs suppress sterol regulatory element binding protein-1c promoter through inhibition of LXR signaling. Mol Endocrinol 17:1240–1254
45. Zhu L, Bakovic M (2008) Liver X Receptor agonists inhibit the phospholipid regulatory gene CTP: Phosphoethanolamine Cytidylyltransferase-Pcyt2. Res Lett Biochem 2008 ID 801849-5p
46. Pan HJ, Lin Y, Chen YE, Vance DE, Leiter EH (2006) Adverse hepatic and cardiac responses to rosiglitazone in a new mouse model of type 2 diabetes: relation to dysregulated phosphatidylcholine metabolism. Vascul Pharmacol 45:65–71
47. Weiss K, Mihály J, Liebisch G, Marosvölgyi T, Frøland L, Schmitz G, Rühl R (2010) Influence of the source of dietary lipid intake on hepatic expression of SCD1 and ELOVL6 and on lipid composition of blood plasma and liver tissue in mice (Submitted)
48. Krey G, Braissant O, L'Horset F, Kalkhoven E, Perroud M, Parker MG, Wahli W (1997) Fatty acids, eicosanoids, and hypolipidemic agents identified as ligands of peroxisome proliferator-activated receptors by coactivator-dependent receptor ligand assay. Mol Endocrinol 11:779–791
49. Marion-Letellier R, Dechelotte P, Iacucci M, Ghosh S (2009) Dietary modulation of peroxisome proliferator-activated receptor gamma. Gut 58:586–593

alterations in the numbers and function of macrophage and dendritic cells in visceral fat [2–4]. Inflammation in visceral adipose tissue is thought to play a central role, with the degree of inflammation being demonstrated to inversely correlate with insulin sensitivity [5–8]. Conversely, treatment of inflammation has been shown to reverse insulin resistance and improve indices of whole body glucose homeostasis. The mechanisms by which a dysregulated immune axis may contribute to IR is multifactorial but a key pathway is through the release of pro-inflammatory cytokines (TNFα and IL-6), and immunoattractant chemokines that further contribute to an adaptive immune response [9–16]. Mice that lack TNFα and CCR-2, the receptor for monocyte chemoattractant protein 1 (MCP-1/CCL-2), have improved insulin sensitivity and glucose metabolism when compared to adiposity-matched controls [13, 17]. Recent studies show that the Toll-like receptor 4 (TLR4) may play a central role in the link among insulin resistance, inflammation, and obesity; TLR4 deficiency prevented insulin resistance and obesity-mediated activation of IκB kinase (IKKb) and c-Jun NH2-terminal kinase (JNK), suggesting that TLR4 is a key modulator in the cross-talk between inflammatory and metabolic pathways [18–22].

Alpha lipoic acid (αLA) is a disulfide derivative of octanoic acid that forms an intra-molecular disulfide bond that is readily reduced to dihydrolipoic acid intra-cellularly [23]. Anorectic effects in rodents have been reported for αLA as well as improved hypertriglyceridemia in Zucker diabetic fatty rats [24]. αLA has been reported to increase insulin sensitivity in the skeletal muscle via AMPK activation in obese rats [25] though other researchers have failed to confirm this finding [24]. αLA has been shown to reduce NF-κB activation in human monocytic cells and reduce inflammation [26]. However the impact of αLA on innate immune inflammation and whether these effects lead to coordinate change in indices of IR/glucose homeostasis have not been investigated. We employed a novel model of diet-induced obesity/IR using transgenic reporter mice that express YFP under control of a c-fms reporter (c-fms^{YFP+}) that allows monocyte specific expression of the reporter and unparalleled ability to track these cells in visceral adipose tissue. In carefully performed pair-fed experiments, we demonstrate that αLA improves key metrics of innate immune activation and IR.

Materials and Methods

Animals

Oral αLA Regimen

c-fms^{YFP+} transgenic mice were generated at the Transgenic Animal Service of Queensland, Brisbane, Queensland, Australia by injection of the transgenes into pronuclei of (C57BL/6 × CBA)F_1 (BCBF1) fertilized eggs [27]. The Committee on Use and Care of Animals from the Ohio State University (OSU) approved all experimental procedures. c-fms^{YFP+} mice of the FVB/N strain were bred and genotyped at OSU and housed in cages individually. YFP^+ males at 6 weeks of age were fed a HFD for 8 weeks (42% energy from fat—Harlan Teklad TD88137) prior to randomized to three dietary groups (5 mice/group): ad libitum, αLA-fed, and pair-fed to αLA. Pair-feeding was employed as αLA is well known to modulate central appetite pathways and reduce food intake. Food intake was monitored every other day by weighing the remaining chow; pair-fed mice were then offered the same amount of food as consumed by the αLA-mice. αLA (2 mg/ml; Sigma Aldrich T5625) was administered in the drinking water (ultrapure 18.2 MΩ) at a pH of 8.0 with NaOH. Pair-fed mice were given ultrapure water at a pH of 8.0. αLA was administered for 8 weeks before mice were sacrificed. Mice consumed approximately 6 mg of αLA per day over the course of the study, which was a dose of 167 mg/kg at time zero, and 157 mg/kg after 8 weeks due to weight gain.

Determining an appropriate oral αLA dose was challenging as there were no published data on plasma αLA levels in mice after oral administration. Thus, we used a dose previously shown to be effective in mice on disease processes, that did not have adverse side effects, and which was reasonable in regards to what plasma levels might be expected. Yi and Maeda [28] used approximately 200 mg/kg via addition to the chow and showed significant abrogation of atherosclerotic lesion development. Additionally, if one considers 50 mg/kg injections in mice resulted in modest plasma levels of 7.6 ± 1.4 μg/ml [29], the oral dose of ∼160 mg/kg used in this study is expected to result in <7 μg/ml plasma concentrations due to bioavailability limits and gastrointestinal metabolism.

IP αLA Regimen

Males at 6 weeks of age were fed a HFD for 8 weeks, before being randomized to αLA or vehicle control groups. A solution of sterile αLA in saline (4 mg/ml) was injected intraperitoneally at a dose of 10 mg/kg once daily, 6 days a week. Mice were weighed daily to ensure accurate dosing. αLA dosing in the mouse was done with attention to the concentration reasonably obtained in human plasma by use of conventional dietary supplements. Healthy human subjects given an average oral dose of 8.25 mg/kg (600 mg) of R-αLA sodium salt dissolved in water were shown to have a mean maximum plasma concentration (C_{max}) of 16.03 μg/ml [30]. However, others have reported a much lower oral bioavailability, with 600 mg of racemic αLA via solid supplement resulting in a C_{max} of 2.85 [31] and

2.7 μg/ml [32]. These data suggest that potassium or sodium salt of lipoic acid have higher oral bioavailability, as was administered in this study. Additionally, a human oral dose of 1,200 mg resulted in plasma C_{max} levels of 3.8 ± 2.6 to 10.3 ± 3.8 μg/ml with area under the curve (AUC) levels from 443.1 ± 283.9 to 848.8 ± 360.5 which was similar to a subcutaneous injection of 50 mg/kg αLA in mice which yielded 7.6 ± 1.4 μg/ml and 223 ± 20 AUC [29]. The dose of 10 mg/kg (daily) and 50 mg/kg (acute) used in this report are reasonable if not conservative in this context.

Serum Cytokine Analysis

Blood was collected via heart puncture under CO_2 anesthesia and allowed to coagulate at room temperature followed by centrifugation. Serum cytokine levels were analyzed using BD™ Cytometric Bead Array, Mouse inflammation kit according to the manufacturer instructions.

Epididymal Fat Pad Digestion and Quantification of ATMs

Epididymal fat pads from c-fms^{YFP+} mice at the end of the treatment phase were excised, minced, washed in 1× PBS, and digested with sterile collagenase type II from *Clostridium histolyticum* (1 mg/ml) in DMEM (10% FBS) at 37 °C with shaking (140 rpm) as detailed previously [4, 33]. The digesta was filtered through a 100 μm nylon cell strainer before centrifugation (300×*g*, 10 min). The resulting pellet was defined as the stromal vascular fraction (SVF). Viable adipose tissue mononuclear cells were isolated from SVF using Lympholyte M (Cedarlane Laboratories Ltd, Burlington, NC). Approximately 10^6 cells were incubated with mouse FcR blocking reagent (Miltenyi Biotec Inc., Auburn CA) in FACS buffer (1× PBS, 5% FBS) for 10 min at 4 °C followed by staining with F4/80-PE-Cy5, CD11b-PE, and isotype control antibodies (Biolegend, San Diego, CA). Cells were washed in FACS buffer 3 times and measured (BD FACS LSR II™ flow cytometer, Becton–Dickinson, San Jose, CA). Data were analyzed using BD FACS Diva 6.0.1 software (Becton–Dickinson, San Jose, CA). Gates were set using the appropriate isotype controls.

Live Confocal Microscopy of Unfixed Adipose Tissue

Epididymal fat was removed using sterile techniques and carefully cut into ~3–4 mm pieces. After rinsing with 1× PBS the tissue was incubated with *Griffonia simplicifolia* isolectin GS-IB4 conjugated to AlexaFluor 488 (10 μg/ml—Molecular Probes), BODIPY 558/568 (5 μM—Molecular Probes), and Hoechst 33342 (40 μM—Molecular Probes) for 1 h in 1× PBS supplemented with 1 mM $CaCl_2$. Isolectin has been shown to be an endothelial cell specific stain in the adipose [34]. Tissue was visualized on a Zeiss laser scanning microscope 510 under 40× water immersion.

Monocyte-Vascular Adhesion as Assessed by Intravital Microscopy

Mice were given αLA IP (50 mg/kg body weight) 24 h before the start of the experiment. TNFα was injected IP (1 μg/kg; 0.9% saline with 1.0% BSA) 4 h before visualization. Under ketamine/xylazine anesthesia, the testicular cremaster muscle was exposed using a dissecting microscope (2×; Nikon SMZ 645, Japan). The cremaster muscle was bathed with Ringers Lactate at 37 °C and monocyte-endothelial interaction was assessed in 15–25 vessels using a Nikon Eclipse FN1 microscope (Nikon, Japan) with a 40×/0.80 W water immersed objective at a 2.0 mm working distance. In all experiments video images were captured and digitalized to 12-bit TIF images using Metamorph software (version 7.1.2.0, Metamorph, Downingtown, USA). Rolling YFP^+ cells were counted per minute for different vessel diameters and vessel segments. All YFP^+ cells, per 100 μm of vessel length, that were immobile for at least 30 s were interpreted as adherent cells [35]. Calculations to determine the number of rolling and adherent cells according to vessel diameter were performed using Opti Test (Version 1.4.1.0).

Bone Marrow Derived Macrophage Culture and Differentiation

Bone marrow was isolated from WT or TLR4 deficient mice and grown in DMEM media supplemented with 10% FBS in the presence of L-cell conditioned media for 5 days. The differentiated macrophages were pretreated with αLA (100 μg/ml) 45 min before LPS (0.5 μg/ml) addition. Post absorption, αLA is rapidly cleared from circulation via renal excretion and tissue uptake. While much is excreted, tissues especially the liver, heart, skeletal muscle, and possibly the brain, accumulate αLA and extensively catabolize to a dozen or more metabolites depending on species [36, 37]. There is also evidence the αLA is rapidly reduced by cells in vitro to DHLA and subsequently excreted [37]. Thus, determining in vitro doses that might be physiologically relevant was challenging. 100 μg/ml (~0.5 mM) αLA was previously shown to prevent LPS-induced TNFα expression in mouse monocytes in vitro and was found to be an optimal dose for Akt phosphorylation [38]. This does is higher than would be obtained in mouse serum, thus it most likely super-physiological but is no more than tenfold higher than what is possible in serum. Also, relative to published in vitro

studies using αLA the dose used herein is conservative [39, 40].

Quantitative-Real-Time PCR Detection of Macrophage Activation Status

RNA was isolated using Absolutely RNA®, Stratagene™ according to the manufacturer's instructions including DNase digestion. RNA quality and quantity were assessed by agarose gel electrophoresis and a Nanodrop™ spectrophotometer. cDNA was reverse transcribed using 800 ng of total RNA according the manufacturer's instructions (Invitrogen Life Technologies—M-MLV reverse transcriptase) using random primers. PCR was performed using SYBR Green I master mix (Roche) on a Roche Lightcycler 480. All real-time reactions had the following profile conditions: 10 min hot start at 95 °C followed by 45 cycles of 94 °C 10 s, 60 °C 20 s, 72 °C 20 s. Reference and target gene dilution standards were run in triplicate for each primer set to calculate PCR efficiency using the above profile. The concentration ratios were determined after PCR efficiency correction by relative quantification analysis using Lightcycler 480 software. All target genes were expressed as fold increase compared to control. Melting/dissociation curves were run on each plate to assure the production of one amplicon of the same melting temperature for each primer set. Real time primers (listed below) were designed to span genomic introns, thus avoiding amplification of genomic DNA possibly present in the RNA samples. "No template," cDNA negative controls were included for each gene set in all PCR reactions to detect contamination. Primers used were: TNFα For 5′-caacggcatggatctcaaagac-3′, Rev 5′-agatagcaaatcggctgacggt-3′; CCR2 For 5′-ttgg gtcatgatccctatgtgg-3′, Rev 5′-ccttcctaatcctgtgaccctt-3′; IL-6 For 5′-attaacacatgttctctgggaaatcgt-3′ Rev 5′-tatatccagtttgg tagcatccatca-3′ MCP-1 For 5′-gcagcaggtgtcccaaagaa-3′ Rev 5′-atttacgggtcaacttcacattcaa-3′ Macrophage galactose *N*-acetyl-galactosamine receptor-specific lectin 1 (Mgl1) For 5′-tggatgggaccgactttgagaa-3′; *Mgl1* Rev 5′-gggac cacctgtagtgatgtg-3′; *Glyceraldehyde-3-phosphate dehydrogenase (GAPDH)* For 5′-gtgaagcaggcatctgaggg-3′; GAPDH Rev 5′-cgaaggtggaagagtgggagt-3′

Chemiluminescent Electrophoretic Mobility Shift Assay

Nuclear extracts for use in EMSAs were performed using the previously published protocol [41, 42]. Oligonucleotides probes (NFκB sense 5′-AGTTGAGGGGACTT TCCCAGGC-3′, NFκB antisense 5′- GCC TGG GAA AGT CCC CTC AAC T-3′) were biotinylated using Biotin 3′ End DNA Labeling Kit (Pierce, Rockford IL #89818) according to manufacturer's instructions. Lightshift™ Chemiluminescent EMSA kit (Peirce, Rockford IL #20148) was used to perform the binding reaction and chemiluminescent detection. Briefly, 5 μg of nuclear extract was incubated at room temperature in a binding reaction which included a final concentration of: 1× binding buffer, 50 ng/μl Poly (dI·dC), 0.05% NP-40, 2.5% glycerol, and 5 mM $MgCl_2$ for 15 min prior to addition of the biotinylated probes. The complex was run on a pre-electrophoresed 6% polyacrylamide gel in 0.5× TBE (pH 8.4) at 100 V for approximately 45 min followed by wet-transfer in 0.5× TBE to Amersham Hybond™ –N+ membrane (GE Healthcare) at 380 mA for 30 min. The transferred DNA was cross-linked to the membrane before continuing with protocol according to manufacturer's instructions. X-ray film was exposed to membrane and developed.

Results

Alpha Lipoic Acid (αla) Administration Improved Markers of Systemic and Local Insulin Sensitivity and Triacylglycerol Metabolism

Oral αLA Regimen

At the end of 8 weeks of HFD feeding, c-fms^{YFP+} transgenic mice were markedly insulin resistant demonstrating evidence of fasting hyperglycemia and hyperinsulinemia. Body weight increased approximately 16 g. Following this period mice were assigned to ad libitum treatment (αLA 2 mg/ml drinking water), or pair-fed groups. c-fms^{YFP+} mice administered αLA-fed mice exhibited improved fasting glucose approaching a high normal level (125 ± 10.6 mg/dl) compared to the pair-fed group (179 ± 15.7 mg/dl) (Fig. 1a). Fasting insulin levels were also significantly lower in αLA-fed mice (0.96 ± 0.21 ng/ml) than the pair-fed group (2.03 ± 0.17 ng/ml) and the ad libitum group (2.23 ± 0.63 ng/ml). Food intake suppression was modest and decreased over time with non-significantly different body weights across groups after 8 weeks of feeding (Ad lib 40.9 ± 1.4 g; Pair-fed 39.8 ± 0.9 g; αLA-fed 38.2 ± 0.8 g). Cholesterol and triglyceride levels were unchanged with αLA feeding. αLA feeding resulted in a significant decrease in serum IL-6 levels (Ad lib 11.9 ± 4.3 ng/ml; Pair-fed 7.4 ± 2.6 ng/ml; αLA-fed 1.1 ± 0.2 ng/ml), an insignificant but measured decrease in MCP-1, and no change in circulating IL-12, TNFα, IFNγ, and IL-10 cytokines (Fig. 1c).

IP αLA Regimen

In contrast to the weight-neutral effects of oral αLA, an IP regimen did have significant weight loss effects. In this

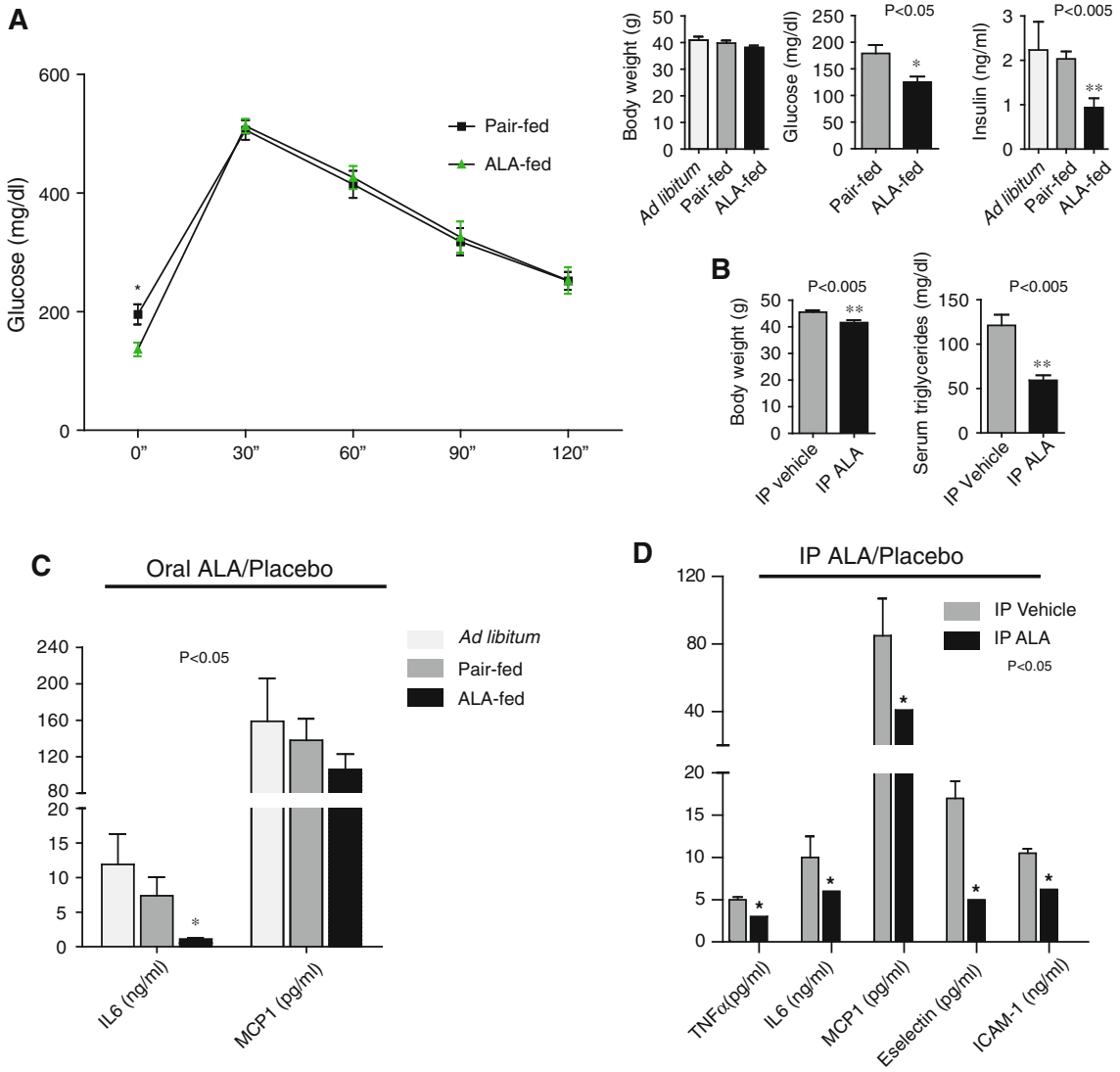

Fig. 1 Effect of α-lipoic acid (αLA) on measures of glucose metabolism. **a** Plasma glucose was measured every 30 min after intra-peritoneal injection of 2 mg/g body weight dextrose after an overnight fast. Fasting glucose and insulin in the αLA-fed mice was significantly lower than the pair-fed control group; $*P < 0.05$; $**P < 0.005$ αLA-fed group compared to pair-fed ($N = 5$/group). However, glucose clearance post-bolus was not improved in the αLA group. **b** IP αLA resulted in significant weight loss, a more dramatic effect on glucose clearance (not shown), and decreased fasting serum triglycerides compared to IP vehicle; $**P < 0.005$. Serum cytokines in HFD fed mice receiving either αLA or placebo by drinking water (**c**) or via intraperitoneal injection (**d**). Oral αLA resulted in a significant decrease in circulating IL6 levels and a nonsignificant decrease in MCP1; there were no changes in serum IL-12, TNFα, IFNγ, and IL-10 cytokine values within the detection the range of the assay. IP αLA administration resulted in a significant decrease in circulating cytokines involved with vascular adhesion and inflammation

experiment as with the oral regimen, after 8 weeks of HFD feeding, mice were randomized to αLA and vehicle control groups. IP αLA resulted in a significant decrease in body weight of 3.9 ± 0.8 g (41.6 ± 0.93 g in IP αLA vs. 45.5 ± 0.73 g in vehicle injected controls). There was no change in plasma total cholesterol but circulating triglycerides were significantly lower in the IP αLA group (59.25 ± 5.7 mg/dl) compared to IP vehicle controls (121 ± 12 mg/dl). IP αLA resulted in significant decreases in serum IL-6, MCP-1, and TNFα. IP αLA also resulted in a significant decrease in serum E-selectin and ICAM-1, markers of monocyte vascular adhesion (Fig. 1d).

In light of its weight neutral effects we proceeded to investigate oral supplementation of αLA at ~160 mg/kg. IP-αLA induced weight loss would have rendered dissociation of weight-loss effects from weight-loss independent effects difficult. Thus continued experimentation focused on the effects of dietary αLA as the effects on food intake

could be more easily addressed and because αLA is most commonly consumed as a dietary supplement.

Dietary αLA Attenuated Visceral Adipose Tissue Macrophage (VATM) Infiltration and In Vivo Macrophage Activation

VATM content of the epididymal adipose of c-fms^{YFP+} mice was quantified using yellow fluorescent protein expression (CD115) in combination with surface staining for CD11b and F4/80, markers for monocytes and mature macrophages, respectively. We found that dietary αLA treatment dramatically decreased the number of YFP$^+$ CD11b$^+$ macrophages per gram of epididymal fat from $6.1 \times 10^5 \pm 0.5$ cells per gram in the ad libitum and $7.4 \times 10^5 \pm 1.7$ in the pair fed group to $1.5 \times 10^5 \pm 0.4$ cells per gram in αLA-fed mice (Fig. 2). This phenomenon was visualized histologically using confocal microscopy of unfixed epididymal adipose collected, stained, and visualized consecutively upon sacrifice. Representative images are provided in Fig. 3a. Assessment of confocal images in the pair-fed mice demonstrate a pattern of crown like structures (CLS) indicative of dead or dying adipocytes [43] and macrophage infiltration. The prevalence of CLS was dramatically decreased in the visceral adipose of the αLA-fed group compared to pair-fed and ad libitum (Fig. 3a). We then examined CD11c$^+$ cells in the stromal vascular fraction of adipose tissue derived from YFP$^+$ animals. αLA-feed significantly attenuated the number of CD11c$^+$ inflammatory macrophages in the visceral adipose with the ad libitum group containing $1.7 \times 10^5 \pm 0.4$ cells per gram, the pair-fed group $1.5 \times 10^5 \pm 0.4$ cells per gram and the αLA-fed group only $0.4 \times 10^5 \pm 0.09$ cells per gram. To further examine the effect of αLA on monocyte/endothelial interactions and monocyte activation pathways, we tested the effects of αLA on TNFα mediated monocyte adhesion using a model of acute inflammation and additionally tested the effects of αLA on monocyte activation in vitro.

αLA Pretreatment Prevented TNFα-Mediated Vascular Adhesion In Vivo

Intravital microscopy of the cremasteric vasculature showed that the number of free-flowing, rolling YFP$^+$ cells was increased by TNFα (Fig. 3b). While αLA did not have an effect of rolling monocytes, αLA pretreatment significantly prevented TNFα-mediated YFP$^+$ cell adherence to vessel walls suggesting that αLA may modulate adhesion molecules involved in firm monocyte adhesion but not

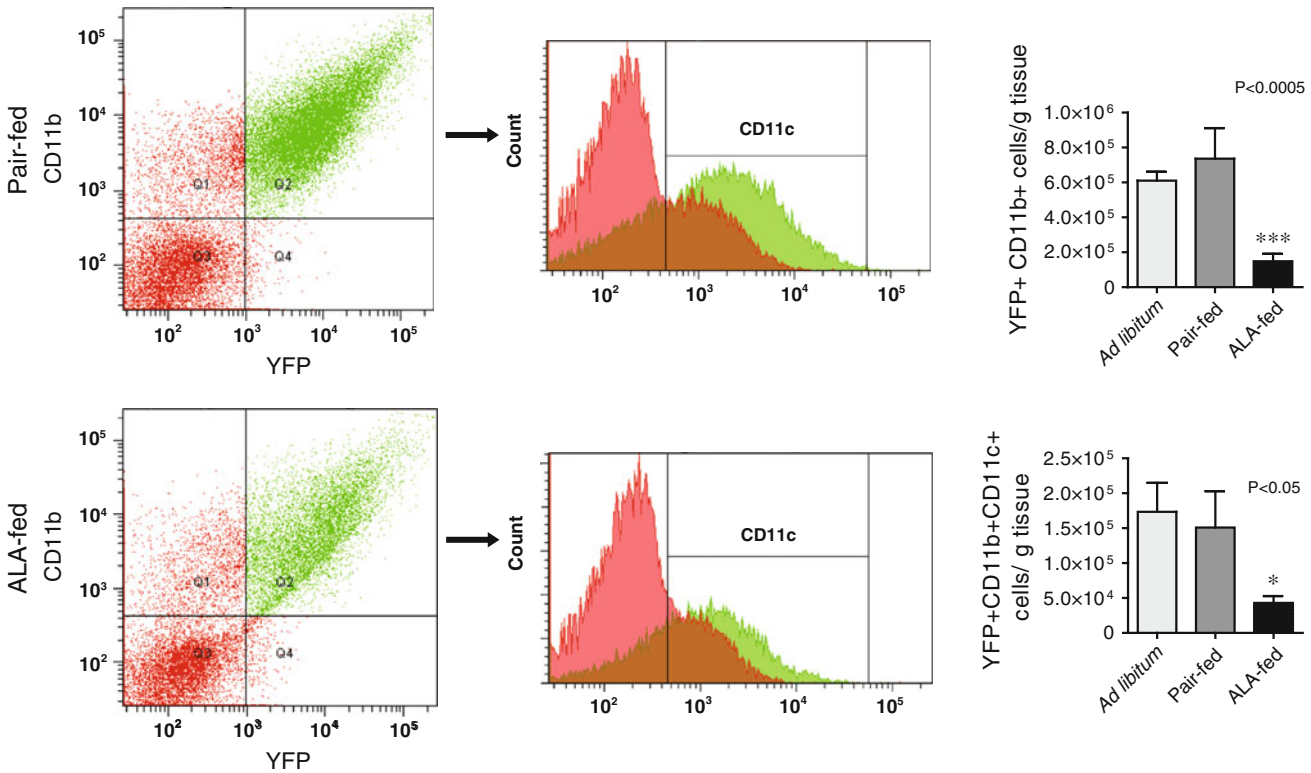

Fig. 2 Macrophage content analysis of the epididymal adipose by flow cytometry. The ad libitum and pair-fed groups had significantly more CD11b$^+$ YFP$^+$ cells per gram of adipose tissue than the αLA fed group, $***P < 0.005$. Oral αLA significantly decreased the number of CD11c positive, inflammatory macrophages, per gram of adipose, $*P < 0.05$ versus pair-fed

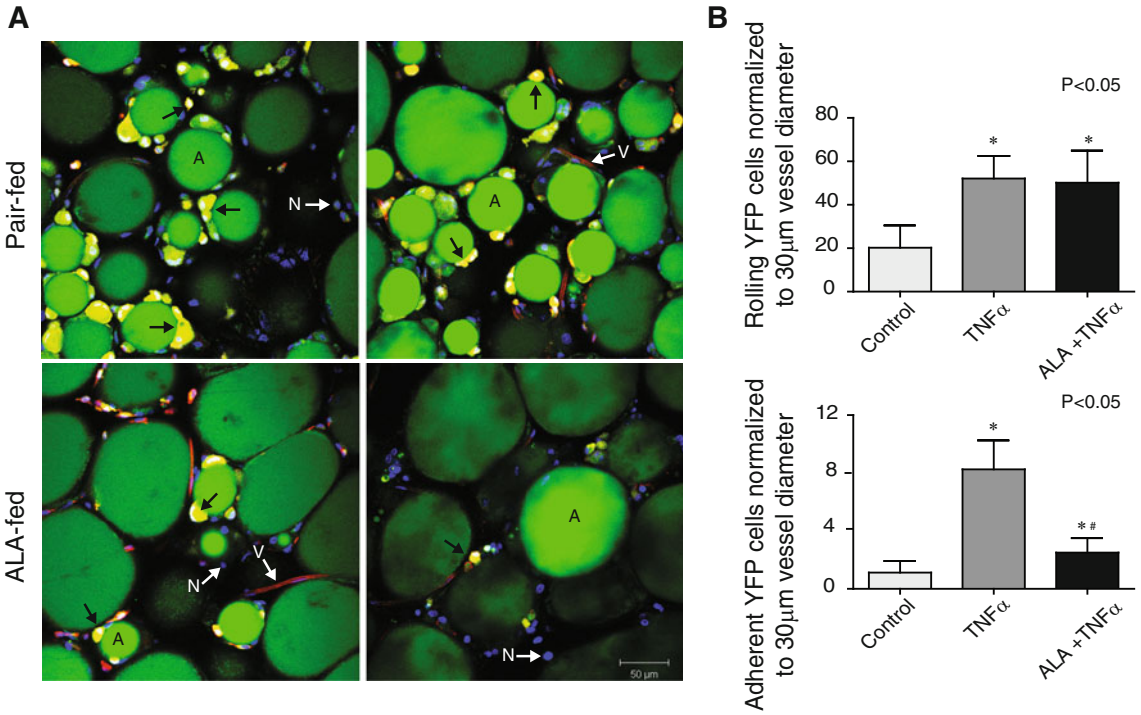

Fig. 3 **a** Representative confocal microscopy images of live epididymal adipose. YFP^+ (*yellow*/indicated by *arrow*) cell infiltration and the prevalence of multiple "crown-like" structures surrounding adipocytes (*green*/indicated by the letter *A*) in the pair-fed and αLA-fed groups. Blood vessels are shown in *red* (indicated by *white arrow V*) due to endothelial staining with *Griffonia simplicifolia* isolectin GS-IB4 conjugated to AlexaFluor 488, most of the YFP expressing cells are outside of the vasculature. The adiposomes are shown in *green* (indicated by the letter *A*) due to BODIPY 558/568 staining and nuclei are *blue* (indicated by *white arrow N*) due to Hoechst 33342 staining. **b** Acute αLA IP pretreatment reduced YFP^+ cell adhesion in cremasteric vessels after injection of TNFα; $^*P < 0.05$ versus control, $^{\#}P < 0.05$ versus TNFα

those involved in rolling. To further examine the effect of αLA on mechanisms by which αLA may modulate excess monocyte infiltration into the adipose we examined the effects of αLA on MCP-1 and CCR-2 in response to a prototypical TLR4 agonist, LPS.

αLA Attenuates MCP-1 Expression on Macrophages via TLR4 Mechanisms

Bone marrow-derived macrophages (BMDM) from wild-type Balb/c mice and toll-like receptor 4 (TLR4) null mice were pretreated with αLA or vehicle control then activated with lipopolysaccharide (LPS), a TLR4 ligand [44]. αLA significantly decreased MCP-1 and TNFα gene expression in response to LPS stimulation but had no effect on IL-6 activation (Fig. 4a). αLA significantly decreased basal TNFα expression in both TLR4 WT and deficient macrophages. The degree of attenuation of LPS-mediated TNFα expression by αLA alone was small but comparable to that seen with $TLR4^{def/def}$. The TNFα and IL-6 response to LPS in $TLR4^{def/def}$ macrophages was significantly blunted compared to the WT cells. MCP-1 induction by LPS was small compared to TNFα and IL6. LPS-mediated MCP-1 expression, however, was potently inhibited by αLA pretreatment. Interestingly, LPS activation had no effect on CCR2 expression, though αLA significantly down-regulated CCR-2 expression in the presence and absence of LPS; suggesting that non-TLR4 pathways are probably involved in CCR2 down-regulation in response to αLA. αLA increased Mgl1 gene expression, a marker of alternative macrophage activation, while LPS decreased expression (data not shown). These data suggest that αLA may function as an anti-inflammatory agent by preventing inflammatory gene expression. Since nuclear factor kappa B (NF-κB) plays a pivotal role in cellular inflammatory processes we decided to assay the effect of αLA on NF-κB-DNA binding in these TLR WT macrophages. An electrophoretic mobility shift assay showed LPS treatment dramatically increased the binding of NF-κB to the oligonucleotide probe. αLA (100 μg/ml) pretreatment of WT BMDM lead to the inhibition of LPS-mediated (0.5 μg/ml) NF-κB activation as measured by binding to probe DNA.

Discussion

Visceral adipose inflammation is believed to play an etiologic role in the development of insulin resistance (IR) in

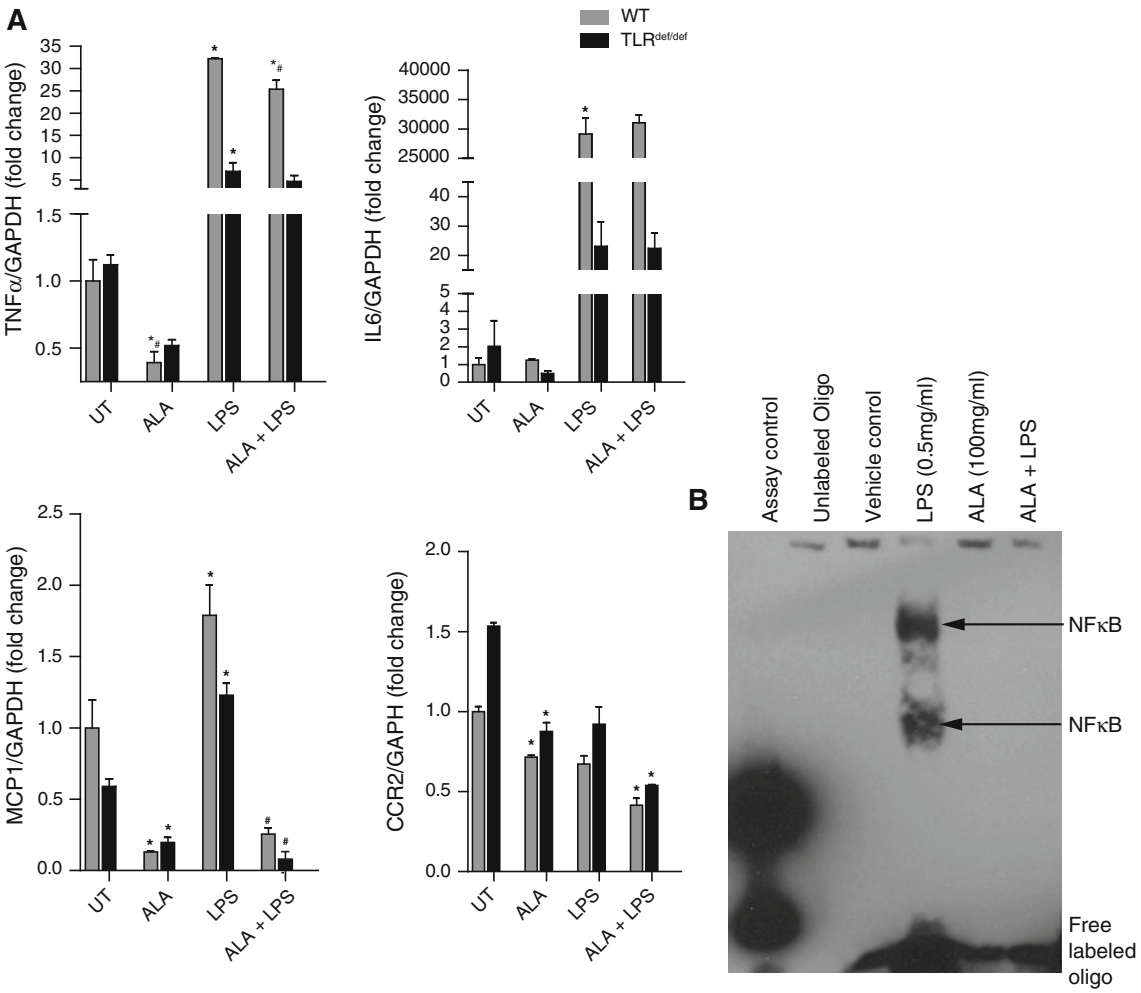

Fig. 4 αLA pretreatment (100 μg/μl) attenuated expression of inflammatory and homing molecules in cultured bone marrow derived macrophages activated with LPS (0.5 μg/μl), $^{*}P < 0.05$ compared to respective untreated (UT) control; $^{\#}P < 0.05$ compared to respective LPS treatment group. TNFα, MCP-1, and CCR2 gene expression is significantly down-regulated by αLA in cultured murine macrophages

obesity and is typified by early, and often dramatic, increases in innate immune cells such as macrophages. With accumulation of neutral lipids in the adiposome, adipocytes hypertrophy and a subset undergo "necrosis-like" cell death resulting in the recruitment of macrophages [45, 46]. The relationship between alterations in innate and adaptive immune cell numbers, their effect on the adipose, and their contribution to the eventual development of obesity is largely attributed to the production and systemic introduction of inflammatory mediators. The pathophysiological processes that develop due to obesity have various putative etiological origins involving multiple tissues, including immune-modulated inflammation of the visceral adipose.

In this study we assessed the effects of αLA on the development of insulin resistance and adipose inflammation in a novel model of murine diet-induced obesity and IR. We demonstrate in pair-feeding experiments that oral αLA exerts beneficial weight loss-independent effects on insulin sensitivity, visceral adipose inflammation, vascular adhesion, and whole body inflammatory cytokine markers. Oral αLA reduced VATM content and activation in insulin resistant, obese mice. αLA also prevented LPS-mediated NF-κB activation and decreased the expression of inflammatory/migratory genes in un-stimulated and LPS-stimulated macrophages. These results suggest that αLA has a potent effect on macrophage activation status and thus may modulate the innate immune response in chronic inflammation in the visceral adipose tissue, a hallmark of type 2 diabetes and the metabolic syndrome.

Though oral αLA was less effective than IP αLA at lowering blood glucose and normalizing markers of insulin resistivity, at the dose used orally, it lacked weight loss effects and obviously prevented its confounding influence in the assessment of results. αLA decreases hypothalamic AMPK activity and causes profound weight loss in rodents by reducing food intake and enhancing energy expenditure [47]. Pair-fed experiments suggest a minimal effect of oral

αLA at ~160 mg/kg on food intake and body weight over 8 weeks in mice. It should be noted that the first week of oral αLA did result in decreased food intake and some weight loss, however, over the subsequent weeks the effect subsided and weights normalized then increased to levels comparable to controls. The reduction in fasting glucose and insulin by oral αLA did not translate into improved glucose bolus clearance, suggesting that αLA did not abrogate the effects of obesity on glucose metabolism in the long term. However, αLA may selectively regulate fasting indices of glucose homeostasis which have been shown to be sensitive to anti-inflammatory measures [48]. Our data suggest that αLA has a moderate effect in already obese mice. The effect may be more dramatic in mice that begin oral αLA prior to a HFD or in mice that are not already overtly insulin resistant.

The marginal effects of post-prandial indices contrasted dramatically with the ability of αLA to reduce the number and activation status of macrophages in the epididymal adipose. Visceral adipose inflammation is a major area of study in obesity and IR, with visceral adipose inflammation being a putative pathophysiological phenomenon with the activation status of VATM being of particular interest. The phenotypic activation state of macrophages is a crucial determinant of functionality and the inflammatory state. Resident tissue macrophages in lean mice display a phenotype that is typical of cells committed to efferocytosis and scavenger functions and are referred to as M2 or "alternatively activated" macrophages expressing anti-inflammatory cytokines (*Il10, Arginase1, Mgl1*) [49] concomitantly with lower levels of M1 genes. High fat diet (HFD) and obesity in mice lead to a M1 or "classically activated" state which have been shown to express CD11c and secrete pro-inflammatory cytokines such as TNFα, IL-6, and IL-12 [4]. This phenotypic shift is now believed to play an important role in the genesis of IR [4]. The dramatic attenuation in VATM numbers and CD11c expression observed by αLA is consistent with an effect on activation status of adipose macrophages. Interestingly, the effects of αLA are similar to those reported in obese CCR2 null mice versus obese wild type (WT) mice [13]. Obese CCR2 null mice also showed a reduction in VATM with a modest decrease in whole body insulin resistance. Our data suggest that modulation of VATM activation and visceral infiltration by αLA in already obese mice decreases systemic markers of inflammation and improves markers of insulin sensitivity.

In separate experiments, we addressed the effects of αLA on the monocyte/macrophage activation state and extravasation by demonstrating that acute αLA administration reduced monocyte adhesion to the endothelium. Homing of macrophages to the visceral adipose may be modified by decreasing vascular adhesion, the first step in extravasation and homing to tissue. Our intravital microscopy data demonstrate a dramatic effect of αLA in reducing monocyte adhesion to venules and supports the hypothesis that αLA may reduce monocyte efflux from the vasculature to tissues due to inflammatory signals. Directly measuring monocyte/macrophage efflux to the epididymal adipose is a preferable method but was not technically possible at the time of these mouse experiments.

To further address the role of αLA on TLR4-mediated macrophage activation and signaling we examined the effects of αLA on bone marrow-derived macrophages from $TLR4^{def/def}$ and WT animals. Recent studies show that the Toll-like receptor 4 (TLR4) may play a central role in the link among insulin resistance, inflammation, and obesity. TLR4 deficiency prevented DIO-mediated insulin resistance and activation of IkB kinase (IKKb) and c-Jun NH2-terminal kinase (JNK), suggesting that TLR4 is a key modulator in the cross-talk between inflammatory and metabolic pathways [18–22]. Recently it was demonstrated that high fat meals can increase circulating LPS levels and may result from increased intestinal permeability to LPS [50, 51]. Additionally, DIO was shown to induce the expression and activation of TLR4 in the adipose of obese rats, while exercise reduced circulating LPS and TLR4 activation [21]. High levels of saturated NEFA, such as palmitate, when combined with hyperinsulinemia, have been shown to activate human monocytes via TLR4 agonism resulting in the production of pro-inflammatory cytokines [52]. Additionally, high glucose conditions may result in oxidative stress-mediated NF-κB activation and subsequent up-regulation of TNFα and MCP-1 [53, 54]. We demonstrated that αLA was an effective inhibitor of NF-κB activation in murine macrophages, a potent transcription factor regulating inflammatory genes including TNFα and IL6 in this cell. We show that αLA pretreatment is capable of preventing TLR4-mediated up-regulation of MCP-1. MCP-1 is the primary cytokine recruiting monocytes, memory T cells, and dendritic cells to sites of tissue injury and inflammation. It has been shown in endothelial cells that αLA prevented high-glucose induced MCP-1 expression via inhibition of reactive oxygen species-mediated NF-κB activation [54]. The cognate receptor for MCP-1, CCR2 is also down-regulated on monocytes by αLA (albeit via non-TLR4 pathways) suggesting that it may make monocytes less responsive to a MCP-1 chemotactic gradient. Interestingly, CCR2 expression was not induced by TLR4 activation, conversely LPS acted synergistically with αLA to further down-regulate CCR2 expression. αLA also potently decreased LPS-stimulated TNFα gene expression demonstrating that αLA can modulated macrophage activation post TLR4 ligation. These data suggest that αLA is a potent modulator of inflammation via TLR4, non-TLR4 and NF-κB pathways.

We acknowledge several important limitations of this study beginning with our focus on adipose-inflammation centric mechanisms. Our study did not investigate the effects of αLA on hepatic glucose generation or adipocyte function. Prior studies with αLA have clearly demonstrated an effect of αLA in improving serum lactate and pyruvate concentrations and improving glucose levels in lean and obese patients with type 2 diabetes [55]. Our experimental design did not clearly examine the effect of αLA on adipocytes themselves. We cannot say whether αLA decreased visceral adipocyte apoptosis and subsequent VATM infiltration or whether αLA prevented monocyte/macrophage activation and infiltration leading to a lower incidence of adipocyte apoptosis. It is also important to note that αLA may have different mechanisms of action based on duration of treatment, route of administration, and maximal plasma concentration thus comparing data between treatment protocols and in vivo and in vitro results is tenuous and must be taken within context. For example, while αLA potently down-regulated TNF, IL6, and MCP-1 gene expression in vitro, the in vivo effects were not nearly as dramatic in the oral αLA group with only IL-6 being significantly down-regulated and more comparable in the IP-αLA mice. It should also be noted that αLA can activate nuclear factor erythroid2-related factor (Nrf2), the principal transcriptional regulator of antioxidant response element (ARE)-mediated gene expression [56] and through these pathways could exert powerful effects on adipose inflammation [57, 58]. Though prior studies have demonstrated important effects on systemic IR and inflammation, a thorough examination of the long-term weight loss-independent effects of αLA on insulin sensitivity and macrophage activation pathways in already obese individuals was needed.

Acknowledgments The primary author was supported by Award Number F32DK083903 from the National Institute of Diabetes and Digestive and Kidney Diseases. The content is solely the responsibility of the authors and does not necessarily represent the official views of the National Institute of Diabetes and Digestive and Kidney Diseases or the National Institutes of Health. The research was also supported in part by Grants to Dr Rajagopalan: R01ES015146, R21DK088522, and R21HL106487.

References

1. Harkins JM, Moustaid-Moussa N, Chung YJ, Penner KM, Pestka JJ, North CM, Claycombe KJ (2004) Expression of interleukin-6 is greater in preadipocytes than in adipocytes of 3T3–L1 cells and C57BL/6J and ob/ob mice. J Nutr 134:2673–2677
2. Xu H, Barnes GT, Yang Q, Tan G, Yang D, Chou CJ, Sole J, Nichols A, Ross JS, Tartaglia LA, Chen H (2003) Chronic inflammation in fat plays a crucial role in the development of obesity-related insulin resistance. J Clin Invest 112:1821–1830
3. Weisberg SP, McCann D, Desai M, Rosenbaum M, Leibel RL, Ferrante AW Jr (2003) Obesity is associated with macrophage accumulation in adipose tissue. J Clin Invest 112:1796–1808
4. Lumeng CN, Bodzin JL, Saltiel AR (2007) Obesity induces a phenotypic switch in adipose tissue macrophage polarization. J Clin Invest 117:175–184
5. Carey DG, Jenkins AB, Campbell LV, Freund J, Chisholm DJ (1996) Abdominal fat and insulin resistance in normal and overweight women: direct measurements reveal a strong relationship in subjects at both low and high risk of NIDDM. Diabetes 45:633–638
6. Cnop M, Landchild MJ, Vidal J, Havel PJ, Knowles NG, Carr DR, Wang F, Hull RL, Boyko EJ, Retzlaff BM, Walden CE, Knopp RH, Kahn SE (2002) The concurrent accumulation of intra-abdominal and subcutaneous fat explains the association between insulin resistance and plasma leptin concentrations: distinct metabolic effects of two fat compartments. Diabetes 51:1005–1015
7. Maeda K, Okubo K, Shimomura I, Mizuno K, Matsuzawa Y, Matsubara K (1997) Analysis of an expression profile of genes in the human adipose tissue. Gene 190:227–235
8. Motoshima H, Wu X, Sinha MK, Hardy VE, Rosato EL, Barbot DJ, Rosato FE, Goldstein BJ (2002) Differential regulation of adiponectin secretion from cultured human omental and subcutaneous adipocytes: effects of insulin and rosiglitazone. J Clin Endocrinol Metab 87:5662–5667
9. Scherer PE (2006) Adipose tissue: from lipid storage compartment to endocrine organ. Diabetes 55:1537–1545
10. Shoelson SE, Lee J, Goldfine AB (2006) Inflammation and insulin resistance. J Clin Invest 116:1793–1801
11. Wellen KE, Hotamisligil GS (2005) Inflammation, stress, and diabetes. J Clin Invest 115:1111–1119
12. Fain JN, Madan AK, Hiler ML, Cheema P, Bahouth SW (2004) Comparison of the release of adipokines by adipose tissue, adipose tissue matrix, and adipocytes from visceral and subcutaneous abdominal adipose tissues of obese humans. Endocrinology 145:2273–2282
13. Weisberg SP, Hunter D, Huber R, Lemieux J, Slaymaker S, Vaddi K, Charo I, Leibel RL, Ferrante AW Jr (2006) CCR2 modulates inflammatory and metabolic effects of high-fat feeding. J Clin Invest 116:115–124
14. Wu H, Ghosh S, Perrard XD, Feng L, Garcia GE, Perrard JL, Sweeney JF, Peterson LE, Chan L, Smith CW, Ballantyne CM (2007) T-cell accumulation and regulated on activation, normal T cell expressed and secreted upregulation in adipose tissue in obesity. Circulation 115:1029–1038
15. Hauner H (2005) Secretory factors from human adipose tissue and their functional role. Proc Nutr Soc 64:163–169
16. Sethi JK, Vidal-Puig AJ (2007) Thematic review series: adipocyte biology adipose tissue function and plasticity orchestrate nutritional adaptation. J Lipid Res 48:1253–1262
17. Uysal KT, Wiesbrock SM, Marino MW, Hotamisligil GS (1997) Protection from obesity-induced insulin resistance in mice lacking TNF-alpha function. Nature 389:610–614
18. Kim F, Pham M, Luttrell I, Bannerman DD, Tupper J, Thaler J, Hawn TR, Raines EW, Schwartz MW (2007) Toll-like receptor-4 mediates vascular inflammation and insulin resistance in diet-induced obesity. Circ Res 100:1589–1596
19. Kopp A, Buechler C, Neumeier M, Weigert J, Aslanidis C, Scholmerich J, Schaffler A (2009) Innate immunity and adipocyte function: ligand-specific activation of multiple Toll-like receptors modulates cytokine, adipokine, and chemokine secretion in adipocytes. Obesity (Silver Spring) 17:648–656
20. Nguyen MT, Favelyukis S, Nguyen AK, Reichart D, Scott PA, Jenn A, Liu-Bryan R, Glass CK, Neels JG, Olefsky JM (2007) A subpopulation of macrophages infiltrates hypertrophic adipose

tissue and is activated by free fatty acids via Toll-like receptors 2 and 4 and JNK-dependent pathways. J Biol Chem 282:35279–35292
21. Oliveira AG, Carvalho BM, Tobar N, Ropelle ER, Pauli JR, Bagarolli RA, Guadagnini D, Carvalheira JB, Saad MJ (2011) Physical exercise reduces circulating lipopolysaccharide and Toll-like receptor 4 activation and improves insulin signaling in tissues of diet-induced obesity rats. Diabetes 60:784–796
22. Song MJ, Kim KH, Yoon JM, Kim JB (2006) Activation of Toll-like receptor 4 is associated with insulin resistance in adipocytes. Biochem Biophys Res Commun 346:739–745
23. Merry BJ, Kirk AJ, Goyns MH (2008) Dietary lipoic acid supplementation can mimic or block the effect of dietary restriction on life span. Mech Ageing Dev 129:341–348
24. Butler JA, Hagen TM, Moreau R (2009) Lipoic acid improves hypertriglyceridemia by stimulating triacylglycerol clearance and downregulating liver triacylglycerol secretion. Arch Biochem Biophys 485:63–71
25. Lee WJ, Song KH, Koh EH, Won JC, Kim HS, Park HS, Kim MS, Kim SW, Lee KU, Park JY (2005) Alpha-lipoic acid increases insulin sensitivity by activating AMPK in skeletal muscle. Biochem Biophys Res Commun 332:885–891
26. Lee HA, Hughes DA (2002) Alpha-lipoic acid modulates NF-kappaB activity in human monocytic cells by direct interaction with DNA. Exp Gerontol 37:401–410
27. Sasmono RT, Oceandy D, Pollard JW, Tong W, Pavli P, Wainwright BJ, Ostrowski MC, Himes SR, Hume DA (2003) A macrophage colony-stimulating factor receptor-green fluorescent protein transgene is expressed throughout the mononuclear phagocyte system of the mouse. Blood 101:1155–1163
28. Yi X, Maeda N (2006) alpha-Lipoic acid prevents the increase in atherosclerosis induced by diabetes in apolipoprotein E-deficient mice fed high-fat/low-cholesterol diet. Diabetes 55:2238–2244
29. Yadav V, Marracci GH, Munar MY, Cherala G, Stuber LE, Alvarez L, Shinto L, Koop DR, Bourdette DN (2010) Pharmacokinetic study of lipoic acid in multiple sclerosis: comparing mice and human pharmacokinetic parameters. Mult Scler 16:387–397
30. Carlson DA, Smith AR, Fischer SJ, Young KL, Packer L (2007) The plasma pharmacokinetics of R-(+)-lipoic acid administered as sodium R-(+)-lipoate to healthy human subjects. Altern Med Rev 12:343–351
31. Teichert J, Kern J, Tritschler HJ, Ulrich H, Preiss R (1998) Investigations on the pharmacokinetics of alpha-lipoic acid in healthy volunteers. Int J Clin Pharmacol Ther 36:625–628
32. Breithaupt-Grogler K, Niebch G, Schneider E, Erb K, Hermann R, Blume HH, Schug BS, Belz GG (1999) Dose-proportionality of oral thioctic acid–coincidence of assessments via pooled plasma and individual data. Eur J Pharm Sci 8:57–65
33. Deiuliis JA, Shin J, Bae D, Azain MJ, Barb R, Lee K (2008) Developmental, hormonal, and nutritional regulation of porcine adipose triglyceride lipase (ATGL). Lipids 43:215–225
34. Nishimura S, Manabe I, Nagasaki M, Hosoya Y, Yamashita H, Fujita H, Ohsugi M, Tobe K, Kadowaki T, Nagai R, Sugiura S (2007) Adipogenesis in obesity requires close interplay between differentiating adipocytes, stromal cells, and blood vessels. Diabetes 56:1517–1526
35. Lim LH, Bochner BS, Wagner EM (2002) Leukocyte recruitment in the airways: an intravital microscopic study of rat tracheal microcirculation. Am J Physiol Lung Cell Mol Physiol 282: L959–L967
36. Harrison EH, McCormick DB (1974) The metabolism of dl-(1,6-14C)lipoic acid in the rat. Arch Biochem Biophys 160:514–522
37. Jones W, Li X, Qu ZC, Perriott L, Whitesell RR, May JM (2002) Uptake, recycling, and antioxidant actions of alpha-lipoic acid in endothelial cells. Free Radic Biol Med 33:83–93
38. Zhang WJ, Wei H, Hagen T, Frei B (2007) Alpha-lipoic acid attenuates LPS-induced inflammatory responses by activating the phosphoinositide 3-kinase/Akt signaling pathway. Proc Natl Acad Sci USA 104:4077–4082
39. Lee CK, Lee EY, Kim YG, Mun SH, Moon HB, Yoo B (2008) Alpha-lipoic acid inhibits TNF-alpha induced NF-kappa B activation through blocking of MEKK1-MKK4-IKK signaling cascades. Int Immunopharmacol 8:362–370
40. Sung MJ, Kim W, Ahn SY, Cho CH, Koh GY, Moon SO, Kim DH, Lee S, Kang KP, Jang KY, Park SK (2005) Protective effect of alpha-lipoic acid in lipopolysaccharide-induced endothelial fractalkine expression. Circ Res 97:880–890
41. Cheshire JL, Baldwin AS Jr (1997) Synergistic activation of NF-kappaB by tumor necrosis factor alpha and gamma interferon via enhanced I kappaB alpha degradation and de novo I kappaB beta degradation. Mol Cell Biol 17:6746–6754
42. Guttridge DC, Albanese C, Reuther JY, Pestell RG, Baldwin AS Jr (1999) NF-kappaB controls cell growth and differentiation through transcriptional regulation of cyclin D1. Mol Cell Biol 19:5785–5799
43. Murano I, Barbatelli G, Parisani V, Latini C, Muzzonigro G, Castellucci M, Cinti S (2008) Dead adipocytes, detected as crown-like structures, are prevalent in visceral fat depots of genetically obese mice. J Lipid Res 49:1562–1568
44. Muroi M, Suzuki T (1993) Role of protein kinase A in LPS-induced activation of NF-kappa B proteins of a mouse macrophage-like cell line, J774. Cell Signal 5:289–298
45. Strissel KJ, Stancheva Z, Miyoshi H, Perfield JW, 2nd, Defuria J, Jick Z, Greenberg AS, Obin MS (2007) Adipocyte death, adipose tissue remodeling and obesity complications. Diabetes 56:2910–2918
46. Cinti S, Mitchell G, Barbatelli G, Murano I, Ceresi E, Faloia E, Wang S, Fortier M, Greenberg AS, Obin MS (2005) Adipocyte death defines macrophage localization and function in adipose tissue of obese mice and humans. J Lipid Res 46:2347–2355
47. Kim MS, Park JY, Namkoong C, Jang PG, Ryu JW, Song HS, Yun JY, Namgoong IS, Ha J, Park IS, Lee IK, Viollet B, Youn JH, Lee HK, Lee KU (2004) Anti-obesity effects of alpha-lipoic acid mediated by suppression of hypothalamic AMP-activated protein kinase. Nat Med 10:727–733
48. Manning PJ, Sutherland WH, Walker RJ, Williams SM, De Jong SA, Ryalls AR, Berry EA (2004) Effect of high-dose vitamin E on insulin resistance and associated parameters in overweight subjects. Diabetes Care 27:2166–2171
49. Charo IF (2007) Macrophage polarization and insulin resistance: PPARgamma in control. Cell Metab 6:96–98
50. Ghanim H, Abuaysheh S, Sia CL, Korzeniewski K, Chaudhuri A, Fernandez-Real JM, Dandona P (2009) Increase in plasma endotoxin concentrations and the expression of Toll-like receptors and suppressor of cytokine signaling-3 in mononuclear cells after a high-fat, high-carbohydrate meal: implications for insulin resistance. Diabetes Care 32:2281–2287
51. Cani PD, Bibiloni R, Knauf C, Waget A, Neyrinck AM, Delzenne NM, Burcelin R (2008) Changes in gut microbiota control metabolic endotoxemia-induced inflammation in high-fat diet-induced obesity and diabetes in mice. Diabetes 57:1470–1481
52. Bunn RC, Cockrell GE, Ou Y, Thrailkill KM, Lumpkin CK Jr, Fowlkes JL (2010) Palmitate and insulin synergistically induce IL-6 expression in human monocytes. Cardiovasc Diabetol 9:73
53. Quan Y, Jiang CT, Xue B, Zhu SG, Wang X (2011) High glucose stimulates TNFalpha and MCP-1 expression in rat microglia via ROS and NF-kappaB pathways. Acta Pharmacol Sin 32:188–193
54. Yang WS, Seo JW, Han NJ, Choi J, Lee KU, Ahn H, Lee SK, Park SK (2008) High glucose-induced NF-kappaB activation occurs via tyrosine phosphorylation of IkappaBalpha in human glomerular endothelial cells: involvement of Syk tyrosine kinase. Am J Physiol Renal Physiol 294:F1065–F1075

55. Konrad T, Vicini P, Kusterer K, Hoflich A, Assadkhani A, Bohles HJ, Sewell A, Tritschler HJ, Cobelli C, Usadel KH (1999) alpha-Lipoic acid treatment decreases serum lactate and pyruvate concentrations and improves glucose effectiveness in lean and obese patients with type 2 diabetes. Diabetes Care 22:280–287
56. Suh JH, Shenvi SV, Dixon BM, Liu H, Jaiswal AK, Liu RM, Hagen TM (2004) Decline in transcriptional activity of Nrf2 causes age-related loss of glutathione synthesis, which is reversible with lipoic acid. Proc Natl Acad Sci USA 101: 3381–3386
57. Itoh K, Chiba T, Takahashi S, Ishii T, Igarashi K, Katoh Y, Oyake T, Hayashi N, Satoh K, Hatayama I, Yamamoto M, Nabeshima Y (1997) An Nrf2/small Maf heterodimer mediates the induction of phase II detoxifying enzyme genes through antioxidant response elements. Biochem Biophys Res Commun 236:313–322
58. Venugopal R, Jaiswal AK (1996) Nrf1 and Nrf2 positively and c-Fos and Fra1 negatively regulate the human antioxidant response element-mediated expression of NAD(P)H:quinone oxidoreductase1 gene. Proc Natl Acad Sci USA 93:14960–14965

energy balance leading to constant weight gain in the form of fat [2]. Since the discovery of leptin in 1994 by Zhang and colleagues [3], the adipocyte and its products have been profoundly studied. Adipose tissue has an important and critical role in the regulation of energy homeostasis, behaving as an endocrine organ that synthesizes molecules involved in the regulation of metabolism [4]. Alterations of both the expression and activity of these molecules also contribute to the development of obesity among other pathologies [4]. IL-15 has been recently described as a cytokine that has important metabolic effects on adipose tissue [5]. IL-15 has pleiotropic functions because it exerts effects on the proliferation, survival, and differentiation of many more distinct cell types than was originally thought [6, 7]. Since the discovery of this cytokine as an anabolic factor for skeletal muscle, several reports have described its important role as a regulator of energy homeostasis [7, 8]. In-vivo studies have shown that chronic IL-15 administration (seven days) results in a 33% decrease of white adipose tissue (WAT) in healthy rats [6]. Additional studies demonstrate that the effects of the cytokine on WAT are partially caused by inhibition of both lipogenesis [9] and LPL activity [10] and by reduced lipid uptake in this tissue [5]. IL-15 also regulates liver lipogenesis, reducing the lipid content of VLDL particles [10], and thermogenesis in brown adipose tissue [11]. Some of the effects of this cytokine are mediated by upregulation of PPARδ [5, 11] a transcription factor involved in fatty acid oxidation and other metabolic adaptations to environmental changes [12]. In summary, IL-15 could be important in the conversion of fat to lean body composition [4, 8, 10, 13].

Inhibition of adipogenesis by IL-15 in 3T3-L1 cells has been reported, suggesting a direct action of the cytokine in adipose tissue [14]. Moreover, in a study using obese rodent models, a correlation was found between the sensitivity to the fat-inhibiting effects of IL-15 and the fat expression of mRNA for signaling subunits of the IL-15 receptor in WAT [15], confirming that IL-15 has a direct effect on this tissue. Thus, it is known that the cytokine signals by activation of two different subunits also present in the IL-2 receptor, and binds specifically to the α subunit of the receptor [7]. The activation of IL-15 receptor triggers different transduction pathways depending on cellular type. Thus, IL-15-mediated signaling involves proteins such as JAK/STAT, the Src family, PI3-Kinase and Akt, MAPK, NFκB, and AP1 in immune cells [16–19]. Regarding its signal transduction in adipose tissue, only one report has suggested that JAK and PKA act as partial mediators of the lipolytic effect that IL-15 exerts on primary pig adipocytes [20].

Taking into account the important effects of the cytokine on lipid metabolism, the objective of this study was to analyze the effects of IL-15 on adipocyte differentiation using the 3T3-L1 preadipose cell line, and to study the signal transduction pathways mediating the effects of the cytokine.

Materials and Methods

Cell Culture and Adipocyte Differentiation

3T3-L1 preadipocytes (ATCC) were cultured in Dulbecco's modified Eagle's medium (DMEM) with high glucose (Invitrogen) supplemented with 10% (*v*/*v*) fetal calf serum (Invitrogen), 25 mM HEPES pH 7.0, 1,000 U/mL penicillin, 1,000 U/mL streptomycin, and 25 μg/mL fungizone (BioWhittaker). To induce adipocyte differentiation, cells were grown for 2 days postconfluence and then treated for 2 days with differentiation medium of DMEM with high glucose supplemented with 10% (*v*/*v*) fetal bovine serum (Invitrogen), 25 mM HEPES pH 7.0, 1,000 U/mL penicillin, 1,000 U/mL streptomycin, and 25 μg/mL fungizone, plus MDI (0.5 mM isobutylmethylxanthine, 0.25 μM dexamethasone and 5 μg/mL insulin). On day 2 the cells were re-fed with differentiation medium that contained insulin (5 μg/mL) instead of MDI, and every 2 days thereafter with differentiation medium alone. The cells were completely differentiated 14 days after induction. 3T3-L1 cells were treated with 10 ng/mL IL-15 (Peprotech) or with PBS for 7 days before inducing differentiation (referred to hereafter as preadipocytes), for 7 days after inducing differentiation (referred to as 7d-adipocytes), and for 7 days after they were differentiated (referred to as 14d-adipocytes). All experimental groups were analyzed at the end of the treatment.

Protein Extraction and Western Blotting

For protein extraction the cells were scraped into ice-cold buffer containing 10 mM Tris pH 7.5, 10 mM EDTA, 400 mM NaCl, 10% glycerol, 0.5% Nonidet P-40, 5 mM NaF, and 0.01 mM sodium orthovanadate, in the presence of protease inhibitors, and then sonicated for 10 s. The samples were then centrifuged at 13,000 rpm for 10 min and the supernatants were collected and protein concentration was determined by use of the BCA method (Pierce, USA). Equal amounts of protein (50 μg) were heat-denatured in sample-loading buffer (50 mM Tris-HCl, pH 6.8, 100 mM DTT, 2% SDS, 0.1% bromophenol blue, 10% glycerol), resolved by SDS–polyacrylamide gel electrophoresis (10% polyacrylamide, 0.1% SDS) and transferred to Immobilon membranes (Immobilon PVDF, Millipore, USA). The filters were blocked with 5% PBS-non-fat dried milk or 5% BSA and then incubated with polyclonal antibodies: anti-phosphoAKT,

anti-phosphoSAPK/JNK, anti-phosphoJAK1, anti-JAK1, anti-phosphoSTAT5, anti-STAT5 (Cell Signaling Technology, Beverly, USA), anti-AKT, anti-SAPK/JNK1, anti-phosphop38 (Santa Cruz Biotechnology, Santa Cruz, CA, USA), and anti-p38 (Calbiochem, Germany). An anti-tubulin polyclonal antibody (Santa Cruz Biotechnology) was used as a control for the different studies. Donkey anti-mouse peroxidase-conjugated IgG (Jackson ImmunoResearch, West Grove, USA), and goat anti-rabbit horseradish peroxidase conjugate (Bio-Rad, USA) were used as secondary antibodies. The membrane-bound immune complexes were detected by use of an enhanced chemiluminescence system (EZ-ECL, Biological Industries, Israel).

Cell-Proliferation Studies

3T3-L1 cells were seeded in multiwells plates and cultured for 24 h for cell attachment. The cells were then serum-starved for 24 h and treated with 10 ng/mL IL-15 or vehicle solution depending on the experimental group. After 24 h of treatment, 1 μCi methyl-[^{3}H]thymidine (Amersham) was added to each well, and cells were incubated for 24 h for thymidine incorporation into DNA [21, 22]. For measuring the cell-proliferation rate, cells were washed twice with PBS, and DNA was precipitated by use of trichloroacetic acid. Finally, cells were homogenized and the total amount of lysate was dissolved in 4 mL liquid-scintillation fluid for total radioactivity estimation in a liquid scintillation counter.

DNA Extraction and Apoptosis

The studies were carried out on 14d-adipocytes. For DNA extraction, cells were resuspended in Kauffman buffer (0.5 M Tris, 2 mM EDTA, 10 mM NaCl, and 1% SDS) and incubated for 12 h in the presence of 200 μg/ml proteinase K. DNA was extracted with phenol–chloroform [23] and apoptosis was measured by LMPCR (ligation-mediated PCR) [24], using the β-actin gene as control. The PCR samples were checked by 1.5% agarose gel electrophoresis and stained with ethidium bromide. The percentage of DNA fragmentation was quantified by scanning densitometry (Phoretix International, Newcastle upon Tyne, UK).

Oil Red O Staining

In order to assess the stage of differentiation, cells were stained by oil red O dye, lipid content being determined in both 7d-adipocytes and 14d-adipocytes. The cells were fixed with 3% paraformaldehyde and stained with the lipophilic dye oil red O (Sigma) dissolved in isopropanol, as previously described [14]. Stained cells were visualized by bright-field microscopy and photographed. Diameter of lipid droplets was measured by bright-field microscopy at ×40.

Annexin V–Propidium Iodide Staining

The staining was performed on 14d-adipocytes. To determine apoptosis by the annexin–propidium iodide method, cells were seeded on coverslips. After 3T3-L1 differentiation, cells were serum-starved for 24 h followed by 24 h-treatment with IL-15 (100 ng/mL). For annexin V–propidium iodide determination, the cells were fixed and stained by use of a commercial kit (rhAnnexin V/FITC/propidium iodide; Bendermedsystems, Pharmingen, San Diego, CA, USA). Apoptosis was assessed by laser-scanning microscopy with a laser wavelength of 495 nm.

DAPI Staining

DAPI staining was carried out using 14d-adipocytes. For analysis of nuclei condensation, the cells were seeded on coverslips. Twenty-four hours after serum deprivation, cells were treated for 24 h with 100 ng/mL IL-15. The cells were then washed with ice-cold PBS, fixed with 70% ethanol for 10 min, stained with a DAPI solution (1 μg/mL) for 20 min, then washed twice and mounted on glass slides with Vectiscilol (Vectashield® Mounting Medium; Vector Laboratoires H-1000, Southfield, MI, USA). DAPI staining was analyzed by use of an epifluorescence microscope (Leica, Solms, Germany).

Real-Time PCR (Polymerase Chain Reaction)

First-strand cDNA was synthesized from total RNA with oligo dT15 primers and random primers pdN6 by using a cDNA synthesis kit (Transcriptor Reverse Transcriptase, Roche, Barcelona, Spain). Analysis of mRNA levels for the genes from the different proteolytic systems was performed with primers designed to detect the following gene products: PPARδ (5′ GAAGCCATCCAGGACACCAT 3′; 3′ AAGG TCTCACTCTCCGTCTT 5′), leptin (5′ TTCACA CACGCAGTCGGTAT 3′; 3′ CATTCA GGGCTAAGGTC CAA 5′) and 18S (5′ GCGAATGGCTCATTAAAT CAGTTA 3′; 3′ GC ACGTAAATAGTCTAGTTTTGGT 5′). To avoid the detection of possible contamination by genomic DNA, primers were designed in different exons. The real-time PCR was performed using a commercial kit (LightCycler™ FastStart DNA Master^{PLUS} SYBR Green I, Roche, Barcelona, Spain). The relative amount of all mRNA was calculated by using the comparative C_T method. The invariant control for all studies was 18S mRNA.

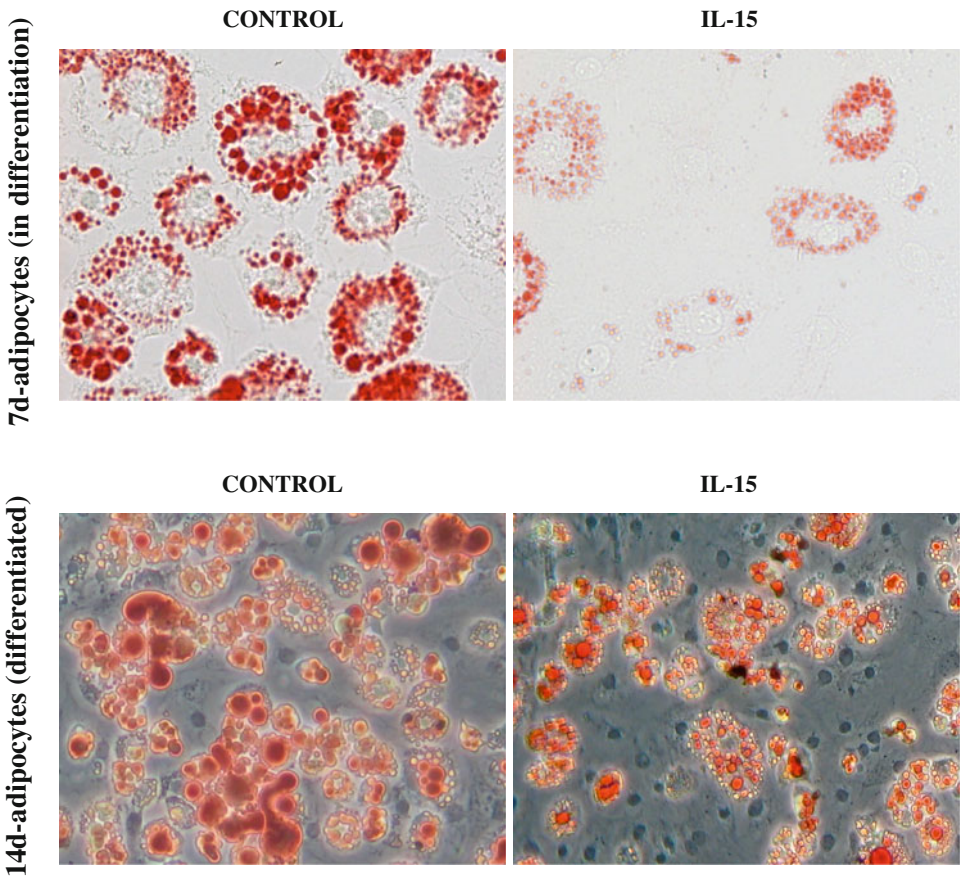

Fig. 1 Oil red O staining of both 7d-adipocytes (in differentiation) and 14d-adipocytes (completely differentiated) after treatment with vehicle or IL-15. Oil red O dye stains lipid content of the cells. These are representative photographs from six independent experiments. The results are means ± SEM for 100 cells and are expressed in μm (diameter of lipid droplets measured by bright-field microscopy at ×40)

Statistical Analysis

All data were analyzed by use of Student's *t* test. Statistical significance of results is indicated by: $*p < 0.05$, $**p < 0.01$, $***p < 0.001$.

Results

To check the degree of adipocyte differentiation, cells were stained with oil red O dye to estimate lipid content (Fig. 1). It can be seen that cells were clearly differentiated and how IL-15 resulted in a significant decrease in lipid content. Levels of different markers (PPAR-γ2 and leptin) also indicated a clear effect of IL-15 on lipid content (Table 1). Because p42/44 MAPK play a central role in the regulation of cell proliferation and cell survival [25–27], their content was analyzed. In preadipocytes, IL-15 treatment caused a significant decrease (60% less than control) of both the phosphorylated form and the total amount of p42/44 MAPK (Fig. 2a) with no differences in the ratio (Fig. 2b). However, IL-15 treatment of early differenciated adipocytes (7 days) caused a strong decrease of the p44 MAPK protein content (84% less than in the control) (Fig. 2a, b). On the other hand, in 14d-adipocytes, IL-15 treatment led to an increase of both forms of p42/44 MAPK (phosphorylated active p44 73% and p42 29%; total amount p44 42% and p42 47%) protein (Fig. 2a).

Table 1 Effects of IL-15 on 7d-adipocytes' mRNA content of the differentiation markers

Experimental group	Control	IL-15
PPARγ	100 ± 48 (5)	26 ± 11 (4)
Leptin	100 ± 30 (5)	17 ± 8 (4)*

For more details see the "Materials and Methods" section. Results are mean ± SEM (*n*) for the number indicated in parentheses. The results are expressed as a percentage of controls. Values that are significantly different by the Student's *t* test from the control group are indicated by $*p < 0.05$

To relate the effects of the cytokine to cell differentiation, the JAK/STAT pathways were examined. The total and activated amount of both JAK and STAT proteins in the different stages of adipocyte differentiation under IL-15 treatment were determined. Despite a significant increase in the total amount of JAK1 and STAT5 proteins in 3T3-L1 preadipocytes (25 and 80% respectively) (Fig. 3a), the ratio between the active or phosphorylated form and the total protein content indicated that there was a significant decrease of active JAK1 protein whereas no significant changes were observed for STAT5 (Fig. 3b). During the

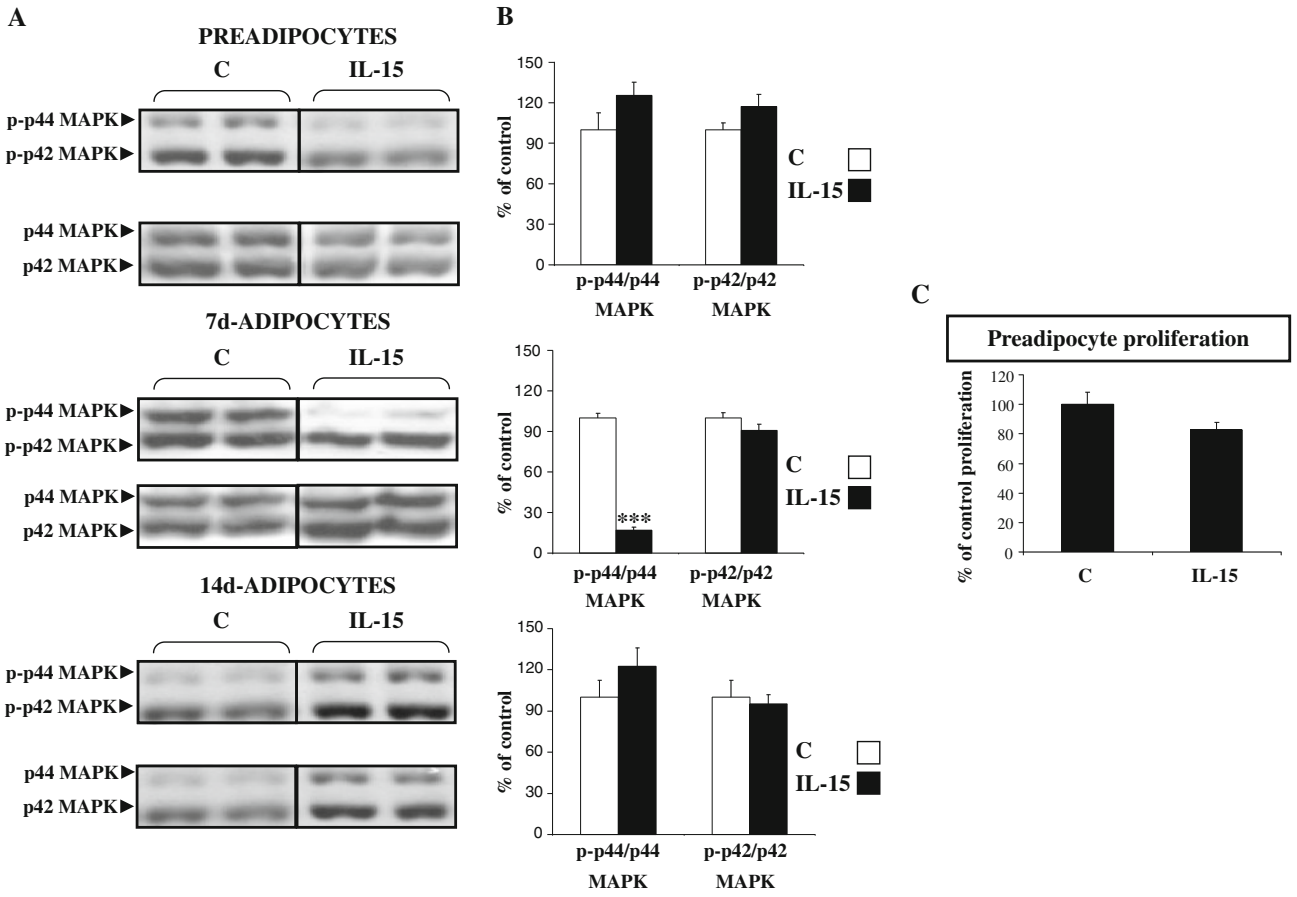

Fig. 2 Effects of IL-15 on MAPK protein content, cell cycle distribution, and proliferation rate. *C* control, *IL-15* IL-15-treated cells. **a** Representative Western blot pattern of both phosphorylated and total p42/p44 MAPK. The images were densitometrically analyzed and corrected for tubulin levels as loading control (images not shown). Data were then statistically analyzed (Student's *t* test). **b** Ratio of densitometric analysis of phosphorylated and total form of p42/p44 MAPK content. The results are means ± SEM for 4 or 5 samples and are expressed as percentages of control values. Values that are significantly different by the Student's *t* test from the control group are indicated by $***p < 0.001$. **c** Effects of IL-15 on proliferation rate of preadipocytes expressed as a percentage of proliferation of control cells

differentiation of 3T3-L1 cells (d7-adipocytes), cytokine treatment induced a decrease in both the active form and the total amount of STAT5 protein, despite no changes were observed in the ratio (Fig. 3a, b). However, in d14-adipocytes, the IL-15 treatment resulted in a significant increase of both JAK1 and STAT5 phosphorylated proteins (127 and 300% respectively) (Fig. 3a) also in the ratio (Fig. 3b), suggesting activation of the JAK/STAT pathway in mature 3T3-L1 adipocytes.

AKT is another important signaling protein for cell proliferation and differentiation [28]. No differences were observed in AKT protein content in 3T3-L1 preadipocytes treated with IL-15 (Fig. 4a). However, treatment with this cytokine induced a significant increase in the total amount of AKT protein (42%) (Fig. 4a) and reduced the ratio (Fig. 4b), therefore modulating the activity of this pathway. Finally, IL-15 caused an increase in both activated and total of AKT protein in 14d-adipocytes (70 and 54%, respectively) (Fig. 4a).

p38 and SAPK/JNK belong to the MAPK signaling pathway and are known to be involved in the regulation of differentiation and cell apoptosis. Interestingly, these proteins can regulate each other [25, 29–32]. In preadipocytes, IL-15 treatment caused a decrease in the total amount of p38 (47%) without affecting its activated phosphorylated form, as shown in Fig. 5a, b. Moreover, in 7d-adipocytes IL-15 treatment also caused a significant reduction in the total amount of p38 (34%), leading to a significant increase of the ratio phospho-p38/p38 (Fig. 5a, b). Finally, in 14d-adipocytes the treatment resulted in a significant decrease in the percentage of activation, but an increase in the total amount of p38 protein (73%). In order to see the effects of IL-15 on the SAPK/JNK pathway, the two proteins that form the dimer (SAPK/JNK54/46) were analyzed. IL-15

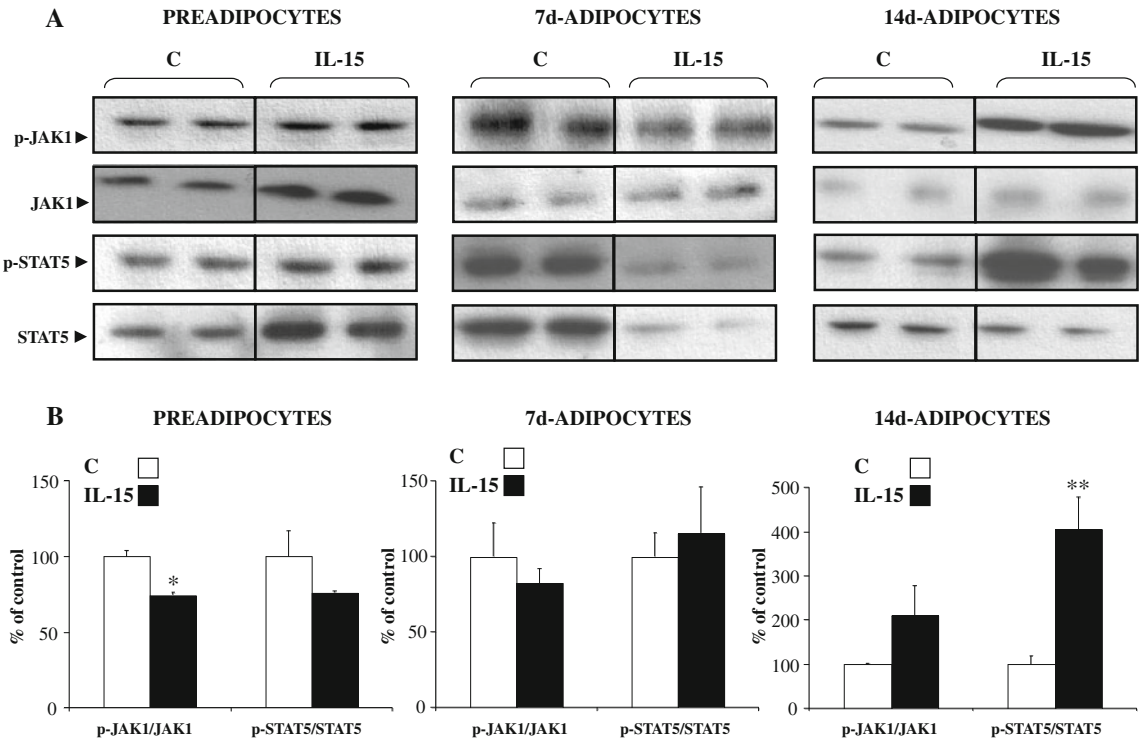

Fig. 3 Effects of IL-15 on JAK1 and STAT5 protein content. *C* control, *IL-15* IL-15-treated cells. **a** Representative Western blot pattern of both phosphorylated and total JAK1 and STAT5. The images were densitometrically analyzed and corrected for tubulin levels as loading control (images not shown). Data were then statistically analyzed (Student's *t* test). **b** Ratio of densitometric analysis of phosphorylated and total form of JAK1 and STAT5 content. The results are means ± SEM for 4 or 5 samples and are expressed as percentages of control values. Values that are significantly different by the Student's *t* test from the control group are indicated by $*p < 0.05$, $**p < 0.01$

treatment caused a significant decrease of the ratio between phospho-SAPK/JNK and SAPK/JNK total (in both JNK54 and 46) in preadipocytes (Fig. 5b). Interestingly, during adipocyte differentiation (14d-adipocytes), the ratio between the active and total forms of these proteins was increased (Fig. 5b).

It is important to note that the increase in p38 and SAPK/JNK in mature 14d-adipocytes has been related to increased apoptosis [25, 31]. Thus, to determine if this could be a satisfactory explanation for the observed increase in the p38 protein, apoptosis was studied by the LMPCR method. Figure 6a shows a clear and significant increase of the DNA ladder levels after IL-15 treatment in 14d-adipocytes, supporting increased apoptosis as a result of the cytokine treatment. DAPI and annexin–propidium iodide analysis confirmed the effects of IL-15 on apoptosis (Fig. 6b, c).

Discussion

The accretion of WAT observed in obese patients can be because of an increase in cell size, cell number or both [33], indicating that the molecular mechanisms that regulate preadipose cell growth, adipose differentiation, and lipogenesis in fat cells, have a key role in controlling the energy balance [33]. Cytokines seem to be major regulators of adipose tissue metabolism [34]. Taking this into consideration, IL-15 is a cytokine of special interest because it causes an important reduction of WAT weight by altering several important processes within this tissue, for example lipogenesis [9, 15], LPL activity, or lipid uptake [5, 10]. Furthermore, it is important to note that our results from oil red O staining confirm that IL-15 is able to inhibit adipogenesis in 3T3-L1 cells as previously described [14].

IL-15 signaling pathways have been widely studied in the immune system since this cytokine was firstly described in immune cells in 1994 [35, 36]. However, very few investigations have been focused on the proteins involved in IL-15 signal transduction in adipose tissue or other non-immune system tissues. Ajuwon and Spurlock [20] described the direct regulation of lipolysis by IL-15 in primary pig adipocytes through a pathway regulated in part by PKA and JAK proteins.

In order to study the signaling of IL-15 on adipocytes, we chose the 3T3-L1 cell line. This is an immortal fibroblast line derived from nonclonal Swiss 3T3 cells that are

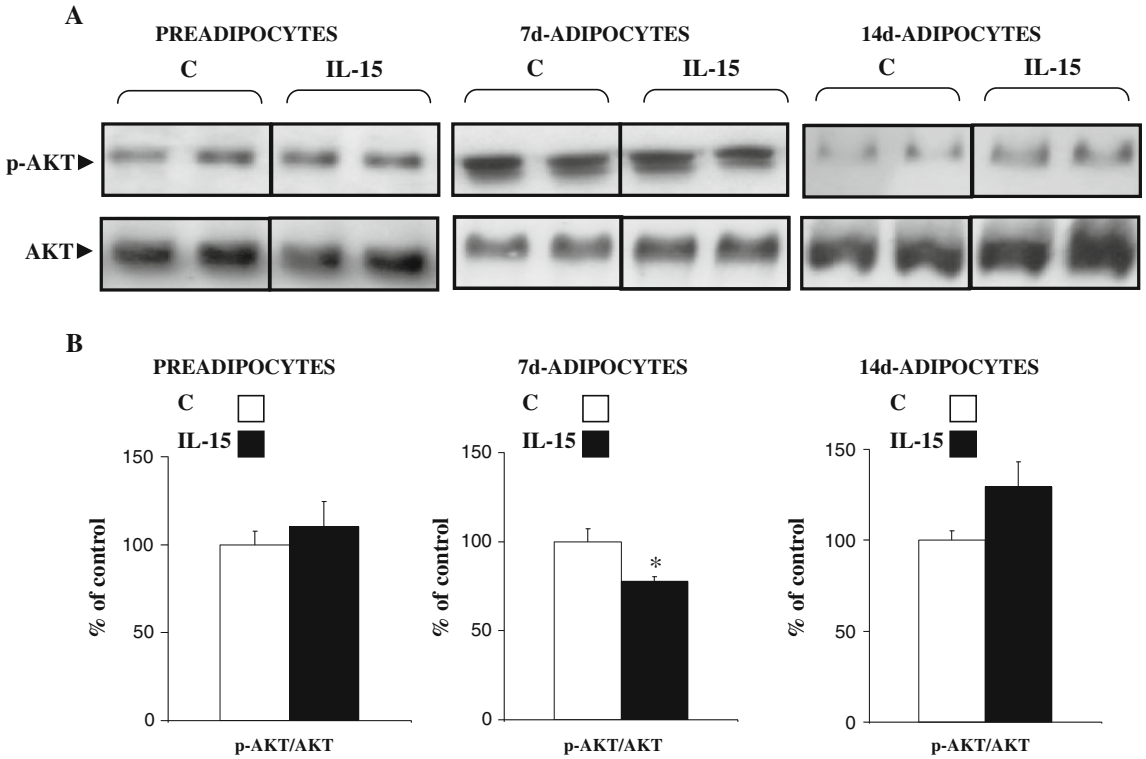

Fig. 4 Effects of IL-15 on AKT protein content. *C* control, *IL-15* IL-15-treated cells. **a** Representative Western blot pattern of both phosphorylated and total AKT. The images were densitometrically analyzed and corrected for tubulin levels as loading control (images not shown). Data were then statistically analyzed (Student's *t* test). **b** Ratio of densitometric analysis of phosphorylated and total form of AKT content. The results are means ± SEM for 4 or 5 samples and are expressed as percentages of control values. Values that are significantly different by the Student's *t* test from the control group are indicated by $*p < 0.05$

already committed to the adipocytic lineage [37]. This cellular model has some limitations, because the adipose tissue matrix has an important role in adipocyte differentiation. However, when these cells receive the appropriate hormonal inducers, they undergo differentiation to mature fat cells [37–39]. In fact, the first stage before differentiation is growth arrest, which is achieved in cultured cells by contact inhibition (named in this study as the preadipocyte group). When the cultured cells receive the differentiation cocktail (isobutylmethylxanthine, dexamethasone, and insulin), they begin the next step of differentiation, called clonal expansion. This is followed by a second growth arrest which is associated with several changes in protein expression. After this, the cells acquire a round morphology, accumulate lipid, become insulin-sensitive, and express typical gene markers (for example PPARγ) of completely differentiated adipocytes [40].

In immune cells, IL-15 signals through several molecules, for example MAPK, AKT, or JAK/STAT. Among these, p42/44 MAPK is highly related to the promotion of cell division [27] and this could be the role of this protein in 3T3-L1 preadipocytes. Indeed, IL-15 seems to downregulate p42/44 MAPK levels in preadipocytes, and it could lead to a tendency of a lower proliferation rate.

The JAK/STAT pathway is a predominant signaling cascade for cytokines including the IL-15 signaling pathway [7]. In addition, it has been described that during adipocyte differentiation, expression levels of STAT5 are highly induced and dysregulation of this cell process attenuates induction of this protein [41]. Floyd and Stephens [42] stated that STAT5A ectopic expression in nonprecursor cells led to fat cell differentiation, confirming the importance of this signaling protein in this adipocyte process. As mentioned in the "Results" section, IL-15 treatment resulted in a decrease in differentiation markers in 7d-adipocytes. Interestingly, treatment of 7d-adipocytes with IL-15 clearly resulted in downregulation of the levels of STAT5 protein, indicating that the effects of IL-15 on adipogenesis could be partly mediated through STAT5 protein. Conversely, in mature adipocytes STAT5 protein has been reported to have an antilipogenic role by inhibiting expression of fatty acid synthase, the central enzyme for de-novo lipogenesis [43]. Furthermore, it has been reported that IL-15 induces loss of adipose tissue partly by inhibiting lipogenesis [9]. Indeed, IL-15 treatment of 14d-adipocytes results in a significant increase in the activity of the JAK/STAT pathway and a decrease in lipid content, suggesting that this cytokine

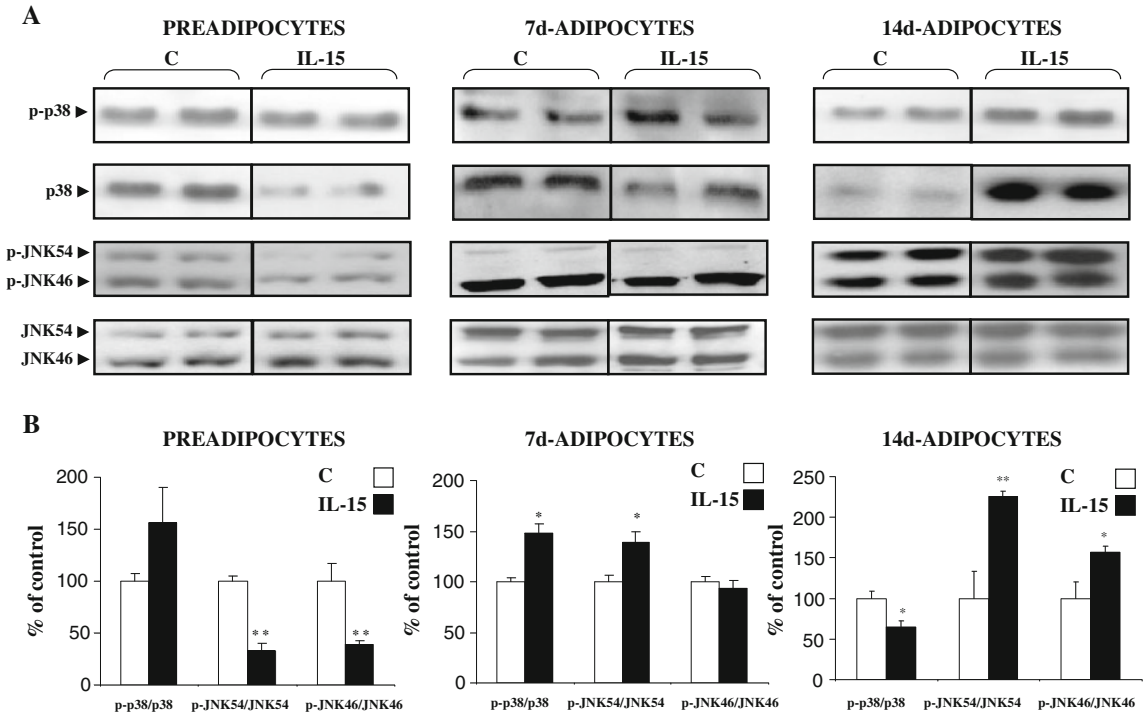

Fig. 5 Effects of IL-15 on p38 and SAPK/JNK protein content. *C* control, *IL-15* IL-15-treated cells. **a** Representative Western blot pattern of both phosphorylated and total p38 and SAPK/JNK. The images were densitometrically analyzed and corrected for tubulin levels as loading control (images not shown). Data were then statistically analyzed (Student's *t* test). **b** Ratio of densitometric analysis of phosphorylated and total form of SAPK/JNK content. The results are means ± SEM for 4 or 5 samples and are expressed as percentages of control values. Values that are significantly different by the Student's *t* test from the control group are indicated by $*p < 0.05$, $**p < 0.01$

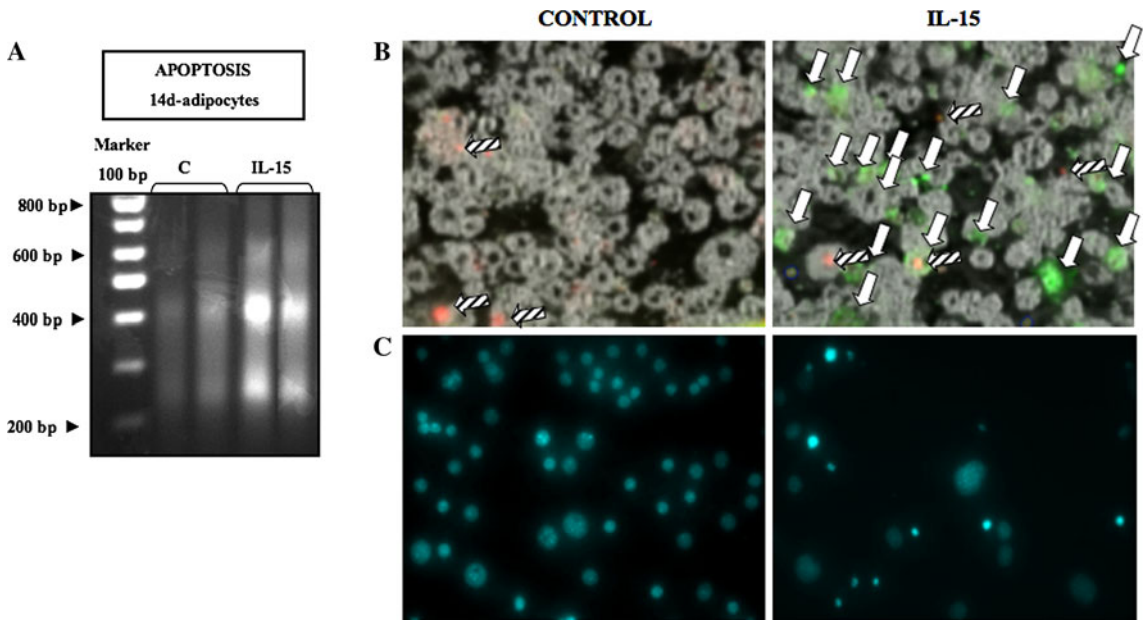

Fig. 6 Effects of IL-15 on apoptosis. *C* control, *IL-15* IL-15-treated cells. **a** DNA fragmentation analysis of adipocytes was assessed by the LMPCR method. **b** Annexin V–propidium iodide stained 3T3-L1 cells observed by laser-scanning microscopy. Cells were detected negative for Annexin V-FITC and PI (viable, or no measurable apoptosis), positive for Annexin V-FITC and negative for PI (*green*-colored and white arrows, early apoptosis, membrane integrity is present), and, finally, Annexin V-FITC and PI positive (*red*-colored and hatched arrows, end-stage apoptosis and death). **c** DAPI stained 3T3-L1 cells observed by epifluorescence microscopy (color figure online)

could also act through these proteins to control adipocyte lipogenesis.

There are contradictory reports on the role of p42/44 MAPK in adipogenesis. On the one hand, some studies have implicated these proteins in the differentiation process [44] and, on the other hand, Font de Mora et al. [45] stated that they are not necessary for this process but rather these proteins exert an antagonizing effect on adipogenesis. However, it is important to note that after insulin treatment—as a differentiation stimulus—the MAPK and AKT pathways are activated [46]. Insulin treatment seems to exert a dual effect on 7d-adipocytes, by inducing mitogenesis in growing cells, and differentiation in confluent cells through p42/44 MAPK and AKT respectively. In our study, the observation that IL-15 inhibited p44 MAPK reinforces the role of this protein in the differentiation process. On the other hand, the activation of p42/44MAPK by IL-15 at day 14 could also be correlated with cytokine blockage of the differentiation process, because p42/44MAPK has been involved in inhibition of terminal adipose conversion. Interestingly, sustained activation of p42/44 MAPK has been demonstrated to inhibit terminal adipose conversion by inhibition of PPARγ, at least [47]. IL-15 could act by blocking the final stages of adipogenesis in 14d-adipocytes by increasing the protein level of p42/44 MAPK and consequently could be blocking PPARγ activity. Additionally, and because the AKT pathway has a key role in adipogenesis, it has been reported that constitutive activation of AKT induces spontaneous adipogenesis in 3T3-L1 cells [28]. The IL-15-induced decrease of the activation ratio at day 7 supports the effects of this cytokine on adipogenesis.

Although previous work established a direct relationship between p38 upregulation and apoptosis in 3T3-L1 adipocytes [29], the results of our study showed upregulation of total p38 in mature adipocytes without affecting the activated protein. In addition, in 14d-adipocytes IL-15 treatment caused a significant increase in SAPK/JNK, which seems to lead to an increment in apoptosis levels as shown in the apoptotic assays (Fig. 6). These results agree with the study of Yang et al. [31], who reported that increased levels of SAPK/JNK are also directly related to apoptosis.

In conclusion, this study expands knowledge of the actions of IL-15 on body fat [8, 10] and confirms the anti-adipose tissue actions of the cytokine. IL-15 could, thus, regulate energy homeostasis by affecting adipose tissue in several cell processes including proliferation, differentiation, lipogenesis, and apoptosis. These actions on adipocytes may be mediated by different signaling pathways: p42/44 MAPK in proliferation and final conversion to adipocytes, STAT5 during differentiation process and lipogenesis, and SAPK/JNK in apoptosis in mature adipocytes. Additional studies are needed to further understand the role of IL-15 in adipogenesis.

Acknowledgments Gemma Fuster was supported by the Dirección General de Investigación Científica y Técnica (BFI2002-02186) of the Ministerio de Educación y Ciencia. Cibely Cristine Fontes-Oliveira was supported by the Programme Alβan, the European Union Programme of High-Level Scholarships for Latin America, scholarship no. E05D059293BR. Contract grant sponsor: Fondo de Investigaciones Sanitarias del Instituto de Salud Carlos III of the Ministerio de Sanidad y Consumo; Contract grant number: 06/0907. Contract grant sponsor: Generalitat de Catalunya (SGR/00108). Contract grant sponsor: Ministerio de Ciencia y Tecnología; Contract grant number: SAF 4744-2005.

Conflict of interest All authors of this research have no conflict of interest related with employment, consultancies, stock ownership, honoraria, paid expert testimony, patent applications/registrations, and grants or other funding.

References

1. Visscher TL, Seidell JC (2001) The public health impact of obesity. Annu Rev Public Health 22:355–375
2. Muoio DM, Newgard CB (2006) Obesity-related derangements in metabolic regulation. Annu Rev Biochem 75:367–401
3. Zhang Y, Hufnagel C, Eiden S, Guo KY, Diaz PA, Leibel R et al (2001) Mechanisms for LEPR-mediated regulation of leptin expression in brown and white adipocytes in rat pups. Physiol Genomics 4:189–199
4. Argiles JM, Lopez-Soriano J, Almendro V, Busquets S, Lopez-Soriano FJ (2005) Cross-talk between skeletal muscle and adipose tissue: a link with obesity? Med Res Rev 25:49–65
5. Almendro V, Busquets S, Ametller E, Carbo N, Figueras M, Fuster G et al (2006) Effects of interleukin-15 on lipid oxidation: disposal of an oral [(14)C]-triolein load. Biochim Biophys Acta 1761:37–42
6. Carbo N, Lopez-Soriano J, Costelli P, Busquets S, Alvarez B, Baccino FM et al (2000) Interleukin-15 antagonizes muscle protein waste in tumour-bearing rats. Br J Cancer 83:526–531
7. Budagian V, Bulanova E, Paus R, Bulfone-Paus S (2006) IL-15/IL-15 receptor biology: a guided tour through an expanding universe. Cytokine Growth Factor Rev 17:259–280
8. Quinn LS (2008) Interleukin-15: a muscle-derived cytokine regulating fat-to-lean body composition. J Anim Sci 86(14 Suppl):E75–83
9. Lopez-Soriano J, Carbo N, Almendro V, Figueras M, Ribas V, Busquets S et al (2004) Rat liver lipogenesis is modulated by interleukin-15. Int J Mol Med 13:817–819
10. Carbo N, Lopez-Soriano J, Costelli P, Alvarez B, Busquets S, Baccino FM et al (2001) Interleukin-15 mediates reciprocal regulation of adipose and muscle mass: a potential role in body weight control. Biochim Biophys Acta 1526:17–24
11. Almendro V, Fuster G, Busquets S, Ametller E, Figueras M, Argiles JM et al (2008) Effects of IL-15 on rat brown adipose tissue: uncoupling proteins and PPARs. Obesity 16:285–289
12. Fredenrich A, Grimaldi PA (2005) PPAR delta: an uncompletely known nuclear receptor. Diabetes Metab 31:23–27
13. Barra NG, Reid S, MacKenzie R, Werstuck G, Trigatti BL, Richards C et al. (2009) Interleukin-15 contributes to the regulation of murine adipose tissue and human adipocytes. Obesity (Silver Spring) 18: 1601–1607
14. Quinn LS, Strait-Bodey L, Anderson BG, Argiles JM, Havel PJ (2005) Interleukin-15 stimulates adiponectin secretion by

3T3–L1 adipocytes: evidence for a skeletal muscle-to-fat signaling pathway. Cell Biol Int 29:449–457
15. Alvarez B, Carbo N, Lopez-Soriano J, Drivdahl RH, Busquets S, Lopez-Soriano FJ et al (2002) Effects of interleukin-15 (IL-15) on adipose tissue mass in rodent obesity models: evidence for direct IL-15 action on adipose tissue. Biochim Biophys Acta 1570:33–37
16. Johnston JA, Bacon CM, Finbloom DS, Rees RC, Kaplan D, Shibuya K et al (1995) Tyrosine phosphorylation and activation of STAT5, STAT3, and Janus kinases by interleukins 2 and 15. Proc Natl Acad Sci USA 92:8705–8709
17. Zhu X, Suen KL, Barbacid M, Bolen JB, Fargnoli J (1994) Interleukin-2-induced tyrosine phosphorylation of Shc proteins correlates with factor-dependent T cell proliferation. J Biol Chem 269:5518–5522
18. Miyazaki T, Liu ZJ, Kawahara A, Minami Y, Yamada K, Tsujimoto Y et al (1995) Three distinct IL-2 signaling pathways mediated by bcl-2, c-myc, and lck cooperate in hematopoietic cell proliferation. Cell 81:223–231
19. Bulanova E, Budagian V, Pohl T, Krause H, Durkop H, Paus R et al (2001) The IL-15R alpha chain signals through association with Syk in human B cells. J Immunol 167:6292–6302
20. Ajuwon KM, Spurlock ME (2004) Direct regulation of lipolysis by interleukin-15 in primary pig adipocytes. Am J Physiol Regul Integr Comp Physiol 287:R608–R611
21. Vitt UA, Mazerbourg S, Klein C, Hsueh AJ (2002) Bone morphogenetic protein receptor type II is a receptor for growth differentiation factor-9. Biol Reprod 67:473–480
22. Spicer LJ, Aad PY, Allen DT, Mazerbourg S, Payne AH, Hsueh AJ (2008) Growth differentiation factor 9 (GDF9) stimulates proliferation and inhibits steroidogenesis by bovine theca cells: influence of follicle size on responses to GDF9. Biol Reprod 78:243–253
23. Almendro V, Carbo N, Busquets S, Figueras M, Tessitore L, Lopez-Soriano FJ et al (2003) Sepsis induces DNA fragmentation in rat skeletal muscle. Eur Cytokine Netw 14:256–259
24. Staley K, Blaschke AJ, Chun J (1997) Apoptotic DNA fragmentation is detected by a semi-quantitative ligation-mediated PCR of blunt DNA ends. Cell Death Differ 4:66–75
25. Ichijo H, Nishida E, Irie K, ten Dijke P, Saitoh M, Moriguchi T et al (1997) Induction of apoptosis by ASK1, a mammalian MAPKKK that activates SAPK/JNK and p38 signaling pathways. Science 275:90–94
26. Grewal JS, Mukhin YV, Garnovskaya MN, Raymond JR, Greene EL (1999) Serotonin 5-HT2A receptor induces TGF-beta1 expression in mesangial cells via ERK: proliferative and fibrotic signals. Am J Physiol 276:F922–F930
27. Meloche S, Pouyssegur J (2007) The ERK1/2 mitogen-activated protein kinase pathway as a master regulator of the G1- to S-phase transition. Oncogene 26:3227–3239
28. Magun R, Burgering BM, Coffer PJ, Pardasani D, Lin Y, Chabot J et al (1996) Expression of a constitutively activated form of protein kinase B (c-Akt) in 3T3–L1 preadipose cells causes spontaneous differentiation. Endocrinology 137:3590–3593
29. Engelman JA, Lisanti MP, Scherer PE (1998) Specific inhibitors of p38 mitogen-activated protein kinase block 3T3–L1 adipogenesis. J Biol Chem 273:32111–32120
30. Engelman JA, Berg AH, Lewis RY, Lin A, Lisanti MP, Scherer PE (1999) Constitutively active mitogen-activated protein kinase kinase 6 (MKK6) or salicylate induces spontaneous 3T3–L1 adipogenesis. J Biol Chem 274:35630–35638
31. Yang JY, Della-Fera MA, Baile CA (2006) Esculetin induces mitochondria-mediated apoptosis in 3T3–L1 adipocytes. Apoptosis 11:1371–1378
32. Qin B, Qiu W, Avramoglu RK, Adeli K (2007) Tumor necrosis factor-alpha induces intestinal insulin resistance and stimulates the overproduction of intestinal apolipoprotein B48-containing lipoproteins. Diabetes 56:450–461
33. Spiegelman BM, Flier JS (1996) Adipogenesis and obesity: rounding out the big picture. Cell 87:377–389
34. Coppack SW, Patel JN, Lawrence VJ (2001) Nutritional regulation of lipid metabolism in human adipose tissue. Exp Clin Endocrinol Diabetes 109(Suppl 2):S202–S214
35. Burton JD, Bamford RN, Peters C, Grant AJ, Kurys G, Goldman CK et al (1994) A lymphokine, provisionally designated interleukin T and produced by a human adult T-cell leukemia line, stimulates T-cell proliferation and the induction of lymphokine-activated killer cells. Proc Natl Acad Sci USA 91:4935–4939
36. Grabstein KH, Eisenman J, Shanebeck K, Rauch C, Srinivasan S, Fung V et al (1994) Cloning of a T cell growth factor that interacts with the beta chain of the interleukin-2 receptor. Science 264:965–968
37. Green H, Meuth M (1974) An established pre-adipose cell line and its differentiation in culture. Cell 3:127–133
38. Green H, Kehinde O (1975) An established preadipose cell line and its differentiation in culture. II. Factors affecting the adipose conversion. Cell 5:19–27
39. Green H, Kehinde O (1976) Spontaneous heritable changes leading to increased adipose conversion in 3T3 cells. Cell 7:105–113
40. Ntambi JM, Young-Cheul K (2000) Adipocyte differentiation and gene expression. J Nutr 130:3122S–3126S
41. Stewart WC, Morrison RF, Young SL, Stephens JM (1999) Regulation of signal transducers and activators of transcription (STATs) by effectors of adipogenesis: coordinate regulation of STATs 1, 5A, and 5B with peroxisome proliferator-activated receptor-gamma and C/AAAT enhancer binding protein-alpha. Biochim Biophys Acta 1452:188–196
42. Floyd ZE, Stephens JM (2003) STAT5A promotes adipogenesis in nonprecursor cells and associates with the glucocorticoid receptor during adipocyte differentiation. Diabetes 52:308–314
43. Hogan JC, Stephens JM (2005) The regulation of fatty acid synthase by STAT5A. Diabetes 54:1968–1975
44. Sale EM, Atkinson PG, Sale GJ (1995) Requirement of MAP kinase for differentiation of fibroblasts to adipocytes, for insulin activation of p90 S6 kinase and for insulin or serum stimulation of DNA synthesis. EMBO J 14:674–684
45. Font de Mora J, Porras A, Ahn N, Santos E (1997) Mitogen-activated protein kinase activation is not necessary for, but antagonizes, 3T3–L1 adipocytic differentiation. Mol Cell Biol 17:6068–6075
46. Rosen ED, Spiegelman BM (2000) Molecular regulation of adipogenesis. Annu Rev Cell Dev Biol 16:145–171
47. Hu E, Kim JB, Sarraf P, Spiegelman BM (1996) Inhibition of adipogenesis through MAP kinase-mediated phosphorylation of PPARgamma. Science 274:2100–2103

of important cellular signaling molecules, termed adipokines. These adipokines have consequences ranging from local autocrine and paracrine effects to systemic endocrine actions. Adipokines also vary widely in both their function and mechanisms of control. One such mechanism of control is the fatty acid composition of adipose tissue which can affect cellular signaling, fatty acid trafficking, gene expression and, consequently, metabolism [1]. Adipose tissue composition varies based on two main effectors: energy balance, which regulates the metabolism of free fatty acids within the adipose tissue, and diet, which will alter the fatty acid profile of the adipose tissue. Although the former has been examined extensively, particularly with regard to leptin expression and adipocyte differentiation, the effects of the latter on endocrine function have only recently begun to be investigated.

Adiponectin is the most highly expressed and secreted adipokine, with beneficial effects on metabolism, inflammation, and vascular function. Adiponectin has a paradoxical expression pattern. As adiposity increases, adiponectin expression and secretion decreases within the adipose tissue [2]. It is believed that this paradox is part of the pathology of obesity, and is symptomatic of dysfunctional adipose tissue. Adiponectin plays a role in insulin sensitivity, LDL oxidation, eNOS activation, inflammation suppression and fatty acid catabolism [3–5]. Thus, hypoadiponectinemia is of interest as a biomarker of both cardiovascular disease and metabolic syndrome.

Another important adipokine that could be stimulated by changes in fatty acid profile is leptin. It was first discovered as the protein encoded by the *obese* gene, named for the phenotype of the double knockout mouse. These mice experience no satiety, and thus eat continuously when fed ad libitum, leading to severe diet-induced obesity. In humans, leptin deficiency has been implicated in cases of morbid obesity, as either a genetic factor or a metabolic insufficiency [6, 7]. Leptin's role in hypothalamic-mediated appetite suppression in response to caloric intake is not its only function. Leptin may also be important in the modulation of T cell activity in the early stages of atherosclerotic development as well as other immune cells [8]. In obesity, leptin may be under-expressed by the adipose tissue in response to a consistently high caloric diet, or, leptin receptors may be down-regulated, thus leading to high plasma leptin levels and leptin resistance [9].

Flaxseed has recently gained popularity as a functional food. Alpha-linolenic acid (ALA) comprises approximately 55% of the total fatty acid content of flaxseed fatty acids [10]. ALA-rich diets, including diets enriched with ground flaxseed, have been shown in interventional and experimental trials to reduce both fatal and non-fatal myocardial infarction [11, 12], cardiac arrhythmias [12–15], and the incidence of atherosclerotic lesions [12, 14, 16, 17]. However, the mechanism whereby ALA and flaxseed induce this cardio-protective action is unclear. Previous data have indicated that ALA from a flaxseed enriched diet is deposited in adipose tissue [18]. It is possible, therefore, that this change in adipose tissue fatty acid content may influence adipose tissue function. We hypothesize that the change in lipid composition in adipose tissue in response to a flaxseed supplemented diet may affect the adipokine signaling from the adipocytes. It is possible, therefore, that the beneficial cardiovascular actions of flaxseed previously observed may be associated with changes in adipokine expression.

Materials and Methods

Diet and Feeding

All experiments were conducted in accordance with the guidelines of the Canadian Council on Animal Care. Sixteen male New Zealand White rabbits (2.8 ± 0.1 kg, Southern Rose Rabbitry) were randomly assigned to receive one of four diets. Diets were prepared as previously described [15, 17] by the addition of components to a regular (RG) rabbit diet (CO-OP Complete Rabbit Ration, Federated Co-operatives): 0.5% cholesterol (CH), or 10% ground flaxseed (FX), or both (CF) for 8 weeks ($n = 4$). The chow was stored at 4 °C and protected from light. The diets differed only in total fat content due to the inclusion of the naturally ALA-rich ground flaxseed (Tables 1, 2). The diet fatty acid composition is outlined in Table 2. Addition of flaxseed to the diet significantly increased the amount of C16:0, C18:0, C18:1 (oleic acid) and C18:3 (ALA) provided. The addition of cholesterol had no significant effect on dietary fatty acids provided in comparison to the RG diet. Rabbits were fed 125 g/day of the diet.

Table 1 Crude dietary composition

	RG	FX	CH	CF
Crude protein (%)	21.3	20.5	20.4	20.5
Carbohydrates (%)	51.4	51.7	52.5	50.6
Crude fat (%)	5.4	8.1	5.2	8.9
Crude fibre (%)	13.5	11.7	13.6	12.4
Ash (%)	8.4	8.1	8.1	7.7
ALA (mg/g of diet)	2.0	20.0	2.1	22.5
Digestible energy (kcal/g)	3.38	3.56	3.37	3.60

RG regular diet, *FX* 10% flaxseed supplemented diet, *CH* 0.5% cholesterol supplemented diet, *CF* 10% flaxseed and 0.5% cholesterol supplemented diet

Table 2 Fatty acid composition of rabbit diets

FAME (mg/g)	RG	FX	CH	CF
C14:0	0.293 ± 0.014	0.371 ± 0.013	0.267 ± 0.002	0.337 ± 0.016
C14:1	0.131 ± 0.001	ND	0.033 ± 0.033	ND
C16:0	6.502 ± 0.247	9.567 ± 0.349*	6.338 ± 0.044	9.364 ± 0.232*
C16:1	0.403 ± 0.024	0.540 ± 0.031	0.354 ± 0.001	0.442 ± 0.004
C18:0	2.200 ± 0.147	3.942 ± 0.157*	2.048 ± 0.006	3.643 ± 0.186*
C18:1 Ol	10.693 ± 0.325	17.055 ± 0.862*	10.292 ± 0.010	16.361 ± 0.840*
C18:1 Vac	1.719 ± 0.148	2.775 ± 0.002*	1.644 ± 0.064	2.611 ± 0.067
C18:2 LA	11.191 ± 0.343	11.781 ± 0.513	12.328 ± 0.170	13.713 ± 0.490
C20:0	0.113 ± 0.011	0.165 ± 0.009	0.117 ± 0.001	0.159 ± 0.025
C18:3n-6 GLA	ND	0.115 ± 0.002	ND	0.125 ± 0.004
C20:1	ND	ND	ND	ND
C18:3n-3 ALA	1.993 ± 0.120	20.077 ± 0.841*	2.119 ± 0.036	22.535 ± 0.679*^
C20:2	0.092 ± 0.012	0.125 ± 0.009	0.087 ± 0.002	0.106 ± 0.007
C22:0	0.160 ± 0.012	0.196 ± 0.002	0.166 ± 0.006	0.199 ± 0.036
C22:1	0.112 ± 0.032	0.292 ± 0.009	0.095 ± 0.009	0.094 ± 0.042
C20:3	ND	ND	ND	0.193 ± 0.003
C22:6 DHA	ND	ND	0.105 ± 0.105	0.115 ± 0.115

Values are means ± SE, as mg of lipid/g of diet. Fatty acids were extracted from rabbit chow

RG regular fed, *FX* 10% flaxseed fed, *CH* 0.5% cholesterol fed, *CF* 0.5% cholesterol plus 10% flaxseed fed, *ND* not detectable amounts present

* $p < 0.05$ versus RG

^ $p < 0.05$ versus FX

Blood Sampling and Analysis

Blood was drawn from the left marginal ear vein of rabbits that were fasted overnight before starting their experimental diets and at 8 weeks. It was collected in vacutainer tubes containing EDTA (Becton–Dickinson). Blood samples were centrifuged at 4,500×*g* at room temperature for 10 min, and plasma was then stored at −80 °C. Before analysis, plasma samples were thawed and centrifuged at 6,800×*g*. Plasma levels of cholesterol and triglycerides were analyzed using a VetTest 8008 blood chemistry analyzer (IDEXX Laboratories). Fatty acids were extracted from plasma and derivatized, as described previously [15, 18].

Tissue Collection

After 8 weeks of dietary treatment, animals were euthanized by 5% isoflurane gas delivered by face mask, followed by cardiac extraction. Retroperitoneal and epididymal adipose tissue were collected. To prevent RNase contamination, the animal and tools were sprayed with RNaseZap (Ambion) both before and during tissue collection. Adipose tissue was immediately placed in RNAlater, and kept overnight at 4 °C, as indicated in the manufacturer's instructions (Ambion). Preliminary testing indicated that there was successful stabilization of mRNA compared to flash freezing or maintenance overnight at 4 °C (as assessed by agarose gel electrophoresis and subsequent qRT-PCR) despite the high lipid content of this tissue. RNAlater was removed from the tissue by suction, and the samples were then flash frozen in liquid nitrogen and stored at −80 °C.

qRT-PCR

RNA was extracted from the adipose tissue in an RNase-free environment. Adipose tissue was homogenized in Trizol reagent (Invitrogen), and fat was removed. Phenol was separated from the solution by washing the solution twice with chloroform. The RNA was precipitated from solution with ethanol, and added to RNeasy columns for further purification (Qiagen). Extracted RNA was quantified and assessed for quality by spectrophotometer and agarose gel electrophoresis. It was then used for qRT-PCR (Quanta Biosystems) using a iQ5 Real-Time PCR Detection System (Bio-Rad). Primers designed using BLAST software (NCBI) and were as follows: Adiponectin: (Forward 5′ACCAGGACAAGAACGTGG AC3′, Reverse 5′TGGAGATGGAATCGTTGACA3′);

Leptin: (Forward 5′GTCGTCGGTTTGGACTTCATC3′, Reverse 5′CGGAGGTTCTCCAGGTCGTTG3′) [19];

GAPDH: (Forward 5′GATGGTGAAGGTCGGAG TGAA3′, Reverse 5′GGTGAAGACGCCAGTGGATT3′) [20].

Primers were validated using NCBI's BLAST software [21]. Unused samples were stored at −80 °C. cDNA was synthesized from 1 ug of RNA with qScript cDNA Supermix (Quanta) via the manufacturer's directions. qPCR proceeded for 2 min at 50 °C, 95 °C for 8.5 min, then 40 cycles of 95 °C for 15 s and 60 °C for 60 s, at which point the data were captured. A melt curve was obtained after cycling with 95 °C for 1 min followed by 55 °C for 1 min,

and 80 10-s capture cycles of 55 + 0.5 °C/cycle. Results were normalized by GAPDH expression and analyzed by the delta–delta-Ct method using iCycler Real-Time Detection Software.

Fatty Acid Extraction and Methylation

Plasma fatty acids were directly extracted and derivatized using a modification of the original method described by Lepage and Roy [22] and later modified by Garg et al. [23]. Briefly, 100 μL of plasma was combined with 2 mL of 4:1 (v/v) methanol:toluene in a borosilicate glass tube. The methanol:toluene solution contained 0.5 mg/ml of the internal standard, C19:0 (Nu-Chek Prep. Inc.). While vortexing, 200 μL of acetyl chloride was slowly added. Tubes were capped with a Teflon lined lid, weighed and then heated at 100 °C for 1 h. Once cooled to room temperature, tubes were re-weighed to ensure no sample loss had occurred. Five milliliters of an aqueous 6% K_2CO_3 solution was then added to terminate and neutralize the reaction. The sample tube was then centrifuged at 5,000 rpm for 5 min at room temperature after which the upper toluene layer was removed and subjected to gas chromatographic analysis using flame ionization detection (GC-FID). Methylation was verified by thin layer chromatography. Fatty acids from approximately 15 mg of adipose tissue were extracted and derivatized using the method outlined by Lepage and Roy [24].

Gas Chromatography

Fatty acid methyl esters (FAME) were injected onto a Varian CP 3800 gas chromatographic system using a Varian CP 8400 autosampler. Analytes were detected using flame ionization detection and analyzed on a Varian MS Workstation (vrs. 6.9.1). One microliter of sample was injected at 250 °C at a split ratio of 50:1 onto a Varian CP-Sil 88 capillary column (60 m × 0.25 mm × 0.20 μm). Helium gas (ultra pure) was used as the carrier gas at a constant flow rate of 1.5 mL/min. The oven temperature was maintained at 111 °C for 1 min then rapidly increased by 20 °C/min to 170 °C. It was then slowly increased at a rate of 5 °C/min to 190 °C and finally by 3 °C/min up to 225 °C where it was maintained for 10 min. FAME were quantified against an external standard, GLC 462 (Nu-Chek Prep, Inc.).

Quantification of Aortic Atherosclerosis

The aorta from the ascending arch to the iliac bifurcation was isolated from peripheral tissues and washed in cold PBS, then opened longitudinally and pinned flat. The aortic lumen was digitally photographed and luminal images were analyzed with Silicon Graphics Imaging software. Fatty streaks and complicated lesions were expressed as a percentile of total luminal surface area.

Statistics

Results were reported as means ± SE, and analyzed with Sigma-Stat software by one-way ANOVA, using Fisher's LSD test. A significant correlation was identified by a *t* test. $p \leq 0.05$ was considered statistically significant.

Results

Body Weight

After 8 weeks of dietary treatment, mean body weight significantly increased from 2.8 ± 0.06 to 3.7 ± 0.09 kg. However, there was no effect on weight with the experimental diets as compared to control diets (data not shown).

Plasma Lipids

There was no significant change in the plasma cholesterol of animals fed a regular or flaxseed supplemented diet after 8 weeks. Supplementation of the diet with dietary cholesterol for 8 weeks induced severe hypercholesterolemia (Fig. 1a). Addition of dietary flaxseed to a cholesterol-enriched diet did not lower the plasma cholesterol values from those observed in animals fed a diet supplemented with cholesterol alone.

Plasma triglycerides were not significantly affected by any of the diets (Fig. 1b). Addition of milled flaxseed to the diet, providing ALA, induced a 17-fold increase in the percentage composition of ALA in the plasma (Fig. 1c). Simultaneous consumption of flaxseed and cholesterol doubled the amount of ALA in the plasma as compared to the consumption of flaxseed alone, comprising 21% of all plasma fatty acids. an eightfold increase in plasma ALA, despite being provided with only 2 mg of ALA/gram, supporting the observation that cholesterol aids in absorption of ALA [15–18].

Atherosclerosis

Animals fed a regular or flaxseed-supplemented diet for 8 weeks did not develop any quantifiable atherosclerosis in the aortic arch (Fig. 2). Inclusion of 0.5% cholesterol in the diet induced atherosclerotic lesions in the aorta, covering 76.3 ± 8.5% of the aortic lumen ($p < 0.05$ vs. RG, $n = 3$). Addition of ground flaxseed to the cholesterol-supplemented diet ameliorated the atherogenic effects of cholesterol, significantly reducing lesions to 28 ± 4.3% of the aortic lumen ($p < 0.05$ vs. CH, $n = 3$).

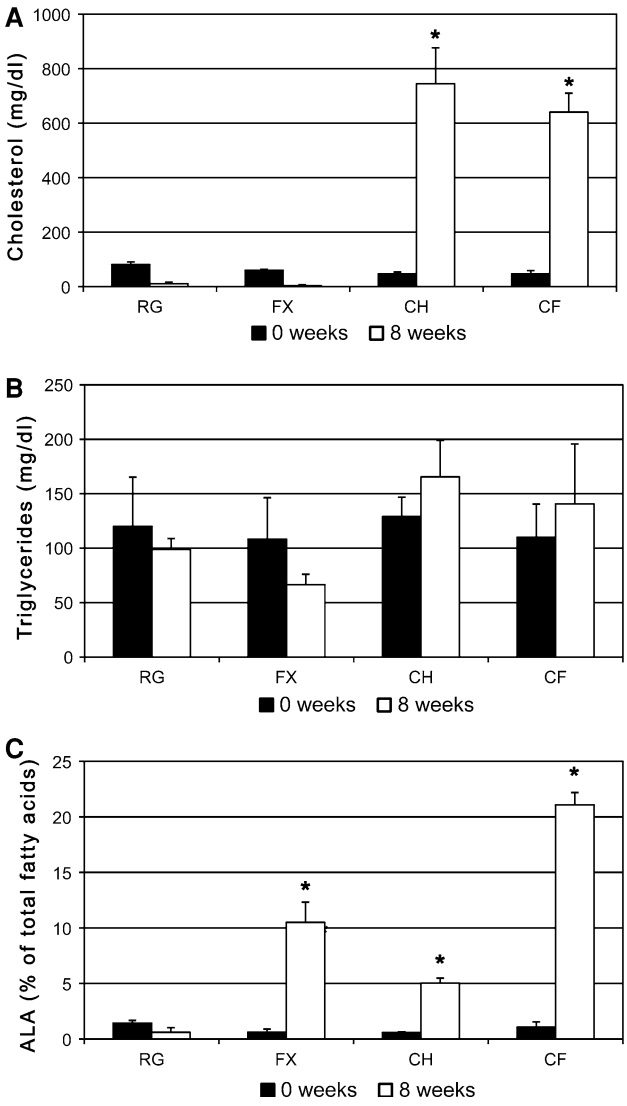

Fig. 1 Plasma cholesterol (**a**), triglycerides (**b**), and alpha-linolenic acid (**c**) levels in male New Zealand White rabbits at baseline and after 8 weeks of dietary treatment. *$p < 0.05$ versus RG; $n = 3$–4. *RG* regular chow, *FX* chow supplemented with 10% flaxseed, *CH* 0.5% cholesterol-supplemented diet, *CF* 10% flaxseed and 0.5% cholesterol-supplemented diet

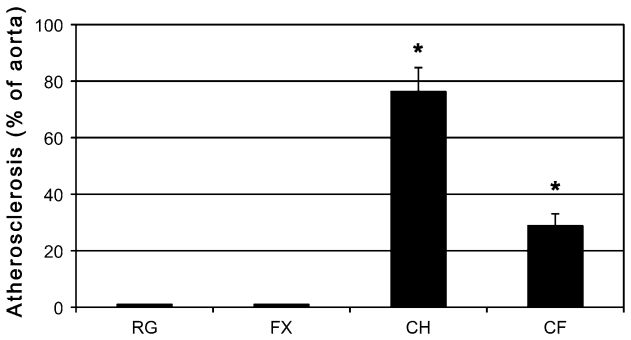

Fig. 2 Development of atherosclerotic lesions on the aorta of New Zealand White rabbits after 8 weeks of dietary treatment. Values are means ± SE; $n = 3$. *$p \leq 0.05$ versus RG; $p \leq 0.05$ versus CH. *RG* regular chow, *FX* chow supplemented with 10% flaxseed, *CH* 0.5% cholesterol-supplemented diet, *CF* 10% flaxseed and 0.5% cholesterol-supplemented diet

Fatty Acid Composition of Adipose Tissue

Total lipids were extracted from two primary sources of visceral fat. Epididymal and retroperitoneal fat consisted of 92.24% lipid by wet weight (range 83.3–99.5%), with no significant changes in total lipid between different dietary treatments, or either adipose source (Tables 3, 4).

The main component of adipose tissue was C18:1, oleic acid, which composed 32.3 ± 1.9% of total fatty acids in the retroperitoneal adipose of RG-fed animals (Table 3). C16:0, palmitic acid, and C18:2, linoleic acid, were also common, comprising 25.2 ± 1.4 and 26.7 ± 1.3% of the total retroperitoneal adipose tissue fatty acid content, respectively. Also stored in appreciable quantities in the retroperitoneal adipose tissue of animals fed a regular diet were ALA (6.34 ± 0.34%), steric acid (6.14 ± 0.57%), palmitoleic acid (2.12 ± 0.08%), vaccenic acid (1.98 ± 0.21%), and myristic acid (1.77 ± 0.12%) (Table 3).

The fatty acid proportions in the epididymal tissue of the animals fed a regular diet were not significantly different than the proportions of fatty acid in retroperitoneal tissue (Table 4). Dietary cholesterol did not significantly affect either total lipids or individual fatty acids as compared to RG. Addition of flaxseed to a regular diet significantly reduced levels of C16:0, C18:1-*cis*, C18:1-*trans*, and C18:2 in the adipose tissue, both in absolute concentrations and relative to total fatty acid content (Tables 3, 4). When consumed in conjunction with 0.5% cholesterol, dietary flaxseed induced a 3.1-fold increase in adipose tissue ALA, a significant increase as compared to RG, but significantly less than animals supplemented only with flaxseed. Dietary cholesterol did not affect any of the other fatty acids observed.

Adipokine Expression

Adiponectin and leptin are the two most highly expressed adipokines in adipose tissue. In epididymal adipose tissue, there was no significant change in either leptin or adiponectin mRNA expression after addition of either flaxseed or cholesterol to the diet (Fig. 3a). Adiponectin expression did not vary with dietary treatment in retroperitoneal adipose tissue (Fig. 3b). However, in retroperitoneal adipose tissue, dietary flaxseed induced a two-fold increase in leptin mRNA ($p < 0.05$ vs. RG). Conversely, dietary cholesterol reduced leptin mRNA expression by about one-half in comparison to control, and the addition of flaxseed to the cholesterol-supplemented diet induced a recovery of leptin expression, increasing expression beyond that of flaxseed alone.

Table 3 Fatty acids in retroperitoneal adipose tissue from rabbits fed diets for 8 weeks

FAME (μmol/g)	Retroperitoneal adipose tissue			
	RG	FX	CH	CF
10:0	ND	ND	ND	ND
12:0	ND	ND	1.54 ± 0.94	1.45 ± 0.87
12:1	ND	ND	ND	ND
14:0	74.40 ± 4.00	50.91 ± 6.76*	66.17 ± 2.12	60.90 ± 1.84
14:1	ND	ND	ND	ND
16:0	945.68 ± 37.82	699.88 ± 15.45*	905.45 ± 40.17	773.21 ± 25.07*
16:1	81.17 ± 7.50	46.95 ± 6.42	90.90 ± 10.74	83.39 ± 13.85
18:0	195.76 ± 12.98	169.31 ± 8.66	179.48 ± 6.93	169.35 ± 4.22
18:1 n-9	1,104.79 ± 75.25	821.93 ± 49.73*	981.88 ± 20.87	962.26 ± 21.53
18:1 *trans*	67.80 ± 7.42	42.39 ± 3.38*	55.96 ± 1.62	49.30 ± 1.26*
18:2 n-6	878.82 ± 26.06	705.14 ± 35.87*	938.47 ± 69.49	778.75 ± 19.54
20:0	0.51 ± 0.38	0.45 ± 0.24	0.88 ± 0.45	ND
18:3 n-6	ND	ND	ND	ND
18:3 n-3	218.96 ± 7.95	895.96 ± 63.33*	184.22 ± 6.98	672.52 ± 78.99*^
20:1	14.49 ± 1.69	11.83 ± 1.16	12.46 ± 1.29	11.14 ± 1.40
20:2	1.68 ± 0.57	0.27 ± 0.18	1.31 ± 0.51	0.60 ± 0.23
22:0	ND	ND	ND	ND
20:3 n-6	ND	ND	ND	ND
20:3 n-3	ND	5.76 ± 0.89	ND	3.32 ± 0.80
22:1	0.68 ± 0.28	0.22 ± 0.15	0.43 ± 0.26	0.83 ± 0.62
20:4 n-6	0.76 ± 0.44	0.38 ± 0.89	1.28 ± 0.75	0.83 ± 0.48
C22:2	ND	ND	ND	ND
C20:5 n-3	ND	ND	ND	ND
C24:0	ND	ND	ND	ND
C24:1	ND	ND	ND	ND
C22:4	ND	ND	ND	ND
C22:5	ND	0.58 ± 0.45	ND	0.48 ± 0.2
C22:6	ND	ND	ND	ND
TL (%)	90.5 ± 0.23	91.4 ± 3.70	95.7 ± 2.02	94.4 ± 1.35

Values are means ± SE. Fatty acids were extracted from retroperitoneal adipose tissue following 8 weeks of feeding ($n = 4$)

RG regular fed, *FX* 10% flaxseed fed, *CH* 0.5% cholesterol fed, *CF* 0.5% cholesterol plus 10% flaxseed fed, *ND* not detectable amounts present, *TL* total mg lipids extracted per mg of tissue

* $p < 0.05$ versus RG

^ $p < 0.05$ versus FX

These changes in leptin expression were positively correlated with plasma ALA and adipose ALA levels (Fig. 4). Plasma ALA correlated with leptin expression in the retroperitoneal adipose tissue ($p < 0.05$), but not in epididymal adipose (Fig. 4a). Adipose tissue ALA exhibited a stronger relationship than plasma ALA with leptin expression in retroperitoneal adipose tissue (Fig. 4b).

Relationship of Leptin Expression to Atherosclerosis

All animals that were not fed cholesterol did not exhibit any atherosclerosis. Consequently, in order to determine if there was a significant relationship between leptin expression and the development of atherosclerotic lesions, linear regression was performed only on data obtained from animals fed a cholesterol-supplemented diet. Increased leptin expression in the retroperitoneal adipose tissue significantly correlated ($p < 0.05$) with decreased atherosclerosis (Fig. 5).

Discussion

One of the primary purposes of this study was to determine if diets of very different lipid composition could influence the expression of leptin or adiponectin in adipose tissue when caloric balance was maintained. It is known that leptin expression varies with caloric balance and adiposity [25–28]. The present study was designed to avoid these potential variables by maintaining the diets in a manner which maintained a consistent level of caloric intake while at the same time insuring diversity in lipid composition. The differences in caloric values between the diets were so minor that they did not induce a significant change in body weight. The data obtained in the present study demonstrates that the lipid composition of the diet can have an important role to play in adipokine expression. The changes in adipokine expression were sensitive to the type of lipid in the diet, the adipose tissue examined and the

Table 4 Fatty acids in epididymal adipose tissue from rabbits fed diets for 8 weeks

FAME (μmol/g)	Epididymal adipose tissue			
	RG	FX	CH	CF
10:0	ND	ND	ND	ND
12:0	ND	1.13 ± 0.85	2.48 ± 1.70	ND
12:1	ND	ND	ND	ND
14:0	79.12 ± 3.28	59.37 ± 4.65	68.03 ± 4.33	57.85 ± 7.95
14:1	0.99 ± 0.52	ND	ND	ND
16:0	919.51 ± 32.27	676.35 ± 20.48*	862.90 ± 46.25	743.00 ± 44.11*
16:1	101.26 ± 11.89	64.76 ± 10.31	89.76 ± 14.79	92.60 ± 21.24
18:0	193.31 ± 7.60	162.54 ± 6.79	169.93 ± 11.23	158.20 ± 7.84
18:1 n-9	1,122.28 ± 38.65	889.86 ± 29.71*	925.11 ± 25.28	917.13 ± 73.87*
18:1 *trans*	69.78 ± 6.12	48.23 ± 1.50*	54.66 ± 3.68	49.07 ± 5.21*
18:2 n-6	893.65 ± 36.57	694.95 ± 22.56*	887.65 ± 17.06	789.54 ± 40.46
20:0	0.88 ± 0.45	ND	1.16 ± 0.61	1.27 ± 0.30
18:3 n-6	ND	ND	ND	ND
18:3 n-3	219.61 ± 7.33	916.35 ± 27.84*	176.76 ± 6.12	569.80 ± 96.29*^
20:1	15.06 ± 1.53	12.81 ± 0.92	11.97 ± 0.45	12.26 ± 0.26
20:2	1.13 ± 0.40	0.48 ± 0.28	0.98 ± 0.57	ND
22:0	ND	ND	ND	ND
20:3 n-6	ND	ND	ND	ND
20:3 n-3	ND	6.58 ± 2.16	ND	0.96 ± 0.81
22:1	1.67 ± 0.64	ND	1.83 ± 0.54	1.78 ± 0.34
20:4 n-6	ND	ND	ND	ND
C22:2	ND	ND	ND	ND
C20:5 n-3	ND	ND	ND	ND
C24:0	ND	ND	ND	ND
C24:1	ND	ND	ND	ND
C22:4	ND	ND	ND	ND
C22:5	ND	ND	ND	ND
C22:6	ND	ND	ND	ND
TL (%)	93.2 ± 2.87	90.5 ± 4.11	88.1 ± 3.36	94.1 ± 2.18

Values are means ± SE. Fatty acids were extracted from epididymal adipose tissue following 8 weeks of feeding ($n = 4$)

RG regular fed, *FX* 10% flaxseed fed, *CH* 0.5% cholesterol fed, *CF* 0.5% cholesterol plus 10% flaxseed fed, *ND* not detectable amounts present, *TL* total mg lipids extracted per mg of tissue

* $p < 0.05$ versus RG

^ $p < 0.05$ versus FX

adipokine studied as well. A high cholesterol diet suppressed leptin expression whereas a diet rich in the omega-3 fatty acid ALA increased leptin expression. Leptin expression was influenced by the diets whereas adiponectin was not. Retroperitoneal but not epididymal adipose tissue was affected by the diets. It is known that the location of the different adipose tissues will influence circulating adipokine levels [29].

The mechanism whereby leptin mRNA expression is regulated by dietary lipids is presently unclear. Although SREBP1c mRNA expression is directly related to polyunsaturated fatty acid content in adipose tissue [30] and an SREBP-like binding element is present in the leptin promoter, it is not responsive to SREBP itself [31]. However, polyunsaturated fatty acids may act as ligands for PPAR gamma to alter adipokine expression [32]. This may occur through an increase in translation [33]. Mason et al. [28] have demonstrated a novel binding site for an adipocyte-specific transcription factor in the -87 position of the leptin promoter which is conserved in both mice and humans, however, the consensus sequence does not match any known transcription factor. This region, termed LP1, presents an interesting possibility for a novel transcription factor which may regulate the response of leptin to dietary lipids in addition to PPAR-gamma.

The observation that the adipose tissue is responding to these diets in a very specific manner suggests that the changes are physiologically important. Increased leptin levels have been identified previously as a risk factor for atherosclerosis [34]. However, data correlating leptin and atherosclerosis have been derived from obese humans and animal models of obesity [35–39]. Our data indicates that in a non-obese population, leptin may have a previously unidentified role in cardioprotection. In support of this hypothesis, leptin expression was significantly correlated in a negative fashion with atherosclerosis. When leptin levels

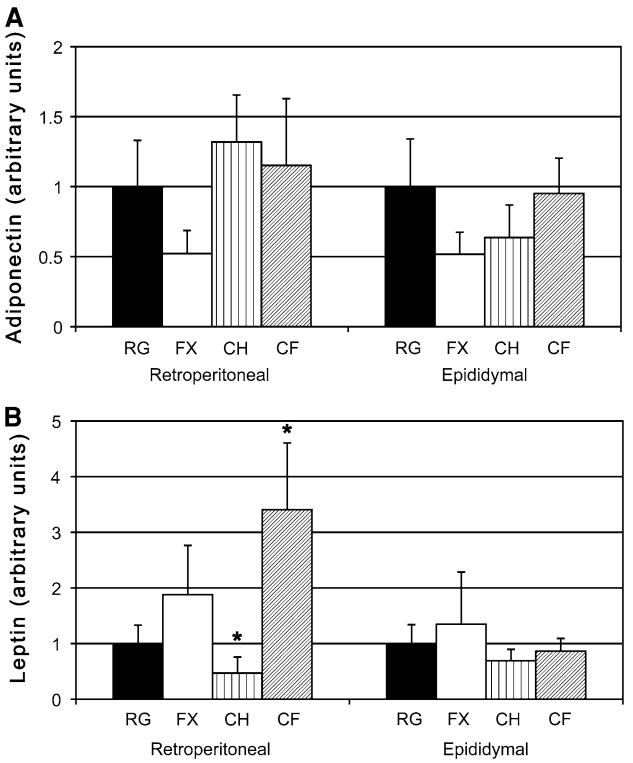

Fig. 3 mRNA expression of adiponectin (**a**) or leptin (**b**) in epididymal and retroperitoneal adipose tissue of New Zealand White rabbits after 8 weeks of dietary treatment, measured by quantitative real-time PCR. Values were normalized by GAPDH expression and expressed as means ± SE; $n = 3$–4. $^*p < 0.05$. *RG* regular chow, *FX* chow supplemented with 10% flaxseed, *CH* 0.5% cholesterol-supplemented diet, *CF* 10% flaxseed and 0.5% cholesterol-supplemented diet

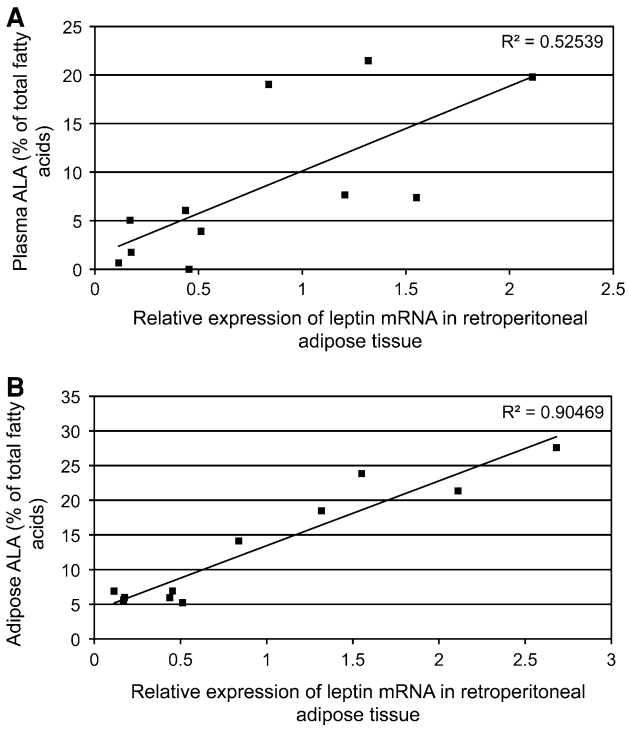

Fig. 4 Correlational analysis of expression of leptin mRNA from retroperitoneal adipose tissue with plasma alpha-linolenic acid (**a**), and adipose alpha-linolenic acid (**b**) of New Zealand White rabbits after 8 weeks of dietary treatment. **a** $^*p < 0.05$; **b** $p < 0.05$

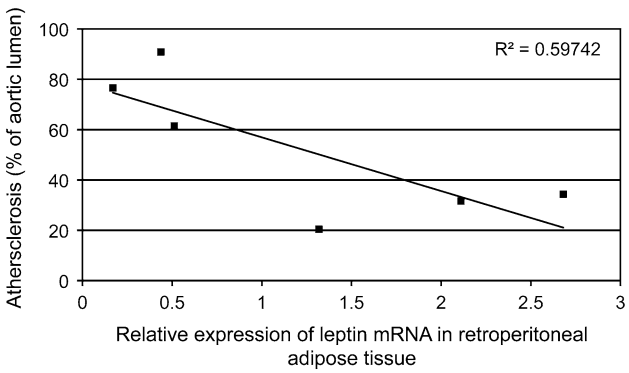

Fig. 5 Correlational analysis of the percentage of the aortic lumen covered with atherosclerotic plaque with leptin mRNA from retroperitoneal adipose tissue of hypercholesterolemic New Zealand White rabbits after 8 weeks of atherogenic dietary treatment. $^*p < 0.05$

were high, atherosclerosis was low and when leptin expression was depressed by circulating cholesterol, atherogenesis was stimulated.

Consumption of flaxseed has previously been shown to improve insulin resistance, hyperlipidemia, atherosclerosis and hypertension and decrease the incidence of cardiac arrhythmias [15–17, 40]. These effects of dietary flaxseed have been attributed, in part, to the rich ALA content of flaxseed [15–17, 40]. Dietary flaxseed provided a source of ALA in the present study which subsequently increased ALA both in the circulation and in the adipose tissue. With the addition of cholesterol to the flaxseed-supplemented diet, plasma ALA increased substantially but adipose tissue levels of ALA did not exhibit further increase beyond those observed when the diet was supplemented with flaxseed alone (Table 3). This could be due to one of several factors. ALA may be deposited in other organs preferentially, such as the heart and liver, as previously observed in the hypercholesterolemic rabbit [18]. Alternatively, a cholesterol-rich diet may direct the ALA to be used directly for beta-oxidation, thus reducing the amount of ALA available for storage [41]. Cholesterol may also induce an efflux of ALA from the adipose tissue, which is greater than the influx of ALA from the plasma, leading to a net decrease in ALA [42]. Further study is required to understand the relative lack of storage of ALA in the adipose tissue when it is presented with such high levels of circulating ALA.

Both beneficial and deleterious cytokines from the adipose tissue may be responsible for many of the links between diet, BMI and cardiovascular disease. The present data demonstrate that dietary cholesterol and flaxseed have

the capacity to alter leptin expression. The cardioprotective effects of flaxseed are thought to be provided in part by its delivery of ALA to the body [16, 40]. However, the mechanism to explain the induction of these effects by ALA remains elusive. In the present study, ALA in the adipose tissue was strongly associated with increased leptin expression and the subsequent reduction of atherosclerosis. Our data, therefore, suggests that flaxseed may induce its anti-atherogenic effects in part via an ALA-mediated modulation of the expression of leptin.

Acknowledgments This study was supported by a grant provided by Canadian Institutes for Health Research and through indirect support provided by the St. Boniface Hospital Foundation. RS McCullough is a Trainee of the Manitoba Health Research Council. AL Edel is a Canadian Institutes for Health Research Banting and Best Doctoral Trainee.

References

1. Gertow K, Rosell M, Sjogren P, Eriksson P, Vessby B, de Faire U, Hamsten A, Hellenius ML, Fisher RM (2006) Fatty acid handling protein expression in adipose tissue, fatty acid composition of adipose tissue and serum, and markers of insulin resistance. Eur J Clin Nutr 60:1406–1413
2. Kern PA, Di Gregorio GB, Lu T, Rassouli N, Ranganathan G (2003) Adiponectin expression from human adipose tissue: relation to obesity, insulin resistance, and tumor necrosis factor-alpha expression. Diabetes 52:1779–1785
3. Haluzik M, Parizkova J, Haluzik MM (2004) Adiponectin and its role in the obesity-induced insulin resistance and related complications. Physiol Res 53:123–129
4. Halleux CM, Takahashi M, Delporte ML, Detry R, Funahashi T, Matsuzawa Y, Brichard SM (2001) Secretion of adiponectin and regulation of apM1 gene expression in human visceral adipose tissue. Biochem Biophys Res Commun 288:1102–1107
5. Iacobellis G, Pistilli D, Gucciardo M, Leonetti F, Miraldi F, Brancaccio G, Gallo P, di Gioia CR (2005) Adiponectin expression in human epicardial adipose tissue in vivo is lower in patients with coronary artery disease. Cytokine 29:251–255
6. Paz-Filho G, Esposito K, Hurwitz B, Sharma A, Dong C, Andreev V, Delibasi T, Erol H, Ayala A, Wong ML, Licinio J (2008) Changes in insulin sensitivity during leptin replacement therapy in leptin-deficient patients. Am J Physiol Endocrinol Metab 295:E1401–E1408
7. Bluher S, Mantzoros CS (2009) Leptin in humans: lessons from translational research. Am J Clin Nutr 89:991S–997S
8. Taleb S, Herbin O, Ait-Oufella H, Verreth W, Gourdy P, Barateau V, Merval R, Esposito B, Clement K, Holvoet P, Tedgui A, Mallat Z (2007) Defective leptin/leptin receptor signaling improves regulatory T cell immune response and protects mice from atherosclerosis. Arterioscler Thromb Vasc Biol 27:2691–2698
9. Dubey H, Das SK, Panda T (2006) Numerical simulation of a fully baffled biological reactor: the differential circumferential averaging mixing plane approach. Biotechnol Bioeng 95:754–766
10. Flax Council 2015 (2009) Flax—A Healthy Food, Flax Council of Canada
11. de Lorgeril M, Renaud S, Mamelle N, Salen P, Martin JL, Monjaud I, Guidollet J, Touboul P, Delaye J (1994) Mediterranean alpha-linolenic acid-rich diet in secondary prevention of coronary heart disease. Lancet 343:1454–1459
12. Albert CM, Oh K, Whang W, Manson JE, Chae CU, Stampfer MJ, Willett WC, Hu FB (2005) Dietary alpha-linolenic acid intake and risk of sudden cardiac death and coronary heart disease. Circulation 112:3232–3238
13. Smith PJ, Blumenthal JA, Babyak MA, Georgiades A, Sherwood A, Sketch MH Jr, Watkins LL (2009) Association between n-3 fatty acid consumption and ventricular ectopy after myocardial infarction. Am J Clin Nutr 89:1315–1320
14. Tziomalos K, Athyros VG, Karagiannis A, Mikhailidis DP (2008) Omega-3 fatty acids: how can they be used in secondary prevention? Curr Atheroscler Rep 10:510–517
15. Ander BP, Weber AR, Rampersad PP, Gilchrist JSC, Pierce GN, Lukas A (2004) Dietary flaxseed protects against ventricular fibrillation induced by ischemia-reperfusion in normal and hypercholesterolemic rabbits. J Nutr 134:3250–3256
16. Dupasquier CM, Dibrov E, Kneesh AL, Cheung PK, Lee KG, Alexander HK, Yeganeh BK, Moghadasian MH, Pierce GN (2007) Dietary flaxseed inhibits atherosclerosis in the LDL receptor-deficient mouse in part through antiproliferative and anti-inflammatory actions. Am J Physiol Heart Circ Physiol 293:H2394–H2402
17. Dupasquier CM, Weber AM, Ander BP, Rampersad PP, Steigerwald S, Wigle JT, Mitchell RW, Kroeger EA, Gilchrist JS, Moghadasian MM, Lukas A, Pierce GN (2006) Effects of dietary flaxseed on vascular contractile function and atherosclerosis during prolonged hypercholesterolemia in rabbits. Am J Physiol Heart Circ Physiol 291:H2987–H2996
18. Ander BP, Edel AL, McCullough RS, Rodriguez-Leyva D, Rampersad P, Gilchrist JSC, Lukas A, Pierce GN (2010) Distribution of omega-3 fatty acids in tissues of rabbits fed a flaxseed-supplemented diet. Metabolism 59:620–627
19. Zhao SP, Wu ZH (2005) Atorvastatin reduces serum leptin concentration in hypercholesterolemic rabbits. Clin Chim Acta 360:133–140
20. Rajagopalan S, Duquaine D, King S, Pitt B, Patel P (2002) Mineralocorticoid receptor antagonism in experimental atherosclerosis. Circulation 105:2212–2216
21. Altschul SF, Gish W, Miller W, Myers EW, Lipman DJ (1990) Basic local alignment search tool. J Mol Biol 215:403–410
22. Lepage G, Roy CC (1986) Direct transesterification of all classes of lipids in a one step reaction. J Lipid Res 27:114–120
23. Garg ML, Leitch J, Blake RJ, Garg R (2006) Long-chain n-3 polyunsaturated fatty acid incorporation into human atrium following fish oil supplementation. Lipids 41:1127–1132
24. Lepage G, Roy CC (1984) Improved recovery of fatty acid through direct transesterification without prior extraction or purification. J Lipid Res 25:1391–1396
25. Farooqi IS, O'Rahilly S (2009) Leptin: a pivotal regulator of human energy homeostasis. Am J Clin Nutr 89:980S–984S
26. Havel PJ (2000) Role of adipose tissue in body-weight regulation: mechanisms regulating leptin production and energy balance. Proc Nutr Soc 59:s359–s371
27. Ingvartsen KL, Boisclair YR (2001) Leptin and the regulation of food intake, energy homeostasis and immunity with special focus on periparturient ruminants. Domest Anim Endocrinol 21:215–250
28. Mason MM, He Y, Chen H, Quon MJ, Reitman M (1998) Regulation of leptin promoter function by Sp1, C/EBP, and a novel factor. Endocrinology 139:1013–1022
29. Turer AT, Khera A, Ayers CR, Turer CB, Grundy SM, Vega GL, Scherer PE (2011) Adipose tissue mass and location affect

circulating adiponectin levels. Diabetologia July 22 (Epub ahead of print)
30. Muhihauser BS, Cook-Johnson R, James M, Miljkovic D, Duthoit E, Gibson R (2010) Opposing effects of omega-3 and omega-6 long chain polyunsaturated fatty acids on the expression of lipogenic genes in omental and retroperitoneal adipose depots in the rat. J Nutr Metab. pii: 927836 Epub
31. Rahmouni K, Sigmund CD (2008) Id3, E47, and SREBP-1c: fat factors controlling adiponectin expression. Circ Res 103:565–567
32. Yu YH, Wu SC, Cheng WT, Mersmann HJ, Shen TL, Ding ST (2011) The function of porcine PPARy and dietary fish oil effect on the expression of lipid and glucose metabolism related genes. J Nutr Biochem 22:179–186
33. Banga A, Unal R, Tripathi P, Pokrovskaya I, Owens RJ, Kern PA, Ranganathan G (2009) Adiponectin translation is increased by the PPARgamma agonists pioglitazone and omega-3 fatty acids. Am J Physiol 296:E480–E489
34. Correia ML, Rahmouni K (2006) Role of leptin in the cardiovascular and endocrine complications of metabolic syndrome. Diabetes Obes Metab 8:603–610
35. Bartels ED, Bang CA, Nielsen LB (2009) Early atherosclerosis and vascular inflammation in mice with diet-induced type 2 diabetes. Eur J Clin Invest 39:190–199
36. Ukkola O, Poykko S, Paivansalo M, Kesaniemi YA (2008) Interactions between ghrelin, leptin and IGF-I affect metabolic syndrome and early atherosclerosis. Ann Med 40:465–473
37. Hoefle G, Saely CH, Risch L, Rein P, Koch L, Schmid F, Aczel S, Marte T, Langer P, Drexel H (2007) Leptin, leptin soluble receptor and coronary atherosclerosis. Eur J Clin Invest 37:629–636
38. Ogawa T, Hirose H, Yamamoto Y, Nishikai K, Miyashita K, Nakamura H, Saito I, Saruta T (2004) Relationships between serum soluble leptin receptor level and serum leptin and adiponectin levels, insulin resistance index, lipid profile, and leptin receptor gene polymorphisms in the Japanese population. Metabolism 53:879–885
39. Chiba T, Shinozaki S, Nakazawa T, Kawakami A, Ai M, Kaneko E, Kitagawa M, Kondo K, Chait A, Shimokado K (2008) Leptin deficiency suppresses progression of atherosclerosis in apoE-deficient mice. Atherosclerosis 196:68–75
40. Bassett CM, Rodriguez-Leyva D, Pierce GN (2009) Experimental and clinical research findings on the cardiovascular benefits of consuming flaxseed. Appl Physiol Nutr Metab 34:965–974
41. Barcelo-Coblijn G, Murphy EJ (2009) Alpha-linolenic acid and its conversion to longer chain n-3 fatty acids: Benefits for human health and a role in maintaining tissue n-3 fatty acid levels. Prog Lipid Res 48:355–357
42. Tang AB, Nishimura KY, Phinney SD (1993) Preferential reduction in adipose tissue alpha-linolenic acid (18:3 omega 3) during very low calorie dieting despite supplementation with 18:3 omega 3. Lipids 28:987–993

PUFA	Polyunsaturated fatty acid(s)
SR	Scavenger Receptor
SR-PSOX	SR for phosphatidylserine and oxidized LDL

Introduction

The accumulation and retention of Apolipoprotein (Apo)B-containing lipoproteins, such as low-density lipoprotein (LDL), within the arterial wall is a major trigger of atherosclerotic plaque development [1, 2]. Along with arterial endothelial activation, LDL retention elicits a chronic inflammatory response whereby monocytes, among other immune cells, are continually recruited to the site of trapped LDL, indicating defective inflammatory resolution [3, 4]. Such monocytes can differentiate into macrophages and, along with those resident in the arterial intima, ingest native and modified forms of LDL through various cellular mechanisms that are usually harnessed in innate immunity to become lipid-rich foam cells [5]. Macrophages were established as critical components of atherosclerotic plaque initiation development in ApoE$^{-/-}$ mice [6]; a well characterized animal model for this disease [7]. The conversion of macrophages into lipid-loaded foam cells is a critical early event in atherosclerosis [1]. The uptake of modified LDL is a key feature of macrophage foam cell formation and involves internalization of modified LDL by a family of scavenger receptors [8, 9] and alternative mechanisms such as macropinocytosis [10] and phagocytosis [11].

There is increasing evidence that dietary intake of long chain n-3 PUFA, such as EPA and DHA, which occur in significant amounts in fish oil, is beneficial against cardiovascular disease. In particular, these fish oil derived n-3 PUFA have been shown to be atheroprotective in different mouse models of the disease [12–16], to reverse defective efferocytosis of apoptotic cells in obese mice [17], to enhance atherosclerotic plaque stability in humans awaiting carotid endarterectomy [18] and to be effective in reducing the risk of cardiac mortality [19, 20]. Nevertheless, despite this evidence, other studies have contradicted some of these results [21–23] although this could be linked to background levels of n-6 PUFA since these can affect the efficacy of n-3 PUFA in atheroprotection [24] and since lowering the n-6:n-3 PUFA ratio in ApoE$^{-/-}$ mice reduces atherosclerotic plaque development [16]. Some of the atheroprotective effects of n-3 PUFA in mice have been shown to involve changes in macrophage function [12, 17] and a recent study found that EPA, delivered from n-3 PUFA ethyl esters, reduced foam cell accumulation in advanced human carotid plaques [25] suggesting that n-3 PUFA not only target macrophage activity but also foam cell formation. It has been found that EPA inhibits cholesteryl ester accumulation in THP-1 [26] and rat peritoneal macrophages [27] with the latter effect attributed to a reduction in acetylated LDL (AcLDL) receptor number. However, it has not been established whether EPA affects direct uptake of modified LDL in human macrophages and whether DHA, another key n-3 PUFA, is also able to regulate this process.

In this present study, we investigated whether the uptake of AcLDL and OxLDL by human macrophages was altered by co-incubation of EPA or DHA. We found that both EPA and DHA inhibited AcLDL uptake in both THP-1 macrophages and primary human monocyte-derived macrophages (HMDMs) whilst DHA, but not EPA, reduced OxLDL uptake. These effects could only partly be explained by changes in the mRNA and protein expression of key scavenger receptors in these cells, thereby suggesting that inhibition of macropinocytosis, as measured by Lucifer Yellow uptake and Syndecan-4 expression, should play an important role in modified LDL uptake.

Materials and Methods

Reagents and Cell Culture

THP-1 cells were maintained in complete RPMI-1640 supplemented with 10% (v/v) heat-inactivated FCS, penicillin (100 U/ml), streptomycin (100 μg/ml) and L-glutamine (2 mmol/l) (all from Invitrogen, Paisley, UK), at 37 °C in a humidified atmosphere containing 5% (v/v) CO_2. HMDMs were isolated from buffy coats supplied by the Welsh Blood service using Ficoll-Hypaque purification [28]. Briefly, blood from the buffy coat was layered over Lymphoprep^{TM} (Nycomed Pharmaceuticals, Oslo, Norway) in Accuspin^{TM} tubes (Sigma–Aldrich, Poole, UK) and centrifuged at 800*g* for 30 min. The resultant mononuclear cell interface was collected and washed 6–8 times in PBS containing 0.4% (v/v) tri-sodium citrate to remove platelets. Monocytes were allowed to adhere to tissue culture plates in complete RPMI-1640 medium containing 5% (v/v) FCS for 10 days to enable macrophage differentiation and permit removal of non-adherent cells. THP-1 cells were differentiated into macrophages using 160 nM phorbol 12-myristate 13-acetate (PMA; Sigma–Aldrich) for 24 h and this ensured high expression levels of scavenger receptors [29]. The stock solutions of EPA and DHA were made up in DMSO at a concentration of 100 mM and were stored at −20 °C. The cells were then incubated for the requisite time with EPA or DHA (both from Nu-Chek-Prep Inc., Elysian, MN, USA) or the same final concentration of DMSO as a vehicle control. For experiments with LY294002, the cells were

pre-treated for 1 h with the inhibitor or vehicle before addition of the lipids.

DiI-AcLDL and Lucifer Yellow Uptake Assays

Cells were incubated for 24 or 48 h with 1,1′-dioctadecyl-3,3,3′,3′-tetramethyllindocarbocyane perchlorate (DiI)-labeled AcLDL (DiI-AcLDL) or oxidized LDL (DiI-OxLDL) (both 10 μg/ml; Intracel, Frederick, MD, USA) or Lucifer Yellow CH dipotassium salt (100 μg/ml; Sigma–Aldrich) in RPMI-1640 containing 0.2% (v/v) fatty-acid free BSA (Sigma–Aldrich) at 37 °C. The concentration of Lucifer Yellow reflects that used routinely in previously reported experiments [30]. DiI-AcLDL and Lucifer Yellow uptake were analyzed by flow cytometry on a FACS Canto (BD Biosciences, Oxford, UK) flow cytometer with at least 10,000 events acquired for each sample. DiI-AcLDL and Lucifer Yellow uptake is represented as a percentage with the DMSO-treated control indicated as 100%.

Real-Time Quantitative PCR

Real-time quantitative PCR analysis was performed using SYBR® Green JumpStart™ *Taq* ReadyMix™ (Sigma–Aldrich) and primers, detailed in the supplementary table, specific for human scavenger receptor (SR)-A (SR-A), CD36, SR for phosphatidylserine and oxidized LDL (SR-PSOX), Syndecan-4, Lipoprotein lipase (LPL), Lectin-like oxidized LDL receptor-1 (LOX-1) and SR-BI using a previously described method [28].

Western Blotting

Total cell lysates were size-fractionated on NuPAGE 4–12% SDS–polyacrylamide gels (Invitrogen) and then analyzed by Western blotting [28]. Antibodies against CD36 (sc-9154) and SR-A (sc-20660) were from Santa Cruz Biotechnology (Santa Cruz, CA) and the antibody to β-actin was from Sigma–Aldrich. Semi-quantitative measurement of Western blots was performed by densitometric analysis using the Gene Tools software (GRI, Braintree, UK).

Fatty Acid Uptake Analysis

Lipids were extracted from cells by a modified Folch method [31] and separated using 1-dimensional thin-layer chromatography on 10 × 10 cm silica gel G plates with double development using toluene/hexane/formic acid (140:60:1, by vol) for the entire plate followed by hexane/diethyl ether/formic acid (60:40:1, by vol) to half height. Plates were sprayed with 0.05% (w/v) 8-anilino-4-naphthosulphonic acid in methanol and viewed under UV light to reveal lipids. The bands corresponding to free fatty acids and total polar lipids were scraped from the TLC plates and their fatty acid compositions and the amounts of incorporated DHA and EPA were determined by gas chromatography using an internal standard of pentadecanoate.

Statistical Analysis

All data are presented as means [± standard deviation, (SD)] on the assigned number of independent experiments. Statistical significance was evaluated using Student's *t* test or by one-way ANOVA with Dunnett's post-hoc test for multiple sample comparison.

Results

EPA and DHA Inhibit AcLDL Uptake by Human Macrophages In Vitro

Macrophage foam cell formation is known to involve the disruption of a homeostatic mechanism that controls cholesterol metabolism and the uptake of modified forms of LDL by macrophages enables rapid, uninhibited conversion into lipid-rich foam cells [5]. One type of modified LDL, AcLDL, is used extensively for in vitro foam cell formation assays since it produces massive intracellular cholesterol accumulation [32]. Considering this, we first investigated the impact of exogenous EPA and DHA incubation (24 h) on the uptake of co-cultured DiI-AcLDL by THP-1 macrophages. Fatty acid uptake analysis showed that 73% of the supplemented EPA and 69% of DHA was taken up by the cells (data not shown). Both acids were partly incorporated into polar lipids and partly located among the pool of cytosolic free fatty acids. EPA and DHA produced a statistically significant decrease in DiI-AcLDL uptake compared to the DMSO-treated control in a concentration-dependent manner (Fig. 1a). The highest concentration, 100 μM, reduced DiI-AcLDL uptake by approximately 40%. Using this same concentration, which lies within the physiological range of human plasma EPA and DHA levels, DiI-AcLDL uptake was also decreased in HMDMs in a statistically significant manner with EPA producing a 28% reduction and DHA a 32% reduction (Fig. 1b). To add to this, EPA produced a comparable reduction in 48 h DiI-AcLDL uptake by THP-1 macrophages (Fig. 1c) whilst DHA was able to produce similar reduction although this change failed to reach significance. In addition, we found that DHA inhibited the uptake of DiI-OxLDL in THP-1 macrophages (Fig. 1d) suggesting that it can also inhibit the uptake of other forms of LDL. Conversely, EPA produced a significant increase in OxLDL uptake (Fig. 1d). These data show that DHA can inhibit both AcLDL and OxLDL uptake by human macrophages

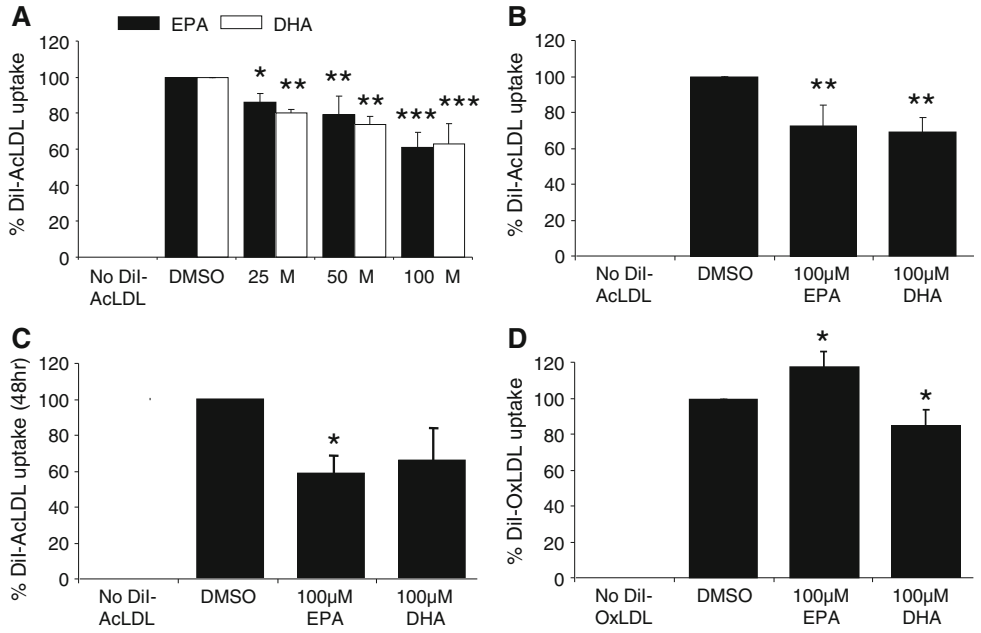

Fig. 1 EPA and DHA regulate the uptake of modified LDL by human macrophages. DiI-AcLDL uptake was measured in 24 h PMA-differentiated THP-1 macrophages following 24 h co-incubation with varying concentrations (25, 50, 100 μM) of EPA (*filled bars*) or DHA (*open bars*) ($n = 4$) (**a**). DiI-AcLDL uptake was measured in 10 day differentiated HMDMs incubated for 24 h with 100 μM EPA or DHA ($n = 4$) (**b**). DiI-AcLDL uptake was measured in 24 h PMA-differentiated THP-1 macrophages co-incubated for 48 h with 100 μM EPA or DHA ($n = 3$) (**c**). DiI-OxLDL uptake was measured in 24 h PMA-differentiated THP-1 macrophages incubated for 24 h with 100 μM EPA or DHA ($n = 4$) (**d**). DMSO was used as a vehicle control in all experiments and the modified LDL uptake in its presence was given an arbitrary value of 100%. Data represent means ± SD. One-way ANOVA with Dunnett's post-hoc test (**a**) or Student's *t* test (**b**–**d**), $*P < 0.05$; $**P < 0.01$; $***P < 0.001$

whilst EPA reduced AcLDL uptake but increased OxLDL in THP-1 cells.

EPA and DHA Do Not Inhibit CD36 and SR-A Expression in Human Macrophages

The uptake of modified LDL into macrophages is principally performed by two scavenger receptors, CD36 and SR-A, which internalize the majority of OxLDL and AcLDL, respectively [8, 9]. We therefore investigated whether the changes in modified LDL uptake in human macrophages by EPA and DHA could be explained by alterations in CD36 and/or SR-A expression. We found that EPA and DHA produced a statistically significant increase in CD36 mRNA levels in THP-1 macrophages and HMDMs but did not produce any significant change in SR-A mRNA expression (Fig. 2a, b). These changes in mRNA expression did not explain the EPA- and DHA-mediated reductions in AcLDL uptake seen in these cells, but may in part explain the observed EPA-mediated increase in OxLDL uptake, particularly since CD36 mRNA expression was increased. We next analyzed the impact of EPA and DHA on the mRNA expression of other scavenger receptors including SR-B1, SR-PSOX and LOX-1, which can take up modified LDL. EPA and DHA did not change the mRNA expression of SR-B1, SR-PSOX and LOX-1 in THP-1 macrophages or HMDMs (Fig. 2a, b). Additionally, EPA and DHA did not alter the mRNA expression of LPL, which is also known to regulate modified LDL uptake (Fig. 2a, b) [33]. Since the reduction in AcLDL uptake by EPA and DHA may involve changes in CD36 and SR-A protein expression rather than mRNA transcripts, we next investigated whether EPA and DHA could inhibit the protein expression of CD36 and SR-A. We found that EPA and DHA increased CD36 protein levels in THP-1 macrophages (Fig. 2c), with the increase by only EPA being statistically significant, but did not alter CD36 protein expression in HMDMs or SR-A protein levels in either THP-1 macrophages or HMDMs (Fig. 2c, d). Collectively, these data show that EPA and DHA do not inhibit CD36 and SR-A expression at either the mRNA or protein level. Therefore, the inhibition of AcLDL uptake by these n-3 PUFA appears to involve a scavenger receptor-independent mechanism in human macrophages whilst EPA may increase OxLDL uptake in THP-1 macrophages via a CD36-dependant mechanism.

EPA and DHA Inhibit Macropinocytosis and Syndecan-4 mRNA Expression

There is evidence documenting scavenger receptor-independent mechanisms of LDL uptake. Native LDL can be

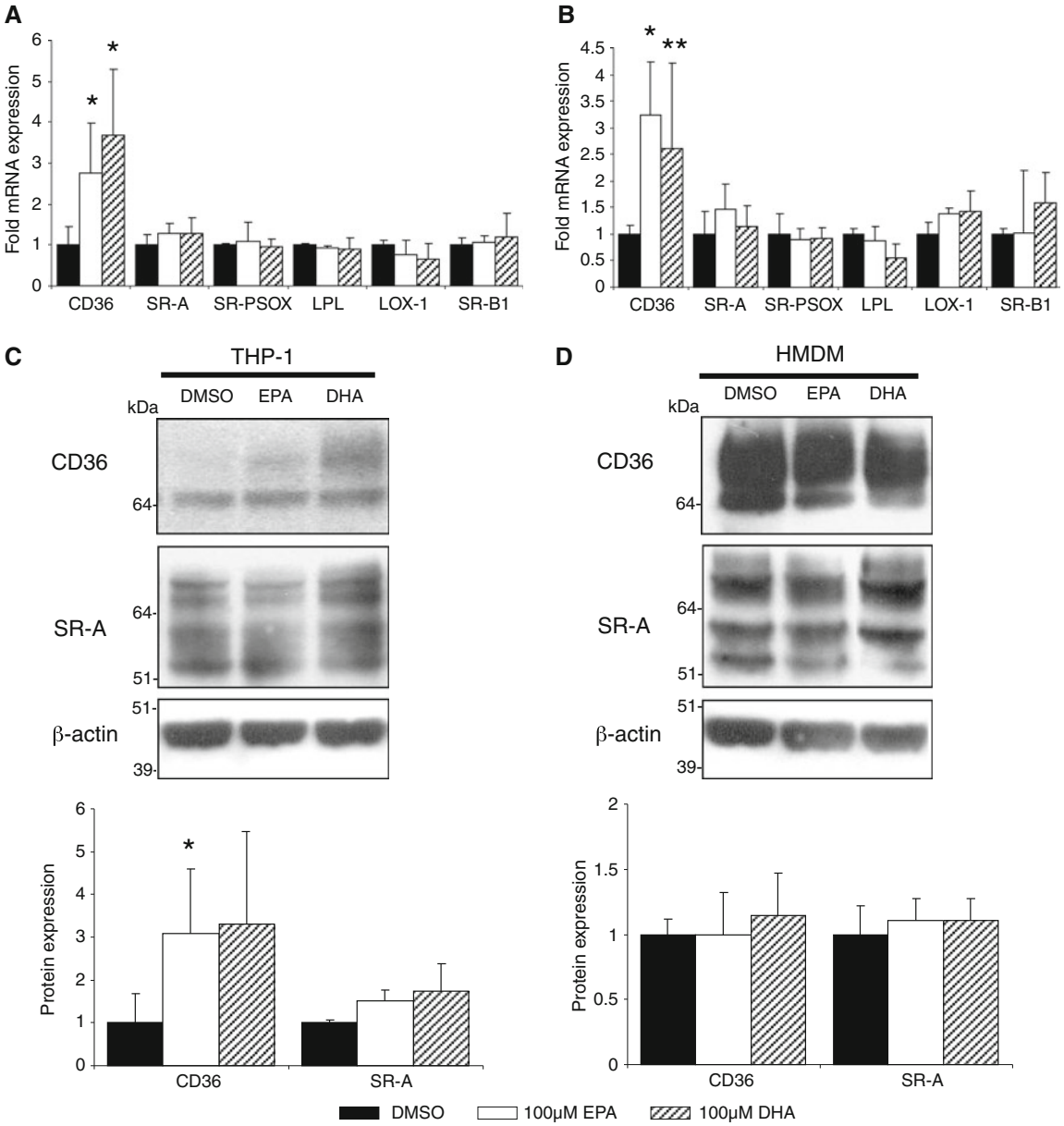

Fig. 2 EPA or DHA do not inhibit mRNA and protein expression of key genes implicated in the uptake of modified lipoproteins in human macrophages. Real-time quantitative PCR for CD36, SR-A, SR-PSOX, LOX-1, LPL and SR-BI was performed on cDNA from 24 h PMA-differentiated THP-1 macrophages (**a**) or 10 day differentiated HMDMs (**b**) incubated for 24 h with DMSO (*filled bars*), 100 μM EPA (*open bars*) or 100 μM DHA (*striped bars*) ($n = 4$). Gene-specific mRNA expression levels were calculated using comparative C_t method and normalized to GAPDH levels with DMSO-treated cells given an arbitrary value of 1. Western blot analysis was performed on total lysates from 24 h PMA-differentiated THP-1 macrophages (**c**) or 10 day differentiated HMDMs (**d**), incubated for 24 h with DMSO (*filled bars*), 100 μM EPA (*open bars*) or 100 μM DHA (*striped bars*) using antibodies against CD36, SR-A or β-actin. Multiple immunoreactive polypeptides for SR-A and CD36 represent different isoforms and/or post-translationally modified products. Semi-quantitative analysis of Western blots was performed by densitometric analysis using the Gene Tools software (GRI) and normalized to β-actin levels (DMSO-treated cells given an arbitrary value of 1). Graphs indicate data from four independent experiments ($n = 4$). All quantitative data represent means ± SD. Student's t test, $^*P < 0.05$; $^{**}P < 0.01$

internalized by the LDL receptor but this mechanism is negatively regulated by rising intracellular cholesterol levels [1]. In addition, it can be taken up by macropinocytosis [34], a form of fluid-phase endocytosis that is phosphoinositide 3-kinase (PI3K)-dependent, involves membrane ruffling and is involved in immune responses such as antigen presentation in dendritic cells [35, 36]. Modified LDLs can also be internalized by macrophages through macropinocytosis [10]. We therefore investigated whether EPA and DHA inhibited macropinocytosis. To do

this, we analyzed the impact of EPA and DHA on the uptake of Lucifer Yellow (LY), a solute marker used to study and quantify macropinocytosis in macrophages [37] by flow cytometry. LY uptake by macrophages was confirmed using confocal microscopy which identified the presence of Lucifer Yellow positive macropinosomes (1–5 μm in diameter) within the cells (data not shown). We found that EPA and DHA inhibited LY uptake by THP-1 macrophages (22 and 24%, respectively) (Fig. 3a) indicating that both EPA and DHA may inhibit macropinocytosis. Furthermore, as seen in Fig. 3b, blockade of macropinocytosis using the PI3 K inhibitor LY294002 [36] completely abolished the EPA- and DHA-mediated inhibition of LY uptake, thereby potentially providing direct evidence for the involvement of macropinocytosis during this process.

In order to further explain these reductions in LY uptake, we next analyzed whether EPA and DHA altered Syndecan-4 expression in these cells. Syndecan-4 is a cell surface heparan sulfate proteoglycan that can be endocytosed through the macropinocytic pathway [38] and can mediate uptake of LPL-enriched LDL [39] and group V secretory phospholipase A_2-modified LDL (GV-LDL) [40]. We found that EPA and DHA produced a statistically significant decrease in Syndecan-4 mRNA expression in THP-1 macrophages (Fig. 3c). The magnitude of this decrease was greater than that seen for LY uptake, which suggested that it might be linked to the inhibition in macropinocytosis. These data suggest that the reduction in macrophage AcLDL uptake triggered by EPA and DHA could involve the inhibition of macropinocytosis and Syndecan-4 expression.

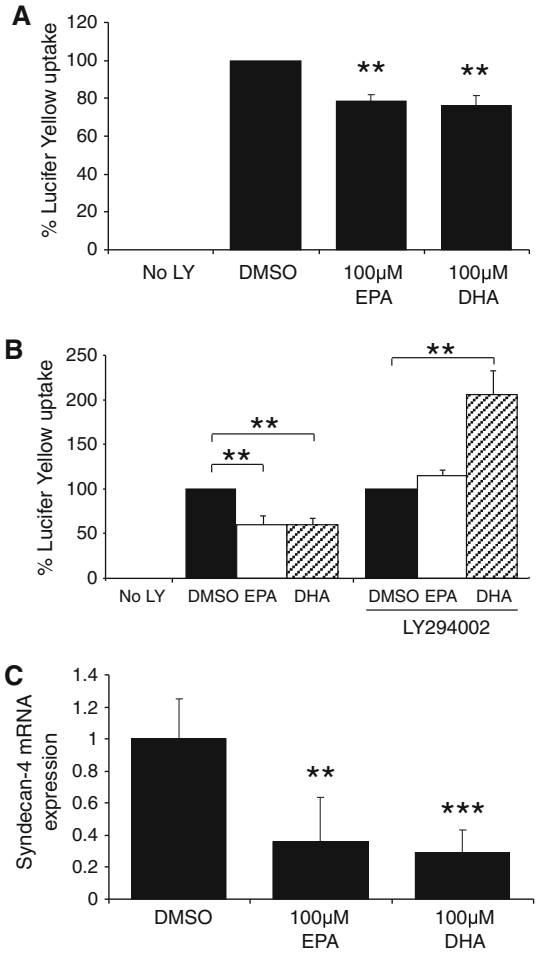

Fig. 3 EPA or DHA inhibit Lucifer Yellow uptake and Syndecan-4 expression in THP-1 macrophages. LY uptake was measured in 24 h PMA-differentiated THP-1 macrophages treated for 24 h with DMSO, 100 μM EPA or 100 μM DHA ($n = 3$–4) (**a**) or DMSO, EPA or DHA in the presence or absence of 100 μM LY294002 stimulation ($n = 3$) (**b**). Lucifer Yellow uptake in the presence of DMSO alone was arbitrarily assigned as 100%. LY294002 produced an approximate 49% inhibition in LY uptake in DMSO-treated cells (i.e., constitutive macropinocytosis). However, to delineate the effect of LY294002 on the EPA- or DHA-mediated inhibition of LY uptake, the relative level of LY uptake in LY294002 treated cells has been arbitrarily assigned as 100%. Syndecan-4 mRNA expression was measured in 24 h PMA-differentiated THP-1 macrophages in response to 24 h treatment with DMSO, 100 μM EPA or 100 μM DHA ($n = 3$) (**c**). Gene-specific mRNA expression levels were calculated using comparative C_t method and normalized to GAPDH levels. The DMSO-treated cells were given an arbitrary value of 1. Data represent means ± SD. Student's t test, $^{**}P < 0.01$; $^{***}P < 0.001$

Discussion

The results reported here supplement evidence describing EPA and DHA, as not only anti-inflammatory but also atheroprotective agents [12–18]. EPA and DHA are known to reduce foam cell accumulation in advanced human carotid plaques [25] and cholesteryl ester levels in THP-1 macrophages [26]. However, here we report that EPA elicits differential effects on the uptake of modified LDL as it reduces the uptake of AcLDL while promoting the uptake of OxLDL. We also report for the first time that DHA is able to regulate a key mechanism in macrophage foam cell formation since it inhibits both AcLDL and OxLDL uptake in human macrophages (Fig. 1). In addition, we show that both EPA and DHA inhibit the uptake of LY by macropinocytosis (Fig. 3).

In our study, the mechanism for EPA- and DHA-mediated inhibition of AcLDL uptake was found to be CD36 and SR-A-independent since their expression was not attenuated by either n-3 PUFA. Indeed, we found that stimulation with EPA or DHA induced the expression CD36 mRNA in both THP-1 macrophages and HMDMs and enhanced CD36 protein expression in only THP-1 macrophages. Clearly, such changes in scavenger receptor expression may be expected to elevate modified LDL uptake. It is possible that the reduction in AcLDL uptake observed in our study may occur as the result of diminished

AcLDL receptor number, as reported in rat peritoneal macrophages [27]. In addition, an inhibition in macropinocytosis and Syndecan-4 expression (Fig. 3) may also explain how AcLDL uptake, and OxLDL uptake in the case of DHA, is reduced independent of changes in the expression of scavenger receptors. Indeed, our data implicate modified LDL as a potential ligand for Syndecan-4 mediated endocytosis since GV-LDL has been identified as a target ligand [40].

As seen in Fig. 2, incubation with EPA induces CD36 mRNA and protein expression in an identical fashion to that observed for DHA. However, this observation contrasts that reported in human monocytic cells [41] and could represent a differential effect of this n-3 PUFA on monocytes compared to macrophages. Nevertheless, increased expression of CD36 mRNA and protein levels could potentially explain the observed increase in OxLDL uptake in response to EPA. Interestingly, EPA has been shown to induce the expression of peroxisome proliferator-activated receptors (PPAR)-α in THP-1 macrophages [26] and numerous studies have used PPAR agonists, such as thiazolidinedione, to delineate an anti-atherogenic role for these ligand-activated transcription factors during foam cell formation [42]. More specifically, it has now been shown that PPAR activation can induce the expression of CD36 [43, 44], which in turn increases the amount of OxLDL internalized [45], while simultaneously promoting cholesterol efflux through the up-regulation of ATP-binding cassette transporter proteins A1 (ABCA-1) and G1 (ABCG-1) in human macrophages [46, 47]. Considering these observations, we may propose that, despite the EPA-mediated up-regulation of OxLDL uptake observed in our study, EPA may still elicit an anti-foam cell phenotype in our system by increasing both OxLDL uptake and cholesterol efflux from the cell, a mode of cholesterol homeostasis also observed during the PPAR-dependant anti-atherogenic actions of interleukin-10 [48]. Furthermore, it has previously been shown that fish oils enhance macrophage reverse cholesterol transport in mice [49], and that AcLDL prepared from LDL isolated from African green monkeys fed on a diet rich in n-3 PUFA increases free cholesterol efflux from THP-1 macrophages [50]. Nevertheless, the role of EPA during cholesterol efflux remains controversial as our own study has shown that EPA does not affect the expression of SR-B1, which contributes to cholesterol efflux, while another study has shown that EPA can reduce ABCA-1-dependent efflux in THP-1 macrophages [51]; a result characteristic of foam cell promoting agents. There have yet to be any reports documenting specific actions of DHA on the above process.

In conclusion, we show that the n-3 PUFA DHA inhibits both AcLDL and OxLDL uptake while EPA reduces AcLDL uptake but increases OxLDL uptake by human macrophages. We also provide data suggesting that DHA and EPA reduce AcLDL uptake, and OxLDL uptake in the case of DHA, through a mechanism that is in part scavenger receptor-independent and may involve inhibition of macropinocytosis and Syndecan-4 expression. Furthermore, despite highlighting a role for CD36 in the EPA-mediated induction of OxLDL uptake, we speculate that EPA has anti-foam cell properties and that both EPA and DHA are capable of inhibiting macrophage foam cell formation. This study adds to evidence describing an atheroprotective role for n-3 PUFA implicating them as potential therapeutic agents for the treatment of clinical atherosclerosis.

Acknowledgments This work was supported by grants from the British Heart Foundation (PG/07/03/22716 and PG/08/073/25520).

Conflicts of interest There are no conflicts of interest

References

1. Lusis AJ (2000) Atherosclerosis. Nature 407:233–241
2. Tabas I, Williams KJ, Borén J (2007) Subendothelial lipoprotein retention as the initiating process in atherosclerosis: update and therapeutic implications. Circulation 116:1832–1844
3. Tabas I (2010) Macrophage death and defective inflammation resolution in atherosclerosis. Nat Rev Immunol 10:36–46
4. McLaren JE, Michael DR, Ashlin TG, Ramji DP (2011) Cytokines, macrophage lipid metabolism and foam cells: implications for cardiovascular disease therapy. Prog Lipid Res 50:331–347
5. Li AC, Glass CK (2002) The macrophage foam cell as a target for therapeutic intervention. Nat Med 8:1235–1242
6. Smith JD, Trogan E, Ginsberg M, Grigaux C, Tian J, Miyata M (1995) Decreased atherosclerosis in mice deficient in both macrophage colony-stimulating factor (op) and apolipoprotein E. Proc Natl Acad Sci USA 92:8264–8268
7. Nakashima Y, Plump AS, Raines EW, Breslow JL, Ross R (1994) ApoE-deficient mice develop lesions of all phases of atherosclerosis throughout the arterial tree. Arterioscler Thromb 14:133–140
8. Plüddemann A, Neyen C, Gordon S (2007) Macrophage scavenger receptors and host-derived ligands. Methods 43:207–217
9. Moore K, Freeman M (2006) Scavenger receptors in atherosclerosis: beyond lipid uptake. Arterioscler Thromb Vasc Biol 26:1702–1711
10. Jones NL, Willingham MC (1999) Modified LDLs are internalized by macrophages in part via macropinocytosis. Anat Rec 255:57–68
11. Tabas I (1999) Nonoxidative modifications of lipoproteins in atherogenesis. Annu Rev Nutr 19:123–139
12. Wang HH, Hung TM, Wei J, Chiang AN (2004) Fish oil increases antioxidant enzyme activities in macrophages and reduces atherosclerotic lesions in apoE-knockout mice. Cardiovasc Res 61:169–176
13. Casós K, Sáiz MP, Ruiz-Sanz JI, Mitjavila MT (2008) Atherosclerosis prevention by a fish oil-rich diet in apoE$^{(-/-)}$ mice is associated with a reduction of endothelial adhesion molecules. Atherosclerosis 201:306–317

14. Matsumoto M, Sata M, Fukuda D, Tanaka K, Soma M, Hirata Y, Nagai R (2008) Orally administered eicosapentaenoic acid reduces and stabilizes atherosclerotic lesions in ApoE-deficient mice. Atherosclerosis 197:524–533
15. Degirolamo C, Kelley KL, Wilson MD, Rudel LL (2010) Dietary n-3 LCPUFA from fish oil but not alpha-linolenic acid-derived LCPUFA confers atheroprotection in mice. J Lipid Res 51:1897–1905
16. Wan JB, Huang LL, Rong R, Tan R, Wang J, Kang JX (2010) Endogenously decreasing tissue n-6/n-3 fatty acid ratio reduces atherosclerotic lesions in apolipoprotein E-deficient mice by inhibiting systemic and vascular inflammation. Arterioscler Thromb Vasc Biol 30:2487–2494
17. Li S, Sun Y, Liang CP, Thorp EB, Han S, Jehle AW, Saraswathi V, Pridgen B, Kanter JE, Li R, Welch CL, Hasty AH, Bornfeldt KE, Breslow JL, Tabas I, Tall AR (2009) Defective phagocytosis of apoptotic cells by macrophages in atherosclerotic lesions of ob/ob mice and reversal by a fish oil diet. Circ Res 105: 1072–1082
18. Thies F, Garry JM, Yaqoob P, Rerkasem K, Williams J, Shearman CP, Gallagher PJ, Calder PC, Grimble RF (2003) Association of n-3 polyunsaturated fatty acids with stability of atherosclerotic plaques: a randomised controlled trial. Lancet 361:477–485
19. Harris WS (2004) Are omega-3 fatty acids the most important nutritional modulators of coronary heart disease risk? Curr Atheroscler Rep 6:447–452
20. Lands B (2008) A critique of paradoxes in current advice on dietary lipids. Prog Lipid Res 47:77–106
21. Ascherio A, Rimm EB, Stampfer MJ, Giovannucci EL, Willett WC (1995) Dietary intake of marine n-3 fatty acids, fish intake, and the risk of coronary disease among men. N Engl J Med 332:977–982
22. Adan Y, Shibata K, Ni W, Tsuda Y, Sato M, Ikeda I, Imaizumi K (1999) Concentration of serum lipids and aortic lesion size in female and male apo E-deficient mice fed docosahexaenoic acid. Biosci Biotechnol Biochem 63:309–313
23. Zampolli A, Bysted A, Leth T, Mortensen A, De Caterina R, Falk E (2006) Contrasting effect of fish oil supplementation on the development of atherosclerosis in murine models. Atherosclerosis 184:78–85
24. Zhang L, Geng Y, Xiao N, Yin M, Mao L, Ren G, Zhang C, Liu P, Lu N, An L, Pan J (2009) High dietary n-6/n-3 PUFA ratio promotes HDL cholesterol level, but does not suppress atherogenesis in apolipoprotein E-null mice 1. J Atheroscler Thromb 16:463–471
25. Cawood AL, Ding R, Napper FL, Young RH, Williams JA, Ward MJ, Gudmundsen O, Vige R, Payne SP, Ye S, Shearman CP, Gallagher PJ, Grimble RF, Calder PC (2010) Eicosapentaenoic acid (EPA) from highly concentrated n-3 fatty acid ethyl esters is incorporated into advanced atherosclerotic plaques and higher plaque EPA is associated with decreased plaque inflammation and increased stability. Atherosclerosis 212:252–259
26. Reza JZ, Doosti M, Salehipour M, Packnejad M, Mojarrad M, Heidari M (2009) Modulation peroxisome proliferators activated receptor alpha (PPAR alpha) and acyl coenzyme A: cholesterol acyltransferase1 (ACAT1) gene expression by fatty acids in foam cell. Lipids Health Dis 8:38
27. Saito I, Saito H, Tamura Y, Yoshida S (1992) Eicosapentaenoic acid inhibits cholesteryl ester accumulation in rat peritoneal macrophages by decreasing the number of specific binding sites of acetyl LDL. Clin Biochem 25:351–355
28. McLaren JE, Michael DR, Salter RC, Ashlin TG, Calder CJ, Miller AM, Liew FY, Ramji DP (2010) IL-33 reduces macrophage foam cell formation. J Immunol 185:1222–1229
29. Grewal T, Priceputu E, Davignon J, Bernier L (2001) Identification of a gamma-interferon-responsive element in the promoter of the human macrophage scavenger receptor A gene. Arterioscler Thromb Vasc Biol 21:825–831
30. Steinberg TH, Newman AS, Swanson JA, Silverstein SC (1987) ATP4- permeabilizes the plasma membrane of mouse macrophages to fluorescent dyes. J Biol Chem 262:8884–8888
31. Garbus J, Deluca HF, Loomans ME, Strong FM (1963) The rapid incorporation of phosphate into mitochondrial lipids. J Biol Chem 238:59–63
32. Goldstein JL, Ho YK, Basu SK, Brown MS (1979) Binding site on macrophages that mediates uptake and degradation of acetylated low density lipoprotein, producing massive cholesterol deposition. Proc Natl Acad Sci U S A 76:333–337
33. Mead JR, Irvine SA, Ramji DP (2002) Lipoprotein lipase: structure, function, regulation, and role in disease. J Mol Med 80:753–769
34. Kruth HS (2002) Sequestration of aggregated low-density lipoproteins by macrophages. Curr Opin Lipidol 13:483–488
35. Norbury CC (2006) Drinking a lot is good for dendritic cells. Immunology 117:443–451
36. Araki N, Johnson MT, Swanson JA (1996) A role for phosphoinositide 3-kinase in the completion of macropinocytosis and phagocytosis by macrophages. J Cell Biol 135:1249–1260
37. Racoosin EL, Swanson JA (1992) M-CSF-induced macropinocytosis increases solute endocytosis but not receptor-mediated endocytosis in mouse macrophages. J Cell Sci 102:867–880
38. Tkachenko E, Lutgens E, Stan RV, Simons M (2004) Fibroblast growth factor 2 endocytosis in endothelial cells proceed via syndecan-4-dependent activation of Rac1 and a Cdc42-dependent macropinocytic pathway. J Cell Sci 117:3189–3199
39. Fuki IV, Kuhn KM, Lomazov IR, Rothman VL, Tuszynski GP, Iozzo RV, Swenson TL, Fisher EA, Williams KJ (1997) The syndecan family of proteoglycans: novel receptors mediating internalization of atherogenic lipoproteins in vitro. J Clin Invest 100:1611–1622
40. Boyanovsky BB, Shridas P, Simons M, van der Westhuyzen DR, Webb NR (2009) Syndecan-4 mediates macrophage uptake of group V secretory phospholipase A2-modified LDL. J Lipid Res 50:641–650
41. Pietsch A, Weber C, Goretzki M, Weber PC, Lorenz RL (1995) N-3 but not N-6 fatty acids reduce the expression of the combined adhesion and scavenger receptor CD36 in human monocytic cells. Cell Biochem Funct 13:211–216
42. Zhang L, Chawla A (2004) Role of PPARgamma in macrophage biology and atherosclerosis. Trends Endocrinol Metab 15:500–505
43. Rios FJ, Jancar S, Melo IB, Ketelhuth DF, Gidlundm M (2008) Role of PPAR-gamma in the modulation of CD36 and FcgammaRII induced by LDL with low and high degrees of oxidation during the differentiation of the monocytic THP-1 cell line. Cell Physiol Biochem 22:549–556
44. Feng J, Han J, Pearce SF, Silverstein RL, Gotto AM, Hajjar DP, Nicholson AC (2000) Induction of CD36 expression by oxidized LDL and IL-4 by a common signaling pathway dependent on protein kinase C and PPAR-gamma. J Lipid Res 41:688–696
45. Tontonoz P, Nagy L, Alvarez JG, Thomazy VA, Evans RM (1998) PPARgamma promotes monocyte/macrophage differentiation and uptake of oxidized LDL. Cell 93:241–252
46. Argmann CA, Sawyez CG, McNeil CJ, Hegele RA, Huff MW (2003) Activation of peroxisome proliferator-activated receptor gamma and retinoid X receptor results in net depletion of cellular cholesteryl esters in macrophages exposed to oxidized lipoproteins. Arterioscler Thromb Vasc Biol 23:475–482
47. Chawla A, Boisvert WA, Lee CH, Laffitte BA, Barak Y, Joseph SB, Liao D, Nagy L, Edwards PA, Curtiss LK, Evans RM, Tontonoz P (2001) A PPAR gamma-LXR-ABCA1 pathway in macrophages is involved in cholesterol efflux and atherogenesis. Mol Cell 7:161–171

48. Han X, Kitamoto S, Lian Q, Boisvert WA (2009) Interleukin-10 facilitates both cholesterol uptake and efflux in macrophages. J Biol Chem 284:32950–32958
49. Nishimoto T, Pellizzon MA, Aihara M, Stylianou IM, Billheimer JT, Rothblat G, Rader DJ (2009) Fish oil promotes macrophage reverse cholesterol transport in mice. Arterioscler Thromb Vasc Biol 29:1502–1508
50. Lada AT, Rudel LL, St Clair RW (2003) Effects of LDL enriched with different dietary fatty acids on cholesteryl ester accumulation and turnover in THP-1 macrophages. J Lipid Res 44:770–779
51. Hu YW, Ma X, Li XX, Liu XH, Xiao J, Mo ZC, Xiang J, Liao DF, Tang CK (2009) Eicosapentaenoic acid reduces ABCA1 serine phosphorylation and impairs ABCA1-dependent cholesterol efflux through cyclic AMP/protein kinase A signaling pathway in THP-1 macrophage-derived foam cells. Atherosclerosis 204:e35–e43

confirmed in randomized phase III clinical trials, the consequences could be considerable by opening up the prospect of systematic adjuvant supplementation during cancer treatment, a significant shift in current cancer therapeutic paradigms.

DHA has been hypothesized to sensitize tumors to anticancer treatments through a variety of mechanisms involving alteration of cellular functions in cancer cells and modifications of the tumor microenvironment [1, 4, 5]. Enrichment of tumor cell membranes with DHA is crucial because it is assumed to be the initial step of these processes. On the basis of animal experiments, clinical trials were carried out in humans, where DHA was supplied to tumor tissues through a dietary supplementation during chemotherapy. Studies in rodents have shown that DHA-enriched diets administered for several weeks significantly increased tumor tissue DHA content in autochthonous mammary tumors [6, 7]. However, beside this observation, little is known about incorporation of preformed DHA in tumor tissue. One pilot study showed that the efficacy of chemotherapy was tightly related to DHA level in plasma phospholipids (PL) during dietary DHA supplementation [2]. In this study, the efficacy of chemotherapy was greater in patients with high plasma levels of DHA compared to patients with low plasma levels of DHA [2]. From these observations, it was hypothesized that blood supply of preformed DHA to tumor tissues varied among patients and that DHA supply to tumors was higher when DHA levels were elevated in plasma PL. It was also hypothesized that plasma could be an indirect indicator of DHA level in tumor tissue. Since all of these hypotheses rely on circumstantial evidences, it appears that the conditions of dietary DHA supplementation needed to obtain optimal DHA accumulation in tumor tissue have to be defined to properly design and interpret studies using dietary DHA intervention aiming at sensitizing tumor tissue to anticancer treatments.

To our knowledge, no study has evaluated the influence of the duration of intake or the dose of DHA on tumor tissue content of DHA, or the use of plasma as a surrogate biomarker. Therefore, we used a model of autochthonous mammary tumors induced by a carcinogen in female rats. This model is relevant to address these issues because carcinomas develop autochthonously in the mammary gland, generating a tumor tissue with features mimicking the complexity of common human breast tumors [8, 9]. Phospholipids and triacylglycerol (TAG) are the main tumor lipid fractions in this model. Herein, we report on the response of tumor PL and TAG fatty acid composition to dietary DHA supplementation over time and to increasing dose of DHA. We also investigated whether DHA level in plasma PL can be a proxy for DHA content in tumors.

Materials and Methods

Animal Procedures

All the work with rats was carried out in accordance with the European guidelines for the care and use of laboratory animals and approved by the local Institutional Animal Care Committee (060NH). Female Sprague–Dawley rats received a single dose of NMU (*n*-methyl-*N*-nitrosourea) by an inguinal subcutaneous injection (25 mg/kg of body weight) at 48 days of age to induce mammary carcinogenesis. Detection of the tumors was performed by palpation twice a week. Tumors developed in the mammary tissue approximately 8 weeks after the induction of carcinogenesis. Diets had the same carbohydrate, protein, mineral, vitamin and total fat content but different fatty acid composition (Table 1). Rats were maintained on a palm oil-based diet (diet 0) until tumor area reached 0.8 cm^2. Then, rats were fed either diet 1 (20 g/day) providing 0.8 g DHA/day for 4 weeks (group 1, $n = 4$) or 9 weeks (group 2, $n = 4$) or diet 2 (20 g/d) providing 1.5 g DHA/day for 4 weeks (group 3, $n = 4$). In group 1, transcutaneous biopsies of one tumor per rat and blood collection (0.4 ml) from the tail were performed under general anaesthesia before switching to a DHA-enriched diet (basal, diet 0) and at week 1 during diet 1. At the end of the study, rats were killed by cervical dislocation. Tumors were rapidly excised, frozen and stored at −80 °C. Blood collected during the study or at sacrifice by cardiac puncture was drawn into EDTA tubes, separated into cells and plasma by centrifugation, and plasma was stored at −80 °C. Palm oil was obtained from the Société Industrielle des Oléagineux (Bougival, France) and DHA was obtained from DHASCO oil (Martek Bioscience, Columbia, MD). The daily doses of DHA given to the rats were 4 g/kg body weight for diet 1 and 8 g/kg body weight for diet 2. If conversions used for drugs apply to nutrients, these amounts would correspond to approximately 700 mg/kg and 1,300 mg/kg respectively in man [10]. These very high dosages of DHA were aimed at experimentally investigating the extent of changes that takes place in the level of DHA in the tumor and plasma.

Fatty Acid Composition Analysis

The fatty acid composition of the experimental diets, plasma and tumors was determined by gas chromatography as previously described [2, 11]. Diet, plasma and tumor tissue lipids were extracted using chloroform/methanol (2:1, by vol; containing 50 mg/L BHT) [12]. PL and TAG were separated by one-dimensional silicagel thin layer chromatography. Fatty acids were

transmethylated with 14% boron trifluoride in methanol at 100 °C for 90 and 30 min, respectively for PL and TAG. FAME were extracted with hexane. Fatty acid methyl esters were resolved on an AS 2000 gas chromatograph (ThermoFinnigan, France) equipped with a cold on-column injector and a 60 meters BPX 70 capillary column, with the aid of an automatic injector. The temperature protocol was adapted from reference [13]. FAME were identified by comparison with authentic standards (Supelco, USA). The peak area was determined using ChromQuest software and results are presented as a percentage of the total peak area.

Statistics

GraphPad Prism (version 4, GraphPad Software, Inc., San Diego, USA) was used for statistical analysis. The effects of time on fatty acid composition were assessed by one-way ANOVA completed with the Bonferroni test. The effects of dose on fatty acid composition were assessed by an unpaired *t* test. The Spearman test was used to analyze the relationship between DHA concentration in plasma and in tumor tissue. Significance was defined as $P < 0.05$ (two-sided).

Results

DHA Accumulation in Tumor PL

The fatty acid composition of tumor PL during dietary DHA supplementation is presented in Table 2. DHA level in tumor PL rose to equilibrate between 2 and 4 weeks. DHA level increased by 2-fold after 4 weeks of intake. No further increase was noted after 4 weeks. When the dose of DHA was doubled, the amount of DHA in tumor PL increased by 1.3-fold. There was a time- and dose-dependent increase in tumor PL EPA content and a time-dependent increase in DPA n-3. No significant change was noted in the amount of ALA. Tumor LA content increased in a time-dependent manner with diet 1 and maintained while on diet 2. There was a reciprocal decrease in tumor PL ARA over time that was enhanced by a higher dose of DHA. Since oleic acid was present in large amounts in the diets, an increase in tumor PL oleic acid content was also noted.

DHA Accumulation in Tumor TAG

The fatty acid composition of tumor TAG during dietary DHA supplementation is presented in Table 3. The DHA

Table 1 Composition of diets

	Diet 0	Diet 1	Diet 2
Peanut oil (g/kg diet)	46.7	46.7	0
Rapeseed oil (g/kg diet)	23.3	23.3	0
Palm oil (g/kg diet)	80	0	0
DHASCO (g/kg diet)	0	80	150
Total SFA (g/kg diet)	62.77 ± 0.58	40.65 ± 0.18	54.61 ± 1.88
Palmitic acid	31.12 ± 1.84	11.16 ± 0.06	11.88 ± 0.39
Stearic acid	24.64 ± 0.17	1.75 ± 0.08	1.04 ± 0.08
Total monounsaturated fatty acids (g/kg diet)	59.77 ± 2.01	60.63 ± 0.67	36.29 ± 0.99
Oleic acid	57.20 ± 2.30	55.21 ± 0.30	30.60 ± 0.59
Total (n-6) fatty acids (g/kg diet)	19.41 ± 0.86	16.34 ± 1.06	1.79 ± 0.07
Linoleic acid	18.86 ± 1.15	15.77 ± 0.64	1.66 ± 0.06
Total (n-3) fatty acids (g/kg diet)	2.94 ± 0.03	30.10 ± 0.33	55.22 ± 1.16
ALA	2.71 ± 0.15	2.07 ± 0.20	0.06 ± 0.00
EPA	ND	0.05 ± 0.01	0.13 ± 0.01
DHA	0.12 ± 0.04	27.66 ± 0.45	54.34 ± 1.05
LA:ALA ratio	6.96	7.62	27.67

Carbohydrates (578 g/kg): corn starch, 372 g/kg; cellulose, 20 g/kg; sugar, 186 g/kg

Proteins (221.6 g/kg): casein, 220 g/kg; methionine, 1.6 g/kg

Mineral mix (40 g/kg, per kg mix): calcium, 8.1 g; phosphorus, 17.1 g; sodium, 3.16 g; chloride, 3.16 g; potassium, 10.8 g; magnesium, 0.9 g; iron, 390 mg; copper, 46 mg; manganese, 230 mg; zinc, 230 mg; cobalt, 1 mg; iodine, 2 mg; selenium, 1 mg; fluorine, 2 mg

Vitamin mix (10 g/kg, per kg mix): retinol, 5,000 UI; cholecalciferol, 2,500 UI; vitamin E (*alpha*-tocopherol), 50 UI; thiamine, 10 mg; riboflavin, 10 mg; pyridoxine, 10 mg; cyanocobalamine, 0.0135 mg; ascorbic acid, 100 mg; menadione, 1 mg; folic acid, 2 mg; nicotinic acid, 45 mg; pantothenic acid, 30 mg; choline, 0.75 mg; inositol, 50 mg; biotin, 0.2 mg

Values are means ± SD, $n = 3$; *ND* not detected

Table 2 Tumor PL fatty acid composition in response to different durations and doses of DHA supplementation

Fatty acid	Diet 0	Diet 1			Diet 2	ANOVA *P*	*t* test *P*
	Basal	Week 1	Week 4	Week 9	Week 4	Time	Dose
16:0	22.91 ± 1.04	24.68 ± 0.63	23.29 ± 1.65	22.66 ± 0.81	23.90 ± 1.09	0.189	0.350
18:0	16.07 ± 1.87	15.13 ± 1.92	14.50 ± 2.20	14.34 ± 1.42	14.03 ± 0.69	0.579	0.555
18:1n-9	11.80 ± 1.04	12.48 ± 0.95	13.19 ± 1.55	15.64 ± 1.01[a,b,c]	15.88 ± 1.99	0.001	0.003
18:2n-6	2.41 ± 0.59	3.12 ± 0.63	5.10 ± 1.32[a]	5.49 ± 0.91[a,b]	4.64 ± 0.93	0.001	0.386
20:4n-6	19.44 ± 0.64	15.44 ± 2.59	12.37 ± 2.69[a]	9.50 ± 2.29[a,b]	6.47 ± 2.45	<0.001	<0.001
18:3n-3	0.01 ± 0.00	0.02 ± 0.00	0.03 ± 0.01	0.03 ± 0.01	0.02 ± 0.01	0.074	0.180
20:5n-3	0.04 ± 0.02	0.43 ± 0.13	1.26 ± 0.34[a,b]	1.56 ± 0.41[a,b]	3.39 ± 0.34	<0.001	<0.001
22:5n-3	0.29 ± 0.06	0.46 ± 0.11	0.75 ± 0.23[a]	0.80 ± 0.18[a]	0.93 ± 0.19	<0.001	0.079
22:6n-3	2.45 ± 0.29	3.47 ± 0.07	5.23 ± 1.23[a,b]	5.11 ± 0.52[a]	6.85 ± 1.04	<0.001	0.018
n-6/n-3 ratio	9.58	4.83	2.66	2.40	1.18		

Values are mean ± SD, $n = 4$ [a] Different from basal, [b]different from week 1, [c]different from week 4, $P < 0.05$

increase in tumor TAG was more progressive and did not equilibrate during the time course of the study compared to tumor PL. The level of 5.5% DHA was reached in 9 weeks in the TAG fraction compared to 4 weeks in the PL fraction. The proportion of DHA in tumor TAG increased 2.6 fold when the dose of DHA was doubled. EPA increased after one week of dietary DHA supplementation to reach a steady state. EPA further increased in response to a higher dose of DHA. DPA n-3 increased in a time- and dose-dependent manner. There was a time-dependent increase in the amount of ALA and LA. Tumor TAG ARA content decreased in a time- and dose-dependent manner. There was also an increase in tumor TAG oleic acid and a decrease in stearic acid.

Relationship Between DHA Concentration in Plasma PL and in Tumor Tissue

DHA increase in plasma PL was rapid and reached a steady state after one week of intake (Table 4). A higher dose of DHA induced a 1.7 fold increase in DHA concentration in plasma PL. The DHA concentration in plasma PL followed a pattern close to that of tumor PL. Changes in EPA and ARA followed a pattern similar to that of tumor PL. An increase of ALA was noted at week 9 during diet 1. The proportion of LA increased during diet 1 but decreased during diet 2 when the amount of LA in the diet was reduced. No significant change in the DPA n-3 level was noticed.

Plasma PL DHA showed a correlation with tumor PL DHA ($r = 0.72$; $P < 0.001$; Fig. 1a) and tumor TAG DHA ($r = 0.64$; $P = 0.003$; Fig. 1b).

Discussion

This study describes the evolution of mammary tumor tissue fatty acids during dietary DHA supplementation over time and with increasing doses of DHA in rats. We found that DHA accumulation in tumor tissue increased in

Table 3 Tumor TAG fatty acid composition in response to different durations and doses of DHA supplementation

Fatty acid	Diet 0	Diet 1			Diet 2	ANOVA *P*	*t* test *P*
	Basal	Week 1	Week 4	Week 9	Week 4	Time	Dose
16:0	23.54 ± 0.79	26.70 ± 4.38	20.14 ± 1.88[b]	21.41 ± 0.91[b]	18.56 ± 2.53	<0.001	0.153
18:0	11.48 ± 1.65	12.42 ± 3.74	7.70 ± 0.94[a,b]	6.02 ± 1.76[a,b]	4.30 ± 1.82	<0.001	<0.001
18:1n-9	29.71 ± 8.74	23.18 ± 8.14	42.73 ± 5.90[a,b]	37.81 ± 4.18[b]	42.51 ± 3.93	<0.001	0.928
18:2n-6	5.82 ± 2.92	4.48 ± 2.16	10.02 ± 1.41[a,b]	12.18 ± 1.66[a,b]	9.05 ± 1.85	<0.001	0.243
20:4n-6	4.28 ± 1.96	5.32 ± 2.53	0.67 ± 0.38[a,b]	0.70 ± 0.37[a,b]	0.25 ± 0.17	<0.001	0.008
18:3n-3	0.27 ± 0.19	0.11 ± 0.05	0.56 ± 0.13[a,b]	0.55 ± 0.18[b]	0.45 ± 0.13	<0.001	0.098
20:5n-3	0.03 ± 0.02	0.18 ± 0.10[a]	0.18 ± 0.09[a]	0.19 ± 0.10[a]	0.32 ± 0.14	0.045	0.027
22:5n-3	0.24 ± 0.15	0.38 ± 0.12	0.23 ± 0.10	0.77 ± 0.32[a,c]	0.55 ± 0.22	0.001	0.005
22:6n-3	1.64 ± 1.01	3.26 ± 1.33	3.40 ± 1.09	5.50 ± 1.95[a]	8.99 ± 1.18	0.004	<0.001
n-6/n-3 ratio	6.65	3.42	2.54	1.81	0.93		

Values are means ± SD, $n = 4$ [a] Different from basal, [b]different from week 1, [c]different from week 4, $P < 0.05$

Table 4 Plasma PL fatty acid composition in response to different durations and doses of DHA supplementation

Fatty acid	Diet 0	Diet 1			Diet 2	ANOVA *P*	*t* test *P*
	Basal	Week 1	Week 4	Week 9	Week 4	Time	Dose
16:0	16.65 ± 1.28	21.34 ± 1.11[a]	23.11 ± 1.05[a]	26.12 ± 1.35[a,b]	27.79 ± 1.91	<0.001	0.015
18:0	42.30 ± 2.96	35.85 ± 1.92[a]	34.14 ± 0.85[a]	36.22 ± 1.75[a]	30.28 ± 2.17	0.003	0.049
18:1n-9	3.71 ± 0.24	4.67 ± 0.43	5.33 ± 0.46[a]	4.51 ± 0.61	5.99 ± 0.41	0.015	0.088
18:2n-6	5.85 ± 1.68	9.08 ± 1.26[a]	11.04 ± 0.38[a]	7.89 ± 0.71	4.74 ± 0.55	0.003	<0.001
20:4n-6	16.59 ± 2.86	6.30 ± 0.83[a]	3.33 ± 0.15[a]	2.15 ± 0.59[a,b]	1.23 ± 0.79	<0.001	0.009
18:3n-3	0.04 ± 0.02	0.04 ± 0.03	0.03 ± 0.03	0.24 ± 0.11[a,b,c]	0.03 ± 0.01	0.004	0.575
20:5n-3	0.10 ± 0.04	2.27 ± 0.95[a]	1.90 ± 0.41[a]	1.82 ± 0.40[a]	4.24 ± 1.17	<0.001	0.032
22:5n-3	0.13 ± 0.02	0.24 ± 0.09	0.25 ± 0.12	0.26 ± 0.03	0.27 ± 0.05	0.250	0.745
22:6n-3	3.70 ± 0.86	6.83 ± 1.67[a]	6.74 ± 2.27[a]	6.04 ± 1.21[a]	11.64 ± 1.47	0.011	0.007
n-6/n-3 ratio	5.20	1.50	1.63	1.19	0.40		

Values are means ± SD, $n = 4$ [a] Different from basal, [b]different from week 1, [c]different from week 4, $P < 0.05$

a time- and dose-dependent manner in response to supplementary dietary DHA and that DHA concentration in plasma PL can serve as a proxy biomarker for tumor DHA.

Enrichment of cancer cell membranes and tumors with DHA has been associated with enhanced efficacy of anticancer treatments and is therefore assumed to be a critical step leading to this effect. Although increased de novo lipogenesis is a property of cancer cells [14], these cells cannot synthesize LCPUFA de novo because mammalian cells cannot introduce double bonds beyond the Δ9 position. Diet is a simple and efficient way to supply DHA to tumors as previously documented in this model [6, 7]. In the present study, we showed that dietary DHA supplementation induced a rapid accumulation of DHA in tumor PL over time. DHA level equilibrated between 2 and 4 weeks of intake in the PL fraction while no steady state was reached within the 9 weeks of intake in the TAG fraction. This suggests that a dietary DHA supplementation for 2–4 weeks would be necessary to significantly increase tumor PL content of DHA. As a practical consequence for future clinical trials, it would be necessary to initiate dietary DHA supplementation at least 2 weeks prior to chemotherapy to ensure optimal DHA accumulation into tumor tissue. When this is not possible, assessment of chemotherapy efficacy should not be performed before one month of dietary DHA supplementation has been achieved.

We provided 0.8 g DHA/day in diet 1 based on previous studies indicating that this dose significantly increased tumor DHA content and sensitized tumors to chemotherapy and radiation therapy in the same model [6, 7]. Despite the saturation of DHA level in tumor PL with this dose of DHA, tumor tissue continued to incorporate DHA in response to the considerable amount of DHA provided by diet 2 (1.5 g/day). DHA accumulation in the TAG fraction was greater than in the PL fraction in response to a higher dose of DHA. These results suggest that tumors have a high propensity to incorporate preformed DHA, even in large amounts. A possible mechanism could be an up-regulation in tumor lipid transporters to meet their high requirement for structural lipids. Whether the rate of growth or proliferation in the tumors could interfere with DHA accumulation in tumor tissue should be examined.

Diet has been considered to be the main source of DHA supplied to tissues including tumors either as preformed DHA or as its precursor, the essential fatty acid α-linolenic acid (18:3n-3, ALA). DHA synthesis from ALA requires elongation, desaturation by Δ6 (EC 1.14.19.3) and Δ5 desaturases (EC 1.14.19.4), and β-oxidation [15]. The activity of the desaturation/elongation pathway in the liver is the most important in terms of supply of ALA metabolites to other tissues. Tumor cells might also contribute to this pathway since several cancer cell lines are capable of processing exogenous essential fatty acids [16, 17]. During diet 0, endogenous synthesis of DHA may be regarded as the likely supply to tumor tissue, since no dietary source of preformed DHA was available. However, this pathway could not have markedly contributed to the increase in DHA level during dietary DHA supplementation because the amount of ALA and the ratio of LA:ALA were approximately similar in diet 1 and diet 0, and diet 2 contained only traces of ALA. The formation of EPA during dietary DHA supplementation, while diets were free from EPA, could be a result of DHA retroconversion [18]. This process mainly takes place in the liver and requires saturation of the Δ4 double bond by Δ4 enoyl CoA reductase (EC 1.3.1.34) and rearrangement of the double bond structure by Δ3, Δ2 enoyl CoA isomerase (EC 5.3.3.8) [19, 20]. The formation of DPA n-3 could be a result of DHA retroconversion or a chain-elongation of the retroconverted EPA. ARA decrease concomitant with increase in LA during dietary DHA supplementation may result from a competition with EPA and a lower conversion

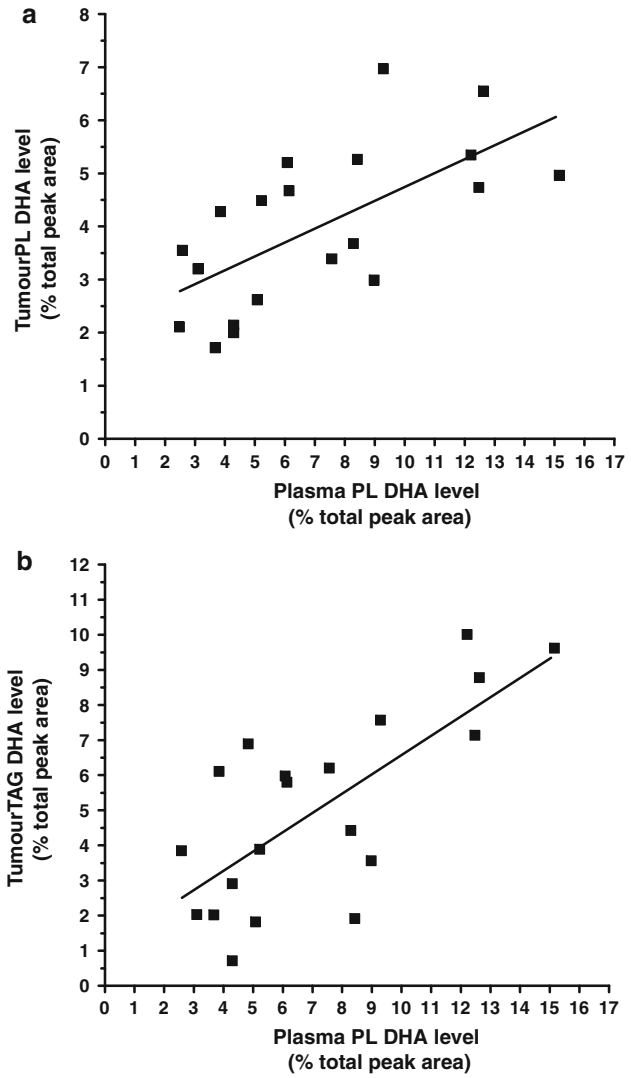

Fig. 1 Positive correlation between tumor PL **(a)**, or TAG **(b)**, DHA levels and DHA concentration in plasma PL. Spearman test results are $r = 0.72$, 95% CI = 0.39–0.88, $P = 0.0003$, $n = 20$ **(a)** and $r = 0.64$, 95% CI = 0.26–0.85, $P = 0.003$, $n = 20$ **(b)**. Lines represent the least-squares regression analysis of best linear fit (GraphPad Prism Software, version 4). Linear regression results are $r^2 = 0.43$, $P = 0.0018$ **(a)** and $r^2 = 0.52$, $P = 0.0003$ **(b)**

from LA. DHA and EPA were shown to downregulate the expression of Δ 5- and Δ 6-desaturases [21]. As a result of ARA changes, there was a dramatic decrease in n-6/n-3 ratio in tumor lipid fractions. Thus, we were able to profoundly modify the fatty acid composition of tumor tissue with a DHA-enriched diet. It is likely that this would have consequences on tumor metabolic pathways, particularly the production of inflammatory eicosanoids.

Blood is the route of delivery of dietary lipids to tissues. Plasma DHA in total lipids has been shown to correlate with DHA accumulation in the brain, retina or liver in experimental animals [22, 23]. We found that DHA accumulation in tumor PL followed a pattern close to that of plasma PL and that DHA in tumor PL and TAG correlated with the DHA level in plasma PL in this model. Studies exploring this issue in cancer patients are difficult to perform because of technical problems and ethical concerns. One study reported that the DHA increase in gastro-intestinal tumors was concomitant with its increase in plasma PL after 5 days of dietary supplementation with fish oil [24]. These results suggest that plasma, beside its use as a biomarker of intake, could be a relevant surrogate biomarker of tumor tissue DHA content.

In conclusion, this study establishes the evolution of tumor tissue fatty acid composition in response to different durations or doses of dietary DHA supplementation and demonstrates that accumulation of preformed DHA into tumor tissue is time- and dose-dependent. These results could provide a basis for a rational design of dietary DHA supplementation in cancer patients.

Acknowledgments DHASCO was graciously provided by Martek Biosciences (Columbia, MD, USA) and palm oil by the Société Industrielle des Oléagineux (Bougival, France). We also thank Pierre Besson for his contribution to this work.

Conflict of interest The authors report no conflict of interest.

References

1. Bougnoux P, Hajjaji N, Maheo K, Couet C, Chevalier S (2010) Fatty acids and breast cancer: sensitization to treatments and prevention of metastatic re-growth. Prog Lipid Res 49:76–86
2. Bougnoux P, Hajjaji N, Ferrasson MN, Giraudeau B, Couet C, Le Floch O (2009) Improving outcome of chemotherapy of metastatic breast cancer by docosahexaenoic acid: a phase II trial. Br J Cancer 101:1978–1985
3. Murphy RA, Mourtzakis M, Chu QS, Baracos VE, Reiman T, Mazurak VC (2011) Supplementation with fish oil increases first-line chemotherapy efficacy in patients with advanced non small cell lung cancer. Cancer doi: 10.1002/cncr.25933
4. Biondo PD, Brindley DN, Sawyer MB, Field CJ (2008) The potential for treatment with dietary long-chain polyunsaturated n-3 fatty acids during chemotherapy. J Nutr Biochem 19:787–796
5. Calviello G, Serini S, Piccioni E, Pessina G (2009) Antineoplastic effects of n-3 polyunsaturated fatty acids in combination with drugs and radiotherapy: preventive and therapeutic strategies. Nutr Cancer 61:287–301
6. Colas S, Paon L, Denis F, Prat M, Louisot P, Hoinard C, Le Floch O, Ogilvie G, Bougnoux P (2004) Enhanced radiosensitivity of rat autochthonous mammary tumors by dietary docosahexaenoic acid. Int J Cancer 109:449–454
7. Colas S, Mahéo K, Denis F, Goupille C, Hoinard C, Champeroux P, Tranquart F, Bougnoux P (2006) Sensitization by dietary docosahexaenoic acid of rat mammary carcinoma to anthracycline: a role for tumor vascularization. Clin Cancer Res 12:5879–5886
8. Gullino PM, Pettigrew HM, Grantham FH (1975) N-Nitrosomethylurea as mammary gland carcinogen in rats. J Natl Cancer Inst 54:401–414

9. Rivera ES, Andrade N, Martin G, Melito G, Cricco G, Mohamad N, Davio C, Caro R, Bergoc RM (1994) Induction of mammary tumors in rat by intraperitoneal injection of NMU: histopathology and estral cycle influence. Cancer Lett 86:223–228
10. Freireich EJ, Gehan EA, Rall DP, Schmidt LH, Skipper HE (1966) Quantitative comparison of toxicity of anticancer agents in mouse, rat, hamster, dog, monkey, and man. Cancer Chemother Rep 50:219–244
11. Chajes V, Lanson M, Fetissof F, Lhuillery C, Bougnoux P (1995) Membrane fatty acids of breast carcinoma: contribution of host fatty acids and tumor properties. Int J Cancer 63:169–175
12. Folch J, Lees M, Sloane Stanley GH (1957) A simple method for the isolation and purification of total lipides from animal tissues. J Biol Chem 226:497–509
13. Childs CE, Romeu-Nadal M, Burdge GC, Calder PC (2010) The polyunsaturated fatty acid composition of hepatic and plasma lipids differ by both sex and dietary fat intake in rats. J Nutr 140:245–250
14. Swinnen JV, Brusselmans K, Verhoeven G (2006) Increased lipogenesis in cancer cells: new players, novel targets. Curr Opin Clin Nutr Metab Care 9:358–365
15. Sprecher H (2002) The roles of anabolic and catabolic reactions in the synthesis and recycling of polyunsaturated fatty acids. Prostaglandins Leukot Essent Fatty Acids 67:79–83
16. Grammatikos SI, Subbaiah PV, Victor TA, Miller WM (1994) Diversity in the ability of cultured cells to elongate and desaturate essential (n-6 and n-3) fatty acids. Ann N Y Acad Sci 745:92–105
17. de Antueno RJ, Allen SJ, Ponton A, Winther MD (2001) Activity and mRNA abundance of Delta-5 and Delta-6 fatty acid desaturases in two human cell lines. FEBS Lett 491:247–251
18. Gronn M, Christensen E, Hagve TA, Christophersen BO (1991) Peroxisomal retroconversion of docosahexaenoic acid (22:6(n-3)) to eicosapentaenoic acid (20:5(n-3)) studied in isolated rat liver cells. Biochim Biophys Acta 1081:85–91
19. Dommes V, Baumgart C, Kunau WH (1981) Degradation of unsaturated fatty acids in peroxisomes. Existence of a 2, 4-dienoyl-CoA reductase pathway. J Biol Chem 256:8259–8262
20. Kunau WH, Dommes P (1978) Degradation of unsaturated fatty acids. Identification of intermediates in the degradation of cis-4-decenoyl-CoA by extracts of beef-liver mitochondria. Eur J Biochem 91:533–544
21. Cho HP, Nakamura M, Clarke SD (1999) Cloning, expression, and fatty acid regulation of the human delta-5 desaturase. J Biol Chem 274:37335–37339
22. Huang MC, Brenna JT, Chao AC, Tschanz C, Diersen-Schade DA, Hung HC (2007) Differential tissue dose responses of (n-3) and (n-6) PUFA in neonatal piglets fed docosahexaenoate and arachidonoate. J Nutr 137:2049–2055
23. Sarkadi-Nagy E, Wijendran V, Diau GY, Chao AC, Hsieh AT, Turpeinen A, Nathanielsz PW, Brenna JT (2003) The influence of prematurity and long chain polyunsaturate supplementation in 4-week adjusted age baboon neonate brain and related tissues. Pediatr Res 54:244–252
24. Senkal M, Haaker R, Linseisen J, Wolfram G, Homann HH, Stehle P (2005) Preoperative oral supplementation with long-chain Omega-3 fatty acids beneficially alters phospholipid fatty acid patterns in liver, gut mucosa, and tumor tissue. J Parenter Enteral Nutr 29:236–240

(multi-deficient diet with 7% protein) may influence brain growth spurt, feeding behavior, ontogeny of reflexes, skeletal muscle mechanical properties and locomotor activity in adult rats [5–7].

Developmental plasticity is now observed when an organism is exposed to very high caloric nutrition before birth [4]. In fact, human studies have shown that high-fat diet availability during gestation and lactation, as well as gestational diabetes, may predispose offspring to increased fat mass and incidence of metabolic syndrome as children and adults [8]. In animals, maternal high fat or cholesterol over-feeding during the perinatal period is associated with long-lasting effects on the offspring such as: dyslipidemia, hyperleptinemia, increased adiposity and blood pressure, elevated blood glucose and triglycerides [9, 10]. Litter size reduction (3 pups/litter) resulted in postnatal overfeeding during the suckling period and elevated blood pressure in adulthood [11]. Previous studies have related early adiposity to faster growth and hyperphagia (suppressed orexigenic signals), as seen in 20-postnatal-day offspring from mothers submitted to a high-fat diet during gestation [12]. Out of this context, the main goal of the present study is to evaluate the long-term effects of a palatable high-fat diet during gestation and lactation on the food intake and lipids profiles of offspring.

Materials and Methods

Animals and Diet

The experimental procedures were approved by the Ethical Committee of the Center of Health Science, Federal University of Bahia (protocol no. 018/2008-13), and followed the Guidelines for the Care and Use of Laboratory Animals [13]. Ten pregnant Wistar rats (aged 90–100 days and weighing 180 ± 11 g) were fed either a control diet (*C*, $n = 5$) or a palatable hyperlipidic diet (HL, $n = 5$) during gestation and lactation. The compositions of the diets are shown in Table 1. The fatty acids were analyzed on a gas chromatograph (Shimadzu GC-9A, Japan) with an FID detector. The column was WAX (25 m × 0.25 mm × 0.2 μm), with a flow of 1.3 mL min^{-1} of helium [14]. During the suckling period, the offspring were kept in groups of 8 pups/litter. At weaning (on the 22th day of age), two male offspring from each mother were randomly chosen and assigned to either control (C_p $n = 10$, pups from control mothers) or palatable hyperlipidic diet (HL_p $n = 10$; pups from HL mothers). The offspring were housed 3–4 per cage and received the animals' standard laboratory chow (Nuvilab® CR1, Brasil) ad libitum.

Table 1 Analysis of fatty acid percentage composition of the diets

Ingredients (g/100 g)	Control diet	Hyperlipidic diet
Carbohydrate	57	46
Protein	22	17
Lipids	4	23
Ashes	9	4
Humidity	8	10
Energy (kcal/g)	3.5	4.5
Individual fatty acids (g/100 g of total fatty acid)		
C12:0	ND	13.81
C14:0	ND	5.81
C16:0	15.86	12.65
C18:0	3.31	6.08
C18:1n-9 *cis*	26.24	34.52
C18:1n-9 *trans*	1.18	0.41
C18:2n-6 *cis*	49.68	21.68
C18:3n-3	3.72	0.27
C20:0	ND	0.77
C20:1n-9	ND	0.80
C22:0	ND	1.58
C24:0	ND	1.01
Total fatty acids		
Total SFA	19.17	41.71
Total MUFA *cis*	26.24	35.32
Total PUFA *cis*	53.4	21.95
Total TFA	1.18	0.41
PUFA:SFA	2.78	0.53
n-6:n-3	13.35	80.3

Control diet included commercial chow (Nuvilab® CR1, Brasil). The palatable food included commercial chow (Nuvilab® CR1, Brasil), peanut, milk chocolate bars, and biscuits in the proportion of 3:2:2:1. The main source of fat in the control diet was soybean oil. The main sources of fat in the HL were lard, animal fat, butter and safflower oil

SFA Saturated fatty acids, *MUFA* Monounsaturated fatty acids, *PUFA* Polyunsaturated fatty acids, *TFA* Trans fatty acids, *ND* Not detected

Measurement of Food Intake and Fasting Serum Glycemia and Cholesterol Profile

On day 76, pups were housed individually for 14 days in a metabolic cage. The first 4 days were designed for adaptation to the cage. Next, the animal's daily food consumption was determined by the difference between the amount of food provided (50 g) at the onset of the light cycle and the amount of food remaining 24 h later. Body and food weights were recorded by a Marte Scale (AS-1000), in increments of 0.01 g [15]. At 100 days old, and after fasting (12 h), serum glucose, total cholesterol, high-density-lipoprotein cholesterol (HDL-C) and triglyceride (TG) levels were determined with commercially available kits (BioSystems, Spain—A 25 Clinical Chemistry

Analyse®). Low-density-lipoprotein cholesterol (LDL-C) and very low-density-lipoprotein cholesterol (VLDL-C) were obtained using Friedwald calculations [16].

Statistical Analyses

Results are presented as means ± standard errors of the mean. Data for all analyses were performed using the statistical program Graphpad Prism 5® (GraphPad Software Inc., La Jolla, CA, USA). For statistical analysis of body weight and food intake, a two-way repeated measures ANOVA was used, with the mother's diet (HL) and time (weeks) as factors. Bonferroni's post hoc test was used, and Student's *t* test was used to compare groups in terms of blood biochemical parameters. Significance was set at $P < 0.05$.

Results and Discussion

Offspring's body weight in the HL_p group was higher than that of the control group throughout the weeks of development (Fig. 1a). The effects of a palatable high-fat diet during the perinatal period and the consequences of offspring body weight have also been seen in previous studies [8, 17]. The present study shows that life-time effects on body weight are seen in rats in response to perinatal (gestation and lactation) and that adult animals fed by mothers that were fed a perinatal high-fat diet were permanently heavier than their controls.

The measurement of food intake during a period of 6 days was higher in the HL_p group (Fig. 1b). High food intake can be associated with a high adiposity, high leptinemia and leptin resistance [18]. There is a correlation between high leptin resistance and the relative food intake per gram of body weight [18]. Although the concentrations of leptin were not evaluated in the present study, previous studies have found that a perinatal high-fat diet or gestational diabetes can lead to hyperinsulinism and a malprogramming in central regulators of body weight and metabolism [17].

Serum total cholesterol, LDL-C, HDL-C, TG, VLDL-C and glycemia were higher in the HL_p group than controls group (Table 2). In addition, these animals were markedly heavier and had significantly increased serum concentrations of glucose, cholesterol, and triglycerides, suggesting impairments in carbohydrate and lipid metabolism. Khan et al. [19] reported an increase in plasma triglycerides and a decrease in HDL-cholesterol concentrations in the female offspring born to mothers fed a rich in lard (25.7% fat) diet 10 days before and throughout pregnancy and lactation, although these changes were only apparent in one-year-old offspring. Although previous studies have used different protocols to induce developmental plasticity by a maternal high-fat diet, our results are in accordance with previously reported results in terms of blood lipid profiles [8, 10, 17,

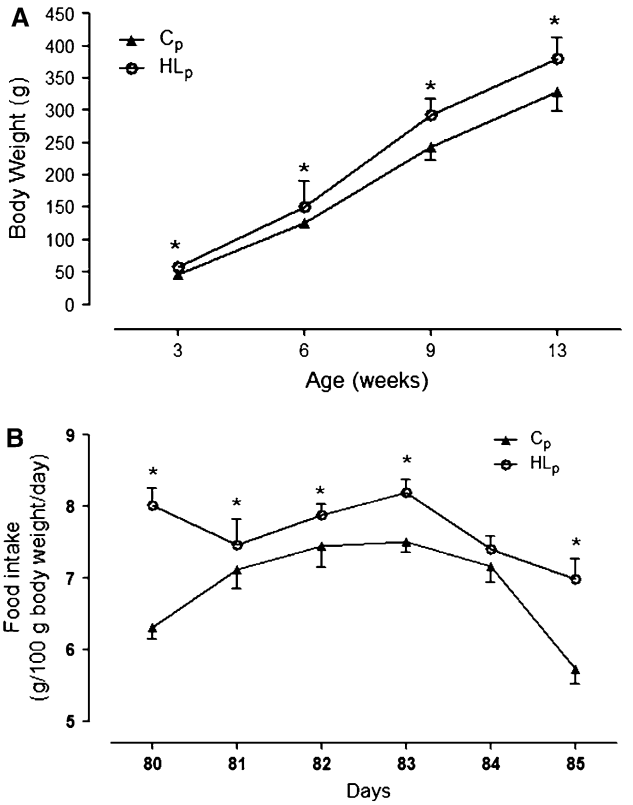

Fig. 1 Body weight of pups from mothers submitted to either a control or a hyperlipidic diet during gestation and lactation (**a**). Body weight was evaluated weekly until the 90th day of life. Food intake by pups at 80 days old from mothers submitted to either a control or a hyperlipidic diet during gestation and lactation (**b**). Food intake was evaluated daily until the 85th day of life. Control (C_p, $n = 10$) and hyperlipidic pups (HL_p, $n = 10$). The values are presented as means + SEM. *$P < 0.05$ using two-way ANOVA and Bonferroni's post hoc test

Table 2 Fasting serum glycemia and cholesterol profile of pups at 90 days old from mothers submitted to either a control or a hyperlipidic diet during gestation and lactation

	C_p	HL_p
Total cholesterol (mg/dL)	35.1 ± 1.0	56.4 ± 3.3*
LDL-C (mg/dL)	9.6 ± 1.1	19.14 ± 2.2*
HDL-C (mg/dL)	16.6 ± 0.7	25.5 ± 1.3*
Triglycerides (mg/dL)	44.2 ± 4.1	58.8 ± 5.5*
VLDL-C (mg/dL)	8.84 ± 0.8	11.76 ± 1.1*
Glycemia (mg/dL)	171.6 ± 11.1	217 ± 10.6*

Control (C_p, $n = 10$) and hyperlipidic pups (HL_p, $n = 10$) were evaluated after 24 h of fasting

LDL-C Low-density-lipoprotein cholesterol, *HDL-C* High-density-lipoprotein cholesterol, *VLDL-C* Very low-density-lipoprotein cholesterol

* $P < 0.05$ by using Student's *t* test

20–22]. The alterations could be associated with the concentration of saturated fatty acids (41.71%) in the mother's diet, even though the post-weaning diet was balanced for both groups in terms of carbohydrates, lipids and protein. The novelty of the present study is that a perinatal high-fat diet induces altered plasma cholesterol and triglyceride levels in the offspring and can predispose the offspring to developing obesity in a manner that is independent of postnatal diet.

Perinatal nutrition-induced hypercholesterolemia has been previously described in animal models, and the offspring's susceptibility to programmed obesity risk has been shown to be dependent on the timing and severity of diet manipulation [3]. Most models have used malnutrition as a stimulus for developmental plasticity, and relatively few studies have seen the effects of a high-fat diet during gestation and lactation. In this regard, we have presented data that confirm our hypothesis by demonstrating that a palatable high-fat diet during perinatal period increases food intake and induces hypercholesterolemia. In conclusion, our observations extend the evidence that both gestation and lactation are critical periods for the development of metabolic disease in later life.

Acknowledgments This study received financial support from the CNPq and FAPESB.

References

1. Barker DJ (2007) The origins of the developmental origins theory. J Intern Med 261:412–417
2. Gluckman PD, Hanson MA, Spencer HG, Bateson P (2005) Environmental influences during development and their later consequences for health and disease: implications for the interpretation of empirical studies. Proc Biol Sci 272:671–677
3. Ozanne SE, Hales CN (2004) Lifespan: catch-up growth and obesity in male mice. Nature 427:411–412
4. Gluckman PD, Hanson MA (2007) Developmental plasticity and human disease: research directions. J Intern Med 261:461–471
5. Barreto-Medeiros JM, Feitoza EG, Magalhaes K, Cabral-Filho JE, Manhaes-De-Castro FM, De-Castro CM, Manhaes-De-Castro R (2004) Malnutrition during brain growth spurt alters the effect of fluoxetine on aggressive behavior in adult rats. Nutr Neurosci 7:49–52
6. Orozco-Solis R, Lopes de Souza S, Barbosa Matos RJ, Grit I, Le Bloch J, Nguyen P, Manhaes de Castro R, Bolanos-Jimenez F (2009) Perinatal undernutrition-induced obesity is independent of the developmental programming of feeding. Physiol Behav 96:481–492
7. Toscano AE, Manhaes-de-Castro R, Canon F (2008) Effect of a low-protein diet during pregnancy on skeletal muscle mechanical properties of offspring rats. Nutrition 24:270–278
8. Shankar K, Harrell A, Liu X, Gilchrist JM, Ronis MJ, Badger TM (2008) Maternal obesity at conception programs obesity in the offspring. Am J Physiol Regul Integr Comp Physiol 294:R528–R538
9. Buckley AJ, Keseru B, Briody J, Thompson M, Ozanne SE, Thompson CH (2005) Altered body composition and metabolism in the male offspring of high fat-fed rats. Metabolism 54:500–507
10. Chechi K, Cheema SK (2006) Maternal diet rich in saturated fats has deleterious effects on plasma lipids of mice. Exp Clin Cardiol 11:129–135
11. Boubred F, Buffat C, Feuerstein JM, Daniel L, Tsimaratos M, Oliver C, Lelievre-Pegorier M, Simeoni U (2007) Effects of early postnatal hypernutrition on nephron number and long-term renal function and structure in rats. Am J Physiol Renal Physiol 293:F1944–F1949
12. Chen H, Morris MJ (2009) Differential responses of orexigenic neuropeptides to fasting in offspring of obese mothers. Obesity (Silver Spring) 17:1356–1362
13. Bayne K (1996) Revised Guide for the Care and Use of Laboratory Animals available. Am Physiol Soc. Physiologist 39:199, 208–111
14. Bligh EG, Dyer WJ (1959) A rapid method of total lipid extraction and purification. Can J Biochem Physiol 37:911–917
15. Lopes de Souza S, Orozco-Solis R, Grit I, Manhaes de Castro R, Bolanos-Jimenez F (2008) Perinatal protein restriction reduces the inhibitory action of serotonin on food intake. Eur J Neurosci 27:1400–1408
16. Friedewald WT, Levy RI, Fredrickson DS (1972) Estimation of the concentration of low-density lipoprotein cholesterol in plasma, without use of the preparative ultracentrifuge. Clin Chem 18:499–502
17. Srinivasan M, Katewa SD, Palaniyappan A, Pandya JD, Patel MS (2006) Maternal high-fat diet consumption results in fetal malprogramming predisposing to the onset of metabolic syndrome-like phenotype in adulthood. Am J Physiol Endocrinol Metab 291:E792–E799
18. Zambrano E, Bautista CJ, Deas M, Martinez-Samayoa PM, Gonzalez-Zamorano M, Ledesma H, Morales J, Larrea F, Nathanielsz PW (2006) A low maternal protein diet during pregnancy and lactation has sex- and window of exposure-specific effects on offspring growth and food intake, glucose metabolism and serum leptin in the rat. J Physiol 571:221–230
19. Khan IY, Taylor PD, Dekou V, Seed PT, Lakasing L, Graham D, Dominiczak AF, Hanson MA, Poston L (2003) Gender-linked hypertension in offspring of lard-fed pregnant rats. Hypertension 41:168–175
20. Tamashiro KL, Moran TH (2010) Perinatal environment and its influences on metabolic programming of offspring. Physiol Behav 100:560–566
21. White CL, Purpera MN, Morrison CD (2009) Maternal obesity is necessary for programming effect of high-fat diet on offspring. Am J Physiol Regul Integr Comp Physiol 296:R1464–R1472
22. Rodrigues AL, de Moura EG, Passos MC, Trevenzoli IH, da Conceicao EP, Bonono IT, Neto JF, Lisboa PC (2011) Postnatal early overfeeding induces hypothalamic higher SOCS3 expression and lower STAT3 activity in adult rats. J Nutr Biochem 22:109–117

lipid-bound state may influence LCAT activity via enzyme binding with the lipid interface, substrate and enzyme activation [5]. Both LCAT-activating and lipid-binding regions in apoA-I has been suggested to exist. The low lipid affinity of 144–186 region has been suggested to be important in LCAT activation [6]. Despite the numerous studies of LCAT reaction with HDL, the quantitative characteristics of the reaction are absent. The study of Verger et al. [7] on phospholipase A catalysis at interface, the identification of the catalytic triad of LCAT as Ser-Asp-His [8] with Ser181 as nucleophile residue in catalysis [9] and consideration of the influence of an added nucleophile at acyl-enzyme deacylation [10] are the seminal keys in the present effort to describe the LCAT reaction at the lipid-water interface of discoidal HDL as a tool for a mechanism-based analysis of enzyme activation by apolipoproteins and the contribution of the HDL structure.

Materials and Methods

Proposed Model of the LCAT Reaction

Two events underlie the kinetic mechanism of cholesteryl ester formation by LCAT with the discoidal HDL particle: (1) the existence of two consecutive equilibria, i.e. enzyme binding to the particle (penetration) and the LCAT reaction with phosphatidylcholine and cholesterol; (2) this reaction at the water-lipid interface proceeds through three steps that involve the formation of an acyl-enzyme intermediate and cholesterol as a nucleophilic agent can compete with water at the deacylation of acyl-enzyme. Indeed, the kinetic analysis of the interfacial catalysis of pancreatic phospholipase A_2 in phospholipid molecular layers has been done [7]. LCAT, in a reaction analogous to that of classical serine-dependent esterases, initially cleaves the *sn*-2 ester bond of phosphatidylcholine with the formation of lysophosphatidylcholine (lysoPtdCho) and an intermediate oxyester. The serine oxyester donates its fatty acyl group to cholesterol, forming a cholesteryl ester and regenerating the nonacylated enzyme [11]. The kinetic scheme 1 combines these events:

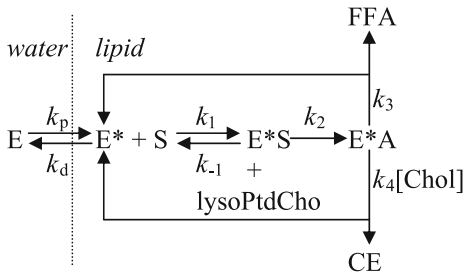

(1)

Kinetic Treatment of the Proposed Model

The balance between different enzyme forms exists (Eq. 2):

$$[E_t] = [E] + [E^*](I/V) + [E^*S](I/V) + [E^*A](I/V) \quad (2)$$

Equations 3–7 satisfy steady state conditions

$$\mathrm{d}[E^*]/\mathrm{dt} = k_p[E] + k_{-1}[E^*S] + (k_3 + k_4[\mathrm{Chol}])[E^*A] - (k_d + k_1[S])[E^*] = 0 \quad (3)$$

$$\mathrm{d}[E^*S]/\mathrm{dt} = k_1[E^*][S] - (k_{-1} + k_2)[E^*S] = 0 \quad (4)$$

$$\mathrm{d}[E^*A]/\mathrm{dt} = k_2[E^*S] - (k_3 + k_4[\mathrm{Chol}])[E^*A] = 0 \quad (5)$$

$$\mathrm{d}[\mathrm{CE}]/\mathrm{dt} = v_i = v_o/(I/V) = k_4[\mathrm{Chol}][E^*A] \quad (6)$$

$$[S] = [S_o]/(I/V) \quad (7)$$

where $[E_t]$ is the total enzyme concentration (mol/volume); $[E]$ is the free enzyme concentration (mol/volume); $[E^*]$ is the penetrated enzyme concentration (mol/surface); $[E^*S]$ is the penetrated enzyme/substrate complex (mol/surface); $[E^*A]$ is the penetrated acyl-enzyme (mol/surface); $[S]$ is the substrate (phosphatidylcholine) concentration (mol/surface); $[S_o]$ is the total substrate concentration in bulk units (mol/volume); [CE] is the product (cholesteryl ester) concentration (mol/surface). I is the total interfacial area (surface) and V the total volume (volume); k_p is the penetration rate constant (volume/surface)(time^{-1}); k_d is the desorption rate constant (time^{-1}); k_1 (mol/surface)$^{-1}$ (time^{-1}); k_{-1} (time^{-1}); k_2 (time^{-1}); k_3 (time^{-1}); k_4 is the second order rate constant (mol/surface)$^{-1}$(time^{-1}); v_i is the interface expression of the velocity (mol/surface·time) and v_o is the bulk expression of the rate (mol/volume·time). Finally (I/V) is the factor for conversion from surface units to bulk units.

Equations 2–7 can be combined to obtain the bulk/interface expression of the velocity v_o/v_i at steady state in terms of the initial surface concentration of substrate $[S]$ (Eq. 8):

$$\frac{v_o}{[E_t]} = \frac{v_i}{[E_t]} \times \frac{I}{V} = \frac{\frac{k_2 \times k_4 \times [\mathrm{Chol}]}{k_2 + k_3 + k_4 \times [\mathrm{Chol}]} \times \frac{I}{V} \times [S]}{\frac{k_3 + k_4 \times [\mathrm{Chol}]}{k_2 + k_3 + k_4 \times [\mathrm{Chol}]} \times K_m^* \times \left(K_d^* + \frac{I}{V}\right) + \frac{I}{V} \times [S]} \quad (8)$$

K_m^* and K_d^* are the interfacial Michaelis–Menten and dissociation constants given by Eqs. 9 and 10, respectively:

$$K_m^* = \frac{k_{-1} + k_2}{k_1} \quad (9)$$

$$K_d^* = \frac{k_d}{k_p} = K_d \times \mathrm{area}_{\mathrm{LCAT}} \times 10^{-14} \times N_A \quad (10)$$

K_d is the dissociation constant of LCAT/disc complex in bulk units (mol/cm^3), $\mathrm{area}_{\mathrm{LCAT}}$ is the accessible area of

LCAT interface recognition region (nm^2), N_A Avogadro' number. K_d should be measured independently.

The interfacial substrate and cholesterol concentrations (mol cm^{-2}) are determined by Eqs. 11 and 12, respectively:

$$[S] = \frac{n_{PC} \times 10^{14}}{(\text{area}_{PC} \times n_{PC} + \text{area}_{Chol} \times n_{Chol}) \times N_A} \quad (11)$$

$$[\text{Chol}] = \frac{n_{Chol} \times 10^{14}}{(\text{area}_{PC} \times n_{PC} + \text{area}_{Chol} \times n_{Chol}) \times N_A} \quad (12)$$

where n_{PC} and n_{Chol} are the number of PC and Chol molecules per disc and area_{PC} and area_{Chol} are the phosphatidylcholine and cholesterol surface areas (nm^2).

Thus the hydrolysis/solvolysis of acyl-LCAT intermediate on the surface of discoidal HDL by water and cholesterol predicts a dependence of the cholesteryl ester formation rate on three variables: the surface substrate concentration [*S*], the surface cholesterol concentration [Chol] and the proportion of interface *I*/*V*. The apparent catalytic rate constant k_{cat}^{app} and Michaelis constant K_m^{app} are defined by Eqs. 13 and 14, respectively:

$$k_{cat}^{app} = \frac{k_2 \times k_4 \times [\text{Chol}]}{k_2 + k_3 + k_4 \times [\text{Chol}]} \quad (13)$$

$$K_m^{app} = \frac{k_3 + k_4 \times [\text{Chol}]}{k_2 + k_3 + k_4 \times [\text{Chol}]} \times K_m^* \left(K_d^* + \frac{I}{V} \right) \quad (14)$$

The individual parameters are derived from double reciprocal plots (Eqs. 15 and 16):

$$\frac{1}{k_{cat}^{app}} = \frac{k_2 + k_3}{k_2 \times k_4} \times \frac{1}{[\text{Chol}]} + \frac{1}{k_2} \quad (15)$$

$$\frac{K_m^{app}}{k_{cat}^{app}} = K_m^* \left(K_d^* + \frac{I}{V} \right) \times \frac{k_3}{k_2 \times k_4} \times \frac{1}{[\text{Chol}]} + \frac{1}{k_2} \times K_m^* \left(K_d^* + \frac{I}{V} \right) \quad (16)$$

Results and Discussion

The raw data of Sparks et al. [12] on apparent kinetic parameters and particle composition for four reconstituted discoidal HDL preparations D4–D26 with two molecules apoA-I per disc were analyzed. The input parameters used in the subsequent calculations are listed in Table 1. It is evident that the interfacial lipid area and the POPC concentration are nearly constant while cholesterol varied at a 6-fold level. The increase in Chol content did not change significantly hydrodynamic diameter of the disks [12]. The k_{cat}^{app} values were normalized to an equal POPC concentration of 2.69×10^{-10} mol cm^{-2}. The $area_{LCAT}$ value calculated with the RVP-net web server [13] for the region between 50 and 74 residues in LCAT sequence, suggested to be involved in interfacial recognition [14], was 6.6 nm^2. The values for molecular surface area area_{PC} and area_{Chol} were chosen as 0.58 and 0.38 nm^2, respectively [15]. These values were obtained for Langmuir-type film at high surface pressures (30–40 mN/m) that mimic a disc bilayer. Even at largest, Chol content in lipid phase of the particle did not exceed 12.5 mol% and Chol-induced POPC area condensation (<5%) was discarded. The bulk K_d value as 3×10^{-10} mol/cm^3, obtained by others [16] for complex analogous to D18, was fixed at the assumption of constant *I*/*V* and [*S*] values for all four complexes. The linear transformation of the input data corresponded well the kinetic mechanism with acyl-enzyme intermediate predicted by Eqs. 15 and 16 (Fig. 1). This treatment allowed the calculation to be made of the complete set of kinetic constants for LCAT-catalyzed cholesteryl ester formation in discoidal HDL (Table 2). The k_2 value is close to phospholipase A_2 LCAT activity with the turnover rate as 40 times/min [17]. The ratio of rate constants of acyl-LCAT hydrolysis/solvolysis by water and cholesterol is 0.66 at 12.5 mol% cholesterol (26 molecules per particle). Cholesterol seems to be an efficient nucleophilic agent at its physiological concentration in discoidal HDL. Also, the amount of cholesterol in native HDL_3 particles varies between 15 and 41 molecules per particle [18], quite comparable to the current values. It should be emphasized that data at high cholesterol content do not indicate a saturation phenomenon, thus giving no evidence for a binding of cholesterol to the enzyme. This would argue against any gross change in the LCAT interfacial recognition region.

Table 1 Compositional and kinetic properties of four discoidal reconstituted HDL

Complex	*I* (nm^2)	POPC $\times 10^{10}$ (mol cm^{-2})	Chol $\times 10^{11}$ (mol cm^{-2})	k_{cat}^{app} (s^{-1})	$K_m^{app} \times 10^8$ (mol POPC cm^{-3})
D4	105	2.82	0.63	0.23	2.2
D8	112	2.79	1.19	0.44	2.5
D18	113	2.69	2.66	0.69	2.5
D26	115	2.62	3.74	0.74	2.5

Numbers in complex name correspond the number of Chol molecules/particle [12]. The raw data for complex composition and for apparent kinetic constants [12] were transformed as input values in Eqs. 15 and 16. The k_{cat}^{app} values were normalized to an equal POPC concentration of 2.69×10^{-10} mol cm^{-2}. POPC and cholesterol surface concentrations were calculated from their molecular areas

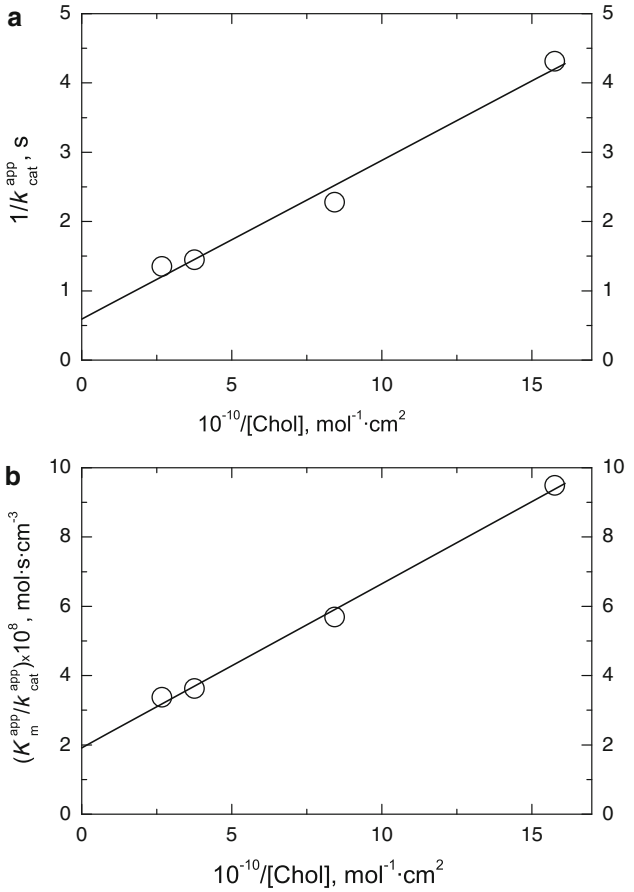

Fig. 1 The relation of apparent kinetic parameters of the LCAT reaction with reconstituted HDL on the cholesterol level. **a** The dependence of the rate constant of cholesteryl ester formation on the cholesterol level in double reciprocal plots. The k_{cat}^{app} values were normalized to an equal POPC concentration of 2.69×10^{-10} mol cm^{-2}. Data were fitted by linear regression $y = a + b \times x$ with $a = 0.59 \pm 0.19$, $b = (2.29 \pm 0.21) \times 10^{-11}$, $r = 0.992$ ($p = 0.008$, $n = 4$); **b** the dependence of kinetic parameters ratio on cholesterol level in double reciprocal plots. The k_{cat}^{app} values were normalized to an equal POPC concentration of 2.69×10^{-10} mol cm^{-2}. Data were fitted by linear regression $y = a + b \times x$ with $a = (1.91 \pm 0.20) \times 10^{-8}$, $b = (4.74 \pm 0.22) \times 10^{-19}$, $r = 0.998$ ($p = 0.002$, $n = 4$)

Table 2 Solvolysis of the acyl-LCAT intermediate by cholesterol and water

k_2 (s^{-1})	k_3 (s^{-1})	$k_4 \times 10^{-11}$ (mol^{-1} cm^2 s^{-1})	K_d^* (cm^{-1})	I/V (cm^{-1})	$K_m^* \times 10^{10}$ (mol cm^{-2})
1.69	3.01	1.22	11.9	93.0	3.08

Errors are ±10%. the K_d^* value was calculated from the bulk K_d and the area of the LCAT interface recognition region. I/V was calculated for the mean value of the bulk K_m and the POPC concentration 2.69×10^{-10} mol cm^{-2}

Early investigations with LCAT also showed that the catalytic activity of the enzyme was sensitive to the amount of cholesterol in the surface of vesicular and discoidal particles [19–21]. In addition, LCAT activity increased at the modest increase of Chol but became independent when Chol level exceeded 20 molecules per particle [22], still comparable with the highest Chol concentration in the present study. Prominent heterogeneity of the complexes in the study of Jonas and McHugh [22] may contribute to the different LCAT kinetics. So, deacylation of acyl-enzyme intermediate by water and cholesterol is not rate-limiting (Table 2) and LCAT activation by apoA-I must involve either activation of the enzyme and/or of the phospholipid molecule. The increased accessibility of the *sn*-2 ester bond of phosphatidylcholine for presentation to the catalytic site of the enzyme may underlie substrate activation by apoA-I [21]. The precise influence of apoA-I domains on phospholipid conformation remains to be established. The calculation of K_m^* value requires the knowledge of K_d^* value determined in turn from the independent measurement of bulk K_d value. K_m^* value agreed well with the analogous parameter for phospholipase A_2 activity toward mixed phosphatidylcholine-detergent micelles when some simplifying assumptions on the dissociation constant, not directly measured, had to be made [23]. However, a difference in K_m^* by two orders of magnitude has been obtained in another study [24] for the same phospholipase A_2-micelle system that weakens the significance of indirectly determined K_d value. The widely used k_{cat}^{app}/K_m^{app} ratio (Eq. 13 divided by Eq. 14) as a measure of LCAT catalytic efficiency is actually a complex function of three rate constants, interfacial Chol concentration and interfacial Michaelis and dissociation constants. All these variables should be introduced into examination of LCAT activity with discoidal HDL. The present analysis may be applied for complexes of apoA-I mutants and other apolipoproteins. This approach will be combined with the consideration of cholesterol radial distribution [25] and apolipoprotein conformational stability [26] in emerging analysis of the contribution of HDL composition and structure into RCT efficiency directed by LCAT at the cholesteryl ester generation step.

Acknowledgments The financial support of the Russian Foundation for Basic Research (grant # 10-04-00270) is gratefully acknowledged.

References

1. Frank PG, Marcel YL (2000) Apolipoprotein A-I: structure-function relationships. J Lipid Res 41:853–872
2. Rousset X, Vaisman B, Amar M, Sethi AA, Remaley AT (2009) Lecithin: cholesterol acyltransferase—from biochemistry to role in cardiovascular disease. Curr Opin Endocrinol Diabetes Obes 16:163–171
3. Jonas A (2000) Lecithin cholesterol acyltransferase. Biochim Biophys Acta 1529:245–256

4. Dergunov AD, Shabrova EV, Dobretsov GE (2010) Composition, structure and substrate properties of reconstituted discoidal HDL with apolipoprotein A-I and cholesteryl ester. Spectrochim Acta A Mol Biomol Spectrosc 75:1100–1107
5. Dolphin PJ (1992) In: Rosseneu M (ed) Structure and function of apolipoproteins. CRC Press, Boca Raton
6. Cho KH, Durbin DM, Jonas A (2001) Role of individual amino acids of apolipoprotein A-I in the activation of lecithin:cholesterol acyltransferase and in HDL rearrangements. J Lipid Res 42:379–389
7. Verger R, Mieras MC, de Haas GH (1973) Action of phospholipase A at interfaces. J Biol Chem 248:4023–4034
8. Peelman F, Vinaimont N, Verhee A, Vanloo B, Verschelde JL, Labeur C, Seguret-Mace S, Duverger N, Hutchinson G, Vandekerckhove J, Tavernier J, Rosseneu M (1998) A proposed architecture for lecithin cholesterol acyl transferase (LCAT): identification of the catalytic triad and molecular modeling. Protein Sci 7:587–599
9. Francone OL, Fielding CJ (1991) Structure–function relationships in human lecithin:cholesterol acyltransferase. Site-directed mutagenesis at serine residues 181 and 216. Biochemistry 30:10074–10077
10. Bender ML, Clement GE, Keizdy FJ (1964) The kinetics of α-chymotrypsin reactions in the presence of added nucleophiles. J Am Chem Soc 86:3697–3703
11. Piran U, Nishida T (1979) Utilization of various sterols by lecithin-cholesterol acyltransferase as acyl acceptors. Lipids 14:478–482
12. Sparks DL, Anantharamaiah GM, Segrest JP, Phillips MC (1995) Effect of the cholesterol content of reconstituted LpA-I on lecithin:cholesterol acyltransferase activity. J Biol Chem 270:5151–5157
13. Ahmad S, Gromiha MM, Sarai A (2003) RVP-net: online prediction of real valued accessible surface area of proteins from single sequences. Bioinformatics 19:1849–1851
14. Adimoolam S, Jonas A (1997) Identification of a domain of lecithin-cholesterol acyltransferase that is involved in interfacial recognition. Biochem Biophys Res Comm 232:783–787
15. Smaby JM, Momsen MM, Brockman HL, Brown RE (1997) Phosphatidylcholine acyl unsaturation modulates the decrease in interfacial elasticity induced by cholesterol. Biophys J 73:1492–1505
16. Bolin DJ, Jonas A (1994) Binding of lecithin:cholesterol acyltransferase to reconstituted high density lipoproteins is affected by their lipid but not apolipoprotein composition. J Biol Chem 269:7429–7434
17. Jauhiainen M, Yuan W, Gelb MH, Dolphin PJ (1989) Human plasma lecithin-cholesterol acyltransferase. Inhibition of the phospholipase A2-like activity by sn-2-difluoroketone phosphatidylcholine analogues. J Biol Chem 264:1963–1967
18. Kumpula LS, Kumpula JM, Taskinen MR, Jauhiainen M, Kaski K, Ala-Korpela M (2008) Reconsideration of hydrophobic lipid distributions in lipoprotein particles. Chem Phys Lipids 155:57–62
19. Aron L, Jones S, Fielding CJ (1978) Human plasma lecithin-cholesterol acyltransferase. Characterization of cofactor-dependent phospholipase activity. J Biol Chem 253:7220–7226
20. Nakagawa M, Nishida T (1973) Role of high density lipoproteins in the lecithin-cholesterol acyltransferase activity with sonicated lecithin-cholesterol dispersions as substrate. Biochim Biophys Acta 296:577–585
21. Yokoyama S, Fukushima D, Kupferberg JP, Ke'zdy FJ, Kaiser ET (1980) The mechanism of activation of lecithin:cholesterol acyltransferase by apolipoprotein A-I and an amphiphilic peptide. J Biol Chem 255:7333–7339
22. Jonas A, McHugh HT (1983) Reaction of lecithin:cholesterol acyltransferase with micellar complexes of apolipoprotein A-I and phosphatidylcholine, containing variable amounts of cholesterol. J Biol Chem 258:10335–10340
23. Deems RA, Eaton BR, Dennis EA (1975) Kinetic analysis of phospholipase A2 activity toward mixed micelles and its implications for the study of lipolytic enzymes. J Biol Chem 250:9013–9020
24. Singh J, Ranganathan R, Hajdu J (2010) Surface dilution kinetics using substrate analog enantiomers as diluents: enzymatic lipolysis by bee venom phospholipase A2. Anal Biochem 407:253–260
25. Dergunov AD, Dobretsov GE, Visvikis S, Siest G (2001) Protein-lipid interactions in reconstituted high density lipoproteins: apolipoprotein and cholesterol influence. Chem Phys Lipids 113:67–82
26. Dergunov AD (2011) Local/bulk determinants of conformational stability of exchangeable apolipoproteins. Biochim Biophys Acta 1814:1169–1177

number of double bonds, with n-3, n-6 and n-9 indicating the position of the first double bond counting from the methyl end

Introduction

Previous reports have shown that, in the rat testis and spermatozoa, sphingomyelin (CerPCho) and ceramide (Cer) contain a high proportion of very long chain (VLC) polyunsaturated fatty acids (PUFA), this including non-hydroxy (n-) and 2-hydroxy (2-OH) VLCPUFA [1, 2]. The association of these unusual lipids with cells of the spermatogenic lineage was indicated by in vivo studies showing that they appear in the testis only after the onset of spermatogenesis and that they gradually disappear from the testis of healthy adult rats in situations that lead to germ cell deprivation with permanence of Sertoli cells [3, 4].

The amount of both types of fatty acids increases in both lipids from the onset of spermatogenesis to adulthood in both sphingolipids, but species with *only* n-VLCPUFA rise during the first few weeks, the species with 2-OH VLCPUFA being the last to be accrued [2]. Conversely, species with n-VLCPUFA disappear from the adult rat testis *before* those with 2-OH VLCPUFA in situations that are known to be damaging to the immature and rapidly dividing germ cell precursors, like doxorubicin treatment [2] and X-ray irradiation [4]. These in vivo changes found an explanation when the acquisition of each type of VLCPUFA was shown to be associated with germ cell differentiation [5]. Thus, virtually only sphingomyelins and ceramides with n-VLCPUFA may be found in the larger and less differentiated pachytene spermatocytes, whereas species with 2-OH VLCPUFA prevail in the smaller but more mature and numerous round spermatids.

After leaving the testis, spermatozoa are known to undergo a series of structural and functional modifications during their passage through the highly convoluted epididymal duct [6, 7]. Progressive motility, a quality obviously associated with the tail, is one of the last properties to be acquired. Epididymal maturation entails changes in many sperm constituents, including proteins and lipids. In several mammalian species, the content of glycerophospholipids (Gpl) per cell decreases as spermatozoa acquire their definite shape and size during their transit from the caput to the caudal segments, this process being associated with a relative increase in choline glycerophospholipids (ChoGpl) [8–11]. In the rat, this concurs with a reduction in the proportion of the major 22:5n-6 in Gpl, and a concomitant increase in that of 22:4n-9, markedly affecting the ChoGpl, but most especially the plamenylcholines (PlsCho) [12].

In contrast to the significant quantitative and qualitative differences observed for the major Gpl, sphingomyelins and ceramides accompany the gametes with little change in their fatty acid profiles from epididymal caput to caudal regions [2]. Moreover, these lipids show similar features in their fatty acids between testicular round spermatids and spermatozoa from epididymal cauda [5]. Both developmental stages contain sphingomyelins with similar proportions of n- and 2-OH VLCPUFA and, intriguingly, high levels of Cer that exclusively contain 2-OH VLCPUFA [5].

A previous study focusing on the species of CerPCho and Cer with nonhydroxy VLCPUFA showed that, as long as care is taken to avoid "spontaneous" hydrolysis of CerPCho during isolation of rat spermatozoa from the epididymal cauda, these gametes contain virtually no Cer [13]. Thus, using divalent cation-free media, most of the n-VLCPUFA-rich species of CerPCho that can be recovered from spermatozoa were found to be located to the head, not only in rat but in bull spermatozoa [13]. It was then intriguing that whole rat spermatozoa contained relatively high levels of Cer with 2-OH VLCPUFA [14], even if isolated in divalent cation-free media [5].

The aim of the present study was to investigate how the sphingomyelins and ceramides that contain both types of VLCPUFA are distributed between head and tail in rat spermatozoa. A comparison with other lipid classes with which these lipids coexist in each of these two regions, focusing on their fatty acids, was also included. Our results show that not only the major Gpl classes and subclasses tend to be unevenly distributed between these two regions, but that sperm sphingomyelins and ceramides are completely segregated.

Materials and Methods

Spermatozoa and Their Parts

Adult (3–4 month-old) Wistar rats, maintained an manipulated in accordance with the Guide for the Care and Use of Laboratory Animals, Institute for Laboratory Animal Research (ILAR), National Academy of Sciences (Bethesda, MD, 1996) were used to obtain the spermatozoa used in this study. Caudal epididymi were excised, freed of their fat pad and blood vessels, and transferred to small dishes containing PBS. After making a few incisions with a scalpel blade, the epididymi were gently incubated under a 95% O_2—5% CO_2 for 15 min at 34 °C to allow release and diffusion of spermatozoa into the medium. The gametes were obtained from such media by centrifugation at $200\times g$, re-suspended in PBS, and subjected to the fractionation procedures. The divalent metal-ion chelator EDTA was incorporated at a concentration of 2.5 mM in

all media used for sperm isolation, from the initial PBS to the sucrose-containing solutions [13]. The study protocol was approved by the Committee on the Care and Use of Research Animals at the University of the South.

To separate the sperm heads from the tails, the gametes were gently suspended in PBS containing 1 mM phenylmethyl-sulfonyl fluoride (PMSF) and the samples were sonicated at 30-s intervals using a Model 250 Branson Sonifier. It was necessary to pool samples of spermatozoa isolated from several rats to obtain sufficient material for lipid analysis. After sonication, the mixture of separated heads and tails was pelleted at 600×*g* at 4 °C, re-suspended in 65% sucrose, loaded onto a step gradient made up of 65, 70 and 75% (w/v) sucrose in PBS-PMSF, and separated in an ultracentrifuge at 4 °C as previously described [13, 15]. The purity of the fractions was verified by light microscopy (Fig. 1).

Lipid Separation and Analysis

Sperm heads and tails were collected from the gradients, gently washed with PBS and pelleted by centrifugation. Lipid extracts were prepared and partitioned using chloroform–methanol mixtures [16]. After evaporating the organic solvents under N_2, the samples were dissolved in chloroform–methanol (2:1 v/v) and aliquots were taken for total lipid phosphorus and phospholipid composition analyses.

For preparative isolation of lipid classes for further analysis, most of the lipid extracts were spotted on TLC plates (500 µm, silica gel G) under N_2, along with commercial standards (Sigma Chemical Co, MO, USA). The polar lipids remained at the origin of the plates, and the neutral lipids were resolved in two steps. Chloroform/methanol/aqueous ammonia (90:10:2 by vol) was run up to the middle of the plates to resolve the ceramides and then hexane/ether (80:20, by vol) up to the top of the plates to separate free cholesterol from other (minor) neutral lipids. After TLC, the zones containing the lipids of interest were located under UV light after spraying with 2′,7′-dichlorofluorescein in methanol and scraped into tubes for elution. This was done by 3 successive extractions of the silica support with chloroform/methanol/water (5:5:1 by vol.), centrifuging, collecting the solvents, and partitioning with four volumes of water to recover the lipids.

The total polar lipid fraction was subjected to further separations and analyses. Choline and ethanolamine glycerophospholipids (ChoGpl, EtnGpl) were resolved into classes by two-dimensional TLC [17]. They were separated into their major subclasses by taking advantage of the lability to acid of the 1-alk-1′-enyl bond present at *sn*-1 in the corresponding plasmalogens and the stability to alkali of the 1-*O*-alkyl bond present in the corresponding glyceryl-ether derivatives [5]. Briefly, the eluted, dried ChoGpl or EtnGpl were gently agitated for 1 min with a small amount of acid acetonitrile (0.5 N HCl). This produced a

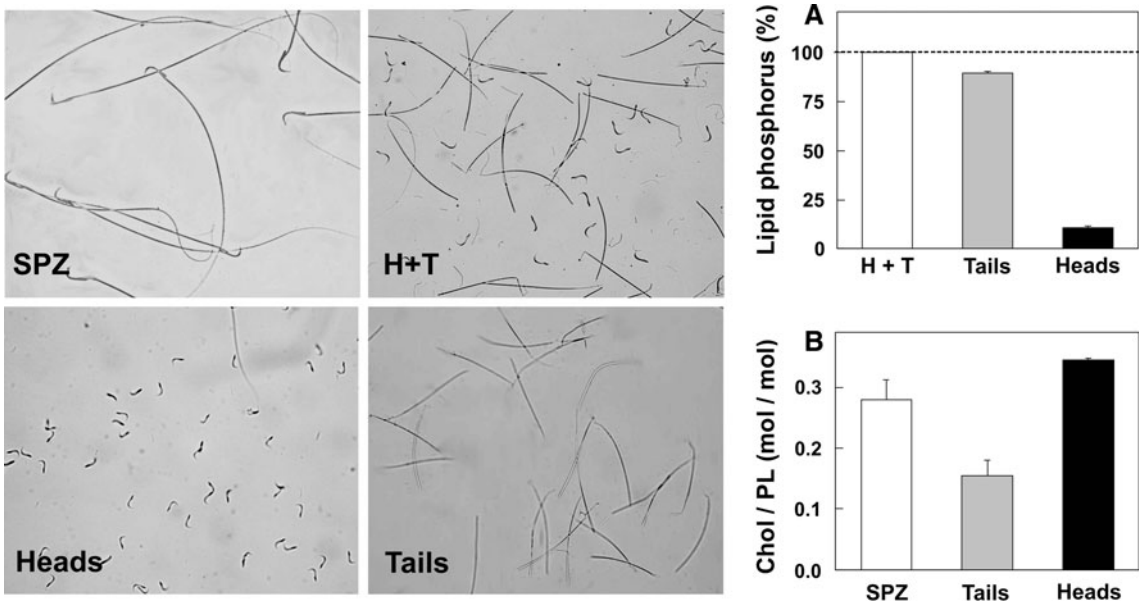

Fig. 1 *Panels on the left*: Phase photomicrographs of intact spermatozoa (SPZ), heads plus tails (H + T), as observed after sperm sonication cycle and before isolation of the two parts, and separate head and tail fractions, obtained after gradient centrifugation. **a** Total lipid phosphorus distribution between head and tail fractions, expressed as percentage of the lipid phosphorus present in the initial H + T fraction. **b** Cholesterol/phospholipid (Chol/PL) ratio in whole sperm and its two main fractions

fatty aldehyde and the corresponding lyso-Gpl, easily separable by TLC (chloroform/methanol/water, 65:25:4, by vol.) from the unchanged lipid (mainly 1,2-diacyl-Gpl plus a small proportion of 1-alkyl-2-acyl-Gpl). After elution, both lipids were subjected to further analysis (phosphorus, fatty acids). An aliquot of the larger band thus obtained was exposed to mild alkali (0.1 N NaOH in methanol) to remove all ester-bound fatty acids, this allowing recovery of the corresponding alkali-stable lysophospholipid, whose phosphorus is representative of the corresponding 1-*O*-alkyl, 2-acyl ChoGpl or EtnGpl subclass.

Sphingomyelin was recovered after TLC using chloroform/methanol/acetic acid/0.15 mM NaCl (50:25:8:2.5 by vol). After elution and drying of this CerPCho (and also of Cer), a similar mild alkali treatment was performed in order to ensure removal from the samples of any potential lipid contaminant containing ester-bound fatty acids [13] and the two lipids were recovered again by TLC.

The fatty acids of all lipid classes were quantified by gas-chromatography (GC). After adding appropriate internal standards, the fatty acids were converted to methyl esters (FAME) by transesterification with 0.5 N H_2SO_4 in anhydrous methanol under N_2 [18], kept overnight at 45 °C in Teflon®-lined, screw-capped tubes. Before GC, FAME were routinely purified by TLC on prewashed (methanol:ethyl ether, 75:25, by vol) silica Gel G plates, using hexane:ether (95:5, by vol for normal FAME and a combination of 80:20 followed by 95:5 by vol of the same solvents) for the cleanup of CerPCho- and Cer-derived FAME and 2-OH-FAME [2]. After elution and drying, the former were analyzed directly by GC and the latter after conversion into O-TMS derivatives.

The nonhydroxy VLCPUFA and the 2-hydroxy VLCPUFA of CerPCho were thoroughly identified by Poulos and colleagues in 1987 and 1992, respectively, using widely accepted lipid methodological procedures including mass spectrometry [19, 20]. More recently, the 2-hydroxy VLCPUFA were also unambiguously characterized in a novel series of glycosphingolipids from mouse testis by Sandhoff and colleagues [21]. Mass spectra of rat germ cell Cer- and CerPCho-derived methyl esters of 28:4n-6 and 30:5n-6 [22] as well as of (intact and hydrogenated) TMS derivatives of 2-OH 28:4 and 2-OH 30:5 [4] appeared in previous articles from our laboratory.

A Varian 3700 Gas Chromatograph equipped with two (2 m × 2 m) glass columns packed with 10% SP 2330 on Chromosorb WAW 100/120 (Supelco, Inc.) was used for fatty acid analysis. The column oven temperature was programmed from 150 to 230 °C at a rate of 5 °C/min for nonhydroxy fatty acids and from 190 to 230 °C in the case of 2-OH fatty acids, the upper temperature being kept for at least 30 min to allow for elution of the longest VLCPUFA (32 carbon in the case of rat testicular lipids). Injector and detector temperatures were set at 220 and 230 °C, respectively, and N_2 (30 ml/min) was the carrier gas. The fatty acids were detected with two flame ionization detectors, operated in the dual-differential mode, connected to a Varian Star Chromatography Workstation (version 4.51).

Statistical analyses- All data are expressed as mean values ± SD, from a number of at least 4 different experiments. Statistical differences between 2 groups were evaluated by unpaired Student's t tests. Statistical analyses were performed using GraphPad Prism 5.0 (GraphPad Software, San Diego, California). All differences tested were statistically significant when assessed at $P < 0.05$.

Results

Spermatozoal Head and Tail Lipids

In comparison with other mammalian species including the mouse, rat spermatozoa are characterized by a long, voluminous tail and a really minute, hook-shaped head (Fig. 1). Of the total lipid phosphorus that was present in the starting homogenate (i.e., the mixture that contained the heads and tails before their separation), the tails contributed on average an 87.5% and the heads a mere 12.5% of the total lipid phosphorus of spermatozoa (Fig. 1a) (tail/head ratio = 7). By the same token, the tails contributed on average a 72% and the heads a 28.5% of the total cholesterol recovered (approximate tail/head ratio = 2.5). In the head, the total cholesterol/total phospholipid ratio (mol/mol) was significantly higher (0.35) than in the tail (0.15), with an intermediate value (0.28) for the whole sperm (Fig. 1b). These data indicate that the concentration of cholesterol with respect to that of phospholipids was more than twice as large in the head as in the tail.

The figures that follow were set to show the quantitative distribution of lipids and their fatty acids between heads and tails. Tables with compositional (%) data may be found in the supplementary material. In the head, choline glycerophospholipids (ChoGpl) constituted the major phospholipid class, followed in a far second place by EtnGpl (60 and 15% of the head phospholipids, respectively) (see supplementary Table 1). In the tail, the proportions of these two lipids were closer but still the ChoGpl predominated (43 and 32%, respectively). The quantitative distribution of phospholipid classes (Fig. 2) showed that all major Gpl appeared in both parts, most predominating in the tail, as expected from the observed head–tail size disparity. The observation that cardiolipin (Ptd_2Gro) was negligible in the head but was the third most abundant phospholipid in the tail fraction (Fig. 2) agrees with the

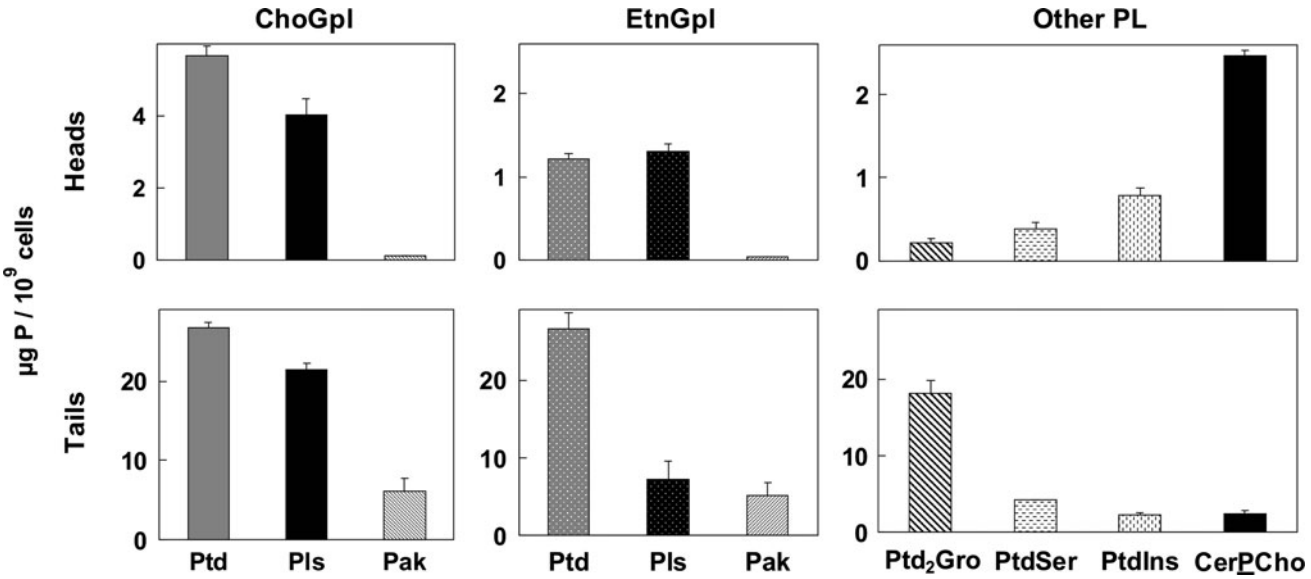

Fig. 2 Distribution of major phospholipids between rat sperm heads and tails. Lipids were quantified on the basis of phosphorus (P) content and expressed on the basis of a given number of cells, taking into account the initial gamete count per sample and the proportion (%) of the total P contributed by each fraction. Note the scale differences. Abbreviations: *ChoGpl* choline glycerophospholipids, *EtnGpl* ethanolamine glycerophospholipids, *Ptd*, *Pls*, and *Pak* the three subclasses (1,2-diacyl-, 1-alk-1′enyl, 2-acyl- and 1-*O*-alkyl, 2-acyl-subclasses, respectively) of ChoGlp or EtnGpl, *Ptd$_2$Gro* diphosphatidylglycerol, *PtdIns* phosphatidylinositol, *PtdSer* phosphatidylserine, *CerPCho* sphingomyelin

fact that the tail contains the middle piece, rich in mitochondria, the inner membrane of which is known to contain cardiolipin.

The different composition of the lipid material present in the two sperm regions was also reflected in the proportions of the three subclasses of ChoGpl and EtnGpl (Fig. 2). Thus, the percentage ratio between phosphatidylcholine (PtdCho), plasmenylcholine (PlsCho), and plasmanylcholine (PakCho) was on average 51:41:8 for whole sperm and quite close (50:39:11) for the tail fraction. The corresponding phosphatidylethanolamine (PtdEtn), plasmenylethanolamine (PlsEtn):plasmenylethanolamine (PakEtn): plasmanylethanolamine (PakEtn) ratios were 64: 27: 9 in whole sperm and 68:19:13 in tails. The proportion of the Pak subclass was somewhat larger in the tail than in whole sperm for both lipid classes because it was virtually undetectable in the head (Fig. 2). The proportion PtdCho:PlsCho and PtdEt:PlsEt in the head were 58:42 and 48:51, respectively. Thus, the head was much richer in plasmalogens than the tail.

In agreement with previous results [13], CerPCho abounded in the head (15% of the phospholipid) but scarcely reached a 2% of total lipid phosphorus in the tail fraction. The amount of CerPCho was therefore similar in tails and heads (Fig. 2), because it comprised a large proportion of the total phospholipid of the (small) head and a small proportion of total phospholipid of the (large) tail.

Distribution of Major Glycerophospholipids

Polyunsaturated fatty acids of the n-6 series with 18–22 carbon atoms collectively constituted the main fatty acids of sperm Gpl (more than half, see Table 2, supplemental material). Although both, heads and tails, were characterized by containing high proportion of 22 carbon PUFA, 22:4n-9 was the main PUFA in the total Gpl of the head fraction, followed by 22:5n-6, while the opposite occurred in the Gpl of the tail, where 22:5n-6 predominated over 22:4n-9. The percentage of species with saturated fatty acids was slightly higher in the total Gpl of heads than of tails, mainly due to 16:0 and 18:0, probably accompanying the mentioned polyenes in Gpl molecules. These characteristics were mostly determined by the fatty acids of the main subclasses of ChoGpl and EtnGpl (Fig. 3).

Although the same fatty acids appeared in PtdCho and PlsCho, their distribution markedly differed between the equivalent lipid of sperm head or tail (Fig. 3). Thus, sperm head PlsCho was markedly richer in 22:4n-9, and showed a much higher 22:4n-9/22:5n-6 ratio, than the PlsCho of the tail. Sperm head PdtCho also contained relatively more 22:4n-9 (and 18:0), and less 22:5n-6 (and 16:0) than the same lipid located in the tail. In quantitative terms, 20% of the total 22:4n-9, in comparison with 10% of the total 22:5n-6 of ChoGpl was in the head (Fig. 3).

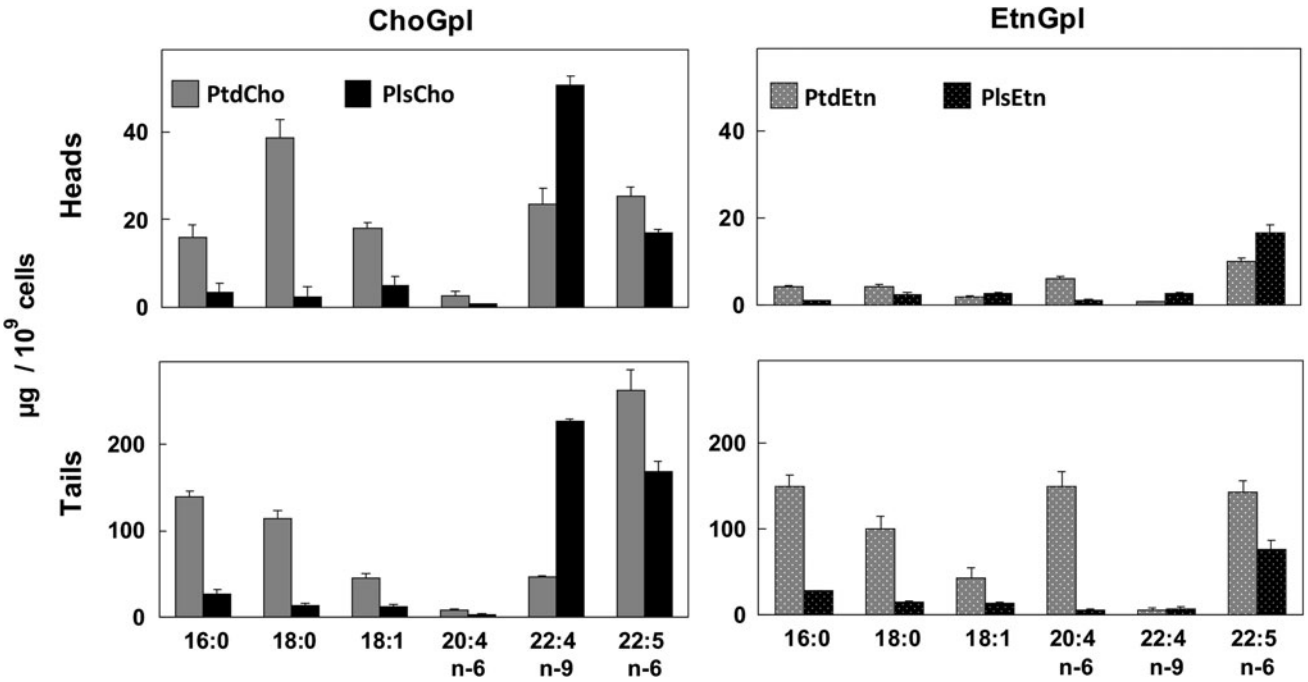

Fig. 3 Amounts of representative fatty acids of the two main subclasses of rat sperm head and tail ChoGpl and EtnGpl. The abbreviations Ptd and Pls indicate phosphatidyl- and plasmenyl-subclasses within each of these lipid classes. Other abbreviations are the same as in Figs. 1 and 2. Note the predominance of 22:5n-6 in tail PtdCho in contrast to that of 22:4n-9 among the PUFA of head PlsCho

The fatty acids of EtnGpl subclasses showed fewer contrasting differences than those of ChoGpl between sperm heads and tails, as long as PlsEtn had 22:5n-6 as its major fatty acid in both fractions. In the tail PtdEtn, 22:5n-6 and 20:4n-6 occurred in similarly large proportions, while 22:4n-9 was a minor fatty acid in relative or absolute terms (Fig. 3).

Distribution of Sphingomyelins and Ceramides

As estimated from its fatty acids, the content per cell of CerPCho was very similar in the head and in the tail (Fig. 4), confirming the distribution of this lipid estimated on the basis of the amount of lipid phosphorus (Fig. 2). However, the fatty acids revealed that the sphingomyelins of the tail contained predominantly saturated fatty acids, while those of the head contained almost exclusively VLCPUFA (Fig. 4). Most of the former were 16:0 and 18:0 (see supplementary Table 3). As for the latter, in addition to the n-VLCPUFA previously reported [13], the 2-OH VLCPUFA were even more abundant (26 and 37% of the total fatty acids, respectively). Both types of VLCPUFA were virtually absent from the CerPCho of the tail and, conversely, little saturates were measurable in the same lipid from the head (Fig. 4).

As previously shown for the ceramides of rat spermatozoa [13], when these gametes were isolated in the presence of EDTA, the total content per cell of Cer was very low in the heads of spermatozoa, as long as the species with n-VLCPUFA are concerned (Fig. 4). However, this did not apply to the Cer present in the tails, which was almost 8 times as high as in the heads, even when both fractions were isolated from the same source and in similar media. Most of this difference was found to be due to the species of Cer that contained 2-OH VLCPUFA as their almost exclusive components (Fig. 4).

As a group, 2-OH VLCPUFA represented more than 80% (see supplementary Table 4) of the fatty acids of the sperm tail-associated Cer in the rat. Considering their large size (Fig. 1), the finding of virtually all of the Cer with 2-OH VLCPUFA located to the tails clarifies why this unique lipid is constitutively so abundant in intact rat spermatozoa (Fig. 4).

The amounts of individual VLCPUFA of Cer and CerPCho involved in this uneven distribution, equivalent on a molar basis to the abundance of the corresponding molecular species, are shown in Fig. 5. The main and virtually only n-VLCPUFA of head CerPCho was 28:4n-6. The main 2-OH VLCPUFA of head CerPCho, and also of

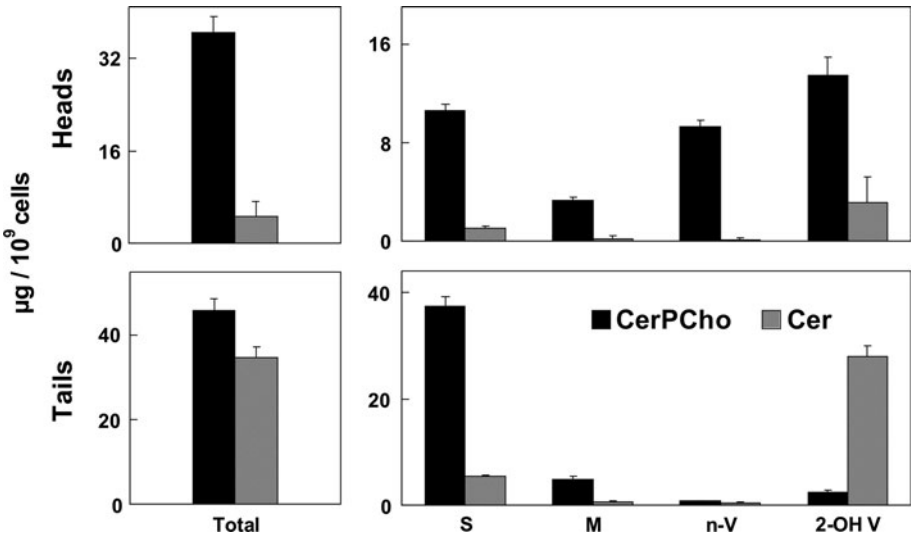

Fig. 4 Amount of sphingomyelins and ceramides, represented by their fatty acids, in rat sperm head and tail fractions. The fatty acids from the two lipids from each fraction were quantified by gas chromatography and are here expressed on the basis of a given number of cells. *Left panels* amounts of total fatty acids; *right panels* amounts of main fatty acids, grouped into saturated (S), monoenoic (M), nonhydroxy VLCPUFA (n-V) and 2-hydroxy VLCPUFA (2-OH V). Note the high total CerPCho/total Cer ratio in the head in comparison to the tail. Note also the predominance of VLCPUFA (n-V plus 2-OH V) in the CerPCho of the head, in contrast to the virtual absence of these fatty acids in the same lipid of tails. The latter contain Cer with almost exclusively 2-OH VLCPUFA

tail Cer, were 2-OH 30:5n-6, 2-OH 28:4n-6, and 2-OH 32:5n-6, in that order (Fig. 5).

Discussion

Because the rat sperm head size is several times smaller than the tail, the fact that the absolute amount of most lipids was larger in the tail than in the head responds to this characteristic. Most lipids of rat spermatozoa showed quantitative and qualitative variations in their proportions and in their fatty acid composition between both regions. A main finding of the present study was that the head contributed virtually all of the VLCPUFA-containing sphingomyelins, while the tail contributed virtually all of the VLCPUFA-containing ceramides, which can be isolated from rat spermatozoa. This observation could be done thanks to the inclusion in the study of the 2-OH VLCPUFA as components of these lipids, and to the strategy of inhibiting the "spontaneous" hydrolysis of membrane lipids, including CerPCho into Cer, by the addition of a divalent cation chelator.

Cholesterol has widespread effects on the behavior of lipid molecules in cell membranes, its best known property being its ability to interact with CerPCho. The relative higher abundance of cholesterol with respect to phospholipids observed here in rat head spermatozoa coincides with the fact that the VLCPUFA-containing species of CerPCho were almost exclusively located to the head, and may in part be a manifestation of this lipid–lipid interaction. However, cholesterol is distributed all over the plasma membrane of spermatozoa, even in the Cer-rich tail, where it interacts also with other lipid classes.

One of the best known functions of sperm sterols, mostly cholesterol, in spermatozoa is to participate in the complex process known as sperm capacitation. Its release to incubation media that contain a suitable cholesterol acceptor (e.g., albumin) during this process is one of the widely accepted prerequisites for sperm capacitation to proceed [23–25]. Zanetti et al. [14] recently showed that during incubation of rat spermatozoa in conditions that lead to their capacitation, the release of cholesterol concurs with a massive hydrolysis of sperm Gpl, with release of plenty of free fatty acids to an albumin-containing medium.

A relatively higher sterol/phospholipid ratio in the head than in the tail has also been observed in gametes from other mammalian species such as the ram and the boar [26], although the opposite seems to be the case in monkey sperm [27]. In addition to obviously wide species-related differences, the diversity of procedures, manipulations and media used in the isolation of the gametes may explain many lipid discrepancies.

The fact that cardiolipin was negligible in the head but abounded in the tail is interpreted to reflect the fact that these lipids normally compose the inner membranes of mitochondria, organelles that remain in the mid-piece that separates together with the tails during the present tail-head separation. It is certainly possible that the CerPCho that contains virtually only saturated and monoenoic fatty acids in the tail (Fig. 4) could also belong to this intracellular

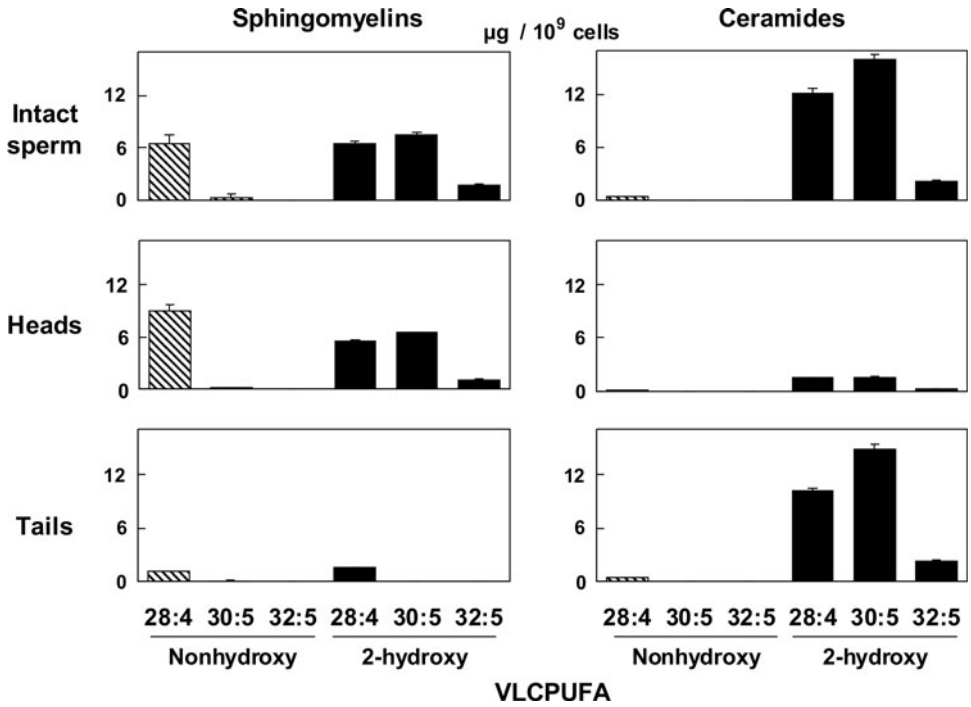

Fig. 5 Amounts of main individual nonhydroxy (*hatched bars*) and 2-hydroxy (*black bars*) VLCPUFA that constitute the CerPCho and Cer of rat spermatozoa and in their head and tail fractions. These (n-6) fatty acids are the main components of the fatty acids that are grouped as n-V and 2-OH V in Fig. 4

structure of the rat tail. The sphingomyelin from a mitochondrial fraction isolated from rat testis showed to be the rich in these two types of fatty acids and poor in VLCPUFA [22]. By the same token, the nuclear and the acrosomal membranes may be expected to contribute their own lipids to the total lipid of the sperm head fraction, in addition to those of the overlying plasma membrane. These intracellular membranes are not easy to isolate and analyze separately in the case of rat sperm head, given its size and fragility of the acrosome. In the case of bovine spermatozoa, sphingomyelin was 10, 13 and 17% of the phospholipids, respectively, in intact spermatozoa, total plasma membrane (i.e., that overlying tails and heads), and the outer acrosomal membrane [28], whereas cardiolipin, originally present in spermatozoa, was absent from both of these membranes.

The high proportion of 22:5n-6 and 22:4n-9 in ChoGpl and the predominance of just 22:5n-6 in EtnGpl, particularly in plasmalogens, is a characteristic of rat spermatozoa. In bovine, ovine, or human spermatozoa, the diacyl- and the abundant alkenyl- subclasses of both lipids, i.e., the four subclasses, are all alike in that they contain 22:6n-3 as their single and predominant PUFA [9, 10, 29, 30]. In this study, the dissimilar fatty acid profiles of ChoGpl and EtnGpl subclasses in rat spermatozoa allowed the observation that they behaved as independent lipids as far as head–tail distribution is concerned (Fig. 3). Notably, the sperm head contained more 22:4n-9-rich PlsCho than did the tail in compositional terms, and the tail contributed more of this Gpl subclass to the total lipid of the gametes in quantitative terms.

In rat sperm, lipid remodeling during epididymal maturation from caput to cauda results in a decrease in sperm head size and total lipid phosphorus, with a concomitant increase in the proportion of plasmenylcholines that contain 22:4n-9 [12]. This specific subclass is absent from the testis, where the PlsCho and PlsEtn of spermatogenic cells increase their proportion of 22:5n-6 with differentiation, but contain no 22:4n-9 [5]. Thus, an important part of the plasmalogens of rat spermatozoa is acquired by these gametes during their passage through the epididymis. The present data allows the inference to be made that this "phospholipid maturation" affects the heads as well as the tails of spermatozoa.

The androgen-dependent epithelial cells of the epididymis contain plenty of peroxisomes and express the enzymes that are required for plasmalogen biosynthesis [31]. Moreover, the synthesis of 22 carbon PUFA that have their first double bond at position 4 (namely, 22:5n-6, 22:6n-3, and also 22:4n-9), requires anabolic enzymes (desaturases, elongases) that are located in the endoplasmic reticulum as well as beta-oxidation enzymes that are located in peroxisomes [32]. In the rat, stearoyl-CoA desaturase 1 (SCD1), stearoyl-CoA desaturase 2 (SCD2), delta5-desaturase, and delta6-desaturase are all actively expressed in the testis and the epididymis [33].

Recently, group III phospholipase A_2 (sPLA$_2$-III), a member of the secreted phospholipase A_2 (sPLA$_2$) family, was shown to be expressed in the mouse proximal epididymal epithelium [34]. Targeted disruption of the gene encoding this protein leads to defects in sperm maturation and fertility. Taken together with the mentioned

biosynthetic activities, this finding suggests that the epididymis may play a role in sperm lipid remodeling by hydrolyzing part of the sperm original Gpl and by delivering PlsCho newly synthesized in situ to the sperm plasma membrane.

After incubation in conditions that lead to sperm capacitation, a significant hydrolysis of ChoGpl occurs that is accompanied by the release of plenty of 22:4n-9 and 22:5n-6 to the media [14], suggesting that plasmalogens participate in this important process. The biological significance that the regionalization of major plasmalogens may have in sperm physiology certainly demands further studies.

The presence of the unique species of Cer that contain 2-OH VLCPUFA in rat sperm tails is consistent with the fact that the proportion of these fatty acids with respect to the rest, and particularly the n-/2-OH VLCPUFA ratio, increase notably in the Cer of whole rat testis from the beginning of spermatogenesis to adulthood [2] and in adults during differentiation from pachytene spermatocytes to spermatids and from these to spermatozoa [5]. Germ cell maturation and differentiation involves the progressive increase in the number and concomitant reduction in size and change in shape from round to elongated forms. In the last phases of spermiation, the size and shape of the head is modified to a larger extent than the tail, which agrees with the fact that the fatty acid composition of Cer is so similar between round spermatids and whole mature spermatozoa [5], and between the latter and isolated sperm tails (present results).

The sharp regionalization observed for these unique species of Cer suggest that they are made in the testis to fulfill a specific function in fertilization that normally involves the sperm tail. One of these functions could be related to sperm motility, as suggested by the fact that mice that lack acid sphingomyelinase have a reduced fertility because their spermatozoa are immotile and have structural defects in their tails [35, 36]. Such a defect was ascribed to an abnormal excess of CerPCho and cholesterol accumulating in the mid-piece, in the tail, or both. The present results reinforce such concept by showing that a certain amount of Cer is required as a normal component of the tail.

The abundance in the sperm head of VLCPUFA-containing sphingomyelins may fulfill a role in sperm physiology that is associated with this region, as it is for instance the acrosomal reaction. It was recently shown [14] that incubation of rat spermatozoa in conditions that evoke this calcium-dependent reaction results in the massive hydrolysis of both (n- and 2-OH VLCPUFA-containing) species of CerPCho, and the concomitant increase in the production of the corresponding species of Cer. The present results, locating these sphingomyelins to the head, are consistent with the acrosomal reaction being a function that exclusively occurs in this sperm area.

The previous finding that the membrane-rich particles known as "residual bodies" of spermiogenesis contain virtually only sphingomyelins with 2-OH-VLCPUFA [5] is consistent with the present results. These structures are formed in the last stages of sperm differentiation in the area of the heads of the condensing spermatids, and are shed from this area as the newly formed spermatozoa are released to seminiferous tubule lumina. The previous observations that epididymal rat spermatozoa [2, 5] constitutively have much more VLCPUFA-containing Cer than CerPCho are also explained by the present findings, since the former are mostly lipids of the large tail, while the latter mostly collect in the small head.

Acknowledgments This work was supported by funds granted by CONICET (Consejo Nacional de Investigaciones Científicas y Técnicas), ANPCyT (Agencia Nacional de Promoción de la Ciencia y la Tecnología), and UNS (Universidad Nacional del Sur), Argentina. G. M. O. and J. M. L. are research fellows from CONICET and the Comisión de Investigaciones Científicas (CIC) of the Province of Buenos Aires, respectively. The collaboration of Pablo L. Ayuza Aresti in the early phases of this work is gratefully acknowledged.

Conflict of interest The authors declare that there is no conflict of interest that could be perceived as prejudicing the impartiality of the research reported.

References

1. Robinson BS, Johnson DW, Poulos A (1992) Novel molecular species of sphingomyelin containing 2-hydroxylated polyenoic very-long-chain fatty acids in mammalian testes and spermatozoa. J Biol Chem 267:1746–1751
2. Zanetti SR, de Los Angeles MM, Rensetti DE, Fornes MW, Aveldano MI (2010) Ceramides with 2-hydroxylated, very long-chain polyenoic fatty acids in rodents: from testis to fertilization-competent spermatozoa. Biochimie 92:1778–1786
3. Furland NE, Luquez JM, Oresti GM, Aveldano MI (2011) Mild testicular hyperthermia transiently increases lipid droplet accumulation and modifies sphingolipid and glycerophospholipid acyl chains in the rat testis. Lipids 46:443–454
4. Oresti GM, Ayuza Aresti PL, Gigola G, Reyes LE, Aveldano MI (2010) Sequential depletion of rat testicular lipids with long-chain and very long-chain polyenoic fatty acids after X-ray-induced interruption of spermatogenesis. J Lipid Res 51:2600–2610
5. Oresti GM, Reyes JG, Luquez JM, Osses N, Furland NE, Aveldano MI (2010) Differentiation-related changes in lipid classes with long-chain and very long-chain polyenoic fatty acids in rat spermatogenic cells. J Lipid Res 51:2909–2921
6. Tsai PS, Gadella BM (2009) Molecular kinetics of proteins at the surface of porcine sperm before and during fertilization. Soc Reprod Fertil Suppl 66:23–36
7. Belleannee C, Belghazi M, Labas V, Teixeira-Gomes AP, Gatti JL, Dacheux JL, Dacheux F (2011) Purification and identification of sperm surface proteins and changes during epididymal maturation. Proteomics 11:1952–1964

8. Nikolopoulou M, Soucek DA, Vary JC (1985) Changes in the lipid content of boar sperm plasma membranes during epididymal maturation. Biochim Biophys Acta 815:486–498
9. Poulos A, Voglmayr JK, White IG (1973) Changes in the phospholipid composition of bovine spermatozoa during their passage through the male reproductive tract. J Reprod Fertil 32:309–310
10. Poulos A, Brown PD, Cox R, White IG (1974) Proceedings: changes in the phospholipid composition of spermatozoa in the reproductive tract of the ram. J Reprod Fertil 36:442–443
11. Rana AP, Majumder GC, Misra S, Ghosh A (1991) Lipid changes of goat sperm plasma membrane during epididymal maturation. Biochim Biophys Acta 1061:185–196
12. Aveldano MI, Rotstein NP, Vermouth NT (1992) Lipid remodelling during epididymal maturation of rat spermatozoa. Enrichment in plasmenylcholines containing long-chain polyenoic fatty acids of the n-9 series. Biochem J 283(Pt 1):235–241
13. Furland NE, Oresti GM, Antollini SS, Venturino A, Maldonado EN, Aveldano MI (2007) Very long-chain polyunsaturated fatty acids are the major acyl groups of sphingomyelins and ceramides in the head of mammalian spermatozoa. J Biol Chem 282:18151–18161
14. Zanetti SR, Monclus ML, Rensetti DE, Fornes MW, Aveldano MI (2010) Differential involvement of rat sperm choline glycerophospholipids and sphingomyelin in capacitation and the acrosomal reaction. Biochimie 92:1886–1894
15. Gitlits VM, Toh BH, Loveland KL, Sentry JW (2000) The glycolytic enzyme enolase is present in sperm tail and displays nucleotide-dependent association with microtubules. Eur J Cell Biol 79:104–111
16. Bligh EG, Dyer WJ (1959) A rapid method of total lipid extraction and purification. Can J Biochem Physiol 37:911–917
17. Rouser G, Fkeischer S, Yamamoto A (1970) Two dimensional then layer chromatographic separation of polar lipids and determination of phospholipids by phosphorus analysis of spots. Lipids 5:494–496
18. Christie WW (1982) Lipid analysis. Pergamon Press, Oxford, UK
19. Poulos A, Johnson DW, Beckman K, White IG, Easton C (1987) Occurrence of unusual molecular species of sphingomyelin containing 28–34-carbon polyenoic fatty acids in ram spermatozoa. Biochem J 248:961–964
20. Robinson BS, Johnson DW, Poulos A (1992) Novel molecular species of sphingomyelin containing 2-hydroxylated polyenoic very-long-chain fatty acids in mammalian testes and spermatozoa. J Biol Chem 267:1746–1751
21. Sandhoff R, Geyer R, Jennemann R, Paret C, Kiss E, Yamashita T, Gorgas K, Sijmonsma TP, Iwamori M, Finaz C, Proia RL, Wiegandt H, Grone HJ (2005) Novel class of glycosphingolipids involved in male fertility. J Biol Chem 280:27310–27318
22. Furland NE, Zanetti SR, Oresti GM, Maldonado EN, Aveldano MI (2007) Ceramides and sphingomyelins with high proportions of very long-chain polyunsaturated fatty acids in mammalian germ cells. J Biol Chem 282:18141–18150
23. Cross NL (2000) Sphingomyelin modulates capacitation of human sperm in vitro. Biol Reprod 63:1129–1134
24. Flesch FM, Brouwers JF, Nievelstein PF, Verkleij AJ, van Golde LM, Colenbrander B, Gadella BM (2001) Bicarbonate stimulated phospholipid scrambling induces cholesterol redistribution and enables cholesterol depletion in the sperm plasma membrane. J Cell Sci 114:3543–3555
25. Shadan S, James PS, Howes EA, Jones R (2004) Cholesterol efflux alters lipid raft stability and distribution during capacitation of boar spermatozoa. Biol Reprod 71:253–265
26. James PS, Wolfe CA, Ladha S, Jones R (1999) Lipid diffusion in the plasma membrane of ram and boar spermatozoa during maturation in the epididymis measured by fluorescence recovery after photobleaching. Mol Reprod Dev 52:207–215
27. Connor WE, Lin DS, Wolf DP, Alexander M (1998) Uneven distribution of desmosterol and docosahexaenoic acid in the heads and tails of monkey sperm. J Lipid Res 39:1404–1411
28. Parks JE, Arion JW, Foote RH (1987) Lipids of plasma membrane and outer acrosomal membrane from bovine spermatozoa. Biol Reprod 37:1249–1258
29. Fuchs B, Muller K, Goritz F, Blottner S, Schiller J (2007) Characteristic oxidation products of choline plasmalogens are detectable in cattle and roe deer spermatozoa by MALDI-TOF mass spectrometry. Lipids 42:991–998
30. Lenzi A, Gandini L, Picardo M, Tramer F, Sandri G, Panfili E (2000) Lipoperoxidation damage of spermatozoa polyunsaturated fatty acids (PUFA): scavenger mechanisms and possible scavenger therapies. Front Biosci 5:E1–E15
31. Reisse S, Rothardt G, Volkl A, Beier K (2001) Peroxisomes and ether lipid biosynthesis in rat testis and epididymis. Biol Reprod 64:1689–1694
32. Sprecher H (2002) The roles of anabolic and catabolic reactions in the synthesis and recycling of polyunsaturated fatty acids. Prostaglandins Leukot Essent Fatty Acids 67:79–83
33. Saether T, Tran TN, Rootwelt H, Christophersen BO, Haugen TB (2003) Expression and regulation of delta5-desaturase, delta6-desaturase, stearoyl-coenzyme A (CoA) desaturase 1, and stearoyl-CoA desaturase 2 in rat testis. Biol Reprod 69:117–124
34. Sato H, Taketomi Y, Isogai Y, Miki Y, Yamamoto K, Masuda S, Hosono T, Arata S, Ishikawa Y, Ishii T, Kobayashi T, Nakanishi H, Ikeda K, Taguchi R, Hara S, Kudo I, Murakami M (2010) Group III secreted phospholipase A2 regulates epididymal sperm maturation and fertility in mice. J Clin Invest 120:1400–1414
35. Butler A, He X, Gordon RE, Wu HS, Gatt S, Schuchman EH (2002) Reproductive pathology and sperm physiology in acid sphingomyelinase-deficient mice. Am J Pathol 161:1061–1075
36. Otala M, Pentikainen MO, Matikainen T, Suomalainen L, Hakala JK, Perez GI, Tenhunen M, Erkkila K, Kovanen P, Parvinen M, Dunkel L (2005) Effects of acid sphingomyelinase deficiency on male germ cell development and programmed cell death. Biol Reprod 72:86–96

atherosclerosis and diabetes develop over time, and risk factors may be detectable early in life [2–6]. Prevention may therefore be possible by targeting factors leading to CVD early in life.

A lipid profile, with high plasma levels of LDL-cholesterol, triacylglycerols (TAG) and apolipoprotein B100 (Apo-B) and a low concentration of HDL-cholesterol and apolipoprotein A1 (Apo-A), increase the risk of atherosclerosis and CVD [7, 8]. Also, plasma LDL particles are comprised of different sub-fractions, differing in chemical composition, size and density, and studies have suggested that particularly the fraction of small dense LDL particles (sdLDL) is associated with CVD [9, 10]. sdLDL is strongly correlated with plasma TAG, and generally the strong correlation between the different lipid fractions makes it difficult to identify the contribution of the separate fractions to the risk of CVD [7, 8, 11].

Fish consumption and supplementation with n-3 polyunsaturated fatty acids (PUFA) in adulthood have been associated with slightly increased levels of HDL cholesterol, lower TAG concentration, and both a lower relative abundance and particle number of sdLDL [12, 13]. Also, fish oil supplementation during infancy has been found to be associated with a decrease in plasma TAG concentration and an increase in the concentration of plasma LDL and total cholesterol [14, 15]. It is, however, not known whether these effects of n-3 PUFA found early in life can track and program the future lipid profile of the child [16].

Breast feeding has also been shown to increase cholesterol concentration in infancy [17]. These short-term effects of breast feeding are, translated into a long-term decrease in total cholesterol in adulthood [17]. This effect is thought to be caused by the relatively high cholesterol concentration of breast milk, leading to a decrease in the endogenous production of cholesterol. However, breast milk also contains high concentrations of n-3 PUFA, which could potentially influence lipid metabolism. To our knowledge, only one study has looked into the long-term effect of fish oil supplementation during early life on the lipid profile in adulthood [18]. In this study, no association between increased dietary intake of n-3 PUFA during the first 5 years of life and lipid profile at the age of 8 years, was found.

We investigated the hypothesis that supplementation with long chain marine n-3 PUFA during fetal life has an impact on the plasma lipid profile in adolescence. This was done by studying offspring from a randomized controlled trial conducted in 1990, where pregnant women were randomized to fish oil, olive oil or no oil [19]. No association between fish oil supplementation during pregnancy and blood lipid profile in the offspring was found.

Methods

The aim of the original study was to investigate the effect of fish oil supplementation on gestational length. The recruitment and randomization of the original study population has previously been described in detail [19].

Briefly, 533 women in gestational week 30 who attended the Midwife Centre in Aarhus, Denmark, were randomized to four 1 g fish oil capsules (FO) (Pikasol: 32% eicosapentaenoic acid and 23% docosahexaenoic acid, corresponding to approximately 2.7 g marine n-3 PUFA) per day ($n = 266$), four similar capsules with olive oil (OO) ($n = 136$) or no capsules (NO) ($n = 131$) in 1990. The women receiving oil were blinded for study interventions, and the capsules and boxes looked identical. The 533 enrolled and randomized women represented 61% of eligible women.

The offspring from the abovementioned randomized controlled trial constituted the study population in the present study. At the time of the study, the offspring were aged between 18 and 19 years. A total of 517 (97%) mother and child pairs were alive and living in Denmark.

All the mothers were contacted by mail and they invited their children to complete a self-administered web-based questionnaire concerning anthropometric measures, health and lifestyle. The offspring were also asked whether they wanted to receive an invitation for a physical examination. Those accepting and those who did not respond were all invited to the physical examination. A total of 382 filled out the questionnaire and 243 participated in the clinical examination (Fig. 1).

At the physical examination, a fasting venous blood sample was drawn, centrifuged and frozen at −80 °C.

Serum TAG and cholesterol fractions (Total, LDL, HDL) were measured according to standard methods on a Modular P from Roche Diagnostics, Basel, Switzerland. Apo-B was measured using antibody from DAKO, Glostrup, Denmark, on an Advia 1650 from Bayer Diagnostics, NY, USA. Interserial variation was 5.5%. Apo-A was measured using antibody from DAKO, Glostrup, Denmark, on an Advia 1650 from Bayer Diagnostics, NY, USA. Interserial variation was 5%.

For the sdLDL analysis, blood, anticoagulated with K3-EDTA 1.6 mg/ml, was centrifuged and plasma stored until analysis. Plasma, adjusted to 1.067 g/L with 60% iodixanol from Optiprep, Axis-Schield PoC As, Oslo, Norway, was prestained with Coomassie blue, under-layered beneath 9% iodixanol and subjected to ultracentrifugation (2½ h, 65.000 rpm 16 °C (341.000 g) in a near vertical rotor (Beckmann NVT65). A digital photograph of LDL subclass profiles was analyzed using Total Lab 1D gel-scan software (Pharmacis, UK). LDL subclass phenotypes A, B and I (Intermediate) were characterized according to the

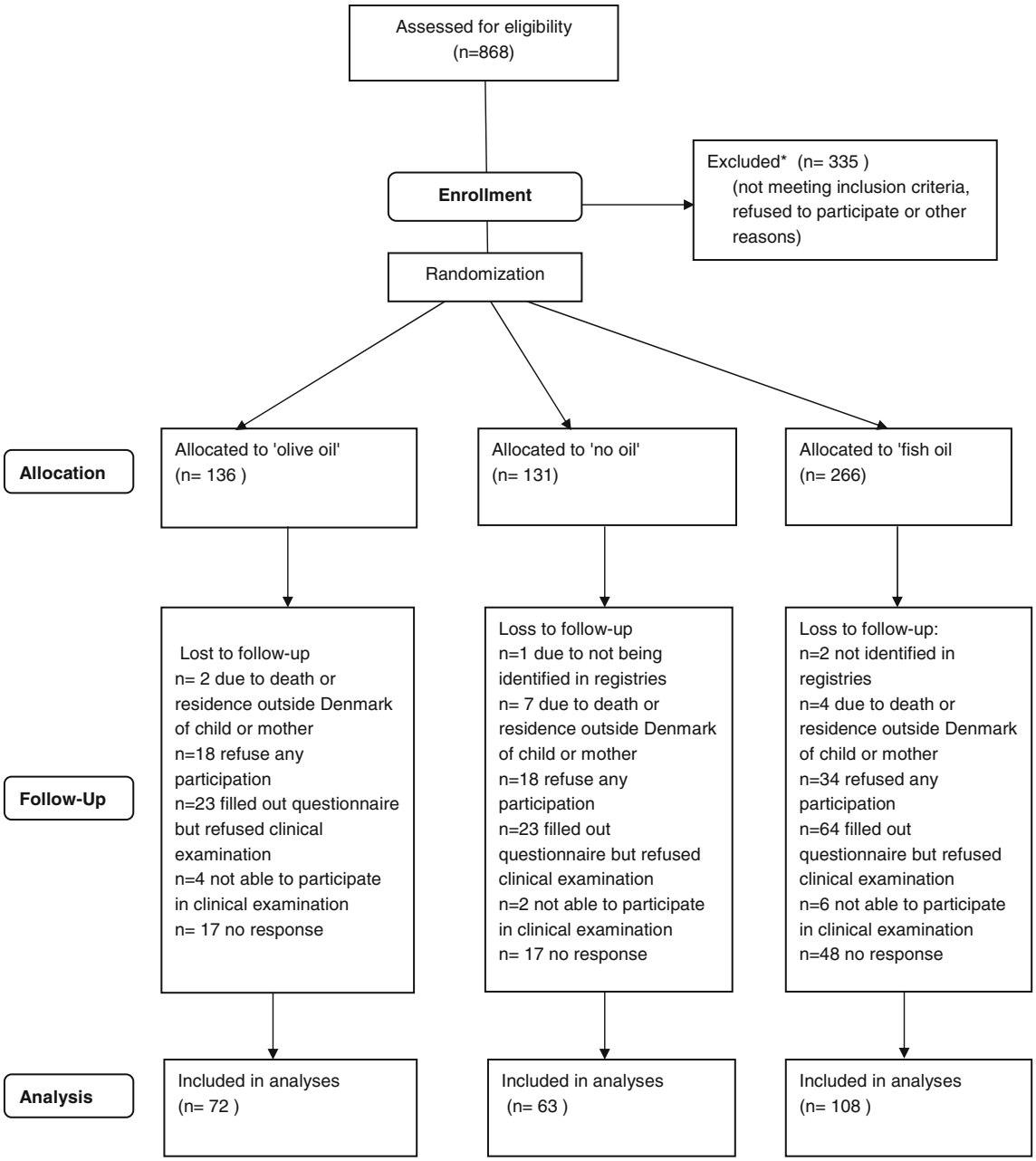

Fig. 1 Flow chart. Nineteen years follow-up of offspring from a randomized controlled trial with fish oil supplementation in pregnancy. Reprinted with permission from Lancet [19] has previously been published [28] and is reprinted with permission from *Am J Clin Nutr*

density and to the area under the curve of B (%AUC B) (sd-LDL) as follows: A: AUC B <40%, I: AUC B 40-50%, B: AUC B >50%. The method has been described in detail previously [20].

Covariates

Information on the mother was collected from the interview and questionnaire during pregnancy. The pregnant women filled out a simple food frequency questionnaire in order to assess their baseline fish consumption, and three categories were defined according to fish consumption. Characteristics of the children were collected from the questionnaire at 18–19 years of age. For this reason, we only had information regarding covariates for the non-participating children who filled out the questionnaire. Information on sex, gestational age and birth weight were collected from medical records.

This study was conducted according to the guidelines laid down in the declaration of Helsinki and all procedures involving human subjects were approved by the local ethics committee (case no.: M-ÅA 20060182) and the

Danish Data Protection Agency (journal no.: 2006-41-6257). Written informed consent was obtained from all subjects.

Statistics

The OO group was used as the reference in the study for the following reasons: (1) the original study showed that blinding worked well in the OO group, indicating that this group was unlikely to have increased their fish consumption during the trial period. (2) It seems reasonable to assume that OO in the supplemented amounts was inert. The results from the NO group are, however, also presented in the tables.

The distribution of biochemical variables was generally skewed, and therefore log transformation was applied to normalize the distribution. Geometric means and interquartile ranges are presented.

Chi-square tests and Student's *t*-tests were used to compare categorical and normally distributed continuous covariates, respectively, between participants and non-participants as well as between the FO and OO groups with two-sided *p*-values <0.05 considered statistically significant. For covariates that were not normally distributed or did not have the same variance in the two groups, Wilcoxon rank sum test was used to test for differences between groups.

Differential programming effects may be found in boys and girls, and therefore the analyses used to estimate the association between fish oil and later lipid profile were initially stratified by sex, using ANOVA. Since the associations were similar in males and females, multiple linear regression modeling adjusting for sex was used to estimate the association. Also, since supplementation with fish oil would be expected to have the largest effect among pregnant women with a low baseline fish intake, the multiple linear regression analyses were also done by only including participants of mothers with a low baseline fish intake ($n = 46$). All associations are reported as percentage difference, since they were all analyzed on the log-scale.

In addition to analyzing the effect on the relative abundance of sdLDL (% of total number of LDL particles) using multiple linear regression, also the effect on the prevalence of LDL subclass B (prevalence of sdLDL >50%) was estimated by logistic regression, adjusting for sex.

Results

Participants

Characteristics of those participating in the clinical examination and the non-participants are given in Table 1. The participants differed from the non-participants with regard to the mother's age during pregnancy, sex and birth weight. Also, the participation rates differed between randomization groups, being lower in the FO group (41%) compared with the OO group (53%). A number of women in the FO group experienced side effects such as gastric reflux during supplementation. When invited to the follow-up, a few mothers reported that they did not think it was relevant for their child to participate since they did not comply with the original study protocol, due to side effects. The women were contacted in writing and the importance of participating was explained, irrespective of compliance. However, among those participating in the clinical examination from the FO group, 1.9% of the mothers took less than 75% of the daily dosage as opposed to 8.6% among non-participants. In the OO group, 2.8% of those participating in the follow-up and 3.2% of non-participants took less than 75% of the daily dosage. There was no information on compliance for 14.6 and 20.9% of the women receiving FO and OO, respectively.

A description of the participants in the three randomization groups is given in Table 2. The three groups were similar with respect to most covariates. The only difference reaching statistical significance was the smoking status in the offspring, with smoking being more prevalent among participants from the OO group compared to the other two groups.

The participants in the study were generally healthy. The median (interquartile range) was 4.0 (3.6; 4.7) mmol/l for total cholesterol, 1.3 (1.1; 1.6) mmol/l for HDL cholesterol, 2.3 (1.8; 2.7) mmol/L for LDL cholesterol and 0.9 (0.6; 1.2) mmol/L for TAG. In light of the recommended lipid levels in healthy subjects from international guidelines a total of 14% had a total cholesterol concentration above 5 mmol/L, 9% an HDL cholesterol concentration less than 1 mmol/L, 18% a LDL cholesterol concentration above 3 mmol/L and only 3% had a TAG concentration above 2 mmol/L.

Fish oil supplementation during pregnancy was not associated with cholesterol concentrations (total cholesterol, LDL, and HDL), TAG concentration or Apo-A1 and Apo-B in the offspring (Table 3). Also, no association was found with relative abundance of sdLDL. However, when restricting the analyses to participants of mothers with a low baseline fish intake, there was a tendency towards a healthier lipid and lipoprotein profile in participants from the FO group compared with the OO group (Table 4). Particularly, TAG, Apo-B and LDL cholesterol tended to be lower in the FO group, but none of the differences were statistically significant.

The distribution of LDL subclass phenotypes A, B and I (Intermediate) in the three randomization groups, stratified by sex, is shown in Fig. 2. There was a tendency towards a

Table 1 Characteristics of participants and non-participants from the follow-up of a randomized controlled trial with fish oil supplementation during pregnancy

	n	Participants	Non-participants	*p*
Mother[a]				
Parity[b]	517			0.82[c]
0		145 (60)	168 (63)	
1		76 (31)	79 (29)	
>1		22 (9)	27 (10)	
Age at giving birth[d]	517	30 ± 4	29 ± 4	0.03[e]
Smoking[b] (yes)	516	67 (28)	93 (34)	0.11[c]
Mother's pre-pregnancy BMI[f] (kg/m^2)	479	21 (20; 23)	21 (20; 23)	0.16[g]
Fish intake[b]	517			0.76[c]
Low		46 (19)	59 (22)	
Medium		141 (58)	155 (57)	
High		56 (23)	60 (22)	
Offspring[h] (19 years)				
Female[b]	517	136 (56)	100 (37)	<0.001[c]
Smokers[b]	370			0.68c[c]
Current		39 (17)	25 (19)	
Ex-smoker		13 (6)	6 (4)	
Occasional smoker		49 (21)	22 (16)	
Never smoker		134 (57)	82 (61)	
Fish hot meal[b]	366			0.09[c]
Never		33 (14)	16 (12)	
1–2 per month		108 (46)	49 (37)	
3–4 per month		71 (31)	46 (35)	
>5 per month		21 (9)	22 (17)	
Fish cold meal[b]	360			0.71[c]
Never		45 (19)	30 (24)	
1–2 per month		95 (41)	45 (36)	
3–4 per month		44 (19)	25 (20)	
>5 per month		50 (21)	26 (21)	
Exercise[b,i]	363	136 (59)	80 (60)	0.95[c]
Parental overweight (yes)				
Mother[b]	366	39 (17)	28 (20)	0.51[c]
Father[b]	356	44 (19)	31 (24)	0.28[c]
Mother or father[b]	355	71 (32)	45 (35)	0.56[c]
Self-reported BMI[d] (kg/m^2)	382	22 ± 3	22 ± 3	0.85[e]
Birth weight[d] (g)	517	3595 ± 486	3485 ± 511	0.01[e]
Gestational age[f] (days)	517	284 (278; 290)	283 (277; 289)	0.20[g]
Randomization code[b]	517			0.04[c]
OO		72 (30)	62 (23)	
NO		63 (26)	60 (22)	
FO		108 (44)	152 (56)	

The table has previously been published [28] and is reprinted with the permission from *Am J Clin Nutr*

OO olive oil, *NO* no oil, *FO* fish oil

[a] Information collected from a self-administered questionnaire to the pregnant women in week 16 of gestation

[b] Presented as number of participants; % in parentheses

[c] Chi-square test

[d] Presented as mean ± SD

[e] Student's *t* test

[f] Presented as median, inter-quartile range in parentheses

[g] Wilcoxon rank sum test

[h] Information collected from a self-administered web-based questionnaire to the offspring at the age of 18–19. Sex and birth weight collected from medical records

[i] Defined as regular exercise of at least 20 min duration, resulting in breathlessness

lower prevalence of phenotype B and larger prevalence of phenotype I in the FO and NO groups compared to the OO group. However, the difference did not reach statistical significance. Sex was significantly associated with LDL phenotype, with phenotype B being more prevalent among males.

Discussion

We found no association between fish oil supplementation during pregnancy and lipid and lipoprotein profile in the 19-year-old offspring. The LDL phenotype in the FO group tended to be healthier in comparison to the

Table 2 Characteristics of mothers and offspring in the olive oil, no oil and fish oil groups from the follow-up of a randomized controlled trial with fish oil supplementation during pregnancy

	OO ($n = 72$)	FO (108)	NO ($n = 63$)	p
Mother[a]				
Parity[b]				0.83[c]
0	42 (58)	65 (60)	38 (60)	
1	24 (33)	32 (30)	20 (32)	
>1	6 (8)	11 (10)	5 (8)	
Age at birth[d]	30 ± 4	30 ± 5	30 ± 4	0.90[b]
Smokers[b] (yes)	18 (25)	28 (26)	21 (33)	0.89[c]
Pre-pregnancy BMI[f] (kg/m^2)	21 (19; 23)	21 (20; 22)	22 (20; 23)	0.58[d]
Offspring[h]				
Female[b]	35 (49)	62 (57)	39 (62)	0.25[c]
Smokers[b]				0.002[c]
Current	19 (27)	13 (13)	7 (12)	
Ex-smoker	6 (9)	1 (1)	6 (10)	
Occasional smoker	10 (14)	27 (26)	12 (20)	
Never smoker	35 (50)	63 (61)	36 (59)	
Fish hot meal[b]				0.80[c]
Never	10 (14)	18 (17)	5 (9)	
1–2 a month	29 (41)	47 (45)	32 (56)	
3–5 a month	23 (32)	30 (29)	18 (32)	
>5 a month	9 (13)	10 (10)	2 (4)	
Fish cold meal[b]				0.09[c]
Never	19 (28)	15 (14)	11 (19)	
1–2 a month	27 (40)	42 (39)	26 (44)	
3–5 a month	8 (12)	22 (21)	14 (24)	
>5 a month	5 (21)	16 (26)	4 (14)	
Exercise[b,i] (yes)	39 (55)	63 (64)	34 (58)	0.98[c]
Parental overweight				
Mother[b]	14 (21)	12 (12)	13 (22)	0.13[c]
Father[b]	11 (16)	21 (20)	12 (21)	0.52[c]
Mother or father[b]	22 (32)	29 (29)	20 (34)	0.64[c]
Birth weight[d] (g)	3543 ± 489	3642 ± 489	3574 ± 476	0.19[e]
Gestational age[f] (days)	283 (277; 289)	284 (280; 291)	285 (277; 291)	0.09[g]

The table has previously been published [28] and is reprinted with permission from *Am J Clin Nutr*

OO olive oil, *FO* fish oil, *NO* no oil

[a] Information collected from a self-administered questionnaire to the pregnant women in week 16 of gestation

[b] Presented as number of participants, % in parentheses

[c] Chi-square test

[d] Presented as mean ± SD

[e] Student's *t* test fish oil versus olive oil

[f] Presented as median, inter-quartile range in parentheses

[g] Wilcoxon rank sum test

[h] Information collected from a self-administered web-based questionnaire to the offspring at the age of 18–19. Sex and birth weight collected from medical records

[i] Defined as regular exercise of at least 20 min duration, resulting in breathlessness

phenotype of the OO group, but the difference was not statistically significant. Finally, there were indications of a healthier lipid profile among offspring of mothers with a low baseline fish intake in the FO group, but with only 46 participants in this group, the confidence intervals were wide and no statistically significant association could be demonstrated.

Loss to follow-up was present overall but significantly higher in the FO group compared to the OO group. This could potentially have led to bias, assuming that a lower participation rate was associated with an unhealthy lipid profile. Participation per se would not be expected to be directly associated with the lipid profile, since most of the participants probably were unaware of their lipid levels, but an unhealthy lipid profile is often associated with a high BMI, and participation could be negatively associated with BMI. However, according to the questionnaire data (Table 1), participation was not associated with BMI. Hence, it is unlikely that the results were biased for BMI.

The larger loss to follow-up in the FO group may partly be caused by differences in compliance. Compliance was higher among participants in the FO group compared to the non-participants. By primarily including participants with high compliance in the analyses, this would strengthen a possible association between FO supplementation and later lipid profile. Hence, this cannot explain the finding of no association in the present study. However, those complying with the study protocol might be different from those not complying, and hence this could introduce some residual confounding.

Participation was associated with exposure and may also be associated with e.g. lifestyle factors which could

Table 3 Concentration of lipid parameters in the three randomization groups and difference in concentrations relative to the olive oil group

	OO ($n = 72$)	NO ($n = 63$)		FO ($n = 108$)	
	Geometric mean[a]	Geometric mean[a]	Difference[b] (%)	Geometric mean[a]	Difference[b] (%)
HDL C (mmol/L)	1.3 (1.1; 1.6)	1.3 (1.1; 1.5)	−2 (−8; 5)	1.4 (1.1; 1.6)	3 (−3; 10)
LDL C (mmol/L)	2.3 (2.0; 2.8)	2.2 (1.8; 2.7)	−6 (−15; 5)	2.3 (1.8; 2.8)	−3 (−11; 7)
Total C (mmol/L)	4.1 (3.6; 4.8)	4.0 (3.6; 4.5)	−4 (−10; 3)	4.1 (3.5; 4.7)	−1 (−6; 5)
TAG (mmol/L)	0.9 (0.6; 1.1)	0.9 (0.6; 1.3)	3 (−12; 20)	0.9 (0.7; 1.2)	−4 (−16; 10)
Apo-A1 (g/L)	1.4 (1.2; 1.5)	1.4 (1.2; 1.6)	−2 (−7; 3)	1.4 (1.2; 1.7)	2 (−2; 7)
Apo-B (g/L)	0.8 (0.7; 0.9)	0.7 (0.6; 0.9)	−5 (−13; 4)	0.8 (0.6; 0.9)	−1 (−9; 7)
sdLDL[c] (%)	36.8 (30.2; 48.5)	33.8 (27.8; 43.5)	−6 (−16; 6)	37.4 (29.2; 43.9)	3 (−7; 15)

No statistically significant difference was found for any of the lipid or lipoprotein fractions

OO olive oil, *NO* no oil, *FO* fish oil, *HDL C* high-density lipoprotein cholesterol, *LDL C* low-density lipoprotein cholesterol, *Total C* total cholesterol, *TAG* triglycerides, *Apo* apolipoprotein, *sdLDL* small dense low-density lipoprotein

[a] Geometric mean, interquartile range in parentheses

[b] Difference (in %) relative to olive oil, adjusted for sex, 95% confidence interval in parentheses

[c] $n = 106$ in FO group

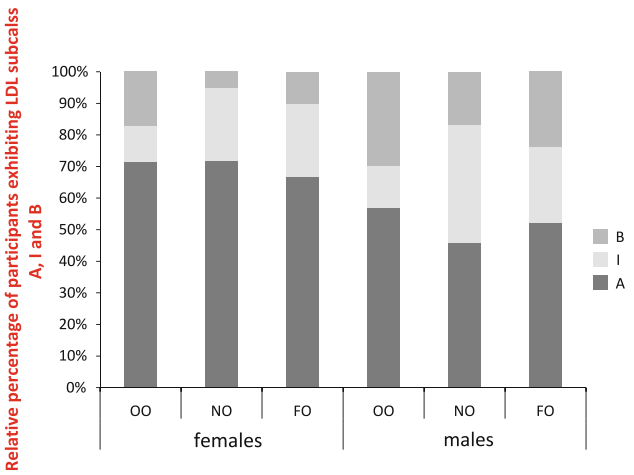

Fig. 2 Distribution of LDL subclass phenotypes A, B and I (Intermediate) in the three randomization groups, stratified by sex. Phenotypes A, B and I were characterized as follows: A: sdLDL <40% of LDL, I: sdLDL 40-50% of LDL particles, B: sdLDL >50% of LDL particles. There was no statistically significant difference in the prevalence of phenotype B between groups

influence lipid profile. Hence, such factors might confound the association between FO supplementation and the lipid profile. In the main analysis we only adjusted for sex. Additional adjustment for offspring smoking and parental overweight did not change estimates.

To our knowledge, no other study has investigated the effect of supplementing with n-3 PUFA during pregnancy on later lipid profile. However, fish oil supplementation during pregnancy has been shown not to affect the lipid profile of the umbilical cord blood speaking against fetal life as the right time window for fish oil supplementation [21]. In another study where term infants were randomized to an intervention aimed at increasing dietary intake of n-3 PUFA and decreasing intake of n-6 PUFA from the time of weaning until the age of 5 years, no association between intervention and lipid profile was found when the children were followed-up at the age of 8 years [18]. The children were, however, very young at follow-up and effects may not be visible until considerably later in life.

Several studies indicate that the lipid profile in adulthood can be influenced, "programmed", by early nutrition. Hence, Barker et al. showed that a low abdominal circumference at birth was associated with higher concentrations of total cholesterol, LDL cholesterol and Apo-B in adulthood [22]. The authors argued that this could be a consequence of impaired liver growth during late gestation due to malnutrition. Accordingly, a study from the Dutch Hunger Winter showed that persons, who were exposed to hunger during early gestation, displayed significantly higher LDL to HDL ratios, and a tendency towards lower plasma concentrations of HDL and Apo-A1 and higher concentrations of LDL and Apo-B compared to persons born before or after the Dutch Hunger Winter [23]. These results, however, contradict results from the Leningrad Siege, where no association between hunger during fetal life or infancy and any of the lipid parameters in adulthood was found [24].

A large body of research on programming of future lipid profile has focused on the effects of breast feeding. The short-term effect of breast feeding in infants is an increase in total cholesterol [17]. However, this effect may be reversed in adulthood, where breastfeeding has been found to be associated with a lower total cholesterol concentration [17]. Hence, a high total cholesterol concentration early in life may be protective later in life.

Table 4 Concentration of lipid parameters in the three randomization groups and difference in concentrations relative to the olive oil group

	OO ($n = 13$)	NO ($n = 9$)		FO ($n = 24$)	
	Geometric mean[a]	Geometric mean[a]	Difference[b] (%)	Geometric mean[a]	Difference[b] (%)
HDL C (mmol/L)	1.4 (1.2; 1.6)	1.2 (1.1; 1.2)	−11 (−26; 7)	1.4 (1.3; 1.7)	6 (−8; 22)
LDL C (mmol/L)	2.6 (2.3; 3.1)	2.5 (1.9; 3.0)	−3 (−24; 24)	2.2 (1.7; 2.6)	−13 (−29; 5)
Total C (mmol/L)	4.5 (4.2; 5.2)	4.2 (3.7; 4.5)	−6 (−20; 10)	4.1 (3.5; 4.7)	−8 (−19; 4)
TAG (mmol/L)	1.1 (0.8; 1.3)	0.8 (0.7; 0.9)	−21 (−47; 17)	0.8 (0.6; 1.25)	−22 (−43; 6)
Apo-A1 (g/L)	1.5 (1.3; 1.6)	1.3 (1.1; 1.3)	−11 (−22; 1)	1.5 (1.3; 1.7)	3 (−7; 14)
Apo-B (g/L)	0.8 (0.7; 1.0)	0.8 (0.6; 0.9)	−3 (−23; 21)	0.7 (0.6; 0.88)	−11 (−26; 6)
sdLDL (%)	35.1 (29.7; 40.2)	32.4 (26.7; 36.4)	−9 (−31; 20)	38.4 (31.4; 42.8)	8 (−13; 34)

Analyses restricted to offspring of mothers with low baseline fish intake during pregnancy

No statistically significant difference was found for any of the lipid or lipoprotein fractions

OO olive oil, *NO* no oil, *FO* fish oil, *HDL C* high-density lipoprotein cholesterol, *LDL C* low-density lipoprotein cholesterol, *Total C* total cholesterol, *TAG* triglycerides, *Apo* apolipoprotein, *sdLDL* small dense low-density lipoprotein

[a] Geometric mean, interquartile range in parentheses

[b] Difference (in %) relative to olive oil, adjusted for sex, 95% confidence interval in parentheses

Also, a study where pre-term infants were randomized to banked breast milk or formulae showed that those receiving banked breast milk had a lower LDL to HDL ratio in adolescence [25]. The mechanism behind the effects of breast-feeding or breast milk on later lipid profile is unknown but may be associated with a lower total energy intake [26] or the higher cholesterol concentration of breast milk compared to infant formulae. The higher cholesterol concentration during early life could potentially suppress endogenous cholesterol production and hence lead to a lower cholesterol concentration later in life [27]. However, breast milk is also high in n-3 PUFA. The short-term effect of supplementing infants with fish oil on serum cholesterol is similar to that of breast feeding [14, 17]. If the effect of breast feeding on later lipid profile is operating through increased cholesterol levels in infancy by inducing decreased endogenous cholesterol production, this could also be the case for fish oil supplementation. Most of the women in the present study had a medium to high baseline fish consumption during pregnancy, and it is possible that this attenuated the effect of fish oil supplementation. Thus, among the offspring of mothers with a low baseline fish intake, there were indications of a beneficial association between fish oil supplementation and later lipid profile. However, as mentioned previously this sub-group analysis contain very few numbers, making it difficult to draw any conclusions. Hence, further studies are needed to confirm this potentially important observation.

Finally, it should be had in mind that very few individuals in early adulthood have an unhealthy lipid profile. Potential benefits of early supplementation with n-3 PUFA on later lipid profile might therefore not be detectable until considerably later in life, and it will be important to follow-up the offspring at later ages.

Conclusion

We found no association between fish oil supplementation during third trimester of pregnancy and offspring plasma lipid and lipoprotein profile in adolescence.

Acknowledgments S.F. Olsen was responsible for the original pregnancy trial and initiated the follow-up of the offspring. D. Rytter, J.H. Christensen, B.H. Bech, S.F. Olsen, E.B. Schmidt and T.B. Henriksen designed the research; D. Rytter and B.H. Bech conducted the research; D. Rytter analyzed the data and wrote the first draft; D. Rytter, J.H. Christensen, S.F. Olsen, E.B. Schmidt, B.H. Bech and T.B. Henriksen wrote the paper; D. Rytter had primary responsibility for the final content. All authors read and approved the final manuscript.

The project described was supported by Award Number R21AT004603 from the National Center For Complementary & Alternative Medicine. The content is solely the responsibility of the authors and does not necessarily represent the official views of the National Center for Complementary & Alternative Medicine or the National Institutes of Health. In addition, the follow-up was supported by the EU FP6 consortium, Early Nutrition Programming Project (EARNEST, Project No. FOOD-CT-2005-007036), The Danish Strategic Research Council, The Danish Heart Foundation, The Novo Nordisk Foundation, The Danish Diabetes Foundation and The Aase and Ejnar Danielsens Foundation. The study sponsors were not involved in the study design; in the collection, analysis, or interpretation of data; in the writing of the report, or in the decision to submit the article for publication.

Conflict of interest All authors declare that there are no conflicts of interest.

References

1. Barker DJ (1997) Fetal nutrition and cardiovascular disease in later life. Br Med Bull 53:96–108
2. Berenson GS, Srinivasan SR, Bao W, Newman WP III, Tracy RE, Wattigney WA (1998) Association between multiple cardiovascular risk factors and atherosclerosis in children and young adults. The Bogalusa heart study. N Engl J Med 338:1650–1656
3. Nguyen QM, Srinivasan SR, Xu JH, Chen W, Berenson GS (2010) Fasting plasma glucose levels within the normoglycemic range in childhood as a predictor of prediabetes and type 2 diabetes in adulthood: the Bogalusa heart study. Arch Pediatr Adolesc Med 164:124–128
4. Baird J, Fisher D, Lucas P, Kleijnen J, Roberts H, Law C (2005) Being big or growing fast: systematic review of size and growth in infancy and later obesity. BMJ 331:929–934
5. Adams C, Burke V, Beilin LJ (2005) Cholesterol tracking from childhood to adult mid-life in children from the Busselton study. Acta Paediatr 94:275–280
6. Elliott WJ (1997) Blood pressure tracking. J Cardiovasc Risk 4:251–256
7. Harchaoui KE, Visser ME, Kastelein JJ, Stroes ES, Dallinga-Thie GM (2009) Triglycerides and cardiovascular risk. Curr Cardiol Rev 5:216–222
8. Di AE, Sarwar N, Perry P, Kaptoge S, Ray KK, Thompson A, Wood AM, Lewington S, Sattar N, Packard CJ, Collins R, Thompson SG, Danesh J (2009) Major lipids, apolipoproteins, and risk of vascular disease. JAMA 302:1993–2000
9. Toft-Petersen AP, Tilsted HH, Aaroe J, Rasmussen K, Christensen T, Griffin BA, Aardestrup IV, Andreasen A, Schmidt EB (2011) Small dense LDL particles—a predictor of coronary artery disease evaluated by invasive and CT-based techniques: a case-control study. Lipids Health Dis 10:21
10. Gazi IF, Tsimihodimos V, Tselepis AD, Elisaf M, Mikhailidis DP (2007) Clinical importance and therapeutic modulation of small dense low-density lipoprotein particles. Expert Opin Biol Ther 7:53–72
11. Stampfer MJ, Krauss RM, Ma J, Blanche PJ, Holl LG, Sacks FM, Hennekens CH (1996) A prospective study of triglyceride level, low-density lipoprotein particle diameter, and risk of myocardial infarction. JAMA 276:882–888
12. Hooper L, Thompson RL, Harrison RA, Summerbell CD, Moore H, Worthington HV, Durrington PN, Ness AR, Capps NE, Davey SG, Riemersma RA, Ebrahim SB (2004) Omega 3 fatty acids for prevention and treatment of cardiovascular disease. Cochrane Database Syst Rev CD003177
13. Griffin BA (2001) The effect of n-3 fatty acids on low density lipoprotein subfractions. Lipids 36(Suppl):S91–S97
14. Damsgaard CT, Schack-Nielsen L, Michaelsen KF, Fruekilde MB, Hels O, Lauritzen L (2006) Fish oil affects blood pressure and the plasma lipid profile in healthy Danish infants. J Nutr 136:94–99
15. Thorsdottir I, Gunnarsdottir I, Palsson GI (2003) Birth weight, growth and feeding in infancy: relation to serum lipid concentration in 12-month-old infants. Eur J Clin Nutr 57:1479–1485
16. Olsen SF (1994) Further on the association between retarded foetal growth and adult cardiovascular disease. Could low intake or marine diets be a common cause? J Clin Epidemiol 47:565–569
17. Owen CG, Whincup PH, Odoki K, Gilg JA, Cook DG (2002) Infant feeding and blood cholesterol: a study in adolescents and a systematic review. Pediatrics 110:597–608
18. Ayer JG, Harmer JA, Xuan W, Toelle B, Webb K, Almqvist C, Marks GB, Celermajer DS (2009) Dietary supplementation with n-3 polyunsaturated fatty acids in early childhood: effects on blood pressure and arterial structure and function at age 8 y. Am J Clin Nutr 90:438–446
19. Olsen SF, Sorensen JD, Secher NJ, Hedegaard M, Henriksen TB, Hansen HS, Grant A (1992) Randomised controlled trial of effect of fish-oil supplementation on pregnancy duration. Lancet 339:1003–1007
20. Davies IG, Graham JM, Griffin BA (2003) Rapid separation of LDL subclasses by iodixanol gradient ultracentrifugation. Clin Chem 49:1865–1872
21. Barden AE, Dunstan JA, Beilin LJ, Prescott SL, Mori TA (2006) n-3 fatty acid supplementation during pregnancy in women with allergic disease: effects on blood pressure, and maternal and fetal lipids. Clin Sci 111:289–294
22. Barker DJ, Martyn CN, Osmond C, Hales CN, Fall CH (1993) Growth in utero and serum cholesterol concentrations in adult life. BMJ 307:1524–1527
23. Roseboom TJ, van der Meulen JH, Osmond C, Barker DJ, Ravelli AC, Bleker OP (2000) Plasma lipid profiles in adults after prenatal exposure to the Dutch famine. Am J Clin Nutr 72: 1101–1106
24. Stanner SA, Bulmer K, Andres C, Lantseva OE, Borodina V, Poteen VV, Yudkin JS (1997) Does malnutrition in utero determine diabetes and coronary heart disease in adulthood? Results from the Leningrad siege study, a cross-sectional study. BMJ 315:1342–1348
25. Singhal A, Cole TJ, Fewtrell M, Lucas A (2004) Breastmilk feeding and lipoprotein profile in adolescents born preterm: follow-up of a prospective randomised study. Lancet 363: 1571–1578
26. Singhal A, Lucas A (2004) Early origins of cardiovascular disease: is there a unifying hypothesis? Lancet 363:1642–1645
27. Wong WW, Hachey DL, Insull W, Opekun AR, Klein PD (1993) Effect of dietary cholesterol on cholesterol synthesis in breast-fed and formula-fed infants. J Lipid Res 34:1403–1411
28. Rytter D, Bech BH, Christensen JH, Schmidt EB, Henriksen TB, Olsen SF (2011) Intake of fish oil during pregnancy and adiposity in the 19-y-old offspring: follow-up on a randomized controlled trial. Am J Clin Nutr. doi:10.3945/ajcn.111.014969

development of infants [1]. For this reason, both DHA and ARA are commonly supplemented in infant formulae. For example, fish oil, which is rich in DHA and eicosapentaenoic acid (EPA, 20:5n-3), is conventionally used as a source of n-3 LC-PUFA in infant formulae in Japan, while DHA-rich microalgal oil (DMO), which is free of EPA, is used to supplement formulae in more than 60 countries worldwide, including the United Kingdom, Mexico, China, United States, and Canada.

A randomized clinical trial has suggested that EPA may be unsuitable for infants because it might reduce ARA levels and delay development [2]. However, maternal milk contains some levels of n-3 LC-PUFA other than DHA, such as 20:3n-3, EPA, and docosapentaenoic acid n-3 (DPAn-3) [3]. Although this suggests that excessive levels of EPA are harmless, the effects of ingestion of trace amounts n-3 LC-PUFA are unknown. Therefore, it is necessary to compare the effects of ingested fish oil and DMO on the fatty acid composition in tissues.

Since available tissue is limited in human studies, animal studies using rodents are useful for elucidating overall LC-PUFA status in target tissues. For example, Moriguchi et al. [4] showed that recovery from the DHA deficiency in the brain and retina caused by n-3 PUFA deficient feeding over two generations takes 8 weeks after initiation of the repletion diet. Animal studies usually employ severe n-3 PUFA deficient conditions, such as long-term n-3 PUFA-deficient diet [4, 5] or artificial rearing conditions with n-3 PUFA-deficient milk [6]. In this study, our interest is the effect of n-3 LC-PUFA on a mildly n-3 PUFA deficient nutritional status because severe n-3 PUFA deficiency is rare in humans, except in such a case as total parenteral nutrition with an inappropriate oil source [7].

In a previous report, we determined the fatty acid composition of serum and liver phospholipids and triglycerides in rat pups from mildly n-3 PUFA-deficient dams who were fed fish oil (FO) or DMO, and found that DMO nearly restored liver EPA levels to those of pups fed a control diet, whereas FO had little effect [8]. However, due to the rapid metabolic turnover in the serum and liver, it is necessary to investigate phospholipid levels in other tissues in order to deduce the overall impact of fish oil and DMO on the LC-PUFA status of human infants.

Here, the fatty acid composition of phospholipids was investigated in five rat tissues, namely the brain, heart,

Table 1 Fatty acid composition (%, [w/w]) of the experimental diets

Fatty acid	Control	n-3 PUFA deficient
16:0	10.3	9.4
18:0	3.8	3.3
20:0	0.3	0.9
22:0	0.4	1.9
24:0	nd	0.8
SFA	14.8	16.1
16:1n-7	0.1	0.1
18:1n-9	24.3	27.5
20:1n-9	0.1	0.6
MUFA	24.5	28.1
18:2n-6	52.7	55.7
18:3n-3	7.9	0.2
Total PUFA	60.6	55.9
n-6/n-3	6.7	278

Fatty acid composition expressed as composition of fatty acid methyl esters

nd not detected (less than 0.1%)

Table 2 Fatty acid composition (%, [w/w]) of the oils fed to rat pups as diet supplements

Fatty acid	FO	DMO
14:0	2.9	11.7
16:0	20.2	10.2
18:0	5.0	0.7
20:0	0.2	0.1
22:0	0.2	0.2
24:0	0.1	0.1
SFA	28.6	23.0
14:1(n-5)	0.1	0.1
16:1(n-7)	3.8	1.5
18:1(n-9)	18.9	23.3
18:1(n-7)	2.4	nd
20:1(n-9)	2	nd
22:1(n-9)	0.3	nd
24:1(n-9)	0.7	nd
MUFA	28.2	24.9
18:2(n-6)	1.2	1.4
20:2(n-6)	0.3	nd
20:3(n-6)	0.1	nd
20:4(n-6)	1.9	nd
22:4(n-6)	0.2	nd
22:5(n-6)	1.0	nd
n-6 PUFA	4.7	1.4
18:3(n-3)	0.5	0.2
20:5(n-3)	7.3	0.1
22:5(n-3)	1.4	0.3
22:6(n-3)	29.3	50.0
n-3 PUFA	38.5	50.6
Total PUFA	43.2	52.0
n-6/n-3	0.12	0.03

Fatty acid composition expressed as composition of fatty acid methyl esters

FO Fish oil, *DMO* DHA-rich microalgal oil, *nd* not detected (less than 0.1%)

kidney, spleen and thymus. We elucidated the effect of pre-weaning supplementation of FO or DMO on tissue fatty acid composition compared to the oil supplement-free condition. FO or DMO was fed to mildly n-3-PUFA-deficient rats pre-weaning and the fatty acid composition of the tissues was determined and compared to the control, namely, pups reared by n-3 PUFA-sufficient dams. The results of this study suggest an important way to improve n-3 PUFA deficiency through supplementation of fish oil and DMO before weaning. This finding is an important consideration in determining how best to accomplish n-3 LC-PUFA supplementation through infant formulae.

Materials and Methods

Animals, Diets, and Supplementation

All animal procedures were performed according to the Regulations for Animal Experiments and Related Activities at Tohoku University (June 27, 2007, Regulation No. 122). Pregnant Sprague-Dawley rats (day 4 of gestation) were purchased from Japan SLC, Inc. (Hamamatsu, Japan).

Two diets were prepared: the AIN-93G diet [9] as a control diet and the n-3 PUFA-deficient diet. The AIN-93G diet composition was the following: 397.5 g/kg cornstarch, 200 g/kg casein, 132 g/kg α-cornstarch, 100 g/kg sucrose, 70 g/kg soybean oil, 50 g/kg cellulose, 35 g/kg mineral mix (AIN-93G), 10 g/kg vitamin mix (AIN-93), 3 g/kg L-cystine and 2.5 g/kg choline bitartrate. The n-3 PUFA-deficient diet was based on the AIN93G diet composition and its oil source from soybean oil was replaced by an n-3-deficient oil which consisted of a mixture of peanut and safflower oils (Table 1). Alpha linolenic acid (ALA, 18:3n-3), was the sole n-3 PUFA source in both diets and was present at a concentration of 0.2% in n-3-deficient oil and 7.9% in soy bean oil for AIN-93G diet. The n-6/n-3 ratio of the n-3 PUFA-deficient oil was 278 and approximately 40-fold higher than that of the soybean oil.

Fatty acid supplements were used as sources of n-3 LC-PUFA (Table 2): FO (Nippon Suisan Kaisha, Ltd., Tokyo, Japan) and DMO (Martek Co., Columbia, MD, USA). The DHA content of FO and DMO was 29.3 and 50.0%, respectively, while EPA was 7.3 and 0.1%, respectively. The oils were emulsified in 1% sodium carboxymethyl cellulose (CELLOGEN F; Dai-ichi Kogyo Seiyaku Co., Kyoto, Japan) solution by sonication to a final concentration of 20% (w/w). The emulsions were freshly prepared daily.

Experimental Procedure

The experimental schedule is shown in Fig. 1. On the day of delivery, the pregnant rats were divided into two diet groups (Table 1): the control diet group ($n = 2$) and the n-3 PUFA-deficient diet group ($n = 6$). Dams were fed the experimental diets through the gestation and lactation

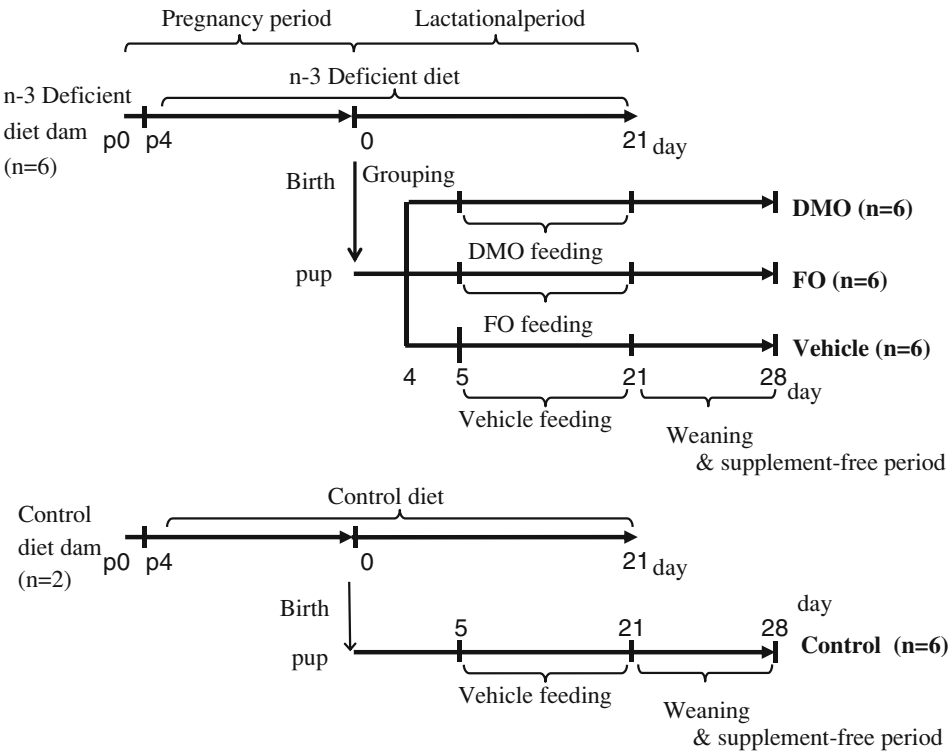

Fig. 1 Schedule of the animal experiment. P0 and P4 indicate days of pregnancy. *DMO* DHA-rich microalgal oil, *FO* fish oil. Vehicle was 1% sodium carboxymethyl cellulose solution

periods. At 4 days of age, pups were weighed and culled to ten individuals from each dam for supplementation experiments. Male pups born to dams fed the n-3 PUFA-deficient diet group were assigned to each of the supplementation treatment groups, and were orally administered fatty acid supplements at 5 μl/g of body weight to pups from 5 to 21 days of age (weaning date): n-3 PUFA-deficient + FO ($n = 6$), n-3 PUFA-deficient + DMO ($n = 6$), and n-3 PUFA-deficient + vehicle ($n = 6$). Male pups ($n = 6$) of dams fed the control diet were also administered the vehicle. The oil or vehicle administration continued for 17 days and ended on the weaning day. After weaning, pups were fed the same diet as their dams for a 1-week without oil or vehicle administration.

After 1-week supplement-free period (28 days of age) pups were sacrificed by decapitation after 12-h food deprivation. Brain, heart, kidney, spleen, and thymus tissues were removed and weighed, and were then immediately frozen and stored at −20 °C until analyzed. For stomach content analysis, pups from another pregnant Sprague-Dawley rat ($n = 10$) fed the control diet ($n = 5$) or n-3 deficient diet ($n = 5$) were bred under the same conditions and sacrificed at 5 days of age.

Fatty Acid Analysis

Total lipids were extracted from stomach contents and tissues using the Bligh-Dyer method [10]. The fatty acid methyl esters (FAME) of lipids from the stomach samples were prepared by treatment with diazomethane followed by sodium methoxide ($NaOCH_3$) [11]. Phospholipids from other tissues were purified by thin layer chromatography (TLC) [12] before preparing FAME using $NaOCH_3$. FAME were analyzed by gas-liquid chromatography (GLC) (GC-380; GL Sciences Inc., Tokyo, Japan) using a CP-Sil 88 WCOT fused silica column (100 m × 0.25 mm i.d., 0.2-m film thickness; Varian, Middelburg, Netherlands) and identified by comparison against commercial external standards. Fatty acid composition was expressed as composition of fatty acid methyl esters.

Statistical Analysis

All data are expressed as the means ± standard deviation (SD). Differences in the stomach content FAME levels of pups from n-3 PUFA-deficient and control groups were detected by the unpaired t test. Dunnett's T3 multiple comparison test was used to determine whether the values of n-3 PUFA deficient + FO, n-3 PUFA deficient + DMO, n-3 PUFA deficient + vehicle, and control groups differed from each other. IBM SPSS Statistic ver. 19 (IBM Corp. Armonk, NY, USA) was used for all statistical calculations.

Table 3 Fatty acid composition (%, [w/w]) of stomach contents of 5-day-old rat pups reared by control dams and mildly n-3 PUFA-deficient dams

Fatty acid	Control	n-3 PUFA deficient
14:0	7.43 ± 1.71	8.36 ± 1.14
16:0	24.97 ± 1.28	25.35 ± 1.06
18:0	4.00 ± 0.23	3.71 ± 0.27
20:0	0.10 ± 0.02*	0.12 ± 0.01
22:0	0.06 ± 0.00***	0.09 ± 0.01
24:0	0.08 ± 0.01**	0.12 ± 0.01
SAF	36.64 ± 2.77	37.75 ± 1.85
16:1(n-7)	2.25 ± 0.32	2.00 ± 0.39
18:1(n-7)	1.99 ± 0.20*	1.63 ± 0.22
18:1(n-9)	25.3 ± 1.81	25.49 ± 0.94
20:1(n-9)	0.45 ± 0.06*	0.61 ± 0.09
22:1(n-9)	0.05 ± 0.01	0.06 ± 0.00
24:1(n-9)	0.05 ± 0.02	0.06 ± 0.00
MUFA	30.10 ± 2.00	29.86 ± 1.09
18:2(n-6)	24.28 ± 1.07	24.99 ± 1.00
18:3(n-6)	0.74 ± 0.22	0.72 ± 0.09
20:2(n-6)	0.94 ± 0.11	1.12 ± 0.27
20:3(n-6)	1.08 ± 0.13	1.31 ± 0.20
20:4(n-6)	2.33 ± 0.42	2.55 ± 0.26
22:4(n-6)	0.62 ± 0.12	0.81 ± 0.20
22:5(n-6)	0.06 ± 0.01***	0.26 ± 0.05
n-6PUFA	30.06 ± 1.47	31.76 ± 1.71
18:3(n-3)	1.79 ± 0.17***	0.20 ± 0.03
20:5(n-3)	0.45 ± 0.08***	0.06 ± 0.01
22:3(n-3)	0.01 ± 0.00	0.01 ± 0.00
22:5(n-3)	0.40 ± 0.04***	0.09 ± 0.02
22:6(n-3)	0.56 ± 0.07***	0.27 ± 0.04
n-3PUFA	3.21 ± 0.16***	0.63 ± 0.09
Total PUFA	33.26 ± 1.55	32.39 ± 1.78
n-6/n-3	9.38 ± 0.50***	51.23 ± 6.22

Fatty acid composition expressed as composition of fatty acid methyl esters

Significant differences between groups as determined by the unpaired t test. (*$P < 0.05$, **$P < 0.01$, ***$P < 0.005$), $n = 5$

Results

Stomach Content

Table 3 shows the fatty acid composition of the stomach contents collected from 5-day-old rat pups. The fatty acid composition of the stomach content reflects that of the dam's milk. Pups reared by dams on the n-3 PUFA-deficient diet had significantly decreased levels of ALA, EPA, docosapentaenoic acid (DPAn-3, 22:5n-3) and DHA levels and significantly increased levels of docosapentaenoic acid (DPAn-6, 22:5n-6) compared to 5-day-old pups reared by

Table 4 Fatty acid composition (%, [w/w]) in brain of rat pups reared by mildly n-3 PUFA-deficient dams with n-3 LC-PUFA-rich oil dietary supplementation

Fatty acid	Control	n-3 PUFA deficient + vehicle	n-3 PUFA deficient + FO	n-3 PUFA deficient + DMO
14:0	0.38 ± 0.25	0.26 ± 0.16	0.44 ± 0.29	0.37 ± 0.15
16:0	24.58 ± 0.63	24.97 ± 2.06	24.10 ± 1.04	24.75 ± 1.04
18:0	19.06 ± 0.48	18.94 ± 0.48	19.11 ± 0.39	19.26 ± 0.56
20:0	0.48 ± 0.12	0.54 ± 0.10	0.53 ± 0.15	0.62 ± 0.09
22:0	0.23 ± 0.09	0.27 ± 0.16	0.36 ± 0.21	0.26 ± 0.23
24:0	0.18 ± 0.06	0.17 ± 0.09	0.19 ± 0.03	0.21 ± 0.04
SFA	44.91 ± 0.54	45.14 ± 1.95	44.74 ± 1.27	45.47 ± 1.18
16:1(n-7)	0.29 ± 0.02	0.27 ± 0.05	0.28 ± 0.02	0.27 ± 0.03
18:1(n-7)	3.14 ± 0.51	3.31 ± 0.59	3.53 ± 0.27	3.19 ± 0.75
18:1(n-9)	15.92 ± 0.41	15.77 ± 1.36	16.36 ± 0.82	16.48 ± 0.66
20:1(n-9)	1.03 ± 0.25	1.01 ± 0.27	1.10 ± 0.27	1.20 ± 0.17
22:1(n-9)	0.15 ± 0.05	0.12 ± 0.10	0.15 ± 0.09	0.16 ± 0.08
MUFA	20.53 ± 0.38	20.48 ± 2.19	21.43 ± 1.39	21.30 ± 1.34
18:2(n-6)	1.34 ± 0.17	1.18 ± 0.09	1.22 ± 0.10	1.32 ± 0.11
20:2(n-6)	0.38 ± 0.06	0.39 ± 0.10	0.39 ± 0.08	0.51 ± 0.09
20:3(n-6)	0.62 ± 0.08	0.53 ± 0.09	0.60 ± 0.06	0.65 ± 0.07
20:4(n-6)	11.32 ± 0.27^{a}	11.40 ± 0.61^{a}	10.95 ± 0.46^{a}	9.95 ± 0.30^{b}
22:4(n-6)	3.94 ± 0.21^{ab}	4.36 ± 0.26^{c}	3.87 ± 0.14^{a}	3.45 ± 0.09^{b}
22:5(n-6)	1.66 ± 0.35^{a}	6.35 ± 0.64^{b}	2.70 ± 0.26^{c}	1.87 ± 0.44^{a}
n-6 PUFA	19.27 ± 0.24^{a}	24.22 ± 0.98^{b}	19.74 ± 0.35^{a}	17.75 ± 0.50^{c}
20:5(n-3)	0.15 ± 0.09	0.10 ± 0.08	0.10 ± 0.09	0.23 ± 0.22
22:5(n-3)	0.57 ± 0.29	0.33 ± 0.17	0.35 ± 0.17	0.56 ± 0.11
22:6(n-3)	14.56 ± 0.74^{ab}	9.72 ± 0.76^{c}	13.65 ± 0.63^{a}	14.69 ± 0.38^{b}
n-3 PUFA	15.29 ± 0.70^{ab}	10.15 ± 0.65^{b}	14.10 ± 0.59^{c}	15.48 ± 0.29^{a}
Total PUFA	34.56 ± 0.74^{a}	34.37 ± 0.94^{ab}	33.84 ± 0.90^{ab}	33.23 ± 0.42^{b}
n-6/n-3	1.26 ± 0.06^{a}	2.40 ± 0.21^{b}	1.40 ± 0.04^{c}	1.15 ± 0.05^{d}

Fatty acid composition expressed as composition of fatty acid methyl esters

DMO DHA-rich microalgal oil, *FO* fish oil

Different lower case letters indicate statistically significant differences, as determined by Dunnett's T3 multiple comparison test (*$P < 0.05$)

dams on the control diet. The level of ARA was not significantly different between the groups.

Brain

DHA content of brain phospholipids in 28-day-old pups was 14.56% in the control diet group, but that in the n-3 PUFA-deficient + vehicle group (9.72%) was significantly lower (0.67-fold lower) than in any other group. For pups in the n-3 PUFA-deficient group, supplementation with DMO gave a significantly greater increase in DHA than FO, and neither was significantly different than the control. DPAn-3 and EPA did not differ significantly among the four groups. ARA was approximately 11% in the control and in the n-3 PUFA-deficient groups with vehicle and FO supplementation, but ARA was slightly decreased (0.9-fold lower than control) in the n-3 PUFA-deficient + DMO group ($P < 0.05$). DPAn-6 showed a 3.8-fold increase from 1.66% in the control group to 6.53% in the n-3 PUFA-deficient + vehicle group ($P < 0.05$). DPAn-6 with FO supplementation was significantly decreased compared to the vehicle, but still 1.6-fold higher than that of the control ($P < 0.05$) (Table 4). DMO supplementation significantly decreased the DPAn-6 content to the control level.

Heart

The DHA content of heart phospholipids was 0.32-fold lower in the n-3 PUFA-deficient diet group (2.80%) than in the control diet group (8.55%)—a significant difference. In the n-3 PUFA-deficient diet groups, FO supplementation restored heart DHA to the control level, while DMO supplementation produced levels that were 1.6-fold greater than the control, a significant difference. DPAn-3 was 3.50% in the control and significantly lower in the other groups (Table 5). EPA was not significantly different among the four groups. ARA in the n-3 PUFA-deficient + DMO group was the lowest in the n-3 PUFA-deficient diet group (24.38%; $P < 0.05$). DPAn-6 was 2.25% in the control group and 7.91% in n-3 PUFA-deficient + vehicle group, a 3.5-fold increase ($P < 0.05$). The DPAn-6 content in the n-3 PUFA-deficient + FO group was significantly lower than in the n-3 PUFA-deficient + vehicle group, but still twice that in the control ($P < 0.05$).

Table 5 Fatty acid composition (%, [w/w]) in heart tissue of rat pups reared by mildly n-3 PUFA-deficient dams with n-3 LC-PUFA-rich oil dietary supplementation

Fatty acid	Control	n-3 PUFA deficient + vehicle	n-3 PUFA deficient + FO	n-3 PUFA deficient + DMO
14:0	0.18 ± 0.18	0.26 ± 0.39	0.11 ± 0.15	0.12 ± 0.10
16:0	14.31 ± 2.52	13.24 ± 1.32	13.02 ± 0.75	13.27 ± 0.94
18:0	23.48 ± 0.72	23.34 ± 0.44	23.18 ± 0.99	23.4 ± 0.91
20:0	0.17 ± 0.17	0.37 ± 0.39	0.19 ± 0.03	0.21 ± 0.04
22:0	0.10 ± 0.14	0.06 ± 0.06	0.07 ± 0.08	0.07 ± 0.10
24:0	0.03 ± 0.08	nd	0.01 ± 0.03	0.03 ± 0.04
SFA	38.26 ± 2.55	37.26 ± 1.77	36.58 ± 0.85	37.11 ± 1.57
14:1(n-5)	nd	0.01 ± 0.03	nd	nd
16:1(n-7)	0.07 ± 0.06	0.11 ± 0.01	0.09 ± 0.05	0.11 ± 0.02
18:1(n-7)	2.86 ± 0.27	2.56 ± 0.15	2.60 ± 0.10	2.62 ± 0.23
18:1(n-9)	2.78 ± 0.24	3.08 ± 0.33	3.14 ± 0.21	3.05 ± 0.36
20:1(n-9)	0.05 ± 0.06	0.16 ± 0.02	0.13 ± 0.07	0.16 ± 0.01
22:1(n-9)	nd	nd	nd	nd
MUFA	5.76 ± 0.39	5.92 ± 0.33	5.97 ± 0.35	5.93 ± 0.56
18:2(n-6)	10.93 ± 1.54	12.02 ± 1.89	12.06 ± 1.87	12.23 ± 1.34
20:2(n-6)	0.52 ± 0.07	0.60 ± 0.04	0.59 ± 0.05	0.60 ± 0.06
20:3(n-6)	0.54 ± 0.07	0.53 ± 0.05	0.58 ± 0.04	0.57 ± 0.05
20:4(n-6)	25.41 ± 1.99^{ab}	26.95 ± 1.37^{a}	27.02 ± 1.06^{a}	24.38 ± 0.29^{b}
22:4(n-6)	4.01 ± 1.92^{abc}	5.14 ± 0.35^{a}	3.90 ± 0.25^{b}	2.49 ± 0.14^{c}
22:5(n-6)	2.25 ± 0.12^{a}	7.91 ± 0.78^{b}	4.47 ± 0.30^{c}	1.89 ± 0.35^{a}
n-6 PUFA	43.66 ± 1.53^{a}	53.15 ± 1.94^{b}	48.61 ± 1.24^{c}	42.16 ± 1.56^{a}
18:3(n-3)	0.05 ± 0.06	nd	nd	nd
20:5(n-3)	0.22 ± 0.08	0.12 ± 0.10	0.07 ± 0.11	0.16 ± 0.15
22:5(n-3)	3.50 ± 0.41^{a}	0.76 ± 0.18 ^{b}	1.06 ± 0.10 ^{c}	0.67 ± 0.11 ^{b}
22:6(n-3)	8.55 ± 1.13^{a}	2.80 ± 0.56^{b}	7.71 ± 0.93^{a}	13.98 ± 1.12^{c}
n-3 PUFA	12.31 ± 1.48^{a}	3.68 ± 0.73^{b}	8.84 ± 1.03^{c}	14.80 ± 1.18^{a}
Total PUFA	55.97 ± 2.24	56.82 ± 1.74	57.45 ± 0.79	56.96 ± 1.45
n-6/n-3	3.59 ± 0.45^{a}	15.06 ± 3.78^{b}	5.59 ± 0.88^{c}	2.87 ± 0.28^{d}

Fatty acid composition expressed as composition of fatty acid methyl esters

nd not detected (less than 0.01%)

DMO DHA-rich microalgal oil, *FO* fish oil

Different lower case letters indicate statistically significant differences, as determined by Dunnett's T3 multiple comparison test (*$P < 0.05$)

DMO supplementation significantly decreased the DPAn-6 content to the control.

Kidney, Spleen, and Thymus

DHA content in the control diet for the kidney (Table 6), spleen (Table 7), thymus (Table 8) phospholipids (2.97, 2.21, 0.81%, respectively) was lower than those for the brain and heart. DHA content in the n-3 PUFA-deficient + vehicle group was 1.09, 0.61, 0.28%, respectively, which is 0.3–0.4-fold lower than in the control group ($P < 0.05$). FO supplementation restored the kidney and thymus DHA levels to the control levels, but the spleen DHA level recovered no further than 0.7-fold that of the positive control ($P < 0.05$). DHA of kidney, spleen, thymus was 1.6, 1.6, 1.9-fold higher respectively for the n-3 PUFA-deficient + DMO group than in the control ($P < 0.05$). Although FO or DMO supplementation significantly restored kidney and spleen DPAn-3 levels compared to the vehicle, was lower than that of the control group ($P < 0.05$). EPA was very low in the n-3 PUFA-deficient + vehicle group in kidney and spleen and was not detected in the thymus. FO or DMO supplementation restored the EPA level in these tissues, and, in particular, the kidney EPA level in the n-3 PUFA deficient + DMO group was not significantly different from the control. Kidney ARA was slightly higher in the n-3 PUFA-deficient diet with vehicle and with FO supplementation than in DMO supplementation group ($P < 0.05$). ARA of spleen and thymus did not significantly differ among the groups. DPAn-6 in the kidney, spleen and thymus was 0.20, 0.44 and 1.43%, respectively, in the control and 2.41, 2.15 and 2.66% in the n-3 PUFA-deficient + vehicle group, representing a 12-, 4.9-, and 1.9-fold increase, respectively ($P < 0.05$). The DPAn-6 content of these tissues in the n-3 PUFA-deficient + FO group was significantly lower than in the n-3 PUFA-deficient + vehicle, but still 4.4-, 3.1- and 1.3-fold that of the positive control. DMO supplementation

Table 6 Fatty acid composition (%, [w/w]) in kidney of rat pups reared by mildly n-3 PUFA-deficient dams a with n-3 LC-PUFA-rich oil dietary supplementation

Fatty acid	Control	n-3 PUFA deficient + vehicle	n-3 PUFA deficient + FO	n-3 PUFA deficient + DMO
14:0	0.53 ± 0.16	0.53 ± 0.2	0.38 ± 0.36	0.60 ± 0.27
16:0	21.60 ± 0.96	21.29 ± 1.25	21.19 ± 1.07	22.06 ± 0.68
18:0	15.98 ± 0.32^{ab}	16.29 ± 0.59^{ab}	16.36 ± 0.46^{a}	15.42 ± 0.43^{b}
20:0	0.23 ± 0.09	0.27 ± 0.15	0.24 ± 0.03	0.21 ± 0.05
22:0	0.11 ± 0.12	0.06 ± 0.09	0.08 ± 0.20	nd
24:0	nd	nd	nd	0.02 ± 0.04
SFA	38.45 ± 0.99	38.44 ± 1.08	38.25 ± 1.75	38.31 ± 0.77
16:1(n-7)	0.54 ± 0.10	0.53 ± 0.10	0.52 ± 0.13	0.49 ± 0.11
18:1(n-7)	2.10 ± 0.33	1.95 ± 0.38	1.92 ± 0.15	1.71 ± 0.12
18:1(n-9)	8.37 ± 1.24	8.4 ± 0.35	8.25 ± 0.42	8.28 ± 0.21
20:1(n-9)	0.16 ± 0.02	0.18 ± 0.02	0.17 ± 0.09	0.19 ± 0.03
22:1(n-9)	nd	nd	nd	nd
MUFA	11.18 ± 1.5	11.05 ± 0.68	10.87 ± 0.51	10.67 ± 0.16
18:2(n-6)	13.1 ± 0.56^{a}	11.72 ± 0.41^{b}	11.93 ± 0.78^{ab}	12.99 ± 0.38^{a}
20:2(n-6)	0.79 ± 0.34	1.04 ± 0.13	1.05 ± 0.17	1.06 ± 0.16
20:3(n-6)	0.98 ± 0.07	1.05 ± 0.12	1.15 ± 0.12	1.14 ± 0.08
20:4(n-6)	29.62 ± 1.34^{ab}	31.37 ± 0.84^{a}	31.13 ± 0.89^{a}	29.22 ± 0.35^{b}
22:4(n-6)	1.13 ± 0.08^{ac}	1.62 ± 0.12^{b}	1.34 ± 0.14^{a}	1.05 ± 0.10^{c}
22:5(n-6)	0.20 ± 0.05^{a}	2.41 ± 0.09^{b}	0.88 ± 0.47^{a}	0.23 ± 0.02^{a}
n-6PUFA	45.81 ± 1.19^{a}	49.19 ± 0.62^{b}	47.49 ± 1.42^{ab}	45.69 ± 0.54^{a}
18:3(n-3)	0.26 ± 0.01	nd	nd	nd
20:5(n-3)	0.33 ± 0.12^{a}	0.04 ± 0.11^{b}	0.14 ± 0.12^{ab}	0.27 ± 0.06^{a}
22:5(n-3)	1.00 ± 0.09^{a}	0.18 ± 0.10^{b}	0.38 ± 0.04^{c}	0.30 ± 0.07^{bc}
22:6(n-3)	2.97 ± 0.22^{a}	1.09 ± 0.17^{b}	2.87 ± 0.23^{a}	4.76 ± 0.22^{c}
n-3PUFA	4.56 ± 0.31^{a}	1.32 ± 0.33^{b}	3.39 ± 0.36^{c}	5.33 ± 0.23^{a}
Total PUFA	50.37 ± 1.45	50.51 ± 0.75	50.88 ± 1.38	51.01 ± 0.74
n-6/n-3	10.07 ± 0.49^{a}	38.91 ± 7.88^{b}	14.16 ± 1.69^{c}	8.59 ± 0.29^{d}

Fatty acid composition expressed as composition of fatty acid methyl esters

nd not detected (less than 0.01%)

DMO DHA-rich microalgal oil, *FO* fish oil

Different lower case letters indicate statistically significant differences, as determined by Dunnett's T3 multiple comparison test (*$P < 0.05$)

significantly decreased the DPAn-6 content compared to the control level.

Discussion

We examined the effect of two common n-3 LC-PUFA supplement sources during the infant period in a rat model. DMO is designed to have the highest breast milk DHA content, i.e. 1.4% of total fatty acids, as reported in a meta-analysis of "DHA and ARA concentrations in breast milk from mothers of term infants" conducted by Brenna et al. [13], as a safe and effective supplemental level. It is difficult to estimate the actual daily fatty acid intake of fat in rat pups that are reared on mother's milk. Based on studies on pups reared on milk replacer [14, 15], 5-day-old pups need 290 mg milk substitute/g body weight with a 12.3% fat content in order to maintain similar body weight to counterparts reared on mother's milk [15]. Based on the calculation that pups at this age ingested 35.7 mg fat/g body weight, the supplementation used in the experiment in this study was set at 1 mg fat/g body weight, corresponding to a 2.8% daily fat intake. The percentage of DHA as a percentage of the total fatty acid intake was calculated to be 1.4% DHA. The supplementation of FO was followed by DMO supplementation and the calculated percentage was 0.82% DHA, 0.04% DPAn-3 and 0.20% EPA of the total fatty acid intake. A supplement-free period at 7 days was set because fatty acids from the oil supplementation are thought to be pooled in the liver and plasma first, it would take more than 4 days to distribute to other tissues [16].

FO supplementation to rat pups of dams fed on a n-3 PUFA-deficient diet nearly restored DHA levels in tissue phospholipids to those of the control group pups; however, tissue phospholipid EPA and DPAn-3 levels did not recover. In addition, the DPAn-6 level, which serves as a reliable index of n-3 PUFA deficiency, did not decrease to the control group level. Taken together, these results indicate that the dosage of FO supplementation to pups in this study was insufficient to completely restore the LC-PUFA status. The low recovery of tissue phospholipid

Table 7 Fatty acid composition (%, [w/w]) in the spleen of rat pups reared by mildly n-3 PUFA-deficient dams with n-3 LC-PUFA-rich oil dietary supplementation

Fatty acid	Control	n-3 PUFA deficient + vehicle	n-3 PUFA deficient + FO	n-3 PUFA deficient + DMO
14:0	0.63 ± 0.18	0.38 ± 0.31	0.55 ± 0.2	0.58 ± 0.22
16:0	28.28 ± 0.98	27.18 ± 2.13	27.71 ± 0.8	28.33 ± 0.86
18:0	15.00 ± 0.35	14.94 ± 1.38	14.85 ± 1.14	14.53 ± 1.12
20:0	0.05 ± 0.08	0.17 ± 0.15	0.16 ± 0.1	0.18 ± 0.05
22:0	nd	0.10 ± 0.13	0.02 ± 0.04	0.02 ± 0.05
24:0	0.01 ± 0.04	0.03 ± 0.06	nd	0.04 ± 0.07
SFA	43.98 ± 0.9	42.8 ± 2.95	43.29 ± 1.28	43.69 ± 1.00
16:1(n-7)	0.46 ± 0.05	0.36 ± 0.19	0.44 ± 0.07	0.45 ± 0.07
18:1(n-7)	2.08 ± 0.12	2.13 ± 0.44	1.98 ± 0.24	1.88 ± 0.12
18:1(n-9)	6.70 ± 0.33	8.89 ± 4.04	7.23 ± 0.32	7.18 ± 0.38
20:1(n-9)	0.37 ± 0.07	0.41 ± 0.23	0.44 ± 0.03	0.43 ± 0.03
22:1(n-9)	0.01 ± 0.03	0.04 ± 0.09	0.02 ± 0.05	0.04 ± 0.06
MUFA	9.63 ± 0.33	11.83 ± 4.71	10.12 ± 0.49	9.99 ± 0.40
18:2(n-6)	9.18 ± 0.38^{a}	8.03 ± 0.4^{b}	8.48 ± 0.22^{bc}	8.89 ± 0.39^{ac}
20:2(n-6)	1.18 ± 0.14	1.25 ± 0.09	1.38 ± 0.07	1.35 ± 0.08
20:3(n-6)	1.04 ± 0.08	0.97 ± 0.12	1.05 ± 0.08	1.06 ± 0.08
20:4(n-6)	25.93 ± 0.40	26.78 ± 1.73	26.82 ± 0.73	25.83 ± 0.35
22:4(n-6)	3.56 ± 0.17^{a}	5.18 ± 0.31^{b}	4.73 ± 0.06^{b}	3.86 ± 0.19^{a}
22:5(n-6)	0.44 ± 0.16^{a}	2.15 ± 0.63^{b}	1.37 ± 0.62^{ab}	0.65 ± 0.4^{a}
n-6 PUFA	41.32 ± 0.76^{a}	44.35 ± 2.05^{ab}	43.84 ± 0.93^{b}	41.64 ± 0.62^{a}
18:3(n-3)	0.02 ± 0.04	0.02 ± 0.06	nd	nd
20:5(n-3)	0.34 ± 0.17^{a}	0.07 ± 0.10^{b}	0.18 ± 0.18^{ab}	0.15 ± 0.16^{ab}
22:5(n-3)	2.50 ± 0.40^{a}	0.33 ± 0.18^{b}	0.88 ± 0.17^{c}	0.91 ± 0.47^{bc}
22:6(n-3)	2.21 ± 0.11^{a}	0.61 ± 0.12^{b}	1.7 ± 0.22^{c}	3.63 ± 0.12^{d}
n-3 PUFA	5.07 ± 0.42^{a}	1.03 ± 0.23^{b}	2.76 ± 0.26^{c}	4.69 ± 0.40^{a}
Total PUFA	46.39 ± 0.92	45.38 ± 2.08	46.59 ± 1.10	46.33 ± 0.64
n-6/n-3	8.19 ± 0.63^{a}	46.06 ± 15.80^{b}	16.01 ± 1.42^{c}	8.94 ± 0.78^{a}

Fatty acid composition expressed as composition of fatty acid methyl esters

nd not detected (less than 0.01%)

DMO DHA-rich microalgal oil, *FO* fish oil

Different lower case letters indicate statistically significant differences, as determined by Dunnett's T3 multiple comparison test ($^{*}P < 0.05$)

EPA and DPAn-3 compared to DHA also suggests that these fatty acids might be preferentially metabolized to DHA in rats.

In the case of DMO supplementation, the brain phospholipid DHA level also recovered to that of the control pups, although the other four tissue phospholipid DHA levels exceeded those of the control group. This finding suggests that the dose of DMO used in this experiment slightly exceeded suitable levels and that brain phospholipid DHA content might be regulated by homeostasis. Tissue phospholipid DPAn-6 was lower compared to the vehicle-feeding group level. Taken together, these results indicate that DMO is more effective than FO for restoring n-3 LC-PUFA status, because DMO contains approximately a 1.3-fold greater total n-3 PUFA than fish oil (Table 2).

Our study showed that both FO and DMO supplementation during the nursing period restored the brain DHA level in pups reared by dams fed a n-3 PUFA-deficient diet, although the brain DHA generally has very slow metabolic turnover. For example, Moriguchi et al. [4] studied the DHA supplementation effect on the tissue fatty acid composition of n-3 PUFA-deficient weaned rats and reported that a full recovery of the DHA level in the brain was not obtained until 8 weeks after initiation of the repletion diet. The following difference in our study might explain this apparently conflicting finding. The one reason n-3 PUFA-deficiency in this study is mild is that the decrease in brain DHA is only one-third of the control level. In addition, infant-stage mammals have an immature brain-blood barrier [17]. Therefore, our experimental design might make it conducive to recovering from the n-3 PUFA deficient condition.

It has been proposed that dietary EPA from fish oil hinders infant development by competing with ARA [2]. However, in the present experiment, FO supplementation did not reduce phospholipid ARA content in nearly any of the examined tissues, a result which may be explained by three possible factors. First, the dosage of FO was appropriate and not excessive to allow recovery of DHA levels in

Table 8 Fatty acid composition (%, [w/w]) in the thymus of rat pups reared by mildly n-3 PUFA-deficient dams with n-3 LC-PUFA-rich oil dietary supplementation

Fatty acid	Control	n-3 PUFA deficient + vehicle	n-3 PUFA deficient + FO	n-3 PUFA deficient + DMO
14:0	1.34 ± 0.42	1.27 ± 0.34	1.26 ± 0.55	1.02 ± 0.36
16:0	26.39 ± 0.59	26.27 ± 0.82	26.09 ± 1.22	25.32 ± 0.58
18:0	15.85 ± 0.51	16.01 ± 0.47	16.31 ± 0.72	16.16 ± 0.69
20:0	0.59 ± 0.26	0.46 ± 0.07	0.57 ± 0.24	0.50 ± 0.18
22:0	0.10 ± 0.11	0.23 ± 0.13	0.14 ± 0.11	0.21 ± 0.15
SFA	44.27 ± 0.79	44.22 ± 0.83	44.37 ± 1.29	43.21 ± 1.25
16:1(n-7)	0.58 ± 0.04	0.56 ± 0.04	0.56 ± 0.04	0.52 ± 0.03
18:1(n-7)	2.22 ± 0.17	2.11 ± 0.15	2.11 ± 0.24	2.39 ± 0.51
18:1(n-9)	8.48 ± 0.40	8.73 ± 0.48	8.89 ± 0.33	9.26 ± 0.53
20:1(n-9)	1.18 ± 0.03^{a}	1.18 ± 0.04^{a}	1.23 ± 0.09^{ab}	1.30 ± 0.07^{ab}
22:1(n-9)	0.16 ± 0.08^{ab}	0.22 ± 0.05^{a}	0.08 ± 0.09^{b}	0.18 ± 0.09^{ab}
MUFA	12.62 ± 0.35	12.8 ± 0.53	12.87 ± 0.58	13.64 ± 1.04
18:2(n-6)	9.59 ± 0.57^{a}	8.37 ± 0.29^{b}	8.9 ± 0.29^{ab}	9.46 ± 0.37^{a}
20:2(n-6)	2.16 ± 0.11	2.10 ± 0.12	2.12 ± 0.25	2.27 ± 0.13
20:3(n-6)	1.52 ± 0.11	1.45 ± 0.20	1.57 ± 0.19	1.81 ± 0.24
20:4(n-6)	23.85 ± 0.60	24.54 ± 0.95	24.14 ± 0.92	23.62 ± 1.06
22:4(n-6)	2.41 ± 0.17^{a}	3.15 ± 0.13^{b}	2.94 ± 0.11^{ab}	2.49 ± 0.35^{a}
22:5(n-6)	1.43 ± 0.41^{a}	2.66 ± 0.18^{b}	1.85 ± 0.38^{a}	1.50 ± 0.42^{a}
n-6 PUFA	40.97 ± 0.36	42.27 ± 0.85	41.52 ± 1.33	41.14 ± 0.93
18:3(n-3)	0.02 ± 0.05	nd	nd	nd
20:5(n-3)	0.32 ± 0.06^{a}	nd	0.09 ± 0.10^{b}	0.06 ± 0.10^{b}
22:5(n-3)	1.00 ± 0.23^{a}	0.42 ± 0.24^{b}	0.31 ± 0.25^{b}	0.38 ± 0.21^{b}
22:6(n-3)	0.81 ± 0.07^{a}	0.28 ± 0.07^{b}	0.84 ± 0.19^{a}	1.56 ± 0.14^{c}
n-3 PUFA	2.14 ± 0.30^{a}	0.70 ± 0.20^{b}	1.24 ± 0.42^{b}	2.01 ± 0.27^{a}
Total PUFA	43.11 ± 0.65	42.97 ± 0.72	42.76 ± 1.44	43.15 ± 1.08
n-6/n-3	19.45 ± 2.57	67.29 ± 31.37	37.06 ± 13.18	20.79 ± 2.45

Fatty acid composition expressed as composition of fatty acid methyl esters

nd not detected (less than 0.01%)

DMO DHA-rich microalgal oil, *FO* fish oil

Different lower case letters indicate statistically significant differences, as determined by Dunnett's T3 multiple comparison test (*$P < 0.05$)

brain phospholipid; second, rat pups could ingest maternal milk that included appropriate levels of ARA; and third, the FO used in this experiment was tuna oil, which has four times more DHA than EPA. Our results are also supported by human studies that have indicated FO with an appropriate level and ratio of DHA and EPA does not affect plasma and erythrocyte ARA status in infants [18, 19].

Contrary to our expectations, DMO supplementation decreased the ARA level in brain phospholipids—0.9% compared to the control level. Although it is unclear whether this slight reduction in brain phospholipid ARA is biologically significant, acute changes in such an important fatty acid would cause metabolic changes in order to maintain fatty acid homeostasis. For example, Kim et al. [20] reported that dietary n-6 PUFA deprivation down-regulates arachidonate metabolizing enzymes in the rat brain such as cytosolic phospholipase A2 and cyclooxygenase-2 decreases ARA consumption. In their experimental conditions, brain ARA content was reduced by 28% [21].

In this study, two sources of n-3 LC-PUFA (FO and DMO) were supplemented to mildly n-3-deficient rat pups to elucidate effects of supplementation on tissue LC-PUFA content. Both FO and DMO improved the DHA level of tissues, particularly the brain. DMO was more effective at increasing tissue DHA status because it is richer in n-3 PUFA than FO. FO had slightly lower PUFA levels than required to completely restore LC-PUFA status to normal levels in this experiment, and EPA did not accumulate in tissues under the conditions tested here. These results demonstrate the effectiveness of ingesting either FO or DMO in the pre-weaning period for improving mild n-3 PUFA deficiency.

Acknowledgments This research is supported in part by Grant-in-Aid for Young Scientists (B) of KAKENHI (20780151), the Ministry of Education, Culture, Sports, Science and Technology (MEXT).

Conflict of interest None.

References

1. Hoffman DR, Boettcher JA, Diersen-Schade DA (2009) Toward optimizing vision and cognition in term infants by dietary

docosahexaenoic and arachidonic acid supplementation: a review of randomized controlled trials, Prostaglandins Leukot Essent Fatty Acids 81:151–158
2. Carlson SE, Cooke RJ, Werkman SH, Tolley EA (1992) First year growth of preterm infants fed standard compared to marine oil n-3 supplemented formula. Lipids 27:901–907
3. Jensen RG (1999) Lipids in human milk. Lipids 34:1243–1271
4. Moriguchi T, Loewke J, Garrison M, Catalan JN, Salem N Jr (2001) Reversal of docosahexaenoic acid deficiency in the rat brain, retina, liver, and serum. J. Lipid Res 42:419–427
5. Harauma A, Salem N Jr, Moriguchi T (2010) Repletion of n-3 fatty acid deficient dams with alpha-linolenic acid: effects on fetal brain and liver fatty acid composition. Lipids 45:659–668
6. Hussein N, Fedorova I, Moriguchi T, Hamazaki K, Kim HY, Hoshiba J, Salem N Jr (2009) Artificial rearing of infant mice leads to n-3 fatty acid deficiency in cardiac, neural and peripheral tissues. Lipids 44:685–702
7. Holman RT (1998) The slow discovery of the importance of omega 3 essential fatty acids in human health. J Nutr 128:427S–433S
8. Kimura F, Ito S, Endo Y, Doisaki N, Koriyama T, Miysazawa T, Fujimoto K (2008) Long-term supplementation of docosahexaenoic acid-Rich, Eicosapentaenoic acid-free microalgal oil in n-3 fatty acid-deficient rat pups. Biosci Biotechnol Biochem 72: 608–610
9. Reeves PG (1997) Components of the AIN-93 diets as improvements in the AIN-76A diet. J Nutr 127:838S–841S
10. Bligh EG, Dyer WJ (1959) A rapid method of total lipid extraction and purification. Can J Biochem Phys 37:911–917
11. Kramer JK, Fellner V, Dugan ME, Sauer FD, Mossoba MM, Yurawecz MP (1997) Evaluating acid and base catalysts in the methylation of milk and rumen fatty acids with special emphasis on conjugated dienes and total *trans* fatty acids. Lipids 32:1219–1228
12. Ohta A, Mayo MC, Kramer N, Lands WE (1990) Rapid analysis of fatty acids in plasma lipids. Lipids 25:742–747
13. Brenna JT, Varamini B, Jensen RG, Diersen-Schade DA, Boettcher JA, Arterburn LM (2007) Docosahexaenoic and arachidonic acid concentrations in human breast milk worldwide. Am J Clin Nutr 85:1457–1464
14. Kimura F, Endo Y, Fujimoto K, Doisaki N, Koriyama T (2005) Administration of two oils rich in n-3 long-chain polyunsaturated fatty acids to rat pups of dams fed a diet high in fat and low in n-3 polyunsaturated fatty acids. Fish Sci 71:431–440
15. Ward GR, Huang YS, Bobik E, Xing HC, Mutsaers L, Auestad N, Montalto M, Wainwright P (1998) Long-chain polyunsaturated fatty acid levels in formulae influence deposition of docosahexaenoic acid and arachidonic acid in brain and red blood cells of artificially reared neonatal rats. J Nutr 128:2473–2487
16. Lin YH, Salem N Jr (2007) Whole body distribution of deuterated linoleic and alpha-linolenic acids and their metabolites in the rat. J Lipid Res 48:2709–2724
17. Viña JR, DeJoseph MR, Hawkins PA, Hawkins RA (1997) Penetration of glutamate into brain of 7-day-old rats. Metab Brain Dis 12:219–227
18. Carlson S (1996) Arachidonic acid status of human infants: influence of gestational age at birth and diets with very long chain n-3 and n-6 fatty acids. J Nutr 26:1092S–1098S
19. Maurage C, Guesnet P, Pinault M, Rochette de Lempdes J, Durand G, Antoine J, Couet C (1998) Effect of two types of fish oil supplementation on plasma and erythrocyte phospholipids in formula-fed term infants. Biol Neonate 74:416–429
20. Kim HW, Rao JS, Rapoport SI, Igarashi M (2011) Dietary n-6 PUFA deprivation downregulates arachidonate but upregulates docosahexaenoate metabolizing enzymes in rat brain. Biochim Biophys Acta 1811:111–117
21. Igarashi M, Gao F, Kim HW, Ma K, Bell JM, Rapoport SI (2009) Dietary n-6 PUFA deprivation for 15 weeks reduces arachidonic acid concentrations while increasing n-3 PUFA concentrations in organs of post-weaning male rats. Biochim Biophys Acta 1791:132–139

DPAn-3	Docosapentaenoic acid (22:5n-3)
EPA	Eicosapentaenoic acid (20:5n-3)
LNA	Linoleic acid (18:2n-6)
LC-PUFA	Long chain polyunsaturated fatty acids (PUFA with 20 or more atoms of carbon)
MUFA	Monounsaturated fatty acids (one double bond)
n-3 LC-PUFA	Long chain polyunsaturated fatty acids (PUFA with 20 or more atoms of carbon) with the first double bond at the 3rd carbon atom from the methyl end of the molecule
n-6 LC-PUFA	Long chain polyunsaturated fatty acids (PUFA with 20 or more atoms of carbon) with the first double bond at the 6th carbon atom from the methyl end of the molecule
PUFA	Polyunsaturated fatty acids (two or more double bonds)
SFA	Saturated fatty acids

Introduction

Fish oil utilization by the aquafeed industry is increasingly recognized by the scientific sector and industry stakeholders as an environmentally unsustainable and economically unviable practice. Thus, a significant global research effort is currently focusing on finding possible remedial strategies; and the use of alternative oils (vegetable oils and animal fats) to replace fish oil in aquafeed formulations is envisaged to be the most practical and easily implemented option [1].

It has been well documented that when fish oil is substituted with alternative oils of terrestrial origin, the resultant fatty acid composition of fish fillet is significantly affected [2, 3]. Specifically, the major detrimental effect of replacing fish oil is the reduction of the overall nutritional qualities of cultured products due to the reduction of health promoting omega-3 long chain polyunsaturated fatty acids (n-3 LC-PUFA; and particularly eicosapentaenoic acid—EPA, 20:5n-3, docosapentaenoic acid—DPAn-3, 22:5n-3 and docosahexaenoic acid—DHA, 22:6n-3) in fish fillet [4]. Therefore, the fatty acid metabolism, and potential fatty acid bioconversion capabilities, of cultured fish is a topic of increasing scientific interest, and major strides have now been achieved in its understanding [5, 6].

On a yearly basis, global salmonid aquaculture is responsible for the exploitation of over 56% fish oil supplies [7]. The high demand for fish oil by the salmonid industry is driven mainly by the market demand/expectation for n-3 LC-PUFA rich products [4, 7], rather than a physiological need of these species. In fact, salmonids such as the Atlantic salmon (*Salmo salar*) and the rainbow trout (*Oncorhynchus mykiss*), are likely better equipped, from a fatty acid metabolism point of view, to cope successfully with fish oil replacement in their diets in comparison to other fish species [8–12]. Rainbow trout in particular, have been shown to be capable of bioconverting large quantities of dietary α-linolenic acid (ALA, 18:3n-3), which can be found in several different vegetable oils, into n-3 LC-PUFA [13]. However, the final n-3 LC-PUFA content of the fillets of trout fed fish oil deprived diets (560 mg per 100 g of fillet) was still significantly lower than that of fish fed with a fish oil-based diet (1,860 mg per 100 g of fillet). Thus, it is important to gain a better understanding of n-3 LC-PUFA biosynthesis in fish, towards more efficiently formulated feeds for maximizing the n-3 LC-PUFA content of fish fillet, when fish oil is not included in dietary formulations.

The enzymes involved in the bioconversion of both n-3 and n-6 C_{18} PUFA to LC-PUFA are the Δ-6 desaturase (EC 1.14.19.3), the Δ-5 desaturase (EC 1.14.19.-) and two elongases (EC 6.2.1.3; Elovl-5 and Elovl-2) [6]. Therefore, it is evident that the proportion of substrate availability (n-3 and n-6 C_{18} PUFA) will ultimately have an effect on the final production of n-3 or n-6 LC-PUFA. As such, it is commonly accepted that the dietary α-linolenic acid (ALA, 18:3n-3)/linoleic acid (LNA, 18:2n-6) ratio plays a major role on fatty acid metabolism. Surprisingly, whilst fish oil deprived diets either rich in 18:3n-3 (i.e. linseed/flaxseed oil, camelina oil, etc.) or 18:2n-6 (i.e soybean oil, sunflower oil, etc.) have been studied in fish in detail [14–16], studies focusing on a sliding 18:3n-3/18:2n-6 ratio are relatively scarce and limited to a few species, including: Coho salmon (*Oncorhynchus kisutch*) [17]; Milkfish (*Chanos chanos*) [18]; silver perch (*Bidyanus bidyanus*) [19]; Eurasian perch (*Perca fluviatilis*) [20]; yellow catfish (*Pelteobagrus fulvidraco*) [21]; and Murray cod (*Maccullochella peelii peelii*) [22, 23]. An early study on rainbow trout also assessed the effect of various 18:3n-3/18:2n-6 ratios in juvenile fish from 0.4 to 4 g of body weight [24]. In this study it was shown that both 18:3n-3 and 18:2n-6 are essential fatty acids for rainbow trout and that trout grew better when receiving a diet richer in 18:3n-3 than 18:2n-6. The authors also suggested that the bioconversion of 18:2n-6 into n-6 LC-PUFA was partially inhibited by dietary 18:3n-3, whilst the bioconversion of 18:3n-3 was also inhibited by dietary 18:2n-6, but to a lesser degree. Importantly, whilst these results are very interesting, it should be noted that in this study, one-month old fish were used, and that prior to the experimentation fish were fed a fat free diet containing fatty acids in a purified free ethyl ester form.

The objective of the present study was to evaluate the effects of different 18:3n-3/18:2n-6 ratios in practical (commercial-like) fish oil deprived diets in rainbow trout over the whole production cycle, with particular attention on the effects on the fatty acid metabolism and the final fatty acid composition of fish fillet.

Materials and Methods

Animals and Husbandry

Juvenile rainbow trout (*Oncorhynchus mykiss*) were obtained from Fisheries Victoria—Department of Primary Industries (Snobs Creek, Victoria, Australia) and transported to Deakin University's Aquaculture Research Facility at the Warrnambool campus. Prior to the commencement of the feeding trial, fish were acclimated to the new environmental conditions in a recirculating aquaculture system (RAS) and maintained on a commercial diet (Skretting, Cambridge, Tasmania, Australia) at 2% of their body weight daily for 5 weeks. The RAS system consisted of 18 (1,000 L) rearing tanks, equipped with inline biological and physical filtration (drum filter with a 60-μm screen; Hydrotech, Vellinge, Sweden), ultra violet (UV) disinfection, oxygen enrichment and temperature and light control. The system was maintained on a 12:12 h light:dark cycle. Fish were held under optimal conditions, the pH (mean 8.26 ± 0.04), dissolved oxygen (mean 9.14 ± 0.30 mg/L) and water temperature (mean 15.0 ± 0.80 °C) were monitored daily. The levels of metabolic waste products, ammonia and nitrite were monitored weekly and recorded values below 0.20 and 0.25 mg L^{-1}, respectively.

Experimental Diets and Study Design

Six iso-proteic and iso-lipidic experimental diets were formulated and manufactured, as previously reported in detail [25], to contain 46% of protein and 18% of lipid and varying only in the dietary lipid source. Fish oil was used as a reference/control diet (CD). Sunflower oil (rich in LA, 18:2n-6) and linseed oil (rich in ALA, 18:3n-3) were blended in variable proportions to obtain five diets with varying ratios of 18:3n-3/18:2n-6, maintaining a constant level of total C_{18} PUFA (58% of total fatty acids). The diets were named ALA72%, ALA54%, ALA36%, ALA18% and ALA2% (indicating the % contribution of 18:3n-3 to total C_{18} PUFA content of the diet). The 18:3n-3/18:2n-6 ratios of five experimental diets were 2.63, 1.19, 0.56, 0.23, and 0.02, respectively.

At the commencement of the experiment, 360 fish with an initial body weight of 29.8 ± 0.21 g were individually weighed and randomly distributed into 18 tanks (20 fish per tank) and randomly assigned to each of the six experimental treatments in triplicate groups.

Fish in each treatment were fed with one of the six experimental diets by hand to apparent satiation twice daily at 0900 h and 1600 h for a 126 day grow out period. Feed consumption was recorded weekly and mortalities were recorded throughout the experimental period.

At the commencement of the experiment, an initial sample of 15 fish was taken and euthanized in excess anaesthetic (AQUI-S, Lower Hutt, New Zealand) for subsequent analysis. Feces were collected during the last week before the termination of the experiment, as previously described in detail [26]. At completion of experimental phase, all fish were individually weighed and eight fish from each tank (24 fish per treatment) were randomly taken, euthanized and stored at −20 °C for future analysis.

All procedures used in this study were approved by the Deakin University Animal Welfare Committee.

Chemical Analysis

Out of the eight fish collected from each replicate tank, four fish per tank were dissected for biometric data and the four left hand fillets were finely chopped, pooled and homogenized before subsequent analysis. The remaining four fish per tank were finely chopped, pooled and homogenized for subsequent chemical analysis. The chemical composition of experimental diets and biological samples was analyzed in triplicate on the pooled samples for each replicate (tank) and conducted according to standard methods. Briefly, moisture was determined by drying samples in an oven at 80 °C to constant weight. Protein content ($N \times 6.25$) was determined using an automated Kjeltech 2300 (Foss Tecator, Geneva, Switzerland). Ash content was determined by incinerating samples (approximately 0.5 g) in a muffle furnace (Wit, C & L Tetlow, Melbourne, Australia) at 550 °C for 18 h. Lipid was determined by chloroform:methanol (2:1) extraction as previously described [27]. Nitrogen free extract (NFE) was calculated by difference and dietary energy content was calculated on the basis of 23.6, 39.5 and 17.2 kJ g^{-1} of protein, fat and carbohydrate, respectively.

Following the lipid extraction, fatty acids were esterified into methyl esters using an acid catalyzed methylation method, and analyzed by gas chromatography according to the methods previously used in the laboratory [27]. Briefly, 0.5 ml of C23:0 (1.5 μg/ml) was added to each sample as an internal standard (Sigma-Aldrich, Inc., St. Louis, MO, USA). Fatty acid methyl esters were isolated and identified using a Shimadzu GC 17A (Shimadzu, Chiyoda-ku, Tokyo, Japan) equipped with an Omegawax 250 capillary column (30 m × 0.25 mm internal diameter, 0.25-μm film thickness; Supelco, Bellefonte, PA, USA), a flame ionisation

detector (FID), a Shimadzu AOC-20i auto injector, and a split injection system (split ratio 50:1). The temperature program was 150–180 °C at 3 °C min^{-1}, then from 180 to 250 °C at 2.5 °C min^{-1} and held at 250 °C for 10 min. The injector and detector temperatures were set at 270 and 280 °C, respectively. The carrier gas was helium at 1.0 ml min^{-1}, at a constant flow. Each of the fatty acids was identified relative to known external standards (37-Component FAME Mix, PUFA No. I-Marine Source, PUFA No. II-Animal Source and PUFA No. III–Menhaden Oil, all from Supleco, Bellefonte, PA, USA). The resulting peaks were then corrected by the theoretical relative FID response factors and quantified relative to the internal standard.

Digestibility and Fatty Acid Metabolism

Chromic oxide in the diets and feces was estimated according to the method of Furukawa and Tsukahara [28]. Estimates of apparent digestibility coefficients (ADC) for dry matter, lipid, total and individual fatty acid were calculated using standard formulas [26].

The in vivo assessment of fish fatty acid metabolism of rainbow trout in this study was performed using the whole-body fatty acid balance method, as described previously in detail [29, 30]. Briefly, this method involves a first step in which the net appearance/disappearance of each individual fatty acid is deduced by means of a mass balance determined by the difference between total fatty acid gain (=final fatty acid content−initial fatty acid content) and the net fatty acid intake (=total fatty acid intake−fatty acid excretion in feces). After the transformation of data from mg to μmol of appeared/disappeared fatty acid per gram of body weight per day, the subsequent second step involves a series of backwards computations along all the known fatty acid bioconversion pathways (n-3 PUFA, n-6 PUFA and SFA + MUFA) so that the fate of each individual fatty acid towards bioconversion, oxidation or deposition, can be determined. Eventually, data relative to apparent in vivo enzyme activity can be reported in absolute terms (μmol g $fish^{-1}$ day^{-1}) or as percentage of substrate availability.

Statistical Analysis

All data were reported as means ± standard error of mean ($n = 3$, $N = 18$). Comparisons amongst treatments were analyzed by one-way analysis of variance (ANOVA) at a significance level of 0.05 following confirmation of normality and homogeneity of variance different statistical tests. Where significant differences were detected by ANOVA, data were subjected to a Student–Newman–Keuls post hoc test for identifying homogeneous subsets. Data were analyzed further by linear regression, where appropriate. The statistical analyses were computed using SPSS v17.0 (SPSS Inc., Chicago, IL, USA).

Results

Diet Compositions

The lipid (∼185 mg/g) and protein (∼465 mg/g) content of the six diets were similar across all treatments, and diets can be considered as iso-proteic, iso-lipidic and iso-energetic (Table 1). The fatty acid composition of the experimental diets reflected the objectives of the formulations (Table 2). CD contained the highest amount of n-3 LC-PUFA, mainly 20:5n-3 (7.6%) and 22:6n-3 (8.9%). The five fish oil deprived experimental diets contained very similar levels of saturated fatty acids (SFA; ∼13.5%), monounsaturated fatty acids (MUFA; ∼23%) and polyunsaturated fatty acids (PUFA; ∼63%). Specifically, total C_{18} PUFA accounted for ∼58%, and the main difference amongst the five diets was the sliding proportion of 18:3n-3/18:2n-6 contributing to total C_{18} PUFA. The resulting 18:3n-3/18:2n-6 ratios were 2.63, 1.19, 0.56, 0.23, and 0.02 for ALA72%, ALA54%, ALA36%, ALA18% and ALA2%, respectively. Amongst these five diets, 20:5n-3 ranged from 2.4 to 2.7% and 22:6n-3 ranged from 2.0 to 2.3% of total fatty acids. These fatty acids were clearly derived from the residual lipid content of the fish meal included in the formulation (Table 2).

Growth Performance, Feed Utilization and Proximate Composition

All experimental diets were readily accepted by fish and no mortality was recorded during the entire feeding trial. No significant differences were found in feed intake, final mean weight or grow rate during the experimental period. Throughout the 126 day experimental period, fish increased their weight by over 1,700% in all treatments. Final mean weights of fish fed the six dietary treatments ranged from 562.2 ± 6.21 to 613.0 ± 7.47 g. FCR was 1.2 in fish fed CD diet and ranged from 1.0 to 1.1 for fish in the other treatments (Table 3). Specific growth rate (SGR) was similar in all experimental groups, varying between 2.3 and 2.4% day^{-1}. No significant differences in condition factor (*K*-value), fat deposition rate (FDR), dress-out percentage (DP), hepatosomatic index (HSI), visceral fat index (VFI) or fillet yield (FY) were found amongst fish fed the different experimental diets (Table 3).

The proximate composition of trout fillets and whole bodies at the commencement and termination of the experiment are reported in Table 4. Small, but statistically

Table 1 Formulation and proximate compositions of experimental diets (mg/g as fed)

	Dietary treatments[a]					
	CD	ALA72%	ALA54%	ALA36%	ALA18%	ALA2%
Fish meal[b]	338.3	338.3	338.3	338.3	338.3	338.3
Defatted soybean meal[b]	338.3	338.3	338.3	338.3	338.3	338.3
Wheat gluten[c]	56.4	56.4	56.4	56.4	56.4	56.4
Wheat flour[d]	110.5	110.5	110.5	110.5	110.5	110.5
Vit + min[b]	3.0	3.0	3.0	3.0	3.0	3.0
Choline[e]	5.0	5.0	5.0	5.0	5.0	5.0
Cr_2O_3[f]	2.0	2.0	2.0	2.0	2.0	2.0
Fish oil[g]	146.6	–	–	–	–	–
Sunflower oil[h]	–	–	36.6	73.3	109.9	146.6
Linseed oil[h]	–	146.6	109.9	73.3	36.6	–
Proximate composition						
Moisture	62.1	67.0	70.1	56.3	67.7	61.0
Protein	464.5	463.5	463.0	466.3	465.7	467.6
Lipid	189.6	185.2	185.9	184.6	186.0	180.4
Ash	84.0	81.3	83.1	83.2	83.6	88.2
NFE[i]	199.7	203.0	197.9	209.6	197.0	202.8
Energy kJ/g[j]	21.89	21.75	21.67	21.90	21.73	21.65

[a] Diet abbreviations: *CD* Control diet 100% fish oil, *ALA72%* diet contains 72% of total C_{18} PUFA in the form of ALA, *ALA54%* diet contains 54% of total C_{18} PUFA in the form of ALA, *ALA36%* diet contains 36% of total C_{18} PUFA in the form of ALA, *ALA18%* diet contains 18% of total C_{18} PUFA in the form of ALA, *ALA2%* diet contains 2% of total C_{18} PUFA in the form of ALA

[b] Ridley Agriproducts, Narangba, Queensland, Australia

[c] Manildra, Auburn, New South Wales, Australia

[d] Black and Gold, NSW, Australia

[e] Choline bitartrate, Sigma-Aldrich, Inc. St. Louis, MO, USA

[f] Chromium oxide, Sigma-Aldrich, Inc. St. Louis, MO, USA

[g] Sceneys veterinary grade, Sceney Chemical PTY., LTD. Sunshine, VIC., Australia

[h] Sceneys refined, Sceney Chemical PTY., LTD. Sunshine, VIC., Australia

[i] Nitrogen free extract

[j] Calculated on the basis of 23.6, 39.5 and 17.2 kJ g^{-1} of protein, fat and carbohydrate, respectively

significant ($P < 0.05$) differences were recorded in ash content of whole bodies and in the moisture, protein and lipid content of fish fillets. The lipid content of fillets of fish fed ALA54% was significantly lower than fish fed ALA72% or CD.

Fillet Fatty Acid Composition

The fatty acid composition of trout fillets at the end of the feeding trial is reported in Table 5. Several statistically significant ($P < 0.05$) differences were recorded and in general the fillet fatty acid make-up was somewhat mirroring that of the corresponding diet. Fillets of fish fed CD contained the highest amount of n-3 LC-PUFA (187.7 ± 0.7 mg g lipid^{-1}), mainly 20:5n-3 (33.9 ± 0.3 mg g lipid^{-1}) and 22:6n-3 (123.1 ± 0.4 mg g lipid^{-1}). The fillets of fish fed the five fish oil deprived experimental diets (from ALA72% to ALA2%) recorded no statistically significant differences in their content of SFA and MUFA, whilst the total PUFA concentration of fish receiving ALA2% (493.2 ± 7.8 mg g lipid^{-1}) was significantly ($P < 0.05$) lower than fish fed ALA72% and ALA54% (536.2 ± 3.7 and 524.9 ± 11.1 mg g lipid^{-1}, respectively). The 18:3n-3 and 18:2n-6 content (and their ratio) in the fillets of fish fed the five fish oil deprived diets were directly proportional to that of their diets with 18:3n-3 varying from 269.2 ± 2.9 to 5.9 ± 0.6 mg g lipid^{-1} and 18:2n-6 varying from 125.2 ± 0.5 to 381.1 ± 8.2 mg g lipid^{-1} in fillets of fish fed ALA72% to ALA2%, respectively.

Despite the five fish oil deprived diets containing almost identical contents of n-3 LC-PUFA, the actual n-3 LC-PUFA of fillets of fish was significantly different with the highest value (110.9 ± 1.7 mg g lipid^{-1}) recorded in ALA72% and the lowest value (50.5 ± 1.2 mg g lipid^{-1}) recorded in ALA2%. The same trend was recorded for individual n-3 LC-PUFA, such as 20:5n-3, 22:5n-3 and 22:6n-3.

Table 2 Fatty acid composition of experimental diets

	Dietary treatments[a]					
	CD	ALA72%	ALA54%	ALA36%	ALA18%	ALA2%
14:0	44.6 (*4.7*)	8.2 (*0.8*)	8.4 (*0.9*)	9.2 (*0.9*)	9.3 (*0.9*)	9.5 (*1.0*)
16:0	140.2 (*14.8*)	75.0 (*7.8*)	77.0 (*8.0*)	82.4 (*8.4*)	84.4 (*8.6*)	85.8 (*9.0*)
18:0	30.4 (*3.2*)	36.1 (*3.7*)	35.4 (*3.7*)	34.4 (*3.5*)	33.6 (*3.4*)	32.0 (*3.3*)
20:0	2.7 (*0.3*)	2.2 (*0.2*)	2.2 (*0.2*)	2.4 (*0.2*)	2.5 (*0.3*)	2.9 (*0.3*)
22:0	1.7 (*0.2*)	1.9 (*0.2*)	2.7 (*0.3*)	3.5 (*0.4*)	4.1 (*0.4*)	4.7 (*0.5*)
24:0	2.5 (0.3)	2.5 (*0.3*)	3.2 (*0.3*)	3.1 (*0.3*)	4.1 (*0.4*)	3.3 (*0.3*)
14:1n-5	0.6 (*0.1*)	–	–	–	–	–
16:1n-7	60.8 (*6.4*)	11.1 (*1.2*)	11.5 (*1.2*)	12.3 (*1.3*)	12.3 (*1.2*)	12.6 (*1.3*)
18:1n-7	33.9 (*3.6*)	13.7 (*1.4*)	14.1 (*1.5*)	15.2 (*1.5*)	15.1 (*1.5*)	14.9 (*1.6*)
18:1n-9	220.0(*23.2*)	173.9 (*18.0*)	182.5 (*18.9*)	192.2 (*19.6*)	201.5 (*20.5*)	201.0 (*21.0*)
20:1n-9	34.2 (*3.6*)	2.6 (*0.3*)	2.5 (*0.3*)	2.6 (*0.3*)	2.6 (*0.3*)	2.7 (*0.3*)
22:1n-9	6.6 (*0.7*)	0.7 (*0.1*)	0.6 (*0.1*)	0.8 (*0.1*)	1.0 (*0.1*)	1.6 (*0.2*)
24:1n-9	1.2 (*0.1*)	2.5 (*0.3*)	1.9 (*0.2*)	1.4 (*0.1*)	0.8 (*0.1*)	–
20:1n-11	4.2 (*0.4*)	0.8 (*0.1*)	0.6 (*0.1*)	0.6 (*0.1*)	0.7 (*0.1*)	0.6 (*0.1*)
22:1n-11	29.6 (*3.1*)	0.9 (*0.1*)	0.9 (*0.1*)	0.4 (*0.0*)	0.5 (*0.0*)	0.7 (*0.1*)
18:2n-6	91.3 (*9.6*)	158.5 (*16.4*)	257.0 (*26.6*)	358.7 (*36.5*)	452.1 (*45.9*)	517.5 (*54.1*)
20:2n-6	4.8 (*0.5*)	0.7 (*0.1*)	0.3 (*0.0*)	0.8 (*0.1*)	0.4 (*0.0*)	0.4 (*0.0*)
22:2n-6	0.4 (*0.0*)	0.8 (*0.1*)	0.7 (*0.1*)	0.3 (*0.0*)	0.1 (*0.0*)	–
18:3n-6	1.3 (*0.1*)	0.1 (*0.0*)	0.3 (*0.0*)	0.6 (*0.1*)	0.8 (*0.1*)	0.9 (*0.1*)
20:3n-6[b]	–	–	–	–	–	–
20:4n-6	6.7 (*0.7*)	2.5 (*0.3*)	2.3 (*0.2*)	2.5 (*0.3*)	1.9 (*0.2*)	2.7 (*0.3*)
22:4n-6	1.8 (*0.2*)	0.4 (*0.0*)	0.4 (*0.0*)	0.4 (*0.0*)	0.4 (*0.0*)	0.4 (*0.0*)
18:3n-3	24.2 (*2.6*)	416.8 (*43.1*)	306.9 (*31.8*)	201.7 (*20.5*)	102.6 (*10.4*)	8.4 (*0.9*)
20:3n-3	2.0 (*0.2*)	0.3 (*0.0*)	0.1 (*0.0*)	–	–	–
18:4n-3	11.3 (*1.2*)	3.7 (*0.4*)	3.2 (*0.3*)	3.2 (*0.3*)	3.0 (*0.3*)	2.6 (*0.3*)
20:4n-3	9.7 (*1.0*)	1.1 (*0.1*)	1.1 (*0.1*)	1.1 (*0.1*)	1.1 (*0.1*)	1.2 (*0.1*)
20:5n-3	71.8 (*7.6*)	23.3 (*2.4*)	24.3 (*2.5*)	26.8 (*2.7*)	24.8 (*2.5*)	23.6 (*2.5*)
22:5n-3	26.5 (*2.8*)	4.8 (*0.5*)	5.1 (*0.5*)	5.6 (*0.6*)	6.0 (*0.6*)	5.7 (*0.6*)
22:6n-3	84.6 (*8.9*)	22.2 (*2.3*)	21.1 (*2.2*)	19.9 (*2.0*)	19.3 (*2.0*)	19.9 (*2.1*)
SFA	222.1 (*23.4*)	125.8 (*13.0*)	128.8 (*13.3*)	135.0 (*13.8*)	138.0 (*14.0*)	138.3 (*14.5*)
MUFA	391.1 (*41.2*)	206.2 (*21.3*)	214.7 (*22.2*)	225.5 (*23.0*)	234.4 (*23.8*)	234.3 (*24.5*)
PUFA	336.4 (*35.4*)	635.2 (*65.7*)	622.9 (*64.5*)	621.6 (*63.3*)	612.4 (*62.2*)	583.3 (*61.0*)
C_{18} n-6 PUFA[c]	92.7 (*9.8*)	158.6 (*16.4*)	257.4 (*26.6*)	359.3 (*36.6*)	452.9 (*46.0*)	518.4 (*54.2*)
C_{18} n-3 PUFA[d]	35.6 (*3.7*)	420.5 (*43.5*)	310.1 (*32.1*)	204.9 (*20.9*)	105.5 (*10.7*)	11.0 (*1.2*)
n-6 LC-PUFA[e]	13.6 (*1.4*)	4.4 (*0.5*)	3.7 (*0.4*)	4.0 (*0.4*)	2.8 (*0.3*)	3.5 (*0.4*)
n-3 LC-PUFA[f]	194.5 (*20.5*)	51.7 (*5.3*)	51.7 (*5.4*)	53.4 (*5.4*)	51.2 (*5.2*)	50.4 (*5.3*)
18:3n-3/18:2n-6[g]	0.27	2.63	1.19	0.56	0.23	0.02

mg per g lipid and w/w % of total fatty acids in parentheses and italics

SFA saturated fatty acids, *MUFA* Monounsaturated fatty acids (1 double bond), *PUFA* Polyunsaturated fatty acids (two or more double bonds)

[a] See Table 1 for diet abbreviations

[b] 20:3n-6 was not detected in any quantifiable amount in the experimental diets, but in consideration it was present in fish tissues, it was reported in the present table for consistency

[c] PUFA with 18 atoms of carbon and the first double bond at the 6th carbon atom from the methyl end of the molecule

[d] PUFA with 18 atoms of carbon and the first double bond at the 3rd carbon atom from the methyl end of the molecule

[e] Long chain polyunsaturated fatty acids (PUFA with 20 or more atoms of carbon) with the first double bond at the 6th carbon atom from the methyl end of the molecule

[f] Long chain polyunsaturated fatty acids (PUFA with 20 or more atoms of carbon) with the first double bond at the 3rd carbon atom from the methyl end of the molecule

[g] Ratio of α-linolenic acid (ALA; 18:3n-3) to linoleic acid (LNA; 18:2n-6)

Table 3 Growth, feed utilization and biometry data of rainbow trout fed the experimental diets for 126 days

	Dietary treatments[a]					
	CD	ALA72%	ALA54%	ALA36%	ALA18%	ALA2%
Initial weight (g)	29.8 ± 0.2	30.3 ± 0.6	30.1 ± 0.4	30.0 ± 0.4	30.2 ± 0.1	30.1 ± 0.3
Final weight (g)	562.2 ± 6.2	586.6 ± 16.2	611.2 ± 24.8	613.0 ± 7.5	563.0 ± 41.2	596.8 ± 31.4
Gain (g/fish)	532.4 ± 6.1	556.3 ± 16.8	581.1 ± 25.2	583.0 ± 7.8	532.8 ± 41.1	566.7 ± 31.2
Gain (%)[b]	1,786 ± 18	1,841 ± 92	1,932 ± 109	1,944 ± 50	1,763 ± 130	1,882 ± 96
Feed intake (g/fish)	627.6 ± 2.9	617.8 ± 9.3	599.6 ± 22.4	608.8 ± 6.8	593.6 ± 12.0	603.9 ± 11.4
SGR (% day^{-1})[c]	2.3 ± 0.0	2.4 ± 0.0	2.4 ± 0.0	2.4 ± 0.0	2.3 ± 0.0	2.4 ± 0.0
FDR (% day^{-1})[d]	3.5 ± 0.0	3.5 ± 0.0	3.5 ± 0.0	3.6 ± 0.0	3.4 ± 0.0	3.5 ± 0.0
FCR[e]	1.2 ± 0.0	1.1 ± 0.0	1.0 ± 0.0	1.0 ± 0.0	1.1 ± 0.1	1.1 ± 0.0
DP (%)[f]	85.2 ± 0.7	84.5 ± 0.8	84.7 ± 0.6	85.0 ± 1.2	84.7 ± 0.6	86.3 ± 0.5
FY (%)[g]	55.8 ± 1.1	55.6 ± 1.4	54.0 ± 1.2	54.6 ± 1.4	53.4 ± 0.8	55.9 ± 1.0
HSI (%)[h]	1.1 ± 0.0	1.2 ± 0.1	1.2 ± 0.1	1.1 ± 0.0	1.1 ± 0.0	1.1 ± 0.0
VFI (%)[i]	7.0 ± 0.8	6.5 ± 0.7	7.4 ± 0.9	8.0 ± 1.0	7.5 ± 0.8	6.1 ± 0.7
K-value[j]	1.9 ± 0.1	2.0 ± 0.1	2.0 ± 0.1	1.9 ± 0.2	1.9 ± 0.1	2.0 ± 0.1

Data represent means ± SEM. Values in the same row with different superscripts are significantly different ($P < 0.05$; ANOVA and Student–Newman–Keuls post hoc test, $n = 3$; $N = 18$)

[a] See Table 1 for diet abbreviations

[b] Weight gain% = (final weight − initial weight) × $(\text{initial weight})^{-1} \times 100$

[c] Specific Growth Rate = [Ln(final weight) − Ln(initial weight)] × $(\text{number of days})^{-1} \times 100$

[d] Fat deposition rate = [Ln(final lipid) − Ln(initial lipid)] × $(\text{number of days})^{-1} \times 100$

[e] Feed conversion ratio = (dry feed fed) × $(\text{wet weight gain})^{-1}$

[f] Dress-out percentage = $(\text{CW} \times \text{BW}^{-1}) \times 100$; where CW is carcass gutted weight (g) and BW is body weight (g)

[g] Fillet yield percentage = $(\text{FW} \times \text{BW}^{-1}) \times 100$; where FW is fillet weight (g)

[h] Hepatosomatic index percent = $(\text{LW} \times \text{BW}^{-1}) \times 100$; where LW is liver weight (g)

[i] Visceral fat index = (Visceral fat weight) × $(\text{total fish weight})^{-1} \times 100$

[j] (Fulton's condition factor) = $(\text{BW} \times \text{L}^{-3}) \times 100$; where *L* is the length (mm)

Table 4 Proximate composition (mg g^{-1} on wet basis) of fillets and whole body of rainbow trout fed the experimental diets for 126 days

Parameters	Initial	Dietary treatments[a]					
		CD	ALA72%	ALA54%	ALA36%	ALA18%	ALA2%
Fillet							
Moisture	787.5	657.6 ± 2.7[a]	656.9 ± 4.4[a]	673.4 ± 3.5[b]	667.4 ± 3.8[ab]	672.4 ± 4.6[b]	664.9 ± 3.3[ab]
Protein	178.4	197.5 ± 2.6[b]	187.9 ± 2.0[a]	198.8 ± 2.5[b]	190.7 ± 1.4[ab]	195.6 ± 2.3[ab]	194.5 ± 2.4[ab]
Lipid	20.0	134.5 ± 3.7[bc]	144.3 ± 3.6[c]	118.2 ± 2.1[a]	131.9 ± 5.2[abc]	123.6 ± 4.5[ab]	130.9 ± 3.8[abc]
Ash	10.8	10.5 ± 1.4	10.9 ± 1.6	9.5 ± 0.7	9.9 ± 0.6	8.3 ± 0.5	9.7 ± 1.2
Whole body							
Moisture	764.7	595.9 ± 2.3	599.7 ± 2.5	595.8 ± 1.5	604.8 ± 6.3	601.1 ± 3.1	604.2 ± 2.1
Protein	68.9	177.3 ± 6.5	170.1 ± 2.7	173.5 ± 2.6	164.4 ± 3.8	169.3 ± 3.2	169.0 ± 1.9
Lipid	51.4	210.3 ± 4.7	211.2 ± 3.6	214.9 ± 2.3	221.1 ± 3.0	211.9 ± 2.6	211.8 ± 3.2
Ash	23.1	16.5 ± 1.5[b]	19.0 ± 1.4[b]	15.8 ± 1.4[b]	9.7 ± 1.6[a]	17.7 ± 0.9[b]	14.9 ± 1.2[b]

Data represent means ± SEM. Values in the same row with different superscripts are significantly different ($P < 0.05$; ANOVA and Student–Newman–Keuls post hoc test, $n = 3$; $N = 18$); Initial values not included in statistical computations

[a] See Table 1 for diet abbreviations

The trout whole bodies were also analyzed for their fatty acid composition (as these values are necessary for the implementation of the whole-body fatty acid balance method), but these data are not reported for simplicity. However, the overall fatty acid composition of trout whole bodies and the specific differences amongst fish fed the

Table 5 Fillet fatty acid composition (mg g lipid^{-1}) of rainbow trout fed the experimental diets for 126 days

	Dietary treatments[a,b]					
	CD	ALA72%	ALA54%	ALA36%	ALA18%	ALA2%
14:0	34.7 ± 0.7^{b}	9.8 ± 0.1^{a}	10.1 ± 0.2^{a}	10.2 ± 0.4^{a}	9.8 ± 0.4^{a}	9.7 ± 0.2^{a}
16:0	157.6 ± 3.2^{b}	114.2 ± 1.2^{a}	112.2 ± 1.5^{a}	115.5 ± 1.0^{a}	113.2 ± 4.2^{a}	115.6 ± 1.3^{a}
18:0	40.4 ± 0.6^{a}	47.5 ± 0.7^{c}	46.4 ± 1.2^{bc}	43.9 ± 1.1^{ab}	43.2 ± 1.2^{ab}	42.6 ± 0.7^{ab}
20:0	1.7 ± 0.1	1.4 ± 0.1	1.5 ± 0.1	1.9 ± 0.4	1.9 ± 0.2	1.8 ± 0.2
22:0	0.9 ± 0.1^{ab}	0.7 ± 0.1^{a}	1.3 ± 0.1^{bc}	1.8 ± 0.1 ^{cd}	1.7 ± 0.3 ^{cd}	2.1 ± 0.1^{d}
24:0	0.6 ± 0.2	0.7 ± 0.4	1.1 ± 0.0	1.2 ± 0.1	0.8 ± 0.4	1.2 ± 0.1
14:1n-5	0.5 ± 0.3	0.2 ± 0.2	0.1 ± 0.1	0.2 ± 0.2	–	0.1 ± 0.1
16:1n-7	65.6 ± 1.7^{b}	22.2 ± 0.5^{a}	19.9 ± 0.4^{a}	21.0 ± 0.5^{a}	18.7 ± 2.4^{a}	22.3 ± 1.3^{a}
18:1n-7	1.7 ± 0.2^{a}	18.0 ± 1.2^{b}	19.1 ± 0.4^{b}	18.5 ± 0.3^{b}	18.1 ± 0.5^{b}	19.8 ± 0.8^{b}
18:1n-9	276.6 ± 5.3^{b}	227.2 ± 2.6^{a}	222.0 ± 3.1^{a}	224.8 ± 1.6^{a}	226.2 ± 10.4^{a}	241.0 ± 3.9^{a}
20:1n-9	34.5 ± 0.2^{c}	10.0 ± 0.5^{a}	9.9 ± 0.3^{a}	10.6 ± 0.4^{a}	10.5 ± 0.6^{a}	12.5 ± 0.3^{b}
22:1n-9	5.2 ± 0.2^{b}	1.3 ± 0.1^{a}	1.0 ± 0.0^{a}	1.1 ± 0.3^{a}	1.2 ± 0.0^{a}	1.3 ± 0.1^{a}
24:1n-9	1.8 ± 0.3	1.2 ± 0.2	1.1 ± 0.1	1.2 ± 0.3	0.6 ± 0.2	1.1 ± 0.4
20:1n-11	4.0 ± 0.1^{b}	0.3 ± 0.2^{a}	0.1 ± 0.0^{a}	0.2 ± 0.2^{a}	–	0.1 ± 0.1^{a}
22:1n-11	17.1 ± 0.3^{b}	0.7 ± 0.1^{a}	0.3 ± 0.0^{a}	0.2 ± 0.2^{a}	–	0.1 ± 0.1^{a}
18:2n-6	82.8 ± 1.4^{a}	125.2 ± 0.5^{b}	198.3 ± 3.2^{c}	266.0 ± 3.5^{d}	329.6 ± 7.0^{e}	381.1 ± 8.2^{f}
20:2n-6	7.6 ± 0.3^{a}	7.6 ± 0.4^{a}	11.2 ± 0.4^{b}	16.0 ± 0.9^{c}	20.8 ± 0.6^{d}	25.7 ± 0.4^{e}
22:2n-6	0.8 ± 0.0^{a}	1.3 ± 0.1^{b}	1.7 ± 0.2^{b}	1.4 ± 0.2^{b}	1.9 ± 0.1^{c}	2.0 ± 0.0^{c}
18:3n-6	1.1 ± 0.2^{a}	1.8 ± 0.3^{ab}	2.4 ± 0.1^{ab}	3.2 ± 0.3^{b}	5.1 ± 0.4^{c}	5.6 ± 1.0^{c}
20:3n-6	2.7 ± 0.2^{a}	2.8 ± 0.2^{a}	4.3 ± 0.0^{b}	6.6 ± 0.4^{c}	8.7 ± 0.3^{d}	11.9 ± 0.8^{e}
20:4n-6	6.2 ± 0.1^{b}	2.9 ± 0.1^{a}	3.5 ± 0.1^{a}	4.0 ± 0.1^{a}	5.2 ± 0.1^{b}	7.6 ± 0.9^{c}
22:4n-6	2.0 ± 0.2^{c}	0.9 ± 0.2^{a}	0.8 ± 0.1^{a}	0.7 ± 0.1^{a}	1.4 ± 0.1^{b}	1.6 ± 0.1^{bc}
18:3n-3	18.9 ± 0.5^{b}	269.2 ± 2.9^{f}	197.5 ± 4.6^{e}	125.1 ± 1.5^{d}	62.7 ± 1.3^{c}	5.9 ± 0.6^{a}
20:3n-3	2.7 ± 0.1^{b}	15.6 ± 0.1^{f}	11.6 ± 0.5^{e}	7.8 ± 0.5^{d}	4.0 ± 0.2^{c}	0.5 ± 0.2^{a}
18:4n-3	5.2 ± 0.1^{c}	13.5 ± 0.5^{f}	8.8 ± 0.2^{e}	6.5 ± 0.4^{d}	4.1 ± 0.1^{b}	1.0 ± 0.1^{a}
20:4n-3	8.4 ± 0.3^{d}	10.6 ± 0.9^{e}	7.5 ± 0.2^{d}	5.7 ± 0.2^{c}	3.3 ± 0.4^{b}	1.0 ± 0.1^{a}
20:5n-3	33.9 ± 0.3^{d}	13.7 ± 0.9^{c}	12.6 ± 0.5^{c}	11.7 ± 0.6^{c}	8.0 ± 0.2^{b}	5.3 ± 0.3^{a}
22:5n-3	19.7 ± 0.1^{d}	7.8 ± 0.2^{c}	6.6 ± 0.4^{bc}	5.8 ± 0.4^{b}	3.2 ± 0.8^{a}	3.1 ± 0.1^{a}
22:6n-3	123.1 ± 0.4^{e}	63.1 ± 0.4^{d}	58.1 ± 2.3^{cd}	54.8 ± 3.6^{c}	48.1 ± 2.1^{b}	40.6 ± 1.0^{a}
SFA	235.9 ± 4.6^{b}	174.4 ± 0.1^{a}	172.6 ± 2.6^{a}	174.7 ± 1.4^{a}	170.6 ± 5.4^{a}	173.1 ± 1.9^{a}
MUFA	407.0 ± 8.3^{b}	281.2 ± 3.7^{a}	273.6 ± 2.6^{a}	277.8 ± 1.0^{a}	275.5 ± 13.0^{a}	298.3 ± 5.8^{a}
PUFA	315.1 ± 2.0^{a}	536.1 ± 1.0^{c}	524.9 ± 11.1^{c}	515.4 ± 3.7^{bc}	506.2 ± 10.1^{bc}	493.2 ± 7.8^{b}
C_{18} n-6 PUFA	83.9 ± 1.4^{a}	127.0 ± 0.6^{b}	200.7 ± 3.1^{c}	269.2 ± 3.5^{d}	334.7 ± 6.7^{e}	386.8 ± 7.5^{f}
C_{18} n-3 PUFA	24.1 ± 0.4^{b}	282.6 ± 2.5^{f}	206.4 ± 4.8^{e}	131.6 ± 1.7^{d}	66.8 ± 1.4^{c}	6.9 ± 0.4^{a}
n-6 LC-PUFA	19.3 ± 0.6^{b}	15.6 ± 0.5^{a}	21.2 ± 0.6^{b}	28.8 ± 1.4^{c}	38.0 ± 0.7^{d}	48.9 ± 1.4^{e}
n-3 LC-PUFA	187.7 ± 0.7^{f}	110.9 ± 1.7^{e}	96.6 ± 3.0^{d}	85.8 ± 5.2^{c}	66.7 ± 2.4^{b}	50.5 ± 1.2^{a}
18:3n-3/18:2n-6	0.23	2.15	1.00	0.47	0.19	0.02

Data represent means ± SEM. Values in the same row with different superscripts are significantly different ($P < 0.05$; ANOVA and Student–Newman–Keuls post hoc test, $n = 3$; $N = 18$)

[a] See Table 1 for diet abbreviations

[b] See Table 2 for fatty acid class abbreviations

different diets were similar and highly consistent with that of the fillets.

The 20:5n-3, 22:5n-3, 22:6n-3 and total n-3 LC-PUFA content of fillets of rainbow trout fed the experimental diets for 126 days, expressed as mg per 100 g of fillet, are depicted in Fig. 1. As expected, the highest content of these fatty acids was recorded in the fillets of fish fed CD. A clear trend towards an increased content of these fatty acids with the increasing dietary supply of 18:3n-3 was present. For example, the 20:5n-3 and 22:6n-3 content of fish fed

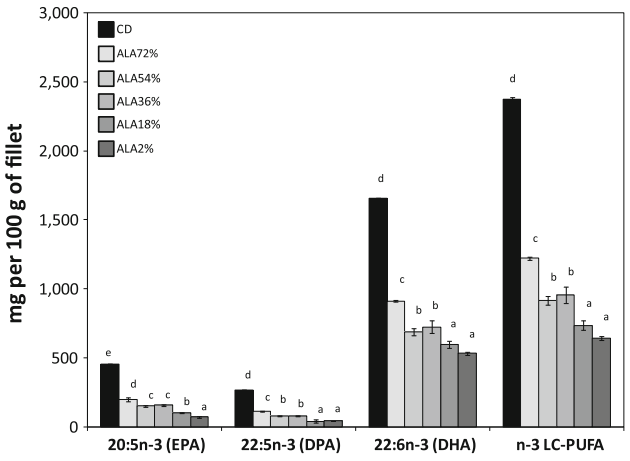

Fig. 1 The EPA (20:5n-3), DPAn-3 (22:5n-3), DHA (22:6n-3) and total n-3 LC-PUFA content of fillets of rainbow trout fed the experimental diets for 126 days (mg per 100 g of fillet)

the ALA2% were 69.2 ± 3.8 and 531.0 ± 12.9 mg per 100 g of fillet, whilst in the ALA72% treatment these values were 197.6 ± 13.6 and 911.3 ± 5.3 mg per 100 g of fillet, respectively.

Lipid and Fatty Acid Digestibility

The dry matter, lipid, total fatty acid and individual fatty acid digestibility are reported in Table 6. In general, all diets recorded high digestibility values, with no significant differences recorded in total dry matter, total lipid and total fatty acid digestibility. Individual fatty acids all recorded relatively high levels of digestibility, and despite a few statistically significant differences, the overall values were numerically similar and within the normal range of values reported for fatty acid digestibility in finfish. The two fatty acids which were quantitatively more variable across all treatments were 18:2n-6 and 18:3n-3, and whilst 18:2n-6 recorded no significant differences in its digestibility across all treatments, 18:3n-3 digestibility in ALA2% (the diet containing the smallest amount of this fatty acid) was significantly lower in comparison to the other diets.

Lipid and Fatty Acid Metabolism

In Table 7 the appearance/disappearance (expressed as mg per fish) of individual fatty acids during the 126 day experimental period are reported. These values are important for the implementation of the whole-body fatty acid balance method but also provide interesting information on its own. In fact, in the five fish oil deprived treatments, 18:2n-6 and 18:3n-3 recorded the highest level of disappearance (proportional to dietary concentration), alongside 20:5n-3. On the other hand, 16:0, 18:1n-9 and 22:6n-3 all recorded a high rate of appearance, clearly indicating that these fatty acids were synthesized by fish during the trial. The resultant apparent in vivo total enzyme activity (μmol g fish^{-1} day^{-1}) in rainbow trout fed the six experimental diets is reported in Table 8. Total apparent in vivo fatty acid de novo biosynthesis was significantly ($P < 0.05$) smaller in the CD treatment compared to the other five treatments, whilst no statistically significant differences were recorded for total apparent in vivo fatty acid β-oxidation. The apparent in vivo fatty acid Δ-9 desaturation was significantly ($P < 0.05$) lower in the CD treatment compared to ALA36%, however, no differences were noted amongst the five fish oil deprived experimental treatments. Total apparent in vivo fatty acid Δ-6 and Δ-5 desaturation both trended towards higher activity in fish receiving higher dietary 18:3n-3 (ALA72% > ALA54% > ALA36% > ALA18% > ALA2%). No apparent in vivo fatty acid Δ-5 desaturation was recorded in fish fed CD.

The apparent in vivo n-6 PUFA and n-3 PUFA bioconversion activity (μmol g fish^{-1} day^{-1}) are reported in Figs. 2 and 3, respectively. Specifically, in these figures the main enzyme activity on the different fatty acid substrates along the n-6 PUFA and n-3 PUFA bioconversion pathway from 18:2n-6 to 22:4n-6 and from 18:3n-3 to 22:6n-3, respectively, are reported. Observing Figs. 2 and 3, it is evident how the enzyme activity was directly proportional to substrate availability: enzyme activity on n-6 PUFA: ALA2% > ALA18% > ALA36% > ALA54% > ALA72%; and enzyme activity on n-3 PUFA: ALA72% > ALA54% > ALA36% > ALA18% > ALA2%. Interestingly, observing Fig. 2, it is evident that the overall enzyme activity was gradually decreasing when moving along the bioconversion pathway (Δ-6 desaturation of 18:2n-6 > elongation of 18:3n-6 > Δ-5 desaturation of 20:3n-6 > elongation of 20:4n-6). This trend was also evident on the n-3 PUFA pathway, but only up to the production of 20:5n-3. In fact, the Δ-6 desaturation of 18:3n-3 was generally higher than the elongation of 18:4n-3, which was higher than the Δ-5 desaturation of 20:4n-3. However, proceeding along the n-3 PUFA bioconversion pathway, the overall elongation of 20:5n-3 to 22:5n-3 was higher than the actual Δ-5 desaturation of 20:4n-3 to 20:5n-3, and similarly, the final elongation, Δ-6 desaturation and chain shortening of 22:5n-3 for the production of 22:6n-3 was even higher. Fish fed the CD treatment recorded an active production of 18:3n-6, 20:3n-6, 22:5n-3 and 22:6n-3, but in no instance was Δ-5 desaturation activity recorded.

In Fig. 4, the Δ-6 desaturase, Elovl-5 elongase Δ-5 desaturase affinity towards n-3 or n-6 fatty acids is reported. Here, the plotted graphs report the relationship between the substrate availability, n-3/n-6 ratio and the ratio of enzyme activity acting on the two substrates (activity on n-3/activity on n-6 ratio). In all three instances, linear regression equations (with a slope of 3.182, 1.122

Table 6 Lipid and fatty acid apparent digestibility (%) in rainbow trout fed the different experimental diets

	Dietary treatments[a,b]					
	CD	ALA72%	ALA54%	ALA36%	ALA18%	ALA2%
14:0	98.2 ± 0.1[b]	97.0 ± 0.4[a]	96.6 ± 0.3[a]	97.0 ± 0.3[a]	97.1 ± 0.2[a]	96.7 ± 0.2[a]
16:0	97.0 ± 0.2[b]	96.1 ± 0.5[ab]	95.8 ± 0.4[ab]	96.6 ± 0.2[ab]	95.7 ± 0.2[ab]	95.4 ± 0.2[a]
18:0	96.1 ± 0.4[c]	95.1 ± 0.6[bc]	94.5 ± 0.3[bc]	95.0 ± 0.2[bc]	93.6 ± 0.5[ab]	92.7 ± 0.5[a]
20:0	96.1 ± 0.3[b]	92.5 ± 0.9[a]	91.1 ± 0.8[a]	91.9 ± 0.6[a]	91.5 ± 0.7[a]	91.6 ± 0.3[a]
22:0	92.6 ± 0.6	90.6 ± 1.5	90.5 ± 0.5	91.9 ± 0.3	90.5 ± 1.0	91.4 ± 1.8
24:0	95.7 ± 1.3	95.7 ± 1.5	95.1 ± 0.8	97.7 ± 1.2	95.0 ± 0.6	97.4 ± 1.7
14:1n-5	100	–	–	–	–	–
16:1n-7	98.8 ± 0.2	98.3 ± 0.3	98.2 ± 0.2	98.5 ± 0.4	98.2 ± 0.1	97.9 ± 0.2
18:1n-7	98.7 ± 0.7	97.7 ± 0.4	97.5 ± 0.4	98.2 ± 0.2	97.8 ± 0.1	97.5 ± 0.2
18:1n-9	98.1 ± 0.2	98.4 ± 0.4	98.4 ± 0.2	98.9 ± 0.0	98.7 ± 0.1	98.3 ± 0.1
20:1n-9	97.3 ± 0.2	96.6 ± 0.6	95.9 ± 0.6	96.8 ± 0.5	96.4 ± 0.4	96.0 ± 0.2
22:1n-9	95.8 ± 0.1	96.2 ± 3.8	95.9 ± 2.5	97.3 ± 2.7	95.1 ± 0.4	94.1 ± 1.0
24:1n-9	100	99.4 ± 0.6	96.4 ± 1.3	99.5 ± 0.5	100	–
20:1n-11	97.3 ± 0.2	100	98.6 ± 1.4	98.0 ± 2.0	97.8 ± 1.1	96.8 ± 1.6
22:1n-11	96.5 ± 0.3	100	100	100	98.7 ± 1.3	96.5 ± 3.5
18:2n-6	98.2 ± 0.5	98.1 ± 0.4	98.5 ± 0.2	99.0 ± 0.0	99.0 ± 0.1	98.8 ± 0.1
20:2n-6	97.1 ± 0.3[e]	90.8 ± 1.6[d]	83.1 ± 2.8[bc]	88.4 ± 1.9[cd]	78.6 ± 0.2[ab]	74.9 ± 2.2[a]
22:2n-6	83.5 ± 2.9	100	98.7 ± 1.3	95.4 ± 4.6	80.6 ± 11.4	–
18:3n-6	98.6 ± 1.4[b]	85.3 ± 7.4[a]	100	100	95.1 ± 0.5[b]	99.0 ± 1.0[b]
20:3n-6	–	–	–	–	–	–
20:4n-6	98.0 ± 0.0	96.4 ± 0.9	96.0 ± 0.2	96.6 ± 0.7	95.7 ± 0.4	96.3 ± 0.3
22:4n-6	96.9 ± 0.4	90.0 ± 3.7	91.0 ± 6.4	88.3 ± 5.9	94.1 ± 0.6	83.9 ± 1.1
18:3n-3	98.3 ± 0.2[b]	99.1 ± 0.2[c]	99.1 ± 0.1[c]	99.3 ± 0.0[c]	99.2 ± 0.1[c]	96.1 ± 0.1[a]
20:3n-3	95.7 ± 0.7	87.6 ± 12.4	88.7 ± 11.3	–	–	–
18:4n-3	99.5 ± 0.2	99.6 ± 0.4	99.5 ± 0.5	99.1 ± 0.1	100.0 ± 0.0	99.1 ± 0.6
20:4n-3	98.3 ± 0.7	93.0 ± 5.8	96.5 ± 1.7	94.9 ± 0.5	95.4 ± 2.7	97.2 ± 0.5
20:5n-3	99.0 ± 0.1	98.4 ± 0.4	98.2 ± 0.1	98.8 ± 0.3	99.0 ± 0.2	98.5 ± 0.3
22:5n-3	99.0 ± 0.1[c]	97.5 ± 0.2[b]	96.4 ± 0.7[b]	96.5 ± 0.3[b]	97.7 ± 0.5[b]	95.0 ± 0.1[a]
22:6n-3	99.7 ± 0.0[b]	98.6 ± 0.5[ab]	98.2 ± 0.6[a]	98.3 ± 0.2[ab]	98.9 ± 0.1[ab]	98.8 ± 0.1[ab]
ADC (DM)[c]	85.3 ± 0.46	81.2 ± 1.47	82.2 ± 1.49	82.6 ± 0.85	83.4 ± 1.01	82.1 ± 0.50
ADC (Lipid)[d]	97.2 ± 0.13	96.6 ± 0.40	96.6 ± 0.29	97.0 ± 0.16	96.7 ± 0.09	96.4 ± 0.13
ADC (FA)[e]	98.1 ± 0.2	98.3 ± 0.3	98.2 ± 0.2	98.5 ± 0.1	98.3 ± 0.1	98.0 ± 0.1

Data represent means ± SEM. Values in the same row with different superscripts are significantly different ($P < 0.05$; ANOVA and Student–Newman–Keuls post hoc test, $n = 3$; $N = 18$)

[a] See Table 1 for diet abbreviations

[b] Apparent nutrient digestibility = 100−[(100(Cr_2O_3 in diet)/(Cr_2O_3 in feces)] × [(% nutrient in feces)/(% nutrient in feed)]

[c] ADC (DM): Apparent dry matter digestibility = 100−[100(Cr_2O_3 in diet)/(Cr_2O_3 in feces)]

[d] ADC (Lipid): Apparent lipid digestibility

[e] ADC (FA): Apparent total fatty acid digestibility

and 8.097 for Δ-6 desaturase, Elovl-5 elongase Δ-5 desaturase, respectively) best described this relationship. It is clearly demonstrated that the Δ-6 desaturase activity acting on 18:3n-3, across either of the experimental treatments (ALA72%–ALA2%), was higher than the activity acting on 18:2n-6 (evident if compared to the line of equity), clearly indicating that the affinity of the Δ-6 desaturase was 3.2-fold higher for 18:3n-3 in comparison to 18:2n-6. Similarly, the Δ-5 desaturase activity acting on 20:4n-3 was much higher than the activity on 20:3n-6, with its affinity being 8-fold higher for 20:4n-3 in comparison to 20:3n-6. Elovl-5 elongase, on the other hand, seemed to have a more balanced affinity between the two substrates, with 18:4n-3 only slightly preferred to 18:3n-6.

Table 7 Individual fatty acid appearance/disappearance (mg per fish) during the 126 day experimental period deduced by the whole-body fatty acid balance method

	Dietary treatments[a]					
	CD	ALA72%	ALA54%	ALA36%	ALA18%	ALA2%
14:0	−1,673.2 ± 123.7^{a}	40.3 ± 33.2^{b}	224.0 ± 85.2^{b}	269.0 ± 19.3^{b}	−5.6 ± 40.6^{b}	60.1 ± 55.5^{b}
16:0	77.9 ± 630.9^{a}	3,381.0 ± 574.9^{b}	4,482.3 ± 839.1^{b}	5,190.8 ± 171.3^{b}	2,639.0 ± 382.4^{b}	4,052.1 ± 605.9^{b}
18:0	789.5 ± 237.5^{a}	1,023.0 ± 190.5^{ab}	1,642.4 ± 414.2^{ab}	2,140.0 ± 154.3^{b}	1,256.0 ± 257.1^{ab}	1,647.7 ± 254.3^{ab}
20:0	−140.9 ± 7.9^{a}	−29.8 ± 31.3^{b}	−43.6 ± 9.8^{b}	−57.4 ± 13.2^{b}	−61.0 ± 28.3^{b}	−96.6 ± 11.0^{ab}
22:0	−130.3 ± 8.9^{bc}	−81.5 ± 7.4^{c}	−110.5 ± 23.0^{bc}	−145.2 ± 8.4^{b}	−207.1 ± 21.6^{a}	−215.3 ± 13.3^{a}
24:0	−230.4 ± 15.8^{b}	−155.6 ± 16.5^{c}	−197.0 ± 25.2^{bc}	−201.3 ± 3.6^{bc}	−320.5 ± 14.9^{a}	−246.0 ± 9.1^{b}
14:1n-5	26.0 ± 11.8	0.0 ± 0.0	13.4 ± 13.4	10.6 ± 10.6	25.6 ± 14.2	12.1 ± 12.1
16:1n-7	−77.4 ± 340.0^{a}	1,149.2 ± 206.8^{b}	1,265.9 ± 235.4^{b}	1,379.9 ± 55.7^{b}	659.1 ± 34.5^{b}	964.7 ± 145.5^{b}
18:1n-7	−4,040.2 ± 61.2^{a}	700.5 ± 103.8^{b}	964.3 ± 247.5^{b}	483.6 ± 417.6^{b}	488.6 ± 156.9^{b}	683.9 ± 151.0^{b}
18:1n-9	4,184.7 ± 1,334.3	5,475.7 ± 1,134.4	7,607.4 ± 2,259.4	9,507.4 ± 545.8	3,457.6 ± 1,422.0	6,753.4 ± 1,567.0
20:1n-9	−193.3 ± 236.7^{a}	816.3 ± 86.6^{b}	1,088.9 ± 167.6^{b}	1,187.1 ± 68.9^{b}	935.2 ± 79.8^{b}	1,063.4 ± 132.4^{b}
22:1n-9	−206.2 ± 22.1^{a}	71.8 ± 11.7^{d}	85.9 ± 10.5^{d}	73.7 ± 2.8^{d}	24.3 ± 4.3^{c}	−15.3 ± 8.8^{b}
24:1n-9	153.4 ± 88.1	0.7 ± 69.4	−14.4 ± 61.7	−11.6 ± 8.7	39.7 ± 52.4	265.0 ± 79.2
20:1n-11	−75.2 ± 14.8	−82.6 ± 10.9	−62.8 ± 10.6	−66.6 ± 2.0	−76.2 ± 2.2	−66.7 ± 2.4
22:1n-11	−1,635.3 ± 66.5^{a}	−74.5 ± 22.7^{b}	−71.7 ± 20.1^{b}	−35.9 ± 8.6^{b}	−33.5 ± 2.5^{b}	−61.9 ± 9.0^{b}
18:2n-6	−1,615.1 ± 365.5^{b}	−3,990.7 ± 345.9^{ab}	−3,882.8 ± 1,939.8^{ab}	−4,020.4 ± 202.6^{ab}	−11,276.1 ± 3,050.1^{a}	−8,832.6 ± 1,803.7^{ab}
20:2n-6	284.3 ± 47.7^{a}	742.5 ± 58.9^{a}	1,400.3 ± 105.2^{b}	2,105.3 ± 110.0^{c}	2,312.3 ± 232.9^{c}	3,098.9 ± 249.7^{d}
22:2n-6	47.3 ± 7.0^{a}	24.1 ± 10.4^{a}	90.4 ± 7.3^{b}	187.0 ± 7.9^{c}	198.5 ± 17.4^{c}	261.3 ± 16.5^{d}
18:3n-6	108.7 ± 35.8^{a}	201.8 ± 21.2^{a}	333.6 ± 18.9^{b}	417.1 ± 31.8^{b}	564.4 ± 24.4^{c}	699.9 ± 51.6^{d}
20:3n-6	297.6 ± 4.6^{a}	322.3 ± 16.5^{a}	524.6 ± 19.3^{a}	853.5 ± 72.4^{b}	1,042.2 ± 48.0^{b}	1,575.4 ± 125.9^{c}
20:4n-6	−97.3 ± 28.4^{a}	17.0 ± 8.6^{b}	88.7 ± 8.7^{c}	215.0 ± 22.5^{d}	419.8 ± 14.5^{e}	587.5 ± 27.4^{f}
22:4n-6	−10.8 ± 18.0^{a}	13.9 ± 21.1^{ab}	75.6 ± 11.8^{bc}	98.2 ± 8.6 ^{cd}	111.5 ± 17.6 ^{cd}	165.5 ± 35.2^{d}
18:3n-3	−836.7 ± 89.4^{d}	−17,152.5 ± 926.4^{a}	−9,978.0 ± 2,120.9^{b}	−5,859.6 ± 242.6^{c}	−4,256.2 ± 617.7^{c}	−256.8 ± 28.8^{d}
20:3n-3	55.0 ± 11.8^{a}	1,854.2 ± 109.0^{e}	1,519.8 ± 131.2^{d}	1,022.3 ± 34.1^{c}	427.5 ± 46.8^{b}	46.4 ± 10.4^{a}
18:4n-3	−781.4 ± 36.2^{a}	1,155.8 ± 93.2^{f}	833.6 ± 26.2^{e}	559.3 ± 57.7^{d}	216.0 ± 40.0^{c}	−176.8 ± 12.7^{b}
20:4n-3	−248.5 ± 10.6^{a}	1,071.7 ± 19.5^{f}	886.5 ± 100.9^{e}	573.2 ± 34.5^{d}	238.0 ± 34.0^{c}	−19.7 ± 13.4^{b}
20:5n-3	−5,331.8 ± 197.0^{a}	−1,228.9 ± 25.6^{d}	−1,348.7 ± 92.5^{d}	−1,738.2 ± 38.6^{c}	−2,063.1 ± 63.4^{b}	−2,144.0 ± 13.0^{b}
22:5n-3	−1,165.7 ± 86.3^{a}	259.5 ± 34.6^{c}	179.3 ± 44.7^{c}	91.8 ± 18.3^{c}	−228.5 ± 28.5^{b}	−294.7 ± 17.9^{b}
22:6n-3	3,284.5 ± 551.9^{ab}	3,731.0 ± 102.0^{b}	3,749.9 ± 430.8^{b}	4,111.8 ± 243.7^{b}	2,696.4 ± 431.6^{ab}	2,040.0 ± 224.9^{a}

Data represent means ± SEM. Values in the same row with different superscripts are significantly different ($P < 0.05$; ANOVA and Student–Newman–Keuls post hoc test, $n = 3$; $N = 18$)

[a] See Table 1 for diet abbreviations

Table 8 Apparent in vivo total enzyme activity (μmol g fish^{-1} day^{-1}) in rainbow trout fed the six experimental diets deduced by the whole-body fatty acid balance method

	Dietary treatments[a]					
	CD	ALA72%	ALA54%	ALA36%	ALA18%	ALA2%
Total fatty acid de novo biosynthesis	0.34 ± 0.23^{a}	1.18 ± 0.19^{b}	1.56 ± 0.33^{b}	1.83 ± 0.07^{b}	0.91 ± 0.18^{ab}	1.40 ± 0.19^{b}
Total fatty acid β-oxidation	1.21 ± 0.18	1.32 ± 0.14	0.63 ± 0.43	0.27 ± 0.02	1.09 ± 0.48	0.42 ± 0.23
Total fatty acid elongation	1.51 ± 0.50^{a}	3.15 ± 0.33^{b}	3.75 ± 0.68^{a}	4.30 ± 0.20^{a}	2.45 ± 0.39^{ab}	3.22 ± 0.38^{ab}
Total fatty acid Δ-9 desaturation	0.43 ± 0.15^{a}	0.75 ± 0.12^{ab}	0.96 ± 0.22^{ab}	1.12 ± 0.04^{b}	0.52 ± 0.13^{ab}	0.85 ± 0.14^{ab}
Total fatty acid Δ-6 desaturation	0.30 ± 0.05^{a}	0.75 ± 0.02^{c}	0.70 ± 0.07^{c}	0.71 ± 0.05^{c}	0.48 ± 0.04^{b}	0.41 ± 0.01^{ab}
Total fatty acid Δ-5 desaturation	n.d.	0.21 ± 0.01^{c}	0.20 ± 0.04^{c}	0.20 ± 0.02^{c}	0.08 ± 0.02^{b}	0.06 ± 0.00^{a}

Data represent means ± SEM. Values in the same row with different superscripts are significantly different ($P < 0.05$; ANOVA and Student–Newman–Keuls post hoc test, $n = 3$; $N = 18$)

[a] See Table 1 for diet abbreviations

n.d. Not detected

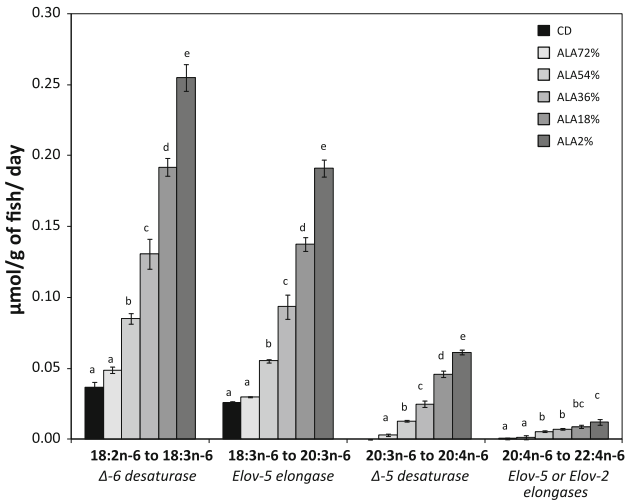

Fig. 2 Apparent in vivo n-6 PUFA bioconversion activity (μmol g fish^{-1} day^{-1}; Δ-6 desaturase, elongase and Δ-5 desaturase) on the different substrates along the n-6 PUFA bioconversion pathway from 18:2n-6 to 22:4n-6 deduced by the whole-body fatty acid balance method

The efficiency of the various apparent in vivo enzyme activities is reported in Table 9 and expressed as product % on total substrate availability (net intake + in vivo production). The efficiency of different enzymes acting on different substrates was somewhat affected by the different dietary treatments, particularly in the two most extreme treatments (CD and ALA2%), whilst values recorded amongst treatments ALA72% to ALA18% were quite consistent.

Discussion

This study could be considered as a practical feeding trial representative of the entire production cycle of rainbow trout, as practical commercial-like experimental diets were used and as juveniles were grown up to commercial size fish (~600 g). However, it also provides specific details towards a better understating of in vivo fatty acid metabolism, and how this can directly impact the final product quality of cultured trout. Thus, it is envisaged that the reported findings could be considered as highly relevant and directly usable by the industry, while at the same time providing valuable insight for researchers investigating fish fatty acid metabolism.

During the feeding trials, fish recorded a weight gain of over 1,700%, with optimal performance (SGR ~2.4 and FCR ~1.1) and no mortality. Whilst some numerical differences were noted amongst various parameters recorded, none were significantly ($P > 0.05$) different, clearly demonstrating that (1) fish oil replacement in rainbow trout practical diets has no negative effect on fish performance, and (2) diets either rich in 18:3n-3 or 18:2n-6 are both equally and favorably utilized by growing trout. These observations are in agreement with the majority of the studies focusing on fish oil replacement in salmonids [2, 3, 8–11, 25] and in several other species, as recently reviewed by Turchini et al. [14]. In direct alignment with the lack of any significant modification to fish performance, there was no effect on overall nutrient digestibility of the different lipid sources recorded in the present study. The individual fatty acid digestibility values recorded were all relatively high (the majority were higher than 95%) and in agreement with the statement that fat and fatty acids are efficiently digested and utilized by fish [31]. In some instances, slight growth retardation has been reported in rainbow trout fed alternative oils, but mainly when the diets were purified or semi-purified, and thus containing little/no fish meal in their formulation [12, 32]. In practical, commercial-like diets, both ALA-rich and LA-rich oils have been suggested to be valid fish oil replacers, as C_{18} PUFA are a good

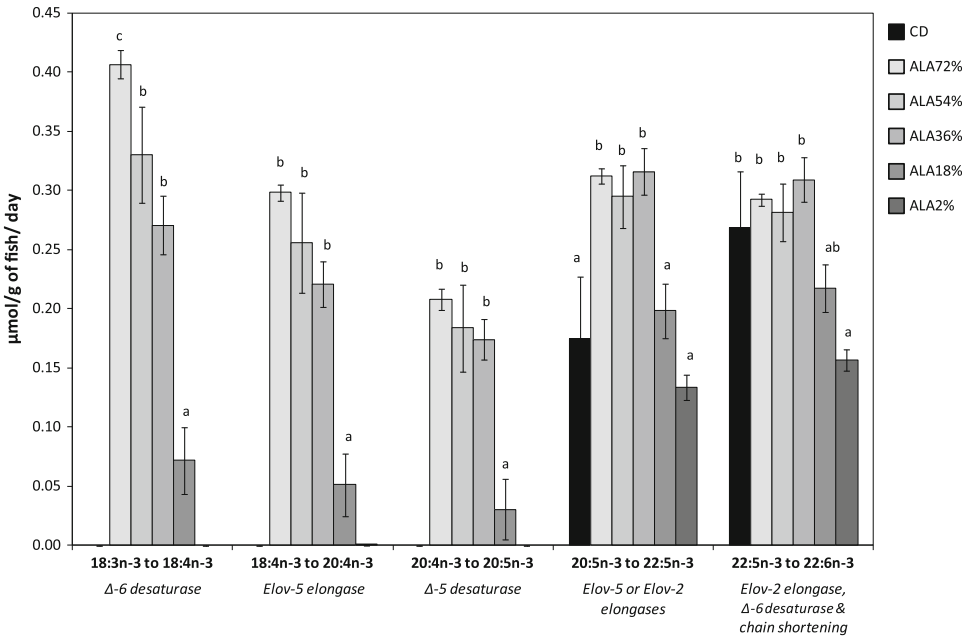

Fig. 3 Apparent in vivo n-3 PUFA bioconversion activity (µmol g fish^{-1} day^{-1}; Δ-6 desaturase, elongase, Δ-5 desaturase and chain shortening) on the different substrates along the n-3 PUFA bioconversion pathway from 18:3n-3 to 22:6n-3 deduced by the whole-body fatty acid balance method

source of available energy for fish growth [15, 16]. However, the dietary availability of 18:3n-3 and 18:2n-6 clearly affects the final fatty acid composition of fish fillets [14], and thus given their different nutritional qualities for human health [33], the use of ALA-rich or LNA-rich oils in aquafeed needs to be carefully evaluated where final eating quality is a concern [4].

Despite numerical differences being noted in the total apparent in vivo β-oxidation of fatty acids in fish under the different dietary treatments, these were, from a statistical point of view, not significantly different. On the contrary, total apparent in vivo fatty acid de novo biosynthesis was markedly and significantly higher in all fish fed the five fish oil deprived diets compared to the fish oil based diet (CD). This was mainly ascribable to a large de novo biosynthesis of SFA and MUFA (which includes fatty acid elongation and Δ-9 desaturation), as previously observed in fish fed diets rich in PUFA and with relatively little dietary SFA and MUFA [12, 34]. Therefore, when making the assumption that the optimal dietary fatty acid composition for a growing animal is the fatty acid composition which minimized in vivo bioconversion and biosynthesis, the theoretical optimal dietary fatty acid composition for farmed rainbow trout should be characterized by a relatively high content of SFA and MUFA, as previously suggested [12].

The PUFA bioconversion pathway in rainbow trout is well established [35, 36], and it is consistent with that of the majority of other vertebrates, involving an alternation of desaturation and elongation steps. The Δ-6 desaturase is the first enzyme involved in the bioconversion of C_{18} PUFA towards longer and more unsaturated LC-PUFA and for this reason it is often considered as the rate-limiting enzyme in the LC-PUFA biosynthetic pathway [37, 38]. However, in the present study it has been shown that a clear trend of progressively less efficient bioconversion of fatty acids to more unsaturated or longer homologues occurs along the n-6 PUFA pathway itself (Fig. 2). This suggests that, more than the existence of a "rate-limiting enzyme", which restricts the LC-PUFA biosynthetic pathway, the pathway has a "funnel-like" efficiency, as previously speculated for rainbow trout [12]. Consistently, it has been reported that the relative activity of each step of the pathway decreases as the chain length increases [39]. Interestingly, this apparent decreasing efficiency was also observed on the n-3 PUFA pathway, but only up to the production of 20:5n-3 (Fig. 3). Hereafter, there was a proportionally higher active production of 22:5n-3 and 22:6n-3 recorded across all treatments (CD included) suggesting an "hourglass-shape" of bioconversion efficiency. This is likely ascribable to the markedly higher substrate availability as all diets contained some 20:5n-3 (the initial substrate for these two last steps) and other n-3 LC-PUFA originating from fish oil in the CD treatment and from the residual oil of the fish meal component of the fish oil deprived experimental diets. This is partially in contrast with a previous study on rainbow trout in which it was reported that the ability of trout hepatocytes to synthesize 22:6n-3 from both 18:3n-3 and 20:5n-3 can be markedly stimulated by eliminating n-3 LC-PUFA from their diets [35]. However, another study on rainbow trout, also reported that fish fed a fish oil based diet, and thus with an abundant dietary supply of 20:5n-3, were still bioconverting this fatty acid up to 22:6n-3 quite efficiently [12].

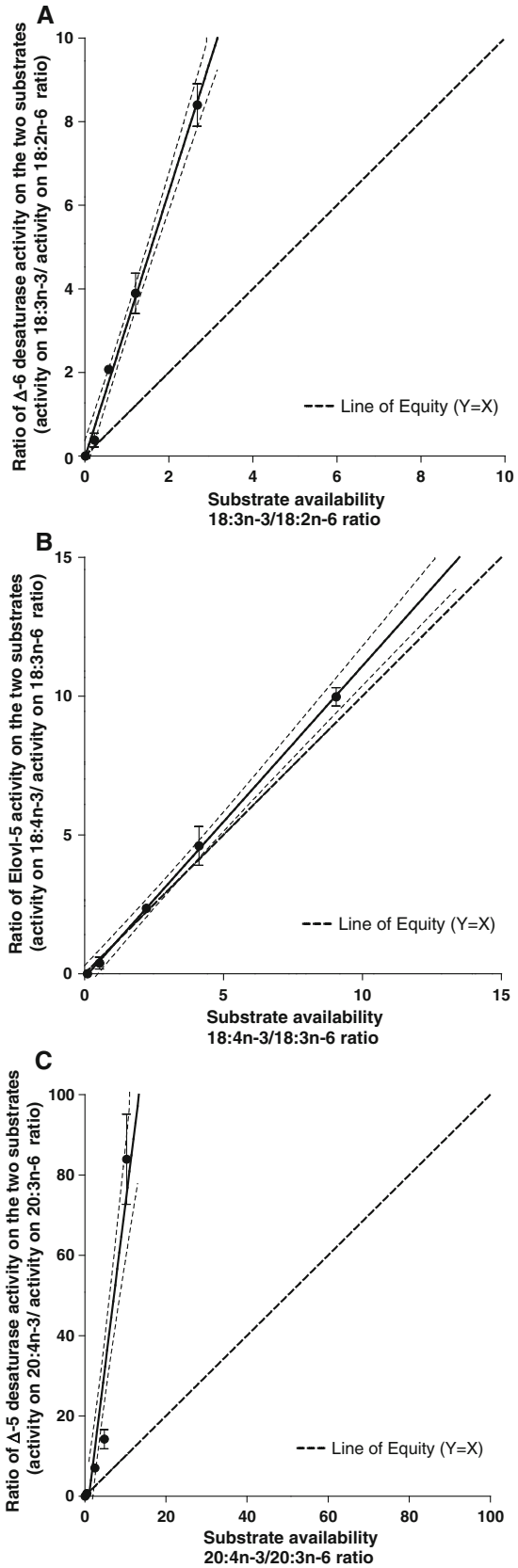

◀ **Fig. 4** Enzyme affinity (substrate preference) towards n-3 or n-6 fatty acids: the relationship between the substrate availability n-3/n-6 ratio and the ratio of the enzyme activity on the two substrates (activity on n-3/activity on n-6 ratio) deduced by the whole-body fatty acid balance method. **a** Affinity of Δ-6 desaturase: relationship between the substrate availability 18:3n-3/18:2n-6 ratio and the ratio of Δ-6 desaturase activity on the two substrates (activity on 18:3n-3/activity on 18:2n-6 ratio). Regression equation: $Y = 3.182X - 0.04168$; $R^2 = 0.97$; **b** Affinity of Elovl-5 elongase: relationship between the substrate availability 18:4n-3/18:3n-6 ratio and the ratio of Elovl-5 elongase activity on the two substrates (activity on 18:4n-3/activity on 18:3n-6 ratio). Regression equation: $Y = 1.122X - 0.1353$; $R^2 = 0.98$; **c** Affinity of Δ-5 desaturase: relationship between the substrate availability 20:4n-3/20:3n-6 ratio and the ratio of Δ-5 desaturase activity on the two substrates (activity on 20:4n-3/activity on 20:3n-6 ratio). Regression equation: $Y = 8.097X - 8.150$; $R^2 = 0.87$. In all graphs, *error bars* represent SEM, *dotted lines* represent 95% confidence band of the regression line, and the lines of equity ($Y = X$) have also been reported for visual reference. In all three linear regressions (**a**, **b** and **c**) the slope deviation from zero was significant ($P < 0.0001$)

Interestingly, the in vivo efficiency of the different enzymes involved in LC-PUFA biosynthesis (expressed as product % on total substrate availability) were quite different relative to the substrate (i.e. n-3 or n-6 PUFA) and relative to the step in the bioconversion pathway (Table 9). Apart from the two most extreme treatments (CD and ALA2%), values recorded amongst treatments ALA72% to ALA18% were quite consistent for a given fatty acid bioconversion step. Observing the middle treatment (ALA36%), it is possible to exemplify more schematically the recorded differences in enzyme efficiency. The efficiency of the apparent in vivo Δ-6 desaturase activity on C_{18} PUFA was generally higher for 18:3n-3 compared to 18:2n-6. In fact in ALA36%, 12.7% of available 18:3n-3 and only 3.5% of available 18:2n-6 were Δ-6 desaturated. Markedly higher values were recorded for the following elongation, with 68.3% of available 18:3n-6 and 72.4% of available 18:4n-3 was elongated in ALA36%. The efficiency of apparent in vivo Δ-5 desaturase activity was then again remarkably different between n-6 and n-3 fatty acids, as 26.4% of available 20:3n-6 was desaturated to 20:4n-6 and over 75.3% of 20:4n-3 was desaturated to 20:5n-3. Similarly, the following elongation recorded much higher efficiency values for n-3 fatty acids compared to n-6 fatty acids, with only 15.3% of available 20:4n-6 and 73.1% of 20:5n-3 been elongated. The final production of 22:6n-3, which involves an elongation, a Δ-6 desaturation and a chain shortening step, recorded very high efficiency values around ~84%, indicating that in general, 22:5n-3 was very efficiently bioconverted to 22:6n-3.

Given 18:3n-3 and 18:2n-6 are both substrates for the Δ-6 desaturase, its affinity towards one or the other is particularly relevant. The above discussed results relative to enzyme efficiency are in agreement with the generally

Table 9 Apparent in vivo enzyme efficiency expressed as product % on total substrate availability (net intake + in vivo production) in rainbow trout fed the six experimental diets deduced by the whole-body fatty acid balance method

	Dietary treatments[a]					
	CD	ALA72%	ALA54%	ALA36%	ALA18%	ALA2%
Δ-6 desaturase						
18:2n-6 to 18:3n-6	3.362 ± 0.37[a]	2.777 ± 0.08[a]	3.186 ± 0.22[a]	3.503 ± 0.25[a]	3.780 ± 0.11[a]	4.759 ± 0.24[b]
18:3n-3 to 18:4n-3	n.d.	8.683 ± 0.28[ab]	10.378 ± 1.93[b]	12.771 ± 1.01[b]	6.490 ± 2.97[a]	n.d.
Elongase (Elovl-5)						
18:3n-6 to 20:3n-6	50.054 ± 3.11[a]	60.296 ± 2.70[b]	62.355 ± 1.63[b]	68.392 ± 1.59[bc]	68.585 ± 0.29[bc]	72.409 ± 1.33[c]
18:4n-3 to 20:4n-3	n.d.	66.505 ± 1.94[c]	69.268 ± 3.96[c]	72.418 ± 0.86[c]	42.468 ± 11.31[b]	0.645 ± 0.64[a]
Δ-5 desaturase						
20:3n-6 to 20:4n-6	n.d.	9.674 ± 2.68[a]	23.213 ± 1.09[b]	26.450 ± 0.39[b]	33.534 ± 1.77[c]	32.117 ± 1.14[c]
20:4n-3 to 20:5n-3	n.d.	67.197 ± 1.68[b]	68.353 ± 2.80[b]	75.339 ± 0.96[b]	32.331 ± 20.87[a]	n.d.
Elongase (Elovl-5 and Elovl-2)						
20:4n-6 to 22:4n-6	0.688 ± 0.69[a]	4.914 ± 4.91[ab]	16.140 ± 2.04[b]	15.301 ± 1.21[b]	13.756 ± 1.79[b]	14.284 ± 2.21[b]
20:5n-3 to 22:5n-3	21.750 ± 6.56[a]	69.821 ± 0.59[b]	70.101 ± 2.36[b]	73.131 ± 1.04[b]	68.324 ± 6.18[b]	59.334 ± 6.94[b]
Elongase (Elovl-2) + Δ-6 desaturase + chain shortening						
22:5n-3 to 22:6n-3	59.738 ± 3.35[a]	81.773 ± 0.38[b]	82.782 ± 1.08[b]	84.872 ± 0.65[b]	85.085 ± 1.19[b]	85.832 ± 0.89[b]

Data represent means ± SEM. Values in the same row with different superscripts are significantly different ($P < 0.05$; ANOVA and Student–Newman–Keuls post hoc test, $n = 3$; $N = 18$)

[a] See Table 1 for diet abbreviations

n.d. Not detected

accepted notion that fatty acid desaturases have a higher affinity towards n-3 PUFA than n-6 PUFA [39]. Accordingly, previous studies using radio-labelled fatty acids in Atlantic salmon hepatocytes observed that the overall level of LC-PUFA synthesis from 18:2n-6 was less than half of that from 18:3n-3, irrespective of the diet [40, 41]. Similarly, using the whole body fatty acid balance method, a 3.2-fold greater Δ-6 desaturase affinity toward 18:3n-3 over 18:2n-6 was recorded in Murray cod [22, 42]. In the present study, an almost identical relationship between substrate availability and Δ-6 desaturase activity was shown (Fig. 4), suggesting that the overall affinity of this enzyme is 3.2-fold greater for 18:3n-3 over 18:2n-6 in rainbow trout. Elovl-5 elongase acting on C_{18} PUFA recorded no difference in affinity, whilst a remarkable 8-fold greater Δ-5 desaturase affinity toward 20:4n-3 over 20:3n-6 was recorded. Thus, if dietary 18:3n-3 and 18:2n-6 are provided in similar amounts (as in diet ALA54%), the amount of 18:4n-3 produced in vivo will be 3-times larger than 18:3n-6. The following Elovl-5 elongase activity, which showed no difference in its affinity, will produce 20:4n-3 and 20:3n-6 roughly maintaining the same ratio of their substrates availability (in this example 3:1). Then, in consideration that Δ-5 desaturase affinity towards 20:4n-3 was 8-fold higher than that acting on 20:3n-6, theoretically it will ultimately produce (3.2 × 8=) ~25.6-fold more 20:5n-3 than 20:4n-6. This difference in substrate preference of the above mentioned enzymes is consistent with previous indications obtained in trout cell culture [43]. To understand how these differences can affect final fatty acid composition of fish tissues, of course, other metabolic pathways (such as further bioconversion and β-oxidation) also need to be considered. However, according to the above discussed results, it is evident that significantly larger amounts of n-3 LC-PUFA, compared to n-6 LC-PUFA, will be found in fish tissues.

The capability of rainbow trout to bioconvert 18:3n-3 into 22:6n-3 in vivo was previously investigated using deuterated (D5)-18:3n-3 ethyl ester [44]. One of the most notable features of this study was the slow rate at which D5-22:6n-3 was synthesized and deposited in tissues. The authors also suggested that in trout, it takes ~4 weeks for a pulse of 18:3n-3 to be fully metabolized to 22:6n-3 and that given the experimental design, it could not be determined whether the PUFA biosynthetic pathway was substrate limited. However, it was also suggested that if more substrate (18:3n-3) had been available the rate of formation of 22:6n-3 might have been increased. Accordingly, in a following study on the same species, it was shown that a relatively large amount of dietary 18:3n-3 was bioconverted up to 22:6n-3, when the diet was deprived of n-3 LC-PUFA and supplied with abundant 18:3n-3 [12]. The results of the present study further confirm the fact that rainbow trout are quite efficient in bioconverting 18:3n-3 to 22:6n-3, and that clearly the PUFA biosynthetic pathway is substrate limited.

When it comes to the eating quality of cultured fish, one of the most important parameters to be considered is the actual quantity of n-3 LC-PUFA in the fish fillets [4, 45]. As expected, in the present trial, the highest content of 20:5n-3, 22:5n-3 and 22:6n-3 (totaling over 2.3 g of n-3LC-PUFA per 100 g of fillet) was recorded in the fillets of fish fed the CD. However, in fish fed the five fish oil deprived diets, a clear trend towards an increased content of these fatty acids with the increasing dietary supply of 18:3n-3 was present, independent of the fact that they were all fed with almost identical amounts of n-3 LC-PUFA. Rainbow trout have been shown previously to be capable of being a net producer of n-3 LC-PUFA [13], and the present study further confirms this. Importantly, it is commonly accepted that when fish oil is replaced in aquafeed, a significant detrimental reduction of total n-3 LC-PUFA occurs in fish fillets [14]. However, the present study highlights the very pertinent point that not all alternative oils are the same, and oils rich in 18:3n-3 can provide significantly higher amounts of total n-3 LC-PUFA in fish fillets in comparison to oils rich in 18:2n-6. For example (Fig. 1), the 20:5n-3 and 22:6n-3 content of fish fed the ALA2% (sunflower oil) were 69.2 ± 3.8 and 531.0 ± 12.9 mg per 100 g of fillet, respectively, whilst in ALA72% (linseed oil) these values were 197.6 ± 13.6 and 911.3 ± 5.3 mg per 100 g of fillet, respectively. Despite an almost identical dietary supply, the fillets of trout fed the diets richest in 18:3n-3 (ALA72%) contained double the amount of n-3 LC-PUFA in comparison to the fillets of fish fed with the diet containing the lowest content of 18:3n-3 (ALA2%). Basically, it was clearly shown that the substitution of fish oil with a proper alternative vegetable oil in aquafeed is an efficient tool that can be easily implemented which has the possibility to transform the salmonid aquaculture industry from a consumer into a net producer of health promoting n-3 LC-PUFA. This will ultimately assist aquaculture to accomplish its role in conserving wild fisheries in the future. However, it is important to highlight that when fish oil is completely replaced by alternative terrestrial oils, and therefore fish are provided with significantly less dietary n-3 LC-PUFA, a remarkable reduction in the n-3 LC-PUFA content in the final product is still unavoidable. Importantly, whilst this study clearly showed that the final n-3 LC-PUFA content in fish fed fish oil deprived diets can be increased by the provision of an abundant dietary supply of 18:3n-3 and the concomitant reduction of total dietary 18:2n-6, the proper balancing of dietary fatty acids with an appropriate amount of SFA and MUFA is also important to guarantee optimal growth performance.

Acknowledgments The authors express their gratitude to Bob Collins for his general and technical support throughout the research project and to Dr. Richard Smullen (RidleyAquafeed, RidleyAgriProducts, Narangba, QLD, Australia) for kindly providing some of the raw materials used in the experimental diets. This research was supported under the Australian Research Council's Discovery Projects funding scheme (project DP1093570). The views expressed herein are those of the authors and are not necessarily those of the Australian Research Council. The first author, Thanuthong, T. is the recipient of a Thai Government scholarship funded by Thai Government, and this support is gratefully acknowledged.

References

1. Turchini GM, Ng WK, Tocher DR (2010) Fish oil replacement and alternative lipid sources in aquaculture feeds. CRC Press, Taylor & Francis Group, Boca Raton, FL, p 551
2. Torstensen BE, Bell JG, Rosenlund G, Henderson RJ, Graff IE, Tocher DR, Lie O, Sargent JR (2005) Tailoring of Atlantic salmon (*Salmo salar* L.) flesh lipid composition and sensory quality by replacing fish oil with a vegetable oil blend. J Agric Food Chem 53(26):10166–10178
3. Bell JG, McGhee F, Campbell PJ, Sargent JR (2003) Rapeseed oil as an alternative to marine fish oil in diets of post-smolt Atlantic salmon (*Salmo salar*): changes in flesh fatty acid composition and effectiveness of subsequent fish oil "wash out". Aquaculture 218(1–4):515–528
4. Rosenlund G, Corraze G, Izquierdo M, Torstensen BE (2010) Fish oil replacement and alternative lipid sources in aquaculture feeds. In: Turchini GM, Ng WK, Tocher DR (eds) The effects of fish oil replacement on nutritional and organoleptic qualities of farmed fish. CRC Press, Taylor & Francis group, Boca Raton, FL, pp 487–522
5. Tocher DR (2010) Fatty acid requirements in ontogeny of marine and freshwater fish. Aquacult Res 41(5):717–732
6. Torstensen BE, Tocher DR (2010) The effects of fish oil replacement on lipid metabolism of fish. In: Turchini GM, Ng WK, Tocher (eds) Fish oil replacement and alternative lipid sources in aquaculture feeds. CRC Press, Taylor & Francis group, Boca Raton, FL, pp 405–438
7. Tacon AGJ, Metian M (2008) Global overview on the use of fish meal and fish oil in industrially compounded aquafeeds: trends and future prospects. Aquaculture 285(1–4):146–158
8. Tocher DR, Bell JG, McGhee F, Dick JR, Fonseca-Madrigal J (2003) Effects of dietary lipid level and vegetable oil on fatty acid metabolism in Atlantic salmon (*Salmo salar* L.) over the whole production cycle. Fish Physiol Biochem 29(3): 193–209
9. Bell JG, Karalazos V, Bendiksen EA (2011) Interactive effects of dietary protein/lipid level and oil source on growth, feed utilisation and nutrient and fatty acid digestibility of Atlantic salmon. Aquaculture 311(1–4):193–200
10. Karalazos V, Bendiksen EA, Dick JR, Bell JG (2007) Effects of dietary protein, and fat level and rapeseed oil on growth and tissue fatty acid composition and metabolism in Atlantic salmon (*Salmo salar* L.) reared at low water temperatures. Aquac Nutr 13(4):256–265
11. Stubhaug I, Lie O, Torstensen BE (2007) Fatty acid productive value and beta-oxidation capacity in Atlantic salmon (*Salmo salar* L.) fed on different lipid sources along the whole growth period. Aquac Nutr 13(2):145–155
12. Turchini GM, Francis DS (2009) Fatty acid metabolism (desaturation, elongation and beta-oxidation) in rainbow trout fed fish oil- or linseed oil-based diets. Br J Nutr 102(1):69–81
13. Turchini GM, Francis DS, Keast RSJ, Sinclair AJ (2011) Transforming salmonid aquaculture from a consumer to a

producer of long chain omega-3 fatty acids. Food Chem 124(2):609–614
14. Turchini GM, Torstensen BE, Ng WK (2009) Fish oil replacement in finfish nutrition. Rev Aquacult 1:10–57
15. Brown PB, Hart S (2010) Soybean oil and other n-6 polyunsaturated fatty acid-rich vegetable oils. In: Turchini GM, Ng WK, Tocher DR (eds) Fish oil replacement and alternative lipid sources in aquaculture feeds. CRC Press, Taylor & Francis group, Boca Raton, FL, pp 133–160
16. Tocher DR, Francis DS, Coupland K (2010) n-3 polyunsaturated fatty acid-rich vegetable oils and blends. In: Turchini GM, Ng WK, Tocher DR (eds) Fish oil replacement and alternative lipid sources in aquaculture feeds. CRC Press, Taylor & Francis group, Boca Raton, FL, pp 209–244
17. Yu TC, Sinnhuber RO (1979) Effect of dietary omega-3 and omega-6 fatty-acids on growth and feed conversion efficiency of coho salmon (*Oncorhynchus-Kisutch*). Aquaculture 16(1):31–38
18. Bautista MN, Delacruz MC (1988) Linoleic (omega-6) and linolenic (omega-3) acids in the diet of fingerling milkfish (Chanos–Chanos Forsskal). Aquaculture 71(4):347–358
19. Smith DM, Hunter BJ, Allan GL, Roberts DCK, Booth MA, Glencross BD (2004) Essential fatty acids in the diet of silver perch (*Bidyanus bidyanus*): effect of linolenic and linoleic acid on growth and survival. Aquaculture 236(1–4):377–390
20. Blanchard G, Makombu JG, Kestemont P (2008) Influence of different dietary 18:3n–3/18:2n–6 ratio on growth performance, fatty acid composition and hepatic ultrastructure in Eurasian perch, *Perca fluviatilis*. Aquaculture 284(1–4):144–150
21. Tan XY, Luo Z, Xie P, Liu XJ (2009) Effect of dietary linolenic acid/linoleic acid ratio on growth performance, hepatic fatty acid profiles and intermediary metabolism of juvenile yellow catfish *Pelteobagrus fulvidraco*. Aquaculture 296(1–2):96–101
22. Senadheera SD, Turchini GM, Thanuthong T, Francis DS (2011) Effects of dietary alpha-linolenic acid (18:3n–3)/linoleic acid (18:2n–6) ratio on fatty acid metabolism in Murray cod (*Maccullochella peelii peelii*). J Agric Food Chem 59(3):1020–1030
23. Senadheera SPSD, Turchini GM, Thanuthong T, Francis DS (2010) Effects of dietary a-linolenic acid (18:3n–3)/linoleic acid (18:2n–6) ratio on growth performance, fillet fatty acid profile and finishing efficiency in Murray cod. Aquaculture 309:222–230
24. Yu TC, Sinnhube RO (1972) Effect of dietary linolenic acid and docosahexaenoic acid on growth and fatty-acid composition of rainbow-trout (Salmo-Gairdneri). Lipids 7(7):450–454
25. Brown TD, Francis DS, Turchini GM (2010) Can dietary lipid source circadian alternation improve omega-3 deposition in rainbow trout? Aquaculture 300(1–4):148–155
26. Francis DS, Turchini GM, Jones PL, De Silva SS (2007) Effects of fish oil substitution with a mix blend vegetable oil on nutrient digestibility in Murray cod, *Maccullochella peelii peelii*. Aquaculture 269(1–4):447–455
27. Palmeri G, Turchini GM, De Silva SS (2007) Lipid characterisation and distribution in the fillet of the farmed Australian native fish, Murray cod (*Maccullochella peelii peelii*). Food Chem 102(3):796–807
28. Furukawa A, Tsukahara H (1966) On the acid digestion method for the determination of chromic oxide as an indicator substance in the study of digestibility in fish. Bull Jap Soc Sci Fish 32:502–506
29. Turchini GM, Francis DS, De Silva SS (2007) A whole body, in vivo, fatty acid balance method to quantify PUFA metabolism (desaturation, elongation and beta-oxidation). Lipids 42(11): 1065–1071
30. Turchini GM, Francis DS, De Silva SS (2008) A whole body, in vivo, fatty acid balance method to quantify PUFA metabolism (desaturation, elongation and beta-oxidation) (vol 42, pg 1065, 2007). Lipids 43(10):977–977
31. Bell JG, Koppe W (2010) Lipids in aquafeeds. In: Turchini GM, Ng WK, Tocher DR (eds) Fish oil replacement and alternative lipid sources in aquaculture feeds. CRC Press, Taylor & Francis group, Boca Raton, FL, pp 21–60
32. Drew MD, Ogunkoya AE, Janz DM, Van Kessel AG (2007) Dietary influence of replacing fish meal and oil with canola protein concentrate and vegetable oils on growth performance, fatty acid composition and organochlorine residues in rainbow trout (*Oncorhynchus mykiss*). Aquaculture 267(1–4):260–268
33. Simopoulos AP (1999) Essential fatty acids in health and chronic disease. Am J Clin Nutr 70(3):560s–569s
34. Turchini GM, Francis DS, de Silva SS (2006) Fatty acid metabolism in the freshwater fish Murray cod (*Maccullochella peelii peelii*) deduced by the whole-body fatty acid balance method. Comp Biochem Physiol B-Biochem Mol Biol 144(1):110–118
35. Buzzi M, Henderson RJ, Sargent JR (1996) The desaturation and elongation of linolenic acid and eicosapentaenoic acid by hepatocytes and liver microsomes from rainbow trout (*Oncorhynchus mykiss*) fed diets containing fish oil or olive oil. Biochimica Et Biophysica Acta—Lipids Lipid Metabol 1299(2):235–244
36. Buzzi M, Henderson RJ, Sargent JR (1997) Biosynthesis of docosahexaenoic acid in trout hepatocytes proceeds via 24-carbon intermediates. Comp Biochem Physiol B-Biochem Mol Biol 116(2):263–267
37. Brenner RR (1981) Nutritional and hormonal factors influencing desaturation of essential fatty acids. Prog Lipid Res 20:41–47
38. Hastings N, Agaba M, Tocher DR, Leaver MJ, Dick JR, Sargent JR, Teale AJ (2001) A vertebrate fatty acid desaturase with delta 5 and delta 6 activities. Proc Natl Acad Sci USA 98(25): 14304–14309
39. Tocher DR (2003) Metabolism and functions of lipids and fatty acids in teleost fish. Rev Fish Sci 11(2):107–184
40. Bell JG, Tocher DR, Farndale BM, Cox DI, McKinney RW, Sargent JR (1997) The effect of dietary lipid on polyunsaturated fatty acid metabolism in Atlantic salmon (*Salmo salar*) undergoing Parr-Smolt transformation. Lipids 32(5):515–525
41. Tocher DR, Bell JG, Dick JR, Sargent JR (1997) Fatty acyl desaturation in isolated hepatocytes from Atlantic salmon (*Salmo salar*): stimulation by dietary borage oil containing gamma-linolenic acid. Lipids 32(12):1237–1247
42. Francis DS, Peters DJ, Turchini GM (2009) Apparent in vivo delta-6 desaturase activity, efficiency, and affinity are affected by total dietary C-18 PUFA in the freshwater fish Murray cod. J Agric Food Chem 57(10):4381–4390
43. Tocher DR, Carr J, Sargent JR (1989) Poly-unsaturated fatty-acid metabolism in fish cells—differential metabolism of (N-3) and (N-6) series acids by cultured-cells originating from a fresh-water Teleost fish and from a marine Teleost fish. Comp Biochem-Physiol B-Biochem Mol Biol 94(2):367–374
44. Bell MV, Dick JR, Porter AEA (2001) Biosynthesis and tissue deposition of docosahexaenoic acid (22 : 6n–3) in rainbow trout (*Oncorhynchus mykiss*). Lipids 36(10):1153–1159
45. Valfre F, Caprino F, Turchini GM (2003) The health benefit of seafood. Vet Res Commun 27:507–512

prey. In spite of this common unique lifestyle and shared morphological features, like a rod shape and a single polar flagellum [3], BALO were found to be a phylogenetically heterogeneous group and, thus, the order *Bdellovibrionales*, to which all BALO belong so far, was split into the two families *Bdellovibrionaceae* and *Bacteriovoracaceae* based on 16S rRNA analyses [4].

The lifecycle of these predatory prokaryotes can be split into several stages, among which the initial interaction between predator and prey determines whether the predator penetrates into the prey or detaches itself. Since the first contact occurs between structures of the cell walls, machineries for attachment, prey recognition and penetration are supposed to be located in the cell wall of the predator. However, the predator–prey interaction mechanisms and therefore the important key structures are still largely unknown.

Beside the outer membrane proteins of BALO [5, 6], lipid structures have previously been analyzed in our group. We elucidated the structures of the lipid A of *B. bacteriovorus* and *B. stolpii*, two distinct BALO strains, and found an unusual structure of the lipid A of *B. bacteriovorus*, which is the first described lipid A structure missing charged residues [7]. *B. stolpii* is a facultative predatory strain that can be grown on prey bacteria but also on rich media. *B. stolpii* possesses a lipid A very different from the *B. bacteriovorus* lipid A, since it carries charged phosphate groups [8]. Very uncommon for prokaryotes, sphingolipids were found in the cell wall of *B. stolpii*, which were shown to be phosphonolipids [9–11]. The only other BALO which has been analyzed so far in respect to its phospholipids is *B. bacteriovorus* [12].

Bacterial cell wall lipids vary to a great extent between organisms, but also between different strains of the same organism. The main phospholipid classes of the model organisms *Escherichia coli* (Gram-negative) and *Bacillus subtilis* (Gram-positive) are phosphatidylethanolamines (PtdEth), phosphatidylglycerols (PtdGro) and cardiolipins (Ptd_2Gro), so these classes are generally believed to be the main membrane-forming lipid classes in all prokaryotes [13]. However, there are bacterial strains containing other phospholipids as major or minor constituents. In some cases, sphingolipids were observed, for the genera *Sphingobacterium* [14] and *Sphingomonas* [15] they are eponymous, but they have also been found in other genera. In the majority of cases, glycerophospholipid structures like phosphatidylcholines (PtdCho) [16], phosphatidylinositol (PtdIns) [17] or amino acid-containing phosphatidylglycerols (PtdGro) or cardiolipins (Ptd_2Gro) [18] are predominant.

In this work we studied the phospholipids of the three BALO strains *B. stolpii*, *B. bacteriovorus* HD100 and *P. starrii*.

Materials and Methods

Bacterial Growth and Lipid Extraction

B. stolpii (DSM 12778) was grown in peptone yeast extract medium at 30 °C for 3–5 days. Cells were harvested by centrifugation. For the obligate prey dependant strains *B. bacteriovorus* HD100 (DSM 50701) and *P. starrii* (DSM 17039), prey bacteria were grown to the stationary phase in liquid Luria-Bertani broth, centrifuged and resuspended in a buffer containing 3 mM ammonium acetate, 3 mM magnesium chloride and 3 mM calcium chloride at pH 7.5. This suspension was infected with the BALO strain. After 2–3 days at 25–27 °C the lysis of the prey bacteria was complete. The cultures were centrifuged at $2{,}000\times g$ for 15 min at 4 °C to minimize the contamination with residual prey bacteria and BALO cells were harvested at $10{,}000\times g$ for 30 min at 4 °C. *B. bacteriovorus* HD100 was grown on *Escherichia coli* K-12 (DSM 423) and *P. starrii* on *Pseudomonas putida* (DSM 50906).

Phospholipids were extracted with the methyl *tert*-butyl ether (MTBE) method described by Matyash et al. [19]. In short, in a glass flask, an aliquot of the cell pellet was resuspended in 0.5 ml of bidistilled water and 3.75 ml of methanol and 12.5 ml of MTBE were added. The mixture was incubated for 1 h at room temperature with shaking. 3.125 ml of bidistilled water were added to separate phases and the organic phase was collected. The water phase was reextracted by addition of 4 ml MTBE, 1.2 ml MeOH and 1 ml bidistilled water. The combined organic phases were evaporated to dryness under a gentle stream of nitrogen.

Analysis of Sphingophosphonolipids

Sphingophosphonolipids (SPNL) were separated from the glycerophospholipid (GPL) species by mild alkaline methanolysis [9] or by incubation of a total phospholipid extract with lipase D (personal communication, Sabine Schiller, Department of Biology, Humboldt-Universität zu Berlin). For the enzymatic assay, 0.3 mg of a total phospholipid extract were dissolved in 183.3 µl of ethyl acetate and 83.3 µl of an acetate buffer (0.2 M sodium acetate, 40 mM calcium chloride, pH 8.0) were added. The solution was heated to 37 °C and 2 µl of a 1 unit μl^{-1} solution of lipase D (Sigma-Aldrich; Steinheim) were added. This mixture was incubated for 2 h at 37 °C. For acetylation, 200 µl of acetic acid anhydride and 2.1 µl of a 5 mg ml^{-1} solution of 4-dimethylaminopyridine in pyridine were added to 420 µl of a solution of SPNL in dry pyridine (approx. 1 mg ml^{-1}). This solution was stirred for 1 h at 60 °C followed by incubation for 16 h at room temperature. The solvent was evaporated under a gentle stream of nitrogen.

The performance of this assay was tested on standard phospholipids (Avanti Polar Lipids, Alabaster).

HPLC–MS

HPLC separation was carried out with an Agilent 1200 system (Agilent, Waldbronn) and a BioBasic-4 column (150 mm × 1 mm i.d., particle size 5 µm, Thermo Scientific, Bremen). Both a LTQ-FT MS Classic equipped with a 6 T superconducting magnet and a LTQ-FT MS Ultra equipped with a 7 T superconducting magnet were used (both Thermo Scientific, Bremen) as detectors. The mass spectrometers were calibrated according to the manufacturer's recommendations and transfer optics were tuned with a lipid standard mixture containing phosphatidylserine (PtdSer; 16:0/18:1), phosphatidylglycerol (PtdGro; 16:0/18:1), phosphatidic acid (PtdOH; 16:0/18:1), phosphatidylethanolamine (PtdEth; 16:0/18:1), phosphatidylcholine (PtdCho; 16:0/18:1) and cardiolipin (Ptd_2Gro; 4×18:1) (Avanti Polar Lipids, Alabaster). The samples were dissolved in acetonitrile/methanol (1:1, by vol.) to a concentration of about 1 mg ml^{-1} and 1–8 µl were injected onto the column.

The HPLC-MS method employed was based on a method by Hein et al. [20]. Eluent A consisted of 95% water and 5% acetonitrile (by vol.), eluent B of 70% acetonitrile, 25% *iso*-propanol and 5% water (by vol.). Both eluents contained 10 mM triethylammonium acetate and 1 mM acetic acid. The gradient elution was started at 70% B and held there for 2 min, after which the % B was linearly increased to 80% in 46 min, then to 100% in 2 min. The % B was held at 100% for 23 min, before it was returned to initial conditions in 2 min, where it was held for 15 min. For more polar lipid classes, the initial conditions of the gradient were changed to 60% B. The separation was performed with a flow rate of 50 µl min^{-1} and the column was heated to 40 °C during separations. All solvents used were of HPLC gradient grade (Mallinckrodt Baker, Deventer). Lipid species were assigned according to their accurate masses in negative electrospray ionization mode and their corresponding fragmentation spectra. The accuracy in the survey scans (FT–MS) was below 2 ppm at all times and fragmentation experiments were carried out in the linear ion trap showing an accuracy of better than ±0.25 Da. All lipid species were detected in the deprotonated form $[M–H]^-$ apart from the PtdCho species, which were detected only as acetate adducts $[M+AcO]^-$. The assignment of the acyl residues to the positions *sn*-1/*sn*-2 was based on intensities of the corresponding fragment ions, as previously published [21].

The mass spectrometric data was processed and evaluated using the Profiler-Merger-Viewer software tool of Hein et al. [22]. Microsoft Excel was used to calculate the masses of the lipid species in the lipid library; PtdSer, PtdGro, PtdIns, PtdOH, PtdEth, mono- and dimethylphosphatidylethanolamines, PtdCho, Ptd_2Gro, sphingophosphonolipids (with AEP, HAEP and APP head group), phosphatidylthreonine, glutamylphosphatidylethanolamine, *N*-acylphosphatidylethanolamine and the corresponding lysoforms were taken into account. Fatty acid (FA) acyl chain lengths from 2–30 carbon atoms with up to 15 double bonds and three hydroxy groups were considered.

Thin-layer Chromatography

One dimensional thin-layer chromatography (1D-TLC) analyses of lipid extracts were carried out on Silica Gel 60 plates (Merck, Darmstadt). The plates were developed with a $CHCl_3$/MeOH/AcOH/H_2O 80:14:12:4 (by vol.) solvent system. Dried plates were stained with a solution of phosphomolybdic acid in ethanol (50 g l^{-1}) and heating. Plates were scanned and images were analyzed densitometrically (ProteomWeaver 2.1.0 software, Definiens AG, München). For re-extraction of the separated lipid classes, dried plates were stained with a solution of primulin in acetone/water 4:1 (by vol.) [23], lipids were re-extracted according to the MTBE protocol described above.

Compositional Analysis

Polar head groups were released by hydrolysis with hydrochloric acid [24]. Fatty acid methyl esters were prepared by dissolving phospholipids in 2 M hydrochloric acid in methanol and stirring for 16 h at 85 °C. Pyrrolidides and picolinyl esters of fatty acids were synthesized as described elsewhere [25, 26]. GC–EI/MS was performed on an electron impact ionization mass spectrometer (Hewlett Packard G1800A) with a fused silica capillary column (HP-5MS, 30 m, inner diameter 0.25 mm, film thickness 0.25 µm). Hydrogen was used as carrier gas at a flow rate of 1 l h^{-1}. Relative abundances were determined from the corresponding peak areas.

Results

Total phospholipid extracts of the organisms *B. stolpii*, *B. bacteriovorus* HD100 and *P. starrii* were separated according to their lipid classes using 1D-TLC (Fig. 1). The relative abundances of the different lipid classes as determined from densitometric analyses of TLC plates are given in Table 1. In all three strains phosphatidylethanolamine, phosphatidylglycerol, and cardiolipin were the most abundant lipid classes. The results for *B. stolpii* are consistent with the data published by Steiner et al. [10]. However, we could not confirm the high proportion of

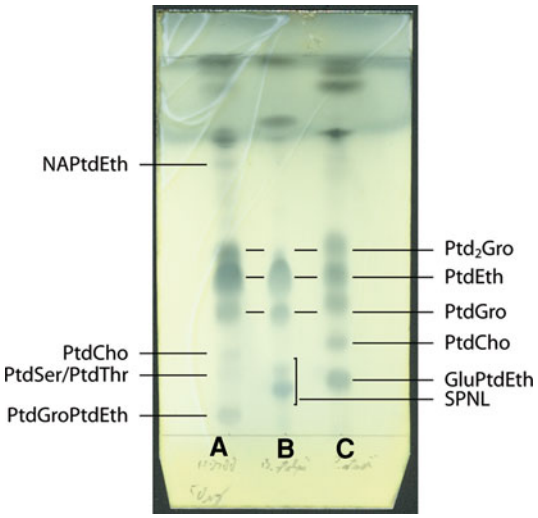

Fig. 1 1D-TLC of total phospholipid extracts of *A B. bacteriovorus* HD100, *B B. stolpii* and *C P. starrii*. The lipids were stained using phosphomolybdic acid. *PtdGroPtdEth* phosphatidylglycerophosphoethanolamine or a phosphatidyl-2(2-aminoethyl)-glycerophosphate, *PtdSer* phosphatidylserine, *PtdThr* phosphatidylthreonine, *PtdCho* phosphatidylcholine, *NAPtdEth* *N*-acylphosphatidylethanolamine, *SPNL* sphingophosphonolipid, *GluPtdEth* glutamylphosphatidylethanolamine, *PtdGro* phosphatidylglycerol, *PtdEth* phosphatidylethanolamine, *Ptd_2Gro* cardiolipin

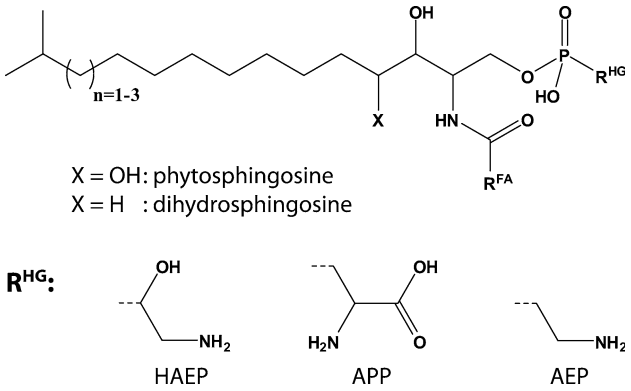

Fig. 2 Chemical structures of the sphingophosphonolipids of *B. stolpii*. *FA* fatty acid, *HG* head group, *HAEP* 1-hydroxy-2-aminoethylphosphonate, *APP* 2-amino-3-phosphonopropanate, *AEP* 2-aminoethylphosphonate

phosphatidylserine found in *B. bacteriovorus* HD100 by Nguyen et al. [12].

Since the SPNL previously found in *B. stolpii* were associated with the predatory life style [10, 11], the three BALO were tested for the presence of sphingolipids. Therefore, total phospholipid extracts were subjected to a mild alkaline methanolysis [9], which is able to cleave the ester linked acyl chains of glycerophospholipids, but not the amide linked acyl chains of sphingolipids. All sphingolipids found in *B. stolpii* proved to be phosphonolipids by incubation with lipase D as well as mass spectrometric characterization after acetylation. Phospholipase D hydrolyzes the phosphodiester bond on the side of the polar head group [27]. Phosphonolipids are not cleaved by phospholipase D since these possess a phosphorus-carbon bond instead of this phosphodiester bond. Like Jayasimhulu et al. [9], we found SPNL comprising phyto- and dihydrosphingosine structures. In addition to the two SPNL head groups 1-hydroxy-2-aminoethylphosphonate (HAEP) and 2-aminoethylphosphonate (AEP) described by Jayasimhulu et al., SPNL with a 2-amino-3-phosphonopropanate (APP) head group were also identified (Fig. 2, Table 2).

In *B. bacteriovorus* HD100 and *P. starrii* no sphingolipid species could be detected. Nevertheless, other unusual lipid structures were found in these two members of the BALO group. Nguyen et al. already reported phosphatidylserines in *B. bacteriovorus* HD100, as well as an additional lipid class for which the identification as *N*-acylphosphatidylethanolamines (NAPtdEth) was proposed [12]. Experimental proof for this assumption other than accurate masses was not provided. With high-resolution mass spectrometry in combination with additional fragmentation experiments, we were able to validate the previously proposed presence of NAPtdEth in *B. bacteriovorus* HD100. Figure 3 shows a typical fragmentation spectrum of a NAPtdEth species. Interestingly, all *N*-acyl chains found in NAPtdEth contained a cyclopropane ring, while mainly 9,10-methylene hexadecanoyl residues were observed.

Table 1 Relative abundances of the phospholipids in cell walls of *B. stolpii*, *B. bacteriovorus* HD100 and *P. starrii*

	% PtdEth	% PtdGro	% Ptd_2Gro	% PtdCho	% PtdSer/PtdThr	% PtdGroPtdEth	% SPNL	% NAPtdEth	% GluPtdEth
B. stolpii	48.3 ± 2.6	20.5 ± 0.9	5.7 ± 1.0				25.6 ± 2.7		
B. bacteriovorus	48.8 ± 1.2	16.6 ± 1.4	19.3 ± 1.5	2.5 ± 0.6	3.2 ± 0.6	4.2 ± 1.2		5.6 ± 1.1	
P. starrii	32.2 ± 2.1	20.2 ± 1.6	20.5 ± 1.2	9.3 ± 1.7					17.8 ± 0.9

Lipid classes were separated with 1D-TLC, stained using phosphomolybdic acid and analyzed densitometrically

PtdEth phosphatidylethanolamine, *PtdGro* phosphatidylglycerol, *Ptd_2Gro* cardiolipin, *PtdCho* phosphatidylcholine, *PtdSer* phosphatidylserine, *PtdThr* phosphatidylthreonine, *PtdGroPtdEth* phosphatidylglycerophosphoethanolamine or phosphatidyl-2(2-aminoethyl)-glycerophosphate, *SPNL* sphingophosphonolipid, *NAPtdEth* *N*-acylphosphatidylethanolamine, *GluPtdEth* glutamylphosphatidylethanolamine

Table 2 Identified sphingophospholipid species of *B. stolpii*

HG	FA	LCB					
		C_{15}		C_{16}		C_{17}	
		Phyto	Dihydro	Phyto	Dihydro	Phyto	Dihydro
	2-OH 13:0	✓	✓	✓	✓	✓	✓
HAEP	2-OH 14:0	✓	✓	✓	✓	✓	✓
	2-OH 15:0	✓	✓	✓	✓	✓	✓
	2-OH 13:0					✓	✓
AEP	2-OH 14:0	✓				✓	✓
	2-OH 15:0	✓		✓		✓	✓
	2-OH 13:0					✓	
APP	2-OH 14:0			✓		✓	
	2-OH 15:0	✓		✓		✓	✓

LCB long-chain base, *HG* head group, *FA* fatty acid, *HAEP* 1-hydroxy-2-aminoethylphosphonate, *AEP* 2-aminoethylphosphonate, *APP* 2-amino-3-phosphonopropanate, *phyto* phytosphingosine, *dihydro* dihydrosphingosine

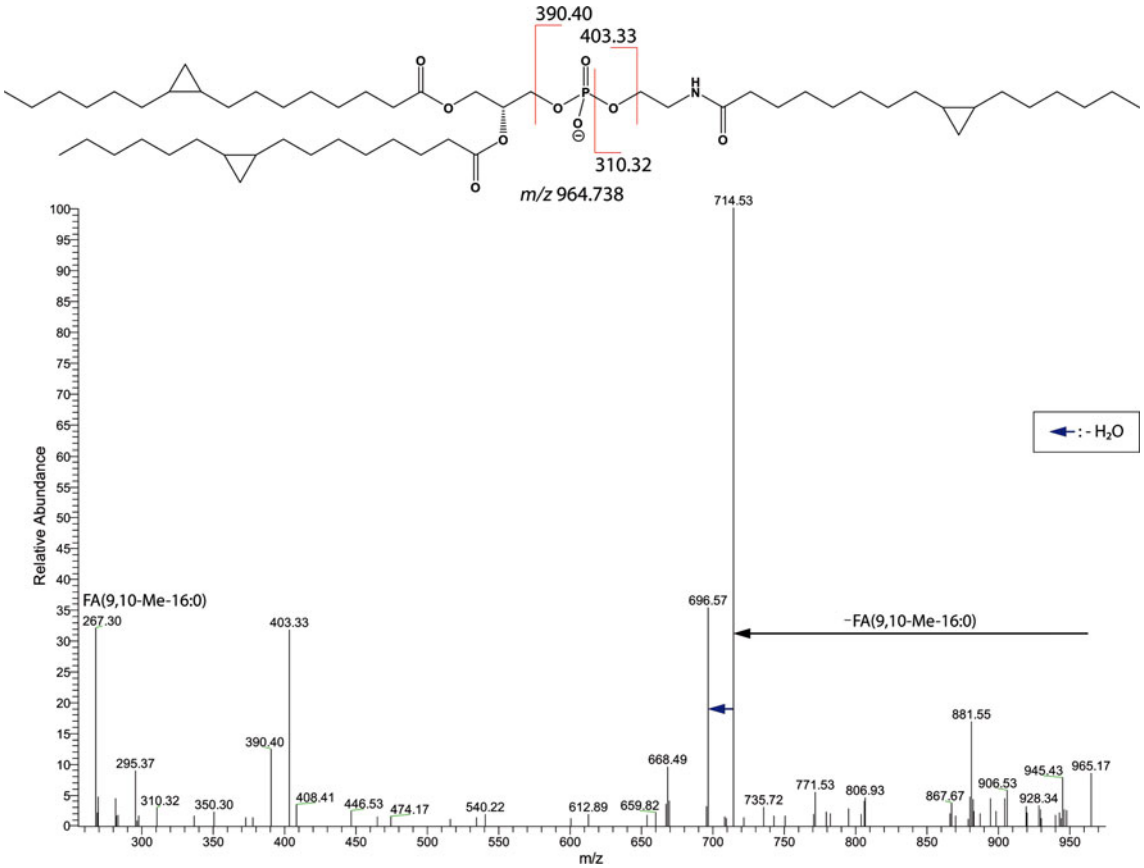

Fig. 3 MS/MS-Spectrum of a NAPtdEth species (*m/z* 964.738) of *B. bacteriovorus* HD100. *FA* fatty acid

Beside PtdSer phospholipids, another lipid class with a head group differing in the mass of one methylene group (CH_2, 14.015 Da) was detected in *B. bacteriovorus* HD100. After hydrolysis a hydrolysis product with a molecular mass of 119.06 Da ($C_4H_9NO_3$) was observed. This sum formula matches threonine, *N*-methylserine and serine methyl ester. The corresponding spectra of the first two were compared (Fig. 4). The third possible structure,

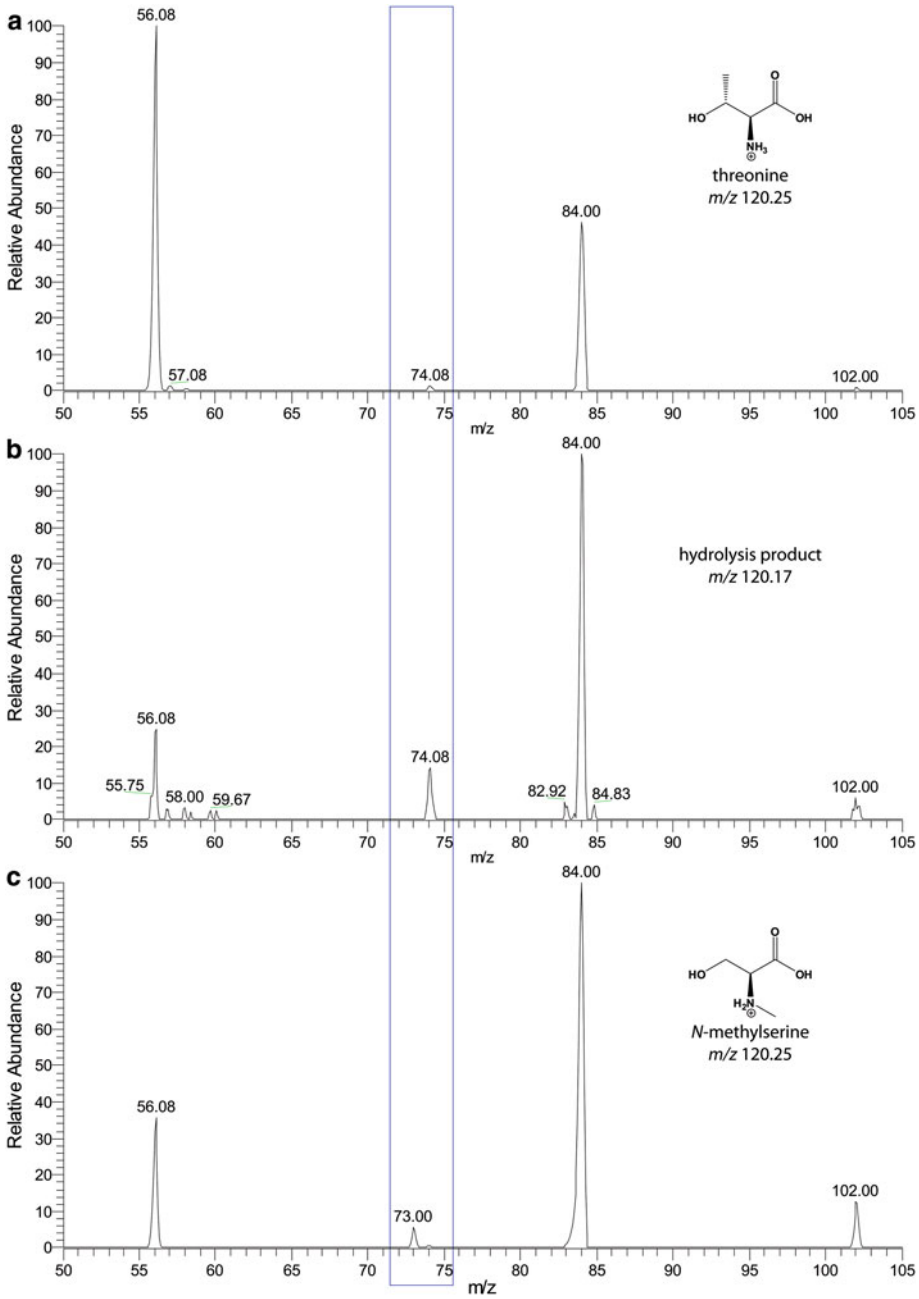

Fig. 4 Comparison of the MS/MS-spectra of **a** threonine, **b** the product with a molecular mass of 119.06 Da of the hydrolysis of the lipid species differing in the mass of one methylene group (CH_2, 14.015 Da) from phosphatidylserines and **c** *N*-methylserine in the positive ion mode

serine methyl ester, was ruled out due to the abundant neutral loss of two water molecules observed in the MS/MS-spectra of the hydrolysis product. By comparison of the fragmentation spectra, the hydrolysis product was identified as threonine and, thus, this new lipid class proved to be phosphatidylthreonines (PtdThr).

Another unknown ninhydrin-positive TLC-spot was apparent after separation of *B. bacteriovorus* HD100 total lipid extracts. In MS/MS-spectra of the reextracted lipids, signals corresponding to PtdGro and phosphatidic acid (PtdOH) could be detected (Fig. 5). Furthermore the loss of ethanolamine (C_2H_7NO, 61.05 Da) and vinylamine (C_2H_5N, 43.04 Da) were apparent. A similar FA distribution in these lipids compared to the PtdGro also supported a structure derived from PtdGro. These findings and the accurate masses of the parent ions strongly suggest PtdGro structures containing an ethanolamine and an additional phosphate residue in the polar head group. In this case either a phosphatidylglycerophosphoethanolamine or a phosphatidyl-2(2-aminoethyl)-glycerophosphate structure (Fig. 6) could be proposed. Additionally, PtdCho species were found in *B. bacteriovorus* HD100 and *P. starrii*.

From *P. starrii* total lipid extracts, TLC spots corresponding to PtdEth, PtdGro, Ptd_2Gro and PtdCho were detected. Furthermore, an additional unknown ninhydrin-positive TLC spot was detected. High resolution MS-spectra

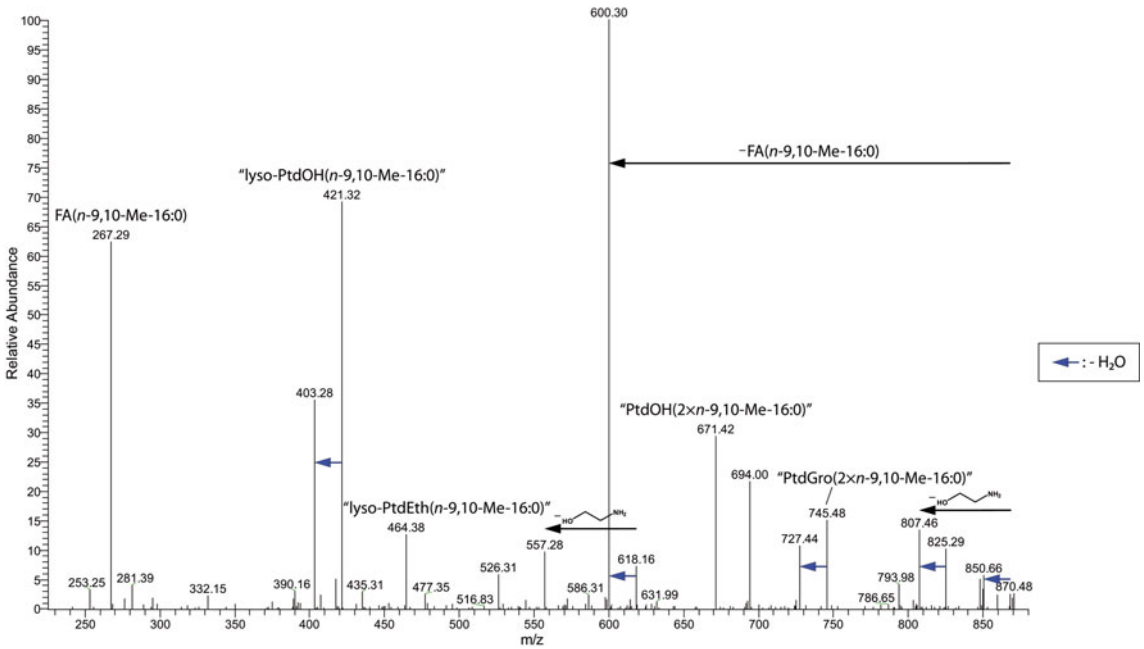

Fig. 5 MS/MS-Spectrum of a lipid species (*m/z* 868.511) of the polar lipid class of *B. bacteriovorus* HD100 for which the characterization as phosphatidylglycerophosphoethanolamines or phosphatidyl-2(2-aminoethyl)-glycerophosphates is proposed. *FA* fatty acid, *PtdOH* phosphatidic acid, *PtdEth* phosphatidylethanolamine, *PtdGro* phosphatidylglycerol

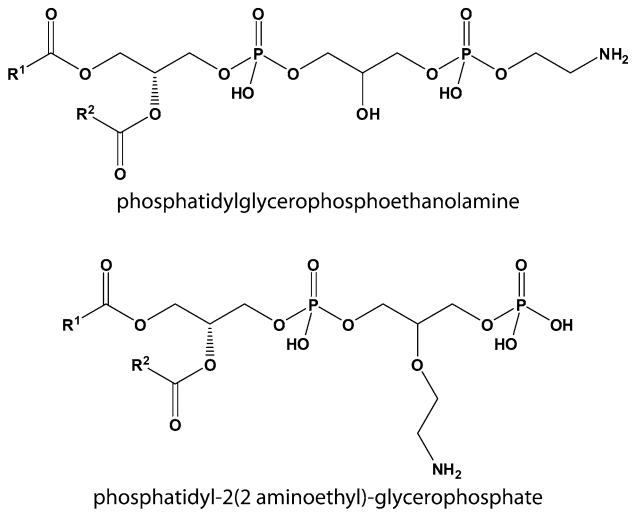

Fig. 6 Potential structures of the polar lipid class (PtdGroPtdEth) of *B. bacteriovorus* HD100. R^1, R^2: alkyl chains, *PtdGroPtdEth* phosphatidylglycerophosphoethanolamine or phosphatidyl-2(2-aminoethyl)-glycerophosphate

and fragmentation experiments performed with the extracted lipids from this TLC spot indicated PtdEth structures containing an *N*-glutamyl residue (Fig. 7). After hydrolysis of these lipids and comparison of the MS/MS-spectra of the hydrolysis product with the molecular mass of 147.05 Da ($C_5H_9NO_4$) with the corresponding fragmentation spectra of glutamic acid, the identification of this lipid class as glutamylphosphatidylethanolamines (GluPtdEth) was verified.

In addition to the mass spectrometric analyses of the TLC separation, we performed HPLC–MS analyses. The most abundant glycerophospholipid species of the identified lipid classes of the three BALO strains *B. stolpii*, *B. bacteriovorus* HD100 and *P. starrii* detected in these experiments are given in Table 3.

The FA compositions of total phospholipid extracts from the three BALO members were determined by GC–EI/MS (Table 4). The FA compositions of the SPNL and glycerophospholipid species of *B. stolpii* were analyzed separately. The FA were converted to methyl esters and analyzed as pyrrolidides after corresponding derivatization. Phospholipid extracts containing cyclopropane FA were analyzed as picolinyl derivates, as acid-catalyzed methanolysis leads to ring openings and formation of methoxy species [29].

C_{13}- up to C_{19}-FA were detected with this methodology, while mainly non hydroxylated fatty acids were detected. The only hydroxy FA present were 2-hydroxy FA in the SPNL of *B. stolpii*, while *B. bacteriovorus* HD100 and *P. starrii* did not show hydroxy FA at all. This is surprising as the lipid A of *B. bacteriovorus* HD100 also contains hydroxy FA as well as the lipid A of *B. stolpii* to a large extent [7, 8]. Hydroxy FA may be labile under some acidic conditions [28]. Nevertheless, we were able to detect hydroxy FA in GC–MS experiments from SPNL after TLC separation and acidic methanolysis. Furthermore, no indications for hydroxy FA were observed in HPLC–MS and MS/MS experiments, apart

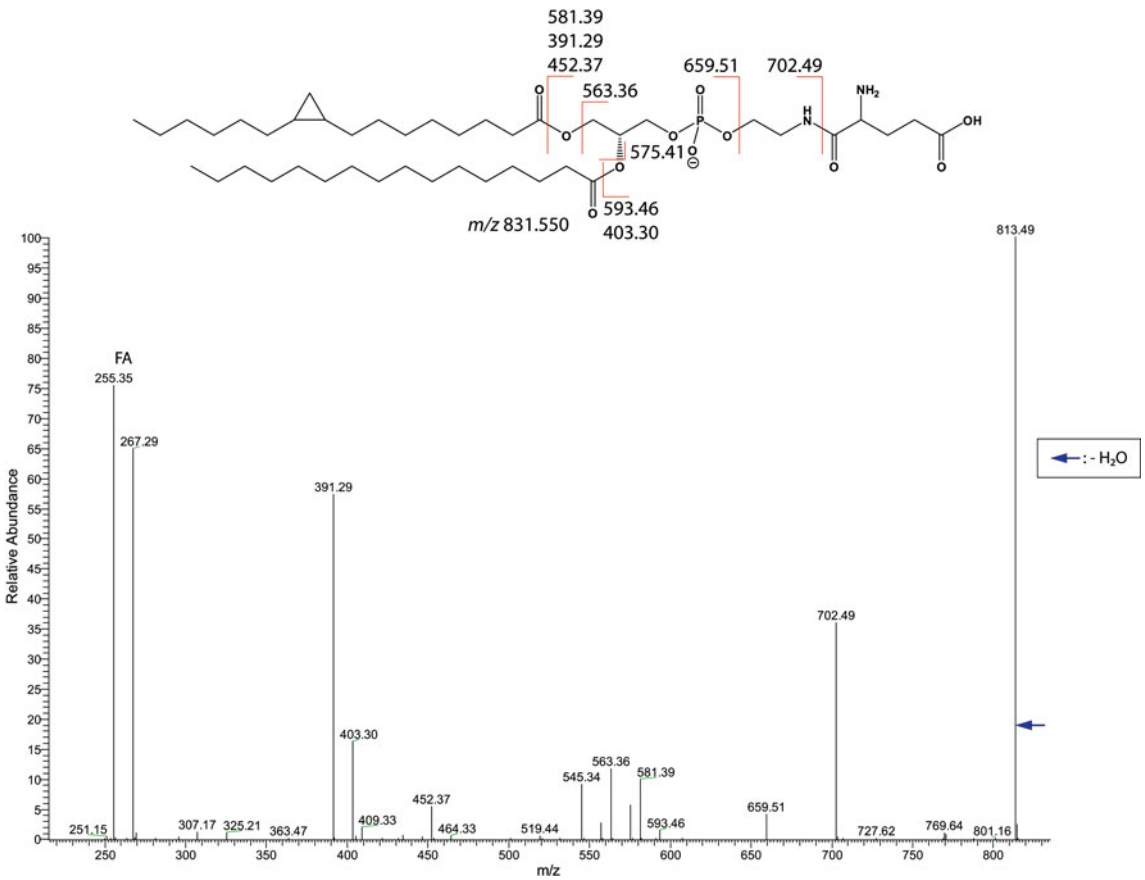

Fig. 7 MS/MS-Spectrum of a glutamylphosphatidylethanolamine species (*m/z* 831.550) of *P. starrii*. *FA* fatty acid

Table 3 Overview of the most abundant species of all identified glycerophospholipid classes from the HPLC-MS analyses containing the most prevalent fatty acid (FA) composition (*sn*-1/*sn*-2)

B. stolpii	PtdEth(15:1/15:0)	PtdGro(15:1/15:0)	Ptd_2Gro(15:0, 15:1; 15:0, 15:1)
	PtdEth(2×15:0)	PtdGro(2 × 115:0)	Ptd_2Gro(2 × 15:0; 15:0, 15:1)
	PtdEth(15:1/13:0)	PtdGro(13:0/15:1)	Ptd_2Gro(13:1, 15:0; 15:1, 15:0)
	PtdEth(15:1/14:0)	PtdGro(2 × 15:1)	$Ptd_2Gro(59:2)$[a]
	PtdEth(13:0/15:0)	PtdGro(14:1/15:0)	Ptd_2Gro(15:0, 15:1; 2 × 15:1)
	PtdEth(2 × 15:1)	PtdGro(13:0/15:0)	$Ptd_2Gro(59:3)$[a]
	PtdEth(14:1/15:1)	PtdGro(14:1/15:1)	
	PtdEth(14:0/15:0)	PtdGro(14:0/15/0)	
	PtdEth(14:1/13:0)	PtdGro(15:0/16:1)	
	PtdEth(13:1/15:1)	PtdGro(13:0/14:1)	
B. bacteriovorus	PtdEth(16:1/17:1)	PtdGro(16:1/17:1)	Ptd_2Gro(16:1, 17:1; 16:1, 17:1)
	PtdEth(15:0/17:1)	PtdGro(2 × 16:1)	Ptd_2Gro(2 × 16:1; 16:1, 17:1)
	PtdEth(16:1/15:0)	PtdGro(2 × 17:1)	Ptd_2Gro(16:0, 16:1; 16:1, 17:1)
	PtdEth(16:0/17:1)	PtdGro(15:1/16:1)	Ptd_2Gro(16:1, 17:1; 15:0, 16:1)
	PtdEth(2 × 15:0)	PtdGro(14:0/17:1)	Ptd_2Gro(16:0, 17:1; 16:1, 17:1)
	PtdEth(2 × 16:1)	PtdGro(15:0/17:1)	Ptd_2Gro(15:1, 17:1; 15:0, 16:1)
	PtdEth(15:1/15:0)	PtdGro(16:0/17:1)	Ptd_2Gro(16:1, 17:1; 16:1, 19:1)
	PtdEth(2 × 17:1)	PtdGro(18:1/17:1)	Ptd_2Gro(15:0, 19:1; 16:1, 17:1)
	PtdEth(17:0/17:1)	PtdGro(17:1/19:1)	Ptd_2Gro(15:0, 17:1; 15:0, 16:1)
	PtdEth(15:1/16:1)	PtdGro(16:0/19:1)	Ptd_2Gro(15:0, 17:1; 16:0, 16:1)

Table 3 continued

	PtdSer(17:1/16:1)	PtdThr(17:1/16:0)	PtdCho(2 × 19:1)
	PtdSer(15:0/19:1)	PtdThr(15:0/17:1)	PtdCho(16:0/19:1)
	PtdSer(15:0/17:1)	PtdThr(17:1/19/1)	PtdCho(18:0/19:1)
	PtdSer(2 × 16:1)	PtdThr(17:1/14:0)	PtdCho(18:0/18:1)
	PtdSer(17:1/16:0)	PtdThr(19:1/16:0)	PtdCho(2×18:1)
	PtdSer(15:0/16:1)	PtdThr(19:1/15:0)	PtdCho(18:1/19:1)
	PtdSer(2 × 17:1)	PtdThr(2 × 17:1)	PtdCho(16:1/18:1)
	PtdSer(18:0/18:1)	PtdThr(17:1/16:1)	PtdCho(2 × 16:1)
	PtdSer(14:0/16:1)	PtdThr(15:1/17:1)	PtdCho(16:0/18:1)
	PtdSer(16:1/19:1)	PtdThr(14:0/16:1)	PtdCho(18:1/17:1)
	NAPtdEth(17:1; 2 × 17:1)		
	NAPtdEth(17:1; 19:1/17:1)		
	NAPtdEth(17:1; 16:0/17:1)		
	NAPtdEth(17:1; 35:1[a])		
	NAPtdEth(17:1; 32:0[a])		
	NAPtdEth(17:1; 17:1/18:1)		
	NAPtdEth(17:1; 17:1/15:0)		
	NAPtdEth(17:1; 34:1[a])		
	NAPtdEth(19:1; 36:2[a])		
	NAPtdEth(17:1; 16:1/17:1)		
P. starrii	PtdEth(16:0/17:1)	PtdGro(16:0/17:1)	Ptd_2Gro(16:0, 17:1; 16:0, 17:1)
	PtdEth(13:0/18:1)	PtdGro(16:0/19:1)	Ptd_2Gro(16:0, 17:1; 17:1, 19:1)
	PtdEth(18:1/16:1)	PtdGro(17:1/19:1)	Ptd_2Gro(16:0, 17:1, 17:1, 18:0)
	PtdEth(19:1/17:1)	PtdGro(2×17:1)	Ptd_2Gro(16:0, 17:1; 17:0, 17:1)
	PtdEth(17:1/15:1)	PtdGro(18:1/17:1)	Ptd_2Gro(16:0, 17:1; 17:1, 18:1)
	PtdEth(13:0/17:1)	PtdGro(18:1/16:0)	Ptd_2Gro(17:1, 19:1; 15:0, 19:1)
	PtdEth(15:0/17:1)	PtdGro(2 × 19:1)	Ptd_2Gro(16:0, 17:1; 2 × 17:1)
	PtdEth(2 × 15:1)	PtdGro(16:0/16:1)	Ptd_2Gro(16:0, 19:1; 17:1, 19:1)
	PtdEth(16:0/19:1)	PtdGro(2 × 16:0)	Ptd_2Gro(2 × 17:1; 17:1, 19:1)
	PtdEth(16:0/18:1)	PtdGro(18:1/19:1)	Ptd_2Gro(2 × 19:1; 2 × 19:1)
	PtdCho(2 × 19:1)	GluPtdEth(17:1/16:0)	
	PtdCho(16:0/19:1)	GluPtdEth(17:1/18:1)	
	PtdCho(18:0/19:1)	GluPtdEth(16:1/16:0)	
	PtdCho(18:1/19:1)	GluPtdEth(16:0/18:1)	
	PtdCho(17:0/19:1)	GluPtdEth(17:1/19:1)	
	PtdCho(16:0/16:1)	GluPtdEth(2 × 17:1)	
	PtdCho(17:1/18:1)	GluPtdEth(16:0/19:1)	
	PtdCho(16:0/17:1)	GluPtdEth(13:0/17:1)	
	PtdCho(2 × 18:1)	GluPtdEth(14:1/15:0)	
	PtdCho(17:1/16:1)	GluPtdEth(14:0/16:0)	

The FA of the two phosphatidyl residues of the Ptd_2Gro species are separated by a semicolon, an assignment to the different *sn*-1 and *sn*-2 positions was not possible; for the NAPtdEth species, first the FA amidically bound to the polar head group, then the FA in positions *sn*-1/*sn*-2 are given

PtdEth phosphatidylethanolamine, *PtdGro* phosphatidylglycerol, *Ptd_2Gro* cardiolipin, *PtdSer* phosphatidylserine, *PtdThr* phosphatidylthreonine, *PtdCho* phosphatidylcholine, *NAPtdEth N*-acylphosphatidylethanolamine, *GluPtdEth* glutamylphosphatidylethanolamine

[a] The designation of the FA composition was not possible, instead the sum of carbon atoms and double bonds is given

from SPNL. These results confirm the absence of hydroxy FA in GPL of *B. bacteriovorus* HD100, *B. stolpii* and *P. starrii*.

All three strains showed *iso*-branched as well as unbranched FA, with a much higher proportion of *iso*-branched FA in *B. stolpii* (73.1%) than in *B. bacteriovorus*

Table 4 Relative abundances of the fatty acids in the phospholipids of BALO strains

B. stolpii	FA	*i*-13:0	*n*-7-13:1	*n*-13:0	*i*-14:0	*n*-7-14:1	*n*-14:0	*i*-7-15:1	*i*-15:0	*n*-7-15:1	*n*-15:0	2-OH *i*-15:0	*n*-16:0
	Total	4.8	1.0	1.2	1.2	3.0	1.7	12.2	51.0	16.3	3.5	3.8	0.3
	GPL	6.9	0.9	1.3	0.9	2.6	1.6	10.0	58.8	13.1	4.0	n. d.	n. d.
		2-OH	2-OH		2-OH	2-OH	2-OH	2-OH					
	FA	*i*-13:0	*n*-13:0	*i*-15:0	*i*-14:0	*n*-14:0	*i*-15:0	*n*-15:0					
	SPNL	14.6	3.2	4.3	1.9	3.2	67.9	4.8					
B. bacteriovorus	FA	*i*-13:0	*i*-14:0	*n*-14:0	*i*-15:0	*n*-9-15:1	*n*-15:0	*n*-9-16:1	*n*-16:0	*n*-9,10-Me-16:0	*n*-11-18:1	*n*-18:0	*n*-11,12-Me-18:0
	Total	0.2	0.4	2.1	11.5	2.4	3.7	16.4	17.3	36.8	2.9	0.1	6.1
					n-7,8-Me-				*n*-9,10-			*n*-11,12-	
P. starrii	FA	*i*-13:0	*n*-14:0	*i*-15:0	14:0	*n*-15:0	*n*-9-16:1	*n*-16:0	Me-16:0	*n*-11-18:1	*n*-18:0	Me-18:0	
	Total	1.1	1.2	0.6	0.8	0.2	3.3	39.3	40.5	5.9	0.8	6.1	

i iso, *n* unbranched, *FA* fatty acid, *GPL* glycerophospholipid, *SPNL* sphingophosphonolipid, *n.d.* not detected

HD100 (12.1%) and *P. starrii* (1.7%). In both of the latter organisms cyclopropane FA in proportions of 42.9% (*B. bacteriovorus* HD100) and 47.4% (*P. starrii*) were found.

Discussion

Besides the known SPNL with HAEP and AEP head groups, SPNL with an APP head group were identified in *B. stolpii* in this study. Lipid-bound APP intermediates were postulated for the biosynthesis of phosphonolipids with AEP head group in various organisms [30, 31], but could not be detected [32–34]. By identifying SPNL with APP and AEP head groups in *B. stolpii*, we were able to detect the proposed lipid-bound APP intermediate of the biosynthesis of the latter. In both of the other analyzed BALO strains, no sphingolipids could be detected. The correlation of the presence of SPNL with the predatory behavior has already been suggested for *B stolpii* [10], but it has been shown that SPNL are not crucial for the predatory behavior of *B. stolpii* [35]. In both *B. bacteriovorus* HD100 and *P. starrii* unusual and previously unidentified lipid structures were found. For the first time, glutamylphosphatidylethanolamines were identified in *P. starrii*. Interestingly, amino acid-containing PtdGro and Ptd_2Gro are known to be present in bacteria, primarily in Gram-positive strains [18], but amino acid-containing PtdEth have not been reported previously. Thus, the presence of glutamylphosphatidylethanolamines in *P. starrii* is unique.

Furthermore, we were able to determine the presence of NAPtdEth in *B. bacteriovorus* HD100, as proposed in another study [12]. In this context, the only amide bound fatty acids found in the NAPtdEth were cyclopropane FA. Additionally, phosphatidylthreonines and another lipid class, probably phosphatidylglycerophosphoethanolamine or phosphatidyl-2(2-aminoethyl)-glycerophosphate, were detected in *B. bacteriovorus* HD100. PtdThr is a rarely observed lipid class, usually found in eukaryotic organisms [24, 36–38]. Nevertheless, the presence of PtdThr lipids has recently been reported in *Clostridium novyi* NT, being the first prokaryotic organism containing PtdThr [39]. Furthermore, in both *B. bacteriovorus* HD100 and *P. starrii* significant amounts of PtdCho have been found.

The role of these under physiological conditions predominant anionic lipids has to be resolved in further studies, especially with regard to a possible involvement in processes relevant for the predatory life style of the BALO. The unusual lipid structures might compose the necessary environment to incorporate important outer membrane proteins (OMP) associated with processes of the predator–prey interaction, or the lipids might even be part of a signalling cascade regulating the OMP function.

From the current point of research, more BALO strains should be analyzed for their lipid composition in order to get a broader view of the presence of specific, partly very unique, lipids in predatory prokaryotes. Although the strains examined so far show distinct lipid structures, a broader view might give insights into the mechanisms of predation and prey recognition employed by predatory prokaryotes.

Acknowledgments The authors gratefully acknowledge financial support by the Deutsche Forschungsgemeinschaft Grant LI309/29-1.

References

1. Stolp H, Petzold H (1962) Untersuchungen über einen obligat parasitischen Mikroorganismus mit lytischer Aktivität für *Pseudomonas*-Bakterien. Phytopathol Z 45:364–390
2. Stolp H, Starr MP (1963) *Bdellovibrio bacteriovorus* gen. et sp. n., a predatory, ectoparasitic, and bacteriolytic microorganism. Antonie Van Leeuwenhoek J Microbiol Serol 29:217–248
3. Jurkevitch E, Davidov Y (2007) Phylogenetic diversity and evolution of predatory prokaryotes. In: Jurkevitch E (ed) Predatory prokaryotes: biology, ecology and evolution, Springer, Berlin, pp 11–56
4. Davidov Y, Jurkevitch E (2004) Diversity and evolution of *Bdellovibrio*-and-like organisms (BALOs), reclassification of *Bacteriovorax starrii* as *Peredibacter starrii* gen. nov., comb. nov., and description of the *Bacteriovorax-Peredibacter* clade as *Bacteriovoracaceae* fam. nov. Int J Syst Evol Microbiol 54:1439–1452
5. Beck S, Schwudke D, Appel B, Linscheid M, Strauch E (2005) Characterization of outer membrane protein fractions of *Bdellovibrionales*. Fems Microbiol Lett 243:211–217
6. Beck S, Schwudke D, Strauch E, Appel B, Linscheid M (2004) *Bdellovibrio bacteriovorus* strains produce a novel major outer membrane protein during predacious growth in the periplasm of prey bacteria. J Bacteriol 186:2766–2773
7. Schwudke D, Linscheid M, Strauch E, Appel B, Zähringer U, Moll H, Müller M, Brecker L, Gronow S, Lindner B (2003) The obligate predatory *Bdellovibrio bacteriovorus* possesses a neutral lipid A containing alpha-D-mannoses that replace phosphate residues—similarities and differences between the lipid As and the lipopolysaccharides of the wild type strain *B. bacteriovorus* HD100 and its host-independent derivative HI100. J Biol Chem 278:27502–27512
8. Müller FD, Beck S, Strauch E, Brecker L, Linscheid MW (2010) Chemical structure of *Bacteriovorax stolpii* lipid A. Lipids 45:189–198
9. Jayasimhulu K, Hunt SM, Kaneshiro ES, Watanabe Y, Giner JL (2007) Detection and identification of *Bacteriovorax stolpii* UKi2 sphingophosphonolipid molecular species. J Am Soc Mass Spectrom 18:394–403
10. Steiner S, Conti SF, Lester RL (1973) Occurrence of Phosphonosphingolipids in *Bdellovibrio bacteriovorus* Strain Uki2. J Bacteriol 116:1199–1211
11. Watanabe Y, Nakajima M, Hoshino T, Jayasimhulu K, Brooks EE, Kaneshiro ES (2001) A novel sphingophosphonolipid head group 1-hydroxy-2-aminoethyl phosphonate in *Bdellovibrio stolpii*. Lipids 36:513–519
12. Nguyen NAT, Sallans L, Kaneshiro ES (2008) The major glycerophospholipids of the predatory and parasitic bacterium *Bdellovibrio bacteriovorus* HID5. Lipids 43:1053–1063
13. Sohlenkamp C, López-Lara IM, Geiger O (2003) Biosynthesis of phosphatidylcholine in bacteria. Prog Lipid Res 42:115–162
14. Naka T, Fujiwara N, Yano I, Maeda S, Doe M, Minamino M, Ikeda N, Kato Y, Watabe K, Kumazawa Y, Tomiyasu I, Kobayashi K (2003) Structural analysis of sphingophospholipids derived from *Sphingobacterium spiritivorum*, the type species of genus *Sphingobacterium*. Biochim Biophys Acta Mol Cell Biol Lipids 1635:83–92
15. White DC, Sutton SD, Ringelberg DB (1996) The genus *Sphingomonas*: physiology and ecology. Curr Opin Biotechnol 7:301–306
16. Aktas M, Wessel M, Hacker S, Klüsener S, Gleichenhagen J, Narberhaus F (2010) Phosphatidylcholine biosynthesis and its significance in bacteria interacting with eukaryotic cells. Eur J Cell Biol 89:888–894
17. Brennan PJ, Lehane DP (1971) Phospholipids of *Corynebacteria*. Lipids 6:401–409
18. Geiger O, González-Silva N, López-Lara IM, Sohlenkamp C (2010) Amino acid-containing membrane lipids in bacteria. Prog Lipid Res 49:46–60
19. Matyash V, Liebisch G, Kurzchalia TV, Shevchenko A, Schwudke D (2008) Lipid extraction by methyl-*tert*-butyl ether for high-throughput lipidomics. J Lipid Res 49:1137–1146
20. Hein EM, Blank LM, Heyland J, Baumbach JI, Schmid A, Hayen H (2009) Glycerophospholipid profiling by high-performance liquid chromatography/mass spectrometry using exact mass measurements and multi-stage mass spectrometric fragmentation experiments in parallel. Rapid Commun Mass Spectrom 23: 1636–1646
21. Vernooij EAAM, Brouwers JFHM, Kettenes-van den Bosch JJ, Crommelin DJA (2002) RP-HPLC/ESI MS determination of acyl chain positions in phospholipids. J Sep Sci 25:285–289
22. Hein EM, Bödeker B, Nolte J, Hayen H (2010) Software tool for mining liquid chromatography/multi-stage mass spectrometry data for comprehensive glycerophospholipid profiling. Rapid Commun Mass Spectrom 24:2083–2092
23. White T, Bursten S, Federighi D, Lewis RA, Nudelman E (1998) High-resolution separation and quantification of neutral lipid and phospholipid species in mammalian cells and sera by multi-one-dimensional thin-layer chromatography. Anal Biochem 258:109–117
24. Mitoma J, Kasama T, Furuya S, Hirabayashi Y (1998) Occurrence of an unusual phospholipid, phosphatidyl-L-threonine, in cultured hippocampal neurons—exogenous L-serine is required for the synthesis of neuronal phosphatidyl-L-serine and sphingolipids. J Biol Chem 273:19363–19366
25. Andersson BA, Holman RT (1974) Pyrrolidides for mass-spectrometric determination of the position of the double bond in monounsaturated fatty acids. Lipids 9:185–190
26. Destaillats F, Angers P (2002) One-step methodology for the synthesis of FA picolinyl esters from intact lipids. J Am Oil Chem Soc 79:253–256
27. Martin SF, DeBlanc RL, Hergenrother PJ (2000) Determination of the substrate specificity of the phospholipase D from *Streptomyces chromofuscus* via an inorganic phosphate quantitation assay. Anal Biochem 278:106–110
28. Brondz I (2002) Development of fatty acid analysis by high-performance liquid chromatography, gas chromatography, and related techniques. Anal Chim Acta 465:1–37
29. Orgambide GG, Reusch RN, Dazzo FB (1993) Methoxylated fatty-acids reported in *Rhizobium* isolates arise from chemical alterations of common fatty-acids upon acid-catalyzed transesterification procedures. J Bacteriol 175:4922–4926
30. Matesic DF, Kaneshiro ES (1984) Incorporation of serine into *Paramecium* ethanolamine phospholipid and phosphonolipid head groups. Biochem J 222:229–233

31. Warren WA (1968) Biosynthesis of phosphonic acids in *Tetrahymena*. Biochim Biophys Acta 156:340–346
32. Horigane A, Horiguchi M, Matsumoto T (1979) Metabolism of 2-amino-3-phosphonopropionic acid in rats. Biochim Biophys Acta 572:385–394
33. Kaneshiro ES (1987) Lipids of *Paramecium*. J Lipid Res 28:1241–1258
34. Rosenberg H (1973) Phosphonolipids. In: Ansell GB, Hawthorne JN, Dawson RMC (eds) Form and function of phospholipids. Elsevier Scientific Publishing Company, Amsterdam, pp 333–344
35. Kaneshiro ES, Hunt SA, Watanabe Y (2008) *Bacteriovorax stolpii* proliferation and predation without sphingophosphonolipids. Biochem Biophys Res Commun 367:21–25
36. Heikinheimo L, Somerharju P (2002) Translocation of phosphatidylthreonine and -serine to mitochondria diminishes exponentially with increasing molecular hydrophobicity. Traffic 3:367–377
37. Ivanova PT, Milne SB, Brown HA (2010) Identification of atypical ether-linked glycerophospholipid species in macrophages by mass spectrometry. J Lipid Res 51:1581–1590
38. Markmalchoff D, Marinetti GV, Hare GD, Meisler A (1978) Characterization of phosphatidylthreonine in polyoma virus transformed fibroblasts. Biochemistry 17:2684–2688
39. Guan Z, Johnston NC, Aygun-Sunar S, Daldal F, Raetz CRH, Goldfine H (2011) Structural characterization of the polar lipids of *Clostridium novyi* NT. Further evidence for a novel anaerobic biosynthetic pathway to plasmalogens. Biochim Biophys Acta Mol Cell Biol Lipids 1811:186–193

Introduction

Phosphatidylcholine (PtdCho) is the major phospholipid (PL) constituent of eukaryotic cells. It is mainly biosynthesized through two pathways: the CDP-choline pathway and the *N*-methylation of phosphatidylethanolamine (PtdEtn) [1]. In mammals, this latter pathway is mainly expressed in the liver [2] where it contributes to the biosynthesis of ~30% of PtdCho [3, 4]. Similar hepatic expression of the PtdEtn *N*-methylation pathway was also demonstrated in euryhaline fish and crustaceans [5]. The physiological significance of the PtdEtn *N*-methylation pathway has long been a matter of debate [6–9], since *Pemt* –/– mice fed a normal diet are viable, fertile and display no obvious phenotype with regards to cognitive functions and behavior [10]. It was suggested that the PtdEtn *N*-methylation was an "accessory" pathway for PtdCho biosynthesis, and that it was conserved during evolution to provide PtdCho on demand when dietary intake of choline is insufficient [7]. Data obtained on *Pemt* –/– mice support that physiological function since the animal fed a choline-deprived diet quickly developed liver steatosis and died [9].

However, some observations suggest that the PtdEtn *N*-methylation pathways may have other physiological functions. Hence it was shown that mitogenic activation of lymphocytes induces an activation of PtdCho synthesis through PtdEtn *N*-methylation [11]. Similar activation of this metabolic pathway has been observed in different cell types including rat reticulocytes exposed to catecholamines [12]. The authors of these studies concluded that the activation of PtdEtn *N*-methylation pathway had a role in signal transduction by facilitating interactions between ß-adrenergic receptors and adenylate cyclase [12–14]. However, in a critical rehearsal of data, Vance and de Kruijff questioned the physiological relevance of PtdEtn *N*-methylation in signal transduction [15]. Other studies demonstrated that the PtdEtn *N*-methylation pathway may have a role in the acclimation of euryhaline species during thermal and salinity changes. Hence, it was shown that acclimation of euryhaline fish and crustaceans to elevated temperatures resulted in an activation of the PtdEtn *N*-methylation pathway in the liver and hepatopancreas of these animals [16–19]. Interestingly, the percentage of PtdCho synthesized in fish liver via the *N*-methylation of PtdEtn was more than doubled in fish adapted to 22 °C than to 12 °C [5]. Furthermore, changes in water salinity were shown to impact PtdCho synthesis in the liver of eels *Anguilla anguilla* with ~35 or ~65% of PtdCho made through PtdEtn *N*-methylation in respectively fresh water- or sea water acclimated animals [17]. We recently reported similar observations in two species of euryhaline crabs, *Carcinus maenas* and *Eriocheir sinensis* [20]. In that study, we demonstrated that acclimation to sea water activates the PtdEtn *N*-methylation pathway in the hepatopancreas and that the newly formed PtdCho is exchanged with the hemolymph of animals. We found that this activation of the PtdEtn *N*-methylation pathway plays an important role in the biosynthesis of betaine (an organic osmolyte derived from choline metabolism) which led us to the conclusion that one of the physiological functions of the PtdEtn *N*-methylation pathway is to provide organic osmolytes (such as betaine) when animals are facing salt stress. However, all these studies were performed in animal models that are considered as good osmoregulators. The euryhaline fish species that were used in these experiments are effectively able to keep their blood osmotic concentrations in a near constant range when salinity of the medium increases. The crustacean species used in the reported studies are also able to regulate their hemolymph osmotic concentration at low salinities and to osmoconform at higher salinity ranges [21]. However, some animals have different strategies to cope with salinity. It is the case of osmoconformers whose blood osmotic concentrations display a direct correlation with salt concentrations in their environment [21]. Some marine molluscs such as the mussel *Mytilus galloprovincialis* are typical osmoconformers. At high salinity, these species have to adjust their intracellular osmotic concentrations to avoid cellular shrinkage. To do so, osmoconformers essentially rely on the accumulation/synthesis of organic osmolytes in order to match their intracellular osmotic concentrations with blood. Interestingly, these animals are known to use betaine as a major organic osmolyte. Knowing the importance of the PtdEtn *N*-methylation pathway in the synthesis of this choline-derived osmolyte in crabs, we hypothesized that this pathway may be expressed in osmoconformers such as the mussel *M. galloprovincialis*. Unfortunately, to our knowledge there are no data on PtdEtn *N*-methylation activity in these animals.

Although the expression of lipids in various tissues of a number of bivalve species has been studied [22, 23], data on their metabolism remain fragmentary. Some information is available in different marine mollusc species on the transport of lipids in the hemolymph in which phospholipids represent 70–90% of total lipids [24–28] and on biosynthesis of fatty acids [29]. Experiments with [^{14}C]-labeled fatty acids suggested the existence of lipid transfer from the blood to various tissues in marine bivalves [27, 28]. However, until now few studies on phospholipids metabolism have been performed in marine molluscs. Using [1-^{3}H]-glycerol, Lubet et al. [30] showed that PtdEtn and PtdCho display the highest turnover rate among phospholipids in all tissues of *M. galloprovincialis*. However, this study did not address PtdEtn *N*-methylation activity in the marine mollusc. The goal of this study was thus to characterize the ability of *M. galloprovincialis* tissues to synthesize PtdCho through this metabolic pathway.

Materials and Methods

Materials

All solvents were of analytical grade and were purchased from SDS (Peypin, France) or Sigma-Aldrich (Saint Quentin Fallavier, France). Silica gel G60 thin layer chromatography (TLC) plates were from Merck (Darmstadt, Germany). Aminopropyl columns (LC–NH_2-500 mg) were from Supelco (Saint Quentin Fallavier, France). L-[3-^{3}H]-serine and [1-^{3}H]-ethanolamine (both with a specific activity of 30 Ci/mmol) were from Amersham, UK. [methyl^{3}H]-adenosylmethionine (specific activity of 80 Ci/mmol) was from American Radiolabeled Chemicals (Saint Louis, MO, USA). PtdEtn and phosphatidyldimethylethanolamine standard and other chemicals were from Sigma–Aldrich.

Animal Experiments

The mussels *M. galloprovincialis* were obtained from a rearing farm in the Bay of Lazaret near Toulon (South of France). Animals were collected in May, at the period of sexual maturity, just before spawning. Female mussels of the same IIIA sexual stage [31] and same age (15 months) were kept in 500 l tanks with running sea water (salinity 38‰) at 17 °C for 2 weeks prior to experimentation. Water was well aerated and filtered.

To test the effect of salinity on PtdEtn *N*-methyltransferase (*Pemt)* activity, animals were acclimated to diluted-sea water (salinity 19‰) for 6 days prior to the experiments.

Mussels were injected in the foot with 10 μCi of [1-^{3}H]-ethanolamine dissolved in sterile sea water. Hemolymph was collected after various incubation times (see results) in plastic centrifuge tubes (coated with complexon K3) by cutting the posterior adductor muscle. Hemocytes were separated from hemolymph by centrifugation at 1,500 g_{av} for 15 min at 10 °C. Animals were rapidly dissected to collect gills, digestive gland and mantle which were weighed before lipid extraction.

In Vitro Incubation of Mussel Tissues

Incubations were performed at 20 °C on 100–200 mg fragments of gills, the mantle or the digestive gland in sterilized sea water containing 10 μCi/ml of [1-^{3}H]-ethanolamine or L-[3-^{3}H] serine. Samples were incubated for 3 h, washed with sea water and lipids analyzed as described below.

In Vitro labeling of Hemocytes

Hemolymph was collected from animals as described above. Hemocytes were labeled for 90 min at 20 °C by addition of 2 μCi of [1-^{3}H]-ethanolamine/ml of hemolymph. At the end of incubation, hemocytes were separated from plasma by centrifugation (1,500 g_{av} – 15 min) and washed twice with non-radioactive plasma. The lipids from hemocytes were extracted and analyzed as described thereafter. Pulse-chase experiments were also performed with [1-^{3}H]-ethanolamine in order to determine the putative exchange of lipids from hemocyte to plasma. In order to do so, hemocytes were labeled with 10 μCi of [1-^{3}H]-ethanolamine/ml of plasma at 20 °C. After 60 min of labeling, hemocytes were separated from plasma by centrifugation and washed twice with non-radioactive plasma. Prelabeled hemocytes (t_{0hr}) were then incubated for 90 min in non-radioactive plasma. At that time, hemocytes were separated from plasma (that was kept for lipid analysis), washed twice with non-radioactive plasma and lipids extracted. Radiolabeling distributions within lipids of the cells and plasma were determined.

Lipid Analysis

Lipids were extracted according to the Folch method [32], and washed according to Chapelle et al. [33] with 0.25% KCl aqueous solution (mass/vol) and deionized water. The chloroform phase was evaporated to dryness with a rotative evaporator along with absolute ethanol to remove traces of water. The sample was further dried overnight in a desiccator. Lipids were weighed, dissolved in benzene/methanol (2:1, vol/vol) and kept at −30 °C until analysis.

Phospholipid determination was performed by measuring phosphate [34] after mineralization of the molecules with sulfuric acid/perchloric acid (2:1, vol/vol) containing 0.1% V_2O_4 (mass/vol) [35]. Individual phospholipids were separated by 2-D TLC according to Portoukalian et al. [36], and detected by the phospholipid specific spray of Dittmer and Lester [37]. Individual phospholipids were quantified as described above. Amino phospholipids and choline-containing phospholipids were revealed, respectively, by ninhydrin spray and the *cis*-aconite reagent of Vaskovky and Suppes [38]. Phosphonolipids[1] were detected according to the Stillway and Harmon procedure [39].

[1] Two spots of phosphonolipids were detected on TLC plates when lipids from *Mytilus galloprovincialis* were separated by the 2D-TLC procedure used herein. ESI–MS and MS/MS analysis showed that both compounds are ceramide aminoethylphosphonate. The full characterization of these two compounds (reported as phosphonolipid X and phosphonolipid Y in this manuscript) will be described elsewhere.

Radioactivity in total lipid extracts was determined on aliquots with a Packard Tricarb ß-spectrometer and Picofluor 30 as scintillation fluid (Packard, US). Water soluble radioactivity was determined on samples of the washing phases.

Labeled phospholipids resolved by 2-D TLC and revealed by Dittmer and Lester's reagent were counted by scraping the spots into scintillation vials in which 3 ml of deionized water/ethanol (1:1, vol/vol) and 8 ml Picofluor 30 were added.

The localization of radioactivity within PtdCho and PtdEtn was performed by acetolysis as described by Renkonen [40]. Briefly, the phospholipids were isolated on a 500 mg aminopropyl column by a modification of the method described by Pietsch and Lorenz [41]. Due to the presence of phosphonolipids, PtdCho and PtdEtn fractions were further chromatographed on TLC plates with chloroform/methanol/acetic acid/water (40:10:10:1, by vol) as the solvent system. PtdCho and PtdEtn spots were visualized with iodine and separately scraped into Teflon screw-capped tubes containing 2 ml of acetic acid/acetic anhydride (3:2, vol/vol). Acetolysis was performed for 5 h at 150 °C. After completion of the reaction the formed bases and diacylglycerol acetate derivatives were extracted with chloroform/methanol/water (8:4:3, by vol). Separation of the aqueous and chloroform phases was facilitated by centrifugation. Radioactivity in the polar moiety of phospholipids was determined by liquid scintillation on an aliquot of the aqueous phase. Radioactivity in the phospholipid hydrophobic moiety was determined after separation of diacylglycerol acetate by TLC with heptane/diisopropyl ether/acetic acid (60:30:3, by vol) as solvent system.

Analysis of fatty acids in PtdCho was performed as follows. PtdCho was isolated on a 500 mg aminopropyl-bonded silica gel column according to the method of Pietsch and Lorenz [41]. The fraction containing PtdCho was dried down under nitrogen and further separated by TLC using chloroform/methanol/acetic acid/water (40:10:10:1, by vol) as solvent system. PtdCho was detected with Dittmer and Lester reagent, scraped into Teflon screw-capped tube and transesterified as previously described [42]. The fatty acid methyl esters were analyzed by gas chromatography on a Chrompack CP 9000 apparatus equipped with a flame ionization detector and a 30 m Omegawax 250 glass capillary column. Nitrogen was used as the carrier gas. Fatty acid methyl esters were separated as previously described [43] and peak areas were calculated using the Maestro integration software from Chrompack.

PtdEtn *N*-Methyltransferase Assay

Pemt was assayed on the microsomal fraction according to the method described by Ridgway and Vance [44]. Briefly, homogenates of mussel tissues were prepared in 10 mM Tris–HCl (pH 7.2) containing 150 mM NaCl and 1 mM each of dithiothreitol, EDTA and phenylmethylsulfonyl fluoride. The tissues were homogenized in a Potter–Elvehjem apparatus. The microsomal fraction obtained by ultracentrifugation at 100,000 g_{av} was kept for *Pemt* assay. *Pemt* activity was performed in 125 mM Tris–HCl (pH 9.2) containing 5 mM dithiothreitol, 1 mM triton X-100, 200 µM [methyl-^{3}H]-AdoMet, 2 mM PtdEtn and 0.4 mM of phosphatidyldimethylethanolamine. The samples were incubated at 37 °C for 30 min. The assay was stopped by addition of 4 ml of chloroform—methanol (2:1, v/v). The lipids were washed as described above and PtdCho was separated from other phospholipids (including phosphatidylmonomethylethanolamine and phospshatidyldimethylethanolamine) by 2-D TLC [36]. Phospholipids were revealed with Dittmer and Lester reagent [37], and radioactivity within PtdCho determined by liquid scintillation. *Pemt* activity was determined on tissues isolated from individual mussels excepted for hemocytes for which activity was assayed on samples pooled from several individuals, due to the limited amount of tissue.

Statistical Analysis

Statistical analysis was performed with SAS software after ratios were transformed to their arcsine [45]. Statistical comparisons between means were performed using one and two-way ANOVA. If the test for normality (Kolmogorov–Smirnov) failed, a non-parametric Kruskal–Wallis one-way ANOVA on ranks was used.

Results

We first determined the phospholipid content in the major tissues of *M. galloprovincialis*. We found that total phospholipids represent 1.12 ± 0.08, 1.42 ± 0.13 and 1.99 ± 0.17% of fresh weight in the gills, the mantle, and the digestive gland, respectively. These data are similar to the one reported for *Mytilus edulis* [23, 46] and *M. galloprovincialis* [30]. Individual phospholipids composition is very similar to the one previously reported by Lubet et al. [30], and are thus not reported herein. PtdCho and PtdEtn were the main phospholipids and represented 70–80% of total phospholipids in the main tissues.

We then studied the in vivo incorporation of [1-^{3}H]-ethanolamine within the tissues and lipids of *M. galloprovincialis*. In all organs most of the radioactivity (between 92 and 95% of total radioactivity) was found in the water soluble and lipid fractions. The radioactivity measured in the chloroform/methanol extract insoluble fraction (mainly made of proteins) accounted for only

5–8% of the total radioactivity in the tissues. Figure 1 shows the kinetics and distributions of [1-^{3}H]-ethanolamine-derived labeling within the waters soluble and lipid fractions in hemolymph, the mantle, the digestive gland and gills during the 72 h following the radio-precursor injection. The highest concentrations of [1-^{3}H]-ethanolamine-derived radioactivity were found in the digestive gland followed by the mantle, the gills and hemolymph. In all tissues, a progressive decrease in labeling in the water soluble fraction was observed with a concomitant radioisotope accumulation in the lipid fraction. Again the digestive gland displayed the highest labeling of lipids. In this tissue, a strong and sustained increase in labeling of lipids was observed up to 72 h following [1-^{3}H]-ethanolamine administration. Similar observation was made in gills where lipid labeling was, within 24 h, increased ~ twofold at a level that remained stable till 72 h. In the hemolymph and the mantle, a maximal lipid labeling was observed 24 h following the administration of [1-^{3}H]-ethanolamine. The increase in labeling observed during the first 24 h was followed by a ~50% decrease of radioactivity level during the next 48 h, showing a different kinetic in these tissues when compared to the one in gills and the digestive gland.

We next examined the distribution of [1-^{3}H]-ethanolamine labeling within the lipids (see Table 1). The distribution of [1-^{3}H]-ethanolamine within the lipids remained relatively constant in each tissue throughout the 72 h of experiments, as shown by the small variation of percentages (Table 1). In all tissues, the radioactivity was mainly incorporated into PtdCho and PtdEtn that concentrated from ~79 to ~92% of the total lipid radioactivity. [1-^{3}H]-ethanolamine-derived labeling was observed in PtdCho in all tissues. Plasma displayed a particularly high proportion of labeled PtdCho (~21% of total lipid radioactivity) when compared to other tissues (from ~7 to ~10% of total lipid radioactivity). The percentage of radioactivity recovered within neutral lipids of plasma and hemocytes was also higher than in other tissues.

This labeling of PtdCho with [1-^{3}H]-ethanolamine suggests that PtdEtn *N*-methylation occurs in the tissues of the mussel *M. galloprovincialis*. However, this PtdCho labeling may also be explained by the putative incorporation of catabolic products of ethanolamine into the fatty acyl and/or glycerol moiety of the phospholipid. To test this possibility acetolysis of PtdEtn and PtdCho was performed and radioactivity within the acetyl-diacylglycerol or head group moieties of the molecules determined. Hence, 48 h after [1-^{3}H]-ethanolamine injection, 55 and 75% of labeling into PtdCho of the digestive gland and plasma were found in the choline moiety of the phospholipid (Fig. 2a). In PtdEtn, 80 and 70% of labeling were detected in the ethanolamine moiety of the molecule isolated from the digestive gland and the plasma respectively (Fig. 2b). These results show that the *N*-methylation pathway of PtdEtn to PtdCho takes place at a significant rate in *M. galloprovincialis.*

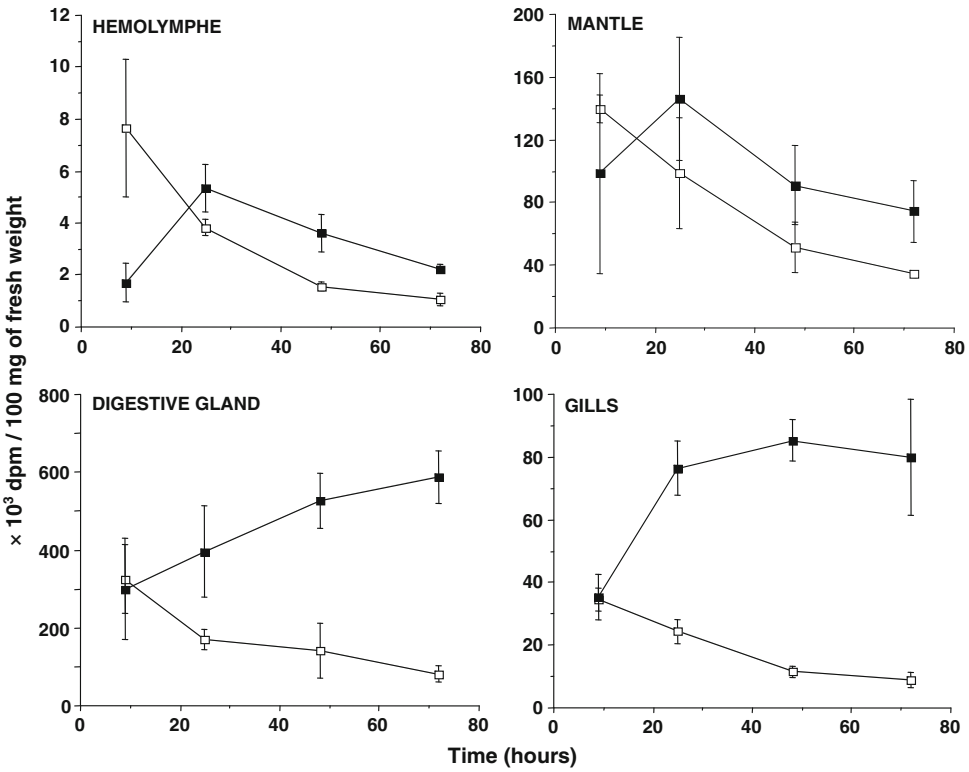

Fig. 1 Distribution of [1-^{3}H]-ethanolamine-derived radioactivity in the water soluble and lipid fractions from *M. galloprovincialis* tissues. Mussels were administered 10 μCi of [1-^{3}H]-ethanolamine as described in the methods section. The different tissues were collected at 9, 24, 48 and 72 h, weighted and lipids were extracted. Radioactivity was determined in the water soluble fraction (*empty squares*) and in the total lipid fraction (*full squares*). Results are averages ± SEM of 5 independent experiments

Table 1 In vivo distribution of [1-^{3}H]-ethanolamine in the lipids *of M. galloprovincialis*

	Mantle	Gills	Digestive gland	Plasma	Hemocytes
Phosphonolipids					
X	4.0 ± 0.8	3.2 ± 0.4	2.4 ± 0.5	2.7 ± 1.6	2.8 ± 1.3
Y	5.0 ± 1.3^{abc}	1.1 ± 0.1^{ad}	1.5 ± 0.3^{b}	1.6 ± 0.6^{c}	3.3 ± 0.9^{d}
Phospholipids					
LysoPtdCho	0.9 ± 0.3^{a}	1.1 ± 0.3^{b}	0.9 ± 0.1^{c}	3.8 ± 0.9^{abcd}	1.2 ± 0.4^{d}
PtdCho	6.7 ± 1.5^{a}	8.6 ± 2.0^{b}	10.1 ± 3.8^{c}	24.8 ± 4.1^{abcd}	9.3 ± 2.3^{d}
PtdEtn	72.0 ± 3.9^{abe}	83 ± 2.5^{acdf}	76.0 ± 2.8^{gh}	54.0 ± 3.8^{bch}	59.4 ± 5.7^{defg}
LysoPtdEtn	–	–	3.1 ± 0.4	–	–
Neutral lipids	3.7 ± 0.7^{abc}	1.2 ± 0.1^{adef}	3.7 ± 0.5^{dgh}	12.1 ± 1.7^{beg}	16.8 ± 4.1^{cfh}

Animals were injected with 10 μCi of [1-^{3}H]-ethanolamine as described in the methods section. After 9, 24, 48, and 72 h the tissues were collected and lipids extracted and purified. The lipids were separated by 2-D TLC and radioactivity determined by liquid scintillation. Results are expressed as the percentage of radioactivity within total lipids. As the distribution of the radioactivity remained the same during the 72 h period, the results are expressed as averages ± SEM (20 animals) between the 9, 24, 48, and 72 h labeling periods. Values with a common superscript show a statistical difference ($p < 0.01$) between tissues in the distribution of radioactivity within an individual lipid

We also determined the specific activity of total phospholipids, PtdEtn and PtdCho in the different tissues of *M. galloprovincialis*. The results (see Table 2) show that the highest specific activities in total phospholipids were observed in the digestive gland and plasma. This was also true for PtdCho that displayed in plasma and the digestive gland a specific activity that was ~5 and ~4.5 times higher than in gills and in the mantle. Interestingly, the specific activity of PtdCho in plasma was very similar to the one in the digestive gland (see Table 2), with a ratio of PtdCho specific activities of ~1.1 between plasma and the digestive gland. This strongly suggests that [1-^{3}H]-ethanolamine-derived PtdCho in plasma is synthesized in the digestive gland through PtdEtn *N*-methylation. This relationship is further illustrated in Fig. 2.

As shown in Fig. 2a, the variation of PtdCho specific radioactivity in hemolymph was correlated ($r = 0.47$, $p < 0.01$) to the one in the digestive gland. The PtdCho specific radioactivity ratios (PtdCho SA in plasma/PtdCho SA in the digestive gland) were effectively not statistically different of 1 after Asin transform (ratios were respectively, 0.87 ± 0.16, 1.42 ± 0.29, 1.20 ± 0.21 and 1.36 ± 0.13 at 9, 24, 48 and 72 h following the label injection). At the opposite, differences were observed in PtdEtn specific activities between plasma and the digestive gland 48 and 72 h following [1-^{3}H]-ethanolamine administration (Fig. 2b). The similar specific activity of [1-^{3}H]-ethanolamine-labeled PtdCho between plasma and the digestive gland strongly suggests that the digestive gland exchanges the newly formed PtdCho with plasma.

We next determined the fatty acid composition of PtdCho purified from the different tissues. The results show that, in all tissues, palmitic (16:0), stearic (18:0), arachidonic (20:4n-6) eicosapentaenoic (20:5n-3) and docosahexaenoic acids (22:6n-3) are the major fatty acids in this phospholipid (see Table 3). These fatty acids accounted for ~76 to ~80% of all fatty acids in PtdCho. The percentage of palmitic and stearic acids was ~1.8-fold higher in plasma and the digestive gland when compared to the mantle and gills. At the opposite, the percentage of docosahexaenoic acid was 2.1-fold lower in plasma and the digestive gland when compared to other tissues. The major observation was that fatty acid composition of PtdCho from plasma is similar to the one of PtdCho isolated from the digestive gland. There was a significant positive correlation between plasma and the digestive gland for 22:6n-3 ($r = 0.53$, $p < 0.001$) the sum of the n-3 PUFA ($r = 0.45$, $p < 0.005$) and n-6/n-3 PUFA ratio ($r = 0.47$, $p < 0.002$).

We then tested the ability of the different tissues to synthesize PtdCho through the PtdEtn *N*-methylation pathway In vitro. In the mantle, gills and the digestive gland, most of [1-^{3}H]-ethanolamine labeling of lipids was recovered into PtdEtn. This phospholipid concentrated from ~87 to ~91% of total lipid radioactivity in these tissues (see Table 4). In the digestive gland, a small but significant part of labeling was observed into PtdCho. Acetolysis of PtdCho purified from the digestive gland showed that ~70% of [1-^{3}H]-ethanolamine-derived labeling was recovered in the choline moiety of the molecule. This was not the case in the mantle and gills where most of PtdCho labeling was detected in the diacylglycerol moiety of the phospholipid. These in vitro observations show that the digestive gland is the place of an active PtdCho synthesis through the PtdEtn *N*-methylation pathway. We also studied the in vitro incorporation of [1-^{3}H]-ethanolamine within the lipids of hemocytes. Surprisingly, the distribution of the precursor in the lipids of these cells was very different when compared to other tissues (see Table 4). Most of the radioactivity (~60%) was found in the neutral

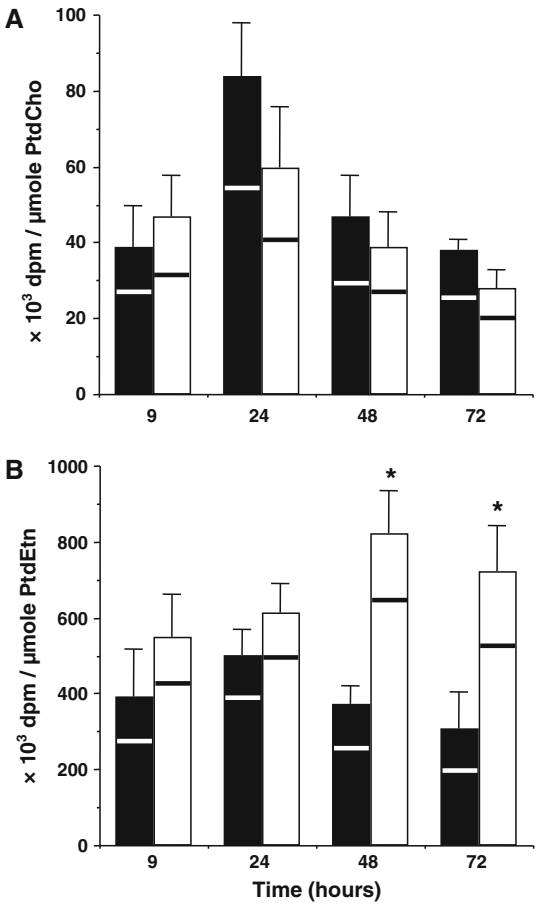

Fig. 2 PtdCho and PtdEtn specific radioactivities in the plasma and the digestive gland of mussels were administered 10 µCi of [1-^{3}H]-ethanolamine as described in methods. Digestive gland and hemolymph were collected at different times after the radio-precursor administration. Plasma was prepared by centrifugation of hemolymph. Lipids were extracted from tissues and phospholipids separated by 2-D TLC. PtdCho and PtdEtn were quantified and radioactivity determined. Panels **A** and **B** respectively, show the specific radioactivities of PtdCho and PtdEtn. Results are averages ± SEM of 5 different experiments and specific radioactivities are expressed as $\times 10^3$ dpm/µmol of PtdCho or PtdEtn. *White* and *black bars* respectively, represent the specific activities in the digestive gland and plasma. The horizontal *black* and *white lines* within the *white* and *black bars*, respectively, represent the extent of labeling recovered within polar head groups (area under the *black* and *white lines*) based on acetolysis of the molecules. *Asterisks* indicate statistical differences between the digestive gland and plasma ($p < 0.01$)

lipid fraction. PtdCho was the phospholipid displaying the highest [1-^{3}H]-ethanolamine-derived labeling along with PtdEtn and the phosphonolipid X. Acetolysis of PtdEtn and PtdCho from hemocytes showed that more than 70% of radioactivity was incorporated into ethanolamine and choline, respectively. These observations demonstrate that, like the digestive gland, hemocytes express an active PtdEtn *N*-methylation pathway. We also found that total phospholipid concentrations are ~5 times higher in hemocytes than in plasma (respectively, 103 ± 69 µg and 17.8 ± 7.8 µg/100 mg of the fresh weight; $n = 5$). Despite this difference we observed that the individual phospholipid composition of hemocytes is similar to the one of plasma except the absence of Diphosphatidylglycerol (Ptd_2Gro) in the latter and that the percentage of Lysophosphatidylcholine (LysoPtdCho) was approximately doubled in plasma compared to cells (see Table 5). We thus performed pulse-chase experiments with [1-^{3}H]-ethanolamine in order to address the occurrence of putative exchange of lipids from hemocytes to plasma. After 60 min of incubation a strong labeling was observed in hemocytes with lipids representing ~1.1% of the total label incorporation (see Table 5). After 90 min of chase in non-radioactive plasma, a transfer of lipids from the cells to the plasma was observed as illustrated by the appearance of radioactivity in the plasma lipid fraction. Interestingly the distribution of [1-^{3}H]-ethanolamine-derived radioactivity within plasmatic lipids was similar with the one in hemocytes at the exception of Phosphatidylinositol (PtdIns) and the phosphonolipid Y that were poorly or not exchanged with plasma (see Table 5). The data also show that the PtdCho synthesized in hemocytes via the PtdEtn *N*-methylation pathway is partly exchanged with plasma inasmuch [1-^{3}H]-ethanolamine-labeled PtdCho was measured in this tissue.

We also performed in vitro labeling experiments with L-[3-^{3}H] serine on the two tissues (digestive gland and hemocytes) in which we observed an active PtdCho synthesis via the PtdEtn *N*-methylation pathway. L-[3-^{3}H] serine was chosen as radio-precursor since it labels a pool of PtdEtn after decarboxylation of Phosphatidylserine (PtdSer). The results in Fig. 3 show that in both tissues an important fraction of L-[3-^{3}H] serine-derived labeling was recovered into PtdCho. Positional analysis of labeling into PtdCho purified from both tissues showed that ~80% of the radioactivity was in the choline moiety of the molecule (Fig. 3). These data show that PtdCho synthesis occurred through the PtdEtn *N*-methylation pathway, confirming the data obtained in vivo and in vitro with [1-^{3}H]-ethanolamine. Figure 3 also demonstrates that in hemocytes most of L-[3-^{3}H] serine labeling was observed into PtdEtn (~73% of total phospholipids labeling), suggesting an active PtdSer decarboxylation in this tissue, at least under our experimental conditions. The phosphonolipids X and Y concentrated also a significant part of L-[3-^{3}H]-serine labeling with respectively ~8 and ~11% of total phospholipids radioactivity in hemocytes and the digestive gland.

We finally determined *Pemt* activity within the tissues of *M. galloprovincialis* acclimated either to sea water or diluted-sea water. Our first attempts on crude tissue homogenates without exogenously supplied PtdEtn and phosphatidyldimethylethanolamine were unsuccessful as

Table 2 Main phospholipids specific radioactivities in the tissues of *M. galloprovincialis*

	Total phospholipids	PtdCho	PtdEtn
Plasma	110.9 ± 15.8	56.4 ± 15	368.6 ± 37.9
Gills	45.6 ± 5.3	11.7 ± 3.1	100.3 ± 11.5
Mantle	63.7 ± 14.9	9.4 ± 3	112.1 ± 11.5
Digestive gland	188.1 ± 25.1	48.8 ± 11.3	655.1 ± 94

Animals were injected with 10 μCi of [1-^{3}H]-ethanolamine as described in the methods section. After 9, 24, 48, and 72 h the lipids were extracted and purified from the different tissues. The phospholipids were separated by 2-D TLC and radioactivity determined by liquid scintillation. Quantification of total lipids, PtdCho and PtdEtn were also performed by phosphate determination as described in the methods section. Specific radioactivity is expressed in $\times 10^3$ dpm/μmol of lipid phosphorus. The values are the means ± SEM (20 animals) of the different determinations undertaken during the 72 h experimental period

Table 3 Fatty acid composition of PtdCho in the tissues of *M. galloprovincialis*

Fatty acid	Plasma	Digestive gland	Mantle	Gills
16:0	33.0 ± 2.4	36.7 ± 3.2	21.5 ± 5.5	18.3 ± 1.4
16:1n-9	1.6 ± 0.6	3.7 ± 0.3	2.4 ± 0.2	1.8 ± 0.2
16:1n-7	0.5 ± 0.2	1.1 ± 0.2	0.5 ± 0.1	0.8 ± 0.3
18:0	15.1 ± 1.6	10.0 ± 0.9	6.1 ± 2.3	6.7 ± 0.1
18:1n-9	2.2 ± 0.5	1.4 ± 0.6	2.1 ± 0.3	1.4 ± 0.1
18:1n-7	2.8 ± 0.8	4.2 ± 0.9	3.6 ± 0.8	2.2 ± 0.2
18:2n-6	1.8 ± 0.5	2.0 ± 0.2	2.1 ± 0.3	1.5 ± 0.5
18:3n-3	1.1 ± 0.4	1.2 ± 0.1	1.2 ± 0.2	0.9 ± 0.1
18:4n-3	1.4 ± 0.5	0.7 ± 0.5	0.5 ± 0.3	0.4 ± 0.1
20:1n-9	2.8 ± 0.6	3.4 ± 0.1	3.2 ± 0.9	2.7 ± 0.1
20:2n-6	0.8 ± 0.4	1.2 ± 0.1	1.3 ± 0.2	1.6 ± 0.6
20:4n-6	6.1 ± 1.2	5.7 ± 0.8	5.9 ± 0.5	10.1 ± 0.7
20:4n-3	0.4 ± 0.2	0.7 ± 0.3	1.0 ± 0.7	N.D
20:5n-3	10.4 ± 0.3	11.8 ± 1.7	19.2 ± 2.3	13.8 ± 0.4
22:5n-3	1.7 ± 0.5	2.1 ± 0.3	2.1 ± 0.2	2.7 ± 0.1
22:6n-3	12.2 ± 0.3	14.0 ± 1.9	23.6 ± 2.8	31.2 ± 1.9

Lipids were extracted and purified from mussel tissues. PtdCho was purified by solid phase extraction on an aminopropyl column and TLC. The phospholipid was transesterified and methyl fatty acids were analyzed by gas chromatography as described in the methods section. The results are expressed as percent of total fatty acids and are average ± SEM of six independent experiments

N.D Not detected

the activity was very low (~0.3–0.4 nmol of methyl group transferred/min/mg of protein in the digestive gland). The activity at 37 °C was much higher than at room temperature (i.e., close to the acclimation temperature of animals) and therefore this temperature was used. We thus determined *Pemt* activity on tissue microsomal fraction according to the procedure described by Ridgway and Vance [44]. Figure 4 shows that the highest *Pemt* activities were recovered within the digestive gland and hemocytes. *Pemt* activities determined within the mantle and gills were respectively ~11 and ~17 lower when compared to the digestive gland from sea water acclimated animals (Fig. 4). We also determined *Pemt* activity on tissues isolated from animals acclimated to diluted-sea water. In these conditions, *Pemt* activities were reduced by respectively, ~36, ~45 and ~55% in gills, hemocytes and the digestive gland when compared to sea water acclimated animals. A ~20% but non-significant decrease ($p = 0.16$) in *Pemt* activity was measured in the mantle of diluted-sea water animals.

Discussion

The major observation of this study is that the mussel *M. galloprovincialis* can synthesize PtdCho through the PtdEtn *N*-methylation pathway in at least two tissues, the digestive gland and the hemocytes. The occurrence of PtdEtn *N*-methylation activity in *M. galloprovincialis* may not be surprising if we consider the fact that biosynthesis of PtdCho by *N*-methylation of PtdEtn is widely expressed throughout evolution, from PtdCho biosynthesizing bacteria to mammals, although enzyme sequences differ substantially between prokaryotes and eukaryotes [1, 47]. In higher vertebrates such as mammals, the PtdEtn *N*-methylation pathway is mainly expressed in the liver [2, 4] with discrete activity in some other tissues such as kidney and cell types such as leucocytes and reticulocytes [11, 48, 49]. We previously showed that the liver/hepatopancreas is also the main site of the PtdEtn *N*-methylation pathway in euryhaline fish and crustaceans [5, 17, 20]. However, there

Table 4 Distribution of [1-^{3}H]-ethanolamine in lipids after in vitro incubation of *M. galloprovincialis* tissues

	Mantle	Gills	Digestive gland	Hemocytes
Phosphonolipids				
X	2.6 ± 0.3	3.3 ± 0.6	2.2 ± 0.4	8.1 ± 0.6
Y	0.3 ± 0.1	0.3 ± 0.1	0.2 ± 0.1	1.9 ± 0.3
Phospholipids				
LysoPtdCho	0.3 ± 0.1	0.1 ± 0.1	0.1 ± 0.1	–
PtdCho	0.5 ± 0.1	0.3 ± 0.1	2.8 ± 0.2*	10.7 ± 1.1*
PtdSer	0.4 ± 0.1	0.4 ± 0.1	0.6 ± 0.2	5.0 ± 0.4
PtdIns	0.6 ± 0.2	0.9 ± 0.2	1.3 ± 0.6	5.7 ± 1.5
PtdEtn	90.7 ± 1.8	90.4 ± 1.1	87.4 ± 1.1	8.5 ± 0.2
Neutral lipids	4.6 ± 0.5	3.2 ± 0.6	3.0 ± 0.8	59.9 ± 1.2

Tissues were incubated in vitro for 3 h at 20 °C with [1-^{3}H]-ethanolamine as described in the methods section. Lipids were extracted, separated by 2-D TLC and analyzed. [1-^{3}H]-ethanolamine-derived radioactivity is expressed as percentage of the total radioactivity recovered on the TLC plate. Acetolysis was also performed on PtdCho as described in the methods section. Asterisks indicate the samples where more than 70% of [1-^{3}H]-ethanolamine-derived radioactivity was recovered within the choline moiety. Results are average ± SD of 3 independent experiments

Table 5 Phospholipid composition of plasma and hemocytes and exchange of [1-^{3}H]-ethanolamine-labeled lipids from hemocytes to plasma in vitro

		Hemocytes	Plasma
Total radioactivity in tissue ($\times 10^3$ dpm)	T_{0hr}	2,521 ± 218	–
	T_{1hr30}	544 ± 28	1,737 ± 138
Radioactivity in total lipids ($\times 10^3$ dpm)	T_{0hr}	29.2 ± 6.8	–
	T_{1hr30}	25.1 ± 3.7	6.1 ± 1.3

Phospholipid composition (% of total lipid phosphorus)			[1-^{3}H]-ethanolamine distribution (% of total dpm)		
	Hemocytes	Plasma		Hemocytes	Plasma
Phosphonolipids			Phosphonolipids		
X	13.4 ± 4.5	10.9 ± 4.7	X	9.2 ± 0.6	7.1 ± 1.0
Y	1.9 ± 0.8	0.7 ± 0.5	Y	2.3 ± 0.2	–
Phospholipids			Phospholipids		
LysoPtdCho	4.1 ± 2.3	11.9 ± 3.7	LysoPtdCho	–	–
PtdCho	34.9 ± 6.9	41.4 ± 6.9	PtdCho	9.6 ± 0.2	9.1 ± 1.0
PtdSer	8.0 ± 3.7	5.9 ± 2.3	PtdSer	6.0 ± 0.3	4.7 ± 0.7
PtdIns	2.3 ± 1.3	4.4 ± 1.9	PtdIns	2.6 ± 0.1	0.4 ± 0.3
PtdEtn	28.6 ± 7.2	24.5 ± 5.3	PtdEtn	5.5 ± 0.3	5.2 ± 1.3
Ptd_2Gro	5.2 ± 3.4	–	Neutral lipids + Ptd_2Gro	64.9 ± 1.2	73.5 ± 0.1

Hemolymph was collected and hemocytes separated from plasma as described in the methods section. The lipids were extracted, phospholipids separated by 2-D TLC and quantified

Phospholipid composition is expressed as percentage of total phosphorus and results are average ± SEM of 5 determinations

Exchange of lipids from hemocytes with plasma was studied as follows. Hemocytes in 10 ml of plasma were labeled with 100 μCi of [1-^{3}H]-ethanolamine for 60 min at 20 °C. Hemocytes were then separated from plasma and washed with non-radioactive plasma. Prelabeled hemocytes (t_{0hr}) were incubated for 90 min in non-radioactive plasma. At that time, hemocytes were separated from plasma, washed and lipids extracted and analyzed. Radiolabeling distribution was determined on the cells and plasma as described in the methods section. [1-^{3}H]-ethanolamine-derived radioactivity is expressed as % of the total radioactivity recovered on the TLC plate. Results are averages ± SD of 3 independent experiments

was no information available on PtdCho biosynthesis by *N*-methylation of PtdEtn in molluscs and the tissues where this metabolic pathway might take place.

The in vivo labeling of *M. galloprovincialis* with [1-^{3}H]-ethanolamine shows that the highest PtdEtn and PtdCho specific activities were observed in the digestive gland and

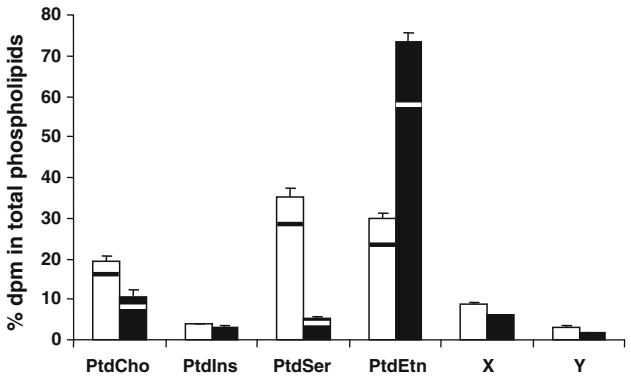

Fig. 3 L-[3-^{3}H]-serine labeling of phospholipids in hemocytes and the digestive gland. The digestive gland and hemocytes were incubated in sterile sea water for 3 h at 20 °C with 10 μCi/ml of L-[3-^{3}H] serine as described in the methods section. The tissues were washed, lipids extracted and phospholipids separated by 2-D TLC. Radioactivity in the different spots was determined by liquid scintillation. *White* and *black* bars respectively, represent the digestive gland and hemocytes. The horizontal *black* and *white lines* within the *white* and *black bars*, respectively, represent the extent of labeling recovered within polar head groups (area under the *black* and *white lines*) based on acetolysis of PtdSer, PtdEtn and PtdCho. The results are averages ± SD of 4 different experiments and the results are expressed as % of total radioactivity recovered in total phospholipids

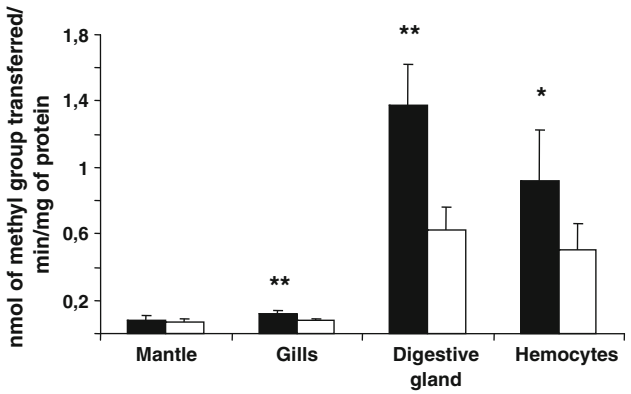

Fig. 4 Effect of salinity on *Pemt* activity in tissues of *M. galloprovincialis* mussels were acclimated to sea water or diluted-sea water for 6 days. Tissues were quickly removed and underwent a *Pemt* assay as described in the methods section. *Black* and *white bars* respectively, represent sea water and diluted-sea water acclimated animals. Data are the averages ± SD of 5 different experiments. *Asterisks* indicate statistical differences between sea water and diluted-sea water acclimated animals (*$p < 0.05$, **$p < 0.001$)

the plasma (Table 2). Phospholipid acetolysis demonstrated that the [1-^{3}H]-ethanolamine-derived labeling was mainly located in the polar head groups of the molecules confirming that the digestive gland can synthesize PtdCho through the PtdEtn *N*-methylation pathway. The PtdCho specific activities in plasma and the digestive gland were very similar suggesting a precursor relationship between these two tissues. We thus compared the kinetics of specific activities into PtdCho from the digestive gland and plasma (Fig. 2a). The results show that, at the opposite of what was observed for PtdEtn (Fig. 2b), no statistical differences could be observed in the specific activities of PtdCho in these two tissues. These observations demonstrate that the [1-^{3}H]-ethanolamine-derived PtdCho, i.e., the PtdCho synthesized by *N*-methylation of PtdEtn in the digestive gland is exchanged with plasma. Our previous results have shown a similar phenomenon in fish and crustaceans where the PtdCho synthesized by *N*-methylation of PtdEtn in the liver/hepatopancreas is exchanged with the plasma of these animals [5, 20]. Interestingly, a role for the PtdEtn *N*-methylation pathway in VLDL lipoprotein secretion has been demonstrated in the liver of *Pemt* –/– mice [50–52]. Fatty acid analysis of PtdCho purified from the digestive gland and plasma also support that there is a precursor relationship between PtdCho synthesized in both tissues of *M. galloprovincialis*. This phospholipid effectively expressed similar fatty acid composition in the two tissues, with a particularly high proportion of palmitic acid and, in contrast, a lower proportion of docosahexaenoic acid when compared to the PtdCho of the mantle and gills (Table 3). Despite these tissue differences in the phospholipid docosahexaenoic acid content, this fatty acid was one of the most expressed, an observation similar to the one reported by others in the mussel *M. edulis* [53]. The metabolic data and PtdCho fatty acid profiles suggest that the digestive gland in the mussel *M. galloprovincialis* insures similar functions in PtdCho synthesis by *N*-methylation of PtdEtn as it is known for the liver in fish and mammals and for the hepatopancreas in crustaceans [20]. The digestive gland is the only tissue where the specific activities of PtdCho and fatty acid composition were similar to the ones in hemolymph.

During in vivo experiments, we also observed a substantial amount of [1-^{3}H]-ethanolamine-derived labeling within Lysophosphatidylethanolamine (LysoPtdEtn) of the digestive gland. In this tissue the lysophospholipid concentrated 3.1 ± 0.4% of radiolabeling. There was no evidence for a LysoPtdEtn-forming activity in other tissues (Table 1) or in vitro (Table 4). The explanation for the specific occurrence of LysoPtdEtn labeling from [1-^{3}H]-ethanolamine within the digestive gland in vivo is not clear. It suggests that the digestive gland may express particularly active metabolic pathway(s) producing this lysophospholipid in vivo. Hax and van Kessel [54] reported the occurrence of LysoPtdEtn within the tissues of the mollusc *Helix pomatia*. Sajiki also reported pH-dependant phospholipase A1 and A2 activities towards PtdEtn in the digestive gland of oysters [55]. Although several biological functions, such as signal transduction, have been attributed to some lysophospholipids (especially lysophosphatidic acid) [56], little is known about LysoPtdEtn [57]. However, antimicrobial activity [58], induction of PC12 cells differentiation [59] and chemotactic migration [60] have been

reported for this lysophospholipid. The occurrence of [1-^{3}H]-ethanolamine-derived labeling within LysoPtdEtn in the digestive gland may simply reflect active remodeling of phospholipids taking place in this tissue which plays a central role in food digestion. Hence LysoPtdEtn expression and labeling in the digestive gland may be the result of concerted actions of phospholipases and reacylation to PtdEtn. A specific LysoPtdEtn acyltransferase has recently been characterized in *Saccharomyces cerevisiae* but the relevance of this observation for animals has still not been established [61].

We also observed that LysoPtdCho relative concentrations in plasma are approximately twice higher than the other tissues (for instance, compare plasma and hemocytes, Table 5). This proportion of LysoPtdCho in plasma is interesting on the basis of what is known about the transport functions that have been ascribed to the lysophospholipid in mammals. When bound to plasma albumin, LysoPtdCho has been shown to be a preferred form of DHA transport to the brain (for a review see [62, 63]). That LysoPtdCho is involved in hemolymph transport of long chain PUFA to tissues in molluscs is thus a tempting hypothesis, but we did not characterize its fatty acid composition.

[1-^{3}H]-Ethanolamine in vitro labeling of tissues strengthens the observations made in vivo. Among the main tissues, the digestive gland was the only one where a significant labeling of PtdCho could be observed, even though the percentage of label recovered within PtdCho was low when compared to in vivo experiments ($\sim$2.8% of total phospholipids radioactivity was recovered into PtdCho when the digestive gland was labeled in vitro versus $\sim$10% in vivo—compare Tables 1 and 4). In vitro, most of the label incorporated into phospholipids was within PtdEtn. Acetolysis of PtdCho isolated from in vitro radiolabeled mantle and gills showed that the low amount of radioactivity recovered in the phospholipid was located in the diacylglycerol moiety of the molecule, the opposite of what was observed in PtdCho purified from the digestive gland.

These different in vitro and in vivo observations point to the digestive gland as the tissue where PtdEtn *N*-methylation is taking place. The in vivo [1-^{3}H]-ethanolamine-derived labeling observed in PtdCho of the mantle and gills may thus be the result of redistribution of the PtdCho synthesized in the digestive gland and exchanged with plasma. Some authors have shown the existence of lipoproteins in the plasma of marine and freshwater bivalves [27, 28]. These authors demonstrated in the pacific oyster (*Crassostrea gigas*) and a freshwater mollusc (*Diplodon delodontus*) that radiolabeled fatty acids were recovered in the plasma lipoproteins and to a lesser extent in hemocytes, and suggested that these structures were involved in lipid transport in molluscs. Our results in *M. galloprovincialis* are in agreement with those reported by these authors on the levels of phospholipids measured in the plasma of *C. gigas* and *D. delodontus*.

However, we were also able to show that, in addition to the digestive gland, PtdEtn *N*-methylation occurs in hemocytes at a significant rate. In vivo radiolabeling of mussels with [1-^{3}H]-ethanolamine showed that $\sim$9.3% of total lipid radioactivity in hemocytes was recovered in PtdCho (see Table 1), with most of the label in the choline moiety of the molecule. In vitro experiments with hemocytes showed that PtdCho concentrated the most [1-^{3}H]-ethanolamine-derived labeling within phospholipids (Table 4). These results demonstrate that an active PtdEtn *N*-methylation pathway is expressed in hemocytes. Pulse-chase experiments with hemocytes indicated that the [1-^{3}H]-ethanolamine-labeled lipids (including PtdCho) synthesized by the cells were partly exchanged with plasma (see Table 5). Thus it appears that plasmatic PtdCho originates from at least two sources: the digestive gland and hemocytes. Unfortunately we were unable to quantify the relative contribution of these tissues in the synthesis of plasmatic PtdCho derived from PtdEtn *N*-methylation. The limited amount of hemocytes enabled us to determine reliably the specific activity of PtdCho in unique samples of these cells. However, it is reasonable to assume that most of [1-^{3}H]-ethanolamine-derived PC in plasma originates from digestive gland because of the close relationship in the specific activities of the phospholipid in these two tissues (Fig. 2a) and because of the low amount of hemocytes in the plasma of *M. galloprovincialis* (we found that less than 1% of hemolymph volume was made of hemocytes).

We also determined *Pemt* activities within the different tissues of *M. galloprovincialis* (Fig. 4). The data confirm that the active PtdEtn *N*-methylation pathway occurs within the digestive gland and hemocytes, strengthening the conclusions based on in vivo and in vitro labeling with [1-^{3}H]-ethanolamine. Acclimation to diluted-sea water caused a reduced *Pemt* activity (Fig. 4). This demonstrates that PC biosynthesis through the PtdEtn *N*-methylation pathway is regulated by environmental salinity, similar to what was reported in fish [5, 19], euryhaline crustaceans [20] and plants facing dryness [64].

Among the few metabolic studies of phospholipids metabolism in molluscs [30, 65, 66] this study is the first to address PtdCho biosynthesis through PtdEtn *N*-methylation in such animals.

Our interest in the PtdEtn *N*-methylation pathway in marine molluscs lies in our previous observations showing that acclimation of euryhaline fish and crustaceans to sea water (i.e., hypertonic conditions with respect to cellular osmolarity) resulted in an activation of *N*-methylation of

PtdEtn into PtdCho that was rapidly exchanged with plasma/hemolymph [5, 17, 20]. We also showed that this PtdCho was used as a precursor for the synthesis of betaine, an important organic osmolyte derived from choline [20]. The PtdEtn *N*-methylation pathway is effectively the only known biosynthetic pathway for choline synthesis in animals [4], whereas plants display active *N*-methylation of phosphorylethanolamine [67]. In the water-stressed barley plant *Hordeum vulgare* Hitz et al. [64] demonstrated a precursor-product relationship between the PtdCho arising from the PtdEtn *N*-methylation pathway and betaine synthesis. In *Pemt* knockout mice a relation between the PtdEtn *N*-methylation pathway and betaine synthesis is suggested by the observations that liver concentrations of this choline metabolite were decreased in female fed a standard diet [68]. Interestingly, *M. galloprovincialis* is known to accumulate high concentrations of betaine when the animal is facing hyperosmotic conditions such as in sea water [69]. These authors demonstrated that moving *M. galloprovincialis* from diluted-sea water (salinity 19‰) to sea water (salinity 38‰) resulted in a 87% increase in tissue betaine concentrations two days after transfer. They also demonstrated that *M. galloprovincialis* displays the ability to synthesize betaine from choline. In similar salinity conditions (see the methods section) we observed a significant effect of salinity on *Pemt* activity (Fig. 4). It is thus tempting to hypothesize that the physiological role described for the PtdEtn *N*-methylation pathway in fish [5, 19] and crustaceans [20] hyperosmotic response may also be relevant in marine molluscs. However, we were unable to measure betaine radiolabeling in plasma during our in vivo experiments due to the small amount of tissue available from animals. The present report characterizing PtdEtn *N*-methylation activity in *M. galloprovincialis* should pave the way to addressing the putative relationship between the PtdEtn *N*-methylation pathway and betaine synthesis in molluscs.

References

1. Kent C (1995) Eukaryotic phospholipid biosynthesis. Annu Rev Biochem 64:315–343
2. Vance DE, Ridgway ND (1988) The methylation of phosphatidylethanolamine. Prog Lipid Res 27:61–79
3. DeLong CJ, Shen YJ, Thomas MJ, Cui Z (1999) Molecular distinction of phosphatidylcholine synthesis between the CDP-choline pathway and phosphatidylethanolamine methylation pathway. J Biol Chem 274:29683–29688
4. Li Z, Vance DE (2008) Phosphatidylcholine and choline homeostasis. J Lipid Res 49:1187–1194
5. Zwingelstein G, Brichon G, Bodennec J, Chapelle S, Abdul-Malak N, El Babili M (1998) Formation of phospholipid nitrogenous bases in euryhaline fish and crustaceans. II. Phosphatidylethanolamine methylation in liver and hepatopancreas. Comp Biochem Physiol 120 B:475–482
6. Mato JM, Alemany S (1983) What is the function of phospholipid *N*-methylation? Biochem J 213:1–10
7. Vance DE, Walkey CJ (1998) Roles for the methylation of phosphatidylethanolamine. Curr Opin Lipidol 9:125–130
8. Vance DE, Walkey CJ, Agellon LB (1998) Why has phosphatidylethanolamine N-methyltransferase survived in evolution? Biochem Soc Trans 26:337–340
9. Walkey CJ, Yu L, Agellon LB, Vance DE (1998) Biochemical and evolutionary significance of phospholipid methylation. J Biol Chem 273:27043–27046
10. Walkey CJ, Donohue LR, Bronson R, Agellon LB, Vance DE (1997) Disruption of the murine gene encoding phosphatidylethanolamine *N*-methyltransferase. Proc Natl Acad Sci USA 94:12880–12885
11. Hirata F, Axelrod J (1980) Phospholipid methylation and biological signal transmission. Science 209:1082–1090
12. Hirata F, Strittmatter WJ, Axelrod J (1979) beta-Adrenergic receptor agonists increase phospholipid methylation, membrane fluidity, and beta-adrenergic receptor-adenylate cyclase coupling. Proc Natl Acad Sci U S A 76:368–372
13. Strittmatter WJ, Hirata F, Axelrod J (1979) Phospholipid methylation unmasks cryptic beta-adrenergic receptors in rat reticulocytes. Science 204:1205–1207
14. Strittmatter WJ, Hirata F, Axelrod J (1981) Regulation of the beta-adrenergic receptor by methylation of membrane phospholipids. Adv Cyclic Nucleotide Res 14:83–91
15. Vance DE, de Kruijff B (1980) The possible functional significance of phosphatidylethanolamine methylation. Nature 288:277–279
16. Zwingelstein G, Abdul Malak N, Brichon G (1978) Effect of environmental temperature on biosynthesis of liver phosphatidylcholine in the trout (*Salmo gairdneri*). J Therm Biol 3:229–233
17. Zwingelstein G, Bodennec J, Brichon G, Abdul Malak N, Chapelle S, El Babili M (1998) Formation of phospholipid nitrogenous bases in euryhaline fish and crustaceans. I. Effects of salinity and temperature on synthesis of phosphatidylserine and its decarboxylation. Comp Biochem Physiol 120 B: 467-473
18. Zwingelstein G, Bodennec J (1998) Phospholipid metabolism in euryhaline fish and crustaceans: Effects of environmental salinity and temperature. Recent Res Devel in Lipids Res 2:39–52
19. Zwingelstein G, Abdul Malak N, Bodennec J, Brichon G (2001) Environmental salinity and phospholipid metabolism in euryhaline fish. Trends in Comparative Biochem & Physiol 8:27–41
20. Athamena A, Brichon G, Trajkovic-Bodennec S, Péqueux A, Chapelle S, Bodennec J, Zwingelstein G (2011) Salinity regulates N-methylation of phosphatidylethanolamine in euryhaline crustaceans hepatopancreas and exchange of newly-formed phosphatidylcholine with hemolymph. J Comp Physiol B. doi: 10.1007/s00360-011-0562-6
21. Péqueux A (1995) Osmotic regulation in crustaceans. J Crustacean Biology 15:1–60
22. Joseph JD (1982) Lipid composition of marine and estuarine invertebrates. Part II: Mollusca. Prog Lipid Res 21:109–153
23. Voogt MT. (1983) Lipids: their distribution and metabolism. In: Wilbur, KM, Hochachka, PW (eds) The Mollusca. Academic Press, pp 329-369
24. Bayne BL (1973) Physiological changes in *Mytilus edulis* L induced by temperature and nutritive stress. J Mar Biol 53:39–58
25. Thompson RJ (1977) Blood chemistry, biochemical composition, and the annual reproductive cycle in the giant scallop, *Placopecten magellanicus*, from southeast Newfoundland. J Fish Res Board Can 34:2104–2116
26. Hoskin GP, Hoskin SP (1977) Partial characterization of the hemolymph lipids of *Mercenaria mercenaria* (Mollusca:

Bivalvia) by thin-layer chromatography and analyses of serum fatty acids during starvation. Biol Bull 152:373–381
27. Allen WV, Conley H (1982) Transport of lipids in the blood of the Pacific oyster, *Crassostrea gigas* (Thunberg). Comp Biochem Physiology 71 B:201–207
28. Pollero RJ, Huca G, Brenner RR (1985) Role of hemocytes and plasma on lipid transport in the freshwater mollusc *Diplodon delodontus*. Comp Biochem Physiol 82 A:339–343
29. de Moreno JEA, Moreno VJ, Brenner RR (1977) Lipid metabolism of the yellow clam, *Mesodesma mactroides*: 3-saturated fatty acids and acetate metabolism. Lipids 12:804–808
30. Lubet P, Brichon G, Besnard JY, Zwingelstein G (1985) Composition and metabolism of lipids in some tissues of the mussel *Mytilus galloprovincialis* L. (Moll. Bivalvia). In vivo and in vitro incorporation of 1 (3)-[^{3}H]-glycerol. Comp Biochem Physiol 82 B:425–431
31. Lubet P (1959) Recherches sur le cycle sexuel et l'émission des gamètes chez les Mytilidae et les pectinidae (Moll. Bivalves). Revue des travaux de l'Office (scientifique et technologique) des Pêches maritimes 23:387–548
32. Folch J, Lees M, Sloane Stanley GH (1957) A simple method for the isolation and purification of total lipides from animal tissues. J Biol Chem 226:497–509
33. Chapelle S, Dandrifosse G, Zwingelstein G (1976) Metabolism of phospholipids of anterior or posterior gills of the crab *Eriocheir sinensis* M EDW, during the adaptation of this animal to media of various salinities. Int J Biochem 7:343–351
34. Bartlett GR (1959) Phosphorous assay in column chromatography. J Biol Chem 234:466–469
35. Buccoliero R, Bodennec J, Van Echten-Deckert G, Sandhoff K, Futerman AH (2004) Phospholipid synthesis is decreased in neuronal tissue in a mouse model of Sandhoff disease. J Neurochem 90:80–88
36. Portoukalian J, Meister R, Zwingelstein G (1978) Improved 2-dimensional solvent system for thin-layer chromatographic analysis of polar lipids on silica-gel 60 precoated plates. J Chromatogr 152:569–574
37. Dittmer JC, Lester RL (1964) A simple, specific spray for the detection of phospholipids on thin-layer chromatograms. J Lipid Res 15:126–127
38. Vaskovsky VE, Suppes ZS (1971) Detection of choline-containing lipids on thin-layer chromatograms. J Chromatogr 63:455–456
39. Stillway LW, Harmon SJ (1980) A procedure for detecting phosphonolipids on thin-layer chromatograms. J Lipid Res 21:1141–1143
40. Renkonen OJ (1966) Altered fatty acid distribution of glycerophosphatides induced by acetolysis. Lipids 1:160–164
41. Pietsch A, Lorenz RL (1993) Rapid separation of the major phospholipid classes on a single aminopropyl cartridge. Lipids 28:945–947
42. Anderton P, Wild TF, Zwingelstein G (1981) Modification of the fatty acid composition of phospholipid in measles virus-persistently infected cells. Biochem Biophys Res Commun 103:285–291
43. Vaisman N, Kaysar N, Zaruk-Adasha Y, Pelled D, Brichon G, Zwingelstein G, Bodennec J (2008) Correlation between changes in blood fatty acid composition and visual sustained attention performance in children with inattention: effect of dietary n-3 fatty acids containing phospholipids. Am J Clin Nutr 87:1170–1180
44. Ridgway ND, Vance DE (1992) Phosphatidylethanolamine N-methyltransferase from rat liver. Methods Enzymol 209:366–374
45. Zar JH (1988) Biostatistical analysis. Prentice-Hall, Englewood Cliffs
46. Lubet P, Delongcamp D (1969) Etude des variations annuelles des constituants lipidiques chez *Mytilus edulis* L à Luc sur Mer. Comptes rendus des séances de la Société de biologie et de ses filiales 163:1110–1112
47. Aktas M, Wessel M, Hacker S, Klusener S, Gleichenhagen J, Narberhaus F (2010) Phosphatidylcholine biosynthesis and its significance in bacteria interacting with eukaryotic cells. Eur J Cell Biol 89:888–894
48. Hirata F, Axelrod J, Crews FT (1979) Concanavalin A stimulates phospholipid methylation and phosphatidylserine decarboxylation in rat mast cells. Proc Natl Acad Sci USA 76:4813–4816
49. Hirata F, Corcoran BA, Venkatasubramanian K, Schiffmann E, Axelrod J (1979) Chemoattractants stimulate degradation of methylated phospholipids and release of arachidonic acid in rabbit leukocytes. Proc Natl Acad Sci USA 76:2640–2643
50. Noga AA, Zhao Y, Vance DE (2002) An unexpected requirement for phosphatidylethanolamine N-methyltransferase in the secretion of very low density lipoproteins. J Biol Chem 277:42358–42365
51. Noga AA, Vance DE (2003) A gender-specific role for phosphatidylethanolamine N-methyltransferase-derived phosphatidylcholine in the regulation of plasma high density and very low density lipoproteins in mice. J Biol Chem 278:21851–21859
52. Vance DE (2008) Role of phosphatidylcholine biosynthesis in the regulation of lipoprotein homeostasis. Curr Opin Lipidol 19:229–234
53. Lin H, Jiang J, Xue CH, Zhang B, Xu JC (2003) Seasonal changes in phospholipids of mussel (*Mytilus edulis* Linné). J Sci Food Agric 83:133–135
54. Hax WM, van Kessel WS (1977) High-performance liquid chromatographic separation and photometric detection of phospholipids. J Chromatogr 142:735–741
55. Sajiki J (1996) Is phospholipase in vinegar oysters a casual agent for human poisoning? J Toxicol Environ Health 47:221–232
56. Choi JW, Lee CW, Chun J (2008) Biological roles of lysophospholipid receptors revealed by genetic null mice: an update. Biochim Biophys Acta 1781:531–539
57. Makide K, Kitamura H, Sato Y, Okutani M, Aoki J (2009) Emerging lysophospholipid mediators, lysophosphatidylserine, lysophosphatidylthreonine, lysophosphatidylethanolamine and lysophosphatidylglycerol. Prost Lip Mediators 89:135–139
58. Meylaers K, Clynen E, Daloze D, Deloof A, Schoofs L (2004) Identification of 1-lysophosphatidylethanolamine (C(16:1)) as an antimicrobial compound in the housefly, *Musca domestica*. Biochem Mol Biol 34:43–49
59. Nishina A, Kimura H, Sekiguchi A, Fukumoto RH, Nakajima S, Furukawa S (2006) Lysophosphatidylethanolamine in *Grifola frondosa* as a neurotrophic activator via activation of MAPK. J Lipid Res 47:1434–1443
60. Park KS, Lee HY, Lee SY (2007) Lysophosphatidylethanolamine stimulates chemotactic migration and cellular invasion in SK-OV3 human ovarian cancer cells: involvement of pertussis toxin-sensitive G-protein coupled receptor. FEBS Lett 581:4411–4416
61. Riekhof WR, Wu J, Jones JL, Voelker DR (2007) Identification and characterization of the major lysophosphatidylethanolamine acyltransferase in *Saccharomyces cerevisiae*. J Biol Chem 282:28344–28352
62. Lagarde M, Bernoud N, Brossard N, Lemaitre-Delaunay D, Thies F, Croset M, Lecerf J (2001) Lysophosphatidylcholine as a preferred carrier form of docosahexaenoic acid to the brain. J Mol Neurosci 16:201–204 discussion 215-221
63. Picq M, Chen P, Perez M, Michaud M, Vericel E, Guichardant M, Lagarde M (2010) DHA metabolism: targeting the brain and lipoxygenation. Mol Neurobiol 42:48–51
64. Hitz WD, Rhodes D, Hanson AD (1981) Radiotracer evidence implicating phosphoryl and phosphatidyl bases as intermediates

in betaine synthesis by water-stressed barley leaves. Plant Physiol 68:814–822
65. Liang CR, Segura LM, Strickla KP (1970) Phospholipid metabolism in molluscs. 2. Activities of choline kinase, ethanolamine kinase, and CTP-phosphorylethanolamine cytidyltransferase in mollusc *Helix-lactea*. Comp Biochem Physiol 48 B:580
66. Lubet P, Brichon G, Besnard JY, Zwingelstein G (1986) Sexual differences in the composition and metabolism of lipids in the mantle of the mussel *Mytilus galloprovincialis* LMK (Mollusca: Bivalvia). Comp Biochem Physiol 84 B:279–285
67. Weretilnyk EA, Smith DD, Wilch GA, Summers PS (1995) Enzymes of Choline Synthesis in Spinach (Response of Phospho-Base N-Methyltransferase Activities to Light and Salinity). Plant Physiol 109:1085–1091
68. Zhu X, Song J, Mar MH, Edwards LJ, Zeisel SH (2003) Phosphatidylethanolamine N-methyltransferase (PEMT) knockout mice have hepatic steatosis and abnormal hepatic choline metabolite concentrations despite ingesting a recommended dietary intake of choline. Biochem J 370:987–993
69. de Vooys CG, Geenevasen JA (2002) Biosynthesis and role in osmoregulation of glycine-betaine in the Mediterranean mussel *Mytilus galloprovincialis* LMK. Comp Biochem Physiol 132 B:409–414

wide range of mono- and disaccharides as well as branched polysaccharides. The optimal temperature for growth is 68 °C (range 50–73 °C) and pH 5.3 (range 4.7–5.8) [2].

The lipid composition of *C. calidirosea* presents a number of unusual features both in the fatty acids and polar lipids. The present publication describes fatty acids of this unique organism, including the discovery of a novel, 5,6-methylene hexadecanoic acid. While polar lipids observed in *C. calidirosea* resembled those reported for *Deinococcus radiodurans*, the polar lipids of the latter contained monoenoic acids only of Δ7, Δ9 and Δ11 series, with up to 11% of unidentified fatty acids [3, 4], and it was highlighted that no cyclopropanoic acids were found [5]. A combination of chemical and instrumental techniques (GC, GCMS, TLC, SPE, preparative HPLC, hydrogenation of unsaturated fatty acids, a cyclopropane ring opening by hydrogenation in glacial acetic acid, formation of DMDS adducts and TMS derivatives, IR, and ^{1}H-NMR) was applied to identify all fatty acids present in the organism at levels above 0.2% of total fatty acids. Characteristic features of *C. calidirosea* seem to be the presence of normal and branched chain *cis*-Δ5 monounsaturated fatty acids and 5,6-methylene hexadecanoic acid. The latter feature makes *C. calidirosea* unique, since cyclopropane fatty acids found in bacteria usually belong to *cis*-9,10-methylene- or *cis*-11,12-methylene families [6], with less common *trans*-4,5-methylene pattern reported for cyanobacteria [7, and references therein].

Materials and Methods

Lipid Extraction

Chthonomonas calidirosea was cultivated as described in [2]. Wet biomass was extracted using the method of Bligh and Dyer [8]. Freeze-dried biomass was extracted by the same method after re-constituting with tenfold excess of water (by weight).

Thin-Layer Chromatography

Neutral lipids were resolved by high performance thin-layer chromatography (HPTLC) on 10 × 10 cm Silica gel 60 glass plates (Merck, Germany) in hexane/diethyl ether/glacial acetic acid (80:20:1, by vol) with the following reference compounds: cholesterol, cholesterol oleate, triolein, 1,2- and 1,3-dipalmitoyl glycerol, 1-monopalmitoyl-glycerol, and oleic acid (Sigma, USA; and IRL own collection of reference lipid compounds). Resolution of diploptene, squalene and partially hydrogenated squalenes was achieved by development of a HPTLC plate with chloroform for 1/3 of height, drying in warm air, followed by development in hexane up to full height [9]. Preparative TLC in hexane was used for isolation of individual neutral lipid classes. Edges of zones were detected by iodine vapours after covering the developed and air-dried plate with a clean glass plate. Zones were each scraped and eluted with 1 ml hexane. Identities of components were established either by direct injections of fractions into GCMS, or by hydrogenation followed by GCMS.

Non-specific detection of organic compounds on TLC plates was performed with the use of iodine vapours or by charring with 5 or 10% (by vol) sulphuric acid in methanol. To improve detection of saturated compounds, charring with molybdate spray [10] was found useful.

Fatty Acids Analysis

Fatty acid methyl esters were prepared from small samples of biomass without lipid extraction and analysed as described by Svetashev et al. [11].

For detailed analysis, fatty acid methyl esters were prepared from the lipid extracts according to the method of Carreau and Dubacq [12], and purified by SPE on a 500 mg Strata SI-1 cartridge (Phenomenex, USA) conditioned with hexane. Hydrocarbons were eluted with 3 ml of hexane and used for diploptene/squalenes detection, and fatty acids methyl esters (FAME) were eluted with 6 ml of hexane-diethyl ether (99:1, by v/v). The method used was identical to the third procedure presented elsewhere [13], with the only exception being the use of a SPE cartridge in place of a Silica gel 60 column.

GC analysis of fatty acid methyl esters was performed on a TraceGC Ultra instrument (ThermoFinnigan, USA), equipped with FID and 30 m, 0.32 mm i.d. BP20 polyethylene glycol capillary column (SGE, Australia). Helium was used as the carrier gas; the split ratio was 1:60. Separation temperature was 195 °C. When non-polar BP1 (60 m, 0.32 mm i.d.) methyl silicone capillary column (SGE, Australia) was used, the separation temperature was maintained at 220 °C. For calculation of equivalent chain length (ECL) of methyl esters of 5- and 6-methyl hexadecanoic acids, the oven temperature was maintained at 150 °C. Fatty acids were identified by the use of reference compounds, the known ECL values for methyl silicone column [14], and by GCMS (see below). Hydrogenation of fatty acid methyl esters was performed according to Appelquist [15]. Dimethyl disulfide (DMDS) adducts formation [16] was used to locate the position of the double bond in monounsaturated fatty acids [17].

To open a cyclopropane ring, hydrogenation of the sample in glacial acetic acid over PtO_2 catalyst [18] was performed for 6 h at room temperature, as described by Saito and Ochiai [19].

Trimethylsilyl derivatives were prepared by dissolving approximately 0.2 mg of the sample in 10 µl of pyridine, and 30 µl of *N*,*O*-bis(trimethylsilyl)trifluoroacetamide with 1% trimethylchlorosilane (Aldrich, USA). The reaction mixture was maintained for 30 min at 60 °C. The sample was either analysed directly, or was evaporated under a stream of argon and re-dissolved in 0.5 ml of hexane prior to the injection.

GCMS analyses were performed on an Agilent 5890N gas chromatograph equipped with a 5973 Inert mass-spectrometric detector and HP-5 capillary column (30 m, 0.32 mm i.d.; Hewlett-Packard, USA). Helium was used as the carrier gas. Analysis of FAME was initiated at 100 °C (hold for 6 min), with the temperature increased at a rate of 5 °C/min up to 160 °C, followed by a rate of 1 °C/min to 240 °C, and then maintained for 25 min. Neutral lipids (diploptene, squalene, and partially hydrogenated squalenes) were analysed in the following temperature programme: 6 min at 100 °C, with the temperature increased at a rate of 5 °C/min up to 160 °C, followed by a rate of 2.5 °C/min to 300 °C, and then this was maintained for 30 min.

Preparative HPLC separation of the *C. calidirosea* free fatty acids was carried out using a Gilson 321 preparative HPLC pump, an Agilent 1100 photodiode array detector (at 205 nm), C12 column (Synergy 4 µ Max-RP 80A 250 × 30.00 mm) with a guard column (Phenomenex SecurityGuard cartridge C12 15 × 30.00 mm). Data were collected and analysed using Gilson Unipoint 3.20 software. Solvents used were: Solvent A: 85% aqueous methanol with 0.05% acetic acid; Solvent B: methanol with 0.05% acetic acid. The eluent flow rate was 15 ml/min. The concentration of injected sample was 200 mg/ml in chloroform, 0.3 ml was injected. The eluent gradient employed was: 0 to 2 min—100% Solvent A; 24 min—35% Solvent A, 65% Solvent B; 69 min—100% Solvent B.

^{1}H-NMR of fatty acid samples was performed in $CDCl_3$ using a Bruker Avance III 500 MHz instrument. Spectra were recorded with the following instrument settings: spectrometer frequency 499.843 MHz, sweep width 10,302 Hz, 65,536 data points, 30° excitation pulse, 32 transients taken, each with a 1-s delay time and f.i.d. acquisition time of 3.18 s. Spectra were processed with a standard exponential weighting function with 0.3 Hz line broadening before Fourier transformation.

IR spectra were recorded with a Spectrum One (Perkin-Elmer) FTIR spectrometer (solvent—CCl_4).

Results

Lipid Content

The lipid content of *C. calidirosea* samples varied between 0.29 and 0.36% of the wet biomass weight, or 7.6–8.8% in the freeze-dried samples. A bright pink pigment was present in all total lipid extracts.

Neutral Lipids

No free fatty acids, wax or sterol or glycerol esters were observed in the total lipids of *C. calidirosea* in our TLC experiments, suggesting that fatty acids, if any, are present as constituents of polar lipids only. Initial analysis of the mixture produced by transmethylation of bacterial biomass without further purification demonstrated the presence of significant quantities of hydrocarbons in the mixture, apart from fatty acid methyl esters. These hydrocarbons were fractionated by preparative TLC (Fig. 1). Individual components were identified by GCMS of intact and hydrogenated samples as squalene, dihydrosqualene, tetrahydrosqualene, hexahydrosqualene, octahydrosqualene and decahydrosqualene (all of these produced squalane upon hydrogenation), and diploptene (hopane was produced upon hydrogenation). An unidentified component, appearing to be partially cyclised squalene with two rings and four double bonds, was also observed. The mass spectrum of this component was similar to that of a known product of an incomplete cyclisation of squalene, γ-polypodatetraene [20], but no further structure elucidation was performed.

Diplopterol, along with barely detectable levels of the methyl ester of β-hydroxy myristic acid were observed when methanolysis products prepared from total lipids [11] were analysed by GCMS in the form of TMS-derivatives.

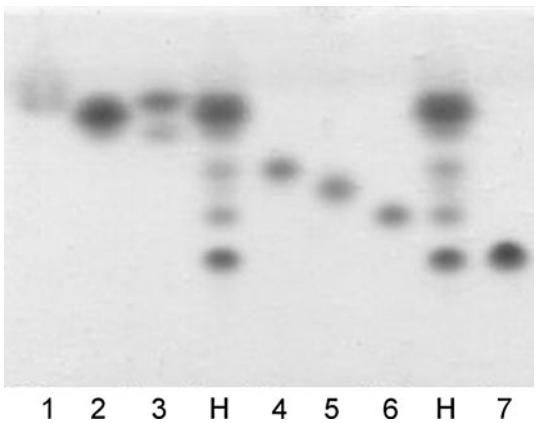

Fig. 1 Fractionation of neutral lipids of *C. calidirosea*. TLC in hexane, detection by iodine vapours. The identities of the components were confirmed by GCMS of fractions before and after hydrogenation (see "Materials and Methods"). *Lanes 1* octahydrosqualene and decahydrosqualene; *2* diploptene and octahydrosqualene; *3* octahydrosqualene, diploptene, and hexahydrosqualene; *H* hexane fraction of *C. calidirosea* neutral lipids; *4* tetrahydrosqualene; *5* unidentified bicyclic tetraene; *6* dihydrosqualene; *7* squalene

Fatty Acids

The only type of unsaturation found in *C. calidirosea* fatty acids was Δ5 with *cis*-configuration. These were identified via GCMS analysis of the DMDS adducts (Fig. 2), and IR spectrometry, resulting in fragments with *m/z* 161, $CH_3SC_5H_7O_2CH_3^+$, and 129 (*m/z* 161-CH_3OH), and no *trans*-unsaturation absorbance at 960–980 cm^{-1} in the IR spectrum.

Comparison of the chromatographic behaviour of the FAME on non-polar and medium polarity phases, along with analysis of hydrogenated samples, allowed the identification of most of the fatty acids present in *C. calidirosea* lipids. Since a BP20 column was unable to separate *ante-iso*-17:0 and *iso*-17:1Δ5 peaks (both components have ECL of 16.68 at 195 °C), a BP1 column was used for fatty acid profiling of cultured samples.

An unidentified fatty acid methyl ester, X, with ECL 16.86 on non-polar column BP1 (Fig. 3), and ECL 17.27 on a medium polarity BP20 column possessed a molecular ion with *m/z* 282, suggesting the presence of a 17:1 fatty acid, but it did not form DMDS adducts and was not affected by mild hydrogenation conditions. MS spectrum of X revealed that it featured an ion pattern characteristic for cyclopropane fatty acids, with the peak at *m/z* 41 of higher intensity than that of *m/z* 43 [21]. ^{1}H-NMR spectra of both polar lipids fraction of *C. calidirosea* lipids, and FAME fraction enriched in X demonstrated a resonance at −0.3 ppm, as well as at 0.6 ppm confirming the presence of a cyclopropane ring with *cis*-stereochemistry [22]. Hydrogenation of X in acetic acid resulted in formation of straight chain 17:0 (ECL 17.00) and two branched FAME with ECL 16.42 and 16.43 on 60 m BP1 column. The former ECL values is close to the one reported by Apon

Fig. 2 Mass-spectrum of DMDS adduct of *i*17:1 methyl ester

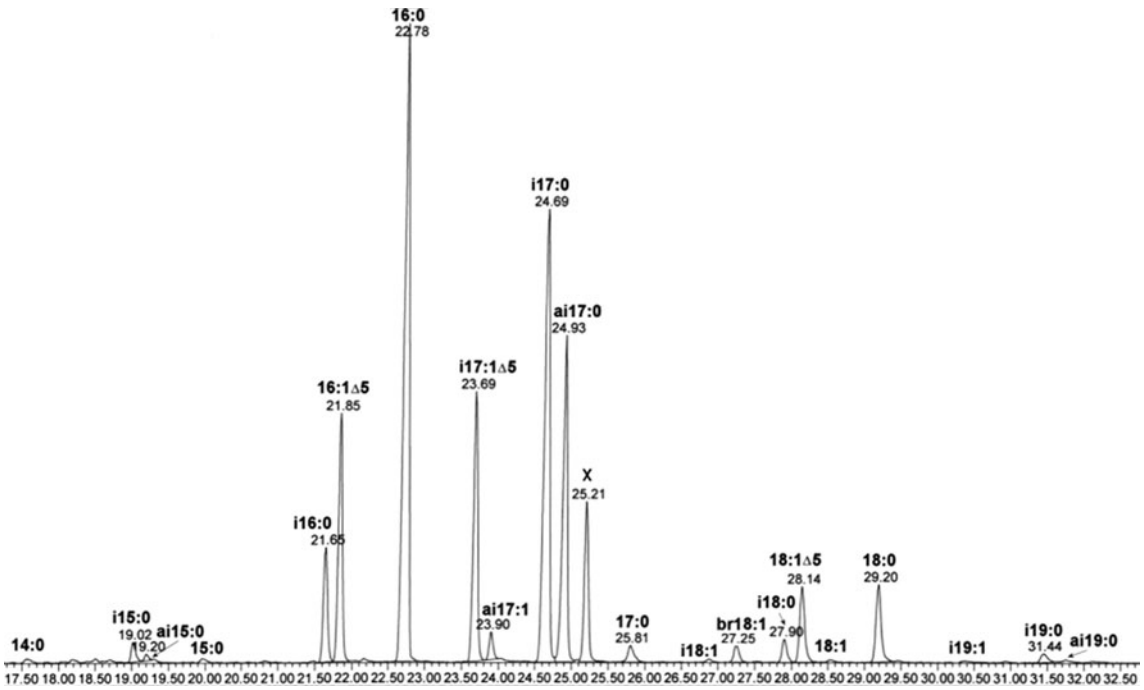

Fig. 3 GC of FAME derived from *C. calidirosea* total lipids on HP-5 capillary column

and Nicolaides [23], who observed the ECL of 16.40 for 6-methyl hexadecanoic acid methyl ester using a home-made 500 or 1,000 ft stainless steel capillary columns coated with Pentasil (a non-polar phase). Unfortunately, they did not report the ECL for 5-methyl hexadecanoic acid methyl ester. In the GCMS experiment these components demonstrated characteristic fragments at *m/z* 115 and 143 (6-methyl 16:0), and at *m/z* 101 and 129 (5-methyl 16:0), correspondingly (Fig. 4), thus confirming 5,6-methylene hexadecanoic acid structure. The presence of a major ion at *m/z* 208 (M-76) in the former spectrum is known to be characteristic for fatty acid methyl esters with a methyl branch at C6 (peak "e" in [18]), while the same fragment may be observed at very low abundance in spectra of 5-methyl- and 7-methyl FAME. A major ion at *m/z* 241 in the latter spectrum originates from the loss of a three carbon fragment from within the chain (ibid.). Overall, MS data for 5-methyl- and 6-methyl-16:0 did match well with those published in Table II of [23], including a peculiar pattern at *m/z* 111 and 112 for 6-methyl-16:0. A satisfactory GC separation of 5-methyl- and 6-methyl hexadecanoic acids was achieved by the use of a 60-m capillary column and reduced temperature of analysis. The level of 5,6-methylene hexadecanoic acid in a solid media-grown sample was 5.2% of total fatty acids (Table 1).

Discussion

Bacterial *cis*-monounsaturated fatty acids of Δ5 series were discovered by Kaneda [24] who found *i*-C16:1Δ5, *n*-C16:1Δ5, *i*-C17:1Δ5, and *ai*-C17:1Δ5 in three species of *Bacillus*, with either *n*-C16:1Δ5 or *ai*-C17:1Δ5 being the major unsaturated component. Later Kaneda commented that the significance of the unusual position of the double bond was not clear, but linked Δ5-unsaturation to aerobic biosynthesis [25].

Cyclopropane fatty acids found in bacteria usually belong to *cis*-9,10-methylene- or *cis*-11,12-methylene families [6]. Less common structures were also reported, e.g., compounds based on *trans*-4,5-methylene pattern were reported for cyanobacteria [7, and references therein]. Since biosynthesis of a cyclopropane ring in fatty acids is accomplished by methylenation of an unsaturated moiety with *S*-adenosylmethionine [26], we expected that the cyclopropane acid found would have a 5,6-methylene

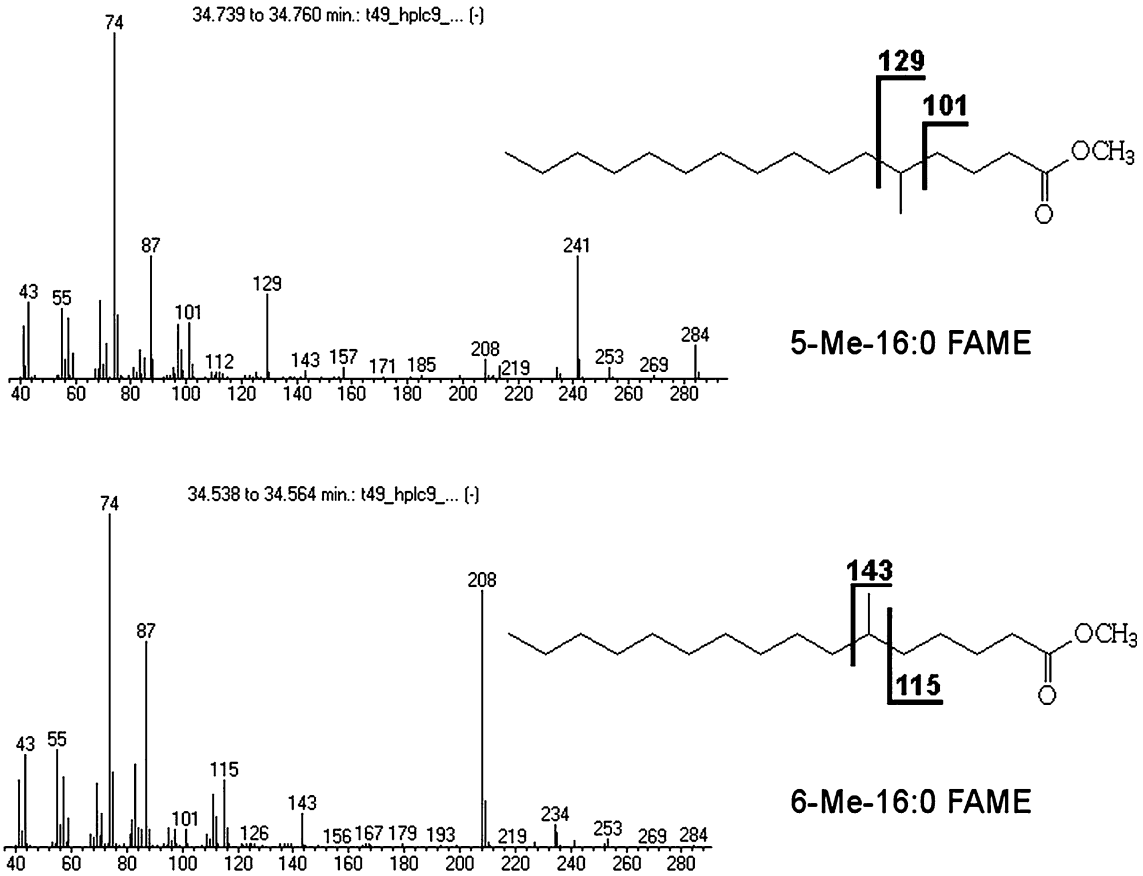

Fig. 4 GCMS of branched acids derived upon cycle opening of compound X: 5-methyl hexadecanoic acid methyl ester (*upper*), and 6-methyl hexadecanoic acid methyl ester (*lower*). The molecular ions of both isomers are situated at *m/z* 284

Table 1 Fatty acid composition of *C. calidirosea*, in weight % of total fatty acids. Only components >0.2% are presented

FA	ECL_{BP1}	ECL_{BP20}	%
14:0	14.00	13.98	0.4
*i*15:0	14.64	14.50	1.0
*ai*15:0	14.74	14.67	0.5
15:0	15.00	15.00	0.4
*i*16:0	15.65	15.52	4.4
16:0[a]	16.00	16.00	25.8
16:1Δ5	15.76	16.16	8.8
*i*17:0	16.65	16.52	19.3
*ai*17:0	16.74	16.68	13.5
*i*17:1Δ5	16.40	16.68	6.8
*ai*17:1Δ5	16.48	16.82	0.7
17:0	17.00	17.00	0.8
5,6-Methylene-16:0 ("X")	16.86	17.27	5.2
*i*18:0	17.65	17.52	1.2
*br*18:1	17.50	17.78	0.9
18:0[a]	18.00	18.00	3.6
18:1Δ5	17.74	18.14	3.2
*i*19:0	18.64	18.51	0.9
*ai*19:0	18.73	18.69	0.3
*i*19:1	18.37	18.69	0.9
Total			98.6

[a] components also present in media

fragment. Indeed, a ring opening study using GCMS analysis of the products confirmed the presence of 5,6-methylene hexadecanoic acid in *C. calidirosea*.

According to the result of a search performed with the use of Reaxys® (Elsevier Properties SA service) and SciFinder® (Chemical Abstracts service), 5,6-methylene hexadecanoic acid has not been reported yet, but a longer chain homologue, 5,6-methylene octadecanoic acid, was synthesised from the corresponding octadecenoic acid [27]. Interestingly, the 2-hydroxy derivative of 5,6-methylene octadecanoic acid is a component of Cepaciamide A, a fungitoxic compound isolated from *Pseudomonas cepacia* [28].

While polar lipids observed in *C. calidirosea* resembled those reported for *Deinococcus radiodurans* (data not shown), the polar lipids of the latter contained monoenoic acids only of Δ7, Δ9 and Δ11 series, with up to 11% of unidentified fatty acids [3, 4], and it was highlighted that no cyclopropanoic acids were found [5]. The prevalence of Δ5 *cis*-monounsaturated and 5,6-methylene hexadecanoic acid provides *C. calidirosea* with a unique set of lipid biomarkers. The fatty acid profile of *Armatimonas rosea*, the only other cultivated bacterium from the phylum Armatimonadetes [29], lacks these markers and suggests that Δ5 *cis*-monounsaturation and 5,6-methylene hexadecanoic acid may only be specific to the class or genus. Additional data on the fatty acid profile of the other bacteria within the *Chthonomonas* genus will provide chemotaxonomic information on these microorganisms and confirm their prevalence.

Acknowledgments The authors are grateful to Dr. Kevin Mitchell for help with HPLC, Dr. Herbert Wong for NMR-spectra recording, Dr. Owen Catchpole for reviewing the manuscript, Alison Speakman for invaluable help in information retrieval (all—IRL), and anonymous reviewers for helping to make this article better. The authors also thank the Tikitere Trust for their on-going support of this research.

Conflict of interest Authors declare that there is no conflict of interest.

References

1. Stott MB, Crowe MA, Mountain BW, Smirnova AV, Hou S, Alam M, Dunfield PF (2008) Isolation of novel bacteria, including a candidate division, from geothermal soils in New Zealand. Environ Microbiol 10:2030–2041
2. Lee KC-Y, Dunfield PF, Morgan XC, Crowe MA, Houghton KM, Vyssotski M, Ryan JLJ, Lagutin K, McDonald IR, Stott MB (2010) Chthonomonas calidirosea gen. nov., sp. nov., an aerobic, pigmented, thermophilic microorganism of a novel bacterial class, Chthonomonadetes classis. nov., of the newly described phylum Armatimonadetes originally designated candidate division OP10. Int J Syst Evol Microbiol. doi:10.1099/ijs.0.027235-0
3. Huang Y, Anderson R (1989) Structure of a novel glucosamine-containing phosphoglycolipid from *Deinococcus radiodurans*. J Biol Chem 264:18667–18672
4. Huang Y, Anderson R (1995) Glucosyl diglyceride lipid structures in *Deinococcus radiodurans*. J Bacteriol 177:2567–2571
5. Anderson R, Huang Y (1992) Fatty acids are precursors of alkylamines in *Deinococcus radiodurans*. J Bacteriol 174:7168–7173
6. Grogan DW, Cronan JE (1997) Cyclopropane ring formation in membrane lipids of bacteria. Microbiol Mol Biol Revs 61:429–441
7. MacMillan JB, Molinski TF (2005) Majusculoic acid, a brominated cyclopropyl fatty acid from a marine cyanobacterial mat assemblage. J Nat Prod 68:604–606
8. Bligh EG, Dyer WJ (1959) A rapid method of total lipid extraction and purification. Can J Biochem Physiol 37:911–917
9. Shigeru Y, Nishino T, Yumoto N, Tokushige M (1991) Hopanoid biosynthesis of *Zymomonas mobilis*. Agric Biol Chem 55:589–591
10. Vaskovsky VE, Kostetsky EY, Vasendin IM (1975) A universal reagent for phospholipid analysis. J Chromatogr 114:129–141
11. Svetashev VI, Vysotskii MV, Ivanova EP, Mikhailov VV (1995) Cellular fatty acids of *Alteromonas* species. Syst Appl Microbiol 18:37–43
12. Carreau JP, Dubacq JP (1978) Adaptation of macro-scale method to the micro-scale for the fatty acid methyl transesterification of biological lipid extracts. J Chromatogr 151:384–390
13. Cyberlipid (2011) Low pressure fractionation of neutral lipids. http://www.cyberlipid.org/fraction/frac0006.htm. Accessed Jan 2011
14. Kaneda T (1977) Fatty acids of the genus *Bacillus*: an example of branched-chain preference. Bacteriol Rev 41:391–418
15. Appelquist LA (1972) A simple and convenient procedure for the hydrogenation of lipids on the micro-and nanomole scale. J Lipid Res 13:146–148

16. Francis GW (1981) Alkylthiolation for the determination of double-bond position in unsaturated fatty acid esters. Chem Phys Lipids 29:369–374
17. Yamamoto K, Shibahara A, Nakayama T, Kajimoto G (1991) Double-bond localization in heneicosapentaenoic acid by a gas chromatography/mass spectrometry (GC/MS) method. Lipids 26:948–950
18. McCloskey JA, Law JH (1967) Ring location in cyclopropane fatty acid esters by a mass spectrometric method. Lipids 2:225–230
19. Saito T, Ochiai H (1998) Fatty acid composition of the cellular slime mold *Polysphondylium pallidum*. Lipids 33:327–332
20. Shiojima K, Arai Y, Masude K, Kamada T, Ageta H (1983) Fern constituents: polypodatetraenes, novel bicyclic triterpenoids, isolated from polypodaceous and aspidiaceous plants. Tetr Lett 24:5733–5736
21. Härtig C (2008) Rapid identification of fatty acid methyl esters using a multidimensional gas chromatography-mass spectrometry database. J Chromatogr A 1177:159–169
22. Knothe G (2006) NMR characterization of dihydrosterculic acid and its methyl ester. Lipids 41:393–396
23. Apon JMB, Nicolaides N (1975) Determination of the position isomers of the methyl branched fatty acid methyl esters by capillary GC/MS. J Chromatogr Sci 13:467–473
24. Kaneda T (1971) Major occurrence of *cis*-Δ^5 fatty acids in three psychrophilic species of *Bacillus*. Biochem Biophys Res Commun 43:298–300
25. Kaneda T (1991) Iso- and anteiso-fatty acids in bacteria: biosynthesis, function, and taxonomic significance. Microbiol Revs 55:288–302
26. Wessjohann LA, Brandt W, Thiemann T (2003) Biosynthesis and metabolism of cyclopropane rings in natural compounds. Chem Rev 103:1625–1647
27. Christie WW, Gunstone FD, Ismail IA, Wade L (1968) Fatty acids, part 17. The synthesis and chromatographic and spectroscopic properties of the cyclopropane esters derived from all the methyl octadecenoates (Δ^2–Δ^{17}). Chem Phys Lipids 2:196–202
28. Jiao Y, Yoshihara T, Ishikuri S, Uchino H, Ichihara A (1996) Structural identification of Cepaciamide A, a novel fungitoxic compound from *Pseudomonas cepacia* D-202. Tetrahedron Lett 37:1039–1042
29. Tamaki H, Tanaka Y, Matsuzawa H, Muramatsu M, Meng X-Y, Hanada S, Mor K, Kamagata Y (2010) *Armatimonas rosea* gen. nov., sp. nov., a Gram-negative, aerobic, chemoheterotrophic bacterium of a novel bacterial phylum, Armatimonadetes phyl. nov., formally called the candidate phylum OP10. Int J Syst Evol Microbiol. doi:10.1099/ijs.0.025643-0

(>12 h). These methods include density gradient ultracentrifugation, nuclear magnetic resonance (NMR) spectroscopy, and polyacrylamide gradient gel electrophoresis (PGGE). Recently, another technique to measure LDL particle size was developed by the Quantimetrix Corporation [9]. This new method, termed the "lipoprint LDL system", allows for the determination of LDL particle size and distribution in <3 h by a polyacrylamide gel electrophoresis system [9]. Although this new method has been used in a variety of clinical trials [10–12], no data on the *agreement* between this new technique and previously validated methods (i.e. PGGE) has been published. Greater insight into the level of agreement between the two methods is of particular importance in view of the increasing application of the lipoprint method in both research and clinical practice. Accordingly, this study evaluated the agreement between LDL particle size and distribution measured by the lipoprint system and PGGE in obese adults at risk for CHD.

Methods

Subjects

Subjects were selected from a 10-week weight loss intervention trial. The study population has been previously described in detail [13]. Inclusion criteria were as follows: males; non-pregnant females; age 35–65 years; BMI between 30 and 39.9 kg/m^2; and not taking glucose or lipid lowering medications. The experimental protocol was approved by the Office for the Protection of Research Subjects at the University of Illinois, Chicago, and all volunteers gave their written informed consent to participate in the trial.

Blood Collection Protocol and Plasma Lipid Analysis

Twelve-hour fasting blood samples were collected between 7.00 am and 9.00 am at baseline (week 1), weeks 3, 6, and 10. Participants were instructed to avoid exercise, alcohol, and coffee for 24 h before each visit. Blood was centrifuged for 15 min at 520×*g* and 4 °C to separate the plasma from the red blood cells. The samples were stored at −80 °C between the time of collection and the time of analysis. Plasma LDL cholesterol and triglyceride concentrations were measured in duplicate using enzymatic kits (Biovision Inc., Moutainview, CA, USA).

Polyacrylamide Gradient Gel Electrophoresis (PGGE)

LDL particle size analysis was performed on whole plasma using nondenaturing 2–16% PGGE, as described previously [14, 15]. All gels were prepared in batches of 8 in our laboratory using a multi-casting chamber (Bio-Rad Laboratories Canada, Mississauga, ON, Canada). Carboxylated latex beads (Duke Science, Palo Alto, CA, USA) were used as standards for molecule size and mass. Plasma samples (3.5 μL) were mixed with a sampling buffer containing 20% sucrose and 0.25% bromophenol blue in a 1:1 (v/v) ratio. Samples were applied to each unique gel in a random fashion. All 64 samples were analyzed in one batch. After a 15-min pre-run, electrophoresis was performed at 150 V for 3 h. Gels were then stained for 1 h with Sudan black (0.07%) and stored in a 0.81% acetic acid/4% methanol solution until analysis. The Imagemaster 1-D Prime computer software (Amersham Pharmacia Biotech, Piscataway, NJ, USA) was used to analyze the gels. Integrated LDL particle size was calculated as the sum of LDL subspecies' diameter multiplied by its relative proportion [14, 15]. The relative proportion of small ($LDL_{<255\ Å}$%), medium ($LDL_{255–260\ Å}$%), and large ($LDL_{>260\ Å}$%) particles was obtained by computing the relative area of the densiometric scan (<255 Å, 255–260 Å, and >260 Å, respectively) [14, 15]. A second batch of plasma samples were analyzed to evaluate the coefficient of variation (CV) between batches. This analysis revealed that measurement of integrated particle size was highly reproducible between batches with a CV of <2%.

Quantimetrix Lipoprint LDL System

This system separates LDL subfractions by a polyacrylamide gel electrophoresis technique [9]. The lipoproteins are separated on the basis of net surface charge and size [9]. The dye used in the lipoprint system binds proportionally to the relative amount of cholesterol in each lipoprotein. High-resolution 3% polyacrylamide gel tubes were used for electrophoresis. LDL subfractionation was performed as described in the lipoprint LDL system product insert. Briefly, 25 μL of sample was mixed with 200 μL of liquid loading gel. All 64 samples were analyzed in duplicate in one batch. The loading gel contained Sudan black dye to stain the lipoproteins. The resulting mixture was added to the top of precast 3% polyacrylamide gel tubes. After photopolymerization at room temperature for 30 min, samples were electrophoresed for 1 h (3 mA/gel tube). The electrophoresis was followed by resting the tubes in the dark for 1 h. Lipoware computer software (Quantimetrix, Redondo Beach, CA, USA) was used to analyze the gels. The software divides the LDL particles into small ($LDL_{<255\ Å}$%), medium ($LDL_{255–260\ Å}$%), and large ($LDL_{>260\ Å}$%) particles. A second batch of plasma samples were analyzed to evaluate the coefficient of variation (CV) between batches. This analysis revealed that measurement of integrated particle size was highly reproducible between batches with a CV of <3%.

Statistics

Results are presented as means ± standard deviations (SD). The intra-subject reliability of the lipoprint duplicate measurements was tested on all samples by calculating the technical error of measurement (TE) as [TE = $\sqrt{(di^2/2N)}$], where *di* represents the difference between measurements on the *i*th sample, and where *N* is equal to the number of samples [16]. Pearson's correlational analysis was implemented to calculate the association between lipoprint and PGGE techniques for integrated LDL particle size, and the proportion of large, medium and small LDL particles. A paired *t* test was used to test for differences in LDL particle size parameters between the lipoprint and PGGE methods. The Bland-Altman test [17] was employed to evaluate the agreement between the two techniques. Tests for normality were undertaken for each variable. A level of statistical significance of $P < 0.05$ was used in all analyses. Data were analyzed using SPSS software (version 18.0 for Mac OS X; SPSS Inc, Chicago, IL, USA).

Results

Sixteen subjects (4 men/12 women) completed the 10-week trial, and LDL particle size was analyzed at 4 different time points. Thus, in total, 64 samples were analyzed by the lipoprint system and PGGE. The mean age and BMI of the subjects at baseline was 46.0 ± 2.4 years and 33.7 ± 1.0 kg/m^2, respectively [13]. Subject ethnicities were as follows: $n = 8$ African Americans, $n = 2$ Caucasians, and $n = 6$ Hispanic Americans. Body weight decreased from 96 ± 5 kg to 91 ± 5 kg over the course of the trial [13]. LDL cholesterol concentrations fell from 102 ± 9 mg/dL to 72 ± 8 mg/dL, while triglyceride levels decreased from 125 ± 15 mg/dL to 88 ± 15 mg/dL [13].

Mean TE for duplicate lipoprint and PGGE measurements was 0.2 ± 0.1 Å (range 0–0.6 Å) and 0.2 ± 0.1 Å (range 0–0.4 Å), respectively, for integrated particle size. These TE values suggest highly reproducible findings for the lipoprint and PGGE techniques. The lipoprint LDL system gave significantly different values for integrated LDL particle size ($P = 0.003$) when compared to the PGGE method (Table 1). In contrast, the two methods gave similar findings for the proportion of large ($P = 0.201$), medium ($P = 0.056$), and small LDL particles ($P = 0.167$). Results of the Bland–Altman test are reported in Fig. 1. The lipoprint system was shown to slightly overestimate integrated LDL particle size by 1.1 ± 3.0 Å. As for the proportion of large, medium, and small LDL particles, there was good agreement between the two methods (i.e. mean difference was <3% for each parameter).

Table 1 LDL particle size as determined by the lipoprint LDL system and polyacrylamide gradient gel electrophoresis (PGGE)

	Lipoprint	PGGE	*P* value[a]
Integrated LDL particle size (Å)	268.9 ± 6.8	267.8 ± 6.0	0.003
Proportion of large LDL particles (%)	70.1 ± 14.6	71.7 ± 17.0	0.201
Proportion of medium LDL particles (%)	19.5 ± 9.2	16.9 ± 8.7	0.056
Proportion of small LDL particles (%)	9.6 ± 7.8	11.4 ± 9.4	0.167

Mean values ± SD of the $n = 64$ samples analyzed

[a] *P* value for difference between methods (Paired *t* test)

Correlational analysis revealed a strong relationship between lipoprint and PGGE for integrated LDL particle size ($r = 0.89$, $P < 0.0001$). Similarly, good relationships between lipoprint and PGGE values were shown for the proportion of large ($r = 0.81$, $P < 0.0001$), medium ($r = 0.67$, $P < 0.0001$), and small ($r = 0.73$, $P < 0.0001$) LDL particles. The bias between lipoprint and PGGE measurements was not correlated with age, body weight, BMI, LDL cholesterol or triglyceride concentrations. Moreover, no difference in the relationship between the two methods was noted when samples with higher concentrations of LDL cholesterol were compared to samples with lower concentrations of LDL cholesterol.

Discussion

Findings from the present validation study suggest that, when compared to the PGGE technique, the lipoprint LDL system is adequate for estimating the proportion small ($LDL_{<255\ Å}$%), medium ($LDL_{255–260\ Å}$%), and large ($LDL_{>260\ Å}$%) particles, but may overestimate integrated LDL particle size. Specifically, we showed here that the mean difference between the two methods for each LDL size subfraction was <3% and non-significant. On the other hand, the lipoprint system was shown to significantly overestimate integrated LDL particle size by 1.1 Å when compared to PGGE. Thus, lipoprint may be an acceptable method for assessing the distribution of LDL particles, but not the absolute size.

To date, three other studies [9, 18, 19] have examined the adequacy of the lipoprint LDL system for the measurement of LDL particle size. For instance, Hoefner et al. [9] and Ensign et al. [18], tested the ability of lipoprint versus PGGE to classify subjects into LDL size phenotypes. In both studies [9, 18], phenotype A was defined as a predominance of large buoyant LDL particles, while phenotype B was defined as a predominance of small dense

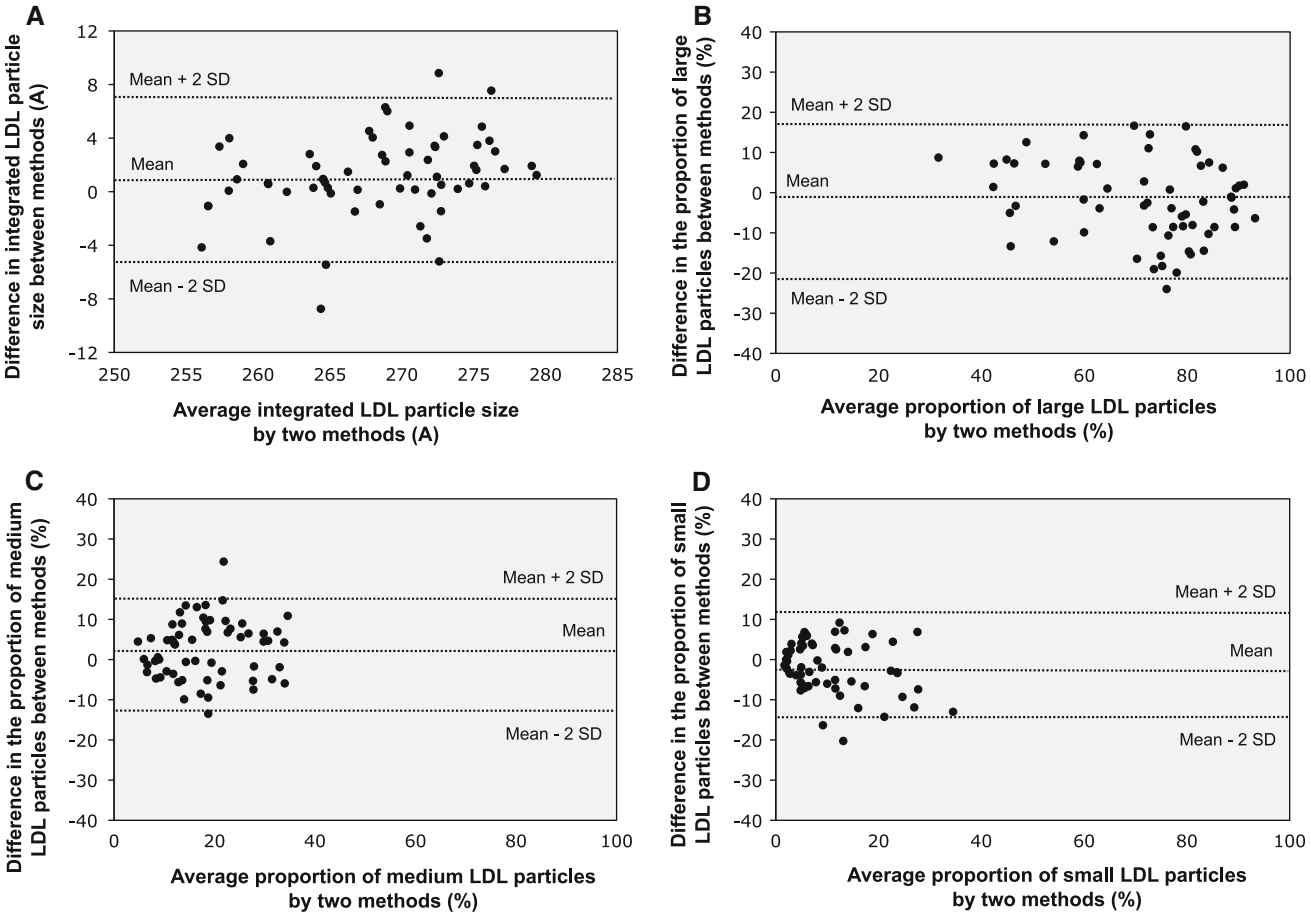

Fig. 1 Bland–Altman plot of the differences between integrated LDL particle size (**a**), and proportion of large (**b**), medium (**c**), and small LDL particles (**d**), predicted by the lipoprint LDL system versus polyacrylamide gradient gel electrophoresis (PGGE). Values for $n = 64$ samples analyzed. Difference between methods calculated as PGGE minus lipoprint values. *Dotted middle line* represents mean difference between methods (bias), and the *outside dotted lines* represent the upper and lower limits of agreement (±2 SD of the mean bias)

LDL particles. Findings from the study by Hoefner et al. [9] revealed a strong correlation between the two methods for their ability to classify individuals as phenotype A, but not as phenotype B. In contrast, Ensign et al. [18] showed a very weak association between methods for LDL size phenotyping. In the trial by Hirany et al. [19], LDL subfractionation was compared between lipoprint and PGGE techniques. Strong correlations between methods were observed for the distribution of large, medium, and small LDL particles in the 102 samples analyzed [19]. Although previous studies have attempted to validate the lipoprint system, it is difficult compare the present findings to what has been reported previously [9, 18, 19] for two main reasons. Firstly, none of the previous trials evaluated integrated particle size, thus a comparison between past and present findings cannot be made for this parameter. Secondly, these previous studies only examined the *association* between the two methods, and not the level of *agreement*. A strong correlation between two methods is simply a sign that the study includes a widespread sample, and gives no indication as to the level of agreement between the two techniques [17]. Since agreement was not measured in any of these previous trials, this statistic cannot be compared between studies. Future studies in this area should therefore aim to implement tests of agreement to complement correlational analyses to compare LDL subfractionation methodologies.

Interestingly, this cohort displayed a very low proportion of small LDL particles (<10%), and a very high proportion of large LDL particles (>70%). One possible explanation for this may be the ethnic distribution of the sample employed. Our cohort consisted of $n = 8$ African Americans, $n = 2$ Caucasians, and $n = 6$ Hispanic Americans. Recent research has shown that African Americans have a more favorable lipoprotein profile (i.e. lower proportion of small LDL particles, and higher proportion of large LDL particles) than Caucasians, despite a higher prevalence of coronary heart disease risk factors

[20]. Since half of the subjects in the study were African American, this may explain why we observed a more favorable lipoprotein profile than what would be expected if the population consisted primarily of Caucasians.

In summary, our findings demonstrate that the lipoprint system may be used as an alternative to the PGGE method for the assessment of LDL size distribution. As for the measurement of absolute size, the validity of the lipoprint system with PGGE is still uncertain. However, it is well known that LDL distribution (particularly the proportion of small LDL particles) is a stronger predictor of CHD risk than absolute size. Thus, this lower concordance between lipoprint and PGGE for absolute LDL size may not be that critical. Moreover, the lipoprint LDL system has several advantages over the PGGE method in that it is less labor-intensive, more cost-effective, faster, and not subject to inter-individual interpretation. Therefore, the lipoprint technique may be viewed as an attractive alternative to PGGE for laboratories that routinely measure LDL particle size distribution for the assessment of CHD risk. Nevertheless, since this study employed a fairly small sample size, more research is required before solid conclusions can be reached.

Acknowledgments We would like to thank the study participants who contributed their time and effort. Departmental grant, Kinesiology and Nutrition, University of Illinois, Chicago.

Conflicts of interest The authors have no conflicts of interest to report.

References

1. Krauss RM (2010) Lipoprotein subfractions and cardiovascular disease risk. Curr Opin Lipidol 21(4):305–311
2. Berneis K, Rizzo M, Spinas GA, Di Lorenzo G, Di Fede G, Pepe I, Pernice V, Rini GB (2009) The predictive role of atherogenic dyslipidemia in subjects with non-coronary atherosclerosis. Clin Chim Acta 406(1–2):36–40
3. Rizzo M, Pernice V, Frasheri A, Di Lorenzo G, Rini GB, Spinas GA, Berneis K (2009) Small, dense low-density lipoproteins (LDL) are predictors of cardio- and cerebro-vascular events in subjects with the metabolic syndrome. Clin Endocrinol (Oxf) 70(6):870–875
4. Norata GD, Raselli S, Grigore L, Garlaschelli K, Vianello D, Bertocco S, Zambon A, Catapano AL (2009) Small dense LDL and VLDL predict common carotid artery IMT and elicit an inflammatory response in peripheral blood mononuclear and endothelial cells. Atherosclerosis 206(2):556–562
5. Rizzo M, Berneis K (2006) Low-density lipoprotein size and cardiovascular risk assessment. QJM 99(1):1–14
6. Fernandez ML, Jones JJ, Ackerman D, Barona J, Calle M, Comperatore MV, Kim JE, Andersen C, Leite JO, Volek JS et al (2010) Low HDL cholesterol is associated with increased atherogenic lipoproteins and insulin resistance in women classified with metabolic syndrome. Nutr Res Pract 4(6):492–498
7. Third Report of the Expert Panel on Detection, Evaluation, and Treatment of High Blood Cholesterol in Adults (ATP III Final Report). In.: NHLBI Publication # 02-5215. National Institutes of Health; 2002:1–280
8. Superko HR, Gadesam RR (2008) Is it LDL particle size or number that correlates with risk for cardiovascular disease? Curr Atheroscler Rep 10(5):377–385
9. Hoefner DM, Hodel SD, O'Brien JF, Branum EL, Sun D, Meissner I, McConnell JP (2001) Development of a rapid, quantitative method for LDL subfractionation with use of the Quantimetrix Lipoprint LDL System. Clin Chem 47(2):266–274
10. Apostolou F, Gazi IF, Kostoula A, Tellis CC, Tselepis AD, Elisaf M, Liberopoulos EN (2009) Persistence of an atherogenic lipid profile after treatment of acute infection with Brucella. J Lipid Res 50(12):2532–2539
11. Lagos KG, Filippatos TD, Tsimihodimos V, Gazi IF, Rizos C, Tselepis AD, Mikhailidis DP, Elisaf MS (2009) Alterations in the high density lipoprotein phenotype and HDL-associated enzymes in subjects with metabolic syndrome. Lipids 44(1):9–16
12. Abbas JM, Chakraborty J, Akanji AO, Doi SA (2008) Hypothyroidism results in small dense LDL independent of IRS traits and hypertriglyceridemia. Endocr J 55(2):381–389
13. Varady KA, Bhutani S, Church EC, Klempel MC (2009) Short-term modified alternate-day fasting: a novel dietary strategy for weight loss and cardioprotection in obese adults. Am J Clin Nutr 90(5):1138–1143
14. St-Pierre AC, Ruel IL, Cantin B, Dagenais GR, Bernard PM, Despres JP, Lamarche B (2001) Comparison of various electrophoretic characteristics of LDL particles and their relationship to the risk of ischemic heart disease. Circulation 104(19): 2295–2299
15. Tchernof A, Lamarche B, Prud'Homme D, Nadeau A, Moorjani S, Labrie F, Lupien PJ, Despres JP (1996) The dense LDL phenotype. Association with plasma lipoprotein levels, visceral obesity, and hyperinsulinemia in men. Diabetes Care 19(6): 629–637
16. Malina RM HP, Lemeshow S (1973) Selected measurements of children 6–11 years. United States (Vital and Health Statistics Series 11, No. 123, U.S.D.H.H.S.). US Government Printing Office, Washington, DC
17. Bland JM, Altman DG (1986) Statistical methods for assessing agreement between two methods of clinical measurement. Lancet 1(8476):307–310
18. Ensign W, Hill N, Heward CB (2006) Disparate LDL phenotypic classification among 4 different methods assessing LDL particle characteristics. Clin Chem 52(9):1722–1727
19. Hirany SV, Othman Y, Kutscher P, Rainwater DL, Jialal I, Devaraj S (2003) Comparison of low-density lipoprotein size by polyacrylamide tube gel electrophoresis and polyacrylamide gradient gel electrophoresis. Am J Clin Pathol 119(3):439–445
20. Miljkovic-Gacic I, Bunker CH, Ferrell RE, Kammerer CM, Evans RW, Patrick AL, Kuller LH (2006) Lipoprotein subclass and particle size differences in Afro-Caribbeans, African Americans, and white Americans: associations with hepatic lipase gene variation. Metabolism 55(1):96–102

lecithin cholesterol acyl transferase mediate the synthesis of CE within cells and in high-density lipoprotein, respectively [5, 6]. Based on the importance of plasma levels of free and esterified cholesterol, it is likely that plasma levels of specific molecular species of CE may have utility as predictors of atherosclerosis, diabetes mellitus, coronary heart disease and cancer [7–9]. It should also be noted that within cells the appearance of CE-enriched lipid droplets is a consequence of impaired metabolism or overnutrition [9, 10]. Furthermore, elevated tissue CE levels are observed in tumors [11].

Mass spectrometry potentially affords rapid high-throughput chemical analysis to interrogate the role of lipids in cellular, tissue and systemic physiological and pathophysiological processes [12, 13]. However, mass spectrometry (MS) of CE is complicated by the presence of other lipids having common isobaric molecular ions (e.g., diacylglycerols), which hinders both the identity and quantification of individual CE by single stage mass spectrometry. Soft ionization techniques have been used in the past for CE analyses, specifically the use of matrix-assisted laser desorption/ionization [14] and electrospray ionization (ESI) [15–17]. It is recognized that ESI can provide efficient quantification of lipid species in complex matrices without the need for derivatization. Although, ammoniated adducts of CE have been used for detection of molecular species using ESI–MS, this adduct produces only moderate levels of MS/MS fragmentation [18, 19]. In this study, ESI–MS/MS strategies were developed and optimized for the species-selective analysis of multiple CE molecular species using sodiated adducts. In comparison to ammoniated adducts of CE, fragmentation of sodiated adducts of a CE result in the loss of a cholestane as a neutral fragment. Based on this fragmentation, neutral loss scanning was developed to quantify sodiated adducts of CE molecular species. This technique was subsequently applied to examine CE molecular species in mouse macrophages supplemented with either linoleic acid or arachidonic acid, as well as in the plasma of mice fed specific diets.

Materials and Methods

Standards and Solvents

Fatty acids and CE molecular species standards, including myristate (14:0), palmitate (16:0), palmitoleate (16:1), heptadecanoate (17:0), stearate (18:0), oleate (18:1), linoleate (18:2), arachidonate (20:4), and docosahexaenoate (22:6) were purchased from NuChek Prep (Elysian, MN). Distearin (18:0–18:0 or 36:0) and diarachidin (20:0–20:0 or 40:0) were also purchased from NuChek Prep (Elysian, MN). Chloroform and methanol were of HPLC grade and were purchased from Burdick and Jackson (Muskegon, MI).

Electrospray Ionization-Mass Spectrometric Analysis

Direct-infusion electrospray ionization mass spectrometry of CE was performed in positive ion mode using a Thermo Fisher TSQ Quantum Ultra with Xcalibur data acquisition software. Samples were analyzed at a flow rate of 3 μL/min. Tune parameters were optimized for CE analyses, and were set at spray voltage = 3,800 V, sheath gas = 8 (arbitrary units), ion sweep gas pressure = 0.5 (arbitrary units), auxiliary gas pressure = 5 (arbitrary units), and capillary temperature = 270 °C. Spectra for survey scans were acquired for five min with a scan rate of 0.5 scans/s. In each MS/MS mode, the collisional energy for the analyses of CE molecular species was set at 25 eV. Spectra for MS/MS scan modes were acquired over 3 min with a scan rate of 0.5 scans/s.

Fatty Acid Supplementation of J774 Cells

J774 cells were a generous gift from Dr. George Rothblat (Children's Hospital of Philadelphia). Mouse J774 monocyte-derived macrophages were maintained at 37 °C with 5% CO_2 in RPMI-1640 (Sigma) supplemented with 10% v/v fetal bovine serum (Atlanta Biologicals) and 1× antibiotic/antimycotic (Sigma). For the fatty acid supplementation, either 50 μM linoleic or arachidonic acid were suspended in media as an ethanol injectate (ethanol <0.1% v/v), and cells were treated with these fatty acids for 24 h followed by a second supplementation with the same concentration of either fatty acid for an additional 24 h. Negative control conditions for the fatty acid-supplementation condition included incubating cells with vehicle-treated media only. Cells were then extracted in the presence of 17:0 CE internal standard by a modified Bligh-Dyer technique [20] with saline in the aqueous phase. The collected chloroform phases were sequentially dried under nitrogen, resuspended in 250 μL of chloroform, and stored under N_2 at −20 °C until analysis. For direct-infusion ESI analysis, 50 μL of the resuspended lipid solution (in chloroform) was added to 200 μL of methanol. NaOH was added to each sample at a concentration of ~10 μM. The ion intensity of each CE molecular species was divided by the ion intensity of the internal standard (CE 17:0), and the mass of each molecular species was determined using parameters from response calibration lines determined for each molecular species in comparison to 17:0 CE. Values for CE molecular species are normalized to cell protein (Bio-Rad Laboratories, Inc., Hercules, CA).

Mouse Feeding Studies

Six week old female C57BL6 mice were started on Western diets (Harlan Teklad 88137) and they remained on this diet for 14 weeks. Control, age-matched female mice were

fed regular chow diet (Teklad 2018S) for the same interval. Blood was collected at the end of this interval by cardiac puncture, and plasma was prepared by centrifugation. Ten microliters of mouse plasma was extracted in the presence of 17:0 CE internal standard by a modified Bligh-Dyer technique [20] with saline in the aqueous phase. Plasma lipid extracts were then subjected to direct infusion ESI–MS for the analyses of CE molecular species.

Preparation of Oxidized Unsaturated CE

Selected CE molecular species (1 nmol) were dried under nitrogen in 12 × 100 mm borosilicate test-tubes and were either immediately resuspended in 250 μL methanol/chloroform (4/1) or were exposed to ambient air for 6 or 15 h prior to being resuspended in 250 μL methanol/chloroform (4/1). For each sample, 1 nmol of 17:0 CE was added as an internal calibrant. Precursor CE molecular species and their oxidized products were subsequently examined by neutral loss scan of 368.5 employing the parameters described above. The CE and CE oxidation species were monitored as sodiated adducts following the addition of NaOH.

Results

Direct Infusion ESI–MS of Sodiated Adducts of Individual CE Molecular Species

As a first step to examine the feasibility of using sodiated adducts of CE for their quantification by mass spectrometry, survey scan spectra and collisionally-activated dissociation (CAD) spectra were collected for 16:0 and 18:2 CE. Data shown in Fig. 1 show the survey scans of sodiated adducts of both 16:0 and 18:2 CE (Panels A & B), and the collisionally-activated dissociation (CAD) spectra of each molecular species with both the cholestane (*m*/z 369.2) and sodiated fatty acid ions (279.04 and 303.08) observed (Panels C & D, Fig. 1). While others have shown that CAD of molecular ions of ammonium adducts of CE yields a robust cholestane positive ion [16, 21, 22], these results show that the sodiated adduct only forms a weak cholestane positive ion and preferentially loses this residue as a neutral in concert with the appearance of an abundant sodiated fatty acyl positive fragment ion. Panels E & F of Fig. 1 show the parent ion (PI) scans using the product ion of the sodiated ion fatty acid (e.g., PI 279.04 and 303.08 for 16:0 CE and 18:2 CE of the sodiated adducts, respectively). It is important to appreciate that the fragmentation of the sodiated CE molecular species to their respective metal ion fatty acyl fragment represents the loss of the neutral fragment cholestane, and this neutral loss can, thus, be potentially useful in uniformly detecting CE. Indeed, Fig. 2 shows the neutral loss (NL) scan of 368.5 of an equimolar mixture of CE molecular species. Importantly, it should be noted that CE with varying degrees of unsaturation have different ionization efficiencies. Positive ions of sodiated adducts of CE molecular species have a greater intensity as the degree of unsaturation increases for sodiated adducts of CE. Accordingly, ionization of the sodiated adduct of each CE molecular species was compared to that of 17:0 CE to determine their relative responses. In addition, 17:0 CE was used in subsequent studies as an internal standard to quantify CE molecular species in biological samples. Table 1 shows the individual calibration constants for the sodiated CE molecular species. Examination of these calibration constants reflect the increased ionization intensities of polyunsaturated CE molecular species with these molecular species having increased slopes compared to the monounsaturated and saturated molecular species. Corrections for disparate ion intensities of these CE molecular species are predominantly dependent on the response factor (slope of calibration lines), and the impact of the *y*-intercepts is generally negligible.

Resolving CE Molecular Species from Isobaric Ions Using the NL 368.5 Scan Mode

NL scanning for 368.5 was used to examine CE in the presence of isobaric diacylglycerol (DAG) molecular species to assess the utility of this NL 368.5 approach for the specific detection of CE molecular species. For this analysis, 16:0 CE and distearin (18:0-18:0 DAG) were examined as sodiated adducts, which both have molecular ions at 647 (Fig. 3). Panels A and D of Fig. 3 show the survey scan and NL 368.5 scan, respectively, for a mixture of 16:0 and 17:0 CE, which have molecular ions at *m*/*z* 647.6 and 661.6, respectively. Panels B and E show the same scans for the analyses of a mixture of 18:0-18:0 DAG and diarachidin (20:0-20:0 DAG), which have molecular ions at 647.5 and 703.6, respectively. These sodiated adducts of the DAGs are not detected with the CE-specific NL 368.5 scan mode (Panel E). Panels C and F show the survey scan and NL 368.5 scan, respectively, for the analyses of all four CE and DAG species in one mixture. In this isobaric mixture, a large *m*/*z* 647 ion was observed in the survey scan (Panel C) due to the presence of the two isobaric lipids. Note that the ion at 647 in the survey scan (Panel C) is greater in intensity than the two internal calibrants (17:0 CE and 20:0-20:0 DAG). However, only the CE molecular species were detected in the NL 368.5 scan (Panel F), and yielded equal ion intensities for this analysis since the saturated CE were present at equimolar concentrations. Thus, these data demonstrate that NL 368.5 scanning can be used to distinguish isobaric CE from DAG molecular species using sodiated adducts.

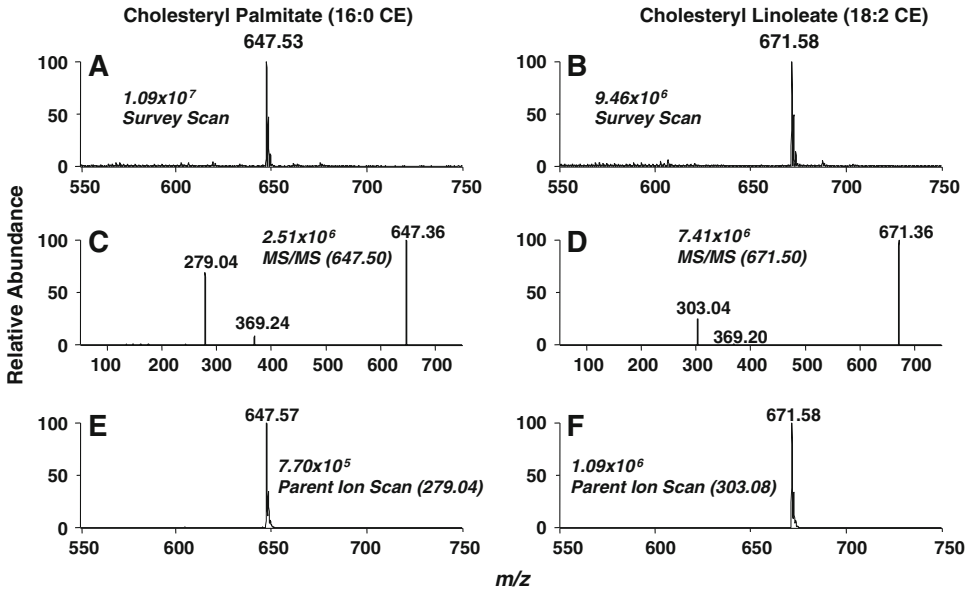

Fig. 1 Survey, CAD, and parent ion scans of sodiated cholesteryl palmitate (16:0 CE) and linoleate (18:2 CE) using direct-infusion ESI–MS analysis. Survey scans (**a**, **b**) were acquired for five min over the *m*/*z* range of 550–750. The CAD analysis (**c**, **d**) was performed at a collisional energy of 25 eV. Parent ion scans (**e**, **f**) were acquired from the sodiated fatty acyl fragment (25 eV). The concentrations of 16:0 and 18:2 CE were 10 μM. The NaOH added prior to ESI analysis was 10 μM

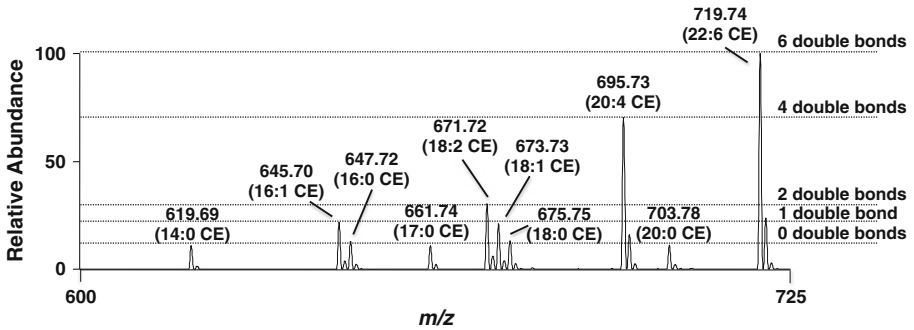

Fig. 2 Neutral loss of 368.5 MS/MS analyses of an equimolar mixture of the cholesteryl esters (each at 2 μM) as sodiated adducts. Spectra were obtained using the neutral loss 368.5 at a collisional energy of 25 eV as described in "Materials and Methods". *Horizontal dashed lines* highlight the disparate ionization efficiencies associated with CE molecular species containing different levels of unsaturation

CE Molecular Species in J774 Cells Supplemented with Specific Fatty Acids in Cell Culture Media

To test the NL 368.5 scan as a technique to quantify CE molecular species of sodiated adducts in biological samples, we treated mouse monocyte-derived macrophages (J774 cells) with media that was supplemented with specific fatty acids to delineate the fatty acid incorporation into CE molecular species. The mass spectra using NL 368.5 for cells without fatty acid treatment revealed that 18:1 CE (673.73) was predominantly present in J774 cells grown in the cell culture media with minimal levels of 18:2 and 20:4 CE present in these cells (Fig. 4, Panel A). In the spectra shown in Fig. 4, *m*/*z* 661.7 is the sodiated adduct of the internal standard, 17:0 CE. Figure 4, Panel B demonstrates that J774 cells supplemented with linoleic acid in the media have increased levels of intracellular 18:2 CE (671.73). Interestingly, as shown in Fig. 4 (Panel C), J774 cells incorporate arachidonic acid into CE pools (*m*/*z* 695.72), and also apparently elongate 20:4 to 22:4 and 24:4 under these cell culture conditions leading to the appearance of 22:4 and 24:4 CE (e.g., 723.76 and 751.84, respectively). Additional analyses showing the accumulation of 22:4 and 24:4 CE molecular species were performed with the addition of both 17:0 CE and 18:3 CE added as internal calibrants (Supplemental Figure). The inclusion of 18:3 CE did not impact the relative spectral intensities of the endogenous CE as well as the 17:0 CE standard. (Supplemental Figure). The amounts of specific CE for J774 cells treated with either linoleic or arachidonic acid compared to cells with no fatty acid treatment are summarized in Fig. 5. With both fatty acid supplementations to the cell culture media, the respective CE molecular species increased with an accompanied decrease in the amount of 18:1 CE. The total CE levels only marginally changed in cells treated with fatty acids due to the accumulation of new molecular species being offset by the decrease in 18:1 CE levels.

Table 1 Calibration line parameters for sodiated adducts of CE molecular species

CE	NL 368.5 $[M + Na]^+$	Line parameters
14:0	619.54	$y = 0.8503x - 0.0073$
16:0	647.57	$y = 1.0642x - 0.0057$
16:1	645.56	$y = 2.3832x + 0.0088$
18:0	675.61	$y = 1.1076x - 0.0258$
18:1	673.59	$y = 1.9934x + 0.0094$
18:2	671.57	$y = 2.7519x - 0.0151$
18:3	669.56	$y = 3.4011x + 0.0379$
20:4	695.57	$y = 4.6394x - 0.1213$
22:6	719.57	$y = 4.8166x - 0.1237$

Linear regression of ion intensity responses for each CE molecular species over a concentration range of 0.1–10 μM was determined. In all cases, the coefficient of determination (R^2) was greater than 0.99. The internal standard, 17:0 CE was constant at 2 μM

Mouse Plasma CE Molecular Species

To further illustrate the utility of NL 368.5 scanning for CE using sodiated adducts, we examined the CE molecular species in the lipid extracts prepared from plasma isolated from female mice fed either normal chow (Panels A & B of Fig. 6) or a Western diet (Panels C & D of Fig. 6). Survey scans in the positive ion mode (Panels A & C) showed CE molecular species amongst other isobaric positive ions, which potentially may preclude an accurate quantification of the CE molecular species. Panels B & D are the same lipid extracts but were subjected to NL 368.5 scanning for CE identification. From these scans, it was readily appreciated that the overall plasma CE levels were elevated and that the CE molecular species profile was much more diverse in mice fed the Western diet (comparing Panels B & D of Fig. 6). Figure 7 summarizes the quantitative data for the plasma CE in mice fed these two diets. In particular, the Western diet led to large increases in both 16:1 and 18:1 CE molecular species. These changes may reflect either increased production of monounsaturated fatty acids that are subsequently incorporated into the CE pool or, alternatively, enrichment of oleic acid in the Western diet (Teklad diet data). Interestingly, the Western diet is not enriched with palmitoleic acid. Also, it should be noted that the Western diet was enriched with cholesterol in comparison to the normal chow diet, which was likely responsible for the almost two-fold increase in total CE levels present in the plasma of these mice.

Oxidative Modification of Unsaturated CE Molecular Species

Studies with arachidonic acid supplementation of J774 cells unexpectedly revealed that arachidonic acid addition led to an increase in elongated CE molecular species, which were observed in the CE pool (Fig. 4). This finding was rapidly determined using the NL 368.5, which is CE class-specific. Similarly this technique was used to examine air oxidation of CE with varying degrees of unsaturation (Fig. 8). NL 368.5 scans of 18:0 CE exposed to ambient air for 15 h indicated that this saturated molecular species was not degraded in an oxidizing environment (Fig. 8, Panel A). In contrast, 18:2, 20:4 and 22:6 CE molecular species were significantly oxidized after exposure to ambient air for 15 h (Panels B–D). Note that in these same analyses, 17:0 CE was added prior to ESI–MS analyses to allow relative

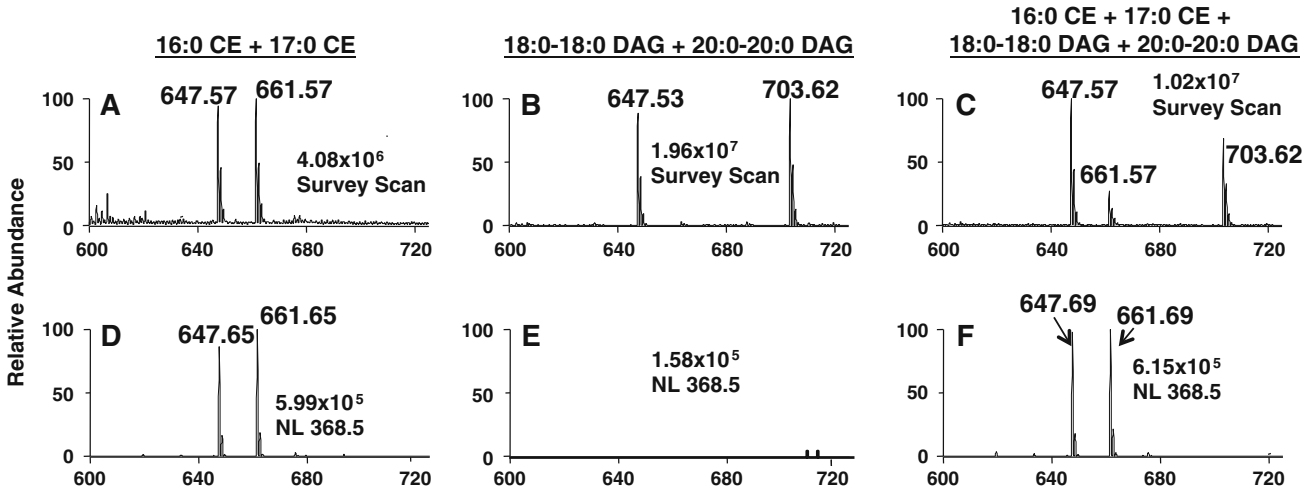

Fig. 3 MS and MS/MS analyses of CE and DAG sodiated adducts. 16:0 CE (*m/z* 647) and 17:0 CE (661) (**a**, **d**), 18:0-18:0 DAG (*m/z* 647) and 20:0-20:0 DAG (703) (**b**, **e**), and a mixture of both CE and DAGs (**c**, **f**) (all lipids present at a concentration of 5 μM) were subjected to direct-infusion ESI–MS analysis. Panels **a**–**c** are survey scans of each lipid mixture over an *m/z* range of 600–725 for five min. Panels **d**–**f** are scans for the neutral loss of 368.5, which were acquired for three min. The collisional energy for the MS/MS analysis of the CE molecular species was 25 eV. The NaOH added prior to ESI analysis was 10 μM

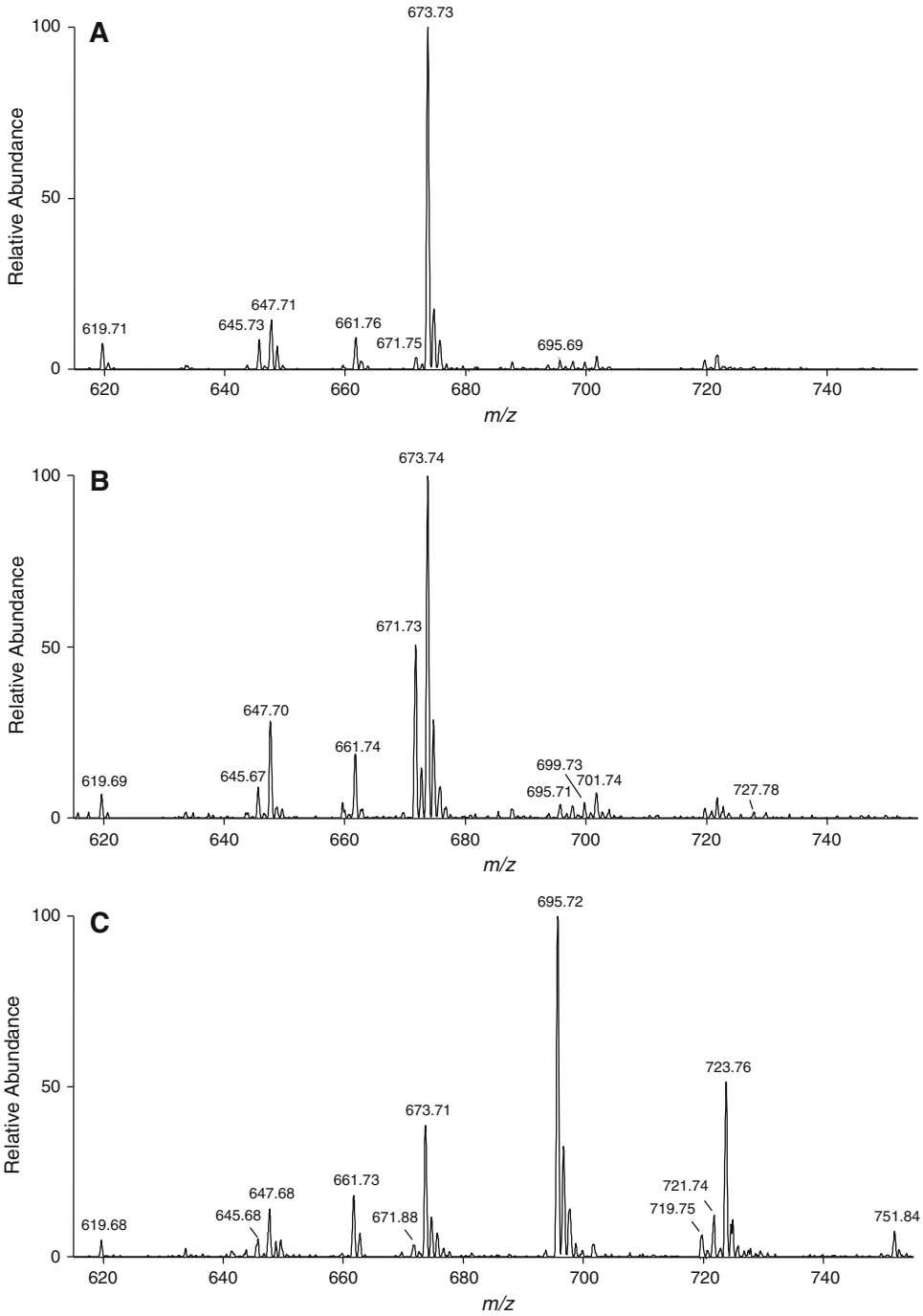

Fig. 4 NL 368.5 scans of sodiated CE present in J774 cells. J774 cells were cultured in the presence of either no fatty acid supplementation (**a**), linoleic acid supplementation (**b**) or arachidonic acid supplementation (**c**). At the end of the cell culture treatment interval, lipids were extracted from J774 cells with 17:0 CE added as an internal standard as described in detail in "Materials and Methods". Neutral loss scans were acquired for five minutes at a collisional energy of 25 eV. NaOH added prior to ESI analysis was 10 μM

comparisons of the parent CE loss due to air oxidation. Close examination of the NL 368.5 scans of 18:2 CE exposed to ambient air revealed oxidation of the parent sodiated adduct of 18:2 CE (671.80) and the appearance of species enriched with one oxygen (*m/z* 685.80 and 687.80) and two oxygens (*m/z* 701.79 and 703.79) (Fig. 8, Panel B). These oxidized molecular species likely reflect the incorporation of oxygen into the parent molecule with 14 and 16 amu increases that likely represent the formation of oxo-ODE and epoxide species, respectively [8, 23]. It is also clear from these studies that as the degree of unsaturation increases in CE (e.g., 20:4 CE and 22:6 CE), the relative rate of CE oxidation increases (Fig. 8). It is envisioned that this rapid analytical method has utility in assessing the oxidation of unsaturated molecular species of CE that are added exogenously in experimental models. Furthermore, the fragmentation of specific species produced in vivo under oxidizing conditions could potentially be detected with this NL technique particularly in conjunction with chromatography.

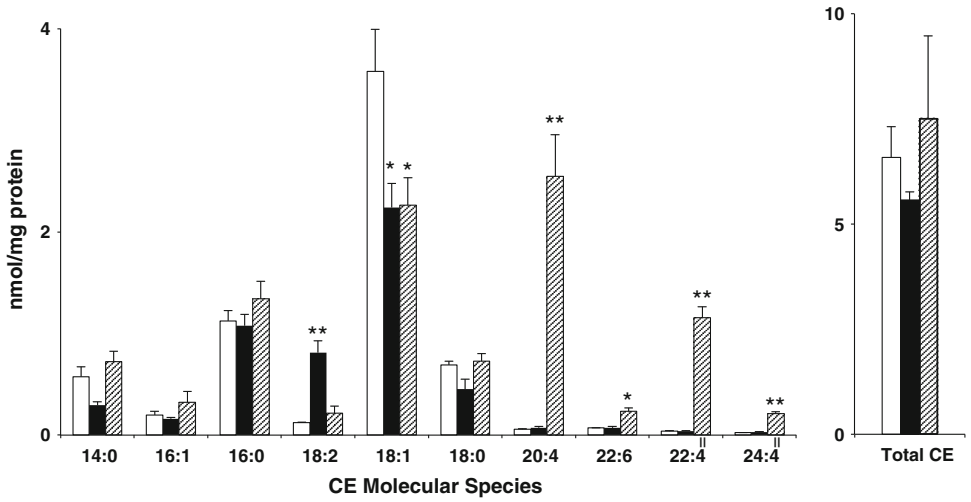

Fig. 5 CE molecular species present in J774 cells. J774 cells were cultured in the presence of either no fatty acid supplementation (*open bars*), linoleic acid supplementation (*black bars*) or arachidonic acid supplementation (*hatched bars*). At the end of the cell culture treatment interval, lipids were extracted from J774 cells with 17:0 CE added as an internal standard, and were subsequently subjected to ESI–MS using NL 368.5 scanning as described in detail in "Materials and Methods". Values are the means + SEM for $n = 3$. All values were corrected by calibration constants in Table 1 with the exception of those indicated (‖), which were corrected with the response factor (slope) of the corresponding shorter chain fatty acid with the same degree of unsaturation. For example, 22:4 and 24:4 CE were corrected using the 20:4 response factor. These elongated CE molecular species were not available to derive response curves. * and ** indicate $p < 0.05$ and $p < 0.005$ for comparisons between no fatty acid supplementation and indicated fatty acid supplementation conditions

Discussion

CE is predominantly found in the core of lipoproteins and lipid droplets [7, 8, 10]. Total plasma cholesterol and its association with specific lipoproteins is an important indicator of cardiovascular risk. Total plasma cholesterol is comprised of both free and esterified cholesterol. Both free cholesterol and CE is carried in plasma by lipoproteins. Despite the importance of CE as an indicator of cardiovascular disease, determining the specific aliphatic fatty acid associated with the CE is often overlooked in both clinical and experimental analyses, which is typically determined by removing the fatty acid by cholesteryl esterase, and then coupling cholesterol oxidase with a colorimetric readout. Using MS, CE molecular species form relatively poor protonated ions compared to other lipids containing class-specific functional groups that ionize [12, 24]. Previous studies have used ammonium acetate to create $[M + NH_4]^+$ ions of lipids using ESI–MS [15–17, 25]. Several groups [16, 21, 22] have examined ammoniated adducts of CE, which under CAD conditions results in predominant cholestane cation fragment. In comparison to the fragmentation of ammoniated adducts of CE, the sodiated adduct had an intense sodiated fatty acid fragment from the neutral loss of the cholestane residue. In addition, lithiated adducts of CE have also been shown to preferentially form lithiated fatty acid fragments in comparison to the cholestane cation observed with ammoniated adducts [26]. It should be appreciated though that the use of sodium to form adducts of CE enables faster workup of samples and is less problematic compared to the use of lithium, which requires extensive back extractions to remove sodium from biological samples.

Overall the goal of this study was to develop an electrospray ionization MS/MS method that could be readily used to quantify CE in biological samples and overcome potential interference and inaccuracies associated with other positive ions that are present in the mass range of biologically relevant CE ($\sim$ m/z 600–750 for sodiated adducts). Data shown in Fig. 3 clearly shows that NL 368.5 scanning specifically detects CE and does not detect isobaric DAG molecular species. Furthermore comparisons of positive ion survey scans and NL 368.5 scans shown in Fig. 6 from lipid extracts of mouse plasma demonstrates the utility of NL 368.5 scanning for detection of CE in complex biological matrices. Similar to other CE adducts that have been assessed in the past [16, 26], CE molecular species with varying degrees of unsaturation were shown to have different ionization efficiencies. CE have a weak dipole that is enhanced in the presence of sodium, and, similar to the dipole of triglycerides and CE with other adducts, the dipole in sodiated CE is dependent on the aliphatic chain length and more specifically the degree of unsaturation of the aliphatic group [12, 15, 16, 27]. Due to the varying degree of chain length and unsaturation for CE present in complex biological samples, it was necessary to generate individual calibration lines for each CE molecular species to correct for disparate responses compared to that of the internal standard (17:0 CE).

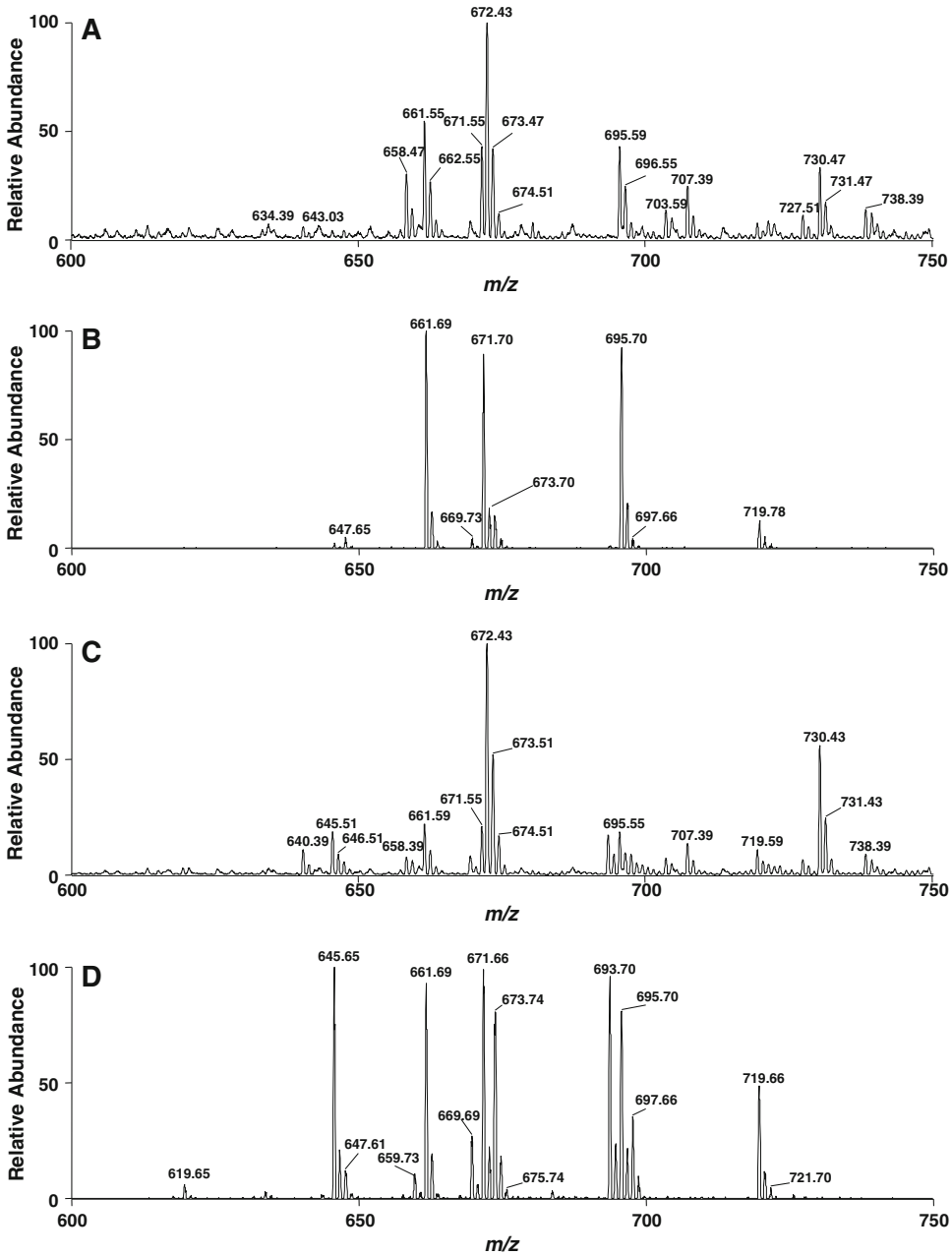

Fig. 6 Survey and NL 368.5 scans of sodiated cholesteryl esters present in mouse plasma. Female mice were fed a diet of either normal chow (**a**, **b**) or Western diet chow (**c**, **d**) for 14 weeks, and plasma was subsequently collected for the analyses of CE molecular species as described in detail in "Materials and Methods". Survey scans (**a**, **c**) and NL 368.5 scans (**b**, **d**) at a collisional energy of 25 eV were each acquired for five min. The NaOH added prior to ESI analysis was 10 μM

It should be appreciated that the use of neutral loss 368.5 scanning for the detection of CE molecular species can also be applied to rapidly determine alterations in the CE molecular species within biological samples, as well as assess fatty acyl decomposition of CE. We performed three experiments that demonstrate the utility of this technique. In the first study, J774 cells were treated with physiological concentrations (50 μM) of either linoleic acid or arachidonic acid, and then we assessed their effect on cellular CE composition. The predominant CE in J774 cells under normal cell culture conditions (control) was 18:1 CE. With addition of either linoleic or arachidonic acid to the cell culture media there was as drop in 18:1 CE levels accompanied by an increase in 18:2 or 20:4 CE respectively. Analyses using NL 368.5 scanning also revealed the somewhat unexpected finding that fatty acid chain elongation products were present in the CE pool of J774 cells treated with arachidonic acid (i.e., 22:4 and 24:4 CE were present). It should be noted that arachidonic acid has previously been shown to undergo elongation, and interestingly 22:4 CE is the predominant CE in the adrenal gland [28, 29]. In the second study, female mice were fed either a normal chow or Western diet for 14 weeks, and plasma CE levels were examined. In the normal chow fed female mouse, the predominant plasma CE were 18:2 and 20:4 CE. In comparison to the chow fed female mice, female

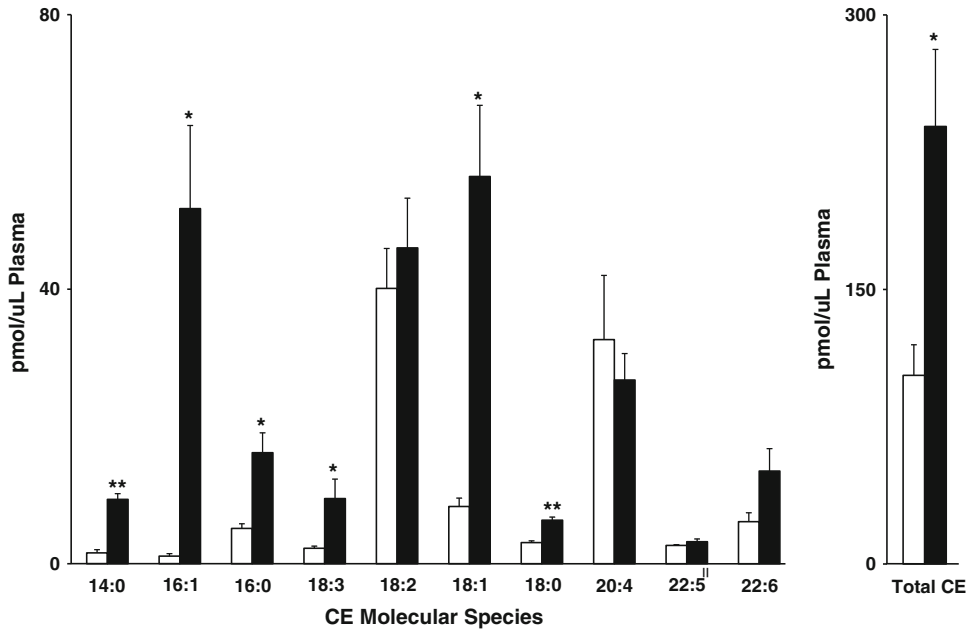

Fig. 7 Plasma CE molecular species in female mice fed either normal chow diet or Western diet. Female mice were fed a diet of either normal chow (*open bars*) or Western diet chow (*black bars*) for 14 weeks, and plasma was subsequently collected for the analysis of CE molecular species using NL 368.5 scans as described in detail in "Materials and Methods". All values were corrected by calibration constants in Table 1 with the exception of 22:5 CE (‖), which was corrected with the response factor (slope) of 20:4 CE. Values are the means + SEM for $n = 3$. * and ** indicate $p < 0.05$ and $p < 0.005$ for comparisons between normal chow diet and the Western diet

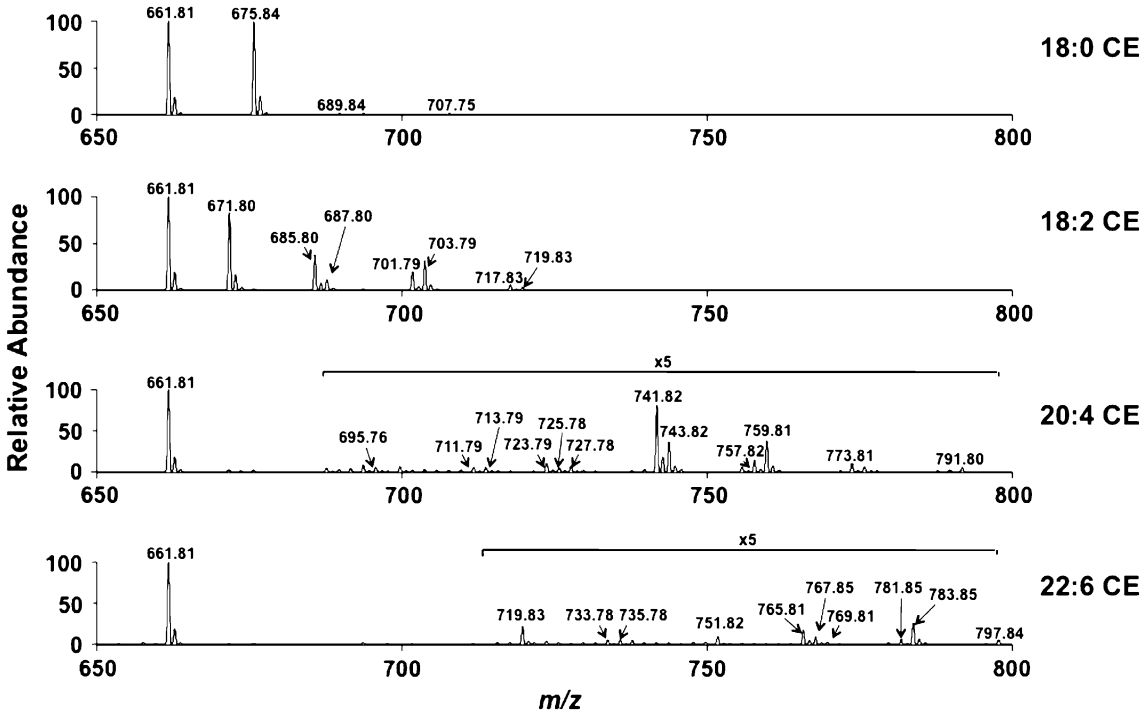

Fig. 8 Comparative oxidation of saturated and unsaturated CE. Indicated CE molecular species (18:0, 18:2, 20:4, and 22:6 molecular species) were dried individually and exposed to ambient air for 15 h. Treatments were terminated by resuspending CE in methanol/chloroform (4/1) containing equimolar 17:0 CE added as an internal calibrant. Each treated CE was subsequently subjected to direct-infusion ESI–MS analyses using neutral loss 368.5 scanning of sodiated adducts as described in "Materials and Methods". In the absence of oxidizing conditions, NL 368.5 analyses showed precursor CE were not decomposed and no oxidized products were observed

mice on a Western diet had nearly the same levels of 18:2 and 20:4 CE, but had a large increase in both 18:1 and 16:1 CE leading to a doubling of the total CE level. In the third study, we examined the air oxidation of several CE standards using the NL 368.5 scan mode to monitor the specific oxidation of CE molecular species. Oxidation of polyunsaturated species of CE is a concern both in the food industry since oxidized CE contribute to the rancid nature of spoiled oils [30], and from a health perspective since oxidized CE molecular species present in lipoproteins are a key contributor to the development of early atherosclerotic fatty streaks [8, 23]. Data herein demonstrates that the neutral loss technique can be used to quantitatively assess the loss of the CE molecular species to oxidation as well as the concomitant qualitative visualization of the oxidized products. It should be appreciated that CE that contain increasing levels of unsaturation are much more susceptible to air oxidation, and saturated CE are relatively stable when exposed to air under the conditions employed. These oxidation studies focused on the oxidation of the aliphatic chain of polyunsaturated molecular species of CE, and not the oxidation of the sterol nucleus. Sterol nucleus oxidation would probably not be detectable by the neutral loss of the cholestane fragment since the cholestane residue would be modified. Additionally, quantifying the oxidized species of CE will require comparing authentic oxidized CE molecular species to an internal standard to obtain species-specific response factors. Taken together, these three experimental approaches illustrate the utility of NL 368.5 scans of the positive ion sodiated adducts of CE in biological samples as well as the verification that the polyunsaturated fatty acid constituents of CE are intact and not oxidized.

In summary, these studies demonstrate the feasibility of forming sodiated adducts of CE molecular species, which can then be specifically detected by NL scanning of 368.5. Sodiated adducts can be readily formed in biological matrices extracted in the presence of saline in the aqueous phase and with the addition of micromolar concentrations of NaOH to samples subjected to direct infusion ESI–MS. Furthermore, since this is a lipid class-specific technique, direct infusion ESI–MS/MS can be used to quantify CE molecular species accurately in the presence of isobaric species in complex or crude biological lipid extracts.

Acknowledgments This research was supported by NIH grants HL074214, HL088073, HL098907 and RR019232 (DAF).

References

1. Brown MS, Ho YK, Goldstein JL (1980) The cholesteryl ester cycle in macrophage foam cells. Continual hydrolysis and re-esterification of cytoplasmic cholesteryl esters. J Biol Chem 255:9344–9352
2. Meng X, Zou D, Shi Z, Duan Z, Mao Z (2004) Dietary diacylglycerol prevents high-fat diet-induced lipid accumulation in rat liver and abdominal adipose tissue. Lipids 39:37–41
3. Schwartz CC, VandenBroek JM, Cooper PS (2004) Lipoprotein cholesteryl ester production, transfer, and output in vivo in humans. J Lipid Res 45:1594–1607
4. Brown MS, Goldstein JL (1997) The SREBP pathway: regulation of cholesterol metabolism by proteolysis of a membrane-bound transcription factor. Cell 89:331–340
5. Francone OL, Gurakar A, Fielding C (1989) Distribution and functions of lecithin:cholesterol acyltransferase and cholesteryl ester transfer protein in plasma lipoproteins. Evidence for a functional unit containing these activities together with apolipoproteins A-I and D that catalyzes the esterification and transfer of cell-derived cholesterol. J Biol Chem 264:7066–7072
6. Suckling KE, Stange EF (1985) Role of acyl-CoA: cholesterol acyltransferase in cellular cholesterol metabolism. J Lipid Res 26:647–671
7. Brecher PI, Chobanian AV (1974) Cholesteryl ester synthesis in normal and atherosclerotic aortas of rabbits and rhesus monkeys. Circ Res 35:692–701
8. Harkewicz R, Hartvigsen K, Almazan F, Dennis EA, Witztum JL, Miller YI (2008) Cholesteryl ester hydroperoxides are biologically active components of minimally oxidized low density lipoprotein. J Biol Chem 283:10241–10251
9. Zock PL, Mensink RP, Harryvan J, de Vries JHM, Katan MB (1997) Fatty acids in serum cholesteryl esters as quantitative biomarkers of dietary intake in humans. Am J Epidemiol 145:1114–1122
10. Mahlberg FH, Glick JM, Jerome WG, Rothblat GH (1990) Metabolism of cholesteryl ester lipid droplets in a J774 macrophage foam cell model. Biochim Biophys Acta 1045:291–298
11. Tosi MR, Bottura G, Lucchi P, Reggiani A, Trinchero A, Tugnoli V (2003) Cholesteryl esters in human malignant neoplasms. Int J Mol Med 11:95–98
12. Han X, Gross RW (2005) Shotgun lipidomics: electrospray ionization mass spectrometric analysis and quantitation of cellular lipidomes directly from crude extracts of biological samples. Mass Spectrom Rev 24:367–412
13. Wenk MR (2005) The emerging field of lipidomics. Nat Rev Drug Discov 4:594–610
14. Schiller J, Süß R, Arnhold J, Fuchs B, Leßig J, Müller M, Petkovic M, Spalteholz H, Zschörnig O, Arnold K (2004) Matrix-assisted laser desorption and ionization time-of-flight (MALDI-TOF) mass spectrometry in lipid and phospholipid research. Prog Lipid Res 43:449–488
15. Hutchins PM, Barkley RM, Murphy RC (2008) Separation of cellular nonpolar neutral lipids by normal-phase chromatography and analysis by electrospray ionization mass spectrometry. J Lipid Res 49:804–813
16. Liebisch G, Binder M, Schifferer R, Langmann T, Schulz B, Schmitz G (2006) High throughput quantification of cholesterol and cholesteryl ester by electrospray ionization tandem mass spectrometry (ESI–MS/MS). Biochim Biophys Acta 1761: 121–128
17. Murphy RC, James PF, McAnoy AM, Krank J, Duchoslav E, Barkley RM (2007) Detection of the abundance of diacylglycerol and triacylglycerol molecular species in cells using neutral loss mass spectrometry. Anal Biochem 366:59–70
18. Duffin KL, Henion JD, Shieh JJ (1991) Electrospray and tandem mass spectrometric characterization of acylglycerol mixtures that are dissolved in nonpolar solvents. Anal Chem 63:1781–1788
19. Murphy RC, Fiedler J, Hevko J (2001) Analysis of nonvolatile lipids by mass spectrometry. Chem Rev 101:479–526
20. Bligh EG, Dyer WJ (1959) A rapid method of total lipid extraction and purification. Can J Biochem Physiol 37:911–917

21. Duffin K, Obukowicz M, Raz A, Shieh JJ (2000) Electrospray/tandem mass spectrometry for quantitative analysis of lipid remodeling in essential fatty acid deficient mice. Anal Biochem 279:179–188
22. Kalo P, Kuuranne T (2001) Analysis of free and esterified sterols in fats and oils by flash chromatography, gas chromatography and electrospray tandem mass spectrometry. J Chromatogr A 935:237–248
23. Fang L, Harkewicz R, Hartvigsen K, Wiesner P, Choi S-H, Almazan F, Pattison J, Deer E, Sayaphupha T, Dennis EA, Witztum JL, Tsimikas S, Miller YI (2010) Oxidized cholesteryl esters and phospholipids in Zebrafish larvae fed a high cholesterol diet. J Biol Chem 285:32343–32351
24. Li YL, Su X, Stahl PD, Gross ML (2007) Quantification of diacylglycerol molecular species in biological samples by electrospray ionization mass spectrometry after one-step derivatization. Anal Chem 79:1569–1574
25. Wewer V, Dombrink I, vom Dorp K, Doermann P (2011) Quantification of sterol lipids in plants by quadrupole time of flight mass spectrometry. J Lipid Res 52:1039–1054
26. Bowden JA, Albert CJ, Barnaby OS, Ford DA (2011) Analysis of cholesteryl esters and diacylglycerols using lithiated adducts and electrospray ionization-tandem mass spectrometry. Anal Biochem 417:202–210
27. Han X, Gross RW (2001) Quantitative analysis and molecular species fingerprinting of triacylglyceride molecular species directly from lipid extracts of biological samples by electrospray ionization tandem mass spectrometry. Anal Biochem 295:88–100
28. Wijendran V, Lawrence P, Diau G-Y, Boehm G, Nathanielsz PW, Brenna JT (2002) Significant utilization of dietary arachidonic acid is for brain adrenic acid in baboon neonates. J Lipid Res 43:762–767
29. Cheng B, Kowal J (1994) Analysis of adrenal cholesteryl esters by reversed phase high performance liquid chromatography. J Lipid Res 35:1115–1121
30. German JB (1999) Food processing and lipid oxidation. Adv Exp Med Biol 459:23–50

sample, for example oleic acid (w/w) [1]. The majority of standard methods proposed by organizations such as the American Oil Chemists Society (AOCS) [2], international Union of Pure and Applied Chemistry (IUPAC) [3] etc., are based on acid–base titration. These methods are time consuming, laborious, have relatively high detection limits and are far from being fully automated [4, 5]. Another shortcoming of the standard methods is the use of toxic solvents, which is not only responsible for increasing the cost of the analysis but also represents a source of potential health risks and environmental pollution [6].

Over the last decade, several methods have been proposed for determining FFA in oils in order to overcome the drawbacks of the official methods. The instrumental determination of individual FFA is carried out usually by gas chromatography (GC), high performance liquid chromatography (HPLC) or capillary electrophoresis (CE), where the sample is subjected to pre-treatments such as liquid–liquid extraction (LLE) or solid-phase extraction and derivatization [7, 8]. Such treatments are necessary either to increase the volatility of the analytes for GC or improve the sensitivity of analytes for HPLC and CE methods.

Recently, Fourier transform infrared (FT-IR) spectroscopy has attracted interest as a method for the determination of FFA in edible oils [9, 10]. However, there are drawbacks to this method. Ismail et al. [11] also proposed a FT-IR method requiring high sample volumes and does not provide the level of speed necessary. Here the main limiting factor is that edible oils have high viscosity.

In recent years, flow injection analysis (FIA) has found wide application as a tool for routine analysis in several fields, including edible oils [1]. The advantages of flow techniques, such as versatility, simplicity and low cost make these procedures excellent choices for the analysis of edible oils because it becomes possible to perform analyses in an organic medium with low liquid waste, in a short period of time and with very high precision [7]. However, few flow injection (FI) methods for the analysis of edible oils and fats have been published. This situation is due to (i) the physical properties of oil samples, (ii) the difficulty of the operation in non-aqueous media, and (iii) difficulty in providing repeatability.

Velasco-Arjona and co-workers [12] described a fully automated robotic method for the determination of acid value (AV) based on the extraction of free fatty acids from olive oil samples into an immiscible phase and subsequent AV determination by monitoring the pH of the sample reagent emulsion using a combined glass-calomel electrode. The method consumes high reagent and sample volumes and requires a long time to complete the analysis, so the use of this method is not recommended. The method proposed by Ekstrom [13] was based on copper soap colorimetry, using one extraction to achieve a reaction of the FFA with copper ions and another to recover copper ions that are subsequently monitored. This method was also modified by others [14, 15] using a phase or membrane separator, and channels and oil samples were injected after being pre-diluted and homogenized with toluene. Nouros et al. [16] suggested an automated FI titrimetric method for the determination of olive oil acidity.

In the present study using a modified HPLC system, a novel method was developed using FIA for the assessment of FFA in corn and sunflower oil samples. An olive oil aliquot was injected into a carrier stream of *n*-propanol containing KOH and a phenolphthalein indicator, and the absorbance of the resulting mixture was monitored continuously. Quantification was performed by taking peak areas measurements into account. The sampling rate was 30–100 h^{-1}, while *n*-propanol consumption was 3–7 mL per run. Almost all of the above-mentioned methods used for FFA determination require some pre-treatments such as dilution with appropriate solvents.

Experimental Section

Samples, Chemicals and Reagents

The chemicals and solvents of chromatographic purity were obtained from Merck (Darmstadt, Germany) and Sigma (St. Louis, USA). Edible oil samples were obtained from the Helvacizade Food Company, manufacturer of edible vegetable oils in Turkey. Oil samples were stored at 4 °C in brown glass bottles and were brought to room temperature before use.

Spectrophotometric Analysis

Initial analyses were performed using a UV detector in order to determine the appropriate wavelength. For this purpose, potassium hydroxide (KOH) and phenolphthalein (PHP) in different concentrations were prepared by dissolving both in *n*-propanol.

Standard Method Analysis

To determine the FFA content in oil samples, the AOCS standard method (Ca-5a-40) was used. According to this method, 0.1000 or 0.2500 N NaOH solutions were used as titrants, and potassium acid phthalate was also used as the primer standard substance to adjust the titrant concentration. The titrant solutions were dissolved in 95% ethyl alcohol, and the indicator solutions (1% PHP) were prepared by dissolving 1 g phenolphthalein in 100 mL 95% ethyl alcohol.

Flow Injection Analysis (FIA)

For the FFA content determination, *n*-propanol was the carrier phase, and KOH and PHP solutions were used as reagents at different concentrations.

Working References Materials (WRM)

Working reference materials supplied by Helvacizade Food Company (Konya, Turkey) were used in the FIA analysis. The contents of FFA% in four sunflower reference oils were 0.07, 0.40, 0.74, 1.40 while in eight corn reference oils the levels of FFA% were 0.09, 0.25, 0.50, 0.75, 1.00, 1.50, 2.00 and 2.42.

Modified HPLC System for FIA Analysis

FIA experiments were performed by using a modified HPLC system (Agilent Technologies Inc., USA) consisting of a G1379A model degasser (B), G1311A model quaternary pump (D), a 7725i model Rheodyne manual injector system with a 20-μL loop (E) and a G1314A model variable wavelength UV detector (I). The temperature of the column was controlled by a G1316A model thermostatted column compartment (F). Data were recorded by a Chemstation 2001 data processor. In addition, a 2-position/6-port selection valve (H) and different reaction coils (G) made in our laboratory from PEEK tubing were adapted into the system. The tubing and fittings used to create the system were obtained from Agilent. Reaction coils are flexible and easy to cut into the desired lengths for the desired degree of reaction. The properties of these coils are given in Table 1. One of the other coils, labeled K in the system, was used to provide the connections. When required for chromatographic analysis, this part of the connection was also used. Coils, shown by the J and K labels in the system, were adapted for later analysis of other oil characteristics. In this study, only G was activated for the formation of the reaction. The single-line manifold system used for determining FFA% content in oil samples is shown in Fig. 1.

Concept of Flow Injection (FI) Analysis for FFA Determination

An alkaline solution, including KOH and PHP, was prepared by dissolution in *n*-propanol and was used as a carrier phase. The method is based on monitoring of changes in the absorbance of the indicators from the basic–acidic–basic form (pink–colorless–pink for PHP) as a result of neutralization of the KOH in the carrier phase by the injected FFA sample. Since the basic properties of the carrier phase decreased in a short time frame, a negative peak occurred. This decrease in the absorbance is proportional to the content of FFA%. Due to the continuous flow of the carrier phase, the absorbance value was increased to the initial absorbance value after a short duration. The negative peak height (h), half-peak width (w) and the area under the peak (A) were utilized to determine the FFA% of the oil samples. The data obtained from the peaks are proportional to the amount of FFA% in the oil samples; the greater the FFA% content in the sample, the more the peak absorbance decreases.

Table 1 Properties of reaction coils used in the FFA% determination tests

	Number of turns of the spiral	Coil length (l) (cm)	Inner diameter of coil (id) (mm)	Inner diameter of tube wrapped of coil (ID) (cm)
Coil 1	74	174	0.50	0.5
Coil 2	42	71	0.50	0.3
Coil 3	19	128	0.25	1.5

Optimizing Experimental Parameters

FIA parameters such as the flow rate of the carrier phase, length, geometry and inner diameter of the reaction coils, and the reagent concentration were optimized. The optimization experiments were performed with sunflower oils with FFA% values ranging between 0.07 and 1.40 and corn oils with FFA% values ranging between 0.09 and 2.42. The analysis was repeated at least five times. The carrier phase flow rate optimization studies were carried out using five different flow rates (0.1, 0.5, 1.0, 2.0, 3.0 mL min^{-1}). In the reaction coil optimization experiments, the effect of three reaction coils (tubing) with different inner diameter, length and geometry was investigated. In the reagent concentration optimization experiments, the effects of the base (KOH) and indicator (PHP) concentrations in the carrier phase were investigated. Reagent concentrations are given in Supplemental Table 1.

Generally, optimization studies investigating the effects of different parameter values on the FFA% experiments were conducted in parallel in order to give a better determination of the cumulative effects of the parameters.

Validating the FIA Method for FFA% Determination

In order to determine the suitability of the FIA method developed for FFA% determination, method validation studies were performed by measuring basic parameters such as precision, accuracy, linear region, LOD and LOQ.

Comparing Standard Methods with the Proposed FIA Method

In order to check the performance of the FIA method, the developed method was applied to real samples and

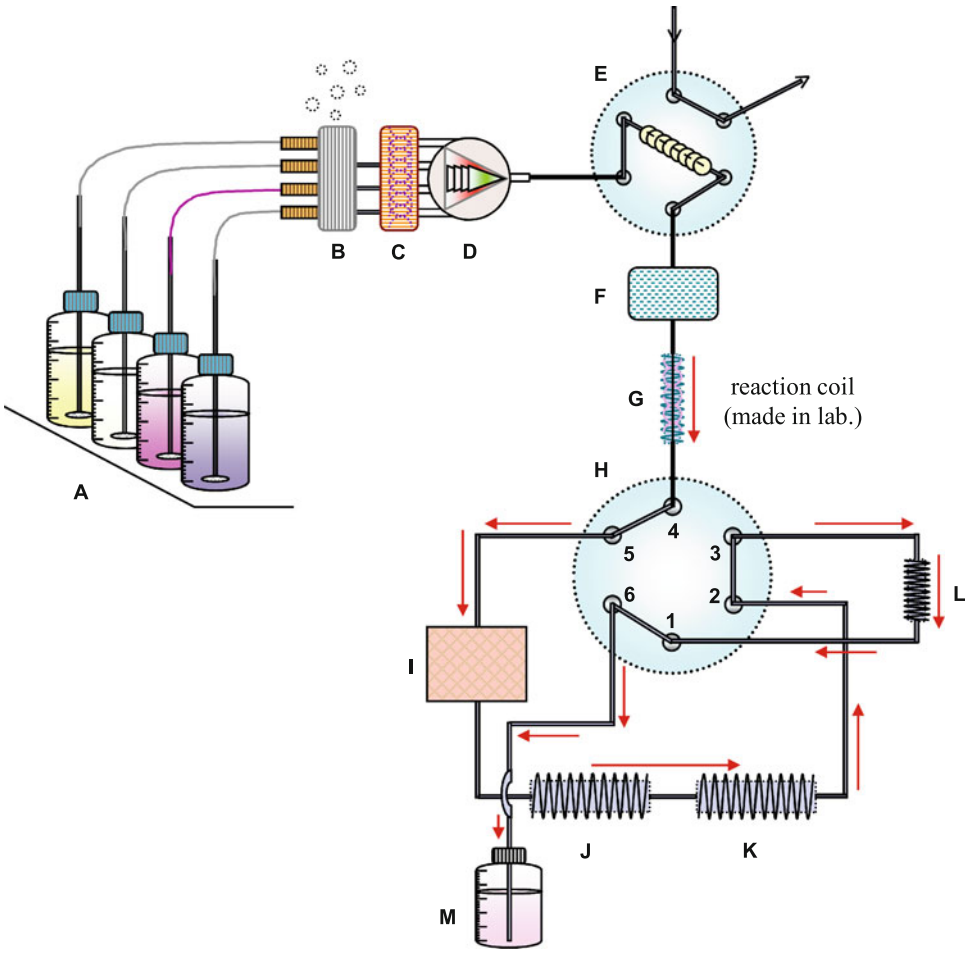

Fig. 1 Modified HPLC system with manual injection for determining FFA% *A* carrier/solvent tray, *B* degasser unit, *C* mixer, *D* quaternary pump, *E* manual injection port, *F* thermostatted column oven, *G* reaction coil (id: 0.25 mm, ID: 1.5 cm), *H* 2-position/6-port selection valve, *I* UV detector, *J–K* 1 mL stainless steel loop (id: 0.76 mm), *L* 50-μL stainless steel loop (id: 0.51 mm), *M* waste

reference material samples of sunflower and corn oils. For real samples, the results were cross checked by the standard AOCS titration method. Data obtained with the two methods were compared using statistical *t* and *F* tests. The *t* test comparing the average values of data groups and the *F* test comparing the variance values of data groups was used for comparison of the methods. The tests were performed using XLSTAT 2010 and statistiXL programs. These tests, applied in accordance with null and alternative hypotheses, were performed as double-sided with a 95% confidence level ($p = 0.05$), and calculated *t* and *F* values were compared with critical *t* and *F* values.

Results and Discussion

Spectrophotometric Analysis

Spectrum scans were collected with a UV detector over a 190–600 nm range. A wavelength of 580 nm showed maximum absorbance and was thus accepted as the appropriate wavelength for FFA measurements.

Flow Injection (FI) Analysis for FFA%

Experiments were carried out with the flow injection system protected from the atmosphere and light, both very important in terms of the reliability of the analysis results. For example, carbon dioxide in the air affects the indicator function due to its acidic properties. Light also triggers the degradation reactions of the oil and may increase the amount of FFA. *n*-Propanol containing the reagent KOH, and indicator (PHP), were used as the carrier phase, and 20-μL oil samples not subjected to any pre-processing were injected into the FIA system. The continuously flowing mobile phase had high absorbance due to the characteristic property of the indicator in basic media. The injected sample reacts with the base (KOH) in the carrier phase and the pH of the carrier phase is lowered for a short period of time. After completion of free fatty acid reactions with the equivalent amounts of base, absorbance returned to the initial value due to the constant stream of fresh carrier phase. The transitory absorbance change presents as a negative peak and is used to calculate the FFA% content since peak intensity increases negatively in proportion to the increased FFA% content.

Optimizing Carrier Flow Rate

The carrier phase flow rate is related directly to the formation of the desired reaction, peak shape, peak size and peak resolution. For this reason, the flow rate of the carrier phase was usually the first parameter optimized in both chromatography and FIA experiments. The peak shape measures the reaction between the analyte and a carrier or reagent. When the desired reaction did not occur, rectangular rather than Gaussian curve-shaped peaks were observed. Although Gaussian-shaped peaks are preferable in chromatography and flow injection analysis, rectangular peaks are also used effectively. Flow rate, peak shape, size and differences in peak absorbance were optimized. After carrying out optimization experiments at five flow rates (0.1, 0.5, 1.0, 2.0, 3.0 mL min^{-1}), the appropriate value for quantitation of FFA was determined to be 2.0 mL min^{-1}. With flow rates lower than 2.0 mL min^{-1}, the desired reaction did not occur and the resultant peaks were spread out too far. When the flow rate was >2.0 mL min^{-1}, the area and height of the obtained peaks decreased. Peaks obtained from the flow rate optimization experiments for each reaction cell are shown in Figs. 2, 3. FFA versus flow rate graphs showed that the highest correlation between measured and reference FFA contents, regardless of oil properties, was obtained with reaction coil 3, the flow rate was 2.0 mL min^{-1} (Table 2).

Optimizing Reaction Coils

The natural properties of oils, especially their viscosity, require that reaction conditions are set up very precisely. For this reason, the type of FIA reaction coils used is very important. Experiments designed to select the best reaction coil were done with various flexible tubes wrapped in a spiral on a cylindrical support. Turbulence associated with a spiral structure accelerated formation of the desired reaction and facilitated the desired degree of dispersion. Also, the internal volume of the tube (reaction coil), the inner diameter of material wrapped around the tube are extremely important factors for selecting the reaction coil. The results revealed that for the reaction to occur to the desired extent, the ratio of the tube's inner diameter (id) to wrapped material's diameter (ID) should be approximately

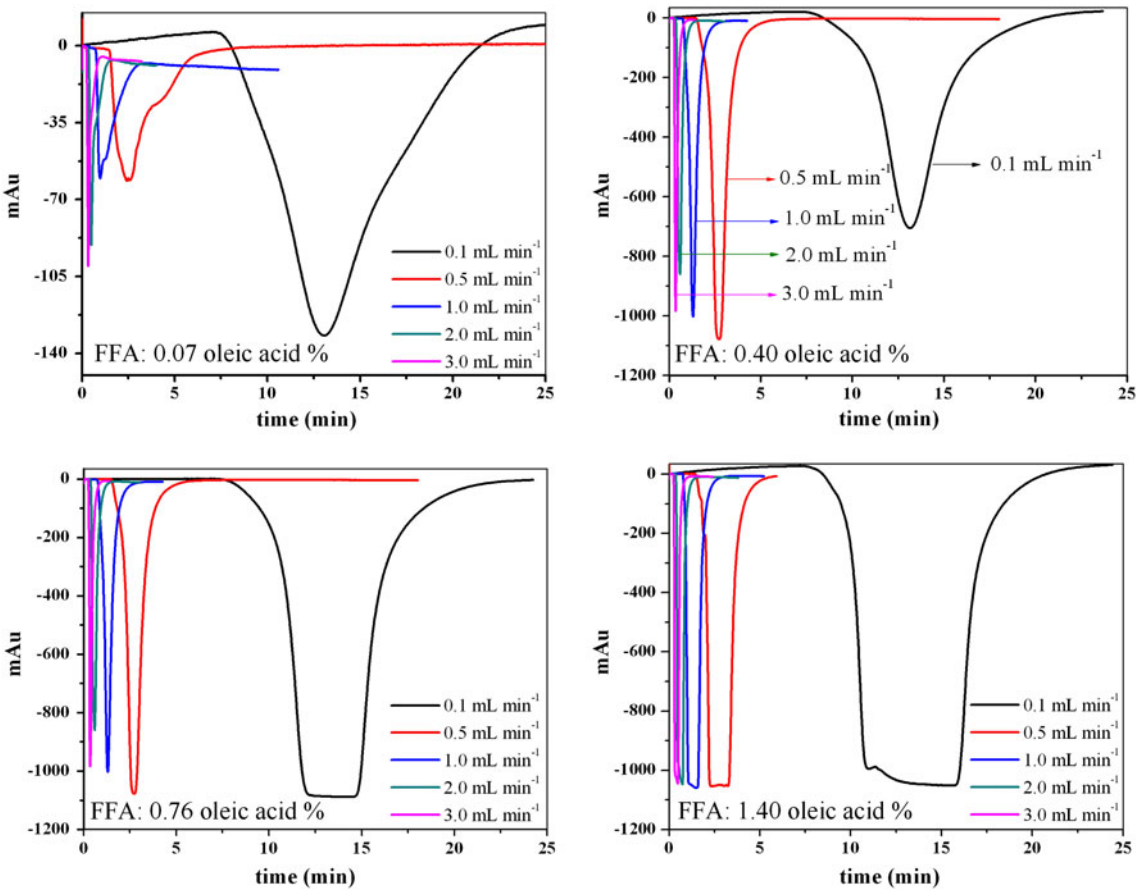

Fig. 2 Peaks obtained from flow rate optimization experiments for sunflower oil samples using coil 1. *Wavelength:* 580 nm

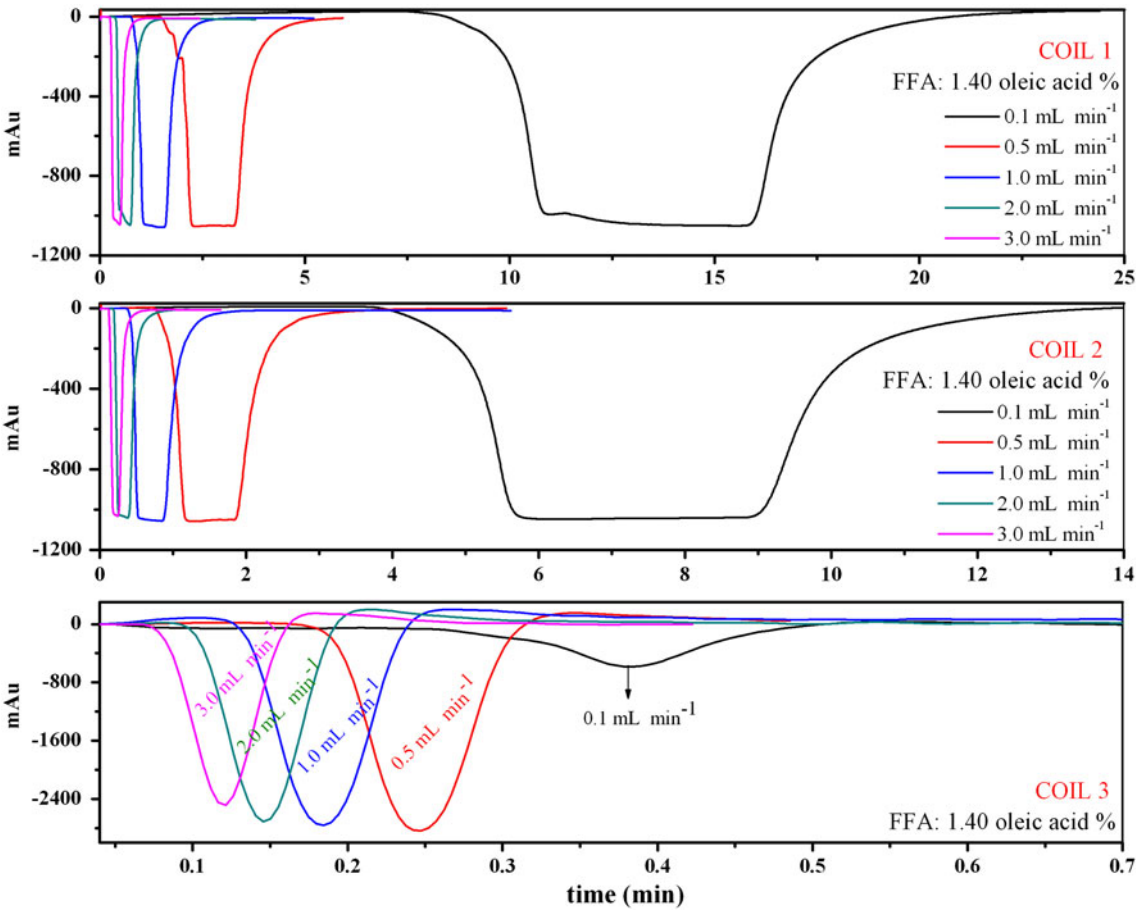

Fig. 3 Peaks obtained from flow rate optimization studies for sunflower oil samples with different reaction coils. *wavelength:* 580 nm

Table 2 Correlation coefficients obtained from Area-FFA% graphs plotted for flow rate and reaction cell studies

	Correlation coefficients of FFA%—flow rate graphs[a]		
Flow rate (mL min^{-1})	Coil 1	Coil 2	Coil 3
0.1	$R^2 = 0.951$	$R^2 = 0.960$	$R^2 = 0.995$
0.5	$R^2 = 0.995$	$R^2 = 0.867$	$R^2 = 0.998$
1.0	$R^2 = 0.989$	$R^2 = 0.859$	$R^2 = 0.997$
2.0	$R^2 = 0.983$	$R^2 = 0.830$	$R^2 = 0.999$
3.0	$R^2 = 0.988$	$R^2 = 0.828$	$R^2 = 0.998$

[a] The experiments were performed using sunflower oils with FFA% values ranging between 0.07 and 1.40 and corn oils with FFA% values ranging between 0.09 and 2.42

1/10. With these conditions, sufficient turbulence can occur and dispersion of the substances can be achieved. Another important factor is the length of the coil. Data obtained with three reaction coils with different lengths and internal diameters, data obtained from these studies show that coil 3, having 19 turns of the spiral, was the most appropriate cell for determining FFA% in different oils (Fig. 3 and Table 2). When coil 1 and coil 2 were used as reaction cells, the peaks necessary for evaluating the results could not be obtained. Namely, oils containing high amounts of FFA did not react sufficiently with the base in the carrier phase. Oils with low amounts of FFA gave distorted peaks due to the length of the reaction cells (Fig. 2).

Optimizing Reagent Concentration

Reagent concentration studies performed with corn oil samples, with FFA% values ranging from 0.09 to 2.42; show that the use of KOH and PHP as reagent and indicator is extremely important to determine the FFA% by FIA. Reagent concentrations used in the experiments must clearly demonstrate peak reductions with increasing FFA content. Reagent concentration studies were carried out with coil 3 at the selected flow rate, 2.0 mL min^{-1}. Many things were taken into consideration when evaluating the results, such as peak separation, symmetry, slope and regression coefficient values of measured FFA% values across samples. Reagent concentration optimization studies were performed using various solutions, with base

concentrations from 2.12×10^{-3} M to 5.00×10^{-3} M and indicator concentrations between 10.63×10^{-5} M and 25.00×10^{-5} M. As can be seen from the peaks plotted for different reagents, best results were obtained when Reagent 2 ($\sim 2.50 \times 10^{-3}$ M KOH and 25.00×10^{-5} M PHP) was used as the reagent (Fig. 4).

Validating the FIA Method for FFA% Determination

Method validation studies were performed by examining basic assay parameters such as precision, accuracy, linear region and dynamic range. The limit of detection (LOD) and the limit of quantification (LOQ) were found from the results of at least five repeat experiments. In order to test the accuracy of the FIA method for the determination of FFA%, three samples of corn and sunflower oil within the range of the calibration curve were analyzed. Accuracy of the FIA method was expressed as relative error (E_r), calculated on the basis of the mean (X_i) and actual values (X_t) of the FFA obtained from five repeated experiments. The mean measured values obtained from the studies were within ±5% of the actual value, thus proving the accuracy of the FIA method. Repeatability of the experiments was determined by carrying out repeat tests in two stages, including intra-day and inter-day tests. Repeatability was measured as the standard deviation (s), relative standard deviation (RSD), variance (s^2) and coefficient of variation (CV), and confidence intervals ($p = 0.05$) for each series (Supplemental Table 2). Regression analysis was carried out by means of a one-way ANOVA analysis and statistical descriptions for the linear range of FIA were obtained (Supplemental Table 3). The scatter plot with fit and residual plot obtained from ANOVA is also shown in Supplemental Fig. 1. The linear measurement ranges for the sunflower and corn oils used in the FFA% analysis were determined to be 0.07–1.40 and 0.09–1.50, respectively. In the calculation of LOD and LOQ, calibration graphs (Area-FFA%) were used, with points plotted for each oil sample. The standard deviations of the areas and FFA% values were calculated by using the slope and intercept of the graph and coefficient of variation (CV) values. FFA values, corresponding to three and ten times the calculated standard deviation value, were regarded as LOD ($3 \times s$) and LOQ ($10 \times s$), respectively. Accordingly, LOD values for corn and sunflower oils were calculated as 7.53×10^{-4} and 7.11×10^{-4} oleic acid %, and LOQ values were calculated as 2.28×10^{-3} and 2.23×10^{-3} oleic acid %, respectively.

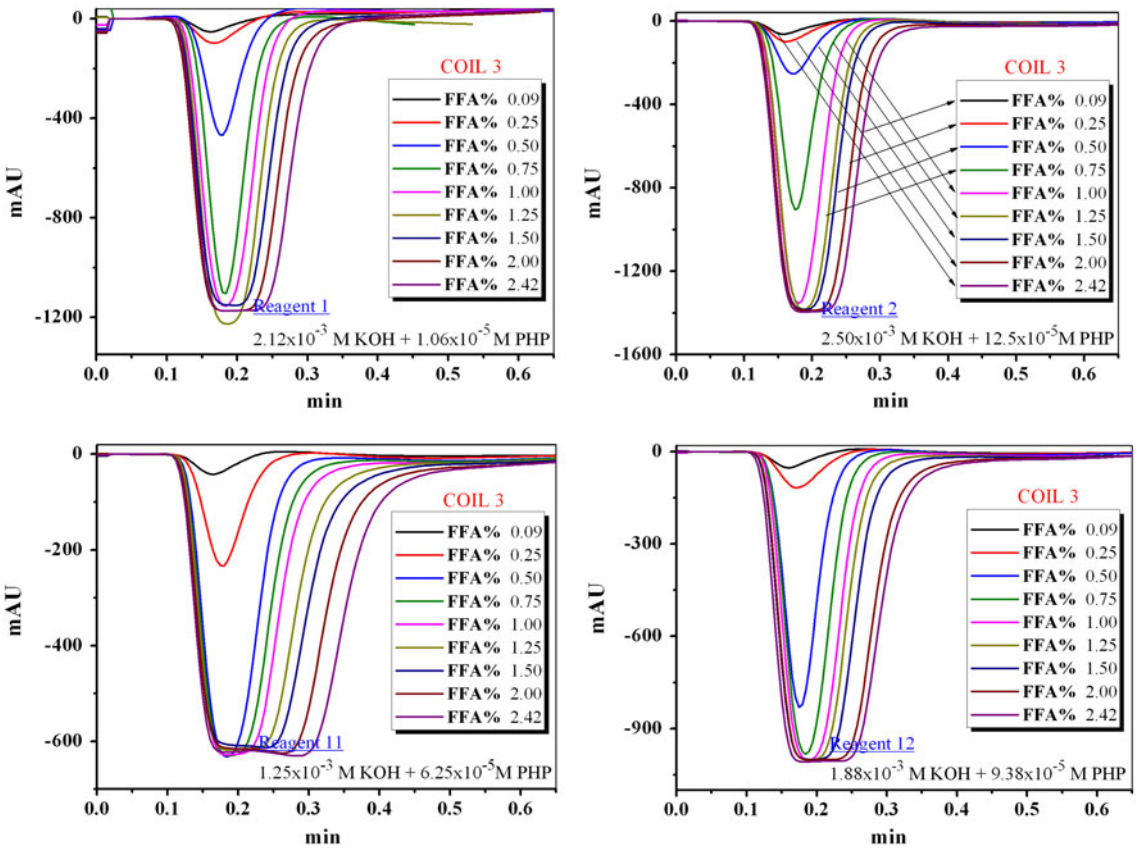

Fig. 4 Peaks obtained from the optimization of reagent concentration studies for corn oil samples

Table 3 Comparison of proposed FIA method with the standard AOCS (Ca-5a-40) method using working reference materials and real oil samples

	By proposed FIA method ($N = 5$)	By standard method ($N = 5$)	
Analysis of oil samples with different FFA% values (FFA% ± s)			
Corn Oil (FFA%: 0.75 ± 0.04)			
$\overline{X}1$: 0.75	0.75	0.74	$\overline{X}1$: 0.75
s: 0.02	0.78	0.81	s: 0.04
	0.73	0.76	
	0.76	0.73	
	0.75	0.71	
Corn oil samples			
Correlation for the two methods ($R^2 = 0.996$)			
WRM oil samples			
1	0.09 ± 0.01	0.09 ± 0.02	
2	0.24 ± 0.01	0.25 ± 0.02	
3	0.49 ± 0.02	0.50 ± 0.03	
4	0.75 ± 0.02	0.75 ± 0.04	
5	1.02 ± 0.03	1.00 ± 0.04	
6	1.49 ± 0.03	1.50 ± 0.04	
7	1.99 ± 0.03	2.00 ± 0.07	
8	1.48 ± 0.02	2.42 ± 0.07	
Real oil samples			$t_{calculated} = 0.09 < t_{critical}$ 2.12
1	0.12 ± 0.02	0.15 ± 0.04	$F_{calculated} = 0.97 < F_{critical} = 4.43$
2	0.25 ± 0.02	0.23 ± 0.06	
3	0.38 ± 0.02	0.42 ± 0.07	
4	0.60 ± 0.03	0.58 ± 0.08	
5	1.06 ± 0.04	1.13 ± 0.11	
6	1.45 ± 0.05	1.60 ± 0.12	
7	1.69 ± 0.05	1.72 ± 0.11	
8	1.80 ± 0.06	1.81 ± 0.13	
9	2.12 ± 0.06	2.13 ± 0.13	
10	2.42 ± 0.08	2.45 ± 0.13	
Sunflower oil samples			
Correlation for the two methods ($R^2 = 0.994$)			
WRM oil samples			
1	0.06 ± 0.01	0.07 ± 0.01	
2	0.41 ± 0.01	0.40 ± 0.02	
3	0.74 ± 0.02	0.74 ± 0.04	
4	1.42 ± 0.01	1.40 ± 0.04	
Real oil samples			$t_{calculated} = 0.08 < t_{critical}$ 2.12
1	0.07 ± 0.01	0.09 ± 0.01	$F_{calculated} = 0.94 < F_{critical} = 4.43$
2	0.15 ± 0.01	0.14 ± 0.01	
3	0.29 ± 0.01	0.20 ± 0.02	
4	0.46 ± 0.01	0.48 ± 0.02	
5	0.58 ± 0.02	0.55 ± 0.03	
6	1.27 ± 0.02	1.30 ± 0.05	
7	0.83 ± 0.02	0.80 ± 0.03	
8	0.97 ± 0.02	0.98 ± 0.04	
9	1.26 ± 0.03	1.24 ± 0.06	
10	1.35 ± 0.03	1.36 ± 0.06	

Evaluating the FIA Method on Working References Materials

The results of the method were also verified on WRM of sunflower and corn oil. Our developed method gave satisfactory results which were comparable to the labelled FFA contents. Therefore, a wide range of FFA contents was covered by analyzing both real samples obtained from industries and the WRM.

Comparing the Standard Method with the Proposed FIA Method

Performance of our developed FIA method was compared statistically with the standard method. Double-sided statistical tests conducted in accordance with Null and alternative hypotheses were found to have a 95% confidence level ($p = 0.05$). The data calculated separately for corn and sunflower oil samples showed that the t and F values calculated from experimental studies were smaller than the critical t and F values ($t_{\text{calculated}} = 0.09 < t_{\text{critical}}$ 2.12 and $F_{\text{calculated}} = 0.97 < F_{\text{critical}} = 4.43$ for corn oils and $t_{\text{calculated}} = 0.08 < t_{\text{critical}}$ 2.12 and $F_{\text{calculated}} = 0.94 < F_{\text{critical}} = 4.43$ for sunflower oils). Consequently, it is very clear from Table 3 that there is no significant difference between the data obtained by the FIA method and the standard method and there is a good correlation between the two methods for both oils ($R^2 = 0.996$ for corn oil and $R^2 = 0.994$ for sunflower oil).

Conclusions

The proposed method was applied successfully to the determination of FFA% content in corn and sunflower oil samples. This novel single-line FIA system is capable of performing many additional important oil analyses such as peroxide value, anisidine value, and iodine value. The developed method, based on a continuous-flow system with manual injection, provides an alternative procedure for quality control of FFA in edible oils compared to the standard reference method. The proposed FIA method requires only 1 ml *n*-propanol, 20 μL of oil sample per analysis and permits the analysis of 120 samples per hour. The superiority of the FIA method presented here is evident in comparison to the total amount of solvent and sample consumed by the standard method (~10 g of oil sample, 50–100 mL ethanol or diethyl ether). Furthermore, the results obtained with the proposed FIA method are highly compatible with those obtained with the standard method ($R^2 = 0.996$ for corn oil and $R^2 = 0.994$ for sunflower oil). Another important advantage of the proposed method is that the oil samples can be injected directly into the system without any pre-treatment. Since our method is simple, accurate, precise, rugged, rapid, cost effective and environmentally friendly, it is directly and easily applicable to other vegetable oils. The procedure is therefore a suitable alternative to the tedious classical method for FFA% determination, and can potentially eliminate more sources of experimental errors. We believe that the proposed method has great potential for a variety of on-line measurements such as peroxide value, anisidine value, and iodine value determination in edible oils. We also suggest that auto injector systems should be examined for their potential to automate FFA analysis.

Acknowledgments This study, a part of Ph.D. thesis entitled "*Improvement of Edible Oil Analysis Methods by Flow Injection Systems*" was supported by Selcuk University Coordination of Scientific Research with SU-BAP 08-101029 project numbers. The authors wish to thank the Principal of Selcuk University and Scientific Research Projects Coordination.

Conflict of interest The authors declare that there is no conflict of interest.

References

1. Thomaidis NS, Georgiou CA (1999) Edible oil analysis by flow injection. Lab Autom Inf Manag 34:101–114
2. AOCS (1998) Official methods and recommended practices of the American oil chemists' society, 4th edn. AOCS Press, Champaign, IL
3. IUPAC (1992) Standard methods for the analysis of oils, fats and derivatives. In: International union of pure and applied chemistry, 1st Supplement to 7th edn. Blackwell Scientific Publications, Oxford
4. Bonastre A, Ors R, Peris M (2004) Advanced automation of a flow injection analysis system for quality control of olive oil through the use of a distributed expert system. Anal Chim Acta 506:189–195
5. Maskula S, Nyman J, Ivaska A (2000) Titration of strong and weak acids by sequential injection analysis technique. Talanta 52:91–99
6. Taljaard RE, van Staden JF (1998) Simultaneous determination of Cobalt(II) and Ni(II) in water and soil samples with sequential injection analysis. Anal Chim Acta 366:177–186
7. Saad B, Ling CW, Jab MS, Lim BP, Mohamad Ali AS, Wai WT, Saleh MI (2007) Determination of free fatty acids in palm oil samples using non-aqueous flow injection titrimetric method. Food Chem 102:1407–1414
8. Makahleh A, Saad B (2011) Flow injection determination of free fatty acids in vegetable oils using capacitively coupled contactless conductivity detection. Anal Chim Acta doi:10.1016/j.aca.2011.03.033
9. Al-Alawi A, van de Voort FR, Sedman J, Ghetler A (2006) Automated FTIR analysis of free fatty acids or moisture in edible oils. J Lab Autom doi:10.1016/j.jala.2005.11.002
10. Canada MJA, Medina AR, Lendl B (2001) Determination of free fatty acids in edible oils by continuous-flow analysis with FT-IR spectroscopic detection. Appl Spectrosc 55(3):356–360

11. Ismail AA, van de Voort FR, Emo G, Sedman J (1993) Rapid quantitative determination of free fatty acids in fats and oils by Fourier transform infrared spectroscopy. J Am Oil Chem Soc 70:335–341
12. Velasco-Arjona A, Luque de Castro MD (1998) A fully robotic method for the determination of acid values in olive oil without titration. J Am Oil Chem Soc 75(12):1849–1853
13. Ekstrom LG (1981) An automatized method for determination of free fatty acids. J Am Oil Chem Soc 58(10):935–938
14. Canham JS, Pacey GE (1987) Automated free fatty acid determination using flow injection analysis solvent extractions. J Am Oil Chem Soc 64(7):1004–1007
15. Puchades R, Suescun A, Maquieira A (1994) Determination of free fatty acids in foods by flow injection. J Sci Food Agr 66(4):473–478
16. Nouros PG, Georgiou CA, Polissiou MG (1997) Automated flow injection spectrophotometric non-aqueous titrimetric determination of the free fatty acid content of olive oil. Anal Chim Acta 351:291–297